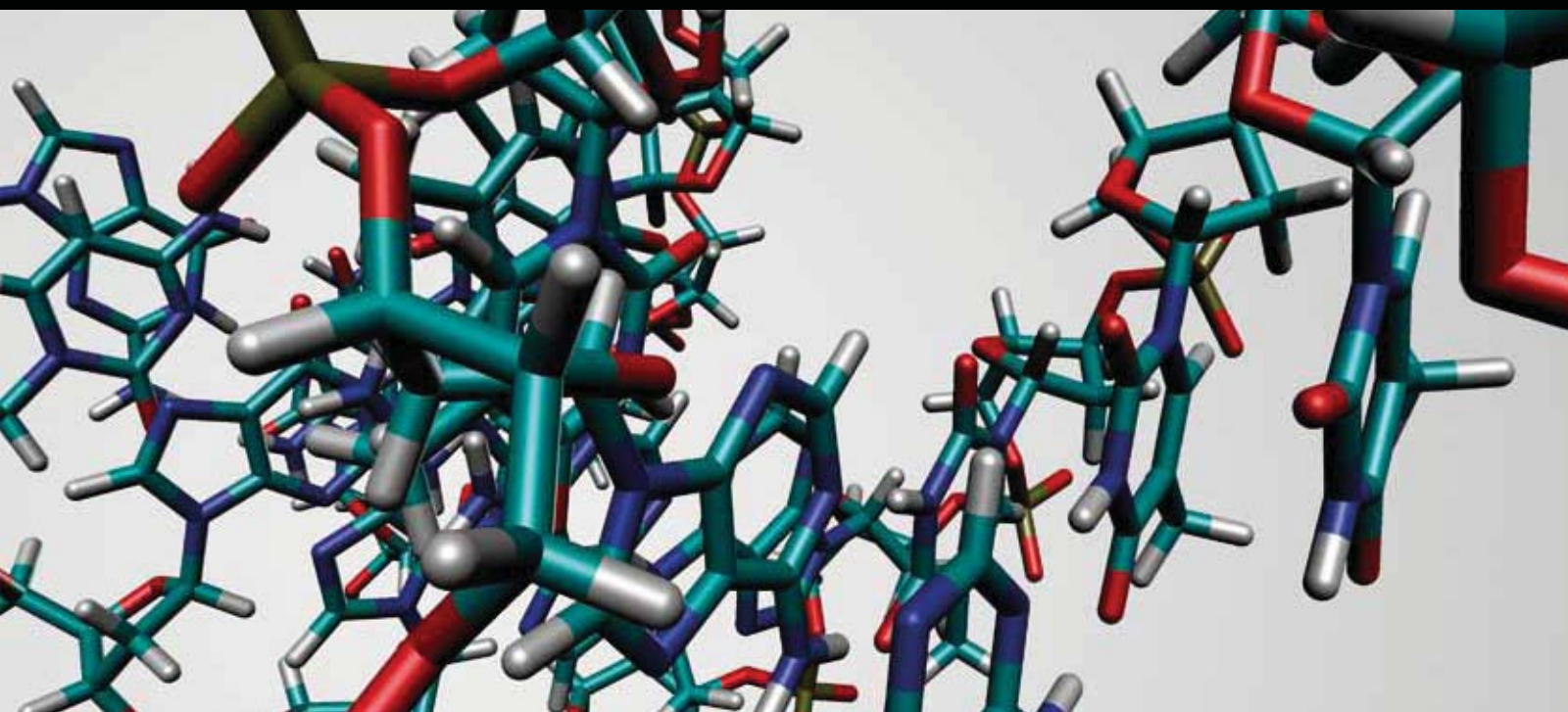


# DNA Damage, Mutagenesis, and DNA Repair

Guest Editors: Ashis Basu, Suse Broyde, Shigenori Iwai, and Caroline Kisker





---

# **DNA Damage, Mutagenesis, and DNA Repair**

Journal of Nucleic Acids

---

## **DNA Damage, Mutagenesis, and DNA Repair**

Guest Editors: Ashis Basu, Suse Broyde, Shigenori Iwai,  
and Caroline Kisker



---

Copyright © 2010 sage-Hindawi Publishing Corporation. All rights reserved.

This is a special issue published in volume 2010 of "Journal of Nucleic Acids." All articles are open access articles distributed under the Creative Commons Attribution License, which permits unrestricted use, distribution, and reproduction in any medium, provided the original work is properly cited.

## Editorial Board

Luigi A. Agrofoglio, France  
Hiroyuki Asanuma, Japan  
Ashis Basu, USA  
Ben Berkhout, The Netherlands  
Ann L. Beyer, USA  
Christiane Branlant, France  
Emery H. Bresnick, USA  
Tom Brown, UK  
Janusz M. Bujnicki, Poland  
Jyoti Chattopadhyaya, Sweden  
Grigory Dianov, UK  
Aidan Doherty, UK  
Joachim Engels, Germany

Ramón Eritja, Spain  
Marina Gottikh, Russia  
John A. Hartley, UK  
Roland K. Hartmann, Germany  
Tapas K Hazra, USA  
Hyouta Himeno, Japan  
Robert Hudson, Canada  
Shigenori Iwai, Japan  
B. H. Kim, Korea  
Jørgen Kjems, Denmark  
Xingguo Liang, Japan  
Luis A. Marky, USA  
Atsushi Maruyama, Japan

P. E. Nielsen, Germany  
Satoshi Obika, Japan  
Tatiana S. Oretskaya, Russia  
Tobias Restle, Germany  
Mitsuo Sekine, Japan  
Jacek Stawinski, Sweden  
Dmitry A. Stetsenko, UK  
Hiroshi Sugiyama, Japan  
Zucaï Suo, USA  
Akio Takenaka, Japan  
Yitzhak Tor, USA  
Dmitry Veprintsev, UK  
Birte Vester, Denmark

# Contents

**DNA Damage, Mutagenesis, and DNA Repair**, Ashis Basu, Suse Broyde, Shigenori Iwai, and Caroline Kisker  
Volume 2010, Article ID 182894, 1 pages

**From DNA Radiation Damage to Cell Death: Theoretical Approaches**, Francesca Ballarini  
Volume 2010, Article ID 350608, 8 pages

**The Biological and Metabolic Fates of Endogenous DNA Damage Products**, Simon Wan Chan and Peter C. Dedon  
Volume 2010, Article ID 929047, 13 pages

**DNA-Destabilizing Agents as an Alternative Approach for Targeting DNA: Mechanisms of Action and Cellular Consequences**, Gaëlle Lenglet and Marie-Hélène David-Cordonnier  
Volume 2010, Article ID 290935, 17 pages

**Structural Determinants of Photoreactivity of Triplex Forming Oligonucleotides Conjugated to Psoralens**, Rajagopal Krishnan and Dennis H. Oh  
Volume 2010, Article ID 523498, 7 pages

**Differential Toxicity of DNA Adducts of Mitomycin C**, Jill Bargonetti, Elise Champeil, and Maria Tomasz  
Volume 2010, Article ID 698960, 6 pages

**Cellular Responses to Cisplatin-Induced DNA Damage**, Alakananda Basu and Soumya Krishnamurthy  
Volume 2010, Article ID 201367, 16 pages

**Intracellular DNA Damage by Lysine-Acetylene Conjugates**, Wang-Yong Yang, Qiang Cao, Catherine Callahan, Catalina Galvis, Qing-Xiang Sang, and Igor V. Alabugin  
Volume 2010, Article ID 931394, 6 pages

**Current Studies into the Genotoxic Effects of Nanomaterials**, Cheng-Teng Ng, Jasmine J. Li, Boon-Huat Bay, and Lin-Yue Lanry Yung  
Volume 2010, Article ID 947859, 12 pages

**Formation and Repair of Tobacco Carcinogen-Derived Bulky DNA Adducts**, Bo Hang  
Volume 2010, Article ID 709521, 29 pages

**Formation, Repair, and Genotoxic Properties of Bulky DNA Adducts Formed from Tobacco-Specific Nitrosamines**, Lisa A. Peterson  
Volume 2010, Article ID 284935, 11 pages

**Smoking, DNA Adducts and Number of Risk DNA Repair Alleles in Lung Cancer Cases, in Subjects with Benign Lung Diseases and in Controls**, Marco Peluso, Armelle Munnia, Sara Piro, Alessandra Armillis, Marcello Ceppi, Giuseppe Matullo, and Riccardo Puntoni  
Volume 2010, Article ID 386798, 7 pages

**Insights into the Structures of DNA Damaged by Hydroxyl Radical: Crystal Structures of DNA Duplexes Containing 5-Formyluracil**, Masaru Tsunoda, Takeshi Sakaue, Satoko Naito, Tomoko Sunami, Naoko Abe, Yoshihito Ueno, Akira Matsuda, and Akio Takénaka  
Volume 2010, Article ID 107289, 10 pages

**Elevated Levels of DNA Strand Breaks Induced by a Base Analog in the Human Cell Line with the P32T ITPA Variant**, Irina S.-R. Waisertreiger, Miriam R. Menezes, James Randazzo, and Youri I. Pavlov  
Volume 2010, Article ID 872180, 11 pages

**SOD1 Is Essential for the Viability of DT40 Cells and Nuclear SOD1 Functions as a Guardian of Genomic DNA**, Eri Inoue, Keizo Tano, Hanako Yoshii, Jun Nakamura, Shusuke Tada, Masami Watanabe, Masayuki Seki, and Takemi Enomoto  
Volume 2010, Article ID 795946, 11 pages

**Mus308 Processes Oxygen and Nitrogen Ethylation DNA Damage in Germ Cells of Drosophila**, Nancy Díaz-Valdés, Miguel A. Comendador, and L. María Sierra  
Volume 2010, Article ID 416364, 7 pages

**Is the Comet Assay a Sensitive Procedure for Detecting Genotoxicity?**, Satomi Kawaguchi, Takanori Nakamura, Ayumi Yamamoto, Gisho Honda, and Yu F. Sasaki  
Volume 2010, Article ID 541050, 8 pages

**Development of a Novel Fluorescence Assay Based on the Use of the Thrombin-Binding Aptamer for the Detection of O<sup>6</sup>-Alkylguanine-DNA Alkyltransferase Activity**, Maria Tintoré, Anna Aviñó, Federico M. Ruiz, Ramón Eritja, and Carme Fàbrega  
Volume 2010, Article ID 632041, 9 pages

**The Emerging Role of Telomerase Reverse Transcriptase in Mitochondrial DNA Metabolism**, Donna M. Gordon and Janine Hertzog Santos  
Volume 2010, Article ID 390791, 7 pages

**Targeting the OB-Folds of Replication Protein A with Small Molecules**, Victor J. Anciano Granadillo, Jennifer N. Earley, Sarah C. Shuck, Millie M. Georgiadis, Richard W. Fitch, and John J. Turchi  
Volume 2010, Article ID 304035, 11 pages

**The Roles of UmuD in Regulating Mutagenesis**, Jaylene N. Ollivierre, Jing Fang, and Penny J. Beuning  
Volume 2010, Article ID 947680, 12 pages

**Error-Prone Translesion DNA Synthesis by *Escherichia coli* DNA Polymerase IV (DinB) on Templates Containing 1,2-dihydro-2-oxoadenine**, Masaki Hori, Shin-Ichiro Yonekura, Takehiko Nohmi, Petr Gruz, Hiroshi Sugiyama, Shuji Yonei, and Qiu-Mei Zhang-Akiyama  
Volume 2010, Article ID 807579, 10 pages

**Architecture of Y-Family DNA Polymerases Relevant to Translesion DNA Synthesis as Revealed in Structural and Molecular Modeling Studies**, Sushil Chandani, Christopher Jacobs, and Edward L. Loechler  
Volume 2010, Article ID 784081, 20 pages

**Characterization of a Y-Family DNA Polymerase  $\epsilon$  from the Eukaryotic Thermophile *Alvinella pompejana***, Sayo Kashiwagi, Isao Kuraoka, Yoshie Fujiwara, Kenichi Hitomi, Quen J. Cheng, Jill O. Fuss, David S. Shin, Chikahide Masutani, John A. Tainer, Fumio Hanaoka, and Shigenori Iwai  
Volume 2010, Article ID 701472, 13 pages

**DNA Polymerase: Structural Homology, Conformational Dynamics, and the Effects of Carcinogenic DNA Adducts**, Richard G. Federley and Louis J. Romano  
Volume 2010, Article ID 457176, 15 pages

**Kinetic Approaches to Understanding the Mechanisms of Fidelity of the Herpes Simplex Virus Type 1 DNA Polymerase**, Yali Zhu, Jason Stroud, Liping Song, and Deborah S. Parris  
Volume 2010, Article ID 631595, 15 pages

**Mechanistic Studies with DNA Polymerases Reveal Complex Outcomes following Bypass of DNA Damage**, Robert L. Eoff, Jeong-Yun Choi, and F. Peter Guengerich  
Volume 2010, Article ID 830473, 12 pages

**Pre-Steady-State Kinetic Analysis of Truncated and Full-Length *Saccharomyces cerevisiae* DNA Polymerase  $\epsilon$** , Jessica A. Brown, Likui Zhang, Shanen M. Sherrer, John-Stephen Taylor, Peter M. J. Burgers, and Zucai Suo  
Volume 2010, Article ID 871939, 11 pages

**Replication Past the  $\gamma$ -Radiation-Induced Guanine-Thymine Cross-Link G[8,5-Me]T by Human and Yeast DNA Polymerase  $\eta$** , Paromita Raychaudhury and Ashis K. Basu  
Volume 2010, Article ID 101495, 10 pages

**The Role of PCNA Posttranslational Modifications in Translesion Synthesis**, Montaser Shaheen, Ilanchezhian Shanmugam, and Robert Hromas  
Volume 2010, Article ID 761217, 8 pages

**Mouse WRN Helicase Domain Is Not Required for Spontaneous Homologous Recombination-Mediated DNA Deletion**, Adam D. Brown, Alison B. Claybon, and Alexander J. R. Bishop  
Volume 2010, Article ID 356917, 6 pages

**The Effect of Mitochondrial Dysfunction on Cytosolic Nucleotide Metabolism**, Claus Desler, Anne Lykke, and Lene Juel Rasmussen  
Volume 2010, Article ID 701518, 9 pages

**BLM Deficiency Is Not Associated with Sensitivity to Hydroxyurea-Induced Replication Stress**, Kenza Lahkim Bennani-Belhaj, Géraldine Buhagiar-Labarchède, Nada Jmari, Rosine Onclercq-Delic, and Mounira Amor-Guélet  
Volume 2010, Article ID 319754, 8 pages

**Rev1, Rev3, or Rev7 siRNA Abolishes Ultraviolet Light-Induced Translesion Replication in HeLa Cells: A Comprehensive Study Using Alkaline Sucrose Density Gradient Sedimentation**, Jun Takezawa, Yukio Ishimi, Naomi Aiba, and Kouichi Yamada  
Volume 2010, Article ID 750296, 12 pages

**Translesion Synthesis Polymerases in the Prevention and Promotion of Carcinogenesis,**

L. Jay Stallons and W. Glenn McGregor

Volume 2010, Article ID 643857, 10 pages

**A Mathematical Model for DNA Damage and Repair,** Philip S. Crooke and Fritz F. Parl

Volume 2010, Article ID 352603, 7 pages

**Base Sequence Context Effects on Nucleotide Excision Repair,** Yuqin Cai, Dinshaw J. Patel, Suse Broyde, and Nicholas E. Geacintov

Volume 2010, Article ID 174252, 9 pages

**True Lies: The Double Life of the Nucleotide Excision Repair Factors in Transcription and DNA Repair,**

Nicolas Le May, Jean-Marc Egly, and Frédéric Coin

Volume 2010, Article ID 616342, 10 pages

**Influence of XRCC1 Genetic Polymorphisms on Ionizing Radiation-Induced DNA Damage and Repair,**

Silvia Sterpone and Renata Cozzi

Volume 2010, Article ID 780369, 6 pages

**Stimulation of DNA Glycosylase Activities by XPC Protein Complex: Roles of Protein-Protein**

**Interactions,** Yuichiro Shimizu, Yasuhiro Uchimura, Naoshi Dohmae, Hisato Saitoh, Fumio Hanaoka, and Kaoru Sugawara

Volume 2010, Article ID 805698, 12 pages

**Coincident *In Vitro* Analysis of DNA-PK-Dependent and -Independent Nonhomologous End Joining,**

Cynthia L. Hendrickson, Shubhadeep Purkayastha, Elzbieta Pastwa, Ronald D. Neumann, and Thomas A. Winters

Volume 2010, Article ID 823917, 11 pages

**Selective Incision of the  $\alpha$ -N<sup>5</sup>-Methyl-Formamidopyrimidine Anomer by *Escherichia coli* Endonuclease**

**IV,** Plamen P. Christov, Surajit Banerjee, Michael P. Stone, and Carmelo J. Rizzo

Volume 2010, Article ID 850234, 10 pages

**Regulation of HuR by DNA Damage Response Kinases,** Hyeon Ho Kim, Kotb Abdelmohsen,

and Myriam Gorospe

Volume 2010, Article ID 981487, 8 pages

**DNA Mismatch Repair in Eukaryotes and Bacteria,** Kenji Fukui

Volume 2010, Article ID 260512, 16 pages

**H2AX Phosphorylation: Its Role in DNA Damage Response and Cancer Therapy,** Monika Podhorecka,

Andrzej Skladanowski, and Przemyslaw Bozko

Volume 2010, Article ID 920161, 9 pages

**Differential Dynamics of ATR-Mediated Checkpoint Regulators,** Danil O. Warmerdam, Roland Kanaar,

and Veronique A. J. Smits

Volume 2010, Article ID 319142, 16 pages

**Role of Topoisomerase II $\beta$  in DNA Damage Response following IR and Etoposide**, Nicola J. Sunter, Ian G. Cowell, Elaine Willmore, Gary P. Watters, and Caroline A. Austin  
Volume 2010, Article ID 710589, 8 pages

**Structural Biology of DNA Repair: Spatial Organisation of the Multicomponent Complexes of Nonhomologous End Joining**, Takashi Ochi, Bancinyane Lynn Sibanda, Qian Wu, Dimitri Y. Chirgadze, Victor M. Bolanos-Garcia, and Tom L. Blundell  
Volume 2010, Article ID 621695, 19 pages

**The Roles of Several Residues of *Escherichia coli* DNA Photolyase in the Highly Efficient Photo-Repair of Cyclobutane Pyrimidine Dimers**, Lei Xu and Guoping Zhu  
Volume 2010, Article ID 794782, 7 pages

**Parameters of Reserpine Analogs That Induce MSH2/MSH6-Dependent Cytotoxic Response**, Aksana Vasilyeva, Jill E. Clodfelter, Michael J. Gorczynski, Anthony R. Gerardi, S. Bruce King, Freddie Salisbury, and Karin D. Scarpinato  
Volume 2010, Article ID 162018, 13 pages

**Early Steps in the DNA Base Excision Repair Pathway of a Fission Yeast *Schizosaccharomyces pombe***, Kyoichiro Kanamitsu and Shogo Ikeda  
Volume 2010, Article ID 450926, 9 pages

**Nonhomologous DNA End Joining in Cell-Free Extracts**, Sheetal Sharma and Sathees C. Raghavan  
Volume 2010, Article ID 389129, 11 pages

**BRCA1 Forms a Functional Complex with  $\gamma$ -H2AX as a Late Response to Genotoxic Stress**, Susan A. Krum, Esther de la Rosa Dalugdugan, Gustavo A. Miranda-Carboni, and Timothy F. Lane  
Volume 2010, Article ID 801594, 9 pages

**Modulation of the Ribonucleotide Reductase-Antimetabolite Drug Interaction in Cancer Cell Lines**, Jun Zhou, Paula Oliveira, Xueli Li, Zhengming Chen, and Gerold Bepler  
Volume 2010, Article ID 597098, 10 pages

**Overview of DNA Repair in *Trypanosoma cruzi*, *Trypanosoma brucei* and *Leishmania major***, Danielle Gomes Passos-Silva, Matheus Andrade Rajão, Pedro Henrique Nascimento de Aguiar, João Pedro Vieira-da-Rocha, Carlos Renato Machado, and Carolina Furtado  
Volume 2010, Article ID 840768, 14 pages

**DNA Damage Induced by Alkylating Agents and Repair Pathways**, Natsuko Kondo, Akihisa Takahashi, Koji Ono, and Takeo Ohnishi  
Volume 2010, Article ID 543531, 7 pages

**Molecular Mechanisms of Ultraviolet Radiation-Induced DNA Damage and Repair**, Rajesh P. Rastogi, Richa, Ashok Kumar, Madhu B. Tyagi, and Rajeshwar P. Sinha  
Volume 2010, Article ID 592980, 32 pages

**Repair of DNA Alkylation Damage by the *Escherichia coli* Adaptive Response Protein AlkB as Studied by ESI-TOF Mass Spectrometry**, Deyu Li, James C. Delaney, Charlotte M. Page, Alvin S. Chen, Cintyu Wong, Catherine L. Drennan, and John M. Essigmann  
Volume 2010, Article ID 369434, 9 pages

**Aflatoxin B<sub>1</sub>-Associated DNA Adducts Stall S Phase and Stimulate Rad51 foci in *Saccharomyces cerevisiae***, Michael Fasullo, Yifan Chen, William Bortcosh, Minzeng Sun, and Patricia A. Egner  
Volume 2010, Article ID 456487, 9 pages

**Expression of O<sup>6</sup>-Alkylguanine-DNA Alkyltransferase in Normal and Malignant Bladder Tissue of Egyptian Patients**, Abir A. Saad, Heba Sh. Kassem, Andrew C. Povey, and Geoffrey P. Margison  
Volume 2010, Article ID 840230, 9 pages

**Lung Cancer Risk and Genetic Polymorphisms in DNA Repair Pathways: A Meta-Analysis**, Chikako Kiyohara, Koichi Takayama, and Yoichi Nakanishi  
Volume 2010, Article ID 701760, 17 pages

**Molecular Mechanisms of the Whole DNA Repair System: A Comparison of Bacterial and Eukaryotic Systems**, Rihito Morita, Shuhei Nakane, Atsuhiko Shimada, Masao Inoue, Hitoshi Iino, Taisuke Wakamatsu, Kenji Fukui, Noriko Nakagawa, Ryoji Masui, and Seiki Kuramitsu  
Volume 2010, Article ID 179594, 32 pages

**Prevention of Mutation, Cancer, and Other Age-Associated Diseases by Optimizing Micronutrient Intake**, Bruce N. Ames  
Volume 2010, Article ID 725071, 11 pages

**Role of Nicotinamide in DNA Damage, Mutagenesis, and DNA Repair**, Devita Surjana, Gary M. Halliday, and Diona L. Damian  
Volume 2010, Article ID 157591, 13 pages

**Preparation of DNA Ladder Based on Multiplex PCR Technique**, Tian-Yun Wang, Li Guo, and Jun-he Zhang  
Volume 2010, Article ID 421803, 3 pages

## Editorial

# DNA Damage, Mutagenesis, and DNA Repair

**Ashis Basu,<sup>1</sup> Suse Broyde,<sup>2</sup> Shigenori Iwai,<sup>3</sup> and Caroline Kisker<sup>4</sup>**

<sup>1</sup> Department of Chemistry, University of Connecticut, Storrs, CT 06269, USA

<sup>2</sup> Department of Biology, New York University, New York, NY 10003, USA

<sup>3</sup> Graduate School of Engineering Science, Osaka University, 1-3 Machikaneyama, Toyonaka, Osaka 560-8531, Japan

<sup>4</sup> Rudolf Virchow Center for Experimental Biomedicine, Institute for Structural Biology, University of Würzburg, 97080 Würzburg, Germany

Correspondence should be addressed to Ashis Basu, ashis.basu@uconn.edu

Received 8 October 2010; Accepted 12 October 2010

Copyright © 2010 Ashis Basu et al. This is an open access article distributed under the Creative Commons Attribution License, which permits unrestricted use, distribution, and reproduction in any medium, provided the original work is properly cited.

This special issue of the *Journal of Nucleic Acids* is dedicated to DNA damage and two important biological consequences provoked by such damage: lesion repair and lesion-induced mutagenesis. These phenomena have attracted broad interest among a large community of scientists that cross disciplines from mathematics, physics, chemistry, and biology to clinical scientists. The importance of DNA damage to human disease, especially cancer, is the common denominator for the widespread fascination with this area, as it spans from the molecular and mechanistic to the cellular, organismal, and therapeutic levels. Hence, papers are presented that showcase the unique strengths that emerge when researchers from a variety of intellectual perspectives focus on basic scientific challenges that must be addressed to improve human health.

The area of DNA damage, mutagenesis, and DNA repair is rapidly evolving. It is, therefore, gratifying to present in one rich volume the most current work from an array of leaders in the field, who offer up-to-date review articles as well as their most recent new research results. Included are DNA damages that may be endogenous, resulting from normal biochemical processes that have unwanted harmful outcomes, or exogenous, stemming from environmental causes such as tobacco smoke. Advanced mass spectrometry methods for damage detection and their processing, a current tour de force that plays a critical role in the field, are presented. Also featured are current molecular understandings of DNA repair mechanisms and mechanisms of damage-processing by DNA polymerases and accessory proteins. On the organismal level, all three kingdoms of life

are represented, and among the eukaryotes the range spans from yeast to protozoa to vertebrates.

Accordingly, we proudly present this special issue of the *Journal of Nucleic Acids*. We thank the contributors for their outstanding work and the many reviewers who served conscientiously and tirelessly to assure an issue that meets the highest standards.

Ashis Basu  
Suse Broyde  
Shigenori Iwai  
Caroline Kisker

## Research Article

# From DNA Radiation Damage to Cell Death: Theoretical Approaches

**Francesca Ballarini**

*Department of Nuclear and Theoretical Physics, INFN-Pavia Section, University of Pavia, via Bassi 6, I-27100 Pavia, Italy*

Correspondence should be addressed to Francesca Ballarini, francesca.ballarini@pv.infn.it

Received 11 May 2010; Accepted 7 September 2010

Academic Editor: Ashis Basu

Copyright © 2010 Francesca Ballarini. This is an open access article distributed under the Creative Commons Attribution License, which permits unrestricted use, distribution, and reproduction in any medium, provided the original work is properly cited.

Some representative models of radiation-induced cell death, which is a crucial endpoint in radiobiology, were reviewed. The basic assumptions were identified, their consequences on predicted cell survival were analyzed, and the advantages and drawbacks of each approach were outlined. In addition to “historical” approaches such as the Target Theory, the Linear-Quadratic model, the Theory of Dual Radiation Action and Katz’ model, the more recent Local Effect Model was discussed, focusing on its application in Carbon-ion hadrontherapy. Furthermore, a mechanistic model developed at the University of Pavia and based on the relationship between cell inactivation and chromosome aberrations was presented, together with recent results; the good agreement between model predictions and literature experimental data on different radiation types (photons, protons, alpha particles, and Carbon ions) supported the idea that asymmetric chromosome aberrations like dicentric and rings play a fundamental role for cell death. Basing on these results, a reinterpretation of the TDRA was also proposed, identifying the TDRA “sublesions” and “lesions” as clustered DNA double-strand breaks and (lethal) chromosome aberrations, respectively.

## 1. Introduction

Cell death is a crucial issue in radiation-induced biological damage, not only because it is widely considered as a reference endpoint to characterize the action of ionizing radiation in different biological targets, but also because cell killing is the main aim for any tumour therapy. In particular, the dependence of cell-death RBE (Relative Biological Effectiveness) on the particle energy is a fundamental information for Carbon-ion therapy; with increasing depth in tissue, the primary-beam energy decreases, thus implying an increase in the radiation LET (Linear Energy Transfer) and in its biological effectiveness.

Many experimental data sets on different cell lines cultured *in vitro* and exposed to different radiation fields are available. These data show that while haploid yeasts, some bacteria and spermatogonia are characterized by a purely exponential dose-response curve, which becomes a straight line in the usual semilogarithmic representation, diploid yeasts and almost all mammalian cells follow a

“sigmoid” survival curve, which in a semilogarithmic plot is characterized by an initial “shoulder” followed by an almost straight portion. The shoulder is generally ascribed to a multiple-track radiation action whereas the straight portion is thought to be due to the action of single tracks. As a consequence, for high-LET radiation, where the intratrack action predominates, the shoulder tends to disappear and high-LET survival curves can be described by a purely exponential dose dependence.

To better understand the mechanisms governing radiation-induced cell death and to allow for predictions where the experimental data are not sufficiently reliable (typically at high doses, where the error bars are generally large due to poor statistics), many theoretical models of radiation-induced cell killing have been proposed [1]. These models have in common a few basic assumptions: (1) cell inactivation is the result of a multistep process, where the first step is an energy absorption in one or more intracellular sensitive volumes; (2) energy absorption in the form of ionizations or excitations in the critical volume(s) will lead

to molecular lesions in the cell; (3) the processing of such lesions causes the cell to lose its ability to carry out normal DNA replication and cell division.

In this paper, some of these models will be presented and discussed, focusing on the assumptions adopted by the authors and on possible model advantages and drawbacks. Far from being exhaustive, this overview will first deal with three “historical” approaches: Lea’s “Target Theory”, which is one of the earliest interpretive models, the “Linear-Quadratic model”, which overcomes some inconsistencies of the Target Theory with mammalian data and explicitly takes into account DNA damage induction and repair, and the Theory of Dual Radiation Action, which leads as well to a linear-quadratic expression for cell survival but starting from a different background with respect to the LQ model. These three general models will be followed by two approaches (the Katz’ model and the more recent Local Effect Model) that are specific for heavy ions; in particular the LEM approach, which allows calculation of heavy-ion cell survival starting from photon experimental data, is applied at GSI in Germany for the biological optimization of Carbon-ion treatment planning. Finally, an original approach developed at the University of Pavia basing on the link between chromosome aberrations and cell death will be presented, together with recent model predictions on the survival of V79 cells exposed to different radiation types. The peculiarity of this approach consists in being mechanistic, since theoretical survival curves are derived from first principles on the biophysical mechanisms underlying DNA damage induction and repair. Importantly, in contrast with many literature mechanistic models including the Linear-Quadratic approach, only two (semi-)free parameters are adopted. Also, the model presented herein works both for low-, intermediate-, and high-LET radiation.

## 2. Lea’s Target Theory

Lea’s “target theory”, which was first developed in 1946 and published in a refined version in 1955 [2], is one of the earliest interpretive models for radiation-induced cell killing and was developed starting from data on microorganisms and bioactive molecules. According to Lea’s model, which is specific for low LET radiation (so that the interaction between distinct events is rare), a cell contains one or more sensitive targets of size  $v$ , which can receive one or more radiation “hits”; a hit is an “active event” occurring within the volume  $v$ , that is an energy absorption event able to induce biological damage such as an ionization or an excitation in the target molecule(s) or in water. The hit probability is then  $\rho = v/V$ , where  $V$  is the *total* cellular volume (that is the product between average cell volume and number of cells at risk). If  $D$  is the total number of active events in the cell population, the probability for a cell to be hit  $h$  times can be expressed as follows:

$$p(\rho, h, D) = \rho^h (1 - \rho)^{(D-h)} {}_D C_h, \quad (1)$$

where  ${}_D C_h$  is the binomial coefficient expressing that  $h$  hits and  $(D - h)$  “misses” can be assigned for  $D$  active events.

Introducing a function  $H(h)$  representing the probability that the cell will survive  $h$  hits (“hit-survival function”), the survival probability after  $h$  hits is

$$P(\rho, h, D) = H(h)p(\rho, h, D) = H(h)\rho^h (1 - \rho)^{(D-h)} {}_D C_h. \quad (2)$$

Since a cell may survive for  $h = 1, 2, 3, \dots, D$ , the total survival probability for the cell, that is the general survival equation according to Lea’s theory, is

$$S(\rho, D) = \sum_h P(\rho, h, D). \quad (3)$$

The case that found the widest applicability in radiobiology is the “multitarget-single-hit” (MTSH) version, according to which the cell contains  $n$  critical targets, each target has the same probability  $q$  of being hit by radiation, and one hit in a given target is sufficient to inactivate that target but not the entire cell. The probability that a cell will survive with  $b$  hits is then

$$P(q, b, n, D) = (1 - e^{-qD})^b (e^{-qD})^{n-b} {}_n C_b B(b), \quad (4)$$

where  $B(b)$ , analogous to  $H(h)$ , is the hit survival function. In the MTSH case, the following limiting conditions can be assigned to  $B(b)$ : (1) if  $b < n$ ,  $B(b)$  assumes a value so that  $P = 1$ ; (2) if  $b \geq n$ ,  $B(b) = 0$  and  $P = 0$ . This means that for  $b < n$  the cell will survive, whereas for  $b \geq n$  the cell will die.

Since the  $n$ th hit assures nonsurvival, the overall survival probability is

$$S(q, n, D) = 1 - (1 - e^{-qD})^n. \quad (5)$$

It is important to observe that, when  $\ln S$  is plotted versus  $D$ , except for the special case of  $n = 1$  each curve has a “shoulder” that increases in breadth with  $n$ . Furthermore, for  $S$  values below about 0.1 each curve becomes a straight line; the extrapolation of this straight line back to the zero-dose ordinate provides the value of  $n$ , called the “target multiplicity”. If the linear portion of the plot is back extrapolated to cross the  $S = 1$  ordinate, that intercept is the “quasi threshold dose”  $D_q$ , which is related to  $n$  and  $D_0$  (where  $D_0 = 1/q$  is the dose for  $1/e$  survival in the linear portion of the plot) by  $D_q = D_0 \ln n$ . Except for  $n = 1$ , the slope at zero dose will be zero, which is one of the main limitations of the model because it is not consistent with the experimental data. To overcome such limitation, a single-target-single-hit term was included, leading to

$$S(p, q, n, D) = e^{-pD} \left[ 1 - (1 - e^{-qD})^n \right], \quad (6)$$

where  $p$  is the inactivation coefficient for the portion of cell killing that is assumed to arise from single hits, whereas  $q$  is the inactivation coefficient for the “usual” MTSH model. Although this equation describes fairly well the behaviour of most mammalian cells, however, it still predicts that the slope of the linear portion of the plot remains constant with increasing dose whereas a more frequent experimental

observation is a constantly increasing slope. This led the investigators to try alternative approaches, also basing on the fact that starting from the 1960s several investigators reported that their data on mammalian cell lines were better described by functions in which the dose appeared both to the first and to the second power.

### 3. The Molecular (or Linear-Quadratic) Model by Chadwick and Leenhouts

The target theory makes no assumption about the induction and repair of the initial DNA damage, which is now known to play a fundamental role for radiation-induced clonogenic death. A number of alternative approaches to Lea's theory have been developed to respond to such objection, and several of these approaches are of a linear-quadratic form. In particular Chadwick and Leenhouts in 1981 [3] developed what they called the "molecular model", which has come to be widely known as the "linear-quadratic" (LQ) model. According to the LQ model, the cell contains certain critical molecules, assumed to be double-stranded DNA, the integrity of which is essential for clonogenic survival; the critical damage is assumed to be a DNA double-strand break (DSB). Ionizing radiation can induce the rupture of DNA molecular bonds ("lesions") that, under certain conditions, are repaired; varying degrees of repair imply different radiobiological effects. If  $N_0$  is the number of DNA molecular bonds available for rupture in the target cell,  $N$  is the number of these bonds that remain intact after a dose  $D$ , and  $K$  is the rupture probability of a single bond per unit dose, then

$$-\frac{dN}{dD} = KN, \quad N = N_0 e^{-KD}. \quad (7)$$

The number of *effective* broken bonds is therefore

$$N_0 - N = fN_0(1 - e^{-KD}), \quad (8)$$

where  $f$  is the fraction of broken bonds that are *not* repaired.

According to Chadwick and Leenhouts, the double helix can undergo a DSB as the result of two different mechanisms: (i) both DNA strands are broken by the same radiation track (or "event"); (ii) each strand is broken independently, but the breaks are close enough in time and space to lead to a DSB. Let  $\Delta$  be the fraction of dose acting through mechanism (i), and  $(1 - \Delta)$  the fraction of dose acting through mechanisms (ii). The number of *unrepaired* DSBs per cell produced by mechanism (ii) is then

$$Q_{ii} = Ef_0 q_1 q_2, \quad (9)$$

where  $E$  is the "effectiveness factor", that is the likelihood for a DSB to occur from two SSBs associated in time and space,  $f_0$  is the fraction of unrepaired DSBs, and  $q_1$  and  $q_2$  are the number of broken bonds on strands 1 and 2, respectively. Therefore,  $q_1 = f_1 n_1 (1 - e^{-k(1-\Delta)D})$  and  $q_2 = f_2 n_2 (1 - e^{-k(1-\Delta)D})$ , where  $n_1$  and  $n_2$  are the number of critical bonds on strands 1 and 2, respectively,  $f_1$  and  $f_2$  are the fractions of unrepaired bonds in strands 1 and 2, and  $k$  is the probability

of bond rupture per bond and per unit dose. Adopting a similar notation, the number of *unrepaired* DSBs induced via mechanism (i) is

$$Q_i = n_0 f_0 [1 - \exp(-k_0 \Delta D)], \quad (10)$$

where  $n_0$  is the number of DNA sites that can sustain a DSB and  $k_0$  is the hit probability constant.

The average number of DSBs per cell is therefore  $Q_i + Q_{ii}$ , and the average number of *lethal* DSBs per cell is

$$Q = p(Q_i + Q_{ii}), \quad (11)$$

where  $p$  is the assumed proportionality constant between the DSB yield and cell death. Lumping constants,

$$Q = p \left[ \chi (1 - e^{-k_0 \Delta D}) + \varphi (1 - e^{-k(1-\Delta)D})^2 \right]. \quad (12)$$

Since according to Poisson-type cell killing the probability of cell survival  $S$  is given by the probability of having 0 lethal lesions, then  $S = e^{-Q}$ . Assuming that  $k$  and  $k_0$  are quite small, one gets the familiar linear-quadratic relationship as follows:

$$S = \exp(-\alpha D - \beta D^2), \quad (13)$$

where  $\alpha = (f_0, n_0, k_0, \Delta)$  and  $\beta = (f_0, E, n_1, n_2, f_1, f_2, k^2, (1 - \Delta)^2)$ . This model represents an attempt to bridge the gap between physics, that is energy deposition by radiation, and biology, that is DNA repair or lack of repair, although the fundamental assumptions are not widely accepted; in particular the hypothesis that the yield of DSBs is proportional to the yield of lethal lesions is not consistent with most experimental data, which in general show that DSBs tend to increase linearly with dose whereas lethal lesions increase with dose in a linear-quadratic fashion. However, the LQ model is widely used in radiobiology since it fits mammalian cell survival data pretty well, overcoming not only the problem of zero slope at zero dose, but also the problem of constant slope at high doses.

### 4. The Theory of Dual Radiation Action by Kellerer and Rossi

The Theory of Dual Radiation Action (TDRA) was proposed by Kellerer and Rossi in 1972 [4], partly to explain the observed increase of neutron RBE at low doses, and partly to incorporate the ideas of microdosimetry. This theory is based on the following assumptions: (1) ionizing radiation induces cellular "sublesions", which are proportional to the radiation dose; (2) the interaction between two sublesions can produce a "lesion", which has a certain fixed probability to lead to cell death. Such interaction is possible only within a "sensitive site"; the interaction probability is 1 for distances smaller than the sensitive site linear dimensions, which according to TDRA are of the order of the micrometer whereas it is 0 for larger distances.

According to the TDRA, the average number of lesions after a dose  $D$  can be expressed as follows:

$$E(D) = \int E(z) f(z, D) dz, \quad (14)$$

where  $f(z, D)dz$  is the probability that, for a dose  $D$ , the specific energy (that is the energy imparted per event and per unit mass) is between  $z$  and  $z + dz$ , and  $E(z)$  is the average number of lesions within a sensitive site. Since  $z$  is a measure of the number of sublesions and since sublesions interact in pairs,  $E(z) = kz^2$  where  $k$  is a biological property of the system. Therefore,

$$E(D) = \int kz^2 f(z, D)dz = k\langle z^2 \rangle. \quad (15)$$

Basing on their microdosimetry experiments, Kellerer and Rossi rewrote this equation by means of the specific-energy spectra, that is,

$$\langle z^2 \rangle = \left( \frac{\int z_1^2 f(z_1) dz_1}{\int z_1 f(z_1) dz_1} \right) D + D^2, \quad (16)$$

where  $f(z_1)$  is the distribution of single-event specific energies.  $E(D)$  can therefore be expressed as follows:

$$E(D) = k(\zeta D + D^2), \quad (17)$$

and the survival probability gets the following linear-quadratic form:

$$S = \exp[-k(\zeta D + D^2)]. \quad (18)$$

This theory has been criticized by various authors in the 1980s considering the LQ approach and results of “event-by-event” radiation track structure studies, according to which the interaction between distinct events occurs at the nm level whereas the TDRA sensitive sites have linear dimensions of the order of the micrometer.

However, an alternative interpretation may be the following: on the basis of the observed relationship between some chromosome aberration types and cell death (see below), sublesions can be thought as DSBs whereas lesions can be thought as lethal chromosome aberrations such as dicentrics and rings; this way a sensitive site of the order of the micrometer becomes consistent with the data, since chromosome aberrations are produced by pairwise interaction of DSBs, and such interaction occurs at the level of interphase chromosome domains, which are known to have linear dimensions of the order of the micrometer.

## 5. Katz’ Amorphous Track Structure Model

In the late 1960s [5], Katz proposed an approach for heavy-ion cell killing (called “amorphous track structure model”) focused on the role of radiation track structure. According to this approach, the critical target in a mammalian cell is assumed to be a “substructure” of the cell nucleus with typical linear dimensions of the order of  $1 \mu\text{m}$ ; the nucleus contains several of these substructures, “like beans in a bag”. The average energy deposition in a given target volume is assumed to be sufficient to determine the biological response, regardless of the target fine structure at lower scales. To represent the photon dose response, Katz adopted the MTSH version of the target theory, according to which the cell

survival probability after a dose  $D$  can be expressed as follows:

$$S_\gamma(D) = 1 - \left[ 1 - \exp\left(-\frac{D}{D_0}\right) \right]^n, \quad (19)$$

where  $n$  is the number of targets and  $D_0$  is the dose for  $1/e$  survival in the linear portion of the plot. Since for heavy ions straight exponential curves are observed, the cell survival probability for heavy ions can be expressed as follows:

$$S_i = e^{-\sigma F}, \quad (20)$$

where  $F$  is the particle fluence and  $\sigma$  is the “inactivation cross section”.

According to Katz’ approach, the transition from the shouldered curves observed at low LET and the high-LET exponential curves is modelled by attributing the dose to two different inactivation modes, that is the “ $\gamma$ -kill” and the “ion-kill”. To determine the relative fractions of energy deposited according to the “ $\gamma$ -kill” or the “ion-kill” mode, the inactivation cross section representing the ion-kill contribution is calculated by

$$\sigma = 2\pi \int \left[ 1 - \exp\left(-\frac{D(r)}{D_0}\right) \right]^n r dr, \quad (21)$$

where  $D(r)$  is the average dose over a (cylindrical) target with typical size of  $1 \mu\text{m}$ . The relative dose contributions for the ion-kill and the “ $\gamma$ -kill” mode are then

$$D_i = \left( \frac{\sigma}{\sigma_0} \right) D, \quad D_\gamma = D - D_i = \left( \frac{1 - \sigma}{\sigma_0} \right) D, \quad (22)$$

where  $\sigma_0$  is a “saturation cross section” that is essentially defined by the projected area of all subtargets in the cell nucleus. The total survival probability is then

$$S = S_i \cdot S_\gamma = e^{-\sigma F} \left[ 1 - \left( 1 - e^{-D_\gamma/D_0} \right)^n \right]. \quad (23)$$

Although in Katz’ model the details at the nm level are not taken into account, it is interesting to note that the linear dimensions of its “critical targets” ( $\sim 1 \mu\text{m}$ ) are of the same order of the dimensions of mammalian cell interphase chromosomes.

## 6. The Local Effect Model (LEM)

A more recent approach, developed and used at GSI for the biological optimization of Carbon-ion treatment planning, is the “Local Effect Model” (LEM) [6]; this model is based on the assumption that the *local* biological effect, that is the damage in a small subvolume (nm) of the cell nucleus, is solely determined by the expectation value of energy deposition in that subvolume, independent of the radiation type. Given a biological target, this implies that differences in the biological action of charged particle beams should be attributed to the different pattern of energy deposition by heavy charged particles with respect to photons, that is radiation track structure at the nm scale. Furthermore, for a given radiation type, differences in the photon response

for different biological targets should lead to differences in the corresponding RBE values. For photons, the volumetric density of *lethal* events per cell can be written as follows:

$$\nu_X(D) = \frac{\langle N_X(D) \rangle}{V_n} = \frac{-\ln S_X(D)}{V_n}, \quad (24)$$

where  $\langle N_X(D) \rangle$  is the average number of lethal events per cell induced by a dose  $D$  of photons,  $V_n$  is the cell nucleus volume, and  $S_X(D)$  is the fraction of surviving cells for photons. Given the complete local dose distribution  $d(x, y, z)$  for ion irradiation, the average number of lethal events per cell by heavy ions can be obtained integrating the local-event density  $\nu_{\text{ion}}(d(x, y, z))$  as follows:

$$\langle N_{\text{ion}} \rangle = \int \nu_{\text{ion}}(d(x, y, z)) dV_n. \quad (25)$$

Since according to the fundamental assumption of LEM  $\nu_{\text{ion}}(d) = \nu_X(d)$ , the average number of lethal events per cell for heavy ions can be written as follows:

$$\langle N_{\text{ion}} \rangle = \int \frac{-\ln S_X(d(x, y, z))}{V_n} dV_n. \quad (26)$$

The integration volume for (26) is given by the volume of the cell nucleus, which is represented as a cylinder with axis parallel to the particle trajectory. Since the integrand is fully determined by the photon biological response, cell killing by heavy ions can be calculated starting from photon experimental data, being the heavy-ion effect “hidden” in the inhomogeneous distribution of local dose  $d(x, y, z)$ . Equation (26), which is the most general formulation of LEM, does not rely on any particular representation of the photon dose response curve and can be applied even if only numerical values of  $S_X$  are available. However, for practical reasons, the authors described the photon response by a (modified) linear-quadratic approach, that is,

$$\langle N_X(D) \rangle = -\ln S_X(D) = \alpha_X D + \beta_X D^2. \quad (27)$$

To take into account that for many biological targets a transition from the shouldered to an exponential shape of the survival curve is observed at high doses, a modified version of the linear-quadratic approach was introduced; according to this version, such transition is described by a parameter  $D_t$ , representing the transition dose to an exponential shape with slope  $s_{\text{max}} = \alpha_X + 2\beta_X D_t$ . The dose response is then given by

$$-\ln S_X(D) = \begin{cases} \alpha_X D + \beta_X D^2, & D \leq D_t, \\ \alpha_X D_t + \beta_X D_t^2 + s_{\text{max}}(D - D_t), & D > D_t. \end{cases} \quad (28)$$

Since for most mammalian cell lines survival curves can be reliably measured only down to  $10^{-3}$ , in general  $D_t$  cannot be directly derived from experimental data, and thus it represents a semifree model parameter; in general, values in the range 15–30 Gy allow consistent descriptions of the data. To perform the numerical integration given

in (26) for a random distribution of particle traversals, a grid has to be used to cope with the rapid variation of the radial dose profile, according to the  $1/r^2$  distribution. Since this leads to computing times that are unacceptable for treatment planning, approximations have been developed to estimate the  $\beta$  parameter. The current version of the model, which recently has been refined taking into account free-radical diffusion, DNA strand-break clustering, and an extension of the inner part of the particle track [7], led to a good agreement with Carbon-ion survival data for different particle energies and different cell lines.

The LEM approach has been implemented in the TRiP treatment planning procedure for the Carbon-ion therapy project at GSI. According to LEM, the biological characteristics of the various target tissues are essentially determined by the  $\alpha/\beta$  ratio for conventional photon irradiation and by  $D_t$ ; values of  $\alpha/\beta = 10$  Gy are frequently reported for early-responding normal and tumoral tissues whereas  $\alpha/\beta = 3$  Gy is reported for late-responding normal tissues. However, the authors themselves emphasize that the photon parameters specific for the considered tissue and the considered endpoint should be used to estimate the RBE. Ideally,  $\alpha/\beta$  values from clinical data would be appropriate; if these are not available, the corresponding data from *in vivo* studies should be used, and if those are not available, *in vitro* experiments may help.

## 7. A Mechanistic Approach Starting from Chromosome Aberrations

At the University of Pavia, a mechanistic model and a Monte Carlo code originally developed for predicting chromosome aberration induction have been recently extended to simulate cell death, starting from the experimentally-observed relationship between some chromosome aberration types (dicentrics, rings, and deletions) and clonogenic inactivation (e.g., [17]).

The model/code for radiation-induced chromosome aberrations, which was initiated more than ten years ago [8], relies on the following basic assumptions: (1) chromosome aberrations arise from DNA breaks that are clustered at the nm level (Cluster Lesions, CLs), each lesion giving rise to two independent chromosome free ends; (2) only pairs of chromosome free ends initially induced within a threshold distance  $d$  can join and thus produce exchange-type aberrations. These assumptions start from the evidence that, on average, 1 Gy of (low-LET) radiation induces about 40 DNA double-strand breaks (DSBs) per cell, but less than 1 chromosome aberration per cell; it is therefore very likely that, among the many initially-induced breaks of the double helix, only those that are severe enough (like those that are clustered at the nm level, assumption 1) and close enough (assumption 2) are involved in the formation of chromosome aberrations, typically *via* the well-known mechanism of nonhomologous end joining (NHEJ). The choice of a step-like function with threshold  $d$  for the free-end rejoining probability reflects the evidence that DNA repair takes place mainly within the channels separating the

various interphase chromosome domains; this evidence was quantitatively “translated” in the simulation code assuming that two chromosome free ends induced with initial distance smaller than a threshold value  $d$  will join with 100% probability whereas two free ends with larger initial distance will never join. The value of  $d$  reflects the average linear dimensions of interphase chromosome territories, that is of the order of  $\sim 1 \mu\text{m}$  for mammalian cells.

The current version of the code can deal either with spherical cell nuclei or with cylindrical nuclei, with dimensions that can be chosen by the user from the input file. The various interphase chromosome territories are modelled as (irregular) intranuclear regions consisting of the union of small adjacent cubic voxels of  $0.2 \mu\text{m}$  side; the volume of each territory, that is the number of voxels constituting that territory, is proportional to the chromosome DNA content. Repetition of chromosome territory construction with different chromosome positions within the cell nucleus provides different interphase nucleus configurations.

The yield of radiation-induced Cluster Lesions (i.e., average number of CLs per Gy and per cell) is the starting point for the simulation of dose-response curves. In terms of biophysical mechanisms, CLs represent those initial DNA breaks that, being clustered and thus severe, can “evolve” into chromosome aberrations; therefore, the yield of CLs primarily depends on radiation quality (that is radiation type and energy), but it can also be modulated by the repair ability of the specific cell line under consideration. In previous works on chromosome aberration induction in lymphocytes exposed to protons or alpha particles, the CLs yields have been taken from “event-by-event” radiation track-structure simulations in which a CL has been defined as “at least two SSBs on each DNA strand within 30 base pairs” [8–11]. In more recent works [12–14] and herein, to take into account not only the radiation quality but also the specific cell response, such yields were left as a semifree parameter; here “semifree” means that only values ranging between  $\sim 1 \text{ CLs Gy}^{-1} \text{ cell}^{-1}$  (low-LET radiation) and  $\sim 10 \text{ CLs Gy}^{-1} \text{ cell}^{-1}$  (high LET) are considered as acceptable.

For a given irradiated cell, for sparsely-ionizing radiation like X- and gamma-rays an actual number of CLs is extracted from a Poisson distribution, and such lesions are then randomly distributed in the nucleus. For light ions like protons and alpha particles, an actual number of particle tracks traversing the nucleus is extracted from a Poisson distribution with average value  $n = SD/(0.16L)$ , where  $S$  is the nucleus cross-sectional area in  $\mu\text{m}^2$ ,  $D$  is the absorbed dose in Gy,  $L$  is the radiation LET in  $\text{keV}/\mu\text{m}$ , and 0.16 is a numerical factor coming from the conversion of eV into Joules. For each nucleus traversal, an actual number of lesions is then extracted from a Poisson distribution with average value  $t \cdot \text{CL}/\mu\text{m}$ , where  $t$  is the traversal length in  $\mu\text{m}$  and  $\text{CL}/\mu\text{m}$  is the average number of lesions per unit length, which is calculated as  $\text{CL}/\mu\text{m} = \text{CLs Gy}^{-1} \text{ cell}^{-1} 0.16 L V^{-1}$ , being  $V$  the cell nucleus volume in  $\mu\text{m}^3$ . For light ions such as protons and alpha particles, the CLs induced by a given particle are randomly distributed along segments representing the primary particle track. The lesions induced by heavy ions

like Carbon, which is nowadays of great interest for tumour hadrontherapy, and Iron, interesting for space radiation research, are located partly along a segment representing the core of the primary track, and partly with a “radial shift” with respect to the track core, to reproduce the effects of energetic secondary electrons (“delta rays”). For a given heavy-ion track, the probability of having a lesion at distance  $r$  from the track core is assumed to be proportional to  $r^{-2}$ .

After assigning the spatial positions of each CL in the cell nucleus, the subsequent simulation steps consist of (1) identification of the chromosome(s) and chromosome arm(s) that have been hit by each CL; (2) pairwise rejoining between chromosome free ends, assuming 100% rejoining probability if the (initial) distance between the two free ends is  $< d$  and no rejoining if the distance is  $> d$ ; accidental rejoining, that is rejoining with the original partner, is allowed; (3) aberration scoring; (4) repetition for a statistically significant number of irradiated cells; (5) repetition for different dose values to obtain a dose-response curve for the main aberration types (dicentric, translocations, rings, deletions, and more than 40 different complex exchanges), directly comparable with experimental data. Specific background (i.e., prior to irradiation) yields for different aberration types can be included by the user (typically, 0.001 whole-genome dicentric/cell and 0.005 whole-genome translocations/cell). Both Giemsa staining and whole-chromosome FISH painting can be simulated, and the scoring of chromosome fragments smaller than a threshold value can be “switched off” by the user, since these fragments can hardly be detected experimentally when chromatin is in its condensed state; a threshold value of 10 Mbp (FISH) or 15 Mbp (Giemsa) has been used until now.

Up to now, the model has been validated for the induction of the main types of chromosome aberrations in lymphocytes exposed to X- and  $\gamma$ -rays [10], protons and alpha particles [9], and Carbon ions and Iron ions [11]. The agreement between model predictions and literature experimental data supports the model assumptions on the mechanisms governing chromosome aberration induction, including the fundamental role of DNA damage clustering at the nm scale and the step-like distance dependence at the  $\mu\text{m}$  scale for the rejoining probability between two (clustered) DNA lesions. Furthermore, the model has been applied to predict the induction of Chronic Myeloid Leukaemia following acute exposure to gamma rays [15] and the induction of chromosome aberrations in astronauts exposed to space radiation [16].

The model/code described above has recently been extended to simulate radiation-induced cell death, starting from the experimentally observed one-to-one relationship between the average number of “lethal aberrations” (that is Giemsa-stained dicentric, rings, and deletions) per cell and  $-\ln S$ , where  $S$  is the fraction of surviving cells [17]. In this extended version, the fraction of surviving cells after a dose  $D$  is then calculated as  $S(D) = e^{-LA(D)}$ , where  $LA(D)$  is the (simulated) average number of lethal aberrations per cell. While the experimental study by Cornforth and Bedford concerns AG1522 cells exposed to X-rays (and subject to delayed plating to allow for potentially-lethal damage repair),

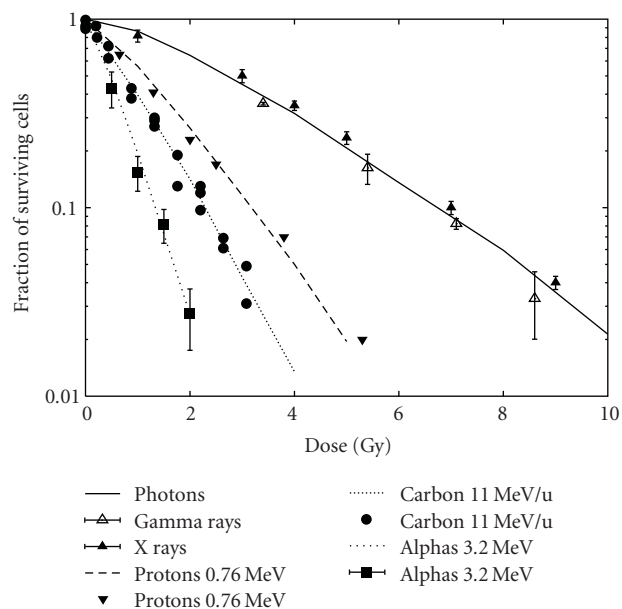


FIGURE 1: From top to bottom: survival of V79 cells exposed to photons, 0.76 MeV protons, 11.0 MeV/u Carbon ions, and 3.2 MeV alpha particles; the lines are model predictions, the points are experimental data taken from [18–21]. The cell nuclei were modelled as right cylinders with height  $6\ \mu\text{m}$  and radius  $6\ \mu\text{m}$  (radius  $5\ \mu\text{m}$  for the Carbon data, basing on personal communication).

the theoretical approach reported herein was applied also to protons,  $\alpha$ -particles, and Carbon ions. The first step of the work consisted of reproducing the experimental outcomes on X-irradiated AG1522 cells; the very good agreement between model predictions and experimental data confirmed the important role of lethal aberrations for radiation-induced cell death [13]. Subsequently, the approach has been extended to V79 cells exposed to X- or gamma-rays, 0.76 MeV protons (LET:  $\sim 30.5\ \text{keV}/\mu\text{m}$ ), and 3.2 MeV  $\alpha$ -particles (LET:  $\sim 120\ \text{keV}/\mu\text{m}$ ). Good agreement with literature experimental data [18–20] was found for all the considered exposure scenarios, indicating that the relationship between lethal aberrations and cell death observed by Cornforth and Bedford can hold not only for AG1522 cells exposed to X-rays but also for other cell types and other radiation types. Very recently, the approach was applied also to 11.0 MeV/u Carbon ions (LET:  $153.5\ \text{keV}/\mu\text{m}$ ).

The results described above are reported in Figure 1, which shows cell survival curves obtained for V79 cells exposed to photons, 0.76 MeV protons, 3.2 MeV  $\alpha$ -particles, and 11.0 MeV/u Carbon ions. The lines are model predictions whereas the points are the corresponding literature data chosen for comparison, that is V79 cells exposed to X-rays [18],  $\gamma$ -rays [19], 0.76 MeV protons [20], 3.2 MeV  $\alpha$ -particles [19], and 11.0 MeV/u Carbon ions [21].

## 8. Conclusions

Some representative theoretical models of radiation-induced cell inactivation were presented and discussed, outlining

the main biophysical assumptions adopted by the various authors and analyzing the consequences of such assumptions in terms of cell survival predictions. More specifically Lea's target theory, which was developed before the discovery of the DNA double helix for microorganisms exposed to low-LET radiation, in its MTS version assumes that there exist  $n$  critical targets in the cell, and that the  $n$ th radiation hit ensures nonsurvival; therefore, the predicted survival curve in the usual semilog scale is characterized by an initial shoulder (with zero slope at zero dose) followed by a straight portion. While the MTS model fits quite well bacteria survival data, most mammalian cell data follow a linear-quadratic behaviour, with negative slope at zero dose and increasing slope at high doses.

Both the Molecular Model and the Theory of Dual Radiation Action lead to a linear-quadratic survival curve, though following different approaches. The Molecular Model considers the DNA double helix as the critical target and takes into account the biophysical mechanisms of DNA damage induction and repair, assuming that the critical damage is a DSB (which can be induced either by a single-track action or by a two-track action) and that the yield of DSBs is proportional to cell inactivation. On the contrary, the TDRA, without specifying the critical target(s) nor the critical damage(s), assumes that radiation induces cellular "sublesions" that interact in pairs to produce "lesions", which in turn lead to cell death with a certain fixed probability; such interaction can take place only within "sensitive sites" of the order of  $\mu\text{m}$ . While these three models focus on the general mechanisms of cell death induced by low-LET radiation, Katz' approach and the LEM model are specific for heavy-ion applications. In particular the LEM model, which describes heavy-ion cell death starting from photon experimental data, is used at GSI in Germany for the biological optimization of Carbon-ion treatment planning.

After reviewing the literature models mentioned above, an approach developed at the University of Pavia was presented together with recent results. The peculiarity of this approach consists in the fact that on one side it is mechanistic (that is the model predictions are derived from a few basic assumptions on the biophysical mechanisms underlying radiation-induced cell death), but at the same time the number of free parameters is kept at a minimum, since only two semifree parameters are adopted: the yield of DNA "Cluster Lesions" and the value of the threshold distance  $d$  for chromosome free-end rejoining. More specifically, the model may be taken as a mechanistic reinterpretation of the TDRA, since the TDRA "sublesions" and "lesions" can be (re-)interpreted as DNA "Cluster Lesions" and (lethal) chromosome aberrations, respectively; CLs, which increase with dose linearly, interact in pairs to produce chromosome aberrations, which increase with dose in a linear-quadratic fashion; such interaction occurs at the level of interphase chromosome domains, which have linear dimensions of the order of the micrometer like the TDRA sensitive sites.

The good agreement between model predictions and literature experimental data on low-, intermediate-, and high-LET radiation (photons, protons, alpha particles, and Carbon ions) supported the idea that asymmetric chromosome

aberrations, such as dicentrics and rings, play a fundamental role in the mechanisms governing radiation-induced cell death. Furthermore, the model may be considered as a predictive tool for potential applications in radiotherapy including therapy with Carbon ions, which is now adopted in various centres worldwide, including the CNAO centre in Pavia.

## Acknowledgments

This work was partially supported by INFN (project “WIDEST1”). The author is also grateful to Michael Cornforth, Marco Durante, Yoshiya Furusawa, Andrea Ottolenghi, Ben Phoenix, Michael Scholz, Maria Antonella Tabocchini, and Wilma Weyrather for useful discussion and/or data sharing.

## References

- [1] E. L. Alpen, *Radiation Biophysics*, Prentice-Hall, Englewood Cliffs, NJ, USA, 1990.
- [2] D. E. Lea, *Actions of Radiations on Living Cells*, Cambridge University Press, New York, NY, USA, 2nd edition, 1955.
- [3] K. H. Chadwick and H. P. Leenhouts, “A molecular theory of cell survival,” *Physics in Medicine and Biology*, vol. 18, no. 1, pp. 78–87, 1973.
- [4] A. M. Kellerer and H. H. Rossi, “A generalized formulation of dual radiation action,” *Radiation Research*, vol. 75, no. 3, pp. 471–488, 1978.
- [5] J. J. Butts and R. Katz, “Theory of RBE for heavy ion bombardment of dry enzymes and viruses,” *Radiation Research*, vol. 30, no. 4, pp. 855–871, 1967.
- [6] M. Scholz and T. Elsässer, “Biophysical models in ion beam radiotherapy,” *Advances in Space Research*, vol. 40, no. 9, pp. 1381–1391, 2007.
- [7] T. Elsässer, M. Krämer, and M. Scholz, “Accuracy of the local effect model for the prediction of biologic effects of carbon ion beams in vitro and in vivo,” *International Journal of Radiation Oncology Biology Physics*, vol. 71, no. 3, pp. 866–872, 2008.
- [8] F. Ballarini, M. Merzagora, F. Monforti et al., “Chromosome aberrations induced by light ions: Monte Carlo simulations based on a mechanistic model,” *International Journal of Radiation Biology*, vol. 75, no. 1, pp. 35–46, 1999.
- [9] F. Ballarini and A. Ottolenghi, “Chromosome aberrations as biomarkers of radiation exposure: modelling basic mechanisms,” *Advances in Space Research*, vol. 31, no. 6, pp. 1557–1568, 2003.
- [10] F. Ballarini, M. Biaggi, A. Ottolenghi et al., “Nuclear architecture and radiation induced chromosome aberrations: models and simulations,” *Radiation Protection Dosimetry*, vol. 99, no. 1–4, pp. 175–182, 2002.
- [11] F. Ballarini, D. Alloni, A. Facoetti, and A. Ottolenghi, “Heavy-ion effects: from track structure to DNA and chromosome damage,” *New Journal of Physics*, vol. 10, Article ID 075008, 2008.
- [12] F. Ballarini, “Chromosome damage by ionizing radiation: a review,” *II Nuovo Cimento B*, vol. 124, no. 4, pp. 443–458, 2009.
- [13] F. Ballarini, J. Bakeine, S. Bortolussi et al., “Nuclear physics meets medicine and biology: Boron neutron capture therapy,” in *Proceedings of the 12th International Conference on Nuclear Reaction Mechanisms, Varenna, June 2009*, F. Cerutti and A. Ferrari, Eds., vol. 2, pp. 561–571, CERN, Geneva, Switzerland, 2010.
- [14] F. Ballarini, S. Bortolussi, A. M. Clerici, C. Ferrari, N. Protti, and S. Altieri, “From radiation-induced chromosome damage to cell death: modelling basic mechanisms and applications to Boron neutron capture therapy,” submitted to *Radiation Protection Dosimetry*.
- [15] F. Ballarini and A. Ottolenghi, “A model of chromosome aberration induction and chronic myeloid leukaemia incidence at low doses,” *Radiation and Environmental Biophysics*, vol. 43, no. 3, pp. 165–171, 2004.
- [16] F. Ballarini and A. Ottolenghi, “A model of chromosome aberration induction: applications to space research,” *Radiation Research*, vol. 164, no. 4, pp. 567–570, 2005.
- [17] M. N. Cornforth and J. S. Bedford, “A quantitative comparison of potentially lethal damage repair and the rejoining of interphase chromosome breaks in low passage normal human fibroblasts,” *Radiation Research*, vol. 111, no. 3, pp. 385–405, 1987.
- [18] Y. Furusawa, K. Fukutsu, M. Aoki et al., “Inactivation of aerobic and hypoxic cells from three different cell lines by accelerated  $^3\text{He}$ -,  $^{12}\text{C}$ - and  $^{20}\text{Ne}$ -Ion beams,” *Radiation Research*, vol. 154, no. 5, pp. 485–496, 2000.
- [19] B. Phoenix, S. Green, M. A. Hill, B. Jones, A. Mill, and D. L. Stevens, “Do the various radiations present in BNCT act synergistically? Cell survival experiments in mixed alpha-particle and gamma-ray fields,” *Applied Radiation and Isotopes*, vol. 67, no. 7–8, pp. S318–S320, 2009.
- [20] M. Belli, F. Cera, R. Cherubini et al., “RBE-LET relationships for cell inactivation and mutation induced by low energy protons in V79 cells: further results at the LNL facility,” *International Journal of Radiation Biology*, vol. 74, no. 4, pp. 501–509, 1998.
- [21] W. K. Weyrather, S. Ritter, M. Scholz, and G. Kraft, “RBE for carbon track-segment irradiation in cell lines of differing repair capacity,” *International Journal of Radiation Biology*, vol. 75, no. 11, pp. 1357–1364, 1999.

## Review Article

# The Biological and Metabolic Fates of Endogenous DNA Damage Products

Simon Wan Chan<sup>1</sup> and Peter C. Dedon<sup>1,2</sup>

<sup>1</sup>Department of Biological Engineering, Massachusetts Institute of Technology, NE47-277, Cambridge, MA 02139, USA

<sup>2</sup>Center for Environmental Health Sciences, Massachusetts Institute of Technology, Cambridge, MA 02139, USA

Correspondence should be addressed to Peter C. Dedon, pcdedon@mit.edu

Received 14 September 2010; Accepted 31 October 2010

Academic Editor: Ashis Basu

Copyright © 2010 S. W. Chan and P. C. Dedon. This is an open access article distributed under the Creative Commons Attribution License, which permits unrestricted use, distribution, and reproduction in any medium, provided the original work is properly cited.

DNA and other biomolecules are subjected to damaging chemical reactions during normal physiological processes and in states of pathophysiology caused by endogenous and exogenous mechanisms. In DNA, this damage affects both the nucleobases and 2-deoxyribose, with a host of damage products that reflect the local chemical pathology such as oxidative stress and inflammation. These damaged molecules represent a potential source of biomarkers for defining mechanisms of pathology, quantifying the risk of human disease and studying interindividual variations in cellular repair pathways. Toward the goal of developing biomarkers, significant effort has been made to detect and quantify damage biomolecules in clinically accessible compartments such as blood and urine. However, there has been little effort to define the biotransformational fate of damaged biomolecules as they move from the site of formation to excretion in clinically accessible compartments. This paper highlights examples of this important problem with DNA damage products.

## 1. Introduction

Endogenous processes of oxidative stress and inflammation cause DNA damage that is mechanistically linked to the pathophysiology of cancer and other human diseases [1]. The DNA damage is comprised of dozens of mutagenic and cytotoxic products [2–4] reflecting the full spectrum of chemical mechanisms, including oxidation, nitrosation, halogenation, and alkylation, as described in numerous published reviews [5–15]. There has been significant interest in developing DNA damage products as biomarkers of disease risk given the strong association between DNA damage and disease pathology [12, 14, 16–22]. However, there has been little consideration given to the biological fate of DNA damage products, such as release from DNA as a result of instability, repair, and reaction with local nucleophiles, and the effect of this fate on the steady-state level of DNA lesions in cells and tissues. Further, the use of tissue-derived DNA for biomarker development poses the problem of accessibility and limits clinical studies, so researchers are exploring the presence of

DNA damage products in other sampling compartments, such as urine (e.g., [16, 23]). These efforts have presumed that DNA repair or cell death leads to dissemination of DNA damage products in blood, with subsequent excretion of specific molecular forms predicted to arise from the various DNA repair or other enzymatic processes. However, one of the major drawbacks to the use of blood or urine as a sampling compartment for development of DNA damage products as biomarkers is the lack of mechanistic information about the fates of the damage products in terms of metabolism and distribution. While information about the metabolic fate and pharmacokinetics of drugs based on nucleobases has been well defined (e.g., [24, 25]), studies of the metabolism of DNA damage products have been limited to a few products such as adducts of ethylene dibromide [26], the pyrimidopurinone adduct of dG, M<sub>1</sub>dG [27–29], and the base propenal and butenedialdehyde species arising from 2-deoxyribose oxidation in DNA [30–32].

The mechanisms governing the fate of endogenous DNA damage products can be viewed from two perspectives,

the first being local reactions that lead to the release of the damage product, such as chemical instability or DNA repair, or the reaction of electrophilic damage products with local nucleophiles. The second perspective is that of drug and xenobiotic metabolism and distribution. In both cases, the release of the damage products from DNA results in their diffusion or transport into extracellular space for subsequent distribution in the blood circulation to the liver and excretory organs. Chemical stability governs the extent and form of distribution of the damage product, with electrophilic species reacting with local nucleophiles and more stable products circulating throughout the body. The damage products may be recognized as substrates for the variety of local or distant metabolic enzymes that cause oxidation, reduction, hydrolysis, and conjugation (e.g., glucuronic acid, sulphate, or glutathione), with metabolites excreted in either urine or bile [33, 34]. We can also view DNA damage products from the perspective of metabolic toxification and detoxification. Metabolic reactions are well known to either reduce the activity of reactive and toxic xenobiotics or to convert unreactive molecules to reactive intermediates that are genotoxic, hepatotoxic, or nephrotoxic [33, 34]. This paradigm applies to DNA damage products that range from relatively stable (e.g., nucleobase deamination products) to highly electrophilic (e.g., base propenals from 2-deoxyribose oxidation in DNA), with metabolic reactions occurring in cells in which the DNA damage occurs or in the liver or other metabolic tissues.

This review addresses the current state of understanding of the metabolic and biological fates of DNA damage products, with an eye on the implications of these fates for mechanisms of toxicity and for development of biomarkers of oxidative stress and inflammation.

## 2. The Spectrum of Nucleic Acid Damage Products

As a prelude to understanding the biological fate of damaged nucleic acids, we must first consider the spectrum of damage products. Nucleobases in DNA, RNA, and the nucleotide pool are subject to damage by a variety of chemical mechanisms related to normal and pathological processes. The superoxide ( $O_2^{\bullet-}$ ) and hydrogen peroxide ( $H_2O_2$ ) generated during aerobic respiration participate in Fenton chemistry to produce hydroxyl radical ( $HO^\bullet$ ), while the activated macrophages and neutrophils of chronic inflammation generate a host of chemically reactive species, including the oxidants peroxynitrite ( $ONOO^-$ ) and nitrosoperoxycarbonate ( $ONOCO_2^-$ ), hypohalous acids ( $HOCl$ ,  $HOBr$ ), and nitrosating agents ( $N_2O_3$ ) [8]. Damage to nucleic acids and nucleotides can occur by direct reaction with these agents or indirectly by reaction with electrophiles generated during oxidation of lipids, carbohydrates, and proteins. Both the nucleobase and sugar moieties are susceptible to attack, with examples of nucleobase damage products shown in Figure 1 and 2-deoxyribose oxidation products shown in Figure 2. The biological and metabolic fates of nucleobase damage products will be addressed first and that of 2-deoxyribose oxidation products later in this chapter.

## 3. The Biological and Metabolic Fates of Damaged Nucleobases

The biological fates of damaged nucleotides and nucleic acids can be viewed from the perspective of either the site of initial damage or from the final sampling compartment used for analysis of the damage products. Among the issues that arise are (1) the reactivity of a damage product and the chemical form of the lesion that is released from the site of generation; (2) the mechanism by which the released damage product reaches the systemic circulation; (3) the potential for the damage product to be chemically modified between the steps of formation and excretion; (4) the mechanism of excretion; (5) the potential for further chemical modification in the excretory compartment. The first of these issues, that of reactivity, is best illustrated by the susceptibility of 8-oxoguanine to further oxidation, as will be discussed shortly, and the deglycosylation of many damaged purines, such as 8-nitroguanine [8], and of purines subjected to  $N^7$ -nitrosation or alkylation [8], both of which have been addressed in detail in the literature. Here we will focus on the metabolic fates of nucleobase damage products.

**3.1. 8-Oxoguanine.** The first consideration of the metabolic fate of a nucleobase damage product is the well-studied 7,8-dihydro-8-oxoguanine (8-oxo-G; Figure 1) [35]. Perhaps the most comprehensive consideration of the biological fate of 8-oxo-G in terms of sources of 8-oxo-G-containing species excreted in the urine is the recent review by Cooke et al. [36], with a very recent review of the utility of 8-oxo-dG as a urinary biomarker [23]. Among the nucleobases in DNA, RNA, and the nucleotide pool, guanine is the most readily oxidized due to its favorable redox potential [35, 37–39] with the spectrum of oxidation products depending on the nature of the oxidant [8, 35] (Figure 1). 8-Oxo-G is one of the major products common to oxidation of guanine by most oxidizing agents, and it has thus been touted as a biomarker of oxidative stress (e.g., [23, 36, 40, 41]). While oxidation of G in DNA is one source of 8-oxo-G, another involves polymerase incorporation of 8-oxo-dGTP formed by oxidation of dGTP in the nucleotide pool [42]. Prokaryotes and eukaryotes are equipped with oxidized purine nucleotide di- and triphosphatases (e.g., *E. coli* MutT, 8-oxo-dGTP triphosphatase) to remove damaged nucleotides from the pool [43].

There are four fates of 8-oxoG in cellular DNA and nucleotides: further oxidation to more stable products, which will be discussed shortly, removal from DNA by repair mechanisms, removal from the nucleotide pool by nucleotide di- and triphosphatases, and eventual release from DNA following cell death. Like many nucleobase oxidation products, 8-oxo-G in DNA is removed by the base excision repair (BER) pathway [44–47], with the ultimate release of free 8-oxo-G nucleobase by N-glycosylase activity. On the other hand, dephosphorylation of 8-oxo-dGTP and dGDP ultimately releases 8-oxo-dGMP and 8-oxodG, which are also the likely forms released from DNA following cell death.

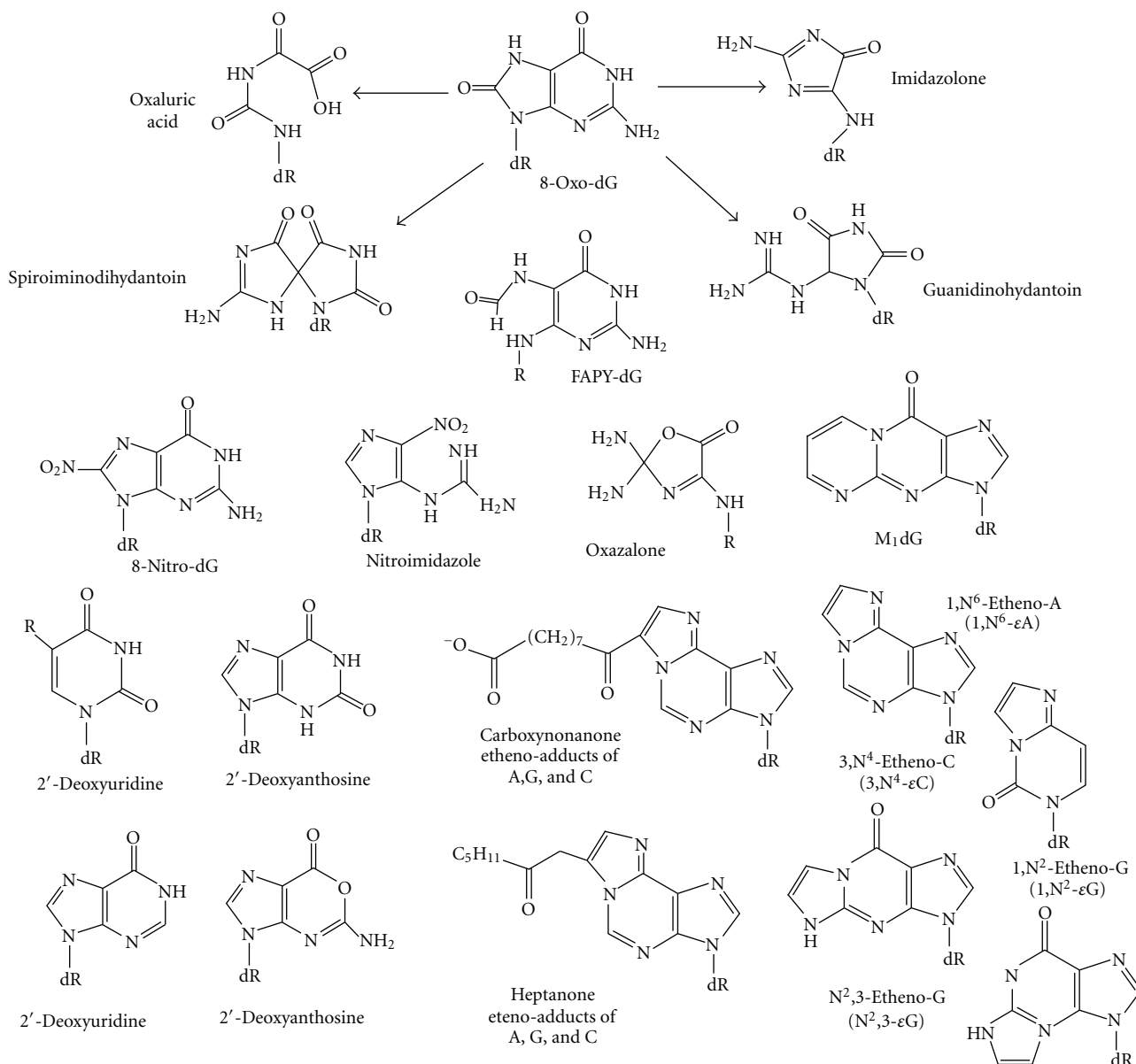


FIGURE 1: Nucleobase damage products.

So, we are faced with the choice of quantifying either 8-oxo-G, 8-oxo-dG, or 8-oxo-dGMP in sampling compartments such as blood and urine. The most abundant of these species appears to be 8-oxo-dG, which is present in human urine at concentrations in the micromolar range. 2-Deoxynucleosides are chromatographically well behaved, and this concentration is amenable to precise and accurate quantification by liquid chromatography-coupled with mass spectrometric methods. While the excretion of 8-oxo-dG may correlate well with conditions of oxidative stress and inflammation [23], the source of this 8-oxo-dG has yet to be established.

Another fate of 8-oxoG in DNA, RNA, and the nucleotide pool, as well as the fate of 8-oxo-G-containing species released from cells, is further oxidation to form a variety

of stable end products, as shown in Figure 1. 8-Oxo-G is significantly more susceptible to further oxidation than G itself (0.74 V versus 1.29 V relative to NHE [39]) and is thus susceptible to reaction with oxidants less potent than hydroxyl radical (2 V versus NHE), such as NO<sub>2</sub><sup>•</sup> (1.04 V versus NHE [48]) and alkyl hydroperoxides (~0.9 V versus NHE [49]). The oxidation of 8-oxo-dG results in the formation of several new products (Figure 1), most of which are more stable than 8-oxo-dG itself and thus potentially better candidates for biomarkers of inflammation and oxidative stress. One must again consider the roles of DNA repair, nucleotide pool cleaning activities, and excretory pathways in finalizing the fate of 8-oxo-G oxidation products.

Finally, recent studies suggest two other confounding factors in the biological fate of 8-oxo-G. The first relates to

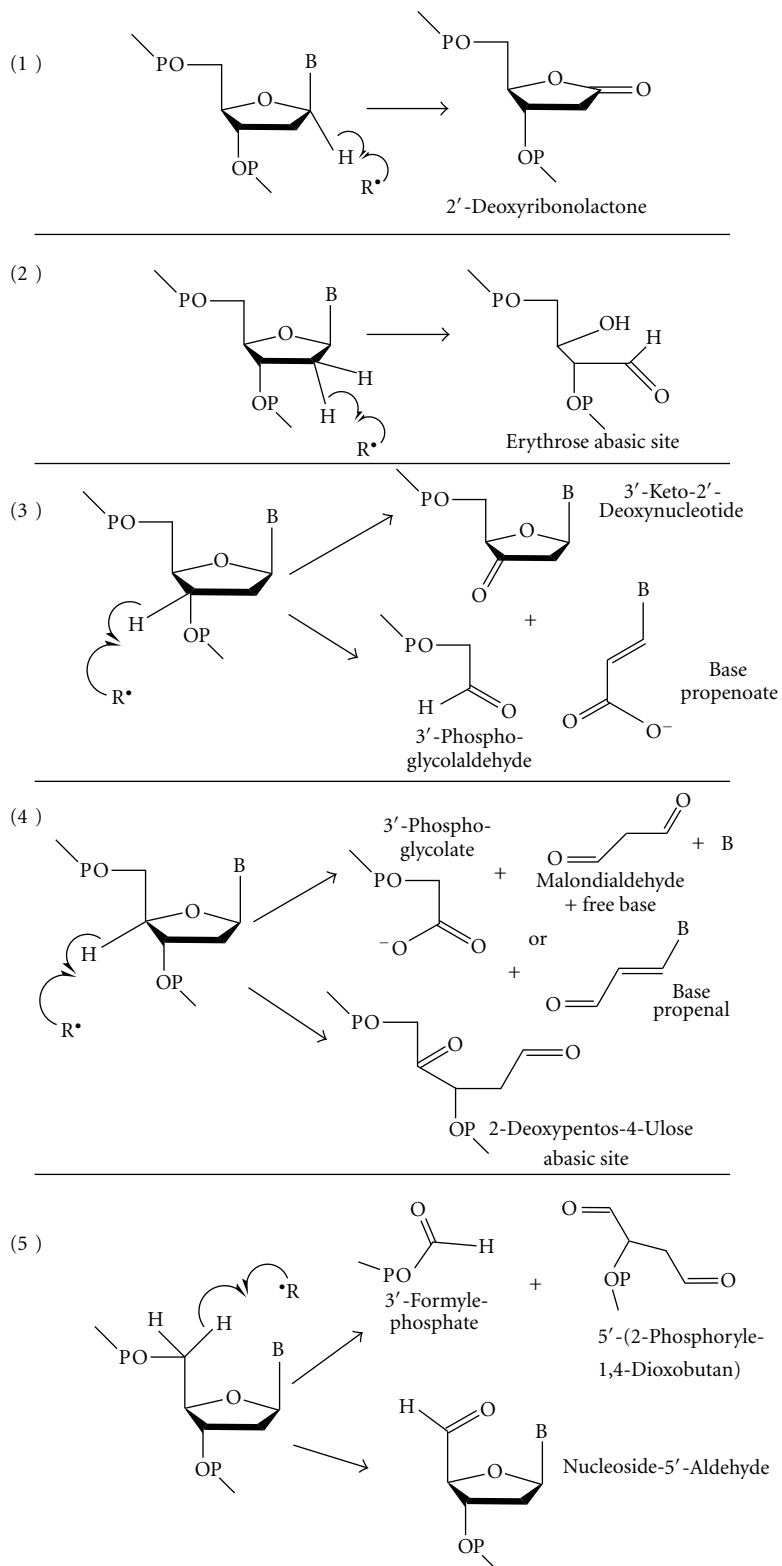


FIGURE 2: 2-Deoxyribose oxidation products.

alternate sources. A study by Tannenbaum and coworkers reveals that 8-oxo-G can arise by further oxidation of species such as 8-nitro-G, which arises from nitrative oxidation of G by  $\text{ONOO}^-$  and  $\text{ONOOCO}_2^-$  [50]. This and other analogous chemistries further confound the assignment of the source of 8-oxo-G-containing species as mechanistic biomarkers. The second confounder involves an alternative fate for 8-oxo-G: deamination to uric acid. Hall et al. have described 8-oxo-G deaminase activity in bacteria [51], which raises the possibility of similar activities in human cells. While we have not observed adventitious deamination of G in our studies of DNA deamination *in vitro* and *in vivo* [52–55], a G deaminase activity cannot be ruled out.

**3.2. Etheno Adducts.** Another major group of DNA lesions with a well-established association with oxidative stress and inflammation involves adducts formed in the reaction of DNA with electrophiles generated by lipid peroxidation [56–58]. This group includes the substituted and unsubstituted etheno nucleobase adducts [58–63] (Figure 1). Extensive study of the urinary excretion of unsubstituted etheno adducts has revealed a strong correlation of excretion with host of human diseases, pathologies, and environmental exposures related to oxidative stress (e.g., see recent studies in [16–21, 64]). Nonetheless, there have been few if any studies aimed at defining the source of the etheno 2-deoxynucleosides measured in these studies.

By analogy to 8-oxo-G, the fate of etheno adducts can be viewed from the perspectives of DNA repair and metabolism. Etheno adducts in DNA are presumed to be repaired by the BER pathway [65], with the release of the free-base adducts. However, biomarker studies again focus on the 2-deoxynucleoside form of the adducts [16–21, 64], which must arise from pathways other than DNA repair. The current focus on quantifying etheno adducts as 2-deoxynucleosides has recently been called into question by the Marnett group's pioneering studies of the metabolism of endogenous DNA adducts [27–29, 66]. With regard to etheno adducts, they incubated 2-deoxynucleoside forms of substituted and unsubstituted etheno adducts in rat liver cytosol and observed an initial deglycosylation of G-derived etheno adducts followed by oxidation of 1,  $N^2$ - $\epsilon$ -G to 2-oxo-1,  $N^2$ - $\epsilon$ -G and of the corresponding substituted adduct, heptanone-1,  $N^2$ - $\epsilon$ -G, to 2-oxoheptanone-1,  $N^2$ - $\epsilon$ -G (Figure 3) [66]. This raises the possibility that urinary biomarker studies may be underestimating the true level of etheno adducts as a result of loss of the 2-deoxynucleoside forms. Further, the oxidized free-base forms may also be useful as biomarkers if they are excreted at high enough levels.

**3.3.  $M_1dG$ .** This mutagenic pyrimidopurinone adduct of dG (Figure 1) forms in reactions of DNA with the lipid peroxidation product, malondialdehyde, and with base propenals derived from 4'-oxidation of 2-deoxyribose in DNA [56, 67–72]. As an endogenous DNA adduct,  $M_1dG$  has been detected at levels ranging from 1 to 1000 lesions per  $10^8$  nucleotides in a variety of organisms, including humans [67, 71, 73–79]. Recent studies suggest that the major source of  $M_1dG$  *in vivo* is base propenals from DNA oxidation [67],

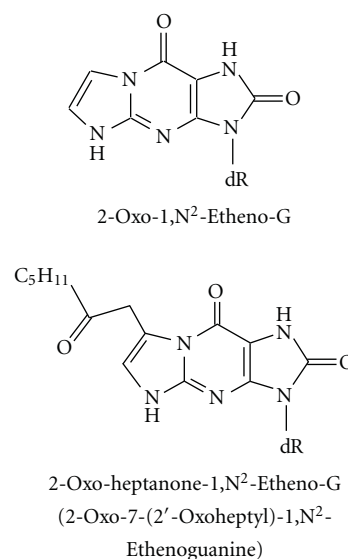


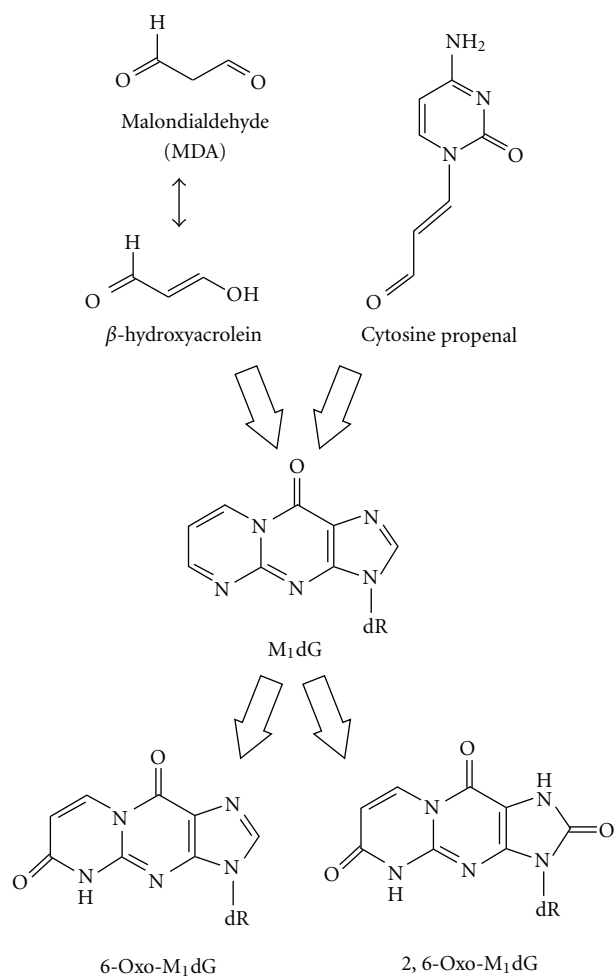
FIGURE 3: Oxidation of substituted etheno adducts.

which is consistent with the higher reactivity of base propenals than malondialdehyde [68, 69] and the proximity of base propenals to dG in DNA. However, contributions from both malondialdehyde and base propenals are likely to occur in an oxidant-, cell-, and tissue-dependent manner [72].

In terms of the biological fate of  $M_1dG$ , the adduct has been demonstrated to be a substrate for nucleotide excision repair (NER) [80, 81], which may explain the appearance of  $M_1dG$  in human and rodent urine [27–29, 79]. However,  $M_1dG$  was detectable in the human urine at levels of 10–20 fmol per kg per 24 h [79], which is a significantly lower excretion rate than other DNA lesions such as 8-oxo-dG (400 pmol per kg per 24 h) [82]. To explore the basis for this low rate of excretion, Marnett and coworkers undertook metabolic and pharmacokinetic studies of  $M_1dG$  in rats [27]. When intravenously administered to rats,  $M_1dG$  was rapidly eliminated from the plasma with a half-life of 10 min [27]. In contrast to the rapid clearance from blood,  $M_1dG$  was found in the urine for more than 24 hr after dosing, which suggested a rapid distribution to tissue followed by slower phase of excretion. Analysis of the urine revealed a metabolite of  $M_1dG$ , 6-oxo- $M_1dG$ , likely derived from hepatic xanthine oxidase activity [27]. Studies in rat liver extracts revealed further oxidation of 6-oxo- $M_1dG$  on the imidazole ring to give 2,6-dioxo- $M_1G$  (Figure 4) [28]. While most of the  $M_1dG$  was excreted unchanged in the urine and the problem of low levels of excretion remains unsolved, these studies point to the importance of defining the biological and metabolic fate of damaged biomolecules in efforts to develop biomarkers of inflammation and oxidative stress.

#### 4. The Biological and Metabolic Fates of 2-Deoxyribose Oxidation Products

In addition to the nucleobases in DNA, the 2-deoxyribose moiety is also subjected to oxidative damage that merits consideration of biological fate and metabolism [9]. As opposed

FIGURE 4: Formation and metabolism of M<sub>1</sub>dG.

to the concept of simple “strand breaks,” growing evidence points to 2-deoxyribose oxidation in DNA as a critical determinant of the toxicity of oxidative stress [9]. Oxidation of each of the five positions in 2-deoxyribose in DNA occurs with an initial hydrogen atom abstraction to form a carbon-centered radical that rapidly adds molecular oxygen to form an unstable peroxy radical. The resulting product spectra for 2-deoxyribose oxidation under aerobic conditions are shown in Figure 2 [9]. Many of these oxidation products are highly electrophilic, with  $\alpha,\beta$ -unsaturated carbonyl motifs, and are thus capable of reacting with proximate nucleophilic sites in DNA, RNA, and proteins to form adducts [9]. This section of the paper will focus on the biological and metabolic or, more broadly, biotransformational fates of 2-deoxyribose oxidation products.

**4.1. DNA Adducts of 2-Deoxyribose Oxidation Products.** One fate of DNA oxidation products is reaction with local electrophiles to form protein and nucleic acids adducts. In this regard, oxidation of 2-deoxyribose in DNA produces a variety of reactive electrophilic species (Figure 2) that readily form adducts with neighboring DNA bases. Oxidation of both the 2'- and 3'-positions of 2-deoxyribose can lead to the formation of the 2-phosphoglycolaldehyde residue

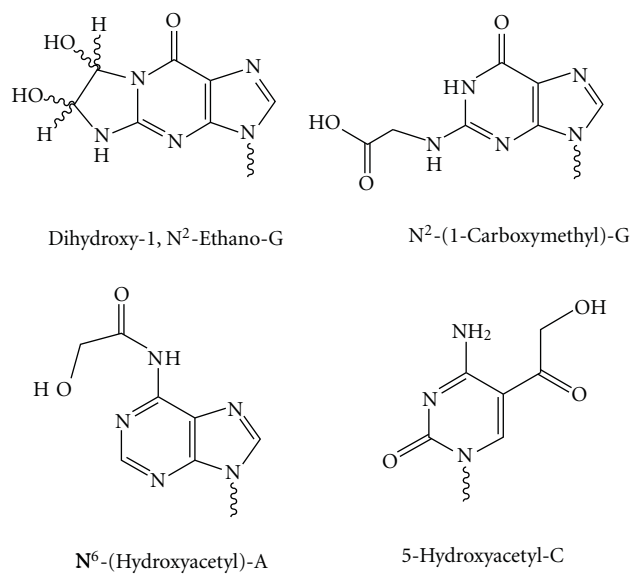


FIGURE 5: Glyoxal adducts of DNA.

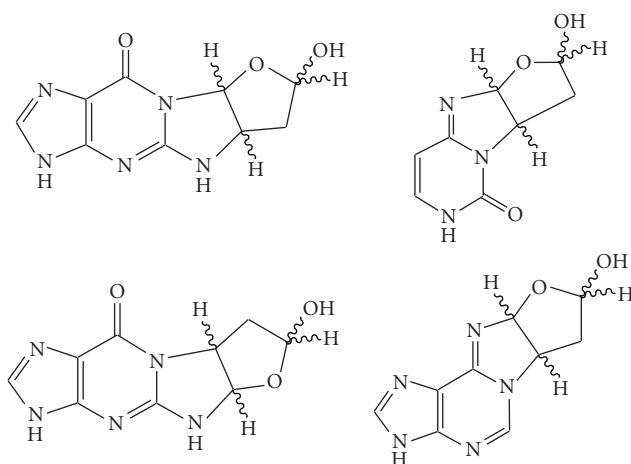


FIGURE 6: Reaction of 1,4-dioxo-2-butene to form bicyclic oxadiazabicyclo-(3.3.0) octamine adducts.

(Figure 2), the latter directly from the oxidation [83, 84] and the former by an induced and indirect oxidation mechanism involving an erythrose intermediate [85, 86]. By either mechanism, 2-phosphoglycolaldehyde undergoes a relatively slow phosphate-phosphonate rearrangement to generate the ubiquitous lipid and carbohydrate oxidation product, glyoxal, that reacts with dG and DNA to form diastereomeric 1,N<sup>2</sup>-glyoxal adducts of dG (Figure 5) [83].

At the 4'- and 5'-positions, 4'-oxidation generates base propenals that readily react with neighboring dG to form the pyrimidopurinone adduct, M<sub>1</sub>dG, as described earlier [67–69]. Oxidation of the 5'-position leads to formation of a 2-phosphoryldioxobutane residue that, possibly following  $\beta$ -elimination to form an  $\alpha,\beta$ -unsaturated *trans*-dioxobutene species, reacts with dC ≫ dG > dA to form bicyclic oxadiazabicyclo-(3.3.0) octamine adducts (Figure 6) [87–91].

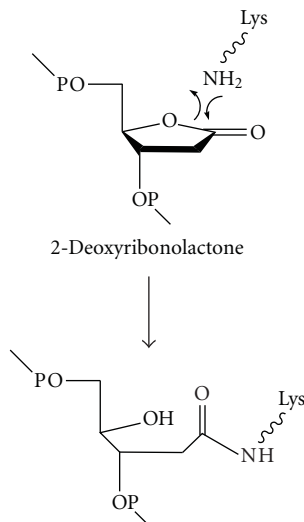


FIGURE 7: Formation of DNA-protein cross-links during repair of 2-deoxyribonolactone abasic sites in DNA.

#### 4.2. Protein Adducts of 2-Deoxyribose Oxidation Products.

In addition to DNA adducts, the electrophiles derived from 2-deoxyribose oxidation react with amino acid side chains in proteins to form a variety of adducts, some with functional consequences. One of the earliest examples of protein adducts from 2-deoxyribose oxidation involves the 1'-position. The 2-deoxyribonolactone abasic site resulting from 1'-oxidation in DNA reacts with DNA repair proteins to form stable protein-DNA cross-links [92, 93]. This phenomenon was first demonstrated by Hashimoto et al. with the *E. coli* DNA BER enzyme endonuclease III [92]. This enzyme normally functions in base excision repair pathways with both an initial N-glycosylase activity against oxidized pyrimidines and a subsequent incision of the resulting abasic site by a lyase activity [94]. Upon binding to the 2-deoxyribonolactone abasic site, however, the active site (lysine 120), which normally forms a Schiff base with the 1'-aldehyde in the ring-opened form of the native abasic site, performs a nucleophilic attack on the carbonyl group of the lactone ring (Figure 7). Unlike a Schiff base, the resulting cross-link is irreversible and complicates the DNA repair process [92]. DeMott et al. observed similar results in which a covalent amide bond was formed by the 1'-carbon of the lactone and the lysine 72 in human polymerase  $\beta$  [93]. Additionally, the 2-deoxyribonolactone undergoes a rate-limiting  $\beta$ -elimination reaction to form a butenolide species with a half-life of 20 h in single-stranded DNA (32–54 h in duplex DNA), followed by a rapid  $\delta$ -elimination to release 5-methylene-2(5H)-furanone [95]. Both the intermediate butenolide and the product methylenefuranone are electrophilic species capable of reaction with nucleophilic sites in DNA and protein, and possibly subject to metabolic reactions such as glutathione conjugation.

Another potential source of protein adducts arises from the variety of  $\alpha,\beta$ -unsaturated carbonyl and dicarbonyl products of 2-deoxyribose oxidation in DNA. The potential here lies in the high concentration of nucleophilic lysine

and arginine residues in histone proteins proximate to the sites of DNA damage and in the well-established reactivity of  $\alpha,\beta$ -unsaturated carbonyl and dicarbonyl species with nucleophilic amino acids, which is perhaps best illustrated by lipid peroxidation products (e.g., [96–103]). Several recent studies have identified specific lysine and histidine adducts of well-defined lipid peroxidation products such as malondialdehyde [100], 4-hydroxynonenal [99], and its oxidation product, 4-oxononenal [97] (Figure 8). The reactions forming these adducts are highly analogous to reactions that could occur with 2-deoxyribose oxidation products, as illustrated in Figure 8. For example, the unsaturated  $\beta$ -elimination product of the 2-deoxypentose-4-ulose product of 4'-oxidation of deoxyribose is a chemical analog of 4-oxononenal derived from lipid peroxidation. It would thus be expected to react with lysines and histidines in histone and other chromatin proteins to form the *bis*-adduct or cross-link observed by observed by Sayre and coworkers [104] and the stable furan derivative observed by observed by Blair and coworkers [97], respectively (Figure 8). Indeed, histones 2A, 2B, and 3 contain 3–5 histidines that have been exploited to cross-link histones to DNA in the classic studies of Mirzabekov and coworkers [105, 106].

The malondialdehyde adducts of lysine, arginine, and histidine represent another protein adduct chemistry with potential parallels between 2-deoxyribose oxidation and lipid peroxidation. The reaction of lysine by nucleophilic substitution yields a moderately stable N-propenal-lysine species (Figure 8) that can react with another lysine to form a propyl-bridged cross-link [107], while the reaction of malondialdehyde with arginine has been shown to produce a stable pyrimidyl-ornithine species (Figure 8) [107]. In both cases, the proportions of modified amino acids are high [108]. Given the analogous reactions of malondialdehyde and base propenals from 4'-oxidation, it is reasonable to expect the formation of propyl-bridged cross-links and pyrimidyl-ornithine species in histone proteins in cells subjected to oxidative stresses.

A final example of protein adducts derived from 2-deoxyribose oxidation products involves N-formylation of lysine by transfer of formyl groups from 3'-formylphosphate residues (Figure 9) [109], among other possible sources such as oxidation of formaldehyde adducts of lysine. N<sup>6</sup>-formyllysine was detected in histone proteins from a variety of sources to the extent of 0.04%–0.1% of all lysines in acid-soluble chromatin proteins including histones, which suggests that the adduct represents an endogenous secondary modification of histones [109]. The chemical analogy of the N-formyl modification to the physiologically important lysine N-acetylation and N-methylation suggests that lysine N-formylation may interfere with signaling mediated by histone and other chromatin protein modifications (e.g., [110, 111]).

In all of these cases, the adducted proteins are subject to degradation, with the potential for the release and excretion of adducted peptides or amino acids. Their potential as biomarkers warrants further study of DNA-derived protein adducts.

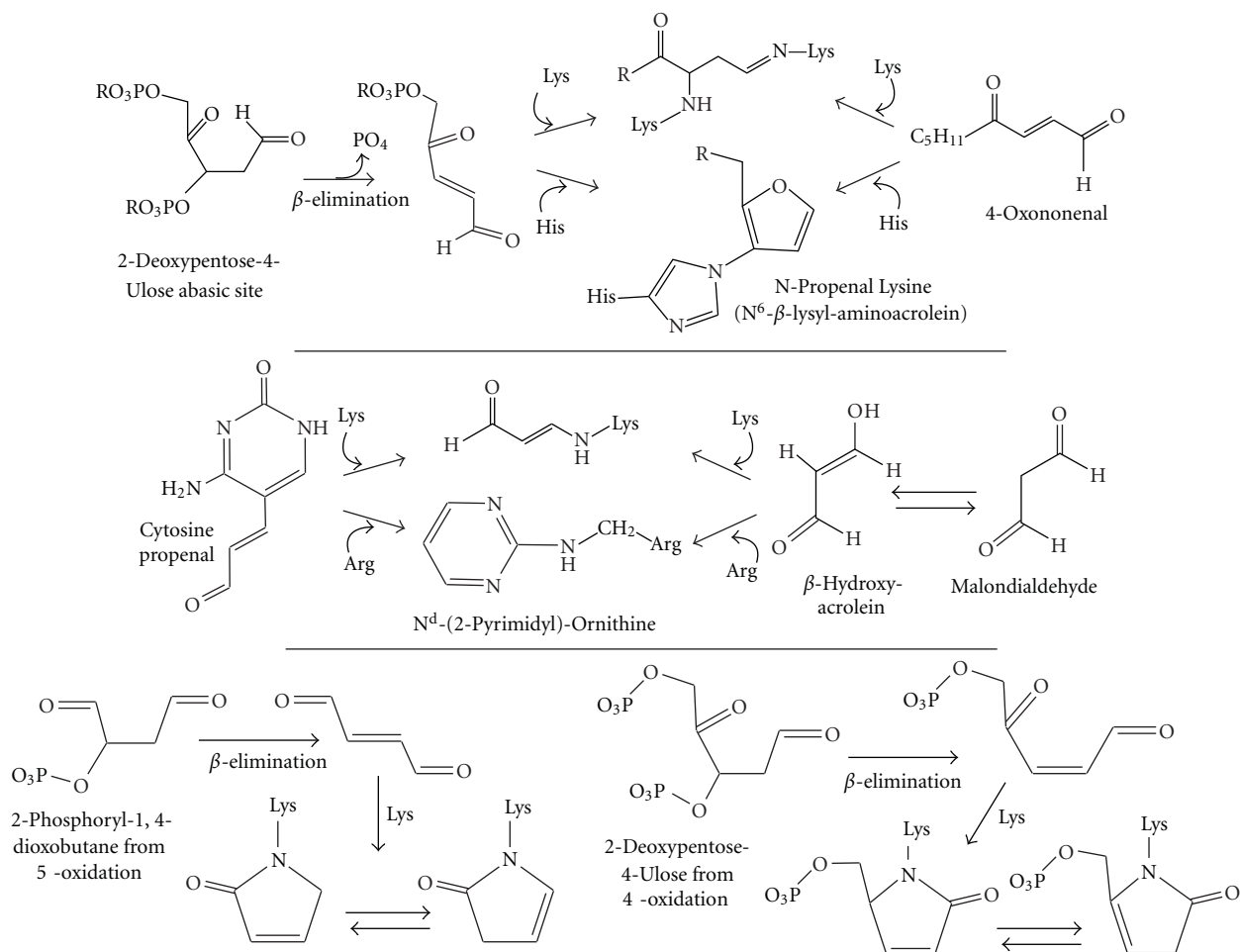


FIGURE 8: Reaction of lipid peroxidation products with lysine.

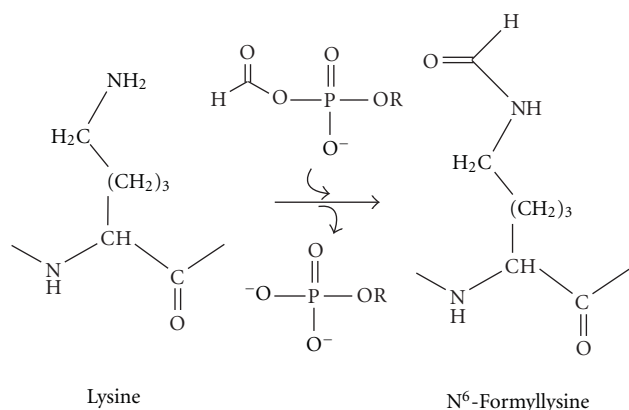


FIGURE 9: Lysine N-formylation by 3'-formylphosphate from 5'-oxidation of 2-deoxyribose.

4.3. *Metabolism of 2-Deoxyribose Oxidation Products.* As in the case of nucleobase lesions, the products of 2-deoxyribose oxidation of DNA must also be considered as substrates for metabolic enzymes and biotransformational reactions. This is all the more apparent given the electrophilic nature of the products, which points to glutathione (GSH) adduct

formation, and the  $\alpha,\beta$ -unsaturated carbonyl structure of many of the products, which makes them ideal substrates for glutathione S-transferases (GST) [34]. Indeed, GSTs have been shown to react with  $\alpha,\beta$ -unsaturated aldehyde-containing lipid peroxidation products, many of which are chemical analogues of 2-deoxyribose oxidation products [9, 68]. Two examples of GST reactions with 2-deoxyribose oxidation products illustrate this biotransformation concept.

The first example involves GSH conjugation of base propenals. One of the classic definitions of GST substrates is that they must react directly with GSH to a measurable extent [34]. This is indeed the case with base propenals, as demonstrated in studies by Berhane et al. in which GSH added to give a Michael adduct and a substitution product with loss of the nucleobase (Figure 10) [30]. In addition, base propenals were found to be among the best substrates for the Pi class of GSTs, producing a single GSH conjugate (Figure 10).

GSH conjugates have also been identified for furan metabolite *cis*-1,4-dioxo-2-butene [31, 32], the conformational isomer of the *trans*-1,4-dioxo-2-butene product of 5'-oxidation (Figure 2). Given the similarity in the reactivity of *cis*- and *trans*-1,4-dioxo-2-butene toward DNA adduct formation [9], it would not be surprising to identify

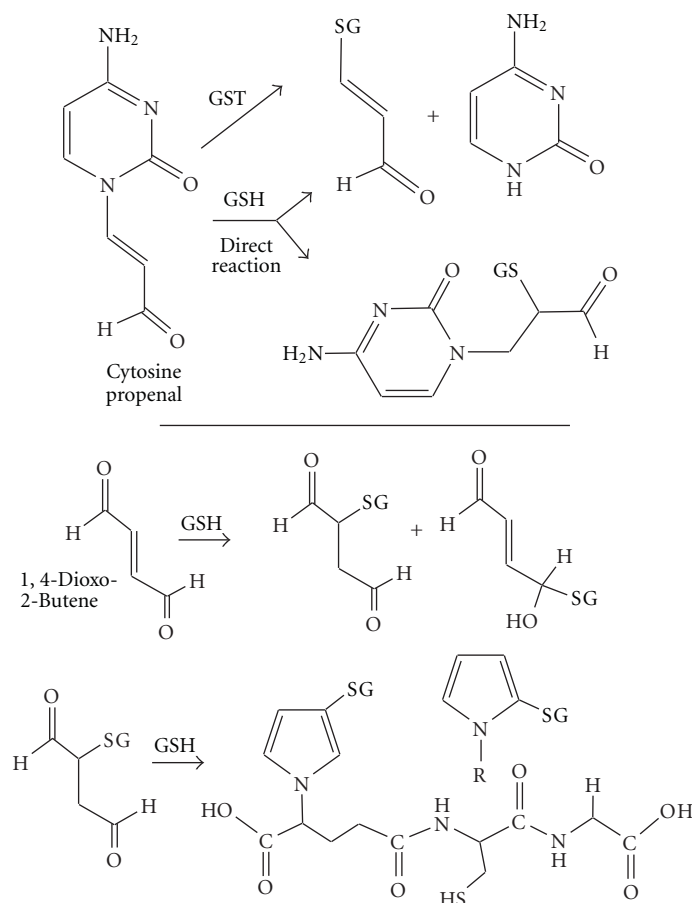


FIGURE 10: Formation of glutathione adducts of 2-deoxyribose oxidation products.

GSH adducts of the *trans*-isomer product of 2-deoxyribose oxidation, as has been observed *in vitro* and *in vivo* with the *cis*-isomer derivative of furan metabolism [31, 32, 112].

## 5. Prospects

Molecules damaged during normal physiological processes and in states of pathology represent a large source of biomarkers with potential clinical utility in defining etiological mechanisms, quantifying the risk of human disease and studying interindividual variations in cellular repair pathways. In spite of this potential, there has been little effort to define the biotransformational fate of damaged biomolecules as they move from the site of formation to excretion in clinically accessible compartments. This paper has highlighted examples of this important problem with DNA damage products. Coupled with the development of more sensitive and specific analytical technologies, there are likely to be major advancements in defining the metabolism of DNA damage products and other damaged biomolecules in the coming years.

## References

- [1] L. A. Loeb and C. C. Harris, "Advances in chemical carcinogenesis: a historical review and prospective," *Cancer Research*, vol. 68, no. 17, pp. 6863–6872, 2008.
- [2] D. E. Barnes and T. Lindahl, "Repair and genetic consequences of endogenous DNA base damage in mammalian cells," *Annual Review of Genetics*, vol. 38, pp. 445–476, 2004.
- [3] J. C. Delaney and J. M. Essigmann, "Biological properties of single chemical-DNA adducts: a twenty year perspective," *Chemical Research in Toxicology*, vol. 21, no. 1, pp. 232–252, 2008.
- [4] G. P. Pfeifer, "Mutagenesis at methylated CpG sequences," *Current Topics in Microbiology and Immunology*, vol. 301, pp. 259–281, 2006.
- [5] R. De Bont and N. van Larebeke, "Endogenous DNA damage in humans: a review of quantitative data," *Mutagenesis*, vol. 19, no. 3, pp. 169–185, 2004.
- [6] B. Epe, "Role of endogenous oxidative DNA damage in carcinogenesis: what can we learn from repair-deficient mice?" *Biological Chemistry*, vol. 383, no. 3-4, pp. 467–475, 2002.
- [7] L. J. Marnett, "Oxyradicals and DNA damage," *Carcinogenesis*, vol. 21, no. 3, pp. 361–370, 2000.
- [8] P. C. Dedon and S. R. Tannenbaum, "Reactive nitrogen species in the chemical biology of inflammation," *Archives of Biochemistry and Biophysics*, vol. 423, no. 1, pp. 12–22, 2004.
- [9] P. C. Dedon, "The chemical toxicology of 2-deoxyribose oxidation in DNA," *Chemical Research in Toxicology*, vol. 21, no. 1, pp. 206–219, 2008.

- [10] D. Pluskota-Karwatka, "Modifications of nucleosides by endogenous mutagens-DNA adducts arising from cellular processes," *Bioorganic Chemistry*, vol. 36, no. 4, pp. 198–213, 2008.
- [11] Y. Wang, "Bulky DNA lesions induced by reactive oxygen species," *Chemical Research in Toxicology*, vol. 21, no. 2, pp. 276–281, 2008.
- [12] U. Nair, H. Bartsch, and J. Nair, "Lipid peroxidation-induced DNA damage in cancer-prone inflammatory diseases: a review of published adduct types and levels in humans," *Free Radical Biology and Medicine*, vol. 43, no. 8, pp. 1109–1120, 2007.
- [13] S. J. Sturla, "DNA adduct profiles: chemical approaches to addressing the biological impact of DNA damage from small molecules," *Current Opinion in Chemical Biology*, vol. 11, no. 3, pp. 293–299, 2007.
- [14] M. S. Cooke, R. Olinski, and S. Loft, "Measurement and meaning of oxidatively modified DNA lesions in urine," *Cancer Epidemiology Biomarkers and Prevention*, vol. 17, no. 1, pp. 3–14, 2008.
- [15] M. D. Evans, M. Dizdaroglu, and M. S. Cooke, "Oxidative DNA damage and disease: induction, repair and significance," *Mutation Research*, vol. 567, no. 1, pp. 1–61, 2004.
- [16] J. Nair, P. Srivatanakul, C. Haas et al., "High urinary excretion of lipid peroxidation-derived DNA damage in patients with cancer-prone liver diseases," *Mutation Research*, vol. 683, pp. 23–28, 2009.
- [17] S. Dechakhamphu, S. Pinlaor, P. Sithithaworn, J. Nair, H. Bartsch, and P. Yongvanit, "Lipid peroxidation and etheno DNA adducts in white blood cells of liver fluke-infected patients: protection by plasma  $\alpha$ -tocopherol and praziquantel," *Cancer Epidemiology Biomarkers and Prevention*, vol. 19, no. 1, pp. 310–318, 2010.
- [18] S. Dechakhamphu, P. Yongvanit, J. Nair, S. Pinlaor, P. Sithithaworn, and H. Bartsch, "High excretion of etheno adducts in liver fluke-infected patients: protection by Praziquantel against DNA damage," *Cancer Epidemiology Biomarkers and Prevention*, vol. 17, no. 7, pp. 1658–1664, 2008.
- [19] M. Meerang, J. Nair, P. Sirankapracha et al., "Increased urinary 1, $N^6$ -ethenodeoxyadenosine and 3, $N^4$ -ethenodeoxycytidine excretion in thalassemia patients: markers for lipid peroxidation-induced DNA damage," *Free Radical Biology and Medicine*, vol. 44, no. 10, pp. 1863–1868, 2008.
- [20] H.-J. C. Chen and C.-F. Kao, "Effect of gender and cigarette smoking on urinary excretion of etheno DNA adducts in humans measured by isotope dilution gas chromatography/mass spectrometry," *Toxicology Letters*, vol. 169, no. 1, pp. 72–81, 2007.
- [21] P. R. Hillestrøm, M.-I. Covas, and H. E. Poulsen, "Effect of dietary virgin olive oil on urinary excretion of etheno-DNA adducts," *Free Radical Biology and Medicine*, vol. 41, no. 7, pp. 1133–1138, 2006.
- [22] J. Son, B. Pang, J. L. McFaline, K. Taghizadeh, and P. C. Dedon, "Surveying the damage: the challenges of developing nucleic acid biomarkers of inflammation," *Molecular BioSystems*, vol. 4, no. 9, pp. 902–908, 2008.
- [23] M. D. Evans, R. Olinski, S. Loft et al., "Toward consensus in the analysis of urinary 8-oxo-7,8-dihydro-2'-deoxyguanosine as a noninvasive biomarker of oxidative stress," *FASEB Journal*, vol. 24, no. 4, pp. 1249–1260, 2010.
- [24] G. B. Elion, A. Kovensky, G. H. Hitchings, E. Metz, and R. W. Rundles, "Metabolic studies of allopurinol, an inhibitor of xanthine oxidase," *Biochemical Pharmacology*, vol. 15, no. 7, pp. 863–880, 1966.
- [25] S. K. Roy, K. R. Korzekwa, F. J. Gonzalez, R. C. Mosche, and M. E. Dolan, "Human liver oxidative metabolism of  $O^6$ -benzylguanine," *Biochemical Pharmacology*, vol. 50, no. 9, pp. 1385–1389, 1995.
- [26] D.-H. Kim and F. P. Guengerich, "Excretion of the mercapturic acid S-[2-( $N^7$ -guanyl)ethyl]N-acetylcysteine in urine following administration of ethylene dibromide to rats," *Cancer Research*, vol. 49, no. 21, pp. 5843–5847, 1989.
- [27] M. B. Otteneeder, C. G. Knutson, J. S. Daniels et al., "In vivo oxidative metabolism of a major peroxidation-derived DNA adduct, M1dG," *Proceedings of the National Academy of Sciences of the United States of America*, vol. 103, no. 17, pp. 6665–6669, 2006.
- [28] C. G. Knutson, D. Akingbade, B. C. Crews, M. Voehler, D. F. Stec, and L. J. Marnett, "Metabolism in vitro and in vivo of the DNA base adduct, M<sub>1</sub>G," *Chemical Research in Toxicology*, vol. 20, no. 3, pp. 550–557, 2007.
- [29] C. G. Knutson, P. L. Skipper, R. G. Liberman, S. R. Tannenbaum, and L. J. Marnett, "Monitoring in vivo metabolism and elimination of the endogenous DNA adduct, M<sub>1</sub>dG 3-(2-Deoxy- $\beta$ -D-erythropentofuranosyl)pyrimido[1,2- $\alpha$ ]purin-10(3H)-one, by accelerator mass spectrometry," *Chemical Research in Toxicology*, vol. 21, no. 6, pp. 1290–1294, 2008.
- [30] K. Berhane, M. Widersten, Å. Engström, J. W. Kozarich, and B. Mannervik, "Detoxication of base propenals and other  $\alpha,\beta$ -unsaturated aldehyde products of radical reactions and lipid peroxidation by human glutathione transferases," *Proceedings of the National Academy of Sciences of the United States of America*, vol. 91, no. 4, pp. 1480–1484, 1994.
- [31] L.-J. Chen, S. S. Hecht, and L. A. Peterson, "Characterization of amino acid and glutathione adducts of cis-2-butene-1,4-dial, a reactive metabolite of furan," *Chemical Research in Toxicology*, vol. 10, no. 8, pp. 866–874, 1997.
- [32] L. A. Peterson, M. E. Cummings, C. C. Vu, and B. A. Matter, "Glutathione trapping to measure microsomal oxidation of furan to cis-2-butene-1,4-dial," *Drug Metabolism and Disposition*, vol. 33, no. 10, pp. 1453–1458, 2005.
- [33] A. F. Nassar and P. F. H. JoAnn Scatina, *Drug Metabolism Handbook*, John Wiley & Sons, River Street Hoboken, NJ, USA, 2009.
- [34] L. J. Casarett, J. Doull, and C. D. Klaassen, *Casarett and Doull's Toxicology: The Basic Science of Poisons*, McGraw-Hill, New York, NY, USA, 7th edition, 2008.
- [35] J. Cadet, T. Douki, and J.-L. Ravanat, "Oxidatively generated damage to the guanine moiety of DNA: mechanistic aspects and formation in cells," *Accounts of Chemical Research*, vol. 41, no. 8, pp. 1075–1083, 2008.
- [36] M. S. Cooke, P. T. Henderson, and M. D. Evans, "Sources of extracellular, oxidatively-modified DNA lesions: implications for their measurement in urine," *Journal of Clinical Biochemistry and Nutrition*, vol. 45, no. 3, pp. 255–270, 2009.
- [37] J. C. Niles, J. S. Wishnok, and S. R. Tannenbaum, "Peroxynitrite-induced oxidation and nitration products of guanine and 8-oxoguanine: structures and mechanisms of product formation," *Nitric Oxide*, vol. 14, no. 2, pp. 109–121, 2006.
- [38] J. Cadet, T. Douki, and J.-L. Ravanat, "One-electron oxidation of DNA and inflammation processes," *Nature Chemical Biology*, vol. 2, no. 7, pp. 348–349, 2006.

- [39] S. Steenken and S. V. Jovanovic, "How easily oxidizable is DNA? One-electron reduction potentials of adenosine and guanosine radicals in aqueous solution," *Journal of the American Chemical Society*, vol. 119, no. 3, pp. 617–618, 1997.
- [40] M. K. Shigenaga, E. N. Aboujaoude, Q. Chen, and B. N. Ames, "Assays of oxidative DNA damage biomarkers 8-oxo-2'-deoxyguanosine and 8-oxoguanine in nuclear DNA and biological fluids by high-performance liquid chromatography with electrochemical detection," *Methods in Enzymology*, vol. 234, pp. 16–33, 1994.
- [41] K. Broedbaek, H. E. Poulsen, A. Weimann et al., "Urinary excretion of biomarkers of oxidatively damaged DNA and RNA in hereditary hemochromatosis," *Free Radical Biology and Medicine*, vol. 47, no. 8, pp. 1230–1233, 2009.
- [42] Y. Nakabeppu, S. Oka, Z. Sheng, D. Tsuchimoto, and K. Sakumi, "Programmed cell death triggered by nucleotide pool damage and its prevention by MutT homolog-1 (MTH1) with oxidized purine nucleoside triphosphatase," *Mutation Research*, vol. 703, no. 1, pp. 51–58, 2010.
- [43] A. G. McLennan, "The Nudix hydrolase superfamily," *Cellular and Molecular Life Sciences*, vol. 63, no. 2, pp. 123–143, 2006.
- [44] T. Paz-Elizur, Z. Sevilya, Y. Leitner-Dagan, D. Elinger, L. C. Roisman, and Z. Livneh, "DNA repair of oxidative DNA damage in human carcinogenesis: potential application for cancer risk assessment and prevention," *Cancer Letters*, vol. 266, no. 1, pp. 60–72, 2008.
- [45] S. Maynard, S. H. Schurman, C. Harboe, N. C. de Souza-Pinto, and V. A. Bohr, "Base excision repair of oxidative DNA damage and association with cancer and aging," *Carcinogenesis*, vol. 30, no. 1, pp. 2–10, 2009.
- [46] J. I. Friedman and J. T. Stivers, "Detection of damaged DNA bases by DNA glycosylase enzymes," *Biochemistry*, vol. 49, no. 24, pp. 4957–4967, 2010.
- [47] S. S. David, V. L. O'Shea, and S. Kundu, "Base-excision repair of oxidative DNA damage," *Nature*, vol. 447, no. 7147, pp. 941–950, 2007.
- [48] D. M. Stanbury, "Reduction potentials involving inorganic free radicals in aqueous solution," *Advances in Inorganic Chemistry*, vol. 33, no. C, pp. 69–138, 1989.
- [49] T. N. Das, T. Dhanasekaran, Z. B. Alfassi, and P. Neta, "Reduction potential of the tert-butylperoxyl radical in aqueous solutions," in *Proceedings of the 4th International Conference on Chemical Kinetics*, National Institute of Standards and Technology, Gaithersburg, Md, USA, 1997.
- [50] J. M. Lee, J. C. Niles, J. S. Wishnok, and S. R. Tannenbaum, "Peroxynitrite reacts with 8-oxipurines to yield 8-oxopurines," *Chemical Research in Toxicology*, vol. 15, no. 1, pp. 7–14, 2002.
- [51] R. S. Hall, A. A. Fedorov, R. Marti-Arbona et al., "The hunt for 8-oxoguanine deaminase," *Journal of the American Chemical Society*, vol. 132, no. 6, pp. 1762–1763, 2010.
- [52] M. Dong and P. C. Dedon, "Relatively small increases in the steady-state levels of nucleobase deamination products in DNA from human TK6 cells exposed to toxic levels of nitric oxide," *Chemical Research in Toxicology*, vol. 19, no. 1, pp. 50–57, 2006.
- [53] M. Dong, C. Wang, W. M. Deen, and P. C. Dedon, "Absence of 2'-deoxyoxanosine and presence of abasic sites in DNA exposed to nitric oxide at controlled physiological concentrations," *Chemical Research in Toxicology*, vol. 16, no. 9, pp. 1044–1055, 2003.
- [54] B. Pang, X. Zhou, H. Yu et al., "Lipid peroxidation dominates the chemistry of DNA adduct formation in a mouse model of inflammation," *Carcinogenesis*, vol. 28, no. 8, pp. 1807–1813, 2007.
- [55] K. Taghizadeh, J. L. McFaline, B. Pang et al., "Quantification of DNA damage products resulting from deamination, oxidation and reaction with products of lipid peroxidation by liquid chromatography isotope dilution tandem mass spectrometry," *Nature Protocols*, vol. 3, no. 8, pp. 1287–1298, 2008.
- [56] L. J. Marnett, "Oxy radicals, lipid peroxidation and DNA damage," *Toxicology*, vol. 181–182, pp. 219–222, 2002.
- [57] T. J. Montine, M. D. Neely, J. F. Quinn et al., "Lipid peroxidation in aging brain and Alzheimer's disease," *Free Radical Biology and Medicine*, vol. 33, no. 5, pp. 620–626, 2002.
- [58] H. Bartsch and J. Nair, "Oxidative stress and lipid peroxidation-derived DNA-lesions in inflammation driven carcinogenesis," *Cancer Detection and Prevention*, vol. 28, no. 6, pp. 385–391, 2004.
- [59] M. V. Williams, H. L. Seon, M. Pollack, and I. A. Blair, "Endogenous lipid hydroperoxide-mediated DNA-adduct formation in min mice," *The Journal of Biological Chemistry*, vol. 281, no. 15, pp. 10127–10133, 2006.
- [60] S. H. Lee, M. V. Williams, R. N. DuBois, and I. A. Blair, "Cyclooxygenase-2-mediated DNA damage," *The Journal of Biological Chemistry*, vol. 280, no. 31, pp. 28337–28346, 2005.
- [61] K. Schmid, J. Nair, G. Winde, I. Velic, and H. Bartsch, "Increased levels of promutagenic etheno-DNA adducts in colonic polyps of FAP patients," *International Journal of Cancer*, vol. 87, no. 1, pp. 1–4, 2000.
- [62] J. Nair, A. Barbin, and H. Bartsch, "Etheno DNA-base adducts from endogenous reactive species," *Mutation Research*, vol. 424, no. 1–2, pp. 59–69, 1999.
- [63] S. H. Lee, J. A. Arora, T. Oe, and I. A. Blair, "4-Hydroperoxy-2-nonenal-induced formation of 1,N<sup>2</sup>-etheno-2'-deoxyguanosine adducts," *Chemical Research in Toxicology*, vol. 18, no. 4, pp. 780–786, 2005.
- [64] H.-J.C. Chen, G.-J. Lin, and W.-P. Lin, "Simultaneous quantification of three lipid peroxidation-derived etheno adducts in human DNA by stable isotope dilution nanoflow liquid chromatography nanospray ionization tandem mass spectrometry," *Analytical Chemistry*, vol. 82, no. 11, pp. 4486–4493, 2010.
- [65] L. Gros, A. A. Ishchenko, and M. Sapparbaev, "Enzymology of repair of etheno-adducts," *Mutation Research*, vol. 531, no. 1–2, pp. 219–229, 2003.
- [66] C. G. Knutson, E. H. Rubinson, D. Akingbade et al., "Oxidation and glycolytic cleavage of etheno and propano DNA base adducts," *Biochemistry*, vol. 48, no. 4, pp. 800–809, 2009.
- [67] X. Zhou, K. Taghizadeh, and P. C. Dedon, "Chemical and biological evidence for base propenals as the major source of the endogenous M<sub>1</sub>dG adduct in cellular DNA," *The Journal of Biological Chemistry*, vol. 280, no. 27, pp. 25377–25382, 2005.
- [68] P. C. Dedon, J. P. Plataras, C. A. Rouzer, and L. J. Marnett, "Indirect mutagenesis by oxidative DNA damage: formation of the pyrimidopyrimidone adduct of deoxyguanosine by base propenal," *Proceedings of the National Academy of Sciences of the United States of America*, vol. 95, no. 19, pp. 11113–11116, 1998.

- [69] J. P. Plastaras, J. N. Riggins, M. Otteneider, and L. J. Marnett, "Reactivity and mutagenicity of endogenous DNA oxopropenylating agents: base propenals, malondialdehyde, and  $N^{\epsilon}$ -oxopropenyllysine," *Chemical Research in Toxicology*, vol. 13, no. 12, pp. 1235–1242, 2000.
- [70] A. K. Basu, S. M. O'Hara, P. Valladier, K. Stone, O. Mols, and L. J. Marnett, "Identification of adducts formed by reaction of guanine nucleosides with malondialdehyde and structurally related aldehydes," *Chemical Research in Toxicology*, vol. 1, no. 1, pp. 53–59, 1988.
- [71] A. K. Chaudhary, M. Nokubo, G. R. Reddy et al., "Detection of endogenous malondialdehyde-deoxyguanosine adducts in human liver," *Science*, vol. 265, no. 5178, pp. 1580–1582, 1994.
- [72] Y.-C. Jeong and J. A. Swenberg, "Formation of  $M_1G$ -dR from endogenous and exogenous ROS-inducing chemicals," *Free Radical Biology and Medicine*, vol. 39, no. 8, pp. 1021–1029, 2005.
- [73] C. A. Rouzer, A. K. Chaudhary, M. Nokubo et al., "Analysis of the malondialdehyde-2'-deoxyguanosine adduct pyrimidopurinone in human leukocyte DNA by gas chromatography/electron capture/negative chemical ionization/mass spectrometry," *Chemical Research in Toxicology*, vol. 10, no. 2, pp. 181–188, 1997.
- [74] A. K. Chaudhary, G. R. Reddy, I. A. Blair, and L. J. Marnett, "Characterization of an  $N^6$ -oxopropenyl-2'-deoxyadenosine adduct in malondialdehyde-modified DNA using liquid chromatography/electrospray ionization tandem mass spectrometry," *Carcinogenesis*, vol. 17, no. 5, pp. 1167–1170, 1996.
- [75] Y.-C. Jeong, R. Sangaiah, J. Nakamura et al., "Analysis of  $M_1G$ -dR in DNA by aldehyde reactive probe labeling and liquid chromatography tandem mass spectrometry," *Chemical Research in Toxicology*, vol. 18, no. 1, pp. 51–60, 2005.
- [76] F. F. Kadlubar, K. E. Anderson, S. Häussermann et al., "Comparison of DNA adduct levels associated with oxidative stress in human pancreas," *Mutation Research*, vol. 405, no. 2, pp. 125–133, 1998.
- [77] C. Leuratti, R. Singh, C. Lagneau et al., "Determination of malondialdehyde-induced DNA damage in human tissues using an immunoslot blot assay," *Carcinogenesis*, vol. 19, no. 11, pp. 1919–1924, 1998.
- [78] P. Yi, X. Sun, D. R. Doerge, and P. P. Fu, "An improved 32P-postlabeling/high-performance liquid chromatography method for the analysis of the malondialdehyde-derived 1, $N^6$ -propanodeoxyguanosine DNA adduct in animal and human tissues," *Chemical Research in Toxicology*, vol. 11, no. 9, pp. 1032–1041, 1998.
- [79] A.-M. Hoberg, M. Otteneider, L. J. Marnett, and H. E. Poulsen, "Measurement of the malondialdehyde-2'-deoxyguanosine adduct in human urine by immuno-extraction and liquid chromatography/atmospheric pressure chemical ionization tandem mass spectrometry," *Journal of Mass Spectrometry*, vol. 39, no. 1, pp. 38–42, 2004.
- [80] S. P. Fink, G. R. Reddy, and L. J. Marnett, "Mutagenicity in *Escherichia coli* of the major DNA adduct derived from the endogenous mutagen malondialdehyde," *Proceedings of the National Academy of Sciences of the United States of America*, vol. 94, no. 16, pp. 8652–8657, 1997.
- [81] L. J. Marnett, "Lipid peroxidation—DNA damage by malondialdehyde," *Mutation Research*, vol. 424, no. 1-2, pp. 83–95, 1999.
- [82] A. Weimann, D. Belling, and H. E. Poulsen, "Quantification of 8-oxo-guanine and guanine as the nucleobase, nucleoside and deoxynucleoside forms in human urine by high-performance liquid chromatography-electrospray tandem mass spectrometry," *Nucleic acids research*, vol. 30, no. 2, p. E7, 2002.
- [83] M. Awada and P. C. Dedon, "Formation of the 1, $N^2$ -glyoxal adduct of deoxyguanosine by phosphoglycolaldehyde, a product of 3'-deoxyribose oxidation in DNA," *Chemical Research in Toxicology*, vol. 14, no. 9, pp. 1247–1253, 2001.
- [84] G. A. Lahoud, A. L. Hitt, and A. C. Bryant-Friedrich, "Aerobic fate of the C-3'-thymidyl radical in single-stranded DNA," *Chemical Research in Toxicology*, vol. 19, no. 12, pp. 1630–1636, 2006.
- [85] H. Sugiyama, Y. Tsutsumi, K. Fujimoto, and I. Saito, "Photoinduced deoxyribose C2' oxidation in DNA. Alkali-dependent cleavage of erythrose-containing sites via a retroaldol reaction," *Journal of the American Chemical Society*, vol. 115, no. 11, pp. 4443–4448, 1993.
- [86] J. Kim, Y. N. Weledji, and M. M. Greenberg, "Independent generation and characterization of a C2'-oxidized basic site in chemically synthesized oligonucleotides," *Journal of Organic Chemistry*, vol. 69, no. 18, pp. 6100–6104, 2004.
- [87] T. Bohnert, L. Gingipalli, and P. C. Dedon, "Reaction of 2'-deoxyribonucleosides with cis- and trans-1,4-dioxo-2-butene," *Biochemical and Biophysical Research Communications*, vol. 323, no. 3, pp. 838–844, 2004.
- [88] B. Chen, T. Bohnert, X. Zhou, and P. C. Dedon, "5'-(2-phosphoryl-1,4-dioxobutane) as a product of 5'-oxidation of deoxyribose in DNA: elimination as trans-1,4-dioxo-2-butene and approaches to analysis," *Chemical Research in Toxicology*, vol. 17, no. 11, pp. 1406–1413, 2004.
- [89] B. Chen, C. C. Vu, M. C. Byrns, P. C. Dedon, and L. A. Peterson, "Formation of 1,4-dioxo-2-butene-derived adducts of 2'-deoxyadenosine and 2'-deoxycytidine in oxidized DNA," *Chemical Research in Toxicology*, vol. 19, no. 8, pp. 982–985, 2006.
- [90] M. C. Byrns, D. P. Predecki, and L. A. Peterson, "Characterization of nucleoside adducts of cis-2-butene-1,4-dial, a reactive metabolite of furan," *Chemical Research in Toxicology*, vol. 15, no. 3, pp. 373–379, 2002.
- [91] M. C. Byrns, C. C. Vu, J. W. Neidigh, J.-L. Abad, R. A. Jones, and L. A. Peterson, "Detection of DNA adducts derived from the reactive metabolite of furan, cis-2-butene-1,4-dial," *Chemical Research in Toxicology*, vol. 19, no. 3, pp. 414–420, 2006.
- [92] M. Hashimoto, M. M. Greenberg, Y. W. Kow, J.-T. Hwang, and R. P. Cunningham, "The 2-deoxyribonolactone lesion produced in DNA by neocarzinostatin and other damaging agents forms cross-links with the base-excision repair enzyme endonuclease III," *Journal of the American Chemical Society*, vol. 123, no. 13, pp. 3161–3162, 2001.
- [93] M. S. Demott, E. Beyret, D. Wong et al., "Covalent trapping of human DNA polymerase  $\beta$  by the oxidative DNA lesion 2-deoxyribonolactone," *The Journal of Biological Chemistry*, vol. 277, no. 10, pp. 7637–7640, 2002.
- [94] S. Boiteux, "Properties and biological functions of the NTH and FPG proteins of *Escherichia coli*: two DNA glycosylases that repair oxidative damage in DNA," *Journal of Photochemistry and Photobiology B*, vol. 19, no. 2, pp. 87–96, 1993.
- [95] Y. Zheng and T. L. Sheppard, "Half-life and DNA strand scission products of 2-deoxyribonolactone oxidative DNA damage lesions," *Chemical Research in Toxicology*, vol. 17, no. 2, pp. 197–207, 2004.

- [96] R. M. LoPachin, T. Gavin, D. R. Petersen, and D. S. Barber, "Molecular mechanisms of 4-hydroxy-2-nonenal and acrolein toxicity: nucleophilic targets and adduct formation," *Chemical Research in Toxicology*, vol. 22, no. 9, pp. 1499–1508, 2009.
- [97] A. K. Yocum, T. Oe, A. L. Yergey, and I. A. Blair, "Novel lipid hydroperoxide-derived hemoglobin histidine adducts as biomarkers of oxidative stress," *Journal of Mass Spectrometry*, vol. 40, no. 6, pp. 754–764, 2005.
- [98] L. M. Sayre, D. A. Zelasko, P. L. R. Harris, G. Perry, R. G. Salomon, and M. A. Smith, "4-Hydroxynonenal-derived advanced lipid peroxidation end products are increased in Alzheimer's disease," *Journal of Neurochemistry*, vol. 68, no. 5, pp. 2092–2097, 1997.
- [99] M. Hashimoto, T. Sibata, H. Wasada, S. Toyokuni, and K. Uchida, "Structural basis of protein-bound endogenous aldehydes: chemical and immunochemical characterizations of configurational isomers of a 4-hydroxy-2-nonenal-histidine adduct," *The Journal of Biological Chemistry*, vol. 278, no. 7, pp. 5044–5051, 2003.
- [100] T. Ishii, S. Kumazawa, T. Sakurai, T. Nakayama, and K. Uchida, "Mass spectroscopic characterization of protein modification by malondialdehyde," *Chemical Research in Toxicology*, vol. 19, no. 1, pp. 122–129, 2006.
- [101] W. Siems and T. Grune, "Intracellular metabolism of 4-hydroxynonenal," *Molecular Aspects of Medicine*, vol. 24, no. 4-5, pp. 167–175, 2003.
- [102] D. L. Carbone, J. A. Doorn, Z. Kiebler, B. R. Ickes, and D. R. Petersen, "Modification of heat shock protein 90 by 4-hydroxynonenal in a rat model of chronic alcoholic liver disease," *Journal of Pharmacology and Experimental Therapeutics*, vol. 315, no. 1, pp. 8–15, 2005.
- [103] S. Yamada, T. Funada, N. Shibata et al., "Protein-bound 4-hydroxy-2-hexenal as a marker of oxidized n-3 polyunsaturated fatty acids," *Journal of Lipid Research*, vol. 45, no. 4, pp. 626–634, 2004.
- [104] W.-H. Zhang, J. Liu, G. Xu, Q. Yuan, and L. M. Sayre, "Model studies on protein side chain modification by 4-Oxo-2-nonenal," *Chemical Research in Toxicology*, vol. 16, no. 4, pp. 512–523, 2003.
- [105] G. A. Nacheva, D. Y. Guschin, O. V. Preobrazhenskaya, V. L. Karpov, K. K. Ebralidse, and A. D. Mirzabekov, "Change in the pattern of histone binding to DNA upon transcriptional activation," *Cell*, vol. 58, no. 1, pp. 27–36, 1989.
- [106] K. K. Ebralidse, S. A. Grachev, and A. D. Mirzabekov, "A highly basic histone H4 domain bound to the sharply bent region of nucleosomal DNA," *Nature*, vol. 331, no. 6154, pp. 365–367, 1988.
- [107] D. A. Slatter, C. H. Bolton, and A. J. Bailey, "The importance of lipid-derived malondialdehyde in diabetes mellitus," *Diabetologia*, vol. 43, no. 5, pp. 550–557, 2000.
- [108] D. A. Slatter, N. C. Avery, and A. J. Bailey, "Identification of a new cross-link and unique histidine adduct from bovine serum albumin incubated with malondialdehyde," *The Journal of Biological Chemistry*, vol. 279, no. 1, pp. 61–69, 2004.
- [109] T. Jiang, X. Zhou, K. Taghizadeh, M. Dong, and P. C. Dedon, "N-formylation of lysine in histone proteins as a secondary modification arising from oxidative DNA damage," *Proceedings of the National Academy of Sciences of the United States of America*, vol. 104, no. 1, pp. 60–65, 2007.
- [110] P. Close, C. Creppe, M. Gillard et al., "The emerging role of lysine acetylation of non-nuclear proteins," *Cellular and Molecular Life Sciences*, vol. 67, no. 8, pp. 1255–1264, 2010.
- [111] X.-J. Yang and E. Seto, "Lysine acetylation: codified crosstalk with other posttranslational modifications," *Molecular Cell*, vol. 31, no. 4, pp. 449–461, 2008.
- [112] L. A. Peterson, K. C. Naruko, and D. P. Predecki, "A reactive metabolite of furan, cis-2-butene-1,4-dial, is mutagenic in the Ames assay," *Chemical Research in Toxicology*, vol. 13, no. 7, pp. 531–534, 2000.

## Review Article

# DNA-Destabilizing Agents as an Alternative Approach for Targeting DNA: Mechanisms of Action and Cellular Consequences

**Gaëlle Lenglet and Marie-Hélène David-Cordonnier**

*INSERM U-837, Jean-Pierre Aubert Research Center (JPARC), Team 4 Molecular and Cellular Targeting for Cancer Treatment, Institute for Research on Cancer of Lille (IRCL), Lille F-59045, France*

Correspondence should be addressed to Marie-Hélène David-Cordonnier, marie-helene.david@inserm.fr

Received 15 April 2010; Revised 27 May 2010; Accepted 3 June 2010

Academic Editor: Ashis Basu

Copyright © 2010 G. Lenglet and M.-H. David-Cordonnier. This is an open access article distributed under the Creative Commons Attribution License, which permits unrestricted use, distribution, and reproduction in any medium, provided the original work is properly cited.

DNA targeting drugs represent a large proportion of the actual anticancer drug pharmacopeia, both in terms of drug brands and prescription volumes. Small DNA-interacting molecules share the ability of certain proteins to change the DNA helix's overall organization and geometrical orientation via tilt, roll, twist, slip, and flip effects. In this ocean of DNA-interacting compounds, most stabilize both DNA strands and very few display helix-destabilizing properties. These types of DNA-destabilizing effect are observed with certain mono- or bis-intercalators and DNA alkylating agents (some of which have been or are being developed as cancer drugs). The formation of locally destabilized DNA portions could interfere with protein/DNA recognition and potentially affect several crucial cellular processes, such as DNA repair, replication, and transcription. The present paper describes the molecular basis of DNA destabilization, the cellular impact on protein recognition, and DNA repair processes and the latter's relationships with antitumour efficacy.

## 1. Introduction

The integrity of DNA is an important aspect of cell survival, since the molecule carries hereditary information and instructs essential biological processes such as transcription and replication of living cells. Alteration of this information can lead to various diseases, including cancer. The various cancer drugs that have been used in chemotherapy over the last 60 years kill cells in different ways. In addition to the targeted therapies developed over the last two decades, many routinely used anticancer agents (topoisomerase I/II inhibitors, DNA alkylating agents, and antimetabolites) target the DNA helix itself. The empirical use of alkylating compounds in cancer treatment started in the 1940s [1]. Watson and Crick's discovery of the DNA double helix in 1953 [2] led to extensive research in the field of the interactions between small molecules (whether of natural or synthetic origin) with nucleic acids. In turn, this work prompted the widespread use of some of these molecules as anticancer agents [3–7].

The interaction between small ligands and DNA involves either (i) nonspecific binding through electrostatic interactions with the negatively charged sugar-phosphate backbone, (ii) intercalation of the ligand's planar aromatic rings between two adjacent base pairs (see Figure 1), or (iii) major- or minor-groove binding. Following DNA recognition by anticancer compounds, the subsequent interaction can either be noncovalent (DNA ligands) or covalent (alkylating agents). Whereas most DNA-interacting compounds stabilize the DNA double helix, a few display the particular ability to destabilize it—leading potentially to various cellular consequences.

## 2. To Be or Not to Be a Helix

The DNA double helix is conventionally illustrated as a spiral staircase, in which the two strands (the handrails) are stabilized by hydrogen bonds between the Watson-Crick base pairs (the steps). However, these “steps” are not stable because their noncovalent interactions are reversible.

Depending on the DNA sequence, denaturation (melting) can be local or widespread [8, 9] and enables various crucial cellular processes (including DNA replication, transcription, and repair) to take place [10–12].

Both sequence specificity and interaction (whether covalent or not) with a small compound or a protein can induce *tilt*, *roll*, and *twist* effects (a rotation of the base pairs in the  $x$ ,  $y$ , or  $z$  axis, respectively—Figure 1) and therefore change the helix's overall organization. Furthermore, *slide* or *flip* effects can also modify the geometrical orientation of the DNA helix (Figure 1). Hence, the *flip* effect and (to a lesser extent) the other above-defined movements modulate the double-strand stability within the helix or at its ends. Indeed, under physiological conditions, local DNA “breathing” has been evidenced at both ends of the DNA helix [14] and B-to-Z DNA structural transitions have been observed in internal DNA regions [15] in a sequence-dependent manner [8, 16–29]. These types of locally open DNA structures are good substrates for specific proteins (such as single-strand binding proteins, SSBPs) which can also induce the opening of a “closed” DNA helix. In addition to naturally occurring DNA breathing, the helix can also be unzipped by cellular proteins and DNA binding compounds (some of which are used in the clinic).

### 3. Protein-Mediated Unzipping

In order to achieve essential cellular processes such as DNA transcription, replication and repair, some cellular proteins are able to naturally unzip the DNA helix [30]. The most well known of these (DNA helicases) are essential players in the above-mentioned processes. The destabilization is obtained through either an active, direct separation of the two DNA strands [31–33] or a passive opening mode in which the helicase binds to the locally single-stranded DNA portion generated by base pairing fluctuation (which mostly depends on the DNA sequence and induces prebent DNA structures) [34–36]. After DNA opening, the helicase partially translocates to the generated single-stranded DNA regions and subsequently moves along the base pairs to unwind the double helix at up to 500–1000 bp·s<sup>-1</sup>. The latter process requires Mg<sup>2+</sup> and ATP [37]. The BLM helicase (the human RecQ helicase responsible for Bloom's syndrome, which is characterized by DNA repair deficiencies) actively destabilizes the DNA duplex and performs rapid, efficient DNA strand separation [38].

Helicases are not the only proteins with intrinsic double-strand DNA opening ability; this is also a property of replication protein A (RPA), a very efficient DNA destabilizing protein involved in many DNA metabolism processes (including repair, replication, and recombination) [39–41]. RPA is a mammalian nuclear SSBP; the SSBP family members (comprising eukaryotic, bacterial and viral proteins) can efficiently destabilize DNA helix by unwinding up to one thousand base pairs. Similarly, the mouse myeloma helix-destabilizing protein, the calf thymus hnRNP-related protein UP1 and the mammalian P8 protein (related to glyceraldehyde-3-phosphate-dehydrogenase) also

present both DNA single-strand binding and DNA helix-destabilizing abilities, as evidenced in thermal denaturation measurements [42–44].

High-mobility group (HMG) proteins are structurally and functionally important chromatin components which also display DNA destabilizing activities. Indeed, melting studies have revealed that both HMG1 and HMG2 destabilize DNA in the presence of 25 to 100 mM NaCl but stabilize DNA in the absence of salt [45, 46]. An HMG-related DNA binding domain with DNA-destabilization properties has been found within c-Abl kinase protein. Moreover, this DNA destabilization was shown to increase the extent of HMG protein binding to DNA in the vicinity of the c-Abl binding site [47, 48].

More recently, it has been reported that the nucleocapsid protein of HIV-1 can destabilize DNA [49] via its DNA-bending activity [50]. More specifically, the DNA-destabilization function involves the protein's first zinc finger, bearing residues Ile24 and Asn27 [51]. Similarly, a DNA destabilization process was attributed to prion protein. The latter's pathological mechanism of action involves translocation to the nucleus, where the protein binds chromatin and converts to insoluble aggregates. Using FRET-coupled DNA-melting temperature studies, prion protein was found to induce significant DNA bending, unwinding, and thus local destabilization of the DNA helix [52].

Although the above-mentioned proteins induce relatively large DNA destabilization effects, small modifications (such as base flipping) could also perturb the local stability of DNA [53]. Various DNA nucleotide excision repair (NER) proteins [54, 55], base excision repair proteins [56–61], and DNA methyltransferases [62, 63] (such as cytosine-C5-methyltransferase [64]) are known to promote base flipping. More recently, base flipping has been described in the recognition of methylated bases by the SET and RING-associated (SRA) domain protein UHRF-1 [65, 66] and DNA binding by the transcription factor NF- $\kappa$ B [67].

### 4. DNA Ligand-Mediated Unzipping

Small compounds that interact noncovalently with DNA can bind to the minor or major groove between the two walls of the DNA helix, via intercalation between two planar “rungs” of the base pair staircase (Figure 1) or covalently as a result of DNA alkylation. Most of the DNA unwinding compounds with well-defined binding modes belong to the intercalating or alkylating groups.

Mono- and bis-intercalators present their intercalative rings between adjacent base pairs in parallel or perpendicular ways. This results in (i) unwinding of the DNA helix by an angle  $x^\circ$ , where  $x^\circ < 36^\circ$  (since  $36^\circ$  is the rotation angle between two adjacent base pairs in native DNA), and (ii) subsequent elongation of the DNA ( $\Delta$ Length). The value of  $x^\circ$  depends on the nature of the interacting compound (the rotated orange arrow in Figure 1).

With DNA alkylating agents, DNA destabilization can arise from DNA bending, base flipping, or much more extensive DNA opening (Figure 1).

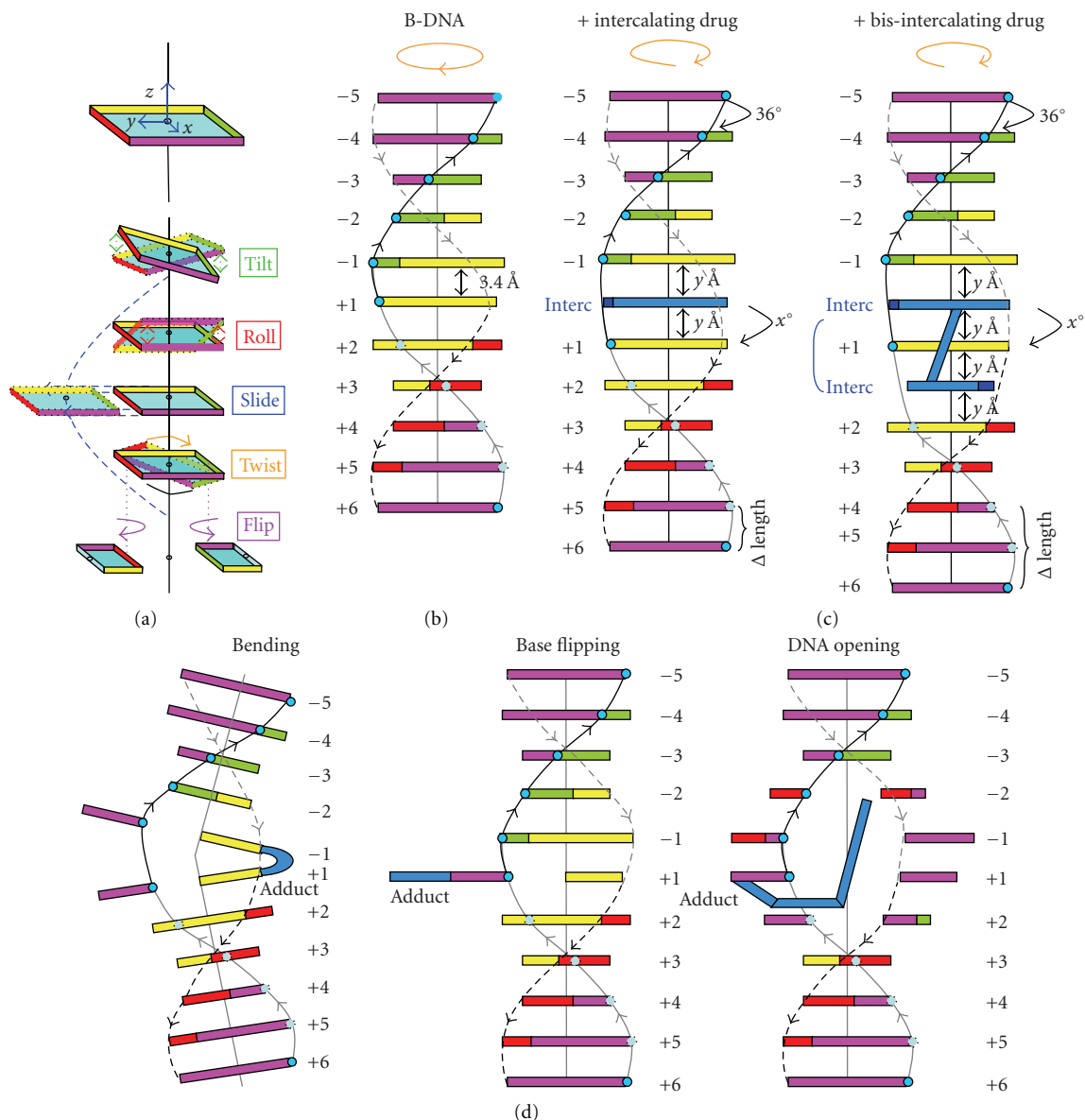


FIGURE 1: Schematic representation of DNA structure. (a) Base pair orientation with  $x$ ,  $y$ , and  $z$  axes result in different kind of rotation (tilt, roll, twist) or slipping of the bases (slide, flip) regarding to the helix central axis. (b) Native B-DNA with nearly 11 base pairs within one helix turn. (c) Mono- or bis-intercalation between adjacent base pairs result in an unwinding of the DNA helix (orange arrow on the top) and a lengthening of the DNA helix ( $\Delta$ Length) depending on the  $x^\circ$  and  $y$  Å values that are specific for a defined DNA intercalating compound. (d) Representation of the DNA bending, base flipping, or double strand opening induced by some DNA destabilizing alkylating agents (adduct). Adapted from Calladine and Drew's schematic boxes representation [13].

**4.1. DNA Intercalators.** DNA-intercalating agents which impair the stability of the helix can be either mono- or bis-intercalators.

**4.1.1. Monointercalating Compounds.** Acridine orange (AO) (Figure 2) is well known for its ability to intercalate between double-stranded DNA but can also bind single-stranded DNA with high affinity. When bound to DNA, AO fluoresces at different wavelengths, depending on the nature of the nucleic acid; green fluorescence occurs after binding to double-strand DNA, whereas red luminescence results from

interaction with single-strand DNA. Thermal denaturation studies suggest that the overall stability of the DNA double helix is increased by AO binding [68]. However, local distortion and denaturation of double-stranded DNA are also generated, as evidenced by formaldehyde and diethylpyrocarbonate (DEPC) probing [69]. DNA denaturation after AO binding was also confirmed by spectral and thermodynamic data [70] and *in situ* experiments [71, 72].

*Ellipticine* and *adriamycin* (Figure 2) also induce local unzipping of the DNA helix; the DNA melting temperature ( $T_m$ ) falls by 5.1 and 4.8°C, respectively, [69, 70, 75]. As with

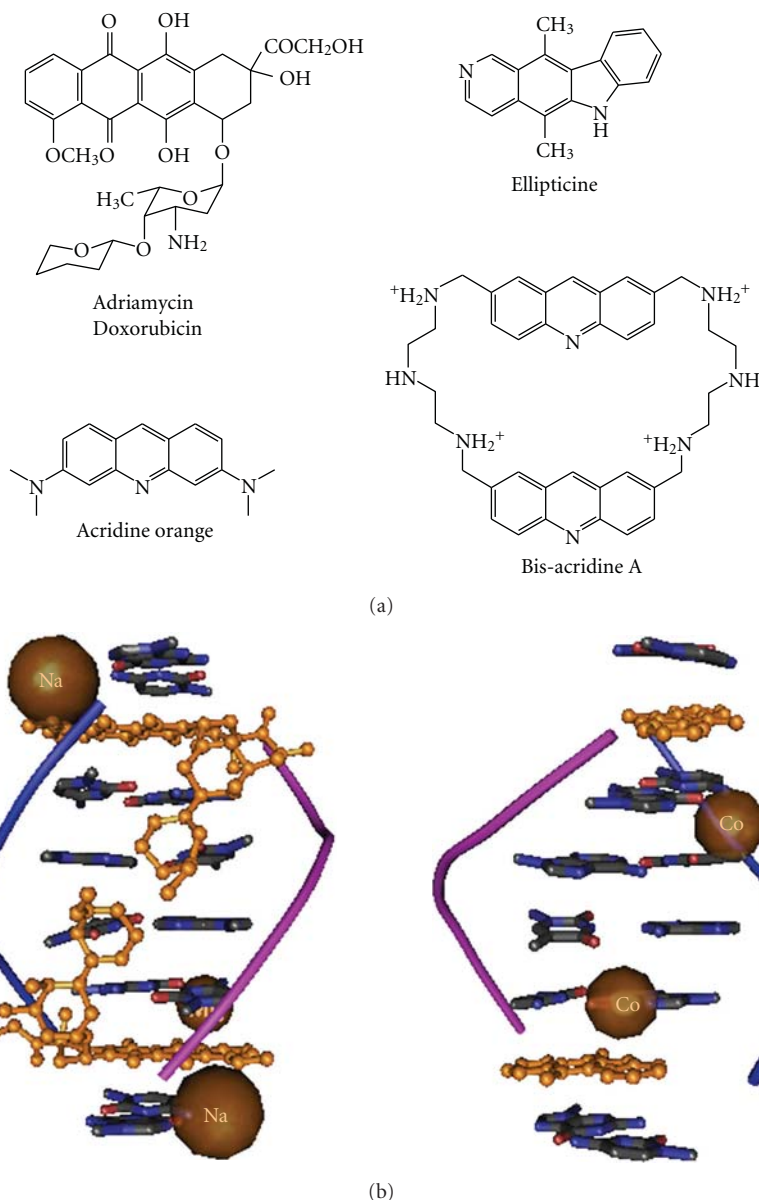


FIGURE 2: Mono- and bis-intercalating compounds inducing local destabilization of the DNA helix. (a) Structure of the compounds. (b) Three-dimensional organisation of *morpholino doxorubicin* bound to d(CGATCG) (left panel) and of *ellipticine* (right panel) intercalated between adjacent base pairs (from crystallographic data [mmdbId:52942] and [mmdbId:52189], respectively, [73, 74]).

AO, these two compounds bind efficiently to single-stranded DNA [76, 77]. This contrasts with *ethidium bromide*'s binding to nucleic acids, which is highly specific for double-stranded DNA and does not destabilize the double helix [78]. *Ellipticine*, *adriamycin*, and AO all intercalate between two adjacent base pairs and then subsequently change their orientation to interact with the single-stranded nucleic acid sections formed locally during DNA breathing. The single-stranded portions within the DNA helix lengthen because of cooperative binding by the intercalator, which thus leads to a higher level of DNA denaturation. This progressive unzipping of the DNA helix has also been observed *in situ* using cytometry, with a direct relationship between

the decrease in green fluorescence and increased concentrations of AO in treated cells or nuclei [72]. Furthermore, post denaturation aggregate formation was observed using electron microscopy, with DNA condensation occurring primarily in heterochromatin, ribosomal, and polysomal structures [71, 72].

**4.1.2. Bis-Intercalating Agents.** Within the *bis*-intercalating group of compounds, the cyclo-*bis*-intercalator *bisacridine A* (*BisA*) (Figure 2) also displayed DNA unwinding properties. This macrocyclic compound is composed of two acridine cores (the DNA-intercalating motifs) linked by polyammonium bridges [79]. By using a variety of complementary

biochemical and biophysical techniques (such as fluorescence, melting temperature studies, and gel electrophoresis), Slama-Schwok et al. nicely demonstrated the ability of the polyaminomacrocyclic *BisA* to shift the equilibrium from duplex DNA towards hairpin nucleic acid structures [80] and to destabilize double-stranded DNA [81] (two properties not observed with monoacridine derivatives). Another characteristic of *BisA* is its potent ability to bind single-stranded DNA. Additionally, when irradiated with light, *BisA* efficiently induces photocleavage through its acridine photoactive core. This activity is greater with single-stranded nucleic acids than with double-stranded nucleic acids [82]. Interestingly, NMR and molecular modelling studies of *BisA* compounds bound to an abasic site-containing DNA show that one acridine ring intercalates between the C·A and T·G base pairs, the second ring lies in the free space of an A·T base pairing and the linker chains are positioned in the major and minor grooves on each side [83]. On the base-pair level, T·G mismatches and AP·T recognition result in base flipping of the thymine—suggesting that *BisA* sterically prevents DNA glycosylases from binding to their specific, base-damaged recognition sites [84].

**4.2. DNA Alkylating Agents.** Intercalating agents are reversible DNA ligands. However, some covalent DNA-binding anticancer drugs can also locally destabilize the DNA helix; these include the well-known alkylating agent *cisplatin* and its derivatives and the recent drug candidate S23906-1 (a *benzo-acronycine* derivative). This contrasts with the DNA stabilization properties of most DNA-alkylating agents (whether used in chemotherapy or not), such as *mitomycin C*, some *psoralen* and dinuclear platinum derivatives, *ecteinascidine 743* and *nitrogen mustards* [85–91].

**4.2.1. Platinated DNA Destabilizing Agents.** *Cisplatin* (cis-diaminedichloridoplatinum(II); Figure 3) was one of the first chemotherapeutic agents to be developed and is still frequently used in the clinic. It is able to form inter- and intrastrand crosslinks and monovalent adducts, primarily through covalent bonding to the N7 atom of guanine residues. The most common lesion is the intra-strand crosslink (occurring preferentially (65%) at the GpG dinucleotide), followed by ApG intrastrand crosslinks (25%). Interstrand crosslinks occur less frequently and depending on the nature of the platinated agent, with 5 to 8% for *cisplatin*, 12% for *transplatin* (Figure 3) and up to 30% for *trans*-PtCl<sub>2</sub>(NH<sub>3</sub>)(*quinoline*) (Figure 3) and *trans*-PtCl<sub>2</sub>(NH<sub>3</sub>)(*thiazole*) derivatives. In comparison, *nitrogen mustards* induce 1 to 5% of inter-strand crosslinks, whereas *nitrosourea* and *mitomycin C* induce 2 to 8% and 5 to 13%, respectively [93–95]. *Cisplatin*-induced intra-strand crosslinks at GpG base pairs result in (i) bending of the DNA axis toward the major groove with an angle of 55–78°, and (ii) DNA distortion, enabling local denaturation of the double helix via destabilization of the Watson-Crick base pairing [96–102]. In comparison, the bending angle for inter-strand crosslinks is 45° and is associated with DNA unwinding of 79 ± 4°. The distortion in platinated-GpG intra-strand crosslinks is different and depends on

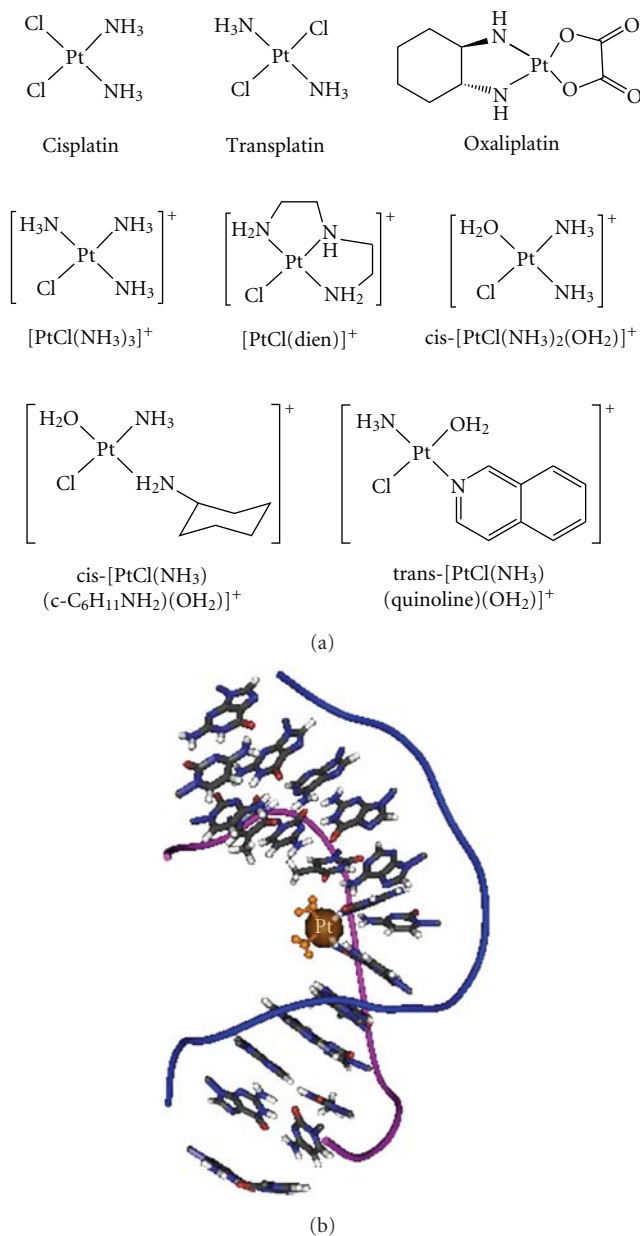


FIGURE 3: Platinum derivatives. (a) Examples of platinated agents inducing local destabilization of the DNA helix. (b) The three-dimensional organization of *cisplatin* bound to DNA are drawn from crystallographic data [mmdbId:47796] [92] and evidenced strong DNA bending induced by *cisplatin* on a duplex DNA decamer oligonucleotide that fits with the L-shape angle of HMG-box DNA-binding domain.

the sequence context, with up to 7 bp for 1,3-intrastrand crosslinks in a TGTGT context [101]. This destabilization was found to be enthalpic (rather than entropic) in origin [101, 103]. Similarly, *cisplatin* adducts occurring at the 5'-TGGT sequence induce a decrease of more than 10°C in the melting temperature—much higher than the decrease of 6°C or so measured for 5'-CGGT and 5'-AGGC sequences [104, 105]. DNA stabilization/destabilization also depends on the pH of the milieu [106]. In contrast to *cisplatin*,

the interstrand crosslinks formed by *transplatin* do not destabilize the DNA helix or correlate with changes in the transition entropy or enthalpy [101, 107].

Interestingly, the third-generation platinum antitumor derivative *oxaliplatin* [(1*R*,2*R*-diamminocyclohexane)-oxalatoplatinum-(II)] (Figure 3) was found to induce greater DNA unwinding, bending and helix destabilization than *cisplatin*. This correlates with the lower degree of cellular DNA damage seen after *oxaliplatin* treatment than after *cisplatin* treatment and the lower HMG protein affinity for *oxaliplatin*-versus *cisplatin*-induced damage [101]; these findings suggest that the two molecules induce different DNA repair processes/efficiencies, depending on the extent of local helix destabilization.

It is noteworthy that some other bifunctional platinum derivatives do not destabilize the DNA duplex. This is the case for pyrazolato-bridged dinuclear platinum(II) complex [(*cis*-{Pt(NH<sub>3</sub>)<sub>2</sub>})<sub>2</sub>(*mu*-OH)(*mu*-pyrazolate)]<sup>2+</sup>, which crosslinks two adjacent guanines and unwinds the DNA by around 15° but does not change the directionality of the helix axis. This absence of bending may explain the lack of DNA destabilization [108].

The DNA sequence is also important; monofunctional platinum adducts exhibit different DNA destabilizing effects depending on the base sequences surrounding the guanine target site [97, 109]. Indeed, when oligonucleotide containing platinum adducts were incubated in the presence of 50 or 500 mM NaCl, the highest DNA destabilization was observed when the guanine target was located within the TGC triplet sequence (with a  $\Delta T_m$  value of -10.6°C and -13.2°C, resp.). For all triplets, the decrease in  $T_m$  was greater in 500 mM NaCl buffer than in 50 mM Na<sup>+</sup> counterion containing buffer. In general, the highest DNA destabilization effect was seen when the monoadduct was positioned between pyrimidine residues. Osmium tetroxide (OsO<sub>4</sub>) and DEPC probing revealed that both thymine and the opposite adenine are crucial for the local distortion of the DNA structure by the platinum mono-adduct positioned within a 5'-TGC triplet but not within a 5'-AGT or 5'-TGA triplet. In contrast, none of these chemical probes reacted with the bifunctional adduct at the 5'-TGGT sequence [110].

Hägerlöf et al. found that the *cisplatin* derivatives *cis*-[PtCl(NH<sub>3</sub>)<sub>2</sub>(OH<sub>2</sub>)]<sup>+</sup>, *cis*-[PtCl(NH<sub>3</sub>)(*c*-C<sub>6</sub>H<sub>11</sub>NH<sub>2</sub>)(OH<sub>2</sub>)]<sup>+</sup>, and *trans*-[PtCl(NH<sub>3</sub>)(*quinoline*)(OH<sub>2</sub>)]<sup>+</sup> destabilized both double-stranded DNA and double-stranded RNA (Figure 3). Indeed, after platination with these compounds, the melting temperatures for both the RNA and DNA hairpins fell. With hairpin RNA, platination induced much weaker destabilization, with a  $\Delta T_m$  of -5°C. In the case of DNA, the platinum-induced destabilization was more pronounced, with  $\Delta T_m$  values of around -11°C [111].

**4.2.2. Ruthenium-Containing Alkylators.** Transition-metal antitumor agents other than platinum compounds also present DNA unwinding activity. This is the case for ruthenium derivatives such as [( $\eta^6$ -*p*-cymene)Ru(II)(en)-(Cl)]<sup>+</sup> (*Ru*-CYM, Figure 4). This organometallic ruthenium(II) arene complex was rationally designed on the basis that changing the metal ion from platinum to ruthenium should

provide additional coordination sites in the octahedral complexes, modify the oxidation rate, and change the ligand affinity and binding kinetics for use in chemotherapy [7, 112–114]. In particular, Brabec and co-workers performed  $T_m$  studies while varying the drug/DNA ratio in buffer containing NaClO<sub>4</sub> concentrations ranging from 0.01 M to 0.2 M [115, 116].  $\Delta T_m$  measurements at a drug/DNA ratio of 0.1 showed a decrease of up to 4°C in the CT-DNA melting temperature at all Na<sup>+</sup> concentrations.

This DNA helix destabilization was also observed using biphenyl (*Ru*-BIP), dihydroanthracene (*Ru*-DHA), and tetrahydroanthracene (*Ru*-THA) (Figure 4) as arenes but only at the highest concentration of NaClO<sub>4</sub> [115]; at lower Na<sup>+</sup>-counterion concentrations, *Ru*-BIP, *Ru*-DHA and *Ru*-THA induced DNA helix stabilization, due to a positive charge effect on the ruthenium moiety and the intercalation process. When compared with the other ruthenium arene complexes, the DNA helix destabilization activity of *Ru*-CYM correlates with a smaller unwinding angle of 7° (versus 14° of unwinding in supercoiled plasmid DNA by *Ru*-BIP, *Ru*-DHA and *Ru*-THA). The *Ru*-CYM-induced DNA-unwinding appears to be consistent with the absence of intercalation of *Ru*-CYM between two adjacent base pairs and the formation of monoadducts on the N7 atom of guanine residues [116]. *Ru*-THA and *Ru*-CYM have been used as models for the repair of DNA-ruthenium complexes the compounds destabilize the DNA helix via different enthalpic effects and differ in terms of their DNA base-pair intercalation propensity. DNA destabilization was also recently evidenced for new ruthenium derivatives, such as *monodentate*-*Ru*(II) [117].

**4.2.3. Psoralen Derivatives.** In terms of DNA stabilization/destabilization properties, the psoralen derivative 4'-(*hydroxymethyl*)-4, 5',8-trimethylpsoralen (HMT) (Figure 5) exerts two effects: (i) monoaddition of a psoralen residue stabilizes the double helix formed by two non-self-complementary oligonucleotides by as much as 1.3 kcal/mol (for a furan-side mono-adduct) or 0.7 kcal/mol (for a pyrone-side mono-adduct) at 25°C in 50 mM NaCl; (ii) mono-addition of a psoralen residue to each of the two thymidines in the double helix in the sequence GGGTACCC destabilizes the helix by 1.8 kcal/mol at 25°C in 1M NaCl—the two HMT molecules at the centre of each strand cause an unfavourable enthalpy change and a favourable entropy change [85].

**4.2.4. Benzopyrene Carcinogens.** In the cell, the environmental and tobacco smoke carcinogen *benzo*[*a*]pyrene (*BaP*) is metabolized into (+/-)-*anti*-*benzo*[*a*]pyrene-7,8-dihydrodiol-9,10-epoxide (*BPDE*) (Figure 5). The (+)-7*R*,8*S*,9*S*,10*R* enantiomer (+)-*anti*-*BPDE* is thought to be the metabolite that is ultimately responsible for mutations, DNA damage, and cancer. By covalently linking to the exocyclic NH<sub>2</sub> group of guanine, *BPDE* forms a bulky DNA adduct in the minor groove of the helix and destabilizes base pairing [120, 121].

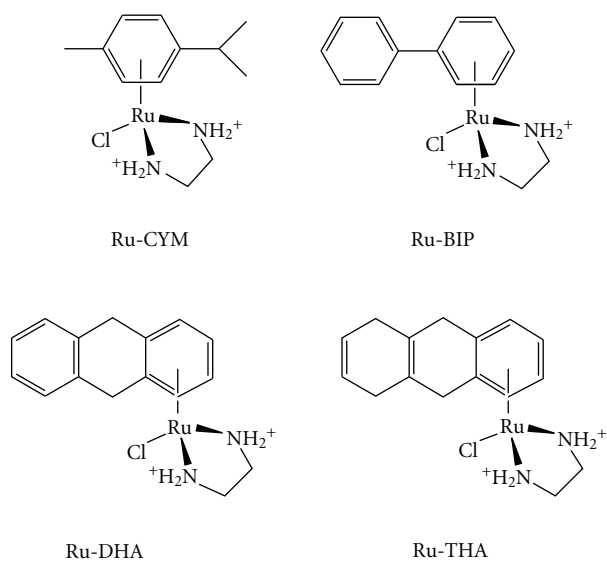


FIGURE 4: Ruthenium derivatives. *Ru-CYM*, *Ru-BIP*, *Ru-DHA*, and *Ru-THA* are examples of ruthenium-containing agents inducing local destabilization of the DNA helix.

Several enantiomers are produced by the alkylation reaction which follows the opening of the epoxide group. The (+)-*anti*-BPDE adducts consist mostly of the carcinogenic 10*S* (+)-*trans-anti*-BPDE (derived from the (+)-7*R*,8*S*,9*S*,10*R* compound) and, to a lesser extent, stereoisomeric 10*R* (+)-*cis*-B [*a*]P-N2-*dG* adducts. The (–)-BPDE enantiomer forms (–)-*trans*-B [*a*]P-N2-*dG* adducts but with lower efficiency. The DNA bonding of the stereoisomeric damage suggests base displaced intercalation or minor groove conformations. Covalent adduct formation prevents the amino group of guanine from hydrogen bonding with the opposite cytosine (which otherwise stabilizes GC base pairs in the native DNA helix). This results in base flipping, with the (+)-*anti*-B [*a*]P-N2-*dG* bulky adduct on the guanine situated in the minor groove and the opposite cytosine aligned with the major groove [122, 123].

Depending on the target sequence, the bulky 10*S* (+)-*trans-anti*-B [*a*]P-N2-*dG* rings point in the 5' direction relative to the alkylated guanine position in each case, although the exact positions are different. Indeed, using 5'-CGG\*C DNA, the 10*S* (+)-*trans-anti*-B [*a*]P-N2-*dG* lesion untwists the DNA significantly and causes a large bend in the DNA helix. In contrast, with a 5'-CG\*GC sequence, no untwisting is seen but the DNA helix is destabilized 5' to the lesion [124]. These structural differences result in differing electrophoretic mobility in polyacrylamide gels and different protein/DNA recognition and DNA repair efficiencies [125].

Although the *BaPs* are environmental mutagens and not antitumor agents, their very particular mode of DNA binding with dual interference on DNA repair processes could highlight useful phenomena involved in the mechanism of action of cancer drugs (such as effects on DNA repair, as described in Section 5).

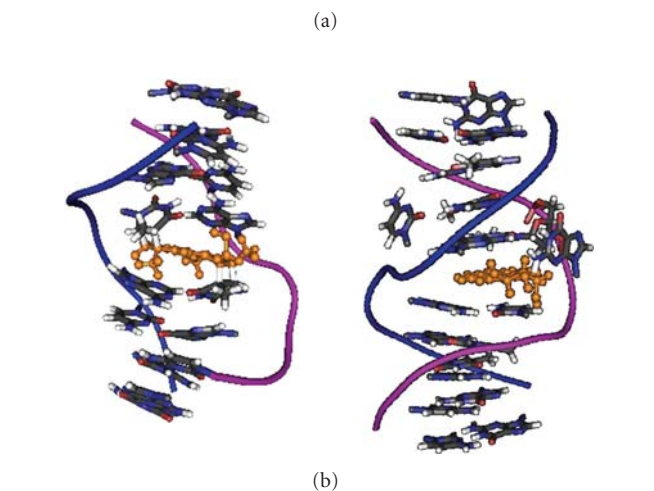
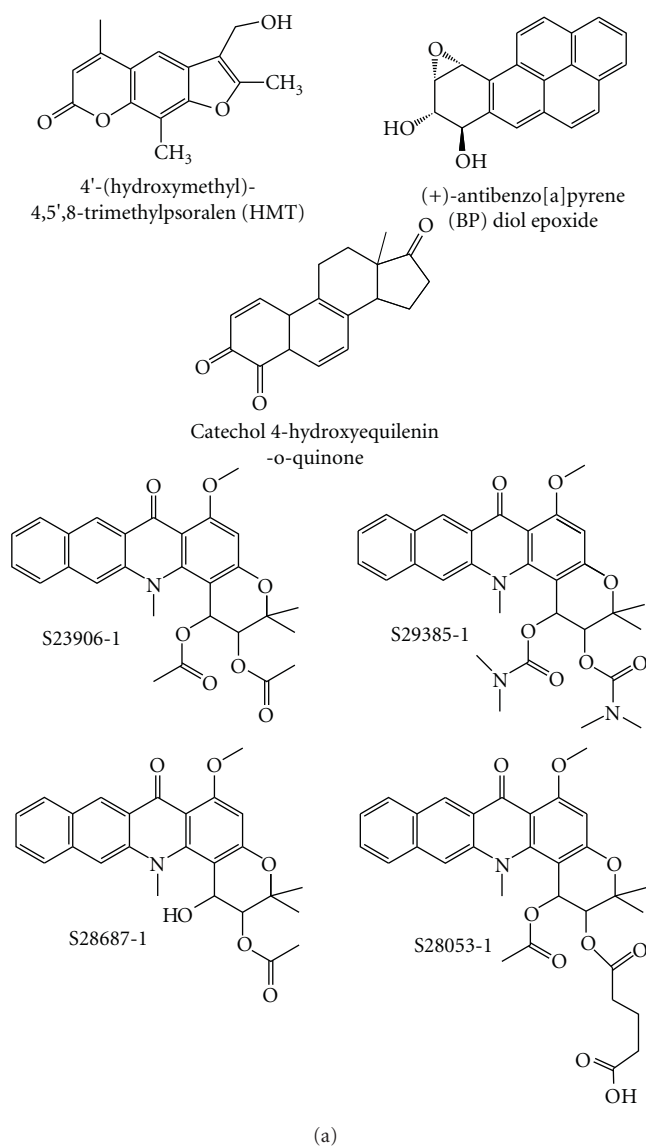


FIGURE 5: Other DNA alkylating agents inducing local destabilization of the DNA helix. (a) Structures of some DNA alkylating molecules that destabilize the DNA helix. (b) Three-dimensional organization of the psoralen derivative *HMT* (a) and (+)-*anti*-BPDE (b) bound to DNA (crystallographic data [mmdbId:52343] [118] and [mmdbId:52106], respectively, [119]).

**4.2.5. 4-Hydroxyequilenin (4-OHEN).** As is the case for *BaP*, 4-OHEN alkylating agents are genotoxic but are not anticancer drugs. 4-OHEN compounds are derived from equine oestrogens (*equilin*, 3-hydroxy-1,3,5(10),7-estratetren-17-one, and *equilenin*, 3-hydroxy-1,3,5(10),6,8-estratetren-17-one) which are present at various concentrations in the hormone substitution therapies used to reduce the side effects of the menopause but which are also thought to contribute to a greater risk of breast cancer in the treated population [126–128]. In the body, both *equilin* and *equilenin* are rapidly converted into the intermediate catechol 4-hydroxyequilenin, which is further oxidized into the reactive 4-hydroxyequilenin-*o*-quinone (Figure 5) [129]. This *ortho*-quinone form of 4-OHEN is a potent cytotoxic and genotoxic agent [130] and forms a bulky lesion on dA, dC, and dG but not T residues [131–134]. This damage can be detected not only in cell culture but also in breast cancer biopsies from patients having undergone hormone substitution therapy [135]. Each of the base adducts are present as four stereoisomers, each of which induces different levels of structural distortion in duplex DNA [136–138].

4-OHEN-C adducts present an unusual cyclic core with the bulky rings pointing along the major or the minor groove depending on whether the glycosidic bond adopts a *syn*- or *anti*conformation, respectively [139]. Alkylation of an 11-bp oligonucleotide at specific dA or dC residues results in a strong decrease in the melting temperature of the double-stranded DNA, compared with the unmodified oligonucleotide. The magnitude of the decrease depends on the position of the adduct within the oligonucleotide: a 6–9°C decrease in  $T_m$  is obtained when the adduct is located 1 or 2-bp from the end of the 11-bp DNA, whereas a large (21–27°C) decrease is induced when the adduct is present more centrally (positions 4 to 8).

The extent of the destabilization also depends on the adduct's stereoisomeric orientation, as defined using circular dichroism measurements [134], thermodynamic analyses and molecular modelling. Indeed, distortions, base-stacking characteristics, and groove sizes were found to vary according to the nature and the stereoisomerism of the bulky DNA lesion [139].

**4.2.6. Benzoacronycine Derivatives.** The compound S23906-1 [(+)-*cis*-1,2-diacetoxy-6-methoxy-3,3,14-trimethyl-1,2,3-14-tetrahydro-7*H*-benzo[*b*]pyrano[3,2-*h*]acridin-7-one] (Figure 5) is a potent DNA-alkylating agent with strong cytotoxic and antitumour properties. On the basis of very promising preclinical trials, it entered clinical trials in 2006 (Servier, France). S23906-1 alkylates DNA on guanine's exocyclic amino group (located in the minor groove of the DNA helix) and thus contrasts with commonly used chemotherapeutic alkylating agents which react at guanine's N7 position in the major groove (*cisplatin*, *nitrosourea*, *nitrogen mustards*, etc.). This nucleophilic point is also targeted by other clinically used antitumour agents, such as *ecteinascidine-743* (*ET-743/trabectedin/Yondelis*) developed by the company PharmaMar (Spain) [140], *mitomycin-C* (a dual alkylating agent which bonds to either the N2 group of

guanine in the minor groove or the N7 group of guanine in the major groove) [141] and *anthramycin* [142].

In contrast to *ET-743*, *mitomycin-C* and the *anthramycins*, the alkylation of double-stranded DNA by S23906-1 results in local destabilization of the DNA helix and thus the formation of a single-stranded DNA portion that can be attacked by single-strand-specific nucleases (such as nuclease S1) [91]. This destabilization was seen with various multiple derivatives of S23906-1 (e.g., esters of the *benzo*[*b*]acronycine core, Figure 5). The dicarbamate derivative S29385-1 had a very strong effect. The DNA destabilization potency of this series was confirmed in a variety of physical and biochemical approaches. For example, quantification of the ratio between the fluorescence of *Picogreen* (a dye which interacts with both double- and single-stranded DNA) and *ethidium bromide* (*BET*) (a double-stranded-specific dye) revealed additional *Picogreen* binding and suggested that S29385-1 generates single-strand DNA (Figure 6(a)). Accordingly, DNA melting temperature studies evidenced a negative  $\Delta T_m$  value, reflecting DNA destabilization (Figure 6(b)).

S23906-1's ability to destabilize DNA was also clearly demonstrated in biochemical approaches, such as electrophoretic mobility shift assays (generating single-stranded DNA form following alkylation of a fully double-stranded DNA fragment) and the use of nuclease-S1 single-strand-specific digestion to map the relative positions of locally DNA openings induced by alkylation (Figure 7 and [91]).

## 5. Drug-Induced DNA Destabilization: Cellular Consequences

Compounds which change the equilibrium between the stable, double-stranded DNA helix and locally destabilized strands could strongly alter protein/DNA recognition and thus have major cellular consequences. Indeed, base kinking, unstacking, and nucleotide extrusion (flipping) induce discontinuities in the double helix and thus facilitate DNA lesion/mismatch recognition [143–145]. The few literature studies to have addressed this point reveal that proteins which recognize damaged DNA are affected by the stabilization or destabilization of the DNA helix; this leads to a major impact on biological parameters such as antitumour activity, transcription factor binding potency, and DNA repair process efficiency [146–148].

This type of cellular impact has been particularly well demonstrated for the platinated adducts recognized by HMG proteins [149]. HMG/platinated DNA recognition is triggered by the strong DNA bending generated by the platinated agent (Figure 2). The large induced bend fits perfectly with the L-shaped structure of HMG DNA binding domain (HMG-box) and reduces the “cost” of DNA bending for the protein [150]. As a consequence, HMG proteins bind less well to *oxaliplatin* adducts than to *cisplatin* adducts because the former agent induces relatively greater DNA bending and thus stronger DNA destabilization [151]. This finding correlates with the lower level of DNA lesions found in cells treated with *oxaliplatin*, relative to *cisplatin*. It is assumed that HMG binding shields the platinated adducts from repair

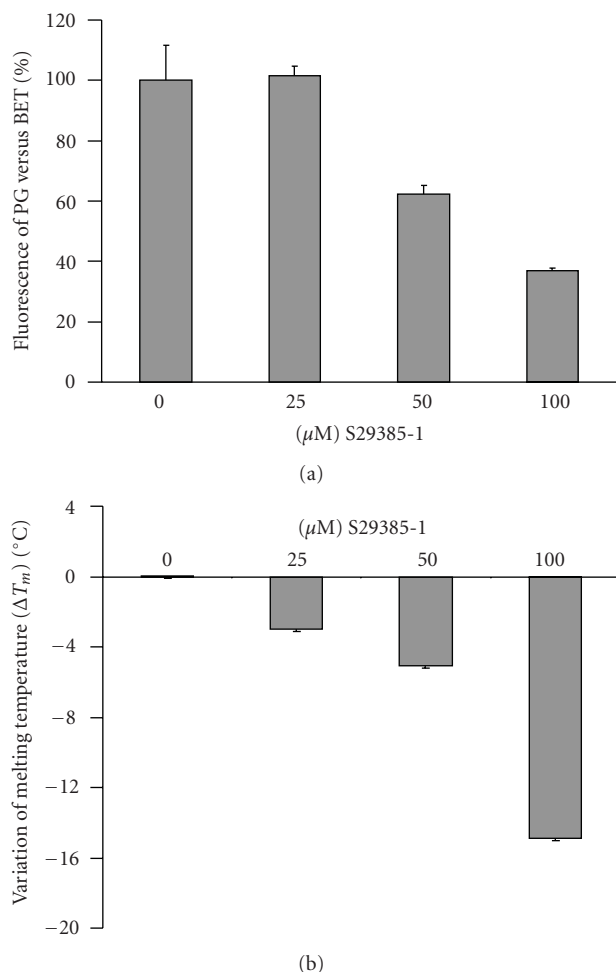


FIGURE 6: DNA destabilization propensities of the benzo-acronycine dicarbamate derivative *S29385-1*. (a) CT-DNA was incubated with increasing concentrations of *S29385-1* prior to the incubation with a mixture of *ethidium bromide* (*BET*) and *Picogreen* (*PG* from Molecular Probes, Invitrogen) to quantify only double-strand DNA or both double-strand and single-stranded DNA, respectively. Results are expressed as the percentage of the peak of emission for *BET* versus *PG*. (b) Variation of the melting temperature studies of a short 24-bp double-strand oligonucleotide incubated for 24 hours alone or with increasing concentrations of *S29385-1* prior to ethanol precipitation of the sample and melting temperature measurement. The results are expressed as the melting temperature for the [DNA+drug] complex minus melting temperature for DNA alone. (Details for the corresponding experimental protocols are described in [91].)

by the human DNA excision machinery [152] and therefore participates in platinated-agent-induced cytotoxicity [153]. However, too strong a bend and greater DNA destabilization lead to a structure that does not fit perfectly with L-shaped HMG-box, thus resulting in a weaker HMG protein binding. The weaker HMG binding to *oxaliplatin* adducts corresponds to weaker protection from DNA repair and so *oxaliplatin*-DNA lesions are more efficiently repaired than *cisplatin*-induced lesions. This results in a lower number of lesions in cells for *oxaliplatin* than for *cisplatin*. Moreover, bent

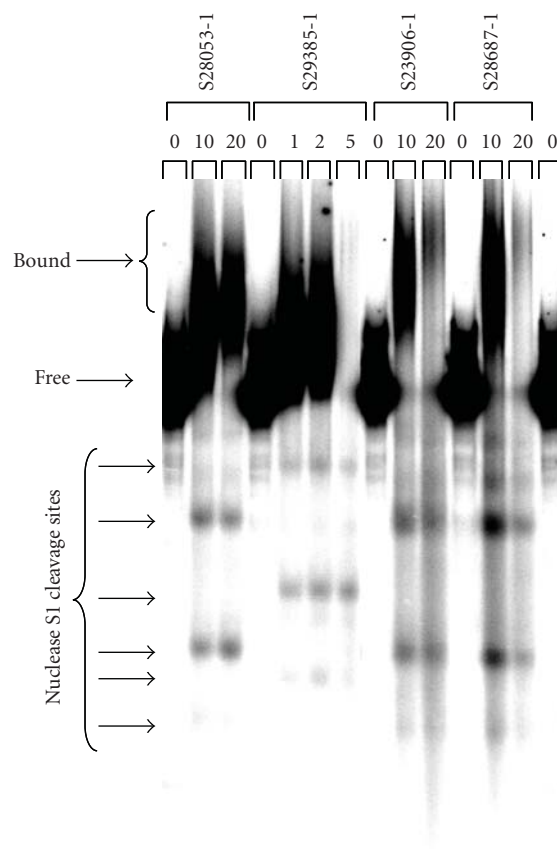


FIGURE 7: Nuclease S1 mapping of locally opened DNA structure. Increasing concentrations of the *benzo-b-acronycine* derivatives presented in Figure 5 were incubated with a radio-labelled 117-bp DNA fragment prior to subsection to nuclease S1 mapping of the induced locally single-stranded DNA portions generated upon DNA alkylation. DNA samples were separated on a 10% native polyacrylamide gel. Concentrations are expressed in  $\mu\text{M}$ . The detailed experimental protocol is described in [91].

platinated-DNA is a good substrate for transcription factors such as SRY and LEF-1 (which belong to the HMG-box family, regarding their DNA-binding domain) and explains the observation of transcriptional changes in treated cells [92, 154–156].

Regarding DNA repair, the local destabilization of the double helix, base flipping and poor base stacking all play a role in the recognition of DNA lesions by repair proteins [157–160]. This has been well demonstrated for the MSH2/MSH6 heterodimer mismatch repair complex (Mut-S alpha), which recognizes not only mismatched bases but also certain DNA lesions, such as *cisplatin* (but not *transplatin*) crosslinks [161–165].

In the case of ruthenium-derivative-induced DNA lesions, the NER machinery appears to be less efficient than for platinum adducts. Interestingly, *Ru-CYM* adducts (which destabilize the DNA helix much more than *Ru-THA* adducts) are excised more efficiently than *Ru-THA* complex adducts. This is consistent with the lower binding by RPA to DNA

containing *Ru-THA* adducts and (to a lesser extent) *Ru-CYM*/DNA damage [166]. The observation that *Ru-THA* was much more cytotoxic than *Ru-CYM* in both A2780 human ovarian cancer cells and the HT29 colon carcinoma cell line suggests that DNA intercalation has a major role in the cytotoxicity of these DNA-destabilizing derivatives.

In prokaryotes, the NER sensor protein UvrB efficiently recognizes *BaP* lesions through lesion-induced local thermodynamic distortion/destabilization and nucleotide flipping [167]. Some variations in the excision efficiency (up to a factor of 3-fold) are observed, depending on the stereoisomeric orientation of the DNA adducts (i.e., (+) or (-), *cis*- or *trans*-) [121]. In eukaryotes, the *BaP* lesions are usually recognized by the NER machinery's "sensor" protein XPC, which then initiates DNA repair in association with the HR23B protein [168, 169]. In particular, it has been suggested that XPC/HR23B's weaker recognition of (+)-*trans-B* [*a*]P-N2-*dG* adducts (relative to the other conformers) contributes to its higher mutagenic and tumorigenic activity [168]. XPC binding requires DNA bending [170] and is facilitated by local conformational flexibility [143, 144, 171] and destabilization of the base pairing, as evidenced by several model DNA lesions (such as thymine-glycol) [172]. This recognition is driven by the "aromatic sensors" Trp690 and Thp733 [41]. On the cellular level, human bronchial epithelial 16HBE cells treated with *BaP* (as a source of reactive *BPDE*) displayed greater expression of the NER proteins XPA and XPG and the heat shock protein Hsp70. Subcellular analysis with confocal microscopy evidenced nuclear colocalization of Hsp70 with XPA and XPG after *BaP* treatment, suggesting that Hsp70 has a role in the cellular DNA repair response [173]. Accordingly, (+/-)-*anti-BPDE* induces chromosome instability and centromere amplification in lung cells [174]. The cellular consequences of (+/-)-*anti-BPDE* treatment were also assessed using a whole-genome microarray technique in normal human amnion epithelial cells; the researchers observed downregulation of the expression of genes involved in signal transduction, cytoskeleton, DNA repair, metabolism and regulation of transcription and the cell cycle, with features similar to those observed after cell irradiation with UV-light [175, 176].

It was recently reported that the structural differences observed for an identical, highly mutagenic, (+)-(7*R*,8*S*,9*S*,10*R*)-7,8-*dihydroxy*-9,10-*epoxy*-7,8,9,10-*tetrahydrobenzo* [*a*]pyrene-DNA lesion lead to different repair processes as a function to the sequence contexts. Indeed, in cell-free human HeLa extracts, destabilized DNA at a 5'-CG\*GC site was more rapidly excised than the bent DNA at a 5'-CGG\*C site [125]. Since the DNA helix is already opened up by alkylation, the DNA repair protein recognition step (including induced base flipping) requires less energy and thus is potentially more rapid for DNA that has already been destabilized (at a 5'-CG\*GC site) than for bent duplex DNA (the 5'-CGG\*C site). This study clearly emphasized the importance of the DNA sequence context for efficient adduct repair [177].

Isomer-dependant DNA repair potency is also assumed to occur with bulky *catechol 4-OHEN*-adducts, which NER proteins excise with an efficiency that depends on the

alkylated base, the stereoisomerism of the adducts and the sequence context. For example, 4-*OHEN*-*dC* adducts are more efficiently excised than 4-*OHEN*-*dA* adducts [178]. Interestingly, it was shown in male zebrafish that 17 $\alpha$ -ethinylestradiol (a source of 4-*OHEN*) is able to decrease NER efficiency and the expression of NER genes such as XPC, XPA, XPD, and XPF (but not HR23B) [179, 180].

In the search for new cancer drugs with novel mechanisms of action and on the basis of promising preclinical testing, the benzoacronycine derivative *S23906-1* has entered Phase I clinical trials as a racemate of two *cis*-diacetylated-enantiomers. As mentioned above, *S23906-1* alkylates DNA in the minor groove and induces strong destabilization of the double helix. Given the presence of two reactive acetate groups on asymmetric carbons, two pairs of enantiomers can be formed: two *cis* (*1R*; *2R* and *1S*; *2S*) and two *trans* (*1R*; *2S* and *1S*; *2R*) structures. Hence, *S23906-1* is a mixture of *1R*; *2R* and *1S*; *2S*. We tested the ability of each of the pure *cis*-enantiomers not only to react with DNA but also to destabilize the DNA helix and thus affect single-stranded endonuclease activity [181]. Our results showed that DNA destabilization depends on the orientation of the adduct core in the open drug/DNA complex and correlates with differing cellular and antitumour effects: the enantiomer with the greatest DNA destabilization presents the highest antitumour activity in animal models [181].

Little is known about the repair of *S23906-1* DNA adducts: the involvement of the NER proteins XPC and CSB was recently found to be related to cell sensitivity to *S23906-1*, associated with both global genome repair and transcription coupled NER [182].

Ongoing work is seeking to identify the proteins involved in *S23906-1*/DNA adduct recognition and evaluate their impact on the compound's cytotoxic activity. On one hand, locally destabilized DNA could favour the recognition of a DNA lesion by the DNA repair "sensor" proteins, leading to an increase in the excision efficiency or rate. Full repair after excision thus results in weaker antitumor activity, unless the DNA repair process is blocked—as has been evidenced for the antitumour activity of *ET-743* (*Yondelis*). In this latter case, the *ET-743*/DNA adduct traps the XPG endonuclease protein involved in the NER machinery and increases the number of single-strand breaks [183]. On the other hand, the wide, local opening of the DNA helix prompted by this particular compound may increase cleavage by single-strand-specific nuclear endonucleases; the greater number of double-strand breaks may then overwhelm the cancer cells' DNA repair capacity.

## 6. Conclusions

Drug-induced destabilization of the DNA helix appears to be part of a novel antitumour mechanism of action and is associated with particular intercalation processes or postalkylation DNA distortions. DNA-destabilizing compounds are relatively rare and represent just a few drops in an ocean of DNA-interacting molecules (which primarily stabilize the double helix). The molecular and cellular consequences of

this original binding mode differ from those induced by DNA-stabilizing compounds. In particular, DNA repair and transcription processes are now known to be affected. The DNA replication machinery may also be affected because DNA opening requires less energy when the double helix is already destabilized by a drug. In view of the little available literature data, researchers are now starting to fill in this gap.

Furthermore, we believe that it is important not to consider DNA destabilization as a unique process. This phenomenon must be considered in relation to (i) the potentially associated bend in the DNA helix (as evidenced by the comparison between *oxaliplatin*- and *cisplatin*-induced distortions of DNA [151] or the effect of the different isomers of *BPDE* [125, 177]), and (ii) the length of the locally destabilized DNA, which varies according to the compound's nature (i.e., the DNA opening induced by *benzoacronycine* derivatives appears to be extensive enough to be susceptible to single-strand-specific nucleases, whereas other modifications are not) [91]. Recent and ongoing studies of the impact of DNA destabilization on DNA repair and cytotoxicity activities illustrate the increasing need for accurate determination of a potential cancer drug's DNA binding mode and subsequent cellular effects. Moreover, DNA-destabilizing compounds may be associated with different drug-induced resistance processes. Further knowledge of three-dimensional structure activity relationships and the cellular consequences (cytotoxicity, DNA repair processes) of treatment with DNA-destabilizing agents will help to clarify the relevance of cancer drug candidates which stabilize or destabilize the DNA helix and will aid the design of potent antitumour agents.

## Acknowledgments

The authors are grateful to the Ligue Nationale Contre le Cancer (Comité du Nord) and the Institut pour la Recherche sur le Cancer de Lille (IRCL) for Grants (Marie-Hélène David-Cordonnier). They thank the Université de Lille 2/Conseil Régional Nord/Pas-de-Calais for a PhD Fellowship (Gaëlle Lenglet). The authors are grateful to Sabine Depauw for technical expertise.

## References

- [1] A. Gilman and F. S. Philips, "The biological actions and therapeutic applications of the B-chloroethyl amines and sulfides," *Science*, vol. 103, no. 2675, pp. 409–436, 1946.
- [2] J. D. Watson and F. H. C. Crick, "Molecular structure of nucleic acids: a structure for deoxyribose nucleic acid," *Nature*, vol. 171, no. 4356, pp. 737–738, 1953.
- [3] M. J. Waring, "DNA modification and cancer," *Annual Review of Biochemistry*, vol. 50, pp. 159–192, 1981.
- [4] B. A. Teicher, Ed., *Cancer Therapeutics: Experimental and Clinical Agents (Cancer Drug Discovery and Development) [Hardcover]*, Humana Press, Clifton, NJ, USA, 1st edition, 1996.
- [5] M. F. Braña, M. Cacho, A. Gradillas, B. de Pascual-Teresa, and A. Ramos, "Intercalators as anticancer drugs," *Current Pharmaceutical Design*, vol. 7, no. 17, pp. 1745–1780, 2001.
- [6] I. Kostova, "Platinum complexes as anticancer agents," *Recent Patents on Anti-Cancer Drug Discovery*, vol. 1, no. 1, pp. 1–22, 2006.
- [7] I. Kostova, "Ruthenium complexes as anticancer agents," *Current Medicinal Chemistry*, vol. 13, no. 9, pp. 1085–1107, 2006.
- [8] U. Dornberger, M. Leijon, and H. Fritzsche, "High base pair opening rates in tracts of GC base pairs," *The Journal of Biological Chemistry*, vol. 274, no. 11, pp. 6957–6962, 1999.
- [9] J. Bode, S. Winkelmann, S. Götze et al., "Correlations between scaffold/matrix attachment region (S/MAR) binding activity and DNA duplex destabilization energy," *Journal of Molecular Biology*, vol. 358, no. 2, pp. 597–613, 2006.
- [10] T. D. Schneider, "Strong minor groove base conservation in sequence logos implies DNA distortion or base flipping during replication and transcription initiation," *Nucleic Acids Research*, vol. 29, no. 23, pp. 4881–4891, 2001.
- [11] C. H. Choi, G. Kalosakas, K. Ø. Rasmussen, M. Hiromura, A. R. Bishop, and A. Usheva, "DNA dynamically directs its own transcription initiation," *Nucleic Acids Research*, vol. 32, no. 4, pp. 1584–1590, 2004.
- [12] M. Gniazdowski, W. A. Denny, S. M. Nelson, and M. Czyz, "Effects of anticancer drugs on transcription factor-DNA interactions," *Expert Opinion on Therapeutic Targets*, vol. 9, no. 3, pp. 471–489, 2005.
- [13] C. R. Calladine and H.R. Drew, *Understanding DNA: The Molecule and How It Works*, Academic Press, San Diego, Calif, USA, 2nd edition, 1997.
- [14] B. F. Putnam, L. L. Van Zandt, E. W. Prohofsky, and W. N. Mei, "Resonant and localized breathing modes in terminal regions of the DNA double helix," *Biophysical Journal*, vol. 35, no. 2, pp. 271–287, 1981.
- [15] S. C. Harvey, "DNA structural dynamics: longitudinal breathing as a possible mechanism for the B  $\rightleftharpoons$  Z transition," *Nucleic Acids Research*, vol. 11, no. 14, pp. 4867–4878, 1983.
- [16] D. R. Kearns, "NMR studies of conformational states and dynamics of DNA," *CRC Critical Reviews in Biochemistry*, vol. 15, no. 3, pp. 237–290, 1984.
- [17] K. J. Breslauer, R. Frank, H. Blocker, and L. A. Marky, "Predicting DNA duplex stability from the base sequence," *Proceedings of the National Academy of Sciences of the United States of America*, vol. 83, no. 11, pp. 3746–3750, 1986.
- [18] R. Beger, Y. Feng, and E. W. Prohofsky, "Vibrational fluctuations of hydrogen bonds in a DNA double helix with alternating TA type inserts," *Biophysical Journal*, vol. 58, no. 2, pp. 437–445, 1990.
- [19] C. J. Benham, "Energetics of the strand separation transition in superhelical DNA," *Journal of Molecular Biology*, vol. 225, no. 3, pp. 835–847, 1992.
- [20] C. J. Benham, "Sites of predicted stress-induced DNA duplex destabilization occur preferentially at regulatory loci," *Proceedings of the National Academy of Sciences of the United States of America*, vol. 90, no. 7, pp. 2999–3003, 1993.
- [21] C. J. Benham, "Duplex destabilization in superhelical DNA is predicted to occur at specific transcriptional regulatory regions," *Journal of Molecular Biology*, vol. 255, no. 3, pp. 425–434, 1996.
- [22] Y. Z. Chen and E. W. Prohofsky, "Sequence and temperature dependence of the interbase hydrogen-bond breathing modes in B-DNA polymers: comparison with low-frequency Raman peaks and their role in helix melting," *Biopolymers*, vol. 35, no. 6, pp. 573–582, 1995.

- [23] A. G. Pedersen, P. Baldi, Y. Chauvin, and S. Brunak, "The biology of eukaryotic promoter prediction—a review," *Computers and Chemistry*, vol. 23, no. 3-4, pp. 191–207, 1999.
- [24] F. Lankaš, J. Šponer, P. Hobza, and J. Langowski, "Sequence-dependent elastic properties of DNA," *Journal of Molecular Biology*, vol. 299, no. 3, pp. 695–709, 2000.
- [25] S. Wärmländer, J. E. Sponer, J. Sponer, and M. Leijoni, "The influence of the thymine C5 methyl group on spontaneous base pair breathing in DNA," *The Journal of Biological Chemistry*, vol. 277, no. 32, pp. 28491–28497, 2002.
- [26] A. Krueger, E. Protozanova, and M. D. Frank-Kamenetskii, "Sequence-dependent basepair opening in DNA double helix," *Biophysical Journal*, vol. 90, no. 9, pp. 3091–3099, 2006.
- [27] T. Ambjörnsson, S. K. Banik, O. Krichevsky, and R. Metzler, "Sequence sensitivity of breathing dynamics in heteropolymer DNA," *Physical Review Letters*, vol. 97, no. 12, Article ID 128105, 4 pages, 2006.
- [28] T. Ambjörnsson, S. K. Banik, O. Krichevsky, and R. Metzler, "Breathing dynamics in heteropolymer DNA," *Biophysical Journal*, vol. 92, no. 8, pp. 2674–2684, 2007.
- [29] C. A. S.A. Minetti, D. P. Remeta, R. Dickstein, and K. J. Breslauer, "Energetic signatures of single base bulges: thermodynamic consequences and biological implications," *Nucleic Acids Research*, vol. 38, no. 1, pp. 97–116, 2010.
- [30] Y.-J. Li, X.-H. Fu, D.-P. Liu, and C.-C. Liang, "Opening the chromatin for transcription," *International Journal of Biochemistry and Cell Biology*, vol. 36, no. 8, pp. 1411–1423, 2004.
- [31] M. D. Betterton and F. Jülicher, "Opening of nucleic-acid double strands by helicases: active versus passive opening," *Physical Review E*, vol. 71, no. 1, Article ID 011904, 11 pages, 2005.
- [32] S. Schuck and A. Stenlund, "ATP-dependent minor groove recognition of TA base pairs is required for template melting by the E1 initiator protein," *Journal of Virology*, vol. 81, no. 7, pp. 3293–3302, 2007.
- [33] C. M. Sanders, "A DNA-binding activity in BPV initiator protein E1 required for melting duplex ori DNA but not processive helicase activity initiated on partially single-stranded DNA," *Nucleic Acids Research*, vol. 36, no. 6, pp. 1891–1899, 2008.
- [34] F. Jelen and E. Palecek, "Nucleotide sequence-dependent opening of double-stranded DNA at an electrically charged surface," *General Physiology and Biophysics*, vol. 4, no. 2, pp. 219–237, 1985.
- [35] T. T. Eckdahl and J. N. Anderson, "Conserved DNA structures in origins of replication," *Nucleic Acids Research*, vol. 18, no. 6, pp. 1609–1612, 1990.
- [36] B. Essevez-Roulet, U. Bockelmann, and F. Heslot, "Mechanical separation of the complementary strands of DNA," *Proceedings of the National Academy of Sciences of the United States of America*, vol. 94, no. 22, pp. 11935–11940, 1997.
- [37] T. M. Lohman and K. P. Bjornson, "Mechanisms of helicase-catalyzed DNA unwinding," *Annual Review of Biochemistry*, vol. 65, pp. 169–214, 1996.
- [38] M. Gyimesi, K. Sarlós, and M. Kovács, "Processive translocation mechanism of the human Bloom's syndrome helicase along single-stranded DNA," *Nucleic Acids Research*, 2010.
- [39] M. S. Wold, "Replication protein A: a heterotrimeric, single-stranded DNA-binding protein required for eukaryotic DNA metabolism," *Annual Review of Biochemistry*, vol. 66, pp. 61–92, 1997.
- [40] S. Waga and B. Stillman, "The DNA replication fork in eukaryotic cells," *Annual Review of Biochemistry*, vol. 67, pp. 721–751, 1998.
- [41] O. Maillard, S. Solyom, and H. Naegeli, "An aromatic sensor with aversion to damaged strands confers versatility to DNA repair," *PLoS Biology*, vol. 5, no. 4, article e79, 2007.
- [42] G. Herrick and B. Alberts, "Nucleic acid helix coil transitions mediated by helix unwinding proteins from calf thymus," *The Journal of Biological Chemistry*, vol. 251, no. 7, pp. 2133–2141, 1976.
- [43] S. R. Planck and S. H. Wilson, "Studies on the structure of mouse helix-destabilizing protein-1. DNA binding and controlled proteolysis with trypsin," *The Journal of Biological Chemistry*, vol. 255, no. 23, pp. 11547–11556, 1980.
- [44] R. L. Karpel and A. C. Burchard, "A basic isozyme of yeast glyceraldehyde-3-phosphate dehydrogenase with nucleic acid helix-destabilizing activity," *Biochimica et Biophysica Acta*, vol. 654, no. 2, pp. 256–267, 1981.
- [45] K. Javaherian, M. Sadeghi, and L. F. Liu, "Nonhistone proteins HMG1 and HMG2 unwind DNA double helix," *Nucleic Acids Research*, vol. 6, no. 11, pp. 3569–3580, 1979.
- [46] A. P. Butler, J. K. W. Mardian, and D. E. Olins, "Nonhistone chromosomal protein HMG 1 interactions with DNA: fluorescence and thermal denaturation studies," *The Journal of Biological Chemistry*, vol. 260, no. 19, pp. 10613–10620, 1985.
- [47] M.-H. David-Cordonnier, M. Hamdane, C. Bailly, and J.-C. D'Halluin, "The DNA binding domain of the human c-Abl tyrosine kinase preferentially binds to DNA sequences containing an AAC motif and to distorted DNA structures," *Biochemistry*, vol. 37, no. 17, pp. 6065–6076, 1998.
- [48] M.-H. David-Cordonnier, D. Payet, J.-C. D'Halluin, M. J. Waring, A. A. Travers, and C. Bailly, "The DNA-binding domain of human c-Abl tyrosine kinase promotes the interaction of a HMG chromosomal protein with DNA," *Nucleic Acids Research*, vol. 27, no. 11, pp. 2265–2270, 1999.
- [49] M. J. Heath, S. S. Derebail, R. J. Gorelick, and J. J. DeStefano, "Differing roles of the N- and C-terminal zinc fingers in human immunodeficiency virus nucleocapsid protein-enhanced nucleic acid annealing," *The Journal of Biological Chemistry*, vol. 278, no. 33, pp. 30755–30763, 2003.
- [50] H. Wang, Y.-S. Yeh, and P. F. Barbara, "HIV-1 nucleocapsid protein bends double-stranded nucleic acids," *Journal of the American Chemical Society*, vol. 131, no. 42, pp. 15534–15543, 2009.
- [51] N. Narayanan, R. J. Gorelick, and J. J. DeStefano, "Structure/function mapping of amino acids in the N-terminal zinc finger of the human immunodeficiency virus type 1 nucleocapsid protein: residues responsible for nucleic acid helix destabilizing activity," *Biochemistry*, vol. 45, no. 41, pp. 12617–12628, 2006.
- [52] A. Bera, A.-C. Roche, and P. K. Nandi, "Bending and unwinding of nucleic acid by prion protein," *Biochemistry*, vol. 46, no. 5, pp. 1320–1328, 2007.
- [53] D. P. Hornby and G. C. Ford, "Protein-mediated base flipping," *Current Opinion in Biotechnology*, vol. 9, no. 4, pp. 354–358, 1998.
- [54] C. Cao, Y. L. Jiang, J. T. Stivers, and F. Song, "Dynamic opening of DNA during the enzymatic search for a damaged base," *Nature structural & Molecular Biology*, vol. 11, no. 12, pp. 1230–1236, 2004.
- [55] E. Malta, G. F. Moolenaar, and N. Goosen, "Base flipping in nucleotide excision repair," *The Journal of Biological Chemistry*, vol. 281, no. 4, pp. 2184–2194, 2006.

- [56] D. J. Hosfield, Y. Guan, B. J. Haas, R. P. Cunningham, and J. A. Tainer, "Structure of the DNA repair enzyme endonuclease IV and its DNA complex: double-nucleotide flipping at abasic sites and three-metal-ion catalysis," *Cell*, vol. 98, no. 3, pp. 397–408, 1999.
- [57] S. R. W. Bellamy, K. Krusong, and G. S. Baldwin, "A rapid reaction analysis of uracil DNA glycosylase indicates an active mechanism of base flipping," *Nucleic Acids Research*, vol. 35, no. 5, pp. 1478–1487, 2007.
- [58] J. L. Tubbs, A. E. Pegg, and J. A. Tainer, "DNA binding, nucleotide flipping, and the helix-turn-helix motif in base repair by O6-alkylguanine-DNA alkyltransferase and its implications for cancer chemotherapy," *DNA Repair*, vol. 6, no. 8, pp. 1100–1115, 2007.
- [59] E. Malta, C. P. Verhagen, G. F. Moolenaar, D. V. Filippov, G. A. Van der Marel, and N. Goosen, "Functions of base flipping in E. coli nucleotide excision repair," *DNA Repair*, vol. 7, no. 10, pp. 1647–1658, 2008.
- [60] C.-G. Yang, C. Yi, E. M. Duguid, et al., "Crystal structures of DNA/RNA repair enzymes AlkB and ABH2 bound to dsDNA," *Nature*, vol. 452, no. 7190, pp. 961–965, 2008.
- [61] S. Jiranusornkul and C. A. Laughton, "Destabilization of DNA duplexes by oxidative damage at guanine: implications for lesion recognition and repair," *Journal of the Royal Society*, vol. 5, supplement 3, pp. 191–198, 2008.
- [62] P. M. Vertino, "Structures and functions," in *S-Adenosylmethionine-dependent methyltransferases*, X. Cheng and R. M. Blumenthal, Eds., pp. 341–372, 1999.
- [63] O. Sundheim, V. A. Talstad, C. B. Vågbø, G. Slupphaug, and H. E. Krokan, "AlkB demethylases flip out in different ways," *DNA Repair*, vol. 7, no. 11, pp. 1916–1923, 2008.
- [64] N. Huang and A. D. MacKerell Jr., "Atomistic view of base flipping in DNA," *Philosophical Transactions of the Royal Society A*, vol. 362, no. 1820, pp. 1439–1460, 2004.
- [65] K. Arita, M. Ariyoshi, H. Tochio, Y. Nakamura, and M. Shirakawa, "Recognition of hemi-methylated DNA by the SRA protein UHRF1 by a base-flipping mechanism," *Nature*, vol. 455, no. 7214, pp. 818–821, 2008.
- [66] H. Hashimoto, J. R. Horton, X. Zhang, M. Bostick, S. E. Jacobsen, and X. Cheng, "The SRA domain of UHRF1 flips 5-methylcytosine out of the DNA helix," *Nature*, vol. 455, no. 7214, pp. 826–829, 2008.
- [67] C. Mura and J. A. McCammon, "Molecular dynamics of a  $\kappa$ B DNA element: base flipping via cross-strand intercalative stacking in a microsecond-scale simulation," *Nucleic Acids Research*, vol. 36, no. 15, pp. 4941–4955, 2008.
- [68] V. Kleinwächter, Z. Balcarová, and J. Boháček, "Thermal stability of complexes of diaminoacridines with deoxyribonucleic acids of varying base content," *Biochimica et Biophysica Acta*, vol. 174, no. 1, pp. 188–201, 1969.
- [69] J. Kapuscinski and Z. Darzynkiewicz, "Increased accessibility of bases in DNA upon binding of acridine orange," *Nucleic Acids Research*, vol. 11, no. 21, pp. 7555–7568, 1983.
- [70] J. Kapuscinski and Z. Darzynkiewicz, "Denaturation of nucleic acids induced by intercalating agents. Biochemical and biophysical properties of acridine orange-DNA complexes," *Journal of Biomolecular Structure and Dynamics*, vol. 1, no. 6, pp. 1485–1499, 1984.
- [71] Z. Darzynkiewicz, D. Evenson, J. Kapuscinski, and M. R. Melamed, "Denaturation of RNA and DNA in situ induced by acridine orange," *Experimental Cell Research*, vol. 148, no. 1, pp. 31–46, 1983.
- [72] Z. Darzynkiewicz, F. Traganos, J. Kapuscinski, and M. R. Melamed, "Denaturation and condensation of DNA in situ induced by acridine orange in relation to chromatin changes during growth and differentiation of Friend erythroleukemia cells," *Cytometry*, vol. 6, no. 3, pp. 195–207, 1985.
- [73] A. Canals, M. Purciolas, J. Aymamí, and M. Coll, "The anticancer agent ellipticine unwinds DNA by intercalative binding in an orientation parallel to base pairs," *Acta Crystallographica Section D*, vol. 61, no. 7, pp. 1009–1012, 2005.
- [74] M. Cirilli, F. Bachechi, G. Ughetto, F. P. Colonna, and M. L. Capobianco, "Interactions between morpholinyl anthracyclines and DNA. The crystal structure of a morpholino doxorubicin bound to d(CGTCAG)," *Journal of Molecular Biology*, vol. 230, no. 3, pp. 878–889, 1993.
- [75] N. C. Garbett and D. E. Graves, "Extending nature's leads: the anticancer agent ellipticine," *Current Medicinal Chemistry—Anti-Cancer Agents*, vol. 4, no. 2, pp. 149–172, 2004.
- [76] F. Zunino, R. Gambetta, A. Di Marco, and A. Zaccara, "Interaction of daunomycin and its derivatives with DNA," *Biochimica et Biophysica Acta*, vol. 277, no. 3, pp. 489–498, 1972.
- [77] K. W. Kohn, M. J. Waring, D. Glaubiger, and C. A. Friedman, "Intercalative binding of ellipticine to DNA," *Cancer Research*, vol. 35, no. 1, pp. 71–76, 1975.
- [78] M. J. Waring, "Structural requirements for the binding of ethidium to nucleic acids," *Biochimica et Biophysica Acta*, vol. 114, no. 2, pp. 234–244, 1966.
- [79] M. P. Teulade-Fichou, J. P. Vigneron, and J. M. Lehn, "Molecular recognition of nucleosides and nucleotides by a water soluble cyclo-bis-intercaland type receptor molecule based on acridine subunits," *Supramolecular Chemistry*, vol. 5, pp. 139–147, 1995.
- [80] A. Slama-Schwok, M.-P. Teulade-Fichou, J.-P. Vigneron, E. Taillandier, and J.-M. Lehn, "Selective binding of a macrocyclic bis-acridine to DNA hairpins," *Journal of the American Chemical Society*, vol. 117, no. 26, pp. 6822–6830, 1995.
- [81] A. Slama-Schwok, F. Peronnet, E. Hantz-Brachet et al., "A macrocyclic bis-acridine shifts the equilibrium from duplexes towards DNA hairpins," *Nucleic Acids Research*, vol. 25, no. 13, pp. 2574–2581, 1997.
- [82] A. J. Blacker, M.-P. Teulade-Fichou, J.-P. Vigneron, M. Fauquet, and J.-M. Lehn, "Selective photocleavage of single-stranded nucleic acids by cyclobisintercaland molecules," *Bioorganic and Medicinal Chemistry Letters*, vol. 8, no. 6, pp. 601–606, 1998.
- [83] M. Jourdan, J. García, J. Lhomme, M.-P. Teulade-Fichou, J.-P. Vigneron, and J.-M. Lehn, "Threading bis-intercalation of a macrocyclic bisacridine at abasic sites in DNA: nuclear magnetic resonance and molecular modeling study," *Biochemistry*, vol. 38, no. 43, pp. 14205–14213, 1999.
- [84] A. David, N. Bleimling, C. Beuck, J.-M. Lehn, E. Weinhold, and M.-P. Teulade-Fichou, "DNA mismatch-specific base flipping by a bisacridine macrocycle," *ChemBioChem*, vol. 4, no. 12, pp. 1326–1331, 2003.
- [85] Y.-B. Shi and J. E. Hearst, "Thermostability of double-stranded deoxyribonucleic acids: effects of covalent additions of a psoralen," *Biochemistry*, vol. 25, no. 20, pp. 5895–5902, 1986.
- [86] M. Tomasz, A. K. Chawla, and R. Lipman, "Mechanism of monofunctional and bifunctional alkylation of DNA by mitomycin C," *Biochemistry*, vol. 27, no. 9, pp. 3182–3187, 1988.

- [87] A. K. Basu, C. J. Hanrahan, S. A. Malia, S. Kumar, R. Bizanek, and M. Tomasz, "Effect of site-specifically located mitomycin C-DNA monoadducts on in vitro DNA synthesis by DNA polymerases," *Biochemistry*, vol. 32, no. 18, pp. 4708–4718, 1993.
- [88] A. J. Warren, A. E. Maccubbin, and J. W. Hamilton, "Detection of mitomycin C-DNA adducts in vivo by 32P-postlabeling: time course for formation and removal of adducts and biochemical modulation," *Cancer Research*, vol. 58, no. 3, pp. 453–461, 1998.
- [89] J. Kašpárková, O. Nováková, O. Vrána, N. Farrell, and V. Brabec, "Effect of geometric isomerism in dinuclear platinum antitumor complexes on DNA interstrand cross-linking," *Biochemistry*, vol. 38, no. 34, pp. 10997–11005, 1999.
- [90] A. S. Fridman, V. Brabec, S. G. Haroutiunian, R. M. Wartell, and D. Y. Lando, "Melting of cross-linked DNA v. cross-linking effect caused by local stabilization of the double helix," *Journal of Biomolecular Structure and Dynamics*, vol. 20, no. 4, pp. 533–545, 2003.
- [91] M.-H. David-Cordonnier, W. Laine, A. Lansiaux et al., "Covalent binding of antitumor benzoacronycines to double-stranded DNA induces helix opening and the formation of single-stranded DNA: unique consequences of a novel DNA-bonding mechanism," *Molecular Cancer Therapeutics*, vol. 4, no. 1, pp. 71–80, 2005.
- [92] A. Gelasco and S. J. Lippard, "NMR solution structure of a DNA dodecamer duplex containing a cis-diammineplatinum(II) d(GpG) intrastrand cross-link, the major adduct of the anticancer drug cisplatin," *Biochemistry*, vol. 37, no. 26, pp. 9230–9239, 1998.
- [93] M. L. G. Dronkert and R. Kanaar, "Repair of DNA interstrand cross-links," *Mutation Research*, vol. 486, no. 4, pp. 217–247, 2001.
- [94] O. D. Schärer, "A molecular basis for damage recognition in eukaryotic nucleotide excision repair," *ChemBioChem*, vol. 9, no. 1, pp. 21–23, 2008.
- [95] D. M. Noll, T. M. Mason, and P. S. Miller, "Formation and repair of interstrand cross-links in DNA," *Chemical Reviews*, vol. 106, no. 2, pp. 277–301, 2006.
- [96] S. F. Bellon, J. H. Coleman, and S. J. Lippard, "DNA unwinding produced by site-specific intrastrand cross-links of the antitumor drug cis-diamminedichloroplatinum(II)," *Biochemistry*, vol. 30, no. 32, pp. 8026–8035, 1991.
- [97] V. Brabec, J. Reedijk, and M. Leng, "Sequence-dependent distortions induced in DNA by monofunctional platinum(II) binding," *Biochemistry*, vol. 31, no. 49, pp. 12397–12402, 1992.
- [98] J.-M. Malinge, C. Pérez, and M. Leng, "Base sequence-independent distortions induced by interstrand cross-links in cis-diamminedichloroplatinum (II)-modified DNA," *Nucleic Acids Research*, vol. 22, no. 19, pp. 3834–3839, 1994.
- [99] J.-M. Malinge, M.-J. Giraud-Panis, and M. Leng, "Interstrand cross-links of cisplatin induce striking distortions in DNA," *Journal of Inorganic Biochemistry*, vol. 77, no. 1-2, pp. 23–29, 1999.
- [100] F. Coste, J.-M. Malinge, L. Serre et al., "Crystal structure of a double-stranded DNA containing a cisplatin interstrand cross-link at 1.63 Å resolution: hydration at the platinated site," *Nucleic Acids Research*, vol. 27, no. 8, pp. 1837–1846, 1999.
- [101] J. Kasparkova, V. Marini, V. Bursova, and V. Brabec, "Biophysical studies on the stability of DNA intrastrand cross-links of transplatin," *Biophysical Journal*, vol. 95, no. 9, pp. 4361–4371, 2008.
- [102] A. S. Fridman, E. N. Galyuk, V. I. Vorob'ev, A. N. Skvortsov, and D. Y. Lando, "Melting of crosslinked DNA: VI. Comparison of influence of interstrand crosslinks and other chemical modifications formed by antitumor compounds on DNA stability," *Journal of Biomolecular Structure and Dynamics*, vol. 26, no. 2, pp. 175–185, 2008.
- [103] N. Poklar, D. S. Pilch, S. J. Lippard, E. A. Redding, S. U. Dunham, and K. J. Breslauer, "Influence of cisplatin intrastrand crosslinking on the conformation, thermal stability, and energetics of a 20-mer DNA duplex," *Proceedings of the National Academy of Sciences of the United States of America*, vol. 93, no. 15, pp. 7606–7611, 1996.
- [104] D. S. Pilch, S. U. Dunham, E. R. Jamieson, S. J. Lippard, and K. J. Breslauer, "DNA sequence context modulates the impact of a cisplatin 1,2-d(GpG) intrastrand cross-link on the conformational and thermodynamic properties of duplex DNA," *Journal of Molecular Biology*, vol. 296, no. 3, pp. 803–812, 2000.
- [105] J. Malina, O. Nováková, M. Vojtkova, G. Natile, and V. Brabec, "Conformation of DNA GG intrastrand cross-link of antitumor oxaliplatin and its enantiomeric analog," *Biophysical Journal*, vol. 93, no. 11, pp. 3950–3962, 2007.
- [106] E. N. Galyuk, A. S. Fridman, V. I. Vorob'ev et al., "Compensation of DNA stabilization and destabilization effects caused by cisplatin is partially disturbed in alkaline medium," *Journal of Biomolecular Structure and Dynamics*, vol. 25, no. 4, pp. 407–417, 2008.
- [107] V. Brabec, M. Sip, and M. Leng, "DNA conformational change produced by the site-specific interstrand cross-link of trans-diamminedichloroplatinum(II)," *Biochemistry*, vol. 32, no. 43, pp. 11676–11681, 1993.
- [108] S. Teletchêa, S. Komeda, J.-M. Teuben, M.-A. Elizondo-Riojas, J. Reedijk, and J. Kozelka, "A pyrazolato-bridged dinuclear platinum(II) complex induces only minor distortions upon DNA-binding," *Chemistry - A European Journal*, vol. 12, no. 14, pp. 3741–3753, 2006.
- [109] V. Bursova, J. Kasparkova, C. Hofr, and V. Brabec, "Effects of monofunctional adducts of platinum(II) complexes on thermodynamic stability and energetics of DNA duplexes," *Biophysical Journal*, vol. 88, no. 2, pp. 1207–1214, 2005.
- [110] A. Schwartz, L. Marrot, and M. Leng, "Conformation of DNA modified at a d(GG) or a d(AG) site by the antitumor drug cis-diamminedichloroplatinum(II)," *Biochemistry*, vol. 28, no. 20, pp. 7975–7979, 1989.
- [111] M. Hägerlöf, P. Papsai, C. S. Chow, and S. K. C. Elmroth, "More pronounced salt dependence and higher reactivity for platination of the hairpin r(CGCGUUGUUCGCG) compared with d(CGCGTTGTTCGCG)," *Journal of Biological Inorganic Chemistry*, vol. 11, no. 8, pp. 974–990, 2006.
- [112] G. Sava, S. Pacor, F. Bregant, V. Ceschia, and G. Mestroni, "Metal complexes of ruthenium: antineoplastic properties and perspectives," *Anti-Cancer Drugs*, vol. 1, no. 2, pp. 99–108, 1990.
- [113] G. Sava, S. Pacor, F. Bregant, and V. Ceschia, "Metal complexes of ruthenium: a potential class of selective anticancer drugs," *Anticancer Research*, vol. 11, no. 3, pp. 1103–1107, 1991.
- [114] C. X. Zhang and S. J. Lippard, "New metal complexes as potential therapeutics," *Current Opinion in Chemical Biology*, vol. 7, no. 4, pp. 481–489, 2003.

- [115] O. Nováková, H. Chen, O. Vrana, A. Rodger, P. J. Sadler, and V. Brabec, "DNA interactions of monofunctional organometallic ruthenium(II) antitumor complexes in cell-free media," *Biochemistry*, vol. 42, no. 39, pp. 11544–11554, 2003.
- [116] O. Nováková, A. A. Nazarov, C. G. Hartinger, B. K. Keppler, and V. Brabec, "DNA interactions of dinuclear Ru(II) arene antitumor complexes in cell-free media," *Biochemical Pharmacology*, vol. 77, no. 3, pp. 364–374, 2009.
- [117] O. Nováková, J. Malina, T. Suchankova, et al., "Energetics, conformation, and recognition of DNA duplexes modified by monodentate Ru(II) complexes containing terphenyl arenes," *Chemistry - A European Journal*, vol. 16, no. 19, pp. 5744–5754, 2010.
- [118] H. P. Spielmann, T. J. Dwyer, J. E. Hearst, and D. E. Wemmer, "Solution structures of psoralen monoadducted and cross-linked DNA oligomers by NMR spectroscopy and restrained molecular dynamics," *Biochemistry*, vol. 34, no. 40, pp. 12937–12953, 1995.
- [119] N. Zhang, C. Lin, X. Huang et al., "Methylation of cytosine at C5 in a CpG sequence context causes a conformational switch of a benzo[a]pyrene diol epoxide-N2-guanine adduct in DNA from a minor groove alignment to intercalation with base displacement," *Journal of Molecular Biology*, vol. 346, no. 4, pp. 951–965, 2005.
- [120] Y. Zou and B. Van Houten, "Strand opening by the UvrA(2)B complex allows dynamic recognition of DNA damage," *The EMBO Journal*, vol. 18, pp. 4889–4901, 1999.
- [121] Y. Zou, C. Luo, and N. E. Geacintov, "Hierarchy of DNA damage recognition in Escherichia coli nucleotide excision repair," *Biochemistry*, vol. 40, no. 9, pp. 2923–2931, 2001.
- [122] M. Cosman, C. De los Santos, R. Fiala, et al., "Solution conformation of the major adduct between the carcinogen (+)-anti-benzo[a]pyrene diol epoxide and DNA," *Proceedings of the National Academy of Sciences of the United States of America*, vol. 89, no. 5, pp. 1914–1918, 1992.
- [123] M. Cosman, C. De Los Santos, R. Fiala et al., "Solution conformation of the (+)-cis-anti-[BP]dG adduct in a DNA duplex: intercalation of the covalently attached benzo[a]pyrenyl ring into the helix and displacement of the modified deoxyguanosine," *Biochemistry*, vol. 32, no. 16, pp. 4145–4155, 1993.
- [124] F. A. Rodríguez, Y. Cai, C. Lin et al., "Exocyclic amino groups of flanking guanines govern sequence-dependent adduct conformations and local structural distortions for minor groove-aligned benzo[α]pyrenyl-guanine lesions in a GG mutation hotspot context," *Nucleic Acids Research*, vol. 35, no. 5, pp. 1555–1568, 2007.
- [125] K. Kropachev, M. Kolbanovskii, Y. Cai et al., "The sequence dependence of human nucleotide excision repair efficiencies of benzo[a]pyrene-derived DNA lesions: insights into the structural factors that favor dual incisions," *Journal of Molecular Biology*, vol. 386, no. 5, pp. 1193–1203, 2009.
- [126] J. L. Bolton, E. Pisha, F. Zhang, and S. Qiu, "Role of quinoids in estrogen carcinogenesis," *Chemical Research in Toxicology*, vol. 11, no. 10, pp. 1113–1127, 1998.
- [127] J. L. Bolton, "Quinoids, quinoid radicals, and phenoxyl radicals formed from estrogens and antiestrogens," *Toxicology*, vol. 177, no. 1, pp. 55–65, 2002.
- [128] J. E. Rossouw, G. L. Anderson, R. L. Prentice et al., "Risks and benefits of estrogen plus progestin in healthy postmenopausal women: principal results from the women's health initiative randomized controlled trial," *Journal of the American Medical Association*, vol. 288, no. 3, pp. 321–333, 2002.
- [129] F. Zhang, Y. Chen, E. Pisha, et al., "The major metabolite of equilin, 4-Hydroxyequilin, autoxidizes to an o-quinone which isomerizes to the potent cytotoxin 4-Hydroxyequilenin-o-quinone," *Chemical Research in Toxicology*, vol. 12, no. 2, pp. 204–213, 1999.
- [130] E. Pisha, X. Lui, A. I. Constantinou, and J. L. Bolton, "Evidence that a metabolite of equine estrogens, 4-hydroxyequilenin, induces cellular transformation in vitro," *Chemical Research in Toxicology*, vol. 14, no. 1, pp. 82–90, 2001.
- [131] L. Shen, S. Qiu, Y. Chen et al., "Alkylation of 2'-deoxynucleosides and DNA by the premarin metabolite 4-hydroxyequilenin semiquinone radical," *Chemical Research in Toxicology*, vol. 11, no. 2, pp. 94–101, 1998.
- [132] F. Zhang, S. M. Swanson, R. B. Van Breemen et al., "Equine estrogen metabolite 4-hydroxyequilenin induces DNA damage in the rat mammary tissues: formation of single-strand breaks, apurinic sites, stable adducts, and oxidized bases," *Chemical Research in Toxicology*, vol. 14, no. 12, pp. 1654–1659, 2001.
- [133] J. Embrechts, F. Lemire, W. Van Dongen, and E. L. Esmans, "Equilenin-2'-deoxynucleoside adducts: analysis with nano-liquid chromatography coupled to nano-electrospray tandem mass spectrometry," *Journal of Mass Spectrometry*, vol. 36, no. 3, pp. 317–328, 2001.
- [134] A. Kolbanovskiy, V. Kuzmin, A. Shastry et al., "Base selectivity and effects of sequence and DNA secondary structure on the formation of covalent adducts derived from the equine estrogen metabolite 4-hydroxyequilenin," *Chemical Research in Toxicology*, vol. 18, no. 11, pp. 1737–1747, 2005.
- [135] J. Embrechts, F. Lemièrre, W. Van Dongen et al., "Detection of estrogen DNA-adducts in human breast tumor tissue and healthy tissue by combined nano LC-nano ES tandem mass spectrometry," *Journal of the American Society for Mass Spectrometry*, vol. 14, no. 5, pp. 482–491, 2003.
- [136] S. Ding, R. Shapiro, N. E. Geacintov, and S. Broyde, "4-Hydroxyequilenin-adenine lesions in DNA duplexes: stereochemistry, damage site, and structure," *Biochemistry*, vol. 46, no. 1, pp. 182–191, 2007.
- [137] S. Ding, R. Shapiro, Y. Cai, N. E. Geacintov, and S. Broyde, "Conformational properties of equilenin—DNA adducts: stereoisomer and base effects," *Chemical Research in Toxicology*, vol. 21, no. 5, pp. 1064–1073, 2008.
- [138] S. Ding, Y. Wang, A. Kolbanovskiy, et al., "Determination of absolute configurations of 4-hydroxyequilenin-cytosine and -adenine adducts by optical rotatory dispersion, electronic circular dichroism, density functional theory calculations, and mass spectrometry," *Chemical Research in Toxicology*, vol. 21, no. 9, pp. 1739–1748, 2008.
- [139] S. Ding, R. Shapiro, N. E. Geacintov, and S. Broyde, "Equilenin-derived DNA adducts to cytosine in DNA duplexes: structures and thermodynamics," *Biochemistry*, vol. 44, no. 44, pp. 14565–14576, 2005.
- [140] Y. Pommier, G. Kohlhagen, C. Bailly, M. Waring, A. Mazumder, and K. W. Kohn, "DNA sequence- and structure-selective alkylation of guanine N2 in the DNA minor groove by ecteinascidin 743, a potent antitumor compound from the caribbean tunicate Ecteinascidia turbinata," *Biochemistry*, vol. 35, no. 41, pp. 13303–13309, 1996.

- [141] M. Tomasz, A. Das, K. S. Tang et al., "The purine 2-amino group as the critical recognition element for sequence-specific alkylation and cross-linking of DNA by mitomycin C," *Journal of the American Chemical Society*, vol. 120, no. 45, pp. 11581–11593, 1998.
- [142] D. E. Thurston, in *Molecular Aspects of Anticancer Drug-DNA Interactions*, S. Neidle and M. J. Waring, Eds., vol. 1, pp. 54–87, Macmillan, London, UK, 1999.
- [143] R. J. Isaacs and H. P. Spielmann, "A model for initial DNA lesion recognition by NER and MMR based on local conformational flexibility," *DNA Repair*, vol. 3, no. 5, pp. 455–464, 2004.
- [144] O. D. Schärer, "A molecular basis for damage recognition in eukaryotic nucleotide excision repair," *ChemBioChem*, vol. 9, no. 1, pp. 21–23, 2008.
- [145] J. L. Tubbs, V. Latypov, S. Kanugula, et al., "Flipping of alkylated DNA damage bridges base and nucleotide excision repair," *Nature*, vol. 459, no. 7248, pp. 808–813, 2009.
- [146] V. Brabec, "DNA Modifications by antitumor platinum and ruthenium compounds: their recognition and repair," *Progress in Nucleic Acid Research and Molecular Biology*, vol. 71, pp. 1–68, 2002.
- [147] V. Brabec and O. Nováková, "DNA binding mode of ruthenium complexes and relationship to tumor cell toxicity," *Drug Resistance Updates*, vol. 9, no. 3, pp. 111–122, 2006.
- [148] T. Bugarcic, O. Nováková, A. Halámiková, et al., "Cytotoxicity, cellular uptake, and DNA interactions of new monodentate ruthenium(II) complexes containing terphenyl arenes," *Journal of Medicinal Chemistry*, vol. 51, no. 17, pp. 5310–5319, 2008.
- [149] R. Reeves and J. E. Adair, "Role of high mobility group (HMG) chromatin proteins in DNA repair," *DNA Repair*, vol. 4, no. 8, pp. 926–938, 2005.
- [150] P. L. Privalov, A. I. Dragan, and C. Crane-Robinson, "The cost of DNA bending," *Trends in Biochemical Sciences*, vol. 34, no. 9, pp. 464–470, 2009.
- [151] J. Kasparkova, M. Vojtiskova, G. Natile, and V. Brabec, "Unique properties of DNA interstrand cross-links of anti-tumor oxaliplatin and the effect of chirality of the carrier ligand," *Chemistry - A European Journal*, vol. 14, no. 4, pp. 1330–1341, 2008.
- [152] J.-C. Huang, D. B. Zamble, J. T. Reardon, S. J. Lippard, and A. Sancar, "HMG-domain proteins specifically inhibit the repair of the major DNA adduct of the anticancer drug cisplatin by human excision nuclease," *Proceedings of the National Academy of Sciences of the United States of America*, vol. 91, no. 22, pp. 10394–10398, 1994.
- [153] A. Sharma, A. Ramanjaneyulu, R. Ray, and M. R. Rajeswari, "Involvement of high mobility group B proteins in cisplatin-induced cytotoxicity in squamous cell carcinoma of skin," *DNA and Cell Biology*, vol. 28, no. 7, pp. 311–318, 2009.
- [154] C. S. Chow, J. P. Whitehead, and S. J. Lippard, "HMG domain proteins induce sharp bends in cisplatin-modified DNA," *Biochemistry*, vol. 33, no. 50, pp. 15124–15130, 1994.
- [155] E. E. Trimmer, D. B. Zamble, S. J. Lippard, and J. M. Essigmann, "Human testis-determining factor SRY binds to the major DNA adduct of cisplatin and a putative target sequence with comparable affinities," *Biochemistry*, vol. 37, no. 1, pp. 352–362, 1998.
- [156] K. Chvátlová, M.-A. Sari, S. Bombard, and J. Kozelka, "LEF-1 recognition of platinated GG sequences within double-stranded DNA. Influence of flanking bases," *Journal of Inorganic Biochemistry*, vol. 102, no. 2, pp. 242–250, 2008.
- [157] M. Fuxreiter, N. Luo, P. Jedlowszky, I. Simon, and R. Osman, "Role of base flipping in specific recognition of damaged DNA by repair enzymes," *Journal of Molecular Biology*, vol. 323, no. 5, pp. 823–834, 2002.
- [158] W. Yang, "Poor base stacking at DNA lesions may initiate recognition by many repair proteins," *DNA Repair*, vol. 5, no. 6, pp. 654–666, 2006.
- [159] W. Yang, "Structure and mechanism for DNA lesion recognition," *Cell Research*, vol. 18, no. 1, pp. 184–197, 2008.
- [160] C.-G. Yang, K. Garcia, and C. He, "Damage detection and base flipping in direct DNA alkylation repair," *ChemBioChem*, vol. 10, no. 3, pp. 417–423, 2009.
- [161] D. R. Duckett, J. T. Drummond, A. I. H. Murchie, et al., "Humnan MutSa recognizes damaged DNA base pairs containing O6-methylguanine, O4-methylthymine, or the cisplatin-d(GpG) adduct," *Proceedings of the National Academy of Sciences of the United States of America*, vol. 93, no. 13, pp. 6443–6447, 1996.
- [162] S. Aebi, B. Kurdi-Haidar, R. Gordon et al., "Loss of DNA mismatch repair in acquired resistance to cisplatin," *Cancer Research*, vol. 56, no. 13, pp. 3087–3090, 1996.
- [163] J. A. Mello, S. Acharya, R. Fishel, and J. M. Essigmann, "The mismatch-repair protein hMSH2 binds selectively to DNA adducts of the anticancer drug cisplatin," *Chemistry and Biology*, vol. 3, no. 7, pp. 579–589, 1996.
- [164] L. Fourrier, P. Brooks, and J.-M. Malinge, "Binding discrimination of MutS to a set of lesions and compound lesions (base damage and mismatch) reveals its potential role as a cisplatin-damaged DNA sensing protein," *The Journal of Biological Chemistry*, vol. 278, no. 23, pp. 21267–21275, 2003.
- [165] M. Castellano-Castillo, H. Kostrhunova, V. Marini et al., "Binding of mismatch repair protein MutS to mispaired DNA adducts of intercalating ruthenium(II) arene complexes," *The Journal of Biological Inorganic Chemistry*, vol. 13, no. 6, pp. 993–999, 2008.
- [166] O. Nováková, J. Kasparkova, V. Bursova et al., "Conformation of DNA modified by monofunctional Ru(II) arene complexes: recognition by DNA binding proteins and repair. Relationship to cytotoxicity," *Chemistry and Biology*, vol. 12, no. 1, pp. 121–129, 2005.
- [167] L. Jia, K. Kropachev, S. Ding, B. Van Houten, N. E. Geacintov, and S. Broyde, "Exploring damage recognition models in prokaryotic nucleotide excision repair with a benzo[a]pyrene-derived lesion in UvrB," *Biochemistry*, vol. 48, no. 38, pp. 8948–8957, 2009.
- [168] V. Mocquet, K. Kropachev, M. Kolbanovskiy et al., "The human DNA repair factor XPC-HR23B distinguishes stereoisomeric benzo[a]pyrenyl-DNA lesions," *The EMBO Journal*, vol. 26, no. 12, pp. 2923–2932, 2007.
- [169] A. Hartwig, "The role of DNA repair in benzene-induced carcinogenesis," *Chemico-Biological Interactions*, vol. 184, no. 1–2, pp. 269–272, 2010.
- [170] A. Janičijević, K. Sugawara, Y. Shimizu et al., "DNA bending by the human damage recognition complex XPC-HR23B," *DNA Repair*, vol. 2, no. 3, pp. 325–336, 2003.
- [171] F. C. Clement, U. Camenisch, J. Fei, N. Kaczmarek, N. Mathieu, and H. Naegeli, "Dynamic two-stage mechanism of versatile DNA damage recognition by xeroderma pigmentosum group C protein," *Mutation Research*, vol. 685, no. 1–2, pp. 21–28, 2010.
- [172] K. L. Brown, M. Roginskaya, Y. Zou, A. Altamirano, A. K. Basu, and M. P. Stone, "Binding of the human nucleotide excision repair proteins XPA and XPC/HR23B

- to the 5R-thymine glycol lesion and structure of the *cis*-(5R,6S) thymine glycol epimer in the 5'-GTgG-3' sequence: destabilization of two base pairs at the lesion site," *Nucleic Acids Research*, vol. 38, no. 2, pp. 428–440, 2009.
- [173] J. Yang, X. Liu, P. Niu, Y. Zou, and Y. Duan, "Correlations and co-localizations of Hsp70 with XPA, XPG in human bronchial epithelia cells exposed to benzo[a]pyrene," *Toxicology*, vol. 265, no. 1-2, pp. 10–14, 2009.
- [174] K. Shinmura, M. Iwaizumi, H. Igarashi et al., "Induction of centrosome amplification and chromosome instability in p53-deficient lung cancer cells exposed to benzo[ $\alpha$ ]pyrene diol epoxide (B[ $\alpha$ ]PDE)," *Journal of Pathology*, vol. 216, no. 3, pp. 365–374, 2008.
- [175] X. Lu, J. Shao, H. Li, and Y. Yu, "Early whole-genome transcriptional response induced by benzo[ $\alpha$ ]pyrene diol epoxide in a normal human cell line," *Genomics*, vol. 93, no. 4, pp. 332–342, 2009.
- [176] X. Lu, J. Shao, H. Li, and Y. Yu, "Temporal gene expression changes induced by a low concentration of benzo[ $\alpha$ ]pyrene diol epoxide in a normal human cell line," *Mutation Research*, vol. 684, no. 1-2, pp. 74–80, 2010.
- [177] Y. Cai, D. J. Patel, N. E. Geacintov, and S. Broyde, "Differential nucleotide excision repair susceptibility of bulky DNA adducts in different sequence contexts: hierarchies of recognition signals," *Journal of Molecular Biology*, vol. 385, no. 1, pp. 30–44, 2009.
- [178] D. Chen, A. Kolbanovskiy, A. Shastry, et al., "Nucleotide excision repair of DNA adducts derived from the binding of the equine estrogen metabolite 4-OHEN to dC and dA adducts in vitro," in *Proceedings of the 97th Annual Meeting of the American Association for Cancer Research*, vol. 47, AACR, Washington, DC, USA, April 2006, abstract no. #5255.
- [179] E. G. Notch, D. M. Miniutti, and G. D. Mayer, "17 $\alpha$ -ethinylestradiol decreases expression of multiple hepatic nucleotide excision repair genes in zebrafish (*Danio rerio*)," *Aquatic Toxicology*, vol. 84, no. 3, pp. 301–309, 2007.
- [180] E. G. Notch and G. D. Mayer, "17 $\alpha$ -ethinylestradiol hinders nucleotide excision repair in zebrafish liver cells," *Aquatic Toxicology*, vol. 95, pp. 273–278, 2009.
- [181] S. Depauw, T. Gaslonde, S. Léonce, et al., "Influence of the stereoisomeric position of the reactive acetate groups of the benzo[*b*]acronycine derivative S23906-1 on its DNA alkylation, helix-opening, cytotoxic, and antitumor activities," *Molecular Pharmacology*, vol. 76, no. 6, pp. 1172–1185, 2009.
- [182] C. J. Rocca, V. Poindessous, D. G. Soares, et al., "The NER proteins XPC and CSB, but not ERCC1, regulate the sensitivity to the novel DNA binder S23906: implications for recognition and repair of antitumor alkylators," *Biochemical Pharmacology*, vol. 80, no. 3, pp. 335–343, 2010.
- [183] A. B. Herrero, C. Martín-Castellanos, E. Marco, F. Gago, and S. Moreno, "Cross-talk between nucleotide excision and homologous recombination DNA repair pathways in the mechanism of action of antitumor trabectedin," *Cancer Research*, vol. 66, no. 16, pp. 8155–8162, 2006.

## Research Article

# Structural Determinants of Photoreactivity of Triplex Forming Oligonucleotides Conjugated to Psoralens

Rajagopal Krishnan<sup>1,2</sup> and Dennis H. Oh<sup>1,2</sup>

<sup>1</sup>Department of Dermatology, University of California at San Francisco, San Francisco, CA 94121, USA

<sup>2</sup>Dermatology Research Unit, San Francisco VA Medical Center, 4150 Clement Street, San Francisco, CA 94121, USA

Correspondence should be addressed to Dennis H. Oh, ohd@derm.ucsf.edu

Received 15 May 2010; Accepted 3 June 2010

Academic Editor: Ashis Basu

Copyright © 2010 R. Krishnan and D. H. Oh. This is an open access article distributed under the Creative Commons Attribution License, which permits unrestricted use, distribution, and reproduction in any medium, provided the original work is properly cited.

Triplex-forming oligonucleotides (TFOs) with both DNA and 2'-O-methyl RNA backbones can direct psoralen photoadducts to specific DNA sequences. However, the functional consequences of these differing structures on psoralen photoreactivity are unknown. We designed TFO sequences with DNA and 2'-O-methyl RNA backbones conjugated to psoralen by 2-carbon linkers and examined their ability to bind and target damage to model DNA duplexes corresponding to sequences within the human *HPRT* gene. While TFO binding affinity was not dramatically affected by the type of backbone, psoralen photoreactivity was completely abrogated by the 2'-O-methyl RNA backbone. Photoreactivity was restored when the psoralen was conjugated to the RNA TFO via a 6-carbon linker. In contrast to the B-form DNA of triplexes formed by DNA TFOs, the CD spectra of triplexes formed with 2'-O-methyl RNA TFOs exhibited features of A-form DNA. These results indicate that 2'-O-methyl RNA TFOs induce a partial B-to-A transition in their target DNA sequences which may impair the photoreactivity of a conjugated psoralen and suggest that optimal design of TFOs to target DNA damage may require a balance between binding ability and drug reactivity.

## 1. Introduction

Psoralens plus ultraviolet A (UVA) therapy are widely used in the treatment of psoriasis and other inflammatory skin diseases. Psoralens intercalate at 5' TA 3' sites and react with thymines upon exposure to UVA. With absorption of the first UVA photon, psoralens form monoadducts (MA), and subsequent exposures may convert furan-sided MA to interstrand crosslinks (XL). This ability to manipulate lesion formation makes psoralens attractive agents for studying DNA damage and repair and for potentially controlling the therapeutic response. Triplex-forming oligonucleotides (TFOs) offer a promising approach to target drugs such as psoralens to specific genes of interest in living cells. However the metabolic activities and electrostatic forces of the cell introduce a major obstacle to this interesting drug delivery system.

In order to overcome barriers to intracellular binding to DNA, TFOs have been extensively engineered. One strategy has been to utilize 2'-O-methyl RNA which has been

reported to significantly enhance the binding affinity relative to DNA-based TFOs [1–5]. It has been suggested that the C3'-endo conformation of the ribose sugar is appropriate for triplex formation [6, 7] and that 2'-O-methyl RNA enhances the TFO association rate without hindering the activity of a psoralen conjugated at the 5' terminus [1, 8]. However, the C3'-endo conformation of an RNA TFO also introduces major structural changes in the major groove and in the helical periodicity of the target sequence [6, 9, 10]. For example, in an intramolecular triplex formed by a 2'-O-methyl RNA pyrimidine-motif TFO, the helical twist increased, and the helical axis was displaced in the purine-Hoogsteen pair, introducing a dominant A-like structure, when compared with the corresponding DNA TFO, where the dominant structure is B-form [6]. In addition, an RNA third strand has also been reported to induce conformational changes in the sugars of the purine strand of duplex DNA, which resulted in a local B-to A-DNA transition [11, 12]. Partial B- to A-DNA transitions have also been observed in triplexes formed by 2'-O-methyl RNA strands [13]. These

TABLE 1: Binding and photoreactive efficiencies for TFOs conjugated to HMT.

TFO	$K_d$		Photoefficiency	
	Nondenaturing gel (nM)	Denaturing gel (nM)	$k_1$ (J/cm <sup>2</sup> ) <sup>-1</sup>	$k_2$ (J/cm <sup>2</sup> ) <sup>-1</sup>
TFO DNA-C2	63 ± 5	7.08 ± 2.6	19 ± 0.5	0.55 ± 0.04
TFO RNA-C2	75 ± 18	—	0	0
TFO RNA-C6	36 ± 4	10.96 ± 2.6	24 ± 4	1.6 ± 0.05

5' TGTACTGATTTTCATTTCTCTTTTCTTCTAGAATGCTTTG  
 Target 3' ACATGACTAAAAGTAAAGAGAAAAGAAGATCTTACAGAAC  
 TFO DNA-C2 TTCGTTTCTCTTTTCTCTCTP 5'  
 TFO RNA-C2 or -C6 UUCGUUUUCUUUUUCUUCUP 5'

FIGURE 1: TFO and target DNA sequences. TFOs composed of either DNA or 2'-O-methyl RNA are depicted. P represents HMT conjugated to the TFO by either a 2- or 6-carbon linker.

induced transitions may potentially alter the activity of TFO-conjugated drugs that interact with the DNA. In this work, we studied the effects of the 2'-O-methyl RNA TFO modification on the photoreactivity of psoralens conjugated to them. We observed that relative to the corresponding DNA TFOs, 2'-O-methyl TFOs can dramatically restrict psoralen reactivity in association with a B- to A-DNA transition in the target sequence.

## 2. Materials and Methods

**2.1. Oligonucleotides.** Synthetic gel-purified oligonucleotides (Oligos Etc., Wilsonville, OR) used as target sequences are shown in Figure 1. The 41 base pair target sequence corresponds to the sequence of the junction between intron 4 and exon 5 of the human hypoxanthine phosphoribosyltransferase (*HPRT*) gene, similar to that targeted in Chinese hamster ovary cells [14]. All TFOs were 20 nucleotide-long pyrimidine-motif sequences that bind parallel to the purine strand of the target DNA duplex and that were conjugated through a saturated 2- or 6-carbon linker to the psoralen derivative, 4'-hydroxymethyl trimethylpsoralen (HMT), at their 5' termini. TFO DNA-C2 contained a DNA backbone with a 2-carbon linker, while RNA-C2 and RNA-C6 possessed 2'-O-methyl RNA backbones with 2- and 6-carbon linkers, respectively.

**2.2. Triplex Formation on Genomic DNA.** Human genomic DNA was purified from HT1080 cells by phenol extraction. 10  $\mu$ M TFO DNA-C2 or TFO RNA-C2 were incubated with 1  $\mu$ g genomic DNA in the presence of binding buffer (10 mM Tris, pH 7.0, 20 mM MgCl<sub>2</sub>, 1 mM spermidine) at room temperature overnight. The mixtures were then irradiated with 0.2 J/cm<sup>2</sup> UVA and analyzed by single-strand ligation PCR as described previously [15]. Briefly, following UVA treatment, the samples were digested with *Dde* I which generates a DNA fragment that includes the TFO binding site. Samples were then subject to primer extension with a biotinylated

primer (5' Biotin-GGGTTGGTTATGATGTGATTTGACTT), and products were captured with streptavidin-coated magnetic beads (Dynal, Oslo, Norway) and ligated at their 3' termini to a ligation oligonucleotide. The ligation products were then amplified using primers 5' GTTATGATGTGATTTGACTTATAATTG (primer 2) and 5' TATGACTATGCATGATCTACGAT (ligation primer) and then linearly amplified with <sup>32</sup>P-end-labeled 5' GATGTGATTTGACTTATAATTGAAAATA (primer 3). The <sup>32</sup>P reaction products were separated on a denaturing gel and quantified by phosphorimaging, and relative intensities of the undamaged and adduct site were calculated.

**2.3. Target Duplex DNA and Triplex Formation.** Synthetic duplex DNA targets containing the TFO binding sites were formed by annealing the complementary target sequences shown in Figure 1. Prior to annealing, the purine strand of the target duplex was labeled at the 5'-terminus with <sup>32</sup>P using T4 polynucleotide kinase (GE Healthcare, Piscataway, NJ). Equimolar quantities of complementary oligonucleotides were mixed in 10 mM Tris, pH 7.5, 1 mM EDTA, heated to 95°C for 5 min, and cooled to room temperature over several hours. 5 nM of the resulting duplex was incubated with TFOs in binding buffer at room temperature overnight. The equilibrium products (duplex and triplex) were separated on a 6% neutral nondenaturing polyacrylamide gel and quantified by phosphorimaging (Bio-Rad GS-360). The dissociation constant,  $K_d$ , was obtained by fitting the bound fraction to a two-state model, as previously described [16]. For studies of photoreactivity, the equilibrium TFO-duplex binding mixture was irradiated with UVA as described previously [16]. The products were separated on a 6% denaturing polyacrylamide gel, quantified by phosphor imaging and an apparent  $K_d$  and the photoefficiency constants for MA and XL formation,  $k_1$  and  $k_2$ , respectively, were obtained by analyzing the product fraction as described before [16].

**2.4. Circular Dichroism (CD).** DNA duplex and triplex samples without <sup>32</sup>P labeling were prepared as described above and transferred to a 2 mm pathlength cuvette. CD spectra were measured in a JASCO J-710 spectropolarimeter equipped with a Xenon lamp. The data from 210 nm to 320 nm were recorded with a sensitivity of 100 mdeg, 1 nm bandwidth, 0.1 nm stepsize, and scan speed of 20 nm/min. The spectral data reported are the average of 5 scans.

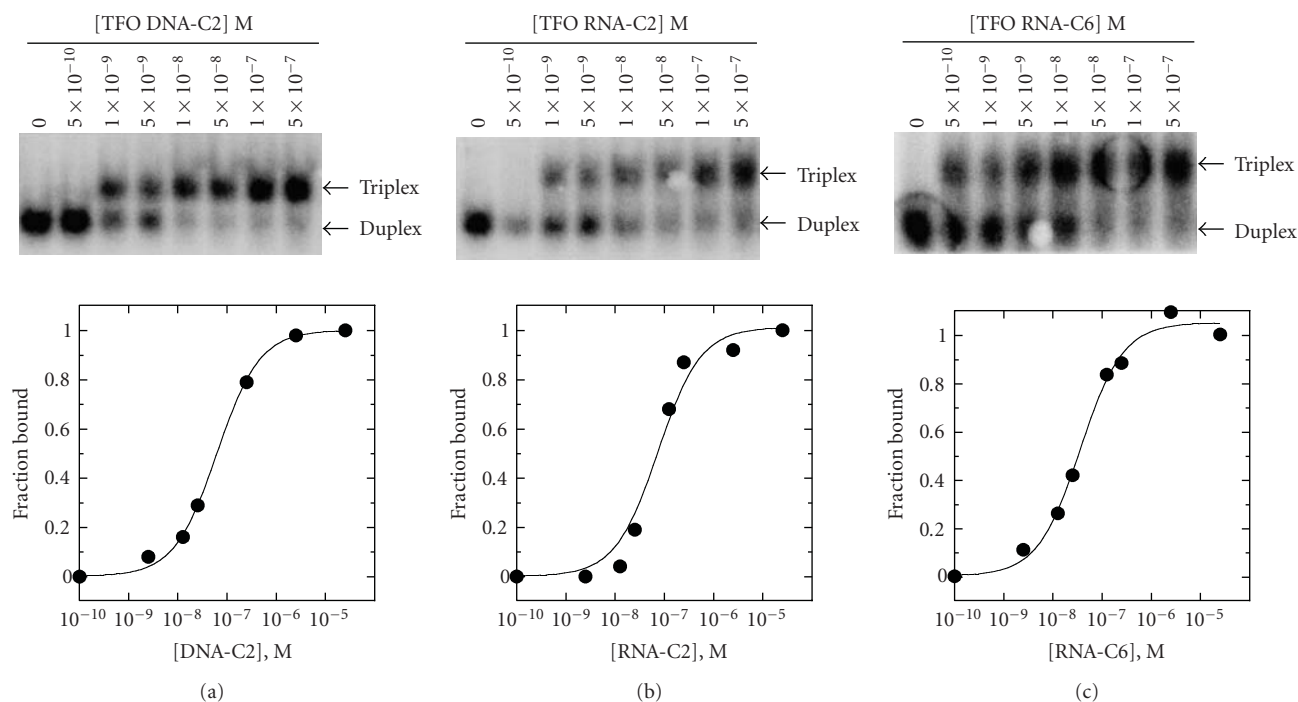


FIGURE 2: Noncovalent binding of TFOs to duplex target. Varying concentrations of (a) TFO DNA-C2, (b) TFO RNA-C2, and (c) TFO RNA-C6 were incubated with 5 nM target DNA duplex overnight before polyacrylamide gel electrophoresis under nondenaturing conditions. Gel bands were quantified and the data was fit with a two-state binding model.

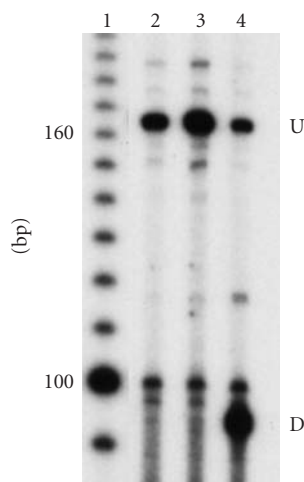


FIGURE 3: Binding of TFOs to genomic DNA targets. 2  $\mu$ M of TFO, either TFO RNA-C2 (lanes 2 and 3) or TFO DNA-C2 (lane 4) were incubated with genomic DNA purified from HT1080 cells and mock irradiated (lane 2) or irradiated with 0.2 J/cm<sup>2</sup> UVA (lanes 3 and 4) and analyzed by single-strand ligation PCR to assay for undamaged (U) and site-specifically damaged (D) DNA. Lane 1 is a 10 base pair DNA ladder.

### 3. Results and Discussion

**3.1. 2'-O-Methyl RNA Backbones Minimally Affects TFO Binding.** As shown in Figure 1, TFOs were designed to target the junction between intron 4 and exon 5 of the human

HPRT gene. TFO DNA-C2 is a DNA TFO conjugated to HMT at the 5' end with 2-carbon linker. TFO RNA-C2 is the corresponding 2'-O-methyl RNA TFO. TFO DNA-C2, when equilibrated with the synthetic DNA duplex target, caused a near-quantitative mobility shift on nondenaturing gel electrophoresis, indicating triplex formation (Figure 2). Quantification of band intensities indicated that TFO DNA-C2 bound with reasonable affinity to the DNA target (Figure 2, Table 1). Under the experimental conditions used, the observed  $K_d$  value of 63 nM for binding of TFO DNA-C2 to human HPRT target is comparable to previously observed values of about 130 nM in rodent DNA [8, 17].

A number of prior reports, however, have indicated that the 3'-endo form of the ribose sugar in an RNA TFO enhances the TFOs binding affinity relative to the corresponding deoxyribose backbone [1–8]. This binding enhancement was attributed to the 3'-endo form being the optimum conformation for Hoogsteen base pairing [6]. Relative to the DNA TFO, the RNA TFO introduces other structural modifications that further enhance TFO binding ability [1–3, 5, 8]. For example, the 2'-O-methyl group positioned between the TFO and duplex purine strand favors the formation of additional van der Waal contacts [6, 18].

In an attempt to improve TFO binding, TFOs RNA-C2 and RNA-C6 were designed to possess 2'-O-methyl ribose backbones and uracil bases instead of thymine and were conjugated to HMT via 2- or 6-carbon linkers, respectively. Although the 2'-O-methyl modified TFOs were expected to bind with higher affinity to the duplex DNA target [1, 5, 8], they actually exhibited binding affinities quite similar to that

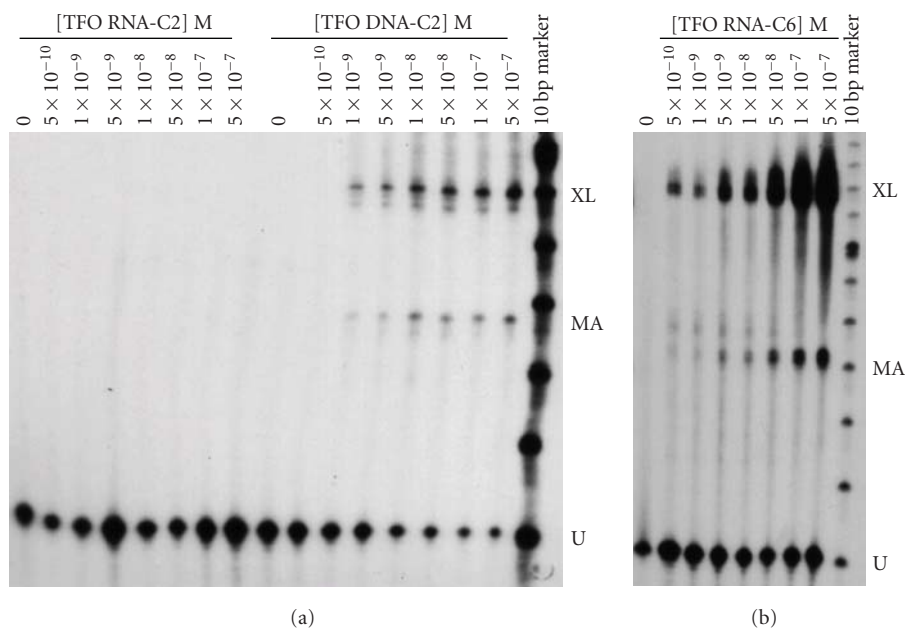


FIGURE 4: Covalent binding of TFOs to duplex target following UVA. Varying concentrations of (a) TFO DNA-C2 or TFO RNA-C2 or of (b) TFO RNA-C6 were incubated with 5 nM target overnight prior to irradiation with  $2\text{ J/cm}^2$  UVA. The products were then analyzed by polyacrylamide gel electrophoresis under denaturing conditions and denoted as unreacted (U), monoadducts (MA), and crosslinks (XL).

of TFO DNA-C2 (Figure 2, Table 1). While TFO RNA-C2 had a  $K_d$  that was not significantly different from that of TFO DNA-C2, a modest reduction in  $K_d$  was observed for TFO RNA-C6, suggesting that the 6-carbon linker further stabilizes binding by allowing better psoralen intercalation, or less likely through direct interactions with the triplex structure, consistent with observations in DNA TFOs [19]. This lack of dramatic enhancement in binding affinity of RNA third strands binding to DNA duplexes has also been observed previously by Han and Dervan [20] and may be due to the RNA TFO's lack of the C-5 methyl group in uridine which likely enhances base stacking and triplex stability [1–3, 18, 21, 22].

**3.2. 2'-O-Methyl RNA Backbones Affect HMT-TFO Photoreactivity.** To detect the binding of TFOs to genomic DNA, we incubated TFOs with human genomic DNA, irradiated the binding mixtures with UVA, and assayed for site-specific psoralen photoadducts using single-stranded ligation PCR. The particular conditions and primers used would be expected to produce PCR amplification products of 163 base pairs for undamaged DNA and of 95 base pairs for DNA damaged by psoralen photoadducts at the TFO target site.

As shown in Figure 3, in the absence of UVA, no site-specific adducts were detected. Following UVA irradiation, TFO DNA-C2 treatment resulted in site-specific photoadduct formation in a significant fraction (87%) of the genomic DNA. In contrast, TFO RNA-C2 treatment followed by UVA irradiation resulted in a barely detectable band at the expected photoadduct site that constituted a much smaller fraction of the total genomic DNA, indicating that little DNA

damage was targeted by TFO RNA-C2. Since the single-strand ligation PCR assay does not clearly discriminate between MA and XL formation and poor binding, we examined the photoproducts more carefully.

Binding of TFOs conjugated to HMT allows the HMT to react with adjacent target thymine. The HPRT duplex target sequence possesses a 5' TpA 3' site immediately adjacent to the 5' terminus of the TFOs, potentially allowing both MA and XL photoadducts to form upon TFO binding and UVA exposure. UVA exposure thus allows covalent capture of all triplex structures in which psoralen photochemistry is possible. Following binding of TFOs to the duplex target, samples were irradiated with UVA and the products were analyzed by denaturing gel electrophoresis. As shown in Figure 4(a), TFO DNA-C2 created dose-dependent covalent photoadducts corresponding to MA and XL. The  $K_d$  for TFO DNA-C2 that was obtained from analysis of photoproducts in denaturing electrophoretic gels was almost ten-fold lower than that obtained from non-denaturing gels (Table 1). The difference in  $K_d$  may signify that psoralen photoadduct formation drives additional binding.

In contrast, upon UVA irradiation, TFO RNA-C2 exhibited a complete inability to deliver photoadducts to the target sequence (Figure 4(a)). TFO concentrations up to  $10\ \mu\text{M}$  were ineffective in producing detectable MA or XL (data not shown). However, photoreactivity could be restored by increasing the linker length between TFO and HMT moieties (Figure 4(b)). TFO RNA-C6 generated dose-dependent MA and XL comparable to TFO DNA-C2, and analysis of the covalent photoadducts resulted in an apparent  $K_d$  that was also similar to TFO DNA-C2. The dependence of photoreactivity when going from 2- to 6-carbon linkers in RNA

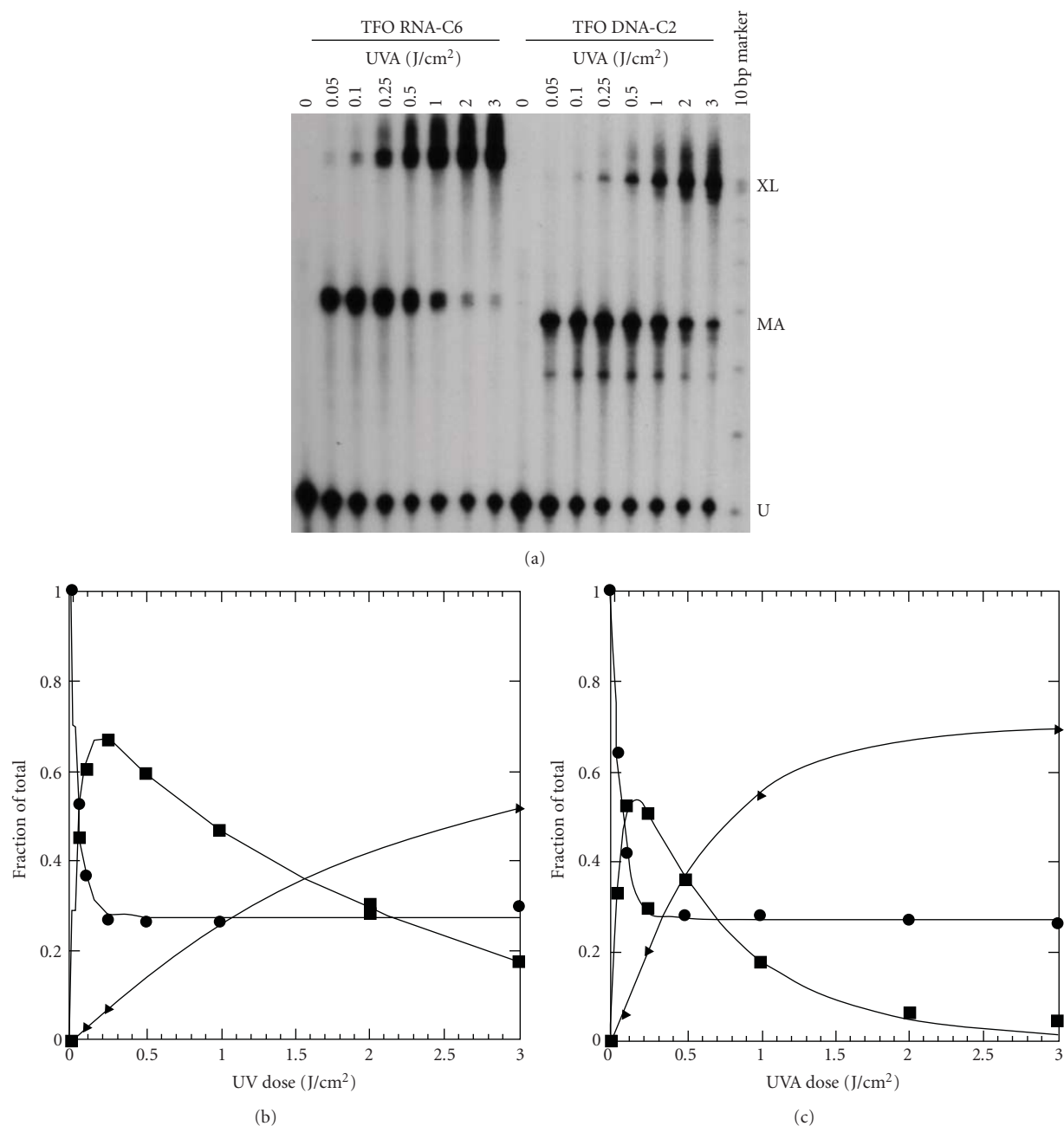


FIGURE 5: Photoreactivity of TFOs conjugated to HMT. 50 nM TFO DNA-C2 or TFO RNA-C6 were incubated with 5 nM duplex target overnight and then irradiated with varying doses of UVA. (a) Separation of reaction products by polyacrylamide gel electrophoresis under denaturing conditions. The products are marked as unreacted (U), monoadducts (MA), and crosslinks (XL). Quantitative analysis (b) TFO DNA-C2 and (c) TFO RNA-C6 for unreacted DNA (circles), MA (squares), and XL (triangles).

TFOs is consistent with a previously reported dependence of mutagenesis on linker length in DNA TFOs [19]. Our results indicate that although TFO backbone composition does not markedly alter TFO binding affinity to the target, it can profoundly affect psoralen photoreactivity.

To assess TFO photoreactivity in further detail, we exposed TFOs bound to the duplex DNA target to varying UVA doses and analyzed the resulting MA and XL photoadducts as a function of UVA dose by modeling the data

with a standard model for psoralen photokinetics [16, 23]. Both TFO DNA-C2 and TFO RNA-C6 reacted with the target DNA duplex by first forming MAs that converted to XLs with subsequent UVA excitation (Figure 5(a)). While MAs formed at approximately similar efficiencies ( $k_1$ ), XL formation ( $k_2$ ) was almost 3-fold more efficient with TFO RNA-C6 (Figures 5(b) and 5(c), Table 1). The ability of a 6-carbon linker to restore psoralen photoreactivity indicates that the 2'-O-methyl sugar is likely not simply causing the

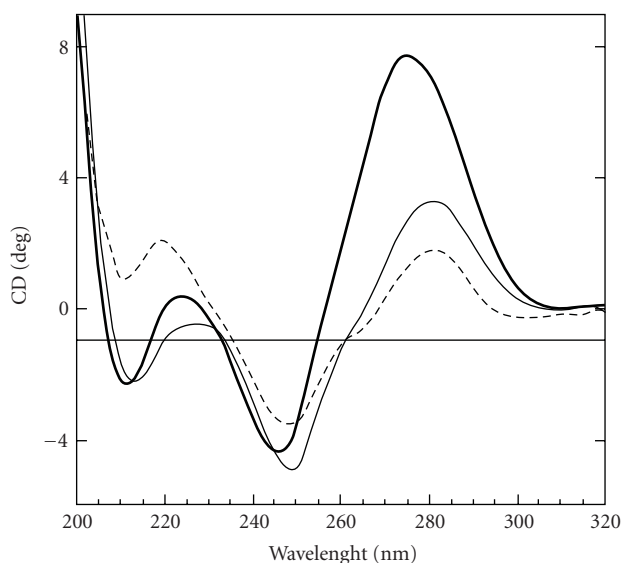


FIGURE 6: CD spectra of TFOs bound to duplex DNA. Shown are spectra for target DNA duplex alone (dashed line) or duplex incubated with TFO DNA-C2 (thin line) or TFO RNA-C2 (bold line).

TpA site to become locally sterically inaccessible. Rather, we speculated that a more global change occurs upon 2'-O-methyl RNA TFO binding that renders the TpA site inaccessible to psoralen when tethered to TFO via a 2-carbon linker, but not a 6-carbon linker.

**3.3. Distortion from B-Form DNA upon Binding of RNA TFOs.** We hypothesized that our 2'-O-methyl RNA TFOs induce a local A-DNA structure in the duplex DNA target under our triplex-forming conditions, as has been previously described for RNA TFOs bound to DNA duplexes [11, 12]. To specifically identify structural changes to the triple helix that might hinder psoralen intercalation and/or photoreactivity, we measured circular dichroism (CD) spectra of our triplexes. As expected and observed previously by others the free DNA and RNA TFO showed CD spectra corresponding to B- and A-Form, respectively [24–26]. The CD spectrum of both the target DNA duplex alone and triplexes formed by target duplex and TFO DNA-C2 each exhibited both a positive peak at 280 nm and a negative peak near 250 nm, and these peak intensities were conserved due to the Cotton effect, indicating that both the DNA duplex and triplex are predominantly in the B-form (Figure 6) [26–29]. If present, the local B- to A-DNA transition might require a large reorientation of psoralen to intercalate into the target site, hindering the psoralen activity. In contrast, the CD spectrum of triplexes formed by TFO RNA-C2 exhibited shifts in the positive peak to 270 nm while the negative peak shifted to 245 nm, and the peaks were non-conserved, indicative of base tilting or distortion. These spectral features are characteristic of A-DNA in which the bases are oriented in a twisted propeller rather than planar configuration [18, 27–29]. In addition, the results are consistent with prior CD

data indicating the presence of the A-DNA conformation in an intramolecular triplex formed with DNA duplex part and 2'-O-methyl RNA third strand [13]. While NMR studies conducted on a similar triplex did not observe A-DNA in 2'-O-methyl RNA-DNA triplexes [6], the number of base pairs per helical twist was found to be near 11 bp which is close to that of A-DNA [6].

In any case, our results indicate that the 2'-O-methyl RNA TFO induces helical transitions that are associated with reduced photoreactivity of psoralen when it is conjugated to the TFO with a 2-carbon linker. Because the helical periodicity increases from 10.5 base pairs per helical turn in B-DNA to 11 base pairs per helical turn in A-DNA, we speculate that the A-form DNA conformations induced by the RNA TFOs move the TpA site out of range of the psoralen when it is conjugated to the TFO by a 2-carbon linker, but not a 6-carbon linker.

## 4. Conclusions

TFOs are promising agents for targeting DNA damage to specific sites in the genome and may be exploited to introduce sequence specific mutations or to alter gene expression [29–31]. The conjugation of psoralens to TFOs can enhance these effects [29]. In general, the enhancement of binding affinity as well as the stability of TFOs by modifications of the sugar and base structure is anticipated to translate into better targeting of DNA damage and biological effects. However, in some cases, enhanced binding affinity *in vitro* due to chemical modifications to the backbone and bases has been associated with diminished biological activity from the conjugated psoralen [7]. Our results indicate that at least certain TFO modifications can result in structural changes that impair psoralen photoreactivity. Therefore, in certain cases, optimal design of TFOs to target DNA damage by psoralen may require a balance between maximizing binding ability and preserving drug reactivity. An additional consideration is that the structural changes induced by different TFO structures may also be differentially recognized and processed by DNA repair pathways.

## Acknowledgments

This work was supported by NIH Grant RO1CA105958 to D. H. Oh. The authors thank Dr. David Agard and Neema Salimi use of the CD spectrometer and assistance with CD measurements. They also thank Christina Butcher for technical assistance and the rest of the Oh Laboratory for helpful discussions.

## References

- [1] S. Wang and E. T. Kool, "Origins of the large differences in stability of DNA and RNA helices: C-5 methyl and 2'-hydroxyl effects," *Biochemistry*, vol. 34, no. 12, pp. 4125–4132, 1995.
- [2] M. Shimizu, T. Koizumi, H. Inoue, and E. Ohtsuka, "Effects of 5-methyl substitution in 2'-O-methyloligo(pyrimidine) nucleotides on triple-helix formation," *Bioorganic and Medicinal Chemistry Letters*, vol. 4, no. 8, pp. 1029–1032, 1994.

- [3] C. Escudé, J.-C. François, J. S. Sun et al., "Stability of triple helices containing RNA and DNA strands: experimental and molecular modeling studies," *Nucleic Acids Research*, vol. 21, no. 24, pp. 5547–5553, 1993.
- [4] R. W. Roberts and D. M. Crothers, "Stability and properties of double and triple helices: dramatic effects of RNA or DNA backbone composition," *Science*, vol. 258, no. 5087, pp. 1463–1466, 1992.
- [5] M. Shimizu, A. Konishi, Y. Shimada, H. Inoue, and E. Ohtsuka, "Oligo(2'-O-methyl)ribonucleotides: effective probes for duplex DNA," *FEBS Letters*, vol. 302, no. 2, pp. 155–158, 1992.
- [6] J. L. Asensio, R. Carr, T. Brown, and A. N. Lane, "Conformational and thermodynamic properties of parallel intramolecular triple helices containing a DNA, RNA, or 2'-OMeDNA third strand," *Journal of the American Chemical Society*, vol. 121, no. 48, pp. 11063–11070, 1999.
- [7] M. D. R. Alam, A. Majumdar, A. K. Thazhathveetil et al., "Extensive sugar modification improves triple helix forming oligonucleotide activity in vitro but reduces activity in vivo," *Biochemistry*, vol. 46, no. 35, pp. 10222–10233, 2007.
- [8] N. Puri, A. Majumdar, B. Cuenoud et al., "Minimum number of 2'-O-(2-aminoethyl) residues required for gene knockout activity by triple helix forming oligonucleotides," *Biochemistry*, vol. 41, no. 24, pp. 7716–7724, 2002.
- [9] J. L. Asensio, T. Brown, and A. N. Lane, "Solution conformation of a parallel DNA triple helix with 5' and 3' triplex-duplex junctions," *Structure*, vol. 7, no. 1, pp. 1–11, 1999.
- [10] C. H. Gotfredsen, P. Schultze, and J. Feigon, "Solution structure of an intramolecular: pyrimidine-purine-pyrimidine triplex containing an RNA third strand," *Journal of the American Chemical Society*, vol. 120, no. 18, pp. 4281–4289, 1998.
- [11] C. Dagneaux, J. Liquier, and E. Taillandier, "Sugar conformations in DNA and RNA-DNA triple helices determined by FTIR spectroscopy: role of backbone composition," *Biochemistry*, vol. 34, no. 51, pp. 16618–16623, 1995.
- [12] J. Liquier, E. Taillandier, R. Klinck, E. Guittet, C. Gouyette, and T. Huynh-Dinh, "Spectroscopic studies of chimeric DNA-RNA and RNA 29-base intramolecular triple helices," *Nucleic Acids Research*, vol. 23, no. 10, pp. 1722–1728, 1995.
- [13] E. R. Kandimalla, G. Venkataraman, V. Sasisekharan, and S. Agrawal, "Single-stranded DNA and RNA targeted triplex-formation: UV, CD and molecular modeling studies of fold-back triplexes containing different RNA, 2'-OMe-RNA and DNA strand combinations," *Journal of Biomolecular Structure and Dynamics*, vol. 14, no. 6, pp. 715–726, 1997.
- [14] A. Majumdar, A. Khorlin, N. Dyatkina et al., "Targeted gene knockout mediated by triple helix forming oligonucleotides," *Nature Genetics*, vol. 20, no. 2, pp. 212–214, 1998.
- [15] D. H. Oh and P. C. Hanawalt, "Triple helix-forming oligonucleotides target psoralen adducts to specific chromosomal sequences in human cells," *Nucleic Acids Research*, vol. 27, no. 24, pp. 4734–4742, 1999.
- [16] D. H. Oh and P. C. Hanawalt, "Binding and photoreactivity of psoralen linked to triple helix-forming oligonucleotides," *Photochemistry and Photobiology*, vol. 72, no. 3, pp. 298–307, 2000.
- [17] N. Puri, A. Majumdar, B. Cuenoud et al., "Targeted gene knockout by 2'-O-aminoethyl modified triplex forming oligonucleotides," *The Journal of Biological Chemistry*, vol. 276, no. 31, pp. 28991–28998, 2001.
- [18] J.-S. Sun and C. Hélène, "Oligonucleotide-directed triple-helix formation," *Current Opinion in Structural Biology*, vol. 3, no. 3, pp. 345–356, 1993.
- [19] M. Raha, L. Lacroix, and P. M. Glazer, "Mutagenesis mediated by triple helix-forming oligonucleotides conjugated to psoralen: effects of linker arm length and sequence context," *Photochemistry and Photobiology*, vol. 67, no. 3, pp. 289–294, 1998.
- [20] H. Han and P. B. Dervan, "Sequence-specific recognition of double helical RNA and RNA·DNA by triple helix formation," *Proceedings of the National Academy of Sciences of the United States of America*, vol. 90, no. 9, pp. 3806–3810, 1993.
- [21] S. Wang, Y. Xu, and E. T. Kool, "Recognition of RNA by triplex formation: divergent effects of pyrimidine C-5 methylation," *Bioorganic and Medicinal Chemistry*, vol. 5, no. 6, pp. 1043–1050, 1997.
- [22] R. A. Cassidy, N. Puri, and P. S. Miller, "Effect of DNA target sequence on triplex formation by oligo-2'-deoxy- and 2'-O-methylribonucleotides," *Nucleic Acids Research*, vol. 31, no. 14, pp. 4099–4108, 2003.
- [23] G. D. Cimino, H. B. Gamper, S. T. Isaacs, and J. E. Hearst, "Psoralens as photoactive probes of nucleic acid structure and function: organic chemistry, photochemistry, and biochemistry," *Annual Review of Biochemistry*, vol. 54, no. 1, pp. 1151–1193, 1985.
- [24] S.-H. Hung, Q. Yu, D. M. Gray, and R. L. Ratliff, "Evidence from CD spectra that d(purine)·r(pyrimidine) and r(purine)·d(pyrimidine) hybrids are in different structural classes," *Nucleic Acids Research*, vol. 22, no. 20, pp. 4326–4334, 1994.
- [25] C. L. Clark, P. K. Cecil, D. Singh, and D. M. Gray, "CD, absorption and thermodynamic analysis of repeating dinucleotide DNA, RNA and hybrid duplexes [d/r(AC)]<sub>12</sub> [d/r(GT/U)]<sub>12</sub> and the influence of phosphorothioate substitution," *Nucleic Acids Research*, vol. 25, no. 20, pp. 4098–4105, 1997.
- [26] J. T. Yang and T. Samejima, "Effect of base tilting on the optical activity of nucleic acids: a hypothesis," *Biochemical and Biophysical Research Communications*, vol. 33, no. 5, pp. 739–745, 1968.
- [27] V. I. Ivanov, L. E. Minchenkova, A. K. Schyolkina, and A. I. Poletayev, "Different conformations of double-stranded nucleic acid in solution as revealed by circular dichroism," *Biopolymers*, vol. 12, no. 1, pp. 89–110, 1973.
- [28] W. C. Johnson and I. Tinoco, "Circular dichroism of polynucleotides: a simple theory," *Biopolymers*, vol. 7, no. 5, pp. 727–749, 1969.
- [29] K. M. Knee, S. B. Dixit, C. E. Aitken, S. Ponomarev, D. L. Beveridge, and I. Mukerji, "Spectroscopic and molecular dynamics evidence for a sequential mechanism for the A-to-B transition in DNA," *Biophysical Journal*, vol. 95, no. 1, pp. 257–272, 2008.
- [30] S. A. Strobel, L. A. D. Stamm, L. Riba, D. E. Housman, and P. B. Dervan, "Site-specific cleavage of human chromosome 4 mediated by triple-helix formation," *Science*, vol. 254, no. 5038, pp. 1639–1642, 1991.
- [31] C. Giovannangeli, S. Diviacco, V. Labrousse, S. Gryaznov, P. Charneau, and C. Helene, "Accessibility of nuclear DNA to triplex-forming oligonucleotides: the integrated HIV-1 provirus as a target," *Proceedings of the National Academy of Sciences of the United States of America*, vol. 94, no. 1, pp. 79–84, 1997.

## Review Article

# Differential Toxicity of DNA Adducts of Mitomycin C

Jill Bargonetti,<sup>1</sup> Elise Champeil,<sup>2</sup> and Maria Tomasz<sup>3</sup>

<sup>1</sup> Department of Biological Sciences, Hunter College, The City University of New York, New York, NY 10021, USA

<sup>2</sup> Department of Science, John Jay College, The City University of New York, New York, NY 10019, USA

<sup>3</sup> Department of Chemistry and Biochemistry, Hunter College, The City University of New York, New York, NY 10021, USA

Correspondence should be addressed to Maria Tomasz, mtomasz@hunter.cuny.edu

Received 9 May 2010; Accepted 10 June 2010

Academic Editor: Ashis Basu

Copyright © 2010 Jill Bargonetti et al. This is an open access article distributed under the Creative Commons Attribution License, which permits unrestricted use, distribution, and reproduction in any medium, provided the original work is properly cited.

The clinically used antitumor agent mitomycin C (MC) alkylates DNA upon reductive activation, forming six covalent DNA adducts in this process. This review focuses on differential biological effects of individual adducts in various mammalian cell cultures, observed in the authors' laboratories. Evidence is reviewed that various adducts are capable of inducing different cell death pathways in cancer cells. This evidence is derived from a parallel study of MC and its derivatives 2,7-diaminomitosene (2,7-DAM) which is the main metabolite of MC and forms two mono-adducts with DNA, and decarbamoyl mitomycin C (DMC), which alkylates and cross-links DNA, predominantly with a chirality opposite to that of the DNA adducts of MC. 2,7-DAM is not cytotoxic and does not activate the p53 pathway while MC and DMC are cytotoxic and able to activate the p53 pathway. DMC is more cytotoxic than MC and can also kill p53-deficient cells by inducing degradation of Checkpoint 1 protein, which is not seen with MC treatment of the p53-deficient cells. This difference in the cell death pathways activated by the MC and DMC is attributed to differential signaling by the DNA adducts of DMC. We hypothesize that the different chirality of the adduct-to-DNA linkage has a modulating influence on the choice of pathway.

The mitomycins are a group of highly potent antibiotics, produced by the microorganism *Streptomyces caespitosus*, as discovered in Japan in the 1950s [1]. The prototype, most studied member of this group is mitomycin C (**1**; MC) (Figure 1). On account of its broad-spectrum antitumor activity, MC has been widely used in clinical cancer chemotherapy [2].

MC has been recognized as a classical DNA damaging agent, on account of its monofunctional and bifunctional DNA alkylating activity. Early studies have revealed an extraordinary property of the mitomycins; they were found to cross-link the complementary strands of DNA *in vivo* and *in vitro* [3]. MC was postulated to have two alkylating centers, the 1,2-aziridine and 10-carbamate groups (Figure 1). The mitomycins were the first natural antibiotics found possessing DNA cross-linking activity; there has been only one other natural cross-linker discovered since, carzinophyllin/azinomycin [4]. Synthetic DNA cross-linkers have become a paradigm of anticancer treatment, however.

Our laboratory has elucidated the structure of the DNA cross-link adduct of MC [5] and five additional monofunctional DNA adducts formed in MC-treated tumor cells as well as their DNA sequence selectivities, as summarized in several reviews (see, [6] and references therein). The structures of the six MC adducts are shown in Figure 2.

Numerous synthetic and natural analogs of the mitomycins have been discovered and studied; the details of which are beyond the scope of this review. However, two closely related derivatives of MC and their DNA adducts are relevant to the present subject, namely, 2,7-diaminomitosene (**2**; 2,7-DAM) and 10-decarbomoyl mitomycin C (**3**; DMC) (Figure 1). Their DNA adducts are described in the context of this review as follows.

2,7-DAM is a major metabolite isolated from cells and tissues treated with MC. It is a byproduct of the reductive activation of MC required for unmasking MC's alkylating activity [7, 8]. Our laboratory found that two of the six DNA adducts formed in MC-treated cells are derived from monofunctional activation of DNA by the nascent metabolite

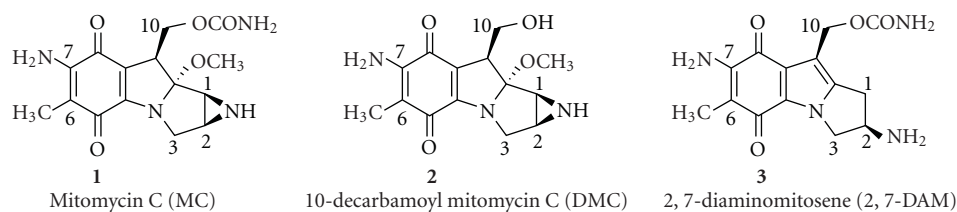


FIGURE 1: Chemical structures of MC, DMC, and 2,7-DAM. (Reproduced with permission from *Chem. Res. Toxicol.* **2008**, *21*, 2370).

of MC, 2,7-DAM [9, 10]. The structures of the two adducts were determined (**5** and **6**; Figure 2) [10, 11]. When tumor cells were treated with 2,7-DAM, the two adducts **5** and **6** were formed at high frequency [10]. Surprisingly, 2,7-DAM was not cytotoxic under aerobic conditions and negligibly cytotoxic under hypoxic treatment relative to MC [12, 13]. Its adduct **5** was specifically shown to be noncytotoxic and nonmutagenic in *E. coli* and simian kidney cells [14]. Consistent with these findings, in cell-free systems template oligonucleotides containing a single 2,7-DAM-dG-N7 adduct directed selective incorporation of cytosine opposite to this adduct in primer strands, catalyzed by Klenow (exo-) DNA polymerase [14]. Although no analogous experiments were performed with 2,7-DAM adduct **6** the nontoxicity and nonmutagenicity of the parent drug [14] predict an outcome similar to that of **5**.

Proof for the cross-link adduct as the critical cytotoxic lesion among the six MC adducts was provided by a study of 10-decarbamoyl mitomycin C (**2**; DMC), an artificial derivative obtained from MC by chemical removal of the 10-carbamoyl group [15]. DMC has long been regarded as an innocuous monofunctional MC derivative, incapable of causing ICLs, on account of lacking its carbamate alkylating center. Accordingly, in two laboratories, incubation of purified DNA and chemically activated DMC yielded only a monofunctional adduct **2a** as the major product, with no evident DNA cross-link adduct detectable [16, 17]. Inconsistent with these findings, however, DMC was reported to be slightly more cytotoxic than MC to hypoxic EMT6 mouse mammary tumor cells as well as to CHO cells [18, 19]. To resolve this paradox, EMT6 cells were treated with MC or DMC under hypoxia at equimolar concentrations and the resulting DNA adducts were determined structurally and quantitatively [20]. DMC treatment generated two stereoisomeric monoadducts **2a** and **2b** (1''-alpha and 1''-beta, resp.) and two ICL adducts, similarly stereoisomeric at the 1'' position **3a** and **3b** (1''-alpha- and 1''-beta isomers, resp.) (Figure 3). In addition, the cytotoxicities of MC, DMC, and 2,7-DAM were determined [20], confirming the earlier results described above. Overall, the adduct frequencies with DMC were much higher (20- to 30-fold) than with MC. Although DMC monoadducts greatly exceeded DMC ICL adducts (approximately 10:1 ratio), the latter were equal or somewhat higher in number than the ICL adducts from MC. The relatively similar cytotoxicities of MC and DMC correlated with the relatively similar ICL adduct frequencies of the two drugs, but not with their relative monoadduct or total adduct frequencies. This correlation may be regarded as

specific experimental evidence that in the EMT6 tumor cell line ICLs rather than monoadducts are the critical factors in the cell death induced by MC [20].

It is important to note, however, that in sharp contrast to the two 2,7-DAM monoadducts **5** and **6**, the MC monoadduct **1a** and MC and DMC common monoadduct **2a** were shown to be highly inhibitory to phage replication after transfection in *E. coli* [21] and strong blocks of DNA synthesis in cell-free systems [22]. Furthermore, monoadduct **1a** was shown to be nonmutagenic in *E. coli*. The biological experiments utilized transfection of single-site adducted M13 phage or synthetic oligonucleotide constructs in *E. coli* strains [22].

Isolation and quantitative analysis of DNA adducts of MC, DMC, and 2,7-DAM formed in tumor cells have been conducted by the Tomasz lab in collaboration with the Sartorelli-Rockwell group at Yale University, using almost exclusively EMT6 mouse mammary tumor cells. Recently, the number of cell lines was expanded in collaboration with the Bargonetti group, and a new method of quantitative analysis of the adducts of MC and DMC was employed, namely, LC/electrospray tandem mass spectrometry [23]. In this work Fanconi Anemia-A cells, normal human fibroblasts, MCF-7 human breast cancer cells, and EMT6 mouse mammary tumor cells were treated with MC or DMC under identical conditions, then the cellular DNA was isolated and analyzed for adducts. In addition to the previously known 1''-alpha isomer adducts of MC the analysis included the new 1''-beta stereoisomers from DMC. The results confirmed the generality of the DMC adduct pattern described above for EMT6 cells [20] in each cell line (Figure 4). It was concluded that DMC shows a stereochemical preference of linkage to the guanine-2-amino group *opposite* from that of MC; it forms two stereoisomeric ICL adducts, and its monoadducts are formed overall at much greater frequencies than its ICLs. The adduct patterns of the Fanconi Anemia-A cells and the control healthy fibroblast cells were identical. This work also provided preliminary evidence for differential removal of adducts upon post-treatment incubation of the cells in drug-free media. However, more work is needed to confirm these preliminary results.

In response to DNA adducts mammalian cells activate a complex signal transduction cascade to activate cell cycle checkpoints, initiate DNA repair, or induce cell death. The Bargonetti group, in collaboration with the Tomasz group, has investigated the biological signaling of mitomycin DNA-adducts using a human tissue culture model [13, 24]. The studies addressed two key areas: the ability of 2,7-DAM, MC,

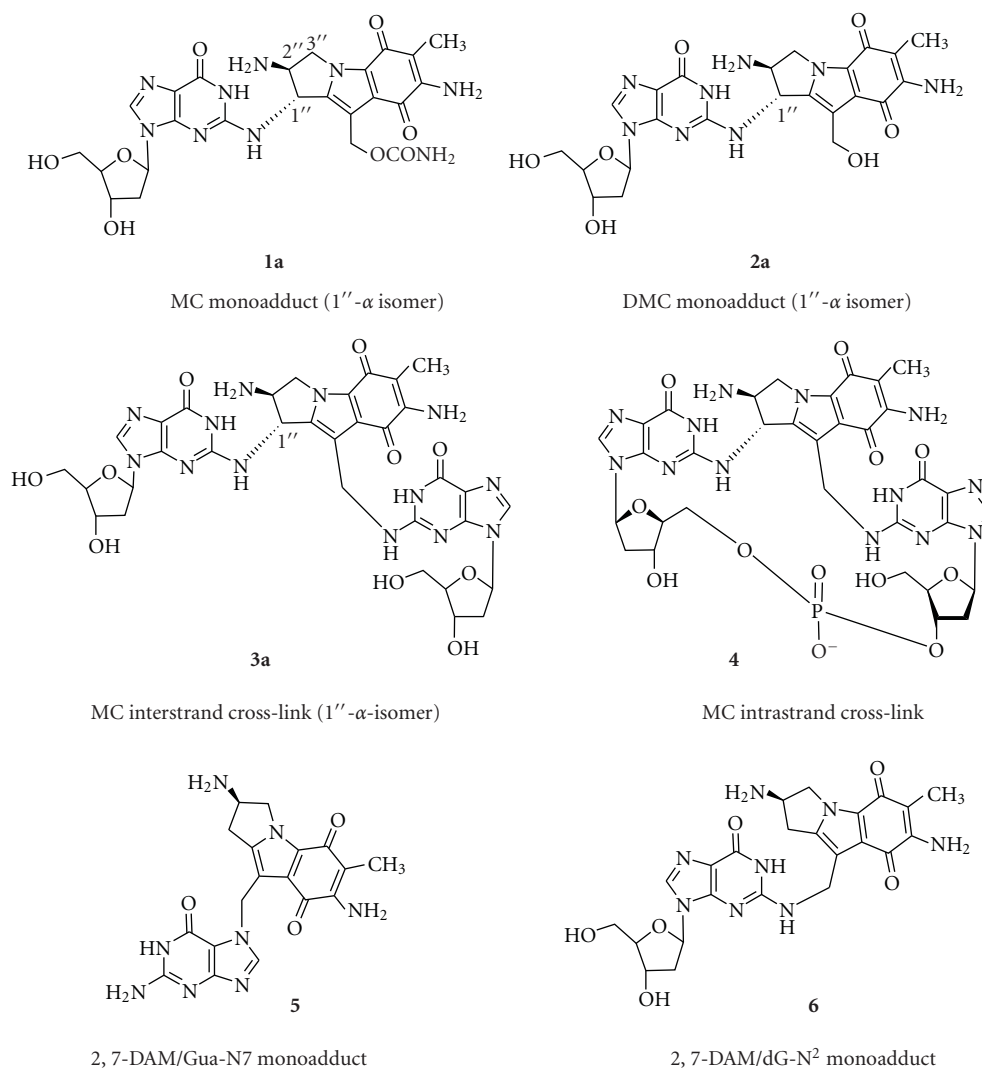


FIGURE 2: Chemical structure of six major adducts of reductively activated MC. (Reproduced with permission from the reference in Figure 1.

and DMC to activate the p53 pathway, and the differing ability of the drugs to induce cell death in either p53-proficient or p53-deficient cells. The p53 protein is a central player in the mammalian cellular response to DNA damage [25]. Following DNA damage the p53 protein is stabilized and functions as a strong transcriptional activator of genes that are required for cell cycle checkpoints, DNA repair, and the induction of cell death [26]. Many cancer cells have lost this response through sporadic mutations that occur in the p53 gene and thus the cells become deficient in the p53-pathway. Over 50 percent of all cancers have sustained mutations to the p53 DNA binding domain and for the purposes of this review we will call them p53-deficient. MC and DMC treatment of mammalian cells that are p53-proficient results in increased p53 protein, activation of the p53-mediated transcriptional activation of p53-pathway genes, and apoptotic cell death [13, 24], while the noncytotoxic mitomycin derivative DAM does not activate the p53 protein or the p53 pathway [13]. This

is in strong keeping with the paradigm of DNA damage-mediated cytotoxicity being associated with the activation of the p53 pathway in p53-proficient cells. DNA damage initiates the activation of DNA repair-related kinases ATR, ATM, Chk1, and Chk2 [27]. Both ATM and ATR kinases are able to phosphorylate and activate p53. The fact that 2,7-DAM does not cause activation of the p53-pathway strongly suggests that the noncytotoxic monoadducts that result following 2,7-DAM treatment (5 and 6) are unable to activate the DNA damage-associated kinase pathways. The comparison of the ability of 2,7-DAM, MC and DMC to activate the p53-pathway demonstrates that 2,7-DAM monoadducts do not activate this critical checkpoint pathway while MC- and DMC-mediated crosslinks are able to do so. DNA interstrand crosslinks (ICLs) are able to use ATR/Chk1 and the Fanconia anemia pathway to signal for cellular checkpoints [28]. Therefore, the 2,7-DAM monoadducts are likely to be repaired using a different pathway.

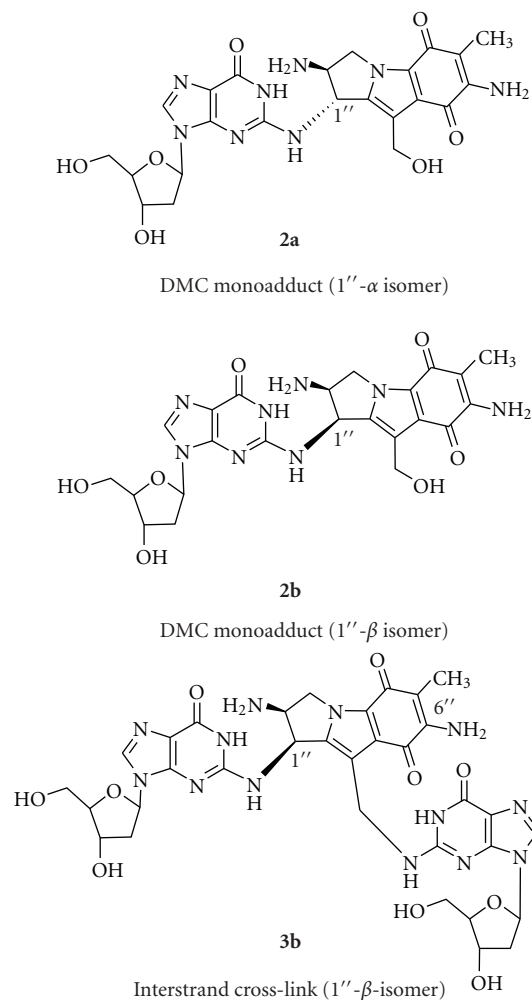


FIGURE 3: Chemical structures of major adducts of DMC. (Reproduced with permission from the reference in Figure 1.)

The ability of mitomycin DNA adducts to sensitize p53-deficient cancer cells to die has been examined by a comparison of the influence of MC and DMC on human cancer cells. Cancer cells that are p53-deficient rely on their ATR/Chk1 checkpoint as their last means of survival and if they lose Chk1 they become more sensitive to death [29, 30]. However, DNA damage can also cause strong activation of ATR that subsequently results in activation of Chk1 ubiquitination and targeted proteolysis of the protein [31]. The loss of Chk1 in p53-deficient cells causes the cells to lose their last remaining cell cycle checkpoint and the cells then die by a caspase 2-mediated pathway [32]. In p53-deficient cells DMC is more cytotoxic than MC [13, 24] and this associates with a reduction in Chk1 upon DMC but not MC treatment [24]. Recent work from the Bargonetti and Tomasz groups suggests that increased cytotoxicity of DMC relative to that of MC might be due to the variable chirality of the DMC/DNA adducts that activate Chk1-mediated proteolysis [23, 33]. Interstrand crosslinks activate the ATR/Chk1 pathway as part of their signal transduction response [28] but variable chirality has yet to be proven to differentially modulate

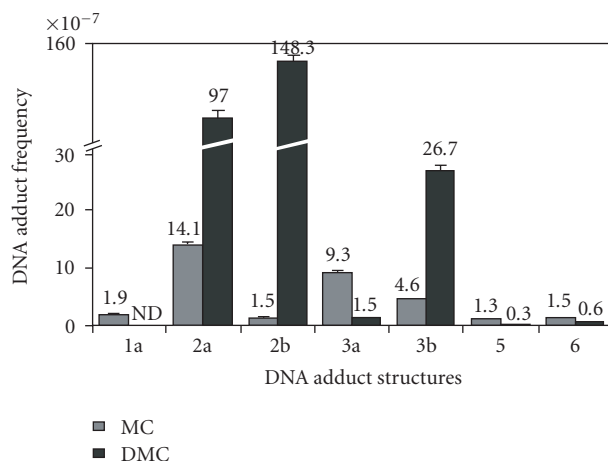


FIGURE 4: Frequencies of DNA adducts formed in MCF-7 human breast cancer cells treated with 10  $\mu$ M MC (gray bars) or 10  $\mu$ M DMC (black bars) for 24 hours under aerobic conditions. The individual frequency values of the bars are indicated above the bar error limits. Error limits are shown in % relative standard deviation units. (Reproduced with permission from the reference in Figure 1.)

such a pathway. However, it has been shown that Fanconi anemia proteins and excision repair proteins participate in recognition of MC DNA adducts [34]. It will be interesting to determine if altered chirality of the mitomycin ICL adducts differentially recruit the DNA damage signaling machinery to the DNA. This could be the consequence of a difference in the alignment of the 1''-alpha and 1''-beta stereoisomeric adducts in DNA. Structural studies in coordination with biochemical techniques to examine specific DNA-protein interactions could further explore this hypothesis.

*In summary.* Using a variety of techniques it has been possible to assign specific biological effects to each of the six DNA adducts of MC in mammalian cell cultures. Critical in this endeavor was the surprising discovery that DMC was slightly more cytotoxic than MC in cell cultures and it produced ICLs which correlated with its cytotoxicity [20]. This served as proof that the ICL was the major cytotoxic lesion of MC and DMC. DMC formed 20–30 times more DNA monoadducts than MC, which were linked to the N<sup>2</sup> atom of guanines with opposite chirality (1''-beta) to that of MC (1''-alpha) [23]. Parallel studies of MC and DMC revealed that DMC is much more cytotoxic to p53-deficient cells than MC [13, 24, 33] and we have shown that it is capable of inducing a cell death pathway involving proteasome-mediated degradation of Checkpoint 1 protein [33]. Future studies in our laboratories aim at elucidating the mechanism of the differential cell death pathways of MC and DMC in the context of the structures of their DNA adducts. More than 50% of human cancers are deficient for p53 function and contain either p53 mutations or oncogenic proteins that functionally inactivate p53. Determining how alternative DNA-adduct chirality can initiate signal transduction pathways for increased cytotoxicity in p53-deficient cancers could become a new paradigm in chemotherapeutic drug discovery.

## Acknowledgments

J. Bargonetti was funded by NIH SCORE Grant (1SC1CA137843) and The Breast Cancer Research Foundation. The paper was facilitated by a NIH Research Centers in Minority Institutions Award from the Division of Research Resources (RR-03037) to Hunter College.

## References

- [1] T. Hata, T. Hoshi, K. Kanamori, et al., "Mitomycin, a new antibiotic from Streptomyces. I," *The Journal of Antibiotics*, vol. 9, pp. 141–146, 1956.
- [2] S. K. Carter and S. T. E. Crooke, *Mitomycin C: Current Status and New Developments*, Academic Press, New York, NY, USA, 1979.
- [3] V. N. Iyer and W. Szybalski, "A molecular mechanism of mitomycin action: linking of complementary DNA strands," *Proceedings of the National Academy of Sciences of the United States of America*, vol. 50, pp. 355–362, 1963.
- [4] R. W. Armstrong, M. E. Salvati, and M. Nguyen, "Novel interstrand cross-links induced by the antitumor antibiotic carzinophilin/azinomycin B," *Journal of the American Chemical Society*, vol. 114, no. 8, pp. 3144–3145, 1992.
- [5] M. Tomasz, R. Lipman, and D. Chowdary, "Isolation and structure of a covalent cross-link adduct between mitomycin C and DNA," *Science*, vol. 235, no. 4793, pp. 1204–1208, 1987.
- [6] M. Tomasz, "Mitomycin C: small, fast and deadly (but very selective)," *Chemistry and Biology*, vol. 2, no. 9, pp. 575–579, 1995.
- [7] M. Tomasz and R. Lipman, "Reductive metabolism and alkylating activity of mitomycin C induced by rat liver microsomes," *Biochemistry*, vol. 20, no. 17, pp. 5056–5061, 1981.
- [8] J. Cummings, V. J. Spanswick, and J. F. Smyth, "Re-evaluation of the molecular pharmacology of Mitomycin C," *European Journal of Cancer Part A*, vol. 31, no. 12, pp. 1928–1933, 1995.
- [9] Y. Palom, M. F. Belcourt, G. S. Kumar et al., "Formation of a major DNA adduct of the mitomycin metabolite 2,7-diaminomitosenone in EMT6 mouse mammary tumor cells treated with mitomycin C," *Oncology Research*, vol. 10, no. 10, pp. 509–521, 1998.
- [10] Y. Palom, M. F. Belcourt, S. M. Musser, A. C. Sartorelli, S. Rockwell, and M. Tomasz, "Structure of adduct X, the last unknown of the six major DNA adducts of mitomycin C formed in EMT6 mouse mammary tumor cells," *Chemical Research in Toxicology*, vol. 13, no. 6, pp. 479–488, 2000.
- [11] G. S. Kumar, S. M. Musser, J. Cummings, and M. Tomasz, "2,7-Diaminomitosenone, a monofunctional mitomycin C derivative, alkylates DNA in the major groove. Structure and base-sequence specificity of the DNA adduct and mechanism of the alkylation," *Journal of the American Chemical Society*, vol. 118, no. 39, pp. 9209–9217, 1996.
- [12] Y. Palom, M. F. Belcourt, L.-Q. Tang et al., "Bioreductive metabolism of mitomycin C in EMT6 mouse mammary tumor cells: cytotoxic and non-cytotoxic pathways, leading to different types of DNA adducts. The effect of dicumarol," *Biochemical Pharmacology*, vol. 61, no. 12, pp. 1517–1529, 2001.
- [13] T. Abbas, M. Olivier, J. Lopez et al., "Differential activation of p53 by the various adducts of mitomycin C," *Journal of Biological Chemistry*, vol. 277, no. 43, pp. 40513–40519, 2002.
- [14] C. D. Utzat, C. C. Clement, L. A. Ramos, A. Das, M. Tomasz, and A. K. Basu, "DNA adduct of the mitomycin C metabolite 2,7-diaminomitosenone is a nontoxic and nonmutagenic DNA lesion in vitro and in vivo," *Chemical Research in Toxicology*, vol. 18, no. 2, pp. 213–223, 2005.
- [15] S. Kinoshita, K. Uzu, K. Nakano, and T. Takahashi, "Mitomycin derivatives. 2. Derivatives of decarbamoylmitosane and decarbamoylmitosenone," *Journal of Medicinal Chemistry*, vol. 14, no. 2, pp. 109–112, 1971.
- [16] A. V. Carrano, L. H. Thompson, and D. G. Stetka, "DNA crosslinking, sister-chromatid exchange and specific mutations," *Mutation Research*, vol. 63, no. 1, pp. 175–188, 1979.
- [17] M. Tomasz, R. Lipman, B. F. McGuinness, and K. Nakanishi, "Isolation and characterization of a major adduct between mitomycin C and DNA," *Journal of the American Chemical Society*, vol. 110, no. 17, pp. 5892–5896, 1988.
- [18] P. R. Hoban, M. I. Walton, C. N. Robson et al., "Decreased NADPH: cytochrome P-450 reductase activity and impaired drug activation in a mammalian cell line resistant to mitomycin C under aerobic but not hypoxic conditions," *Cancer Research*, vol. 50, no. 15, pp. 4692–4697, 1990.
- [19] S. Rockwell and S. Y. Kim, "Cytotoxic potential of monoalkylation products between mitomycins and DNA: studies of decarbamoyl mitomycin C in wild-type and repair-deficient cell lines," *Oncology Research*, vol. 7, no. 1, pp. 39–47, 1995.
- [20] Y. Palom, G. S. Kumar, L.-Q. Tang et al., "Relative toxicities of DNA cross-links and monoadducts: new insights from studies of decarbamoyl mitomycin C and mitomycin C," *Chemical Research in Toxicology*, vol. 15, no. 11, pp. 1398–1406, 2002.
- [21] L. A. Ramos, R. Lipman, M. Tomasz, and A. K. Basu, "The major mitomycin C-DNA monoadduct is cytotoxic but not mutagenic in *Escherichia coli*," *Chemical Research in Toxicology*, vol. 11, no. 1, pp. 64–69, 1998.
- [22] A. K. Basu, C. J. Hanrahan, S. A. Malia, S. Kumar, R. Bizanek, and M. Tomasz, "Effect of site-specifically located mitomycin C-DNA monoadducts on in vitro DNA synthesis by DNA polymerases," *Biochemistry*, vol. 32, no. 18, pp. 4708–4718, 1993.
- [23] M. M. Paz, S. Ladwa, E. Champeil et al., "Mapping DNA adducts of mitomycin C and decarbamoyl mitomycin C in cell lines using liquid chromatography/electrospray tandem mass spectrometry," *Chemical Research in Toxicology*, vol. 21, no. 12, pp. 2370–2378, 2008.
- [24] E. K. Boamah, D. E. White, K. E. Talbott et al., "Mitomycin-DNA adducts induce p53-dependent and p5-independent cell death pathways," *ACS Chemical Biology*, vol. 2, no. 6, pp. 399–407, 2007.
- [25] T. D. Halazonetis, V. G. Gorgoulis, and J. Bartek, "An oncogene-induced DNA damage model for cancer development," *Science*, vol. 319, no. 5868, pp. 1352–1355, 2008.
- [26] K. H. Vousden and C. Prives, "Blinded by the light: the growing complexity of p53," *Cell*, vol. 137, no. 3, pp. 413–431, 2009.
- [27] B. B. Zhou, H. J. Anderson, and M. Roberge, "Targeting DNA checkpoint kinases in cancer therapy," *Cancer Biology & Therapy*, vol. 2, no. 4, pp. S16–S22, 2003.
- [28] M. Ben-Yehoyada, L. C. Wang, I. D. Kozekov, C. J. Rizzo, M. E. Gottesman, and J. Gautier, "Checkpoint signaling from a single DNA interstrand crosslink," *Molecular Cell*, vol. 35, no. 5, pp. 704–715, 2009.
- [29] H. C. Reinhardt, A. S. Aslanian, J. A. Lees, and M. B. Yaffe, "p53-deficient cells rely on ATM- and ATR-mediated checkpoint signaling through the p38MAPK/MK2 pathway

- for survival after DNA damage,” *Cancer Cell*, vol. 11, no. 2, pp. 175–189, 2007.
- [30] Q. Liu, S. Guntuku, X.-S. Cui et al., “Chk1 is an essential kinase that is regulated by Atr and required for the G2/M DNA damage checkpoint,” *Genes and Development*, vol. 14, no. 12, pp. 1448–1459, 2000.
- [31] Y.-W. Zhang, D. M. Otterness, G. G. Chiang et al., “Genotoxic stress targets human Chk1 for degradation by the ubiquitin-proteasome pathway,” *Molecular Cell*, vol. 19, no. 5, pp. 607–618, 2005.
- [32] S. Sidi, T. Sanda, R. D. Kennedy et al., “Chk1 suppresses a caspase-2 apoptotic response to DNA damage that bypasses p53, Bcl-2, and caspase-3,” *Cell*, vol. 133, no. 5, pp. 864–877, 2008.
- [33] E. K. Boamah, A. Brekman, M. Tomasz, et al., “DNA adducts of decarbamoyl mitomycin C efficiently kill cells with compromised p53 resulting from proteasome-mediated degradation of Chk1,” *Chemical Research in Toxicology*, vol. 23, no. 7, pp. 1151–1162, 2010.
- [34] X. Shen, H. Do, Y. Li et al., “Recruitment of fanconi anemia and breast cancer proteins to DNA damage sites is differentially governed by replication,” *Molecular Cell*, vol. 35, no. 5, pp. 716–723, 2009.

## Review Article

# Cellular Responses to Cisplatin-Induced DNA Damage

**Alakananda Basu and Soumya Krishnamurthy**

*Department of Molecular Biology & Immunology, University of North Texas Health Science Center and Institute for Cancer Research, 3500 Camp Bowie Boulevard, Fort Worth, TX 76107, USA*

Correspondence should be addressed to Alakananda Basu, alakananda.basu@unthsc.edu

Received 12 May 2010; Accepted 28 June 2010

Academic Editor: Ashis Basu

Copyright © 2010 A. Basu and S. Krishnamurthy. This is an open access article distributed under the Creative Commons Attribution License, which permits unrestricted use, distribution, and reproduction in any medium, provided the original work is properly cited.

Cisplatin is one of the most effective anticancer agents widely used in the treatment of solid tumors. It is generally considered as a cytotoxic drug which kills cancer cells by damaging DNA and inhibiting DNA synthesis. How cells respond to cisplatin-induced DNA damage plays a critical role in deciding cisplatin sensitivity. Cisplatin-induced DNA damage activates various signaling pathways to prevent or promote cell death. This paper summarizes our current understandings regarding the mechanisms by which cisplatin induces cell death and the bases of cisplatin resistance. We have discussed various steps, including the entry of cisplatin inside cells, DNA repair, drug detoxification, DNA damage response, and regulation of cisplatin-induced apoptosis by protein kinases. An understanding of how various signaling pathways regulate cisplatin-induced cell death should aid in the development of more effective therapeutic strategies for the treatment of cancer.

## 1. Introduction

Cisplatin was discovered fortuitously by Dr. Rosenberg in 1965 while he was examining the effect of electromagnetic field on bacterial cell growth [1, 2]. Since the active principle that inhibited bacterial cell division was identified to be cisplatin, he anticipated that it would also inhibit the proliferation of rapidly dividing cancer cells. Cisplatin was indeed demonstrated to possess antitumor activity in a mouse model [3] and was first used in the clinical trial almost 30 years ago. Since its approval by the Food and Drug administration in 1978, cisplatin continues to be one of the most effective anticancer drugs used in the treatment of solid tumors.

Cisplatin has been used as a first-line therapy for several cancers, including testicular, ovarian, cervical, head, and neck and small-cell lung cancers either alone or in combination with other anticancer agents. It is also used as an adjuvant therapy following surgery or radiation. In addition to cisplatin, its analogs, such as carboplatin and oxaliplatin, are also currently being used in the clinic. However, patients who initially respond to cisplatin therapy often develop resistance to the drug during the course of the treatment.

The success of cisplatin therapy is compromised due to dose-limiting toxicity, especially nephrotoxicity as well as resistance by tumor cells to cisplatin. Cellular resistance to cisplatin could be either intrinsic or acquired. The clinically acquired resistance can be caused by decreased drug accumulation which includes reduced uptake or increased efflux of cisplatin, increased drug detoxification by cellular thiols, increased DNA repair or tolerance of cisplatin-damaged DNA and the ability of the cancer cells to evade cisplatin-induced cell death. Numerous studies have focused on the drug-target interactions, cellular pharmacology, and pharmacokinetics of cisplatin. Another active area of research has been to develop analogs of cisplatin to minimize toxicity and circumvent cisplatin resistance.

The antitumor activity of cisplatin is believed to be due to its interaction with chromosomal DNA [4]. Only a small fraction of cisplatin, however, actually interacts with DNA and the inhibition of DNA replication cannot solely account for its biological activity [5]. In addition, the efficacy of chemotherapeutic drugs depends not only on their ability to induce DNA damage but also on the cell's ability to detect and respond to DNA damage [6]. Following DNA damage, cells may either repair the damage and start

progressing through the cell cycle or if they cannot repair the damage, cells proceed to die [5]. Cisplatin, like many other chemotherapeutic drugs, can induce apoptosis. Thus, the signaling pathways that regulate apoptosis have significant impact on deciding cellular responsiveness to cisplatin. There are many excellent reviews on cisplatin and its analogues [7–15]. In this paper, we primarily focused on recent studies on cellular responses to cisplatin-induced DNA damage although we briefly discussed steps leading to cisplatin-induced DNA damage. This comprehensive paper should not only benefit researchers in the field of cisplatin but also benefit those interested in mechanisms of chemoresistance and targeted therapy.

## 2. Biotransformation of Cisplatin

Cisplatin or *cis*-diamminedichloroplatinum(II) is a neutral, square-planar, coordination complex of divalent Pt [8]. The *cis* configuration is required for its antitumor activity [16]. It has two labile chloride groups and two relatively inert amine ligands. Cisplatin undergoes hydrolysis in water. The chloride concentration is an important factor in determining the hydrolysis or aquation of cisplatin. The high chloride concentration (~103 mM) of blood plasma prevents the hydrolysis of cisplatin. Upon entering the cell, the chloride concentration drops down to 4 mM which facilitates the aquation process [17]. The aquated form of cisplatin is a potent electrophile and reacts with a variety of nucleophiles, including nucleic acids and sulfhydryl groups of proteins.

## 3. Accumulation of Cisplatin Inside Cells

Cisplatin and its analogues were initially thought to enter cells by passive diffusion because cisplatin uptake was linear, nonsaturable and could not be competed with platinum analogs [4–6, 17]. Although decreased accumulation of cisplatin is often associated with acquired resistance to cisplatin, few or no changes were observed in the plasma membrane function in the cisplatin-resistant cell lines as compared to the parental cells [18–20]. In 1981, it was first proposed that cisplatin could be transported actively via the carrier-mediated transport [21]. Several transporters, including the Na<sup>+</sup>, K<sup>+</sup>-ATPase [22] and members of solute carrier (SLC) transporters [11] have been implicated in facilitating the entry of cisplatin into the cells. The plasma membrane copper transporter-1 (CTR1), a member of the SLC family, gained particular attention since a defect in *Ctr1* gene decreased cisplatin accumulation in yeast [23, 24]. In addition, cisplatin and carboplatin accumulation was attenuated in mouse embryonic fibroblasts from *ctr1*<sup>-/-</sup> animals compared to wild-type animals [18]. Interestingly, both copper and cisplatin were shown to cause rapid downregulation of CTR1 in ovarian cancer cells by the proteasome-mediated pathway [19]. While CTR1 appears to transport cisplatin and its analogs, there is little decrease in CTR1 when cells acquire resistance to cisplatin. A recent study demonstrated that copper transporter-2 or CTR2 limits accumulation of cisplatin and the level of CTR2

correlates with the sensitivity of ovarian carcinoma cells to cisplatin [25]. The organic cationic transporters SLC22 family of proteins have also been shown to participate in cisplatin influx [11]. Thus, cisplatin can enter cells by passive or facilitated diffusion and by active transport. Depending on the cellular context, multiple transporters may be involved in cisplatin uptake. Therefore, it is difficult to correlate cisplatin sensitivity/resistance with a particular transporter.

Many cell lines with acquired resistance to cisplatin often exhibit reduced drug accumulation. Unlike multidrug resistance (MDR), drug efflux does not appear to be the major cause of cisplatin resistance. Kawai et al. first reported that a 200-kDa plasma membrane glycoprotein is overexpressed in murine thymic lymphoma cells selected for resistance to cisplatin, which correlated with reduced accumulation of cisplatin in the cells [26]. The increased expression of this protein correlated with the degree of cisplatin resistance [26]. There was, however, no follow-up study to establish the importance of this protein in conferring cisplatin resistance. The ATP-dependent glutathione-conjugated efflux pump and copper transporters ATP7A and ATP7B have been implicated in cisplatin export [20]. It is generally believed that reduced cisplatin accumulation in cisplatin resistant cells is due to decrease in uptake of cisplatin rather than an increase in drug efflux [7, 27].

## 4. Formation and Repair of Cisplatin DNA Adduct

DNA is thought to be the primary biological target of cisplatin [17, 28, 29]. The platinum atom of cisplatin forms covalent bonds with the N<sup>7</sup> position of purine bases to form 1,2- or 1,3-intrastrand crosslinks and a lower percentage of interstrand crosslinks. Cisplatin resembles bifunctional alkylating agents. The intrastrand crosslink between two adjacent G residues is believed to be the critical lesion responsible for cisplatin cytotoxicity. Formation of cisplatin-DNA adducts interferes with DNA replication and transcription. The interstrand and intrastrand crosslinks disrupt the structure of the DNA. This alteration in the structure is recognized by the cellular proteins to repair cisplatin-induced DNA damage. Increased repair of cisplatin-induced DNA damage has been associated with cisplatin resistance.

**4.1. Cisplatin and Nucleotide Excision Repair Pathway.** Since the intrastrand cross-link is the major lesion caused by cisplatin-induced DNA damage, it is primarily repaired via the nucleotide excision repair (NER) system. Xeroderma Pigmentosum (XP) is a disorder caused by deficiency of genes involved in NER. Cells derived from XP patients are exquisitely sensitive to cisplatin [30]. In addition, the favorable response of testicular cancer to cisplatin was associated with low levels of XP complementation group A (XPA) and excision repair cross-complementation group I (ERCCI), which participate in NER [31, 32]. A number of studies correlated the overexpression of ERCC1 or XPA proteins with cisplatin resistance [31–34]. The existence of ERCC1 exon VIII alternative splicing was observed in ovarian

cancer cells [35]. Although this splicing did not affect the level of ERCC1, it decreased its excision repair function. In addition, epigenetic changes, such as hypermethylation of ERCC1, which inversely correlated with ERCC1 mRNA levels, have been suggested as a mechanism for enhanced cisplatin sensitivity [36]. A recent study demonstrated that XPA binding domain of ERCC1 was required for the repair of cisplatin-damaged DNA [37]. A double knockdown of XPF/ERCC1 complex was shown to be very effective in enhancing cisplatin sensitivity in non-small cell lung cancer cells [38]. An antisense DNA against XPA sensitized lung adenocarcinoma cells to cisplatin [34]. Recently, it has been reported that treatment of rat spiral ganglion neurons with cisplatin induced the mRNA levels of XPA and XPC along with nuclear translocation of these enzymes, thus decreasing the rate limiting step in the NER pathway [39]. This can provide a plausible mechanism by which cisplatin induces NER. Kang et al. made an interesting observation that XPA was regulated in a circadian fashion in the mouse liver, but not in the testis [40]. Removal of cisplatin-DNA adducts also followed a circadian pattern in the extracts derived from the liver. The authors proposed that chronochemotherapy could be more effective in the treatment of cancers in which XPA removes cisplatin-DNA adducts in a circadian fashion. Thus, the cisplatin-induced DNA repair employing the NER process is multilayered including epigenetic, transcriptional, and posttranslational regulation.

NER is also linked to the cellular signaling pathways. It has been reported that the NER process may prevent cisplatin-induced apoptosis by activating the ataxia telangiectasia mutated (ATM) pathway which is recruited to the damaged DNA through XPC [41]. Lack of functional p53 has been associated with persistence of cisplatin-induced intrastrand cross-links, suggesting the importance of p53 in regulating NER of cisplatin-damaged DNA [42]. Functional NER was also required for cisplatin-induced transcription of Bcl-xL via nuclear factor-kappa B (NF- $\kappa$ B) [43].

In addition to NER, cisplatin can also induce transcription-coupled repair (TCR). The intrastrand crosslink stalls RNA polymerase II to trigger TCR [44]. It has been reported that p53 protects against cisplatin-induced apoptosis in a TCR-dependent manner [30]. In addition, the homology-directed DNA repair (HR) that allows error-free repair of the double-strand breaks caused by the excision of cisplatin-DNA adducts has been implicated in the repair of cisplatin-induced DNA damage [45]. It has been reported that mouse mammary tumors containing irreparable null alleles of *Brca1* gene, which is involved in DNA double strand break repair, do not become resistant to cisplatin. Bypass of cisplatin-DNA adduct has also been associated with cisplatin resistance. DNA polymerase-eta could replicate across intrastrand cross-link between cisplatin and two adjacent G residues [46].

**4.2. Cisplatin and Mismatch Repair Pathway.** Mismatch repair (MMR) system recognizes cisplatin-induced DNA damage, but instead of increasing cell viability, MMR system was shown to be important for cisplatin-mediated cytotoxicity [47]. DNA mismatch repair protein, MutS $\alpha$  recognized

DNA lesions formed by cisplatin [48–50], and mutations in MSH1 or MLH1 genes of the MMR system were observed in cisplatin-resistant cells [51–53]. Recently, the proapoptotic function of cisplatin was shown to be mediated in an MSH2/MSH6-dependent manner [54]. MLH1-proficient cells were more sensitive to cisplatin compared to MLH1-deficient cells. Cell death by cisplatin was associated with significant proteolysis of MLH1, caused by destabilization of X-linked inhibitor of apoptosis protein (XIAP), resulting in caspase activation [55]. The repair function of MMR proteins has been reported to be uncoupled from their function in mediating cisplatin-induced cell death [56–58]. Since the primary mechanism of cisplatin involves DNA damage and p53 is also involved in DNA damage signaling, there are many studies that correlate cisplatin and DNA damage and repair with p53 activity [59–62]. It has been reported that cisplatin enhances the interaction between mismatch repair protein MLH1/postmeiotic segregation increased 2 (PMS2) and p73 triggering apoptosis in mismatch repair-proficient cells [60].

## 5. Interaction of Cisplatin with Cellular Thiols

Although the major target of cisplatin is the nuclear DNA, it exhibits a high affinity towards sulfur donors such as cysteines and methionines forming stable Pt-S bonds. This competes with the affinity towards the nitrogen atom in the DNA thus contributing towards resistance against the cytotoxic action of cisplatin [63]. The abundant intracellular thiols involved in the drug resistance are glutathione and metallothionein.

**5.1. Interaction of Cisplatin with Glutathione.** When cancer cells are exposed to cisplatin, the platinum atom in cisplatin is chelated by glutathione (GSH) and the glutathione-Pt complex is effluxed from the cell in an ATP-dependent manner by the glutathione transporter family, termed the GS-X pumps [64]. It was initially noted that cells that are resistant to cisplatin have elevated levels of glutathione [65]. However, recent studies with cisplatin-resistant cancer cell lines seem to suggest otherwise [66, 67]. Based on NMR studies, Kasherman et al. reported that the higher levels of GSH do not correlate with decreased sensitivity to cisplatin [68]. In agreement with this study, Chen et al. suggested that increased levels of GSH might sensitize cells to cisplatin by upregulation of the copper transporter hCtr1 [69]. Therefore, whether overexpression of glutathione contributes to or combats cisplatin resistance is still under debate.

Apart from GSH, the glutathione S-transferase P1-1 (GSTP1-1) enzyme has also been associated with resistance to cisplatin-based chemotherapy [70, 71]. Pasello et al. demonstrated that increased levels of GSTP1 were associated with cisplatin resistance in osteosarcoma cell lines and a higher relapse rate and poor prognosis in high-grade osteosarcoma patients [72]. In contrast, a recent study by Peklak-Scott et al. suggested that a high level of cisplatin resistance may not be due to conjugation of

cisplatin to glutathione by GSTP1 [73]. Other enzymes in the glutathione transferase family, such as the GST $\mu$  or the GSTO1-1, have also been implicated in contributing towards cisplatin resistance [74, 75]. Thus, although a great deal of work has been focused on the correlation of glutathione and its conjugating enzymes towards cisplatin resistance, further studies are needed to explore this in detail.

**5.2. Interaction of Cisplatin with Metallothionein.** Metallothioneins (MT) are cysteine-rich proteins, which consist of 61-68 amino acids of which 20 are cysteines. The four isoforms of MTs (MT1-MT4) are ubiquitously expressed in humans and are inducible by a variety of drugs, including cisplatin [76]. They are involved in zinc and copper homeostasis, heavy metal detoxification, and protection from apoptosis. Initial reports observed an increased expression of metallothionein correlating with cisplatin resistance in ovarian carcinoma cell lines [77]. We have also seen that a wide variety of human cancer cell lines with acquired resistance to cisplatin overexpressed metallothionein and ectopic expression of metallothionein conferred cisplatin resistance [78]. Recent reports also suggest that the increased expression of metallothionein correlates with cellular resistance against cisplatin [79–81].

The ubiquitously occurring metallothionein isoforms, MT-1 and MT-2, have been shown to react faster with cisplatin [82], compared to glutathione [83, 84]. The basal levels of MT-1 and MT-2 are often significantly increased in cancer cells [78, 85], resulting in even stronger scavenging of divalent platinum, and contributing to acquired resistance against cisplatin [78, 86, 87]. MT-3 isoform was initially thought to be unresponsive to the platinum drugs [81]. Recent reports, however, suggest that MT-3 is overexpressed in hypoxic conditions, and the reaction between MT-3 and Pt(II) is kinetically preferred [81]. The authors further proposed that the Zn(II) released from this reaction can result in the upregulation of the MT-1 and MT-2 isoforms. Thus, metallothionein isoforms play an important role in contributing towards cisplatin resistance.

## 6. Cisplatin and DNA Damage Signaling

Various stress signals generate DNA lesions that may lead to mutations and genomic instability. Following DNA damage, cell cycle checkpoints are activated to delay cell-cycle progression to provide time for DNA repair or eliminate genetically unstable cells by inducing cell death. It is now recognized that inhibition of DNA replication is not sufficient to explain cisplatin cytotoxicity. How cells respond to cisplatin-induced DNA damage plays a major role in the ultimate decision whether a cell should live or die following cisplatin treatment.

**6.1. p53 and Cisplatin-Induced DNA Damage Response.** The tumor suppressor protein p53 is considered as the “guardian of genome”. It plays a critical role in eliciting cellular responses to DNA damage. p53 is a short-lived protein

which is primarily degraded via the ubiquitin proteasome-mediated pathway [30, 88]. The E3 ubiquitin ligase Mdm2 is a transcriptional target of p53 and regulates p53 expression via a negative feedback loop [30]. DNA damage results in the activation of ATM and/or ATM- and Rad3-related (ATR), resulting in phosphorylation and stabilization of p53 [88]. p53 can transactivate genes involved in cell cycle progression (e.g., p21), DNA repair (e.g., growth arrest and DNA damage-inducible 45, GADD45), and apoptosis (e.g., Bax) [89].

Fujiwara et al. first demonstrated that adenoviral-mediated delivery of p53 into small-cell lung cancer cells induced massive apoptosis both in monolayer cultures and in tumor xenografts upon treatment with cisplatin [90]. Introduction of wild-type p53 by adenovirus vector also sensitized ovarian cancer cells to cisplatin [91–93]. Several proteins, including cyclin-dependent kinase inhibitor p21, ATR, and checkpoint kinase (CHK2) have been implicated in p53-mediated apoptosis [94–97]. In addition, tumor cells lacking functional p53 were more resistant to cisplatin than cells that contained functional p53 and the resistant cell lines were sensitized to cisplatin upon reconstitution with wild-type p53 [98, 99]. p53 itself has been shown to bind cisplatin-modified DNA [100]. In addition, cisplatin was shown to induce nitrosylation of p53 preventing its mitochondrial translocation [101].

p53 can regulate cisplatin-induced cell death by several mechanisms. Degradation of FLIP (FLICE-like inhibitory protein) has been reported to be necessary for p53-induced apoptosis in response to cisplatin [102, 103]. p53 also promotes cisplatin-induced apoptosis by directly binding and counteracting the antiapoptotic function of Bcl-xL [104]. Although the phosphatase and tensin homolog (PTEN) is believed to inhibit phosphoinositide 3-kinase (PI3K)/Akt, overexpression of PTEN was shown to involve p53-mediated apoptotic cascade in cisplatin-resistant ovarian cancer cells independent of PI3K/Akt pathway [105]. The nutrient-sensor AMP-kinase (AMPK) was shown to be activated by cisplatin in AGS and HCT-116 cancer cells and inhibition of AMPK enhanced cisplatin-induced apoptosis by causing hyperinduction of p53 [106].

One of the major side effects of cisplatin therapy is nephrotoxicity and the involvement of p53 in cisplatin-induced nephrotoxicity has been investigated. p53 induced proapoptotic Bcl-2 family member PUMA $\alpha$  in renal tubular cells upon treatment with cisplatin, and dominant-negative p53 suppressed the expression of PUMA $\alpha$ . This study was extended in C57 mice. Acute renal failure upon cisplatin treatment was abrogated in p53-deficient C57 mice and this was associated with little or no induction of PUMA $\alpha$  [107]. CHK2 has also been implicated in apoptosis of renal cells and tissues as a result of cisplatin-induced p53 activation [94]. A study by Yang et al. revealed that caspase-6 and -7 are transcriptional targets of p53 [108]. Thus, induction of p53 by cisplatin resulted in the activation of these caspases contributing to nephrotoxicity [108]. Inhibition of p53 by pharmacological inhibitor or knockout of p53 in mice suppressed caspase-6 and -7 transactivation and protected against nephrotoxicity. Recently, microRNAs have also been

shown to play a major role in cisplatin nephrotoxicity. miR-34a is induced by cisplatin via p53 and plays a cytoprotective role in the survival of proximal tubular cells [109].

Although a plethora of literature exists on the role of p53 in contributing towards cisplatin cytotoxicity, p53 has also been associated with cisplatin resistance. MCF-7 breast cancer cells containing wild-type p53 are highly resistant to cisplatin but disruption of p53 by the introduction of human papilloma virus (HPV) in MCF-7 cells sensitized these cells to cisplatin [110]. Ovarian cancer cells selected for cisplatin resistance exhibited higher levels of p53 compared to cisplatin-sensitive counterpart [111]. Although p53 level is low in HeLa cells due to degradation of p53 by HPV, it was elevated in cisplatin-resistant HeLa cells [112]. Studies have also shown that mutations in p53 contributed to cisplatin resistance in different cancer models [113–116].

Although p53 plays an important role in cisplatin-induced DNA damage response, p53-negative cells also respond to cisplatin-induced DNA damage, suggesting alternate pathways of sensing cisplatin-induced DNA damage.

#### 6.2. *c-Abl and Cisplatin-Induced DNA Damage Response.*

The tyrosine kinase *c-Abl* plays an important role in stress response to DNA damaging agents. It belongs to the non-receptor tyrosine kinases and contains nuclear localization motifs and nuclear export signals. Thus, it can shuttle between the nucleus and cytoplasm. Nuclear import of *c-Abl* was shown to be necessary for DNA damage-induced apoptosis [117]. It is activated in response to cisplatin causing activation of *c-Jun*-N-terminal kinase (JNK)/stress-activated protein kinase (SAPK) [118]. *c-Abl*-deficient cells fail to activate JNK. Nuclear *c-Abl* can associate with and phosphorylate MEK kinase 1 (MEKK1) in response to DNA damage resulting in the activation of JNK/SAPK [119]. Nehmé et al. [120] demonstrated that activation of *c-Abl* and JNK is contingent upon the recognition of cisplatin-induced DNA damage by the MMR system since *c-Abl* response is absent in MMR-deficient cells. They further demonstrated that the activation by these pathways is specific to cisplatin and not to the cisplatin analogue oxaliplatin, thus highlighting the importance of the MMR system to specifically recognize cisplatin-DNA adducts [120, 121].

Interestingly, MMR/*c-Abl* cooperates with p73, a member of the p53 family, to trigger apoptosis [122]. Cisplatin caused induction of p73 in several cancer cell lines and in mouse embryonic fibroblasts (MEF), which were proficient in mismatch DNA-repair pathway but not in MEF deficient in *c-Abl* or MMR [122]. Activation of *c-Abl* in response to cisplatin led to phosphorylation and stabilization of p73 [123, 124]. Phosphorylation of p73 can also increase its proapoptotic function by dissociating itself from p63, another member of the p53 family. p63 can bind to and counteract the proapoptotic function of p73 [125]. In addition, *c-Jun* was shown to enhance p73 stability and transactivation activity by preventing its degradation via the proteasomal pathway [126]. Binding of the transcription coactivator Yap1 also prevents proteasomal degradation of p73 and results in the recruitment of p300 to trigger transcription of proapoptotic genes. *c-Abl* can directly

phosphorylate Yap1, increasing its stability and affinity for p73 [127]. Phosphorylation of Yap1 can dictate whether p73 will transactivate proapoptotic or growth arrest genes [127]. A recent study suggests that *c-Abl* can regulate the function of p63. Phosphorylation of p63 at Tyr residue by *c-Abl* stabilizes it causing an increase in its proapoptotic function [128].

Cisplatin can trigger cleavage of *c-Abl* which is a substrate for caspase and proteolytic cleavage of *c-Abl* was shown to be important for cisplatin-induced apoptosis [129]. Activation of p38 MAPK is critical for regulating cisplatin activity. Galan-Moya et al. [130] recently reported that *c-Abl* activates p38 MAPK independent of its tyrosine-kinase activity but by stabilizing MKK6, the upstream kinase of p38 MAPK. This study provides an explanation why the *c-Abl* inhibitor imatinib fails to inhibit p38 MAPK [130]. Thus, *c-Abl* is an important mediator of cisplatin-induced DNA damage response and acts in cooperation with the siblings of p53 and MAPK pathways to trigger cisplatin-induced apoptosis.

## 7. Regulation of Cisplatin-Induced Cell Death by Protein Kinases

Cisplatin primarily induces cell death by apoptosis and a defect in apoptotic signaling could also confer cisplatin resistance. There are two major pathways of cell death [131, 132]. The extrinsic pathway is initiated when ligands bind to the tumor necrosis factor- $\alpha$  (TNF $\alpha$ ) receptor superfamily followed by oligomerization and recruitment of procaspase-8 via adaptor molecules to form the death-inducing signaling complex (DISC). The intrinsic pathway is initiated by cellular stress, such as DNA damage, resulting in release of cytochrome-c from the mitochondria causing activation of procaspase-9 through the interaction with apoptosis promoting activating factor-1 (APAF-1) and formation of an active apoptosome complex. Bcl-2 family proteins regulate DNA damage-induced apoptosis by regulating the release of mitochondrial cytochrome c in response to DNA damage. Cisplatin-induced genotoxic stress activates multiple signal transduction pathways, which can contribute to apoptosis or chemoresistance.

**7.1. Cisplatin and Protein Kinase C.** Protein kinase C (PKC) is a family of closely related phospholipid-dependent enzymes that play critical roles in signal transduction and cell regulation [133–136]. Based on the structure and biochemical properties they are grouped as conventional ( $\alpha$ ,  $\beta$ I,  $\beta$ II, and  $\gamma$ ), novel ( $\delta$ ,  $\epsilon$ ,  $\eta$ , and  $\theta$ ) and atypical ( $\zeta$  and  $\iota$ ) PKCs. Tumor-promoting phorbol esters are potent activators of PKCs but persistent treatment with phorbol esters can induce downregulation or degradation of phorbol ester-sensitive conventional and novel PKCs.

We inadvertently found that the PKC signal transduction pathway can regulate cisplatin sensitivity. In the meantime, Hofmann et al. reported that inhibition of PKC by quercetin or downregulation of PKC by the phorbol ester, 12-*O*-tetradecanoylphorbol-13-acetate (TPA) could enhance the antiproliferative activity of cisplatin [137]. In contrast,

Isonishi et al. [138] and we [139] simultaneously reported that activation of PKC by phorbol esters could enhance sensitivity of human ovarian cancer 2008 and human cervical cancer HeLa cells to cisplatin. There were contrasting reports whether activation or downregulation of PKC was necessary for cisplatin sensitization [138, 140]. Although TPA is a useful tool as a pharmacological agent to study PKC function, it is a tumor promoter and therefore cannot be used in the clinic. We first showed that bryostatin 1, a partial PKC agonist which lacks tumor promoting activity, also sensitized HeLa cells to cisplatin [141]. Based on the preclinical studies, Phase II trial using combination of bryostatin 1 and cisplatin was initiated in advanced recurrent cervical carcinoma but was not very effective [142]. Combination of bryostatin 1 and cisplatin had minimal toxicity in patients with refractory nonhematological malignancies although only four patients achieved an objective response [143]. This may be because bryostatin 1 is a partial agonist and its regulation is complex. One of the caveats with these earlier studies to define the role of PKC in regulating cisplatin sensitivity was that PKC activation and downregulation was monitored based on PKC activity assay which does not discriminate among PKC isozymes. We now know that PKC isozymes may have distinct and even opposite effects on cisplatin-induced cell death [144]. Another shortcoming with these studies was the use of pharmacological agents that lack absolute specificity to PKC.

An increase in novel PKC $\delta$  or  $\epsilon$  and a decrease in conventional PKCs have been associated with acquired resistance to cisplatin [145]. However, inhibition of PKC $\alpha$  by Gö 6976 and depletion of PKC $\alpha$  by siRNA enhanced sensitivity of both parental and cisplatin-resistant HeLa cells to cisplatin [146]. Antisense oligonucleotides against PKC $\alpha$  enhanced the antitumor activity of cisplatin against human breast cancer MCF-7, prostate cancer PC3, and human small cell carcinoma H69 cells transplanted in nude mice [147]. Additionally, antisense oligonucleotide against PKC $\alpha$  in combination with cisplatin was effective in patients with non-small cell lung cancer [148]. Furthermore, although PKC $\alpha$  was downregulated in cisplatin-resistant A2780 cells, introduction of PKC $\alpha$  in these cells attenuated cisplatin sensitivity [149]. A recent study demonstrated that inhibition of PKC $\beta$  by enzastaurin enhanced cisplatin sensitivity via dephosphorylation of p90 ribosomal S6 kinase and Bad [150]. These results suggest that conventional PKC $\alpha$  and  $\beta$  function as antiapoptotic proteins. It is not clear why a decrease rather than an increase in cPKCs was associated with cisplatin resistance.

The observation that PKC $\delta$  is a substrate for caspase-3 [151] established the importance of this PKC isozyme in apoptotic signaling. It has been reported that treatment of cisplatin-resistant human squamous cell carcinoma SCC-25 (SCC25/CP) cells to cisplatin failed to induce caspase-3 activation and cleavage of PKC $\delta$  due to an increase in antiapoptotic Bcl-xL [152]. Interestingly, the effect of bryostatin 1 on caspase activation and PKC $\delta$  downregulation followed similar biphasic concentration response in both parental and cisplatin-resistant HeLa cells [146, 153]. We have shown that PKC $\delta$  not only acts downstream of caspase-3 but it

can also regulate cisplatin-induced activation of caspase-3 [154]. These studies were based on the effect of rottlerin, a pharmacological inhibitor of PKC $\delta$  on cisplatin-induced apoptosis [155]. Although rottlerin caused downregulation of caspase-2 and inhibition of cisplatin-induced apoptosis, the effect of rottlerin on caspase-2 downregulation was not due to inhibition of PKC $\delta$  [156]. The effect of PKC $\delta$  on cisplatin-induced apoptosis depends on the cellular context. In gastric cancer MKN28 cells, PKC $\delta$  was shown to enhance cisplatin-induced caspase activation and cell death via p53 [157]. Overexpression of PKC $\delta$  or caspase cleavage-resistant mutant of PKC $\delta$  had little effect on cisplatin-induced cell death in human small-cell lung cancer H69 cells which have mutated p53 [158]. On the other hand, knockdown of PKC $\delta$  enhanced cisplatin-induced cell death in thyroid cancer by decreasing fos expression [159].

We have shown that overexpression of PKC $\epsilon$  contributes to cisplatin resistance by inhibiting cisplatin-induced apoptosis [160]. Integrative genomic approach has identified PKC $\iota$  as a potential oncogene for ovarian carcinoma [161]. It has also been associated with chemoresistance of glioblastoma multiforme, an aggressive form of brain cancer [162]. The mechanism of PKC $\iota$ -mediated chemoresistance involved inhibition of p38 MAPK [162]. A recent study suggests that atypical PKC $\zeta$  can counteract the ability of cisplatin to decrease matrix metalloproteinase-2 secretion [163]. Thus, the effects of PKC on cellular sensitivity/resistance to cisplatin depend on the pattern of the PKC isozymes as well as on the cellular context.

**7.2. Cisplatin and MAPK.** Mitogen-activated protein kinases (MAPK) are a family of structurally-related serine/threonine protein kinases that coordinate various extracellular signals to regulate cell growth and survival [164–166]. There are three major subfamilies of MAPK: extracellular signal-regulated kinase (ERK)-1 and -2, stress-activated protein kinase (SAPK)/c-Jun N-terminal kinase (JNK) and p38 MAPK. All three MAPKs have been implicated in regulating cisplatin-induced cell death.

ERK is activated in response to growth factors and mitogens. Cisplatin has been shown to cause activation of ERK in several cell types although there are controversies whether activation of ERK prevents or contributes to cisplatin-induced cell death [167–173]. ERK has been shown to function as a prosurvival protein in ovarian cancer [102, 174], melanoma [175], cervical cancer SiHA [176], human myeloid leukemic [177], and gastric cancer [178] cells. High basal nuclear phospho-ERK2 was associated with cisplatin resistance of ovarian cancer OVCAR-3 cells [179]. Furthermore, nanoparticle-mediated delivery of MEK inhibitor PD98059 enhanced antitumor activity of cisplatin in melanoma-bearing mice [180]. Cisplatin-induced ERK activation precedes p53-mediated DNA damage response since ERK directly phosphorylates p53 causing upregulation of p21, GADD45, and Mdm2 [181]. Thus, activation of ERK may cause cell cycle arrest allowing time for the repair of cisplatin-induced DNA damage via p53. ERK also induced phosphorylation of BAD at Ser112 site in response to cisplatin in ovarian cancer cells, and

inhibition of ERK by PD98059 or mutation of Ser112 to Ala sensitized cells to cisplatin [174]. In SiHA cells, phosphorylation and activation of NF- $\kappa$ B were associated with the prosurvival function of ERK [176]. Glutathione-mediated cisplatin transport and GSTP1 expression also contributed to the antiapoptotic function of ERK in human myeloid leukemic cells [177] and gastric cancer cells [178], respectively. Recently, it has been reported that ovarian cancer cells grown in three-dimensional cultures acquired resistance to anoikis and apoptosis when exposed to clinically relevant concentrations of cisplatin [167]. This resistance was mediated by the ERK1/2 signaling and the PI3K/Akt pathway. ERK signaling was also shown to be activated when stimulated by inducers such as the cigarette smoke-carcinogen NNK [4-(methylnitrosamino)-1-(3-pyridyl)-1-butanone], causing cisplatin resistance [182].

ERK activation was also shown to be required for cisplatin-induced apoptosis in cervical cancer HeLa cells [168, 169, 173], osteosarcoma and neuroblastoma cells [183], testicular germ cell tumors [184], glioma cells [185], renal epithelial cells [186], nasopharyngeal carcinoma cells [187], and human small cell lung cancer cells [188]. Decrease in ERK level/phosphorylation was associated with cisplatin resistance in HeLa cells [168, 173]. Cisplatin-induced activation of p53 was associated with proapoptotic effect of ERK1/2 in B104 cells [189], whereas cisplatin-induced acute renal failure (ARF) in mice was attributed to increase in TNF $\alpha$  gene expression by ERK and activation of caspase-3 [190]. We have found that knockdown of PKC $\delta$  attenuates cisplatin-induced ERK activation and apoptosis [173], suggesting that PKC $\delta$  acts upstream of ERK1/2 to trigger cisplatin-induced apoptosis.

**7.3. Cisplatin and JNK.** c-Jun N-terminal kinase or stress-activated protein kinase is activated by various stress stimuli, including DNA damage. The involvement of the JNK pathway in cisplatin-induced apoptosis began when it was seen that cells defective in JNK pathway were resistant to cisplatin [191]. Although both cis and transplatin activated the JNK pathway, the kinetics of JNK activation was distinct [192]. Slow and persistent activation of JNK by cisplatin as opposed to rapid and transient activation of JNK by transplatin may explain the ability of cisplatin to induce cell death. The observation that p73, a proapoptotic member of the p53 family, forms a complex with JNK leading to cisplatin-induced apoptosis, provides a mechanistic basis of how JNK activation leads to cisplatin-induced apoptosis [193]. A mutation in the binding sites of JNK reduced p73-mediated apoptosis. In addition, JNK has been involved in cisplatin-induced cytotoxicity mediated by the latent membrane protein-1 (LMP-1) of the Epstein-Barr virus [190, 194] and phospholipase A2-activating protein (PLAA) [195]. Furthermore, inhibition of TWIST [196], Snail [197], cytokeratin-8 [198], and the RNA-dependent protein kinase (PKR) [199] has been reported to induce JNK activation leading to cisplatin-mediated cytotoxicity. Studies have also implicated activation of JNK pathway following recognition of cisplatin-induced DNA damage by the MMR [121, 200]. JNK and c-Abl were proposed to be signal transducers

involved in MMR system that recognizes the cisplatin-DNA adducts and induce cell death [121]. In addition to its role in regulating anticancer activity of cisplatin, JNK pathway has also been implicated in the nephrotoxicity induced by cisplatin. Inhibition of the JNK pathway was cytoprotective restricting renal cell death and inflammation [201]. Recently, the JNK pathway was also shown to mediate cisplatin-induced nephrotoxicity driven by the Toll-like receptor, TLR4 [202].

**7.4. Cisplatin and p38 MAPK.** The p38 MAPK family is activated by environmental stress and inflammatory cytokines and is an important mediator of cisplatin-induced apoptosis. The activation of this pathway by cisplatin has been seen in different experimental model systems, resulting in a cisplatin-sensitive phenotype [203]. Inhibition of p38 MAPK rendered cells resistant to cisplatin and restimulation of the p38 MAPK along with JNK sensitized cisplatin resistant ovarian cancer 2008/C13\* cells by increasing the expression of FasL [204]. Akt2 has been shown to negatively regulate the p38 MAPK pathway by binding to and phosphorylating one of the p38 family members ASK1, resulting in the inhibition of this pathway and rendering the cells resistant to cisplatin [205]. The p38 MAPK pathway was shown to be activated in response to agents such as curcumin which induced apoptosis in cisplatin-resistant ovarian cancer cells [206]. Thus, the activation of p38 MAPK regardless of the upstream signaling pathway seems to be important in mediating cisplatin-induced cytotoxicity. Winograd-Katz and Levitzki identified EGFR as a substrate for p38 MAPK and cisplatin-induced receptor internalization was triggered by p38-mediated phosphorylation of the receptor [207]. p38 MAPK has been shown to mediate its effect via p18(Hamlet), a p38 MAPK-regulated protein, which interacts with p53 and stimulates the transcription of proapoptotic genes PUMA and NOXA to induce apoptosis [208]. Like JNK, p38 MAPK has also been implicated in contributing to nephrotoxicity possibly via TNF $\alpha$  [209, 210]. Thus, the p38 MAPK pathway plays a critical role in regulating cisplatin-induced apoptosis.

**7.5. Cisplatin and Akt.** Akt belongs to a family of serine/threonine kinases which act downstream of phosphoinositide 3-kinase (PI3K) and plays a critical role in cell survival [211]. Several studies have established the involvement of Akt in contributing to the acquired resistance to cisplatin in several cancers, including ovarian [174, 212], uterine [213], small-cell lung cancer [214], nonsmall-cell lung cancer [215] and hepatoblastoma [216]. Hayakawa et al. first demonstrated that cisplatin-induced DNA damage caused phosphorylation of BAD at Ser136 via Akt and inhibition of Akt sensitized ovarian cancer cells to cisplatin [174]. Asselin et al. provided evidence that the X-linked inhibitor of apoptosis (XIAP) inhibits cisplatin-mediated cell death in cisplatin-sensitive A2780 ovarian cancer cells via phosphorylation and activation of Akt [217]. On the other hand, Dan et al. demonstrated that XIAP is a substrate for Akt and phosphorylation of XIAP by Akt prevents its ubiquitination and degradation in response to cisplatin, suggesting

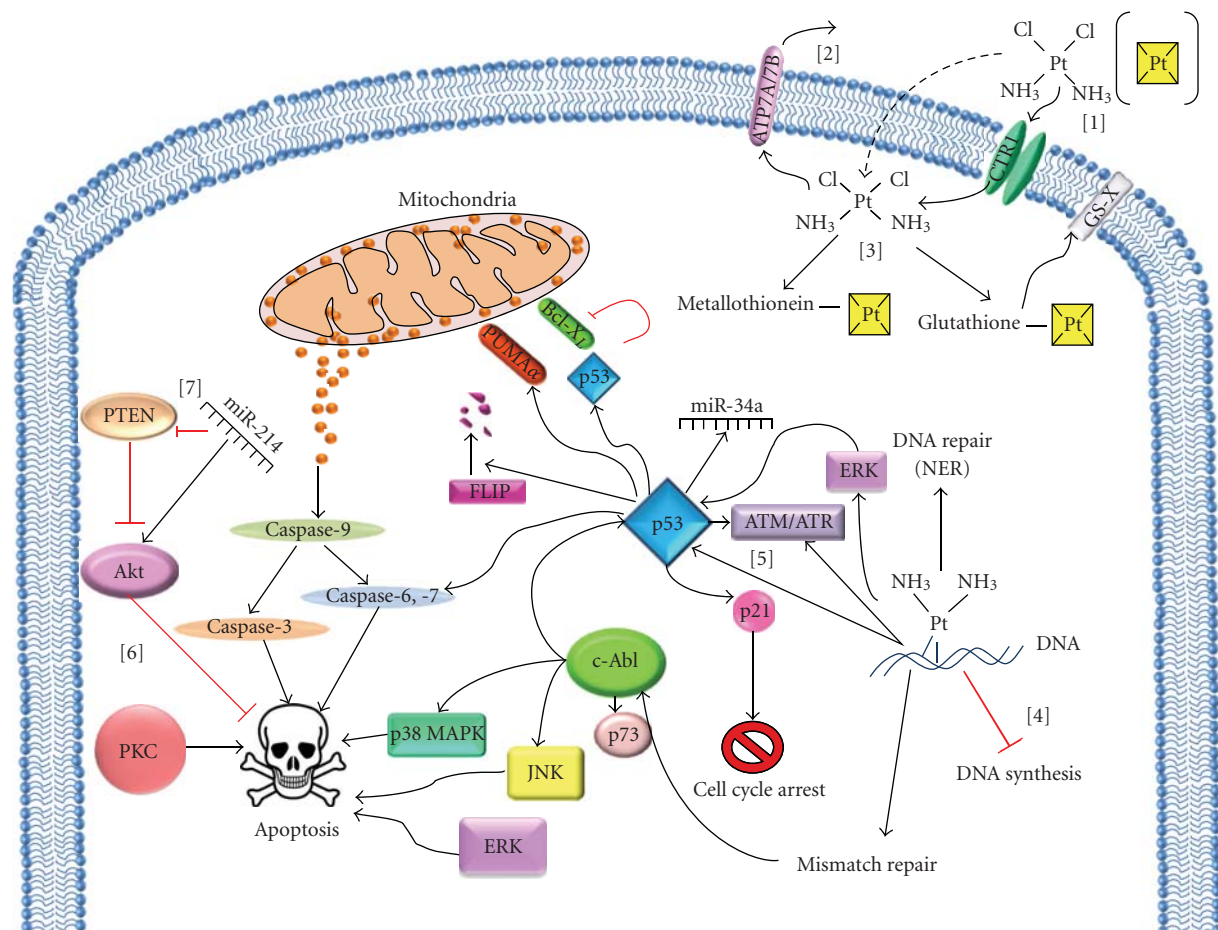


FIGURE 1: Cellular responses to cisplatin-induced DNA damage. [1] Entry of cisplatin into cells by passive diffusion (indicated by dotted arrows), carrier-mediated transport, employing copper transporter-1 (CTR1). [2] Efflux of cisplatin from the cells by the ATP-dependent transporters, ATP7A and ATP7B. [3] Cisplatin binds to cellular thiols, such as glutathione and metallothionein. The glutathione-cisplatin conjugates are further transported from the cells by the ATP-dependent, GS-X pumps. [4] Once cisplatin interacts with DNA, it stalls cell proliferation by inhibiting DNA synthesis, followed by activation of DNA damage response. [5] Cisplatin-DNA adducts is primarily repaired via the nucleotide excision repair (NER) system and also induces cell-cycle arrest. The DNA damage response is transduced mainly via p53 and c-Abl. Cisplatin-induced DNA damage activates p53, leading to the induction of p21, GADD45, proapoptotic PUMA $\alpha$ , caspase-6, -7, and microRNAs such as miR-34a. p53 also promotes cisplatin-induced apoptosis by binding and inhibiting the antiapoptotic Bcl-xL and also by degradation of FLIP. Cisplatin-DNA adducts activates the mismatch repair system which further activates c-Abl, leading to the activation of JNK and p38 MAPK and stabilization of p73 resulting in apoptosis. [6] Kinases such as PKC, ERK, and Akt are also involved in the regulation of cisplatin-induced cell death. [7] miR-214 promotes cisplatin resistance by downregulating PTEN and activating Akt.

that XIAP promotes cell survival acting downstream of Akt [218]. In small-cell lung cancer cells, the antiapoptotic protein survivin appears to mediate the effect of Akt in protecting against cisplatin-induced cell death [214].

PI3K/Akt inhibitor not only sensitized ovarian cancer cells to cisplatin *in vitro* but also enhanced the antitumor activity of cisplatin in nude mice implanted with Caov-3 human ovarian cancer xenograft [212]. Cisplatin increased p53 and decreased XIAP in cisplatin-sensitive ovarian cancer 2008 cells but not in cisplatin-resistant variant 2008/C13\* cells unless Akt was inhibited. The status of p53 also influenced the ability of Akt inhibitors to potentiate cisplatin sensitivity. Ectopic expression of the tumor suppressor PTEN which inhibits PI3K/Akt pathway sensitized cisplatin-resistant ovarian cancer 2008/C13\* cells

containing wild-type p53 but not in A2780/CP cells containing mutant p53 [105]. It has been suggested that Akt promotes chemoresistance by decreasing p53 phosphorylation and PUMA upregulation [219]. Heat shock protein, HSP27 which is often overexpressed in cisplatin-resistant cells enhanced cisplatin-induced Akt phosphorylation, suggesting that HSP27 may contribute to chemoresistance via the Akt pathway [220]. Among the Akt isoforms, Akt2 has been associated with chemoresistance of ovarian and uterine cancers [205, 213, 221]. However, acquisition of resistance by human lung cancer cells was associated with Akt1 overexpression and gene amplification [222]. Abedini et al. demonstrated that Akt confers cisplatin resistance via inhibition of p53-dependent ubiquitination and degradation of FLIP in response to cisplatin [223]. Claerhout et al. raised

the possibility that autophagy plays an important role in contributing to cisplatin resistance [224]. In a progressive model of cutaneous squamous cell carcinoma cell lines, inhibition of autophagy by 3-methyladenine or by ATG5 knockdown, along with inhibition of Akt enhanced the cytotoxicity of cisplatin [224]. Recently, it has been reported that several microRNAs are deregulated in ovarian cancer and miR-214 promotes cell survival and cisplatin resistance by downregulating PTEN and activating Akt [225]. Thus, Akt/PTEN pathway plays an important role in cisplatin resistance and could be intervened to reverse the resistant phenotype.

## 8. Conclusion

Despite significant advancements in drug development and molecular-targeted therapy, traditional chemotherapy continues to be the major treatment option. For more than thirty years, cisplatin serves as one of the most important anticancer drugs used clinically. However, cisplatin resistance continues to be the major hurdle in cancer chemotherapy. As depicted in Figure 1, cellular sensitivity to cisplatin is not only regulated by its uptake, efflux or interaction with its target DNA but cellular responses to cisplatin-induced DNA damage also play a major role in deciding the ultimate cell fate. Cells can activate protective responses to inhibit cell cycle progression and repair cisplatin-induced DNA damage. Although extensive DNA damage can induce cell death by apoptosis, several signaling pathways, including Akt, PKC, and MAPKs (e.g., ERK, JNK, and p38 MAPK) can regulate cisplatin-induced apoptosis. The tumor suppressor protein p53 play a critical role in regulating cell cycle arrest, DNA repair and apoptosis. The nonreceptor tyrosine kinase c-Abl can also participate in DNA damage response by activating various MAPKs and interacting with p53 and p73. Recent evidence suggests that microRNAs can also regulate cisplatin sensitivity. Since various signaling pathways regulate cisplatin sensitivity, one way to improve the efficacy of cisplatin is to use it in combination with agents that target the signaling pathways and contribute to cisplatin resistance. Additionally, combining cisplatin with molecular-targeted therapy should lower the dosage of cisplatin currently employed and thus help in alleviating its side effects such as nephrotoxicity. As discussed in this paper, the cellular context has significant impact in deciding the ultimate response to cisplatin and may vary from one patient to another. Thus, the major challenge is to develop individualized therapy options that will be tailor-made to benefit a particular patient. Given the uncertainty with the success of any newly developed drug and the success of cisplatin as a chemotherapeutic agent, this approach may be more feasible and should be actively pursued.

## Acknowledgments

The authors sincerely apologize if they inadvertently left out any major contribution in this field. This paper was supported by the Grant CA071727 (AB) from the National

Cancer Institute. S. Krishnamurthy is supported by the Predoctoral Traineeship Award BC083099 from DOD BCRP.

## References

- [1] B. Rosenberg, "Fundamental studies with cisplatin," *Cancer*, vol. 55, no. 10, pp. 2303–2316, 1985.
- [2] B. Rosenberg, L. Van Camp, and T. Krigas, "Inhibition of cell division in *Escherichia coli* by electrolysis products from a platinum electrode," *Nature*, vol. 205, no. 4972, pp. 698–699, 1965.
- [3] B. Rosenberg, L. VanCamp, J. E. Trosko, and V. H. Mansour, "Platinum compounds: a new class of potent antitumor agents," *Nature*, vol. 222, no. 5191, pp. 385–386, 1969.
- [4] S. E. Sherman, D. Gibson, A. H.-J. Wang, and S. J. Lippard, "X-ray structure of the major adduct of the anticancer drug cisplatin with DNA: cis-[Pt(NH<sub>3</sub>)<sub>2</sub>{d(pGpG)}]," *Science*, vol. 230, no. 4724, pp. 412–417, 1985.
- [5] A. Eastman, "Activation of programmed cell death by anticancer agents: cisplatin as a model system," *Cancer Cells*, vol. 2, no. 8-9, pp. 275–280, 1990.
- [6] J. F. R. Kerr, C. M. Winterford, and B. V. Harmon, "Apoptosis: its significance in cancer and cancer therapy," *Cancer*, vol. 73, no. 8, pp. 2013–2026, 1994.
- [7] L. Kelland, "The resurgence of platinum-based cancer chemotherapy," *Nature Reviews Cancer*, vol. 7, no. 8, pp. 573–584, 2007.
- [8] R. C. Todd and S. J. Lippard, "Inhibition of transcription by platinum antitumor compounds," *Metallomics*, vol. 1, no. 4, pp. 280–291, 2009.
- [9] A. Rebillard, D. Lagadic-Gossmann, and M.-T. Dimanche-Boitrel, "Cisplatin cytotoxicity: DNA and plasma membrane targets," *Current Medicinal Chemistry*, vol. 15, no. 26, pp. 2656–2663, 2008.
- [10] H. Zorbas and B. K. Keppler, "Cisplatin damage: are DNA repair proteins saviors or traitors to the cell?" *ChemBioChem*, vol. 6, no. 7, pp. 1157–1166, 2005.
- [11] M. D. Hall, M. Okabe, D.-W. Shen, X.-J. Liang, and M. M. Gottesman, "The role of cellular accumulation in determining sensitivity to platinum-based chemotherapy," *Annual Review of Pharmacology and Toxicology*, vol. 48, pp. 495–535, 2008.
- [12] M. Kartalou and J. M. Essigmann, "Recognition of cisplatin adducts by cellular proteins," *Mutation Research*, vol. 478, no. 1-2, pp. 1–21, 2001.
- [13] S. B. Howell, R. Safaei, C. A. Larson, and M. J. Sailor, "Copper transporters and the cellular pharmacology of the platinum-containing cancer drugs," *Molecular Pharmacology*, vol. 77, no. 6, pp. 887–894, 2010.
- [14] D. Wang and S. J. Lippard, "Cellular processing of platinum anticancer drugs," *Nature Reviews Drug Discovery*, vol. 4, no. 4, pp. 307–320, 2005.
- [15] M. Kartalou and J. M. Essigmann, "Mechanisms of resistance to cisplatin," *Mutation Research*, vol. 478, no. 1-2, pp. 23–43, 2001.
- [16] D. B. Zamble and S. J. Lippard, "Cisplatin and DNA repair in cancer chemotherapy," *Trends in Biochemical Sciences*, vol. 20, no. 10, pp. 435–439, 1995.
- [17] Y. Sedletska, M.-J. Giraud-Panis, and J.-M. Malinge, "Cisplatin is a DNA-damaging antitumor compound triggering multifactorial biochemical responses in cancer cells: importance of apoptotic pathways," *Current Medicinal Chemistry: Anti-Cancer Agents*, vol. 5, no. 3, pp. 251–265, 2005.

- [18] A. K. Holzer, G. H. Manorek, and S. B. Howell, "Contribution of the major copper influx transporter CTR1 to the cellular accumulation of cisplatin, carboplatin, and oxaliplatin," *Molecular Pharmacology*, vol. 70, no. 4, pp. 1390–1394, 2006.
- [19] A. K. Holzer, K. Katano, L. W. J. Klomp, and S. B. Howell, "Cisplatin rapidly down-regulates its own influx transporter hCTR1 in cultured human ovarian carcinoma cells," *Clinical Cancer Research*, vol. 10, no. 19, pp. 6744–6749, 2004.
- [20] R. Safaei, A. K. Holzer, K. Katano, G. Samimi, and S. B. Howell, "The role of copper transporters in the development of resistance to Pt drugs," *Journal of Inorganic Biochemistry*, vol. 98, no. 10, pp. 1607–1613, 2004.
- [21] J. E. Byfield and P. M. Calabro-Jones, "Carrier-dependent and carrier-independent transport of anti-cancer alkylating agents," *Nature*, vol. 294, no. 5838, pp. 281–283, 1981.
- [22] P. A. Andrews, S. C. Mann, H. H. Huynh, and K. D. Albright, "Role of the Na<sup>+</sup>, K<sup>+</sup>-adenosine triphosphatase in the accumulation of cis-diamminedichloroplatinum(II) in human ovarian carcinoma cells," *Cancer Research*, vol. 51, no. 14, pp. 3677–3681, 1991.
- [23] S. Ishida, J. Lee, D. J. Thiele, and I. Herskowitz, "Uptake of the anticancer drug cisplatin mediated by the copper transporter Ctr1 in yeast and mammals," *Proceedings of the National Academy of Sciences of the United States of America*, vol. 99, no. 22, pp. 14298–14302, 2002.
- [24] R. Safaei and S. B. Howell, "Copper transporters regulate the cellular pharmacology and sensitivity to Pt drugs," *Critical Reviews in Oncology/Hematology*, vol. 53, no. 1, pp. 13–23, 2005.
- [25] B. G. Blair, C. Larson, R. Safaei, and S. B. Howell, "Copper transporter 2 regulates the cellular accumulation and cytotoxicity of cisplatin and carboplatin," *Clinical Cancer Research*, vol. 15, no. 13, pp. 4312–4321, 2009.
- [26] K. Kawai, N. Kamatani, E. Georges, and V. Ling, "Identification of a membrane glycoprotein overexpressed in murine lymphoma sublines resistant to cis-diamminedichloroplatinum(II)," *Journal of Biological Chemistry*, vol. 265, no. 22, pp. 13137–13142, 1990.
- [27] D. P. Gately and S. B. Howell, "Cellular accumulation of the anticancer agent cisplatin: a review," *British Journal of Cancer*, vol. 67, no. 6, pp. 1171–1176, 1993.
- [28] E. R. Jamieson and S. J. Lippard, "Structure, recognition, and processing of cisplatin-DNA adducts," *Chemical Reviews*, vol. 99, no. 9, pp. 2467–2498, 1999.
- [29] A. Eastman, "The formation, isolation and characterization of DNA adducts produced by anticancer platinum complexes," *Pharmacology and Therapeutics*, vol. 34, no. 2, pp. 155–166, 1987.
- [30] B. C. McKay, C. Becerril, and M. Ljungman, "P53 plays a protective role against UV- and cisplatin-induced apoptosis in transcription-coupled repair proficient fibroblasts," *Oncogene*, vol. 20, no. 46, pp. 6805–6808, 2001.
- [31] C. Welsh, R. Day, C. McGurk, J. R. W. Masters, R. D. Wood, and B. Köberle, "Reduced levels of XPA, ERCC1 and XPF DNA repair proteins in testis tumor cell lines," *International Journal of Cancer*, vol. 110, no. 3, pp. 352–361, 2004.
- [32] B. Köberle, J. R. W. Masters, J. A. Hartley, and R. D. Wood, "Defective repair of cisplatin-induced DNA damage caused by reduced XPA protein in testicular germ cell tumours," *Current Biology*, vol. 9, no. 5, pp. 273–276, 1999.
- [33] R. Rosell, M. Taron, A. Barnadas, G. Scagliotti, C. Sarries, and B. Roig, "Nucleotide excision repair pathways involved in cisplatin resistance in non-small-cell lung cancer," *Cancer Control*, vol. 10, no. 4, pp. 297–305, 2003.
- [34] X. Wu, W. Fan, S. Xu, and Y. Zhou, "Sensitization to the cytotoxicity of cisplatin by transfection with nucleotide excision repair gene xeroderma pigmentosum group A antisense RNA in human lung adenocarcinoma cells," *Clinical Cancer Research*, vol. 9, no. 16, part 1, pp. 5874–5879, 2003.
- [35] Y. Sun, T. Li, K. Ma et al., "The impacts of ercc1 gene exon VIII alternative splicing on cisplatin-resistance in ovarian cancer cells," *Cancer Investigation*, vol. 27, no. 9, pp. 891–897, 2009.
- [36] H.-Y. Chen, C.-J. Shao, F.-R. Chen, A.-L. Kwan, and Z.-P. Chen, "Role of ERCC1 promoter hypermethylation in drug resistance to cisplatin in human gliomas," *International Journal of Cancer*, vol. 126, no. 8, pp. 1944–1954, 2010.
- [37] B. Orelli, T. B. McClendon, O. V. Tsodikov, T. Ellenberger, L. J. Niedernhofer, and O. D. Schärer, "The XPA-binding domain of ERCC1 is required for nucleotide excision repair but not other DNA repair pathways," *Journal of Biological Chemistry*, vol. 285, no. 6, pp. 3705–3712, 2010.
- [38] S. Arora, A. Kothandapani, K. Tillison, V. Kalman-Maltese, and S. M. Patrick, "Downregulation of XPF-ERCC1 enhances cisplatin efficacy in cancer cells," *DNA Repair*, vol. 9, no. 7, pp. 745–753, 2010.
- [39] O. W. Guthrie, H.-S. Li-Korotky, J. D. Durrant, and C. Balaban, "Cisplatin induces cytoplasmic to nuclear translocation of nucleotide excision repair factors among spiral ganglion neurons," *Hearing Research*, vol. 239, no. 1-2, pp. 79–91, 2008.
- [40] T.-H. Kang, L. A. Lindsey-Boltz, J. T. Reardon, and A. Sancar, "Circadian control of XPA and excision repair of cisplatin-DNA damage by cryptochrome and HERC2 ubiquitin ligase," *Proceedings of the National Academy of Sciences of the United States of America*, vol. 107, no. 11, pp. 4890–4895, 2010.
- [41] S. L. Colton, X. S. Xu, Y. A. Wang, and G. Wang, "The involvement of ataxia-telangiectasia mutated protein activation in nucleotide excision repair-facilitated cell survival with cisplatin treatment," *Journal of Biological Chemistry*, vol. 281, no. 37, pp. 27117–27125, 2006.
- [42] S. Bhana and D. R. Lloyd, "The role of p53 in DNA damage-mediated cytotoxicity overrides its ability to regulate nucleotide excision repair in human fibroblasts," *Mutagenesis*, vol. 23, no. 1, pp. 43–50, 2008.
- [43] S. L. Lomonaco, X. S. Xu, and G. Wang, "The role of Bcl-x(L) protein in nucleotide excision repair-facilitated cell protection against cisplatin-induced apoptosis," *DNA and Cell Biology*, vol. 28, no. 6, pp. 285–294, 2009.
- [44] G. E. Damsma, A. Alt, F. Brueckner, T. Carell, and P. Cramer, "Mechanism of transcriptional stalling at cisplatin-damaged DNA," *Nature Structural and Molecular Biology*, vol. 14, no. 12, pp. 1127–1133, 2007.
- [45] P. Borst, S. Rottenberg, and J. Jonkers, "How do real tumors become resistant to cisplatin?" *Cell Cycle*, vol. 7, no. 10, pp. 1353–1359, 2008.
- [46] A. Alt, K. Lammens, C. Chiochini et al., "Bypass of DNA lesions generated during anticancer treatment with cisplatin by DNA polymerase  $\eta$ ," *Science*, vol. 318, no. 5852, pp. 967–970, 2007.
- [47] Y. Sedletska, L. Fourrier, and J.-M. Malinge, "Modulation of MutS ATP-dependent functional activities by DNA containing a cisplatin compound lesion (base damage and mismatch)," *Journal of Molecular Biology*, vol. 369, no. 1, pp. 27–40, 2007.
- [48] M. Yamada, E. O'Regan, R. Brown, and P. Karran, "Selective recognition of a cisplatin-DNA adduct by human mismatch

- repair proteins,” *Nucleic Acids Research*, vol. 25, no. 3, pp. 491–496, 1997.
- [49] L. Fourrier, P. Brooks, and J.-M. Malinge, “Binding discrimination of MutS to a set of lesions and compound lesions (base damage and mismatch) reveals its potential role as a cisplatin-damaged DNA sensing protein,” *Journal of Biological Chemistry*, vol. 278, no. 23, pp. 21267–21275, 2003.
- [50] E. Papouli, P. Cejka, and J. Jiricny, “Dependence of the cytotoxicity of DNA-damaging agents on the mismatch repair status of human cells,” *Cancer Research*, vol. 64, no. 10, pp. 3391–3394, 2004.
- [51] J. T. Drummond, J. Genschel, E. Wolf, and P. Modrich, “DHFR/MSH3 amplification in methotrexate-resistant cells alters the hMutSa/hMutS $\beta$  ratio and reduces the efficiency of base-base mismatch repair,” *Proceedings of the National Academy of Sciences of the United States of America*, vol. 94, no. 19, pp. 10144–10149, 1997.
- [52] R. Brown, G. L. Hirst, W. M. Gallagher et al., “hMLH1 expression and cellular responses of ovarian tumour cells to treatment with cytotoxic anticancer agents,” *Oncogene*, vol. 15, no. 1, pp. 45–52, 1997.
- [53] S. Aebi, B. Kurdi-Haidar, R. Gordon et al., “Loss of DNA mismatch repair in acquired resistance to cisplatin,” *Cancer Research*, vol. 56, no. 13, pp. 3087–3090, 1996.
- [54] R. P. Topping, J. C. Wilkinson, and D. Scarpinato, “Mismatch repair protein deficiency compromises cisplatin-induced apoptotic signaling,” *Journal of Biological Chemistry*, vol. 284, no. 21, pp. 14029–14039, 2009.
- [55] X. Ding, A. B. Mohd, Z. Huang et al., “MLH1 expression sensitises ovarian cancer cells to cell death mediated by XIAP inhibition,” *British Journal of Cancer*, vol. 101, no. 2, pp. 269–277, 2009.
- [56] E. Avdievich, C. Reiss, S. J. Scherer et al., “Distinct effects of the recurrent Mlh1G67R mutation on MMR functions, cancer, and meiosis,” *Proceedings of the National Academy of Sciences of the United States of America*, vol. 105, no. 11, pp. 4247–4252, 2008.
- [57] D. P. Lin, Y. Wang, S. J. Scherer et al., “An Msh2 point mutation uncouples DNA mismatch repair and apoptosis,” *Cancer Research*, vol. 64, no. 2, pp. 517–522, 2004.
- [58] G. Yang, S. J. Scherer, S. S. Shell et al., “Dominant effects of an Msh6 missense mutation on DNA repair and cancer susceptibility,” *Cancer Cell*, vol. 6, no. 2, pp. 139–150, 2004.
- [59] X. Lin and S. B. Howell, “DNA mismatch repair and p53 function are major determinants of the rate of development of cisplatin resistance,” *Molecular Cancer Therapeutics*, vol. 5, no. 5, pp. 1239–1247, 2006.
- [60] H. Shimodaira, A. Yoshioka-Yamashita, R. D. Kolodner, and J. Y. J. Wang, “Interaction of mismatch repair protein PMS2 and the p53-related transcription factor p73 in apoptosis response to cisplatin,” *Proceedings of the National Academy of Sciences of the United States of America*, vol. 100, no. 5, pp. 2420–2425, 2003.
- [61] X. Lin, K. Ramamurthi, M. Mishima, A. Kondo, R. D. Christen, and S. B. Howell, “p53 modulates the effect of loss of DNA mismatch repair on the sensitivity of human colon cancer cells to the cytotoxic and mutagenic effects of cisplatin,” *Cancer Research*, vol. 61, no. 4, pp. 1508–1516, 2001.
- [62] P. Branch, M. Masson, G. Aquilina, M. Bignami, and P. Karran, “Spontaneous development of drug resistance: mismatch repair and p53 defects in resistance to cisplatin in human tumor cells,” *Oncogene*, vol. 19, no. 28, pp. 3138–3145, 2000.
- [63] V. Cepeda, M. A. Fuertes, J. Castilla, C. Alonso, C. Quevedo, and J. M. Pérez, “Biochemical mechanisms of cisplatin cytotoxicity,” *Anti-Cancer Agents in Medicinal Chemistry*, vol. 7, no. 1, pp. 3–18, 2007.
- [64] T. Ishikawa and F. Ali-Osman, “Glutathione-associated cis-diamminedichloroplatinum(II) metabolism and ATP-dependent efflux from leukemia cells. Molecular characterization of glutathione-platinum complex and its biological significance,” *Journal of Biological Chemistry*, vol. 268, no. 27, pp. 20116–20125, 1993.
- [65] A. K. Godwin, A. Meister, P. J. O’Dwyer, C. S. Huang, T. C. Hamilton, and M. E. Anderson, “High resistance to cisplatin in human ovarian cancer cell lines is associated with marked increase of glutathione synthesis,” *Proceedings of the National Academy of Sciences of the United States of America*, vol. 89, no. 7, pp. 3070–3074, 1992.
- [66] Boubakari, K. Bracht, C. Neumann, R. Grünert, and P. J. Bednarski, “No correlation between GSH levels in human cancer cell lines and the cell growth inhibitory activities of platinum diamine complexes,” *Archiv der Pharmazie*, vol. 337, no. 12, pp. 668–671, 2004.
- [67] K. Bracht, Boubakari, R. Grünert, and P. J. Bednarski, “Correlations between the activities of 19 anti-tumor agents and the intracellular glutathione concentrations in a panel of 14 human cancer cell lines: comparisons with the National Cancer Institute data,” *Anti-Cancer Drugs*, vol. 17, no. 1, pp. 41–51, 2006.
- [68] Y. Kasherman, S. Sturup, and D. Gibson, “Is glutathione the major cellular target of cisplatin? A study of the interactions of cisplatin with cancer cell extracts,” *Journal of Medicinal Chemistry*, vol. 52, no. 14, pp. 4319–4328, 2009.
- [69] H. H. W. Chen, I.-S. Song, A. Hossain et al., “Elevated glutathione levels confer cellular sensitization to cisplatin toxicity by up-regulation of copper transporter hCtr1,” *Molecular Pharmacology*, vol. 74, no. 3, pp. 697–704, 2008.
- [70] N. Ban, Y. Takahashi, T. Takayama et al., “Transfection of glutathione S-transferase (GST)- $\pi$  antisense complementary DNA increases the sensitivity of a colon cancer cell line to adriamycin, cisplatin, melphalan, and etoposide,” *Cancer Research*, vol. 56, no. 15, pp. 3577–3582, 1996.
- [71] M. Miyazaki, K. Kohno, Y. Saburi et al., “Drug resistance to cis-diamminedichloroplatinum(II) in Chinese hamster ovary cell lines transfected with glutathione S-transferase pi gene,” *Biochemical and Biophysical Research Communications*, vol. 166, no. 3, pp. 1358–1364, 1990.
- [72] M. Pasello, F. Michelacci, I. Scionti et al., “Overcoming glutathione S-transferase P1-related cisplatin resistance in osteosarcoma,” *Cancer Research*, vol. 68, no. 16, pp. 6661–6668, 2008.
- [73] C. Pecklak-Scott, P. K. Smitherman, A. J. Townsend, and C. S. Morrow, “Role of glutathione S-transferase P1-1 in the cellular detoxification of cisplatin,” *Molecular Cancer Therapeutics*, vol. 7, no. 10, pp. 3247–3255, 2008.
- [74] E. W. LaPensee, S. J. Schwemberger, C. R. LaPensee, E. M. Bahassi, S. E. Afton, and N. Ben-Jonathan, “Prolactin confers resistance against cisplatin in breast cancer cells by activating glutathione-S-transferase,” *Carcinogenesis*, vol. 30, no. 8, pp. 1298–1304, 2009.
- [75] S. Piaggi, C. Raggi, A. Corti et al., “Glutathione transferase omega 1-1 (GSTO1-1) plays an anti-apoptotic role in cell resistance to cisplatin toxicity,” *Carcinogenesis*, vol. 31, no. 5, pp. 804–811, 2010.

- [76] A. Basu and J. S. Lazo, "A hypothesis regarding the protective role of metallothioneins against the toxicity of DNA interactive anticancer drugs," *Toxicology Letters*, vol. 50, no. 2-3, pp. 123-135, 1990.
- [77] P. A. Andrews, M. P. Murphy, and S. B. Howell, "Metallothionein-mediated cisplatin resistance in human ovarian carcinoma cells," *Cancer Chemotherapy and Pharmacology*, vol. 19, no. 2, pp. 149-154, 1987.
- [78] S. L. Kelley, A. Basu, B. A. Teicher, M. P. Hacker, D. H. Hamer, and J. S. Lazo, "Overexpression of metallothionein confers resistance to anticancer drugs," *Science*, vol. 241, no. 4874, pp. 1813-1815, 1988.
- [79] P. Surowiak, V. Materna, A. Maciejczyk et al., "Nuclear metallothionein expression correlates with cisplatin resistance of ovarian cancer cells and poor clinical outcome," *Virchows Archiv*, vol. 450, no. 3, pp. 279-285, 2007.
- [80] T. Suzuki, S. Ohata, T. Togawa, S. Himeno, and S. Tanabe, "Arsenic accumulation decreased in metallothionein null cisplatin-resistant cell lines," *Journal of Toxicological Sciences*, vol. 32, no. 3, pp. 321-328, 2007.
- [81] A. V. Karotki and M. Vařák, "Reaction of human metallothionein-3 with cisplatin and transplatin," *Journal of Biological Inorganic Chemistry*, vol. 14, no. 7, pp. 1129-1138, 2009.
- [82] J. Hidalgo, M. Aschner, P. Zatta, and M. Vařák, "Roles of the metallothionein family of proteins in the central nervous system," *Brain Research Bulletin*, vol. 55, no. 2, pp. 133-145, 2001.
- [83] G. Chu, "Cellular responses to cisplatin. The roles of DNA-binding proteins and DNA repair," *Journal of Biological Chemistry*, vol. 269, no. 2, pp. 787-790, 1994.
- [84] D. Hagrman, J. Goodisman, J. C. Dabrowiak, and A.-K. Souid, "Kinetic study on the reaction of cisplatin with metallothionein," *Drug Metabolism and Disposition*, vol. 31, no. 7, pp. 916-923, 2003.
- [85] E. S. Woo, A. Monks, S. C. Watkins, A. S. Wang, and J. S. Lazo, "Diversity of metallothionein content and subcellular localization in the National Cancer Institute tumor panel," *Cancer Chemotherapy and Pharmacology*, vol. 41, no. 1, pp. 61-68, 1997.
- [86] M. G. Cherian, A. Jayasurya, and B.-H. Bay, "Metallothioneins in human tumors and potential roles in carcinogenesis," *Mutation Research*, vol. 533, no. 1-2, pp. 201-209, 2003.
- [87] S. E. Theocharis, A. P. Margeli, J. T. Kljanienko, and G. P. Kouraklis, "Metallothionein expression in human neoplasia," *Histopathology*, vol. 45, no. 2, pp. 103-118, 2004.
- [88] A. Efeyan and M. Serrano, "p53: guardian of the genome and policeman of the oncogenes," *Cell Cycle*, vol. 6, no. 9, pp. 1006-1010, 2007.
- [89] V. De Laurenzi and G. Melino, "Evolution of functions within the p53/p63/p73 family," *Annals of the New York Academy of Sciences*, vol. 926, pp. 90-100, 2000.
- [90] T. Fujiwara, E. A. Grimm, T. Mukhopadhyay, W.-W. Zhang, L. B. Owen-Schaub, and J. A. Roth, "Induction of chemosensitivity in human lung cancer cells in vivo by adenovirus-mediated transfer of the wild-type p53 gene," *Cancer Research*, vol. 54, no. 9, pp. 2287-2291, 1994.
- [91] J. Horowitz, "Adenovirus-mediated p53 gene therapy: overview of preclinical studies and potential clinical applications," *Current Opinion in Molecular Therapeutics*, vol. 1, no. 4, pp. 500-509, 1999.
- [92] J. Kigawa, S. Sato, M. Shimada et al., "p53 gene status and chemosensitivity in ovarian cancer," *Human Cell*, vol. 14, no. 3, pp. 165-171, 2001.
- [93] K. Song, K. H. Cowan, and B. K. Sinha, "In vivo studies of adenovirus-mediated p53 gene therapy for cisplatin-resistant human ovarian tumor xenografts," *Oncology Research*, vol. 11, no. 3, pp. 153-159, 1999.
- [94] N. Pabla, S. Huang, Q.-S. Mi, R. Daniel, and Z. Dong, "ATR-Chk2 signaling in p53 activation and DNA damage response during cisplatin-induced apoptosis," *Journal of Biological Chemistry*, vol. 283, no. 10, pp. 6572-6583, 2008.
- [95] S. Kondo, B. P. Barna, Y. Kondo et al., "WAF1/CIP1 increases the susceptibility of p53 non-functional malignant glioma cells to cisplatin-induced apoptosis," *Oncogene*, vol. 13, no. 6, pp. 1279-1285, 1996.
- [96] D. B. Zamble, T. Jacks, and S. J. Lippard, "p53-dependent and -independent responses to cisplatin in mouse testicular teratocarcinoma cells," *Proceedings of the National Academy of Sciences of the United States of America*, vol. 95, no. 11, pp. 6163-6168, 1998.
- [97] X. Yang, M. Fraser, U. M. Moll, A. Basak, and B. K. Tsang, "Akt-mediated cisplatin resistance in ovarian cancer: modulation of p53 action on caspase-dependent mitochondrial death pathway," *Cancer Research*, vol. 66, no. 6, pp. 3126-3136, 2006.
- [98] Y. Kanamori, J. Kigawa, Y. Minagawa et al., "A newly developed adenovirus-mediated transfer of a wild-type p53 gene increases sensitivity to cis-diamminedichloroplatinum (II) in p53-deleted ovarian cancer cells," *European Journal of Cancer*, vol. 34, no. 11, pp. 1802-1806, 1998.
- [99] J. Kigawa, S. Sato, M. Shimada, Y. Kanamori, H. Itamochi, and N. Terakawa, "Effect of p53 gene transfer and cisplatin in a peritonitis carcinomatosus model with p53-deficient ovarian cancer cells," *Gynecologic Oncology*, vol. 84, no. 2, pp. 210-215, 2002.
- [100] C. C. Wetzel and S. J. Berberich, "p53 binds to cisplatin-damaged DNA," *Biochimica et Biophysica Acta*, vol. 1517, no. 3, pp. 392-397, 2001.
- [101] E. Hernlund, O. Kutuk, H. Basaga, S. Linder, T. Panaretakis, and M. Shoshan, "Cisplatin-induced nitrosylation of p53 prevents its mitochondrial translocation," *Free Radical Biology and Medicine*, vol. 46, no. 12, pp. 1607-1613, 2009.
- [102] D. L. Persons, E. M. Yazlovitskaya, and J. C. Pelling, "Effect of extracellular signal-regulated kinase on p53 accumulation in response to cisplatin," *Journal of Biological Chemistry*, vol. 275, no. 46, pp. 35778-35785, 2000.
- [103] M. R. Abedini, E. J. Muller, J. Brun, R. Bergeron, D. A. Gray, and B. K. Tsang, "Cisplatin induces p53-dependent FLICE-like inhibitory protein ubiquitination in ovarian cancer cells," *Cancer Research*, vol. 68, no. 12, pp. 4511-4517, 2008.
- [104] O. Kutuk, E. D. Arisan, T. Tezil, M. C. Shoshan, and H. Basaga, "Cisplatin overcomes Bcl-2-mediated resistance to apoptosis via preferential engagement of Bak: critical role of Noxa-mediated lipid peroxidation," *Carcinogenesis*, vol. 30, no. 9, pp. 1517-1527, 2009.
- [105] X. Yan, M. Fraser, Q. Qiu, and B. K. Tsang, "Over-expression of PTEN sensitizes human ovarian cancer cells to cisplatin-induced apoptosis in a p53-dependent manner," *Gynecologic Oncology*, vol. 102, no. 2, pp. 348-355, 2006.
- [106] H.-S. Kim, J.-T. Hwang, H. Yun et al., "Inhibition of AMP-activated protein kinase sensitizes cancer cells to cisplatin-induced apoptosis via hyper-induction of p53," *Journal of Biological Chemistry*, vol. 283, no. 7, pp. 3731-3742, 2008.
- [107] M. Jiang, Q. Wei, J. Wang et al., "Regulation of PUMA- $\alpha$  by p53 in cisplatin-induced renal cell apoptosis," *Oncogene*, vol. 25, no. 29, pp. 4056-4066, 2006.

- [108] C. Yang, V. Kaushal, R. S. Haun, R. Seth, S. V. Shah, and G. P. Kaushal, "Transcriptional activation of caspase-6 and -7 genes by cisplatin-induced p53 and its functional significance in cisplatin nephrotoxicity," *Cell Death and Differentiation*, vol. 15, no. 3, pp. 530–544, 2008.
- [109] K. Bhatt, L. Zhou, Q. S. Mi, et al., "microRNA-34a is induced via p53 during cisplatin nephrotoxicity and contributes to cell survival," *Molecular Medicine*, 2010.
- [110] S. Fan, M. L. Smith, D. J. Rivet II et al., "Disruption of p53 function sensitizes breast cancer MCF-7 cells to cisplatin and pentoxifylline," *Cancer Research*, vol. 55, no. 8, pp. 1649–1654, 1995.
- [111] R. Brown, C. Clugston, P. Burns et al., "Increased accumulation of p53 protein in cisplatin-resistant ovarian cell lines," *International Journal of Cancer*, vol. 55, no. 4, pp. 678–684, 1993.
- [112] C. L. Johnson, D. Lu, J. Huang, and A. Basu, "Regulation of p53 stabilization by DNA damage and protein kinase C," *Molecular Cancer Therapeutics*, vol. 1, no. 10, pp. 861–867, 2002.
- [113] P. Perego, M. Giarola, S. C. Righetti et al., "Association between cisplatin resistance and mutation of p53 gene and reduced bax expression in ovarian carcinoma cell systems," *Cancer Research*, vol. 56, no. 3, pp. 556–562, 1996.
- [114] S. C. Righetti, G. Della Torre, S. Pilotti et al., "A comparative study of p53 gene mutations, protein accumulation, and response to cisplatin-based chemotherapy in advanced ovarian carcinoma," *Cancer Research*, vol. 56, no. 4, pp. 689–693, 1996.
- [115] A. Vekris, D. Meynard, M.-C. Haaz, M. Bayssas, J. Bonnet, and J. Robert, "Molecular determinants of the cytotoxicity of platinum compounds: the contribution of in silico research," *Cancer Research*, vol. 64, no. 1, pp. 356–362, 2004.
- [116] B. Piovesan, N. Pennell, and N. L. Berinstein, "Human lymphoblastoid cell lines expressing mutant p53 exhibit decreased sensitivity to cisplatin-induced cytotoxicity," *Oncogene*, vol. 17, no. 18, pp. 2339–2350, 1998.
- [117] M. Preyer, C.-W. Shu, and J. Y. J. Wang, "Delayed activation of Bax by DNA damage in embryonic stem cells with knock-in mutations of the Abl nuclear localization signals," *Cell Death and Differentiation*, vol. 14, no. 6, pp. 1139–1148, 2007.
- [118] S. Kharbanda, R. Ren, P. Pandey et al., "Activation of the c-Abl tyrosine kinase in the stress response to DNA-damaging agents," *Nature*, vol. 376, no. 6543, pp. 785–788, 1995.
- [119] S. Kharbanda, P. Pandey, T. Yamauchi et al., "Activation of MEK kinase 1 by the c-Abl protein tyrosine kinase in response to DNA damage," *Molecular and Cellular Biology*, vol. 20, no. 14, pp. 4979–4989, 2000.
- [120] A. Nehmé, R. Baskaran, S. Nebel et al., "Induction of JNK and c-Abl signalling by cisplatin and oxaliplatin in mismatch repair-proficient and -deficient cells," *British Journal of Cancer*, vol. 79, no. 7-8, pp. 1104–1110, 1999.
- [121] A. Nehmé, R. Baskaran, S. Aebi et al., "Differential induction of c-Jun NH2-terminal kinase and c-Abl kinase in DNA mismatch repair-proficient and -deficient cells exposed to cisplatin," *Cancer Research*, vol. 57, no. 15, pp. 3253–3257, 1997.
- [122] J. Gong, A. Costanzo, H.-Q. Yang et al., "The tyrosine kinase c-Abl regulates p73 in apoptotic response to cisplatin-induced DNA damage," *Nature*, vol. 399, no. 6738, pp. 806–809, 1999.
- [123] K. K. C. Tsai and Z.-M. Yuan, "c-Abl stabilizes p73 by a phosphorylation-augmented interaction," *Cancer Research*, vol. 63, no. 12, pp. 3418–3424, 2003.
- [124] T. Truong, G. Sun, M. Doorly, J. Y. J. Wang, and M. A. Schwartz, "Modulation of DNA damage-induced apoptosis by cell adhesion is independently mediated by p53 and c-Abl," *Proceedings of the National Academy of Sciences of the United States of America*, vol. 100, no. 18, pp. 10281–10286, 2003.
- [125] C.-O. Leong, N. Vidnovic, M. P. DeYoung, D. Sgroi, and L. W. Ellisen, "The p63/p73 network mediates chemosensitivity to cisplatin in a biologically defined subset of primary breast cancers," *Journal of Clinical Investigation*, vol. 117, no. 5, pp. 1370–1380, 2007.
- [126] W. H. Toh, M. M. Siddique, L. Boominathan, K. W. Lin, and K. Sabapathy, "c-Jun regulates the stability and activity of the p53 homologue, p73," *Journal of Biological Chemistry*, vol. 279, no. 43, pp. 44713–44722, 2004.
- [127] D. Levy, Y. Adamovich, N. Reuven, and Y. Shaul, "Yap1 phosphorylation by c-Abl is a critical step in selective activation of proapoptotic genes in response to DNA damage," *Molecular Cell*, vol. 29, no. 3, pp. 350–361, 2008.
- [128] S. Gonfloni, L. Di Tella, S. Caldarola et al., "Inhibition of the c-Abl-TAp63 pathway protects mouse oocytes from chemotherapy-induced death," *Nature Medicine*, vol. 15, no. 10, pp. 1179–1185, 2009.
- [129] N. Machuy, K. Rajalingam, and T. Rudel, "Requirement of caspase-mediated cleavage of c-Abl during stress-induced apoptosis," *Cell Death and Differentiation*, vol. 11, no. 3, pp. 290–300, 2004.
- [130] E. M. Galan-Moya, J. Hernandez-Losa, C. I. Aceves Luquero et al., "c-Abl activates p38 MAPK independently of its tyrosine kinase activity: implications in cisplatin-based therapy," *International Journal of Cancer*, vol. 122, no. 2, pp. 289–297, 2008.
- [131] G. Nuñez, M. A. Benedict, Y. Hu, and N. Inohara, "Caspases: the proteases of the apoptotic pathway," *Oncogene*, vol. 17, no. 25, pp. 3237–3245, 1998.
- [132] F. C. Kischkel, S. Hellbardt, I. Behrmann et al., "Cytotoxicity-dependent APO-1 (Fas/CD95)-associated proteins form a death-inducing signaling complex (DISC) with the receptor," *EMBO Journal*, vol. 14, no. 22, pp. 5579–5588, 1995.
- [133] A. Basu and U. Sivaprasad, "Protein kinase C $\epsilon$  makes the life and death decision," *Cellular Signalling*, vol. 19, no. 8, pp. 1633–1642, 2007.
- [134] A. C. Newton, "Regulation of the ABC kinases by phosphorylation: protein kinase C as a paradigm," *Biochemical Journal*, vol. 370, no. 2, pp. 361–371, 2003.
- [135] A. Basu, "The potential of protein kinase C as a target for anticancer treatment," *Pharmacology and Therapeutics*, vol. 59, no. 3, pp. 257–280, 1993.
- [136] Y. Nishizuka, "Intracellular signaling by hydrolysis of phospholipids and activation of protein kinase C," *Science*, vol. 258, no. 5082, pp. 607–614, 1992.
- [137] J. Hofmann, W. Doppler, A. Jakob et al., "Enhancement of the antiproliferative effect of cis-diamminedichloroplatinum(II) and nitrogen mustard by inhibitors of protein kinase C," *International Journal of Cancer*, vol. 42, no. 3, pp. 382–388, 1988.
- [138] S. Isonishi, P. A. Andrews, and S. B. Howell, "Increased sensitivity to cis-diamminedichloroplatinum(II) in human ovarian carcinoma cells in response to treatment with 12-O-tetradecanoylphorbol 13-acetate," *Journal of Biological Chemistry*, vol. 265, no. 7, pp. 3623–3627, 1990.
- [139] A. Basu, B. A. Teicher, and J. S. Lazo, "Involvement of protein kinase C in phorbol ester-induced sensitization of HeLa cells

- to cis-diamminedichloroplatinum(II)," *Journal of Biological Chemistry*, vol. 265, no. 15, pp. 8451–8457, 1990.
- [140] J. Hirata, Y. Kikuchi, T. Kita et al., "Modulation of sensitivity of human ovarian cancer cells to cis-diamminedichloroplatinum(II) by 12-O-tetradecanoylphorbol-13-acetate and D,L-buthionine-S,R-sulphoximine," *International Journal of Cancer*, vol. 55, no. 3, pp. 521–527, 1993.
- [141] A. Basu and J. S. Lazo, "Sensitization of human cervical carcinoma cells to cis-diamminedichloroplatinum(II) by bryostatin 1," *Cancer Research*, vol. 52, no. 11, pp. 3119–3124, 1992.
- [142] F. Nezhat, S. Wadler, F. Muggia et al., "Phase II trial of the combination of bryostatin-1 and cisplatin in advanced or recurrent carcinoma of the cervix: a New York Gynecologic Oncology Group study," *Gynecologic Oncology*, vol. 93, no. 1, pp. 144–148, 2004.
- [143] A. C. Pavlick, J. Wu, J. Roberts et al., "Phase I study of bryostatin 1, a protein kinase C modulator, preceding cisplatin in patients with refractory non-hematologic tumors," *Cancer Chemotherapy and Pharmacology*, vol. 64, no. 4, pp. 803–810, 2009.
- [144] A. Basu, A. P. Kozikowski, K. Sato, and J. S. Lazo, "Cellular sensitization to cis-diamminedichloroplatinum(II) by novel analogues of the protein kinase C activator lyngbyatoxin A," *Cancer Research*, vol. 51, no. 10, pp. 2511–2514, 1991.
- [145] A. Basu and K. M. Weixel, "Comparison of protein kinase C activity and isoform expression in cisplatin-sensitive and -resistant ovarian carcinoma cells," *International Journal of Cancer*, vol. 62, no. 4, pp. 457–460, 1995.
- [146] S. Mohanty, J. Huang, and A. Basu, "Enhancement of cisplatin sensitivity of cisplatin-resistant human cervical carcinoma cells by bryostatin 1," *Clinical Cancer Research*, vol. 11, no. 18, pp. 6730–6737, 2005.
- [147] T. Geiger, M. Müller, N. M. Dean, and D. Fabbro, "Antitumor activity of a PKC- $\alpha$  antisense oligonucleotide in combination with standard chemotherapeutic agents against various human tumors transplanted into nude mice," *Anti-Cancer Drug Design*, vol. 13, no. 1, pp. 35–45, 1998.
- [148] G. Tortora and F. Ciardiello, "Antisense strategies targeting protein kinase C: preclinical and clinical development," *Seminars in Oncology*, vol. 30, no. 4, pp. 26–31, 2003.
- [149] S. C. Righetti, P. Perego, N. Carenini et al., "Molecular alterations of cells resistant to platinum drugs: role of PKC $\alpha$ ," *Biochimica et Biophysica Acta*, vol. 1763, no. 1, pp. 93–100, 2006.
- [150] K.-W. Lee, G. K. Sang, H.-P. Kim et al., "Enzastaurin, a protein kinase C $\beta$  inhibitor, suppresses signaling through the ribosomal S6 kinase and bad pathways and induces apoptosis in human gastric cancer cells," *Cancer Research*, vol. 68, no. 6, pp. 1916–1926, 2008.
- [151] T. Ghayur, M. Hugunin, R. V. Talanian et al., "Proteolytic activation of protein kinase C  $\delta$  by an ICE/CED 3-like protease induces characteristics of apoptosis," *Journal of Experimental Medicine*, vol. 184, no. 6, pp. 2399–2404, 1996.
- [152] E. Segal-Bendirdjian and A. Jacquemin-Sablon, "Cisplatin resistance in a murine leukemia cell line is associated with a defective apoptotic process," *Experimental Cell Research*, vol. 218, no. 1, pp. 201–212, 1995.
- [153] J. Huang, S. Mohanty, and A. Basu, "Cisplatin resistance is associated with deregulation in protein kinase C- $\delta$ ," *Biochemical and Biophysical Research Communications*, vol. 316, no. 4, pp. 1002–1008, 2004.
- [154] A. Basu and G. R. Akkaraju, "Regulation of caspase activation and cis-diamminedichloroplatinum(II)-induced cell death by protein kinase C," *Biochemistry*, vol. 38, no. 14, pp. 4245–4251, 1999.
- [155] A. Basu, M. D. Woolard, and C. L. Johnson, "Involvement of protein kinase C- $\delta$  in DNA damage-induced apoptosis," *Cell Death and Differentiation*, vol. 8, no. 9, pp. 899–908, 2001.
- [156] A. Basu, B. Adkins, and C. Basu, "Down-regulation of caspase-2 by rottlerin via protein kinase C- $\delta$ -independent pathway," *Cancer Research*, vol. 68, no. 8, pp. 2795–2802, 2008.
- [157] Y. Iioka, K. Mishima, N. Azuma et al., "Overexpression of protein kinase C $\delta$  enhances cisplatin-induced cytotoxicity correlated with p53 in gastric cancer cell line," *Pathobiology*, vol. 72, no. 3, pp. 152–159, 2005.
- [158] S. D. Persaud, V. Hoang, J. Huang, and A. Basu, "Involvement of proteolytic activation of PKC $\delta$  in cisplatin-induced apoptosis in human small cell lung cancer H69 cells," *International Journal of Oncology*, vol. 27, no. 1, pp. 149–154, 2005.
- [159] A. Muscella, L. Urso, N. Calabriso et al., "Anti-apoptotic effects of protein kinase C- $\delta$  and c-fos in cisplatin-treated thyroid cells," *British Journal of Pharmacology*, vol. 156, no. 5, pp. 751–763, 2009.
- [160] A. Basu and J. S. Cline, "Oncogenic transformation alters cisplatin-induced apoptosis in rat embryo fibroblasts," *International Journal of Cancer*, vol. 63, no. 4, pp. 597–603, 1995.
- [161] L. Zhang, J. Huang, N. Yang et al., "Integrative genomic analysis of protein kinase C (PKC) family identifies PKC $\epsilon$  as a biomarker and potential oncogene in ovarian carcinoma," *Cancer Research*, vol. 66, no. 9, pp. 4627–4635, 2006.
- [162] R. M. Baldwin, M. Garratt-Lalonde, D. A. E. Parolin, P. M. Krzyzanowski, M. A. Andrade, and I. A. J. Lorimer, "Protection of glioblastoma cells from cisplatin cytotoxicity via protein kinase C $\epsilon$ -mediated attenuation of p38 MAP kinase signaling," *Oncogene*, vol. 25, no. 20, pp. 2909–2919, 2006.
- [163] L. Urso, A. Muscella, N. Calabriso et al., "Effects of cisplatin on matrix metalloproteinase-2 in transformed thyroid cells," *Biochemical Pharmacology*, vol. 79, no. 6, pp. 810–816, 2010.
- [164] L. Chang and M. Karin, "Mammalian MAP kinase signalling cascades," *Nature*, vol. 410, no. 6824, pp. 37–40, 2001.
- [165] G. L. Johnson and R. Lapadat, "Mitogen-activated protein kinase pathways mediated by ERK, JNK, and p38 protein kinases," *Science*, vol. 298, no. 5600, pp. 1911–1912, 2002.
- [166] C. J. Marshall, "Specificity of receptor tyrosine kinase signaling: transient versus sustained extracellular signal-regulated kinase activation," *Cell*, vol. 80, no. 2, pp. 179–185, 1995.
- [167] M. K. S. Tang, H. Y. Zhou, J. W. P. Yam, and A. S. T. Wong, "c-Met overexpression contributes to the acquired apoptotic resistance of nonadherent ovarian cancer cells through a cross talk mediated by phosphatidylinositol 3-kinase and extracellular signal-regulated kinase 1/2," *Neoplasia*, vol. 12, no. 2, pp. 128–138, 2010.
- [168] X. Wang, J. L. Martindale, and N. J. Holbrook, "Requirement for ERK activation in cisplatin-induced apoptosis," *Journal of Biological Chemistry*, vol. 275, no. 50, pp. 39435–39443, 2000.
- [169] P. Y. Yeh, S.-E. Chuang, K.-H. Yeh, Y. C. Song, C.-K. Ea, and A.-L. Cheng, "Increase of the resistance of human cervical carcinoma cells to cisplatin by inhibition of the MEK to ERK signaling pathway partly via enhancement of anticancer drug-induced NF $\kappa$ B activation," *Biochemical Pharmacology*, vol. 63, no. 8, pp. 1423–1430, 2002.
- [170] G. Nowak, "Protein kinase C- $\alpha$  and ERK1/2 mediate mitochondrial dysfunction, decreases in active Na<sup>+</sup> transport,

- and cisplatin-induced apoptosis in renal cells," *Journal of Biological Chemistry*, vol. 277, no. 45, pp. 43377–43388, 2002.
- [171] J. Hayakawa, M. Ohmichi, H. Kurachi et al., "Inhibition of extracellular signal-regulated protein kinase or c-Jun N-terminal protein kinase cascade, differentially activated by cisplatin, sensitizes human ovarian cancer cell line," *Journal of Biological Chemistry*, vol. 274, no. 44, pp. 31648–31654, 1999.
- [172] D. L. Persons, E. M. Yazlovitskaya, W. Cui, and J. C. Pelling, "Cisplatin-induced activation of mitogen-activated protein kinases in ovarian carcinoma cells: Inhibition of extracellular signal-regulated kinase activity increases sensitivity to cisplatin," *Clinical Cancer Research*, vol. 5, no. 5, pp. 1007–1014, 1999.
- [173] A. Basu and H. Tu, "Activation of ERK during DNA damage-induced apoptosis involves protein kinase C $\delta$ ," *Biochemical and Biophysical Research Communications*, vol. 334, no. 4, pp. 1068–1073, 2005.
- [174] J. Hayakawa, M. Ohmichi, H. Kurachi et al., "Inhibition of BAD phosphorylation either at serine 112 via extracellular signal-regulated protein kinase cascade or at serine 136 via Akt cascade sensitizes human ovarian cancer cells to cisplatin," *Cancer Research*, vol. 60, no. 21, pp. 5988–5994, 2000.
- [175] A. Mandic, K. Viktorsson, T. Heiden, J. Hansson, and M. C. Shoshan, "The MEK1 inhibitor PD98059 sensitizes C8161 melanoma cells to cisplatin-induced apoptosis," *Melanoma Research*, vol. 11, no. 1, pp. 11–19, 2001.
- [176] P. Y. Yeh, K.-H. Yeh, S.-E. Chuang, Y. C. Song, and A.-L. Cheng, "Suppression of MEK/ERK signaling pathway enhances cisplatin-induced NF- $\kappa$ B activation by protein phosphatase 4-mediated NF- $\kappa$ B p 65 Thr dephosphorylation," *Journal of Biological Chemistry*, vol. 279, no. 25, pp. 26143–26148, 2004.
- [177] D. Amrán, P. Sancho, C. Fernández et al., "Pharmacological inhibitors of extracellular signal-regulated protein kinases attenuate the apoptotic action of cisplatin in human myeloid leukemia cells via glutathione-independent reduction in intracellular drug accumulation," *Biochimica et Biophysica Acta*, vol. 1743, no. 3, pp. 269–279, 2005.
- [178] Y. Zhang, X. Qu, W. Jing et al., "GSTP1 determines cisplatin cytotoxicity in gastric adenocarcinoma MGC803 cells: regulation by promoter methylation and extracellular regulated kinase signaling," *Anti-Cancer Drugs*, vol. 20, no. 3, pp. 208–214, 2009.
- [179] S. Lee, S. Yoon, and D.-H. Kim, "A high nuclear basal level of ERK2 phosphorylation contributes to the resistance of cisplatin-resistant human ovarian cancer cells," *Gynecologic Oncology*, vol. 104, no. 2, pp. 338–344, 2007.
- [180] S. Basu, R. Harfouche, S. Soni, G. Chimote, R. A. Mashelkar, and S. Sengupta, "Nanoparticle-mediated targeting of MAPK signaling predisposes tumor to chemotherapy," *Proceedings of the National Academy of Sciences of the United States of America*, vol. 106, no. 19, pp. 7957–7961, 2009.
- [181] R. D. DeHaan, E. M. Yazlovitskaya, and D. L. Persons, "Regulation of p53 target gene expression by cisplatin-induced extracellular signal-regulated kinase," *Cancer Chemotherapy and Pharmacology*, vol. 48, no. 5, pp. 383–388, 2001.
- [182] T. Nishioka, J. Guo, D. Yamamoto, L. Chen, P. Huppi, and C. Y. Chen, "Nicotine, through upregulating pro-survival signaling, cooperates with NNK to promote transformation," *Journal of Cellular Biochemistry*, vol. 109, no. 1, pp. 152–161, 2010.
- [183] W. Woessmann, X. Chen, and A. Borkhardt, "Ras-mediated activation of ERK by cisplatin induces cell death independently of p53 in osteosarcoma and neuroblastoma cell lines," *Cancer Chemotherapy and Pharmacology*, vol. 50, no. 5, pp. 397–404, 2002.
- [184] S. Schweyer, A. Soruri, O. Meschter et al., "Cisplatin-induced apoptosis in human malignant testicular germ cell lines depends on MEK/ERK activation," *British Journal of Cancer*, vol. 91, no. 3, pp. 589–598, 2004.
- [185] B. K. Choi, C. H. Choi, H. L. Oh, and Y. K. Kim, "Role of ERK activation in cisplatin-induced apoptosis in A172 human glioma cells," *NeuroToxicology*, vol. 25, no. 6, pp. 915–924, 2004.
- [186] Y. K. Kim, H. J. Kim, C. H. Kwon et al., "Role of ERK activation in cisplatin-induced apoptosis in OK renal epithelial cells," *Journal of Applied Toxicology*, vol. 25, no. 5, pp. 374–382, 2005.
- [187] L. F. Sheu, Z. H. Young, W. C. Lee, Y. F. Chen, W. Y. Kao, and A. Chen, "STI571 sensitizes nasopharyngeal carcinoma cells to cisplatin: sustained activation of ERK with improved growth inhibition," *International Journal of Oncology*, vol. 30, no. 2, pp. 403–411, 2007.
- [188] R. Dhar and A. Basu, "Constitutive activation of p70 S6 kinase is associated with intrinsic resistance to cisplatin," *International Journal of Oncology*, vol. 32, no. 5, pp. 1133–1137, 2008.
- [189] S. A. Park, H. J. Park, B. I. Lee, Y. H. Ahn, S. U. Kim, and K. S. Choi, "Bcl-2 blocks cisplatin-induced apoptosis by suppression of ERK-mediated p53 accumulation in B104 cells," *Molecular Brain Research*, vol. 93, no. 1, pp. 18–26, 2001.
- [190] S.-K. Jo, W. Y. Cho, S. A. Sung, H. K. Kim, and N. H. Won, "MEK inhibitor, U0126, attenuates cisplatin-induced renal injury by decreasing inflammation and apoptosis," *Kidney International*, vol. 67, no. 2, pp. 458–466, 2005.
- [191] B. W. Zanke, K. Boudreau, E. Rubie et al., "The stress-activated protein kinase pathway mediates cell death following injury induced by cis-platinum, UV irradiation or heat," *Current Biology*, vol. 6, no. 5, pp. 606–613, 1996.
- [192] I. Sánchez-Perez, J. R. Murguía, and R. Perona, "Cisplatin induces a persistent activation of JNK that is related to cell death," *Oncogene*, vol. 16, no. 4, pp. 533–540, 1998.
- [193] E. V. Jones, M. J. Dickman, and A. J. Whitmarsh, "Regulation of p73-mediated apoptosis by c-Jun N-terminal kinase," *Biochemical Journal*, vol. 405, no. 3, pp. 617–623, 2007.
- [194] X. Zhang, D. Sanmun, L. Hu, B. Fadeel, and I. Ernberg, "Epstein-Barr virus-encoded LMP1 promotes cisplatin-induced caspase activation through JNK and NF- $\kappa$ B signaling pathways," *Biochemical and Biophysical Research Communications*, vol. 360, no. 1, pp. 263–268, 2007.
- [195] F. Zhang, G. Suarez, J. Sha, J. C. Sierra, J. W. Peterson, and A. K. Chopra, "Phospholipase A2-activating protein (PLAA) enhances cisplatin-induced apoptosis in HeLa cells," *Cellular Signalling*, vol. 21, no. 7, pp. 1085–1099, 2009.
- [196] W.-L. Zhuo, Y. Wang, X.-L. Zhuo, Y.-S. Zhang, and Z.-T. Chen, "Short interfering RNA directed against TWIST, a novel zinc finger transcription factor, increases A549 cell sensitivity to cisplatin via MAPK/mitochondrial pathway," *Biochemical and Biophysical Research Communications*, vol. 369, no. 4, pp. 1098–1102, 2008.
- [197] W. Zhuo, Y. Wang, X. Zhuo, Y. Zhang, X. Ao, and Z. Chen, "Knockdown of Snail, a novel zinc finger transcription factor, via RNA interference increases A549 cell sensitivity to

- cisplatin via JNK/mitochondrial pathway," *Lung Cancer*, vol. 62, no. 1, pp. 8–14, 2008.
- [198] Y. Wang, Q.-Y. He, S.-W. Tsao, Y.-H. Cheung, A. Wong, and J.-F. Chiu, "Cytokeratin 8 silencing in human nasopharyngeal carcinoma cells leads to cisplatin sensitization," *Cancer Letters*, vol. 265, no. 2, pp. 188–196, 2008.
- [199] A. Pataer, S. G. Swisher, J. A. Roth, C. J. Logothetis, and P. Corn, "Inhibition of RNA-dependent protein kinase (PKR) leads to cancer cell death and increases chemosensitivity," *Cancer Biology and Therapy*, vol. 8, no. 3, pp. 245–252, 2009.
- [200] O. Potapova, A. Haghghi, F. Bost et al., "The Jun kinase/stress-activated protein kinase pathway functions to regulate DNA repair and inhibition of the pathway sensitizes tumor cells to cisplatin," *Journal of Biological Chemistry*, vol. 272, no. 22, pp. 14041–14044, 1997.
- [201] H. D. C. Francescato, R. S. Costa, F. B. Júnior, and T. M. Coimbra, "Effect of JNK inhibition on cisplatin-induced renal damage," *Nephrology Dialysis Transplantation*, vol. 22, no. 8, pp. 2138–2148, 2007.
- [202] B. Zhang, G. Ramesh, S. Uematsu, S. Akira, and W. B. Reeves, "TLR4 signaling mediates inflammation and tissue injury in nephrotoxicity," *Journal of the American Society of Nephrology*, vol. 19, no. 5, pp. 923–932, 2008.
- [203] J. H. Losa, C. P. Cobo, J. G. Viniegra, V. J. Sánchez-Arevalo Lobo, S. Ramón y Cajal, and R. Sánchez-Prieto, "Role of the p38 MAPK pathway in cisplatin-based therapy," *Oncogene*, vol. 22, no. 26, pp. 3998–4006, 2003.
- [204] A. Mansouri, L. D. Ridgway, A. L. Korapati et al., "Sustained activation of JNK/p38 MAPK pathways in response to cisplatin leads to Fas ligand induction and cell death in ovarian carcinoma cells," *Journal of Biological Chemistry*, vol. 278, no. 21, pp. 19245–19256, 2003.
- [205] Z.-Q. Yuan, R. I. Feldman, G. E. Sussman, D. Coppola, S. V. Nicosia, and J. Q. Cheng, "AKT2 inhibition of cisplatin-induced JNK/p38 and bax activation by phosphorylation of ASK1. Implication of AKT2 in chemoresistance," *Journal of Biological Chemistry*, vol. 278, no. 26, pp. 23432–23440, 2003.
- [206] N. M. Weir, K. Selvendiran, V. K. Kutala et al., "Curcumin induces G2/M arrest and apoptosis in cisplatin-resistant human ovarian cancer cells by modulating Akt and p38 MAPK," *Cancer Biology and Therapy*, vol. 6, no. 2, pp. 178–184, 2007.
- [207] S. E. Winograd-Katz and A. Levitzki, "Cisplatin induces PKB/Akt activation and p38MAPK phosphorylation of the EGF receptor," *Oncogene*, vol. 25, no. 56, pp. 7381–7390, 2006.
- [208] A. Cuadrado, V. Lafarga, P. C. F. Cheung et al., "A new p38 MAP kinase-regulated transcriptional coactivator that stimulates p53-dependent apoptosis," *EMBO Journal*, vol. 26, no. 8, pp. 2115–2126, 2007.
- [209] H. D. C. Francescato, R. S. Costa, C. G. A. da Silva, and T. M. Coimbra, "Treatment with a p38 MAPK inhibitor attenuates cisplatin nephrotoxicity starting after the beginning of renal damage," *Life Sciences*, vol. 84, no. 17–18, pp. 590–597, 2009.
- [210] G. Ramesh and W. B. Reeves, "p38 MAP kinase inhibition ameliorates cisplatin nephrotoxicity in mice," *American Journal of Physiology*, vol. 289, no. 1, pp. F166–F174, 2005.
- [211] D. P. Brazil and B. A. Hemmings, "Ten years of protein kinase B signalling: a hard Akt to follow," *Trends in Biochemical Sciences*, vol. 26, no. 11, pp. 657–664, 2001.
- [212] T. Ohta, M. Ohmichi, T. Hayasaka et al., "Inhibition of phosphatidylinositol 3-kinase increases efficacy of cisplatin in in vivo ovarian cancer models," *Endocrinology*, vol. 147, no. 4, pp. 1761–1769, 2006.
- [213] V. Gagnon, I. Mathieu, E. Sexton, K. Leblanc, and E. Asselin, "AKT involvement in cisplatin chemoresistance of human uterine cancer cells," *Gynecologic Oncology*, vol. 94, no. 3, pp. 785–795, 2004.
- [214] L. L. Belyanskaya, S. Hopkins-Donaldson, S. Kurtz et al., "Cisplatin activates Akt in small cell lung cancer cells and attenuates apoptosis by survivin upregulation," *International Journal of Cancer*, vol. 117, no. 5, pp. 755–763, 2005.
- [215] M. W. Lee, D. S. Kim, N. Y. Min, and H. T. Kim, "Akt1 inhibition by RNA interference sensitizes human non-small cell lung cancer cells to cisplatin," *International Journal of Cancer*, vol. 122, no. 10, pp. 2380–2384, 2008.
- [216] W. Hartmann, J. Küchler, A. Koch et al., "Activation of phosphatidylinositol-3'-kinase/AKT signaling is essential in hepatoblastoma survival," *Clinical Cancer Research*, vol. 15, no. 14, pp. 4538–4545, 2009.
- [217] E. Asselin, G. B. Mills, and B. K. Tsang, "XIAP regulates Akt activity and caspase-3-dependent cleavage during cisplatin-induced apoptosis in human ovarian epithelial cancer cells," *Cancer Research*, vol. 61, no. 5, pp. 1862–1868, 2001.
- [218] H. C. Dan, M. Sun, S. Kaneko et al., "Akt phosphorylation and stabilization of X-linked inhibitor of apoptosis protein (XIAP)," *Journal of Biological Chemistry*, vol. 279, no. 7, pp. 5405–5412, 2004.
- [219] V. Gagnon, C. Van Themsche, S. Turner, V. Leblanc, and E. Asselin, "Akt and XIAP regulate the sensitivity of human uterine cancer cells to cisplatin, doxorubicin and taxol," *Apoptosis*, vol. 13, no. 2, pp. 259–271, 2008.
- [220] Y. Zhang and X. Shen, "Heat shock protein 27 protects L929 cells from cisplatin-induced apoptosis by enhancing Akt activation and abating suppression of thioredoxin reductase activity," *Clinical Cancer Research*, vol. 13, no. 10, pp. 2855–2864, 2007.
- [221] M. Fraser, B. M. Leung, X. Yan, H. C. Dan, J. Q. Cheng, and B. K. Tsang, "p53 is a determinant of X-linked inhibitor of apoptosis protein/Akt-mediated chemoresistance in human ovarian cancer cells," *Cancer Research*, vol. 63, no. 21, pp. 7081–7088, 2003.
- [222] L.-Z. Liu, X.-D. Zhou, G. Qian, X. Shi, J. Fang, and B.-H. Jiang, "AKT1 amplification regulates cisplatin resistance in human lung cancer cells through the mammalian target of rapamycin/p70s6K1 pathway," *Cancer Research*, vol. 67, no. 13, pp. 6325–6332, 2007.
- [223] M. R. Abedini, E. J. Muller, R. Bergeron, D. A. Gray, and B. K. Tsang, "Akt promotes chemoresistance in human ovarian cancer cells by modulating cisplatin-induced, p53-dependent ubiquitination of FLICE-like inhibitory protein," *Oncogene*, vol. 29, no. 1, pp. 11–25, 2010.
- [224] S. Claerhout, L. Verschooten, S. Van Kelst, et al., "Concomitant inhibition of AKT and autophagy is required for efficient cisplatin-induced apoptosis of metastatic skin carcinoma," *International Journal of Cancer*, 2010.
- [225] H. Yang, W. Kong, L. He et al., "MicroRNA expression profiling in human ovarian cancer: miR-214 induces cell survival and cisplatin resistance by targeting PTEN," *Cancer Research*, vol. 68, no. 2, pp. 425–433, 2008.

## Research Article

# Intracellular DNA Damage by Lysine-Acetylene Conjugates

**Wang-Yong Yang, Qiang Cao, Catherine Callahan, Catalina Galvis, Qing-Xiang Sang, and Igor V. Alabugin**

*Department of Chemistry and Biochemistry, Florida State University, Tallahassee, FL 32306-4390, USA*

Correspondence should be addressed to Igor V. Alabugin, alabugin@chem.fsu.edu

Received 25 April 2010; Revised 26 June 2010; Accepted 6 July 2010

Academic Editor: Ashis Basu

Copyright © 2010 Wang-Yong Yang et al. This is an open access article distributed under the Creative Commons Attribution License, which permits unrestricted use, distribution, and reproduction in any medium, provided the original work is properly cited.

Previously, we reported the design and properties of alkyne C-lysine conjugates, a powerful and tunable family of DNA cleaving reagents. We also reported that, upon photoactivation, these molecules are capable of inducing cancer cells death. To prove that the cell death stems from DNA cleavage by the conjugates, we investigated intracellular DNA damage induced by these molecules in LNCap cancer cells using single cell gel electrophoresis (SCGE) assays. The observation of highly efficient DNA damage confirmed that lysine acetylene conjugate is capable of cleaving the densely compacted intracellular DNA. This result provides a key mechanistic link between efficient DNA cleavage and cytotoxicity towards cancer cells for this family of light-activated anticancer agents.

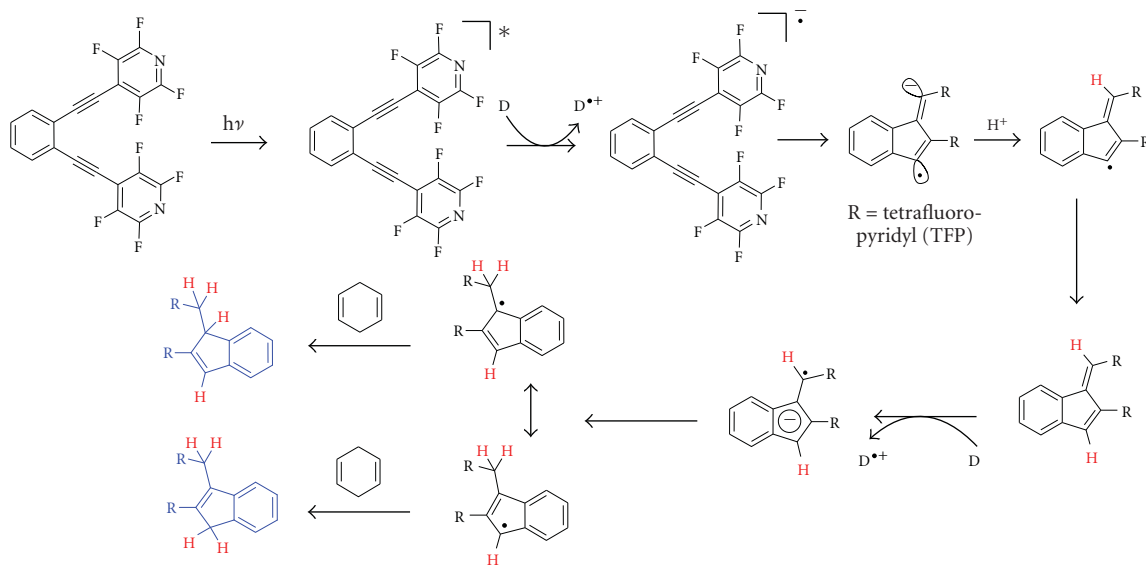
## 1. Introduction

Because double stranded (ds) DNA cleavage is much harder to repair than single stranded (ss) DNA cleavage, ds damage is particularly efficient in inducing self-programmed cell death or apoptosis [1]. A particularly striking example of this efficiency is provided by natural enediyne antibiotics [2]. These compounds, often hailed as the most potent family of anticancer agents [3], produce cleavage of both strands of DNA duplex via two hydrogen abstractions from two opposite strands of DNA backbone by a reactive biradical, *p*-benzyne, generated from the enediyne core via a process, called the Bergman cyclization [4–6]. However, natural enediynes not only lack selectivity towards cancer cells, but also do not cause the ds cleavage with 100% efficiency. Even the best of them, calicheamicin leads to only 25% cleavage [7]. Thus, design of compounds which are capable of more efficient ds DNA cleavage and combine this efficiency with selectivity towards cancer cells remains the focal point of the anticancer therapeutic agents targeting DNA.

We have found that DNA damaging potential of enediynes can be increased if their reactivity is tuned towards C1–C5 photocyclizations, a new reaction discovered in our

lab which leads to incorporation of four rather than two hydrogen atoms from the environment [8, 9].

Because C1–C5 cyclization proceeds under photochemical conditions for thermal C1–C5 cyclization, see [10, 11], it takes advantage of the high degree of spatial and temporal controls over reactivity inherent to the photochemical activation. The use of tissue-penetrating light allows for efficient, and selective, spatial and temporal control over prodrug activation as light can be delivered directly to the tumor when it contains a high concentration of the prodrug. Skin cancer is the most obvious target for this therapy and, in 2006, the UK National Institute of Health and Clinical Excellence (NICE) recommended PDT for basal cell carcinoma. However, PDT can be also used to treat tumors on the lining of internal organs or cavities. Other tumors can be targeted with low-energy tissue penetrating photons, especially if the three-dimensional control of activation is provided by the two-photon excitation mode. For two photon excitation of enediynes, see [12–14]. In addition, this radical-anionic C1–C5 cyclization of enediynes is triggered by photoinduced electron transfer (PET). This mechanistic feature increases cellular selectivity because activation is possible only in the direct vicinity of a suitable electron



SCHEME 1: C1–C5 photocyclization of bis-TFP-enediyne and proposed mechanism in the proximity to DNA (four abstracted hydrogens are shown in red, TFP = tetrafluoropyridine).

donor such as DNA to occur. In the absence of such a donor, TFP-substituted enediynes (Scheme 1) are unreactive, both thermally and photochemically.

We have also found that related TFP-substituted monoacetylenes are capable of photochemical alkylation of electron rich  $\pi$ -systems [15–17] and investigated whether this reaction can be also used for controlled DNA-modification. A priori, efficient DNA-cleavage by monoalkynes incapable of the Bergman or C1–C5 cyclizations can involve several possible mechanisms like base alkylation, hydrogen abstraction, generation of reactive oxygen species as well as PET.

In order to increase solubility of TFP-warheads in water and their affinity to DNA, we combined them with lysine via carboxyl moiety of the amino acid, Figure 1 [18].

Importantly, this mode of attachment leaves both amino groups of lysine available for an acid-base reaction which converts them into cationic ammonium groups. We found that DNA-damaging ability of such hybrid molecules can be fine-tuned in the narrow range of physiological pH conditions which results in a dramatic increase in reactivity at the lower pH of hypoxic tumor cells [19]. Less basic  $\alpha$ -amino group is protonated at the lower pH than 7 and this protonation not only prevents quenching the excited state of the chromophore but also provides tighter binding to negatively charged DNA. Remarkably, the change in reactivity occurs at a relatively narrow and predefined pH point ( $\sim$ pH 6). These DNA-photocleavers provide the DNA cleavage ratios of up to the 1 : 2 ds : ss at pH 5.5 at concentrations and irradiation times where almost no ds cleavage is observed at the pH of healthy cells. This dramatic increase of ds DNA cleavage at the lower pH renders these molecules more efficient ds DNA cleavers than calicheamicin under the conditions suitable for selective targeting of acidic cancer tissues (Figure 2(a)). We also found that the C-lysine conjugates bind selectively

to nicks and gaps in a DNA duplex and, upon photochemical activation, transform the easily repairable ss-DNA damage into much more therapeutically important ds-DNA damage [20] (Figure 2(b)).

The medicinal potential of these molecules has been illustrated by a >90% LNCap cancer cell death induced by photochemically activated TFP-acetylene-lysine conjugate **3** in one treatment at concentrations as low as 10 nM. Notably, at these concentrations, toxicity without light is negligible. Similar increases in reactivity upon activation with light were observed in parallel experiments with UMRC3, UMRC6, and 786-O cancer cell lines [19].

In summary, our previous work led to the development of a family of powerful and tunable DNA cleaving reagents which have been shown to cleave both plasmid DNA and DNA oligomers outside of cells [15, 18]. We have also proven that these reagents can induce cancer cells death at the low concentrations. However, our previous work offered no evidence for DNA-damage by TFP-enediynes and acetylenes inside of cells. Such evidence is important because cell death can result from mechanisms other than DNA cleavage and because DNA-cleavage of intracellular DNA should be more difficult since this DNA is compactly organized around histone proteins. The aim of this work is to test the efficiency of our light-activated ds-DNA-cleavers towards intracellular DNA using single cell gel electrophoresis assay which can measure DNA damage in individual eukaryote cells [21–25]. This assay has been used as a standard technique for evaluation of DNA damage/repair, biomonitoring, and genotoxicity testing [26–33]. The alkaline SCGE assay detects both ss and ds DNA damages. The cleaved DNA fragments are able to migrate out of the cell under an electric field after lysis and alkali treatments while undamaged DNA moves slower and remains with the confines of the nucleoid.

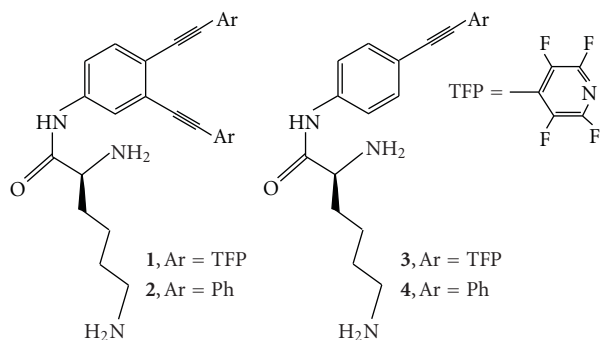


FIGURE 1: Structures of C-lysine conjugate.

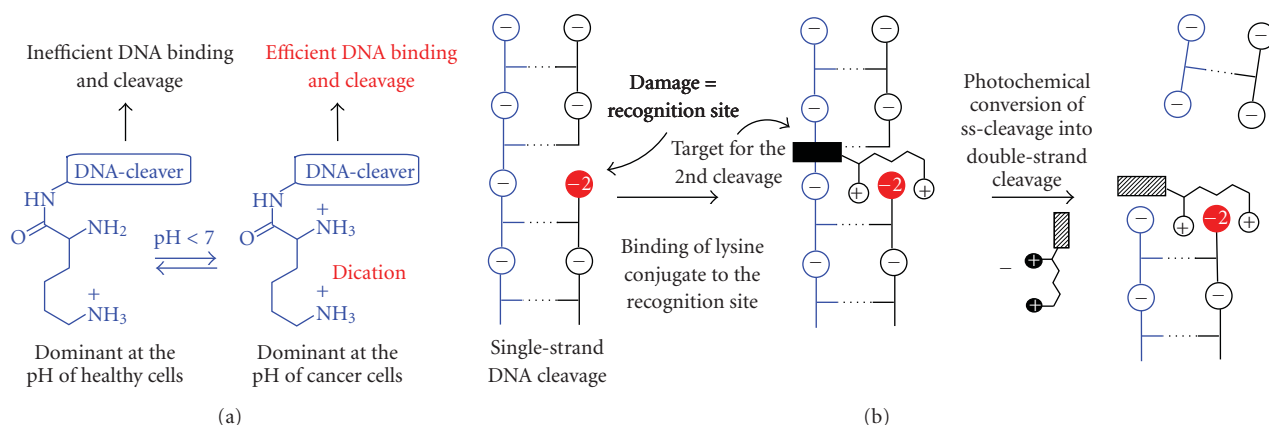


FIGURE 2: (a) Design of pH-dependent DNA-cleavers based on different stages of protonation of the lysine side chain, (b) photochemical conversion of ss-DNA cleavage into more therapeutically important ds-DNA cleavage through lysine-phosphate monoester recognition of the initial damage site.

## 2. Materials and Methods

**2.1. General Information.** Reagent kit for single cell gel electrophoresis assay kit, CometAssay, and control cells containing different levels of DNA damage, CometAssay Control Cell, were purchased from Trevigen, Inc. The CC0 sample corresponds to cells with undamaged DNA whereas CC1, CC2, and CC3 have different levels of DNA-cleavage induced with Etoposide [34]. Miligel FisherBiotech Horizontal Electrophoresis System was used for electrophoresis. Olympus BX61 microscope attached with the DP71 color digital camera was used to take fluorescence images of SCGE assay. The images were qualified by Comet Score 1.5 software (Tritec). Tail moment, the ratio of tail length to head diameter (L/H), DNA percentage in tail, and tail length were used to estimate DNA damage. The tail moment has been regarded as an appropriate index of induced DNA damage by computerized image analysis. It represents both the amount of damaged DNA and the distance of migration by a single number. The tail moment was calculated by multiplying the percentage of DNA in the tail by the tail length; see [35].

**2.2. Preparation of LNCap Cells and Their Treatment with Conjugate 3.** LNCap cells (P.35) were plated in 6 (100 mm) plates at density of 250,000 cells/well and were maintained in

RPMI 1640 medium supplemented with 10% FBS, sodium bicarbonate (2 g/L). When they reach 70% confluence, compound 3 was dissolved in serum-free RPMI 1640 medium supplemented with sodium bicarbonate (2 g/L). After the RPMI 1640, medium containing the compound 3 (0, 10, and 50  $\mu$ M) were added to the cells and the cells were placed in the incubator for 4 hours. The cells were exposed to UV with cover removed for maximum exposure for 10 minutes and were trypsinized and counted. Solutions in ice cold 1 $\times$  PBS ( $\text{Ca}^{2+}$  and  $\text{Mg}^{2+}$  free), with  $1 \times 10^5$  cells/mL, were prepared based on CometAssay instruction from Trevigen, Inc.

**2.3. Alkaline Single Cell Gel Electrophoresis Assay.** LMAgarose was melt in boiling water bath for 5 minutes and placed in 37 $^\circ$ C water bath for at least 20 minutes to cool. Cells at  $1 \times 10^5$ /mL were combined with molten LMAgarose at a ratio of 1 : 10 (v/v) and 50  $\mu$ L of the mixture was transferred on CometSlides. The slides were placed at 4 $^\circ$ C in the dark for 30 minutes and they were immersed in prechilled lysis solution. After 30-minute immersion at 4 $^\circ$ C, the slides were immersed in alkaline solution prepared freshly with NaOH (0.6 g), 200 mM EDTA (250  $\mu$ L), and dH<sub>2</sub>O (49.75 mL) for 20 minutes at room temperature, in the dark. Then, the slides were removed from alkaline solution and washed by immersing in 1 $\times$  TBE buffer for 5 minutes twice. After

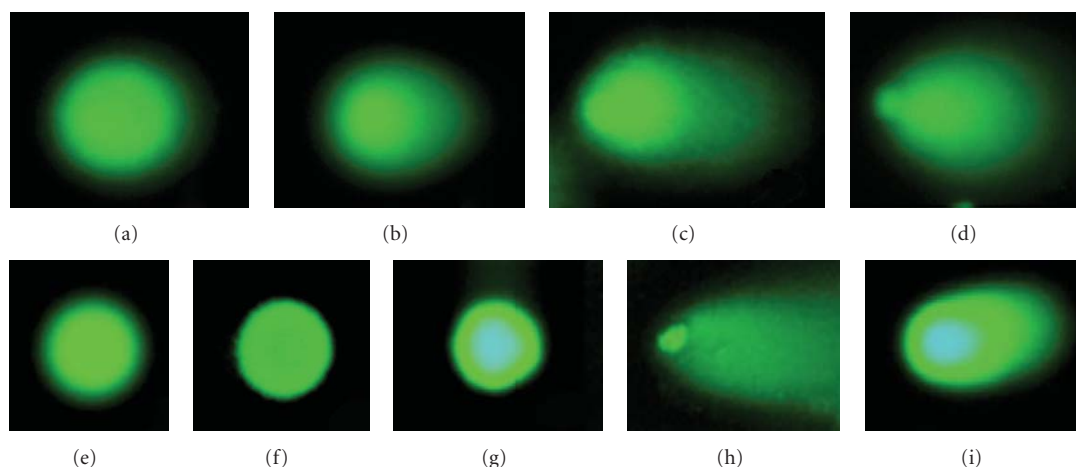


FIGURE 3: Images of SCGE assays. Controls: (a) Undamaged control cell, (b)–(d) Control cells with variable amount of DNA damage. LNCap Cells: (e) No compound + No UV; (f) No compound + UV; (g) **3** (50  $\mu$ M) + No UV; (h) **3** (50  $\mu$ M) + UV; (i) **3** (10  $\mu$ M) + UV. All UV irradiations were carried out for 10 minutes.

TABLE 1: Qualified data from SCGE assays.

Exp.	Tail moment	L/H	%DNA in tail	Tail length (px)
(a)	0	0	$0.3 \pm 0.3$	0
(b)	$9.9 \pm 0.9$	$0.4 \pm 0.1$	$33.2 \pm 2.9$	$29.7 \pm 1.5$
(c)	$22.1 \pm 2.0$	$0.8 \pm 0.1$	$47.0 \pm 5.5$	$47.7 \pm 9.3$
(d)	$107.3 \pm 7.8$	$6.8 \pm 1.4$	$96.8 \pm 1.3$	$110.8 \pm 6.9$
(e)	0	0	$0.9 \pm 1.2$	$0.2 \pm 0.4$
(f)	$0.1 \pm 0.1$	0	$2.0 \pm 2.3$	$2.2 \pm 2.0$
(g)	0	0	1.3	0
(h)	$155.3 \pm 62.6$	$4.6 \pm 2.0$	$92.0 \pm 4.1$	$167.0 \pm 62.2$
(i)	$26.1 \pm 10.1$	$0.7 \pm 0.1$	$41.4 \pm 9.0$	$61.2 \pm 12.8$

adding  $1\times$  TBE buffer not to exceed 0.5 cm above slides in electrophoresis tank, the voltage at 1 volt per cm was applied for 10 minutes. The slides were immersed in  $dH_2O$  twice for 10 minutes, then in 70% ethanol for 5 minutes. The samples were dried at  $\leq 45^\circ C$  for 15 minutes and 100  $\mu$ L of diluted SYBR Green I was placed on the gels and the slides were stored at refrigerator. After 5 minutes, excess SYBR solution was removed by gentle tapping and the slides were completely dried at room temperature in the dark. The fluorescence images were taken by epifluorescence microscopy.

### 3. Results and Discussion

The control SCGE assay results for undamaged cells (CC0) and commercially obtained cells with variable amount of DNA damage (CC1–3) are summarized in the top part of Figure 3 (entries (a)–(d)). As expected, while SCGE assay with healthy cells showed no tails indicative of DNA damage, the assays with the damaged cells produced characteristic tails, the size of which correlates with the extent of DNA damage in these cells. Qualified data of the assays are given in Table 1. With the pretreated control cells (Table 1, (b)–(d)),

33, 47, and 98% of DNA were detected in tails, respectively. Tail moment values are also consistent with different levels of DNA damage.

After confirming that assay conditions work in the control cells, we proceed to investigate DNA damage induced by conjugate **3** in LNCap cancer cells. To find whether UV itself or thermal reactions of compound **3** may be responsible for the DNA cleavage in cancer, we included two control experiments with cells exposed to UV for 10 minutes in the absence of a DNA-cleaver (Figure 3(f)) and with cells treated with 50  $\mu$ M of compound **3** for 4 hours without photochemical activation (Figure 3(g)). No DNA damage is observed in the control cases. This result confirms that neither UV nor compound **3** in the dark can damage DNA under these experimental conditions. In contrast, photochemical activation of 50  $\mu$ M of compound **3** produced very efficient DNA damage (more than 90% DNA in the tail, Table 1) in individual cells (Figure 3(h)). Irradiation in the presence of 10  $\mu$ M of compound **3** also showed significant DNA damage ( $\sim 40\%$  DNA in the tail, Figure 3(i)). These results confirm that compound **3** can penetrate into the nucleus of the cancer cell and damage highly compacted DNA photochemically.

The concentrations of lysine conjugates used in our comet experiments are significantly higher than  $>0.01$  mM concentrations sufficient to cause significant photocytotoxicity to several cancer cells lines. This difference is not limited to the comet assay—our earlier experiments with pure DNA also required micromolar concentrations of the conjugate to observe the cleavage [18, 19]. The observation has two consequences. First, it suggests (somewhat surprisingly) that the efficiency of cleavage for isolated plasmid DNA and compacted cellular DNA is not drastically different, thus indicating that our compounds should accumulate in the cell nucleus rather efficiently.

Second, this observation may indicate the presence of an additional, even more efficient, mechanism for cytotoxicity which may not be based on DNA cleavage. Alternatively, it

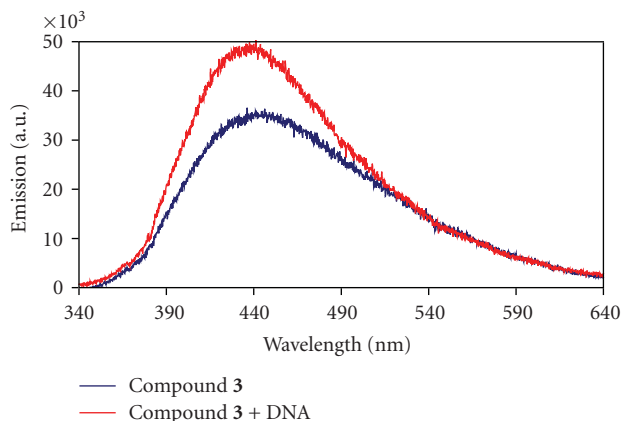


FIGURE 4: Emission spectrum of **3** ( $10\ \mu\text{M}$ ) in phosphate buffer at pH 7. Blue: without DNA, Red: with  $30\ \mu\text{M/b.p}$  of Calf thymus DNA.

may also mean that even small amount of DNA cleavage (which is not detected by the conventional, relatively insensitive assays) is still sufficient for causing apoptosis. Although we cannot distinguish between these two mechanisms at this point, this mechanistic ambiguity renders important the observation that lysine-acetylene conjugate can indeed target and damage cellular DNA.

Interestingly, the fluorescence images of cells treated with compound **3** (Figures 3(g) and 3(i)) showed blue fluorescence in the nucleus region on top of the green fluorescence from the DNA-staining dye, SYBR Green I. Because this blue fluorescence is not observed in control cells without the conjugate, the emission is likely to result either from compound **3** itself which has the maximum emission at 440 nm (Figure 4) or from one of the respective photoproducts derived from the DNA-photocleaver. This observation provides additional evidence that conjugate **3** can be uptaken into the nucleus of cancer cells. It is also interesting that there is no residual blue fluorescence in Figure 3(h), where the DNA is broken completely.

#### 4. Conclusions

SCGE assays confirm the occurrence of efficient cleavage of highly compacted *intracellular* DNA by a light-activated C-lysine acetylene conjugate. This result provides a key mechanistic link between efficient DNA cleavage and significant cytotoxicity in cell proliferation assays.

#### Acknowledgments

The authors are grateful to the National Science Foundation (CHE-0848686) and TTCP Grant from the James and Ester King Florida Biomedical Research Program to IVA, and DOD Grant W81XWH-07-1-0225 from US Congressionally Directed Medical Research Programs to QXS for partial support of this research.

#### References

- [1] M. Stanulla, J. Wang, D. S. Chervinsky, S. Thandla, and P. D. Aplan, "DNA cleavage within the MLL breakpoint cluster region is a specific event which occurs as part of higher-order chromatin fragmentation during the initial stages of apoptosis," *Molecular and Cellular Biology*, vol. 17, no. 7, pp. 4070–4079, 1997.
- [2] K. C. Nicolaou, A. L. Smith, and E. W. Yue, "Chemistry and biology of natural and designed enediynes," *Proceedings of the National Academy of Sciences of the United States of America*, vol. 90, no. 13, pp. 5881–5888, 1993.
- [3] U. Galm, M. H. Hager, S. G. Van Lanen, J. Ju, J. S. Thorson, and B. Shen, "Antitumor antibiotics: bleomycin, enediynes, and mitomycin," *Chemical Reviews*, vol. 105, no. 2, pp. 739–758, 2005.
- [4] R. R. Jones and R. G. Bergman, "*p*-Benzyne. Generation as an intermediate in a thermal isomerization reaction and trapping evidence for the 1,4-benzenediyl structure," *Journal of the American Chemical Society*, vol. 94, no. 2, pp. 660–661, 1972.
- [5] R. G. Bergman, "Reactive 1,4-dehydroaromatics," *Accounts of Chemical Research*, vol. 6, no. 1, pp. 25–31, 1973.
- [6] I. Alabugin, B. Breiner, and M. Manoharan, "Cycloaromatization reactions: the testing ground for theory and experiment," *Advances in Physical Organic Chemistry*, vol. 42, pp. 1–33, 2007.
- [7] K. Elmroth, J. Nygren, S. Mårtensson, I. H. Ismail, and O. Hammarsten, "Cleavage of cellular DNA by calicheamicin  $\gamma_1$ ," *DNA Repair*, vol. 2, no. 4, pp. 363–374, 2003.
- [8] I. V. Alabugin and S. V. Kovalenko, "C1–C5 photochemical cyclization of enediynes," *Journal of the American Chemical Society*, vol. 124, no. 31, pp. 9052–9053, 2002.
- [9] I. V. Alabugin and M. Manoharan, "Radical-anionic cyclizations of enediynes: remarkable effects of benzannulation and remote substituents on cycloaromatization reactions," *Journal of the American Chemical Society*, vol. 125, no. 15, pp. 4495–4509, 2003.
- [10] M. Prall, A. Wittkopp, and P. R. Schreiner, "Can fulvenes form from enediynes? A systematic high-level computational study on parent and benzannulated enediyne and enyne-allene cyclizations," *Journal of Physical Chemistry A*, vol. 105, no. 40, pp. 9265–9274, 2001.
- [11] C. Vavilala, N. Byrne, C. M. Kraml, D. M. Ho, and R. A. Pascal Jr., "Thermal C1–C5 diradical cyclization of enediynes," *Journal of the American Chemical Society*, vol. 130, no. 41, pp. 13549–13551, 2008.
- [12] J. F. Kauffman, J. M. Turner, I. V. Alabugin et al., "Two-photon excitation of substituted enediynes," *Journal of Physical Chemistry A*, vol. 110, no. 1, pp. 241–251, 2006.
- [13] N. J. Turro, A. Evenzahav, and K. C. Nicolaou, "Photochemical analogue of the Bergman cycloaromatization reaction," *Tetrahedron Letters*, vol. 35, no. 44, pp. 8089–8092, 1994.
- [14] A. Evenzahav and N. J. Turro, "Photochemical rearrangement of enediynes: is a "photo-Bergman" cyclization a possibility?" *Journal of the American Chemical Society*, vol. 120, no. 8, pp. 1835–1841, 1998.
- [15] B. Breiner, J. C. Schlatterer, S. V. Kovalenko, N. L. Greenbaum, and I. V. Alabugin, "Protected  $^{32}\text{P}$ -labels in deoxyribonucleotides: investigation of sequence selectivity of DNA photocleavage by enediyne-, fulvene-, and acetylene-lysine conjugates," *Angewandte Chemie. International Edition*, vol. 45, no. 22, pp. 3666–3670, 2006.

- [16] T. A. Zeidan, S. V. Kovalenko, M. Manoharan, R. J. Clark, I. Ghiviriga, and I. V. Alabugin, "Triplet acetylenes as synthetic equivalents of 1,2-bicarbenes: phantom  $n, \pi^*$  state controls reactivity in triplet photocycloaddition," *Journal of the American Chemical Society*, vol. 127, no. 12, pp. 4270–4285, 2005.
- [17] T. A. Zeidan, R. J. Clark, S. V. Kovalenko, I. Ghiviriga, and I. V. Alabugin, "Triplet acetylenes as synthetic equivalents of 1,2-bicarbenes, part II: new supramolecular scaffolds from photochemical cycloaddition of diarylacetylenes to 1,4-cyclohexadienes," *Chemistry—A European Journal*, vol. 11, no. 17, pp. 4953–4960, 2005.
- [18] S. V. Kovalenko and I. V. Alabugin, "Lysine-enediynes conjugates as photochemically triggered DNA double-strand cleavage agents," *Chemical Communications*, no. 11, pp. 1444–1446, 2005.
- [19] W.-Y. Yang, B. Breiner, S. V. Kovalenko et al., "C-lysine conjugates: pH-controlled light-activated reagents for efficient double-stranded DNA cleavage with implications for cancer therapy," *Journal of the American Chemical Society*, vol. 131, no. 32, pp. 11458–11470, 2009.
- [20] B. Breiner, J. C. Schlatterer, S. V. Kovalenko, N. L. Greenbaum, and I. V. Alabugin, "DNA damage-site recognition by lysine conjugates," *Proceedings of the National Academy of Sciences of the United States of America*, vol. 104, no. 32, pp. 13016–13021, 2007.
- [21] O. Ostling and K. J. Johanson, "Microelectrophoretic study of radiation-induced DNA damages in individual mammalian cells," *Biochemical and Biophysical Research Communications*, vol. 123, no. 1, pp. 291–298, 1984.
- [22] N. P. Sing, M. T. McCoy, R. R. Tice, and E. L. Schneider, "A simple technique for quantitation of low levels of DNA damage in individual cells," *Experimental Cell Research*, vol. 175, no. 1, pp. 184–191, 1988.
- [23] P. L. Olive, J. P. Banath, and R. E. Durand, "Heterogeneity in radiation-induced DNA damage and repair in tumor and normal cells measured using the "comet" assay," *Radiation Research*, vol. 122, no. 1, pp. 86–94, 1990.
- [24] V. J. McKelvey-Martin, M. H. L. Green, P. Schmezer, B. L. Pool-Zobel, M. P. De Meo, and A. Collins, "The single cell gel electrophoresis assay (comet assay): a European review," *Mutation Research*, vol. 288, no. 1, pp. 47–63, 1993.
- [25] E. Rojas, M. C. Lopez, and M. Valverde, "Single cell gel electrophoresis assay: methodology and applications," *Journal of Chromatography B*, vol. 722, no. 1-2, pp. 225–254, 1999.
- [26] P. Virag, I. Brie, I. D. Postescu et al., "Comparative study of two evaluation methods for the genotoxic effects of environmental heavy metals on normal cells," *Toxicology and Industrial Health*, vol. 25, no. 4-5, pp. 253–258, 2009.
- [27] M. V. Coronas, T. S. Pereira, J. A. V. Rocha et al., "Genetic biomonitoring of an urban population exposed to mutagenic airborne pollutants," *Environment International*, vol. 35, no. 7, pp. 1023–1029, 2009.
- [28] A. Azqueta, S. Shaposhnikov, and A. R. Collins, "DNA oxidation: investigating its key role in environmental mutagenesis with the comet assay," *Mutation Research: Genetic Toxicology and Environmental Mutagenesis*, vol. 674, no. 1-2, pp. 101–108, 2009.
- [29] G. Wirzinger, L. Weltje, J. Gercken, and H. Sordyl, "Genotoxic damage in field-collected three-spined sticklebacks (*Gasterosteus aculeatus* L.): a suitable biomonitoring tool?" *Mutation Research: Genetic Toxicology and Environmental Mutagenesis*, vol. 628, no. 1, pp. 19–30, 2007.
- [30] L. Migliore, R. Colognato, A. Naccarati, and E. Bergamaschi, "Relationship between genotoxicity biomarkers in somatic and germ cells: findings from a biomonitoring study," *Mutagenesis*, vol. 21, no. 2, pp. 149–152, 2006.
- [31] B.-S. Kim, J. J. Park, L. Edler et al., "New measure of DNA repair in the single-cell gel electrophoresis (comet) assay," *Environmental and Molecular Mutagenesis*, vol. 40, no. 1, pp. 50–56, 2002.
- [32] F. Kassie, W. Parzefall, and S. Knasmüller, "Single cell gel electrophoresis assay: a new technique for human biomonitoring studies," *Mutation Research: Reviews in Mutation Research*, vol. 463, no. 1, pp. 13–31, 2000.
- [33] V. Garaj-Vrhovac and N. Kopjar, "The comet assay—a new technique for detection of DNA damage in genetic toxicology studies and human biomonitoring," *Periodicum Biologorum*, vol. 100, no. 3, pp. 361–365, 1998.
- [34] S. A. S. Walles, R. Zhou, and E. Liliemark, "DNA damage induced by etoposide; a comparison of two different methods for determination of strand breaks in DNA," *Cancer Letters*, vol. 105, no. 2, pp. 153–159, 1996.
- [35] B. Hellman, H. Vaghef, and B. Bostrom, "The concepts of tail moment and tail inertia in the single cell gel electrophoresis assay," *Mutation Research*, vol. 336, no. 2, pp. 123–131, 1995.

## Review Article

# Current Studies into the Genotoxic Effects of Nanomaterials

**Cheng-Teng Ng,<sup>1,2</sup> Jasmine J. Li,<sup>1,2</sup> Boon-Huat Bay,<sup>1</sup> and Lin-Yue Lanry Yung<sup>2</sup>**

<sup>1</sup> Department of Anatomy, Yong Loo Lin School of Medicine, National University of Singapore, 4 Medical Drive, Block MD10, Singapore 117597

<sup>2</sup> Department of Chemical and Biomolecular Engineering, National University of Singapore, 4 Engineering Drive 4, Block E5 no. 02-09, Singapore 117576

Correspondence should be addressed to Boon-Huat Bay, antbaybh@nus.edu.sg and Lin-Yue Lanry Yung, cheyly@nus.edu.sg

Received 24 May 2010; Revised 20 July 2010; Accepted 20 July 2010

Academic Editor: Shigenori Iwai

Copyright © 2010 Cheng-Teng Ng et al. This is an open access article distributed under the Creative Commons Attribution License, which permits unrestricted use, distribution, and reproduction in any medium, provided the original work is properly cited.

Nanotechnology has created opportunities for engineers to manufacture superior and more efficient devices and products. Nanomaterials (NMs) are now widely used in consumer products as well as for research applications. However, while the lists of known toxic effects of nanomaterials and nanoparticles (NPs) continue to grow, there is still a vast gap in our knowledge about the genotoxicity of NMs. In this paper, we highlight some NMs of interest and discuss the current *in vivo* and *in vitro* studies into genotoxic effects of NMs.

## 1. Introduction

Materials in the nanoscale are used in many commercial products and industrial practices in the new millennium. They are now increasingly found in plastic wares, clothing, cosmetics, electrical appliances, and even food products. Their applications also extend into the biomedical field and healthcare, particularly in medical imaging and diagnosis, pharmaceuticals, drug delivery, and therapy [1]. The demand for nanomaterials (NMs) in the market in the areas defined above is escalating and estimated to reach sales of up to US\$1 trillion by 2015 [2]. The recent burgeoning research interest and development of NMs, nanotechnology, and nanomedicine have led to a vast potential for novel ways of rapid disease diagnosis, treatment, and enhancement of the quality of life. NMs consist of one or more components present in various forms that possess at least one-dimensional structure of diameters in the range of 1 to 100 nm [3]. Engineered NMs, including nanoparticles (NPs) and nanofibres, are generally categorized into four classes, which include carbon-based materials, metal-based materials (quantum dots, nanosilver, and nanogold), dendrimers (nanosized polymers), and composites. Their characteristic features are durability, high conductivity, and reactivity [4].

Many researchers have commented that in actuality, there is still much more to be understood about nanomaterials, especially with regard to the health risks and hazards. The Royal Society and Royal Academy of Engineering first raised this concern in 2004 [5]. This has paved the way for a rapid increase in investigational studies in the toxicity of nanobased materials, in particular, genotoxicity studies of NMs and nanoparticles (NP). A quick search through the Pubmed literature database shows that the bulk of the research articles on NM genotoxicity were published within the past 3 years. As the development of nanotechnological applications continue to grow, it is anticipated that there will be an even greater demand for safety and health and risk assessments studies in the coming years. There have been excellent reviews regarding the methodologies for studying NM-induced toxicity [6–8].

In this paper, we would like to briefly discuss the methodologies currently available for genotoxic studies and present a survey of the *in vitro* and *in vivo* genotoxicological studies of NMs conducted in recent years.

## 2. Methodologies in Genotoxicity Studies

The study of NM toxicology has its roots in ultrafine particle study, mostly starting out as particulate matter (PM10) and

carbon black. The first wave of nanotoxicological studies were assessments of NM cytotoxicity which had been comprehensively outlined by Lewinski et al. [9]. Currently, there is an increasing focus on specific nanotoxic effects, and thus the advent of a subfield called “nanogenotoxicology” [10] which generally refers to the study of toxic effects of NMs on genomic stability and integrity. Common *in vitro* tests for measuring insults to DNA would centre on single-strand and double-strand breaks, mutations, deletions, chromosomal aberrations, impairment in DNA repair and cell-cycle while tumorigenesis and carcinogenicity are the main focus in *in vivo* studies. There are as many different kinds of NMs as there are elements and compounds. NMs, depending on the size, shape, elemental materials, and the surface functional groups were observed to have a range of detrimental effects on cells. Compounding the difficulties in toxicological studies, Stone et al. [6] and Landsiedel et al. [7] reiterated that based on existing knowledge, specific NMs probably induce definitive genotoxic effects. Nevertheless, some of the more common tests used in current genotoxic studies are described below.

### 2.1. In Vitro Techniques and Approaches

**2.1.1. Ames Test (Bacterial Reversion Mutation Test).** This test is used to assess the mutagenicity of a chemical compound [11]. Various strains of the histidine dependent bacterium, *Salmonella typhimurium*, contain mutations in the genes that impair synthesis of histidine required for cell growth. Test substances or compounds are added to different areas on the agar plate, and the bacterium is then plated onto the minimal histidine media. The test compound is deemed to have mutagenic potential if it is able to cause mutations that allow the bacterium to revert back its histidine synthesis ability. The downside of this test is that it is difficult to translate prokaryotic data for eukaryotic genotoxicity testing, and the test is known to generate false positive results [12]. Specific to NM toxicity testing, there are doubts if the Ames test is accurately representative of genotoxicity. Some NMs are not able to cross the bacterial wall, and some kill the test organism as they are bactericidal [7]. Therefore, data should be followed up with other tests after the initial screening.

**2.1.2. Comet Assay (Single-Cell Gel Electrophoresis Assay).** This is a simple, inexpensive, and sensitive technique to test for DNA damage. It was first described in 1988 by Singh et al. [13] and has since become the standard test for DNA damage. Cell samples from *in vitro* or *in vivo* experiments are first suspended in low melting point agarose and cast onto microscope slides. The cells are lysed so that only the DNA remains, which is then made to undergo electrophoresis in order to separate the DNA strands based on molecular weight. The DNA strands are subsequently stained with, for example, SYBR green dye and viewed under a fluorescence microscope. Under specific conditions, this test is able to distinguish single- and double-strand breaks in DNA. It is a quick way to assess DNA lesions and extent of genotoxicity in individual eukaryotic cells. However, due

to its sensitivity, samples should be handled appropriately to ensure reproducibility of the results.

**2.1.3. Micronucleus Test (MN)/Cytokinesis Block Micronucleus Test (CBMN).** This assay is based on scoring the number of micronuclei (MNI) in treated cells [14]. MNI are formed during anaphase from chromosomal fragments or whole chromosomes that are left behind when the nucleus divides. Over time, the assay has evolved to include a pretreatment with cytochalasin-B (Cyt-B), a cytokinesis blocking agent that inhibits cell-division, thereby giving the cells a binucleated appearance. This enables more accurate scoring and the ability to sieve out the dividing cells (where MNI would be found) from the nondividing ones, thereby reducing the incidence of false positives. The CBMN method is now routinely used for measuring chromosome breakage, impairment in DNA repair, chromosome loss, nondisjunction, necrosis, apoptosis and cytostasis.

**2.1.4. Hydroxy-Deoxyguanosine (8-OHdG) Analysis.** Oxidative stress is considered one of the foremost reasons for DNA damage. Reactive oxygen species (ROS) generated in metabolizing cells could attack DNA base guanine forming the 8-OHdG lesions, which is known to have mutagenic potential and hence used routinely as a biomarker for carcinogenesis [15]. There are a few methods to measure the extent of 8-OHdG lesions and the most established is HPLC (high-performance liquid chromatography), which is often coupled with mass spectrometry, also known as the HPLC-MS/MS. Other methods include performing antibody probes for DNA repair proteins or posttreatment with the enzyme formamidopyrimidine DNA N-glycosylase before quantitative analysis with the comet assay to determine DNA strand breaks [16].

**2.2. In Vivo Approaches.** There is a need for validation of animal models for studies in NM toxicity. The difficulties lie in devising the correct approach in interpreting the studies and deciding on the parameters that should be considered in examining NM toxicity in *in vivo* systems. Many investigators have administered NMs through inhalation exposure or orally, ingestion by feed or water supply, and direct instillation or injection into the body. Usually, the subsequent bioavailability and translocation of the NMs are evaluated, including the organ of entry as well as in other organs where accumulation is more significant. The tests used for assessment of genotoxicity are similar to those used in the *in vitro* studies.

## 3. Nanomaterials and their Genotoxic Status

A summary of some of the current genotoxic studies in nanomaterials are shown in Tables 1 and 2, which display the *in vivo* and *in vitro* studies, respectively.

**3.1. Carbon Fullerenes.** Carbon fullerenes, which are ultra-fine particulate matter, are one of the most ubiquitous NMs found [46]. They are generally present in polluted air as

TABLE 1: Selected *in vivo* genotoxicity studies on NMs.

Type of NP	Size and form	Experimental design/genotoxic tests	Summary of findings	References
C60 fullerenes	spheres	Bone marrow micronucleus test on ICR mice	No <i>in vivo</i> clastogenic ability of C <sub>60</sub> up to 88 mg/kg	Shinohara et al.; 2009 [17]
C60 Single-walled carbon nanotubes (SWCNT)	spheres	Oral administration at doses of 0.064 and 0.64 mg/kg of body weight. 8-OHdG analysis	Both NPs were associated with increase in 8-OHdG in liver and lungs. No impairment of DNA repair system	Folkmann et al.; 2009 [18]
SWCNT Multi-walled carbon nanotubes (MWCNT)	nanotubes	Oral administration and urinary samples collected for Ames test	No urinary mutagenicity	Szendi and Varga 2008 [19]
Carbon black (CB) C60 SWCNT AuNP Cd quantum dots (QDs)	nanospheres	Apo E knockout mice Timepoints at 3 and 24 hours; NP administered by instillation	Increase in cytokines gene expression. ApoE $-/-$ mice are sensitive to particle induced inflammation. DNA damage in order of. QD>CB>SWCNT> C <sub>60</sub> , Au	Jacobsen et al.; 2009 [20]
TiO <sub>2</sub>	anatase/rutile 21 nm	TiO <sub>2</sub> ingested through drinking water at concentrations of 60, 120, 300, 600 $\mu$ g/mL. Comet assay MN test gamma-H2AX immunostaining 8-OHdG analysis	Increase in 8-OHdG and gamma-H2AX foci. indicative of DNA double-strand breaks. MN. shows increase in DNA deletions.	Trouiller et al.; 2009 [21]
Ag	60 nm	Oral administration in Sprague-Dawley rats over a period of 28 days; doses at 30, 300 and 1000 mg/kg.	No significant genotoxicity in bone marrow. (micronucleated erythrocytes)	Kim et al.; 2008 [22]
Silica	amorphous 37 and 83 nm	Inhalation study where mice were exposed to $3.7 \times 10^7$ and $1.8 \times 10^8$ particles/cm <sup>3</sup>	No significant pulmonary, inflammatory, genotoxic or adverse lung histopathological effects	Sayes et al.; 2010 [23]

they are often released in soot resulting from the process of fuel combustion. Engineered carbon fullerenes are stable, soccer ball-like carbon atoms with hexagonal and pentagonal shapes. The most notable fullerene would be C60, a highly reactive biomolecules that has the ability to cross blood brain barrier (BBB) [47]. C60 fullerene is highly used in industry as catalysts, reactive oxygen species scavengers [48] and tools in drug delivery systems [49].

Since the early 1990s, there have been concerns about the potential dermal and inhalation effects of fullerenes due to their strong oxidizing and phototoxic properties [50]. *In vitro* experiments have shown C60 to be generally noncytotoxic with no mutagenic response [17, 24] in Chinese hamster ovary (CHO-K1) cells and mouse lung epithelial cells [28] using the Ames test and CBMN tests, respectively. Another report has found that C60 treatment

also increases formamidopyrimidine [fapy]-DNA glycosylase (FPG) sensitive sites, accounting for short-term DNA strand damage. Xu et al. observed that C60 induced an increase in mutation yield in primary mouse embryo fibroblast cells and dose-dependent formation of free radical ONOO<sup>-</sup> [25] using dihydrorhodamine radical probes. However, in the *in vivo* setting, C60 treatment was found to be associated with increased DNA damage 8-hydroxydeoxyguanosine (8-OHdG) in mouse lung and liver [18]. Not surprisingly, inflammatory cytokines such as the interleukins and MIP and MCP genes were found to be upregulated although C60 extent of damage was lower as compared to other NMs.

**3.2. Carbon Nanotubes.** Carbon nanotubes are the byproducts of combustion, which are commonly present in air pollution and soot. Engineered carbon nanotubes can also

TABLE 2: Selected *in vitro* genotoxicity studies on NMs.

Type of NP	Size and form	Experimental design/genotoxic tests	Summary of findings	References
<b>Carbons</b>				
C <sub>60</sub>	0.92 m <sup>2</sup> /g surface area	Ames test	No mutagenic response, and no incidence of chromosomal aberration	Shinohara et al.; 2009 [17]
C <sub>60</sub>	polyhydroxylated	CHO-K1 cells chromosome aberration assay CBMN test	No genotoxicity at all doses (11–221 μM)	Mrdanović et al., 2009 [24]
C <sub>60</sub>	nanospheres	Mouse primary embryo fibroblasts Dihydrorhodamine 123 radical probe	Increased mutation yield and induces kilo-based pair deletion mutations in transgenic mouse cells. Dose-dependent formation of ONOO <sup>-</sup>	Xu et al.; 2009 [25]
SWCNT -MWSCNT	nanotubes	Human lymphocytes in culture CBMN test Sister Chromatid Exchange (SCE) assay	No genotoxicity effects but SWCNT induces mitotic inhibition	Szendi and Varga; 2008 [19]
MWSCNT	agglomerates	V79 cells treated for 18 h and 30 h at 2.5, 5 and 10 μg/mL. Chromosome aberration test Ames test	No mutagenic or clastogenic effects	Wirnitzer et al., 2009 [26]
MWSCNT	nanotubes	Ames test on <i>Salmonella typhimurium</i> TA 98 and TA 100 strains, and on <i>Escherichia coli</i> WP2uvrA strain, in presence and in absence of the metabolic activation system S9	No mutagenic effects	Di Sotto et al.; 2009, [27]
C <sub>60</sub> SWCNT Carbon black (CB)	0.7 nm (C60) 0.9–1.7 nm (SWCNT) 14 nm (CB)	FE1-muta trademark mouse lung epithelial cell line comet assay FE1-MML mutagenicity analysis c11 mutation analysis	No cell death. Slower proliferation and cell-cycle arrest at G <sub>1</sub> with SWCNT. Mutant frequency unaffected by 576 h exposure	Jacobsen et al., 2008 [28]
<b>Metals</b>				
Alumina (Al <sub>2</sub> O <sub>3</sub> ) Cobalt Chromium alloy (CoCr)	bare	Human primary fibroblasts over 5 days CBMN assay gamma-H2AX immunostaining cytogenetic analysis (FISH)	At 24 h, Al <sub>2</sub> O <sub>3</sub> increase micronucleus binucleated cells, chromosomal loss, gain, and polyploidy. At 24 h, CoCr induce dose-dependent increase in micronucleus binucleated cells, chromosomal loss, gain, deletions, and polyploidy.	Tsaousi et al.; 2010, [29]
Co	20 nm 500 nm	Balb/3T3 cells at 1–100 μM dose concentrations. CBMN test Comet assay	Significant results for CBMN and comet assay but no dose-dependency. Increase of type III foci	Ponti et al.; 2009 [30]
Co	100–500 nm	Peripheral blood leucocytes at 24, 48 h timepoints in 10 <sup>-5</sup> M and 10 <sup>-4</sup> M dose concentrations CBMN test Comet assay	Induces DNA damage Genotoxic effects modulated by donor characteristics and/or Co2+ release.	Colognato et al.; 2008 [31]

TABLE 2: Continued.

Type of NP	Size and form	Experimental design/genotoxic tests	Summary of findings	References
Al <sub>2</sub> O <sub>3</sub> TiO <sub>2</sub>	nanoparticles	CHO-K1 cells Micronucleus (MN) test Sister chromatid exchange (SCE)	MN frequencies increase at 0.5 and 1 µg/mL TiO <sub>2</sub> and 0.5–10 µg/mL Al <sub>2</sub> O <sub>3</sub> . SCE higher at 1–5 µg/mL TiO <sub>2</sub> treatment, and at 1–25 µg/mL Al <sub>2</sub> O <sub>3</sub>	Di Virgillio et al.; 2010 [32]
TiO <sub>2</sub>	rutile/anatase fine rutile	Human bronchial epithelial cells (BEAS 2B) with 1–100 µg/cm <sup>2</sup> at 24, 48, and 72 h. Comet assay MN test	Both induce DNA damage at all treatment times. Only nanosize rutile increase frequency of MN cells at 10, 60 µg/cm <sup>2</sup> , 72 h.	Falck et al.; 2009 [33]
TiO <sub>2</sub>	with p,p'-DDT	Human embryo L-02 hepatocyte 0.01, 0.1, 1 µg/mL treatment concentrations Flow cytometry with DCFH-DA probe 8OHdG analysis Comet assay MN test	TiO <sub>2</sub> enhances photocatalysis. Increases oxidative stress, DNA adducts, DNA strand breaks, and chromosome damage	Shi et al.; 2010 [34]
TiO <sub>2</sub>	2–30 nm (mean at 15 nm)	NIH3T3 human fibroblasts HFW cells Short-term treatment at 24, 48 and 72 h. Long-term treatment, cell passage every 3 days with NP media. Flow cytometry with H2DCFDA probes  Cell-cycle analysis Cell-division analysis Confocal microscopy	Short-term increased cell survival and growth. Long-term G <sub>2</sub> /M delay and slower cell-division with aberrant multipolar spreads. Overall disturbance in cell-cycle progression, duplicate genome segregation, and chromosomal instability	Huang et al.; 2009 [35]
TiO <sub>2</sub> Fe <sub>2</sub> O <sub>3</sub>	anatase <100 nm <100 nm	Human lung fibroblasts IMR-90 and BEAS-2B cells Electron paramagnetic resonance (EPR) 8-OHdG analysis	TiO <sub>2</sub> treatment showed no DNA breakage, DNA adduct nor free radical generation. Fe <sub>2</sub> O <sub>3</sub> had significant DNA damage after 24 h in IMR-90 cells	Bhattacharya et al.; 2009 [36]
TiO <sub>2</sub>	nanoparticles rutile anatase	Mouse primary embryo fibroblasts Dihydrorhodamine 123 radical probe	Increased mutation yield and induces kilo-based pair deletion mutations in transgenic mouse cells. Dose-dependent formation of ONOO <sup>-</sup>	Xu et al.; 2009 [25]
TiO <sub>2</sub>	100 nm	Human lymphoblastoid cells. Treatment with 26, 65, 130 µg/mL at 6, 24, 48 h. CBMN test Comet assay Hypoxanthine-guanine phosphoribosyltransferase (HPRT) gene mutation assay	130 µg/mL treatment increases MNBC frequency 2-3 folds and 2.5 fold in mutation frequency. 65 µg/mL treatment induce 5 fold increase in comet tail moments	Wang et al.; 2007 [37]

TABLE 2: Continued.

Type of NP	Size and form	Experimental design/genotoxic tests	Summary of findings	References
ZnO	nanospheres	Human epidermal cell line (A431) Treatment at 0.8, 0.008g/mL Comet assay	Significant DNA damage in comet assay. Induces oxidative stress	Sharma et al.; 2009 [38]
Ag	30 nm, nanospheres	Medaka fish cell lines Treatment at 0.05, 0.1, 0.3 $\mu\text{g}/\text{cm}^2$	Chromosomal aberration and aneuploidy	Wise et al.; 2010 [39]
Ag	6–20 nm starch coated	IMR-90 and human glioblastoma cells U251 Comet assay CBMN Annexin V propidium iodide staining	DNA aberrations more prominent in cancer cells with more chromosomal aberrations.	Asharani et al.; 2009 [40]
Ag	25 nm polysaccharide surface functionalized and uncoated nanospheres	Mouse embryonic stem cells and embryonic fibroblasts Immuno blot Immunofluorescence	Upregulation of p53, Rad 51 and phosphorylated H2AX protein expression. Coated AgNP show more severe damage than uncoated AgNP	Ahamed et al.; 2008 [41]
Au	20 nm Serum coated	Human fetal lung fibroblasts cells (MRC-5) treated with nAu at 0, 0.5 and 1 nm concentrations. 8-OHdG analysis	Significant DNA damage in 1 nm treatment compared to control.	Li et al.; 2008 [42]
Platinum (Pt NP)	5–8 nm capped with poly-vinyl alcohol	Human cell line	p53 activation, p21 downregulation. Increase of DNA damage, arrest at cell-cycle S phase and apoptosis	Asharani et al.; 2010 [43]
<b>Other Nanomaterials</b>				
Nanoceria ( $\text{CeO}_2$ )	nanoparticles	Human lens epithelial cells at 5, 10 $\mu\text{g}/\text{mL}$ concentrations SCE Comet assay (alkaline)	No DNA damage nor SCE	Pierscionek et al.; 2010 [44]
Polymer NP	lyophilized PELGE and PLGANp	CHO cells MN test SCE	No significant difference in MN assay and no cell-cycle delay. SCE found to be higher in 5 kinds of PELGE-NP than in negative controls	He et al.; 2009 [45]

come in a variety of shapes and conformations, with the most common being the single-walled carbon nanotubes (SWCNTs) and the multiwalled carbon nanotubes (MWCNTs). They are also found in a wide range of applications in the industry as composites, polymers, as well as in the biomedical and pharmaceutical fields. Great physical strength, flexibility, electrical conductivity, insolubility and nonbiodegradability are among the valued properties of carbon nanotubes [51]. On the other hand, it has been postulated that these nanotubes could possess health hazards upon inhalation as their durability, biopersistence, and long and thin shape resembling asbestos fibers [52]. In

addition, trace contaminations with iron and nickel have been reported to be the major cause of toxicity in carbon nanotubes [53].

There is a scarcity of information regarding SWCNTs and genotoxicity. SWCNTs have been reported to induce slower proliferation rate and cell-cycle arrest at G1 phase in mice lung epithelial cells [28] and mitotic inhibition in human lymphocyte cultures [19]. In *in vivo* experiments, oral administration of SWCNTs in mice is found to be associated with increase in 8-OHdG levels in liver and lung [18]. SWCNTs, compared to carbon black, only causes moderate inflammation in ApoE knockout mice [20]. However,

agglomerates of MWCNTs were found to possess neither clastogenic nor mutagenic effects [19, 26, 27] when put under the Ames test and chromosome aberration test.

**3.3. Titanium Dioxide and Zinc Oxide Nanoparticles ( $\text{TiO}_2$  and  $\text{ZnO}$  NPs).**  $\text{TiO}_2$  and  $\text{ZnO}$  NPs, which have the properties of high refractive index and brightness, are regularly used as whitening pigments or reflective optical coats [54]. These specific properties lead to the application in commercial products such as paint and whitening agents in food products [55]. Nanoparticulate suspensions of  $\text{ZnO}$  and  $\text{TiO}_2$  also appear transparent in air and liquid under visible light. As such, ultrafine  $\text{TiO}_2$  is also extensively used in cosmetics, skin care, and sunscreen products, as their application does not leave unsightly white residue on skin unlike bulk  $\text{TiO}_2$  [56].  $\text{ZnO}$  is quite well known to be cytotoxic to cells in culture [57], while the toxicity of  $\text{TiO}_2$ NP is rapidly gaining attention due to the increased use and applications in many accessible medical and cosmetic products.  $\text{TiO}_2$ NP comes in two common shapes, namely, the rutile and anatase forms. Although both are found to be genotoxic, one study showed that the anatase form induced greater DNA damage in human bronchial epithelium [33].  $\text{TiO}_2$ NP could also increase cell sensitivity to phototoxicity [34], as well as induce more DNA adducts, strand breaks, base-pair mutations and chromosomal damage [21, 25, 37]. Interestingly, Huang et al. reported that while long-term exposure to  $\text{TiO}_2$ NP slowed down cell-division and induced aberrant multipolar spreads, chromatin alignment, and segregation, short-term exposure increased cell survival and growth and number of multinucleated cells [35]. Another group of investigators did not observe DNA breakage under  $\text{TiO}_2$ NP treatment but found positive DNA adduct formation and free radical generation [36].

Although ZnONPs are probably the less studied of the two, there is also evidence to suggest that they may also induce significant DNA damage through oxidative stress, albeit with less obvious effects than in  $\text{TiO}_2$ NPs [38].

**3.4. Aluminium Oxide Nanoparticles ( $\text{Al}_2\text{O}_3$ NPs).**  $\text{Al}_2\text{O}_3$ NP, or alumina NP as it is commonly known, belongs to a class of materials known as nanoceramics. It is widely used in industrial and medical product such as orthopaedic parts and composite repellant. However, the toxic and genotoxic effects of  $\text{Al}_2\text{O}_3$ NP are not well known, and there are very few research studies on the toxicity of this material. Thus far,  $\text{Al}_2\text{O}_3$ NPs were found to significantly increase micronucleus frequencies, chromosomal loss, and gain mutations as well as polyploidy but no sister chromatid exchanges were found to take place [29, 32].

**3.5. Cobalt and Cobalt-Chromium Nanoparticles (CoNPs and CoCrNPs).** Cobalt and its alloy are commonly used in hip joint replacements and other orthopedic joint replacements. Unfortunately, the friction produced in movement of the replacement joints generate NPs of the metal which could reach out and affect the surrounding tissue and even lymphocytes, thereby lead to some concerns regarding the

genotoxicity observed from clinical studies [58]. Hence, much interest was generated to study the effects of these wear particles and a significant amount of research into Co and CoCr NPs are centered around these issues. The results, although not surprising, are generally aligned to positive indications of genotoxicity. Analysis of peripheral blood leukocytes of patients with cobalt alloy joint replacements showed positive DNA damage in comet assays [31]. However, it was also suggested that these results could possibly be modulated by donor characteristics and may be due to  $\text{Co}^{2+}$  release instead of CoNPs per se. Recent studies show that by 24 h, CoCrNPs induced a dose-dependant increase in micronucleus containing cells as well as chromosomal loss, gains, deletions, and polyploidy [29]. In a separate study with CoNPs on Balb/3T3 cells, there were significant results in micronuclei and comet assay for NP induced DNA damage but the results were not dose-dependent [30].

**3.6. Quantum Dots.** Quantum dots are crystalline semi-conducting NPs. They are comprised of a metalloid crystalline core and a “cap” or “shell” that shields the core or renders the dots biologically compatible [4]. The metalloid crystalline core is normally made up of heavy metals like cadmium and lead or sometimes from other semiconductor, noble, and transition metals. These are also quantum dots that are coated with materials such as polyethylene glycol, zinc sulphide, or polyacrylate [59]. Quantum dots are used in composites, paints, inks, solar cells, and optoelectronics [4]. Due to their bright fluorescence, narrow emission, broad UV excitation, and photostability, they have been used as alternative fluorescent dyes for labeling cell structure *in vitro* and for fluorescence imaging *in vivo* [60].

They are considered one of the most toxic of substances and there are many studies showing the acute cytotoxicity of quantum dots [61]. The cadmium and lead metals themselves are considered potent human carcinogens. Cadmium induces DNA damage and mutation through ROS production and inhibition of DNA repair and methylation [62]. It also incites disruption of E-cadherin cell-to-cell adhesion which could lead to tumor formation. Lead and its compounds are listed under group 2B of possible human carcinogens in IARC reports [63], as they are found to induce lipid peroxidation and inhibit enzymes and antioxidants thereby putting the cell under an environment of oxidative stress [64]. However, few have ventured into exploring the genotoxicity of such QDs. One experiment with Apo E knockout mice showed that such mice were more sensitized to QD-induced inflammation, upregulating gene expressions of cytokines, IL-6, Mip 2 and Mip signaling molecules [20].

**3.7. Silver and Gold Nanoparticles (AgNPs and AuNPs).** AgNPs and AuNPs are the most marketable NPs and widely used in consumer products. AgNPs are particularly known for their antimicrobial qualities, while AuNPs are used in bioimaging and diagnosis applications. They are also easily synthesized from their salt compounds and are convenient

to handle, which also makes them another popular choice of NMs to work with. What is of concern is that several studies have found AgNPs to be toxic in aquatic animals [65] and AuNPs to possess some degree of toxicity *in vitro* [66]. Many researchers have focused on AgNPs because of the acute toxicity shown *in vitro* experiments. AgNPs were found to induce DNA damage in human glioblastoma cells as well as chromosomal aberrations in human fibroblast cells [40]. Other genotoxic reactions include upregulation of p53 and DNA repair protein Rad51 observed in mouse embryonic stem cells and fibroblasts [41]. In the same study, AgNP when functionalized with polysaccharide on its surface was more DNA damaging than uncoated AgNPs. In long-term rodent studies, oral administration of high-dose AgNPs for 28 days resulted in liver damage but no significant genotoxicity in erythrocytes and bone marrow [22]. A number of studies have also shown that AgNP treatment induced DNA damaging effects on aquatic and plant cells with impairment of cell-division [39, 65]. Although less dramatic than AgNPs, AuNPs are also able to induce DNA damage in the form of single-strand lesions in human lung fibroblasts [42].

**3.8. Other Nanoparticles.** There are a few research groups working with new types of NPs. The rare earth metal cerium oxide NPs (nanoceria) is one example. Researchers have found nanoceria to be a radical scavenger with antiinflammatory effects [67] which causes no DNA damage [44]. They are currently being developed for application in human lens epithelium. Although this is a promising NM for future applications, it has also been reported that nanoceria exerts differential growth in soybean seedlings [68]. Silica NPs, or often known as mesoporous silica, are also popular materials for development of drug delivery and cell-imaging systems [69, 70]. There are few genotoxicity studies on silica NPs but a notable one by Sayes et al. [23] has shown that there are no significant inflammatory or genotoxic effects in mouse lungs on short-term exposure. Metal NPs such as platinum NPs (PtNPs) and iron oxide  $\text{Fe}_2\text{O}_3$ NPs are also popular alternatives. There is one report on PtNP toxicity which showed an increase in DNA damage concurrent with p53, p21 downregulation, and cell-cycle arrest at the S-phase [43]. Fe and  $\text{Fe}_2\text{O}_3$ NPs are also known to be toxic and can cause significant DNA damage [36].

Other particles of note are the nanopolymers. Although there is a wide variety of such nanopolymers, they are generally known as a family of compounds that consists of chain units, which could be fashioned into nano-sized particles. These are also largely being developed for use in drug delivery [71]. Current genotoxicity studies suggest that some of these nanopolymers show antiinflammatory properties and also non or limited DNA damage [45, 72]. However, a recent report has implicated long-term nanopolymer exposure to pulmonary fibrosis and granuloma formation, resulting in two fatal deaths [73]. This case cannot be taken in isolation and others have raised the concern that the workplace condition as well as health or other pre-dispositions of the workers involved should be considered [74].

## 4. NMs and Carcinogenesis

While it has been shown in many *in vitro* experiments that NMs are able to induce DNA damage and some form of mutagenesis, there is still a lack of evidence for tumorigenicity of NPs. Of note, *in vivo* studies involving MWCNT has demonstrated formation of mesotheliomas in rodents in works by Takagi and colleagues [75] and Sakamoto et al. [76]. Wide spread deposition of MWCNTs were observed in the peritoneal cavity where the nanotubes were injected. In the study by Sakamoto et al., they have even found mesotheliomas in the peritoneal cavity away from the original site of injection, suggesting that MWCNTs may easily translocate and also exert effects away from organ of exposure. Both studies emphasized on the persistency, size and shape on the carcinogenic potential of MWCNTs. While such studies may provide some insight into the outcome of NM toxicity, one must take into account the differences in how the nanotubes were prepared as well as the experimental design. Muller et al. conducted similar tests on MWCNTs but reported no carcinogenicity after a 2 year period of exposure [77]. They speculate that tumor formation could be dependent on size and length of the nanotubes administered and the p53 knockout mice used in the Takagi study produced a more sensitive carcinogenic reaction. However, NMs can induce oxidative stress and trigger inflammatory responses, which could form the starting point for carcinogenesis to occur. NMs that are highly reactive are also more likely to absorb endogenous substances, react with proteins and enzymes, trigger cytokine release. This would mediate inflammatory responses and potentially initiate a series of toxic responses far from the initial site of deposition [78, 79]. C60 fullerene, for example, was reported to cause photo-induced DNA damage by interacting with biological reducing agents such as NADH to cleave supercoiled DNA [80]. Similarly, exposure to carbon nanotubes in atmospheric air pollution has been associated with adverse cardiovascular effects by causing aortic DNA damage, platelet aggregation and enhances vascular thrombosis through inflammatory events [81].

Biopersistence of NMs pose a certain degree of adverse health effect. For instance, when the clearance rate is slower than the accumulative rate, the NMs will remain in the lungs; and those containing mutagenic substances will increase the risk of developing cancer. To address this concern, Sera et al. conducted a mutagenicity test using 3 different strains of *Salmonella* and found C60 Fullerene to exert mutagenic activity due to the oxidized phospholipids in rat liver microsoms [82].

There are also certain shortcomings in the current research field. The short-term nature of toxicology tests in the treatment period for NMs generally lasts only up to three days, which implies that testing is limited to acute toxicity. *In vitro* and *in vivo* genotoxicity testing will have to be conducted for longer periods to observe if there are long-term effects of NMs such as tumour formation and carcinogenesis. Treatment intervals will have to go beyond days to weeks or even months in animal studies. It will also be useful to look at the clearance of NMs from the body and

to study if there is a preference for accumulation in certain organs and any effect from biopersistence of such NMs.

On the public front, safety measures have been implemented to safeguard the public health. The International Agency for Research on Cancer (IARC) recently classified TiO<sub>2</sub> as a potential Group 2B human carcinogen. This decision was made on the experimental animal carcinogenicity data [83]. There had been four previous epidemiological studies conducted among the male production workers at TiO<sub>2</sub> industry from Western Europe and North America. After comparing the risk for lung and kidney cancer with the general population, they concluded that these data were not supportive enough to conclude the association between occupational exposure of TiO<sub>2</sub> and cancer risk. Hence, data collected were inadequate in classifying TiO<sub>2</sub> as potential carcinogen. However, there was sufficient animal carcinogenicity data that provided evidence of TiO<sub>2</sub>-induced carcinogenicity. Several TiO<sub>2</sub> exposure routes were chosen for experimental animal studies. These include oral, inhalation, intratracheal, subcutaneous injection, and intraperitoneal administration. Researchers observed an increase in tumor incidence in these experimental animals upon TiO<sub>2</sub> exposure. After considering other relevant data such as clearance kinetics of TiO<sub>2</sub> and micronucleus formation, a conclusion that TiO<sub>2</sub> possess possible carcinogenicity to human was made.

## 5. Conclusion

The field of nanotoxicology, besides investigations on the adverse effects of NMs, also include continuous monitoring and risk assessment of NMs. Despite the many nanotoxicological studies that are ongoing, there are questions that need to be answered and addressed. There is difficulty in interpreting data in view of variable parameters utilized in the study, for example, the sizes of the NMs and its composing materials. The most critical research gap is the lack of studies on real-time NM exposure. Moreover, there is a need for long-term nanomaterials exposure assessment for studies on tumourigenesis. At the industry level, close monitoring and followup on the levels of emissions from NM production industries are essential in protecting public health and our environment. However, there still exists a lack of appropriate epidemiological studies and equipment for accurate collection of data in assessing the real risk of NM exposure in the workplace. Despite the promising applications of NMs, there are still doubts regarding their safety. There is some certainty that NMs do pose a certain degree of health risk that would require further investigation. A proper guideline on NM usage is imperative to ensure the safety of NMs for consumer usage and environment.

## Acknowledgments

The paper was supported by the Singapore Ministry of Education Academic Research Fund Tier 2 via grant MOE2008-T2-1-046 and the National University of Singapore (NUS)

Environmental Research Institute (NERI) via Grant no. R706000002646.

## References

- [1] B. Nowack and T. D. Bucheli, "Occurrence, behavior and effects of nanoparticles in the environment," *Environmental Pollution*, vol. 150, no. 1, pp. 5–22, 2007.
- [2] M. C. Roco, "Environmentally responsible development of nanotechnology," *Environmental Science and Technology*, vol. 39, no. 5, pp. 106A–112A, 2005.
- [3] D. B. Warheit, C. M. Sayes, K. L. Reed, and K. A. Swain, "Health effects related to nanoparticle exposures: environmental, health and safety considerations for assessing hazards and risks," *Pharmacology and Therapeutics*, vol. 120, no. 1, pp. 35–42, 2008.
- [4] M. C. Powell and M. S. Kanarek, "Nanomaterial health effects—part 1: background and current knowledge," *Wisconsin Medical Journal*, vol. 105, no. 2, pp. 16–20, 2006.
- [5] The Royal Society and the Royal Academy of Engineering, "Environmental applications and impacts of nanotechnology: summary of evidence presented to nanotechnology working group," 2003.
- [6] V. Stone, H. Johnston, and R. P. F. Schins, "Development of in vitro systems for nanotoxicology: methodological considerations in vitro methods for nanotoxicology Vicki Stone et al," *Critical Reviews in Toxicology*, vol. 39, no. 7, pp. 613–626, 2009.
- [7] R. Landsiedel, M. D. Kapp, M. Schulz, K. Wiench, and F. Oesch, "Genotoxicity investigations on nanomaterials: methods, preparation and characterization of test material, potential artifacts and limitations-many questions, some answers," *Mutation Research*, vol. 681, no. 2-3, pp. 241–258, 2009.
- [8] N. Singh, B. Manshian, G. J. S. Jenkins et al., "NanoGenotoxicology: the DNA damaging potential of engineered nanomaterials," *Biomaterials*, vol. 30, no. 23-24, pp. 3891–3914, 2009.
- [9] N. Lewinski, V. Colvin, and R. Drezek, "Cytotoxicity of nanoparticles," *Small*, vol. 4, no. 1, pp. 26–49, 2008.
- [10] K. Donaldson, V. Stone, C. L. Tran, W. Kreyling, and P. J. A. Borm, "Nanotoxicology," *Occupational and Environmental Medicine*, vol. 61, no. 9, pp. 727–728, 2004.
- [11] K. Mortelmans and E. Zeiger, "The Ames Salmonella/microsome mutagenicity assay," *Mutation Research*, vol. 455, no. 1-2, pp. 29–60, 2000.
- [12] N. Khandoudi, P. Porte, S. Chtourou, F. Nessler, D. Marzin, and F. Le Curieux, "The presence of arginine may be a source of false positive results in the Ames test," *Mutation Research*, vol. 679, no. 1-2, pp. 65–71, 2009.
- [13] N. P. Singh, M. T. McCoy, R. R. Tice, and E. L. Schneider, "A simple technique for quantitation of low levels of DNA damage in individual cells," *Experimental Cell Research*, vol. 175, no. 1, pp. 184–191, 1988.
- [14] M. Fenech, "Cytokinesis-block micronucleus cytome assay," *Nature Protocols*, vol. 2, no. 5, pp. 1084–1104, 2007.
- [15] P. Karihtala, Y. Soini, L. Vaskivuo, R. Bloigu, and U. Puistola, "DNA adduct 8-hydroxydeoxyguanosine, a novel putative marker of prognostic significance in ovarian carcinoma," *International Journal of Gynecological Cancer*, vol. 19, no. 6, pp. 1047–1051, 2009.
- [16] A. Valavanidis, T. Vlachogianni, and C. Fiotakis, "8-hydroxy-2'-deoxyguanosine (8-OHdG): a critical biomarker of oxidative stress and carcinogenesis," *Journal of Environmental Science and Health. Part C*, vol. 27, no. 2, pp. 120–139, 2009.

- [17] N. Shinohara, K. Matsumoto, S. Endoh, J. Maru, and J. Nakanishi, "In vitro and in vivo genotoxicity tests on fullerene C60 nanoparticles," *Toxicology Letters*, vol. 191, no. 2-3, pp. 289–296, 2009.
- [18] J. K. Folkmann, L. Risom, N. R. Jacobsen, H. Wallin, S. Loft, and P. Møller, "Oxidatively damaged DNA in rats exposed by oral gavage to C60 fullerenes and single-walled carbon nanotubes," *Environmental Health Perspectives*, vol. 117, no. 5, pp. 703–708, 2009.
- [19] K. Szendi and C. Varga, "Lack of genotoxicity of carbon nanotubes in a pilot study," *Anticancer Research*, vol. 28, no. 1, pp. 349–352, 2008.
- [20] N. R. Jacobsen, P. Møller, K. A. Jensen et al., "Lung inflammation and genotoxicity following pulmonary exposure to nanoparticles in ApoE-/- mice," *Particle and Fibre Toxicology*, vol. 6, article 2, 2009.
- [21] B. Trouiller, R. Reliene, A. Westbrook, P. Solaimani, and R. H. Schiestl, "Titanium dioxide nanoparticles induce DNA damage and genetic instability in vivo in mice," *Cancer Research*, vol. 69, no. 22, pp. 8784–8789, 2009.
- [22] Y. S. Kim, J. S. Kim, H. S. Cho et al., "Twenty-eight-day oral toxicity, genotoxicity, and gender-related tissue distribution of silver nanoparticles in Sprague-Dawley rats," *Inhalation Toxicology*, vol. 20, no. 6, pp. 575–583, 2008.
- [23] C. M. Sayes, K. L. Reed, K. P. Glover et al., "Changing the dose metric for inhalation toxicity studies: short-term study in rats with engineered aerosolized amorphous silica nanoparticles," *Inhalation Toxicology*, vol. 22, no. 4, pp. 348–354, 2010.
- [24] J. Mrdanović, S. Šolajić, V. Bogdanović, K. Stankov, G. Bogdanović, and A. Djordjević, "Effects of fullereneol C60(OH)24 on the frequency of micronuclei and chromosome aberrations in CHO-K1 cells," *Mutation Research*, vol. 680, no. 1-2, pp. 25–30, 2009.
- [25] A. Xu, Y. Chai, T. Nohmi, and T. K. Hei, "Genotoxic responses to titanium dioxide nanoparticles and fullerene in gpt delta transgenic MEF cells," *Particle and Fibre Toxicology*, vol. 6, article 3, 2009.
- [26] U. Wirtzner, B. Herbold, M. Voetz, and J. Ragot, "Studies on the in vitro genotoxicity of baytubes®, agglomerates of engineered multi-walled carbon-nanotubes (MWCNT)," *Toxicology Letters*, vol. 186, no. 3, pp. 160–165, 2009.
- [27] A. Di Sotto, M. Chiaretti, G. A. Carru, S. Bellucci, and G. Mazzanti, "Multi-walled carbon nanotubes: lack of mutagenic activity in the bacterial reverse mutation assay," *Toxicology Letters*, vol. 184, no. 3, pp. 192–197, 2009.
- [28] N. R. Jacobsen, G. Pojana, P. White et al., "Genotoxicity, cytotoxicity, and reactive oxygen species induced by single-walled carbon nanotubes and C60 fullerenes in the FE1-Muta™ mouse lung epithelial cells," *Environmental and Molecular Mutagenesis*, vol. 49, no. 6, pp. 476–487, 2008.
- [29] A. Tsaousi, E. Jones, and C. P. Case, "The in vitro genotoxicity of orthopaedic ceramic (Al2O3) and metal (CoCr alloy) particles," *Mutation Research*, vol. 697, no. 1-2, pp. 1–9, 2010.
- [30] J. Ponti, E. Sabbioni, B. Munaro et al., "Genotoxicity and morphological transformation induced by cobalt nanoparticles and cobalt chloride: an in vitro study in Balb/3T3 mouse fibroblasts," *Mutagenesis*, vol. 24, no. 5, pp. 439–445, 2009.
- [31] R. Colognato, A. Bonelli, J. Ponti et al., "Comparative genotoxicity of cobalt nanoparticles and ions on human peripheral leukocytes in vitro," *Mutagenesis*, vol. 23, no. 5, pp. 377–382, 2008.
- [32] A. L. Di Virgilio, M. Reigosa, P. M. Arnal, and M. Fernández Lorenzo de Mele, "Comparative study of the cytotoxic and genotoxic effects of titanium oxide and aluminium oxide nanoparticles in Chinese hamster ovary (CHO-K1) cells," *Journal of Hazardous Materials*, vol. 177, no. 1-3, pp. 711–718, 2010.
- [33] G. C. M. Falck, H. K. Lindberg, S. Suhonen et al., "Genotoxic effects of nanosized and fine TiO2," *Human and Experimental Toxicology*, vol. 28, no. 6-7, pp. 339–352, 2009.
- [34] Y. Shi, J.-H. Zhang, M. Jiang, L.-H. Zhu, H.-Q. Tan, and B. Lu, "Synergistic genotoxicity caused by low concentration of titanium dioxide nanoparticles and p,p'-DDT in human hepatocytes," *Environmental and Molecular Mutagenesis*, vol. 51, no. 3, pp. 192–204, 2010.
- [35] S. Huang, P. J. Chueh, Y.-W. Lin, T.-S. Shih, and S.-M. Chuang, "Disturbed mitotic progression and genome segregation are involved in cell transformation mediated by nano-TiO2 long-term exposure," *Toxicology and Applied Pharmacology*, vol. 241, no. 2, pp. 182–194, 2009.
- [36] K. Bhattacharya, M. Davoren, J. Boertz, R. P. F. Schins, E. Hoffmann, and E. Dopp, "Titanium dioxide nanoparticles induce oxidative stress and DNA-adduct formation but not DNA-breakage in human lung cells," *Particle and Fibre Toxicology*, vol. 6, article 17, 2009.
- [37] J. J. Wang, B. J. S. Sanderson, and H. Wang, "Cyto- and genotoxicity of ultrafine TiO2 particles in cultured human lymphoblastoid cells," *Mutation Research*, vol. 628, no. 2, pp. 99–106, 2007.
- [38] V. Sharma, R. K. Shukla, N. Saxena, D. Parmar, M. Das, and A. Dhawan, "DNA damaging potential of zinc oxide nanoparticles in human epidermal cells," *Toxicology Letters*, vol. 185, no. 3, pp. 211–218, 2009.
- [39] J. P. Wise Sr., B. C. Goodale, S. S. Wise et al., "Silver nanospheres are cytotoxic and genotoxic to fish cells," *Aquatic Toxicology*, vol. 97, no. 1, pp. 34–41, 2010.
- [40] P. V. AshaRani, G. L. K. Mun, M. P. Hande, and S. Valiyaveetil, "Cytotoxicity and genotoxicity of silver nanoparticles in human cells," *ACS Nano*, vol. 3, no. 2, pp. 279–290, 2009.
- [41] M. Ahamed, M. Karns, M. Goodson et al., "DNA damage response to different surface chemistry of silver nanoparticles in mammalian cells," *Toxicology and Applied Pharmacology*, vol. 233, no. 3, pp. 404–410, 2008.
- [42] J. J. Li, L. Zou, D. Hartono, C.-N. Ong, B.-H. Bay, and L.-Y. L. Yung, "Gold nanoparticles induce oxidative damage in lung fibroblasts in vitro," *Advanced Materials*, vol. 20, no. 1, pp. 138–142, 2008.
- [43] P. V. Asharani, N. Xinyi, M. P. Hande, and S. Valiyaveetil, "DNA damage and p53-mediated growth arrest in human cells treated with platinum nanoparticles," *Nanomedicine*, vol. 5, no. 1, pp. 51–64, 2010.
- [44] B. K. Pierscionek, Y. Li, A. A. Yasseen, L. M. Colhoun, R. A. Schachar, and W. Chen, "Nanoceria have no genotoxic effect on human lens epithelial cells," *Nanotechnology*, vol. 21, no. 3, Article ID 035102, 2010.
- [45] L. He, L. Yang, Z.-R. Zhang et al., "In vitro evaluation of the genotoxicity of a family of novel MeO-PEG-poly(D,L-lactico-co-glycolic acid)-PEG-OMe triblock copolymer and PLGA nanoparticles," *Nanotechnology*, vol. 20, no. 45, Article ID 455102, 2009.
- [46] G. D. Nielsen, M. Roursgaard, K. A. Jensen, S. S. Poulsen, and S. T. Larsen, "In vivo biology and toxicology of fullerenes and their derivatives," *Basic and Clinical Pharmacology and Toxicology*, vol. 103, no. 3, pp. 197–208, 2008.
- [47] F. Lao, L. Chen, W. Li et al., "Fullerene nanoparticles selectively enter oxidation-damaged cerebral microvessel endothelial cells inhibit JNK-related apoptosis," *ACS Nano*, vol. 3, no. 11, pp. 3358–3368, 2009.

- [48] Z. Hu, W. Guan, W. Wang, L. Huang, H. Xing, and Z. Zhu, "Synthesis of  $\beta$ -alanine C60 derivative and its protective effect on hydrogen peroxide-induced apoptosis in rat pheochromocytoma cells," *Cell Biology International*, vol. 31, no. 8, pp. 798–804, 2007.
- [49] B. Sitharaman, T. Y. Zakharian, A. Saraf et al., "Water-soluble fullerene (C60) derivatives as nonviral gene-delivery vectors," *Molecular Pharmaceutics*, vol. 5, no. 4, pp. 567–578, 2008.
- [50] C. S. Foote, F. N. Diederich, R. Whetten, and F. Wudl, "Buckminsterfullerene," *Chemical and Engineering News*, vol. 68, no. 51, p. 2, 1990.
- [51] R. C. Aitken, K. S. Creely, and C. L. Tran, *Nanoparticles: An Occupational Hygiene Review*, HSE Books, Suffolk, UK, 2004.
- [52] S. Moreira, N. B. Silva, J. Almeida-Lima et al., "BC nanofibres: in vitro study of genotoxicity and cell proliferation," *Toxicology Letters*, vol. 189, no. 3, pp. 235–241, 2009.
- [53] K. Pulskamp, S. Diabaté, and H. F. Krug, "Carbon nanotubes show no sign of acute toxicity but induce intracellular reactive oxygen species in dependence on contaminants," *Toxicology Letters*, vol. 168, no. 1, pp. 58–74, 2007.
- [54] N. S. Allen, M. Edge, G. Sandoval, J. Verran, J. Stratton, and J. Maltby, "Photocatalytic coatings for environmental applications," *Photochemistry and Photobiology*, vol. 81, no. 2, pp. 279–290, 2005.
- [55] M. J. Jackson and A. Waqar, *Titanium Dioxide Coatings in Medical Devices*, Springer, New York, NY, USA, 2007.
- [56] M. C. Powell and M. S. Kanarek, "Nanomaterial health effects—part 2: uncertainties and recommendations for the future," *Wisconsin Medical Journal*, vol. 105, no. 3, pp. 18–23, 2006.
- [57] I.-S. Kim, M. Baek, and S.-J. Choi, "Comparative Cytotoxicity of  $\text{Al}_2\text{O}_3$ ,  $\text{CeO}_2$ ,  $\text{TiO}_2$  and ZnO nanoparticles to human lung cells," *Journal of Nanoscience and Nanotechnology*, vol. 10, no. 5, pp. 3453–3458, 2010.
- [58] C. P. Case, "Chromosomal changes after surgery for joint replacement," *The Journal of Bone and Joint Surgery—Series B*, vol. 83, no. 8, pp. 1093–1095, 2001.
- [59] R. Hardman, "A toxicologic review of quantum dots: toxicity depends on physicochemical and environmental factors," *Environmental Health Perspectives*, vol. 114, no. 2, pp. 165–172, 2006.
- [60] A. M. Deraus, W. C. W. Chan, and S. N. Bhatia, "Probing the cytotoxicity of semiconductor quantum dots," *Nano Letters*, vol. 4, no. 1, pp. 11–18, 2004.
- [61] K. G. Li, J. T. Chen, S. S. Bai et al., "Intracellular oxidative stress and cadmium ions release induce cytotoxicity of unmodified cadmium sulfide quantum dots," *Toxicology in Vitro*, vol. 23, no. 6, pp. 1007–1013, 2009.
- [62] M. Waisberg, P. Joseph, B. Hale, and D. Beyersmann, "Molecular and cellular mechanisms of cadmium carcinogenesis," *Toxicology*, vol. 192, no. 2–3, pp. 95–117, 2003.
- [63] M.-C. Rousseau, K. Straif, and J. Siemiatycki, "IARC carcinogen update," *Environmental Health Perspectives*, vol. 113, no. 9, pp. A580–A581, 2005.
- [64] S. J. S. Flora, M. Mittal, and A. Mehta, "Heavy metal induced oxidative stress & its possible reversal by chelation therapy," *Indian Journal of Medical Research*, vol. 128, no. 4, pp. 501–523, 2008.
- [65] M. Kumari, A. Mukherjee, and N. Chandrasekaran, "Genotoxicity of silver nanoparticles in *Allium cepa*," *Science of the Total Environment*, vol. 407, no. 19, pp. 5243–5246, 2009.
- [66] Y. Pan, A. Leifert, D. Ruau et al., "Gold nanoparticles of diameter 1.4 nm trigger necrosis by oxidative stress and mitochondrial damage," *Small*, vol. 5, no. 18, pp. 2067–2076, 2009.
- [67] S. M. Hirst, A. S. Karakoti, R. D. Tyler, N. Sriranganathan, S. Seal, and C. M. Reilly, "Anti-inflammatory properties of cerium oxide nanoparticles," *Small*, vol. 5, no. 24, pp. 2848–2856, 2009.
- [68] M. L. López-Moreno, G. de la Rosa, and J. A. Hernandez-Viezas, "Evidence of the differential biotransformation and genotoxicity of ZnO and CeO(2) nanoparticles on Soybean (*Glycine max*) plants," *Environmental Science & Technology*. In press.
- [69] Q. He, J. Shi, F. Chen, M. Zhu, and L. Zhang, "An anticancer drug delivery system based on surfactant-templated mesoporous silica nanoparticles," *Biomaterials*, vol. 31, no. 12, pp. 3335–3346, 2010.
- [70] M. Liong, J. Lu, M. Kovochich et al., "Multifunctional inorganic nanoparticles for imaging, targeting, and drug delivery," *ACS Nano*, vol. 2, no. 5, pp. 889–896, 2008.
- [71] V. Piddubnyak, P. Kurcok, A. Matuszowicz et al., "Oligo-3-hydroxybutyrates as potential carriers for drug delivery," *Biomaterials*, vol. 25, no. 22, pp. 5271–5279, 2004.
- [72] A. S. Chauhan, P. V. Diwan, N. K. Jain, and D. A. Tomalia, "Unexpected in vivo anti-inflammatory activity observed for simple, surface functionalized poly(amidoamine) dendrimers," *Biomacromolecules*, vol. 10, no. 5, pp. 1195–1202, 2009.
- [73] Y. Song, X. Li, and X. Du, "Exposure to nanoparticles is related to pleural effusion, pulmonary fibrosis and granuloma," *European Respiratory Journal*, vol. 34, no. 3, pp. 559–567, 2009.
- [74] J. D. Brain, W. Kreyling, and P. Gehr, "To the editors: express concern about the recent paper by Song et al," *The European Respiratory Journal*, vol. 35, no. 1, pp. 226–227, 2010.
- [75] A. Takagi, A. Hirose, T. Nishimura et al., "Induction of mesothelioma in p53+/- mouse by intraperitoneal application of multi-wall carbon nanotube," *Journal of Toxicological Sciences*, vol. 33, no. 1, pp. 105–116, 2008.
- [76] Y. Sakamoto, D. Nakae, N. Fukumori et al., "Induction of mesothelioma by a single intrascrotal administration of multi-wall carbon nanotube in intact male Fischer 344 rats," *Journal of Toxicological Sciences*, vol. 34, no. 1, pp. 65–76, 2009.
- [77] J. Muller, M. Delos, N. Panin, V. Rabolli, F. Huaux, and D. Lison, "Absence of carcinogenic response to multiwall carbon nanotubes in a 2-year bioassay in the peritoneal cavity of the rat," *Toxicological Sciences*, vol. 110, no. 2, pp. 442–448, 2009.
- [78] E. Bergamaschi, O. Bussolati, A. Magrini et al., "Nanomaterials and lung toxicity: interactions with airways cells and relevance for occupational health risk assessment," *International Journal of Immunopathology and Pharmacology*, vol. 19, supplement 4, pp. 3–10, 2006.
- [79] P. J. A. Borm and W. Kreyling, "Toxicological hazards of inhaled nanoparticles—potential implications for drug delivery," *Journal of Nanoscience and Nanotechnology*, vol. 4, no. 5, pp. 521–531, 2004.
- [80] D. Wang, L. Sun, W. Liu, W. Chang, X. Gao, and Z. Wang, "Photoinduced DNA cleavage by  $\alpha$ -,  $\beta$ -, and  $\gamma$ -cyclodextrin-bicapped C60 supramolecular complexes," *Environmental Science and Technology*, vol. 43, no. 15, pp. 5825–5829, 2009.
- [81] A. Radomski, P. Jurasz, D. Alonso-Escolano et al., "Nanoparticle-induced platelet aggregation and vascular thrombosis," *British Journal of Pharmacology*, vol. 146, no. 6, pp. 882–893, 2005.
- [82] N. Sera, H. Tokiwa, and N. Miyata, "Mutagenicity of the fullerene C60-generated singlet oxygen dependent formation

of lipid peroxides," *Carcinogenesis*, vol. 17, no. 10, pp. 2163–2169, 1996.

- [83] R. Baan, K. Straif, Y. Grosse, B. Secretan, F. El Ghissassi, and V. Cogliano, "Carcinogenicity of carbon black, titanium dioxide, and talc," *The Lancet Oncology*, vol. 7, no. 4, pp. 295–296, 2006.

## Review Article

# Formation and Repair of Tobacco Carcinogen-Derived Bulky DNA Adducts

**Bo Hang**

*Life Sciences Division, Department of Cancer and DNA Damage Responses, Lawrence Berkeley National Laboratory, Berkeley, CA 94720, USA*

Correspondence should be addressed to Bo Hang, bo.hang@lbl.gov

Received 20 May 2010; Revised 16 July 2010; Accepted 17 September 2010

Academic Editor: Ashis Basu

Copyright © 2010 Bo Hang. This is an open access article distributed under the Creative Commons Attribution License, which permits unrestricted use, distribution, and reproduction in any medium, provided the original work is properly cited.

DNA adducts play a central role in chemical carcinogenesis. The analysis of formation and repair of smoking-related DNA adducts remains particularly challenging as both smokers and nonsmokers exposed to smoke are repetitively under attack from complex mixtures of carcinogens such as polycyclic aromatic hydrocarbons and *N*-nitrosamines. The bulky DNA adducts, which usually have complex structure, are particularly important because of their biological relevance. Several known cellular DNA repair pathways have been known to operate in human cells on specific types of bulky DNA adducts, for example, nucleotide excision repair, base excision repair, and direct reversal involving *O*<sup>6</sup>-alkylguanine DNA alkyltransferase or AlkB homologs. Understanding the mechanisms of adduct formation and repair processes is critical for the assessment of cancer risk resulting from exposure to cigarette smoke, and ultimately for developing strategies of cancer prevention. This paper highlights the recent progress made in the areas concerning formation and repair of bulky DNA adducts in the context of tobacco carcinogen-associated genotoxic and carcinogenic effects.

## 1. Introduction

Tobacco was traded from North America to the world about 500 years ago. Since then, tobacco use by smoking cigarettes, cigars, and pipes, or by chewing, has wreaked havoc on mankind. Nearly 1.3 billion people are active smokers worldwide [1], who also pose a threat of indirect exposure to even more nonsmokers through secondhand smoke (SHS, also known as environmental tobacco smoke, ETS). Cigarette smoke accounts for 30% of all cancer deaths. Based on the International Agency for Research on Cancer (IARC), cigarette smoking is associated with cancers in many organs/tissues such as lung, head, neck, and bladder [2]. The lung is particularly vulnerable as ~90% of lung cancer cases are caused by cigarette smoking. Cigarette smoke causes other diseases as well, including pulmonary disorders, cardiovascular diseases and stroke, and developmental defects. There is also sufficient evidence in recent years that SHS causes lung cancer [3]. In US nonsmokers, SHS is responsible for about 3,000 lung cancer deaths, 46,000 cardiac-related illnesses, and 430 sudden infant death syndrome (SIDS) per year [4].

Four types of smoke have been classified so far [5]: (1) Mainstream smoke (MSS), created by tobacco combustion at approximately 1,200–1,600°C, when smokers inhale the tobacco smoke from a burning cigarette, (2) Sidestream smoke (SSS), emanating from the smouldering end of a lit cigarette at ~900°C when no active smoking occurs while the smoker pauses before taking the next puff, (3) SHS, a mixture of about 85% of SSS and 15% of exhaled MSS, and (4) Thirdhand smoke (THS), a newly emerged type, defined as residual tobacco smoke adsorbed onto indoor surfaces after active smoking has ceased, where the semivolatile and nonvolatile components undergo chemical transformation to produce new toxicants [6–8].

In the last 50 years, many studies have been performed to identify chemical toxicants in cigarette smoke, which may represent the most rich resource of exogenous human mutagens and carcinogens. MSS contains more than 4,000 chemicals. Among them, over 60 have been classified by IARC as carcinogens [9]. These include 10 polycyclic aromatic hydrocarbons (PAHs), 6 hydrocarbons, 10 nitrosamines, 13 aromatic amines, 2 aldehydes, 3 phenolic compounds, 4 volatile hydrocarbons, 3 nitro compounds,

12 miscellaneous organic compounds, and 9 inorganic and metals compounds [10]. This list contains some of the strong animal and/or human carcinogens, such as PAHs, *N*-nitrosamines, and aromatic amines, all of which react with DNA to form adducts [11–13]. The most prevalent ones in the vapor phase are aldehydes, benzene, and butadiene. It should be emphasized that SSS or SHS also contains several thousand individual compounds as does MSS [5], and most of the above-mentioned carcinogens are also present in SSS/SHS [12]. Since such a carcinogenic source, that is, cigarette smoke, is preventable, and DNA adduct levels correlate with cigarette consumption [13], tobacco smoke provides a unique model for understanding the cause-effect or environment-gene relationship in smoking-related cancer development. However, the real assessment of such relationships is very difficult due to multiple reasons [14]. For example, Metabolic activation imposes an additional level of complexity for such assessment. In addition, cigarette smoke contains co-carcinogens and tumor promoters that are also crucial for tumorigenicity of smoke condensates [12, 15, 16].

Although certain carcinogens in cigarette smoke, such as formaldehyde and  $\alpha,\beta$ -unsaturated aldehydes (enals), directly react with DNA to form covalent adducts, most of carcinogenic compounds are so-called procarcinogens that must be metabolically activated to form ultimate carcinogens [12]. These metabolites are usually electrophilic that react with the nucleophilic sites on DNA bases. The well-studied microsomal cytochrome P450 (CYP) system [17] activates many tobacco carcinogens such as PAHs, *N*-nitrosamines, aromatic amines, and benzene [18–20]. Therefore, carcinogen metabolism is often a double-edged sword in that it not only detoxifies and excretes toxicants but may also convert them into harmful reactive species. The individual variation in metabolic activation such as genetic polymorphisms in carcinogen-metabolizing genes is an important determinant of DNA adduct levels and is used to identify smokers with increased cancer risk [21, 22].

Most chemical carcinogens react with cellular DNA as the ultimate target. Cigarette smoke condensates were initially known to have mutagenic activity by the 1970s [23], and adducts were detected in cellular DNA from smokers in the 1980s [24]. Since then, many tobacco carcinogen-derived adducts have been identified *in vitro* and *in vivo*, owing to the development of highly sensitive analytical detection methods, such as  $^{32}\text{P}$ -postlabeling and mass spectrometry (MS) [25, 26]. It has been shown that cigarette smokers have higher levels of DNA adducts than nonsmokers [12, 13, 27, 28]. Studies have also shown that current smokers have higher adduct levels compared with former smokers [13]. With some exceptions of inconsistency, many epidemiologic and clinical studies have shown an association between the *in vivo* levels of DNA adducts resulting from cigarette smoke and the occurrence of tobacco-related cancers in lung, head and neck, and bladder [13]. There are numerous reviews specifically related to the relationships between tobacco carcinogen exposure, DNA adduct formation, carcinogen/adduct mutagenic potential, and increased cancer risk related to smoking [13, 19, 26, 27, 29–32].

Tobacco carcinogens generate a broad spectrum of DNA lesions ranging from sugar damage, apurinic/apyrimidinic (AP) sites, small modified bases (e.g.,  $\text{O}^6\text{-mG}$  and 8-oxoG), and bulky base adducts to more deleterious lesions such as DNA crosslinks and strand breaks. The so-called bulky DNA adducts are formed by the covalent binding of those chemical carcinogens with large size, such as PAHs and aromatic amines, to various sites on DNA bases. These adducts also include exocyclic DNA bases such as the etheno, propano, and benzetheno adducts formed by respective bifunctional compounds [33, 34]. These bulky adducts represent a major and important class of DNA damage originating from exposure to cigarette smoke. One characteristic of these bulky adducts is that they tend to significantly disrupt the DNA helical structure and block Watson-Crick base pairing [35, 36]. They are usually highly mutagenic, as exemplified by the PAH-DNA adducts [30] and exocyclic DNA adducts [34, 37]. Some of them may not be repaired (e.g., benzo[*c*]phenanthrene  $\text{N}^6\text{-dA}$  adducts [38]) or only poorly repaired (e.g., two dibenzo[*a,l*]pyrene-induced DNA adduct [39]), thus leading to their persistence in genomic DNA. Smokers with high levels of these bulky adducts have been shown to be associated with an increased risk of cancers [40, 41]. In fact, most of the compelling data on the connection of DNA adducts with cancer have been obtained with bulky DNA adducts and their respective carcinogens. For example, PAH- and acrolein-DNA adducts are preferentially formed in the same mutational hotspots of *p53* in the lung cancers of smokers [30, 42, 43]. This tumor suppressor gene is frequently mutated in ~40% of lung cancer cases. There is also evidence that a high level of bulky DNA adducts in tissues, such as those caused by PAHs and vinyl chloride (VC), is associated with an increased risk of tumor in humans and animals [40, 44–46]. It should be pointed out that tobacco smoke also produces reactive oxygen species (ROS) and induces oxidative stress [11, 47]. Those lesions that arise directly from ROS attack of a base (e.g., 8-oxoG) or deoxyribose (e.g., base propenals) [48, 49] could also play a role in tobacco carcinogenesis.

Cigarette smoking can cause complex biological responses. If unrepaired, DNA adducts may block replication and transcription. There is evidence that only a single BPDE-DNA adduct can effectively block expression of a reporter gene [50]. DNA damage can either activate checkpoint signaling pathways leading to cell cycle arrest or induce cell apoptosis by recruitment of immunologic and inflammatory responses [31]. More importantly, persistence of DNA adducts such as those formed by tobacco carcinogens PAHs and *N*-nitrosamines plays a central role in tobacco-induced carcinogenesis [27]. These adducts not only represent a very early event by inducing specific genetic changes that are a prerequisite to the initiation of cancer, but also occur during the continuum of the carcinogenic process [31]. DNA adducts can lead to nucleotide misincorporation, thus causing gene mutations. Mutations in the *p53* gene are more commonly observed in lung cancers from smokers than nonsmokers [51, 52]. Exposure to smoking has been associated with activating mutations in proto-oncogenes (e.g., the *ras* gene family) and inactivation of tumor

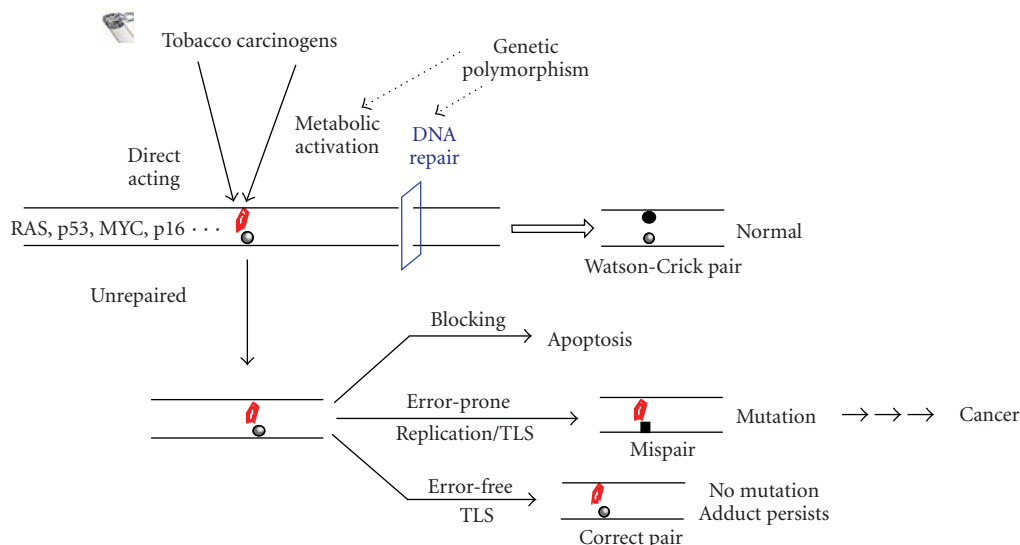


FIGURE 1: Schematic presentation of the formation, repair and mutagenic potential of tobacco carcinogen-induced bulky adducts in genomic DNA. The formation of a bulky DNA adduct (marked in red), if not repaired or poorly repaired, results in multiple genetic changes such as cell death and gene mutation. TLS (translesion DNA synthesis) can prevent a mutation by error-free incorporation opposite the adduct. Error-prone incorporation at the adduct site by replicative or translesional DNA pols is the source for mutation. Only those adducts that finally escape all the defense mechanisms may lead to biologically important mutations.

suppressor genes (e.g., *p53* and *p16*) in cancers [53–56]. Microarray-based analyses also reveal that cigarette smoking alters expression of many genes involved in other functions [57]. In addition to point mutations, there are correlations between DNA adduct levels and other somatic alterations, for example, loss of heterozygosity (LOH) that may occur at the very early stages of tobacco carcinogenesis [58, 59]. In addition, epigenetic changes such as abnormal promoter methylation of certain genes also occur more frequently in lung tumors from smokers than in never-smokers or may appear in healthy individuals who start to smoke [60, 61], highlighting the importance of both genetic and epigenetic changes in tobacco carcinogenesis. Tobacco carcinogens can also contribute to tumorigenesis by interacting with proteins, RNA, and lipids, in addition to DNA.

To avoid tobacco carcinogen-induced DNA damage, quitting smoking or avoiding exposure is the first and foremost important approach. However, once such damage is formed, DNA repair is the next major defense mechanism (Figure 1). Organisms from prokaryotes to mammals have evolved a number of repair pathways, including direct reversal, base excision repair (BER), nucleotide excision repair (NER), mismatch repair (MMR), and double-strand break (DSB) repair [62–64]. In model systems, such as cultured cells and genetically manipulated organisms, these pathways have been shown to operate on specific types of DNA lesions. NER is the major pathway for the repair of various duplex-distorting bulky DNA lesions such as those induced by PAHs. Small alkylated and oxidized lesions, including those arising from endogenous sources, are excised by the BER pathway which also repairs certain single-ring exocyclic DNA adducts. For certain alkylated bases and etheno adducts, they can be repaired through direct reversal

carried out by specialized repair proteins. In general, the understanding of damage recognition and mechanism of repair is important to gain insight into the specific roles of tobacco DNA adducts in the development of cancer and other chronic diseases since, at the end, the overall cellular repair capacity in response to exposure is critically related to the levels of DNA adducts in the genome or mutations in genes. The role of individual variability in repair, for example, polymorphisms in repair genes, has been related to the increased cancer risk in smokers [22, 65, 66]. Ultimately, it is the impaired or poor repair of DNA adducts (e.g., those bulky adducts and oxidized bases with cytotoxicity and mutagenicity) that is expected to be most important in the etiology of smoking-related cancer and other disorders.

Studies in the last decade have revealed that if a DNA adduct is unrepaired or irreparable, cells may use translesion DNA synthesis (TLS) to bypass the adduct to ensure the continuum of DNA replication [67–69]. TLS is performed by various specialized DNA polymerases (pols), mostly from the Y-family, with the possibility of nucleotide misincorporation [70, 71]. These enzymes possess an open and preformed active site, enabling accommodation of a broad spectrum of DNA adducts with different structures [69]. In studies reported in literature, error-prone incorporations opposite an adducted nucleotide appear to occur commonly or co-exist with error-free incorporations [72–74]. However, in some other cases, TLS pols perform error-free bypass on damaged DNA templates such as the efficient and correct nucleotide incorporation at the acrolein adduct  $\gamma$ -HO-PdG by pol  $\iota$  and subsequent extension of replication by pol  $\kappa$  [75]. The fidelity of TLS observed in these experiments tends to depend on the individual pol tested as well as the structure of the target adduct. In general, the primary roles of these pols

and how they operate in the cell with regard to interacting with replication and repair machineries remain to be further understood.

This paper will focus on the formation and repair of bulky/exocyclic DNA adducts induced by the major tobacco carcinogens in relation to tobacco mutagenesis and carcinogenesis. For small base lesions induced by tobacco chemical carcinogens, see previous reviews by Singer [76] and Shrivastav et al. [77]. In general, the literature so far on the covered review topics has been extensive. Therefore, only selected published data are used to illustrate the relevant areas, ideas, and concepts. I regret that this review does not permit acknowledgment of the many researchers who made the original findings in these important areas.

## 2. Formation and Repair of Bulky DNA Adducts by Tobacco Carcinogens

*2.1. Formation of Bulky DNA Adducts: An Overview.* Since smokers are repetitively exposed to complex mixtures of genotoxic carcinogens, the collective formation of DNA adducts is very complex as reflected by their chemical types and cellular levels. Although this paper is focused on bulky DNA adducts, other types of DNA lesions by tobacco carcinogens may be equally or more important than bulky DNA adducts for a given carcinogen or cancer type. DNA adduct levels are normally analyzed in target tissues in order to elucidate the relationship between tobacco carcinogens and cancer development. These levels should reach steady state such that the number of newly formed adducts equals the number of adducts lost every day which are related to a number of factors including carcinogen reactivity, exposure doses, timing of exposure, metabolic processes, and DNA repair capacity [13]. Understanding of DNA adducts with regard to their formation, isolation, and identification can be critical in several ways: (1) to understand the mechanism of tobacco carcinogens; for example, the analysis of formation of DNA adduct at gene mutational hotspots [30, 78] has provided important insight into the cancer etiology; (2) to assess the biologically effective doses of tobacco carcinogens [25]; (3) to assess DNA repair capacity (DRC) towards the adducts [13, 79]; (4) to find biomarkers of tobacco genotoxicity and uptake/metabolism of specific carcinogens [12, 13].

Many types of DNA adducts, including those formed by benzo[*a*]pyrene (B[*a*]P), 4-(methylnitrosamino)-1-(3-pyridyl)-1-butanone (NNK), *N'*-nitrosonornicotine (NNN), and 4-aminobiphenyl (4-ABP), have been detected from tissues of smokers as well as nonsmokers exposed to SHS [11–13, 80–82]. The common tobacco carcinogens and related metabolites that give rise to bulky DNA adducts are listed in Figure 2. In tissues, the typical adduct levels are at about 1 adduct in  $10^6$ – $10^7$  normal bases [27, 83]. In general, DNA adduct levels as low as 1 in  $10^6$ – $10^{12}$  normal bases can be significant with definite biological consequences [84]. Although  $^{32}\text{P}$ -postlabeling and immunoassay have been extensively utilized for adduct analysis, the detection and identification of DNA adducts at these or even lower levels have been greatly facilitated by the highly sensitive/specific

and new types of techniques [11, 12, 25, 26] such as HPLC with fluorescence, mass spectrometry (MS), and electrochemical detection, particularly the coupling of liquid chromatography (LC) to MS and electrospray ionization (ESI), that is, LC-ESI-MS [25]. The number of compounds/DNA adducts in Figure 2 is expected to grow when more of such studies are carried out. It should be emphasized that SHS also contains all of the common carcinogenic compounds listed in Figure 2, albeit with varying concentrations. Some of the significantly existing chemical carcinogens in SHS are NNK, NNN, B[*a*]P, benz[*a*]anthracene, benzene, 1,3-butadiene, 4-ABP, and 2-naphthylamine [5].

In addition to being directly formed by tobacco carcinogens, DNA adducts can be generated through inflammation, particularly by ROS and reactive nitrogen species (RNS). Due to the direct surface exposure, cigarette smoking triggers an inflammatory response in human lung and causes chronic obstructive pulmonary disease (COPD) [85], which has been shown to possess significant abnormalities in inflammatory pathways [86–89]. Smokers are known to have elevated levels of oxidative stress [11, 47], which is increasingly linked to cancer and neurological diseases [90, 91]. Cigarette smoke may induce oxidative stress by several mechanisms [11, 47]: (1) it contains oxidizing compounds and ROS; (2) the ROS-generating redox cycling by quinone-hydroquinone complex as well as PAH quinones and their corresponding catechols; (3) smoking may weaken the antioxidant defense system. The elevated oxidative stress in smokers is accompanied by lipid peroxidation (LPO) [11] which results from reactions of reduced oxygen species with polyunsaturated fatty acids (PUFAs). It is well documented that LPO produces enals, including acrolein, crotonaldehyde, and *trans*-4-hydroxy-2-nonenal (HNE) [92–94]. These compounds react with DNA to produce etheno ( $\epsilon$ )-adducts as well as propano adducts [92–94]. This explains why chronic inflammation in humans is accomplished by increased levels of such adducts [94]. It should be noted that these adducts are also present in tissues of humans and untreated animals at very low levels as background lesions [92–94].

To understand the chemistry between a carcinogen and DNA bases is instrumental in revealing the molecular mechanism of mutagenicity and carcinogenicity of the carcinogen [18]. A single carcinogen can cause several different types of DNA damage, mainly due to the process of metabolism that can yield several or many reactive metabolites. All the carcinogens listed in Figure 2 can form more than one type of DNA adducts. For example, NNK can form both simple methylated and bulky pyridyloxobutyl (POB) adducts [80, 84]. A single electrophilic carcinogen can form multiple adducts of the same nature by reacting with all four DNA bases. For example, benzene metabolites, hydroquinone (HQ) and para-benzoquinone (*p*-BQ), form exocyclic adducts on dA, dC, and dG [95–98]. BPDE, by way of another example, can generate both dG and dA adducts. Different carcinogens preferentially react with different sites on the bases [18]. For dG, PAHs predominantly bind to its 2-NH<sub>2</sub> group, alkylating agents such as tobacco-specific nitrosamines (TSNAs) mainly react at the *N*-7 or O<sup>6</sup> position, and aromatic amines tend to bind to the 8-carbon

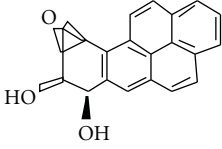
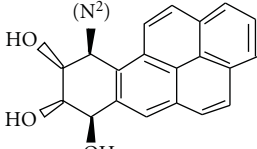
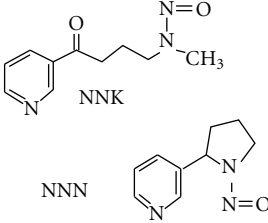
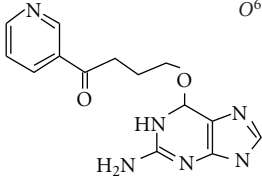
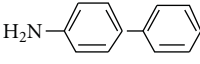
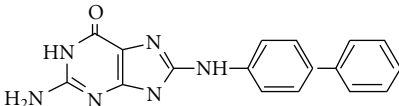
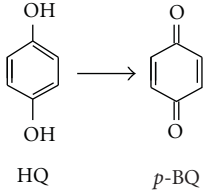
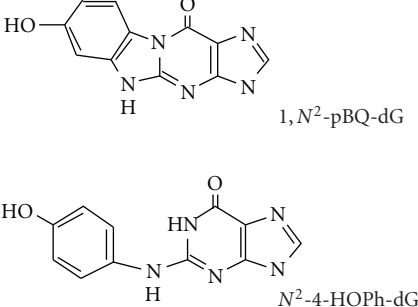
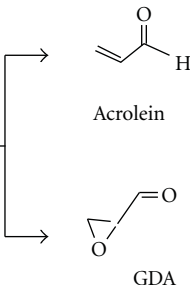
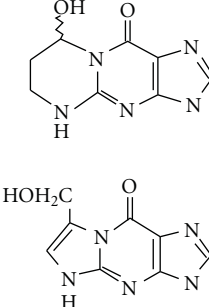
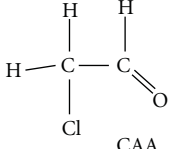
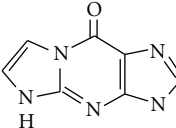
Carcinogen	Metabolite	Adduct Structure
B[ $\alpha$ ]P	 (-)-anti-BPDE	 (+)-trans-BPDE-N <sup>2</sup> -dG
TSNAs	 NNK NNN	 O <sup>6</sup> -POB-dG
ABP	 4-ABP	 dG-C8-ABP
Benzene	 HQ p-BQ	 1,N <sup>2</sup> -pBQ-dG N <sup>2</sup> -4-HOPh-dG
Acrolein	 Acrolein GDA	 $\gamma$ -OH-PdG 1,N <sup>2</sup> -hm- $\epsilon$ G
VC	 CAA	 1,N <sup>2</sup> - $\epsilon$ G

FIGURE 2: Structures of tobacco carcinogens, metabolites, and bulky dG adducts. These are only the partial list of DNA reactive carcinogens in cigarette smoke. The dG adducts listed are representatives of the adducts formed by the corresponding metabolites. Note that the stereochemistry of BPDE-DNA adducts is complex (see text). Acrolein can form two propano dG isomers,  $\gamma$ -HO-PdG (major), and  $\alpha$ -HO-PdG (minor). CAA forms angular  $N^2,3$ - $\epsilon$ G, an isomer for  $1,N^2$ - $\epsilon$ G.

position [25]. All oxygen and nitrogen sites on DNA bases are actually reactive with alkylating agents *in vitro* under physiological conditions [18].

Of the DNA adducts formed by tobacco carcinogens, exocyclic adducts have been extensively studied for their chemistry of formation [34, 99]. Bifunctional electrophilic compounds such as HQ and *p*-BQ, acrolein, and VC metabolites, are all able to form exocyclic adducts [44]. The common sites for forming an exocyclic ring are *N*-1 and *N*<sup>6</sup> of dA, *N*-3 and *N*<sup>4</sup> of dC, *N*-1 and *N*<sup>2</sup> of dG as well as *N*<sup>2</sup> and *N*-3 of dG (superscript indicates exocyclic oxygen or nitrogen) [100]. Adducts may be promutagenic if formed at coding sites of the bases, including *O*<sup>6</sup>, *N*-1, and *N*<sup>2</sup> of dG, *N*-1 and *N*<sup>6</sup> of dA, *O*<sup>2</sup>, *N*-3, and *N*<sup>4</sup> of dC, and *O*<sup>4</sup> and *N*-3 of T [101]. Structurally, exocyclic adducts are analogous but can differ in ring structure such as size (e.g., 5- versus 6-membered), number (e.g., one ring versus two rings), angularity (e.g., linear versus angular), substituents' nature (e.g., -OH versus -CH<sub>2</sub>OH), and location (e.g.,  $\alpha$ -HO-PdG versus  $\gamma$ -HO-PdG) [34, 102]. The structural features of specific adducts may define the specificity and efficiency of their repair, as discussed below, as well as their mutagenicity.

**2.2. Repair of Bulky DNA Adducts: An Overview.** In the last two decades or so, considerable progress has been made in understanding the specificity, mechanism of action, and *in vivo* importance of many repair enzymes and pathways. This has been greatly facilitated by major advances in discovery of new enzymes or novel activities, synthesis of site-directed damage-containing oligonucleotides, construction of damage-containing shuttle vectors and viral genomes for *in vivo* studies, determination of high-resolution structures of repair enzymes and damaged DNA, development of gene mutant models, identification of protein interaction networks, gene analyses such as mutation spectrum mapping and single nucleotide polymorphisms (SNPs), and by the latest studies using omic profiling technology. There are many excellent reviews specifically related to the complete process as well as specific repair pathways that restore DNA to its normal state [62–64, 103–108].

Several major mechanisms have been shown to be involved in the repair of bulky DNA adducts that can be induced by tobacco carcinogens, as discussed below in detail. It is important to determine which adducts are removed efficiently or poorly, as those adducts that persist may cause a greater long-term mutagenic potential. Excision repair, whether it is base (BER) or nucleotide excision (NER), has to be at least a two-step process in which the damage recognition and excision is followed by DNA replication, whereas direct reversal, catalyzed by *O*<sup>6</sup>-alkylguanine DNA alkyltransferase (AGT, also known as MGMT) or AlkB homologs (ABHs), restores the normal base without excision [64]. Multiple repair mechanisms could be involved in the removal of various DNA adducts produced by a single compound. As will be described below, the benzetheno adducts of HQ/*p*-BQ are substrates for AP endonuclease, and the hydroxyphenyl dG adduct formed by the same compounds is repaired by NER. In some cases, more than one enzyme or mechanism can act on the same adduct,

which may serve as backups or operate with different functions in the cell. For example, 3, *N*<sup>4</sup>-ethenocytosine ( $\epsilon$ C) is excised by three different DNA glycosylases and repaired by two different repair pathways, BER and ABH2. Although the mismatch repair (MMR) pathway appears not to be directly implicated yet as significantly as the above pathways in response to the bulky adducts, MutS protein has been shown to bind to the propano dG and M<sub>1</sub>G adducts [109], suggesting that MutS can bind to exocyclic adducts and may trigger a MMR-mediated response.

Although certain repair data come from research using prokaryotic enzymes, this paper will concentrate on mammalian/human repair enzymes whenever possible. In principle, the analogous enzymes and general mechanisms exist in both prokaryotes and eukaryotes, and such conservation has provided a solid foundation for our understanding of mammalian repair. It should also be pointed out that much of the repair data concerning tobacco carcinogen-derived adducts was not directly obtained from tobacco-related studies, but rather based on reports focusing on chemical carcinogens *per se*.

### 2.3. Repair of Specific DNA Adducts by Different Pathways

**2.3.1. Nucleotide Excision Repair (NER).** NER is the most versatile repair pathway in the cell and the primary mechanism for the removal of chemical carcinogen-induced bulky DNA adducts that significantly distort the DNA helix structure [64, 107, 110, 111]. The molecular mechanism of NER is now well understood. Its pathway in eukaryotes consists of at least 30 gene products [112] and can be reconstituted with purified key proteins *in vitro* [113, 114]. Mutations in some of these NER genes may lead to xeroderma pigmentosum (XP), a genetic disorder with seven complementation groups (from XPA to XPG), and a higher incidence of skin cancer [64]. The steps in NER consist of sequential assembly of proteins that perform different functions: damage recognition by XPC-HR23B, opening of a denaturation bubble by TFIIH, incision of the damaged strand by XPG and ERCC1-XPF, displacement and excision of the lesion-containing oligonucleotide (24–32 base long), repair synthesis by DNA polymerase  $\delta/\epsilon$ , and DNA ligation by ligase III. There are two subsets of the pathway: global genomic repair (GGR) and transcription-coupled repair (TCR) that differ in the mode of damage recognition and are regulated by differential cellular mechanisms [105, 107, 110, 111]. GGR is involved in repair of DNA lesions from the transcriptionally silent regions of the genome and the nontranscribed strand of the active genes. GGR probes for DNA lesions that cause structural distortion or chemical alteration. TCR preferentially repairs the distorting lesions on the transcribed strand in active genes in order to avoid a stalled RNA polymerase II. The mammalian NER activity appears to be mostly modulated by posttranslational modifications and by protein-protein interactions.

NER activity can be measured in cell-free extracts by the cleavage of site-directed oligonucleotide containing an adduct or by the extent of DNA repair synthesis in damaged plasmid DNA. Figure 3 shows the structures of important

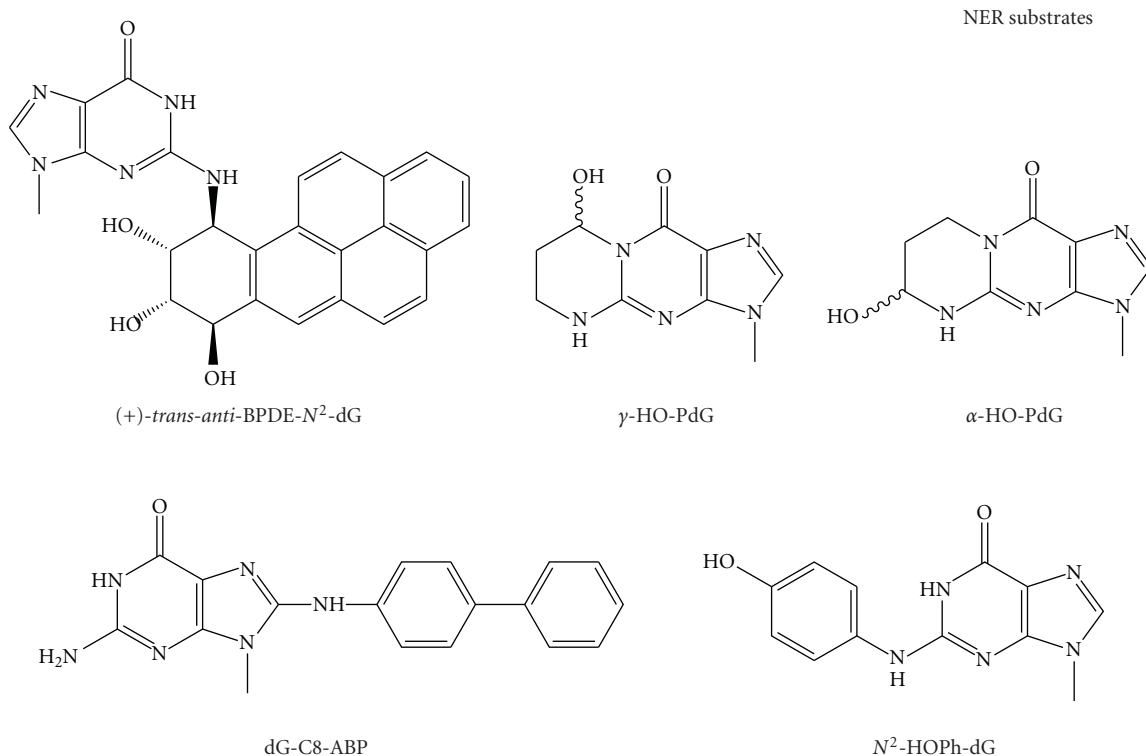


FIGURE 3: Structures of smoking-induced bulky DNA adducts that are substrates for NER.

toxic and mutagenic bulky adducts as NER substrates which are formed by those major carcinogens in cigarette smoke, including PAHs, acrolein, 4-ABP, and benzene. NER also processes endogenous bulky DNA adducts formed by enals from LPO [115]. In addition, intra- and interstrand crosslinks such as those generated by UV light and cisplatin are usually repaired by NER [64]. These crosslinks could also be formed by bifunctional tobacco chemicals such as acrolein and crotonaldehyde [116]. Therefore, NER is a critical repair pathway for protecting against the tobacco carcinogen-induced mutagenesis and carcinogenesis.

(1) *Formation and Repair of PAH-Derived DNA Adducts.* PAHs are thought to be the major contributors to the etiology of smoke-induced cancers, particularly lung cancer. B[a]P was the first carcinogen to be found in cigarette smoke [117] and has been extensively studied as a surrogate for PAHs. It is present in cigarette smoke at low levels (10–50 ng/cigarette) but is higher than other PAHs [11]. In one well studied metabolic pathway mediated by successive P450/epoxide hydrolase/P450, B[a]P yields active carcinogenic epoxides, mainly B[a]P-7,8-diol-9,10-epoxide (BPDE) [18, 118]. The diol epoxide exists as two diastereoisomers, *anti*- and *syn*-BPDE, each of which can be resolved into (+)- and (–)-enantiomers. The isomer (+)-*anti*-BPDE has the greatest tumorigenicity *in vivo* [119]. The latter reacts at the *N*<sup>2</sup> of dG to yield either *trans*- or *cis*-ring opening of the epoxide ring, forming (+)-*trans*- and (+)-*cis*-BPDE-*N*<sup>2</sup>-dG adducts [120, 121]. Similarly, (–)-*anti*-BPDE forms (–)-*trans*- and (–)-*cis*-BPDE-*N*<sup>2</sup>-dG adducts.

Of these four stereoisomeric adducts, (+)-*trans*-BPDE-*N*<sup>2</sup>-dG is the most abundant, which is also the major adduct identified *in vivo* [122, 123] and was detected in 45% of smokers' lung [124]. A second path for the activation of B[a]P involves P450-mediated activation to yield free cations [125] that can induce unstable adducts leading to AP sites. A third metabolic pathway is through aldo-keto reductase superfamily-mediated oxidation of B[a]P-7,8-diol to catechol that enters into a redox cycle to form a reactive B[a]P-7,8-quinone (BPQ) [126, 127]. Although a recent study did not support that BPQ forms stable DNA adducts in mice [128], there is evidence that this pathway operates in human lungs leading to ROS-mediated genotoxicity such as causing G to T transversions that inactivate *p53* [127, 129]. So far, the relative importance of these pathways in cancer development remains to be determined.

BPDE-DNA adducts are recognized and repaired by *E. coli* NER complex UvrABC nuclease [130] and human NER [131–133]. Taking advantage of the stereochemistry involved in the formation of these bulky adducts, a number of studies addressed the effects of adduct conformation, base pairing, and sequence context on DNA repair. For example, using an *in vitro* repair system with oligonucleotides containing one of the four BPDE-*N*<sup>2</sup>-dG adducts described above Hess et al. showed that the rates of human NER repair of these adducts are dependent on their different stereochemical configurations [131]. The rates of excision were found to vary over 100-fold among these dG adducts, and the *cis*-adducts of dG are repaired more rapidly than the *trans*-adducts [131]. It was later found that different conformations of these adducts

are recognized differentially by the NER lesion recognition complex XPC-HR23B, which can be correlated with the relatively low repair of (+)-*trans*-BPDE- $N^2$ -dG [121]. Similar correlations were observed with UvrABC nuclease [134]. To further show the importance of local DNA conformation, the nature of the base opposite a BPDE adduct is found to be critical in modulating the repair rates [38]. As will be discussed below in Section 2.5, the processing of BPDE-DNA adducts by both UvrABC and human NER is also sequence dependent. BPDE forms  $N^6$ -dA adducts in native DNA as well, although relatively inefficiently [135, 136], which exhibit differential conformation and perturbation of DNA duplex than the BPDE-dG adducts [35]. Using cell extracts, human NER activity has been shown for the (+)- or (-)-*trans-anti*-BPDE-dA adducts [38, 131].

Several early studies showed that repair of BPDE-DNA adducts occurs much faster in the transcribed strand than in the nontranscribed strand of *HPRT* or *p53* genes, indicating that these adducts are subject to TCR [137, 138]. These adducts block human RNA pol II elongation on the transcribed strand, which could be a signal for initiating TCR, also in a stereochemistry- and sequence-dependent manner [139]. A later work shows that common genetic variations in Cockayne syndrome A (CSA) and B (CSB) proteins are associated with NER repair capacity of BPDE-induced DNA damage in smokers [140]. Mutations with CSA and CSB result in Cockayne syndrome with impaired TCR [64]. Taken together, this strand preference in repair may contribute to the mutational property of the human lung cancer *p53* gene in response to BPDE exposure: repair of BPDE adducts along the nontranscribed strand of *p53* is consistently slower than repair in the transcribed strand, and repair at the major damage hotspots in the nontranscribed strand is 2–4 times slower than repair at other damage sites [138].

Dibenzo[*a,l*]pyrene (DB[*a,l*]P) is another PAH that has been found to be present in tobacco smoke particulates and is the most potent carcinogen of the PAHs tested to date in rodent systems. Similar to the B[*a*]P-derived adducts, the bulky adducts formed by ( $\pm$ )-*anti*-DBPDE possess different structures and adopt different conformations [141]. They are differentially repaired by NER in human cells with some being poorly removed, as shown by a recent study [39]. The repair of DBPDE-DNA adducts by NER has been shown to be slower than the repair of BPDE-DNA adducts [142]. In general, the poor repair by NER of DBPDE-DNA adducts, at least some of them, may account for the high carcinogenicity of the parent compound.

(2) *Formation and Repair of DNA Adducts of Aromatic Amine 4-ABP*. Chemicals in this class such as 4-ABP bind to DNA bases mainly at C-8 position. Adducts can also be formed at  $N^2$ - and  $O^6$ - of dG and  $N^6$ - of dA [30]. 4-ABP has been established as a major human bladder carcinogen [143]. 4-ABP forms DNA adducts after *N*-hydroxylation by P450 to the mutagenic metabolite *N*-hydroxy-4-aminobiphenyl (*N*-OH-4-ABP). *N*-(deoxyguanosin-8-yl)-4-aminobiphenyl (dG-C8-ABP) (Figure 2) is the major adduct of 4-ABP, and the minor adduct is *N*-(deoxyadenosin-8-yl)-4-ami-

nobiphenyl (dA-C8-ABP) [144]. The major adduct has been detected in the human cells after exposure to *N*-OH-4-ABP [145]. This adduct was also identified from DNA of the bladder biopsy samples from smokers and is quantitatively related to smoking status [146]. dG-C8-ABP adducts have been identified from human bladder cancer tissues [147, 148]. Moreover, higher levels of DNA adducts correlated with more invasive tumors (higher tumor grades) [147]. The unique binding pattern of 4-ABP in the *p53* gene, that is, the *p53* mutational hotspots in bladder cancer at several codons are also the preferential sites for 4-ABP adduct formation, links 4-ABP to the etiology of bladder cancer [149].

Although the detailed molecular mechanism of the repair of 4-ABP-DNA adducts is not clear, DNA fragments modified with *N*-OH-4-ABP were shown to be incised by *E. coli* NER complex, the UvrABC nuclease [150]. An early study investigated the rate of disappearance of dG-C8-ABP in human transitional cell carcinomas of the bladder and showed that the majority of the adducts can be removed within 48 hours after treatment with 4-ABP [151]. Another study showed that dG-ABP was repaired rapidly while dA-ABP persisted in human uroepithelial cells [144]. There is evidence of the human NER pathway involvement in the repair of these adducts, as the host cell reactivation (HCR) assays performed in NER-deficient cells showed reduced repair of DNA lesions from plasmid treated with 4-ABP [152]. In addition, it was shown that loss of function of the *p53* gene in human bladder epithelial cancer cells reduces the efficiency of repair of dG-C8-ABP, suggesting that *p53* may modulate its repair in target cells [151, 153]. The relationship between deficient DNA repair of 4-ABP-DNA adducts and increased bladder cancer risk was supported by the findings that such repair capacity was significantly lower in bladder cancer cases than in controls, and ever-smokers with low DNA repair capacity exhibited a 6-fold increased risk compared with never smokers with normal repair capacity [152].

(3) *Formation and Repair of Propano Adducts of  $\alpha,\beta$ -Unsaturated Aldehydes (Enals)*. Enals can arise from both cigarette smoking and endogenous LPO [154]. Cigarette smoke contains relatively high concentrations of acrolein and crotonaldehyde. HNE is a unique product of  $\omega$ -6 of PUFAs [92]. Acrolein is the simplest enal and is a model chemical for this class of carcinogens. Acrolein is one of the most abundant compounds in MSS (60–100  $\mu$ g/cigarette) and is also present in SSS at high concentrations [5]. It is highly reactive without metabolic activation. Acrolein forms exocyclic adducts on DNA bases, predominantly 1, $N^2$ -dG adducts [155, 156]. The principal adduct is  $\gamma$ -hydroxypropano-2'-deoxyguanosine ( $\gamma$ -OH-PdG) that exists as a mixture of C8-OH epimers (Figure 3) [157], and the other adduct is  $\alpha$ -hydroxypropano-2'-deoxyguanosine ( $\alpha$ -OH-PdG). The mutagenicity of  $\alpha$ -OH-PdG is well established, while the mutagenicity of  $\gamma$ -OH-PdG has been reported with mixed results [158, 159]. Both adducts were recently found in human lungs using LC-ESI-MS/MS [160]. Acrolein-DNA adducts have been detected in the tissues of cigarette smokers with significantly higher levels than those of nonsmokers

[161, 162]. Likewise, both crotonaldehyde and HNE also form stereoisomeric propano dG adducts, and increased crotonaldehyde-dG adduct levels were observed in smokers [163]. HNE adducts have also been detected in rodent and human tissues [163, 164]. The mutagenic potential of these dG adducts were recently summarized by Minko et al. [157].

$\gamma$ -HO-PdG is a substrate for *E. coli* UvrABC nuclease [43, 165]. In humans, NER of this adduct has been reported [158]. There is also biochemical evidence that the HNE-DNA adducts are repaired by UvrABC [92] and mammalian NER in cell-free extracts [92, 166]. A recent study revealed that NER and recombination, but not MMR, are involved in repair of HNE-treated phage DNA replicating in *E. coli* [167]. Moreover, the repair rates were shown to be affected by the adduct stereochemistry when four HNE-dG isomers were tested [166]. Interestingly, although BER is able to excise the  $1,N^2$ - $\epsilon$ G adduct, it appears to have no *in vitro* activity towards the structurally analogous adducts  $\gamma$ -OH-PdG,  $\alpha$ -OH-PdG, and PdG [168] and no *in vivo* protective role in a mutagenesis assay based on the vector containing a  $\gamma$ -OH-PdG [169].

Recent findings also pointed to the role of highly accurate TLS in protecting cells from the potential genotoxicity of the acrolein-DNA adducts [158, 165]. Previous *in vivo* site-specific mutagenicity studies have shown an efficient error-free bypass of the  $\gamma$ -HO-PdG adduct [165, 170]. Work from *E. coli* indicated that NER, recombination repair, and error-free TLS are all involved in the cellular response to this major acrolein-dG adduct [165].

(4) *Formation and Repair of In Vivo HQ-/p-BQ-Induced Hydroxyphenyl Adducts.* Benzene is a well-established human carcinogen and is associated with an increased risk of leukemia [171]. It is a significant volatile compound in the vapor phase (12–48  $\mu$ g/cigarette) [5]. In one major metabolic pathway, benzene is converted by P450 to benzene oxide which is further converted to phenol, catechol (CAT) and various derivatives [20, 172] (Figure 4). One biologically important stable metabolite is *p*-BQ, an oxidation product of HQ [20, 172]. A number of bulky DNA adducts have been detected *in vitro* and *in vivo* when exposed to HQ or *p*-BQ [95–98, 173–177]. Reaction of *p*-BQ or HQ with DNA *in vitro* has been shown to result in the formation of two ring exocyclic benzetheno adducts on dC, dA, and dG [95–98]. These adducts are highly mutagenic as tested *in vitro* with human pols involved in TLS and in yeast by site-directed mutagenesis [178]. The Bodell group has found that the DNA adducts formed in animals after benzene administration are identical to those produced in cells treated with HQ, suggesting that HQ is the main benzene metabolite causing adduct formation *in vivo* [177]. By  $^{32}$ P-postlabeling, the principal DNA adduct caused by HQ or *p*-BQ corresponds to  $N^2$ -(4-hydroxyphenyl)-2'-dG( $N^2$ -4-HOPh-dG) [173, 177]. Exocyclic adducts were also detected *in vitro* from reactions of *trans,trans*-muconaldehyde (MUC), a reactive ring-opened diene dialdehyde formed from a minor metabolic route [179, 180]. It is still unclear as to what role the above covalent DNA adducts may play in benzene-induced carcinogenesis, since benzene also induces

other types of DNA damage as well as chromosomal damage. For example, oxidized bases such as 8-oxoG can be caused through the quinone/hydroquinone redox cycling [11] (also see Section 2.1). Benzene also generates DNA strand breaks [181, 182] through direct attack by ROS or unstable DNA adducts. As shown in Figure 4, catechol *o*-quinones can react with DNA by 1,4-Michael addition to yield major N3A and N7G adducts which are unstable and generate AP sites [183].

We recently reported the repair of  $N^2$ -4-HOPh-dG *E. coli* UvrABC nuclease [184]. The specificity of such repair was also compared with those of DNA glycosylases and damage-specific endonucleases of *E. coli* both of which were found to have no detectable activity toward this adduct. We also showed that *p*-BQ-modified plasmid is efficiently cleaved by UvrABC, indicating the involvement of NER in repair of benzene-derived DNA damage [184]. The role of NER in the repair of HQ/*p*-BQ-induced DNA damage was also suggested in another mutagenesis study using HQ- or *p*-BQ-treated plasmid containing the supF reporter gene in NER-deficient (XPA) human cells [185]. Note that HQ- and *p*-BQ-derived exocyclic adducts are repaired by a different mechanism called nucleotide incision repair (NIR), as discussed below. In general, although benzene metabolites show relatively low DNA binding activity *in vivo*, their induced DNA damage and repair seem to be complex [186].

2.3.2. *Base Excision Repair (BER).* BER is the primary repair mechanism for the removal of small DNA lesions such as alkylated, oxidized, and deaminated bases from endogenous sources or environmental carcinogens [64, 187–191]. The steps of the BER pathway have been well characterized [64]: it is initiated by a damage-specific DNA glycosylase that recognizes a modified base and cleaves the *N*-glycosylic bond between the base and the sugar moiety. Glycosylases can be divided into monofunctional, for example, alkylpurine-DNA glycosylase (AAG, also MPG, APNG, and ANPG) and thymine-DNA glycosylase (TDG), and bifunctional (with an AP lyase activity), for example, OGG1, endonuclease III homolog 1 (NTH1), and endonuclease VIII-like glycosylases (NEILs). Each DNA glycosylase has its unique specificity, but overlapping activities are common among various DNA glycosylases that may have different structures and/or catalytic mechanisms [191]. After glycosylase, the resulting AP site is processed by 5' AP endonuclease, AP lyase, and DNA polymerase activities to cleave the AP site, trim strand break intermediates, and catalyze repair synthesis. A DNA ligase finally completes the process by sealing the remaining nick. The basic BER mechanism described above is complicated by the identification of subpathways (i.e., the short-patch and long-patch BER) in mammalian systems [192]. There is also a network of protein-protein interactions involving numerous proteins inside and outside of BER, which is thought to play a key role in coordination of BER components as well as in regulation of cellular BER functions [193–195]. Evidence has emerged to support that BER deficiency is an important contributing factor of cancer susceptibility, as shown in both animal models and human studies [196].

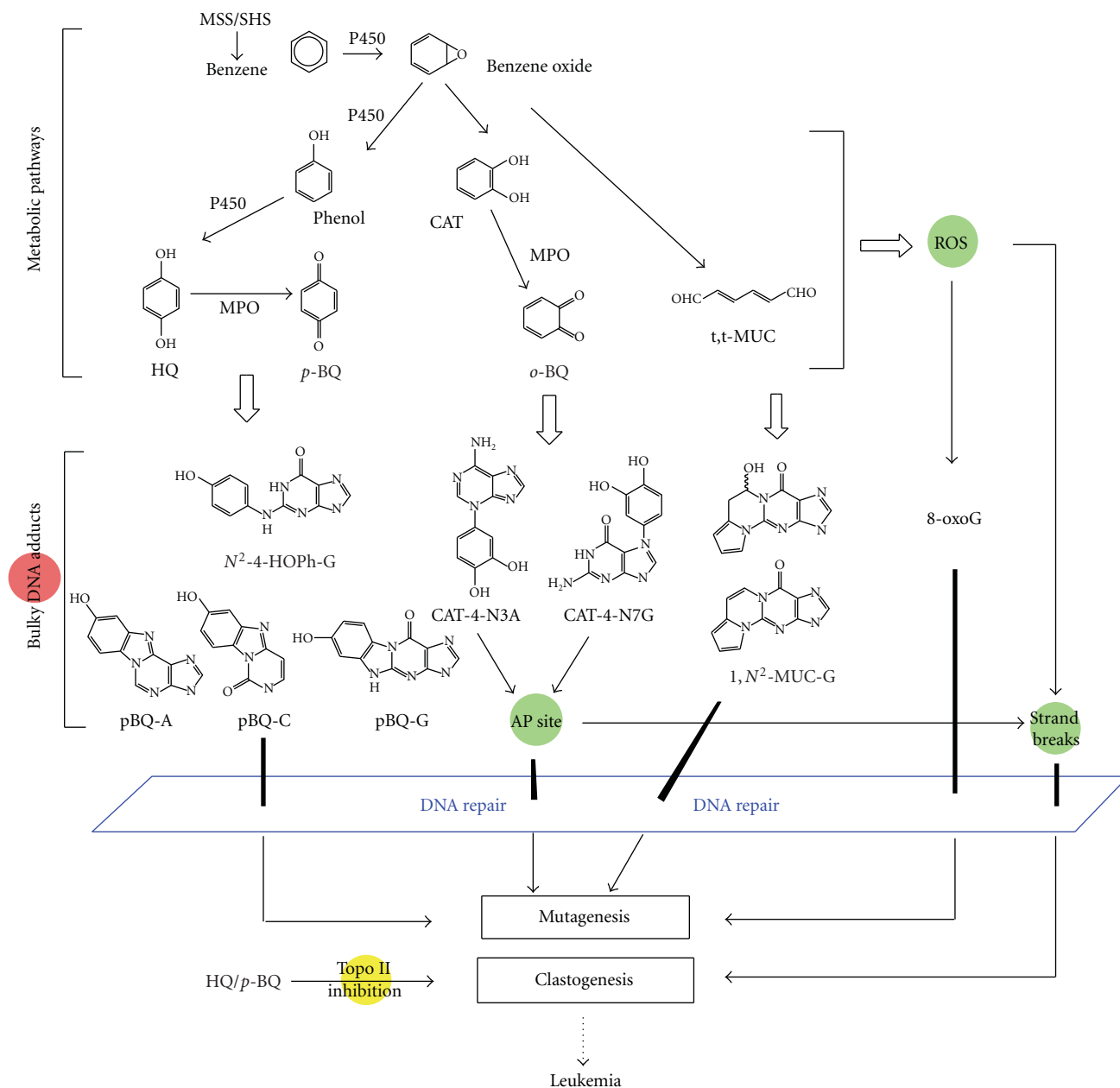


FIGURE 4: Multiple benzene metabolites, different types of DNA lesions, and proposed biological effects. Benzene has a complex metabolism and the listed metabolites are not a complete list. The adducts formed include those identified *in vitro* and *in vivo*, stable and unstable, bulky and oxidized adducts. DSBs are one of the most severe DNA lesions caused directly and indirectly by benzene metabolites. Repair of benzene-DNA adducts may include multiple mechanisms such as BER, NER, and NIR. Only those adducts that finally escape all the defense mechanisms such as repair, or are misrepaired, may lead to mutations. Persistence or coexistence of different types of lesions could form a broad-based attack on the genomic stability. It is also known that a number of benzene metabolites can inhibit topoisomerase II (topo II) activity, which may represent a potential mechanism for benzene's clastogenic effects [326].

Surveying the activities of known glycosylases indicates that many of them are able to excise tobacco carcinogen-induced DNA adducts, including the common alkylated and oxidized bases and some exocyclic adducts. The tobacco carcinogen-derived exocyclic DNA adducts listed in Figure 5 are known substrates for respective glycosylases as described below. It should be noted that a crucial role of BER is to repair an AP site which is mutagenic because of its

noncoding nature [197, 198]. As stated above, certain tobacco carcinogens generate unstable DNA adducts that are an important source of the AP sites in the genome.

(1) *Formation and Repair of Etheno DNA Adducts.* Etheno ( $\epsilon$ ) adducts are the most extensively studied exocyclic adducts [34, 199] which are formed by the attack of bifunctional aldehydes or epoxides at a nitrogen of the base, followed

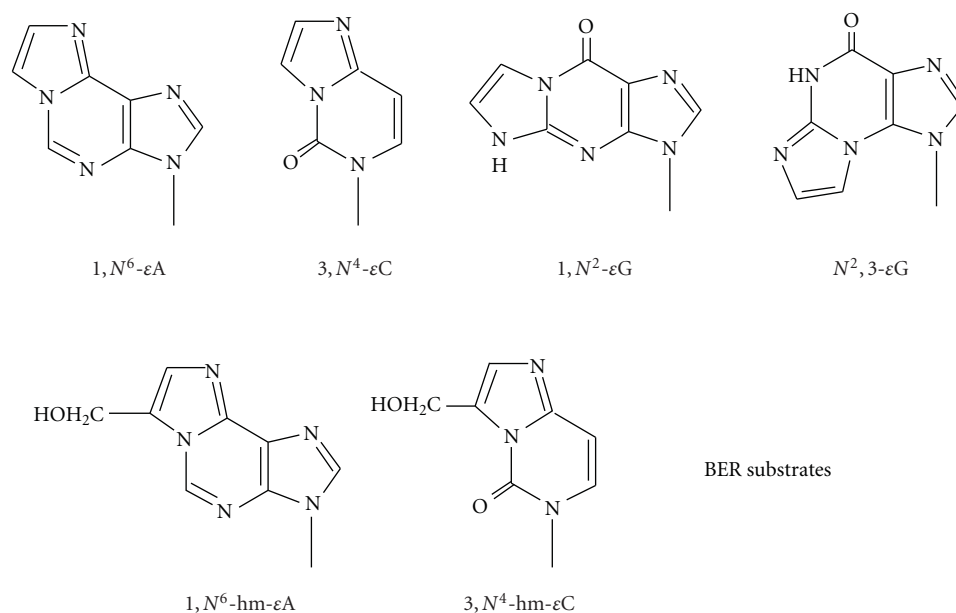


FIGURE 5: Structures of smoking-induced bulky DNA adducts that are substrates for BER.

by dehydration and ring closure [34]. Cigarette smoke is a significant source for these adducts as shown by the urinary levels of  $\epsilon\text{C}$  [200] and  $1,N^2\text{-}\epsilon\text{G}$  [201] in smokers. These adducts could be formed by VC in cigarette smoke (5–30 ng/cigarette) as well as LPO products [94]. VC is processed by P450 yield unstable chloroethylene oxide (CEO), which quickly converts to chloroacetaldehyde (CAA) [202, 203]. Both CEO and CAA can form  $\epsilon$ -adducts. In experimental animals and in humans exposed to VC, liver angiosarcomas are the most common type of tumors. CAA has been studied extensively in terms of forming  $\epsilon$ -adducts, [18, 99], and the quantitative relationships in double-stranded DNA treated with CAA are as follows:  $3,N^4\text{-}\epsilon\text{C} \geq 1,N^6\text{-}\epsilon\text{A} > N^2,3\text{-}\epsilon\text{G} \gg 1,N^2\text{-}\epsilon\text{G}$  [204]. The mutagenic properties of these adducts have been established [37], and there is evidence that  $\epsilon$ -adducts may be responsible for *ras* and *p53* mutations in liver tumors of VC-exposed humans [33].

Studies on repair of exocyclic adducts have largely been focused on BER, except for propano-dG adducts that are repaired by NER.  $\epsilon$ -Adducts are repaired by BER, initiated mainly by two human DNA glycosylases: AAG and TDG [34]. In *E. coli*, they are repaired by functional homologs of AAG and TDG: AlkA (m<sup>3</sup>A-DNA glycosylase II) and mismatch uracil-DNA glycosylase (Mug), respectively [34].

**Excision of  $\epsilon\text{A}$ .** Human AAG excises this adduct from double-stranded [205, 206] and single-stranded DNA [207]. The crystal structure of human AAG bound to DNA containing an  $\epsilon\text{A}$  has been solved [208, 209]. AAG is also the major activity against  $\epsilon\text{A}$  *in vivo*, as shown in *Aag*<sup>-/-</sup> knockout mice [210, 211]. Increased mutations were observed in the *hprt* gene, and levels of  $\epsilon\text{A}$  were significantly higher and persisted longer in DNA from *Aag*<sup>-/-</sup> mice than those from wild-type mice when treated with vinyl carbamate [210,

211]. Moreover  $\epsilon\text{A}$  and  $\epsilon\text{C}$  accumulated to higher levels in *Aag*<sup>-/-</sup> mice following stimulation of colonic inflammation, indicating that the repair of such adducts formed by LPO is important for protection against chronic inflammation-induced ROS and carcinogenesis [212]. As described below, the AlkB/ABH pathway is also involved in the repair of  $\epsilon\text{A}$  and  $\epsilon\text{C}$  adducts. NER is not involved in its repair [213].

**Excision of  $\epsilon\text{C}$ .** We and Saparbaev et al. independently found that the  $\epsilon\text{C}$  activity resides in both human TDG and *E. coli* Mug proteins [214, 215]. The main biological role of TDG appears to remove thymine from a T:G mismatch resulting from the deamination of 5-methylcytosine (5-mC) in a CpG site, which could be involved in active DNA demethylation when in combination with a deaminase that converts 5-mC to T leading to a T:G mismatch [216]. *In vitro* assays have shown that the activity of TDG is most efficient when T:G or  $\epsilon\text{C}$ :G is in a CpG sequence context [217, 218]. Recently, the crystal structure of TDG (the catalytic domain) complexed with DNA containing an AP site was reported [219]. Other studies have also shown low excision of  $\epsilon\text{C}$  by human single-strand-selective monofunctional uracil-DNA glycosylase (SMUG1) [220] and methyl-CpG binding domain protein (MBD4 or MED1) [221].

**Excision of  $\epsilon\text{G}$  adducts.** In rodents,  $N^2,3\text{-}\epsilon\text{G}$  represents the predominant  $\epsilon$ -adduct and is readily induced in hepatic nonparenchymal cells by VC, the target cells for this compound [222]. There is a correlation between the levels of this adduct and the incidence of VC-induced angiosarcoma [222]. *E. coli* AlkA excises  $N^2,3\text{-}\epsilon\text{G}$  from CAA-treated DNA [223]. Both *in vitro* [224] and animal studies [222] showed that the human removal of  $N^2,3\text{-}\epsilon\text{G}$  is slow. It was also shown that repair capacity would be different in various

cell types in liver in that the expression of AAG mRNA was induced in the hepatocytes of rat exposed to VC, while the nonparenchymal cells had only 20% of the AAG mRNA of hepatocytes, indicating that the target cells for VC had much lower expression of this glycosylase [225]. It should be noted that  $N^2,3$ - $\epsilon$ G is also an endogenous adduct arising from LPO [225].  $1,N^2$ - $\epsilon$ G, an isomer of  $N^2,3$ - $\epsilon$ G, is a substrate for both *E. coli* Mug and human AAG as tested *in vitro* [207, 226].

*Excision of hydroxymethyl  $\epsilon$ -adducts.* We recently studied *in vitro* repair of two exocyclic adducts formed by acrolein metabolite glycidaldehyde (GDA), a potent mutagen and animal carcinogen. 7-(Hydroxymethyl)- $1,N^6$ -ethenoadenine (7-hm- $\epsilon$ A), the main adduct, can be found in skin cells of mice treated topically with GDA [227]. Minor adducts with guanosine and deoxyguanosine were also found [228]. The 8-hm- $\epsilon$ C adduct has only been identified *in vitro* [229]. These  $\epsilon$  analogs are expected to be as promutagenic as the corresponding  $\epsilon$ -adducts, and 8-hm- $\epsilon$ C has been shown to miscode when tested with mammalian DNA pols [230]. Biochemical assays have shown that 7-hm- $\epsilon$ A is primarily repaired by AAG [231]. While 8-hm- $\epsilon$ C is excised by *E. coli* Mug and human TDG [232], these excision activities were from half-to a few-fold lower than the corresponding  $\epsilon$  activities, which could be attributed to the extra  $-\text{CH}_2\text{OH}$  group on the  $\epsilon$ -ring [231].

### 2.3.3. Direct Reversal of DNA Damage

(1) *Formation and Repair of Pyridyloxobutyl (POB)-DNA Adducts of TSNAs.* Tobacco-specific nitrosamines (TSNAs) are exclusively found in cigarette smoke and are formed through *N*-nitrosation of nicotine during tobacco curing and processing [233]. Common TSNAs found in cigarette smoke particles include NNK, NNN, and *N*-nitrosoanatabine (NAB). NNK has a strong affinity for the lung and is a systematic lung carcinogen [234]. NNK is among the most potent lung cancer carcinogens in tobacco smoke [27]. TSNAs require activation by the P450 system [80]. In one pathway, NNK is activated to form mutagenic  $O^6$ -mG [235]. In addition, NNK- and NNN-generated reactive intermediates form bulky POB-DNA adducts, including the 7- and  $O^6$ -positions of dG and the  $O^2$ -position of dC and T [84]. Four of them have been recently characterized and detected in NNK- or NNN-treated animals [236]. One of them,  $O^6$ -[4-(3-pyridyl)-4-oxobut-1-yl]-2'-dG ( $O^6$ -POB-dG) [237–239] (Figure 2), will be discussed here, which has been shown to be mutagenic in both *E. coli* and human cells using a site-specific mutagenesis assay and is considered a critical lesion in NNK/NNN carcinogenesis [240]. Higher levels of adducts are found in lung and tracheobronchial tissues of smokers than in nonsmokers, by the detection of 4-hydroxy-1-(3-pyridyl)-1-butanone (HPB), a product from acid hydrolysis of the POB-DNA adducts [80]. Most recently, 1-(*N*-methyl-*N*-nitrosamino)-1-(3-pyridinyl)-4-butanal (NNA) was identified from thirdhand smoke (THS) as the major product resulting from the reaction of nicotine with nitrous acid (HONO), along with NNK and NNN [241] (see Section 3.2).

Both  $O^6$ -mG and  $O^6$ -POB-dG adducts have been shown to be substrates for AGT [106, 237, 242]. However, the repair of the bulky POB adducts has been much less studied compared to  $O^6$ -mG. AGT primarily repairs  $O^6$ -alkylguanine adducts and protects against mutagenicity of respective alkylating agents [106]. It is not an enzyme but an alkyl group acceptor. Repair occurs by transfer of the alkyl group at the  $O^6$  position of G to a cysteine residue at its active site of the protein, which results in a protein conformational change that signals for its degradation [243]. AGT reaction is stoichiometric with  $O^6$ -mG acting as a suicide substrate; therefore, the cellular repair capacity is limited by the constitutive levels of AGT that can be also depleted under overdose of alkylating agents [106].

$O^6$ -POB-dG has been shown to be repaired by AGT both *in vitro* [237] and *in vivo* [244]. This adduct is efficiently repaired by mammalian AGTs but poorly repaired by bacterial counterparts, AdaC and Ogt [235, 244]. Since both  $O^6$ -mG and  $O^6$ -POB-dG may have implications in NNK-induced carcinogenesis, the relative repair rates of these two adducts by AGT should be an important factor in determining the levels and biological importance of these two lesions. Studies by Mijal et al. [235] demonstrated that human AGT showed an  $\sim 2$ -fold preference for the removal of  $O^6$ -mG over  $O^6$ -POB-dG, rodent AGTs exhibited the same rate, and the bacterial proteins reacted poorly with  $O^6$ -POB-dG. These data indicate the high importance of protein structure with respect to substrate efficiency. In conclusion, AGT is expected to be critical in the repair of  $O^6$ -alkylguanine adducts formed by tobacco-derived *N*-nitrosamines. It should be noted that cytotoxicity and mutagenesis studies suggest a NER involvement in the removal of NNK-derived DNA damage [236, 245]. A very weak but time-dependent *in vitro* NER activity was also detected using oligonucleotide containing an  $O^6$ -POB-dG and reconstituted human excision nuclease [236].

(2) *Repair of Etheno Adducts by AlkB Homologs.* It was reported in 2005 that *E. coli* AlkB protein and its human homolog, ABH3, repair  $\epsilon$ A and  $\epsilon$ C *in vitro* [246, 247]. Later, ABH2 was shown to exhibit robust activity for  $\epsilon$ A and is the principal dioxygenase for removal of  $\epsilon$ A *in vivo* as shown by *Abh2*<sup>-/-</sup> mouse studies [248]. Further experiments showed that ABH2, but not ABH3, is able to complement the *E. coli* alkB mutant which is defective in the repair of  $\epsilon$ -adducts [248]. AlkB is a member of the superfamily of iron- $\alpha$ -ketoglutarate-dependent dioxygenases. Using bioinformatics, eight mammalian homologs of AlkB, ABH1 to ABH8, have been identified [249]. The direct reversal mechanism for their action involves a unique iron-mediated reaction with cofactor  $\alpha$ -ketoglutarate that could epoxidize the exocyclic double bond of the  $\epsilon$ -adducts [246, 247]. The epoxide generated can be hydrolyzed to form the lesion-free base and glyoxal. In addition to  $\epsilon$ A and  $\epsilon$ C, these proteins also repair other methylated/ethylated bases [250, 251]. They can act on both single- and double-stranded DNA substrates and may play different/complementary roles to the glycosylases as mentioned above. In general, single-strand

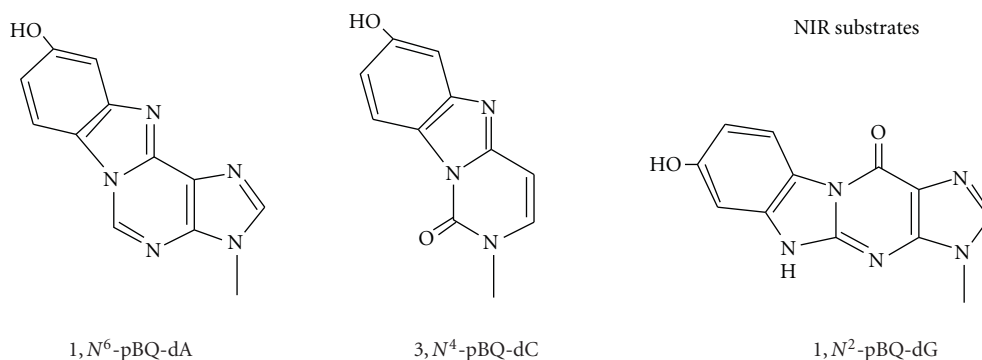


FIGURE 6: Structures of smoking-induced bulky DNA adducts that are substrates for NIR.

specificity suggests repair of lesions in single-stranded DNA regions that are transiently generated during replication and transcription.

Given that DNA glycosylases also act on  $\epsilon$ -adducts (see Section 2.3.2(1)), at least two repair pathways may act on these adducts *in vivo*. This may explain why the incidences of carcinomas were similar between wild-type and *Aag*-knockout mice treated with vinyl carbamate [252]. Genetic studies using *AlkA*-proficient and -deficient cells show that *AlkB* is important for counteracting the mutagenicity of the  $\epsilon$ -adducts [246]. A study comparing the repair efficiency of *AlkB* versus *AlkA* in *E. coli* shows that *AlkA* seems to be the more important enzyme in response to exposure to CAA [246]. Similar data were obtained from knockout mice [248], which showed that the *Abh2* activity is not sufficient for the removal of spontaneously produced  $\epsilon$ A adducts in *Aag*<sup>-/-</sup> mouse liver, whereas mouse *Aag* activity is sufficient to repair spontaneously produced  $\epsilon$ A lesions in *Abh2*<sup>-/-</sup> mouse liver. These results suggest that both *AAG* and *ABH2/3* proteins can play a role in the cellular response to the exposure of tobacco carcinogens that generate these  $\epsilon$ -adducts.

**2.3.4. Nucleotide Incision Repair (NIR).** The exocyclic benzotheno *p*-BQ adducts are bulkier than the  $\epsilon$ -adducts, with an additional five-membered ring and a hydroxy group. As might be expected, such bulky adducts hinder replication *in vitro* and *in vivo* and cause frameshift deletions and base mispairing [178]. In the past years, we have studied repair of three major *in vitro* adducts formed by HQ and *p*-BQ (designated as pBQ adducts), 1,  $N^6$ -pBQ-dA, 3,  $N^4$ -pBQ-dC, and 1,  $N^2$ -pBQ-dG (Figure 6). Our initial study discovered that these adducts are recognized by the major human AP endonuclease (APE1, also known as HAP1, APEX, and Ref-1) as well as *E. coli* exonuclease III and endonuclease IV [253, 254]. Mechanistic studies showed that human APE1 hydrolyzes the phosphodiester bond 5' next to the adduct, leaving the *p*-BQ derivative on the 5'-terminal of the 3' fragment as a "dangling base" [253, 255, 256]. This mode of incision was later named nucleotide incision pathway [257, 258], which also acts on several oxidized DNA bases. While the AP site is the preferred substrate for APE1, cleavage of the pBQ-dC adduct requires the same catalytic center as the AP

site as shown from mutant APE1 proteins [256]. Molecular dynamics simulations [36] suggest that APE1 utilizes a reaction mechanism for phosphodiester bond cleavage of DNA containing pBQ-dC similar to that reported for the AP site [259]. Given that these adducts have not been reported to be present *in vivo*, the biological role of these adducts as well their repair by NIR awaits further investigation.

**2.3.5. Summary.** The repair mechanisms for representative bulky DNA adducts discussed above are summarized in Figure 7. It should be emphasized that most of the repair studies in the past have applied a single compound for modification or exposure, and results from such studies cannot be simply extrapolated to real exposures. However, the information on repair specificity and efficiency from such studies provides the framework for further evaluation of potential relationships among repair deficiencies, carcinogen mutagenicity, and human susceptibility to cigarette smoke. Also, as stated above, tobacco carcinogens are able to generate other specific DNA lesions in addition to bulky DNA adducts. The importance of bulky DNA adducts relative to other types of DNA lesions needs further investigation, and in any case, a combined action from different types of DNA/chromosomal damage, as demonstrated in Figure 4 for benzene' biological effects, is expected to be the basis of genotoxicity conferred by many tobacco carcinogens.

**2.4. Molecular Structure of DNA Adducts and DNA Repair.** A crucial question in repair is how repair proteins recognize DNA adducts, since repair specificity has both biochemical and biological implications. A related question is "what are the factors responsible for good and poor repair?" To date, we have learned a great deal with regard to what structural factors of adducts and repair proteins determine the specificity and rate of repair, mainly based on biochemical data atomic resolution structures of adducted DNA and repair proteins [64, 102, 260, 261].

The study of how a DNA adduct affects the structure of DNA and how it interacts with its repair protein is essential in order to develop a theory for both why only some adducts are repaired and the specific mode of repair. When surveying the multiplicity of DNA substrates for NER, the primary repair

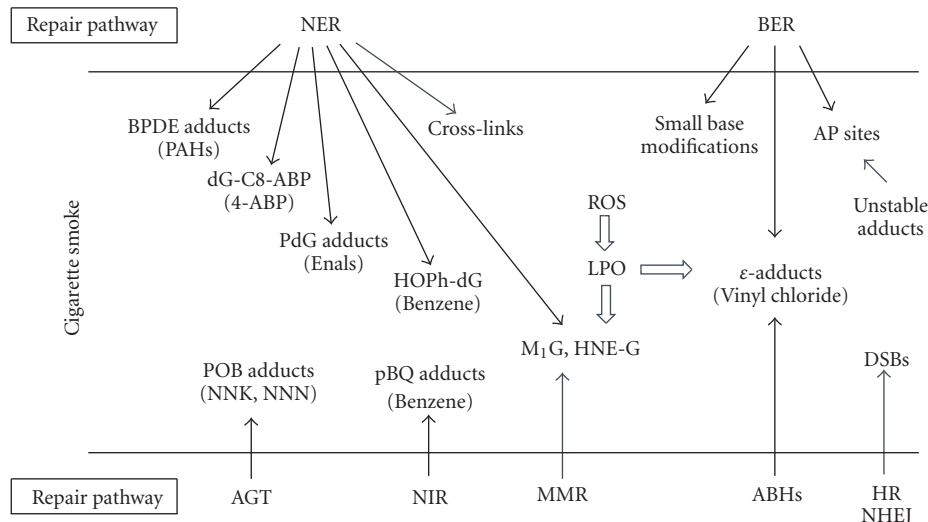


FIGURE 7: Summary of specificity of repair of tobacco carcinogen-induced bulky DNA adducts by the major DNA repair pathways. Some of the nonbulky DNA lesions and their repair mechanisms are also presented. For example, DSBs caused by cigarette smoke are repaired by nonhomologous end joining (NHEJ) and homologous recombination (HR). Note that overlapping substrate specificity is common.

pathway for many bulky DNA adducts, one basic question is how NER recognizes these chemically diverse substrates through the common structural features of the recognition unit XPC-HR23B. Moreover, what is the basis for the fact that the repair rates of different bulky adducts by NER can vary by several orders of magnitude [111, 262]? It should be recognized that, as described above, the complexity of these adducts is enormous, including those adducts that are formed by compounds with stereochemical properties (e.g., BPDE, acrolein, and HNE). Recognition and repair rates of such stereoisomeric adducts generally reflect or depend on adduct conformation. In the case of BPDE- $N^2$ -dG adducts, both their removal by human NER [131] and patterns of helix opening by XPC-HR23B [121] are stereochemistry dependent. Recently, crystal structures of NER proteins, that is, bacterial UvrB [263] and yeast Rad4 (human XPC homolog) [264], complexed with damaged DNA, have been described, both of which suggest a mode of action involving strand separation and nucleotide flipping for the bulky DNA lesions.

As for BER, a number of high-resolution structures of glycosylases, including those complexed with DNA lesions, have provided a valuable insight into adduct selection as well as mechanisms of base flipping and catalysis [260, 261, 265]. In addition, molecular modeling studies such as molecular dynamics simulations have offered additional information about the structural features of DNA substrates and their interactions with repair enzymes [36, 266]. Some common features of recognition by DNA glycosylases can be summarized based on the reported structural studies: (1) adduct shape, hydrogen-bonding potential, and electric charge distribution are key for recognition; (2) base unstacking is present at the lesion site; (3) the target nucleotide has to be flipped out of the DNA duplex and fit in the active site of a glycosylase [261]. Similarly, AP endonucleases flip an AP

site out into their active sites, as shown by the co-crystal structures [259, 267]. Early on, we had some puzzling questions for this pathway and its glycosylases. For example, why are structurally related adducts repaired differentially? for instance, BER excises the 5-membered unsaturated exocyclic  $\epsilon$ G but not the 6-membered propano-dG [34, 157]. Also, why can lesions with largely diverse structures be processed by the same protein, as seen by human APE1 acting on both AP site and pBQ-dC [253, 255, 256]? In general, the key to the specificity of recognition has been known to be not only the primary adduct structure, but the localized effect of each adduct on DNA structure as well as on thermodynamics, and, moreover, the structure and function of the repair protein. Since most repair enzymes act on adducts in double-stranded DNA, each adduct may cause differing distortion and flexibility as a result of factors such as being in the major or minor groove, *syn* or *anti*, planar or angular, adjacent base pair tilting, propeller twist, and helical twist [102]. Ultimately, it is hoped that we can predict repair specificity/efficiency as well as identify structural hallmarks of mutagenic lesions in the genome, using appropriate computational and/or screening approaches. This can only be done after a large amount of structural and theoretical data have been acquired, which relate adduct structural features with outcomes of repair and mutagenesis.

**2.5. Nucleic Acid Sequence, Mutational Hotspots, and DNA Repair.** The sequence-dependent repair infers that local DNA structures adjacent to an adducted nucleotide are important determinants of repair specificity and efficiency. The study of the role of sequence in base modification was started mainly in the 1980s in terms of sequence selectivity for mutational events which were generally induced by environmental agents [268]. Extensive work on relating sequence-dependent adduct formation and mutation has

been done using chemical modification (e.g., BPDE) of genomic DNA, followed by determination of the mutation pattern and spectra [268]. These data were among the first used to substantiate the concept of “hotspots”; that is, for a given reagent, there was site specificity for DNA modification. An example is that *in vivo*, only the second guanine residue in codon 12 (GGA) of the *H-ras* gene was modified by an alkylating agent, leading to G:C to A:T mutations [269], which is consistent with other studies demonstrating the sequence-dependent formation of  $O^6$ -alkylguanine in DNA [270, 271].

In addition to preferential DNA adduct formation at specific sites, poor repair is another major determinant of mutational hotspots [30]. Many studies have highlighted the importance of sequence context in influencing the rate and extent of repair [268]. Examples among the tobacco carcinogen-induced bulky DNA adducts are BPDE-DNA adducts [134, 138, 272–274], POB-DNA adducts [242],  $\epsilon$ A [275], and  $\epsilon$ C [232], whose repair efficiencies could vary over manyfold when present in different neighbor sequences. These examples involve repair systems including at least NER, BER, NIR, and AGT [268]. A review by Singer and Hang commented on many enzymes in these pathways with regard to the role of adduct, neighbor bases, and repair rate [268]. Also, Donigan and Sweasy recently summarized the known sequence context-specific activities of several glycosylases and polymerase  $\beta$  in BER [276]. It can be concluded now that sequence-dependent repair tends to be predominant, instead of being a random phenomenon.

Mechanistically, the structural factors that modulate sequence-dependent repair have been well studied with certain adducts such as BPDE-DNA adducts [274, 277]. An NMR study using a sequence containing a natural GG mutational hotspot showed that the presence of the major BPDE-derived dG adduct at one of the two neighboring G positions resulted in significantly different local structural distortions, especially bending or kinking at the adduct position and destabilization of Watson-Crick hydrogen bonding of the flanking base pairs [35]. Using the same sequences, Kropachev et al. demonstrated that such hydrogen bonding destabilization elicits the most significant NER response, while the flexible kink is less important in such interaction [274]. It is also apparent that the chemical nature of a DNA adduct itself can affect the effect of neighbor sequences. For example, the repair of a POB adduct by AGT is more strongly influenced by its neighbor bases than that of the smaller methylated base substrate [242].

Regardless of the nature of the specific structural differences discussed above, current evidence also supports that thermodynamic stability of lesion-containing oligonucleotides plays an important role in sequence-dependent repair [268, 274, 278]. In the case of BPDE-DNA adducts, the degree of local thermodynamic destabilization was related to the degree of recognition of duplex sequences containing a bulky adduct by the NER machinery [262, 274, 279]. Both of our studies on sequence-dependent repair of  $\epsilon$ A [275] and AP site [280] also demonstrated a role of thermodynamic properties in influencing double-strandedness of the substrates and repair their efficiency.

Recent studies have discovered a strong coincidence of mutational hotspots in human lung cancers and the sites of preferential binding of BPDE [42, 281] and acrolein [43] in the *p53* gene. The overall prevalence of *p53* mutations is higher in cigarette smokers than in nonsmokers [51, 52]. A number of hotspots have been found along *p53* in lung cancer which are generally G to T transversions [30]. It has been reported that in PAH- or acrolein-treated cells the same positions of their mutation hotspots are also major hotspots for mutations observed in human lung cancers from smokers, strongly suggesting a role of DNA adducts in etiology of these cancers [30]. As discussed above, poor/slow repair of DNA adducts at these sites may be a major factor for their occurrence and persistence at these mutational hotspots. To further support this notion several groups in the mid-1990s examined the *in vivo* repair rates along a gene fragment using the ligation-mediated PCR technique [282]. As for BPDE adducts in human *HPRT* and *p53* genes, Wei et al. [272] found that repair rates can differ markedly from site to site over a time period, as measured by the percentage of adduct remaining. Moreover, very slow repair was observed at certain positions that are frequently mutated after BPDE treatment [272]. These studies clearly indicate a correlation between inefficient DNA repair and the occurrence of mutation hotspots. Finally, in addition to site-specific preferential formation of DNA adducts and sequence context of DNA repair, the biological selection of induced mutations is also considered important for the hotspot phenomenon, which gives cells with specific mutation(s) a growth advantage and results in dominant mutations in cancer cells [283, 284].

**2.6. Interindividual Variations in Response to Tobacco Carcinogens and Cancer Risk.** It has long been recognized that only a small percent of cigarette smokers develop cancer, for example, ~11%–24% of smokers develop lung cancer [285], which suggested that interindividual variability in key cellular processes is crucial in response to tobacco carcinogens. Many molecular and epidemiological studies have been revealing a multifactorial nature of such variability [286–289]. One top aim of the target cancer prevention programs is to identify smokers and nonsmokers exposed to SHS with higher susceptibility. The interindividual differences discussed below will be focused on those genotypes and phenotypes involving DNA repair capacity (DRC) in relation to the mutagenicity and carcinogenicity of tobacco-induced bulky adducts.

Considerable progress has been made towards a better understanding of the association between individual tobacco carcinogens and tumor development in specific organs/tissues [12], as exemplified by the following cases: NNK and PAH are potent lung carcinogens; aromatic amines such as 4-ABP are the main cause of bladder cancer in smokers; benzene induces acute myelogenous leukemia (AML). Whether reduced or deficient DRC for tobacco carcinogen-derived DNA damage is associated with somatic mutation and susceptibility to cancer has been a subject of investigation. A commonly used approach is to measure the repair or levels of specific DNA adducts which serve as

an intermediate end-point of genotoxicity [14]. Decreased repair activities for bulky DNA adducts have been observed in cells/tissues of cancer patients. For example, epidemiologic studies using the HCR assay showed that low cellular DRC in response to BPDE-induced DNA damage is associated with increased risk of lung, head, and neck cancers [65, 286, 290]. Biochemical studies also showed that reduced repair of  $\epsilon$ A and  $\epsilon$ C adducts was present in lung adenocarcinomas [291]. In principle, the phenotypes of DNA repair must be characterized for mutagenic adducts and any newly identified adducts in smokers and nonsmokers exposed to SHS.

Deficient repair towards tobacco smoking-related DNA adducts may occur under various mechanisms. A common one is polymorphisms in relevant DNA repair genes, such as those identified in the NER, BER, and AGT pathways [289, 292, 293]. It has been shown that cellular levels of DNA adducts such as those arising from BPDE exposure can be affected in some of those genetic variants [132, 294]. In the last decade, although mixed or discrepant results have been reported, positive results on numerous polymorphisms in DNA repair genes, along with those in metabolic genes, have been revealed and are continuously being found in the context of cigarette smoking and cancer [22, 295, 296]. It seems that polymorphisms in tobacco metabolism and/or repair should lead to differences in both local carcinogen levels and/or DNA adduct levels *in vivo* [14]. Another mechanism that can cause the loss of DNA repair capacity is LOH; for instance, LOH at the human 8-oxoG-DNA glycosylase (OGG1) gene locus is a frequent event in lung cancer, which would increase the mutational load from 8-oxoG due to ROS in smokers [297].

DRC could also be influenced by nongenetic factors that cause a phenotypic reduction/ablation of repair activities. Examples of such factors include those that are disease related, for example, NER deficiency in XP and Cockayne syndrome patients [64, 140], and those that are repair-inhibition based. For the latter, carcinogen-mediated effects on proteins play an important role. Two types of tobacco chemicals can cause protein damage and inhibit repair. There are at least 30 metals in cigarette smoke, including arsenic, cadmium, nickel, and chromium, which have been shown to inhibit various DNA repair enzymes and pathways [298–302]. For instance, both arsenic and nickel compounds interfere with the repair of BPDE-DNA adducts [298, 299]. Cadmium and chromium (VI) are also known as effective DNA repair inhibitors and play a similar role in influencing adduct levels in smokers [303, 304]. Therefore, coexposure to these heavy metals by smokers may enhance the mutagenic potential of genotoxic tobacco carcinogens [305]. In addition to metals, certain tobacco carcinogens themselves have been found to inhibit DNA repair, as exemplified by acrolein inhibiting NER repair of BPDE-DNA adducts [43]. Similar to metals, the coexistence of these chemicals in cigarette smoke is also expected to lead to more persistent or severe DNA damage as a result of suppressed DNA repair.

In addition to tissue differences in bioactivation of tobacco carcinogens [306, 307], recent studies in rodents suggest that the DRC in a given organ/tissue/cell type may play a role in organoselectivity of tobacco carcinogens.

For example, both AGT [308] and NER [309] activities are related to the interorgan differences in response to NNK treatment, which could be an important factor in determining organ-specific susceptibility to NNK-induced carcinogenesis. Another example is benzene which targets the bone marrow. DNA adduct levels in the bone marrow of benzene-treated mice are significantly higher than those in liver, as shown by tissue distribution studies [310]. Interestingly, although no repair capacity has been tested for a particular benzene adduct *in vivo*, when treated with alkylating agents, the DRC of primary human hematopoietic CD34<sup>+</sup> cells from bone marrow was significantly lower than more differentiated CD34<sup>-</sup> cells of the same donor [311]. In general, the tissue- or cell type-specific responses to tobacco exposure and their mechanisms are not well understood and await more extensive investigation.

### 3. From the Known to the Unknown: Future and Perspective

**3.1. Uncharacterized Adducts and Repair.** The bulky DNA adducts discussed here are only a small list of representatives derived from tobacco carcinogens. We need not only more information on these important bulky adducts, but also more knowledge of those other adducts that are still not understood. (1) There are many other chemicals in cigarette smoke that have not yet been evaluated for DNA adduct-forming ability. For instance, there are 18 *N*-nitrosamines and 106 aldehydes present in cigarette smoke [10]. (2) Chemicals may be neglected only because of their lower concentrations in cigarette smoke. For example, some PAHs exist in cigarette smoke at low amounts relative to B[a]P. Some of these compounds may even have stronger carcinogenic effect [30]. (3) The research attention tends to be more focused on the effect of the major adducts of a chemical carcinogen. However, in some cases, the minor adducts are substantially more mutagenic than the major ones. For example, the biological response of *N*-nitrosamines could be correlated with minor forms of DNA damage [312]. However, the repair specificity and kinetics of these DNA lesions are still unknown. (4) Many bulky adducts have been identified *in vitro* under physiological conditions but have not been detected yet *in vivo*. Examples include a number of exocyclic adducts formed by benzene metabolites (Figure 4). Although many *in vitro* studies have been focused on the HQ- and *p*-BQ-derived benzetheno adducts [313] and MUC-DNA adducts [179], no conclusion can yet be drawn on whether they are formed in cells/tissues. (5) In some cases, bulky DNA adducts are detected from the tissues of exposed humans or animals using <sup>32</sup>P-postlabeling, but their chemical structures have not been elucidated. These adducts were generally described in the literature as “aromatic or hydrophobic adducts”. (6) Endogenous DNA adducts can be formed as a result of cigarette smoke, which is currently attributed to the formation of LPO products [92–94]. Further research is needed to learn the dose-response relationship with regard to the formation of these adducts as well as their relative importance in smoking-induced carcinogenesis. The complexity of such analysis

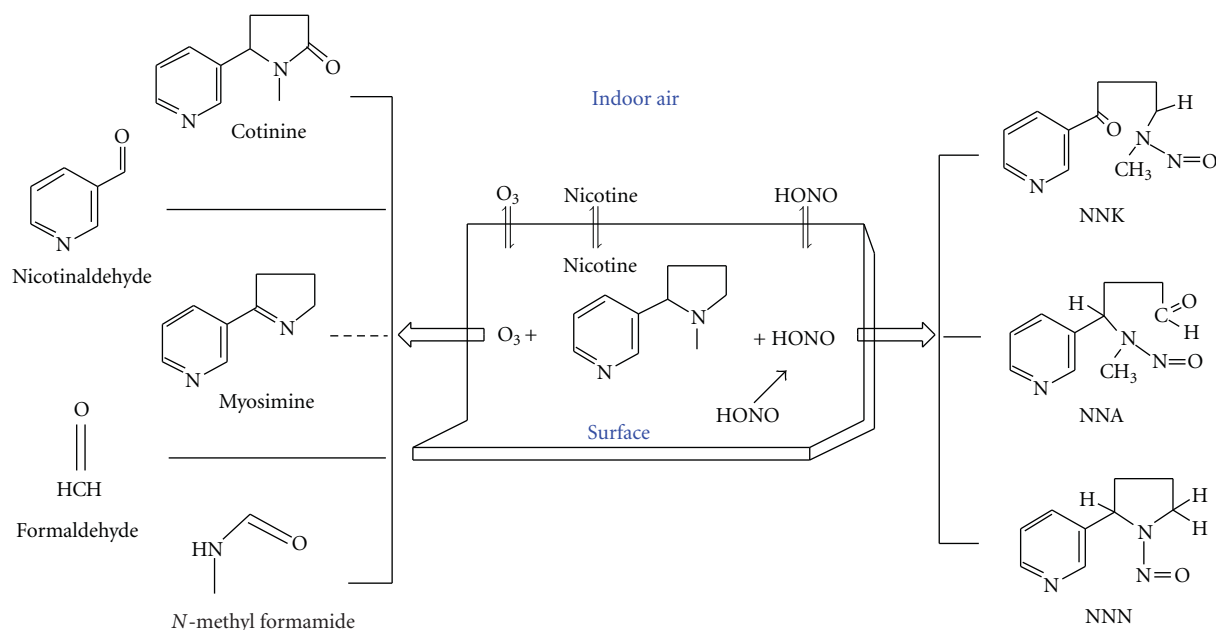


FIGURE 8: Stable nicotine-derived secondary products after reacting with ozone ( $O_3$ ) or nitrous acid (HONO). All the structures illustrated were positively identified except for myosimine that was tentatively identified. HONO can be adsorbed from air source or derived from surface-catalyzed reaction. Adopted from the work by Destaillets et al. [317] and Sleiman et al. [241].

is that the same DNA adducts, for example, the  $\epsilon$ -DNA adducts, are generated by both tobacco carcinogens and endogenously formed compounds, even though they can be chemically different [49]. (7) Although the majority of studies on adducts and cancer have focused on stable ones, many adducts formed by tobacco carcinogens are chemically unstable, for example, the benzene-derived CAT-4-N3A and CAT-4-N7G [183], and the potential effects of such adducts versus stable adducts are largely unknown. (8) Many DNA adducts have been detected, some in cells/tissues, but not yet characterized with respect to their repair. An example is that the epoxides of 1,3-butadiene [314, 315], a tobacco carcinogen in both MSS and SSS, cause the formation of *N*-1-(2,3,4-trihydroxybutyl) adenine adduct in human samples [316], but its repair is unknown. (9) Sometimes cellular repair has been detected using repair-deficient cells/animals in combination with mutagenesis assays, but detailed biochemical properties of such repair have not been elucidated. In other cases, repair studies have only been performed *in vitro*, such as the *p*-BQ-derived benzetheno adducts [253, 255]. Although animal studies have limitations with significant differences from humans, many important experiments on the formation and repair of carcinogenic adducts can only be performed in appropriate animals. The major difference is that *in vivo*, enzymes may be inducible and become saturated at the carcinogen dose used, and in the genome, there can be preferential repair as well as organ and cell variations and there may be cooperative repair mechanisms which have not been well understood. This is only a partial list of the reasons why repair specificity and efficiency discovered *in vitro* have to be validated *in vivo*.

**3.2. SHS and THS Carcinogens and DNA Adducts.** To investigate the relationship between cigarette smoking and DNA damage, understanding of the chemical and biophysical properties of various forms of tobacco smoke is also critical. For instance, although a great deal is known about the chemistry and toxicity of MSS and SHS, little is known about the identity and molecular toxicology of toxicants produced *de novo* in THS [6, 7]. However, it has been well established that indoor surfaces significantly adsorb semi- and nonvolatile SHS compounds, for example, nicotine, 3-ethenylpyridine, naphthalene, cresols, and phenol which are slowly reemitted into the air [317–320]. Therefore, all of these compounds can be significant components in THS. Moreover, compounds sorbed onto a surface can undergo chemical transformations by reacting with common reactive atmospheric species. Recent indoor chemistry studies have elegantly revealed that nicotine reacts with ozone ( $O_3$ ) to yield aldehydes and possibly myosimine [317] and with nitrous acid (HONO) to form NNA, NNN, and NNK [241] (Figure 8). NNA was identified as the major product, which is absent in freshly emitted tobacco smoke but found in *in vitro* reaction of nicotine with  $NaNO_2$  [321]. NNA has a mutagenic activity similar to that of NNN [322], but its tumorigenic activity in animals was not conclusive [323, 324]. So far, nothing has been tested for its potential to form DNA adducts, but it is expected to be reactive with DNA due to its aldehyde group. Therefore, it would be important to assess its intake and biological properties. Based on their chemical structure, all of the by-products shown in Figure 8 are anticipated or have already been known to form DNA adducts.

As stated earlier, SSS and SHS, the precursors of THS, contain thousands of chemicals, including nicotine and well-defined carcinogens, partitioned between the gas and particulate phases. The secondary analysis by Schick's group of animal experimental data from the past documents of Philip Morris available at University of California, San Francisco (UCSF) concluded that the mature and "aged" SSS is several-folds more toxic than the fresh SSS [325]. Such evidence constitutes compelling and sufficient rationale to determine the chemical composition of unique toxicants produced in THS *de novo* and to detect new/different types of DNA adducts formed by "aged" SSS. In conclusion, this is a new and important research area with regard to developing strategies and methods to identify the chemical components SHS aging and THS and to assess currently unknown genotoxic potential and biomarker availability through DNA adduct studies.

**3.3. Future Directions.** Understanding the mechanisms of formation and repair of bulky DNA adducts is critical for analysis and management of tobacco-induced mutagenesis and carcinogenesis. It is hoped that continued studies will provide more information about the structural and biological implications of specific bulky DNA adducts and the broader range of their effects during the pathogenesis. Future efforts should be made to identify and characterize novel compounds and adducts, such as those produced in aged SHS and THS, to identify those highly mutagenic adducts that are refractory to DNA repair, to find adducts as reliable biomarkers for measuring exposure, especially for SHS and THS, to explore new potential biological functions of adducts, such as their interactions with cellular signaling networks, impact on stem cells of target tissues, and roles in epigenetic changes, and to find effective ways to inhibit DNA adduct formation in target organs. Innovative study designs along with more comprehensive approaches (e.g., systems biology) and new technology development (e.g., high-throughput analysis) will be important for achieving these goals. Ultimately, a better knowledge of the mechanisms by which the chemical carcinogen exposure increases cancer risk in smokers and individuals exposed to SHS/THS could lead to new strategies for cancer prevention and could serve as the experimental evidence for framing and enforcing tobacco control policies in order to minimize health hazards and protect vulnerable populations.

## Abbreviations

MSS:	Mainstream smoke
SSS:	Sidestream smoke
SHS:	Secondhand smoke
ETS:	Environmental tobacco smoke
THS:	Thirdhand smoke
PAH:	Polycyclic aromatic hydrocarbon
B[a]P:	Benz[a]pyrene
BPDE:	Benzo[a]pyrene diol epoxide
TSNAs:	Tobacco-specific nitrosamines
NNK:	4-(Methylnitrosamino)-1-(3-pyridyl)-1-butanone

NNN:	<i>N'</i> -Nitrosornnicotine
NNA:	1-( <i>N</i> -methyl- <i>N</i> -nitrosamino)-1-(3-pyridinyl)-4-butanal
POB:	Pyridyloxobutyl
O <sup>6</sup> -POB-dG:	O <sup>6</sup> -[4-(3-Pyridyl)-4-oxobut-1-yl]-2'-dG
4-ABP:	4-Aminobiphenyl
dG-C8-ABP:	<i>N</i> -(Deoxyguanosin-8-yl)-4-aminobiphenyl
enals:	$\alpha,\beta$ -Unsaturated aldehydes
PdG:	1, <i>N</i> <sup>2</sup> -Propanoguanine
<i>p</i> -BQ:	para-Benzoquinone
HQ:	Hydroquinone
<i>N</i> <sup>2</sup> -4-HOPh-dG:	<i>N</i> <sup>2</sup> -(4-Hydroxyphenyl)-2'-dG
MUC:	<i>trans,trans</i> -Muconaldehyde
VC:	Vinyl chloride
CEO:	Chloroethylene oxide
CAA:	Chloroacetaldehyde
HNE:	<i>trans</i> -4-Hydroxy-2-nonenal
$\epsilon$ :	Etheno
hm:	Hydroxymethyl
M <sub>1</sub> G:	Pyrimido[1,2- $\alpha$ ]-purin-10(3 <i>H</i> )-one
O <sup>6</sup> -mG:	O <sup>6</sup> -Methylguanine
8-oxoG:	7,8-Dihydro-8-oxoguanine
DSB:	Double-strand break
ROS:	Reactive oxygen species
LPO:	Lipid peroxidation
AGT:	O <sup>6</sup> -Alkylguanine-DNA alkyltransferase
ABH:	AlkB homolog
NER:	Nucleotide excision repair
GGR:	Global genomic repair
TCR:	Transcription-coupled repair
BER:	Base excision repair
NIR:	Nucleotide incision repair
MMR:	Mismatch repair
AP:	Apurinic/aprimidinic
Mug:	Mismatch-specific uracil-DNA glycosylase
TDG:	Thymine-DNA glycosylase
AlkA:	<i>E. coli</i> 3-methyladenine DNA glycosylase II
AAG:	Alkylpurine DNA glycosylase
OGG1:	8-Oxoguanine DNA glycosylase
APE1:	Major human AP endonuclease
pol:	Polymerase
HCR:	Host-cell reactivation
DRC:	DNA repair capacity
SNP:	Single nucleotide polymorphism.

## Acknowledgments

The work was supported by the Grant 19XT-0070 (B.H.) from the Tobacco-Related Disease Research Program (TRD RP) of the State of California. The research on chemistry and biochemistry of DNA adducts in our laboratory was previously supported by the NIH/NCI Grant R01CA72079 (to B.H.) and by the Laboratory Directed Research and Development Program (LDRD) of Lawrence Berkeley National Laboratory under U.S. Department of Energy Contract no. DE-AC02-05CH11231.

## References

- [1] WHO, "The World Health Report," Shaping the Future. pp.91–94, 2003.
- [2] IARC, "Tobacco Smoke and Involuntary Smoking," in *IARC Monographs on the Evaluation of the Carcinogenic Risks of Chemicals to Humans*, vol. 83, pp. 121–844, IARC, Lyon, France, 2004.
- [3] IARC, "Tobacco Smoke and Involuntary Smoking," in *IARC Monographs on the Evaluation of the Carcinogenic Risks of Chemicals to Humans*, vol. 83, pp. 1189–413, IARC, Lyon, France, 2004.
- [4] "The Health Consequences of Involuntary Exposure to Tobacco Smoke," A Report of the Surgeon General, US Department of Health and Human Services, Center for Disease Control and Prevention, Atlanta, Ga, USA, 2006.
- [5] CEPA. California Environmental Protection Agency, Proposed Identification of Environmental Tobacco Smoke as a Toxic Air Contaminant, 2005.
- [6] G. E. Matt, "Thirdhand smoke: new frontiers in the protection of nonsmokers," in *Proceedings of the Rocky Mountain Smoke-Free Conference*, Jackson, Wyo, USA, 2007.
- [7] J. P. Winickoff, J. Friebely, S. E. tanski et al., "Beliefs about the health effects of "thirdhand" smoke and home smoking bans," *Pediatrics*, vol. 123, no. 1, pp. e74–e79, 2009.
- [8] K. Asotra, "Thirdhand smoke: an unappreciated public health hazard," Proceeding of the University of California Riverside Symposium on Tobacco-Related Disease, September 2009, <http://www.trdrp.org/>.
- [9] C. J. Smith, T. A. Perfetti, R. Garg, and C. Hansch, "IARC carcinogens reported in cigarette mainstream smoke and their calculated log P values," *Food and Chemical Toxicology*, vol. 41, no. 6, pp. 807–817, 2003.
- [10] D. Hoffmann, I. Hoffmann, and K. El-Bayoumy, "The less harmful cigarette: a controversial issue. A tribute to Ernst L. Wynder," *Chemical Research in Toxicology*, vol. 14, no. 7, pp. 767–790, 2001.
- [11] S. S. Hecht, "Tobacco smoke carcinogens and lung cancer," *Journal of the National Cancer Institute*, vol. 91, no. 14, pp. 1194–1210, 1999.
- [12] S. S. Hecht, "Tobacco carcinogens, their biomarkers and tobacco-induced cancer," *Nature Reviews Cancer*, vol. 3, no. 10, pp. 733–744, 2003.
- [13] J. K. Wiencke, "DNA adduct burden and tobacco carcinogenesis," *Oncogene*, vol. 21, no. 48, pp. 7376–7391, 2002.
- [14] E. Taioli, "Gene-environment interaction in tobacco-related cancers," *Carcinogenesis*, vol. 29, no. 8, pp. 1467–1474, 2008.
- [15] D. Hoffmann and E. L. Wynder, "A study of tobacco carcinogenesis. XI. Tumor initiators, tumor accelerators, and tumor promoting activity of condensate fractions," *Cancer*, vol. 27, no. 4, pp. 848–864, 1971.
- [16] B. L. Van Duuren, C. Katz, and B. M. Goldschmidt, "Cocarcinogenic agents in tobacco carcinogenesis," *Journal of the National Cancer Institute*, vol. 51, no. 2, pp. 703–705, 1973.
- [17] F. P. Guengerich, "Common and uncommon cytochrome P450 reactions related to metabolism and chemical toxicity," *Chemical Research in Toxicology*, vol. 14, no. 6, pp. 611–650, 2001.
- [18] B. Singer and D. Grunberger, *Molecular Biology of Mutagens and Carcinogens*, Plenum Press, New York, NY, USA, 1983.
- [19] S. S. Hecht, "Progress and challenges in selected areas of tobacco carcinogenesis," *Chemical Research in Toxicology*, vol. 21, no. 1, pp. 160–171, 2008.
- [20] M. R. Lovern, C. E. Cole, and P. M. Schlosser, "A review of quantitative studies of benzene metabolism," *Critical Reviews in Toxicology*, vol. 31, no. 3, pp. 285–311, 2001.
- [21] S. D. Spivack, M. J. Fasco, V. E. Walker, and L. S. Kaminisky, "The molecular epidemiology of lung cancer," *Critical Reviews in Toxicology*, vol. 27, no. 4, pp. 319–365, 1997.
- [22] X. Wu, H. Zhao, R. Suk, and D. C. Christiani, "Genetic susceptibility to tobacco-related cancer," *Oncogene*, vol. 23, no. 38, pp. 6500–6523, 2004.
- [23] L. D. Kier, E. Yamasaki, and B. N. Ames, "Detection of mutagenic activity in cigarette smoke condensates," *Proceedings of the National Academy of Sciences of the United States of America*, vol. 71, no. 10, pp. 4159–4163, 1974.
- [24] S. S. Hecht, "Cigarette smoking: cancer risks, carcinogens, and mechanisms," *Langenbeck's Archives of Surgery*, vol. 391, no. 6, pp. 603–613, 2006.
- [25] R. Singh and P. B. Farmer, "Liquid chromatography-electrospray ionization-mass spectrometry: the future of DNA adduct detection," *Carcinogenesis*, vol. 27, no. 2, pp. 178–196, 2006.
- [26] P. B. Farmer and R. Singh, "Use of DNA adducts to identify human health risk from exposure to hazardous environmental pollutants: the increasing role of mass spectrometry in assessing biologically effective doses of genotoxic carcinogens," *Mutation Research*, vol. 659, no. 1-2, pp. 68–76, 2008.
- [27] S. S. Hecht, "Cigarette smoking and lung cancer: chemical mechanisms and approaches to prevention," *Lancet Oncology*, vol. 3, no. 8, pp. 461–469, 2002.
- [28] D. H. Phillips, "Smoking-related DNA and protein adducts in human tissues," *Carcinogenesis*, vol. 23, no. 12, pp. 1979–2004, 2002.
- [29] G. N. Wogan, S. S. Hecht, J. S. Felton, A. H. Conney, and L. A. Loeb, "Environmental and chemical carcinogenesis," *Seminars in Cancer Biology*, vol. 14, no. 6, pp. 473–486, 2004.
- [30] G. P. Pfeifer, M. F. Denissenko, M. Olivier, N. Tretyakova, S. S. Hecht, and P. Hainaut, "Tobacco smoke carcinogens, DNA damage and p53 mutations in smoking-associated cancers," *Oncogene*, vol. 21, no. 48, pp. 7435–7451, 2002.
- [31] L. A. Loeb and C. C. Harris, "Advances in chemical carcinogenesis: a historical review and prospective," *Cancer Research*, vol. 68, no. 17, pp. 6863–6872, 2008.
- [32] D. M. DeMarini, "Genotoxicity of tobacco smoke and tobacco smoke condensate: a review," *Mutation Research*, vol. 567, no. 2-3, pp. 447–474, 2004.
- [33] H. Bartsch and B. Singer, *Exocyclic DNA Adducts in Mutagenesis and Carcinogenesis*, vol. 150, IARC Scientific Publications, Lyon, France, 1999.
- [34] B. Hang, "Repair of exocyclic DNA adducts: rings of complexity," *BioEssays*, vol. 26, no. 11, pp. 1195–1208, 2004.
- [35] N. E. Geacintov, M. Cosman, B. E. Hingerty, S. Amin, S. Broyde, and D. J. Patel, "NMR solution structures of stereoisomeric covalent polycyclic aromatic carcinogen-DNA adducts: principles, patterns, and diversity," *Chemical Research in Toxicology*, vol. 10, no. 2, pp. 111–146, 1997.
- [36] A. B. Guliaev, B. Hang, and B. Singer, "Structural insights by molecular dynamics simulations into specificity of the major human AP endonuclease toward the benzene-derived DNA adduct, pBQ-C," *Nucleic Acids Research*, vol. 32, no. 9, pp. 2844–2852, 2004.
- [37] A. Barbin, "Etheno-adduct-forming chemicals: from mutagenicity testing to tumor mutation spectra," *Mutation Research*, vol. 462, no. 2-3, pp. 55–69, 2000.

- [38] T. Buterin, M. T. Hess, N. Luneva et al., "Unrepaired fjord region polycyclic aromatic hydrocarbon-DNA adducts in ras codon 61 mutational hot spots," *Cancer Research*, vol. 60, no. 7, pp. 1849–1856, 2000.
- [39] W. A. Spencer, J. Singh, and D. K. Orren, "Formation and differential repair of covalent DNA adducts generated by treatment of human cells with (+/-)-anti-dibenzo[a,l]pyrene-11,12-diol-13, 14-epoxide," *Chemical Research in Toxicology*, vol. 22, no. 1, pp. 81–89, 2009.
- [40] F. Veglia, G. Matullo, and P. Vineis, "Bulky DNA adducts and risk of cancer: a meta-analysis," *Cancer Epidemiology Biomarkers and Prevention*, vol. 12, no. 2, pp. 157–160, 2003.
- [41] G. Matullo, S. Guarrera, S. Carturan et al., "DNA repair gene polymorphisms, bulky DNA adducts in white blood cells and bladder cancer in a case-control study," *International Journal of Cancer*, vol. 92, no. 4, pp. 562–567, 2001.
- [42] M. F. Denissenko, A. Pao, M.-S. Tang, and G. P. Pfeifer, "Preferential formation of benzo[a]pyrene adducts at lung cancer mutational hotspots in P53," *Science*, vol. 274, no. 5286, pp. 430–432, 1996.
- [43] Z. Feng, W. Hu, Y. Hu, and M.-S. Tang, "Acrolein is a major cigarette-related lung cancer agent: preferential binding at p53 mutational hotspots and inhibition of DNA repair," *Proceedings of the National Academy of Sciences of the United States of America*, vol. 103, no. 42, pp. 15404–15409, 2006.
- [44] H. Bartsch, "Keynote address: exocyclic adducts as new risk markers for DNA damage in man," *IARC Scientific Publications*, no. 150, pp. 1–16, 1999.
- [45] S. Nesnow, J. A. Ross, M. J. Mass, and G. D. Stoner, "Mechanistic relationships between DNA adducts, oncogene mutations, and lung tumorigenesis in strain a mice," *Experimental Lung Research*, vol. 24, no. 4, pp. 395–405, 1998.
- [46] A. M. Jarabek, L. H. Pottenger, L. S. Andrews et al., "Creating context for the use of DNA adduct data in cancer risk assessment: I. Data organization," *Critical Reviews in Toxicology*, vol. 39, no. 8, pp. 659–678, 2009.
- [47] E. Burlakova, G. Zhizhina, S. Gurevich et al., "Biomarkers of oxidative stress and smoking in cancer patients," *Journal of Cancer Research and Therapeutics*, vol. 6, no. 1, pp. 47–53, 2010.
- [48] P. C. Dedon, J. P. Plataras, C. A. Rouzer, and L. J. Marnett, "Indirect mutagenesis by oxidative DNA damage: formation of the pyrimidopurinone adduct of deoxyguanosine by base prepenal," *Proceedings of the National Academy of Sciences of the United States of America*, vol. 95, no. 19, pp. 11113–11116, 1998.
- [49] R. de Bont and N. van Larebeke, "Endogenous DNA damage in humans: a review of quantitative data," *Mutagenesis*, vol. 19, no. 3, pp. 169–185, 2004.
- [50] K. S. Koch, R. G. Fletcher, M. P. Grond et al., "Inactivation of plasmid reporter gene expression by one benzo(a)pyrene diol-epoxide DNA adduct in adult rat hepatocytes," *Cancer Research*, vol. 53, no. 10, pp. 2279–2286, 1993.
- [51] M. S. Greenblatt, W. P. Bennett, M. Hollstein, and C. C. Harris, "Mutations in the p53 tumor suppressor gene: clues to cancer etiology and molecular pathogenesis," *Cancer Research*, vol. 54, no. 18, pp. 4855–4878, 1994.
- [52] T. M. Hernandez-Boussard and P. Hainaut, "A specific spectrum of p53 mutations in lung cancer from smokers: review of mutations compiled in the IARC p53 database," *Environmental Health Perspectives*, vol. 106, no. 7, pp. 385–391, 1998.
- [53] S. H. Reynolds and M. W. Anderson, "Activation of proto-oncogenes in human and mouse lung tumors," *Environmental Health Perspectives*, vol. 93, pp. 145–148, 1991.
- [54] G. Akopyan and B. Bonavida, "Understanding tobacco smoke carcinogen NNK and lung tumorigenesis," *International journal of oncology*, vol. 29, no. 4, pp. 745–752, 2006.
- [55] K. K. Divine, L. C. Pulling, P. G. Marron-Terada et al., "Multiplicity of abnormal promoter methylation in lung adenocarcinomas from smokers and never smokers," *International Journal of Cancer*, vol. 114, no. 3, pp. 400–405, 2005.
- [56] W. H. Westra, R. J. C. Slebos, G. J. A. Offerhaus et al., "K-ras oncogene activation in lung adenocarcinomas from former smokers: evidence that K-ras mutations are an early and irreversible event in the development of adenocarcinoma of the lung," *Cancer*, vol. 72, no. 2, pp. 432–438, 1993.
- [57] T. M. Penning and C. Lerman, "Genomics of smoking exposure and cessation: lessons for cancer prevention and treatment," *Cancer prevention research (Philadelphia, Pa.)*, vol. 1, no. 2, pp. 80–83, 2008.
- [58] S. Zienolddiny, D. Ryberg, M. O. Arab, V. Skaug, and A. Haugen, "Loss of heterozygosity is related to p53 mutations and smoking in lung cancer," *British Journal of Cancer*, vol. 84, no. 2, pp. 226–231, 2001.
- [59] T. Hirao, H. H. Nelson, T. D. S. Ashok et al., "Tobacco smoke-induced DNA damage and an early age of smoking initiation induce chromosome loss at 3p21 in lung cancer," *Cancer Research*, vol. 61, no. 2, pp. 612–615, 2001.
- [60] D.-H. Kim, H. H. Nelson, J. K. Wiencke et al., "p16(INK4a) and histology-specific methylation of CpG islands by exposure to tobacco smoke in non-small cell lung cancer," *Cancer Research*, vol. 61, no. 8, pp. 3419–3424, 2001.
- [61] Y. T. Ma, S. Collins, L. Young, P. Murray, and C. Woodman, "Smoking-induced p16 methylation in young women," 35th ESMO Congress, Poster 160, Milan, Italy, 2010.
- [62] R. D. Wood, M. Mitchell, and T. Lindahl, "Human DNA repair genes, 2005," *Mutation Research*, vol. 577, no. 1-2, pp. 275–283, 2005.
- [63] T. Lindahl and R. D. Wood, "Quality control by DNA repair," *Science*, vol. 286, no. 5446, pp. 1897–1905, 1999.
- [64] E. C. Friedberg, G. C. Walker, W. Siede, R. D. Wood, R. A. Schultz, and T. Ellenberger, *DNA Repair and Mutagenesis*, ASM Press, Herndon, Va, USA, 2006.
- [65] L. -E. Wang, Z. Hu, E. M. Sturgis et al., "Reduced DNA repair capacity for removing tobacco carcinogen-induced DNA adducts contributes to risk of head and neck cancer but not tumor characteristics," *Clinical Cancer Research*, vol. 16, no. 2, pp. 764–774, 2010.
- [66] A. S. Neumann, E. M. Sturgis, and Q. Wei, "Nucleotide excision repair as a marker for susceptibility to tobacco-related cancers: a review of molecular epidemiological studies," *Molecular Carcinogenesis*, vol. 42, no. 2, pp. 65–92, 2005.
- [67] R. Woodgate, "A plethora of lesion-replicating DNA polymerases," *Genes and Development*, vol. 13, no. 17, pp. 2191–2195, 1999.
- [68] R. E. Johnson, M. T. Washington, S. Prakash, and L. Prakash, "Bridging the gap: a family of novel DNA polymerases that replicate faulty DNA," *Proceedings of the National Academy of Sciences of the United States of America*, vol. 96, no. 22, pp. 12224–12226, 1999.
- [69] W. Yang and R. Woodgate, "What a difference a decade makes: insights into translesion DNA synthesis," *Proceedings of the National Academy of Sciences of the United States of America*, vol. 104, no. 40, pp. 15591–15598, 2007.

- [70] H. Ohmori, E. C. Friedberg, R. P. P. Fuchs et al., "The Y-family of DNA Polymerases," *Molecular Cell*, vol. 8, no. 1, pp. 7–8, 2001.
- [71] C. Guo, J. N. Kosarek-Stancel, T.-S. Tang, and E. C. Friedberg, "Y-family DNA polymerases in mammalian cells," *Cellular and Molecular Life Sciences*, vol. 66, no. 14, pp. 2363–2381, 2009.
- [72] R. L. Levine, H. Miller, A. Grollman et al., "Translesion DNA Synthesis Catalyzed by Human Pol  $\eta$  and Pol  $\kappa$  across 1,N<sup>6</sup>-Ethenodeoxyadenosine," *Journal of Biological Chemistry*, vol. 276, no. 22, pp. 18717–18721, 2001.
- [73] O. Rechkoblit, Y. Zhang, D. Guo et al., "trans-lesion synthesis past bulky benzo[a]pyrene diol epoxide N<sup>2</sup>-dG and N<sup>6</sup>-dA lesions catalyzed by DNA bypass polymerases," *Journal of Biological Chemistry*, vol. 277, no. 34, pp. 30488–30494, 2002.
- [74] D. Chiapperino, M. Cai, J. M. Sayer et al., "Error-prone translesion synthesis by human DNA polymerase  $\eta$  on DNA-containing deoxyadenosine adducts of 7,8-dihydroxy-9,10-epoxy-7,8,9,10- tetrahydrobenzo[a]pyrene," *Journal of Biological Chemistry*, vol. 280, no. 48, pp. 39684–39692, 2005.
- [75] M. T. Washington, I. G. Minko, R. E. Johnson et al., "Efficient and error-free replication past a minor-groove DNA adduct by the sequential action of human DNA polymerases  $\iota$  and  $\kappa$ ," *Molecular and Cellular Biology*, vol. 24, no. 13, pp. 5687–5693, 2004.
- [76] B. Singer, "DNA damage: chemistry, repair, and mutagenic potential," *Regulatory Toxicology and Pharmacology*, vol. 23, no. 1 I, pp. 2–13, 1996.
- [77] N. Shrivastav, D. Li, and J. M. Essigmann, "Chemical biology of mutagenesis and DNA repair: cellular responses to DNA alkylation," *Carcinogenesis*, vol. 31, no. 1, pp. 59–70, 2009.
- [78] A. Besaratinia and G. P. Pfeifer, "Investigating human cancer etiology by DNA lesion footprinting and mutagenicity analysis," *Carcinogenesis*, vol. 27, no. 8, pp. 1526–1537, 2006.
- [79] C. Li, L.-E. Wang, and Q. Wei, "DNA repair phenotype and cancer susceptibility-A mini review," *International Journal of Cancer*, vol. 124, no. 5, pp. 999–1007, 2009.
- [80] S. S. Hecht, "DNA adduct formation from tobacco-specific N-nitrosamines," *Mutation Research*, vol. 424, no. 1-2, pp. 127–142, 1999.
- [81] F. P. Perera, D. Tang, V. Rauh et al., "Relationship between polycyclic aromatic hydrocarbon-DNA adducts, environmental tobacco smoke, and child development in the World Trade Center Cohort," *Environmental Health Perspectives*, vol. 115, no. 10, pp. 1497–1502, 2007.
- [82] D. H. Phillips, "Smoking-related DNA and protein adducts in human tissues," *Carcinogenesis*, vol. 23, no. 12, pp. 1979–2004, 2002.
- [83] K. Szyfter, J. Banaszewski, P. Jałoszyński, M. Pabiszczak, W. Szyfter, and Z. Szmęja, "Carcinogen:DNA adducts in tobacco smoke-associated cancer of the upper respiratory tract," *Acta Biochimica Polonica*, vol. 46, no. 2, pp. 275–287, 1999.
- [84] S. J. Sturla, "DNA adduct profiles: chemical approaches to addressing the biological impact of DNA damage from small molecules," *Current Opinion in Chemical Biology*, vol. 11, no. 3, pp. 293–299, 2007.
- [85] K. F. Rabe, S. Hurd, A. Anzueto et al., "Global strategy for the diagnosis, management, and prevention of chronic obstructive pulmonary disease: GOLD executive summary," *American Journal of Respiratory and Critical Care Medicine*, vol. 176, no. 6, pp. 532–555, 2007.
- [86] C. Smith, T. Perfetti, and J. King, "Perspectives on pulmonary inflammation and lung cancer risk in cigarette smokers," *Inhalation Toxicology*, vol. 18, no. 9, pp. 667–677, 2006.
- [87] V. Kim, T. J. Rogers, and G. J. Criner, "New concepts in the pathobiology of chronic obstructive pulmonary disease," *Proceedings of the American Thoracic Society*, vol. 5, no. 4, pp. 478–485, 2008.
- [88] P. R. Reynolds, M. G. Cosio, and J. R. Hoidal, "Cigarette smoke-induced Egr-1 upregulates proinflammatory cytokines in pulmonary epithelial cells," *American Journal of Respiratory Cell and Molecular Biology*, vol. 35, no. 3, pp. 314–319, 2006.
- [89] T. Walser, X. Cui, J. Yanagawa et al., "Smoking and lung cancer: the role of inflammation," *Proceedings of the American Thoracic Society*, vol. 5, no. 8, pp. 811–815, 2008.
- [90] J. E. Klaunig and L. M. Kamendulis, "The role of oxidative stress in carcinogenesis," *Annual Review of Pharmacology and Toxicology*, vol. 44, pp. 239–267, 2004.
- [91] S. P. Hussain and C. C. Harris, "Inflammation and cancer: an ancient link with novel potentials," *International Journal of Cancer*, vol. 121, no. 11, pp. 2373–2380, 2007.
- [92] F. -L. Chung, J. Pan, S. Choudhury, R. Roy, W. Hu, and M. -S. Tang, "Formation of trans-4-hydroxy-2-nonenal- and other enal-derived cyclic DNA adducts from  $\omega$ -3 and  $\omega$ -6 polyunsaturated fatty acids and their roles in DNA repair and human p53 gene mutation," *Mutation Research*, vol. 531, no. 1-2, pp. 25–36, 2003.
- [93] L. J. Marnett, "Oxy radicals, lipid peroxidation and DNA damage," *Toxicology*, vol. 181-182, pp. 219–222, 2002.
- [94] H. Bartsch and J. Nair, "Accumulation of lipid peroxidation-derived DNA lesions: potential lead markers for chemoprevention of inflammation-driven malignancies," *Mutation Research*, vol. 591, no. 1-2, pp. 34–44, 2005.
- [95] L. Jowa, S. Winkle, G. Kalf, G. Witz, and R. Snyder, "Deoxyguanosine adducts formed from benzoquinone and hydroquinone," *Advances in Experimental Medicine and Biology*, vol. 197, pp. 825–832, 1986.
- [96] K. Pongracz and W. J. Bodell, "Detection of 3'-hydroxy-1,N<sup>6</sup>-benzetheno-2'-deoxyadenosine 3'-phosphate by <sup>32</sup>P post-labeling of DNA reacted with p-benzoquinone," *Chemical Research in Toxicology*, vol. 4, no. 2, pp. 199–202, 1991.
- [97] K. Pongracz, S. Kaur, A. L. Burlingame, and W. J. Bodell, "Detection of (3'-hydroxy)-3,N<sup>4</sup>-benzetheno-2'-deoxycytidine-3'-phosphate by <sup>32</sup>P-postlabeling of DNA reacted with p-benzoquinone," *Carcinogenesis*, vol. 11, no. 9, pp. 1469–1472, 1990.
- [98] M. Gaskell, R. Jukes, D. J. L. Jones, E. A. Martin, and P. B. Farmer, "Identification and characterization of (3'',4''-dihydroxy)-1,N<sup>2</sup>- benzetheno-2'-deoxyguanosine 3'-monophosphate, a novel DNA adduct formed by benzene metabolites," *Chemical Research in Toxicology*, vol. 15, no. 8, pp. 1088–1095, 2002.
- [99] B. Singer and H. Bartsch, *Exocyclic DNA Adducts in Mutagenesis and Carcinogenesis*, IARC Scientific Publications, Lyon, France, 1999.
- [100] N. J. Leonard, "Etheno-substituted nucleotides and coenzymes: fluorescence and biological activity," *CRC Critical Reviews in Biochemistry*, vol. 15, no. 2, pp. 125–199, 1984.
- [101] R. J. Albertini and L. M. Sweeney, "Propylene oxide: genotoxicity profile of a rodent nasal carcinogen," *Critical Reviews in Toxicology*, vol. 37, no. 6, pp. 489–520, 2007.
- [102] B. Singer and B. Hang, "What structural features determine repair enzyme specificity and mechanism in chemically modified DNA?" *Chemical Research in Toxicology*, vol. 10, no. 7, pp. 713–732, 1997.

- [103] A. Memisoglu and L. Samson, "Base excision repair in yeast and mammals," *Mutation Research*, vol. 451, no. 1-2, pp. 39–51, 2000.
- [104] P. Modrich and R. Lahue, "Mismatch repair in replication fidelity, genetic recombination, and cancer biology," *Annual Review of Biochemistry*, vol. 65, pp. 101–133, 1996.
- [105] P. C. Hanawalt, "Subpathways of nucleotide excision repair and their regulation," *Oncogene*, vol. 21, no. 58, pp. 8949–8956, 2002.
- [106] A. E. Pegg, "Repair of  $O^6$ -alkylguanine by alkyltransferases," *Mutation Research*, vol. 462, no. 2-3, pp. 83–100, 2000.
- [107] J. H. J. Hoeijmakers, "DNA damage, aging, and cancer," *New England Journal of Medicine*, vol. 361, no. 15, pp. 1475–1485, 2009.
- [108] J. T. Reardon and A. Sancar, "Nucleotide excision repair," *Progress in Nucleic Acid Research and Molecular Biology*, vol. 79, pp. 183–235, 2005.
- [109] K. A. Johnson, M. L. Mierzwa, S. P. Fink, and L. J. Marnett, "MutS recognition of exocyclic DNA adducts that are endogenous products of lipid oxidation," *Journal of Biological Chemistry*, vol. 274, no. 38, pp. 27112–27118, 1999.
- [110] T. Nouspikel, "DNA repair in mammalian cells: nucleotide excision repair: variations on versatility," *Cellular and Molecular Life Sciences*, vol. 66, pp. 994–1009, 2009.
- [111] L. C. J. Gillet and O. D. Schärer, "Molecular mechanisms of mammalian global genome nucleotide excision repair," *Chemical Reviews*, vol. 106, no. 2, pp. 253–276, 2006.
- [112] M. K.K. Shivji, "Nucleotide excision repair DNA synthesis by DNA polymerase  $\epsilon$  in the presence of PCNA, RFC, and RPA," *Biochemistry*, vol. 34, no. 15, pp. 5011–5017, 1995.
- [113] A. Aboussekhra, M. Biggerstaff, M. K. K. Shivji et al., "Mammalian DNA nucleotide excision repair reconstituted with purified protein components," *Cell*, vol. 80, no. 6, pp. 859–868, 1995.
- [114] D. Mu, C.-H. Park, T. Matsunaga, D. S. Hsu, J. T. Reardon, and A. Sancar, "Reconstitution of human DNA repair excision nuclease in a highly defined system," *Journal of Biological Chemistry*, vol. 270, no. 6, pp. 2415–2418, 1995.
- [115] L. J. Marnett and J. P. Plastaras, "Endogenous DNA damage and mutation," *Trends in Genetics*, vol. 17, no. 4, pp. 214–221, 2001.
- [116] M. P. Stonez, Y.-J. Cho, H. Huang et al., "Interstrand DNA cross-links induced by  $\alpha,\beta$ -unsaturated aldehydes derived from lipid peroxidation and environmental sources," *Accounts of Chemical Research*, vol. 41, no. 7, pp. 793–804, 2008.
- [117] R. L. Cooper, A. J. Lindsey, and R. E. Waller, "The presence of 3,4-benzopyrene in cigarette smoke," *Chemical Industry*, vol. 46, p. 1418, 1954.
- [118] W. Xue and D. Warshawsky, "Metabolic activation of polycyclic and heterocyclic aromatic hydrocarbons and DNA damage: a review," *Toxicology and Applied Pharmacology*, vol. 206, no. 1, pp. 73–93, 2005.
- [119] M. K. Buening, P. G. Wislocki, H. Levin et al., "Tumorigenicity of the optical enantiomers of the diastereomeric benzo[a]pyrene 7,8-diol-9,10-epoxides in newborn mice: exceptional activity of (+)-7 $\beta$ ,8 $\alpha$ -dihydroxy-9 $\alpha$ ,10 $\alpha$ -epoxy-7,8,9,10-tetrahydrobenzo[a]pyrene," *Proceedings of the National Academy of Sciences of the United States of America*, vol. 75, no. 11, pp. 5358–5361, 1978.
- [120] J. Szeliga and A. Dipple, "DNA adduct formation by polycyclic aromatic hydrocarbon dihydrodiol epoxides," *Chemical Research in Toxicology*, vol. 11, no. 1, pp. 1–11, 1998.
- [121] V. Mocquet, K. Kropachev, M. Kolbanovskiy et al., "The human DNA repair factor XPC-HR23B distinguishes stereoisomeric benzo[a]pyrenyl-DNA lesions," *EMBO Journal*, vol. 26, no. 12, pp. 2923–2932, 2007.
- [122] I. B. Weinstein, A. M. Jeffrey, K. W. Jennette et al., "Benzo[a]pyrene diol epoxides as intermediates in nucleic acid binding in vitro and in vivo," *Science*, vol. 193, no. 4253, pp. 592–594, 1976.
- [123] M. Koreeda, P. D. Moore, P. Wislocki et al., "Binding of benzo[a]pyrene 7,8-diol-9,10-epoxides to DNA, RNA, and protein of mouse skin occurs with high stereoselectivity," *Science*, vol. 199, no. 4330, pp. 778–781, 1978.
- [124] G. Boysen and S. S. Hecht, "Analysis of DNA and protein adducts of benzo[a]pyrene in human tissues using structure-specific methods," *Mutation Research*, vol. 543, no. 1, pp. 17–30, 2003.
- [125] E. L. Cavalieri and E. G. Rogan, "Central role of radical cations in metabolic activation of polycyclic aromatic hydrocarbons," *Xenobiotica*, vol. 25, no. 7, pp. 677–688, 1995.
- [126] T. M. Penning, M. E. Burczynski, C.-F. Hung, K. D. McCoull, N. T. Palackal, and L. S. Tsuruda, "Dihydrodiol dehydrogenases and polycyclic aromatic hydrocarbon activation: generation of reactive and redox active o-quinones," *Chemical Research in Toxicology*, vol. 12, no. 1, pp. 1–18, 1999.
- [127] J.-H. Park, D. Mangal, K. A. Tacka et al., "Evidence for the aldo-keto reductase pathway of polycyclic aromatic trans-dihydrodiol activation in human lung A549 cells," *Proceedings of the National Academy of Sciences of the United States of America*, vol. 105, no. 19, pp. 6846–6851, 2008.
- [128] S. Nesnow, G. Nelson, W. T. Padgett et al., "Lack of contribution of covalent benzo[a]pyrene-7,8-quinone-DNA adducts in benzo[a]pyrene-induced mouse lung tumorigenesis," *Chemico-Biological Interactions*, vol. 186, no. 2, pp. 157–165, 2010.
- [129] D. Yu, J. A. Berlin, T. M. Penning, and J. Field, "Reactive oxygen species generated by PAH o-quinones cause change-in-function mutations in p53," *Chemical Research in Toxicology*, vol. 15, no. 6, pp. 832–842, 2002.
- [130] M.-S. Tang, J. R. Pierce, R. P. Doisy, M. E. Nazimiec, and M. C. MacLeod, "Differences and similarities in the repair of two benzo[a]pyrene diol epoxide isomers induced DNA adducts by uvrA, uvrB, and uvrC gene products," *Biochemistry*, vol. 31, no. 36, pp. 8429–8436, 1992.
- [131] M. T. Hess, D. Gunz, N. Luneva, N. E. Geacintov, and H. Naegeli, "Base pair conformation-dependent excision of benzo[a]pyrene diol epoxide-guanine adducts by human nucleotide excision repair enzymes," *Molecular and Cellular Biology*, vol. 17, no. 12, pp. 7069–7076, 1997.
- [132] R. Pastorelli, A. Cerri, M. Mezzetti, E. Consonni, and L. Airoldi, "Effect of DNA repair gene polymorphisms on BPDE-DNA adducts in human lymphocytes," *International Journal of Cancer*, vol. 100, no. 1, pp. 9–13, 2002.
- [133] R. Meschini, E. Marotta, A. Berni et al., "DNA repair deficiency and BPDE-induced chromosomal alterations in CHO cells," *Mutation Research*, vol. 637, no. 1-2, pp. 93–100, 2008.
- [134] Y. Zou, S. M. Shell, C. D. Utzat et al., "Effects of DNA adduct structure and sequence context on strand opening of repair intermediates and incision by UvrABC nuclease," *Biochemistry*, vol. 42, no. 43, pp. 12654–12661, 2003.
- [135] T. Meehan and K. Straub, "Double stranded DNA stereoselectively binds benzo(a)pyrene diol epoxides," *Nature*, vol. 277, no. 5695, pp. 410–412, 1979.

- [136] A. M. Jeffrey, K. Grzeskowiak, I. B. Weinstein, K. Nakanishi, P. Roller, and R. G. Harvey, "Benzo(a)pyrene-7,8-dihydrodiol 9,10-oxide adenosine and deoxyadenosine adducts: structure and stereochemistry," *Science*, vol. 206, no. 4424, pp. 1309–1311, 1979.
- [137] R.-H. Chen, V. M. Maher, J. Brouwer, P. van de Putte, and J. J. McCormick, "Preferential repair and strand-specific repair of benzo[a]pyrene diol epoxide adducts in the HPRT gene of diploid human fibroblasts," *Proceedings of the National Academy of Sciences of the United States of America*, vol. 89, no. 12, pp. 5413–5417, 1992.
- [138] M. F. Denissenko, A. Pao, G. P. Pfeifer, and M.-S. Tang, "Slow repair of bulky DNA adducts along the nontranscribed strand of the human p53 gene may explain the strand bias of transversion mutations in cancers," *Oncogene*, vol. 16, no. 10, pp. 1241–1247, 1998.
- [139] R. A. Perlow, A. Kolbanovskii, B. E. Hingerty, N. E. Geacintov, S. Brody, and D. A. Scicchitano, "DNA adducts from a tumorigenic metabolite of benzo[a]pyrene block human RNA polymerase II elongation in a sequence- and stereochemistry-dependent manner," *Journal of Molecular Biology*, vol. 321, no. 1, pp. 29–47, 2002.
- [140] S. Leng, A. Bernauer, C. A. Stidley et al., "Association between common genetic variation in Cockayne syndrome A and B genes and nucleotide excision repair capacity among smokers," *Cancer Epidemiology Biomarkers and Prevention*, vol. 17, no. 8, pp. 2062–2069, 2008.
- [141] R. Jankowiak, F. Ariese, A. Hewer et al., "Structure, conformations, and repair of DNA adducts from dibenzo[a,l]pyrene:  $^{32}\text{P}$ -postlabeling and fluorescence studies," *Chemical Research in Toxicology*, vol. 11, no. 6, pp. 674–685, 1998.
- [142] A. Lagerqvist, D. Håkansson, G. Prochazka et al., "Both replication bypass fidelity and repair efficiency influence the yield of mutations per target dose in intact mammalian cells induced by benzo[a]pyrene-diol-epoxide and dibenzo[a,l]pyrene-diol-epoxide," *DNA Repair*, vol. 7, no. 8, pp. 1202–1212, 2008.
- [143] F. F. Kadlubar and A. F. Badawi, "Genetic susceptibility and carcinogen-DNA adduct formation in human urinary bladder carcinogenesis," *Toxicology Letters*, vol. 82–83, pp. 627–632, 1995.
- [144] S. Swaminathan, J. F. Hatcher, S. M. Frederickson, C. A. Reznikoff, and J. C. Pink, "The relationship between DNA-adduct formation and induction of mutations in the hypoxanthine-guanine phosphoribosyl transferase (HGPRT) locus in human uroepithelial cells," *Polycyclic Aromatic Compounds*, vol. 6, pp. 43–52, 1994.
- [145] E. M., Ricicki, W. Luo, W. Fan, L. P. Zhao, H. Zarbl, and P. Vouros, "Quantification of N-(deoxyguanosin-8-yl)-4-aminobiphenyl adducts in human lymphoblastoid TK6 cells dosed with N-hydroxy-4-acetylaminobiphenyl and their relationship to mutation, toxicity, and gene expression profiling," *Analytical Chemistry*, vol. 78, pp. 6422–6432, 2006.
- [146] G. Talaska, A. Z. S. S. Al-Juburi, and F. F. Kadlubar, "Smoking related carcinogen-DNA adducts in biopsy samples of human urinary bladder: identification of N-(deoxyguanosin-8-yl)-4-aminobiphenyl as a major adduct," *Proceedings of the National Academy of Sciences of the United States of America*, vol. 88, no. 12, pp. 5350–5354, 1991.
- [147] L. Airoidi, F. Orsi, C. Magagnotti et al., "Determinants of 4-aminobiphenyl-DNA adducts in bladder cancer biopsies," *Carcinogenesis*, vol. 23, no. 5, pp. 861–866, 2002.
- [148] B. Zayas, S. W. Stillwell, J. S. Wishnok et al., "Detection and quantification of 4-ABP adducts in DNA from bladder cancer patients," *Carcinogenesis*, vol. 28, no. 2, pp. 342–349, 2007.
- [149] Z. Feng, W. Hu, W. N. Rom, F. A. Beland, and M.-S. Tang, "4-Aminobiphenyl is a major etiological agent of human bladder cancer: evidence from its DNA binding spectrum in human p53 gene," *Carcinogenesis*, vol. 23, no. 10, pp. 1721–1727, 2002.
- [150] Z. Feng, W. Hu, W. N. Rom, F. A. Beland, and M.-S. Tang, "N-hydroxy-4-aminobiphenyl-DNA binding in human p53 gene: sequence preference and the effect of C5 cytosine methylation," *Biochemistry*, vol. 41, no. 20, pp. 6414–6421, 2002.
- [151] J. L. Torino, M. S. Burger, C. A. Reznikoff, and S. Swaminathan, "Role of TP53 in repair of N-(deoxyguanosin-8-yl)-4-aminobiphenyl adducts in human transitional cell carcinoma of the urinary bladder," *Carcinogenesis*, vol. 22, no. 1, pp. 147–154, 2001.
- [152] J. Lin, F. F. Kadlubar, M. R. Spitz, H. Zhao, and X. Wu, "A modified host cell reactivation assay to measure DNA repair capacity for removing 4-aminobiphenyl adducts: a pilot study of bladder cancer," *Cancer Epidemiology Biomarkers and Prevention*, vol. 14, no. 7, pp. 1832–1836, 2005.
- [153] S. Swaminathan, J. L. Torino, and M. S. Burger, "Human urinary bladder epithelial cells lacking wild-type p53 function are deficient in the repair of 4-aminobiphenyl-DNA adducts in genomic DNA," *Mutation Research*, vol. 499, no. 1, pp. 103–117, 2002.
- [154] J. F. Stevens and C. S. Maier, "Acrolein: sources, metabolism, and biomolecular interactions relevant to human health and disease," *Molecular Nutrition and Food Research*, vol. 52, no. 1, pp. 7–25, 2008.
- [155] F.-L. Chung, R. Young, and S. S. Hecht, "Formation of cyclic 1,N<sup>2</sup>-propanodeoxyguanosine adducts in DNA upon reaction with acrolein or crotonaldehyde," *Cancer Research*, vol. 44, no. 3, pp. 990–995, 1984.
- [156] R. G. Nath and F.-L. Chung, "Detection of exocyclic 1,N<sup>2</sup>-propanodeoxyguanosine adducts as common DNA lesions in rodents and humans," *Proceedings of the National Academy of Sciences of the United States of America*, vol. 91, no. 16, pp. 7491–7495, 1994.
- [157] I. G. Minko, I. D. Kozekov, T. M. Harris, C. J. Rizzo, R. S. Lloyd, and M. P. Stone, "Chemistry and biology of DNA containing 1,N(2)-deoxyguanosine adducts of the  $\alpha,\beta$ -unsaturated aldehydes acrolein, crotonaldehyde, and 4-hydroxynonenal," *Chemical Research in Toxicology*, vol. 22, no. 5, pp. 759–778, 2009.
- [158] S.-I. Kim, G. P. Pfeifer, and A. Besaratinia, "Lack of mutagenicity of acrolein-induced DNA adducts in mouse and human cells," *Cancer Research*, vol. 67, no. 24, pp. 11640–11647, 2007.
- [159] H.-T. Wang, S. Zhang, Y. Hu, and M.-S. Tang, "Mutagenicity and sequence specificity of acrolein-DNA adducts," *Chemical Research in Toxicology*, vol. 22, no. 3, pp. 511–517, 2009.
- [160] S. Zhang, P. W. Villalta, M. Wang, and S. S. Hecht, "Detection and quantitation of acrolein-derived 1,N<sup>2</sup>-propanodeoxyguanosine adducts in human lung by liquid chromatography- electrospray ionization-tandem mass spectrometry," *Chemical Research in Toxicology*, vol. 20, no. 4, pp. 565–571, 2007.
- [161] R. G. Nath, J. E. Ocando, J. B. Guttenplan, and F.-L. Chung, "1,N<sup>2</sup>-propanodeoxyguanosine adducts: potential

- new biomarkers of smoking-induced DNA damage in human oral tissue," *Cancer Research*, vol. 58, no. 4, pp. 581–584, 1998.
- [162] L. J. Marnett, "DNA adducts of  $\alpha,\beta$ -unsaturated aldehydes and dicarbonyl compounds," *IARC Scientific Publications*, no. 125, pp. 151–163, 1994.
- [163] F. L. Chung, L. Zhang, J. E. Ocando, and R. G. Nath, "Role of 1,N<sup>2</sup>-propanodeoxyguanosine adducts as endogenous DNA lesions in rodents and humans," *IARC Scientific Publications*, no. 150, pp. 45–54, 1999.
- [164] F.-L. Chung, R. G. Nath, J. Ocando, A. Nishikawa, and L. Zhang, "Deoxyguanosine adducts of t-4-Hydroxy-2-nonenal are endogenous DNA lesions in rodents and humans: detection and potential sources," *Cancer Research*, vol. 60, no. 6, pp. 1507–1511, 2000.
- [165] I.-Y. Yang, M. Hossain, H. Miller et al., "Responses to the major acrolein-derived deoxyguanosine adduct in *Escherichia coli*," *Journal of Biological Chemistry*, vol. 276, no. 12, pp. 9071–9076, 2001.
- [166] S. Choudhury, J. Pan, S. Amin, F.-L. Chung, and R. Roy, "Repair kinetics of trans-4-Hydroxynonenal-induced cyclic 1,N<sup>2</sup>-propanodeoxyguanine DNA adducts by human cell nuclear extracts," *Biochemistry*, vol. 43, no. 23, pp. 7514–7521, 2004.
- [167] B. Janowska, M. Komisarowski, P. Prorok et al., "Nucleotide excision repair and recombination are engaged in repair of trans-4-hydroxy-2-nonenal adducts to DNA bases in *Escherichia coli*," *International Journal of Biological Sciences*, vol. 5, no. 6, pp. 611–620, 2009.
- [168] I.-Y. Yang, G. Chan, H. Miller et al., "Mutagenesis by acrolein-derived propanodeoxyguanosine adducts in human cells," *Biochemistry*, vol. 41, no. 46, pp. 13826–13832, 2002.
- [169] L. A. van der Veen, M. F. Hashim, L. V. Nechev, T. M. Harris, C. M. Harris, and L. J. Marnett, "Evaluation of the mutagenic potential of the principal DNA adduct of acrolein," *Journal of Biological Chemistry*, vol. 276, no. 12, pp. 9066–9070, 2001.
- [170] I.-Y. Yang, F. Johnson, A. P. Grollman, and M. Moriya, "Genotoxic mechanism for the major acrolein-derived deoxyguanosine adduct in human cells," *Chemical Research in Toxicology*, vol. 15, no. 2, pp. 160–164, 2002.
- [171] IARC, *IARC Monographs on the Evaluation of the Carcinogenic Risk of Chemicals to Humans: Some Industrial Chemicals and Dyestuffs*, vol. 29, International Agency for Research on Cancer, Lyon, France, 1982.
- [172] R. Snyder and C. C. Hedli, "An overview of benzene metabolism," *Environmental Health Perspectives*, vol. 104, supplement 6, pp. 1165–1171, 1996.
- [173] G. Levay, K. Pongracz, and W. J. Bodell, "Detection of DNA adducts in HL-60 cells treated with hydroquinone and p-benzoquinone by <sup>32</sup>P-postlabeling," *Carcinogenesis*, vol. 12, no. 7, pp. 1181–1186, 1991.
- [174] H. Bauer, E. A. Dimitriadis, and R. Snyder, "An in vivo study of benzene metabolite DNA adduct formation in liver of male New Zealand rabbits," *Archives of Toxicology*, vol. 63, no. 3, pp. 209–213, 1989.
- [175] M. V. Reddy, G. R. Blackburn, C. A. Schreiner, M. A. Mehlman, and C. R. Mackerer, "<sup>32</sup>P analysis of DNA adducts in tissues of benzene-treated rats," *Environmental Health Perspectives*, vol. 82, pp. 253–257, 1989.
- [176] E. Krewet, C. Verkoyen, G. Muller, C. Schell, W. Popp, and K. Norpoth, "Studies on guanine adducts excreted in rat urine after benzene exposure," *Carcinogenesis*, vol. 14, no. 2, pp. 245–250, 1993.
- [177] W. J. Bodell, D. N. Pathak, G. Lévy, Q. Ye, and K. Pongracz, "Investigation of the DNA adducts formed in B6C3F1 mice treated with benzene: implications for molecular dosimetry," *Environmental Health Perspectives*, vol. 104, supplement 6, pp. 1189–1193, 1996.
- [178] Z. Xie, Y. Zhang, A. B. Guliaev et al., "The p-benzoquinone DNA adducts derived from benzene are highly mutagenic," *DNA Repair*, vol. 4, no. 12, pp. 1399–1409, 2005.
- [179] G. Witz, Z. Zhang, and B. D. Goldstein, "Reactive ring-opened aldehyde metabolites in benzene hematotoxicity," *Environmental Health Perspectives*, vol. 104, supplement 6, pp. 1195–1199, 1996.
- [180] B. T. Golding and W. P. Watson, "Possible mechanisms of carcinogenesis after exposure to benzene," *IARC Scientific Publications*, no. 150, pp. 75–88, 1999.
- [181] R. P. Amin and G. Witz, "DNA-protein crosslink and DNA strand break formation in HL-60 cells treated with trans,trans-muconaldehyde, hydroquinone and their mixtures," *International Journal of Toxicology*, vol. 20, no. 2, pp. 69–80, 2001.
- [182] M. Shen, Q. Lan, L. Zhang et al., "Polymorphisms in genes involved in DNA double-strand break repair pathway and susceptibility to benzene-induced hematotoxicity," *Carcinogenesis*, vol. 27, no. 10, pp. 2083–2089, 2006.
- [183] E. L. Cavalieri, K. -M. Li, N. Balu et al., "Catechol orthoquinones: the electrophilic compounds that form depurinating DNA adducts and could initiate cancer and other diseases," *Carcinogenesis*, vol. 23, no. 6, pp. 1071–1077, 2002.
- [184] B. Rodriguez, Y. Yang, A. B. Guliaev, A. Chenna, and B. Hang, "Benzene-derived N<sup>2</sup>-(4-hydroxyphenyl)-deoxyguanosine adduct: UvrABC incision and its conformation in DNA," *Toxicology Letters*, vol. 193, no. 1, pp. 26–32, 2010.
- [185] M. Gaskell, K. I. E. McLuckie, and P. B. Farmer, "Comparison of the repair of DNA damage induced by the benzene metabolites hydroquinone and p-benzoquinone: a role for hydroquinone in benzene genotoxicity," *Carcinogenesis*, vol. 26, no. 3, pp. 673–680, 2005.
- [186] A. Hartwig, "The role of DNA repair in benzene-induced carcinogenesis," *Chemico-Biological Interactions*, vol. 184, no. 1–2, pp. 269–272, 2010.
- [187] S. S. David and S. D. Williams, "Chemistry of glycosylases and endonucleases involved in base-excision repair," *Chemical Reviews*, vol. 98, no. 3, pp. 1221–1261, 1998.
- [188] J. L. Huffman, O. Sundheim, and J. A. Tainer, "DNA base damage recognition and removal: new twists and grooves," *Mutation Research*, vol. 577, no. 1–2, pp. 55–76, 2005.
- [189] B. Dalhus, J. K. Laerdahl, P. H. Backe, and M. Bjørås, "DNA base repair—recognition and initiation of catalysis," *FEMS Microbiology Reviews*, vol. 33, no. 6, pp. 1044–1078, 2009.
- [190] B. Hang, *Base Excision Repair*, World Scientific Publishing Co. Pte. Ltd, Singapore, 2006.
- [191] J. C. Fromme and G. L. Verdine, "Base excision repair," *Advances in Protein Chemistry*, vol. 69, pp. 1–41, 2004.
- [192] A. B. Robertson, A. Klungland, T. Rognes, and I. Leiros, "DNA repair in mammalian cells: base excision repair: the long and short of it," *Cellular and Molecular Life Sciences*, vol. 66, pp. 981–993, 2009.
- [193] B. Hang and B. Singer, "Protein-protein interactions involving DNA glycosylases," *Chemical Research in Toxicology*, vol. 16, no. 10, pp. 1181–1195, 2003.
- [194] I. V. Kovtun and C. T. McMurray, "Crosstalk of DNA glycosylases with pathways other than base excision repair," *DNA Repair*, vol. 6, no. 4, pp. 517–529, 2007.

- [195] J. Fan and D. M. Wilson III, "Protein-protein interactions and posttranslational modifications in mammalian base excision repair," *Free Radical Biology and Medicine*, vol. 38, no. 9, pp. 1121–1138, 2005.
- [196] J. Baute and A. Depicker, "Base excision repair and its role in maintaining genome stability," *Critical Reviews in Biochemistry and Molecular Biology*, vol. 43, no. 4, pp. 239–276, 2008.
- [197] D. M. Wilson III and D. Barsky, "The major human abasic endonuclease: formation, consequences and repair of abasic lesions in DNA," *Mutation Research*, vol. 485, no. 4, pp. 283–307, 2001.
- [198] S. Boiteux and M. Guillet, "Abasic sites in DNA: repair and biological consequences in *Saccharomyces cerevisiae*," *DNA Repair*, vol. 3, no. 1, pp. 1–12, 2004.
- [199] L. Gros, A. A. Ishchenko, and M. Saparbaev, "Enzymology of repair of etheno-adducts," *Mutation Research*, vol. 531, no. 1-2, pp. 219–229, 2003.
- [200] H.-J. C. Chen, C.-L. Hong, C.-F. Wu, and W.-L. Chiu, "Effect of cigarette smoking on urinary 3,N<sup>4</sup>-ethenocytosine levels measured by gas chromatography/mass spectrometry," *Toxicological Sciences*, vol. 76, no. 2, pp. 321–327, 2003.
- [201] H.-J. C. Chen and W.-L. Chiu, "Association between cigarette smoking and urinary excretion of 1,N<sup>2</sup>-ethenoguanine measured by isotope dilution liquid chromatography-electrospray ionization/tandem mass spectrometry," *Chemical Research in Toxicology*, vol. 18, no. 10, pp. 1593–1599, 2005.
- [202] P. J. Gehring, P. G. Watanabe, and C. N. Park, "Resolution of dose-response toxicity data for chemicals requiring metabolic activation: example—vinyl chloride," *Toxicology and Applied Pharmacology*, vol. 44, no. 3, pp. 581–591, 1978.
- [203] F. P. Guengerich, D.-H. Kim, and M. Iwasaki, "Role of human cytochrome P-450 IIE1 in the oxidation of many low molecular weight cancer suspects," *Chemical Research in Toxicology*, vol. 4, no. 2, pp. 168–179, 1991.
- [204] J. T. Kuśmierk and B. Singer, "1,N<sup>2</sup>-ethenodeoxyguanosine: properties and formation in chloroacetaldehyde-treated polynucleotides and DNA," *Chemical Research in Toxicology*, vol. 5, no. 5, pp. 634–638, 1992.
- [205] M. K. Dosanjh, R. Roy, S. Mitra, and B. Singer, "1,N<sup>6</sup>-Ethenoadenine is preferred over 3-methyladenine as substrate by a cloned human N-methylpurine-DNA glycosylase (3-methyladenine-DNA glycosylase)," *Biochemistry*, vol. 33, no. 7, pp. 1624–1628, 1994.
- [206] M. Saparbaev, K. Kleibl, and J. Laval, "Escherichia coli, Saccharomyces cerevisiae, rat and human 3-methyladenine DNA glycosylases repair 1,N<sup>6</sup>-ethenoadenine when present in DNA," *Nucleic Acids Research*, vol. 23, no. 18, pp. 3750–3755, 1995.
- [207] C.-Y. I. Lee, J. C. Delaney, M. Kartalou et al., "Recognition and processing of a new repertoire of DNA substrates by human 3-methyladenine DNA glycosylase (AAG)," *Biochemistry*, vol. 48, no. 9, pp. 1850–1861, 2009.
- [208] A. Y. Lau, O. D. Schärer, L. Samson, G. L. Verdine, and T. Ellenberger, "Crystal structure of a human alkylbase-DNA repair enzyme complexed to DNA: mechanisms for nucleotide flipping and base excision," *Cell*, vol. 95, no. 2, pp. 249–258, 1998.
- [209] A. Y. Lau, M. D. Wyatt, B. J. Glassner, L. D. Samson, and T. Ellenberger, "Molecular basis for discriminating between normal and damaged bases by the human alkyladenine glycosylase AAG," *Proceedings of the National Academy of Sciences of the United States of America*, vol. 97, no. 25, pp. 13573–13578, 2000.
- [210] R. H. Elder, J. G. Jansen, R. J. Weeks et al., "Alkylpurine-DNA-N-glycosylase knockout mice show increased susceptibility to induction of mutations by methyl methanesulfonate," *Molecular and Cellular Biology*, vol. 18, no. 10, pp. 5828–5837, 1998.
- [211] B. P. Engelward, G. Weeda, M. D. Wyatt et al., "Base excision repair deficient mice lacking the Aag alkyladenine DNA glycosylase," *Proceedings of the National Academy of Sciences of the United States of America*, vol. 94, no. 24, pp. 13087–13092, 1997.
- [212] L. B. Meira, J. M. Bugni, S. L. Green et al. et al., "DNA damage induced by chronic inflammation contributes to colon carcinogenesis in mice," *Journal of Clinical Investigation*, vol. 118, no. 7, pp. 2516–2525, 2008.
- [213] S. Choudhury, S. Adhikari, A. Cheema, and R. Roy, "Evidence of complete cellular repair of 1,N<sup>6</sup>-ethenoadenine, a mutagenic and potential damage for human cancer, revealed by a novel method," *Molecular and Cellular Biochemistry*, vol. 313, no. 1-2, pp. 19–28, 2008.
- [214] B. Hang, M. Medina, H. Fraenkel-Conrat, and B. Singer, "A 55-kDa protein isolated from human cells shows dna glycosylase activity toward 3,N<sup>4</sup>-ethenocytosine and the G/T mismatch," *Proceedings of the National Academy of Sciences of the United States of America*, vol. 95, no. 23, pp. 13561–13566, 1998.
- [215] M. Saparbaev and J. Laval, "3,N<sup>4</sup>-ethenocytosine, a highly mutagenic adduct, is a primary substrate for Escherichia coli double-stranded uracil-DNA glycosylase and human mismatch-specific thymine-DNA glycosylase," *Proceedings of the National Academy of Sciences of the United States of America*, vol. 95, no. 15, pp. 8508–8513, 1998.
- [216] J. -K. Zhu, "Active DNA demethylation mediated by DNA glycosylases," *Annual Review of Genetics*, vol. 43, pp. 143–166, 2009.
- [217] S. , P. Gallinari, Y.-Z. Xu et al., "Base analog and neighboring base effects on substrate specificity of recombinant human G:T mismatch-specific thymine-DNA-glycosylase," *Biochemistry*, vol. 35, no. 39, pp. 12926–12932, 1996.
- [218] T. R. Waters and P. F. Swann, "Thymine-DNA glycosylase and G to A transition mutations at CpG sites," *Mutation Research*, vol. 462, no. 2-3, pp. 137–147, 2000.
- [219] A. Maiti, M. T. Morgan, E. Pozharski, and A. C. Drohat, "Crystal structure of human thymine DNA glycosylase bound to DNA elucidates sequence-specific mismatch recognition," *Proceedings of the National Academy of Sciences of the United States of America*, vol. 105, no. 26, pp. 8890–8895, 2008.
- [220] B. Kavli, O. Sundheim, M. Akbari et al., "hUNG2 is the major repair enzyme for removal of uracil from U:A matches, U:G mismatches, and U in single-stranded DNA, with hSMUG1 as a broad specificity backup," *Journal of Biological Chemistry*, vol. 277, no. 42, pp. 39926–39936, 2002.
- [221] F. Petronzelli, A. Riccio, G. D. Markham et al., "Investigation of the substrate spectrum of the human mismatch-specific DNA N-glycosylase MED1 (MBD4): fundamental role of the catalytic domain," *Journal of Cellular Physiology*, vol. 185, no. 3, pp. 473–480, 2000.
- [222] J. A. Swenberg, M. S. Bogdanffy, A. Ham et al., "Formation and repair of DNA adducts in vinyl chloride- and vinyl fluoride-induced carcinogenesis," *IARC Scientific Publications*, no. 150, pp. 29–43, 1999.

- [223] Z. Matijasevic, M. Sekiguchi, and D. B. Ludlum, "Release of N<sup>2</sup>,3-ethenoguanine from chloroacetaldehyde-treated DNA by Escherichia coli 3-methyladenine DNA glycosylase II," *Proceedings of the National Academy of Sciences of the United States of America*, vol. 89, no. 19, pp. 9331–9334, 1992.
- [224] M. K. Dosanjh, A. Chenna, E. Kim, H. Fraenkel-Conrat, L. Samson, and B. Singer, "All four known cyclic adducts formed in DNA by the vinyl chloride metabolite chloroacetaldehyde are released by a human DNA glycosylase," *Proceedings of the National Academy of Sciences of the United States of America*, vol. 91, no. 3, pp. 1024–1028, 1994.
- [225] S. Holt, G. Roy, S. Mitra, P. B. Upton, M. S. Bogdanffy, and J. A. Swenberg, "Deficiency of N-methylpurine-DNA-glycosylase expression in nonparenchymal cells, the target cell for vinyl chloride and vinyl fluoride," *Mutation Research*, vol. 460, no. 2, pp. 105–115, 2000.
- [226] M. Sapparbaev, S. Langouët, C. V. Privezentzev et al., "1,N<sup>2</sup>-ethenoguanine, a mutagenic DNA adduct, is a primary substrate of Escherichia coli mismatch-specific uracil-DNA glycosylase and human alkylpurine-DNA-N-glycosylase," *Journal of Biological Chemistry*, vol. 277, no. 30, pp. 26987–26993, 2002.
- [227] S. Steiner, A. E. Crane, and W. P. Watson, "Molecular dosimetry of DNA adducts in C3H mice treated with glycidaldehyde," *Carcinogenesis*, vol. 13, no. 1, pp. 119–124, 1992.
- [228] B. M. Goldschmidt, T. P. Blazej, and B. L. Van Duuren, "The reaction of guanosine and deoxyguanosine with glycidaldehyde," *Tetrahedron Letters*, vol. 9, no. 13, pp. 1583–1586, 1968.
- [229] Y. Kohwi, "Non-B DNA structure: preferential target for the chemical carcinogen glycidaldehyde," *Carcinogenesis*, vol. 10, no. 11, pp. 2035–2042, 1989.
- [230] B. Singer, M. Medina, Y. Zhang, Z. Wang, A. B. Guliaev, and B. Hang, "8-(Hydroxymethyl)-3,N<sup>4</sup>-etheno-C, a potential carcinogenic glycidaldehyde product, miscodes in vitro using mammalian DNA polymerases," *Biochemistry*, vol. 41, no. 6, pp. 1778–1785, 2002.
- [231] P. Wang, A. B. Guliaev, R. H. Elder, and B. Hang, "Alkylpurine-DNA-N-glycosylase excision of 7-(hydroxymethyl)-1,N<sup>6</sup>-etheno-adenine, a glycidaldehyde-derived DNA adduct," *DNA Repair*, vol. 5, no. 1, pp. 23–31, 2006.
- [232] B. Hang and A. B. Guliaev, "Substrate specificity of human thymine-DNA glycosylase on exocyclic cytosine adducts," *Chemico-Biological Interactions*, vol. 165, no. 3, pp. 230–238, 2007.
- [233] D. Hoffmann, K. D. Brunnemann, B. Prokopczyk, and M. V. Djordjevic, "Tobacco-specific N-nitrosamines and Arecaderived N-nitrosamines: chemistry, biochemistry, carcinogenicity, and relevance to humans," *Journal of Toxicology and Environmental Health*, vol. 41, no. 1, pp. 1–52, 1994.
- [234] S. S. Hecht, "Tobacco carcinogens, their biomarkers and tobacco-induced cancer," *Nature Reviews Cancer*, vol. 3, no. 10, pp. 733–744, 2003.
- [235] R. S. Mijal, N. M. Thomson, N. L. Fleischer et al., "The repair of the tobacco specific nitrosamine derived adduct O<sup>6</sup>-[4-oxo-4-(3-pyridyl)butyl]guanine by O<sup>6</sup>-alkylguanine-DNA alkyltransferase variants," *Chemical Research in Toxicology*, vol. 17, no. 3, pp. 424–434, 2004.
- [236] L. Li, J. Perdigo, A. E. Pegg et al., "The influence of repair pathways on the cytotoxicity and mutagenicity induced by the pyridyloxobutyl pathway of tobacco-specific nitrosamines," *Chemical Research in Toxicology*, vol. 22, no. 8, pp. 1464–1472, 2009.
- [237] L. Wang, T. E. Spratt, X.-K. Liu, S. S. Hecht, A. E. Pegg, and L. A. Peterson, "Pyridyloxobutyl adduct O<sup>6</sup>-[4-oxo-4-(3-pyridyl)butyl]guanine is present in 4-(acetoxymethylnitrosamino)-1-(3-pyridyl)-1-butanone-treated DNA and is a substrate for O<sup>6</sup>-alkylguanine-DNA alkyltransferase," *Chemical Research in Toxicology*, vol. 10, no. 5, pp. 562–567, 1997.
- [238] S. Zhang, M. Wang, P. W. Villalta, B. R. Lindgren, Y. Lao, and S. S. Hecht, "Quantitation of pyridyloxobutyl DNA adducts in nasal and oral mucosa of rats treated chronically with enantiomers of N'-nitrosornicotine," *Chemical Research in Toxicology*, vol. 22, no. 5, pp. 949–956, 2009.
- [239] R. S. Mijal, N. A. Loktionova, C. C. Vu, A. E. Pegg, and L. A. Peterson, "O<sup>6</sup>-pyridyloxobutylguanine adducts contribute to the mutagenic properties of pyridyloxobutylating agents," *Chemical Research in Toxicology*, vol. 18, no. 10, pp. 1619–1625, 2005.
- [240] G. T. Pauly, L. A. Peterson, and R. C. Moschel, "Mutagenesis by O<sup>6</sup>-[4-oxo-4-(3-pyridyl)butyl]guanine in Escherichia coli and human cells," *Chemical Research in Toxicology*, vol. 15, no. 2, pp. 165–169, 2002.
- [241] M. Sleiman, L. A. Gundel, J. F. Pankow, P. Jacob III, B. C. Singer, and H. Destailats, "Formation of carcinogens indoors by surface-mediated reactions of nicotine with nitrous acid, leading to potential thirdhand smoke hazards," *Proceedings of the National Academy of Sciences of the United States of America*, vol. 107, no. 15, pp. 6576–6581, 2010.
- [242] R. S. Mijal, S. Kanugula, C. C. Vu, Q. Fang, A. E. Pegg, and L. A. Peterson, "DNA sequence context affects repair of the tobacco-specific adduct O<sup>6</sup>-[4-oxo-4-(3-pyridyl)butyl]guanine by human O<sup>6</sup>-alkylguanine-DNA alkyltransferases," *Cancer Research*, vol. 66, no. 9, pp. 4968–4974, 2006.
- [243] M. Xu-Welliver and A. E. Pegg, "Degradation of the alkylated form of the DNA repair protein, O<sup>6</sup>-alkylguanine-DNA alkyltransferase," *Carcinogenesis*, vol. 23, no. 5, pp. 823–830, 2002.
- [244] N. M. Thomson, P. M. Kenney, and L. A. Peterson, "The pyridyloxobutyl DNA adduct, O<sup>6</sup>-[4-Oxo-4-(3-pyridyl)butyl]guanine, is detected in tissues from 4-(methylnitrosamino)-1-(3-pyridyl)-1-butanone-treated A/J mice," *Chemical Research in Toxicology*, vol. 16, no. 1, pp. 1–6, 2003.
- [245] P. J. Brown, L. L. Bedard, and T. E. Massey, "Repair of 4-(methylnitrosamino)-1-(3-pyridyl)-1-butanone-induced DNA pyridyloxobutylation by nucleotide excision repair," *Cancer Letters*, vol. 260, no. 1–2, pp. 48–55, 2008.
- [246] J. C. Delaney, L. Smeester, C. Wong et al., "AlkB reverses etheno DNA lesions caused by lipid oxidation in vitro and in vivo," *Nature Structural and Molecular Biology*, vol. 12, no. 10, pp. 855–860, 2005.
- [247] Y. Mishina, C.-G. Yang, and C. He, "Direct repair of the exocyclic DNA adduct 1,N<sup>6</sup>-etheno-adenine by the DNA repair AlkB proteins," *Journal of the American Chemical Society*, vol. 127, no. 42, pp. 14594–14595, 2005.
- [248] J. Ringvoll, M. N. Moen, L. M. Nordstrand et al., "AlkB homologue 2-mediated repair of etheno-adenine lesions in mammalian DNA," *Cancer Research*, vol. 68, no. 11, pp. 4142–4149, 2008.
- [249] M. A. Kurowski, A. S. Bhagwat, G. Papaj, and J. M. Bujnicki, "Phylogenomic identification of five new human homologs

- of the DNA repair enzyme AlkB," *BMC Genomics*, vol. 4, article no. 48, 2003.
- [250] T. Duncan, S. C. Trewick, P. Koivisto, P. A. Bates, T. Lindahl, and B. Sedgwick, "Reversal of DNA alkylation damage by two human dioxygenases," *Proceedings of the National Academy of Sciences of the United States of America*, vol. 99, no. 26, pp. 16660–16665, 2002.
- [251] J. C. Delaney and J. M. Essigmann, "Mutagenesis, genotoxicity, and repair of 1-methyladenine, 3-alkylcytosines, 1-methylguanine, and 3-methylthymine in alkB *Escherichia coli*," *Proceedings of the National Academy of Sciences of the United States of America*, vol. 101, no. 39, pp. 14051–14056, 2004.
- [252] A. Barbin, R. Wang, P. J. O'Connor, and R. H. Elder, "Increased formation and persistence of 1,N<sup>6</sup>-ethenoadenine in DNA is not associated with higher susceptibility to carcinogenesis in alkylpurine-DNA-N-glycosylase knockout mice treated with vinyl carbamate," *Cancer Research*, vol. 63, no. 22, pp. 7699–7703, 2003.
- [253] B. Hang, A. Chenna, H. Fraenkel-Conrat, and B. Singer, "An unusual mechanism for the major human apurinic/aprimidinic (AP) endonuclease involving 5' cleavage of DNA containing a benzene-derived exocyclic adduct in the absence of an AP site," *Proceedings of the National Academy of Sciences of the United States of America*, vol. 93, no. 24, pp. 13737–13741, 1996.
- [254] A. Chenna, B. Hang, B. Rydberg et al., "The benzene metabolite p-benzoquinone forms adducts with DNA bases that are excised by a repair activity from human cells that differs from an ethenoadenine glycosylase," *Proceedings of the National Academy of Sciences of the United States of America*, vol. 92, no. 13, pp. 5890–5894, 1995.
- [255] B. Hang, D. G. Rothwell, J. Sagi, I. D. Hickson, and B. Singer, "Evidence for a common active site for cleavage of an AP site and the benzene-derived exocyclic adduct, 3,N<sup>4</sup>-benzetheno-dC, in the major human AP endonuclease," *Biochemistry*, vol. 36, no. 49, pp. 15411–15418, 1997.
- [256] D. G. Rothwell, B. Hang, M. A. Gorman, P. S. Freemont, B. Singer, and I. D. Hickson, "Substitution of Asp-210 in HAP1 (APE/Ref-1) eliminates endonuclease activity but stabilises substrate binding," *Nucleic Acids Research*, vol. 28, no. 11, pp. 2207–2213, 2000.
- [257] A. A. Ischenko and M. K. Saparbaev, "Alternative nucleotide incision repair pathway for oxidative DNA damage," *Nature*, vol. 415, no. 6868, pp. 183–187, 2002.
- [258] L. Gros, A. A. Ishchenko, H. Ide, R. H. Elder, and M. K. Saparbaev, "The major human AP endonuclease (Ape1) is involved in the nucleotide incision repair pathway," *Nucleic Acids Research*, vol. 32, no. 1, pp. 73–81, 2004.
- [259] C. D. Mol, T. Izumi, S. Mitra, and J. A. Tainer, "DNA-bound structures and mutants reveal abasic DNA binding by APE1 and DNA repair coordination [corrected]," *Nature*, vol. 403, pp. 451–456, 2000.
- [260] K. Hitomi, S. Iwai, and J. A. Tainer, "The intricate structural chemistry of base excision repair machinery: implications for DNA damage recognition, removal, and repair," *DNA Repair*, vol. 6, no. 4, pp. 410–428, 2007.
- [261] W. Yang, "Structure and mechanism for DNA lesion recognition," *Cell Research*, vol. 18, no. 1, pp. 184–197, 2008.
- [262] D. Gunz, M. T. Hess, and H. Naegeli, "Recognition of DNA adducts by human nucleotide excision repair. Evidence for a thermodynamic probing mechanism," *Journal of Biological Chemistry*, vol. 271, no. 41, pp. 25089–25098, 1996.
- [263] J. J. Truglio, E. Karakas, B. Rhau et al., "Structural basis for DNA recognition and processing by UvrB," *Nature Structural and Molecular Biology*, vol. 13, no. 4, pp. 360–364, 2006.
- [264] J.-H. Min and N. P. Pavletich, "Recognition of DNA damage by the Rad4 nucleotide excision repair protein," *Nature*, vol. 449, no. 7162, pp. 570–575, 2007.
- [265] J. C. Fromme, A. Banerjee, and G. L. Verdine, "DNA glycosylase recognition and catalysis," *Current Opinion in Structural Biology*, vol. 14, no. 1, pp. 43–49, 2004.
- [266] R. Shapiro, S. Ellis, B. E. Hingerty, and S. Broyde, "Effect of ring size on conformations of aromatic amine-DNA adducts: the aniline-C8 guanine adduct resides in the B-DNA major groove," *Chemical Research in Toxicology*, vol. 11, no. 4, pp. 335–341, 1998.
- [267] D. J. Hosfield, Y. Guan, B. J. Haas, R. P. Cunningham, and J. A. Tainer, "Structure of the DNA repair enzyme endonuclease IV and its DNA complex: double-nucleotide flipping at abasic sites and three-metal-ion catalysis," *Cell*, vol. 98, no. 3, pp. 397–408, 1999.
- [268] B. Singer and B. Hang, "Nucleic acid sequence and repair: role of adduct, neighbor bases and enzyme specificity," *Carcinogenesis*, vol. 21, no. 6, pp. 1071–1078, 2000.
- [269] S. Sukumar, V. Notario, D. Martin Zanca, and M. Barbacid, "Induction of mammary carcinomas in rats by nitrosomethylurea involves malignant activation of H-ras-1 by single point mutations," *Nature*, vol. 306, no. 5944, pp. 658–661, 1983.
- [270] F. C. Richardson, J. A. Boucheron, T. R. Skopek, and J. A. Swenberg, "Formation of O<sup>6</sup>-methyldeoxyguanosine at specific sites in a synthetic oligonucleotide designed to resemble a known mutagenic hotspot," *Journal of Biological Chemistry*, vol. 264, no. 2, pp. 838–841, 1989.
- [271] M. E. Dolan, M. Oplinger, and A. E. Pegg, "Sequence specificity of guanine alkylation and repair," *Carcinogenesis*, vol. 9, no. 11, pp. 2139–2143, 1988.
- [272] D. Wei, V. M. Maher, and J. J. McCormick, "Site-specific rates of excision repair of benzo[a]pyrene diol epoxide adducts in the hypoxanthine phosphoribosyltransferase gene of human fibroblasts: correlation with mutation spectra," *Proceedings of the National Academy of Sciences of the United States of America*, vol. 92, no. 6, pp. 2204–2208, 1995.
- [273] Z. Feng, W. Hu, J. X. Chen et al., "Preferential DNA damage and poor repair determine ras gene mutational hotspot in human cancer," *Journal of the National Cancer Institute*, vol. 94, no. 20, pp. 1527–1536, 2002.
- [274] K. Kropachev, M. Kolbanovskii, Y. Cai et al., "The sequence dependence of human nucleotide excision repair efficiencies of benzo[a]pyrene-derived DNA lesions: insights into the structural factors that favor dual incisions," *Journal of Molecular Biology*, vol. 386, no. 5, pp. 1193–1203, 2009.
- [275] B. Hang, J. Sági, and B. Singer, "Correlation between sequence-dependent glycosylase repair and the thermal stability of oligonucleotide duplexes containing 1,N<sup>6</sup>-ethenoadenine," *Journal of Biological Chemistry*, vol. 273, no. 50, pp. 33406–33413, 1998.
- [276] K. A. Donigan and J. B. Sweasy, "Sequence context-specific mutagenesis and base excision repair," *Molecular Carcinogenesis*, vol. 48, no. 4, pp. 362–368, 2009.
- [277] Q. Ruan, T. Liu, A. Kolbanovskiy et al., "Sequence context- and temperature-dependent nucleotide excision repair of a benzo[a]pyrene diol epoxide-guanine DNA adduct catalyzed by thermophilic UvrABC proteins," *Biochemistry*, vol. 46, no. 23, pp. 7006–7015, 2007.

- [278] Y. Cai, K. Kropachev, R. Xu et al., "Distant neighbor base sequence context effects in human nucleotide excision repair of a benzo[a]pyrene-derived DNA lesion," *Journal of Molecular Biology*, vol. 399, no. 3, pp. 397–409, 2010.
- [279] N. E. Geacintov, S. Broyde, T. Buterin et al., "Thermodynamic and structural factors in the removal of bulky DNA adducts by the nucleotide excision repair machinery," *Biopolymers*, vol. 65, no. 3, pp. 202–210, 2002.
- [280] J. Sági, B. Hang, and B. Singer, "Sequence-dependent repair of synthetic AP sites in 15-mer and 35-mer oligonucleotides: role of thermodynamic stability imposed by neighbor bases," *Chemical Research in Toxicology*, vol. 12, no. 10, pp. 917–923, 1999.
- [281] L. E. Smith, M. F. Denissenko, W. P. Bennett et al., "Targeting of lung cancer mutational hotspots by polycyclic aromatic hydrocarbons," *Journal of the National Cancer Institute*, vol. 92, no. 10, pp. 803–811, 2000.
- [282] M.-S. Tang, J. B. Zheng, M. F. Denissenko, G. P. Pfeifer, and Y. Zheng, "Use of UvrABC nuclease to quantify benzo[a]pyrene diol epoxide-DNA adduct formation at methylated versus unmethylated CpG sites in the p53 gene," *Carcinogenesis*, vol. 20, no. 6, pp. 1085–1089, 1999.
- [283] S. N. Rodin and A. S. Rodin, "Origins and selection of p53 mutations in lung carcinogenesis," *Seminars in Cancer Biology*, vol. 15, no. 2, pp. 103–112, 2005.
- [284] J.-H. Park, S. Gelhaus, S. Vedantam et al., "The pattern of p53 mutations caused by PAH o-quinones is driven by 8-oxo-dGuo formation while the spectrum of mutations is determined by biological selection for dominance," *Chemical Research in Toxicology*, vol. 21, no. 5, pp. 1039–1049, 2008.
- [285] M. J. Thun, S. J. Henley, and E. E. Calle, "Tobacco use and cancer: an epidemiologic perspective for geneticists," *Oncogene*, vol. 21, no. 48, pp. 7307–7325, 2002.
- [286] Q. Wei, L. Cheng, C. I. Amos et al., "Repair of tobacco carcinogen-induced DNA adducts and lung cancer risk: a molecular epidemiologic study," *Journal of the National Cancer Institute*, vol. 92, no. 21, pp. 1764–1772, 2000.
- [287] R. M. Santella, M. Gammon, M. Terry et al., "DNA adducts, DNA repair genotype/phenotype and cancer risk," *Mutation Research*, vol. 592, no. 1-2, pp. 29–35, 2005.
- [288] R. Ankathil, "Tobacco, genetic susceptibility and lung cancer," *Tobacco Use Insights*, vol. 3, pp. 1–15, 2010.
- [289] A. G. Schwartz, G. M. Prysak, C. H. Bock, and M. L. Cote, "The molecular epidemiology of lung cancer," *Carcinogenesis*, vol. 28, no. 3, pp. 507–518, 2007.
- [290] L. Cheng, S. A. Eicher, Z. Guo, W. K. Hong, M. R. Spitz, and Q. Wei, "Reduced DNA repair capacity in head and neck cancer patients," *Cancer Epidemiology Biomarkers and Prevention*, vol. 7, no. 6, pp. 465–468, 1998.
- [291] E. Speina, M. Zielińska, A. Barbin et al., "Decreased repair activities of 1,N<sup>6</sup>-ethenoadenine and 3,N<sup>4</sup>-ethenocytosine in lung adenocarcinoma patients," *Cancer Research*, vol. 63, no. 15, pp. 4351–4357, 2003.
- [292] M. C. Miller III, H. W. Mohrenweiser, and D. A. Bell, "Genetic variability in susceptibility and response to toxicants," *Toxicology Letters*, vol. 120, no. 1-3, pp. 269–280, 2001.
- [293] A. C. Povey, G. P. Margison, and M. F. Santibáñez-Koref, "Lung cancer risk and variation in MGMT activity and sequence," *DNA Repair*, vol. 6, no. 8, pp. 1134–1144, 2007.
- [294] M. B. Terry, M. D. Gammon, F. F. Zhang et al., "Polymorphism in the DNA repair gene XPD, polycyclic aromatic hydrocarbon-DNA adducts, cigarette smoking, and breast cancer risk," *Cancer Epidemiology Biomarkers and Prevention*, vol. 13, no. 12, pp. 2053–2058, 2004.
- [295] C. Kiyohara and K. Yoshimasu, "Genetic polymorphisms in the nucleotide excision repair pathway and lung cancer risk: a meta-analysis," *International Journal of Medical Sciences*, vol. 4, no. 2, pp. 59–71, 2007.
- [296] H. Hoffmann, C. Isner, J. Högel, and G. Speit, "Genetic polymorphisms and the effect of cigarette smoking in the comet assay," *Mutagenesis*, vol. 20, no. 5, pp. 359–364, 2005.
- [297] H. Wikman, A. Risch, F. Klimek et al., "hOGG1 polymorphism and loss of heterozygosity (LOH): significance for lung cancer susceptibility in a Caucasian population," *International Journal of Cancer*, vol. 88, no. 6, pp. 932–937, 2000.
- [298] T. Schwerdtle, I. Walter, and A. Hartwig, "Arsenite and its biomethylated metabolites interfere with the formation and repair of stable BPDE-induced DNA adducts in human cells and impair XPAzf and Fpg," *DNA Repair*, vol. 2, no. 12, pp. 1449–1463, 2003.
- [299] A. Hartwig and T. Schwerdtle, "Interactions by carcinogenic metal compounds with DNA repair processes: toxicological implications," *Toxicology Letters*, vol. 127, no. 1–3, pp. 47–54, 2002.
- [300] A. Witkiewicz-Kucharczyk and W. Bal, "Damage of zinc fingers in DNA repair proteins, a novel molecular mechanism in carcinogenesis," *Toxicology Letters*, vol. 162, no. 1, pp. 29–42, 2006.
- [301] D. R. McNeill, A. Narayana, H.-K. Wong, and D. M. Wilson III, "Inhibition of Ape1 nuclease activity by lead, iron, and cadmium," *Environmental Health Perspectives*, vol. 112, no. 7, pp. 799–804, 2004.
- [302] P. Wang, A. B. Guliaev, and B. Hang, "Metal inhibition of human N-methylpurine-DNA glycosylase activity in base excision repair," *Toxicology Letters*, vol. 166, no. 3, pp. 237–247, 2006.
- [303] R. Godschalk, J. Hogervorst, H. Albering et al., "Interaction between cadmium and aromatic DNA adducts in hprt mutagenesis during foetal development," *Mutagenesis*, vol. 20, no. 3, pp. 181–185, 2005.
- [304] W. Hu, Z. Feng, and M. -S. Tang, "Chromium(VI) enhances (+/-)-anti-7 $\beta$ ,8 $\alpha$ -dihydroxy-9 $\alpha$ , 10 $\alpha$ -epoxy-7,8,9,10-tetrahydrobenzo[a]pyrene-induced cytotoxicity and mutagenicity in mammalian cells through its inhibitory effect on nucleotide excision repair," *Biochemistry*, vol. 43, no. 44, pp. 14282–14289, 2004.
- [305] V. Sipinen, J. Laubenthal, A. Baumgartner et al., "In vitro evaluation of baseline and induced DNA damage in human sperm exposed to benzo[a]pyrene or its metabolite benzo[a]pyrene-7,8-diol-9,10-epoxide, using the comet assay," *Mutagenesis*, vol. 25, no. 4, pp. 417–425, 2010.
- [306] H. Tjalve, "The tissue distribution and the tissue specificity of bioactivation of some tobacco-specific and some other N-nitrosamines," *Critical Reviews in Toxicology*, vol. 21, no. 4, pp. 265–294, 1991.
- [307] A. A. Elfarra, R. J. Krause, and R. A. Kemper, "Cellular and molecular basis for species, sex and tissue differences in 1,3-butadiene metabolism," *Chemico-Biological Interactions*, vol. 135-136, pp. 239–248, 2001.
- [308] L. A. Peterson, N. M. Thomson, D. L. Crankshaw, E. E. Donaldson, and P. J. Kenney, "Interactions between methylating and pyridyloxobutylating agents in A/J mouse lungs: implications for 4-(methylnitrosamino)-1-(3-pyridyl)-1-butanone-induced lung tumorigenesis," *Cancer Research*, vol. 61, no. 15, pp. 5757–5763, 2001.
- [309] P. J. Brown and T. E. Massey, "In vivo treatment with 4-(methylnitrosamino)-1-(3-pyridyl)-1-butanone (NNK)

- induces organ-specific alterations in in vitro repair of DNA pyridyloxobutylation," *Mutation Research*, vol. 663, no. 1-2, pp. 15–21, 2009.
- [310] M. R. Creek, C. Mani, J. S. Vogel, and K. W. Turteltaub, "Tissue distribution and macromolecular binding of extremely low doses of [<sup>14</sup>C]-benzene in B6C3F1 mice," *Carcinogenesis*, vol. 18, no. 12, pp. 2421–2427, 1997.
- [311] C. Buschfort-Papewalis, T. Moritz, B. Liedert, and J. Thomale, "Down-regulation of DNA repair in human CD34+ progenitor cells corresponds to increased drug sensitivity and apoptotic response," *Blood*, vol. 100, no. 3, pp. 845–853, 2002.
- [312] F. A. Beland and M. C. Poirier, "Significance of DNA adduct studies in animal models for cancer molecular dosimetry and risk assessment," *Environmental Health Perspectives*, vol. 99, pp. 5–10, 1993.
- [313] B. Singer and B. Hang, "Mammalian enzymatic repair of etheno and para-benzoquinone exocyclic adducts derived from the carcinogens vinyl chloride and benzene," *IARC Scientific Publications*, no. 150, pp. 233–247, 1999.
- [314] R. R. Selzer and A. A. Elfarra, "Synthesis and biochemical characterization of N<sup>1</sup>-, N<sup>2</sup>-, and N<sup>7</sup>-guanosine adducts of butadiene monoxide," *Chemical Research in Toxicology*, vol. 9, no. 1, pp. 126–132, 1996.
- [315] R. R. Selzer and A. A. Elfarra, "In vitro reactions of butadiene monoxide with single- and double-stranded DNA: characterization and quantitation of several purine and pyrimidine adducts," *Carcinogenesis*, vol. 20, no. 2, pp. 285–292, 1999.
- [316] C. Zhao, P. Vodicka, R. J. Šrám, and K. Hemminki, "Human DNA adducts of 1,3-butadiene, an important environmental carcinogen," *Carcinogenesis*, vol. 21, no. 1, pp. 107–111, 2000.
- [317] H. Destaillets, B. C. Singer, S. K. Lee, and L. A. Gundel, "Effect of ozone on nicotine desorption from model surfaces: evidence for heterogeneous chemistry," *Environmental Science and Technology*, vol. 40, no. 6, pp. 1799–1805, 2006.
- [318] M. Sleiman, R. L. Maddalena, L. A. Gundel, and H. Destaillets, "Rapid and sensitive gas chromatography-ion-trap tandem mass spectrometry method for the determination of tobacco-specific N-nitrosamines in secondhand smoke," *Journal of Chromatography A*, vol. 1216, no. 45, pp. 7899–7905, 2009.
- [319] B. C. Singer, A. T. Hodgson, and W. W. Nazaroff, "Gas-phase organics in environmental tobacco smoke: 2. Exposure-relevant emission factors and indirect exposures from habitual smoking," *Atmospheric Environment*, vol. 37, no. 39-40, pp. 5551–5561, 2003.
- [320] M. D. van Loy, W. J. Riley, J. M. Daisey, and W. W. Nazaroff, "Dynamic behavior of semivolatile organic compounds in indoor air. 2. Nicotine and phenanthrene with carpet and wallboard," *Environmental Science and Technology*, vol. 35, no. 3, pp. 560–567, 2001.
- [321] D. Hoffmann and S. S. Hecht, "Nicotine-derived N-nitrosamines and tobacco-related cancer: current status and future directions," *Cancer Research*, vol. 45, no. 3, pp. 935–944, 1985.
- [322] C. L. Crespi, B. W. Penman, H. V. Gelboin, and F. J. Gonzalez, "A tobacco smoke-derived nitrosamine, 4(methylnitrosamino)-1-(3-pyridyl)-1-butanone, is activated by multiple human cytochrome P450s including the polymorphic human cytochrome P4502D6," *Carcinogenesis*, vol. 12, no. 7, pp. 1197–1201, 1991.
- [323] A. Castonguay, D. Lin, G. D. Stoner et al., "Comparative carcinogenicity in A/J mice and metabolism by cultured mouse peripheral lung of N<sup>7</sup>-nitrosornicotine, 4-(methylnitrosamino)-1-(3-pyridyl)-1-butanone, and their analogues," *Cancer Research*, vol. 43, no. 3, pp. 1223–1229, 1983.
- [324] IARC, *Monographs on the Evaluation of the Carcinogenic Risk of Chemicals to Humans*, IARC, Lyon, France, 1985.
- [325] S. Schick and S. A. Glantz, "Sidestream cigarette smoke toxicity increases with aging and exposure duration," *Tobacco Control*, vol. 15, no. 6, pp. 424–429, 2006.
- [326] A. M. Hutt and G. F. Kalf, "Inhibition of human DNA topoisomerase II by hydroquinone and p-benzoquinone, reactive metabolites of benzene," *Environmental Health Perspectives*, vol. 104, supplement 6, pp. 1265–1269, 1996.

## Review Article

# Formation, Repair, and Genotoxic Properties of Bulky DNA Adducts Formed from Tobacco-Specific Nitrosamines

**Lisa A. Peterson**

*Division of Environmental Health Sciences, Masonic Cancer Center, Mayo Mail Code 806, 420 Delaware St SE, Minneapolis, MN 55455, USA*

Correspondence should be addressed to Lisa A. Peterson, peter431@umn.edu

Received 7 June 2010; Accepted 8 July 2010

Academic Editor: Ashis Basu

Copyright © 2010 Lisa A. Peterson. This is an open access article distributed under the Creative Commons Attribution License, which permits unrestricted use, distribution, and reproduction in any medium, provided the original work is properly cited.

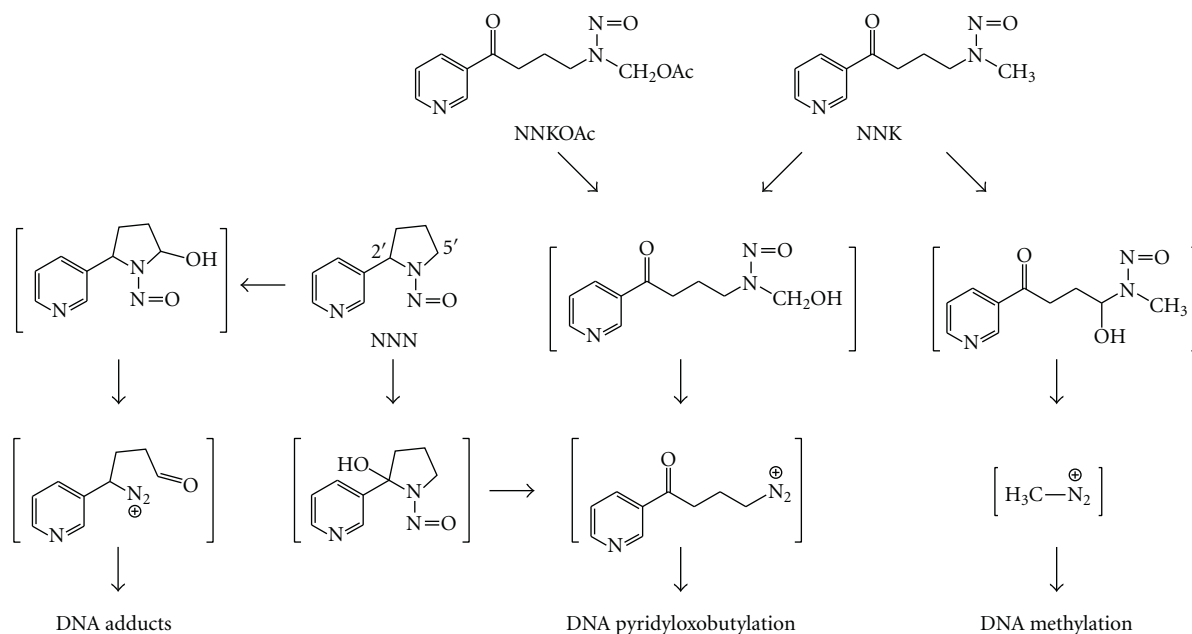
4-(Methylnitrosamino)-1-(3-pyridyl)-1-butanone (NNK) and *N'*-nitrosornicotine (NNN) are tobacco-specific nitrosamines present in tobacco products and smoke. Both compounds are carcinogenic in laboratory animals, generating tumors at sites comparable to those observed in smokers. These Group 1 human carcinogens are metabolized to reactive intermediates that alkylate DNA. This paper focuses on the DNA pyridyloxobutylation pathway which is common to both compounds. This DNA route generates 7-[4-(3-pyridyl)-4-oxobut-1-yl]-2'-deoxyguanosine, *O*<sup>2</sup>-[4-(3-pyridyl)-4-oxobut-1-yl]-2'-deoxycytosine, *O*<sup>2</sup>-[4-(3-pyridyl)-4-oxobut-1-yl]-2'-deoxythymidine, and *O*<sup>6</sup>-[4-(3-pyridyl)-4-oxobut-1-yl]-2'-deoxyguanosine as well as unstable adducts which dealkylate to release 4-hydroxy-1-{3-pyridyl}-1-butanone or depyriminidate/depurinate to generate abasic sites. There are multiple repair pathways responsible for protecting against the genotoxic effects of these adducts, including adduct reversal as well as base and nucleotide excision repair pathways. Data indicate that several DNA adducts contribute to the overall mutagenic properties of pyridyloxobutylating agents. Which adducts contribute to the carcinogenic properties of this pathway are likely to depend on the biochemistry of the target tissue.

## 1. Introduction

Tobacco use has been linked to a variety of human cancers, including lung, oral cavity, esophagus, pharynx, larynx, urinary bladder, pancreas, and liver cancers [1]. Lung cancer alone is responsible for the deaths of 1.3 million people annually worldwide [2]. It is the leading cause of cancer deaths in the United States, with 80%–90% of this cancer associated with tobacco use [1]. Environmental tobacco smoke (second-hand smoke) has also been associated with human lung cancer but the risks are significantly lower than those associated with smoking [1].

There are more than 5000 identified chemicals present in cigarette smoke [1, 3–5]. More than 60 of these compounds are demonstrated chemical carcinogens in animal models [1, 3, 4, 6]. An important group of tobacco carcinogens are the tobacco-specific nitrosamines. These compounds are formed from tobacco alkaloids like nicotine during the curing process of tobacco [7]. 4-(Methylnitrosamino)-1-(3pyridyl)-1-butanone (NNK) and *N'*-nitrosornicotine (NNN) are

two of the most potent tobacco-specific nitrosamines present in tobacco products and smoke [8]. Both compounds are carcinogenic in laboratory animals, generating tumors at sites comparable to those observed in smokers [8]. NNK is a potent lung carcinogen, which also induces liver and nasal tumors [9–11]. This compound induces lung adenocarcinomas in rodents at lifetime doses that are comparable to those experienced by smokers [8]. Adenocarcinoma is now the most common type of lung cancer observed in humans, having surpassed squamous cell carcinoma [12–16]. This shift in histology has been attributed not to improvements in diagnoses but rather to changing cigarette design, which has changed smoking behavior resulting in increased uptake of tobacco-specific nitrosamines by smokers [14]. Metabolic products of NNK have been detected in urine of smokers and individuals exposed to second-hand smoke, indicating that humans are exposed to and metabolize this carcinogen [17–20]. NNN is carcinogenic to the esophagus, nasal cavity, and respiratory tract in laboratory animals [8]. This nitrosamine is present in higher amounts than any other esophageal



SCHEME 1: Pathways of bioactivation of NNK, NNN, and model pyridyloxobutylating agent, NNKOAc.

carcinogen in tobacco smoke [8]. It and/or its glucuronide conjugate have been detected in the urine and toenails of smokers and smokeless tobacco users [21–25]. Based on animal studies, NNK and NNN are listed as Group 1 human carcinogens by the International Agency for Cancer Research [6, 8].

NNK and NNN require metabolism to exert their toxicological properties [8]. NNK-induced carcinogenesis requires cytochrome P450 catalyzed metabolic activation to DNA reactive metabolites [26]. NNK is metabolized to either a methylating or a pyridyloxobutylating agent (Scheme 1). The methylation pathway generates well-characterized methyl DNA adducts, such as 7-methylguanine (7-mG), O<sup>6</sup>-methylguanine (O<sup>6</sup>-mG), and O<sup>4</sup>-methylthymidine (O<sup>4</sup>-mT) [27–31]. The dominant mutagenic adduct is O<sup>6</sup>-mG [32, 33]. The repair mechanisms and genotoxic properties of this adduct have been extensively reviewed [34–37] and will not be a focus of this paper. The formation, repair, and genotoxic properties of the pyridyloxobutyl adducts will be discussed below.

NNN also has two pathways to form DNA adducts, 2'- and 5'-hydroxylation [8]. (S)-NNN, the dominant enantiomer in tobacco products [38], undergoes primarily 2'-hydroxylation whereas (R)-NNN undergoes both 2'- and 5'-hydroxylation [39]. 2'-Hydroxylation generates the same pyridyloxobutylating agent as methyl hydroxylation of NNK (Scheme 1). 5'-Hydroxylation generates a reactive metabolite that can also alkylate DNA (Scheme 1) [40, 41]. However, no data exist for the levels of these adducts *in vivo*. For the purpose of this paper, we will focus on the pyridyloxobutylation pathway.

## 2. Structure of Pyridyloxobutyl DNA Adducts

The pyridyloxobutylation pathway leads to a variety of adducts, four of which have been recently identified (Scheme 2). They are 7-[4-(3-pyridyl)-4-oxobut-1-yl]-2'-deoxyguanosine (7-pobdG) [42], O<sup>2</sup>-[4-(3-pyridyl)-4-oxobut-1-yl]-2'-deoxycytosine (O<sup>2</sup>-pobdC) [43], O<sup>2</sup>-[4-(3-pyridyl)-4-oxobut-1-yl]-2'-deoxythymidine (O<sup>2</sup>-pobdT) [43], and O<sup>6</sup>-[4-(3-pyridyl)-4-oxobut-1-yl]-2'-deoxyguanosine (O<sup>6</sup>-pobdG) [42–44]. Both 7-pobdG and O<sup>2</sup>-pobdC readily release the corresponding nucleobases, 7[4-(3-pyridyl)-4-oxobut-1-yl]-guanine (7-pobG) and O<sup>2</sup>-[4-(3-pyridyl)-4-oxobut-1-yl]-cytosine (O<sup>2</sup>-pobC), respectively, leaving behind an abasic site [42, 43]. In addition, some pyridyloxobutyl DNA adducts are unstable and dealkylate to release 4-hydroxy-1-(3-pyridyl)-1-butanone (HPB) (Scheme 2) [31, 45]. HPB-releasing adducts include O<sup>2</sup>-pobdC [43] and 7-pobdG [42]. Quantitation of the specific pyridyloxobutyl DNA adducts in calf thymus DNA treated with a model pyridyloxobutylating agent, 4-(acetoxymethylnitrosamino)-1-(3-pyridyl)-1-butanone (NNKOAc, Scheme 1), demonstrates that HPB-releasing adducts are the major adducts present in pyridyloxobutylated DNA [46]. They represent approximately 65% of the total adducts formed. The relative levels of the specific adducts making up the remainder are 7-pobG > O<sup>6</sup>-pobdG > O<sup>2</sup>-pobdT ≥ O<sup>2</sup>-pobC.

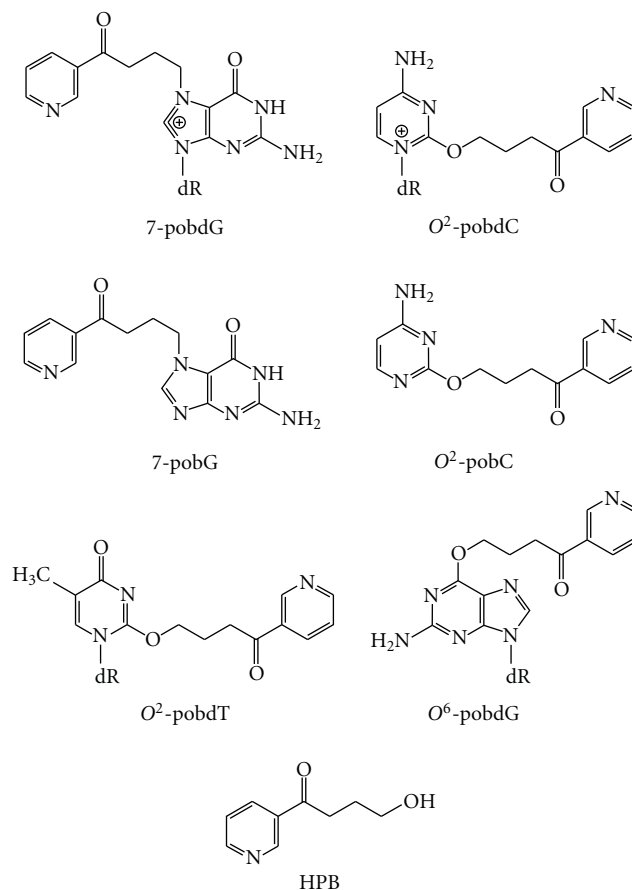
Conflicting evidence exists for the formation of phosphate adducts in pyridyloxobutylated DNA. HPB is not released from pyridyloxobutylated DNA when heated under basic conditions [45]. This observation is not consistent with the presence of pyridyloxobutyl phosphate esters. However, the 3'-termini of NNKOAc-induced strand breaks

are resistant to  $^{32}\text{P}$ -endlabeling in the presence of T4 DNA polymerase even after incubating with endonuclease IV which removes 3'-phosphate or 3'-phosphoglycolate groups [47]. This observation suggests that there may be an adduct on the 3'-phosphate group. However, the nucleobase adduct,  $O^6$ -pobdG, has been reported to inhibit 3'-exonuclease degradation of DNA [48]. Therefore, it is possible this adduct or other pyridyloxobutyl DNA adducts inhibits endonuclease IV as well. Also supporting the formation of pyridyloxobutyl phosphate adducts is the detection of a 4-(3-[ $^3\text{H}$ ]pyridyl)-4-hydroxy-2-butylcobalam complex when enzymatic digests of DNA from [ $^3\text{H}$ ]NNK-treated animals were reacted with cob(I)alamin followed by sodium borohydride [49]. This reaction product accounted for up to 22% of the total pyridyloxobutyl adducts detected. Cob(I)alamin selectively reacts with alkyl phosphate adducts [50]. However, the pyridyloxobutyl group might be more reactive with this reagent than a simple alkyl group and the product may be formed from adducts other than alkyl phosphates. This possibility requires further testing.

### 3. Levels of Pyridyloxobutyl DNA Adducts in NNK- or NNN-Treated Rodents

Pyridyloxobutyl DNA adducts have been observed in DNA isolated from the tissues of NNK- or NNN-treated animals. HPB-releasing adducts have been detected in target tissues and have been shown to persist [8, 52]. They have also been linked to tumor formation in the rat [53]. More recent studies have reported the levels of specific adducts in target and nontarget tissues of NNK- or NNN-treated rodents. One of the first studies demonstrated that  $O^6$ -pobdG was present at very low levels in lung and liver DNA from [ $^3\text{H}$ ]NNK-treated A/J mice [54]. Subsequent experiments have employed sensitive LC-MS/MS assays [55, 56] for their detection of DNA from *in vivo* sources. Table 1 displays the levels of pyridyloxobutyl DNA adducts detected in lung and liver DNA following four subcutaneous doses of NNK [51]. In this study, the relative adduct distribution was  $O^2$ -pobdT  $\geq$  7-pobG  $>$   $O^2$ -pobC  $\gg$   $O^6$ -pobdG in lung DNA and  $O^2$ -pobdT = 7-pobG  $\geq$   $O^2$ -pobC  $\gg$   $O^6$ -pobdG in liver DNA. The levels of 7-pobG,  $O^2$ -pobC and  $O^2$ -pobdT were higher in liver relative to lung DNA whereas the levels of  $O^6$ -pobdG were higher in lung relative to liver.  $O^2$ -pobdT was also the dominant adduct detected when rats were chronically treated with a lower dose of NNK (10 ppm in drinking water) (Table 2) [57, 58]. The relative distribution of pyridyloxobutyl DNA adducts was  $O^2$ -pobdT  $>$  7-pobG  $\gg$   $O^2$ -pobC  $\gg$   $O^6$ -pobdG in lung DNA and  $O^2$ -pobdT  $\gg$  7-pobG  $>$   $O^2$ -pobC in liver DNA;  $O^6$ -pobdG was not observed in liver DNA from these animals [57]. Pyridyloxobutyl DNA adducts were also observed in nasal respiratory mucosa, nasal olfactory mucosa, oral mucosa, and pancreas from NNK-treated rats [59]. The relative levels of total pyridyloxobutyl DNA adducts is lung  $>$  liver  $>$  nasal respiratory mucosa  $>$  nasal olfactory mucosa  $\approx$  oral mucosa  $\approx$  pancreas [59].

Similar studies have been performed in NNN-treated rats [60, 61]. Chronic treatment of F344 rats with (*R*)-



SCHEME 2: Structures of pyridyloxobutyl DNA adducts and HPB.

NNN or (*S*)-NNN in the drinking water (10 ppm, 1–20 weeks) led to adduct formation in lungs, liver, nasal respiratory mucosa, nasal olfactory, and oral mucosa [60, 61]. Target tissues (nasal olfactory, respiratory mucosa, and esophagus) had the highest levels of pyridyloxobutyl DNA adducts whereas the nontarget tissues (lung and liver) had the lowest levels. The enantiomers gave different levels of pyridyloxobutyl DNA adducts in the various tissues. (*R*)-NNN produced the highest levels in lung nasal olfactory and nasal respiratory tissue whereas (*S*)-NNN generated higher levels in esophagus, liver, and oral mucosa [60, 61]. These tissue-dependent differences are likely due to tissue differences in the cytochrome P450 enzymes responsible for the bioactivation of these two enantiomers [60, 61].

As with NNK,  $O^2$ -pobdT was a major adduct observed in DNA from various NNN-exposed tissues such as nasal olfactory mucosa ( $O^2$ -pobdT  $>$  7-pobG  $\gg$   $O^2$ -pobC  $>$   $O^6$ -pobdG), respiratory mucosa ( $O^2$ -pobdT  $>$  7-pobG  $\gg$   $O^2$ -pobC  $>$   $O^6$ -pobdG), and oral mucosa ( $O^2$ -pobdT  $\approx$  7-pobG  $\gg$   $O^2$ -pobC  $>$   $O^6$ -pobdG) as well as liver and lung ( $O^2$ -pobdT  $\gg$  7-pobG  $\geq$   $O^2$ -pobC). In the rat esophagus, 7-pobG was the dominant adduct (7-pobG  $\geq$   $O^2$ -pobdT  $\approx$   $O^2$ -pobC).  $O^6$ -pobdG was not detected in lung, liver or esophageal DNA [60].

TABLE 1: Adduct levels in NNK-treated rats [51].

Tissue	NNK Dose (mmol/kg) <sup>a</sup>	Mean $\pm$ S.D., $N = 5$ (fmol/mg DNA)			
		7-pobG	O <sup>2</sup> -pobdT	O <sup>2</sup> -pobC	O <sup>6</sup> -pobG
Lung	saline control	N.D. <sup>b</sup>	N.D.	N.D.	N.D.
	0.025	933 $\pm$ 89	1120 $\pm$ 66	483 $\pm$ 36	251 $\pm$ 26
	0.1	1800 $\pm$ 478	2020 $\pm$ 483	840 $\pm$ 169	487 $\pm$ 101
Liver	saline control	N.D.	N.D.	N.D.	N.D.
	0.025	3550 $\pm$ 1600	3530 $\pm$ 725	2930 $\pm$ 521	28 $\pm$ 17
	0.1	12200 $\pm$ 1600	12300 $\pm$ 1690	7800 $\pm$ 1680	140 $\pm$ 25

<sup>a</sup>Administered by s.c. injection daily for 4 days.

<sup>b</sup>N.D.: not detected (detection limit, 3 fmol/mg DNA).

#### 4. Formation of Pyridyloxobutyl DNA Adducts in Humans

While there is no information regarding the levels of the four individual pyridyloxobutyl DNA adducts in humans, HPB-releasing adducts have been detected in human tissue samples. Levels of these adducts were significantly higher ( $P < .0001$ ) in self-reported smokers who had lung cancer than in self-reported nonsmokers who had lung cancer ( $404 \pm 258$  versus  $59 \pm 56$  fmol HPB released/mg DNA, resp.) [62]. Since HPB-releasing adducts accumulate in normal lung tissues of lung cancer patients but not in normal smoking controls [62, 63], these data support a hypothesis that smokers who accumulate pyridyloxobutyl DNA adducts may be at increased risk of lung cancer.

#### 5. Repair Pathways for Pyridyloxobutyl DNA Adducts

DNA adduct repair protects a cell against the toxic and genotoxic effects of DNA damage. There are multiple pathways involved in the removal of alkylated DNA bases generated by reactive alkanediazohydroxides. These include direct base repair by alkyltransferases and excision of the DNA damage by base excision repair (BER) or nucleotide excision repair (NER). Mismatch repair is involved in the detection and repair of mismatched DNA adducts. Below is a review of the pathways thought to be involved in the repair of pyridyloxobutyl DNA damage.

**5.1. Adduct Reversal.** O<sup>6</sup>-Alkylguanine DNA alkyltransferase (AGT) is a suicide protein that repairs O<sup>6</sup>-alkylguanine adducts by facilitating the transfer of the alkyl group from the O<sup>6</sup>-position of guanine to a cysteine residue in the protein's active site [35]. This alkylation reaction inactivates the protein and triggers a conformational change [64] which leads to its degradation [65]. Consequently, the initial repair capacity of a cell is determined by its constitutive levels of AGT.

While O<sup>6</sup>-pobdG is readily repaired by mammalian AGTs, it is not a good substrate for the bacterial AGTs *ada*

and *ogt* [66]. The ability of AGT orthologs to repair this bulky O<sup>6</sup>-alkylguanine adduct is likely determined by the size of the protein's adduct binding site. Rodent AGT has the largest binding site and repairs O<sup>6</sup>-pobdG faster than human AGT which has a smaller binding pocket [66]. The bacterial AGTs have an even smaller binding pocket, explaining the inability of these proteins to repair this damage [66]. This adduct reversal pathway is a major repair pathway for O<sup>6</sup>-pobdG in mammalian cells [54, 66, 67].

**5.2. Base Excision Repair.** Base excision repair (BER) is another important pathway for the repair of nitrosamine-derived DNA damage. This pathway is involved in the repair of single strand breaks, small alkyl guanine damage, and oxidized DNA bases as well as abasic sites [68, 69]. It is a multistep process that is initiated when damaged bases are removed by glycosylases, leaving abasic sites in DNA. The abasic sites are removed by an endonuclease. The missing nucleoside is then replaced and ligation occurs. It is likely that NNK-derived methyl adducts such as 7-methylguanine and N<sup>3</sup>-methyladenine are removed by base excision repair [70]. The ability of pyridyloxobutyl adducts to serve as substrates for BER glycosylases has not been studied. It is possible that they could serve as substrates since the structurally similar adduct, O<sup>6</sup>-butylguanine, appears to be repaired in part by BER *in vivo* [71]. It is likely that abasic sites formed by the depurination/depyrimidination of 7-pobG and O<sup>2</sup>-pobC, respectively, are repaired by this pathway.

While little is known about the role of BER in the repair of pyridyloxobutyl DNA damage, two observations suggest that BER may be important. First, incubation of lysate from NNKOAc-treated cells with formamidopyrimidine glycosylase prior to the COMET assay results in a small but significant increase in strand breaks [72]. This observation indicates that there are pyridyloxobutyl DNA adducts that are substrates for this glycosylase. Second, loss of XRCC1, an important scaffold protein in BER [73], increases the mutagenic and toxic effects of NNKOAc [67]. The loss of this protein does not affect the rate of removal of specific pyridyloxobutyl DNA adducts from DNA [67]. However, the observed increase in toxicity and mutagenicity indicates

TABLE 2: Comparative DNA adduct levels in lung and liver of F344 rats treated with 10 ppm NNK in the drinking water and sacrificed at various intervals [57, 58].

		Adduct Levels fmol/mg DNA (mean $\pm$ S.D.)					
Week		1	2	5	10	16	20
Lung	O <sup>6</sup> -mG	976 $\pm$ 342	1020 $\pm$ 423	2550 $\pm$ 263	1020 $\pm$ 314	729 $\pm$ 57.5	1910 $\pm$ 615
	O <sup>6</sup> -pobdG	45 $\pm$ 7 <sup>a</sup>	50 $\pm$ 5 <sup>a</sup>	46 $\pm$ 13 <sup>a</sup>	44 $\pm$ 14 <sup>a</sup>	34 $\pm$ 17 <sup>a</sup>	20 $\pm$ 5 <sup>a</sup>
	7-pobG	750 $\pm$ 95	1180 $\pm$ 131	1360 $\pm$ 214 <sup>a</sup>	2220 $\pm$ 864	1700 $\pm$ 175 <sup>a</sup>	1060 $\pm$ 169
	O <sup>2</sup> -pobdT	1080 $\pm$ 99	2020 $\pm$ 150	3890 $\pm$ 648	8260 $\pm$ 2730 <sup>a</sup>	6720 $\pm$ 606 <sup>a</sup>	5070 $\pm$ 1060 <sup>a</sup>
	O <sup>2</sup> -pobC	240 $\pm$ 23	250 $\pm$ 18	400 $\pm$ 87 <sup>a</sup>	730 $\pm$ 211	810 $\pm$ 152	940 $\pm$ 175
Liver	Week	1	2	5	10	16	20
	O <sup>6</sup> -mG	3830 $\pm$ 865	7120 $\pm$ 2080	2310 $\pm$ 946	564 $\pm$ 250	637 $\pm$ 59	891 $\pm$ 379
	O <sup>6</sup> -pobdG	n.d.	n.d.	n.d.	n.d.	n.d.	n.d.
	7-pobG	490 $\pm$ 104 <sup>a</sup>	880 $\pm$ 182 <sup>a</sup>	1050 $\pm$ 90	1460 $\pm$ 625	1170 $\pm$ 86 <sup>a</sup>	730 $\pm$ 225
	O <sup>2</sup> -pobdT	650 $\pm$ 121 <sup>a</sup>	1230 $\pm$ 272 <sup>a</sup>	2190 $\pm$ 174	3740 $\pm$ 1170 <sup>a</sup>	3540 $\pm$ 643 <sup>a</sup>	2680 $\pm$ 643 <sup>a</sup>
O <sup>2</sup> -pobC	170 $\pm$ 43 <sup>a</sup>	140 $\pm$ 25 <sup>a</sup>	240 $\pm$ 17	580 $\pm$ 214	350 $\pm$ 152	490 $\pm$ 146	

n.d., not detected.

<sup>a</sup>Significantly different from O<sup>6</sup>-mG,  $P < .05$ .

that XRCC1 plays an important role in protecting a cell against the harmful effects of these adducts. Together, these observations provide evidence for the role of BER in the repair of pyridyloxobutyl DNA damage.

**5.3. Nucleotide Excision Repair.** Another important pathway for the repair of bulky DNA damage is nucleotide excision repair (NER) [74, 75]. Like BER, NER is a multiprotein mediated repair pathway. However, in this pathway a whole section of the damaged DNA strand is removed in several steps. A new strand is then synthesized by DNA polymerase using the undamaged strand as a template.

Several pieces of experimental data support the importance of NER in the repair of pyridyloxobutyl DNA adducts. In one study, [ $\alpha$ -<sup>32</sup>P]TTP was incorporated into NNKOAc-treated plasmid DNA when incubated with extracts from normal human lymphoid cells in an ATP-dependent fashion [76]. This activity was significantly lower in cell extracts from XPA- and XPC-deficient cell lines. XPA and XPC are two important proteins involved in the initiation of the NER pathway [74, 75] so their absence significantly impacts the efficiency of NER.

A second study examined the removal of specific pyridyloxobutyl DNA adducts from DNA in NNKOAc-treated Chinese hamster ovary cells [67]. The rate of removal of these adducts was compared between the parental cell line, AA8, which has functional NER but not AGT, and UV5 cells which lacks both functional NER [loss of ERCC-2 (XPD)] and AGT [77]. O<sup>2</sup>-pobdT was the only adduct whose removal was affected by the loss of ERCC-2. Its repair was significantly slower in the absence of this protein, suggesting the importance of NER in the removal of this adduct. Since there were several reports indicating that larger

O<sup>6</sup>-alkylguanine adducts appear to be preferentially repaired by nucleotide excision repair [78–82], O<sup>6</sup>-pobdG repair was also expected to be reduced in cells lacking NER. However, O<sup>6</sup>-pobdG was a poor substrate for this pathway in CHO cells as well as in an *in vitro* human NER repair assay [67].

**5.4. Mismatch Repair.** Mismatch repair (MMR) is another important guard against genotoxic stress. In the case of alkylating agents, this pathway plays a critical role in the cytotoxicity mediated by these compounds [70, 83–85]. When alkylation is extensive, MMR is involved in triggering cell death which protects against the mutagenic activity of these agents. For example, MMR recognizes O<sup>6</sup>-mG-T mismatch that occur when AGT is overwhelmed [83]. Unrepaired O<sup>6</sup>-mG is toxic [36]; absence of MMR removes the toxicity of methylating agents indicating that this repair pathway is involved in the mechanism of toxicity [34]. MMR is initiated when the MSH2-MSH6 heterodimer (Mut $\alpha$ ) binds to the mismatch. The MLH1-PMS2 heterodimer then binds to Mut $\alpha$  and triggers removal of the mismatched base. In the case of damaged bases, the mismatch process enters a futile cycle if the adduct is not repaired since polymerases repeatedly insert the wrong base opposite the modified base. This futile cycle can trigger apoptosis [70, 85]. This futile cycle can be thwarted by homologous recombination, a multiprotein pathway that uses the sister chromatid as the template to circumvent replication-halting DNA adducts [85, 86].

The role of mismatch repair in a cell's response to pyridyloxobutyl DNA adducts has not been explored. Preliminary data indicate that O<sup>6</sup>-pobdG may not be a very toxic adduct. Repair of O<sup>6</sup>-pobdG by human AGT in bacteria did not influence the toxicity of the model pyridyloxobutylating

TABLE 3: Levels of  $O^6$ -mG and  $O^6$ -pobG in lung and livers of NNK-treated wild-type and AGT knockout mice<sup>a</sup> [88].

AGT status	pmol adducts/ $\mu$ mol guanine			
	lung		liver	
$O^6$ -mG	24 h	4 weeks	24 h	4 weeks
Wildtype	42 $\pm$ 12	55 $\pm$ 9	17 $\pm$ 11	5.3 $\pm$ 0.7
Knockout	65 $\pm$ 19	110 $\pm$ 20	210 $\pm$ 110	380 $\pm$ 80 <sup>b</sup>
$O^6$ -pobG				
Wildtype	1.7 $\pm$ 0.5	0.8 $\pm$ 0.2	1.4 $\pm$ 0.5	$\leq$ 0.3
Knockout	2.9 $\pm$ 0.6	2.5 $\pm$ 0.3	2.7 $\pm$ 1.2	4.9 $\pm$ 1.4

<sup>a</sup>Mice received either a single dose of NNK (~250 mg/kg) and sacrificed 24 h postinjection or three weekly doses of NNK (~250 mg/kg each week) and sacrificed 1 week after the third treatment. Numbers represent the average of five samples  $\pm$  SD.

<sup>b</sup>Three samples  $\pm$  SD. Two other samples were analyzed and these two animals had  $O^6$ -mG levels of 26 and 31 pmol  $O^6$ -mG/ $\mu$ mol guanine. The liver 7-mG adduct levels for all five animals were similar: 134  $\pm$  17 pmol 7-mG/ $\mu$ mol guanine.

agent, NNKOAc [87]. This observation differs starkly from that observed with methylating agents where the toxicity of a methylating agent is markedly reduced when AGT is expressed [87]. Similar results were observed in CHO cells; AGT expression only minimally reduced the cytotoxicity of NNKOAc while repairing almost 100% of the  $O^6$ -pobdG formed by this pyridyloxobutylating agent [67]. The reduced toxicity of  $O^6$ -pobdG may cause it to more greatly contribute to the overall mutagenic activity of a pyridyloxobutylating agent since cell death protects against the mutagenic activity of DNA alkylating agents.

**5.5. In Vivo Repair.** For both NNK and NNN, the relative distribution of the four pyridyloxobutyl DNA adducts in tissues from exposed rats was significantly different from that observed in DNA treated with a model pyridyloxobutylating agent *in vitro* [56, 57, 59–61]. This difference likely results from the active repair of specific adducts. Further support for this hypothesis is the observed tissue variation in relative adduct distribution [57, 59–61].

One adduct that appears to be well-repaired *in vivo* is  $O^6$ -pobdG [56, 57, 59–61]. The levels of this adduct are very low relative to the other adducts (Tables 1 and 2). In NNK-treated animals, the levels of  $O^6$ -mG were much greater than the levels of  $O^6$ -pobdG and in the range of the other pyridyloxobutyl DNA adducts [58]. This observation suggests that the larger adduct,  $O^6$ -pobdG, is more readily repaired than  $O^6$ -mG *in vivo*. AGT is one pathway clearly responsible for the repair of  $O^6$ -pobdG *in vivo* [54]. However, other repair pathways may also be involved since this adduct does not accumulate in lungs of AGT knockout mice whereas  $O^6$ -mG does (Table 3) [88]. This conclusion is further supported by data in wild-type mice which indicates that AGT is inactivated in mouse lung following exposure to NNK [89].

The most persistent adduct *in vivo* is  $O^2$ -pobdT [56, 57, 59–61]. This adduct is a minor adduct in the absence of repair ( $7$ -pobG >  $O^6$ -pobdG >  $O^2$ -pobdT  $\geq$   $O^2$ -pobC) [46]. This is somewhat surprising since this adduct is repaired by

NER in cell line models [67]. A recent study indicated that NER is reduced in the lungs of NNK-treated mice providing an explanation for the persistence of this adduct *in vivo* [90]. The mechanism of this reduction is unknown.

## 6. Mutagenic Activity of Pyridyloxobutyl DNA Adducts

Pyridyloxobutylating agents are mutagenic in a variety of test systems [67, 87, 91, 92]. However, our knowledge of which pyridyloxobutyl adducts are causing mutations is still rudimentary. Site-specific mutagenesis studies have only been performed for one adduct,  $O^6$ -pobdG [93]. In bacteria, it produces exclusively GC to AT transitional mutations. In human kidney cell line 293 cells, it produces primarily GC to AT transitional mutations with some GC to TA transversions and deletions as well as a number of more complex mutations.

A few studies have begun to link the overall mutagenic activity of pyridyloxobutyl DNA damage to specific adducts through exploring the impact of various DNA repair pathways on the mutagenic properties of the model pyridyloxobutylating agent, NNKOAc. The earliest studies were performed in bacteria. NNKOAc is mutagenic in *Salmonella typhimurium* tester strains TA100, TA1535, and TA98, but not TA102 [92]. Reversion of TA100 and TA1535 requires mutations at a GC base pair and reversion of TA98 requires a frameshift mutation near a CG base pair [94]. TA102 has an AT base pair at the site of reversion [94]. Based on these observations, it was concluded that pyridyloxobutyl DNA adducts formed at GC base pairs were mutagenic, at least in bacteria. However, we cannot rule out that adducts at AT base pairs are not mutagenic in this study since TA102 has an active NER system [94] that could be repairing any mutagenic adducts at AT base pairs. TA100, TA1535, and TA98 lack UvrB and, as a result, do not have an functional NER system [94].

One candidate adduct for the mutagenicity observed in TA100 and TA1535 is  $O^6$ -pobdG. This adduct is poorly

repaired by bacterial AGT [66]. Consistent with its possible role in NNKOAc-induced mutagenicity is the observation that the mutagenic activity of NNKOAc was reduced by roughly 80% in bacteria expressing human AGT [87]. These studies were performed in *S. typhimurium* strain YG7108 which is a derivative of TA1535 that lacks both bacterial AGT genes, *ada* and *ogt* [95]. Since the levels of  $O^6$ -pobdG were reduced in the strain expressing human AGT by about 66% [87], these data are consistent with the hypothesis that  $O^6$ -pobdG is a significant contributor to the mutagenic activity of pyridyloxobutylating agents at GC base pairs. Other contributors may include  $O^2$ -pobC and 7-pobG. However, these two adducts are not substrates for human AGT.

NNKOAc also induced mutations in the *hprt* gene in Chinese hamster ovary (CHO) cells [67]. Analysis of the mutational spectrum indicated that the bulk of the mutations occurred at AT base pairs [67]. Most of the AT mutations were AT to CG transversion mutations. There were also a small portion of AT to TA transversions and AT to GC transitional mutations. Approximately 20% of the mutations were at GC base pairs with the majority of these being GC to AT transitional mutations.

Loss of NER through ERCC-2 mutation results in an increase in mutation frequency induced by NNKOAc in CHO cells [67]. This loss reduced the rate of  $O^2$ -pobdT repair in these cells. In addition, there was a corresponding increase in the frequency of AT to TA mutations relative to the control cell line. Therefore, it is likely that  $O^2$ -pobdT triggers AT to TA mutations. This conclusion is supported by the observation that another  $O^2$ -alkyl-2'-deoxythymidine adduct,  $O^2$ -ethyl-2'-deoxythymidine, also induces AT to TA mutations [96]. Loss of BER through loss of XRCC1 also led to an increase in AT to TA mutations [67], suggesting that this repair pathway is involved in repair of pyridyloxobutyl DNA damage at AT base pairs. One possibility is that  $O^2$ -pobdT is a substrate for BER glycosylases and the result abasic sites are responsible for observed increase in AT to TA mutations observed in the cells lacking BER. This hypothesis is supported by the report that site-specifically incorporated abasic sites primarily induce transversion mutations with AT to TA mutations being more abundant than AT to GC mutations [97].

Expression of human AGT in CHO cells did not significantly impact the mutation frequency of NNKOAc [67]. However, mutations at GC base pairs represented only approximately 20% of the detected mutations. There was a reduction in the GC to AT mutations in these cells but this reduction did not significantly affect the mutation frequency. Since there was almost complete repair of  $O^6$ -pobdG, these data support the hypothesis that  $O^6$ -pobdG is responsible for the GC to AT transitional mutations triggered by pyridyloxobutyl DNA adducts.

*In vivo* studies investigating the mutagenic properties of the pyridyloxobutyl pathway are limited. Mutations were observed in the 12th codon of *K-ras* in lung tumors of A/J mice receiving multiple doses of NNKOAc [98]. Since these mutations were GC to AT transitions and GC to TA transversions, it is likely that  $O^6$ -pobdG is responsible, in part, for these mutations. Both NNK and

NNN have been shown to be mutagenic in target tissues in *lacZ* and *lacI* transgenic mice [88, 99–101]. The resulting transgene mutation spectra have only been reported for NNK [88, 101]. NNK induced an increased rate of GC to AT transitional mutations at non-CpG sites as well as AT to TA transitional mutations and a mixture of transversion mutations (AT to GC, AT to CG, GC to CG, and GC to TA). Since NNK both methylates and pyridyloxobutylates DNA, it is difficult to associate specific mutations with specific adducts. However, it is clear that the mutational spectrum is substantially more complicated than that observed for simple methylating nitrosamines like dimethylnitrosamine, which primarily induces GC to AT transitional mutations at non-CpG sites [102–104].

Collectively, the data presented above indicate that there are several mutagenic DNA adducts formed upon pyridyloxobutylation of DNA. These include  $O^6$ -pobdG and  $O^2$ -pobdT. Other adducts likely contribute as well. Which adducts contribute to the carcinogenic properties of this pathway are likely to depend on the biological system. If mutations at AT base pairs are required to produce proteins with oncogenic function, the formation of  $O^2$ -pobdT and its repair is probably important for tumor initiation by this pathway. On the other hand, if mutations at GC base pairs are important for triggering the carcinogenic process, the formation and persistence of  $O^6$ -pobdG will be linked to tumor formation. For example, GC to AT and GC to TA mutations were observed in the 12th codon of *K-ras* in lung tumors of A/J mice receiving multiple doses of NNKOAc [98]. It is likely that  $O^6$ -pobdG is responsible, in part, for these mutations. Future studies are required to better define the toxicological properties of all pyridyloxobutyl adducts and to determine the repair pathways responsible for protecting against their genotoxic effects. An understanding of these fundamental biochemical issues may help in understanding the individual differences in susceptibility to lung cancer risk associated with tobacco use.

## Acknowledgment

The research in the Peterson Laboratory has been funded by CA-59887 and CA-115309.

## References

- [1] International Agency for Research on Cancer, *Tobacco Smoke and Involuntary Smoking*, IARC, Lyon, France, 83rd edition, 2004.
- [2] World Health Organization, "Cancer," Fact Sheet No. 297. 2009 <http://www.who.int/mediacentre/factsheets/fs297/en/print.html>.
- [3] D. Hoffmann and S. Hecht, "Advances in tobacco carcinogenesis," in *Handbook of Experimental Pharmacology*, C. S. Cooper and P. L. Grover, Eds., pp. 63–102, Springer, Berlin, Germany, 1990.
- [4] G. N. Wogan, S. S. Hecht, J. S. Felton, A. H. Conney, and L. A. Loeb, "Environmental and chemical carcinogenesis," *Seminars in Cancer Biology*, vol. 14, no. 6, pp. 473–486, 2004.
- [5] A. Rodgman and T. A. Perfetti, *The Chemical Components of Tobacco and Tobacco Smoke*, CRC Press, Boca Rotan, Fla, USA, 2009.

- [6] S. S. Hecht, "Tobacco smoke carcinogens and lung cancer," *Journal of the National Cancer Institute*, vol. 91, no. 14, pp. 1194–1210, 1999.
- [7] S. S. Hecht and D. Hoffmann, "Tobacco-specific nitrosamines, an important group of carcinogens in tobacco and tobacco smoke," *Carcinogenesis*, vol. 9, no. 6, pp. 875–884, 1988.
- [8] S. S. Hecht, "Biochemistry, biology, and carcinogenicity of tobacco-specific *N*-nitrosamines," *Chemical Research in Toxicology*, vol. 11, no. 6, pp. 559–603, 1998.
- [9] S. S. Hecht, C. B. Chen, T. Ohmori, and D. Hoffmann, "Comparative carcinogenicity in F344 rats of the tobacco-specific nitrosamines, *N'*-nitrososornicotine and 4-(*N*-methyl-*N*-nitrosamino)-1-(3-pyridyl)-1-butanone," *Cancer Research*, vol. 40, no. 2, pp. 298–302, 1980.
- [10] A. Rivenson, D. Hoffmann, B. Prokopczyk, S. Amin, and S. S. Hecht, "Induction of lung and exocrine pancreas tumors in F344 rats by tobacco-specific and areca-derived *N*-nitrosamines," *Cancer Research*, vol. 48, no. 23, pp. 6912–6917, 1988.
- [11] S. S. Hecht, M. A. Morse, S. Amin et al., "Rapid single-dose model for lung tumor induction in A/J mice by 4-(methylnitrosamino)-1-(3-pyridyl)-1-butanone and the effect of diet," *Carcinogenesis*, vol. 10, no. 10, pp. 1901–1904, 1989.
- [12] S. S. Devesa, F. Bray, A. P. Vizcaino, and D. M. Parkin, "International lung cancer trends by histologic type: male:female differences diminishing and adenocarcinoma rates rising," *International Journal of Cancer*, vol. 117, no. 2, pp. 294–299, 2005.
- [13] F. Chen, W. F. Bina, and P. Cole, "Declining incidence rate of lung adenocarcinoma in the United States," *Chest*, vol. 131, no. 4, pp. 1000–1005, 2007.
- [14] M. J. Thun, C. A. Lally, J. T. Flannery, E. E. Calle, W. D. Flanders, and C. W. Heath Jr., "Cigarette smoking and changes in the histopathology of lung cancer," *Journal of the National Cancer Institute*, vol. 89, no. 21, pp. 1580–1586, 1997.
- [15] D. Hoffmann, A. Rivenson, S. E. Murphy, F.-L. Chung, S. Amin, and S. S. Hecht, "Cigarette smoking and adenocarcinoma of the lung: the relevance of nicotine-derived *N*-nitrosamines," *Journal of Smoking-Related Disorders*, vol. 4, no. 3, pp. 165–189, 1993.
- [16] E. L. Wynder and D. Hoffmann, "Smoking and lung cancer: scientific challenges and opportunities," *Cancer Research*, vol. 54, no. 20, pp. 5284–5295, 1994.
- [17] S. S. Hecht, S. G. Carmella, S. E. Murphy, S. Akerkar, K. D. Brunemann, and D. Hoffmann, "A tobacco-specific lung carcinogen in the urine of men exposed to cigarette smoke," *New England Journal of Medicine*, vol. 329, no. 21, pp. 1543–1546, 1993.
- [18] W. D. Parsons, S. G. Carmella, S. Akerkar, L. E. Bonilla, and S. S. Hecht, "A metabolite of the tobacco-specific lung carcinogen 4-(methylnitrosamino)-1-(3-pyridyl)-1-butanone in the urine of hospital workers exposed to environmental tobacco smoke," *Cancer Epidemiology Biomarkers and Prevention*, vol. 7, no. 3, pp. 257–260, 1998.
- [19] G. M. Lackmann, U. Salzberger, U. Töllner, M. Chen, S. G. Carmella, and S. S. Hecht, "Metabolites of a tobacco-specific carcinogen in urine from newborns," *Journal of the National Cancer Institute*, vol. 91, no. 5, pp. 459–465, 1999.
- [20] S. S. Hecht, "Carcinogen biomarkers for lung or oral cancer chemoprevention trials," *IARC Scientific Publications*, vol. 154, pp. 245–255, 2001.
- [21] I. Stepanov and S. S. Hecht, "Tobacco-specific nitrosamines and their pyridine-*N*-glucuronides in the urine of smokers and smokeless tobacco users," *Cancer Epidemiology Biomarkers and Prevention*, vol. 14, no. 4, pp. 885–891, 2005.
- [22] I. Stepanov and S. S. Hecht, "Detection and quantitation of *N'*-nitrososornicotine in human toenails by liquid chromatography-electrospray ionization-tandem mass spectrometry," *Cancer Epidemiology Biomarkers and Prevention*, vol. 17, no. 4, pp. 945–948, 2008.
- [23] I. Stepanov, S. G. Carmella, S. Han et al., "Evidence for endogenous formation of *N'*-nitrososornicotine in some long-term nicotine patch users," *Nicotine and Tobacco Research*, vol. 11, no. 1, pp. 99–105, 2009.
- [24] D. Kavvadias, G. Scherer, M. Urban et al., "Simultaneous determination of four tobacco-specific *N*-nitrosamines (TSNA) in human urine," *Journal of Chromatography B*, vol. 877, no. 11–12, pp. 1185–1192, 2009.
- [25] D. Kavvadias, G. Scherer, F. Cheung, G. Errington, J. Shepherd, and M. McEwan, "Determination of tobacco-specific *N*-nitrosamines in urine of smokers and non-smokers," *Biomarkers*, vol. 14, no. 8, pp. 547–553, 2009.
- [26] Y. Weng, C. Fang, R. J. Turesky, M. Behr, L. S. Kaminisky, and X. Ding, "Determination of the role of target tissue metabolism in lung carcinogenesis using conditional cytochrome P450 reductase-null mice," *Cancer Research*, vol. 67, no. 16, pp. 7825–7832, 2007.
- [27] S. A. Belinsky, C. M. White, and J. A. Boucheron, "Accumulation and persistence of DNA adducts in respiratory tissue of rats following multiple administrations of the tobacco specific carcinogen 4-(*N*-methyl-*N*-nitrosamino)-1-(3-pyridyl)-1-butanone," *Cancer Research*, vol. 46, no. 3, pp. 1280–1284, 1986.
- [28] S. S. Hecht, N. Trushin, A. Castonguay, and A. Rivenson, "Comparative tumorigenicity and DNA methylation in F344 rats by 4-(methylnitrosamino)-1-(3-pyridyl)-1-butanone and *N*-nitrosodimethylamine," *Cancer Research*, vol. 46, no. 2, pp. 498–502, 1986.
- [29] S. A. Belinsky, J. F. Foley, C. M. White, M. W. Anderson, and R. R. Maronpot, "Dose-response relationship between *O*<sup>6</sup>-methylguanine formation in Clara cells and induction of pulmonary neoplasia in the rat by NNK," *Cancer Research*, vol. 50, no. 12, pp. 3772–3780, 1990.
- [30] S. E. Murphy, A. Palomino, S. S. Hecht, and D. Hoffmann, "Dose-response study of DNA and hemoglobin adduct formation by 4-(methylnitrosamino)-1-(3-pyridyl)-1-butanone in F344 rats," *Cancer Research*, vol. 50, no. 17, pp. 5446–5452, 1990.
- [31] L. A. Peterson and S. S. Hecht, "*O*<sup>6</sup>-Methylguanine is a critical determinant of 4-(methylnitrosamino)-1-(3-pyridyl)-1-butanone tumorigenesis in A/J mouse lung," *Cancer Research*, vol. 51, no. 20, pp. 5557–5564, 1991.
- [32] E. L. Loechler, C. L. Green, and J. M. Essigmann, "In vivo mutagenesis by *O*<sup>6</sup>-methylguanine built into a unique site in a viral genome," *Proceedings of the National Academy of Sciences of the United States of America*, vol. 81, pp. 6271–6275, 1984.
- [33] R. E. Bishop, G. T. Pauly, and R. C. Moschel, "*O*<sup>6</sup>-Ethylguanine and *O*<sup>6</sup>-benzylguanine incorporated site-specifically in codon 12 of the rat *H-ras* gene induce semi-targeted as well as targeted mutations in Rat4 cells," *Carcinogenesis*, vol. 17, no. 4, pp. 849–856, 1996.

- [34] B. Kaina, M. Christmann, S. Naumann, and W. P. Roos, "MGMT: key node in the battle against genotoxicity, carcinogenicity and apoptosis induced by alkylating agents," *DNA Repair*, vol. 6, no. 8, pp. 1079–1099, 2007.
- [35] A. E. Pegg, "Repair of  $O^6$ -alkylguanine by alkyltransferases," *Mutation Research*, vol. 462, no. 2-3, pp. 83–100, 2000.
- [36] M. Bignami, M. O'Driscoll, G. Aquilina, and P. Karran, "Unmasking a killer: DNA  $O^6$ -methylguanine and the cytotoxicity of methylating agents," *Mutation Research*, vol. 462, no. 2-3, pp. 71–82, 2000.
- [37] P. F. Swann, "Why do  $O^6$ -alkylguanine and  $O^4$ -alkylthymine miscode? The relationship between the structure of DNA containing  $O^6$ -alkylguanine and  $O^4$ -alkylthymine and the mutagenic properties of these bases," *Mutation Research*, vol. 233, no. 1-2, pp. 81–94, 1990.
- [38] S. G. Carmella, E. J. McIntee, M. Chen, and S. S. Hecht, "Enantiomeric composition of  $N'$ -nitrosornicotine and  $N'$ -nitrosoanatabine in tobacco," *Carcinogenesis*, vol. 21, no. 4, pp. 839–843, 2000.
- [39] E. J. McIntee and S. S. Hecht, "Metabolism of  $N'$ -nitrosornicotine enantiomers by cultured rat esophagus and in vivo in rats," *Chemical Research in Toxicology*, vol. 13, no. 3, pp. 192–199, 2000.
- [40] P. Upadhyaya, E. J. McIntee, P. W. Villalta, and S. S. Hecht, "Identification of adducts formed in the reaction of 5'-acetoxy- $N'$ -nitrosornicotine with deoxyguanosine and DNA," *Chemical Research in Toxicology*, vol. 19, no. 3, pp. 426–435, 2006.
- [41] P. Upadhyaya and S. S. Hecht, "Identification of adducts formed in the reactions of 5'-acetoxy- $N'$ -nitrosornicotine with deoxyadenosine, thymidine, and DNA," *Chemical Research in Toxicology*, vol. 21, no. 11, pp. 2164–2171, 2008.
- [42] M. Wang, G. Cheng, S. J. Sturla et al., "Identification of adducts formed by pyridyloxobutylation of deoxyguanosine and DNA by 4-(acetoxyethylnitrosamino)-1-(3-pyridyl)-1-butanone, a chemically activated form of tobacco specific carcinogens," *Chemical Research in Toxicology*, vol. 16, no. 5, pp. 616–626, 2003.
- [43] S. S. Hecht, P. W. Villalta, S. J. Sturla et al., "Identification of  $O^2$ -substituted pyrimidine adducts formed in reactions of 4-(Acetoxymethylnitrosamino)-1-(3-pyridyl)-1-butanone and 4-(Acetoxymethylnitrosamino)-1-(3-pyridyl)-1-butanol with DNA," *Chemical Research in Toxicology*, vol. 17, no. 5, pp. 588–597, 2004.
- [44] L. Wang, T. E. Spratt, X.-K. Liu, S. S. Hecht, A. E. Pegg, and L. A. Peterson, "Pyridyloxobutyl adduct  $O^6$ -[4-oxo-4-(3-pyridyl)butyl]guanine is present in 4-(acetoxyethylnitrosamino)-1-(3-pyridyl)-1-butanone-treated DNA and is a substrate for  $O^6$ -alkylguanine-DNA alkyltransferase," *Chemical Research in Toxicology*, vol. 10, no. 5, pp. 562–567, 1997.
- [45] S. S. Hecht, T. E. Spratt, and N. Trushin, "Evidence for 4-(3-pyridyl)-4-oxobutylation of DNA in F344 rats treated with the tobacco-specific nitrosamines 4-(methylnitrosamino)-1-(3-pyridyl)-1-butanone and  $N'$ -nitrosornicotine," *Carcinogenesis*, vol. 9, no. 1, pp. 161–165, 1988.
- [46] S. J. Sturla, J. Scott, Y. Lao, S. S. Hecht, and P. W. Villalta, "Mass spectrometric analysis of relative levels of pyridyloxobutylation adducts formed in the reaction of DNA with a chemically activated form of the tobacco-specific carcinogen 4-(methylnitrosamino)-1-(3-pyridyl)-1-butanone," *Chemical Research in Toxicology*, vol. 18, no. 6, pp. 1048–1055, 2005.
- [47] J.-F. Cloutier, R. Drouin, M. Weinfeld, T. R. O'Connor, and A. Castonguay, "Characterization and mapping of DNA damage induced by reactive metabolites of 4-(methylnitrosamino)-1-(3-pyridyl)-1-butanone (NNK) at nucleotide resolution in human genomic DNA," *Journal of Molecular Biology*, vol. 313, no. 3, pp. 539–557, 2001.
- [48] S. Park, M. Seetharaman, A. Ogdie, D. Ferguson, and N. Tretyakova, "3'-Exonuclease resistance of DNA oligodeoxynucleotides containing  $O^6$ -[4-oxo-4-(3-pyridyl)butyl]guanine," *Nucleic Acids Research*, vol. 31, no. 7, pp. 1984–1994, 2003.
- [49] J. Haglund, A. P. Henderson, B. T. Golding, and M. Törnqvist, "Evidence for phosphate adducts in DNA from mice treated with 4-( $N$ -methyl- $N$ -nitrosamino)-1-(3-pyridyl)-1-butanone (NNK)," *Chemical Research in Toxicology*, vol. 15, no. 6, pp. 773–779, 2002.
- [50] J. Haglund, A. Rafiq, L. Ehrenberg, B. T. Golding, and M. Törnqvist, "Transalkylation of phosphotriesters using Cob(I)alamin: toward specific determination of DNA-phosphate adducts," *Chemical Research in Toxicology*, vol. 13, no. 4, pp. 253–256, 2000.
- [51] M. Wang, G. Cheng, P. W. Villalta, and S. S. Hecht, "Development of liquid chromatography electrospray ionization tandem mass spectrometry methods for analysis of DNA adducts of formaldehyde and their application to rats treated with  $N$ -nitrosodimethylamine or 4-(methylnitrosamino)-1-(3-pyridyl)-1-butanone," *Chemical Research in Toxicology*, vol. 20, no. 8, pp. 1141–1148, 2007.
- [52] S. S. Hecht, "DNA adduct formation from tobacco-specific  $N$ -nitrosamines," *Mutation Research*, vol. 424, no. 1-2, pp. 127–142, 1999.
- [53] M. E. Staretz, P. G. Foiles, L. M. Miglietta, and S. S. Hecht, "Evidence for an important role of DNA pyridyloxobutylation in rat lung carcinogenesis by 4-(methylnitrosamino)-1-(3-pyridyl)-1-butanone: effects of dose and phenethyl isothiocyanate," *Cancer Research*, vol. 57, no. 2, pp. 259–266, 1997.
- [54] N. M. Thomson, P. M. Kenney, and L. A. Peterson, "The pyridyloxobutyl DNA adduct,  $O^6$ -[4-oxo-4-(3-pyridyl)butyl]guanine, is detected in tissues from 4-(methylnitrosamino)-1-(3-pyridyl)-1-butanone-treated A/J mice," *Chemical Research in Toxicology*, vol. 16, no. 1, pp. 1–6, 2003.
- [55] N. M. Thomson, R. S. Mijal, R. Ziegel et al., "Development of a quantitative liquid chromatography/electrospray mass spectrometric assay for a mutagenic tobacco specific nitrosamine-derived DNA adduct,  $O^6$ -[4-oxo-4-(3-pyridyl)butyl]-2'-deoxyguanosine," *Chemical Research in Toxicology*, vol. 17, no. 12, pp. 1600–1606, 2004.
- [56] Y. Lao, P. W. Villalta, S. J. Sturla, M. Wang, and S. S. Hecht, "Quantitation of pyridyloxobutyl DNA adducts of tobacco-specific nitrosamines in rat tissue DNA by high-performance liquid chromatography-electrospray ionization-tandem mass spectrometry," *Chemical Research in Toxicology*, vol. 19, no. 5, pp. 674–682, 2006.
- [57] Y. Lao, N. Yu, F. Kassie, P. W. Villalta, and S. S. Hecht, "Formation and accumulation of pyridyloxobutyl DNA adducts in F344 rats chronically treated with 4-(methylnitrosamino)-1-(3-pyridyl)-1-butanone and enantiomers of its metabolite, 4-(methylnitrosamino)-1-(3-pyridyl)-1-butanol," *Chemical Research in Toxicology*, vol. 20, no. 2, pp. 235–245, 2007.
- [58] P. Upadhyaya, B. R. Lindgren, and S. S. Hecht, "Comparative levels of  $O^6$ -methylguanine, pyridyloxobutyl-, and

- pyridylhydroxybutyl-DNA adducts in lung and liver of rats treated chronically with the tobacco-specific carcinogen 4-(methylnitrosamino)-1-(3-pyridyl)-1-butanone," *Drug Metabolism and Disposition*, vol. 37, no. 6, pp. 1147–1151, 2009.
- [59] S. Zhang, M. Wang, P. W. Villalta et al., "Analysis of pyridyloxobutyl and pyridylhydroxybutyl DNA adducts in extrahepatic tissues of F344 rats treated chronically with 4-(methylnitrosamino)-1-(3-pyridyl)-1-butanone and enantiomers of 4-(methylnitrosamino)-1-(3-pyridyl)-1-butanol," *Chemical Research in Toxicology*, vol. 22, no. 5, pp. 926–936, 2009.
- [60] Y. Lao, N. Yu, F. Kassie, P. W. Villalta, and S. S. Hecht, "Analysis of pyridyloxobutyl DNA adducts in F344 rats chronically treated with (R)- and (S)-N'-nitrosornicotine," *Chemical Research in Toxicology*, vol. 20, no. 2, pp. 246–256, 2007.
- [61] S. Zhang, M. Wang, P. W. Villalta, B. R. Lindgren, Y. Lao, and S. S. Hecht, "Quantitation of pyridyloxobutyl DNA adducts in nasal and oral mucosa of rats treated chronically with enantiomers of N'-nitrosornicotine," *Chemical Research in Toxicology*, vol. 22, no. 5, pp. 949–956, 2009.
- [62] D. Hölzle, D. Schlöbe, A. R. Tricker, and E. Richter, "Mass spectrometric analysis of 4-hydroxy-1-(3-pyridyl)-1-butanone-releasing DNA adducts in human lung," *Toxicology*, vol. 232, no. 3, pp. 277–285, 2007.
- [63] D. Schlöbe, D. Hölzle, D. Hatz, L. von Meyer, A. R. Tricker, and E. Richter, "4-Hydroxy-1-(3-pyridyl)-1-butanone-releasing DNA adducts in lung, lower esophagus and cardia of sudden death victims," *Toxicology*, vol. 245, no. 1-2, pp. 154–161, 2008.
- [64] D. S. Daniels, C. D. Mol, A. S. Arvai, S. Kanugula, A. E. Pegg, and J. A. Tainer, "Active and alkylated human AGT structures: a novel zinc site, inhibitor and extrahelical base binding," *EMBO Journal*, vol. 19, no. 7, pp. 1719–1730, 2000.
- [65] M. Xu-Welliver and A. E. Pegg, "Degradation of the alkylated form of the DNA repair protein, O<sup>6</sup>-alkylguanine-DNA alkyltransferase," *Carcinogenesis*, vol. 23, no. 5, pp. 823–830, 2002.
- [66] R. S. Mijal, N. M. Thomson, N. L. Fleischer et al., "The repair of the tobacco specific nitrosamine derived adduct O<sup>6</sup>-[4-oxo-4-(3-pyridyl)butyl]guanine by O<sup>6</sup>-alkylguanine-DNA alkyltransferase variants," *Chemical Research in Toxicology*, vol. 17, no. 3, pp. 424–434, 2004.
- [67] L. Li, J. Perdigo, A. E. Pegg et al., "The influence of repair pathways on the cytotoxicity and mutagenicity induced by the pyridyloxobutyl pathway of tobacco-specific nitrosamines," *Chemical Research in Toxicology*, vol. 22, no. 8, pp. 1464–1472, 2009.
- [68] J. C. Fromme, A. Banerjee, and G. L. Verdine, "DNA glycosylase recognition and catalysis," *Current Opinion in Structural Biology*, vol. 14, no. 1, pp. 43–49, 2004.
- [69] P. Fortini, B. Pascucci, E. Parlanti, M. D'Errico, V. Simonelli, and E. Dogliotti, "The base excision repair: mechanisms and its relevance for cancer susceptibility," *Biochimie*, vol. 85, no. 11, pp. 1053–1071, 2003.
- [70] M. D. Wyatt and D. L. Pittman, "Methylating agents and DNA repair responses: methylated bases and sources of strand breaks," *Chemical Research in Toxicology*, vol. 19, no. 12, pp. 1580–1594, 2006.
- [71] L. Airoidi, C. Magagnotti, M. Bonfanti et al., "Detection of O<sup>6</sup>-butyl- and O<sup>6</sup>-(4-hydroxybutyl)guanine in urothelial and hepatic DNA of rats given the bladder carcinogen N-nitrosobutyl(4-hydroxybutyl)amine," *Carcinogenesis*, vol. 15, no. 10, pp. 2297–2301, 1994.
- [72] S. Lacoste, A. Castonguay, and R. Drouin, "Formamidopyrimidine adducts are detected using the comet assay in human cells treated with reactive metabolites of 4-(methylnitrosamino)-1-(3-pyridyl)-1-butanone (NNK)," *Mutation Research*, vol. 600, no. 1-2, pp. 138–149, 2006.
- [73] J. Fan and D. M. Wilson III, "Protein-protein interactions and posttranslational modifications in mammalian base excision repair," *Free Radical Biology and Medicine*, vol. 38, no. 9, pp. 1121–1138, 2005.
- [74] C. Petit and A. Sancar, "Nucleotide excision repair: from E. coli to man," *Biochimie*, vol. 81, no. 1-2, pp. 15–25, 1999.
- [75] A. Sancar, L. A. Lindsey-Boltz, K. Ünsal-Kaçmaz, and S. Linn, "Molecular mechanisms of mammalian DNA repair and the DNA damage checkpoints," *Annual Review of Biochemistry*, vol. 73, pp. 39–85, 2004.
- [76] P. J. Brown, L. L. Bedard, and T. E. Massey, "Repair of 4-(methylnitrosamino)-1-(3-pyridyl)-1-butanone-induced DNA pyridyloxobutylation by nucleotide excision repair," *Cancer Letters*, vol. 260, no. 1-2, pp. 48–55, 2008.
- [77] L. H. Thompson, K. W. Brookman, and L. E. Dillehay, "Hypersensitivity to mutation and sister-chromatid-exchange induction in CHO cell mutants defective in incising DNA containing UV lesions," *Somatic Cell Genetics*, vol. 8, no. 6, pp. 759–773, 1982.
- [78] R. W. Chambers, E. Sledziewska-Gojska, S. Hirani-Hojatti, and H. Borowy-Borowski, "uvrA and recA mutations inhibit a site-specific transition produced by a single O<sup>6</sup>-methylguanine in gene G of bacteriophage ΦX174," *Proceedings of the National Academy of Sciences of the United States of America*, vol. 82, no. 21, pp. 7173–7177, 1985.
- [79] R. W. Chambers, E. Sledziewska-Gojska, and S. Hirani-Hojatti, "In vivo effect of DNA repair on the transition frequency produced from a single O<sup>6</sup>-methyl- or O<sup>6</sup>-n-butyl-guanine in a T:G base pair," *Molecular & General Genetics*, vol. 213, no. 2-3, pp. 325–331, 1988.
- [80] S. A. M. Bol, H. van Steeg, C. T. H. M. van Oostrom et al., "Nucleotide excision repair modulates the cytotoxic and mutagenic effects of N-butyl-N-nitrosourea in cultured mammalian cells as well as in mouse splenocytes *in vivo*," *Mutagenesis*, vol. 14, no. 3, pp. 317–322, 1999.
- [81] J. M. Boyle, R. Saffhill, G. P. Margison, and M. Fox, "A comparison of cell survival, mutation and persistence of putative promutagenic lesions in Chinese hamster cells exposed to BNU or MNU," *Carcinogenesis*, vol. 7, no. 12, pp. 1981–1985, 1986.
- [82] J. M. Boyle, G. P. Margison, and R. Saffhill, "Evidence for the excision repair of O<sup>6</sup>-n-butyldeoxyguanosine in human cells," *Carcinogenesis*, vol. 7, no. 12, pp. 1987–1990, 1986.
- [83] D. R. Duckett, J. T. Drummond, A. I. H. Murchie, et al., "Human MutSα recognizes damaged DNA base pairs containing O<sup>6</sup> methylguanine, O<sup>4</sup>-methylthymine, or the cisplatin d(GpG) adduct," *Proceedings of the National Academy of Sciences of the United States of America*, vol. 93, pp. 6443–6447, 1996.
- [84] J. Wu, L. Gu, H. Wang, N. E. Geacintov, and G.-M. Li, "Mismatch repair processing of carcinogen-DNA adducts triggers apoptosis," *Molecular and Cellular Biology*, vol. 19, no. 12, pp. 8292–8301, 1999.
- [85] M. Christmann, M. T. Tomcic, W. P. Roos, and B. Kaina, "Mechanisms of human DNA repair: an update," *Toxicology*, vol. 193, no. 1-2, pp. 3–34, 2003.
- [86] J. H. J. Hoeijmakers, "Genome maintenance mechanisms for preventing cancer," *Nature*, vol. 411, no. 6835, pp. 366–374, 2001.

- [87] R. S. Mijal, N. A. Loktionova, C. C. Vu, A. E. Pegg, and L. A. Peterson, "*O*<sup>6</sup>-pyridyloxobutylguanine adducts contribute to the mutagenic properties of pyridyloxobutylating agents," *Chemical Research in Toxicology*, vol. 18, no. 10, pp. 1619–1625, 2005.
- [88] L. E. Sandercock, J. N. Hahn, L. Li et al., "Mgmt deficiency alters the in vivo mutational spectrum of tissues exposed to the tobacco carcinogen 4-(methylnitrosamino)-1-(3-pyridyl)-1-butanone (NNK)," *Carcinogenesis*, vol. 29, no. 4, pp. 866–874, 2008.
- [89] L. A. Peterson, N. M. Thomson, D. L. Crankshaw, E. E. Donaldson, and P. J. Kenney, "Interactions between methylating and pyridyloxobutylating agents in A/J mouse lungs: implications for 4-(methylnitrosamino)-1-(3-pyridyl)-1-butanone-induced lung tumorigenesis," *Cancer Research*, vol. 61, no. 15, pp. 5757–5763, 2001.
- [90] P. J. Brown and T. E. Massey, "In vivo treatment with 4-(methylnitrosamino)-1-(3-pyridyl)-1-butanone (NNK) induces organ-specific alterations in in vitro repair of DNA pyridyloxobutylation," *Mutation Research*, vol. 663, no. 1-2, pp. 15–21, 2009.
- [91] S. S. Hecht, D. Lin, and A. Castonguay, "Effects of  $\alpha$ -deuterium substitution on the mutagenicity of 4-(methylnitrosamino)-1-(3-pyridyl)-1-butanone (NNK)," *Carcinogenesis*, vol. 4, no. 3, pp. 305–310, 1983.
- [92] P. G. Foiles, L. A. Petersen, L. M. Miglietta, and Z. Ronai, "Analysis of mutagenic activity and ability to induce replication of polyoma DNA sequences by different model metabolites of the carcinogenic tobacco-specific nitrosamine 4-(methylnitrosamino)-1-(3-pyridyl)-1-butanone," *Mutation Research*, vol. 279, no. 2, pp. 91–101, 1992.
- [93] G. T. Pauly, L. A. Peterson, and R. C. Moschel, "Mutagenesis by *O*<sup>6</sup>-[4-oxo-4-(3-pyridyl)butyl]guanine in *Escherichia coli* and human cells," *Chemical Research in Toxicology*, vol. 15, no. 2, pp. 165–169, 2002.
- [94] D. M. Maron and B. N. Ames, "Revised methods for the salmonella mutagenicity test," *Mutation Research*, vol. 113, no. 3-4, pp. 173–215, 1983.
- [95] M. Yamada, B. Sedgwick, T. Sofuni, and T. Nohmi, "Construction and characterization of mutants of *Salmonella typhimurium* deficient in DNA repair of *O*<sup>6</sup>-methylguanine," *Journal of Bacteriology*, vol. 177, no. 6, pp. 1511–1519, 1995.
- [96] O. S. Bhanot, P. C. Grevatt, J. M. Donahue, C. N. Gabrielides, and J. J. Solomon, "In vitro DNA replication implicates *O*<sup>2</sup>-ethyldeoxythymidine in transversion mutagenesis by ethylating agents," *Nucleic Acids Research*, vol. 20, no. 3, pp. 587–594, 1992.
- [97] V. Simonelli, L. Narciso, E. Dogliotti, and P. Fortini, "Base excision repair intermediates are mutagenic in mammalian cells," *Nucleic Acids Research*, vol. 33, no. 14, pp. 4404–4411, 2005.
- [98] Z. A. Ronai, S. Gradia, L. A. Peterson, and S. S. Hecht, "G to A transitions and G to T transversions in codon 12 of the *Ki-ras* oncogene isolated from mouse lung tumors induced by 4-(methylnitrosamino)-1-(3-pyridyl)-1-butanone (NNK) and related DNA methylating and pyridyloxobutylating agents," *Carcinogenesis*, vol. 14, no. 11, pp. 2419–2422, 1993.
- [99] M. D. M. von Pressentin, W. Kosinska, and J. B. Guttenplan, "Mutagenesis induced by oral carcinogens in lacZ mouse (MutaMouse) tongue and other oral tissues," *Carcinogenesis*, vol. 20, no. 11, pp. 2167–2170, 1999.
- [100] M. D. M. von Pressentin, M. Chen, and J. B. Guttenplan, "Mutagenesis induced by 4-(methylnitrosamino)-1-(3-pyridyl)-1-butanone-4-(methylnitrosamino)-1-(3-pyridyl)-1-butanone and N-nitrosornicotine in lacZ upper aerodigestive tissue and liver and inhibition by green tea," *Carcinogenesis*, vol. 22, no. 1, pp. 203–206, 2001.
- [101] K. Hashimoto, K.-I. Ohsawa, and M. Kimura, "Mutations induced by 4-(methylnitrosamino)-1-(3-pyridyl)-1-butanone (NNK) in the lacZ and cII genes of Muta Mouse," *Mutation Research*, vol. 560, no. 2, pp. 119–131, 2004.
- [102] X. Wang, T. Suzuki, T. Itoh et al., "Specific mutational spectrum of dimethylnitrosamine in the lacZ transgene of big blue C57BL/6 mice," *Mutagenesis*, vol. 13, no. 6, pp. 625–630, 1998.
- [103] V. L. Souliotis, J. H. M. van Delft, M.-J. S. T. Steenwinkel, R. A. Baan, and S. A. Kyrtpoulos, "DNA adducts, mutant frequencies and mutation spectra in *lacZ* transgenic mice treated with *N*-nitrosodimethylamine," *Carcinogenesis*, vol. 19, no. 5, pp. 731–739, 1998.
- [104] B. S. Shane, D. L. Smith-Dunn, J. G. de Boer, B. W. Glickman, and M. L. Cunningham, "Mutant frequencies and mutation spectra of dimethylnitrosamine (DMN) at the lacI and cII loci in the livers of Big Blue transgenic mice," *Mutation Research*, vol. 452, no. 2, pp. 197–210, 2000.

## Research Article

# Smoking, DNA Adducts and Number of Risk DNA Repair Alleles in Lung Cancer Cases, in Subjects with Benign Lung Diseases and in Controls

Marco Peluso,<sup>1</sup> Armelle Munnia,<sup>1</sup> Sara Piro,<sup>1</sup> Alessandra Armillis,<sup>1</sup> Marcello Ceppi,<sup>2</sup> Giuseppe Matullo,<sup>3,4</sup> and Riccardo Puntoni<sup>2</sup>

<sup>1</sup> Cancer Risk Factor Branch, Analytical and Biomolecular Cytology Unit, ISPO—Cancer Prevention and Research Institute, Via Cosimo il Vecchio N.2, 50139 Florence, Italy

<sup>2</sup> Molecular Epidemiology Unit, National Cancer Research Institute, 16132 Genoa, Italy

<sup>3</sup> Department of Genetics, Biology and Biochemistry, Faculty of Medicine and Surgery, University of Turin, 10124 Turin, Italy

<sup>4</sup> Section of Epidemiology, ISI Foundation—Institute for Scientific Interchange, Villa Gualino, 10133 Turin, Italy

Correspondence should be addressed to Marco Peluso, m.peluso@ispo.toscana.it

Received 14 May 2010; Revised 8 July 2010; Accepted 28 July 2010

Academic Editor: Shigenori Iwai

Copyright © 2010 Marco Peluso et al. This is an open access article distributed under the Creative Commons Attribution License, which permits unrestricted use, distribution, and reproduction in any medium, provided the original work is properly cited.

Smoke constituents can induce DNA adducts that cause mutations and lead to lung cancer. We have analyzed DNA adducts and polymorphisms in two DNA repair genes, for example, XRCC1 Arg194Trp and Arg399Gln genes and XRCC3 Thr241Met gene, in 34 lung cancer cases in respect to 30 subjects with benign lung cancer disease and 40 healthy controls. When the study population was categorized in base to the number of risk alleles, adducts were significantly increased in individuals bearing 3-4 risk alleles (OR = 4.1 95% C.I. 1.28–13.09,  $P = .009$ ). A significant association with smoking was noticed in smokers for more than 40 years carrying 3-4 risk alleles (OR = 36.38, 95% C.I. 1.17–1132.84,  $P = .040$ ). A not statistically significant increment of lung cancer risk was observed in the same group (OR = 4.54, 95% C.I. 0.33–62.93,  $P = .259$ ). Our results suggest that the analysis of the number of risk alleles predicts the interindividual variation in DNA adducts of smokers and lung cancer cases.

## 1. Introduction

Lung cancer is a leading cause of cancer death in the world [1]. Advances in the treatment of locally advanced lung cancer had no impact on overall 5-year survival rates from this disease that remains only of 15%. Although the rates of lung cancer mortality have started to decrease in countries where smoking habits have been modified, the projections are not optimistic because of the recent surge in tobacco consumption among young people. In addition, even if smoking habits could be modified significantly, the long lag time between peak of tobacco consumption and the development of lung cancer will assure a long life for this epidemic.

The role of tobacco smoking in the aetiology of lung cancer has been widely evaluated [2]. Many compounds present in the smoke of cigarettes, such as the polycyclic

aromatic hydrocarbons (PAH), induce DNA adducts after metabolic activation [3]. Unrepaired DNA adducts can cause mutations, including mutational hot spots in p53 tumour suppressor gene [4], and lead to unregulated cell growth and cancer. Increased DNA adduct levels have been suggested to be predictive of lung cancer risk, reflecting both the environmental exposure to carcinogens than individual susceptibility [5–8].

It has been hypothesized that interindividual difference in lung cancer risk may be due to differences in DNA repair. In support of this hypothesis, different studies have indicated that DNA variation in DNA repair genes may influence cancer susceptibility [9]. Our group has conducted a number of studies that have shown associations between DNA polymorphisms in DNA repair genes, mainly in XRCC1 (X-ray repair cross complementing) and XRCC3 genes, cancer, and/or DNA adducts [10–14] and unpublished results.

Thus, we have decided to extend our analysis to the individuals included in a lung cancer case-control study.

In this study, we have analyzed the levels of DNA adducts and DNA polymorphisms in two DNA repair genes, for example, XRCC1 Arg194Trp and XRCC1 Arg399Gln, and XRCC3 Thr241Met polymorphisms, representing the base excision repair (BER) and the double-strand breaks repair (DSB) pathways, in lung cancer cases in respect to individuals with benign lung disease and to healthy controls. Then, we decided to investigate the combination of the variant allele/s of XRCC1 Arg194Trp and Arg399Gln polymorphisms with the wild type allele of XRCC3 Thr241Met. The analysis of the effects of different combinations of DNA repair polymorphisms on DNA adducts has been done under the assumption that the combination of polymorphisms can have additive or more than additive effects on DNA adduct formation.

## 2. Materials and Methods

**2.1. Study Population.** Peripheral blood samples were collected, after written informed consent to participate in the present study, from 34 nonsmall cell lung cancer patients (26 males and 8 females, mean age 63.4 years) and from 30 (22 males and 8 females, mean age 63.5 years) subjects with benign lung diseases admitted to the National Cancer Institute and San Martino Hospital, Genoa, Italy. 40 controls (25 males and 15 females, mean age 63.4 years) were recruited from a group of blood donors. Lung cancer cases were asked to participate in the study after the diagnosis, but before radio and chemotherapy. The group of benign lung diseases was formed by subjects affected by Chronic Obstructive Pulmonary Disease (COPD), asthma, and pneumoconiosis. A standard questionnaire was administered to all volunteers by personal interview at the time of blood collection. Smoking status was defined as smoker, within the last year, former smoker, at least one year before diagnosis, and nonsmoker.

**2.2. DNA Adduct and Polymorphism Analyses.** Peripheral blood lymphocytes (PBLs) were separated from 5 mL freshly collected whole blood by centrifugation on a Ficoll gradient. PBL DNA was extracted and purified using a method that requires RNA and protein digestion and extraction with organic solvents [13]. DNA samples were stored at  $-80^{\circ}\text{C}$  until laboratory analysis. PBL DNA adducts were analysed using the nuclease P1 modification of the  $^{32}\text{P}$ -postlabelling technique [13]. DNA samples (1–5  $\mu\text{g}$ ) were digested with micrococcal nuclease (32.17 mU) and spleen phosphodiesterase (21.6 mU). Hydrolyzed DNA was treated with nuclease P1 (110 mU) for 30'. The nuclease P1 resistant DNA samples were then labelled by incubation with 25  $\mu\text{Ci}$  of carrier-free  $[\gamma\text{-}^{32}\text{P}]\text{ATP}$  (3000 Ci/mM) and T4-polynucleotide kinase (112.5 mU). The obtained  $^{32}\text{P}$ -labelled samples were analysed using 1.0 M sodium phosphate, pH 6.8. DNA adduct resolution was achieved using 4.0 M lithium formate, 7.5 M urea, pH 3.5 and 0.65 M lithium chloride, 0.45 M Tris base, 7.7 M urea, pH 8.0. Chromatograms were

finally developed using 1.7 M sodium phosphate pH 5.0. Detection and quantification of PBL DNA adducts and normal nucleotides (nn) were obtained by storage phosphor imaging techniques employing intensifying screens [15]. After background subtraction, the levels of DNA adducts were expressed such as relative adduct labelling (RAL) = screen pixel in adducted nucleotides/screen pixel in nn.

Polymerase Chain Reaction followed by enzymatic digestion was used for the genotyping of XRCC1 Arg194Trp and Arg399Gln, and XRCC3 Thr241Met [12].

**2.3. Statistical Analysis.** Logistic regression analysis was carried out to calculate Odds Ratios (ORs) adjusted for different covariates (i.e., age, sex, smoking, and DNA polymorphisms, as appropriate) categorizing DNA adduct levels by RAL median value (above/below 0.1 DNA adducts per  $10^8$  nn). A multiple regression analysis has also been performed grouping individuals according to the number of at risk alleles. A *P*-value less than or equal to 5% was considered significant. All the analyses were performed by the statistical package SPSS.

## 3. Results and Discussion

Genotype and allele frequencies were calculated by counting, and genotype distributions were in Hardy-Weinberg equilibrium. Genotype frequencies were, respectively: XRCC1 Arg194Arg = 88.8%, Arg194Trp = 11.2%, XRCC1 Arg399Arg = 38.5%, Arg399Gln = 49%, Gln399Gln = 12.5%, XRCC3 Thr241Thr = 40%, Thr241Met = 41%, and Met241Met = 19%, in keeping with those reported previously [9].

Characteristics of the study population are summarized in Table 1. PBL DNA adducts were increased in former and current smokers in respect to nonsmokers. The highest levels of DNA adducts were detected in individuals that reported to smoke for more than 40 years. A slightly increment of DNA damage was observed in benign lung disease and lung cancer patients in respect to controls.

Multiple regression analysis shows an increased frequency of PBL DNA adducts in smokers for more than 40 years (OR = 5.28, 95% confidence interval (C.I.) 1.00–27.72, *P* = .049). A significant trend with increasing number of smoked cigarettes was found (*P* for trend <.05). After the previous cited adjustments, no differences were observed comparing controls with benign lung diseases and lung cancer patients.

When the associations of DNA adducts with DNA polymorphisms were considered, a null association with XRCC1 Arg194Trp and Arg388Gln polymorphisms was found (OR = 4.08, 95% C.I. 0.77–21.48, *P* = .098 and OR = 1.32, 95% C.I. 0.34–5.18; *P* = .689, resp.). Conversely, a statistically significant inverse effect was observed with XRCC3 Thr241Met polymorphism (OR = 0.17, 95% C.I. 0.05–0.61, *P* = .006).

Then, we investigated the combination of the variant allele/s of XRCC1 Arg194Trp and Arg399Gln polymorphisms with the wild type allele of XRCC3 Thr241Met.

TABLE 1: Means of DNA adducts  $\pm$  standard error (SE) for different variables considered in the study plus the parameter estimates of the multivariate regression model.

	N <sup>a</sup>	Means <sup>b</sup> $\pm$ S.E.	Odds Ratio	C.I.	P-value
Gender					
Woman <sup>c</sup>	31	1.2 $\pm$ 0.3	1		
Male	73	1.3 $\pm$ 0.2	0.65	0.19–2.16	.480
Age (years)					
Per unit	104	1.3 $\pm$ 0.2	1.02	0.97–1.06	.516
Smoking habit					
Nonsmoker <sup>c</sup>	21	0.8 $\pm$ 0.4	1		
Former smoker	44	1.0 $\pm$ 0.3	1.60	0.39–6.58	.517
Smoker <40 years	11	1.5 $\pm$ 0.7	2.38	0.41–13.90	.336
Smoker $\geq$ 40 years	27	2.0 $\pm$ 0.5	5.28	1.00–27.72	.049
Status					
Controls <sup>c</sup>	40	1.0 $\pm$ 0.3	1		
Benign lung disease	30	1.3 $\pm$ 0.4	0.93	0.28–3.03	.898
Lung cancer	34	1.5 $\pm$ 0.4	1.17	0.39–3.47	.783
XRCC1 Arg194Trp					
Arg/Arg <sup>c</sup>	87	1.1 $\pm$ 0.2	1		
Arg/Trp	11	2.6 $\pm$ 1.1	4.08	0.77–21.48	.098
XRCC1 Arg399Gln					
Arg/Arg <sup>c</sup>	37	0.9 $\pm$ 0.2	1		
Arg/Gln	47	1.4 $\pm$ 0.3	0.93	0.36–2.39	.882
Gln/Gln	12	1.8 $\pm$ 1.0	1.32	0.34–5.18	.689
XRCC3 Thr241Met					
Thr/Thr <sup>c</sup>	40	1.5 $\pm$ 0.4	1		
Thr/Met	41	1.2 $\pm$ 0.3	0.38	0.15–0.97	.043
Met/Met	19	0.7 $\pm$ 0.4	0.17	0.05–0.61	.006
Number of risk alleles					
0-1 <sup>c</sup>	25	0.8 $\pm$ 0.4	1		
2	31	1.0 $\pm$ 0.3	0.92	0.31–2.69	.877
3-4	38	2.0 $\pm$ 0.5	4.1	1.28–13.09	.009

<sup>a</sup>Some figures do not add up to the total because of missing values.

<sup>b</sup>Levels per 10<sup>8</sup> normal nucleotides.

<sup>c</sup>Reference level.

The choice was based on the different association of XRCC1 and XRCC3 polymorphisms with lung cancer risk, for example, positive for XRCC1 Arg194Trp and Arg399Gln and negative for XRCC3 Met241Met [9, 16, 17]. The analysis of the effect of different combinations of DNA repair single nucleotide polymorphisms on DNA adducts has been performed under the assumption that the combination of different polymorphisms can have additive or more than additive effects.

When the study population was categorized in base to the number of risk alleles, the levels of DNA adducts were statistically significantly increased in individuals bearing three-four risk alleles (OR=4.1 95% C.I. 1.28–13.09,  $P = .009$ ). A significant association with smoking was noticed in smokers for more than 40 years carrying 3-4 risk alleles (OR=36.38, 95% C.I. 1.17-1132.84,  $P = .040$ ). A not

statistically significant increment of lung cancer risk was observed in the same group (OR = 4.54, 95% C.I. 0.33–62.93,  $P = .259$ ). A significant trend with increasing the number of risk alleles was also observed ( $P$  for trend <.05). Any association with benign lung diseases was not found.

Tobacco smoking is recognised as the primary preventable cause of human cancer. Therefore, many studies have explored the influence of smoking on the levels of DNA adducts in nucleated blood cells in order to identify an early and sensitive biomarker of effective intake of tobacco carcinogens [18].

In our study, we have analyzed PBLs as surrogate and more accessible tissues than bronchial biopsies, and we compared the levels of DNA adducts in patients with lung cancer in respect to those with benign lung diseases and controls. Our aim was to evaluate whether the levels of

TABLE 2: Means of DNA adducts  $\pm$  standard error (SE) case-control status considering the number of DNA repair risk alleles plus the parameter estimates of the multivariate regression model.

	$N^a$	Means <sup>b</sup> $\pm$ S.E.	Odds Ratio	C.I.	$P$ -value
0-1 risk alleles					
Smoking habit					
Nonsmoker <sup>c</sup>	6	1.7 $\pm$ 1.5	1		
Former smoker	12	0.4 $\pm$ 0.1	0.08	0.00–9.76	.302
Smoker <40 years	2	0.3 $\pm$ 0.2	0.33	0.00–67.26	.686
Smoker $\geq$ 40 years	5	1.3 $\pm$ 1.1	0.16	0.00–27.05	.480
Status					
Controls <sup>c</sup>	13	1.3 $\pm$ 0.7	1		
Benign lung disease	4	0.4 $\pm$ 0.1	1.23	0.08–19.30	.884
Lung cancer	8	0.5 $\pm$ 0.2	0.43	0.05–4.00	.458
2 risk alleles					
Smoking habit					
Nonsmoker <sup>c</sup>	7	0.4 $\pm$ 0.1	1		
Former smoker	10	0.7 $\pm$ 0.4	2.46	0.12–50.98	.560
Smoker <40 years	5	0.8 $\pm$ 0.6	0.86	0.03–28.37	.933
Smoker $\geq$ 40 years	9	1.7 $\pm$ 0.6	20.91	0.62–709.04	.091
Status					
Controls <sup>c</sup>	12	0.5 $\pm$ 0.2	1		
Benign lung disease	7	1.1 $\pm$ 0.6	1.11	0.12–10.00	.928
Lung cancer	12	1.3 $\pm$ 0.5	2.39	0.25–22.62	.447
3-4 risk alleles					
Smoking habit					
Nonsmoker <sup>c</sup>	5	0.4 $\pm$ 0.2	1		
Former smoker	20	1.7 $\pm$ 0.7	9.47	0.52–173.16	.130
Smoker $\geq$ 40 years	9	2.9 $\pm$ 1.3	36.38	1.17–1132.84	.040
Status					
Controls <sup>c</sup>	12	1.5 $\pm$ 0.6	1		
Benign lung disease	15	2.1 $\pm$ 0.9	0.45	0.06–3.69	.460
Lung cancer	11	2.3 $\pm$ 1.1	4.54	0.33–62.93	.259

<sup>a</sup>Some figures do not add up to the total because of missing values.

<sup>b</sup>Levels per  $10^8$  normal nucleotides.

<sup>c</sup>Reference level.

DNA adducts were associated with benign or malignant lung chronic diseases. The question of the utility of PBLs as a valid surrogate for a specific organ like lung, representing the events occurring in the target tissue, is still open [19]. Nevertheless, some studies have indicated that the use of PBLs such as a biological marker, may help in the identification of subjects at elevated risk [6–8]. PBLs are considered suitable to monitor environmental and occupational carcinogen exposure and to estimate the burden of DNA adducts in respiratory tissue [5, 20–22]. In fact, increased amount of PBL DNA adducts have been found among subjects heavily exposed to air pollution [21]. The relationship with target tissue DNA adducts may vary between type of carcinogen and target tissue although significant correlations have been seen between the levels of DNA damage in PBLs and bronchial mucosa [20].

Uppermost, we have considered the effect of smoking on DNA adduct levels. Our findings show that the levels of DNA adducts of smokers were higher than those of former and nonsmokers. Our finding shows that PBL DNA adduct may reflect exposures to carcinogens, such as those contained in tobacco smoke better than other surrogate tissues, such as leukocyte DNA adducts. However, discrepant results have been also reported with PBLs [18]. This is probably due to methodical differences in the  $^{32}\text{P}$ -DNA postlabelling protocol applied from research laboratories.

Next results show that the effect of smoking on DNA damage was more marked in the subjects that reported to smoke for more than 40 years. Although detailed information on smoking history, for example, number of pack of cigarettes smoked per years was missing, our findings

support the hypothesis that the formation of DNA adducts is significantly influenced by chronic carcinogen exposure. Furthermore, when study population was subgrouped for the number of risk alleles, a significant association with smoking was observed in the subjects carrying three or more risk alleles who reported to smoke for more than 40 years. Conversely, no effect of smoking was observed in smokers bearing one or less risk allele.

The contribution of duration of exposure to cigarette smoke has important implications for both research studies and prevention strategies. It has been shown that the age at first exposure and duration are associated influences to the levels of DNA adducts [23]. Smoking during adolescence has been shown to produce physiological changes leading to increased persistence of DNA adducts less, and subjects who begin smoking very early in life tend to be heavy smokers [23]. Two large epidemiological studies demonstrated that duration is more important than intensity of cigarette smoking in predicting lung cancer risk [24, 25]. Herein reported results support in part this hypothesis, thus shedding light on the mechanisms involved in the aetiology of smoking related cancers. It is likely that a plateau of the formation of DNA adducts is reached at these time points [5]. In fact, the persistence of DNA adducts in PBLs is less than one decade, which is the maximum lifespan for long-living lymphocytes.

Our next results show that DNA adduct levels were comparable in individuals with benign lung disease or with lung cancer and in controls. However, when specific combinations of variant alleles were investigated, a not significant increased lung cancer risk was observed in individuals bearing the same number of risk alleles.

In a meta-analysis of cancer and bulky DNA adducts [26], DNA damage has been reported to be predictive of lung cancer, particularly in smokers. In Veglia's meta-analysis, smokers presented a significant difference between lung cancer cases and controls, with patients having 83% higher amount of DNA adducts than controls. We know that the interpretation of the meta-analysis is limited by the fact that in case-control studies, the level of biomarker may reflect the presence of cancer disease rather than its aetiology. However, an exception is represented by three cohort studies, in which DNA adducts have been found to be prospectively predictive of lung cancer outcome [6–8]. The importance of these studies is based on the fact that biomarker measurement in PBLs collected several years before cancer onset ruled out the possibility that the higher levels of DNA damage were reflecting metabolic changes associated with cancer.

No increment of DNA adducts has been found in subjects with different benign bronchial pathologies, such as COPD, asthma, and pneumoconiosis, characterized by important inflammatory processes in respect to controls. However, such inflammatory phenomena can influence DNA adduct levels in lung target cells by increasing the biologically effective dose of PAH [27]. This hypothesis is consistent with a previous case-control study where the levels of DNA adducts in individuals with inflammatory diseases were significantly higher than those of controls [28].

DNA damage primarily reflects exposures to carcinogens but is modulated by inherited and acquired susceptibilities. Age, gender, and life-style and dietary habits have been reported to influence levels of DNA adducts [5, 29, 30]. DNA adducts may be also influenced by the individual's ability to remove DNA adducts undergoing from interindividual variability [31]. Although the main pathway for removal of bulky DNA adducts is nucleotide excision repair, it has been shown that BER and DSB repair mechanisms may participate in bulky DNA adduct repair, supporting the association of XRCC1 and XRCC3 polymorphisms with such kind of DNA damage [32, 33]. In this study we observed an effect of XRCC3 Thr241Met polymorphism on DNA adducts. Positive nonstatistically significant associations with XRCC1 Arg194Trp and Gln399Gln genotypes were found whereas an inverse significant association was detected in XRCC3 Met241Met carriers. Our findings are in keeping with previous studies showing that the variant alleles of the XRCC1 Arg399Gln polymorphism is associated with DNA adducts [10, 12, 13]. A recent pooled analysis has shown a protective effect conferred by XRCC3 241Met allele carriers against lung cancer [16]. However, other studies have reported higher levels of DNA damage in individuals with XRCC1 Arg194Arg and XRCC3 Met241Met genotypes [12, 33]. Our results suggest that case-control studies are more indicative for the determination of genetic susceptibility than cross-sectional studies.

To study the effect of different combinations of DNA repair single nucleotide polymorphisms on DNA adducts, we have investigated the combination of the variant allele/s of XRCC1 Arg194Trp and Arg399Gln polymorphisms with the wild type allele of XRCC3 Thr241Met. This was based on the different association of XRCC1 and XRCC3 polymorphisms with lung cancer risk, for example, positive for XRCC1 Arg194Trp and Arg399Gln and negative for XRCC3 Thr241Met [9, 16, 17, 34]. Our findings show that the combination of different polymorphisms can have additive effects on the levels of DNA adducts. In fact, when the number of risk alleles was analyzed, DNA adducts were higher in individuals carrying three-four risk alleles. Furthermore, when our population was categorized in base to the number of risk alleles, the association between smoking and lung cancer risk tended to be present in the same individuals bearing three-four risk alleles. Although statistical significances were seen in our analyses, our study is underpowered, and larger studies are needed to confirm the associations between DNA polymorphisms, cancer, and DNA adducts.

Furthermore, a previous report has shown that smoking is strong harmful factor that can eliminate the effect of DNA polymorphisms of DNA repair genes on lung cancer susceptibility [34]. Smoking could lead to cancer due to its toxic effect regardless of whether individuals have polymorphisms with low repair proficiency. Thus, the examination of the effect of different combinations of DNA polymorphisms for the prediction of lung cancer susceptibility could be more useful in nonsmokers exposed to relatively minor environmental factors.

## 4. Conclusions

The results of the present study support the utilisation of PBLs as surrogate and more accessible tissues than bronchial biopsies. In fact, we have observed a stronger effect of smoking on DNA adducts of 40 years smokers. When study population was subgrouped for number of risk alleles, the association with smoking was concentrated in carriers of 3-4 risk alleles that reported to have smoked for more than 40 years. A nonsignificant increased lung cancer risk was observed in individuals bearing the same number of risk alleles. Our results suggest that analysis of risk alleles can predict the interindividual variation in DNA adduct levels observed in smokers and lung cancer cases.

## Acknowledgments

This study was partially supported from the Associazione Italiana per la Ricerca sul Cancro (AIRC), Milan, Italy. The authors are grateful to Rosa Filiberti, Donatella Ugolini, Monica Neri, and Andrea Ardizzoni for their efforts in specimens collection.

## References

- [1] S. Dubey and C. A. Powell, "Update in lung cancer 2006," *American Journal of Respiratory and Critical Care Medicine*, vol. 175, no. 9, pp. 868–874, 2007.
- [2] IARC, *Monographs on the Evaluation of Carcinogenic Risks to Humans. Tobacco Smoke and Involuntary Smoking*, IARC Scientific Publications, no. 83, IARC, Lyon, France, 1996.
- [3] J. K. Wiencke, "DNA adduct burden and tobacco carcinogenesis," *Oncogene*, vol. 21, no. 48, pp. 7376–7391, 2002.
- [4] L. E. Smith, M. F. Denissenko, W. P. Bennett et al., "Targeting of lung cancer mutational hotspots by polycyclic aromatic hydrocarbons," *Journal of the National Cancer Institute*, vol. 92, no. 10, pp. 803–811, 2000.
- [5] M. Peluso, M. Ceppi, A. Munnia, R. Puntoni, and S. Parodi, "Analysis of 13 32P-DNA postlabeling studies on occupational cohorts exposed to air pollution," *American Journal of Epidemiology*, vol. 153, no. 6, pp. 546–558, 2001.
- [6] D. Tang, D. H. Phillips, M. Stampfer et al., "Association between carcinogen-DNA adducts in white blood cells and lung cancer risk in the physicians health study," *Cancer Research*, vol. 61, no. 18, pp. 6708–6712, 2001.
- [7] M. Peluso, A. Munnia, G. Hoek et al., "DNA adducts and lung cancer risk: a prospective study," *Cancer Research*, vol. 65, no. 17, pp. 8042–8048, 2005.
- [8] H. Bak, H. Autrup, B. L. Thomsen et al., "Bulky DNA adducts as risk indicator of lung cancer in a Danish case-cohort study," *International Journal of Cancer*, vol. 118, no. 7, pp. 1618–1622, 2006.
- [9] S. Zienolddiny, D. Campa, H. Lind et al., "Polymorphisms of DNA repair genes and risk of non-small cell lung cancer," *Carcinogenesis*, vol. 27, no. 3, pp. 560–567, 2006.
- [10] D. Palli, A. Russo, G. Masala et al., "DNA adducts levels and DNA repair polymorphisms in traffic-exposed workers and a general population," *International Journal of Cancer*, vol. 94, pp. 121–127, 2001.
- [11] G. Matullo, S. Guarrera, S. Caturan et al., "DNA repair gene polymorphisms, bulky DNA adducts in white blood cells and bladder cancer in a case control study," *International Journal of Cancer*, vol. 92, pp. 562–567, 2001.
- [12] G. Matullo, D. Palli, M. Peluso et al., "XRCC1, XRCC3, XPD gene polymorphisms, smoking and 32P-DNA adducts in a sample of healthy subjects," *Carcinogenesis*, vol. 22, no. 9, pp. 1437–1445, 2001.
- [13] G. Matullo, M. Peluso, S. Polidoro et al., "Combination of DNA repair gene single nucleotide polymorphisms and increased levels of DNA adducts in a population-based study," *Cancer Epidemiology Biomarkers and Prevention*, vol. 12, no. 7, pp. 674–677, 2003.
- [14] G. Matullo, A. M. Dunning, S. Guarrera et al., "DNA repair polymorphisms and cancer risk in non-smokers in a cohort study," *Carcinogenesis*, vol. 27, no. 5, pp. 997–1007, 2006.
- [15] M. Peluso, P. Srivatanakul, A. Munnia et al., "DNA adduct formation among workers in a Thai industrial estate and nearby residents," *Science of the Total Environment*, vol. 389, no. 2-3, pp. 283–288, 2008.
- [16] R. J. Hung, D. C. Christiani, A. Risch et al., "International lung cancer consortium: pooled analysis of sequence variants in DNA repair and cell cycle pathways," *Cancer Epidemiology Biomarkers and Prevention*, vol. 17, no. 11, pp. 3081–3089, 2008.
- [17] Z. Yin, B. Zhou, Q. He, M. Li, P. Guan, and X. Li, "Association between polymorphisms in DNA repair genes and survival of non-smoking female patients with lung adenocarcinoma," *BMC Cancer*, vol. 9, article 439, 2009.
- [18] D. H. Phillips, "Smoking-related DNA and protein adducts in human tissues," *Carcinogenesis*, vol. 23, no. 12, pp. 1979–2004, 2002.
- [19] A. Besaratinia, L. M. Maas, E. M. C. Brouwer, J. C. S. Kleinjans, and F. J. Van Schooten, "Comparison between smoking-related DNA adduct analysis in induced sputum and peripheral blood lymphocytes," *Carcinogenesis*, vol. 21, pp. 1335–1340, 2000.
- [20] M. Peluso, M. Neri, G. Margarino et al., "Comparison of DNA adduct levels in nasal mucosa, lymphocytes and bronchial mucosa of cigarette smokers and interaction with metabolic gene polymorphisms," *Carcinogenesis*, vol. 25, no. 12, pp. 2459–2465, 2004.
- [21] P. Vineis and K. Husgafvel-Pursiainen, "Air pollution and cancer: biomarker studies in human populations," *Carcinogenesis*, vol. 26, no. 11, pp. 1846–1855, 2005.
- [22] L. Godderis, M. De Boeck, V. Haufroid et al., "Influence of genetic polymorphisms on biomarkers of exposure and genotoxic effects in styrene-exposed workers," *Environmental and Molecular Mutagenesis*, vol. 44, no. 4, pp. 293–303, 2004.
- [23] J. K. Wiencke, S. W. Thurston, K. T. Kelsey et al., "Early age at smoking initiation and tobacco carcinogen DNA damage in the lung," *Journal of the National Cancer Institute*, vol. 91, no. 7, pp. 614–619, 1999.
- [24] R. Doll and R. Peto, "Cigarette smoking and bronchial carcinoma: dose and time relationships among regular smokers and lifelong non-smokers," *Journal of Epidemiology and Community Health*, vol. 32, no. 4, pp. 303–313, 1978.
- [25] W. D. Flanders, C. A. Lally, B.-P. Zhu, S. J. Henley, and M. J. Thun, "Lung cancer mortality in relation to age, duration of smoking, and daily cigarette consumption: results from cancer prevention study II," *Cancer Research*, vol. 63, no. 19, pp. 6556–6562, 2003.

- [26] F. Veglia, G. Matullo, and P. Vineis, "Bulky DNA adducts and risk of cancer: a meta-analysis," *Cancer Epidemiology Biomarkers and Prevention*, vol. 12, no. 2, pp. 157–160, 2003.
- [27] P. J. Borm, A. M. Knaapen, R. P. Schins, R. W. Godschalk, and F. J. Schooten, "Neutrophils amplify the formation of DNA adducts by benzo[a]pyrene in lung target cells," *Environmental Health Perspectives*, vol. 105, pp. 1089–1093, 1997.
- [28] C. Sacerdote, M. Peluso, A. Munnia, C. Malaveille, and P. Vineis, "The choice of controls in a case-control study on WBC-DNA adducts and metabolic polymorphisms," *Biomarkers*, vol. 5, no. 4, pp. 307–313, 2000.
- [29] P. Vineis and F. Perera, "DNA adducts as markers of exposure to carcinogens and risk of cancer," *International Journal of Cancer*, vol. 88, no. 3, pp. 325–328, 2000.
- [30] D. Palli, G. Masala, M. Peluso et al., "The effects of diet on DNA bulky adduct levels are strongly modified by GSTM1 genotype: a study on 634 subjects," *Carcinogenesis*, vol. 25, no. 4, pp. 577–584, 2004.
- [31] M. Berwick and P. Vineis, "Markers of DNA repair and susceptibility to cancer in humans: an epidemiologic review," *Journal of the National Cancer Institute*, vol. 92, no. 11, pp. 874–897, 2000.
- [32] E. Braithwaite, X. Wu, and Z. Wang, "Repair of DNA lesions induced by polycyclic aromatic hydrocarbons in human cell-free extracts: involvement of two excision repair mechanisms in vitro," *Carcinogenesis*, vol. 19, no. 7, pp. 1239–1246, 1998.
- [33] Y. Wang, M. R. Spitz, Y. Zhu, Q. Dong, S. Shete, and X. Wu, "From genotype to phenotype: correlating XRCC1 polymorphisms with mutagen sensitivity," *DNA Repair*, vol. 2, no. 8, pp. 901–908, 2003.
- [34] Y. Tanaka, Y. Maniwa, V. P. Bermudez et al., "Nonsynonymous single nucleotide polymorphisms in DNA damage repair pathways and lung cancer risk," *Cancer*, vol. 116, pp. 896–902, 2010.

## Research Article

# Insights into the Structures of DNA Damaged by Hydroxyl Radical: Crystal Structures of DNA Duplexes Containing 5-Formyluracil

Masaru Tsunoda,<sup>1</sup> Takeshi Sakaue,<sup>2,3</sup> Satoko Naito,<sup>2,4</sup> Tomoko Sunami,<sup>2,5</sup> Naoko Abe,<sup>6,7</sup> Yoshihito Ueno,<sup>6,8</sup> Akira Matsuda,<sup>6</sup> and Akio Takénaka<sup>1,2,9</sup>

<sup>1</sup> Faculty of Pharmacy, Iwaki Meisei University, Chuodai-Iino, Iwaki 970-8551, Japan

<sup>2</sup> Graduate School of Bioscience and Biotechnology, Tokyo Institute of Technology, Midori-ku, Yokohama 226-8501, Japan

<sup>3</sup> Teijin Institute for Biomedical Research, Teijin Ltd., 4-3-2 Asahigaoka, Hino, Tokyo 191-0053, Japan

<sup>4</sup> Discovery Technology Research Laboratories, Eisai Co. Ltd., 13 Tokodai 5-chome, Tsukuba-shi, Ibaraki 300-2635, Japan

<sup>5</sup> Kansai Photon Science Institute, JAEA, 8-1-7 Umemidai, Kizugawa 619-0215, Japan

<sup>6</sup> Graduate School of Pharmaceutical Sciences, Hokkaido University, Kita-ku, Sapporo 060-0812, Japan

<sup>7</sup> Nano Medical Engineering Laboratory, Advanced Science Institute, RIKEN 2-1, Hirosawa, Wako-Shi, Saitama 351-0198, Japan

<sup>8</sup> Faculty of Engineering, Gifu University, 1-1 Yanagido, Gifu 501-1193, Japan

<sup>9</sup> Graduate School of Science and Technology, Iwaki Meisei University, Chuodai-Iino, Iwaki 970-8551, Japan

Correspondence should be addressed to Akio Takénaka, atakenak@bio.titech.ac.jp

Received 7 June 2010; Revised 19 July 2010; Accepted 15 August 2010

Academic Editor: Ashis Basu

Copyright © 2010 Masaru Tsunoda et al. This is an open access article distributed under the Creative Commons Attribution License, which permits unrestricted use, distribution, and reproduction in any medium, provided the original work is properly cited.

Hydroxyl radicals are potent mutagens that attack DNA to form various base and ribose derivatives. One of the major damaged thymine derivatives is 5-formyluracil (fU), which induces pyrimidine transition during replication. In order to establish the structural basis for such mutagenesis, the crystal structures of two kinds of DNA d(CGCGRATfUCGCG) with R = A/G have been determined by X-ray crystallography. The fU residues form a Watson-Crick-type pair with A and two types of pairs (wobble and reversed wobble) with G, the latter being a new type of base pair between ionized thymine base and guanine base. *In silico* structural modeling suggests that the DNA polymerase can accept the reversed wobble pair with G, as well as the Watson-Crick pair with A.

## 1. Introduction

Hydroxyl radicals, activated from hydrogen peroxide and hydrogen superoxide anion under light radiation, are well known as potent mutagens that attack DNA and convert them to many different kinds of base and ribose derivatives [1, 2]. Every aerobic organism possesses several enzymes to remove such toxic oxides, as well as to recover the damaged DNA. However, when an excess amount of the radicals attacks DNA, the thymine base is oxidized at the 5-methyl group to form 5-formyluracil base (hereafter 2'-deoxy-5-formyluridine residue is referred to as fU) as a major product. (The four characters, A, T, G, and C, represent the respective nucleotide residues in DNA sequence.

The other abbreviations used are fU for 5-formyluracil or 2'-deoxy-5-formyluridine residue, dfUTP for 2'-deoxy-5-formyluridine 5'-triphosphate, HPLC for high pressure liquid chromatography, fUA for d(CGCGAATfUCGCG), and fUG for d(CGCGGATfUCGCG). It was demonstrated that 2'-deoxy-5-formyluridine triphosphate (dfUTP) was incorporated against both A and G templates, possibly forming fU:A and fU:G base pairs during *in vitro* DNA replication [3, 4]. On the other hand, it was reported that dfUTP-induced pyrimidine transitions, G:C → A:T and A:T → G:C, as well as a gene transversion from G:C to T:A, could occur *in vivo* [5, 6]. These results suggest that fU can behave as C, A, and G in addition to its original property of T.

TABLE 1: Crystallization conditions.

Crystals	fUA <sup>1</sup>	fUA <sup>2</sup>	fUA <sup>3</sup>	fUA <sup>4</sup>	fUG <sup>1</sup>	fUG <sup>2</sup>	fUG <sup>3</sup>
Droplet							
Sodium cacodylate buffer solution (mM)	20	20	20	20	20 <sup>a</sup>	20	20
pH	6.5	6.0	7.0	6.0	8.1	7.0	7.0
DNA (mM)	0.5	0.5	0.5	0.5	0.5	0.5	0.5
Spermine 4HCl (mM)	6	6	6	6	6	6	6
Sodium chloride (mM)	6	40	40	6	—	40	40
Potassium chloride(mM)	60	—	—	40	—	—	—
Magnesium chloride(mM)	6	10	—	—	—	10	10
Barium chloride(mM)	—	—	10	—	—	—	—
MPD (% in v/v)	5	5	5	5	5	5	5
Hoechst 33258 (mM)	—	—	—	—	—	0.5	—
DAPI (mM)	—	—	—	—	—	—	0.5
Reservoir solution							
MPD (%)	40	40	40	40	40	35	40
Temperature (K)	277	277	277	277	277	277	277

MPD: 2-methyl-2,4- pentanediol.

Hoechst 33258: 2'-(4-hydroxyphenyl)-6-(4- methyl-1-piperazinyl)-2,6'-bi-1*H*-benzimidazole.

DAPI: 4',6-diamidino-2-phenylindole.

<sup>a</sup>Buffer solution of fUG<sup>1</sup> is 3-[4-(2-Hydroxyethyl)-1-piperazinyl]propanesulfonic acid.

In order to reveal the interaction geometry of the modified base fU, we performed X-ray analyses on fU-containing DNA duplexes. The fU residues were introduced into the self-complementary Dickerson-Drew-type dodecamer sequence, which is expected to be easy to crystallize. The DNAs used in this study are d(CGCGAATfUCGCG) and d(CGCGGATfUCGCG) and will be referred to as fUA and fUG, respectively. The fU base faces either an adenine or a guanine at the two sites in each duplex. Four fUA crystals and three fUG crystals were obtained under different conditions. Their crystal structures have been successfully determined at resolutions ranging from 1.5 to 3.0 Å. In the preliminary papers [7, 8], magnesium ion effects on crystallizations of fUA were discussed, but the detailed structure of base-pair formations and its biological significance were not published. In this paper we describe the structures of the base pairs formed between fU and G and between fU and A, based on which the pyrimidine transition induced by the oxidized thymine base will be discussed.

## 2. Materials and Methods

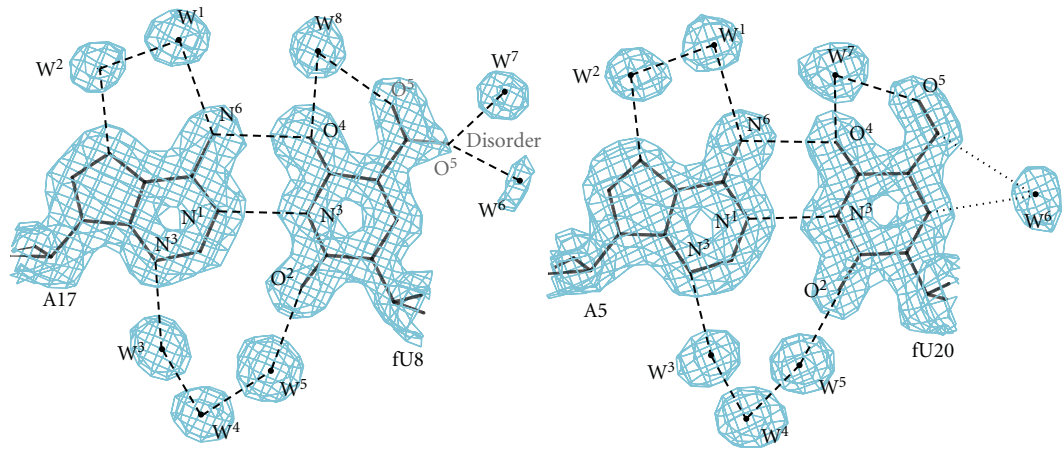
**2.1. Oligodeoxyribonucleotide Synthesis.** fUA and fUG were synthesized by the solid phase phosphoramidite method as described previously in [9] and were purified by reverse-phase column chromatography and reverse-phase and anion-exchange HPLCs. After NaIO<sub>4</sub> treatment, the oligonucleotides with fU were further purified by reverse-phase and anion-exchange HPLCs.

**2.2. Crystallization and Data Collection.** Initial screenings of crystallization conditions were performed using the hanging

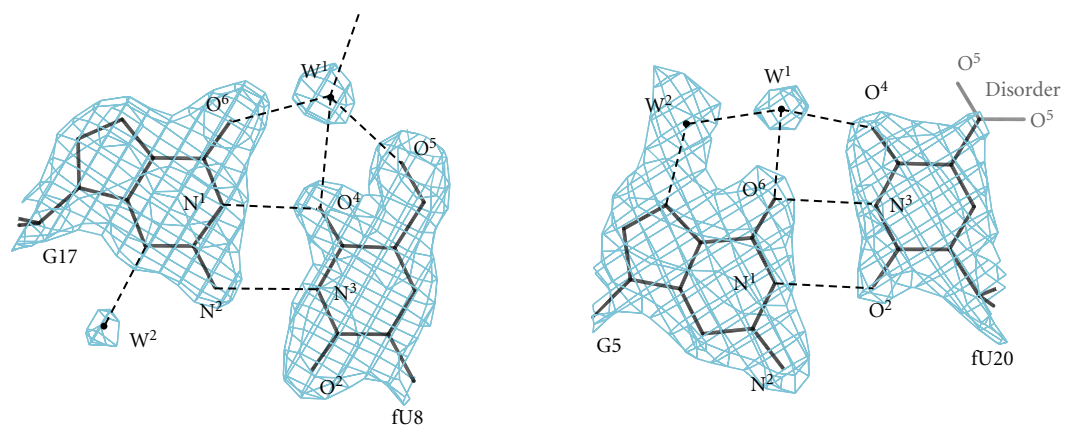
drop vapor diffusion method, equilibrating 2 μl droplets against 1 ml of the reservoir solution. The optimized conditions for growing the four different crystals of fUA (fUA<sup>1</sup>, fUA<sup>2</sup>, fUA<sup>3</sup>, and fUA<sup>4</sup>) and three different crystals of fUG are given in Table 1. As the fUG<sup>1</sup> crystal was too small, two kinds of dyes, Hoechst 33258 and DAPI, were added to stabilize the duplex formation (fUG<sup>2</sup> and fUG<sup>3</sup>).

Crystals suitable for X-ray data collections were picked up from their mother liquors using a nylon loop (Hampton Research) and transferred into liquid nitrogen. All X-ray experiments for the seven crystals were performed with synchrotron radiation at the Photon Factory in Tsukuba. Diffraction patterns of the fUA crystals, which were recorded on imaging plates, were processed subsequently using the programs *DENZO* and *Scalepack* [10] and those of the fUG crystals, recorded on Quantum 4 CCD, with the program *DPS/MOSFLM* [11]. Low-resolution data around the 10 Å resolution shell were truncated because they did not fit well into the diffraction profile. The crystal data and the statistics of data collection are summarized in Table 2.

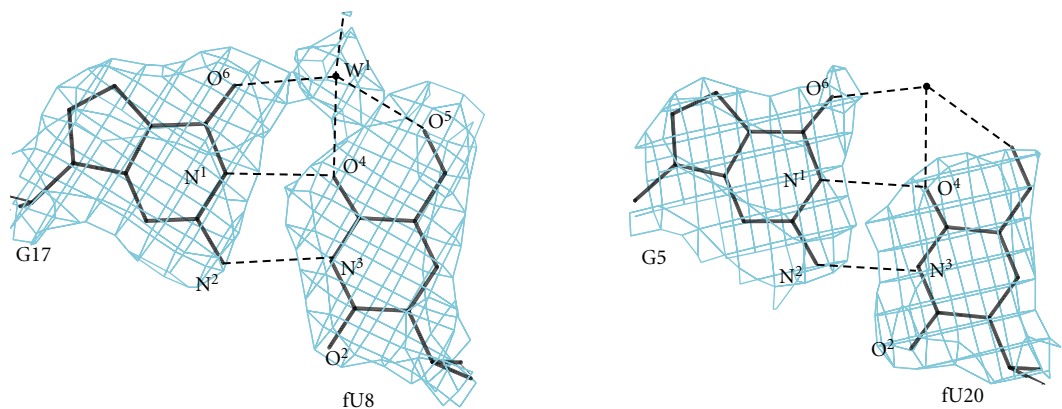
**2.3. Structure Determination and Refinement.** Initial phases were derived by molecular replacement with the program *AMoRe* [12] using the atomic coordinates of the corresponding unmodified DNA duplex (PDB ID 355D, see [13]) as structural probes. The molecular structures were constructed and modified on a graphic workstation with the program *Coot* [14] in the CCP4 program suite [15]. The atomic parameters were refined with the program *Refmac* [16] in CCP4 [15] with maximum-likelihood techniques, followed by interpretation of an omit map at every nucleotide residue. Newly defined patches were prepared for partially applying



(a)



(b)



(c)

FIGURE 1: The final  $2|F_o| - |F_c|$  maps around the fU residues in the fUA<sup>2</sup> (a), the fUG<sup>2</sup> (b), and the fUG<sup>3</sup> (c) crystals. The maps are contoured at  $1\sigma$  level by the program *DINO* [18]. Those of the fUG<sup>1</sup> crystal are omitted due to similarity to (c). Values indicate possible hydrogen bond distances. Characters N, O, and W indicate nitrogen, oxygen, and water oxygen atoms, respectively.

TABLE 2: Crystal data and statistical information on data collection and processing and on structure determination.

Crystals	fUA <sup>1</sup>	fUA <sup>2</sup>	fUA <sup>3</sup>	fUA <sup>4</sup>	fUG <sup>1</sup>	fUG <sup>2</sup>	fUG <sup>3</sup>
Wavelength (Å)	1.00	0.90	1.00	1.00	1.00	1.00	1.00
Beamline (at PF)	BL-18B	BL-6B	BL-18B	BL-6B	BL-18B	BL-18B	BL-18B
Oscillation ranges(°)	5	3	5	5	3	2	2
Frames	72	60	34	36	60	90 × 2 <sup>c</sup>	90
Space group	<i>P</i> 2 <sub>1</sub> 2 <sub>1</sub> 2 <sub>1</sub>						
<i>a</i> (Å)	25.8	26.0	25.2	25.3	24.6	25.3	25.0
<i>b</i> (Å)	39.3	39.5	41.2	41.7	40.0	40.3	40.5
<i>c</i> (Å)	65.0	65.7	65.4	66.0	68.5	66.0	66.8
<i>Z</i> <sup>a</sup>	1	1	1	1	1	1	1
Matthews coefficient (Å <sup>3</sup> Da <sup>-1</sup> )	2.15	2.20	2.22	2.28	2.28	2.28	2.29
Solvent content (%)	42.9	44.2	44.6	45.9	46.0	46.1	46.3
Resolution (Å)	1.57	1.5	1.7	1.8	3.0	1.95	2.6
Completeness (%)	97.1	99.4	97.7	99.3	99.3	99.9	99.9
<i>R</i> <sub>merge</sub> <sup>b</sup> (%)	3.1	4.8	2.9	2.8	11.4	4.0	6.3
Observed reflections	87588	66227	31872	45728	16654	72307	38399
Unique reflections	9502	10301	7779	6881	1531	5312	2342
Redundancy	9.22	6.43	4.10	6.65	10.9	13.6	16.4
<i>Structure refinement</i> <sup>f</sup>							
Resolution range (Å)	10.0–1.57	10.0–1.55	10.0–1.85	10.0–1.80	15.0–3.02	10.0–1.95	10.0–2.70
<i>R</i> -factor (%) <sup>d</sup>	18.3	18.3	21.6	19.3	18.8	20.3	21.1
<i>R</i> <sub>free</sub> (%) <sup>e</sup>	23.2	22.5	26.0	23.1	22.9	26.1	27.8
R.m.s. deviation							
Bond distances (Å)	0.027	0.028	0.019	0.021	0.005	0.019	0.007
Bond angles (°)	3.8	3.6	3.2	3.4	0.9	3.1	1.0
No. of ions	1Mg <sup>2+</sup> , 1K <sup>+</sup>	1Mg <sup>2+</sup>	—	—	—	1Mg <sup>2+</sup>	1Mg <sup>2+</sup>
No. of additive molecules	—	—	—	—	—	1Hoechst33258	1DAPI
No. of water molecules	150	185	82	142	27	123	45
PDB-ID	1G75	1G8N	1G8U	1G8V	3AJJ	3AJK	3AJL

<sup>a</sup>Number of duplexes in the asymmetric unit. <sup>b</sup> $R_{\text{merge}} = 100 \times \sum_{\mathbf{h}j} |I_{\mathbf{h}j} - \langle I_{\mathbf{h}} \rangle| / \sum_{\mathbf{h}j} I_{\mathbf{h}j}$ , where  $I_{\mathbf{h}j}$  is the  $j$ th measurement of the intensity of reflection  $\mathbf{h}$  and  $\langle I_{\mathbf{h}} \rangle$  is its mean value. <sup>c</sup>Two data sets were taken for a crystal by changing exposure time to compensate overloaded reflections. <sup>d</sup> $R$ -factor =  $100 \times \sum (|F_o| - |F_c|) / \sum |F_o|$ , where  $|F_o|$  and  $|F_c|$  are the observed and calculated structure factor amplitudes, respectively. <sup>e</sup>Calculated using a random set containing 10% of observations that were not included throughout refinement [17].

structural restrains to the modified residue. Water, ion, and dye molecules were assigned and included in the refinements. The program *CNS* [17] was used in the final refinements of fUG<sup>1</sup> and fUG<sup>3</sup> to stabilize the base pairs containing X with hydrogen bonds. The statistics of structure refinements are summarized in Table 2. Examples of the quality of the final electron density maps are depicted in Figure 1. Helical and local base-pair parameters [19], as well as the torsion angles and pseudorotation phase angles of sugar rings [19], were calculated using the program *3DNA* [20]. Some of them are shown in Table 3 and Figure 4.

**2.4. Coordinates.** Atomic coordinates and structure factors have been deposited in the Protein Data Bank with accession

codes 1G75, 1G8N, 1G8U, 1G8V, 3AJJ, 3AJK, and 3AJL for fUA<sup>1</sup>, fUA<sup>2</sup>, fUA<sup>3</sup>, fUA<sup>4</sup>, fUG<sup>1</sup>, fUG<sup>2</sup>, and fUG<sup>3</sup>, respectively.

### 3. Results

**3.1. Quality of X-ray Analyses.** All the crystals are isomorphous to the orthorhombic form of the unmodified duplex crystal. Crystallization of fUA was easy as expected, and the crystals obtained diffracted within the 1.5–1.8 Å resolution range. In every crystal, the formyl group of the fU8 residue on one of the two chains was disordered between the two alternative conformers, *anti* and *syn*, while that in the other chain adopted only the *syn* conformation. Relative occupancies of the disordered oxygen atoms, estimated

TABLE 3: A comparison of the local base-pair parameters at the modified pairs, calculated with the program 3DNA [20].

	Pair	fUA <sup>1</sup>	fUA <sup>2</sup>	fUA <sup>3</sup>	fUA <sup>4</sup>	fUG <sup>1</sup>	fUG <sup>2</sup>	fUG <sup>3</sup>	Ave	Unm
Shear (Å)	fU8:R	0.01	-0.03	-0.05	-0.08	-2.00	-2.24	-2.19	-0.94	-0.11
	R:fU20	0.05	0.08	-0.04	-0.01	1.90	-2.08	2.15	0.29	-0.04
Stretch (Å)	fU8:R	-0.19	-0.13	-0.08	-0.10	0.15	0.00	0.08	-0.04	-0.12
	R:fU20	-0.10	-0.11	-0.16	-0.16	0.13	-0.58	0.10	-0.13	-0.11
Stagger (Å)	fU8:R	0.10	0.11	-0.06	0.08	-0.33	-0.08	0.03	-0.02	-0.00
	R:fU20	0.09	0.00	0.00	0.10	-0.06	0.10	-0.05	0.03	0.01
Buckle (°)	fU8:R	-6.04	-4.89	-2.68	-4.97	-5.62	-10.56	-9.96	-6.39	-1.56
	R:fU20	8.11	6.02	9.91	9.34	6.78	8.68	4.50	7.62	4.72
Propeller (°)	fU8:R	-12.4	-12.4	-12.5	-11.9	-9.1	-16.3	-13.3	-12.6	-16.4
	R:fU20	-14.3	-14.5	-15.2	-15.3	-18.8	-14.6	-13.9	-15.2	-15.3
C1' . . . C1' (Å)	fU8:R	10.4	10.5	10.4	10.4	11.0	11.2	11.0	10.5(WC)	10.5
	R:fU20	10.5	10.6	10.3	10.4	11.1	10.6	11.1	11.1(rw)	10.5

R: a purine residue, A or G, Ave: average, Unm: unmodified duplex [14], WC: Watson-Crick type and rw: reversed wobble.

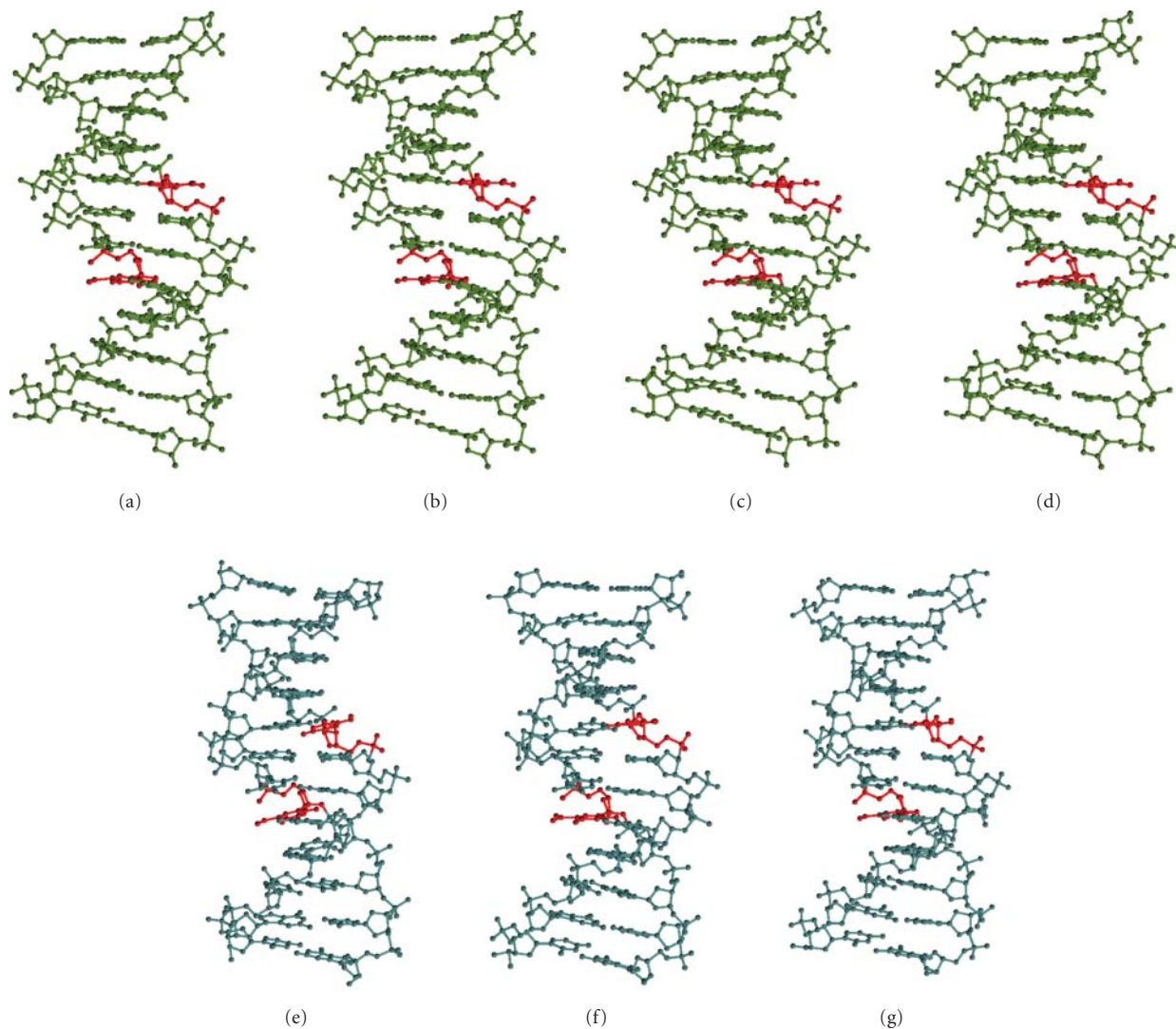


FIGURE 2: The overall structures of DNA duplexes containing fU, (a) fUA<sup>1</sup>, (b) fUA<sup>2</sup>, (c) fUA<sup>3</sup>, (d) fUA<sup>4</sup>, (e) fUG<sup>1</sup>, (f) fUG<sup>2</sup>, and (g) fUG<sup>3</sup>. The fU residues are colored red. Hoechst33258 and DAPI are omitted for clarity.

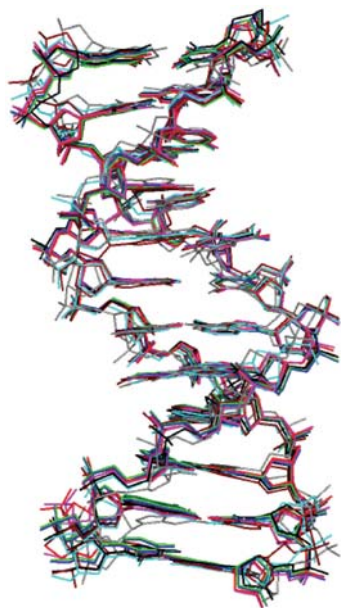


FIGURE 3: Superimposition of the fUA<sup>1</sup>(green), fUA<sup>2</sup>(blue), fUA<sup>3</sup>(red), fUA<sup>4</sup>(violet), fUG<sup>1</sup>(gray), fUG<sup>2</sup>(brown), and fUG<sup>3</sup>(cyan) duplexes onto the unmodified duplex (black) for comparison of the duplex conformations.

from the electron densities, were assumed in the structure refinements. (The residue numbering is 1 ~ 12 for one chain and 13 ~ 24 for another chain.)

On the other hand, fUG was difficult to crystallize. Attempts to crystallize fUG under conditions similar to those for fUA, that is, at neutral or slightly acidic pH, were unsuccessful. Small single crystals of fUG<sup>2</sup> appeared at basic pH (pH 8.1) but they poorly diffracted X-rays. Cocrystallization with several dyes was then attempted with the hope of stabilizing duplex formation. This approach led to the successful crystallization of fUG<sup>2</sup> and fUG<sup>3</sup> although the resolution of the fUG<sup>3</sup> crystal was still quite low. Hoechst 33258 and DAPI were found to be bound in the central region of the minor grooves of fUG<sup>2</sup> and fUG<sup>3</sup>, respectively, in a manner similar to the other DNA duplexes containing such dyes [21–27]. Interestingly, during refinements of fUG<sup>2</sup>, it was found that the two fU bases moved to different directions, one toward the minor groove side and the other toward the major groove side from the canonical Watson-Crick-type pairing position, and the resulting electron density also showed the same movements. In the case of fUG<sup>1</sup> and fUG<sup>3</sup>, however, the two fU bases moved to the same direction toward the minor groove side, and the electron densities, though poor, also supported the movements.

**3.2. Overall Structures.** The local helical parameters show that all the fUA and the fUG duplexes adopt the B-form conformation even in complex with dyes, as shown in Figure 2. Superimpositions of the present structures onto the unmodified duplex structure are shown in Figure 3 and yield an average root mean square deviation of 1.4 Å.

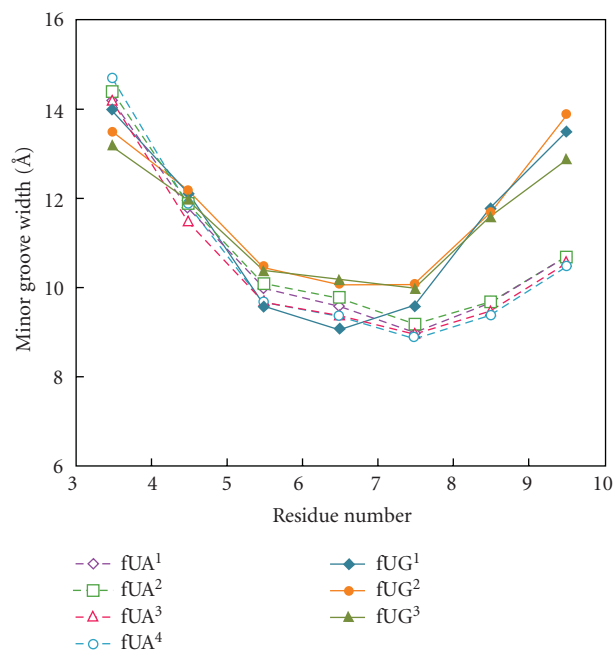


FIGURE 4: The minor groove widths in the fU-substituted and unmodified duplexes. The minor groove calculations were performed with the program 3DNA [20]. The widths are wider at the central regions in fUG<sup>2</sup> and fUG<sup>3</sup> compared with those in fUA<sup>1</sup>, fUA<sup>2</sup>, fUA<sup>3</sup>, fUA<sup>4</sup>, and fUG<sup>1</sup> because Hoechst33258 and DAPI are bound in the grooves.

Closer inspection of the superimposed structures reveals no drastic differences between the modified and the unmodified duplexes. However, the minor groove widths (see Figure 4) indicate that fUG<sup>2</sup> and fUG<sup>3</sup> are wider at the center compared with those of the other DNA duplexes. These changes in the DNA conformation are presumably due to the binding of DAPI and Hoechst33258 rather than the fU introductions. Another feature is that, at residues 3–5, the minor groove width is wider. This is typical of Dickerson-Drew-type DNA duplexes that are packed in the orthorhombic cell. The widening occurs because the duplex accepts the end of a neighboring duplex along the c axis through two hydrogen bonds to form a C:G:G:C quartet. The other end (the residues 8–10) is not widened. However, the corresponding width of every fUG crystal is wider, as discussed later.

**3.3. Hydrogen Bonding Schemes of Base Pairs.** In every crystal, the two DNA strands are associated to each other through base-pair formations, and all the bases, except for the modified bases and their counter bases positioned on the opposite strands in the duplexes, form the canonical Watson-Crick base pairs. All the pairing geometries of fU residues are shown in Figure 5. As depicted in Figure 1(a), the electron densities clearly show that the fU residues in fUA<sup>2</sup> are paired with the opposite A residues in the Watson-Crick geometry. Those of other fUA crystals also show the same paired structures. These results indicate that the oxidized T residue (fU) still has an ability to form a Watson-Crick-type base pair

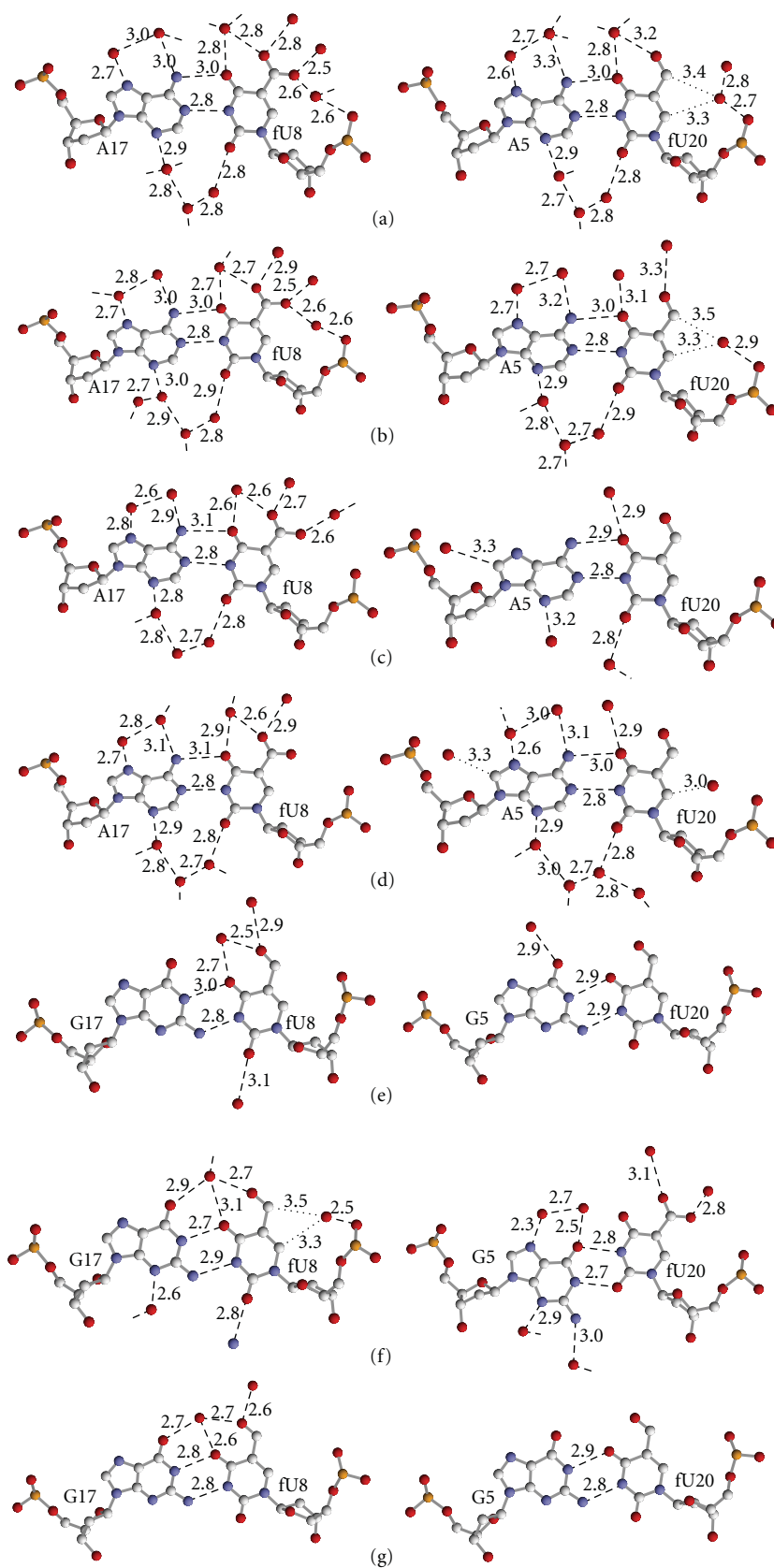


FIGURE 5: The pair formation geometry of fU residues found in (a) fUA<sup>1</sup>, (b) fUA<sup>2</sup>, (c) fUA<sup>3</sup>, (d) fUA<sup>4</sup>, (e) fUG<sup>1</sup>, (f) fUG<sup>2</sup>, and (g) fUG<sup>3</sup>. Broken and dotted lines indicate possible hydrogen bonds and CH $\cdots$ O interactions, respectively, and values indicate atomic distances in Å. The pictures are drawn by the program RASMOL [28].

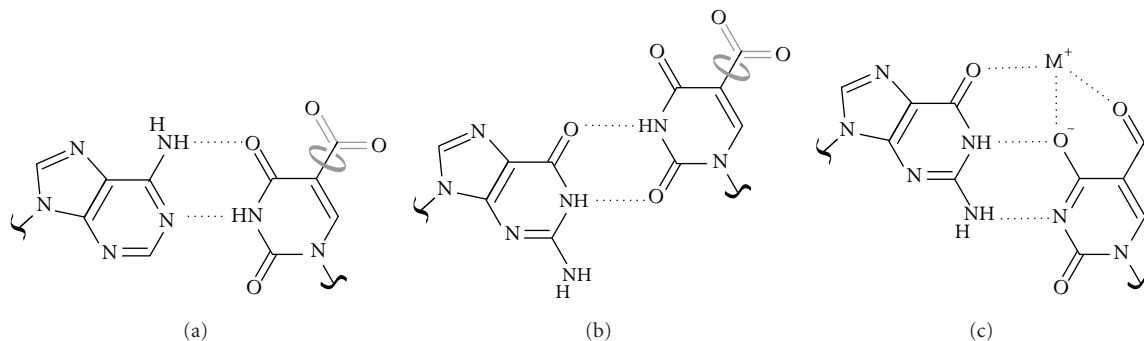


FIGURE 6: Hydrogen bonding schemes with chemical structures of the observed base pairs: (a) Watson-Crick type, (b) wobble type, and (c) reversed wobble type. M indicates a hydronium or sodium ion.

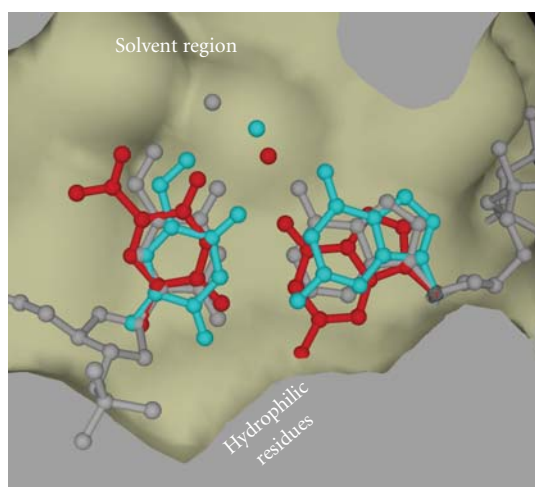


FIGURE 7: Models of the Watson-Crick-type fU:A (gray) and the reversed wobble fU:G (blue) pairs bound in DNA polymerase I (PDB-ID 3EZ5, see [30]), constructed by fitting the paired bases to the observed pair. The template residues and incoming NTP molecules are bound in the binding pocket of the enzyme, the hydrophilic residues of which may interact to the atoms at the edges of the two bases. The guanine N<sup>2</sup> and C<sup>2</sup> atoms of the wobble fU:G pair (red) are too close to the protein atoms.

with A. The formyl groups of fU could either adopt the *anti* or *syn* conformations depending on the surrounding water structure.

On the other hand, the most interesting features can be seen in the interaction geometries between fU and G in the fUG crystals. In the fUG<sup>2</sup> crystal, the fU20 residue forms a typical wobble pair with G5 through the N<sup>3</sup>H ··· O<sup>6</sup> and O<sup>2</sup> ··· HN<sup>1</sup> hydrogen bonds, and the formyl group is disordered between *syn* and *anti* conformations. However the fU8 residue forms a new type of pair with the opposite G17 residue through the two hydrogen bonds, O<sup>4</sup> ··· HN<sup>1</sup> and N<sup>3</sup> ··· HN<sup>2</sup>. In the pairing, the G base moves to the major groove side and the fU8 base moves to the minor groove side. Compared to the wobble pair, these bases move in the reverse direction. An atom was located on the electron density map (see Figure 1), and it is within hydrogen distance

of the O<sup>4</sup> and O<sup>5</sup> atoms of fU8 and the O<sup>6</sup> atom of G17. As the density of the atoms was of almost the same level as those of other water molecules, a water molecule was temporarily positioned at the peak for further structure refinements. In other words, it seems that a water molecule is trapped in the space surrounded by the three oxygen atoms to stabilize the pair formation. In the fUG<sup>3</sup> crystal, the two fU residues at the different sites also form the respective pairs with the opposite G residues. The geometries are, however, both in the new reversed wobble type, as shown in Figure 1(c). Water molecules are also assigned at the positions similarly surrounded by the three oxygen atoms, as described above, though the corresponding electron density at the fU20 site is rather poor due perhaps to low resolution. Furthermore, in the fUG<sup>1</sup> crystal obtained at pH 8.1 without the help of dyes, the electron density, though again at low resolution, suggests that the two fU residues form pairs with the opposite G residues in a similar manner to those found in fUG<sup>3</sup> obtained with DAPI. Therefore it is considered that the presence of dyes stabilizes duplex structure but does not affect the pairing modes.

#### 4. Discussion

Figure 6 summarizes the pairing modes with their chemical structures, found in the fUA and fUG crystals. It is noteworthy that an oxygen atom always exists at the center almost equidistant from the three surrounding oxygen atoms (O<sup>4</sup> and O<sup>5</sup> of fU and O<sup>6</sup> of G) in the reversed wobble geometry. Because of this pairing, the N<sup>1</sup> atom of fU should be deprotonated and the O<sup>4</sup> atom of fU might be ionized so that the central pocket must accept a hydronium ion instead of a water molecule to stabilize the pair formation. This is consistent with the fact that the fUG<sup>1</sup> crystal was obtained in alkaline state without the help of dyes. The pK<sub>a</sub> value decreases from 9.7 to 8.1 in response to the formylation by T oxidation [29]. A sodium ion but not a potassium could also be accommodated, judging from the size of the pocket.

A comparison of the local base-pair parameters at the modified pairs is given in Table 3. As the sequence is basically palindromic, the duplex has a twofold axis at the centre of the duplex perpendicular to the helical axis. Therefore,

the base pairs at fU8 and fU20 exhibit buckle angles and shear distances with signs (+/−) different between the positions related by the twofold symmetry, but propeller twist angles with the same sign though their absolute values are affected by crystal packing. All of the fU:A pairs satisfy these conditions. (The shear values fluctuate around zero in the standard B-form duplex.) The fUG duplexes also adopt this geometrical rule, except for the shear parameter. In the fUG<sup>2</sup> duplex, the two fU:G pairs have the shear values with the same sign (fU8 −2.24 Å and fU20 −2.08 Å). This means that the G17 and G5 bases which are paired with fU8 and fU20 move in the different directions along the X-axis [see the definition in [19]], that is, G17 shifts up toward the major groove side and G5 shifts down toward the minor groove side (or fU8 moves down toward the minor groove and fU20 moves up toward the major groove). These movements are just ascribed to the reversed wobbling and the normal wobbling, respectively. Another feature of the fU:G reversed wobbling can be seen in the C<sup>1′</sup>-C<sup>1′</sup> distance which is longer by 0.6 Å, as compared with those of the Watson-Crick pairing. This expansion is also reflected in the wider minor groove widths found in every fU:G duplexes.

The present work has clarified a total of three interaction modes, a Watson-Crick type for fU:A pairing and two wobble types (wobble and reversed wobble) for fU:G pairing. It has been believed that the DNA polymerase accepts base pairs only with the Watson-Crick geometries. The wobble pairing easily occurs between G and T, but the DNA polymerase [30] eliminates such a pair by sieving the shape of the pairs. In order to examine the possibility that a reversed wobble pair could also be accepted by the enzyme the pairing geometry was modeled into the enzyme *in silico*. As seen in Figure 7, the reversed wobble pair is reasonably accommodated without atomic collisions by slightly rotating the pair. On the contrary, a wobble pair, rotated in the opposite direction, would still collide with atoms of the enzyme. Thus, it could be concluded that G forms a pair with fU in the ionized form and A forms a Watson-Crick pair with fU and that the reversed wobble pair is allowed to be bound in the DNA polymerase. This tolerance explains the occurrence of mis-incorporation during replication and leads to pyrimidine transition mutagenesis.

Methoxyamine is also well known as a potent mutagen. N<sup>6</sup>-methoxyl-adenine [31, 32] and N<sup>4</sup>-methoxyl-cytosine [33–35] residues in the damaged DNAs adopt the imino tautomer to form mismatched base pairs, which mimic the Watson-Crick pair geometries. In contrast, fU derived from thymine oxidation forms a reversed wobble pair, which is also acceptable to the DNA polymerase.

The focus of the present work is on pyrimidine transition mutation and not gene transversion. The atomic mechanism of the latter will be revealed by similar X-ray studies.

## Acknowledgments

This work was supported in part by a grant for the RFTF Project from the Japanese Society for the Promotion of Science and by Grants-in-Aid for Scientific Research from

the Ministry of Education, Culture, Sports, Science and Technology of Japan. The authors thank N. Igarashi and S. Wakatsuki for facilities and help during data collection.

## References

- [1] S. S. Wallace, "Enzymatic processing of radiation-induced free radical damage in DNA," *Radiation Research*, vol. 150, no. 5, pp. S60–S79, 1998.
- [2] B. Halliwell and O. I. Aruoma, "DNA damage by oxygen-derived species. Its mechanism and measurement in mammalian systems," *FEBS Letters*, vol. 281, no. 1–2, pp. 9–19, 1991.
- [3] M. Yoshida, K. Makino, H. Morita, H. Terato, Y. Ohyama, and H. Ide, "Substrate and mispairing properties of 5-formyl-2'-deoxyuridine 5'-triphosphate assessed by *in vitro* DNA polymerase reactions," *Nucleic Acids Research*, vol. 25, no. 8, pp. 1570–1577, 1997.
- [4] H. Terato, A. Masaoka, M. Kobayashi et al., "Enzymatic repair of 5-formyluracil. II. Mismatch formation between 5-formyluracil and guanine during DNA replication and its recognition by two proteins involved in base excision repair (AlkA) and mismatch repair (MutS)," *The Journal of Biological Chemistry*, vol. 274, no. 35, pp. 25144–25150, 1999.
- [5] K. Fujikawa, H. Kamiya, and H. Kasai, "The mutations induced by oxidatively damaged nucleotides, 5-formyl-dUTP and 5-hydroxy-dCTP, in *Escherichia coli*," *Nucleic Acids Research*, vol. 26, no. 20, pp. 4582–4587, 1998.
- [6] H. Kamiya, N. Murata-Kamiya, N. Karino, Y. Ueno, A. Matsuda, and H. Kasai, "Induction of T→G and T→A transversions by 5-formyluracil in mammalian cells," *Mutation Research*, vol. 513, no. 1–2, pp. 213–222, 2002.
- [7] M. Tsunoda, N. Karino, Y. Ueno, A. Matsuda, and A. Takénaka, "Crystallization and preliminary X-ray analysis of a DNA dodecamer containing 2'-deoxy-5-formyluridine; what is the role of magnesium cation in crystallization of Dickerson-type DNA dodecamers?" *Acta Crystallographica Section D*, vol. 57, no. 2, pp. 345–348, 2001.
- [8] M. Tsunoda, J. Kondo, N. Karino, Y. Ueno, A. Matsuda, and A. Takenaka, "Water mediated Dickerson-Drew-type crystal of DNA dodecamer containing 2'-deoxy-5-formyluridine," *Biophysical Chemistry*, vol. 95, no. 3, pp. 227–233, 2002.
- [9] H. Sugiyama, S. Matsuda, K. Kino, Q.-M. Zhang, S. Yonei, and I. Saito, "New synthetic method of 5-formyluracil-containing oligonucleotides and their melting behavior," *Tetrahedron Letters*, vol. 37, no. 50, pp. 9067–9070, 1996.
- [10] Z. Otwinowski and W. Minor, "Processing of X-ray diffraction data collected in oscillation mode," *Methods in Enzymology*, vol. 276, pp. 307–326, 1997.
- [11] M. G. Rossmann and C. G. van Beek, "Data processing," *Acta Crystallographica Section D*, vol. 55, no. 10, pp. 1631–1640, 1999.
- [12] J. Navaza and P. Saludjian, "AMoRe: an automated package for molecular replacement," *Acta Crystallographica A*, vol. 50, pp. 157–163, 1994.
- [13] X. Shui, L. McFail-Isom, G. G. Hu, and L. D. Williams, "The B-DNA dodecamer at high resolution reveals a spine of water on sodium," *Biochemistry*, vol. 37, no. 23, pp. 8341–8355, 1998.
- [14] P. Emsley and K. Cowtan, "Coot: model-building tools for molecular graphics," *Acta Crystallographica Section D*, vol. 60, no. 12, pp. 2126–2132, 2004.
- [15] "Collaborative Computational Project," Number 4, 1994.
- [16] G. N. Murshudov, A. A. Vagin, and E. J. Dodson, "Refinement of macromolecular structures by the maximum-likelihood

- method," *Acta Crystallographica Section D*, vol. 53, no. 3, pp. 240–255, 1997.
- [17] A. T. Brünger, P. D. Adams, G. M. Clore et al., "Crystallography & NMR system: a new software suite for macromolecular structure determination," *Acta Crystallographica Section D*, vol. 54, no. 5, pp. 905–921, 1998.
- [18] A. Philippsen, "DINO: Visualizing Structural Biology," 2002, <http://www.dino3d.org/>.
- [19] W. K. Olson, M. Bansal, S. K. Burley et al., "A standard reference frame for the description of nucleic acid base-pair geometry," *Journal of Molecular Biology*, vol. 313, no. 1, pp. 229–237, 2001.
- [20] X.-J. Lu and W. K. Olson, "3DNA: a software package for the analysis, rebuilding and visualization of three-dimensional nucleic acid structures," *Nucleic Acids Research*, vol. 31, no. 17, pp. 5108–5121, 2003.
- [21] E. C. M. Juan, S. Shimizu, X. Ma et al., "Insights into the DNA stabilizing contributions of a bicyclic cytosine analogue: crystal structures of DNA duplexes containing 7,8-dihydropyrido[2,3-*d*]pyrimidin-2-one," *Nucleic Acids Research*, vol. 2010, pp. 1–9, 2010.
- [22] M. K. Teng, N. Usman, C. A. Frederick, and A. H. Wang, "The molecular structure of the complex of Hoechst 33258 and the DNA dodecamer d(CGCGAATTCGCG)," *Nucleic Acids Research*, vol. 16, no. 6, pp. 2671–2690, 1988.
- [23] J. R. Quintana, A. A. Lipanov, and R. E. Dickerson, "Low-temperature crystallographic analyses of the binding of Hoechst 33258 to the double-helical DNA dodecamer C-G-C-G-A-A-T-T-C-G-C-G," *Biochemistry*, vol. 30, no. 42, pp. 10294–10306, 1991.
- [24] M. Sriram, G. A. van der Marel, H. L. P. F. Roelen, J. H. Van Boom, and A. H.-J. Wang, "Conformation of B-DNA containing O6-ethyl-G-C base pairs stabilized by minor groove binding drugs: molecular structure of d(CGC[e6G]AATTCGCG complexed with Hoechst 33258 or Hoechst 33342," *EMBO Journal*, vol. 11, no. 1, pp. 225–232, 1992.
- [25] G. R. Clark, C. J. Squire, E. J. Gray, W. Leupin, and S. Neidle, "Designer DNA-binding drugs: the crystal structure of a meta-hydroxy analogue of Hoechst 33258 bound to d(CGCGAATTCGCG)<sub>2</sub>," *Nucleic Acids Research*, vol. 24, no. 24, pp. 4882–4889, 1996.
- [26] T. A. Larsen, D. S. Goodsell, D. Cascio, K. Grzeskowiak, and R. E. Dickerson, "The structure of DAPI bound to DNA," *Journal of Biomolecular Structure and Dynamics*, vol. 7, no. 3, pp. 477–491, 1989.
- [27] D. Vlieghe, J. Sponer, and L. Van Meervelt, "Crystal structure of d(GGCCAATTGG) complexed with DAPI reveals novel binding mode," *Biochemistry*, vol. 38, no. 50, pp. 16443–16451, 1999.
- [28] R. A. Sayle and E. J. Milner-White, "RASMOL: biomolecular graphics for all," *Trends in Biochemical Sciences*, vol. 20, no. 9, pp. 374–376, 1995.
- [29] E. J. Privat and L. C. Sowers, "A proposed mechanism for the mutagenicity of 5-formyluracil," *Mutation Research*, vol. 354, no. 2, pp. 151–156, 1996.
- [30] A. A. Golosov, J. J. Warren, L. S. Beese, and M. Karplus, "The mechanism of the translocation step in DNA replication by DNA polymerase I: a computer simulation analysis," vol. 18, no. 1, pp. 83–93, 2010.
- [31] T. Chatake, A. Ono, Y. Ueno, A. Matsuda, and A. Takénaka, "Crystallographic studies on damaged DNAs. I. An N<sup>6</sup>-methoxyadenine residue forms a Watson-Crick pair with a cytosine residue in a B-DNA duplex," *Journal of Molecular Biology*, vol. 294, no. 5, pp. 1215–1222, 1999.
- [32] T. Chatake, T. Hikima, A. Ono, Y. Ueno, A. Matsuda, and A. Takénaka, "Crystallographic studies on damaged DNAs. II. N<sup>6</sup>-methoxyadenine can present two alternate faces for Watson-Crick base-pairing, leading to pyrimidine transition mutagenesis," *Journal of Molecular Biology*, vol. 294, no. 5, pp. 1223–1230, 1999.
- [33] M. T. Hossain, T. Sunami, M. Tsunoda et al., "Crystallographic studies on damaged DNAsIV. N<sup>4</sup>-methoxycytosine shows a second face for Watson-Crick base-pairing, leading to purine transition mutagenesis," *Nucleic Acids Research*, vol. 29, no. 19, pp. 3949–3954, 2001.
- [34] M. T. Hossain, T. Chatake, T. Hikima et al., "Crystallographic studies on damaged DNAs: III. N<sup>4</sup>-methoxycytosine can form both Watson-Crick type and wobbled base pairs in a B-form duplex," *Journal of Biochemistry*, vol. 130, no. 1, pp. 9–12, 2001.
- [35] M. Tofazzal Hossain, J. Kondo, Y. Ueno, A. Matsuda, and A. Takénaka, "X-Ray analysis of d(CGCGAATTXGCG)<sub>2</sub> containing a 2'-deoxy-N<sup>4</sup>-methoxycytosine residue at X: a characteristic pattern of sugar puckers in the crystalline state of the Dickerson-Drew type DNA dodecamers," *Biophysical Chemistry*, vol. 95, no. 1, pp. 69–77, 2002.

## Research Article

# Elevated Levels of DNA Strand Breaks Induced by a Base Analog in the Human Cell Line with the P32T ITPA Variant

Irina S.-R. Waisertreiger,<sup>1,2</sup> Miriam R. Menezes,<sup>1</sup> James Randazzo,<sup>3</sup> and Youri I. Pavlov<sup>1</sup>

<sup>1</sup> Eppley Institute for Research in Cancer, University of Nebraska Medical Center, Omaha, NE 68198-6805, USA

<sup>2</sup> Institute of Cytology, Russian Academy of Sciences, St. Petersburg 194064, Russia

<sup>3</sup> Department of Pharmaceutical Sciences, University of Nebraska Medical Center, Omaha, NE 68198-6025, USA

Correspondence should be addressed to Youri I. Pavlov, ypavlov@unmc.edu

Received 26 April 2010; Accepted 11 July 2010

Academic Editor: Ashis Basu

Copyright © 2010 Irina S.-R. Waisertreiger et al. This is an open access article distributed under the Creative Commons Attribution License, which permits unrestricted use, distribution, and reproduction in any medium, provided the original work is properly cited.

Base analogs are powerful antimetabolites and dangerous mutagens generated endogenously by oxidative stress, inflammation, and aberrant nucleotide biosynthesis. Human inosine triphosphate pyrophosphatase (ITPA) hydrolyzes triphosphates of noncanonical purine bases (i.e., ITP, dITP, XTP, dXTP, or their mimic: 6-hydroxyaminopurine (HAP) deoxynucleoside triphosphate) and thus regulates nucleotide pools and protects cells from DNA damage. We demonstrate that the model purine base analog HAP induces DNA breaks in human cells and leads to elevation of levels of ITPA. A human polymorphic allele of the *ITPA*, 94C->A encodes for the enzyme with a P32T amino-acid change and leads to accumulation of nonhydrolyzed ITP. The polymorphism has been associated with adverse reaction to purine base-analog drugs. The level of both spontaneous and HAP-induced DNA breaks is elevated in the cell line with the *ITPA* P32T variant. The results suggested that human *ITPA* plays a pivotal role in the protection of DNA from noncanonical purine base analogs.

## 1. Introduction

Modified bases in DNA pose a severe threat for genome integrity [1], (Figure 1). DNA could be directly damaged by environmental factors such as ionizing radiation, chemical mutagens or endogenous factors, such as oxidative stress and inflammation [2–4]. Many of these factors also damage nucleotides in DNA precursor pools [5–7]. Additionally, cellular metabolism *per se* also contributes to the contamination of pools by nucleobase-analogs. Base-analogs in the deoxyribonucleoside triphosphate form are incorporated into DNA by DNA polymerases and are the source of genetic changes [8]. Potent repair systems remove not only the lesions from DNA, but also the harmful triphosphates from the DNA precursor pools (Figure 1, [1, 8]). Defects of these protection mechanisms lead to hypermutagenesis [9] or hyperrecombination [10–12] and result in genome instability, which predisposes individuals to diseases like cancer [13, 14]. Base-analogs are clinically important and are widely used as immunosuppressants as well, antiviral

and anticancer agents. The determination of the reasons for individual sensitivity/resistance is of high priority.

The major mutagenic modified purine bases include 8-oxoguanine and 2-hydroxyadenine [15]. The 8-oxoguanine in deoxyribonucleoside triphosphate form can be incorporated into DNA by replicative as well as specialized DNA polymerases [16–18]. It can form base pairs with cytosine and adenine and, therefore, can lead to transversion mutations [19]. The MutT protein of *E. coli* hydrolyzes 8-oxodGTP to 8-oxodGMP, preventing incorporation into DNA [17]. Mutational inactivation of this gene leads to a 10,000-fold increase in the rates of transversions [20], but no elevation of DNA fragmentation is detected in *mutT* strains [21]. The 2-hydroxyadenine also has strong mutagenic potential [3]. Deamination of normal purines, as well as dysregulation of the purine biosynthesis, leads to contamination of nucleotide pools with deoxyinosine triphosphate and deoxyxanthine triphosphate. Inflammation induces various types of base damage from oxidative stress and elevated lipid peroxidation [22]. The latter can

generate mutagenic derivatives of adenine and guanine, HAP and its 2-amino derivative *in vitro* [23]. HAP might be generated by monooxygenation of adenine [24]. HAP also can be generated by adenylosuccinate synthase, an enzyme of the *de novo* purine biosynthesis pathway wherein hydroxylamine is provided instead of aspartate in the reaction with IMP [25]. Thus, HAP can be a natural contaminant of dNTP pools [23, 26], however the literature does not report direct measurements of HAP derivatives in nucleotide pools. HAP is strongly mutagenic in bacteria and yeast [26, 27]. The dHAPTP is incorporated into DNA by various DNA polymerases *in vitro* [28, 29]. Overwhelming indirect genetic evidence in microorganisms suggests that the mutagenic effect is mediated by dHAPTP incorporation into DNA [26]. There is only fragmentary information about the effects of endogenous and exogenous base-analogs, such as HAP, in multicellular eukaryotes.

There are a number of evolutionarily conserved enzymatic systems that sanitize the nucleotide pool by selectively breaking deoxynucleoside triphosphate forms of base-analog DNA precursors, either to monophosphate [17, 30] or to nucleoside [31, 32] or diphosphate [33]. Additional systems affect quality of dNTP pools [34]. One of them, NUDT16, destroys abnormal diphosphates [35]. Polymorphisms in the genes encoding protective enzymes are associated with an increased risk of cancer [36], a predisposition to base-analog-associated adverse drug reactions [37] or a modulation of response to therapy in hepatitis C patients [38].

ITPA is a prominent enzyme protecting from base-analogs [27, 39]. ITPA orthologs from humans, yeast (encoded by the *HAM1* gene), and bacteria (encoded by the *rdgB* gene) control levels of ITP, dITP and dHAPTP by hydrolyzing ITP/dITP to PPi and IMP/dIMP [27, 30, 40]. One report documents that yeast ITPA can hydrolyze pyrimidine analogs as well [41]. ITPA is highly conserved among species [26, 40, 42]. In *E. coli*, the *rdgB* mutation is synthetically lethal with the *recA* mutation abolishing homologous recombination [27, 39]. The *rdgB* mutation sensitizes to the mutagenic and recombinogenic effects of HAP in molybdenum-cofactor defective strain background (another system protecting from HAP [43–45]) because of a massive accumulation of breaks in DNA [27, 39, 46]. DNA damage is caused by intermediates in the repair of base-analogs in DNA by Endo V encoded by the *nfi* gene. This has been proven by the viability of triple *rdgB recA nfi* mutants [27].

HAP is very mutagenic in yeast but does not induce recombination [48]. A defect in the yeast homolog of ITPA, Ham1, leads to elevated HAPmutagenesis, but it does not affect spontaneous mutagenesis [49]. The natural substrate, dITP, seems to be non-mutagenic when it is incorporated in DNA, because hypoxanthine base pairs properly with cytosine [50], and yeast apparently do not possess an enzyme able to recognize hypoxanthine, xanthine and HAP in DNA similar to Endo V. Therefore, DNA with these bases is not nicked and no recombination and DNA breakage are seen. The situation in yeast might be atypical. Inosine and xanthine in DNA are recognized in most organisms by a specialized repair system initiated by the orthologs of

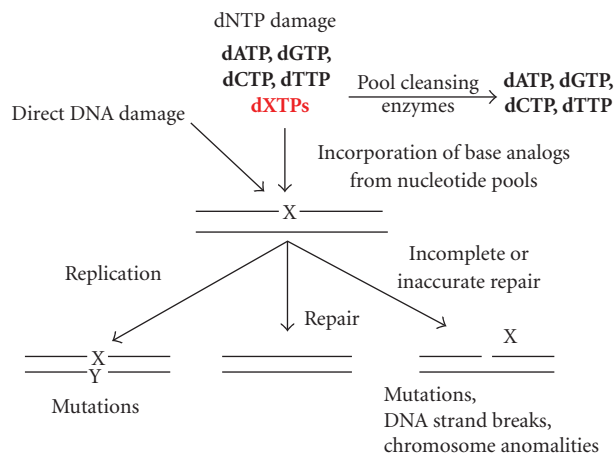


FIGURE 1: Base-analog DNA cycle. Environmental and intrinsic mutagens can damage DNA directly or can damage DNA precursor pools. When cleansing is inefficient, base-analogs are incorporated into DNA. Damaged bases lead to mutations in replication cycles or can be correctly repaired by base excision repair. Intermediates of this repair can lead to mutagenesis, DNA breaks, and chromosome changes.

endonuclease V [51] and elicit DNA repair reactions that lead to DNA fragmentation and genomic instability when the level of analogues is high [3, 39, 46].

The repair of purine base-analogs in humans has not been studied. Mutations in the human ITPA gene lead to the accumulation of ITP in erythrocytes but do not show a clear disease phenotype, perhaps due to compensation by other cleansing enzymes [52, 53]. Human ITPA P32T variant, abolishing the ITPA activity in erythrocytes, has been associated in most publications with adverse reactions to purine analogues used in the treatment of blood cancers, transplant, and inflammatory bowel diseases [37, 54–59]. The ITPA P32T variant causes sensitivity to mercaptopurine used for the treatment of acute lymphoblastic leukemia [60].

Knockout of the *Itpa* gene in mice is lethal primarily because of heart failure [53]. Primary embryonic fibroblasts exhibit moderate chromosome instability phenotype [61], and the inviability of the *Itpa* knockout mice suggests that the enzyme performs essential functions in addition to the prevention of the misincorporation of purine base-analogs in DNA. If we assume that the role of ITPA is the same in humans, the ITPA P32T variant should result in an incomplete loss of activity, at least in the heart. Indeed, ITPA with the change possesses enzymatic activity but is thermally unstable [62, 63], suggesting a possibility that the levels of the protein and its activity could vary among tissues.

In this study, we demonstrate by comet assay that the model purine base-analog, HAP, induces DNA strand breaks in three different human cell lines. This suggests that there is active recognition of incorporated base-analogs and nicking of DNA. The inducibility of the system of HAP repair was indicated by the shape of HAP dose response on the frequency of DNA strand breaks. We suggest and provide the evidence that one component of the repair

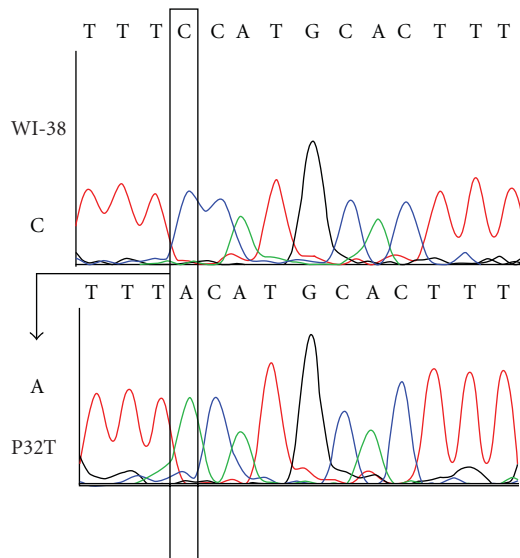
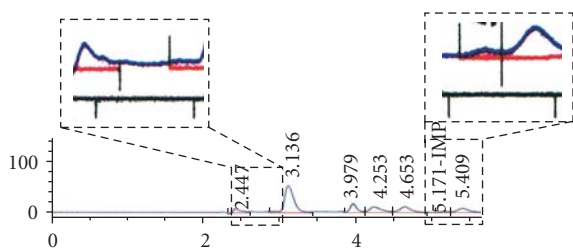
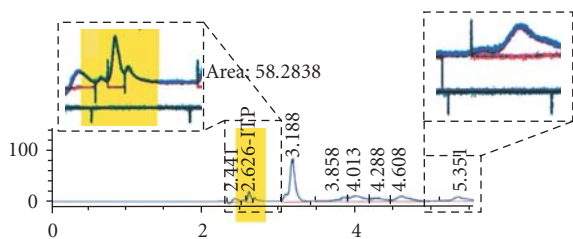


FIGURE 2: Verification of the genotype of the P32T cell line. Electropherogram of the DNA sequence of the region with C94A mutation is shown. The experiment was performed as described in Section 2.



(a) HPLC analysis of WI-38 extract.



(b) HPLC analysis of P32T extract.

FIGURE 3: Accumulation of ITP in the P32T cell line. Areas of chromatogram corresponding to ITP and IMP are enlarged in boxes above the actual printout. Whole-cell lysates corresponding to 100  $\mu$ g of protein were deproteinized by acid extraction with 1 N HCl followed by alkali treatment with an equal volume of 1 N NaOH. The samples were centrifuged at 14,000 RPM for 10 min. The volume of aqueous fraction (supernatant) was adjusted to 500  $\mu$ L with HPLC-grade water. The samples were run on an Alltech hypersil BDS C18 5 $\mu$  column. The HP 1100 HPLC connected to an autosampler and a DAD detector (which was set at 262 nm) was used. Flow rate was kept constant at 1.1 mL/min, and a gradient flow was used: 0 to 5 minutes, 100% (a), 5–5 : 10 ramp up to 100% (b), 5 : 10–8 : 10, 100% (b), 8 : 10–8 : 20 ramp down to 100% (a). In the preliminary experiments we have determined the retention of pure 0.5 mM solutions of ITP (~2.6) and IMP (~5.2).

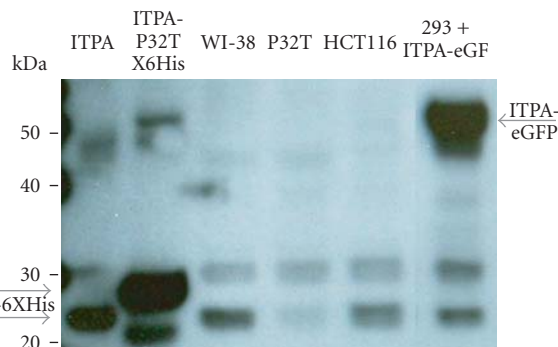


FIGURE 4: Specificity of polyclonal antibodies against ITPA in Western blot. Western blots were performed as described in Section 2. Antibodies against ITPA react largely with ITPA (a band closer to 20 kDa marker, see compared with lane where pure ITPA was loaded, and predicted molecular mass was 21.4 kDa) and, less intense, with an unrelated protein running at 30 kDa. The level of ITPA, but not of this non-specific protein, is decreased almost 10-fold in the soluble fraction of the P32T cell line. In the control reprobing experiment the amount of GAPDH was the same in all three cell lines (not shown). The position of the immunoreactive band was shifted up, closer to the 30 kDa marker in the lane with the 6 His-tagged pure ITPA-P32T (predicted molecular mass 23.6 kDa [47]). We also analyzed the extracts of 293 cell lines transfected with expressing ITPA-EGFP fusion protein (51.4 kDa) and have found that the major band was detected at a position corresponding to 50 kDa.

system is ITPA. Consistent with this, the level of spontaneous and base-analog-induced DNA damage was elevated in cell line P32T with compromised ITPA activity. The levels and distribution of ITPA P32T as determined by immunostaining have been changed in the P32T cell line. The results suggest that patients with the 94C->A polymorphism in the *ITPA*

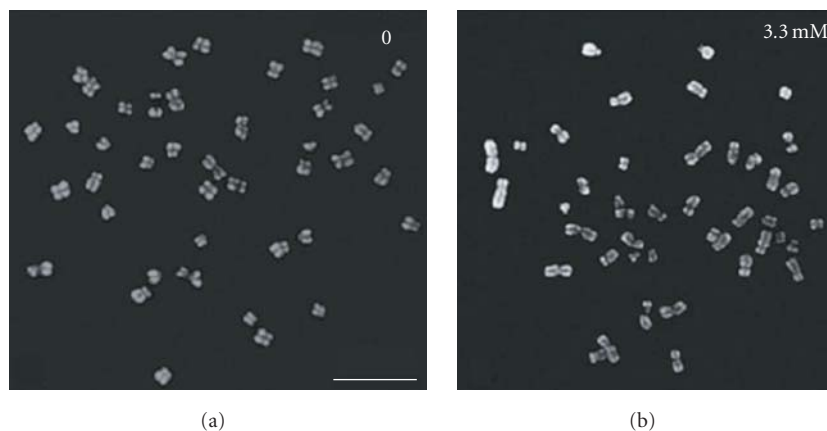


FIGURE 5: HAP does not induce massive chromosome fragmentation. The untreated HCT116 metaphase spreads (a) and HCT116 metaphase spreads obtained at the end of treatment by 3.3 mM HAP (b) were counterstained with DAPI (grey). Bar—10  $\mu$ m.

in addition to drug intolerance might possess increased predisposition to diseases resulting from DNA repair defects.

## 2. Materials and Methods

**2.1. Human Cell Cultures.** The normal, diploid, human lung fibroblast cell line, WI-38, (ATCC CCL-75) was kindly provided by Dr. Vera Gorbunova (University of Rochester, NY). The human fibroblast cell line (Coriell Institute Biorepository (GMO1617), called here P32T, is homozygous for a C>A transversion of nucleotide 94 (94C>A) in exon 2 of the ITPA gene. This leads to a proline to threonine substitution at codon 32 (P32T). These untransformed cell lines were cultivated as a monolayer in MEM (Invitrogen, USA) supplemented with 10% fetal calf serum (GIBCO) and 1 mM sodium pyruvate (Invitrogen, USA) at 37°C in a 5% CO<sub>2</sub> atmosphere. For the fibroblasts, cells at early passages (<25 passages) were used in all experiments to avoid complications of replicative senescence because WI-38 cells have a mean lifespan of approximately 45 to 60 population doublings.

The epithelial colorectal cancer cell line HCT116 (ATCC, CCL247, kindly provided by Dr. Robert E. Lewis, UNMC), was cultivated in DMEM (Invitrogen, USA) containing 10% fetal calf serum at 37°C in a 5% CO<sub>2</sub> atmosphere. The colorectal cancer HCT116 cells are defective in mismatch repair due to a nonsense mutation in the *MLH1* gene [64]. For the experiment addressing the specificity of our antibodies against ITPA, we transfected colorectal carcinoma 293 cells by pEGFP plasmid (obtained from Dr. A. Rizzino, UNMC) with ITPA cloned into BamHI-EcoRI sites in frame with EGFP.

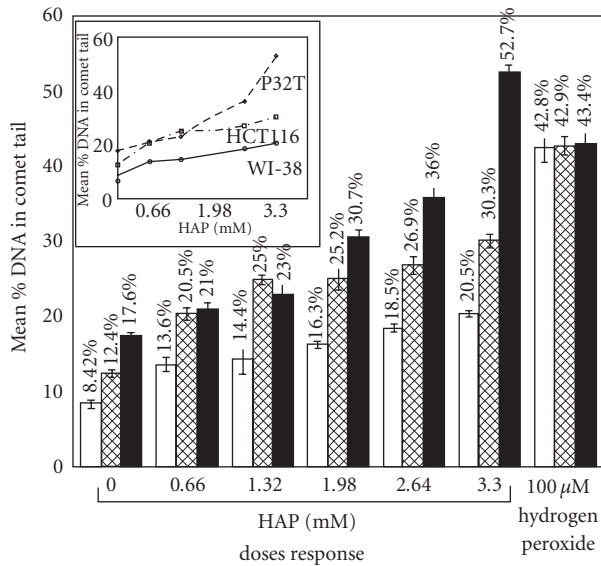
**2.2. Characterization of P32T Fibroblast Cell Line.** We verified the presence of the 94C->A change in the *ITPA* gene by sequencing of exon 2 amplified from genomic DNA (as exon 2–4 fragment) or from RNA. For genomic DNA isolation,  $1 \times 10^6$  cells were harvested for fibroblasts bearing wild-type (WI-38) or mutant (P32T) *ITPA*, and DNA was isolated

according to the Fermentas Inc. protocol: (<http://www.fermentas.com/en/support/application-protocols>). Briefly, cell pellets were lysed with SDS and Proteinase K. After incubation with NaCl, DNA was phenol:chloroform extracted and precipitated with ethanol. DNA pellets thus obtained were resuspended in nuclease-free water. For RNA extraction we have used the RNeasy kit (Qiagen, USA). The cDNA synthesis was performed using the qScript DNA synthesis kit (Quanta Biosciences #95047-025).

For amplification of the specific ITPA region encompassing the site of the 94C->A change, either genomic DNA or cDNA was diluted 100-fold and exons 2 through 4 were amplified using Exons 2, 3, 4 forward and reverse primers and conditions [65]. Sequencing of the genomic fragment was performed by the same primers and the sequence of the cDNA fragment was performed using ITPA-sN 5'TCATTGGTGGGGAAGAAGATC and ITPA-sC 5'AAGCTGCCAAACTGCCAAA. The sequencing confirmed that the P32T cell line possesses 94C->A transversions (Figure 2).

We also detected the hallmark accumulation of ITP in the P32T cell line by HPLC, confirming that ITPA activity is compromised in this cell line [65] (Figure 3).

**2.3. The Alkaline Comet Assay.** All the required chemicals were purchased from Trevigen, Inc. (USA). The comet assay was carried out under alkaline conditions, as described in the attached Trevigen instructions. Cells (WI-38, HCT116 and P32T) with or without H<sub>2</sub>O<sub>2</sub> or HAP treatment were suspended in 1% low melting point agarose in 1xPBS, pH 7.4, at 37°C and immediately pipetted onto a CometSlide. The agarose was allowed to set at 4°C for 10–30 min and the slide was immersed in a lysis solution at 4°C for 50 min to remove cellular proteins. Slides were then placed at 0.3 M NaOH and 1 mM EDTA for 45 min at room temperature before electrophoresis at 300 mA for 60 min at 4°C. The slides were then washed two times for 10 min each with water and then dehydrated in 70% ethanol for 5 min before staining with 1xSYBR Green I staining solution. To prevent background DNA damage, handling samples and all the steps



WI-38  
 HCT116  
 P32T

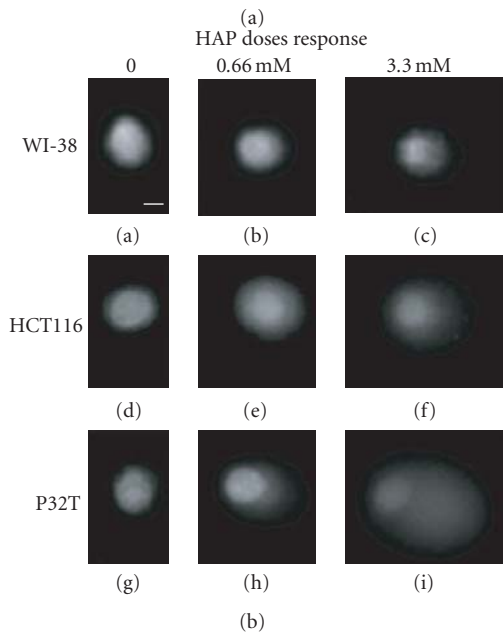
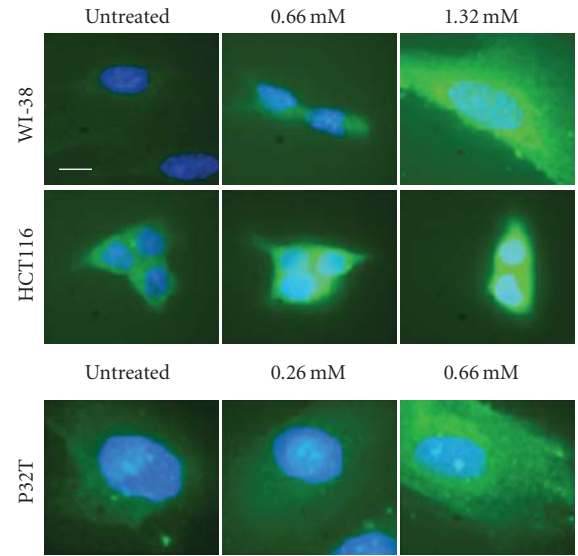
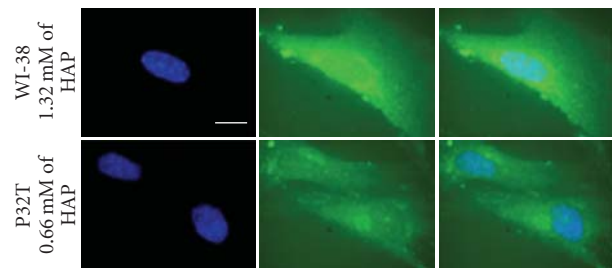


FIGURE 6: HAP induces DNA breaks in human cells. The effect of HAP and 100  $\mu$ M hydrogen peroxide on the frequency of single-stranded breaks recorded at the end of treatment in WI-38, HCT116 and P32T cell cultures by single-cell electrophoresis at pH > 13. (a) Analysis of the concentration-dependent effects of HAP and hydrogen peroxide on the frequency of DNA strand breaks in WI-38, HCT116 and P32T cells. The damaging DNA-agent dose responses are plotted on the x-axis. The mean percent DNA in the comet tail is plotted on the y-axis as a ratio of the amount of DNA in the comet tail/the amount of DNA in the whole comet. The insert in the upper part of the plot is a linear plot of this correlation for each culture. Results are shown as means  $\pm$  standard error of results of six different experiments. The level of statistical significance was set at  $P < .05$ . (b) Micrographs of WI-38 (a, b, c), HCT116 (d, e, f), and P32T (g, h, i) cells treated with different doses of HAP: 0 (a, d, g), 0.66 mM (b, e, h) and 3.3 mM (c, f, i) for 24 hr. Bar—10  $\mu$ m.



(a)



(b)

FIGURE 7: Intracellular localization and induction of ITPA. (a) The effect of HAP on ITPA levels and distribution in the WI-38, HCT116 and P32T cells. Immunofluorescence of ITPA in the WI-38, upper row, HCT116, middle row and P32T, lower row. Immunostaining and counterstaining were performed with antirabbit monoclonal antibody (green) and DAPI (blue), respectively. Bar—10  $\mu$ m Representative images are shown. (b) Details of immunofluorescence pattern of ITPA in the HAP-treated WI-38 (upper row, 1.32 mM HAP) and P32T (lower row, 0.66 mM HAP) cells. Left column—DAPI only, middle column—detection of ITPA antibodies, and right column—merged picture.

included in the preparation of the slides for the comet assay were conducted under yellow light or in the dark.

The slides were examined using an epifluorescence microscope “Nikon Eclipse 80i.” A total of 100 comets per slide were scored. Comets were randomly captured at a constant depth of the gel, avoiding the edges of the gel, occasional dead cells, and superimposed comets. The percent (%) of DNA in the comet tail was used in this study as the measure of DNA damage. Consistent with the Trevigen Inc. application guide, the average content of DNA in the comet tail of untreated normal cells is less than ten percent. The amount of DNA in the comet tail was estimated by computerized image analysis of selected comets using CometScore software. Six independent experiments were performed. Then, the average and standard error was

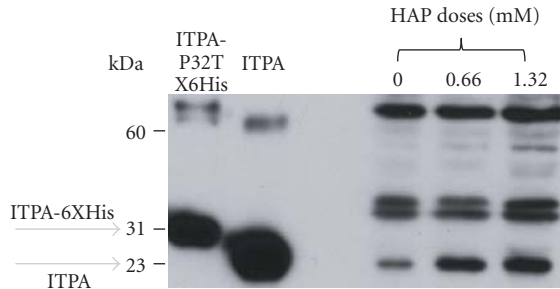


FIGURE 8: HAP treatment leads to the increase of ITPA levels in HCT116 cell extracts. Western blots were performed as described in Section 2. Two controls are in the left part: first lane—His-tagged pure ITPA (30 kDa), second lane:—pure ITPA (23 kDa). Third, fourth, and fifth lane shows the levels of ITPA (23 kDa) in extract of untreated cells, and cells treated by 0.66 mM HAP and 1.32 mM HAP. To estimate the induction of ITPA, we measured the ratio of the intensity of the band corresponding to monomeric ITPA to nonspecific bands. Estimated by this method, the induction relative to the control was 2.2 times at 0.66 mM and 2.6 times at 1.32 mM.

determined. The statistical significance of differences was estimated by Student's *t*-criterion.

**2.4. Chromosome Analysis.** For metaphase chromosome spreads, WI-38, HCT116, and P32T cells (treated for 23 h with DMSO or HAP in DMSO) were arrested in metaphase by a 1 h treatment with 0.5  $\mu\text{g}/\text{ml}$  colcemide (Gibco URL, USA), treated hypotonically with 0.075 M KCl, fixed three times in a 3:1 methanol-acetic acid mixture, spread on glass slides, and air dried. Twenty spreads for each culture were analyzed by CytoVision software (Genetix Corp., CA); only the total number and size of the chromosomes were determined.

**2.5. Western Blot Analysis.** HCT116, WI-38, and P32T cells were cultivated until subconfluence ( $5 \times 10^5$  cells per plate). The cells were harvested and resuspended in the lysis buffer (1xPBS containing a protease inhibitor cocktail (Roche Biochemicals, IN, USA), pH = 7.4). Each pellet was mechanically sheared using a pestle. The lysate was cleared by centrifugation and protein content determined by Bradford reagent from BioRad. The lysate equivalent to 100  $\mu\text{g}$  of protein was boiled in Laemli's buffer (Invitrogen, USA). The protein samples were resolved on a 10%–20% Tris-Glycine gel (Invitrogen, USA) by SDS-PAGE and transferred to nitrocellulose membranes. Membranes were blocked overnight in commercially available blocking buffer (Thermo Scientific, USA). Membranes were then incubated in 1:500 dilutions of primary antibody against ITPA (the in-house polyclonal antibodies against ITPA are described elsewhere [55]) and GAPDH (Cell Signaling #2118) for one hour at room temperature. The membranes were then washed with commercially available washing buffer (Thermoscientific, USA) five times for 10 min each. This was followed by incubation with secondary antibody (1:1500 dilution) (Cell signaling #7074) for 40 min at room temperature. This was followed by washing (5 times for 10 min each) and detection

by the ECL system (ThermoScientific, USA) according to the manufacturer's instructions. The results are presented in Figure 4. A major visible band, corresponding to ITPA (compare with lane with pure ITPA), is prominent in WI-38 fibroblasts, and cancer HCT116 cell extracts (gray arrow) but is less pronounced in P32T cells, as we described before [55]. The intensity of the non-specific 30 kDa band is similar in all three cell lines. The position of the immunoreactive band was shifted up, closer to the 30 kDa marker, in lane with 6 His-tagged pure ITPA-P32T (predicted molecular mass 23.6 kDa [47]). We also analyzed the extract of 293 cell lines transfected with a plasmid expressing the gene for ITPA-EGFP fusion protein (51.4 kDa) and have found that a major band was detected at a position corresponding to 50 kDa. The data unequivocally prove that antibodies react primarily with ITPA.

For the analysis of ITPA induction by HAP by Western blots we cultivated HCT116 cells with or without HAP until subconfluence ( $5 \times 10^5$  cells per plate). The cells were harvested and resuspended in the lysis buffer (50 mM Tris, pH = 8.0, 1 mM PMSF, 10% (v/v) glycerol, 0.5% Triton X-100) and disrupted and processed as before with the following modifications to improve the quality and resolution. The lysate equivalent to 30  $\mu\text{g}$  of protein was boiled in Laemli's buffer containing 100 mM DTT and loaded on a 10%–20% Tris-Glycine gel by SDS-PAGE. After trial run and Coomassie staining the amount of extracts was further adjusted to produce equal amount of loaded protein in the control and treatment and run in the new gel. After transfer, nitrocellulose membranes were blocked overnight in 5% dry milk/1x PBST. Membranes were incubated in 1:2000 dilutions of primary antibody against ITPA described above for one hour at room temperature. The membranes were washed with 1x PBST three times for 15 min each, and, incubated with secondary HRP-linked antibody (1:100000 dilution) (Cell Signaling #7074) for 1 hour at room temperature. Membrane was washed three times for 15 min each and signals were detected by SuperSignal West Femto Maximum Sensitivity Substrate (ThermoScientific, USA) according to the manufacturer's instructions.

**2.6. Immunocytochemistry.** Cells (WI-38, HCT116 and P32T) with or without HAP treatment were fixed with methanol acetic acid mixture (3:1). All procedures were performed at room temperature. To prevent non-specific binding in the consequent antibody detection, samples were blocked in 1xPBS containing 5% BSA and 0.05% Tritone X-100. We have used the primary antibodies against ITPA described in the previous section and a goat-antirabbit antibody Alexa Fluor 488 nm conjugated (Thermoscientific, USA). Both antibodies were diluted 1:1000 in 1xPBS containing 5% BSA and 0.05% Triton X-100. Slides were washed three times in 1xPBST buffer between incubations with primary and secondary antibodies and after incubations. After washing, the cells were counterstained with DAPI, mounted in antifade medium and analyzed by fluorescent microscopy. No fluorescence was detected when primary antibodies were omitted from the protocol, and very low signal was detected when preimmune rabbit serum was used

in place of primary antibody, suggesting that fluorescence signals were absolutely dependent on antiITPA antibodies. Three independent repeats of this experiment have been done.

**2.7. Microscopy and Image Analysis.** After the comet assay or immunocytochemistry procedures, cells were examined on a Nikon Eclipse 80i microscope. Images were recorded separately by a CCD device Photometrics CoolSnap cf and merged using Adobe Photoshop software.

### 3. Results

**3.1. HAP Does not Cause Chromosome Hyperfragmentation in Three Human Cell Lines.** It has been reported previously that treatment of human epidermoid carcinoma cells with 1 mM HAP lead to massive chromosome fragmentation (Figure 2 in [66]). We examined HAP effects on chromosomes in WI-38, HCT116, and P32T lines. We studied chromosome spreads of untreated WI-38, HCT116, and P32T cells versus the same cells treated with 3.3 mM HAP. There were no more chromosomal abnormalities after treatment with 3.3 mM HAP than in the untreated HCT116 chromosome spreads (Figure 5). We did not observe any striking differences in the rates of chromosomal abnormalities in WI-38 and P32T chromosome spreads as well (data not shown). It is possible that the cell line used in earlier studies was hypersensitive to HAP.

**3.2. The Increase in HAP Dose Proportionally Elevated the Rate of DNA Breaks in WI-38, HCT116, and P32T Cells.** We investigated the effect of 24 h treatment by different HAP concentrations on the frequency of single-stranded breaks in WI-38, HCT116 and P32T cell cultures by single cell electrophoresis at pH > 13. Under our experimental conditions and with doses of mutagens used, no substantial cell killing occurred. The percent of DNA in the comet tail (thereafter named tail DNA) of the total DNA was used in the study as the estimate of the amount of single-stranded breaks. The mean tail DNA was statistically significantly different in the three lines: 8.42% in untreated normal WI-38 fibroblasts, 12.4% in colorectal cancer cell culture HCT116, and the highest 17.6%, in P32T fibroblast cell culture, a large change for this type of assay two-fold increase over normal fibroblasts (Figure 6(a)). The increased level of tail DNA in untreated cells likely indicates persistent unrepaired endogenous damage in HCT116 and P32T cells.

WI-38 normal fibroblasts were quite resistant to HAP: the highest concentration of 3.3 mM HAP increased tail DNA two-fold to 20.5%, much less than the positive control hydrogen peroxide (42.8% tail DNA) (Figure 6(a)). The induction curve had quite a gentle slope with a small hump/plateau of resistance when the dose increased from 0.66 to 1.32 (seen clearly in the insert in Figure 6(a)). The comet tails in WI-38 cells after treatment with 0.66 mM–3.3 mM of HAP were the shortest among the variables studied (Figure 6(b)). The response of the HCT116 cells to the hydrogen peroxide treatment was similar to that of the WI-38 cells (tail DNA

was 42.9%). HAP produced more DNA damage than in WI-38 cells. An initial eight percent increase at 0.66 mM was followed by the plateau of around 25% tail DNA at doses 1.32 mM–2.64 mM (Figure 6(a), insert). This apparent resistance to the induction of breaks was finally concurred by 3.3 mM of HAP and tail DNA reached 30.3% (Figure 6(a)). P32T cells were most sensitive to HAP, while the sensitivity to hydrogen peroxide was similar to other cell lines (43.4%). The lowest dose of HAP induced as much tail DNA in P32T as the highest dose in normal fibroblasts (21%). The 1.98 mM HAP produced 30.7% tail DNA in P32T, exceeding the maximum of tail DNA induced by HAP in other cell cultures studied at the same dose. After 3.3 mM HAP treatment of these cells, the level of tail DNA reached 52.7% and the tail was much longer than in WI-38 and HCT116 under the same conditions (Figures 6(a) and 6(b)). In summary, HAP induced DNA breaks in human cells. HAP was moderately active in normal WI-38 fibroblasts, HCT116 cancer cells were more sensitive than WI-38 cells and P32T ITPA-deficient fibroblasts were the most susceptible.

**3.3. ITPA Cellular Levels and Distribution Change Differently after HAP Treatment of WI-38, HCT116 and P32T Lines.** The presence of the plateau in the dose-response curves for HAP indicated that wild-type cells might possess an inducible protection system, which is activated at 0.66–1.32 mM HAP. One possible candidate is ITPA and we studied ITPA distribution after HAP treatment in WI-38, HCT116 and P32T cells by whole-cell immunostaining with specific antibodies against ITPA (specificity of antibodies has been verified by Western Blot, because of the shift of detected GFP-tagged ITPA to higher position, Figure 4).

ITPA was not readily detected in untreated WI-38 fibroblasts, and cells were stained very weakly (Figure 7(a)). The detected ITPA amount increased after the treatment with 0.66 mM and 1.32 mM HAP. The untreated HCT116 cancer cells were stained with antibody against ITPA somewhat more efficiently than WI-38 cells (Figure 7(a)). The ITPA amount increased after 0.66 mM and 1.32 mM HAP treatment, the latter dose producing strikingly bright cytoplasm (Figure 7(a)). Maybe this phenomenon simply relates to the smaller size of cytoplasm relative to nucleus. Some ITPA was detected in untreated ITPA-deficient P32T fibroblasts, similar to HCT116 cells (Figure 7(a), lower row). After treatment with 0.66 mM HAP, the ITPA amount increased, so induction occurred at lower dose.

Fluorescence in all cases was mostly in cytoplasm and was generally uneven. The brighter fluorescent regions in WI-38 cells were of three types. One type resembled a net structure adjacent to nuclei. Another type was small granules localized in nuclei (Figure 7(b), upper row). The third was one big bright granule, typically at the border of nuclei and cytoplasm or localized in the nuclei close to its edge. In HCT116, the heterogeneity was less pronounced and the net structure was not observed (compare to Figure 7(a)). It is possible that it is undetectable due to a small cytoplasmic part of the cell and very bright fluorescence. In P32T fibroblasts the distribution was different. Net-like structure has not been observed. Some brighter regions adjacent to

nuclei were present but they were unstructured (Figure 7(b), lower row).

We also have used Western blot analysis in HCT116 cells to confirm and quantify induction of ITPA by HAP (Figure 8). Clearly, HAP treatment leads to up to 2.6-fold elevation of the amount of ITPA.

## 4. Discussion

**4.1. Response of Human Cells to Base-analog HAP Treatment.** It is known that HAP is mutagenic, clastogenic and carcinogenic in hamster cells [67, 68]. Using Comet assay we have shown that HAP produced DNA breaks in the human cell lines tested. The most logical explanation of this and other currently available data is that the base-analog was incorporated into DNA and either human Endo V homolog (encoded by the LOC284131, see description of closely related mouse homolog in [51]) or other an unknown glycosylase/endonuclease recognized incorporated HAP and incised DNA strands (Figure 1).

Analysis of the dose-response curves revealed a hump/plateau region indicative of the induction of a cellular protective response/repair system. The HAP-treated WI-38 fibroblasts with wild-type ITPA had the lowest rates of DNA breaks, and untreated WI-38 cells had the lowest levels of spontaneous breaks among cell lines studied. The hump in the dose-response curve indicated that there is an induction of the repair activity at 0.66–1.32 mM HAP.

We found moderately elevated levels of spontaneous breaks in HCT116. It remains to be determined whether this effect is related to the defect of a mismatch-repair system. The levels of DNA breaks by HAP in HCT116 cells were higher than in WI-38 fibroblasts and the analysis of the dose-response curve indicated that the repair system most likely was activated completely only by 1.32 mM HAP.

The P32T ITPA-deficient fibroblasts were the most sensitive to the induction of DNA breaks by HAP treatment. We propose that deoxyribonucleoside triphosphates of HAP, usually removed by ITPA in wild-type cell lines, remain in the detectable amount in the DNA precursor pools of ITPA P32T fibroblasts. They are incorporated in DNA causing the excess of DNA breaks. This observation correlates well with the accumulation of ITP only in this cell line (Figure 3). It is known that ITPA P32T produced ectopically protects bacteria and yeast from HAP to the same extent as wild-type ITPA, but the level of ITPA P32T in human cell extracts is much lower than in normal fibroblasts [62]. Apparently, the human repair system does not work properly in P32T cells alleviating DNA damage by downstream repair enzymes. The spontaneous level of DNA breaks in this cell line was the highest, raising the possibility that there is persistent endogenous DNA damage in these cells. It is tempting to speculate that the damage is caused by endogenous dITP/dXTP.

The next set of experiments explored one possible component of the HAP-induced repair system.

**4.2. ITPA Levels and Distribution in HAP Treated Human Cells.** We have analyzed in detail the levels and intracellular

distribution of ITPA. We confirmed that the enzyme is located mainly in cytoplasm [69]. We have found that ITPA levels increased significantly upon treatment with HAP in all the investigated cells, although it was significantly lower in the ITPA P32T fibroblasts than in WI-38 and HCT116 cells. P32T ITPA-deficient fibroblasts responded by the production of ITPA to much lower doses of HAP, because the destruction of dHAPTP is less efficient in these cells and effective concentrations of substrates for the ITPA are higher.

The antibody staining revealed a net-like structure adjacent to nuclei and other, granular structures in the WI-38 normal fibroblasts, when ITPA is induced by HAP. This is consistent with previous analyses of the localization of ITPA to purine biosynthetic complexes. It has been shown previously that human enzymes involved in *de novo* purine biosynthesis (for example, hTrifGART protein, and formylglycinamide ribonucleotide synthase, PRPP amidotransferase, hPAICS, adenylosuccinate lyase and hATIC), colocalize and cluster in human cell cytoplasm [70]. This is consistent with the hypothesis that these clusters represent a “purinosome”—an organoid essential for purine biosynthesis. Usually these clusters localized throughout the whole cytoplasm volume but there were one or two big clusters on the border of nuclei and cytoplasm. One possible interpretation of our results is that ITPA, the enzyme of purine “salvage” pathway, constitutes a part of this purinosome. The candidate structure is a big fluorescent granule. Further colocalization experiments are needed to test our hypothesis.

Hypothetically, the net-like structure described here may represent a factory checking quality of dNTP pools. It is possible that this abnormal ITPA distribution is one of the reasons for a lack of ITPA function in P32T individuals, despite almost normal activity of the enzyme [62].

Taken together, our results suggest that human cells possess a repair system for purine base-analogs similar, in part, to bacteria. The genetically active derivative of HAP is deoxyribonucleoside triphosphate. Cells are protected from dHAPTP by hydrolysis by ITPA. Some dHAPTP is presumably incorporated into DNA, and subsequent repair of HAP leads to DNA strand breaks.

## Acknowledgments

The authors are grateful to Dr. S. Kozmin, Dr. I. M. Spivak, and Dr. N. E. Erukashvili for critical reading of the manuscript and helpful comments. They thank Coriell Repository for the P32T cell line. The work was supported by an NE DHHS LB506 Grant, by a UNMC Eppley Cancer Center 010107 Pilot Grant, and in part, by NCI Grant R01 CA129925 to Youri I. Pavlov. Miriam R. Menezes was supported by a UNMC graduate student fellowship. I. S.-R. Waisertreiger and M. R. Menezes contributed equally to this work.

## References

- [1] E. C. Friedberg, *DNA Repair and Mutagenesis*, ASM Press, Washington, DC, USA, 2006.

- [2] B. N. Ames and L. S. Gold, "Endogenous mutagens and the causes of aging and cancer," *Mutation Research*, vol. 250, no. 1-2, pp. 3-16, 1991.
- [3] H. Kamiya, "Mutagenic potentials of damaged nucleic acids produced by reactive oxygen/nitrogen species: approaches using synthetic oligonucleotides and nucleotides," *Nucleic Acids Research*, vol. 31, no. 2, pp. 517-531, 2003.
- [4] P. C. Dedon and S. R. Tannenbaum, "Reactive nitrogen species in the chemical biology of inflammation," *Archives of Biochemistry and Biophysics*, vol. 423, no. 1, pp. 12-22, 2004.
- [5] M. Hori, C. Ishiguro, H. Harashima, and H. Kamiya, "In vivo mutagenicities of damaged nucleotides produced by nitric oxide and ionizing radiation," *Biological and Pharmaceutical Bulletin*, vol. 28, no. 3, pp. 520-522, 2005.
- [6] S. Haghdoost, L. Sjölander, S. Czene, and M. Harms-Ringdahl, "The nucleotide pool is a significant target for oxidative stress," *Free Radical Biology and Medicine*, vol. 41, no. 4, pp. 620-626, 2006.
- [7] H. Ohshima, T. Sawa, and T. Akaike, "8-Nitroguanine, a product of nitrative DNA damage caused by reactive nitrogen species: formation, occurrence, and implications in inflammation and carcinogenesis," *Antioxidants and Redox Signaling*, vol. 8, no. 5-6, pp. 1033-1045, 2006.
- [8] C. K. Mathews, "DNA precursor metabolism and genomic stability," *FASEB Journal*, vol. 20, no. 9, pp. 1300-1314, 2006.
- [9] R. G. Fowler and R. M. Schaaper, "The role of the *mutT* gene of *Escherichia coli* cell in maintaining replication fidelity," *FEMS Microbiology Reviews*, vol. 21, no. 1, pp. 43-54, 1997.
- [10] E. A. Kouzminova and A. Kuzminov, "Chromosomal fragmentation in dUTPase-deficient mutants of *Escherichia coli* and its recombinational repair," *Molecular Microbiology*, vol. 51, no. 5, pp. 1279-1295, 2004.
- [11] E. A. Kouzminova and A. Kuzminov, "Fragmentation of replicating chromosomes triggered by uracil in DNA," *Journal of Molecular Biology*, vol. 355, no. 1, pp. 20-33, 2006.
- [12] E. A. Kouzminova and A. Kuzminov, "Patterns of chromosomal fragmentation due to uracil-DNA incorporation reveal a novel mechanism of replication-dependent double-stranded breaks," *Molecular Microbiology*, vol. 68, no. 1, pp. 202-215, 2008.
- [13] A. L. Jackson and L. A. Loeb, "The mutation rate and cancer," *Genetics*, vol. 148, no. 4, pp. 1483-1490, 1998.
- [14] P. Rai, T. T. Onder, J. J. Young et al., "Continuous elimination of oxidized nucleotides is necessary to prevent rapid onset of cellular senescence," *Proceedings of the National Academy of Sciences of the United States of America*, vol. 106, no. 1, pp. 169-174, 2009.
- [15] T. Nunoshiba, T. Watanabe, Y. Nakabeppu, and K. Yamamoto, "Mutagenic target for hydroxyl radicals generated in *Escherichia coli* mutant deficient in Mn- and Fe-superoxide dismutases and Fur, a repressor for iron-uptake systems," *DNA Repair*, vol. 1, no. 5, pp. 411-418, 2002.
- [16] K. C. Cheng, D. S. Cahill, H. Kasai, S. Nishimura, and L. A. Loeb, "8-Hydroxyguanine, an abundant form of oxidative DNA damage, causes G → T and A → C substitutions," *The Journal of Biological Chemistry*, vol. 267, no. 1, pp. 166-172, 1992.
- [17] H. Maki and M. Sekiguchi, "MutT protein specifically hydrolyses a potent mutagenic substrate for DNA synthesis," *Nature*, vol. 355, no. 6357, pp. 273-275, 1992.
- [18] Y. I. Pavlov, D. T. Minnick, S. Izuta, and T. A. Kunkel, "DNA replication fidelity with 8-oxodeoxyguanosine triphosphate," *Biochemistry*, vol. 33, no. 15, pp. 4695-4701, 1994.
- [19] M. L. Michaels and J. H. Miller, "The GO system protects organisms from the mutagenic effect of the spontaneous lesion 8-hydroxyguanine (7,8-dihydro-8-oxoguanine)," *Journal of Bacteriology*, vol. 174, no. 20, pp. 6321-6325, 1992.
- [20] E. C. Cox, "Mutator gene studies in *Escherichia coli*: the *mutT* gene," *Genetics*, vol. 73, no. 1973, pp. 67-80, 1973.
- [21] E. Rotman and A. Kuzminov, "The *mutT* defect does not elevate chromosomal fragmentation in *Escherichia coli* because of the surprisingly low levels of MutM/MutY-recognized DNA modifications," *Journal of Bacteriology*, vol. 189, no. 19, pp. 6976-6988, 2007.
- [22] B. Pang, X. Zhou, H. Yu et al., "Lipid peroxidation dominates the chemistry of DNA adduct formation in a mouse model of inflammation," *Carcinogenesis*, vol. 28, no. 8, pp. 1807-1813, 2007.
- [23] T. Simandan, J. Sun, and T. A. Dix, "Oxidation of DNA bases, deoxyribonucleosides and homopolymers by peroxy radicals," *Biochemical Journal*, vol. 335, no. 2, pp. 233-240, 1998.
- [24] B. Clement and T. Kunze, "Hepatic microsomal N-hydroxylation of adenine to 6-N-hydroxylaminopurine," *Biochemical Pharmacology*, vol. 39, no. 5, pp. 925-933, 1990.
- [25] I. Lieberman, "Enzymatic synthesis of adenosine-5'-phosphate from inosine-5'-phosphate," *The Journal of Biological Chemistry*, vol. 223, no. 1, pp. 327-339, 1956.
- [26] S. G. Kozmin, R. M. Schaaper, P. V. Shcherbakova et al., "Multiple antimutagenesis mechanisms affect mutagenic activity and specificity of the base analog 6-N-hydroxylaminopurine in bacteria and yeast," *Mutation Research*, vol. 402, no. 1-2, pp. 41-50, 1998.
- [27] N. E. Burgis, J. J. Brucker, and R. P. Cunningham, "Repair system for noncanonical purines in *Escherichia coli*," *Journal of Bacteriology*, vol. 185, no. 10, pp. 3101-3110, 2003.
- [28] M. T. Abdul-Masih and M. J. Bessman, "Biochemical studies on the mutagen, 6-N-hydroxylaminopurine. Synthesis of the deoxynucleoside triphosphate and its incorporation into DNA in vitro," *The Journal of Biological Chemistry*, vol. 261, no. 5, pp. 2020-2026, 1986.
- [29] Y. I. Pavlov, V. V. Suslov, P. V. Shcherbakova et al., "Base analog N6-hydroxylaminopurine mutagenesis in *Escherichia coli*: genetic control and molecular specificity," *Mutation Research*, vol. 357, no. 1-2, pp. 1-15, 1996.
- [30] N. E. Burgis and R. P. Cunningham, "Substrate specificity of RdgB protein, a deoxyribonucleoside triphosphate pyrophosphohydrolase," *The Journal of Biological Chemistry*, vol. 282, no. 6, pp. 3531-3538, 2007.
- [31] S. Quirk, S. K. Bhathnagar, and M. J. Bessman, "Primary structure of the deoxyguanosine triphosphate triphosphohydrolase-encoding gene (*dgt*) of *Escherichia coli*," *Gene*, vol. 89, no. 1, pp. 13-18, 1990.
- [32] D. Gawel, M. D. Hamilton, and R. M. Schaaper, "A novel mutator of *Escherichia coli* carrying a defect in the *dgt* gene, encoding a dGTP triphosphohydrolase," *Journal of Bacteriology*, vol. 190, no. 21, pp. 6931-6939, 2008.
- [33] J. Zheng, V. K. Singh, and Z. Jia, "Identification of an ITPase/XTPase in *Escherichia coli* by structural and biochemical analysis," *Structure*, vol. 13, no. 10, pp. 1511-1520, 2005.
- [34] B. Budke and A. Kuzminov, "Production of clastogenic DNA precursors by the nucleotide metabolism in *Escherichia coli*," *Molecular Microbiology*, vol. 75, no. 1, pp. 230-245, 2010.
- [35] T. Iyama, N. Abolhassani, D. Tsuchimoto, M. Nonaka, and Y. Nakabeppu, "NUDT16 is a (deoxy)inosine diphosphatase, and its deficiency induces accumulation of single-strand breaks in

- nuclear DNA and growth arrest," *Nucleic Acids Research*, vol. 2010, p. 12, 2010.
- [36] T. Kohno, H. Kunitoh, K. Toyama et al., "Association of the OGG1-Ser326Cys polymorphism with lung adenocarcinoma risk," *Cancer Science*, vol. 97, no. 8, pp. 724–728, 2006.
- [37] A. M. Marinaki, J. A. Duley, M. Arenas et al., "Mutation in the ITPA gene predicts intolerance to azathioprine," *Nucleosides, Nucleotides and Nucleic Acids*, vol. 23, no. 8-9, pp. 1393–1397, 2004.
- [38] J. Fellay, A. J. Thompson, D. Ge et al., "ITPA gene variants protect against anaemia in patients treated for chronic hepatitis C," *Nature*, vol. 464, no. 7287, pp. 405–408, 2010.
- [39] J. S. Bradshaw and A. Kuzminov, "RdgB acts to avoid chromosome fragmentation in *Escherichia coli*," *Molecular Microbiology*, vol. 48, no. 6, pp. 1711–1725, 2003.
- [40] S. Lin, A. G. McLennan, K. Ying et al., "Cloning, expression, and characterization of a human inosine triphosphate pyrophosphatase encoded by the itpa gene," *The Journal of Biological Chemistry*, vol. 276, no. 22, pp. 18695–18701, 2001.
- [41] S. Takayama, M. Fujii, A. Kurosawa, N. Adachi, and D. Ayusawa, "Overexpression of HAM1 gene detoxifies 5-bromodeoxyuridine in the yeast *Saccharomyces cerevisiae*," *Current Genetics*, vol. 52, no. 5-6, pp. 203–211, 2007.
- [42] K. Y. Hwang, J. H. Chung, S.-H. Kim, Y. Sun Han, and Y. Cho, "Structure-based identification of a novel NTPase from *Methanococcus jannaschii*," *Nature Structural Biology*, vol. 6, no. 7, pp. 691–696, 1999.
- [43] S. G. Kozmin, Y. I. Pavlov, R. L. Dunn, and R. M. Schaaper, "Hypersensitivity of *Escherichia coli D(uvrB-bio)* mutants to 6-hydroxylaminopurine and other base analogs is due to a defect in molybdenum cofactor biosynthesis," *Journal of Bacteriology*, vol. 182, no. 12, pp. 3361–3367, 2000.
- [44] S. G. Kozmin and R. M. Schaaper, "Molybdenum cofactor-dependent resistance to N-hydroxylated base analogs in *Escherichia coli* is independent of MobA function," *Mutation Research*, vol. 619, no. 1-2, pp. 9–15, 2007.
- [45] S. G. Kozmin, P. Leroy, Y. I. Pavlov, and R. M. Schaaper, "YcbX and yjiM, two novel determinants for resistance of *Escherichia coli* to N-hydroxylated base analogues," *Molecular Microbiology*, vol. 68, no. 1, pp. 51–65, 2008.
- [46] L. Lukas and A. Kuzminov, "Chromosomal fragmentation is the major consequence of the *rdgB* defect in *Escherichia coli*," *Genetics*, vol. 172, no. 2, pp. 1359–1362, 2006.
- [47] J. Porta, C. Kolar, S. G. Kozmin, Y. I. Pavlov, and G. E. O. Borgstahl, "Structure of the orthorhombic form of human inosine triphosphate pyrophosphatase," *Acta Crystallographica Section F*, vol. 62, no. 11, pp. 1076–1081, 2006.
- [48] I. I. Pavlov, "Mutants of *Saccharomyces cerevisiae* supersensitive to the mutagenic effect of 6-N-hydroxylaminopurine," *Genetika*, vol. 22, no. 9, pp. 2235–2243, 1986.
- [49] V. N. Noskov, K. Staak, P. V. Shcherbakova et al., "HAM1, the gene controlling 6-N-hydroxylaminopurine sensitivity and mutagenesis in the yeast *Saccharomyces cerevisiae*," *Yeast*, vol. 12, no. 1, pp. 17–29, 1996.
- [50] B. Budke and A. Kuzminov, "Hypoxanthine incorporation is nonmutagenic in *Escherichia coli*," *Journal of Bacteriology*, vol. 188, no. 18, pp. 6553–6560, 2006.
- [51] A. Moe, J. Ringvoll, L. M. Nordstrand et al., "Incision at hypoxanthine residues in DNA by a mammalian homologue of the *Escherichia coli* antimutator enzyme endonuclease V," *Nucleic Acids Research*, vol. 31, no. 14, pp. 3893–3900, 2003.
- [52] M. Y. Galperin, O. V. Moroz, K. S. Wilson, and A. G. Murzin, "House cleaning, a part of good housekeeping," *Molecular Microbiology*, vol. 59, no. 1, pp. 5–19, 2006.
- [53] M. Behmanesh, K. Sakumi, N. Abolhassani et al., "ITPase-deficient mice show growth retardation and die before weaning," *Cell Death and Differentiation*, vol. 16, no. 10, pp. 1315–1322, 2009.
- [54] J. A. Duley, A. M. Marinaki, M. Arenas, and T. H. J. Florin, "Do ITPA and TPMT genotypes predict the development of side effects to AZA?" *Gut*, vol. 55, no. 7, pp. 1048–1049, 2006.
- [55] J. M. van Dieren, A. J. van Vuuren, J. G. Kusters, E. E. S. Nieuwenhuis, E. J. Kuipers, and C. J. Van Der Woude, "ITPA genotyping is not predictive for the development of side effects in AZA treated inflammatory bowel disease patients," *Gut*, vol. 54, no. 11, p. 1664, 2005.
- [56] A. M. Marinaki, A. Ansari, J. A. Duley et al., "Adverse drug reactions to azathioprine therapy are associated with polymorphism in the gene encoding inosine triphosphate pyrophosphatase (ITPase)," *Pharmacogenetics*, vol. 14, no. 3, pp. 181–187, 2004.
- [57] T. Maeda, S. Sumi, A. Ueta et al., "Genetic basis of inosine triphosphate pyrophosphohydrolase deficiency in the Japanese population," *Molecular Genetics and Metabolism*, vol. 85, no. 4, pp. 271–279, 2005.
- [58] M. Shipkova, K. Lorenz, M. Oellerich, E. Wieland, and N. Von Ansen, "Measurement of erythrocyte inosine triphosphate pyrophosphohydrolase (ITPA) activity by HPLC and correlation of ITPA genotype-phenotype in a Caucasian population," *Clinical Chemistry*, vol. 52, no. 2, pp. 240–247, 2006.
- [59] N. von Ahsen, V. W. Armstrong, C. Behrens et al., "Association of inosine triphosphatase 94C>A and thiopurine S-methyltransferase deficiency with adverse events and study drop-outs under azathioprine therapy in a prospective Crohn disease study," *Clinical Chemistry*, vol. 51, no. 12, pp. 2282–2288, 2005.
- [60] G. Stocco, M. H. Cheok, K. R. Crews et al., "Genetic polymorphism of inosine triphosphate pyrophosphatase is a determinant of mercaptopurine metabolism and toxicity during treatment for acute lymphoblastic leukemia," *Clinical Pharmacology and Therapeutics*, vol. 85, no. 2, pp. 164–172, 2009.
- [61] N. Abolhassani, T. Iyama, D. Tsuchimoto et al., "NUDT16 and ITPA play a dual protective role in maintaining chromosome stability and cell growth by eliminating dIDP/IDP and dITP/ITP from nucleotide pools in mammals," *Nucleic Acids Research*, vol. 38, no. 9, pp. 2891–2903, 2010.
- [62] E. I. Stepchenkova, E. R. Tarakhovskaya, K. Spitler et al., "Functional study of the P32T ITPA variant associated with drug sensitivity in humans," *Journal of Molecular Biology*, vol. 392, no. 3, pp. 602–613, 2009.
- [63] G. Herting, K. Barber, M. R. Zappala, R. P. Cunningham, and N. E. Burgis, "Quantitative in vitro and in vivo characterization of the human P32T mutant ITPase," *Biochimica et Biophysica Acta*, vol. 1802, pp. 269–274, 2009.
- [64] S. Jacob, M. Aguado, D. Fallik, and F. Praz, "The role of the DNA mismatch repair system in the cytotoxicity of the topoisomerase inhibitors camptothecin and etoposide to human colorectal cancer cells," *Cancer Research*, vol. 61, no. 17, pp. 6555–6562, 2001.
- [65] S. Sumi, A. M. Marinaki, M. Arenas et al., "Genetic basis of inosine triphosphate pyrophosphohydrolase deficiency," *Human Genetics*, vol. 111, no. 4-5, pp. 360–367, 2002.
- [66] J. J. Biesele, "Some morphological effects of alkylating agents," *Experimental Cell Research*, vol. 9, supplement, pp. 525–534, 1963.
- [67] J. C. Barrett, "Induction of gene mutation in and cell transformation of mammalian cells by modified purines:

- 2-aminopurine and 6-N-hydroxylaminopurine," *Proceedings of the National Academy of Sciences of the United States of America*, vol. 78, no. 9, pp. 5685–5689, 1981.
- [68] T. Tsutsui, H. Maizumi, and J. C. Barrett, "Induction by modified purines (2-aminopurine and 6-N-hydroxylaminopurine) of chromosome aberrations and aneuploidy in Syrian hamster embryo cells," *Mutation Research*, vol. 148, no. 1-2, pp. 107–112, 1985.
- [69] M. Behmanesh, K. Sakumi, D. Tsuchimoto et al., "Characterization of the structure and expression of mouse Itpa gene and its related sequences in the mouse genome," *DNA Research*, vol. 12, no. 1, pp. 39–51, 2005.
- [70] S. An, R. Kumar, E. D. Sheets, and S. J. Benkovic, "Reversible compartmentalization of de novo purine biosynthetic complexes in living cells," *Science*, vol. 320, no. 5872, pp. 103–106, 2008.

## Research Article

# SOD1 Is Essential for the Viability of DT40 Cells and Nuclear SOD1 Functions as a Guardian of Genomic DNA

Eri Inoue,<sup>1</sup> Keizo Tano,<sup>2</sup> Hanako Yoshii,<sup>2</sup> Jun Nakamura,<sup>3</sup> Shusuke Tada,<sup>1</sup>  
Masami Watanabe,<sup>2</sup> Masayuki Seki,<sup>1</sup> and Takemi Enomoto<sup>1,4</sup>

<sup>1</sup> Molecular Cell Biology Laboratory, Graduate School of Pharmaceutical Sciences,  
Tohoku University, Aoba 6-3, Aramaki, Aoba-ku, Sendai 980-8578, Japan

<sup>2</sup> Research Reactor Institute, Kyoto University, Kumatori 590-0494, Japan

<sup>3</sup> Department of Environmental Sciences and Engineering, University of North Carolina at Chapel Hill,  
Chapel Hill, NC 27599, USA

<sup>4</sup> Research Institute of Pharmaceutical Sciences, Faculty of Pharmacy, Musashino University,  
1-1-20 Shinmachi, Nishitokyo-shi, Tokyo 202-8585, Japan

Correspondence should be addressed to Masayuki Seki, seki@mail.pharm.tohoku.ac.jp and  
Takemi Enomoto, t.eno@musashino-u.ac.jp

Received 19 April 2010; Accepted 4 June 2010

Academic Editor: Shigenori Iwai

Copyright © 2010 Eri Inoue et al. This is an open access article distributed under the Creative Commons Attribution License, which permits unrestricted use, distribution, and reproduction in any medium, provided the original work is properly cited.

Reactive oxygen species (ROSs) are produced during normal cellular metabolism, particularly by respiration in mitochondria, and these ROSs are considered to cause oxidative damage to macromolecules, including DNA. In our previous paper, we found no indication that depletion of mitochondrial superoxide dismutase, SOD2, resulted in an increase in DNA damage. In this paper, we examined SOD1, which is distributed in the cytoplasm, nucleus, and mitochondrial intermembrane space. We generated conditional *SOD1* knockout cells from chicken DT40 cells and analyzed their phenotypes. The results revealed that SOD1 was essential for viability and that depletion of SOD1, especially nuclear SOD1, increased sister chromatid exchange (SCE) frequency, suggesting that superoxide is generated in or near the nucleus and that nuclear SOD1 functions as a guardian of the genome. Furthermore, we found that ascorbic acid could offset the defects caused by SOD1 depletion, including cell lethality and increases in SCE frequency and apurinic/aprimidinic sites.

## 1. Introduction

Superoxide is produced during normal cellular metabolism, particularly by respiration in mitochondria, and reactive oxygen species (ROSs) derived from superoxide are considered to cause oxidative damage to macromolecules including DNA [1, 2]. Superoxide dismutases (SODs) convert superoxide into hydrogen peroxide and molecular oxygen [3]. SODs are classified into three species in vertebrate cells: copper- and zinc-dependent SOD or SOD1, manganese-dependent SOD or SOD2, and copper-dependent SOD or SOD3 [4]. SOD1 is present in the cytoplasm, the nucleus, and the intermembrane space of mitochondria [5–7], SOD2 is present in the mitochondrial matrix [8, 9], and SOD3 is a

secreted protein found in the extracellular matrix of tissues [4, 10].

The importance of SOD2 in organisms has been clearly shown with *Sod2* knockout mice. In one case, *Sod2* knockout mice survived only up to three weeks of age and exhibited several novel pathologic phenotypes, including severe anemia, degeneration of neurons, and progressive motor disturbances [11]. Moreover, the *Sod2* knockout mice older than seven days exhibited extensive mitochondrial injury within degenerating neurons and cardiac myocytes. In the second case of *Sod2* knockout, mice were born alive but died within ten days with severe cardiomyopathy [12]. In our previous study, we investigated the events occurring shortly after the loss of SOD2 in vertebrate

cells by generating conditional *SOD2* knockout cells using chicken DT40 cells [13]. By monitoring the frequency of sister chromatid exchange (SCE), a very sensitive assay for detecting DNA lesions [14], we found that depletion of *SOD2* had no impact on the integrity of genomic DNA.

In the case of *SOD1*, high levels of *SOD1* have been detected in the central nervous system, liver, and kidney in mammals. In some cases, *SOD1* is referred to as cytoplasmic SOD because of its high distribution in the cytoplasm, but it is also detected in cellular organelles including nucleus [5, 6]. Recent studies show that *SOD1* may act as a nuclear protein as well. *SOD1* interacts with estrogen receptor  $\alpha$  (*ER* $\alpha$ ), a ligand-activated transcription factor, and influences the expression of estrogen responsive genes [15]. Moreover, since it is reported that *SOD1*-deficient mice show increased mutagenesis and cancer risk [16, 17], it seems likely that *SOD1* functions in the nucleus besides the regulation of transcription. However, little attention has been paid to the role of *SOD1* in the nucleus, especially as a guardian of the genome.

In this study, we generated conditional *SOD1* knockout cells from DT40 cells and examined their phenotypes. Our results indicated that *SOD1* is essential for viability in DT40 cells, and that nuclear *SOD1* functions as a guardian of the genome by scavenging superoxide generated in or near the nucleus.

## 2. Materials and Methods

**2.1. Plasmid Construction.** DNA containing *SOD1* exons I–V was obtained by PCR from DT40 genomic DNA using the Easy-DNA Kit (Invitrogen, Carlsbad, California, USA) and Ex-Taq polymerase (Takara Bio Inc., Otsu, Shiga, Japan). The chicken targeting constructs for *SOD1*, *SOD1*-blastcidin<sup>r</sup> and *SOD1*-puromycin<sup>r</sup>, were made by replacing the exons I–III with blastcidin (Bsr) or puromycin (Puro) selection marker cassette. To construct an expression plasmid carrying a human *SOD1* cDNA with the tet-off promoter (*hSOD1*), the human *SOD1* cDNA was obtained by reverse transcription-PCR (RT-PCR) from HeLa cells using SuperScript III Reverse Transcriptase (Invitrogen) and inserted into the pUHG 10-3 vector [18].

To construct a plasmid carrying a localization signal combined with *hSOD1*, *hSOD1* cDNA alone, or *hSOD1* cDNA combined with either nuclear localization signal (NLS) derived from SV40 large tumor antigen or nuclear export signal (NES) derived from chicken, HDAC3 [19] was inserted into the EGFP-C1 vector (BD Biosciences, San Jose, California, USA).

**2.2. Cell Culture.** Cells were cultured in Roswell Park Memorial Institute medium (RPMI)1640 supplemented with 10% fetal bovine serum, 1% chicken serum, and 100  $\mu$ g/mL kanamycin at 39°C. To generate a growth curve, cells ( $1 \times$

$10^5$ ) were inoculated and cultured at 39°C for the specified time periods, and the number of cells was counted in a representative field using a Bürker-Türk line counting chamber. Ascorbic acid phosphoric ester magnesium salt (APM) (Wako Pure Chemical Industries Ltd., Osaka, Japan) was dissolved in phosphate buffered saline (PBS; 137 mM NaCl, 2.68 mM KCl, 8.04 mM Na<sub>2</sub>HPO<sub>4</sub>, and 1.47 mM KH<sub>2</sub>PO<sub>4</sub>) and then diluted with culture medium at the time of assay.

**2.3. Gene Disruption.** For gene targeting, DT40 cells ( $1 \times 10^7$ ) were electroporated with a Gene Pulser (BioRad, Hercules, California, USA) at 550 V and 25  $\mu$ F in the presence of 30  $\mu$ g linearized targeting constructs. Drug-resistant colonies were selected in 96-well plates with medium containing 30  $\mu$ g/mL blastcidin S or 0.5  $\mu$ g/mL puromycin. Gene disruption was confirmed by Southern blotting, genomic PCR, and RT-PCR.

**2.4. Southern Blotting.** Southern blotting was performed according to the manual of Rediprime II Random Prime Labelling System (GE Healthcare UK Ltd. Amersham Place, Little Chalfont, Buckinghamshire, UK). Genomic DNA (40  $\mu$ g) was digested with *Nde* I, separated in a 1% agarose gel, transferred to a nylon membrane (GE Healthcare UK Ltd.) using 20  $\times$  standard saline citrate (20  $\times$  SSC; 3 M NaCl, 0.3 M sodium citrate), and then hybridized with the 771 bp <sup>32</sup>P-labeled probe indicated in Figure 1(b).

**2.5. Western Blotting.** Cells that had been cultured in the presence or absence of doxycycline (Dox), a derivative of tetracycline, for 0, 24, 48, 72, and 96 hours were harvested, washed with PBS, precipitated, and suspended in SDS sample buffer (50 mM Tris-HCl (pH 6.8), 10% glycine, 2% SDS, 0.1% bromophenol blue and 0.1 M DTT). Samples prepared from  $7.5 \times 10^4$  cells were fractionated in a linear 4% to 14% gradient SDS-polyacrylamide gel. Proteins were transferred onto a Immun-Blot PVDF Membrane (BioRad) and immunoblotted with primary antibodies (anti-Cu/Zn Superoxide Dismutase (Assay Designs, Inc., Ann Arbor, Michigan, USA)), anti-LaminB1 (Invitrogen), anti- $\alpha$ -tubulin (Sigma-Aldrich, St. Louis, Missouri, USA), and anti- $\beta$ -actin (Sigma-Aldrich), followed by a horseradish peroxidase-conjugated antirabbit or antimouse IgG secondary antibody (New England Biolabs, Ipswich, Massachusetts, USA). Bands were visualized using enhanced chemiluminescence (ECL) (GE Healthcare).

**2.6. Cell Cycle Analysis.** Cells were prepared using the CycleTEST PLUS DNA Reagent Kit (Becton Dickinson, Franklin Lakes, New Jersey, USA). Subsequent flow-cytometric analysis was performed with FACScan (Becton Dickinson). Data were analyzed using CellFIT software (Becton Dickinson).

**2.7. Superoxide Assay.** Intracellular generation of ROS was detected by BES-So-AM (Wako Pure Chemical Industries Ltd.), a highly specific fluorescent probe for superoxide [20].

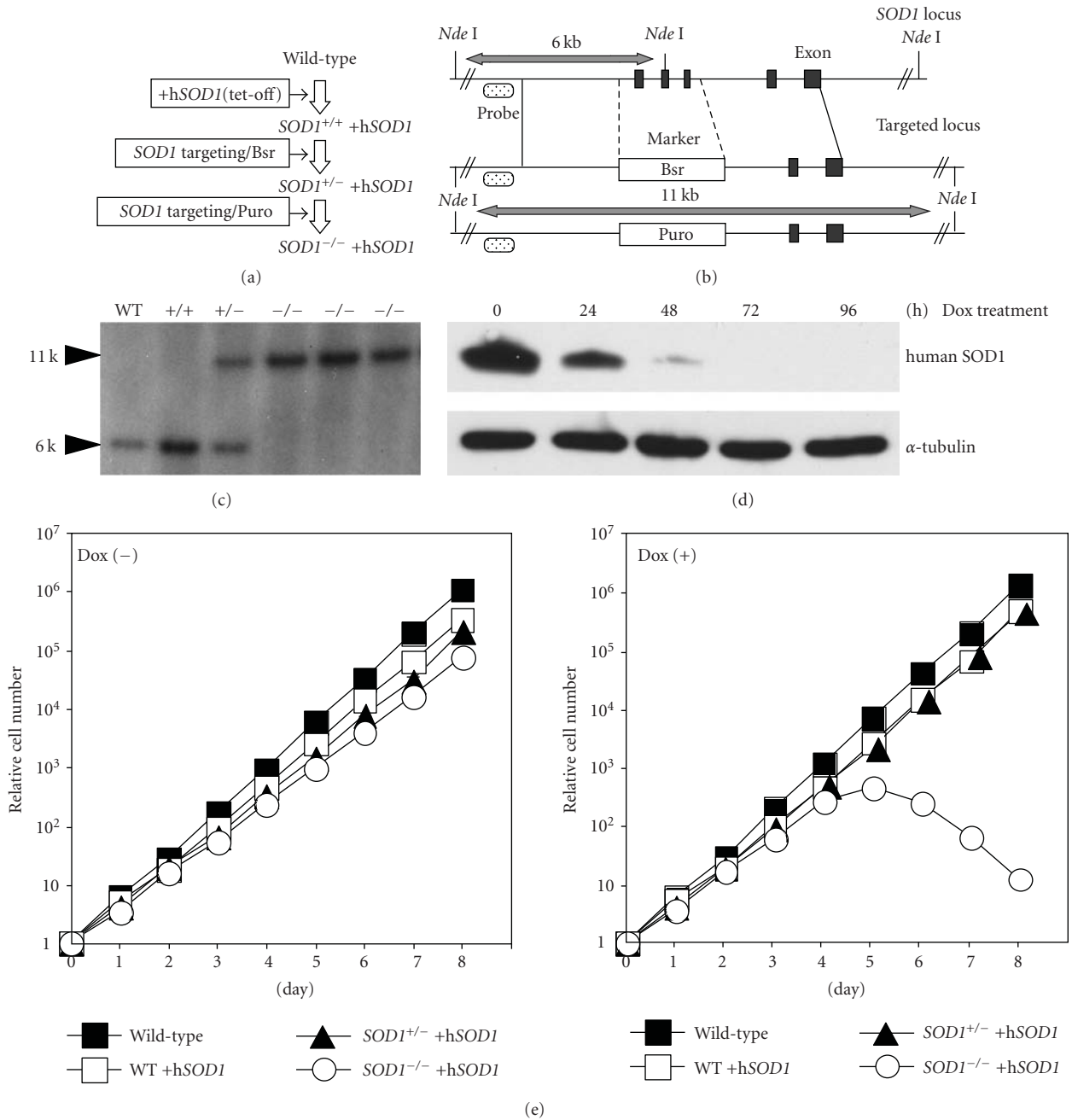


FIGURE 1: Generation of *SOD1*<sup>-/-</sup> cells expressing human *SOD1* from the tet-off promoter. (a) Schematic representation of the generation of DT40 *SOD1*<sup>-/-</sup> + h*SOD1* cells. (b) Schematic representation of the *SOD1* genomic locus and configuration of the targeted locus. (c) Southern blot analysis for the confirmation of the status of the *SOD1* wild-type (WT), WT + human *SOD1* (+/+), heterozygous (+/-), and homozygous (-/-) cells, using *Nde*I digested genomic DNA and the probe indicated in (b). (d) Dox-dependent disappearance of human *SOD1*, as confirmed by western blot analysis, with  $\alpha$ -tubulin used as the loading control. (e) Growth curves of indicated genotype cells. Indicated mutant cells were cultured in the presence or absence of 1  $\mu$ g/mL Dox. Dox had no effect on the growth or viability of wild-type cells.

The agent was dissolved in dimethyl sulfoxide and diluted with culture medium at the time of assay. Cells were treated with 5  $\mu$ M (final concentration) BES-So-AM for 20 min. After washing twice with PBS, the cells were suspended in PBS, and fluorescent intensity was measured using FACScan (Becton Dickinson).

2.8. Measurement of Sister Chromatid Exchange. To measure the frequency of sister chromatid exchange (SCE), cells (1 ~ 2  $\times$  10<sup>6</sup>) were cultured for two cycle periods in medium containing 10  $\mu$ M BrdU with or without paraquat (Sigma-Aldrich) and pulsed with 0.1  $\mu$ g/mL colcemid (Wako Pure Chemical Industries Ltd.) for 2 hours. The cells were

harvested and treated with 75 mM KCl for 18 min at room temperature and then fixed with methanol-acetic acid (3 : 1) for 30 min. The cell suspension was then dropped onto ice-cold wet glass slides and air-dried. The cells on the slides were incubated with 10  $\mu$ g/mL Hoechst 33258 in phosphate buffer (pH 6.8) for 20 min and rinsed with MacIlvaine solution (164 mM Na<sub>2</sub>HPO<sub>4</sub>, 16 mM citric acid, pH 7.0). The cells were then exposed to black light ( $\lambda = 352$  nm) at a distance of 1 cm for 20 min, incubated in 2X SSC (0.3 M NaCl, 0.03 M sodium citrate) at 58°C for 20 min, and then stained with 3% Giemsa solution for 20 min.

**2.9. Aldehyde Reactive Probe (ARP) Slot Blot Analysis.** AP sites were measured as previously described in [21] by aldehyde reactive probe (ARP, Dojindo Molecular Technology, Gaithersburg, MD, USA) labeling and slot blot (PMID: 9443396).

### 3. Results

**3.1. Generation of Conditional SOD1-Knockout Cells.** To investigate the events occurring shortly after depletion of SOD1, we generated cells in which the expression of the SOD1 gene could be turned off by Dox treatment, using chicken DT40 cells. First, DT40 wild-type cells were transfected with a plasmid expressing a human SOD1 cDNA driven by the tet-off promoter (Figure 1(a)). Then, SOD1 genes were disrupted as shown in Figure 1(b). Disruption was confirmed by Southern blotting (Figure 1(c)) using the probe shown in the Figure 1(b). Treatment of these cells with Dox suppressed expression of the hSOD1 protein (Figure 1(d)). The hSOD1 protein level reached a limit of detection at 96 hours after Dox addition as measured by western blotting, even in the case of overexposure (data not shown).

Even in the absence of Dox, the growth rate of SOD1<sup>-/-</sup> + hSOD1 cells was slightly lower than that of wild-type cells. Although fibroblasts derived from the SOD1 knockout mouse are reportedly viable [22], the SOD1 gene knockout DT40 cells developed in this study died after depletion of SOD1. As mentioned above, hSOD1 disappeared within 96 hours after Dox addition, and cells ceased exponential growth on the 5th day and died soon after (Figure 1(e)).

**3.2. Analyses of Cell Death in SOD1-Depleted Cells.** We next analyzed the mode of cell death of hSOD1-depleted cells. Flow cytometric analysis showed that hSOD1-depleted cells died gradually without arresting in a specific phase of the cell cycle (Figure 2(a)). Microscopic observation revealed the appearance of apoptotic bodies (Figure 2(b)). In agreement with this observation, cleavage of the apoptotic marker lamin B1 was detected from two days after Dox addition (Figure 2(c)). Interestingly, five days after Dox addition, the proportion of cells in the M phase decreased, with a concomitant increase in the number of cells with "hypercondensed chromatin" (Figure 2(b)), resembling the

hypercondensed chromatin, that appears in colcemid-treated cells arrested for long periods in the M phase [23].

**3.3. Depletion of SOD1 Increases Superoxide Levels and Affects Genome Integrity.** To understand the influence of hSOD1 depletion on the level of superoxide in the cell, intracellular levels of superoxide were measured using BES-So-AM, a fluorescent probe used to detect cell-derived superoxide with high selectivity [20]. The intracellular level of superoxide in the hSOD1-depleted cells cultured in the presence of Dox for 108 hours was twofold higher than that in the SOD1<sup>-/-</sup> + hSOD1 cells expressing hSOD1 (Figure 3(a)).

Since SOD1 reportedly exists in the nucleus, we next addressed its possible function in genome integrity. When DNA damage occurs, under normal conditions, the genome is repaired immediately and properly using appropriate DNA repair pathways. When cells are treated with DNA damaging agents such as Mitomycin C or UV irradiation, elevated sister chromatid exchange (SCE) frequencies can be observed at much lower doses of the agents than those to cause lethality because some DNA repair pathways include recombination processes [14, 24, 25]. Therefore, SCE is considered a very sensitive indicator of the existence of DNA lesions. SCE frequencies were measured to detect whether or not SOD1 participates in protecting DNA from attack from superoxide. SCE frequency in hSOD1-depleted cells cultured in the presence of Dox for 120 hours was increased approximately fourfold compared with that in hSOD1-expressing cells (Figure 3(b)).

Oxidative DNA damage is repaired mainly by a base-excision repair pathway that generates apurinic/apyrimidinic (AP) sites during its repair process [26]. Therefore, an increase in AP sites indicates an increase in oxidative DNA damage. As shown in Figure 3(c), the number of AP sites in SOD1-depleted cells was about twofold that in hSOD1-expressing cells. These phenotypes observed in SOD1-depleted cells, elevated SCE frequency and increased AP sites suggest that SOD1 could serve to provide protection for genomic DNA against ROS.

**3.4. Ascorbic Acid Offsets the Absence of SOD1.** Defense mechanisms against oxidative stress caused by ROS involve both enzymatic and nonenzymatic antioxidants. Ascorbic acid is a representative non-enzymatic antioxidant and its phosphoric ester magnesium salt (APM) is known to exert anti-mutagenic effects by scavenging organic radicals [27, 28].

The phenomena observed in SOD1-depleted cells seem to be caused directly or indirectly by the increase in superoxide, but do not appear to be due to the depletion of SOD1 protein itself. To test this, SOD1-depleted cells were cultured in the presence of APM (Figure 4(a)). SOD1-depleted cells proliferated normally in the presence of APM, and no growth defect was observed after culturing cells longer than 10 days (data not shown). It must be noted that the suppression of expression of SOD1 by Dox is not affected by APM addition (Figure 4(a); lower panel). The superoxide level in the cells cultured in the presence of Dox,

but also with APM for 108 h, was reduced to the level of the cells expressing hSOD1 (Figure 3(a)). Furthermore, APM completely compensated for depletion of SOD1 with regard to the number of AP sites and SCE frequency (Figures 3(c) and 4(b)).

**3.5. Nuclear Localization of SOD1 Is Important for Its Function in Reducing DNA Lesions.** Mitochondria are the major superoxide-producing organelles in the cell and contain an intrinsic SOD, SOD2. In our previous study, we found that depletion of SOD2 had no impact on SCE frequency. It is possible that superoxide produced in or near the nucleus could cause DNA lesions, and that SOD1 in the nucleus could therefore reduce these lesions. To confirm the above possibility, we generated cells expressing hSOD1 fused with a nuclear localization signal (NLS) or nuclear export signal (NES) and green fluorescent protein (GFP) for visualization. The expression vectors GFP-NLS-hSOD1, GFP-NES-hSOD1, and GFP-hSOD1 were transfected into *SOD1*<sup>-/-</sup> + hSOD1 cells. Their expression and localization were confirmed by GFP, which tagged the N-terminal of hSOD1 (Figure 5(a)). The hSOD1 without localization signals was distributed throughout the cell. In contrast, the hSOD1 fused with NLS was found mainly in the nucleus and the hSOD1 fused with NES was found mainly in the cytoplasm. Although, in the presence of Dox, cells expressing NLS-hSOD1 or NES-hSOD1 grew slightly slower than the cells expressing hSOD1, NLS-hSOD1 and NES-hSOD1 did suppress lethality (Figure 5(b)).

To test whether DNA damage could be increased by excluding nuclear SOD1, SCE frequency was measured in the cells expressing NES-hSOD1 as well as the cells expressing NLS-hSOD1 or hSOD1 without any localization signal. As mentioned above, the *SOD2*<sup>-/-</sup> + hSOD2 cells did not show any difference in SCE frequency between Dox-treated and untreated cells (Figure 5(c)). Cells expressing NES-hSOD1 showed a slight increase in SCE frequency in the presence of Dox while cells expressing NLS-hSOD1 or hSOD1 showed no difference in SCE frequency in the presence or absence of Dox. The limited increase in SCE frequency in the cells expressing NES-hSOD1 compared with that in SOD1-depleted cells may be due to the incomplete exclusion of SOD1 from the nucleus (Figure 5(a)). The importance of nuclear SOD1 for protecting DNA from lesions was more clearly shown when these cells were treated with a superoxide-generating agent, paraquat. As shown in Figure 5(d), the cells expressing NES-hSOD1 showed a prominent increase in SCE frequency in the presence of Dox, but the cells expressing NLS-hSOD1 or hSOD1 did not.

## 4. Discussion

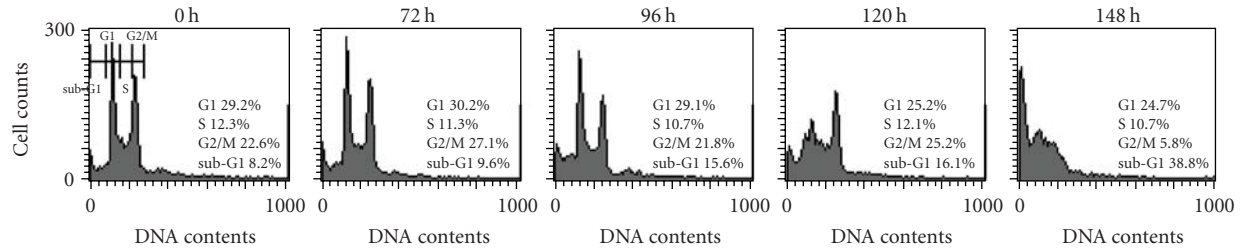
In this study, we analyzed the phenotypes of conditional *SOD1* knockout cells after depletion of SOD1 in order to understand the cellular functions of SOD1. We found that SOD1 was essential for viability and that nuclear SOD1 protected the genome. In addition, we found that ascorbic acid recovered cell viability and suppressed increases in SCE

frequency and AP sites, two phenotypes observed in SOD1-depleted cells.

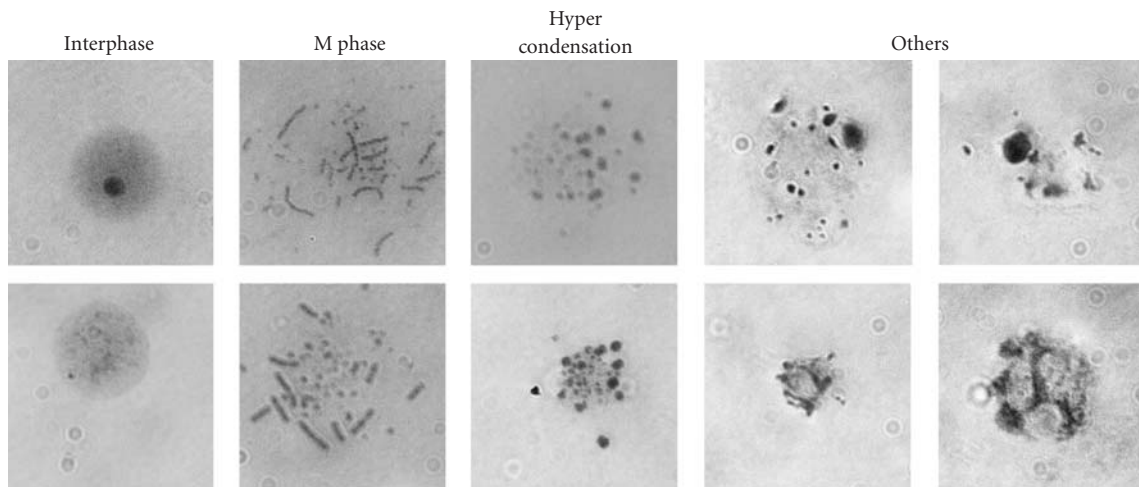
The lethality of the SOD1-depleted cells seems to conflict with the previous observation that an *SOD1* knockout mouse is viable, albeit with a shortened life span [29, 30]. This conflict could be explained as follows. The detrimental effects seen in the *SOD1* knockout mouse caused by SOD1 depletion could have been opposed by the effects of other antioxidants, including ascorbic acid, which the mouse produces in the liver [31] in sufficient quantities for the retention of viability. In addition, the concentration of oxygen in the tissues or cells *in vivo* is much lower than that in the cell cultures. In fact, lowering the oxygen concentration in the cell cultures partially retarded the lethality in SOD1-depleted DT40 cells (data not shown).

The main source of superoxide production is the mitochondria. During energy transduction, a small number of electrons “leak” to oxygen prematurely, forming the oxygen free radical superoxide, which has been implicated in the pathophysiology of a variety of diseases [32]. In spite of these implications, superoxide is not highly reactive [33], and it is membrane impermeable, so it is highly compartmentalized within the cell, that is, there is no flux between the pools of matrix and cytoplasmic superoxide [34, 35]. However, more reactive secondary ROS, such as hydrogen peroxide and hydroxyl radicals, are derived from superoxide, and these are able to penetrate biological membranes [33, 35]. The hydroxyl radical is known to react with all components of the DNA molecule, damaging both the purine and pyrimidine bases, and also the deoxyribose backbone [36]. It therefore seems reasonable that nuclear DNA is damaged more by ROS derived from unscavenged superoxide than by superoxide itself. However, the fact that SOD2-depleted DT40 cells showed no increase in the frequency of SCE indicates that ROS derived from unscavenged, mitochondria-generated superoxide seem to have little impact on the integrity of genomic DNA.

Superoxide is also generated by several enzymes, such as NADPH oxidase, xanthine oxidase, flavoenzymes, and cytochrome P-450, in addition to enzymes of the mitochondrial respiratory chain [35, 37]. The relatively ubiquitous distribution of SOD1 in the cell seems to indicate that SOD1 scavenges superoxide at the site where it is generated. In this context, it is interesting that the cells expressing NES-hSOD1 showed a relatively high frequency of SCE. This suggests that nuclear SOD1 could function to mitigate DNA lesions caused directly or indirectly by superoxide generated in or near the nucleus. At present, it is not clear how superoxide is generated there, but NADPH oxidase is one candidate. NADPH oxidase produces superoxide in phagocytes, and a significant proportion of the NADPH oxidase subunits in unstimulated cells is present as a fully preassembled and functional ROS-generating complex associated with the intracellular cytoskeleton, particularly in a perinuclear distribution [35]. Furthermore, the highest level of NADPH oxidase complex-dependent superoxide generation has been detected in the nuclei-enriched fraction among several subcellular fractions differentiated by centrifugation [37].



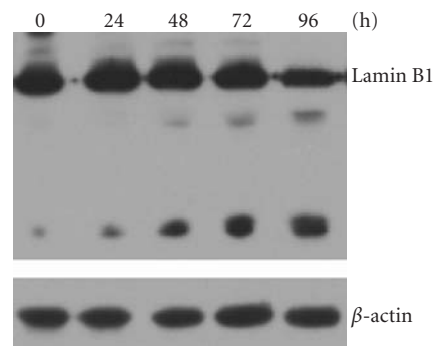
(a)



	Wild-type	<i>SOD1</i> <sup>-/-</sup> +h <i>SOD1</i>		
		No treatment	Dox (+) 96 h	Dox (+) 128 h
Interphase	91.3	93.5	80.1	67.7
M phase	8.2	5.6	4.1	1.1
Hypercondensation	0	0.4	0.2	5
Others	0.5	0.5	15.7	26.2

:Percentage

(b)



(c)

FIGURE 2: Phenomena appearing after depletion of *SOD1*. (a) Cell cycle analysis of *SOD1*<sup>-/-</sup> cells. Cell cycle was analyzed using flow cytometry. Distribution patterns of asynchronous culture of Dox-treated cells for the indicated timepoints. The percentages of cells in each cell cycle phase and dead cells are shown on the right side of each panel. (b) Categorization of Giemsa-stained cells. Cells not having interphase nucleus, mitotic chromosomes, or hypercondensed chromosomes are classified into others in which apoptotic cells are included. Cells were harvested and treated with 75 mM KCl and fixed with methanol-acetic acid (3 : 1). The cell suspension was dropped onto wet glass slides, air dried, and stained with Giemsa solution (upper row). Percentages of cells exhibiting select phenomena were based on the categorization detailed in the boxes above the micrographs. At least 500 cells were counted in each sample. (c) Western blotting analysis of Lamin B1, with  $\beta$ -actin used as loading control.

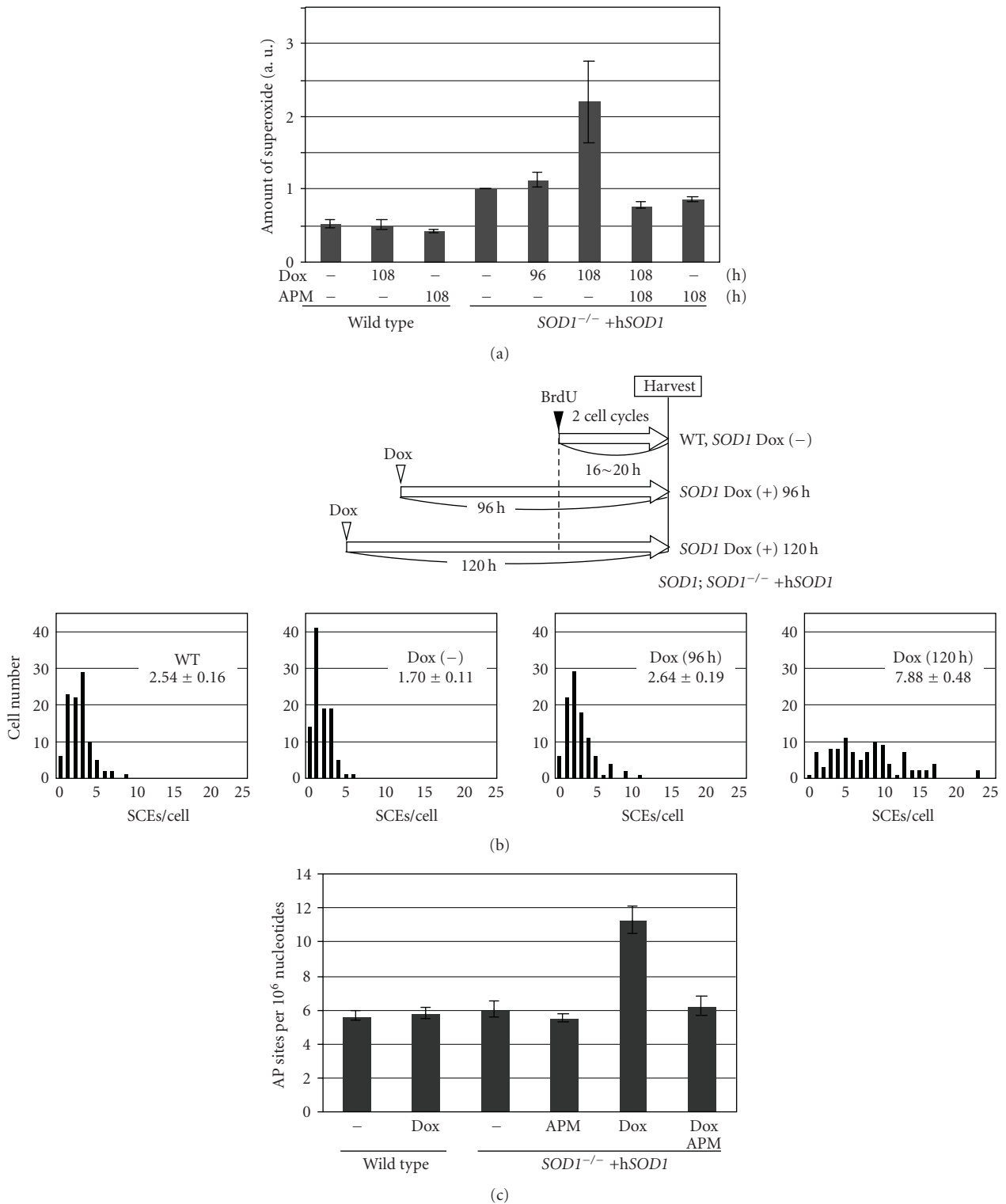


FIGURE 3: Increases in superoxide, SCE frequency, and AP sites upon depletion of SOD1. (a) Superoxide level. Levels of superoxide were measured with BES-So-AM. The intensity of *SOD1*<sup>-/-</sup> +h*SOD1* cells not treated with Dox was used as the standard (a.u.; arbitrary unit = 1). Error bars indicate standard errors based on three independent experiments. (b) SCE frequency. Schematic representation of cell treatment is depicted in upper panel. Cells were cultured for two cell cycles in a medium containing BrdU. Histograms represent SCEs in wild-type cells and in *SOD1*<sup>-/-</sup> cells treated with Dox for the indicated timepoints. The mean and standard error are shown in the upper right corner. (c) AP sites. Scanning densitometric analysis of slot blots of endogenous AP sites was performed as described previously in [21]. Some cells were treated with Dox and/or APM for 112 hours. Bars indicate standard errors.

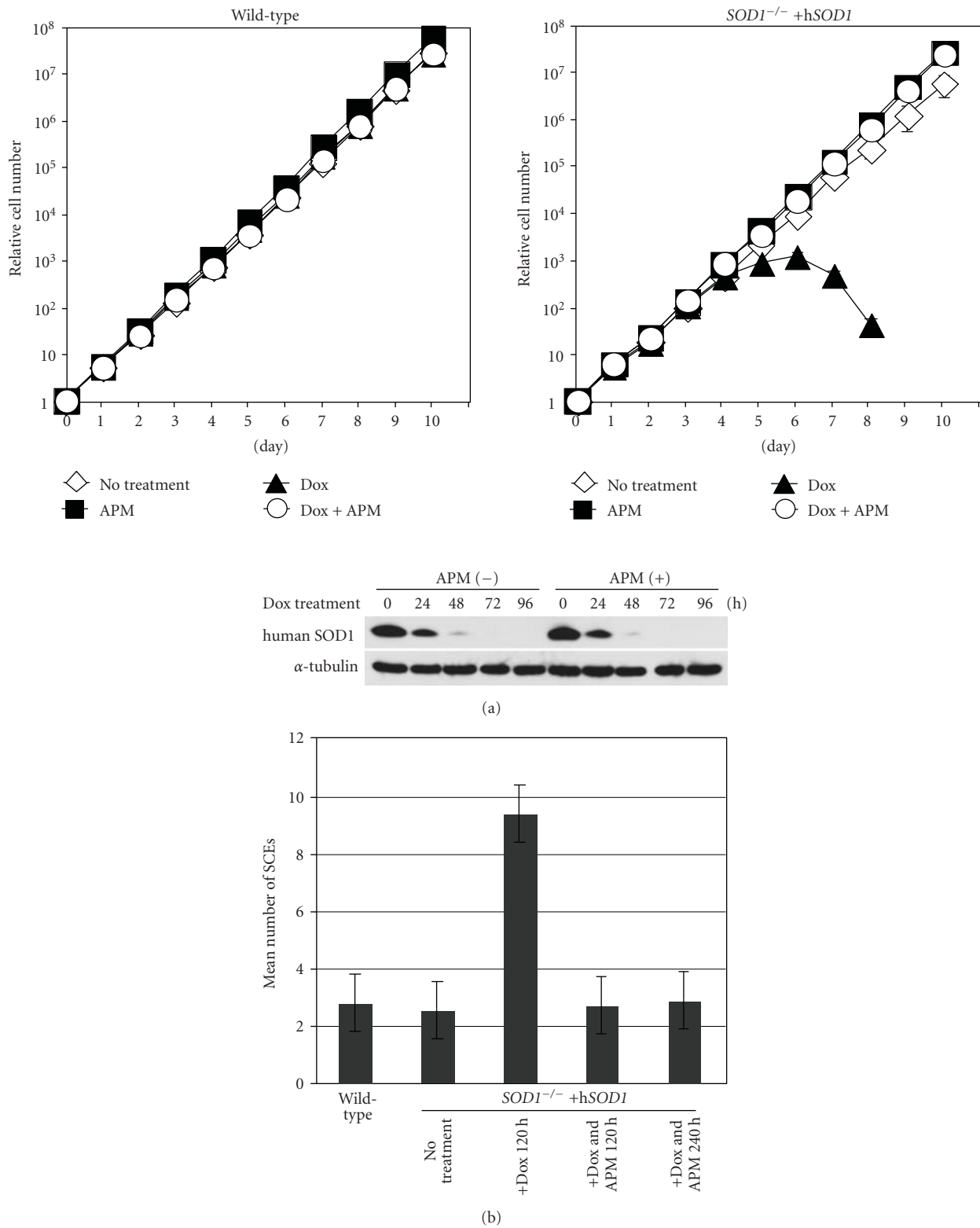
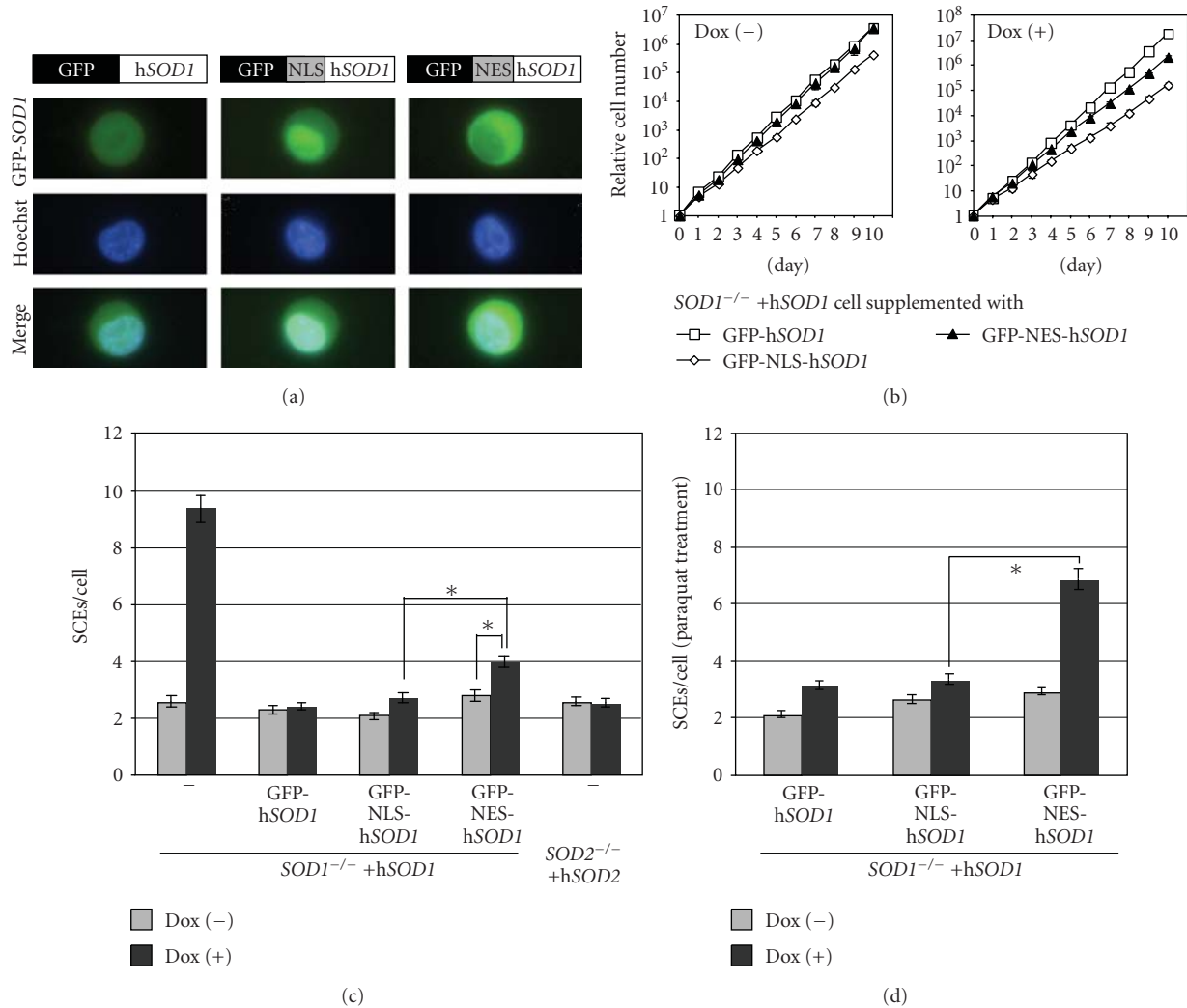


FIGURE 4: Suppression of lethality and increase in SCE frequency in cells depleted of SOD1 by APM (a) Upper panel: growth curves of cells of the indicated genotypes. Cells were cultured with or without 1  $\mu$ g/mL Dox and/or 200  $\mu$ M APM. Lower panel: disappearance of hSOD1 was confirmed by western blotting. (b) SCE frequencies of cells treated with Dox and APM for 0, 120, or 240 hours. A total of 100 metaphase cells was counted in each sample. Bars indicate standard errors.



**FIGURE 5: Exclusion of SOD1 from nuclei increases SCE.** (a) Distribution of SOD1 with NLS or NES localization signal. Upper panels show the subcellular localization of GFP-hSOD1 with and without localization signals. The middle and lower panels indicate Hoechst staining and merged images, respectively. (b) Growth curves of  $SOD1^{-/-}$  + hSOD1 cells complemented with indicated hSOD1. Cells were cultured in the presence or absence of 1  $\mu\text{g}/\text{mL}$  Dox. (c) SCE frequency. SCE frequencies of  $SOD1^{-/-}$  + hSOD1 cells expressing the indicated hSOD1 or those of  $SOD2^{-/-}$  + hSOD2 cells cultured in the presence or absence of 1  $\mu\text{g}/\text{mL}$  Dox for 120 hours were measured. Bars indicate standard errors. \*, student  $t$ -test,  $P < .01$ . (d) SCE frequency in the presence of paraquat. Paraquat was added at a final concentration of 100  $\mu\text{M}$  to the culture medium 20 hours prior to harvesting. SCE frequencies of  $SOD1^{-/-}$  + hSOD1 cells expressing the indicated hSOD1 in the presence or absence of 1  $\mu\text{g}/\text{mL}$  Dox for 120 hours were measured. Bars indicate standard errors. \*, student  $t$ -test,  $P < .01$ .

SOD1 is a very abundant protein in the cell and may play roles other than the dismutation of superoxide. For example, SOD1 interacts with  $\text{ER}\alpha$ , a ligand-activated transcription factor, and influences the expression of estrogen responsive genes [15]. Therefore, it is conceivable that some of the observed phenotypes of SOD1-depleted cells are caused by depletion of SOD1 protein itself and not by a defect in superoxide dismutase activity. However, this possibility is unlikely, since ascorbic acid suppressed all of the phenotypes of SOD1-depleted cells, including cell lethality.

Although depletion of SOD1 causes DNA lesions, as indicated by increases in SCE frequency and AP sites, the major cause for lethality in SOD1-depleted cells is not the increase in DNA lesions, since the increases in SCE frequency

and AP sites are moderate and since NES-SOD1 suppresses lethality. The appearance of "hyper condensed chromatin" suggests hindrance of microtubules formation. Noteworthy, the level of superoxide and SCE frequency increased in SOD1 depleted cell around 108–120 h after addition of Dox (Figures 3(a) and 4(b)). In contrast, apoptotic cells appeared at 96 hours after addition of Dox. We speculate that superoxide level begins to increase earlier than 96 hours after addition of Dox although it is too little to be detected. Since ascorbic acid suppressed the phenotypes observed at 96 hours after addition of Dox, an increase in superoxide even at a low level may influence something more sensitive cellular components other than nuclear genome. Preliminary experiments indicated disordered microtubules construction

in SOD1-depleted cells (data not shown). The next direction for our study will therefore to address the major cause for the lethality seen in SOD1-depleted cells.

## 5. Conclusions

SOD1 is essential for cell viability, and depletion of SOD1 causes elevated SCE and increased AP sites. Ascorbic acid suppresses the increase in SCE frequency and AP sites in SOD1-depleted cells. Since elevated spontaneous and paraquat-induced SCE is suppressed by nuclear but not cytoplasmic SOD1, this study represents the first evidence that nuclear SOD1 has a role in guarding the genome against oxidative stress. Taken together, these results clearly demonstrate the importance of the nuclear distribution of SOD1 and ascorbic acid in the maintenance of genome stability.

## Acknowledgments

This paper was supported by Grants-in-Aid for Scientific Research and for Scientific Research in Priority Areas from the ministry of Education, Science, Sports, and Culture of Japan. This paper was also supported in part by the US NIEHS P42-ES05948 and P30-ES10126.

## References

- [1] T. Finkel and N. J. Holbrook, "Oxidants, oxidative stress and the biology of ageing," *Nature*, vol. 408, no. 6809, pp. 239–247, 2000.
- [2] L. J. Marnett and J. P. Plataras, "Endogenous DNA damage and mutation," *Trends in Genetics*, vol. 17, no. 4, pp. 214–221, 2001.
- [3] J. M. McCord and I. Fridovich, "Superoxide dismutase. An enzymic function for erythrocyte hemocuprein," *Journal of Biological Chemistry*, vol. 244, no. 22, pp. 6049–6055, 1969.
- [4] I. N. Zelko, T. J. Mariani, and R. J. Folz, "Superoxide dismutase multigene family: a comparison of the CuZn-SOD (SOD1), Mn-SOD (SOD2), and EC-SOD (SOD3) gene structures, evolution, and expression," *Free Radical Biology and Medicine*, vol. 33, no. 3, pp. 337–349, 2002.
- [5] L.-Y. Chang, J. W. Slot, H. J. Geuze, and J. D. Crapo, "Molecular immunocytochemistry of the CuZn superoxide dismutase in rat hepatocytes," *Journal of Cell Biology*, vol. 107, no. 6 I, pp. 2169–2179, 1988.
- [6] J. D. Crapo, T. Oury, C. Rabouille, J. W. Slot, and L.-Y. Chang, "Copper,zinc superoxide dismutase is primarily a cytosolic protein in human cells," *Proceedings of the National Academy of Sciences of the United States of America*, vol. 89, no. 21, pp. 10405–10409, 1992.
- [7] L. A. Sturtz, K. Diekert, L. T. Jensen, R. Lill, and V. C. Culotta, "A fraction of yeast Cu,Zn-superoxide dismutase and its metallochaperone, CCS, localize to the intermembrane space of mitochondria. A physiological role for SOD1 in guarding against mitochondrial oxidative damage," *Journal of Biological Chemistry*, vol. 276, no. 41, pp. 38084–38089, 2001.
- [8] R. A. Weisiger and I. Fridovich, "Superoxide dismutase. Organelle specificity," *Journal of Biological Chemistry*, vol. 248, no. 10, pp. 3582–3592, 1973.
- [9] R. A. Weisiger and I. Fridovich, "Mitochondrial superoxide dismutase. Site of synthesis and intramitochondrial localization," *Journal of Biological Chemistry*, vol. 248, no. 13, pp. 4793–4796, 1973.
- [10] S. L. Marklund, E. Holme, and L. Hellner, "Superoxide dismutase in extracellular fluids," *Clinica Chimica Acta*, vol. 126, no. 1, pp. 41–51, 1982.
- [11] R. M. Lebovitz, H. Zhang, H. Vogel et al., "Neurodegeneration, myocardial injury, and perinatal death in mitochondrial superoxide dismutase-deficient mice," *Proceedings of the National Academy of Sciences of the United States of America*, vol. 93, no. 18, pp. 9782–9787, 1996.
- [12] Y. Li, T.-T. Huang, E. J. Carlson et al., "Dilated cardiomyopathy and neonatal lethality in mutant mice lacking manganese superoxide dismutase," *Nature Genetics*, vol. 11, no. 4, pp. 376–381, 1995.
- [13] S. Takada, E. Inoue, K. Tano et al., "Generation and characterization of cells that can be conditionally depleted of mitochondrial SOD2," *Biochemical and Biophysical Research Communications*, vol. 379, no. 2, pp. 233–238, 2009.
- [14] R. J. Albertini, D. Anderson, G. R. Douglas et al., "IPCS guidelines for the monitoring of genotoxic effects of carcinogens in humans," *Mutation Research*, vol. 463, no. 2, pp. 111–172, 2000.
- [15] A. K. Rao, Y. S. Ziegler, I. X. McLeod, J. R. Yates, and A. M. Nardulli, "Effects of Cu/Zn superoxide dismutase on estrogen responsiveness and oxidative stress in human breast cancer cells," *Molecular Endocrinology*, vol. 22, no. 5, pp. 1113–1124, 2008.
- [16] R. A. Busuttill, A. M. Garcia, C. Cabrera et al., "Organ-specific increase in mutation accumulation and apoptosis rate in CuZn-superoxide dismutase-deficient mice," *Cancer Research*, vol. 65, no. 24, pp. 11271–11275, 2005.
- [17] S. Elchuri, T. D. Oberley, W. Qi et al., "CuZnSOD deficiency leads to persistent and widespread oxidative damage and hepatocarcinogenesis later in life," *Oncogene*, vol. 24, no. 3, pp. 367–380, 2005.
- [18] M. Gossen and H. Bujard, "Tight control of gene expression in mammalian cells by tetracycline-responsive promoters," *Proceedings of the National Academy of Sciences of the United States of America*, vol. 89, no. 12, pp. 5547–5551, 1992.
- [19] Y. Takami and T. Nakayama, "N-terminal region, C-terminal region, nuclear export signal, and deacetylation activity of histone deacetylase-3 are essential for the viability of the DT40 chicken B cell line," *Journal of Biological Chemistry*, vol. 275, no. 21, pp. 16191–16201, 2000.
- [20] H. Maeda, K. Yamamoto, I. Kohno et al., "Design of a practical fluorescent probe for superoxide based on protection-deprotection chemistry of fluoresceins with benzenesulfonyl protecting groups," *Chemistry*, vol. 13, no. 7, pp. 1946–1954, 2007.
- [21] P. D. Chastain 2nd, J. Nakamura, J. Swenberg, and D. Kaufman, "Nonrandom AP site distribution in highly proliferative cells," *FASEB Journal*, vol. 20, no. 14, pp. 2612–2614, 2006.
- [22] T.-T. Huang, M. Yasunami, E. J. Carlson et al., "Superoxide-mediated cytotoxicity in superoxide dismutase-deficient fetal fibroblasts," *Archives of Biochemistry and Biophysics*, vol. 344, no. 2, pp. 424–432, 1997.
- [23] D. F. Hudson, P. Vagnarelli, R. Gassmann, and W. C. Earnshaw, "Condensin is required for nonhistone protein assembly and structural integrity of vertebrate mitotic chromosomes," *Developmental Cell*, vol. 5, no. 2, pp. 323–336, 2003.
- [24] E. Sonoda, M. S. Sasaki, C. Morrison, Y. Yamaguchi-Iwai, M. Takata, and S. Takeda, "Sister chromatid exchanges are

- mediated by homologous recombination in vertebrate cells," *Molecular and Cellular Biology*, vol. 19, no. 7, pp. 5166–5169, 1999.
- [25] M. Otsuki, M. Seki, E. Inoue et al., "Analyses of functional interaction between RECQL1, RECQL5, and BLM which physically interact with DNA topoisomerase III $\alpha$ ," *Biochimica et Biophysica Acta*, vol. 1782, no. 2, pp. 75–81, 2008.
- [26] J. Nakamura and J. A. Swenberg, "Endogenous apurinic/aprimidinic sites in genomic DNA of mammalian tissues," *Cancer Research*, vol. 59, no. 11, pp. 2522–2526, 1999.
- [27] S. Koyama, S. Kodama, K. Suzuki, T. Matsumoto, T. Miyazaki, and M. Watanabe, "Radiation-induced long-lived radicals which cause mutation and transformation," *Mutation Research*, vol. 421, no. 1, pp. 45–54, 1998.
- [28] T. Harada, G. Kashino, K. Suzuki, N. Matsuda, S. Kodama, and M. Watanabe, "Different involvement of radical species in irradiated and bystander cells," *International Journal of Radiation Biology*, vol. 84, no. 10, pp. 809–814, 2008.
- [29] M. M. Matzuk, L. Dionne, Q. Guo, T. R. Kumar, and R. M. Lebovitz, "Ovarian function in superoxide dismutase 1 and 2 knockout mice," *Endocrinology*, vol. 139, no. 9, pp. 4008–4011, 1998.
- [30] S. Elchuri, T. D. Oberley, W. Qi et al., "CuZnSOD deficiency leads to persistent and widespread oxidative damage and hepatocarcinogenesis later in life," *Oncogene*, vol. 24, no. 3, pp. 367–380, 2005.
- [31] I. B. Chatterjee, "Evolution and the biosynthesis of ascorbic acid," *Science*, vol. 182, no. 4118, pp. 1271–1272, 1973.
- [32] M. Valko, D. Leibfritz, J. Moncol, M. T. D. Cronin, M. Mazur, and J. Telser, "Free radicals and antioxidants in normal physiological functions and human disease," *International Journal of Biochemistry and Cell Biology*, vol. 39, no. 1, pp. 44–84, 2007.
- [33] J. Nordberg and E. S. J. Arnér, "Reactive oxygen species, antioxidants, and the mammalian thioredoxin system," *Free Radical Biology and Medicine*, vol. 31, no. 11, pp. 1287–1312, 2001.
- [34] F. Missirlis, J. Hu, K. Kirby, A. J. Hilliker, T. A. Rouault, and J. P. Phillips, "Compartment-specific protection of iron-sulfur proteins by superoxide dismutase," *Journal of Biological Chemistry*, vol. 278, no. 48, pp. 47365–47369, 2003.
- [35] J.-M. Li and A. M. Shah, "Endothelial cell superoxide generation: regulation and relevance for cardiovascular pathophysiology," *American Journal of Physiology*, vol. 287, no. 5, pp. R1014–R1030, 2004.
- [36] B. Halliwell and J. M. C. Gutteridge, *Free Radicals in Biology and Medicine*, Oxford University Press, Oxford, UK, 3rd edition, 1999.
- [37] J.-M. Li and A. M. Shah, "Intracellular localization and preassembly of the NADPH oxidase complex in cultured endothelial cells," *Journal of Biological Chemistry*, vol. 277, no. 22, pp. 19952–19960, 2002.

## Research Article

# Mus308 Processes Oxygen and Nitrogen Ethylation DNA Damage in Germ Cells of *Drosophila*

Nancy Díaz-Valdés,<sup>1,2</sup> Miguel A. Comendador,<sup>1</sup> and L. María Sierra<sup>1</sup>

<sup>1</sup>Área de Genética, Departamento de Biología Funcional e Instituto Universitario de Oncología del Principado de Asturias (IUOPA), University of Oviedo, 33006 Oviedo, Spain

<sup>2</sup>Área de Hepatología y Terapia Génica, Centro de Investigación Médica Aplicada (CIMA), University of Navarra, 31008 Pamplona, Spain

Correspondence should be addressed to L. María Sierra, lmsierra@uniovi.es

Received 13 May 2010; Revised 27 July 2010; Accepted 2 September 2010

Academic Editor: Shigenori Iwai

Copyright © 2010 Nancy Díaz-Valdés et al. This is an open access article distributed under the Creative Commons Attribution License, which permits unrestricted use, distribution, and reproduction in any medium, provided the original work is properly cited.

The *D. melanogaster mus308* gene, highly conserved among higher eukaryotes, is implicated in the repair of cross-links and of O-ethylpyrimidine DNA damage, working in a DNA damage tolerance mechanism. However, despite its relevance, its possible role on the processing of different DNA ethylation damages is not clear. To obtain data on mutation frequency and on mutation spectra in *mus308* deficient (*mus308*<sup>-</sup>) conditions, the ethylating agent diethyl sulfate (DES) was analysed in postmeiotic male germ cells. These data were compared with those corresponding to *mus308* efficient conditions. Our results indicate that Mus308 is necessary for the processing of oxygen and N-ethylation damage, for the survival of fertilized eggs depending on the level of induced DNA damage, and for an influence of the DNA damage neighbouring sequence. These results support the role of *mus308* in a tolerance mechanism linked to a translesion synthesis pathway and also to the alternative end-joining system.

## 1. Introduction

Among the genes identified so far in *Drosophila melanogaster* that play a role in DNA damage repair, *mus308* presents some unique properties, because its cDNA sequence shows motifs characteristic of DNA helicase and DNA polymerases [1]. The putative product of this gene was indeed isolated as a new DNA polymerase, homologue to the *Escherichia coli* DNA polymerase I, carrying as well a DNA helicase domain at the N terminus region [2]. Orthologues of this gene have been found in *Caenorhabditis elegans* [1], *Arabidopsis thaliana* [3, 4], and mammals [3, 5–9]. In humans, three genes encoding proteins with sequence similarities to Mus308—one similar to Mus308 helicase, HEL308 [3], and two similar to the Mus308 polymerase, POLQ [5, 7] and POLN [6]—have been identified to date. POLQ, the most studied of these proteins, has also an ATPase/helicase domain at the N terminus and is able to perform DNA synthesis past an abasic site, following the A-rule [10]; however,

there are contradictory results about its fidelity in a normal nondamaged template [10, 11].

The *mus308* gene is involved in the repair of cross-linking adducts [12, 13] and also of monofunctional damage [13], probably persistent and difficult to repair by other systems, such as the O-ethylpyrimidine damage induced by N-ethyl-N-nitrosourea (ENU) in postmeiotic male germ cells [14]. In addition, at least parts of ENU- and diethyl sulphate- (DES-) induced damages were repaired by Mus308 in female germ cells of *Drosophila* [15]. This protein works in a damage bypass mechanism [1, 13], which was originally related to homologous recombination, HR [14, 16]. Nevertheless, the isolation of the DNA polymerase encoded by this locus [2], its possible ability for DNA synthesis through abasic sites [10, 11], and the requirement of a functional Mus308 protein to prevent damage-induced DNA strand breaks in vivo in somatic cells of *Drosophila* [17], pointing to a translesion synthesis (TLS) mechanism as the activity of this protein [17]. In summary, along these years the

work of our laboratory have demonstrated that Mus308 works in the repair/processing of cross-links and oxygen ethylation damage [13–15, 17] whereas N-ethylation damage is apparently not substrate of this system, because no effect of methyl methanesulphonate (MMS) was detected either in germ cells [13] or in somatic ones [17]. Additionally, its mechanism of action is poorly understood, because it could be related to HR [14, 16] or to TSL [17]. Because of this, we have proposed that the *mus308* locus works in a bypass-mediated tolerance mechanism, BTM [15, 17].

Given the conservation of *mus308* among higher eukaryotic organisms, this locus is likely a part of a repair system relevant to DNA damage processing. Therefore, it would be important to elucidate what types of DNA damage, apart from cross-links and O-ethylpyrimidine adducts, are substrate of this system and to get information about which of the two possible mechanisms of action, HR or TLS, is actually involved in the damage bypass process.

To have more information about the role of Mus308 in the processing of DNA ethylation damage, we have studied here the effect of DES in postmeiotic male germ cells, analysing maternal repair and using the vermilion system [18]. This system combines the analysis of induced mutation frequencies, both at a single locus (*vermilion*, with a specific locus test) and at multiloci (700 loci in the X-chromosome, with the recessive lethal test), with the generation and analysis of mutation spectra [18]. Our data, together with other already published, indicate that Mus308 protein is involved in the processing of all types of oxygen ethylation damage, that it is also involved in the processing of nitrogen ethylation damage, that it prevents cell death at least when the amount of DNA damage is high, and that this protein could be working in a TLS mechanism as well as in an alternative end-joining system (alt-EJ).

## 2. Material and Methods

**2.1. Chemicals.** DES (CAS no. 64–67-5), obtained from Sigma Química (Spain), was dissolved in a solution of 3% ethanol-1% Tween-80 in 33.1 mM phosphate buffer (16.5 mM Na<sub>2</sub>HPO<sub>4</sub>, 16.6 mM KH<sub>2</sub>PO<sub>4</sub>, pH 6.8), containing 5% sucrose.

**2.2. RL Test and Isolation of Vermilion Mutants.** 1-2-days old *brown (bw)* males, in groups of 30 individuals, were placed in glass tubes, with eight layers of glass microfiber paper (Whatmann, GF/A) at the bottom, soaked with 0.9 ml of different DES concentrations. Negative controls were carried out treating males only with the solvent solution. After 3 hours treatment, males were mated to *In(1)sc<sup>S1</sup>L sc<sup>R</sup>In(1)dl<sup>pr</sup> – ” 49, y, sc<sup>S1</sup>sc<sup>R</sup>, v; bw; mus308<sup>D2</sup> (I, v; bw; mus308)* virgin females (for marker descriptions see [19]). Protocols for fractionation the progeny in mature sperm and spermatids for the recessive lethal (RL) test and for isolation of F<sub>1</sub> and F<sub>2</sub>*vermilion (v)* mutants were described elsewhere [14].

At least five different experiments were carried out for each concentration and, since there were no differences

among them, data were pooled. Statistical analysis of RL results was performed comparing mutant frequencies in treated flies with their respective negative controls, using the Fisher exact test.

The influence of *mus308* in the repair or processing of ethylation-induced damage was measured through the mutability index (MI) [20], and the statistical analysis of Aguirrezabalaga et al. [13] was carried out to determine whether MI values significantly differed from 1.

**2.3. Molecular Analysis of Mutations.** For each transmissible *vermilion* mutant, a homozygous strain was established to carry out the molecular analysis. All the isolated mutants were analysed.

The isolation of DNA and PCR amplifications were as described [21]. Mutant *vermilion* genes were cloned in the *M13mp19* vector or in a *pUC18* plasmid [22]. Sequencing reactions for the coding region were carried out using the dideoxy method, with a set of 10 internal primers. A fragment of about 1.8 Kb, localized upstream of the coding region, was analyzed as described before [21] in those mutants which did not show changes in the coding sequence. In order to exclude Taq polymerase-introduced errors, at least two plaques or colonies from independent PCR reactions were sequenced for each mutant.

Statistical analyses of differences between mutation spectra were carried out using the hypergeometric test for comparison of samples from mutational spectra [23, 24].

## 3. Results and Discussion

**3.1. RL and Vermilion Mutation Frequencies.** The RL and *vermilion* mutation frequencies, both spontaneous and induced by the different DES concentrations under *mus308* deficient (*mus308*<sup>−</sup>) conditions, are presented in Table 1. Pooled data from mature sperm and spermatids are shown, because no differences between them were found in any case (not shown).

All chemically induced RL mutation frequencies are statistically higher than the spontaneous one, although their values decrease as DES concentration increases. Comparisons with the results previously obtained in *mus308* proficient (*mus308*<sup>+</sup>) conditions [25] reveal two relevant differences (Table 1). First, the spontaneous RL frequency is statistically lower in *mus308*<sup>−</sup> than in *mus308*<sup>+</sup> conditions. Second, in *mus308*<sup>−</sup> conditions, a decrease in RL frequencies is induced as DES concentration increases, whereas the opposite, that is an increase was detected in efficient repair conditions. Consequently, the value of the mutability index (MI) for 10 mM DES is statistically higher than 1 whereas for 15 mM and 25 mM the MIs are lower than 1 (Table 1).

To analyse the dose range between 10 and 15 mM DES, and to compare both repair conditions in the same experiment, a new and small experiment was carried out with 12 mM concentration. The obtained results confirmed that when the amount of DNA damage is low or moderate, hypermutability is obtained (4.8% and 8.2% RL mutation frequencies in *mus308*<sup>+</sup> and in *mus308*<sup>−</sup>, respectively, with

TABLE 1: Recessive lethal (RL) and  $\nu$  mutation frequencies induced by DES on postmeiotic male germ cells of *D. melanogaster*, under *mus308* deficient (*mus308*<sup>-</sup>) and efficient (*mus308*<sup>+</sup>) conditions. Values of mutability index (MI) and their statistical signification are also presented.

Repair status	Treat.	Dose (mM)	F <sub>1</sub> Analysis			F <sub>2</sub> Analysis				MI <sup>(b)</sup> ( <i>Mmus308</i> <sup>-</sup> / <i>Mmus308</i> <sup>+</sup> )
			Offspring	$\nu$ mutants	Freq. ( $\times 10^{-4}$ )	Offspring <sup>(a)</sup>	$\nu$ mutants	Freq. ( $\times 10^{-4}$ )	%RL	
<i>mus308</i> <sup>-</sup>	Control		24002	0	0	15698	0	0	0.17	
	DES	10	19582	0	0	12576	0	0	3.04***	1.55***
		15	154737	2	0.13	56093	11	1.96	2.91***	0.13***
		25	10092	0	0	6925	0	0	0.51***	0.01***
<i>mus308</i> <sup>+</sup>	Control		8678	0	0	6766	0	0	0.28	
	DES <sup>(c)</sup>	10	54175	0	0	13090	2	1.53	2.13***	
		15	23209	4	1.72	9101	13	14.28	20.78***	
		25	15853	6	3.78	4703	5	10.63	29.22***	

(a) The F<sub>2</sub> offspring is the number of nonsterile treated X-chromosomes(b) MI: mutation frequency induced in *mus308*<sup>-</sup> / mutation frequency induced in *mus308*<sup>+</sup>(c) Data from Sierra et al. [25]. One experiment was carried out mating the treated males to *I, $\nu$ ;bw* females to check the validity of these previous data for comparisons.\**P* < .05; \*\**P* < .01; \*\*\**P* < .001.TABLE 2: Molecular characterization of  $\nu$  mutants induced by DES in postmeiotic male germ cells, under *mus308*<sup>-</sup> conditions.

Mutant	Brood	Position	Mutation	Change	Sequence (5'–3') <sup>(a)</sup>
D8-4	F <sub>2</sub> -1B	92–556	464 bp deletion		
D8-5	F <sub>2</sub> -1B	566	CG-TA	Leu-Phe	ACAG C TCCTG
D8-6	F <sub>2</sub> -1B	6	TA-AT	Ser-Arg	TCAG T TCGC
		129	TA-CG	intron	tcag t tctg
		323	TA-CG	intron	tgag t aggt
		398	CG-AT	Gln-Lys	CAAG C AGAT
		416	GC-TA	Asp-Tyr	GTTC G ACTC
D8-7	F <sub>2</sub> -1B	1167	GC-AT	Trp-STOP	AAGT G GAGA
D8-8	F <sub>2</sub> -2C	648	CG-TA	Ser-Phe	GCAT C TGGT
D8-9	F <sub>2</sub> -1A		No mutation		
D8-11	F <sub>2</sub> -1C	-944	AT-TA		TATA A ATAT
		-243	TA-AT		TCAG T TATT
D8-12	F <sub>2</sub> -1A	492	GC-AT	Arg-Gln	AACC G AGTG
D8-14	F <sub>2</sub> -2A	494	GC-AT	Val-Met	CCGA G TGGT
D8-18	F <sub>2</sub> -2A	1128	TA-CG	Leu-Pro	TTGC T CACC
		1168	GC-AT	Trp-STOP	AGTG G AGAT
D8-19	F <sub>2</sub> -2A	596	AT-GC	Thr-Ala	GGAG A CCAT
D8-21	F <sub>2</sub> -2A	974	CG-TA	Arg-STOP	GAAG C GACG
D8-23	F <sub>2</sub> -2A	656	CG-TA	Gln-STOP	TTTT C AGTC
D8-26 <sup>(b)</sup>	F <sub>2</sub> -2A	promotor			
D8-27	F <sub>2</sub> -1C	322	GC-AT	intron	gtga g tag
D8-29	F <sub>2</sub> -2C	875	CG-TA	Gln-STOP	GTTT C AGGA
D8-30	F <sub>1</sub> -2B	974	CG-TA	Arg-STOP	GAAG C GACG
D8-31	F <sub>1</sub> -2C	-323	TA-AT		TCAG T TATT
		-945–935	10 bp deletion		

(a) Since for some mutation types the damaged base could not be identified, the sequence surrounding the detected change in the coding strand is presented. Intron sequences are shown in lower case letters, exon sequences in capitals.

(b) See text for details.

TABLE 3: Relative and absolute mutation frequencies ( $F_1$  and  $F_2$  values expressed as mutation frequencies  $\times 10^{-5}$ ) of the different mutation types constituting the mutation spectra induced by DES in postmeiotic male germ cells, in  $mus308^-$  and  $mus308^+$  conditions.

Chemical	Mutation type	$mus308^-$			$mus308^{+(a)}$		
		Relative frequency %	Absolute frequency ( $\times 10^{-5}$ ) $F_1$ $F_2$		Relative frequency %	Absolute frequency ( $\times 10^{-5}$ ) $F_1$ $F_2$	
DES	GC-AT	47.8	0.5	7.9	73.3	6.8	49.0
	AT-GC	17.4	—	5.3	3.3	—	3.3
	AT-TA	17.4	0.5	4.0	10.0	1.9	3.3
	AT-CG	—	—	—	6.7	1.0	3.3
	GC-TA	8.7	—	2.6	—	—	—
	Deletions	8.7	0.5	1.3	6.7	—	6.5

<sup>(a)</sup>Data of  $mus308^+$  conditions are from Sierra et al. [25]. One experiment was carried out mating the treated males to  $I;v;bw$  females to check the validity of the previous data for comparisons.

a statistically significant MI of 1.7). It is noticeable that the very high rise in mutation frequency was detected between 10–12 mM and 15 mM DES in efficient repair conditions, but it is not unusual to find such a narrow window of increased activity in a chemical [26].

The obtained results demonstrate that Mus308 detects and processes DES-induced DNA damages. On one hand, low effectiveness DES doses, such as 10–12 mM (inducing low mutation frequencies), cause DNA damage, mostly oxygen alkylations [27], that seems to be processed through an error-free pathway, as pointed by the observed hypermutability. On the other hand, with high effectiveness DES doses (such as 15 and 25 mM), able to induce also considerable nitrogen alkylations [27], the obtained results indicate hypomutability; this fact, together with a decreased induced fertility, suggest that a functional Mus308 protein is necessary for the survival of the fertilized eggs.

The analysis of *vermilion* mutation frequencies (Table 1) show that, under  $mus308^-$  conditions and considering all concentrations together, 2 mutants were isolated in  $F_1$  ( $0.11 \times 10^{-4}$  mutation frequency) while most  $v$  mutants, 11, were isolated among the  $F_2$  offspring ( $1.46 \times 10^{-4}$  mutation frequency). Other 5  $v$  mutants were isolated from mass cultures, but they are not included in the mutation frequency estimations. Additionally, another mutant induced by DES was identified by genetic analysis as a translocation between the X and Y chromosomes that does not include the  $v$  locus. A comparison of these data with those obtained under  $mus308$  proficient conditions [25] reveals that the  $F_1$  and  $F_2$  induced mutation frequencies are much lower in  $mus308^-$  than in  $mus308^+$  conditions, indicating that the hypomutability observed with RL frequencies also extends to  $v$  mutation frequencies.

These results are in agreement with those previously obtained with ENU in the same cell type and under the same repair conditions. In that case, hypermutability was observed with a concentration that induced a moderate level of DNA damage (1 mM ENU), and similar results were found in RL and *vermilion* mutation frequencies analysis [14].

Results obtained here are consistent with a HR-mediated bypass of DNA damage if at least part of this damage induces cell mortality. However, a bypass tolerance system mediated by TLS could be also implicated in the processing of DES

induced damaged. Thus, a DNA polymerase could process error-free some DNA damage, like oxygen alkylation, when the amount of DNA damage is low, but the processing of other types of induced DNA lesions, especially when they are present in high amounts (because other repair systems are saturated or inactive), like nitrogen alkylation, could be error-prone [28].

Moreover, there is another tolerance system, the alternative end-joining process (alt-EJ), independent of ligase 4 [29]. *mus308* was very recently discovered to be involved in this system [30], which processes DNA double strand breaks generated by replication blockage. Our results are compatible also with this system because nitrogen alkylations can be the source of DNA strand breaks [27].

**3.2. Mutation Spectra.** Details of DES-induced mutants are shown in Table 2. In D8-9 no mutation was found, and the same mutation was present in the independent mutants D8-21 and D8-30, as previously reported for other *vermilion* spectra [14, 18, 21, 31, 32]. In D8-26 no mutation was detected in the coding region nor in the proximal part of the promoter, but the distal part of the promoter could not be amplified, suggesting the presence of a mutation. Additionally, D8-6 presented five different mutations none of which was found in any other mutant. No mutants were isolated either from the 24002  $F_1$  and 15698  $F_2$  flies analysed in the concurrent control experiments or in the historical control; therefore, we consider that the observed mutations were induced by DES. The  $v$  mutation spectrum, constituted by the 23 obtained mutations, is summarized in Table 3 and includes two deletions (8.7%) and 21 base pair changes, distributed as follows: 11 GC-AT (47.8%) and 4 AT-GC (17.4%) transitions, and 4 AT-TA (17.4%) and 2 GC-TA (8.7%) transversions.

The pairing up of these mutations with the several adducts induced by DES indicates that: (i) the GC-AT and AT-GC transitions in the DES spectrum should be, respectively, the consequence of the O<sup>6</sup>-ethylguanine and O<sup>4</sup>-ethylthymine adducts [33–36], induced by this chemical [37–39]; (ii) AT-TA transversions are most probably due to N-ethylation [40], like the rest of transversions and the deletions [25, 27], because DES does not ethylate

O<sup>2</sup>-thymine [37]. The two found deletions occur between direct repeats and, as the translocation, they can be indirectly generated from N-ethylation, as described before [27].

Comparison of the relative mutation frequencies of this *mus308*<sup>-</sup> spectrum with those previously obtained under *mus308*<sup>+</sup> conditions (Table 3) reveals clear differences ( $P = .07$ , with the hypergeometric test, and lower if the translocation is considered), including a strong decrease in the frequency of GC-AT transitions, and increases in the frequencies of AT-GC transitions, transversions and deletions under *mus308*<sup>-</sup> conditions. These results confirm that Mus308 is processing O<sup>6</sup>-ethylguanine and O<sup>4</sup>-ethylthymine, as indicated before [14], and reveal that this protein is also processing N-ethylation damage.

O<sup>6</sup>-ethylguanine, like O<sup>6</sup>-methylguanine, is a stable DNA lesion [37] that can mispair with T to produce GC-AT transitions as indicated but can also pair correctly with C [41] or can even block DNA polymerases [41, 42]. Therefore, O<sup>6</sup>-ethylguanine can fit as a substrate of Mus308. O<sup>4</sup>-ethylthymine is a DNA damage with a long half-life [37], difficult to repair in mammals [43–45]. Although it is not considered a lethal lesion [33, 36], it is able to block DNA replication in mammalian cells in a NER deficient background [46]. NER is apparently implicated in its repair in *Drosophila* [27, 32], although rather inefficiently, because AT-GC transitions are one of the most frequently ENU-induced damages in the repair-active premeiotic germ cells of this organism [21, 31]. Therefore, this adduct fits with the proposed requirements for the substrates of Mus308 [13, 14].

Since at least part of the N-ethylation damage can be persistent and can block DNA synthesis [37], its detection as substrate of Mus308, especially when the level of DNA damage is very high and repair is difficult, is not unexpected or strange. Additionally, it can be considered that N-ethylation is a source of DNA strand breaks [27], and this type of DNA damage is substrate of Mus308 in the alt-EJ system [30].

The sequence specificity of DES- induced mutations was studied determining the base pairs 5' and 3' of the damaged nucleotide (Table 2). The results of this analysis show that AT pairs are present at 5' in 64% of GC-AT mutations in *mus308*<sup>-</sup> conditions whereas 64%–70% of this type of mutations is preceded by GC pairs at 5' in *mus308*<sup>+</sup> conditions [25] and in NER deficient conditions [27], respectively. This means that the neighbouring sequences 5' to O<sup>6</sup>-ethylguanine change depending on the Mus308 status, which is in good accordance with the proposed polymerase function of Mus308, specially considering that no influence of surrounding sequences was found before for this chemical in this locus [25, 27], nor were expected for an S<sub>N</sub>1/S<sub>N</sub>2 alkylating agent [47].

In summary, the results presented in this paper demonstrate that Mus308 processes oxygen and nitrogen alkylations, and they support its role in a tolerance mechanism that is especially relevant in case of high DNA damage levels, because it prevents cell death. Additionally, these results suggest that this protein could act through a TLS pathway, because of (i) the detected neighbouring sequence influence, and (ii) its DNA polymerase activity. Finally, these results also agree with the Mus308 role in the alt-EJ system, for the

processing of DNA damage-inducing strand breaks, which can be compatible with the TLS pathway [30].

## Acknowledgments

This work was supported by Grants PB95/1043 and PB98/1561, sponsored by the DGES-Spanish Ministry of Education and Science. N.D-Valdes. was granted by FICYT (Asturias) with a predoctoral fellowship. The authors thank Drs. L. Alvarez, F. Barros, M. Sierra, and J.A. Ferreiro for critically reading the manuscript and HERO-España and Agua de Cuevas for providing glass and plastic material.

## References

- [1] P. V. Harris, O. M. Mazina, E. A. Leonhardt, R. B. Case, J. B. Boyd, and K. C. Burtis, "Molecular cloning of *Drosophila mus308*, a gene involved in DNA cross-link repair with homology to prokaryotic DNA polymerase I genes," *Molecular and Cellular Biology*, vol. 16, no. 10, pp. 5764–5771, 1996.
- [2] M. Oshige, N. Aoyagi, P. V. Harris, K. C. Burtis, and K. Sakaguchi, "A new DNA polymerase species from *Drosophila melanogaster*: a probable *mus308* gene product," *Mutation Research*, vol. 433, no. 3, pp. 183–192, 1999.
- [3] F. Marini and R. D. Wood, "A human DNA helicase homologous to the DNA cross-link sensitivity protein *mus308*," *Journal of Biological Chemistry*, vol. 277, no. 10, pp. 8716–8723, 2002.
- [4] S. Inagaki, T. Suzuki, M.-A. Ohto et al., "Arabidopsis TEBICHI, with helicase and DNA polymerase domains, is required for regulated cell division and differentiation in meristems," *Plant Cell*, vol. 18, no. 4, pp. 879–892, 2006.
- [5] F. S. Sharief, P. J. Vojta, P. A. Ropp, and W. C. Copeland, "Cloning and chromosomal mapping of the human DNA polymerase  $\theta$  (POLQ), the eighth human DNA polymerase," *Genomics*, vol. 59, no. 1, pp. 90–96, 1999.
- [6] F. Marini, N. Kim, A. Schuffert, and R. D. Wood, "POLN, a nuclear PolA family DNA polymerase homologous to the DNA cross-link sensitivity protein *mus308*," *Journal of Biological Chemistry*, vol. 278, no. 34, pp. 32014–32019, 2003.
- [7] M. Seki, F. Marini, and R. D. Wood, "POLQ (Pol  $\theta$ ), a DNA polymerase and DNA-dependent ATPase in human cells," *Nucleic Acids Research*, vol. 31, no. 21, pp. 6117–6126, 2003.
- [8] N. Shima, S. A. Hartford, T. Duffy, L. A. Wilson, K. J. Schimenti, and J. C. Schimenti, "Phenotype-based identification of mouse chromosome instability mutants," *Genetics*, vol. 163, no. 3, pp. 1031–1040, 2003.
- [9] N. Shima, R. J. Munroe, and J. C. Schimenti, "The mouse genomic instability mutation *chaos1* is an allele of Polq that exhibits genetic interaction with *Atm*," *Molecular and Cellular Biology*, vol. 24, no. 23, pp. 10381–10389, 2004.
- [10] M. Seki, C. Masutani, L. W. Yang et al., "High-efficiency bypass of DNA damage by human DNA polymerase Q," *EMBO Journal*, vol. 23, no. 22, pp. 4484–4494, 2004.
- [11] G. Maga, I. Shevelev, K. Ramadan, S. Spadari, and U. Hübscher, "DNA polymerase  $\theta$  purified from human cells is a high-fidelity enzyme," *Journal of Molecular Biology*, vol. 319, no. 2, pp. 359–369, 2002.
- [12] J. B. Boyd, K. Sakaguchi, and P. V. Harris, "*mus308* Mutants of *Drosophila* exhibit hypersensitivity to DNA cross-linking agents and are defective in a deoxyribonuclease," *Genetics*, vol. 125, no. 4, pp. 813–819, 1990.

- [13] I. Aguirrezabalaga, L. M. Sierra, and M. A. Comendador, "The hypermutability conferred by the *mus308* mutation of *Drosophila* is not specific for cross-linking agents," *Mutation Research*, vol. 336, no. 3, pp. 243–250, 1995.
- [14] L. Tosal, M. A. Comendador, and L. M. Sierra, "The *mus308* locus of *Drosophila melanogaster* is implicated in the bypass of ENU-induced O-alkylpyrimidine adducts," *Molecular and General Genetics*, vol. 263, no. 1, pp. 144–151, 2000.
- [15] J. Hernando, L. Álvarez, J. A. Ferreiro, I. Sancho, M. A. Comendador, and L. M. Sierra, "Female germ cell mutagenicity of model chemicals in *Drosophila melanogaster*: mechanistic information and analysis of repair systems," *Mutation Research*, vol. 545, no. 1–2, pp. 59–72, 2004.
- [16] J. J. Sekelsky, K. C. Burtis, and R. S. Hawley, "Damage control: the pleiotropy of DNA repair genes in *Drosophila melanogaster*," *Genetics*, vol. 148, no. 4, pp. 1587–1598, 1998.
- [17] C. Bilbao, J. A. Ferreiro, M. A. Comendador, and L. M. Sierra, "Influence of *mus201* and *mus308* mutations of *Drosophila melanogaster* on the genotoxicity of model chemicals in somatic cells in vivo measured with the comet assay," *Mutation Research*, vol. 503, no. 1–2, pp. 11–19, 2002.
- [18] M. J. M. Nivard, I. Aguirrezabalaga, L. A. P. Ballering, A. Pastink, L. M. Sierra, and E. W. Vogel, "Evaluation of the database on mutant frequencies and DNA sequence alterations of vermilion mutations induced in germ cells of *Drosophila* shows the importance of a neutral mutation detection system," *Mutation Research*, vol. 431, no. 1, pp. 39–57, 1999.
- [19] L. D. Lindsley and G. G. Zimm, *The Genome of Drosophila melanogaster*, Academic Press, San Diego, Calif, USA, 1992.
- [20] E. W. Vogel, "Nucleophilic selectivity of carcinogens as a determinant of enhanced mutational response in excision repair-defective strains in *Drosophila*: effects of 30 carcinogens," *Carcinogenesis*, vol. 10, no. 11, pp. 2093–2106, 1989.
- [21] L. Álvarez, M. A. Comendador, and L. M. Sierra, "O-ethylthymidine adducts are the most relevant damages for mutation induced by N-ethyl-N-nitrosourea in female germ cells of *Drosophila melanogaster*," *Environmental and Molecular Mutagenesis*, vol. 40, no. 2, pp. 143–152, 2002.
- [22] L. Álvarez, M. A. Comendador, and L. M. Sierra, "Effect of nucleotide excision repair on ENU-induced mutation in female germ cells of *Drosophila melanogaster*," *Environmental and Molecular Mutagenesis*, vol. 41, no. 4, pp. 270–279, 2003.
- [23] W. T. Adams and T. R. Skopek, "Statistical test for the comparison of samples from mutational spectra," *Journal of Molecular Biology*, vol. 194, no. 3, pp. 391–396, 1987.
- [24] N. F. Cariello, W. W. Piegorsch, W. T. Adams, and T. R. Skopek, "Computer program for the analysis of mutational spectra application to p53 mutations," *Carcinogenesis*, vol. 15, no. 10, pp. 2281–2285, 1994.
- [25] L. M. Sierra, A. Pastink, M. J. M. Nivard, and E. W. Vogel, "DNA base sequence changes induced by diethyl sulfate in postmeiotic male germ cells of *Drosophila melanogaster*," *Molecular and General Genetics*, vol. 237, no. 3, pp. 370–374, 1993.
- [26] D. Brusick, *Principles of Genetic Toxicology*, Plenum Press, New York, NY, USA, 2nd edition, 1987.
- [27] L. M. Sierra, M. M. J. Nivard, and E. W. Vogel, "Influence of nucleotide excision repair and of dose on the types of vermilion mutations induced by diethyl sulfate in postmeiotic male germ cells of *Drosophila*," *Mutation Research*, vol. 431, no. 1, pp. 69–79, 1999.
- [28] E. C. Friedberg, W. J. Feaver, and V. L. Gerlach, "The many faces of DNA polymerases: strategies for mutagenesis and for mutational avoidance," *Proceedings of the National Academy of Sciences of the United States of America*, vol. 97, no. 11, pp. 5681–5683, 2000.
- [29] M. McVey and S. E. Lee, "MMEJ repair of double-strand breaks (director's cut): deleted sequences and alternative endings," *Trends in Genetics*, vol. 24, no. 11, pp. 529–538, 2008.
- [30] S. H. Chan, A. M. Yu, and M. McVey, "Dual roles for DNA polymerase theta in alternative end-joining repair of double-strand breaks in *Drosophila*," *PLOS Genet*, vol. 6, Article ID e1001005, 2010.
- [31] L. Tosal, M. A. Comendador, and L. M. Sierra, "N-Ethyl-N-nitrosourea predominantly induces mutations at AT base pairs in pre-meiotic germ cells of *Drosophila* males," *Mutagenesis*, vol. 13, no. 4, pp. 375–380, 1998.
- [32] L. Tosal, M. A. Comendador, and L. M. Sierra, "In vivo repair of ENU-induced oxygen alkylation damage by the nucleotide excision repair mechanism in *Drosophila melanogaster*," *Molecular and General Genetics*, vol. 265, no. 2, pp. 327–335, 2001.
- [33] R. Saffhill, G. P. Margison, and P. J. O'Connor, "Mechanisms of carcinogenesis induced by alkylating agents," *Biochimica et Biophysica Acta*, vol. 823, no. 2, pp. 111–145, 1985.
- [34] K. S. Ellison, E. Dogliotti, T. D. Connors, A. K. Basu, and J. M. Essigmann, "Site-specific mutagenesis by O<sup>6</sup>-alkylguanines located in the chromosomes of mammalian cells: influence of the mammalian O<sup>6</sup>-alkylguanine-DNA alkyltransferase," *Proceedings of the National Academy of Sciences of the United States of America*, vol. 86, no. 22, pp. 8620–8624, 1989.
- [35] J. C. Klein, M. J. Bleeker, J. T. Lutgerink et al., "Use of shuttle vectors to study the molecular processing of defined carcinogen-induced DNA damage: mutagenicity of single O<sup>4</sup>-ethylthymine adducts in HeLa cells," *Nucleic Acids Research*, vol. 18, no. 14, pp. 4131–4137, 1990.
- [36] M. K. Dosanjh, P. Menichini, R. Eritja, and B. Singer, "Both O<sup>4</sup>-methylthymine and O<sup>4</sup>-ethylthymine preferentially form alkyl T·G pairs that do not block in vitro replication in a defined sequence," *Carcinogenesis*, vol. 14, no. 9, pp. 1915–1919, 1993.
- [37] D. T. Beranek, "Distribution of methyl and ethyl adducts following alkylation with monofunctional alkylating agents," *Mutation Research*, vol. 231, no. 1, pp. 11–30, 1990.
- [38] M. Bignami, A. Vitelli, A. Di Muccio et al., "Relationship between specific alkylated bases and mutations at two gene loci induced by ethylnitrosourea and diethyl sulfate in CHO cells," *Mutation Research*, vol. 193, no. 1, pp. 43–51, 1988.
- [39] P. Fortini, A. Calcagnile, A. Di Muccio, M. Bignami, and E. Dogliotti, "Quantitative relationship between ethylated DNA bases and gene mutation at two loci in CHO cells," *Environmental and Molecular Mutagenesis*, vol. 21, no. 2, pp. 154–159, 1993.
- [40] L. A. Loeb and B. D. Preston, "Mutagenesis by apurinic/apyrimidinic sites," *Annual Review of Genetics*, vol. 20, pp. 201–230, 1986.
- [41] M. K. Dosanjh, E. L. Loechler, and B. Singer, "Evidence from in vitro replication that O<sup>6</sup>-methylguanine can adopt multiple conformations," *Proceedings of the National Academy of Sciences of the United States of America*, vol. 90, no. 9, pp. 3983–3987, 1993.
- [42] G. T. Pauly, S. H. Hughes, and R. C. Moschel, "Mutagenesis in *Escherichia coli* by three O<sup>6</sup>-substituted guanines in double-stranded or gapped plasmids," *Biochemistry*, vol. 34, no. 27, pp. 8924–8930, 1995.
- [43] S. M. Bronstein, T. R. Skopek, and J. A. Swenberg, "Efficient repair of O<sup>6</sup>-ethylguanine, but not O<sup>4</sup>-ethylthymine or O<sup>2</sup>-ethylthymine, is dependent upon O<sup>6</sup>-alkylguanine-DNA

- alkyltransferase and nucleotide excision repair activities in human cells," *Cancer Research*, vol. 52, no. 7, pp. 2008–2011, 1992.
- [44] C. W. Op Het Veld, S. Van Hees-Stuivenberg, A. A. Van Zeeland, and J. G. Jansen, "Effect of nucleotide excision repair on hprt gene mutations in rodent cells exposed to DNA ethylating agents," *Mutagenesis*, vol. 12, no. 6, pp. 417–424, 1997.
- [45] A. E. Pegg, "Repair of O<sup>6</sup>-alkylguanine by alkyltransferases," *Mutation Research*, vol. 462, no. 2-3, pp. 83–100, 2000.
- [46] J. C. Klein, M. J. Bleeker, H. C. P. F. Roelen et al., "Role of nucleotide excision repair in processing of O<sup>4</sup>-alkylthymines in human cells," *Journal of Biological Chemistry*, vol. 269, no. 41, pp. 25521–25528, 1994.
- [47] M. J. Horsfall, A. J. E. Gordon, P. A. Burns, M. Zielenska, G. M. E. Van der Vliet, and B. W. Glickman, "Mutational specificity of alkylating agents and the influence of DNA repair," *Environmental and Molecular Mutagenesis*, vol. 15, no. 2, pp. 107–122, 1990.

## Research Article

# Is the Comet Assay a Sensitive Procedure for Detecting Genotoxicity?

Satomi Kawaguchi,<sup>1</sup> Takanori Nakamura,<sup>2</sup> Ayumi Yamamoto,<sup>1</sup> Gisho Honda,<sup>2</sup> and Yu F. Sasaki<sup>1</sup>

<sup>1</sup>Laboratory of Genotoxicity, Faculty of Chemical and Biological Engineering, Hachinohe National College of Technology, Uwanotai 16-1, Hachinohe, Aomori 039-1192, Japan

<sup>2</sup>Department of Pharmaceutical Health Care, Faculty of Pharmaceutical Sciences, Himeji Dokkyo University, Kamiohno 7-2-1, Himeji, Hyogo 670-8524, Japan

Correspondence should be addressed to Yu F. Sasaki, yfsasakiaugsta@yahoo.co.jp

Received 30 May 2010; Revised 9 September 2010; Accepted 4 October 2010

Academic Editor: Shigenori Iwai

Copyright © 2010 Satomi Kawaguchi et al. This is an open access article distributed under the Creative Commons Attribution License, which permits unrestricted use, distribution, and reproduction in any medium, provided the original work is properly cited.

Although the Comet assay, a procedure for quantitating DNA damage in mammalian cells, is considered sensitive, it has never been ascertained that its sensitivity is higher than the sensitivity of other genotoxicity assays in mammalian cells. To determine whether the power of the Comet assay to detect a low level of genotoxic potential is superior to those of other genotoxicity assays in mammalian cells, we compared the results of Comet assay with those of micronucleus test (MN test). WTK1 human lymphoblastoid cells were exposed to methyl nitrosourea (MNU), ethyl nitrosourea (ENU), methyl methanesulfonate (MMS), ethyl methanesulfonate (EMS), bleomycin (BLM), or UVC. In Comet assay, cells were exposed to each mutagen with (Comet assay/araC) and without (Comet assay) DNA repair inhibitors (araC and hydroxyurea). Furthermore, acellular Comet assay (acellular assay) was performed to determine how single-strand breaks (SSBs) as the initial damage contributes to DNA migration and/or to micronucleus formation. The lowest genotoxic dose (LGD), which is defined as the lowest dose at which each mutagen causes a positive response on each genotoxicity assay, was used to compare the power of the Comet assay to detect a low level of genotoxic potential and that of MN test; that is, a low LGD indicates a high power. Results are summarized as follows: (1) for all mutagens studied, LGDs were MN test  $\leq$  Comet assay; (2) except for BLM, LGDs were Comet assay/araC  $\leq$  MN test; (3) except for UVC and MNU, LGDs were acellular assay  $\leq$  Comet assay/araC  $\leq$  MN test  $\leq$  Comet assay. The following is suggested by the present findings: (1) LGD in the Comet assay is higher than that in MN test, which suggests that the power of the MN test to detect a low level of genotoxic potential is superior to that of the Comet assay; (2) for the studied mutagens, all assays were able to detect all mutagens correctly, which suggests that the sensitivity of the Comet assay and that of the MN test were exactly identical; (3) the power of the Comet assay to detect a low level of genotoxic potential can be elevated to a level higher than that of MN test by using DNA synthesis inhibitors, such as araC and HU.

## 1. Introduction

Many methods have been used to identify genotoxic substances, including the detection of DNA damage, chromosome aberrations, and gene mutations both *in vitro* and *in vivo*. The Comet assay, which can detect single-strand breaks (SSBs) as initial damage and those developed from alkali-labile sites under alkaline condition (pH > 12.6), is a rapid and sensitive procedure for detecting genotoxicity in mammalian cells [1, 2]. When the sensitivity of a

genotoxicity testing method is regarded as high, it means that it can detect wide variety of compounds with unknown genotoxic potential and that the assay can detect a low level of genotoxic potential by known genotoxic compounds. The former is very important in order to avoid pseudonegative results. In general, therefore, compounds with unknown genotoxic potential are assayed at a high dose, including maximum tolerated (subtoxic) dose. The genotoxic dose response curve for genotoxic compounds is thought to reach zero without having a no-response level at a low

dose. This statement forms the basis of the “nonthreshold concept” in the risk assessment, which describes the absence of a threshold in genotoxic potential. The “nonthreshold concept” for genotoxic compounds means that these agents could have an influence on humans even at very low-levels [3]. Therefore, it is important to detect low level genotoxicity.

Although the Comet assay is considered highly sensitive [1, 2], it has not been well ascertained whether its sensitivity to detect genotoxicity is higher than that of other procedures. Although the Comet assay is essentially a method of detecting single-strand breaks (SSBs), we have shown that a low level of SSB as the initial damage cannot be detected by the Comet assay because these SSBs disappear following a repair event and that SSBs as initial DNA damage can be well detected in the acellular Comet assay (acellular assay) [4]. The Comet assay can directly detect not only SSBs as initial DNA damage but also SSBs that develop from alkali-labile sites under alkaline condition ( $\text{pH} > 12.6$ ) and that formed during repair of base adducts or alkylated bases, which are not initial DNA damage [5]. The micronucleus test (MN test) is a standard procedure that can detect structural chromosome aberrations derived from initial damage in the S phase and/or numerical chromosome aberrations due to aneuploidic effects in the M phase [6, 7]. Pfau et al. [8] conducted combined experiments with MLC5 cells including Comet assay and MN test and showed that the genotoxicity of heterocyclic amines was observed at concentrations that were 2000-fold lower on MN test than on Comet assay. However, Van Goethem et al. showed that the lowest genotoxic concentrations of pure cobalt powder, a cobalt-containing alloy, and cobalt-tungsten carbide were lower on Comet assay than on MN test [9]. Hartmann et al. [10] tested 36 pharmaceutical compounds with unknown genotoxic potential comparatively in the Comet assay and MN test using V79 Chinese hamster cells and reported that more compounds were positive in the MN test than in the Comet assay. Kawaguchi et al. [11] conducted combined experiments with TK6 and WTK1 cells including the Comet assay, chromosome aberration assay, and *TK* mutation assay and showed that the genotoxicity of kojic acid was observed at  $\geq 2500 \mu\text{g/mL}$  on Comet assay and the chromosome aberration test and at  $\geq 1250 \mu\text{g/mL}$  on *TK* mutation assay. However, the exposure conditions used in some of those studies differed among different assays (Pfau et al. [8] exposed cells for 30 min and 24 h in the Comet assay and MN test, resp.) and model mutagens with well-characterized action mechanisms were not used, making it difficult to systematically compare the sensitivities of those assays including the Comet assay. In our series of studies using well-known mutagens, we showed that SSBs as initial damage can be well detected by acellular assay but not by Comet assay under standard condition [4] and that the response of Comet assay to mutagens inducing DNA damage that can be repaired by the excision repair system tended to be affected by *p53* status [12]. Here, to discuss whether that the power of the Comet assay to detect a low level of genotoxic potential is superior to that of MN test, we conducted combined experiments with TK6 cells including (standard) Comet assay, acellular assay, and MN test under identical exposure conditions.

## 2. Materials and Methods

**2.1. Chemicals.** Methyl methanesulfonate (MMS) and ethyl methanesulfonate (EMS) were obtained from Sigma Chemicals Inc., St. Louis, MO (U.S.A.). Methyl nitrosourea (MNU) and ethyl nitrosourea (ENU) were purchased from Nacalai Tesque, Inc., Kyoto (Japan). They were dissolved in dimethyl sulfoxide (DMSO, Wako Pure Chemical Industries, Ltd., Osaka). Bleomycin (BLM, Wako Pure Chemical Industries, Ltd.) was dissolved in physiological saline. The DNA repair inhibitors hydroxyurea (HU) and cytosine-1- $\beta$ -D-arabinofuranoside (araC), purchased from Wako Pure Chemical Industries, Ltd., were dissolved in physiological saline. Regular (GP-42) and low melting point (LGT) agarose were obtained from Nacalai Tesque, Inc. and were diluted to 1% in physiological saline.

**2.2. Cells.** *TK*<sup>+/-</sup> heterozygote of the TK6 human lymphoblastoid cells exhibiting wild-type *p53* (generously donated by Dr. Honma, National Institute of Health Sciences, Tokyo) were used. Cells were maintained in logarithmic growth using RPMI 1640 medium (Nissui Pharmaceutical Co., Ltd.) supplemented with 10% horse serum (SAFC Biosciences), 200  $\mu\text{g/mL}$  sodium pyruvate, and 200  $\mu\text{g/mL}$  streptomycin at 37°C under a 5% CO<sub>2</sub> atmosphere.

**2.3. Cell Treatment with Mutagens.** Cells were centrifuged and resuspended in a culture medium at a concentration of  $5 \times 10^5$  cells/mL, and 1 mL of cell suspensions containing each chemical mutagen were incubated for 2 h in the presence (Comet assay/araC) or absence (Comet assay) of the DNA repair inhibitors araC (1.8 mM) and HU (10 mM). (The two inhibitors were used at concentrations that did not induce significant reductions in cell viability [12].) On Comet assay and Comet assay/araC, exposed cells were sampled immediately after chemical treatment, and the percentage of viable cells was measured by the trypan blue exclusion test. Relative survival (survival under each concentration compared with that of an untreated control) was obtained. For UVC irradiation, 1 mL of cell suspension in saline ( $5 \times 10^5$  cells/mL) in a 6-cm dish was irradiated with a germicide lamp (National GL15, 15W, Matsushita Electric Industrial Co., Japan), as the UVC source from a distance of 15 cm. Irradiated cells were incubated for 2 h in fresh medium with (Comet assay/araC) or without (Comet assay) DNA repair inhibitors (araC and HU) and then sampled.

**2.4. Comet Preparation.** Treated cells were suspended in 1% agarose-LGT at  $5 \times 10^5$  cells/75  $\mu\text{L}$ , and 75  $\mu\text{L}$  of cell suspension was immediately deposited on a fully frosted slide (Matsunami Glass Ind., Ltd., Osaka, Japan) which was coated with 1% agarose GP-42 and then covered with another slide glass. Although 0.5% LGT agarose is generally used, 1% LGT agarose (Nacalai Tesque, Inc.) was used in this study. In the case of LGT agarose obtained from Nacalai Tesque, Inc., 0.5% LGT is too soft to be used routinely in this assay. Although DNA migration tended to be lower in 1% LGT than in 0.5% LGT, there was no qualitative difference in the responses of

this assay in 0.5% and 1% (Figure 4), which is why 0.5% LGT agarose was used.

The slides were placed so as to allow the agarose to gel. The samples on the slides were then immediately exposed to a lysing solution (pH 10) of 2.5 M NaCl, 100 mM EDTA disodium ( $\text{Na}_2\text{EDTA}$ ), 10 mM Trizma, 1% sarkosyl, 10% DMSO, and 1% Triton X-100 and incubated at 4°C for 1 h. The slides were then placed on a horizontal gel electrophoresis platform and covered with pH > 13 alkaline solution composed of 300 mM NaOH and 1 mM  $\text{Na}_2\text{EDTA}$ . The slides were left in solution at 0°C for 20 min to allow unwinding of the DNA and expression of alkali-labile sites to occur. The power supply was set at 1 V/cm and 250 mA. The DNA was subjected to electrophoresis at 0°C for 20 min, and the slides were rinsed with 400 mM Trizma (pH 7.5) to neutralize the excess alkalinity. Each slide was stained with 50  $\mu\text{L}$  of 20  $\mu\text{g}/\text{mL}$  ethidium bromide (Wako Pure Chemical Industries, Ltd.) and covered with a coverslip. One hundred cells on two slides per dose (two slides were prepared for each dose) were examined and photographed (black and white ASA 400 Fuji film) at 200x magnification using a fluorescence microscope (Olympus) equipped with G filter. The whole length of the Comet (“migration”) was measured.

The measures of DNA migration include many parameters [13]: % of damaged cells (i.e., cells with tails), damaged categories (classified into various types or intensities based on shape), length of DNA migration (total or tail), and tail moment (e.g., amount of tail DNA x tail length). Although the use of % tail DNA is recommended [13], we used the whole length of the Comet as a unique parameter. Although the Comet image length is likely to be quantitatively inferior to % tail DNA, its qualitative power to differentiate positive and negative responses is not unsuitable and no parameters are unacceptable [13]. In this study, the responses on Comet assay were not analyzed quantitatively. LGDs for two versions of the Comet assay and MN test were obtained from qualitative analysis of the results (differentiation between positive and negative responses at each dose). Therefore, use of the whole length of the Comet as a unique parameter is not considered to have affected the results of this study.

The effect of chemical treatment on migration was analyzed using ANOVA and Dunnett test. The lowest genotoxic dose (LGD) was defined as the lowest dose where DNA migration increased significantly. In this study, LGD was used to compare the power of each assay to detect a low level of genotoxic potential of each mutagen; that is, low LGD shows high power.

**2.5. Acellular Comet Assay (Acellular Assay).** Slides for the Comet assay from untreated TK6 cells were prepared as outlined above and the slides were lysed immediately in a lysing solution at 4°C for one hour as described above. Lysed slides were neutralized in 400 mM Tris HCl buffer (pH 7.5) for 15 min and exposed to RPMI 1640 medium with 10% horse serum containing different concentrations of the test agents for 2 h at 37°C in the dark. After the treatment period, the slides were rinsed by immersion in cold distilled water, and then the slides were electrophoresed at pH > 13 and

0°C for 20 min after unwinding of the DNA at pH > 13 for 20 min. The power supply was set at 1 V/cm and 250 mA. In the Comet assay, although SSBs could be differentiated from alkali-labile lesions derived from base lesions; SSBs could be detected by electrophoresis at pH 12.1 and both SSBs and alkali-labile lesions by electrophoresis at pH > 13 [14]. DNA damage detected under the acellular condition at both pH 12 and pH > 13 were shown to be SSBs but not alkali-labile lesions, and there were no differences in the responses of the acellular assay at pH > 13 from those at pH 12 [15], which is why electrophoresis was conducted at pH > 13. For UVC irradiation, neutralized slides were irradiated by a germicide lamp (National GL15, 15W, Matsushita Electric Industrial Co., Japan) from a distance of 15 cm. Irradiated slides were incubated for 2 h in 400 mM Tris HCl buffer immediately after UVC-irradiation, and then the slides were electrophoresed at pH > 13 as described above.

**2.6. Micronucleus Test (MN Test).** Cells were exposed to each mutagen as described above. At the end of a treatment period, the cells were washed with Hanks’ BSS and cultured for 24 h in medium containing cytochalasin B at 3  $\mu\text{g}/\text{mL}$ , and then cells were sampled. For UVC irradiation, 1 mL of cell suspension in saline ( $1 \times 10^6$  cells/mL) in 6-cm dish was irradiated by a germicide lamp (National GL15, 15W, Matsushita Electric Industrial Co., Japan) as the UVC source from a distance of 15 cm. Irradiated cells were incubated for 24 h in medium containing cytochalasin B at 3  $\mu\text{g}/\text{mL}$ , and then cells were sampled. The collected cells were suspended in 0.075 M KCl hypotonic solution for 15 min, the cell suspension was concentrated to a volume of 1 mL, mixed with 1 mL of 10% neutral buffered formalin solution and then concentrated to a volume of 100  $\mu\text{L}$ . The cell suspension was further mixed with 100  $\mu\text{L}$  of 0.05 w/v% aqueous solution of acridine orange, and then 50  $\mu\text{L}$  of cell suspension was placed on a slide glass and mounted with 24  $\times$  48 mm cover slips. Binuclei cells with micronuclei (MNBNC) per 2000 binuclei cells (BNC) and BNC per 2000 cells were scored with the aid of fluorescence microscope (Olympus at 600x magnification) equipped with a B filter. The prevalence of MNBNC was analyzed statistically by  $\chi^2$  test. The lowest genotoxic dose (LGD) was defined as the lowest dose at which MNBNC increased significantly.

### 3. Results

Results of the Comet assay and Comet assay/araC are shown in Figure 1. Results of acellular assay and MN test are shown in Figures 2 and 3, respectively. LGDs are summarized in Table 1.

Both in Comet assay and Comet assay/araC, BLM, alkylating agents (MMS, EMS, MNU, and ENU), and UVC increased DNA migration significantly. In general, detection of DNA migration was greater on Comet assay/araC than on Comet assay. Both in the Comet assay and Comet assay/araC, relative survivals were >70% in the dose range of studied mutagens (data not shown). On acellular assay, BLM and alkylating agents, but not UVC, increased DNA migration

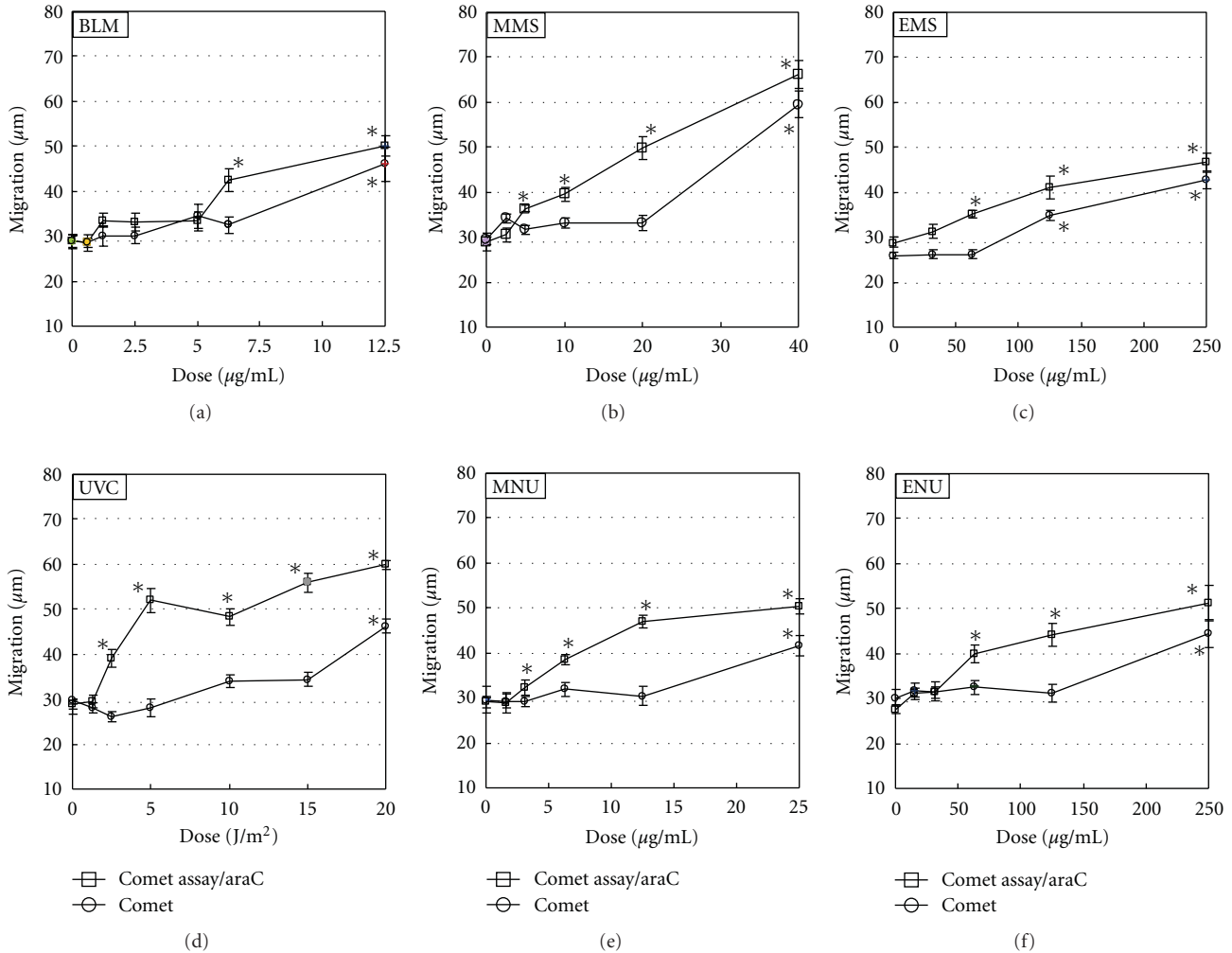


FIGURE 1: Comet assay and Comet assay/araC in TK6 cells. Slides for Comet assay were prepared immediately after the exposure to chemical mutagens for 2 h with or without araC/HU, or 2 h culture with or without araC/HU after UVC irradiation. Electrophoresis was conducted at pH > 13. Reproducibility was ascertained by three independent experiments, and representative data are shown. The error bars indicate standard errors of the mean. \*Significant difference from untreated control:  $P < .05$ .

TABLE 1: LGDs for Comet assay, Comet assay/araC, acellular assay, and MN test using TK6 cells.

Mutagen	LGD ( $\mu\text{g/mL}$ or $\text{J/m}^2$ )			Ratio of LGD	
	Comet assay	Comet assay/araC	acellular assay	MN test	(Comet assay: MN test)
UVC	20	2.5	—	15	1.3
MNU	25	3.125	6.25	12.5	2
ENU	250	62.5	31.3	125	2
MMS	40	20	10	20	2
EMS	125	62.5	62.5	125	1
BLM	12.5	6.25	0.0625	5	2.5

significantly. On MN test, BLM, alkylating agents, and UVC increased MNBNC significantly.

For BLM, LGDs were  $12.5 \mu\text{g/mL}$ ,  $6.25 \mu\text{g/mL}$ ,  $0.0625 \mu\text{g/mL}$ , and  $5 \mu\text{g/mL}$  in the Comet assay, Comet assay/araC, acellular assay, and MN test, respectively; that is, LGDs were acellular assay < MN test < Comet assay/araC < Comet assay. For MMS, LGDs were  $40 \mu\text{g/mL}$ ,  $20 \mu\text{g/mL}$ ,  $10 \mu\text{g/mL}$ ,

and  $20 \mu\text{g/mL}$  on Comet assay, Comet assay/araC, acellular assay, and MN test, respectively; that is, acellular assay < Comet assay/araC = MN test < Comet assay. For EMS, LGDs were  $125 \mu\text{g/mL}$ ,  $62.5 \mu\text{g/mL}$ ,  $62.5 \mu\text{g/mL}$ , and  $125 \mu\text{g/mL}$  on Comet assay, Comet assay/araC, acellular assay, and MN test, respectively; that is, acellular assay = Comet assay/araC < MN test = Comet assay. For MNU, LGDs

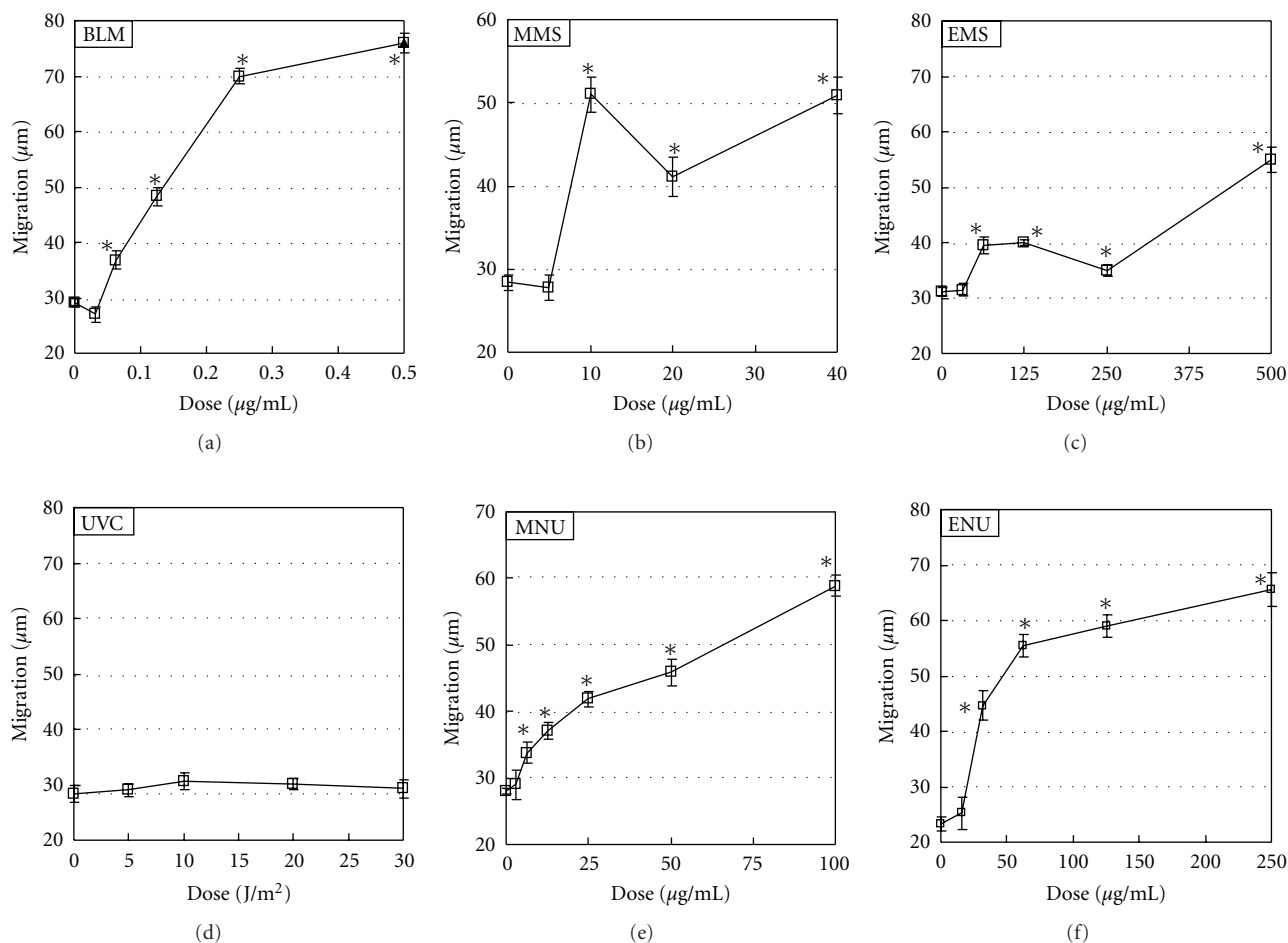


FIGURE 2: Acellular assay in TK6 cells. Slides for Comet assay were exposed to each chemical mutagen for 2 h or irradiated with UVC, and then electrophoresis was conducted at pH > 13 immediately after exposure to the chemical mutagen or 2 h after UVC irradiation. Reproducibility was ascertained by three independent experiments and representative data are shown. The error bars indicate standard errors of the mean. \*Significant difference from untreated control:  $P < .05$ .

were 25  $\mu\text{g/mL}$ , 3.125  $\mu\text{g/mL}$ , 6.25  $\mu\text{g/mL}$ , and 12.5  $\mu\text{g/mL}$  on Comet assay, Comet assay/araC, acellular assay, and MN test, respectively; that is, Comet assay/araC < acellular assay < MN test < Comet assay. For ENU, LGDs were 250  $\mu\text{g/mL}$ , 62.5  $\mu\text{g/mL}$ , 31.3  $\mu\text{g/mL}$ , and 125  $\mu\text{g/mL}$  on Comet assay, Comet assay/araC, acellular assay, and MN test, respectively; that is, acellular assay < Comet assay/araC < MN test < Comet assay. For UVC, LGDs were 20  $\text{J/m}^2$ , 2.5  $\text{J/m}^2$ , and 15  $\mu\text{g/mL}$  on Comet assay, Comet assay/araC, and MN test, respectively; that is, Comet assay/araC < MN test < Comet assay.

#### 4. Discussion

The present results are summarized as follows: (1) for all mutagens studied, LGDs were MN test  $\leq$  comet assay; (2) except for BLM, LGDs were Comet assay/araC  $\leq$  MN test; (3) except for UVC and MNU, LGDs were acellular assay  $\leq$  Comet assay/araC  $\leq$  MN test  $\leq$  Comet assay. Therefore, despite the belief in the high sensitivity of Comet assay, its power in detecting a low level of genotoxicity was lower

than that of MN test. Although the development of initial damage into alkali-labile sites following repair events is an important factor supporting the sensitivity of Comet assay, it is easily assumed that DNA resynthesis and rejoining events following SSB formation reduce the sensitivity of Comet assay in detecting DNA damage such as alkylated bases and bulky base adducts. In this study, we used two methods of canceling the effects of DNA resynthesis and/or rejoining events. One is acellular assay [16] and the other is the use of DNA repair inhibitors (araC and HU) [5, 17]. Acellular assay is a modified version of Comet assay, in which lysed cells are exposed to test compounds, there are no biological events acting on the formation and/or disappearance of SSBs [4, 16]. In our previous study, where positive responses on Comet and acellular assays were detected at pH 12 and >13, there were no apparent pH effects on acellular assay, suggesting that SSBs as initial DNA damage are detected on acellular assay at pH 12 and pH > 13 [15].

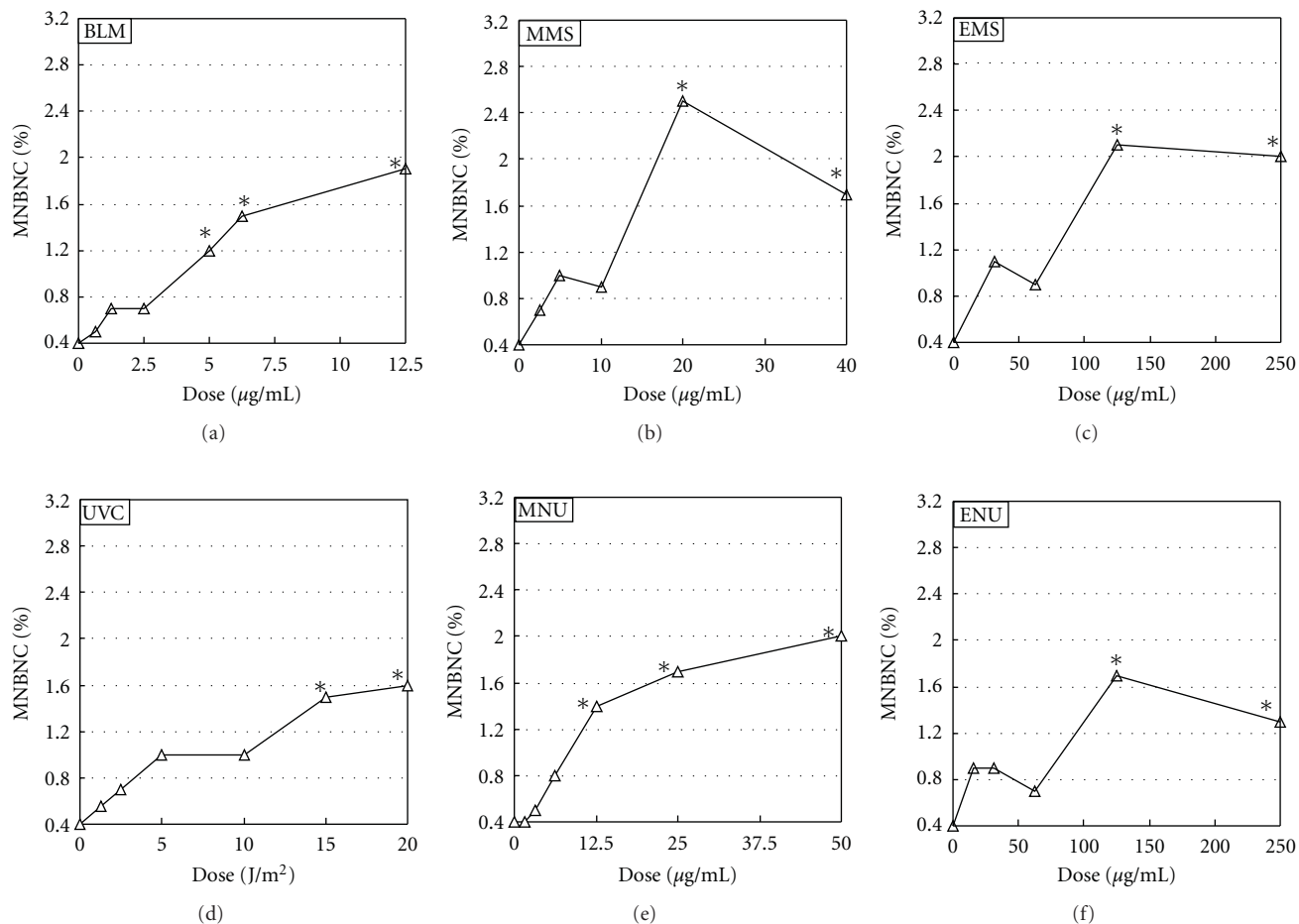


FIGURE 3: MN test in TK6 cells. TK6 cells were exposed to each chemical mutagen for 2 h or irradiated with UVC and were incubated for 24 h with cytochalasin B, and then slides for MN test were prepared. Reproducibility was ascertained by three independent experiments and representative data are shown. \*Significant difference from untreated control:  $P < .05$ .

When SSBs as initial DNA lesions are not rejoined, they would be responsible for DNA migration on Comet assay. For SSB-inducers such as BLM [18]; therefore, migration would be observed on acellular assay, while rejoining of SSBs before the preparation of the Comet assay would reduce positive response on Comet assay. If the level of SSBs as initial DNA damage is high enough to persist until the preparation of the Comet assay, migration would be observed in Comet assay. While BLM led to positive responses at  $\geq 0.0625 \mu\text{g/mL}$  on acellular assay, it led to negative responses at  $\leq 1.25 \mu\text{g/mL}$  on Comet assay. This discrepancy would be explained as follows. Although rejoining of BLM-induced SSBs before the preparation of the Comet assay reduces positive responses on Comet assay, rejoining of BLM-induced SSBs does not occur on acellular assay where none of the cellular functions remain active. The induction of SSBs by BLM at  $\leq 1.25 \mu\text{g/mL}$  would be too low to persist until the preparation of the Comet assay, which would be responsible for the negative and positive responses at  $\leq 1.25 \mu\text{g/mL}$  on Comet and acellular assays, respectively. The Comet assay detects SSBs as initial damage and SSBs formed through repairing process of initial damage other than SSBs [1, 2, 4], while MN test

detects structural chromosome aberrations that are derived from primary damage in the S phase and/or numerical chromosome aberrations due to aneugenic effects in the M phase [6, 7]. Therefore, even if the SSB-induction level by BLM is too low to persist until the preparation of the Comet assay, SSBs that can persist until the start of the S phase could form micronuclei, which could explain why LGDs are detected on the order of MN test  $\leq$  Comet assay.

Comet assay detects SSBs produced as initial damage as well as those generated during the repair of initial damage such as alkylated bases, bulky base adducts, and pyrimidine dimers [1, 2]. Therefore, in the case of mutagens forming DNA adduct, the sensitivity of the Comet assay is supported by the conversion efficiency of initial damage into alkali-labile sites through the repair processes [1, 2]. Pyrimidine dimers, which are well known to be induced by UVC, are removed by the nucleotide excision repair, which involves incision of the DNA strand, excision of the damaged nucleotide, gap filling by DNA resynthesis, and rejoining by ligation. As shown by the negative responses on acellular assay, it is considered that UVC does not induce SSBs as initial damage [4]. As shown by the positive responses

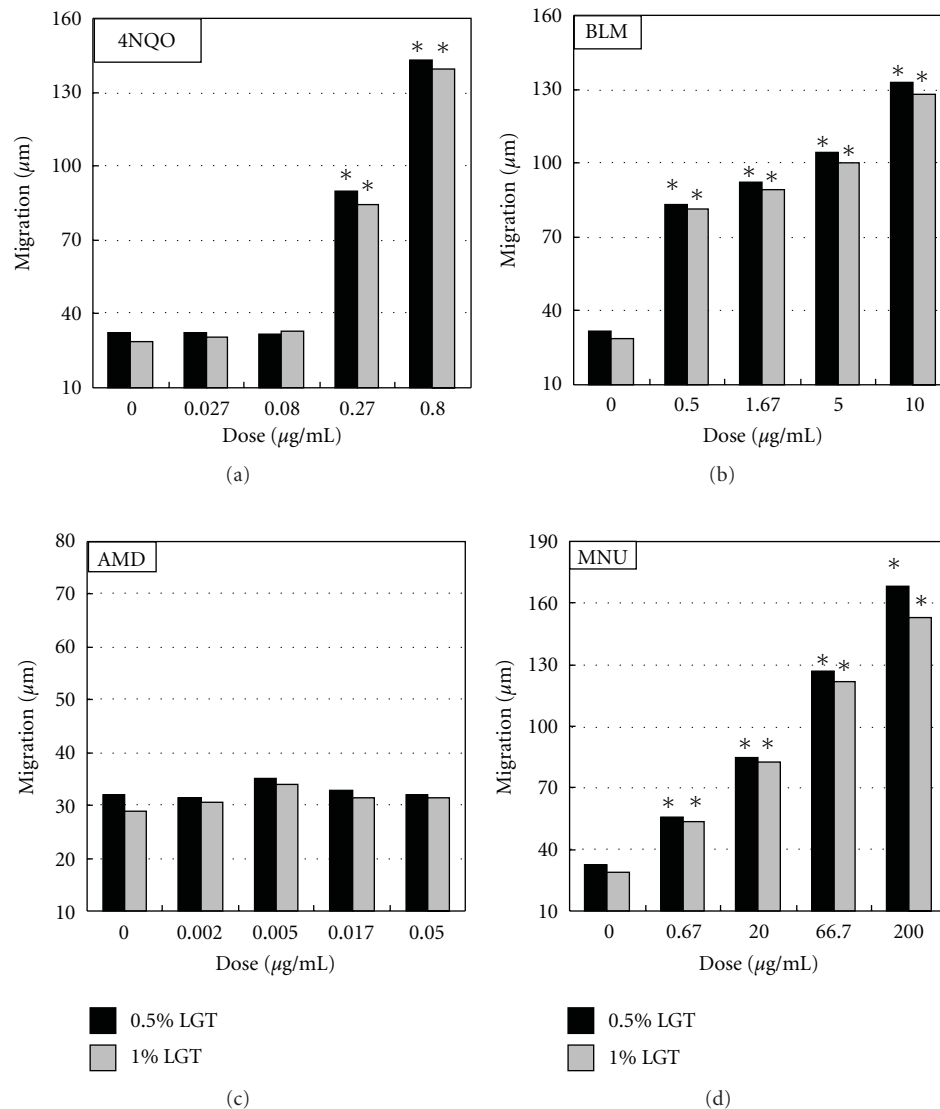


FIGURE 4: Comet assay in 0.5% LGT and 1% LGT. Chinese hamster CHO cells were exposed to each chemical mutagen for 1 h, and then slides for Comet assay were prepared immediately after the exposure. Electrophoresis was conducted at  $\text{pH} > 13$ . 4NQO, 4-nitroquinoline-1-oxide; AMD, actinomycin D \*Significant difference from untreated control:  $P < .05$ .

on acellular assay; however, it is considered that not only alkylated bases as initial damage but also SSBs as initial damage are induced by alkylating agents [4]. (SSBs as initial damage would not contribute markedly to positive responses on Comet assay [4].) SSBs that are formed during the process of repairing pyrimidine dimers and alkylated bases are responsible for the DNA migration observed on Comet assay [4]. SSB-rejoining, which reduces DNA migration, can be canceled by incubation with DNA synthesis inhibitors such as HU and araC, which block DNA resynthesis [5, 17]. LGDs of UVC and alkylating agents were MN test < Comet assay, suggesting that SSBs formed from pyrimidine dimers and alkylated bases that do not persist until the preparation of the Comet assay can form micronuclei. However, LGDs of UVC and alkylating agents were detected in the order of Comet assay/araC < MN test, suggesting that not all unrejoined SSBs form micronuclei and that the inhibition

of the rejoining step during excision repair can elevate the power of the Comet assay to detect a low level of genotoxic potential to a level higher than that of MN test.

LGDs of BLM and studied mutagens except for BLM were 2.5-fold and  $\leq 2$ -fold higher on Comet assay than on MN test, respectively, which would suggest that the power of the Comet assay to detect a low level of genotoxic potential tended to be lower than that on MN test for mutagens that easily produce SSBs as the initial damage. This suggests that SSBs as initial damage might make a greater contribution to micronucleus formation than to DNA migration, considering our previous discussion that SSBs as the initial damage would not contribute markedly to positive responses on Comet assay [4]. Furthermore, it is considered that the second step of repair events includes gap filling by DNA resynthesis followed by ligation, which reduces the sensitivity on Comet assay to a level below that of

MN test, though the progression of initial damage to alkali-labile sites during the repair process is an important factor contributing to the sensitivity on Comet assay.

In conclusion, the power of Comet assay to detect a low level of genotoxicity is lower than that of MN test, which concurs with the results reported by Pfau et al. [8]. For the studied mutagens, all assays (except for acellular assay for UVC) were able to detect all mutagens correctly, suggesting that the sensitivities of Comet assay and MN test were exactly identical. For the studied mutagens; however, LGDs on Comet assay were higher than those on MN test, suggesting that the power of MN test to detect low level of genotoxic potential is superior to that of Comet assay. Higher LGDs on MN test would depend on the selection of different spectra of damage by the Comet assay and MN test; that is, the formation of SSBs during repairing process is an important factor leading to positive responses on Comet assay and whether cells with unrepaired DNA damage can enter the S phase to form structural chromosome aberrations would be an important factor leading to positive responses on MN test. Furthermore, whether LGDs on Comet assay are lower or higher than those on MN test would depend on which compounds are examined. Despite the lower power of the Comet assay to detect a low level of genotoxic potential, one of the most important advantages of the Comet assay is that DNA damage can be measured in any cell type [19], while the MN test is limited to cells having mitotic activity. Furthermore, the power of Comet assay to detect a low level of genotoxicity can be elevated to a level higher than that of MN test by using DNA resynthesis inhibitors, such as araC and HU.

## References

- [1] N. P. Singh, M. T. McCoy, R. R. Tice, and E. L. Schneider, "A simple technique for quantitation of low levels of DNA damage in individual cells," *Experimental Cell Research*, vol. 175, no. 1, pp. 184–191, 1988.
- [2] D. W. Fairbairn, P. L. Olive, and K. L. O'Neill, "The Comet assay: a comprehensive review," *Mutation Research*, vol. 339, no. 1, pp. 37–59, 1995.
- [3] S. Fukushima, A. Kakehshi, M. Wei, and H. Wanibuchi, "Existence of a threshold for genotoxic carcinogens: evidence from mechanism-based carcinogenicity studies," *Genes and Environment*, vol. 32, pp. 33–36, 2009.
- [4] S. Kawaguchi, T. Nakamura, G. Honda, N. Yokohama, and Y. F. Sasaki, "Detection of DNA single strand breaks induced by chemical mutagens using the acellular Comet assay," *Genes and Environment*, vol. 30, pp. 77–88, 2008.
- [5] A. R. Collins, "The Comet assay for DNA damage and repair: principles, applications, and limitations," *Molecular Biotechnology*, vol. 26, no. 3, pp. 249–261, 2004.
- [6] G. Obe, P. Pfeiffer, J. R. K. Savage et al., "Chromosomal aberrations: formation, identification and distribution," *Mutation Research*, vol. 504, no. 1-2, pp. 17–36, 2002.
- [7] M. Fenech and A. A. Morley, "Measurement of micronuclei in lymphocytes," *Mutation Research*, vol. 147, no. 1-2, pp. 29–36, 1985.
- [8] W. Pfau, F. L. Martin, K. J. Cole et al., "Heterocyclic aromatic amines induce DNA strand breaks and cell transformation," *Carcinogenesis*, vol. 20, no. 4, pp. 545–551, 1999.
- [9] F. Van Goethem, D. Lison, and M. Kirsch-Volders, "Comparative evaluation of the in vitro micronucleus test and the alkaline single cell gel electrophoresis assay for the detection of DNA damaging agents: genotoxic effects of cobalt powder, tungsten carbide and cobalt-tungsten carbide," *Mutation Research - Genetic Toxicology and Environmental Mutagenesis*, vol. 392, no. 1-2, pp. 31–43, 1997.
- [10] A. Hartmann, A. Elhajouji, E. Kiskinis et al., "Use of the alkaline Comet assay for industrial genotoxicity screening: comparative investigation with the micronucleus test," *Food and Chemical Toxicology*, vol. 39, no. 8, pp. 843–858, 2001.
- [11] S. Kawaguchi, T. Nakamura, G. Honda, and Y. F. Sasaki, "Evaluation of in vitro genotoxic potential of kojic acid in human lymphoblastoid cells," *Genes and Environment*, vol. 29, pp. 153–158, 2007.
- [12] T. Nakamura, A. Yamamoto, G. Honda, S. Kawaguchi, N. Yokohama, and Y. F. Sasaki, "Does p53 status affect the sensitivity of the Comet assay?" *Genes and Environment*, vol. 32, pp. 14–20, 2010.
- [13] R. R. Tice, E. Agurell, D. Anderson et al., "Single cell gel/Comet assay: guidelines for in vitro and in vivo genetic toxicology testing," *Environmental and Molecular Mutagenesis*, vol. 35, no. 3, pp. 206–221, 2000.
- [14] Y. Miyamae, K. Iwasaki, N. Kinae et al., "Detection of DNA lesions induced by chemical mutagens using the single-cell gel electrophoresis (Comet) assay. 2. Relationship between DNA migration and alkaline condition," *Mutation Research - Genetic Toxicology and Environmental Mutagenesis*, vol. 393, no. 1-2, pp. 107–113, 1997.
- [15] S. Kawaguchi, T. Nakamura, G. Honda, N. Yokohama, and Y. F. Sasaki, "Detection of DNA single strand breaks induced by chemical mutagens using the acellular Comet assay," *Genes and Environment*, vol. 30, pp. 77–88, 2008.
- [16] T. Kasamatsu, K. Kohda, and Y. Kawazoe, "Comparison of chemically induced DNA breakage in cellular and subcellular systems using the Comet assay," *Mutation Research*, vol. 369, no. 1, pp. 1–6, 1996.
- [17] E. Rojas, M. C. Lopez, and M. Valverde, "Single cell gel electrophoresis assay: methodology and applications," *Journal of Chromatography B: Biomedical Sciences and Applications*, vol. 722, no. 1-2, pp. 225–254, 1999.
- [18] B. K. Vig and R. Lewis, "Genetic toxicology of bleomycin," *Mutation Research*, vol. 49, pp. 189–238, 1978.
- [19] Y. F. Sasaki, K. Sekihashi, F. Izumiyama et al., "The Comet assay with multiple mouse organs: comparison of Comet assay results and carcinogenicity with 208 chemicals selected from the IARC monographs and U.S. NTP carcinogenicity database," *Critical Reviews in Toxicology*, vol. 30, no. 6, pp. 629–799, 2000.

## Research Article

# Development of a Novel Fluorescence Assay Based on the Use of the Thrombin-Binding Aptamer for the Detection of O<sup>6</sup>-Alkylguanine-DNA Alkyltransferase Activity

Maria Tintoré,<sup>1</sup> Anna Aviñó,<sup>1</sup> Federico M. Ruiz,<sup>2</sup> Ramón Eritja,<sup>1</sup> and Carme Fàbrega<sup>1</sup>

<sup>1</sup> Institute for Research in Biomedicine (IRB Barcelona) IQAC-CSIC, CIBER-BBN Networking Centre on Bioengineering Biomaterials and Nanomedicine, Cluster Building, Baldri i Reixac 10, 08028 Barcelona, Spain

<sup>2</sup> Chemical and Physical Biology CIB (CSIC), Ramiro de Maeztu 9, 28040 Madrid, Spain

Correspondence should be addressed to Carme Fàbrega, carme.fabrega@irbbarcelona.org

Received 11 June 2010; Accepted 17 July 2010

Academic Editor: Ashis Basu

Copyright © 2010 Maria Tintoré et al. This is an open access article distributed under the Creative Commons Attribution License, which permits unrestricted use, distribution, and reproduction in any medium, provided the original work is properly cited.

Human O<sup>6</sup>-alkylguanine-DNA alkyltransferase (hAGT) is a DNA repair protein that reverses the effects of alkylating agents by removing DNA adducts from the O<sup>6</sup> position of guanine. Here, we developed a real-time fluorescence hAGT activity assay that is based on the detection of conformational changes of the thrombin-binding aptamer (TBA). The quadruplex structure of TBA is disrupted when a central guanine is replaced by an O<sup>6</sup>-methyl-guanine. The sequence also contains a fluorophore (fluorescein) and a quencher (dabsyl) attached to the opposite ends. In the unfolded structure, the fluorophore and the quencher are separated. When hAGT removes the methyl group from the central guanine of TBA, it folds back immediately into its quadruplex structure. Consequently, the fluorophore and the quencher come into close proximity, thereby resulting in decreased fluorescence intensity. Here, we developed a new method to quantify the hAGT without using radioactivity. This new fluorescence resonance energy transfer assay has been designed to detect the conformational change of TBA that is induced by the removal of the O<sup>6</sup>-methyl group.

## 1. Introduction

Alkylating agents are chemotherapeutic anticancer drugs that produce their cytotoxic effect by generating adducts at multiple sites in DNA [1]. A subset of alkylating agents, which includes nitrosoureas and temozolamide, have a preference for alkylating guanine at the O<sup>6</sup> position, which is the most relevant in terms of mutagenesis and carcinogenesis [2–9]. In particular, 1,3-bis-(2-chloroethyl)-1-nitrosourea (BCNU) attacks initially at the O<sup>6</sup> guanine position, causing its rearrangement in a cyclic intermediate thus giving rise to N<sup>1</sup>,O<sup>6</sup>-ethanoguanine [10]. Finally, a cross-link with the opposite cytosine is formed, and, as a consequence, DNA replication is blocked, producing G2/M arrest [11]. In addition to the well-known side effects and limitations of chemotherapeutic agents, these substances also present problems of acquired tumor resistance. In particular, the DNA-repair human O<sup>6</sup>-alkylguanine DNA alkyltransferase

(hAGT or MGMT) is responsible for removing alkyl adducts from the O<sup>6</sup> position of guanines, thereby blocking the cytotoxic effects of the alkylating agents and making a crucial contribution to the resistance mechanism [12–14]. It is well established that tumor cells show greater expression of this protein than healthy cells. Thus, this increased expression appears to be predictive of a poor response to chemotherapeutic drugs. This effect has been observed in a large number of cancers, ranging from colon cancer, lung tumors, breast cancer, pancreatic tumors, non-Hodgkin's lymphoma, myeloma, and glioblastoma multiforme, among others [15–17]. In addition methylation of the hAGT promoter and consequently the complete depletion of hAGT, it has been associated with longer survival in patients with gliomas undergoing combined radiation-chemotherapy treatment [18, 19]. Therefore, pharmacological inhibition of hAGT has the potential to enhance the cytotoxicity of a diverse range of anticancer agents [20].

hAGT is a 22-kDa (207 AA) DNA-binding protein that contains a highly conserved internal cysteine, which acts as the acceptor site for alkyl groups. The S-alkyl-Cys formed is not regenerated and the protein, which behaves as a suicidal enzyme, inactivates itself in the dealkylation process [21, 22]. This single turnover of hAGT renders it vulnerable to inactivation. On the basis of this observation, intense research effort has been devoted to the identification of small molecules capable of inhibiting hAGT activity and significantly enhancing the cytotoxic effect of BCNU in prostate, breast, colon, and lung tumor cells [20].

Several methods are available to characterize the mechanism of action of hAGT and its activity. Moreover, they also have the capacity to evaluate the capacity of small molecules to inhibit hAGT. Most of these methods are based on radioactivity assays while others are based on multiple-step enzymatic reactions [23–26].

G-quadruplexes are a family of four-stranded DNA structures stabilized by the stacking of guanine tetrads, in which four planar guanines form a cyclic array of hydrogen bonds [27]. These G-rich regions are connected by lateral, central, or diagonal loops of diverse sizes and composition that form base-pairing alignments, which in turn stack with the terminal G-tetrads, thus further stabilizing G-quadruplex structures [28]. Another key element in G-quadruplex formation is the presence of monovalent cations, which stabilize the negative electrostatic potential created by the guanine O<sup>6</sup> oxygen atoms within the quadruplex core [29, 30]. However, most divalent cations have the capacity to induce the dissociation of G-quadruplex structures [31]. Finally, modifications in the base composition of the tetrads are poorly tolerated by these structures. As an example, inosine [32] and O<sup>6</sup>-methylguanine [33], both nonnatural bases can form a smaller number of hydrogen bonds and thus destabilize the G-quadruplex.

Given the potential relevance of hAGT as a prognostic marker of cancer and as a therapeutic target, and that its substrate O<sup>6</sup>-methylguanine disrupts the formation of G-quadruplex structures [33], here, we developed a new fluorescence activity assay for hAGT. For this purpose, we selected the thrombin-binding aptamer (TBA) as our G-quadruplex model. TBA is a well-known 15 mer that adopts a chair-like structure consisting of two G-tetrads connected by two lateral TT loops and a central TGT loop [34]. The modification of its sequence in positions 5 or 6 by replacing a guanine of the tetrad for an O<sup>6</sup>-methylguanine disrupts folding, leaving it in an extended conformation. Giving that the two conformations bring the two ends of TBA together take them further apart, our working hypothesis was that the incorporation of fluorescence probes results in a measurable change in intensity. The final aim of this fluorescence assay was to measure the DNA repair activity of hAGT and thus facilitate the search for new and more potent inhibitors which enhance chemotherapeutic drugs. Although several methods have been described to quantify hAGT activity [23–26], none of them use the conformational change of G-quadruplex for this purpose. Here, we describe the development of a straightforward, rapid, one-step fluorescence resonance energy transfer (FRET) assay.

## 2. Materials and Methods

**2.1. Chemicals.** 5'-Fluorescein CE phosphoramidite (6-FAM), 3'-Dabsyl CPG, O<sup>6</sup>-methylguanine (O<sup>6</sup>-MeG) and G<sup>dmf</sup> phosphoramidites were purchased from Link technologies (UK) and Glen Research (USA). O<sup>6</sup>-methylguanine was protected with the isobutyryl group [35]. Standard phosphoramidites and ancillary reagents were purchased from Applied Biosystems (Europe).

The matrices for MALDI-TOF experiments were 2',4',6'-trihydroxyacetophenone monohydrate (THAP) and ammonium citrate dibasic.

Solvents for chromatographic analysis were prepared using triethylamine, acetic acid, and acetonitrile as mobile phase. All other chemicals were of analytical reagent grade and were used as supplied. Ultrapure water (Millipore, USA) was used in all experiments.

**2.2. Instrumentation.** Semipreparative reverse phase (RP) HPLC was performed on a Waters chromatography system using Nucleosil semipreparative 120 C18 (250 × 8 mm) columns. Analytical RP-HPLC was performed using an XBridge OST C18 2.5 μm column and a Nucleosil Analytical column 120 C18 (250 × 4 mm). Oligonucleotides were detected by UV absorption at 260 nm. Mass spectra were recorded on a MALDI Voyager DE<sup>TM</sup> RP time-of-flight (TOF) spectrometer (Applied Biosystems, USA) with a nitrogen laser at 337 nm using a 3-ns pulse. Fluorometric measurements were performed on a spectrofluorometer multidetection microplate reader Biotek FL × 800 and a Jasco FP6200. Molecular absorption spectra between 220 and 550 nm were recorded with a Jasco V650 spectrophotometer. The temperature was controlled with a Jasco ETC 272T Peltier device. Hellma quartz cuvettes (0.5 and 1.0 cm path length, 500 or 1000 μL volume) were used.

**2.3. Oligonucleotide Synthesis.** Oligonucleotide sequences (shown in Table 1) were synthesized on an ABI 3400 DNA Synthesizer (Applied Biosystems, USA) using a 200-nmol scale synthesis and following the standard protocols. We used dimethylformamido-protected guanine G<sup>dmf</sup> phosphoramidite for all the syntheses. 5'-Fluorescein CE phosphoramidite (6-FAM), O<sup>6</sup>-methylguanine (O<sup>6</sup>-MeG) and G<sup>dmf</sup> phosphoramidites were from commercial sources. The isobutyryl group was used to protect the amino group of O<sup>6</sup>-MeG [35]. The quencher group was introduced at the 3' end using the controlled pore glass functionalized with a 3'-Dabsyl derivative CPG. O<sup>6</sup>-MeG-containing oligonucleotides were deblocked using concentrated aqueous ammonia overnight at room temperature following the manufacturer's instructions. The resulting products were desalted by Sephadex G-25 (NAP-10, GE Healthcare, USA) and purified by reversed-phase HPLC using Nucleosil columns. The yields and purities obtained for the products were around 85% for 5-O<sup>6</sup>-MeG-TBA and 6-O<sup>6</sup>-MeG-TBA, and >98% for the rest of the sequences. The length and homogeneity of the oligonucleotides were checked by MALDI-TOF.

TABLE 1: Sequences of TBA oligonucleotide derivatives used in the development of the hAGT fluorescence assay. <sup>Me</sup>G represents O<sup>6</sup>-methylguanine. MB represents the fluorophore group (FAM), labelled in the 5' end, and the quencher group (Dabsyl), labelled in the 3' end of the sequence.

Abbreviation	Sequence
TBA	5'-GGT TGG TGT GGT TGG-3'
5-O <sup>6</sup> -MeG-TBA	5'-GGT T <sup>Me</sup> GG TGT GGT TGG-3'
6-O <sup>6</sup> -MeG-TBA	5'-GGT TG <sup>Me</sup> GTGT GGT TGG-3'
C-TBA	5'-CCA ACC ACA CCA ACC-3'
MB-TBA	5'-FAM-GGT TGG TGT GGT TGG-Dabsyl-3'
MB-5-O <sup>6</sup> -MeG-TBA	5'-FAM-GGT T <sup>Me</sup> GG TGT GGT TGG- Dabsyl-3'
MB-6-O <sup>6</sup> -MeG-TBA	5'-FAM-GGT TG <sup>Me</sup> G TGT GGT TGG- Dabsyl-3'
3-HP-TBA	5'-A CCT TTT GGT TGG TGT GGT TGG-3'
6-HP-TBA	5'-C CAA CCT TTT GGT TGG TGT GGT TGG-3'
9-HP-TBA	5'-A CAC CAA CCT TTT GGT TGG TGT GGT TGG-3'

5-O<sup>6</sup>-MeG-TBA [M] = 4731.7 (expected 4737.8), 6-O<sup>6</sup>-MeG-TBA [M] = 4729.9 (expected 4737.8), MB-5-O<sup>6</sup>-MeG-TBA [M] = 5828.49 (expected 5826.0), MB-6-O<sup>6</sup>-MeG-TBA [M] = 5826.80 (expected 5826.0).

The DNA-strand concentration was determined by absorbance measurements (260 nm) by calculating extinction coefficients. Oligonucleotide samples were kept at 4°C until further use. Double-stranded O<sup>6</sup>-MeG-TBA was formed by annealing equimolar concentrations of complementary oligonucleotide strands at 72°C for 5 min and then allowed to slowly cool to room temperature.

**2.4. Melting Temperature Studies.** Melting curves were measured by monitoring the absorbance hyperchromicity at 295 and 495 nm in a JASCO V650 spectrophotometer equipped with a Peltier temperature-controlling unit. UV/Vis absorption spectra were recorded at 1°C/min intervals, with a 1-min equilibration time at each temperature; the sample was heated over the range 20–80°C. The buffer solutions used were 10 mM sodium cacodylate pH 7.0 and 100 mM KCl. Sample concentration was around 4 μM. Each sample was allowed to equilibrate at the initial temperature without any external control of temperature for 5 min before the melting experiment began. The melting temperatures (T<sub>m</sub>) are the average value of at least one pair of T<sub>m</sub> experiments.

**2.5. CD Spectra.** Samples were prepared as described for the melting experiments by UV spectroscopy. Measurements were conducted in 10 mM sodium cacodylate pH 7.0 and 100 mM KCl. Sample concentration was between 1–4 μM. The CD spectra were recorded on a Jasco J-810 spectropolarimeter attached to a Julabo F/25HD circulating water bath in 1 cm path-length quartz cylindrical cells. Spectra were recorded at room temperature using a 100 nm/min scan rate, a spectral band width of 1 nm and a time constant of 4 s. All the spectra were corrected with the buffer blank and plotted using Origin software.

**2.6. Human Recombinant hAGT Protein.** Full-length hAGT was overexpressed and purified as previously described [36].

Briefly, hAGT protein cloned in the pet-21a (+) (Novagen) vector was expressed in the *E. coli* strain Rosetta. Once the culture reached an OD<sub>600</sub> value of 0.98, hAGT was induced by adding 1 mM IPTG (Sigma) and left for 4 h at 30°C. The pellet from a 1-L culture was disrupted by sonication and centrifuged. The supernatant was filtered, loaded into a HiTrap FF column (GE Healthcare) with buffer 350 mM NaCl, 20 mM Tris pH 8, 20 mM imidazole, and 1 mM BME, and then eluted with an imidazole (Fluka) gradient up to 500 mM in the same buffer. Finally, the protein was loaded into a Superdex 75 16/60 column (GE Healthcare) with the following buffer: 200 mM NaCl (Merck), 20 mM Tris pH 8.0 (Merck), 10 mM DTT (Sigma) and 0.1 mM EDTA (Sigma). The protein was concentrated to 2 mg/mL in this buffer and kept at –20°C in the presence of 40 % glycerol. The same protocol was used for the purification of the inactive mutant hAGT-C145S, cloned in the pet-28a (+) vector (Novagen), and expressed in the *E. coli* strain BL21.

**2.7. HPLC hAGT Assay.** Assays were conducted using double-stranded 5-O<sup>6</sup>-MeG and 6-O<sup>6</sup>-MeG TBA paired with TBA complementary sequence or using single-stranded 5-O<sup>6</sup>-MeG and 6-O<sup>6</sup>-MeG TBA.

In order to measure the dealkylation of O<sup>6</sup>-MeG, 50 pmol of the O<sup>6</sup>-MeG-TBA substrates were incubated with a range of concentration of hAGT (16 nM to 1.6 μM) to a final volume of 120 μL in a reaction buffer (200 mM NaCl, 50 mM Tris pH 8.0, 1 mM DTT, and 5 mM EDTA). Several incubation times were tested (30, 60, 90, 120, 360, and 1440 min) at 37°C and the reaction was stopped by heating the samples at 72°C for 5 min. The reaction products were analyzed by HPLC on a Nucleosil analytical column at 60°C or room temperature, depending on the substrates used in the experiment (double- or single-stranded TBA). The HPLC flow rate was 1 mL/min, and a gradient of 10%–40% acetonitrile for 20 min was used.

**2.8. Fluorescence Assay for hAGT Activity.** The fluorescence assay was performed in a multidetection microplate reader biotek FLx800 in optical 96-well Optical btm reaction plates

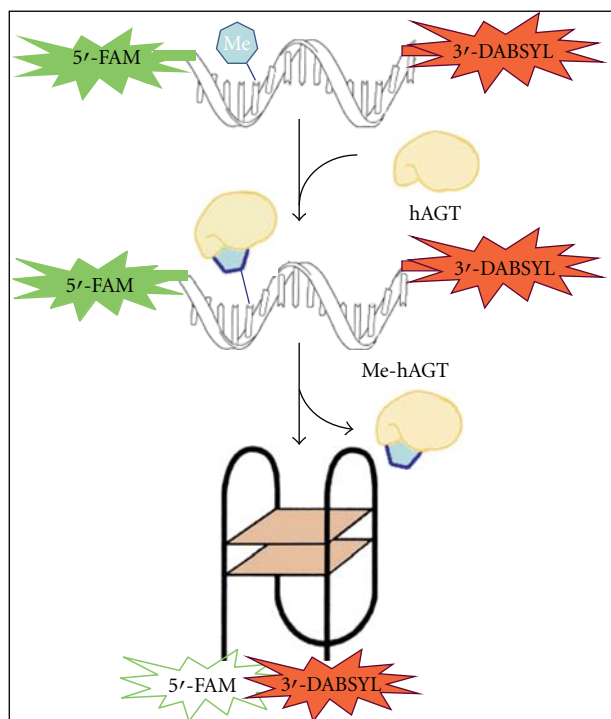


FIGURE 1: Scheme of fluorescence-based hAGT assay. The substrate is the thrombin-binding aptamer modified by an O<sup>6</sup>-methylguanine (Me) in extended conformation, with a fluorophore and quencher in the opposite ends of the sequence. The refold of the G-quadruplex structure of TBA is dependent on the removal of the methyl adduct by alkyl-guanine-DNA-O<sup>6</sup>-alkyltransferase (hAGT). This repair moves the quencher and the fluorophore molecules in close proximity and blocks fluorescence.

(Nunc, USA). Full-length hAGT recombinant protein (207 amino acids) was used for the assay and the hAGT-C145S inactive mutant was used as a negative control. The reaction was performed in a total volume of 50  $\mu$ L in each well, incubating increasing concentrations of hAGT (5, 10, 20, 40, 60, and 80 nM) enzyme in reaction buffer (200 mM NaCl, 50 mM Tris pH 8.0, 1 mM DTT, 5 mM EDTA, and 20 mM KCl). The assay of hAGT was then initiated by the addition of 5  $\mu$ L of different concentrations (5, 10, 25, and 50 nM) of fluorescently labelled MB-O<sup>6</sup>-MeG-TBA substrate and this solution was then placed in a microplate reader system. Fluorescence was measured every minute for 20 min or 40 min at excitation and emission wavelengths of 485 and 535 nm, respectively. Averages over three readings were taken for each condition tested. Each experiment was performed in triplicate.

### 3. Results and Discussion

The aim of this study was to develop a real-time hAGT activity assay based on the detection of differences between extended and folded conformations of TBA. Our working hypothesis was that the quadruplex structure of TBA is

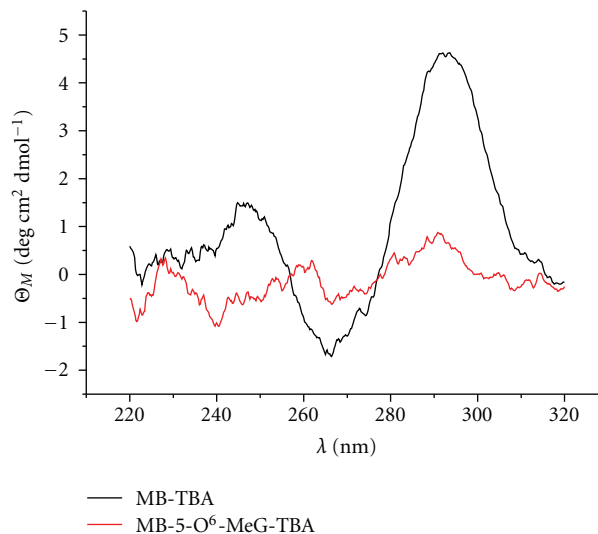


FIGURE 2: CD spectra of MB-TBA and MB-5-O<sup>6</sup>-MeG-TBA at 25°C. Buffer conditions: 10 mM sodium cacodylate pH 7.0 and 100 mM KCl, sample concentration 1  $\mu$ M.

disrupted when a central guanine is replaced by an O<sup>6</sup>-methylguanine. The TBA sequence also contains a fluorophore and a quencher group attached to 5' or 3' end, respectively. In the presence of O<sup>6</sup>-methylguanine, methylated TBA unfolds and the fluorophore and the quencher become physically separated beyond the Förster distance. When the repair protein hAGT is added to the methylated aptamer, the enzyme removes the methyl group from the mutated guanine, thus allowing TBA to fold back into its chair-like conformation. As a result, the quencher comes closer to the fluorophore and blocks its fluorescence, as illustrated in Figure 1. This loss of fluorescence is quantified as a direct measurement of hAGT activity.

**3.1. Synthesis of Modified G-Quadruplex Sequences.** The G-quadruplex sequences used in this study are shown in Table 1. Oligonucleotide synthesis was performed by the solid-phase 2'-cyanoethyl-phosphoramidite method [37]. Ammonia treatment was performed at room temperature overnight to minimize decomposition of O<sup>6</sup>-methylguanine. For the same reason, the dimethylformamidino group was selected for the protection of 2'-deoxyguanosine [38]. The sequences were characterized by HPLC and mass spectrometry, which provided the expected molecular weights. The yields of the isolated molecular beacon oligonucleotides after HPLC purification and desalting were in the range of those obtained for unmodified oligonucleotides.

**3.2. Thermal Stability of Methylguanine-Modified TBA.** In order to induce the unfolding of the quadruplex structure of TBA, we introduced an O<sup>6</sup>-methyl-guanine at position 5 or 6 of TBA. Melting curves of the modified sequences were performed by UV spectroscopy and compared with the unmodified sequence. These experiments were carried

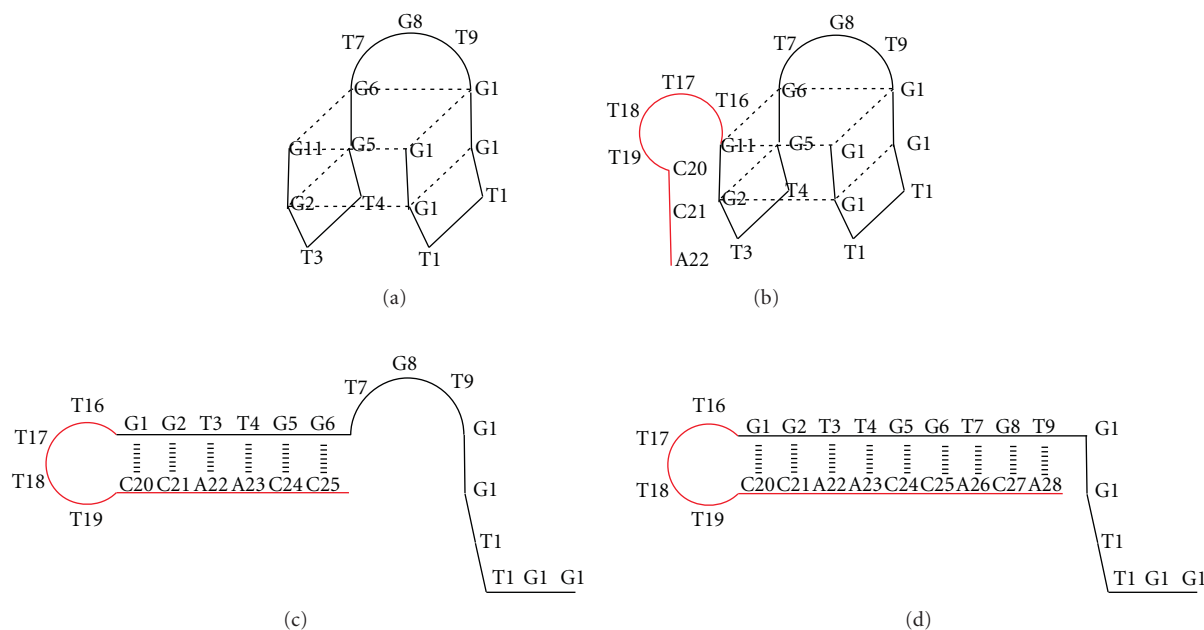


FIGURE 3: Schematic representation of the structure of several derivatives of thrombin-binding aptamers (TBAs) prepared in this study. TBA sequence is shown in black, and T4 loop with different sizes of the complementary sequences are shown in red. (a) Native TBA; (b) TBA-hairpin containing three overhanging complementary nucleotides (3-HP-TBA); (c) TBA-hairpin containing six overhanging complementary nucleotides (6-HP-TBA); (d) TBA-hairpin containing nine overhanging complementary nucleotides (9-HP-TBA). Between 3–6 complementary nucleotides are required to disrupt the intramolecular quadruplex to form an intramolecular duplex.

out at pH 7 in buffer containing 10 mM sodium cacodylate and 100 mM KCl, which is predicted to stabilize G-quadruplex structures. We did not observe a melting temperature at 295 nm for 5-O<sup>6</sup>-MeG-TBA or 6-O<sup>6</sup>-MeG-TBA and the corresponding molecular beacons (see Figures S1–S4 in Supplementary Data Material available online at doi: 10.4061/2010/632041). The absence of this transition is consistent with the disruption of the quadruplex structure. These results contrast with the melting temperature of native TBA ( $T_m$  48°C) and MB-TBA ( $T_m$  46°C). Moreover, circular dichroism of methylated-TBA derivatives did not show the presence of the maximum at 295 nm, which is characteristic of the antiparallel quadruplex of TBA (Figure 2 and Figure S5). These results confirmed that methylation of guanine in either of the two positions of the TBA sequence prevents the formation of the chair structure. This observation confirms our working hypothesis.

Given that the DNA repair activity exerted by hAGT is higher in double-stranded DNA than single-stranded DNA [39], we studied the stability and the quadruplex formation of elongated self-complementary TBA derivatives (see Table 1). We designed several TBA oligonucleotides elongated in their 3' end with a subset of self-complementary sequences of diverse sizes. The purpose of these elongations was to check whether the extended sequences have the capacity to form a double strand helix of different lengths and strengths with themselves without disrupting the chair-like structure. For 6-HP-TBA and 9-HP-TBA, we found that the corresponding  $T_m$  at 260 nm were 63°C and 71.8°C, respectively. This observation confirms our hypothesis of a double helix structure that increases in strength as the

sequence length increases. However, we did not detect a melting temperature of these two sequences at 295 nm. The absence of a transition at 295 nm is consistent with the absence of an antiparallel quadruplex structure. In contrast, 3-HP-TBA, corresponding to an overhang of only 3 nucleotides, gave a melting temperature of 46°C at 295 nm, which is slightly but similar to that obtained for natural TBA. This result indicates that 3-HP-TBA forms an antiparallel quadruplex instead of a duplex because the overhang is too short to break the chair-like structure. Circular dichroism confirms the quadruplex structure of 3-HP-TBA and the absence of quadruplex structure in 6-HP-TBA and 9-HP-TBA (Figure S6). Models of all these structures are shown in Figure 3.

**3.3. HPLC Analysis of DNA Repair Activity of hAGT.** In order to observe the efficiency of hAGT to remove alkyl groups from single-stranded oligonucleotides, we performed several assays to determine the optimal conditions of the reaction.

For this purpose, the full-length hAGT was first over-expressed and purified as described previously [36]. Increasing concentrations of the protein were incubated with double-stranded 5-O<sup>6</sup>-MeG and 6-O<sup>6</sup>-MeG TBA, annealed with its complementary sequence. Figure 4(a) shows the HPLC profile of the final product of the reaction with double-stranded 5-O<sup>6</sup>-MeG-TBA. In order to separate the two strands of the TBA substrate (Figure 4(a) top right panel), HPLC analyses were done at 60°C. After incubation with hAGT, we detected a peak with a shorter retention time, which corresponds to the restored TBA sequence caused by

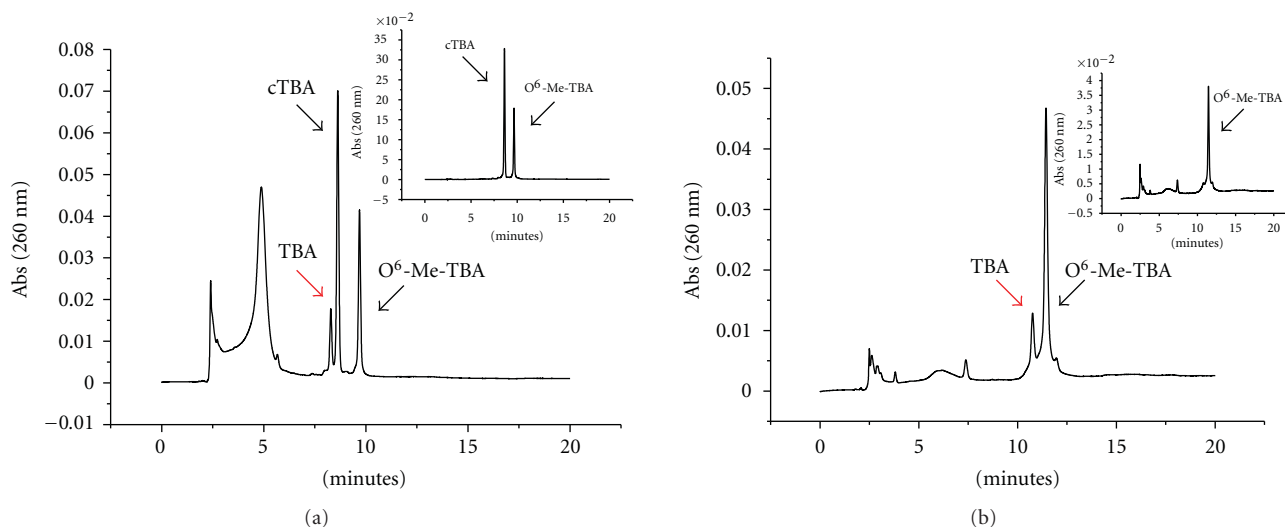


FIGURE 4: HPLC analysis of hAGT activity over double- and single-stranded TBA before and after incubation with hAGT. (a) Repair of double-stranded 5-O<sup>6</sup>-MeG-TBA by hAGT. The peak labelled as cTBA corresponds to the complementary sequence of 5-O<sup>6</sup>-MeG-TBA. The top right panel shows HPLC chromatogram in absence of hAGT. The gradient was from 10%–40% acetonitrile for 20 min at 60°C. (b) Repair of single-stranded 5-O<sup>6</sup>-MeG-TBA by hAGT. The inserted panel shows HPLC chromatogram in the absence of hAGT. Gradient used: 10%–40% acetonitrile, 20 min at room temperature.

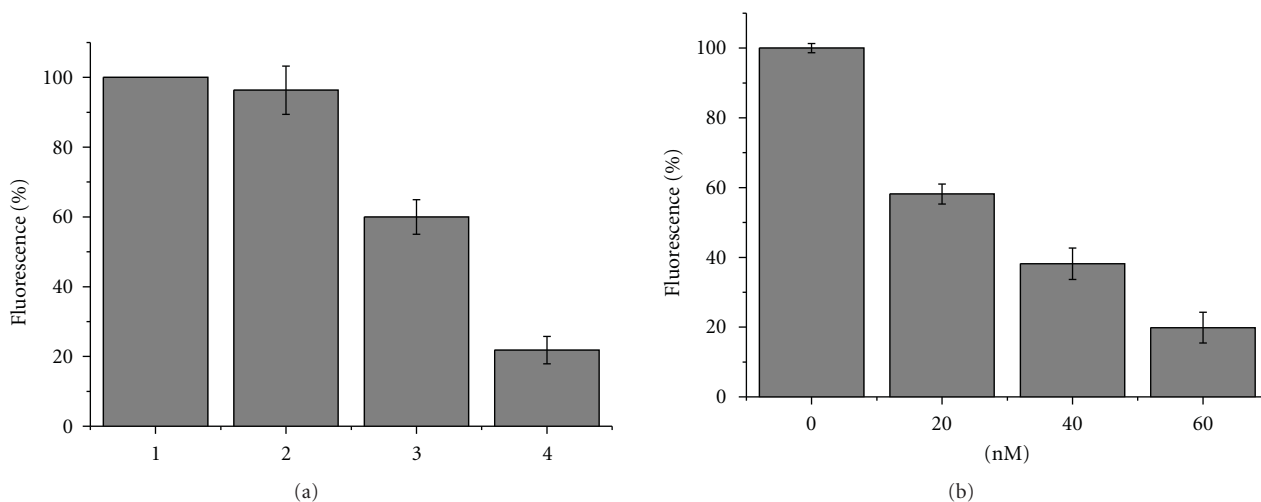


FIGURE 5: Fluorescence intensity of the real-time hAGT assay, measured at excitation and emission wavelengths of 485 nm and 535, respectively. (a) Illustration of the different controls with 5 nM MB-5-O<sup>6</sup>-MeG-TBA: (1) Positive control of MB-5-O<sup>6</sup>-MeG-TBA in the absence of hAGT; (2) Intensity in presence of the inactive mutant hAGT-C145S; (3) Decrease in fluorescence when adding 40 nM active hAGT; and (4) basal fluorescence of 5 nM of MB-TBA. (b) Decrease in intensity caused by the activity of hAGT at a range of concentrations (0, 20, 40, and 60 nM), in all of them the basal fluorescence of MB-TBA was subtracted.

the removal of the methyl group. We obtained the same results when we used double-stranded 6-O<sup>6</sup>-MeG-TBA as a substrate (data not shown). As expected, hAGT activity was not affected by the position of the alkyl group within the sequence. We then tested hAGT activity over single-stranded methylated TBA in the previously optimized conditions and obtained similar results to those shown in Figure 4(b). The top right panel shows the HPLC chromatogram in the absence of hAGT. In this case, the HPLC analyses were performed at room temperature because the substrate was single-stranded TBA. Our results confirmed that hAGT has

the capacity to remove methyl groups from single- or double-stranded TBA with the same efficacy. Therefore, we selected single-stranded TBA as substrate for the development of our fluorescence assay.

**3.4. Fluorescence hAGT Activity Assay.** On the basis of the results obtained in the melting temperature and the HPLC experiments, we tested the effectiveness of our proposed model to the DNA repair activity of hAGT by means of fluorescence. First of all, we determined the minimum amount of TBA required to achieve a detectable and reliable

difference in intensity compared to the background. As expected, the negative control natural TBA quadruplex gave low background fluorescence, because of the proximity of the fluorophore and the quencher groups in the chair-like structure (Figure 5(a)). Although the fluorescence of MB-TBA was low, this fluorescence was subtracted from the fluorescence value in each experiment. The concentration of 5 nM of fluorescently labelled MB-O<sup>6</sup>-MeG-TBA was considered the optimal concentration as the fluorescence signal was intense and only a small amount of hAGT protein was required to achieve a substantial decrease in fluorescence in 20–40 min. In the optimal conditions, the presence of hAGT produced a remarkable decrease in fluorescence intensity, caused by the demethylation of the O<sup>6</sup> position of guanines, thereby allowing the TBA to form its typical quadruplex structure, which brings together the fluorophore and the quencher groups, as occurred in the negative control. The rate of decrease in fluorescence intensity correlated directly with the amount of hAGT in the reaction mixture (Figure 5(b)). Moreover, the inactive mutant hAGT-C145S did not exhibit any decrease in fluorescence (Figure 5(a)). This result was expected because of the inability of this mutated protein to repair the modified TBA. Figure 5(b) shows the fluorescence intensities for the real time hAGT assay. All these observations are consistent with the hypothesis and design of our FRET method.

#### 4. Conclusion

Although radioactivity has been widely used in the search of potential inhibitors of hAGT [23, 24], this technique does not allow real-time data acquisition and, in addition, requires radioactive materials. Here, we developed a sensitive fluorescence method that allows the quantification of hAGT activity in a single step and in a straightforward manner. Although another fluorescence method has already been developed for this purpose [25], it requires the addition of a restriction enzyme, followed by the addition of an exonuclease after the hAGT activity reaction. Consequently, although it is a real-time assay, a three-step reaction is required before observing an increase in fluorescence. In contrast, in our assay, a change in fluorescence is detected in a single step (homogeneous), and this method does not depend on the activity of two additional enzymes.

Our assay is based on the detection of conformational changes of TBA in the presence or absence of O<sup>6</sup>-methylguanines in its structure. The quadruplex structure of TBA is disrupted when a central guanine is replaced by an O<sup>6</sup>-methylguanine. Fluorophore groups can be added to the modified sequence in order to detect the conformational changes by fluorescence. The variation in fluorescence can be quantified as a direct measurement of hAGT activity. In addition, this technique requires lower amounts of substrate and does not call for the use of radioactive materials. Furthermore, this method can be easily transferred to a high throughput experiment for the evaluation of small molecules as potential hAGT inhibitors [36]. Research in this direction is currently underway in the laboratory.

#### Abbreviations

BME:	2-mercaptoethanol
Dabsyl:	3-(N-4'-sulfonyl-4-(dimethylamino)-azobenzene)-3-aminopropyl
dmf:	Dimethylformamidino group
DTT:	Dithiothreitol
EDTA:	Ethylenediaminetetraacetic acid
FAM:	Fluoresceine
AGT:	O <sup>6</sup> -alkylguanine-DNA alkyltransferase
hAGT:	Human AGT
HPLC:	High performance liquid chromatography
IPTG:	Isopropyl $\beta$ -D-1-thiogalactopyranoside
MB:	Molecular Beacon
O <sup>6</sup> -MeG:	O <sup>6</sup> -methylguanine
TBA:	Thrombin-binding aptamer
cTBA:	Complementary TBA
TEAA:	Triethylammonium acetate
TFA:	Trifluoroacetic acid
Tris:	Tris(hydroxymethyl)aminomethane
Tm:	Melting temperature
UV:	Ultraviolet.

#### Acknowledgments

This work was supported by the Fondo de Investigaciones Sanitarias (Grant PI06/1250), by the Dirección General de Investigación Científica y Técnica (Grant BFU2007-63287, CTQ2010-20541), the Generalitat de Catalunya (2009/SGR/208), the COST project (G4-net, MP0802), the Instituto de Salud Carlos III (CIBER-BNN, CB06\_01\_0019), and a SNS Miguel Servet contract from the Instituto de Salud Carlos III. The authors thank Tanya Yates for editing the paper and the reviewer for the detailed revision of the paper. This work is dedicated to the memory of Ángel Ramírez Ortiz who was a great mentor, colleague, and friend.

#### References

- [1] M. R. Middleton and G. P. Margison, "Improvement of chemotherapy efficacy by inactivation of a DNA-repair pathway," *Lancet Oncology*, vol. 4, no. 1, pp. 37–44, 2003.
- [2] A. Sabharwal and M. R. Middleton, "Exploiting the role of O<sup>6</sup>-methylguanine-DNA-methyltransferase (MGMT) in cancer therapy," *Current Opinion in Pharmacology*, vol. 6, no. 4, pp. 355–363, 2006.
- [3] A. E. Pegg and B. Singer, "Is O<sup>6</sup>-alkylguanine necessary for initiation of carcinogenesis by alkylating agents?" *Cancer Investigation*, vol. 2, p. 18, 1984.
- [4] R. Saffhill, G. P. Margison, and P. J. O'Connor, "Mechanisms of carcinogenesis induced by alkylating agents," *Biochimica et Biophysica Acta*, vol. 823, no. 2, pp. 111–145, 1985.
- [5] B. Singer, "O-Alkyl pyrimidines in mutagenesis and carcinogenesis: occurrence and significance," *Cancer Research*, vol. 46, no. 10, pp. 4879–4885, 1986.
- [6] K. A. Jaeckle, H. J. Eyre, J. J. Townsend et al., "Correlation of tumor O<sup>6</sup> methylguanine-DNA methyltransferase levels with survival of malignant astrocytoma patients treated with bis-chloroethylnitrosourea: a Southwest Oncology Group study," *Journal of Clinical Oncology*, vol. 16, no. 10, pp. 3310–3315, 1998.

- [7] M. Belanich, M. Pastor, T. Randall et al., "Retrospective study of the correlation between the DNA repair protein alkyltransferase and survival of brain tumor patients treated with carmustine," *Cancer Research*, vol. 56, no. 4, pp. 783–788, 1996.
- [8] R. S. Foote, S. Mitra, and B. C. Pal, "Demethylation of O<sup>6</sup>-methylguanine synthetic DNA polymer by an inducible activity in *Escherichia coli*," *Biochemical and Biophysical Research Communications*, vol. 97, no. 2, pp. 654–659, 1980.
- [9] A. E. Pegg, "Mammalian O<sup>6</sup>-alkylguanine-DNA alkyltransferase: regulation and importance in response to alkylating carcinogenic and therapeutic agents," *Cancer Research*, vol. 50, no. 19, pp. 6119–6129, 1990.
- [10] W. P. Tong, M. C. Kirk, and D. B. Ludlum, "Formation of the cross-link 1-[N<sup>3</sup>-deoxycytidyl],2-[N<sup>1</sup>-deoxyguanosinyl]ethane in DNA treated with N,N'-bis(2-chloroethyl)-N-nitrosourea," *Cancer Research*, vol. 42, no. 8, pp. 3102–3105, 1982.
- [11] L. Yan, J. R. Donze, and L. Liu, "Inactivated MGMT by O<sup>6</sup>-benzylguanine is associated with prolonged G2/M arrest in cancer cells treated with BCNU," *Oncogene*, vol. 24, no. 13, pp. 2175–2183, 2005.
- [12] T. P. Brent, P. J. Houghton, and J. A. Houghton, "O<sup>6</sup>-alkylguanine-DNA alkyltransferase activity correlates with the therapeutic response of human rhabdomyosarcoma xenografts to 1-(2-chloroethyl)-3-(trans-4-methylcyclohexyl)-1-nitrosourea," *Proceedings of the National Academy of Sciences of the United States of America*, vol. 82, no. 9, pp. 2985–2989, 1985.
- [13] G. Tagliabue, L. Citti, G. Massazza, G. Damia, R. Giavazzi, and M. D'Incalci, "Tumour levels of O<sup>6</sup>-alkylguanine-DNA-alkyltransferase and sensitivity to BCNU of human xenografts," *Anticancer Research*, vol. 12, no. 6B, pp. 2123–2125, 1992.
- [14] R. Pepponi, G. Marra, M. P. Fuggetta et al., "The effect of O<sup>6</sup>-alkylguanine-DNA alkyltransferase and mismatch repair activities on the sensitivity of human melanoma cells to temozolomide, 1,3-bis(2-chloroethyl)1-nitrosourea, and cisplatin," *Journal of Pharmacology and Experimental Therapeutics*, vol. 304, no. 2, pp. 661–668, 2003.
- [15] S. L. Gerson, "Clinical relevance of MGMT in the treatment of cancer," *Journal of Clinical Oncology*, vol. 20, no. 9, pp. 2388–2399, 2002.
- [16] G. P. Margison, A. C. Povey, B. Kaina, and M. F. Santibáñez Koref, "Variability and regulation of O<sup>6</sup>-alkylguanine-DNA alkyltransferase," *Carcinogenesis*, vol. 24, no. 4, pp. 625–635, 2003.
- [17] S. L. Gerson, "MGMT: its role in cancer aetiology and cancer therapeutics," *Nature Reviews Cancer*, vol. 4, no. 4, pp. 296–307, 2004.
- [18] M. E. Hegi, A.-C. Diserens, T. Gorlia et al., "MGMT gene silencing and benefit from temozolomide in glioblastoma," *The New England Journal of Medicine*, vol. 352, no. 10, pp. 997–1003, 2005.
- [19] M. Esteller, J. Garcia-Foncillas, E. Andion et al., "Inactivation of the DNA-repair gene MGMT and the clinical response of gliomas to alkylating agents," *The New England Journal of Medicine*, vol. 343, no. 19, pp. 1350–1354, 2000.
- [20] A. E. Pegg, K. Swenn, M.-Y. Chae, M. E. Dolan, and R. C. Moschel, "Increased killing of prostate, breast, colon, and lung tumor cells by the combination of inactivators of O<sup>6</sup>-alkylguanine-DNA alkyltransferase and N,N'-bis(2-chloroethyl)-N-nitrosourea," *Biochemical Pharmacology*, vol. 50, no. 8, pp. 1141–1148, 1995.
- [21] K. S. Srivenugopal, X.-H. Yuan, H. S. Friedman, and F. Ali-Osman, "Ubiquitination-dependent proteolysis of O<sup>6</sup>-methylguanine-DNA methyltransferase in human and murine tumor cells following inactivation with O<sup>6</sup>-benzylguanine or 1,3-bis(2-chloroethyl)-1-nitrosourea," *Biochemistry*, vol. 35, no. 4, pp. 1328–1334, 1996.
- [22] M. Xu-Welliver and A. E. Pegg, "Degradation of the alkylated form of the DNA repair protein, O<sup>6</sup>-alkylguanine-DNA alkyltransferase," *Carcinogenesis*, vol. 23, no. 5, pp. 823–830, 2002.
- [23] B. D. Wilson, M. Strauss, B. J. Stickells, E. G. Hoal-van Helden, and P. D. Van Helden, "An assay for O<sup>6</sup>-alkylguanine-DNA alkyltransferase based on restriction endonuclease inhibition and magnetic bead separation of products," *Carcinogenesis*, vol. 15, no. 10, pp. 2143–2148, 1994.
- [24] M. E. Dolan, D. Schicchitano, and A. E. Pegg, "Use of oligodeoxynucleotides containing O<sup>6</sup>-alkylguanine for the assay of O<sup>6</sup>-alkylguanine-DNA-alkyltransferase activity," *Cancer Research*, vol. 48, no. 5, pp. 1184–1188, 1988.
- [25] A. M. Moser, M. Patel, H. Yoo, F. M. Balis, and M. E. Hawkins, "Real-time fluorescence assay for O<sup>6</sup>-alkylguanine-DNA alkyltransferase," *Analytical Biochemistry*, vol. 281, no. 2, pp. 216–222, 2000.
- [26] R. S. Wu, S. Hurst-Calderone, and K. W. Kohn, "Measurement of O<sup>6</sup>-alkylguanine-DNA alkyltransferase activity in human cells and tumor tissues by restriction endonuclease inhibition," *Cancer Research*, vol. 47, no. 23, pp. 6229–6235, 1987.
- [27] J. L. Huppert, "Four-stranded nucleic acids: structure, function and targeting of G-quadruplexes," *Chemical Society Reviews*, vol. 37, no. 7, pp. 1375–1384, 2008.
- [28] S. Neidle, "The structures of quadruplex nucleic acids and their drug complexes," *Current Opinion in Structural Biology*, vol. 19, no. 3, pp. 239–250, 2009.
- [29] N. V. Hud, F. W. Smith, F. A. L. Anet, and J. Feigon, "The selectivity for K<sup>+</sup> versus Na<sup>+</sup> in DNA quadruplexes is dominated by relative free energies of hydration: a thermodynamic analysis by 1H NMR," *Biochemistry*, vol. 35, no. 48, pp. 15383–15390, 1996.
- [30] S. Burge, G. N. Parkinson, P. Hazel, A. K. Todd, and S. Neidle, "Quadruplex DNA: sequence, topology and structure," *Nucleic Acids Research*, vol. 34, no. 19, pp. 5402–5415, 2006.
- [31] S. W. Blume, V. Guarcello, W. Zacharias, and D. M. Miller, "Divalent transition metal cations counteract potassium-induced quadruplex assembly of oligo(dG) sequences," *Nucleic Acids Research*, vol. 25, no. 3, pp. 617–625, 1997.
- [32] A. G. Petrovic and P. L. Polavarapu, "Quadruplex structure of polyriboinosinic acid: dependence on alkali metal ion concentration, pH and temperature," *Journal of Physical Chemistry B*, vol. 112, no. 7, pp. 2255–2260, 2008.
- [33] C. S. Mekmaysy, L. Petraccone, N. C. Garbett et al., "Effect of O<sup>6</sup>-methylguanine on the stability of G-quadruplex DNA," *Journal of the American Chemical Society*, vol. 130, no. 21, pp. 6710–6711, 2008.
- [34] R. F. Macaya, P. Schultze, F. W. Smith, J. A. Roe, and J. Feigon, "Thrombin-binding DNA aptamer forms a unimolecular quadruplex structure in solution," *Proceedings of the National Academy of Sciences of the United States of America*, vol. 90, no. 8, pp. 3745–3749, 1993.
- [35] O. S. Bhanot and A. Ray, "The in vivo mutagenic frequency and specificity of O<sup>6</sup>-methylguanine in  $\phi$ X174 replicative form DNA," *Proceedings of the National Academy of Sciences of the United States of America*, vol. 83, no. 19, pp. 7348–7352, 1986.

- [36] F. M. Ruiz, R. Gil-Redondo, A. Morreale, Á. R. Ortiz, C. Fábrega, and J. Bravo, "Structure-based discovery of novel non-nucleosidic DNA alkyltransferase inhibitors: virtual screening and in vitro and in vivo activities," *Journal of Chemical Information and Modeling*, vol. 48, no. 4, pp. 844–854, 2008.
- [37] M. H. Caruthers, A. D. Barone, S. L. Beaucage et al., "Chemical synthesis of deoxyoligonucleotides by the phosphoramidite method," *Methods in Enzymology*, vol. 154, pp. 287–313, 1987.
- [38] H. Vu, C. McCollum, C. Lotys, and A. Andrus, "New reagents and solid support for automated oligonucleotide synthesis," *Nucleic Acids Symposium Series*, no. 22, pp. 63–64, 1990.
- [39] J. J. Rasimas, A. E. Pegg, and M. G. Fried, "DNA-binding mechanism of O<sup>6</sup>-alkylguanine-DNA alkyltransferase: effects of protein and DNA alkylation on complex stability," *Journal of Biological Chemistry*, vol. 278, no. 10, pp. 7973–7980, 2003.

## Review Article

# The Emerging Role of Telomerase Reverse Transcriptase in Mitochondrial DNA Metabolism

**Donna M. Gordon<sup>1</sup> and Janine Hertzog Santos<sup>2</sup>**

<sup>1</sup> *Department of Biological Sciences, Mississippi State University, 114 Harned Hall, 295 Lee Boulevard, Mississippi State, MS 39762, USA*

<sup>2</sup> *Department of Pharmacology and Physiology, New Jersey Medical School of UMDNJ, 185 South Orange Avenue, Medical Sciences Building, H653, Newark, NJ 07103, USA*

Correspondence should be addressed to Janine Hertzog Santos, santosja@umdnj.edu

Received 14 May 2010; Revised 26 July 2010; Accepted 31 August 2010

Academic Editor: Ashis Basu

Copyright © 2010 D. M. Gordon and J. H. Santos. This is an open access article distributed under the Creative Commons Attribution License, which permits unrestricted use, distribution, and reproduction in any medium, provided the original work is properly cited.

Telomerase is a reverse transcriptase specialized in telomere synthesis. The enzyme is primarily nuclear where it elongates telomeres but recent reports have shown that it also localizes to mitochondria. The function of TERT in mitochondria is largely unknown but the available findings point to a role in mitochondrial DNA metabolism. This paper discusses the available data on mitochondrial telomerase with particular emphasis on its effects upon the organellar DNA.

## 1. Introduction

Telomerase is a reverse transcriptase well recognized for its function at telomeres, protein-DNA structures essential for the stability of linear chromosomes. The enzyme is composed minimally of two different subunits, a catalytic core (TERT) responsible for DNA catalysis and an RNA component (TERC) that is used as template for telomeric DNA synthesis. Whereas the RNA is present in both somatic and germ cells constitutively, expression of TERT is tightly regulated. Telomerase activity is high during embryogenesis and in the vast majority of tumors but is low or non-existent in most adult somatic cells [1]. Both TERT mRNA and protein have been reported in telomerase-negative cells albeit at low levels [2, 3].

In recent years many different reports have indicated that the reverse transcriptase component of telomerase has additional cellular functions beyond telomere stabilization. For instance, TERT has been shown to play a role in chromatin remodeling and in DNA damage response and to act as a transcriptional modulator of the Wnt/beta-catenin signaling pathways [4, 5]. More recently it was shown to acquire properties of an RNA-dependent RNA polymerase when in a complex with the RNA component

of the mitochondrial endoribonuclease MRP; such activity is not involved in the maintenance of telomeres but rather in regulation of gene expression [6].

In line with the idea that TERT has extratelomeric functions, we were the first to show that the human protein (hTERT) is also mitochondrial [7, 8]. The mitochondrial localization of endogenous and ectopically expressed hTERT was subsequently reproduced by others [9–12]. The presence of hTERT in mitochondria was surprising given the well-established role of telomerase in telomere maintenance and the lack of a telomeric structure on the mitochondrial DNA (mtDNA). However, it was not entirely unexpected as cytoplasmic localization of telomerase had been previously reported [13–17] and, as described above, other functions outside telomere maintenance have been increasingly ascribed to hTERT.

This paper focuses on the localization of TERT to mitochondria and its putative role in mtDNA metabolism. We review findings regarding the effects of mitochondrial hTERT upon genotoxic stress and recent evidence demonstrating the impact of TERT (or lack thereof) to mitochondrial biology under nonstress conditions. The impact of mitochondrial telomerase to aging and telomere maintenance is not discussed as it has been reviewed

elsewhere [18]. More information about the noncanonical and/or extratelomeric activities of telomerase can be found in other recent reviews [19–21].

## 2. Mitochondrial Localization of TERT

*2.1. Endogenous and Ectopically Expressed TERT Are Mitochondrial.* The first evidence that TERT was a mitochondrial protein came from studies done by us initially identifying a mitochondrial-targeting signal (MTS) at its N-terminus [7]. Using software packages that predict MTSs, we identified the first 20 amino acid residues of TERT to be a putative mitochondrial targeting peptide. We found the MTS to be conserved among higher eukaryotes such as plants, fish, and mammals but not present in lower species such as yeast and tetrahymena [7]. Fusion of EGFP to the C-terminus of full-length wild-type (WT) human TERT showed that the recombinant protein was localized to mitochondria. Addition of only the MTS to the N-terminus of EGFP rendered the fluorescent protein completely mitochondrial and mutations of two amino acid residues within the MTS abolished hTERT's mitochondrial localization, indicating that the MTS was sufficient and required to target hTERT to mitochondria [7, 8]. Telomerase enzymatic activity was also detected in purified mitochondrial extracts from various human cells [7], collectively providing strong evidence that hTERT was a mitochondrial protein. Subsequently, others have confirmed the presence of endogenous hTERT in mitochondria by immunofluorescence and Western blotting [9–12]. Of note, a recent study showed that hTERT is found in purified mitochondria of primary umbilical vein endothelial cells [12], underscoring that the mitochondrial localization of hTERT is not an artifact of protein overexpression or associated with cellular transformation. In this context, our unpublished work shows that a fraction of endogenous rat and mouse TERT is mitochondrial as well (Green et al. in preparation).

The content of hTERT in cancer cells has been estimated to range from 20 to 50 molecules [22]. According to recent reports [11, 12] and to our unpublished data, we estimate that ~10–20% of the total cellular hTERT is mitochondrial under nonstress conditions, which is equivalent to 3–10 molecules of hTERT/mitochondrion at least in cancer cells. It is not surprising then that many have missed the mitochondrial localization of TERT. The unequal subcellular distribution of dually targeted proteins is a wide spread phenomenon and has been termed “eclipsed distribution” [23]. Many of these proteins have been shown to have distinct functions in the different subcellular compartments [23–26] similar to what is predicted for TERT activity.

*2.2. Submitochondrial Localization of TERT.* To gain insight into the molecular function of a mitochondrial protein it is necessary to define its submitochondrial localization since its presence in the mitochondrial membrane (inner or outer) or in the matrix would predict different biological functions. Haendeler et al. [11] identified the submitochondrial localization of hTERT by immunoblots and co-immunoprecipitations. The authors isolated mitochondria

from Hek293, treated the purified organelles with proteinase K, and probed for hTERT by Western blots. Using this approach they concluded that hTERT was mostly localized to the mitochondrial matrix. Their claims were substantiated by experiments demonstrating that overexpressed myc-tagged hTERT co-immunoprecipitated with TOM20, TOM40, and TIM23 [11]. TOM20, TOM40, and TIM23 are protein translocases of the outer (TOM20 and TOM40) and inner (TIM23) mitochondrial import machinery [24]. These results are consistent with experiments showing that hTERT binds mtDNA (see below), which resides in the matrix.

## 3. Regulation of hTERT's Subcellular Distribution

It is now recognized that the dual targeting of proteins can be regulated, induced, or rebalanced in response to cellular signaling or to changes in extracellular conditions [26]. While much is still unknown about how the subcellular distribution of TERT is achieved, the available data suggest that it is tightly regulated. In this section, we review published information regarding the signals that target TERT to the nucleus and mitochondria and the role of oxidative stress in redistributing hTERT within the cell. An excellent review about mechanisms, regulation, and function of dual targeting of proteins has been recently published [26].

*3.1. TERT's Targeting Signals.* It is clear that at basal levels TERT is primarily nuclear with only a small fraction present in mitochondria. However, it is currently unknown what regulates the intracellular distribution of TERT. In addition to its N-terminal MTS, hTERT has a nuclear export signal (NES) spanning amino acids 978–987 [14, 27]. Several nuclear localization signals (NLSs) are predicted but they have not yet been mapped out onto the protein [14]. No splicing variants involving the MTS or the NES of hTERT have been reported neither have variants that change its subcellular distribution been identified. It therefore seems likely that the dual targeting of TERT is based on a single translation product containing different targeting signals. In such a case, the balance between the mitochondrial and nuclear pools of the protein may be determined by various competing factors, including the affinity of each signal for its target or, alternatively, the accessibility of the target signal for specific receptor binding [26].

*3.2. Regulation of TERT's Distribution by Oxidative Stress.* The intracellular distribution of hTERT changes upon specific stimuli, and many different proteins have been associated with its shuttling between nucleus and cytoplasm (including mitochondria) [10, 12, 14, 16, 28–32]. Under oxidative stress, the distribution of hTERT is regulated by posttranslational modifications. Indeed, Src kinase has been shown to control the export of hTERT from the nucleus into the cytoplasm upon oxidative stress [10, 16]. Dephosphorylation of hTERT by the phosphatase Shp-2 reversed this process [28]. Increased localization of hTERT to mitochondria upon oxidative stress was also reported [10].

High levels of mitochondrial hTERT were observed within hours of exposure to hydrogen peroxide ( $H_2O_2$ ) but several days were required in the case of hyperoxia. Although it took weeks, this redistribution of hTERT under hyperoxia was found to be a reversible process [10]. Together these data suggest that the intracellular redistribution of hTERT under oxidative stress likely relies on *de novo* protein synthesis but the current data do not exclude protein relocalization. Carrying out similar experiments in the presence of cycloheximide will help clarify this issue.

Büchner et al. [12] recently suggested that Src kinase also controls mitochondrial levels of hTERT upon oxidative stress similar to what has been shown for nuclear hTERT. The authors found that while levels of WT hTERT decreased in mitochondria upon  $H_2O_2$  exposure, no changes occurred in a mutant version of hTERT (Y707F) that is not phosphorylated by Src kinase. They concluded that oxidative stress resulted in the Src-dependent mitochondrial downregulation of hTERT [12].

While it is possible that Src is involved in regulating nuclear and mitochondrial levels of hTERT under oxidative stress, the above data should be taken with some caution. The conclusions were based on targeting WT and Y707F hTERT to mitochondria by cloning it into a mitochondrial shooter vector, which essentially adds another MTS to the N-terminus of hTERT [11]. However, no data showing the degree of mitochondrial localization of this construct was provided, which is required for proper interpretation of the data since levels of hTERT were assayed in total lysates prior to and after  $H_2O_2$  treatment [12]. If under oxidative stress TERT indeed relocalizes to mitochondria, lack of complete mitochondrial localization of mitoTERT may skew interpretation of the results. Assaying levels of mitoTERT in isolated mitochondria under the same experimental conditions [11] could easily address this concern.

Regardless of the role of Src, the downregulation of mitochondrial hTERT could also stem from increased degradation of hTERT, decreased affinity of the mutant protein for the mitochondrial import machinery, or promotion of protein folding, which would compete for translocation [23–26]. Clearly, additional studies are required to better understand how the intracellular distribution and mitochondrial localization of hTERT are regulated, and whether the other stimuli reported to induce the subcellular shuttling of hTERT also influence the balance between mitochondrial and nuclear localization of the protein.

#### 4. hTERT and Its Role in mtDNA Metabolism

Direct proof that TERT works in mtDNA metabolism is still missing but the ability of hTERT to modulate mtDNA damage induced by various agents, coupled with the recent demonstration that hTERT binds to mtDNA, strongly supports such a function. In this section we review evidence that mitochondrial hTERT promotes, protects, or does not interfere with mtDNA damage induced by different types of genotoxins. Taken together, the data indicate that the modulation of mtDNA damage caused by TERT is genotoxin-dependent and likely related to the type of lesion

present on the mtDNA. The exact mechanism(s) through which hTERT modulates mtDNA damage has yet to be elucidated. We also discuss findings about the interaction of hTERT with the organellar DNA. However, we do not touch on the role of hTERT in stress-mediated cell death as this has been recently reviewed [18].

**4.1. Mitochondrial hTERT Modulates Oxidative Damage on the mtDNA.** As reviewed above, oxidative stress alters hTERT levels in mitochondria. Why under such conditions mitochondrial hTERT levels fluctuate is not clear but the available data suggest that it may respond to oxidative damage to mtDNA. Major controversy is observed regarding modulation of oxidative stress-mediated mtDNA damage, with evidence demonstrating that hTERT either exacerbates or protects against this type of insult [7, 8, 10]. The reasons for the opposing results are still unclear but they could reflect differences in the cellular backgrounds, in antioxidant defenses, and/or in the dose/length of the stress (see below).

We were the first to show that hTERT modulates mtDNA damage caused by  $H_2O_2$  (200  $\mu$ M for either 15 minutes or 1 hour). Specifically, we demonstrated that cells expressing WT hTERT were more sensitive to  $H_2O_2$ -mediated mtDNA damage than the telomerase negative controls. Using 7 different cell lines expressing ectopic or endogenous hTERT and the respective non-hTERT isogenic controls, we showed that levels of mtDNA damage were significantly increased by the presence of the WT protein [7]. The promotion of damage was specific for hTERT because when hTERT was cloned flanked by *lox p* and excised using *cre* recombinase the effects were reversed [8]. All cells showed similar kinetics of  $H_2O_2$  breakdown; however, we detected an increase in bioavailable iron in cells overexpressing hTERT [7]. Iron can drive Fenton chemistry and more iron could increase the levels of hydroxyl radical generation, potentially explaining our results [7].

Subsequently, we established that the promotion of  $H_2O_2$ -induced mtDNA damage was strictly dependent on the presence of hTERT in mitochondria [8]. Stable expression of a nonmitochondrial mutant (R3E/R6EhTERT) completely abolished the promotion of mtDNA damage caused by 200  $\mu$ M  $H_2O_2$ , leading to levels of lesions that were either not different from or even below their non-hTERT counterparts. Similar findings were observed using a catalytically inactive hTERT mutant, indicating that the promotion of mtDNA damage relied on reverse transcriptase activity. These results were obtained in different cellular backgrounds, demonstrating that the effects of mitochondrial hTERT were general and did not rely on a particular cell type. Together, these data led to the conclusion that telomerase must be active and in mitochondria to promote  $H_2O_2$ -induced mtDNA damage [7, 8].

Interestingly, work by Ahmed et al. in 2008 contradicts these findings. Using MRC-5 and MRC-5 stably expressing hTERT, they showed less damage in cells expressing exogenous hTERT when compared to the non-hTERT counterpart after treatment with 500  $\mu$ M  $H_2O_2$  for 3 hours. A similar trend was observed for cells put under hyperoxia conditions (40% oxygen) for up to 70 days. While levels of

hyperoxia-induced mtDNA damage plateaued in MRC-5 cells from days 20 to 70, in MRC-5 hTERT the mtDNA damage was entirely eliminated after day 40, when hTERT was solely mitochondrial localized [10]. These data suggest that (i) mtDNA repair was either not operating or was overwhelmed in MRC-5 cells by the (likely) constant levels of damage induced by hyperoxia and (ii) that repair or turnover of hyperoxia-induced mtDNA damage was modulated by hTERT but only when the protein was in mitochondria. It is worth noting that the protection afforded by hTERT in this study could result from upregulation of antioxidant defenses since an increase in at least one antioxidant enzyme was detected in MRC-5 hTERT by gene expression profiles [10].

**4.2. Effects of hTERT on mtDNA Damage Induced by Other Genotoxins.** Methyl methanesulfonate (MMS) is a methylating agent that preferentially alkylates the N-7 position of guanine. This lesion is converted into an abasic site and transiently into a single DNA strand break (SSB, [33]). Such lesions are repaired on the mitochondrial genome through the base excision repair pathway (BER, [34]). When hTERT overexpressing cells and their non-hTERT isogenic counterparts were exposed to MMS, no differences in the levels of either nuclear or mtDNA damage were observed. On the contrary, the trend pointed to a decrease in damage in both genomes in the presence of WT hTERT, which did not reach statistical significance [8].

As observed with H<sub>2</sub>O<sub>2</sub>, mtDNA damage induced by etoposide was promoted by hTERT. Indeed, a slight but significant enhancement in mtDNA damage was observed in NHF hTERT cells exposed to 1 μM etoposide, which was not observed in NHF controls [8]. Etoposide, like H<sub>2</sub>O<sub>2</sub>, not only causes DNA double-strand breaks (DSBs) but induces oxidative stress as well [35]. Note that the majority of DNA breaks provoked by H<sub>2</sub>O<sub>2</sub> are SSBs. In mitochondria, oxidized DNA and SSBs are repaired by BER whereas to date no system to correct DSBs has been identified in the mammalian organelle [34].

Mitochondrial hTERT was also proposed to protect mtDNA against UV damage. Using *in vitro* assays it was shown that preincubation of isolated DNA with *in vitro* translated hTERT protected the DNA against UV exposure. To show that this effect was physiologically relevant and involved the mitochondrial function of TERT, lung fibroblasts from WT and TERT knockout (KO) animals were exposed to increasing doses of UV and mitochondrial function assessed based on the MTT assay. Significantly less MTT conversion was observed in the KO cells with increasing doses of UV, leading to the conclusion that mitochondrial TERT protects mtDNA *in vitro* and mitochondrial function *in vivo* from UV damage [11]. Since nuclear TERT is also absent in the KO animals, further studies are required to define whether the protection afforded by TERT against UV damage indeed relies on its mitochondrial activity.

Likewise, expression of WT hTERT alleviated mtDNA depletion caused by low doses of ethidium bromide (EtBr) treatment. This rescue effect was more pronounced with expression of a mitochondrially targeted hTERT [11].

Potential mechanisms through which hTERT could be protecting the mtDNA from damage induced by UV and EtBr that cause, respectively, pyrimidine dimers and inter- and intrastrand crosslinks are unknown. Repair systems to remove these complex lesions have not been identified in mitochondria [34]. Based on the notion that mtDNA molecules containing nonrepairable lesions are targeted for degradation, one could speculate that hTERT may promote mtDNA turnover. Such activity is consistent with our previously proposed role for hTERT in mitochondrial quality control [8]. Other proposed that means through which TERT may modulate mtDNA damage are (i) modulation of BER, (ii) increase in intracellular bioavailable iron, (iii) changes in antioxidant defenses, and/or (iv) processing of mitochondrial DSBs. More studies are required to define the exact mechanism(s) through which TERT alters mtDNA damage and, importantly, what kinds of lesions are impacted by TERT.

**4.3. hTERT Associates with mtDNA.** If TERT was involved in mtDNA metabolism, one would predict that it binds mtDNA. Indeed, recent studies demonstrate that hTERT interacts with the mitochondrial genome. Using chromatin immunoprecipitations in cultured cells, Haendeler and colleagues demonstrated that hTERT interacts with mtDNA, consistent with its presence in the mitochondrial matrix. Surprising, however, was the fact that only two regions of the mtDNA were pulled down with hTERT: ND1 and ND2 of complex I [11]. Why only these two regions were identified as bound to TERT, which has been shown to have preference for telomeric DNA sequences [36], is not clear. While mtDNA does not have a telomeric structure, it does contain 22 telomeric-like repeats distributed across the two strands of the genome [7]. Such sequences could potentially be recognized by mitochondrial TERT and justify the preference for ND1 and ND2 binding. However, analysis of these gene sequences revealed no TTAGGG repeats (data not shown). Other potential explanations for hTERT association with mtDNA may relate to the oxidative state of the mitochondria during the experiments or the use of transient hTERT expression. Regardless, the binding of hTERT to the mitochondrial genome certainly strengthens its putative role in mtDNA metabolism. It will be interesting to define whether other regions of the mtDNA bind to TERT when the protein is stably expressed and, more importantly, whether such interaction changes upon genotoxic stress.

## 5. TERT and Mitochondrial Biology

MtDNA integrity is intimately related to mitochondrial function. Once mtDNA is damaged, expression of critical protein components of the electron transport chain (ETC) is decreased leading to increased reactive oxygen species (ROS) generation and decreased mitochondrial membrane potential ( $\Delta\Psi_m$ ). Such events lead to a vicious cycle of mitochondrial damage, ultimately affecting mitochondrial import, calcium homeostasis, and ATP production among other processes [37–39]. Consistent with a role for TERT in mtDNA metabolism, recent work has shown that the absence

of hTERT is associated with mitochondrial dysfunction. For instance, cells lacking hTERT showed higher mitochondrial ROS and decreased respiratory chain efficiency when compared to controls [10, 11, 27]. This section reviews evidence regarding the impact of hTERT on various mitochondrial parameters under basal conditions. Together the data reinforce the emerging role of hTERT in mitochondrial biology.

**5.1. hTERT and ROS Production.** Using mitoSOX and dihydrorhodamine (DHR) to detect mitochondrial superoxide ( $O_2^{\bullet-}$ ) and cellular peroxides (such as  $H_2O_2$ ) it was shown that fluorescence from both dyes was decreased in MRC-5 hTERT cells when compared to MRC-5. These data indicate that the presence of hTERT was associated with decreased mitochondrial ROS production [10]. In agreement, overexpression of WT hTERT in Hek293 decreased levels of ROS when compared to empty-vector control or a catalytically inactive mutant [11]. In complementary experiments, siRNA knockdown of hTERT in HUVEC and Hek293 cells showed increased production of  $O_2^{\bullet-}$  and  $H_2O_2$ , confirming the notion that hTERT lowers the basal levels of ROS generation [10, 11].

Recently, we showed that expression of a mutant hTERT ( $_{NES}$ -hTERT) that is unable to shuttle between subcellular compartments exhibited decreased mtDNA integrity and increased mitochondrial ROS [27]. These data are consistent with the above-mentioned work [10, 11] and suggest that nonnuclear hTERT is associated with improved mitochondrial function. However, our data did not rule out the possibility that the mitochondrial defects observed upon expression of  $_{NES}$ -hTERT were associated with the senescent phenotype of the cells or to the defect in shuttling of hTERT itself [27]. It is important to note that these data were collected under nonstress conditions and therefore do not contradict our previous findings which were obtained under  $H_2O_2$  exposure [7, 8]. Although it would be interesting to submit  $_{NES}$ -hTERT-expressing cells to oxidative stress, the data obtained will need to be interpreted with caution given the high degree of telomere damage and premature senescence triggered by expression of this mutant hTERT [27].

**5.2. hTERT and Respiratory Chain Activity.** The energy released by the transport of electrons through the ETC also provides protons used to establish an electrochemical gradient across the inner mitochondrial membrane [39]. Using JC-1 and confocal microscopy, it was shown that MRC-5 hTERT cells had significantly higher  $\Delta\Psi_m$  at normoxic conditions when compared to its isogenic non-hTERT control [10]. However, this seemed in apparent contradiction with the lower levels of ROS in these cells given there is more chance of ROS generation when the  $\Delta\Psi_m$  is high [40, 41]. The authors suggested that the mitochondria of hTERT cells are tightly coupled, which explains the low ROS levels [10]. Indeed we recently showed that cells expressing WT hTERT have highly coupled mitochondria [27].

The activity of the ETC was directly evaluated using cells expressing either WT hTERT or a catalytically inactive mutant. Overall succinate-dependent respiratory function

was 30% lower in the mutant while complex I activity was higher in cells carrying the WT protein. The increased respiratory capacity detected in cultured cells was confirmed *in vivo*. Respiratory function in intact heart and liver mitochondria isolated from WT and KO TERT animals was analyzed. Complex I activity was lower in the heart of the KO animals; however, no changes were detected in liver mitochondria. These data led to the hypothesis that *in vivo* the impact of mitochondrial TERT may be more prominent in cells that have high-energy requirements and less regenerative capacity [11].

The improvement in complex I function was attributed to the direct binding of hTERT to ND1 and ND2, which could potentially increase expression of these proteins [11]. Recent data in yeast suggest that enhanced mitochondrial respiration may be mediated by increased number of oxidative phosphorylation (OXPHOS) complexes per organelle as opposed to increasing the total number of mitochondria per cell [42]. It will be interesting to test whether this is the case in mammalian cells and, if so, which OXPHOS complexes are modulated by hTERT in mitochondria.

Two TERT KO mouse models have been generated, and no gross defects have been observed in early generations [43, 44], inconsistent with a major role for TERT in mtDNA metabolism. It is important to note that results observed with cells grown in culture were mild, and it is possible that subtle differences have been overlooked when not specifically investigating mitochondrial function in these animals. Alternatively, it is feasible that compensatory mechanisms were activated in the KO animals. Interestingly, late generation mTERT KO animals had accelerated infertility, which was initially ascribed to the short telomeres present in the animals. However, mice heterozygous for TERT, while having very short telomeres, did not show the same phenotype, leading the authors to conclude that the dosage of TERT was important for genomic stability [45]. It is known that proper mitochondrial function plays an important role in fertility [46]. In light of the latest findings, it is tempting to speculate that the impact of the lack of mitochondrial TERT contributed to the infertility previously observed in the KO animals. Certainly, it seems worth revisiting the mouse models available to address whether mitochondrial abnormalities are present in these animals. Of particular interest will be to measure mitochondrial function in the KO animals under conditions that require a high-energy demand. Of note, TERT KO animals have been submitted to physical exercise, and an important role for telomerase has been ascertained in the heart and in aortic endothelial cells [47, 48]. However, no direct assessment of mitochondrial function such as cytochrome c oxidase activity or ATP production was conducted nor was a connection to mitochondrial biology or to telomerase function in mitochondria established [47, 48], all worth addressing in future studies.

## 6. Concluding Remarks

Mitochondrial function is key to cellular homeostasis, and maintenance of mitochondrial quality has major impact in health and disease. A role for TERT in mitochondria is clearly

emerging although its exact mechanism of action remains largely unknown. Years of work done *in vitro* and *in vivo* have established telomerase as a main player in aging and cancer primarily due to its action upon the telomeres. The mitochondrial localization and function of TERT bring yet another layer of complexity to the already intricate scenario of telomerase multitasking in the cell. More experiments are certainly required to differentiate the mitochondrial effects of TERT as dependent on its nuclear versus mitochondrial localization and to establish the biological significance of TERT in mitochondria *in vivo*. The next years will be very exciting for both the mitochondrial and telomerase fields as more details about the function of TERT in the organelle are unveiled. Such studies will allow for a better understanding of the overall role of telomerase in cellular function and will lay foundation for new therapeutic approaches to aging, age- and mitochondrial-related diseases, and cancer.

## Acknowledgments

The authors thank Dr. Patricia L. Opresko from the Department of Environmental and Occupational Health and Dr. Hong Wang from the Department of Pharmacology and Chemical Biology of the University of Pittsburgh for critical review of the paper. They also thank the support from the Department of Defense through the Army Research Office (Award no. 56027LS to J. H. Santos).

## References

- [1] J. W. Shay and W. E. Wright, "Senescence and immortalization: role of telomeres and telomerase," *Carcinogenesis*, vol. 26, no. 5, pp. 867–874, 2005.
- [2] A. Kilian, D. D. L. Bowtell, H. E. Abud et al., "Isolation of a candidate human telomerase catalytic subunit gene, which reveals complex splicing patterns in different cell types," *Human Molecular Genetics*, vol. 6, no. 12, pp. 2011–2019, 1997.
- [3] K. Masutomi, E. Y. Yu, S. Khurts et al., "Telomerase maintains telomere structure in normal human cells," *Cell*, vol. 114, no. 2, pp. 241–253, 2003.
- [4] K. Masutomi, R. Possemato, J. M. Y. Wong et al., "The telomerase reverse transcriptase regulates chromatin state and DNA damage responses," *Proceedings of the National Academy of Sciences of the United States of America*, vol. 102, no. 23, pp. 8222–8227, 2005.
- [5] J.-I. Park, A. S. Venteicher, J. Y. Hong et al., "Telomerase modulates Wnt signalling by association with target gene chromatin," *Nature*, vol. 460, no. 7251, pp. 66–72, 2009.
- [6] Y. Maida, M. Yasukawa, M. Furuuchi et al., "An RNA-dependent RNA polymerase formed by TERT and the RMRP RNA," *Nature*, vol. 461, no. 7261, pp. 230–235, 2009.
- [7] J. H. Santos, J. N. Meyer, M. Skorvaga, L. A. Annab, and B. Van Houten, "Mitochondrial hTERT exacerbates free-radical-mediated mtDNA damage," *Aging Cell*, vol. 3, no. 6, pp. 399–411, 2004.
- [8] J. H. Santos, J. N. Meyer, and B. Van Houten, "Mitochondrial localization of telomerase as a determinant for hydrogen peroxide-induced mitochondrial DNA damage and apoptosis," *Human Molecular Genetics*, vol. 15, no. 11, pp. 1757–1768, 2006.
- [9] D. Del Bufalo, A. Rizzo, D. Trisciuglio et al., "Involvement of hTERT in apoptosis induced by interference with Bcl-2 expression and function," *Cell Death and Differentiation*, vol. 12, no. 11, pp. 1429–1438, 2005.
- [10] S. Ahmed, J. F. Passos, M. J. Birket et al., "Telomerase does not counteract telomere shortening but protects mitochondrial function under oxidative stress," *Journal of Cell Science*, vol. 121, no. 7, pp. 1046–1053, 2008.
- [11] J. Haendeler, S. Dröse, N. Büchner et al., "Mitochondrial telomerase reverse transcriptase binds to and protects mitochondrial DNA and function from damage," *Arteriosclerosis, Thrombosis, and Vascular Biology*, vol. 29, no. 6, pp. 929–935, 2009.
- [12] N. Büchner, T. -C. Zschauer, M. Lukosz, J. Altschmied, and J. Haendeler, "Downregulation of mitochondrial telomerase reverse transcriptase induced by H<sub>2</sub>O<sub>2</sub> is Src kinase dependent," *Experimental Gerontology*, vol. 45, no. 7-8, pp. 558–562, 2010.
- [13] G. B. Morin, "The human telomere terminal transferase enzyme is a ribonucleoprotein that synthesizes TTAGGG repeats," *Cell*, vol. 59, no. 3, pp. 521–529, 1989.
- [14] H. Seimiya, H. Sawada, Y. Muramatsu et al., "Involvement of 14-3-3 proteins in nuclear localization of telomerase," *EMBO Journal*, vol. 19, no. 11, pp. 2652–2661, 2000.
- [15] B. N. Armbruster, S. S. R. Banik, C. Guo, A. C. Smith, and C. M. Counter, "N-terminal domains of the human telomerase catalytic subunit required for enzyme activity *in vivo*," *Molecular and Cellular Biology*, vol. 21, no. 22, pp. 7775–7786, 2001.
- [16] J. Haendeler, J. Hoffmann, R. P. Brandes, A. M. Zeiher, and S. Dimmeler, "Hydrogen peroxide triggers nuclear export of telomerase reverse transcriptase via Src kinase family-dependent phosphorylation of tyrosine 707," *Molecular and Cellular Biology*, vol. 23, no. 13, pp. 4598–4610, 2003.
- [17] J. Haendeler, J. Hoffmann, J. F. Diehl et al., "Antioxidants inhibit nuclear export of telomerase reverse transcriptase and delay replicative senescence of endothelial cells," *Circulation Research*, vol. 94, no. 6, pp. 768–775, 2004.
- [18] G. Saretzki, "Telomerase, mitochondria and oxidative stress," *Experimental Gerontology*, vol. 44, no. 8, pp. 485–492, 2009.
- [19] C. Belgiovine, I. Chiodi, and C. Mondello, "Telomerase: cellular immortalization and neoplastic transformation. Multiple functions of a multifaceted complex," *Cytogenetic and Genome Research*, vol. 122, no. 3-4, pp. 255–262, 2009.
- [20] F. M. Bollmann, "The many faces of telomerase: emerging extratelomeric effects," *BioEssays*, vol. 30, no. 8, pp. 728–732, 2008.
- [21] Y. Cong and J. W. Shay, "Actions of human telomerase beyond telomeres," *Cell Research*, vol. 18, no. 7, pp. 725–732, 2008.
- [22] S. B. Cohen, M. E. Graham, G. O. Lovrecz, N. Bache, P. J. Robinson, and R. R. Reddel, "Protein composition of catalytically active human telomerase from immortal cells," *Science*, vol. 315, no. 5820, pp. 1850–1853, 2007.
- [23] N. Regev-Rudzki and O. Pines, "Eclipsed distribution: a phenomenon of dual targeting of protein and its significance," *BioEssays*, vol. 29, no. 8, pp. 772–782, 2007.
- [24] A. Naamati, N. Regev-Rudzki, S. Galperin, R. Lill, and O. Pines, "Dual targeting of Nfs1 and discovery of its novel processing enzyme, Icp55," *Journal of Biological Chemistry*, vol. 284, no. 44, pp. 30200–30208, 2009.
- [25] N. Regev-Rudzki, O. Yogev, and O. Pines, "The mitochondrial targeting sequence tilts the balance between mitochondrial and cytosolic dual localization," *Journal of Cell Science*, vol. 121, no. 14, pp. 2423–2431, 2008.

- [26] O. Yogev and O. Pines, "Dual targeting of mitochondrial proteins: mechanism, regulation and function," *Biochimica et Biophysica Acta*. In press.
- [27] O. A. Kovalenko, M. J. Caron, P. Ulema et al., "A mutant telomerase defective in nuclear-cytoplasmic shuttling fails to immortalize cells and is associated with mitochondrial dysfunction," *Aging Cell*, vol. 9, no. 2, pp. 203–219, 2010.
- [28] S. Jakob, P. Schroeder, M. Lukosz et al., "Nuclear protein tyrosine phosphatase Shp-2 is one important negative regulator of nuclear export of telomerase reverse transcriptase," *Journal of Biological Chemistry*, vol. 283, no. 48, pp. 33155–33161, 2008.
- [29] M. Akiyama, T. Hideshima, T. Hayashi et al., "Nuclear factor- $\kappa$ B p65 mediates tumor necrosis factor  $\alpha$ -induced nuclear translocation of telomerase reverse transcriptase protein," *Cancer Research*, vol. 63, no. 1, pp. 18–21, 2003.
- [30] K. Liu, R. J. Hodes, and N.-P. Weng, "Cutting edge: telomerase activation in human T lymphocytes does not require increase in telomerase reverse transcriptase (hTERT) protein but is associated with hTERT phosphorylation and nuclear translocation," *Journal of Immunology*, vol. 166, no. 8, pp. 4826–4830, 2001.
- [31] A. Kimura, M. Ohmichi, J. Kawagoe et al., "Induction of hTERT expression and phosphorylation by estrogen via Akt cascade in human ovarian cancer cell lines," *Oncogene*, vol. 23, no. 26, pp. 4505–4515, 2004.
- [32] R. Ram, O. Uziel, O. Eldan et al., "Ionizing radiation up-regulates telomerase activity in cancer cell lines by post-translational mechanism via ras/phosphatidylinositol 3-kinase/Akt pathway," *Clinical Cancer Research*, vol. 15, no. 3, pp. 914–923, 2009.
- [33] S. H. Wilson, "Mammalian base excision repair and DNA polymerase beta," *Mutation Research*, vol. 407, no. 3, pp. 203–215, 1998.
- [34] B. S. Mandavilli, J. H. Santos, and B. Van Houten, "Mitochondrial DNA repair and aging," *Mutation Research*, vol. 509, no. 1-2, pp. 127–151, 2002.
- [35] P. Meresse, E. Dechaux, C. Monneret, and E. Bertounesque, "Etoposide: discovery and medicinal chemistry," *Current Medicinal Chemistry*, vol. 11, no. 18, pp. 2443–2466, 2004.
- [36] D. C. F. Sealey, L. Zheng, M. A. S. Taboski, J. Cruickshank, M. Ikura, and L. A. Harrington, "The N-terminus of hTERT contains a DNA-binding domain and is required for telomerase activity and cellular immortalization," *Nucleic Acids Research*, vol. 38, no. 6, pp. 2019–2035, 2009.
- [37] B. Van Houten, V. Woshner, and J. H. Santos, "Role of mitochondrial DNA in toxic responses to oxidative stress," *DNA Repair*, vol. 5, no. 2, pp. 145–152, 2006.
- [38] D. C. Wallace, "Mitochondria as chi," *Genetics*, vol. 179, no. 2, pp. 727–735, 2008.
- [39] D. C. Wallace and W. Fan, "The pathophysiology of mitochondrial disease as modeled in the mouse," *Genes and Development*, vol. 23, no. 15, pp. 1714–1736, 2009.
- [40] R. S. Balaban, S. Nemoto, and T. Finkel, "Mitochondria, oxidants, and aging," *Cell*, vol. 120, no. 4, pp. 483–495, 2005.
- [41] M. P. Murphy, "How mitochondria produce reactive oxygen species," *Biochemical Journal*, vol. 417, no. 1, pp. 1–13, 2009.
- [42] G. S. Shadel and Y. Pan, "Multi-faceted regulation of mitochondria by TOR," *Cell Cycle*, vol. 8, no. 14, p. 2143, 2009.
- [43] X. Yuan, S. Ishibashi, S. Hatakeyama et al., "Presence of telomeric G-strand tails in the telomerase catalytic subunit TERT knockout mice," *Genes to Cells*, vol. 4, no. 10, pp. 563–572, 1999.
- [44] Y. Liu, B. E. Snow, M. P. Hande et al., "The telomerase reverse transcriptase is limiting and necessary for telomerase function in vivo," *Current Biology*, vol. 10, no. 22, pp. 1459–1462, 2000.
- [45] N. Erdmann, Y. Liu, and L. Harrington, "Distinct dosage requirements for the maintenance of long and short telomeres in mTert heterozygous mice," *Proceedings of the National Academy of Sciences of the United States of America*, vol. 101, no. 16, pp. 6080–6085, 2004.
- [46] M. Terzioglu and N.-G. Larsson, "Mitochondrial dysfunction in mammalian ageing," *Novartis Foundation Symposium*, vol. 287, pp. 197–208, 2007.
- [47] C. Werner, M. Hanhoun, T. Widmann et al., "Effects of physical exercise on myocardial telomere-regulating proteins, survival pathways, and apoptosis," *Journal of the American College of Cardiology*, vol. 52, no. 6, pp. 470–482, 2008.
- [48] C. Werner, T. Fürster, T. Widmann et al., "Physical exercise prevents cellular senescence in circulating leukocytes and in the vessel wall," *Circulation*, vol. 120, no. 24, pp. 2438–2447, 2009.

## Research Article

# Targeting the OB-Folds of Replication Protein A with Small Molecules

Victor J. Anciano Granadillo,<sup>1</sup> Jennifer N. Earley,<sup>1</sup> Sarah C. Shuck,<sup>1,2,3</sup> Millie M. Georgiadis,<sup>2</sup> Richard W. Fitch,<sup>4</sup> and John J. Turchi<sup>1,2</sup>

<sup>1</sup>Department of Medicine/Hematology and Oncology, Indiana University School of Medicine, Joseph E. Walther Hall, R3-C562, 980 W. Walnut Street, Indianapolis, IN 46202, USA

<sup>2</sup>Department of Biochemistry and Molecular Biology, Indiana University School of Medicine, Joseph E. Walther Hall, R3-C562, 980 W. Walnut Street, Indianapolis, IN 46202, USA

<sup>3</sup>Department of Biochemistry, Vanderbilt University School of Medicine, 850 Robinson Research Building, Nashville, TN 37209, USA

<sup>4</sup>Department of Chemistry and Physics, Indiana State University, Terre Haute, IN 47809, USA

Correspondence should be addressed to John J. Turchi, jturchi@iupui.edu

Received 19 August 2010; Accepted 27 September 2010

Academic Editor: Ashis Basu

Copyright © 2010 Victor J. Anciano Granadillo et al. This is an open access article distributed under the Creative Commons Attribution License, which permits unrestricted use, distribution, and reproduction in any medium, provided the original work is properly cited.

Replication protein A (RPA) is the main eukaryotic single-strand (ss) DNA-binding protein involved in DNA replication and repair. We have identified and developed two classes of small molecule inhibitors (SMIs) that show *in vitro* inhibition of the RPA-DNA interaction. We present further characterization of these SMIs with respect to their target binding, mechanism of action, and specificity. Both reversible and irreversible modes of inhibition are observed for the different classes of SMIs with one class found to specifically interact with DNA-binding domains A and B (DBD-A/B) of RPA. In comparison with other oligonucleotide/oligosaccharide binding-fold (OB-fold) containing ssDNA-binding proteins, one class of SMIs displayed specificity for the RPA protein. Together these data demonstrate that the specific targeting of a protein-DNA interaction can be exploited towards interrogating the cellular activity of RPA as well as increasing the efficacy of DNA-damaging chemotherapeutics used in cancer treatment.

## 1. Introduction

Replication protein A (RPA) is an essential protein involved in numerous DNA metabolic pathways including replication, repair, and recombination. RPA's activity in these pathways is in part a function of its single-stranded DNA (ssDNA) binding activity. RPA is a heterotrimeric protein comprised of 70-, 34-, and 14-kDa subunits [1] and binds to DNA through interactions with a series of OB-folds that display a high affinity for ssDNA [2]. OB-folds are found in numerous proteins, specifically those that perform their function through the interaction with single-stranded nucleic acid structures including tRNA synthetases, telomeres, and replication and repair intermediates [3]. The human telomeric DNA-binding proteins, POT1 and TPP1, both use OB-folds to recognize and bind the 3' ssDNA overhang of telomeres

[4, 5]. The breast cancer susceptibility protein, BRCA2, has three OB-folds that confer binding to ssDNA, which stimulates RAD51-mediated recombination [6]. The OB-fold, also referred to as a Greek key motif [3], consists of two three-stranded antiparallel  $\beta$ -sheets in which one strand is shared between them, forming a  $\beta$ -barrel structure. An  $\alpha$ -helix is typically located between strands 3 and 4, which packs against the bottom of the  $\beta$ -barrel [7]. The RPA 70-kDa subunit contains four putative OB-folds, two of which (A and B) comprise the central DNA binding domain (DBD-A/B), which contributes the majority of the ssDNA binding activity of the heterotrimeric protein. While other DNA binding domains within RPA include zinc ribbons and helix-turn-helix motifs [8], the OB-folds of DBD-A/B possess aromatic amino acid residues (F238 and F269 in DBD-A and W361 and F386 in DBD-B) that provide critical base-stacking

interactions [9]. A recombinant construct containing the DBD-A/B of RPA has been expressed, purified, and shown to be sufficient to bind DNA [9].

The importance of RPA in DNA replication has been demonstrated by genetic studies in yeast [10], genetic knockdown studies in human cells [11] and more recently in chemical genomic studies with an SMI of RPA [12]. RPA plays multiple roles in DNA replication including assembly of prereplication complexes and stabilization of ssDNA following helicase-catalyzed unwinding [13]. Moreover, very recent data demonstrating that RPA can unwind duplex DNA has led to a model where RPA may help in maintaining double-stranded DNA stability throughout replication [14]. Inhibition of any one of these steps is likely to have deleterious effects on DNA replication and ultimately cell viability.

RPA inhibition with a recently identified SMI of RPA, TDRL-505, has been demonstrated to synergize with cisplatin in a human lung cancer cell model [12]. This effect is likely to be a function of alterations in DNA repair, specifically nucleotide excision repair (NER), though effects on homologous recombination cannot be ruled out. Cisplatin [*cis*-diamminedichloroplatinum (II)] is commonly used as a chemotherapeutic drug in cancer treatment that forms cytotoxic intra- and interstrand DNA-cisplatin adducts. DNA-cisplatin adducts are repaired mainly through the NER pathway, and RPA has been shown to preferentially bind to duplex cisplatin-damaged DNA compared to undamaged DNA through the development of ssDNA [15–17]. RPA is also responsible for the recognition of interstrand cross-links caused by cisplatin treatment [17, 18]. Cisplatin resistant cancers have been linked to enhanced DNA repair, and thus the ability to impact DNA repair efficiency via modulation of RPA's DNA-binding activity is of potential clinical use to treat cancer in conjunction with platinum agents [19]. Etoposide, a common chemotherapeutic drug that induces replication fork stalling by inhibiting topoisomerase II, was also demonstrated to synergize with the RPA SMI TDRL-505 [12]. This synergistic activity is predicted to increase the toxic effects exerted by etoposide both in the context of DNA replication and repair. RPA's role in homologous recombination may be mediating this effect where DNA double-strand breaks are processed to generate a 3' ssDNA overhang to which RPA binds to help catalyze RAD51-dependent strand exchange [20]. In *Saccharomyces cerevisiae*, mutations within the DNA binding domain and protein-protein interaction regions of ScRPA lead to highly decreased meiotic recombination [21].

To further investigate the mechanisms of small molecule inhibition of RPA, we have analyzed the *in vitro* activity of a series of SMIs and their interactions with various RPA constructs. We assessed binding and interaction with full-length heterotrimeric RPA and a construct comprised of just DBD-A/B. The data presented suggest different modes of binding and interactions between the various classes of compounds and RPA, indicating that they potentially target different OB-folds or different regions of the protein structure. We also present data demonstrating that one class of SMIs does appear to have limited specificity; however another class of

SMIs is highly specific for the RPA protein-DNA interaction and does not inhibit the interaction between ssDNA and other OB-fold-containing proteins.

## 2. Materials and Methods

**2.1. Materials.** Phosphocellulose matrix was obtained from Sigma. Radiolabeled nucleotides were purchased from Perkin-Elmer Life Science (Boston, MA). All oligonucleotide substrates were purchased from Integrated DNA Technology (Coralville, IA) and gel purified by 12% polyacrylamide, 7 M urea preparative denaturing gel electrophoresis. The 3Pc3 sequence is 5'-GGA GAC CGA AGA GGA AAA GAA GGA GAG AGG-3', the 34-mer is 5'-CTA GAA AGG GGG AAG AAA GGG AAG AGG CCA GAG A-3', and the 15-mer is 5'-GGT TAC GGT TAC CCC-3'.

**2.2. Small Molecule Inhibitors.** TDRL-505 was obtained from Exclusive Chemistry (Obninsk, Russia) and CheSS19 was prepared as described in [22]. (+/-) isobornyl haloesters were prepared by the following general procedure. Briefly, to an ice-cooled solution of (+/-)-isoborneol (1.00 g, 6.48 mmol) in dry CH<sub>2</sub>Cl<sub>2</sub> (25 mL) in a Schlenk tube under N<sub>2</sub> was added dicyclohexylcarbodiimide (1.60 g, 7.76 mmol), followed by the corresponding haloacid (7.15 mmol) and 4-dimethylaminopyridine (77 mg, 0.63 mmol). The clear colorless solution was stirred 18–24 hours at which time TLC analysis indicated complete consumption of isoborneol (R<sub>f</sub> 0.26, 9:1 hexanes/EtOAc), and precipitates of dicyclohexylurea were evident. Diethyl ether (25 mL) was added, precipitating the bulk of the dicyclohexylurea. The mixture was filtered and the filter cake washed with ether (2 × 25 mL). The filtrate which had developed additional precipitate was refiltered and the solvent removed by rotary evaporation. Kugelrohr distillation of the residue afforded the haloesters as colorless oils of greater than 90% purity. Details concerning the synthesis and chemical characterization of MCI13E and MCI13F are presented in Supplementary Material available online at doi:10.4061/2010/304035.

### 2.3. Protein Expression and Purification

**RPA.** Human full-length, untagged heterotrimeric RPA (RPA) was purified as previously described in [17].

**DBD-A/B.** The sequence encoding the RPA p70 DNA-binding domains A and B was subcloned from the hrRPA plasmid (provided by Dr. Marc Wold, University of Iowa) into the pET15b (Novagen) vector, and the protein was expressed in BL21(DE3) cells (Stratagene) as previously described in [9]. Briefly, cells were grown to an OD<sub>600</sub> of 0.8, induced with 0.5 mM isopropyl-1-thio-β-D-galactopyranoside (IPTG) at 37°C for 2–3 hours. Small-scale DBD-A/B preparations were obtained from 1 L cultures, and, following induction, cells were harvested by centrifugation at 700 × g for 30 minutes at 4°C. The pellets were suspended in Buffer A (20 mM Tris, pH 7.5, 10% glycerol, 500 mM NaCl,

10 mM  $\beta$ -mercaptoethanol (BME), and 1  $\mu$ g/mL phenylmethanesulfonyl fluoride (PMSF), leupeptin, and pepstatin) at 1 mL/gram of cells. The cells were lysed by sonication and insoluble material sedimented at  $15,000 \times g$  for 30 minutes at 4°C. The supernatant was then loaded onto a 10 mL phosphocellulose column, equilibrated with Buffer A, and the flow-through material collected. Imidazole was added to the flow-through to a final concentration of 5 mM, which was then loaded onto a 2 mL nickel-NTA-agarose column. The column was then washed with Buffer A containing 50 mM imidazole after which protein was eluted from the column using a gradient from 50–500 mM imidazole. Fractions were analyzed for protein content using Bradford and SDS-PAGE analysis in addition to assessment of DNA binding activity as determined by anisotropy. Fractions containing the DBD-A/B protein were pooled and dialyzed overnight in Buffer B (1 mM HEPES, pH 7.2, 10 mM dithiothreitol (DTT), 50 mM NaCl, and 1  $\mu$ g/mL PMSF, pepstatin, and leupeptin) and aliquots stored at  $-80^\circ\text{C}$ .

**2.4. Fluorescence Polarization.** Fluorescence polarization experiments were performed as previously described in [23]. Reactions contained 20 nM F-dT<sub>12</sub>, and increasing concentrations of RPA and DBD-A/B as indicated in the figure legends. SMIs were diluted in H1 buffer (10 mM HEPES, pH 7.2, 1 mM DTT, 0.01% NP-40, and 100 mM NaCl), and the final DMSO concentration was kept below 1%.

#### 2.5. Electrophoretic Mobility Shift Assay (EMSA)

**RPA and DBD-A/B Binding.** EMSAs were performed as previously described in [16] using a purine rich ssDNA substrate (3Pc3). Briefly, reactions contained 12.5 nM 5'-[<sup>32</sup>P]-labeled 3Pc3 ssDNA and the indicated concentrations of RPA or DBD-A/B. Protein was preincubated with the indicated concentration of SMI for 30 minutes at 37°C. DNA was then added and reactions incubated for additional 5 minutes at room temperature in a final reaction volume of 40  $\mu$ L. Reactions were then resolved on a 6% native polyacrylamide gel and electrophoresed at 170 volts for 1 hour. Gels were dried and quantified via phosphorimager analysis and ImageQuant software (Molecular Dynamics).

**E. coli SSB Binding Assay.** These EMSAs were performed similarly to those for the RPA constructs, with the following exceptions. Reactions contained 25 nM of 5'-[<sup>32</sup>P]-labeled 3Pc3 ssDNA and 3.3 nM (assuming homotetramer formation) SSB protein (Enzymatics, Beverly, MA). Reactions (20  $\mu$ L) were carried out in 20 mM HEPES, pH 7.5, 1 mM DTT, 0.01% NP-40, 100 mM NaCl and resolved by 6% native polyacrylamide gel electrophoresis at 25 mA for 2 hours. Gels were dried and quantified via phosphorimager analysis as described above.

**Schizosaccharomyces pombe Pot1(DBD) Binding Assay.** EMSAs were performed as described above for *Ec*SSB. Reactions contained 25 nM of 5'-[<sup>32</sup>P]-labeled 15-mer

ssDNA and 20 nM Pot1(DBD) protein (generously provided by Dr. Deborah Wuttke, University of Colorado, Boulder). Reactions (20  $\mu$ L) were carried out in 20 mM HEPES, pH 7.5, 1 mM DTT, 0.01% NP-40, 100 mM NaCl, at room temperature, and resolved by 6% native polyacrylamide gel electrophoresis at 25 mA for 2 hours. Gels were dried and quantified via phosphorimager analysis as described above.

**2.6. Analysis of Reversible Inhibition.** To assess the reversibility of select SMIs, the indicated SMI was preincubated with RPA or the DBD-A/B construct for 30 minutes at room temperature. The resulting solution was dialyzed versus 500 mL H1 buffer at 4°C using 0.5 ml, 12,000 molecular weight cut-off dialysis cassettes (Pierce). The resulting protein was recovered and concentration determined by Bradford analysis. Analysis of DNA binding activity was performed either by EMSA or FP. In each series of experiments, there was no loss of DNA binding activity in vehicle control-treated protein.

## 3. Results

**3.1. TDRL-505 Targets the Central OB-Folds of RPA.** Previous work from our laboratory has identified two classes of RPA SMIs [12, 22, 24]. The first class of SMIs was identified from screening and analysis of structure activity relationships (SARs) of the ChemDiv library [12]. From this analysis, TDRL-505 was identified and contains a substituted dihydropyrazole with a 4-oxo-butanoic acid at N1, a bromophenyl substituent at C3, and 2-chloro 7-ethoxyquinoline at C5 (Figure 1(a)). Previous *in vitro* analysis suggested that this SMI was potentially interacting with the central OB-folds found in RPA p70, DBD-A/B, as it was capable of blocking RPA binding to a 12-base ssDNA [12]. RPA binding to this short of DNA substrate is primarily through the DBD-A/B domain. In addition, molecular modeling analysis revealed a thermodynamically favorable interaction between TDRL-505 and this domain [12]. DBD-A/B extends from amino acids 181–432. It has been purified and retains DNA binding activity, albeit at approximately 5% of that observed for the full-length heterotrimer [25]. A similar construct of this region, containing amino acids 181–422, was crystallized in complex with a (dC)<sub>8</sub> DNA substrate and the structure solved in addition to a DNA-free structure of the 181–432 amino acid region [26, 27]. In order to examine the effect of TDRL-505 on the DBD-A/B region alone, we subcloned amino acids 181–432 of human RPA p70. The DBD-A/B construct was overexpressed and purified to near homogeneity, via metal affinity chromatography, as determined by SDS-PAGE (Figure 2(a)). DNA-binding activity was assessed by EMSA and 125 nM DBD-A/B selected for analysis, which represented approximately 50% DNA binding of the 34-base DNA substrate (data not shown). Increasing concentrations of TDRL-505 resulted in a concentration-dependent decrease in DNA binding activity as assessed by EMSA (Figure 2(b)). Quantification of the results demonstrates a half-maximal inhibition of approximately 40  $\mu$ M (Figure 2(c)), about twice that observed for the intact heterotrimer [12]. These data

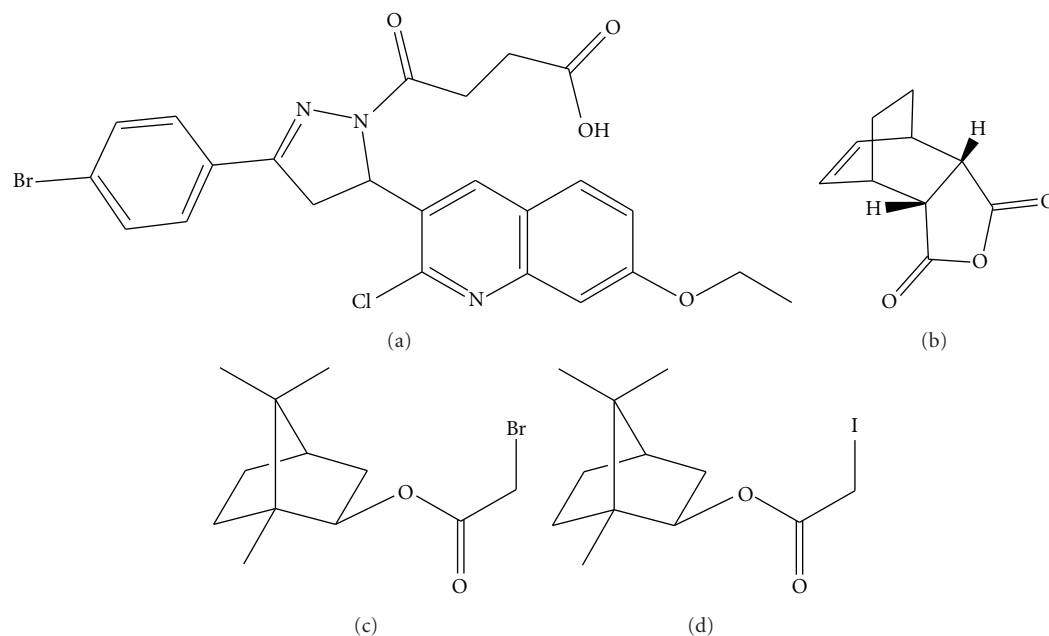


FIGURE 1: Chemical structure of RPA small molecule inhibitors. (a) TDRL-505; (b) CheSS19; (c) MCI13E; (d) MCI13F.

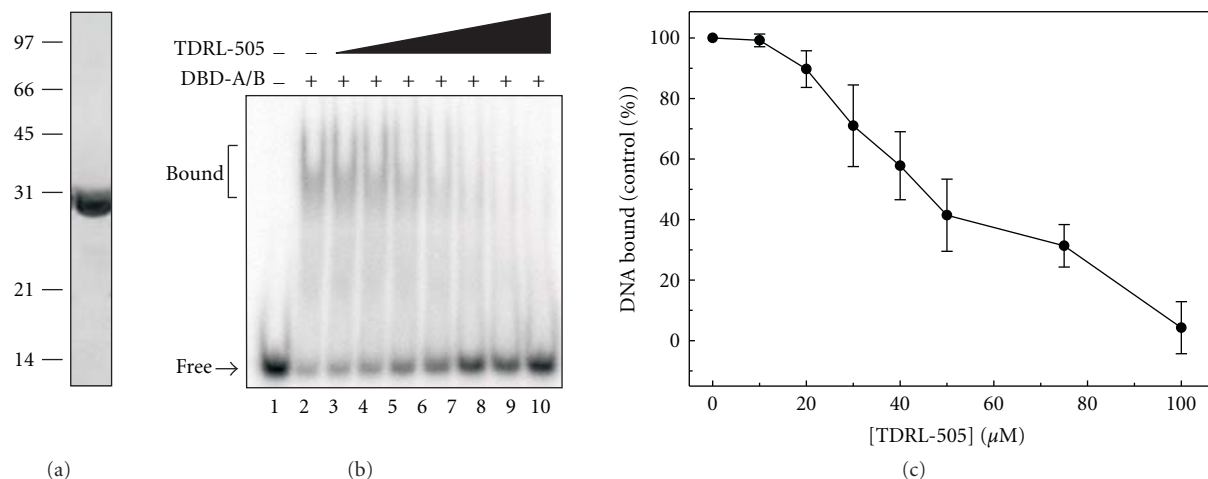


FIGURE 2: TDRL-505 inhibits RPA DBD-A/B-DNA interactions. (a) SDS-PAGE analysis of purified RPA DBD-A/B. DBD-A/B was purified as described in “Section 2” and analyzed by electrophoresis on a 12% NuPAGE Bis-Tris Gel. The gel was stained with Coomassie blue. (b) EMSA analysis of TDRL-505 inhibition of DBD-A/B DNA binding activity. Assays were performed as described in “Section 2” with increasing concentrations of TDRL-505 from 10–100  $\mu\text{M}$  in reactions with 12.5 nM DNA and 125 nM DBD-A/B. Products were analyzed by nondenaturing gel electrophoresis, dried, and imaged by phosphorimager analysis. The arrow indicates the position of the free DNA and the bracket the position of the bound DBD-A/B-DNA complex. (c) Quantification of EMSA binding data from Panel (b). The signal representing the RPA-bound and free fractions of DNA was quantified using ImageQuant software, and values represent the mean and SD of triplicate determinations.

support a model whereby TDRL-505 inhibits RPA's DNA binding activity via blocking the protein-DNA interactions at the central OB-folds in RPA p70.

**3.2. CheSS19 Inhibits Both WT RPA and RPA AB Region Interactions with DNA.** The second class of SMIs we identified contain a bicyclic-isobornyl ester which was initially identified as a hit in a screen of the NCI diversity set and

analogous identified in a subsequent screen of the NCI developmental therapeutics general library [24]. Initial SAR analysis indicated that variation in the bridging structure had minimal effects on RPA inhibitory activity while creating reactive anhydrides greatly increased activity [22]. To ascertain if the tricyclic anhydride, CheSS19 (Figure 1(b)), also inhibited DNA binding via an interaction with the central DBD-A/B, we compared its inhibitory activity towards the DBD-A/B construct and full-length heterotrimeric RPA using EMSA

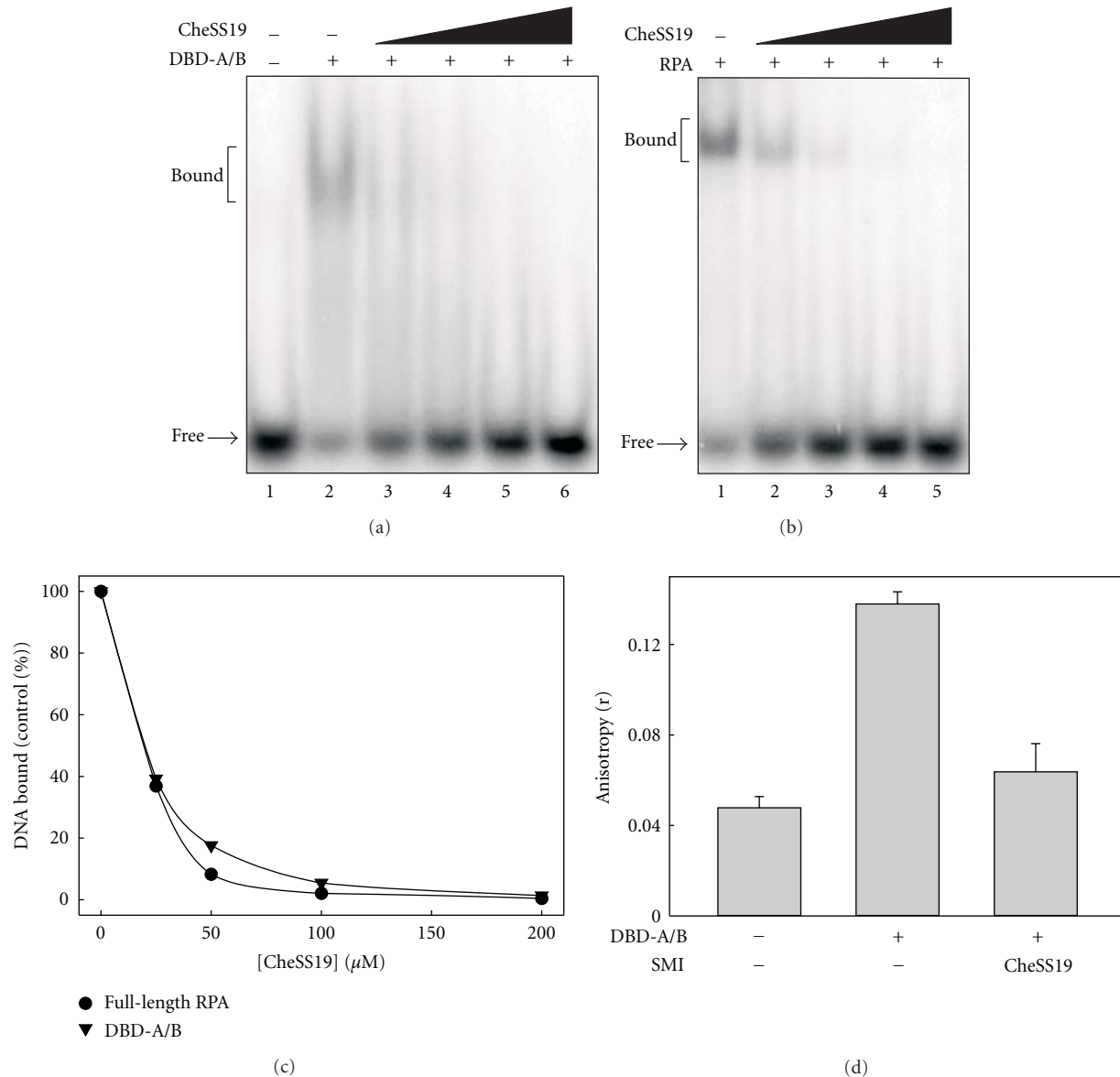


FIGURE 3: Irreversible inhibition of RPA DBD-A/B-DNA-binding activity by CheSS19. (a) EMSA analysis of CheSS19 inhibition of RPA DBD-A/B. Assays were performed as described in the legend to Figure 2. Reactions contained 12.5 mM DNA, 50 nM DBD-A/B and 0, 25, 50, 100 and 200  $\mu\text{M}$  CheSS19 (Lanes, 2-6, resp.) (b) CheSS19 inhibition of full-length heterotrimeric RPA as assessed by EMSA. Reactions were identical to those in panel (a) except contained 25 nM full-length RPA. (c) Quantification of the binding data presented in panels (a) and (b). (d) Fluorescence polarization analysis of CheSS19 inactivated RPA DBD-A/B. RPA DBD-A/B was preincubated with vehicle (1% DMSO) or CheSS19 (1 pmol in 1% DMSO) for 30 minutes at 37°C. Following incubation, the reaction mix was dialyzed versus H1 buffer overnight at 4°C. The protein was recovered, and DNA-binding activity measured by FP analysis of binding to an F-dT12 substrate was performed as described in “Section 2”. Bar 1: DNA control, Bar 2: control vehicle-treated DBD-A/B, and Bar 3: CheSS19-treated DBD-A/B. Control vehicle did not show inhibition of binding before dialysis similarly to Figure 5 Lane 3. The data represent the mean and range of two independent experiments.

analysis. The results demonstrate that CheSS19 inhibits the DNA binding activity of the DBD-A/B construct with similar potency to the heterotrimeric RPA preparation (Figures 3(a)–3(c)). Our prior observation that CheSS19 irreversibly inhibited full-length RPA prompted us to examine its interaction with the smaller DBD-A/B construct to refine where it covalently binds [22]. In this experiment, DBD-A/B was incubated with CheSS19 and then the reaction mix

dialyzed overnight to remove dissociable inhibitor. Following dialysis, the protein was assessed for binding in a fluorescence polarization assay. Data demonstrates that dialyzed DBD-A/B that had been preincubated with CheSS19 was able to inhibit DBD-A/B DNA-binding activity as compared to protein incubated with DMSO vehicle (Figure 3(d)). These results are consistent with CheSS19 inhibiting DBD-A/B in an irreversible manner.

**3.3. Analysis of Isobornyl Haloesters.** While the anhydride groups in the active CheSS series are effective at inhibiting RPA, no cellular activity was observed following treatment with this series of compounds (data not shown). This is potentially a result of the highly reactive anhydride non-specifically bonding with other components or hydrolyzing to an inactive dicarboxylic acid prior to encountering RPA in the cell nucleus. We therefore employed a less reactive substituent to assess *in vitro* inhibition and analyzed a series of haloester derivatives of Isobornyl. Synthesis and analysis with the bromo- and iodoesters MCI13E and F, respectively (Figures 1(c) and 1(d)), revealed inhibition of the full-length heterotrimer RPA in EMSA analysis with the iodo-containing compound (MCI13F) being slightly more effective (Figure 4(a)). The isobornyl haloesters, MCI13E and MCI13F, had calculated  $IC_{50}$  of  $16.1 \pm 2.8 \mu\text{M}$  and  $10.1 \pm 1.0 \mu\text{M}$ , respectively. Interestingly, when we assessed inhibition of DBD-A/B, neither MCI13E nor MCI13F compounds inhibited DNA binding of this protein construct (Figure 4(b)). Due to lack of inhibition, the  $IC_{50}$ 's for the inhibition of the DBD-A/B with the isobornyl haloesters were not calculable. Considering the differential inhibition observed between the anhydride and haloesters with respect to specificity, we sought to determine if the isobornyl haloesters inhibited full-length RPA in an irreversible fashion. Full-length RPA was mixed with MCI13E or vehicle control, and then the reaction mixture was dialyzed overnight. Analysis of the resulting protein-DNA complex (Figure 5, lanes 5 and 6) showed that, in reactions where RPA was incubated with MCI13E, inhibition was not reversed by dialysis as would be expected from a reversible inhibitor. In fact, the degree of inhibition was similar to that observed for the MCI13E treated RPA before dialysis (Figure 5, lanes 3 and 4). These results indicate a mode of MCI13E inhibition of RPA that involved a covalent adduct between the MCI13E and RPA. These data suggest that the different chemical reactivity of the isobornyl haloester derivatives alkylate RPA in a different way that likely does not include the DBD-A/B region. Where anhydrides preferentially react with amine residues or hydrolyze in the aqueous medium, alkyl halides are more reactive with sulfur nucleophiles such as Cys residues or hydrogen-bonded OH groups such as Ser/Thr/Tyr. The isobornyl bromoester has been used previously for labeling cysteines. [28]. Furthermore, analysis of cellular activity reveals that, unlike the isobornyl haloesters, the tricyclic anhydride does not display any cellular activity (data not shown).

**3.4. SMI Specificity.** To determine the specificity of the TDRL-505, CheSS19, and MCI13E/F compounds, we examined their effects on two ssDNA-binding proteins which use OB-folds for recognition and binding of ssDNA, *E. coli* SSB [3], and the *Schizosaccharomyces pombe* Pot1(DBD) domain [29]. The *EcSSB* protein is a non-sequence-specific ssDNA binding protein, whereas the *SpPot1*(DBD) protein is a telomere-specific, ssDNA binding protein. In these experiments, protein was preincubated with the SMIs, as was done for the RPA experiments, prior to addition of radiolabeled ssDNA to the reactions. TDRL-505 was

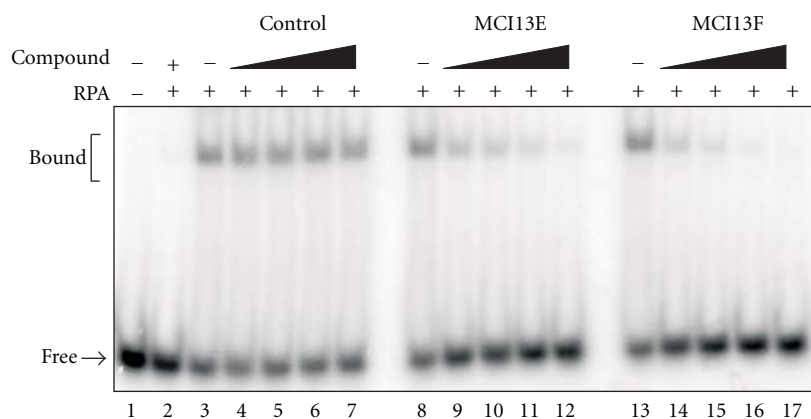
shown to be ineffective in blocking *EcSSB* binding to a ssDNA substrate (Figures 6(a) and 6(b)). While there is a slight decrease (~20%) in binding observed at the highest concentration of TDRL-505 tested ( $100 \mu\text{M}$ ), this is minimal compared to the nearly 90% inhibition observed for RPA [12] and the RPA DBD-A/B (Figure 2). Similarly, *EcSSB* binding was unaffected by CheSS19 and the MCI13E and MCI13F compounds (Figures 6(d) and 6(e)). In all cases, the  $IC_{50}$  of the compounds examined in relation to *EcSSB* binding is greater than  $100 \mu\text{M}$ .

To further validate the specificity of TDRL-505, we examined its influence on the *SpPot1*(DBD) construct. The mode of ssDNA binding by *SpPot1*(DBD) is quite different compared to that of the hRPA protein; however, they both contain ssDNA-binding domains, which are responsible for the majority of the observed DNA-binding activity of the full-length proteins. The *SpPot1*(DBD) protein was found to be inhibited by TDRL-505 (Figure 7) with an  $IC_{50}$  of  $15.7 \pm 1.6 \mu\text{M}$ . Together, these data demonstrate that while the RPA SMIs, CheSS19, and MCI13E/F inhibit the interaction of RPA with ssDNA, TDRL-505 compound seems to inhibit eukaryotic ssDNA-binding OB-fold interactions as demonstrated with two different protein-ssDNA complexes.

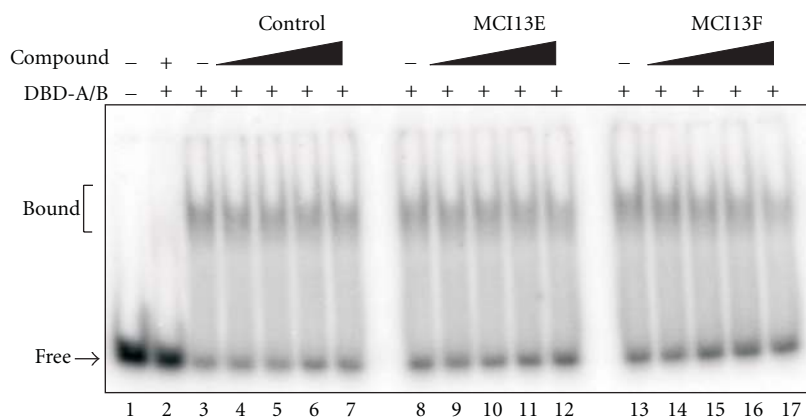
## 4. Discussion

The six OB-folds distributed throughout three subunits of RPA have been implicated in numerous aspects of DNA metabolism via RPA DNA binding as well as interactions with other proteins [11, 25]. Inhibition of DNA binding activity by targeting the OB-folds with SMIs has the potential to provide a separation of function and elucidate the contribution of the various domains in the numerous pathways in which RPA participates. Thus, targeting a particular OB-fold or other interaction domain may allow for pathway-specific targeting of RPA. For instance, one could inhibit RPA's activity in nucleotide excision repair (NER) and not in replication, which would present clinical utility in cancer treatment to allow synergy with DNA damaging chemotherapeutic agents while potentially limiting toxicity. It has been suggested that the OB-folds beyond the DBD-A/B region contribute to full-length RPA's ssDNA interaction, which stems from the observation that while DBD-A/B can accommodate a  $(\text{dC})_8$  DNA substrate, variations in binding are observed dependent on DNA sequence length [1]. Our observation that TDRL-505 can inhibit the DBD-A/B region of RPA p70 from binding to ssDNA supports our previously published molecular modeling data, in which energetically favorable binding was observed within DBD-A and DBD-B as well as the interdomain region [12].

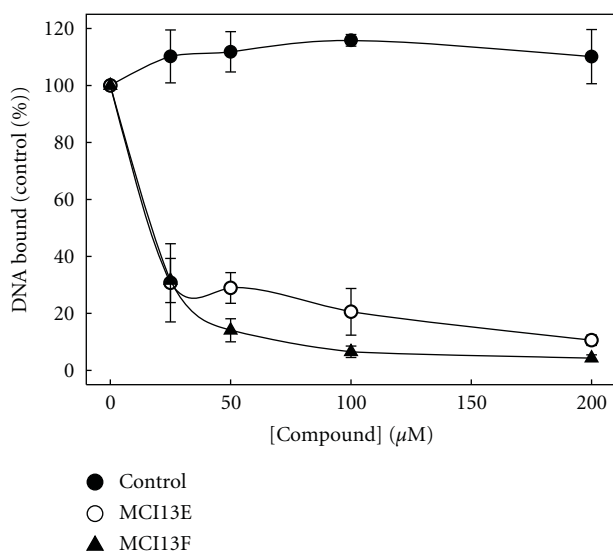
We have further demonstrated that, while not an RPA-specific inhibitor, TDRL-505 displays specificity for eukaryotic ssDNA binding activity of OB-fold containing proteins as no significant inhibition of the related ssDNA binding protein, *EcSSB*, was observed. Although the *EcSSB* and *SpPot1*(DBD) proteins contain OB-folds, and in this regard, are structurally related to full-length RPA p70 and the DBD-A/B, the mechanism of ssDNA binding by these proteins is very different. As shown in Figure 8(a), the



(a)



(b)



(c)

FIGURE 4: Inhibition of full-length heterotrimeric RPA but not DBD-A/B-DNA-binding activity by the MCI13 series of bicyclic isoborneol haloesters. The control used is a distillate of the reaction components of the synthesis of the MCI13 compounds diluted in equal concentration of DMSO as the MCI13, inhibitors. (a) Increasing concentrations of control compound, MCI13E, or MCI13F (25, 50, 100, and 200  $\mu\text{M}$ ) were titrated in DNA binding reactions containing full-length heterotrimeric RPA. Binding to  $[^{32}\text{P}]$ -ss 30-base 3Pc3 DNA was assessed by EMSA as described in “Section 2.” (b) The same inhibitor concentrations were assessed in reactions measuring the binding of DBD-A/B to a 30-mer substrate. (c) Analysis of control, MCI13E, and MCI13F inhibition of full length RPA. Average of three independent experiments is shown with Standard Deviation as error bars. From this graph,  $\text{IC}_{50}$  were calculated. MCI13E had a calculated  $\text{IC}_{50}$  of  $16.06 \pm 2.78 \mu\text{M}$ , while MCI13F had a calculated  $\text{IC}_{50}$  of  $10.11 \pm 1.0 \mu\text{M}$ .

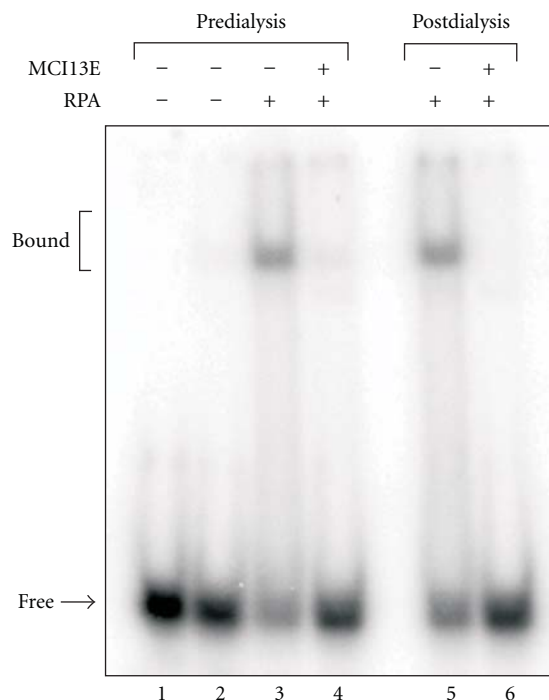


FIGURE 5: Irreversible inactivation of full-length heterotrimeric RPA by MCI13E. Incubation of RPA with MCI13E, dialysis, and recovery were performed as described in the legend to Figure 3. DNA binding activity of the resulting protein was assessed by EMSA using a 5'-[<sup>32</sup>P]-ss 34-base DNA as described in "Section 2." Lanes 1–4 predialysis, lanes 5 and 6 postdialysis.

*EcSSB* protein contains a single OB-fold, yet, forms a homotetramer yielding a functional molecule containing four OB-folds. The *EcSSB* protein also has been shown to bind nucleic acid in the reverse polarity compared to RPA [3]. On the other hand, the ssDNA-binding modes of RPA and SpPot1 are more similar. With this in mind, our demonstration that TDRL-505 displays inhibitory effects on both RPA and SpPot1(DBD) is not surprising. However, if the affinity of TDRL-505 was achieved through the common structural elements of OB-folds, specificity of the inhibitor would be less likely. The SpPot1(DBD) construct has been biochemically characterized and, by analogy to hPot1, binds ssDNA with the same 5' to 3' polarity as RPA p70 [30]. Structurally, residues 1–187 have been shown to contain an OB-fold, and residues 188–389 have been postulated to contain a second OB-fold, similar to the hPot1 protein [4] and the RPA DBD-A/B construct. Although ssDNA-binding interactions are mediated by similar structural elements within each OB-fold domain in these proteins, the resulting complexes differ significantly in the overall trajectory of the ssDNA on the surface of the protein and the specific hydrophobic stacking interactions of aromatic residues in the protein with the bases of the ssDNA (Figure 8). Thus, as each of the proteins presents a distinct binding site for ssDNA, the specificity of TDRL-505 seems to be limited relative to the other SMIs tested (CheSS19 and MCI13E/F) for inhibition of RPA as compared to other OB-fold-related proteins. Despite

the limited specificity, it would appear that TDRL-505 may be specific to eukaryotic OB-fold-ssDNA interactions as it fails to inhibit the *EcSSB*-ssDNA interaction.

The series of compounds based on a bicyclic framework (MCI13E, MCI13F, and CheSS19) showed inhibition of full-length heterotrimeric RPA. Interestingly the less reactive derivatives containing a haloester (MCI13E and F) displayed no inhibitory activity in DNA binding assays with purified DBD-A/B while the more reactive tricyclic anhydride derivative, CheSS19, showed potent inhibitory activity against both full-length RPA and the DBD-A/B construct. The mode of RPA inhibition with the tricyclic anhydride and isborneol derivatives was found to be irreversible, consistent with the reactive anhydride and haloester functional groups. None of the isborneol compounds were found to significantly inhibit the ssDNA binding activity of *EcSSB* suggesting that this class of compounds is specific for RPA. Together these data provide evidence suggestive of specific targeting of different functional domains of RPA that can be used to exploit and interrogate their importance in the various metabolic pathways in which RPA participates. Previous data demonstrated that inhibition of RPA with SMIs results in cell cycle arrest and sensitization to DNA-damaging agents, cisplatin and etoposide [12]. These data suggest that exploitation of this chemical genetic approach can ultimately aid in the elucidation of the mechanism of RPA action in critical DNA metabolic pathways including DNA replication, recombination, and repair.

## 5. Conclusions

Small molecule inhibitors have proved to be invaluable in the interrogation of biochemical pathways, protein activity, and cellular function. While targeting macromolecular protein-protein and protein-DNA interactions is somewhat more complex than targeting an enzyme-substrate interaction, recent work has yielded some success in this regard [12, 32–34]. In this paper, we provide evidence for TDRL-505 inhibition of RPA-DNA binding via an interaction with the central OB-folds of RPA p70, DBD-A/B. This mechanism of inhibition is likely to impact all DNA metabolic events where RPA exerts its activity by high affinity binding to ssDNA. The demonstration that MCI13E and MCI13F do not inhibit the DBD-A/B construct while showing potent inhibition of the full-length RPA heterotrimer points to other critical interactions between RPA and DNA that are essential for its DNA binding activity. While the elucidation of the specific sites of interaction of each SMI and RPA remains, the irreversible inactivation of full-length RPA by MCI13E provides a potential mechanism to identify the specific amino acids being modified and hence determine the subunit and potential DNA-binding domain targeted by this SMI. The identification of the specific site of TDRL-505 interaction within DBD-A/B is being pursued via high-resolution structural analyses, and together, will provide a framework for the further elucidation of the mechanisms of inhibition and how this impairment in DNA binding activity influences cellular DNA metabolism.

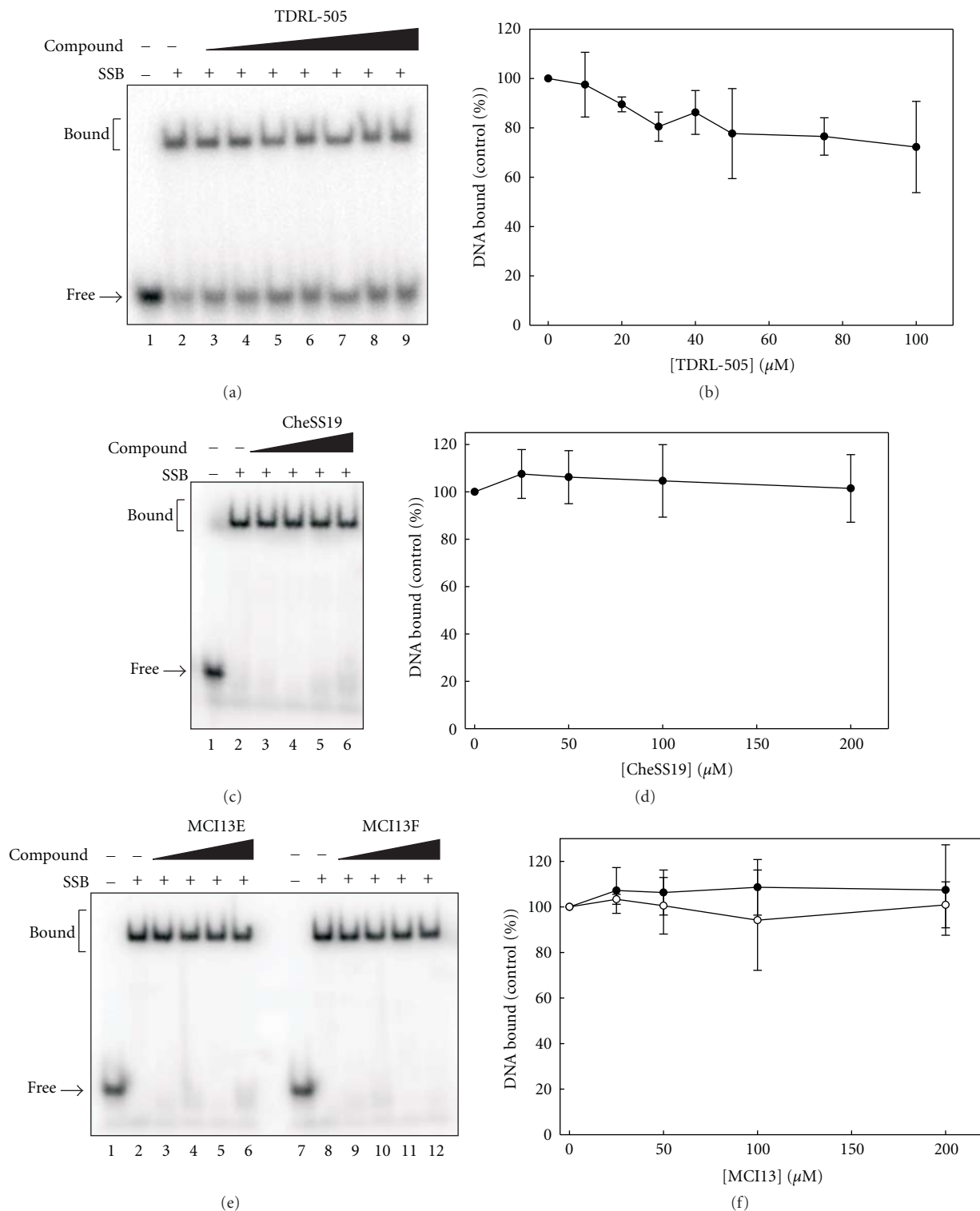


FIGURE 6: *EcSSB* protein-ssDNA interaction is not affected by the RPA inhibitors. (a) Titration of TDRL-505 in *EcSSB* DNA-binding reactions. TDRL-505 (0, 10, 20, 30, 40, 50, 75, and 100  $\mu\text{M}$ ) was preincubated with *EcSSB*, and binding to a 30-base pair ssDNA was assessed by EMSA as described in “Section 2.” (b) Analysis of TDRL-505 inhibition of *EcSSB*. The average of three independent experiments is presented with SD. (c) CheSS19 titration in *EcSSB* DNA-binding reactions. CheSS19 (0, 25, 50, 100, and 200  $\mu\text{M}$ ) was preincubated with *EcSSB*, and binding reactions were carried out as in (a). (d) Analysis of CheSS19 inhibition of *EcSSB*. The average of three independent experiments is presented with SD. (e) Titration of MCI13E and MCI13F in *EcSSB* DNA-binding reactions. Concentrations of MCI13E/F used were 0, 25, 50, 100, and 200  $\mu\text{M}$ . (f) Analysis of MCI13E/F inhibition of *EcSSB*. The average of three independent experiments is presented with SD. Data for MCI13E is shown as filled circles, and MCI13F is shown as open circles. In panels (a), (c), and (e), the “Free” ssDNA is indicated with an arrow, and the “Bound” ssDNA is indicated by brackets. All reactions were performed in the same order and manner as the RPA-binding reactions.

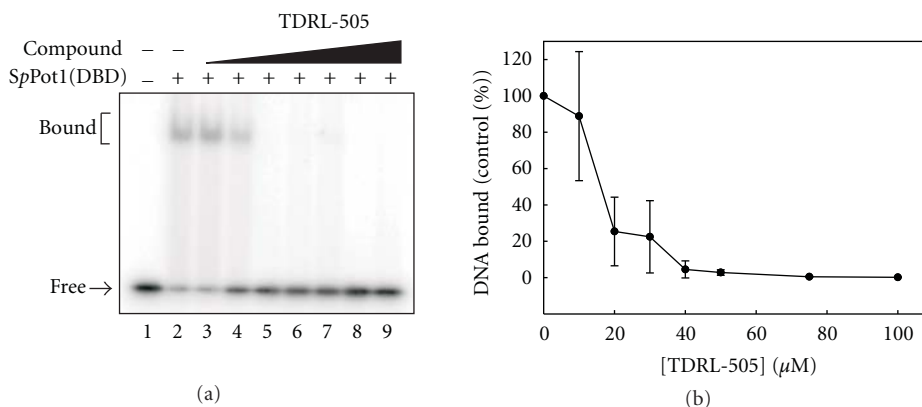


FIGURE 7: TDRL-505 inhibits *SpPot1*(DBD) ssDNA binding. (a) Titration of TDRL-505 in ssDNA-binding reactions with *SpPot1*(DBD). TDRL-505 was preincubated with *SpPot1*(DBD) (0, 25, 50, 100 μM) prior to EMSA analysis of binding to the 15-mer oligonucleotide. “Free” ssDNA is indicated with an arrow, and the “Bound” ssDNA is indicated by a bracket. (b) Analysis of TDRL-505 inhibition of *SpPot1*(DBD). The average of three independent experiments is presented with SD.

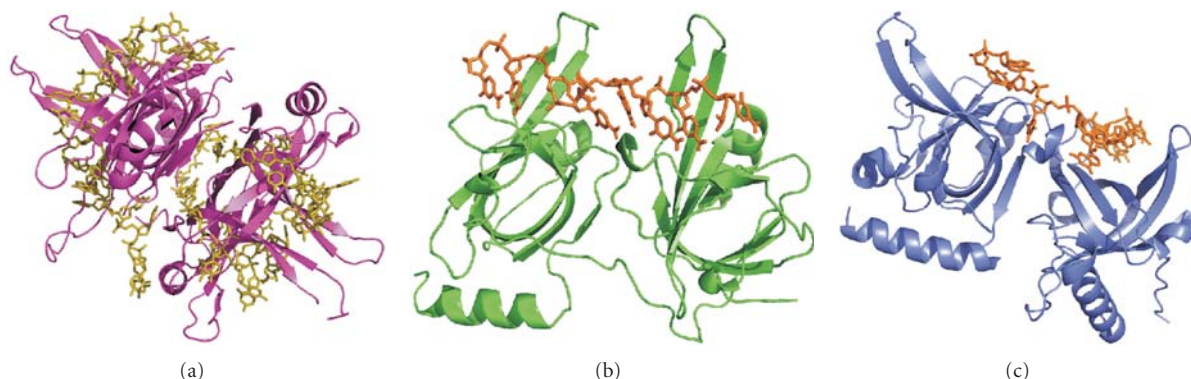


FIGURE 8: Comparison of the ssDNA-binding interface of OB-fold containing proteins. Proteins are shown as cartoon and ssDNA as stick renderings. (a) Structure of the homotetramer of *EcSSB* (1EYG); DNA is shown in gold [31]. (b) Structure of the RPA DBD-A/B (1JMC); DNA is shown in orange [27]. (c) Structure of the human Pot1(DBD) (1XJV); DNA is shown in orange [4]. Each structure is shown in the same orientation to highlight the different ssDNA binding interfaces used by each of these proteins for their specific functions.

## Acknowledgments

The authors thank all members of the Turchi lab for the helpful discussion and Dr. Deborah Wuttke for providing the *SpPot1*(DBD) protein. This paper was supported by NIH award CA082741 to JJT and the National Science Foundation award CHE0521075 for the 400 MHz NMR spectrometer at Indiana State University.

## References

- [1] M. S. Wold, “Replication protein A: a heterotrimeric, single-stranded DNA-binding protein required for eukaryotic DNA metabolism,” *Annual Review of Biochemistry*, vol. 66, pp. 61–92, 1997.
- [2] A. Bochkarev and E. Bochkareva, “From RPA to BRCA2: lessons from single-stranded DNA binding by the OB-fold,” *Current Opinion in Structural Biology*, vol. 14, no. 1, pp. 36–42, 2004.
- [3] D. L. Theobald, R. M. Mitton-Fry, and D. S. Wuttke, “Nucleic acid recognition by OB-fold proteins,” *Annual Review of Biophysics and Biomolecular Structure*, vol. 32, pp. 115–133, 2003.
- [4] M. Lei, E. R. Podell, and T. R. Cech, “Structure of human POT1 bound to telomeric single-stranded DNA provides a model for chromosome end-protection,” *Nature Structural & Molecular Biology*, vol. 11, no. 12, pp. 1223–1229, 2004.
- [5] F. Wang, E. R. Podell, A. J. Zaugg et al., “The POT1-TPP1 telomere complex is a telomerase processivity factor,” *Nature*, vol. 445, no. 7127, pp. 506–510, 2007.
- [6] H. Yang, P. D. Jeffrey, J. Miller et al., “BRCA2 function in DNA binding and recombination from a BRCA2-DSS1-ssDNA structure,” *Science*, vol. 297, no. 5588, pp. 1837–1848, 2002.
- [7] A. G. Murzin, “OB(oligonucleotide/oligosaccharide binding)-fold: common structural and functional solution for non-homologous sequences,” *EMBO Journal*, vol. 12, pp. 861–867, 1993.
- [8] E. Bochkareva, S. Korolev, S. P. Lees-Miller, and A. Bochkarev, “Structure of the RPA trimerization core and its role in the multistep DNA-binding mechanism of RPA,” *EMBO Journal*, vol. 21, no. 7, pp. 1855–1863, 2002.

- [9] R. A. Pfuetzner, A. Bochkarev, L. Frappier, and A. M. Edwards, "Replication protein A: characterization and crystallization of the DNA binding domain," *Journal of Biological Chemistry*, vol. 272, no. 1, pp. 430–434, 1997.
- [10] K. Umezū, N. Sugawara, C. Chen, J. E. Haber, and R. D. Kolodner, "Genetic analysis of yeast RPA1 reveals its multiple functions in DNA metabolism," *Genetics*, vol. 148, no. 3, pp. 989–1005, 1998.
- [11] S. J. Haring, A. C. Mason, S. K. Binz, and M. S. Wold, "Cellular functions of human RPA1: multiple roles of domains in replication, repair, and checkpoints," *Journal of Biological Chemistry*, vol. 283, no. 27, pp. 19095–19111, 2008.
- [12] S. C. Shuck and J. J. Turchi, "Targeted inhibition of Replication Protein A reveals cytotoxic activity, synergy with chemotherapeutic DNA-damaging agents, and insight into cellular function," *Cancer Research*, vol. 70, no. 8, pp. 3189–3198, 2010.
- [13] S. Waga and B. Stillman, "The DNA replication fork in eukaryotic cells," *Annual Review of Biochemistry*, vol. 67, pp. 721–751, 1998.
- [14] I. de Vlaminck, I. Vidic, M. T. J. van Loenhout, R. Kanaar, J. H. G. Lebbink, and C. Dekker, "Torsional regulation of hRPA-induced unwinding of double-stranded DNA," *Nucleic Acids Research*, vol. 38, no. 12, pp. 4133–4142, 2010.
- [15] D. B. Zamble, D. Mu, J. T. Reardon, A. Sancar, and S. J. Lippard, "Repair of cisplatin-DNA adducts by the mammalian excision nuclease," *Biochemistry*, vol. 35, no. 31, pp. 10004–10013, 1996.
- [16] S. M. Patrick and J. J. Turchi, "Xeroderma pigmentosum complementation group A protein (XPA) modulates RPA-DNA interactions via enhanced complex stability and inhibition of strand separation activity," *Journal of Biological Chemistry*, vol. 277, no. 18, pp. 16096–16101, 2002.
- [17] S. M. Patrick and J. J. Turchi, "Replication protein a (RPA) binding to duplex cisplatin-damaged DNA is mediated through the generation of single-stranded DNA," *Journal of Biological Chemistry*, vol. 274, no. 21, pp. 14972–14978, 1999.
- [18] S. M. Patrick, K. Tillison, and J. M. Horn, "Recognition of cisplatin-DNA interstrand cross-links by replication protein A," *Biochemistry*, vol. 47, no. 38, pp. 10188–10196, 2008.
- [19] E. Reed, "Platinum-DNA adduct, nucleotide excision repair and platinum based anti-cancer chemotherapy," *Cancer Treatment Reviews*, vol. 24, no. 5, pp. 331–344, 1998.
- [20] M. E. Stauffer and W. J. Chazin, "Physical interaction between replication protein A and Rad51 promotes exchange on single-stranded DNA," *Journal of Biological Chemistry*, vol. 279, no. 24, pp. 25638–25645, 2004.
- [21] C. Soustelle, M. Vedel, R. Kolodner, and A. Nicolas, "Replication protein A is required for meiotic recombination in *Saccharomyces cerevisiae*," *Genetics*, vol. 161, no. 2, pp. 535–547, 2002.
- [22] J. J. Turchi, S. C. Shuck, E. A. Short, and B. J. Andrews, "Targeting nucleotide excision repair as a mechanism to increase cisplatin efficacy," in *Platinum and Other Heavy Metal Compounds in Cancer Chemotherapy*, A. Bonetti, R. Leone, F. M. Muggia, and S. B. Howell, Eds., Humana Press, New York, NY, USA, 2009.
- [23] B. J. Andrews, J. A. Lehman, and J. J. Turchi, "Kinetic analysis of the Ku-DNA binding activity reveals a redox-dependent alteration in protein structure that stimulates dissociation of the Ku-DNA complex," *Journal of Biological Chemistry*, vol. 281, no. 19, pp. 13596–13603, 2006.
- [24] B. J. Andrews and J. J. Turchi, "Development of a high-throughput screen for inhibitors of replication protein A and its role in nucleotide excision repair," *Molecular Cancer Therapeutics*, vol. 3, no. 4, pp. 385–391, 2004.
- [25] I. M. Wyka, K. Dhar, S. K. Binz, and M. S. Wold, "Replication Protein A interactions with DNA: differential binding of the core domains and analysis of the DNA interaction surface," *Biochemistry*, vol. 42, no. 44, pp. 12909–12918, 2003.
- [26] E. Bochkareva, V. Belegu, S. Korolev, and A. Bochkarev, "Structure of the major single-stranded DNA-binding domain of replication protein A suggests a dynamic mechanism for DNA binding," *EMBO Journal*, vol. 20, no. 3, pp. 612–618, 2001.
- [27] A. Bochkarev, R. A. Pfuetzner, A. M. Edwards, and L. Frappier, "Structure of the single-stranded-DNA-binding domain of replication protein A bound to DNA," *Nature*, vol. 385, no. 6612, pp. 176–181, 1997.
- [28] R. I. Murray, I. C. Gunsalus, and K. M. Dus, "Active site studies of cytochrome P=450CAM. I. Specific cysteine labeling with the affinity reagent isobornyl bromoacetate as a model for substrate binding," *Journal of Biological Chemistry*, vol. 257, no. 21, pp. 12517–12525, 1982.
- [29] M. Lei, E. R. Podell, P. Baumann, and T. R. Cech, "DNA self-recognition in the structure of Pot1 bound to telomeric single-stranded DNA," *Nature*, vol. 426, no. 6963, pp. 198–202, 2003.
- [30] J. E. Croy, E. R. Podell, and D. S. Wuttke, "A new model for *Schizosaccharomyces pombe* telomere recognition: the telomeric single-stranded DNA-binding Activity of Pot1-389," *Journal of Molecular Biology*, vol. 361, no. 1, pp. 80–93, 2006.
- [31] S. Raghunathan, A. G. Kozlov, T. M. Lohman, and G. Waksman, "Structure of the heterodimeric complex between CAD domains of CAD and ICAD," *Nature Structural Biology*, vol. 7, no. 8, pp. 658–662, 2000.
- [32] P. Y. Ng, Y. Tang, W. M. Knosp, H. S. Stadler, and J. T. Shaw, "Synthesis of diverse lactam carboxamides leading to the discovery of a new transcription-factor inhibitor," *Angewandte Chemie*, vol. 46, no. 28, pp. 5352–5355, 2007.
- [33] R. E. Moellering, M. Cornejo, T. N. Davis et al., "Direct inhibition of the NOTCH transcription factor complex," *Nature*, vol. 462, no. 7270, pp. 182–188, 2009.
- [34] M. N. Saha, H. Jiang, J. Jayakar, D. Reece, D. R. Branch, and H. Chang, "MDM2 antagonist nutlin plus proteasome inhibitor velcade combination displays a synergistic anti-melanoma activity," *Cancer Biology and Therapy*, vol. 9, no. 11, pp. 937–945, 2010.

## Review Article

# The Roles of UmuD in Regulating Mutagenesis

Jaylene N. Ollivierre,<sup>1</sup> Jing Fang,<sup>1</sup> and Penny J. Beuning<sup>1,2</sup>

<sup>1</sup> Department of Chemistry and Chemical Biology, Northeastern University, 360 Huntington Avenue, 102 Hurtig Hall, Boston, MA 02115, USA

<sup>2</sup> Center for Interdisciplinary Research on Complex Systems, Northeastern University, 360 Huntington Avenue, 102 Hurtig Hall, Boston, MA 02115, USA

Correspondence should be addressed to Penny J. Beuning, beuning@neu.edu

Received 13 June 2010; Accepted 1 August 2010

Academic Editor: Ashis Basu

Copyright © 2010 Jaylene N. Ollivierre et al. This is an open access article distributed under the Creative Commons Attribution License, which permits unrestricted use, distribution, and reproduction in any medium, provided the original work is properly cited.

All organisms are subject to DNA damage from both endogenous and environmental sources. DNA damage that is not fully repaired can lead to mutations. Mutagenesis is now understood to be an active process, in part facilitated by lower-fidelity DNA polymerases that replicate DNA in an error-prone manner. Y-family DNA polymerases, found throughout all domains of life, are characterized by their lower fidelity on undamaged DNA and their specialized ability to copy damaged DNA. Two *E. coli* Y-family DNA polymerases are responsible for copying damaged DNA as well as for mutagenesis. These DNA polymerases interact with different forms of UmuD, a dynamic protein that regulates mutagenesis. The UmuD gene products, regulated by the SOS response, exist in two principal forms: UmuD<sub>2</sub>, which prevents mutagenesis, and UmuD<sub>2</sub><sup>'</sup>, which facilitates UV-induced mutagenesis. This paper focuses on the multiple conformations of the UmuD gene products and how their protein interactions regulate mutagenesis.

## 1. Mutagenesis Due to Y-Family DNA Polymerases

The observation of nonmutable phenotypes of *E. coli umu* (UV-nonmutable) mutants led to the discovery that mutagenesis in *E. coli* is an active process [1–4]. The mutagenesis process utilizes specialized DNA polymerases belonging to the Y family [5]. Y-family DNA polymerases are found in all domains of life and have the specialized ability to replicate damaged DNA, a process known as translesion synthesis (TLS) [5–8]. This specialized ability comes at the cost of lower fidelity in replicating undamaged DNA compared to replicative DNA polymerases. Indeed, Y-family polymerases are from one to several orders of magnitude less accurate than replicative DNA polymerases [9–11]. Moreover, Y-family polymerases lack intrinsic 3'-5'-exonuclease activity and have inherent low processivity [6, 8, 12–14]. Because the cellular functions of Y-family DNA polymerases are potentially mutagenic, their activities are tightly regulated. *E. coli* has two members of the Y family, DNA pol IV (DinB, encoded by the *dinB* gene) [15] and pol V (UmuD<sub>2</sub>C, encoded by the UmuD and UmuC genes) [16, 17], whose

functions are regulated on multiple levels. A key feature of their regulation is their interactions with products of the UmuD gene.

## 2. SOS Regulation

The UmuD gene is found in an operon with UmuC [18, 19]. The expression of these genes, as well as the *dinB* gene, is negatively regulated by the LexA repressor as part of the SOS response [7, 20]. LexA binds to a sequence in the operator region of regulated genes called the “SOS box,” with a consensus sequence of 5' taCTGtatatatataCAGta, where the most conserved residues are in capital letters [21]. Upon DNA damage, a region of single-stranded DNA (ssDNA) forms due to the inability to continue replication of the damaged DNA. RecA polymerizes on the ssDNA, forming a RecA/ssDNA nucleoprotein filament, which is the inducing signal for the SOS response (Figure 1) [22]. Upon binding to the RecA/ssDNA filament, LexA undergoes a conformational change that stimulates its latent ability to cleave itself [23]. LexA cleavage inactivates it as a repressor and exposes a

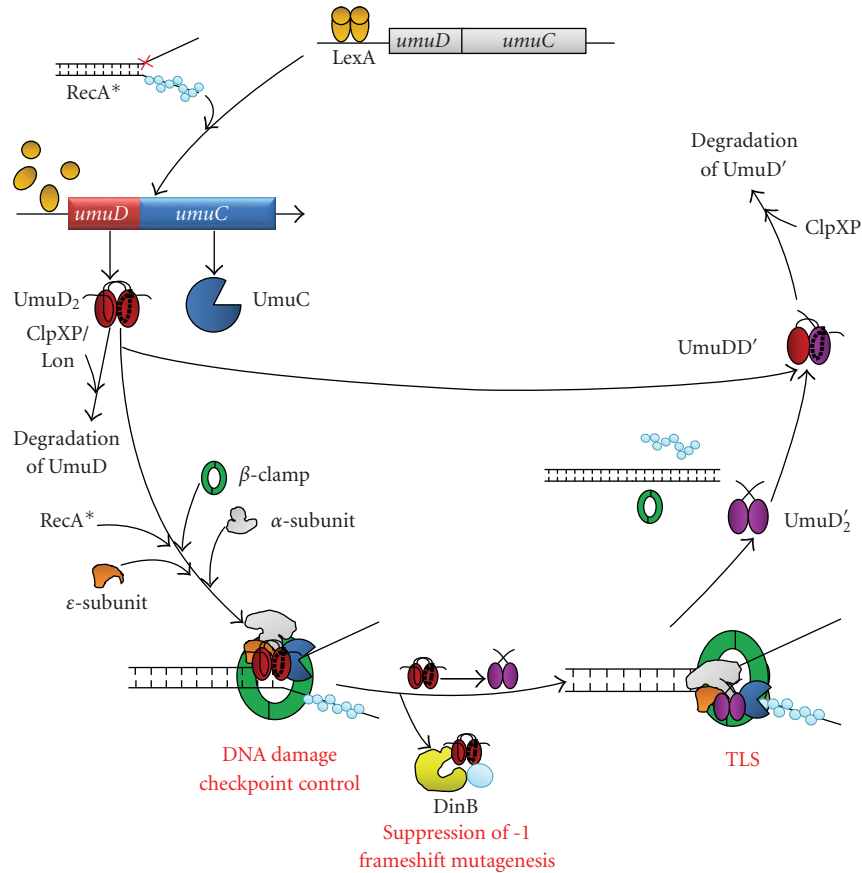


FIGURE 1: Life cycle and interactions of UmuD gene products. Details are described in the text.

proteolysis signal sequence, leading to degradation of LexA [24] and to increased expression of at least 57 SOS-regulated genes, including UmuD [20]. The cellular levels of UmuD, UmuC, and DinB all increase approximately 10-fold upon SOS induction, with UmuD increasing from ~180 to ~2400 molecules, UmuC increasing from ~15 to ~200 molecules, and DinB increasing from ~250 to ~2500 molecules per cell [25, 26]. The products of SOS-regulated genes are involved in DNA repair, DNA damage tolerance, and regulation of cell division. As the cell recovers from genotoxic stresses, it is presumed that the concentration of ssDNA is reduced, resulting in a decrease of RecA/ssDNA filament in the cell. This occurrence allows intact LexA to accumulate, thereby diminishing the SOS response [4].

### 3. UmuD is a Molecular Adaptor That Regulates Mutagenesis

Following initiation of the SOS response, UmuD<sub>2</sub> is the predominant form of the protein for 20–30 minutes [27]. The presence of UmuD and UmuC protects the cell from the potential deleterious effects of the error-prone DNA damage response pathway, a function which is genetically distinct from their role in SOS mutagenesis [27, 28]. UmuD<sub>2</sub>, together with UmuC, may act in a primitive DNA damage

checkpoint, as they specifically inhibit DNA replication without an effect on transcription or translation when present at elevated levels in cells grown at 30°C [27, 29]. UmuD and UmuC also slow the resumption of DNA replication after UV irradiation [27]. Therefore, UmuDC acts in a noncatalytic fashion by delaying SOS mutagenesis and thereby allowing accurate pathways such as nucleotide excision repair time to proceed [27, 28]. Moreover, UmuD interacts with DinB and inhibits its mutagenic -1 frameshift activity [30].

UmuD<sub>2</sub> interacts with the RecA/ssDNA filament, which stimulates the ability of UmuD to cleave itself, removing its N-terminal 24 amino acids [31–33]. UmuD is homologous to the C-terminal domain of LexA, and their cleavage reactions are remarkably similar: both proteins utilize a Ser-Lys (S60-K97 in UmuD) catalytic dyad, which is also similar to the reaction carried out by signal peptidases [34]. By analogy to signal peptidases, K97 is proposed to deprotonate S60, which is then capable of nucleophilic attack on the peptide backbone [34]. Therefore, UmuD<sub>2</sub> and LexA also undergo autodigestion at elevated pH [23, 33]. The kinetics of cleavage are remarkably different for UmuD<sub>2</sub> and LexA, with cleavage of LexA much more efficient than that of UmuD<sub>2</sub> in both RecA- and alkaline-mediated cleavage [33]. Moreover, LexA undergoes intramolecular cleavage [35] while UmuD<sub>2</sub> is capable of intermolecular cleavage [36–38].

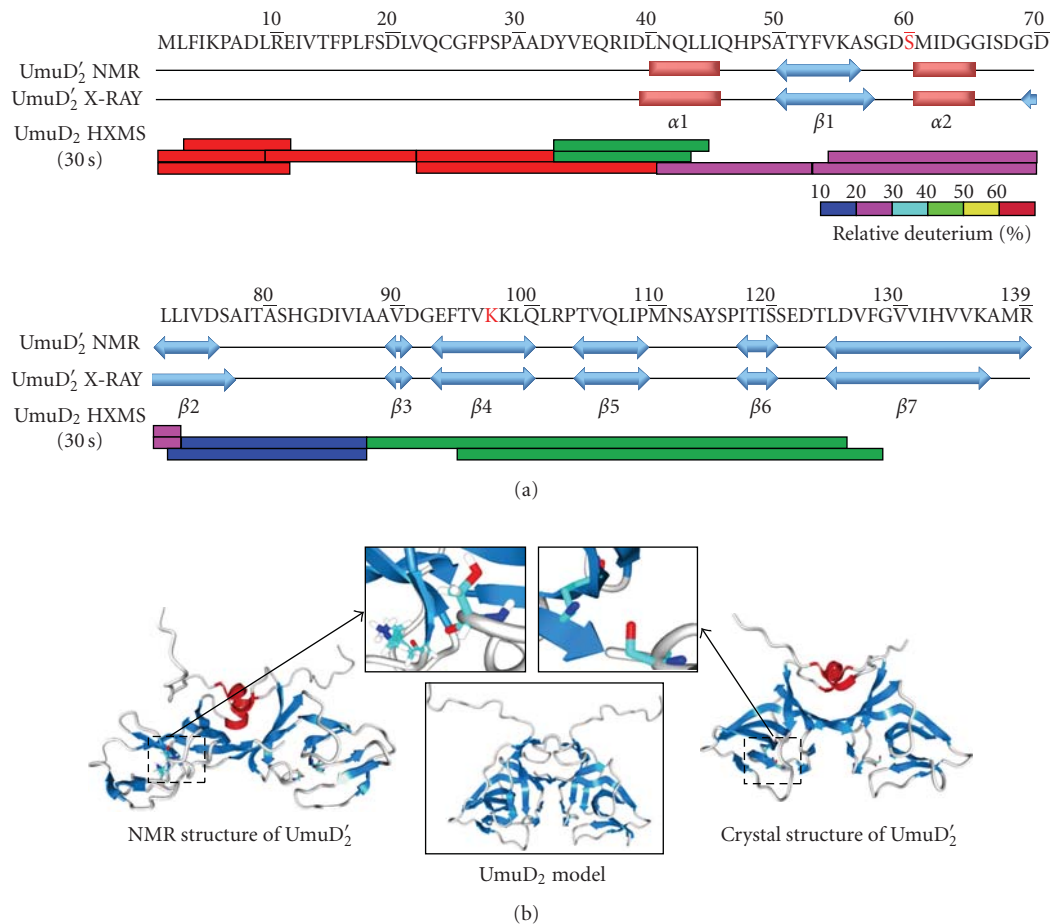


FIGURE 2: The secondary and tertiary structure of UmuD<sub>2</sub> and UmuD'<sub>2</sub>. (a) Secondary structure comparison between the UmuD'<sub>2</sub> NMR [44, 45] and crystal [46] structures. The  $\alpha$  helices are shown in red, and  $\beta$  sheets are shown in blue. Relative deuterium incorporation of UmuD<sub>2</sub> at 30 sec labeling in HXMS experiments is shown, and the colors are based on the relative deuterium percentage scale shown [51]. (b) Comparison of the NMR [44, 45] and crystal [46] structures of UmuD'<sub>2</sub>. The color of the  $\alpha$  helices and  $\beta$  sheets is consistent with (a). The active site regions are boxed and shown in the insets. A model of full-length UmuD<sub>2</sub> is shown [52].

RecA-facilitated cleavage of UmuD to UmuD' occurs 20–40 minutes after the induction of SOS and serves to initiate TLS [4, 27]. UmuD' together with UmuC forms the TLS polymerase Pol V that is active in the damage tolerance mechanism SOS mutagenesis [4, 16, 17, 39, 40]. Additionally, UmuD' and UmuC inhibit RecA-dependent homologous recombination as a result of the direct interaction of UmuD'C with the RecA/ssDNA nucleoprotein filament, thereby preventing accurate recombination repair [41–43]. Taken together, these results support a model in which full-length UmuD acts to prevent mutagenesis while UmuD' facilitates it.

#### 4. Structure and Dynamics of UmuD

Since the UmuD gene products play crucial roles in managing the biological responses to DNA damage, the conformation and dynamics of UmuD<sub>2</sub> and UmuD'<sub>2</sub> are of great interest. To date, the structure of full-length UmuD<sub>2</sub> has not been amenable to crystallization or NMR analysis.

However, the NMR [44, 45] and crystal [46] structures (Figure 2) of UmuD'<sub>2</sub> have been solved. Both structures show that UmuD'<sub>2</sub> is a homodimer with a C<sub>2</sub> axis of symmetry and show similar secondary structures: UmuD'<sub>2</sub> is composed primarily of  $\beta$ -strands with two short  $\alpha$ -helices in each monomer. The C-terminal globular domain (residues 40–139) is mainly composed of curved antiparallel  $\beta$ -strands connected by tight turns with a long C-terminal strand,  $\beta$ 7, that spans both monomers (Figure 2). Residues between positions 132–139 in  $\beta$ 7 in UmuD and UmuD' show the strongest interdimer cross-linking of their monocysteine derivatives [47]. The  $\alpha$ 1 helices pack against each other in the dimer interface. Both UmuD<sub>2</sub> and UmuD'<sub>2</sub> are exceptionally tight dimers with equilibrium dissociation constants  $K_{D^s} < 10$  pM [48]. The active site residue K97 is in the middle of strand  $\beta$ 4 while S60 is in helix  $\alpha$ 2 (Figure 2) [44, 46]. In both structures, the short N-terminal arms that remain after cleavage (residues 25–39) are largely unstructured [45, 46].

The differences between the X-ray and NMR structures of UmuD' are not insignificant [44]. The RMSD of the backbone atoms (residues 40–139) between the two

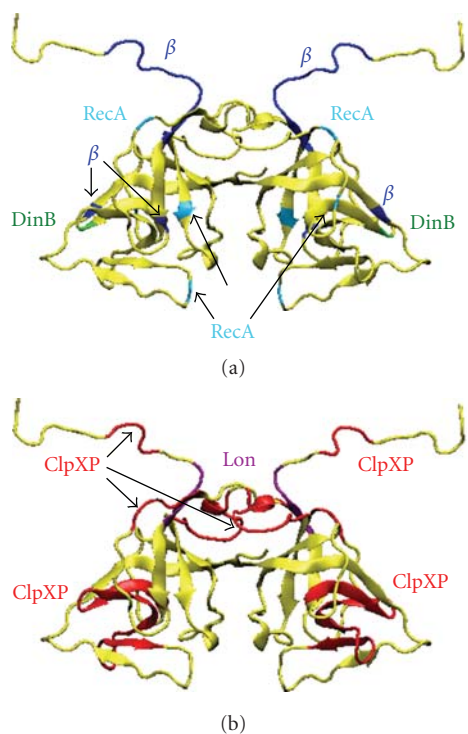


FIGURE 3: Protein interaction sites on UmuD. (a) The  $\beta$  clamp interacts with residues 14–19, 24, 52, and 126 (blue) [53]. RecA interacts with residues 34, 81, 57, 67, and 112 (cyan) [49]. DinB interacts with residue 91 on UmuD (green) [30]. (b) ClpXP interacts with residues 9–12, 33–37, 41–51, and 85–109 (red) [123]. Lon binds to regions close to the residues that are important for interaction with ClpXP, residues 15–19 (violet) [125].

structures of UmuD<sub>2</sub> is 4.59 Å [44]. Moreover, the active site in the crystal structure appears correctly positioned for catalysis, while in the NMR structure, the catalytic residues Ser60 and Lys97 are over 7 Å apart and are not positioned appropriately (Figure 2) [44, 46]. It has been suggested that the conformation of UmuD<sub>2</sub> in the crystal structure is similar to the conformation of UmuD<sub>2</sub> bound to the RecA/ssDNA nucleoprotein filament [44], which might indicate the mechanism whereby RecA/ssDNA acts as a coprotease in facilitating UmuD cleavage. Several residues on the outer loops and the surface of UmuD<sub>2</sub>, specifically Val34, Ser57, Ser67, Ser81, and Ser112, each when changed to single cysteines, have been shown to cross-link to RecA and therefore are likely sites of interaction between the two proteins (Figure 3) [49]. The structure of UmuD<sub>2</sub>C-RecA/ssDNA complex determined by using cryo-electron microscopy shows UmuD<sub>2</sub>C bound deep in the groove of the RecA/ssDNA nucleoprotein filament and a second binding mode with UmuD<sub>2</sub>C at the end of the RecA/ssDNA filament [50].

The differences in the X-ray and NMR structures of UmuD' and other findings suggested that UmuD and UmuD' may be quite dynamic proteins. Indeed, UmuD<sub>2</sub> and UmuD<sub>2</sub>' were recently found to be intrinsically disordered proteins [48]. Despite the predominantly  $\beta$ -sheet character

in the solved structures of UmuD', the circular dichroism spectra of both UmuD' and UmuD at physiological concentrations (5  $\mu$ M) in solution are more characteristic of a random coil than of  $\beta$  sheets [48]. Higher concentrations of UmuD or UmuD' (2 mM) or incubation with crowding agents or partner proteins including DinB or the  $\beta$  clamp induced CD spectra more characteristic of a predominantly  $\beta$ -sheet structure [48].

An analysis of the dynamics of UmuD using hydrogen-deuterium exchange mass spectrometry (HXMS) found that many regions of UmuD<sub>2</sub> were highly dynamic in solution, especially its N-terminal arms (Figure 2), consistent with previous suggestions [36, 44, 51]. In addition, the comparison of the conformations and dynamics of UmuD<sub>2</sub> and UmuD<sub>2</sub>' in solution by HXMS indicated that the N-terminal arm was a key factor governing the dynamics of UmuD<sub>2</sub> and UmuD<sub>2</sub>'. In the absence of the N-terminal 24 residues in UmuD<sub>2</sub>', regions of the globular domain likely to contact the arm underwent more exchange than in UmuD<sub>2</sub> [51]. The predicted dimer interface of UmuD<sub>2</sub> was the most resistant to deuteration indicating that this region is the most stable and structured part of the protein. The results of HXMS were consistent both with the proposed model of UmuD<sub>2</sub> [52] and with the observation that UmuD<sub>2</sub> is relatively unstructured [48].

Gas-phase hydrogen-deuterium exchange experiments, which specifically detect side-chain hydrogen exchange at msec time scales, show that when the arm is truncated, in UmuD<sub>2</sub>', more side-chain sites can be labeled, reinforcing the idea that the arm protects part of the globular domain of the protein from interactions with solvent [51]. Therefore, the flexible N-terminal arm and the extended binding interface are potential sites for UmuD<sub>2</sub> to interact with other partner proteins. Indeed, the  $\beta$  processivity clamp has been shown to interact with specific amino acids in both the N-terminal arm and the globular domain of UmuD<sub>2</sub> [53].

Also in support of the dynamic nature of UmuD, it was found that Leu101 and Arg102 are important for proper positioning of the Ser/Lys active site dyad upon interaction with the RecA/ssDNA filament [54]. HXMS experiments showed that the peptides including these residues (89–125 and 95–128) are highly deuterated (Figure 2) [51]. Additionally, from molecular modeling experiments four distinct conformations of UmuD<sub>2</sub> were calculated; all four were isoenergetic, suggesting that all four conformations may be physiologically relevant [52]. Thus, the flexibility of UmuD<sub>2</sub> is likely to be a key feature governing its cleavage activity as well as interactions with its numerous protein partners.

Not only are the monomer units of UmuD and UmuD' highly flexible, but multiple dimeric forms are also observed. Homodimers of UmuD<sub>2</sub> and UmuD<sub>2</sub>' readily exchange to form the UmuDD' heterodimer, which has been found to be the most thermodynamically stable dimeric form [55]. Additionally, the X-ray structure of UmuD<sub>2</sub>' suggested two possible dimer interfaces [46, 56]. Much biochemical data, as well as solution NMR and HXMS experiments, are consistent with the dimer interface shown in Figure 2 [45, 47, 51]. However, some experiments suggest that the other dimer

interface (not shown) may also form [56]. Both dimer interfaces may be present in solution, as indicated by the observation of higher order cross-linked UmuD multimers of molecular weights consistent with tetramers and hexamers and larger complexes [28, 56]. UmuD and UmuD' appear to be intrinsically highly dynamic proteins that can adopt multiple dimeric, and possibly higher order, forms.

## 5. The Interactions of the UmuD Gene Products with the $\alpha$ , $\beta$ , and $\epsilon$ Subunits of DNA Polymerase III

DNA pol III is the 10-subunit complex responsible for most DNA replication in *E. coli* [57, 58]. Although pol III and UmuD<sub>2</sub>C reduce the primer extension activity of each other by competing for DNA primer termini, they also appear to directly interact as UmuD<sub>2</sub>C enhances the polymerase activity of pol III with a temperature-sensitive  $\alpha$  protein *in vitro* [17, 59, 60]. UmuD<sub>2</sub> and UmuD<sub>2</sub>' directly interact with components of the replicative DNA polymerase III, including the  $\alpha$  catalytic,  $\beta$  processivity, and  $\epsilon$  proofreading subunits [28, 61]. The UmuD gene products display differential interactions with these components of the replisome. UmuD<sub>2</sub> binds more strongly to the  $\beta$  processivity clamp than UmuD<sub>2</sub>' does whereas UmuD<sub>2</sub>' binds more strongly to the  $\alpha$  polymerase subunit than UmuD<sub>2</sub> does, which is consistent with the UmuD gene products serving temporally separate roles in coordinating the replication machinery in response to DNA damage [61].

The  $\epsilon$  subunit possesses 3' to 5' exonuclease activity and serves as the proofreading subunit of the replicative DNA polymerase [57]. Both UmuD<sub>2</sub> and UmuD<sub>2</sub>' interact with the C-terminal domain of  $\epsilon$ , which is the same region of  $\epsilon$  that contacts  $\alpha$  [61–63]. The overexpression of the  $\epsilon$  subunit suppresses UmuDC-mediated cold sensitivity whereas overexpression of any of the other pol III subunits does not [62].

By far, the best characterized interactions of UmuD or UmuD' with the replisome are the interactions between UmuD or UmuD' and the  $\beta$  processivity clamp. Overexpression of the  $\beta$  processivity clamp exacerbates UmuDC-mediated cold sensitivity, which was used as the basis of selection to identify additional sites of interaction between UmuD', UmuC, and the  $\beta$  clamp [62, 64, 65]. It was suggested that the exacerbation of the cold sensitive phenotype is due to an exaggerated checkpoint response [61, 64].

UmuD<sub>2</sub> binds to  $\beta$  in the vicinity of the same hydrophobic pocket region where other  $\beta$ -binding proteins interact [53, 66]. As the  $\beta$  clamp is a homodimer, it has two such interaction sites per functional protein. However, there is still likely to be a hierarchy or competition for binding to the clamp because at least eight proteins are likely to interact with the  $\beta$  clamp at the same site, some of which possess different affinities for the  $\beta$  clamp (Table 1) [66–74]. By using site-directed mutagenesis and cross-linking experiments, it was reported that UmuD<sub>2</sub>, UmuD<sub>2</sub>', and the  $\alpha$  catalytic subunits of Pol III share some common contacts with  $\beta$ , but each of these proteins possesses a different

TABLE 1: *E. coli* proteins that interact with the  $\beta$  clamp via the  $\beta$ -binding pentapeptide motif QL[SD]LF or similar sequence [67].

$\beta$ -interacting proteins	$\beta$ -binding sequence	References
UmuD	<sup>14</sup> TFPLF <sup>18</sup>	[52, 53] <sup>(1)</sup>
DNA Pol V (UmuC)	<sup>357</sup> QLNLF <sup>361</sup>	[127, 128]
DNA Pol IV (DinB)	<sup>346</sup> QLVLGL <sup>351</sup>	[68, 127, 129]
DNA Pol II (Pol B)	<sup>779</sup> QLGLF <sup>783</sup>	[127]
DNA Pol III ( $\alpha$ -subunit)	<sup>920</sup> QADMF <sup>924</sup>	[130]
$\delta$ -subunit Clamp Loader	<sup>70</sup> AMSLF <sup>74</sup>	[131]
MutS	<sup>812</sup> QMSLL <sup>816</sup>	[132]
Hda	<sup>6</sup> QLSLPL <sup>11</sup>	[133]

<sup>(1)</sup>Although these residues reside in an important region for interactions with the  $\beta$  clamp, their identity is not required for UmuD to interact with  $\beta$  (see text Section 5).

affinity for  $\beta$  [66]. The N-terminal region of UmuD<sub>2</sub> contains a canonical  $\beta$  clamp-binding motif (<sup>14</sup>TLPLF<sup>18</sup>) (Figures 2 and 3, Table 1); this motif is used by a number of proteins to bind to the hydrophobic pocket on the  $\beta$  clamp (Figure 3) [67]. By constructing truncations of UmuD, it was determined that the residues between 9 and 19 are critical for interactions with the  $\beta$  clamp [53]. A UmuD<sub>2</sub> variant containing mutations in the canonical  $\beta$  clamp interaction motif was found to bind  $\beta$  with the same affinity as wild-type UmuD but with a different tryptophan fluorescence emission spectrum of  $\beta$  [52], which indicates that the motif itself is not necessary for the interaction, but it likely indicates a conformational change in the  $\beta$  clamp upon UmuD binding [6]. Additionally, residues in the C-terminal globular domain of UmuD and UmuD' are also involved in interactions with the  $\beta$  clamp (Figure 3) [53]. Therefore, UmuD<sub>2</sub> interacts with the  $\beta$  clamp by both its N-terminal arm and C-terminal globular domain.

## 6. Molecular Interactions of UmuD with Y-Family DNA Polymerases UmuC and DinB

**6.1. Molecular Interactions of umuD Gene Products with UmuC.** Disruptions to the *umuDC* operon result in non-mutability by UV, 4-nitroquinoline 1-oxide (4-NQO), methyl methanesulfonate (MMS), and other agents [1–4], presumably due to the lack of TLS by pol V. Pol V has a base substitution error frequency of  $10^{-3}$ – $10^{-5}$  on undamaged DNA, compared to  $10^{-4}$ – $10^{-6}$  for the replicative DNA polymerase pol III [75, 76]. Pol V copies DNA-containing lesions such as abasic sites, thymine-thymine cyclobutane pyrimidine dimers, (6-4) photoproducts, as well as the C<sup>8</sup>-dG adduct of *N*-2-acetylaminofluorene, while preferentially misincorporating dG opposite the 3' T of the thymine-thymine (6-4) photoproducts [16, 17, 59, 75, 77, 78]. This specific mutagenic bypass of the (6-4) photoproduct is a major contributor to the observed UmuC-dependent SOS mutagenesis [75, 79]. UmuC contains intrinsic DNA polymerase activity and is therefore capable of DNA synthesis on undamaged DNA, but TLS activity requires the formation of the UmuD'C complex and the presence of RecA [16, 80].

Other cofactors, including SSB and the  $\beta$  processivity clamp and clamp loader, also support TLS by pol V [16, 17, 59, 75, 80–86].

Whereas UmuD' is required for TLS by UmuC, full-length UmuD does not support TLS [16, 87]. Cells expressing UmuD and UmuC at elevated levels exhibit a cold sensitive for growth phenotype that is not yet well understood [29]. Full-length UmuD also plays a role together with UmuC in inhibiting the recovery of DNA replication after UV exposure [27]. Moreover, full-length UmuD that cannot be cleaved because it harbors the S60A active site mutation causes a dramatic reduction in UV-induced mutagenesis while UmuD'-S60A shows only a modest decrease in UV-induced mutagenesis [32]. Cells expressing UmuC together with noncleavable UmuD-S60A are sensitive to UV relative to cells expressing wild-type UmuD and UmuC but are resistant to killing by UV irradiation relative to cells that are  $\Delta$ umuDC [27, 52, 55]. Taken together, these findings suggest that full-length UmuD specifically prevents mutagenesis, presumably at least in part by preventing UmuC from engaging in mutagenic TLS.

Due to the difficulty in acquiring large quantities of pure, active UmuC and pol V, protein interaction studies have been somewhat limited, especially considering that the UmuC gene was identified in the 1970s. However, the physical interaction between UmuD' and UmuC was confirmed using immunoprecipitation, yeast two-hybrid assay and glycerol gradient analysis [88, 89]. Additionally, the interaction between full-length UmuD and UmuC was verified by using affinity chromatography and velocity sedimentation in glycerol gradients, but not immunoprecipitation from cell extracts [88]. From this, it was concluded that UmuC associates strongly with UmuD' *in vivo* whereas, *in vitro*, UmuC interacts efficiently with both forms of the UmuD gene products [88]. The likely stoichiometry was determined to be one UmuC with either a dimeric UmuD or UmuD' [88]. UmuD and UmuD' appear to interact with the C-terminus of UmuC, as a UmuC construct lacking its C-terminal 25 residues showed dramatically reduced binding to both UmuD and UmuD' [28]. In addition to the UmuD and UmuD' homodimers, UmuC also interacts with the UmuDD' heterodimer, which acts to inhibit SOS mutagenesis, possibly by titrating out the dimeric UmuD' species that is active in TLS [88–91].

**6.2. Molecular Interactions of UmuD and DinB.** The *dinB* (damage-inducible) gene encoding DNA pol IV (DinB) was discovered in a screen using reporter fusions to identify DNA damage-inducible genes [92]. DinB (Pol IV) is the other Y-family lesion bypass polymerase in *E. coli* and is the only Y-family polymerase that is conserved throughout all domains of life [5, 15]. The expression level of chromosomal DinB under DNA damaging conditions is 6–12 times higher than that of UmuC or PolB (DNA pol II) with about 2500 molecules of DinB in an SOS-induced cell [25]. DinB is also found on the recombinant F' plasmid that was constructed to determine mutation spectra of specific revertible *lac*<sup>-</sup> alleles [25, 93]. The expression level of DinB in an uninduced state

from the F' plasmid in *E. coli* strain CC108 is approximately 750 molecules, as compared to 250 molecules expressed from the chromosome in the absence of SOS induction [25]. DinB has a misincorporation error frequency of  $10^{-3}$ – $10^{-5}$  [94]. Unlike UmuD'C, DinB elongates templates with bulged structures causing potentially deleterious -1 frameshift mutations [95, 96]. It was also shown that DinB and its eukaryotic ortholog Pol  $\kappa$  can accurately and efficiently perform TLS on templates containing N<sup>2</sup>-deoxyguanosine (N<sup>2</sup>-dG) adducts, suggesting that these proteins are specialized for relatively accurate TLS over some N<sup>2</sup>-dG adducts [97–99].

UmuD, UmuD', and RecA play important roles in the regulation of DinB, and direct physical interactions between DinB and UmuD, UmuD', and RecA have been detected [30]. Although this may have initially seemed surprising, the expression levels of UmuD (180 molecules uninduced; 2400 molecules in SOS-induced cells) and DinB (250 molecules uninduced; 2500 molecules in SOS-induced cells) before and after SOS induction align [25, 26]. The stoichiometry of the complex was found to be one DinB molecule to one UmuD<sub>2</sub> dimer [30]. DinB and UmuD<sub>2</sub> bind with a  $K_D$  of 0.62  $\mu$ M [30]. It was also determined that DinB, RecA, and UmuD<sub>2</sub> form a stable ternary complex under physiological conditions *in vitro* [30]. Genetic and biochemical analysis shows that full-length UmuD as well as the noncleavable UmuD variant UmuD S60A strongly inhibits the -1 frameshift mutator effect of DinB [30]. UmuD and UmuD' also inhibit DinB activity in adaptive mutagenesis [30]. Presteady-state kinetics experiments led to the proposal that DinB bound to DNA containing a repetitive sequence is in equilibrium between a template slipped conformation, which leads to frameshift mutagenesis and a nonslipped conformation [100]. UmuD appears to prevent DinB-dependent frameshift mutagenesis by favoring the nonslipped conformation upon binding to DinB [100]. UmuD also modulates DinB function by facilitating efficient extension of correctly paired primer termini while blocking extension of mismatched termini [30, 100].

Using peptide array mapping and structural homology models of both DinB and UmuD, it was proposed that UmuD interacts with several hydrophobic residues on the surface of DinB in the thumb and finger domains. DinB residue F172 in the thumb domain was identified as a likely site of interaction with UmuD. Indeed, DinB F172A has lower affinity for UmuD ( $K_D$  reduced ~56-fold) and exhibits less UmuD-dependent -1 frameshift suppression *in vivo* and *in vitro* than wild-type DinB [30]. The DinB interacting surface on UmuD is a discontinuous surface when mapped onto a model of *trans*-UmuD [47, 52]. Alternatively, isoenergetic models of UmuD in which the N-terminal arms are in a noncleavable conformation provide alternative interacting surfaces across the side of UmuD [52]. UmuD D91, on the outer surface of UmuD, was proposed as a likely residue to be important for interaction with DinB (Figure 3). UmuD D91A has reduced affinity for DinB ( $K_D$  reduced by over 24-fold) and dramatically reduced suppression of -1 frameshift mutagenesis compared to wild-type UmuD [30]. This suggests that there may be multiple biologically relevant

conformations of UmuD that can interact with DinB or other polymerases [48, 51, 52, 101]. These interactions may aid in the suppression of frameshift mutagenesis by blocking the open active site that is needed to elongate bulged templates [13, 14, 30, 102]. By creating a ternary complex model of DinB, UmuD<sub>2</sub>, and RecA, it was suggested that UmuD<sub>2</sub> and RecA work together in restricting the open active site of DinB thereby preventing -1 frameshift mutagenesis on bulged templates [30, 100]. Therefore, the presence of full-length UmuD actually enhances accurate TLS by DinB while suppressing extension of bulged templates that would cause frameshift mutagenesis.

## 7. Molecular Interactions of UmuD and UmuD' with Lon and ClpXP Proteases

Regulation of UmuD protein levels by ClpXP and Lon proteases is an important part of the SOS response to DNA damage. Proteolytic degradation of the UmuD gene products is involved in cessation of SOS mutagenesis [4, 103, 104]. ClpXP is composed of the ATP-dependent unfoldase ClpX hexamer and the double-ringed, 14-subunit serine protease, ClpP [105–109]. The domain structure of the Lon protease is quite similar in that it contains an ATPase domain, a sensor and substrate discrimination domain (SSD), and a protease domain [110]. The mechanism of degradation begins when ClpX unfolds the substrates using repeated cycles of ATP hydrolysis and translocates the unfolded peptide into the ClpP chamber where proteolysis occurs. Substrate recognition involves the N- or C-terminal regions of the target protein binding to the substrate-processing site on ClpX [111, 112]. These signals may become apparent after cleavage, as in the case of LexA, or upon a conformational change in the target protein [113, 114]. However, the addition of an 11-amino acid (AANDENYALAA) *ssrA* tag to improperly translated nascent polypeptides will result in direct targeting to ClpXP for degradation [107, 108, 115–118]. This C-terminal *ssrA* tag is encoded by the *ssrA* transfer mRNA and is added cotranslationally to proteins translated without an in-frame stop codon [117, 118]. In addition, substrate recognition by ClpXP involves the interaction of tethering sites with adaptor proteins. These adaptor proteins are not degraded themselves but work to enhance the degradation of the target protein [119, 120]. One example is the SspB-mediated degradation of *ssrA*-tagged protein. Here, one part of the target protein binds the tethering site on ClpX while the SspB protein interacts with the *ssrA* tag enabling efficient delivery to ClpXP for degradation [121, 122].

Similar to SspB-facilitated degradation of *ssrA*-tagged target proteins, UmuD' is a substrate for ClpXP but is only degraded when bound to full-length UmuD [123, 124]. Therefore, the preferential formation of UmuDD' heterodimer specifically leads to a decrease in the steady-state levels of UmuD' *in vivo* [123]. Although the residues found within the N-terminal 24 amino acids of UmuD serve as the degradation signal for ClpXP degradation of UmuD', UmuD serves as an adaptor and is not itself degraded [124]. UmuD also serves as an adaptor in the context of

UmuD<sub>2</sub> homodimers, leading to degradation of one UmuD in the dimer [123]. UmuD residues 9–12 are necessary for UmuD' instability and therefore protease recognition (Figure 3) [124]. Amino acids 15–19 of UmuD are also implicated in the degradation of the UmuDD' heterodimer by ClpXP (Figure 3) [124]. On the other hand, while residues 15–19 are also important for Lon-mediated degradation of UmuD, residues 9–12 are not involved in recognition by Lon [125]. ClpXP recognition sites can also be found on the surface of UmuD', in particular, residues 33–37, 41–51, and 85–109 were found to interact robustly with ClpXP (Figure 3) [124]. The UmuD-facilitated degradation of UmuD' can be impeded by the SspB-tethering peptide, and the SspB-tethering motif is interchangeable with the sequence in UmuD. Because the N-terminal domain of ClpX mediates interactions with both SspB and UmuD, it was determined that UmuD acts as a ClpX delivery factor that is critical in tethering itself and UmuD' to ClpX. This seems to be a primary mechanism for bringing SOS mutagenesis to an end [126].

## 8. Conclusions

Although the UmuD gene was discovered over 30 years ago, new findings regarding how the UmuD gene products regulate mutagenesis have been made even within the last few years. This is despite the fact that there is still no high-resolution structure of full-length UmuD. The extremely dynamic nature of UmuD and UmuD' has only recently come to light and provides insights into the large number of specific protein interactions of which the UmuD gene products are capable. Because of the role of UmuD in regulating mutagenesis, it could be important in bacterial evolution and is therefore potentially an important drug target.

## Acknowledgments

Jaylene N. Ollivierre and Jing Fang contributed equally in this work. The authors are pleased to acknowledge generous financial support from a New Faculty Award from the Camille & Henry Dreyfus Foundation (PJB), the NSF (CAREER Award, MCB-0845033 to PJB), and the NU Office of the Provost (PJB). P. J. Beuning is a Cottrell Scholar of the Research Corporation for Science Advancement.

## References

- [1] A. Bagg, C. J. Kenyon, and G. C. Walker, "Inducibility of a gene product required for UV and chemical mutagenesis in *Escherichia coli*," *Proceedings of the National Academy of Sciences of the United States of America*, vol. 78, no. 9, pp. 5749–5753, 1981.
- [2] T. Kato and Y. Shinoura, "Isolation and characterization of mutants of *Escherichia coli* deficient in induction of mutations by ultraviolet light," *Molecular and General Genetics*, vol. 156, no. 2, pp. 121–131, 1977.
- [3] G. Steinborn, "Uvm mutants of *Escherichia coli* K12 deficient in UV mutagenesis. I. Isolation of *uvm* mutants and their

- phenotypical characterization in DNA repair and mutagenesis," *Molecular and General Genetics*, vol. 165, no. 1, pp. 87–93, 1978.
- [4] E. C. Friedberg, G. C. Walker, W. Siede, R. D. Wood, R. A. Schultz, and T. Ellenberger, *DNA Repair and Mutagenesis*, ASM Press, Washington, DC, USA, 2nd edition, 2005.
  - [5] H. Ohmori, E. C. Friedberg, R. P. P. Fuchs et al., "The Y-family of DNA polymerases," *Molecular Cell*, vol. 8, no. 1, pp. 7–8, 2001.
  - [6] D. F. Jarosz, P. J. Beuning, S. E. Cohen, and G. C. Walker, "Y-family DNA polymerases in *Escherichia coli*," *Trends in Microbiology*, vol. 15, no. 2, pp. 70–77, 2007.
  - [7] K. Schlacher and M. F. Goodman, "Lessons from 50 years of SOS DNA-damage-induced mutagenesis," *Nature Reviews Molecular Cell Biology*, vol. 8, no. 7, pp. 587–594, 2007.
  - [8] W. Yang and R. Woodgate, "What a difference a decade makes: insights into translesion DNA synthesis," *Proceedings of the National Academy of Sciences of the United States of America*, vol. 104, no. 40, pp. 15591–15598, 2007.
  - [9] A. Maor-Shoshani, N. B. Reuven, G. Tomer, and Z. Livneh, "Highly mutagenic replication by DNA polymerase V (UmuC) provides a mechanistic basis for SOS untargeted mutagenesis," *Proceedings of the National Academy of Sciences of the United States of America*, vol. 97, no. 2, pp. 565–570, 2000.
  - [10] S. D. McCulloch and T. A. Kunkel, "The fidelity of DNA synthesis by eukaryotic replicative and translesion synthesis polymerases," *Cell Research*, vol. 18, no. 1, pp. 148–161, 2008.
  - [11] S. Kobayashi, M. R. Valentine, P. Pham, M. O'Donnell, and M. F. Goodman, "Fidelity of *Escherichia coli* DNA polymerase IV: preferential generation of small deletion mutations by dNTP-stabilized misalignment," *Journal of Biological Chemistry*, vol. 277, no. 37, pp. 34198–34207, 2002.
  - [12] M. T. Washington, K. D. Carlson, B. D. Freudenthal, and J. M. Pryor, "Variations on a theme: eukaryotic Y-family DNA polymerases," *Biochimica et Biophysica Acta*, vol. 1804, no. 5, pp. 1113–1123, 2010.
  - [13] W. Yang, "Damage repair DNA polymerases Y," *Current Opinion in Structural Biology*, vol. 13, no. 1, pp. 23–30, 2003.
  - [14] W. Yang, "Portraits of a Y-family DNA polymerase," *FEBS Letters*, vol. 579, no. 4, pp. 868–872, 2005.
  - [15] J. Wagner, P. Gruz, S.-R. Kim et al., "The *dinB* gene encodes a novel *E. coli* DNA polymerase, DNA pol IV, involved in mutagenesis," *Molecular Cell*, vol. 4, no. 2, pp. 281–286, 1999.
  - [16] N. B. Reuven, G. Arad, A. Maor-Shoshani, and Z. Livneh, "The mutagenesis protein UmuC is a DNA polymerase activated by UmuD', RecA, and SSB and is specialized for translesion replication," *Journal of Biological Chemistry*, vol. 274, no. 45, pp. 31763–31766, 1999.
  - [17] M. Tang, X. Shen, E. G. Frank, M. O'Donnell, R. Woodgate, and M. F. Goodman, "UmuD<sub>2</sub>C is an error-prone DNA polymerase, *Escherichia coli* pol V," *Proceedings of the National Academy of Sciences of the United States of America*, vol. 96, no. 16, pp. 8919–8924, 1999.
  - [18] S. J. Elledge and G. C. Walker, "Proteins required for ultraviolet light and chemical mutagenesis: identification of the products of the *umuC* locus of *Escherichia coli*," *Journal of Molecular Biology*, vol. 164, no. 2, pp. 175–192, 1983.
  - [19] H. Shinagawa, T. Kato, T. Ise, K. Makino, and A. Nakata, "Cloning and characterization of the *umu* operon responsible for inducible mutagenesis in *Escherichia coli*," *Gene*, vol. 23, no. 2, pp. 167–174, 1983.
  - [20] L. A. Simmons, J. J. Foti, S. E. Cohen, and G. C. Walker, "The SOS regulatory network," in *EcoSal—Escherichia coli and Salmonella: Cellular and Molecular Biology*, A. Bock III, R. C. Kaper, J. B. Karp et al., Eds., chapter 5.4.3., ASM Press, Washington, DC, USA, 2008.
  - [21] J. Courcelle, A. Khodursky, B. Peter, P. O. Brown, and P. C. Hanawalt, "Comparative gene expression profiles following UV exposure in wild-type and SOS-deficient *Escherichia coli*," *Genetics*, vol. 158, no. 1, pp. 41–64, 2001.
  - [22] M. Sassanfar and J. W. Roberts, "Nature of the SOS-inducing signal in *Escherichia coli*. The involvement of DNA replication," *Journal of Molecular Biology*, vol. 212, no. 1, pp. 79–96, 1990.
  - [23] J. W. Little, "Autodigestion of *lexA* and phage  $\lambda$  repressors," *Proceedings of the National Academy of Sciences of the United States of America*, vol. 81, no. 3, pp. 1375–1379, 1984.
  - [24] S. B. Neher, J. M. Flynn, R. T. Sauer, and T. A. Baker, "Latent ClpX-recognition signals ensure LexA destruction after DNA damage," *Genes and Development*, vol. 17, no. 9, pp. 1084–1089, 2003.
  - [25] S.-R. Kim, K. Matsui, M. Yamada, P. Gruz, and T. Nohmi, "Roles of chromosomal and episomal *dinB* genes encoding DNA pol IV in targeted and untargeted mutagenesis in *Escherichia coli*," *Molecular Genetics and Genomics*, vol. 266, no. 2, pp. 207–215, 2001.
  - [26] R. Woodgate and D. G. Ennis, "Levels of chromosomally encoded Umu proteins and requirements for *in vivo* UmuD cleavage," *Molecular and General Genetics*, vol. 229, no. 1, pp. 10–16, 1991.
  - [27] T. Opperman, S. Murli, B. T. Smith, and G. C. Walker, "A model for a *umuDC*-dependent prokaryotic DNA damage checkpoint," *Proceedings of the National Academy of Sciences of the United States of America*, vol. 96, no. 16, pp. 9218–9223, 1999.
  - [28] M. D. Sutton and G. C. Walker, "*umuDC*-mediated cold sensitivity is a manifestation of functions of the UmuD<sub>2</sub>C complex involved in a DNA damage checkpoint control," *Journal of Bacteriology*, vol. 183, no. 4, pp. 1215–1224, 2001.
  - [29] L. Marsh and G. C. Walker, "Cold sensitivity induced by overproduction of UmuDC in *Escherichia coli*," *Journal of Bacteriology*, vol. 162, no. 1, pp. 155–161, 1985.
  - [30] V. G. Godoy, D. F. Jarosz, S. M. Simon, A. Abyzov, V. Ilyin, and G. C. Walker, "UmuD and RecA directly modulate the mutagenic potential of the Y family DNA polymerase *dinB*," *Molecular Cell*, vol. 28, no. 6, pp. 1058–1070, 2007.
  - [31] H. Shinagawa, H. Iwasaki, T. Kato, and A. Nakata, "RecA protein-dependent cleavage of UmuD protein and SOS mutagenesis," *Proceedings of the National Academy of Sciences of the United States of America*, vol. 85, no. 6, pp. 1806–1810, 1988.
  - [32] T. Nohmi, J. R. Battista, L. A. Dodson, and G. C. Walker, "RecA-mediated cleavage activates UmuD for mutagenesis: mechanistic relationship between transcriptional derepression and posttranslational activation," *Proceedings of the National Academy of Sciences of the United States of America*, vol. 85, no. 6, pp. 1816–1820, 1988.
  - [33] S. E. Burckhardt, R. Woodgate, R. H. Scheuermann, and H. Echols, "UmuD mutagenesis protein of *Escherichia coli*: overproduction, purification, and cleavage by RecA," *Proceedings of the National Academy of Sciences of the United States of America*, vol. 85, no. 6, pp. 1811–1815, 1988.

- [34] M. Paetzel and N. C. J. Strynadka, "Common protein architecture and binding sites in proteases utilizing a Ser/Lys dyad mechanism," *Protein Science*, vol. 8, no. 11, pp. 2533–2536, 1999.
- [35] S. N. Slilaty, J. A. Rupley, and J. W. Little, "Intramolecular cleavage of LexA and phage  $\lambda$  repressors: dependence of kinetics on repressor concentration, pH, temperature, and solvent," *Biochemistry*, vol. 25, no. 22, pp. 6866–6875, 1986.
- [36] J. P. McDonald, T. S. Peat, A. S. Levine, and R. Woodgate, "Intermolecular cleavage by UmuD-like enzymes: identification of residues required for cleavage and substrate specificity," *Journal of Molecular Biology*, vol. 285, no. 5, pp. 2199–2209, 1999.
- [37] J. P. McDonald, E. G. Frank, A. S. Levine, and R. Woodgate, "Intermolecular cleavage by UmuD-like mutagenesis proteins," *Proceedings of the National Academy of Sciences of the United States of America*, vol. 95, no. 4, pp. 1478–1483, 1998.
- [38] J. P. McDonald, E. E. Maury, A. S. Levine, and R. Woodgate, "Regulation of UmuD cleavage: role of the amino-terminal tail," *Journal of Molecular Biology*, vol. 282, no. 4, pp. 721–730, 1998.
- [39] I. Bruck, R. Woodgate, K. McEuntee, and M. F. Goodman, "Purification of a soluble UmuD' C complex from *Escherichia coli*: cooperative binding of UmuD' C to single-stranded DNA," *Journal of Biological Chemistry*, vol. 271, no. 18, pp. 10767–10774, 1996.
- [40] R. Woodgate, M. Rajagopalan, C. Lu, and H. Echols, "UmuC mutagenesis protein of *Escherichia coli*: purification and interaction with UmuD and UmuD'," *Proceedings of the National Academy of Sciences of the United States of America*, vol. 86, no. 19, pp. 7301–7305, 1989.
- [41] W. M. Rehrauer, P. E. Lavery, E. L. Palmer, R. N. Singh, and S. C. Kowalczykowski, "Interaction of *Escherichia coli* RecA protein with LexA repressor. I. LexA repressor cleavage is competitive with binding of a secondary DNA molecule," *Journal of Biological Chemistry*, vol. 271, no. 39, pp. 23865–23873, 1996.
- [42] S. Sommer, A. Bailone, and R. Devoret, "The appearance of the UmuD' C protein complex in *Escherichia coli* switches repair from homologous recombination to SOS mutagenesis," *Molecular Microbiology*, vol. 10, no. 5, pp. 963–971, 1993.
- [43] H. Szpilewska, P. Bertrand, A. Bailone, and M. Dutreix, "In vitro inhibition of RecA-mediated homologous pairing by UmuD' C proteins," *Biochimie*, vol. 77, no. 11, pp. 848–853, 1995.
- [44] A. E. Ferentz, G. C. Walker, and G. Wagner, "Converting a DNA damage checkpoint effector (UmuD<sub>2</sub>C) into a lesion bypass polymerase (UmuD<sub>2</sub>C)," *EMBO Journal*, vol. 20, no. 15, pp. 4287–4298, 2001.
- [45] A. E. Ferentz, T. Opperman, G. C. Walker, and G. Wagner, "Dimerization of the UmuD' protein in solution and its implications for regulation of SOS mutagenesis," *Nature Structural Biology*, vol. 4, no. 12, pp. 979–983, 1997.
- [46] T. S. Peat, E. G. Frank, J. P. McDonald, A. S. Levine, R. Woodgate, and W. A. Hendrickson, "Structure of the UmuD' protein and its regulation in response to DNA damage," *Nature*, vol. 380, no. 6576, pp. 727–730, 1996.
- [47] M. D. Sutton, A. Guzzo, I. Narumi et al., "A model for the structure of the *Escherichia coli* SOS-regulated UmuD<sub>2</sub> protein," *DNA Repair*, vol. 1, no. 1, pp. 77–93, 2002.
- [48] S. M. Simon, F. J. R. Sousa, R. Mohana-Borges, and G. C. Walker, "Regulation of *Escherichia coli* SOS mutagenesis by dimeric intrinsically disordered *umuD* gene products," *Proceedings of the National Academy of Sciences of the United States of America*, vol. 105, no. 4, pp. 1152–1157, 2008.
- [49] M. H. Lee and G. C. Walker, "Interactions of *Escherichia coli* UmuD with activated RecA analyzed by cross-linking UmuD monocysteine derivatives," *Journal of Bacteriology*, vol. 178, no. 24, pp. 7285–7294, 1996.
- [50] E. G. Frank, N. Cheng, C. C. Do et al., "Visualization of two binding sites for the *Escherichia coli* UmuD<sub>2</sub>C complex (DNA pol V) on RecA-ssDNA filaments," *Journal of Molecular Biology*, vol. 297, no. 3, pp. 585–597, 2000.
- [51] J. Fang, K. D. Rand, M. C. Silva, T. E. Wales, J. R. Engen, and P. J. Beuning, "Conformational dynamics of the *Escherichia coli* DNA polymerase manager proteins UmuD and UmuD'," *Journal of Molecular Biology*, vol. 398, no. 1, pp. 40–53, 2010.
- [52] P. J. Beuning, S. M. Simon, A. Zemla, D. Barsky, and G. C. Walker, "A non-cleavable UmuD variant that acts as a UmuD' mimic," *Journal of Biological Chemistry*, vol. 281, no. 14, pp. 9633–9640, 2006.
- [53] M. D. Sutton, I. Narumi, and G. C. Walker, "Posttranslational modification of the *umuD*-encoded subunit of *Escherichia coli* DNA polymerase V regulates its interactions with the  $\beta$  processivity clamp," *Proceedings of the National Academy of Sciences of the United States of America*, vol. 99, no. 8, pp. 5307–5312, 2002.
- [54] M. D. Sutton, M. Kim, and G. C. Walker, "Genetic and biochemical characterization of a novel *umuD* mutation: insights into a mechanism for UmuD self-cleavage," *Journal of Bacteriology*, vol. 183, no. 1, pp. 347–357, 2001.
- [55] J. R. Battista, T. Ohta, T. Nohmi, W. Sun, and G. C. Walker, "Dominant negative *umuD* mutations decreasing RecA-mediated cleavage suggest roles for intact UmuD in modulation of SOS mutagenesis," *Proceedings of the National Academy of Sciences of the United States of America*, vol. 87, no. 18, pp. 7190–7194, 1990.
- [56] T. S. Peat, E. G. Frank, J. P. McDonald, A. S. Levine, R. Woodgate, and W. A. Hendrickson, "The UmuD' protein filament and its potential role in damage induced mutagenesis," *Structure*, vol. 4, no. 12, pp. 1401–1412, 1996.
- [57] Z. Kelman and M. O'Donnell, "DNA polymerase III holoenzyme: structure and function of a chromosomal replicating machine," *Annual Review of Biochemistry*, vol. 64, pp. 171–200, 1995.
- [58] C. S. McHenry, "Chromosomal replicases as asymmetric dimers: studies of subunit arrangement and functional consequences," *Molecular Microbiology*, vol. 49, no. 5, pp. 1157–1165, 2003.
- [59] S. Fujii, V. Gasser, and R. P. Fuchs, "The biochemical requirements of DNA polymerase V-mediated translesion synthesis revisited," *Journal of Molecular Biology*, vol. 341, no. 2, pp. 405–417, 2004.
- [60] S. Fujii, A. Isogawa, and R. P. Fuchs, "RecFOR proteins are essential for Pol V-mediated translesion synthesis and mutagenesis," *EMBO Journal*, vol. 25, no. 24, pp. 5754–5763, 2006.
- [61] M. D. Sutton, T. Opperman, and G. C. Walker, "The *Escherichia coli* SOS mutagenesis proteins UmuD and UmuD' interact physically with the replicative DNA polymerase," *Proceedings of the National Academy of Sciences of the United States of America*, vol. 96, no. 22, pp. 12373–12378, 1999.
- [62] M. D. Sutton, S. Murli, T. Opperman, C. Klein, and G. C. Walker, "*umuDC-dnaQ* interaction and its implications for cell cycle regulation and SOS mutagenesis in *Escherichia coli*," *Journal of Bacteriology*, vol. 183, no. 3, pp. 1085–1089, 2001.

- [63] S. A. Taft-Benz and R. M. Schaaper, "The C-terminal domain of DnaQ contains the polymerase binding site," *Journal of Bacteriology*, vol. 181, no. 9, pp. 2963–2965, 1999.
- [64] M. D. Sutton, M. F. Farrow, B. M. Burton, and G. C. Walker, "Genetic interactions between the *Escherichia coli* *umuDC* gene products and the  $\beta$  processivity clamp of the replicative DNA polymerase," *Journal of Bacteriology*, vol. 183, no. 9, pp. 2897–2909, 2001.
- [65] P. J. Beuning, S. Chan, L. S. Waters, H. Addepalli, J. N. Ollivierre, and G. C. Walker, "Characterization of novel alleles of the *Escherichia coli* *umuDC* genes identifies additional interaction sites of UmuC with the beta clamp," *Journal of Bacteriology*, vol. 191, no. 19, pp. 5910–5920, 2009.
- [66] J. M. Duzen, G. C. Walker, and M. D. Sutton, "Identification of specific amino acid residues in the *E. coli*  $\beta$  processivity clamp involved in interactions with DNA polymerase III, UmuD and UmuD'," *DNA Repair*, vol. 3, no. 3, pp. 301–312, 2004.
- [67] B. P. Dalrymple, K. Kongsuwan, G. Wijffels, N. E. Dixon, and P. A. Jennings, "A universal protein-protein interaction motif in the eubacterial DNA replication and repair systems," *Proceedings of the National Academy of Sciences of the United States of America*, vol. 98, no. 20, pp. 11627–11632, 2001.
- [68] D. Y. Burnouf, V. Olieric, J. Wagner et al., "Structural and biochemical analysis of sliding clamp/ligand interactions suggest a competition between replicative and translesion DNA polymerases," *Journal of Molecular Biology*, vol. 335, no. 5, pp. 1187–1197, 2004.
- [69] J. M. H. Heltzel, R. W. Maul, S. K. Scouten Ponticelli, and M. D. Sutton, "A model for DNA polymerase switching involving a single cleft and the rim of the sliding clamp," *Proceedings of the National Academy of Sciences of the United States of America*, vol. 106, no. 31, pp. 12664–12669, 2009.
- [70] J. M. H. Heltzel, S. K. Scouten Ponticelli, L. H. Sanders et al., "Sliding clamp-DNA interactions are required for viability and contribute to DNA polymerase management in *Escherichia coli*," *Journal of Molecular Biology*, vol. 387, no. 1, pp. 74–91, 2009.
- [71] R. W. Maul, S. K. Scouten Ponticelli, J. M. Duzen, and M. D. Sutton, "Differential binding of *Escherichia coli* DNA polymerases to the  $\beta$ -sliding clamp," *Molecular Microbiology*, vol. 65, no. 3, pp. 811–827, 2007.
- [72] S. K. Scouten Ponticelli, J. M. Duzen, and M. D. Sutton, "Contributions of the individual hydrophobic clefts of the *Escherichia coli*  $\beta$  sliding clamp to clamp loading, DNA replication and clamp recycling," *Nucleic Acids Research*, vol. 37, no. 9, pp. 2796–2809, 2009.
- [73] M. D. Sutton and J. M. Duzen, "Specific amino acid residues in the  $\beta$  sliding clamp establish a DNA polymerase usage hierarchy in *Escherichia coli*," *DNA Repair*, vol. 5, no. 3, pp. 312–323, 2006.
- [74] G. Wijffels, B. P. Dalrymple, P. Prosselkov et al., "Inhibition of protein interactions with the  $\beta_2$  sliding clamp of *Escherichia coli* DNA polymerase III by peptides from  $\beta_2$ -binding proteins," *Biochemistry*, vol. 43, no. 19, pp. 5661–5671, 2004.
- [75] M. Tang, P. Pham, X. Shen et al., "Roles of *E. coli* DNA polymerases IV and V in lesion-targeted and untargeted SOS mutagenesis," *Nature*, vol. 404, no. 6781, pp. 1014–1018, 2000.
- [76] L. B. Bloom, X. Chen, D. K. Fygenon, J. Turner, M. O'Donnell, and M. F. Goodman, "Fidelity of *Escherichia coli* DNA polymerase III holoenzyme: the effects of  $\beta$ ,  $\gamma$  complex processivity proteins and  $\epsilon$  proofreading exonuclease on nucleotide misincorporation efficiencies," *Journal of Biological Chemistry*, vol. 272, no. 44, pp. 27919–27930, 1997.
- [77] N. B. Reuven, G. Tomer, and Z. Livneh, "The mutagenesis proteins UmuD' and UmuC prevent lethal frameshifts while increasing base substitution mutations," *Molecular Cell*, vol. 2, no. 2, pp. 191–199, 1998.
- [78] S. Fujii and R. P. Fuchs, "Defining the position of the switches between replicative and bypass DNA polymerases," *EMBO Journal*, vol. 23, no. 21, pp. 4342–4352, 2004.
- [79] O. J. Becherel and R. P. P. Fuchs, "SOS mutagenesis results from up-regulation of translesion synthesis," *Journal of Molecular Biology*, vol. 294, no. 2, pp. 299–306, 1999.
- [80] K. Schlacher, K. Leslie, C. Wyman, R. Woodgate, M. M. Cox, and M. F. Goodman, "DNA polymerase V and RecA protein, a minimal mutasome," *Molecular Cell*, vol. 17, no. 4, pp. 561–572, 2005.
- [81] K. Schlacher, M. M. Cox, R. Woodgate, and M. F. Goodman, "RecA acts in trans to allow replication of damaged DNA by DNA polymerase V," *Nature*, vol. 442, no. 7105, pp. 883–887, 2006.
- [82] A. Maor-Shoshani and Z. Livneh, "Analysis of the stimulation of DNA polymerase V of *Escherichia coli* by processivity proteins," *Biochemistry*, vol. 41, no. 48, pp. 14438–14446, 2002.
- [83] N. B. Reuven, G. Arad, A. Z. Stasiak, A. Stasiak, and Z. Livneh, "Lesion bypass by the *Escherichia coli* DNA polymerase V requires assembly of a RecA nucleoprotein filament," *Journal of Biological Chemistry*, vol. 276, no. 8, pp. 5511–5517, 2001.
- [84] P. Pham, E. M. Seitz, S. Saveliev et al., "Two distinct modes of RecA action are required for DNA polymerase V-catalyzed translesion synthesis," *Proceedings of the National Academy of Sciences of the United States of America*, vol. 99, no. 17, pp. 11061–11066, 2002.
- [85] Q. Jiang, K. Karata, R. Woodgate, M. M. Cox, and M. F. Goodman, "The active form of DNA polymerase v is UmuD' 2 C-RecA-ATP," *Nature*, vol. 460, no. 7253, pp. 359–363, 2009.
- [86] G. Arad, A. Hendel, C. Urbanke, U. Curth, and Z. Livneh, "Single-stranded DNA-binding protein recruits DNA polymerase V to primer termini on RecA-coated DNA," *Journal of Biological Chemistry*, vol. 283, no. 13, pp. 8274–8282, 2008.
- [87] M. Rajagopalan, C. Lu, R. Woodgate, M. O'Donnell, M. F. Goodman, and H. Echols, "Activity of the purified mutagenesis proteins UmuC, UmuD', and RecA in replicative bypass of an abasic DNA lesion by DNA polymerase III," *Proceedings of the National Academy of Sciences of the United States of America*, vol. 89, no. 22, pp. 10777–10781, 1992.
- [88] R. Woodgate, M. Rajagopalan, C. Lu, and H. Echols, "UmuC mutagenesis protein of *Escherichia coli*: purification and interaction with UmuD and UmuD'," *Proceedings of the National Academy of Sciences of the United States of America*, vol. 86, no. 19, pp. 7301–7305, 1989.
- [89] P. Jonczyk and A. Nowicka, "Specific *in vivo* protein-protein interactions between *Escherichia coli* SOS mutagenesis proteins," *Journal of Bacteriology*, vol. 178, no. 9, pp. 2580–2585, 1996.
- [90] M. Rajagopalan, C. Lu, R. Woodgate, M. O'Donnell, M. F. Goodman, and H. Echols, "Activity of the purified mutagenesis proteins UmuC, UmuD', and RecA in replicative bypass of an abasic DNA lesion by DNA polymerase III," *Proceedings of the National Academy of Sciences of the United States of America*, vol. 89, no. 22, pp. 10777–10781, 1992.

- [91] I. Bruck, R. Woodgate, K. McEuntee, and M. F. Goodman, "Purification of a soluble UmuD'C complex from *Escherichia coli*: cooperative binding of UmuD'C to single-stranded DNA," *Journal of Biological Chemistry*, vol. 271, no. 18, pp. 10767–10774, 1996.
- [92] C. J. Kenyon and G. C. Walker, "DNA-damaging agents stimulate gene expression at specific loci in *Escherichia coli*," *Proceedings of the National Academy of Sciences of the United States of America*, vol. 77, no. 5, pp. 2819–2823, 1980.
- [93] B. S. Strauss, R. Roberts, L. Francis, and P. Pouryazdanparast, "Role of the *dinB* gene product in spontaneous mutation in *Escherichia coli* with an impaired replicative polymerase," *Journal of Bacteriology*, vol. 182, no. 23, pp. 6742–6750, 2000.
- [94] S. Kobayashi, M. R. Valentine, P. Pham, M. O'Donnell, and M. F. Goodman, "Fidelity of *Escherichia coli* DNA polymerase IV. Preferential generation of small deletion mutations by dNTP-stabilized misalignment," *Journal of Biological Chemistry*, vol. 277, no. 37, pp. 34198–34207, 2002.
- [95] J. Wagner, P. Gruz, S.-R. Kim et al., "The *dinB* gene encodes a novel *E. coli* DNA polymerase, DNA pol IV, involved in mutagenesis," *Molecular Cell*, vol. 4, no. 2, pp. 281–286, 1999.
- [96] S.-R. Kim, K. Matsui, M. Yamada, P. Gruz, and T. Nohmi, "Roles of chromosomal and episomal *dinB* genes encoding DNA pol IV in targeted and untargeted mutagenesis in *Escherichia coli*," *Molecular Genetics and Genomics*, vol. 266, no. 2, pp. 207–215, 2001.
- [97] D. F. Jarosz, V. G. Godoy, J. C. Delaney, J. M. Essigmann, and G. C. Walker, "A single amino acid governs enhanced activity of *dinB* DNA polymerases on damaged templates," *Nature*, vol. 439, no. 7073, pp. 225–228, 2006.
- [98] R. Napolitano, R. Janel-Bintz, J. Wagner, and R. P. P. Fuchs, "All three SOS-inducible DNA polymerases (Pol II, Pol IV and Pol V) are involved in induced mutagenesis," *EMBO Journal*, vol. 19, no. 22, pp. 6259–6265, 2000.
- [99] N. Lenne-Samuel, R. Janel-Bintz, A. Kolbanovskiy, N. E. Geacintov, and R. P. P. Fuchs, "The processing of a Benzo(a)pyrene adduct into a frameshift or a base substitution mutation requires a different set of genes in *Escherichia coli*," *Molecular Microbiology*, vol. 38, no. 2, pp. 299–307, 2000.
- [100] J. J. Foti, A. M. DeLucia, C. M. Joyce, and G. C. Walker, "UmuD<sub>2</sub> inhibits a non-covalent step during *dinB*-mediated template slippage on homopolymeric nucleotide runs," *Journal of Biological Chemistry*, vol. 285, no. 30, pp. 23086–23095, 2010.
- [101] P. J. Beuning, S. M. Simon, V. G. Godoy, D. F. Jarosz, and G. C. Walker, "Characterization of *Escherichia coli* translesion synthesis polymerases and their accessory factors," *Methods in Enzymology*, vol. 408, pp. 318–340, 2006.
- [102] H. Ling, F. Boudsocq, R. Woodgate, and W. Yang, "Crystal structure of a Y-family DNA polymerase in action: a mechanism for error-prone and lesion-bypass replication," *Cell*, vol. 107, no. 1, pp. 91–102, 2001.
- [103] M. Gonzalez and R. Woodgate, "The "tale" of umuD and its role in SOS mutagenesis," *BioEssays*, vol. 24, no. 2, pp. 141–148, 2002.
- [104] E. G. Frank, D. G. Ennis, M. Gonzalez, A. S. Levine, and R. Woodgate, "Regulation of SOS mutagenesis by proteolysis," *Proceedings of the National Academy of Sciences of the United States of America*, vol. 93, no. 19, pp. 10291–10296, 1996.
- [105] S. Gottesman, W. P. Clark, V. De Crecy-Lagard, and M. R. Maurizi, "ClpX, an alternative subunit for the ATP-dependent Clp protease of *Escherichia coli*. Sequence and in vivo activities," *Journal of Biological Chemistry*, vol. 268, no. 30, pp. 22618–22626, 1993.
- [106] M. R. Maurizi, W. P. Clark, Y. Katayama et al., "Sequence and structure of Clp P, the proteolytic component of the ATP-dependent Clp protease of *Escherichia coli*," *Journal of Biological Chemistry*, vol. 265, no. 21, pp. 12536–12545, 1990.
- [107] Y.-I. Kim, R. E. Burton, B. M. Burton, R. T. Sauer, and T. A. Baker, "Dynamics of substrate denaturation and translocation by the ClpXP degradation machine," *Molecular Cell*, vol. 5, no. 4, pp. 639–648, 2000.
- [108] S. K. Singh, R. Grimaud, J. R. Hoskins, S. Wickner, and M. R. Maurizi, "Unfolding and internalization of proteins by the ATP-dependent proteases ClpXP and ClpAP," *Proceedings of the National Academy of Sciences of the United States of America*, vol. 97, no. 16, pp. 8898–8903, 2000.
- [109] J. Wang, J. A. Hartling, and J. M. Flanagan, "The structure of ClpP at 2.3 Å resolution suggests a model for ATP-dependent proteolysis," *Cell*, vol. 91, no. 4, pp. 447–456, 1997.
- [110] C. K. Smith, T. A. Baker, and R. T. Sauer, "Lon and Clp family proteases and chaperones share homologous substrate-recognition domains," *Proceedings of the National Academy of Sciences of the United States of America*, vol. 96, no. 12, pp. 6678–6682, 1999.
- [111] M. Gonciarz-Swiatek, A. Wawrzynow, S.-J. Um et al., "Recognition, targeting, and hydrolysis of the λ O replication protein by the ClpP/ClpX protease," *Journal of Biological Chemistry*, vol. 274, no. 20, pp. 13999–14005, 1999.
- [112] J. M. Flynn, S. B. Neher, Y.-I. Kim, R. T. Sauer, and T. A. Baker, "Proteomic discovery of cellular substrates of the ClpXP protease reveals five classes of ClpX-recognition signals," *Molecular Cell*, vol. 11, no. 3, pp. 671–683, 2003.
- [113] K. R. Marshall-Batty and H. Nakai, "trans-targeting of the phage Mu repressor is promoted by conformational changes that expose its ClpX recognition determinant," *Journal of Biological Chemistry*, vol. 278, no. 3, pp. 1612–1617, 2003.
- [114] S. B. Neher, J. M. Flynn, R. T. Sauer, and T. A. Baker, "Latent ClpX-recognition signals ensure LexA destruction after DNA damage," *Genes and Development*, vol. 17, no. 9, pp. 1084–1089, 2003.
- [115] B. M. Burton, T. L. Williams, and T. A. Baker, "ClpX-mediated remodeling of Mu transpososomes: selective unfolding of subunits destabilizes the entire complex," *Molecular Cell*, vol. 8, no. 2, pp. 449–454, 2001.
- [116] J. A. Kenniston, T. A. Baker, J. M. Fernandez, and R. T. Sauer, "Linkage between ATP consumption and mechanical unfolding during the protein processing reactions of an AAA+ degradation machine," *Cell*, vol. 114, no. 4, pp. 511–520, 2003.
- [117] A. W. Karzai, E. D. Roche, and R. T. Sauer, "The SsrA-SmpB system for protein tagging, directed degradation and ribosome rescue," *Nature Structural Biology*, vol. 7, no. 6, pp. 449–455, 2000.
- [118] D. Dulebohn, J. Choy, T. Sundermeier, N. Okan, and A. W. Karzai, "Trans-translation: the tmRNA-mediated surveillance mechanism for ribosome rescue, directed protein degradation, and nonstop mRNA decay," *Biochemistry*, vol. 46, no. 16, pp. 4681–4693, 2007.
- [119] I. Levchenko, R. A. Grant, D. A. Wah, R. T. Sauer, and T. A. Baker, "Structure of a delivery protein for an AAA+ protease in complex with a peptide degradation tag," *Molecular Cell*, vol. 12, no. 2, pp. 365–372, 2003.
- [120] I. Levchenko, M. Seidel, R. T. Sauer, and T. A. Baker, "A specificity-enhancing factor for the ClpXP degradation machine," *Science*, vol. 289, no. 5488, pp. 2354–2356, 2000.

- [121] D. A. Wah, I. Levchenko, T. A. Baker, and R. T. Sauer, "Characterization of a specificity factor for an AAA+ ATPase: assembly of SspB dimers with *ssrA*-tagged proteins and the ClpX hexamer," *Chemistry and Biology*, vol. 9, no. 11, pp. 1237–1245, 2002.
- [122] D. A. Wah, I. Levchenko, G. E. Rieckhof, D. N. Bolon, T. A. Baker, and R. T. Sauer, "Flexible linkers leash the substrate binding domain of SspB to a peptide module that stabilizes delivery complexes with the AAA+ ClpXP protease," *Molecular Cell*, vol. 12, no. 2, pp. 355–363, 2003.
- [123] S. B. Neher, R. T. Sauer, and T. A. Baker, "Distinct peptide signals in the UmuD and UmuD' subunits of UmuD/D' mediate tethering and substrate processing by the ClpXP protease," *Proceedings of the National Academy of Sciences of the United States of America*, vol. 100, no. 23, pp. 13219–13224, 2003.
- [124] M. Gonzalez, F. Rasulova, M. R. Maurizi, and R. Woodgate, "Subunit-specific degradation of the UmuD/D' heterodimer by the ClpXP protease: the role of *trans* recognition in UmuD' stability," *EMBO Journal*, vol. 19, no. 19, pp. 5251–5258, 2000.
- [125] M. Gonzalez, E. G. Frank, A. S. Levine, and R. Woodgate, "Lon-mediated proteolysis of the *Escherichia coli* UmuD mutagenesis protein: *in vitro* degradation and identification of residues required for proteolysis," *Genes and Development*, vol. 12, no. 24, pp. 3889–3899, 1998.
- [126] M. D. Sutton, "Damage signals triggering the *Escherichia coli* SOS response," in *DNA Damage and Recognition*, Y. W. K. Wolfram Seide and P. W. Doetsch, Eds., pp. 781–802, Taylor & Francis, New York, NY, USA, 2006.
- [127] O. J. Becherel, R. P. P. Fuchs, and J. Wagner, "Pivotal role of the  $\beta$ -clamp in translesion DNA synthesis and mutagenesis in *E. coli* cells," *DNA Repair*, vol. 1, no. 9, pp. 703–708, 2002.
- [128] P. J. Beuning, D. Sawicka, D. Barsky, and G. C. Walker, "Two processivity clamp interactions differentially alter the dual activities of UmuC," *Molecular Microbiology*, vol. 59, no. 2, pp. 460–474, 2006.
- [129] K. A. Bunting, S. M. Roe, and L. H. Pearl, "Structural basis for recruitment of translesion DNA polymerase Pol IV/*dinB* to the  $\beta$ -clamp," *EMBO Journal*, vol. 22, no. 21, pp. 5883–5892, 2003.
- [130] P. R. Dohrmann and C. S. McHenry, "A bipartite polymerase-processivity factor interaction: only the internal  $\beta$  binding site of the  $\alpha$  subunit is required for processive replication by the DNA polymerase III holoenzyme," *Journal of Molecular Biology*, vol. 350, no. 2, pp. 228–239, 2005.
- [131] D. Jeruzalmi, O. Yurieva, Y. Zhao et al., "Mechanism of processivity clamp opening by the delta subunit wrench of the clamp loader complex of *E. coli* DNA polymerase III," *Cell*, vol. 106, no. 4, pp. 417–428, 2001.
- [132] F. J. López de Saro and M. O'Donnell, "Interaction of the  $\beta$  sliding clamp with MutS, ligase, and DNA polymerase I," *Proceedings of the National Academy of Sciences of the United States of America*, vol. 98, no. 15, pp. 8376–8380, 2001.
- [133] M. Kurz, B. Dalrymple, G. Wijffels, and K. Kongsuwan, "Interaction of the sliding clamp  $\beta$ -subunit and Hda, a DnaA-related protein," *Journal of Bacteriology*, vol. 186, no. 11, pp. 3508–3515, 2004.

## Research Article

# Error-Prone Translesion DNA Synthesis by *Escherichia coli* DNA Polymerase IV (DinB) on Templates Containing 1,2-dihydro-2-oxoadenine

Masaki Hori,<sup>1</sup> Shin-Ichiro Yonekura,<sup>1,2</sup> Takehiko Nohmi,<sup>3</sup> Petr Gruz,<sup>3</sup> Hiroshi Sugiyama,<sup>4</sup> Shuji Yonei,<sup>1</sup> and Qiu-Mei Zhang-Akiyama<sup>1</sup>

<sup>1</sup>Laboratory of Stress Response Biology, Graduate School of Science, Kyoto University, Kitashirakawa-Oiwakecho, Sakyo-ku, Kyoto 606-8502, Japan

<sup>2</sup>Institute of Molecular and Cellular Biosciences, The University of Tokyo, Yayoi, Bunkyo-ku, Tokyo 113-0032, Japan

<sup>3</sup>Division of Genetics and Mutagenesis, National Institute of Health Science, 1-18-1, Kamiyoga, Setagaya-ku, Tokyo 158-8501, Japan

<sup>4</sup>Laboratory of Biological Chemistry, Graduate School of Science, Kyoto University, Kitashirakawa-Oiwakecho, Sakyo-ku, Kyoto 606-8502, Japan

Correspondence should be addressed to Qiu-Mei Zhang-Akiyama, qmzhang@kingyo.zool.kyoto-u.ac.jp

Received 13 May 2010; Revised 14 July 2010; Accepted 5 August 2010

Academic Editor: Ashis Basu

Copyright © 2010 Masaki Hori et al. This is an open access article distributed under the Creative Commons Attribution License, which permits unrestricted use, distribution, and reproduction in any medium, provided the original work is properly cited.

*Escherichia coli* DNA polymerase IV (Pol IV) is involved in bypass replication of damaged bases in DNA. Reactive oxygen species (ROS) are generated continuously during normal metabolism and as a result of exogenous stress such as ionizing radiation. ROS induce various kinds of base damage in DNA. It is important to examine whether Pol IV is able to bypass oxidatively damaged bases. In this study, recombinant Pol IV was incubated with oligonucleotides containing thymine glycol (dTg), 5-formyluracil (5-fodU), 5-hydroxymethyluracil (5-hmdU), 7,8-dihydro-8-oxoguanine (8-oxodG) and 1,2-dihydro-2-oxoadenine (2-oxodA). Primer extension assays revealed that Pol IV preferred to insert dATP opposite 5-fodU and 5-hmdU, while it inefficiently inserted nucleotides opposite dTg. Pol IV inserted dCTP and dATP opposite 8-oxodG, while the ability was low. It inserted dCTP more effectively than dTTP opposite 2-oxodA. Pol IV's ability to bypass these lesions decreased in the order: 2-oxodA > 5-fodU ~ 5-hmdU > 8-oxodG > dTg. The fact that Pol IV preferred to insert dCTP opposite 2-oxodA suggests the mutagenic potential of 2-oxodA leading to A:T → G:C transitions. Hydrogen peroxide caused an ~2-fold increase in A:T → G:C mutations in *E. coli*, while the increase was significantly greater in *E. coli* overexpressing Pol IV. These results indicate that Pol IV may be involved in ROS-enhanced A:T → G:C mutations.

## 1. Introduction

In recent years, novel types of DNA polymerase have been characterized in prokaryotes and eukaryotes. They share significant amino acid sequence identity and are characterized by their low fidelity and low processivity of DNA synthesis [1–3] and are classified as Y-family DNA polymerases. These DNA polymerases have the ability to catalyze synthesis past DNA lesions that otherwise block replication [1–3]. This process is termed translesion DNA synthesis (TLS). Y-family DNA polymerases have been identified in nearly all organisms. In *Escherichia coli*, two DNA polymerases, Pol IV and Pol V, have been classified into the Y-family polymerases

[1–4]. They are induced in the SOS response when *E. coli* cells encounter environmental stresses such as UV light and are involved in induction of mutations [4–8].

The *dinB* gene product has been shown to possess DNA synthesizing activity and is named DNA polymerase IV (Pol IV) [4]. Recent studies revealed an important role of the Y family of DNA polymerases in tolerance mechanisms towards various types of DNA damage [1–3, 9–11]. Napolitano et al. [7] found that Pol IV is able to bypass benzo(α)pyrene-adducts in DNA via both error-free and error-prone pathways. Jarosz et al. [9] reported that Pol IV is responsible for TLS over potentially lethal nitrofurazone-induced DNA adducts. In addition, Pol IV can synthesize

accurately across N2-furfuryl-guanine lesions. Recently, Yuan et al. [10] found that Pol IV efficiently and accurately bypassed N2-(1-carboxyethyl)-2'-deoxyguanosine, one of the major byproducts of the glycolysis pathway. Furthermore, Pol IV has the ability to bypass acrolein-mediated guanine DNA-peptide crosslinks [11]. These findings indicate that Pol IV contributes to the replicative bypass of lesions that block synthesis by replicative DNA polymerases and thereby helps to minimize the generation of DNA strand breaks, chromosome aberrations, and cell death.

In aerobic organisms, reactive oxygen species (ROS) are continuously produced during normal metabolism and by exogenous agents such as ionizing radiation. ROS react with DNA, proteins, and lipids and thereby cause harmful effects on cells. When cellular DNA is attacked by ROS, various types of DNA damage are generated [12–15] and might be involved in aging and many diseases including cancer [14, 15]. Oxidatively damaged bases produced by ROS have abnormal structures that induce several kinds of biological consequences. Bacterial and eukaryotic cells have DNA repair systems to remove damaged bases and restore DNA to its normal sequence [12, 16, 17]. If unrepaired, damaged bases would block DNA replication or cause the insertion of “incorrect” nucleotides opposite the lesion to form mismatches.

In this study, we examined whether Pol IV can bypass oxidatively damaged bases and is involved in mutation induction at the damaged sites. The primer extension assay revealed that Pol IV did not bypass the thymine glycol-(dTg-) containing DNA, while Pol IV preferred to insert dATP opposite 5-formyluracil (5-fodU) and 5-hydroxymethyluracil (5-hmdU), major oxidative products of thymine. dCTP and dATP were inserted opposite 7,8-dihydro-8-oxoguanine (8-oxodG) but the insertion ability was low. Pol IV more efficiently inserted dCTP than dTTP opposite 1,2-dihydro-2-oxoadenine (2-oxodA) in the template DNA, suggesting the mutagenic potential of 2-oxodA leading to A:T → G:C mutations. Pol IV's ability to handle these lesions decreased in the order: 2-oxodA > 5-fodU~5-hmdU > 8-oxodG > dTg. It was also found that hydrogen peroxide treatment caused an increase in A:T → G:C mutations in *E. coli*, while the increase was significantly greater in *E. coli* overexpressing Pol IV. These results indicate that Pol IV may be involved in these ROS-enhanced A:T → G:C mutations.

## 2. Materials and Methods

**2.1. Chemicals and Enzymes.** Ampicillin and isopropyl-β-D-thiogalactopyranoside (IPTG) were purchased from Wako Pure Chemicals (Osaka, Japan). T4 polynucleotide kinase, Taq DNA polymerase, and restriction enzymes were obtained from Takara Shuzo (Kyoto, Japan) and Toyobo (Osaka, Japan). [ $\gamma$ -<sup>32</sup>P]ATP (>148 TBq/mmol) was obtained from ICN Biomedicals Inc. (Costa Mesa, CA). Columns used for column chromatography and high performance liquid chromatography (HPLC) were purchased from Pharmacia (Uppsala, Sweden).

**2.2. Synthesis of Substrate Oligonucleotides Containing Oxidatively Damaged Bases.** 24-mer oligonucleotide containing 2-oxodA was synthesized as previously described by Sugiyama et al. [18]. 24-mer oligonucleotide containing dTg was synthesized as described by Dianov et al. [17]. 22-mer oligonucleotides containing 5-fodU and 5-hmdU were synthesized and purified as previously described [19]. 24-mer oligonucleotides containing 8-oxodG was obtained from Trevigen (Gaithersburg, MD). The structures of the studied oxidatively damaged bases are illustrated in Figure 1. Primers were synthesized and purified by Takara Shuzo (Kyoto, Japan). The nucleotide sequences of template and primer oligonucleotides used in this study are shown in Table 1.

**2.3. Expression and Purification of Pol IV with Histidine Tag.** Pol IV was overproduced and purified from *E. coli* BL21(DE3)/pLysS carrying pET16B-DinB, as described by Wagner et al. [4]. The cells were grown in M9 minimal medium containing 50 μg/mL ampicillin and 30 μg/mL chloramphenicol. Overnight cultures (5 mL) were inoculated into 500 mL of prewarmed LB medium containing 50 μg/mL ampicillin. The culture was incubated with shaking at 37°C until the optical density at 600 nm reached about 0.9, and expression of the proteins was induced by adding IPTG to a final concentration of 1 mM. After 30 min of incubation at 30°C, rifampicin was added to a final concentration of 100 μg/mL, and incubation was continued for an additional 3 hr at 30°C. *E. coli* cells were then harvested, washed once in ice-cold buffer A (50 mM Tris-HCl (pH 8.0), 300 mM NaCl and 20 mM imidazole), resuspended in a total volume of 8 mL of the same buffer, and frozen in dry ice/ethanol bath. Frozen cells were thawed and supplemented with 1 mg of chicken egg lysozyme, 0.4 mg of pefabloc SC, and β-mercaptoethanol (EtSH) to a final concentration of 20 mM. Chromosomal DNA was sheared by sonication, and lysates were treated with DNase I at 40 mg/mL and RNase TI at 130 U/mL for 10 min at room temperature. The final volume was then adjusted to 15 mL with buffer A supplemented with 20 mM EtSH, and the cell lysate was cleared by centrifugation at 13,000 × g. The supernatant was applied to a 2-mL column connected to a FPLC system. The column was washed with 20 mL of NaCl and then developed with a linear gradient of imidazole up to 1 M. DinB protein started to elute at approximately 300 mM imidazole. Fractions containing His-tag DinB were combined and concentrated to about 2.6 mL containing 5.6 mg/mL His-tag DinB (fraction 2). Fraction 2 was then applied to a Superdex 75 XK 16/60 column connected to an FPLC system equilibrated with 20 mM HEPES (pH 7.4), 150 mM NaCl, 0.1 mM EDTA, 10% w/v glycerol, and 1 mM dithiothreitol (DTT). Fractions corresponding to the DinB peak, which eluted at an approximate molecular weight of 32 kDa, were combined together to give a total volume of 3 mL containing 8 mg of pure HT-dinB. The purified protein was stored at -80°C.

**2.4. In Vitro DNA Synthesis.** Primers were labeled at the 5'-end with [ $\gamma$ -<sup>32</sup>P]ATP by T4 polynucleotide kinase and annealed with the appropriate template oligonucleotides.

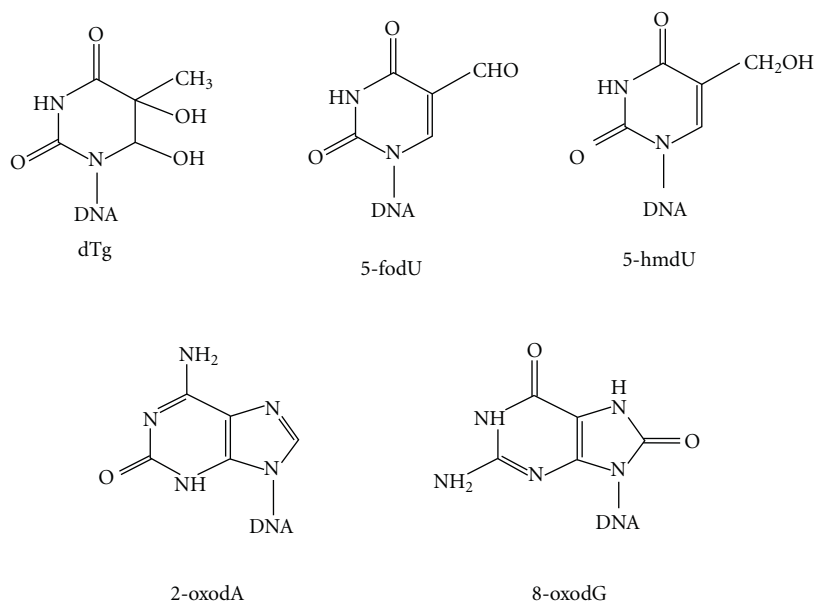


FIGURE 1: The structures of the studied oxidatively damaged bases, thymine glycol (dTg), 5-formyluracil (5-fodU), 5-hydroxymethyluracil (5-hmdU), 1,2-dihydro-2-oxoadenine (2-oxodA), and 7,8-dihydro-8-oxoguanine (8-oxodG).

TABLE 1: Nucleotide sequences of oligonucleotides used in this study.

Template 1	3'-CGTCGGGCCCCCTA <u>A</u> GTGATCAAG-5'
Template 2	3'-CGTCGGGCCCCCTA <u>2</u> GTGATCAAG-5'
Template 3	3'-CGTCGGGCCCCCTA <u>G</u> GTGATCAAG-5'
Template 4	3'-CGTCGGGCCCCCTA <u>8</u> GTGATCAAG-5'
Template 5	3'-ACGTCCAGCTCACATC <u>T</u> CCTAG-5'
Template 6	3'-ACGTCCAGCTCACATC <u>F</u> CCTAG-5'
Template 7	3'-ACGTCCAGCTCACATC <u>H</u> CCTAG-5'
Template 8	3'-CGACGGGCCCCCA <u>A</u> TGAGAACAAG-5'
Template 9	3'-CGACGGGCCCCCA <u>X</u> GAGAACAAG-5'
Primer 1	5'- <sup>32</sup> P-GCTGCCCGGGGGTT-3'
Primer 2	5'- <sup>32</sup> P-TGCAGGTCGACTCTAG-3'
Primer 3	5'- <sup>32</sup> P-GCAGCCCGGGGGAT-3'

2, F, H, 8, and X represent 1,2-dihydro-2-oxoadenine (2-oxodA), 5-formyluracil (5-fodU), 5-hydroxymethyluracil (5-hmdU), 7,8-dihydro-8-oxoguanine (8-oxodG), and thymine glycol (dTg), respectively.

The substrates thus prepared were incubated with purified Pol IV in a reaction mixture (10  $\mu$ l) containing 30 mM  $\text{KH}_2\text{PO}_4$  (pH 7.4), 7.5 mM  $\text{MgCl}_2$ , 1 mM DTT, 5 mM NaCl, 0.1 mg/mL BSA, 5% glycerol, and 150 mM of the specified deoxyribonucleotide(s). The amount of Pol IV and incubation time are described in the figure legends. After incubation at 20°C, the reaction was terminated by addition of stop solution (95% formamide, 20 mM EDTA, 0.1% bromophenol blue, and 0.1% xylene cyanol). The samples were then heated at 95°C for 5 min, and immediately cooled on ice and then loaded onto 20% polyacrylamide gels in 90 mM Tris-borate (pH 8.3) containing 7 M urea and 2 mM EDTA. After electrophoresis at 1,300 V, the gels were dried

and autoradiographed using Fuji RX films at  $-80^\circ\text{C}$ . The intensity of each band was determined using an imaging analyzer (Fuji BAS 1800II).

**2.5. In Vivo Mutagenesis.** Single colonies of *E. coli* CC101, CC105, and CC106 [20] transformed with a plasmid encoding wild-type pDinB or a mutant Pol IV (pDinB003) [4] were inoculated into a minimal glucose medium containing 50  $\mu\text{g}/\text{mL}$  of ampicillin and incubated at 37°C for 40 hr. The mutant Pol IV was generated by site-specific mutagenesis replacing aspartic acid in position 103 with asparagine [4]. The cultures were centrifuged, resuspended in the same medium with 1 mM of IPTG, and further incubated for 5 hr at 37°C. Hydrogen peroxide ( $\text{H}_2\text{O}_2$ ) was added to the cultures at a final concentration of 10 mM, followed by incubation at 37°C for 1 hr. The cultures were centrifuged, washed, and resuspended in prewarmed LB medium. After incubation to stationary phase and appropriate dilution, the cell suspensions were spread on both duplicate minimal lactose plates and minimal glucose plates for the detection of lactose-fermenting ( $\text{Lac}^+$ ) revertants and viable cells, respectively. Mutant colonies on the plate were counted after incubation overnight. The mutation frequency was expressed as number of mutants/ $10^8$  viable cells.

### 3. Results

**3.1. Replication of DNA Containing dTg by Pol IV.** In this study, primer extension assays were performed with Pol IV purified by affinity chromatography to examine whether Pol IV could bypass oxidatively damaged bases. Oligonucleotides containing dTg, 5-fodU, 5-hmdU, 8-oxodG, or 2-oxodA (Table 1) were annealed to appropriate primers and

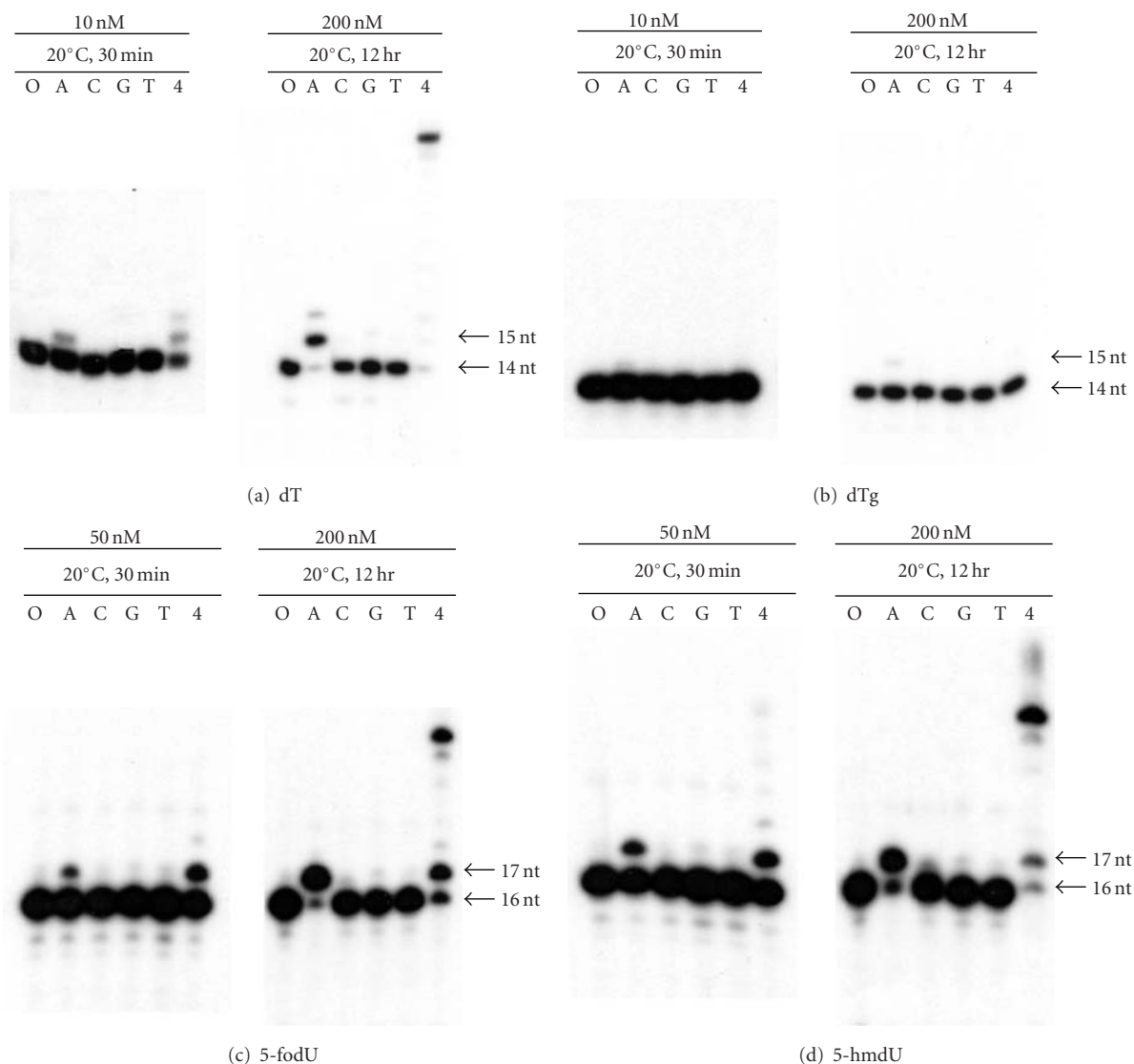


FIGURE 2: Primer extension assay for Pol IV to bypass dTg, 5-fodU, and 5-hmdU in the template oligonucleotides. Primers were labeled at the 5'-terminal by polynucleotide kinase and annealed with appropriate template oligonucleotide. Primer/templates (50 fmol) in a 10- $\mu$ l reaction mixture was incubated at 20°C with purified Pol IV at 50 nM for 30 min (left) and at 200 nM for 12 hr (right), followed by polyacrylamide gel electrophoresis. (a) dT (primer 1/template 8), (b) dTg (primer 1/template 9), (c) 5-fodU (primer 2/template 6), and (d) 5-hmdU (primer 2/template 7).

incubated with purified Pol IV. Pol IV was added to the reaction mixture at 50 and 200 nM.

dTg is a major oxidative product of thymine in DNA and blocks DNA synthesis by most DNA polymerases [12, 15]. However, certain TLS polymerases such as a human Pol Nu can occasionally bypass dTg and thereby continue DNA replication beyond the lesion [12, 21–23]. Hence, it was of interest to examine whether Pol IV has the ability to bypass dTg. In this study, we prepared oligonucleotide containing dTg by osmium tetroxide treatment [17]. Pol IV replicated the oligonucleotides containing undamaged thymine (Figure 2(a)). As shown in Figure 2(b), we could not detect the insertion of dNTPs opposite the lesion, while a faint band of dATP inserted was seen when the oligonucleotide was incubated with Pol IV reacted at 200 nM for 12 hr.

**3.2. Insertion of dATP and dCTP opposite 8-oxodG in the Template DNA by Pol IV.** 8-oxodG is a major oxidative product of guanine and has high miscoding potential [12–16, 24]. Replicative DNA polymerases insert dATP as frequently as dCTP opposite 8-oxodG in the template. Therefore, G:C  $\rightarrow$  T:A transversions occur at the site of 8-oxodG [12–16].

In this study, when Pol IV was incubated at 50 nM with the template oligonucleotide containing 8-oxodG for 30 min, no nucleotides were inserted opposite the lesion. However, when added at 200 nM and incubated with the substrate for 12 hr, Pol IV inserted both dCTP and dATP opposite 8-oxodG (Figure 3(a)). These results indicate that Pol IV could bypass over 8-oxodG through both error-free and error-prone processes. However, the Pol IV's insertion ability was very low.

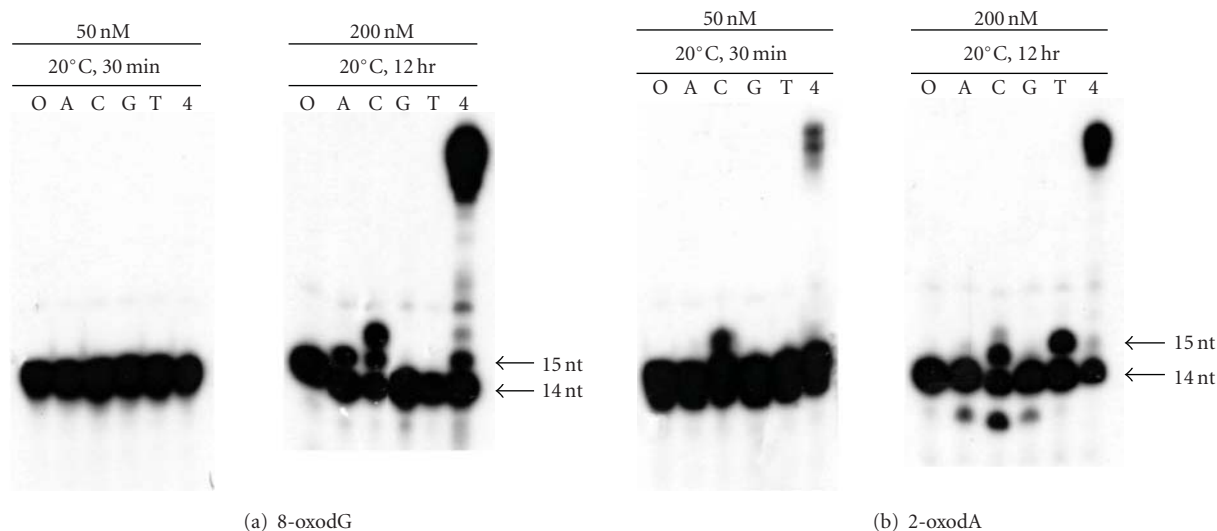


FIGURE 3: Primer extension assay for Pol IV to bypass 8-oxodG and 2-oxodA in the template oligonucleotide. Primer 3 was labeled at the 5'-terminal by polynucleotide kinase and annealed with appropriate template oligonucleotides. Primer 3/templates (50 fmol) in a 10- $\mu$ l reaction mixture were incubated at 20°C with purified Pol IV at 50 nM for 30 min (left) and at 200 nM for 12 hr (right), followed by polyacrylamide gel electrophoresis. (a) 8-oxodG (primer 3/template 4), (b) 2-oxodA (primer 3/template 2).

3.3. *Replication of DNA Containing 5-fodU and 5-hmdU by Pol IV.* 5-fodU and 5-hmdU are major products of oxidative damage of the methyl group of thymine [12, 19, 25]. Attack of hydroxyl radicals on the 5-methyl group generates 5-hydroperoxymethyluracil, the most stable thymine hydroperoxide [12]. It decomposes to the more stable products 5-fodU and 5-hmdU [12, 25]. Recent studies showed that 5-fodU is a potentially mutagenic lesion [25, 26]. It directs insertion of mismatched bases opposite the lesion during DNA synthesis *in vitro* [27]. We previously showed that Klenow fragment with and without 3'  $\rightarrow$  5' exonuclease (KFexo<sup>+</sup> and KFexo<sup>-</sup>, resp.), *Thermus thermophilus* (Tth) DNA polymerase (exonuclease-deficient) and *Pyrococcus furiosus* (Pfu) DNA polymerase (exonuclease-proficient) read through the site of 5-fodU in the template [27]. 5-fodU directs insertion of dCMP and dGMP in addition to dATP opposite the lesion by these DNA polymerases. Furthermore, KFexo<sup>-</sup> and Tth can bypass the 5-hmdU template via the insertion of dAMP opposite the 5-hmdU [27].

The primer extension assays for the templates containing 5-fodU and 5-hmdU showed that Pol IV preferred to insert dATP opposite 5-fodU and 5-hmdU, while other dNTP insertions were <5% (Figures 2(c) and 2(d)). Pol IV synthesized full-length duplex 22-mer oligonucleotides when added at 200 nM and incubated for 12 hr (Figures 2(c) and 2(d)).

3.4. *Bypass of 2-oxodA by Pol IV.* 2-oxodA is a common product of adenine generated by ROS [12, 28]. Previous studies showed that replicative DNA polymerases and KFexo<sup>-</sup> mainly insert dATP and dGTP opposite 2-oxodA during DNA synthesis *in vitro* [12, 29, 30]. It is important to elucidate the mechanism of bypass 2-oxodA by Pol IV.

TABLE 2: The insertion kinetics of dCTP and dTTP opposite 1,2-dihydro-2-oxoadenine (2-oxodA) by Pol IV.

Substrate	Km (fmol/ mL /min)	$V_{max}$ (min <sup>-1</sup> )	$k_{cat}$	$k_{cat}/Km$
dCTP	8.5	217.4	$4.4 \times 10^{-3}$	$5.2 \times 10^{-4}$
dTTP	25.6	42.9	$8.6 \times 10^{-4}$	$3.4 \times 10^{-5}$

Primer 3 was labeled at the 5'-terminal by polynucleotide kinase and annealed with appropriate template oligonucleotides. Primer 3/template 2 (50 fmol) in a 10- $\mu$ l reaction mixture was incubated at 20°C for 60 min with purified Pol IV (50 nM) in the presence of dTTP or dCTP at various concentrations (0.02~500  $\mu$ M), followed by polyacrylamide gel electrophoresis.

2-oxodA significantly reduced the rate of DNA synthesis by KFexo<sup>-</sup> (data not shown). When incubated with templates containing 2-oxodA, Pol IV inserted both dTTP and dCTP opposite 2-oxodA. It was evident that Pol IV inserted dCTP more efficiently than dTTP (Figure 3(b)). The results were obtained by a comparison of the full-length products obtained by *in vitro* DNA synthesis in the presence of the four nucleotides. We determined the insertion kinetics of Pol IV for dTTP and dCTP opposite 2-oxodA. Comparing the  $k_{cat}/Km$  values revealed that Pol IV inserted dCTP opposite 2-oxodA with nearly 30 fold greater catalytic efficiency than dTTP (Table 2). It is suggested that 2-oxodA in DNA induces A:T  $\rightarrow$  G:C transitions.

3.5. *Overexpression of Pol IV Causes A:T  $\rightarrow$  G:C Transitions In Vivo.* To clarify the roles of Pol IV in mutation induction *in vivo*, we carried out the *in vivo* mutagenesis assay with *E. coli* strains bearing a F'lac containing a *lacZ* allele, which codes for inactive  $\beta$ -galactosidase [20]. Unless base

TABLE 3: Frequencies of mutations to Lac<sup>+</sup> in *E. coli* CC101~CC106 strains with overexpressed *dinB* gene after incubation with hydrogen peroxide.

Strain	Base substitution	Plasmid	Mutants/10 <sup>8</sup> viable cells		Increase in mutation frequency (b – a)	Fold increase in mutation frequency (b/a)
			No H <sub>2</sub> O <sub>2</sub> <sup>a</sup>	10 mM H <sub>2</sub> O <sub>2</sub> <sup>b</sup>		
CC101	A:T → C:G	pDinB	1.9	4.2	2.3	2.2
		pDinB003	1.5	1.8	0.3	1.2
CC105	A:T → T:A	pDinB	3.6	4.4	0.8	1.2
		pDinB003	1.5	3.4	1.9	2.3
CC106	A:T → G:C	pDinB	1.1	11.6	10.5	10.5
		pDinB003	0.8	1.8	1.0	2.3

*E. coli* CC101, CC105, and CC106 transformed with a plasmid wild-type plasmid (pDinB) and a mutant Pol IV (pDinB003) in stationary phase were incubated at 37°C with 1 mM of IPTG for 5 hr, followed by the treatment 10 mM H<sub>2</sub>O<sub>2</sub> for 1 hr. The mutant Pol IV (DinB003) was generated by site-specific mutagenesis replacing aspartic acid in position 103 with asparagine [4]. The mutation frequency was expressed as number of mutants/10<sup>8</sup> viable cells.

substitution mutations occur, these *E. coli* cells cannot grow on lactose minimal medium. To determine the type of base substitutions caused by overexpression of Pol IV, we constructed *E. coli* CC101, CC105, and CC106 strains [20] with pDinB or a mutant Pol IV [4], where these *dinB* genes were overexpressed. The mutant Pol IV was generated by site-specific mutagenesis replacing aspartic acid in position 103 with asparagine [4].

2-oxodA has been shown to occur in DNA by treatment of cells with hydrogen peroxide (H<sub>2</sub>O<sub>2</sub>) [12, 28]. Hence, the *E. coli* cells were exposed to H<sub>2</sub>O<sub>2</sub> and the Lac<sup>+</sup> reversion frequency was measured. Compared with CC101 and CC105, CC106 with the pDinB plasmid showed a significant increase in the frequency of Lac<sup>+</sup> reversions when exposed to hydrogen peroxide (Table 3). Hydrogen peroxide treatment caused an ~2-fold increase in A:T → G:C mutations in *E. coli*, while the increase was significantly greater (~10-fold) in *E. coli* overexpressing Pol IV. The overexpression of Pol IV had its greater effect on A:T → G:C mutations than A:T → C:G and A:T → T:A mutations. The enhancement of A:T → G:C mutations depended on the Pol IV ability, since the expression of a mutant Pol IV lacking the polymerase activity did not increase the mutation frequency in *E. coli* CC106 exposed to H<sub>2</sub>O<sub>2</sub>. As *E. coli* CC106 can reverse Lac<sup>+</sup> only through A:T → G:C transitions [20], these results indicate that A:T → G:C transitions are induced via an error-prone translesion DNA synthesis by Pol IV in *E. coli* cells.

#### 4. Discussion

Recent progress in research about novel types of DNA polymerase in prokaryotes and eukaryotes has given us much information about the mechanism of bypass replication of damaged bases in DNA and mutation induction. DNA polymerases of the Y-family are involved in translesion DNA synthesis [1–3, 7–11]. Replication prevention is caused by base modifications induced by various DNA-damaging agents, such as ROS [1–3, 12, 15, 29, 30]. Purine and pyrimidine bases in DNA are easily oxidized by ROS, which leads to abnormal DNA behavior, including DNA replication prevention. In addition, damaged bases induce several types

of mutations, including base substitutions. Replication errors must occur at the sites of damaged bases to be fixed as mutations. Certain TLS DNA polymerases, such as Pol IV, catalyze the insertion of nucleotides opposite damaged bases and thereby may play a role in mutation induction [4–8]. Continuing of DNA replication beyond the lesion is required for maintenance of the genome integrity.

dTg blocks DNA synthesis by many prokaryotic and eukaryotic DNA polymerases one nucleotide before and opposite the lesion site [12, 15, 31]. On the other hand, some DNA polymerases inefficiently insert noncognate nucleotides opposite dTg [12, 22]. DNA polymerase  $\eta$  and  $\kappa$  are able to continue synthesis after having inserted dATP opposite the lesion [12, 21–23]. Pol  $\zeta$  also contributes to the bypass of dTg as well as other lesions that block synthesis by replicative DNA polymerases [32]. In contrast, Pol IV did not have the ability to bypass dTg (Figure 2(b)).

There are four diastereomers of dTg [31, 33]. dTg exists in solution as either the 5R *cis-trans* pair or the 5S *cis-trans* pair, due to epimerization at the C<sub>6</sub> position. The bypass over dTg by Y-family DNA polymerases is stereospecific [21–23, 32]. Pol  $\zeta$  bypasses the 5R epimers more efficiently [32], while Pol  $\kappa$  bypasses the 5S epimers more efficiently [22]. Pol Nu has been shown to be particularly adept at efficient and accurate translesion DNA synthesis past a 5S-thymine glycol [21].

8-oxodG is not a replicative block for replicative DNA polymerases, which incorporate dATP as frequently as dCTP opposite 8-oxodG in the template [12–16, 24]. As a result, G:C → T:A transversions occur at the site of 8-oxoG. We showed here that Pol IV inserted dATP opposite 8-oxoG in the template, but the insertion efficiency was very low (Figure 3(a)). These results indicate that Pol IV preferred to insert dCTP opposite 8-oxodG. Recently, Maga et al. [34] also reported that DNA polymerases  $\lambda$  and  $\eta$  can bypass 8-oxodG by insertion of dCTP opposite 8-oxodG in the template. Therefore, it is likely that these Pols are a principal player in mutation induction by template 8-oxodG.

Oxidation of the 5-methyl group of thymine produces the stable products 5-fodU and 5-hmdU in DNA [12, 25]. When 5-fodU is produced in a template DNA, base substitutions are induced at the site of the lesion [25, 26].

We previously showed that 5-fodU is removed from DNA in *E. coli* by three DNA glycosylases, MutM, endonuclease III (Nth), and endonuclease VIII [35]. The frequency of spontaneous mutations is significantly enhanced in *E. coli* *mutM nth nei* triple mutant compared with the wild-type strain [35]. The results in Figure 2(c) demonstrate, for the first time, that if 5-fodU remains in the template strand, Pol IV prefers to insert dATP opposite the lesion and hence induces no mutations.

5-hmU directs the insertion of only dATP during normal DNA replication [12, 15, 27]. The present results indicate that Pol IV preferred to insert dATP at the site of 5-hmdU (Figure 2(d)) and as a result does not make base substitutions. The results are in accord with the finding that a *Bacillus subtilis* bacteriophage (SPO1) has 5-hmdU in its DNA instead of thymine and 5-hmdU:dA base-pairs show the same behavior as T:A [36]. On the other hand, *E. coli* and mammalian cells have DNA glycosylases that remove 5-hmdU from DNA [12, 37, 38]. Why do cells possess repair enzymes for 5-hmdU that forms stable base pairs with adenine? There is another pathway of 5-hmdU generation: oxidation and deamination of 5-methylcytosine (5-mdC). 5-mC occurs naturally in DNA as a product of cytosine methylation [37]. Therefore, a normal base pair between 5-mdC and dG generates a mismatched base pair of 5-hmdU:dG, which would cause 5-mC (C):G to T:A transitions. Recently, we found that a 5-hmdU DNA glycosylase activity of MutM and Nth removes 5-hmdU from 5-hmdU:dG mispairs with 37~58 times greater efficiency, respectively, than that from 5-hmdU:dA base pairs [38].

2-oxodA (isoguanine) is a common lesion of adenine produced by ROS and ionizing radiation. It is a replicative block for several DNA polymerases [12]. However, 2-oxodA has a mutational potential comparable to that of 8-oxodG in bacteria and mammalian cells. Barone et al. [39] found that insertion opposite 2-oxodA is difficult for both K<sub>1</sub>Exo<sup>-</sup> and the replicative Pol  $\alpha$ . A template 2-oxodA might cause a transient replication block, thereby provoking recruitment of TLS polymerases. Archeal Dpo4 is efficient to insert nucleotides opposite 2-oxodA, while human Pol  $\eta$  inefficient [39]. Replication of a template 2-oxodA by these polymerases is mutagenic and causes base substitutions. On the other hand, Crespan et al. [40] showed that 2-oxodA can be efficiently and faithfully bypassed by a human DNA Pol  $\lambda$  in combination with proliferating cell nuclear antigen (PCNA) and replication protein A (RP-A). Thus, the efficiency and fidelity of TLS on the 2-oxodA template depend upon the DNA polymerase used.

We found that “incorrect” dCTP was effectively incorporated opposite 2-oxodA by Pol IV (Figure 3(b)), suggesting a stable base pair between 2-oxodA and dC. Thermodynamic analysis also showed that 2-oxodA forms a stable base pair with cytosine, guanine, and thymine, and to a lesser extent with adenine [18, 39]. The base-pairing scheme of 2-oxodA (isoguanine):dC has been postulated [41]. 2-oxodA:dC is a potent inducer of parallel-stranded DNA duplex structure. All imino protons associated with the 2-oxodA:dC basepairs are consistent with the formation of a stable duplex suggested by  $T_m$  measurements [18]. 2-oxodA might form stable

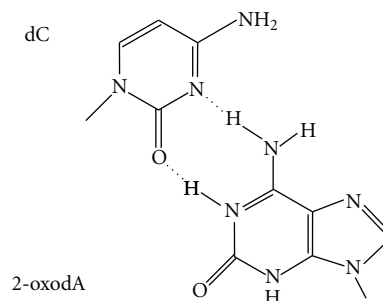


FIGURE 4: Possible wobble structure for base pairing of the 1,2-dihydro-2-oxoadenine (2-oxodA):dC.

reverse Watson-Crick basepair with the normal dC [41]. However, the base pairing would not be present in the active site of a DNA polymerase, as the sugar-triphosphate moiety could not fit properly in the active site. Even if it could fit, the sugar-triphosphate moiety would not be properly oriented for catalysis. Alternatively, a wobble structure with two hydrogen bonds is possible as shown in Figure 4. No equivalent structure is possible for 2-oxodA:dT.

2-oxodA is as mutagenic as 8-oxodG when a double-stranded shuttle vector DNA containing 2-oxodA is replicated in *E. coli* and mammalian cells. Bypass of 2-oxodA results in the formation of A:T  $\rightarrow$  G:C transitions and A:T  $\rightarrow$  T:A transversions during leading strand synthesis [12, 29, 30]. Moreover, we observed here that a template 2-oxodA directs the insertion of “incorrect” dCTP more efficiently than that of “correct” dTTP (Figure 3(b)) *in vitro*. Based on this together with the *in vivo* mutagenesis data (Table 3), we conclude that Pol IV has the ability to bypass 2-oxodA and induce A:T  $\rightarrow$  G:C transitions at the site of 2-oxodA. Pol IV overexpression has its greater effect on A:T  $\rightarrow$  G:C mutations than A:T  $\rightarrow$  C:G and A:T  $\rightarrow$  T:A mutations. The facts may reflect that Pol IV is accurately handling a lesion leading A:T  $\rightarrow$  C:G and A:T  $\rightarrow$  T:A mutations that some other DNA Pol tends to handle inaccurately. To prevent mutation induction, *E. coli* MutY and human MUTYH proteins have been shown to remove 2-oxodA from double-stranded DNA *in vitro* [42, 43].

The generation of 2-oxodA in double-stranded DNA by a Fenton-like reagent is less efficient than 8-oxodG [12, 30]. On the other hand, the yield of 2-oxodA is similar to that of 8-oxodG in the monomeric form [12, 30]. Thus, it is likely that most 2-oxodA that occurs in DNA arises through insertion of 2-oxo-dATP generated in the nucleotide pool. 2-oxo-dATP is inserted opposite G and T in the template by DNA polymerase III and DNA polymerase I *in vitro* [30, 44, 45]. On the other hand, calf thymus Pol  $\alpha$  inserts 2-oxo-dATP opposite noncognant C in addition to cognant T, which would cause induction of G:C  $\rightarrow$  A:T transitions *in vivo*. Hydrogen peroxide treatment caused a ~2-fold increase in A:T  $\rightarrow$  G:C mutations in *E. coli*, while the increase was significantly greater (~10-fold) in *E. coli* overexpressing Pol IV (Table 3). These results indicate that Pol IV may involved in these ROS-enhanced A:T  $\rightarrow$  G:C mutations. It is also likely that the UmuDC gene products may play a critical role in the

mutagenesis by damaged nucleotides, such as 2-oxodA, that block DNA replication.

Pol IV is relatively efficient on 2-oxodA, 5-fodU and 5-hmdU, but inefficient on dTg and 8-oxodG. Of these five lesions, Pol IV is most efficient with 2-oxodA. In 2-oxodA the  $\text{-C=O}$  is at C2 and in the minor groove. Pol IV has consistently proven to be relatively effective at handling bulky N2-dG adducts, which is the same positioning as the extra oxygen in 2-oxodA. This may be achieved by stabilization of the 2-oxodA conformation in the active site through specific interactions between Pol IV and 2-oxodA. The other lesions have bulk in the major groove. The 5-position of pyrimidines is relatively away from the DNA backbone, which might explain the ability of Pol IV to handle 5-fodU and 5-hmdU. While dTg has extra bulk at C5, it also has bulk at C4, and 8-oxodG has bulk at C8G. Both C4T and C8G are closer to the DNA backbone. Pol IV may have something in its structure that cause a steric impediment in the cases of the extra bulk at C4 in dTg and at C8 in 8-oxodG.

Certain TLS polymerases can perform proficient and moderately accurate bypass of particular types of DNA damage, while some other polymerases continue synthesis after having inserted "incorrect" bases opposite the lesion. The differences in the chemical structure of the lesions and the association between polymerases and the lesion and nucleotides inserted may affect how for that structural information in the altered bases contributes to nucleotide selection during insertion opposite these lesions by these polymerases.

## 5. Conclusion

In this paper, we examined whether Pol IV can bypass oxidatively damaged bases and is involved in mutation induction at the damaged sites. Recombinant Pol IV was incubated *in vitro* with chemically synthesized oligonucleotides containing dTg, 5-fodU, 5-hmdU, 8-oxodG, and 2-oxodA. Pol IV preferred to insert dA opposite 5-fodU and 5-hmdU, while it did not insert any nucleotides opposite dTg. Pol IV inserted dA and dC opposite template 8-oxodG, while the Pol IV's ability was low. Pol IV inserted dCTP more efficiently than dTTP opposite 2-oxodA in DNA, suggesting that 2-oxodA in the template DNA has mutagenic potential leading to A:T  $\rightarrow$  G:C transitions. Hydrogen peroxide treatment caused a  $\sim$ 2-fold increase in A:T  $\rightarrow$  G:C mutations in *E. coli*, while the increase was significantly greater ( $\sim$ 10-fold) in *E. coli* overexpressing Pol IV. These results indicate that Pol IV may play an important role in mutagenesis by 2-oxodA in *E. coli*.

## Acknowledgments

The authors thank Dr. Elizabeth Nakajima for critically reading the paper. The authors wish to express their gratitude to the reviewers for helpful and excellent comments and discussion. This paper was financially supported in part by Grants-in-Aid for Science Research nos. 19510056, 21510056 from the Ministry of Education, Culture, Sports, Science and Technology of Japan (to Q-M. Zhang-Akiyama) and Global

Center of Excellence Program "Formation of a Strategic Base for Biodiversity and Evolutionary Research (A06): from Genome to Ecosystem". The authors are also grateful to Takeda Science Foundation (Osaka) and the Central Research Institute of Electric Power Industry (Tokyo) for supporting Q-M. Zhang-Akiyama.

## References

- [1] H. Ohmori, E. C. Friedberg, R. P. P. Fuchs et al., "The Y-family of DNA polymerases," *Molecular Cell*, vol. 8, no. 1, pp. 7–8, 2001.
- [2] D. F. Jarosz, P. J. Beuning, S. E. Cohen, and G. C. Walker, "Y-family DNA polymerases in *Escherichia coli*," *Trends in Microbiology*, vol. 15, no. 2, pp. 70–77, 2007.
- [3] A. R. Lehmann, A. Niimi, T. Ogi et al., "Translesion synthesis: Y-family polymerases and the polymerase switch," *DNA Repair*, vol. 6, no. 7, pp. 891–899, 2007.
- [4] J. Wagner, P. Gruz, S.-R. Kim et al., "The dinB gene encodes a novel *E. coli* DNA polymerase, DNA pol IV, involved in mutagenesis," *Molecular Cell*, vol. 4, no. 2, pp. 281–286, 1999.
- [5] M. Tang, P. Pham, X. Shen et al., "Roles of *E. coli* DNA polymerases IV and V in lesion-targeted and untargeted SOS mutagenesis," *Nature*, vol. 404, no. 6781, pp. 1014–1018, 2000.
- [6] R. S. Galhardo, R. Do, M. Yamada et al., "DinB upregulation is the sole role of the SOS response in stress-induced mutagenesis in *Escherichia coli*," *Genetics*, vol. 182, no. 1, pp. 55–68, 2009.
- [7] R. Napolitano, R. Janel-Bintz, J. Wagner, and R. P. P. Fuchs, "All three SOS-inducible DNA polymerases (Pol II, Pol IV and Pol V) are involved in induced mutagenesis," *EMBO Journal*, vol. 19, no. 22, pp. 6259–6265, 2000.
- [8] S.-R. Kim, K. Matsui, M. Yamada, P. Gruz, and T. Nohmi, "Roles of chromosomal and episomal dinB genes encoding DNA pol IV in targeted and untargeted mutagenesis in *Escherichia coli*," *Molecular Genetics and Genomics*, vol. 266, no. 2, pp. 207–215, 2001.
- [9] D. F. Jarosz, V. G. Godoy, J. C. Delaney, J. M. Essigmann, and G. C. Walker, "A single amino acid governs enhanced activity of DinB DNA polymerases on damaged templates," *Nature*, vol. 439, no. 7073, pp. 225–228, 2006.
- [10] B. Yuan, H. Cao, Y. Jiang, H. Hong, and Y. Wang, "Efficient and accurate bypass of N2-(1-carboxyethyl)-2'-deoxyguanosine by DinB DNA polymerase in vitro and in vivo," *Proceedings of the National Academy of Sciences of the United States of America*, vol. 105, no. 25, pp. 8679–8684, 2008.
- [11] A. Kumari, I. G. Minko, M. B. Harbut, S. E. Finkel, M. F. Goodman, and R. S. Lloyd, "Replication bypass of interstrand cross-link intermediates by *Escherichia coli* DNA polymerase IV," *Journal of Biological Chemistry*, vol. 283, no. 41, pp. 27433–27437, 2008.
- [12] S. Bjelland and E. Seeberg, "Mutagenicity, toxicity and repair of DNA base damage induced by oxidation," *Mutation Research*, vol. 531, no. 1-2, pp. 37–80, 2003.
- [13] J. Cadet, T. Delatour, T. Douki et al., "Hydroxyl radicals and DNA base damage," *Mutation Research*, vol. 424, no. 1-2, pp. 9–21, 1999.
- [14] B. N. Ames, M. K. Shigenaga, and T. M. Hagen, "Oxidants, antioxidants, and the degenerative diseases of aging," *Proceedings of the National Academy of Sciences of the United States of America*, vol. 90, no. 17, pp. 7915–7922, 1993.

- [15] S. S. Wallace, "Biological consequences of free radical-damaged DNA bases," *Free Radical Biology and Medicine*, vol. 33, no. 1, pp. 1–14, 2002.
- [16] S. S. David, V. L. O'Shea, and S. Kundu, "Base-excision repair of oxidative DNA damage," *Nature*, vol. 447, no. 7147, pp. 941–950, 2007.
- [17] G. L. Dianov, T. Thybo, I. I. Dianova, L. J. Lipinski, and V. A. Bohr, "Single nucleotide patch base excision repair is the major pathway for removal of thymine glycol from DNA in human cell extracts," *Journal of Biological Chemistry*, vol. 275, no. 16, pp. 11809–11813, 2000.
- [18] H. Sugiyama, S. Ikeda, and I. Saito, "Remarkably stable parallel-stranded oligonucleotides containing 5-methylisocytosine and isoquinine," *Journal of the American Chemical Society*, vol. 118, no. 41, pp. 9994–9995, 1996.
- [19] H. Sugiyama, S. Matsuda, K. Kino, Q.-M. Zhang, S. Yonei, and I. Saito, "New synthetic method of 5-formyluracil-containing oligonucleotides and their melting behavior," *Tetrahedron Letters*, vol. 37, no. 50, pp. 9067–9070, 1996.
- [20] C. G. Cupples and J. H. Miller, "A set of *lacZ* mutations in *Escherichia coli* that allow rapid detection of each of the six base substitutions," *Proceedings of the National Academy of Sciences of the United States of America*, vol. 86, no. 14, pp. 5345–5349, 1989.
- [21] K.-I. Takata, T. Shimizu, S. Iwai, and R. D. Wood, "Human DNA polymerase N (POLN) is a low fidelity enzyme capable of error-free bypass of 5S-thymine glycol," *Journal of Biological Chemistry*, vol. 281, no. 33, pp. 23445–23455, 2006.
- [22] P. L. Fischhaber, V. L. Gerlach, W. J. Feaver, Z. Hatahet, S. S. Wallace, and E. C. Friedberg, "Human DNA polymerase  $\kappa$  bypasses and extends beyond thymine glycols during translesion synthesis in vitro, preferentially incorporating correct nucleotides," *Journal of Biological Chemistry*, vol. 277, no. 40, pp. 37604–37611, 2002.
- [23] R. Kusumoto, C. Masutani, S. Iwai, and F. Hanaoka, "Translesion synthesis by human DNA polymerase  $\eta$  across thymine glycol lesions," *Biochemistry*, vol. 41, no. 19, pp. 6090–6099, 2002.
- [24] G. W. Hsu, M. Ober, T. Carell, and L. S. Beese, "Error-prone replication of oxidatively damaged DNA by a high-fidelity DNA polymerase," *Nature*, vol. 431, no. 7005, pp. 217–221, 2004.
- [25] S. Bjelland, H. Ånensen, I. Knævelsrud, and E. Seeberg, "Cellular effects of 5-formyluracil in DNA," *Mutation Research*, vol. 486, no. 2, pp. 147–154, 2001.
- [26] I. Miyabe, Q.-M. Zhang, H. Sugiyama, K. Kino, and S. Yonei, "Mutagenic effects of 5-formyluracil on a plasmid vector during replication in *Escherichia coli*," *International Journal of Radiation Biology*, vol. 77, no. 1, pp. 53–58, 2001.
- [27] Q.-M. Zhang, H. Sugiyama, I. Miyabe et al., "Replication in vitro and cleavage by restriction endonuclease of 5-formyluracil- and 5-hydroxymethyluracil-containing oligonucleotides," *International Journal of Radiation Biology*, vol. 75, no. 1, pp. 59–65, 1999.
- [28] Z. Nackerdien, K. S. Kasprzak, G. Rao, B. Halliwell, and M. Dizdaroglu, "Nickel(II)- and cobalt(II)-dependent damage by hydrogen peroxide to the DNA bases in isolated human chromatin," *Cancer Research*, vol. 51, no. 21, pp. 5837–5842, 1991.
- [29] H. Kamiya and H. Kasai, "Mutations induced by 2-hydroxyadenine on a shuttle vector during leading and lagging strand syntheses in mammalian cells," *Biochemistry*, vol. 36, no. 37, pp. 11125–11130, 1997.
- [30] H. Kamiya, "Mutagenicities of 8-hydroxyguanine and 2-hydroxyadenine produced by reactive oxygen species," *Biological and Pharmaceutical Bulletin*, vol. 27, no. 4, pp. 475–479, 2004.
- [31] H. Miller, A. S. Fernandes, E. Zaika et al., "Stereoselective excision of thymine glycol from oxidatively damaged DNA," *Nucleic Acids Research*, vol. 32, no. 1, pp. 338–345, 2004.
- [32] R. E. Johnson, S.-L. Yu, S. Prakash, and L. Prakash, "Yeast DNA polymerase zeta ( $\zeta$ ) is essential for error-free replication past thymine glycol," *Genes and Development*, vol. 17, no. 1, pp. 77–87, 2003.
- [33] K. L. Brown, T. Adams, V. P. Jasti, A. K. Basu, and M. P. Stone, "Interconversion of the cis-5R,6S- and trans-5R,6R-thymine glycol lesions in duplex DNA," *Journal of the American Chemical Society*, vol. 130, no. 35, pp. 11701–11710, 2008.
- [34] G. Maga, G. Villani, E. Crespan et al., "8-oxo-guanine bypass by human DNA polymerases in the presence of auxiliary proteins," *Nature*, vol. 447, no. 7144, pp. 606–608, 2007.
- [35] Q.-M. Zhang, I. Miyabe, Y. Matsumoto, K. Kino, H. Sugiyama, and S. Yonei, "Identification of repair enzymes for 5-formyluracil in DNA: nth, nei, and mutM proteins of *Escherichia coli*," *Journal of Biological Chemistry*, vol. 275, no. 45, pp. 35471–35477, 2000.
- [36] R. G. Kallen, M. Simon, and J. Marmur, "The occurrence of a new pyrimidine base replacing thymine in a bacteriophage DNA: 5-hydroxymethyl uracil," *Journal of Molecular Biology*, vol. 5, pp. 248–250, 1962.
- [37] V. Rusmintratrip and L. C. Sowers, "An unexpectedly high excision capacity for mispaired 5-hydroxymethyluracil in human cell extracts," *Proceedings of the National Academy of Sciences of the United States of America*, vol. 97, no. 26, pp. 14183–14187, 2000.
- [38] M. Hori, S. Yonei, H. Sugiyama, K. Kino, K. Yamamoto, and Q.-M. Zhang, "Identification of high excision capacity for 5-hydroxymethyluracil mispaired with guanine in DNA of *Escherichia coli* MutM, Nei and Nth DNA glycosylases," *Nucleic Acids Research*, vol. 31, no. 4, pp. 1191–1196, 2003.
- [39] F. Barone, S. D. McCulloch, P. Macpherson et al., "Replication of 2-hydroxyadenine-containing DNA and recognition by human MutS $\alpha$ ," *DNA Repair*, vol. 6, no. 3, pp. 355–366, 2007.
- [40] E. Crespan, U. Hübscher, and G. Maga, "Error-free bypass of 2-hydroxyadenine by human DNA polymerase  $\lambda$  with proliferating cell nuclear antigen and replication protein A in different sequence contexts," *Nucleic Acids Research*, vol. 35, no. 15, pp. 5173–5181, 2007.
- [41] X.-L. Yang, H. Sugiyama, S. Ikeda, I. Saito, and A. H.-J. Wang, "Structural studies of a stable parallel-stranded DNA duplex incorporating isoguanine: cytosine and isocytosine: guanine basepairs by nuclear magnetic resonance spectroscopy," *Biophysical Journal*, vol. 75, no. 3, pp. 1163–1171, 1998.
- [42] Y. Ushijima, Y. Tominaga, T. Miura, D. Tsuchimoto, K. Sakumi, and Y. Nakabeppu, "A functional analysis of the DNA glycosylase activity of mouse MUTYH protein excising 2-hydroxyadenine opposite guanine in DNA," *Nucleic Acids Research*, vol. 33, no. 2, pp. 672–682, 2005.
- [43] K. Hashiguchi, Q. M. Zhang, H. Sugiyama, S. Ikeda, and S. Yonei, "Characterization of 2-hydroxyadenine DNA glycosylase activity of *Escherichia coli* MutY protein," *International Journal of Radiation Biology*, vol. 78, no. 7, pp. 585–592, 2002.

- [44] H. Kamiya, H. Maki, and H. Kasai, "Two DNA polymerases of *Escherichia coli* display distinct misinsertion specificities for 2-Hydroxy-dATP during DNA synthesis," *Biochemistry*, vol. 39, no. 31, pp. 9508–9513, 2000.
- [45] K. Satou, H. Harashima, and H. Kamiya, "Mutagenic effects of 2-hydroxy-dATP on replication in a HeLa extract: induction of substitution and deletion mutations," *Nucleic Acids Research*, vol. 31, no. 10, pp. 2570–2575, 2003.

## Review Article

# Architecture of Y-Family DNA Polymerases Relevant to Translesion DNA Synthesis as Revealed in Structural and Molecular Modeling Studies

Sushil Chandani,<sup>1</sup> Christopher Jacobs,<sup>2</sup> and Edward L. Loechler<sup>1</sup>

<sup>1</sup>Biology Department, Boston University, Boston, MA 02215, USA

<sup>2</sup>Graduate Program in Bioinformatics, Boston University, Boston, MA 02215, USA

Correspondence should be addressed to Edward L. Loechler, loechler@bu.edu

Received 6 July 2010; Accepted 26 July 2010

Academic Editor: Ashis Basu

Copyright © 2010 Sushil Chandani et al. This is an open access article distributed under the Creative Commons Attribution License, which permits unrestricted use, distribution, and reproduction in any medium, provided the original work is properly cited.

DNA adducts, which block replicative DNA polymerases (DNAPs), are often bypassed by lesion-bypass DNAPs, which are mostly in the Y-Family. Y-Family DNAPs can do non-mutagenic or mutagenic dNTP insertion, and understanding this difference is important, because mutations transform normal into tumorigenic cells. Y-Family DNAP architecture that dictates mechanism, as revealed in structural and modeling studies, is considered. Steps from adduct blockage of replicative DNAPs, to bypass by a lesion-bypass DNAP, to resumption of synthesis by a replicative DNAP are described. Catalytic steps and protein conformational changes are considered. One adduct is analyzed in greater detail: the major benzo[a]pyrene adduct (B[a]P-N<sup>2</sup>-dG), which is bypassed non-mutagenically (dCTP insertion) by Y-family DNAPs in the IV/ $\kappa$ -class and mutagenically (dATP insertion) by V/ $\eta$ -class Y-Family DNAPs. Important architectural differences between IV/ $\kappa$ -class versus V/ $\eta$ -class DNAPs are discussed, including insights gained by analyzing ~400 sequences each for bacterial DNAPs IV and V, along with sequences from eukaryotic DNAPs kappa, eta and iota. The little finger domains of Y-Family DNAPs do not show sequence conservation; however, their structures are remarkably similar due to the presence of a core of hydrophobic amino acids, whose exact identity is less important than the hydrophobic amino acid spacing.

## 1. Introduction

DNA damaging agents (genotoxins) cause mutations that initiate tumor formation, which makes sense given that tumor cells have mutations in key growth control genes that lead to improperly regulated cell growth [1, 2]. The steps leading to mutagenesis vary depending on the genotoxin, but the paradigm in Figure 1 illustrates many of the typical steps using one particularly well-studied chemical carcinogen benzo[a]pyrene [3–5]. At the apex of this process are DNA adducts, which, if they are not removed by DNA repair, usually block replicative DNA polymerases (DNAPs). To overcome such potentially lethal blockage, cells have DNAPs that do translesion synthesis (TLS) past these DNA lesions/adducts [6–22].

Cells possess many DNAPs; for example, human cells, yeast (*S. cerevisiae*) and *E. coli* have at least fifteen, eight

and five, respectively, [6–22]. Most TLS-DNAPs are in the Y-Family [6–22], where humans have three template-directed members (hDNAPs  $\eta$ ,  $\iota$ , and  $\kappa$ ), yeast has one (scDNAP  $\eta$ ), and *E. coli* has two (ecDNAPs IV and V). Y-Family DNAPs have a conserved ~350 aa core, which includes the polymerase active site (representative references [23–40]). As with all DNA polymerases, Y-Family members resemble a right-hand with thumb, palm, and fingers domains, although their “stubby” fingers and thumb result in more solvent accessible surface around the template/dNTP binding pocket [19], which is undoubtedly the case to accommodate the bulky and/or deforming DNA adducts/lesions that protrude into these open spaces during bypass. Y-Family DNAPs grip DNA with an additional domain, which is usually called the “little finger domain” or the “polymerase-associated domain” (PAD) [23–25].

Y-Family DNAPs are found in all three domains of life, bacteria, archaea, and eukaryotes, which undoubtedly reflects the fact that all cells face the same issues when confronting the need to replicate past DNA damage. The pattern of TLS is often strikingly similar in different cell types. For example, human DNAP  $\kappa$  was originally discovered because its sequence closely resembles *E. coli* DNAP IV [41–43], and dNTP insertion opposite a variety of adducts/lesions is remarkably similar for the DNAP IV/ $\kappa$  pair (Table 1), suggesting they are functional orthologs (discussed in [44]). *E. coli* DNAP V and human DNAP  $\eta$  are also functional orthologs, based on their similarity of dNTP insertion opposite a variety of adducts/lesions (Table 1, [44]). Cases have been made that the IV/ $\kappa$ -class is present in cells to bypass endogenously generated N<sup>2</sup>-dG adducts, and the V/ $\eta$ -class is present to bypass UV-induced photoproducts, as discussed below.

B-Family DNAPs can also be involved in TLS, such as DNAP II in *E. coli* and REV3 (the polymerase subunit of DNAP  $\zeta$ ), which is present in most eukaryotes [6, 7, 13–15]. B-family TLS-DNAPs are involved in a DNA repair process involving some interstrand DNA cross-links [45–49] and in TLS of some adduct/lesions (see below).

Herein, we reflect principally on how structural architecture of Y-family DNAPs might affect their mechanism as it relates to cellular function, in particular why lesion-bypass is sometimes nonmutagenic and other times it is mutagenic. Extensive reviews that focus more on the cell biology, regulation and phenomenology have appeared recently for Y-Family DNAPs from bacteria [21, 22] and eukaryotes [7–12].

## 2. Translesion Synthesis DNA Polymerases in *E. coli*

*E. coli* has proven to be an excellent model system to study many aspects of the bypass of DNA adducts/lesions by TLS-DNAPs. *E. coli* has two Y-Family DNA polymerases: DNAP IV (*dinB* gene, 351 aa, 39.5 kDa) and DNAP V, which consists of one subunit of UmuC (*umuC* gene, 422 aa, 47.7 kDa) and two subunits of UmuD' (see below). UmuD' is derived from UmuD (*umuD* gene, 139 aa, 15 kDa) following autodigestive removal of its 24 N-terminal aa, when stimulated by RecA\* [13, 14, 21, 22, 50]. DNAP II (*polB* gene, 783 aa, 90 kDa) is a B-Family lesion bypass DNAP. DNAPs II, IV and V are each induced as part of the SOS response, which is triggered by DNA damage and leads to the induction of ~40 proteins that help *E. coli* cope with the damage [50]. The basal and SOS-induced levels are different for each polymerase, where the [uninduced/induced] levels are [~40/~280] for DNAP II, [~250/~2500] for DNAP IV and [~15/~200] for DNAP V [51–53]. It seems likely that each of these TLS-DNAP is present in *E. coli* principally to overcome the cellular problems presented by a lesion commonly encountered in cells as discussed next.

Although DNAP V replicates undamaged templates with relatively low fidelity ( $10^{-3}$  to  $10^{-4}$ ) [54], one striking quality is its ability to accurately bypass UV photoproducts; for example, it inserts dATP opposite TT-CPDs [54]. Analysis

of insertion tendencies opposite a variety of adducts/lesions led to the observation that DNAP V may have two insertion modes: (i) correct dNTP insertion, and (ii) default dATP insertion [44]. UV light is a frequently encountered form of DNA damage for which a TLS-DNAP might be important, and since TT-CPDs are the major UV lesion [55], a default dATP insertion mode might help minimize UV mutagenesis. However, the utilization of this second mode in other circumstances may have drawbacks. For example, UV mutagenesis also depends on the *umuD/C* genes, implying that DNAP V is required for UV mutagenesis, where C → T mutations in 5'-PyC sequences predominate, which also implies dATP insertion (discussed in reference [56]). DNAP V is involved in other mutagenesis pathways; for example, it inserts dATP opposite +BP in the G → T mutational pathway [57], as discussed below. In fact, the preferential mutagenic insertion of dATP opposite a variety of DNA lesions in *E. coli* has been called the “A-rule” (see [58, 59] and references therein), and it seems likely that this is attributable to DNAP V's tendency to insert dATP [44]. Based on lesion-bypass specificity (Table 1), *E. coli* DNAP V appears to be the functional ortholog of human DNAP  $\eta$  [36], which is almost certainly responsible for correct bypass of UV-lesions in human cells and minimizing UV-light mutagenesis that leads to skin cancer [60–65].

On its own, UmuC, which is the polymerase subunit of DNAP V, either misfolds or aggregates and is found in inclusion bodies [22, 50, 66]. UmuC copurifies with UmuD', though the yield is invariably low [22, 50, 66]. RecA is also required for efficient DNAP V activity, and recently, the “DNAP V mutasome” was shown to be a UmuC/UmuD'<sub>2</sub>/RecA heterotetramer [67, 68]. The RecA monomer is added from the 3'-end of a RecA filament either in *cis* or in *trans*, where the former seems intuitively more likely, since UmuC/UmuD'<sub>2</sub> would encounter a 3'-*cis*-RecA at a lesion site, given that RecA filaments coat ss-DNA on the downstream side of a lesion-blocked replication fork. To form RecA filaments on ss-DNA, SSB must first be removed, which is accomplished by RecFOR [69]. Interestingly, some evidence suggests that the RecA eukaryotic homolog Rad51 is able to stimulate DNAP  $\eta$ , which is the DNAP V ortholog [70].  $\beta$ -clamp also plays a significant role with DNAP V as discussed below.

DNAP IV replicates undamaged DNA only ~5-fold less accurately than the catalytic  $\alpha$ -subunit of DNAP III [54]. It is prone to making –1 frameshift mutations in homopolymeric runs of six or more G:C base pairs, and base substitutions also result [22, 71]. DNAP IV's most striking quality is its ability to accurately bypass a variety of N<sup>2</sup>-dG adducts [72–77]. Methylglyoxal is produced nonenzymatically from various cellular trioses and forms N<sup>2</sup>-(1-carboxyethyl)-2'-dG as its major stable adduct, which is bypassed accurately by DNAP IV [76]. Oxidative metabolism forms reactive oxygen species that generate lipid peroxidation products that give exocyclic adducts, some of which can ring-open to N<sup>2</sup>-dG adducts in ds-DNA [78] and might be bypassed by DNAP IV, though this has not been investigated experimentally. These observations have led several groups to speculate that the cellular rationale for the genesis of the IV/ $\kappa$ -class of Y-Family

TABLE 1: Dominant dNTP insertions opposite various DNA adducts/lesions by *E. coli* DNAPs IV and V, and human DNAPs  $\kappa$  and  $\eta$ .<sup>†</sup>

Lesion	DNAP V	DNAP $\eta$	DNAP IV	DNAP $\kappa$
[+ta]-BP-N <sup>2</sup> -dG	A/C	A $\geq$ G	C	C
AAF-C8-dG	C	C	C/T	C/T
AF-C8-dG	—	—	C	C
TT-CPD	AA	AA	n	n
T(6-4)T	AG	nG	n	n
AP site	A	A	n	A*

<sup>†</sup> Dominant dNTP insertion using purified DNAPs, where “n” indicates “no” or low activity, “A\*” indicates bypass by an unusual mechanism, and “—” indicates data unavailable. Data, as reviewed in [44].

DNAPs is the accurate bypass of N<sup>2</sup>-dG adducts derived from various endogenous mechanisms [72, 76].

No analogous story vis-a-vis adducts/lesions has yet emerged to provide a rationale for the presence of B-family DNAP II in cells, though one possibility is its involvement in an accurate DNA repair pathway for interstrand cross-links [45]. An analogous pathway involving B-family DNAP  $\xi$  exists in eukaryotic cells, and a pathway has been proposed [46–49]. As discussed below, DNAP II functions in other TLS pathways.

UmuD<sub>2</sub>C (not UmuD’<sub>2</sub>C) is thought to slow down normal DNA replication in response to DNA damage, thus allowing additional time for lesion removal, which is considered a DNA damage checkpoint analogous to what happens in eukaryotic cells [79]. Another mechanism to accomplish this was recently described: DNAP II or IV can associate with the DnaB helicase and slow down the replication fork [80].

The TLS-DNAPs also confer selective advantage on *E. coli* during long periods in stationary phase, the so-called “growth advantage in stationary phase” (GASP) phenotype [81]. Finally, DNAP IV is particularly elevated in stationary phase ( $\sim 7500$ /cell) and is implicated in adaptive mutagenesis [82].

### 3. Eukaryotic Y-Family DNAPs

Extensive reviews of the cell biology, regulation, and phenomenology of eukaryotic Y-Family DNAPs have appeared recently [7–12]. Herein, we focus on structural considerations that relate to lesion bypass, though we briefly describe each of the four subclasses of eukaryotic Y-Family DNAPs: REV1, DNAP  $\kappa$ , DNAP  $\eta$ , and DNAP  $\iota$ .

REV1 is not a traditional template-directed polymerase and does not use base-base hydrogen bonding. Rather REV1 is a dCTP insertase that flips template dGs out of the helix, after which dCTP insertion is directed by hydrogen bonding to a REV1 arginine residue [83]. REV1 seems to play a central role in many lesion bypass events as a structural component, and DNAPs  $\kappa$ ,  $\eta$ , and  $\iota$  each have REV1 binding domains [9].

DNAP  $\kappa$  is the eukaryotic ortholog of DNAP IV (Table 1), and they seem to be present in cells to accurately insert opposite N<sup>2</sup>-dG adducts [84], for example, DNAP  $\kappa$  deficient cells are sensitized to killing by benzo[a]pyrene, which

predominantly forms an N<sup>2</sup>-dG adducts [85]. DNAP  $\kappa$  uniquely has an N-terminal extension of 100 aa called the “N-clasp” [35]. The N-clasp has three  $\alpha$ -helices in a U-shape, one of which ( $\sim$ aa30–50) binds on the surface of the fingers domain, the second of which ( $\sim$ aa50–75) links the fingers and thumb domains and lies diagonally across the duplex region of DNA, and the third traverses the thumb domain to the usual site of the N-terminus in Y-Family DNAPs. Removal of the N-clasp significantly decreases DNAP  $\kappa$  polymerase activity [35]. The presence of the N-clasp has implications for lesion bypass; for example, DNAP  $\kappa$  does not bypass the N<sup>6</sup>-dA adduct of benzo[a]pyrene [86], which has been attributed to a steric clash between the N-clasp and the pyrene moiety, as revealed in a molecular modeling study [87]. DNAP  $\kappa$  structure is considered below.

A major role of DNAP  $\eta$  is nonmutagenic bypass of UV lesions, such as TT-CPDs, and humans deficient in DNAP  $\eta$  have the cancer-prone syndrome Xeroderma pigmentosum variant (XPV), which leads to a high incidence of UV-induced skin cancer [60–65]. Both human and yeast DNAP  $\eta$  preferentially insert dATP opposite the 5’-T and 3’-T of a TT-CPD, with misinsertion being higher at the 3’-T, where dGTP is incorporated  $\sim 3\%$  of the time [88, 89]. Recently, X-ray structures of a TT-CPD in the active site of yeast DNAP  $\eta$  [39] and human DNAP  $\eta$  [40] have emerged. These findings are presented in a separate section (Section 8), after certain principles about Y-Family DNAPs structure have been discussed. DNAP  $\eta$  also plays a role in accurate bypass of the oxidative lesion 8oxoG [90] and adducts formed by the anticancer drug *cis*-platinum [91].

The role of DNAP  $\iota$  in cells is more enigmatic, though the fact that deficient cells show enhanced sensitivity to oxidative damage may be revealing [92]. One interesting feature of DNAP  $\iota$  is its propensity to use *syn*-purines in the template to form Hoogsteen base pairs *syn*-A:T and *syn*-G:C [36, 37]. A cellular rationale for this is the following. Oxidative damage leads to lipid peroxidation products, which form exocyclic adducts that block the Watson-Crick *antiface* of the DNA bases. Exocyclic purine adducts in the *syn*-configuration can still base pair through their Hoogsteen face. The *syn*-A:T base pair has two hydrogen bonds, just like *anti*-A:T. However, both *syn*-G:C and *syn*-G:T base pairs have only one hydrogen bond, unless a proton is trapped. In a *syn*-GH<sup>+</sup>:C base pair the trapped proton is between N7G and N3C, whose pKa values are relatively

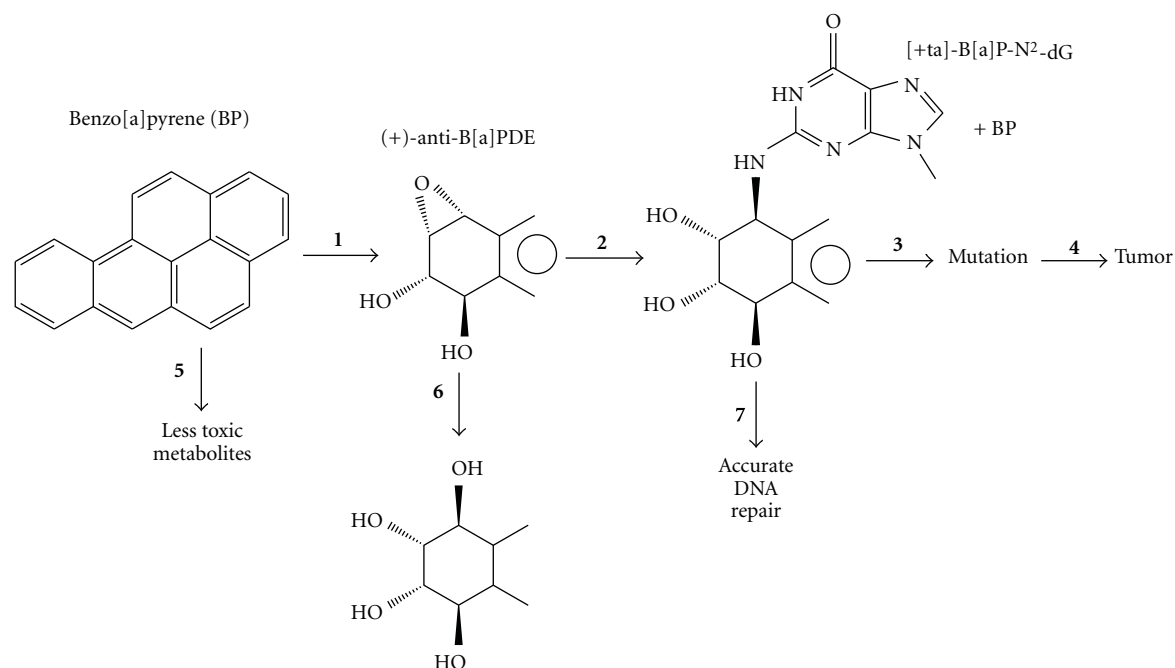


FIGURE 1: Mutagenesis/carcinogenesis paradigm with benzo[a]pyrene. Steps in the horizontal direction lead toward carcinogenicity, and include metabolic activation (step 1), reaction with DNA (step 2), adduct mutagenesis (step 3), and tumorigenesis (step 4). Steps in the vertical direction lead to diminished carcinogenicity, and include metabolic detoxification (step 5), carcinogen deactivation (step 6), and DNA repair (step 7). Diminished carcinogenicity is also associated with other cellular processes, such as delaying the cell cycle and apoptosis [1].

high ( $\sim 3$ ), while a trapped proton in a *syn*-GH<sup>+</sup>:T base pair would be between O<sup>6</sup>G and O<sup>4</sup>T, whose pKa values are much lower. Thus, a *syn*-GH<sup>+</sup>:T base pair is expected to be less stable than a *syn*-GH<sup>+</sup>:C base. Evidence for DNAP  $\iota$  using *syn*-GH<sup>+</sup>:C base pairing exists [37]. 1,N<sup>6</sup>-etheno-A directs both dCTP and dTTP incorporation, and in this case both require a trapped proton [38], where the pKa values of the relevant atoms trapping the proton are more equal. While such thinking is considered satisfying [12], one finding suggests that the situation can be more complex. DNAP  $\iota$  preferentially incorporates dCTP opposite the major adduct of 2-acetylaminofluorene (AAF-C8-dG) [93], *Syn*-AAF-C8-dG places the bulky AAF-moiety in the minor groove, where molecular modeling showed that it does not fit, while *anti*-AAF-C8-dG:C pairing, which places the AAF-moiety in the spacious major groove side of DNAP  $\iota$ , is possible [94]. The authors propose that purine adducts with bulk on the minor groove side probably use *syn*-purine pairing, but that purine adducts with bulk on the major groove side probably use *antipurine* pairing. *Anti*-AAF-C8-dG:C pairing requires a modest change in sugar pucker (from C3'-endo to C1'-exo), as noted in modeling studies with both DNAP  $\iota$  [94] and Dpo4 [95].

Base substitution rates on undamaged templates are relatively high with all of these polymerases:  $\gamma$ DNAP  $\eta$  ( $\sim 10^{-2}$ ), hDNAP  $\eta$  ( $\sim 3.5 \times 10^{-3}$ ), hDNAP  $\kappa$  ( $\sim 6 \times 10^{-4}$ ), and hDNAP  $\iota$  actually prefers to form template-dT:dGTP; indel mutation rates are all in the same range ( $\sim 1\text{--}2.4 \times 10^{-3}$ ) (reviewed in [7]).

#### 4. Y-Family DNAP Mechanistic Steps

A number of comprehensive reviews have appeared that analyze the structures of Y-Family DNAPs [10–12, 32, 33]. In this section, we focus on what is known about protein structural changes that occur during DNA synthesis as probed via X-ray structural analysis and other techniques, principally with Dpo4. The chemistry of catalysis is also considered.

Upon DNA binding to Apo-Dpo4, the thumb/palm/fingers domains do not change their structure dramatically. However, the little finger domain acts like a door, which is open in Apo-Dpo4, and then rotates  $\sim 130^\circ$  to close around DNA; in particular, it binds in the major groove in the duplex region from about L + 3 to L + 8 [33]. This motion is facilitated by the fact that the little finger is connected to the rest of the protein by a simple ten amino acid tether. Once binary-Dpo4 is formed, the palm, fingers and little finger translate  $\sim 3.3 \text{ \AA}$  along the helix as the next template base slides into the active site, which opens the space into which the complementary dNTP binds to give ternary-Dpo4 [32]. The thumb domain, however, does not move in this step, but, rather, moves either before, during, or after the subsequent covalent reaction step. A variety of subtler changes in Dpo4 structure are also reported to accompany these steps [32, 33]. Kinetic studies reveal that Y-Family DNAPs have a rate-determining conformational change before dNTP incorporation [10, 96], and three conformational states E, E', and E'' have been reported, where the E'  $\rightarrow$  E'' conformational transition is rate

determining, though the nature of these states have not been identified. Recently, hydrogen-deuterium exchange in tandem with mass spectrometry has been used to study conformational changes in Dpo4 brought about by dNTP binding [30]. Correct dNTP binding affects the structure of a loop between the B-helix and the C-helix above the Dpo4 active site. (The positioning of these features can be inferred from the UmuC(V) sequence in Figure 2.) Another conformational change was also detected in the H-helix, which contacts the primer strand and was proposed to move away from the active site in conjunction with ds-DNA movement to permit room for correct dNTP binding. The F-helix also moves, but this motion is not specific for the correct dNTP. In terms of lesion bypass, Dpo4 showed decreased catalytic efficiency with increasing bulk of N<sup>2</sup>-dG adducts, which was attributed more to the effects of the bulky lesion on the rate of the catalytic step than on the rate of the conformational steps [31].

Several studies have shown that dNTP incorporation is more dependent on base:base hydrogen bonding for Y-Family DNAPs than for DNAPs in other families during the replication of both undamaged and damaged DNA [97–99].

The steps in covalent catalysis by Dpo4 have been explored using a combination of molecular modeling/dynamics and ab initio QM/MM minimizations; a novel water-mediated and substrate-assisted mechanism was proposed [100]. In the first step, a water molecule in the active site serves as a conduit to deprotonate the primer 3'-OH and protonate an oxygen on the  $\alpha$ -phosphate of the dNTP. In the second step, a second water molecule in the active site serves as a conduit to deprotonate the oxygen on the  $\alpha$ -phosphate of the dNTP and to protonate an oxygen on the  $\gamma$ -phosphate. Following these two steps the deprotonated 3'-O<sup>-</sup> of the primer is a stronger nucleophile and attacks the  $\alpha$ -phosphate, while the second water molecule serves as a conduit again—this time to deprotonate the  $\gamma$ -phosphate of the dNTP and to protonate the  $\beta$ -phosphate, which is on the pyrophosphate leaving group, thus facilitating its removal.

## 5. The Steps Leading to Translesion Synthesis in *E. coli*

A well-developed model for the steps in translesion synthesis has emerged for *E. coli* [107]. Replicative DNAP III stalls at many adducts. For example, in the case of AAF-C8-dG, the 3' → 5' exonuclease activity of DNAP III competes with its polymerase activity, such that [L-1] : [L0] ratio is ~10 : 1 ratio of primers, as determined in vitro [66]. A TLS-DNAP probably helps dissociate a stalled DNAP III from the lesion site (see below). DNAP III reinitiates replication hundreds to thousands of base pairs downstream of the adduct/lesion at the next primosome assembly site in a process called “replication restart,” either on the lagging strand using the normal lagging strand machinery (i.e., PriA/B/C, DnaB/C/T, and primase), or on the leading strand, whose details are being worked out [108, 109]. This leaves an ss-gap between the lesion site and the site where DNAP III did replication restart. This gap is either filled via recombination or via DNA

replication, which begins with the action of TLS-DNAPs [15, 108, 109].

DNAP IV binds  $\beta$ -clamp to help release a stalled DNAP III from the same  $\beta$ -clamp, leaving DNAP IV/ $\beta$ -clamp at the site of the lesion [110]. This process is rapid ( $t < 15$  s). Presumably, a similar mechanism operates for each TLS-DNAP (II, IV and V), which all have  $\beta$ -clamp binding sites (consensus: QLxLF) that are required for them to be active in *E. coli* [111]. An X-ray structure shows that the underlined amino acids QLVLGL at the C-terminus of DNAP IV form the main interactions with a “cleft” in the  $\beta$ -clamp [112]. The  $\alpha$ -subunit of DNAP III and the  $\delta$ -subunit of the  $\gamma$ -complex also bind to the cleft in the  $\beta$ -clamp. DNAP IV and V can also bind to a site in the “rim” of the  $\beta$ -clamp, but this seems unimportant for TLS [113–115]. In vitro studies show that  $\beta$ -clamp stimulates both polymerase activity and processivity of TLS-DNAPs: the addition of  $\beta$ -clamp in vitro increases DNAP IV activity ~2000-fold and processivity from 1 nucleotide to ~400 nucleotides, and also increases DNAP V activity ~100-fold and processivity from 1-2 nucleotides to ~18 nucleotides [22].

What factors affect the choice about which TLS-DNAP will insert opposite a particular lesion? Several lines of evidence suggest that *E. coli* has a hierarchy for the replication of normal, unadducted DNA when DNAP III is inactivated: DNAP II > IV > V [116]. (The assays did not permit an assessment of DNAP I.) Since this order (III > II > IV > V) does not reflect the relative concentration of these DNAPs in cells (see above), another mechanism for decision making was suggested, such as relative DNAP affinity for the  $\beta$ -clamp. This order does reflect relative fidelity of these DNAPs and would be a sensible order for *E. coli* to allow TLS-DNAPs to initially sample adducts/lesions prior to a decision about which will do TLS. But the ultimate decision is probably predominantly controlled by which TLS-DNAP is most efficient at bypassing a particular adduct/lesion biochemically.

After insertion opposite the lesion, additional extension synthesis by a TLS-DNAP is required, or else DNAP III's proof-reading 3' → 5' exonuclease activity will remove the inserted nucleotides back to the site of the lesion [66, 117]. The amount of extension required before DNAP III can resume normal synthesis appears to be pathway dependent, where it is [L + 4] for the AAF-C8-dG nonmutagenic pathway with DNAP V, and [L + 3] for the AAF-C8-dG -2 frameshift pathway with DNAP V [66, 83, 117].

## 6. Two Case Studies Showing the Interplay of Y-Family DNAPs in Translesion Synthesis

More is known about the details of TLS for the major adduct of *N*-2-acetylaminofluorene (AAF-C8-dG), and N<sup>2</sup>-dG adducts in *E. coli* than for any other adducts/lesions in any other model system. In these cases, multiple translesion DNAPs are involved in both the nonmutagenic and mutagenic pathways, as outlined in this section.

AAF was originally developed as a potential pesticide, but it was abandoned when it was found to be a potent rat carcinogen [118]. Following activation, AAF principally binds at



Secondary Consensus Percent AA type <i>E. coli</i>	181	190										200										210										220										225									
V	G	D	V	W	G	I	G	R	R	I	S	K	K	L	N	A	M	G	I	K	T	A	L	D	L	A	D	A	D	P	R	F	I	R	K	R	H	F	N	V	V	L	E	R	T						
71	28	45	69	98	96	53	98	70	59	31	32	45	47	91	20	34	38	84	82	24	76	69	47	58	84	50	23	35	34	32	20	19	46	75	58	18	65	35	78	1	63	63	86	72							
17	25	3	0	0	0	0	1	15	101	62	11	0	41	139	10	0	0	0	0	0	0	284	41	22	0	206	22	142	10	33	48	17	45	9	30	16	9	0	5	5	7	38	1	2							
2	0	0	1	0	0	0	2	0	0	0	0	0	0	20	0	0	0	0	0	0	0	0	0	0	0	0	0	0	0	0	0	0	0	0	0	0	0	0	0	0	0	0	0	0	0	0					
0	157	186	0	0	0	0	0	2	0	0	6	7	0	1	26	8	3	4	1	24	3	0	0	1	238	0	0	96	0	140	20	25	5	0	0	0	0	0	0	0	0	0	0	0	0	0	0				
0	101	178	0	0	0	0	0	0	0	0	29	34	4	0	64	20	6	7	0	12	0	0	0	6	38	0	0	56	0	0	0	0	0	0	0	0	0	0	0	0	0	0	0	0	0	0	0				
0	0	1	0	0	0	0	0	0	0	1	2	1	14	6	0	4	6	0	0	2	0	0	0	20	0	0	56	0	0	0	0	0	0	0	0	0	0	0	0	0	0	0	0	0	0	0	0	0			
0	116	2	0	0	0	0	396	1	402	8	6	0	31	7	5	0	15	5	346	0	0	0	0	0	0	0	0	0	0	0	0	0	0	0	0	0	0	0	0	0	0	0	0	0	0	0	0	0			
0	1	2	0	0	0	0	0	0	25	0	0	0	14	2	13	18	0	14	2	13	0	38	0	10	3	0	1	9	5	8	0	18	13	0	3	76	0	9	0	1	0	0	0	0	0	0	0	0			
66	2	0	97	0	1	216	0	0	4	106	0	0	0	13	10	1	1	338	5	0	20	1	0	4	6	0	9	0	40	2	24	188	9	1	2	0	65	27	24	7	1	20	0	0	0	0					
0	18	18	0	0	0	0	0	25	70	3	9	183	194	0	24	22	15	0	100	7	0	19	3	0	4	2	10	11	7	2	37	2	3	44	237	0	0	6	1	0	9	24	0	0	0						
18	0	1	18	1	0	0	0	0	127	7	7	11	372	4	39	76	0	5	15	1	1	194	1	346	4	10	35	0	21	6	79	75	2	31	37	0	3	12	178	4	3	68	0	0	0						
3	0	1	2	0	0	0	0	1	18	0	0	7	5	2	12	156	0	2	2	2	6	10	0	0	0	0	3	11	75	0	2	14	35	3	6	36	0	7	32	14	0	0	0	0							
0	52	32	0	0	0	0	0	2	327	382	14	28	307	4	0	8	36	3	0	58	3	58	3	1	1	1	0	0	0	0	0	0	0	0	0	0	0	0	0	0	0	0	0	0	0	0	0				
3	0	0	0	0	0	0	0	15	0	0	0	0	0	0	0	0	0	0	0	0	0	1	1	0	2	0	0	0	91	133	10	8	0	0	0	0	3	1	2	0	0	0	0	0	0	0	0	0			
0	7	3	0	0	0	0	0	0	4	69	5	6	19	22	0	55	16	27	2	0	12	0	1	98	0	6	52	28	0	5	7	19	0	14	39	52	0	0	0	0	0	0	0	0	0	0	0	0			
0	6	3	0	0	0	0	0	1	287	243	0	6	30	89	0	41	17	47	2	0	46	1	0	27	2	0	68	51	4	4	9	83	14	0	307	42	47	0	0	0	0	0	0	0	0	0	0				
0	40	3	0	0	0	0	0	5	8	1	15	130	5	2	0	14	42	3	1	0	13	39	0	0	0	0	0	0	0	0	0	0	0	0	0	0	0	0	0	0	0	0	0	0	0	0	0	0			
11	13	2	0	0	0	0	0	1	61	57	13	4	0	8	36	3	0	0	2	41	311	2	0	0	0	0	0	0	0	0	0	0	0	0	0	0	0	0	0	0	0	0	0	0	0	0	0	0			
290	0	0	0	0	0	0	0	2	3	31	0	0	0	0	0	0	0	0	0	0	0	0	0	0	0	0	0	0	0	0	0	0	0	0	0	0	0	0	0	0	0	0	0	0	0	0	0	0	0		
0	0	0	0	0	0	0	0	0	9	0	0	0	0	0	0	0	0	0	0	0	0	0	0	0	0	0	0	0	0	0	0	0	0	0	0	0	0	0	0	0	0	0	0	0	0	0	0	0	0		
0	0	0	0	0	0	0	0	0	9	0	0	0	0	0	0	0	0	0	0	0	0	0	0	0	0	0	0	0	0	0	0	0	0	0	0	0	0	0	0	0	0	0	0	0	0	0	0	0	0	0	
HYDRO	399	31	7	410	410	6	410	2	36	22	307	128	85	71	410	74	225	280	3	407	75	4	404	329	24	411	243	59	282	101	240	117	298	408	32	35	76	394	3	395	305	287	118	5	114						
LONG	97	8	2	100	100	1	100	0	9	5	75	31	21	17	100	18	55	68	1	99	18	1	98	80	6	100	59	14	69	25	58	28	73	99	8	9	186	1	96	74	70	29	1	80	0	0					
SHORT	0	103	8	0	0	0	0	0	0	0	83	3	7	60	75	0	49	15	24	11	0	49	13	0	12	25	0	24	40	10	20	7	35	9	1	89	79	45	0	26	1	5	34	595	0	0					
	11	105	37	0	0	0	0	0	0	0	336	383	90	215	265	313	0	225	403	2	255	403	2	48	106	0	167	183	123	141	112	191	68	3	367	344	231	7	294	16	66	12	3	94	297						
	3	26	9	0	0	0	0	2	2	82	93	22	52	64	76	0	54	34	25	12	0	62	98	0	12	26	0	41	45	30	34	27	46	17	1	89	84	56	2	72	4	16	3	8	96	72					

FIGURE 2: Continued.



been reported [32]. Regrettably, the structures do not reveal insights about how dCTP might be inserted opposite AF-C8-dG, but they do offer a glimpse of more-or-less normal Watson-Crick AF-C8-dG:dC base pairing in the L + 1, which has the AF moiety in the opening on the major groove side of Dpo4, and in the L + 2 position, in which the AF-moiety is accommodated by a modest rearrangement in the little finger domain.

Benzo[a]pyrene (B[a]P) is a well-studied DNA damaging agent that is a potent mutagen/carcinogen and an example of a polycyclic aromatic hydrocarbon (PAH), a class of ubiquitous environmental substances produced by incomplete combustion [120, 121]. PAHs in general and B[a]P in particular induce the kinds of mutations thought to be relevant to carcinogenesis and may be important in human cancer [122–128]. B[a]P mutational spectra were established with the major metabolite that reacts with DNA (i.e., (+)-*anti*-B[a]PDE), in *E. coli* [129], yeast [130, 131] and mammalian (CHO) cells [132]. Mutagenesis has also been studied with [+ta]-B[a]P-N<sup>2</sup>-dG (+BP, Figure 1), the major adduct of (+)-*anti*-B[a]PDE, and G → T mutations predominate in most cases (see [133] and references therein).

DNAPs IV and V of *E. coli* are both involved in TLS with B[a]P-N<sup>2</sup>-dG adducts, although they play very different roles. In studies with purified proteins, DNAP IV inserted dCTP (>99%) opposite both +BP and its mirror image –BP ([–ta]-B[a]P-N<sup>2</sup>-dG) in a 5′-CGA sequence, while DNAP V inserted dATP (>99%) [77]. This tendency is evident in *E. coli*. DNAP IV is required in the nonmutagenic pathway with +BP [72–75], –BP [75] and other N<sup>2</sup>-dG adducts [72, 76]. An amino acid change (F12I) at the conserved “steric gate” (which excludes rNTPs) decreases dCTP insertion in vitro opposite several N<sup>2</sup>-dG adducts and similarly decreases TLS in vivo, which argues that DNAP IV does dCTP insertion in vivo [72]. In the nonmutagenic pathway DNAP V is required in addition to DNAP IV with +BP [73–75]. Why are two DNAPs required for nonmutagenic TLS with +BP: certain lesions need one DNAP for insertion and a second for extension [134, 135]. Thus, if DNAP IV does dCTP insertion [72–77], then DNAP V must do extension, which is sensible given kinetic findings with purified proteins show that DNAP V can be significantly better than DNAP IV at the step directly following adduct-G:C formation (i.e., extension) in the case of +BP compared to –BP (discussed in greater detail in reference [75]). Regarding the nonmutagenic pathway with –BP, only DNAP IV is required for efficient TLS [75], suggesting it does both insertion and extension. In a 5′-TGT sequence, DNAP V is required in the G → T pathway for +BP, while DNAPs II and IV are not, implying that DNAP V must do insertion and extension [57]. However, in a 5′-GGA sequence, G → T mutations were shown not dependent on DNAP V and were not enhanced by SOS induction, which implies no lesion-bypass DNAP involvement and led the authors to propose that DNAP III was involved in dATP insertion opposite +BP [73, 74]. Random mutagenesis studies with [+anti]-B[a]PDE also showed the existence of a non-SOS-inducible G → T pathway (discussed in [57]), though the major G → T pathway did require SOS-induction, implying involvement of a lesion-bypass DNAP.

## 7. Architecture of Y-Family DNAPs

Table 1 [44] shows that dNTP insertion opposite a variety of adducts/lesions, including +BP, is remarkably similar for the DNAP IV and DNAP  $\kappa$  pair, suggesting they are functional orthologs. Insertion is also remarkably similar for the DNAP V and DNAP  $\eta$  pair, suggesting they are also functional orthologs. There must be structural reasons for the insertion preferences of these DNAPs, though the key elements are not obvious, given that in alignments, for example, UmuC(V) shares only 20% amino acid identity with its functional ortholog hDNAP  $\eta$ , which is about the same as the 21% identity that it shares with its nonfunctional ortholog hDNAP  $\kappa$  [44]. The extent of this dilemma is further revealed by the fact that hDNAP  $\eta$  is no more identical to scDNAP  $\eta$  (24%) than it is to hDNAP  $\kappa$  (24%). Nevertheless, a careful examination of Y-Family DNAP structure suggests that key structural features do exist.

A variety of architectural features are revealed by considering how B[a]P-N<sup>2</sup>-dG adducts must sit in the active sites of Y-family DNAPs and how these structures might relate to adduct processing [136]. To form an adduct-dG:dCTP base pair, the B[a]P moiety must be in the developing minor groove, since the adduction site (N<sup>2</sup>-dG) is in the minor groove in a Watson-Crick base pair. On the minor groove side, Y-Family DNAPs have an opening (or gap) next to the active site between the fingers and little finger domains. This opening looks like an elliptical hole of varying sizes in Dpo4 [24–32], Dbh [23], hDNAP  $\iota$  [36–38] and in models of DNAP IV and UmuC(V) [44], while it looks like a slot in hDNAP  $\kappa$  [35]. It is not unreasonable to think that the size and shape of this opening might influence dNTP insertional mechanism given that the bulky B[a]P moiety must interact with this opening on the minor groove side.

The character of this opening can be analyzed based on a simple analogy to a “chimney.” Three regions of the protein contribute to the chimney as shown in Figure 3(a) for our model of DNAP IV: an upper lip (aa33–36, turquoise) and a left lip (aa73–76, blue), which are in the fingers domain, while the lower lip (blue, aa244–247), is in the little finger domain [136]. The UmuC(V) chimney is shown in Figure 3(b).

Two features control the size and character of this opening. (1) The amino acid side chains in the upper lip (aa33–36 in DNAP IV) can be thought of as a “flue,” which either plug the chimney leaving a small opening or do not plug the chimney leaving a large opening. The flue amino acids are present in all Y-Family DNAPs. (2) A “cap” may lie over the top of the chimney opening. The cap is formed by an insert of amino acids in the left lip of the chimney and is only present in DNAP  $\eta$  [39, 40].

First, we consider how the “flue” amino acid side chains influence the character of the “chimney.” Why do we think that the chimney is a key structural feature that is likely to be important for protein function? If the chimney is important, then evidence for its importance should exist, even in the case of UmuC where no X-ray structure exists. We aligned 408 UmuC(V) sequences, and Figure 2 shows the total number of each of the twenty amino acids that are

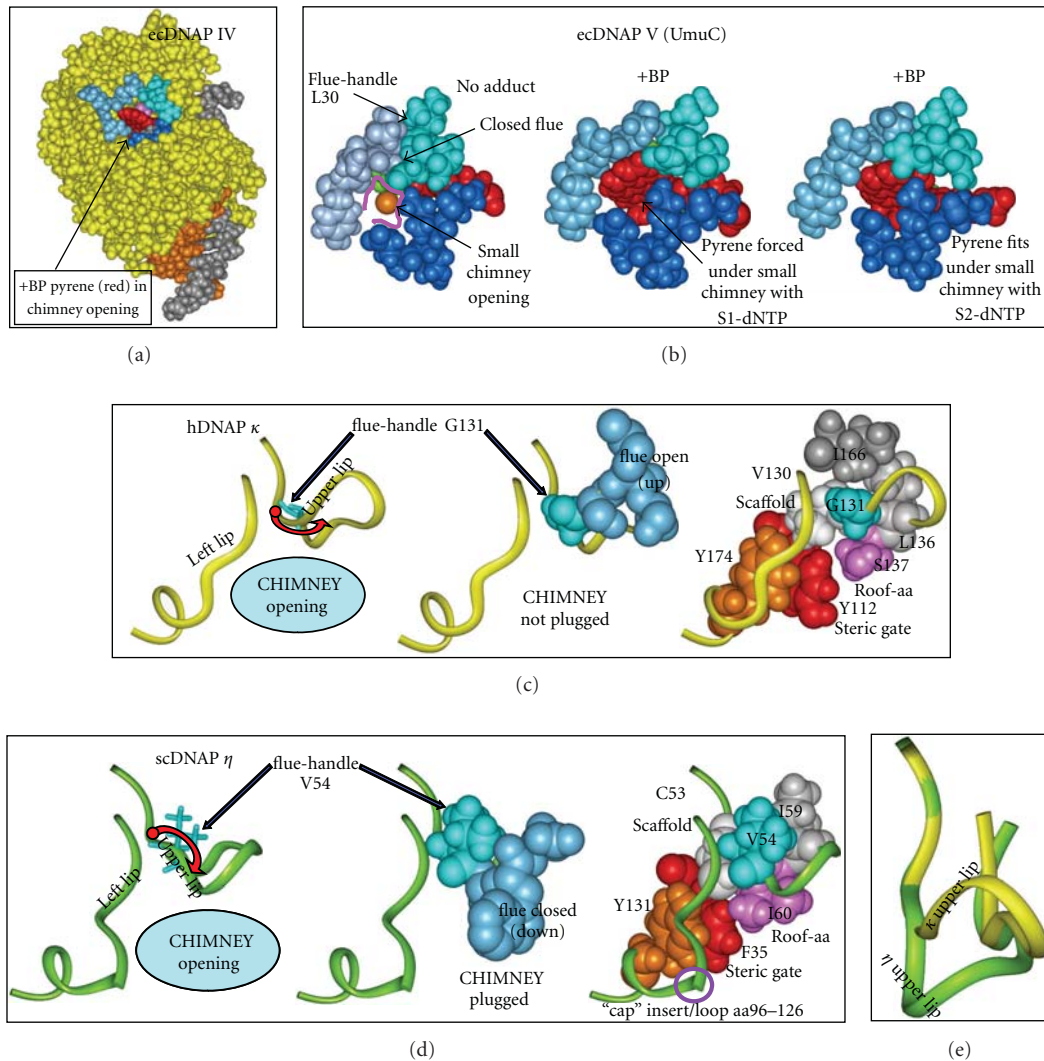


FIGURE 3: Structures of regions of ecDNAP IV (a), ecUmuC(V) (b), hDNAP  $\kappa$  (c), scDNAP  $\eta$  (d). (a) View from the minor groove side of DNAP IV (yellow), showing the "chimney" opening (left or hole), which is defined by the upper lip (turquoise, aa33–36), left lip (blue, aa73–76) and lower lip (dark blue, aa244–247). The chimney opening in DNAP IV is large enough to accommodate the pyrene moiety of +BP (red). In DNAP IV, the dG moiety of +BP can base pair comfortably with dCTP in the canonical S1-dNTP shape. (Neither the dG moiety of +BP nor the dCTP are visible.) The template (gray) and primer (brown) are also shown. (b) Models of UmuC(V) with no adduct (B/left) or +BP paired with dCTP in the canonical "chair-like" S1-dNTP shape (b/center) or +BP paired with dCTP in the non-canonical, "goat-tail-like" S2-dNTP shape (b/right). The chimney opening is small (b/left) and the pyrene moiety of +BP does not fit into the chimney such that the S1-dNTP shape is possible (b/center). In contrast, the pyrene moiety of +BP fits under the chimney opening in the case of pairing with dCTP in the S2-dCTP shape (b/right), because it sits lower down in the active site compared to S1-dNTP. (c) Regions of hDNAP  $\kappa$ . Y-Family DNAPs in the IV/ $\kappa$ -class have a glycine "flue-handle," such as G131 (turquoise, c/left) in hDNAP  $\kappa$  G131 adopts  $\phi/\varphi$ -angles that lead to upward curvature of the protein backbone in the chimney upper lip (red arrow, c/left) and results in the "flue" amino acids (S132/M133, blue, c/center) pointing away from the chimney, giving a large opening. The c/right structure shows V130 (white) that serves as a scaffold to organize the chimney's upper lip and left lip (yellow ribbons), along with the roof-aa (S137, purple), the steric gate (Y112, red) and a conserved tyrosine (Y174, brown), which stacks on the backbone of the left lip and helps orient it. V130 forms a square with the G131 flue-handle, L136 (gray) and the S137 roof (pink) upon which I166 stacks (dark gray). (d) Regions in scDNAP  $\eta$ . Y-Family DNAPs in the V/ $\eta$  class have a bulky "flue-handle," such as V54 in scDNAP  $\eta$  (turquoise, d/left), which causes downward curvature of the chimney upper lip (red arrow, d/center), and results in the "flue" amino acids (Q33/W34, blue, d/center) plugging the chimney, giving a small opening. The structure in d/right shows scaffold C53 (white) organizing the chimney's upper lip and left lip (green ribbons in (c)), along with the roof-aa (I60, purple), the steric gate (F35, red) and a conserved tyrosine (Y131, brown), which stacks on the backbone of the left lip and orients it. C53 forms a square with the V54 flue-handle (turquoise), I59 (gray) and the I60 roof (pink). scDNAP  $\eta$  has a large insert/loop (aa96–126) in the left lip, which is represented as a discontinuity. (e) The upper lip for hDNAP  $\kappa$  (yellow) is superimposed on the upper lip for scDNAP  $\eta$  (green), which clearly shows the differences in curvature. X-ray coordinates are from 2OH2 for hDNAP  $\kappa$  [29] and from 1JIH for scDNAP  $\eta$  [27], where hydrogens were added using insightII.

found at each aa position. Positions with  $\geq 90\%$  aa homology or with clusters of high homology are highlighted in pink and red. Many of the first  $\sim 20$  aa show high homology, including the presumptive catalytically essential aspartate (D6), and the steric gate (Y11). The region around the catalytically essential aspartate/glutamate pair (D101/E102) is also highly conserved. These and other regions that are conserved in all Y-family DNAPs are highlighted in pink in Figure 2. Regions conserved in UmuC(V), but not in other Y-Family DNAPs, are highlighted in red in Figure 2. One such conserved region is V29-C36, which is part of a loop that includes one edge of the chimney lip (S31-D34). (This loop is discussed at greater length in Section 7.1). A second conserved region is S71-Y77, which includes the second lip of the chimney, as well as other features discussed below. This conservation is strong evidence that the nature of the chimney opening is important. The third edge of the chimney (E255-T258) is in the little finger domain, and in our model of UmuC the third lip is farther from the active site and appears less likely to impinge on adducts protruding from the minor groove. Consistent with this view the third lip of the chimney is less well conserved. Preliminary analysis of the chimney lips of large collections of DNAPs IV,  $\kappa$ , and  $\eta$  sequences also reveal considerable amino acid conservation of the chimney lips.

**7.1. Structural Basis for a Large versus a Small Chimney Opening.** DNAP IV has a large chimney opening (Figure 3(a)), which can accommodate the pyrene thus allowing +BP to readily pair with dCTP when dCTP adopts the canonical shape observed in all other families of DNAPs [136, 137]. In contrast, UmuC(V) has a small chimney opening (Figure 3(b)), which forces +BP downward in the active site into a position where catalysis seems unlikely to be facile [136, 137]. What structural difference(s) in DNAP IV versus UmuC(V) might result in a large versus a small chimney opening, and is this structural difference(s) conserved in other Y-Family DNAPs in the IV/ $\kappa$ -class versus the DNAP V/ $\eta$ -class?

The chimney upper lip (turquoise, Figure 3(a)) is closest to the active site, and principally defines whether the chimney can accommodate the bulky B[a]P moiety. The first amino acid in the upper lip of *E. coli* DNAP IV is glycine (G32). We have collected 434 DNAP IV sequences from the literature, and 418 have glycine at this position. Furthermore, 13/13 DNAP  $\kappa$  proteins from different species have glycine at this position. The one X-ray structure for the IV/ $\kappa$ -class is hDNAP  $\kappa$  [29], which shows that this glycine (G131, turquoise, Figure 3(c)), is followed by upward curvature of the chimney upper lip (red arrow, Figure 3(c)/left). This glycine can be thought of as a “flue-handle” whose  $\phi/\varphi$ -angles permit this upward curvature (see below), with the consequence being that the R-groups on the next several amino acids (the “flue”; S132/R133, blue in Figure 3(c)/middle) point away from the chimney opening, which remains open. Our models of DNAP IV also have this upward curvature (Figure 3(a)) with an open flue, which depends on the analogous glycine flue-handle (G32).

In contrast, leucine (L30 in Figure 2) is the flue-handle in UmuC(V) in 370/408 cases. Furthermore, 11/11 DNAP

$\eta$  proteins from different species have a bulky valine at the flue-handle position. The X-ray structure of scDNAP  $\eta$  [25], which is in the V/ $\eta$ -class, shows that its bulky V54 flue-handle (turquoise, Figure 3(d)/left) is associated with downward curvature of the chimney upper lip (red arrow), which forces the “flue” (Q55/Y56, blue in Figure 3(d)/middle) to plug the chimney. Figure 3(e) shows the upward curvature of the upper lip of hDNAP  $\kappa$  (yellow) superimposed on the downward curvature for scDNAP  $\eta$  (green). In UmuC(V) the sequence is slightly different (VLSN), though the outcome is the same: the bulky L30 flue-handle causes downward curvature, and an asparagine (N32) plugs the chimney giving a closed flue (Figure 3(b)).

Upward versus downward curvature of the chimney upper lip can be traced to the  $\phi/\varphi$ -angles adopted by the flue-handle [136]. The  $\phi/\varphi$ -angles for the nonglycine flue-handles in scDNAP  $\eta$ , hDNAP  $\eta$ , hDNAP  $\iota$ , UmuC(V), and Dpo4 are all similar, resulting in downward curvature of the chimney’s upper lip, causing the flue to plug the chimney and the chimney opening to be small. In contrast, Glycine has greater flexibility in its  $\phi/\varphi$ -angles compared to all other amino acids, and the glycine flue-handles in hDNAP  $\kappa$  and DNAP IV adopt  $\phi/\varphi$ -angles unique to glycine that allow upward curvature of the chimney’s upper lip, which keeps the nearby flue amino acids away from the chimney opening.

**7.2. Roof-aa and Roof-Neighbor-aa.** Another key difference between the IV/ $\kappa$ -class and the V/ $\eta$ -class is the bulk of the roof-aa (pink in Figures 3(c)/right and 3(d)/right), which is a positionally conserved residue that lies above the nucleobase of the dNTP, as seen in the active site of Dpo4 [24–32], yDNAP  $\eta$  [34], hDNAP  $\iota$  [36–38], hDNAP  $\kappa$  [35], and hDNAP  $\eta$  [39, 40]. Isoleucine is the dominant roof-aa in UmuC(V) (227/408), with valine (156/408) being the next most prevalent aa (Figure 2). In fact, compared to *E. coli* wt-UmuC (100%), the mutant I38V-UmuC (137%) is slightly more active in the nonmutagenic pathway with +BP, while amino acids that do not branch at the  $\beta$ -carbon, including leucine, show much lower activity [138]. Immediately after the roof-aa in UmuC(V), principally alanine is found (346/408). In the case of DNAP  $\eta$  from different species, the [roof-aa/next-aa] is [I/A] in 10/11 cases. In the yDNAP  $\eta$  X-ray structure [I60/A61] form a hydrophobic layer above the nucleobase of the dNTP.

In the collection of 434 DNAP IV sequences, there is more variability at the equivalent [roof-aa/next-aa] positions: [S/T] is preferred (238/434, 59%), though any of the nonbulky amino acids S, A, or T can be found at both the roof-aa (434/434) and the next-aa (406/434). For DNAP  $\kappa$ , the roof position is also principally S, A, or T (10/13) and the next amino acid is always threonine (13/13). In X-ray structures the threonine methyl group in Dpo4 (T45) and in hDNAP  $\kappa$  (T138) sit near the roof-aa (A44 and S137, resp.), and the hydroxyl of the threonine forms a hydrogen bond with a nonbonded oxygen on P $\beta$  of the dNTP.

When the [roof/next-aa] were mutated in wt-UmuC(V) from [I38/A39] to the single mutants [I38A/A39] or [I38/A39T], polymerase activity declined significantly; however, the double mutant [I38A/A39T], is nearly as active

as wild type UmuC(V) [138]. I38A/A39T-UmuC has the same sequence as wt-Dpo4 (A44/T45), which is in the IV/ $\kappa$ -class. These findings show the importance to activity of the coupling of the identity of the [roof-aa/next-aa].

**7.3. The Interconnected Architecture of the Chimney and Roof Regions.** To understand the interconnected architecture of the chimney/roof regions of Y-Family DNAPs, it is useful to focus on a bulky aliphatic amino acid, which is highly conserved V29 (374/408) in our collection of UmuC(V) sequences. (In the equivalent position, all 434 DNAP IV sequences have either valine or isoleucine; valine is present in 10/11 DNAP  $\eta$  sequences and in 13/13 DNAP  $\kappa$  sequences.) This amino acid plays a scaffolding role as revealed in X-ray structures [23–38] and in models [44, 136, 138]. Using hDNAP  $\kappa$  [35] as an example, this scaffolding valine (V130, white in Figure 3(c)/right) is the beginning of a loop that ends with the roof-aa, and the two form a backbone hydrogen bond (scaffold-C=O:HN-roof). This backbone hydrogen bond is also observed in X-ray structures from Dpo4 [24–32], scDNAP  $\eta$  [35], hDNAP  $\kappa$  [35], and hDNAP  $\iota$  [36–38]. The scaffold-V130 also contacts the flue-handle (G131) and L136 (Figure 3(c)/right, gray). Thus, the base of this loop is anchored by a square of four amino acids (V130/G131/L136/S137). In scDNAP  $\eta$ , this region looks similar with C53/V54/I59/I60 (Figure 3(d)/right). The square includes I31/G32/I41/S42 in DNAP IV, and V29/L30/V37/I38 in UmuC(V). Evidence suggests that V29 and I38 are likely to be in contact in UmuC(V) [138].

Scaffold-V130 in hDNAP  $\kappa$  (white, Figure 3(c)/right) also helps organize the steric gate (Y12, red), which face-stacks with Y174 (brown), a highly conserved tyrosine whose other aromatic face contacts the backbone of the left lip of the chimney (i.e., aa168–171 in hDNAP  $\kappa$ ), thus helping to orient it. A tyrosine is found at this position in 406/408 UmuC(V) sequences, in 432/434 DNAP IV sequences, in 11/11 DNAP  $\eta$  sequences, and in 13/13 DNAP  $\kappa$  sequences.

**7.4. The Chimney “Cap”.** The interconnection between the roof and chimney regions are similar in scDNAP  $\eta$  (Figure 3(d)/right). However, the left chimney lip has an insert (aa93–127), which is not shown in Figure 3(c) but is indicated by a circle. In spite of this insert/loop, the chimney left lip of scDNAP  $\eta$  resembles the left lip of hDNAP  $\kappa$  (Figure 3(c)/right) and of other Y-Family DNAPs. This insert serves as a “cap” over the chimney opening, such that the chimney is completely closed. DNAP  $\eta$  always has a cap, though its size varies (e.g., aa81–87 in hDNAP  $\eta$ ). Speculation about a role for the DNAP  $\eta$  chimney cap is in the next section.

## 8. DNAP $\eta$ Structures with TT-CPDs

Recently, X-ray structures of yeast DNAP  $\eta$  [39] and human DNAP  $\eta$  [40] with a TT-CPD were published, and remarkable insights have emerged. Two template bases are in the active site, with the base on the 3'-side base pairing with the dNTP. When the 3'-T of the TT-CPD interacts

with dATP, the 5'-T of the TT-CPD is also in the active site, and when the 5'-T of the TT-CPD is interacting with dATP, then the normal base on its 5'-side is in the active site. Undamaged DNA appears similarly. The T-bases of a TT-CPD lie at an angle of  $\sim 30^\circ$  with respect to each other and lack the usual twist between the base pairs; however, the impact of these distortions are minimized by the protein, such that the TT-CPD looks remarkably similar to a normal pair of adjacent thymines. Watson-Crick pairing is observed between the dATP and each T-base of the TT-CPD.

dATP adopts the canonical chair-like shape found in all families of DNAPs (see Section 10), though the shape is nuanced; for example, the angle of the A-base is tilted slightly downward compared to other dNTPs in Y-Family DNAPs in order to pair with the 3'-T of the TT-CPD. In hDNAP  $\eta$ , the guanidinium of R61 interacts with phosphate-oxygens on both the  $\alpha$ - and  $\beta$ -positions of dATP, which is a unique interaction among Y-Family DNAPs. Interestingly, the equivalent R73 in  $\gamma$ DNAP  $\eta$  is flexible and can be in this position, or it can face the opposite direction and pair with the extra template base in the active site; that is, the base not paired with the dNTP. This arginine is one of the most conserved amino acids in DNAP  $\eta$ , though the R73A mutation in  $\gamma$ DNAP  $\eta$  retains normal kinetics with respect to both undamaged and damaged DNA, which suggests that its most important role is not being revealed in studies with a TT-CPD. In UmuC(V), which is the bacterial ortholog of DNAP  $\eta$ , methionine (M51) is usually at the equivalent position, though arginine or lysine are frequently present (42/408) (Figure 2). The other highly conserved amino acid in DNAP  $\eta$  is a glutamine (Q38 in hDNAP  $\eta$  and Q55 in  $\gamma$ DNAP  $\eta$ ), which sits in the minor groove and interacts with both O<sup>2</sup>-positions on the T-bases of the TT-CPD.

Why is DNAP  $\kappa$  inactive on CPDs, while DNAP  $\eta$  is active? A number of structural elements no doubt contribute, but one important feature is that M135 in DNAP  $\kappa$ , which lies two positions before the roof-aa, is too bulky to accommodate both template-Ts of the TT-CPD. In the equivalent position, hDNAP  $\eta$  has a glycine (G46) and  $\gamma$ DNAP  $\eta$  has a serine (S58), whose smaller size permits TT-CPD in the active site. Thus, DNAP  $\kappa$  may have an amino acid (i.e., M135) to minimize its activity on substrates meant for the V $\eta$ -class of DNAPs. Similarly, one of the functions of the flue and the cap for V/ $\eta$ -class DNAPs may be to minimize its activity on adducts that protrude into the minor groove, which are substrates for IV/ $\kappa$ -class DNAPs.

## 9. Architecture of the Y-Family Little Finger Domain

Y-Family DNAPs show considerable amino acid homology in the thumb/palm/fingers domains (approximately aa1–230), which makes alignment in this region, including for UmuC(V), unambiguous [44]. However, alignment of the little finger domain is more problematic. X-ray structures exist for the little finger domain of seven Y-Family DNAPs, and their fundamental structure is similar. They show a conserved secondary structure of  $\beta 1-\alpha 1-\beta 2-\beta 3-\alpha 2-\beta 4$ , where

the four  $\beta$ -strands are aligned and anti-parallel, while the two  $\alpha$ -helices are aligned, antiparallel and cross-diagonally over the  $\beta$ -strands. In spite of this structural conservation, standard sequence alignment algorithms (e.g., ClustalW or MUSCLE) do not correctly align the little finger domains of these seven proteins.

Figure 4 shows the correct alignment based on the X-ray structures (as described in the legend), including the little finger domain of DNAP IV [112]. What features of these sequences allow the structures to be conserved, even though their primary amino acid sequences are not conserved? An inspection of the X-ray structures reveals that little finger domains are held together by a core of about twenty-one hydrophobic residues, which are highlighted in turquoise in the alignment in Figure 4 (H1–H21) and are shown in a Dpo4 structure (Figure 5). Though hydrophobicity is conserved at these twenty-one positions, the exact amino acid is not. Dpo4, Dbh, DNAP  $\kappa$ , DNAP IV, DNAP  $\iota$ , yDNAP  $\eta$ , and hDNAP  $\eta$  have 19, 19, 17, 20, 20, 20, and 20 hydrophobic residues, respectively, at these 21 positions (Figure 4).

A comparison of these seven proteins reveals that the little finger domain has thirteen positions where an amino acid side-chain can interact with a phosphate-oxygen. Nine positions have a consensus lysine, arginine, asparagine or glutamine, which can interact with a phosphate-oxygen in the DNA backbone; they are designated L1–L9 in the alignment in Figure 4 (red) to indicate that their R-groups are “long.” They are also shown in the Dpo4 structure in Figure 5 (red). Four positions have a consensus serine or threonine that can interact with a phosphate-oxygen; they are designated S1–S4 to indicate that their R-groups are “short” in Figure 4 (pink). They are also shown for Dpo4 in Figure 5 (pink).

In terms of DNA interactions, there are some nuances. In several cases amino acids with longer R-groups can also serve at the S1–S4 positions (e.g., K301 in Dbh). Regarding S3, S297/Dpo4, S297/Dbh and S359/DNAP  $\iota$  clearly interact with the P + 6 phosphate-oxygen; however, T469/DNAP  $\kappa$  looks like a rotation would be required for it to interact properly, though it was counted as a positive. Q296 in DNAP IV might be able to interact with P + 5, though DNA is not present for definitive assessment and it is noncanonical, so it is not counted. R285/DNAP IV and R283/Dbh (instead of N340) might interact with P + 8, though DNA is not present for definitive assessment and it is non-canonical, so neither is counted.

Of the thirteen sites that can interact with phosphate-oxygens (i.e., L1–L9 and S1–S4), Dpo4 and Dbh have an appropriate amino acid at 13/13 sites and 11/13 sites, respectively. In contrast, hDNAP  $\kappa$ , DNAP IV, hDNAP  $\iota$ , yDNAP  $\eta$  and hDNAP  $\eta$  have an appropriate amino acid at 9, 8, 7, 8, and 7 sites, respectively. The higher level of conformity for Dpo4 and Dbh undoubtedly reflects the need for more interactions with DNA given that they are from thermophilic bacteria and must operate at elevated temperatures. The similar number of residues ( $\sim$ 8) for the other DNAPs probably reflects that they operate at a similar but lower temperature (i.e., 37°C), and if they had more

interactions they might bind DNA too tightly. We note that an increase in hydrophobic residues in the hydrophobic core was not expected for Dpo4 and Dbh, because hydrophobic interactions strengthen as temperature increases.

## 10. How Y-Family Architecture Influences dCTP versus dATP Insertion Opposite B[a]P Adducts

DNAP IV can pair dCTP with the dG moiety of +BP, importantly because the bulky pyrene can be accommodated in DNAP IV's large chimney opening (Figure 3(a)). For phosphoester bond formation to occur the distance between primer-O3' and P $\alpha$ -dCTP must be reaction-ready and can be compared to the closest possible distance, a van der Waals' contact ( $\sim$ 3.5 Å). In models of +BP in DNAP IV [136], the distance between primer-O3' and P $\alpha$ -dCTP was  $\sim$ 3.7 Å, which approximates a van der Waals' contact, and, thus, can be thought of as being “reaction ready.” The no-adduct control had a similar primer-O3' and P $\alpha$ -dCTP distance ( $\sim$ 3.7 Å).

In contrast, UmuC(V) does not give a satisfactory structure when +BP is paired with dCTP (Figure 3(b)/center), because UmuC(V)'s small chimney opening forces the bulky pyrene moiety downward. Asparagine-32 is the main problem, and its side chain plugs the UmuC(V) chimney leading to a clash with +BP. In the unadducted structure (Figure 3(b)/left), N32 adopts its lowest energy rotational conformer with respect to the C $\alpha$ –C $\beta$  bond. The presence of +BP leads to a rotation about the C $\alpha$ –C $\beta$  bond (Figure 3(b)/center); however, no other rotation can get N32 any farther out of the way. Consequently, UmuC(V)'s small chimney forces the +BP-dG in the template and its paired dCTP to move downward such that the primer-O3'/dCTP-P $\alpha$  distance is elongated to  $\sim$ 5.0 Å, which is a nonreaction-ready distance.

These observations provide a reasonable rationale for why DNAP IV preferentially does cellular dCTP insertion in cells: DNAP IV's large chimney opening permits a reasonable adduct-dG:dCTP structure with reaction-ready distances between primer-O3' and P $\alpha$ -dCTP.

If UmuC(V)'s small chimney enforces a non-reaction-ready distance between the primer-O3'/dNTP-P $\alpha$ , then how could UmuC(V) insert any dNTP opposite +BP? Recently, we offered a hypothesis [136].

X-ray structures from all DNAP families show a canonical dNTP shape that has been called “chair-like,” and its structure from T7 DNA polymerase is shown in Figure 6 (blue insert), which is also observed in most of the X-ray structures of Y-Family DNAPs, including Dpo4 (“S1-dNTP shape,” Figure 6, green). However, a second non-canonical “goat-tail-like” shape (“S2-dNTP”, Figure 6, yellow) has also been observed [26]. The goat-tail-like S2-dNTP shape can lie lower down in the active site, and +BP paired with dCTP in the S2-dNTP shape allows the pyrene to lie comfortably under the small chimney opening of UmuC(V), which allows the primer-O3'/dNTP-P $\alpha$  distance to be reaction-ready ( $\sim$ 3.8 Å).



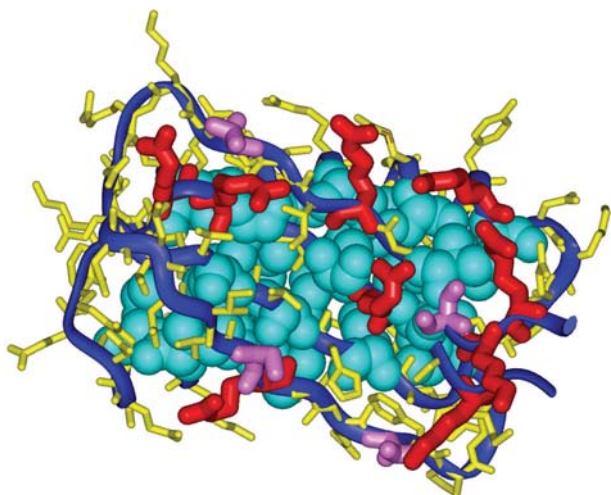


FIGURE 5: The little finger domain of Dpo4, showing amino acids whose R-groups contribute to the hydrophobic core (H1–H21, turquoise). Furthermore, lysine/arginine/asparagine/glutamine residues that interact with phosphate-oxygens are shown in red (L1–L9), and serine/threonine residues that interact with phosphate-oxygens are shown in pink (S1–S4). The view is toward the four anti-parallel  $\beta$ 1– $\beta$ 4 strands, and  $\beta$ 1 begins to the right, while the last amino acid in  $\beta$ 4 is shown just below it. The view is also into the face that binds duplex DNA, where the helix axis is approximately vertical. The Dpo4 coordinates are from 1SOM-B.

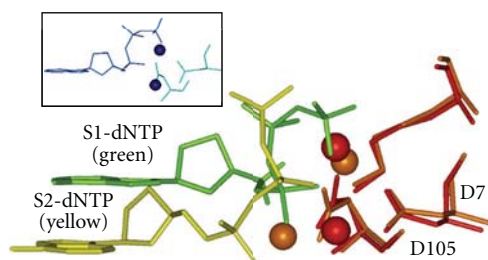


FIGURE 6: Side view of a dNTP in the “chair-like” shape S1-dNTP (green) versus the “goat-tail-like” shape S2-dNTP (yellow). Key amino acids (only D7, D105, and K159 are shown) from a Dpo4 structure adopting the S1-dNTP shape were superimposed on the same amino acids in a Dpo4 structure adopting the S2-dNTP. Spheres are divalent cations (S1-dNTP/red and S2-dNTP/brown). S1-dATP from T7 DNA polymerase is also shown (insert, blue). X-ray coordinates are from 1SOM-B for Dpo4/S1-dNTP, 1RYS-A for Dpo4/S2-dNTP, and 1T7P for T7 DNAP.

## 11. Unusual Architectural Features of Dpo4

Dpo4 is by far the best studied Y-Family DNAP, both structurally and biochemically. Based on biochemical and X-ray findings [28], Dpo4 insertion opposite +BP was proposed to follow a “dislocation” or “templated” pathway. Dislocation/templated insertion (see [135, 136] and references therein) involves DNAP stalling at an adduct, slippage to the next 5′-base along the template, which directs incorporation (e.g., dATP insertion opposite the 5′-T in a 5′-TG sequence context), whereupon the newly incorporated

dA slips back to form an adduct-G:A mispair, from which extension yields the mispair that ultimately gives a G→T mutation. Dpo4 preferentially inserted dCTP, dTTP, dATP and dGTP opposite +BP in 5′-GG, 5′-AG, 5′-TG and 5′-CG sequences, respectively, [28], which is consistent with a dislocation/templated mechanism.

Though the dislocation/templated mechanism is attractive for Dpo4, considerable evidence both in vitro and in vivo suggest that neither DNAP IV nor DNAP V follow a dislocation/templated mechanism with +BP, as discussed extensively in [136] and references therein.

Why might Dpo4 be different than DNAPs IV and V? Dpo4 is in the IV/ $\kappa$ -class, and it has a nonbulky roof-aa and roof-neighbor-aa [A44/A57], as expected for the IV/ $\kappa$ -class. However, Dpo4 has a very small chimney opening (discussed below), which is associated with for the V/ $\eta$ -class. Thus, Dpo4 is a hybrid with a roof similar to the IV/ $\kappa$ -class and a chimney similar to the V/ $\eta$ -class.

Dpo4 has a small chimney opening, because its bulky flue-handle (C31) causes downward curvature of the chimney upper lip and leads to a closed flue (V32) [136]. In fact, Dpo4’s chimney is exceedingly blocked: (1) the V32 flue is inserted deeper into the chimney than, for example, the N32 flue of UmuC(V), and (2) M76, which is the second amino acid in Dpo4’s left lip, also plugs the chimney. DNAP IV and UmuC(V) have non-bulky G74 and S72, respectively, in the position equivalent to M76 in Dpo4. Thus, the excessively plugged chimney of Dpo4 forces the pyrene moiety of +BP so far from the active site that base pairing via either S1-dCTP or S2-dCTP is impossible; consequently, both the pyrene and the dG moieties of +BP are forced to be extrahelical with consequence being that pairing cannot occur with its complementary dC [28].

As mentioned above, DNAPs  $\eta$ , IV,  $\eta$ , and  $\iota$  have an appropriate amino acid at 9, 8, 7, and 8, respectively, of the thirteen sites that can interact with phosphate-oxygens (L1–L9 and S1–S4). In contrast, Dpo4 and Dbh conform 13/13 and 11/13, respectively, which undoubtedly reflects the need for more interactions with DNA given that they are from thermophilic bacteria and must operate at an elevated temperature. Thus, Dpo4 studied at 37°C, which is typical, may give results that do not reflect correctly on aspects of the mechanism of other Y-Family DNAPs, which have evolved to operate at 37°C.

This analysis suggests reasons for caution when applying conclusions from Dpo4 to other Y-Family DNAPs, especially those purely in the IV/ $\kappa$ -class or the V/ $\eta$ -class. Perhaps Dpo4 evolved its hybrid roof/chimney structure to bypass a unique set of lesions encountered by a thermophilic bacteria. Alternatively, perhaps the structure of Dpo4 at physiologically relevant elevated temperatures is different than at the temperature at which it was crystallized (room temperature.) and assayed (37°C), and this affects its structure and behavior.

## 12. Structure of B-Family Lesion-Bypass DNAPs

This paper has focused on Y-Family DNAPs, though some lesion bypass DNAPs are in the B-Family, including DNAP

II in *E. coli* and REV3 of DNAP  $\xi$  in many eukaryotic cells. DNAP II inserts and extends the  $-2$  frameshift intermediate of AAF-C8-dG [66, 117], which must have two looped out nucleotides as well as the AAF moiety protruding into the major groove. Data also suggests that DNAP II and DNAP  $\xi$  are involved in the bypass of interstrand crosslinks [45–49], which must have a large oligonucleotide protruding into the major groove during TLS. Though B-Family DNAPs completely surround DNA, the structure on the minor and major groove sides are very different, as revealed in structures of both *E. coli* DNAP II [139] and Rb69 DNAP [140]. B-family DNAPs have a helical protein component that follows and contacts the minor groove side of duplex DNA. On the major groove side, however, a protein dome is present that leaves a large open cavity. Though Y-Family DNAPs are open to solvent on their major groove side, the solvent-exposed DNA surface inside the cavity for DNAP II ( $\sim 400 \text{ \AA}^2$ , when considering, for example, the template: dNTP base pair plus the L + 1 base pair) is actually larger than with either DNAP IV ( $\sim 230 \text{ \AA}^2$ ) or UmuC(V) ( $\sim 130 \text{ \AA}^2$ ). It seems likely that the large cavity and solvent exposed region on the major groove side of B-Family DNAPs may be essential for their ability to accomplish TLS on lesions having bulky protrusions into the major groove.

## Abbreviations

B[a]P:	Benzo[a]pyrene
+BP:	[+ta]-B[a]P-N <sup>2</sup> -dG (Figure 1)
–BP:	[–ta]-B[a]P-N <sup>2</sup> -dG
TT-CPD:	Thymine-thymine cyclopyrimidine dimer
TLS:	Translesion synthesis, which includes the insertion of a base opposite a DNA adduct, as well as subsequent elongation
DNAP:	DNA polymerase
S1-dNTP:	The “chair-like” dNTP shape
S2-dNTP:	The “goat-tail-like” dNTP shape
aa:	Amino acid.

## References

- [1] R. A. Weinberg, *The Biology of Cancer*, Garland Science, Taylor & Francis, New York, NY, USA, 2007.
- [2] A. Luch, “Nature and nurture—lessons from chemical carcinogenesis,” *Nature Reviews Cancer*, vol. 5, no. 2, pp. 113–125, 2006.
- [3] B. Singer and D. Grunberger, *Molecular Biology of Mutagens and Carcinogens*, Plenum Press, New York, NY, USA, 1983.
- [4] A. Balmain, R. Brown, and C. C. Harris, Eds., “The twentieth anniversary special issue contains reviews of many carcinogenesis topics,” *Carcinogenesis*, vol. 21, pp. 339–531, 2000.
- [5] A. H. Conney, “Induction of microsomal enzymes for foreign chemicals and carcinogenesis by polycyclic aromatic hydrocarbons: G.H.A. Clowes Memorial Lecture,” *Cancer Research*, vol. 42, no. 12, pp. 4875–4917, 1982.
- [6] S. D. McCulloch and T. A. Kunkel, “The fidelity of DNA synthesis by eukaryotic replicative and translesion synthesis polymerases,” *Cell Research*, vol. 18, no. 1, pp. 148–161, 2008.
- [7] S. D. McCulloch and T. A. Kunkel, “The fidelity of DNA synthesis by eukaryotic replicative and translesion synthesis polymerases,” *Cell Research*, vol. 18, no. 1, pp. 148–161, 2008.
- [8] C. Guo, J. N. Kosarek-Stancel, T.-S. Tang, and E. C. Friedberg, “Y-family DNA polymerases in mammalian cells,” *Cellular and Molecular Life Sciences*, vol. 66, no. 14, pp. 2363–2381, 2009.
- [9] L. S. Waters, B. K. Minesinger, M. E. Wiltrout, S. D’Souza, R. V. Woodruff, and G. C. Walker, “Eukaryotic translesion polymerases and their roles and regulation in DNA damage tolerance,” *Microbiology and Molecular Biology Reviews*, vol. 73, no. 1, pp. 134–154, 2009.
- [10] J. D. Pata, “Structural diversity of the Y-family DNA polymerases,” *Biochimica et Biophysica Acta*, vol. 1804, no. 5, pp. 1124–1135, 2010.
- [11] S. Schneider, S. Schorr, and T. Carell, “Crystal structure analysis of DNA lesion repair and tolerance mechanisms,” *Current Opinion in Structural Biology*, vol. 19, no. 1, pp. 87–95, 2009.
- [12] M. T. Washington, K. D. Carlson, B. D. Freudenthal, and J. M. Pryor, “Variations on a theme: eukaryotic Y-family DNA polymerases,” *Biochimica et Biophysica Acta*, vol. 1804, no. 5, pp. 1113–1123, 2010.
- [13] K. Bebenek and T. A. Kunkel, “Functions of DNA polymerases,” *Advances in Protein Chemistry*, vol. 69, pp. 137–165, 2004.
- [14] P. J. Rothwell and G. Waksman, “Structure and mechanism of DNA polymerases,” *Advances in Protein Chemistry*, vol. 71, pp. 401–440, 2005.
- [15] E. C. Friedberg, G. W. Walker, W. Siede, R. D. Wood, R. A. Schultz, and T. Ellenberger, *DNA Repair and Mutagenesis*, American Society for Microbiology, Washington, DC, USA, 2nd edition, 2006.
- [16] W. Yang and R. Woodgate, “What a difference a decade makes: insights into translesion DNA synthesis,” *Proceedings of the National Academy of Sciences of the United States of America*, vol. 104, no. 40, pp. 15591–15598, 2007.
- [17] H. Ohmori, E. C. Friedberg, R. P. P. Fuchs et al., “The Y-family of DNA polymerases,” *Molecular Cell*, vol. 8, no. 1, pp. 7–8, 2001.
- [18] T. Nohmi, “Environmental stress and lesion-bypass DNA polymerases,” *Annual Review of Microbiology*, vol. 60, pp. 231–253, 2006.
- [19] W. Yang, “Damage repair DNA polymerases Y,” *Current Opinion in Structural Biology*, vol. 13, no. 1, pp. 23–30, 2003.
- [20] S. Prakash, R. E. Johnson, and L. Prakash, “Eukaryotic translesion synthesis DNA polymerases: specificity of structure and function,” *Annual Review of Biochemistry*, vol. 74, pp. 317–353, 2005.
- [21] D. F. Jarosz, P. J. Beuning, S. E. Cohen, and G. C. Walker, “Y-family DNA polymerases in *Escherichia coli*,” *Trends in Microbiology*, vol. 15, no. 2, pp. 70–77, 2007.
- [22] R. P. Fuchs, S. Fujii, and J. Wagner, “Properties and functions of *Escherichia coli*: Pol IV and Pol V,” *Advances in Protein Chemistry*, vol. 69, pp. 229–264, 2004.
- [23] B.-L. Zhou, J. D. Pata, and T. A. Steitz, “Crystal structure of a DinB lesion bypass DNA polymerase catalytic fragment reveals a classic polymerase catalytic domain,” *Molecular Cell*, vol. 8, no. 2, pp. 427–437, 2001.
- [24] H. Ling, F. Boudsocq, R. Woodgate, and W. Yang, “Crystal structure of a Y-family DNA polymerase in action: a mechanism for error-prone and lesion-bypass replication,” *Cell*, vol. 107, no. 1, pp. 91–102, 2001.

- [25] H. Ling, F. Boudsocq, B. S. Plosky, R. Woodgate, and W. Yang, "Replication of a cis-syn thymine dimer at atomic resolution," *Nature*, vol. 424, no. 6952, pp. 1083–1087, 2003.
- [26] A. Vaisman, H. Ling, R. Woodgate, and W. Yang, "Fidelity of Dpo4: effect of metal ions, nucleotide selection and pyrophosphorolysis," *EMBO Journal*, vol. 24, no. 17, pp. 2957–2967, 2005.
- [27] O. Rechtkoblit, L. Malinina, Y. Cheng et al., "Stepwise translocation of Dpo4 polymerase during error-free bypass of an oxoG lesion," *PLoS Biology*, vol. 4, no. 1, pp. 25–42, 2006.
- [28] J. Bauer, G. Xing, H. Yagi, J. M. Sayer, D. M. Jerina, and H. Ling, "A structural gap in Dpo4 supports mutagenic bypass of a major benzo [a]pyrene dG adduct in DNA through template misalignment," *Proceedings of the National Academy of Sciences of the United States of America*, vol. 104, no. 38, pp. 14905–14910, 2007.
- [29] J. H. Wong, K. A. Fiala, Z. Suo, and H. Ling, "Snapshots of a Y-family DNA polymerase in replication: substrate-induced conformational transitions and implications for fidelity of Dpo4," *Journal of Molecular Biology*, vol. 379, no. 2, pp. 317–330, 2008.
- [30] R. L. Eoff, R. Sanchez-Ponce, and F. P. Guengerich, "Conformational changes during nucleotide selection by *Sulfolobus solfataricus* DNA polymerase Dpo4," *Journal of Biological Chemistry*, vol. 284, no. 31, pp. 21090–21099, 2009.
- [31] H. Zhang and F. P. Guengerich, "Effect of N<sup>2</sup>-guanyl modifications on early steps in catalysis of polymerization by *Sulfolobus solfataricus* P2 DNA polymerase Dpo4 T239W," *Journal of Molecular Biology*, vol. 395, no. 5, pp. 1007–1018, 2010.
- [32] O. Rechtkoblit, A. Kolbanovskiy, L. Malinina, N. E. Geacintov, S. Broyde, and D. J. Patel, "Mechanism of error-free and semitargeted mutagenic bypass of an aromatic amine lesion by Y-family polymerase Dpo4," *Nature Structural and Molecular Biology*, vol. 17, no. 3, pp. 379–388, 2010.
- [33] J. Trincao, R. E. Johnson, C. R. Escalante, S. Prakash, L. Prakash, and A. K. Aggarwal, "Structure of the catalytic core of *S. cerevisiae* DNA polymerase eta: implications for translesion DNA synthesis," *Molecular Cell*, vol. 8, no. 2, pp. 417–426, 2001.
- [34] A. Alt, K. Lammens, C. Chiochini et al., "Bypass of DNA lesions generated during anticancer treatment with cisplatin by DNA polymerase  $\eta$ ," *Science*, vol. 318, no. 5852, pp. 967–970, 2007.
- [35] S. Lone, S. A. Townson, S. N. Uljon et al., "Human DNA polymerase kappa encircles DNA: implications for mismatch extension and lesion bypass," *Molecular Cell*, vol. 25, no. 4, pp. 601–614, 2007.
- [36] D. T. Hair, R. E. Johnson, S. Prakash, L. Prakash, and A. K. Aggarwal, "Replication by human DNA polymerase- $\iota$  occurs by Hoogsteen base-pairing," *Nature*, vol. 430, no. 6997, pp. 377–380, 2004.
- [37] D. T. Nair, R. E. Johnson, L. Prakash, S. Prakash, and A. K. Aggarwal, "Human DNA polymerase  $\iota$  incorporates dCTP opposite template G via a G.C+ Hoogsteen base pair," *Structure*, vol. 13, no. 10, pp. 1569–1577, 2005.
- [38] D. T. Nair, R. E. Johnson, L. Prakash, S. Prakash, and A. K. Aggarwal, "Hoogsteen base pair formation promotes synthesis opposite the 1,N<sup>6</sup>-ethenodeoxyadenosine lesion by human DNA polymerase  $\iota$ ," *Nature Structural and Molecular Biology*, vol. 13, no. 7, pp. 619–625, 2006.
- [39] T. D. Silverstein, R. E. Johnson, R. Jain, L. Prakash, S. Prakash, and A. K. Aggarwal, "Structural basis for the suppression of skin cancers by DNA polymerase," *Nature*, vol. 465, no. 7301, pp. 1039–1043, 2010.
- [40] C. Biertümpfel, Y. Zhao, Y. Kondo et al., "Structure and mechanism of human DNA polymerase," *Nature*, vol. 465, no. 7301, pp. 1044–1048, 2010.
- [41] R. E. Johnson, S. Prakash, and L. Prakash, "The human DINB1 gene encodes the DNA polymerase Pol $\theta$ ," *Proceedings of the National Academy of Sciences of the United States of America*, vol. 97, no. 8, pp. 3838–3843, 2000.
- [42] E. Ohashi, T. Ogi, R. Kusumoto et al., "Error-prone bypass of certain DNA lesions by the human DNA polymerase  $\kappa$ ," *Genes and Development*, vol. 14, no. 13, pp. 1589–1594, 2000.
- [43] Y. Zhang, F. Yuan, X. Wu et al., "Error-free and error-prone lesion bypass by human DNA polymerase  $\kappa$  in vitro," *Nucleic Acids Research*, vol. 28, no. 21, pp. 4138–4146, 2000.
- [44] C. H. Lee, S. Chandani, and E. L. Loechler, "Homology modeling of four Y-family, lesion-bypass DNA polymerases: the case that *E. coli* Pol IV and human Pol  $\kappa$  are orthologs, and *E. coli* Pol V and human Pol  $\eta$  are orthologs," *Journal of Molecular Graphics and Modelling*, vol. 25, no. 1, pp. 87–102, 2006.
- [45] M. Berardini, W. Mackay, and E. L. Loechler, "A site-specific study of a plasmid containing single nitrogen mustard interstrand cross-link: evidence for a second, recombination-independent pathway for the DNA repair of interstrand cross-links," *Biochemistry*, vol. 36, pp. 3506–3513, 1997.
- [46] S. Sarkar, A. A. Davies, H. D. Ulrich, and P. J. McHugh, "DNA interstrand crosslink repair during G1 involves nucleotide excision repair and DNA polymerase  $\zeta$ ," *EMBO Journal*, vol. 25, no. 6, pp. 1285–1294, 2006.
- [47] P. J. McHugh and S. Sarkar, "DNA interstrand cross-link repair in the cell cycle: a critical role for polymerase  $\zeta$  in G1 phase," *Cell Cycle*, vol. 5, no. 10, pp. 1044–1047, 2006.
- [48] P. Lehoczký, P. J. McHugh, and M. Chovanec, "DNA interstrand cross-link repair in *Saccharomyces cerevisiae*," *FEMS Microbiology Reviews*, vol. 31, no. 2, pp. 109–133, 2007.
- [49] M. Räschle, P. Knipsheer, M. Enoiu et al., "Mechanism of replication-coupled DNA interstrand crosslink repair," *Cell*, vol. 134, no. 6, pp. 969–980, 2008.
- [50] K. Schlacher and M. F. Goodman, "Lessons from 50 years of SOS DNA-damage-induced mutagenesis," *Nature Reviews Molecular Cell Biology*, vol. 8, no. 7, pp. 587–594, 2000.
- [51] Z. Qiu and M. F. Goodman, "The *Escherichia coli* polB locus is identical to dinA, the structural gene for DNA polymerase II: characterization of pol II purified from a polB mutant," *Journal of Biological Chemistry*, vol. 272, no. 13, pp. 8611–8617, 1997.
- [52] S.-R. Kim, K. Matsui, M. Yamada, P. Gruz, and T. Nohmi, "Roles of chromosomal and episomal dinB genes encoding DNA pol IV in targeted and untargeted mutagenesis in *Escherichia coli*," *Molecular Genetics and Genomics*, vol. 266, no. 2, pp. 207–215, 2001.
- [53] R. Woodgate and D. G. Ennis, "Levels of chromosomally encoded Umu proteins and requirements for in vivo UmuD cleavage," *Molecular and General Genetics*, vol. 229, no. 1, pp. 10–16, 1991.
- [54] M. Tang, P. Pham, X. Shen et al., "Roles of *E. coli* DNA polymerases IV and V in lesion-targeted and untargeted SOS mutagenesis," *Nature*, vol. 404, no. 6781, pp. 1014–1018, 2000.
- [55] D. E. Brash and W. A. Haseltine, "UV-induced mutation hotspots occur at DNA damage hotspots," *Nature*, vol. 298, no. 5870, pp. 189–192, 1982.
- [56] M. F. Goodman, "Error-prone repair DNA polymerases in prokaryotes and eukaryotes," *Annual Review of Biochemistry*, vol. 71, pp. 17–50, 2002.

- [57] J. Yin, K. Y. Seo, and E. L. Loechler, "A role for DNA polymerase V in G→T mutations from the major benzo[a]pyrene N<sup>2</sup>-dG adduct when studied in a 5'-TGT sequence in *E. coli*," *DNA Repair*, vol. 3, no. 3, pp. 323–334, 2004.
- [58] B. S. Strauss, "The "A" rule revisited: polymerases as determinants of mutational specificity," *DNA Repair*, vol. 1, no. 2, pp. 125–135, 2002.
- [59] E. L. Loechler, "Mechanism by which aflatoxins and other bulky carcinogens induce mutations," in *The Toxicology of Aflatoxins: Human Health, Veterinary, and Agricultural Significance*, D. L. Eaton and J. D. Groopman, Eds., chapter 8, pp. 149–178, Academic Press, Orlando, Fla, USA, 1994.
- [60] C. Masutani, R. Kusumoto, A. Yamada et al., "The XPV (xeroderma pigmentosum variant) gene encodes human DNA polymerase  $\eta$ ," *Nature*, vol. 399, no. 6737, pp. 700–704, 1999.
- [61] R. E. Johnson, S. Prakash, and L. Prakash, "Efficient bypass of a thymine-thymine dimer by yeast DNA polymerase, Poleta," *Science*, vol. 283, no. 5404, pp. 1001–1004, 1999.
- [62] R. E. Johnson, C. M. Kondratyck, S. Prakash, and L. Prakash, "hRAD30 mutations in the variant form of xeroderma pigmentosum," *Science*, vol. 285, no. 5425, pp. 263–265, 1999.
- [63] M. T. Washington, R. E. Johnson, S. Prakash, and L. Prakash, "Fidelity and processivity of *Saccharomyces cerevisiae* DNA polymerase  $\eta$ ," *Journal of Biological Chemistry*, vol. 274, no. 52, pp. 36835–36838, 1999.
- [64] M. T. Washington, R. E. Johnson, S. Prakash, and L. Prakash, "Accuracy of thymine-thymine dimer bypass by *Saccharomyces cerevisiae* DNA polymerase  $\eta$ ," *Proceedings of the National Academy of Sciences of the United States of America*, vol. 97, no. 7, pp. 3094–3099, 2000.
- [65] R. E. Johnson, M. T. Washington, S. Prakash, and L. Prakash, "Fidelity of human DNA polymerase  $\eta$ ," *Journal of Biological Chemistry*, vol. 275, no. 11, pp. 7447–7450, 2000.
- [66] S. Fujii and R. P. Fuchs, "Interplay among replicative and specialized DNA polymerases determines failure or success of translesion synthesis pathways," *Journal of Molecular Biology*, vol. 372, no. 4, pp. 883–893, 2007.
- [67] Q. Jiang, K. Karata, R. Woodgate, M. M. Cox, and M. F. Goodman, "The active form of DNA polymerase  $\nu$  is UmuD' 2 C-RecA-ATP," *Nature*, vol. 460, no. 7253, pp. 359–363, 2009.
- [68] M. Patel, Q. Jiang, R. Woodgate, M. M. Cox, and M. F. Goodman, "A new model for SOS-induced mutagenesis: how RecA protein activates DNA polymerase V," *Critical Reviews in Biochemistry and Molecular Biology*, vol. 45, no. 3, pp. 171–184, 2010.
- [69] S. Fujii, A. Isogawa, and R. P. Fuchs, "RecFOR proteins are essential for Pol V-mediated translesion synthesis and mutagenesis," *EMBO Journal*, vol. 25, no. 24, pp. 5754–5763, 2006.
- [70] M. J. McIlwraith, A. Vaisman, Y. Liu, E. Fanning, R. Woodgate, and S. C. West, "Human DNA polymerase  $\epsilon$  promotes DNA synthesis from strand invasion intermediates of homologous recombination," *Molecular Cell*, vol. 20, pp. 783–792, 2005.
- [71] S. Kobayashi, M. R. Valentine, P. Pham, M. O'Donnell, and M. F. Goodman, "Fidelity of *Escherichia coli* DNA polymerase IV. Preferential generation of small deletion mutations by dNTP-stabilized misalignment," *Journal of Biological Chemistry*, vol. 277, no. 37, pp. 34198–34207, 2002.
- [72] D. F. Jarosz, V. G. Godoy, J. C. Delaney, J. M. Essigmann, and G. C. Walker, "A single amino acid governs enhanced activity of DinB DNA polymerases on damaged templates," *Nature*, vol. 439, no. 7073, pp. 225–228, 2006.
- [73] N. Lenne-Samuel, R. Janel-Bintz, A. Kolbanovskiy, N. E. Geacintov, and R. P. P. Fuchs, "The processing of a Benzo(a)pyrene adduct into a frameshift or a base substitution mutation requires a different set of genes in *Escherichia coli*," *Molecular Microbiology*, vol. 38, no. 2, pp. 299–307, 2000.
- [74] R. Napolitano, R. Janel-Bintz, J. Wagner, and R. P. P. Fuchs, "All three SOS-inducible DNA polymerases (Pol II, Pol IV and Pol V) are involved in induced mutagenesis," *EMBO Journal*, vol. 19, no. 22, pp. 6259–6265, 2000.
- [75] K. Y. Seo, A. Nagalingam, S. Miri et al., "Mirror image stereoisomers of the major benzo[a]pyrene N<sup>2</sup>-dG adduct are bypassed by different lesion-bypass DNA polymerases in *E. coli*," *DNA Repair*, vol. 5, no. 4, pp. 515–522, 2006.
- [76] B. Yuan, H. Cao, Y. Jiang, H. Hong, and Y. Wang, "Efficient and accurate bypass of N<sup>2</sup>-(1-carboxyethyl)-2'-deoxyguanosine by DinB DNA polymerase in vitro and in vivo," *Proceedings of the National Academy of Sciences of the United States of America*, vol. 105, no. 25, pp. 8679–8684, 2008.
- [77] X. Shen, J. M. Sayer, H. Kroth et al., "Efficiency and accuracy of SOS-induced DNA polymerases replicating benzo[a]pyrene-7,8-diol 9,10-epoxide A and G adducts," *Journal of Biological Chemistry*, vol. 277, no. 7, pp. 5265–5274, 2002.
- [78] L. J. Marnett, "Oxyradicals and DNA damage," *Carcinogenesis*, vol. 21, no. 3, pp. 361–370, 2000.
- [79] T. Opperman, S. Murli, B. T. Smith, and G. C. Walker, "A model for a umuDC-dependent prokaryotic DNA damage checkpoint," *Proceedings of the National Academy of Sciences of the United States of America*, vol. 96, no. 16, pp. 9218–9223, 1999.
- [80] C. Indiani, L. D. Langston, O. Yurieva, M. F. Goodman, and M. O'Donnell, "Translesion DNA polymerases remodel the replisome and alter the speed of the replicative helicase," *Proceedings of the National Academy of Sciences of the United States of America*, vol. 106, no. 15, pp. 6031–6038, 2009.
- [81] B. Yeiser, E. D. Pepper, M. F. Goodman, and S. E. Finkel, "SOS-induced DNA polymerases enhance long-term survival and evolutionary fitness," *Proceedings of the National Academy of Sciences of the United States of America*, vol. 99, no. 13, pp. 8737–8741, 2002.
- [82] J. D. Tompkins, J. L. Nelson, J. C. Hazel, S. L. Leugers, J. D. Stumpf, and P. L. Foster, "Error-prone polymerase, DNA polymerase IV, is responsible for transient hypermutation during adaptive mutation in *Escherichia coli*," *Journal of Bacteriology*, vol. 185, no. 11, pp. 3469–3472, 2003.
- [83] D. T. Nair, R. E. Johnson, L. Prakash, S. Prakash, and A. K. Aggarwal, "Rev1 employs a novel mechanism of DNA synthesis using a protein template," *Science*, vol. 309, no. 5744, pp. 2219–2222, 2006.
- [84] S. Avkin, M. Goldsmith, S. Velasco-Miguel, N. Geacintov, E. C. Friedberg, and Z. Livneh, "Quantitative analysis of translesion DNA synthesis across a benzo[a]pyrene-guanine adduct in mammalian cells: the role of DNA polymerase," *Journal of Biological Chemistry*, vol. 279, no. 51, pp. 53298–53305, 2004.

- [85] T. Ogi, Y. Shinkai, K. Tanaka, and H. Ohmori, "Polk protects mammalian cells against the lethal and mutagenic effects of benzo[a]pyrene," *Proceedings of the National Academy of Sciences of the United States of America*, vol. 99, no. 24, pp. 15548–15553, 2002.
- [86] O. Rechkoblit, Y. Zhang, D. Guo et al., "trans-lesion synthesis past bulky benzo[a]pyrene diol epoxide N<sup>2</sup>-dG and N6-dA lesions catalyzed by DNA bypass polymerases," *Journal of Biological Chemistry*, vol. 277, no. 34, pp. 30488–30494, 2002.
- [87] L. Jia, N. E. Geacintov, and S. Broyde, "The N-clasp of human DNA polymerase  $\kappa$  promotes blockage or error-free bypass of adenine- or guanine-benzo[a]pyrenyl lesions," *Nucleic Acids Research*, vol. 36, no. 20, pp. 6571–6584, 2008.
- [88] S. D. McCulloch, A. Wood, P. Garg, P. M. J. Burgers, and T. A. Kunkel, "Effects of accessory proteins on the bypass of a cis-syn thymine-thymine dimer by *Saccharomyces cerevisiae* DNA polymerase  $\eta$ ," *Biochemistry*, vol. 46, no. 30, pp. 8888–8896, 2007.
- [89] S. D. McCulloch, R. J. Kokoska, C. Masutani, S. Iwai, F. Hanaoka, and T. A. Kunkel, "Preferential cis-syn thymine dimer bypass by DNA polymerase  $\eta$  occurs with biased fidelity," *Nature*, vol. 428, no. 6978, pp. 97–100, 2004.
- [90] L. Haracska, S.-L. Yu, R. E. Johnson, L. Prakash, and S. Prakash, "Efficient and accurate replication in the presence of 7,8-dihydro-8-oxoguanine by DNA polymerase  $\eta$ ," *Nature Genetics*, vol. 25, no. 4, pp. 458–461, 2000.
- [91] A. Vaisman, C. Masutani, F. Hanaoka, and S. G. Chaney, "Efficient translesion replication past oxaliplatin and cisplatin GpG adducts by human DNA polymerase  $\eta$ ," *Biochemistry*, vol. 39, no. 16, pp. 4575–4580, 2000.
- [92] T. B. Petta, S. Nakajima, A. Zlatanou et al., "Human DNA polymerase iota protects cells against oxidative stress," *EMBO Journal*, vol. 27, no. 21, pp. 2883–2895, 2008.
- [93] Y. Zhang, F. Yuan, X. Wu, J.-S. Taylor, and Z. Wang, "Response of human DNA polymerase  $\iota$  to DNA lesions," *Nucleic Acids Research*, vol. 29, no. 4, pp. 928–935, 2001.
- [94] K. Donny-Clark, R. Shapiro, and S. Broyde, "Accommodation of an N-(deoxyguanosin-8-yl)-2-acetylaminofluorene adduct in the active site of human DNA polymerase  $\iota$ : Hoogsteen or Watson–Crick base pairing?" *Biochemistry*, vol. 48, no. 1, pp. 7–18, 2009.
- [95] L. Wang and S. Broyde, "A new anti conformation for N-(deoxyguanosin-8-yl)-2-acetylaminofluorene (AAF-dG) allows Watson-Crick pairing in the *Sulfolobus solfataricus* P2 DNA polymerase IV (Dpo4)," *Nucleic Acids Research*, vol. 34, no. 3, pp. 785–795, 2006.
- [96] C. Xu, B. A. Maxwell, J. A. Brown, L. Zhang, and Z. Suo, "Global conformational dynamics of a Y-family DNA polymerase during catalysis," *PLoS Biology*, vol. 7, no. 10, Article ID e1000225, 2009.
- [97] M. A. Booher, S. Wang, and E. T. Kool, "Base pairing and steric interactions between pyrimidine strand bridging loops and the purine strand in DNA pyrimidine-purine-pyrimidine triplexes," *Biochemistry*, vol. 33, no. 15, pp. 4645–4651, 1994.
- [98] M. T. Washington, S. A. Helquist, E. T. Kool, L. Prakash, and S. Prakash, "Requirement of Watson-Crick hydrogen bonding for DNA synthesis by yeast DNA polymerase  $\eta$ ," *Molecular and Cellular Biology*, vol. 23, no. 14, pp. 5107–5112, 2003.
- [99] W. T. Wolfle, M. T. Washington, E. T. Kool et al., "Evidence for a Watson-Crick hydrogen bonding requirement in DNA synthesis by human DNA polymerase  $\kappa$ ," *Molecular and Cellular Biology*, vol. 25, no. 16, pp. 7137–7143, 2005.
- [100] L. Wang, X. Yu, P. Hu, S. Broyde, and Y. Zhang, "A water-mediated and substrate-assisted catalytic mechanism for *Sulfolobus solfataricus* DNA polymerase IV," *Journal of the American Chemical Society*, vol. 129, no. 15, pp. 4731–4737, 2007.
- [101] I. Letunic, L. Goodstadt, N. J. Dickens et al., "Recent improvements to the SMART domain-based sequence-annotation resource," *Nucleic Acids Research*, vol. 30, no. 1, pp. 242–244, 2002.
- [102] A. Bairoch, R. Apweiler, C. H. Wu et al., "The universal protein resource (UniProt)," *Nucleic Acids Research*, vol. 33, pp. D154–D159, 2005.
- [103] T. Lima, A. H. Auchincloss, E. Coudert et al., "HAMAP: a database of completely sequenced microbial proteome sets and manually curated microbial protein families in UniProtKB/Swiss-Prot," *Nucleic Acids Research*, vol. 37, no. 1, pp. D471–D478, 2009.
- [104] R. C. Edgar, "MUSCLE: multiple sequence alignment with high accuracy and high throughput," *Nucleic Acids Research*, vol. 32, no. 5, pp. 1792–1797, 2004.
- [105] Y. Ye and A. Godzik, "Flexible structure alignment by chaining aligned fragment pairs allowing twists," *Bioinformatics*, vol. 19, supplement 2, pp. ii246–ii255, 2003.
- [106] A. R. Ortiz, C. E. M. Strauss, and O. Olmea, "MAMMOTH (matching molecular models obtained from theory): an automated method for model comparison," *Protein Science*, vol. 11, no. 11, pp. 2606–2621, 2002.
- [107] S. Fujii and R. P. Fuchs, "Biochemical basis for the essential genetic requirements of RecA and the  $\beta$ -clamp in Pol V activation," *Proceedings of the National Academy of Sciences of the United States of America*, vol. 106, no. 35, pp. 14825–14830, 2009.
- [108] R. C. Heller and K. J. Marians, "Replisome assembly and the direct restart of stalled replication forks," *Nature Reviews Molecular Cell Biology*, vol. 7, no. 12, pp. 932–943, 2006.
- [109] L. D. Langston and M. O'Donnell, "DNA replication: keep moving and don't mind the gap," *Molecular Cell*, vol. 23, no. 2, pp. 155–160, 2006.
- [110] A. Furukohri, M. F. Goodman, and H. Maki, "A dynamic polymerase exchange with *Escherichia coli* DNA polymerase IV replacing DNA polymerase III on the sliding clamp," *Journal of Biological Chemistry*, vol. 283, no. 17, pp. 11260–11269, 2008.
- [111] O. J. Becherel, R. P. P. Fuchs, and J. Wagner, "Pivotal role of the  $\beta$ -clamp in translesion DNA synthesis and mutagenesis in *E. coli* cells," *DNA Repair*, vol. 4, no. 9, pp. 703–708, 2002.
- [112] K. A. Bunting, S. M. Roe, and L. H. Pearl, "Structural basis for recruitment of translesion DNA polymerase Pol IV/DinB to the  $\beta$ -clamp," *EMBO Journal*, vol. 22, no. 21, pp. 5883–5892, 2003.
- [113] J. M. H. Heltzel, R. W. Maul, S. K. Scouten Ponticelli, and M. D. Sutton, "A model for DNA polymerase switching involving a single cleft and the rim of the sliding clamp," *Proceedings of the National Academy of Sciences of the United States of America*, vol. 106, no. 31, pp. 12664–12669, 2009.
- [114] J. M. H. Heltzel, S. K. Scouten Ponticelli, L. H. Sanders et al., "Sliding clamp-DNA interactions are required for viability and contribute to DNA polymerase management in *Escherichia coli*," *Journal of Molecular Biology*, vol. 387, no. 1, pp. 74–91, 2009.
- [115] J. Wagner, H. Etienne, R. P. Fuchs, A. Cordonnier, and D. Burnouf, "Distinct  $\beta$ -clamp interactions govern the activities of the  $\gamma$  family PolIV DNA polymerase," *Molecular Microbiology*, vol. 74, no. 5, pp. 1143–1151, 2009.

- [116] S. Delmas and I. Matic, "Interplay between replication and recombination in *Escherichia coli*: impact of the alternative DNA polymerases," *Proceedings of the National Academy of Sciences of the United States of America*, vol. 103, no. 12, pp. 4564–4569, 2006.
- [117] R. P. Fuchs and S. Fujii, "Translesion synthesis in *Escherichia coli*: lessons from the NarI mutation hot spot," *DNA Repair*, vol. 6, no. 7, pp. 1032–1041, 2007.
- [118] R. H. Heflich and R. E. Neft, "Genetic toxicity of 2-acetylaminofluorene, 2-aminofluorene and some of their metabolites and model metabolites," *Mutation Research*, vol. 318, no. 2, pp. 73–174, 1994.
- [119] L. Wang and S. Broyde, "A new anti conformation for N-(deoxyguanosin-8-yl)-2-acetylaminofluorene (AAF-dG) allows Watson-Crick pairing in the *Sulfolobus solfataricus* P2 DNA polymerase IV (Dpo4)," *Nucleic Acids Research*, vol. 34, no. 3, pp. 785–795, 2006.
- [120] R. G. Harvey, *Polycyclic Aromatic Hydrocarbons: Chemistry and Cancer*, Wiley-VCH, New York, NY, USA, 1997.
- [121] A. Dipple, "Polycyclic aromatic hydrocarbon carcinogens," in *Polycyclic Aromatic Hydrocarbons and Carcinogenesis*, R. G. Harvey, Ed., pp. 1–17, American Chemical Society Press, Washington, DC, USA, 1985.
- [122] M. F. Denissenko, A. Pao, M.-S. Tang, and G. P. Pfeifer, "Preferential formation of benzo[a]pyrene adducts at lung cancer mutational hotspots in P53," *Science*, vol. 274, no. 5286, pp. 430–432, 1996.
- [123] M. F. Denissenko, A. Pao, G. P. Pfeifer, and M.-S. Tang, "Slow repair of bulky DNA adducts along the nontranscribed strand of the human p53 gene may explain the strand bias of transversion mutations in cancers," *Oncogene*, vol. 16, no. 10, pp. 1241–1247, 1998.
- [124] M.-S. Tang, J. B. Zheng, M. F. Denissenko, G. P. Pfeifer, and Y. Zheng, "Use of UvrABC nuclease to quantify benzo[a]pyrene diol epoxide-DNA adduct formation at methylated versus unmethylated CpG sites in the p53 gene," *Carcinogenesis*, vol. 20, no. 6, pp. 1085–1089, 1999.
- [125] G. P. Pfeifer and M. F. Denissenko, "Formation and repair of DNA lesions in the p53 gene: relation to cancer mutations?" *Environmental and Molecular Mutagenesis*, vol. 31, no. 3, pp. 197–205, 1998.
- [126] G. P. Pfeifer, M. F. Denissenko, M. Olivier, N. Tretyakova, S. S. Hecht, and P. Hainaut, "Tobacco smoke carcinogens, DNA damage and p53 mutations in smoking-associated cancers," *Oncogene*, vol. 21, no. 48, pp. 7435–7451, 2002.
- [127] L. E. Smith, M. F. Denissenko, W. P. Bennett et al., "Targeting of lung cancer mutational hotspots by polycyclic aromatic hydrocarbons," *Journal of the National Cancer Institute*, vol. 92, no. 10, pp. 803–811, 2000.
- [128] G. P. Pfeifer and P. Hainaut, "On the origin of G → T transversions in lung cancer," *Mutation Research*, vol. 526, no. 1-2, pp. 39–43, 2003.
- [129] H. Rodriguez and E. L. Loechler, "Mutagenesis by the (+)-anti-diol epoxide of benzo[a]pyrene: what controls mutagenic specificity?" *Biochemistry*, vol. 32, no. 7, pp. 1759–1769, 1993.
- [130] Z. Xie, E. Braithwaite, D. Guo, B. Zhao, N. E. Geacintov, and Z. Wang, "Mutagenesis of benzo[a]pyrene diol epoxide in yeast: requirement for DNA polymerase  $\zeta$  and involvement of DNA polymerase  $\eta$ ," *Biochemistry*, vol. 42, no. 38, pp. 11253–11262, 2003.
- [131] J.-H. Yoon, C.-S. Lee, and G. P. Pfeifer, "Simulated sunlight and benzo[a]pyrene diol epoxide induced mutagenesis in the human p53 gene evaluated by the yeast function assay: lack of correspondence to tumor mutation spectra," *Carcinogenesis*, vol. 24, no. 1, pp. 113–119, 2003.
- [132] M. Schiltz, X. X. Cui, Y.-P. Lu et al., "Characterization of the mutational profile of (+)-7R,8S-dihydroxy-9S,10R-epoxy-7,8,9,10-tetrahydrobenzo[a] at the hypoxanthine (guanine) phosphoribosyltransferase gene in repair-deficient Chinese hamster V-H1 cells," *Carcinogenesis*, vol. 20, no. 12, pp. 2279–2285, 1999.
- [133] K.-Y. Seo, A. Nagalingam, M. Tiffany, and E. L. Loechler, "Mutagenesis studies with four stereoisomeric N<sup>2</sup>-dG benzo[a]pyrene adducts in the identical 5'-CGC sequence used in NMR studies: G → T mutations dominate in each case," *Mutagenesis*, vol. 20, no. 6, pp. 441–448, 2005.
- [134] R. E. Johnson, M. T. Washington, L. Haracska, S. Prakash, and L. Prakash, "Eukaryotic polymerases  $\iota$  and  $\zeta$  act sequentially to bypass DNA lesions," *Nature*, vol. 406, no. 6799, pp. 1015–1019, 2000.
- [135] F. Yuan, Y. Zhang, D. K. Rajpal et al., "Specificity of DNA lesion bypass by the yeast DNA polymerase  $\eta$ ," *Journal of Biological Chemistry*, vol. 275, no. 11, pp. 8233–8239, 2000.
- [136] S. Chandani and E. L. Loechler, "Y-family DNA polymerases may use two different dNTP shapes for insertion: a hypothesis and its implications," *Journal of Molecular Graphics and Modelling*, vol. 27, no. 7, pp. 759–769, 2009.
- [137] S. Chandani and E. L. Loechler, "Molecular modeling benzo[a]pyrene N<sup>2</sup>-dG adducts in the two overlapping active sites of the Y-family DNA polymerase Dpo4," *Journal of Molecular Graphics and Modelling*, vol. 25, no. 5, pp. 658–670, 2007.
- [138] K. Y. Seo, J. Yin, P. Donthamsetti, S. Chandani, C. H. Lee, and E. L. Loechler, "Amino acid architecture that influences dNTP insertion efficiency in Y-family DNA polymerase V of *E. coli*," *Journal of Molecular Biology*, vol. 392, no. 2, pp. 270–282, 2009.
- [139] F. Wang and W. Yang, "Structural insight into translesion synthesis by DNA Pol II," *Cell*, vol. 139, no. 7, pp. 1279–1289, 2009.
- [140] M. Hogg, S. S. Wallace, and S. Doublé, "Crystallographic snapshots of a replicative DNA polymerase encountering an abasic site," *EMBO Journal*, vol. 23, no. 7, pp. 1483–1493, 2004.

## Research Article

# Characterization of a Y-Family DNA Polymerase $\eta$ from the Eukaryotic Thermophile *Alvinella pompejana*

Sayo Kashiwagi,<sup>1</sup> Isao Kuraoka,<sup>1</sup> Yoshie Fujiwara,<sup>1</sup> Kenichi Hitomi,<sup>1,2,3</sup> Quen J. Cheng,<sup>3,4</sup> Jill O. Fuss,<sup>3</sup> David S. Shin,<sup>2,3</sup> Chikahide Masutani,<sup>5</sup> John A. Tainer,<sup>2,3</sup> Fumio Hanaoka,<sup>6</sup> and Shigenori Iwai<sup>1</sup>

<sup>1</sup> Graduate School of Engineering Science, Osaka University, 1-3 Machikaneyama, Toyonaka, Osaka 560-8531, Japan

<sup>2</sup> Department of Molecular Biology and The Skaggs Institute for Chemical Biology, The Scripps Research Institute, La Jolla, CA 92037, USA

<sup>3</sup> Life Science Division, Lawrence Berkeley National Laboratory, Berkeley, CA 94720, USA

<sup>4</sup> University of California San Diego, 9500 Gilman Drive no. 0613C, La Jolla, CA 92093, USA

<sup>5</sup> Graduate School of Frontier Biosciences, Osaka University, 1-3 Yamadaoka, Suita, Osaka 565-0871, Japan

<sup>6</sup> Faculty of Science, Gakushuin University, 1-5-1 Mejiro, Toshima-ku, Tokyo 171-8588, Japan

Correspondence should be addressed to Shigenori Iwai, iwai@chem.es.osaka-u.ac.jp

Received 13 May 2010; Accepted 29 June 2010

Academic Editor: Ashis Basu

Copyright © 2010 Sayo Kashiwagi et al. This is an open access article distributed under the Creative Commons Attribution License, which permits unrestricted use, distribution, and reproduction in any medium, provided the original work is properly cited.

Human DNA polymerase  $\eta$  (HsPol $\eta$ ) plays an important role in translesion synthesis (TLS), which allows for replication past DNA damage such as UV-induced *cis-syn* cyclobutane pyrimidine dimers (CPDs). Here, we characterized ApPol $\eta$  from the thermophilic worm *Alvinella pompejana*, which inhabits deep-sea hydrothermal vent chimneys. ApPol $\eta$  shares sequence homology with HsPol $\eta$  and contains domains for binding ubiquitin and proliferating cell nuclear antigen. Sun-induced UV does not penetrate *Alvinella*'s environment; however, this novel DNA polymerase catalyzed efficient and accurate TLS past CPD, as well as 7,8-dihydro-8-oxoguanine and isomers of thymine glycol induced by reactive oxygen species. In addition, we found that ApPol $\eta$  is more thermostable than HsPol $\eta$ , as expected from its habitat temperature. Moreover, the activity of this enzyme was retained in the presence of a higher concentration of organic solvents. Therefore, ApPol $\eta$  provides a robust, human-like Pol $\eta$  that is more active after exposure to high temperatures and organic solvents.

## 1. Introduction

Although genomic DNA contains genetic information that should be error-free for proper cellular function, it is continually subjected to ubiquitous DNA-damaging agents of both environmental and endogenous origins, such as UV and ionizing radiation and reactive oxygen species (ROS) [1–3]. To maintain genomic integrity, cells possess several repair pathways, including nucleotide excision repair (NER), base excision repair (BER), and recombination repair, to cope with the various resulting lesions. However, some lesions are not repaired and are encountered by the replication machinery. During DNA replication, these lesions block high-fidelity replicative DNA polymerases, and if not processed correctly, eventually lead to mutagenesis, carcinogenesis, or

cell death. To avoid such catastrophic consequences, cells have a translesion DNA synthesis (TLS) mechanism that allows efficient and accurate DNA synthesis past lesions [4–6].

The importance of TLS in humans has been indicated by studies of an inherited human disease called xeroderma pigmentosum variant (XP-V), which is characterized by the hypersensitivity of skin to sunlight and the high incidence of sunlight-induced skin cancer [7, 8]. The *XPV* gene encodes human DNA polymerase  $\eta$  (HsPol $\eta$ ), a 713 amino acid protein that is a member of the Y-family DNA polymerases that includes human DNA polymerases  $\iota$ ,  $\kappa$ , and Rev1 [6, 9, 10]. Cells from XP-V patients are defective in the replication of damaged DNA and show hypermutability after exposure to UV radiation or DNA-damaging agents. These results

indicate that HsPol $\eta$  is at least involved in the accurate translesion pathway to avoid mutations by UV-induced lesions *in vivo*. Consistent with these observations, biochemical studies revealed that HsPol $\eta$ , unlike the replicative Pol $\delta$  and Pol $\epsilon$ , was able to catalyze efficient and accurate TLS past a UV-induced *cis-syn* cyclobutane pyrimidine dimer (CPD). In contrast, DNA containing other UV-induced lesions, such as the pyrimidine(6–4)pyrimidone photoproduct (6–4 pp) and its Dewar valence isomer (Dewar), which are efficiently repaired by NER *in vivo* [11, 12], is not replicated by HsPol $\eta$  [13, 42].

Furthermore, this enzyme was reportedly able to bypass not only UV-induced lesions but also various other lesions induced by both environmental and endogenous reactive oxygen species. For instance, HsPol $\eta$  bypasses 7,8-dihydro-8-oxoguanine (8-oxoG), 5R-thymine glycol (5R-Tg), and 5S-thymine glycol (5S-Tg), but not an apurinic/aprimidinic (AP) site [13–19], although these lesions, which have small alterations in their chemical structures, are mainly repaired by BER *in vivo*. Thus, these findings indicate that HsPol $\eta$  also plays an important function in the replication of DNA containing ROS-induced lesions *in vivo*.

In addition to its role in TLS, HsPol $\eta$  can extend DNA synthesis from D-loop recombination intermediates, and its activity is stimulated by Rad51 recombinase [20]. Moreover, Pol $\eta$ -disrupted DT40 cells show significant decreases in the frequencies of both immunoglobulin-variable gene conversion and double-strand break-induced homologous recombination [21]. Taken together, these reports indicate that Pol $\eta$  is involved in homologous recombination repair, and thus, Pol $\eta$  seems to be important for DNA damage tolerance in living cells.

*Alvinella pompejana* is a polychaetous annelid that inhabits active deep-sea hydrothermal vent sites along the East Pacific Rise, where it colonizes the walls of actively venting high-temperature chimneys. The average temperature is about 68°C, with spikes up to 81°C, and thus exceeds the predicted 55°C limit for the survival of eukaryotes [22, 23]. The ability of this worm to survive in such an extreme environment suggests that *A. pompejana* may contain highly stable proteins that can be used for biology, biotechnology, and industry. Several proteins have been characterized from *A. pompejana* and the analyses have revealed the proteins have enhanced thermostability [24–26], which include *A. pompejana* superoxide dismutase (SOD) and U2AF65, which are more stable than their human homologs.

In this study, we cloned an *A. pompejana* gene with homology to the HsPol $\eta$  gene. The encoded full-length recombinant protein was produced in *Escherichia coli*. Characterization of ApPol $\eta$  revealed that it had the ability to bypass CPD, 8-oxoG, 5R-Tg, and 5S-Tg, but did not bypass either 6–4 pp, Dewar, or an AP site analog. This substrate specificity is similar to that of the HsPol $\eta$ , yet ApPol $\eta$  is comparatively more thermostable than HsPol $\eta$  and retains activity in the presence of organic solvents. Therefore, ApPol $\eta$  is a robust human-like Pol $\eta$  that is useful to complement and expand ideas on TLS mechanisms by virtue of its eukaryotic origin and enhanced stability.

## 2. Materials and Methods

**2.1. Materials.** Recombinant HsPol $\eta$  tagged with (His)<sub>6</sub> at its C-terminal end was produced in Sf9 insect cells using the baculovirus expression system and was purified by sequential column chromatography on HiTrap Q, Ni-NTA agarose, and MonoS, as described previously [17]. Klenow fragment 3′–5′ exonuclease minus (KF) and T7 DNA polymerase were purchased from New England Biolabs and USB, respectively. Oligonucleotides containing CPD [27], 6–4 pp [28], Dewar [29], 5R-Tg [30], and 5S-Tg [31] were synthesized on an Applied Biosystems 3400 DNA synthesizer, as described, and those containing 8-oxoG and the AP site analog (dSpacer) were synthesized using phosphoramidite building blocks purchased from Glen Research.

**2.2. Cloning of the ApPol $\eta$  Gene.** Full-length ApPol $\eta$  cDNA was isolated by RACE PCR, using cDNA prepared with the GeneRacer kit (Invitrogen) from total RNA isolated from frozen whole worm samples. A 2.5 cm frozen section of the posterior end of *A. pompejana* collected with the DSV Alvin submersible [23] was ground using a mortar and pestle in liquid nitrogen. The ground tissue was aliquoted into eppendorf tubes, and after the addition of Trizol (Invitrogen) (1.4 mL), the mixture was incubated at room temperature for 10 minutes. After centrifugation at 12,000 ×g for 10 minutes, the supernatant (1 mL) was mixed with chloroform (250  $\mu$ l), and was incubated at room temperature for 2 minutes. The samples were then centrifuged at 12,000 ×g for 15 minutes to separate the total RNA into the aqueous layer. The RNA was then precipitated by adding isopropanol (500  $\mu$ l) to the aqueous solution (600  $\mu$ l), and was incubated at 4°C for 1.5 hours. After centrifugation at 12,000 ×g for 10 minutes at 4°C, the pellet was washed with 75% ethanol (1.4 mL) and then stored in 75% ethanol (1 mL) at –80°C. The stored RNA was pelleted by centrifugation and resuspended in diethylpyrocarbonate-treated water (20  $\mu$ l), and the concentration was determined by measuring the absorbance at 280 nm. A 5  $\mu$ g portion of the total RNA was used to prepare cDNA using the GeneRacer kit (Invitrogen), according to the manufacturer's instructions. In brief, total RNA was dephosphorylated using calf intestinal alkaline phosphatase, extracted with phenol-chloroform, and precipitated with ethanol. The RNA was decapped using tobacco acid pyrophosphatase, extracted, and precipitated, and then the GeneRacer 5′ oligo was ligated to the 5′ ends. Finally, the RNA was subjected to the reverse transcription reaction using a poly-T primer containing the GeneRacer 3′ oligo sequence, to generate a single-stranded cDNA library with known 5′ and 3′ sequences.

The amino acid sequence of HsPol $\eta$  was used for an in-house TBLASTN search of a translated *A. pompejana* expressed sequence tag (EST) database comprised of sequences derived from collaborations with the Joint Genome Institute (Walnut Creek, CA) and Genome Therapeutics (Waltham, MA). A positive hit at the 5′ end of the gene was identified on EST CAGA3172. The 3′ sequence was determined from the prepared *A. pompejana* GeneRacer cDNA library by 3′ RACE PCR, using a gene specific primer

(AlviXPVF1 5'GG GAC TGG TCT GTG CTG GCC GTG GAA AT 3') and the GeneRacer 3' oligo primer, together with the touchdown PCR strategy and KOD polymerase (Novagen). The PCR product was TOPO cloned into the pCR2.1 vector (Invitrogen) and was analyzed by restriction enzyme digestion and sequencing. The full-length ApPol $\eta$  gene was amplified from the cDNA library, using two gene-specific primers, AlviXPVF1 (the above sequence) and AlviXPVR2 (5' GGG ATG ATT CTA CAC TTT GCT GAA AAA TCT ATC CA 3'), and KOD polymerase under the standard PCR conditions. The 2.2 kb product was gel-purified and TOPO cloned into the pCR4 vector (Invitrogen) and was analyzed by restriction enzyme digestion and sequencing. Restriction sites were added to the ends by a subsequent round of PCR and TOPO cloning. The full-length ApPol $\eta$  cDNA was then subcloned into pET21a (Novagen), using the *Nde* I and *Eco* RI restriction nucleases and T4 DNA ligase, and was analyzed by restriction enzyme digestion and sequencing.

**2.3. Expression and Purification of the ApPol $\eta$  Protein.** Recombinant ApPol $\eta$  gene was expressed in *E. coli* Rosetta2 (DE3) (Novagen). The cells were grown at 37°C to an absorbance at 600 nm of 0.6. The cultures were placed in an ice slurry for 20 minutes, and then isopropyl- $\beta$ -D-thiogalactopyranoside was added to a final concentration of 0.5 mM. After the cultures were incubated at 12°C for 40 hours, the cells were collected by centrifugation, rinsed with buffer A containing 10 mM sodium phosphate (pH 7.4), 10% glycerol, and 300 mM NaCl, and resuspended in buffer A containing *p*-amidinophenylmethanesulfonyl fluoride hydrochloride and a protease inhibitor cocktail (complete, EDTA free (Roche)). The lysate mixtures were mixed with powdered lysozyme at a final concentration of 2 mg/mL for 10 minutes on ice, and then were subjected to ultrasonication. The lysates were centrifuged, and the supernatants were mixed with Talon resin (Clontech) (50% w/v, equilibrated with lysis buffer containing 10 mM sodium phosphate (pH 7.4), 10% glycerol, 300 mM NaCl, and 5 mM imidazole). The resin was washed with the same buffer, and the bound proteins were eluted with eluate buffer (lysis buffer containing 300 mM imidazole). The eluate was diluted and applied to a HiTrap Heparin HP column (GE Healthcare) equilibrated with buffer B (50 mM sodium phosphate (pH 7.4), 1 mM EDTA, 1 mM  $\beta$ -mercaptoethanol, and 0.01% Triton X-100) containing 0.1 M NaCl. Elution was performed by a stepwise gradient of 0.2 M to 0.6 M NaCl in buffer B. The peak fractions containing ApPol $\eta$  eluted at 0.5 M NaCl, and were stored at -80°C.

**2.4. TLS Reactions.** The 5'-<sup>32</sup>P-labeled primer-template was prepared by mixing a 16-mer primer labeled at its 5' end with each of the 30-mer templates, at a molar ratio of 1 : 1. Standard reaction mixtures (10  $\mu$ l), containing 40 mM Tris-HCl (pH 8.0), 1 mM MgCl<sub>2</sub>, 100 mM dNTPs, 10 mM DTT, 0.24 mg/mL BSA, 60 mM KCl, 2.5% glycerol, 40 nM 5'-<sup>32</sup>P-labeled primer-template, and purified ApPol $\eta$ , were incubated at 37°C. The reaction times and the enzyme amounts

are indicated in the figure legends. The reactions were terminated by the addition of stop solution (8  $\mu$ l), containing 95% formamide, 20 mM EDTA, 0.025% bromophenol blue, and 0.025% xylene cyanol. The protein was denatured by boiling, and the products were separated by electrophoresis on a denaturing 16% polyacrylamide gel. Dried gels were analyzed on a FUJIFILM BAS 1800 bioimage analyzer.

**2.5. Thermostability of ApPol $\eta$ .** The relative thermostabilities of ApPol $\eta$  and HsPol $\eta$  were compared by heating each enzyme to temperatures ranging between 37°C and 58°C for 5 minutes. An aliquot of each enzyme was then used for the standard 20 minutes TLS reaction at 37°C to measure the incorporation of a single nucleotide, dCMP, opposite the template G residue (see the TLS reactions described above). The enzyme concentrations used in the reactions were initially determined by making serial dilutions of each enzyme and identifying the concentration necessary to give the same extension level of the labeled primer. These amounts were 1.8 and 5.9 fmol for HsPol $\eta$  and ApPol $\eta$ , respectively. The ability of each enzyme to extend the primer was quantified with MultiGauge software (FUJIFILM), and the specific activity, compared to the activity of each enzyme heated to 37°C, was calculated. The specific activity was plotted as a function of the temperature to which the enzyme was exposed.

### 3. Results

**3.1. Amino Acid Sequence of ApPol $\eta$ .** A cDNA sequence with homology to that of HsPol $\eta$  was cloned from an *A. pompejana* cDNA library by RACE PCR. The open reading frame encoded a predicted product of 745 amino acid residues, with a calculated molecular mass of 83 kDa. Alignment of the amino acid sequence against HsPol $\eta$  revealed 38.1% identity and 57.6% similarity overall (identities = 283/708 (39%), positives = 414/708 (58%), gaps = 68/708 (9%)). The alignment (Figure 1(a)) also indicated the high conservation within the N-terminal region and the presence of the four structural domains (finger, palm, thumb, and little finger) that are the hallmarks of the Y-family translesion DNA polymerases [32, 33]. Ubiquitin (Ub)-binding domains [34–36] and a proliferating cell nuclear antigen (PCNA)-binding domain [37, 38], located in the C-terminal region of Pol $\eta$ , were identified in the ApPol $\eta$  amino acid sequence, suggesting that Ub and/or PCNA regulate this protein.

The Y-family DNA polymerases  $\iota$  (Pol $\iota$ ) and  $\kappa$  (Pol $\kappa$ ) and the B-family DNA polymerase  $\zeta$  (Pol $\zeta$ ) are known to share sequence homology with the Y-family HsPol $\eta$ . To analyze the relationship between this *A. pompejana* protein and other translesion DNA polymerases, a phylogenetic tree was produced on the basis of the amino acid sequences of these DNA polymerases, by the unweighted pair group method with arithmetic mean (UPGMA). The tree revealed that this protein was not related to Pol $\kappa$ , Pol $\iota$ , or Pol $\zeta$ , but was more closely related to Pol $\eta$  (Figure 1(b)). Therefore, we concluded that this protein is a member of the DNA polymerase  $\eta$

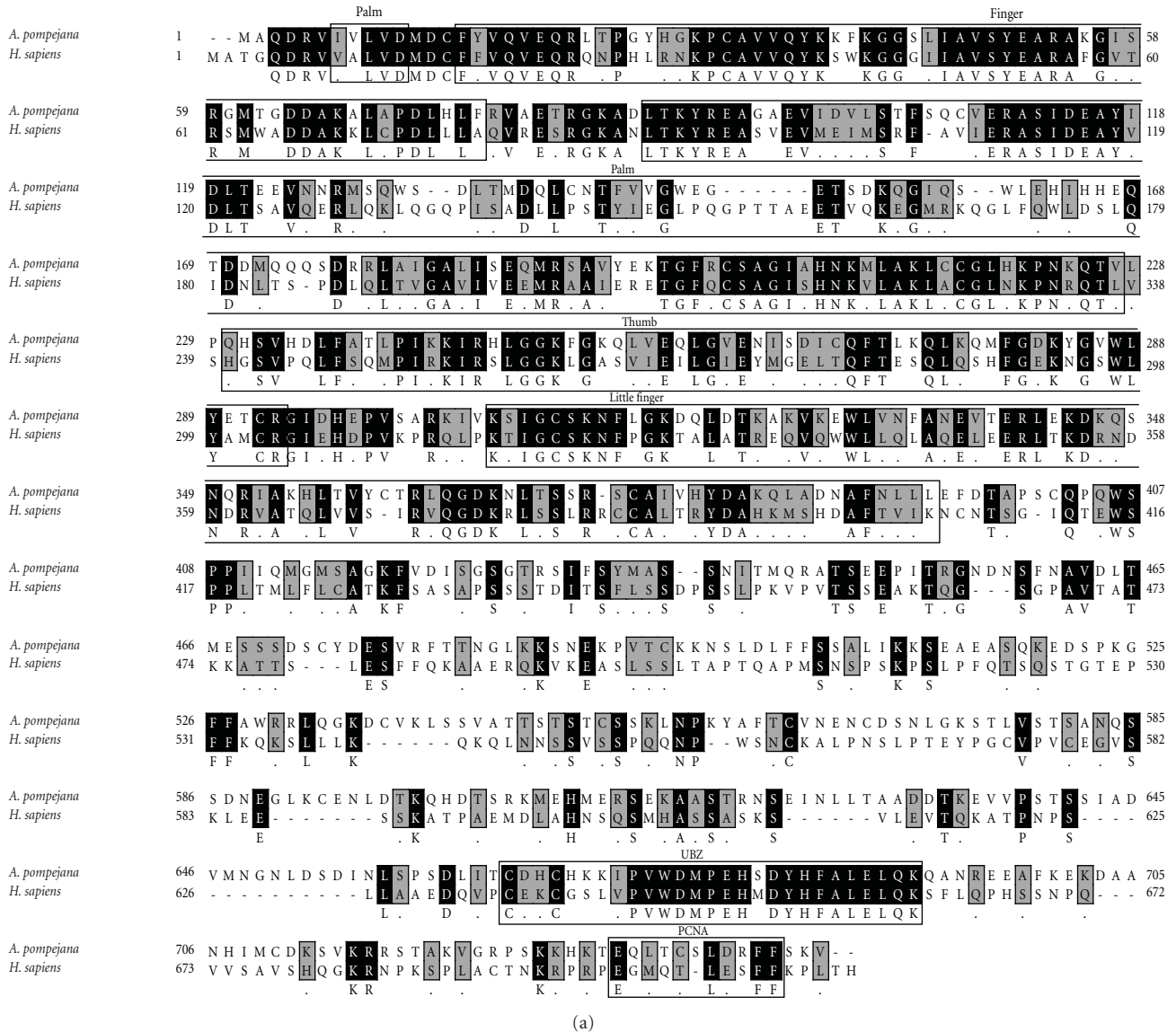


FIGURE 1: (a) Alignment of the amino acid sequences of ApPol $\eta$  and HsPol $\eta$  (NP\_006493.1). Identical and similar residues between the two enzymes are indicated in black and grey, respectively. (b) Phylogenetic analysis of TLS polymerases. A phylogenetic tree was constructed by the UPGMA method, based on the amino acid sequences of the ApPol $\eta$  and other Y- and B-family DNA polymerases.

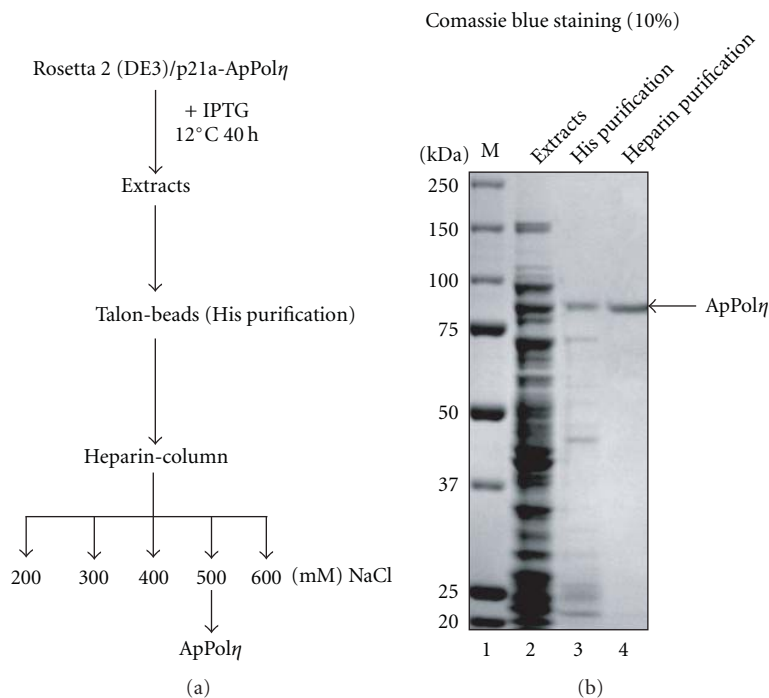


FIGURE 2: Purification of the recombinant ApPol $\eta$  protein. Aliquots from various steps of the purification were subjected to 10% SDS-PAGE analysis, and the proteins were visualized by staining with Coomassie Brilliant Blue. ApPol $\eta$  has a molecular mass of 85 kDa. Lane 1, markers; lane 2, cell extract; lane 3, Talon eluate; lane 4, HiTrap Heparin HP eluate.

group, and thus referred to the protein as *A. pompejana* DNA polymerase  $\eta$ .

**3.2. Purification of ApPol $\eta$ .** To examine the biological activities of the protein encoded by the ApPol $\eta$  cDNA, we prepared the recombinant ApPol $\eta$  protein with a C-terminal (His) $_6$  tag in *E. coli*. The extract was first fractionated on Talon beads, and then purified on a Heparin column. The recombinant protein was eluted by a step gradient of NaCl (Figure 2(a)). As expected from the calculated relative molecular mass, the purified recombinant ApPol $\eta$  bearing the (His) $_6$  tag migrated as a single band of approximately 85 kDa in the SDS-PAGE analysis (Figure 2(b)), and exhibited DNA polymerase activity (Figure 3(a)). The recombinant human Y-family polymerases, for example, Pol $\eta$ , Pol $\iota$ , and Pol $\kappa$ , are usually prepared from baculovirus-infected insect cells, as reported previously [13, 17, 39, 40]. In the present study, the incubation of the cultures at a low temperature after induction enabled the production of full-length ApPol $\eta$  in *E. coli*, as was also reported by Hoffman et al. [41] for Pol $\eta$  from other species. The yield of the purified protein was 15.5  $\mu$ g per liter of the culture.

**3.3. TLS Past UV-Induced Photoproducts by ApPol $\eta$ .** UV irradiation induces the formation of pyrimidine dimers, namely, CPD and 6–4 pp. The latter is isomerized to Dewar by exposure to UVA/B. HsPol $\eta$  catalyzed efficient and accurate TLS past CPD [13], but not 6–4 pp [13] and Dewar (unpublished results). To examine whether ApPol $\eta$  possessed TLS activity for UV-induced lesions, 30-mer oligonucleotide

templates containing a single lesion were hybridized to a 5'- $^{32}$ P-labeled 16-mer oligonucleotide primer, and these duplexes were employed for the TLS reactions (Figure 3). Klenow fragment (KF) inserted one nucleotide opposite CPD, but did not elongate the primer (Figure 3(b), lane 1), whereas ApPol $\eta$  could efficiently elongate the primer up to the end of the 30-mer, in an enzyme concentration-dependent manner (Figure 3(b), lanes 3–7). Similar experiments were performed with other UV-induced lesions, 6–4 pp and Dewar. ApPol $\eta$  could insert one nucleotide opposite these lesions, but elongation of the primers was not observed (Figures 3(c) and 3(d)), in a manner similar to HsPol $\eta$  [13, 42].

To examine the preference for nucleotide incorporation opposite the lesion by ApPol $\eta$ , the polymerization reactions were performed in the presence of only a single deoxyribonucleoside triphosphate (Figure 4). Although HsPol $\eta$  replicates undamaged DNA with low fidelity [43, 44], it can accurately incorporate dATP opposite the TT sequence of CPD [13]. On the undamaged template, ApPol $\eta$  preferred to incorporate dATP correctly, and dGTP was incorporated less frequently (Figure 4(a)), indicating that ApPol $\eta$ , like HsPol $\eta$ , replicates undamaged DNA with low fidelity. When the template contained CPD, ApPol $\eta$  incorporated dATP exclusively (Figure 4(b), lane 4), indicating that ApPol $\eta$ , like HsPol $\eta$ , can accurately perform TLS past CPD. For both 6–4 pp and Dewar, primers that were elongated with dAMP and dGMP by ApPol $\eta$  were detected, although the elongation efficiency was very low (Figures 4(c) and 4(d)). While we are able to test these activities biochemically, establishing the

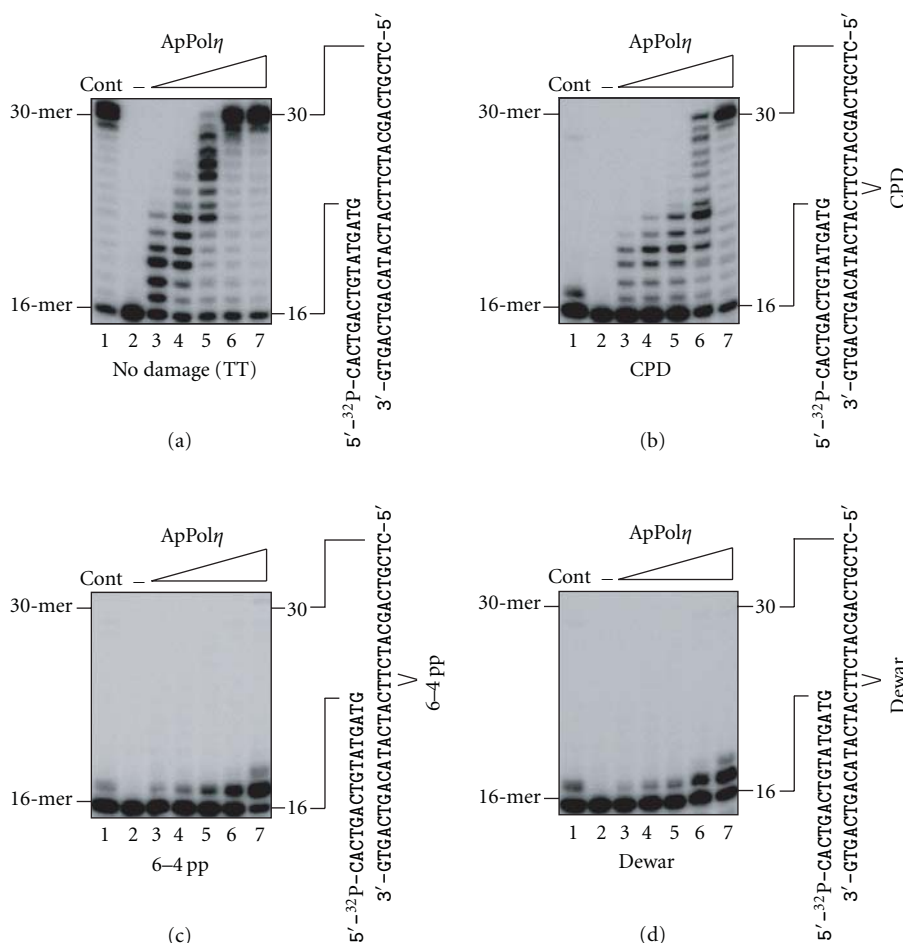


FIGURE 3: TLS by ApPol $\eta$  past CPD, 6–4 pp, and Dewar. Increasing amounts of ApPol $\eta$  (12, 24, 59, 118, and 588 fmol in lanes 3–7, resp.) were incubated with 40 nM of the primer-templates indicated beside each panel. The templates contained undamaged TT (a), CPD (b), 6–4 pp (c), and Dewar (d). The samples for lanes 1 and 2 contained 0.1 U KF and no enzyme, respectively. The reactions were incubated at 37°C for 20 minutes, and then were subjected to 15% polyacrylamide/7.5 M urea gel electrophoresis. The autoradiograms of the gels are shown.

biological roles of ApPol $\eta$  would require additional assays such as genetic complementation, however these results were also similar to those obtained for HsPol $\eta$ .

**3.4. TLS Past Oxidative Lesions by ApPol $\eta$ .** Since *A. pompejana* inhabits deep sea thermal vent regions that are in excess of 1.5 km under the ocean surface where UV-rays from the sun do not penetrate [45, 46], we thought that CPD containing DNA may not be a major template for ApPol $\eta$ . Other candidates were assumed to be oxidative lesions, because the high temperature and the solutes at the hydrothermal vent sites might induce oxidative stress. Tg is one of the major DNA lesions produced by ROS, and two isomeric forms, 5R-Tg and 5S-Tg, are produced in DNA. Tg often blocks DNA replication by replicative DNA polymerases [40], but rarely induces mutation [41]. However, HsPol $\eta$  can catalyze efficient and accurate TLS past each Tg isomer [17].

Using the 30-mer oligonucleotides containing a single lesion at the 17th nucleotide from its 3' end as templates, we examined the ability of ApPol $\eta$  to replicate DNA past

5R-Tg and 5S-Tg. At both lesions, the replicative T7 DNA polymerase was blocked completely (Figures 5(a) and 5(b), lane 1), but ApPol $\eta$  efficiently catalyzed the replication reaction (Figures 5(a) and 5(b), lanes 3–7). To examine the preference of nucleotide incorporation opposite each Tg isomer, the polymerization reactions were tested in the presence of only a single deoxyribonucleoside triphosphate (Figures 6(a) and 6(b)). ApPol $\eta$  preferred to incorporate dATP (Figures 6(a) and 6(b), lane 4). Although dGTP was incorporated in the absence of the other nucleotides (lane 6), this product, which exhibited slightly slower migration in the PAGE analysis, was not detected when the four nucleotides were added (lane 3). These results indicated that ApPol $\eta$  had the ability to catalyze TLS accurately past both 5R-Tg and 5S-Tg.

Another major oxidative DNA lesion induced by ROS is 8-oxoG, which is an important promutagen *in vivo* and *in vitro* [1]. Similar experiments were performed with a template containing 8-oxoG, instead of Tg. No insertion of any nucleotide opposite the lesion by T7 DNA polymerase was observed (Figure 5(d), lane 1), whereas ApPol $\eta$  could

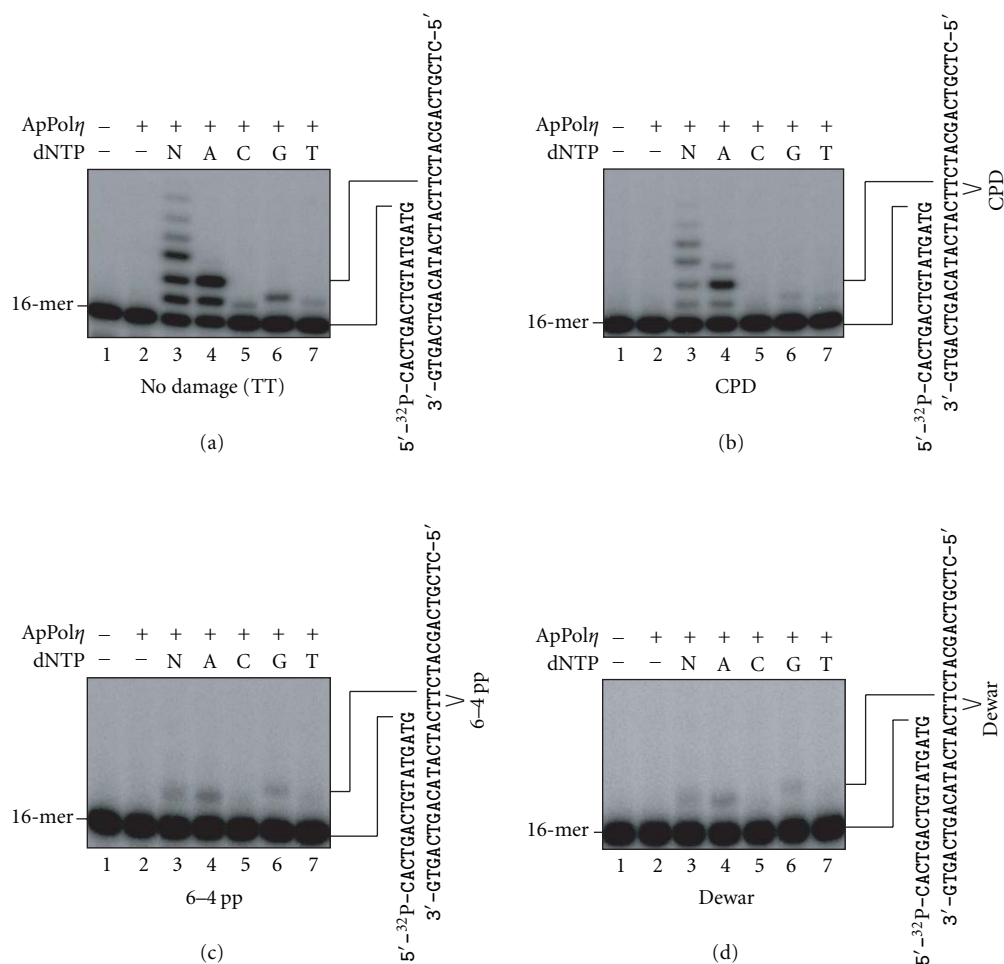


FIGURE 4: Selectivity of nucleotide incorporation by ApPol $\eta$  opposite undamaged TT (a), CPD (b), 6-4 pp (c), and Dewar (d). ApPol $\eta$  (12 fmol in lanes 2-7) was incubated with each primer-temple in the presence of the four dNTPs (lane 3), the indicated dNTP (lanes 4-7), or the absence of dNTP (lane 2). Lane 1 contained no enzyme. The reactions were incubated at 37°C for 5 minutes, and then were subjected to 15% polyacrylamide/7.5 M urea gel electrophoresis. The autoradiograms of the gels are shown.

bypass 8-oxoG efficiently (Figure 5(d), lanes 3-7). For the nucleotide preference, ApPol $\eta$  preferred to incorporate the correct dCTP opposite the undamaged template G (Figure 6(c)), whereas it mainly incorporated the incorrect dATP opposite 8-oxoG (Figure 6(d)). Thus, this enzyme replicates DNA containing 8-oxoG efficiently but incorrectly, leading to frequent G·C to T·A transversions. In addition, we investigated whether ApPol $\eta$  has TLS activity on a template containing the AP site analog. However, like the other Y-family DNA polymerases, this enzyme was unable to catalyze TLS past this lesion (data not shown).

**3.5. In Vitro Stability of ApPol $\eta$ .** As *A. pompejana* colonizes the walls of actively venting high-temperature chimneys [23, 45, 46], we hypothesized that its enzymes may be more thermostable than those found in mesophilic organisms, as shown for other TLS polymerases derived from single cellular hyperthermophilic organisms such as *Sulfolobus solfataricus* DNA polymerase 4 (Dpo4) [47, 48]. To test this possibility, we compared the activity of ApPol $\eta$  along

with that of HsPol $\eta$  after heating both enzymes to various temperatures for 5 minutes. After this treatment, we tested the ability of both enzymes to incorporate a single dCMP opposite a template G. As shown in Figure 7, ApPol $\eta$  retained the activity even after it was heated to 49°C. In contrast, the activity of HsPol $\eta$  diminished rapidly after heating to temperatures higher than 43°C. Therefore, ApPol $\eta$  is relatively more thermostable than HsPol $\eta$ .

**3.6. Stability of ApPol $\eta$  in Organic Solvents.** As a further test of ApPol $\eta$  stability, we tested the ability of ApPol $\eta$  to incorporate dCMP opposite a template G in the presence of various organic solvents. In these assays, dimethyl sulfoxide (DMSO), ethanol, and isopropanol (IPA) were used at concentrations of 20% (v/v). Similar experiments were performed in a study on TLS past a benzo[*a*]pyrene adduct by another thermostable Y-family DNA polymerase, archaeal Dpo4, although the organic solvents were added to stabilize the benzo[*a*]pyrene moiety in the major groove, rather than to test the protein stability [45]. As shown in Figure 8(a),

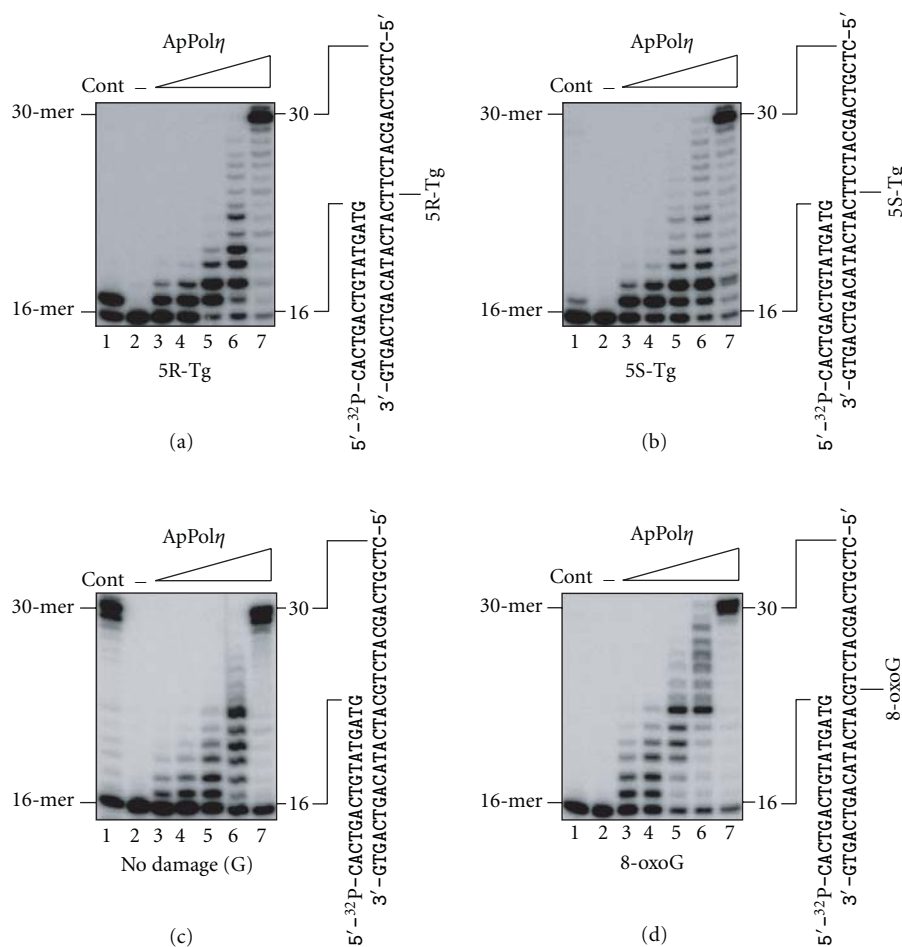


FIGURE 5: TLS by ApPol $\eta$  past 5R-Tg, 5S-Tg, and 8-oxoG. Increasing amounts of ApPol $\eta$  (12, 24, 59, 118, 588 fmol in lanes 3–7, resp.) were incubated with 40 nM of the primer-templates indicated beside each panel. The templates contained 5R-Tg (a), 5S-Tg (b), undamaged G (c), and 8-oxoG (d). The samples for lanes 1 and 2 contained 0.1 U T7 DNA polymerase and no enzyme, respectively. The reactions were incubated at 37°C for 20 minutes, and then were subjected to 15% polyacrylamide/7.5 M urea gel electrophoresis. The autoradiograms of the gels are shown.

ApPol $\eta$  exhibited higher activity than HsPol $\eta$  in the presence of all of the solvents used in this study, although IPA greatly reduced the enzyme activity. In the presence of DMSO, ApPol $\eta$  retained the full activity, even when the reaction mixture contained this solvent at a concentration of 20% (Figure 8(b)). These results support our conclusion that the full-length ApPol $\eta$  protein is more stable than its human homolog.

## 4. Discussion

**4.1. CPD and Tg in TLS by ApPol $\eta$ .** In this study, we cloned the cDNA encoding the novel thermostable DNA polymerase  $\eta$  from *A. pompejana*, which colonizes deep-sea hydrothermal vents. This enzyme was produced in *E. coli*, and was purified as a full-length recombinant protein (85 kDa) bearing a (His)<sub>6</sub> tag. The purified ApPol $\eta$  protein displayed DNA polymerase activity. This enzyme catalyzed TLS past CPD, 5R-Tg, 5S-Tg, and 8-oxoG, but not past 6–4 pp, Dewar, or the AP site analog, in a similar manner to

TABLE 1: Comparison of nucleotide incorporation into lesion-containing template-primers between HsPol $\eta$  and ApPol $\eta$ .

DNA lesion	HsPol $\eta$	ApPol $\eta$
CPD	AA [7–10]	AA
6–4 pp	— <sup>a</sup> [9, 10]	— <sup>a</sup>
Dewar	— <sup>a,b</sup>	— <sup>a</sup>
5R-Tg	A [15]	A
5S-Tg	A [15]	A
8-oxoG	C/A [16, 17]	C/A
AP site analog	— <sup>a</sup> [10, 17]	— <sup>a</sup>

<sup>a</sup>no incorporation; <sup>b</sup>unpublished result.

HsPol $\eta$  (Table 1). We also demonstrated that ApPol $\eta$  was more stable than HsPol $\eta$ .

Despite the fact that *A. pompejana* inhabits the deep sea, where UV-rays do not penetrate, the UV-induced CPD was found to be an excellent template for ApPol $\eta$ . Considering

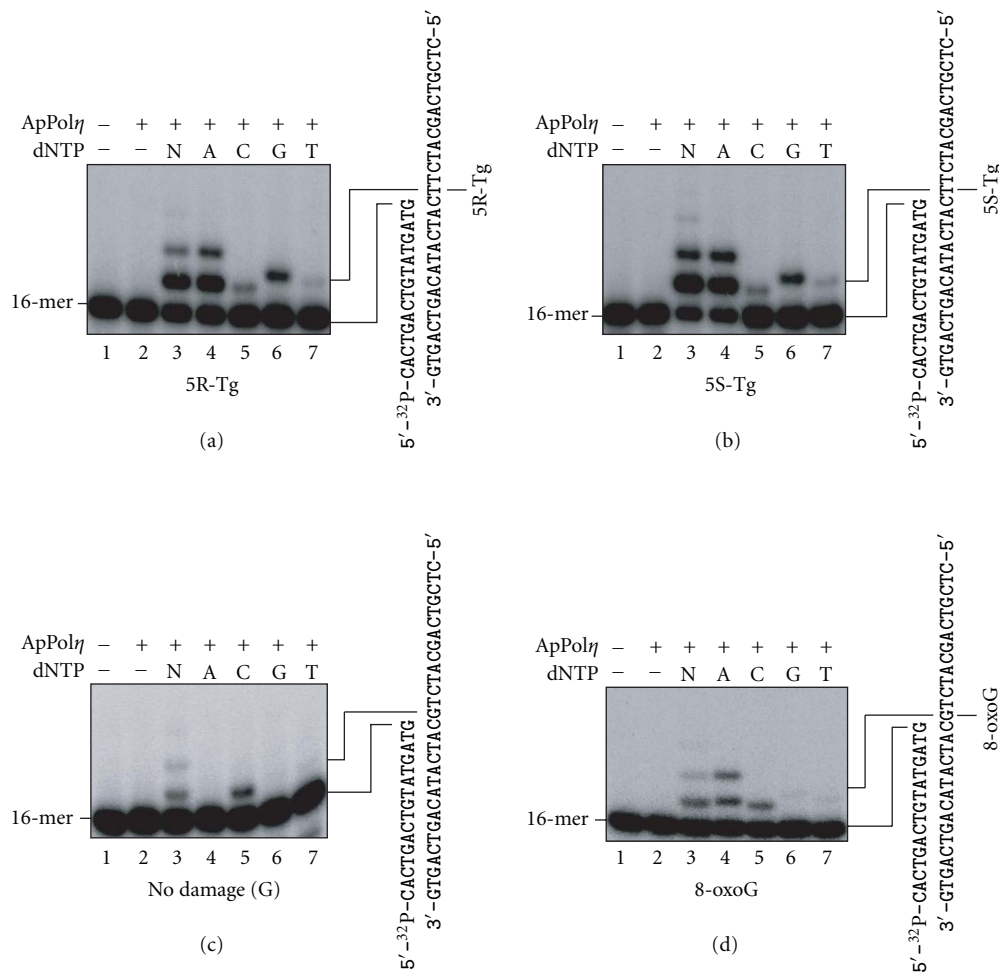


FIGURE 6: Selectivity of nucleotide incorporation by ApPol $\eta$  opposite 5R-Tg (a), 5S-Tg (b), undamaged G (c), and 8-oxoG (d). ApPol $\eta$  (12 fmol in lanes 2–7) was incubated with each primer-temple in the presence of the four dNTPs (lane 3), the indicated dNTP (lanes 4–7), or the absence of dNTP (lane 2). Lane 1 contained no enzyme. The reactions were incubated at 37°C for 5 minutes, and then were subjected to 15% polyacrylamide/7.5 M urea gel electrophoresis. The autoradiograms of the gels are shown.

that a genetic defect in the HsPol $\eta$  gene results in the XP-V syndrome, and that XP-V patients are sensitive to sunlight and highly prone to cancer development, the critical role of HsPol $\eta$  is thought to be error-free TLS across CPD in human cells. As *A. pompejana*'s environment is significantly less subject to UV radiation produced by the sun, we speculate that the inclusion of the TLS polymerase system within the organism may arise from specific environmental adaptations. Evidence for photosynthetic events at hydrothermal vent sites has been noted [49], where energy for the reactions may arise from vent activity. Moreover, the vent area is sporadically subject to periods of intense volcanic and geothermal activity that may cause production of bulky DNA lesions within these organisms. The presence of ApPol $\eta$  may also play a role in protecting developing embryos, as embryos pass through a period of developmental arrest when passing from one colony site to another before renewed growth [50]. In these cases, they may experience periods of geothermal light during passage and during their development at their new colonization site. Thus, these Pol $\eta$  proteins may protect the

embryo until it becomes more self-motile and can build its housing tube.

Here, we also showed that this polymerase catalyzes efficient and accurate TLS past both 5R-Tg and 5S-Tg, which are generated by ROS. Since Tg can block DNA replication by replicative DNA polymerases and also induces cell death, the critical role of ApPol $\eta$  might be error-free TLS across Tg in *A. pompejana* cells.

**4.2. Stability of ApPol $\eta$ .** Since *A. pompejana* inhabits hydrothermal vent sites at temperatures that often measure within the representative classifications for thermophilic (40–60°C) and hyperthermophilic organisms (60°C and higher), we expected that ApPol $\eta$  would be thermostable. In agreement with these expectations, we found that ApPol $\eta$  was more thermostable than HsPol $\eta$  (Figure 7), but less stable than an archaeal DinB-like polymerase from the hyperthermophile *S. solfataricus* P2 [47, 51] which lives at higher temperatures (>75°C) than *A. pompejana*. Posttranslational modification of proteins is sometimes important for

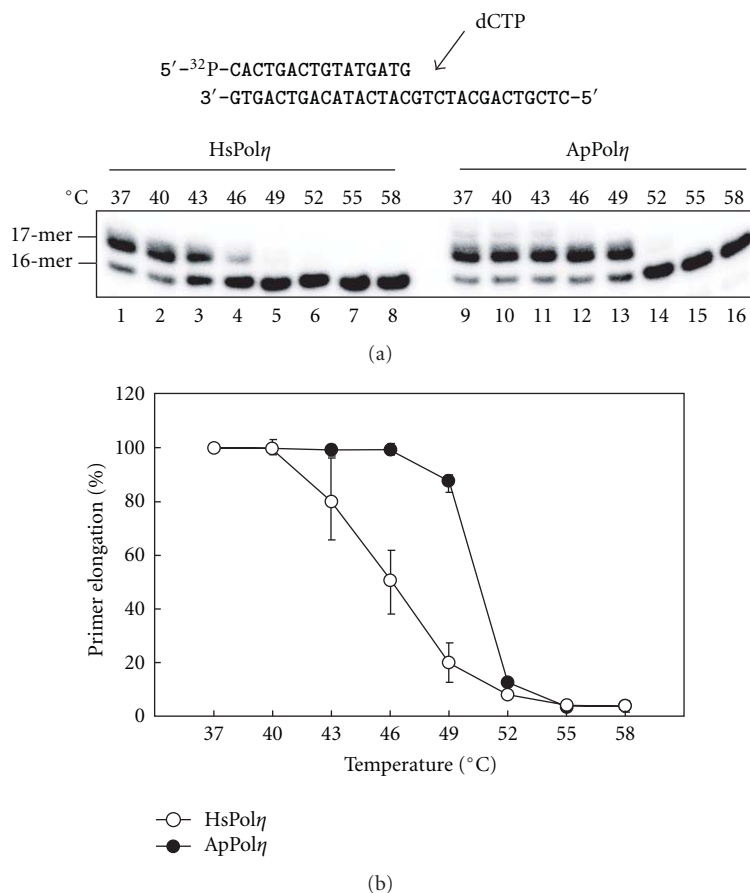


FIGURE 7: Thermostability of ApPol $\eta$ . (a) Aliquots of ApPol $\eta$  (closed circles) and HsPol $\eta$  (open circles) were heated to the indicated temperature for 5 minutes. The effect of this treatment on the polymerase activity was subsequently determined by analyzing the respective enzyme's ability to extend a radiolabeled primer by incorporating dCMP opposite the template G. Replication assays were performed at 37°C for 20 minutes. (b) The ability of each enzyme to extend the primer was quantified, and the specific activity compared to that of each enzyme heated at 37°C was calculated and subsequently plotted as a function of the temperature to which the enzyme was initially exposed.

their structure and function. Since the ApPol $\eta$  used in this study was produced in *E. coli*, the measured thermostability was that without eukaryotic post-translational modifications. We expected that this enzyme may be modified in insect cells, which are more closely related to *A. pompejana* cells than to *E. coli* cells, and thus might gain higher thermostability. Therefore, we prepared ApPol $\eta$  in Sf9 insect cells using the baculovirus expression system. The ApPol $\eta$  protein produced in Sf9 cells could catalyze DNA synthesis at 37°C, but lacked translesion activity after it was heated to 55°C (data not shown).

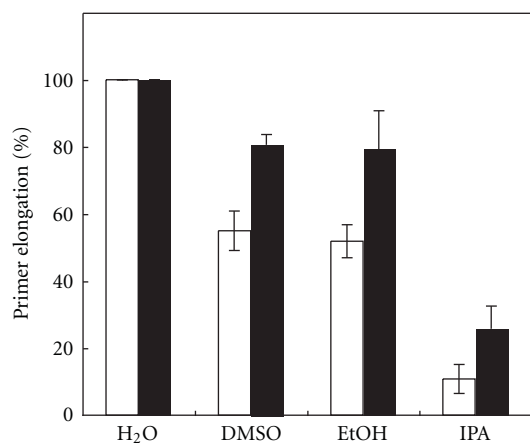
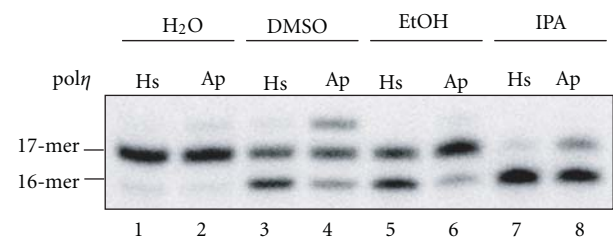
There might be several reasons why ApPol $\eta$  is not even more thermostable. (1) It has been reported that Pol $\eta$  functions in a replication complex during TLS [37, 38, 52]. Thus, it is possible that ApPol $\eta$  becomes more heat resistant with the help of other thermostable replication proteins in *A. pompejana* cells. In fact, ApPol $\eta$  has a PCNA binding motif (Figure 1(a)), indicating that ApPol $\eta$  may exist in a replication complex with PCNA. (2) Y-family DNA polymerases replicate undamaged DNA in an error-prone manner [34–36, 38]. Hence, to maintain genetic integrity, it might not be favorable for cells to have an extremely stable

mutator polymerase. The present study is the starting point for the elucidation of the temperature preference of each *A. pompejana* enzyme and its biological significance, which will further our understanding of the ecology of this unique living organism.

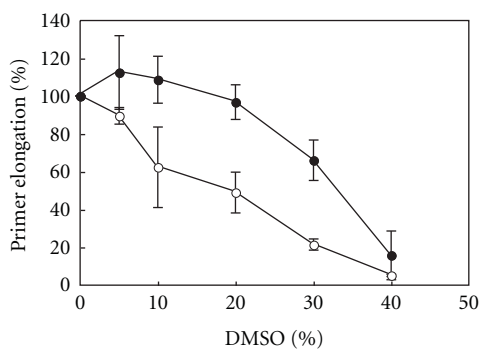
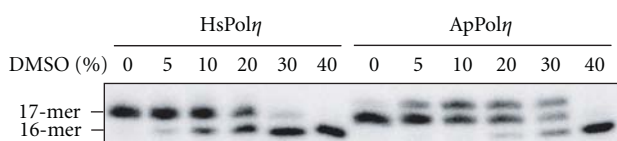
ApPol $\eta$  could be useful for *in vitro* studies as a new paradigm system to understand TLS mechanisms and also could be a starting material for the development of a more stable eukaryotic-like TLS polymerase by directed evolution. Such an enzyme will enable us to amplify heavily damaged DNA, such as ancient DNA, by PCR-like methods.

## 5. Conclusions

In this study, we cloned an *A. pompejana* gene with homology to the HsPol $\eta$  gene. The primary structure of the protein indicated the conservation of the PCNA binding domain and the ubiquitin-binding zinc finger motif. The encoded full-length recombinant protein, ApPol $\eta$ , was readily produced in *Escherichia coli* and purified. We demonstrated that ApPol $\eta$  could bypass CPD, 8-oxoG, 5R-Tg, and 5S-Tg, but not



(a)



(b)

FIGURE 8: Activity of ApPol $\eta$  in organic solvent-containing solutions. (a) Incorporation of dCMP in the presence of DMSO, ethanol, and IPA at a concentration of 20% (v/v) was analyzed, using the primer-template shown in Figure 7. Replication assays were performed at 30°C for 10 minutes. (b) The same assays were performed with various concentrations of DMSO.

6–4 pp, Dewar, or any AP site analog revealing a similar spectrum of activities to those of the human homolog. ApPol $\eta$ 's properties of higher stability with human-like activities offer advantages over other known eukaryotic TLS polymerases for future basic and practical applications.

## Acknowledgments

The authors thank S. C. Cary and B. R. Chapados for technical support. They thank the R/V Atlantis and DSV Alvin crews in aiding *A. pompejana* sample collection and the Department of Energy (DOE) Joint Genome Institute for partial EST sequencing for this work. This work was supported by Human Frontier Science Program (J. A. Tainer, F. Hanaoka, S. Iwai), by the 3rd Annual Incyte Discovery Award (D. S. Shin, J. A. Tainer), by the US National Institutes of Health Grants GM46312 (JAT), and by DOE program Integrated Diffraction Analysis Technologies (J. A. Tainer) and DOE Community Sequence Program award (D. S. Shin, J. A. Tainer). D. S. Shin and K. Hitomi were supported in part by Skaggs Institute for Chemical Biology, and D. S. Shin was further supported in part by a Ruth L. Kirschstein NSRA Fellowship. Bulky lesion repair in the Tainer lab is supported by NIH grant R01 CA112093. J. O. Fuss and Q. J. Cheng were supported in part by the US National Cancer Institute Grant CA112093 and the US Department of Energy Molecular Assemblies: Genes and Genomes Integrated Efficiently Project (DE-FG0207ER64326), plus the NRSA Fellowship 1F32CA108393 to J. O. Fuss.

## References

- [1] E. C. Friedberg, G. C. Walker, W. Siede, R. D. Wood, R. A. Schultz, and T. Ellenberger, *DNA Repair and Mutagenesis*, American Society for Microbiology, Washington, DC, USA, 2nd edition, 2005.
- [2] J. H. J. Hoeijmakers, "Genome maintenance mechanisms for preventing cancer," *Nature*, vol. 411, no. 6835, pp. 366–374, 2001.
- [3] T. Lindahl and R. D. Wood, "Quality control by DNA repair," *Science*, vol. 286, no. 5446, pp. 1897–1905, 1999.
- [4] E. C. Friedberg, A. R. Lehmann, and R. P. P. Fuchs, "Trading places: how do DNA polymerases switch during translesion DNA synthesis?" *Molecular Cell*, vol. 18, no. 5, pp. 499–505, 2005.
- [5] A. R. Lehmann, A. Niimi, T. Ogi et al., "Translesion synthesis: Y-family polymerases and the polymerase switch," *DNA Repair*, vol. 6, no. 7, pp. 891–899, 2007.
- [6] H. Ohmori, E. C. Friedberg, R. P. P. Fuchs et al., "The Y-family of DNA polymerases," *Molecular Cell*, vol. 8, no. 1, pp. 7–8, 2001.
- [7] A. M. Cordonnier and R. P. P. Fuchs, "Replication of damaged DNA: molecular defect in Xeroderma pigmentosum variant cells," *Mutation Research*, vol. 435, no. 2, pp. 111–119, 1999.
- [8] A. R. Lehmann, S. Kirk Bell, and C. F. Arlett, "Xeroderma pigmentosum cells with normal levels of excision repair have a defect in DNA synthesis after UV irradiation," *Proceedings of the National Academy of Sciences of the United States of America*, vol. 72, no. 1, pp. 219–223, 1975.

- [9] R. E. Johnson, C. M. Kondratick, S. Prakash, and L. Prakash, "hRAD30 mutations in the variant form of xeroderma pigmentosum," *Science*, vol. 285, no. 5425, pp. 263–265, 1999.
- [10] C. Masutani, R. Kusumoto, A. Yamada et al., "The XPV (xeroderma pigmentosum variant) gene encodes human DNA polymerase  $\eta$ ," *Nature*, vol. 399, no. 6737, pp. 700–704, 1999.
- [11] J. T. Reardon, A. F. Nichols, S. Keeney et al., "Comparative analysis of binding of human damaged DNA-binding protein (XPE) and Escherichia coli damage recognition protein (UvrA) to the major ultraviolet photoproducts: T[c,s]T, T[t,s]T, T[6-4]T, and T[Dewar]T," *Journal of Biological Chemistry*, vol. 268, no. 28, pp. 21301–21308, 1993.
- [12] A. van Hoffen, J. Venema, R. Meschini, A. A. van Zeeland, and L. H. F. Mullenders, "Transcription-coupled repair removes both cyclobutane pyrimidine dimers and 6-4 photoproducts with equal efficiency and in a sequential way from transcribed DNA in xeroderma pigmentosum group C fibroblasts," *EMBO Journal*, vol. 14, no. 2, pp. 360–367, 1995.
- [13] C. Masutani, R. Kusumoto, S. Iwai, and F. Hanaoka, "Mechanisms of accurate translesion synthesis by human DNA polymerase  $\eta$ ," *EMBO Journal*, vol. 19, no. 12, pp. 3100–3109, 2000.
- [14] M. B. de Moura, B. L. F. Schamber-Reis, D. G. P. Silva et al., "Cloning and characterization of DNA polymerase  $\eta$  from Trypanosoma cruzi: roles for translesion bypass of oxidative damage," *Environmental and Molecular Mutagenesis*, vol. 50, no. 5, pp. 375–386, 2009.
- [15] L. Haracska, M. T. Washington, S. Prakash, and L. Prakash, "Inefficient bypass of an abasic site by DNA polymerase  $\eta$ ," *Journal of Biological Chemistry*, vol. 276, no. 9, pp. 6861–6866, 2001.
- [16] L. Haracska, S.-L. Yu, R. E. Johnson, L. Prakash, and S. Prakash, "Efficient and accurate replication in the presence of 7,8-dihydro-8-oxoguanine by DNA polymerase  $\eta$ ," *Nature Genetics*, vol. 25, no. 4, pp. 458–461, 2000.
- [17] R. Kusumoto, C. Masutani, S. Iwai, and F. Hanaoka, "Translesion synthesis by human DNA polymerase  $\eta$  across thymine glycol lesions," *Biochemistry*, vol. 41, no. 19, pp. 6090–6099, 2002.
- [18] S. D. McCulloch, R. J. Kokoska, P. Garg, P. M. Burgers, and T. A. Kunkel, "The efficiency and fidelity of 8-oxo-guanine bypass by DNA polymerases  $\delta$  and  $\eta$ ," *Nucleic Acids Research*, vol. 37, no. 9, pp. 2830–2840, 2009.
- [19] Y. Zhang, F. Yuan, X. Wu et al., "Error-prone lesion bypass by human DNA polymerase  $\eta$ ," *Nucleic Acids Research*, vol. 28, no. 23, pp. 4717–4724, 2000.
- [20] M. J. McIlwraith, A. Vaisman, Y. Liu, E. Fanning, R. Woodgate, and S. C. West, "Human DNA polymerase  $\eta$  promotes DNA synthesis from strand invasion intermediates of homologous recombination," *Molecular Cell*, vol. 20, no. 5, pp. 783–792, 2005.
- [21] T. Kawamoto, K. Araki, E. Sonoda et al., "Dual roles for DNA polymerase  $\eta$  in homologous DNA recombination and translesion DNA synthesis," *Molecular Cell*, vol. 20, no. 5, pp. 793–799, 2005.
- [22] S. C. Cary, T. Shank, and J. Stein, "Worms bask in extreme temperatures," *Nature*, vol. 391, no. 6667, pp. 545–546, 1998.
- [23] D. S. Shin, M. DiDonato, D. P. Barondeau et al., "Super-oxide dismutase from the eukaryotic thermophile Alvinella pompejana: structures, stability, mechanism, and insights into amyotrophic lateral sclerosis," *Journal of Molecular Biology*, vol. 385, no. 5, pp. 1534–1555, 2009.
- [24] T. V. Burjanadze, "New analysis of the phylogenetic change of collagen thermostability," *Biopolymers*, vol. 53, no. 6, pp. 523–528, 2000.
- [25] K. L. Henscheid, D. S. Shin, S. C. Cary, and J. A. Berglund, "The splicing factor U2AF65 is functionally conserved in the thermotolerant deep-sea worm Alvinella pompejana," *Biochimica et Biophysica Acta*, vol. 1727, no. 3, pp. 197–207, 2005.
- [26] P. Piccino, F. Viard, P.-M. Sarradin, N. Le Bris, D. Le Guen, and D. Jollivet, "Thermal selection of PGM allozymes in newly founded populations of the thermotolerant vent polychaete Alvinella pompejana," *Proceedings of the Royal Society B*, vol. 271, no. 1555, pp. 2351–2359, 2004.
- [27] T. Murata, S. Iwai, and E. Ohtsuka, "Synthesis and characterization of a substrate for T4 endonuclease V containing a phosphorodithioate linkage at the thymine dimer site," *Nucleic Acids Research*, vol. 18, no. 24, pp. 7279–7286, 1990.
- [28] S. Iwai, M. Shimizu, H. Kamiya, and E. Ohtsuka, "Synthesis of a phosphoramidite coupling unit of the pyrimidine (6-4) pyrimidone photoproduct and its incorporation into oligodeoxynucleotides," *Journal of the American Chemical Society*, vol. 118, no. 32, pp. 7642–7643, 1996.
- [29] J. Yamamoto, K. Hitomi, T. Todo, and S. Iwai, "Chemical synthesis of oligodeoxyribonucleotides containing the Dewar valence isomer of the (6-4) photoproduct and their use in (6-4) photolyase studies," *Nucleic Acids Research*, vol. 34, no. 16, pp. 4406–4415, 2006.
- [30] S. Iwai, "Synthesis of thymine glycol containing oligonucleotides from a building block with the oxidized base," *Angewandte Chemie*, vol. 39, no. 21, pp. 3874–3876, 2000.
- [31] T. Shimizu, K. Manabe, S. Yoshikawa, Y. Kawasaki, and S. Iwai, "Preferential formation of (5S,6R)-thymine glycol for oligodeoxyribonucleotide synthesis and analysis of drug binding to thymine glycol-containing DNA," *Nucleic Acids Research*, vol. 34, no. 1, pp. 313–321, 2006.
- [32] B. C. Broughton, A. Cordonnier, W. J. Kleijer et al., "Molecular analysis of mutations in DNA polymerase  $\eta$  in xeroderma pigmentosum-variant patients," *Proceedings of the National Academy of Sciences of the United States of America*, vol. 99, no. 2, pp. 815–820, 2002.
- [33] H. Ling, F. Boudsocq, R. Woodgate, and W. Yang, "Crystal structure of a Y-family DNA polymerase in action: a mechanism for error-prone and lesion-bypass replication," *Cell*, vol. 107, no. 1, pp. 91–102, 2001.
- [34] M. Bienko, C. M. Green, N. Crosetto et al., "Ubiquitin-binding domains in Y-family polymerases regulate translesion synthesis," *Science*, vol. 310, no. 5755, pp. 1821–1824, 2005.
- [35] S. Sabbioneda, C. M. Green, M. Bienko, P. Kannouche, I. Dikic, and A. R. Lehmann, "Ubiquitin-binding motif of human DNA polymerase  $\nu$  is required for correct localization," *Proceedings of the National Academy of Sciences of the United States of America*, vol. 106, no. 8, p. E20, 2009.
- [36] N. Acharya, J.-H. Yoon, H. Gali et al., "Reply to sabbioneda et al.: Role of ubiquitin-binding motif of human DNA polymerase  $\nu$  in translesion synthesis," *Proceedings of the National Academy of Sciences of the United States of America*, vol. 106, no. 8, p. E21, 2009.
- [37] L. Haracska, R. E. Johnson, I. Unk et al., "Physical and functional interactions of human DNA polymerase  $\eta$  with PCNA," *Molecular and Cellular Biology*, vol. 21, no. 21, pp. 7199–7206, 2001.
- [38] P. L. Kannouche, J. Wing, and A. R. Lehmann, "Interaction of human DNA polymerase  $\eta$  with monoubiquitinated PCNA:

- a possible mechanism for the polymerase switch in response to DNA damage,” *Molecular Cell*, vol. 14, no. 4, pp. 491–500, 2004.
- [39] E. Ohashi, T. Ogi, R. Kusumoto et al., “Error-prone bypass of certain DNA lesions by the human DNA polymerase  $\kappa$ ,” *Genes and Development*, vol. 14, no. 13, pp. 1589–1594, 2000.
- [40] A. Tissier, E. G. Frank, J. P. McDonald, S. Iwai, F. Hanaoka, and R. Woodgate, “Misinsertion and bypass of thymine-thymine dimers by human DNA polymerase  $\iota$ ,” *EMBO Journal*, vol. 19, no. 19, pp. 5259–5266, 2000.
- [41] P. D. Hoffman, M. J. Curtis, S. Iwai, and J. B. Hays, “Biochemical evolution of DNA polymerase  $\eta$ : properties of plant, human, and yeast proteins,” *Biochemistry*, vol. 47, no. 16, pp. 4583–4596, 2008.
- [42] R. E. Johnson, L. Haracska, S. Prakash, and L. Prakash, “Role of DNA polymerase  $\eta$  in the bypass of a (6-4) TT photoproduct,” *Molecular and Cellular Biology*, vol. 21, no. 10, pp. 3558–3563, 2001.
- [43] R. E. Johnson, M. T. Washington, S. Prakash, and L. Prakash, “Fidelity of human DNA polymerase  $\eta$ ,” *Journal of Biological Chemistry*, vol. 275, no. 11, pp. 7447–7450, 2000.
- [44] T. Matsuda, K. Bebenek, C. Masultanl, F. Hanaoka, and T. A. Kunkel, “Low fidelity DNA synthesis by human DNA polymerase- $\eta$ ,” *Nature*, vol. 404, no. 6781, pp. 1011–1013, 2000.
- [45] B. J. Campbell, J. L. Stein, and S. C. Cary, “Evidence of chemolithoautotrophy in the bacterial community associated with *Alvinella pompejana*, a hydrothermal vent polychaete,” *Applied and Environmental Microbiology*, vol. 69, no. 9, pp. 5070–5078, 2003.
- [46] S. C. Cary, M. T. Cottrell, J. L. Stein, F. Camacho, and D. Desbruyères, “Molecular identification and localization of filamentous symbiotic bacteria associated with the hydrothermal vent annelid *Alvinella pompejana*,” *Applied and Environmental Microbiology*, vol. 63, no. 3, pp. 1124–1130, 1997.
- [47] F. Boudsocq, S. Iwai, F. Hanaoka, and R. Woodgate, “*Sulfolobus solfataricus* P2 DNA polymerase IV (Dp04): an archaeal DinB-like DNA polymerase with lesion-bypass properties akin to eukaryotic pol $\eta$ ,” *Nucleic Acids Research*, vol. 29, no. 22, pp. 4607–4616, 2001.
- [48] J. P. McDonald, A. Hall, D. Gasparutto, J. Cadet, J. Ballantyne, and R. Woodgate, “Novel thermostable Y-family polymerases: applications for the PCR amplification of damaged or ancient DNAs,” *Nucleic Acids Research*, vol. 34, no. 4, pp. 1102–1111, 2006.
- [49] J. T. Beatty, J. Overmann, M. T. Lince et al., “An obligately photosynthetic bacterial anaerobe from a deep-sea hydrothermal vent,” *Proceedings of the National Academy of Sciences of the United States of America*, vol. 102, no. 26, pp. 9306–9310, 2005.
- [50] F. Pradillon, B. Shillito, C. M. Young, and F. Gaill, “Developmental arrest in vent worm embryos,” *Nature*, vol. 413, no. 6857, pp. 698–699, 2001.
- [51] H. Ling, F. Boudsocq, R. Woodgate, and W. Yang, “Snapshots of replication through an abasic lesion: structural basis for base substitutions and frameshifts,” *Molecular Cell*, vol. 13, no. 5, pp. 751–762, 2004.
- [52] S. Shachar, O. Ziv, S. Avkin et al., “Two-polymerase mechanisms dictate error-free and error-prone translesion DNA synthesis in mammals,” *EMBO Journal*, vol. 28, no. 4, pp. 383–393, 2009.

## Review Article

# DNA Polymerase: Structural Homology, Conformational Dynamics, and the Effects of Carcinogenic DNA Adducts

**Richard G. Federley and Louis J. Romano**

*Department of Chemistry, Wayne State University, Detroit, MI 48202, USA*

Correspondence should be addressed to Louis J. Romano, [ljr@chem.wayne.edu](mailto:ljr@chem.wayne.edu)

Received 14 May 2010; Accepted 30 June 2010

Academic Editor: Ashis Basu

Copyright © 2010 R. G. Federley and L. J. Romano. This is an open access article distributed under the Creative Commons Attribution License, which permits unrestricted use, distribution, and reproduction in any medium, provided the original work is properly cited.

DNA replication is vital for an organism to proliferate and lying at the heart of this process is the enzyme DNA polymerase. Most DNA polymerases have a similar three dimensional fold, akin to a human right hand, despite differences in sequence homology. This structural homology would predict a relatively unvarying mechanism for DNA synthesis yet various polymerases exhibit markedly different properties on similar substrates, indicative of each type of polymerase being prescribed to a specific role in DNA replication. Several key conformational steps, discrete states, and structural moieties have been identified that contribute to the array of properties the polymerases exhibit. The ability of carcinogenic adducts to interfere with conformational processes by directly interacting with the protein explicates the mutagenic consequences these adducts impose. Recent studies have identified novel states that have been hypothesised to test the fit of the nascent base pair, and have also shown the enzyme to possess a lively quality by continually sampling various conformations. This review focuses on the homologous structural changes that take place in various DNA polymerases, both replicative and those involved in adduct bypass, the role these changes play in selection of a correct substrate, and how the presence of bulky carcinogenic adducts affects these changes.

## 1. Introduction

Accurate replication of genomic DNA is imperative for the successful proliferation of an organism. The enzyme DNA polymerase is responsible for catalyzing the template-directed addition of a deoxyribonucleoside-5'-triphosphate (dNTP<sup>1</sup>) to a growing DNA strand and must do so rapidly and with high fidelity. It is known that the thermodynamics of base pairing alone are insufficient to account for the incredibly low error rates achieved during DNA synthesis [1], and that the DNA polymerase imposes constraints on the selection of a correct nucleotide for incorporation into the primer. Utilizing the thermodynamics of base pairing alone can only account for an accuracy of 1 mistake in 150 nucleotides incorporated, whereas polymerases are known to have error frequencies ranging from  $10^{-3}$  to  $10^{-5}$  [2, 3]. DNA polymerases must not only ensure accurate synthesis through selection of a correct dNTP, but they also must prevent the incorporation of incorrect substrates such as ribonucleoside-5'-triphosphates (rNTPs). Therefore,

a stringent mechanism must be in place for rejection of correctly base pairing nucleotides having a ribose 2' hydroxyl. In addition, some DNA polymerases must cope with reading templates containing DNA adducts that have evaded nucleotide or base excision repair. These roadblocks to replication, such as the well studied DNA adducts 2-aminofluorene (AF) and *N*-acetyl-2-aminofluorene (AAF), present a tough challenge to the polymerase by altering the template structure, often causing a misincorporation event to occur, the generation of a frameshift, or simply place a stringent block to the advancement of replication [4, 5].

Normally, DNA replication proceeds via nucleotide synthesis performed by replicative polymerases. These polymerases are efficient at incorporating bases that allow proper Watson-Crick hydrogen bonding and also fulfil strict geometric constraints within the polymerase active site. However, the replication past the aforementioned DNA adducts presents a special problem to the tight constraints of a replicative polymerase's active site. To alleviate these roadblocks, a special class of polymerases exist to fill such a

niche. The bypass or translesion synthesis (TLS) polymerases have the ability to accommodate a vast array of DNA lesions and perform either incorporation or extension in regions where replicative polymerases stall or fail completely. This paper will focus on the homologous conformational changes that take place in various DNA polymerases, the role these changes play in selection of a correct substrate, and how the presence of bulky carcinogenic adducts affects these changes.

## 2. A Face for a Name

*E. coli* DNA polymerase I plays a role in the repair of damaged duplex DNA and the processing of Okazaki fragments in *E. coli* [3]. This polymerase consists of a multidomain architecture housing not only the 5'-3' polymerization activity required for DNA replication, but also 3'-5' and 5'-3' exonuclease activities. The 3'-5' exonuclease, or proofreading activity, allows greater fidelity to be achieved by removing incorrectly incorporated nucleotides from the growing DNA primer strand resulting in another opportunity to incorporate the correct base before continuing on with synthesis. The 5'-3' exonuclease does not directly function in increasing fidelity but instead is involved with processing of Okazaki fragments by the excision of RNA primers situated on the lagging strand.

A very useful proteolytic digest of DNA polymerase I produces a truncated enzyme termed Klenow fragment. Klenow fragment houses the 5'-3' polymerase activity required for DNA synthesis and the 3'-5' exonuclease proofreading activity, but is devoid of the 5'-3' domain responsible for the excision of RNA primers. In addition, a single D424A point mutation within Klenow fragment's 3'-5' exonuclease domain almost abolishes the exonuclease activity, making this polymerase an excellent choice for DNA synthesis studies without the complication of exonuclease action [9]. Klenow fragment has been a model enzyme for the study of DNA replication for the last four decades, and the solution of the crystal structure in 1985 by Ollis et al. aided in providing a structural overview of the enzymatic domains [10].

The crystal structure of Klenow fragment revealed a two domain architecture, with the smaller 200 amino acid N-terminus forming the 3'-5' exonuclease domain and the larger 400 amino acid C-terminal domain folding to form the polymerization domain. The general shape of the Klenow fragment polymerization domain, being akin to a right hand, has proven to be strikingly universal among DNA polymerases. Klenoq1, the analogous Klenow fragment portion of thermophilic *Thermus aquaticus* DNA polymerase I, showed a C-terminal fold nearly identical to that of Klenow fragment and can be seen in Figure 1(a) [7]. The polymerase domain can be further divided into three subdomains consisting of the fingers, thumb, and palm, all of which form a cleft of approximately 20–24 Å wide and 25–35 Å deep [10]. Based on previous biochemical studies identifying catalytically important residues in Klenow fragment, the active site of the C-terminal polymerization domain was mapped to the base of the cleft within the palm of the enzyme, with the 3'-5' exonuclease active site located

about 35 Å away. The cleft was noted to be of the approximate size to bind DNA, but it would not be until 1993 when Beese et al. published a cocrystal structure of Klenow fragment bound to duplex DNA that the orientation and structure of the duplex within the enzyme would be known [11].

The cocrystal structure of Klenow bound to duplex DNA gave the first glimpse into the arrangement of the DNA within the polymerase and evidence of the first conformational change that takes place within the enzyme. In this structure, the DNA was situated within the polymerase at right angles to the cleft containing the active polymerase site however, the 3' primer terminus was melted from the template and situated within the exonuclease site in an editing complex. Despite being in an editing complex, the authors modeled the primer strand at the polymerase active site and concluded that the primer could alternate between the exonuclease and polymerase sites, without dissociation of the enzyme. Interestingly, Beese et al. noted in their modeling that some distortion of the DNA duplex terminus or protein would be required in order to achieve binding at the polymerase site and that this distortion of the DNA would make the equilibrium between single-stranded and double-stranded DNA more sensitive to mismatches. Irrespective of the mode of binding, many important observations were noted from this structure and further confirmed in later crystal structures of Klenoq (Figure 1(b)) [8]. One such observation was the small DNA-induced closing motion the thumb region undergoes upon formation of the binary complex. A region of the thumb, residues 558 to 637 in Klenow fragment, executes a shift (12 Å at the N-terminus of helix I) towards the 3'-5' exonuclease domain to form direct contacts with the DNA [11]. Chemical modification studies also showed that Lys635 (Lys540 in Klenoq), which is a highly conserved residue among the Pol I family, is directly involved in DNA binding [12]. In addition to the thumb, extensive contacts are formed between the enzyme and the DNA, although virtually all contacts are nonspecific in nature, forming interactions with the phosphate backbone of the DNA, or to the universal hydrogen bond donors and acceptors of the minor groove. This is important to ensure that the polymerase will bind all DNA equally, irrespective of the sequence. The small closing movement of the thumb upon DNA binding proved to be the first of at least two conformational changes to take place. The initial description of Klenow fragment in terms of a hand, and specifically the naming of the subdomains as fingers and thumb, proved to be somewhat serendipitous due to their anthropomorphic motions upon forming a binary complex, and as was later shown, a catalytically competent ternary complex.

## 3. Hold on Tight

In order to successfully replicate DNA, an active ternary complex must be formed with the proper geometric alignment of the polymerase catalytic residues, the metal ions, the primer-template DNA duplex, and the correctly chosen dNTP. The first crystal structure solutions for the ternary complexes were of Rat DNA polymerase  $\beta$ , Klenoq1, the

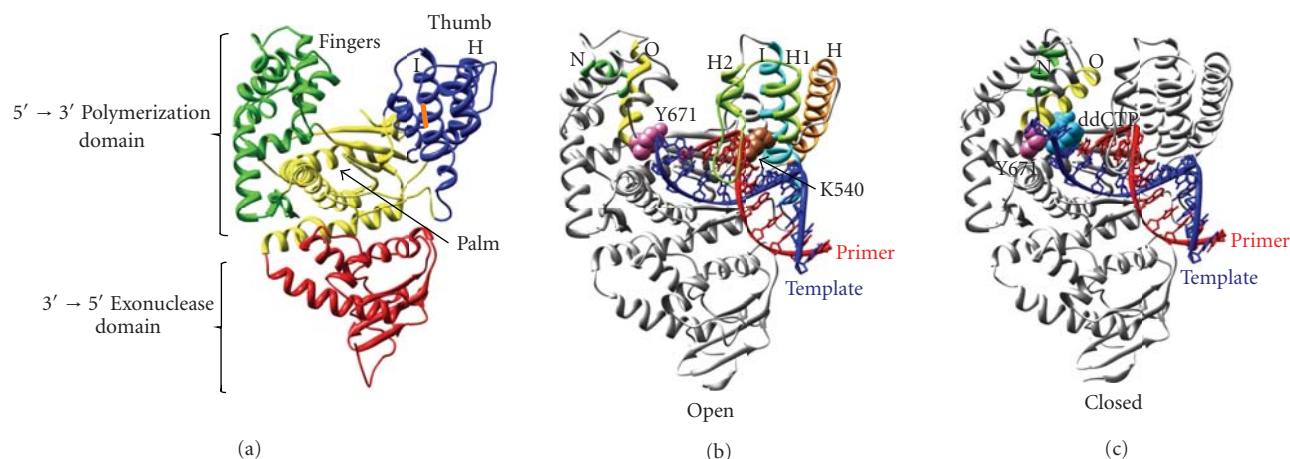


FIGURE 1: Structure of Klenotaq1 (a) Structure of Klenotaq1 in the absence of DNA (PDB #1KTQ) [7]. The overall structure of polymerases resembles that of a human right hand forming palm (yellow), fingers (green), and thumb (blue) domains. The palm domain houses the active site residues responsible for the 5' to 3' polymerase activity, and the 3' to 5' exonuclease domain (red) allows excision of misincorporated bases. The H1H2 Loop is disordered and missing from the structure (ends connected with orange line). (b) Klenotaq1 open binary complex (PDB #4KTQ) [8]. The DNA is situated in the cleft formed between the fingers, thumb, and palm domains. The Y671 residue (pink) is stacked on top of the template (dark blue). K540 (brown) makes nonspecific interactions with the minor groove to aid in holding the polymerase bound to the DNA. Helices I (cyan) and H (orange) make small movements relative to their positions in the open complex, and the H1H2 loop (light green) now becomes ordered and visible in the structure. The remainder of the colors are as follows primer (red), H1 and H2 helix (light green), O helix (yellow), and N helix (green). (c) Klenotaq1 closed ternary complex (PDB #3KTQ) [8]. A correctly base pairing ddCTP (light blue) is located within the active site inducing a large conformational change of the O (yellow) and N (green) helices (compare with positions in (b)). Y671 is now flipped out of its stacking arrangement with the template and the templating base forms Watson-Crick base pairs with the ddCTP. Molecular graphics images were produced using the UCSF Chimera package from the Resource for Biocomputing, Visualization, and Informatics at the University of California, San Francisco (supported by NIH P41 RR-01081) [6].

replicative DNA polymerase of bacteriophage T7, and *Bacillus stearothermophilus* DNA polymerase I [8, 13–15]. These structures revealed a great deal of information regarding the location of dNTP binding and catalytically active residues, a large conformational change in the protein, and a two metal ion mechanism for nucleotidyl transfer. Despite the wide breadth of organisms these polymerases were obtained from, all exhibited the now stereotypical polymerase architecture of a human right hand and share a similar geometry of the polymerase active site. What follows is a general culmination of information for most observed structures.

The ternary complex is defined by binding of a dNTP into the polymerase cleft alongside the DNA. The incoming dNTP is aligned within the active site by interactions of the nonbridging oxygens of the phosphate moiety to positively charged residues along and near the O helix, placing the phosphate moiety roughly parallel to the O helix. These phosphate interactions are suggested as the primary recognition segment of the incoming dNTP, which is based upon crystal structures of binary complexes of Klenotaq1 with all four dNTPs, showing the phosphates of all four dNTPs aligned in similar positions [16]. However, the base and ribose moieties were in slightly different orientations for the four structures. Most interestingly, the formation of the ternary complex in the presence of the next correct dNTP for base pairing with the first single stranded template base is accompanied by a large conformational change in the fingers of the polymerase (Figure 1(c)). In the case of

Klenotaq, this change is an inward rotation of the O helix by approximately  $46^\circ$  ( $41^\circ$  in T7) towards the primer-template [8, 14]. The formation of the closed ternary complex has the effect of clamping down the dNTP into the active site, effectively sealing off the crevice formed by the thumb, palm, and fingers, resulting in the proper geometric alignment of catalytic residues to complete a nucleotidyl transfer reaction.

Further elaboration by Dzantiev and Romano showed that the closed tertiary complex could only be observed in the presence of the next correct nucleotide and not in the presence of incorrectly base pairing nucleotides [17]. Using a tryptic digestion analysis they showed that trypsin was capable of cleaving Klenow fragment near the active site of the polymerization domain in its open form. However, upon incubation of Klenow fragment with a correctly base pairing dNTP the cleavage was inhibited, presumably due to the conformational change of the enzyme protecting the region near the active site from proteolytic cleavage. Further, a correctly base pairing ribonucleotide substrate also did not trigger this conformational change as evidence by the formation of trypsin cleavage products. This suggested that only a correctly base pairing dNTP could conform to the close fitting active site of the polymerase and any deviation from the ideal active site geometry would not allow the conformational change to take place. Indeed, the crystal structures of the closed ternary complexes showed the dNTP situated in a tightly surrounded environment as it stacks between the 3' base of the primer strand and

residues of the O helix [14]. The dNTP binds such that it can form a Watson-Crick base pair with the first single-stranded templating base. The dNTP is further coordinated and positioned by interactions to two metal ions located within the active site.

The alignment of the dNTP in the closed conformation allows a two metal ion mechanism for the nucleotidyl transfer to occur. The two metal ions, positioned approximately 3.6 Å apart, are octahedrally coordinated by all three phosphates of the dNTP, the highly conserved side chain residues of the enzyme, and two water molecules (Figure 2). Metal ion A functions to lower the ribose's 3'OH affinity for its hydrogen. This makes the attack on the  $\alpha$  phosphate of the dNTP by the primer's 3' O<sup>-</sup> possible. Metal B serves to support the leaving of the pyrophosphate and together both metals stabilize the negative charge of the pentavalent transition state. It appears that all polymerases studied to date, as well as enzymes such as HIV -1 reverse transcriptase, utilize this same two metal ion mechanism for nucleotide addition (minireview in [18]).

Similar to the changes within the enzyme during binding, the DNA undergoes several changes from its typical solution based linear B-form duplex structure [8, 13–15]. The DNA in the ternary complex remains held in place by the small conformational change of the thumb. This maintenance of the closed thumb conformation ensures that despite continued dissociation and reassociation of incoming dNTPs during the selection process, the transient binary DNA-Pol complex remains relatively stable and the propensity for dissociation during these transient events does not increase dramatically. The polymerase-DNA interactions are almost exclusively nonspecific in nature, binding to the nonsequence-specific minor groove while providing no interactions to the sequence specific major groove, with the small exception of those bases located near the active site. Despite the wide breadth of organisms the polymerases were obtained from, the DNA is mostly B-form yet transitions to A-form DNA as it nears the active site [8, 13–15]. The B-form DNA has an ordered spine of water molecules along the minor groove interacting with the N3's of purines and O2's of pyrimidines [15]. Both proper A-T and G-C base pairs display the correct N3 and O2 along the minor groove required for this interaction, whereas misincorporations will cause a disturbance in these interactions, possibly providing a mechanism by which misincorporations can be detected upstream of the active site. These highly ordered water molecules are intentionally disrupted along the minor groove as it nears the active site, giving rise to A-form DNA and a widening of the minor groove with a decreased helical twist in this region. The DNA is further contorted forming a slight "S" shape, with the first bend being induced by interactions with the palm domain, and the second from interactions with the closed thumb [14].

As the conformational change from the open to closed ternary complex occurs, another interesting movement takes place regarding the templating base and an aromatic residue at the base of the O helix (Tyr766 in Klenow Fragment, Tyr671 in Klentaq, Tyr530 in T7). In both the open binary and open ternary complexes, the templating base is

twisted almost 90° away from the nucleotide binding site (Figure 2(a)), and in its place the aforementioned Tyr671 of the O helix is stacked on top of the template of the terminal base pair [8]. At first glance, this appears to be illogical since the template base must be base-paired with the incoming nucleotide to direct its proper selection. However, this unique positioning of the templating base in the open conformation is thought to allow an incoming dNTP to "preview" the template prior to reaching the full depth of the binding pocket and has thus been coined the preinsertion site [19]. This preview in the preinsertion site may facilitate selection of a correct dNTP early on in the incorporation process. Upon binding of a correct dNTP to the complex, the conformational closing movement of the O helix induces a movement of the tyrosine side chain out of its stacking arrangement on the template, allowing the flipped out templating base to rotate back into its typical stacking arrangement with the template (Figure 2(b)) [8]. The exchange of positions of the tyrosine side chain with that of the templating base in the closed conformation allows the templating base to form its typical Watson-Crick hydrogen bonding alignment with the incoming dNTP. Given a correct fit, the subsequent alignment of catalytic residues takes place and phosphodiester bond formation can ensue.

However, selection of a proper nucleotide is no trivial matter considering the onslaught of correctly base pairing ribonucleotides and mismatched deoxyribonucleotides that must be rejected in order to find the correctly matching substrate. Utilizing a FRET-based stopped flow and chemical quench assay, Joyce et al. studied the mechanism by which each of these incorrect substrates are selected against during the process of replication [20]. In this assay, a fluorophore donor was positioned on a mobile portion of the fingers of Klenow fragment and a fluorescence quencher was positioned on the DNA. This allowed monitoring of a change in position of the fingers relative to the DNA and the formation of a correctly paired ternary complex. A concentration-dependent decrease in fluorescence was seen in the presence of the next correct dNTP, indicating that fingers closing was occurring. Mismatching dNTPs as well as mismatching rNTPs showed little fluorescence change, suggesting that they are selected against early on in the process, prior to fingers closing. This implied that a large discrimination against mismatching nucleotides (dNTPs and rNTPs) occurs directly in the open conformation. Addition of a correctly base pairing rNTP caused the conformational change to a closed complex to become significantly hampered, yet still occur to a marginal extent. This reduction in conformational change had previously been identified as a direct clash between the 2'-OH of the incoming ribonucleotide and the steric gate side chain Glu710 of Klenow fragment (Glu615 of Klentaq, see Figure 2) [21]. Similarly, Doublé et al. postulated, based on their crystal structure of T7 DNA polymerase, that the corresponding Glu480 residue along with Tyr526 forms a hydrophobic pocket that would preclude the 2'-OH of ribonucleotides [14].

Taken together, this indicates that the selection of a correctly pairing substrate occurs first, followed by a selection against ribonucleotides. This specific order for the

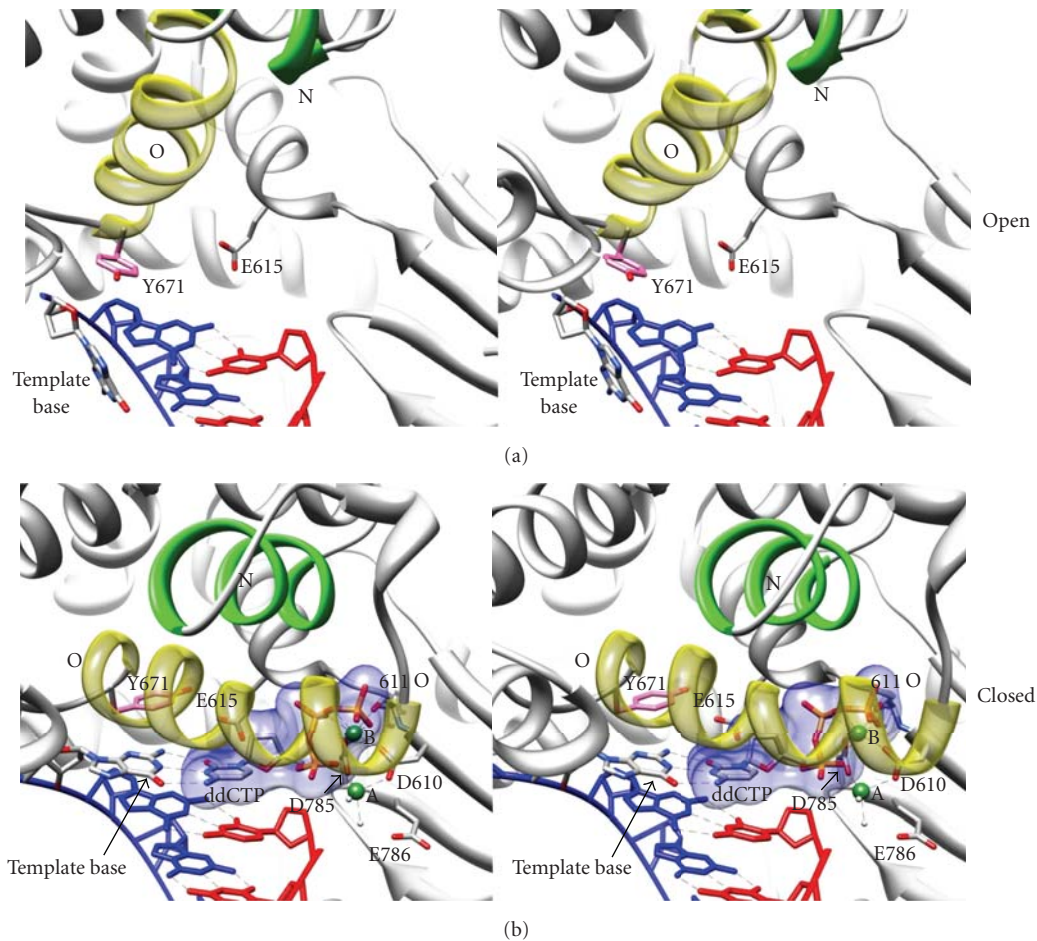


FIGURE 2: Stereoview (cross-eyed viewing) of Klentaq1 active site in the open binary (a) (PDB #4KTQ) and closed ternary (b) (PDB #3KTQ) conformations from the same view point [8]. (a) Open conformation: The O (yellow) and N (green) helices are in an open conformation allowing incoming dNTPs to reach the active site. The templating base (colored by element) is flipped out and Y671 (pink) occupies a stacked arrangement with the template (dark blue). (b) Closed conformation: The O and N helices have undergone a large conformational change and closed off the nucleotide binding pocket, which a ddCTP (colored by element with blue space filling) now occupies. The Y671 residue has flipped away from the template allowing the templating base to form a Watson-Crick base-pair with the ddCTP. The position of E615 allows screening of rNTPs via a steric clash with what would be a 2'OH of an incoming rNTP. The metal ions A and B (green spheres) form interactions with the phosphates of the ddCTP, and Klentaq residues D610, 611 O, D785, and 2 waters (grey spheres). The missing binding partner of metal A is hypothesised to be the missing 3'OH of the dideoxy-terminated primer terminus.

stepwise selection of a proper substrate provides a more efficient pathway for replication. By initially constraining downstream processing of a substrate to only correctly base pairing molecules, six of the eight possible substrates will be selected against. This provides an efficient first step to screen out as many incompatible substrates as possible, thereby limiting downstream processing of incompatible substrates. In essence, only one incorrect substrate (the correctly pairing ribonucleotide) of the initial eight nucleotide substrates will see further unnecessary processing. Conversely, if the ribonucleotide was selected against first, four of the eight substrates (all dNTPs) would need to be screened for in downstream processing prior to catalysis, and any additional time spent in their processing would be wasted three out of the four times. Overall, the conformationally-induced changes in the thumb upon binding DNA, and the large

changes in the fingers, function to grip the DNA and dNTP substrate, respectively. This provides a means for testing the nascent base pair for correct alignment and ensuring that only compatible dNTPs are incorporated.

#### 4. Roadblocks to Replication

The mechanism by which a correct nucleotide is chosen is clearly a complex process even under ideal conditions. However, DNA is under constant assault from both endogenous and exogenous agents that alter the DNA template by modifying the bases, resulting in distortions in the DNA structure or changes in the base electrostatics. Due to their disrupting nature, DNA damage can act as roadblocks to DNA polymerases or result in nucleotide misincorporations

and generation of frameshifts. One class of DNA damage that has been well-studied is that formed when experimental animals are treated with *N*-acetyl-2-aminofluorene (AAF). This compound, originally patented as an insecticide, has been shown to induce the formation of tumors in a variety of organs and was subsequently never introduced to market [22]. Metabolic activation and reaction of these compounds with DNA results in the attachment of the AAF or the related AF counterpart to the C8 position of guanine as the major DNA adducts.

Structural, biochemical, and theoretical studies all indicate that the dG-C8-AF structure causes much less distortion in duplex DNA compared with the dG-C8-AAF adduct. NMR experiments show that the guanine bearing the AAF adduct rotates from an *anti*- to *syn* conformation (Figure 3) in the double stranded DNA helix so that the fluorine moiety becomes inserted into the helix (base displacement model) [23]. This contrasts with the dG-C8-AF adduct that can adopt interchangeable conformations: (i) in the major structure, the fluorene remains outside the helix (outside binding model) and (ii) while the minor conformation has the fluorene ring stacked within the helix [24, 25]. These different conformations presumably are related to the differences observed in the biological properties of these two adducts. Utilizing primer extension assays, numerous studies have shown that a dG-C8-AAF adduct at the templating position poses a strong block to DNA synthesis by high-fidelity polymerases, whereas a dG-C8-AF adduct in the same sequence is more easily bypassed [26]. When the adducts are positioned on the template downstream single-stranded region at the +1 and +2 templating positions little to no effect from either adduct is noted. (For clarity, due to the various formats utilized to describe the positions of nucleotides, the numbering scheme used here is such that the first single-stranded templating base found within the insertion site of the polymerase during normal replication is signified position 0 (this is the current base being replicated). Downstream single-stranded template DNA is given consecutive positive numbers beginning with the +1 template base found in the preinsertion site, and upstream duplex DNA already replicated is given consecutive negative numbers starting with the first duplexed base pair in the postinsertion site (-1 position). This scheme is used to allow a direct visualization of the nucleotide position being discussed in relation to the polymerase, and is also the primary numbering schematic used when discussing crystal structures [27].) In contrast to positioning of the adduct at the +1 and +2 positions, positioning at the postinsertion site (position -1) or in regions of the DNA upstream of the postinsertion site (at the -2 and -3 positions relative to the insertion site) leads to diminished synthesis [28]. This indicates that the specific placement of the adduct within the polymerase active site was guiding its behaviour [28, 29].

It is interesting to note that despite the block posed by the presence of the dG-C8-AAF adduct, gel shift binding experiments utilizing Klenow fragment showed that polymerase binding to the AAF modified template was an order of magnitude greater than to native DNA [26]. In addition, unlike native DNA where addition of a correctly base pairing

dNTP induces a tighter binding, the identity and presence of any dNTP had little to no effect on this already strengthened binding. To remedy this counterintuitive discovery, Dzantiev and Romano postulated that the AAF moiety was interacting with hydrophobic amino acid residues located within or near the active site of the polymerase. This interaction was thought to strengthen the binary DNA-polymerase complex and also preclude binding of a dNTP within the active site. Further, the authors postulated that the adduct may block the conformational change seen in the presence of the next correctly base pairing nucleotide, thereby removing any further energetic contribution that the dNTP would bestow upon the complex.

A subsequent paper by the same authors explored more directly the conformational change of Klenow fragment in the presence of these two adducts [29]. Utilizing the same tryptic digestion assay discussed above for unmodified DNA, it was shown that the conformational change typically induced by the presence of the next correct dNTP was in fact inhibited by the presence of the dG-C8-AAF adduct, as predicted. The tryptic digestion band indicative of the open conformation was maintained despite the presence of any dNTP. However, this was only observed when the adduct was in the templating position. When the dG-C8-AAF adduct was moved one nucleotide to the +1 templating position (the preinsertion site), the dNTP-induced conformational change was again observed. Conversely, placement of a dG-C8-AF adduct in the templating position (insertion site) only partially inhibited the conformational change to a closed ternary complex. This difference was attributed to the dissimilar conformations that each adduct adopts within the polymerase active site and further strengthened the proposition that the AAF adduct was inducing interactions within the polymerase-DNA complex in a way that precluded the conformational changes necessary for competent nucleotide binding [29].

Picking up on this line of investigation, in 2003 Lone and Romano utilized a Klenow mutant, Y766S, to focus on the specific interactions responsible for the effect of the AAF adducts on this inhibition [30]. In the native protein the tyrosine at position 766 is located at the base of the O helix near the junction of the fingers and palm domain and is thought to function in maintaining active site geometry. This tyrosine stacks with the templating base in the open conformation and swings away during formation of the closed complex (similar to Figure 2(b)), (see more detailed description in Section 3). Mutations at this position have been shown to both increase the rate of insertions of incorrect nucleotides and reduce the ability to extend from these misincorporations [31]. Under identical conditions, the wild-type Klenow fragment predominantly stalled one nucleotide prior to the dG-C8-AAF adduct, incorporating across from the adduct approximately 20%, and extending past the AAF adduct to yield 6% full extension. Interestingly, the Y766S mutant showed a higher (40%) incorporation across from the AAF adduct, but gave only 1% full extension [30]. In addition, the Y766S mutant showed a 16-fold higher  $V_{\max}/K_m$  for incorporation of a correct dC across from the dG-C8-AAF adduct and also displayed a much greater

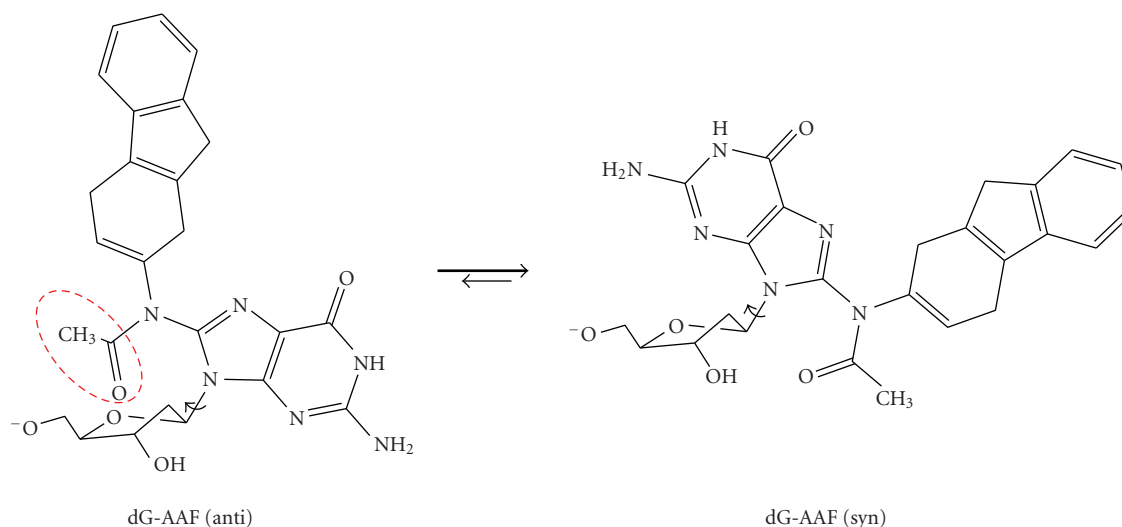


FIGURE 3: Conformations of a dG-C8-AAF adduct. Native DNA favors the *anti* conformation that allows Watson-Crick base pairs to form with the opposing strand while a dG-C8-AAF in the *anti* conformation results in a steric clash between the acetyl moiety (circled red) and the ribose. This causes the conformational equilibrium to shift towards the more favorable *syn* conformation. dG-C8-AAF adducts differ from dG-C8-AF adducts by having a smaller hydrogen in place of the circled acetyl moiety. This avoids the steric clash and allows both the *syn*- and *anti* conformations to be sampled.

propensity to misincorporate nucleotides on unmodified DNA. Together, this illustrated the importance placed upon the tyrosine residue for discrimination of a correct base pair and also shows that the Y766S mutation allowed the accommodation of the AAF-C8-dG lesion, possibly because of a more open active site that allows improper base pairs to form during synthesis [30].

Using gel shift analyses and the tryptic digestion assay, the ability of the Y766S mutant to undergo a conformational change was examined [30]. Similar to wild-type, the Y766S mutant showed an increased binding to native DNA in the presence of the next correct dNTP. The binding of the mutant polymerase to a dG-C8-AAF adduct was also increased, again similar to wild-type. However, where the wild-type showed no further increase in binding strength to dG-C8-AAF containing primer-templates in the presence of a correctly pairing dCTP, the mutant polymerase did show increased binding. In fact, the presence of any nucleotide appeared to increase the binding strength of the mutant, indicating a possible conformational change was occurring. This was confirmed utilizing the tryptic digestion analysis in which it was shown that the presence of dCTP caused protection of the cleavage site whereas other dNTPs reduced cleavage, indicating a conformational change was taking place despite the presence of the dG-C8-AAF adduct [30]. The ability of the mutant Y766S to undergo a conformational change even in the presence of a bulky dG-C8-AAF adduct is indicative of the more open active site and the importance the tyrosine residue plays in this conformational transition. Interestingly, the Y family of bypass polymerases that specialize in synthesis past bulky adducts also display a markedly open active site [33]. It is thought that this open nature better accommodates lesions by reducing the propensity of steric clashes, although at the expense of reduced fidelity.

## 5. What You See Is What You Get

It has long been thought that the conformations adopted within the active site by various DNA adducts will account for the array of biological effects and mutagenic consequences that the adducts display [22, 34]. Direct evidence for the predicted mechanism of inhibition of the conformational change for wild-type Klenow fragment in the presence of dG-C8-AAF, along with the increased binding affinity to these substrates, came in the form a crystal structure published in 2004 [32]. Dutta et al. were successful in obtaining functionally relevant crystal structures of bacteriophage T7 DNA polymerase bound to DNA duplexes containing either a dG-C8-AAF or dG-C8-AF at the templating position. The crystal structure of the dG-C8-AAF adduct has several key features that correlate with the aforementioned results obtained by Romano et al. First, the polymerase complex with dG-C8-AAF modified DNA is in a distorted open conformation and no nucleotide is bound to the complex despite the fact that crystals were grown in the presence of ddCTP (Figure 4(a)). The modified nucleoside is in a *syn* conformation, flipped out of the active site and bound to the surface of the fingers. The AAF moiety is positioned in a hydrophobic pocket behind the O helix stacking alongside Phe528, which is usually buried within the fingers (Figure 4(b)). Further stabilizing the position of the AAF moiety are hydrogen bonds between the adducted guanine's N2 and N7 with Asp534 and Arg566, respectively. The AAF interactions with the O helix pushes the helix towards the active site, forcing Tyr530 (analogous Tyr766 of Klenow fragment and Tyr671 of Klentaq) partially into the nucleotide binding site [32]. The positioning of the AAF and its various direct interactions with the polymerase, as well as the inability to bind nucleotide due to the positioning

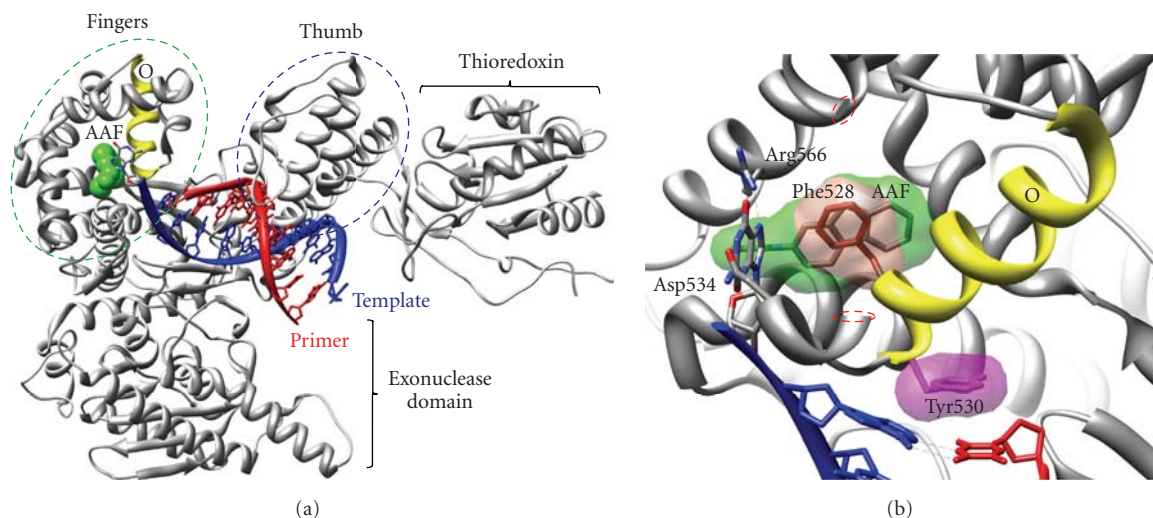


FIGURE 4: Structure of bacteriophage T7 polymerase bound to a DNA primer-template containing a dG-AAF adduct at the templating position (PDB# 1X9M) [32]. (a) The overall shape of T7 polymerase resembles a human right hand forming fingers (green circle), thumb (blue circle), and palm (not highlighted). T7 also contains thioredoxin, a processivity factory, in addition to the polymerase and exonuclease domains. The AAF adduct (green) inserts behind the O helix (yellow), locking the helix in a distorted open conformation, inhibiting the binding of dNTPs. (b) Close-up view of active site. The AAF moiety (grey with green space filling) is inserted into a hydrophobic pocket behind the O helix stacking with a flipped out Phe528 (brown, with brown space filling), which is buried in the native structure. The adducted guanine is in an *anti* conformation placing the hydrogen bond acceptors and donors away from the nucleotide binding position. This position is further stabilized by hydrogen bonds to Arg566 and Asp534. The AAF moiety pushes the O helix forward, causing Tyr530 (pink with pink space filling) to stack on top of the DNA, occupying the nucleotide binding site which occludes a dNTP from binding. Residues 537–557 have been removed for simplified visualization (ends are circled red).

of Tyr530, explain why the adduct places a strong block on replication as well as its increased binding affinity. This also confirms the previous experiments performed using Y766S that showed that the presence of the smaller serine allowed the conformational change to a closed ternary complex to occur.

The crystal structure containing the analogously positioned dG-C8-AF adduct showed similar conformations as the AAF adduct, but with a few significant differences. The AF residue was not positioned in the same hydrophobic pocket as its AAF counterpart, but instead the electron density of this moiety was either of poor quality or absent [32]. Despite limited quality of the electron density around the AF adduct, it could be established that the AF moiety was also not binding to the active site of the polymerase. This is indicative of a fluctuation between various conformations, possibly a transition from *anti*- to *syn* conformations. The amino acid residues forming the hydrophobic pocket of the AAF complex were oriented in more native-like positions within the AF containing structure. Also, the important Tyr530 was found to occupy the binding site of the template base in the closed ternary complex. The authors modeled the positions of the AF adduct in both *syn*- and *anti*- conformations of the nucleoside [32]. The *anti* conformation was shown to be able to form a closed complex with no significant steric clashes with the AF adduct. However, the *syn* conformation was shown to place the AF adduct stacked in the active site. This stacking arrangement will effectively compete with the stacking arrangement of guanine

in the alternative *anti* conformation. The positioning of the adducted guanine in the *syn* conformation would not allow base pairing with an incoming nucleotide and would subsequently stall synthesis when in this conformation.

A paper published by Hsu et al. in the same year was successful in crystallizing thermophilic *Bacillus* DNA polymerase I fragment in the presence of an AF and AAF adduct, and provided direct visualization of the effects of a dG-C8-AF adduct [35]. *Bacillus* DNA polymerase I fragment has the ability to catalyze nucleotide addition within the crystal, allowing snapshots to be taken of the adducted guanine within the pre- and postinsertion sites [13]. Capture of a dG-C8-AF adduct within the preinsertion site showed the adducted template base within the preinsertion site in a *syn* conformation, with the fluorene moiety also buried within the confines of the same site. The presence of the adduct induced a perturbation of the O1 helix, yet the O helix maintained its position in an open conformation. The remainder of the protein and the DNA was unaltered by the presence of the dG-C8-AF adduct. This showed that prior to incorporation of a dCTP the dG-C8-AF was positioned within the preinsertion site, whereas the catalytic site, the O helix, and postinsertion site remained unaffected and presumably capable of performing the transfer of the template base from the preinsertion site to the insertion site. The relatively ordered structure allows nucleotide incorporation to occur opposite the dG-C8-AF adduct, albeit to a reduced extent relative to unmodified DNA.

After a dCTP had been incorporated within the complex, the dG-C8-AF adopts an *anti* conformation, placing the AF moiety within the major groove while the dG forms cognate Watson-Crick hydrogen bonds with the dC within the postinsertion site. The polymerase is able to accommodate this structure because the adduct is solvent exposed within the major groove, unlike what would occur if its placement was into the minor groove where many interactions between the DNA and the polymerase are found. This conformation is similar to the outside model that places the AAF moiety outside the duplex DNA helix [24, 25]. This structure also showed a much greater degree of distortion that ultimately affects DNA replication. The dG-C8-AF:dC induces distortions to the template that relocate the  $n - 1$  template base causing perturbations to the minor groove, the O and O1 helicies, and placing the AF moiety obscuring the preinsertion site to the next template base. This conveniently explains the ability of polymerases to incorporate across from an AF adduct, yet exhibit difficulty in extending further. Conversely, the dG-C8-AAF adduct-containing structure in the pre- and postinsertion sites were indistinguishable, and hence a dCTP was absent from the postinsertion structure. In both structures the protein was in an open conformation with an empty preinsertion site as the AAF-adducted guanine is somewhat disordered and placed over the preinsertion site. The duplex DNA, as well as the protein's catalytic, pre- and postinsertion sites were undisturbed. Again, this inability to perform incorporation could presumably be due to the inability of a dG-C8-AAF adduct to adopt an *anti* conformation. In general, the observed crystal structures Dutta et al. [32] and of Hsu et al. [35] correlated well with the previous results and provided further support for the premise that the effects of these adducts are related to the conformations that they adopt within the polymerase active site. However, the crystal structures of Dutta et al. and Hsu et al. show that the conformations adopted by the adducts are also dependent upon the polymerase they are bound to, yet still correlate well with the previously observed results.

## 6. Not All Sequences Are Created Equal

The stark difference in the mutagenic properties of AAF and AF adducts are further influenced by the sequence of bases surrounding the adduct. AAF's ability to induce frameshifts is targeted to repetitive sequences such as the *NarI* restriction recognition sequence (5'-G<sub>1</sub>G<sub>2</sub>CG<sub>3</sub>CC-3') (*NarI* sequence reviewed in [36]) [37]. In bacteria, when an AAF adduct is positioned at G<sub>3</sub> a dinucleotide GC deletion is produced, while an AF adduct at this same position does not yield the deletion product [37, 38]. The dinucleotide deletion is thought to be induced via a slipped displaced structure where during synthesis the primer is capable of misaligning with the template within the polymerase active site. These misaligned looped out structures are further stabilized by Watson-Crick base pairing of adjacent nucleotides, allowing the polymerase to skip the nucleotides in proximity to the adduct. Gill and Romano explored this

possibility utilizing primer extension analysis and gel shift binding assays of various primers along the *NarI* restriction recognition sequence [39]. By positioning various primers along the AAF modified template and examining which nucleotide best complemented binding of Klenow fragment, along with the ability to extend the substrate, it was shown that the formation of a GC dinucleotide bulge was induced. Interestingly, where the AAF adduct previously had caused a significant increase in binding to non-*NarI* sequences, an AAF adduct positioned at G<sub>3</sub> of the *NarI* sequence showed no increase in binding affinity over the unmodified *NarI* sequence. In fact, both the binding of Klenow fragment to AAF modified and unmodified *NarI* sequences showed decreases over non-*NarI* sequences [39]. This indicated that a possible different conformation with the AAF modified *NarI* sequence existed within the polymerase active site than had previously been noted in the non-*NarI* sequence of the T7 or *Bacillus* fragment crystal structures. Similar to non-*NarI* sequences modified with AAF, the addition of nucleotides did not enhance Klenow fragment binding. However, the presence of dGTP, dATP, or dTTP did decrease the binding affinity. This was indicative of a destabilizing effect these nucleotides had on the complex, presumably due to an incorrect base pair match.

Taken together, these results indicated a specific two-step mechanism for formation of the dinucleotide deletion (Figure 5). The first step has a dCTP be incorporated across from the AAF modified base, followed by a structural rearrangement that places the AAF modified base along with the upstream 3'C in a dinucleotide bulge. The primer's 5' upstream guanine and the cytosine initially incorporated across from the adduct now base pair downstream of the templates adducted guanine. This two-step mechanism also suggests that the frameshift extension product could be generated *in vivo* by two different polymerases, one better suited for incorporation across from the bulky AAF adduct followed by another more suited for extension from the adduct (reviewed in [40]). This two enzyme stepwise mechanism has been postulated for both bacterial and eukaryotic polymerases and provides a mechanism to reconcile the different properties required of a polymerase for replicative DNA synthesis, and the specialized niche of performing replication in proximity to bulky DNA adducts. This process is exacerbated by specific sequences such as *NarI* that preferentially adopt structures to induce frameshift mutations after incorporation of a nucleotide opposite the adducted base.

## 7. Bypassing Roadblocks

A class of polymerases capable of performing nucleotide incorporation in the presence of such distorting adducts as AF and AAF are the bypass or translesion synthesis (TLS) polymerases [42]. TLS polymerases are characterized by their open active sites that are capable of accommodating bulky lesions and the DNA distortions they produce. For example, yeast Pol $\eta$  ( $\gamma$ Pol $\eta$ ) has a more open active site

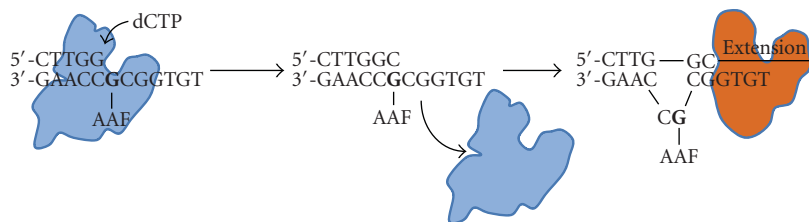


FIGURE 5: Mechanism for bypass of a dG-C8-AAF adduct in the *NarI* sequence. A polymerase more suited for incorporation across from the adduct places a proper dCTP:G base pair at the adducted position followed by incorporation, then dissociation of the enzyme. A subsequent rearrangement of the DNA to form a 2 nucleotide budge ensues, allowing a possible second polymerase to perform extension from this slipped structure, resulting in a  $-2$  deletion frameshift product.

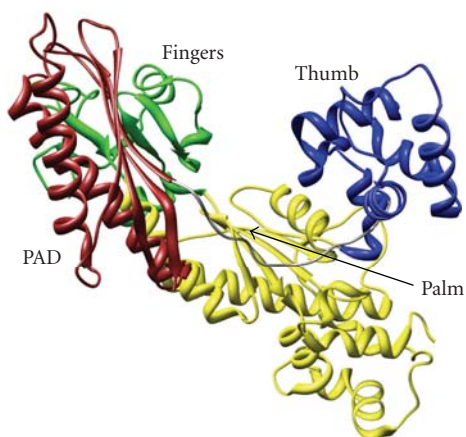


FIGURE 6: Structural overview of the TLS yeast polymerase eta (PDB# 1JIH, molecule A) [41].  $\gamma$ Pol $\eta$  contains stubby fingers (green), and thumb (blue) domains, a palm (yellow), as well as a polymerase associated domain (PAD) (brown). The open nature of the active site allows two nucleotides to be accommodated during synthesis, as well as bulky carcinogenic adducts and DNA distorting lesions.

caused by stubby fingers and thumb domains, as well as an additional polymerase associated domain (PAD) (Figure 6).  $\gamma$ Pol $\eta$  belongs to the Y-family of polymerases and also contains a little finger domain that is unique to this class of polymerases. The more open active site allows Pol $\eta$  in both humans and yeast to correctly synthesis past a *cis-syn* thymine-thymine UV-induced dimer [43]. Unlike the solvent-excluded tight constraints of replicative polymerases, the active sites of Y-family polymerases are solvent exposed and thus capable of accommodating many distorting lesions. However, the open active site comes at the cost of low fidelity, orders of magnitude lower than replicative polymerases [44, 45]. Bypass polymerases typically also do not possess high processivity, indicative of their brief role in synthesis past a lesion then allowing a more precise replicative polymerase to continue synthesis [46].

Prakash and co-workers were the first to present evidence that  $\gamma$ Pol $\eta$  was capable of undergoing a conformational change step prior to chemistry occurring [41]. Utilizing presteady state kinetics and measuring the elemental effect of a sulfur substituted for an oxygen at the  $\alpha$ -phosphate of

the nucleotide they showed that  $\gamma$ Pol $\eta$  undergoes an induced fit mechanism for nucleotide incorporation.  $\gamma$ Pol $\eta$  poorly discriminates between correct and incorrect nucleotides both at the initial nucleotide binding step and during the induced conformational change. A more direct FRET-based method was used to visualize the global conformational dynamics of another similar Y family polymerase, Dpo4, in a paper published by Xu and co-workers [47]. Here, FRET pairs were positioned at various locations around Dpo4 allowing movement of specific locations to be tracked during real time measurements. Assemblage of all movements along with the rates of the corresponding FRET changes allowed the authors to assemble global movements of the enzyme. Upon binding of a correct nucleotide, a concerted global rearrangement of all four domains (fingers, little fingers, thumb, and palm) takes place where the little fingers domain moved in opposing directions to the polymerase core domains. The movement was relatively small compared to those of T7, being only a few angstroms, yet form similar fingers and thumb closing motions as mentioned previously for various other polymerases.

On unmodified DNA, gel shift binding assays with  $\gamma$ Pol $\eta$  showed increased binding in the presence of the next correct nucleotide [48]. This is consistent with a dNTP-induced conformational change resulting in a closed ternary complex, just as what had been shown previously for Klenow fragment. Addition of an incorrectly base pairing dGTP was noted to have a destabilizing effect on the complex, presumably due to an incompatible fit within the enzyme, again similar to that previously observed for Klenow fragment.

Extension assays showed that  $\gamma$ Pol $\eta$  is capable of fully bypassing a dG-C8-AAF adduct and while incorporation occurred across from a dG-C8-AAF adduct, extension past this position was inhibited [48]. These results are similar to that observed for the Klenow mutant Y766S, which, similar to  $\gamma$ Pol $\eta$ , also has a more open active site. Interestingly, where Klenow fragment was unable to become more stable upon addition of any dNTP across from a dG-C8-AAF adduct, binding was stabilized with  $\gamma$ Pol $\eta$  in the presence of dCTP, consistent with the formation of a closed ternary complex. Also, consistent with the lack of extension after incorporation across from the AAF adduct, no enhanced binding was observed at this position in the presence of the next correct nucleotide. Despite the structural

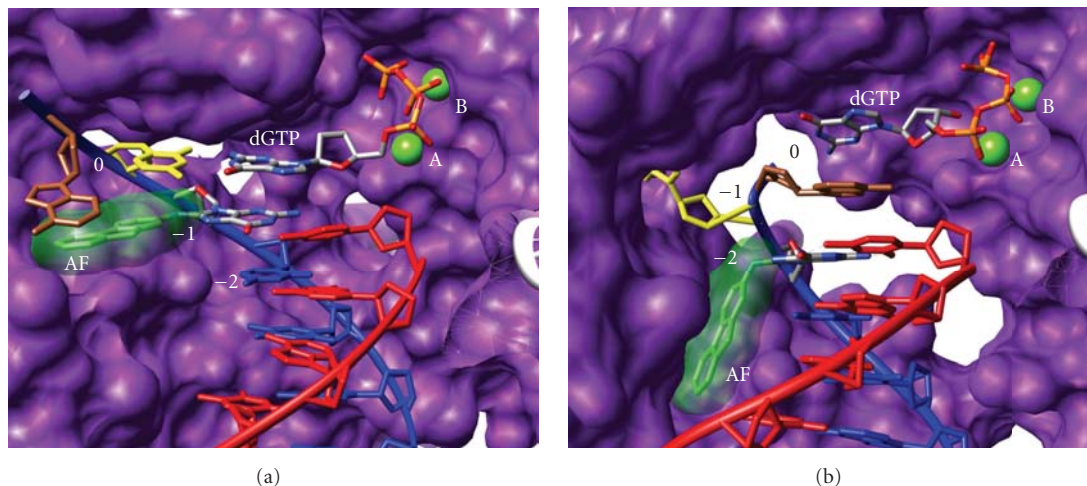


FIGURE 7: Two structures of Dpo4 ternary complexes in the presence of a dG-C8-AF adducted template, one forming a correctly aligned primer-template and a second forming a looped out structure of the template (PDB# 3KHH) [27]. (a) Correctly aligned primer template with the dGTP and corresponding template dC correctly at the 0 position. The adducted dG retains base pairing with its corresponding dC while the AF is positioned towards the major groove and stacks in a pocket of the little fingers domain. The +1 templating base stacks on top of the AF adduct and is in alignment with the 0 position. (b) The misaligned structure contains the templating base in a looped out structure. The looped out base slides into a pocket, rotated away from the active site. As a consequence the +1 templating base rotates and stacks on top of the adducted dG base, and the DNA is shifted downwards as the +1 base now occupies the -1 position within the polymerase. The AF adduct is rotated downwards and placed into a hydrophobic pocket within the little fingers domain. The dGTP does not contain any Watson-Crick binding partner as it occupies the 0 position and stacks onto of the template base below.

and behavioral differences between replicative polymerases and lesion bypass polymerases, a common conformational change in the mechanism appears to be shared in this case. It should be noted, however, that studies of some polymerase such as Dbh have not been able to detect a conformational change [49]. Although it is conceivable that smaller undetected conformational changes are performing the analogous function as the larger scale rearrangements seen in replicative polymerases or that these motions have yet to be detected.

The open active site of Y-family polymerases is not necessary only to accommodate DNA lesions, but also able to allow various primer-template alignments that may favor the replication of the adducted template. As mentioned previously, the formation of frameshift mutations in the *NarI* sequence occur via a template misalignment and this misaligned structure must be accommodated within the polymerase active site. A recent crystal structure by Rechkoblit et al. of the Y family polymerase Dpo4 in the presence of an dG-C8-AF adduct shows such a complex and how it can be accommodated and stabilized within the polymerase [27].

In this study, two molecular structures were obtained in one asymmetric unit of the crystal: (1) a correct alignment with the dG-C8-AF adduct base pairing with a dC at the -1 position (dG-AF:dC at the postinsertion site) and a typical correctly forming dC:dGTP pair of the adjacent base (5' template side of adduct at position 0, the insertion site) (Figure 7(a)) and (2) a misaligned structure with the dG-C8-AF adduct base pairing with a dC shifted to the -2 position (1 position upstream of the postinsertion site) and

the adjacent 5' C of the template looping out (Figure 7(b)). More specifically, in the correctly aligned molecule 1 the dG containing the AF is in an *anti* conformation and the AF is placed on the major groove side of the duplex within a pocket buried from solvent, and stabilized by interactions to the little finger domain. This is similar to the conformation of the AF adduct in *Bacillus* fragment, with the exception that Dpo4 contains interactions to the little fingers domain that stabilize the adducts position, a caveat that is impossible in *Bacillus* fragment due to the lack of a little fingers domain [35]. The template C 5' of the adduct (at position 0, the insertion site) is base paired with an incoming dGTP, yet is shifted from its typical stacking arrangement over the postinsertion site base pair, and is instead poised partially over the AF adduct with the dGTP over the center of the postinsertion site base pair. In addition, the next downstream template base (0 position, which would typically be within the insertion site) is flipped out and stacks on top of the AF adduct in alignment with the templating C base and the incoming dGTP at the 0 position (insertion site). In the misaligned structure of molecule 2 the dG-C8-AF: dC base pair is shifted upstream relative to the polymerase to the -2 position, as the adjacent 5' template C loops out of the helix towards the major groove, stacking with the little fingers domain (Figure 7(b)). Again, the AF adduct is on the side of the major groove and situated within a pocket on the little fingers. The 0 template base is rotated back into the helix and occupies the postinsertion site (-1 position) as the incoming dGTP stacks on top of it in the insertion site (occupying the 0 position). Consequently, the incoming nucleotide does not possess a Watson-Crick hydrogen binding partner.

Interestingly, the correctly pairing ternary structure of molecule 1 was poised in resemblance to a binary like state which is incapable of performing catalysis without additional rearrangements. However, the misaligned structure of molecule 2 showed an uncanny resemblance to the ternary complex of Dpo4, with protein-DNA interactions similar to that of the ternary complex. It should be noted however that the misaligned structure of molecule 2, despite being arranged similar to a ternary complex, would also require further rearrangements in order to achieve a catalytic state.

The ability of Dpo4 to not only accommodate the bulky AF lesion but also to stabilize its position by binding to the little fingers domain that only Y family polymerases possess, is indicative of its design for its role in lesion bypass. In addition, Dpo4's ability to further utilize its specialized little finger domain to stabilize primer-template misalignments strengthens its ability to cope with distorting lesions, albeit at the expense of increasing mutagenicity. This paper also shows that misaligned structures are not only stabilized by the Watson-Crick base pairing of the misaligned structure, but also, and possibly more so by direct interactions of the polymerase with the misaligned complex [27].

## 8. Always on the Move

Recently, a new picture regarding the conformational dynamics of polymerases has begun to emerge. Single-molecule assays allow the direct monitoring of individual molecules and can reveal properties that are otherwise masked by ensemble averaging of large populations of molecules. Nonsynchronous fluctuations that appear in fleeting moments of time go unseen in ensemble averages yet become obvious when viewed at the single molecule level. Single-molecule FRET (smFRET) experiments where a FRET donor was positioned on the template of a duplex DNA strand, and a FRET acceptor was positioned on Klenow fragment, allowed the direct visualization of DNA synthesis as it proceeded through incorporation of three nucleotides [50]. The movement of the DNA to the exonuclease domain, as well as the movements during synthesis, could also be viewed. As expected, discrete steps in the FRET traces were observed for each nucleotide incorporation event. Further, a few individual molecules were noted to have the primer transition directly from the polymerization site to the exonuclease site, and vice versa, without dissociation of the binary complex. This correlated well with the proposition made during the modeling of the crystal structure in 1993 by Beese et al. [11]. In addition, following each incorporation event the polymerase appeared to move one nucleotide further downstream than was necessary to place the following nucleotide in the preinsertion site. This was immediately followed by a return back to the expected FRET level for the ensuing preinsertion site. This transient drop was routinely observed in the presence of the next correct nucleotide and was never observed in the presence of an incorrectly base pairing nucleotide. The ubiquitous nature of this novel step led the authors to conclude that this

was indeed an integral step in nucleotide incorporation and that it might be involved in checking for proper base pair formation. Movement to this site might be part of the routine proofreading process that results in movement of a misincorporation to the exonuclease domain. This transitioning process to the exonuclease domain was observed when experiments were performed using mismatched primer-template termini [50]. Alternatively, it was also suggested that the transient state could represent an equilibrium between the preinsertion and insertion complexes or it could represent a further conformational rearrangement that is part of the polymerase mechanism. Regardless, the smFRET based discovery of this novel motion of the polymerase shows new dynamics previously unobserved in bulk biochemical experiments.

Further demonstration of the lively dynamic nature of these enzymes comes from new evidence regarding the continual conformational changes that polymerases undergo during nucleotide incorporation and the identification of yet another conformational state [51]. Santoso et al. utilized alternating-laser excitation (ALEX) smFRET with both members of the FRET pair placed on Klenow fragment to directly monitor conformational changes of the polymerase in real-time. More specifically, one fluorophore was positioned on residue 744 of the fingers domain of Klenow fragment, and the other on residue 550 of the thumb. Using a femtoliter observation volume where individual molecules diffuse freely, the conformational changes of the enzyme could be accurately tracked. Observations of Klenow fragment bound to DNA in a binary complex revealed that despite the lack of dNTP, the enzyme was found to occupy both the open and closed states, with the open conformation existing 66% of the time. The large occupancy of polymerases in a closed binary complex is a fascinating proposition and adds an active quality to the crystal structure snapshot of the binary complex published almost two decades previously [11]. Upon addition of the next correctly base pairing dNTP, the closed conformation dominated 84% of the time [51]. Addition of incorrectly base pairing dNTPs revealed a third conformation of the enzyme that was distinct from the open and closed complexes identified previously. Similarly, addition of rNTPs also showed the formation of a third state. Despite the similarities observed in the third conformational state observed with incorrect dNTPs and rNTPs the authors advocate that they cannot be the exact same state, because as noted earlier the rejection of an incorrectly base pairing dNTP occurs at a different step along the reaction pathway than does the rejection of rNTPs. Regardless, the third state is thought to more closely resemble an open KF-dNTP complex where the interactions of the triphosphate moiety induce a subtle rearrangement of the residues along the O helix, yielding the third FRET state. This process would allow the complementarity of the templating base with the incoming dNTP to be tested in the open conformation. Provided a good fit is obtained the polymerase would then move the pair to the active site via rearrangements of the O-helix as the closed conformation is formed, whereas mispairing nucleotides would be rejected in the open conformation. More striking than the identification

of the novel third conformational state was the observations that the unbound enzyme was found to be continually fluctuating between various conformational states despite the lack of a DNA template or dNTPs [51]. These conformational transitions were incredibly rapid, occurring in the low millisecond range. The ability of the polymerase to continually sample its conformational states in the absence of substrate further exemplifies the dynamic nature of this enzyme.

## 9. Conclusions

DNA polymerases are remarkable enzymes that are able to match a dNTP with the template base, reject the rNTP that is present at a much higher concentration, accommodate four different base pair orientations in their active sites and do all of this at an incredible rate. The overall three-dimensional structure of various polymerases, mainly their anthropomorphic projection of a human right hand, has proven to be strikingly similar from different organisms. Along with these structural similarities, the identification of several key conformational changes appears to be common. These include the subtle rearrangements of the thumb domain of the polymerase to strengthen the grasp on the DNA upon formation of a binary complex and the large nucleotide-induced conformational change of the O and N helices upon formation of a ternary complex. The conformational change of the O helix has been associated with various steps of the mechanism: the alignment of the catalytic residues and the positioning of the DNA; the positioning of indexing residues such as Tyr766 of Klenow fragment; the positioning of the dNTP substrate to lock it in the proper orientation for catalysis; and obstructing incompatible residues such as rNTPs from achieving catalytic competency. DNA adducts have been shown to inhibit DNA synthesis and the ability of adducts such as AF and AAF, to induce radically different effects during synthesis has been linked to the structures they adopt within the active site of polymerase and their ability to disrupt or block conformational changes. The sequence surrounding an adduct further contributes to the mutagenic properties, as is seen with the GGCGCC *NarI* sequence containing an AAF adduct. Lastly, the view of these enzymes exhibiting stopped motion as they progress through discreetly identified steps is changing. Single-molecule studies have revealed properties masked before in ensemble averaging. Identification of obligate novel intermediates along the mechanistic pathway, coupled with the dynamic nature of these enzymes to sample multiple states, even in the absence of substrates, are two new discoveries that open the door for future studies. It is hoped that future experiments examining these novel changes in the presence of bulky carcinogenic adducts will identify additional conformational checkpoints, and in keeping with anthropomorphic qualities, areas of indecision by polymerases which contribute to mutagenesis.

## Abbreviations

dNTP <sup>1</sup> :	Deoxyribonucleoside 5'-triphosphate
DNA:	Deoxyribonucleic acid
rNTP:	Ribonucleoside 5'-triphosphate
ddNTP:	Dideoxyribonucleoside 5'-triphosphate
AF:	2-aminofluorene
AAF:	N-acetyl-2-aminofluorene
dG-C8-AF:	N-(2'-deoxyguanosin-8-yl)-2-aminofluorene
dG-C8-AAF:	N-(2'-deoxyguanosin-8-yl)-N-acetyl-2-aminofluorene
TLS:	Trans lesion synthesis
RNA:	Ribonucleic acid
FRET:	Förster resonance energy transfer
smFRET:	Single molecule Förster resonance energy transfer
ALEX:	Alternating laser excitation.

## Acknowledgment

This paper was supported by Public Health Service Grant CA40605 awarded by the Department of Health and Human Services.

## References

- [1] T. A. Kunkel and K. Bebenek, "DNA replication fidelity," *Annual Review of Biochemistry*, vol. 69, pp. 497–529, 2000.
- [2] K. Bebenek, C. M. Joyce, M. P. Fitzgerald, and T. A. Kunkel, "The fidelity of DNA synthesis catalyzed by derivatives of *Escherichia coli* DNA polymerase I," *Journal of Biological Chemistry*, vol. 265, no. 23, pp. 13878–13887, 1990.
- [3] A. Kornberg, *DNA Replication*, W. H. Freeman, San Francisco, Calif, USA, 1980.
- [4] P. K. Gupta, D. L. Johnson, T. M. Reid, M.-S. Lee, L. J. Romano, and C. M. King, "Mutagenesis by single site-specific arylamine-DNA adducts. Induction of mutations at multiple sites," *Journal of Biological Chemistry*, vol. 264, no. 33, pp. 20120–20130, 1989.
- [5] S. Shibutani and A. P. Grollman, "Nucleotide misincorporation on DNA templates containing N-(deoxyguanosin-N2-yl)-2-(acetyl-amino)fluorene," *Chemical Research in Toxicology*, vol. 6, no. 6, pp. 819–824, 1993.
- [6] E. F. Pettersen, T. D. Goddard, C. C. Huang et al., "UCSF Chimera—a visualization system for exploratory research and analysis," *Journal of Computational Chemistry*, vol. 25, no. 13, pp. 1605–1612, 2004.
- [7] S. Korolev, M. Nayal, W. M. Barnes, E. Di Cera, and G. Waksman, "Crystal structure of the large fragment of *Thermus aquaticus* DNA polymerase I at 2.5-Å resolution: structural basis for thermostability," *Proceedings of the National Academy of Sciences of the United States of America*, vol. 92, no. 20, pp. 9264–9268, 1995.
- [8] Y. Li, S. Korolev, and G. Waksman, "Crystal structures of open and closed forms of binary and ternary complexes of the large fragment of *Thermus aquaticus* DNA polymerase I: structural basis for nucleotide incorporation," *EMBO Journal*, vol. 17, no. 24, pp. 7514–7525, 1998.
- [9] V. Derbyshire, N. D. F. Grindley, and C. M. Joyce, "The 3'-5' exonuclease of DNA polymerase I of *Escherichia coli*:

- contribution of each amino acid at the active site to the reaction," *EMBO Journal*, vol. 10, no. 1, pp. 17–24, 1991.
- [10] D. L. Ollis, P. Brick, R. Hamlin, N. G. Xuong, and T. A. Steitz, "Structure of large fragment of *Escherichia coli* DNA polymerase I complexed with dTMP," *Nature*, vol. 313, no. 6005, pp. 762–766, 1985.
- [11] L. S. Beese, V. Derbyshire, and T. A. Steitz, "Structure of DNA polymerase I Klenow fragment bound to duplex DNA," *Science*, vol. 260, no. 5106, pp. 352–355, 1993.
- [12] S. Basu, A. Basu, and M. J. Modak, "Pyridoxal 5'-phosphate mediated inactivation of *Escherichia coli* DNA polymerase I: identification of lysine-635 as an essential residue for the processive mode of DNA synthesis," *Biochemistry*, vol. 27, no. 18, pp. 6710–6716, 1988.
- [13] J. R. Kiefer, C. Mao, J. C. Braman, and L. S. Beese, "Visualizing DNA replication in a catalytically active *Bacillus* DNA polymerase crystal," *Nature*, vol. 391, no. 6664, pp. 304–307, 1998.
- [14] S. Doublé, S. Tabor, A. M. Long, C. C. Richardson, and T. Ellenberger, "Crystal structure of a bacteriophage T7 DNA replication complex at 2.2 Å resolution," *Nature*, vol. 391, no. 6664, pp. 251–258, 1998.
- [15] H. Pelletier, M. R. Sawaya, A. Kumar, S. H. Wilson, and J. Kraut, "Structures of ternary complexes of rat DNA polymerase  $\beta$ , a DNA template-primer, and ddCTP," *Science*, vol. 264, no. 5167, pp. 1891–1903, 1994.
- [16] Y. Li, Y. Kong, S. Korolev, and G. Waksman, "Crystal structures of the Klenow fragment of *Thermus aquaticus* DNA polymerase I complexed with deoxyribonucleoside triphosphates," *Protein Science*, vol. 7, no. 5, pp. 1116–1123, 1998.
- [17] L. Dzantiev and L. J. Romano, "A conformational change in *E. coli* DNA polymerase I (Klenow fragment) is induced in the presence of a dNTP complementary to the template base in the active site," *Biochemistry*, vol. 39, no. 2, pp. 356–361, 2000.
- [18] S. Doublé, M. R. Sawaya, and T. Ellenberger, "An open and closed case for all polymerases," *Structure*, vol. 7, no. 2, pp. R31–R35, 1999.
- [19] S. J. Johnson, J. S. Taylor, and L. S. Beese, "Processive DNA synthesis observed in a polymerase crystal suggests a mechanism for the prevention of frameshift mutations," *Proceedings of the National Academy of Sciences of the United States of America*, vol. 100, no. 7, pp. 3895–3900, 2003.
- [20] C. M. Joyce, O. Potapova, A. M. DeLucia, X. Huang, V. P. Basu, and N. D. F. Grindley, "Fingers-closing and other rapid conformational changes in DNA polymerase I (Klenow fragment) and their role in nucleotide selectivity," *Biochemistry*, vol. 47, no. 23, pp. 6103–6116, 2008.
- [21] M. Astatke, K. Ng, N. D. F. Grindley, and C. M. Joyce, "A single side chain prevents *Escherichia coli* DNA polymerase I (Klenow fragment) from incorporating ribonucleotides," *Proceedings of the National Academy of Sciences of the United States of America*, vol. 95, no. 7, pp. 3402–3407, 1998.
- [22] R. H. Heflich and R. E. Neft, "Genetic toxicity of 2-acetylaminofluorene, 2-aminofluorene and some of their metabolites and model metabolites," *Mutation Research*, vol. 318, no. 2, pp. 73–174, 1994.
- [23] S. F. O'Handley, D. G. Sanford, and R. Xu, "Structural characterization of an N-acetyl-2-aminofluorene (AAF) modified dna oligomer by NMR, energy minimization, and molecular dynamics," *Biochemistry*, vol. 32, no. 10, pp. 2481–2497, 1993.
- [24] L. M. Eckel and T. R. Krugh, "2-aminofluorene modified DNA duplex exists in two interchangeable conformations," *Nature Structural Biology*, vol. 1, no. 2, pp. 89–94, 1994.
- [25] L. M. Eckel and T. R. Krugh, "Structural characterization of two interchangeable conformations of a 2-aminofluorene-modified DNA oligomer by NMR and energy minimization," *Biochemistry*, vol. 33, no. 46, pp. 13611–13624, 1994.
- [26] L. Dzantiev and L. J. Romano, "Interaction of *Escherichia coli* DNA polymerase I (Klenow fragment) with primer-templates containing N-acetyl-2-aminofluorene or N-2-aminofluorene adducts in the active site," *Journal of Biological Chemistry*, vol. 274, no. 6, pp. 3279–3284, 1999.
- [27] O. Rechkoblit, A. Kolbanovskiy, L. Malinina, N. E. Geacintov, S. Brodye, and D. J. Patel, "Mechanism of error-free and semitargeted mutagenic bypass of an aromatic amine lesion by Y-family polymerase Dpo4," *Nature Structural and Molecular Biology*, vol. 17, no. 3, pp. 379–388, 2010.
- [28] H. Miller and A. P. Grollman, "Kinetics of DNA polymerase I (Klenow fragment exo-) activity on damaged dna templates: effect of proximal and distal template damage on DNA synthesis," *Biochemistry*, vol. 36, no. 49, pp. 15336–15342, 1997.
- [29] L. Dzantiev and L. J. Romano, "Differential effects of N-acetyl-2-aminofluorene and N-2-aminofluorene adducts on the conformational change in the structure of DNA polymerase I (Klenow fragment)," *Biochemistry*, vol. 39, no. 17, pp. 5139–5145, 2000.
- [30] S. Lone and L. J. Romano, "Mechanistic insights into replication across from bulky DNA adducts: a mutant polymerase I allows an N-acetyl-2-aminofluorene adduct to be accommodated during DNA synthesis," *Biochemistry*, vol. 42, no. 13, pp. 3826–3834, 2003.
- [31] J. B. Bell, K. A. Eckert, C. M. Joyce, and T. A. Kunkel, "Base miscoding and strand misalignment errors by mutator Klenow polymerases with amino acid substitutions at tyrosine 766 in the O helix of the fingers subdomain," *Journal of Biological Chemistry*, vol. 272, no. 11, pp. 7345–7351, 1997.
- [32] S. Dutta, Y. Li, D. Johnson et al., "Crystal structures of 2-acetylaminofluorene and 2-aminofluorene in complex with T7 DNA polymerase reveal mechanisms of mutagenesis," *Proceedings of the National Academy of Sciences of the United States of America*, vol. 101, no. 46, pp. 16186–16191, 2004.
- [33] J. Trincão, R. E. Johnson, C. R. Escalante, S. Prakash, L. Prakash, and A. K. Aggarwal, "Structure of the Catalytic Core of *S. cerevisiae* DNA polymerase  $\eta$ : implications for translesion DNA synthesis," *Molecular Cell*, vol. 8, no. 2, pp. 417–426, 2001.
- [34] B. Singer and D. Grunberger, *Molecular Biology of Mutagens and Carcinogens*, Plenum Press, New York, NY, USA, 1983.
- [35] G. W. Hsu, J. R. Kiefer, D. Burnouf, O. J. Becherel, R. P. P. Fuchs, and L. S. Beese, "Observing translesion synthesis of an aromatic amine DNA adduct by a high-fidelity DNA polymerase," *Journal of Biological Chemistry*, vol. 279, no. 48, pp. 50280–50285, 2004.
- [36] R. P. Fuchs and S. Fujii, "Translesion synthesis in *Escherichia coli*: lessons from the NarI mutation hot spot," *DNA Repair*, vol. 6, no. 7, pp. 1032–1041, 2007.
- [37] N. Koffel-Schwartz, J.-M. Verdier, M. Bichara, et al., "Carcinogen-induced mutation spectrum in wild-type, uvrA and umuC strains of *Escherichia coli*. Strain specificity and mutation-prone sequences," *Journal of Molecular Biology*, vol. 177, no. 1, pp. 33–51, 1984.
- [38] R. S. Tebbs and L. J. Romano, "Mutagenesis at a site-specifically modified NarI sequence by acetylated and deacetylated aminofluorene adducts," *Biochemistry*, vol. 33, no. 30, pp. 8998–9006, 1994.

- [39] J. P. Gill and L. J. Romano, "Mechanism for N-acetyl-2-aminofluorene-induced frameshift mutagenesis by *Escherichia coli* DNA polymerase I (Klenow fragment)," *Biochemistry*, vol. 44, no. 46, pp. 15387–15395, 2005.
- [40] E. C. Friedberg, A. R. Lehmann, and R. P. P. Fuchs, "Trading places: how do DNA polymerases switch during translesion DNA synthesis?" *Molecular Cell*, vol. 18, no. 5, pp. 499–505, 2005.
- [41] M. T. Washington, L. Prakash, and S. Prakash, "Yeast DNA polymerase  $\eta$  utilizes an induced-fit mechanism of nucleotide incorporation," *Cell*, vol. 107, no. 7, pp. 917–927, 2001.
- [42] S. Prakash, R. E. Johnson, and L. Prakash, "Eukaryotic translesion synthesis DNA polymerases: specificity of structure and function," *Annual Review of Biochemistry*, vol. 74, pp. 317–353, 2005.
- [43] R. E. Johnson, S. Prakash, and L. Prakash, "Efficient bypass of a thymine-thymine dimer by yeast DNA polymerase, Pol $\eta$ ," *Science*, vol. 283, no. 5404, pp. 1001–1004, 1999.
- [44] T. Matsuda, K. Bebenek, C. Masultani, F. Hanaoka, and T. A. Kunkel, "Low fidelity DNA synthesis by human DNA polymerase- $\eta$ ," *Nature*, vol. 404, no. 6781, pp. 1011–1013, 2000.
- [45] M. T. Washington, R. E. Johnson, S. Prakash, and L. Prakash, "Fidelity and processivity of *Saccharomyces cerevisiae* DNA polymerase  $\eta$ ," *Journal of Biological Chemistry*, vol. 274, no. 52, pp. 36835–36838, 1999.
- [46] M. T. Washington, R. E. Johnson, S. Prakash, and L. Prakash, "Accuracy of thymine-thymine dimer bypass by *Saccharomyces cerevisiae* DNA polymerase  $\eta$ ," *Proceedings of the National Academy of Sciences of the United States of America*, vol. 97, no. 7, pp. 3094–3099, 2000.
- [47] C. Xu, B. A. Maxwell, J. A. Brown, L. Zhang, and Z. Suo, "Global conformational dynamics of a Y-family DNA polymerase during catalysis," *PLoS Biology*, vol. 7, no. 10, Article ID e1000225, 2009.
- [48] V. Vooradi and L. J. Romano, "Effect of N-2-acetylaminofluorene and 2-aminofluorene adducts on DNA binding and synthesis by yeast DNA polymerase  $\eta$ ," *Biochemistry*, vol. 48, no. 19, pp. 4209–4216, 2009.
- [49] J. Cramer and T. Restle, "Pre-steady-state kinetic characterization of the DinB homologue DNA polymerase of *Sulfolobus solfataricus*," *Journal of Biological Chemistry*, vol. 280, no. 49, pp. 40552–40558, 2005.
- [50] T. D. Christian, L. J. Romano, and D. Rueda, "Single-molecule measurements of synthesis by DNA polymerase with base-pair resolution," *Proceedings of the National Academy of Sciences of the United States of America*, vol. 106, no. 50, pp. 21109–21114, 2009.
- [51] Y. Santoso, C. M. Joyce, O. Potapova et al., "Conformational transitions in DNA polymerase I revealed by single-molecule FRET," *Proceedings of the National Academy of Sciences of the United States of America*, vol. 107, no. 2, pp. 715–720, 2010.

## Review Article

# Kinetic Approaches to Understanding the Mechanisms of Fidelity of the Herpes Simplex Virus Type 1 DNA Polymerase

Yali Zhu,<sup>1</sup> Jason Stroud,<sup>2</sup> Liping Song,<sup>1</sup> and Deborah S. Parris<sup>1,2</sup>

<sup>1</sup>Department of Molecular Virology, Immunology, and Medical Genetics, The Ohio State University, 2198 Graves Hall, 333 West Tenth Avenue, Columbus, OH 43210, USA

<sup>2</sup>Department of Molecular Genetics, The Ohio State University, 2198 Graves Hall, 333 West Tenth Avenue, Columbus, OH 43210, USA

Correspondence should be addressed to Deborah S. Parris, parris.1@osu.edu

Received 17 June 2010; Revised 13 August 2010; Accepted 30 September 2010

Academic Editor: Ashis Basu

Copyright © 2010 Yali Zhu et al. This is an open access article distributed under the Creative Commons Attribution License, which permits unrestricted use, distribution, and reproduction in any medium, provided the original work is properly cited.

We discuss how the results of presteady-state and steady-state kinetic analysis of the polymerizing and excision activities of herpes simplex virus type 1 (HSV-1) DNA polymerase have led to a better understanding of the mechanisms controlling fidelity of this important model replication polymerase. Despite a poorer misincorporation frequency compared to other replicative polymerases with intrinsic 3' to 5' exonuclease (exo) activity, HSV-1 DNA replication fidelity is enhanced by a high kinetic barrier to extending a primer/template containing a mismatch or abasic lesion and by the dynamic ability of the polymerase to switch the primer terminus between the exo and polymerizing active sites. The HSV-1 polymerase with a catalytically inactivated exo activity possesses reduced rates of primer switching and fails to support productive replication, suggesting a novel means to target polymerase for replication inhibition.

## 1. Introduction and Overview

Maintaining fidelity of DNA replication is essential to the survival of even the simplest organisms. Based on mammalian models, lack of faithful DNA replication by DNA polymerases is associated with a large number of human diseases including, but not limited to, cancer and a variety of precancerous conditions [1–7]. A number of repair mechanisms exist to correct errors that occur during DNA synthesis, including mismatch repair, base and nucleotide excision repair, and recombination repair, and these mechanisms have been reviewed recently elsewhere [8–11]. Despite the existence of these repair mechanisms, a major determinant of replication fidelity is the ability of the replicative DNA polymerase to faithfully copy DNA. This ability is promoted not only by the high fidelity with which the polymerase selects correct versus incorrect nucleotide, but also by the reduced capacity for the polymerase to extend or replicate through primer/templates (P/Ts) containing distortions such as mismatches, abasic (AP) sites, or oxidative or bulky lesions [12–17]. This kinetic barrier to extension causes the

replicative polymerase to stall. In many organisms, including prokaryotes, archaea, and eukaryotes, stalling of the replicative polymerase is required to permit a short-term exchange with a low-fidelity polymerase (including one or more Y-family polymerases, or the B-family DNA polymerase  $\zeta$ ). This occurs via exclusive interactions of the respective polymerases with processivity factor in order to permit lesion bypass [18–27]. Although these lesion bypass polymerases are generally more error-prone and do not repair the lesion, they rescue the organism from lethal replication failure when DNA is damaged [28, 29]. The stalling of a replicative polymerase at DNA lesions or following misincorporation also appears to be important for self-correction by allowing engagement of the intrinsic 3' to 5' exonuclease (exo) activity to “proof-read” replication errors as they occur or to sense the presence of DNA lesions [14, 30–37]. Pre-steady-state and steady-state kinetic analysis of polymerases with or without a functional exo activity have been instrumental in understanding the mechanisms that permit DNA polymerases to copy DNA with high fidelity, as well as how they

avoid the permanent mutagenic effects of misincorporated nucleotides or DNA damage [14, 15, 33, 34, 38–40].

This review analyzes the different mechanisms that control replication fidelity that are intrinsic to replicative DNA polymerases, with a specific focus on those that are utilized by the polymerase encoded by herpes simplex virus type 1 (HSV-1)—the prototypic member of a family of viruses which cause high morbidity in the human population. Because of the ease with which they can be genetically manipulated, viruses have also proven to be excellent models to better understand the functions required for faithful genome duplication [41–45]. Moreover, viral polymerases, including the HSV-1 DNA polymerase and the human immunodeficiency virus (HIV) reverse transcriptase, are important therapeutic targets of antiviral drugs [46–48]. A summary of studies that have reported the pre-steady-state and steady-state kinetics of HSV-1 DNA polymerase are provided and compared to those of other replicative polymerases to gain insight into the similarities and differences by which these polymerases control fidelity. By understanding how activities required for high-fidelity DNA replication are modulated and coordinated by the HSV-1 DNA polymerase, it may be possible to design novel antiviral approaches to thwart replication of this important human pathogen.

## 2. General Parameters that Control Polymerase Fidelity

**2.1. Nucleotide Selectivity.** The single most important contributor to fidelity of most DNA polymerases is nucleotide selectivity—that is, the propensity with which the polymerase incorporates correctly versus incorrectly base-paired nucleotide [33, 34, 38, 49–53]. For replicative polymerases, nucleotide selectivity has been shown to account for an error rate in the range of  $>10^{-3}$  to  $10^{-5}$  [33, 34, 49, 52]. The structures of a variety of replicative DNA polymerases have been solved, including the structures for the A-type polymerases that replicate T7 bacteriophage [54] and mammalian mitochondria (pol  $\gamma$ ; [55]), and the B-type replicative polymerases of the T4-related bacteriophage RB69 [56], HSV-1 [57], and yeast (*Saccharomyces cerevisiae*) DNA polymerase  $\delta$  [58]. It is clear that the nucleotide-binding pocket is able to accommodate or snugly “fit” the correctly paired nucleotide via space and geometry [59, 60]. This promotes a higher ground-state binding affinity of the correct, compared to incorrect, nucleotide. In addition, evidence points to an induced fit model, whereby the binding of correct nucleotide better promotes the conformational change necessary to form the closed structure required for catalysis [34, 49, 50, 54, 56, 61]. For the bulk of these polymerases, it is this conformational change, rather than the chemical catalytic step, which is rate-limiting for correct nucleotide incorporation under pre-steady-state conditions [34, 39, 62–64]. For incorrect nucleotide incorporation, there may be contributions from conformational and chemical steps as well as from the propensity for rapid dissociation of mispaired dNTP from the polymerase [65]. By contrast, the structure of the active site of the Y-family polymerases

reveals that the relatively high frequency for mismatch incorporation ( $>10^{-3}$ ) and for bypass of DNA lesions can be attributed to a more open active site than that formed by A or B type polymerases [66–69].

**2.2. Proofreading by 3′-5′ Exonuclease Activity.** Most replicative polymerases possess or are closely associated with a 3′ to 5′ exo activity, and loss of this inherent or associated activity results in an increased mutation frequency *in vitro* and *in vivo* [70–74]. The contribution of the exo activity to increasing overall fidelity of DNA replication varies for different sequence contexts, but is on the order of 10- to 100-fold for most of the replicative polymerases [31, 33, 51, 63, 75, 76]. The importance of polymerase-associated exo activity in maintaining genomic stability in higher eukaryotes is also confirmed by the increased cancer incidence in transgenic mice containing an exo-deficient polymerase  $\delta$  [5, 6] and by the premature aging that occurs in transgenic mice containing an exo-deficient pol  $\gamma$  [3].

Because the exo activity competes with the polymerizing activity for the 3′ primer terminus, high-fidelity replication in its presence might be expected to have a real cost in terms of polymerizing speed and/or efficiency. However, pre-steady-state kinetic experiments have demonstrated that the means by which both rapid polymerization and correct nucleotide incorporation can be maintained reflects the ability of a polymerase to partition the primer terminus to the polymerizing or exo sites as needed [15, 31, 33, 34, 62, 63, 77]. The relative efficiencies for polymerization and proofreading during active DNA synthesis are influenced by a variety of parameters, including the relative affinities of a matched or mismatched primer terminus for the polymerizing or exo site, the rates of polymerization at matched versus mismatched primer termini, the rates of excision of matched versus mismatched primer termini, and the ability of a primer end to switch between the polymerizing and exo site with or without dissociation of the template from the polymerase.

Donlin and coworkers [33] demonstrated that the T7 DNA polymerase holoenzyme (with *E. coli* thioredoxin processivity factor) possesses the same binding affinity for matched or mismatched P/T although the T7 pol binds P/T tighter to the polymerization domain than to the exo site. In addition, the polymerization rate of incorporation of correct nucleotides is fast (300/sec) and the excision rate on ssDNA is even faster ( $>700$ /sec) [33, 62]. However, transfer of the primer to the physically distinct exo site is slower by 10-fold when the DNA is matched compared to when it is mismatched. When a misincorporation event occurs, the polymerization rate for T7 polymerase is slowed, permitting a transfer of the primer strand from the pol to the exo site. The rapid transfer of the mismatched nucleotide to the exo site permits excision of that nucleotide. For the T7 holoenzyme, the transfer of the now-matched P/T back to the polymerization site occurs without dissociation. Thus, the kinetic partitioning of the primer between the polymerizing and exo sites, without a rate-limiting dissociation of

TABLE 1: Summary of presteady-state kinetics of nucleotide incorporation by HSV-1 DNA polymerase.

Enzyme	Primer/template end after incorp.	dNTP:Template N <sup>a</sup>	$k_{\text{pol}}$ (sec <sup>-1</sup> ) <sup>b</sup>	$K_d$ (dNTP) apparent( $\mu\text{M}$ ) <sup>c</sup>	Efficiency ( $\mu\text{M}^{-1}$ sec <sup>-1</sup> )(inverse rel. discrim) <sup>d</sup>
WT pol	Matched	dATP:dT	258 $\pm$ 38 <sup>h,j</sup> (estimated)	ND <sup>e</sup>	ND
		dTTP:dA	157 $\pm$ 31 <sup>f</sup>	12.2 $\pm$ 5.7 <sup>f</sup>	12.9 $\pm$ 2.5
	Mismatched	dATP:dA	106 $\pm$ 9 <sup>f</sup>	279 $\pm$ 83 <sup>f</sup>	0.38 $\pm$ 0.03 (34)
	Abasic	dATP:Sp[0]	209 $\pm$ 33 <sup>h</sup>	75 $\pm$ 37 <sup>h</sup>	2.8 $\pm$ 0.44 (4.6)
Exo <sup>-</sup> pol	Matched	dTTP:dA	199 $\pm$ 26 <sup>i</sup>	4.8 $\pm$ 2.1 <sup>i</sup>	41.5 $\pm$ 5.4
	Mismatched	dATP:dA	8.7 $\pm$ 0.5 <sup>j</sup>	131 $\pm$ 24 <sup>j</sup>	0.07 $\pm$ 0.004 (600)
WT pol/UL42	Matched	dATP:dT	261 $\pm$ 26 <sup>f</sup> (estimated)	ND	ND
	Mismatched	dATP:dA	137 $\pm$ 21 <sup>f</sup>	6.4 $\pm$ 2.8 <sup>f</sup>	21.4 $\pm$ 3.3
Exo <sup>-</sup> pol/UL42	Matched	dGTP:dC	640 $\pm$ 60 <sup>g</sup> (estimated)	8 $\pm$ 2 <sup>g</sup>	80 $\pm$ 7.5
	Chain term	ACV-TP:dC	10.1 $\pm$ 0.8 <sup>g</sup>	6 $\pm$ 1 <sup>g</sup>	1.7 $\pm$ 0.3 (48)

<sup>a</sup>Refers to incoming dNTP for incorporation opposite the templating residue (N) indicated. <sup>b</sup>Rate constant at unlimiting incoming dNTP concentration determined by the equation  $k_{\text{obs}} = k_{\text{pol}}[\text{dNTP}]/([\text{dNTP}] + K_d)$ . <sup>c</sup>Apparent ground-state dissociation constant of dNTP determined according to the function indicated above. <sup>d</sup>Efficiency for incorporation of dNTP was calculated as  $k_{\text{pol}}/K_d(\text{dNTP})$ . Relative discrimination was estimated by dividing the efficiency for formation of a matched terminus by that for formation of mismatched, abasic, or chain terminator (acyclovir triphosphater, ACV-TP) primer/template interface. Number shown in parentheses is inverse of relative discrimination for formation of that terminus. <sup>e</sup>Not Done (ND). <sup>f</sup>From [64]. <sup>g</sup>From [78]. <sup>h</sup>From [79]. <sup>i</sup>From [75]. <sup>j</sup>From [80]

the holoenzyme from the P/T, permits rapid repair with little cost to overall rate of extension [33].

The structurally similar A-type mitochondrial polymerase (pol  $\gamma$ ) possesses an inherently poorer fidelity than the T7 polymerase [31, 63]. Compared to T7 polymerase, excision of mismatched DNA occurs at a much slower maximum rate (9/sec). Nevertheless, error correction without enzyme dissociation occurs with an efficiency of 80% [31]. By contrast, another A-type enzyme, Klenow fragment of DNA polymerase I, has an even slower rate of excision (0.003/sec), which would favor dissociation when that enzyme stalls at a mismatch [15, 77]. The latter results suggest that proofreading by Klenow is a less efficient means for error correction than by either bacteriophage T7 DNA polymerase or mammalian pol  $\gamma$ .

The T4 DNA polymerase catalytic subunit (a B-type polymerase) also incorporates correct nucleotides at a rapid rate (>400/sec) whereas the exo activity excises ssDNA at a rate of approximately 100/sec [34]. As for the T7 polymerase, transfer of primer from the polymerization to the exo site is slower (5-fold for T4 polymerase) for matched compared to mismatched P/T. However, because the rate constant for dissociation of the T4 polymerase catalytic subunit from the P/T (6–8/sec) competes with that for transfer of a mismatched primer to the exo site (5/sec), direct editing can occur only 40% of the time. Therefore, editing by the T4 polymerase catalytic subunit is less efficient than by the T7 DNA polymerase holoenzyme [33, 34].

As shown for the T4-like RB69 bacteriophage DNA polymerase, the ability of a mispaired end to access the exo site requires a  $\sim 40^\circ$  rotation relative to its position at the polymerase active site [56, 81]. Because the template

strand is not firmly anchored during this movement to the exo site for Klenow enzyme, the DNA must diffuse to the exo site, although one-way diffusion could be facilitated by retention of the primer in the thumb domain during the conformational change [56, 82]. A  $\beta$ -hairpin within the exo domain of the B-type polymerase encoded by bacteriophage RB69 has been proposed to hold the template in place as the primer terminus is transferred from the polymerizing to the exo active sites [83]. The analogous hairpin of *S. cerevisiae* pol  $\delta$  interacts extensively with the template strand which could stabilize the enzyme-DNA interaction during the conformational transition [58]. By contrast, the  $\beta$ -hairpin of RB69 polymerase does not associate with normal DNA and interacts with only a portion of the ssDNA template containing an abasic site [56, 58]. This could account for the relative inefficiency by which the RB69-like T4 DNA polymerase can edit mismatched DNA in a single association event [34, 58, 84].

*2.3. Alternative Mechanisms by Which the Exo Activity Enhances Polymerase Fidelity.* It is becoming increasingly clear that the exo activity associated with polymerases increases fidelity by mechanisms in addition to nucleotide editing. For example, the presence of exo activity also appears to be important for preventing translesion DNA synthesis or strand displacement synthesis by a number of polymerases, including those of pol  $\delta$ , bacteriophage T4, and HSV-1 [14, 85–89]. This is because the ability of a polymerase to partition the DNA primer between the polymerizing and exo sites allows the enzyme to engage in idling turnover—that is, successive rounds of excision and incorporation, with or without dissociation—whenever

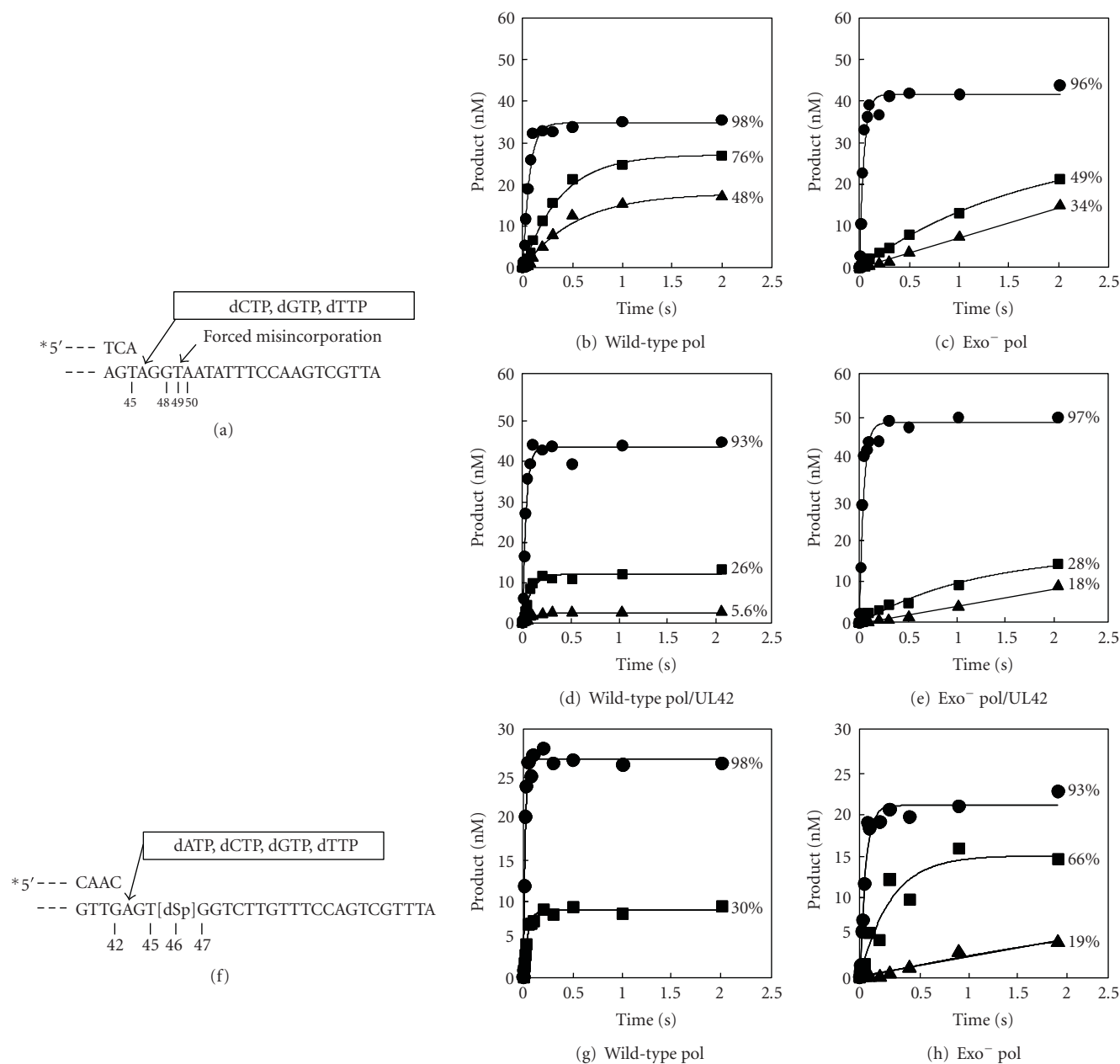


FIGURE 1: Running-start single-turnover kinetics for extension of mismatched or damaged P/Ts by HSV-1 DNA polymerase. Panels (a)–(e) represent forced misincorporation and extension reactions and are adapted from [75] whereas panels (f)–(h) show extension of AP-containing P/Ts and are adapted from [79]. (a) A partial sequence of the P/T (5' end-labeled 45 nt primer annealed to 67 nt template) is shown. The dNTPs added lacked dATP to force misincorporation opposite position 49 in reactions containing the wild-type pol (b), exo<sup>-</sup> pol (c), wild-type pol/UL42 (d), or exo<sup>-</sup> pol/UL42 (e). Reactions were performed with 50 nM enzyme, 100 nM P/T, and 250  $\mu$ M of each dNTP indicated and single-turnover conditions were ensured by the addition of nonradioactive activated calf-thymus DNA trap (500  $\mu$ g/ml) at the time of initiation. Reactions were terminated by the addition of EDTA, products were separated on denaturing polyacrylamide gels, gels were exposed to storage phosphor screens, and bands were quantified as previously described [75, 79]. (b)–(e) show plots of the concentration of products formed greater than or equal to 48 (●), 49 (■), or 50 (▲) nt in length. Except as indicated, the data were fit to the burst equation [extension product] =  $A(1 - e^{-kt})$ , where  $A$  is the burst amplitude,  $k$  is the observed rate constant, and  $t$  is the reaction time. The plots for formation of 50 nt product by the exo<sup>-</sup> pol or exo<sup>-</sup> pol/UL42 were produced by fitting the data to a linear function. The percentages next to each curve represent the amounts of primer  $\geq$  to that length compared to the amount of P/T actively engaged by the respective polymerases (i.e., that were extended by at least 1 nt). (f) A partial sequence of the P/T is shown. A dSpacer (dSp) was placed at position 46 from the 3' end of the template to mimic an abasic site. Reactions were performed as indicated above except that all four dNTPs were included for extension by wild-type pol (g) or exo<sup>-</sup> pol (h). Products representing primers extended to position 45 located 1 nt upstream (–1) of the AP site and beyond (●), products extended to the AP site and beyond (■), and products that were extended 1 or more nucleotides past the AP site (▲) are shown. The data in the plots were fit to the burst equation or to a linear function as indicated for plots (b)–(e). The numbers to the right of the curves represent the percentage of primers extended at least to this site compared to the number that were actively engaged by the respective polymerases.

it encounters a kinetic barrier to extension. This idling-behavior increases overall DNA replication fidelity because it prevents extension through abasic sites or oxidized nucleotides, such as 8-oxyguanine, which would have a high probability for introducing mutations [13]. Idling turnover by a polymerase also limits strand displacement synthesis. Failure to limit strand displacement synthesis by yeast pol  $\delta$  during Okazaki fragment maturation has been shown to lead to the production of aberrant or improperly processed lagging strand intermediates in vitro and higher mutation frequency in vivo [86, 87].

#### 2.4. Role of Processivity Factors in Fidelity of DNA Replication.

There has been much disagreement concerning the role of polymerase accessory proteins in maintaining fidelity. Parameters that could be altered by processivity factors include kinetic barriers to extending a mismatch or bypassing a lesion, the ability of the polymerase to partition its activity between the physically distinct exo and pol sites, the relative accessibility of the exo and pol sites, and dissociation of polymerase upon encountering a barrier to extension [33, 72, 76, 90, 91]. Capson et al. [34] proposed that the T4 polymerase processivity factor would enhance fidelity by limiting the dissociation of enzyme from mismatched P/T, thereby increasing the efficiency for direct editing by the enzyme. However, for several polymerases, an inverse relationship was shown between processivity or DNA binding and fidelity, at least under some circumstances [90–93]. For T7 DNA polymerase, the processivity factor was found to enhance fidelity by retaining the polymerase long enough to edit misincorporated nucleotides [33]. For T4 DNA polymerase, the addition of processivity factors to the wild-type enzyme had no impact on fidelity of DNA replication and did not permit lesion bypass. However the addition of processivity factors to an exo-deficient T4 polymerase did permit lesion bypass with low concentrations of enzyme, which did not permit efficient translesion synthesis in the absence of processivity factors [91]. Proliferating cell nuclear antigen (PCNA) was also demonstrated to increase misinsertion frequency and to promote the ability of mammalian pol  $\delta$  to bypass DNA lesions [90, 93, 94], thereby reducing fidelity. Likewise, the addition of processivity factor to mitochondrial polymerase (pol  $\gamma$ ) reduced the incorporation fidelity of both the wild-type and exo-deficient enzyme in gap-filling assays, predominantly by enhancing the efficiency for extending mismatches [76].

### 3. Herpes Simplex Virus Type 1 as a Model Eukaryotic Replicative DNA Polymerase

**3.1. Properties of the HSV-1 DNA Polymerase.** HSV-1 encodes a B-type DNA-dependent DNA polymerase that is the product of the UL30 gene and is essential for origin-dependent DNA synthesis in cell culture and for the production of infectious progeny virus in vivo [95–100]. In vitro, the HSV-1 DNA polymerase is also required together with 5 other viral encoded proteins for leading strand synthesis on model templates [101]. In addition to a 5' to 3' polymerizing

activity, the polymerase catalytic subunit (pol) possesses an intrinsic 3' to 5' exo domain [57, 99, 102, 103]. In infected cells, HSV-1 pol forms a stable heterodimer with the product of the UL42 gene (UL42) [104–106]. The UL42 protein is a double-stranded DNA-binding protein that serves as an accessory protein to increase the processivity of the HSV-1 pol catalytic subunit [104, 107, 108]. The ability of the UL42 processivity subunit to form a stable heterodimer with the HSV-1 pol catalytic subunit resembles the type of arrangement observed for the A-type polymerases, T7 bacteriophage DNA polymerase and mitochondrial pol  $\gamma$ , with their respective processivity factors. However, the structure of HSV-1 UL30 pol catalytic subunit most closely resembles that for the eukaryotic replicative polymerase, pol  $\delta$  [57, 58]. Interestingly, the structure of the UL42 processivity factor resembles that for a subunit of the pol  $\delta$  processivity factor, PCNA [109, 110]. However, the two globular domains of HSV-1 UL42 are oriented differently from those of a PCNA monomer such that they could not easily form the toroidal structure of the homotrimeric PCNA processivity factor [109]. The co-crystal structure of UL42 with a pol C-terminal peptide suggests a flexible attachment to the unstructured C-terminal tail of HSV-1 pol, similar to what has been observed for other processivity factors with their cognate B-type polymerase [56–58, 81, 82, 109]. Since the UL42 processivity factor does not require energy or other proteins to load it onto DNA or to form the heterodimeric holoenzyme [104, 105, 107, 111], it is easier to investigate the role of processivity factor in controlling the fidelity of this viral replicative polymerase compared to that of its close homolog, pol  $\delta$ .

**3.2. Genetic Analysis of HSV-1 Replication Fidelity.** Epidemiological studies suggest that HSV-1 DNA replication is not as faithful as that of its human host. For example, mutations occur frequently during HSV-1 replication in vivo, such that many nucleotide polymorphisms can be observed even in epidemiologically related strains of virus [112–114]. The genetic diversity of viral progeny that results from this poor fidelity is likely to contribute to selection of virus “mutants” capable of evading natural host immune mechanisms as well as antiviral drugs. Indeed, clinical isolates from humans not exposed to antiviral drugs have been shown to contain a preexisting subpopulation of virus resistant to high concentrations of acyclovir [115]. For random HSV-1 isolates from Japan, the average number of nucleotide differences observed in the 1,131 bp thymidine kinase (tk) gene was 3.3 [114]. In another study, the HSV-1 tk gene mutation frequency (estimated at  $5 \times 10^{-5}$ ) was determined by measuring the average frequency of acyclovir-resistant plaques that arose under nonselective growth conditions during a single replication cycle for independent cultures of an acyclovir-sensitive (wild-type) laboratory strain of HSV-1 [116].

Examining the role of the 3'-5' exo activity in maintaining the fidelity of HSV-1 DNA replication in culture has been challenging since it has not been possible to isolate viral mutants by altering conserved residues within either

TABLE 2: Summary of presteady-state kinetics of excision by wild-type HSV-1 polymerase.

Enzyme	P/T interface	Fast burst rate constant (sec <sup>-1</sup> )	P/T excised at fast rate (%)	Slow burst rate constant (sec <sup>-1</sup> )	P/T excised at slow rate (%)
WT pol <sup>a</sup>	dA/dT (matched)	59 ± 18 <sup>b</sup>	6 <sup>b</sup>	2.2 ± 0.7 <sup>b</sup>	26 <sup>b</sup>
	dA/dA (mismatched)	113 ± 7 <sup>c</sup>	29 <sup>c</sup>	NA	NA
	dA/AP (abasic)	130 ± 0 <sup>c</sup>	39 <sup>c</sup>	NA	NA
WT pol/UL42 <sup>d</sup>	dG/dC (matched)	12 ± 6 <sup>b</sup>	12.5 <sup>b</sup>	0.25 ± 0.02 <sup>b</sup>	87.5 <sup>b</sup>
	dG (8 nt frayed)	125 ± 7 <sup>b</sup>	73 <sup>b</sup>	1.3 ± 0.2 <sup>b</sup>	27 <sup>b</sup>
	ACV/dC (matched)	(5.1 ± 0.4) × 10 <sup>-3c</sup>	96 <sup>c</sup>	NA	NA
	ACV (8 nt frayed)	≥ 0.3 <sup>c</sup>	100 <sup>c</sup>	NA	NA
	ACV/dC + dNTP	(2 ± 0.6) × 10 <sup>-4c</sup>	94 <sup>c</sup>	NA	NA
	ACV (8 nt frayed) + dNTP	≥ 0.3 <sup>c</sup>	100 <sup>c</sup>	NA	NA

<sup>a</sup> The wild-type pol catalytic subunit (25 nM) was incubated in the presence of EDTA with 10 nM of a 46 nt primer annealed to a 67 nt template differing only at the primer/template (P/T) interface as indicated. Single turnover conditions were achieved by initiating reactions with MgCl<sub>2</sub> plus activated calf thymus DNA to trap dissociating pol (from [79]). All kinetic constants are apparent.

<sup>b</sup> The amount of full-length primer remaining was plotted as a function of time and the data were fit to the five-parameter double exponential decay function [intact primer] =  $ae^{-bt} + ce^{-dt} + f$ , where  $a$  and  $b$  are the amplitude and burst rate constant, respectively, during the fast phase, and  $c$  and  $d$  are the amplitude and burst rate constant during the slow phase of excision. The  $f$  constant represents the amount of unexcised primer remaining due to dissociation of the enzyme from the P/T or to failure of the enzyme to bind all of the P/T prior to initiation.

<sup>c</sup> The amount of full-length primer remaining was plotted as a function of time and the data were fit to a three-parameter single exponential decay function [intact primer] =  $ae^{-bt} + c$  due to the absence of a slower phase. NA, not applicable for single exponential functions.

<sup>d</sup> The wild-type pol/UL42 heterodimer (100 nM) was incubated in the presence of EDTA under single turnover conditions with 90 nM 26 nt primer containing the 3' nucleotide dGMP (dG) or acyclovir monophosphate (ACV) annealed to a 45 nt template prepared as described [78]. In some cases as indicated, the P/T contained 8 mismatches at the 3' end of the primer (frayed), the last of which was ACV. When added, the concentration of dNTPs was 100 μM (from [78]). All kinetic constants are apparent.

the Exo I or Exo II sites [117, 118]. Most of the HSV-1 Exo II site pol mutations created by Gibbs and coworkers failed to complement the replication of a pol null virus or to synthesize any viral DNA in these complementation assays [118]. Biochemical analysis of similar Exo II mutants by another group revealed that these mutations compromised not only the exo activity, but also the extension activity of the polymerase, perhaps accounting for their lethal phenotype [119]. Mutations that map in the conserved Exo I residues that are involved in the coordination of the metal ions required for catalysis (e.g., D368A and E370A) also possess little if any exo activity, though their polymerase activities are similar to or greater than that of the wild-type HSV-1 pol [75, 119]. Nevertheless, the D368A Exo I mutation was lethal for virus replication [117]. It has been suggested that the exo and polymerizing domains of the HSV-1 pol may be fundamentally different and less distinct from each other than those domains for other polymerases [118]. However, the resolved crystal structure of the HSV-1 pol shows that the organization of the exo domain with respect to the palm, fingers, and thumb subdomains is similar to that shown for *S. cerevisiae* pol δ [57, 58].

The only exo-deficient HSV-1 polymerases capable of supporting virus replication are those that map to the conserved Exo III site [116]. These Exo III site mutant proteins (e.g., Y577H, a double mutant Y577H/D581A, and Y577F) were somewhat compromised for polymerizing activity, but the 3' to 5' exo activity was reduced from 6- to 50-fold, depending on the mutation [116, 119]. Transient expression of the Y577H and Y577H/D581A mutant pol genes complemented the replication of an HSV-1 pol null

mutant virus, and viable virus progeny could be isolated when the mutations were introduced into the viral genome [116]. These viruses displayed a mutator phenotype with mutation frequencies that were 300- and 800-fold higher, respectively, than that for the parental wild-type virus [116]. The mutator phenotype of Exo III mutant viruses clearly demonstrates an important role for the intrinsic exo activity of the HSV-1 DNA polymerase in maintaining fidelity of viral DNA replication in culture. However, the inability of other exo-deficient polymerases to support virus replication, particularly the Exo I site mutants with wild-type polymerizing activity, suggests a more complex role for this domain during viral DNA replication.

**3.3. Discrimination between Correct versus Incorrect Nucleotide for Incorporation by HSV-1 DNA Polymerase.** Presteady-state kinetic analysis can provide a better understanding of the complex interactions between the polymerizing and exo functional domains by determining the individual parameters that control correct and incorrect nucleotide incorporation with undamaged template or a template with a noninformative lesion, such as an AP site. Table 1 summarizes the results of several different presteady-state kinetic studies of single nucleotide incorporation by various HSV-1 polymerases—that is, the wild-type and the Exo I site mutant (D368A) pols with or without the UL42 processivity factor. For better comparisons, only the apparent  $K_d$ s for dNTP are shown since true  $K_d$  for dNTP was determined in only one study [64]. The rate constants for correct nucleotide incorporation by the wild-type HSV-1 pol in the absence or

presence of UL42 processivity factor were not significantly different in two different sequence contexts (Table 1 and [64]). This contrasts with the ability of PCNA to increase the rates of polymerization by mammalian pol  $\delta$  approximately 3-fold [39].

For wild-type HSV-1 pol, the rate constant for misincorporation of dATP opposite dA template (106/sec) was only moderately less than for correct incorporation of dTTP (157/sec) into the same P/T (Table 1). Discrimination between the correct and incorrect nucleotide for HSV-1 pol occurs predominantly at the level of ground state binding affinity of dNTP, as indicated by a >20-fold decrease in affinity of dATP (incorrect) compared to dTTP (correct) for dA-containing template. Although the processivity factor slowed the rate of incorporation of mismatched dNTP by the wild-type pol approximately 4-fold, the pol/UL42 complex had an even greater difference in affinity between incorrect and correct dNTP compared to the wild-type pol catalytic subunit. Thus, HSV-1 pol, with or without processivity factor, discriminates between correct versus incorrect dNTP with similar relative efficiencies (Table 1). The relative discrimination values shown in Table 1 (34 and 130) differ somewhat from published values, since the latter used the lower true  $K_d$  (dNTP) values to estimate a misincorporation frequency of 1 in 300 for both pol and pol/UL42 [64]. This misincorporation frequency is approximately 10 times higher than that reported for the exo-deficient Klenow fragment of *E. coli* DNA polymerase I [53], suggesting that HSV-1 pol is one of the least faithful DNA polymerases with intrinsic exo activity [64]. It is interesting to note that a misincorporation frequency of 1 in 300 is similar to the nucleotide variation within the HSV-1 tk locus (an average of 3.3 changes for a gene of ~1,000 bp) noted among Japanese isolates [114]. Most other studies that have estimated lower HSV-1 mutation frequencies (between  $5 \times 10^{-5}$  and  $5 \times 10^{-4}$ ) have relied on the frequencies for isolating mutations in genes that are scored by function, such as acyclovir-resistance [116] or plaque color due to mutation in a lac Z locus introduced into the viral genome [120, 121]. Such studies naturally underestimate misincorporation frequency because they fail to score silent mutations that do not alter phenotype.

The D368A mutation renders the polymerase completely deficient in exo function but with a pre-steady-state polymerization rate constant for incorporation of correct nucleotide that is approximately 20% higher for the mutant catalytic subunit (199/sec) compared to the wild-type pol on the same P/T (Table 1). Although the relative differences in ground state binding affinity for mismatched versus matched nucleotide were similar for the exo<sup>-</sup> and wild-type pols, the pre-steady-state rate constant for incorporating an incorrect nucleotide by this mutant pol was 23 times lower than that for incorporating a correct one (Table 1). This results in an overall 600-fold reduced efficiency for incorporation of incorrect compared to correct dNTP by the exo<sup>-</sup> pol. Overall, the HSV-1 exo<sup>-</sup> pol misincorporates nucleotides >5-times less efficiently than does the wild-type pol using the same P/T (Table 1). Thus, the HSV-1 exo<sup>-</sup> pol misincorporation efficiency differs from that of exo-deficient Klenow enzyme

by a factor of only 2 [53]. As discussed in detail in a subsequent section, the lower misincorporation efficiencies observed by the HSV-1 exo<sup>-</sup> pol, compared to the wild-type pol, may reflect a defect in the ability of the enzyme, or enzyme:incorrect dNTP ternary complex, to transfer the primer terminus between the polymerizing and exo sites.

The specific impact of the UL42 processivity factor on the efficiency with which the exo-deficient pol can discriminate between incorrect and correct nucleotides for incorporation cannot be determined from Table 1. However, the ground-state binding affinity of the antiviral compound, acyclovir (ACV) triphosphate, for the exo<sup>-</sup> pol/UL42 complex, is roughly the same as the affinity of dGTP for incorporation opposite a dC templating residue [78, 122] (Table 1). By contrast, the rate constant for incorporation of ACV-TP by the exo<sup>-</sup> pol/UL42 complex is considerably slower than the rate constant for incorporation of matched dNTP by the exo<sup>-</sup> pol, but similar to that for incorporation of mismatched nucleotide by the exo<sup>-</sup> catalytic subunit (Table 1). Thus, it is likely that the slow rate-limiting step for incorporation of ACV-TP by the exo<sup>-</sup> pol/UL42 reflects a slow conformational change and/or chemistry step, as suggested for mismatched dNTP incorporation [50].

**3.4. Kinetics of Nucleotide Incorporation at AP Sites by HSV-1 DNA Polymerase.** The kinetic parameters that govern nucleotide incorporation by the HSV-1 pol opposite an AP site on the template differ from those for either correct or incorrect incorporation with undamaged templates. For example, for wild-type pol, there is no significant difference in the rate constant for incorporation ( $k_{\text{pol}}$ ) of dATP opposite the matched dT compared to that for incorporation opposite an AP site (Table 1). Pre-steady-state kinetic experiments also revealed that the productive binding of the HSV-1 pol to a P/T containing an AP site located 1 nucleotide downstream (+1) from the P/T interface (true  $K_d$  (DNA) =  $42.1 \pm 7.4$  nM; [79]) was indistinguishable from that for undamaged P/T (true  $K_d$  (DNA) =  $44 \pm 3.0$  nM; [64]). These results suggest that the enzyme cannot sense the AP site on the template strand ahead of attempts at incorporation. Nevertheless, the ground state binding affinity for dATP opposite the noncoding AP site ( $1/K_d$ ) was reduced approximately 5-fold for wild-type pol compared to that for incorporation opposite a matched nucleotide (Table 1).

**3.5. Presteady-State Kinetics of Excision by the HSV-1 DNA Polymerase.** Under single turnover conditions in which the wild-type pol is bound to P/T at equilibrium and excision is initiated by the addition of MgCl<sub>2</sub> with high-excess cold DNA trap, the kinetics for excision of a mismatched P/T, or a P/T containing dA opposite an AP site, approach that for excision of frayed ssDNA ends by the wild-type pol/UL42 holoenzyme (Table 2, [64, 78]). The fast burst rate constant for excision of matched P/T by wild-type pol is considerably slower than that for mismatched or A:AP P/Ts (Table 2). In addition, a smaller proportion of matched primer was cleaved, compared to primer opposite a mismatched or AP-containing template. Wild-type pol/UL42 also cleaved

a smaller proportion of matched ends compared to frayed ones, and with a smaller burst rate constant (Table 2). These results indicate that most of the matched P/T is held at equilibrium in the polymerization site with little difference in the relative distribution in the presence (12.5%) versus absence (6%) of processivity factor. Because the presence of excess unlabeled DNA trap prevents access of labeled P/T to any polymerase that dissociates, the slow burst rate constant for excision, when present, is indicative of the rate by which the primer strand is destabilized and transferred to the exo active site in a single association event (2.2/sec for pol and 0.25/sec for pol/UL42; Table 2). From these data alone, it is difficult to determine whether the differences observed in both fast and slow burst rate constants for cleavage of a dA/dT matched P/T by pol, compared to those for cleavage of dG/dC matched P/T by pol/UL42, reflect a greater thermal stability of the dG/dC base-pair or a significant slowing of excision rate by UL42. However, in side-by-side comparisons on the same matched P/T, Chaudhuri et al. [64] demonstrated no more than a 2-fold reduction in fast burst rates for cleavage of matched P/T in the presence versus the absence of UL42.

Although HSV-1 pol excises the 3' nucleotide from mismatched or A:AP P/Ts at rates similar to those for ssDNA (unpublished results, but exemplified by the fast rates of excision of frayed ends by pol/UL42), only a portion of the P/Ts occupied by the pol are cleaved at the fast burst rate in a single-turnover (Table 2). Since no slow burst rate was observed for wild-type pol with either P/T, the results indicate that the remainder of the P/Ts were either not bound to the enzyme or dissociated from it at a rate faster than that required to transfer the 3' primer terminus from the polymerizing to the exo site. In the presence of pol/UL42, not only is a large proportion of frayed primer cleaved with a fast burst rate constant, but the remainder that bound initially at the polymerization site (27%; Table 2) was transferred to the exo active site for cleavage prior to dissociation. These results suggest that UL42 might increase the overall fidelity of DNA synthesis by increasing the probability that a mismatched P/T will be excised prior to its dissociation from wild-type pol during processive synthesis, when most of the primer would be expected to be located at the polymerizing site.

As previously indicated by steady-state kinetic analysis [122], pre-steady-state kinetic analysis reveals that the excision of ACV-TP opposite the matched dC template is extremely slow, with a burst rate constant approximately 2000-fold slower than for the fast burst rate constant for excision of dG on matched template [78] (Table 2). Excision is slowed another 25-fold when dNTP is present. In all cases, the excision rate is slower than the rate of transfer from the pol to the exo site and/or the rate of dissociation from the P/T since no slower burst rate was observed. The association of next correct dNTP has been reported to lock the polymerase into a dead-end complex with ACV-TP [122]. However, the comparatively small difference in excision burst rate constants in the presence versus absence of dNTP following ACV incorporation may suggest that the dNTP stabilizes a replicating P/T within the polymerizing site, thereby reducing its rate of transfer from the pol to

exo site [57, 78]. Taken together, these results suggest the importance of the HSV-1 pol to possess a dynamic ability to switch the P/T between the polymerizing and exo sites for its ability to function properly, and a role for UL42 in preventing dissociation of pol from a mismatched primer terminus during active DNA extension.

*3.6. Mismatch Extension by HSV-1 Pol during Processive Synthesis.* Early steady-state experiments were used to determine the ability of the HSV-1 pol to extend mismatches [123]. Despite potent exo activity, the wild-type HSV-1 pol was observed to extend mismatches at high concentrations of next correct single nucleotide. However, the efficiency ( $V_{\max}/K_m$ ) for wild-type pol extension of mismatches with next correct nucleotide was considerably lower than for the exo<sup>-</sup> pol [75, 123]. This was due in large part to cleavage of the mismatched primer terminus by the exo activity of the wild-type pol, resulting in an incorrectly matched P/T for extension with the tested nucleotide. Indeed, when the template nucleotide located at position -1 with respect to the mismatched primer terminus was complementary to the incoming nucleotide, efficiency for extending the "mismatched" P/T was virtually the same as for matched [75, 119]. Because dissociation would effectively reduce the  $V_{\max}$ , these results demonstrate the effective ability of the wild-type HSV-1 pol to switch the primer to the exo site, cleave the mismatch, switch it back to the polymerizing site, and incorporate new nucleotide, all without dissociating. It also suggests that with this kinetic partitioning, there is little cost to extension efficiency when proof-reading by the HSV-1 polymerase is required. Nevertheless, steady-state experiments do not provide an accurate measure of the ability of a polymerase to extend uncorrected mismatches.

Running-start single-turnover experiments have been used to gain a better understanding of the kinetic barrier for HSV-1 pol to extend mismatches and how the polymerase responds to misincorporation during active polymerization [75]. The data in [75] have been adapted and included in Figure 1 for comparative purposes. In these experiments, the terminus of a 5' end-labeled primer was located 3 nucleotides upstream (-3) of a target site that forced misincorporation due to the absence of matched nucleotide in the pool (Figure 1(a)). Critical to these experiments was (1) a saturating or close to saturating concentration of all other nucleotides, (2) equilibrium binding of the polymerase to the P/T prior to initiation (in the presence of EDTA), and (3) initiation of reactions with MgCl<sub>2</sub> and excess DNA to trap any polymerase molecules that dissociate from the P/T following initiation [75]. Because active polymerization would occur for several nucleotides, the P/T would be expected to be firmly bound to the polymerase active site for several cycles of processive correct nucleotide incorporations prior to a forced misincorporation event. Surprisingly, three-fourths of the P/T productively engaged by the wild-type pol misincorporated nucleotide at the target position, and two-thirds of those were extended by at least one additional nucleotide prior to dissociation (accounting for 48% of total P/T productively bound by

the pol, see Figure 1(b)). The presence of a strong pause site [75] suggests that the wild-type pol switches the primer end to the exo site, cleaves the mismatch to form a matched P/T, then rapidly switches back to the pol site for another forced misincorporation event. Repeated cycles of excision and incorporation (idling) then ensue in a single association of the pol catalytic subunit with P/T, until the mismatch is successfully extended (Figure 1(b)). These results indicate that the rate of transfer of the mismatched primer terminus between the polymerizing and exo sites (one or more times) is greater than the rate of dissociation of the wild-type pol from the P/T during forced misincorporation.

The  $\text{exo}^-$  HSV-1 pol also misincorporated and extended mismatches, but the kinetics for misincorporation were markedly slower compared with wild-type pol, with only half of the productively engaged  $\text{exo}^-$  pol misincorporating within 2 sec (Figure 1(c)). The latter results are in excellent agreement with the less efficient ability of the  $\text{exo}^-$  pol, compared to the wild-type pol, in incorporating an incorrect nucleotide in standing start experiments (Table 1). However, a similar proportion of available mismatched P/T was extended by the  $\text{exo}^-$  pol, compared with the wild-type pol, albeit at a slower rate. The near linear kinetics for mismatch extension by the  $\text{exo}^-$  pol are not the result of multiple turnovers of enzyme with P/T because of the presence of DNA trap. Instead, the absence of a burst likely indicates that the rate-limiting step is the slow rate of primer switching ( $\sim 0.24/\text{sec}$  [75]) from the polymerizing to the exo site and back when the mismatch cannot be cleaved.

The impact of the UL42 processivity factor in preventing mismatch extension is clearly observed in these running start experiments. Not only do fewer mismatched P/T accumulate in the presence (26%) versus absence (76%) of UL42, but only 5.6% of all P/T (21% of those that misincorporated) are extended one nucleotide beyond the mismatch and none were extended further (Figure 1(d); [75]). Because the rates of incorporation of incorrect nucleotide and excision of mismatches or frayed ends (Tables 1 and 2, resp.) do not differ substantially for wild-type HSV-1 pol in the presence or absence of processivity factor, the results suggest that UL42 increases the efficiency and/or rates by which the mismatched/frayed primer terminus is transferred between the polymerizing and exo sites in a single association event during active replication.

**3.7. Failure of the HSV-1 DNA Polymerase to Bypass AP Lesions during Active Replication.** Similar running-start single-turnover experiments have been performed on P/Ts in which the target site on the template was an AP site, located 4 nt downstream of the primer terminus (Figure 1(f)). The data have been adapted from a previously published report [79] to permit side-by-side comparisons with mismatch extension data [75]. The wild-type HSV-1 pol extended the primer to the AP target site with more rapid burst kinetics than it did to a misincorporation target (compare Figures 1(g) and 1(b)). However, compared to mismatches, AP sites posed a greater kinetic barrier to extension by the wild-type HSV-1 pol, since no lesion bypass was detected

(Figure 1(g); [79]). With such a high kinetic barrier, the rate of dissociation of the pol from the damaged P/T exceeded that required for extension, resulting in a smaller percentage (30%) of primer extended to the AP target site (Figure 1(g)) compared to that which resulted from misincorporation (76%; Figure 1(b)).

The absence of exo activity prevents excision of the residue that is incorporated opposite an AP site and, as observed following misincorporation, this slows the transfer of primer between the exo and polymerizing sites. Although the  $\text{exo}^-$  pol was able to bypass AP lesions, bypass synthesis was extremely inefficient (Figure 1(h)). These results are in agreement with the requirement for exo-deficiency in order for the HSV-1 pol to incorporate nucleotide opposite a cisplatin cross-link [88]. It was also shown in those studies that neither the wild-type nor  $\text{exo}^-$  pol, with or without UL42 processivity subunit, could completely bypass the cisplatin lesion. However, UL42 did increase the ability of HSV-1  $\text{exo}^-$  pol to incorporate nucleotide opposite the cisplatin lesion [88]. No studies to date have examined the ability of UL42 to permit AP lesion bypass synthesis.

AP sites have been shown to be present in HSV-1 replicating and virion DNA at a frequency of 2.8–5.9/genome equivalent [79]. Given that wild-type pol is unable to bypass these lesions, there must be other mechanisms to permit synthesis through or around AP lesions, such as recombination or repair. The newly discovered AP and 5'-deoxyribose phosphate lyase activities of the HSV-1 pol, both of which are involved in base excision repair, might perform such a task to repair AP lesions [124]. It is also possible that other viral DNA replication components would permit lesion bypass.

**3.8. Importance of Kinetic Partitioning between the Polymerizing and exo Sites for Fidelity.** The kinetic barrier to extending a mismatched P/T prevents most misincorporation events from becoming fixed mutations. The exo activity of the HSV-1 pol reinforces the kinetic barrier by permitting excision of the mismatched primer terminus when the polymerase “stalls”. In reality, the polymerase does not truly stall when it encounters a kinetic barrier, but rather engages in idling at that site through successive rounds of incorporation and excision, even in the absence of the UL42 processivity factor. The idling activity is made possible by the ability of the polymerase to dynamically switch the P/T from the polymerizing site to the exo site and back. Pre-steady-state kinetic analysis has demonstrated that UL42 increases the processivity of the HSV-1 pol from  $\sim 1700$  to  $>5,000$  per association event [64]. UL42 also increases the efficiency of excision of mismatches formed during processive DNA synthesis by increasing the rate and/or efficiency of transfer of the mismatched primer between the polymerizing and exo active sites. This makes UL42 an unusual fidelity factor because it affects neither the rates of polymerization nor the rates of excision [64]. Moreover, UL42 does not promote mismatch extension or lesion bypass, distinguishing it from the functions of the processivity factors of polymerases in the

same family, such as T4 DNA polymerase and mammalian pol  $\delta$  [90, 91, 94].

Mounting evidence suggests that altering the ability of the HSV-1 pol to switch between the exo and pol active sites will have an impact on fidelity. It is interesting to note that mutations in UL42 that either increase or decrease affinity for DNA result in decreased replication fidelity and reduced numbers of viable virus progeny [120, 121]. Although classical measures of this idling activity depend on the presence of a functional exo activity [85], the running-start single-turnover experiments described in Figure 1 demonstrate the ability of the HSV-1 polymerase to switch the primer terminus between the exo and pol sites even in the absence of exo catalytic activity. However, the increased affinity of the exo site for mismatched primer (ssDNA), and the corresponding decreased affinity of mismatched DNA for the polymerizing site, renders the catalytically inactivated Exo I site mutant pol (D368A) less efficient in switching behavior and in extending mismatched primers [75, 123]. The fact that the Exo I mutant pol is also slower in its ability to incorporate incorrect dNTP than the wild-type pol suggests that binding of an incorrectly matched dNTP to the HSV-1 pol may destabilize the association of the primer terminus with the polymerizing active site. UL42 slows the rate of switching of the exo<sup>-</sup> pol on mismatched termini during processive synthesis even more (Figure 1(e); and [75]). If the rate of switching is slower than that for dissociation of the polymerase from the P/T, then extension would be disfavored, which could explain why no viable progeny have been isolated with this particular mutation [117].

Mutations outside the exo domain may also impact P/T switching by the HSV-1 pol. Kinetic analysis of HSV-1 pol containing a finger domain mutation (L774F) showed significant stalling during normal elongation and a decreased efficiency for extending mismatches [125, 126]. When introduced into the pol gene of the virus, this mutation increased fidelity of DNA synthesis compared to that of the parental virus, regardless of the presence or absence of an Exo III site mutation [125, 126]. These properties are consistent with enhanced idling-turnover ability and increased primer switching compared to the wild-type pol. For T4 DNA polymerase, mutations that increase the switching rate have also been shown to possess antimutator activity [41], consistent with the importance of the ability of the pol to efficiently transfer the primer end between the polymerizing and exo active sites to maintain fidelity. Since the T4 switch mutations do not map to the same domain as the HSV-1 L774F mutation, additional studies will be required to ascertain the mechanism by which the HSV-1 finger domain mutant enhances replication fidelity.

**3.9. Kinetic Partitioning and Virus Viability.** The ability of the HSV-1 DNA polymerase to engage in dynamic switching of P/T between the pol and exo sites when kinetic barriers to extension are encountered is likely to be essential to the viability of virus. It is interesting to note that part of the effectiveness of the chain-terminator, acyclovir, now appears

to be its influence on the ability of the HSV-1 pol to switch the primer terminus between the polymerizing and exo sites. As suggested by Hanes et al. [78], the addition of dNTP to an HSV-1 pol that has incorporated ACV may favor retention of the ACV-containing P/T at the pol site, making ACV less likely to be removed by the exo activity.

We propose that compounds that specifically target the HSV-1 pol exo activity for inactivation, or that significantly inhibit the ability of replicating viral DNA to be transferred between the polymerizing and exo sites, would be effective antiviral agents. By holding the primer terminus in the exo site, extension by the polymerase would be slowed and could lead to chain termination and replication failure. Holding the primer in the polymerase active site would be expected to decrease the ability of the polymerase to excise mismatches that are frequently formed by the polymerase and to increase the probability for mismatch extension. This would lead to the accumulation of a lethal number of mutations during replication. Due to the conserved nature of the polymerase among the herpesvirus family members [99], it should be possible to target other herpesvirus polymerases in the same way, particularly those for which no effective nontoxic inhibitor has been identified to date.

## Acknowledgments

This work was supported in part by parent Grant GM 034930 and American Reinvestment and Recovery Act Supplemental GM 034930-04S1 from the National Institutes of Health (D.S.P.). During part of this work, Y. Zhu was supported by a training Grant from the National Cancer Institute (CA 09338). Core services were provided by the Ohio State University Comprehensive Cancer Center and the Department of Molecular Virology, Immunology, and Medical Genetics.

## References

- [1] J. P. Wittschieben, S. C. Reshmi, S. M. Gollin, and R. D. Wood, "Loss of DNA polymerase  $\zeta$  causes chromosomal instability in mammalian cells," *Cancer Research*, vol. 66, no. 1, pp. 134–142, 2006.
- [2] R. N. Venkatesan, P. M. Treuting, E. D. Fuller et al., "Mutation at the polymerase active site of mouse DNA polymerase  $\delta$  increases genomic instability and accelerates tumorigenesis," *Molecular and Cellular Biology*, vol. 27, no. 21, pp. 7669–7682, 2007.
- [3] A. Trifunovic, A. Wredenberg, M. Falkenberg et al., "Premature ageing in mice expressing defective mitochondrial DNA polymerase," *Nature*, vol. 429, no. 6990, pp. 417–423, 2004.
- [4] Q. Lin, A. B. Clark, S. D. McCulloch et al., "Increased susceptibility to UV-induced skin carcinogenesis in polymerase  $\eta$ -deficient mice," *Cancer Research*, vol. 66, no. 1, pp. 87–94, 2006.
- [5] R. E. Goldsby, N. A. Lawrence, L. E. Hays et al., "Defective DNA polymerase- $\delta$  proofreading causes cancer susceptibility in mice," *Nature Medicine*, vol. 7, no. 6, pp. 638–639, 2001.
- [6] R. E. Goldsby, L. E. Hays, X. Chen et al., "High incidence of epithelial cancers in mice deficient for DNA polymerase  $\delta$  proofreading," *Proceedings of the National Academy of Sciences*, vol. 100, no. 12, pp. 7100–7105, 2003.

- Sciences of the United States of America*, vol. 99, no. 24, pp. 15560–15565, 2002.
- [7] C. A. Dumstorf, A. B. Clark, Q. Lin et al., “Participation of mouse DNA polymerase  $\iota$  in strand-biased mutagenic bypass of UV photoproducts and suppression of skin cancer,” *Proceedings of the National Academy of Sciences of the United States of America*, vol. 103, no. 48, pp. 18083–18088, 2006.
- [8] A. B. Robertson, A. Klungland, T. Rognes, and I. Leiros, “DNA repair in mammalian cells: base excision repair: the long and short of it,” *Cellular and Molecular Life Sciences*, vol. 66, no. 6, pp. 981–993, 2009.
- [9] T. A. Kunkel and D. A. Erie, “DNA mismatch repair,” *Annual Review of Biochemistry*, vol. 74, pp. 681–710, 2005.
- [10] J. Jiricny, “The multifaceted mismatch-repair system,” *Nature Reviews Molecular Cell Biology*, vol. 7, no. 5, pp. 335–346, 2006.
- [11] P. C. Hanawalt, “Paradigms for the three Rs: DNA replication, recombination, and repair,” *Molecular Cell*, vol. 28, no. 5, pp. 702–707, 2007.
- [12] A. M. Woodside and F. P. Guengerich, “Misincorporation and stalling at  $O^6$ -methylguanine and  $O^6$ -benzylguanine: evidence for inactive polymerase complexes,” *Biochemistry*, vol. 41, no. 3, pp. 1039–1050, 2002.
- [13] L. G. Lowe and F. P. Guengerich, “Steady-state and pre-steady-state kinetic analysis of dNTP insertion opposite 8-oxo-7,8-dihydroguanine by *Escherichia coli* polymerases I  $exo^-$  and II  $exo^-$ ,” *Biochemistry*, vol. 35, no. 30, pp. 9840–9849, 1996.
- [14] N. Tanguy Le Gac, E. Delagoutte, M. Germain, and G. Villani, “Inactivation of the 3’-5’ exonuclease of the replicative T4 DNA polymerase allows translesion DNA synthesis at an abasic site,” *Journal of Molecular Biology*, vol. 336, no. 5, pp. 1023–1034, 2004.
- [15] R. D. Kuchta, P. Benkovic, and S. J. Benkovic, “Kinetic mechanism whereby DNA polymerase I (Klenow) replicates DNA with high fidelity,” *Biochemistry*, vol. 27, no. 18, pp. 6716–6725, 1988.
- [16] M. F. Goodman and D. K. Fygenon, “DNA polymerase fidelity: from genetics toward a biochemical understanding,” *Genetics*, vol. 148, no. 4, pp. 1475–1482, 1998.
- [17] H. Echols and M. F. Goodman, “Fidelity mechanisms in DNA replication,” *Annual Review of Biochemistry*, vol. 60, pp. 477–511, 1991.
- [18] P. Stelter and H. D. Ulrich, “Control of spontaneous and damage-induced mutagenesis by SUMO and ubiquitin conjugation,” *Nature*, vol. 425, no. 6954, pp. 188–191, 2003.
- [19] S. Prakash and L. Prakash, “Translesion DNA synthesis in eukaryotes: a one- or two-polymerase affair,” *Genes and Development*, vol. 16, no. 15, pp. 1872–1883, 2002.
- [20] S. D. McCulloch and T. A. Kunkel, “The fidelity of DNA synthesis by eukaryotic replicative and translesion synthesis polymerases,” *Cell Research*, vol. 18, no. 1, pp. 148–161, 2008.
- [21] C. Hoegge, B. Pfander, G.-L. Moldovan, G. Pyrowolakis, and S. Jentsch, “RAD6-dependent DNA repair is linked to modification of PCNA by ubiquitin and SUMO,” *Nature*, vol. 419, no. 6903, pp. 135–141, 2002.
- [22] L. Haracska, I. Unk, R. E. Johnson et al., “Stimulation of DNA synthesis activity of human DNA polymerase  $\kappa$  by PCNA,” *Molecular and Cellular Biology*, vol. 22, no. 3, pp. 784–791, 2002.
- [23] L. Haracska, I. Unk, R. E. Johnson et al., “Roles of yeast DNA polymerases  $\delta$  and  $\zeta$  of Rev 1 in the bypass of abasic sites,” *Genes and Development*, vol. 15, no. 8, pp. 945–954, 2001.
- [24] L. Haracska, S. Prakash, and L. Prakash, “Yeast DNA polymerase  $\zeta$  is an efficient extender of primer ends opposite from 7,8-dihydro-8-oxoguanine and  $O^6$ -methylguanine,” *Molecular and Cellular Biology*, vol. 23, no. 4, pp. 1453–1459, 2003.
- [25] L. Haracska, L. Prakash, and S. Prakash, “Role of human DNA polymerase  $\kappa$  as an extender in translesion synthesis,” *Proceedings of the National Academy of Sciences of the United States of America*, vol. 99, no. 25, pp. 16000–16005, 2002.
- [26] L. Haracska, C. M. Kondratick, I. Unk, S. Prakash, and L. Prakash, “Interaction with PCNA is essential for yeast DNA polymerase  $\eta$  function,” *Molecular Cell*, vol. 8, no. 2, pp. 407–415, 2001.
- [27] L. Haracska, R. E. Johnson, I. Unk et al., “Targeting of human DNA polymerase  $\iota$  to the replication machinery via interaction with PCNA,” *Proceedings of the National Academy of Sciences of the United States of America*, vol. 98, no. 25, pp. 14256–14261, 2001.
- [28] M. F. Goodman, “Error-prone repair DNA polymerases in prokaryotes and eukaryotes,” *Annual Review of Biochemistry*, vol. 71, pp. 17–50, 2002.
- [29] E. C. Friedberg, R. Wagner, and M. Radman, “Specialized DNA polymerases, cellular survival, and the genesis of mutations,” *Science*, vol. 296, no. 5573, pp. 1627–1630, 2002.
- [30] L. J. Reha-Krantz, “Regulation of DNA polymerase exonucleolytic proofreading activity: studies of bacteriophage T4 ‘antimutator’ DNA polymerases,” *Genetics*, vol. 148, no. 4, pp. 1551–1557, 1998.
- [31] A. A. Johnson and K. A. Johnson, “Exonuclease proofreading by human mitochondrial DNA polymerase,” *Journal of Biological Chemistry*, vol. 276, no. 41, pp. 38097–38107, 2001.
- [32] F. Foury and S. Vanderstraeten, “Yeast mitochondrial DNA mutators with deficient proofreading exonucleolytic activity,” *EMBO Journal*, vol. 11, no. 7, pp. 2717–2726, 1992.
- [33] M. J. Donlin, S. S. Patel, and K. A. Johnson, “Kinetic partitioning between the exonuclease and polymerase sites in DNA error correction,” *Biochemistry*, vol. 30, pp. 538–546, 1991.
- [34] T. L. Capson, J. A. Peliska, B. F. Kaboord et al., “Kinetic characterization of the polymerase and exonuclease activities of the gene 43 protein of bacteriophage T4,” *Biochemistry*, vol. 31, no. 45, pp. 10984–10994, 1992.
- [35] A. J. Berdis, “Dynamics of translesion DNA synthesis catalyzed by the bacteriophage T4 exonuclease-deficient DNA polymerase,” *Biochemistry*, vol. 40, no. 24, pp. 7180–7191, 2001.
- [36] A. Bebenek, G. T. Carver, H. K. Dressman et al., “Dissecting the fidelity of bacteriophage RB69 DNA polymerase: site-specific modulation of fidelity by polymerase accessory proteins,” *Genetics*, vol. 162, no. 3, pp. 1002–1018, 2002.
- [37] M. Hogg, S. S. Wallace, and S. Doublé, “Crystallographic snapshots of a replicative DNA polymerase encountering an abasic site,” *EMBO Journal*, vol. 23, no. 7, pp. 1483–1493, 2004.
- [38] R. D. Kuchta, V. Mizrahi, P. A. Benkovic, K. A. Johnson, and S. J. Benkovic, “Kinetic mechanism of DNA polymerase I (Klenow),” *Biochemistry*, vol. 26, no. 25, pp. 8410–8417, 1987.
- [39] H. J. Einolf and F. P. Guengerich, “Kinetic analysis of nucleotide incorporation by mammalian DNA polymerase

- $\delta$ ," *Journal of Biological Chemistry*, vol. 275, no. 21, pp. 16316–16322, 2000.
- [40] M. Hogg, W. Cooper, L. Reha-Krantz, and S. S. Wallace, "Kinetics of error generation in homologous B-family DNA polymerases," *Nucleic Acids Research*, vol. 34, no. 9, pp. 2528–2535, 2006.
- [41] S. A. Stocki, R. L. Nonay, and L. J. Reha-Krantz, "Dynamics of bacteriophage T4 DNA polymerase function: identification of amino acid residues that affect switching between polymerase and 3' → 5' exonuclease activities," *Journal of Molecular Biology*, vol. 254, no. 1, pp. 15–28, 1995.
- [42] L. J. Reha-Krantz and M. J. Bessman, "Studies on the biochemical basis of mutation VI. Selection and characterization of a new bacteriophage T4 mutator DNA polymerase," *Journal of Molecular Biology*, vol. 145, no. 4, pp. 677–695, 1981.
- [43] N. Muzyczka, R. L. Poland, and M. J. Bessman, "Studies on the biochemical basis of spontaneous mutation. I. A comparison of the deoxyribonucleic acid polymerases of mutator, antimutator, and wild type strains of bacteriophage T4," *Journal of Biological Chemistry*, vol. 247, no. 22, pp. 7116–7122, 1972.
- [44] M. S. Hershfield, "On the role of deoxyribonucleic acid polymerase in determining mutation rates. Characterization of the defect in the T4 deoxyribonucleic acid polymerase caused by the ts L88 mutation," *Journal of Biological Chemistry*, vol. 248, no. 4, pp. 1417–1423, 1973.
- [45] A. R. Fersht, "Fidelity of replication of phage  $\phi$ X174 DNA by DNA polymerase III holoenzyme: Spontaneous mutation by misincorporation," *Proceedings of the National Academy of Sciences of the United States of America*, vol. 76, no. 10, pp. 4946–4950, 1979.
- [46] H. Mitsuya, R. F. Jarrett, and M. Matsukura, "Long-term inhibition of human T-lymphotropic virus type III/lymphadenopathy-associated virus (human immunodeficiency virus) DNA synthesis and RNA expression in T cells protected by 2',3'-dideoxynucleosides in vitro," *Proceedings of the National Academy of Sciences of the United States of America*, vol. 84, no. 7, pp. 2033–2037, 1987.
- [47] P. A. Furman, J. A. Fyfe, M. H. St. Clair et al., "Phosphorylation of 3'-azido-3'-deoxythymidine and selective interaction of the 5'-triphosphate with human immunodeficiency virus reverse transcriptase," *Proceedings of the National Academy of Sciences of the United States of America*, vol. 83, no. 21, pp. 8333–8337, 1986.
- [48] G. B. Elion, "The biochemistry and mechanism of action of acyclovir," *Journal of Antimicrobial Chemotherapy*, vol. 12, pp. 9–17, 1983.
- [49] I. Wong, "An induced-fit kinetic mechanism for DNA replication fidelity: direct measurement by single-turnover kinetics," *Biochemistry*, vol. 30, no. 2, pp. 526–537, 1991.
- [50] Y.-C. Tsai and K. A. Johnson, "A new paradigm for DNA polymerase specificity," *Biochemistry*, vol. 45, no. 32, pp. 9675–9687, 2006.
- [51] T. A. Kunkel and K. Bebenek, "DNA replication fidelity," *Annual Review of Biochemistry*, vol. 69, pp. 497–529, 2000.
- [52] W. M. Kati, K. A. Johnson, L. F. Jerva, and K. S. Anderson, "Mechanism and fidelity of HIV reverse transcriptase," *Journal of Biological Chemistry*, vol. 267, no. 36, pp. 25988–25997, 1992.
- [53] J. G. Bertram, K. Oertell, J. Petruska, and M. F. Goodman, "DNA polymerase fidelity: comparing direct competition of right and wrong dNTP substrates with steady state and pre-steady state kinetics," *Biochemistry*, vol. 49, no. 1, pp. 20–28, 2010.
- [54] S. Doublé, S. Tabor, A. M. Long, C. C. Richardson, and T. Ellenberger, "Crystal structure of a bacteriophage T7 DNA replication complex at 2.2 Å resolution," *Nature*, vol. 391, no. 6664, pp. 251–258, 1998.
- [55] Y.-S. Lee, W. D. Kennedy, and Y. W. Yin, "Structural insight into processive human mitochondrial DNA synthesis and disease-related polymerase mutations," *Cell*, vol. 139, no. 2, pp. 312–324, 2009.
- [56] M. C. Franklin, J. Wang, and T. A. Steitz, "Structure of the replicating complex of a pol  $\alpha$  family DNA polymerase," *Cell*, vol. 105, no. 5, pp. 657–667, 2001.
- [57] S. Liu, J. D. Knafels, J. S. Chang et al., "Crystal structure of the herpes simplex virus 1 DNA polymerase," *Journal of Biological Chemistry*, vol. 281, no. 26, pp. 18193–18200, 2006.
- [58] M. K. Swan, R. E. Johnson, L. Prakash, S. Prakash, and A. K. Aggarwal, "Structural basis of high-fidelity DNA synthesis by yeast DNA polymerase  $\delta$ ," *Nature Structural and Molecular Biology*, vol. 16, no. 9, pp. 979–986, 2009.
- [59] S. Moran, R. X.-F. Ren, and E. T. Kool, "A thymidine triphosphate shape analog lacking Watson-Crick pairing ability is replicated with high sequence selectivity," *Proceedings of the National Academy of Sciences of the United States of America*, vol. 94, no. 20, pp. 10506–10511, 1997.
- [60] M. F. Goodman, "Hydrogen bonding revisited: geometric selection as a principal determinant of DNA replication fidelity," *Proceedings of the National Academy of Sciences of the United States of America*, vol. 94, no. 20, pp. 10493–10495, 1997.
- [61] L. S. Beese, V. Derbyshire, and T. A. Steitz, "Structure of DNA polymerase I Klenow fragment bound to duplex DNA," *Science*, vol. 260, no. 5106, pp. 352–355, 1993.
- [62] S. S. Patel, "Pre-steady-state kinetic analysis of processive DNA replication including complete characterization of an exonuclease-deficient mutant," *Biochemistry*, vol. 30, no. 2, pp. 511–525, 1991.
- [63] A. A. Johnson and K. A. Johnson, "Fidelity of nucleotide incorporation by human mitochondrial DNA polymerase," *Journal of Biological Chemistry*, vol. 276, no. 41, pp. 38090–38096, 2001.
- [64] M. Chaudhuri, L. Song, and D. S. Parris, "The herpes simplex virus type 1 DNA polymerase processivity factor increases fidelity without altering pre-steady-state rate constants for polymerization or excision," *Journal of Biological Chemistry*, vol. 278, no. 11, pp. 8996–9004, 2003.
- [65] Y.-C. Tsai and K. A. Johnson, "A new paradigm for DNA polymerase specificity," *Biochemistry*, vol. 45, no. 32, pp. 9675–9687, 2006.
- [66] B.-L. Zhou, J. D. Pata, and T. A. Steitz, "Crystal structure of a DinB lesion bypass DNA polymerase catalytic fragment reveals a classic polymerase catalytic domain," *Molecular Cell*, vol. 8, no. 2, pp. 427–437, 2001.
- [67] W. Yang, "Portraits of a Y-family DNA polymerase," *FEBS Letters*, vol. 579, no. 4, pp. 868–872, 2005.
- [68] J. Trincão, R. E. Johnson, C. R. Escalante, S. Prakash, L. Prakash, and A. K. Aggarwal, "Structure of the catalytic core of *S. cerevisiae* DNA polymerase  $\eta$ : implications for translesion DNA synthesis," *Molecular Cell*, vol. 8, no. 2, pp. 417–426, 2001.
- [69] H. Ling, F. Boudsocq, R. Woodgate, and W. Yang, "Crystal structure of a Y-family DNA polymerase in action: a

- mechanism for error-prone and lesion-bypass replication," *Cell*, vol. 107, no. 1, pp. 91–102, 2001.
- [70] T. A. Kunkel, L. A. Loeb, and M. F. Goodman, "On the fidelity of DNA replication. The accuracy of T4 DNA polymerases in copying  $\phi$ X174 DNA in vitro," *Journal of Biological Chemistry*, vol. 259, no. 3, pp. 1539–1545, 1984.
- [71] L. C. Kroutil, K. Register, K. Bebenek, and T. A. Kunkel, "Exonucleolytic proofreading during replication of repetitive DNA," *Biochemistry*, vol. 35, no. 3, pp. 1046–1053, 1996.
- [72] L. C. Kroutil, M. West Frey, B. F. Kaboord, T. A. Kunkel, and S. J. Benkovic, "Effect of accessory proteins on T4 DNA polymerase replication fidelity," *Journal of Molecular Biology*, vol. 278, no. 1, pp. 135–146, 1998.
- [73] M. W. Frey, N. G. Nossal, T. L. Capson, and S. J. Benkovic, "Construction and characterization of a bacteriophage T4 DNA polymerase deficient in 3' → 5' exonuclease activity," *Proceedings of the National Academy of Sciences of the United States of America*, vol. 90, no. 7, pp. 2579–2583, 1993.
- [74] L. B. Bloom, X. Chen, D. K. Fygenon, J. Turner, M. O'Donnell, and M. F. Goodman, "Fidelity of *Escherichia coli* DNA polymerase III holoenzyme: the effects of  $\beta$ ,  $\gamma$  complex processivity proteins and  $\epsilon$  proofreading exonuclease on nucleotide misincorporation efficiencies," *Journal of Biological Chemistry*, vol. 272, no. 44, pp. 27919–27930, 1997.
- [75] L. Song, M. Chaudhuri, C. W. Knopf, and D. S. Parris, "Contribution of the 3' → 5'-exonuclease activity of herpes simplex virus type 1 DNA polymerase to the fidelity of DNA synthesis," *Journal of Biological Chemistry*, vol. 279, no. 18, pp. 18535–18543, 2004.
- [76] M. J. Longley, D. Nguyen, T. A. Kunkel, and W. C. Copeland, "The fidelity of human DNA polymerase  $\gamma$  with and without exonucleolytic proofreading and the p55 accessory subunit," *Journal of Biological Chemistry*, vol. 276, no. 42, pp. 38555–38562, 2001.
- [77] C. M. Joyce, "How DNA travels between the separate polymerase and 3'-5'-exonuclease sites of DNA polymerase I (Klenow fragment)," *Journal of Biological Chemistry*, vol. 264, no. 18, pp. 10858–10866, 1989.
- [78] J. W. Hanes, Y. Zhu, D. S. Parris, and K. A. Johnson, "Enzymatic therapeutic index of acyclovir: viral versus human polymerase  $\gamma$  specificity," *Journal of Biological Chemistry*, vol. 282, no. 34, pp. 25159–25167, 2007.
- [79] Y. Zhu, L. Song, J. Stroud, and D. S. Parris, "Mechanisms by which herpes simplex virus DNA polymerase limits translesion synthesis through abasic sites," *DNA Repair*, vol. 7, no. 1, pp. 95–107, 2008.
- [80] L. Song, *The role of the associated 3' to 5' exonuclease activity and processivity factor (UL42) of herpes simplex virus type 1 DNA polymerase on the fidelity of DNA replication*, Ph.D. dissertation, The Ohio State University, Columbus, Ohio, USA, 2004.
- [81] Y. Shamoo and T. A. Steitz, "Building a replisome from interacting pieces: Sliding clamp complexed to a peptide from DNA polymerase and a polymerase editing complex," *Cell*, vol. 99, no. 2, pp. 155–166, 1999.
- [82] J. Wang, A. K. M. A. Sattar, C. C. Wang, J. D. Karam, W. H. Konigsberg, and T. A. Steitz, "Crystal structure of a pol  $\alpha$  family replication DNA polymerase from bacteriophage RB69," *Cell*, vol. 89, no. 7, pp. 1087–1099, 1997.
- [83] M. Hogg, P. Aller, W. Konigsberg, S. S. Wallace, and S. Doublié, "Structural and biochemical investigation of the role in proofreading of a  $\beta$  hairpin loop found in the exonuclease domain of a replicative DNA polymerase of the B family," *Journal of Biological Chemistry*, vol. 282, no. 2, pp. 1432–1444, 2007.
- [84] E. Fidalgo da Silva and L. J. Reha-Krantz, "DNA polymerase proofreading: active site switching catalyzed by the bacteriophage T4 DNA polymerase," *Nucleic Acids Research*, vol. 35, no. 16, pp. 5452–5463, 2007.
- [85] Y. Zhu, K. S. Trego, L. Song, and D. S. Parris, "3' to 5' exonuclease activity of herpes simplex virus type 1 DNA polymerase modulates its strand displacement activity," *Journal of Virology*, vol. 77, no. 18, pp. 10147–10153, 2003.
- [86] Y. H. Jin, R. Obert, P. M. J. Burgers, T. A. Kunkel, M. A. Resnick, and D. A. Gordenin, "The 3' → 5' exonuclease of DNA polymerase  $\delta$  can substitute for the 5' flap endonuclease Rad27/Fen1 in processing Okazaki fragments and preventing genome instability," *Proceedings of the National Academy of Sciences of the United States of America*, vol. 98, no. 9, pp. 5122–5127, 2001.
- [87] Y. H. Jin, R. Ayyagari, M. A. Resnick, D. A. Gordenin, and P. M. J. Burgers, "Okazaki fragment maturation in yeast: II. Cooperation between the polymerase and 3'-5'-exonuclease activities of Pol  $\delta$  in the creation of a ligatable nick," *Journal of Biological Chemistry*, vol. 278, no. 3, pp. 1626–1633, 2003.
- [88] M. E. Arana, L. Song, N. T. Le Gac, D. S. Parris, G. Villani, and P. E. Boehmer, "On the role of proofreading exonuclease in bypass of a 1,2 d(GpG) cisplatin adduct by the herpes simplex virus-1 DNA polymerase," *DNA Repair*, vol. 3, no. 6, pp. 659–669, 2004.
- [89] V. Khare and K. A. Eckert, "The proofreading 3' → 5' exonuclease activity of DNA polymerases: a kinetic barrier to translesion DNA synthesis," *Mutation Research*, vol. 510, no. 1-2, pp. 45–54, 2002.
- [90] D. J. Mozzherin, S. Shibutani, C.-K. Tan, K. M. Downey, and P. A. Fisher, "Proliferating cell nuclear antigen promotes DNA synthesis past template lesions by mammalian DNA polymerase  $\delta$ ," *Proceedings of the National Academy of Sciences of the United States of America*, vol. 94, no. 12, pp. 6126–6131, 1997.
- [91] G. Blanca, E. Delagoutte, N. Tanguy Le Gac, N. P. Johnson, G. Baldacci, and G. Villani, "Accessory proteins assist exonuclease-deficient bacteriophage T4 DNA polymerase in replicating past an abasic site," *Biochemical Journal*, vol. 402, no. 2, pp. 321–329, 2007.
- [92] D. T. Minnick, M. Astatke, C. M. Joyce, and T. A. Kunkel, "A thumb subdomain mutant of the large fragment of *Escherichia coli* DNA polymerase I with reduced DNA binding affinity, processivity, and frameshift fidelity," *Journal of Biological Chemistry*, vol. 271, no. 40, pp. 24954–24961, 1996.
- [93] K. Hashimoto, K. Shimizu, N. Nakashima, and A. Sugino, "Fidelity of DNA polymerase  $\delta$  holoenzyme from *Saccharomyces cerevisiae*: the sliding clamp proliferating cell nuclear antigen decreases its fidelity," *Biochemistry*, vol. 42, no. 48, pp. 14207–14213, 2003.
- [94] S. S. Daube, G. Tomer, and Z. Livneh, "Translesion replication by DNA polymerase  $\delta$  depends on processivity accessory proteins and differs in specificity from DNA polymerase  $\beta$ ," *Biochemistry*, vol. 39, no. 2, pp. 348–355, 2000.
- [95] C. A. Wu, N. J. Nelson, D. J. McGeoch, and M. D. Challberg, "Identification of herpes simplex virus type 1 genes required for origin-dependent DNA synthesis," *Journal of Virology*, vol. 62, no. 2, pp. 435–443, 1988.
- [96] S. W. Wong, A. F. Wahl, P. M. Yuan et al., "Human DNA polymerase alpha gene expression is cell proliferation

- dependent and its primary structure is similar to both prokaryotic and eukaryotic replicative DNA polymerases," *EMBO Journal*, vol. 7, no. 1, pp. 37–47, 1988.
- [97] D. J. M. Purifoy, R. B. Lewis, and K. L. Powell, "Identification of the herpes simplex virus DNA polymerase gene," *Nature*, vol. 269, no. 5629, pp. 621–623, 1977.
- [98] A. I. Marcy, D. R. Yager, and D. M. Coen, "Isolation and characterization of herpes simplex virus mutants containing engineered mutations at the DNA polymerase locus," *Journal of Virology*, vol. 64, no. 5, pp. 2208–2216, 1990.
- [99] C. W. Knopf, "Evolution of viral DNA-dependent DNA polymerases," *Virus Genes*, vol. 16, no. 1, pp. 47–58, 1998.
- [100] J. T. Jofre, P. A. Schaffer, and D. S. Parris, "Genetics of resistance to phosphonoacetic acid in strain KOS of herpes simplex virus type 1," *Journal of Virology*, vol. 23, no. 3, pp. 833–836, 1977.
- [101] M. Falkenberg, I. R. Lehman, and P. Elias, "Leading and lagging strand DNA synthesis in vitro by a reconstituted herpes simplex virus type 1 replisome," *Proceedings of the National Academy of Sciences of the United States of America*, vol. 97, no. 8, pp. 3896–3900, 2000.
- [102] A. I. Marcy, P. D. Olivo, M. D. Challberg, and D. M. Coen, "Enzymatic activities of overexpressed herpes simplex virus DNA polymerase purified from recombinant baculovirus-infected insect cells," *Nucleic Acids Research*, vol. 18, no. 5, pp. 1207–1215, 1990.
- [103] K. W. Knopf, "Properties of herpes simplex virus DNA polymerase and characterization of its associated exonuclease activity," *European Journal of Biochemistry*, vol. 98, no. 1, pp. 231–244, 1979.
- [104] J. Gottlieb, A. I. Marcy, D. M. Coen, and M. D. Challberg, "The herpes simplex virus type 1 UL42 gene product: a subunit of DNA polymerase that functions to increase processivity," *Journal of Virology*, vol. 64, no. 12, pp. 5976–5987, 1990.
- [105] M. L. Gallo, D. H. Jackwood, M. Murphy, H. S. Marsden, and D. S. Parris, "Purification of the herpes simplex virus type 1 65-kilodalton DNA-binding protein: properties of the protein and evidence of its association with the virus-encoded DNA polymerase," *Journal of Virology*, vol. 62, no. 8, pp. 2874–2883, 1988.
- [106] J. J. Crute and I. R. Lehman, "Herpes simplex-1 DNA polymerase. Identification of an intrinsic 5' → 3' exonuclease with ribonuclease H activity," *Journal of Biological Chemistry*, vol. 264, no. 32, pp. 19266–19270, 1989.
- [107] T. R. Hernandez and I. R. Lehman, "Functional interaction between the herpes simplex-1 DNA polymerase and UL42 protein," *Journal of Biological Chemistry*, vol. 265, no. 19, pp. 11227–11232, 1990.
- [108] M. L. Gallo, D. I. Dorsky, C. S. Crumpacker, and D. S. Parris, "The essential 65-kilodalton DNA-binding protein of herpes simplex virus stimulates the virus-encoded DNA polymerase," *Journal of Virology*, vol. 63, no. 12, pp. 5023–5029, 1989.
- [109] H. J. Zuccola, D. J. Filman, D. M. Coen, and J. M. Hogle, "The crystal structure of an unusual processivity factor, herpes simplex virus UL42, bound to the C terminus of its cognate polymerase," *Molecular Cell*, vol. 5, no. 2, pp. 267–278, 2000.
- [110] T. S. R. Krishna, X.-P. Kong, S. Gary, P. M. Burgers, and J. Kuriyan, "Crystal structure of the eukaryotic DNA polymerase processivity factor PCNA," *Cell*, vol. 79, no. 7, pp. 1233–1244, 1994.
- [111] J. Gottlieb and M. D. Challberg, "Interaction of herpes simplex virus type 1 DNA polymerase and the UL42 accessory protein with a model primer template," *Journal of Virology*, vol. 68, no. 8, pp. 4937–4945, 1994.
- [112] B. Roizman and M. Tognon, "Restriction endonuclease patterns of herpes simplex virus DNA: application to diagnosis and molecular epidemiology," *Current Topics in Microbiology and Immunology*, vol. 104, pp. 273–286, 1983.
- [113] B. Roizman and T. Buchman, "The molecular epidemiology of herpes simplex viruses," *Hospital Practice*, vol. 14, no. 1, pp. 94–104, 1979.
- [114] E. Kudo, H. Shiota, T. Naito, K. Satake, and M. Itakura, "Polymorphisms of thymidine kinase gene in herpes simplex virus type 1: analysis of clinical isolates from herpetic keratitis patients and laboratory strains," *Journal of Medical Virology*, vol. 56, no. 2, pp. 151–158, 1998.
- [115] D. S. Parris and J. E. Harrington, "Herpes simplex virus variants resistant to high concentrations of acyclovir exist in clinical isolates," *Antimicrobial Agents and Chemotherapy*, vol. 22, no. 1, pp. 71–77, 1982.
- [116] Y. T. Hwang, B. U.-Y. Liu, D. M. Coen, and C. B. C. Hwang, "Effects of mutations in the exo III motif of the herpes simplex virus DNA polymerase gene on enzyme activities, viral replication, and replication fidelity," *Journal of Virology*, vol. 71, no. 10, pp. 7791–7798, 1997.
- [117] J. D. Hall, K. L. Orth, K. L. Sander, B. M. Swihart, and R. A. Senese, "Mutations within conserved motifs in the 3'-5' exonuclease domain of herpes simplex virus DNA polymerase," *Journal of General Virology*, vol. 76, no. 12, pp. 2999–3008, 1995.
- [118] J. S. Gibbs, K. Weisshart, P. Digard, A. DeBruynkops, D. M. Knipe, and D. M. Coen, "Polymerization activity of an  $\alpha$ -like DNA polymerase requires a conserved 3'-5' exonuclease active site," *Molecular and Cellular Biology*, vol. 11, no. 9, pp. 4786–4795, 1991.
- [119] F. J. P. Kühn and C. W. Knopf, "Herpes simplex virus type 1 DNA polymerase: mutational analysis of the 3'-5'-exonuclease domain," *Journal of Biological Chemistry*, vol. 271, no. 46, pp. 29245–29254, 1996.
- [120] C. Jiang, G. Komazin-Meredith, W. Tian, D. M. Coen, and C. B. C. Hwang, "Mutations that increase DNA binding by the processivity factor of herpes simplex virus affect virus production and DNA replication fidelity," *Journal of Virology*, vol. 83, no. 15, pp. 7573–7580, 2009.
- [121] C. Jiang, Y. T. Hwang, J. C. W. Randell, D. M. Coen, and C. B. C. Hwang, "Mutations that decrease DNA binding of the processivity factor of the herpes simplex virus DNA polymerase reduce viral yield, alter the kinetics of viral DNA replication, and decrease the fidelity of DNA replication," *Journal of Virology*, vol. 81, no. 7, pp. 3495–3502, 2007.
- [122] J. E. Reardon and T. Spector, "Herpes simplex virus type 1 DNA polymerase. Mechanism of inhibition by acyclovir triphosphate," *Journal of Biological Chemistry*, vol. 264, no. 13, pp. 7405–7411, 1989.
- [123] R. O. Baker and J. D. Hall, "Impaired mismatch extension by a herpes simplex DNA polymerase mutant with an editing nuclease defect," *Journal of Biological Chemistry*, vol. 273, no. 37, pp. 24075–24082, 1998.
- [124] F. Bogani and P. E. Boehmer, "The replicative DNA polymerase of herpes simplex virus 1 exhibits apurinic/aprimidinic and 5'-deoxyribose phosphate lyase activities," *Proceedings of the National Academy of Sciences of the United States of America*, vol. 105, no. 33, pp. 11709–11714, 2008.
- [125] W. Tian, Y. T. Hwang, Q. Lu, and C. B. C. Hwang, "Finger domain mutation affects enzyme activity, DNA replication efficiency, and fidelity of an exonuclease-deficient DNA

polymerase of herpes simplex virus type 1," *Journal of Virology*, vol. 83, no. 14, pp. 7194–7201, 2009.

- [126] W. Tian, Y. T. Hwang, and C. B. C. Hwang, "The enhanced DNA replication fidelity of a mutant herpes simplex virus type 1 DNA polymerase is mediated by an improved nucleotide selectivity and reduced mismatch extension ability," *Journal of Virology*, vol. 82, no. 17, pp. 8937–8941, 2008.

## Review Article

# Mechanistic Studies with DNA Polymerases Reveal Complex Outcomes following Bypass of DNA Damage

Robert L. Eoff,<sup>1</sup> Jeong-Yun Choi,<sup>2</sup> and F. Peter Guengerich<sup>1</sup>

<sup>1</sup>Department of Biochemistry and Center in Molecular Toxicology, Vanderbilt University School of Medicine, 638 Robinson Research Building, 2200 Pierce Avenue, Nashville, TN 37232-0146, USA

<sup>2</sup>Department of Pharmacology, School of Medicine, Ewha Womans University, Seoul 158-710, Republic of Korea

Correspondence should be addressed to F. Peter Guengerich, f.guengerich@vanderbilt.edu

Received 6 May 2010; Accepted 12 August 2010

Academic Editor: Ashis Basu

Copyright © 2010 Robert L. Eoff et al. This is an open access article distributed under the Creative Commons Attribution License, which permits unrestricted use, distribution, and reproduction in any medium, provided the original work is properly cited.

DNA is a chemically reactive molecule that is subject to many different covalent modifications from sources that are both endogenous and exogenous in origin. The inherent instability of DNA is a major obstacle to genomic maintenance and contributes in varying degrees to cellular dysfunction and disease in multi-cellular organisms. Investigations into the chemical and biological aspects of DNA damage have identified multi-tiered and overlapping cellular systems that have evolved as a means of stabilizing the genome. One of these pathways supports DNA replication events by in a sense adopting the mantra that one must “make the best of a bad situation” and tolerating covalent modification to DNA through less accurate copying of the damaged region. Part of this so-called DNA damage tolerance pathway involves the recruitment of specialized DNA polymerases to sites of stalled or collapsed replication forks. These enzymes have unique structural and functional attributes that often allow bypass of adducted template DNA and successful completion of genomic replication. What follows is a selective description of the salient structural features and bypass properties of specialized DNA polymerases with an emphasis on Y-family members.

## 1. Introduction

The ability to replicate covalently modified or “damaged” DNA and unusual secondary structures in template DNA (i.e., non-B DNA conformations) is critical to the survival and evolution of all biological systems. Highly accurate B-family DNA polymerases are the primary means of replicating eukaryotic genomes with few mistakes (e.g., error rates of  $10^{-4}$ – $10^{-7}$ ), although subsequent mismatch repair activity improves the fidelity of replication about 100-fold. Covalent modification of nucleic acids can disrupt normal replication processing of the heritable material. Of course, damage to DNA can be recognized and removed from the genome prior to replication but this repair capacity is not perfect and lesions do persist in the genome during S-phase. Damage signals that occur during replication (S-phase) and postreplication (G2/M phase) can activate signaling pathways that ultimately recruit a set of specialized DNA polymerases to the replication fork. These enzymes provide the cell with a means of “tolerating” the modified residue

by catalyzing DNA synthesis opposite a number of different lesions, as well as non-B form DNA secondary structures that can inhibit normal replication. The outcome of this specialized DNA synthesis reaction can be accurate and promote cell survival or it can be mutagenic, which often proves deleterious to cellular homeostasis. A precise description of how bypass polymerases from different organisms function to tolerate damage to the genome is a fundamental aspect of understanding mechanisms of mutagenesis. We describe results that have helped define the potential ramifications of certain DNA lesions to the replication machinery.

Life is dependent upon accurate replication or “copying” of DNA by enzymes called DNA polymerases [1–3]. The same chemical reaction is utilized to replicate the genome of all organisms studied to date, namely, nucleophilic attack of a deprotonated 3'-oxygen atom on the primer terminus upon the  $\alpha$ -phosphate of an incoming dNTP [4]. Related organisms tend to share more similarities in terms of the enzymes and proteins associated with copying DNA, with some features more highly conserved than others. Enzymatic

redundancy with functional distinction and complex pathway overlap are overarching themes describing how cells tolerate DNA damage [5, 6]. A careful balance is needed to ensure that mechanisms primarily retained to “protect” the genome do not result in unnecessary mutagenic events and/or cell death.

Numerous types of chemical modifications to DNA have been identified (Figure 1) and many agents that are known to damage DNA are also carcinogens [8, 9]. Biochemical analysis of DNA polymerase activity has shown that these enzymes utilize a series of molecular checkpoints that typically promote formation of “Watson-Crick” base pairing geometry and, therefore, stable propagation of DNA [10]. One can easily imagine that changing the chemical structure of DNA will alter the catalytic properties of DNA polymerases. Some DNA polymerases show less tolerance to covalent modification of DNA, including the B-family DNA polymerases such as, pols  $\delta$  and  $\epsilon$ , both of which possess exonuclease activity. These enzymes are able to bypass certain DNA lesions [11, 12] and this bypass activity probably bears relevance towards what occurs *in vivo* (Figure 2). When considering translesion DNA synthesis in general, it is believed that nonessential DNA polymerases, such as the Y-family, perform bypass more efficiently than the so-called “high fidelity” exonuclease containing enzymes. The most important questions to ask related to DNA adduct bypass pertain to how the presence of DNA adducts produce changes in nucleotide selectivity (i.e., fidelity) due to altered structural features and/or changes in catalytic rate constants for individual DNA polymerases. Most research on translesion DNA synthesis attempts to focus on DNA modifications that have been correlated with increased mutagenesis and/or the manifestation of disease [13]. Much of the work done during the last decade has focused on understanding how nonessential polymerases, most of which do not possess exonuclease activity, catalyze DNA synthesis opposite damaged DNA [14]. Numerous exemplary efforts from the groups of Woodgate, W. Yang, Friedberg, Lehmann, Loeb, Geacintov, Levneh, Nohmi, Walker, Goodman, the Prakashes, Burgers, Lloyd, and Kunkel and our long-time collaborators at Vanderbilt—M. Egli, C. J. Rizzo, L. J. Marnett, T. M. Harris, and M. P. Stone—to name a few individuals have increased our understanding of translesion DNA synthesis in tremendous ways. Of the nonessential pols studied to date, the Y-family DNA polymerases seem to be the primary means of tolerating genotoxic insults through direct bypass of adducts during S-phase and the G2/M phase transition, although the B-family members pol II and pol  $\xi$  also play important roles in prokaryotic and eukaryotic cells, respectively. While the activity of nonessential or “specialized” DNA polymerases can suppress damage-induced mutagenesis [15], this suppression at sites of damage can still lead to nontargeted mutations elsewhere [16]. Indeed, the misregulation of their activity is believed to participate in mutagenic events and antagonistic pleiotropy associated with tumorigenesis and aging because they do not possess exonuclease “proofreading” ability and they are generally more likely to make mistakes on undamaged template DNA (Figure 2) [17–24]. These specialized DNA

polymerases generally share the following attributes: (i) they possess no intrinsic exonuclease activity (except for pol II), (ii) they have spacious active sites with fewer structural and kinetic checks upon the nascent base pair, (iii) they exhibit reduced processivity, (iv) the error rates with unmodified template DNA are higher than for replicative counterparts, and (v) there are damage-inducible signaling pathways that recruit them to replication foci. Structurally speaking, the overall domain architecture of Y-family DNA polymerases is similar to that of other polymerases, including B-family members (Figure 2). However, there are several important differences that are obvious from the crystal structures. For example, the active site of Y-family DNA polymerases is much larger and more exposed to solvent than B-family counterparts. The Y-family also possesses the unique “little finger” domain, as well as N-terminal extensions such as the N-digit of REV1 and the N-clasp of human pol  $\kappa$  [14]. Some elements of so-called translesion or specialized DNA synthesis events are relatively clear now. For example, the genetic, biological, and biochemical data supporting the pre-eminent importance of human pol  $\eta$  in the largely accurate bypass of UV-induced cyclobutane pyrimidine dimers (CPDs) is very strong [25–28]. Still, there remain many outstanding questions of interest related to mechanisms that promote DNA damage tolerance. Following is a summary of the literature concerning how these specialized DNA polymerases perform synthesis across DNA adducts.

## 2. Bypass of Abasic Sites and Small Oxidative Lesions

Perhaps the most prevalent form of genetic insult in cells is loss of a purine/pyrimidine base to generate an abasic site (Figure 1(a)) [29, 30]. Generation of abasic sites can occur enzymatically through the action of glycosylases, from spontaneous hydrolysis at the glycosidic bond or from reactions with exogenous chemical agents [31, 32]. Abasic sites provide no purinic or pyrimidinic moiety for DNA polymerases to use as a template during replication. Naturally occurring deoxyribose abasic sites exist in equilibrium between the ring-closed  $\alpha$ - and  $\beta$ -hemiacetals (99%) and ring-opened aldehyde or hydrated aldehyde (<1%), which has led to the common practice of studying a stable tetrahydrofuran (THF) moiety instead of a true abasic site. Mechanistic studies with the THF analogue (of natural abasic sites) highlight the concept that if the enzyme does not encounter a base then the normal catalytic pathway is diverted into a chemical path that generally results in the incorporation of dATP opposite the THF abasic site (i.e., the “A-rule”) [33]. In *Escherichia coli* cells, pol V appears to provide the most efficient means of bypassing abasic THF sites, with insertion of dATP being the preferred catalytic event [34]. In contrast to events in *E. coli*, eukaryotic cells appear to rely upon a combination of DNA polymerases to bypass abasic moieties. DNA polymerases  $\delta$  and REV1, in combination with pol  $\xi$ , bypass abasic sites *in vitro* and *in vivo* [35, 36]. Recently, yeast pol  $\epsilon$  was reported to bypass abasic sites *in vitro* [37]. Dpo4 inserts dATP opposite the THF moiety

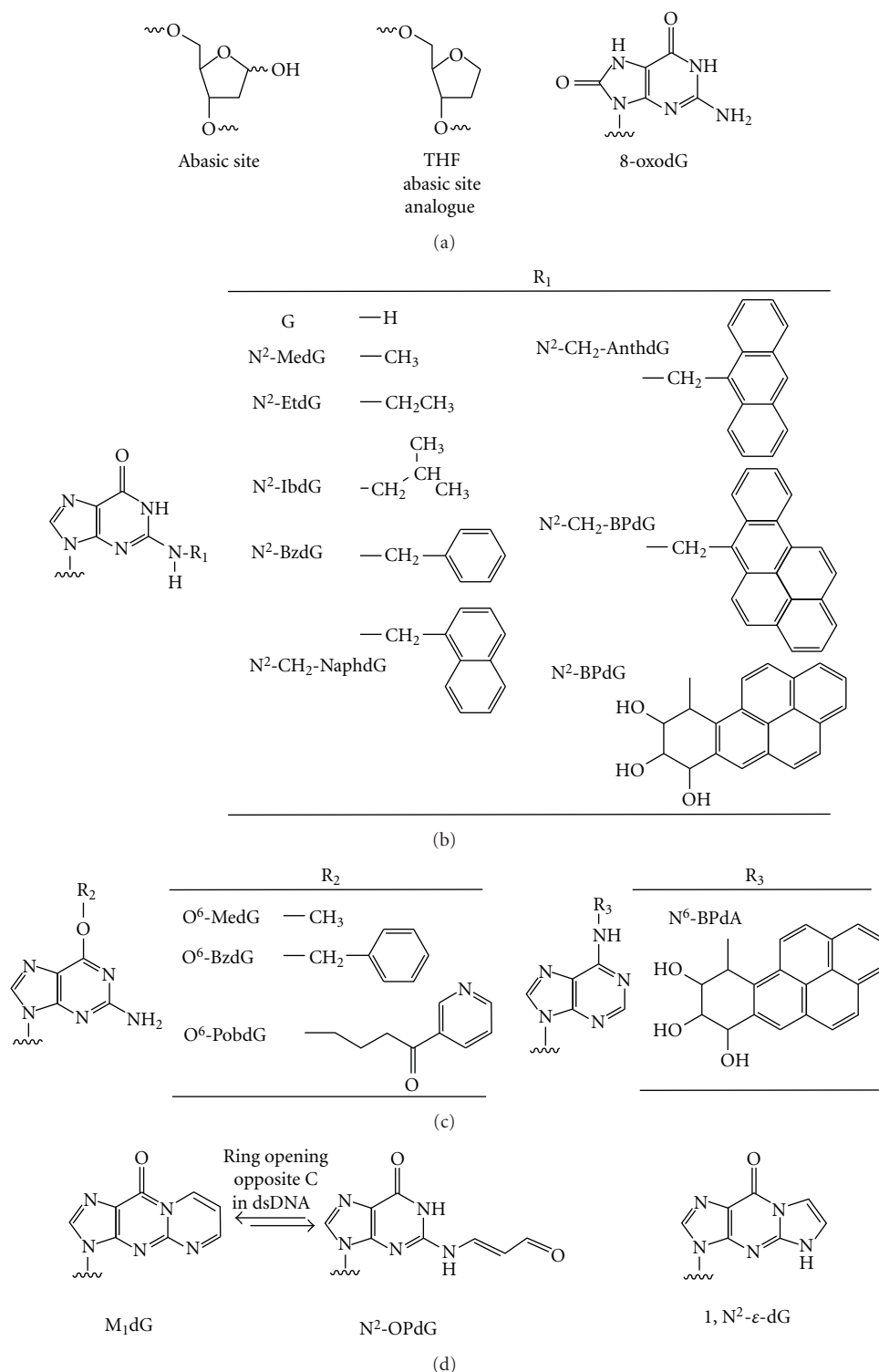


FIGURE 1: Overview of DNA adducts. The number of DNA adducts formed through interactions with reactive chemicals or ionizing radiation is vast, and more thorough reviews have been performed elsewhere [7]. We have chosen to focus on some of the most thoroughly studied DNA adducts, in terms of how the adduct affects DNA polymerase structure and function. A, abasic sites and 8-oxodG; B, minor groove N<sup>2</sup>-dG adducts; C, major groove O<sup>6</sup>-dG and N<sup>6</sup>-dA adducts; D, exocyclic dG adducts. Adduct stereospecificity is not shown in structures of B[a]P DNA adducts.

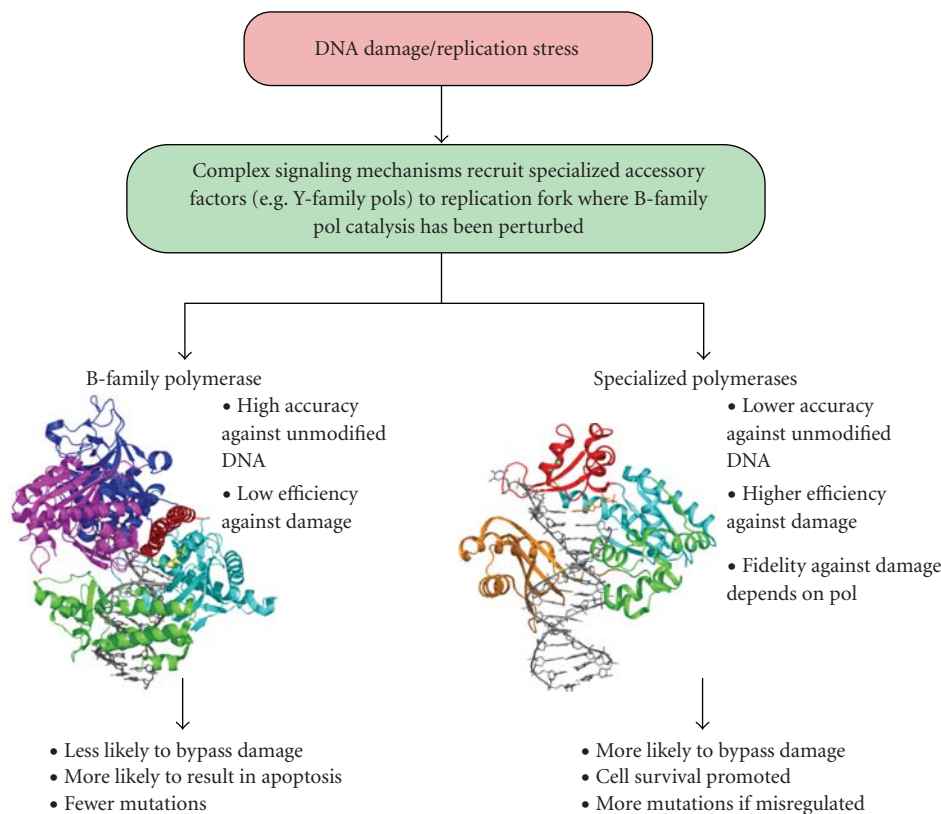


FIGURE 2: Schematic overview of DNA damage tolerance and two families of DNA polymerases that are partitioned at the replication fork during translesion DNA synthesis. Genotoxic insults can lead to damage that stalls or slows the replication fork. Signaling through the ATM and ATR kinases leads to the recruitment of nonessential “bypass” polymerases. The Y-family pols appear to be the primary means of synthesizing past DNA lesions at stalled or collapsed replication forks but misregulation of these enzymes can lead to events that promote mutagenesis and ultimately tumorigenesis. The exquisite regulation of Y-family DNA polymerases is vital to cellular survival in the face of DNA damage and in the prevention excessive mutagenesis. Two DNA polymerase structures are shown, that of the catalytic subunit of the B-family member yeast pol  $\delta$  in ternary complex with 12/16-mer DNA (gray) and an incoming dCTP (yellow) (pdb id code 3IAY; [42]). The Y-family polymerase Dpo4 from *S. solfataricus* is also shown in ternary complex with 13/18-mer DNA (gray) and an incoming ddATP (pdb id code 1JX4; [43]). Both enzymes possess the core the palm (cyan), finger (red), and thumb (green) domains. Pol  $\delta$  also has a 3' to 5' exonuclease domain (magenta), as well as the N-terminal domain (dark blue). The little finger domain (orange) is unique to the Y-family.

with  $\sim 100$ -fold reduction in catalytic efficiency [38]. Both human and yeast pol  $\eta$  preferentially insert dGTP opposite THF with a large ( $\sim 10^3$ ) decrease in efficiency, but the preference for dGTP is only very small for human  $\eta$ , as dATP insertion opposite THF is about the same as dGTP [39]. Human pol  $\kappa$  catalytic efficiency decreases  $\sim 10^4$  when attempting to insert opposite THF, although the addition of accessory factors such as PCNA, RFC, and RPA increases the efficiency  $\sim 40$ -fold [40]. Human pol  $\iota$  inserts either dGTP or dTTP opposite THF with  $\sim 10$ -fold reduction in efficiency [41].

One issue with the THF studies is that bypass of natural abasic sites involves primarily accurate bypass (the “C-rule”), which appears to depend on the action of REV1 (Figure 3) [44]. Because depurination is much more frequent than depyrimidination and guanine is the base more likely to depurinate (generating an abasic site), there is an intellectual attraction to the concept that an enzyme that primarily inserts dCTP (regardless of the template base identity) would

be involved in bypass of abasic sites. This model highlights the role of the deoxycytidyl transferase activity of REV1 in “accurate” bypass of abasic sites. REV1 catalyzes phosphoryl transfer in a protein template-dependent manner by using an arginine residue to pair with dCTP [45]. Consequently, the REV1 enzyme primarily (but not exclusively) catalyzes incorporation of dCTP, regardless of the identity of the template sequence.

Cells are constantly exposed to exogenous and endogenous sources of oxidative damage to DNA [31, 46, 47]. Guanine is the most readily oxidized base in the genome and 7,8-dihydro-8-oxo-2'-deoxyguanosine (8-oxodG) (Figure 1(a)) has long been considered a classical marker of oxidative damage to the genetic code [48]. The 8-oxodG adduct is strongly mutagenic in bacterial and eukaryotic cells, inducing primarily G to T transversions [49]. At least four pathways prevent 8-oxodG adducts or 8-oxodG:A mispairs from accumulating in the eukaryotic genome [50–54]. *In vitro* analysis of DNA and RNA polymerase activity opposite

	Abasic (THF)	8-oxoG	O <sup>6</sup> -MeG	O <sup>6</sup> -BzG	N <sup>2</sup> -MeG	N <sup>2</sup> -BPG	M <sub>1</sub> dG
<i>S. solfataricus</i> Dpo4 • Most likely product • Relative efficiency	• dA insertion or -1 frameshift • Reduced 100x	• dC insertion • Increased 2x	• Mostly dC some dT • Reduced 1000x	• Mostly dC some dT and dA • Reduced 5000x	• dC insertion • Reduced 3x	• dATP slightly preferred • Reduced	• dA insertion or -1 frameshift • Reduced 300x
Human polymerase $\eta$ • Most likely product • Relative efficiency	• dG and dA equal • Reduced 1000x	• dC insertion • Unchanged	• dC and dT equal • Reduced 10x	• dC and dT equal • Reduced 50x	• dC insertion • Reduced 3x	• dA 2-fold better than dC • Reduced 200x	• dATP insertion or -1 frameshift • Reduced 7x
Human polymerase $\iota$ • Most likely product • Relative efficiency	• dG and dT equal • Reduced 100x	• dC insertion • Reduced 6x	• dT insertion • Increased 2x	• dT insertion • Unchanged	• dC 2-fold better than dT • Reduced 10x	• dC and dT equal • Reduced 20x	• dC insertion • Reduced 2x
Human polymerase $\kappa$ • Most likely product • Relative efficiency	• dA insertion • Reduced 10 <sup>4</sup> x	• dATP insertion • Unchanged	• dC and dT equal • Reduced 100x	• dC slightly better than dT • Reduced 900x	• dC insertion • Reduced 3x	• dC insertion • Reduced 25x	• dC insertion • Reduced 30x
Human REV1 • Most likely product • Relative efficiency	• dC insertion • Unchanged	• dC insertion • Reduced 2x	• dC insertion • Reduced 16x	• dC insertion • Reduced 4x	• dC insertion • Reduced 3x	• dC insertion • Unchanged	• dC insertion • Reduced 2x

FIGURE 3: Summary of DNA adduct bypass capabilities for selected DNA polymerases. The table attempts to summarize the effect of different DNA adducts on Y-family DNA polymerase catalytic efficiency and makes note of the most likely dNTP insertion event for each lesion. Please see the main text for the corresponding references.

the lesion has provided some insight into mechanisms of 8-oxodG bypass. In general, most DNA polymerases tested show either a preference for incorrect insertion of dATP or are kinetically indifferent to dCTP or dATP [55–60]. Some notable exceptions to this rule have been documented: (i) *Saccharomyces cerevisiae* DNA polymerase  $\eta$  [61–63] and (ii) Dpo4, the *dinB* homologue from the crenarchaeote *Sulfolobus solfataricus* [64–66]. These enzymes are at least 20-fold more efficient at accurate bypass of 8-oxodG than incorrect insertion of dATP (Figure 3). It is also notable that the fidelity of 8-oxodG bypass by human pols  $\lambda$  and  $\eta$  is increased (100-fold and 27-fold, resp.) by the inclusion of the accessory factors PCNA and RPA [63]. Both human pol  $\iota$  and REV1 perform relatively accurate bypass of 8-oxodG by preferentially inserting dCTP with only moderate loss of efficiency [67, 68].

The apparent functional superiority of Dpo4 and pol  $\eta$  at maintaining genomic integrity during bypass of 8-oxodG is at least partly due to an electrostatic contact between the little finger domain and the O8 atom of 8-oxodG [64]. Crystal structures with Dpo4 in complex with 8-oxodG modified DNA template reveal that Arg-332 forms a hydrogen bond with the O8 atom of 8-oxodG, which apparently stabilizes the normal *anti* conformation around the glycosidic bond and presents the unperturbed Watson-Crick face of the base to the incoming dNTP. Super-imposition of yeast pol  $\eta$  with Dpo4 suggests that Lys-498 may provide a similar function to Arg-332. At the nucleoside level, 8-oxoG preferentially

adopts the *syn* orientation that will present the Hoogsteen edge of the base to the incoming dNTP in the active site of polymerases [69]. The *syn* 8-oxodG:dA pairing mode has been observed for many polymerases, including Dpo4 [55, 66]. However, stabilization of the *anti* mode for 8-oxodG by Dpo4 results in an energy of activation value that is actually lower for Dpo4-catalyzed insertion of dCTP opposite 8-oxodG than dCTP insertion opposite dG, thereby favoring accurate bypass [66].

In contrast to Dpo4, the human DinB homologue pol  $\kappa$  is quite error-prone at bypass of 8-oxoG, preferentially inserting dATP opposite the lesions [70]. There are at least three distinct molecular features that distinguish the activities of Dpo4 and pol  $\kappa$  during insertion opposite 8-oxodG [70]. The first distinction can be found in the little finger residue Arg-332 that stabilizes *anti* 8-oxodG in Dpo4. In pol  $\kappa$  the analogous residue is Leu-508, which obviously cannot mediate electrostatic stabilization of *anti* 8-oxodG. Mutating Leu-508 to lysine shifts the kinetic preference towards accurate insertion of dCTP opposite 8-oxodG. The second distinction resides in the fact that the active site of pol  $\kappa$  is sterically more constrained than Dpo4, especially in considering the residues that form the “roof” over the nascent base pair. Residues Phe-155, Ser-134, Pro-153, Met-135, and Ala-151 from the finger domain of pol  $\kappa$  correspond to Val-62, Gly-41, Pro-60, Ala-42, and Gly-58 in Dpo4. The active site of pol  $\kappa$  only accommodates a single template residue. The third distinction between

pol  $\kappa$  and Dpo4-catalyzed bypass of 8-oxodG is inferred from kinetic and structural differences between these two enzymes. The most striking structural difference between pol  $\kappa$  and Dpo4 is the N-terminal extension called the “N-clasp” in pol  $\kappa$  that is vital to polymerase activity. Dpo4 has no analogous domain. The N-clasp sits atop the DNA binding cleft, encircling the DNA, and serves to stabilize the position of the little finger domain relative to the polymerase core domains. The contacts made between the N-clasp, the finger, and little finger domains are presumably limiting conformational fluctuations near the template DNA binding region. Thus, the more thermodynamically stable *syn* orientation of 8-oxoG will therefore be more difficult to shift back to the *anti* form (i.e., the mode ideal for accurate insertion of dCTP) in the pol  $\kappa$  active site relative to Dpo4.

### 3. Major and Minor Groove DNA Adducts

The site of adduct formation on heterocyclic purine/pyrimidine residues is an important determinant of whether the lesion will be blocking or whether a given polymerase will perform synthesis in an accurate or inaccurate manner. Most replicative DNA polymerases have contacts with the hydrogen bond accepting atoms of purines and pyrimidines on the minor groove portion of the dsDNA (N3 for purines and O2 for pyrimidines) near the active site and are consequently strongly impeded by minor groove adducts [71]. Y-family polymerases do not possess an analogous minor groove check upon base pair geometry, which when combined with a more spacious active site results in a greater ability to tolerate bulky minor groove DNA adducts.

The N2 atom of guanine is located on the minor groove side of double-stranded (ds) DNA and is susceptible to modification by  $\alpha,\beta$ -unsaturated aldehydes such as, acrolein, crotonaldehyde, malondialdehyde, and *trans*-4-hydroxynonenal, as well as oxidation products of heterocyclic aromatic amines (e.g., *N*-hydroxy-2-amino-3-methylimidazo[4,5-*f*]quinoline) and polycyclic aromatic hydrocarbons (e.g., benzo[*a*]pyrene) [72–75]. The effect of minor groove adduct bulk on the kinetics of Y-family or replicative polymerase catalysis has been studied in a systematic manner by increasing the size of a series of dG adducts from N<sup>2</sup>-methyl(Me)dG to N<sup>2</sup>-methylene(6-benzo[*a*]pyrenyl)dG (N<sup>2</sup>-BPdG) (Figure 1(b)) [76–80]. Of course, adducts can also form on the major groove [81]. The effect of adduct size on the major groove side was studied for the Y-family and replicative polymerases using O<sup>6</sup>-(Ar)alkyl-dG adducts ranging in size from O<sup>6</sup>-methyl-dG (O<sup>6</sup>-MedG) to O<sup>6</sup>-pyridyloxobutyl-dG (O<sup>6</sup>-PobdG) (Figure 1(c)) [80, 82].

Kinetic and structural work with the model Y-family DNA polymerase Dpo4 provides an initial framework for understanding bypass of minor groove DNA adducts. Unlike model replicative polymerases (i.e., A- and B-family polymerases from model organisms such as, bacteriophage T7 and RB69), which are severely inhibited by even the small N<sup>2</sup>-MeG adduct, Dpo4 is able to bypass a series

of minor groove adducts with negligible inhibitory effects on catalytic efficiency and moderate effects upon fidelity [83]. Two crystal structures of Dpo4 in complex with the bulky N<sup>2</sup>-methylene(2-naphthyl)-dG (N<sup>2</sup>-CH<sub>2</sub>-Naph-dG) adducted DNA have been reported [83]. Interestingly, the N<sup>2</sup>-CH<sub>2</sub>-Naph-dG adduct was found to adopt two distinct postinsertion orientations in complexes that should be identical. One structure placed N<sup>2</sup>-CH<sub>2</sub>-Naph-dG in the *anti*-orientation, which forces the cytosine residue at the primer terminus out of the active site into the growing minor groove face. The second structure revealed N<sup>2</sup>-CH<sub>2</sub>-Naph-dG rotated into the *syn* orientation, which allows the N4 exocyclic amino group of cytosine to form a bifurcated Hoogsteen pair with the N7 and O6 atoms of N<sup>2</sup>-CH<sub>2</sub>-Naph-dG. Since the fidelity of Dpo4 bypass of N<sup>2</sup>-CH<sub>2</sub>-Naph-dG is only diminished ~2-fold relative to dG, it seems likely that the productive conformation involves the *anti* oriented adduct paired in normal Watson-Crick mode with dCTP and that the crystal structures failed to reveal the true active conformation. These structural results are indicative of the conformational heterogeneity that most likely accompanies many DNA adduct bypass events.

Like Dpo4, all four human Y-family DNA polymerases show fairly remarkable tolerance of minor groove DNA adducts when compared to model replicative enzymes. The efficiency and fidelity of pol  $\eta$  bypass are not reduced much by N<sup>2</sup>-bulk equal to or smaller than the N<sup>2</sup>-CH<sub>2</sub>-Naph-dG adduct, but it is severely perturbed by N<sup>2</sup>-dG adducts larger than a methylene(9-anthracenyl) group in the minor groove [76–78, 80]. REV1 and pol  $\kappa$  provide the most accurate and catalytically tolerant means of bypassing of minor groove bulk at the guanine N<sup>2</sup> atom at least up to a benzo[*a*]pyrene group (N<sup>2</sup>-CH<sub>2</sub>-BPdG) (Figure 3) [76, 80] but probably for different molecular reasons. The REV1 catalytic efficiency ( $k_{\text{cat}}/K_{\text{m,dNTP}}$ ) is barely reduced at all during dCTP insertion opposite N<sup>2</sup>-CH<sub>2</sub>-BPdG relative to dG [80], presumably due to the fact that REV1 uses the N-terminal domain called the “N-digit” to flip the template base out of the polymerase active site, which results in the pairing of dCTP opposite an arginine in the N-digit. Pol  $\kappa$ , on the other hand, is most likely stabilizing the N<sup>2</sup>-(ar)alkyl dG adducts in the minor groove through an interaction with the N-clasp. In contrast to the N-digit of REV1 (which resides on the minor groove side of the DNA binding cleft), the N-clasp sits on top of the polymerase active site [84]. An *in vitro* comparison of pol  $\kappa$ -catalyzed bypass of N<sup>2</sup>-BPdG and N<sup>6</sup>-BPdA adducts clearly showed that the minor groove N<sup>2</sup>-BPdG was bypassed efficiently (regardless of adduct stereochemistry), while N<sup>6</sup>-BPdA was a complete block to pol  $\kappa$  activity [85]. The results from a recent molecular modeling study are consistent with the idea that the N-clasp of pol  $\kappa$  plays a central role in facilitating accurate bypass of N<sup>2</sup>-BPdG adducts [86]. The modeling work suggests that *anti*-oriented N<sup>2</sup>-BPdG is stabilized in the minor groove because there are close contacts with the N-clasp if N<sup>2</sup>-BPdG is positioned in the major groove by adopting the *syn*-orientation. Moreover, there appears to be a phenylalanine residue conserved only in pol  $\kappa$  (Phe-151) and REV1 (Phe-543) that may form base-stacking

interactions with the benzo[*a*]pyrene ring system, favoring minor groove stabilization during accurate bypass of the adduct.

Bypass of major groove O<sup>6</sup>-(Ar)alkyl-dG DNA adducts, at least up to O<sup>6</sup>-benzyl-dG (O<sup>6</sup>-BzdG), is performed efficiently by human pol  $\iota$  (Figure 3) but this reaction is highly error-prone (i.e., insertion of dTTP is the major product for both O<sup>6</sup>-MedG and O<sup>6</sup>-BzdG), and pol  $\iota$  efficiency is decreased 300-fold by O<sup>6</sup>-PobdG [82]. Other DNA polymerases, including pol  $\delta$  (with PCNA), are able to bypass adducts in the major groove but the catalytic efficiency of these events appears to be more perturbed than with pol  $\iota$ . Human replicative pol  $\delta$  (with PCNA) appears to better accommodate and bypass major groove O<sup>6</sup>-BzdG adducts [82] than minor groove N<sup>2</sup>-BzdG adducts [77–80, 82]. In contrast, most of human Y-family DNA polymerases except for pol  $\iota$  can bypass minor groove N<sup>2</sup>-G adducts [76–80] much more efficiently than major groove O<sup>6</sup>-G adducts [82]. Human pol  $\kappa$  was found to be the DNA polymerase most inhibited by the major groove-protruding O<sup>6</sup>-(Ar)alkyl dG adducts, consistent with the N<sup>6</sup>-BPdA results and further suggesting a role for the N-clasp in pol  $\kappa$  functionality. Dpo4 can bypass O<sup>6</sup>-MedG and O<sup>6</sup>-BzdG adducts in a catalytically perturbed (i.e., the efficiency is decreased 14- to 62-fold for each of the adducts) but mostly accurate manner (~70% accurate insertion of dCTP) [87, 88]. The efficiency of Dpo4-catalyzed bypass of bulky N<sup>6</sup>-adenyl polycyclic aromatic hydrocarbon (PAH) adducts is reduced several hundred fold and results in a mixture of error-free and error-prone products [89]. By way of comparison, the high-fidelity bacteriophage T7<sup>-</sup> DNA polymerase is inhibited over 2,000-fold by N<sup>6</sup>-dA-PAH adducts [90]. Crystal structures of Dpo4 in complex with O<sup>6</sup>-(Ar)alkyl-dG modified DNA reveal that accurate bypass of these adducts proceeds through a “wobble” base pairing between dC and the O<sup>6</sup>-(ar)alkyl-dG adduct. Work with the (+)-*trans* and (–)-*trans*-N<sup>6</sup>-BPdA adducts indicated that human pol  $\eta$  was quite efficient at bypassing the (+)-*trans* stereoisomer in what appears to be an accurate manner but was essentially blocked by the (–)-*trans* stereoisomer of the N<sup>6</sup>-BPdA adduct [85]. The exact structural rationale for the results with pol  $\eta$  and major groove dA adducts remains unknown. Interestingly, pol  $\eta$  but not pol  $\iota$  nor  $\kappa$  can copy past O<sup>6</sup>-PobdG [82] as well as the C<sup>8</sup>-dG adduct of 2-amino-3-methylimidazo[4,5-*f*]quinoline (IQ) [61], indicating the versatile bypass activity of pol  $\eta$  past various DNA lesions such as major and minor groove DNA adducts, ring-closed exocyclic DNA adducts (*vide infra*), as well as pyrimidine dimers.

#### 4. Exocyclic DNA Adducts

Exocyclic DNA adducts can be formed through many of the same chemical and biological processes that form major/minor groove adducts, namely, electrophilic lipid oxidation products and products arising from oxidation of DNA [73, 91]. Of particular interest is the 3-(2'-deoxy- $\beta$ -D-erythro-pentofuranosyl)pyrimido[1,2-*a*]purin-10(3*H*)-one (M<sub>1</sub>dG) adduct (Figure 1(d)) arising from exposure to

the bis-electrophile malondialdehyde or base propenals that arise following treatment with chemicals such as bleomycin [92–94]. The M<sub>1</sub>dG adduct has been detected at levels of 5,400 adducts per liver cell in the DNA of healthy humans [95]. This adduct is a particularly insidious impediment to genomic integrity because it can ring-open when paired opposite cytosine in dsDNA [96], which may mask its presence from detection by DNA repair pathways. In single-stranded (ss) DNA, the ring-opened N<sup>2</sup>-oxopropenyl-2'-deoxyguanosine (N<sup>2</sup>-OPdG) form closes to M<sub>1</sub>dG, blocking the Watson-Crick edge of the guanine base. M<sub>1</sub>dG is mutagenic in both bacterial and mammalian cells, producing mainly G to T transversions but also resulting in –1 frameshift deletions [97]. Studies with Y-family DNA polymerases indicate that pol  $\eta$  is the most likely candidate for producing the G to T transversions in mammalian systems (Figure 3) [98]. Both pols  $\iota$  and  $\kappa$  are relatively accurate when bypassing M<sub>1</sub>dG, and while pol  $\kappa$  showed preferential insertion of dCTP there was a strong level of inhibition relative to catalysis opposite dG (Maddukuri, L., Eoff, R.L., Choi, J-Y., Rizzo, C. J., Guengerich, F. P., and Marnett, L.J., *Biochemistry in press*). Crystal structures have been solved with Dpo4 in complex with M<sub>1</sub>dG modified template DNA [99]. Like human pol  $\eta$ , Dpo4 preferentially inserts dATP opposite M<sub>1</sub>dG, although the catalytic efficiency of this reaction is diminished 260- to 430-fold relative to normal insertion of dCTP opposite template dG. The M<sub>1</sub>dG adduct is in the ring-closed form in both Dpo4 ternary structures reported, even though the primer in one complex was designed to pair a 3'-terminal cytosine residue with M<sub>1</sub>dG.

1,N<sup>2</sup>-Etheno ( $\epsilon$ ) dG (Figure 1(d)) is another mutagenic exocyclic DNA adduct formed through the reaction of DNA with reactive chemicals (e.g., epoxides formed from oxidation of vinyl chloride and urethane) and endogenous products of lipid peroxidation [100–103]. The 1,N<sup>2</sup>- $\epsilon$ -dG adduct, like the ring-closed M<sub>1</sub>dG adduct, blocks the Watson-Crick edge of guanine. Similar to M<sub>1</sub>dG bypass, human pols  $\eta$  and  $\iota$  can bypass 1,N<sup>2</sup>- $\epsilon$ -dG and generate misinsertion errors (G and T, resp.), but pol  $\kappa$  was severely inhibited in catalysis [76]. Biochemical studies with Dpo4 showed that the major products arising from bypass of 1,N<sup>2</sup>- $\epsilon$ -dG are dATP misinsertions and –1 frameshift deletions [104]. In the same study, crystal structures revealed that Dpo4 readily skips past the 1,N<sup>2</sup>- $\epsilon$ -dG adduct with no major perturbations to the polymerase active site. A similar so-called “type II” structure was solved for Dpo4 in complex with M<sub>1</sub>dG-containing template DNA [99]. As noted earlier, there are no hydrogen bonds between the purine/pyrimidine rings of the nascent base pair and amino acid side chains in the Dpo4 active site to influence base pair geometry. Recent work has highlighted the importance of base-stacking between the primer-template junction and the nascent base pair during Dpo4-catalyzed generation of –1 frameshift deletions [83]. Presumably the same phenomenon is playing a significant role in determining the outcome of Dpo4-catalyzed bypass of exocyclic DNA adducts and perhaps other Y-family DNA polymerases.

## 5. Summary and Outlook

Many questions remain regarding the biological importance of individual DNA polymerases during bypass of specific DNA lesions. *In vitro* experimentation with purified recombinant enzymes can certainly establish what is possible in nature but may not represent what is most likely to occur *in vivo*. The mechanisms that regulate how and when specialized DNA polymerases gain access to damaged template DNA are complex, and many elements of these pathways remain to be elucidated. Mechanistic studies related to adduct bypass in different sequence contexts might also be very helpful in developing a greater understanding of mutations hotspots and the relationship of mutations to cancer. Finally, the importance of Y-family DNA polymerases in the processing of non-B form DNA is an area of active interest because these types of structures are intimately linked to the manifestation of fragile sites in the genome, as well as in rearrangements that occur in the promoter regions of tumor suppressors and oncogenes.

## Abbreviations

G:	Guanine
A:	Adenine
C:	Cytosine
dG:	2'-deoxyguanosine
THF:	Tetrahydrofuran
8-oxodG:	7,8-dihydro-8-oxo-1'-deoxyguanosine
dNTP:	Deoxynucleoside triphosphate
pol:	DNA polymerase
Dpo4:	<i>Sulfolobus solfataricus</i> DNA Polymerase IV
PCNA:	Proliferating cell nuclear antigen
RFC:	Replication factor C
RPA:	Replication protein A
PAH:	Polycyclic aromatic hydrocarbon
BP:	Benzo[ <i>a</i> ]pyrene
Me:	Methyl
Et:	Ethyl
ib:	Isobutyl
Bz:	Benzyl
N <sup>2</sup> -CH <sub>2</sub> -Naph:	N <sup>2</sup> -methylene(2-naphthyl)
N <sup>2</sup> -CH <sub>2</sub> -Anth:	N <sup>2</sup> -methylene(9-anthracenyl)
N <sup>2</sup> -CH <sub>2</sub> -BP:	N <sup>2</sup> -methylene(6-benzo[ <i>a</i> ]pyrenyl)
Pob:	4-oxo-4-(3-pyridyl)butyl
exo <sup>-</sup> :	Exonuclease deficient
IQ:	2-amino-3-methylimidazo[4,5- <i>f</i> ]quinoline (IQ)
M <sub>1</sub> dG:	3-(2'-deoxy-β-D-erythro-Pentofuranosyl)pyrimido[1,2- <i>a</i> ]Purin-10(3 <i>H</i> )-one
N <sup>2</sup> -OP:	N <sup>2</sup> -oxopropenyl
ds:	Double-stranded
ss:	Single-stranded
1,N <sup>2</sup> -ε:	1,N <sup>2</sup> -etheno.

## Acknowledgment

This work was supported in part by United States Public Health Service Grants R01 ES010375 (F.P.G.), K99 GM084460 (R.L.E.), and P30 ES000267 (F.P.G.).

## References

- [1] U. Hübscher, G. Maga, and S. Spadari, "Eukaryotic DNA polymerases," *Annual Review of Biochemistry*, vol. 71, pp. 133–163, 2002.
- [2] C. M. Joyce and T. A. Steitz, "Function and structure relationships in DNA polymerases," *Annual Review of Biochemistry*, vol. 63, pp. 777–822, 1994.
- [3] L. A. Loeb and R. J. Monnat Jr., "DNA polymerases and human disease," *Nature Reviews Genetics*, vol. 9, no. 8, pp. 594–604, 2008.
- [4] K. A. Johnson, "The kinetic and chemical mechanism of high-fidelity DNA polymerases," *Biochimica et Biophysica Acta*, vol. 1804, no. 5, pp. 1041–1048, 2010.
- [5] D. J. Chang and K. A. Cimprich, "DNA damage tolerance: when it's OK to make mistakes," *Nature Chemical Biology*, vol. 5, no. 2, pp. 82–90, 2009.
- [6] E. C. Friedberg, G. C. Walker, W. Siede, R. D. Wood, R. A. Shultz, and T. Ellenberger, *DNA Repair and Mutagenesis*, ASM Press, Washington, DC, USA, 2nd edition, 2006.
- [7] N. Geacintov and S. Broyde, Eds., *The Chemical Biology of DNA Damage*, Wiley-VCH, Weinheim, Germany, 2010.
- [8] B. N. Ames, "Identifying environmental chemicals causing mutations and cancer," *Science*, vol. 204, no. 4393, pp. 587–593, 1979.
- [9] P. D. Lawley, "Chemical Carcinogens," in *Chemical Carcinogens*, C. E. Searle, Ed., pp. 325–484, American Chemical Society, Washington, DC, USA, 1984.
- [10] C. M. Joyce and S. J. Benkovic, "DNA polymerase fidelity: kinetics, structure, and checkpoints," *Biochemistry*, vol. 43, no. 45, pp. 14317–14324, 2004.
- [11] N. Sabouri, J. Viberg, D. K. Goyal, E. Johansson, and A. Chabes, "Evidence for lesion bypass by yeast replicative DNA polymerases during DNA damage," *Nucleic Acids Research*, vol. 36, no. 17, pp. 5660–5667, 2008.
- [12] M. W. Schmitt, Y. Matsumoto, and L. A. Loeb, "High fidelity and lesion bypass capability of human DNA polymerase δ," *Biochimie*, vol. 91, no. 9, pp. 1163–1172, 2009.
- [13] F. P. Guengerich, "Interactions of carcinogen-bound DNA with individual DNA polymerases," *Chemical Reviews*, vol. 106, no. 2, pp. 420–452, 2006.
- [14] W. Yang and R. Woodgate, "What a difference a decade makes: Insights into translesion DNA synthesis," *Proceedings of the National Academy of Sciences of the United States of America*, vol. 104, no. 40, pp. 15591–15598, 2007.
- [15] J. P. McDonald, A. S. Levine, and R. Woodgate, "The *Saccharomyces cerevisiae* RAD30 gene, a homologue of *Escherichia coli* dinB and umuC, is DNA damage inducible and functions in a novel error-free postreplication repair mechanism," *Genetics*, vol. 147, no. 4, pp. 1557–1568, 1997.
- [16] S. G. Kozmin, Y. I. Pavlov, T. A. Kunkel, and E. Sage, "Roles of *Saccharomyces cerevisiae* DNA polymerases Polη and Polζ in response to irradiation by simulated sunlight," *Nucleic Acids Research*, vol. 31, no. 15, pp. 4541–4552, 2003.

- [17] M. R. Albertella, C. M. Green, A. R. Lehmann, and M. J. O'Connor, "A role for polymerase  $\eta$  in the cellular tolerance to cisplatin-induced damage," *Cancer Research*, vol. 65, no. 21, pp. 9799–9806, 2005.
- [18] M. R. Albertella, A. Lau, and M. J. O'Connor, "The overexpression of specialized DNA polymerases in cancer," *DNA Repair*, vol. 4, no. 5, pp. 583–593, 2005.
- [19] A. Alt, K. Lammens, C. Chiocchini et al., "Bypass of DNA lesions generated during anticancer treatment with cisplatin by DNA polymerase  $\eta$ ," *Science*, vol. 318, no. 5852, pp. 967–970, 2007.
- [20] C. Bavoux, J. S. Hoffmann, and C. Cazaux, "Adaptation to DNA damage and stimulation of genetic instability: the double-edged sword mammalian DNA polymerase  $\kappa$ ," *Biochimie*, vol. 87, no. 7, pp. 637–646, 2005.
- [21] C. Bavoux, A. M. Leopoldino, V. Bergoglio et al., "Up-regulation of the error-prone DNA polymerase  $\kappa$  promotes pleiotropic genetic alterations and tumorigenesis," *Cancer Research*, vol. 65, no. 1, pp. 325–330, 2005.
- [22] F. Lemée, C. Bavoux, M. J. Pillaire et al., "Characterization of promoter regulatory elements involved in downexpression of the DNA polymerase  $\kappa$  in colorectal cancer," *Oncogene*, vol. 26, no. 23, pp. 3387–3394, 2007.
- [23] A. Tissier, J. P. McDonald, E. G. Frank, and R. Woodgate, "pol $\iota$ , a remarkably error-prone human DNA polymerase," *Genes and Development*, vol. 14, no. 13, pp. 1642–1650, 2000.
- [24] J. Yang, Z. Chen, Y. Liu, R. J. Hickey, and L. H. Malkas, "Altered DNA polymerase  $\iota$  expression in breast cancer cells leads to a reduction in DNA replication fidelity and a higher rate of mutagenesis," *Cancer Research*, vol. 64, no. 16, pp. 5597–5607, 2004.
- [25] C. Biertumpfel, Y. Zhao, Y. Kondo et al., "Structure and mechanism of human DNA polymerase  $\eta$ ," *Nature*, vol. 465, no. 7301, pp. 1044–1048, 2010.
- [26] C. Masutani, R. Kusumoto, A. Yamada et al., "The XPV (xeroderma pigmentosum variant) gene encodes human DNA polymerase  $\eta$ ," *Nature*, vol. 399, no. 6737, pp. 700–704, 1999.
- [27] T. D. Silverstein, R. E. Johnson, R. Jain, L. Prakash, S. Prakash, and A. K. Aggarwal, "Structural basis for the suppression of skin cancers by DNA polymerase  $\eta$ ," *Nature*, vol. 465, no. 7301, pp. 1039–1043, 2010.
- [28] M. T. Washington, L. Prakash, and S. Prakash, "Mechanism of nucleotide incorporation opposite a thymine-thymine dimer by yeast DNA polymerase  $\eta$ ," *Proceedings of the National Academy of Sciences of the United States of America*, vol. 100, no. 21, pp. 12093–12098, 2003.
- [29] T. Lindahl and B. Nyberg, "Rate of depurination of native deoxyribonucleic acid," *Biochemistry*, vol. 11, no. 19, pp. 3610–3618, 1972.
- [30] J. Nakamura, V. E. Walker, P. B. Upton, S.-Y. Chiang, Y. W. Kow, and J. A. Swenberg, "Highly sensitive apurinic/aprimidinic site assay can detect spontaneous and chemically induced depurination under physiological conditions," *Cancer Research*, vol. 58, no. 2, pp. 222–225, 1998.
- [31] D. E. Barnes and T. Lindahl, "Repair and genetic consequences of endogenous DNA base damage in mammalian cells," *Annual Review of Genetics*, vol. 38, pp. 445–476, 2004.
- [32] L. A. Loeb and B. D. Preston, "Mutagenesis by apurinic/aprimidinic sites," *Annual Review of Genetics*, vol. 20, pp. 201–230, 1986.
- [33] S. Shibutani, M. Takeshita, and A. P. Grollman, "Translesional synthesis on DNA templates containing a single abasic site: a mechanistic study of the "a rule"," *Journal of Biological Chemistry*, vol. 272, no. 21, pp. 13916–13922, 1997.
- [34] M. Tang, P. Pham, X. Shen et al., "Roles of *E. coli* DNA polymerases IV and V in lesion-targeted and untargeted SOS mutagenesis," *Nature*, vol. 404, no. 6781, pp. 1014–1018, 2000.
- [35] P. E. M. Gibbs, J. McDonald, R. Woodgate, and C. W. Lawrence, "The relative roles *in vivo* of *Saccharomyces cerevisiae* Pol  $\eta$ , Pol  $\zeta$ , Rev1 protein and Pol32 in the bypass and mutation induction of an abasic site, T-T (6-4) photoadduct and T-T *cis-syn* cyclobutane dimer," *Genetics*, vol. 169, no. 2, pp. 575–582, 2005.
- [36] L. Haracska, I. Unk, R. E. Johnson et al., "Roles of yeast DNA polymerases  $\delta$  and  $\zeta$  and Rev 1 in the bypass of abasic sites," *Genes and Development*, vol. 15, no. 8, pp. 945–954, 2001.
- [37] N. Sabouri and E. Johansson, "Translesion synthesis of abasic sites by yeast DNA polymerase  $\epsilon$ ," *Journal of Biological Chemistry*, vol. 284, no. 46, pp. 31555–31563, 2009.
- [38] F. Boudsocq, S. Iwai, F. Hanaoka, and R. Woodgate, "*Sulfolobus solfataricus* P2 DNA polymerase IV (Dpo4): an archaeal DinB-like DNA polymerase with lesion-bypass properties akin to eukaryotic pol $\eta$ ," *Nucleic Acids Research*, vol. 29, no. 22, pp. 4607–4616, 2001.
- [39] L. Haracska, M. T. Washington, S. Prakash, and L. Prakash, "Inefficient bypass of an abasic site by DNA polymerase  $\eta$ ," *Journal of Biological Chemistry*, vol. 276, no. 9, pp. 6861–6866, 2001.
- [40] L. Haracska, I. Unk, R. E. Johnson et al., "Stimulation of DNA synthesis activity of human DNA polymerase  $\kappa$  by PCNA," *Molecular and Cellular Biology*, vol. 22, no. 3, pp. 784–791, 2002.
- [41] R. E. Johnson, M. T. Washington, L. Haracska, S. Prakash, and L. Prakash, "Eukaryotic polymerases  $\iota$  and  $\zeta$  act sequentially to bypass DNA lesions," *Nature*, vol. 406, no. 6799, pp. 1015–1019, 2000.
- [42] M. K. Swan, R. E. Johnson, L. Prakash, S. Prakash, and A. K. Aggarwal, "Structural basis of high-fidelity DNA synthesis by yeast DNA polymerase  $\delta$ ," *Nature Structural and Molecular Biology*, vol. 16, no. 9, pp. 979–986, 2009.
- [43] H. Ling, F. Boudsocq, R. Woodgate, and W. Yang, "Crystal structure of a Y-family DNA polymerase in action: a mechanism for error-prone and lesion-bypass replication," *Cell*, vol. 107, no. 1, pp. 91–102, 2001.
- [44] C. Otsuka, S. Sanadai, Y. Hata et al., "Difference between deoxyribose- and tetrahydrofuran-type abasic sites in the *in vivo* mutagenic responses in yeast," *Nucleic Acids Research*, vol. 30, no. 23, pp. 5129–5135, 2002.
- [45] D. T. Nair, R. E. Johnson, L. Prakash, S. Prakash, and A. K. Aggarwal, "Biochemistry: rev1 employs a novel mechanism of DNA synthesis using a protein template," *Science*, vol. 309, no. 5744, pp. 2219–2222, 2005.
- [46] B. N. Ames, "Dietary carcinogens and anticarcinogens. Oxygen radicals and degenerative diseases," *Science*, vol. 221, no. 4617, pp. 1256–1263, 1983.
- [47] M. Valko, H. Morris, and M. T. D. Cronin, "Metals, toxicity and oxidative stress," *Current Medicinal Chemistry*, vol. 12, no. 10, pp. 1161–1208, 2005.
- [48] C. G. Fraga, M. K. Shigenaga, J.-W. Park, P. Degan, and B. N. Ames, "Oxidative damage to DNA during aging: 8-Hydroxy-2'-deoxyguanosine in rat organ DNA and urine," *Proceedings of the National Academy of Sciences of the United States of America*, vol. 87, no. 12, pp. 4533–4537, 1990.

- [49] M. Abul Kalam, K. Haraguchi, S. Chandani et al., "Genetic effects of oxidative DNA damages: comparative mutagenesis of the imidazole ring-opened formamidopyrimidines (Fapy lesions) and 8-oxo-purines in simian kidney cells," *Nucleic Acids Research*, vol. 34, no. 8, pp. 2305–2315, 2006.
- [50] S. Boiteux and J. P. Radicella, "The human OGG1 gene: structure, functions, and its implication in the process of carcinogenesis," *Archives of Biochemistry and Biophysics*, vol. 377, no. 1, pp. 1–8, 2000.
- [51] M. L. Michaels, C. Cruz, A. P. Grollman, and J. H. Miller, "Evidence that MutY and MutM combine to prevent mutations by an oxidatively damaged form of guanine in DNA," *Proceedings of the National Academy of Sciences of the United States of America*, vol. 89, no. 15, pp. 7022–7025, 1992.
- [52] M. L. Michaels and J. H. Miller, "The GO system protects organisms from the mutagenic effect of the spontaneous lesion 8-hydroxyguanine (7,8-dihydro-8-oxoguanine)," *Journal of Bacteriology*, vol. 174, no. 20, pp. 6321–6325, 1992.
- [53] M. L. Michaels, J. Tchou, A. P. Grollman, and J. H. Miller, "A repair system for 8-oxo-7,8-dihydrodeoxyguanine," *Biochemistry*, vol. 31, no. 45, pp. 10964–10968, 1992.
- [54] M. P. Gallego and A. Sarasin, "Transcription-coupled repair of 8-oxoguanine in human cells and its deficiency in some DNA repair diseases," *Biochimie*, vol. 85, no. 11, pp. 1073–1082, 2003.
- [55] L. G. Brieba, B. F. Eichman, R. J. Kokoska, S. Doublé, T. A. Kunkel, and T. Ellenberger, "Structural basis for the dual coding potential of 8-oxoguanosine by a high-fidelity DNA polymerase," *EMBO Journal*, vol. 23, no. 17, pp. 3452–3461, 2004.
- [56] H. J. Einolf and F. P. Guengerich, "Fidelity of nucleotide insertion at 8-oxo-7,8-dihydroguanine by mammalian DNA polymerase  $\delta$ : steady-state and pre-steady-state kinetic analysis," *Journal of Biological Chemistry*, vol. 276, no. 6, pp. 3764–3771, 2001.
- [57] H. J. Einolf, N. Schnetz-Boutaud, and F. P. Guengerich, "Steady-state and pre-steady-state kinetic analysis of 8-oxo-7,8-dihydroguanosine triphosphate incorporation and extension by replicative and repair DNA polymerases," *Biochemistry*, vol. 37, no. 38, pp. 13300–13312, 1998.
- [58] L. L. Furge and F. P. Guengerich, "Analysis of nucleotide insertion and extension at 8-oxo-7,8-dihydroguanine by replicative T7 polymerase exo- and human immunodeficiency virus-1 reverse transcriptase using steady-state and pre-steady-state kinetics," *Biochemistry*, vol. 36, no. 21, pp. 6475–6487, 1997.
- [59] L. G. Lowe and F. P. Guengerich, "Steady-state and pre-steady-state kinetic analysis of dNTP insertion opposite 8-oxo-7,8-dihydroguanine by *Escherichia coli* I exo- and II exo-," *Biochemistry*, vol. 35, no. 30, pp. 9840–9849, 1996.
- [60] S. Shibutani, M. Takeshita, and A. P. Grollman, "Insertion of specific bases during DNA synthesis past the oxidation-damaged base 8-oxodG," *Nature*, vol. 349, no. 6308, pp. 431–434, 1991.
- [61] K. D. Carlson and M. T. Washington, "Mechanism of efficient and accurate nucleotide incorporation opposite 7,8-dihydro-8-oxoguanine by *Saccharomyces cerevisiae* DNA polymerase  $\eta$ ," *Molecular and Cellular Biology*, vol. 25, no. 6, pp. 2169–2176, 2005.
- [62] L. Haracska, S.-L. Yu, R. E. Johnson, L. Prakash, and S. Prakash, "Efficient and accurate replication in the presence of 7,8-dihydro-8-oxoguanine by DNA polymerase  $\eta$ ," *Nature Genetics*, vol. 25, no. 4, pp. 458–461, 2000.
- [63] G. Maga, G. Villani, E. Crespan et al., "8-oxo-guanine bypass by human DNA polymerases in the presence of auxiliary proteins," *Nature*, vol. 447, no. 7144, pp. 606–608, 2007.
- [64] R. L. Eoff, A. Irimia, K. C. Angel, M. Egli, and F. P. Guengerich, "Hydrogen bonding of 7,8-dihydro-8-oxodeoxyguanosine with a charged residue in the little finger domain determines miscoding events in *Sulfolobus solfataricus* DNA polymerase Dpo4," *Journal of Biological Chemistry*, vol. 282, no. 27, pp. 19831–19843, 2007.
- [65] O. Rechkoblit, L. Malinina, Y. Cheng et al., "Stepwise translocation of Dpo4 polymerase during error-free bypass of an oxoG lesion," *PLoS Biology*, vol. 4, no. 1, p. e11, 2006.
- [66] H. Zang, A. Irimia, J.-Y. Choi et al., "Efficient and high fidelity incorporation of dCTP opposite 7,8-dihydro-8-oxodeoxyguanosine by *Sulfolobus solfataricus* DNA polymerase Dpo4," *Journal of Biological Chemistry*, vol. 281, no. 4, pp. 2358–2372, 2006.
- [67] A. Vaisman and R. Woodgate, "Unique misinsertion specificity of pol  $\eta$  may decrease the mutagenic potential of deaminated cytosines," *EMBO Journal*, vol. 20, no. 22, pp. 6520–6529, 2001.
- [68] Y. Zhang, X. Wu, O. Rechkoblit, N. E. Geacintov, J.-S. Taylor, and Z. Wang, "Response of human REV1 to different DNA damage: preferential dCMP insertion opposite the lesion," *Nucleic Acids Research*, vol. 30, no. 7, pp. 1630–1638, 2002.
- [69] S. Uesugi and M. Ikehara, "Carbon-13 magnetic resonance spectra of 8-substituted purine nucleosides. Characteristic shifts for the *syn* conformation," *Journal of the American Chemical Society*, vol. 99, no. 10, pp. 3250–3253, 1977.
- [70] A. Irimia, R. L. Eoff, F. P. Guengerich, and M. Egli, "Structural and functional elucidation of the mechanism promoting error-prone synthesis by human DNA polymerase  $\kappa$  opposite the 7,8-dihydro-8-oxo-2'-deoxyguanosine adduct," *Journal of Biological Chemistry*, vol. 284, no. 33, pp. 22467–22480, 2009.
- [71] M. Hogg, S. S. Wallace, and S. Doublé, "Bumps in the road: how replicative DNA polymerases see DNA damage," *Current Opinion in Structural Biology*, vol. 15, no. 1, pp. 86–93, 2005.
- [72] S. C. Cheng, B. D. Hilton, J. M. Roman, and A. Dipple, "DNA adducts from carcinogenic and noncarcinogenic enantiomers of benzo[a]pyrene dihydrodiol epoxide," *Chemical Research in Toxicology*, vol. 2, no. 5, pp. 334–340, 1989.
- [73] M. H. G. Medeiros, "Exocyclic DNA adducts as biomarkers of lipid oxidation and predictors of disease. Challenges in developing sensitive and specific methods for clinical studies," *Chemical Research in Toxicology*, vol. 22, no. 3, pp. 419–425, 2009.
- [74] T. Meehan and K. Straub, "Double stranded DNA stereoselectively binds benzo(a)pyrene diol epoxides," *Nature*, vol. 277, no. 5695, pp. 410–412, 1979.
- [75] I. G. Minko, I. D. Kozekov, T. M. Harris, C. J. Rizzo, R. S. Lloyd, and M. P. Stone, "Chemistry and biology of DNA containing 1,N<sup>2</sup>-deoxyguanosine adducts of the  $\alpha,\beta$ -unsaturated aldehydes acrolein, crotonaldehyde, and 4-hydroxynonenal," *Chemical Research in Toxicology*, vol. 22, no. 5, pp. 759–778, 2009.
- [76] J.-Y. Choi, K. C. Angel, and F. P. Guengerich, "Translesion synthesis across bulky N<sup>2</sup>-alkyl guanine DNA adducts by human DNA polymerase  $\kappa$ ," *Journal of Biological Chemistry*, vol. 281, no. 30, pp. 21062–21072, 2006.
- [77] J.-Y. Choi and F. P. Guengerich, "Analysis of the effect of bulk at N<sup>2</sup>-alkylguanine DNA adducts on catalytic efficiency and fidelity of the processive DNA polymerases bacteriophage

- T7 exonuclease- and HIV-1 reverse transcriptase,” *Journal of Biological Chemistry*, vol. 279, no. 18, pp. 19217–19229, 2004.
- [78] J.-Y. Choi and F. P. Guengerich, “Adduct size limits efficient and error-free bypass across bulky  $N^2$ -guanine DNA lesions by human DNA polymerase  $\eta$ ,” *Journal of Molecular Biology*, vol. 352, no. 1, pp. 72–90, 2005.
- [79] J.-Y. Choi and F. P. Guengerich, “Kinetic evidence for inefficient and error-prone bypass across bulky  $N^2$ -guanine DNA adducts by human DNA polymerase,” *Journal of Biological Chemistry*, vol. 281, no. 18, pp. 12315–12324, 2006.
- [80] J.-Y. Choi and F. P. Guengerich, “Kinetic analysis of translesion synthesis opposite bulky  $N^2$ - and  $O^6$ -alkylguanine DNA adducts by human DNA polymerase REV1,” *Journal of Biological Chemistry*, vol. 283, no. 35, pp. 23645–23655, 2008.
- [81] K. S. Gates, “An overview of chemical processes that damage cellular DNA: spontaneous hydrolysis, alkylation, and reactions with radicals,” *Chemical Research in Toxicology*, vol. 22, no. 11, pp. 1747–1760, 2009.
- [82] J.-Y. Choi, G. Chowdhury, H. Zang et al., “Translesion synthesis across  $O^6$ -alkylguanine DNA adducts by recombinant human DNA polymerases,” *Journal of Biological Chemistry*, vol. 281, no. 50, pp. 38244–38256, 2006.
- [83] H. Zhang, R. L. Eoff, I. D. Kozekov, C. J. Rizzo, M. Egli, and F. P. Guengerich, “Versatility of  $\gamma$ -family *Sulfolobus solfataricus* DNA polymerase Dpo4 in translesion synthesis past bulky  $N^2$ -alkylguanine adducts,” *Journal of Biological Chemistry*, vol. 284, no. 6, pp. 3563–3576, 2009.
- [84] S. Lone, S. A. Townson, S. N. Uljon et al., “Human DNA polymerase kappa encircles DNA: implications for mismatch extension and lesion bypass,” *Molecular Cell*, vol. 25, no. 4, pp. 601–614, 2007.
- [85] O. Rechkoblit, Y. Zhang, D. Guo et al., “*trans*-lesion synthesis past bulky benzo[a]pyrene diol epoxide  $N^2$ -dG and  $N^6$ -dA lesions catalyzed by DNA bypass polymerases,” *Journal of Biological Chemistry*, vol. 277, no. 34, pp. 30488–30494, 2002.
- [86] L. Jia, N. E. Geacintov, and S. Broyde, “The N-clasp of human DNA polymerase  $\kappa$  promotes blockage or error-free bypass of adenine- or guanine-benzo[a]pyrenyl lesions,” *Nucleic Acids Research*, vol. 36, no. 20, pp. 6571–6584, 2008.
- [87] R. L. Eoff, K. C. Angel, M. Egli, and F. P. Guengerich, “Molecular basis of selectivity of nucleoside triphosphate incorporation opposite  $O^6$ -benzylguanine by *Sulfolobus solfataricus* DNA polymerase Dpo4: steady-state and pre-steady-state kinetics and X-ray crystallography of correct and incorrect pairing,” *Journal of Biological Chemistry*, vol. 282, no. 18, pp. 13573–13584, 2007.
- [88] R. L. Eoff, A. Irimia, M. Egli, and F. P. Guengerich, “*Sulfolobus solfataricus* DNA polymerase Dpo4 is partially inhibited by “Wobble” pairing between  $O^6$ -methylguanine and cytosine, but accurate bypass is preferred,” *Journal of Biological Chemistry*, vol. 282, no. 2, pp. 1456–1467, 2007.
- [89] H. Zang, G. Chowdhury, K. C. Angel, T. M. Harris, and F. P. Guengerich, “Translesion synthesis across polycyclic aromatic hydrocarbon diol epoxide adducts of deoxyadenosine by *Sulfolobus solfataricus* DNA polymerase Dpo4,” *Chemical Research in Toxicology*, vol. 19, no. 6, pp. 859–867, 2006.
- [90] H. Zang, T. M. Harris, and F. P. Guengerich, “Kinetics of nucleotide incorporation opposite polycyclic aromatic hydrocarbon-DNA adducts by processive bacteriophage T7 DNA polymerase,” *Chemical Research in Toxicology*, vol. 18, no. 2, pp. 389–400, 2005.
- [91] H. Bartsch and B. Singer, Eds., *Exocyclic DNA Adducts in Mutagenesis and Carcinogenesis*, vol. 150, IARC Scientific Publications, International Agency for Research on Cancer, Lyon, France, 1999.
- [92] A. K. Basu, S. M. O’Hara, P. Valladier, K. Stone, O. Mols, and L. J. Marnett, “Identification of adducts formed by reaction of guanine nucleosides with malondialdehyde and structurally related aldehydes,” *Chemical Research in Toxicology*, vol. 1, no. 1, pp. 53–59, 1988.
- [93] P. C. Dedon, J. P. Plataras, C. A. Rouzer, and L. J. Marnett, “Indirect mutagenesis by oxidative DNA damage: formation of the pyrimidopurinone adduct of deoxyguanosine by base propenal,” *Proceedings of the National Academy of Sciences of the United States of America*, vol. 95, no. 19, pp. 11113–11116, 1998.
- [94] H. Seto, T. Okuda, T. Takesue, and T. Ikemura, “Reaction of malonaldehyde with nucleic acid. I. Formation of fluorescent pyrimido[1,2-a]purin-10(3H)-one nucleosides,” *Bulletin of the Chemical Society of Japan*, vol. 56, no. 6, pp. 1799–1802, 1983.
- [95] A. K. Chaudhary, M. Nokubo, L. J. Marnett, and I. A. Blair, “Analysis of the malondialdehyde-2’-deoxyguanosine adduct in rat liver DNA by gas chromatography/electron capture negative chemical ionization mass spectrometry,” *Biological Mass Spectrometry*, vol. 23, no. 8, pp. 457–464, 1994.
- [96] H. Mao, N. C. Schnetz-Boutaud, J. P. Weisenseel, L. J. Marnett, and M. P. Stone, “Duplex DNA catalyzes the chemical rearrangement of a malondialdehyde deoxyguanosine adduct,” *Proceedings of the National Academy of Sciences of the United States of America*, vol. 96, no. 12, pp. 6615–6620, 1999.
- [97] L. A. VanderVeen, M. F. Hashim, Y. Shyr, and L. J. Marnett, “Induction of frameshift and base pair substitution mutations by the major DNA adduct of the endogenous carcinogen malondialdehyde,” *Proceedings of the National Academy of Sciences of the United States of America*, vol. 100, no. 2, pp. 14247–14252, 2003.
- [98] J. B. Stafford, R. L. Eoff, A. Kozekova, C. J. Rizzo, P. Guengerich, and L. J. Marnett, “Translesion DNA synthesis by human DNA polymerase  $\eta$  on templates containing a pyrimidopurinone deoxyguanosine adduct, 3-(2’-deoxy- $\beta$ -D-erythro-pentofuranosyl)pyrimido-[1,2-a]purin-10(3H)-one,” *Biochemistry*, vol. 48, no. 2, pp. 471–480, 2009.
- [99] R. L. Eoff, J. B. Stafford, J. Szekely et al., “Structural and functional analysis of *Sulfolobus solfataricus* Y-family DNA polymerase Dpo4-catalyzed bypass of the malondialdehyde-deoxyguanosine adduct,” *Biochemistry*, vol. 48, no. 30, pp. 7079–7088, 2009.
- [100] F. P. Guengerich, S. Langouët, A. N. Mican, S. Akasaka, M. Müller, and M. Persmark, “Formation of etheno adducts and their effects on DNA polymerases,” in *Exocyclic DNA Adducts in Mutagenesis and Carcinogenesis*, B. Singer and H. Bartsch, Eds., vol. 150, pp. 137–145, IARC Scientific Publications, International Agency for Research on Cancer, Lyon, France, 1999.
- [101] F. P. Guengerich, M. Persmark, and W. G. Humphreys, “Formation of 1, $N^2$ - and  $N^2,3$ -ethenoguanine from 2-haloalkoxiranes: isotopic labeling studies and isolation of a hemiaminal derivative of  $N^2$ -(2-oxoethyl)guanine,” *Chemical Research in Toxicology*, vol. 6, no. 5, pp. 635–648, 1993.
- [102] S. S. Hecht, R. Young-Sciame, and F.-L. Chung, “Reaction of  $\alpha$ -acetoxy-*N*-nitrosopiperidine with deoxyguanosine: oxygen-dependent formation of 4-oxo-2-pentenal and a 1, $N^2$ -ethenodeoxyguanosine adduct,” *Chemical Research in Toxicology*, vol. 5, no. 5, pp. 706–712, 1992.

- [103] R. S. Sodum and F.-L. Chung, "1,*N*<sup>2</sup>-Ethenodeoxyguanosine as a potential marker for DNA adduct formation by trans-4-hydroxy-2-nonenal." *Cancer Research*, vol. 48, no. 2, pp. 320–323, 1988.
- [104] H. Zang, A. K. Goodenough, J.-Y. Choi et al., "DNA adduct bypass polymerization by *Sulfolobus solfataricus* DNA polymerase Dpo4: analysis and crystal structures of multiple base pair substitution and frameshift products with the adduct 1,*N*<sup>2</sup>-ethenoguanine," *Journal of Biological Chemistry*, vol. 280, no. 33, pp. 29750–29764, 2005.

## Research Article

# Pre-Steady-State Kinetic Analysis of Truncated and Full-Length *Saccharomyces cerevisiae* DNA Polymerase Eta

Jessica A. Brown,<sup>1</sup> Likui Zhang,<sup>1</sup> Shanen M. Sherrer,<sup>1</sup> John-Stephen Taylor,<sup>2</sup>  
Peter M. J. Burgers,<sup>3</sup> and Zucui Suo<sup>1</sup>

<sup>1</sup>Department of Biochemistry, The Ohio State University, Columbus, OH 43210, USA

<sup>2</sup>Department of Chemistry, Washington University, St. Louis, MO 63130, USA

<sup>3</sup>Department of Biochemistry and Molecular Biophysics, Washington University School of Medicine, St. Louis, MO 63110, USA

Correspondence should be addressed to Zucui Suo, suo.3@osu.edu

Received 11 March 2010; Accepted 30 April 2010

Academic Editor: Ashis Basu

Copyright © 2010 Jessica A. Brown et al. This is an open access article distributed under the Creative Commons Attribution License, which permits unrestricted use, distribution, and reproduction in any medium, provided the original work is properly cited.

Understanding polymerase fidelity is an important objective towards ascertaining the overall stability of an organism's genome. *Saccharomyces cerevisiae* DNA polymerase  $\eta$  ( $\gamma$ Pol $\eta$ ), a Y-family DNA polymerase, is known to efficiently bypass DNA lesions (e.g., pyrimidine dimers) in vivo. Using pre-steady-state kinetic methods, we examined both full-length and a truncated version of  $\gamma$ Pol $\eta$  which contains only the polymerase domain. In the absence of  $\gamma$ Pol $\eta$ 's C-terminal residues 514–632, the DNA binding affinity was weakened by 2-fold and the base substitution fidelity dropped by 3-fold. Thus, the C-terminus of  $\gamma$ Pol $\eta$  may interact with DNA and slightly alter the conformation of the polymerase domain during catalysis. In general,  $\gamma$ Pol $\eta$  discriminated between a correct and incorrect nucleotide more during the incorporation step (50-fold on average) than the ground-state binding step (18-fold on average). Blunt-end additions of dATP or pyrene nucleotide 5'-triphosphate revealed the importance of base stacking during the binding of incorrect incoming nucleotides.

## 1. Introduction

DNA polymerases are organized into seven families: A, B, C, D, X, Y, and reverse transcriptase [1, 2]. Among these families, DNA polymerases are involved in DNA replication, DNA repair, DNA lesion bypass, antibody generation, and sister chromatid cohesion [3]. Despite these diverse roles, DNA polymerases catalyze the nucleotidyl transfer reaction using a two divalent metal ion mechanism [4] with at least one positively charged residue [5] that functions as a general acid [6] at their active site, follow a similar minimal kinetic pathway [7], and share a similar structural architecture consisting of the fingers, palm, and thumb subdomains [8, 9]. Surprisingly, the polymerization fidelity of eukaryotic DNA polymerases spans a wide range: one error per one to one billion nucleotide incorporations ( $10^0$  to  $10^{-9}$ ) [10].

The Y-family DNA polymerases are known for catalyzing nucleotide incorporation with low fidelity and poor processivity. These enzymes are specialized for translesion DNA synthesis which involves nucleotide incorporation opposite and downstream of a damaged DNA site. Lesion bypass can be either error-free or error-prone depending on the DNA polymerase and DNA lesion combination. To accommodate a distorted DNA substrate, Y-family DNA polymerases utilize several features: a solvent-accessible [11] and conformationally flexible active site [12], smaller fingers and thumb subdomains [11], an additional subdomain known as the little finger [11], the little finger and polymerase core domains move in opposite directions during a catalytic cycle [13], and a lack of 3'  $\rightarrow$  5' exonuclease activity [14]. Unfortunately, these features, which facilitate lesion bypass, may also contribute to the low fidelity of a Y-family DNA polymerase during replication of a damaged or undamaged

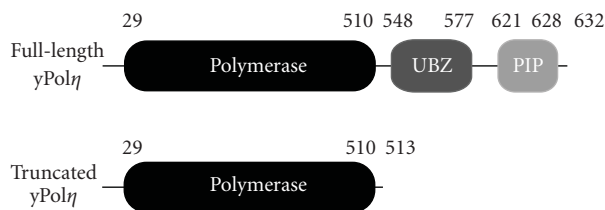


FIGURE 1: Schematic illustration of  $\gamma$ Pol $\eta$ . The polymerase domain of  $\gamma$ Pol $\eta$  is at the N-terminus while a ubiquitin-binding zinc finger (UBZ) domain and PCNA-interacting peptide (PIP) motif is at the C-terminus. Residue numbers are denoted above each region. For this study, the truncated construct contains only the polymerase domain.

DNA template. Thus, it is important to understand the mechanism and fidelity of the Y-family DNA polymerases.

*Saccharomyces cerevisiae* DNA polymerase  $\eta$  ( $\gamma$ Pol $\eta$ ), a Y-family DNA polymerase, is critical for the error-free bypass of UV-induced DNA damage such as a *cis-syn* thymine-thymine dimer [15–19]. To date, Pol $\eta$  remains the only Y-family DNA polymerase with a confirmed biological function [20].  $\gamma$ Pol $\eta$  is organized into a polymerase domain, ubiquitin-binding zinc finger (UBZ) domain, and proliferating cell nuclear antigen- (PCNA) interacting peptide (PIP) motif (Figure 1). X-ray crystal structures of  $\gamma$ Pol $\eta$ 's catalytic core have been solved alone [21] as well as in complex with a cisplatin-DNA adduct and an incoming nucleotide [22]. Due to a lack of structures for full-length  $\gamma$ Pol $\eta$ , it is unclear if the C-terminal residues 514–632 interact with DNA and contribute to the polymerase function of  $\gamma$ Pol $\eta$ . Using pre-steady-state kinetic techniques, we have measured the base-substitution fidelity of full-length and truncated  $\gamma$ Pol $\eta$  (Figure 1) catalyzing nucleotide incorporation into undamaged DNA. In addition, we have determined the DNA binding affinity of both full-length and truncated  $\gamma$ Pol $\eta$ . Our results show that the C-terminus of  $\gamma$ Pol $\eta$  has a minor effect on the DNA binding affinity and the base substitution fidelity of this lesion bypass DNA polymerase.

## 2. Materials and Methods

**2.1. Materials.** Materials were purchased from the following companies: [ $\gamma$ - $^{32}$ P] ATP, MP Biomedicals (Solon, OH); Biospin columns, Bio-Rad Laboratories (Herclues, CA); dNTPs, GE Healthcare (Piscataway, NJ); oligodeoxyribonucleotides, Integrated DNA Technologies, Inc. (Coralville, IA); and OptiKinase, USB (Cleveland, OH).

**2.2. Preparation of Substrates and Enzymes.** The synthetic oligodeoxyribonucleotides listed in Table 1 were purified as described previously [23]. The primer strand 21-mer or blunt-end 16-mer was 5'-radiolabeled with [ $\gamma$ - $^{32}$ P]ATP and OptiKinase. Then, the 21-mer was annealed to the appropriate 41 mer template (Table 1) and the palindromic blunt-end substrates were annealed as described previously [23]. The catalytic core of  $\gamma$ Pol $\eta$  (1–513) containing an N-terminal

TABLE 1: Sequences of DNA substrates<sup>a</sup>.

D-1	5'–CGCAGCCGTCCAACCAACTCA–3' 3'–GCGTCGGCAGGTTGGTTGAGTAGCAGCTAGGTTACGGCAGG–5'
D-6	5'–CGCAGCCGTCCAACCAACTCA–3' 3'–GCGTCGGCAGGTTGGTTGAGTGGCAGCTAGGTTACGGCAGG–5'
D-7	5'–CGCAGCCGTCCAACCAACTCA–3' 3'–GCGTCGGCAGGTTGGTTGAGTGCAGCTAGGTTACGGCAGG–5'
D-8	5'–CGCAGCCGTCCAACCAACTCA–3' 3'–GCGTCGGCAGGTTGGTTGAGTCGAGCTAGGTTACGGCAGG–5'
F-8	5'–CGCAGCCGTCCAACCAACTCA–3' 3'–GCGTCGGCAGGTTGGTTGAGTCXCAGCTAGGTTACGGCAGG–5'
BE1	5'–ATGAGTTGCAACTCAT–3' 3'–TACTCAACGTTGAGTA–5'
BE2	5'–TTGAGTTGCAACTCAA–3' 3'–AACTCAACGTTGAGTT–5'
BE3	5'–CTGAGTTGCAACTCAG–3' 3'–GACTCAACGTTGAGTC–5'
BE4	5'–GTGAGTTGCAACTCAC–3' 3'–CACTCAACGTTGAGTG–5'

<sup>a</sup>The template base highlighted in bold is unique to each strand and X denotes 2-aminopurine.

MGSSH<sub>6</sub>SSGLVPRGSH tag was purified as described previously [24]. The full-length  $\gamma$ Pol $\eta$  (1–632) was expressed and purified from yeast [25]. Pyrene 5'-triphosphate (dPTP) was synthesized as described previously [26].

**2.3. Pre-Steady-State Kinetic Assays.** All experiments were performed in reaction buffer A which contained 40 mM Tris-HCl pH 7.5 at 23°C, 5 mM MgCl<sub>2</sub>, 1 mM DTT, 10  $\mu$ g/mL BSA, and 10% glycerol. A rapid chemical-quench flow apparatus (KinTek, PA, USA) was used for fast reactions. For burst assays, a preincubated solution of  $\gamma$ Pol $\eta$  (320 nM) and 5'-[ $^{32}$ P]-labeled D-1 DNA (480 nM) was mixed with dTTP·Mg<sup>2+</sup> (100  $\mu$ M). To measure the dissociation rate of the  $\gamma$ Pol $\eta$ ·DNA binary complex, a preincubated solution of  $\gamma$ Pol $\eta$  (50 nM) and 5'-[ $^{32}$ P]-labeled D-1 DNA (100 nM) was mixed with a molar excess of unlabeled D-1 DNA (2.5  $\mu$ M) for various time intervals prior to initiating the polymerization reaction with dTTP·Mg<sup>2+</sup> (150 and 400  $\mu$ M for truncated and full-length  $\gamma$ Pol $\eta$ , resp.) for 15 s. For single-turnover kinetic assays, a preincubated solution of  $\gamma$ Pol $\eta$  (150 nM) and 5'-[ $^{32}$ P]-labeled DNA (30 nM) was mixed with an incoming dNTP·Mg<sup>2+</sup> (0.4–800  $\mu$ M). Reactions were quenched at the designated time by adding 0.37 M EDTA. Reaction products were analyzed by sequencing gel electrophoresis (17% acrylamide, 8 M urea, 1  $\times$  TBE running buffer), visualized using a Typhoon TRIO (GE Healthcare), and quantitated with ImageQuant software (Molecular Dynamics).

**2.4. DNA Binding Assays.** The equilibrium dissociation constant ( $K_d^{\text{DNA}}$ ) of the  $\gamma$ Pol $\eta$ ·DNA binary complex was determined using two techniques. First, an electrophoretic mobility shift assay (EMSA) was employed by adding increasing concentrations of  $\gamma$ Pol $\eta$  (10–450 nM) into a fixed concentration of 5'-[ $^{32}$ P]-labeled D-1 DNA (10 nM) in

buffer A. The solution established equilibrium during a 20-minute incubation period. Then, the binary complex was separated from unbound DNA using a 4.5% native polyacrylamide gel and running buffer as previously described except the final concentration of Tris was adjusted to 40 mM [27]. Second, a fluorescence titration assay was used. Increasing concentrations of  $\gamma$ Pol $\eta$  (2–300 nM) were titrated into a fixed concentration of F-8 DNA (25 nM) in buffer A (devoid of BSA). The F-8 DNA substrate (Table 1) was excited at a wavelength of 312 nm with emission and excitation slit widths of 5 nm. The emission spectra were collected at 1 nm intervals from 320 to 500 nm using a Fluoromax-4 (Jobin Jvon Horiba). Emission background from the buffer and intrinsic protein fluorescence were subtracted from each spectrum.

**2.5. Data Analysis.** For the pre-steady-state burst assay, the product concentration was graphed as a function of time ( $t$ ) and the data were fit to the burst equation (1) using the nonlinear regression program, KaleidaGraph (Synergy Software):

$$[\text{Product}] = A[1 - \exp(-k_1 t) + k_2 t]. \quad (1)$$

$A$  represents the fraction of active enzyme,  $k_1$  represents the observed burst rate constant, and  $k_2$  represents the observed steady-state rate constant.

Data for the EMSA were graphed by plotting the concentration of the binary complex as a function of enzyme concentration ( $E_0$ ) and fitting it to a quadratic equation (2):

$$[\text{E} \cdot \text{DNA}] = 0.5 \left( K_d^{\text{DNA}} + E_0 + D_0 \right) - 0.5 \left[ \left( K_d^{\text{DNA}} + E_0 + D_0 \right)^2 - 4E_0 D_0 \right]^{1/2}. \quad (2)$$

$D_0$  is the DNA concentration.

For the fluorescence titration experiments, a modified quadratic equation (3) was applied to a plot of the fluorescence intensity ( $F$ ) measured at 370 nm versus enzyme concentration:

$$[F] = F_{\max} + \left[ \frac{F_{\min} - F_{\max}}{2D_0} \right] \times \left\{ \left( K_d^{\text{DNA}} + E_0 + D_0 \right) - \left[ \left( K_d^{\text{DNA}} + E_0 + D_0 \right)^2 - 4E_0 D_0 \right]^{1/2} \right\}. \quad (3)$$

$F_{\max}$  and  $F_{\min}$  represent the maximum and minimum fluorescence intensity, respectively.

For the rate of DNA dissociation from the binary complex, a single-exponential equation (4) was applied to a plot of product concentration versus time:

$$[\text{Product}] = A[\exp(-k_{\text{off}} t)] + C. \quad (4)$$

$A$  represents the reaction amplitude,  $k_{\text{off}}$  is the observed rate constant of DNA dissociation, and  $C$  is the concentration of

the radiolabeled DNA product in the presence of a DNA trap for unlimited time.

For the single-turnover kinetic assays, a plot of product concentration versus time was fit to a single-exponential equation (5) to extract the observed rate constant of nucleotide incorporation ( $k_{\text{obs}}$ ):

$$[\text{Product}] = A[1 - \exp(-k_{\text{obs}} t)]. \quad (5)$$

To measure the maximum rate constant of incorporation ( $k_p$ ) and the apparent equilibrium dissociation constant ( $K_d$ ) of an incoming nucleotide, the extracted  $k_{\text{obs}}$  values were plotted as a function of nucleotide concentration and fit to a hyperbolic equation (6):

$$[k_{\text{obs}}] = \frac{k_p [\text{dNTP}]}{(K_d + [\text{dNTP}])}. \quad (6)$$

The free energy change ( $\Delta\Delta G$ ) for a correct and incorrect nucleotide substrate dissociating from the E·DNA·dNTP complex was calculated according to (7).

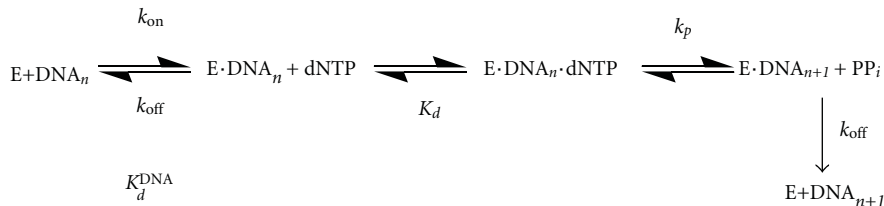
$$\Delta\Delta G = RT \ln \left[ \frac{(K_d)_{\text{incorrect}}}{(K_d)_{\text{correct}}} \right]. \quad (7)$$

Here,  $R$  is the universal gas constant and  $T$  is the reaction temperature in Kelvin.

### 3. Results and Discussion

**3.1. Truncated and Full-Length  $\gamma$ Pol $\eta$  Display Biphasic Kinetics.** Previously, transient state kinetic techniques have been used to characterize full-length  $\gamma$ Pol $\eta$  at 30°C [28]. Therefore, we first performed a burst assay (see Section 2) to ensure that our purified proteins, truncated and full-length  $\gamma$ Pol $\eta$  (Figure 1), behaved in a similar manner at 23°C. Compared to wild-type  $\gamma$ Pol $\eta$ , the truncated construct contains only the polymerase domain (Figure 1). A preincubated solution of  $\gamma$ Pol $\eta$  (320 nM) and 5'-[<sup>32</sup>P]-labeled 21/41 mer D-1 DNA (480 nM) was mixed with dTTP·Mg<sup>2+</sup> (100  $\mu$ M) and quenched with EDTA at various times. Product concentration was plotted as a function of time and was fit to (1), since there were two distinct kinetic phases: a rapid, exponential phase and a slow, linear phase (data not shown). These burst results were similar to those previously published [28]. Biphasic kinetics of nucleotide incorporation indicated that the first turnover rate was the rate of nucleotide incorporation occurring at the enzyme's active site while subsequent turnovers (i.e., linear phase) were likely limited by the DNA product release step as demonstrated by full-length  $\gamma$ Pol $\eta$  at 30°C [28] and other DNA polymerases [23, 29, 30].

**3.2. The C-Terminal 119 Residues Slightly Enhance DNA Binding Affinity of  $\gamma$ Pol $\eta$ .** The equilibrium dissociation constant for the binary complex of  $\gamma$ Pol $\eta$ ·DNA ( $K_d^{\text{DNA}}$ ) was measured to determine if the C-terminus of  $\gamma$ Pol $\eta$  affects DNA binding affinity (Scheme 1). First, the  $K_d^{\text{DNA}}$  was estimated using the EMSA (see Section 2). For example, varying concentrations



SCHEME 1

of full-length  $\gamma\text{Pol}\eta$  (10–450 nM) were incubated with a fixed concentration of 5'-[ $^{32}\text{P}$ ]-labeled D-1 DNA (10 nM) before separating the binary complex from the unbound DNA on a native gel (Figure 2(a)). Then, a quadratic equation (2) was applied to a plot of the binary complex concentration versus  $\gamma\text{Pol}\eta$  concentration which resolved a  $K_d^{\text{DNA}}$  of  $16 \pm 1$  nM (Figure 2(b) and Table 2). Under similar reaction conditions, the  $K_d^{\text{DNA}}$  of truncated  $\gamma\text{Pol}\eta$  was estimated to be  $34 \pm 3$  nM, a binding affinity ( $1/K_d^{\text{DNA}}$ ) value that is 2-fold weaker than that of full-length  $\gamma\text{Pol}\eta$  (Table 2).

To corroborate these estimated  $K_d^{\text{DNA}}$  values, we measured the true  $K_d^{\text{DNA}}$  for the  $\gamma\text{Pol}\eta$ -DNA complex using a fluorescence titration assay. An analog of dA, 2-aminopurine, was embedded into the 41 mer template of F-8 DNA which is identical to 21/41 mer D-8 DNA except that 2-aminopurine flanks the 5' end of the templating dC base (Table 1). The F-8 DNA substrate (25 nM) was excited at 312 nm, and the emission spectrum was collected from 320 to 500 nm. After serial additions of full-length or truncated  $\gamma\text{Pol}\eta$  in independent titrations, a decrease in the fluorescence intensity of F-8 was observed. These changes in fluorescence intensity at 370 nm were plotted as a function of the  $\gamma\text{Pol}\eta$  concentration and were fit to (3) to extract a  $K_d^{\text{DNA}}$  equal to  $7 \pm 4$  nM for full-length  $\gamma\text{Pol}\eta$  (Figure 2(c)) and  $13 \pm 5$  nM for truncated  $\gamma\text{Pol}\eta$  (Table 2). These  $K_d^{\text{DNA}}$  measurements were tighter than those determined using EMSA, since the fluorescence titration assay allows  $\gamma\text{Pol}\eta$  to associate and dissociate during data collection. In contrast, EMSA does not maintain a constant equilibrium because dissociated  $\gamma\text{Pol}\eta$  cannot reassociate with DNA during electrophoresis separation. Nonetheless, there was a confirmed  $\sim 2$ -fold difference in the DNA binding affinity between full-length and the catalytic core of  $\gamma\text{Pol}\eta$  which indicates that the C-terminal 119 amino acid residues of  $\gamma\text{Pol}\eta$  slightly enhance the binding of the enzyme to DNA.

Next, we directly measured the rate of DNA dissociation from the  $\gamma\text{Pol}\eta$ -DNA complex (see Section 2). A preincubated solution of  $\gamma\text{Pol}\eta$  (50 nM) and 5'-radiolabeled D-1 DNA (100 nM) was combined with a 50-fold molar excess of unlabeled D-1 DNA for various time intervals before dTTP was added for 15 s to allow ample extension of the labeled D-1 DNA that remained in complex with  $\gamma\text{Pol}\eta$ . A plot of product concentration versus the incubation time with the unlabeled DNA trap (data not shown) was fit to (4) which yielded DNA dissociation rates ( $k_{\text{off}}$ ) of  $0.008 \pm 0.001 \text{ s}^{-1}$  and  $0.0041 \pm 0.0008 \text{ s}^{-1}$  for truncated

TABLE 2: Rate and equilibrium dissociation constants for the binary complex  $\gamma\text{Pol}\eta$ -DNA at 23°C.

Kinetic Parameter	Truncated $\gamma\text{Pol}\eta$	Full-length $\gamma\text{Pol}\eta$
$k_{\text{on}}$ ( $\mu\text{M}^{-1} \text{ s}^{-1}$ ) <sup>a</sup>	0.62	0.59
$k_{\text{off}}$ ( $\text{s}^{-1}$ )	$0.008 \pm 0.001$	$0.0041 \pm 0.0008$
$K_d^{\text{DNA}}$ (nM) <sup>b</sup>	$34 \pm 3$	$16 \pm 1$
$K_d^{\text{DNA}}$ (nM) <sup>c</sup>	$13 \pm 5$	$7 \pm 4$

<sup>a</sup>Calculated as  $k_{\text{on}}/K_d^{\text{DNA}}$ . The  $K_d^{\text{DNA}}$  value was measured from a fluorescence titration assay.

<sup>b</sup>Estimated using EMSA.

<sup>c</sup>Measured using a fluorescence titration assay.

and full-length  $\gamma\text{Pol}\eta$ , respectively (Table 2 and Scheme 1). Interestingly, the rate of DNA dissociation from full-length  $\gamma\text{Pol}\eta$  is 2-fold slower than that from truncated  $\gamma\text{Pol}\eta$ , which indicated that the C-terminus of  $\gamma\text{Pol}\eta$  may slightly contribute to this polymerase's DNA binding affinity.

Based on the measured  $K_d^{\text{DNA}}$  from Figure 2(c) and  $k_{\text{off}}$  values, the apparent second-order association rate constant ( $k_{\text{on}} = k_{\text{off}}/K_d^{\text{DNA}}$ ) of the binary complex  $\gamma\text{Pol}\eta$ -DNA was calculated to be 0.62 and  $0.59 \mu\text{M}^{-1} \text{ s}^{-1}$  for truncated and full-length  $\gamma\text{Pol}\eta$ , respectively (Table 2). These similar  $k_{\text{on}}$  values indicate that the slightly stronger DNA binding affinity of full-length  $\gamma\text{Pol}\eta$  is mainly due to a slightly slower rate of DNA dissociation ( $k_{\text{off}}$ ). Taken together, the data in Table 2 suggest that the C-terminal 119 amino acid residues of  $\gamma\text{Pol}\eta$  slightly hinder the dissociation of DNA from the binary complex  $\gamma\text{Pol}\eta$ -DNA. This hindrance is through either direct physical interactions between the C-terminus of  $\gamma\text{Pol}\eta$  and DNA, modulation of the conformation of the polymerase domain by the C-terminus of  $\gamma\text{Pol}\eta$ , or both.

**3.3. Base Substitution Fidelity of Truncated  $\gamma\text{Pol}\eta$ .** Since a pre-steady-state burst was observed for truncated  $\gamma\text{Pol}\eta$ , we continued to investigate the nucleotide incorporation efficiency ( $k_p/K_d$ ) by measuring the maximum rate of nucleotide incorporation ( $k_p$ ) and the apparent equilibrium dissociation constant ( $K_d$ ) of an incoming nucleotide under single-turnover conditions [31]. By performing these experiments with  $\gamma\text{Pol}\eta$  in molar excess over DNA, the conversion of D-DNA<sub>n</sub> to D-DNA<sub>n+1</sub> (Scheme 1) was directly observed in a single pass through the enzymatic pathway [32]. A preincubated solution of truncated  $\gamma\text{Pol}\eta$  (150 nM) and 5'-[ $^{32}\text{P}$ ]-labeled D-7 DNA (30 nM) was mixed with varying concentrations of dATP·Mg<sup>2+</sup> (0.4–80  $\mu\text{M}$ ) and quenched with EDTA at

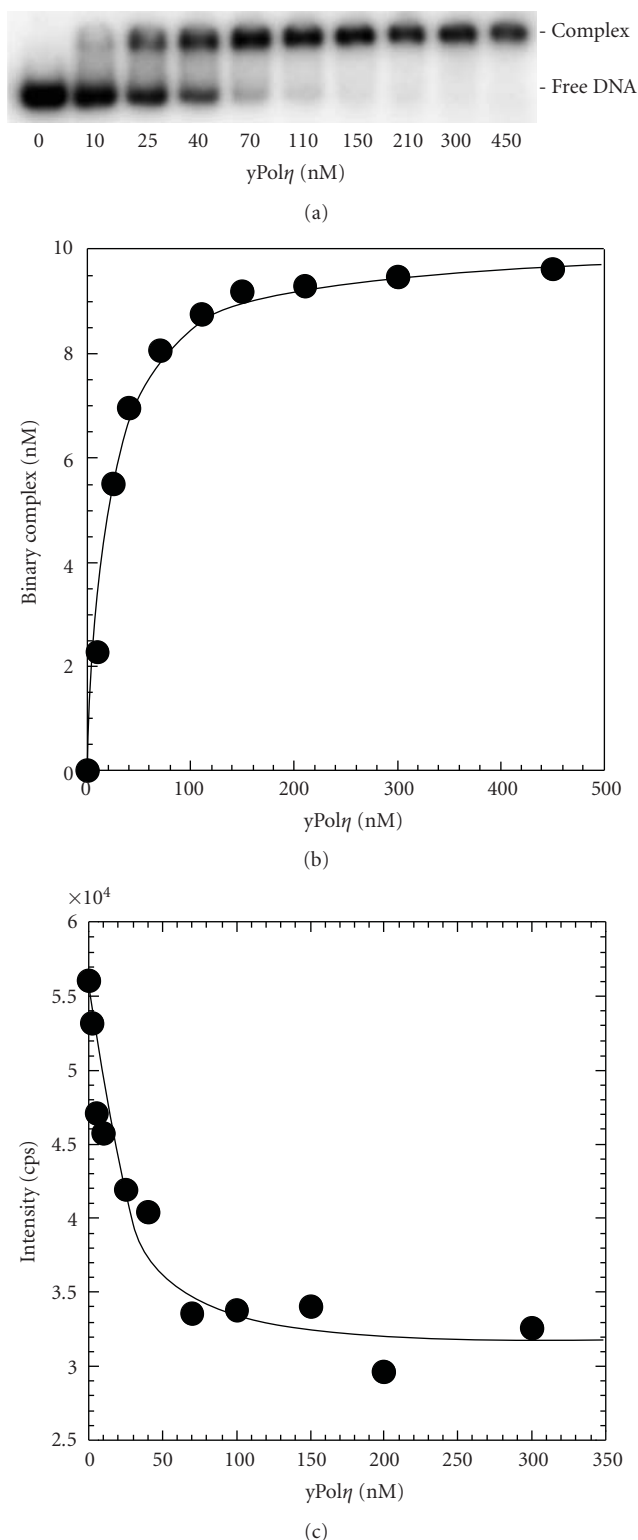


FIGURE 2: Equilibrium dissociation constant for full-length yPol $\eta$ . (a) Gel image showing binary complex formation at various concentrations of full-length yPol $\eta$  (10–450 nM) in the presence of 5′-[<sup>32</sup>P]-labeled D-1 DNA (10 nM). (b) The concentration of the binary complex was plotted as a function of full-length yPol $\eta$  concentration and fit to (2) to yield a  $K_d^{\text{DNA}} = 16 \pm 1$  nM. (c) For the fluorescence titration assay, a plot of fluorescence intensity versus full-length yPol $\eta$  concentration was fit to (3) which resolved a  $K_d^{\text{DNA}} = 7 \pm 4$  nM.

various times (see Section 2). A plot of product concentration versus time was fit to (5) to extract the observed rate constant ( $k_{\text{obs}}$ ) for dATP incorporation (Figure 3(a)). Then, the  $k_{\text{obs}}$  values were plotted as a function of dATP concentration and fit to a hyperbolic equation (6) which resolved a  $k_p$  of  $6.9 \pm 0.4$  s<sup>-1</sup> and an apparent  $K_d$  of  $17 \pm 3$   $\mu$ M (Figure 3(b)). The pre-steady-state kinetic parameters for the remaining 15 possible dNTP:dN base pair combinations were determined under single-turnover conditions and were used to calculate the substrate specificity constant ( $k_p/K_d$ ), discrimination factor ( $(k_p/K_d)_{\text{correct}}/(k_p/K_d)_{\text{incorrect}}$ ), and fidelity ( $(k_p/K_d)_{\text{incorrect}}/[(k_p/K_d)_{\text{correct}} + (k_p/K_d)_{\text{incorrect}}]$ ) of truncated yPol $\eta$  (Table 3).

Overall, the base substitution fidelity of truncated yPol $\eta$  was in the range of  $10^{-2}$  to  $10^{-4}$  which translates into 1 misincorporation per 100 to 10,000 nucleotide incorporations (Table 3). Depending on the mispair, truncated yPol $\eta$  catalyzed a misincorporation with 30- to 2,700-fold (640-fold on average) lower efficiency than the corresponding correct base pair. To better understand the mechanistic basis of truncated yPol $\eta$ 's fidelity, the equation for polymerase fidelity can be simplified as follows:

$$\begin{aligned} \text{Fidelity} &= \frac{(k_p/K_d)_{\text{incorrect}}}{[(k_p/K_d)_{\text{correct}} + (k_p/K_d)_{\text{incorrect}}]} \\ &\approx \frac{(k_p/K_d)_{\text{incorrect}}}{(k_p/K_d)_{\text{correct}}} \\ &= \left[ \frac{(k_p)_{\text{incorrect}}}{(k_p)_{\text{correct}}} \right]^{-1} \left[ \frac{(K_d)_{\text{correct}}}{(K_d)_{\text{incorrect}}} \right]^{-1} \\ &= (\text{rate difference})^{-1} (\text{binding affinity difference})^{-1}. \end{aligned} \quad (8)$$

Thus, fidelity is inversely proportional to the rate difference and apparent binding affinity difference between correct and incorrect nucleotide incorporation. In general, the mechanistic basis of yPol $\eta$ 's discrimination was due to a 3- to 68-fold (18-fold on average) weaker apparent binding affinity ( $1/K_d$ ) and 5- to 220-fold (50-fold on average) slower rate constant of incorporation for a mismatched dNTP.

**3.4. Kinetic Significance of Base Stacking Contributing to the Binding Affinity of an Incoming Nucleotide.** Although all four correct dNTPs were bound with similarly high affinity (Table 3), mismatched purine deoxyribonucleotides have 2- to 6-fold lower apparent  $K_d$  values than mismatched pyrimidine deoxyribonucleotides. Because 5′-protruding purines have been found to have stronger stacking interactions with a terminal DNA base pair than 5′-protruding pyrimidines [33], the difference in apparent  $K_d$  values suggests that base-stacking interactions between an incorrect dNTP and the terminal primer/template base pair dA:dT (Table 1) play a role on the binding of dNTP by truncated yPol $\eta$ . Interestingly, we have previously demonstrated that the preferred nucleotide for template-independent nucleotide

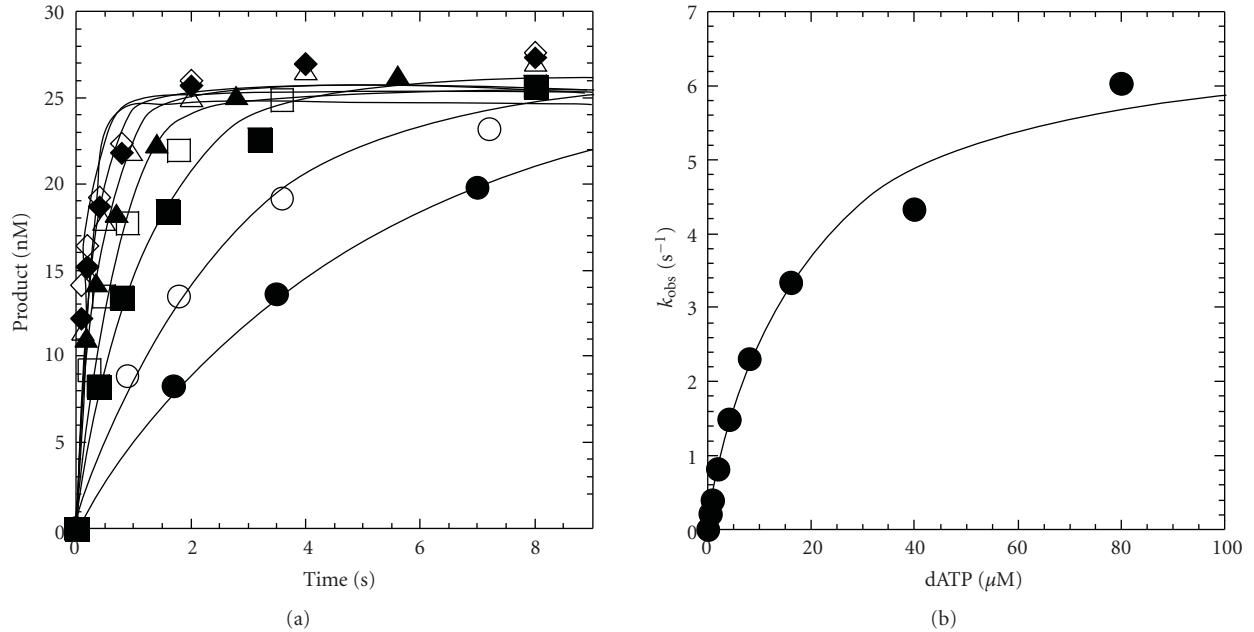


FIGURE 3: Concentration dependence on the pre-steady-state rate constant of nucleotide incorporation catalyzed by truncated yPol $\eta$ . (a) A preincubated solution of truncated yPol $\eta$  (150 nM) and 5'-[<sup>32</sup>P]-labeled D-7 DNA (30 nM) was mixed with dATP·Mg<sup>2+</sup> (0.4 μM, ●; 0.8 μM, ○; 2 μM, ■; 4 μM, □; 8 μM, ▲; 16 μM, △; 40 μM, ◆; 80 μM, ◇) and quenched with EDTA at various time intervals. The solid lines are the best fits to a single-exponential equation which determined the observed rate constant,  $k_{\text{obs}}$ . (b) The  $k_{\text{obs}}$  values were plotted as a function of dATP concentration. The data (●) were then fit to a hyperbolic equation, yielding a  $k_p$  of  $6.9 \pm 0.4 \text{ s}^{-1}$  and a  $K_d$  of  $17 \pm 3 \mu\text{M}$ .

TABLE 3: Kinetic parameters of nucleotide incorporation into D-DNA catalyzed by truncated yPol $\eta$  at 23°C.

dNTP	$k_p$ (s <sup>-1</sup> )	$K_d$ (μM)	$k_p/K_d$ (μM <sup>-1</sup> s <sup>-1</sup> )	Discrimination Factor <sup>a</sup>	Fidelity <sup>b</sup>
<i>Template dA (D-1)</i>					
dTTP	$3.9 \pm 0.2$	$15 \pm 2$	$2.6 \times 10^{-1}$		
dATP	$0.089 \pm 0.005$	$80 \pm 20$	$1.1 \times 10^{-3}$	230	$4.3 \times 10^{-3}$
dCTP	$0.43 \pm 0.06$	$210 \pm 60$	$2.0 \times 10^{-3}$	130	$7.8 \times 10^{-3}$
dGTP	$0.15 \pm 0.01$	$80 \pm 20$	$1.9 \times 10^{-3}$	140	$7.2 \times 10^{-3}$
<i>Template dG (D-6)</i>					
dCTP	$15.6 \pm 0.3$	$11.2 \pm 0.8$	1.4		
dATP	$0.071 \pm 0.002$	$138 \pm 9$	$5.1 \times 10^{-4}$	2700	$3.7 \times 10^{-4}$
dGTP	$0.116 \pm 0.006$	$80 \pm 10$	$1.5 \times 10^{-3}$	960	$1.0 \times 10^{-3}$
dTTP	$0.92 \pm 0.07$	$330 \pm 40$	$2.8 \times 10^{-3}$	500	$2.0 \times 10^{-3}$
<i>Template dT (D-7)</i>					
dATP	$6.9 \pm 0.4$	$17 \pm 3$	$4.1 \times 10^{-1}$		
dCTP	$1.00 \pm 0.04$	$210 \pm 20$	$4.8 \times 10^{-3}$	85	$1.2 \times 10^{-2}$
dGTP	$0.55 \pm 0.01$	$46 \pm 3$	$1.2 \times 10^{-2}$	30	$2.9 \times 10^{-2}$
dTTP	$0.62 \pm 0.02$	$280 \pm 20$	$2.2 \times 10^{-3}$	180	$5.4 \times 10^{-3}$
<i>Template dC (D-8)</i>					
dGTP	$6.3 \pm 0.1$	$6.8 \pm 0.4$	$9.3 \times 10^{-1}$		
dATP	$0.087 \pm 0.003$	$90 \pm 10$	$9.7 \times 10^{-4}$	960	$1.0 \times 10^{-3}$
dCTP	$0.127 \pm 0.007$	$200 \pm 30$	$6.4 \times 10^{-4}$	1500	$6.9 \times 10^{-4}$
dTTP	$1.39 \pm 0.06$	$460 \pm 40$	$3.0 \times 10^{-3}$	310	$3.3 \times 10^{-3}$

<sup>a</sup>Calculated as  $(k_p/K_d)_{\text{correct}} / (k_p/K_d)_{\text{incorrect}}$ .

<sup>b</sup>Calculated as  $(k_p/K_d)_{\text{incorrect}} / [(k_p/K_d)_{\text{correct}} + (k_p/K_d)_{\text{incorrect}}]$ .

TABLE 4: Kinetic parameters for nucleotide incorporation onto blunt-end DNA catalyzed by truncated yeast Pol $\eta$  at 23°C.

DNA (Terminal base pair)	dNTP	$k_p$ (s $^{-1}$ )	$K_d$ ( $\mu$ M)	$k_p/K_d$ ( $\mu$ M $^{-1}$ s $^{-1}$ )	Efficiency Ratio <sup>a</sup>
BE1 (dT:dA)	dATP	0.026 $\pm$ 0.002	1200 $\pm$ 200	2.2 $\times$ 10 $^{-5}$	—
	dPTP	1.27 $\pm$ 0.08	60 $\pm$ 10	2.1 $\times$ 10 $^{-2}$	980
BE2 (dA:dT)	dATP	0.036 $\pm$ 0.002	220 $\pm$ 30	1.6 $\times$ 10 $^{-4}$	—
	dPTP	0.68 $\pm$ 0.03	23 $\pm$ 3	3.0 $\times$ 10 $^{-2}$	180
BE3 (dG:dC)	dATP	0.0087 $\pm$ 0.0003	360 $\pm$ 30	2.4 $\times$ 10 $^{-5}$	—
	dPTP	0.22 $\pm$ 0.01	9 $\pm$ 2	2.4 $\times$ 10 $^{-2}$	1000
BE4 (dC:dG)	dATP	0.032 $\pm$ 0.001	930 $\pm$ 70	3.4 $\times$ 10 $^{-5}$	—
	dPTP	0.74 $\pm$ 0.03	12 $\pm$ 2	6.2 $\times$ 10 $^{-2}$	1800

<sup>a</sup>Calculated as  $(k_p/K_d)_{\text{dPTP}}/(k_p/K_d)_{\text{dATP}}$ .

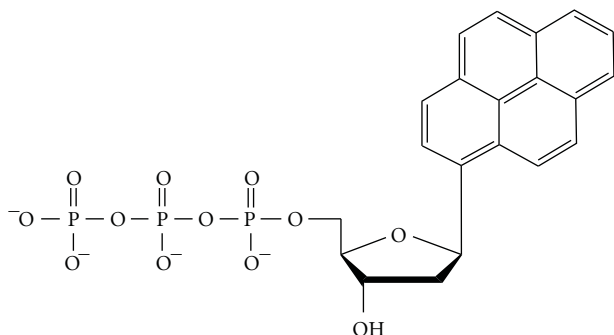


FIGURE 4: Chemical structure of a nonnatural nucleotide analog, dPTP.

incorporation catalyzed by Dpo4, another Y-family DNA polymerase, is dATP mainly due to its strong intrahelical base-stacking ability [26]. To further evaluate the role of base stacking, we first examined if truncated  $\gamma$ Pol $\eta$  can catalyze template-independent nucleotide incorporation of dATP or dPTP (Figure 4) onto four palindromic, blunt-end DNA substrates (BE1, BE2, BE3, and BE4 in Table 1). The base of dPTP, a dNTP analog, has four conjugated benzene rings but possesses no hydrogen-bonding abilities. The DNA substrates possess all four possible terminal base pairs and each molecule of them can be bound by a single polymerase molecule. Our radioactive experiments showed that truncated  $\gamma$ Pol $\eta$  was able to incorporate dATP and dPTP (data not shown). Then, we individually measured the kinetic parameters for dATP and dPTP incorporation under single-turnover reaction conditions (Table 4). Interestingly, the apparent  $K_d$  values of dATP were 3- to 5-fold smaller with a purine than those with a pyrimidine on the primer's 3'-base, indicating that base stacking is also important for the binding of dATP to the binary complex of  $\gamma$ Pol $\eta$ -blunt-end DNA. This base-stacking effect is more dramatic for dPTP incorporation onto blunt-end DNA because the apparent  $K_d$  values of dPTP are 10- to 80-fold tighter than dATP incorporation onto the same blunt-end DNA substrate (Table 4). Thus, the binding free energy difference between dATP and dPTP is 1.4 to 2.6 kcal/mol. Previously, we have obtained a comparable binding free energy difference of 2.3 kcal/mol for similar blunt-end dATP and dPTP incorporation at 37°C

catalyzed by Dpo4 [26]. Although neither dATP nor dPTP forms any hydrogen bonds with a template base when bound by  $\gamma$ Pol $\eta$ -blunt-end DNA, the bases of these two nucleotides should have different base-stacking interactions with a terminal base pair of a blunt-end DNA substrate considering that a dangling pyrene base (1.7 kcal/mol) has previously been found to possess a higher base-stacking free energy than a dangling adenosine (1.0 kcal/mol) [33]. However, the base-stacking free energy difference (0.7 kcal/mol) between pyrene and adenosine is smaller than the aforementioned binding free energy difference (1.4–2.6 kcal/mol) between dPTP and dATP. Thus, other sources likely contribute to the tighter binding of dPTP over dATP. One possible source is favorable van der Waals interactions between pyrene and active site residues of truncated  $\gamma$ Pol $\eta$ . In addition, the base-stacking effect and van der Waals interactions may stabilize the ternary complex of  $\gamma$ Pol $\eta$ -blunt-end DNA-nucleotide and facilitate catalysis, leading to much higher  $k_p$  values with dPTP than those with dATP (Table 4). Due to the differences in  $k_p$  and apparent  $K_d$ , the substrate specificity values of dPTP are 100- to 1,000-fold higher than those of dATP with blunt-end DNA (Table 4) and 10- to 100-fold higher than mismatched dATP with regular DNA (Table 3).

**3.5. Base Substitution Fidelity of Full-Length  $\gamma$ Pol $\eta$ .** The base substitution fidelities of full-length and truncated  $\gamma$ Pol $\eta$  may differ because the C-terminal, nonenzymatic regions may alter the polymerization fidelity. For example, the proline-rich domain of human DNA polymerase  $\lambda$  has been shown to upregulate the polymerase fidelity up to 100-fold [34]. To determine if the C-terminus of  $\gamma$ Pol $\eta$  influences polymerization fidelity, we measured the pre-steady-state kinetic parameters for dNTP incorporation into D-1 DNA (template dA) catalyzed by full-length  $\gamma$ Pol $\eta$  (Table 5). The fidelity was calculated to be in the range of  $(1.4 \text{ to } 2.6) \times 10^{-3}$  for full-length  $\gamma$ Pol $\eta$  (Table 5). Relative to the fidelity of truncated  $\gamma$ Pol $\eta$  with D-1 (Table 3), full-length  $\gamma$ Pol $\eta$  has a 3-fold higher fidelity. Therefore, the C-terminus of  $\gamma$ Pol $\eta$  slightly affects the base substitution fidelity. Moreover, truncated  $\gamma$ Pol $\eta$  discriminated between a correct and incorrect dNTP by  $\sim$ 30-fold on average based on the  $k_p$  difference while the discrimination for full-length  $\gamma$ Pol $\eta$  was  $\sim$ 170-fold on average for incorporation into D-1 DNA (Tables 3 and 5). The incorporation rate constant for correct dTTP was

TABLE 5: Kinetic parameters of nucleotide incorporation into D-1 DNA catalyzed by full-length  $\gamma$ Pol $\eta$  at 23°C.

dNTP	$k_p$ (s <sup>-1</sup> )	$K_d$ ( $\mu$ M)	$k_p/K_d$ ( $\mu$ M <sup>-1</sup> s <sup>-1</sup> )	Discrimination Factor <sup>a</sup>	Fidelity <sup>b</sup>
<i>Template dA (D-1)</i>					
dTTP	4.2 $\pm$ 0.5	40 $\pm$ 10	1.1 $\times$ 10 <sup>-1</sup>		
dATP	0.0235 $\pm$ 0.0003	156 $\pm$ 7	1.5 $\times$ 10 <sup>-4</sup>	700	1.4 $\times$ 10 <sup>-3</sup>
dCTP	0.019 $\pm$ 0.001	70 $\pm$ 10	2.7 $\times$ 10 <sup>-4</sup>	390	2.6 $\times$ 10 <sup>-3</sup>
dGTP	0.043 $\pm$ 0.003	170 $\pm$ 40	2.5 $\times$ 10 <sup>-4</sup>	420	2.4 $\times$ 10 <sup>-3</sup>

<sup>a</sup> Calculated as  $(k_p/K_d)_{\text{correct}}/(k_p/K_d)_{\text{incorrect}}$ .

<sup>b</sup> Calculated as  $(k_p/K_d)_{\text{incorrect}}/[(k_p/K_d)_{\text{correct}} + (k_p/K_d)_{\text{incorrect}}]$ .

$\sim 4$  s<sup>-1</sup> for both  $\gamma$ Pol $\eta$  enzymes, but the misincorporation rate was 3- to 23-fold faster for truncated  $\gamma$ Pol $\eta$ . This rate enhancement for truncated  $\gamma$ Pol $\eta$  is partially offset by a greater discrimination at the apparent ground-state binding level so that the fidelity of truncated  $\gamma$ Pol $\eta$  was only 3-fold lower than that of full-length  $\gamma$ Pol $\eta$ .

**3.6. Effect of the Nonenzymatic C-Terminus of  $\gamma$ Pol $\eta$  on Its Polymerase Activity.** Our above studies demonstrated that the C-terminus of  $\gamma$ Pol $\eta$  enhances this enzyme's DNA binding affinity and base substitution fidelity by 2- and 3-fold, respectively. These results suggest that the nonenzymatic, C-terminal region of  $\gamma$ Pol $\eta$  (Figure 1) has a mild impact on the N-terminal polymerase domain and its activity. This conclusion is inconsistent with previous studies which have qualitatively demonstrated that mutations or deletions in the UBZ domain or PIP motif do not affect polymerase activity [35–37]. However, these reported qualitative assays are not sufficiently sensitive to detect the small perturbation on polymerase activity as described in this paper. The presence of the C-terminal 119 residues of  $\gamma$ Pol $\eta$  may either interact with DNA, slightly alter the conformation of the polymerase domain, or both (see above discussion), thereby enhancing its DNA binding affinity and polymerase fidelity.

**3.7. Kinetic Comparison among Y-Family DNA Polymerases.** The fidelity of several Y-family DNA polymerases synthesizing undamaged DNA has been determined by employing steady-state [38–48], pre-steady-state [28, 30, 49–53], or M13-based mutation assays [39, 41, 42, 45, 54, 55]. From these studies, the fidelity ranges from 10<sup>0</sup> to 10<sup>-4</sup>. Under steady-state reaction conditions, the base substitution fidelity of  $\gamma$ Pol $\eta$  and human Pol $\eta$  has been measured to be in the range from 10<sup>-2</sup> to 10<sup>-4</sup> and 10<sup>-2</sup> to 10<sup>-3</sup>, respectively [38, 40], which is similar to our pre-steady-state kinetic results. Consistently, Pol $\eta$  displays the highest substrate specificity for the dCTP:dG base pair under both steady-state and pre-steady-state reaction conditions (Table 3 and unpublished data, Brown and Suo) [38, 40]. This may seem surprising, since Pol $\eta$  participates in the efficient bypass of UV-induced DNA damage such as a *cis-syn* thymine-thymine dimer (i.e., a dATP:dT base pair) [15–20, 56, 57]. However, Pol $\eta$  has also been shown to be efficient at bypassing guanine-specific damage such as 8-oxo-7,8-dihydro-dG [58, 59], 1,2-*cis*-diammineplatinum(II)-d(GpG) intrastrand cross-links [60–63], and various N2-dG lesions [64, 65].

Among the four eukaryotic Y-family DNA polymerases (i.e., Pol $\eta$ , DNA polymerase  $\kappa$ , DNA polymerase  $\iota$  (Pol $\iota$ ), and Rev1), Rev1 exhibits low fidelity on undamaged DNA due to its strong preference for inserting dCTP [46, 52] while Pol $\iota$  has an unusual preference for dGTP:dT mispairs over dATP:dT due to Hoogsteen base pair formation [51, 69]. Interestingly, the lowest fidelity base pair for truncated  $\gamma$ Pol $\eta$  was dGTP:dT (Table 3). This observation likely results from the formation of a wobble base pair. The two hydrogen bonds established in the wobble base pair may enhance the catalytic efficiency of  $\gamma$ Pol $\eta$  since hydrogen bonding is important for the efficiency and accuracy of  $\gamma$ Pol $\eta$  [70]. Also noteworthy, the truncated versions of eukaryotic Y-family DNA polymerases have been used for many biochemical studies in literature. Based on our quantitative kinetic analysis of  $\gamma$ Pol $\eta$ , these results suggested the nonenzymatic regions of Y-family DNA polymerases do not alter the polymerase activity significantly.

**3.8. Fidelity Comparison among Various DNA Polymerase Families.** As a Y-family DNA polymerase,  $\gamma$ Pol $\eta$  displays low fidelity on undamaged DNA (Tables 3 and 5) [38]. In contrast, replicative DNA polymerases in the A- and B-families have a polymerization fidelity that is 1–3 orders of magnitude greater than the Y-family DNA polymerases (Table 6). DNA polymerases with higher fidelity are more proficient at using the ground-state binding affinity to discriminate between a correct and incorrect dNTP. The Y-family DNA polymerases provide little to no discrimination based on the  $K_d$  difference while replicative DNA polymerases discriminate up to almost three orders of magnitude. This lack of selection in the ground state by the Y-family DNA polymerases may be due to the relatively loose and solvent-accessible active site which has minimal contacts with the nascent base pair [11, 21, 71]. Moreover, nucleotide selection by the Y-family DNA polymerases in the ground state may be mainly governed by Watson-Crick base pairing, since the calculated  $\Delta\Delta G$  values (0.95–1.7 kcal/mol) are similar to the free energy differences between correct and incorrect base pairs (0.3–1.0 kcal/mol at 37°C) at the primer terminus based on DNA melting studies (Table 6) [72]. However, with  $\Delta\Delta G$  values  $\geq 3.0$  kcal/mol, the replicative DNA polymerases harness the additional 2.0 kcal/mol of energy from other sources such as a tight active site or close contacts with the nascent base pair. One common fidelity checkpoint among DNA polymerases is the varying rate differences between a matched and mismatched

TABLE 6: Comparison of base substitution fidelity for various DNA polymerases.

Polymerase	Polymerase Family	Fidelity <sup>a</sup>	$K_d$ Difference <sup>b</sup>	$k_p$ Difference <sup>b</sup>	$\Delta\Delta G$ (kcal/mol) <sup>c</sup>
Truncated $\gamma$ Pol $\eta$ <sup>d</sup>	Y	$3.7 \times 10^{-4}$ to $2.9 \times 10^{-2}$	3 to 68	5 to 220	1.6
Dpo4 <sup>e</sup>	Y	$1.5 \times 10^{-4}$ to $3.2 \times 10^{-3}$	1 to 18	240 to 1700	0.95
rPol $\beta$ <sup>f</sup>	X	$1.1 \times 10^{-5}$ to $5.9 \times 10^{-4}$	35 to 342	28 to 708	3.0
PolB1 exo- <sup>g</sup>	B	$3.5 \times 10^{-6}$ to $1.2 \times 10^{-4}$	109 to 918	4 to 589	3.7
hPol $\gamma$ <sup>h</sup>	A	$4.6 \times 10^{-7}$ to $2.9 \times 10^{-4}$	42 to 900	39 to 12000	3.4

<sup>a</sup>Calculated as  $(k_p/K_d)_{\text{incorrect}} / [(k_p/K_d)_{\text{correct}} + (k_p/K_d)_{\text{incorrect}}]$ . <sup>b</sup>Calculated as defined in equation (8). <sup>c</sup>Calculated using equation (7). <sup>d</sup>At 23°C (this work).

<sup>e</sup>At 37°C [50]. <sup>f</sup>At 37°C [66]. <sup>g</sup>At 37°C, excluding the fidelity contribution from the 3' → 5' exonuclease activity [67]. <sup>h</sup>At 37°C, excluding the fidelity contribution from the 3' → 5' exonuclease activity [68].

base pair. These large differences may correspond to different rate-limiting steps (e.g., protein conformational change, or phosphodiester bond formation) during nucleotide incorporation [9, 30, 71]. For  $\gamma$ Pol $\eta$ , kinetic data suggest that correct and incorrect dNTPs are limited by a conformational step preceding chemistry, although, additional studies are needed to confirm these results [28].

#### 4. Conclusions

This work presents the mechanistic basis of the base substitution fidelity of  $\gamma$ Pol $\eta$  on undamaged DNA, which examined all possible dNTP:dN base pair combinations for the first time.  $\gamma$ Pol $\eta$  discriminates against incorrect nucleotides at both the ground-state nucleotide binding and incorporation steps. Furthermore, base stacking contributes to tighter binding for a misincorporation. Finally, the 119 residues at the C-terminus have a mild impact on the kinetic mechanism of  $\gamma$ Pol $\eta$ .

#### Abbreviations

BSA: Bovine serum albumin  
dNTP: 2'-deoxynucleoside 5'-triphosphate  
Dpo4: *Sulfolobus solfataricus* P2 DNA polymerase IV  
dPTP: Pyrene 5'-triphosphate  
EMSA: Electrophoretic mobility shift assay  
HPol $\gamma$ : Human mitochondrial DNA polymerase gamma  
PCNA: Proliferating cell nuclear antigen  
PIP: PCNA-interacting peptide  
PolB1: Exonuclease-deficient DNA polymerase B1 from *sulfolobus solfataricus* P2  
PolI: DNA polymerase iota  
rPol $\beta$ : Rat DNA polymerase beta  
TBE: Tris/boric acid/EDTA  
UBZ: Ubiquitin-binding zinc finger  
YPol $\eta$ : *Saccharomyces cerevisiae* DNA polymerase eta.

#### Acknowledgments

This work was supported by the National Institutes of Health Grants CA040463 (to Zucui Suo and John-Stephen Taylor) and GM032431 (to Peter M.J. Burgers). Jessica A. Brown was supported by an American Heart Association Pre-doctoral Fellowship (Grant 0815382D). Shanen M. Sherrer

was supported by a Predoctoral Fellowship from the National Institutes of Health Chemistry-Biology Interface Program at The Ohio State University (Grant 5 T32 GM008512-13). Brown and Zhang contributed equally to this work.

#### References

- [1] J. D. Fowler and Z. Suo, "Biochemical, structural, and physiological characterization of terminal deoxynucleotidyl transferase," *Chemical Reviews*, vol. 106, no. 6, pp. 2092–2110, 2006.
- [2] M. Garcia-Diaz and K. Bebenek, "Multiple functions of DNA polymerases," *Critical Reviews in Plant Sciences*, vol. 26, no. 2, pp. 105–122, 2007.
- [3] P. M. J. Burgers, E. V. Koonin, E. Bruford et al., "Eukaryotic DNA polymerases: proposal for a revised nomenclature," *Journal of Biological Chemistry*, vol. 276, no. 47, pp. 43487–43490, 2001.
- [4] T. A. Steitz, "DNA- and RNA-dependent DNA polymerases," *Current Opinion in Structural Biology*, vol. 3, no. 1, pp. 31–38, 1993.
- [5] J. D. Fowler, J. A. Brown, M. Kvaratskhelia, and Z. Suo, "Probing conformational changes of human DNA polymerase lambda using mass spectrometry-based protein footprinting," *Journal of Molecular Biology*, vol. 390, no. 3, pp. 368–379, 2009.
- [6] C. Castro, E. D. Smidansky, J. J. Arnold et al., "Nucleic acid polymerases use a general acid for nucleotidyl transfer," *Nature Structural and Molecular Biology*, vol. 16, no. 2, pp. 212–218, 2009.
- [7] A. A. Johnson, K. A. Fiala, and Z. Suo, "DNA polymerases and their interactions with DNA and nucleotides," in *Nucleoside Triphosphates and Their Analogs: Chemistry, Biotechnology, and Biological Applications*, M. M. Vaghefi, Ed., pp. 133–168, Taylor & Francis, Boca Raton, Fla, USA, 2005.
- [8] T. A. Steitz, "DNA polymerases: structural diversity and common mechanisms," *Journal of Biological Chemistry*, vol. 274, no. 25, pp. 17395–17398, 1999.
- [9] C. M. Joyce and S. J. Benkovic, "DNA polymerase fidelity: kinetics, structure, and checkpoints," *Biochemistry*, vol. 43, no. 45, pp. 14317–14324, 2004.
- [10] S. D. McCulloch and T. A. Kunkel, "The fidelity of DNA synthesis by eukaryotic replicative and translesion synthesis polymerases," *Cell Research*, vol. 18, no. 1, pp. 148–161, 2008.
- [11] H. Ling, F. Boudsocq, R. Woodgate, and W. Yang, "Crystal structure of a Y-family DNA polymerase in action: a mechanism for error-prone and lesion-bypass replication," *Cell*, vol. 107, no. 1, pp. 91–102, 2001.

- [12] S. Mizukami, T. W. Kim, S. A. Helquist, and E. T. Kool, "Varying DNA base-pair size in subangstrom increments: evidence for a loose, not large, active site in low-fidelity Dpo4 polymerase," *Biochemistry*, vol. 45, no. 9, pp. 2772–2778, 2006.
- [13] C. Xu, B. A. Maxwell, J. A. Brown, L. Zhang, and Z. Suo, "Global conformational dynamics of a Y-family DNA polymerase during catalysis," *PLoS Biology*, vol. 7, Article ID e1000225, 2009.
- [14] H. Ohmori, E. C. Friedberg, R. P. P. Fuchs et al., "The Y-family of DNA Polymerases," *Molecular Cell*, vol. 8, no. 1, pp. 7–8, 2001.
- [15] J. P. McDonald, A. S. Levine, and R. Woodgate, "The *Saccharomyces cerevisiae* RAD30 gene, a homologue of *Escherichia coli* dinB and umuC, is DNA damage inducible and functions in a novel error-free postreplication repair mechanism," *Genetics*, vol. 147, no. 4, pp. 1557–1568, 1997.
- [16] R. E. Johnson, S. Prakash, and L. Prakash, "Requirement of DNA polymerase activity of yeast Rad30 protein for its biological function," *Journal of Biological Chemistry*, vol. 274, no. 23, pp. 15975–15977, 1999.
- [17] A. A. Roush, M. Suarez, E. C. Friedberg, M. Radman, and W. Siede, "Deletion of the *Saccharomyces cerevisiae* gene RAD30 encoding an *Escherichia coli* DinB homolog confers UV radiation sensitivity and altered mutability," *Molecular and General Genetics*, vol. 257, no. 6, pp. 686–692, 1998.
- [18] R. E. Johnson, S. Prakash, and L. Prakash, "Efficient bypass of a thymine-thymine dimer by yeast DNA polymerase, Pol $\eta$ ," *Science*, vol. 283, no. 5404, pp. 1001–1004, 1999.
- [19] S.-L. Yu, R. E. Johnson, S. Prakash, and L. Prakash, "Requirement of DNA polymerase  $\eta$  for error-free bypass of UV-induced CC and TC photoproducts," *Molecular and Cellular Biology*, vol. 21, no. 1, pp. 185–188, 2001.
- [20] C. Masutani, R. Kusumoto, A. Yamada et al., "The XPV (xeroderma pigmentosum variant) gene encodes human DNA polymerase  $\eta$ ," *Nature*, vol. 399, no. 6737, pp. 700–704, 1999.
- [21] J. Trincão, R. E. Johnson, C. R. Escalante, S. Prakash, L. Prakash, and A. K. Aggarwal, "Structure of the catalytic core of *S. cerevisiae* DNA polymerase  $\eta$ : implications for translesion DNA synthesis," *Molecular Cell*, vol. 8, no. 2, pp. 417–426, 2001.
- [22] A. Alt, K. Lammens, C. Chiochini et al., "Bypass of DNA lesions generated during anticancer treatment with cisplatin by DNA polymerase  $\eta$ ," *Science*, vol. 318, no. 5852, pp. 967–970, 2007.
- [23] K. A. Fiala and Z. Suo, "Mechanism of DNA polymerization catalyzed by *Sulfolobus solfataricus* P2 DNA polymerase IV," *Biochemistry*, vol. 43, no. 7, pp. 2116–2125, 2004.
- [24] V. J. Cannistraro and J.-S. Taylor, "DNA-thumb interactions and processivity of T7 DNA polymerase in comparison to yeast polymerase  $\eta$ ," *Journal of Biological Chemistry*, vol. 279, no. 18, pp. 18288–18295, 2004.
- [25] P. Garg, C. M. Stith, J. Majka, and P. M. J. Burgers, "Proliferating cell nuclear antigen promotes translesion synthesis by DNA polymerase  $\zeta$ ," *Journal of Biological Chemistry*, vol. 280, no. 25, pp. 23446–23450, 2005.
- [26] K. A. Fiala, J. A. Brown, H. Ling et al., "Mechanism of template-independent nucleotide incorporation catalyzed by a template-dependent DNA polymerase," *Journal of Molecular Biology*, vol. 365, no. 3, pp. 590–602, 2007.
- [27] K. A. Fiala, C. D. Hypes, and Z. Suo, "Mechanism of abasic lesion bypass catalyzed by a Y-family DNA polymerase," *Journal of Biological Chemistry*, vol. 282, no. 11, pp. 8188–8198, 2007.
- [28] M. T. Washington, L. Prakash, and S. Prakash, "Yeast DNA polymerase  $\eta$  utilizes an induced-fit mechanism of nucleotide incorporation," *Cell*, vol. 107, no. 7, pp. 917–927, 2001.
- [29] J. A. Brown and Z. Suo, "Elucidating the kinetic mechanism of DNA polymerization catalyzed by *Sulfolobus solfataricus* P2 DNA polymerase B1," *Biochemistry*, vol. 48, no. 31, pp. 7502–7511, 2009.
- [30] K. A. Fiala, S. M. Sherrer, J. A. Brown, and Z. Suo, "Mechanistic consequences of temperature on DNA polymerization catalyzed by a Y-family DNA polymerase," *Nucleic Acids Research*, vol. 36, no. 6, pp. 1990–2001, 2008.
- [31] Y.-C. Tsai and K. A. Johnson, "A new paradigm for DNA polymerase specificity," *Biochemistry*, vol. 45, no. 32, pp. 9675–9687, 2006.
- [32] K. A. Johnson, "Transient-state kinetic analysis of enzyme reaction pathways," *Enzymes*, vol. 20, pp. 1–61, 1992.
- [33] K. M. Guckian, B. A. Schweitzer, R. X.-F. Ren, C. J. Sheils, D. C. Tahmassebi, and E. T. Kool, "Factors contributing to aromatic stacking in water: evaluation in the context of DNA," *Journal of the American Chemical Society*, vol. 122, no. 10, pp. 2213–2222, 2000.
- [34] K. A. Fiala, W. W. Duym, J. Zhang, and Z. Suo, "Up-regulation of the fidelity of human DNA polymerase  $\lambda$  by its non-enzymatic proline-rich domain," *Journal of Biological Chemistry*, vol. 281, no. 28, pp. 19038–19044, 2006.
- [35] L. Haracska, C. M. Kondratick, I. Unk, S. Prakash, and L. Prakash, "Interaction with PCNA is essential for yeast DNA polymerase  $\eta$  function," *Molecular Cell*, vol. 8, no. 2, pp. 407–415, 2001.
- [36] N. Acharya, A. Brahma, L. Haracska, L. Prakash, and S. Prakash, "Mutations in the ubiquitin binding UBZ motif of DNA polymerase  $\eta$  do not impair its function in translesion synthesis during replication," *Molecular and Cellular Biology*, vol. 27, no. 20, pp. 7266–7272, 2007.
- [37] Z. Zhuang, R. E. Johnson, L. Haracska, L. Prakash, S. Prakash, and S. J. Benkovic, "Regulation of polymerase exchange between Pol $\eta$  and Pol $\delta$  by monoubiquitination of PCNA and the movement of DNA polymerase holoenzyme," *Proceedings of the National Academy of Sciences of the United States of America*, vol. 105, no. 14, pp. 5361–5366, 2008.
- [38] M. T. Washington, R. E. Johnson, S. Prakash, and L. Prakash, "Fidelity and processivity of *Saccharomyces cerevisiae* DNA polymerase  $\eta$ ," *Journal of Biological Chemistry*, vol. 274, no. 52, pp. 36835–36838, 1999.
- [39] T. Matsuda, K. Bebenek, C. Masutani, F. Hanaoka, and T. A. Kunkel, "Low fidelity DNA synthesis by human DNA polymerase- $\eta$ ," *Nature*, vol. 404, no. 6781, pp. 1011–1013, 2000.
- [40] R. E. Johnson, M. T. Washington, S. Prakash, and L. Prakash, "Fidelity of human DNA polymerase  $\eta$ ," *Journal of Biological Chemistry*, vol. 275, no. 11, pp. 7447–7450, 2000.
- [41] Y. Zhang, F. Yuan, H. Xin et al., "Human DNA polymerase  $\kappa$  synthesizes DNA with extraordinarily low fidelity," *Nucleic Acids Research*, vol. 28, no. 21, pp. 4147–4156, 2000.
- [42] E. Ohashi, K. Bebenek, T. Matsuda et al., "Fidelity and processivity of DNA synthesis by DNA polymerase  $\kappa$ , the product of the human DINB1 gene," *Journal of Biological Chemistry*, vol. 275, no. 50, pp. 39678–39684, 2000.
- [43] A. Tissier, J. P. McDonald, E. G. Frank, and R. Woodgate, "pol $\iota$ , a remarkably error-prone human DNA polymerase," *Genes and Development*, vol. 14, no. 13, pp. 1642–1650, 2000.
- [44] F. Boudsocq, S. Iwai, F. Hanaoka, and R. Woodgate, "*Sulfolobus solfataricus* P2 DNA polymerase IV (Dp04): an

- archaeal DinB-like DNA polymerase with lesion-bypass properties akin to eukaryotic pol $\eta$ ,” *Nucleic Acids Research*, vol. 29, no. 22, pp. 4607–4616, 2001.
- [45] R. J. Kokoska, K. Bebenek, F. Boudsocq, R. Woodgate, and T. A. Kunkel, “Low fidelity DNA synthesis by a Y family DNA polymerase due to misalignment in the active site,” *Journal of Biological Chemistry*, vol. 277, no. 22, pp. 19633–19638, 2002.
- [46] L. Haracska, S. Prakash, and L. Prakash, “Yeast Rev1 protein is a G template-specific DNA polymerase,” *Journal of Biological Chemistry*, vol. 277, no. 18, pp. 15546–15551, 2002.
- [47] A. Vaisman, H. Ling, R. Woodgate, and W. Yang, “Fidelity of Dpo4: effect of metal ions, nucleotide selection and pyrophosphorolysis,” *EMBO Journal*, vol. 24, no. 17, pp. 2957–2967, 2005.
- [48] Y. Zhang, X. Wu, O. Rechkoblit, N. E. Geacintov, J.-S. Taylor, and Z. Wang, “Response of human REV1 to different DNA damage: preferential dCMP insertion opposite the lesion,” *Nucleic Acids Research*, vol. 30, no. 7, pp. 1630–1638, 2002.
- [49] M. T. Washington, R. E. Johnson, L. Prakash, and S. Prakash, “The mechanism of nucleotide incorporation by human DNA polymerase  $\eta$  differs from that of the yeast enzyme,” *Molecular and Cellular Biology*, vol. 23, no. 22, pp. 8316–8322, 2003.
- [50] K. A. Fiala and Z. Suo, “Pre-steady-state kinetic studies of the fidelity of *Sulfolobus solfataricus* P2 DNA polymerase IV,” *Biochemistry*, vol. 43, no. 7, pp. 2106–2115, 2004.
- [51] M. T. Washington, R. E. Johnson, L. Prakash, and S. Prakash, “Human DNA polymerase  $\iota$  utilizes different nucleotide incorporation mechanisms dependent upon the template base,” *Molecular and Cellular Biology*, vol. 24, no. 2, pp. 936–943, 2004.
- [52] C. A. Howell, S. Prakash, and M. T. Washington, “Pre-steady-state kinetic studies of protein-template-directed nucleotide incorporation by the yeast Rev1 protein,” *Biochemistry*, vol. 46, no. 46, pp. 13451–13459, 2007.
- [53] S. M. Sherrer, J. A. Brown, L. R. Pack et al., “Mechanistic studies of the bypass of a bulky single-base lesion catalyzed by a Y-family DNA polymerase,” *Journal of Biological Chemistry*, vol. 284, no. 10, pp. 6379–6388, 2009.
- [54] O. Potapova, N. D. F. Grindley, and C. M. Joyce, “The mutational specificity of the Dbh lesion bypass polymerase and its implications,” *Journal of Biological Chemistry*, vol. 277, no. 31, pp. 28157–28166, 2002.
- [55] F. Boudsocq, R. J. Kokoska, B. B. Plosky et al., “Investigating the role of the little finger domain of Y-family DNA polymerases in low fidelity synthesis and translesion replication,” *Journal of Biological Chemistry*, vol. 279, no. 31, pp. 32932–32940, 2004.
- [56] R. E. Johnson, C. M. Kondratick, S. Prakash, and L. Prakash, “hRAD30 mutations in the variant form of xeroderma pigmentosum,” *Science*, vol. 285, no. 5425, pp. 263–265, 1999.
- [57] M. T. Washington, L. Prakash, and S. Prakash, “Mechanism of nucleotide incorporation opposite a thymine-thymine dimer by yeast DNA polymerase  $\eta$ ,” *Proceedings of the National Academy of Sciences of the United States of America*, vol. 100, no. 21, pp. 12093–12098, 2003.
- [58] L. Haracska, S.-L. Yu, R. E. Johnson, L. Prakash, and S. Prakash, “Efficient and accurate replication in the presence of 7,8-dihydro-8-oxoguanine by DNA polymerase  $\eta$ ,” *Nature Genetics*, vol. 25, no. 4, pp. 458–461, 2000.
- [59] K. D. Carlson and M. T. Washington, “Mechanism of efficient and accurate nucleotide incorporation opposite 7,8-dihydro-8-oxoguanine by *Saccharomyces cerevisiae* DNA polymerase  $\eta$ ,” *Molecular and Cellular Biology*, vol. 25, no. 6, pp. 2169–2176, 2005.
- [60] A. Vaisman, C. Masutani, F. Hanaoka, and S. G. Chaney, “Efficient translesion replication past oxaliplatin and cisplatin GpG adducts by human DNA polymerase  $\eta$ ,” *Biochemistry*, vol. 39, no. 16, pp. 4575–4580, 2000.
- [61] C. Masutani, R. Kusumoto, S. Iwai, and F. Hanaoka, “Mechanisms of accurate translesion synthesis by human DNA polymerase  $\eta$ ,” *EMBO Journal*, vol. 19, no. 12, pp. 3100–3109, 2000.
- [62] E. Bassett, A. Vaisman, K. A. Tropea et al., “Frameshifts and deletions during in vitro translesion synthesis past Pt-DNA adducts by DNA polymerases  $\beta$  and  $\eta$ ,” *DNA Repair*, vol. 1, no. 12, pp. 1003–1016, 2002.
- [63] E. Bassett, A. Vaisman, J. M. Havener, C. Masutani, F. Hanaoka, and S. G. Chaney, “Efficiency of extension of mismatched primer termini across from cisplatin and oxaliplatin adducts by human DNA polymerases  $\beta$  and  $\eta$  in vitro,” *Biochemistry*, vol. 42, no. 48, pp. 14197–14206, 2003.
- [64] J.-Y. Choi and F. P. Guengerich, “Adduct size limits efficient and error-free bypass across bulky N 2-guanine DNA lesions by human DNA polymerase  $\eta$ ,” *Journal of Molecular Biology*, vol. 352, no. 1, pp. 72–90, 2005.
- [65] J.-Y. Choi, H. Zang, K. C. Angel et al., “Translesion synthesis across 1,N2-ethenoguanine by human DNA polymerases,” *Chemical Research in Toxicology*, vol. 19, no. 6, pp. 879–886, 2006.
- [66] J. Ahn, V. S. Kraynov, X. Zhong, B. G. Werneburg, and M.-D. Tsai, “DNA polymerase  $\beta$ : effects of gapped DNA substrates on dNTP specificity, fidelity, processivity and conformational changes,” *Biochemical Journal*, vol. 331, part 1, pp. 79–87, 1998.
- [67] L. Zhang, J. A. Brown, S. A. Newmister, and Z. Suo, “Polymerization fidelity of a replicative DNA polymerase from the hyperthermophilic archaeon *Sulfolobus solfataricus* P2,” *Biochemistry*, vol. 48, no. 31, pp. 7492–7501, 2009.
- [68] H. R. Lee and K. A. Johnson, “Fidelity of the human mitochondrial DNA polymerase,” *Journal of Biological Chemistry*, vol. 281, no. 47, pp. 36236–36240, 2006.
- [69] D. T. Nair, R. E. Johnson, S. Prakash, L. Prakash, and A. K. Aggarwal, “Replication by human DNA polymerase- $\iota$  occurs by Hoogsteen base-pairing,” *Nature*, vol. 430, no. 6997, pp. 377–380, 2004.
- [70] M. T. Washington, S. A. Helquist, E. T. Kool, L. Prakash, and S. Prakash, “Requirement of Watson-Crick hydrogen bonding for DNA synthesis by yeast DNA polymerase  $\eta$ ,” *Molecular and Cellular Biology*, vol. 23, no. 14, pp. 5107–5112, 2003.
- [71] J. H. Wong, K. A. Fiala, Z. Suo, and H. Ling, “Snapshots of a Y-family DNA polymerase in replication: substrate-induced conformational transitions and implications for fidelity of Dpo4,” *Journal of Molecular Biology*, vol. 379, no. 2, pp. 317–330, 2008.
- [72] J. Petruska, M. F. Goodman, M. S. Boosalis, L. C. Sowers, C. Cheong, and I. Tinoco Jr., “Comparison between DNA melting thermodynamics and DNA polymerase fidelity,” *Proceedings of the National Academy of Sciences of the United States of America*, vol. 85, no. 17, pp. 6252–6256, 1988.

## Research Article

# Replication Past the $\gamma$ -Radiation-Induced Guanine-Thymine Cross-Link G[8,5-Me]T by Human and Yeast DNA Polymerase $\eta$

Paromita Raychaudhury and Ashis K. Basu

Department of Chemistry, University of Connecticut, Storrs, CT 06269, USA

Correspondence should be addressed to Ashis K. Basu, ashis.basu@uconn.edu

Received 9 June 2010; Accepted 2 July 2010

Academic Editor: Shigenori Iwai

Copyright © 2010 P. Raychaudhury and A. K. Basu. This is an open access article distributed under the Creative Commons Attribution License, which permits unrestricted use, distribution, and reproduction in any medium, provided the original work is properly cited.

$\gamma$ -Radiation-induced intrastrand guanine-thymine cross-link, G[8,5-Me]T, hinders replication *in vitro* and is mutagenic in mammalian cells. Herein we report *in vitro* translesion synthesis of G[8,5-Me]T by human and yeast DNA polymerase  $\eta$  (hPol  $\eta$  and yPol  $\eta$ ). dAMP misincorporation opposite the cross-linked G by yPol  $\eta$  was preferred over correct incorporation of dCMP, but further extension was 100-fold less efficient for G\*:A compared to G\*:C. For hPol  $\eta$ , both incorporation and extension were more efficient with the correct nucleotides. To evaluate translesion synthesis in the presence of all four dNTPs, we have developed a plasmid-based DNA sequencing assay, which showed that yPol  $\eta$  was more error-prone. Mutational frequencies of yPol  $\eta$  and hPol  $\eta$  were 36% and 14%, respectively. Targeted G  $\rightarrow$  T was the dominant mutation by both DNA polymerases. But yPol  $\eta$  induced targeted G  $\rightarrow$  T in 23% frequency relative to 4% by hPol  $\eta$ . For yPol  $\eta$ , targeted G  $\rightarrow$  T and G  $\rightarrow$  C constituted 83% of the mutations. By contrast, with hPol  $\eta$ , semi-targeted mutations (7.2%), that is, mutations at bases near the lesion, occurred at equal frequency as the targeted mutations (6.9%). The kind of mutations detected with hPol  $\eta$  showed significant similarities with the mutational spectrum of G[8,5-Me]T in human embryonic kidney cells.

## 1. Introduction

DNA-DNA interstrand and intrastrand cross-links are strong blocks of DNA replication, and understanding the details of polymerase bypass of these complex lesions is of major interest [1–5]. The double base DNA lesions are formed at substantial frequency by ionizing radiation and by metal-catalyzed H<sub>2</sub>O<sub>2</sub> reactions (reviewed in [6]). A major DNA damage, in anoxic conditions, is an intrastrand cross-linked species in which C8 of Gua is linked to the 5-methyl group of an adjacent thymine, but the G[8,5-Me]T cross-link is formed at a much higher rate than the T[5-Me,8]G cross-link (Figure 1) [7]. Additional thymine-purine cross-links have been isolated from  $\gamma$ -irradiated DNA in oxygen-free aqueous solution [8]. Wang and coworkers identified structurally similar guanine-cytosine and guanine-5-methylcytosine cross-links in DNA exposed to  $\gamma$ - or X-rays [9–11]. The G[8,5-Me]T cross-link is formed in a dose-dependent manner in human cells when exposed to  $\gamma$ -rays [12], and the G[8,5]C cross-link is formed at a slightly lower level [13].

These intrastrand cross-links destabilize the DNA double helix [14], and UvrABC, the excision nuclease proteins from *Escherichia coli*, can excise them [15, 16]. Using purified DNA polymerases, it was shown that G[8,5-Me]T and G[8,5]C are strong blocks of replication *in vitro* [12, 17]. For G[8,5-Me]T, primer extension is terminated after incorporation of dAMP opposite the 3'-T by exo-free Klenow fragment and Pol IV (dinB) of *Escherichia coli* whereas Taq polymerase is completely blocked at the nucleotide preceding the cross-link [17]. However, yeast polymerase  $\eta$  (yPol  $\eta$ ), a member of the Y-family DNA polymerase from *Saccharomyces cerevisiae*, can bypass both G[8,5-Me]T and G[8,5]C cross-links with reduced efficiency [12, 18]. For both these two lesions, nucleotide incorporation opposite the 3'-base of the cross-link is accurate, but the incorporation of dAMP and dGMP is favored opposite the cross-linked G by yPol  $\eta$  over that of the correct nucleotide, dCMP [12, 18].

We have recently compared translesion synthesis of G[8,5-Me]T with T[5-Me,8]G in simian and human embryonic kidney cells and found that both cross-links are strongly

mutagenic and that the two lesions show interesting pattern of mutations, which included high frequency of semitargeted mutations that occurred a few bases 5' or 3' to the cross-link [19]. One can anticipate a role of one or more Y-family DNA polymerases in bypassing these replication blocking lesions, and we noted that purified human DNA polymerase  $\eta$  (hPol  $\eta$ ) incorporates dCMP preferentially opposite the G of G[8,5-Me]T cross-link, in contrast to  $\gamma$ Pol  $\eta$  which incorporates dAMP and dGMP much more readily [12, 19]. However, the previous preliminary studies did not examine the kinetics of polymerase extension beyond the lesion site; nor were the full-length extension products analyzed. The kinetics of nucleotide incorporations are influenced by DNA damages, not only at the lesion site but at least up to 3 bases 5' to the lesion [20]. Therefore, incorporation pattern opposite the lesion provides only part of the information on lesion bypass. In the current paper, we have evaluated translesion synthesis of the G[8,5-Me]T cross-link by these two DNA polymerases more critically by determining single nucleotide incorporation kinetics and characterizing the full-length extension products in the presence of all four dNTPs. We report herein that G[8,5-Me]T bypass by  $\gamma$ Pol  $\eta$  is much more error-prone than hPol  $\eta$ . We also show that the mutational signatures of these two polymerases are different.

## 2. Materials and Methods

**2.1. Materials.** [ $\gamma$ -<sup>32</sup>P] ATP was supplied by Du Pont New England Nuclear (Boston, MA). Recombinant human and yeast DNA polymerases  $\eta$  were purchased from Enzymax, LLC. (Lexington, KY). *EcoR* V restriction endonuclease, T4 DNA ligase, and T4 polynucleotide kinase were obtained from New England Biolabs (Beverly, MA). *E. coli* DL7 (AB1157, *lac* $\Delta$ U169, *uvr*<sup>+</sup>) was from J. Essigmann (MIT, Cambridge, MA). The pMS2 phagemid was a gift from Masaaki Moriya (SUNY, Stony Brook, NY).

### 2.2. Methods

**2.2.1. Synthesis and Characterization of Oligonucleotides.** The lesions containing oligonucleotides have been synthesized and characterized as reported in [15]. Unmodified oligonucleotides were analyzed by MALDI-TOF MS analysis, which gave a molecular ion with a mass within 0.005% of theoretical whereas adducted oligonucleotides were analyzed by ESI-MS in addition to digestion followed by HPLC analysis.

**2.2.2. Construction of 26-mer and 36-mer Containing G[8,5-Me]T Cross-Link.** The 26-mer G[8,5-Me]T template, 5'-GTGCG<sup>+</sup>TGTTTGTATCGCTTGCAGGGG-3', was constructed by ligating a 5'-phosphorylated 14-mer, 5'-ATC-GCTTGCAGGGG-3' (~7.5 nmol), to the G[8,5-Me]T cross-linked 12-mer, 5'-GTGCG<sup>+</sup>TGTTTGT-3' (~5 nmol), in the presence of an 18-nucleotide complementary oligonucleotide, 5'-GCAAGCGATACAAACACG-3' (~7.5 nmol),

as described [19, 21]. Similarly, a 12-mer, 5'-CCUGGA-AGCGAU-3' (~7.5 nmol), a 5'-phosphorylated G[8,5-Me]T 12-mer (~5 nmol), and a 5'-phosphorylated 12-mer, 5'-AUCGCUGCUACC-3' (~7.5 nmol), were annealed to a complementary 26-mer, 5'-GCAGCGATACAAACACGC-ACATCGCT-3' (~7.5 nmol), and ligated in the presence of T4 DNA ligase to prepare a G[8,5-Me]T cross-linked 36-mer, 5'-CCUGGAAGCGAUGTGCG<sup>+</sup>TGTTTGTATCGCUGCUACC-3'. The oligonucleotides were separated by electrophoresis on a 16% polyacrylamide-8 M urea gel. The ligated product bands were visualized by UV shadowing and excised. The 26-mers and the 36-mers were desalted on a Sephadex G-25 (Sigma) column and stored at -20°C until further use.

### 2.2.3. In Vitro Nucleotide Incorporation and Chain Extension.

To determine the nucleotide preferentially incorporated opposite G[8,5-Me]T cross-link, the steady-state kinetic analyses were performed by the method of Goodman and coworkers [22, 23]. The primed template was obtained by annealing 5-fold molar excess of the modified or control 26-mer template (~20 ng) to a complementary 5'-<sup>32</sup>P-labeled primer. Primer extension under standing start conditions was carried out with hPol  $\eta$  or  $\gamma$ Pol  $\eta$  (6.4 nM) with individual dNTPs or a mixture of all four dNTPs in 25 mM Tris-HCl buffer (pH 7.5), 5 mM MgCl<sub>2</sub>, and 5 mM dithiothreitol at 37°C for various times. The reactions were terminated by adding an equal volume of 95% (v/v) formamide, 20 mM EDTA, 0.02% (w/v) xylene cyanol, and 0.02% (w/v) bromophenol blue and heating at 90°C for 2 min, and the products were resolved on a 20% polyacrylamide gel containing 8 M urea. The DNA bands were visualized and quantitated using a Phosphorimager. The dNTP concentration and time of incubation were optimized to ensure that primer extension was less than 20%. The  $K_m$  and  $k_{cat}$  were extrapolated from the Michaelis-Menten plot of the kinetic data.

### 2.2.4. Analysis of the Full-Length Bypass Products Using pMS2 Vector.

The ss pMS2 shuttle vector DNA (58 pmols, 100  $\mu$ g) was digested with an excess of *EcoR* V (300 pmol, 4.84  $\mu$ g) for 1 h at 37°C followed by room temperature overnight. A 36-mer scaffold oligonucleotide containing the G[8,5-Me]T cross-link (or a control) was annealed overnight at 16°C to form the gapped DNA. The gapped plasmid was incubated with hPol  $\eta$  or  $\gamma$ Pol  $\eta$  and a mixture of all four dNTPs (25 mM each) in 25 mM Tris-HCl buffer (pH 7.5), 5 mM MgCl<sub>2</sub>, and 5 mM dithiothreitol at 37°C for various times. DNA ligase (200 units) was added, and the pMS2 mixture containing the DNA polymerase, dNTPs, and so forth, was ligated overnight at 16°C. The scaffold oligonucleotide was digested by treatment with uracil glycosylase and exonuclease III, the proteins were extracted with phenol/chloroform, and the DNA was precipitated with ethanol. The final construct was dissolved in deionized water and used to transform *E. coli* DL7 cells. The transformants were randomly picked and analyzed by DNA sequencing.

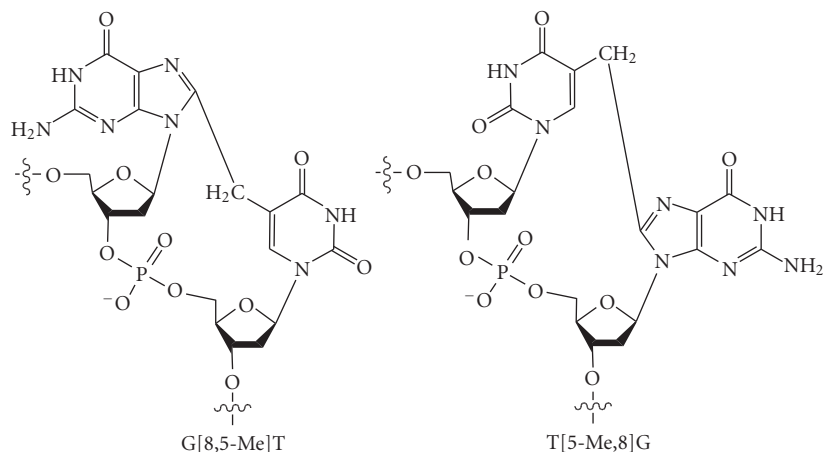


FIGURE 1: Chemical structures of the two  $\gamma$ -radiation-induced intrastrand cross-links, G[8,5-Me]T and T[5-Me,8]G.

### 3. Results

**3.1. In Vitro Bypass by DNA Polymerase  $\eta$ .** A 26-mer template, 5'-GTGCG<sup>^</sup>TGTTTGTATCGCTTGCAGGGG-3', which contained the G[8,5-Me]T cross-link (G<sup>^</sup>T) at the 5th and 6th bases from the 5' end, was constructed. The DNA sequence of the first 12-nucleotides in this template was taken from codon 272–275 of the *p53* gene, in which the G[8,5-Me]T cross-link was incorporated at the second and third nucleotide of codon 273, a well-known mutational hotspot for human cancer [24]. We used both running start and standing start conditions to evaluate bypass of the cross-link. Template-primer complex (50 nM) was incubated with increasing concentration of hPol  $\eta$  and yPol  $\eta$  at 37°C for 30 min in the presence of all four dNTPs (100  $\mu$ M). For the running start experiments, a 5'-<sup>32</sup>P-radiolabeled 14-mer primer, 5'-CTGCAAGCGATAACA-3', was annealed to the template so that it was 3 bases 3' to the cross-link. As shown in Figure 2, G[8,5-Me]T was a strong block of both DNA polymerases. With 5 nM hPol  $\eta$ , 80% of the control template extended to a 22-mer and a 23-mer (full-length) products whereas for G[8,5-Me]T less than 1% extended to the full-length product, and a major block was at the cross-linked G (19-mer). With 20 nM hPol  $\eta$ , nearly 75% was blocked after incorporating a base opposite the cross-linked G (19-mer), and the full-length product increased only to ~10%. The full-length product increased to ~18% with 50 nM hPol  $\eta$ . In similar experiment using yPol  $\eta$ , unlike the human enzyme, the major blocks were at 19-mer and 20-mer (i.e., opposite the cross-linked G and its 5' neighbor). With 50 nM yPol  $\eta$ , 8% of the primer extended to full-length 23-mer product.

With concentrations of hPol  $\eta$  and yPol  $\eta$  at 50 nM, a substantial fraction (18% and 8%, resp.) of the primer extended to full-length products in 30 min. So we chose to use 50 nM Pol  $\eta$  concentrations for the subsequent experiment. As shown in Figure 3, in the presence of all four dNTPs, extension of a 14-mer primer on the control template rapidly generated a full-length extension product (a 23-mer) as well as a blunt-end addition product (a 24-mer) in 5 min with 50 nM hPol  $\eta$  whereas the extension of

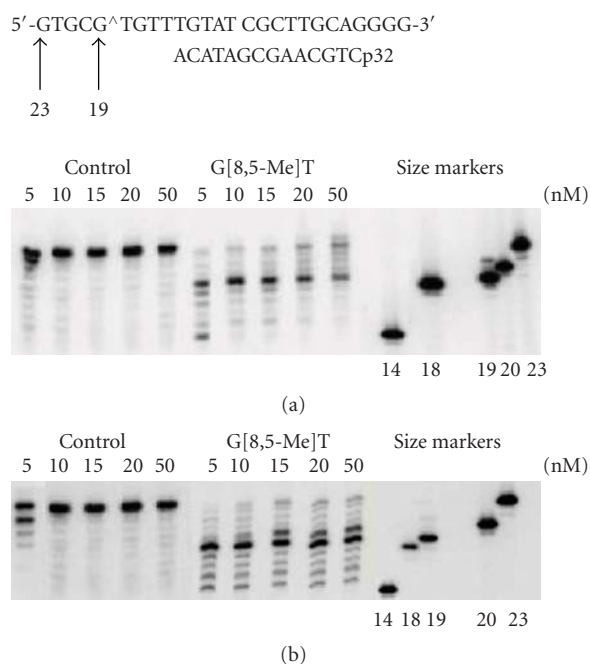


FIGURE 2: Extension of a 14-mer primer by varying concentration (5, 10, 15, 20, and 50 nM) of hPol  $\eta$  (a) and yPol  $\eta$  (b) on control and G[8,5-Me]T templates in the presence of all four dNTPs. The experiments were carried out at 37°C for 30 min.

the primer stalled after adding a base opposite the cross-linked T and G, generating a 19-mer. It is interesting that hPol  $\eta$  did not stall before either of the cross-linked bases, but it was unable to continue synthesis only after incorporating a dNMP opposite the cross-linked G. Longer incubation allowed further extension, including a small fraction of full-length product, but even after 2 h the 19-mer band was the most pronounced extension product. The result was qualitatively similar with yPol  $\eta$ , except that the extent of full-length product was only marginally increased with time and it stalled both after incorporation of a nucleotide opposite

TABLE 1: Kinetic parameters for dCTP and dATP incorporation and chain extension by human DNA polymerase  $\eta$  (6.4 nM) on an undamaged and G[8,5-Me]T cross-link containing substrate.

dNTP	$k_{\text{cat}}$ ( $\text{min}^{-1}$ )	$K_m$ ( $\mu\text{M}$ )	$k_{\text{cat}}/K_m$ ( $\mu\text{M}^{-1} \text{min}^{-1}$ )	$F_{\text{inc}}^a$	X:G	$k_{\text{cat}}$ ( $\text{min}^{-1}$ )	$K_m$ ( $\mu\text{M}$ )	$k_{\text{cat}}/K_m$ ( $\mu\text{M}^{-1} \text{min}^{-1}$ )	$F_{\text{ext}}^a$	
	5'-GTGCG <sup>^</sup> TGTTTGTATCGCTTGCAGGGG-3' ACAAACATAGCGAACp32 Nucleotide Incorporation					5'-GTGCG <sup>^</sup> TGTTTGTATCGCTTGCAGGGG-3' X ACAAACATAGCGAACp32 Chain Extension <sup>b</sup>				
Undamaged substrate										
dCTP	$7.6 \pm 0.1$	$0.02 \pm 0.003$	380	1.0	C:G	$3.9 \pm 0.2$	$0.09 \pm 0.005$	43.4	1.0	
dATP	$6.25 \pm 0.01$	$6.5 \pm 0.03$	0.96	$2.5 \times 10^{-3}$	A:G	$4.7 \pm 0.1$	$5.1 \pm 0.03$	0.9	$2.1 \times 10^{-2}$	
G[8,5-Me]T-containing substrate										
dCTP	$2.43 \pm 0.02$	$0.11 \pm 0.002$	22.1	$5.8 \times 10^{-2}$	C:G*	$2.0 \pm 0.02$	$0.24 \pm 0.004$	8.3	0.2	
dATP	$1.75 \pm 0.1$	$1.07 \pm 0.01$	1.63	$4.2 \times 10^{-3}$	A:G*	$1.7 \pm 0.01$	$2.6 \pm 0.03$	0.65	$1.5 \times 10^{-2}$	

<sup>a</sup>Fidelity ( $F$ ) of incorporation or extension was determined by the following equation:  $(k_{\text{cat}}/K_m)_{\text{incorrect}}/(k_{\text{cat}}/K_m)_{\text{correct}}$ .

<sup>b</sup>Steady-state kinetics for dGTP incorporation opposite C immediately following the X:G or X:G\* pair was determined.

TABLE 2: Kinetic parameters for dCTP and dATP incorporation and chain extension by yeast DNA polymerase  $\eta$  (6.4 nM) on an undamaged and G[8,5-Me]T cross-link containing substrate.

dNTP	$k_{\text{cat}}$ ( $\text{min}^{-1}$ )	$K_m$ ( $\mu\text{M}$ )	$k_{\text{cat}}/K_m$ ( $\mu\text{M}^{-1} \text{min}^{-1}$ )	$F_{\text{inc}}^a$	X:G	$k_{\text{cat}}$ ( $\text{min}^{-1}$ )	$K_m$ ( $\mu\text{M}$ )	$k_{\text{cat}}/K_m$ ( $\mu\text{M}^{-1} \text{min}^{-1}$ )	$F_{\text{ext}}^a$	
	5'-GTGCG <sup>^</sup> TGTTTGTATCGCTTGCAGGGG-3' ACAAACATAGCGAACp32 Nucleotide Incorporation					5'-GTGCG <sup>^</sup> TGTTTGTATCGCTTGCAGGGG-3' X ACAAACATAGCGAACp32 Chain Extension <sup>b</sup>				
Undamaged substrate										
dCTP	$7.3 \pm 0.02$	$0.04 \pm 0.002$	182.5	1.0	C:G	$4.4 \pm 0.04$	$0.07 \pm 0.001$	62.8	1.0	
dATP	$5.3 \pm 0.03$	$9.5 \pm 0.002$	0.56	$3.1 \times 10^{-3}$	A:G	$3.7 \pm 0.04$	$1.3 \pm 0.01$	2.8	$4.4 \times 10^{-2}$	
G[8,5-Me]T-containing substrate										
dCTP	$1.99 \pm 0.001$	$11.2 \pm 0.01$	0.17	$9.3 \times 10^{-4}$	C:G*	$1.6 \pm 0.1$	$0.31 \pm 0.002$	5.2	$8.2 \times 10^{-2}$	
dATP	$2.2 \pm 0.01$	$0.59 \pm 0.005$	3.72	$2.0 \times 10^{-2}$	A:G*	$1.2 \pm 0.009$	$22.0 \pm 1.0$	0.05	$7.9 \times 10^{-4}$	

<sup>a</sup>Fidelity ( $F$ ) of incorporation or extension was determined by the following equation:  $(k_{\text{cat}}/K_m)_{\text{incorrect}}/(k_{\text{cat}}/K_m)_{\text{correct}}$ .

<sup>b</sup>Steady-state kinetics for dGTP incorporation opposite C immediately following the X:G or X:G\* pair was determined.

the cross-linked G (19-mer) and after incorporation of a nucleotide opposite its 5'-neighbor (20-mer). Standing start experiments were carried out, and the amount of extension of the primer by one nucleotide was plotted with increasing dNTP concentration to determine the initial velocity of the polymerase-catalyzed reaction, which is shown in Figure 4. From these plots, the steady-state kinetic parameters,  $K_m$  and  $k_{\text{cat}}$ , for nucleotide incorporation opposite cross-linked G and the same for the control were determined (Tables 1 and 2). For hPol  $\eta$ , catalytic efficiency ( $k_{\text{cat}}/K_m$ ) of dCMP incorporation was 17-fold decreased opposite the cross-linked G whereas extension to the next base was decreased 5-fold relative to control. By contrast, for yPol  $\eta$  dCMP incorporation was decreased 1,000-fold, and extension to the next base was decreased 12-fold relative to control. This suggests

that yPol  $\eta$  had more difficulty in bypassing G[8,5-Me]T than hPol  $\eta$ . As was reported before [12, 19], in contrast to hPol  $\eta$ , which incorporates the correct nucleotide preferentially opposite G[8,5-Me]T, yPol  $\eta$  was much more error-prone, and insertion of dAMP opposite the cross-linked G was favored over that of the correct nucleotide, dCMP (Tables 1 and 2). In fact, dAMP misincorporation opposite the cross-linked G was more than 20-times more efficient than dCMP incorporation by yPol  $\eta$ . However, with yPol  $\eta$  the extension was 100-fold slower for G\*:A pair compared to G\*:C pair whereas the same for hPol  $\eta$  was about 13-fold slower. In each case, the higher catalytic efficiency was due to a much smaller  $K_m$ . When nucleotide incorporation fidelity opposite the cross-linked G and its 5' base was considered, dCMP incorporation over dAMP misincorporation was 200-fold more

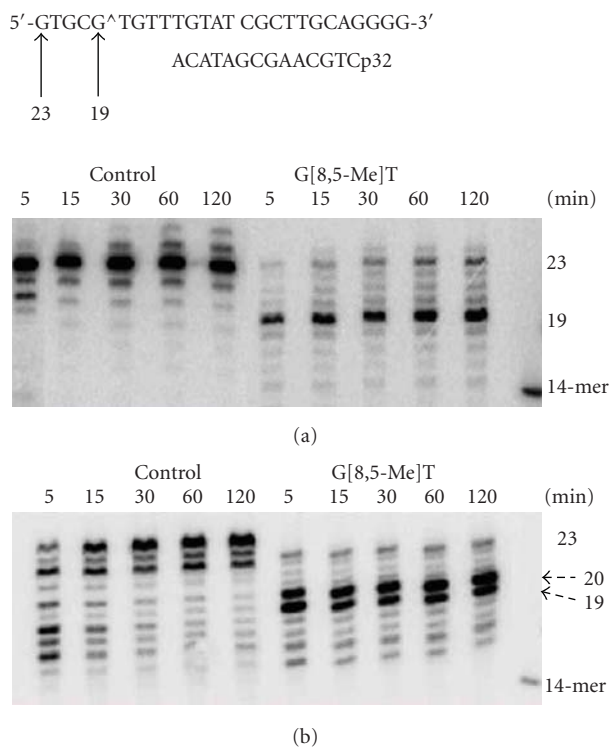


FIGURE 3: Extension of a 14-mer primer by 50 nM hPol  $\eta$  (a) and yPol  $\eta$  (b) on control and G[8,5-Me]T templates in the presence of all four dNTPs for the indicated time at 37°C.

efficient for hPol  $\eta$  whereas the same was only 5-fold more efficient for yPol  $\eta$ . Nevertheless, it seems that dCMP was preferred opposite the cross-linked G for bypass of G[8,5-Me]T by both DNA polymerases although the ability to discriminate against the wrong nucleotide by yPol  $\eta$  was not high.

**3.2. Analysis of the Full-Length Bypass Products.** Although steady-state kinetics provides useful information on the ability to incorporate a nucleotide opposite a lesion and further extension, it is important to determine the sequences of full-length bypass products in the presence of all four dNTPs. In mammalian cells, replication of G[8,5-Me]T-containing DNA also generates significant level of semi-targeted mutations [19], and it would be of interest to determine if pol  $\eta$  causes errors not only opposite the cross-link but also near the lesion. Guengerich and colleagues have developed an elegant LC-ESI/MS/MS-based method to analyze the polymerase extension products [25–30]. In the current paper, we report a plasmid-based approach to accomplish the same goal. The principle of this approach is shown in Scheme 1. The pMS2 plasmid was linearized by digestion with *EcoR* V. A scaffold 36-mer, containing two 12-nucleotide regions complementary to the two ends of the digested plasmid, was annealed to generate a gapped circular DNA, in which the G[8,5-Me]T cross-link was located in the

middle of a 12-nucleotide gap. The scaffold G[8,5-Me]T-36-mer contained the same local DNA sequence near the G[8,5-Me]T cross-link as the 26-mer used in the steady-state kinetic assay. It also contained several uracils replacing thymines at the two ends where it annealed with the plasmid. The circular scaffold plasmid DNA was incubated with 50 nM hPol  $\eta$  or yPol  $\eta$  and a mixture of all four dNTPs (25 mM each) in 25 mM Tris-HCl buffer (pH 7.5), 5 mM MgCl<sub>2</sub>, and 5 mM dithiothreitol at 37°C for various times. We expected a large fraction of the control construct to extend to full-length circular product whereas a much smaller fraction of the cross-linked construct was able to do the same. The full-length extension product extended up to the 3' end of the circular DNA, and the nick between the two ends was sealed by ligation overnight at 16°C in the presence of an excess of T4 DNA ligase to generate covalently closed circular ss plasmid. Although the DNA polymerase was not inactivated, both hPol  $\eta$  and yPol  $\eta$  were inefficient in continuing further extension at 16°C (data not shown). The scaffold 36-mer was digested by treatment with uracil DNA glycosylase and exonuclease III. The removal of the lesion-containing scaffold was considered critical to avoid any potential *in vivo* replication of the lesion. Therefore, we analyzed the products by agarose gel electrophoresis after uracil DNA glycosylase followed by exonuclease III treatment and confirmed that the plasmid was quantitatively linearized when either Pol  $\eta$  or DNA ligase was absent (data not shown). The proteins were extracted with phenol and chloroform, and the DNA was precipitated with ethanol. The DNA was used to transform repair-competent *E. coli* DL7, and the transformants were analyzed by DNA sequencing.

The number of colonies recovered upon transformation in *E. coli* of the plasmid incubated with hPol  $\eta$  for different times is shown in Figure 5. Since linear ss DNA is inefficient in transfecting *E. coli*, no colonies were recovered from the zero time point from both the control and the G[8,5-Me]T scaffold whereas increasing numbers of colonies were recovered as incubation times with the DNA polymerase were increased. The number of colonies reflected the extent of full-length product that was ligated, and relative to the control 36-mer scaffold, the G[8,5-Me]T scaffold generated only 9% progeny at 15 min, which increased to 18% at 30 min and to 27% after 2 h (Figure 4). (For this calculation, the number of colonies obtained from the 120 min extension of the control 36-mer was considered 100%.) This suggests that with increased time of incubation, more DNA polymerase can bypass the G[8,5-Me]T cross-link, as we have also noted in the primer extension experiment with the G[8,5-Me]T 26-mer.

DNA sequencing results of the 2 h incubation products from two independent experiments with hPol  $\eta$  and yPol  $\eta$  are shown in Figure 6. The types and numbers of mutants from two different experiments are shown in Figure 6(a) whereas Figure 6(b) shows the combined result in a bar graph. As noted in the kinetic studies, yPol  $\eta$  was found to be more error-prone than hPol  $\eta$ . Mutational frequencies of yPol  $\eta$  and hPol  $\eta$  were 36% and 14%, respectively, for the G[8,5-Me]T cross-link whereas no mutants were recovered from the control after sequencing in excess of

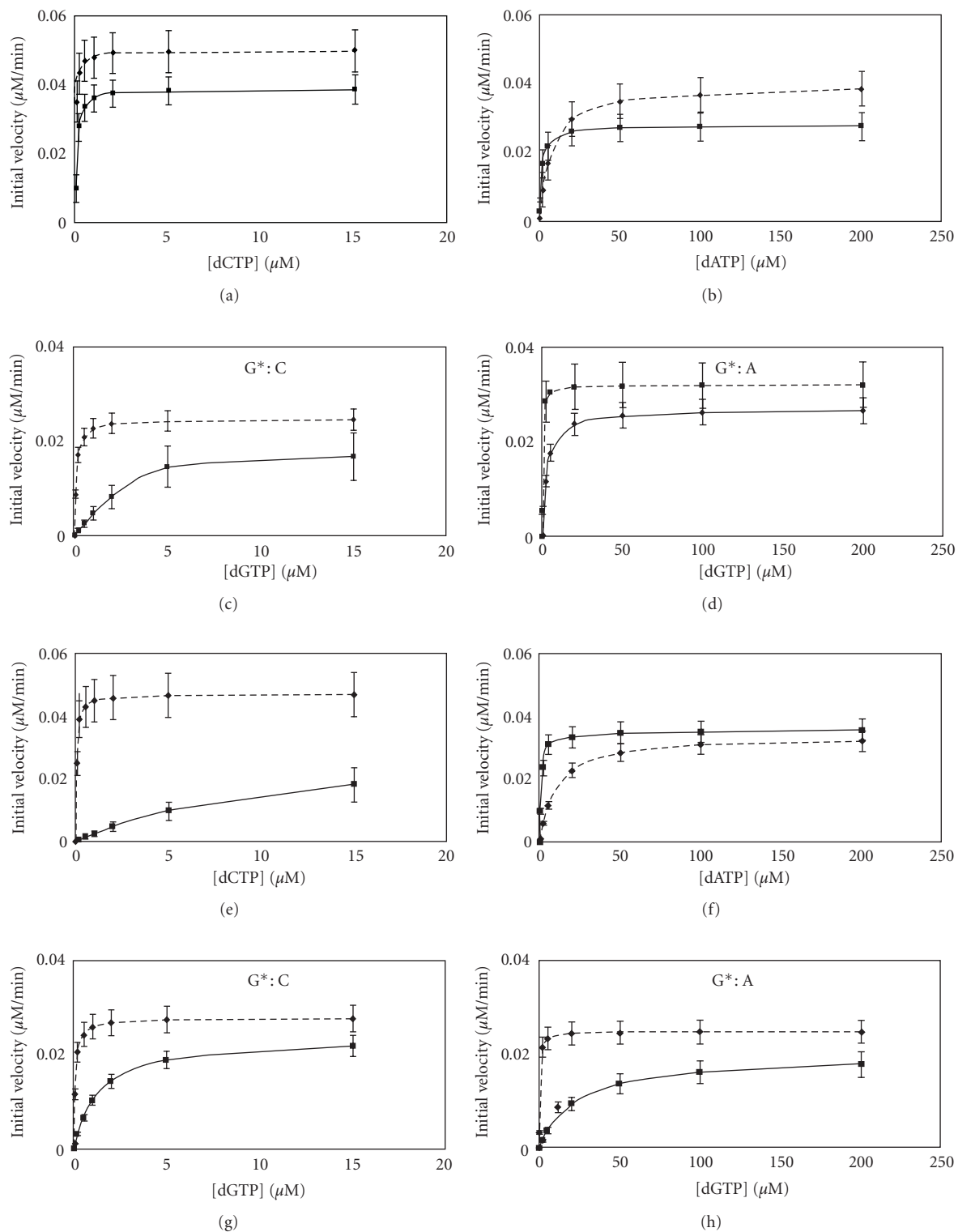
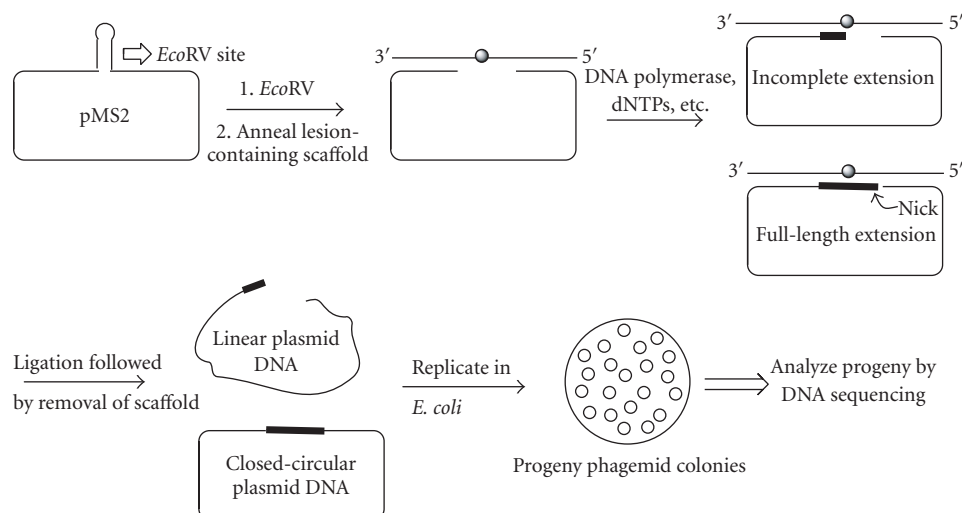


FIGURE 4: Single nucleotide incorporation and extension assay. Template-primer (50 nM) was incubated with 6.4 nM hPol  $\eta$  or yPol  $\eta$  for various times with increasing concentrations of dNTP. Steady-state kinetics for single nucleotide incorporation opposite cross-linked (G) (solid line) or control (G) (dashed line) are shown in (a), (b), (e), and (f). (a) and (b) represent dCTP and dATP incorporations, respectively, for hPol  $\eta$  whereas (e) and (f) represent the same for yPol  $\eta$ . Steady-state kinetics for dGTP incorporation opposite (C) immediately following the cross-linked (G) (solid line) or control (G) (dashed line) are shown in (c), (d), (g), and (h). (c) and (d) represent extension of G\*:C and G\*:A pairs, respectively, for hPol  $\eta$  whereas (g) and (h) represent the same for yPol  $\eta$ . Error bars show the standard deviation of at least three experiments.



SCHEME 1: General protocol for analyzing the full-length extension products.

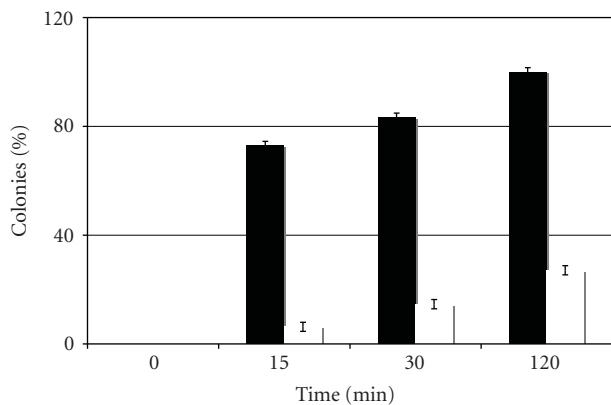


FIGURE 5: The number of colonies obtained from extension by hPol  $\eta$  of a control scaffold (black) was compared with the G[8,5-Me]T scaffold (white) at different time points in the bar graph. The number of colonies obtained from the 120 min extension of the control 36-mer was arbitrarily considered 100%. The zero time point showing no colonies ensures that colonies only originated from the extension products.

one hundred colonies following extension with each DNA polymerase. The pattern of mutagenesis from the G[8,5-Me]T cross-link was significantly different for these two polymerases.  $\gamma$ Pol  $\eta$  induced targeted G  $\rightarrow$  T as the major mutagenic event, followed by targeted G  $\rightarrow$  C; these two base substitutions, taken together, constituted 83% of the mutations. By contrast, in the case of hPol  $\eta$ , semitargeted mutations (7.2%) occurred at equal frequency as the targeted mutations (6.9%). With hPol  $\eta$ , though most frequent mutation was G  $\rightarrow$  T (4%), approximately half as many G  $\rightarrow$  A (2.2%) was also detected. It is interesting that even a single targeted G  $\rightarrow$  A could not be detected in the extension by  $\gamma$ Pol  $\eta$ . Similarly, targeted G  $\rightarrow$  C was completely absent with hPol  $\eta$ . For the cross-linked T,  $\gamma$ Pol  $\eta$  bypass was completely error-free whereas low (0.6%) level

of T  $\rightarrow$  G transversions was detected with hPol  $\eta$ . With  $\gamma$ Pol  $\eta$ , semitargeted mutations were restricted to the immediate 5'-C and 3'-G of the cross-link, but with hPol  $\eta$ , errors were noted as far as two bases 5' and five bases 3' to the cross-link. In sum, despite the similarity of targeted G  $\rightarrow$  T transversions, the mutational profile of the two Y-family DNA polymerases exhibited distinct patterns.

#### 4. Discussion

In earlier studies it was shown that hPol  $\eta$  preferentially incorporates the correct nucleotide opposite each of the cross-linked bases whereas  $\gamma$ Pol  $\eta$ , though accurately incorporates dAMP opposite the cross-linked T, is highly error-prone in nucleotide incorporation opposite the cross-linked G [12, 19]. However, neither the kinetics of further extension of the primer nor the sequences of the full-length extension products were determined. Miller and Grollman [20] have shown that DNA polymerase functions can be affected by replication-blocking lesions remote from the lesion site. In the current investigation, using steady-state kinetics, we determined that though dAMP incorporation opposite the G of G[8,5-Me]T by  $\gamma$ Pol  $\eta$  was more than 20-fold preferred over dCMP incorporation, further extension of the G\*:A pair was 100-fold less efficient than extension of the G\*:C pair. As a result, dCMP incorporation followed by further extension was 5-times as efficient as dAMP incorporation by  $\gamma$ Pol  $\eta$ . For hPol  $\eta$ , on the other hand, it was nearly 200-times as efficient.

In order to characterize the full-length extension products in the presence of all four dNTPs, we developed a novel method to sequence them. In this approach, as shown in Scheme 1, a single-stranded plasmid (e.g., pMS2) containing a restriction endonuclease site in a hairpin region is digested and linearized by the enzyme. A DNA adduct containing scaffold is annealed to the linear DNA to create a gapped plasmid, in which the lesion is situated in the middle of this gap. A DNA polymerase is allowed to extend the

h POL $\eta$	
Trial 1: Mutations 27/179 (15%)	T(3) T(5) A(4) T(8) G(1) $\Delta$ (3) C(3)
Trial 2: Mutations 18/140 (13%)	T(2) T(3) A(3) T(5) G(1) $\Delta$ (2) C(2)
5'...G T G C G ^ T G T T T G T...-3'	
Trial 1: Mutations 33/90 (37%)	T(2) T(21) T(1) G(1) C(7) C(1)
Trial 2: Mutations 43/123 (35%)	T(4) T(27) T(1) G(2) C(8) C(1)

y POL  $\eta$

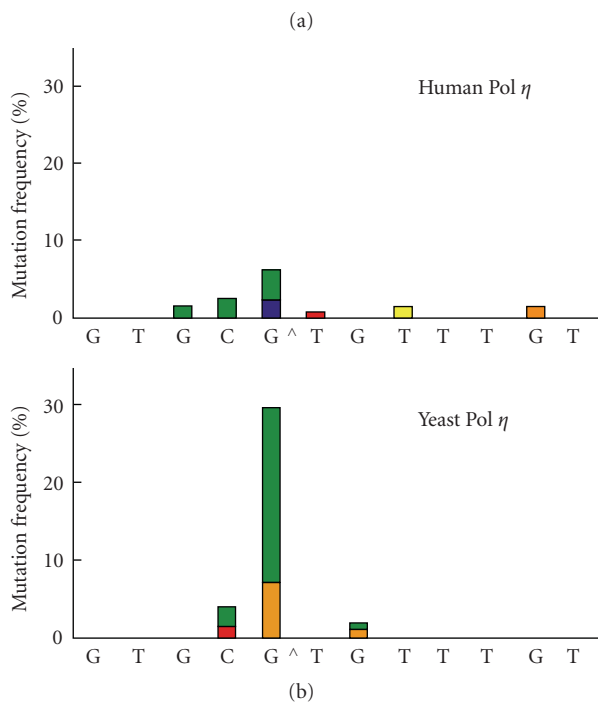


FIGURE 6: (a) Types and frequencies of mutations induced by G[8,5-Me]T as determined from the full-length extension products generated by hPol  $\eta$  (top) and yPol  $\eta$  (bottom). It is noteworthy that no mutants were isolated from the control batches after sequencing in excess of one hundred colonies. (b) The combined data in (a) is represented in bar graph showing the percentages of each type of single-base substitution or deletion induced by G[8,5-Me]T by hPol  $\eta$  (top) and yPol  $\eta$  (bottom). The colors represent T (green), A (blue), G (red), C (orange), and one-base deletion (yellow). The T deletion in a run of three thymines by hPol  $\eta$  was arbitrarily shown here at the T closest to the lesion.

3'-end of the plasmid to fill in the gap, which is then enzymatically ligated to create a closed-circular plasmid or viral genome. The ss circular DNA is replicated in *E. coli*, and the progeny is subjected to DNA sequencing. The scaffold is quantitatively removed prior to transformation in *E. coli* to avoid biological processing of the lesion *in vivo*. The DNA sequencing result of the area which originally contained the gap provides the nature of extension products. It is worth mentioning that other plasmid-based sequencing techniques using PCR amplification have been developed and successfully used in recent years [31, 32]. However,

we believe that the hallmark of our current approach is its simplicity. It neither requires expensive instrumentation nor is technically demanding. While the sensitivity of the mass spectral analysis is limited by the signal to noise ratio, which varies from experiment to experiment, the plasmid-based sequencing approach enables determination of misincorporations occurring at a level of less than 1% frequency. However, the sequence determination is dependent on the efficiency of ligation, which is only proficient with full-length extension products. As a result, a limitation of the current plasmid-based approach is that it does not offer any

information on the incomplete extension products, which may be readily available by the MS approach. Using this method of sequencing, we showed that  $\gamma$ Pol  $\eta$  was much more error-prone in bypassing G[8,5-Me]T than hPol  $\eta$ . The targeted G  $\rightarrow$  T was the major type of mutation by both DNA polymerases, but  $\gamma$ Pol  $\eta$  induced it nearly 6-times more efficiently than hPol  $\eta$ . With hPol  $\eta$ , semitargeted mutations, that is, mutations near the lesion, occurred at approximately equal frequency as the targeted mutations whereas more than 80% of the mutations were targeted mutations with  $\gamma$ Pol  $\eta$ .

Several studies have established differences between the yeast and the human enzyme. For translesion synthesis of  $\gamma$ -hydroxypropanodeoxyguanosine,  $\gamma$ Pol  $\eta$  synthesizes past the adduct relatively accurately whereas hPol  $\eta$  discriminates poorly between incorporation of correct and wrong nucleotides opposite the adduct [33]. The mechanistic basis of these two enzymes has been examined, which showed that they differ in several important respects [34]. hPol  $\eta$  has a 50-fold-faster rate of nucleotide incorporation than  $\gamma$ Pol  $\eta$  but binds the nucleotide with an approximately 50-fold-lower level of affinity. It is unclear how these differences influence the nucleotide incorporation opposite the G[8,5-Me]T cross-link.

When the hPol  $\eta$  mutational spectrum was compared with the mutations detected in human embryonic kidney cells [19], significant similarities in the two results are apparent. Notably, the high frequency of G  $\rightarrow$  T followed by G  $\rightarrow$  A and the semitargeted mutations 5' to the cross-link such as 5'-C  $\rightarrow$  T and 5'-G  $\rightarrow$  T reflect a similar pattern in the *in vitro* studies using purified DNA hPol  $\eta$  and the cellular studies. These similarities notwithstanding, certain variations in the mutation profiles are also noteworthy. Targeted T  $\rightarrow$  A and substitutions at adjacent 3'-G and the thymines noted in the mammalian cells were absent in the hPol  $\eta$  extensions. It was suggested that in a cell the binding to proliferating cell nuclear antigen (PCNA) via its PCNA-interacting protein domain is a prerequisite for hPol  $\eta$ 's ability to function in translesion synthesis in human cells [35]. Therefore, certain differences between bypass of a DNA damage by a purified hPol  $\eta$  *in vitro* and that in a cell should be anticipated. Although there is insufficient evidence to conclude that hPol  $\eta$  is responsible for the observed mutations of G[8,5-Me]T in human cells, it seems reasonable to postulate that this Y-family DNA polymerase is one of the DNA polymerases involved in the cellular bypass of this cross-link.

## Abbreviations

- G[8,5-Me]T or G<sup>⋈</sup>T: Guanine-thymine intrastrand cross-link where C8 of guanine is covalently bonded to the methyl carbon of the 3'-thymine
- T[5-Me,8]G or T<sup>⋈</sup>G: Thymine-guanine intrastrand cross-link where C8 of guanine is covalently bonded to the methyl carbon of the 5'-thymine
- hPol  $\eta$  and  $\gamma$ Pol  $\eta$ : Represent human and yeast DNA polymerase  $\eta$ , respectively.

## Acknowledgment

This paper was supported by the National Institute of Environmental Health Sciences, NIH (Grant ES013324).

## References

- [1] J. A. Brown, S. A. Newmister, K. A. Fiala, and Z. Suo, "Mechanism of double-base lesion bypass catalyzed by a Y-family DNA polymerase," *Nucleic Acids Research*, vol. 36, no. 12, pp. 3867–3878, 2008.
- [2] A. Vaisman and S. G. Chaney, "The efficiency and fidelity of translesion synthesis past cisplatin and oxaliplatin GpG adducts by human DNA polymerase  $\beta$ ," *Journal of Biological Chemistry*, vol. 275, no. 17, pp. 13017–13025, 2000.
- [3] A. Vaisman, C. Masutani, F. Hanaoka, and S. G. Chaney, "Efficient translesion replication past oxaliplatin and cisplatin GpG adducts by human DNA polymerase  $\eta$ ," *Biochemistry*, vol. 39, no. 16, pp. 4575–4580, 2000.
- [4] M. Kanuri, L. V. Nechev, S. E. Kiehna et al., "Evidence for *Escherichia coli* polymerase II mutagenic bypass of intrastrand DNA crosslinks," *DNA Repair*, vol. 4, no. 12, pp. 1374–1380, 2005.
- [5] A. Kumari, I. G. Minko, M. B. Harbut, S. E. Finkel, M. F. Goodman, and R. S. Lloyd, "Replication bypass of interstrand cross-link intermediates by *Escherichia coli* DNA polymerase IV," *Journal of Biological Chemistry*, vol. 283, no. 41, pp. 27433–27437, 2008.
- [6] H. C. Box, J. B. Dawidzik, and E. E. Budzinski, "Free radical-induced double lesions in DNA," *Free Radical Biology and Medicine*, vol. 31, no. 7, pp. 856–868, 2001.
- [7] H. C. Box, H. B. Patrzyc, J. B. Dawidzik et al., "Double base lesions in DNA X-irradiated in the presence or absence of oxygen," *Radiation Research*, vol. 153, no. 4, pp. 442–446, 2000.
- [8] S. Bellon, J.-L. Ravanat, D. Gasparutto, and J. Cadet, "Cross-linked thymine-purine base tandem lesions: synthesis, characterization, and measurement in  $\gamma$ -irradiated isolated DNA," *Chemical Research in Toxicology*, vol. 15, no. 4, pp. 598–606, 2002.
- [9] Q. Zhang and Y. Wang, "Independent generation of the 5-hydroxy-5,6-dihydrothymidin-6-yl radical and its reactivity in dinucleoside monophosphates," *Journal of the American Chemical Society*, vol. 126, no. 41, pp. 13287–13297, 2004.
- [10] Q. Zhang and Y. Wang, "The reactivity of the 5-hydroxy-5,6-dihydrothymidin-6-yl radical in oligodeoxyribonucleotides," *Chemical Research in Toxicology*, vol. 18, no. 12, pp. 1897–1906, 2005.
- [11] Q. Q. Zhang and Y. Wang, "Generation of 5-(2'-deoxycytidyl)methyl radical and the formation of intrastrand cross-link lesions in oligodeoxyribonucleotides," *Nucleic Acids Research*, vol. 33, no. 5, pp. 1593–1603, 2005.
- [12] Y. Jiang, H. Hong, H. Cao, and Y. Wang, "In vivo formation and in vitro replication of a guanine-thymine intrastrand cross-link lesion," *Biochemistry*, vol. 46, no. 44, pp. 12757–12763, 2007.
- [13] H. Hong, H. Cao, and Y. Wang, "Formation and genotoxicity of a guanine-cytosine intrastrand cross-link lesion in vivo," *Nucleic Acids Research*, vol. 35, no. 21, pp. 7118–7127, 2007.
- [14] C. Gu and Y. Wang, "Thermodynamic and in vitro replication studies of an intrastrand G[8-5]C cross-link lesion," *Biochemistry*, vol. 44, no. 24, pp. 8883–8889, 2005.
- [15] Z. Yang, L. C. Colis, A. K. Basu, and Y. Zou, "Recognition and incision of  $\gamma$ -radiation-induced cross-linked guanine-thymine

- tandem lesion G[8,5-Me]T by UvrABC nuclease," *Chemical Research in Toxicology*, vol. 18, no. 9, pp. 1339–1346, 2005.
- [16] C. Gu, Q. Zhang, Z. Yang, Y. Wang, Y. Zou, and Y. Wang, "Recognition and incision of oxidative intrastrand cross-link lesions by UvrABC nuclease," *Biochemistry*, vol. 45, no. 35, pp. 10739–10746, 2006.
- [17] S. Bellon, D. Gasparutto, C. Saint-Pierre, and J. Cadet, "Guanine-thymine intrastrand cross-linked lesion containing oligonucleotides: from chemical synthesis to in vitro enzymatic replication," *Organic and Biomolecular Chemistry*, vol. 4, no. 20, pp. 3831–3837, 2006.
- [18] C. Gu and Y. Wang, "LC-MS/MS Identification and yeast polymerase  $\eta$  bypass of a novel  $\gamma$ -irradiation-induced intrastrand cross-link lesion G[8-5]C," *Biochemistry*, vol. 43, no. 21, pp. 6745–6750, 2004.
- [19] L. C. Colis, P. Raychaudhury, and A. K. Basu, "Mutational specificity of  $\gamma$ -radiation-induced guanine-thymine and thymine-guanine intrastrand cross-links in mammalian cells and translesion synthesis past the guanine-thymine lesion by human DNA polymerase  $\eta$ ," *Biochemistry*, vol. 47, no. 31, pp. 8070–8079, 2008.
- [20] H. Miller and A. P. Grollman, "Kinetics of DNA polymerase I (Klenow fragment exo-) activity on damaged dna templates: effect of proximal and distal template damage on DNA synthesis," *Biochemistry*, vol. 36, no. 49, pp. 15336–15342, 1997.
- [21] J. M. McNulty, B. Jerkovic, P. H. Bolton, and A. K. Basu, "Replication inhibition and miscoding properties of DNA templates containing a site-specific cis-thymine glycol or urea residue," *Chemical Research in Toxicology*, vol. 11, no. 6, pp. 666–673, 1998.
- [22] M. S. Boosalis, J. Petruska, and M. F. Goodman, "DNA polymerase insertion fidelity. Gel assay for site-specific kinetics," *Journal of Biological Chemistry*, vol. 262, no. 30, pp. 14689–14696, 1987.
- [23] L. V. Mendelman, J. Petruska, and M. F. Goodman, "Base mispair extension kinetics. Comparison of DNA polymerase  $\alpha$  and reverse transcriptase," *Journal of Biological Chemistry*, vol. 265, no. 4, pp. 2338–2346, 1990.
- [24] M. Hollstein, B. Shomer, M. Greenblatt et al., "Somatic point mutations in the p53 gene of human tumors and cell lines: updated compilation," *Nucleic Acids Research*, vol. 24, no. 1, pp. 141–146, 1996.
- [25] J. S. Stover, G. Chowdhury, H. Zang, F. P. Guengerich, and C. J. Rizzo, "Translesion synthesis past the C8- and N2-deoxyguanosine adducts of the dietary mutagen 2-amino-3-methylimidazo[4,5-f]quinoline in the NarI recognition sequence by prokaryotic DNA polymerases," *Chemical Research in Toxicology*, vol. 19, no. 11, pp. 1506–1517, 2006.
- [26] H. Zang, A. K. Goodenough, J.-Y. Choi et al., "DNA adduct bypass polymerization by *Sulfolobus solfataricus* DNA polymerase Dpo4: analysis and crystal structures of multiple base pair substitution and frameshift products with the adduct 1,N2-ethenoguanine," *Journal of Biological Chemistry*, vol. 280, no. 33, pp. 29750–29764, 2005.
- [27] R. L. Eoff, K. C. Angel, M. Egli, and F. P. Guengerich, "Molecular basis of selectivity of nucleoside triphosphate incorporation opposite O6-benzylguanine by *Sulfolobus solfataricus* DNA polymerase Dpo4: steady-state and pre-steady-state kinetics and X-ray crystallography of correct and incorrect pairing," *Journal of Biological Chemistry*, vol. 282, no. 18, pp. 13573–13584, 2007.
- [28] R. L. Eoff, A. Irimia, K. C. Angel, M. Egli, and F. P. Guengerich, "Hydrogen bonding of 7,8-dihydro-8-oxodeoxyguanosine with a charged residue in the little finger domain determines miscoding events in *Sulfolobus solfataricus* DNA polymerase Dpo4," *Journal of Biological Chemistry*, vol. 282, no. 27, pp. 19831–19843, 2007.
- [29] R. L. Eoff, A. Irimia, M. Egli, and F. P. Guengerich, "*Sulfolobus solfataricus* DNA polymerase Dpo4 is partially inhibited by "Wobble" pairing between O6-methylguanine and cytosine, but accurate bypass is preferred," *Journal of Biological Chemistry*, vol. 282, no. 2, pp. 1456–1467, 2007.
- [30] P. P. Christov, K. C. Angel, F. P. Guengerich, and C. J. Rizzo, "Replication past the N5-methyl-formamidopyrimidine lesion of deoxyguanosine by DNA polymerases and an improved procedure for sequence analysis of in vitro bypass products by mass spectrometry," *Chemical Research in Toxicology*, vol. 22, no. 6, pp. 1086–1095, 2009.
- [31] K. A. Fiala and Z. Suo, "Sloppy bypass of an abasic lesion catalyzed by a Y-family DNA polymerase," *Journal of Biological Chemistry*, vol. 282, no. 11, pp. 8199–8206, 2007.
- [32] H. Fang and J.-S. Taylor, "Serial analysis of mutation spectra (SAMS): a new approach for the determination of mutation spectra of site-specific DNA damage and their sequence dependence," *Nucleic Acids Research*, vol. 36, no. 18, pp. 6004–6012, 2008.
- [33] I. G. Minko, M. T. Washington, M. Kanuri, L. Prakash, S. Prakash, and R. S. Lloyd, "Translesion synthesis past acrolein-derived DNA adduct,  $\gamma$ -hydroxypropanodeoxyguanosine, by yeast and human DNA polymerase  $\eta$ ," *Journal of Biological Chemistry*, vol. 278, no. 2, pp. 784–790, 2003.
- [34] M. T. Washington, R. E. Johnson, L. Prakash, and S. Prakash, "The mechanism of nucleotide incorporation by human DNA polymerase  $\eta$  differs from that of the yeast enzyme," *Molecular and Cellular Biology*, vol. 23, no. 22, pp. 8316–8322, 2003.
- [35] N. Acharya, J.-H. Yoon, H. Gali et al., "Roles of PCNA-binding and ubiquitin-binding domains in human DNA polymerase  $\eta$  in translesion DNA synthesis," *Proceedings of the National Academy of Sciences of the United States of America*, vol. 105, no. 46, pp. 17724–17729, 2008.

## Review Article

# The Role of PCNA Posttranslational Modifications in Translesion Synthesis

**Montaser Shaheen, Ilanchezhian Shanmugam, and Robert Hromas**

*Department of Internal Medicine and the University of New Mexico Cancer Center, University of New Mexico Health Science Center, MSC08 4630, 900 Camino de Salud, Albuquerque, NM 87131, USA*

Correspondence should be addressed to Robert Hromas, rhromas@salud.unm.edu

Received 16 April 2010; Revised 17 June 2010; Accepted 1 July 2010

Academic Editor: Ashis Basu

Copyright © 2010 Montaser Shaheen et al. This is an open access article distributed under the Creative Commons Attribution License, which permits unrestricted use, distribution, and reproduction in any medium, provided the original work is properly cited.

Organisms are predisposed to different types in DNA damage. Multiple mechanisms have evolved to deal with the individual DNA lesions. Translesion synthesis is a special pathway that enables the replication fork to bypass blocking lesions. Proliferative Cell Nuclear Antigen (PCNA), which is an essential component of the fork, undergoes posttranslational modifications, particularly ubiquitylation and sumoylation that are critical for lesion bypass and for filling of DNA gaps which result from this bypass. A special ubiquitylation system, represented by the Rad6 group of ubiquitin conjugating and ligating enzymes, mediates PCNA mono- and polyubiquitylation in response to fork stalling. The E2 SUMO conjugating enzyme Ubc9 and the E3 SUMO ligase Siz1 are responsible for PCNA sumoylation during undisturbed S phase and in response to fork stalling as well. PCNA monoubiquitylation mediated by Rad6/Rad18 recruits special polymerases to bypass the lesion and fill in the DNA gaps. PCNA polyubiquitylation achieved by *ubc13-mms2/Rad 5* in yeast mediates an error-free pathway of lesion bypass likely through template switch. PCNA sumoylation appears required for this error-free pathway, and it plays an antirecombinational role during normal replication by recruiting the helicase Srs2 to prevent sister chromatid exchange and hyper-recombination.

## 1. Introduction

DNA damage is an unavoidable aspect of existence that results from both endogenous metabolism and exogenous insults. These include reactive oxygen species and DNA replication errors, in addition to ionizing radiation, UV light and mutagenic chemicals. There are multiple specialized DNA repair pathways that correct various DNA lesions, such as abasic nucleotides [1], mismatched bases [2], single strand defects or lesions [3], and double strand breaks (DSBs) [4]. In certain conditions, the DNA damage may persist unrepaired until a replication fork collides with it. This is seen often with DNA interstrand cross-linking (ICL) lesions which are some of the most toxic types of DNA damage. ICL lesions are usually repaired in S-Phase, after replication forks encounter them [5]. Other types of DNA damage observed at the single strand level, resulting from UV exposure or certain chemicals, can also block the replication fork.

The arrested fork usually deals with such collision utilizing a potentially mutagenic process named Translesion Synthesis (TLS) [6, 7]. This type of DNA synthesis ensures relatively uninterrupted replication even in the face of DNA injury. TLS was initially described in prokaryotes, and termed Post-Replication Repair (PRR) [8]. In *E. coli* TLS leaves behind single stranded gaps that are repaired at a subsequent cell cycle stage. Similar gaps have been described in Eukaryotes as well [9, 10]. When a replication fork collides with an ICL or a single strand lesion, a one-ended DSB may form. This could trigger homology-based repair, also termed Homologous Recombination (HR), which is another pathway the fork utilizes to repair DNA lesions particularly ICLs [11]. The classic DNA polymerases that mediate undisturbed replication cannot bypass most ssDNA lesions, and several alternative (atypical) polymerases that mediate lesion bypass in TLS have been described. The key regulator of TLS is the replication sliding clamp Proliferative Cell

Nuclear Antigen (PCNA). The PCNA trimer holds multiple proteins that participate in both normal replication and TLS. The role of PCNA in TLS is governed by posttranslational modifications that occur to it in response to an arrested fork. In this brief paper we describe the process of PCNA ubiquitylation and sumoylation in response to replication fork stalling and the impact of these modifications on TLS.

## 2. PCNA Ubiquitylation in Response to Fork Stalling Lesions

PCNA has been described as the coordinator of the replicating fork [12]. It mediates the recruitment of multiple factors required for DNA replication and repair. In a seminal paper, the Jentsch group described the involvement of PCNA ubiquitylation and sumoylation in TLS [13]. This Ubiquitylation is mediated by the Rad6 group TLS factors [13]. It had been known for a long time that Rad6 family was involved in TLS in Eukaryotes, and that most of its members display ubiquitin conjugating and ligating activities [14–16]. Protein ubiquitylation has emerged as a widespread process that impacts a myriad of cellular processes in eukaryotes [17]. This process starts with binding of the conserved 76 aa peptide ubiquitin to E1 ubiquitin activating enzyme. This transfers ubiquitin to an E2 conjugating enzyme, which interacts with an E3 ligase to transfer ubiquitin to a specific substrate. The E3 ligase is the determinant of the specificity of the substrate to which ubiquitin is attached. Rad6/Rad18 are the E2/E3 complex that mediates PCNA ubiquitylation at a conserved Lysine164 [13]. It has been shown that this modification increases affinity of TLS DNA polymerases to PCNA which contributes to lesion bypass [18]. This was initially demonstrated for the human TLS Polymerase  $\eta$  (pol $\eta$ ) but later was shown to apply to other eukaryotic polymerases of the Y family, including polymerases  $\iota$  and  $\kappa$  which are not present in yeast [19, 20]. This enhanced affinity for PCNA by the Y family of TLS DNA polymerases is due to presence of ubiquitin-binding domains of the UBM or UBZ types [21] in these polymerases which interact with the monoubiquitin on PCNA (Figure 1). The major TLS polymerases in yeast include Rad30, Rev1, Rev3, and Rev7 (Rev7 is the regulatory unit, and Rev3 is the catalytic unit of Polymerase zeta.) Further discussion of the detailed role of each TLS polymerase can be found elsewhere [6, 7].

PCNA undergoes further ubiquitylation on the same Lysine 164 to generate a ubiquitin chain [13]. This polyubiquitin chain formation is dependent on the presence of the monoubiquitin species mediated by Rad6/Rad18 [13]. The ubiquitin molecules within this chain bind each other through the lysine 63 (K63) of each ubiquitin. This type of ubiquitin chain is different from that of the canonical ubiquitin chains bound through K48 which are responsible for substrate degradation by the proteasome system [17]. Although a K63 ubiquitin chain could lead to protein degradation, it has mainly been implicated in non-degradation pathways such as vesicle excretion, signaling, the immune response, and different forms of DNA repair [17]. PCNA polyubiquitylation is mediated by another E2/E3 complex

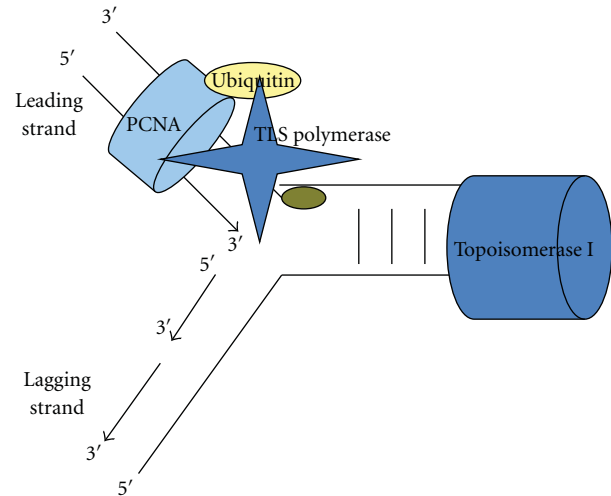


FIGURE 1: Fork stalling results in monoubiquitylation of the replication clamp PCNA which increases its affinity to a TLS polymerase. The latter replaces the high-fidelity replicative polymerase and it can accommodate the lesion even with the risk of generating mutations in certain circumstances. This Polymerase binds PCNA through its PIP box and a ubiquitin binding domain.

in the Rad6 pathway of PRR, namely *ubc13-mms2*/Rad 5 in yeast [13]. A mammalian *ubc13-mms2* homologue has been known for years [15], and two mammalian homologues of Rad5 with E3 ligase and helicase activities (HLTF and SHPRH) were recently described [22–24]. PCNA polyubiquitylation in the setting of fork-blocking lesions results in a form of error-free repair believed to be mediated by template switching (Figure 2) [25]. The exact mechanism of such template switching is unknown, but it appears (at least in yeast) that there are two pathways: one is Rad52 dependent and the other is Rad52 independent [26]. A recent study indicated that Rad5-mediated template switch is appreciated as X-shaped DNA structure on 2-gel electrophoresis, and it appears to involve holiday junctions (recombination intermediates) and HR proteins [27]. Another potential scenario for this error-free pathway is through fork regression after stalling which has been demonstrated *in vitro* [28]. Rad5 appears to promote this fork regression. However, since competent replication checkpoint prevents such fork regression, it is believed to be unlikely mechanism to mediate this pathway [29]. Mutant Rad5 or *ubc13* yeast strains lack such error-free repair [13, 25]. PCNA monoubiquitylation at K164 has been described across all eukaryotic cells, from budding [13, 30] and fission yeast [31] to humans [18], and includes chicken DT40 cells [32, 33] and *Xenopus laevis* egg extracts [34]. This monoubiquitylation is seen during normal replication in DT40 and mammalian cells [31, 32]. It is induced by DNA damage in human cells, and is observed only after DNA damage in budding yeast [13, 30]. PCNA polyubiquitylation is clearly seen in yeast after DNA damage, but has been difficult to demonstrate in mammalian systems, and often requires over-expression of the E3 ligases to be observed [22–24]. Evidence of the existence of an error-free



and ubiquitination, and also it is genetically stable. The other pathway operates when the first pathway is defective, and depends on Rad51 recombination and it is genetically unstable, and could lead to chromosomal translocation [43–45]. Another investigation demonstrated that sumoylation of PCNA could interfere with its association with another protein, Eco1 which is important for the establishment of chromatid cohesion during replication [46]. Blocking PCNA sumoylation partially rescues the temperature sensitivity of some Eco1 mutants [47]. It is also believed that the binding of the E2 SUMO ligase Ubc9 to PCNA on a critical region may block the binding of other PCNA interacting proteins [12]. All the above may indicate that sumoylation of PCNA also plays a key regulatory role in recombination and thus genomic stability.

#### 4. What Types of DNA Lesions Do Trigger PCNA Modification?

PCNA ubiquitylation and sumoylation are triggered by a wide variety of DNA lesions that block the replication fork, such as the ones caused by alkylating chemicals (e.g., methylmethanesulfonate (MMS) and 4-nitroquinoline oxide), bulky adducts such as benzo[a]pyrene dihydrodiol epoxide (BPDE), hydrogen peroxide (which produces oxidative damage), UV light (producing photoproducts) and ICL agents [13, 30, 47]. Nucleotide depletion such as the one achieved by hydroxyurea (HU), which causes a fork stalling and subsequent collapse, can also induce PCNA modification. However, HU is a weaker trigger of PCNA monoubiquitylation when compared to ICL or alkylating agents [48]. PCNA modification is tightly connected to replication since chemicals that cause direct DNA DSBs, such as bleomycin, do not cause PCNA ubiquitination or sumoylation [47, 49]. The topoisomerase I inhibitor camptothecin does not trigger PCNA ubiquitylation even though it blocks fork progression, by collision with the camptothecin/Topo I complex [47, 49]. This led to the suggestion that the uncoupling of fork helicase activity and polymerase movement is the actual trigger of PCNA ubiquitylation [50]. This uncoupling creates ssDNA that binds the Replication Protein A (RPA), which recruits Rad18, to the stalled fork. RPA has been shown to be required for TLS to proceed across multiple types of DNA lesions [44, 46]. Camptothecin triggers some PCNA ubiquitylation in *S. pombe* [31], but this modification is minimally above the normal S-phase ubiquitin signal that is seen in this organism. Ionizing Radiation (IR) triggers PCNA ubiquitylation in budding and fission yeast [30, 31] but not in mammalian cells [18, 49]. As mentioned above, in *S. cerevisiae*, PCNA is sumoylated in S phase without DNA damage while PCNA ubiquitylation is noted during S phase in *S. Pombe*, and higher eukaryotes including humans [13, 30, 31, 47, 49].

#### 5. The Relation between PCNA Ubiquitylation and the Kinetics of TLS

Traditionally, TLS is envisioned as an alternative replication process by which the stalled fork can bypass a lesion. PCNA

ubiquitylation is imagined as facilitating this bypass by recruiting low-fidelity polymerases. However, recent lines of evidence suggest that PCNA ubiquitylation may play its major role in filling in the gaps generated in PRR by utilizing these TLS polymerases. One study, using 2-D gel and electron microscopy to probe repair intermediates, revealed that UV-irradiated *S. cerevisiae* cells uncouple leading and lagging strand replication at irreparable UV lesions, thus generating long ssDNA regions on one side of the fork [51]. Small ssDNA gaps accumulate along the replicated duplexes, likely resulting from repriming events on both leading and lagging strands. It was concluded that TLS and homologous recombination factors counteract gap accumulation without affecting fork progression [51]. Recent work revealed that limiting the mutagenic or error-free pathways of TLS to the G<sub>2</sub>/M phases of the cell-cycle promote efficiently lesion tolerance indicating that both branches of the DNA damage tolerance operate effectively after chromosomal replication, outside S phase [52]. Another elegant study using an inducible system of DNA damage bypass in *S. cerevisiae* demonstrated that TLS occur predominantly during S-phase but it is separable in time and space from genome replication [53]. The same study found that both during and after S phase, ultraviolet-radiation-induced lesions are bypassed predominantly via error-prone translesion synthesis whereas the error-free pathway functions as a backup system. The process of bypassing the lesion itself may rely more on other factors rather than on modified PCNA. For instance, using the genetically tractable chicken cell line DT40, it was shown that TLS at stalled replication forks requires both Rev1 translesion polymerase-interaction domain and ubiquitin-binding domain in its C terminus. Surprisingly, however, PCNA ubiquitylation was not required to maintain normal fork progression on damaged DNA. Conversely, PCNA ubiquitylation was essential for filling PRR gaps [54]. Rev1 may recruit other essential TLS components through its multifunctional domains required for lesion bypass. On the other hand, it was demonstrated that the level of Rev1 protein is extremely low during G<sub>1</sub> and rises slowly throughout early and mid-S phase but begins to increase rapidly only in late S phase, reaching a maximum level in G<sub>2</sub>. Its level is then maintained at a high intracellular concentration throughout mitosis until after telophase [55]. DNA damage causes Rev1 to accumulate earlier in S phase without significantly affecting the level reached in G<sub>2</sub>/M phase. This is also suggestive of a role in PRR in G<sub>2</sub> rather than S phase, as would be predicted [55]. This cell cycle regulation of Rev1 is seen mainly in yeast and has not been demonstrated in higher eukaryotes. Notice that, Rev1 catalytic activity may be dispensable for TLS [56], and this protein may play its major role in TLS as a scaffold that attracts other TLS polymerases [57]. Overall, the picture is still nebulous regarding the exact kinetics of TLS/PRR in eukaryotes. Future studies may shed light on the detailed mechanisms of lesion bypass.

With the sequence of events that build up at the stalled fork, it was shown that Rad18 binds ssDNA [58], but this binding is much weaker compared to the binding of RPA to ssDNA. Thus, it appears that RPA recruits Rad18 to ssDNA

[47]. Rad18 in turn binds directly to Rad6 [58, 59] to initiate PCNA monoubiquitylation, and it also directly binds Rad5 [60], which together with MMS2/Ubc13 [16] mediate PCNA polyubiquitylation. Fluorescence-based biophysical methods revealed that mammalian Rad18 becomes immobilized in nuclear foci only in S phase cells, and that its physical association with Rad6 or Polymerase  $\eta$  is appreciated only in these foci upon DNA damage [61].

## 6. Other Functions of the Rad6/Rad18 in DNA Repair

The 9-1-1 checkpoint clamp is a complex with structural similarity of PCNA. It is implicated in signaling from ssDNA at the stalled fork to the checkpoint proteins, particularly Chk1, to activate the replication checkpoint [62, 63]. One recent report identified 9-1-1 as a target of Rad6/Rad18 monoubiquitylation in budding yeast upon triggering DNA damage [64]. This ubiquitylation is involved in control of global gene regulation in a way reminiscent of the bacterial SOS response to DNA damage which enhances DNA repair gene transcription, translesion synthesis, and recombination [64]. Rad18 was also shown to be recruited to sites of DNA DSB probably through interaction of its Ubiquitin Binding domain with ubiquitin chains deposited at the DSB site [65]. It is shown that Rad18 contributes to homologous recombination repair of DSB probably through direct interaction with the recombinase RAD51C [65]. Furthermore, evidence implicates Rad18 in HR since chicken T40 deficient in Rad18 show aberrant gene conversion (the main form of HR) [66]. In addition, the HR pathway that gets activated in the absence of rad18 is a defective one and may lead to genetic instability [43, 66]. Rad18 appears to suppress an NHEJ pathway when DSB is induced at the fork level to promote repair by HR [67]. It seems from all the above that Rad6/Rad18 play key roles in coordinating several DNA damage response pathways through ubiquitylation of two DNA clamps, PCNA and 9-1-1, as well as other unidentified targets.

## 7. The Role of USP1 in PCNA Deubiquitylation

USP1 was identified in a screen for the ubiquitin protease which mediates the removal of monoubiquitin from ubiquitylated Fanconi anemia group D2 (Fancd2 is ubiquitylated in response to fork stalling, and it contributes to TLS, particularly in response to ICL lesions.) [68]. Subsequently, USP1 was identified as a deubiquitylating enzyme for monoubiquitylated PCNA as well [48]. USP1 gets cleaved, and subsequently degraded by the proteasome system in response to UV light exposure, but not to alkylating or cross-linking agents [48, 68]. It is believed that there is a steady-state level of PCNA ubiquitylation by Rad6-Rad18 which is continuously antagonized by USP1, and when USP1 level goes down post-UV exposure, this leads to detectable PCNA ubiquitylation. Contrary to prediction, USP1 deletion leads to DNA damage sensitivity [69], and mice deficient in USP1 display DNA damage phenotype

reminiscent of Fanconi anemia [70]. This defective DNA repair is associated with constitutively chromatin-bound monoubiquitylated FANCD2. In contrast, persistent PCNA monoubiquitylation has negligible impact on DNA repair or mutagenesis [69]. The molecular mechanism of this phenotype is uncertain. It is worth mentioning that PCNA ubiquitylation occurs earlier after UV light than that after chemical exposure, and it persists for a long time (at least 48 hours) after a single exposure to different DNA damaging agents ([48, 49], and our observation).

## 8. Does the Replication Checkpoint Activate PCNA Ubiquitylation?

The replication checkpoint gets activated in response to situations that cause replication fork stalling in S phase. ATR (Ataxia Telangiectasia and Rad3-related) protein plays a central role in activating this checkpoint. The exposed ssDNA at the fork recruits RPA, which, in turn, recruits ATRIP (ATR-Interacting Protein), and that brings in ATR, which phosphorylates and activates Chk1 [62, 63]. The PCNA-like replication clamp (the 9-1-1 complex), whose loader interacts with RPA, also contributes to ATR and Chk1 activation. ATR and Chk1 phosphorylate multiple proteins to among other functions stabilize the stalled fork, suppress the late-firing origins of replications, halt cell cycle progression, and induce repair pathways, [62, 63]. In yeast and lower eukaryotes, it has been shown that this checkpoint activation does not alter the status of PCNA ubiquitylation [31, 47, 50]. In other words, checkpoint activation in yeast could be prevented by suppressing ATR or Chk1 without impacting PCNA ubiquitylation in response to fork stalling. In mammalian systems, the picture is less clearer. One report demonstrated 60% reduction in PCNA monoubiquitylation triggered by chemical DNA damage when ATR or Chk1 levels were reduced by siRNA [20]. Another study failed to show a change in the PCNA-monoubiquitin level upon reducing ATR levels [49], but did find a reduction when RPA was reduced. Thus, RPA appears to be instrumental for PCNA ubiquitylation to be induced [47, 49]. PTIP/Swift, an adaptor protein for the checkpoint kinases ATM and ATR, appears to contribute to PCNA ubiquitylation in human cells and *X. laevis* egg extracts since depletion of PTIP/Swift results in a reduction in this modification [71]. The cell cycle inhibitor p21 binds PCNA, and its down-regulation is required for PCNA monoubiquitylation upon DNA damage [72]. On the other hand, a contradictory study showed that depleting p21 or p53 results in a decrease in PCNA monoubiquitylation post-UV exposure [73]. The mechanisms of these conflicting effects are unknown, but it is worth mentioning that one of these two studies exogenously over-expressed p21 and this could have contributed to the difference in outcome [72]. One report indicated that replication checkpoint proteins are dispensable for TLS to proceed in yeast [74]; however, if there is a deficiency of NER, then repair of ssDNA lesions is heavily tilted toward TLS, and checkpoint proteins enhance the repair by TLS in this situation [74, 75].

## 9. Summary and Future Directions

Research in TLS/PRR has progressed through multiple stages over the past 5 decades, from its description in bacteria and then eukaryotes, to discovering its mechanisms in bacteria and yeast. A key step in this field was the identification of Rad6 as essential for TLS in eukaryotes. This led to the report [13] that described the fundamental role of the Rad6 group in ubiquitylating PCNA. The identification of PCNA posttranslational modifications opened the door for a cascade of other studies into the role of modified PCNA in TLS and the mechanism of that. However, there are questions that remain to be answered about the details of the error-free pathway of TLS, and the timing of events that take place at the stalled fork. There is no doubt that ongoing research in this area will come up with explanations for all these questions that may or may not agree with current predictions. It is noteworthy to mention that research in this field has also enriched our understanding of the mechanisms of mutagenesis, and the implications of that in carcinogenesis and cancer therapy.

## References

- [1] A. B. Robertson, A. Klungland, T. Rognes, and I. Leiros, "Base excision repair: the long and short of it," *Cellular and Molecular Life Sciences*, vol. 66, no. 6, pp. 981–993, 2009.
- [2] G.-M. Li, "Mechanisms and functions of DNA mismatch repair," *Cell Research*, vol. 18, no. 1, pp. 85–98, 2008.
- [3] T. Nospikel, "DNA repair in mammalian cells: nucleotide excision repair: variations on versatility," *Cellular and Molecular Life Sciences*, vol. 66, no. 6, pp. 994–1009, 2009.
- [4] C. Wyman and R. Kanaar, "DNA double-strand break repair: all's well that ends well," *Annual Review of Genetics*, vol. 40, pp. 363–383, 2006.
- [5] M. Räschle, P. Knipsheer, M. Enoiu et al., "Mechanism of replication-coupled DNA interstrand crosslink repair," *Cell*, vol. 134, no. 6, pp. 969–980, 2008.
- [6] E. C. Friedberg, "Suffering in silence: the tolerance of DNA damage," *Nature Reviews Molecular Cell Biology*, vol. 6, no. 12, pp. 943–953, 2005.
- [7] A. R. Lehmann, A. Niimi, T. Ogi et al., "Translesion synthesis: Y-family polymerases and the polymerase switch," *DNA Repair*, vol. 6, no. 7, pp. 891–899, 2007.
- [8] W. D. Rupp and P. Howard-Flanders, "Discontinuities in the DNA synthesized in an excision-defective strain of *Escherichia coli* following ultraviolet irradiation," *Journal of Molecular Biology*, vol. 31, no. 2, pp. 291–304, 1968.
- [9] L. Prakash, "Characterization of postreplication repair in *Saccharomyces cerevisiae* and effects of *rad6*, *rad18*, *rev3* and *rad52* mutations," *Molecular and General Genetics*, vol. 184, no. 3, pp. 471–478, 1981.
- [10] C. Lawrence, "The *RAD6* DNA repair pathway in *Saccharomyces cerevisiae*: what does it do, and how does it do it?" *BioEssays*, vol. 16, no. 4, pp. 253–258, 1994.
- [11] X. Li and W.-D. Heyer, "Homologous recombination in DNA repair and DNA damage tolerance," *Cell Research*, vol. 18, no. 1, pp. 99–113, 2008.
- [12] G.-L. Moldovan, B. Pfander, and S. Jentsch, "PCNA, the maestro of the replication fork," *Cell*, vol. 129, no. 4, pp. 665–679, 2007.
- [13] C. Hoege, B. Pfander, G.-L. Moldovan, G. Pyrowolakis, and S. Jentsch, "*RAD6*-dependent DNA repair is linked to modification of PCNA by ubiquitin and SUMO," *Nature*, vol. 419, no. 6903, pp. 135–141, 2002.
- [14] S. Jentsch, J. P. McGrath, and A. Varshavsky, "The yeast DNA repair gene *RAD6* encodes a ubiquitin-conjugating enzyme," *Nature*, vol. 329, no. 6135, pp. 131–134, 1987.
- [15] R. M. Hofmann and C. M. Pickart, "Noncanonical *MMS2*-encoded ubiquitin-conjugating enzyme functions in assembly of novel polyubiquitin chains for DNA repair," *Cell*, vol. 96, no. 5, pp. 645–653, 1999.
- [16] H. D. Ulrich and S. Jentsch, "Two RING finger proteins mediate cooperation between ubiquitin-conjugating enzymes in DNA repair," *The EMBO Journal*, vol. 19, no. 13, pp. 3388–3397, 2000.
- [17] C. M. Pickart and M. J. Eddins, "Ubiquitin: structures, functions, mechanisms," *Biochimica et Biophysica Acta*, vol. 1695, no. 1–3, pp. 55–72, 2004.
- [18] P. L. Kannouche, J. Wing, and A. R. Lehmann, "Interaction of human DNA polymerase  $\eta$  with monoubiquitinated PCNA: a possible mechanism for the polymerase switch in response to DNA damage," *Molecular Cell*, vol. 14, no. 4, pp. 491–500, 2004.
- [19] B. S. Plosky, A. E. Vidal, A. R. F. de Henestrosa et al., "Controlling the subcellular localization of DNA polymerases  $\iota$  and  $\eta$  via interactions with ubiquitin," *The EMBO Journal*, vol. 25, no. 12, pp. 2847–2855, 2006.
- [20] X. Bi, L. R. Barkley, D. M. Slater et al., "Rad18 regulates DNA polymerase  $\kappa$  and is required for recovery from S-phase checkpoint-mediated arrest," *Molecular and Cellular Biology*, vol. 26, no. 9, pp. 3527–3540, 2006.
- [21] M. Bienko, C. M. Green, N. Crosetto et al., "Biochemistry: ubiquitin-binding domains in Y-family polymerases regulate translesion synthesis," *Science*, vol. 310, no. 5755, pp. 1821–1824, 2005.
- [22] I. Unk, I. Hajdú, K. Fátýol et al., "Human HLTf functions as a ubiquitin ligase for proliferating cell nuclear antigen polyubiquitination," *Proceedings of the National Academy of Sciences of the United States of America*, vol. 105, no. 10, pp. 3768–3773, 2008.
- [23] I. Unk, I. Hajdú, K. Fátýol et al., "Human SHPRH is a ubiquitin ligase for Mms2-Ubc13-dependent polyubiquitylation of proliferating cell nuclear antigen," *Proceedings of the National Academy of Sciences of the United States of America*, vol. 103, no. 48, pp. 18107–18112, 2006.
- [24] A. Motegi, H.-J. Liaw, K.-Y. Lee et al., "Polyubiquitination of proliferating cell nuclear antigen by HLTf and SHPRH prevents genomic instability from stalled replication forks," *Proceedings of the National Academy of Sciences of the United States of America*, vol. 105, no. 34, pp. 12411–12416, 2008.
- [25] H. Zhang and C. W. Lawrence, "The error-free component of the *RAD6/RAD18* DNA damage tolerance pathway of budding yeast employs sister-strand recombination," *Proceedings of the National Academy of Sciences of the United States of America*, vol. 102, no. 44, pp. 15954–15959, 2005.
- [26] V. Gangavarapu, S. Prakash, and L. Prakash, "Requirement of *RAD52* group genes for postreplication repair of UV-damaged DNA in *Saccharomyces cerevisiae*," *Molecular and Cellular Biology*, vol. 27, no. 21, pp. 7758–7764, 2007.
- [27] E. C. Minca and D. Kowalski, "Multiple Rad5 activities mediate sister chromatid recombination to bypass DNA damage at stalled replication forks," *Molecular Cell*, vol. 38, no. 5, pp. 649–661, 2010.

- [28] A. Blastyák, L. Pintér, I. Unk, L. Prakash, S. Prakash, and L. Haracska, "Yeast Rad5 protein required for postreplication repair has a DNA helicase activity specific for replication fork regression," *Molecular Cell*, vol. 28, no. 1, pp. 167–175, 2007.
- [29] J. M. Sogo, M. Lopes, and M. Foiani, "Fork reversal and ssDNA accumulation at stalled replication forks owing to checkpoint defects," *Science*, vol. 297, no. 5581, pp. 599–602, 2002.
- [30] P. Stelter and H. D. Ulrich, "Control of spontaneous and damage-induced mutagenesis by SUMO and ubiquitin conjugation," *Nature*, vol. 425, no. 6954, pp. 188–191, 2003.
- [31] J. Frampton, A. Irmisch, C. M. Green et al., "Postreplication repair and PCNA modification in *Schizosaccharomyces pombe*," *Molecular Biology of the Cell*, vol. 17, no. 7, pp. 2976–2985, 2006.
- [32] H. Arakawa, G.-L. Moldovan, H. Saribasak, N. N. Saribasak, S. Jentsch, and J.-M. Buerstedde, "A role for PCNA ubiquitination in immunoglobulin hypermutation," *PLoS Biology*, vol. 4, no. 11, pp. 1947–1956, 2006.
- [33] L. J. Simpson, A.-L. Ross, D. Szüts et al., "RAD18-independent ubiquitination of proliferating-cell nuclear antigen in the avian cell line DT40," *EMBO Reports*, vol. 7, no. 9, pp. 927–932, 2006.
- [34] C. A. Leach and W. M. Michael, "Ubiquitin/SUMO modification of PCNA promotes replication fork progression in *Xenopus laevis* egg extracts," *Journal of Cell Biology*, vol. 171, no. 6, pp. 947–954, 2005.
- [35] K. Terai, T. Abbas, A. A. Jazaeri, and A. Dutta, "CRL4<sup>Cdt2</sup> E3 ubiquitin ligase monoubiquitinates PCNA to promote translesion DNA synthesis," *Molecular Cell*, vol. 37, no. 1, pp. 143–149, 2010.
- [36] S. Sarkar, A. A. Davies, H. D. Ulrich, and P. J. McHugh, "DNA interstrand crosslink repair during G1 involves nucleotide excision repair and DNA polymerase  $\zeta$ ," *The EMBO Journal*, vol. 25, no. 6, pp. 1285–1294, 2006.
- [37] E. S. Johnson, "Protein modification by SUMO," *Annual Review of Biochemistry*, vol. 73, pp. 355–382, 2004.
- [38] J. M. P. Desterro, M. S. Rodriguez, and R. T. Hay, "SUMO-1 modification of I $\kappa$ B $\alpha$  inhibits NF- $\kappa$ B activation," *Molecular Cell*, vol. 2, no. 2, pp. 233–239, 1998.
- [39] L. Haracska, C. A. Torres-Ramos, R. E. Johnson, S. Prakash, and L. Prakash, "Opposing effects of ubiquitin conjugation and SUMO modification of PCNA on replicational bypass of DNA lesions in *Saccharomyces cerevisiae*," *Molecular and Cellular Biology*, vol. 24, no. 10, pp. 4267–4274, 2004.
- [40] R. H. Schiestl, S. Prakash, and L. Prakash, "The SRS2 suppressor of rad6 mutations of *Saccharomyces cerevisiae* acts by channeling DNA lesions into the RAD52 DNA repair pathway," *Genetics*, vol. 124, no. 4, pp. 817–831, 1990.
- [41] B. Pfander, G.-L. Moldovan, M. Sacher, C. Hoege, and S. Jentsch, "SUMO-modified PCNA recruits Srs2 to prevent recombination during S phase," *Nature*, vol. 436, no. 7049, pp. 428–433, 2005.
- [42] E. Papouli, S. Chen, A. A. Davies et al., "Crosstalk between SUMO and ubiquitin on PCNA is mediated by recruitment of the helicase Srs2p," *Molecular Cell*, vol. 19, no. 1, pp. 123–133, 2005.
- [43] D. Branzei, F. Vanoli, and M. Foiani, "SUMOylation regulates Rad18-mediated template switch," *Nature*, vol. 456, no. 7224, pp. 915–920, 2008.
- [44] A. Motegi, R. Sood, H. Moinova, S. D. Markowitz, P. P. Liu, and K. Myung, "Human SHPRH suppresses genomic instability through proliferating cell nuclear antigen polyubiquitination," *Journal of Cell Biology*, vol. 175, no. 5, pp. 703–708, 2006.
- [45] A. Motegi, K. Kuntz, A. Majeed, S. Smith, and K. Myung, "Regulation of gross chromosomal rearrangements by ubiquitin and SUMO ligases in *Saccharomyces cerevisiae*," *Molecular and Cellular Biology*, vol. 26, no. 4, pp. 1424–1433, 2006.
- [46] G.-L. Moldovan, B. Pfander, and S. Jentsch, "PCNA controls establishment of sister chromatid cohesion during S phase," *Molecular Cell*, vol. 23, no. 5, pp. 723–732, 2006.
- [47] A. A. Davies, D. Huttner, Y. Daigaku, S. Chen, and H. D. Ulrich, "Activation of ubiquitin-dependent DNA damage bypass is mediated by replication protein A," *Molecular Cell*, vol. 29, no. 5, pp. 625–636, 2008.
- [48] T. T. Huang, S. M. B. Nijman, K. D. Mirchandani et al., "Regulation of monoubiquitinated PCNA by DUB autocleavage," *Nature Cell Biology*, vol. 8, no. 4, pp. 339–347, 2006.
- [49] A. Niimi, S. Brown, S. Sabbioneda et al., "Regulation of proliferating cell nuclear antigen ubiquitination in mammalian cells," *Proceedings of the National Academy of Sciences of the United States of America*, vol. 105, no. 42, pp. 16125–16130, 2008.
- [50] D. J. Chang, P. J. Lupardus, and K. A. Cimprich, "Monoubiquitination of proliferating cell nuclear antigen induced by stalled replication requires uncoupling of DNA polymerase and mini-chromosome maintenance helicase activities," *Journal of Biological Chemistry*, vol. 281, no. 43, pp. 32081–32088, 2006.
- [51] M. Lopes, M. Foiani, and J. M. Sogo, "Multiple mechanisms control chromosome integrity after replication fork uncoupling and restart at irreparable UV lesions," *Molecular Cell*, vol. 21, no. 1, pp. 15–27, 2006.
- [52] G. I. Karras and S. Jentsch, "The RAD6 DNA damage tolerance pathway operates uncoupled from the replication fork and is functional beyond S phase," *Cell*, vol. 141, no. 2, pp. 255–267, 2010.
- [53] Y. Daigaku, A. A. Davies, and H. D. Ulrich, "Ubiquitin-dependent DNA damage bypass is separable from genome replication," *Nature*, vol. 465, no. 7300, pp. 951–955, 2010.
- [54] C. E. Edmunds, L. J. Simpson, and J. E. Sale, "PCNA ubiquitination and REV1 define temporally distinct mechanisms for controlling translesion synthesis in the avian cell line DT40," *Molecular Cell*, vol. 30, no. 4, pp. 519–529, 2008.
- [55] L. S. Waters and G. C. Walker, "The critical mutagenic translesion DNA polymerase Rev1 is highly expressed during G<sub>2</sub>/M phase rather than S phase," *Proceedings of the National Academy of Sciences of the United States of America*, vol. 103, no. 24, pp. 8971–8976, 2006.
- [56] A.-L. Ross, L. J. Simpson, and J. E. Sale, "Vertebrate DNA damage tolerance requires the C-terminus but not BRCT or transferase domains of REV1," *Nucleic Acids Research*, vol. 33, no. 4, pp. 1280–1289, 2005.
- [57] C. Guo, P. L. Fischhaber, M. J. Luk-Paszyc et al., "Mouse Rev1 protein interacts with multiple DNA polymerases involved in translesion DNA synthesis," *The EMBO Journal*, vol. 22, no. 24, pp. 6621–6630, 2003.
- [58] V. Bailly, J. Lamb, P. Sung, S. Prakash, and L. Prakash, "Specific complex formation between yeast RAD6 and RAD18 proteins: a potential mechanism for targeting RAD6 ubiquitin-conjugating activity to DNA damage sites," *Genes and Development*, vol. 8, no. 7, pp. 811–820, 1994.
- [59] V. Bailly, S. Lauder, S. Prakash, and L. Prakash, "Yeast DNA repair proteins Rad6 and Rad18 form a heterodimer that has ubiquitin conjugating, DNA binding, and ATP hydrolytic activities," *Journal of Biological Chemistry*, vol. 272, no. 37, pp. 23360–23365, 1997.
- [60] H. D. Ulrich and S. Jentsch, "Two RING finger proteins mediate cooperation between ubiquitin-conjugating enzymes

- in DNA repair," *The EMBO Journal*, vol. 19, no. 13, pp. 3388–3397, 2000.
- [61] N. B. Watson, E. Nelson, M. Digman, J. A. Thornburg, B. W. Alphenaar, and W. G. McGregor, "RAD18 and associated proteins are immobilized in nuclear foci in human cells entering S-phase with ultraviolet light-induced damage," *Mutation Research*, vol. 648, no. 1-2, pp. 23–31, 2008.
- [62] S. P. Jackson and J. Bartek, "The DNA-damage response in human biology and disease," *Nature*, vol. 461, no. 7267, pp. 1071–1078, 2009.
- [63] D. Branzei and M. Foiani, "Maintaining genome stability at the replication fork," *Nature Reviews Molecular Cell Biology*, vol. 11, no. 3, pp. 208–219, 2010.
- [64] Y. Fu, Y. Zhu, K. Zhang, M. Yeung, D. Durocher, and W. Xiao, "Rad6-Rad18 mediates a eukaryotic SOS response by ubiquitinating the 9-1-1 checkpoint clamp," *Cell*, vol. 133, no. 4, pp. 601–611, 2008.
- [65] J. Huang, M. S.Y. Huen, H. Kim et al., "RAD18 transmits DNA damage signalling to elicit homologous recombination repair," *Nature Cell Biology*, vol. 11, no. 5, pp. 592–603, 2009.
- [66] D. Szüts, L. J. Simpson, S. Kabani, M. Yamazoe, and J. E. Sale, "Role for RAD18 in homologous recombination in DT40 cells," *Molecular and Cellular Biology*, vol. 26, no. 21, pp. 8032–8041, 2006.
- [67] A. Saberi, H. Hohegger, D. Szüts et al., "RAD18 and poly(ADP-ribose) polymerase independently suppress the access of nonhomologous end joining to double-strand breaks and facilitate homologous recombination-mediated repair," *Molecular and Cellular Biology*, vol. 27, no. 7, pp. 2562–2571, 2007.
- [68] S. M. B. Nijman, T. T. Huang, A. M. G. Dirac et al., "The deubiquitinating enzyme USP1 regulates the fanconi anemia pathway," *Molecular Cell*, vol. 17, no. 3, pp. 331–339, 2005.
- [69] V. H. Oestergaard, F. Langevin, H. J. Kuiken et al., "Deubiquitination of FANCD2 is required for DNA crosslink repair," *Molecular Cell*, vol. 28, no. 5, pp. 798–809, 2007.
- [70] J. M. Kim, K. Parmar, M. Huang et al., "Inactivation of murine Usp1 results in genomic instability and a Fanconi anemia phenotype," *Developmental Cell*, vol. 16, no. 2, pp. 314–320, 2009.
- [71] T. Göhler, I. M. Munoz, J. Rouse, and J. J. Blow, "PTIP/Swift is required for efficient PCNA ubiquitination in response to DNA damage," *DNA Repair*, vol. 7, no. 5, pp. 775–787, 2008.
- [72] G. Soria, O. Podhajcer, C. Prives, and V. Gottifredi, "P21Cip1/WAF1 downregulation is required for efficient PCNA ubiquitination after UV irradiation," *Oncogene*, vol. 25, no. 20, pp. 2829–2838, 2006.
- [73] S. Avkin, Z. Sevilya, L. Toube et al., "p53 and p21 regulate error-prone DNA repair to yield a lower mutation load," *Molecular Cell*, vol. 22, no. 3, pp. 407–413, 2006.
- [74] V. Pagès, S. R. Santa Maria, L. Prakash, and S. Prakash, "Role of DNA damage-induced replication checkpoint in promoting lesion bypass by translesion synthesis in yeast," *Genes and Development*, vol. 23, no. 12, pp. 1438–1449, 2009.
- [75] A. G. Paulovich, C. D. Armour, and L. H. Hartwell, "The *Saccharomyces cerevisiae* RAD9, RAD17, RAD24 and MEC3 genes are required for tolerating irreparable, ultraviolet-induced DNA damage," *Genetics*, vol. 150, no. 1, pp. 75–93, 1998.

## Research Article

# Mouse WRN Helicase Domain Is Not Required for Spontaneous Homologous Recombination-Mediated DNA Deletion

Adam D. Brown,<sup>1,2</sup> Alison B. Claybon,<sup>1</sup> and Alexander J. R. Bishop<sup>1,2</sup>

<sup>1</sup>Greehey Children's Cancer Research Institute, The University of Texas Health Science Center at San Antonio, San Antonio, TX 78229, USA

<sup>2</sup>Department of Cellular and Structural Biology, The University of Texas Health Science Center at San Antonio, San Antonio, TX 78229, USA

Correspondence should be addressed to Alexander J. R. Bishop, bishopa@uthscsa.edu

Received 16 May 2010; Accepted 7 July 2010

Academic Editor: Ashis Basu

Copyright © 2010 Adam D. Brown et al. This is an open access article distributed under the Creative Commons Attribution License, which permits unrestricted use, distribution, and reproduction in any medium, provided the original work is properly cited.

Werner syndrome is a rare disorder that manifests as premature aging and age-related diseases. *WRN* is the gene mutated in WS, and is one of five human RecQ helicase family members. WS cells exhibit genomic instability and altered proliferation, and *in vitro* studies suggest that WRN has a role in suppressing homologous recombination. However, more recent studies propose that other RecQ helicases (including WRN) promote early events of homologous recombination. To study the role of WRN helicase on spontaneous homologous recombination, we obtained a mouse with a deleted WRN helicase domain and combined it with the *in vivo* pink-eyed unstable homologous recombination system. In this paper, we demonstrate that WRN helicase is not necessary for suppressing homologous recombination *in vivo* contrary to previous reports using a similar mouse model.

## 1. Introduction

Werner syndrome (WS) is a rare autosomal recessive disease associated with premature age-related phenotypes such as cancer, osteoporosis, diabetes mellitus and early graying of the hair (review [1]). The gene responsible for WS (*WRN*) is one of a five human RecQ helicases including BLM, RECQL1, RECQL4, and RECQ5. Like WS, the absence of BLM and RECQL4 gives rise to the clinically distinct diseases, Bloom's syndrome (BS) and Rothmund-Thomson syndrome, respectively. Although a variety of different *WRN* mutations have been discovered, many result in a truncated nonfunctional WRN (summarized in [2]). Cells from WS patients depict an aging phenotype including reduced proliferation associated with an increase in S-phase [3] and early passage senescence [3, 4]. Furthermore, WS cells show increased levels of genomic instability thought to be caused from increased levels of illegitimate recombination. These observations lead us to investigate the role of WRN *in vivo*.

For this study we used a WRN mouse model with a deleted helicase domain [5] in combination with the well-established murine pink-eyed unstable ( $p^{un}$ ) mouse model

that can be used to determine changes in the spontaneous frequency of somatic homologous recombination (HR) events [6–8]. Though rare, this particular *Wrn* mutation has been found in a small population of WS patients [9, 10] and is therefore relevant to the human disease. The  $p^{un}$  assay is based on an HR-mediated deletion of one copy of a 70 kb DNA duplication that encompasses exons 6–18 of the *p* gene [11]. The exact deletion of one copy of the repeated region will restore the function of this pigmentation gene, and this can be observed as somatic events in pigmented tissues such as the fur and the retinal pigment epithelium (RPE) [8, 12]. The further development of the  $p^{un}$  eye spot assay which identifies  $p^{un}$  reversion events on a monolayer of clear RPE cells has proven to be significantly more sensitive and informative than the fur spot assay [6].

Studies in yeast using a similar duplication/deletion assay to the  $p^{un}$  reversion assay have identified several possible mechanisms of HR that may mediate this type of deletion event. These include intrachromatid exchange, one-sided strand invasion, unequal sister chromatid exchange (SCE), sister chromatid conversion, and single-strand annealing (SSA) [13]. Excluding SSA, each of these HR mechanisms

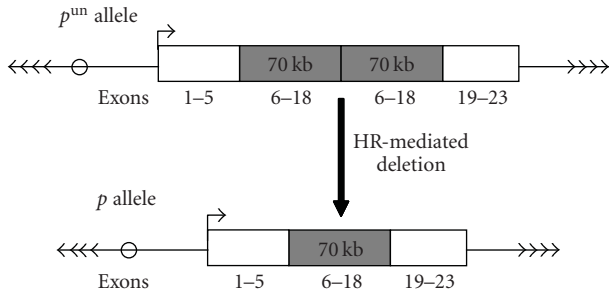


FIGURE 1: HR-mediated reversion of the  $p^{un}$  allele. Schematic of the  $p^{un}$  mutation (tandem duplication of exons 6–18), where an HR event mediates the deletion of one copy rendering a functional  $p$  gene allowing pigmentation of RPE cells. Circles and arrowheads represent centromere and telomere DNA, respectively.

is considered RAD51-dependent. RAD51-dependent HR is considered a high fidelity DNA repair mechanism that is frequently associated with DNA replication (review [14]). For example, replication forks can stall or collapse when the replication machinery encounters DNA damage like a single strand break, and HR is capable of repairing the damaged DNA template and restoring the replication fork [15]. Claybon et al. recently reported that in the absence of PARP1, somatic HR events, measured by the  $p^{un}$  system, are highly elevated and that a majority of these events were large clonally expanded cells [16]. These authors went on to suggest that these clonally expanded populations of cells are the result of an HR-mediated deletion that occurred during replication, probably in a RAD51-dependent mechanism (as compared to SSA). The utility of the helicase domain of mouse WRN is discussed below.

## 2. Materials and Methods

**2.1. Mouse Lines and PCR Genotyping.** WRN helicase mutant ( $Wrn^{\Delta hel/+}$ ) [5] mice on an FVB strain background were obtained from Dr. P. Leder, and C57BL/6J and C57BL/6J  $p^{un/un}$  mice were obtained from the Jackson Laboratory (Bar Harbor, ME). In order to obtain congenic C57BL/6J  $p^{un/un} Wrn^{\Delta hel/+}$  mice (hereafter called  $Wrn^{\Delta hel/+}$ ),  $Wrn^{\Delta hel/+}$  mice were backcrossed 5 times to C57BL/6J followed by two additional crosses to C57BL/6J  $p^{un/un}$  mice. All mice were maintained with  $p^{un/un}$  mutation. Control ( $Wrn^{+/+}$ ) and experimental ( $Wrn^{\Delta hel/\Delta hel}$ ) animals result from crossing  $Wrn^{\Delta hel/+}$  mice together. The  $p^{un/un}$  allele was genotyped by the identification of the phenotypic dilute coat color. Genotypes for the  $Wrn$  allele were determined by a PCR amplification protocol obtained from Aya Leder, Harvard Medical School, MA consisting of the following 3 primers: (1) 5'-GTTTCCTCTATCATCTGTAACAGG-3', (2) 5'-GCCAAGGAGCAAAGCTGCTAT-3' and (3) 5'-AGTGAGACATGTATGACTACC-3' and the thermo profile: 1 cycle of 94°C for 5 min; 30 cycles of 94°C for 30 s, 60°C for 30 s, and 72°C for 1 min; 1 cycle of 72°C for 3 min. Amplicon size for the wt PCR product is 350 bp and  $Wrn$  mutant 450 bp. When necessary, genomic DNA was isolated

from fixed RPE using the Qiagen DNeasy Blood and Tissue kit according to manufacture's recommendations.

**2.2. Dissection, Visualizing, and Scoring Eye Spots on the Retinal Pigment Epithelium.** Harvesting of the eye and dissection of the RPE were carried out as previously described in [7]. RPE whole mounts were visualized and imaged using a Zeiss Lumar V.12 stereomicroscope, Zeiss Axiovision MRm camera, and Zeiss Axiovision 4.6 software (Thornwood, NY).  $p^{un}$  reversion events were identified on the transparent monolayer of the RPE as pigmented cells or eye spots. Total number of eye spots and number of cells making up that eye spot were recorded for each RPE according to the criteria set forth by Bishop et al. in [7]. Additionally, the relative distance from the optic nerve of each eye spot was recorded. This was done by using the measurement tool in Adobe Photoshop, by first measuring from the center of the optic nerve to the proximal edge of the eye spot and then from the center of the optic nerve to the edge of the RPE. The relative distance is then determined by dividing the former by the latter.

**2.3. Statistical Analysis.** All statistics were carried using GraphPad Prism (La Jolla, CA). These include tests for normality (Shapiro-Wilk test), equal variances (Fmax test), two group comparisons (Mann-Whitney test), and contingency tables (Fisher's exact test).

## 3. Results

**3.1. Loss of WRN Helicase Activity Does Not Affect the Overall Frequency of Spontaneous Homologous Recombination in Mouse RPE In Vivo.** The frequency of spontaneous HR for mice with helicase domain-deficient WRN protein was previously reported as being increased 2-fold using the  $p^{un}$  fur spot assay [17]. Though the  $p^{un}$  fur spot assay can be considered a faithful assay for measuring HR frequency *in vivo*, the  $p^{un}$  eye spot assay affords many advantages, including being more sensitive to changes in HR frequency [8] and can reveal information about the timing of events during development [7], developmental patterning [18], and even information about whether the HR events are associated with replication [16]. Therefore, we set out to recapitulate the fur spot study and to determine whether we might be able to reveal any additional phenotypes associated with the  $Wrn^{\Delta hel}$  HR events. Surprisingly, when we compared the number of eye spots per RPE in  $Wrn^{+/+}$  versus  $Wrn^{\Delta hel/\Delta hel}$  (Table 1 and Figure 2(a)), we were unable to detect a significant increase in the overall frequency of HR events ( $P = .35$ , Mann-Whitney test) (Figure 2(b)). The nonparametric Mann Whitney test was used because our data was found to be not normal (data not shown) with unequal variances using a Fmax test ( $P < .0001$ ). Of interest, the variance within the  $Wrn^{+/+}$  RPE was larger than expected due to three RPEs with higher than usual numbers of reversion events. To determine whether the lack of difference in HR frequency between  $Wrn^{+/+}$  and  $Wrn^{\Delta hel/\Delta hel}$  was due to the wild-type RPE with elevated HR frequency, we compared the frequency of eye spots of our WRN wild-type RPEs with an

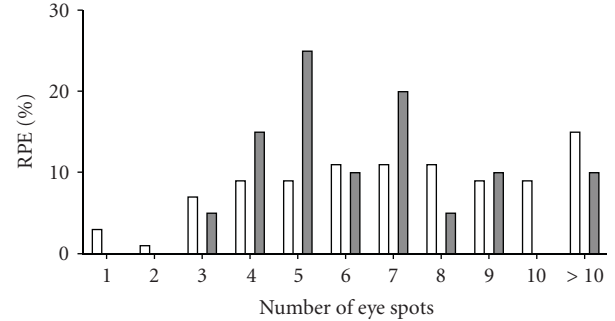
TABLE 1: Summary of RPE examined and  $p^{un}$  reversion frequency by *Wrn* genotype.

Genotype	Number of RPE	Total number of eye spots	Avg. number of eye spots per RPE	Avg. eye spot size (cell number)
<i>Wrn</i> <sup>+/+</sup>	53	522	10	6
<i>Wrn</i> <sup>Δhel/Δhel</sup>	20	152	8	4

independent wild-type data set that was recently reported by our laboratory [16]. No statistical difference in  $p^{un}$  reversion frequency was observed between these two groups of wild-type RPE (data not shown). We therefore combined these wild-type datasets, compared their combined  $p^{un}$  reversion eyespot frequency with *Wrn*<sup>Δhel/Δhel</sup>, and still did not observe any statistical difference between genotypes (Figure 2(b)). Therefore, it appears that WRN helicase activity is not required for HR, and no additional HR events are instigated by the WRN mutation.

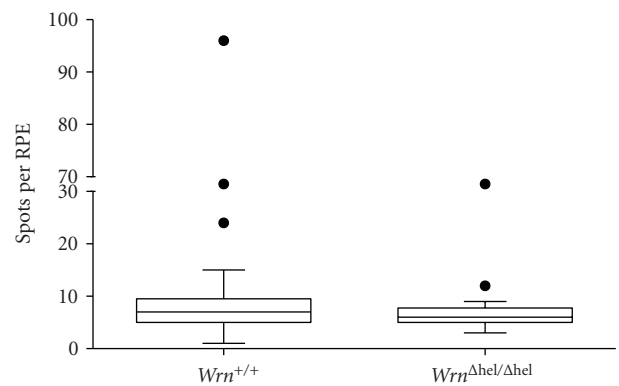
**3.2. Single- and Multicell Eye Spots in Mouse RPE Are Not Affected by WRN Helicase.** We classify eye spots as having either single (1 cell) or multi-cell ( $\geq 2$  cells) events [8]. Due to the edge-biased proliferation of the RPE [19] and the apparent “position shift” between single-cell and multi-cell eye spots [7], we speculate that multi-cell (clonally expanded)  $p^{un}$  reversion events are associated with DNA replication (discussed below). Approximately 60% of eye spots are normally single cell events. Even though we did not observe an overall difference in HR frequency, we wanted to see if WRN helicase activity affected the clonal expansion of  $p^{un}$  reversion events. Here we found no significant difference between single versus multi-cell eye spots when comparing *Wrn*<sup>+/+</sup> versus *Wrn*<sup>Δhel/Δhel</sup> RPE ( $P = .39$ , Fisher’s exact test Figure (3)). These data indicate that the helicase activity of WRN does not affect clonal expansion of mouse RPE cells following HR.

**3.3. Distribution of HR Events during RPE Development Is Not Affected by WRN Helicase Mutation.** The mouse RPE develops radially outward from the optic nerve with an edge-biased pattern of proliferation [19]. The RPE begins to form in the developing eye cup at  $\sim 8.5$  dpc and continues through the first week of postnatal development [20, 21]. Much like the age of a tree that can be determined using its concentric rings, the retrospective mapping of an eye spot onto an RPE suggests when during development a  $p^{un}$  reversion event occurred [7]. Previously we have reported mutant genotypes that affected either the timing of  $p^{un}$  reversion events during RPE development or the pattern of RPE development by examining eye spot patterns [6, 18]. In order to determine if WRN helicase function has a role in HR at a specific point during murine development, each RPE was divided into 10 concentric rings where the inner most ring contains the optic nerve depicting the beginning of RPE development (0.0-0.1) to the outer most ring at the edge of the RPE (0.9-1.0).



□ *Wrn*<sup>+/+</sup>  
■ *Wrn*<sup>Δhel/Δhel</sup>

(a)



(b)

FIGURE 2: Frequency of HR in mouse RPE. (a) Population distribution of eye spots per RPE in wild-type (open boxes) and *Wrn*<sup>Δhel/Δhel</sup> (grey boxes). (b) Overall frequency of eye spots per RPE shown as a box and whisker plot. No statistical difference in HR was detected between wild-type and *Wrn*<sup>Δhel/Δhel</sup> groups ( $P = .35$ ).

At each interval, the pattern of positional distribution was similar for both *Wrn*<sup>+/+</sup> and *Wrn*<sup>Δhel/Δhel</sup> for all eye spots ( $P = .22$ , Chi-square test, Figure 4). Of note, the positional analysis of the eye spots measures the distance from the center of the optic nerve to the most proximal cell of an eye spot, irrespective of the number of cells that constitutes the eye spot. These results suggest that the effect of the WRN helicase mutation on HR does not alter the timing or distribution of  $p^{un}$  reversion events during mouse RPE.

## 4. Discussion

In summary, mice expressing a helicase-deficient *Wrn* allele did not have an increase in the frequency of spontaneous HR. Our results differ substantially from earlier work done using this same mouse model with the less sensitive  $p^{un}$  fur spot assay which observed at least a 2-fold increase in  $p^{un}$  reversion events [17]. In our experience we have never observed a discrepancy in  $p^{un}$  reversion frequency between the neural crest-derived melanocyte-dependent fur spot assay and the neural epithelium-derived RPE-based eye spot assay.

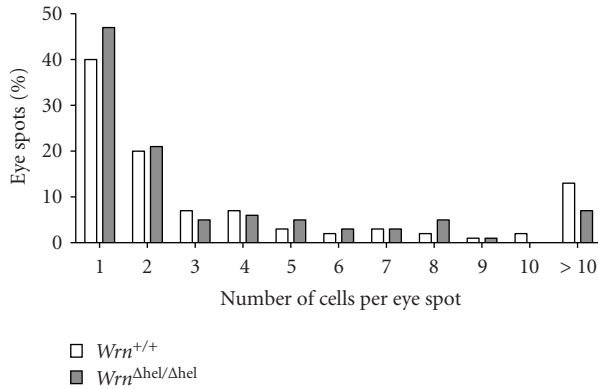


FIGURE 3: Frequency of the different sizes of eye spot (number of cells per eye spot) in mouse RPE. *Wrn*<sup>Δhel/Δhel</sup> (grey boxes) does not affect cell size distribution compared to wild-type (open boxes) ( $P = .39$ ).

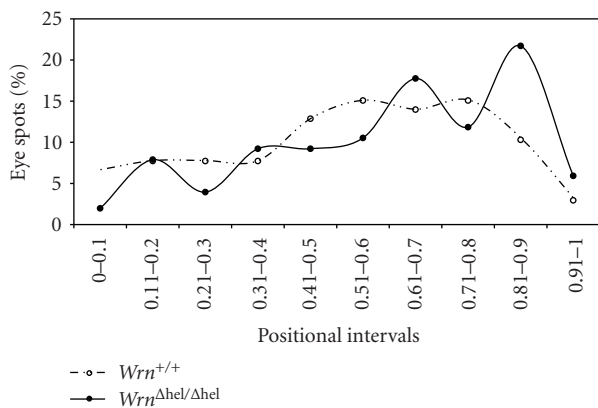


FIGURE 4: Positional distribution of all eye spots. WRN helicase does not affect positional or pattern distribution ( $P = .22$ ). Wild type (open circles with dash line) and *Wrn*<sup>Δhel/Δhel</sup> (closed circles with solid line) RPE.

However, it should be noted that we have not examined the frequency of  $p^{\text{un}}$  fur spots in our C57BL/6/J congenic animals, and it is formally possible that the difference may be due to difference in strain background. Our result also differs from a more recent report using the  $p^{\text{un}}$  eye spot assay with the expression of a transgenic dominant negative human WRN allele [22]. This latter report observed a 30% increase in eye spots (from an average of 6 to 8 eye spots per RPE in wild-type and WRN impaired, resp.), a relatively slight, though significant increase for the  $p^{\text{un}}$  eye spot assay, that could be simply explained by sample size; Yamamoto et al. [22] used approximately 50 RPE per group compared to our 20 RPE. Alternately, the difference could be due to a difference in using a mouse helicase deficient *Wrn* mutant mouse and a mouse model that expressed a transgenic dominant negative allele of human WRN.

The  $p^{\text{un}}$  fur spot assay is reliant upon detecting large clonal expansions of melanocytes following  $p^{\text{un}}$  reversion that are visible in the fur (at least 1 mm<sup>2</sup>). In contrast, the  $p^{\text{un}}$  eye spot assay can detect both single cell and clonally expanded (multi-cell) reversion events. Additionally, the  $p^{\text{un}}$

eye spot assay can be used to determine any differences in the timing of HR events during embryonic development. In this study we found that the helicase activity of mouse WRN does not affect the frequency of single versus multi-cell events and nor does it affect the timing of spontaneous HR events during mouse embryonic development.

Although WS cells are described as having genomic instability, there is some discrepancy as to the role WRN plays in HR. In support of WRN as a suppressor of illegitimate HR, WS patients exhibit variegated chromosomal translocations [23], elevated recombination levels between microhomology plasmids [24], approximate 2-fold increase of RAD51 focus formation [25], and sensitivity to agents that lead to replication stress [5, 26–28]. Additionally, WRN is known to associate with proteins tied to replication machinery like RPA [29–32], PCNA [33–35], Pol $\delta$  [36, 37], and RAD52 [38]. In contrast though, WS cells do not have elevated amounts of SCE which are the hallmark of BS [39].

More recent studies have begun to show that RecQ helicases (e.g., WRN) promote HR via mechanisms like DNA resection. Following double-strand breaks (DSBs), the helicase domain of Sgs1 (yeast RecQ orthologue of WRN) is required for resection of DNA ends to produce single strand DNA substrates for RAD51 [40, 41]. Additionally, the helicase function of Sgs1 is required for normal kinetics of HR at the *MAT* locus, and yeast mutants for Sgs1 and Exo1 nuclease exhibit sensitivity to DNA damaging at similar levels to Rad52 mutants (which are diminished for HR repair) [42]. These same authors subsequently went on to demonstrate that the RecQ helicase BLM also has some DNA resection functions following Camptothecin-induced DSBs and that BLM function of DSB resection is in parallel with an EXO1-dependent pathway [42]. A separate study investigated the role of WRN following exposure to chromium(VI), an agent known to induce DSBs, and found that chromium(VI) treated human cells depleted of WRN and WS cells had delayed or absent RAD51 focus formation [43]. This study again suggests that WRN is important for promoting HR, potentially in early steps of this process (e.g., initiation via resection) following DNA damage. Unlike the other human RecQ helicase members, WRN also has exonuclease activity, so understanding which enzymatic function of WRN is involved in promoting HR is valuable to our knowledge of this protein, as well as insightful to the syndrome. As it pertains to this study, we found that the helicase function of WRN is neither necessary for, nor suppresses spontaneous HR. With regard to other RecQ helicases, we recently found HR to be significantly elevated in the absence of BLM using the  $p^{\text{un}}$  eye spot assay (data not shown). Considering the lack of effect observed in our study, and only a mild suppressive effect in the Yamamoto et al. study [21] compared to a deficiency in BLM (data not shown), it would appear that WRN only plays a minor role in suppressing HR, possibly the result of redundancy amongst the different RecQ family members. Together, these studies give insight into the potential differences between two of the known five human RecQ helicases and suggest that future studies are warranted to better understanding the functions of WRN (and BLM) in HR.

## Acknowledgment

This paper was supported by the National Institutes of Health [K22ES012264 to A. J. R. Bishop] and National Institute of Aging [T32AG021890 A. D. Brown]. A. D. Brown and A. B. Claybon contributed equally to this work.

## References

- [1] B. A. Kudlow, B. K. Kennedy, and R. J. Monnat Jr., "Werner and Hutchinson-Gilford progeria syndromes: mechanistic basis of human progeroid diseases," *Nature Reviews Molecular Cell Biology*, vol. 8, no. 5, pp. 394–404, 2007.
- [2] M. Muftuoglu, J. Oshima, C. von Kobbe, W.-H. Cheng, D. F. Leistriz, and V. A. Bohr, "The clinical characteristics of Werner syndrome: molecular and biochemical diagnosis," *Human Genetics*, vol. 124, no. 4, pp. 369–377, 2008.
- [3] F. Takeuchi, F. Hanaoka, M. Goto, M. Yamada, and T. Miyamoto, "Prolongation of S phase and whole cell cycle in Werner's syndrome fibroblasts," *Experimental Gerontology*, vol. 17, no. 6, pp. 473–480, 1982.
- [4] R. G. A. Faragher, I. R. Kill, J. A. A. Hunter, F. M. Pope, C. Tannock, and S. Shall, "The gene responsible for Werner syndrome may be a cell division "counting" gene," *Proceedings of the National Academy of Sciences of the United States of America*, vol. 90, no. 24, pp. 12030–12034, 1993.
- [5] M. Lebel and P. Leder, "A deletion within the murine Werner syndrome helicase induces sensitivity to inhibitors of topoisomerase and loss of cellular proliferative capacity," *Proceedings of the National Academy of Sciences of the United States of America*, vol. 95, no. 22, pp. 13097–13102, 1998.
- [6] A. J. R. Bishop, M. C. Hollander, B. Kosaras, R. L. Sidman, A. J. Fornace Jr., and R. H. Schiestl, "Atm-, p53-, and Gadd45a-deficient mice show an increased frequency of homologous recombination at different stages during development," *Cancer Research*, vol. 63, no. 17, pp. 5335–5343, 2003.
- [7] A. J. R. Bishop, B. Kosaras, N. Carls, R. L. Sidman, and R. H. Schiestl, "Susceptibility of proliferating cells to benzo[a]pyrene-induced homologous recombination in mice," *Carcinogenesis*, vol. 22, no. 4, pp. 641–649, 2001.
- [8] A. J. R. Bishop, B. Kosaras, R. L. Sidman, and R. H. Schiestl, "Benzo(a)pyrene and X-rays induce reversions of the pink-eyed unstable mutation in the retinal pigment epithelium of mice," *Mutation Research*, vol. 457, no. 1–2, pp. 31–40, 2000.
- [9] C.-E. Yu, J. Oshima, Y.-H. Fu et al., "Positional cloning of the Werner's syndrome gene," *Science*, vol. 272, no. 5259, pp. 258–262, 1996.
- [10] C.-E. Yu, J. Oshima, E. M. Wijsman et al., "Mutations in the consensus helicase domains of the Werner syndrome gene. Werner's Syndrome Collaborative Group," *American Journal of Human Genetics*, vol. 60, no. 2, pp. 330–341, 1997.
- [11] Y. Gondo, J. M. Gardner, Y. Nakatsu et al., "High-frequency genetic reversion mediated by a DNA duplication: the mouse pink-eyed unstable mutation," *Proceedings of the National Academy of Sciences of the United States of America*, vol. 90, no. 1, pp. 297–301, 1993.
- [12] R. H. Schiestl, F. Khogali, and N. Carls, "Reversion of the mouse pink-eyed unstable mutation induced by low doses of X-rays," *Science*, vol. 266, no. 5190, pp. 1573–1576, 1994.
- [13] A. Galli and R. H. Schiestl, "On the mechanism of UV and  $\gamma$ -ray induced intrachromosomal recombination in yeast cells synchronized in different stages of the cell cycle," *Molecular and General Genetics*, vol. 248, no. 3, pp. 301–310, 1995.
- [14] F. Pâques and J. E. Haber, "Multiple pathways of recombination induced by double-strand breaks in *Saccharomyces cerevisiae*," *Microbiology and Molecular Biology Reviews*, vol. 63, no. 2, pp. 349–404, 1999.
- [15] C. Arnaudeau, C. Lundin, and T. Helleday, "DNA double-strand breaks associated with replication forks are predominantly repaired by homologous recombination involving an exchange mechanism in mammalian cells," *Journal of Molecular Biology*, vol. 307, no. 5, pp. 1235–1245, 2001.
- [16] A. B. Claybon, B. Karia, C. Bruce, and A. J. R. Bishop, "PARP1 suppresses homologous recombination events in mice in vivo," *Nucleic Acids Research*, pp. 1–8, 2010.
- [17] M. Lebel, "Increased frequency of DNA deletions in pink-eyed unstable mice carrying a mutation in the Werner syndrome gene homologue," *Carcinogenesis*, vol. 23, no. 1, pp. 213–216, 2002.
- [18] A. J. R. Bishop, B. Kosaras, M. C. Hollander, A. Fornace Jr., R. L. Sidman, and R. H. Schiestl, "p21 controls patterning but not homologous recombination in RPE development," *DNA Repair*, vol. 5, no. 1, pp. 111–120, 2006.
- [19] L. Bodenstern and R. L. Sidman, "Growth and development of the mouse retinal pigment epithelium. I. Cell and tissue morphometrics and topography of mitotic activity," *Developmental Biology*, vol. 121, no. 1, pp. 192–204, 1987.
- [20] A. V. Ershov and O. G. Stroeve, "Post-natal pattern of cell proliferation in retinal pigment epithelium of mice studied with tritiated thymidine autoradiography," *Cell Differentiation and Development*, vol. 28, no. 3, pp. 173–177, 1989.
- [21] A. Nakayama, M.-T. T. Nguyen, C. C. Chen, K. Opdecamp, C. A. Hodgkinson, and H. Arnheiter, "Mutations in microphthalmia, the mouse homolog of the human deafness gene MITE, affect neuroepithelial and neural crest-derived melanocytes differently," *Mechanisms of Development*, vol. 70, no. 1–2, pp. 155–166, 1998.
- [22] M. L. Yamamoto, R. Reliene, J. Oshima, and R. H. Schiestl, "Effects of human Werner helicase on intrachromosomal homologous recombination mediated DNA deletions in mice," *Mutation Research*, vol. 644, no. 1–2, pp. 11–16, 2008.
- [23] D. Salk, K. Au, H. Hoehn, and G. M. Martin, "Cytogenetics of Werner's syndrome cultured skin fibroblasts: variegated translocation mosaicism," *Cytogenetics and Cell Genetics*, vol. 30, no. 2, pp. 92–107, 1981.
- [24] R. Z. Cheng, S. Murano, B. Kurz, and R. J. Shmookler Reis, "Homologous recombination is elevated in some Werner-like syndromes but not during normal in vitro or in vivo senescence of mammalian cells," *Mutation Research*, vol. 237, no. 5–6, pp. 259–269, 1990.
- [25] P. Pichierri, A. Franchitto, P. Mosesso, and F. Palitti, "Werner's syndrome protein is required for correct recovery after replication arrest and DNA damage induced in S-phase of cell cycle," *Molecular Biology of the Cell*, vol. 12, no. 8, pp. 2412–2421, 2001.
- [26] R. Elli, L. Chessa, A. Antonelli, P. Petrinelli, R. Ambra, and L. Marcucci, "Effects of topoisomerase II inhibition in lymphoblasts from patients with progeroid and "chromosome instability" syndromes," *Cancer Genetics and Cytogenetics*, vol. 87, no. 2, pp. 112–116, 1996.
- [27] M. Okada, M. Goto, Y. Furuichi, and M. Sugimoto, "Differential effects of cytotoxic drugs on mortal and immortalized B-lymphoblastoid cell lines from normal and Werner's syndrome patients," *Biological & Pharmaceutical Bulletin*, vol. 21, pp. 235–239, 1998.

- [28] M. Poot, K. A. Gollahon, and P. S. Rabinovitch, "Werner syndrome lymphoblastoid cells are sensitive to camptothecin-induced apoptosis in S-phase," *Human Genetics*, vol. 104, no. 1, pp. 10–14, 1999.
- [29] J.-C. Shen, M. D. Gray, J. Oshima, and L. A. Loeb, "Characterization of Werner syndrome protein DNA helicase activity: directionality, substrate dependence and stimulation by replication protein A," *Nucleic Acids Research*, vol. 26, no. 12, pp. 2879–2885, 1998.
- [30] R. M. Brosh Jr., D. K. Orren, J. O. Nehlin et al., "Functional and physical interaction between WRN helicase and human replication protein A," *Journal of Biological Chemistry*, vol. 274, no. 26, pp. 18341–18350, 1999.
- [31] K. M. Doherty, J. A. Sommers, M. D. Gray et al., "Physical and functional mapping of the replication protein A interaction domain of the Werner and Bloom syndrome helicases," *Journal of Biological Chemistry*, vol. 280, no. 33, pp. 29494–29505, 2005.
- [32] J.-C. Shen, Y. Lao, A. Kamath-Loeb, M. S. Wold, and L. A. Loeb, "The N-terminal domain of the large subunit of human replication protein A binds to Werner syndrome protein and stimulates helicase activity," *Mechanisms of Ageing and Development*, vol. 124, no. 8-9, pp. 921–930, 2003.
- [33] M. Lebel, E. A. Spillare, C. C. Harris, and P. Leder, "The Werner syndrome gene product co-purifies with the DNA replication complex and interacts with PCNA and topoisomerase I," *Journal of Biological Chemistry*, vol. 274, no. 53, pp. 37795–37799, 1999.
- [34] S. Huang, S. Beresten, B. Li, J. Oshima, N. A. Ellis, and J. Campisi, "Characterization of the human and mouse WRN 3' → 5' exonuclease," *Nucleic Acids Research*, vol. 28, no. 12, pp. 2396–2405, 2000.
- [35] A. M. Rodríguez-López, D. A. Jackson, J. O. Nehlin, F. Iborra, A. V. Warren, and L. S. Cox, "Characterisation of the interaction between WRN, the helicase/exonuclease defective in progeroid Werner's syndrome, and an essential replication factor, PCNA," *Mechanisms of Ageing and Development*, vol. 124, no. 2, pp. 167–174, 2003.
- [36] A. S. Kamath-Loeb, E. Johansson, P. M. J. Burgers, and L. A. Loeb, "Functional interaction between the Werner syndrome protein and DNA polymerase  $\delta$ ," *Proceedings of the National Academy of Sciences of the United States of America*, vol. 97, no. 9, pp. 4603–4608, 2000.
- [37] A. S. Kamath-Loeb, L. A. Loeb, E. Johansson, P. M. J. Burgers, and M. Fry, "Interactions between the Werner syndrome helicase and DNA polymerase  $\delta$  specifically facilitate copying of tetraplex and hairpin structures of the d(CGG)<sub>n</sub> trinucleotide repeat sequence," *Journal of Biological Chemistry*, vol. 276, no. 19, pp. 16439–16446, 2001.
- [38] K. Baynton, M. Otterlei, M. Björås, C. Von Kobbe, V. A. Bohr, and E. Seeberg, "WRN interacts physically and functionally with the recombination mediator protein RAD52," *Journal of Biological Chemistry*, vol. 278, no. 38, pp. 36476–36486, 2003.
- [39] M. I. Melaragno, D. Pagni, and M. D. A. C. Smith, "Cytogenetic aspects of Werner's syndrome lymphocyte cultures," *Mechanisms of Ageing and Development*, vol. 78, no. 2, pp. 117–122, 1995.
- [40] E. P. Mimitou and L. S. Symington, "Sae2, Exo1 and Sgs1 collaborate in DNA double-strand break processing," *Nature*, vol. 455, no. 7214, pp. 770–774, 2008.
- [41] Z. Zhu, W.-H. Chung, E. Y. Shim, S. E. Lee, and G. Ira, "Sgs1 helicase and two nucleases Dna2 and Exo1 resect DNA double-strand break ends," *Cell*, vol. 134, no. 6, pp. 981–994, 2008.
- [42] S. Gravel, J. R. Chapman, C. Magill, and S. P. Jackson, "DNA helicases Sgs1 and BLM promote DNA double-strand break resection," *Genes and Development*, vol. 22, no. 20, pp. 2767–2772, 2008.
- [43] A. Zecevic, H. Menard, V. Gurel, E. Hagan, R. DeCaro, and A. Zhitkovich, "WRN helicase promotes repair of DNA double-strand breaks caused by aberrant mismatch repair of chromium-DNA adducts," *Cell Cycle*, vol. 8, no. 17, pp. 2769–2778, 2009.

## Review Article

# The Effect of Mitochondrial Dysfunction on Cytosolic Nucleotide Metabolism

Claus Desler,<sup>1</sup> Anne Lykke,<sup>2</sup> and Lene Juel Rasmussen<sup>1</sup>

<sup>1</sup> Center for Healthy Aging, Faculty of Health Sciences, University of Copenhagen, 2200 Copenhagen, Denmark

<sup>2</sup> Department of Science, Systems and Models, Roskilde University, 4000 Roskilde, Denmark

Correspondence should be addressed to Lene Juel Rasmussen, ljr@mitosci.net

Received 15 June 2010; Accepted 19 July 2010

Academic Editor: Ashis Basu

Copyright © 2010 Claus Desler et al. This is an open access article distributed under the Creative Commons Attribution License, which permits unrestricted use, distribution, and reproduction in any medium, provided the original work is properly cited.

Several enzymes of the metabolic pathways responsible for metabolism of cytosolic ribonucleotides and deoxyribonucleotides are located in mitochondria. Studies described in this paper suggest dysfunction of the mitochondria to affect these metabolic pathways and limit the available levels of cytosolic ribonucleotides and deoxyribonucleotides, which in turn can result in aberrant RNA and DNA synthesis. Mitochondrial dysfunction has been linked to genomic instability, and it is possible that the limiting effect of mitochondrial dysfunction on the levels of nucleotides and resulting aberrant RNA and DNA synthesis in part can be responsible for this link. This paper summarizes the parts of the metabolic pathways responsible for nucleotide metabolism that can be affected by mitochondrial dysfunction.

## 1. Introduction

Mitochondria are semiautonomous organelles present in almost all eukaryotic cells in quantities ranging from a single copy to several thousand per cell. Important mitochondrial functions include ATP production by oxidative phosphorylation,  $\beta$ -oxidation of fatty acids, and metabolism of amino acids and lipids. Furthermore, mitochondria have a prominent role in apoptosis. Mitochondrial dysfunction has been linked to genomic instability, and mutations in mitochondrial DNA (mtDNA) have been shown in a wide array of tumors [1, 2].

The focus of this paper is on the consequences of mitochondrial function for metabolism of cytosolic ribonucleotides and deoxyribonucleotides. Several of the rate-limiting steps of these metabolic pathways take place in the mitochondria and can be affected by the fitness of the organelle. Disturbance of mitochondrial function therefore has the potential to affect the cytosolic levels of ribonucleotides and deoxyribonucleotides, which in turn can affect the genomic stability.

Where deoxyribonucleotides are exclusively destined for DNA synthesis in the form of deoxyribonucleotides

triphosphates (dNTP), ribonucleotides have a multitude of uses in RNA synthesis in the form of ribonucleotide triphosphates (rNTP), as chemical energy transporters in the form of adenine-5'-triphosphate (ATP) and to form the basis of second messenger molecules. Disruption of the intracellular levels of deoxyribonucleotides or ribonucleotides is unfavorable for the cell. Imbalance of the dNTP pools can induce a variety of genetic changes such as base substitutions, frameshift mutations, delay of replication fork progression and DNA replication, as well as increase the frequency of fragile sites [3–9]. Decreased levels of rNTP pools inhibits RNA synthesis, likely by inhibiting the initiation frequency of RNA polymerase I, and thereby inhibiting the synthesis of rRNA [10]. Furthermore, inhibition of purine and pyrimidine synthesis induces a potentially p53-mediated cell cycle arrest and inhibits proliferation, which ultimately leads to increased cytotoxicity [11–14].

The total number of genes encoding mitochondrial proteins is estimated to 1013 [15]. Mitochondria contain their own autonomous genome, which encodes 13 polypeptides. The remainder is encoded by nuclear DNA and imported into mitochondria. Mitochondrial dysfunction can therefore be the result of mutations in either the mitochondrial or

nuclear genome. Mitochondria are enclosed by a double-membrane where the electron transport chain (ETC) maintains an electrochemical potential gradient between the intermembrane space and the matrix of the mitochondria. The ETC is constituted of four membrane bound enzyme complexes (complex I-IV) and two electron carriers (ubiquinone and cytochrome c) and is located in the inner membrane of the mitochondria. The electrochemical gradient is utilized by the ATP synthase (complex V) to generate ATP by oxidative phosphorylation.

The 13 polypeptides encoded by mtDNA constitute critical subunits of the ETC and ATP synthase [16, 17]. Mitochondrial dysfunction resulting from mutations in the mitochondrial genome therefore affects the function of the ETC, the electrochemical gradient and the generation of ATP by oxidative phosphorylation whereas mitochondrial dysfunctions caused by mutations in nuclear encoded proteins can affect all mitochondrial processes.

Several studies have demonstrated a correlation between different types of mitochondrial dysfunction and aberrant synthesis of cytosolic ribonucleotides and deoxyribonucleotides [18–21]. In the following, we will review mitochondrial pathways that are involved in the metabolism of cytosolic ribonucleotides and deoxyribonucleotides. Exempt from this paper is any direct link between aberrant production of ATP from oxidative phosphorylation and synthesis of cytosolic ribonucleotides and deoxyribonucleotides. Most metabolic pathways are dependent on ATP and a review of these processes in response to an insufficient ATP synthesis is outside the scope of this paper.

## 2. Dihydroorotate Dehydrogenase Links Mitochondria to the *de novo* Pyrimidine Biosynthesis

The flavoenzyme dihydroorotate dehydrogenase (DHODHase) catalyzes the conversion of dihydroorotate to orotate by oxidation, making DHODHase an integral step of the *de novo* synthesis of pyrimidines. Subsequent catalytic steps convert orotate into uridine monophosphates which can be further converted to UTP and CTP, and ultimately, dTTP and dCTP. DHODHase is located in the inner membrane of the mitochondria with the active site facing the inner membrane [22]. DHODHase is functionally connected to the ETC by a flavin prosthetic group that couples dihydroorotate oxidation to respiratory ubiquinone reduction [23]. From ubiquinol, the reduced form of ubiquinone, the flow of electrons continues through the ETC (see Figure 1).

As a result of the connection between DHODHase and the ETC, it has been suggested that any dysfunction of the ETC-lack of oxygen, presence of inhibitors or mutations of complex III and IV, would entail impairments of the *de novo* UMP synthesis and a subsequent decrease in the *de novo* synthesis of pyrimidines and, thereby, the cytosolic ribonucleotide pool [24]. Along this line, it has been suggested that mitochondrial dysfunction will lead to an imbalance of the cytosolic dNTP pool caused by inhibition of the DHODHase [25]. The relationship between DHODHase and the ETC

has been described using the two ETC inhibitors, rotenone and sodium cyanide, on mitochondria isolated from rat liver, kidney, and heart. Rotenone inhibits the transfer of electrons from complex I of the ETC to ubiquinone whereas sodium cyanide inhibits complex IV. In isolated mitochondria, treatment with sodium cyanide abolishes the activity of DHODHase while treatment with rotenone does not seem to have an effect [24]. This indicates that only an inhibition or impairment of the complexes of ETC that causes a build up of ubiquinol has an inhibitory effect on the DHODHase. A functional ETC is not only necessary for correct function of DHODHase, but also for correct localization of the protein. DHODHase is encoded by nDNA and the import into the membrane of the mitochondria is dependent on a targeting signal in the N-terminal segment of the protein. It has been demonstrated that import of rat DHODHase into yeast mitochondria was abolished by an uncoupling of the mitochondrial membrane indicating the requirement of a membrane potential for correct positioning of DHODHase [26].

The importance of a functional DHODHase for the *de novo* synthesis of pyrimidines is emphasized by the effect of inhibitors of DHODHase. Leflunomide and brequinar are two examples of DHODHase inhibitors that bind to the quinone-binding site of DHODHase, thereby, blocking interaction between ubiquinone and the flavin prosthetic group of DHODHase [27]. Treatment of human lymphocytes with leflunomide or brequinar arrests the cells in G1 phase and inhibits both RNA and DNA synthesis [28–30]. The inhibitory effects are suppressed by addition of uridine, which can be salvaged to UMP whereby the *de novo* synthesis of pyrimidines is bypassed. Treating the human leukemic cell line CCRF.CEM with leflunomide or brequinar cause a significant reduction in the levels of CTP and UTP, while the levels of purine nucleotides are unaffected after treatment with leflunomide or increased after treatment with brequinar [31].

Chloramphenicol is an antimicrobial agent that inhibits mitochondrial protein synthesis [32]. Treatment of cells with chloramphenicol therefore mimics an mtDNA induced mitochondrial dysfunction and impaired ETC activity. Treatment of chick embryo cells with chloramphenicol inhibits activity of DHODHase as well as cell growth [33]. Growth of Ehrlich Ascites tumor cells under hypoxic conditions inhibited the ETC and caused reduced activity of the DHODHase and resulted in a G1 arrest [34]. For both the chloramphenicol treated chick embryo cells and hypoxic Ehrlich Ascites tumor cells, growth inhibition was reversed by addition of pyrimidines to the growth media. This indicates that mitochondrial dysfunction affecting the ETC has an inhibitory effect on DHODHase activity that is comparable to inhibition with leflunomide or brequinar. This conclusion is substantiated by the fact that cultured mammalian cells devoid of mtDNA are auxotrophic for pyrimidines and must be routinely grown in the presence of a uridine supplement [21].

An inhibition of DHODHase has been demonstrated to result in decreased levels of pyrimidine ribonucleotides and has been proposed to result in imbalanced dNTP

pools [24, 25]. The activity of DHODHase is coupled to the activity of ETC and mitochondrial dysfunctions affecting the activity of the ETC is therefore likely to affect the activity of the DHODase and the *de novo* synthesis of pyrimidine ribo- and deoxyribonucleotides. In concordance, we have previously demonstrated the human cancer cells depleted of mtDNA had lowered dNTP levels when compared with parental cell lines with functional mtDNA [18]. Furthermore, unpublished data indicates that a leflunomide-mediated inhibition of DHODHase in a human cervical cancer cell line results in decreased levels of dTTP and dCTP (data not shown). It is therefore possible that damage to the ETC can affect the cytosolic levels of pyrimidine nucleotides through the activity of the DHODHase.

### 3. Mitochondrial Production of One-Carbon Units Links Mitochondria to the *de novo* Purine Biosynthesis

Serine is a major source of one-carbon units required for the synthesis of glycine, thymidylate, methionine, several methylation reactions, and, most important for this paper, purine synthesis (see Figure 1). In mammals, serine is derived from the diet and is synthesized from glycolysis via 3-phosphoglycerate. Serine is reversibly converted into glycine in a process catalyzed by serine hydroxymethyltransferase (SHMT) [35]. There are two isoenzymes of SHMT, a cytosolic (cSHMT) and a mitochondrial (mSHMT) [36]. It is generally believed that the process catalyzed by mSHMT is the primary pathway for conversion of serine to glycine. This is substantiated by studies using Chinese Hamster Ovary (CHO) cells where loss of mSHMT activity was demonstrated to result in an accumulation of intracellular serine leading to a 15-fold higher serine concentration. Nevertheless, the net flux through cSHMT was still in the direction of serine synthesis [37]. Furthermore, CHO cells deficient in mSHMT activity are glycine auxotrophs [38], and the auxotrophy can be suppressed by transfection with a human version of mSHMT, suggesting that the primary role of mSHMT but not cSHMT is to generate glycine [39].

During the mSHMT catalyzed conversion of serine to glycine, a methyl group is transferred from serine to tetrahydrofolate (THF), yielding glycine and 5,10-methylene-THF [35]. Within the mitochondrial compartment, 5,10-methylene-THF is converted into formate in a series of enzymatic conversions initiated by the conversion of 5,10-methylene-THF into 5-methyl-THF and subsequently into 10-formyl-THF, in  $\text{NAD}^+$ -dependent reactions catalyzed by the bifunctional enzyme methylene-THF-dehydrogenase. 10-formyl-THF is converted into formate in a reaction catalyzed by 10-formyl-THF-synthase and formate can be exported from mitochondria to the cytosol, where it is converted back to 10-formyl-THF in an ATP dependent reaction catalyzed by 10-formyl-THF-synthetase. Cytosolic 10-formyl-THF is an essential one-carbon unit donor for the *de novo* synthesis of purine nucleotides, requiring 2 moles of 10-formyl-THF per mole of purine ring formed. Reviewed in [40, 41]. The role of mitochondrial formate is

demonstrated using radioactive labeled variants of formate and serine in murine fibroblasts and human breast cancer cells. Labeled one-carbon units could be traced into both RNA and DNA and their origin could be traced to originate from serine imported to the mitochondria and exported as formate [19, 42].

The contribution of mitochondrial formate to purine synthesis is not existing in all cell types. The rate limiting enzyme methylene-THF-dehydrogenase is expressed in transformed and embryonic cell lines as well as undifferentiated cells from bone marrow, thymus, and spleen but not in differentiated tissue from brain, heart, skeletal muscle, liver, or kidney where the mitochondrial production of formate therefore is absent [43]. Even though a supply of mitochondrial produced formate is not necessarily an indispensable carbon source for purine synthesis, a blocked production of formate is demonstrated to inhibit cell-cycle progression in mouse fibroblasts and in phytohemagglutinin stimulated splenocytes accompanied by significant decreases in both cellular deoxyribonucleotide and ribonucleotide pools [19, 20]. Furthermore, mouse embryos that do not express methylene-THF-dehydrogenase and therefore are unable to generate mitochondrial formate are not viable [44], underlining the importance of the mitochondrial production for formate on nucleotide synthesis in exposed cells.

The proteins necessary for mitochondrial production of one-carbon units and export of formate are all nuclear encoded. This eliminates the possibility of any direct involvement of mitochondrial encoded proteins in this pathway. It is, however, possible that mutations of the mitochondrial genome that will result in a decreased function of the ETC, turnover of intermediates or the production of ATP can have an indirect effect on the mitochondrial production of one-carbon units and formate export. Loss of mtDNA and resulting damaged ETC has been argued to cause a decrease in mitochondrial NADH oxidation to  $\text{NAD}^+$  and a resulting inhibition on mitochondrial processes dependent on  $\text{NAD}^+$  [45]. Since methylene-THF-dehydrogenase is a  $\text{NAD}^+$ -dependent enzyme, lack of  $\text{NAD}^+$  could limit the production of mitochondrial formate, and it is therefore possible that loss of mtDNA indirectly can influence the production of mitochondrial formate and thereby cytosolic purine synthesis. By comparing human osteosarcoma cells devoid of mtDNA with their parental mtDNA containing cells, it was found that both cell lines grew equally well in complete and glycine-deficient media, demonstrating that the cells without mtDNA were not glycine auxotrophs [19]. This indicates that loss of mtDNA does not abolish purine synthesis, however, it does not remove the possibility that loss of mtDNA limits the production of mitochondrial formate and results in lowered levels of cytosolic purine levels.

### 4. Mitochondrial Production of Nitric Oxide Indirectly Affects the Nucleotide Metabolism

Nitric oxide (NO) is an uncharged and highly diffusible inorganic signal molecule with a wide variety of roles in the organism. Mitochondrial nitric oxide synthase (mtNOS)

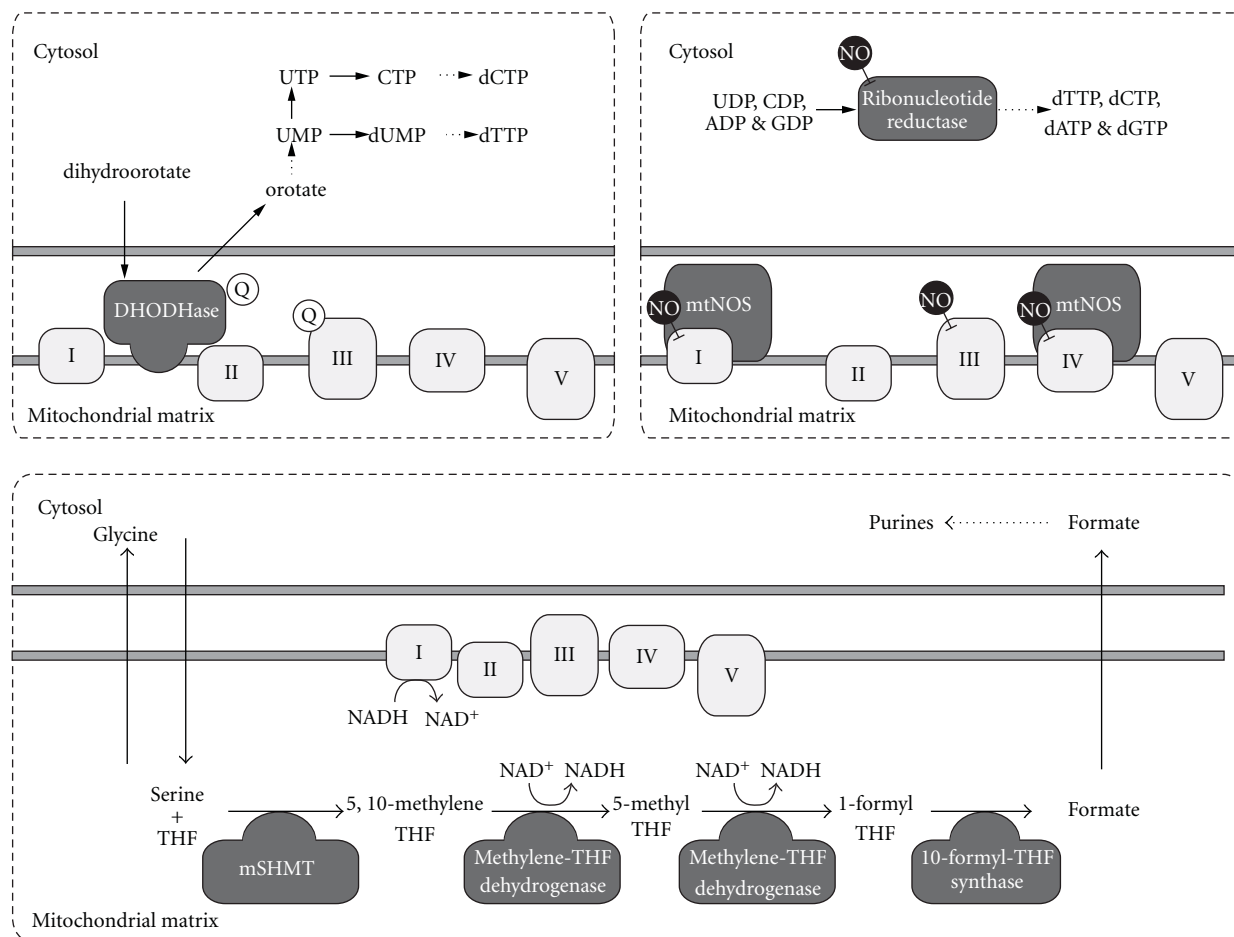


FIGURE 1: Overview of metabolic pathways responsible for nucleotide metabolism that can be affected by mitochondrial dysfunction. The illustration depicts the outer and inner mitochondrial membrane. Complexes of the electron transport chain are illustrated with boxes marked with numerals I-IV. Boxes marked with V depict ATP synthase. Darkened boxes illustrate enzymes of interest. Upper left: Dihydroorotate (DHODHase) is an integral enzyme in the *de novo* synthesis of pyrimidines. The enzyme is located in the inner mitochondrial membrane and its activity is dependent on an active electron transport chain. Upper right: Mitochondrial nitric oxide synthase (mtNOS) creates NO in a  $\text{Ca}^{2+}$  dependent reaction. The enzyme is located in the inner mitochondrial membrane where it interacts with both complexes I and IV of the electron transport chain. The activity of mtNOS is linked to the mitochondrial membrane potential. NO has the potential to inhibit the activity of Complexes I, III, and IV, but also ribonucleotide reductase in the cytosol. Lower: Illustration of the mitochondrial production of one-carbon units and mitochondrial export of formate. See text for details.

is a constitutively expressed nuclear encoded enzyme that generates NO in a  $\text{Ca}^{2+}$ -dependent reaction. Furthermore, judging from proven properties of other nitric oxide synthases, production of NO by mtNOS is likely regulated by acetylation and phosphorylation of the enzyme [reviewed in 46]. MtNOS is located in the inner membrane of the mitochondria, [46] where it physically interacts with both complexes I and IV of the ETC (See Figure 1) [47, 48]. NO has at sub-micromolar concentrations been demonstrated to act as a competitive inhibitor of complex IV and to inhibit electron transport at complex III. Furthermore, complex I is inhibited after long-term exposure to NO [49–51]. As a result of the inhibitory effects of NO on different sites of the ETC, both the activities of DHODHase and ATP synthase have been demonstrated to be inhibited in response to increased NO levels [52, 53]. Both the localization of mtNOS and the inhibitory effects of NO on the generation of ATP by

oxidative phosphorylation have led to the general belief that the purpose of mtNOS is to regulate the oxygen uptake according to the energy requirement of the cell in a short-term fashion. Besides a direct regulatory effect on oxygen uptake, NO has in turn the potential of indirectly inhibiting the synthesis of nucleotides through its inhibitory effects on the DHODHase as discussed previously.

Efflux of NO from the mitochondria is maximal after treatment with oligomycin and minimal after treatment of CCCP. Treatment with oligomycin inhibits the ATP synthase and produces a hyperpolarization of the mitochondrial membrane. Conversely, treatment with CCCP uncouples the membrane. This led to the hypothesis that mtNOS is a voltage-dependent enzyme, whose activity is regulated by mitochondrial membrane potential [54, 55]. Very little is known about any possible deregulation of mtNOS resulting from mitochondrial dysfunction. If the activity of mtNOS

is linked to the membrane potential and a depolarization inactivates the enzyme, damage to the ETC will therefore inactivate the protein. Conversely inhibition of the ATP synthase leading to a hyperpolarization will activate mtNOS. Examples of mutations affecting the ATP synthase are known. The ATP synthase has been demonstrated to be severely impaired in patients with mutated versions of the mtDNA encoded ATPase 6 subunit of the ATP synthase [56]. The influence of this and other damages to the ATP synthase on mtNOS has, however, not been investigated.

Nitric oxide produced by mtNOS is most likely not constricted to the mitochondria, but may serve a role in the cytosolic compartment. Efflux of NO from the mitochondria to the cytosol has been demonstrated. This efflux is correlated with the membrane potential of the mitochondria and has been hypothesized to function as a mitochondrial signal to the cytosol, reporting on the energy status of the mitochondria [54, 55]. By using mitochondria extracted from different rat tissue, the fraction of cytosolic NO resulting from a mitochondrial efflux was calculated to range from 61% in heart tissue to 18% in brain tissue [54]. The role of an efflux of NO from the mitochondria into the cytosol is unknown however, it has been suggested that it may serve a regulatory role in cell metabolism and proliferation [54, 57]. In this case, an imbalance of the dNTP pool demonstrated in cells with a mitochondrial dysfunction could be caused by a resulting error in this pleiotropic regulation of cell metabolism. However, NO have several targets in the cellular compartment, and depending on the amount of NO emanating from the mitochondria, these could provide a more direct relationship between the mitochondria and dNTP balance. During the *de novo* pathway the reduction of ribonucleotides to 2'-deoxyribonucleotides is catalyzed by the rate limiting enzyme ribonucleotide reductase. The reductase constitutes the major regulator of the *de novo* dNTP synthesis [58] mediating a reduction of the 2'-hydroxy group in the ribose of the ribonucleotides [59]. The resulting deoxyribonucleotides dADP, dCDP, and dGDP undergo phosphorylation yielding the corresponding dNTPs; however, dTTP is synthesized from dCDP, and dUDP and requires additional steps. Ribonucleotide reductase has been demonstrated to be directly inhibited by NO resulting in a depletion of dNTP proportional to the amount of NO. Treatment of a human lymphoblastoid cell line with different NO prodrugs induced a dNTP imbalance that was comparable to the dNTP profile after treatment with the ribonucleotide reductase inhibitor hydroxy urea [60]. Inhibition of the reductase by NO was demonstrated to induce a decrease of dATP and dCTP levels whereas the dTTP levels were transiently increased [60].

## 5. Flux of Deoxyribonucleotides between Mitochondria and the Cytosol Is Unlikely to Cause a Cytosolic dNTP Imbalance

The cellular content of rNTP and dNTP is sequestered into two pools, a mitochondrial and a cytosolic, separated by the mitochondrial double membrane [61]. The existence of a

mitochondrial salvage pathway of dNTP is well-established whereas the existence of a mitochondrial *de novo* pathway of dNTP is debated [62]. The mitochondrial inner membrane is impermeable to charged molecules, and consequently, there is no direct exchange of rNTP or dNTP between the cytosolic and mitochondrial compartments. However, several studies have shown a facilitated transport of dNTP between the two compartments reviewed in [62]. Furthermore, export of dNTP from mitochondria and incorporation into nDNA has been demonstrated [63]. It can, therefore, be speculated that the mitochondrial production of dNTP complements the cytosolic dNTP pools and dysfunction of mitochondrial dNTP synthesis results in a cytosolic dNTP imbalance.

Both *de novo* and salvage pathways carry out synthesis of cytosolic dNTP, while only the salvage pathway has been demonstrated in mitochondria. The replication of mtDNA is not synchronized with the synthesis of nDNA [64] and therefore this organelle requires a constant supply of dNTP. Mitochondria are able to synthesize dNTP by a specific salvage pathway where imported deoxyribonucleosides are phosphorylated by the two rate-determining deoxyribonucleoside kinases: thymidine kinase 2 (TK2) and deoxyguanosine kinase (dGK) yielding deoxyribonucleoside mono-phosphates, which in turn can be further phosphorylated to their corresponding di- and triphosphates or be dephosphorylated to deoxyribonucleosides again by mitochondrial deoxyribonucleotidases [65, 66]. The presence of a mitochondrial located ribonucleotide reductase has been proposed [62, 66], opening for the possibility of a mitochondrial *de novo* synthesis of dNTP. The contribution of this pathway to the mitochondrial and cytosolic pool of dNTP is however unknown.

Export of deoxyribonucleotides from the mitochondrial to the cytosolic compartment has been demonstrated. In cells lacking essential enzymes of the cytosolic salvage pathway, an exogenous source of labeled thymidine was imported into the mitochondria and phosphorylated exclusively by the mitochondrial salvage pathway, resulting in a mitochondrial pool of labeled dTTP. Efflux to the cytosolic compartment and incorporation of labeled dTTP into nDNA could be demonstrated, confirming an export of mitochondrial deoxyribonucleotides. Even though the cells lacked a functional cytosolic salvage pathway the contribution of the labeled dTTP only constituted a fraction of the cytosolic pool of dNTP, indicating a strong dominance of dNTP produced by the *de novo* pathway, demonstrating that the mitochondrial contribution to the cytosolic pool of dNTP is negligible [63].

In nondividing tissue, loss of function mutations of TK2 has been demonstrated to result in mitochondrial dNTP imbalance and consequently deletions and depletions of mtDNA [67]. Furthermore, even minor impairment of TK2 activity has been reported to result in a decreased mitochondrial dNTP pool [68]. Using a human cervical cancer cell line that can be induced to express lower levels of TK2, it was possible to reduce the activity of TK2 in the cell with 47% [69]. The activity was assayed by the ability of TK2 to phosphorylate thymidine- $\beta$ -D-araboside. Decreasing the activity of the mitochondrial salvage pathway

by lowering the level of TK2 did not alter the cytosolic dNTP pools, supporting the small contribution of mitochondrial dNTP export to the cellular dNTP pool [69].

Whereas the mitochondrial export of dNTP, most likely is an insignificant contribution to the cytosolic dNTP pools, import of dNTP to the mitochondria is essential for the fidelity of mtDNA. In cycling cells, the majority of the intramitochondrial deoxynucleotides are synthesized in the cytosol and imported into mitochondria [63]. The p53 inducible small subunit of the ribonucleotide reductase p53R2 is believed to allow *de novo* synthesis of dNTP outside the S-phase in response to DNA damage [70]. Mutations of p53R2 have been demonstrated to result in mtDNA depletion, likely caused by insufficient mitochondrial dNTP pools [71]. This indicates that mitochondria is dependent of cytosolic dNTP in all phases of cell cycle.

In summary, published data from the literature show that export of mitochondrial-produced dNTP is negligible compared to the cytosolic dNTP synthesis and the flux of dNTP is most likely in the direction of from the cytosol to the mitochondria. Furthermore, inhibition of the mitochondrial salvage pathway has no effect on the cytosolic dNTP pools. Together, this strongly suggests that dysfunction of mitochondrial salvage, or potentially *de novo*, synthesis of dNTP is unlikely to cause a cytosolic dNTP imbalance by deficient export or excessive import of deoxyribonucleotides.

## 6. Conclusion

In this paper we describe three mitochondrial pathways involved in the synthesis of cytosolic rNTP and dNTP. These three pathways encompass (1) DHODHase-mediated conversion of dihydroorotate to orotate, a rate limiting step of *de novo* synthesis of pyrimidines; (2) export of mitochondrial one carbon units in the form of formate, used in the production of cytosolic purine nucleotides; and (3) mitochondrial produced NO acting as an effector with both intra mitochondrial and cytosolic targets involved in the cytosolic synthesis of rNTP and dNTP.

The mitochondrial production and export of formate diverge from the pathways involving DHODHase and mitochondrial NO. All components responsible for mitochondrial production and export of formate are nuclear encoded and the pathway is sensitive to mutations in the nuclear genes encoding these. However, even though the pathway can be limited by comprehensive damage to the ETC, the pathway is most likely substrate-dependent and not regulated by the overall activity of the mitochondria. In contrast, the activity of DHODHase is directly dependent on the activity of the ETC and the membrane potential. In this regard, the activity of DHODHase reflects the activity of the mitochondria. Even though DHODHase is nuclear encoded, the ETC consists of both mitochondrial and nuclear encoded subunits. A degradation of mtDNA as seen in a multitude of pathological conditions including cancer [1, 2], or as demonstrated in aged tissue [72] will therefore affect the activity of DHODHase and consequently

the synthesis of pyrimidine nucleotides. In contrast, mitochondrial export of formate and related purine synthesis will likely be unaffected by nothing less than a complete degradation of mtDNA and the ETC. NO produced from mtNOS targets both the DHODHase and ATPase and is proposed to be a metabolic feedback mechanism regulated by the mitochondrial membrane potential. By inhibiting the DHODHase, mtNOS indirectly affects the *de novo* synthesis of pyrimidines. MtNOS also releases NO into the cytosolic compartment and can potentially target the ribonucleotide reductase and thereby inhibit the major regulator of the *de novo* synthesis of dNTP. It was demonstrated that mtNOS is activated by hyper polarization of the mitochondrial membrane. A mitochondrial dysfunction, like damage to the ATP synthase, that allows an excessive build up of mitochondrial membrane potential is therefore likely to activate mtNOS whereas a general degradation of mtDNA and/or the ETC leads to a depolarization of the mitochondrial membrane and inactivate the enzyme.

The effect of especially DHODHase, but also mtNOS and to some extent mitochondrial production of formate, is dependent on the activity of ETC and mitochondrial membrane potential. In functional cells, this pathway probably constitutes a feedback mechanism, where synthesis of RNA and DNA is regulated by the mitochondrial activity. However, in a pathological context, this relationship has the potential of affecting the genomic stability of the nuclear genome. Mutations affecting the activity of the ETC can lead to a detrimental effect on the cytosolic dNTP levels, and in turn imbalanced dNTP pools can cause genetic instability in the nuclear genome. In accordance, we have demonstrated that human cell lines devoid of mtDNA showed decreased and imbalanced levels of dNTP as well as increased frequency of chromosomal instability compared to parental cell lines with functional mtDNA [18, 73]. Chromosomal instability has been demonstrated to occur in human osteosarcoma cell lines devoid of mtDNA. Furthermore, the cells were demonstrated to have tumorigenic properties measured by an increased anchorage independent growth when compared to parental cells with functional mtDNA. It was reported that the reintroduction of functional mitochondria with mtDNA could suppress the tumorigenic phenotype [74]. These observations and others define a role for dysfunctional mitochondria in the progression of cancer. It will be important to further elucidate the role of the mitochondrial function on the dNTP regulation in the detrimental relationship between dysfunctional mitochondria and cancer due to the known mutagenic effects of dNTP imbalance.

## References

- [1] J. S. Penta, F. M. Johnson, J. T. Wachsman, and W. C. Copeland, "Mitochondrial DNA in human malignancy," *Mutation Research*, vol. 488, no. 2, pp. 119–133, 2001.
- [2] J. S. Modica-Napolitano and K. K. Singh, "Mitochondria as targets for detection and treatment of cancer," *Expert Reviews in Molecular Medicine*, vol. 4, no. 9, pp. 1–19, 2002.

- [3] P.-Y. Ke, Y.-Y. Kuo, C.-M. Hu, and Z.-F. Chang, "Control of dTTP pool size by anaphase promoting complex/cyclosome is essential for the maintenance of genetic stability," *Genes and Development*, vol. 19, no. 16, pp. 1920–1933, 2005.
- [4] P. Reichard, "Interactions between deoxyribonucleotide and DNA synthesis," *Annual Review of Biochemistry*, vol. 57, pp. 349–374, 1988.
- [5] K. Bebenek and T. A. Kunkel, "Frameshift errors initiated by nucleoside misincorporation," *Proceedings of the National Academy of Sciences of the United States of America*, vol. 87, no. 13, pp. 4946–4950, 1990.
- [6] P. B. Jacky, B. Beek, and G. R. Sutherland, "Fragile sites in chromosomes: possible model for the study of spontaneous chromosome breakage," *Science*, vol. 220, no. 4592, pp. 69–70, 1983.
- [7] B. A. Kunz and S. E. Kohalmi, "Modulation of mutagenesis by deoxyribonucleotide levels," *Annual Review of Genetics*, vol. 25, pp. 339–359, 1991.
- [8] R. G. Wickremasinghe and A. V. Hoffbrand, "Reduced rate of DNA replication fork movement in megaloblastic anemia," *Journal of Clinical Investigation*, vol. 65, no. 1, pp. 26–36, 1980.
- [9] B. Golos and J. Malec, "Comparison of the effect of hydroxyurea and methotrexate on DNA fragmentation at various reaction conditions," *Neoplasma*, vol. 38, no. 6, pp. 559–564, 1991.
- [10] I. Grummt and F. Grummt, "Control of nucleolar RNA synthesis by the intracellular pool sizes of ATP and GTP," *Cell*, vol. 7, no. 3, pp. 447–453, 1976.
- [11] M. Kondo, T. Yamaoka, S. Honda et al., "The rate of cell growth is regulated by purine biosynthesis via ATP production and G1 to S phase transition," *Journal of Biochemistry*, vol. 128, no. 1, pp. 57–64, 2000.
- [12] L. Quéméneur, L.-M. Gerland, M. Flacher, M. Ffrench, J.-P. Revillard, and L. Genestier, "Differential control of cell cycle, proliferation, and survival of primary T lymphocytes by purine and pyrimidine nucleotides," *Journal of Immunology*, vol. 170, no. 10, pp. 4986–4995, 2003.
- [13] S. P. Linke, K. C. Clarkin, A. Di Leonardo, A. Tsou, and G. M. Wahl, "A reversible, p53-dependent G0/G1 cell cycle arrest induced by ribonucleotide depletion in the absence of detectable DNA damage," *Genes and Development*, vol. 10, no. 8, pp. 934–947, 1996.
- [14] L. L. Bennett Jr., D. Smithers, and L. M. Rose, "Inhibition of synthesis of pyrimidine nucleotides by 2-hydroxy-3-(3,3-dichloroallyl)-1,4-naphthoquinone," *Cancer Research*, vol. 39, no. 12, pp. 4868–4874, 1979.
- [15] D. J. Pagliarini, S. E. Calvo, B. Chang et al., "A mitochondrial protein compendium elucidates complex I disease biology," *Cell*, vol. 134, no. 1, pp. 112–123, 2008.
- [16] D. C. Wallace, "Mitochondrial diseases in man and mouse," *Science*, vol. 283, no. 5407, pp. 1482–1488, 1999.
- [17] S. DiMauro and E. A. Schon, "Mitochondrial respiratory-chain diseases," *The New England Journal of Medicine*, vol. 348, no. 26, pp. 2656–2668, 2003.
- [18] C. Desler, B. Munch-Petersen, T. Stevnsner et al., "Mitochondria as determinant of nucleotide pools and chromosomal stability," *Mutation Research*, vol. 625, no. 1-2, pp. 112–124, 2007.
- [19] H. Patel, E. Di Pietro, and R. E. MacKenzie, "Mammalian fibroblasts lacking mitochondrial NAD<sup>+</sup>-dependent methylenetetrahydrofolate dehydrogenase-cyclohydrolase are glycine auxotrophs," *The Journal of Biological Chemistry*, vol. 278, no. 21, pp. 19436–19441, 2003.
- [20] S. J. James, B. J. Miller, D. R. Cross, L. J. McGarrity, and S. M. Morris, "The essentiality of folate for the maintenance of deoxynucleotide precursor pools, DNA synthesis, and cell cycle progression in PHA-stimulated lymphocytes," *Environmental Health Perspectives*, vol. 101, no. 5, pp. 173–178, 1993.
- [21] M. P. King and G. Attardi, "Human cells lacking mtDNA: repopulation with exogenous mitochondria by complementation," *Science*, vol. 246, no. 4929, pp. 500–503, 1989.
- [22] M. E. Jones, "The genes for and regulation of the enzyme activities of two multifunctional proteins required for the de novo pathway for UMP biosynthesis in mammals," *Molecular Biology, Biochemistry, and Biophysics*, vol. 32, pp. 165–182, 1980.
- [23] B. Bader, W. Knecht, M. Fries, and M. Löffler, "Expression, purification, and characterization of histidine-tagged rat and human flavoenzyme dihydroorotate dehydrogenase," *Protein Expression and Purification*, vol. 13, no. 3, pp. 414–422, 1998.
- [24] M. Löffler, J. Jöckel, G. Schuster, and C. Becker, "Dihydroorotat-ubiquinone oxidoreductase links mitochondria in the biosynthesis of pyrimidine nucleotides," *Molecular and Cellular Biochemistry*, vol. 174, no. 1-2, pp. 125–129, 1997.
- [25] K. K. Singh, "Mitochondria damage checkpoint in apoptosis and genome stability," *FEMS Yeast Research*, vol. 5, no. 2, pp. 127–132, 2004.
- [26] J. Rawls, W. Knecht, K. Diekert, R. Lill, and M. Löffler, "Requirements for the mitochondrial import and localization of dihydroorotate dehydrogenase," *European Journal of Biochemistry*, vol. 267, no. 7, pp. 2079–2087, 2000.
- [27] S. Liu, E. A. Neidhardt, T. H. Grossman, T. Ocain, and J. Clardy, "Structures of human dihydroorotate dehydrogenase in complex with antiproliferative agents," *Structure*, vol. 8, no. 1, pp. 25–33, 2000.
- [28] A. S.-F. Chong, K. Rezai, H. M. Gebel et al., "Effects of leflunomide and other immunosuppressive agents on T cell proliferation in vitro," *Transplantation*, vol. 61, no. 1, pp. 140–145, 1996.
- [29] K. Rückemann, L. D. Fairbanks, E. A. Carrey et al., "Leflunomide inhibits pyrimidine de novo synthesis in mitogen-stimulated T-lymphocytes from healthy humans," *The Journal of Biological Chemistry*, vol. 273, no. 34, pp. 21682–21691, 1998.
- [30] S. Greene, K. Watanabe, J. Braatz-Trulson, and L. Lou, "Inhibition of dihydroorotate dehydrogenase by the immunosuppressive agent leflunomide," *Biochemical Pharmacology*, vol. 50, no. 6, pp. 861–867, 1995.
- [31] H. M. Cherwinski, N. Byars, S. J. Ballaron, G. M. Nakano, J. M. Young, and J. T. Ransom, "Leflunomide interferes with pyrimidine nucleotide biosynthesis," *Inflammation Research*, vol. 44, no. 8, pp. 317–322, 1995.
- [32] B. Storrie and G. Attardi, "Expression of the mitochondrial genome in HeLa cells. IX. Effect of inhibition of mitochondrial protein synthesis on mitochondrial formation," *Journal of Cell Biology*, vol. 56, no. 3, pp. 819–831, 1973.
- [33] M. Grégoire, R. Morais, M. A. Quilliam, and D. Gravel, "On auxotrophy for pyrimidines of respiration-deficient chick embryo cells," *European Journal of Biochemistry*, vol. 142, no. 1, pp. 49–55, 1984.
- [34] M. Löffler, "On the role of dihydroorotate dehydrogenase in growth cessation of Ehrlich ascites tumor cells cultured under oxygen deficiency," *European Journal of Biochemistry*, vol. 107, no. 1, pp. 207–215, 1980.

- [35] L. Schirch, "Serine hydroxymethyltransferase," *Advances in Enzymology and Related Areas of Molecular Biology*, vol. 53, pp. 83–112, 1982.
- [36] T. A. Garrow, A. A. Brenner, V. M. Whitehead et al., "Cloning of human cDNAs encoding mitochondrial and cytosolic serine hydroxymethyltransferases and chromosomal localization," *The Journal of Biological Chemistry*, vol. 268, no. 16, pp. 11910–11916, 1993.
- [37] M. R. Narkewicz, S. D. Sauls, S. S. Tjoa, C. Teng, and P. V. Fennessey, "Evidence for intracellular partitioning of serine and glycine metabolism in Chinese hamster ovary cells," *Biochemical Journal*, vol. 313, no. 3, pp. 991–996, 1996.
- [38] W. Pfendner and L. I. Pizer, "The metabolism of serine and glycine in mutant lines of Chinese hamster ovary cells," *Archives of Biochemistry and Biophysics*, vol. 200, no. 2, pp. 503–512, 1980.
- [39] P. J. Stover, L. H. Chen, J. R. Suh, D. M. Stover, K. Keyomarsi, and B. Shane, "Molecular cloning, characterization, and regulation of the human mitochondrial serine hydroxymethyltransferase gene," *The Journal of Biological Chemistry*, vol. 272, no. 3, pp. 1842–1848, 1997.
- [40] D. R. Appling, "Compartmentation of folate-mediated one-carbon metabolism in eukaryotes," *FASEB Journal*, vol. 5, no. 12, pp. 2645–2651, 1991.
- [41] F. Depeint, W. R. Bruce, N. Shangari, R. Mehta, and P. J. O'Brien, "Mitochondrial function and toxicity: role of B vitamins on the one-carbon transfer pathways," *Chemico-Biological Interactions*, vol. 163, no. 1–2, pp. 113–132, 2006.
- [42] T.-F. Fu, J. P. Rife, and V. Schirch, "The role of serine hydroxymethyltransferase isozymes in one-carbon metabolism in MCF-7 cells as determined by  $^{13}\text{C}$  NMR," *Archives of Biochemistry and Biophysics*, vol. 393, no. 1, pp. 42–50, 2001.
- [43] N. R. Mejia and R. E. MacKenzie, "NAD-dependent methylenetetrahydrofolate dehydrogenase is expressed by immortal cells," *The Journal of Biological Chemistry*, vol. 260, no. 27, pp. 14616–14620, 1985.
- [44] E. Di Pietro, J. Sirois, M. L. Tremblay, and R. E. MacKenzie, "Mitochondrial NAD-dependent methylenetetrahydrofolate dehydrogenase-methylenetetrahydrofolate cyclohydrolase is essential for embryonic development," *Molecular and Cellular Biology*, vol. 22, no. 12, pp. 4158–4166, 2002.
- [45] R. K. Naviaux, "Mitochondrial control of epigenetics," *Cancer Biology and Therapy*, vol. 7, no. 8, pp. 1191–1193, 2008.
- [46] A. Tatoyan and C. Giulivi, "Purification and characterization of a nitric-oxide synthase from rat liver mitochondria," *The Journal of Biological Chemistry*, vol. 273, no. 18, pp. 11044–11048, 1998.
- [47] T. Persichini, V. Mazzone, F. Polticelli et al., "Mitochondrial type I nitric oxide synthase physically interacts with cytochrome c oxidase," *Neuroscience Letters*, vol. 384, no. 3, pp. 254–259, 2005.
- [48] M. C. Franco, V. G. Antico Arciuch, J. G. Peralta et al., "Hypothyroid phenotype is contributed by mitochondrial complex I inactivation due to translocated neuronal nitric-oxide synthase," *The Journal of Biological Chemistry*, vol. 281, no. 8, pp. 4779–4786, 2006.
- [49] M. W. J. Cleeter, A. M. Cooper, B. M. Darley-Usmar, D. Moncada, and A. H. V. Schapira, "Reversible inhibition of cytochrome c oxidase, the terminal enzyme of the mitochondrial respiratory chain, by nitric oxide," *FEBS Letters*, vol. 345, no. 1, pp. 50–54, 1994.
- [50] J. J. Poderoso, M. C. Carreras, C. Lisdero, N. Riobó, F. Schöpfer, and A. Boveris, "Nitric oxide inhibits electron transfer and increases superoxide radical production in rat heart mitochondria and submitochondrial particles," *Archives of Biochemistry and Biophysics*, vol. 328, no. 1, pp. 85–92, 1996.
- [51] N. A. Riobó, E. Clementi, M. Melani et al., "Nitric oxide inhibits mitochondrial NADH:ubiquinone reductase activity through peroxynitrite formation," *Biochemical Journal*, vol. 359, no. 1, pp. 139–145, 2001.
- [52] C. Beuneu, R. Auger, M. Löffler, A. Guissani, G. Lemaire, and M. Lepoivre, "Indirect inhibition of mitochondrial dihydroorotate dehydrogenase activity by nitric oxide," *Free Radical Biology and Medicine*, vol. 28, no. 8, pp. 1206–1213, 2000.
- [53] P. S. Brookes, J. P. Bolaños, and S. J. R. Heales, "The assumption that nitric oxide inhibits mitochondrial ATP synthesis is correct," *FEBS Letters*, vol. 446, no. 2–3, pp. 261–263, 1999.
- [54] A. Boveris, L. B. Valdez, T. Zaobornyj, and J. Bustamante, "Mitochondrial metabolic states regulate nitric oxide and hydrogen peroxide diffusion to the cytosol," *Biochimica et Biophysica Acta*, vol. 1757, no. 5–6, pp. 535–542, 2006.
- [55] L. B. Valdez, T. Zaobornyj, and A. Boveris, "Mitochondrial metabolic states and membrane potential modulate mtNOS activity," *Biochimica et Biophysica Acta*, vol. 1757, no. 3, pp. 166–172, 2006.
- [56] A. Baracca, S. Barogi, V. Carelli, G. Lenaz, and G. Solaini, "Catalytic activities of mitochondrial ATP synthase in patients with mitochondrial DNA T8993G mutation in the ATPase 6 gene encoding subunit a," *The Journal of Biological Chemistry*, vol. 275, no. 6, pp. 4177–4182, 2000.
- [57] A. Boveris, L. E. Costa, E. Cadenas, and J. J. Poderoso, "Regulation of mitochondrial respiration by adenosine diphosphate, oxygen, and nitric oxide," *Methods in Enzymology*, vol. 301, pp. 188–198, 1998.
- [58] A. Jordan and P. Reichard, "Ribonucleotide reductases," *Annual Review of Biochemistry*, vol. 67, pp. 71–98, 1998.
- [59] A. Larsson and P. Reichard, "Allosteric effects and substrate specificity of the ribonucleoside diphosphate reductase system from *Escherichia coli* B," *Biochimica et Biophysica Acta*, vol. 113, no. 2, pp. 407–408, 1966.
- [60] B. Roy, O. Guittet, C. Beuneu, G. Lemaire, and M. Lepoivre, "Depletion of deoxyribonucleoside triphosphate pools in tumor cells by nitric oxide," *Free Radical Biology and Medicine*, vol. 36, no. 4, pp. 507–516, 2004.
- [61] D. Bogenhagen and D. A. Clayton, "Mouse 1 cell mitochondrial DNA molecules are selected randomly for replication throughout the cell cycle," *Cell*, vol. 11, no. 4, pp. 719–727, 1977.
- [62] C. K. Mathews and S. Song, "Maintaining precursor pools for mitochondrial DNA replication," *FASEB Journal*, vol. 21, no. 10, pp. 2294–2303, 2007.
- [63] G. Pontarin, L. Gallinaro, P. Ferraro, P. Reichard, and V. Bianchi, "Origins of mitochondrial thymidine triphosphate: dynamic relations to cytosolic pools," *Proceedings of the National Academy of Sciences of the United States of America*, vol. 100, no. 21, pp. 12159–12164, 2003.
- [64] A. F. Davis and D. A. Clayton, "In situ localization of mitochondrial DNA replication in intact mammalian cells," *Journal of Cell Biology*, vol. 135, no. 4, pp. 883–893, 1996.
- [65] S. Eriksson, B. Munch-Petersen, K. Johansson, and H. Ecklund, "Structure and function of cellular deoxyribonucleoside kinases," *Cellular and Molecular Life Sciences*, vol. 59, no. 8, pp. 1327–1346, 2002.

- [66] V. Bianchi and J. Sychala, "Mammalian 5'-nucleotidases," *The Journal of Biological Chemistry*, vol. 278, no. 47, pp. 46195–46198, 2003.
- [67] A. Saada, A. Shaag, H. Mandel, Y. Nevo, S. Eriksson, and O. Elpeleg, "Mutant mitochondrial thymidine kinase in mitochondrial DNA depletion myopathy," *Nature Genetics*, vol. 29, no. 3, pp. 342–344, 2001.
- [68] L. Wang, A. Saada, and S. Eriksson, "Kinetic properties of mutant human thymidine kinase 2 suggest a mechanism for mitochondrial DNA depletion myopathy," *The Journal of Biological Chemistry*, vol. 278, no. 9, pp. 6963–6968, 2003.
- [69] C. Desler, B. Munch-Petersen, and L. J. Rasmussen, "The role of mitochondrial dNTP levels in cells with reduced TK2 activity," *Nucleosides, Nucleotides and Nucleic Acids*, vol. 25, no. 9#8211;11, pp. 1171–1175, 2006.
- [70] H. Tanaka, H. Arakawa, T. Yamaguchi et al., "A ribonucleotide reductase gene involved in a p53-dependent cell-cycle checkpoint for DNA damage," *Nature*, vol. 404, no. 6773, pp. 42–49, 2000.
- [71] A. Bourdon, L. Minai, V. Serre et al., "Mutation of RRM2B, encoding p53-controlled ribonucleotide reductase (p53R2), causes severe mitochondrial DNA depletion," *Nature Genetics*, vol. 39, no. 6, pp. 776–780, 2007.
- [72] R. L. Delsite, L. J. Rasmussen, A. K. Rasmussen, A. Kalen, P. C. Goswami, and K. K. Singh, "Mitochondrial impairment is accompanied by impaired oxidative DNA repair in the nucleus," *Mutagenesis*, vol. 18, no. 6, pp. 497–503, 2003.
- [73] V. W. S. Liu, C. Zhang, and P. Nagley, "Mutations in mitochondrial DNA accumulate differentially in three different human tissues during ageing," *Nucleic Acids Research*, vol. 26, no. 5, pp. 1268–1275, 1998.
- [74] K. K. Singh, M. Kulawiec, I. Still, M. M. Desouki, J. Geradts, and S.-I. Matsui, "Inter-genomic cross talk between mitochondria and the nucleus plays an important role in tumorigenesis," *Gene*, vol. 354, no. 1-2, pp. 140–146, 2005.

## Research Article

# BLM Deficiency Is Not Associated with Sensitivity to Hydroxyurea-Induced Replication Stress

**Kenza Lahkim Bennani-Belhaj,<sup>1,2</sup> Géraldine Buhagiar-Labarchède,<sup>1,2</sup> Nada Jmari,<sup>1,2</sup> Rosine Onclercq-Delic,<sup>1,2</sup> and Mounira Amor-Guélet<sup>1,2</sup>**

<sup>1</sup>Institut Curie, Centre de Recherche, Centre Universitaire, Bât. 110, 91405 Orsay, France

<sup>2</sup>CNRS, UMR 3348, 91405 Orsay, France

Correspondence should be addressed to Mounira Amor-Guélet, mounira.amor@curie.u-psud.fr

Received 11 May 2010; Accepted 19 July 2010

Academic Editor: Ashis Basu

Copyright © 2010 Kenza Lahkim Bennani-Belhaj et al. This is an open access article distributed under the Creative Commons Attribution License, which permits unrestricted use, distribution, and reproduction in any medium, provided the original work is properly cited.

Bloom's syndrome (BS) displays one of the strongest known correlations between chromosomal instability and a high risk of cancer at an early age. BS cells combine a reduced average fork velocity with constitutive endogenous replication stress. However, the response of BS cells to replication stress induced by hydroxyurea (HU), which strongly slows the progression of replication forks, remains unclear due to publication of conflicting results. Using two different cellular models of BS, we showed that BLM deficiency is not associated with sensitivity to HU, in terms of clonogenic survival, DSB generation, and SCE induction. We suggest that surviving BLM-deficient cells are selected on the basis of their ability to deal with an endogenous replication stress induced by replication fork slowing, resulting in insensitivity to HU-induced replication stress.

## 1. Introduction

Bloom's syndrome (BS) combines marked genetic instability with an increase in the risk of cancer development and results from mutations in the *BLM* gene, which encodes BLM, a RecQ 3'-5' DNA helicase [1]. BS cells have very high frequencies of sister chromatid exchanges (SCEs) mediated by RAD51-dependent homologous recombinations [2–4]. Physical and functional links between BLM, replication and HR have been found. BLM deficiency is associated with replication abnormalities [5–9] and with an increase in HR, including a higher frequency of spontaneous symmetric quadriradial interchanges, SCEs, and an increase in the generation of homozygosity [10]. Following replication arrest, BLM coprecipitates with RAD51 [11, 12] and the primary mediators of the S-phase checkpoint, ATR and Chk1 [13]. BLM and RAD51 are colocalized during replication fork stalling and reside in a matrix-bound complex [14, 15]. During replication stress, BLM, 53BP1, and RAD51 form a complex; Chk1-mediated phosphorylation of 53BP1 enhances its binding to BLM and is required for the accumulation of 53BP1 at the site of stalled replication, and BLM

enhances the colocalization of 53BP1 and RAD51 during replication arrest [16]. BLM-deficient cells display constitutively large numbers of RAD51-containing foci. Both BLM and 53BP1 abolish the formation of endogenous RAD51 foci and disrupt RAD51 polymerization [11, 16]. SUMOylation of BLM regulates its association with RAD51 by promoting its recruitment and/or retention to damaged replication forks [17]. BLM also acts downstream from RAD51 to rescue anaphase bridges resulting from RAD51 deficiency, probably at difficult-to-replicate DNA sequences such as fragile sites [4]. *In vitro*, BLM unwinds DNA structures mimicking replication forks and HR intermediates, such as D-loops, and catalyzes the branch migration of Holliday junctions [18–20]. It resolves double Holliday junctions, together with topoisomerase III $\alpha$ , Rmi1/BLAP75, and Rmi2 [21, 22], and catalyzes the regression of replication forks [23, 24]. BLM inhibits the D-loop formation catalyzed by RAD51, by displacing RAD51 from single-stranded DNA, thereby disrupting nucleoprotein filaments [25]. Several models of the maintenance of genome integrity by BLM during DNA replication have been developed, most suggesting that BLM restarts replication after the stalling of the fork [26, 27]. In

the absence of BLM, cells display a slowing of replication fork progression associated with constitutive replication stress [9]. This raises questions about the response of BLM-deficient cells to an exogenous replicative stress slowing the progression of replication still further, such as hydroxyurea (HU). HU inhibits the ribonucleotide reductase commonly used to induce replicational stress which slows fork rate progression with respect to the temporal programme of origin activation [28]. Conflicting data have been reported concerning the sensitivity of BLM-deficient cells to HU. BLM-deficient cells generated from the chicken DT40 B-cell line display normal sensitivity to HU [29] whereas BS lymphoblastoid cells are resistant to HU-induced apoptosis [30], and BS GM08505 fibroblast cells are hypersensitive to HU [31]. In this paper, we used two different cellular models of BS to investigate the sensitivity of BLM-deficient cells to HU-induced replication stress. We show that BLM deficiency is not associated with sensitivity to HU, in terms of clonal growth, DSB generation, and SCE induction. We discuss these results in light of the reported cellular responses of BLM-deficient cells to replication stress.

## 2. Materials and Methods

**2.1. Cell Cultures and Transfections.** The SV40-transformed BS fibroblast cell line GM08505B and HeLa cells were used as previously described [32]. HeLaV cells and HeLash cells were obtained as described elsewhere [4]. For transient transfection assay siRNAs,  $3\text{--}4 \times 10^5$  cells were used to seed 3 ml of DMEM in six-well plates. Cells were transfected with siRNAs specific for BLM (ON-TARGETplus, SMARTpool, Dharmacon), or negative control siRNAs (ON-TARGETplus siCONTROL Nontargeting Pool, Dharmacon) at a final concentration of 100 nM using DharmaFect 1<sup>TM</sup> (Dharmacon), according to the manufacturer's instructions.

BS-GFP and BS-GFP-BLM cells were obtained by transfecting BS GM08505B cells with the EGFP-C1 vector alone (Clontech, Mountain View, CA), or with this vector containing the full length BLM cDNA [33], respectively, using JetPEI reagent (Ozyme). After 48 hours, selection with 800 to 1600  $\mu\text{g}/\text{ml}$  of G418 (Invitrogen) was applied. Individual colonies were isolated and maintained in DMEM containing 500  $\mu\text{g}/\text{ml}$  G418.

**2.2. Chemicals.** Hydroxyurea (HU) (Sigma) was used at a final concentration of 2 mM or 5 mM.

**2.3. Western Blot Analysis.** Cells were lysed in 350 mM NaCl, 50 mM Tris-HCl pH 7.5, 1% NP-40, 1 mM NaF, and protease inhibitors for 30 min on ice, sonicated and heated. Samples equivalent to 15 or 30  $\mu\text{g}$  of protein were subjected to electrophoresis in Novex 4–12% Bis-Tris precast gels (Invitrogen). The procedures used for gel electrophoresis and immunoblotting were as previously described [34].

**2.4. Flow Cytometry Analysis.** Cells were fixed with 70% ethanol at  $-20^\circ\text{C}$  for at least 30 min. After 2 washes, cells were incubated for 30 min at  $37^\circ\text{C}$  in PBS containing

100  $\mu\text{g}/\text{ml}$  RNase A (Sigma) and 10  $\mu\text{g}/\text{ml}$  propidium iodide (Sigma). The DNA content was determined by measuring fluorescent intensities on FACS-calibur flow cytometer (Becton Dickinson). Data were processed with Cell Quest software.

**2.5. Antibodies.** All the commercial antibodies were used according to the manufacturers' specifications. The primary antibodies used against BLM were ab476 (1:1000; rabbit, Abcam) and C18 (1:150; goat, Santa-Cruz Biotechnology). We used rabbit polyclonal antibodies against Chk1 ser317, Chk2 threonine 68, and H2AX serine 139 (1:1000; Cell Signaling),  $\beta$ -actin (1:10000; Sigma), and GAPDH (1:5000; Millipore).

Horseradish peroxidase-conjugated goat antimouse IgG and goat antirabbit IgG (Santa Cruz Biotechnology) were used as secondary antibodies, at dilutions of 1:5000 and 1:10000.

**2.6. Sister Chromatid Exchange Assays.** Cells were left untreated or were transfected as indicated. After 24 h of transfection with siRNA, cells were left untreated or were treated with HU, transferred to slides and cultured in the presence of 10 mM 5-bromodeoxyuridine (Sigma) at  $37^\circ\text{C}$ , under an atmosphere containing 5%  $\text{CO}_2$ . After 40 h (HeLaV and HeLashBLM cells) or 50 h (BS-GFP or BS-GFP-BLM) of incubation, colchicine (Sigma) was added to a final concentration of 0.1 mg/ml, and the cells were incubated for 1 hour. They were then incubated in hypotonic solution (1:6 (vol/vol) FCS-distilled water) and fixed by incubation with a 3:1 (vol/vol) mixture of methanol and acetic acid. Cells were then stained by incubation with 10 mg/ml Hoechst 33258 (Sigma) in distilled water for 20 minutes, rinsed with  $2 \times \text{SSC}$  (Euromedex), exposed to UV light at 365 nm and at a distance of 10 cm for 105 minutes, rinsed in distilled water, stained by incubation with 2% Giemsa solution (VWR) for 16 minutes, rinsed in distilled water, dried, and mounted. Chromosomes were observed with a Leica DMRB microscope at 100x magnification. Metaphases were captured with a SONY DXC 930 P camera, and SCEs were analyzed.

**2.7. Clonogenic Survival Assays.** Untreated or HU-treated cells were plated in drug-free medium at 3 densities, in triplicate, for the counting of 30 to 300 clones depending on expected survival. Alternatively, cells were plated and treated as previously described [31]. After 14 to 21 days of incubation colonies were fixed and stained with methylene blue (5 g/l in 50% water and 50% methanol) and scored. Only experiments giving a linear correlation between the different dilutions were considered. Cell survival was estimated by dividing the number of colony-forming units in treated samples by the number of colony-forming units in untreated samples, with control cell survival defined as 1. The percentage of cell survival is indicated within each histogram.

**2.8. Comet Assays.** BS-GFP and BS-GFP-BLM cells or HeLashBLM and HeLaV transfected as in Figure 1(a) were left untreated or were treated with 2 mM HU for 16 h or 48 h.

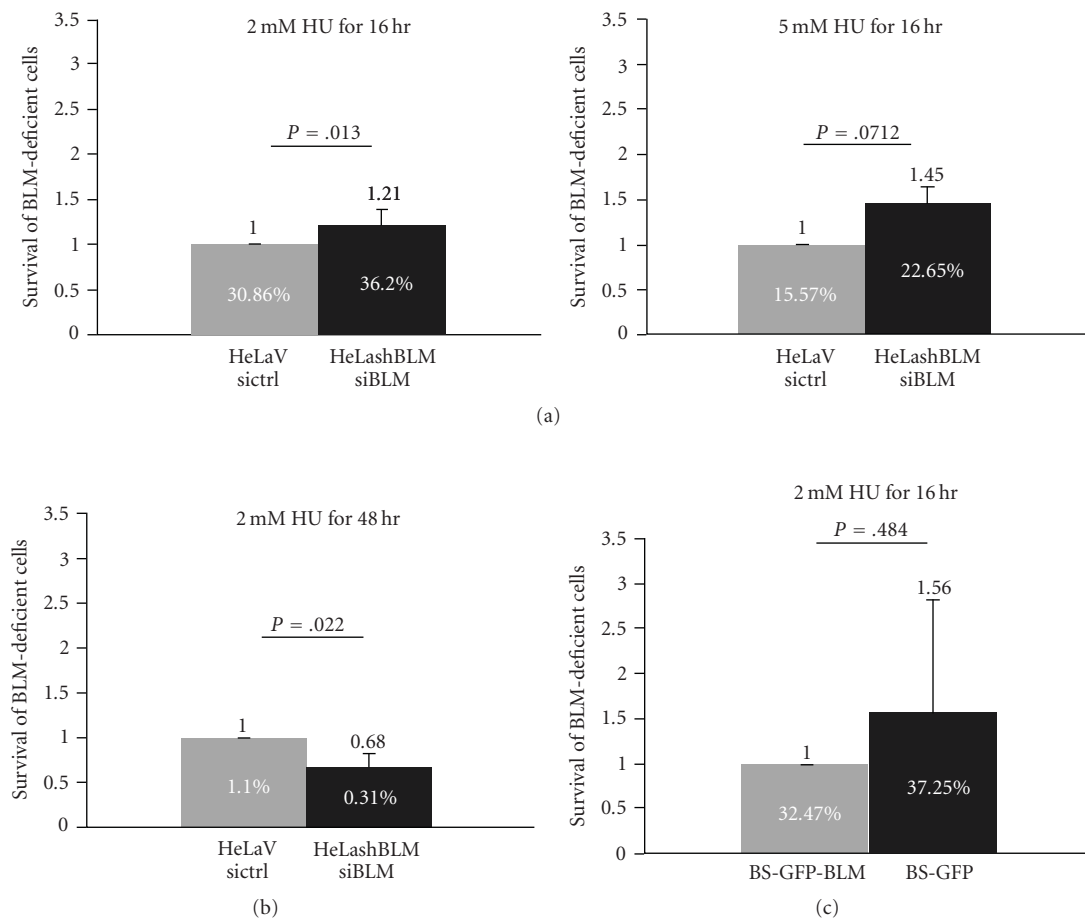


FIGURE 1: BLM-downregulated HeLa cells and BS cells are insensitive to HU-induced replication stress. (a) HeLaV and HeLashBLM cells were transfected with 100 nM of a negative control siRNA (ctrl) or with 100 nM of siRNA targeting the BLM mRNA (BLM), respectively. After 24 h, cells were left untreated or were treated with 2 mM or 5 mM HU for 16 h. Cells were then plated in triplicate at three densities in drug-free medium. The means of six independent experiments for 2 mM HU and of two independent experiments for 5 mM HU are shown. The error bars indicate SD. (b) As in (a) except that cells were treated with 2 mM HU for 48 hr, the means of 3 independent experiments are shown. (c) BS-GFP and BS-GFP-BLM cell lines were left untreated or were treated with 2 mM HU for 16 h and plated as in (a). The means of 3 independent experiments are shown.

After 24 h, cells were left untreated or were treated with 2 mM HU for 16 h or 48 h. At the end of the treatment period, the cells were treated with Accutase (PAA). Aliquots of cell suspension were mixed with an equal volume of 1% low-melting-point agarose in DMEM to obtain a suspension of cells in 0.5% agarose, which was then dispensed onto microscope slides (with frosted ends) coated with a layer of 0.5% normal-melting-point agarose. Slides were incubated in lysis solution [2.5 mol/L NaCl, 100 mmol/L EDTA, 10 mmol/L Tris, 1% sodium lauryl sarcosinate, 10% DMSO, and 1% TritonX-100 (pH 10)] at 4°C for 1 h, then denatured in alkali buffer (0.3 mol/L NaOH, pH 13 and 1 mmol/L EDTA) for 40 minutes at 20°C and subjected to electrophoresis for 25 min at 25 V (300 mA). Slides were immersed in neutralization buffer (400 mmol/L Tris-HCl, pH 7.5) for at least 5 minutes. They were then drained, rinsed carefully with distilled water, and stained with ethidium bromide staining solution (20 µg/ml) before being covered with a coverslip. For the visualization of DNA damage, ethidium bromide-

stained DNA was observed at a magnification of x20, under a fluorescence microscope. Between 100 and 110 cells per sample and per experiment were analyzed in Comet Assay 2 software (Perceptive Instrument).

2.9. *Statistical Methods.* Significance was assessed with Student's *t*-test. For all tests,  $P < .05$  was considered statistically significant.

### 3. Results

3.1. *Both HeLa Cells with BLM Downregulation and BS Cells Are Insensitive to HU-Induced Replication Stress.* We investigated whether BLM downregulation was associated with changes in the sensitivity of cells to HU-induced replication stress. We first used a new cellular model for BS consisting of HeLa cells constitutively expressing an shRNA specific for BLM and transiently transfected with a pool of siRNAs directed against sequences other than that targeted

by shBLM (HeLash-siBLM), together with the corresponding control cells (HeLaV-sictrl) [4]. We assessed HeLash-siBLM sensitivity to HU in clonogenic survival assays. BLM mRNA levels and SCE frequency were assessed in all experiments with HeLash-siBLM (data not shown). After treatment with 2 or 5 mM HU for 16 hr, HeLash-siBLM cells were either less sensitive or displayed similar levels of sensitivity to HU than control cells, respectively (Figure 1(a)). As BS cell hypersensitivity was reported after 48 h of exposure to HU concentrations from 0.01 to 10 mM in a previous study [31], we repeated the experiments after 48 h of exposure to 2 mM HU. The clonogenic survival of both HeLa cells with BLM downregulation and control cells was strongly decreased, with BLM-downregulated cells significantly more sensitive to 48 h of exposure to HU than control cells (Figure 1(b)). These experiments were repeated with BS GM08505 fibroblasts (BS-GFP) and their complemented counterparts (BS-GFP-BLM) (see Section 2). The clonogenic survival of BS cells and control cells was similar after 16 h of exposure to HU (Figure 1(c)). After 48 h of exposure to HU, we detected no clones, for either BS cells or BLM-complemented cells. Increasing the number of cells plated by a factor 10 and using two different protocols did not affect the results obtained. This indicates that the BS cell line we used behaves differently from the one used by Davies et al. [31], potentially because one of them derived in culture due to the mutator and hyper-rec phenotype of BS cells [1]. Altogether our results indicate that in terms of clonal survival, BLM deficiency is not associated with an increase in the sensitivity to 16 h of treatment with HU. However, BLM-downregulated HeLa cells are significantly more sensitive to 48 h of HU treatment than control cells are.

**3.2. Levels of HU-Induced DSBs Are Similar in BLM-Deficient Cells and in Control Cells.** The prolonged treatment of cells with HU results in the accumulation of DSBs [35]. We carried out a time-course study of the effect of HU on DSB levels in BLM-downregulated HeLa cells and in control cells. DSB induction was assessed by evaluating levels of histone H2AX phosphorylated at serine 139 ( $\gamma$ -H2AX) and of checkpoint kinase 2 phosphorylated at threonine 68 (Chk2 pT68). Chk1 activation and BLM accumulation were induced by blocking replication [34, 36]. We therefore determined the levels of activated Chk1 phosphorylated at serine 345 (Chk1 pS345) and BLM. The progressive accumulation of BLM in control cells was observed, with the highest levels after 16 to 24 h of exposure to HU (Figure 2(a)). No BLM was detected in HeLash-siBLM cells, as expected. The efficiency of replication blockade by HU was confirmed by FACS analysis and by the detection of activated Chk1 in both control cells and BLM-depleted HeLa cells. Significantly higher levels of accumulation of  $\gamma$ -H2AX and activated Chk2 were observed in control cells and in BLM-downregulated HeLa cells after 48 h of HU exposure than after 16 h (Figure 2(a)). The amounts of  $\gamma$ -H2AX and of Chk2pT68 detected in response to HU treatment were similar in BLM-deficient cells and in control cells. In BS-GFP cells and their complemented counterparts,  $\gamma$ -H2AX

accumulation was also stronger after 48 h of HU treatment than after 16 h (Figure 2(b)).

We evaluated HU genotoxicity in BLM-deficient cells further, by carrying out an *in vitro* alkaline DNA comet assay [37]. The mean tail moment (a numerical measurement of the DNA damage defined as the product of the tail length and the fraction of total DNA in the tail) was similar in BLM-deficient cells (HeLash-siBLM or BS-GFP) and in control cells (HeLaV-sictrl or BS-GFP-BLM, respectively), whether untreated or treated with 2 mM HU for 16 h (Figures 2(c), 2(d), and 2(e)). However, the mean tail moment was significantly higher after 48 h of HU treatment than in the absence of treatment or after 16 h of treatment, by a factor of about two in both BS cells and their complemented counterparts (Figure 2(e)), and by factors of four to ten in BLM-downregulated HeLa cells and their controls (Figure 2(d)). Thus, 16 h of treatment with 2 mM HU activates the Chk1-mediated replication checkpoint but does not generate a significant increase in DNA damage whereas 48 h of treatment with 2 mM HU leads to a significant increase in DNA damage, to similar levels in BLM-deficient cells control cells. BLM deficiency is not therefore associated with an increase in DSB induction in response to HU.

**3.3. HU Treatment Induces a Similar Increase in the Frequency of SCEs in BLM-Deficient Cells and Control Cells.** HU treatment efficiently induces SCEs formation [38]. We analyzed the effect of HU-induced replication stress on SCEs levels in BLM-deficient cells and in control cells. We found a slight but significant increase in SCE levels in both BLM-downregulated HeLa cells (x1.4) and in BS cells (x1.3) this increase is similar to that observed in the corresponding control cells (x1.7 and x1.4, resp.) (Figures 3(a) and 3(b)). Thus, BLM deficiency is not associated with an increase in SCEs induction in response to HU.

## 4. Discussion

We used hydroxyurea to investigate the cellular consequences of HU-induced replication stress in two cellular models of BS. We found that although BLM-deficient cells have a strong increase in SCE frequency due to BLM deficiency, the further increase in the SCE frequency induced by the treatment with HU was similar to that of control cells. Thus, BLM deficiency is not associated with sensitivity to HU in terms of SCE induction. We also showed that BLM-deficient cells were insensitive to HU induced replication stress (2 or 5 mM HU for 16 h), consistent with the normal sensitivity to HU of the BLM-defective chicken DT40 cells [29]. By contrast, Davies et al. [31] showed that BS cells were hypersensitive to prolonged exposure to HU. We also found that BLM-downregulated HeLa cells were significantly more sensitive to treatment with HU for 48 h than control cells were. We investigated the reasons for this sensitivity of BLM-deficient cells to 48 h of HU treatment but not to 16 h of treatment, by analyzing the effects of HU on DSB induction. We found that 48 h of HU treatment generated numerous DSBs whereas

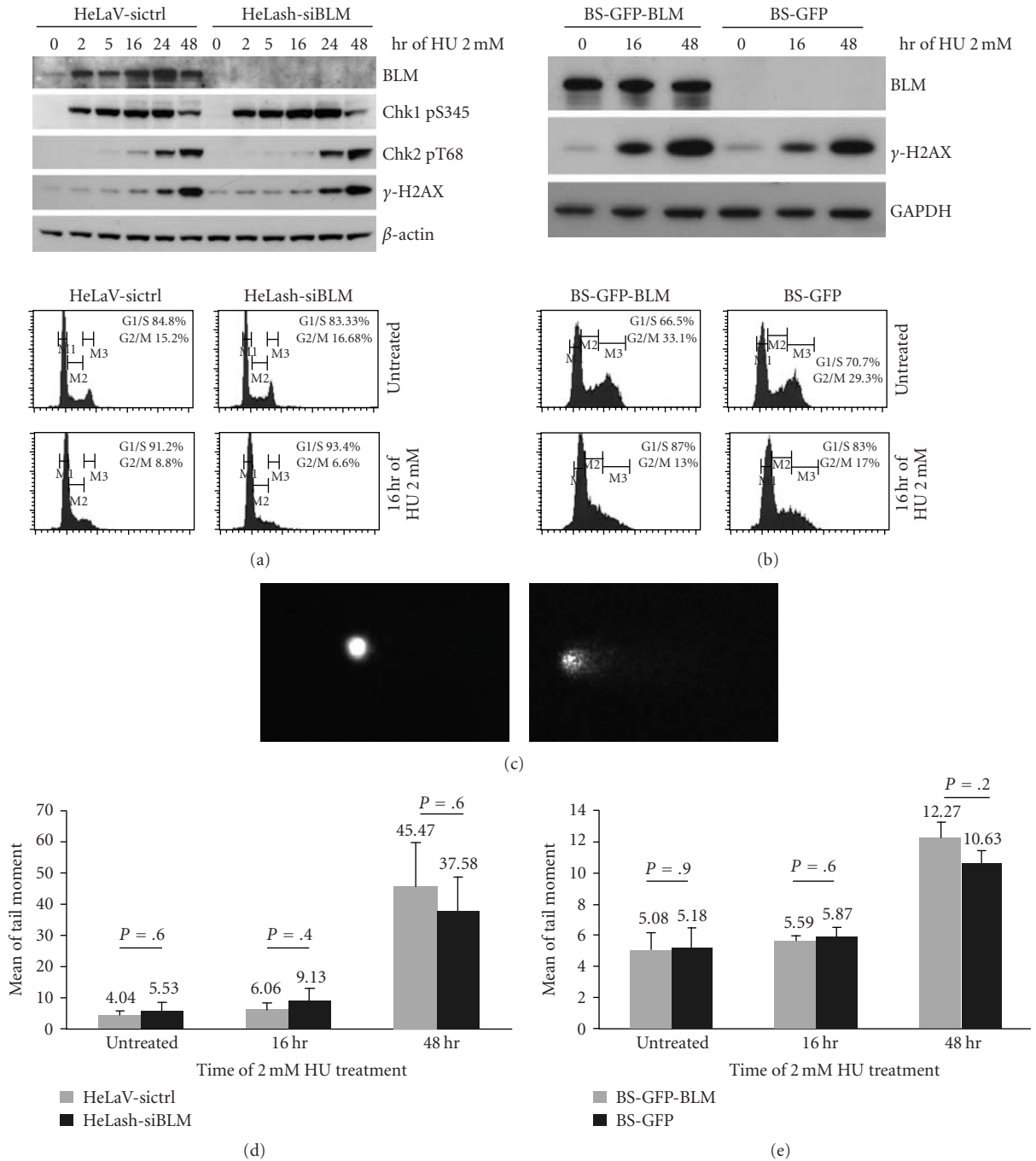


FIGURE 2: Levels of HU-induced DSBs are similar in BLM-deficient cells and control cells. (a) HeLaV and HeLashBLM cells were transfected as in Figure 1(a). Upper panel: After 24 h, cells were left untreated (0) or were treated with 2 mM HU for the indicated times. Protein extracts were subjected to SDS-PAGE. The membrane was probed with anti-BLM (C18), anti-Chk1 pS345, anti-Chk2 pT68, and anti- $\gamma$ -H2AX antibodies, and with anti- $\beta$ -actin antibody, as a loading control. The membrane was stripped and reblocked between successive antibody incubations. Lower panel: After 24 h, cells left untreated or treated with 2 mM HU for 16 h were harvested, fixed, and analyzed by FACS. (b) BS-GFP and BS-GFP-BLM cells were left untreated or were treated with 2 mM HU for the indicated times. Protein extracts were subjected to SDS-PAGE and the bands were transferred to a membrane. The membrane was probed with anti-BLM (C18), anti- $\gamma$ -H2AX antibodies, and with anti-GAPDH antibody, as a loading control. Lower panel: After 24 h, cells left untreated or treated with 2 mM HU for 16 h were harvested, fixed, and analyzed by FACS. (c) Representative images of HeLa cells in the comet assays. (Left) Untreated cell. (Right) Example of cell displaying an increase in DNA migration after 48 h of HU treatment, due to DNA breaks. (d) The effect of 2 mM HU treatment on DNA migration (tail moment) in the comet assays with HeLaV and HeLash BLM cells transfected as in Figure 1(a). After 24 h of transfection, cells were left untreated or were treated with 2 mM HU for 16 h or 48 h. The cells were subjected to comet assays (see Section 2). Two independent experiments were analyzed for each set of conditions. Between 100, and 110 cells were scored for each set of conditions, in each experiment. Error bars represent standard errors of the mean. (e) As in (d), using BS-GFP-BLM or BS-GFP cells left untreated or treated with 2 mM HU for 16 h or 48 h.

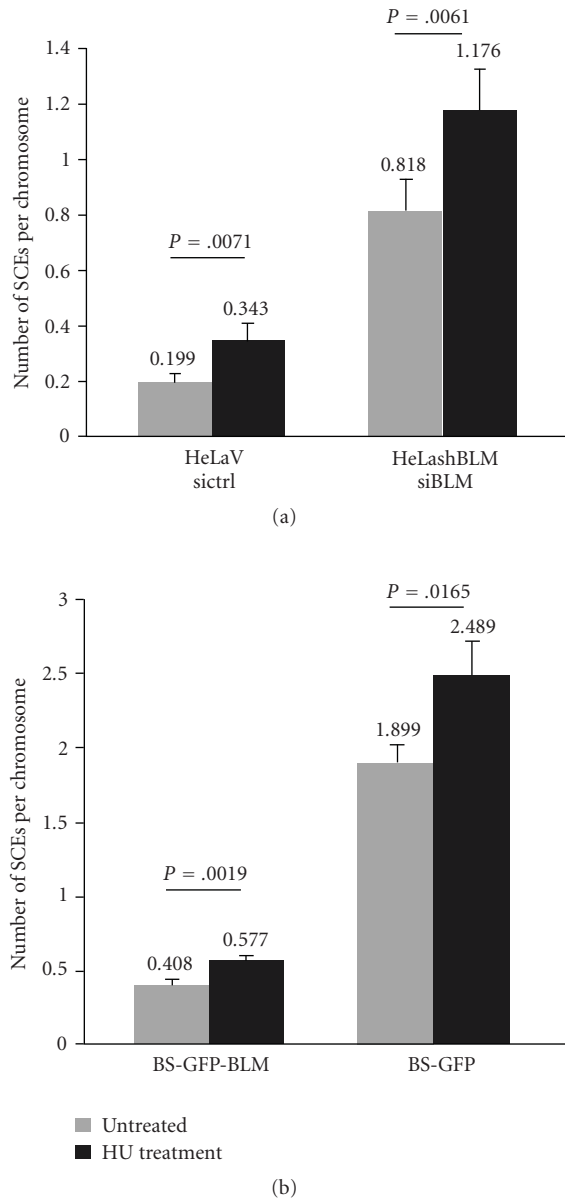


FIGURE 3: Levels of HU-induced SCEs are similar in BLM-deficient cells and control cells. (a) Number of SCEs per chromosome in HeLaV or in HeLashBLM cells transfected as in Figure 1(a), left untreated or treated with 2 mM HU for 16 h. Between 2174 and 4314 chromosomes from 5 independent experiments were analyzed for each set of conditions. Errors bars represent standard errors of the means. (b) Number of SCEs per chromosome in BS-GFP-BLM and BS-GFP cells left untreated or treated as in (a). Between 1864 and 2255 chromosomes from 4 independent experiments were analyzed for each set of conditions. Errors bars represent standard errors of the means.

16 h of treatment did not, as expected [35]. However, the DSB levels determined on the basis of  $\gamma$ -H2AX detection or in comet assays were found to be similar in BLM-deficient cells and in control cells treated with HU, indicating a lack of association between BLM deficiency and an increase in DSB induction by HU. These results are consistent with the data

reported by Rao et al. [39] showing that despite the delay in H2AX phosphorylation on serine 139 observed in BLM-deficient cells treated with HU (1 mM) or camptothecin (1  $\mu$ M), the number of  $\gamma$ -H2AX foci per nucleus reaches that of control cells 6 h after either of these treatments. Camptothecin induces replication-associated DSBs [40], and BS cells are hypersensitive to camptothecin [39]. These results indicate that the reported differences in the sensitivity of BLM-deficient cells to HU reflect differences in their sensitivity to HU-induced DSBs; this sensitivity depends on the numbers of DSBs generated by the HU treatment, but not on HU-induced replication stress *per se* that is associated with few DNA breaks. Indeed, unstressed BLM-deficient cells have DNA replication defects, resulting in spontaneously arrested replication forks and a decrease in the distance between origins [8, 9]. Such inhibition of the progress of replication forks may render BS cells susceptible to some DNA breaks, accounting for constitutive endogenous ATM-Chk2- $\gamma$ H2AX checkpoint activation detected only by immunofluorescence [9]. Such checkpoint activation has been found in clinical specimens from human tumours at various stages and in cultured cells subjected to replication stress [41, 42]. Endogenous ATM-Chk2- $\gamma$ H2AX activation in BS cells is thus thought to reflect a precancerous state, with replication stress associated with few DNA breaks [9]. If BS cells were hypersensitive to such replication stress, they would not survive this constitutive replication defect. We therefore suggest that surviving BLM-deficient cells have been selected on the basis of their ability to survive in the presence of a constitutive replication stress associated with few DNA breaks.

## 5. Conclusion

We showed that the clonogenic survival of BLM-deficient cells was insensitive to hydroxyurea (HU)-induced replication stress. Gamma-H2AX detection and comet assays revealed the numbers of DNA double-strand breaks (DSB) generated by HU treatment to be similar in BLM-deficient cells and control cells. Moreover, BLM deficiency did not further increase the frequency of HU-induced sister chromatid exchanges (SCEs). We propose that BLM-deficient cells are selected to survive with an endogenous replication stress induced by replication fork slowing, resulting in insensitivity to HU-induced replication stress.

## Acknowledgments

The authors thank Nathan Ellis for providing them with the BLM-GFP construct. They also thank Dr. Marie Dutreix (Institut Curie) for advices and helpful discussions and Christophe Roulin (Institut Curie) for expert assistance with comet assays. This paper was supported by Grants from the Institut Curie (PIC), the CNRS, the INCa (PL333), the Cancéropôle/Région Ile-de-France, and the ARC, and by a fellowship from the Cancéropôle/Région Ile-de-France, Association pour la Recherche sur le Cancer, and Ligue Nationale contre le Cancer (Comité de l'Essonne) (K. L. B-B).

## References

- [1] N. A. Ellis, J. Groden, T.-Z. Ye et al., "The Bloom's syndrome gene product is homologous to RecQ helicases," *Cell*, vol. 83, no. 4, pp. 655–666, 1995.
- [2] M. Otsuki, M. Seki, E. Inoue et al., "Functional interactions between BLM and XRCC3 in the cell," *Journal of Cell Biology*, vol. 179, no. 1, pp. 53–63, 2007.
- [3] E. Sonoda, M. S. Sasaki, C. Morrison, Y. Yamaguchi-Iwai, M. Takata, and S. Takeda, "Sister chromatid exchanges are mediated by homologous recombination in vertebrate cells," *Molecular and Cellular Biology*, vol. 19, no. 7, pp. 5166–5169, 1999.
- [4] K. L. Bennani-Belhaj, S. Rouzeau, G. Buhagiar-Labarchède et al., "The Bloom syndrome protein limits the lethality associated with RAD51 deficiency," *Molecular Cancer Research*, vol. 8, no. 3, pp. 385–394, 2010.
- [5] R. Hand and J. German, "A retarded rate of DNA chain growth in Bloom's syndrome," *Proceedings of the National Academy of Sciences of the United States of America*, vol. 72, no. 2, pp. 758–762, 1975.
- [6] F. Giannelli, P. F. Benson, S. A. Pawsey, and P. E. Polani, "Ultra-violet light sensitivity and delayed DNA chain maturation in Bloom's syndrome fibroblasts," *Nature*, vol. 265, no. 5593, pp. 466–469, 1977.
- [7] U. Lonn, S. Lonn, U. Nylen, G. Winblad, and J. German, "An abnormal profile of DNA replication intermediates in Bloom's syndrome," *Cancer Research*, vol. 50, no. 11, pp. 3141–3145, 1990.
- [8] S. L. Davies, P. S. North, and I. D. Hickson, "Role for BLM in replication-fork restart and suppression of origin firing after replicative stress," *Nature Structural and Molecular Biology*, vol. 14, no. 7, pp. 677–679, 2007.
- [9] V. A. Rao, C. Conti, J. Guirouilh-Barbat et al., "Endogenous  $\gamma$ -H2AX-ATM-Chk2 checkpoint activation in Bloom's syndrome helicase-deficient cells is related to DNA replication arrested forks," *Molecular Cancer Research*, vol. 5, no. 7, pp. 713–724, 2007.
- [10] J. German, "Bloom's syndrome," *Dermatologic Clinics*, vol. 13, no. 1, pp. 7–18, 1995.
- [11] L. Wu, S. L. Davies, N. C. Levitt, and I. D. Hickson, "Potential role for the BLM helicase in recombinational repair via a conserved interaction with RAD51," *The Journal of Biological Chemistry*, vol. 276, no. 22, pp. 19375–19381, 2001.
- [12] V. Tripathi, T. Nagarjuna, and S. Sengupta, "BLM helicase-dependent and -independent roles of 53BP1 during replication stress-mediated homologous recombination," *Journal of Cell Biology*, vol. 178, no. 1, pp. 9–14, 2007.
- [13] S. Sengupta, A. I. Robles, S. P. Linke et al., "Functional interaction between BLM helicase and 53BP1 in a Chk1-mediated pathway during S-phase arrest," *Journal of Cell Biology*, vol. 166, no. 6, pp. 801–813, 2004.
- [14] O. Bischof, S.-H. Kim, J. Irving, S. Beresten, N. A. Ellis, and J. Campisi, "Regulation and localization of the Bloom syndrome protein in response to DNA damage," *Journal of Cell Biology*, vol. 153, no. 2, pp. 367–380, 2001.
- [15] S. Sengupta, S. P. Linke, R. Pedoux et al., "BLM helicase-dependent transport of p53 to sites of stalled DNA replication forks modulates homologous recombination," *EMBO Journal*, vol. 22, no. 5, pp. 1210–1222, 2003.
- [16] V. Tripathi, S. Kaur, and S. Sengupta, "Phosphorylation-dependent interactions of BLM and 53BP1 are required for their anti-recombinogenic roles during homologous recombination," *Carcinogenesis*, vol. 29, no. 1, pp. 52–61, 2008.
- [17] K. J. Ouyang, L. L. Woo, J. Zhu, D. Huo, M. J. Matunis, and N. A. Ellis, "SUMO modification regulates BLM and RAD51 interaction at damaged replication forks," *PLoS Biology*, vol. 7, no. 12, Article ID e1000252, 2009.
- [18] J. K. Karow, A. Constantinou, J.-L. Li, S. C. West, and I. D. Hickson, "The Bloom's syndrome gene product promotes branch migration of Holliday junctions," *Proceedings of the National Academy of Sciences of the United States of America*, vol. 97, no. 12, pp. 6504–6508, 2000.
- [19] A. J. van Brabant, T. Ye, M. Sanz, J. L. German III, N. A. Ellis, and W. K. Holloman, "Binding and melting of D-loops by the Bloom syndrome helicase," *Biochemistry*, vol. 39, no. 47, pp. 14617–14625, 2000.
- [20] C. Z. Bachrati, R. H. Borts, and I. D. Hickson, "Mobile D-loops are a preferred substrate for the Bloom's syndrome helicase," *Nucleic Acids Research*, vol. 34, no. 8, pp. 2269–2279, 2006.
- [21] S. Raynard, W. Bussen, and P. Sung, "A double holliday junction dissolvosome comprising BLM, topoisomerase III $\alpha$ , and BLAP75," *The Journal of Biological Chemistry*, vol. 281, no. 20, pp. 13861–13864, 2006.
- [22] L. Wu, C. Z. Bachrati, J. Ou et al., "BLAP75/RMI1 promotes the BLM-dependent dissolution of homologous recombination intermediates," *Proceedings of the National Academy of Sciences of the United States of America*, vol. 103, no. 11, pp. 4068–4073, 2006.
- [23] A. Machwe, L. Xiao, J. Groden, and D. K. Orren, "The Werner and Bloom syndrome proteins catalyze regression of a model replication fork," *Biochemistry*, vol. 45, no. 47, pp. 13939–13946, 2006.
- [24] C. Ralf, I. D. Hickson, and L. Wu, "The Bloom's syndrome helicase can promote the regression of a model replication fork," *The Journal of Biological Chemistry*, vol. 281, no. 32, pp. 22839–22846, 2006.
- [25] D. V. Bugreev, X. Yu, E. H. Egelman, and A. V. Mazin, "Novel pro- and anti-recombination activities of the Bloom's syndrome helicase," *Genes and Development*, vol. 21, no. 23, pp. 3085–3094, 2007.
- [26] M. Amor-Gu eret, "Bloom syndrome, genomic instability and cancer: the SOS-like hypothesis," *Cancer Letters*, vol. 236, no. 1, pp. 1–12, 2006.
- [27] L. Wu, "Role of the BLM helicase in replication fork management," *DNA Repair*, vol. 6, no. 7, pp. 936–944, 2007.
- [28] G. M. Alvino, D. Collingwood, J. M. Murphy, J. Delrow, B. J. Brewer, and M. K. Raghuraman, "Replication in hydroxyurea: it's a matter of time," *Molecular and Cellular Biology*, vol. 27, no. 18, pp. 6396–6406, 2007.
- [29] O. Imamura, K. Fujita, A. Shimamoto et al., "Bloom helicase is involved in DNA surveillance in early S phase in vertebrate cells," *Oncogene*, vol. 20, no. 10, pp. 1143–1151, 2001.
- [30] M. Ababou, V. Dumaire, Y. L ecluse, and M. Amor-Gu eret, "Cleavage of BLM and sensitivity of Bloom's syndrome cells to hydroxyurea and UV-C radiation," *Cell Cycle*, vol. 1, no. 4, pp. 262–266, 2002.
- [31] S. L. Davies, P. S. North, A. Dart, N. D. Lakin, and I. D. Hickson, "Phosphorylation of the Bloom's syndrome helicase and its role in recovery from S-phase arrest," *Molecular and Cellular Biology*, vol. 24, no. 3, pp. 1279–1291, 2004.
- [32] S. Dutertre, M. Ababou, R. Onclercq et al., "Cell cycle regulation of the endogenous wild type Bloom's syndrome DNA helicase," *Oncogene*, vol. 19, no. 23, pp. 2731–2738, 2000.
- [33] S. Eladad, T.-Z. Ye, P. Hu et al., "Intra-nuclear trafficking of the BLM helicase to DNA damage-induced foci is regulated by SUMO modification," *Human Molecular Genetics*, vol. 14, no. 10, pp. 1351–1365, 2005.

- [34] M. Ababou, V. Dumaire, Y. Lécluse, and M. Amor-Guélet, "Bloom's syndrome protein response to ultraviolet-C radiation and hydroxyurea-mediated DNA synthesis inhibition," *Oncogene*, vol. 21, no. 13, pp. 2079–2088, 2002.
- [35] Y. Saintigny, F. Delacôte, G. Varès et al., "Characterization of homologous recombination induced by replication inhibition in mammalian cells," *EMBO Journal*, vol. 20, no. 14, pp. 3861–3870, 2001.
- [36] H. Zhao and H. Piwnica-Worms, "ATR-mediated checkpoint pathways regulate phosphorylation and activation of human Chk1," *Molecular and Cellular Biology*, vol. 21, no. 13, pp. 4129–4139, 2001.
- [37] G. Speit and P. Schütz, "The effect of inhibited replication on DNA migration in the comet assay in relation to cytotoxicity and clastogenicity," *Mutation Research*, vol. 655, no. 1-2, pp. 22–27, 2008.
- [38] A. Matsuoka, C. Lundin, F. Johansson et al., "Correlation of sister chromatid exchange formation through homologous recombination with ribonucleotide reductase inhibition," *Mutation Research*, vol. 547, no. 1-2, pp. 101–107, 2004.
- [39] V. A. Rao, A. M. Fan, L. Meng et al., "Phosphorylation of BLM, dissociation from topoisomerase III $\alpha$ , and colocalization with  $\gamma$ -H2AX after topoisomerase I-induced replication damage," *Molecular and Cellular Biology*, vol. 25, no. 20, pp. 8925–8937, 2005.
- [40] Y.-H. Hsiang, M. G. Lihou, and L. F. Liu, "Arrest of replication forks by drug-stabilized topoisomerase I-DNA cleavable complexes as a mechanism of cell killing by camptothecin," *Cancer Research*, vol. 49, no. 18, pp. 5077–5082, 1989.
- [41] J. Bartkova, Z. Hořejší, K. Koed et al., "DNA damage response as a candidate anti-cancer barrier in early human tumorigenesis," *Nature*, vol. 434, no. 7035, pp. 864–870, 2005.
- [42] V. G. Gorgoulis, L.-V. F. Vassiliou, P. Karakaidos et al., "Activation of the DNA damage checkpoint and genomic instability in human precancerous lesions," *Nature*, vol. 434, no. 7035, pp. 907–913, 2005.

## Research Article

# Rev1, Rev3, or Rev7 siRNA Abolishes Ultraviolet Light-Induced Translesion Replication in HeLa Cells: A Comprehensive Study Using Alkaline Sucrose Density Gradient Sedimentation

Jun Takezawa,<sup>1</sup> Yukio Ishimi,<sup>2</sup> Naomi Aiba,<sup>1</sup> and Kouichi Yamada<sup>1</sup>

<sup>1</sup> Division of Genetic Biochemistry, The National Institute of Health and Nutrition, Shinjuku-ku, Tokyo 162-8636, Japan

<sup>2</sup> Faculty of Science, Ibaraki University, Mito-shi, Ibaraki-ken 310-8512, Japan

Correspondence should be addressed to Kouichi Yamada, kouichi@nih.go.jp

Received 14 May 2010; Revised 13 July 2010; Accepted 17 September 2010

Academic Editor: Shigenori Iwai

Copyright © 2010 Jun Takezawa et al. This is an open access article distributed under the Creative Commons Attribution License, which permits unrestricted use, distribution, and reproduction in any medium, provided the original work is properly cited.

When a replicative DNA polymerase stalls upon encountering a lesion on the template strand, it is relieved by other low-processivity polymerase(s), which insert nucleotide(s) opposite the lesion, extend by a few nucleotides, and dissociate from the 3'-OH. The replicative polymerase then resumes DNA synthesis. This process, termed translesion replication (TLS) or replicative bypass, may involve at least five different polymerases in mammals, although the participating polymerases and their roles have not been entirely characterized. Using siRNAs originally designed and an alkaline sucrose density gradient sedimentation technique, we verified the involvement of several polymerases in ultraviolet (UV) light-induced TLS in HeLa cells. First, siRNAs to Rev3 or Rev7 largely abolished UV-TLS, suggesting that these 2 gene products, which comprise Pol $\zeta$ , play a main role in mutagenic TLS. Second, Rev1-targeted siRNA also abrogated UV-TLS, indicating that Rev1 is also indispensable to mutagenic TLS. Third, Pol $\eta$ -targeted siRNA also prevented TLS to a greater extent than our expectations. Fourth, although siRNA to Pol $\iota$  had no detectable effect, that to Pol $\kappa$  delayed UV-TLS. To our knowledge, this is the first study reporting apparent evidence for the participation of Pol $\kappa$  in UV-TLS.

## 1. Introduction

Multiple systems have evolved to manage the genomic photoproducts generated by harmful UV light. One such system is nucleotide excision repair (NER), which eliminates photoproducts from DNA strands by dual incision on both sides of a damaged base. The NER system cannot, however, remove all UV-damaged bases. When a replicative DNA polymerase stalls upon encountering a residual photoproduct on the template strand, it is relieved by other low-processivity polymerase(s), which incorporate nucleotide(s) opposite the lesion, extend by a few nucleotides and dissociate from the 3'-OH. The replicative polymerase then resumes DNA synthesis. This process, termed translesion replication (TLS) or replicative bypass (reviewed in [1]), is also one of the subtle systems that have evolved for the management of genomic photoproducts.

UV-C (100–290 nm wavelength) induces 2 main photoproducts [2]: the more frequent cyclobutane pyrimi-

dine dimer (CPD) and the several-fold lower pyrimidine-pyrimidone (6-4) photoproduct ((6-4)PP). *cis-syn* CPD, a predominant form of the multiple configurations, contains 2 adjacent pyrimidines that are covalently linked in parallel. Although the frequency of CPD varies with nucleotide composition, a ratio of T-T to C-T to T-C to C-C of 68 : 13 : 16 : 3 is obtained from UV-irradiated plasmid DNA. Cytosines within CPD are unstable, and are deaminated to uracil or 5-methylcytosine, and further deaminated to thymine [3]. The helical distortion caused by CPD is so inconspicuous that almost half of the lesions remain unrepaired by NER, even 6 hours after UV irradiation in the case of CHO cells [2].

The (6-4)PPs from T-C, C-C, and, less frequently, T-T sequences are detected in UV-irradiated DNA whereas that of C-T are not. In (6-4)PP, linkage between C-6 of one pyrimidine and C-4 of the adjacent pyrimidine cause the 2 bases to be in nearly perpendicular position. Consequently, formation of this lesion causes a major distortion in the double helix. NER preferentially removes (6-4)PP more

rapidly than it removes CPD from the genome in human and rodent cells [4].

At least 5 mammalian DNA polymerases are suggested to be implicated in UV-induced TLS: Pols  $\eta$ ,  $\iota$ ,  $\zeta$ ,  $\kappa$ , and Rev1, all of which belong to the Y family except for Pol $\zeta$  (B family) (reviewed in [1, 5, 6]). However, the participating polymerases and their roles have not been entirely characterized.

Patients with the autosomal recessive disorder, xeroderma pigmentosum variant (XP-V), have a predisposition to skin cancer, and XP-V cells demonstrate hypermutability after UV irradiation (reviewed in [7]). The defective gene in XP-V encodes Pol $\eta$ , which was first purified from a HeLa cell extract as an activity that complements TLS defect in XP-V cell extract [8]. Human Pol $\eta$  catalysed DNA synthesis past TT-CPD very efficiently and in a relatively accurate manner, as demonstrated by the lesion-bypass assay [7, 9]. When template DNA contained a (6-4)TT-PP, Pol $\eta$  incorporated one (random) nucleotide opposite the first thymine and another nucleotide opposite the second thymine of the lesion, but rarely continued across the lesion [7, 9].

Human Pol $\eta$  was also identified via a search for the homolog of yeast *Saccharomyces cerevisiae* *Rad30* gene, which encodes an error-free bypass protein [10]. Various XP-V causative mutations have been found in the Pol $\eta$  gene, *hRAD30A*, of XP-V patients [10, 11].

Pol $\iota$  (*RAD30B*) is the other mammalian homolog of yeast Pol $\eta$ , isolated by a similar approach [12]. In contrast to Pol $\eta$ , Pol $\iota$  is less efficient and less accurate [13].

Pol $\kappa$  was obtained by cloning of a human homolog of the *E. coli dinB* gene, encoding DNA Pol IV [14]. Pol $\kappa$  was reported to be unable to bypass either CPD or (6-4)PP [15, 16].

Originally, Rev1, 3, and 7 were cloned from *S. cerevisiae* isolates, in which the frequency of UV-induced reversion from *cyc1* mutations was reduced [17]. Human and mouse homologs (*Rev1*, 3, 7 gene) were later isolated [18–20]. Pol $\zeta$  is a complex of the *Rev3* and *Rev7* gene products, which act as the catalytic and regulatory subunit, respectively. Yeast Pol $\zeta$  is shown to be responsible for 98% of UV-induced base substitutions and 90% of frameshift mutations, in addition to spontaneous mutations [21]. Nonetheless, yeast Pol $\zeta$  itself was revealed to be too faithful to incorporate opposite CPD. Instead, it can efficiently extend from a matched or mismatched 3'-end (reviewed in [5, 6]). Human or mouse Pol $\zeta$  is assumed to have similar enzymatic properties to that of yeast, because several lines of antisense RNA expression or siRNA knockdown experiments in human or mouse cells have proven that Pol $\zeta$  is involved in mutagenic TLS [22–24].

Yeast and human Rev1 encode highly specialized DNA polymerases that preferentially insert a C residue opposite an abasic site in the template. This deoxycytidyl (dC) transferase activity is, however, unlikely to be required for UV-TLS, judging by observation in a yeast *rev1-1* mutant strain [25], which retains much of its dC transferase activity, but has a missense mutation (G193R) in the N-terminal BRCT domain. Rev1 protein also contains ubiquitin-binding motifs (UBMs) that interact with monoubiquitinated PCNA (a DNA polymerase sliding clamp) [26]. In the downstream C-terminal region, Rev1 interacts not only with Rev7 but also

with other bypass-polymerases [27], suggesting that Rev1 acts as a mediator and physical bridges between PCNA and Pol $\zeta$ .

Following DNA damage, such as that caused by UV and MMS, monoubiquitins are conjugated to PCNA arrested at the lesion-site by RAD6/RAD18 and recruit bypass-polymerases [28, 29]. In addition to Rev1, Pols  $\eta$ ,  $\iota$ , and  $\kappa$  possess UBMs and physically interact with PCNA [1, 5, 6]. Stalled replicative Pol $\delta$  is replaced, in turn, with one of these bypass polymerases bound on the PCNA by yet unknown “polymerase switching” mechanisms (reviewed in [1, 30]).

Translesion replication is typically detected with an alkaline sucrose density gradient centrifugation (ASDG) technique. Pulse-labelled replication products are smaller in UV-irradiated XP-V cells than in unirradiated cells; however, on prolonged incubation, the replication products in the irradiated cells eventually attain a high molecular weight similar to that in unirradiated cells. This conversion is interpreted that DNA synthesis is temporarily retarded by UV photoproducts, and then continues beyond the lesion, leaving a gap that is subsequently sealed [31]. The initial size of the newly synthesized DNA is approximately equal to the average distance between lesions in the template strands [32]. This means the gaps in the newly synthesized DNA are opposite the photoproducts [33]. Therefore, sealing of the gaps, by translesion or other postreplication repair mechanisms, can be observed by monitoring the molecular weight of labelled DNA.

Using a modified ASDG technique [34], we precisely detected the elongation of pulse-labelled replication products in the irradiated XP-V cells, showing that UV-TLS is delayed in the cells, but not completely abolished [35]. The marginal TLS is markedly prevented by caffeine at millimolar concentrations, as Lehmann et al. pointed out [31], and by proteasome inhibitors as well (unpublished results). In contrast, these agents do not retard UV-TLS in normal diploid cells. To know more about the inefficient polymerase(s) *in vivo*, we added specific DNA polymerase inhibitors. Butylphenyldeoxyguanosine (BuPGdR) inhibited TLS in XP-V cells [35], suggesting that Pol $\zeta$  may be involved in this Pol $\eta$ -independent bypass.

We recently reported that caffeine or proteasome inhibitors inhibit UV-TLS also in human cancer cells [36], and that, similar to XP-V cells, UV-TLS was much slower than in normal cells. These results suggested that UV bypass in cancer cells is predominantly of the Pol $\eta$ -independent type. Therefore, we expected that Pol $\zeta$  plays a major part in UV-TLS in cancer cells. Although Pol $\eta$  exists in normal quantity in these cells, it was supposed to be inactivated by some reasons. We explored these hypotheses here.

## 2. Materials and Methods

**2.1. Design of siRNAs.** All siRNAs duplexes were synthesized by JBioS (Japan) (Table 1). We designed the sequences for siRNA according to the JBioS guide (<http://www.JBioS.co.jp/RNAselect.htm>). Selection of target sequence for each siRNA proceeds as follows: first, an AAG or AAC sequence is found at least 75 nucleotides (nt) downstream from the start codon; the AAG (or AAC) and the following 18 nt sequence

TABLE 1: siRNAs used.

siRNA	Sense strand <sup>(a),(b)</sup>	Antisense strand <sup>(a),(b)</sup>	Prevention of UV-TLS (result)
siRev3-A	gcuuuacaugagauacaaaTT	uuuguaucauguaaaagcTT	significant
siRev3-B	gacaguuuucagucaagauTT	aucuugacugaaaacugucTT	significant
siRev3-C	gagguaugauccugauuuTT	aaauacaggaucauaccucTT	significant
siRev3-D	guauugacuuaugucggauTT	auccgacauaagucaauacTT	significant
siRev3cont-A (6nt mismatches)	<b>gg</b> uuugag <u>ua</u> augu <b>ac</b> gauTT	auc <b>gu</b> acau <b>ua</b> cuca <b>aac</b> TT	no effect
siRev3cont-B (4nt mismatches)	<b>gg</b> auugag <u>uu</u> augu <b>ac</b> gauTT	auc <b>gu</b> acau <b>aa</b> cuca <b>auc</b> TT	no effect
siRev3cont-C (2nt mismatches)	guauugag <u>uu</u> auguc <b>cg</b> auTT	auc <b>gg</b> acau <b>aa</b> cuca <b>au</b> acTT	no effect
siRev7-A	gauccaggucaucaaggauTT	auccuugaugaccuggaucTT	partial
siRev7-B	gaugcagcuuuacguggaaTT	uuccaccguaaagcugcaucTT	significant
siRev7-C	cacugucugucuaaaauacTT	guauuugagacagacagugTT	significant
siRev7cont-A	gaugcag <u>uu</u> uacgucgaaTT	uuc <b>g</b> acg <b>ua</b> aa <b>acc</b> ugcaucTT	no effect
siRev1-A	cacauuuuuugccacaaaTT	uuuguggcauuuuuugugTT	significant
siRev1-B	gaagauugaaacggaaaaTT	auuuuuccguuucaauucTT	significant
siRev1-C	ccuucagacugcauuuuuaTT	uaaaauugcagucugaaggTT	significant
siRev1-D	gugugaauugacugaguuuTT	aaacucagucaauucacacTT	significant
siRev1cont-E	ccuucac <b>accg</b> ca <b>acg</b> uuuTT	ua <b>acg</b> uug <b>cg</b> gugugaaggTT	little to no effect
siPol $\eta$ -4	uaaaccuugugcaguuuaTT	uacaacugcacaaguuuaTT	partial
siPol $\eta$ -A	gaaguuuuguccagauuuTT	aagaucuggacauaacuucTT	significant
siPol $\eta$ -B	gcuucgcuuucacucuuuTT	uaagagauagaaagcgaagcTT	significant
siPol $\eta$ cont-A	uaaaccu <b>gg</b> ugcagucgaaTT	uac <b>g</b> acug <b>cacc</b> agguuuTT	no effect
siPol $\iota$ -A	gccucauacagugaguuuTT	uaaucucacuguaugaggcTT	no effect
siPol $\iota$ -5	aaguguccacaguuguuuTT	auaccaacuguggacacuuTT	no effect
siPolk-A	gagaaaauuacaaaauuTT	uaauuuuguuuuuuucucTT	partial
siPolk-B	gaauaaacaaauggacaaTT	uuguccauuuugguuuuucTT	partial
siPolk-C	cuguuaccuuuaguugaaTT	uucaacuuaaugguuacagTT	considerable
siPolkcont-B	gagaaa <b>g</b> ua <b>aca</b> g <b>cu</b> uaTT	ua <b>agc</b> u <b>gu</b> ua <b>cu</b> uuuucTT	little to no effect

<sup>(a)</sup>Small letters mean ribonucleotides, and large letters mean deoxyribonucleotides.

<sup>(b)</sup>Mismatched bases are illustrated in bold and italic letters.

(N18) are picked up. Ideally, the 2 nt following the N18 are TT, TN, NT, or AA. GC content of N18 is recommended to be about 40% to 50%. If GC content is less than 30%, or greater than 70%, avoid the sequence. The N18 had better be AT-rich in the 3' half and especially at the 3' end (2 nt).

**2.2. HeLa Cell Culture and siRNA Treatment.** HeLa cells were maintained in monolayers in Dulbecco's modified Eagle's medium (D'MEM) supplemented with 10% fetal calf serum (FCS) ("normal" medium), trypsinized and seeded into culture dishes ( $2 \times 10^5$  cells/ $\phi$  60 mm dish). About 6–8 hours later, the cells were treated with micelles of siRNA and OligofectAMINE (Invitrogen), formed according to the manufacturer's protocol, except Opti-MEM was replaced with D'MEM. The siRNA concentration used in RT-PCR analysis and western blot analysis was 5 nM.

**2.3. UV Irradiation and Translesion Replication.** Forty hours after siRNA addition, HeLa cells were exposed to UV light ( $10 \text{ J/m}^2$ ) from a germicidal lamp (Toshiba GL15) at

$0.6 \text{ J/m}^2$  per s. After 30 minutes in culture, the medium was changed to labeling medium consisting of D'MEM supplemented with 10% FCS and  $10 \mu\text{Ci/mL}$  of [ $U$ - $^{14}\text{C}$ ]thymidine (Moravek MC267,  $470 \text{ mCi/mmol}$ ). UV-irradiated cells were pulse-labelled for 1 hour, while nonirradiated cells were labelled for 30 minutes. The medium was changed to normal medium, and the cells were chased for 5 hours. These cells were harvested by trypsinisation and examined by ASDG [34].

**2.4. Alkaline Sucrose Density Gradient Centrifugation (ASDG).** Cells (about  $1 \times 10^5$  in  $50 \mu\text{L}$  PBS) were gently layered onto  $50 \mu\text{L}$  of 1% sucrose in PBS, which was overlaid on  $100 \mu\text{L}$  of lysis solution (0.6 M KOH, 2.0 M KCl, 10 mM EDTA, and 1% *N*-lauroylsarcosine), which was placed on top of a 4.35 mL alkaline 5–20% sucrose gradient (0.3 M KOH, 2.0 M KCl, 1 mM EDTA, and 0.1% *N*-lauroylsarcosine) with 0.4 mL of alkaline 80% sucrose as a cushion at the bottom. The gradient was centrifuged at 6,000 rpm ( $4,320 \times g$ ) for 15.6 hours at  $15^\circ\text{C}$  in a Beckman SW 50.1 rotor. The gradient was fractionated onto 30 circles of no. 17 paper

(Whatman). The paper circles were dried, immersed in cold 5% trichloroacetic acid for 10 minutes, washed 3 times with ethanol and once with acetone, and dried; radioactivity was then measured. As a molecular weight marker, [ $^{14}\text{C}$ ]-labelled T4 DNA phage particles were placed on the lysis layer and sedimented in a parallel run. The approximate fragment length of each fraction was estimated on the basis of the position of the T4 DNA marker and that of *E. coli* DNA and adjusted by sucrose density curve [34]. Average fragment length (in megabase(Mb)) of each profile is shown in Figures as fragment length of the median fraction [35]. (Median fraction is the middle fraction that separates the higher half of the profile from the lower half.)

**2.5. RT-PCR.** Total RNA was isolated using an RNeasy spin column (QIAGEN). One  $\mu\text{g}$  of total RNA was treated with DNase I (Invitrogen), reverse-transcribed using SuperScript II (Invitrogen) with random hexamers or PrimeScript II (TaKaRa) with oligo(dT) primers, followed by treatment with *E. coli* RNase H (Invitrogen). The PCR mixture contained cDNA templates, dNTPs, rTaq Pol (TOYOBO), anti-Taq (TOYOBO), and appropriate primers. Primers to assess knockdown of each gene were as follows: Rev3, 5'-GGAACGTCAACAGGAGCAAC-3' and 5'-GGAGCAATCCAACACCTGC-3'; Rev7, 5'-TGCTGTCCATCAGCTCAGAC-3' and 5'-AGAGCACTTGGAAATCAGGGC-3'; Rev1, 5'-CTCCTGCAGAGAAACCCCTG-3' and 5'-ACAAGCACTTATGGCACAGCT-3'; Pol $\eta$ , 5'-CCCAGGCAACTACCCAAAAC-3' and 5'-GGGCTCAGTTCCTGTACTTTG-3'; Pol $\iota$ , 5'-ATGATCAAGTGTGCCACAC-3' and 5'-ACATGACCCGACACAGTCAC-3'; Pol $\kappa$ , 5'-AGACAAGAATACCGCCAGCC-3' and 5'-AGGAAGGATTATTGCACTTGCC-3'; GAPDH, 5'-ACCACAGTCCATGCCATCAC-3' and 5'-TCCACCACCCTGTTGCTGTA-3'. All PCR reactions were carried out for 27 cycles, with the exception of GAPDH (25 cycles). PCR products were subjected to a MultiNA microtip electrophoresis DNA/RNA analyzer (Shimadzu Biotech).

**2.6. Western Blotting.** Cells were rinsed with PBS, lysed with  $1 \times$  SDS-PAGE loading buffer and collected by scraping. Cell lysate was boiled for 10 minutes, sonicated for 30 seconds and centrifuged at  $20,000 \times g$  for 10 minutes. The supernatant was used for western blotting after measuring protein content by Bradford method. The supernatant (60  $\mu\text{g}$  protein) was separated on 5–20% (Rev7, Rev1 and Pol $\iota$ ) or 3–10% (the rest) SDS-polyacrylamide gels (Wako) and transferred onto Immobilon-P<sup>SQ</sup> membranes (Millipore). The membranes were incubated with antibodies to bypass-polymerases (Rev1, Santa Cruz Biotechnology sc-48806; Rev7, BD Transduction Laboratories 612266; Pol $\eta$ , Santa Cruz Biotechnology sc-17770; Pol $\iota$ , Abnova H00011201-M01; Pol $\kappa$ , a kind gift from Dr. Tomoo Ogi, Nagasaki University), and then with horseradish peroxidase-conjugated secondary antibodies (anti mouse IgG, DAKO PO-0447; anti-rabbit IgG, DAKO PO-0448). Antibodies were diluted with CanGetSignal (TOYOBO) to enhance immunoreactivity. The signals were developed with ECL-Plus (GE Healthcare),

and blots were stripped for reprobing with anti  $\alpha$ -tubulin antibody (Sigma T5168).

### 3. Results

**3.1. Effect of siRNAs to Rev3 or Rev7 on HeLa UV-TLS.** We selected 4 target sites from the human Rev3 mRNA sequence (NCBI locus: NM\_002912), according to the JBioS guide. All the Rev3 siRNAs (Table 1) effectively knocked down expression of Rev3 (Figure 1(a)) and, at 5 nM, abolished UV-TLS in HeLa cells (Figure 1(b)). Replication products immediately after UV irradiation were sedimented as a sharp peak, illustrated by a thin line in Figure 1(b), slightly larger in size than the T4 phage DNA marker. When only Oligofectamine-treated cells were chased in normal medium for 5 hours, the products joined to form larger DNA with lengths in the order of megabases (Mb), illustrated by a thick line. In Rev3 siRNA-transfected cells, the products remain in smaller size, as depicted by a thin line with open marks, demonstrating these siRNAs prevent UV-TLS (Figure 1(b)).

We assessed how many mismatched nucleotides (nt) are necessary at minimum for the negative control siRNA (Figure 1(c)) and found that siRev3cont-C, designed from siRev3-D with 2 nt mismatches, did not prevent UV-TLS, indicating that these Rev3 siRNAs degrade Rev3 mRNA with high specificity. The dose-response profile of siRev3-D, shows that only 1 nM siRNA sufficiently inhibited UV-TLS (Figure 1(d)). The siRev3-D siRNA had no effect on normal replication (Figure 1(e)).

We selected 3 target sites from the human Rev7 mRNA sequence (NM\_006341) (Table 1), and found that all siRNAs effectively reduced Rev7 expression (Figure 2(a)); 5 nM siRev7-B or siRev7-C completely abolished UV-TLS (siRev7-A elicited only partial prevention) (Figure 2(b)). The siRev7cont-A, designed from siRev7-B with 2 nt mismatches, had no effect (ibid). The dose-response profile of siRev7-B shows that 1 nM siRNA was sufficient to inhibit UV-TLS (Figure 2(c)); Rev7 siRNAs had no effect on normal replication (Figure 2(d)).

**3.2. SiRNAs to Rev1 Significantly Abrogated UV-TLS.** For knockdown of Rev1 expression, we selected 4 sites from the human Rev1 mRNA sequence (NM\_016316) (Table 1) (Figure 3(a)). The siRNAs (5 nM) targeted to these sites abolished UV-TLS in HeLa cells (Figure 3(b)). The siRev1cont-E, designed from siRev1-C with 4 nt mismatches, had little to no effect. The dose-response profile of siRev1-C shows that 1 nM of the siRNA was enough to inhibit UV-TLS (Figure 3(c)); siRev1-C or siRev1-D siRNA had no effect on normal replication (Figure 3(d)).

**3.3. SiRNAs to Pol $\eta$  Prevented UV-TLS to a Great Extent.** First, we tested the siRNA described by Choi and Pfeifer [37], siPol $\eta$ -4, which partially inhibited UV-TLS (Figure 4(a)). The negative control, siPol $\eta$ cont-A, was designed from siPol $\eta$ -4 with 2 nt mismatches, had no effect (ibid). We added 2 Pol $\eta$  siRNAs of new design (human Pol $\eta$  mRNA sequence: NM\_006502) (Table 1), and these siRNAs also effectively

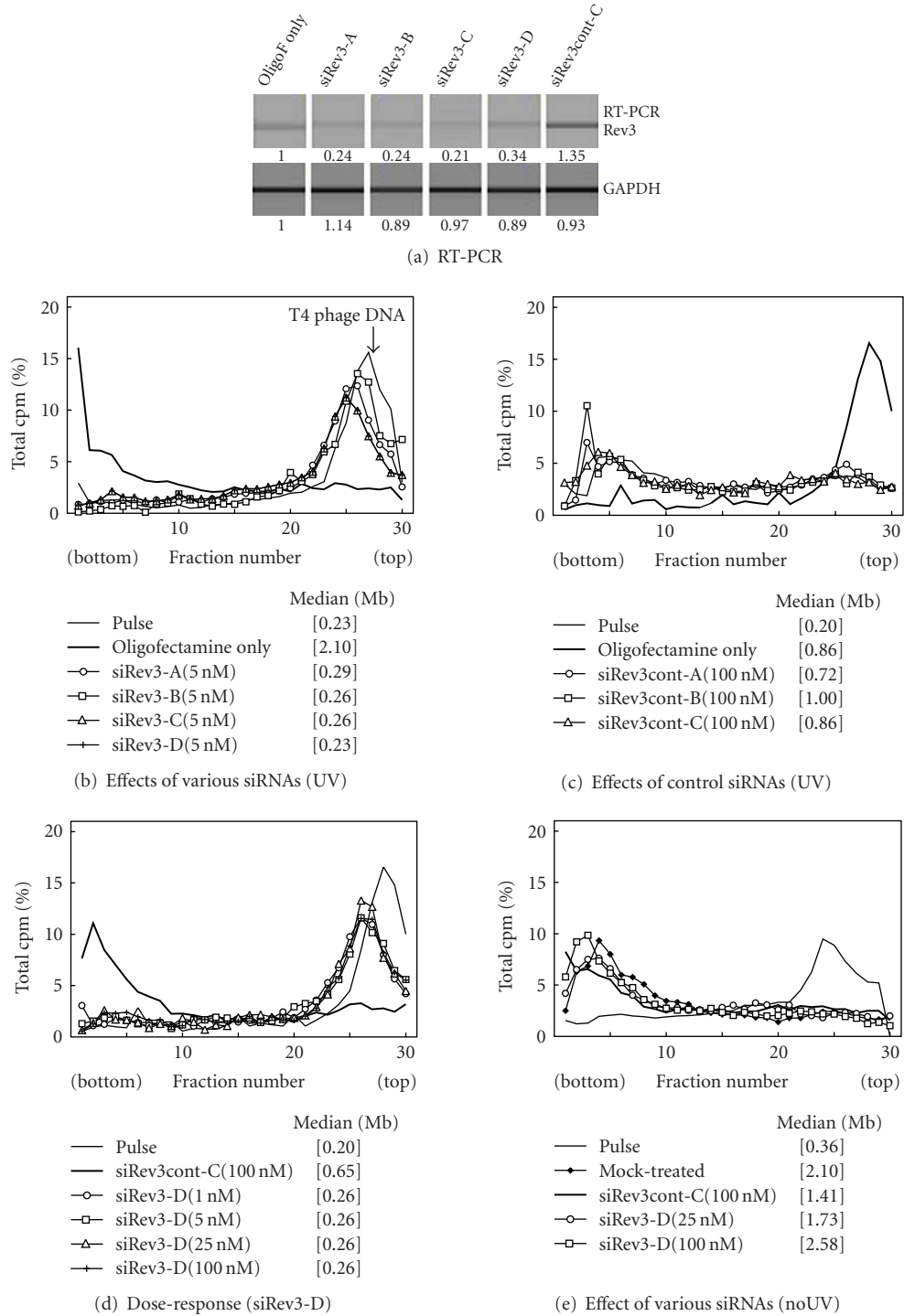


FIGURE 1: Efficient knockdown by Rev3 siRNAs and their effects on UV-induced TLS in HeLa cells (ASDG profiles of replication products). (a) Efficiency of knockdown on Rev3 expression (RT-PCR analysis); (b) Effects of various Rev3 siRNAs; (c) Effects of Rev3 control siRNAs; (d) Dose-response of siRev3-D; (e) Effect of various Rev3 siRNAs (no UV control). Twenty-four hours after Rev3 siRNA transfection, total RNA was isolated and Rev3 RNA was quantified by RT-PCR. Results were shown in MultiNA gel images and the expression level was presented under the panel (a). Forty hours after Rev3 siRNA transfection, cells were UV-irradiated ( $10 \text{ J/m}^2$ ), incubated in normal medium for 30 minutes, pulse-labelled with  $10 \mu\text{Ci/mL}$  of [ $^{14}\text{C}$ ]thymidine for 1 hour, washed twice with PBS, and incubated for 5 hours at  $37^\circ\text{C}$  in normal medium (b, c, d). siRev3cont-A, 6 nt mismatches; siRev3cont-B, 4 nt mismatches; siRev3cont-C, 2 nt mismatches (c). Forty hours after Rev3 siRNA transfection, cells were not UV-irradiated, pulse-labelled with  $10 \mu\text{Ci/mL}$  of [ $^{14}\text{C}$ ]thymidine for 30 minutes, washed twice with PBS, and incubated at  $37^\circ\text{C}$  in normal medium for 1 hour (e). Some of these profiles overlap (c, d, e). Sedimentation is from right to left. The arrow indicates the position of T4 phage DNA (166 kb, i.e., approximately  $5.5 \times 10^7 \text{ Da}$ /single strand). Labelled *E.coli* DNA (approximately 4 Mb) sedimented near the bottom (fractions 3–6) (4). Average fragment length (in Mb) of each profile is shown in square brackets as fragment length of the median fraction.

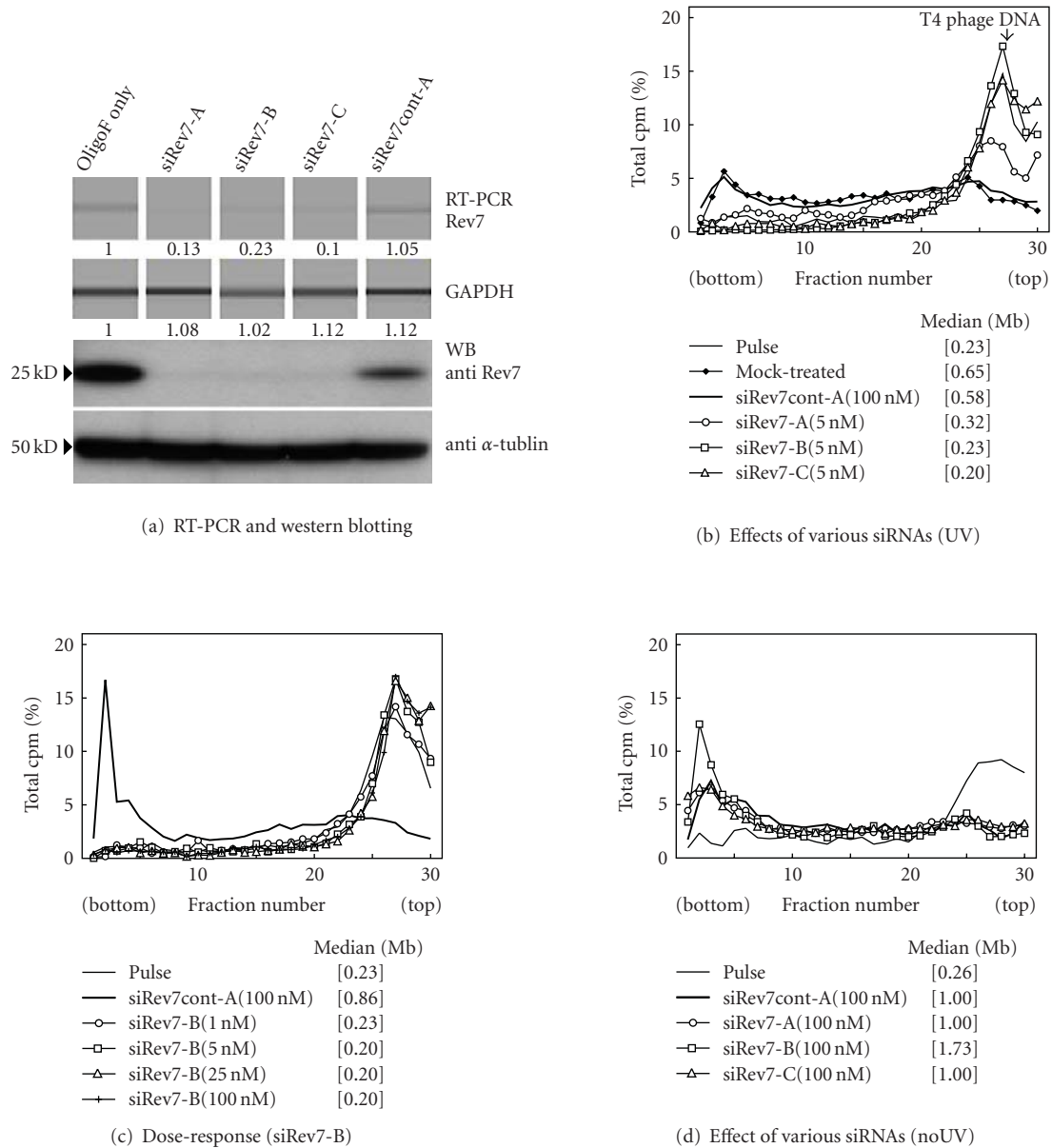


FIGURE 2: Efficient knockdown by Rev7 siRNAs and their effects on UV-induced TLS in HeLa cells (ASDG profiles of replication products). (a) Efficiency of knockdown on Rev7 expression (RT-PCR analysis and western blot analysis); (b) Effects of various Rev7 siRNAs; (c) Dose-response of siRev7-B; (d) Effect of various Rev7 siRNAs (no UV control). Twenty-four hours after Rev7 siRNA transfection, total RNA was isolated and Rev7 RNA was quantified by RT-PCR. Results were shown in MultiNA gel images and the expression level was presented under the panel (a). Forty hours after Rev7 siRNA transfection, whole cell extracts were prepared and Rev7 protein was quantified by western blot analysis (a). Forty hours after Rev7 siRNA transfection, cells were UV-irradiated ( $10 \text{ J/m}^2$ ), incubated in normal medium for 30 minutes, pulse-labelled with  $10 \mu\text{Ci/mL}$  of  $[^{14}\text{C}]$ thymidine for 1 hour, washed twice with PBS, and incubated at  $37^\circ\text{C}$  in normal medium (b, c). Forty hours after Rev7 siRNA transfection, cells were not UV-irradiated, pulse-labelled with  $10 \mu\text{Ci/mL}$  of  $[^{14}\text{C}]$ thymidine for 30 minutes, washed twice with PBS, and incubated at  $37^\circ\text{C}$  in normal medium for 1 hour (d). Some of these profiles overlap (c, d). Sedimentation is from right to left. The arrow indicates the position of T4 phage DNA (166 kb, i.e., approximately  $5.5 \times 10^7$  Da/single strand). Average fragment length (in Mb) of each profile is shown in square brackets.

knocked down Pol $\eta$  expression (Figure 4(b)). These latter siRNAs at 5 nM abolished UV-TLS to a greater extent than siPol $\eta$ -4 (Figure 4(c)). The Pol $\eta$  siRNAs had no effect on normal replication (Figure 4(d)).

3.4. Polk siRNAs Delayed UV-TLS, While siRNAs to Pol $\iota$  Did Not. Although Pol $\iota$  siRNAs efficiently prevented Pol $\iota$  expression (Figure 5(a)), we could not detect these effects on ASDG profiles (Figure 5(b)). The siPol $\iota$ -5 was reported by

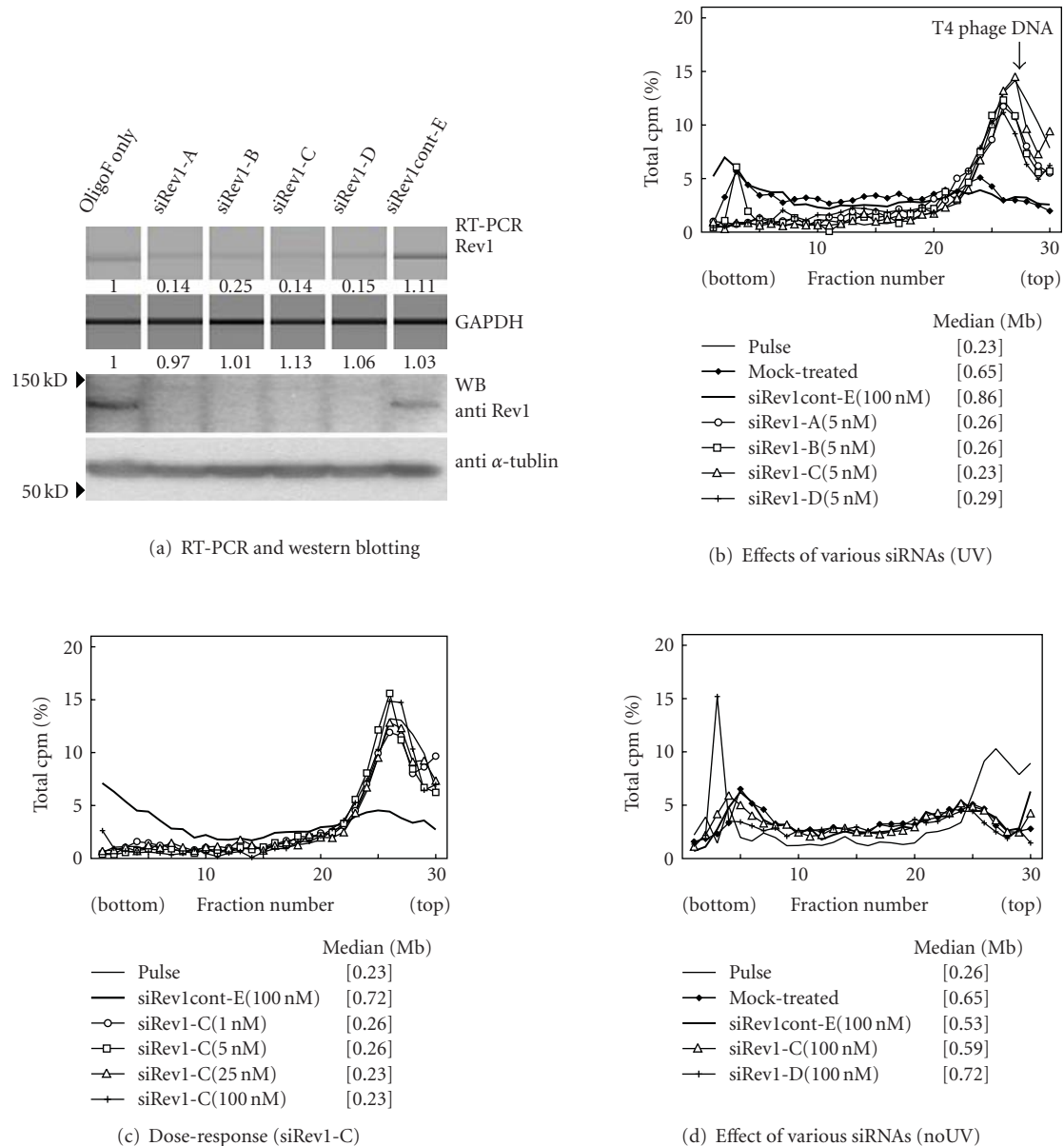


FIGURE 3: Efficient knockdown by Rev1 siRNAs and their effects on UV-induced TLS in HeLa cells (ASDG profiles of replication products). (a) Efficiency of knockdown on Rev1 expression (RT-PCR analysis and western blot analysis); (b) Effects of various Rev1 siRNAs on UV-TLS; (c) Dose-response of siRev1-C on UV-TLS; (d) Effect of various siRNAs (no UV control). Twenty-four hours after Rev1 siRNA transfection, total RNA was isolated and Rev1 RNA was quantified by RT-PCR. Results were shown in MultiNA gel images and the expression level was presented under the panel (a). Forty hours after Rev1 siRNA transfection, whole cell extracts were prepared and Rev1 protein was quantified by western blot analysis (a). Forty hours after Rev1 siRNA transfection, cells were UV-irradiated ( $10 \text{ J/m}^2$ ), incubated in normal medium for 30 minutes, pulse-labelled with  $10 \mu\text{Ci/mL}$  of  $^{14}\text{C}$ thymidine for 1 hour, then washed twice with PBS, and incubated for 5 hours at  $37^\circ\text{C}$  in normal medium (b, c). Forty hours after Rev1 siRNA transfection, cells were not UV-irradiated, pulse-labelled with  $10 \mu\text{Ci/mL}$  of  $^{14}\text{C}$ thymidine for 30 minutes, washed twice with PBS, and incubated at  $37^\circ\text{C}$  in normal medium for 1 hour (d). Some of these profiles overlap (b, c). Sedimentation is from right to left. The arrow indicates the position of T4 phage DNA (166 kb, i.e., approximately  $5.5 \times 10^7 \text{ Da}$ /single strand). Average fragment length (in Mb) of each profile is shown in square brackets.

Choi et al. [38], and the target sequence of siPol $\alpha$ -A was 4 nt downstream from the one reported by Machida et al. [39] (human Pol $\alpha$  mRNA sequence: NM.007195).

We prepared 3 siRNAs for knockdown of Pol $\kappa$  mRNA (NM.016218) (Figure 6(a)). In contrast to siPol $\alpha$ , these Pol $\kappa$  siRNAs (5 nM) delayed UV-TLS in HeLa cells

(Figure 6(b)). The siPol $\kappa$ cont-B, from siPol $\kappa$ -A with 3 nt mismatches, had little to no effect. The dose-response profile of siPol $\kappa$ -A shows that the molecule sufficiently inhibited UV-TLS at 1 nM (Figure 6(c)). The Pol $\kappa$  siRNAs had no effect on normal replication (Figure 6(d)).

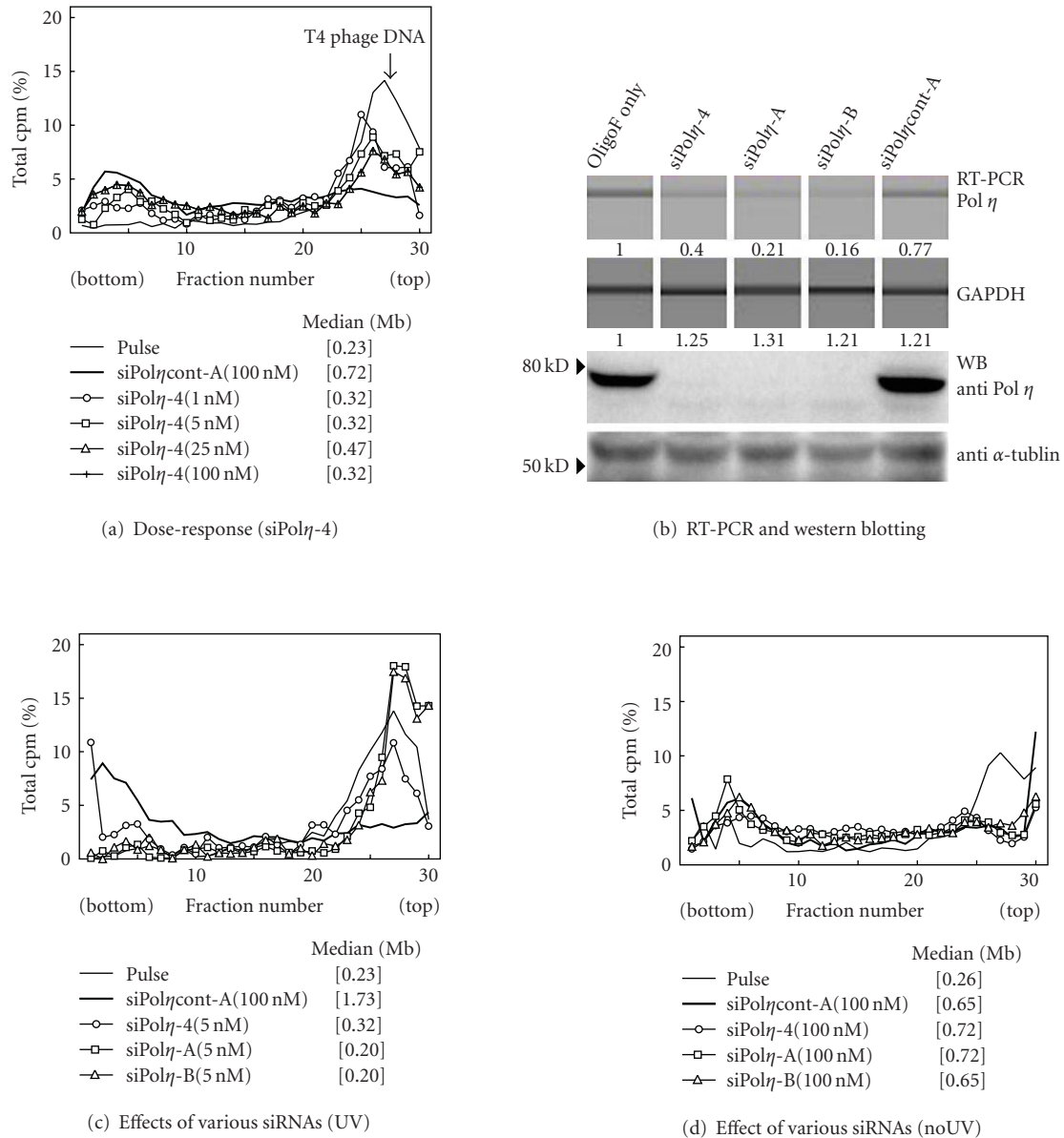


FIGURE 4: Efficient knockdown by Pol $\eta$  siRNAs and the effects on UV-induced TLS in HeLa cells (ASDG profiles of replication products). (a) Dose-response of siPol $\eta$ -4 on UV-TLS, Efficiency of knockdown on Pol $\eta$  expression; (b) RT-PCR analysis and western blot analysis, (c) Effects of various Pol $\eta$  siRNAs on UV-TLS, (d) Effect of various Pol $\eta$  siRNAs (no UV control). Twenty-four hours after Pol $\eta$  siRNA transfection, total RNA was isolated and Pol $\eta$  RNA was quantified by RT-PCR. Results were shown in MultiNA gel images and the expression level was presented under the panel (b). Forty hours after Pol $\eta$  siRNA transfection, whole cell extracts were prepared and Pol $\eta$  protein was quantified by western blot analysis (b). Forty hours after Pol $\eta$  siRNA transfection, cells were UV-irradiated (10 J/m<sup>2</sup>), incubated in normal medium for 30 minutes, pulse-labelled with 10  $\mu$ Ci/mL of [<sup>14</sup>C]thymidine for 1 hour, then washed twice with PBS, and incubated for 5 hours at 37°C in normal medium (a, c). Forty hours after Pol $\eta$  siRNA transfection, cells were not UV-irradiated, pulse-labelled with 10  $\mu$ Ci/mL of [<sup>14</sup>C]thymidine for 30 minutes, washed twice with PBS, and incubated at 37°C in normal medium for 1 hour (d). Some of these profiles overlap (d). Sedimentation is from right to left. The arrow indicates the position of T4 phage DNA (166 kb, i.e., approximately  $5.5 \times 10^7$  Da/single strand). Average fragment length (in Mb) of each profile is shown in square brackets.

#### 4. Discussion

We verified the involvement of multiple bypass polymerases in UV-TLS in HeLa cells using original siRNAs and ASDG

technique, which is consistent with the recent model of 2 polymerase mechanisms [40, 41]. Rev3 and Rev7, which comprise Pol $\zeta$ , were confirmed to participate in mutagenic UV-TLS. Also, Rev1 was suggested to play an important role

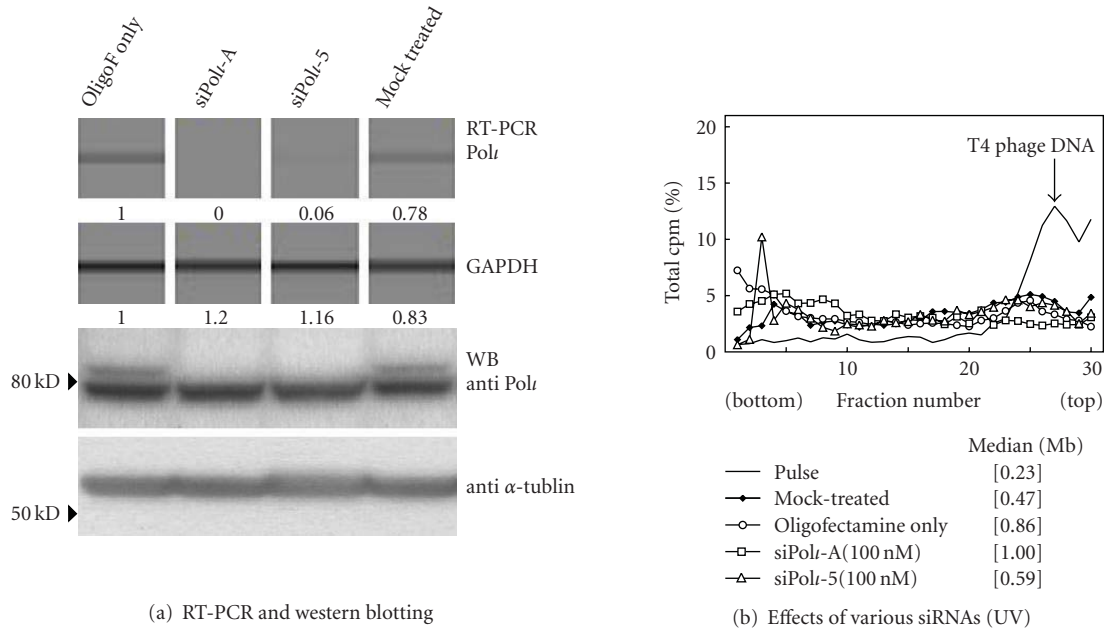


FIGURE 5: Efficient knockdown by *Polι* siRNAs and the effects on UV-induced TLS in HeLa cells (ASDG profiles of replication products). (a) Efficiency of knockdown on *Polι* expression (RT-PCR analysis and western blot analysis); (b) Effects of two *Polι* siRNAs on UV-TLS. Twenty-four hours after *Polι* siRNA transfection, total RNA was isolated and *Polι* RNA was quantified by RT-PCR. Results were shown in MultiNA gel images and the expression level was presented under the panel (a). Forty hours after *Polι* siRNA transfection, whole cell extracts were prepared and *Polι* protein was quantified by western blot analysis (a). Forty hours after *Polι* siRNA transfection, cells were UV-irradiated ( $10\text{ J/m}^2$ ), incubated in normal medium for 30 minutes, pulse-labelled with  $10\ \mu\text{Ci/mL}$  of [ $^{14}\text{C}$ ]thymidine for 1 hour, then washed twice with PBS, and incubated for 5 hours at  $37^\circ\text{C}$  in normal medium (b). Sedimentation is from right to left. The arrow indicates the position of T4 phage DNA (166 kb, i.e., approximately  $5.5 \times 10^7$  Da/single strand). Average fragment length (in Mb) of each profile is shown in square brackets.

in human TLS, although in avian DT40 cells, Rev1 may have a distinct role [42]. We were surprised to find that siRNAs against *Polη* prevented TLS to a great extent. TLS was delayed in *Polκ* siRNA-transfected cells, but not in si*Polι*-transfected cells.

We anticipated a limited participation of *Polη*, because UV-TLS in HeLa cells is very slow (i.e., inefficient) and caffeine-sensitive [35]. However, siRNAs against *Polη*, particularly si*Polη*-A and si*Polη*-B, prevented TLS to a great extent. Since both Rev3 and Rev7 siRNAs also significantly abolished UV-TLS, these results suggest that the *Polζ*-dependent TLS pathway and the *Polη*-dependent process are not mutually exclusive but overlapped.

Enzymology of yeast *Polζ* revealed that this polymerase is too faithful to insert nucleotides opposite a CPD, although it efficiently extends from a matched or mismatched 3' end [5, 6]. Therefore, we assumed that mutagenic (error-prone) TLS proceeded through the insertion by *Polι* or *Polκ* of mismatched nucleotides opposite UV photoproducts, followed by extension by *Polζ*. Our data showed, however, that si*Polι* had no effect, and si*Polκ* partially prevented TLS. These results suggest that in some cases, *Polη*, and to a lesser extent *Polκ*, may insert nucleotide(s) opposite UV photoproducts, followed by extension by *Polζ*.

*Polη* is capable of bypassing a CPD without aid of other TLS polymerases. Both yeast and human *Polη*, however, incorporate wrong nucleotide at a fairly high rate and can

extend these mismatched primer termini with only a frequency of  $\sim 10^{-2}$  to  $10^{-3}$  relative to extension from matched primer termini [6, 43]. Plausibly, *Polη* dissociates from there and the proof-reading exonuclease of *Polδ* removes the wrong nucleotide [44]. To the primer termini, *Polη* is recruited again and incorporates a new nucleotide. This cycle is repeated until *Polη* incorporates a correct nucleotide. We suppose that disruption or malfunction of this cooperation renders mismatched primer termini accessible to *Polζ*.

Recently, Yoon et al. published 2 papers describing the effects of siRNA knockdown on the efficiency of TLS at TT-CPD [45] or (6-4)TT PP [46] on duplex plasmids in human cells. They also reported the effects of siRNA knockdown on mutation frequencies in the  $\lambda$  phage *cII* gene lysogenized in mouse cells expressing a (6-4)PP photolyase [45] or CPD photolyase [46]. The results of this tremendous and detailed study demonstrated that Pals  $\eta$ ,  $\kappa$ , and  $\zeta$  contribute to CPD bypass, wherein Pals  $\kappa$  and  $\zeta$  promote mutagenic TLS and *Polη* executes error-free bypasses (*Polι* siRNA had no effect) [45]. As for (6-4)PP bypass, Pals  $\eta$  and  $\iota$  provide alternate pathways for mutagenic TLS, and *Polζ* acts in a predominantly error-free manner (*Polκ* siRNA had no effect) [46].

The participation of Pals  $\kappa$  or  $\iota$  in CPD bypass was similarly demonstrated by our results and those of Yoon et al. [45]. Because (6-4)PP is a minor photoproduct, which is removed predominantly by NER, and because HeLa cells

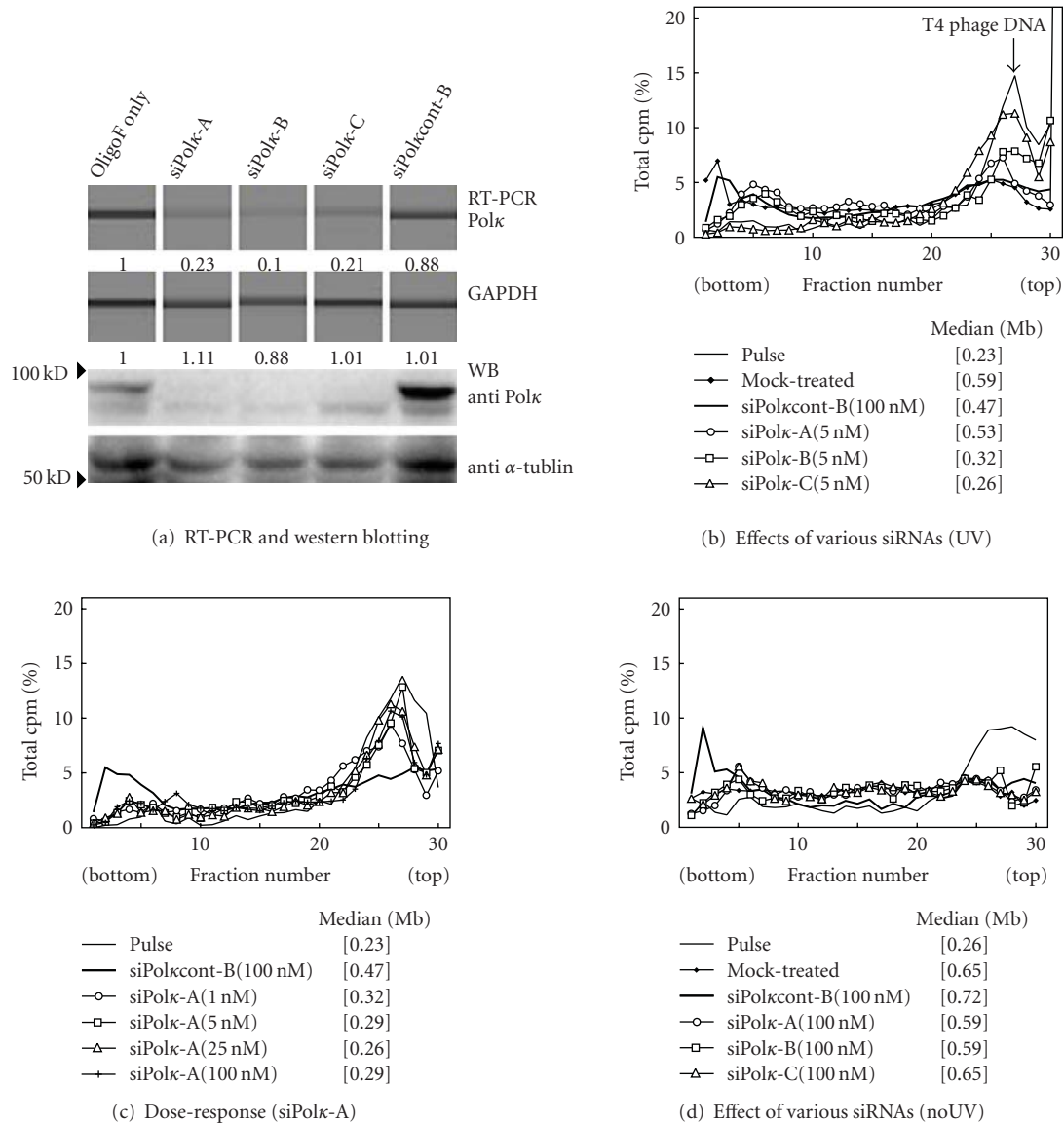


FIGURE 6: Efficient knockdown by *Polk* siRNAs and the effects on UV-induced TLS in HeLa cells (ASDG profiles of replication products). (a) Efficiency of knockdown on *Polk* expression (RT-PCR analysis and western blot analysis), (b) Effects of various *Polk* siRNAs on UV-TLS, (c) Dose-response of siPolk-A on UV-TLS, (d) Effect of various *Polk* siRNAs (no UV control). Twenty-four hours after *Polk* siRNA transfection, total RNA was isolated and *Polk* RNA was quantified by RT-PCR. Results were shown in MultiNA gel images and the expression level was presented under the panel (a). Forty hours after *Polk* siRNA transfection, whole cell extracts were prepared, and *Polk* protein was quantified by western blot analysis (a). Forty hours after *Polk* siRNA transfection, cells were UV-irradiated ( $10 \text{ J/m}^2$ ), incubated in normal medium for 30 minutes, pulse-labelled with  $10 \mu\text{Ci/mL}$  of  $^{14}\text{C}$ thymidine for 1 hour, then washed twice with PBS, and incubated for 5 hours at  $37^\circ\text{C}$  in normal medium (b, c). Forty hours after *Polk* siRNA transfection, cells were not UV-irradiated, pulse-labelled with  $10 \mu\text{Ci/mL}$  of  $^{14}\text{C}$ thymidine for 30 minutes, washed twice with PBS, and incubated at  $37^\circ\text{C}$  in normal medium for 1 hour (d). Some of these profiles overlap (c, d). Sedimentation is from right to left. The arrow indicates the position of T4 phage DNA (166 kb, i.e., approximately  $5.5 \times 10^7 \text{ Da}$ /single strand). Average fragment length (in Mb) of each profile is shown in square brackets.

possess high NER activity (unpublished observation), it is reasonable to conclude that our phenomena observed in HeLa cells by ASDG are largely attributable to CPD, although we have not yet determined the extent of remaining (6-4)PP.

We may also conclude that Rev1 is indispensable for TLS across CPD. Thus far, it is unknown if Rev1 is equally involved in TLS across CPD and (6-4)PP, or if it exhibits

some preference. Nelson et al. [25] demonstrated that Rev1p participates in UV-TLS across (6-4)PP, based on yeast transfected with a (6-4)PP-carrying plasmid; only slight differences were observed with a CPD-carrying plasmid.

*In vitro* lesion-bypass assay showed that Pol $\eta$  alone accomplishes bypass across TT-CPD as above (i.e., both insertion and extension) [8, 9]. However, Yoon et al.

presented complex results showing involvement of multiple bypass polymerases. They used SV-untransformed XP-A and XP-V cells, but did not include SV-untransformed normal fibroblasts, wherein we detected quick and caffeine-insensitive UV-TLS [35, 36]. It is possible that the kind of damage, as well as cell status (normal, transformed, or cancerous) may determine the participation of bypass polymerase(s).

We have presented the first apparent evidence that Pol $\kappa$  participates in UV-TLS. Pol $\kappa$  knockout mouse embryonic cells are known to be UV sensitive [47], but the mechanism had not yet been determined. Pol $\kappa$  is also thought to play a part in the repair-synthesis step of NER [48, 49]. From the results of lesion-bypass assays, human Pol $\kappa$  was suggested to be unable to bypass CPD or (6-4)PP. Because the outcomes of such *in vitro* assays depend on the assay conditions [12], these results must be validated *in vivo*, such as by ASDG analysis.

## 5. Conclusions

Using siRNAs originally designed and ASDG technique, we verified the participation of multiple bypass polymerases in UV-induced TLS in HeLa cells, which is the consistent with recent model of 2 polymerase mechanisms. UV-TLS was largely abolished by siRNAs to Rev3 or Rev7, suggesting that these 2 proteins, which constitute Pol $\zeta$ , play a primary role in mutagenic TLS. Rev1-targeted siRNAs also significantly abolished UV-TLS, consistent with prior suggestions that Rev1 is indispensable in mammalian mutagenic TLS. Unexpectedly, siRNAs to Pol $\eta$  prevented TLS to a great extent, implying that the Pol $\eta$ - and Pol $\zeta$ -dependent processes do not alternate but overlap. Pol $\kappa$  siRNAs, but not siRNAs to Pol $\iota$ , delayed TLS; this is the first apparent evidence for the participation of Pol $\kappa$  in UV-TLS.

## Acknowledgments

The authors are grateful to Dr. Hisao Masai (Tokyo Metropolitan Institute of Medical Science) for kind advice to siRNA design and transfection. This work was supported in part by Grants for Nuclear Research and Scientific Research from the Ministry of Education, Culture, Sports, Science, and Technology, Japan and by a Grant from the Mishima Kaiun Memorial Foundation. The author have no financial conflict of interests.

## References

- [1] A. R. Lehmann, A. Niimi, T. Ogi et al., "Translesion synthesis: Y-family polymerases and the polymerase switch," *DNA Repair*, vol. 6, no. 7, pp. 891–899, 2007.
- [2] E. C. Friedberg, G. C. Walker, and W. Siede, *DNA Repair and Mutagenesis*, ASM Press, Washington, DC, USA, 1995.
- [3] M. J. Horsfall, A. Borden, and C. W. Lawrence, "Mutagenic properties of the T-C cyclobutane dimer," *Journal of Bacteriology*, vol. 179, no. 9, pp. 2835–2839, 1997.
- [4] D. L. Mitchell and R. S. Nairn, "The biology of the (6-4) photoproduct," *Photochemistry and Photobiology*, vol. 49, no. 6, pp. 805–819, 1989.
- [5] S. Prakash and L. Prakash, "Translesion DNA synthesis in eukaryotes: a one- or two-polymerase affair," *Genes and Development*, vol. 16, no. 15, pp. 1872–1883, 2002.
- [6] S. Prakash, R. E. Johnson, and L. Prakash, "Eukaryotic translesion synthesis DNA polymerases: specificity of structure and function," *Annual Review of Biochemistry*, vol. 74, pp. 317–353, 2005.
- [7] J. E. Cleaver and K. H. Kraemer, "Xeroderma pigmentosum and cockayne syndrome," in *The Metabolic and Molecular Basis of Inherited Disease*, C. R. Scriver, A. L. Beaudet, W. S. Sly, and D. Valle, Eds., vol. 3, pp. 4393–4419, McGraw-Hill, New York, NY, USA, 7th edition, 1995.
- [8] C. Masutani, R. Kusumoto, S. Iwai, and F. Hanaoka, "Mechanisms of accurate translesion synthesis by human DNA polymerase  $\eta$ ," *EMBO Journal*, vol. 19, no. 12, pp. 3100–3109, 2000.
- [9] C. Masutani, R. Kusumoto, A. Yamada et al., "Xeroderma pigmentosum variant: from a human genetic disorder to a novel DNA polymerase," *Cold Spring Harbor Symposia on Quantitative Biology*, vol. 65, pp. 71–80, 2000.
- [10] S. Prakash, R. E. Johnson, M. T. Washington, L. Haracska, C. M. Kondratieck, and L. Prakash, "Role of yeast and human DNA polymerase  $\eta$  in error-free replication of damaged DNA," *Cold Spring Harbor Symposia on Quantitative Biology*, vol. 65, pp. 51–59, 2000.
- [11] C. Masutani, R. Kusumoto, A. Yamada et al., "The XPV (xeroderma pigmentosum variant) gene encodes human DNA polymerase  $\eta$ ," *Nature*, vol. 399, no. 6737, pp. 700–704, 1999.
- [12] J. P. McDonald, V. Rapić-Otrin, J. A. Epstein et al., "Novel human and mouse homologs of *Saccharomyces cerevisiae* DNA polymerase  $\eta$ ," *Genomics*, vol. 60, no. 1, pp. 20–30, 1999.
- [13] A. Tissier, E. G. Frank, J. P. McDonald, S. Iwai, F. Hanaoka, and R. Woodgate, "Misinsertion and bypass of thymine-thymine dimers by human DNA polymerase  $\iota$ ," *EMBO Journal*, vol. 19, no. 19, pp. 5259–5266, 2000.
- [14] V. L. Gerlach, W. J. Feaver, P. L. Fischhaber et al., "Human DNA polymerase  $\kappa$ : a novel DNA polymerase of unknown biological function encoded by the *DINB1* gene," *Cold Spring Harbor Symposia on Quantitative Biology*, vol. 65, pp. 41–49, 2000.
- [15] E. Ohashi, T. Ogi, R. Kusumoto et al., "Error-prone bypass of certain DNA lesions by the human DNA polymerase  $\kappa$ ," *Genes and Development*, vol. 14, no. 13, pp. 1589–1594, 2000.
- [16] E. Ohashi, K. Bebenek, T. Matsuda et al., "Fidelity and processivity of DNA synthesis by DNA polymerase  $\kappa$ , the product of the human *DINB1* gene," *Journal of Biological Chemistry*, vol. 275, no. 50, pp. 39678–39684, 2000.
- [17] C. W. Lawrence and R. B. Christensen, "Ultraviolet-induced reversion of *cyc1* alleles in radiation-sensitive strains of yeast. III. rev3 mutant strains," *Genetics*, vol. 92, no. 2, pp. 397–408, 1979.
- [18] P. E. M. Gibbs, X.-D. Wang, Z. Li et al., "The function of the human homolog of *Saccharomyces cerevisiae* REV1 is required for mutagenesis induced by UV light," *Proceedings of the National Academy of Sciences of the United States of America*, vol. 97, no. 8, pp. 4186–4191, 2000.
- [19] P. E. M. Gibbs, W. G. McGregor, V. M. Maher, P. Nisson, and C. W. Lawrence, "A human homolog of the *Saccharomyces cerevisiae* REV3 gene, which encodes the catalytic subunit of DNA polymerase  $\zeta$ ," *Proceedings of the National Academy of Sciences of the United States of America*, vol. 95, no. 12, pp. 6876–6880, 1998.
- [20] Y. Murakumo, T. Roth, H. Ishii et al., "A human REV7 homolog that interacts with the polymerase  $\zeta$  catalytic subunit

- hREV3 and the spindle assembly checkpoint protein hMAD2,” *Journal of Biological Chemistry*, vol. 275, no. 6, pp. 4391–4397, 2000.
- [21] C. W. Lawrence, “Cellular roles of DNA polymerase  $\zeta$  and Rev1 protein,” *DNA Repair*, vol. 1, no. 6, pp. 425–435, 2002.
- [22] Z. Li, H. Zhang, T. P. McManus, J. J. McCormick, C. W. Lawrence, and V. M. Maher, “hREV3 is essential for error-prone translesion synthesis past UV or benzo[a]pyrene diol epoxide-induced DNA lesions in human fibroblasts,” *Mutation Research*, vol. 510, no. 1-2, pp. 71–80, 2002.
- [23] K. McNally, J. A. Neal, T. P. McManus, J. J. McCormick, and V. M. Maher, “hRev7, putative subunit of hPol $\zeta$ , plays a critical role in survival, induction of mutations, and progression through S-phase, of UV(254 nm)-irradiated human fibroblasts,” *DNA Repair*, vol. 7, no. 4, pp. 597–604, 2008.
- [24] M. Diaz, N. B. Watson, G. Turkington, L. K. Verkoczy, N. R. Klinman, and W. G. McGregor, “Decreased frequency and highly aberrant spectrum of ultraviolet-induced mutations in the hprt gene of mouse fibroblasts expressing antisense RNA to DNA polymerase  $\zeta$ ,” *Molecular Cancer Research*, vol. 1, no. 11, pp. 836–847, 2003.
- [25] J. R. Nelson, P. E. M. Gibbs, A. M. Nowicka, D. C. Hinkle, and C. W. Lawrence, “Evidence for a second function for *Saccharomyces cerevisiae* Rev1p,” *Molecular Microbiology*, vol. 37, no. 3, pp. 549–554, 2000.
- [26] C. Guo, T.-S. Tang, M. Bienko et al., “Ubiquitin-binding motifs in REV1 protein are required for its role in the tolerance of DNA damage,” *Molecular and Cellular Biology*, vol. 26, no. 23, pp. 8892–8900, 2006.
- [27] C. Guo, P. L. Fischhaber, M. J. Luk-Paszyc et al., “Mouse Rev1 protein interacts with multiple DNA polymerases involved in translesion DNA synthesis,” *EMBO Journal*, vol. 22, no. 24, pp. 6621–6630, 2003.
- [28] P. L. Kannouche, J. Wing, and A. R. Lehmann, “Interaction of human DNA polymerase  $\eta$  with monoubiquitinated PCNA: a possible mechanism for the polymerase switch in response to DNA damage,” *Molecular Cell*, vol. 14, no. 4, pp. 491–500, 2004.
- [29] K. Watanabe, S. Tateishi, M. Kawasuji, T. Tsurimoto, H. Inoue, and M. Yamaizumi, “Rad18 guides pol $\eta$  to replication stalling sites through physical interaction and PCNA monoubiquitination,” *EMBO Journal*, vol. 23, no. 19, pp. 3886–3896, 2004.
- [30] P. L. Fischhaber and E. C. Friedberg, “How are specialized (low-fidelity) eukaryotic polymerases selected and switched with high-fidelity polymerases during translesion DNA synthesis?” *DNA Repair*, vol. 4, no. 2, pp. 279–283, 2005.
- [31] A. R. Lehmann, S. Kirk Bell, C. F. Arlett et al., “Xeroderma pigmentosum cells with normal levels of excision repair have a defect in DNA synthesis after UV irradiation,” *Proceedings of the National Academy of Sciences of the United States of America*, vol. 72, no. 1, pp. 219–223, 1975.
- [32] A. R. Lehmann, “Postreplication repair of DNA in ultraviolet-irradiated mammalian cells,” *Journal of Molecular Biology*, vol. 66, no. 3, pp. 319–337, 1972.
- [33] A. R. Lehmann, “Postreplication repair of DNA in mammalian cells,” *Life Sciences*, vol. 15, no. 12, pp. 2005–2016, 1974.
- [34] K. Yamada, Y. Kameyama, and S. Inoue, “An improved method of alkaline sucrose density gradient sedimentation to detect less than one lesion per 1 Mb DNA,” *Mutation Research*, vol. 364, no. 2, pp. 125–131, 1996.
- [35] K. Yamada, J. Takezawa, and O. Ezaki, “Translesion replication in cisplatin-treated xeroderma pigmentosum variant cells is also caffeine-sensitive: features of the error-prone DNA polymerase(s) involved in UV-mutagenesis,” *DNA Repair*, vol. 2, no. 8, pp. 909–924, 2003.
- [36] J. Takezawa, Y. Ishimi, and K. Yamada, “Proteasome inhibitors remarkably prevent translesion replication in cancer cells but not normal cells,” *Cancer Science*, vol. 99, no. 5, pp. 863–871, 2008.
- [37] J.-H. Choi and G. P. Pfeifer, “The role of DNA polymerase  $\eta$  in UV mutational spectra,” *DNA Repair*, vol. 4, no. 2, pp. 211–220, 2005.
- [38] J.-H. Choi, A. Besaratinia, D.-H. Lee, C.-S. Lee, and G. P. Pfeifer, “The role of DNA polymerase  $\iota$  in UV mutational spectra,” *Mutation Research*, vol. 599, no. 1-2, pp. 58–65, 2006.
- [39] K. Machida, K. T.-N. Cheng, V. M.-H. Sung et al., “Hepatitis C virus induces a mutator phenotype: enhanced mutations of immunoglobulin and protooncogenes,” *Proceedings of the National Academy of Sciences of the United States of America*, vol. 101, no. 12, pp. 4262–4267, 2004.
- [40] S. Shachar, O. Ziv, S. Avkin et al., “Two-polymerase mechanisms dictate error-free and error-prone translesion DNA synthesis in mammals,” *EMBO Journal*, vol. 28, no. 4, pp. 383–393, 2009.
- [41] J. K. Hicks, C. L. Chute, M. T. Paulsen et al., “Differential roles for DNA polymerases eta, zeta, and REV1 in lesion bypass of intrastrand versus interstrand DNA cross-links,” *Molecular and Cellular Biology*, vol. 30, no. 5, pp. 1217–1230, 2010.
- [42] C. E. Edmunds, L. J. Simpson, and J. E. Sale, “PCNA ubiquitination and REV1 define temporally distinct mechanisms for controlling translesion synthesis in the avian cell line DT40,” *Molecular Cell*, vol. 30, no. 4, pp. 519–529, 2008.
- [43] T. Matsuda, K. Bebenek, C. Masutani, F. Hanaoka, and T. A. Kunkel, “Low fidelity DNA synthesis by human DNA polymerase- $\eta$ ,” *Nature*, vol. 404, no. 6781, pp. 1011–1013, 2000.
- [44] K. Bebenek, T. Matsuda, C. Masutani, F. Hanaoka, and T. A. Kunkel, “Proofreading of DNA polymerase  $\eta$ -dependent replication errors,” *Journal of Biological Chemistry*, vol. 276, no. 4, pp. 2317–2320, 2001.
- [45] J.-H. Yoon, L. Prakash, and S. Prakash, “Highly error-free role of DNA polymerase  $\eta$  in the replicative bypass of UV-induced pyrimidine dimers in mouse and human cells,” *Proceedings of the National Academy of Sciences of the United States of America*, vol. 106, no. 43, pp. 18219–18224, 2009.
- [46] J.-H. Yoon, L. Prakash, and S. Prakash, “Error-free replicative bypass of (6–4) photoproducts by DNA polymerase  $\zeta$  in mouse and human cells,” *Genes and Development*, vol. 24, no. 2, pp. 123–128, 2010.
- [47] T. Ogi, Y. Shinkai, K. Tanaka, and H. Ohmori, “Polk protects mammalian cells against the lethal and mutagenic effects of benzo[a]pyrene,” *Proceedings of the National Academy of Sciences of the United States of America*, vol. 99, no. 24, pp. 15548–15553, 2002.
- [48] T. Ogi and A. R. Lehmann, “The Y-family DNA polymerase  $\kappa$  (pol  $\kappa$ ) functions in mammalian nucleotide-excision repair,” *Nature Cell Biology*, vol. 8, no. 6, pp. 640–642, 2006.
- [49] T. Ogi, S. Limsirichaikul, R. M. Overmeer et al., “Three DNA polymerases, recruited by different mechanisms, carry out NER repair synthesis in human cells,” *Molecular Cell*, vol. 37, no. 5, pp. 714–727, 2010.

## Review Article

# Translesion Synthesis Polymerases in the Prevention and Promotion of Carcinogenesis

L. Jay Stallons<sup>1</sup> and W. Glenn McGregor<sup>1,2,3</sup>

<sup>1</sup>Department of Pharmacology and Toxicology, James Graham Brown Cancer Center, University of Louisville School of Medicine, Louisville, KY 40202, USA

<sup>2</sup>Department of Medicine (Medical Oncology), James Graham Brown Cancer Center, University of Louisville School of Medicine, Louisville, KY 40202, USA

<sup>3</sup>Clinical and Translational Research, 505 S. Hancock Street, Louisville, KY 40202, USA

Correspondence should be addressed to W. Glenn McGregor, wgmcmgregor@louisville.edu

Received 16 June 2010; Accepted 13 August 2010

Academic Editor: Ashis Basu

Copyright © 2010 L. J. Stallons and W. G. McGregor. This is an open access article distributed under the Creative Commons Attribution License, which permits unrestricted use, distribution, and reproduction in any medium, provided the original work is properly cited.

A critical step in the transformation of cells to the malignant state of cancer is the induction of mutations in the DNA of cells damaged by genotoxic agents. Translesion DNA synthesis (TLS) is the process by which cells copy DNA containing unrepaired damage that blocks progression of the replication fork. The DNA polymerases that catalyze TLS in mammals have been the topic of intense investigation over the last decade. DNA polymerase  $\eta$  (Pol  $\eta$ ) is best understood and is active in error-free bypass of UV-induced DNA damage. The other TLS polymerases (Pol  $\iota$ , Pol  $\kappa$ , REV1, and Pol  $\zeta$ ) have been studied extensively *in vitro*, but their *in vivo* role is only now being investigated using knockout mouse models of carcinogenesis. This paper will focus on the studies of mice and humans with altered expression of TLS polymerases and the effects on cancer induced by environmental agents.

## 1. Introduction

Tumorigenesis is a multistep process beginning with the transformation of a single cell by the accumulation of at least six distinct characteristics. These include infinite lifespan, resistance to antigrowth signals, resistance to apoptosis, autocrine production of growth signals, sustained angiogenesis, and tissue invasion [1]. Most environmental carcinogens induce transformation by causing mutations in the DNA that alter the activity of protooncogenes or tumor suppressors. These mutations are formed when residual, unrepaired DNA damage stalls progression of the replication fork during S phase. Stalled replication forks are most frequently resolved using error-free mechanisms that include homologous recombination or use of the homologous nascent strand as a template. Nevertheless, replication may proceed using the damaged strand as a template in an error-prone process known as translesion DNA synthesis (TLS). TLS is defined as the incorporation of a nucleotide across from DNA damage followed by extension of the potentially

mispaired primer-template, and can be error-free or error-prone. Cellular commitment to error-free, recombinatorial damage avoidance or error-prone TLS is modulated by the molecular switch PCNA (Figure 1). Cells presumably risk mutations caused by TLS to relieve replication fork blockage at DNA adducts and to avoid the potential formation of extremely cytotoxic double strand breaks (DSB). Although it accounts for less than 10% of all bypass synthesis events in yeast [2], the frequency of potentially mutagenic TLS may be as high as 50% in higher eukaryotes [3–5]. The propensity and mutagenic potential of TLS explain why it is etiologic in most environmentally-induced cancers and has been the focus of numerous investigations over the past decade.

TLS is performed by a relatively new category of accessory DNA polymerases. Polymerase  $\eta$  (Pol  $\eta$ ), Pol  $\iota$ , Pol  $\kappa$ , and REV1 in the Y-family [6] and Pol  $\zeta$  in the B-family [7, 8] are responsible for most TLS in mammalian cells. These proteins have active sites that are larger and more open than those of the high-fidelity replicative DNA polymerases (Pol  $\alpha$ ,  $\delta$ , and  $\epsilon$ ), allowing accommodation of and synthesis past

DNA templates with large, helix-distorting lesions [9]. This unique ability to synthesize DNA opposite bulky adducts helps cells avoid double strand breaks associated with replication fork stalling, but can also lead to mutagenesis by incorrect base addition. It is important to note that polymerases in the Y-family are expressed in all three kingdoms of life, indicating a critical and evolutionarily conserved role for these proteins [6]. The obviously conflicting roles of these enzymes in both preventing and promoting genetic instability are reflected in the tight cellular control of the TLS pathway (Figure 1). Although extensive *in vitro* studies have given us a better understanding of their role in the cell, much less is known about the function of TLS polymerases in living animals. Limited epidemiological studies have been conducted to associate single nucleotide polymorphisms (SNPs) with cancer risk in humans. Knockout mice have been generated for each gene, and carcinogenesis studies are published or underway. Importantly, studies in mice and humans have shown that TLS polymerases, particularly Pol  $\eta$ , are involved in immunoglobulin gene hypermutation. Readers are directed to reviews by Reynaud et al. and Diaz et al. for an exploration of this function of TLS polymerases [10, 11]. This review will focus on the rapidly progressing connection of TLS and cancer research in knockout mice and human populations.

## 2. REV1

REV1 was discovered in budding yeast by the Lawrence group in 1989 as a component of the Pol  $\zeta$  complex [17]. The catalytic activity of REV1 is limited to insertion of dCMP across from a template dG [18]. The human homolog was cloned in 1999 and has the same template-dependent dCMP transferase catalytic activity on an undamaged template or an abasic site [19]. One locus used in eukaryotic cells to measure mutation frequency is *HPRT*, a gene involved in the purine salvage pathway. In this forward mutation assay, cells with loss-of-function mutations in *HPRT* are resistant to the drug 6-thioguanine (TG). REV1 is required for carcinogen-induced *HPRT* mutagenesis in human cells [20–22], but the catalytic activity appears to be dispensable for the induction of UV-induced mutations [23, 24], indicating that this protein probably plays a structural rather than catalytic role in UV mutagenesis.

Cells from mice with a targeted deletion of the BRCA1 C-terminal (BRCT) homology domain of Rev1 (*Rev1<sup>B/B</sup>*) have a reduced UV-induced mutation frequency at the *Hprt* locus [25]. However, the animals have a paradoxically decreased latency of squamous cell carcinoma (SCC) formation and only marginally reduced p53 mutagenesis in the skin after UV exposure [26]. Despite *Rev1<sup>B/B</sup>* cells showing a moderate increase in chromatid breaks and exchanges after UV *in vitro* [25], comparative genomic hybridization of UV-induced SCC and normal skin DNA reveals no increase in the frequency of gross genomic alterations in *Rev1<sup>B/B</sup>* SCC [26]. If point mutations and chromosomal rearrangements are near normal levels in BRCT-deleted *Rev1<sup>B/B</sup>* mice, what is the reason for accelerated SCC development? Acute UV exposure

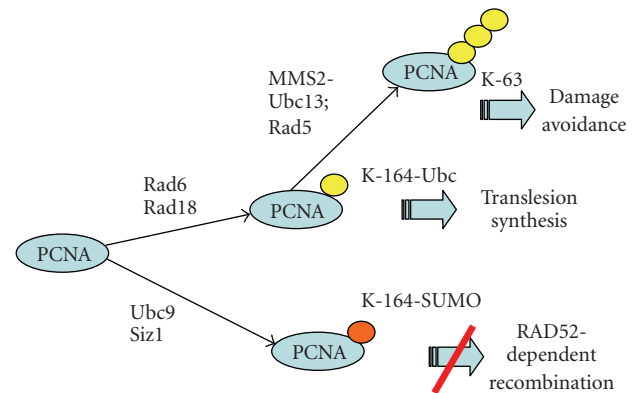


FIGURE 1: Regulation of DNA lesion bypass in *Saccharomyces cerevisiae* and humans. Bulky DNA lesions can cause blockage of replicative polymerases and replication fork stalling. The ubiquitin conjugase/ubiquitin ligase pair Rad6/Rad18 is recruited to stalled replication forks where the proteins catalyze monoubiquitylation of PCNA at lysine 164. TLS proteins such as REV1 and Pol  $\eta$  have increased affinity for monoubiquitylated PCNA, which facilitates their recruitment and the completion of TLS. In yeast, Rad5 and the MMS2-Ubc13 complex (UBE2V2-UBE2N in humans) can catalyze polyubiquitylation of PCNA via lysine 63 of ubiquitin, which blocks TLS and activates error-free damage avoidance. Damage avoidance includes template switching, during which the nascent DNA strand from the sister duplex is used as an undamaged homologous template to replicate past the lesion. Humans express two Rad5 homologs, SHPRH and HLF1, and both catalyze K-63-linked polyubiquitylation of PCNA in human cells [12–15]. In yeast, Ubc9-Siz1 can attach the small ubiquitin-like modifier (SUMO) to lysine 164 of PCNA in a reaction that competes with Rad6/Rad18-mediated monoubiquitylation. PCNA SUMOylation at K-164 attracts the helicase Srs2 and prevents error-prone RAD52-dependent recombination. Reproduced with permission from Watson et al. [16].

of these *Rev1*-mutant mice induces enhanced Atr signaling, senescence, and apoptosis in the skin. However, long-term low-dose UV exposure causes a mitogenic response, as evidenced by epidermal hyperplasia, decreased apoptosis, and increased proliferation of CPD-containing keratinocytes [26]. Based on literature reports of the etiological role of IL-6 in carcinogenesis and elevated IL-6 levels in the skin after a single subtoxic UV dose, the authors conclude that error-prone TLS of UV-induced DNA damage is responsible for suppressing the proinflammatory, tumor-promoting effects of UV in the skin. However, more direct immunological studies are needed to confirm that Rev1 suppresses UV-induced inflammation and tumor suppression.

REV1 has also been implicated in TLS across other types of DNA lesions. Benzo[a]pyrenedi-oxide (BPDE) is the primary carcinogenic metabolite of B[a]P and causes point mutations in a REV1-dependent manner [22, 27]. BPDE-induced *Hprt* mutations are dramatically decreased in primary mouse fibroblasts after ribozyme-mediated *Rev1*-knockdown. When a plasmid expressing this ribozyme is delivered to the lungs of A/J mice by aerosol nebulization,

*Rev1* mRNA is reduced by ~ %50 in the bronchial epithelium. This targeted gene therapy causes a ~ %40 reduction in the lung tumor multiplicity after B[a]P treatment. In addition, only 73% of ribozyme-treated mice develop lung adenomas after B[a]P, compared with 100% penetrance in control animals [28]. This report highlights the potential for interrupting translesion synthesis as a chemoprevention strategy.

Although no human disorder involving *REV1* deficiency is known, there are 16 SNPs in humans that result in nonsynonymous amino acid changes. The F257S SNP, which lies outside of all known functional domains of the protein, has been associated with an increased risk of squamous cell carcinoma of the lung in patients who have ever smoked cigarettes [29]. However, this association remains controversial [30]. The same F257S SNP was associated with decreased risk of cervical cancer, and N373S within the catalytic domain was associated with increased risk of cervical cancer. Both effects were specific for squamous cell carcinoma and not relevant for adenocarcinoma of the cervix [31]. Although the functional consequences of these polymorphisms are unknown, these studies support a role for *REV1* in the formation of multiple internal cancers.

### 3. Pol $\eta$

The study of translesion synthesis in mammals began in 1999 with the discovery of the molecular defect that results in Xeroderma Pigmentosum (XP) variant syndrome. All XP patients have dramatically increased susceptibility to UV-induced skin cancer [32]. Patients in complementation groups A through G are deficient in nucleotide excision repair (NER), the major pathway for removal of helix-distorting lesions, including those induced by UV. However, the XP variant subset of patients has normal NER activity [33, 34], yet displays the skin cancer-prone phenotype of NER-deficient patients. The XP variant mystery persisted for nearly three decades. Intensive investigations indicate that after UV-irradiation cells from these patients have difficulty exiting S-phase that is exacerbated by caffeine [35, 36]. Further, these cells are extremely hypermutable after UV [37]. In 1999, two groups independently discovered that XP variant patients carry autosomal recessive mutations in *POLH*, the human gene coding for Pol  $\eta$ , and that the enzyme can catalyze error-free DNA synthesis across from a template TT cyclobutane pyrimidine dimer (CPD) [38–40]. The dramatic increase in skin cancer risk of XP variant patients could now be explained by the absence of a critical translesion DNA polymerase. UV principally induces photoaddition products between intrastrand adjacent pyrimidines, the most frequent of which are TT CPD. These lesions block progression of the replication fork. Data indicate that helicase activity may continue in spite of the blocked replication complex, resulting in single-stranded DNA that is rapidly coated with replication protein A (RPA). This appears to attract the ubiquitin ligase RAD18, which has binding sites for the ubiquitin conjugase RAD6, Pol  $\eta$ , and RPA. One target of

ubiquitylation is PCNA. Since Pol  $\eta$  has a ubiquitin binding domain, Pol  $\eta$  is now thought to be preferentially attracted to the stalled fork because it is chaperoned directly by RAD18 and binds to the ubiquitylated PCNA (Figure 1) [41]. Data indicate that Pol  $\eta$  then incorporates AA across from TT CPD in the template. In the absence of Pol  $\eta$ , another translesion polymerase, which is potentially error-prone when bypassing these common UV-induced lesions, accesses the damaged template (reviewed in [42, 43]). Generation of Pol  $\eta$ -knockout mice shows that the highly homologous mouse Pol  $\eta$  protein functions similarly in UV-induced mutagenesis and carcinogenesis. Pol  $\eta$ -deficient mice develop squamous cell carcinoma with 100% penetrance at a UV fluence that does not cause any tumors in wild-type littermates. In addition, approximately one-third of heterozygous mice develop cancer after UV exposure [44]. This raises the possibility that humans carrying heterozygous mutations in the *POLH* gene may have an increased risk of developing skin cancer. However, this speculation has not been clinically investigated.

There is evidence that XP variant patients develop internal cancers faster than Pol  $\eta$ -proficient individuals [45, 46], raising the possibility that Pol  $\eta$ -deficiency is involved in the formation of multiple human cancers caused by DNA damaging agents other than UV. Six SNPs in *POLH* have been found to date that result in nonsynonymous amino acid substitutions, but their functional significance is unknown. There is a single study evaluating the effects on cancer risk of *POLH* polymorphisms. Flanagan and colleagues found no significant changes in coding-region SNPs of *POLH* among 40 basal cell carcinoma and squamous cell carcinoma patients in a fair-skinned Irish population [47]. It is clear that larger epidemiological studies of *POLH* status are needed to evaluate the effects of *POLH* polymorphisms.

### 4. Pol $\iota$

DNA polymerase  $\iota$  (Pol  $\iota$ ) was discovered in 1999 as a novel homolog of Pol  $\eta$  in mammals and is encoded by the human *POLI* gene [48]. *In vitro* studies with purified enzyme indicate error-prone TLS function on almost all substrates examined, perhaps due to the still controversial ability of Pol  $\iota$  to incorporate incoming nucleotides using Hoogsteen base pairing [49, 50]. Exhaustive characterization of the error-prone replication properties of Pol  $\iota$  has lent credibility to the hypothesis that *Poli* is a candidate gene for the Pulmonary adenoma resistance 2 (*Par2*) locus in mice [51–53]. The *Par2* locus was identified in 1996 by chromosomal linkage mapping between BALB/cJ and A/J mouse strains and plays a major role in the relative resistance of BALB mice versus the A/J strain to developing urethane-induced lung adenomas [54]. Wang et al. identified ten amino acid-substitution polymorphisms between A/J and BALB mice that produce changes in substrate recognition of Pol  $\iota$ ; while the enzyme from both strains is functional, the isoform expressed in BALB mice may be more accurate on certain undamaged templates [52]. These studies

suggest that Pol  $\iota$  acts to suppress urethane-induced lung adenomas. It has been hypothesized that this activity is due to the augmentation of base excision repair (BER) by Pol  $\iota$ , because the enzyme has 5′ deoxyribose phosphate (dRP) lyase activity and can partially reconstitute the BER-deficiency of Pol  $\beta$ -null cells *in vitro* [55]. It is possible that after urethane-induced DNA damage, which produces 1,  $N^6$ -ethenoadenine adducts [56] that are primarily repaired by BER [57], Pol  $\iota$  acts in the gap-filling step of lesion repair. If the isoform of Pol  $\iota$  expressed in A/J mice is more likely to add the incorrect G opposite a template T in the gap-filling step of BER, as was found *in vitro* [52], this could explain the increased incidence of lung adenomas in A/J mice. In support of this hypothesis, nearly all urethane-induced adenomas in mice have a CAA → CGA transition in codon 61 of *Kras2* [51]. In addition, 129-derived mouse strains that carry a SNP in codon 27 of *Poli* resulting in a severely truncated protein [58] display extreme sensitivity to urethane-induced lung adenomas [53]. In the absence of Pol  $\iota$ , it has been hypothesized that another DNA polymerase, such as Pol  $\beta$ , inserts the incorrect base during gap filling in the repair of urethane-induced DNA damage. However, normal mouse Pol  $\iota$  displays extremely error-prone properties during synthesis opposite all four undamaged template bases *in vitro* [58], making it unlikely to prevent mutations during BER in mice that are Pol  $\iota$ -competent. Further studies must be completed to determine the tumor suppression mechanism of Pol  $\iota$  in mouse lung carcinogenesis.

A growing body of evidence suggests that Pol  $\iota$  is involved in error-prone TLS of UV-induced DNA damage *in vivo*. The heightened UV mutagenesis of Pol  $\eta$ -null (XP variant) human cells has been attributed to TLS by Pol  $\iota$  [59]. Loss of the functional *Poli* gene in dermal cells results in a dramatically reduced UV-induced mutation frequency at the *Hprt* locus in both wild-type and Pol  $\eta$ -deficient mice (Figure 2). Remarkably, however, the decreased UV-induced mutagenesis observed due to loss of the error-prone Pol  $\iota$  from Pol  $\eta$ -deficient mice is associated with increased cancer risk after UV exposure (Figure 3) [60]. This result was confirmed and extended by Ohkumo and colleagues who showed that *Poli*<sup>-/-</sup> mice are more likely to develop aggressive mesenchymal tumors after UV than *Poli*-proficient siblings [61]. These apparently contradictory findings speak to the fact that cancer etiology is more complex than the point mutations scored by the *Hprt* assay, and that one cannot use cell biology alone to accurately predict cancer risk in a TLS model. Indeed, they suggest a tumor suppressor role for Pol  $\iota$  that could be separate from its role as a TLS polymerase prone to induce single base-substitution mutations. It is also possible that Pol  $\iota$  is error-free when bypassing a minor UV adduct, or that it is involved in error-free BER of the minimal oxidative damage induced by UVB used in these studies [62], but more detailed experiments must be performed to evaluate these possibilities.

The role of Pol  $\iota$  in the induction of cancer induced by other carcinogens has not been systematically studied to date. It is interesting to note that Newcomb et al. found

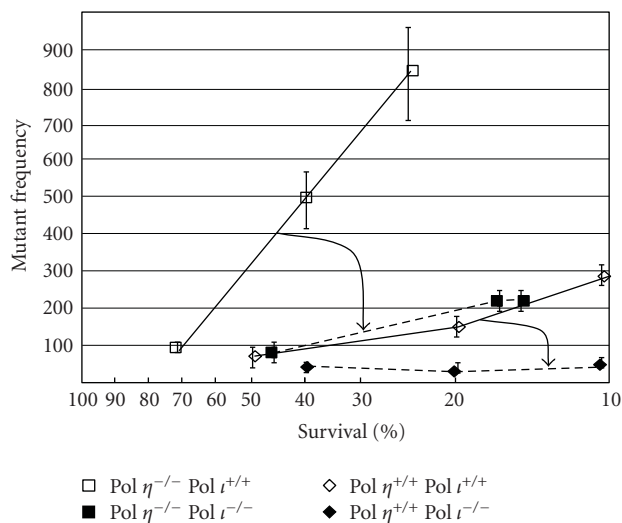


FIGURE 2: Frequency of 6-thioguanine-resistant ( $TG^r$ ) clones as a function of survival after UV irradiation. Cells were plated on three 150-mm-diameter dishes at a density of  $10^4 \text{ cm}^{-2}$  to determine mutant frequency or at cloning density to determine survival. After attachment, plates were irradiated with UV fluences to yield 20%–40% survival. The actual survival in the mutagenesis experiments was determined by refeeding the survival plates at one week and staining with crystal violet after two weeks. Percent survival for each UV fluence was corrected for replating and plotted on the x-axis. The corresponding mutant frequency at each survival is plotted on the y-axis. Each point represents the mean of three independent dishes at the indicated survival,  $\pm 1$  SD. Mutant frequency at the *Hprt* locus is defined as the number of  $TG^r$  clones per million clonable cells. Each data point represents independent experiments in which  $2\text{--}4 \times 10^6$  surviving cells were selected after UV irradiation and an 8- to 9-day expression period. The data have been corrected for cloning efficiency on the day of selection, and the spontaneous background mutant frequency ( $1 \times 10^{-5}$ ) has been subtracted. The arrows indicate the reduction in mutant frequency when Pol  $\iota$  is disrupted in the Pol  $\eta$ -deficient background (larger arrow) and in the Pol  $\eta$ -proficient background (smaller arrow). Reproduced with permission from Dumstorf et al. [60].

that Pol  $\iota$ -deficient 129 mice are resistant to  $\gamma$ -irradiation-induced thymic lymphoma but sensitive to methylating agent-induced thymic lymphoma [63].  $\gamma$ -Irradiation induces DNA strand breaks and oxidative damage, and Pol  $\iota$  is known to protect cells from oxidative stress [64]. It is therefore possible that increased cell death after  $\gamma$ -irradiation protects *Poli*<sup>-/-</sup> 129 mice from lymphomagenesis. However, Pol  $\iota$  does not affect the sensitivity of Pol  $\beta$ -null cells to methylating agents [65], so the sensitivity of 129 mice to thymic lymphoma induced in this way is still unexplained.

There is no known human disorder involving deficiency for Pol  $\iota$ . However, Pol  $\iota$  is overexpressed in some lung cancer cell lines [52] as well as in primary human gliomas [66]. The T706A SNP was found to increase the risk of adenocarcinoma and squamous cell carcinoma of the lung in persons < 61 years of age [29]. However, this association was not confirmed by another independent study [67] and failed to show significance in a meta-analysis [68].

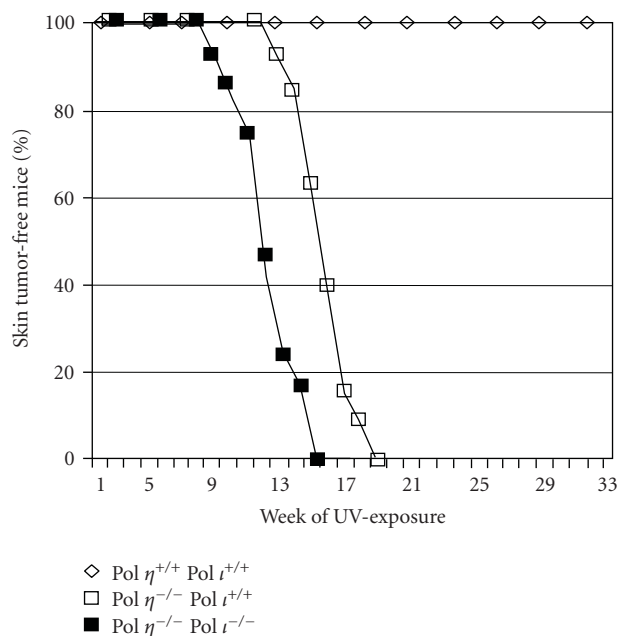


FIGURE 3: UV light-induced skin cancer in mice. Mice were shaved once per week and irradiated three times per week with 3.75 kJ/m<sup>2</sup> for 20 weeks or until the first skin tumor arose. Mice were inspected weekly for the development of skin tumors. All 12 homozygous *Polh* knockout mice (open diamonds) developed skin tumors by 18 weeks, while all 12 *Polh*<sup>-/-</sup>*Poli*<sup>-/-</sup> mice (open circles) developed skin tumors by 13 weeks. This *Poli*-dependent decrease in tumor latency is highly significant ( $P < .0002$ ). No difference was found in the histological analysis of skin tumors among the groups. Reproduced with permission from Dumstorf et al. [60].

Another SNP in human *POLI*, F532S, is associated with prostate cancer patients whose tumors display *TMPRSS2-ERG* fusion with a highly significant odds ratio of 4.6 [69]. The protooncogenic transcription factor *ERG* was identified as the most frequently overexpressed gene in human prostate cancers [70], and fusion with the androgen-responsive serine protease *TMPRSS2* by chromosomal rearrangement was found in >90% of *ERG*-overexpressing cases [71]. Threonine 706 and serine 532, the two residues altered by these SNPs in Pol  $\iota$ , are located in the noncanonical ubiquitin-binding motifs UBM2 and UBM1, respectively [72]. These two polymorphisms could therefore affect binding of Pol  $\iota$  to ubiquitinated PCNA, which is required for its recruitment to stalled replication forks following DNA damage. In the case of prostate cancer, the F532S variant of Pol  $\iota$  may promote chromosomal instability by causing replication fork stalling and double-strand break (DSB) formation. DSB formed in this way could promote cellular transformation by causing chromosomal rearrangements that place the protooncogene *ERG* under control of the androgen-responsive promoter elements of *TMPRSS2* and lead to *ERG*-overexpression as is found in many prostate cancers [71]. Evidence supports the suppression of skin and lung cancers by Pol  $\iota$  in humans and mice, and new studies suggest that other cancers could be

affected by this protein, making it a promising candidate for future investigation.

## 5. Pol $\kappa$

The fourth member of the Y-family is DNA polymerase  $\kappa$ . Pol  $\kappa$  performs faithful TLS of BPDE-induced DNA damage *in vitro* by inserting dC opposite a template BPDE-adducted G [73–75]. Pol  $\kappa$  is required for recovery from a novel BPDE-induced intra-S phase checkpoint, and the protein relocates to stalled replication forks after BPDE-induced DNA damage [76, 77]. *Polk*<sup>-/-</sup> mouse embryonic fibroblasts (MEFs) show persistent S-phase arrest after BPDE exposure, which results in increased DSB formation at stalled replication forks and increased toxicity in cells without functional Pol  $\kappa$  [77]. Avkin and colleagues measured TLS efficiency and fidelity in *Polk*<sup>-/-</sup> MEFs using a shuttle vector technique. TLS efficiency on a plasmid containing a site-specific BPDE-*N*<sup>2</sup>-dG adduct is reduced nearly threefold in *Polk*<sup>-/-</sup> MEFs, and mutagenic TLS is increased from 29% to 50% in knockout cells, supporting a role for Pol  $\kappa$  in the efficient and error-free bypass of BPDE DNA damage [78]. siRNA-mediated *POLK*-knockdown also reduces the efficiency of TLS past BPDE-*N*<sup>2</sup>-dG in human U2OS cells [79]. This body of evidence suggests that Pol  $\kappa$  could have an important role in cancers caused by bulky chemical carcinogens like BPDE. Pol  $\kappa$  has also recently been linked to nucleotide excision repair. *Polk*<sup>-/-</sup> MEFs have reduced levels of NER of UV damage, including reduced repair synthesis and removal of 6-4 photoproducts after UV. Both of these phenotypes are largely corrected by expressing wild-type Pol  $\kappa$ , but not a catalytically inactive mutant [80]. Pol  $\kappa$  carries out NER repair synthesis and is recruited to sites of NER through its interaction with XRCC1 and ubiquitinated PCNA [81]. These remarkable studies highlight the ability of TLS polymerases to function in multiple cellular pathways and the likelihood that *Polk* plays an important role in preventing DNA damage-induced carcinogenesis. While *Polk*-knockout mice have been generated [82, 83] and show increased spontaneous mutagenesis in kidney, liver, and lung [84], no cancer studies have yet been reported using these models.

Pol  $\kappa$  is overexpressed in ~70% of nonsmall cell lung cancers (NSCLC) examined [85], and this overexpression correlates with mutation status of *TP53* [86] which is itself an indicator of poor prognosis [87]. In addition, *POLK* promoter activity is increased in *TP53*<sup>-/-</sup> cells, and p53 protein suppresses *POLK* promoter activity *in vitro*. These reports suggest that Pol  $\kappa$  overexpression in NSCLC could be secondary to loss of functional p53, but the correlation between these two events must be investigated to rule out an etiological role for Pol  $\kappa$  in lung cancer. Much stronger epidemiological evidence shows that Pol  $\kappa$  is overexpressed in gliomas. Multivariate analysis indicates that Pol  $\kappa$  overexpression is an independent prognostic factor for the assessment of glioma patient outcomes (Figure 4) [66]. Although the potential role of Pol  $\kappa$  in the etiology of brain tumors is unclear, Pol  $\kappa$  is clearly a candidate for

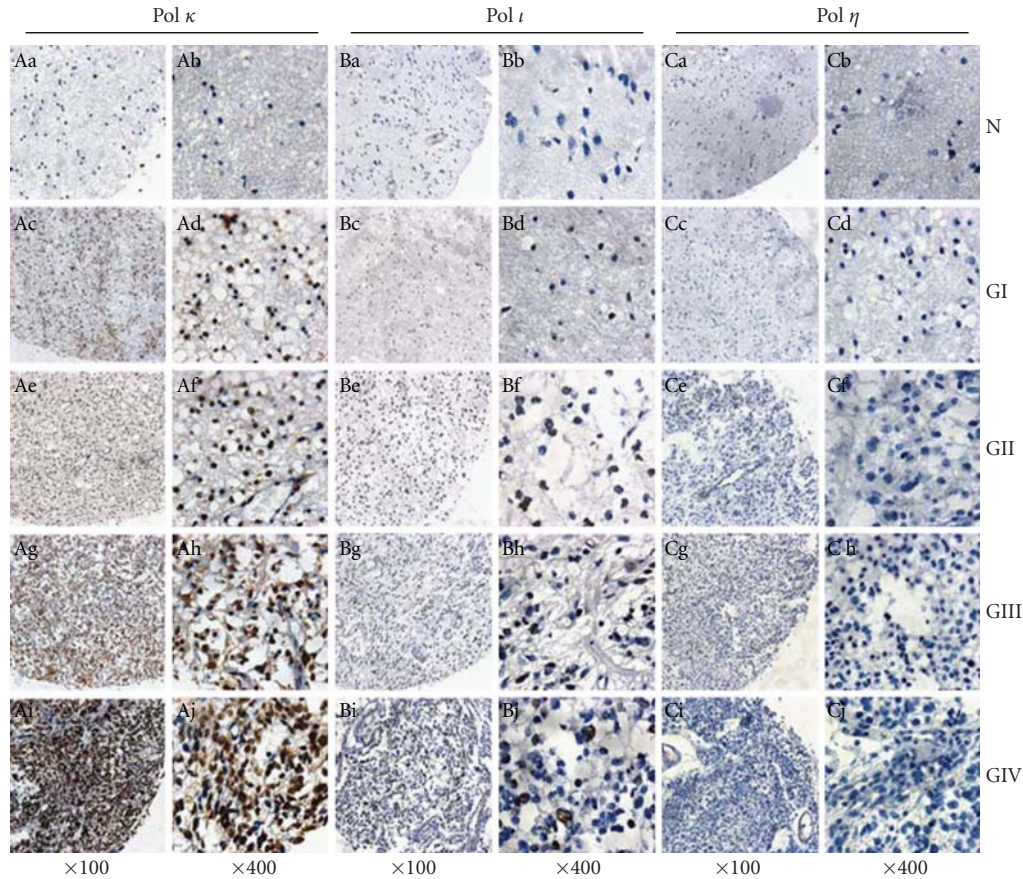


FIGURE 4: Immunohistochemical analysis of Pol  $\kappa$ , Pol  $\iota$ , and Pol  $\eta$  expression in primary glioma tissues (g) and normal brain tissues (n). Paraffin-embedded tissue microarrays comprising 104 primary glioma specimens from WHO grades I-IV were stained for Pol  $\kappa$ , Pol  $\iota$ , or Pol  $\eta$ . Representative images of Pol  $\kappa$ , Pol  $\iota$ , and Pol  $\eta$  expression: Aa, Ab, Ba, Bb, Ca, and Cb, normal brain tissue; Ac, Ad, Bc, Bd, Cc, and Cd, pilocytic astrocytoma (WHO grade I); Ae, Af, Be, Bf, Ce, and Cf, diffuse astrocytoma (WHO grade II); Ag, Ah, Bg, Bh, Cg, and Ch, anaplastic astrocytomas (WHO grade III); Ai, Aj, Bi, Bj, Ci, and Cj, glioblastoma multiforme (WHO grade IV); magnification: X100 (Aa, Ac, Ae, Ag, Ai, Ba, Bc, Be, Bg, Bi, Ca, Cc, Ce, Cg, and Ci) and X400 (Ab, Ad, Af, Ah, Aj, Bb, Bd, Bf, Bh, Bj, Cb, Cd, Cf, Ch, and Cj). Reproduced with permission from Wang et al. [66].

investigation of cancer risk and chemoprevention of multiple tumor types.

## 6. Pol $\zeta$

The human homolog of yeast DNA Polymerase  $\zeta$  is required for mutagenesis by UV, BPDE, and other carcinogens [7, 88]. Pol  $\zeta$  belongs to the B-family of DNA polymerases and contains a large catalytic subunit encoded by the *REV3* gene in humans [7] along with the much smaller regulatory protein REV7 [89]. Early investigations in *Saccharomyces cerevisiae* showed that rev3 mutant strains have reduced rates of spontaneous mutation [90], indicating that Pol  $\zeta$  is involved in the mutagenic processing of spontaneous and UV-induced mutations. Studies in mammalian cells indicate that Pol  $\zeta$  has a role in both repair of double strand breaks and base substitution mutagenesis, the latter likely involving extension of mispaired primer termini after initial TLS by another polymerase [91, 92]. Pol  $\zeta$  is the only

TLS polymerase required for development, and complete *Rev3*-knockout results in mitotic catastrophe and lethality at mouse embryonic day 10.5 [93–95]. However, conditional *Rev3*-knockout mice have been generated and are viable and fertile. While *Rev3*-deficiency alone is insufficient to promote cancer formation, conditional *Rev3* knockout accelerates the spontaneous formation of lymphoma in *Trp53*<sup>-/-</sup> mice. In humans, *REV3* gene expression is reduced by twofold in 40 of 74 (54%) colon carcinomas compared to matched normal tissue [96]. However, normal expression is found in much smaller sample sets of gastric, colon, lung, and renal cancers [97], and the gene is not mutated in primary tumors or cell lines from breast and colon cancers [89]. The expression levels of *REV3* in human cancers, particularly colon carcinoma, must be revisited using larger sample sizes to draw firm conclusions about the correlation of gene expression and cancer progression. No studies are published investigating the 25 nonsynonymous SNPs in human *REV3*, but the possibility exists that functional changes in human Pol  $\zeta$  could alter the risk of cancer formation.

## 7. Conclusions

The importance of translesion DNA synthesis in preventing human cancer is well understood from the example of XP variant, in which patients lacking the Y-family DNA polymerase  $\eta$  are prone to develop UV-induced skin cancers due to an extremely hypermutable phenotype. However, we understand very little about how the other polymerases involved in TLS affect human health and cancer risk. Recently developed mouse models have so far provided conflicting results; ribozyme-mediated knockdown of total Rev1 and removal of the BRCT domain both result in reduced mutagenesis by BPDE or UV, respectively. As expected, when *Rev1* mRNA is knocked down using the same ribozyme delivered to the lungs of mice, multiplicity of B[a]P-induced lung adenomas decreases [28]. In contrast, Rev1 BRCT-null mice develop UV-induced squamous cell carcinomas *faster* than wild-type controls [26]. In a similarly paradoxical finding, mice lacking both Pol  $\eta$  and Pol  $\iota$  have decreased UV-induced mutations in their dermal fibroblasts and accelerated development of squamous cell carcinoma after UV treatment compared to Pol  $\iota$ -proficient animals [60]. While it is understood that the mutations induced by these polymerases are etiological in many environmentally-induced cancers, it is clear from these studies that simply blocking TLS is not sufficient to reduce cancer risk, and in fact may cause an acceleration of carcinogenesis. More detailed studies are needed using existing mouse models to determine the effects of TLS polymerase activity on cancer development after diverse carcinogen exposures. In addition, molecular epidemiological studies must be conducted to evaluate the functional consequences of the many nonsynonymous SNPs in TLS polymerase genes, some of which have already been associated with cancer risk or protection. After a decade of intense research, there are still critical gaps in our understanding of the role of TLS in human health and cancer risk.

## Acknowledgments

The authors wish to thank Alden Klarer for thoughtful discussion of the manuscript. This work was partially supported by USPHS Grant T32-E011564, by a predoctoral fellowship to L. Jay Stallons, and by USPHS Grant R01-CA112197 to W. Glenn McGregor.

## References

- [1] D. Hanahan and R. A. Weinberg, "The hallmarks of cancer," *Cell*, vol. 100, no. 1, pp. 57–70, 2000.
- [2] K. Baynton, A. Bresson-Roy, and R. P. P. Fuchs, "Analysis of damage tolerance pathways in *Saccharomyces cerevisiae*: a requirement for Rev3 DNA polymerase in translesion synthesis," *Molecular and Cellular Biology*, vol. 18, no. 2, pp. 960–966, 1998.
- [3] S. Adar, L. Izhar, A. Hendel, N. Geacintov, and Z. Livneh, "Repair of gaps opposite lesions by homologous recombination in mammalian cells," *Nucleic Acids Research*, vol. 37, no. 17, pp. 5737–5748, 2009.
- [4] K. M. Vasquez, K. Marburger, Z. Intody, and J. H. Wilson, "Manipulating the mammalian genome by homologous recombination," *Proceedings of the National Academy of Sciences of the United States of America*, vol. 98, no. 15, pp. 8403–8410, 2001.
- [5] M. J. Shulman, C. Collins, A. Connor, L. R. Read, and M. D. Baker, "Interchromosomal recombination is suppressed in mammalian somatic cells," *EMBO Journal*, vol. 14, no. 16, pp. 4102–4107, 1995.
- [6] H. Ohmori, E. C. Friedberg, R. P. P. Fuchs et al., "The Y-family of DNA polymerases," *Molecular Cell*, vol. 8, no. 1, pp. 7–8, 2001.
- [7] P. E. M. Gibbs, W. G. McGregor, V. M. Maher, P. Nisson, and C. W. Lawrence, "A human homolog of the *Saccharomyces cerevisiae* REV3 gene, which encodes the catalytic subunit of DNA polymerase  $\zeta$ ," *Proceedings of the National Academy of Sciences of the United States of America*, vol. 95, no. 12, pp. 6876–6880, 1998.
- [8] W. Lin, X. Wu, and Z. Wang, "A full-length cDNA of hREV3 is predicted to encode DNA polymerase  $\zeta$  for damage-induced mutagenesis in humans," *Mutation Research*, vol. 433, no. 2, pp. 89–98, 1999.
- [9] S. D. McCulloch and T. A. Kunkel, "The fidelity of DNA synthesis by eukaryotic replicative and translesion synthesis polymerases," *Cell Research*, vol. 18, no. 1, pp. 148–161, 2008.
- [10] C.-A. Reynaud, F. Delbos, A. Faili, Q. Gueranger, S. Aoufouchi, and J.-C. Weill, "Competitive repair pathways in immunoglobulin gene hypermutation," *Philosophical Transactions of the Royal Society B*, vol. 364, no. 1517, pp. 613–619, 2009.
- [11] M. Diaz and C. Lawrence, "An update on the role of translesion synthesis DNA polymerases in Ig hypermutation," *Trends in Immunology*, vol. 26, no. 4, pp. 215–220, 2005.
- [12] A. Motegi, H.-J. Liaw, K.-Y. Lee et al., "Polyubiquitination of proliferating cell nuclear antigen by HLTf and SHPRH prevents genomic instability from stalled replication forks," *Proceedings of the National Academy of Sciences of the United States of America*, vol. 105, no. 34, pp. 12411–12416, 2008.
- [13] A. Motegi, R. Sood, H. Moinova, S. D. Markowitz, P. P. Liu, and K. Myung, "Human SHPRH suppresses genomic instability through proliferating cell nuclear antigen polyubiquitination," *Journal of Cell Biology*, vol. 175, no. 5, pp. 703–708, 2006.
- [14] I. Unk, I. Hajdú, K. Fátýol et al., "Human HLTf functions as a ubiquitin ligase for proliferating cell nuclear antigen polyubiquitination," *Proceedings of the National Academy of Sciences of the United States of America*, vol. 105, no. 10, pp. 3768–3773, 2008.
- [15] I. Unk, I. Hajdú, K. Fátýol et al., "Human SHPRH is a ubiquitin ligase for Mms2-Ubc13-dependent polyubiquitylation of proliferating cell nuclear antigen," *Proceedings of the National Academy of Sciences of the United States of America*, vol. 103, no. 48, pp. 18107–18112, 2006.
- [16] N. B. Watson, S. Mukhopadhyay, and W. G. McGregor, "Translesion DNA replication proteins as molecular targets for cancer prevention," *Cancer Letters*, vol. 241, no. 1, pp. 13–22, 2006.
- [17] F. W. Larimer, J. R. Perry, and A. A. Hardigree, "The REV1 gene of *Saccharomyces cerevisiae*: isolation, sequence, and functional analysis," *Journal of Bacteriology*, vol. 171, no. 1, pp. 230–237, 1989.
- [18] J. R. Nelson, C. W. Lawrence, and D. C. Hinkle, "Deoxycytidyl transferase activity of yeast REV1 protein," *Nature*, vol. 382, no. 6593, pp. 729–731, 1996.

- [19] M. Diaz, J. Velez, M. Singh, J. Cerny, and M. F. Flajnik, "Mutational pattern of the nurse shark antigen receptor gene (NAR) is similar to that of mammalian Ig genes and to spontaneous mutations in evolution: the translesion synthesis model of somatic hypermutation," *International Immunology*, vol. 11, no. 5, pp. 825–833, 1999.
- [20] P. E. M. Gibbs, X.-D. Wang, Z. Li et al., "The function of the human homolog of *Saccharomyces cerevisiae* REV1 is required for mutagenesis induced by UV light," *Proceedings of the National Academy of Sciences of the United States of America*, vol. 97, no. 8, pp. 4186–4191, 2000.
- [21] D. R. Clark, W. Zacharias, L. Panaitescu, and W. G. McGregor, "Ribozyme-mediated REV1 inhibition reduces the frequency of UV-induced mutations in the human HPRT gene," *Nucleic Acids Research*, vol. 31, no. 17, pp. 4981–4988, 2003.
- [22] S. Mukhopadhyay, D. R. Clark, N. B. Watson, W. Zacharias, and W. G. McGregor, "REV1 accumulates in DNA damage-induced nuclear foci in human cells and is implicated in mutagenesis by benzo[a]pyrenediol epoxide," *Nucleic Acids Research*, vol. 32, no. 19, pp. 5820–5826, 2004.
- [23] C. W. Lawrence, P. E. M. Gibbs, R. S. Murante et al., "Roles of DNA polymerase  $\zeta$  and Rev1 protein in eukaryotic mutagenesis and translesion replication," in *Proceedings of the Cold Spring Harbor Symposia on Quantitative Biology*, vol. 65, pp. 61–69, 2000.
- [24] A.-L. Ross, L. J. Simpson, and J. E. Sale, "Vertebrate DNA damage tolerance requires the C-terminus but not BRCT or transferase domains of REV1," *Nucleic Acids Research*, vol. 33, no. 4, pp. 1280–1289, 2005.
- [25] J. G. Jansen, A. Tsaalbi-Shtylik, P. Langerak et al., "The BRCT domain of mammalian Rev1 is involved in regulating DNA translesion synthesis," *Nucleic Acids Research*, vol. 33, no. 1, pp. 356–365, 2005.
- [26] A. Tsaalbi-Shtylik, J. W. A. Verspuy, J. G. Jansen et al., "Error-prone translesion replication of damaged DNA suppresses skin carcinogenesis by controlling inflammatory hyperplasia," *Proceedings of the National Academy of Sciences of the United States of America*, vol. 106, no. 51, pp. 21836–21841, 2009.
- [27] B. Zhao, J. Wang, N. E. Geacintov, and Z. Wang, "Pol $\eta$ , Pol $\zeta$  and Rev1 together are required for G to T transversion mutations induced by the (+)- and (-)-*trans-anti-BPDE-N*<sup>2</sup>-dG DNA adducts in yeast cells," *Nucleic Acids Research*, vol. 34, no. 2, pp. 417–425, 2006.
- [28] C. A. Dumstorf, S. Mukhopadhyay, E. Krishnan, B. Haribabu, and W. G. McGregor, "REV1 is implicated in the development of carcinogen-induced lung cancer," *Molecular Cancer Research*, vol. 7, no. 2, pp. 247–254, 2009.
- [29] T. Sakiyama, T. Kohno, S. Mimaki et al., "Association of amino acid substitution polymorphisms in DNA repair genes TP53, POLI, REV1 and LIG4 with lung cancer risk," *International Journal of Cancer*, vol. 114, no. 5, pp. 730–737, 2005.
- [30] R. P. Young, R. J. Hopkins, B. A. Hay et al., "A gene-based risk score for lung cancer susceptibility in smokers and ex-smokers," *Postgraduate Medical Journal*, vol. 85, no. 1008, pp. 515–524, 2009.
- [31] X. He, F. Ye, J. Zhang, Q. Cheng, J. Shen, and H. Chen, "REV1 genetic variants associated with the risk of cervical carcinoma," *European Journal of Epidemiology*, vol. 23, no. 6, pp. 403–409, 2008.
- [32] K. H. Kraemer and H. Slor, "Xeroderma pigmentosum," *Clinics in Dermatology*, vol. 3, no. 1, pp. 33–69, 1985.
- [33] J. E. Cleaver, "Xeroderma pigmentosum: variants with normal DNA repair and normal sensitivity to ultraviolet light," *Journal of Investigative Dermatology*, vol. 58, no. 3, pp. 124–128, 1972.
- [34] B. S. Tung, W. G. McGregor, Y.-C. Wang, V. M. Maher, and J. J. McCormick, "Comparison of the rate of excision of major UV photoproducts in the strands of the human HPRT gene of normal and xeroderma pigmentosum variant cells," *Mutation Research*, vol. 362, no. 1, pp. 65–74, 1996.
- [35] A. R. Lehmann, S. Kirk Bell, and C. F. Arlett, "Xeroderma pigmentosum cells with normal levels of excision repair have a defect in DNA synthesis after UV irradiation," *Proceedings of the National Academy of Sciences of the United States of America*, vol. 72, no. 1, pp. 219–223, 1975.
- [36] J. C. Boyer, W. K. Kaufmann, B. P. Brylawski, and M. Cordeiro-Stone, "Defective postreplication repair in xeroderma pigmentosum variant fibroblasts," *Cancer Research*, vol. 50, no. 9, pp. 2593–2598, 1990.
- [37] V. M. Maher, L. M. Ouellette, R. D. Curren, and J. J. McCormick, "Frequency of ultraviolet light-induced mutations is higher in xeroderma pigmentosum variant cells than in normal human cells," *Nature*, vol. 261, no. 5561, pp. 593–595, 1976.
- [38] C. Masutani, R. Kusumoto, A. Yamada et al., "The XPV (xeroderma pigmentosum variant) gene encodes human DNA polymerase  $\eta$ ," *Nature*, vol. 399, no. 6737, pp. 700–704, 1999.
- [39] R. E. Johnson, C. M. Kondratick, S. Prakash, and L. Prakash, "hRAD30 mutations in the variant form of xeroderma pigmentosum," *Science*, vol. 285, no. 5425, pp. 263–265, 1999.
- [40] C. Masutani, M. Araki, A. Yamada et al., "Xeroderma pigmentosum variant (XP-V) correcting protein from HeLa cells has a thymine dimer bypass DNA polymerase activity," *EMBO Journal*, vol. 18, no. 12, pp. 3491–3501, 1999.
- [41] K. Watanabe, S. Tateishi, M. Kawasuji, T. Tsurimoto, H. Inoue, and M. Yamaizumi, "Rad18 guides pol $\eta$  to replication stalling sites through physical interaction and PCNA monoubiquitination," *EMBO Journal*, vol. 23, no. 19, pp. 3886–3896, 2004.
- [42] C. Guo, J. N. Kosarek-Stancel, T.-S. Tang, and E. C. Friedberg, "Y-family DNA polymerases in mammalian cells," *Cellular and Molecular Life Sciences*, vol. 66, no. 14, pp. 2363–2381, 2009.
- [43] L. S. Waters, B. K. Minesinger, M. E. Wiltrout, S. D'Souza, R. V. Woodruff, and G. C. Walker, "Eukaryotic translesion polymerases and their roles and regulation in DNA damage tolerance," *Microbiology and Molecular Biology Reviews*, vol. 73, no. 1, pp. 134–154, 2009.
- [44] Q. Lin, A. B. Clark, S. D. McCulloch et al., "Increased susceptibility to UV-induced skin carcinogenesis in polymerase  $\eta$ -deficient mice," *Cancer Research*, vol. 66, no. 1, pp. 87–94, 2006.
- [45] K. Kuwamoto, H. Miyauchi-Hashimoto, T. Isei, and T. Horio, "Xeroderma pigmentosum variant associated with multiple cancers," *Photodermatology Photoimmunology and Photomedicine*, vol. 15, no. 3–4, pp. 127–132, 1999.
- [46] K. H. Kraemer, M. M. Lee, and J. Scotto, "DNA repair protects against cutaneous and internal neoplasia: evidence from xeroderma pigmentosum," *Carcinogenesis*, vol. 5, no. 4, pp. 511–514, 1984.
- [47] A. M. Flanagan, G. Rafferty, A. O'Neill et al., "The human POLH gene is not mutated, and is expressed in a cohort of patients with basal or squamous cell carcinoma of the skin," *International Journal of Molecular Medicine*, vol. 19, no. 4, pp. 589–596, 2007.
- [48] J. P. McDonald, V. Rapić-Otrin, J. A. Epstein et al., "Novel human and mouse homologs of *Saccharomyces cerevisiae* DNA polymerase," *Genomics*, vol. 60, no. 1, pp. 20–30, 1999.

- [49] D. T. Nair, R. E. Johnson, S. Prakash, L. Prakash, and A. K. Aggarwal, "Replication by human DNA polymerase- $\iota$  occurs by Hoogsteen base-pairing," *Nature*, vol. 430, no. 6997, pp. 377–380, 2004.
- [50] J. Wang, "DNA polymerases: hoogsteen base-pairing in DNA replication?" *Nature*, vol. 437, no. 7057, pp. E6–E7, 2005.
- [51] G.-H. Lee, H. Nishimori, Y. Sasaki, H. Matsushita, T. Kitagawa, and T. Tokino, "Analysis of lung tumorigenesis in chimeric mice indicates the Pulmonary adenoma resistance 2 (Par2) locus to operate in the tumor-initiation stage in a cell-autonomous manner: detection of polymorphisms in the Poli gene as a candidate for Par2," *Oncogene*, vol. 22, no. 15, pp. 2374–2382, 2003.
- [52] M. Wang, T. R. Devereux, H. G. Vikis et al., "Pol  $\iota$  is a candidate for the mouse pulmonary adenoma resistance 2 locus, a major modifier of chemically induced lung neoplasia," *Cancer Research*, vol. 64, no. 6, pp. 1924–1931, 2004.
- [53] G.-H. Lee and H. Matsushita, "Genetic linkage between Poli deficiency and increased susceptibility to lung tumors in mice," *Cancer Science*, vol. 96, no. 5, pp. 256–259, 2005.
- [54] M. Obata, H. Nishimori, K. Ogawa, and G.-H. Lee, "Identification of the Par2 (Pulmonary adenoma resistance) locus on mouse chromosome 18, a major genetic determinant for lung carcinogen resistance in BALB/cByJ mice," *Oncogene*, vol. 13, no. 8, pp. 1599–1604, 1996.
- [55] K. Bebenek, A. Tissier, E. G. Frank et al., "5'-deoxyribose phosphate lyase activity of human DNA polymerase  $\iota$  in vitro," *Science*, vol. 291, no. 5511, pp. 2156–2159, 2001.
- [56] R. C. Fernando, J. Nair, A. Barbin, J. A. Miller, and H. Bartsch, "Detection of 1,N6-ethenodeoxyadenosine and 3,N4-ethenodeoxycytidine by immunoaffinity/32P-postlabelling in liver and lung DNA of mice treated with ethyl carbamate (urethane) or its metabolites," *Carcinogenesis*, vol. 17, no. 8, pp. 1711–1718, 1996.
- [57] S. Choudhury, S. Adhikari, A. Cheema, and R. Roy, "Evidence of complete cellular repair of 1,N6-ethenoadenine, a mutagenic and potential damage for human cancer, revealed by a novel method," *Molecular and Cellular Biochemistry*, vol. 313, no. 1-2, pp. 19–28, 2008.
- [58] J. P. McDonald, E. G. Frank, B. S. Plosky et al., "129-Derived strains of mice are deficient in DNA polymerase  $\iota$  and have normal immunoglobulin hypermutation," *Journal of Experimental Medicine*, vol. 198, no. 4, pp. 635–643, 2003.
- [59] Y. Wang, R. Woodgate, T. P. McManus, S. Mead, J. J. McCormick, and V. M. Maher, "Evidence that in xeroderma pigmentosum variant cells, which lack DNA polymerase  $\eta$ , DNA polymerase  $\iota$  causes the very high frequency and unique spectrum of UV-induced mutations," *Cancer Research*, vol. 67, no. 7, pp. 3018–3026, 2007.
- [60] C. A. Dumstorf, A. B. Clark, Q. Lin et al., "Participation of mouse DNA polymerase  $\iota$  in strand-biased mutagenic bypass of UV photoproducts and suppression of skin cancer," *Proceedings of the National Academy of Sciences of the United States of America*, vol. 103, no. 48, pp. 18083–18088, 2006.
- [61] T. Ohkumo, Y. Kondo, M. Yokoi et al., "UV-B radiation induces epithelial tumors in mice lacking DNA polymerase  $\eta$  and mesenchymal tumors in mice deficient for DNA polymerase  $\iota$ ," *Molecular and Cellular Biology*, vol. 26, no. 20, pp. 7696–7706, 2006.
- [62] D. L. Mitchell, J. Jen, and J. E. Cleaver, "Relative induction of cyclobutane dimers and cytosine photohydrates in DNA irradiated in vitro and in vivo with ultraviolet-C and ultraviolet-B light," *Photochemistry and Photobiology*, vol. 54, no. 5, pp. 741–746, 1991.
- [63] E. W. Newcomb, L. E. Diamond, S. R. Sloan, M. Corominas, I. Guerrero, and A. Pellicer, "Radiation and chemical activation of ras oncogenes in different mouse strains," *Environmental Health Perspectives*, vol. 81, pp. 33–37, 1989.
- [64] T. B. Petta, S. Nakajima, A. Zlatanou et al., "Human DNA polymerase iota protects cells against oxidative stress," *EMBO Journal*, vol. 27, no. 21, pp. 2883–2895, 2008.
- [65] V. Poltoratsky, J. K. Horton, R. Prasad, W. A. Beard, R. Woodgate, and S. H. Wilson, "Negligible impact of pol  $\iota$  expression on the alkylation sensitivity of pol  $\beta$ -deficient mouse fibroblast cells," *DNA Repair*, vol. 7, no. 6, pp. 830–833, 2008.
- [66] H. Wang, W. Wu, H. W. Wang et al., "Analysis of specialized DNA polymerases expression in human gliomas: association with prognostic significance," *Neuro-Oncology*, vol. 12, no. 7, pp. 679–686, 2010.
- [67] S. Zienolddiny, D. Campa, H. Lind et al., "Polymorphisms of DNA repair genes and risk of non-small cell lung cancer," *Carcinogenesis*, vol. 27, no. 3, pp. 560–567, 2006.
- [68] P. Vineis, M. Manuguerra, F. K. Kavvoura et al., "A field synopsis on low-penetrance variants in DNA repair genes and cancer susceptibility," *Journal of the National Cancer Institute*, vol. 101, no. 1, pp. 24–36, 2009.
- [69] M. Luedeke, C. M. Linnert, M. D. Hofer et al., "Predisposition for TMPRSS2-ERG fusion in prostate cancer by variants in DNA repair genes," *Cancer Epidemiology Biomarkers and Prevention*, vol. 18, no. 11, pp. 3030–3035, 2009.
- [70] G. Petrovics, A. Liu, S. Shaheduzzaman et al., "Frequent overexpression of ETS-related gene-1 (ERG1) in prostate cancer transcriptome," *Oncogene*, vol. 24, no. 23, pp. 3847–3852, 2005.
- [71] S. A. Tomlins, D. R. Rhodes, S. Perner et al., "Recurrent fusion of TMPRSS2 and ETS transcription factor genes in prostate cancer," *Science*, vol. 310, no. 5748, pp. 644–648, 2005.
- [72] M. Bienko, C. M. Green, N. Crosetto et al., "Ubiquitin-binding domains in Y-family polymerases regulate translesion synthesis," *Science*, vol. 310, no. 5755, pp. 1821–1824, 2005.
- [73] N. Suzuki, E. Ohashi, A. Kolbanovskiy et al., "Translesion synthesis by human DNA polymerase  $\kappa$  on a DNA template containing a single stereoisomer of dG-(+)- or dG-(-)-anti-N<sup>2</sup>-BPDE (7,8-dihydroxy-anti-9,10-epoxy-7,8,9,10-tetrahydrobenzo[a]pyrene)," *Biochemistry*, vol. 41, no. 19, pp. 6100–6106, 2002.
- [74] O. Rechkoblit, Y. Zhang, D. Guo et al., "trans-lesion synthesis past bulky benzo[a]pyrene diol epoxide N<sup>2</sup>-dG and N<sup>6</sup>-dA lesions catalyzed by DNA bypass polymerases," *Journal of Biological Chemistry*, vol. 277, no. 34, pp. 30488–30494, 2002.
- [75] Y. Zhang, X. Wu, D. Guo, O. Rechkoblit, and Z. Wang, "Activities of human DNA polymerase  $\kappa$  in response to the major benzo[a]pyrene DNA adduct: error-free lesion bypass and extension synthesis from opposite the lesion," *DNA Repair*, vol. 1, no. 7, pp. 559–569, 2002.
- [76] N. Guo, D. V. Faller, and C. Vaziri, "Carcinogen-induced S-phase arrest is Chk1 mediated and caffeine sensitive," *Cell Growth and Differentiation*, vol. 13, no. 2, pp. 77–86, 2002.
- [77] X. Bi, D. M. Slater, H. Ohmori, and C. Vaziri, "DNA polymerase kappa is specifically required for recovery from the benzo[a]pyrene-dihydrodiol epoxide (BPDE)-induced S-phase checkpoint," *The Journal of Biological Chemistry*, vol. 280, pp. 22343–22355, 2005.
- [78] S. Avkin, M. Goldsmith, S. Velasco-Miguel, N. Geacintov, E. C. Friedberg, and Z. Livneh, "Quantitative analysis of translesion DNA synthesis across a benzo[a]pyrene-guanine adduct in

- mammalian cells: the role of DNA polymerase," *Journal of Biological Chemistry*, vol. 279, no. 51, pp. 53298–53305, 2004.
- [79] S. Shachar, O. Ziv, S. Avkin et al., "Two-polymerase mechanisms dictate error-free and error-prone translesion DNA synthesis in mammals," *EMBO Journal*, vol. 28, no. 4, pp. 383–393, 2009.
- [80] T. Ogi and A. R. Lehmann, "The Y-family DNA polymerase  $\kappa$  (pol  $\kappa$ ) functions in mammalian nucleotide-excision repair," *Nature Cell Biology*, vol. 8, no. 6, pp. 640–642, 2006.
- [81] T. Ogi, S. Limsirichaikul, R. M. Overmeer et al., "Three DNA polymerases, recruited by different mechanisms, carry out NER repair synthesis in human cells," *Molecular Cell*, vol. 37, no. 5, pp. 714–727, 2010.
- [82] D. Schenten, V. L. Gerlach, C. Guo et al., "DNA polymerase K deficiency does not affect somatic hypermutation in mice," *European Journal of Immunology*, vol. 32, no. 11, pp. 3152–3160, 2002.
- [83] T. Shimizu, Y. Shinkai, T. Ogi, H. Ohmori, and T. Azuma, "The absence of DNA polymerase  $\kappa$  does not affect somatic hypermutation of the mouse immunoglobulin heavy chain gene," *Immunology Letters*, vol. 86, no. 3, pp. 265–270, 2003.
- [84] J. N. K. Stancel, L. D. McDaniel, S. Velasco, J. Richardson, C. Guo, and E. C. Friedberg, "Polk mutant mice have a spontaneous mutator phenotype," *DNA Repair*, vol. 8, no. 12, pp. 1355–1362, 2009.
- [85] J. O-Wang, K. Kawamura, Y. Tada et al., "DNA polymerase  $\kappa$ , implicated in spontaneous and DNA damage-induced mutagenesis, is overexpressed in lung cancer," *Cancer Research*, vol. 61, no. 14, pp. 5366–5369, 2001.
- [86] Y. Wang, M. Seimiya, K. Kawamura et al., "Elevated expression of DNA polymerase kappa in human lung cancer is associated with p53 inactivation: Negative regulation of POLK promoter activity by p53," *International Journal of Oncology*, vol. 25, no. 1, pp. 161–165, 2004.
- [87] V. Skaug, D. Ryberg, E. H. Kure et al., "p53 Mutations in defined structural and functional domains are related to poor clinical outcome in non-small cell lung cancer patients," *Clinical Cancer Research*, vol. 6, no. 3, pp. 1031–1037, 2000.
- [88] M. Diaz, N. B. Watson, G. Turkington, L. K. Verkoczy, N. R. Klinman, and W. G. McGregor, "Decreased frequency and highly aberrant spectrum of ultraviolet-induced mutations in the hprt gene of mouse fibroblasts expressing antisense RNA to DNA polymerase  $\zeta$ ," *Molecular Cancer Research*, vol. 1, no. 11, pp. 836–847, 2003.
- [89] Y. Murakumo, T. Roth, H. Ishii et al., "A human REV7 homolog that interacts with the polymerase  $\zeta$  catalytic subunit hREV3 and the spindle assembly checkpoint protein hMAD2," *Journal of Biological Chemistry*, vol. 275, no. 6, pp. 4391–4397, 2000.
- [90] S. K. Quah, R. C. Von Borstel, and P. J. Hastings, "The origin of spontaneous mutation in *Saccharomyces cerevisiae*," *Genetics*, vol. 96, no. 4, pp. 819–839, 1980.
- [91] P. P. H. Van Sloun, I. Varlet, E. Sonneveld et al., "Involvement of mouse Rev3 in tolerance of endogenous and exogenous DNA damage," *Molecular and Cellular Biology*, vol. 22, no. 7, pp. 2159–2169, 2002.
- [92] J. P. Wittschieben, S. C. Reshmi, S. M. Gollin, and R. D. Wood, "Loss of DNA polymerase  $\zeta$  causes chromosomal instability in mammalian cells," *Cancer Research*, vol. 66, no. 1, pp. 134–142, 2006.
- [93] M. Bemark, A. A. Khamlichi, S. L. Davies, and M. S. Neuberger, "Disruption of mouse polymerase  $\zeta$  (Rev3) leads to embryonic lethality and impairs blastocyst development in vitro," *Current Biology*, vol. 10, no. 19, pp. 1213–1216, 2000.
- [94] J. Wittschieben, M. K. K. Shivji, E. Lalani et al., "Disruption of the developmentally regulated Rev31 gene causes embryonic lethality," *Current Biology*, vol. 10, no. 19, pp. 1217–1220, 2000.
- [95] G. Esposito, I. Godin, U. Klein, M.-L. Yaspo, A. Cumano, and K. Rajewsky, "Disruption of the Rev31-encoded catalytic subunit of polymerase  $\zeta$  in mice results in early embryonic lethality," *Current Biology*, vol. 10, no. 19, pp. 1221–1224, 2000.
- [96] J.-M. Brondello, M. J. Pillaire, C. Rodriguez et al., "Novel evidences for a tumor suppressor role of Rev3, the catalytic subunit of Pol  $\zeta$ ," *Oncogene*, vol. 27, no. 47, pp. 6093–6101, 2008.
- [97] K. Kawamura, J. O-Wang, R. Bahar et al., "The error-prone DNA polymerase zeta catalytic subunit (Rev3) gene is ubiquitously expressed in normal and malignant human tissues," *International Journal of Oncology*, vol. 18, no. 1, pp. 97–103, 2001.

## Research Article

# A Mathematical Model for DNA Damage and Repair

Philip S. Crooke<sup>1</sup> and Fritz F. Parl<sup>2</sup>

<sup>1</sup>Department of Mathematics, Vanderbilt University, Nashville, TN 37240, USA

<sup>2</sup>Department of Pathology, Vanderbilt University, Nashville, TN 37232, USA

Correspondence should be addressed to Fritz F. Parl, fritz.parl@vanderbilt.edu

Received 13 April 2010; Accepted 27 May 2010

Academic Editor: Ashis Basu

Copyright © 2010 P. S. Crooke and F. F. Parl. This is an open access article distributed under the Creative Commons Attribution License, which permits unrestricted use, distribution, and reproduction in any medium, provided the original work is properly cited.

In cells, DNA repair has to keep up with DNA damage to maintain the integrity of the genome and prevent mutagenesis and carcinogenesis. While the importance of both DNA damage and repair is clear, the impact of imbalances between both processes has not been studied. In this paper, we created a combined mathematical model for the formation of DNA adducts from oxidative estrogen metabolism followed by base excision repair (BER) of these adducts. The model encompasses a set of differential equations representing the sequence of enzymatic reactions in both damage and repair pathways. By combining both pathways, we can simulate the overall process by starting from a given time-dependent concentration of  $17\beta$ -estradiol ( $E_2$ ) and 2'-deoxyguanosine, determine the extent of adduct formation and the correction by BER required to preserve the integrity of DNA. The model allows us to examine the effect of phenotypic and genotypic factors such as different concentrations of estrogen and variant enzyme haplotypes on the formation and repair of DNA adducts.

## 1. Introduction

Estrogens are known carcinogens recognized as prime risk factor for the development of breast cancer [1]. The principal enzyme controlling estrogen metabolism in breast tissue is cytochrome P450 1B1 (CYP1B1), which sequentially oxidizes  $E_2$  to 4-OHE<sub>2</sub> and the estrogen quinone ( $E_2$ -3,4-Q, Figure 1). The highly reactive quinone nonenzymatically attacks DNA and forms covalent adducts with bases, such as 4-OHE<sub>2</sub>-N7-Gua ( $GUA_{\text{adduct}}$ ), which undergoes depurination by hydrolysis of the N-glycosylic bond between base and sugar, leaving an apurinic (AP) site in the double-stranded DNA. AP sites are repaired by the base excision repair (BER) pathway in a sequence of enzymatic reactions. AP endonuclease APE1 cleaves 5' to the AP site to generate a nick with 3'-OH and 5'-deoxyribose phosphate termini. DNA polymerase (Pol) catalyzes the release of the deoxyribose phosphate residue and DNA synthesis to fill the gap, which is then sealed by DNA ligase (Figure 1). This reaction sequence is carried out in one of two pathways, "short-patch" and "long-patch", which differ in the number of inserted nucleotides and the protein components.

In this paper, we present a mathematical model for the formation of DNA adducts from oxidative estrogen metabolism followed by BER of these adducts. The modeling is initially done in two stages: (1) formation of estrogen-deoxyribonucleoside adducts, and (2) repair of adducts in the BER. By combining both stages, we can simulate the overall process by starting from a given time-dependent concentration of  $E_2$  and 2'-deoxyguanosine, determine the extent of adduct formation and the correction by BER required to preserve the integrity of DNA.

## 2. Mathematical Model

The mathematical model is constructed in stages. Stage 1 deals with the formation of DNA adducts from estrogen metabolism and Stage 2 encompasses the repair of adducts. In the differential equations that will constitute the model,  $E_2$  denotes  $17\beta$ -estradiol, 4-OHE<sub>2</sub> the catechol estrogen,  $E_2$ -3,4-Q the estrogen quinone, GUA the deoxyribonucleoside 2'-deoxyguanosine, and  $GUA_{\text{adduct}}$  the estrogen adduct 4-OHE<sub>2</sub>-N7-Gua over time  $t$ . We assume that the starting

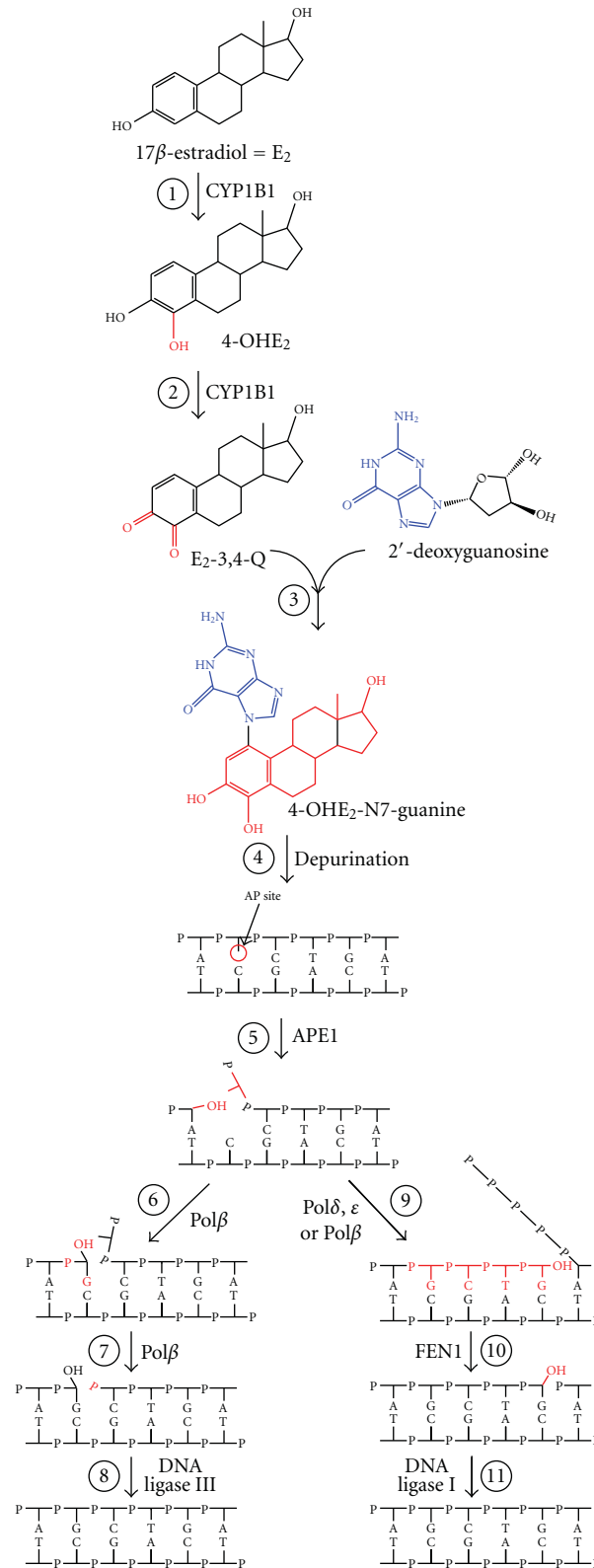


FIGURE 1: Overview of estrogen metabolism-induced DNA adduct formation and subsequent DNA repair by BER. The top sequence of reactions shows the CYP1B1-mediated oxidative estrogen metabolism resulting in estrogen-deoxyribonucleoside adduct formation. The bottom sequence of reactions shows the BER pathway with its two branches, the predominant short-patch pathway (left) and the alternate long-patch pathway (right). Not shown is the formation of the catechol estrogen 2-OHE<sub>2</sub>, which yields stable adducts, and the redox cycling of catechol estrogens and estrogen quinones, which generates reactive oxygen species capable of producing oxidative DNA adducts.

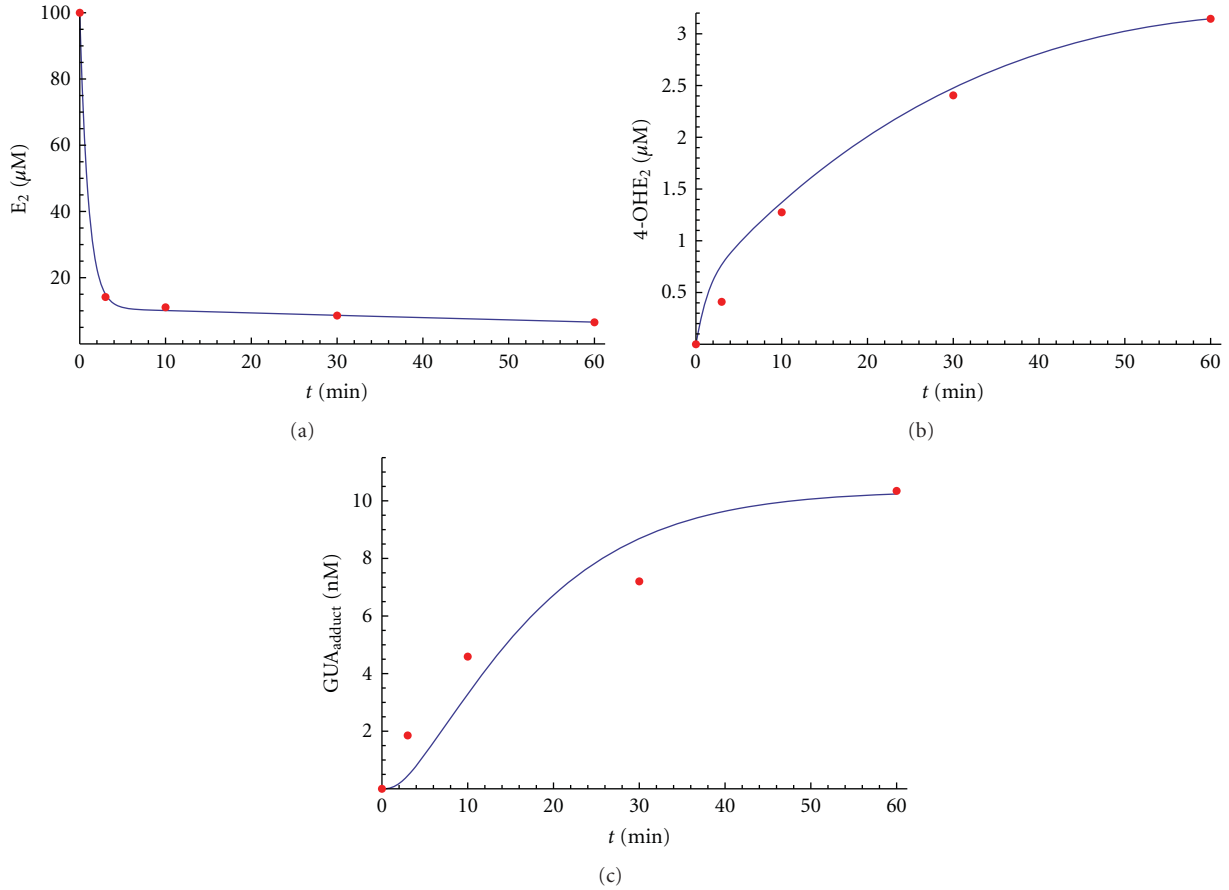
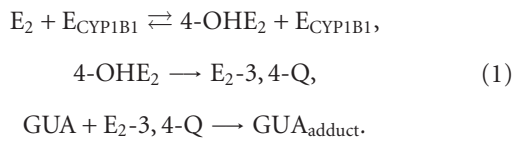


FIGURE 2: Comparison of stage 1 mathematical model (DNA damage) with experimental data. The metabolism of  $E_2$  (a),  $4\text{-OHE}_2$  (b), and  $\text{GUA}_{\text{adduct}}$  (c) is shown as a function of time. In each graph the dots represent the experimental data [2], and the curves are derived from the mathematical model.

points for the dynamic model are the initial concentration of  $\text{GUA}(0) = \text{GUA}_0$  and a prescribed time series is given for  $E_2$ .

The first stage of the model is based on the first three steps of the reaction sequence shown in Figure 1. As chemical reactions, these steps are



In the first reaction, the production of  $4\text{-OHE}_2$  from  $E_2$  is an enzymatic reaction mediated by CYP1B1 that follows Michaelis-Menten kinetics with parameters  $K_{m_1}$  and  $k_{\text{cat}_1}$  [3]. In the second reaction,  $E_2\text{-3,4-Q}$  is produced from  $4\text{-OHE}_2$  according to Hill-type kinetics. It has been shown that  $E_2\text{-3,4-Q}$  is highly reactive and will spontaneously form adducts with DNA without enzyme involvement [2]. Thus, in the third reaction, the formation of adducts is proportional to the levels of the quinone and the deoxyribonucleoside with a rate constant denoted by  $k_Q$ . Estrogen-DNA adducts have been detected in normal and malignant human breast tissues

[4, 5], and we have recently provided direct experimental evidence that oxidative metabolism of the parent hormone  $E_2$  leads to the formation of  $4\text{-OHE}_2$  and deoxyribonucleoside adducts, such as  $4\text{-OHE}_2\text{-N7-Gua}$  [2]. Using a compartmental analysis we created a mathematical model for reaction sequence (1). Figure 2 shows superimposed the experimental data (dots) and the model simulations (curves) for  $E_2$ ,  $4\text{-OHE}_2$ , and  $\text{GUA}_{\text{adduct}}$ .

The second stage of the model is based on the BER pathway (Figure 1) and uses a compartmental analysis with Michaelis-Menten kinetics to simulate the enzymatic reactions in the pathway [6]. The enzymes include the endonucleases APE1 and FEN1, DNA polymerases  $\beta$  and  $\delta$  ( $\text{Pol}\beta$ ,  $\text{Pol}\delta$ ), and ligases 1 and 3 ( $\text{Lig1}$ ,  $\text{Lig3}$ ). The dynamic process is modeled by a system of nonlinear differential equations.  $S(t)$  denotes the concentration of DNA adducts. We define the source and removal function for the repair cycle functions,  $S(t)$  and  $R(t)$ , as  $S(t) = k_s \text{GUA}_{\text{adduct}}$  and  $R(t) = k_r (E_2\text{-3,4-Q}) y_9$ . Here,  $k_s$  is a modeling parameter expressed in  $[1/\text{min}]$  which reflects the rate at which  $\text{GUA}_{\text{adduct}}$  enters the repair cycle. The parameter  $k_r$  is the rate at which  $y_9(t)$  interacts with  $E_2\text{-3,4-Q}$  to form  $\text{GUA}_{\text{adduct}}$ . The two parameters,  $k_s$  and  $k_r$ , can be used to control the rates of entering and exiting of adducts and

TABLE 1: Parameters for System of Differential Equations [6].

Reaction subscript ( <i>i</i> )	$k_{\text{cat}_i}$ [1/min]	$K_{m_i}$ [nmol/L]
5	192.168	34.7
6	4.500	500
7	49.020	210
8,11	1.278	56.7
9	36.000	100
10	8.130	39

repaired lesions, respectively. For the simulations, we have chosen,  $k_r = k_s = 1$ ,

$$\begin{aligned}
\frac{dy_4}{dt} &= S(t) - \frac{k_{\text{cat}_5} E_{\text{APE1}} y_4}{K_{m_5} + y_2}, \\
\frac{dy_5}{dt} &= \frac{k_{\text{cat}_5} E_{\text{APE1}} y_4}{K_{m_5} + y_4} - \frac{k_{\text{cat}_6} E_{\text{Pol}\beta} y_5}{K_{m_6} + y_5} - \frac{k_{\text{cat}_9} E_{\text{Pol}\delta} y_5}{K_{m_9} + y_5}, \\
\frac{dy_6}{dt} &= \frac{k_{\text{cat}_7} E_{\text{Pol}\beta} y_7}{K_{m_7} + y_7} - \frac{k_{\text{cat}_6} E_{\text{Pol}\beta} y_6}{K_{m_6} + y_6}, \\
\frac{dy_7}{dt} &= \frac{k_{\text{cat}_6} E_{\text{Pol}\beta} y_5}{K_{m_6} + y_5} - \frac{k_{\text{cat}_7} E_{\text{Pol}\beta} y_7}{K_{m_7} + y_7}, \\
\frac{dy_8}{dt} &= \frac{k_{\text{cat}_6} E_{\text{Pol}\beta} y_6}{K_{m_6} + y_6} - \frac{k_{\text{cat}_{11}} E_{\text{Lig1}} y_8}{K_{m_{11}} + y_8} - \frac{k_{\text{cat}_8} E_{\text{Lig3}} y_8}{K_{m_8} + y_8}, \\
\frac{dy_9}{dt} &= \frac{k_{\text{cat}_{11}} E_{\text{Lig1}} y_{11}}{K_{m_{11}} + y_{11}} + \frac{k_{\text{cat}_8} E_{\text{Lig3}} y_{11}}{K_{m_8} + y_{11}} \\
&\quad + \frac{k_{\text{cat}_{11}} E_{\text{Lig1}} y_8}{K_{m_{11}} + y_8} + \frac{k_{\text{cat}_8} E_{\text{Lig3}} y_8}{K_{m_8} + y_8} - R(t), \\
\frac{dy_{10}}{dt} &= \frac{k_{\text{cat}_9} E_{\text{Pol}\delta} y_5}{K_{m_9} + y_5} - \frac{k_{\text{cat}_{10}} E_{\text{FEN1}} y_{10}}{K_{m_{10}} + y_{10}}, \\
\frac{dy_{11}}{dt} &= \frac{k_{\text{cat}_{10}} E_{\text{FEN1}} y_{10}}{K_{m_{10}} + y_{10}} - \frac{k_{\text{cat}_{11}} E_{\text{Lig1}} y_{11}}{K_{m_{11}} + y_{11}} - \frac{k_{\text{cat}_8} E_{\text{Lig3}} y_{11}}{K_{m_8} + y_{11}}.
\end{aligned} \tag{2}$$

There are several Michaelis-Menten parameters,  $k_{\text{cat}_i}$  and  $K_{m_i}$ , for which experimental values have been estimated or measured (Table 1) [6]. The enzyme levels are denoted by  $E_{\text{APE1}}$ ,  $E_{\text{FEN1}}$ ,  $E_{\text{Pol}\beta}$ ,  $E_{\text{Pol}\delta}$ ,  $E_{\text{Lig1}}$ , and  $E_{\text{Lig3}}$ . The variable,  $y_9(t)$ , represents the repaired  $\text{GUA}_{\text{adduct}}$ , and if we set its initial condition in the system of differential equations as  $y_9(0) = \text{GUA}_0$ , it has the same meaning as  $\text{GUA}(t)$ . AP endonucleases, such as AP endonuclease 1 (APE1), are quite abundant in most cells, ranging from 200,000 to 7,000,000 APE1 molecules per cell in fibroblasts and HeLa cells, respectively [7, 8]. Thus, the minimal concentration of APE1 in nuclear extract can be assumed to be 2000 nM [6]. The equivalent estimated concentrations of  $\text{Pol}\beta$ ,  $\text{Pol}\delta$ , FEN1, Lig1, and Lig3 are 419, 600, 450, 254, and 254 nM, respectively [6, 9, 10].

It is estimated that AP sites are also generated spontaneously at an estimated rate of 2,000 to 10,000 per cell per day [11, 12]. We used (2) to determine the time necessary to repair these AP sites. In Figure 3 we demonstrate that the repair of lesions is a nonlinear process. For small values of

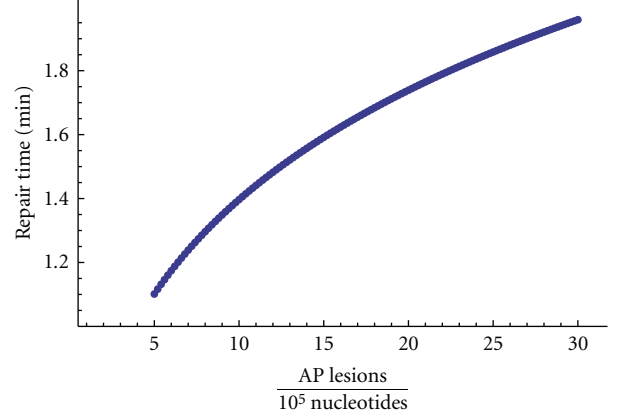


FIGURE 3: Stage 2 mathematical model of BER. The plot shows the time required to repair a fixed number of AP sites per  $10^5$  nucleotides with wild-type BER enzymes. The horizontal axis represents the starting number of AP sites per  $10^5$  nucleotides and the vertical axis the time for this number of sites to be repaired.

the ratio (AP lesions/ $10^5$  Nucleotides), the slope of the repair time function is relatively large as compared to larger values of the ratio. Figure 3 captures the dynamics of only the repair part of the model, that is, it shows the repair times for a fixed amount of AP lesions.

In the experiments addressed mathematically in Stage 1 of the model, we demonstrated that the CYP1B1-mediated oxidation of  $E_2$  resulted in the formation of approximately 10 nmol/L 4-OHE<sub>2</sub>-N7-Gua, which translates into 10 adducts per  $10^5$  nucleotides per hour [2]. Since the formation of 4-OHE<sub>2</sub>-N7-Gua leads to spontaneous depurination [13], we can assume an equal number of AP sites formed as a result of oxidative estrogen metabolism. This is one order of magnitude higher than the number of AP sites formed in normal leukocytes and fibroblasts, 10 AP sites per  $10^6$  nucleotides per hour [13]. The living cell depends on efficient enzymatic repair of the continuous chemical damage inflicted on genomic DNA. Therefore, in the last stage of the model we combine the adduct formation model (Stage 1) and the adduct repair model (Stage 2). The mathematical model used in Stage 1 was chosen to fit batch data (a fixed amount of  $E_2$ ). However, we consider the case when  $E_2$  is continuously available and can vary over time and hence, there is continuous adduct formation and repair. In our modification of the Stage 1 model, we assume that the total amount of 2'-deoxyguanosine is fixed, and it exists in two states: damaged ( $\text{GUA}_{\text{adduct}}$ ) and undamaged or repaired ( $y_9$ ). The modified Stage 1 model, which accounts for the continuous nature of damage and repair, is then given by the following system of ordinary differential equations

$$\begin{aligned}
\frac{d(4\text{-OHE}_2)}{dt} &= \frac{k_{\text{cat}_1} E_{\text{CYP1B1}} E_2}{K_{m_1} + E_2} - \frac{V_{\text{maxQ}} 4\text{-OHE}_2}{K_{m_Q} + 4\text{-OHE}_2}, \\
\frac{d(E_2\text{-3, 4-Q})}{dt} &= \frac{V_{\text{maxQ}} 4\text{-OHE}_2}{K_{m_Q} + 4\text{-OHE}_2} - k_Q E_2\text{-3, 4-Q}, \\
\frac{d(\text{GUA}_{\text{adduct}})}{dt} &= k_r (E_2\text{-3, 4-Q}) y_7 - k_s \text{GUA}_{\text{adduct}}.
\end{aligned} \tag{3}$$

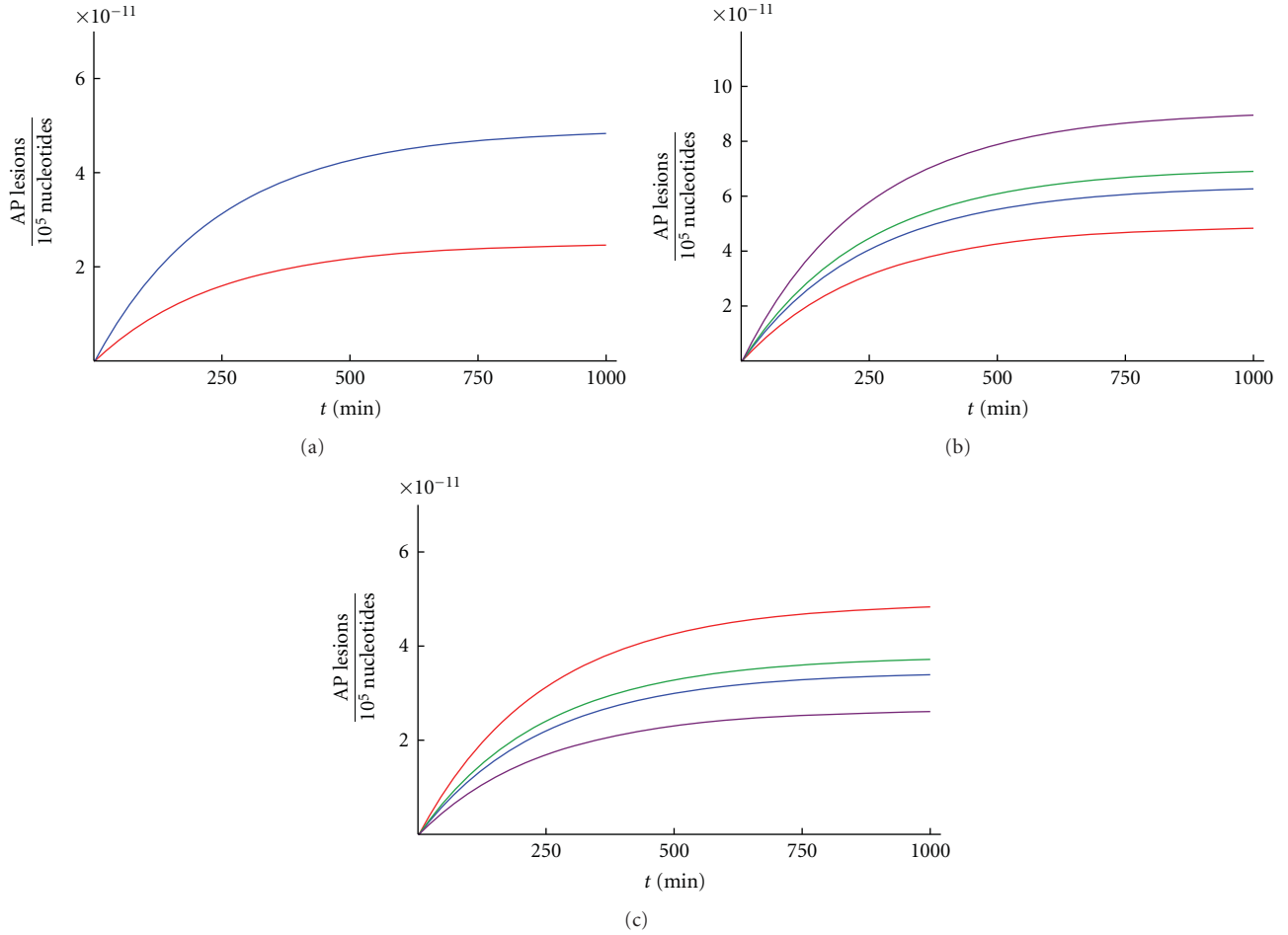


FIGURE 4: Effects of different concentrations of estrogen and variant haplotypes of CYP1B1 and APE1 on the formation and repair of DNA adducts. (a) Shows the effect of doubling the concentration of  $E_2$  on the number of AP lesions per  $10^5$  nucleotides over time using  $E_2 = 1$  (red curve) and  $E_2 = 2$  (blue curve). (b) Shows the effect of variant haplotypes of CYP1B1 and APE1 leading to an increase in the number of AP lesions per  $10^5$  nucleotides relative to wild-type enzymes. Each curve uses different assumptions about the kinetic constant,  $k_{cat}$ , for the CYP1B1 and APE1 enzymes. The red curve depicts the wild-types with  $k_{cat_1} = 1.6$  (CYP1B1) and  $k_{cat_5} = 192.168$  (APE1). The blue curve uses a 30% increase in  $k_{cat_1}$ , keeping  $k_{cat_5} = 192.168$ . The green curve employs a 30% reduction in  $k_{cat_1}$ , keeping  $k_{cat_5} = 192.168$ . Finally, the purple curve uses both a 30% increase in  $k_{cat_1}$  and a 30% reduction in  $k_{cat_5}$ . (c) Shows the effect of different variant haplotypes of CYP1B1 and APE1 that cause a decrease in the number of AP lesions per  $10^5$  nucleotides relative to wild-type enzymes. The wild-type is shown in red, a 30% decrease of CYP1B1 activity with APE1 activity held at its wild-type level in blue, 30% increase of APE1 activity with CYP1B1 activity held at its wild-type level in green, and a 30% decrease in CYP1B1 activity with a 30% increase of APE1 activity in purple.

The endpoint of the repair process is  $y_9(t)$  which is the concentration of  $GUA(t)$ . The term,  $R(t) = k_r y_9(E_2-3, 4-Q)$  where  $k_r$  is a constant, is the term that connects (2) and (3). In case the AP sites are not generated spontaneously but produced by DNA glycosylases, we can easily incorporate the enzymatic reaction catalyzed by glycosylases, which is not rate limiting for BER [9].

The combined Stage 3 model is composed of the differential in (2) and (3) along with their initial conditions. One can easily show that the system has a conservation law

$$\frac{GUA_{adduct}(t)}{GUA_0} = 1 - \frac{1}{GUA_0} \sum_{i=4}^{11} y_i(t). \quad (4)$$

Since this equation holds for all times, it calculates, at least in theory, the steady-state value of the unrepaired ratio.

### 3. Discussion

Numerous epidemiological studies have implicated estrogens in the development of breast cancer [1]. A pooled analysis of nine prospective studies of serum estrogen levels and breast cancer in over 2,400 postmenopausal women revealed a strong association of serum  $E_2$  concentrations with breast cancer risk [14]. In Figure 4(a), we show the results of the combined model for a constant source of estrogen,  $E_2(t) \equiv 1$ , on the number of AP sites per  $10^5$  nucleotides as well as the effect of doubling the  $E_2$  level,  $E_2(t) \equiv 2$ . Clinical studies estimate that the doubling of serum  $E_2$  levels confers a 1.3-fold increase in the risk of breast cancer [14]. Our model predicts a larger increase in the number of AP sites, indicating the involvement of other factors, such as enzyme activities. Enzymes involved in the production of

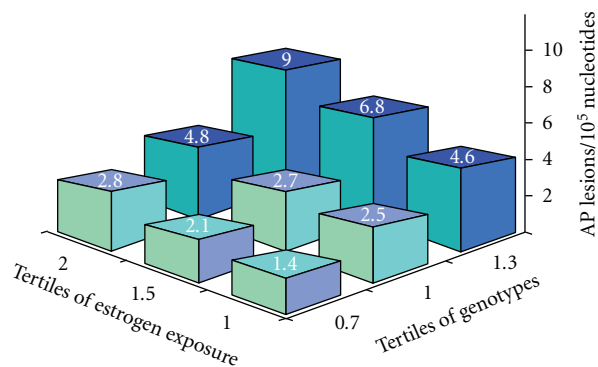


FIGURE 5: Three-dimensional graph displaying the interaction of estrogen exposure, enzyme genotypes, and resulting AP sites per  $10^5$  nucleotides. We display estrogen exposure in tertiles on the  $x$ -axis. Estrogen exposure can be represented by actual  $E_2$  values, measured in pmol/L, in combination with semiquantitative estimates of each woman's overall exposure to estrogen. The latter can be derived by taking into account her total years of ovulation as a function of current age, age at menarche, age at menopause, numbers of full-term pregnancies, and the dosage and duration of the use of exogenous estrogens. Thus, as far as the model is concerned, exogenous and endogenous estrogens can be combined although their precise contribution to estrogen exposure is presently unknown. The  $y$ -axis represents the combined effects of wild-type and variant enzyme haplotypes in the oxidative estrogen metabolism and BER pathways on AP levels. In theory, all enzyme genotype combinations shown in Figures 4(b) and 4(c) could be plotted. However for clarity, we have plotted only the wild-type and the lowest and highest variant haplotypes, separated into tertiles based on their respective AP sites per  $10^5$  nucleotides, which is represented on the  $z$ -axis. (The authors acknowledge Eric Parl for the design of this figure.)

DNA-damaging carcinogens and in repair of the resulting adducts are critical in maintaining the integrity of genomic DNA. Genetic variants of these enzymes, which occur in the general population, have been shown to play a role in altering specific reactions catalyzed by the individual enzymes. For example, we have shown that commonly occurring variants of CYP1B1 differ in their activity of producing 4-OHE<sub>2</sub> from the parent hormone  $E_2$  [3, 15]. Similarly, the APE1 gene contains over 20 polymorphic sites, which have been assessed functionally as recombinant proteins or based on structural predictions [16, 17]. Several APE1 variants are associated with substantially reduced or increased activities. For example, L104R, E126D, and R237A exhibit 50% and D283G 90% reduction in repair capacity [16]. In view of these associations we used the model to examine the effect of variant enzyme haplotypes on the formation and repair of DNA adducts. In Figure 4(b), we illustrate the effect of replacing wild-type CYP1B1 with a variant having a 30% greater  $k_{cat}$  and wild-type APE1 with a variant having a 30% lower  $k_{cat}$ . As expected, the more active CYP1B1 variant increases DNA damage, and the less active APE1 variant results in decreased repair, which is reflected in higher levels of AP lesions for each. Their combined occurrence has an additive effect on AP lesions. Figure 4(c) shows the effect

of different variants of CYP1B1 and APE1, which cause a decrease in number of AP sites relative to the wild-type enzymes. The panels in Figure 4 demonstrate the number the DNA adducts, which are constantly being created and repaired as modeled in (2) and (3), approaching steady values in the integrated process of adduct formation and repair.

A limitation of the model is its focus on BER and the omission of other DNA repair pathways. While the majority of adducts derived from 4-OHE<sub>2</sub> and  $E_2$ -3, 4-Q are depurinating N7 guanine adducts susceptible to BER, other stable, bulky DNA adducts that do not depurinate are also formed. However, the level of the stable adducts is three to four orders of magnitude lower than the level of depurinating adducts justifying the emphasis on BER [13, 18]. A vast number of depurination events occur under normal conditions involving not just guanine but other bases as well [19]. The importance of depurinating adducts derived from oxidative estrogen metabolism relative to the total spectrum of depurination events is presently unknown.

A critical strength of the model is that it can readily incorporate additional enzymes involved in the metabolism, as we have shown for CYP1A1, catechol-O-methyl transferase, and glutathione S-transferase P1 in the estrogen metabolism pathway [20]. Moreover, the model incorporates both phenotypic measures of estrogen exposure and genotypic data. This is schematically shown in Figure 5, which displays the interaction of estrogens, enzyme genotypes, and resulting AP sites per  $10^5$  nucleotides as a three-dimensional graph. In designing Figure 5, we assumed that the difference in estrogen exposure between individual women is no more than twofold, with the tertiles 1.0, 1.5, and 2.0 used for the  $x$ -axis. This range is conservative since up to fivefold differences in breast tissue concentrations have been reported in [21]. Regardless of the scale used for the  $x$ -axis, the production of AP sites would be expected to be greater in women with more endogenous (more ovulatory cycles) or exogenous (hormone replacement therapy, oral contraceptives) estrogen exposure. The effect of wild-type and variant enzyme haplotypes on AP sites is displayed on the  $y$ -axis. It is evident from Figure 5 that the combined phenotypic and genotypic factors exert not just an additive but multiplicative effect on AP site levels, which are shown on the  $z$ -axis.

In conclusion, we modeled the dynamic interaction between the estrogen-mediated DNA damage pathway and the DNA BER pathway in order to assess the overall impact on carcinogenesis. The model encompasses a set of differential equations representing the sequence of enzymatic reactions in both damage and repair pathways. The model allows us to examine the effect of phenotypic and genotypic factors such as different concentrations of estrogen and variant enzyme haplotypes on the formation and repair of DNA adducts. As a practical application, the model can be used to explore genetic factors in the damage-repair cycle (through the rate constants and estrogen levels) as a first step in understanding why some women develop breast cancer while others with similar circumstances do not. As better information about the kinetics in the model (e.g., rate constants for different haplotypes) becomes available,

predictions about breast cancer risk will improve. Thus, the model may be useful for the construction of breast cancer risk models.

## Acknowledgments

This work was supported by NIH (U54CA113007) and the Vanderbilt Integrative Cancer Biology Center.

## References

- [1] B. E. Henderson and H. S. Feigelson, "Hormonal carcinogenesis," *Carcinogenesis*, vol. 21, no. 3, pp. 427–433, 2000.
- [2] A. R. Belous, D. L. Hachey, S. Dawling, N. Roodi, and F. F. Parl, "Cytochrome P450 1B1-mediated estrogen metabolism results in estrogen-deoxyribonucleoside adduct formation," *Cancer Research*, vol. 67, no. 2, pp. 812–817, 2007.
- [3] I. H. Hanna, S. Dawling, N. Roodi, F. P. Guengerich, and F. F. Parl, "Cytochrome P450 1B1 (CYP1B1) pharmacogenetics association of polymorphisms with functional differences in estrogen hydroxylation activity," *Cancer Research*, vol. 60, no. 13, pp. 3440–3444, 2000.
- [4] J. Embrechts, F. Lemièrre, W. Van Dongen et al., "Detection of estrogen DNA-adducts in human breast tumor tissue and healthy tissue by combined nano LC-nano ES tandem mass spectrometry," *Journal of the American Society for Mass Spectrometry*, vol. 14, no. 5, pp. 482–491, 2003.
- [5] Y. Markushin, W. Zhong, E. L. Cavalieri et al., "Spectral characterization of catechol estrogen quinone (CEQ)-derived DNA adducts and their identification in human breast tissue extract," *Chemical Research in Toxicology*, vol. 16, no. 9, pp. 1107–1117, 2003.
- [6] B. A. Sokhansanj and D. M. Wilson III, "Estimating the effect of human base excision repair protein variants on the repair of oxidative DNA base damage," *Cancer Epidemiology Biomarkers and Prevention*, vol. 15, no. 5, pp. 1000–1008, 2006.
- [7] E. Cappelli, T. Hazra, J. W. Hill, G. Slupphaug, M. Bogliolo, and G. Frosina, "Rates of base excision repair are not solely dependent on levels of initiating enzymes," *Carcinogenesis*, vol. 22, no. 3, pp. 387–393, 2001.
- [8] D. S. Chen, T. Herman, and B. Demple, "Two distinct human DNA diesterases that hydrolyze 3'-blocking deoxyribose fragments from oxidized DNA," *Nucleic Acids Research*, vol. 19, no. 21, pp. 5907–5914, 1991.
- [9] D. K. Srivastava, I. Husain, C. L. Arteaga, and S. H. Wilson, "DNA polymerase  $\beta$  expression differences in selected human tumors and cell lines," *Carcinogenesis*, vol. 20, no. 6, pp. 1049–1054, 1999.
- [10] A. E. Tomkinson, D. D. Lasko, G. Daly, and T. Lindahl, "Mammalian DNA ligases. Catalytic domain and size of DNA ligase I," *Journal of Biological Chemistry*, vol. 265, no. 21, pp. 12611–12617, 1990.
- [11] H. Atamna, I. Cheung, and B. N. Ames, "A method for detecting abasic sites in living cells: age-dependent changes in base excision repair," *Proceedings of the National Academy of Sciences of the United States of America*, vol. 97, no. 2, pp. 686–691, 2000.
- [12] T. Lindahl and B. Nyberg, "Rate of depurination of native deoxyribonucleic acid," *Biochemistry*, vol. 11, no. 19, pp. 3610–3618, 1972.
- [13] E. L. Cavalieri, D. E. Stack, P. D. Devanesan et al., "Molecular origin of cancer: catechol estrogen-3,4-quinones as endogenous tumor initiators," *Proceedings of the National Academy of Sciences of the United States of America*, vol. 94, no. 20, pp. 10937–10942, 1997.
- [14] T. J. Key, "Endogenous sex hormones and breast cancer in postmenopausal women: reanalysis of nine prospective studies," *Journal of the National Cancer Institute*, vol. 94, no. 8, pp. 606–616, 2002.
- [15] P. S. Crooke, M. D. Ritchie, D. L. Hachey, S. Dawling, N. Roodi, and F. F. Parl, "Estrogens, enzyme variants, and breast cancer: a risk model," *Cancer Epidemiology Biomarkers and Prevention*, vol. 15, no. 9, pp. 1620–1629, 2006.
- [16] M. Z. Hadi, M. A. Coleman, K. Fidelis, H. W. Mohrenweiser, and D. M. Wilson III, "Functional characterization of Ape1 variants identified in the human population," *Nucleic Acids Research*, vol. 28, no. 20, pp. 3871–3879, 2000.
- [17] T. Xi, I. M. Jones, and H. W. Mohrenweiser, "Many amino acid substitution variants identified in DNA repair genes during human population screenings are predicted to impact protein function," *Genomics*, vol. 83, no. 6, pp. 970–979, 2004.
- [18] K.-M. Li, R. Todorovic, P. Devanesan et al., "Metabolism and DNA binding studies of 4-hydroxyestradiol and estradiol-3,4-quinone in vitro and in female ACI rat mammary gland in vivo," *Carcinogenesis*, vol. 25, no. 2, pp. 289–297, 2004.
- [19] T. Lindahl, "Instability and decay of the primary structure of DNA," *Nature*, vol. 362, no. 6422, pp. 709–715, 1993.
- [20] S. Dawling, D. L. Hachey, N. Roodi, and F. F. Parl, "In vitro model of mammary estrogen metabolism: structural and kinetic differences between catechol estrogens 2- and 4-hydroxyestradiol," *Chemical Research in Toxicology*, vol. 17, no. 9, pp. 1258–1264, 2004.
- [21] E. G. Rogan, A. F. Badawi, P. D. Devanesan et al., "Relative imbalances in estrogen metabolism and conjugation in breast tissue of women with carcinoma: potential biomarkers of susceptibility to cancer," *Carcinogenesis*, vol. 24, no. 4, pp. 697–702, 2003.

## Review Article

# Base Sequence Context Effects on Nucleotide Excision Repair

Yuqin Cai,<sup>1</sup> Dinshaw J. Patel,<sup>2</sup> Suse Broyde,<sup>1</sup> and Nicholas E. Geacintov<sup>3</sup>

<sup>1</sup> Department of Biology, New York University, New York, NY 10003, USA

<sup>2</sup> Structural Biology Program, Memorial Sloan-Kettering Cancer Center, New York, NY 10021, USA

<sup>3</sup> Department of Chemistry, New York University, New York, NY 10003, USA

Correspondence should be addressed to Nicholas E. Geacintov, ng1@nyu.edu

Received 16 May 2010; Accepted 16 June 2010

Academic Editor: Ashis Basu

Copyright © 2010 Yuqin Cai et al. This is an open access article distributed under the Creative Commons Attribution License, which permits unrestricted use, distribution, and reproduction in any medium, provided the original work is properly cited.

Nucleotide excision repair (NER) plays a critical role in maintaining the integrity of the genome when damaged by bulky DNA lesions, since inefficient repair can cause mutations and human diseases notably cancer. The structural properties of DNA lesions that determine their relative susceptibilities to NER are therefore of great interest. As a model system, we have investigated the major mutagenic lesion derived from the environmental carcinogen benzo[*a*]pyrene (B[*a*]P), 10*S* (+)-*trans-anti*-B[*a*]P-*N*<sup>2</sup>-dG in six different sequence contexts that differ in how the lesion is positioned in relation to nearby guanine amino groups. We have obtained molecular structural data by NMR and MD simulations, bending properties from gel electrophoresis studies, and NER data obtained from human HeLa cell extracts for our six investigated sequence contexts. This model system suggests that disturbed Watson-Crick base pairing is a better recognition signal than a flexible bend, and that these can act in concert to provide an enhanced signal. Steric hindrance between the minor groove-aligned lesion and nearby guanine amino groups determines the exact nature of the disturbances. Both nearest neighbor and more distant neighbor sequence contexts have an impact. Regardless of the exact distortions, we hypothesize that they provide a local thermodynamic destabilization signal for repair.

## 1. Introduction

Nucleotide excision repair (NER) plays a central role in preserving the genome of prokaryotes and eukaryotes. This versatile repair system removes structurally and chemically diverse bulky DNA lesions, including those induced by exposure to UV light and environmental chemical carcinogens [1, 2]. The vital importance of this mechanism is demonstrated by several human NER-deficiency syndromes including xeroderma pigmentosum (XP), cockayne syndrome (CS), and trichothiodystrophy (TTD) [3]. XP, for example, is characterized by high photosensitivity, hyperpigmentation, premature skin ageing, and proneness to developing skin cancer [4]. Furthermore, the capacity of the NER pathway is important in cancer chemotherapy [5]: NER diminishes the efficacy of chemotherapeutic agents such as cisplatin, which act via the formation of bulky DNA adducts. A better understanding of the mechanisms of recognition of DNA lesions by the NER system may lead to the design of improved chemotherapeutic drugs that can modulate the repair response. Recent findings reveal that polymorphisms

in human NER repair genes have an impact on the repair of DNA lesions and cancer susceptibility [6, 7], as well as on chemotherapeutic efficacy [8].

The eukaryotic NER pathway is a biologically complicated process and consists of two sub-pathways with different substrate specificity: global genome NER (GG-NER) [9, 10] and transcription-coupled repair (TCR) [11–14]. Both sub-pathways consist of ordered multistep processes, which differ in the early steps, when the DNA lesions are recognized, but converge in the later steps. In GG-NER, the focus of our present interest, the whole genome is scanned for bulky lesions to initiate the repair process. Two independent complexes, one involving the XPC/HR23B/Centrin 2 proteins [15–17] and the other involving the DDB1/DDB2 heterodimer [18–21], have been implicated in the early steps of base-damage recognition during NER [9]. By contrast, the TCR sub-pathway is activated by a stalled RNA polymerase during transcription [12]. Once the lesion is detected, the two sub-pathways proceed in an essentially identical manner to excise it: the multisubunit transcription factor, TFIIH, containing helicases XPB, and XPD, is recruited to the

lesion site, followed by XPA, the single-strand DNA binding protein RPA, and the two nucleases XPG and XPF-ERCC1. Once assembled, a 24–32 oligonucleotide stretch containing the lesion is excised from the damaged strand. This 24–32 oligonucleotide stretch is the hallmark of a successful NER event. Finally, gap resynthesis by DNA polymerases  $\delta$ ,  $\epsilon$ , and  $\kappa$  [22] and ligation by DNA ligase I complete the NER process [23].

One remarkable characteristic of the NER pathway is its ability to excise an astounding variety of chemically and structurally diverse lesions [2], and the rates of repair can vary over several orders of magnitude. However, the differences in the structural and thermodynamic properties of the lesions that control the diverse NER efficiencies have remained elusive. It has been suggested that the NER factors do not recognize the lesion itself, but rather the local distortions and destabilizations in the DNA that are associated with it [24–30]. A number of different properties of damaged DNA that elicit the NER response have been proposed. These include disruption of Watson-Crick hydrogen bonding [24, 31], kinks in the damaged DNA [32], thermodynamic destabilization [24, 29, 33], diminished base stacking [34, 35], local conformational flexibility [36], and flipped-out bases in the unmodified complementary strand [37–40]. A crystal structure of yeast Rad4/Rad23, the homolog of the human NER recognition factor XPC/HR23B, bound to DNA containing a cyclobutane pyrimidine dimer, shows that Rad4/Rad23 inserts a  $\beta$ -hairpin through the DNA duplex and expels two mismatched thymines in the undamaged strand out of the duplex to bind with the enzyme (PDB ID: 2QSG) [41]. This structure suggests that lesions which thermodynamically destabilize the DNA duplex and facilitate the flipping of base pairs and the intrusion of the beta-hairpin are good substrates to the NER machinery: the more locally destabilized the lesion, the better it is repaired.

The modulation of NER susceptibility for the same lesion by neighboring base sequence context, is however, a relatively unexplored area. If a lesion is better repaired in one sequence context than the other, a lesion-induced mutational hotspot could result. In order to elucidate the relationship between NER efficiency and base sequence-governed DNA distortion and destabilization induced by a bulky DNA adduct, we have employed as a model system the major lesion derived from the cancer-causing compound benzo[*a*]pyrene (B[*a*]P) [42]. B[*a*]P is the most well-studied member in a family of ubiquitous environmental pollutants known as polycyclic aromatic hydrocarbons. The tumorigenic metabolite of B[*a*]P [43] is the diol epoxide *r7*, *t8*-dihydroxy-*t9*,10-epoxy-7,8,9,10-tetrahydrobenzo[*a*]pyrene (B[*a*]PDE). This intermediate reacts with DNA and RNA; the most abundantly stable adduct produced in mammalian cells [44–46] is the 10S (+)-*trans-anti*-B[*a*]P-*N*<sup>2</sup>-dG adduct ([G\*]) (Figure 1(a)), the focus of our work. This adduct, unless removed by DNA repair mechanisms [47], is highly mutagenic [48, 49].

We have investigated the identical 10S (+)-*trans-anti*-B[*a*]P-*N*<sup>2</sup>-dG adduct in the six sequence contexts shown in Figure 1(b), utilizing an array of approaches: NER in human HeLa cell extracts, ligation and polyacrylamide gel electrophoresis techniques to assess bending properties of

the modified duplexes, and structural studies utilizing high resolution NMR methods as well as unrestrained molecular dynamics (MD) simulations. The position of the B[*a*]P ring system in the B-DNA minor groove, directed 5' along the modified strand, was first determined by NMR in the 5'-...C[G\*]C-I... sequence in 1992 [50], but sequence-governed structural details as well as dynamic properties remained to be elucidated. One important motivation for our work was to explore the role of nearby guanine amino groups on the structural properties and NER susceptibilities of these duplexes. The key difference in these duplexes is the presence and positioning of guanines flanking the [G\*], either immediately adjacent to the lesion or beyond: the B[*a*]P rings compete for space with the bulky amino group of guanine on the minor groove side of B-DNA, which we anticipated would differentially impact the structures of the damaged duplexes in a sequence context-dependent manner. A further motivation was to explore the role of differing sequence contexts beyond the lesion that vary in intrinsic flexibility. We hypothesized that subtle but critical structural effects governed by sequence context would manifest themselves by impacting NER efficiencies. Our results determined that sequence context could cause an up to four-fold difference in relative NER susceptibility, with even distant neighbors influencing NER. Locally disturbed Watson-Crick hydrogen bonding and flexible bending are two key sequence-governed structural distortions caused by this lesion that the NER machinery appears to recognize with different efficiencies. More generally, different lesions in varied sequence contexts will cause different kinds of distortions; thus, the extent of the local thermodynamic destabilization will also vary; we hypothesize that it is the extent and type of destabilization that determines the relative NER efficiency.

## 2. Nearest Neighbor Base Sequence Context Impacts NER of the 10S (+)-*trans-anti*-B[*a*]P-*N*<sup>2</sup>-dG Adduct

*The 5'-...C[G\*]G..., 5'-...G[G\*]C..., and 5'-...I[G\*]C... Sequences.* High resolution NMR solution studies have shown that the bulky aromatic B[*a*]P residue is positioned in the minor groove on the 5'-side of [G\*] [51] in the 5'-...C[G\*]G... and 5'-...G[G\*]C... duplexes (Figure 2). However, there are sequence-governed differences in some of the structural features. Specifically, in the 5'-...C[G\*]G... duplex, NMR studies revealed that the C : G base pair on the 5'-side of [G\*] is severely disturbed. In the case of the sequence-isomer 5'-...G[G\*]C... duplex, this perturbation is not observed. On the other hand, analyses of MD simulations [51, 52] based on the NMR data revealed significant unwinding near the lesion site combined with an anomalously enlarged *Roll* (Figure 3), not observed in the 5'-...C[G\*]G... duplex. Polyacrylamide gel electrophoresis techniques revealed an unusual slow electrophoretic mobility of the 5'-...G[G\*]C... duplex, which is a manifestation of a kink [53] that is highly flexible [54]. This flexible bend is caused on a molecular level by the severe untwisting

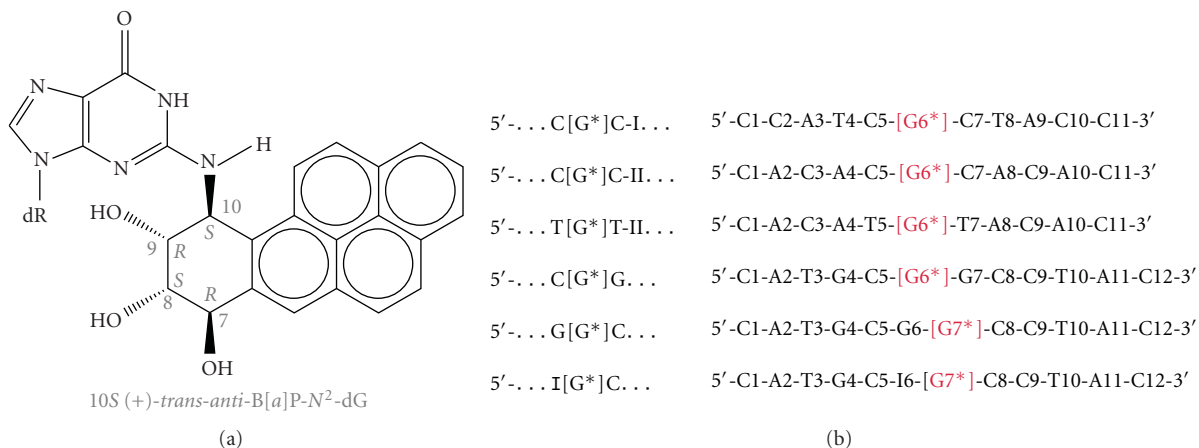


FIGURE 1: (a) Chemical structure of the 10S (+)-*trans-anti*-B[a]P-*N*<sup>2</sup>-dG adduct. (b) Base sequence contexts investigated. For 5'-...I[G\*]C..., formally, inosine is the nucleoside, while hypoxanthine is the correct name for the corresponding base; for simplicity we utilize the term inosine.

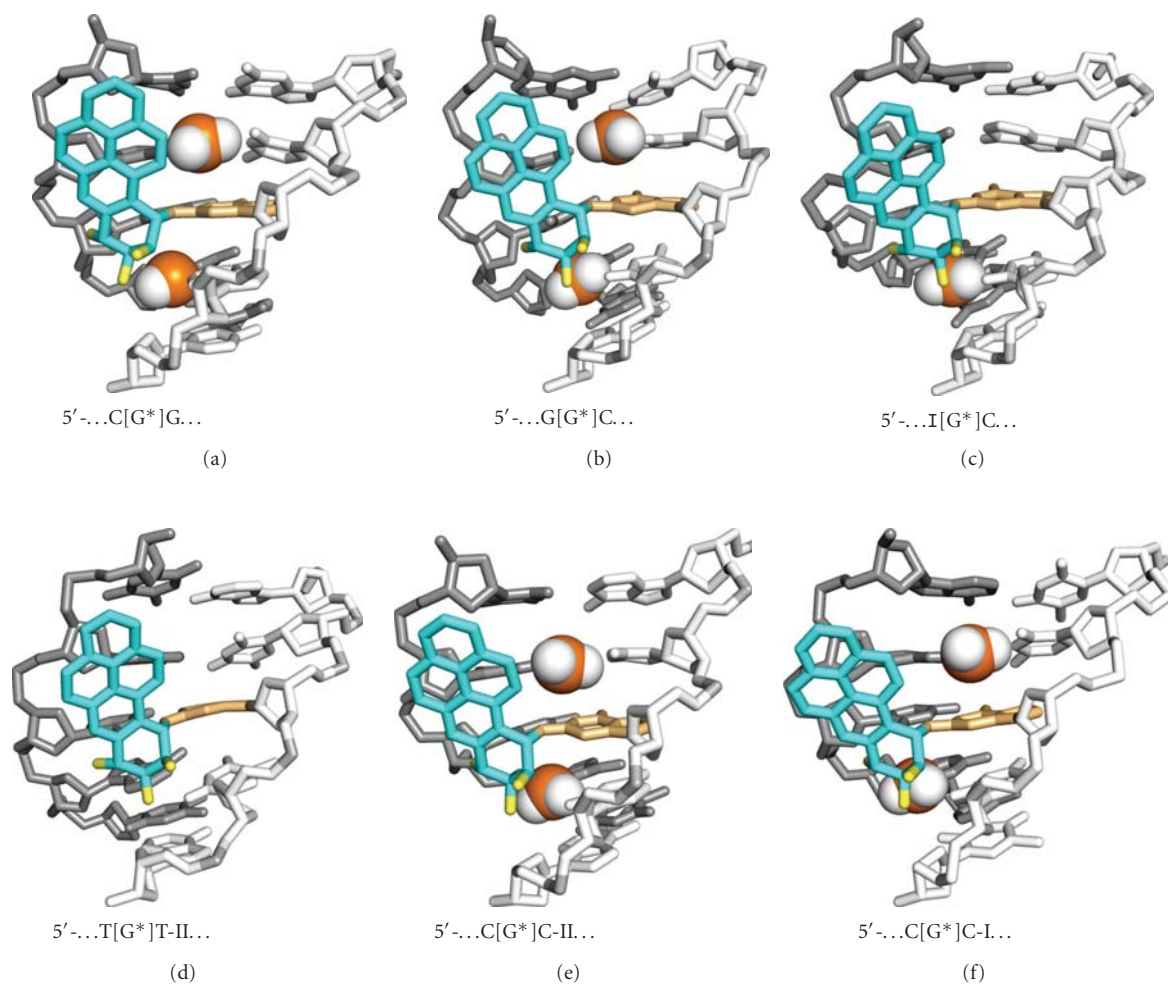


FIGURE 2: Effects of nearby guanine amino groups on the positioning of the 10S (+)-*trans-anti*-B[a]P-*N*<sup>2</sup>-dG adduct in the minor groove of the lesion-containing duplexes. The presence or absence and exact location of the guanine amino groups is governed by the base sequence contexts and determines the structural distortion/destabilization of the damaged duplexes. The damaged strand is light grey, and the partner is dark grey.

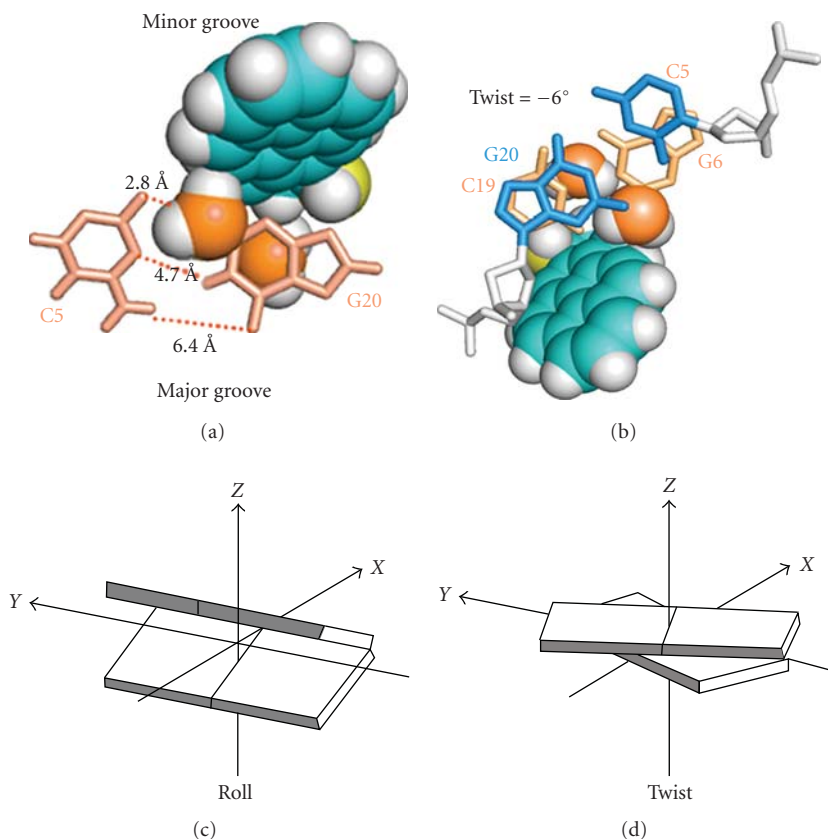


FIGURE 3: (a) In the 5'-. . .C[G\*]G... sequence context, steric hindrance between the B[a]P moiety and nearby guanine amino groups causes the episodic denaturation of the C5 : G20 Watson-Crick hydrogen bond. (b) In the 5'-. . .G[G\*]C... sequence context, steric hindrance between the B[a]P moiety and nearby guanine amino groups causes untwisting, manifested as a bend. (c) and (d) Definition of DNA duplex helicoidal parameters *Roll* and *Twist*, respectively. These cartoons are adapted with permission from Lu et al., *Nucleic Acids Res.* **31** (17): 5108–5121, Figure 1, Copyright 2003, Oxford University Press.

and enlarged *Roll* determined by MD from the NMR data: DNA bending is largely caused by increased *Roll*, which is correlated with untwisting [55–57]. The underlying structural reasons for the disturbed Watson-Crick hydrogen bond in the 5'-. . .C[G\*]G... case and the flexible bend in the 5'-. . .G[G\*]C... duplex were revealed from MD simulations: for 5'-. . .C[G\*]G..., the bulky amino group on G20 (Figure 3), which is partner to the C on the 5' side of [G\*], is sterically crowded by the B[a]P ring system since both are on the minor groove side, and hence this C5 : G20 base pair is episodically denatured (Figure 3(a)); for the 5'-. . .G[G\*]C... case, the B[a]P rings crowd the G6 amino group, and in this case the crowding is relieved by the severe untwisting accompanied by the increased *Roll*, which produces the flexible bend observed by gel electrophoresis. Investigations with the 5'-. . .I[G\*]C... sequence context substantiated the critical role of the guanine amino group since “I” (Figure 1(b)) lacks this group: the gel electrophoretic manifestation of a flexible bend was abolished. The NMR data showed conformational heterogeneity in minor groove conformations [51], and the MD simulations showed episodic denaturation of one of the two hydrogen bonds at the I:C base pair, explaining the heterogeneity.

The repair efficiency relative to 5'-. . .C[G\*]C-I..., the standard sequence utilized in many NMR and NER studies [53, 58], is  $4.1 \pm 0.2$ ,  $1.7 \pm 0.2$  and  $1.3 \pm 0.2$  for the 5'-. . .C[G\*]G..., 5'-. . .G[G\*]C... and 5'-. . .I[G\*]C... duplexes, respectively (Figure 4). In the 5'-. . .C[G\*]G... duplex, dynamic episodic denaturation of Watson-Crick base pairing flanking the lesion on the 5' side correlates with the greatest NER susceptibility while the flexible bend in 5'-. . .G[G\*]C... is a less pronounced NER recognition signal, and the disturbance to one hydrogen bond in the 5'-. . .I[G\*]C... case provides a still lesser signal [52, 53] in this series.

*The 5'-. . .C[G\*]C-II... and 5'-. . .T[G\*]T-II... Sequence Contexts.* The 5'-. . .C[G\*]C-II... and 5'-. . .T[G\*]T-II... sequences (Figure 1(b)) are of unusual interest for several reasons. While a single, well-defined minor groove adduct conformation is observed in 5'-. . .C[G\*]C... duplexes [50], in the 5'-. . .T[G\*]T-II... sequence context, the minor groove-aligned adduct conformation is heterogeneous [59]. Furthermore, polyacrylamide gel electrophoresis studies showed that the adduct induces a rigid bend in the 5'-. . .C[G\*]C-II... DNA duplex [60], while in the 5'-. . .T[G\*]T-II... sequence context, the lesion induces a

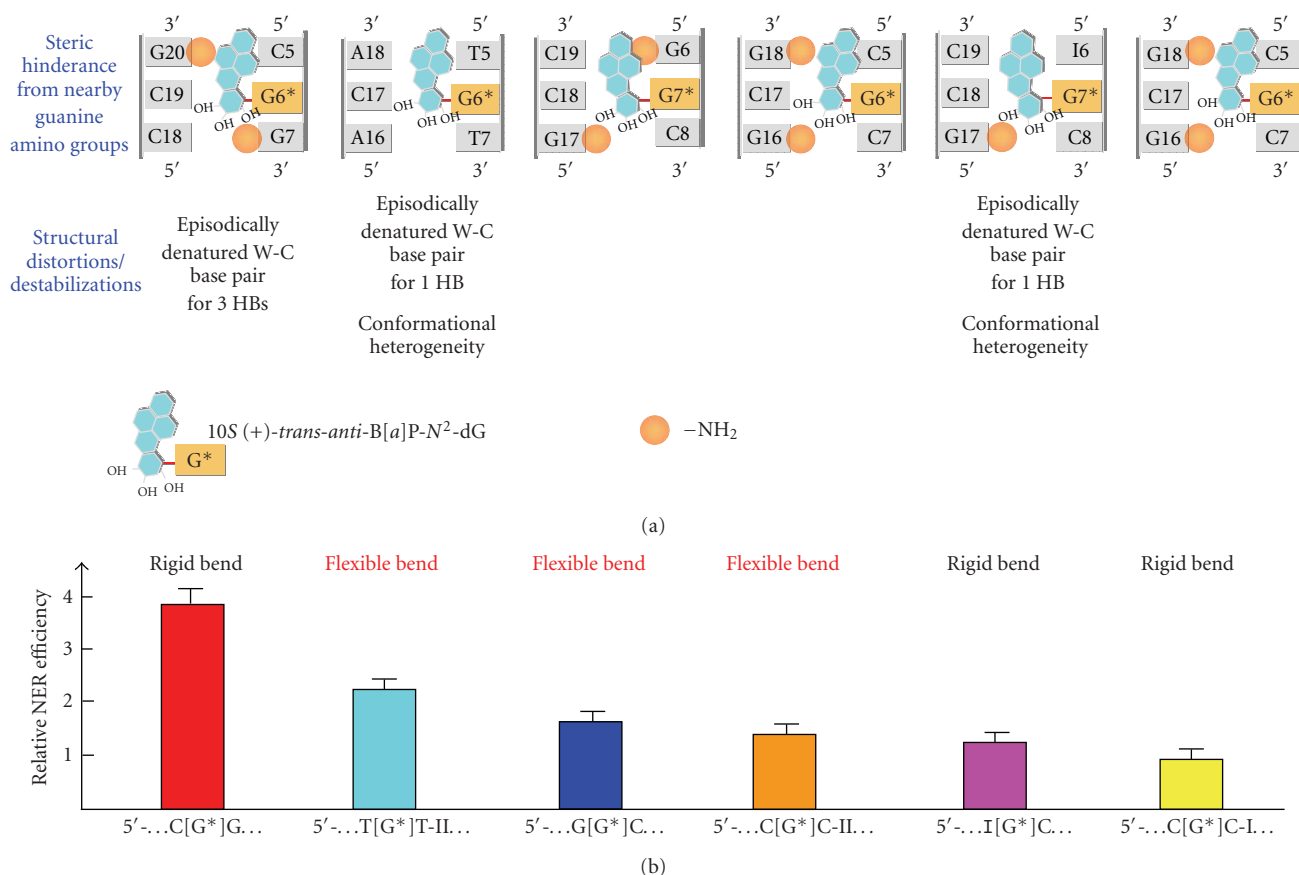


FIGURE 4: Hierarchy of NER recognition signals for the 10S (+)-*trans-anti-B[a]P-N<sup>2</sup>-dG* adduct in various sequence contexts.

highly flexible bend [59, 60]. Also, the 5'...T[G\*]T-II... 11-mer duplex has a lower thermal melting point than the 11-mer 5'...C[G\*]C-II... duplex (the exact difference depends on sequence length) [61] as expected from the thermodynamic properties of T:A and C:G Watson-Crick base pairs [62, 63]. Molecular insights on these experimental observations [64] were provided by MD simulations for the 5'...T[G\*]T-II... and 5'...C[G\*]C-II... duplexes. Consistent with the conformational heterogeneity observed in the NMR studies [59], it was found that the 5'...T[G\*]T-II... duplex is much more dynamic than the 5'...C[G\*]C-II... duplex: the highly dynamic base pair on the 5'-side of the lesion exhibits episodic denaturation of one of the two Watson-Crick hydrogen bonds, in agreement with the partial rupturing of this base pair observed by the NMR methods [59]; also, the 5'...T[G\*]T-II... duplex shows somewhat increased and more dynamic *Roll* and untwisting compared to the 5'...C[G\*]C-II... duplex, consistent with the flexible bend observed only for the 5'...T[G\*]T-II... case; in addition, the B[a]P ring system exhibits greater mobility and the duplex groove dimensions are more variable. The differences are accounted for by a coupled series of properties: the intrinsically weaker stacking of T-G compared to C-G steps allows for greater flexibility in the 5'...T[G\*]T-II... duplex; the weaker T:A pair, with only two hydrogen bonds, compared to the C:G pair, with three bonds, provides

enhanced flexibility; moreover, the absence of guanine amino groups adjacent to the [G\*] in the 5'...T[G\*]T-II... case allows for greater mobility for the B[a]P ring system. Overall, the greater flexibility of the 5'...T[G\*]T-II... sequence is attributable to the absence of the guanine amino group.

The rates of incision in the human HeLa cell assay relative to 5'...C[G\*]C-I... is  $2.4 \pm 0.2$  and  $1.6 \pm 0.2$  for the 5'...T[G\*]T-II... and the 5'...C[G\*]C-II... duplexes, respectively [53], corresponding to a  $1.5 \pm 0.2$ -fold higher-repair efficiency for the 5'...T[G\*]T-II... case relative to 5'...C[G\*]C-II... The better repair susceptibility in the 5'...T[G\*]T-II... case is consistent with the overall enhanced dynamics manifested in various structural properties, notably Watson-Crick hydrogen bonding and bending.

### 3. Distant Neighbor Base Sequence Context Affects NER of the 10S (+)-*trans-anti-B[a]P-N<sup>2</sup>-dG* Adduct

The 5'...C[G\*]C-I... and 5'...C[G\*]C-II... sequences (Figure 1(b)) differ in the sequences beyond the nearest neighbors to [G\*].

Since different sequence steps are known to be differentially flexible [57, 65], we hypothesized that the same minor groove lesion [50, 64] with different distant neighbors would

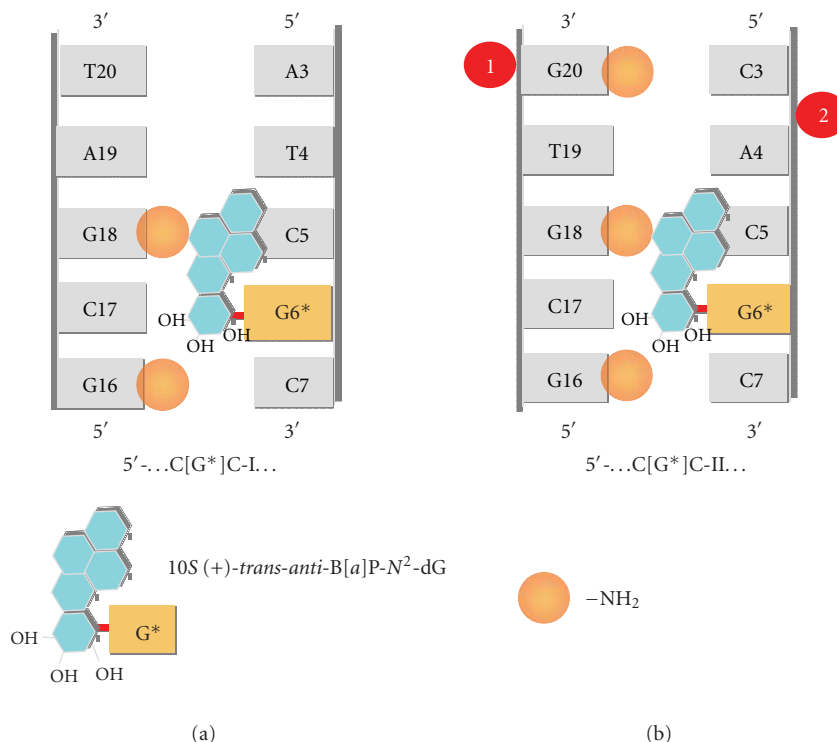


FIGURE 5: Cartoon representation of the lesion-containing duplexes (a) 5'...C[G\*]C-I... and (b) 5'...C[G\*]C-II... Note that 5'...C[G\*]C-I... and 5'...C[G\*]C-II... differ beginning with the next nearest neighbor to [G\*] and beyond. The locations of the key guanine amino group “1” and highly flexible dinucleotide C-A step “2”, present only in the 5'...C[G\*]C-II... sequence, are marked in red balloons.

be differentially repaired. Polyacrylamide gel electrophoresis and self-ligation circularization experiments revealed that the 5'...C[G\*]C-II... duplex is more bent and suggested that it has more torsional flexibility than the 5'...C[G\*]C-I... duplex [66]. Our MD simulations revealed the underlying structural origins to this bending difference. The key role is played by the unique -C3-A4-C5- segment in the 5'...C[G\*]C-II... duplex. The more torsionally flexible bend observed for the 5'...C[G\*]C-II... duplex originates from the guanine amino group at the C3:G20 pair (Figure 5). This amino group acts as a wedge to open the minor groove; facilitated by the highly deformable local -C3-A4- base step, the amino group allows the B[a]P ring system to better bury its hydrophobic surface within the groove walls. This produces a yet more enlarged minor groove which is coupled with more local untwisting and more enlarged and flexible *Roll* [67], causing the greater bend in 5'...C[G\*]C-II... [66] (Figure 5).

The NER efficiencies are  $1.6 \pm 0.2$  times greater in the 5'...C[G\*]C-II... than in the 5'...C[G\*]C-I... sequence context [66] showing that distant neighbors to [G\*] modulate the NER susceptibility. The greater NER susceptibility for the 5'...C[G\*]C-I... duplex is explained by its greater bending with enhanced flexibility: the intrinsic minor groove enlargement caused by both the guanine amino groups [55, 68] and the great flexibility of pyrimidine-purine steps, including the C-A step [57, 69–72] allow the B[a]P moiety (Figure 5) to more favorably position itself, but at the expense of the greater bend that makes it more repair-susceptible.

#### 4. Understanding Repairability Differences: the Degree of Local Thermodynamic Destabilization Is a Unifying Hypothesis

We have carried out a series of studies with the same 10S (+)-*trans-anti-B[a]P-N<sup>2</sup>-dG* lesion in a number of sequence contexts that differ in how the lesion is positioned in relation to nearby guanine amino groups. Additionally, we have considered differences in intrinsic flexibility of sequences flanking the lesion. These are model systems for gaining understanding of NER lesion recognition factors. We have obtained molecular structural data by NMR and MD simulations, bending properties from gel electrophoresis studies, and NER data from human HeLa cell extracts for all of our investigated sequence contexts (Figure 1(b)). Figure 4 summarizes our key findings and enables us to infer a hierarchy of NER recognition signals for the series of sequences and the single lesion we explored. We point out here that a variety of structural disturbances are found in each case, which are correlated. Examples include impaired Watson-Crick pairing that is accompanied by diminished base stacking, and DNA bending towards the major groove, that is induced by a minor groove lesion and is accompanied by minor groove enlargement. Our present model system suggests that disturbed Watson-Crick base pairing is a better recognition signal than a flexible bend, and that these can act in concert to provide an enhanced signal: for example, for 5'...T[G\*]T-II... one episodically ruptured Watson-Crick hydrogen bond combined with the flexible bend results

in better repair than just one disturbed hydrogen bond as in 5'-...I[G\*]C..., or the flexible bend alone in 5'-...G[G\*]C... (Figure 4). For our system, steric hindrance between the minor groove-aligned lesion and nearby guanine amino groups, if present, determines the exact nature of the disturbances, depending on exactly where the guanine amino groups are situated. The intrinsic flexibility of the specific base steps also plays an important role in causing the differential disturbances. Both the nearest neighbor and the more distant neighbor sequence contexts have an impact.

More globally, different lesions may cause different types of distortions depending on the specific nature of the lesion and its sequence context. However, regardless of exactly what these distortions are, we hypothesize that they must provide a *local* thermodynamic destabilization signal for repair to ensue, and the greater the extent of destabilization, the better the repair. The destabilization would facilitate the strand separation, base-flipping, and  $\beta$ -hairpin insertion by the XPC/HR23B recognition factor [41, 73] needed to initiate NER. In this way, the NER machinery would excise a large variety of lesions with different efficiencies, by recognizing the thermodynamic impact of the lesions rather than the lesions themselves [24, 29, 41, 73]. Lesions that resist NER present a great hazard, as they survive to the replication step and produce a mutagenic outcome; such NER-resistant lesions provide an important opportunity for gaining further understanding of the mechanism utilized by the NER apparatus to recognize different lesions [74].

## Abbreviations

B[a]P:	benzo[a]pyrene
B[a]PDE:	benzo[a]pyrene diol epoxide
(+)- <i>anti</i> -B[a]PDE:	(+)-(7R,8S,9S,10R)-7,8-dihydroxy-9,10-epoxy-7,8,9,10-tetrahydrobenzo[a]pyrene
NER:	nucleotide excision repair
MD:	molecular dynamics.

## Acknowledgments

The experimental portion of this paper was supported by NIH Grant CA-099194 (Nicholas E. Geacintov), and the computational aspects were supported by Grant CA-28038 (S. Broyde). Partial support for computational infrastructure and system's management was also provided by CA75449 (S. Broyde). Support for this paper to Dinshaw J. Patel. was provided by CA-046533. The content is solely the responsibility of the authors and does not necessarily represent the official views of the National Cancer Institute or the National Institutes of Health.

## References

[1] E. C. Friedberg, G. C. Walker, et al., *DNA Repair and Mutagenesis*, ASM Press, Washington, DC, USA, 2006.

[2] L. C. J. Gillet and O. D. Schärer, "Molecular mechanisms of mammalian global genome nucleotide excision repair," *Chemical Reviews*, vol. 106, no. 2, pp. 253–276, 2006.

[3] K. H. Kraemer, N. J. Patronas, R. Schiffmann, B. P. Brooks, D. Tamura, and J. J. DiGiovanna, "Xeroderma pigmentosum, trichothiodystrophy and Cockayne syndrome: a complex genotype-phenotype relationship," *Neuroscience*, vol. 145, no. 4, pp. 1388–1396, 2007.

[4] J. E. Cleaver, "Cancer in xeroderma pigmentosum and related disorders of DNA repair," *Nature Reviews Cancer*, vol. 5, no. 7, pp. 564–573, 2005.

[5] L. P. Martin, T. C. Hamilton, and R. J. Schilder, "Platinum resistance: the role of DNA repair pathways," *Clinical Cancer Research*, vol. 14, no. 5, pp. 1291–1295, 2008.

[6] C. Li, L. E. Wang, and Q. Wie, "DNA repair phenotype and cancer susceptibility—a mini review," *International Journal of Cancer*, vol. 124, no. 5, pp. 999–1007, 2009.

[7] F. Wang, Y. He, H. Guo et al., "Genetic variants of nucleotide excision repair genes are associated with DNA damage in coke oven workers," *Cancer Epidemiology Biomarkers and Prevention*, vol. 19, no. 1, pp. 211–218, 2010.

[8] P. A. Bradbury, M. H. Kulke, R. S. Heist et al., "Cisplatin pharmacogenetics, DNA repair polymorphisms, and esophageal cancer outcomes," *Pharmacogenetics and Genomics*, vol. 19, no. 8, pp. 613–625, 2009.

[9] T. Nouspikel, "Nucleotide excision repair: variations on versatility," *Cellular and Molecular Life Sciences*, vol. 66, no. 6, pp. 994–1009, 2009.

[10] K. Sugawara, "Regulation of damage recognition in mammalian global genomic nucleotide excision repair," *Mutation Research*, vol. 685, no. 1–2, pp. 29–37, 2010.

[11] D. A. Scicchitano, "Transcription past DNA adducts derived from polycyclic aromatic hydrocarbons," *Mutation Research*, vol. 577, no. 1–2, pp. 146–154, 2005.

[12] P. C. Hanawalt and G. Spivak, "Transcription-coupled DNA repair: two decades of progress and surprises," *Nature Reviews Molecular Cell Biology*, vol. 9, no. 12, pp. 958–970, 2008.

[13] S. Tornaletti, "DNA repair in mammalian cells: transcription-coupled DNA repair: directing your effort where it's most needed," *Cellular and Molecular Life Sciences*, vol. 66, no. 6, pp. 1010–1020, 2009.

[14] K. Dreij, J. A. Burns, et al., "DNA damage and transcription elongation: consequences and RNA Integrity," in *The Chemical Biology of DNA Damage*, N. E. Geacintov and S. Broyde, Eds., WILEY-VCH, Weinheim, Germany, 2010.

[15] K. Sugawara, J. M. Y. Ng, C. Masutani et al., "Xeroderma pigmentosum group C protein complex is the initiator of global genome nucleotide excision repair," *Molecular Cell*, vol. 2, no. 2, pp. 223–232, 1998.

[16] M. Volker, M. J. Moné, P. Karmakar et al., "Sequential assembly of the nucleotide excision repair factors in vivo," *Molecular Cell*, vol. 8, no. 1, pp. 213–224, 2001.

[17] T. Riedl, F. Hanaoka, and J.-M. Egly, "The comings and goings of nucleotide excision repair factors on damaged DNA," *EMBO Journal*, vol. 22, no. 19, pp. 5293–5303, 2003.

[18] M. E. Fitch, S. Nakajima, A. Yasui, and J. M. Ford, "In vivo recruitment of XPC to UV-induced cyclobutane pyrimidine dimers by the DDB2 gene product," *Journal of Biological Chemistry*, vol. 278, no. 47, pp. 46906–46910, 2003.

[19] J. Moser, M. Volker, H. Kool et al., "The UV-damaged DNA binding protein mediates efficient targeting of the nucleotide excision repair complex to UV-induced photo lesions," *DNA Repair*, vol. 4, no. 5, pp. 571–582, 2005.

- [20] K. Sugawara, Y. Okuda, M. Saijo et al., "UV-induced ubiquitylation of XPC protein mediated by UV-DDB-ubiquitin ligase complex," *Cell*, vol. 121, no. 3, pp. 387–400, 2005.
- [21] R. Nishi, S. Alekseev, C. Dinant et al., "UV-DDB-dependent regulation of nucleotide excision repair kinetics in living cells," *DNA Repair*, vol. 8, no. 6, pp. 767–776, 2009.
- [22] T. Ogi, S. Limsirichaikul, R. M. Overmeer et al., "Three DNA polymerases, recruited by different mechanisms, carry out NER repair synthesis in human cells," *Molecular Cell*, vol. 37, no. 5, pp. 714–727, 2010.
- [23] C. Guo, T.-S. Tang, and E. C. Friedberg, "SnapShot: nucleotide excision repair," *Cell*, vol. 140, no. 5, pp. 754–754.e1, 2010.
- [24] D. Gunz, M. T. Hess, and H. Naegeli, "Recognition of DNA adducts by human nucleotide excision repair. Evidence for a thermodynamic probing mechanism," *Journal of Biological Chemistry*, vol. 271, no. 41, pp. 25089–25098, 1996.
- [25] E. Evans, J. G. Moggs, J. R. Hwang, J.-M. Egly, and R. D. Wood, "Mechanism of open complex and dual incision formation by human nucleotide excision repair factors," *EMBO Journal*, vol. 16, no. 21, pp. 6559–6573, 1997.
- [26] Y. Fujiwara, C. Masutani, T. Mizukoshi, J. Kondo, F. Hanaoka, and S. Iwai, "Characterization of DNA recognition by the human UV-damaged DNA-binding protein," *Journal of Biological Chemistry*, vol. 274, no. 28, pp. 20027–20033, 1999.
- [27] R. D. Wood, "DNA damage recognition during nucleotide excision repair in mammalian cells," *Biochimie*, vol. 81, no. 1–2, pp. 39–44, 1999.
- [28] K. Sugawara, T. Okamoto, Y. Shimizu, C. Masutani, S. Iwai, and F. Hanaoka, "A multistep damage recognition mechanism for global genomic nucleotide excision repair," *Genes and Development*, vol. 15, no. 5, pp. 507–521, 2001.
- [29] N. E. Geacintov, S. Broyde, T. Buterin et al., "Thermodynamic and structural factors in the removal of bulky DNA adducts by the nucleotide excision repair machinery," *Biopolymers*, vol. 65, no. 3, pp. 202–210, 2002.
- [30] K. Sugawara, Y. Shimizu, S. Iwai, and F. Hanaoka, "A molecular mechanism for DNA damage recognition by the xeroderma pigmentosum group C protein complex," *DNA Repair*, vol. 1, no. 1, pp. 95–107, 2002.
- [31] M. T. Hess, D. Gunz, N. Luneva, N. E. Geacintov, and H. Naegeli, "Base pair conformation-dependent excision of benzo[a]pyrene diol epoxide-guanine adducts by human nucleotide excision repair enzymes," *Molecular and Cellular Biology*, vol. 17, no. 12, pp. 7069–7076, 1997.
- [32] M. Missura, T. Buterin, R. Hindges et al., "Double-check probing of DNA bending and unwinding by XPA-RPA: an architectural function in DNA repair," *EMBO Journal*, vol. 20, no. 13, pp. 3554–3564, 2001.
- [33] N. E. Geacintov, H. Naegeli, et al., "Structural aspects of polycyclic aromatic carcinogen-damaged DNA and its recognition by NER proteins," in *DNA Damage and Recognition*, W. Siede, Y. W. Kow, and P. W. Doetsch, Eds., Taylor & Francis, London, UK, 2006.
- [34] W. Yang, "Poor base stacking at DNA lesions may initiate recognition by many repair proteins," *DNA Repair*, vol. 5, no. 6, pp. 654–666, 2006.
- [35] W. Yang, "Structure and mechanism for DNA lesion recognition," *Cell Research*, vol. 18, no. 1, pp. 184–197, 2008.
- [36] R. J. Isaacs and H. P. Spielmann, "A model for initial DNA lesion recognition by NER and MMR based on local conformational flexibility," *DNA Repair*, vol. 3, no. 5, pp. 455–464, 2004.
- [37] T. Buterin, C. Meyer, B. Giese, and H. Naegeli, "DNA quality control by conformational readout on the undamaged strand of the double helix," *Chemistry and Biology*, vol. 12, no. 8, pp. 913–922, 2005.
- [38] E. Malta, G. F. Moolenaar, and N. Goosen, "Base flipping in nucleotide excision repair," *Journal of Biological Chemistry*, vol. 281, no. 4, pp. 2184–2194, 2006.
- [39] J. J. Truglio, E. Karakas, B. Rhau et al., "Structural basis for DNA recognition and processing by UvrB," *Nature Structural and Molecular Biology*, vol. 13, no. 4, pp. 360–364, 2006.
- [40] F. C. Clement, U. Camenisch, J. Fei, N. Kaczmarek, N. Mathieu, and H. Naegeli, "Dynamic two-stage mechanism of versatile DNA damage recognition by xeroderma pigmentosum group C protein," *Mutation Research*, vol. 685, no. 1–2, pp. 21–28, 2010.
- [41] J.-H. Min and N. P. Pavletich, "Recognition of DNA damage by the Rad4 nucleotide excision repair protein," *Nature*, vol. 449, no. 7162, pp. 570–575, 2007.
- [42] A. Luch, "Nature and nurture—lessons from chemical carcinogenesis," *Nature Reviews Cancer*, vol. 5, no. 2, pp. 113–125, 2005.
- [43] M. K. Buening, P. G. Wislocki, and H. Levin, "Tumorigenicity of the optical enantiomers of the diastereomeric benzo[a]pyrene 7,8-diol-9,10-epoxides in newborn mice: exceptional activity of (+)-7 $\beta$ ,8 $\alpha$ -dihydroxy-9 $\alpha$ ,10 $\alpha$ -epoxy-7,8,9,10-tetrahydrobenzo[a]pyrene," *Proceedings of the National Academy of Sciences of the United States of America*, vol. 75, no. 11, pp. 5358–5361, 1978.
- [44] I. B. Weinstein, A. M. Jeffrey, and K. W. Jennette, "Benzo[a]pyrene diol epoxides as intermediates in nucleic acid binding in vitro and in vivo," *Science*, vol. 193, no. 4253, pp. 592–594, 1976.
- [45] M. Koreeda, P. D. Moore, and P. Wislocki, "Binding of benzo[a]pyrene 7,8-diol-9,10-epoxides to DNA, RNA, and protein of mouse skin occurs with high stereoselectivity," *Science*, vol. 199, no. 4330, pp. 778–781, 1978.
- [46] I. B. Weinstein, A. M. Jeffrey, and K. W. Jennette, "Benzo[a]pyrene diol epoxides as intermediates in nucleic acid binding in vitro and in vivo," *Science*, vol. 193, no. 4253, pp. 592–594, 1976.
- [47] D. Wei, V. M. Maher, and J. J. McCormick, "Site-specific rates of excision repair of benzo[a]pyrene diol epoxide adducts in the hypoxanthine phosphoribosyltransferase gene of human fibroblasts: correlation with mutation spectra," *Proceedings of the National Academy of Sciences of the United States of America*, vol. 92, no. 6, pp. 2204–2208, 1995.
- [48] A. Fernandes, T. Liu, S. Amin, N. E. Geacintov, A. P. Grollman, and M. Moriya, "Mutagenic potential of stereoisomeric bay region (+)- and (-)-*cis-anti*-benzo[a]pyrene diol epoxide-*N*<sup>2</sup>-2'-deoxyguanosine adducts in *Escherichia coli* and Simian kidney cells," *Biochemistry*, vol. 37, no. 28, pp. 10164–10172, 1998.
- [49] K. Y. Seo, A. Nagalingam, M. Tiffany, and E. L. Loechler, "Mutagenesis studies with four stereoisomeric *N*<sup>2</sup>-dG benzo[a]pyrene adducts in the identical 5'-CGC sequence used in NMR studies: G  $\rightarrow$  T mutations dominate in each case," *Mutagenesis*, vol. 20, no. 6, pp. 441–448, 2005.
- [50] M. Cosman, C. de los Santos, R. Fiala et al., "Solution conformation of the major adduct between the carcinogen (+)-*anti*-benzo[a]pyrene diol epoxide and DNA," *Proceedings of the National Academy of Sciences of the United States of America*, vol. 89, no. 5, pp. 1914–1918, 1992.

- [51] F. A. Rodríguez, Y. Cai, C. Lin et al., "Exocyclic amino groups of flanking guanines govern sequence-dependent adduct conformations and local structural distortions for minor groove-aligned benzo[*a*]pyrenyl-guanine lesions in a GG mutation hotspot context," *Nucleic Acids Research*, vol. 35, no. 5, pp. 1555–1568, 2007.
- [52] Y. Cai, D. J. Patel, N. E. Geacintov, and S. Broyde, "Differential nucleotide excision repair susceptibility of bulky DNA adducts in different sequence contexts: hierarchies of recognition signals," *Journal of Molecular Biology*, vol. 385, no. 1, pp. 30–44, 2009.
- [53] K. Kropachev, M. Kolbanovskii, Y. Cai et al., "The sequence dependence of human nucleotide excision repair efficiencies of benzo[*a*]pyrene-derived DNA lesions: insights into the structural factors that favor dual incisions," *Journal of Molecular Biology*, vol. 386, no. 5, pp. 1193–1203, 2009.
- [54] J. Xu, *Sequence dependence of carcinogen-induced DNA bending*, Ph.D. thesis, New York University, New York, NY, USA, 1999.
- [55] A. A. Gorin, V. B. Zhurkin, and W. K. Olson, "B-DNA twisting correlates with base-pair morphology," *Journal of Molecular Biology*, vol. 247, no. 1, pp. 34–48, 1995.
- [56] R. E. Dickerson, "DNA bending: the prevalence of kinkiness and the virtues of normality," *Nucleic Acids Research*, vol. 26, no. 8, pp. 1906–1926, 1998.
- [57] W. K. Olson, A. A. Gorin, X.-J. Lu, L. M. Hock, and V. B. Zhurkin, "DNA sequence-dependent deformability deduced from protein-DNA crystal complexes," *Proceedings of the National Academy of Sciences of the United States of America*, vol. 95, no. 19, pp. 11163–11168, 1998.
- [58] N. E. Geacintov, M. Cosman, B. E. Hingerty, S. Amin, S. Broyde, and D. J. Patel, "NMR solution structures of stereoisomeric covalent polycyclic aromatic carcinogen-DNA adducts: Principles, patterns, and diversity," *Chemical Research in Toxicology*, vol. 10, no. 2, pp. 111–146, 1997.
- [59] R. Xu, B. Mao, S. Amin, and N. E. Geacintov, "Bending and circularization of site-specific and stereoisomeric carcinogen-DNA adducts," *Biochemistry*, vol. 37, no. 2, pp. 769–778, 1998.
- [60] H. Tsao, B. Mao, P. Zhuang, R. Xu, S. Amin, and N. E. Geacintov, "Sequence dependence and characteristics of bends induced by site-specific polynuclear aromatic carcinogen-deoxyguanosine lesions in oligonucleotides," *Biochemistry*, vol. 37, no. 14, pp. 4993–5000, 1998.
- [61] Q. Ruan, T. Liu, A. Kolbanovskiy et al., "Sequence context- and temperature-dependent nucleotide excision repair of a benzo[*a*]pyrene diol epoxide-guanine DNA adduct catalyzed by thermophilic UvrABC proteins," *Biochemistry*, vol. 46, no. 23, pp. 7006–7015, 2007.
- [62] K. J. Breslauer, R. Frank, H. Blocker, and L. A. Marky, "Predicting DNA duplex stability from the base sequence," *Proceedings of the National Academy of Sciences of the United States of America*, vol. 83, no. 11, pp. 3746–3750, 1986.
- [63] J. SantaLucia Jr., H. T. Allawi, and P. A. Seneviratne, "Improved nearest-neighbor parameters for predicting DNA duplex stability," *Biochemistry*, vol. 35, no. 11, pp. 3555–3562, 1996.
- [64] Y. Cai, D. J. Patel, N. E. Geacintov, and S. Broyde, "Dynamics of a benzo[*a*]pyrene-derived guanine DNA lesion in TGT and CGC sequence contexts: enhanced mobility in TGT explains conformational heterogeneity, flexible bending, and greater susceptibility to nucleotide excision repair," *Journal of Molecular Biology*, vol. 374, no. 2, pp. 292–305, 2007.
- [65] E. J. Gardiner, C. A. Hunter, M. J. Packer, D. S. Palmer, and P. Willett, "Sequence-dependent DNA Structure: a database of octamer structural parameters," *Journal of Molecular Biology*, vol. 332, no. 5, pp. 1025–1035, 2003.
- [66] Y. Cai, K. Kropachev, R. Xu et al., "Distant neighbor base sequence context effects in human nucleotide excision repair of a benzo[*a*]pyrene-derived DNA lesion," *Journal of Molecular Biology*, vol. 399, no. 3, pp. 397–409, 2010.
- [67] R. C. Johnson, S. Stella, et al., "Bending and compaction of DNA by proteins," in *Protein-Nucleic Acid Interactions*, P. A. Rice and C. C. Correll, Eds., The Royal Society of Chemistry, Cambridge, UK, 2008.
- [68] C. R. Calladine, "Mechanics of sequence-dependent stacking of bases in B-DNA," *Journal of Molecular Biology*, vol. 161, no. 2, pp. 343–352, 1982.
- [69] M. A. el Hassan and C. R. Calladine, "Conformational characteristics of DNA: empirical classifications and a hypothesis for the conformational behaviour of dinucleotide steps," *Philosophical Transactions of the Royal Society A*, vol. 355, no. 1722, pp. 43–100, 1997.
- [70] M. A. el Hassan and C. R. Calladine, "Two distinct modes of protein-induced bending in DNA," *Journal of Molecular Biology*, vol. 282, no. 2, pp. 331–343, 1998.
- [71] M. J. Packer, M. P. Dauncey, and C. A. Hunter, "Sequence-dependent DNA structure: dinucleotide conformational maps," *Journal of Molecular Biology*, vol. 295, no. 1, pp. 71–83, 2000.
- [72] T. M. Okonogi, S. C. Alley, A. W. Reese, P. B. Hopkins, and B. H. Robinson, "Sequence-dependent dynamics of duplex DNA: the applicability of a dinucleotide model," *Biophysical Journal*, vol. 83, no. 6, pp. 3446–3459, 2002.
- [73] O. D. Schärer, "A molecular basis for damage recognition in eukaryotic nucleotide excision repair," *ChemBioChem*, vol. 9, no. 1, pp. 21–23, 2008.
- [74] T. Buterin, M. T. Hess, N. Luneva et al., "Unrepaired fjord region polycyclic aromatic hydrocarbon-DNA adducts in ras codon 61 mutational hot spots," *Cancer Research*, vol. 60, no. 7, pp. 1849–1856, 2000.

## Review Article

# True Lies: The Double Life of the Nucleotide Excision Repair Factors in Transcription and DNA Repair

**Nicolas Le May, Jean-Marc Egly, and Frédéric Coin**

*Department of Functional Genomics, IGBMC, CNRS/INSERM/Université de Strasbourg, BP 163, 67404 Illkirch Cedex, Strasbourg, France*

Correspondence should be addressed to Frédéric Coin, fredr@igbmc.fr

Received 12 April 2010; Accepted 21 May 2010

Academic Editor: Ashis Basu

Copyright © 2010 Nicolas Le May et al. This is an open access article distributed under the Creative Commons Attribution License, which permits unrestricted use, distribution, and reproduction in any medium, provided the original work is properly cited.

Nucleotide excision repair (NER) is a major DNA repair pathway in eukaryotic cells. NER removes structurally diverse lesions such as pyrimidine dimers, arising upon UV irradiation or bulky chemical adducts, arising upon exposure to carcinogens and some chemotherapeutic drugs. NER defects lead to three genetic disorders that result in predisposition to cancers, accelerated aging, neurological and developmental defects. During NER, more than 30 polypeptides cooperate to recognize, incise, and excise a damaged oligonucleotide from the genomic DNA. Recent papers reveal an additional and unexpected role for the NER factors. In the absence of a genotoxic attack, the promoters of RNA polymerases I- and II-dependent genes recruit XPA, XPC, XPG, and XPF to initiate gene expression. A model that includes the growth arrest and DNA damage 45 $\alpha$  protein (Gadd45 $\alpha$ ) and the NER factors, in order to maintain the promoter of active genes under a hypomethylated state, has been proposed but remains controversial. This paper focuses on the double life of the NER factors in DNA repair and transcription and describes the possible roles of these factors in the RNA synthesis process.

## 1. Introduction

A number of DNA repair pathways protect us from the deleterious effects of DNA damage. The importance of these mechanisms is highlighted by the existence of genetic disorders in which impaired DNA repair mechanisms predispose patients to cancer and early onset of aging. A major advance in our understanding of these DNA repair mechanisms has been to uncover the tangled connection existing between these systems and other fundamental cellular processes such as DNA replication and transcription. These cellular processes are not only highly connected with DNA repair pathways but they also share common factors with them. This complexity leads to new hypothesis about the cause of the phenotypes displayed by patients suffering from DNA repair disorders and may even force us to re-evaluate the place of the repair factors in cellular homeostasis.

## 2. The NER Pathway: The Fountain of Youth of Our Genome

We do not live forever young. We all have to experience aging, a functional decline coupled to an increased mortality risk from diseases such as cancer. The molecular origins of aging can be sought, at least in part, in an alteration of the expression of our genes that results from the physicochemical constitution of DNA, which does not guarantee life-long stability (for reviews see [1, 2]). Over time, DNA accumulates a tremendous diversity of lesions that, if unrepaired, lead to mutations that dysregulate the function of proteins. DNA lesions originate from environmental agents such as the ultraviolet (UV) component of sunlight, ionizing radiation, and numerous genotoxic chemicals, and also from the products of normal cellular metabolism. Aging is a relatively slow process for most of us, but unfortunately premature appearance of multiple symptoms of aging can be observed in a growing family of human syndromes [3, 4]. Among

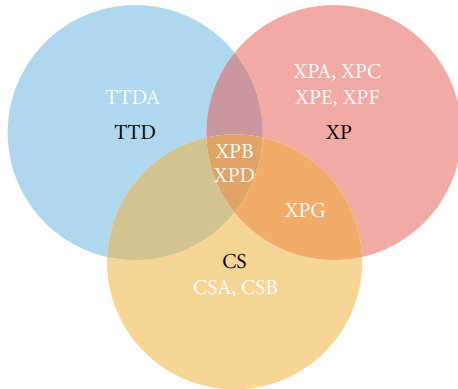


FIGURE 1: Three disorders for nine genes. Mutations in ten genes are responsible for the *xeroderma pigmentosum* (XP), the *trichothiodystrophy* (TTD) or the Cockayne syndrome (CS). XPA, XPC, XPE and XPF are only involved in XP; CSA and CSB are only involved in CS; XPG is involved in pure XP or in a combined XP/CS syndrome; XPB and XPD are involved in TTD, XP, or in a combined XP/CS syndrome. TTDA is only involved in TTD.

them, the *xeroderma pigmentosum* (XP), *trichothiodystrophy* (TTD), and Cockayne syndrome (CS) are remarkable as they all include two distinct phenotypes: either a 1000-fold elevated suninduced skin cancer risk, for XP patients, or a segmental progeria without an increase in cancer incidence, for CS and TTD [5]. These syndromes uncover what our lives would be if a “fountain of youth” was not protecting our genome day after day from endogenous and exogenous assaults. Indeed, the main molecular defect of the XP, CS, and TTD patients resides in a defect in the nucleotide excision repair (NER) pathway [6]. NER is an evolutionarily conserved DNA repair caretaker pathway involving about 30 proteins, ten of which (designated XPA to G; TTDA, CSA, and CSB) are differentially associated with XP, CS, or TTD disorders in an intricate network (Figure 1). NER is divided into two subpathways, which differentially remove damages from our genome depending on their location [7]. In the Global Genome NER (GGNER), the XPChHR23B complex recognizes damages. The DNA is then opened by the XPD and XPB helicasecontaining transcription/repair complex TFIIH together with XPA and RPA to generate the damaged single stranded DNA ready for incision by the specific endonucleases XPG and ERCC1-XPE. DNA gap filling is done by the replicative DNA polymerases  $\delta$  and  $\epsilon$  or the translesional polymerase  $k$ , in the presence of PCNA, RFC, and RPA [8] (Figure 2). In transcription-coupled NER (TC-NER), blockage of transcribing RNA Polymerase II (RNA-Pol II) on the damaged DNA template is thought to initiate the repair reaction in a process that requires, in addition to TFIIH, XPA, XPG, and ERCC1-XPE, the TCR-specific proteins CSB and CSA [9] (Figure 2). Although CSB is required to recruit NER factors to the stalled RNA-Pol II, CSA is coming later and is not needed for the formation of the TCR complex [10] (Figure 2).

Next to the basal NER machinery, additional factors modulate the efficiency of the NER reaction but are not

required to incise a damaged oligonucleotide *in vitro*. The GG-NER damage recognition factor, XPC, forms *in vivo* a heterotrimeric complex involving one of the two human homologs of *S.cerevisiae* Rad23p (hHR23B) and centrin 2, a centrosomal protein [11]. The role of centrin 2 and hHR23B in NER has been elusive but they seem to increase the damage recognition capacity of XPC [12]. The XPE complex, mutated in XP-E patients, is another accessory NER factor composed of DDB1 and DDB2. The role of the XPE protein remains unclear, but it could participate in the recognition of lesions together with XPC [13]. Another NER factor, XPA-binding protein 2 (XAB2), was identified by virtue of its ability to interact with XPA [14]. XAB2 also associates with the TC-NER specific proteins CSA and CSB, as well as with RNA-Pol II, after UV irradiation and is specifically involved in the TC-NER subpathway [15]. Finally, the DDB2 and CSA polypeptides can be found integrated into nearly identical complexes containing cullin 4A, Roc1, and COP9 that seem to favor NER [16]. Although limited today, the list of proteins that modulate the NER reaction should increase in a near future and benefit from high throughput technologies. The study of these cofactors will constitute an important challenge, as the modulation of the efficiency of NER to eliminate DNA lesions may explain some cancer predispositions in healthy people. Moreover, identifying the complete set of proteins that participate in NER is a crucial aspect of cancer therapy since the resistance to chemotherapy treatment could partially rely on the capacities of the cell to eliminate drug-induced DNA lesions.

### 3. The NER Pathway in a Chromatin Context: Take Old Factors to Make Them New

New DNA repair players have also emerged from the study of NER in the chromatin context. Reorganisation of nucleosome structure following NER was observed over 30 years ago [17], and many studies demonstrate that chromatin acts as a barrier for the recognition of the lesions by NER factors [18]. Not surprisingly, chromatin remodelers identified in NER were already known to promote accessibility to the DNA for the transcription machinery. The ATP-dependent chromatin remodelling complexes SWI/SNF or ISW2 have been shown to act on UV-damaged nucleosomes and to stimulate repair *in vitro* [19]. In yeast, UV irradiation increases contacts between SWI/SNF and the homologs of XPC-hHR23B, and inactivation of SWI-SNF leads to a slow removal of CPD lesions [20]. Finally, the ATP-dependent chromatin assembly factor-1 (CAF-1) is required to restore the chromatin conformation after the removal of the lesions [21].

Apart from ATP-dependent nucleosome remodelling, many forms of histones modifications have been unveiled after UV irradiation. Histone acetylation was the first modification to be shown to play a role in NER. Treatment of nonreplicating human cells with the histone deacetylase inhibitor sodium butyrate enhances NER [22]. PCNA, the replicative protein involved in the DNA resynthesis step of NER, interacts with the p300 histone acetyltransferase

following UV irradiation [23]. On the other hand, a complex containing the damaged DNA-binding protein DDB1, the CREB-binding protein CBP, and p300 has been isolated *in vivo* [24]. Another complex, TBP-free-TAFII complex (TFTC), directs histone H3 acetylation by hGCN5 after UV irradiation and facilitates access of DNA repair machinery to lesions within chromatin [25]. In addition to histone acetylation, UV damage also induces histone H2A monoubiquitination in the vicinity of DNA lesions [26]. Monoubiquitination of H2A depends on functional NER and occurs after incision [27].

Overall, these data show that histone modifications form part of the cellular response to UV damage and clearly play a role in chromatin remodelling during DNA repair. However, the exact nature of the modified histones and residues as well as the role of these modifications in the facilitation of DNA damage access or in the DNA damage response not clear. Much remains to be done to define a histone code in NER, comparable to that acquired in other fundamental cellular processes like transcription or double-strand break repair.

#### 4. The Unveiled Side of the XP, CS, and TTD Syndromes

Although the UV sensitivity and/or cancer predisposition of XP, CS, and TTD patients can be explained by defects in NER, some other of their phenotypes (including neurological and developmental defects) are more difficult to rationalize. For instance, some group A patients show the most severe progressive neurological disorders while the XPA protein is only known for its role in the verification of the damages [5]. Thus, several studies have aimed to discover additional processes that may be disrupted in these pathologies and at a first glance have found evidence for transcription defect in TFIIH-, XPG-, and CSB-mutated cells.

TFIIH is a ten-subunit complex composed of a core (XPB, p62, p52, p44, p34, and TTDA) coupled to the Cdk-activating kinase complex (CAK) through the XPD subunit [28]. A recent study showed that CAK does not participate to NER and is released from the core TFIIH during the formation of the preincision complex following the recruitment of XPA [29] (see also Figure 2). As a component of TFIIH, CAK phosphorylates both the carboxyl terminal domain of RNA-Pol II and some nuclear receptors (NRs) including the retinoic acid receptors (RAR $\alpha$  and  $\gamma$ ) [30], the thyroid hormone receptor (TR) [31], and the peroxysome proliferator-activated receptor (PPAR) [32]. Phosphorylation of these NRs is required for the transactivation of specific genes. Cdk7 also activates the vitamin D receptor indirectly, by phosphorylating the Ets1 coactivator [33] (Table 1).

Patients with mutations in XPB and XPD display a transcriptional defect in specific genes, which may help clarifying the origin of their developmental or neurological problems. In TTD-XPD cells, mutations in XPD destabilize the CAK complex from TFIIH leading to defects in the phosphorylation of RAR, ER, and PPAR. In XP-B patients, two mutations in XPB (F99S and fs740) lead to the combined

XP/CS defect with a very low level of residual NER activity [34]. However, only the fs740 mutation is cancer prone [35]. It was shown that this mutation specifically blocks transcription activation by the FUSE-Binding Protein (FBP), a regulator of c-myc expression, and inhibition by the FBP-Interacting Repressor (FIR) [36]. The fact that the regulation by FBP and FIR is impaired could directly affect proper regulation of c-myc expression and explain the development of malignancy in the corresponding patient. The XPB and XPD subunits of TFIIH are not the only NER polypeptides to be involved in transcription.

The first evidence for an involvement of XPG in transcription came from a study in yeast. RAD2, the *S.cerevisiae* counterpart of XPG, was shown to be required in promoting efficient RNA-Pol II transcription [37]. Later, it was demonstrated that mutations in human XPG, as found in XP-G/CS patient cells, prevent the association of XPG with TFIIH, resulting in the dissociation of the CAK and XPD from the core TFIIH [38]. This dissociation leads to an impair transactivation of the NR-dependent responsive genes.

The TCR-specific CSB protein belongs to the ATP-dependent SWI2/SNF2 family of chromatin remodeling proteins and has been shown to play a role in both remodeling the chromatin structure and disrupting protein-DNA interactions [39]. Besides its role in TCR, CSB is involved in the transcription recovery of housekeeping genes after UV irradiation [40]. CSB is specifically recruited to the promoters of these genes and helps in the recruitment of both the RNA-Pol II and the associated basal transcription factors, probably through its chromatin remodeling activity (Table 1).

Altogether, these data show that the transcription defect in XP/CS, CS, or TTD is subtle and more difficult to evaluate than the NER defect because this defect targets specific genes, under specific conditions, and probably in a cell-specific manner. However, the involvement of transcription dysregulation in aging and cancer makes these studies very important for the understanding of these diseases. Interestingly, a picture emerges from these studies, which shows that mutations in XP factors lead to a modification of the expression of specific genes by possibly two means; either through the accumulation of unrepaired lesions that will lead to mutations or through a direct involvement of repair factors in gene expression. However, a piece of the puzzle is missing. Even though a clear involvement of XPB, XPD, XPG, or CSB in transcription was documented, it has been more difficult to assign a transcriptional role to XPC, XPA, or ERCC1-XPF until the recent works discussed below.

#### 5. Behind the Evidence: A Transcriptional Role for the NER Factors

Protein coding genes expression is the result of an acute process that starts at the promoter of a given gene and involves, in the addition to the RNA-Pol II and the basal transcription factors, a cocktail of proteins such as the NR, coactivators, mediator, and histone-modifying enzymes. A study from our group [41] shows that some NER factors are associated with the transcription machinery at the promoter

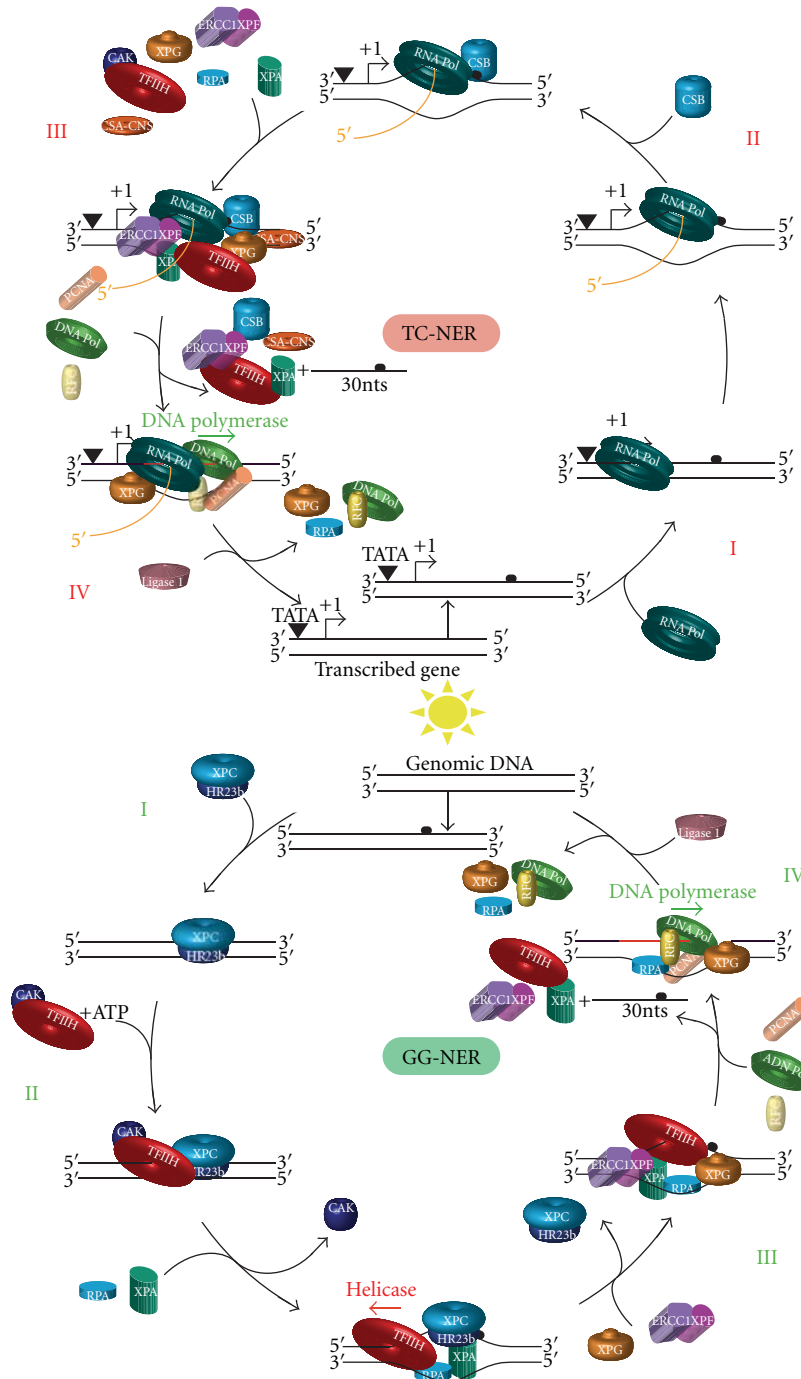


FIGURE 2: The two subpathways of mammalian NER. Physical or chemical agents like UV, cis-platin, or benzopyrene can damage DNA and induce damage-mediated helix distortions anywhere in the genome (GG-NER in green, bottom panel) or on the transcribed strand of a gene (TC-NER in red, top panel). Bottom panel: (I) XPC-RAD23B recognizes and binds to DNA damage-mediated helix distortion to initiate GG-NER. (II) TFIIH is recruited in an ATP-dependent manner, followed by XPA and RPA, which verify the presence of the lesion. During this step, the CAK module of TFIIH is released from the preincision complex [29]. (III) Within the preincision complex, ERCC1-XPF and XPG structure-specific endonucleases incise the damaged strand on the 5' and 3' sides of the lesion, respectively. Following incision, NER factors are released from the DNA, except XPG and RPA that favour the recruitment of the replication machinery composed of PCNA, RFC, and the DNA Polymerases  $\delta$ ,  $\epsilon$ , or  $\kappa$  (ref). (IV) Following replication of the gap, the DNA is sealed by the ligase 1 (or the ligase III-XRCC1 complex in nondividing cells). Top Panel: (I) TC-NER is triggered by DNA damage-mediated blockage of RNA-Pol II (Top panel). (II) CSB is then recruited to the stalled RNA-Pol II enzyme and triggers the recruitment of the NER factors TFIIH, XPA, RPA, ERCC1-XPF, and XPG together with the CSA-CNS complex (III). (IV) Following the excision of the damaged oligonucleotide, the same DNA replication machinery of the GG-NER subpathway fills the gap created by the incision/excision step.

TABLE 1: Repair/transcription factors and their functions.

Factors	Role in NER	Role in transcription
TFIIH	Opens DNA around the damage. Favors 5' incision by ERCC1-XPF.	Opens DNA around the promoter. Phosphorylates the CTD of RNA-Pol II. Phosphorylates NR and coactivators.
XPG	Incises DNA in 3' from the lesion	Involved in NR-dependent transcription. Stabilizes the interaction of CAK to the core TFIIH.
CSB	TC-NER-specific factor. Recruits NER factors to stalled RNA-Pol II.	Chromatin-remodeling factor (SWI-SNF family). Reinitiates transcription after DNA damage removal.
<b>XPC</b>	<b>Recognition of lesions</b>	<b>Involved in NR-dependent transcription.</b> <b>Removal of 5meC</b> <b>Chromatin modification?</b>
<b>XPA</b>	<b>Verification of lesions</b>	<b>Involved in NR-dependent transcription.</b> <b>Removal of 5meC</b> <b>Chromatin modification?</b>
<b>XPF</b>	<b>Incises DNA in 3' from the lesion</b>	<b>Involved in NR-dependent transcription.</b> <b>Removal of 5meC,</b> <b>Chromatin modification?</b> <b>Incision?</b>

In bold, the new NER factors involved in transcription.

of several activated NR-dependent genes. The recruitment occurs in a sequential order after the formation of the preinitiation complex (PIC) and induces XPC, CSB, XPA, and the XPG and ERCC1-XPF endonucleases. The transcriptional complex equipped with NER factors is formed in the absence of any exogenous genotoxic attack and is distinct from a repair complex, since it is specifically sensitive to transcription inhibitors and can be formed in the absence of the TCR specific-CSB protein (Figure 3). Following transcription initiation, NER factors escort the RNA-Pol II during the elongation step to form a complex that does not include XPC but requires CSB (Figure 3). These observations suggest a different function for the NER factors located at promoters in respect to those located at distal regions of the gene; while the latter may represent a pre-TCR complex ready to remove lesions on transcribed genes, the former may play an active role in transcription. In line with this hypothesis, patient cell lines mutated in XPC, XPA, or XPG show a dysregulation of the NR-dependent genes that results from a defect in the association of the NER factors with the transcription machinery. Although the corresponding XPC, XPA, XPG, and ERCC1-XPF repair factors are not essential for PIC formation, it remains that they optimize the efficiency of transcription.

## 6. Insight into the Function of the NER Factor in Transcription

How do NER factors favor NR-dependent genes transcription? Several studies have reported a controversial role for Gadd45 $\alpha$  in association with the endonuclease activity of XPG in transcription: the active demethylation of CpGs islands localized at proximal promoters [42–44]. Recent works support these findings and demonstrate that the recruitment of XPC, XPA, XPG, and ERCC1-XPF on the promoter of active RNA-Pol I- and II-dependent genes

allows the association of Gadd45 $\alpha$  to the PIC and induce the demethylation of promoters [41, 44]. Mutations in XPC, XPA and XPG found in XP patients dysregulate the corecruitment of the NER factors and Gadd45 $\alpha$  to active promoters, thereby abolishing the active demethylation step and thus affecting transcription.

How can the NER factors demethylate DNA? Similar to a classical NER lesion, 5'-methylcytosine (meC) combined to the specific chromatin environment during transcription initiation could be recognized and eliminated by the NER machinery [45] (Figure 4(a)). Indeed, a previous study demonstrated a faster repair rates near the transcription initiation site linked to increased local concentrations of DNA repair factors associated with basal transcription factors [46]. The sequential recruitment of NER factors could help the incision and the replacement of meC with unmethylated nucleotides. Even if incision by XPG on the promoter of RNA Pol I-dependent genes has been reported [44], this hypothesis is highly controversial, and several groups propose other alternatives to explain the demethylation of meC. Recent studies have supported a model involving at least two steps [43, 47] (Figure 4(b)). The model predicts the conversion of meC to cytosine by the direct removal of the methyl group or by the hydrolytic deamination of meC to thymine further excised by a DNA repair enzyme. The first step concerns the deamination reaction and implies apolipoprotein B mRNA editing enzyme (APOBECS) proteins such as activation-induced cytidine deaminase (AID) and APOBEC1, which function in sequence specific context. Alternatively, it has also been suggested that enzymes called DNA methyltransferases (DNMTs) exhibit dual and opposite actions, not only to methylate CpG islands but also to deaminate them [48]. The second step is related to the action of a DNA glycosylase such as Mdb4 or TDG that remove thymine from G/T mismatches to generate abasic sites rapidly cleaved through the activity of apurinic/apyrimidinic

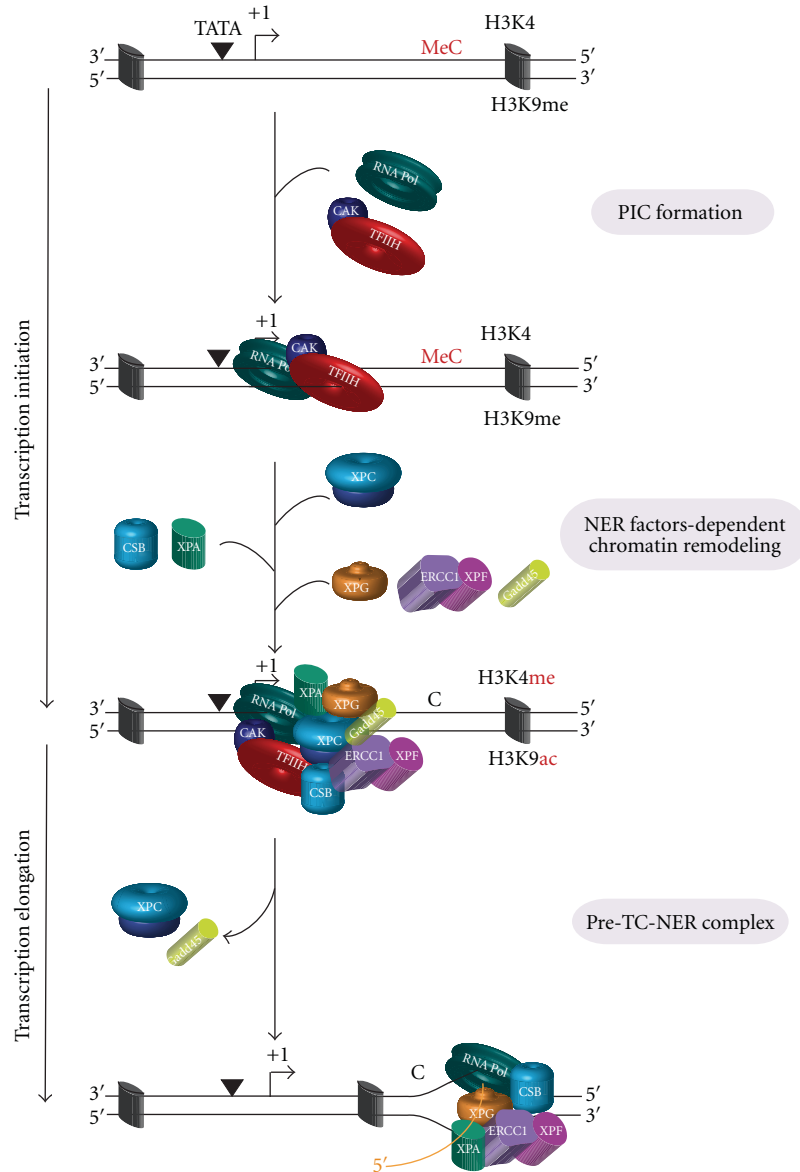


FIGURE 3: NER factors and gene transcription. Upon gene activation, the formation of preinitiation complex (PIC) precedes the recruitment of XPC, which allows the sequential arrival of the other NER factors in the following order CSB, XPA/RPA, XPG/ERCC1-XPF, and Gadd45 $\alpha$ . The association of NER factors and Gadd45 $\alpha$  with the transcription machinery leads to a cascade of histone PTMs. Concomitantly, an active demethylation of 5' CpG islands occurs.

endonuclease (APE) (Figure 4(b)) [43]. It was recently shown that Mdb4 is corecruited to active promoters with proteins from base-excision-repair (BER) process such as APE-1, DNA ligase I, or polymerase  $\delta$  [48]. Even though the role of Gadd45 $\alpha$  is controversial, it clearly increases the efficiency of the demethylation process.

The results obtained recently by several groups lead us to propose another hypothesis that could account for the active demethylation of promoters during transcription and involves both the NER and the BER factors. Active DNA demethylation at promoters is intimately linked with histones posttranslational modifications (PTMs) [49]. Di/tri

methylation of H3K4 (H3K4me) and di/trimethylation of H3K9 (H3K9me) correlate with active transcription and heterochromatin, respectively. In a repressed status, the methyltransferase G9a catalyzes the methylation of H3K9, which allows the binding of the heterochromatin protein 1 (HP1) to facilitate the local formation of heterochromatin. The G9a-containing complex also recruits the DNA methyltransferases DNMT3A and DNMT3B that catalyze the *de novo* methylation of DNA at promoters. Conversely, during active transcription and concomitantly to demethylation/acetylation of H3K9, methylation of H3K4 inhibits contacts between nucleosome and DNMT3 to facilitate active

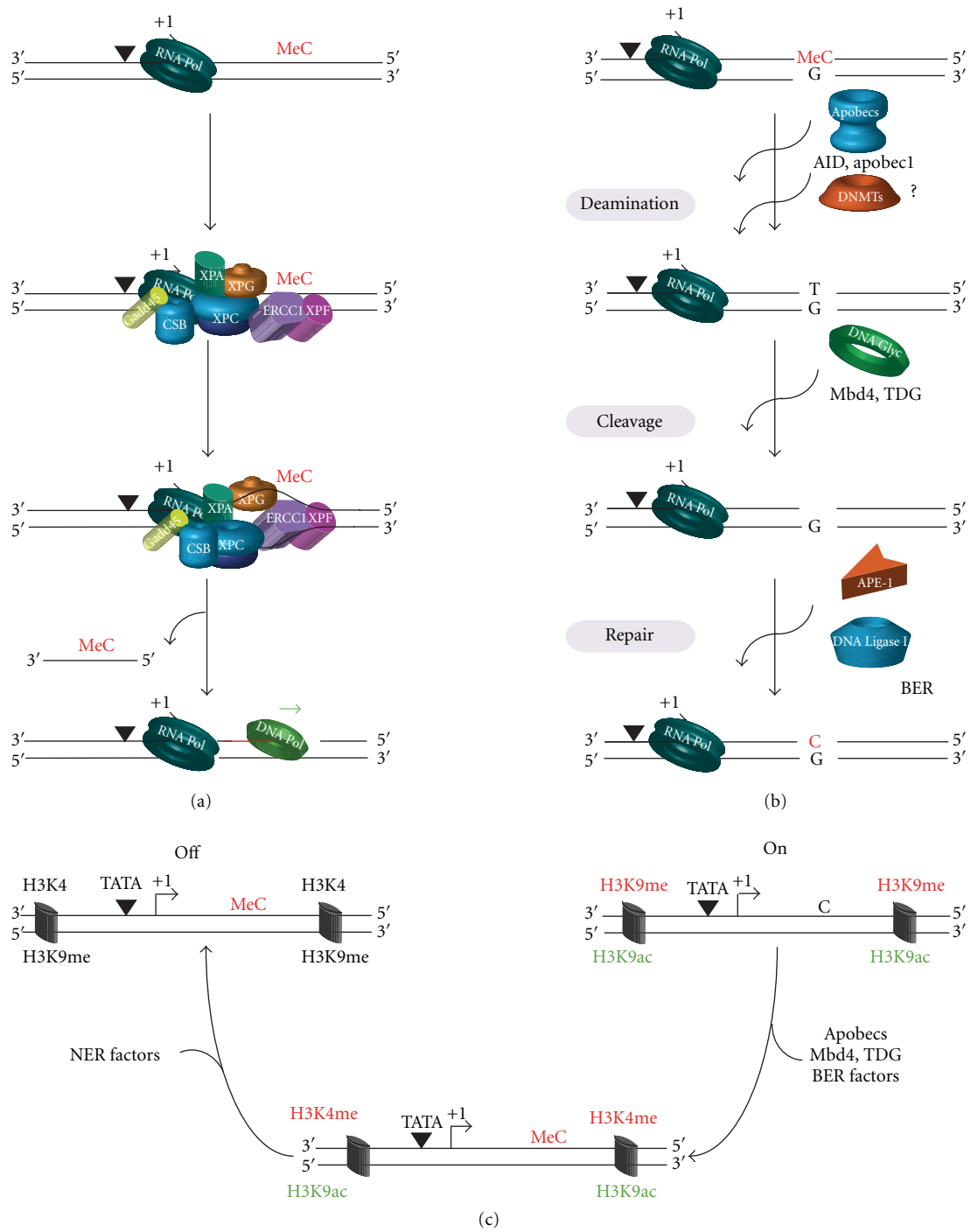


FIGURE 4: Potential mechanisms of cytosine demethylation. (a) The NER machinery, recruited to the preinitiation complex, can recognize the 5-methyl cytosine (meC) as a NER-specific substrate, in the presence of Gadd45 $\alpha$ , and eliminate it in a process closely related to the canonical NER process with the incision/excision of the oligonucleotide containing the meC. (b) Another pathway involves two steps; first, the deamination of 5-methylcytosine (meC) to thymine, which involves proteins from Apobec family such as AID or APOBEC1. A role in deamination has been also suggested for DNMTs proteins. Consequently, the impairment of the thymine with the guanine in the opposite strand induces the recruitment of DNA glycosylases such as Mbd4 or TDG that remove thymine through cleavage of the glycosidic bond. Following the action of DNA glycosylases, it remains an apyrimidinic site, which is cleaved by an AP endonuclease such as APE1 and repaired through the polymerase  $\beta$  and DNA ligases. NER factors and Gadd45 $\alpha$  are involved in this mechanism but their roles are not determined. (c) We propose that NER factors control the epigenetic environment of the promoter favouring the demethylation of H3K9 and the methylation of H3K4. Following the action of the NER factors, Apobec proteins and BER factors demethylate the meC in a process similar to (b).

DNA demethylation [50]. NR-dependent altered transcription observed in XP-C, XP-A, or XP-G cells is accompanied by dysregulation of PTMs of histones. The hypermethylated status of these promoters in these cells is associated with absence of H3K4me and maintenance of the H3K9me marks. These observations imply that the promoter of NR-dependent genes persists in a heterochromatin environment, despite the formation of the RNA-Pol II machinery, thereby impairing optimal transcription. There is no evidence of a direct role of repair factors in the regulation of histones PTMs or histone-modifying enzymes; it can be hypothesised that NER factors function upstream of the BER factors to help to maintain a euchromatin environment characterised by a demethylation of H3K9 and a methylation of H3K4 (Figure 4(c)).

## 7. Conclusion

Almost twenty years after the discovery that the basal transcription factor TFIID was also involved in NER [51], a new age arises from the discovery that basal NER factors are involved in activated transcription. The emergence of repair factors in transcription forces us to modify our approach for the understanding of the broad clinical features described for the so-called XP, TTD, and CS “repair syndromes”, but it also represents a breakthrough in gene expression studies. Indeed, the effects of DNA methylation variations on gene expression have been largely studied, but the mechanisms that promote active demethylation combined to histones modifications are just appearing with the finding that DNA repair factors may participate to this process.

Besides the 2D space organisation of a gene, one has also to consider the 3D space organisation of the nucleus. Transcription is deeply associated to genome organization; the location of a gene within the chromosome territories influences its ability to be reached by the suitable machinery [52]. Since the PTMs of histone and the methylated status of genomic DNA are connected to the dynamic topological regulation of chromatin, we have to consider that NER factors could contribute to transcription through a role in the nonrandom organization of the nucleus. Surprisingly, besides the DNA repair disorders, a second group of diseases that are characterized by accelerated aging comprises the Hutchinson-Gilford syndrome (or Progeria) that is due to a point mutation in Lamin A [53, 54]. This protein is a structural component of the nuclear matrix that plays a role in the 3D organization of the genome. It is then tempting to propose that changes in the nuclear architecture in these disorders participate in the modification of the transcription program and possibly to the impairment of the repair of some lesions, that altogether lead to accelerated aging and cancer.

## Acknowledgments

The authors are more than grateful to Renier Velez Cruz, and Emmanuel Compe for the critical reading of this paper and for their suggestion. Frédéric Coin and Jean-Marc Egly are

funded by the Institut National du Cancer (INCA-2008-041), the French National Research Agency (ANR-08-GENOPAT-042), and ERC advanced Grant (ERC-2008-ADG233077). Nicolas Le May is supported by the INSERM.

## References

- [1] J. H. J. Hoeijmakers, “DNA damage, aging, and cancer,” *The New England Journal of Medicine*, vol. 361, no. 15, pp. 1475–1485, 2009.
- [2] J. Q. Svejstrup, “The interface between transcription and mechanisms maintaining genome integrity,” *Trends in Biochemical Sciences*, vol. 35, no. 6, pp. 333–338, 2010.
- [3] B. Schumacher, G. A. Garinis, and J. H. J. Hoeijmakers, “Age to survive: DNA damage and aging,” *Trends in Genetics*, vol. 24, no. 2, pp. 77–85, 2008.
- [4] Y. Kamenisch and M. Berneburg, “Progeroid syndromes and UV-induced oxidative DNA damage,” *Journal of Investigative Dermatology Symposium Proceedings*, vol. 14, no. 1, pp. 8–14, 2009.
- [5] A. R. Lehmann, “DNA repair-deficient diseases, xeroderma pigmentosum, Cockayne syndrome and trichothiodystrophy,” *Biochimie*, vol. 85, no. 11, pp. 1101–1111, 2003.
- [6] J. E. Cleaver, E. T. Lam, and I. Revet, “Disorders of nucleotide excision repair: the genetic and molecular basis of heterogeneity,” *Nature Reviews Genetics*, vol. 10, no. 11, pp. 756–768, 2009.
- [7] P. C. Hanawalt, “Subpathways of nucleotide excision repair and their regulation,” *Oncogene*, vol. 21, no. 58, pp. 8949–8956, 2002.
- [8] T. Ogi, S. Limsirichaikul, R. M. Overmeer et al., “Three DNA polymerases, recruited by different mechanisms, carry out NER repair synthesis in human cells,” *Molecular Cell*, vol. 37, no. 5, pp. 714–727, 2010.
- [9] M. Fousteri and L. H. F. Mullenders, “Transcription-coupled nucleotide excision repair in mammalian cells: molecular mechanisms and biological effects,” *Cell Research*, vol. 18, no. 1, pp. 73–84, 2008.
- [10] G. Spivak, R. A. Cox, and P. C. Hanawalt, “New applications of the Comet assay: Comet-FISH and transcription-coupled DNA repair,” *Mutation Research*, vol. 681, no. 1, pp. 44–50, 2009.
- [11] M. Araki, C. Masutani, M. Takemura et al., “Centrosome protein centrin 2/caltractin 1 is part of the xeroderma pigmentosum group C complex that initiates global genome nucleotide excision repair,” *Journal of Biological Chemistry*, vol. 276, no. 22, pp. 18665–18672, 2001.
- [12] R. Nishi, Y. Okuda, E. Watanabe et al., “Centrin 2 stimulates nucleotide excision repair by interacting with xeroderma pigmentosum group C protein,” *Molecular and Cellular Biology*, vol. 25, no. 13, pp. 5664–5674, 2005.
- [13] T. Itoh and D. Bennett, “The XPE gene of xeroderma pigmentosum, its product and biological roles,” *Advances in Experimental Medicine and Biology*, vol. 637, pp. 57–64, 2008.
- [14] Y. Nakatsu, H. Asahina, E. Citterio et al., “XAB2, a novel tetratricopeptide repeat protein involved in transcription-coupled DNA repair and transcription,” *Journal of Biological Chemistry*, vol. 275, no. 45, pp. 34931–34937, 2000.
- [15] I. Kuraoka, S. Ito, T. Wada et al., “Isolation of XAB2 complex involved in pre-mRNA splicing, transcription, and transcription-coupled repair,” *Journal of Biological Chemistry*, vol. 283, no. 2, pp. 940–950, 2008.

- [16] R. Groisman, J. Polanowska, I. Kuraoka et al., "The ubiquitin ligase activity in the DDB2 and CSA complexes is differentially regulated by the COP9 signalosome in response to DNA damage," *Cell*, vol. 113, no. 3, pp. 357–367, 2003.
- [17] M. J. Smerdon and M. W. Lieberman, "Nucleosome rearrangement in human chromatin during UV-induced DNA repair synthesis," *Proceedings of the National Academy of Sciences of the United States of America*, vol. 75, no. 9, pp. 4238–4241, 1978.
- [18] R. Hara, J. Mo, and A. Sancar, "DNA damage in the nucleosome core is refractory to repair by human excision nuclease," *Molecular and Cellular Biology*, vol. 20, no. 24, pp. 9173–9181, 2000.
- [19] H. Menoni, D. Gasparutto, A. Hamiche et al., "ATP-dependent chromatin remodeling is required for base excision repair in conventional but not in variant H2A.Bbd nucleosomes," *Molecular and Cellular Biology*, vol. 27, no. 17, pp. 5949–5956, 2007.
- [20] F. Gong, D. Fahy, and M. J. Smerdon, "Rad4-Rad23 interaction with SWI/SNF links ATP-dependent chromatin remodeling with nucleotide excision repair," *Nature Structural and Molecular Biology*, vol. 13, no. 10, pp. 902–907, 2006.
- [21] P.-H. L. Gaillard, E. M.-D. Martini, P. D. Kaufman, B. Stillman, E. Moustacchi, and G. Almouzni, "Chromatin assembly coupled to DNA repair: a new role for chromatin assembly factor I," *Cell*, vol. 86, no. 6, pp. 887–896, 1996.
- [22] M. J. Smerdon, S. Y. Lan, R. E. Calza, and R. Reeves, "Sodium butyrate stimulates DNA repair in UV-irradiated normal and xeroderma pigmentosum human fibroblasts," *Journal of Biological Chemistry*, vol. 257, no. 22, pp. 13441–13447, 1982.
- [23] S. Hasan, P. O. Hassa, R. Imhof, and M. O. Hottiger, "Transcription coactivator p300 binds PCNA and may have a role in DNA repair synthesis," *Nature*, vol. 410, no. 6826, pp. 387–391, 2001.
- [24] A. Datta, S. Bagchi, A. Nag et al., "The p48 subunit of the damaged-DNA binding protein DDB associates with the CBP/p300 family of histone acetyltransferase," *Mutation Research*, vol. 486, no. 2, pp. 89–97, 2001.
- [25] M. Brand, J. G. Moggs, M. Oulad-Abdelghani et al., "UV-damaged DNA-binding protein in the TFIIIC complex links DNA damage recognition to nucleosome acetylation," *The EMBO Journal*, vol. 20, no. 12, pp. 3187–3196, 2001.
- [26] M. G. Kapetanaki, J. Guerrero-Santoro, D. C. Bisi, C. L. Hsieh, V. Rapić-Otrin, and A. S. Levine, "The DDB1-CUL4A/DDB2 ubiquitin ligase is deficient in xeroderma pigmentosum group E and targets histone H2A at UV-damaged DNA sites," *Proceedings of the National Academy of Sciences of the United States of America*, vol. 103, no. 8, pp. 2588–2593, 2006.
- [27] S. Bergink, F. A. Salomons, D. Hoogstraten et al., "DNA damage triggers nucleotide excision repair-dependent monoubiquitylation of histone H2A," *Genes and Development*, vol. 20, no. 10, pp. 1343–1352, 2006.
- [28] M. Zurita and C. Merino, "The transcriptional complexity of the TFIIH complex," *Trends in Genetics*, vol. 19, no. 10, pp. 578–584, 2003.
- [29] F. Coin, V. Oksenysh, V. Mocquet, S. Groh, C. Blattner, and J. M. Egly, "Nucleotide excision repair driven by the dissociation of CAK from TFIIH," *Molecular Cell*, vol. 31, no. 1, pp. 9–20, 2008.
- [30] A. Keriell, A. Sary, A. Sarasin, C. Rochette-Egly, and J.-M. Egly, "XPD mutations prevent TFIIH-dependent transactivation by nuclear receptors and phosphorylation of RAR $\alpha$ ," *Cell*, vol. 109, no. 1, pp. 125–135, 2002.
- [31] E. Compe, M. Malerba, L. Soler, J. Marescaux, E. Borrelli, and J.-M. Egly, "Neurological defects in trichothiodystrophy reveal a coactivator function of TFIIH," *Nature Neuroscience*, vol. 10, no. 11, pp. 1414–1422, 2007.
- [32] E. Compe, P. Drané, C. Laurent et al., "Dysregulation of the peroxisome proliferator-activated receptor target genes by XPD mutations," *Molecular and Cellular Biology*, vol. 25, no. 14, pp. 6065–6076, 2005.
- [33] P. Drané, E. Compe, P. Catez, P. Chymkowitz, and J.-M. Egly, "Selective regulation of vitamin D receptor-responsive genes by TFIIH," *Molecular Cell*, vol. 16, no. 2, pp. 187–197, 2004.
- [34] W. Vermeulen, R. J. Scott, S. Rodgers et al., "Clinical heterogeneity within xeroderma pigmentosum associated with mutations in the DNA repair and transcription gene ERCC3," *American Journal of Human Genetics*, vol. 54, no. 2, pp. 191–200, 1994.
- [35] G. Weeda, R. C. A. van Ham, W. Vermeulen, D. Bootsma, A. J. van der Eb, and J. H. J. Hoeijmakers, "A presumed DNA helicase encoded by ERCC-3 is involved in the human repair disorders xeroderma pigmentosum and Cockayne's syndrome," *Cell*, vol. 62, no. 4, pp. 777–791, 1990.
- [36] J. Liu, S. Akoulitchev, A. Weber et al., "Defective interplay of activators and repressors with TFIIH in xeroderma pigmentosum," *Cell*, vol. 104, no. 3, pp. 353–363, 2001.
- [37] S.-K. Lee, S.-L. Yu, L. Prakash, and S. Prakash, "Requirement of yeast RAD2, a homolog of human XPG gene, for efficient RNA polymerase II transcription: implications for Cockayne syndrome," *Cell*, vol. 109, no. 7, pp. 823–834, 2002.
- [38] S. Ito, I. Kuraoka, P. Chymkowitz et al., "XPG stabilizes TFIIH, allowing transactivation of nuclear receptors: implications for cockayne syndrome in XP-G/CS patients," *Molecular Cell*, vol. 26, no. 2, pp. 231–243, 2007.
- [39] E. Citterio, V. Van Den Boom, G. Schnitzler et al., "ATP-dependent chromatin remodeling by the Cockayne syndrome B DNA repair-transcription-coupling factor," *Molecular and Cellular Biology*, vol. 20, no. 20, pp. 7643–7653, 2000.
- [40] L. Proietti-De-Santis, P. Drané, and J.-M. Egly, "Cockayne syndrome B protein regulates the transcriptional program after UV irradiation," *The EMBO Journal*, vol. 25, no. 9, pp. 1915–1923, 2006.
- [41] N. Le May, D. Mota-Fernandes, R. Vélez-Cruz, I. Iltis, D. Biard, and J. M. Egly, "NER factors are recruited to active promoters and facilitate chromatin modification for transcription in the absence of exogenous genotoxic attack," *Molecular Cell*, vol. 38, no. 1, pp. 54–66, 2010.
- [42] G. Barreto, A. Schäfer, J. Marhold et al., "Gadd45a promotes epigenetic gene activation by repair-mediated DNA demethylation," *Nature*, vol. 445, no. 7128, pp. 671–675, 2007.
- [43] K. Rai, I. J. Huggins, S. R. James, A. R. Karpf, D. A. Jones, and B. R. Cairns, "DNA demethylation in zebrafish involves the coupling of a deaminase, a glycosylase, and Gadd45," *Cell*, vol. 135, no. 7, pp. 1201–1212, 2008.
- [44] K.-M. Schmitz, N. Schmitt, U. Hoffmann-Rohrer, A. Schäfer, I. Grummt, and C. Mayer, "TAF12 recruits Gadd45a and the nucleotide excision repair complex to the promoter of rRNA genes leading to active DNA demethylation," *Molecular Cell*, vol. 33, no. 3, pp. 344–353, 2009.
- [45] D. K. Ma, J. U. Guo, G.-L. Ming, and H. Song, "DNA excision repair proteins and Gadd45 as molecular players for active DNA demethylation," *Cell Cycle*, vol. 8, no. 10, pp. 1526–1531, 2009.

- [46] Y. Tu, S. Tornaletti, and G. P. Pfeifer, "DNA repair domains within a human gene: selective repair of sequences near the transcription initiation site," *The EMBO Journal*, vol. 15, no. 3, pp. 675–683, 1996.
- [47] C. Popp, W. Dean, S. Feng et al., "Genome-wide erasure of DNA methylation in mouse primordial germ cells is affected by AID deficiency," *Nature*, vol. 463, no. 7284, pp. 1101–1105, 2010.
- [48] R. Métivier, R. Gallais, C. Tiffoche et al., "Cyclical DNA methylation of a transcriptionally active promoter," *Nature*, vol. 452, no. 7183, pp. 45–50, 2008.
- [49] H. Cedar and Y. Bergman, "Linking DNA methylation and histone modification: patterns and paradigms," *Nature Reviews Genetics*, vol. 10, no. 5, pp. 295–304, 2009.
- [50] S. K. T. Ooi, C. Qiu, E. Bernstein et al., "DNMT3L connects unmethylated lysine 4 of histone H3 to de novo methylation of DNA," *Nature*, vol. 448, no. 7154, pp. 714–717, 2007.
- [51] L. Schaeffer, R. Roy, S. Humbert et al., "DNA repair helicase: a component of BTF2 (TFIIH) basic transcription factor," *Science*, vol. 259, no. 5104, pp. 58–63, 1993.
- [52] T. Cremer, M. Cremer, S. Dietzel, S. Müller, I. Solovei, and S. Fakan, "Chromosome territories—a functional nuclear landscape," *Current Opinion in Cell Biology*, vol. 18, no. 3, pp. 307–316, 2006.
- [53] A. De Sandre-Giovannoli, R. Bernard, P. Cau et al., "Lamin A truncation in Hutchinson-Gilford progeria," *Science*, vol. 300, no. 5628, p. 2055, 2003.
- [54] M. Eriksson, W. T. Brown, L. B. Gordon et al., "Recurrent de novo point mutations in lamin A cause Hutchinson-Gilford progeria syndrome," *Nature*, vol. 423, no. 6937, pp. 293–298, 2003.

## Review Article

# Influence of *XRCC1* Genetic Polymorphisms on Ionizing Radiation-Induced DNA Damage and Repair

**Silvia Sterpone and Renata Cozzi**

*Department of Biology, University of "Roma TRE", Viale Guglielmo Marconi 446, 00146 Rome, Italy*

Correspondence should be addressed to Renata Cozzi, [cozzi@uniroma3.it](mailto:cozzi@uniroma3.it)

Received 3 March 2010; Accepted 19 May 2010

Academic Editor: Ashis Basu

Copyright © 2010 S. Sterpone and R. Cozzi. This is an open access article distributed under the Creative Commons Attribution License, which permits unrestricted use, distribution, and reproduction in any medium, provided the original work is properly cited.

It is well known that ionizing radiation (IR) can damage DNA through a direct action, producing single- and double-strand breaks on DNA double helix, as well as an indirect effect by generating oxygen reactive species in the cells. Mammals have evolved several and distinct DNA repair pathways in order to maintain genomic stability and avoid tumour cell transformation. This review reports important data showing a huge interindividual variability on sensitivity to IR and in susceptibility to developing cancer; this variability is principally represented by genetic polymorphisms, that is, DNA repair gene polymorphisms. In particular we have focussed on single nucleotide polymorphisms (SNPs) of *XRCC1*, a gene that encodes for a scaffold protein involved basically in Base Excision Repair (BER). In this paper we have reported and presented recent studies that show an influence of *XRCC1* variants on DNA repair capacity and susceptibility to breast cancer.

## 1. Introduction

During evolution, mammalian cells have optimised distinct pathways to repair DNA preserving genome integrity and avoiding fixing of harmful mutations. DNA lesions could be caused by external insults as well as by exposure to mutagenic substances. They could also be produced endogenously, for example, by reactive oxygen species generated during physiological processes.

Five main different repair mechanisms have been described in humans: MMR (Mismatch Repair), BER (Base Excision Repair), NER (Nucleotide Excision Repair), HRR (Homologous Recombination Repair), and NHEJ (Nonhomologous End Joining).

MMR is a postreplicative mechanism that ensures the application of the Watson-Crick base pairing principle on DNA double helix, discriminating mismatches resulting from DNA polymerase errors, and rectifying them to avoid mutation [1].

Generally, BER corrects DNA base lesions due to oxidative, alkylation, deamination damages via two general pathways: short patch and long patch [2]; NER is a more versatile pathway that senses the distortion caused by a base

damaged by chemical (i.e., cross-linking agents) or physical (i.e., UV) agents and excises a tract of few nucleotides around the lesion [3].

In BER and NER mechanisms, single-strand breaks (SSBs) are an enzymatic consequence of the repair of damaged DNA but they could represent a serious risk for cells if they are not filled by a polymerase and rejoined by DNA ligase. In fact during DNA replication SSBs could be converted to more lethal DNA double-strand breaks (DSBs). DSBs could generate deletions, chromosome translocations, hence genomic instability [4, 5] and in some circumstances induce cell cycle arrest and apoptosis [6, 7].

Homologous Recombination Repair (HRR) and Non-homologous DNA-End Joining (NHEJ) are the two major pathways of DSBs repair. A third system, single-strand annealing (SSA), shares HRR and NHEJ components. The fundamental difference between HRR and NHEJ is the dependence on DNA homology template [8].

All DNA repair pathways are finely regulated and many of the genes involved in these mechanisms are highly conserved from bacteria to humans. This high conservation degree indicates the importance of repair pathways in living organisms.

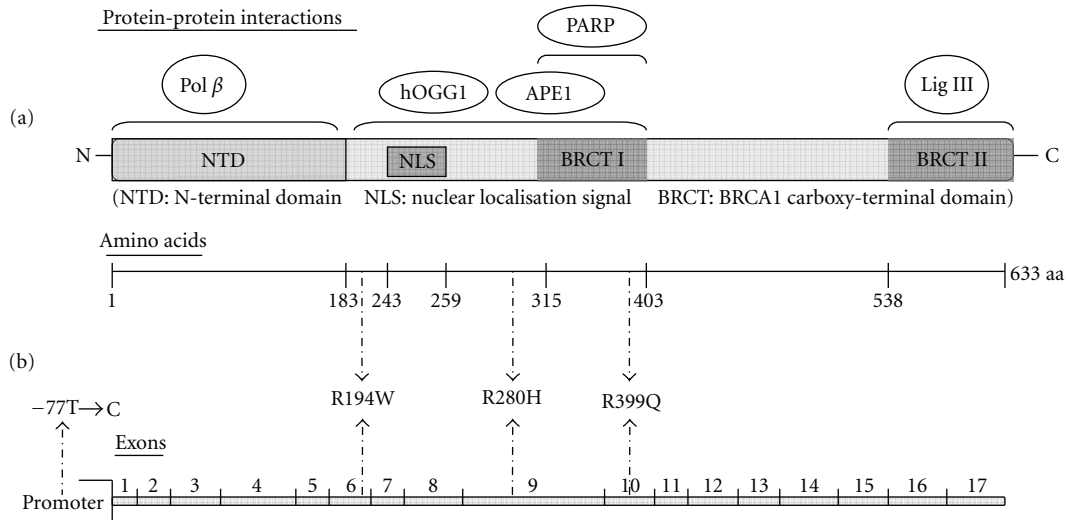


FIGURE 1: Human XRCC1 protein and gene structure. (a) The diagram shows XRCC1 domains and the regions of interaction with other components of BER. (b) The diagram shows the structure of the gene with the most common and studied single nucleotide polymorphisms (SNPs): -77 T  $\rightarrow$  C, R194W, R280H and R399Q. Each of them is detailed in the text.

In literature it has been well documented that defects in DNA repair are associated with human disorders. Several genetic diseases are linked to mutations in genes involved in DNA repair, that is, XP Xeroderma Pigmentosum, CS Cockayne Syndrome, FA Fanconi Anemia, and NBS Nijmegen Breakage Syndrome. Furthermore, studies conducted on knockout and mutant animal models have suggested the key function of specific components of DNA repair machineries.

Despite the lack of a pathological phenotype, humans bearing variant alleles of DNA repair genes could show a different individual response to DNA damage.

The principal source of interindividual variability is represented by genetic polymorphisms. The presence of polymorphic alleles in DNA repair genes may alter the repair capacity modifying the biological responses to exogenous and endogenous DNA insults, both at cellular and tissue level, and the individual susceptibility in developing different kind of disease, such as cancer.

In this review we focussed on the influence of DNA repair polymorphisms on human individual sensitivity to Ionising Radiation (IR) treatment and susceptibility to cancer; in particular we are interested in better understanding whether SNPs in *XRCC1* gene, encoding, for a scaffold protein involved basically in BER pathway, could impair DNA repair efficiency so increasing the risk to develop tumour, such as sporadic breast cancer.

## 2. XRCC1 Polymorphisms and IR Exposure

XRCC genes, abbreviation of X-ray cross complementing, are components of several different damage recovery pathways, and XRCC proteins do not show similarity in biochemical functions.

The human *XRCC1* (X-ray repair cross-complementing group 1) gene, located on chromosome 19q13.2, encodes for a 633aa protein (Figure 1) that plays an important role in

BER and single-strand breaks repair (SSBR), following exposure to endogenous reactive oxygen species, IR or alkylating agents [9, 10]. Additionally, XRCC1 seems to take part also in DSBs repair [11, 12]. Lévy et al. [11] demonstrated that the DNA-dependent protein kinase (DNA-PK), a key factor in NHEJ, is able to phosphorylate XRCC1 (Ser 371) after ionizing radiation that causes XRCC1 dimer dissociation. This posttranslational modification seems to be important for rejoining DSBs in response to DNA damage caused by IR, as also showed by the failure of S371L mutant XRCC1 to rescue DSBs repair defect in deficient EM9 cells.

In 2004 Audebert et al. showed an involvement of the XRCC1/Lig III complex in DSBs rejoining. The complex, otherwise involved in BER, could act in an alternative end-joining mechanism that complements DNA-PK/XRCC4/Lig IV dependent NHEJ [12].

A lot of information about XRCC1 function has been derived from mutant mammalian cell lines; *XRCC1* mutants were initially identified in the AA8 strain of Chinese hamster ovary (CHO) cells, and four of these, denoted EM7, EM9, EM-C11 and EM-C12, represent a model to study the consequence of the lack or a reduced level of this protein [13].

The XRCC1 is a scaffold protein that interacts with other many components of BER as DNA polymerase  $\beta$ , APE1, hOGG1, poly-(ADP-ribose) polymerase and DNA ligase III in the NH<sub>2</sub>-terminal, central, and COOH-terminal regions, respectively, as resumed in Figure 1 [14–16].

In 1998 Shen et al. [17] described three polymorphisms of *XRCC1* gene, which resulted in non-conservative amino-acid changes at evolutionary conserved regions: C  $\rightarrow$  T substitution in codon 194 of exon 6 (Arg to Trp); G  $\rightarrow$  A substitution in codon 280 of exon 9 (Arg to His) and G  $\rightarrow$  A substitution in codon 399 of exon 10 (Arg to Gln). (Figure 1)

Recently, Hao et al. [18] identified, in Chinese population, another variant in the *XRCC1* gene located in the

5'UTR (5'-untranslated region),  $-77 \text{ T} \rightarrow \text{C}$ . (Figure 1). Afterwards this polymorphism was also confirmed to be present, with a higher frequency, in Caucasian population [19, 20].

All these single nucleotide polymorphisms (SNPs) could alter the XRCC1 function and impair DNA repair efficiency or accuracy. In 1983, Setlow [21] claimed that healthy subjects differ in their intrinsic capacity in repairing DNA damage and this variation could be a result of variants in DNA repair genes that consequently can modify the individual susceptibility to radiation exposure.

A report by Lunn et al. [22] suggested that XRCC1 codon 399 polymorphism located within the BRCT domain [23] which interacts with PARP, may result in deficient DNA repair. More recently, Taylor et al. (2002) showed that although BRCT1 domain is critical for efficient single-strand break repair and cell survival, 399 polymorphism located within this domain did not appear to significantly affect XRCC1 function. On the contrary, by using molecular dynamics techniques Monaco et al. (2007) predicted the structure of wild-type and polymorphic form of BRCT1 domain of XRCC1 demonstrating that the polymorphism in exon 10 changed the XRCC1's secondary structure. These contrasting results call for further investigations to clarify whether the Arg  $\rightarrow$  Gln substitution in codon 399 could affect DNA repair capability [24, 25].

Hu and co-workers (2001) evaluated whether amino acid substitution variants of DNA repair genes, that is, XRCC1-399, contribute to ionizing radiation (IR) susceptibility as measured by prolonged cell cycle G<sub>2</sub> delay. In  $\gamma$ -irradiated lymphocytes from disease-free controls, they found a higher mitotic delay in subjects with Arg/Gln and Gln/Gln genotypes than homozygous wild-type ones. The difference, however, was not statistically significant. In conclusion, they indicated that the XRCC1 Arg/Gln genotype may influence cellular response to IR, particularly in women with positive family history (FH) of breast cancer [26].

In order to elucidate the influence of the most common SNP of XRCC1 (Arg399Gln) on the individual DNA repair capacity, Cornetta et al. [27] assessed the repair capacity through alkaline Comet assay in human peripheral blood cells of healthy subjects treated *in vitro* with X rays. They observed that subjects with XRCC1 variant Gln/Gln genotype exhibited lower values of DNA damage than those with homozygous wild-type (Arg/Arg) and heterozygous (Arg/Gln) genotypes, both at basal level and after treatment. On the contrary, the baseline DNA damage, measured as Tail Moment, was found to be increased in healthy individuals bearing the XRCC1 399Gln variant allele in Weng and colleagues' work [28].

Hence, Cornetta et al. [27] concluded that individuals bearing Gln/Gln genotype had fewer DNA breaks and resolved open breaks faster than homozygote wt and heterozygote subjects. Anyway, as they noticed, the Comet assay does not provide information about the fidelity of DNA repair and misrepaired lesions could lead to chromosomal-type damage. Angelini et al. [29] demonstrated that subject exposed to IR (both X- and  $\gamma$ -rays) with XRCC1 variant genotypes had a higher frequency of micronuclei (MN) with

respect to wild type ones. Furthermore, a high chromosomal damage could trigger off apoptosis in cells with 399 polymorphic genotypes consequently resulting protective through the elimination of potentially transformed cells. This hypothesis is supported by Seedhouse et al. [30] who showed a protective effect of XRCC1-399 variant allele against the development of therapy-related acute myeloblastic leukemia (t-AML).

On the contrary, Aka et al., [31] showed that XRCC1-399 polymorphism resulted in higher residual DNA values, measured by Comet assay, after  $\gamma$ -ray treatment and Godderis et al., [32] in collusion with Rzeszowska-Wolny et al. [33], performing Comet assay and MN analysis, concluded that XRCC1-399 did not seem to influence DNA damage repair after  $\gamma$ -rays exposure.

The individual susceptibility to IR can also differ in subjects affected by cancer, as interindividual variation in therapeutic exposure to ionising radiation response revealed. Moreover, cancer patients seem to be more radiosensitive than healthy persons: Scott et al. [34] found that about 40% of breast cancer (BC) patients are radiosensitive in comparison to about 9% of healthy controls.

Recently, our group analysed the response to IR exposure in sporadic BC patients and healthy controls by measuring DNA damage through alkaline Comet assay [35]. We did not observe a great interindividual variation in either group but we found that BC patients were more radiosensitive and exhibited a significantly higher mean of basal and IR-induced DNA damage when compared to healthy controls. Anyhow, in this study the impairment of BC repair capacity did not result to be associated with XRCC1-399 polymorphism. But, interestingly the reduced repair ability in BC patients was related to high degrees of tissue side effects.

This is in agreement with results reported by Alapetite and colleagues who observed that BC patients with most severe complications showed impaired rejoining as analysed through alkaline Comet assay [36].

### 3. XRCC1 Polymorphisms and Risk of Developing Cancer

Related to an impaired DNA repair capacity and an increased mutagenesis, polymorphisms in DNA repair genes could also modify the risk of developing cancer. Epidemiological studies were focussed on assessing a possible link between genetic factors, in particular low penetrance genes as well as SNPs, and increased/decreased risk of tumour. Along this line Breast Cancer (BC) is a very interesting field of research.

It is the most common cause of cancer death in women worldwide. Most etiologic factors are established [37–39], but concerning the association between DNA repair SNPs and the sporadic form of this tumour, literature data are often contradictory.

Recently, in 2009, Huang et al. [40] performed a meta-analysis that collected data about the association between breast cancer and the XRCC1 polymorphisms Arg194Trp (9411 cases and 9783 controls), Arg399Gln (22 481 cases and 23 905 controls) and Arg280His (6062 cases and 5864 controls) in different inheritance models [dominant model:

TABLE 1: Reported studies about the association of *XRCC1*-399 polymorphism and DNA repair capacity.

<i>XRCC1</i> -399 GENOTYPE	IR EXPOSURE	EFFECTS ON DNA REPAIR CAPACITY	REFERENCES
Variant	$\gamma$ -rays	Higher mitotic delay index	Hu et al., 2001 [26]
Variant	X-and $\gamma$ -rays	Higher MN frequency	Angelini et al., 2005 [29]
Variant	$\gamma$ -rays	No-one on DNA damage values (Comet) Higher background frequency of MN	Rzeszowska et al., 2005 [33]
Variant	$\gamma$ -rays	Higher residual damage (Comet)	Aka et al., 2006 [31]
Gln399Gln	X-rays	Lower DNA damage (Comet)	Cornetta et al., 2006 [27]
Variant	$\gamma$ -rays	No-one on DNA damage values (Comet) and MNCB	Godderis et al., 2006 [32]
Variant	No	Higher basal DNA damage (Comet)	Weng et al., 2009 [28]

Variant= Arg399Gln + Gln399Gln.

TABLE 2: Reported studies about the association of *XRCC1*-399 and BC risk.

Protective effect	Breast Cancer Association Consortium, 2006 [41]
	Saadat et al., 2008 [42]
Risk factor	Duel et al., 2001 [43]
	Moullan et al., 2003 [44]
	Smith et al., 2003 [39]
	Zhang et al., 2006 [45]
	Huang et al., 2009 [40]
	Sterpone et al., 2010 [20]

homozygous wild-type versus (homozygous mutant+heterozygous) and recessive model: (homozygous wild-type+heterozygous) versus homozygous mutant).

Reference to SNPs in codon 194 and 280, they did not appear to be risk factors for breast cancer but case-control studies on Arg399Gln have provided conflicting results.

About *XRCC1* Arg399Gln polymorphism, in 2006, Breast Cancer Association Consortium [41] reported that there was no evidence of an association of BC with this SNP and with a large meta-analysis Saadat et al. [42] concluded that this polymorphism was associated with BC risk in studies from Asian countries but not from Western countries, when using a recessive model. On the other hand, Huang [40] suggested that both under recessive and dominant models, the Arg399Gln was associated with a trend of increased breast cancer risk, regardless of ethnic subgroups division. In agreement with this conclusion and several other studies [39, 43–45], our group showed a slightly increase of BC risk in Caucasians using dominant model: women bearing at least one *XRCC1*-399 variant allele seem to be at higher risk of developing this tumour [20].

Additionally, we found that the presence of variant allele at codon 399 combined with the variant allele in the promoter,  $-77$  C which alone was not associated with BC, determined a significantly higher risk of developing this cancer: this combination could affect strand breaks repair as a consequence of the reduced availability of *XRCC1* transcript, even in the variant form.

To date, only one other study reported the analysis of haplotypes considering the promoter SNP together with 194, 280 and 399 polymorphisms in BC patients and healthy controls. In collusion with our analysis [20], Brem et al. did not find any association between BC and promoter polymorphism; BC risk was positively associated with  $-77$ , 194, and 399 wild-type alleles and 280 variant allele haplotype, even if the *P* value was not significant [19].

The haplotype risk association could be an interesting and more complete approach than association studies in which only individual *XRCC1* SNPs are considered, thus leading to errors in risk estimation.

#### 4. Conclusions

In this review we have focussed on the effect of genetic basis on interindividual differences in response to DNA damaging agents. In particular we have considered DNA damage caused by ionizing radiation, commonly used in the care of tumour.

The consequences of IR exposure could be very serious and radiation injury may develop months to years later after treatment with numerous and individual manifestations. Hence, radiation-induced DNA damage and its repair play a critical role for the susceptibility of patients affected by cancer to side effects after radiotherapy.

In conclusion, as the reported studies want to support (see Table 1 and Table 2), it is an important goal of biological

and clinical research to detect genetic components like DNA repair gene polymorphisms as possible indicators of radiosensitivity in order to adjust radiotherapy protocols for both sensitive and resistant patients.

## Acknowledgment

The authors thank Tommaso Cornetta and Antonella Testa for the helpful discussions.

## References

- [1] C. Kunz, Y. Saito, and P. Schär, "Mismatched repair: variations on a theme," *Cellular and Molecular Life Sciences*, vol. 66, no. 6, pp. 1021–1038, 2009.
- [2] A. B. Robertson, A. Klungland, T. Rognes, and I. Leiros, "Base excision repair: the long and short of it," *Cellular and Molecular Life Sciences*, vol. 66, no. 6, pp. 981–993, 2009.
- [3] T. Nospikel, "Nucleotide excision repair: variations on versatility," *Cellular and Molecular Life Sciences*, vol. 66, no. 6, pp. 994–1009, 2009.
- [4] B. Elliott and M. Jasin, "Human genome and diseases: review double-strand breaks and translocations in cancer," *Cellular and Molecular Life Sciences*, vol. 59, no. 2, pp. 373–385, 2002.
- [5] L. H. Thompson and D. Schild, "Recombinational DNA repair and human disease," *Mutation Research*, vol. 509, no. 1-2, pp. 49–78, 2002.
- [6] S. P. Jackson, "Detecting, signalling and repairing DNA double-strand breaks," *Biochemical Society Transactions*, vol. 29, no. 6, pp. 655–661, 2001.
- [7] C. J. Norbury and I. D. Hickson, "Cellular responses to DNA damage," *Annual Review of Pharmacology and Toxicology*, vol. 41, pp. 367–401, 2001.
- [8] K. Valerie and L. F. Povirk, "Regulation and mechanisms of mammalian double-strand break repair," *Oncogene*, vol. 22, no. 37, pp. 5792–5812, 2003.
- [9] E. J. Duell, J. K. Wiencke, T.-J. Cheng et al., "Polymorphisms in the DNA repair genes XRCC1 and ERCC2 and biomarkers of DNA damage in human blood mononuclear cells," *Carcinogenesis*, vol. 21, no. 5, pp. 965–971, 2000.
- [10] L. H. Thompson and M. G. West, "XRCC1 keeps DNA from getting stranded," *Mutation Research*, vol. 459, no. 1, pp. 1–18, 2000.
- [11] N. Lévy, A. Martz, A. Bresson, C. Spenlehauer, G. de Murcia, and J. Ménessier-de Murcia, "XRCC1 is phosphorylated by DNA-dependent protein kinase in response to DNA damage," *Nucleic Acids Research*, vol. 34, no. 1, pp. 32–41, 2006.
- [12] M. Audebert, B. Salles, and P. Calsou, "Involvement of poly(ADP-ribose) polymerase-1 and XRCC1/DNA ligase III in an alternative route for DNA double-strand breaks rejoining," *Journal of Biological Chemistry*, vol. 279, no. 53, pp. 55117–55126, 2004.
- [13] K. W. Caldecott, "XRCC1 and DNA strand break repair," *DNA Repair*, vol. 2, no. 9, pp. 955–969, 2003.
- [14] A. E. Vidal, S. Boiteux, I. D. Hickson, and J. P. Radicella, "XRCC1 coordinates the initial and late stages of DNA abasic site repair through protein-protein interactions," *EMBO Journal*, vol. 20, no. 22, pp. 6530–6539, 2001.
- [15] S. Marsin, A. E. Vidal, M. Sossou et al., "Role of XRCC1 in the coordination and stimulation of oxidative DNA damage repair initiated by the DNA glycosylase hOGG1," *Journal of Biological Chemistry*, vol. 278, no. 45, pp. 44068–44074, 2003.
- [16] R. Brem and J. Hall, "XRCC1 is required for DNA single-strand break repair in human cells," *Nucleic Acids Research*, vol. 33, no. 8, pp. 2512–2520, 2005.
- [17] M. R. Shen, I. M. Jones, and H. Mohrenweiser, "Nonconservative amino acid substitution variants exist at polymorphic frequency in DNA repair genes in healthy humans," *Cancer Research*, vol. 58, no. 4, pp. 604–608, 1998.
- [18] B. Hao, H. Wang, K. Zhou et al., "Identification of genetic variants in base excision repair pathway and their associations with risk of esophageal squamous cell carcinoma," *Cancer Research*, vol. 64, no. 12, pp. 4378–4384, 2004.
- [19] R. Brem, D. G. Cox, B. Chapot et al., "The XRCC1 –77T → C variant: haplotypes, breast cancer risk, response to radiotherapy and the cellular response to DNA damage," *Carcinogenesis*, vol. 27, no. 12, pp. 2469–2474, 2006.
- [20] S. Sterpone, V. Mastellone, L. Padua et al., "Single-nucleotide polymorphisms in BER and HRR genes, XRCC1 haplotypes and breast cancer risk in Caucasian women," *Journal of Cancer Research and Clinical Oncology*, vol. 136, no. 4, pp. 631–636, 2010.
- [21] R. B. Setlow, "Variations in DNA repair among humans," in *Human Carcinogenesis*, C. C. Harris and H. N. Autrup, Eds., pp. 231–254, Academic Press, New York, NY, USA, 1983.
- [22] R. M. Lunn, R. G. Langlois, L. L. Hsieh, C. L. Thompson, and D. A. Bell, "XRCC1 polymorphisms: effects on aflatoxin B1-DNA adducts and glycoprotein A variant frequency," *Cancer Research*, vol. 59, no. 11, pp. 2557–2561, 1999.
- [23] X. Zhang, S. Moréra, P. A. Bates et al., "Structure of an XRCC1 BRCT domain: a new protein-protein interaction module," *EMBO Journal*, vol. 17, no. 21, pp. 6404–6411, 1998.
- [24] R. M. Taylor, A. Thistlethwaite, and K. W. Caldecott, "Central role for the XRCC1 BRCT I domain in mammalian DNA single-strand break repair," *Molecular and Cellular Biology*, vol. 22, no. 8, pp. 2556–2563, 2002.
- [25] R. Monaco, R. Rosal, M. A. Dolan, M. R. Pincus, and P. W. Brandt-Rauf, "Conformational effects of a common codon 399 polymorphism on the BRCT1 domain of the XRCC1 protein," *Protein Journal*, vol. 26, no. 8, pp. 541–546, 2007.
- [26] J. J. Hu, T. R. Smith, M. S. Miller, H. W. Mohrenweiser, A. Golden, and L. D. Case, "Amino acid substitution variants of APE1 and XRCC1 genes associated with ionizing radiation sensitivity," *Carcinogenesis*, vol. 22, no. 6, pp. 917–922, 2001.
- [27] T. Cornetta, F. Festa, A. Testa, and R. Cozzi, "DNA damage repair and genetic polymorphisms: assessment of individual sensitivity and repair capacity," *International Journal of Radiation Oncology Biology Physics*, vol. 66, no. 2, pp. 537–545, 2006.
- [28] H. Weng, Z. Weng, Y. Lu, K. Nakayama, and K. Morimoto, "Effects of cigarette smoking, XRCC1 genetic polymorphisms, and age on basal DNA damage in human blood mononuclear cells," *Mutation Research*, vol. 679, no. 1-2, pp. 59–64, 2009.
- [29] S. Angelini, R. Kumar, F. Carbone et al., "Micronuclei in humans induced by exposure to low level of ionizing radiation: influence of polymorphisms in DNA repair genes," *Mutation Research*, vol. 570, no. 1, pp. 105–117, 2005.
- [30] C. Seedhouse, R. Bainton, M. Lewis, A. Harding, N. Russell, and E. Das-Gupta, "The genotype distribution of the XRCC1 gene indicates a role for base excision repair in the development of therapy-related acute myeloblastic leukemia," *Blood*, vol. 100, no. 10, pp. 3761–3766, 2002.
- [31] P. Aka, R. Mateuca, J.-P. Buchet, H. Thierens, and M. Kirsch-Volders, "Are genetic polymorphisms in OGG1, XRCC1 and XRCC3 genes predictive for the DNA strand break repair phenotype and genotoxicity in workers exposed to low dose

- ionising radiations?" *Mutation Research*, vol. 556, no. 1-2, pp. 169–181, 2004.
- [32] L. Godderis, P. Aka, R. Mateuca, M. Kirsch-Volders, D. Lison, and H. Veulemans, "Dose-dependent influence of genetic polymorphisms on DNA damage induced by styrene oxide, ethylene oxide and gamma-radiation," *Toxicology*, vol. 219, no. 1–3, pp. 220–229, 2006.
- [33] J. Rzeszowska-Wolny, J. Polanska, M. Pietrowska et al., "Influence of polymorphisms in DNA repair genes XPD, XRCC1 and MGMT on DNA damage induced by gamma radiation and its repair in lymphocytes in vitro," *Radiation Research*, vol. 164, no. 2, pp. 132–140, 2005.
- [34] D. Scott, J. B. P. Barber, E. L. Levine, W. Burrill, and S. A. Roberts, "Radiation-induced micronucleus induction in lymphocytes identifies a high frequency of radiosensitive cases among breast cancer patients: a test for predisposition?" *British Journal of Cancer*, vol. 77, no. 4, pp. 614–620, 1998.
- [35] S. Sterpone, T. Cornetta, L. Padua et al., "DNA repair capacity and acute radiotherapy adverse effects in Italian breast cancer patients," *Mutation Research*, vol. 684, no. 1-2, pp. 43–48, 2010.
- [36] C. Alapetite, P. Thirion, A. De La Rochefordière, J.-M. Cosset, and E. Moustacchi, "Analysis by alkaline comet assay of cancer patients with severe reactions to radiotherapy: defective rejoining of radioinduced DNA strand breaks in lymphocytes of breast cancer patients," *International Journal of Cancer*, vol. 83, no. 1, pp. 83–90, 1999.
- [37] R. Parshad, F. M. Price, V. A. Bohr, K. H. Cowans, J. A. Zujewski, and K. K. Sanford, "Deficient DNA repair capacity, a predisposing factor in breast cancer," *British Journal of Cancer*, vol. 74, no. 1, pp. 1–5, 1996.
- [38] J. J. Hu, T. R. Smith, M. S. Miller, K. Lohman, and L. D. Case, "Genetic regulation of ionizing radiation sensitivity and breast cancer risk," *Environmental and Molecular Mutagenesis*, vol. 39, no. 2-3, pp. 208–215, 2002.
- [39] T. R. Smith, M. S. Miller, K. Lohman et al., "Polymorphisms of XRCC1 and XRCC3 genes and susceptibility to breast cancer," *Cancer Letters*, vol. 190, no. 2, pp. 183–190, 2003.
- [40] Y. Huang, L. Li, and L. Yu, "XRCC1 Arg399Gln, Arg194Trp and Arg280His polymorphisms in breast cancer risk: a meta-analysis," *Mutagenesis*, vol. 24, no. 4, pp. 331–339, 2009.
- [41] Breast Cancer Association Consortium, "Commonly studied single-nucleotide polymorphisms and breast cancer: results from the Breast Cancer Association Consortium," *Journal of the National Cancer Institute*, vol. 98, no. 19, pp. 1382–1396, 2006.
- [42] M. Saadat and M. Ansari-Lari, "Polymorphism of XRCC1 (at codon 399) and susceptibility to breast cancer, a meta-analysis of the literatures," *Breast Cancer Research and Treatment*, vol. 115, pp. 137–144, 2008.
- [43] E. J. Duell, R. C. Millikan, G. S. Pittman et al., "Polymorphisms in the DNA repair gene XRCC1 and breast cancer," *Cancer Epidemiology Biomarkers and Prevention*, vol. 10, no. 3, pp. 217–222, 2001.
- [44] N. Moullan, D. G. Cox, S. Angèle, P. Romestaing, J.-P. Gérard, and J. Hall, "Polymorphisms in the DNA repair gene XRCC1m breast cancer risk, and response to radiotherapy," *Cancer Epidemiology Biomarkers and Prevention*, vol. 12, no. 11, pp. 1168–1174, 2003.
- [45] Y. Zhang, P. A. Newcomb, K. M. Egan et al., "Genetic polymorphisms in base-excision repair pathway genes and risk of breast cancer," *Cancer Epidemiology Biomarkers and Prevention*, vol. 15, no. 2, pp. 353–358, 2006.

## Research Article

# Stimulation of DNA Glycosylase Activities by XPC Protein Complex: Roles of Protein-Protein Interactions

Yuichiro Shimizu,<sup>1,2</sup> Yasuhiro Uchimura,<sup>3</sup> Naoshi Dohmae,<sup>4</sup> Hisato Saitoh,<sup>3</sup>  
Fumio Hanaoka,<sup>1,2</sup> and Kaoru Sugasawa<sup>1,5</sup>

<sup>1</sup> Cellular Physiology Laboratory, RIKEN Discovery Research Institute, Wako, Saitama 351-0198, Japan

<sup>2</sup> Graduate School of Frontier Biosciences, Osaka University, Suita, Osaka 565-0871, Japan

<sup>3</sup> Department of Biological Sciences, Graduate School of Science and Technology, Kumamoto University, Kumamoto 860-8555, Japan

<sup>4</sup> Biomolecular Characterization Team, RIKEN Discovery Research Institute, Wako, Saitama 351-0198, Japan

<sup>5</sup> Biosignal Research Center, Organization of Advanced Science and Technology, Kobe University, Kobe, Hyogo 657-8501, Japan

Correspondence should be addressed to Kaoru Sugasawa, ksugasawa@garnet.kobe-u.ac.jp

Received 30 April 2010; Accepted 9 June 2010

Academic Editor: Ashis Basu

Copyright © 2010 Yuichiro Shimizu et al. This is an open access article distributed under the Creative Commons Attribution License, which permits unrestricted use, distribution, and reproduction in any medium, provided the original work is properly cited.

We showed that XPC complex, which is a DNA damage detector for nucleotide excision repair, stimulates activity of thymine DNA glycosylase (TDG) that initiates base excision repair. XPC appeared to facilitate the enzymatic turnover of TDG by promoting displacement from its own product abasic site, although the precise mechanism underlying this stimulation has not been clarified. Here we show that XPC has only marginal effects on the activity of *E. coli* TDG homolog (*EcMUG*), which remains bound to the abasic site like human TDG but does not significantly interact with XPC. On the contrary, XPC significantly stimulates the activities of sumoylated TDG and SMUG1, both of which exhibit quite different enzymatic kinetics from unmodified TDG but interact with XPC. These results point to importance of physical interactions for stimulation of DNA glycosylases by XPC and have implications in the molecular mechanisms underlying mutagenesis and carcinogenesis in XP-C patients.

## 1. Introduction

DNA, which carries the genetic information, is liable to alterations by various agents of endogenous and environmental origin. In order to prevent the deleterious effects yielded by such DNA lesions and to maintain the integrity of the genome and cellular functions, cells are equipped with several DNA repair systems, such as base excision repair (BER), nucleotide excision repair (NER), and mismatch repair (for review, see [1]). BER is one of the most versatile repair pathways that can deal with base lesions resulting mainly from alkylation, oxidation, deamination, and replication errors. This pathway is initiated by damage-specific DNA glycosylases that release the altered or inappropriate bases by cleavage of the *N*-glycosylic bond from the phosphate-sugar backbone, thereby resulting in production of the apurinic/apyrimidinic (AP) sites (reviewed in [2, 3]). The phosphodiester bond 5' to the AP site is then nicked by

AP endonucleases. A class of DNA glycosylases, designated bifunctional DNA glycosylases, possess additional AP lyase activity that further cleaves the phosphodiester bond 3' to the AP site generated by its own glycosylase activity. When BER is initiated by such bifunctional DNA glycosylases, AP endonuclease removes 3'-unsaturated aldehyde left behind by the AP lyase activity. As a consequence of either pathways, 3'-OH end is generated which is suitable for the following DNA repair synthesis.

Unlike BER that mainly repairs base lesions, NER deals with a wide variety of helix-distorting lesions, including ultraviolet (UV) light-induced pyrimidine photodimers as well as intrastrand crosslinks and bulky adducts induced by numerous chemical compounds. Xeroderma pigmentosum (XP) is one of the autosomal recessive disorders that are associated with defective NER and clinically characterized by severe photosensitivity against UV exposure and a high risk of skin cancer. To date, seven NER-deficient XP

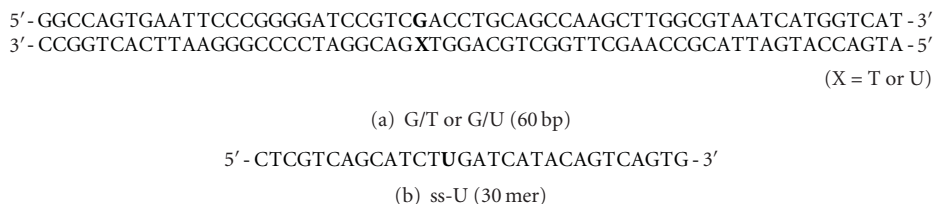


FIGURE 1: DNA substrates used in this study.

genetic complementation groups have been identified (XP-A through -G), for each of which the responsible gene has been cloned [4]. Unlike most of the other XP groups, XP-C patients show defects only in one of the two NER subpathways, that is, global genome NER that covers the entire genome. The other subpathway is referred to as transcription-coupled NER, which repairs transcription-blocking lesions on the transcribed strand of active genes. The XPC protein, the responsible gene product for the XP group C, plays an essential role in DNA damage recognition and the following initiation of global genome NER [5–7]. It forms *in vivo* a stable heterotrimeric complex with either RAD23A or RAD23B, one of the two mammalian homologues of *Saccharomyces cerevisiae* Rad23p, and centrin 2, which is known also as a component of the centrosome [8–10]. RAD23 stabilizes the XPC protein *in vivo* [11, 12], and the XPC-RAD23 heterodimer is sufficient to reconstitute the cell-free NER reaction [13, 14], whereas centrin 2 appears to potentiate the damage-specific DNA binding activity of the XPC complex [15]. Biochemical and structural analyses revealed that this complex recognizes a specific DNA secondary structure containing a junction between double-stranded DNA and a single-stranded 3'-overhang [16–18]. After the DNA binding by XPC, ATPase/helicase activities of TFIIH (exerted by the XPB and XPD subunits) open DNA duplex and demarcate damage, probably with the aid of XPG, XPA, and replication protein A (RPA). The damaged strand is then cleaved in both sides of the lesion by two structure-specific NER endonucleases, ERCC1-XPF and XPG, and the resulting gap is refilled with the DNA repair synthesis [19].

We have previously shown that XPC interacts directly with one of the DNA glycosylases, thymine DNA glycosylase (TDG) [20]. TDG removes thymine or uracil residues from G/T or G/U mismatches, which are mainly derived from hydrolytic deamination of 5-methylcytosines or cytosines, respectively (for review, see [21]). TDG is unique in that it cannot dissociate from the substrate DNA by itself after accomplishing its enzymatic activity [22, 23]. Crystal structure of the *E. coli* homolog of TDG, the mismatch-specific uracil DNA glycosylase (*EcMUG*), demonstrated that the inability to turnover is due to its tight interaction with the guanine opposite the AP site [24, 25]. Extensive biochemical analyses have suggested that this feature may be applicable also to the human TDG [22, 23, 26]. Since continuous attachment of TDG to AP sites must interfere with the following BER process, it has been conceivable that there should be certain factors that promote dissociation of TDG from the processed DNA. One candidate for such factors relieving TDG of the product inhibition is AP

endonuclease 1 (APE1), which acts in the BER pathway immediately after the DNA glycosylases [22, 27–29]. Another factor would be sumoylation of TDG, which occurs at a single specific site (Lys330 in human TDG) [30]. The X-ray crystal structure of sumoylated TDG revealed that this modification induces a significant conformational change in the C-terminal domain of TDG, which seems to sterically prevent its interaction with DNA [31]. Thus, it has been proposed that the sumoylation following base excision may promote the enzymatic turnover of TDG [32], although precise timing and regulation of the modification *in vivo* still remain to be elucidated. In addition, we have previously shown that XPC-RAD23B forms a ternary complex with TDG bound to the substrate DNA and promote dissociation of TDG from the AP site [20]. Like TDG and APE1, XPC can recognize and bind to AP sites, although the observed affinity is relatively low if opposite base is guanine [20]. Therefore, two notions have been conceivable concerning molecular mechanisms underlying the stimulation of TDG turnover by XPC: direct physical interaction and competition for the AP site. More recently, it has been reported that XPC interacts with and stimulates the activity of OGG1, a major DNA glycosylase that removes various oxidative base lesions including 8-oxoguanine [33]. Here we further investigate possible involvement of the XPC protein complex in BER by using various DNA glycosylases as well as a sumoylated form of TDG, which gives further insights to the molecular mechanisms for the TDG stimulation.

## 2. Materials and Methods

**2.1. Purification of Recombinant Proteins.** Purification of recombinant human XPC and His-tagged RAD23B (RAD23B-His) was carried out [34, 35], and the XPC-RAD23B-His heterodimer was reconstituted *in vitro* as described previously [17]. His-TDG, GST-TDG, GST, and His-SMUG1 were also purified as described elsewhere [20, 36].

*EcMUG* and UNG2, both fused to the N-terminal His-tag, were expressed in *E. coli* strain BL21 (DE3) using the pET-28a vector (Novagen). Expression of His-*EcMUG* was induced with 1 mM isopropyl- $\beta$ -D-thiogalactopyranoside (IPTG) at 37°C for 3 hours. The bacterial cell pellets were sonicated in buffer A [25 mM sodium phosphate (pH 7.5), 1 mM EDTA, 25 mM NaCl, 0.01% Nonidet P-40, 1 mM dithiothreitol (DTT), 0.25 mM phenylmethylsulfonyl fluoride (PMSF), protease inhibitor cocktail (Complete; Roche Diagnostics)] and centrifuged for 30 minutes at 100,000 g.

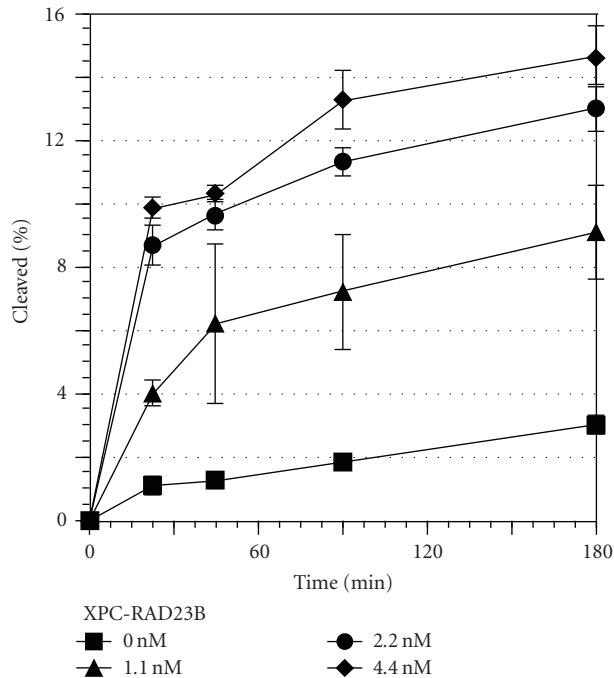


FIGURE 2: XPC stimulates the activity of TDG that cleaves uracil from G/U mismatches. The activity of TDG was measured by using 1.6 nM of 60-bp DNA containing a single G/U mismatch as a substrate. The reaction was done at 30°C for the indicated time with 0.42 nM His-TDG in the presence of various concentrations of XPC-RAD23B. The DNA samples were then purified and subjected to alkali-treatment to cleave the resulting AP sites and separated with denaturing PAGE. The ratio of the cleaved product was calculated and plotted as a graph. The mean values and standard errors were calculated from at least two independent experiments.

The supernatant was loaded onto a phosphocellulose column (P-11; Whatman) equilibrated with buffer B [20 mM sodium phosphate (pH 7.5), 10% glycerol, 0.01% Triton X-100, 0.25 mM PMSF] containing 0.1 M NaCl. After the resin was washed thoroughly with the same buffer, bound proteins were eluted stepwise with buffer B containing 0.2 and 1 M NaCl. Proteins recovered in the 1 M NaCl fraction were then applied to a column packed with TALON resin (Clontech) equilibrated with buffer C [20 mM Tris-HCl (pH 7.5), 10% glycerol, 0.1 M NaCl, 0.01% Triton X-100, 0.25 mM PMSF] containing 5 mM imidazole. The column was then washed extensively with the same buffer, followed by stepwise elution of the bound proteins with buffer C containing 20, 100, and 250 mM imidazole. Finally, the 100 mM imidazole fraction containing His-*EcMUG* was dialyzed against buffer D [20 mM sodium phosphate (pH 7.5), 1 mM EDTA, 10% glycerol, 0.01% Triton X-100, 1 mM DTT, 0.25 mM PMSF] containing 0.2 M NaCl.

Expression of His-UNG2 was induced with 1 mM IPTG at 30°C for 3 hours. The bacterial cell extract was prepared as described above and loaded onto a HiLoad 16/10 SP Sepharose HP column (GE Healthcare Biosciences) equilibrated with buffer B containing 0.1 M NaCl. After washing the resin with the same buffer, bound proteins were eluted

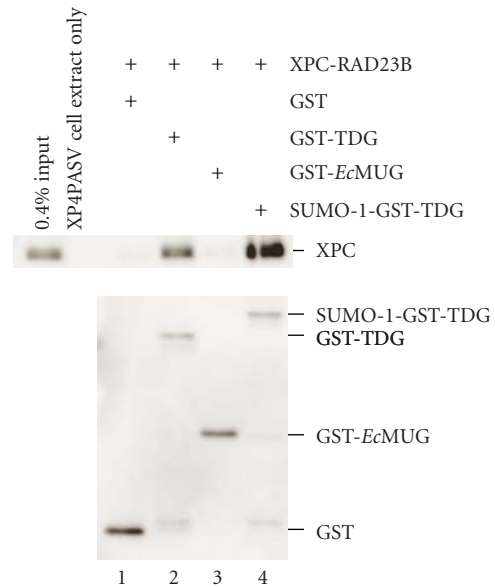


FIGURE 3: XPC physically interacts with SUMO-1-conjugated TDG, but not with *EcMUG*. Glutathione-Sepharose beads (20  $\mu$ l) were incubated in 100  $\mu$ l of the binding mixture containing 10 nM of GST (negative control), GST-TDG (positive control), GST-*EcMUG*, or SUMO-1-GST-TDG in the presence of the same concentration of XPC-RAD23B. After extensive washing, bound proteins were eluted with buffer containing 10 mM glutathione. One-fourth of each eluate was mixed with whole cell extract from XP4PASV cells which do not express XPC and subjected to 8% SDS-PAGE followed by immunoblotting with anti-XPC antibody (upper panel). The same samples were also subjected to 12% SDS-PAGE followed by immunoblotting with anti-GST antibody (lower panel).

stepwise with buffer B containing 0.5 and 1 M NaCl. His-UNG2 recovered in the 0.5 M NaCl fraction was further purified with TALON resin, exactly as described above for His-*EcMUG*. The 250 mM imidazole fraction was then loaded onto a Mono S PC 1.6/5 column equilibrated with buffer D containing 0.1 M NaCl. The column was developed with a linear gradient of 0.1–0.7 M NaCl in buffer D and His-UNG2 was eluted around 0.4 M NaCl. Finally, the sample was subjected to gel filtration chromatography using a Superdex 75 PC 3.2/30 column (GE Healthcare Biosciences) equilibrated with buffer D containing 0.2 M NaCl.

Sumoylation of His-TDG was conducted in *E. coli* strain BL21 (DE3) as described [37]. After induction of protein expression with 1 mM IPTG at 30°C for 3 hours, bacterial cell extract was prepared and fractionated on SP Sepharose and TALON columns exactly as described above for His-UNG2. The 250 mM imidazole fraction from the TALON column containing SUMO-1-His-TDG was subsequently loaded onto a Mono Q HR 5/5 column (GE Healthcare Biosciences) equilibrated with buffer E [20 mM Tris-HCl (pH 7.5), 1 mM EDTA, 10% glycerol, 0.01% Triton X-100, 1 mM DTT, 0.25 mM PMSF] containing 0.1 M NaCl. The column was developed with a linear gradient of 0.1–0.5 M NaCl in buffer E and SUMO-1-His-TDG was eluted around

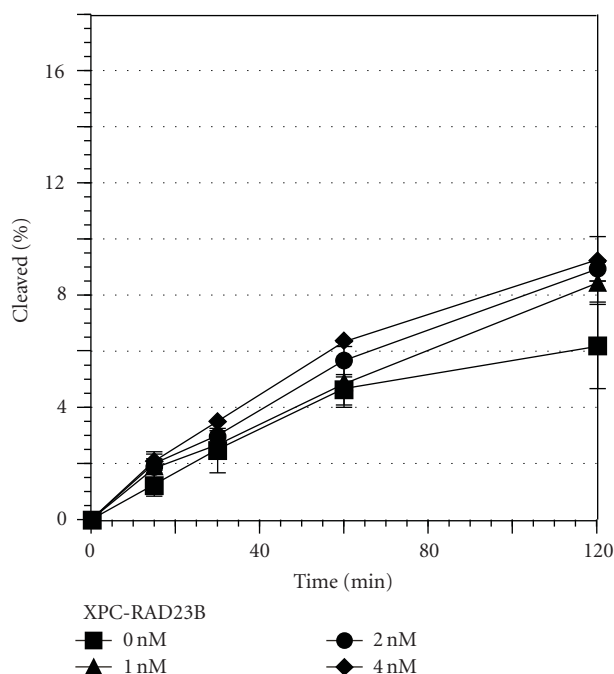


FIGURE 4: The effect of XPC on the activity of *EcMUG* that cleaves uracil from G/U mismatches. The activity of *EcMUG* was measured by using 1.6 nM of 60-bp DNA containing a single G/U mismatch as a substrate. The reaction was done at 30°C for the specified time with 0.8 nM His-*EcMUG* and indicated concentrations of XPC-RAD23B. The DNA samples were then purified and subjected to alkali-treatment to cleave the resulting AP sites and separated with denaturing PAGE. The ratio of the cleaved product was calculated and plotted as a graph. The mean values and standard errors were calculated from at least two independent experiments.

0.2 M NaCl. Finally, proteins were loaded onto a Mono S PC 1.6/5 column equilibrated with buffer D containing 0.1 M NaCl and then eluted with a linear gradient of 0.1–0.5 M NaCl in buffer D. SUMO-1-His-TDG was collected from the fractions around 0.2 M NaCl.

GST-fusion proteins were expressed in *E. coli* strain BL21 (DE3) using the expression vector pGEX4T3 and purified through two successive chromatography procedures using a GSTrap column (GE Healthcare Biosciences) and then a Mono S PC 1.6/5 column.

Flag-tagged MBD4 (Flag-MBD4) was expressed in insect cells using the Bac-to-Bac baculovirus expression system (Invitrogen). High Five cells were infected with the recombinant baculovirus, and proteins were extracted from the cells with buffer F [25 mM Tris-HCl (pH 8.0), 1 mM EDTA, 0.3 M NaCl, 10% glycerol, 1% Nonidet P-40, 1 mM DTT, 0.25 mM PMSE, protease inhibitor cocktail (Complete)] and dialyzed against buffer D containing 0.1 M NaCl. Samples were then loaded onto a HiLoad 16/10 SP Sepharose HP column (GE Healthcare Biosciences) equilibrated with buffer D containing 0.1 M NaCl. After washing the column with the same buffer, bound proteins were eluted stepwise with buffer D containing 0.5 and 1 M NaCl. The 0.5 M NaCl fraction was subsequently loaded to an anti-Flag M2-agarose column

(Sigma-Aldrich) and eluted with buffer D plus 1 M NaCl and 0.1 mg/ml 3 × Flag-peptide (Sigma-Aldrich). The eluate was adjusted at 0.3 M NaCl by dilution with buffer B and then loaded to a HiTrap heparin HP column (GE Healthcare Biosciences) equilibrated with buffer D containing 0.3 M NaCl. Bound proteins were eluted stepwise with buffer D containing 0.5 and 1 M NaCl, and Flag-MBD4 appeared in the 1 M NaCl fraction. Finally, the fraction was diluted by buffer D in order to decrease the NaCl concentration to 0.3 M again and subjected to a Mono S PC 1.6/5 column equilibrated with buffer D containing 0.3 M NaCl. The elution of the bound protein was conducted with a linear gradient of 0.3–1 M NaCl in buffer D, where Flag-MBD4 was collected from the fractions around 0.5 M NaCl.

**2.2. Nicking Assay.** The enzymatic activities of DNA glycosylases in the presence or absence of XPC-RAD23B were measured as described previously [20]. Substrates used (G/T, G/U, and ss-U) are shown in Figure 1.

**2.3. GST Pull-Down Assay.** Glutathione-Sepharose 4 fast flow (GE Healthcare Biosciences: 20  $\mu$ l) was mixed with recombinant proteins as indicated in 100  $\mu$ l of the binding buffer 20 mM sodium phosphate (pH 7.4), 1 mM EDTA, 150 mM NaCl, 1 mM DTT, 5% glycerol, 0.01% Triton X-100, 100  $\mu$ g/ml bovine serum albumin. After incubation on ice for 1 hour with occasional agitation, the beads were washed eight times with 500  $\mu$ l of the binding buffer and the proteins retained on the beads were eluted using 20  $\mu$ l of the binding buffer containing 10 mM glutathione. Since purified XPC has a tendency to aggregate when boiled in the presence of SDS, each eluate was mixed before denaturation with the whole cell extract (0.4  $\mu$ g protein) from XP4PASV cells that do not express endogenous XPC [20]. An aliquote of each eluate mixed with XP4PASV cell extract was subjected to 8% SDS-PAGE and analyzed by immunoblotting using polyclonal anti-XPC or anti-GST antibodies.

**2.4. Antibodies.** The polyclonal antibodies against XPC and TDG were raised as described previously [20, 35]. The polyclonal anti-GST (GE Healthcare Biosciences) and anti-SUMO-1 (Santa Cruz Biotechnology) antibodies were purchased.

### 3. Results

**3.1. XPC Stimulates the Repair of G/U Mismatches Initiated by TDG.** We first examined whether XPC can stimulate the enzymatic activity of TDG that removes uracils from the G/U mismatches by the conventional DNA glycosylase assay involving the substrate shown in Figure 1(a). We have previously shown by using the DNA substrate containing a single G/T mismatch that XPC-RAD23B stimulates the activity of TDG by promoting dissociation of the enzyme from the AP site [20]. Although TDG has been shown to exhibit significantly higher activity with G/U than G/T mismatches, the severe product inhibition has been also observed with the G/U substrate [23]. In this point of

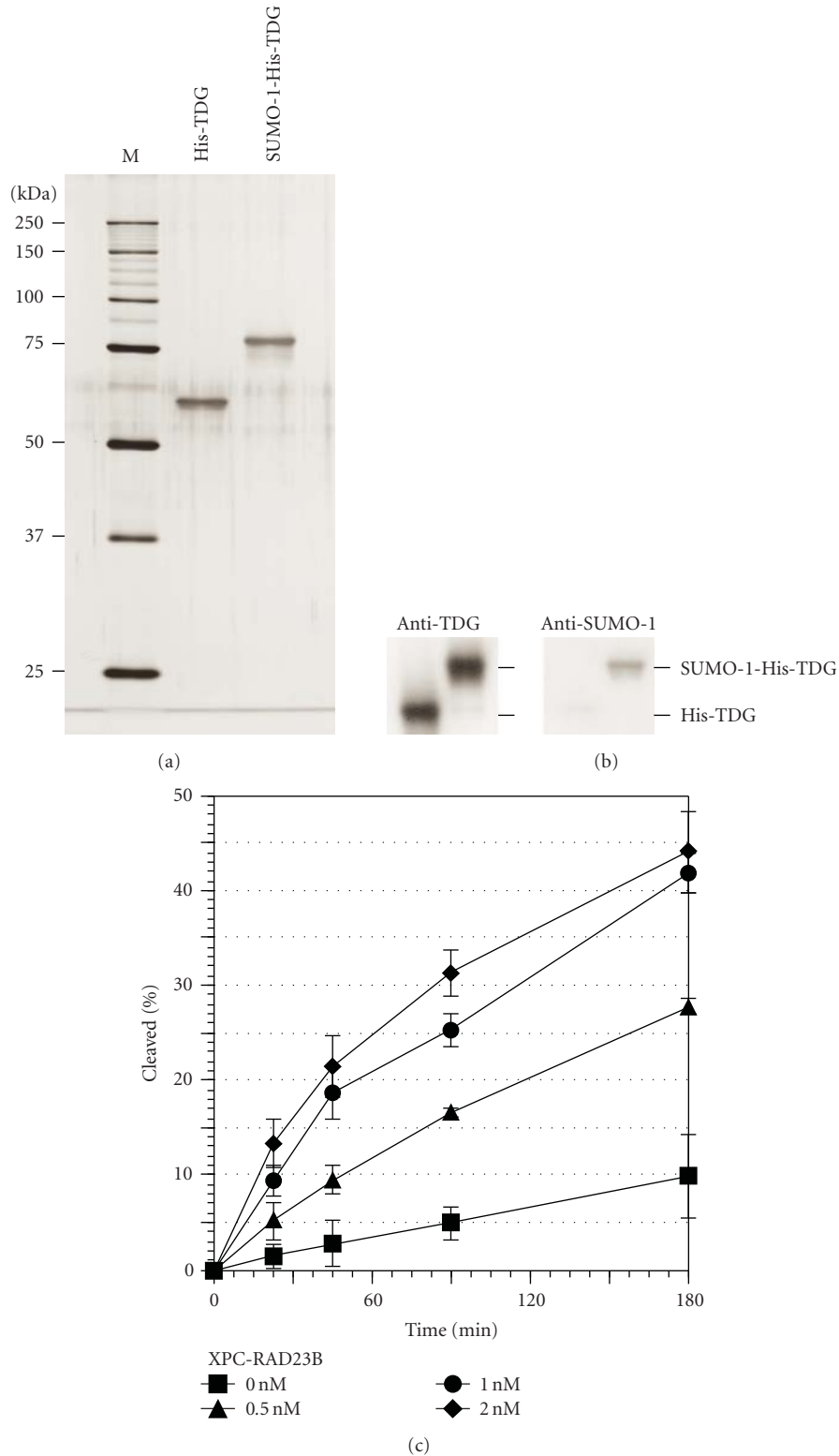


FIGURE 5: The effect of XPC on the activity of SUMO-1-modified TDG that cleaves uracil from G/U mismatches. (a) Silver staining of the purified recombinant nonmodified His-TDG and SUMO-1-modified His-TDG. M represents the size marker. (b) The sumoylation of TDG was verified with western blot analyses using anti-TDG antibody (left) or anti-SUMO-1 antibody (right). (c) The activity of sumoylated His-TDG was measured by using 1.6 nM of 60-bp DNA containing a single G/U mismatch as a substrate. The reaction was done at 30°C for the time indicated with 2 nM SUMO-1-conjugated His-TDG in the presence of XPC-RAD23B. The DNA samples were then purified and subjected to alkali-treatment to cleave the resulting AP sites and separated with denaturing PAGE. The ratio of the cleaved product was calculated and plotted as a graph. The mean values and standard errors were calculated from at least two independent experiments.

view, the effect of XPC on TDG may be similar regardless of which substrate is used, because the AP site opposite guanine is in any way produced as a result of the enzymatic action. Compared with the reaction kinetics of TDG alone, addition of XPC-RAD23B stimulated the activity of TDG on G/U mismatches up to 5-fold in a dose-dependent manner (Figure 2), exactly as expected.

**3.2. XPC Has Only a Marginal Effect on the Activity of *E. coli* Homolog of TDG.** In order to test the significance of protein-protein interaction between XPC and TDG for the stimulation, we purified an *E. coli* homolog of TDG, the mismatch-specific uracil-DNA glycosylase (*EcMUG*) [38]. Unlike TDG, which is involved in correction of both G/T and G/U mismatches, *EcMUG* is primarily G/U-specific, with very low activity toward G/T mismatches [24]. However, *EcMUG* resembles human TDG in that, after cleavage of the particular bases, it remains tightly bound to the AP site generated after exhibiting the glycosylase activity [22–25]. We first tested the presence or absence of physical interaction between XPC and *EcMUG* fused to glutathione S-transferase (GST-*EcMUG*). Ten nanomolar each of GST-*EcMUG*, GST-TDG as a positive control, or GST alone as a negative control was mixed with the equal concentration of XPC-RAD23B, and proteins were pulled down with glutathione-Sepharose beads. Immunoblot analyses revealed that a significant amount of XPC was bound to GST-TDG whereas only little amount of XPC was bound to GST alone as expected (Figure 3, compare lanes 1 and 2; see also [20]). It should be noted that the amount of GST-TDG recovered in the bound fraction was only ~20% of GST. Meanwhile, the binding between XPC and *EcMUG* was as much as the background level (Figure 3, compare lanes 1 to 3), indicating that XPC-RAD23B does not interact with *EcMUG* *in vitro* under the conditions tested.

We next added XPC into the nicking assay using the G/U substrate in order to see whether it influences the activity of *EcMUG*. Although significant physical interaction could not be detected (Figure 3), it was possible that XPC-RAD23B may still stimulate the activity of *EcMUG* by displacing the glycosylase from the AP site, since XPC itself also seems to have a binding affinity toward the AP site [20]. As shown in Figure 4, however, XPC hardly affected the enzymatic activity of *EcMUG*; while 0.8 nM *EcMUG* processed about 6% of the substrate DNA (1.6 nM) within 120 minutes, ~9% of the uracil was removed from the G/U mismatched-DNA in the presence of 4 nM XPC-RAD23B. Although there might be thus a very weak stimulation, the effect of XPC on *EcMUG* activity was much less pronounced than that on TDG.

**3.3. XPC Stimulates the Activity of Sumoylated TDG.** A covalent modification of TDG by SUMO-1 was shown to dramatically affect its DNA binding properties [30, 32]. Consequently, TDG appears to lose its activity on G/T mismatches, whereas the excision of uracils from G/U substrates is even enhanced upon sumoylation. The stimulation of the uracil cleavage seemed to be due to relief of TDG from the product inhibition via SUMO-1 conjugation [30].

Given that the sumoylated TDG may not be bound to the AP site so stably, it was of our great interest to know whether XPC can interact with and stimulate the activity of the modified enzyme. To test this idea, we prepared SUMO-1-conjugated TDG by expressing E1 (Aos1-Uba2), E2 (Ubc9), SUMO-1, and TDG (His- or GST-tagged) in *E. coli* simultaneously, which enables efficient sumoylation of TDG within bacteria [37]. The sumoylated His-TDG (Figure 5(a)) and GST-TDG (data not shown) were purified to near homogeneity. We confirmed that the purified protein specifically reacts with both anti-TDG and anti-SUMO-1 antibodies (Figure 5(b)). Analysis of the protease-digested fragments with mass spectrometry and peptide sequencing further demonstrated that SUMO-1 is conjugated exactly to the predicted site (Lys330 of TDG; data not shown).

At first, we tested a protein-protein interaction between XPC and the sumoylated TDG by GST pull-down assay. As shown in Figure 3, a significant amount of XPC was coprecipitated with SUMO-1-GST-TDG if compared to GST alone, and approximately 2-fold more XPC appeared to bind to SUMO-1-GST-TDG than to nonmodified GST-TDG. This indicates that XPC can bind to TDG regardless of the presence or absence of modification by SUMO-1. We then examined whether XPC can affect the activity of SUMO-1-TDG. As reported by Hardeland et al. [30], the purified recombinant SUMO-1-TDG had only marginal activity for G/T mismatches (data not shown). On the other hand, SUMO-1-TDG showed nearly linear kinetics of uracil removal from G/U mismatches up to 120-minute incubation, suggesting that the product inhibition was much less pronounced as described previously (Figure 5(c); [30]). Interestingly, this activity of SUMO-1-TDG was further stimulated by the addition of XPC in a dose-dependent manner (Figure 5(c)). Incubation of 4 nM XPC-RAD23B resulted in ~5-fold processing of the G/U mismatch in 120 minutes, and this ratio was comparable to the stimulation of nonmodified TDG cleaving the same substrate (Figure 5(c)). Thus, these results demonstrate that XPC can upregulate the activity of not only nonmodified TDG but also SUMO-1-modified TDG *in vitro*.

**3.4. Effects of XPC on Other DNA Glycosylases.** Since it has been reported that XPC stimulates OGG1 in addition to TDG, we next investigated the effect of XPC on various DNA glycosylases, especially the monofunctional DNA glycosylases that are involved in G/T and/or G/U mismatch repair, including UNG2, MBD4 (also referred to as MED1), and SMUG1. UNG2 and SMUG1 mainly remove uracils not only from double-stranded DNA but also from single-stranded DNA, whereas MBD4 as well as TDG is more or less specialized toward correction of G/T and G/U mismatches particularly in the CpG context. As shown in Figure 6, XPC showed no obvious effect on the activity of UNG2 against G/U mismatch (Figure 6(a)), that of MBD4 against G/T mismatch (Figure 6(b)), or that of MBD4 against G/U mismatch (data not shown). Although the activities of both UNG2 and MBD4 were somewhat reduced in the presence of XPC, this may be due to the nonspecific

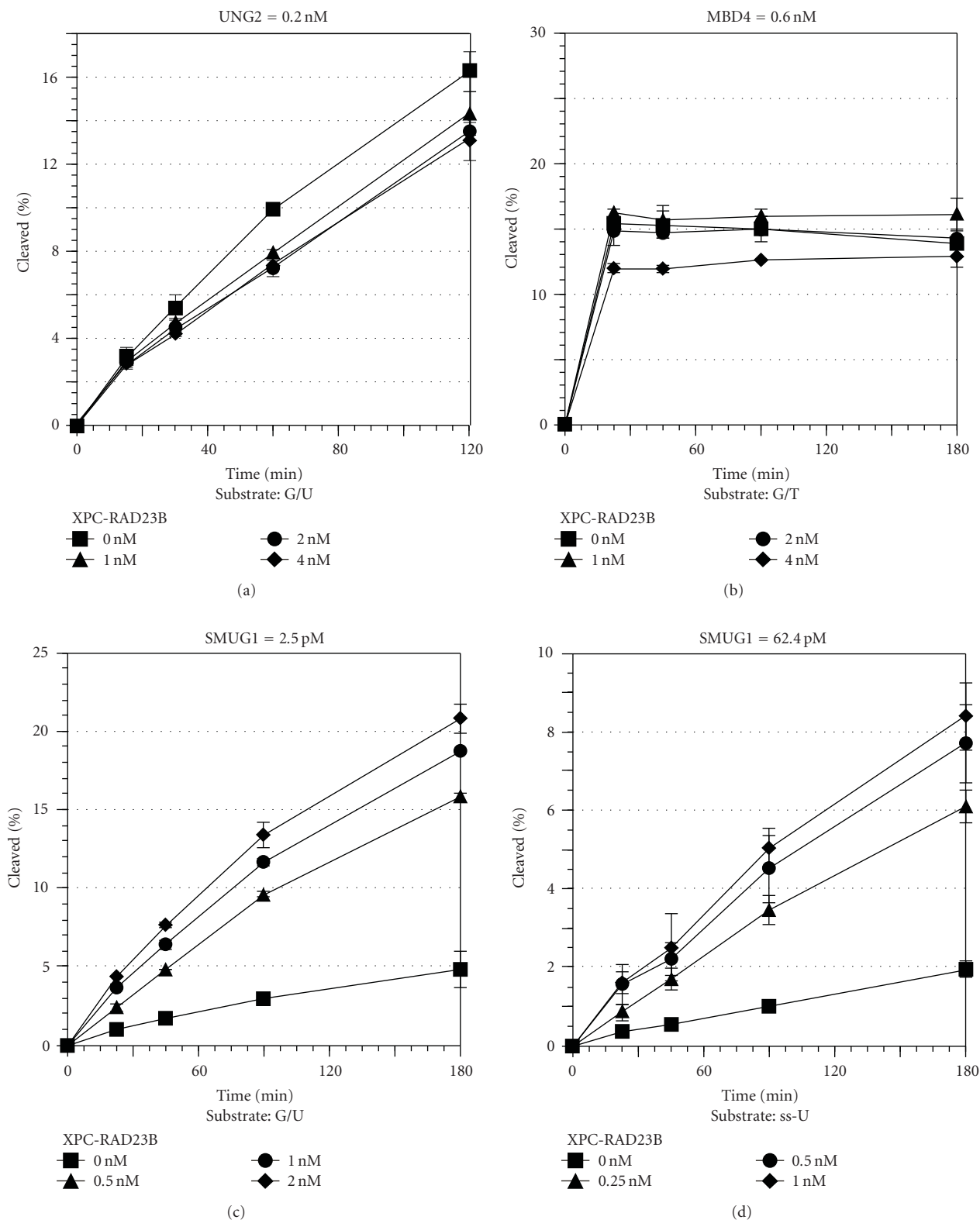


FIGURE 6: The effect of XPC on the activity of other DNA glycosylases involved in G/T and/or G/U mismatch repair. The activity of UNG2 (a), MBD4 (b), or SMUG1 ((c) and (d)) was measured in the presence of various amounts of XPC-RAD23B. In each reaction, 1.6 nM of 60-bp DNA containing a single G/U mismatch ((a) and (c)), G/T mismatch (b), or single stranded 30-mer oligonucleotide containing a single uracil residue (d) was used as the substrate. The reaction was done at 30°C for the time indicated with specified concentration of purified recombinant proteins as shown. The DNA samples were then purified and subjected to alkali-treatment to cleave the resulting AP sites and separated with denaturing PAGE. The ratio of the cleaved product was calculated and plotted as a graph. The mean values and standard errors were calculated from at least two independent experiments.

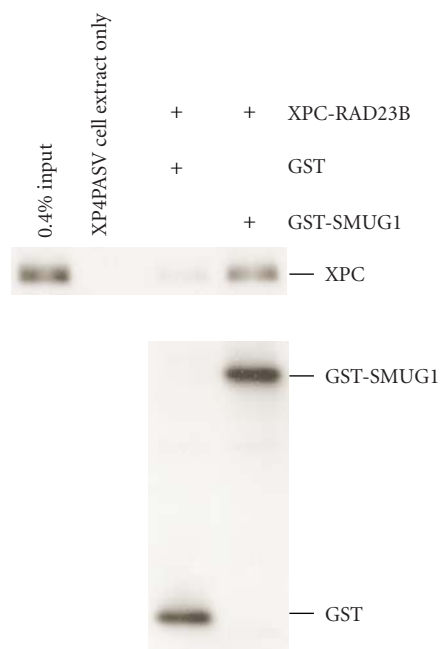


FIGURE 7: XPC interacts physically with SMUG1 *in vitro*. Glutathione-Sepharose beads (20  $\mu$ l) were incubated in 100  $\mu$ l of the binding mixture with 10 nM of either GST or GST-TDG in the presence of the same concentration of XPC-RAD23B. After extensive washing, bound proteins were eluted with buffer containing 10 mM glutathione. One-fourth of each eluate was mixed with whole cell extract from XP4PASV cells which do not express XPC and subjected to 8% SDS-PAGE followed by immunoblotting with anti-XPC antibody (upper panel). The same samples were also subjected to 12% SDS-PAGE followed by immunoblotting with anti-GST antibody (lower panel).

binding of XPC to DNA. On the contrary, XPC showed a striking stimulation on the activity of SMUG1 against G/U mismatch in a dose-dependent manner (Figure 6(c)). In the absence of XPC, 2.5 pM SMUG1 processed about 5% of 1.6 nM G/U-mismatched DNA in 120 minutes under the conditions tested. Meanwhile, the presence of 2 nM XPC-RAD23B boosted the SMUG1 activity up to 4-fold under the equivalent conditions. This stimulation was also observed when a single-stranded 30-mer oligonucleotide containing a single uracil residue was used as a substrate (Figures 1 and 6(d)). While 62.4 pM SMUG1 cleaved about 2% of the substrate (1.6 nM) in 120 minutes, addition of 1 nM XPC-RAD23B stimulated the cleavage up to 8% under the same conditions. Although SMUG1 is known to remove uracils more efficiently from single-stranded DNA than from double-stranded DNA, our results showed the opposite pattern. This might be due to the difference in length of the substrate DNA between G/U-mismatched double-stranded DNA (60 bp) and single-stranded DNA (30 mer) [39]. These results suggest that XPC functionally interacts not only with TDG but also with SMUG1.

**3.5. XPC Physically Interacts with SMUG1.** Since our results indicate that XPC could stimulate the activity of SMUG1

*in vitro*, we tested the existence of the protein-protein interaction between XPC and SMUG1 by using the GST-pull down assay (Figure 7). Ten nanomolar each of GST or GST-fused SMUG1 was incubated with an equimolar amount of XPC-RAD23B, and then bound to the glutathione-Sepharose beads. After eluting the bound protein with glutathione, the presence of GST and GST-SMUG1 or XPC was visualized by immunoblotting using anti-GST or anti-XPC antibody, respectively. While equivalent molar amounts of GST and GST-SMUG1 were observed within the eluates, only little amount of XPC was bound to the control GST. On the other hand, a significant amount of XPC was pulled-down with GST-SMUG1. Although this protein-protein interaction seems to be relatively weak (only ~0.4% of the input was bound to XPC), these results indicate presence of a direct interaction between XPC and SMUG1.

## 4. Discussion

**4.1. Mechanistic Implications on the Enzymatic Turnover of TDG Promoted by XPC.** In this study, we have further examined the molecular mechanisms of interaction between XPC and TDG that facilitate the enzymatic turnover of TDG. In our previous studies, XPC appeared to promote dissociation of TDG from the AP site that is generated by its own glycosylase activity on G/T mismatch [20]. At least two possible mechanisms have been considered, which could contribute to the displacement of TDG from the abasic reaction product: (1) protein-protein interaction between XPC and TDG weakens the binding affinity of TDG to the substrate DNA, and (2) XPC and TDG compete for the same AP site, and thus TDG is pushed out. In order to examine which factor is more critical for the enhanced enzymatic turnover, *EcMUG*, an *E. coli* homolog of mammalian TDG, was utilized as a model that can bind to the AP site as well as TDG [24, 25] but cannot interact with XPC (Figure 3). Our results indicate that the stimulation of *EcMUG* by XPC is almost negligible when compared to human TDG (Figure 4). Although there might be very weak stimulation of *EcMUG*, which could be due to competitive displacement of the enzyme from the AP site by XPC-RAD23B, these results point to importance of the protein-protein interaction for the stimulation of TDG by XPC. In agreement with this idea, we show here that XPC also stimulates the activities of sumoylated TDG and SMUG1, both of which interact physically with XPC (Figures 3 and 7).

Our present data also indicate that very stable association of DNA glycosylase with the produced AP site is not a prerequisite for stimulation by XPC. It has been reported that modification of TDG by SUMO alters its structure in the C-terminal domain, which leads to the release of TDG from the AP site and therefore induces accelerated enzymatic turnover [30–32]. In fact, in contrast to the immediately saturating reaction patterns of unmodified TDG, the sumoylated enzyme exhibited a nearly linear kinetics of uracil removal from G/U mismatches. Even under these conditions, intriguingly, XPC has an ability to further stimulate the activity of SUMO-1-TDG. It is possible that,

like the reported case for OGG1, XPC may stimulate loading of certain DNA glycosylases to substrate DNA. Although competition with XPC for the AP site may not be sufficient by itself to displace the tightly bound DNA glycosylase, our data do not exclude that the binding affinity of XPC to the AP site may still contribute to promotion of the enzymatic turnover. Considering the fact that XPC and APE1 stimulate the activity of TDG in an additive fashion [20] and that APE1 also further stimulates the activity of SUMO-1-TDG [30], XPC, sumoylation, and APE1 might be collaborating to control the repair of G/T and G/U mismatches positively *in vivo*. To understand the relationship between these three factors in detail, *in vivo* regulation of the TDG sumoylation should be clarified in the future experiments. In addition, it has been shown that XPC undergoes *in vivo* posttranslational modifications, such as ubiquitylation [40, 41], sumoylation [41], and phosphorylation [42, 43]. Although the observed stimulation of DNA glycosylases seemed to occur in the absence of these modifications, it is still possible that one or more of these modifications may affect interaction with and/or stimulation of some DNA glycosylases. Future studies would be necessary to address such intriguing possibility.

**4.2. Possible Roles of Interactions between XPC and TDG/SMUG1 in Prevention of Mutagenesis and Carcinogenesis.** Mammalian cells contain at least four nuclear DNA glycosylases that can correct G/U and/or G/T mismatches, that is, TDG, UNG2, MBD4, and SMUG1. Although precise niche for each of these DNA glycosylases remains to be clarified, their biological roles have been suggested through observations of *in vivo* behaviors and through interacting partners. UNG2 seems to be specialized in counteracting U:A base pairs formed by misincorporation of dUTP during DNA replication. Among the uracil-DNA glycosylases, only UNG2 specifically accumulates in the replication foci during the S phase, thereby colocalizing with proliferating cell nuclear antigen (PCNA) and RPA [44]. On the other hand, SMUG1 was first identified by *in vitro* expression cloning [39] and also independently found to be a backup enzyme for UNG2 [45, 46]. Unlike UNG2, SMUG1 may account for the repair of replication-independent premutagenic G/U mispairs resulting from cytosine deamination *in vivo*, since it is expressed similarly in nonproliferating and proliferating cells [45] and it does not colocalize with PCNA during the S phase [47]. TDG and MBD4 apparently have very similar substrate specificities: G/T and G/U mispairs that are spontaneously generated by deamination of cytosines in CpG dinucleotides. Besides its function in BER, TDG is also known to interact with and regulate several transcription factors [48–51]. MBD4 interacts with a mismatch repair protein MLH1 [52], which may be involved in regulation of some DNA damage response pathways [53]. Interestingly, human UNG, TDG, and SMUG1 genes are closely located within the long arm of chromosome 12, and these genes are believed to be the derivatives from an identical ancestral gene [54]. In fact, structural studies revealed that they contain several common folds despite rather low (~10%) amino acid sequence homology [55, 56]. In these points of view, TDG

and SMUG1 might still possess the common surface that might be the remnant of the ancestor to interact with XPC.

It has been reported that TDG is able to process certain oxidative pyrimidine lesions, such as thymine glycol, 5-hydroxyuracil, and 5-hydroxymethyluracil, when paired with guanine [21]. In addition, SMUG1 was shown to be a primary repair enzyme for a subset of oxidized uracil derivatives such as 5-formyluracil, 5-hydroxymethyluracil, and 5-hydroxyuracil in both single- and double-stranded DNA [57, 58]. Taken together with the recent report showing that XPC stimulates the activity of OGG1 [33], these findings suggest that XPC might be involved in repair of diverse oxidative DNA lesions. In fact, lack of endogenous XPC seems to result in inefficient repair of spontaneous oxidative DNA damage. Interestingly, while a significant amount of H<sub>2</sub>O<sub>2</sub> is produced upon UV irradiation in most of the complementation groups of the XP cells including XP-C compared to normal cells [59], plasmid reactivation assays revealed that only XP-C cells exhibited markedly reduced repair capacity for some singlet oxygen-induced DNA lesions [60]. Furthermore, extensive mutational analyses of the *Trp53* of UVB-induced skin tumors in *Xpc*<sup>-/-</sup> mice revealed a mutational hotspot at a nondipyrimidinic CpG site in codon 122 [61, 62]. At this site, C to T transition has been frequently detected specifically in *Xpc*<sup>-/-</sup> mice (not in *Xpa*<sup>-/-</sup> or *Csa*<sup>-/-</sup> mice), which is plausibly explained by reduced TDG activity in the absence of functional XPC protein. However, the tandem mutations AC > TT and AC > CT have been also found at the same site, which cannot be attributed either to UV-induced dipyrimidinic photolesions or to deamination of the cytosine alone. In addition, it has been reported that age-dependent spontaneous mutations significantly accumulate in *Xpc*<sup>-/-</sup> mice even without UV exposure [63], and *p53* gene mutations were identified in internal tumors of XP-C patients [64]. Many of these mutations are less likely to be the result of defects in correction of G/T and/or G/U mismatches. It could be possible that impaired repair of certain types of oxidative damage may be involved in occurrence of these mutations.

## 5. Conclusions

Here we show that XPC stimulates activities of a certain spectrum of DNA glycosylases, for which protein-protein interactions seem to be important, rather than competition for AP sites. In order to clarify the significance of interaction between XPC and TDG or SMUG1 *in vivo*, it should be necessary to understand the precise physiological roles of the different thymine- and uracil-DNA glycosylases. Further studies would reveal novel and important aspects in understanding the mutagenesis and carcinogenesis in XP-C patients.

## Acknowledgments

The authors thank L. Lan, M. Takao, and A. Yasui (Tohoku University) for MBD4 cDNA and purified NEIL1 protein and M. Shirakawa (Kyoto University) for information on the

sumoylation system in bacteria. This work was supported by Grants-in-Aid from the Ministry of Education, Culture, Sports, Science and Technology of Japan.

## References

- [1] E. C. Friedberg, G. C. Walker, W. Siede, R. D. Wood, R. A. Schultz, and T. Ellenberger, *DNA Repair and Mutagenesis*, ASM Press, Washington, DC, USA, 2nd edition, 2006.
- [2] A. K. McCullough, M. L. Dodson, and R. S. Lloyd, "Initiation of base excision repair: glycosylase mechanisms and structures," *Annual Review of Biochemistry*, vol. 68, pp. 255–285, 1999.
- [3] O. D. Schärer and J. Jiricny, "Recent progress in the biology, chemistry and structural biology of DNA glycosylases," *BioEssays*, vol. 23, no. 3, pp. 270–281, 2001.
- [4] D. Bootsma, K. H. Kraemer, J. E. Cleaver, and J. H. J. Hoeijmakers, "Nucleotide excision repair syndromes: xeroderma pigmentosum, Cockayne syndrome, and trichothiodystrophy," in *The Metabolic and Molecular Basis of Inherited Disease*, C. R. Scriver, A. L. Beaudet, W. S. Sly, and D. Valle, Eds., pp. 677–703, McGraw-Hill, New York, NY, USA, 2001.
- [5] T. Riedl, F. Hanaoka, and J.-M. Egly, "The comings and goings of nucleotide excision repair factors on damaged DNA," *EMBO Journal*, vol. 22, no. 19, pp. 5293–5303, 2003.
- [6] K. Sugawara, J. M. Y. Ng, C. Masutani et al., "Xeroderma pigmentosum group C protein complex is the initiator of global genome nucleotide excision repair," *Molecular Cell*, vol. 2, no. 2, pp. 223–232, 1998.
- [7] M. Volker, M. J. Moné, P. Karmakar et al., "Sequential assembly of the nucleotide excision repair factors in vivo," *Molecular Cell*, vol. 8, no. 1, pp. 213–224, 2001.
- [8] M. Araki, C. Masutani, M. Takemura et al., "Centrosome protein centrin 2/caltractin 1 is part of the xeroderma pigmentosum group C complex that initiates global genome nucleotide excision repair," *The Journal of Biological Chemistry*, vol. 276, no. 22, pp. 18665–18672, 2001.
- [9] C. Masutani, K. Sugawara, J. Yanagisawa et al., "Purification and cloning of a nucleotide excision repair complex involving the xeroderma pigmentosum group C protein and a human homologue of yeast RAD23," *EMBO Journal*, vol. 13, no. 8, pp. 1831–1843, 1994.
- [10] M. K. K. Shivji, A. P. M. Eker, and R. D. Wood, "DNA repair defect in xeroderma pigmentosum group C and complementing factor from HeLa cells," *The Journal of Biological Chemistry*, vol. 269, no. 36, pp. 22749–22757, 1994.
- [11] J. M. Y. Ng, W. Vermeulen, G. T. J. van der Horst et al., "A novel regulation mechanism of DNA repair by damage-induced and RAD23-dependent stabilization of xeroderma pigmentosum group C protein," *Genes and Development*, vol. 17, no. 13, pp. 1630–1645, 2003.
- [12] Y. Okuda, R. Nishi, J. M. Y. Ng et al., "Relative levels of the two mammalian Rad23 homologs determine composition and stability of the xeroderma pigmentosum group C protein complex," *DNA Repair*, vol. 3, no. 10, pp. 1285–1295, 2004.
- [13] S. J. Araújo, F. Tirode, F. Coin et al., "Nucleotide excision repair of DNA with recombinant human proteins: definition of the minimal set of factors, active forms of TFIIH, and modulation by CAK," *Genes and Development*, vol. 14, no. 3, pp. 349–359, 2000.
- [14] D. Mu, C.-H. Park, T. Matsunaga, D. S. Hsu, J. T. Reardon, and A. Sancar, "Reconstitution of human DNA repair excision nuclease in a highly defined system," *The Journal of Biological Chemistry*, vol. 270, no. 6, pp. 2415–2418, 1995.
- [15] R. Nishi, Y. Okuda, E. Watanabe et al., "Centrin 2 stimulates nucleotide excision repair by interacting with xeroderma pigmentosum group C protein," *Molecular and Cellular Biology*, vol. 25, no. 13, pp. 5664–5674, 2005.
- [16] J.-H. Min and N. P. Pavletich, "Recognition of DNA damage by the Rad4 nucleotide excision repair protein," *Nature*, vol. 449, no. 7162, pp. 570–575, 2007.
- [17] K. Sugawara, T. Okamoto, Y. Shimizu, C. Masutani, S. Iwai, and F. Hanaoka, "A multistep damage recognition mechanism for global genomic nucleotide excision repair," *Genes and Development*, vol. 15, no. 5, pp. 507–521, 2001.
- [18] K. Sugawara, Y. Shimizu, S. Iwai, and F. Hanaoka, "A molecular mechanism for DNA damage recognition by the xeroderma pigmentosum group C protein complex," *DNA Repair*, vol. 1, no. 1, pp. 95–107, 2002.
- [19] L. C. J. Gillet and O. D. Schärer, "Molecular mechanisms of mammalian global genome nucleotide excision repair," *Chemical Reviews*, vol. 106, no. 2, pp. 253–276, 2006.
- [20] Y. Shimizu, S. Iwai, F. Hanaoka, and K. Sugawara, "Xeroderma pigmentosum group C protein interacts physically and functionally with thymine DNA glycosylase," *EMBO Journal*, vol. 22, no. 1, pp. 164–173, 2003.
- [21] D. Cortázar, C. Kunz, Y. Saito, R. Steinacher, and P. Schär, "The enigmatic thymine DNA glycosylase," *DNA Repair*, vol. 6, no. 4, pp. 489–504, 2007.
- [22] T. R. Waters, P. Gallinari, J. Jiricny, and P. F. Swann, "Human thymine DNA glycosylase binds to apurinic sites in DNA but is displaced by human apurinic endonuclease 1," *The Journal of Biological Chemistry*, vol. 274, no. 1, pp. 67–74, 1999.
- [23] T. R. Waters and P. F. Swann, "Kinetics of the action of thymine DNA glycosylase," *The Journal of Biological Chemistry*, vol. 273, no. 32, pp. 20007–20014, 1998.
- [24] T. E. Barrett, R. Savva, G. Panayotou et al., "Crystal structure of a G:T/U mismatch-specific DNA glycosylase: mismatch recognition by complementary-strand interactions," *Cell*, vol. 92, no. 1, pp. 117–129, 1998.
- [25] T. E. Barrett, O. D. Schärer, R. Savva et al., "Crystal structure of a thwarted mismatch glycosylase DNA repair complex," *EMBO Journal*, vol. 18, no. 23, pp. 6599–6609, 1999.
- [26] U. Hardeland, M. Bentele, J. Jiricny, and P. Schar, "Separating substrate recognition from base hydrolysis in human thymine DNA glycosylase by mutational analysis," *The Journal of Biological Chemistry*, vol. 275, no. 43, pp. 33449–33456, 2000.
- [27] M. Abu and T. R. Waters, "The main role of human thymine-DNA glycosylase is removal of thymine produced by deamination of 5-methylcytosine and not removal of ethenocytosine," *The Journal of Biological Chemistry*, vol. 278, no. 10, pp. 8739–8744, 2003.
- [28] M. E. Fitzgerald and A. C. Drohat, "Coordinating the initial steps of base excision repair: apurinic/apyrimidinic endonuclease 1 actively stimulates thymine DNA glycosylase by disrupting the product complex," *The Journal of Biological Chemistry*, vol. 283, no. 47, pp. 32680–32690, 2008.
- [29] C. V. Privezentzev, M. Saparbaev, and J. Laval, "The HAP1 protein stimulates the turnover of human mismatch-specific thymine-DNA-glycosylase to process 3,N4-ethenocytosine residues," *Mutation Research*, vol. 480–481, pp. 277–284, 2001.
- [30] U. Hardeland, R. Steinacher, J. Jiricny, and P. Schär, "Modification of the human thymine-DNA glycosylase by ubiquitin-like proteins facilitates enzymatic turnover," *EMBO Journal*, vol. 21, no. 6, pp. 1456–1464, 2002.

- [31] D. Baba, N. Maita, J.-G. Jee et al., "Crystal structure of thymine DNA glycosylase conjugated to SUMO-1," *Nature*, vol. 435, no. 7044, pp. 979–982, 2005.
- [32] R. Steinacher and P. Schär, "Functionality of human thymine DNA glycosylase requires SUMO-regulated changes in protein conformation," *Current Biology*, vol. 15, no. 7, pp. 616–623, 2005.
- [33] M. D'Errico, E. Parlanti, M. Teson et al., "New functions of XPC in the protection of human skin cells from oxidative damage," *EMBO Journal*, vol. 25, no. 18, pp. 4305–4315, 2006.
- [34] C. Masutani, M. Araki, K. Sugawara et al., "Identification and characterization of XPC-binding domain of hHR23B," *Molecular and Cellular Biology*, vol. 17, no. 12, pp. 6915–6923, 1997.
- [35] K. Sugawara, C. Masutani, A. Uchida et al., "HHR23B, a human Rad23 homolog, stimulates XPC protein in nucleotide excision repair in vitro," *Molecular and Cellular Biology*, vol. 16, no. 9, pp. 4852–4861, 1996.
- [36] K. Kino, Y. Shimizu, K. Sugawara, H. Sugiyama, and F. Hanaoka, "Nucleotide excision repair of 5-formyluracil in vitro is enhanced by the presence of mismatched bases," *Biochemistry*, vol. 43, no. 10, pp. 2682–2687, 2004.
- [37] Y. Uchimura, M. Nakamura, K. Sugawara, M. Nakao, and H. Saitoh, "Overproduction of eukaryotic SUMO-1- and SUMO-2-conjugated proteins in *Escherichia coli*," *Analytical Biochemistry*, vol. 331, no. 1, pp. 204–206, 2004.
- [38] P. Gallinari and J. Jiricny, "A new class of uracil-DNA glycosylases related to human thymine-DNA glycosylase," *Nature*, vol. 383, no. 6602, pp. 735–738, 1996.
- [39] K. A. Haushalter, P. T. Stukenberg, M. W. Kirschner, and G. L. Verdine, "Identification of a new uracil-DNA glycosylase family by expression cloning using synthetic inhibitors," *Current Biology*, vol. 9, no. 4, pp. 174–185, 1999.
- [40] K. Sugawara, Y. Okuda, M. Saijo et al., "UV-induced ubiquitylation of XPC protein mediated by UV-DDB-ubiquitin ligase complex," *Cell*, vol. 121, no. 3, pp. 387–400, 2005.
- [41] Q.-E. Wang, Q. Zhu, G. Wani, M. A. El-Mahdy, J. Li, and A. A. Wani, "DNA repair factor XPC is modified by SUMO-1 and ubiquitin following UV irradiation," *Nucleic Acids Research*, vol. 33, no. 13, pp. 4023–4034, 2005.
- [42] S. A. Beausoleil, M. Jedrychowski, D. Schwartz et al., "Large-scale characterization of HeLa cell nuclear phosphoproteins," *Proceedings of the National Academy of Sciences of the United States of America*, vol. 101, no. 33, pp. 12130–12135, 2004.
- [43] S. Matsuoka, B. A. Ballif, A. Smogorzewska et al., "ATM and ATR substrate analysis reveals extensive protein networks responsive to DNA damage," *Science*, vol. 316, no. 5828, pp. 1160–1166, 2007.
- [44] M. Otterlei, E. Warbrick, T. A. Nagelhus et al., "Post-replicative base excision repair in replication foci," *EMBO Journal*, vol. 18, no. 13, pp. 3834–3844, 1999.
- [45] H. Nilsen, K. A. Haushalter, P. Robins, D. E. Barnes, G. L. Verdine, and T. Lindahl, "Excision of deaminated cytosine from the vertebrate genome: role of the SMUG1 uracil-DNA glycosylase," *EMBO Journal*, vol. 20, no. 15, pp. 4278–4286, 2001.
- [46] H. Nilsen, I. Rosewell, P. Robins et al., "Uracil-DNA glycosylase (UNG)-deficient mice reveal a primary role of the enzyme during DNA replication," *Molecular Cell*, vol. 5, no. 6, pp. 1059–1065, 2000.
- [47] B. Kavli, O. Sundheim, M. Akbari et al., "hUNG2 is the major repair enzyme for removal of uracil from U:A matches, U:G mismatches, and U in single-stranded DNA, with hSMUG1 as a broad specificity backup," *The Journal of Biological Chemistry*, vol. 277, no. 42, pp. 39926–39936, 2002.
- [48] D. Chen, M. J. Lucey, F. Phoenix et al., "T:G mismatch-specific thymine-DNA glycosylase potentiates transcription of estrogen-regulated genes through direct interaction with estrogen receptor  $\alpha$ ," *The Journal of Biological Chemistry*, vol. 278, no. 40, pp. 38586–38592, 2003.
- [49] C. Missero, M. T. Pirro, S. Simeone, M. Pischetola, and R. Di Lauro, "The DNA glycosylase T:G mismatch-specific thymine DNA glycosylase represses thyroid transcription factor-1-activated transcription," *The Journal of Biological Chemistry*, vol. 276, no. 36, pp. 33569–33575, 2001.
- [50] M. Tini, A. Benecke, S.-J. Um, J. Torchia, R. M. Evans, and P. Chambon, "Association of CBP/p300 acetylase and thymine DNA glycosylase links DNA repair and transcription," *Molecular Cell*, vol. 9, no. 2, pp. 265–277, 2002.
- [51] S. Um, M. Harbers, A. Benecke, B. Pierrat, R. Losson, and P. Chambon, "Retinoic acid receptors interact physically and functionally with the T:G mismatch-specific thymine-DNA glycosylase," *The Journal of Biological Chemistry*, vol. 273, no. 33, pp. 20728–20736, 1998.
- [52] A. Bellacosa, L. Cicchillitti, F. Schepis et al., "MED1, a novel human methyl-CpG-binding endonuclease, interacts with DNA mismatch repair protein MLH1," *Proceedings of the National Academy of Sciences of the United States of America*, vol. 96, no. 7, pp. 3969–3974, 1999.
- [53] S. Cortellino, D. Turner, V. Masciullo et al., "The base excision repair enzyme MED1 mediates DNA damage response to antitumor drugs and is associated with mismatch repair system integrity," *Proceedings of the National Academy of Sciences of the United States of America*, vol. 100, no. 25, pp. 15071–15076, 2003.
- [54] H. E. Krokan, M. Otterlei, H. Nilsen et al., "Properties and functions of human uracil-DNA glycosylase from the UNG gene," *Progress in Nucleic Acid Research and Molecular Biology*, vol. 68, pp. 365–386, 2001.
- [55] L. H. Pearl, "Structure and function in the uracil-DNA glycosylase superfamily," *Mutation Research*, vol. 460, no. 3-4, pp. 165–181, 2000.
- [56] J. E. A. Wibley, T. R. Waters, K. Haushalter, G. L. Verdine, and L. H. Pearl, "Structure and specificity of the vertebrate anti-mutator uracil-DNA glycosylase SMUG1," *Molecular Cell*, vol. 11, no. 6, pp. 1647–1659, 2003.
- [57] R. J. Boorstein, A. Cummings Jr., D. R. Marenstein et al., "Definitive Identification of Mammalian 5-Hydroxymethyluracil DNA N-Glycosylase Activity as SMUG1," *The Journal of Biological Chemistry*, vol. 276, no. 45, pp. 41991–41997, 2001.
- [58] A. Masaoka, M. Matsubara, R. Hasegawa et al., "Mammalian 5-formyluracil-DNA glycosylase. 2. Role of SMUG1 uracil-DNA glycosylase in repair of 5-formyluracil and other oxidized and deaminated base lesions," *Biochemistry*, vol. 42, no. 17, pp. 5003–5012, 2003.
- [59] M. Vuillaume, L. Daya-Grosjean, P. Vincens et al., "Striking differences in cellular catalase activity between two DNA repair-deficient diseases: xeroderma pigmentosum and trichothiodystrophy," *Carcinogenesis*, vol. 13, no. 3, pp. 321–328, 1992.
- [60] T. M. Runger, B. Epe, and K. Moller, "Repair of Ultraviolet B and singlet oxygen-induced DNA damage in xeroderma pigmentosum cells," *Journal of Investigative Dermatology*, vol. 104, no. 1, pp. 68–73, 1995.
- [61] D. Nahari, L. D. McDaniel, L. B. Task, R. L. Daniel, S. Velasco-Miguel, and E. C. Friedberg, "Mutations in the Trp53 gene

of UV-irradiated Xpc mutant mice suggest a novel Xpc-dependent DNA repair process," *DNA Repair*, vol. 3, no. 4, pp. 379–386, 2004.

- [62] A. M. Reis, D. L. Cheo, L. B. Meira et al., "Genotype-specific Trp53 mutational analysis in ultraviolet B radiation- induced skin cancers in Xpc and Xpc Trp53 mutant mice," *Cancer Research*, vol. 60, no. 6, pp. 1571–1579, 2000.
- [63] S. W. P. Wijnhoven, H. J. M. Kool, L. H. F. Mullenders et al., "Age-dependent spontaneous mutagenesis in Xpc mice defective in nucleotide excision repair," *Oncogene*, vol. 19, no. 43, pp. 5034–5037, 2000.
- [64] G. Giglia, N. Dumaz, C. Drougard, M.-F. Avril, L. Daya-Grosjean, and A. Sarasin, "p53 Mutations in skin and internal tumors of xeroderma pigmentosum patients belonging to the complementation group C," *Cancer Research*, vol. 58, no. 19, pp. 4402–4409, 1998.

## Research Article

# Coincident *In Vitro* Analysis of DNA-PK-Dependent and -Independent Nonhomologous End Joining

Cynthia L. Hendrickson,<sup>1,2</sup> Shubhadeep Purkayastha,<sup>1</sup> Elzbieta Pastwa,<sup>3</sup>  
Ronald D. Neumann,<sup>1</sup> and Thomas A. Winters<sup>1</sup>

<sup>1</sup>Radiology & Imaging Sciences Department, Nuclear Medicine Section, Warren G. Magnuson Clinical Center, National Institutes of Health, Bethesda, MD 20892, USA

<sup>2</sup>Applied Biosystems, Advanced Genetic Applications, 500 Cummings Center, Suite 2450, Beverly, MA 01915, USA

<sup>3</sup>Molecular Genetics Department, Medical University of Lodz, Lodz 92-215, Poland

Correspondence should be addressed to Thomas A. Winters, twinters@mail.nih.gov

Received 15 May 2010; Accepted 6 June 2010

Academic Editor: Ashis Basu

Copyright © 2010 Cynthia L. Hendrickson et al. This is an open access article distributed under the Creative Commons Attribution License, which permits unrestricted use, distribution, and reproduction in any medium, provided the original work is properly cited.

In mammalian cells, DNA double-strand breaks (DSBs) are primarily repaired by nonhomologous end joining (NHEJ). The current model suggests that the Ku 70/80 heterodimer binds to DSB ends and recruits DNA-PK<sub>cs</sub> to form the active DNA-dependent protein kinase, DNA-PK. Subsequently, XRCC4, DNA ligase IV, XLF and most likely, other unidentified components participate in the final DSB ligation step. Therefore, DNA-PK plays a key role in NHEJ due to its structural and regulatory functions that mediate DSB end joining. However, recent studies show that additional DNA-PK-independent NHEJ pathways also exist. Unfortunately, the presence of DNA-PK<sub>cs</sub> appears to inhibit DNA-PK-independent NHEJ, and *in vitro* analysis of DNA-PK-independent NHEJ in the presence of the DNA-PK<sub>cs</sub> protein remains problematic. We have developed an *in vitro* assay that is preferentially active for DNA-PK-independent DSB repair based solely on its reaction conditions, facilitating coincident differential biochemical analysis of the two pathways. The results indicate the biochemically distinct nature of the end-joining mechanisms represented by the DNA-PK-dependent and -independent NHEJ assays as well as functional differences between the two pathways.

## 1. Introduction

DNA double-strand breaks (DSBs) constitute the most cytotoxic form of DNA damage in the genome. DSBs are generated not only by exogenous sources, such as ionizing radiation, radiomimetic compounds, and topoisomerase inhibitors but also from endogenous cellular processes that generate reactive oxygen species [1, 2]. In mammalian cells, one of the major pathways for the repair of DSBs is nonhomologous end joining (NHEJ) [3, 4]. The principle proteins that participate in this DNA end joining pathway both *in vitro* [5–7] and *in vivo* [8–10] are the Ku 70/80 heterodimer, DNA-PK<sub>cs</sub>, XRCC4, DNA ligase IV and XLF (XRCC4-like factor; also called Cernunnos) that has recently been identified as a binding partner of the DNA ligase IV-XRCC4 complex and as necessary for efficient ligation via NHEJ [11, 12]. Subsets of NHEJ may involve other factors

such as Artemis [13]. Together with the Artemis protein, DNA-PK<sub>cs</sub> can stimulate processing of the DNA ends [14, 15]. Additional proteins, including DNA polymerases  $\mu$  and  $\lambda$ , TDP1 (tyrosyl-DNA phosphodiesterase), PNK (polynucleotide kinase), and WRN (Werner's syndrome helicase) are also likely to play a role in DSB repair [16]. Recent reports suggest that numerous other proteins, including ATM, histones H1 and H2AX, NBS1, and Mre11 may also have some influence on the NHEJ pathway [17–19]. NHEJ is a complex, multistep process initiated by the binding of a heterodimeric complex composed of Ku70 and Ku80 subunits (encoded by the XRCC5 and XRCC6 genes, respectively) to both ends of the broken DNA molecule with high specificity and affinity [20]. Ku binds DNA DSB ends and recruits DNA-PK<sub>cs</sub>, which is a 460 kDa serine/threonine protein kinase, to the ends [21]. Ku then translocates inward, approximately 14 bp on the DNA, allowing DNA-PK<sub>cs</sub> to contact DNA [22].

The resulting DNA-PK holoenzyme (Ku/DNA-PKcs) has a serine/threonine protein kinase activity that is necessary for efficient repair [23]. A current model of NHEJ suggests that inward translocation of Ku allows DNA-PKcs molecules on opposing DSB ends to interact across the DSB and form a molecular “bridge” or synapse between the two DNA ends [24], and end-joining may then be completed by ligation of the DNA ends by DNA ligase IV/XRCC4/XLF complex [25].

Therefore, DNA-PK has important roles in NHEJ that include its DNA end-bridging activity [24], and its function in regulating DSB end processing enzymes, such as the structure-dependent nuclease Artemis [15] and its requirement for the stable recruitment of the DNA ligase IV/XRCC4 complex [26]. In support of this DNA-PK-dependent NHEJ model, previous studies have shown that DNA-PK binds XRCC4-ligase IV [26, 27], but not the other mammalian DNA ligases (I or III) *in vitro* [28]. It has also been shown that wortmannin, a chemical inhibitor of DNA-PK, [29] inhibits NHEJ [5] in a way similar to that seen in cells expressing kinase deficient DNA-PKcs [23]. However, the role of DNA-PK kinase activity in NHEJ has not yet been fully understood. Although DNA-PKcs binds to Ku at DNA DSB sites, disruption of these DNA-PK complexes by autophosphorylation [30, 31] is required for subsequent ligation of the DNA ends [32, 33]. It has been established that DNA-dependent protein kinase (DNA-PK) undergoes a series of autophosphorylation events that facilitate successful completion of nonhomologous end joining [32]. DNA-PKcs is phosphorylated at multiple sites *in vivo* in response to DNA damage, including serine 2056 [34], a cluster of sites between residues 2609–2647 (referred to as the ABCDE or Thr-2609 cluster), and threonine 3950 [35]. Although DNA-PKcs in which the ABCDE sites have been mutated to alanine has normal protein kinase activity, its ability to dissociate from the Ku-DNA complex is reduced *in vitro* [36] and *in vivo* [37], suggesting that phosphorylation of the ABCDE sites plays a major role in regulating disassembly of the initial DNA-PK complex. DNA-PK also phosphorylates the Ku subunits [38] and XRCC4 [39], but mutation of these phosphorylation sites does not inhibit NHEJ [26, 40]. It has been suggested that activation of the kinase may be required for mobilization of the DNA ligase IV/XRCC4 complex [41], but the mechanism for mobilization is unknown. It has also been suggested that phosphorylation of histone H1 by DNA-PK, which reduces the affinity of the histone for DNA is required for NHEJ [42]. Alternatively, it has also been proposed that DNA-PKcs stimulates, but is not essential to, NHEJ [10, 18]. Recent studies have revealed the overall structural architecture of DNA-PKcs and Ku with DNA under conditions that mimic DSBs and DNA-PKcs autophosphorylation [43]. The results indicate that efficient association and dissociation of the DNA-PKcs at DSBs is regulated by Ku and DNA-PKcs autophosphorylation that induces dramatic conformational changes in the protein. Recently, a three-dimensional crystal structure of purified DNA-PKcs in complex with C-terminal fragments of Ku80 has been determined and reveals irregular regions of repetitive structures ( $\alpha$ -helical HEAT repeats) that might provide a flexible cradle to promote DNA DSB repair [44]. Conceivably, individual phosphorylation events

have different effects on DNA-PKcs structure and function, both *in vitro* and *in vivo*, which in turn influences the assembly and disassembly of the initial NHEJ complex that regulates the accessibility of the DSB to other repair factors as well as pathway progression [3, 33, 45]. The DNA-PK dependent pathway could thus be characterized as the principle NHEJ pathway that employs the products of DNA-PKcs, Ku70/80, DNA ligase IV, XRCC4, XLF, and Artemis. Defects in the components of this pathway have been implicated in genomic instability and development of cancer [46, 47]. The possibility however of the presence of alternative pathways for NHEJ was suggested by early experiments in which cells deficient in DNA-PKcs, Ku, DNA ligase IV, or XRCC4 showed a high potential of end joining with preferential use of microhomologies [48]. The presence of at least one alternate pathway was first indicated by the observation that DNA-PK mutant M059J cells, which do not express DNA-PKcs, retain the ability to repair DNA DSBs [8] and exhibit wild-type end-joining activity *in vitro* [49], suggesting the involvement of a DNA-PK-independent end-joining pathway in these cells. At least two NHEJ mechanisms have also been identified in cells with DNA-PKcs *in vivo*: an immediate, high-fidelity end joining that occurs within two hours, followed by an error-prone DSB repair with slower kinetics [49, 50]. A study of cell lines with and without DNA-PKcs, M059K, and M059J, respectively, suggests that the first, faster NHEJ pathway is DNA-PKcs-dependent and the second, slower NHEJ pathway is DNA-PKcs-independent [51, 52]. DNA-PK-dependent and -independent repair has also been indicated *in vivo* as a function of cell cycle [53]. Recent studies have confirmed the operation of alternative pathways of NHEJ in the absence of the DNA-PK/LigIV/XRCC4 complex, in which another ligase partially substitutes for DNA ligase IV [54, 55]. Although Pol $\beta$ , XRCC1, PARP-1, and DNA ligase III contribute predominantly to base excision repair (BER) and SSB repair [56], these proteins are also considered to be candidate components for backup pathways for NHEJ in which ligase III provides the major ligation activity [57, 58]. Indeed, PARP-1 has been shown to compete with Ku for repair of DNA double-strand breaks but apparently through distinct NHEJ pathways [59]. These backup pathways are not typically detectable in the presence of DNA-PKcs, suggesting that the binding of the protein to the DNA inhibits DNA-PK-independent NHEJ [49, 54]. A more recent work has identified histone H1 as an additional putative factor that operates preferentially within these backup pathways [60]. Although there is a significant evidence *in vivo* and *in vitro* of a DNA-PKcs-independent NHEJ pathway, this DNA end-joining mechanism has only been reported *in vitro* in the absence of the kinase subunit due to the apparent inhibition of alternate pathways by DNA-PKcs [54]. In this study, we have identified *in vitro* reaction conditions that optimize the repair of DNA DSBs via a DNA-PK-independent pathway in the presence of functional DNA-PKcs. We also evaluated DSB end-joining efficiency and DNA-PK activity in extracts treated with wortmannin, which is a potent and selective inhibitor of phosphatidylinositol 3-kinases (PI3K) as well as the PI3K-like DNA-PK and has a pronounced effect on DNA DSB repair [61, 62]. Under these

same conditions, we have found that DNA-PK is active in the absence of wortmannin and inhibited in the presence of wortmannin but that inhibition of DNA-PK's kinase activity does not inhibit NHEJ. Results also confirm that under reaction conditions that favor DNA-PK-dependent NHEJ, wortmannin completely inhibits DNA end joining. We have found that the individual activities of the two NHEJ repair pathways are differentially affected by reaction conditions. Furthermore, as evidenced in earlier studies [49, 50], we have observed decreased DSB repair fidelity under reaction conditions that favor DNA-PK-independent NHEJ.

## 2. Materials and Methods

**2.1. Materials.** T4 DNA ligase (10 U/ $\mu$ L) was purchased from Invitrogen (Carlsbad, CA.). Wortmannin was from Sigma (St. Louis, MO). Restriction enzymes were from New England Biolabs (Beverly, MA). Vistra Green was obtained from Amersham Biosciences (Piscataway, NJ). Antibodies to Ku80, XRCC4, GAPDH, PARP-1, histone H1 (IgG<sub>2a</sub>), DNA-PK<sub>cs</sub>, and ATM were purchased from Abcam, Inc. (Cambridge, MA). Antibodies to DNA ligase I, Mre11, Rad50, and NBS1 were from GeneTex, Inc. (San Antonio, TX). Antibodies to DNA ligase III were from Novus Biologicals (Littleton, CO). All antibodies were of isotype IgG<sub>1</sub> except where noted. The DNA-PK peptide substrate was purchased from Promega (Madison, WI). Plasmid pSP189 was a gift from Dr. Michael Seidman (National Institute of Aging, Baltimore, MD).

**2.2. Cellular Extraction.** Unless otherwise indicated, cervical cancer (HeLa) cells, fibroblast (WI-38) cells, and malignant glioma (M059K) cells ( $8 \times 10^7$  cells/mL) were extracted by triplicate rounds of freezing and thawing in B1 lysis buffer (10 mM HEPES pH 7.9, 60 mM KCl, 1 mM EDTA pH 8.0, 1 mM DTT, and 1 mM PMSF). Lysates were cleared by centrifugation at  $16,000 \times g$  for 30 min at 4°C and the supernatants constituting the WCEs were stored as aliquots at -80°C.

**2.3. DSB End-Joining Assays.** Reactions (50  $\mu$ L; 50 mM Tris-HCl, pH 7.6, 5 mM MgCl<sub>2</sub>, 1 mM DTT, 1  $\mu$ g/mL aprotinin, 1  $\mu$ g/mL leupeptin, 10  $\mu$ g/mL bestatin, 1 mM pepabloc, 1 mM ATP, 100 ng StuI-cut pSP189 plasmid DNA unless otherwise indicated, and with or without 5% (w/v) polyethylene glycol, MW ~8 kDa, ((PEG) also where indicated) were initiated with the addition of 15  $\mu$ g WCE. Reactions were incubated at 30°C for the times indicated. Experiments with wortmannin were prepared and incubated on ice for 10 min before heating to 30°C. All reactions were stopped with the addition of SDS (0.4%) and incubation at 65°C for 15 min. DNA was recovered by phenol: chloroform extraction and ethanol precipitation, separated on 1% agarose gels, and stained with Vistra Green for 1 hr. Images were digitized with a FluorImager 595 system and quantified densitometrically using GelPro v2.0 software (Media Cybernetics, Gaithersburg, MD).

DSB repair fidelity experiments employed a modification of the end-joining assay described above. Repair fidelity was

measured as a function of restriction enzyme recleavage efficiency for the end-joined DNA products recovered from the assay described above. Standard end-joining reactions were run with pSP189 DNA linearized with StuI, EcoRI, PvuI, or Hin1I (producing blunt, 4 nucleotide 5'-overhang, 2 nucleotide 5'-overhang, or 2 nucleotide 3'-overhang DSB ends, respectively). DNA recovered from these reactions in the ethanol precipitation step was redissolved in 20  $\mu$ L of the appropriate manufacturer's restriction enzyme reaction buffer and split into two 10  $\mu$ L aliquots. One aliquot was incubated at 37°C for 2 h with 2.5 U of the restriction enzyme originally used to linearize the plasmid. Following this redigestion step, both aliquots were electrophoresed and analyzed as described above for the end-joining assay. All DSB repair fidelity reactions were run in triplicate.

**2.4. Kinase Assays.** Kinase activity was assayed under the same conditions as DNA end joining, except for the addition of 5  $\mu$ g peptide substrate (EPPLSQEAFADLWKK) and 0.2  $\mu$ Ci [ $\gamma$ -<sup>32</sup>P] ATP. Reactions were incubated at 30°C for 10 min then quenched as described for the end-joining assay. The peptide substrate was isolated on 16% Tris-Tricine SDS PAGE gels and analyzed by autoradiography.

**2.5. Immunodepletions.** WCE (700  $\mu$ g) was incubated with antibody (70  $\mu$ g) for 1 hr on ice. Antibody-bound protein was removed by adding either Sepharose A or G in binding buffer (50 mM Tris-HCl, pH 7.6; 0.1 mg/mL BSA), and rotating for 1 hr at 4°C. Unbound proteins were recovered by filtration through a 0.22  $\mu$ m cellulose acetate membrane and stored at -80°C. Target protein depletion was confirmed by western blot, following 4–12% Tris-Glycine SDS gradient PAGE. Immunodepletion of DNA ligase IV was performed using antibodies to XRCC4 due to the lack of ligase IV-specific antibodies. It has been reported that only trace ligase IV is found unbound to XRCC4 due to the instability of free DNA ligase IV [63]. In our hands, immunodepletion of XRCC4 resulted in nearly complete removal of the ligase.

## 3. Results and Discussion

**3.1. Determination of Preferential Reaction Conditions for DNA-PK-Dependent, and DNA-PK-Independent Nonhomologous End-Joining Pathways.** In previous studies, both DNA-PK dependent and independent NHEJ pathways have been observed *in vivo* [5, 49–51, 58], however, no *in vitro* reaction conditions in the presence of a functional DNA-PK<sub>cs</sub> protein have been reported to date that favor DNA-PK-independent DNA end joining. Several studies have noted the role of polymers such as PEG in stabilizing and enhancing the binding of proteins to the DNA through a macromolecular crowding effect [64]. Earlier works had shown that in the presence of high concentrations of macromolecules such as PEG, T4 DNA ligase as well as DNA ligase preparations from rat liver nuclei or from Escherichia coli actively catalyze blunt end ligations, in contrast to the poor activity of these enzymes on such substrates under conventional assay conditions [65]. These and other studies have argued that

such macromolecular crowding or confinement may perhaps play a more essential role in cell biology and physiology than otherwise noted and could well be a more adequate model for intracellular, *in vivo* conditions [66].

We observe that, in the presence of 5% polyethylene glycol (PEG), DNA end joining is insensitive to wortmannin, a potent and selective inhibitor of DNA-PK [29] that covalently binds to the protein. Whole cell extracts (WCE) from HeLa, WI-38, and M059K cells were assayed for DNA end-joining activity with and without 5% PEG and 10  $\mu$ M wortmannin. The WCEs were assayed for the ability to end-join blunt-end *StuI*-cut plasmid DNA (which we have previously shown to be NHEJ-dependent [67]) and produce plasmid dimers and trimers that were detected on agarose gels stained with Vista Green (Figure 1(a)). After 2 hrs at 30°C in the absence of PEG, the WCEs generated 5 to 25% product, depending on cell type (Figure 1(b)). The same reactions run with 10  $\mu$ M wortmannin reduced the total amount of product to between 0 to 4%, also depending on cell type. The assay was repeated in the presence of 5% PEG, resulting in 12 to 24% product in the absence of wortmannin. For HeLa and WI-38 WCEs, product yield increased up to 2-fold with the addition of PEG, while addition of 10  $\mu$ M wortmannin resulted in little or no decrease in product. However, an approximately 60% decrease in product was observed with M059K WCE in the presence of PEG and wortmannin, which though significantly less than the wortmannin inhibition observed with this extract in reactions without PEG still indicated that a fraction of the NHEJ was wortmannin-sensitive even in the presence of PEG. It could be argued that a residual amount of the end-joined product is due to DNA-PK-dependent NHEJ or that alternatively, DNA-PK<sub>cs</sub> may be playing a structural and/or stimulatory role in the organization of the initial NHEJ complex [43].

The end-joining reactions were repeated with HeLa WCE, 1% DMSO, and 0.1 to 10  $\mu$ M wortmannin in 1% DMSO (Figure 2(a)). Complete inhibition of DNA end joining was observed in the absence of PEG with 1.5  $\mu$ M wortmannin. In contrast, in the presence of 5% PEG, only a 15 to 20% reduction in product was observed with 1.5  $\mu$ M wortmannin. No further inhibition was observed with up to 10  $\mu$ M wortmannin. To determine the effective concentration of PEG required to favor wortmannin-insensitive NHEJ, the DNA end-joining assay was repeated for 1 hr at 30°C with 0 to 5% PEG with and without 10  $\mu$ M wortmannin (Figure 2(b)). In the absence of wortmannin, a steady increase in product formation was observed with the addition of up to 4% PEG, after which, a trend towards a small decrease in product formation was observed. Conversely, in the presence of wortmannin, a minimum of 3% PEG was required for the generation of end-joined product and at 5% PEG, little or no wortmannin inhibition was observed. Presumably, at a concentration of 5% PEG, the product is being formed by a wortmannin-insensitive, DNA-PK-independent NHEJ pathway.

It has been reported previously that blunt-ended DNA activates DNA-PK less efficiently than DNA DSBs with 3' - or 5' -overhangs [68]. Therefore, we wished to confirm DNA-PK

activity under our end-joining reaction conditions in the absence of PEG and wortmannin and also determine whether the loss of wortmannin sensitivity in the presence of PEG was due to the operation of a DNA-PK-independent pathway or simply due to the inability of wortmannin to inhibit DNA-PK in the presence of PEG. DNA-PK kinase activity was assayed under the same reaction conditions as those used for the end-joining assays (Figure 2(c)). Reactions were prepared in the same manner as the DNA end-joining reactions, but with the addition of 5  $\mu$ g of a peptide DNA-PK-phosphorylation substrate and [ $\gamma$ -<sup>32</sup>P] ATP. The reactions were prepared with and without DNA, 5% PEG, and 10  $\mu$ M wortmannin, and incubated at 30°C for 5 minutes. As is typical with the peptide substrate-based DNA-PK activity assay, nonspecific background kinase activity is observed for samples in the absence of added activator DNA, regardless of the presence or absence of PEG. A 2.5- to 3-fold DNA-dependent increase in kinase activity was observed following addition of the blunt-ended end-joining substrate DNA, and no difference in activity was observed between reactions with and without PEG. The addition of 10  $\mu$ M wortmannin inhibited all detectable kinase activity in both reactions, indicating that the PEG did not affect the ability of wortmannin to inhibit DNA-PK kinase activity. Therefore, PEG did not inhibit DNA binding, kinase activation, or wortmannin-mediated inhibition of DNA-PK. Consequently, even though DNA-PK kinase is active in the presence of PEG, DNA end joining seems to be independent of this kinase activity, since addition of 10  $\mu$ M wortmannin, which completely inhibits kinase activity, does not inhibit NHEJ in the presence of PEG. Thus, in the presence of 5% PEG, *in vitro* reaction conditions are established in which the NHEJ proceeds via a DNA-PK-independent pathway or at least one that is independent of the kinase activity of DNA-PK. This result argues for a much broader role for DNA-PK in the context of the structural architecture of the initial NHEJ complex in addition to the role it plays in catalyzing phosphorylation of several other repair proteins [43, 44].

*3.2. Survey of Proteins Involved in DNA-PK-Dependent and -Independent Nonhomologous End Joining.* We wished to determine the contribution of individual proteins to either of the two NHEJ pathways. To this end, a variety of proteins were individually immunodepleted from the HeLa WCE and DNA end-joining assays were conducted (with and without 5% PEG) to detect depletion-dependent reductions in end-joining activity (Figure 3). Immunodepletion of Ku80 and DNA ligase IV resulted in an almost complete loss of DNA end-joining efficiency for reactions both in the presence or absence of 5% PEG. This supports our earlier observations [69] and indicates the indispensable role that Ku plays in the initial recognition and binding of DSB ends and that of ligase IV in the final ligation step of the NHEJ process. Immunodepletion of NBS1 and histone H1 resulted in a significant loss of DNA-PK-dependent DNA end-joining activity in reactions without PEG (Figure 3(a)). In comparison, in reactions with 5% PEG, only a minimal loss of presumed DNA-PK-independent activity was observed with immunodepletion of NBS1 and histone H1

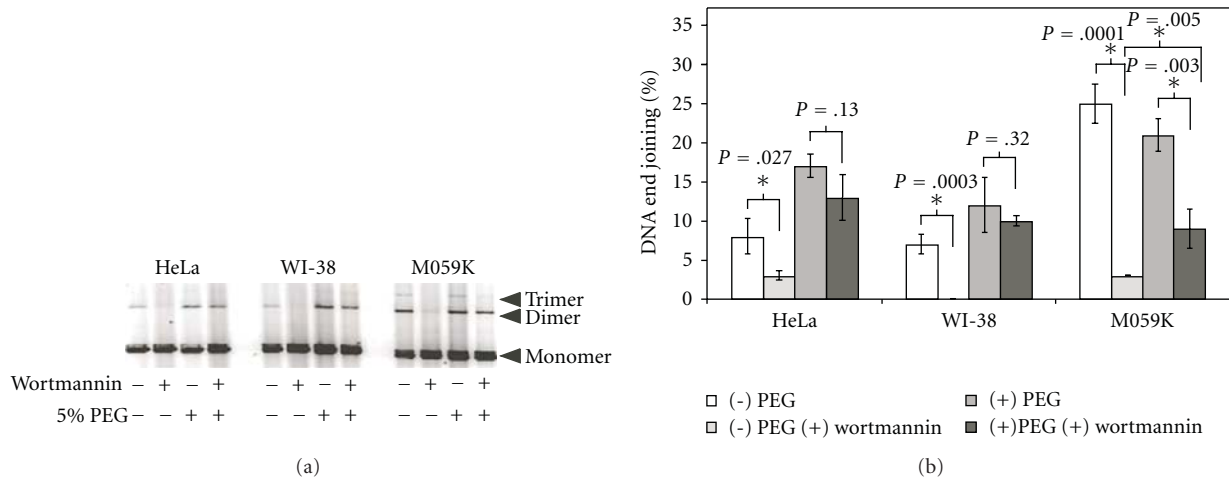


FIGURE 1: DNA end joining with HeLa, WI-38, and M059K WCEs with and without 5% PEG and/or 10  $\mu$ M wortmannin. (a) Agarose gel image showing typical DNA end-joining reaction results. Dimer and trimer DNA end-joining product yields are calculated as a fraction of the total DNA in the lane and reported graphically as shown in panel B. (b) Graphical depiction of results for triplicate end-joining reactions run with the three cell extracts under each of the conditions indicated. Error bars indicate the standard deviation for triplicate reactions. Significant differences, as determined by the Student *t*-test, are indicated by an asterisk. The *P*-values for each pairing are given above the brackets.

(Figure 3(b)). This is an interesting result in the context of the supposed stimulatory role of NBS1 and histone H1 in the backup pathways of NHEJ, where histone H1 enhances the activity of both DNA ligase III and PARP-1 [60]. Immunodepletion of DNA-PK<sub>cs</sub> resulted in a 30% reduction in the efficiency of the end-joining reactions without PEG, with little reduction observed in the presence of PEG. In addition, immunodepletion of Poly (ADP-ribose) polymerase 1 (PARP) and DNA ligase III consistently resulted in a trend toward increased efficiency for both the presumed DNA-PK-dependent and -independent NHEJ over the course of multiple experiments. This observation suggests the operation of backup pathways under these conditions and supports the hypothesis that these proteins may compete for repair at the DSB ends through alternate NHEJ pathways [58, 59]. Perrault et al. reported that DNA-PK independent DNA end joining is observed after immunodepletion of DNA-PK<sub>cs</sub> [54]. To confirm that the DNA end joining observed after immunodepletion of DNA-PK<sub>cs</sub> is actually DNA-PK-independent, the immunodepleted extract was assayed for activity with and without 10  $\mu$ M wortmannin (Figure 3(c)). End joining by the WCE was inhibited in the presence of 10  $\mu$ M wortmannin; whereas the DNA end-joining activity of the DNA-PK<sub>cs</sub> immunodepleted extract was wortmannin-insensitive, indicating that a DNA-PK-independent process formed the product.

From an examination of the immunodepletion data, only Ku and ligase IV-XRCC4 complex could be specifically identified as participating in the DNA-PK-independent NHEJ in this system, while Ku, DNA-PK<sub>cs</sub>, ligase IV-XRCC4, NBS1, and histone H1 are implicated in the DNA-PK-dependent NHEJ. These results support a previous model proposed by Riballo et al., in which one pathway consists of Ku and ligase IV-XRCC4 that can be stimulated by DNA-PK<sub>cs</sub>, and

a second, DNA-PK<sub>cs</sub>-dependent pathway that requires NBS1 [18].

**3.3. The *In Vitro* DNA-PK-Dependent and -Independent Non-homologous End-Joining Pathways Exhibit Different Optimal Reaction Conditions.** Several groups have reported *in vitro* assays for DNA DSB repair but reaction conditions differ considerably. To investigate if reaction conditions could be established for the end-joining assay that favor one pathway over the other, we tested the DNA end-joining activity of HeLa WCE with and without 5% PEG under a variety of reaction conditions. Two separate buffers were used. Buffer A is composed of 50 mM Tris-HCl, pH 7.6, and 75 mM KOAc along with 5 mM MgCl<sub>2</sub>, 1 mM DTT, and a protease inhibitor cocktail. Buffer B includes bis-tris-propane, pH 8.2, and 75 mM KCl with 5 mM MgCl<sub>2</sub>, 1 mM DTT, and a protease inhibitor cocktail as before (see Materials and Methods for details). DSB end joining with HeLa WCE under these two conditions were measured over time with and without 5% PEG. In the absence of PEG, buffer A produced a small but consistently higher yield of DNA end-joining products over time compared to reactions in buffer B, and under both conditions, a linear increase in product was generated during the first 5 hours (data not shown). With PEG, an increase in end joining was observed with buffer B compared to buffer A (Figure 4(a)). However, under both conditions, product formation appeared to plateau after about 3 hours. Buffer A therefore, seemed to provide the most optimal reaction conditions for the DNA-PK-dependent (without PEG) end-joining whereas Buffer B seemed to provide the same for the DNA-PK-independent (with PEG) end-joining pathway in our system.

This observation was also reported by Ramsden et al., who demonstrated a modest increase in Ku-dependent ligation of DNA lacking DNA-PK<sub>cs</sub> on increasing the

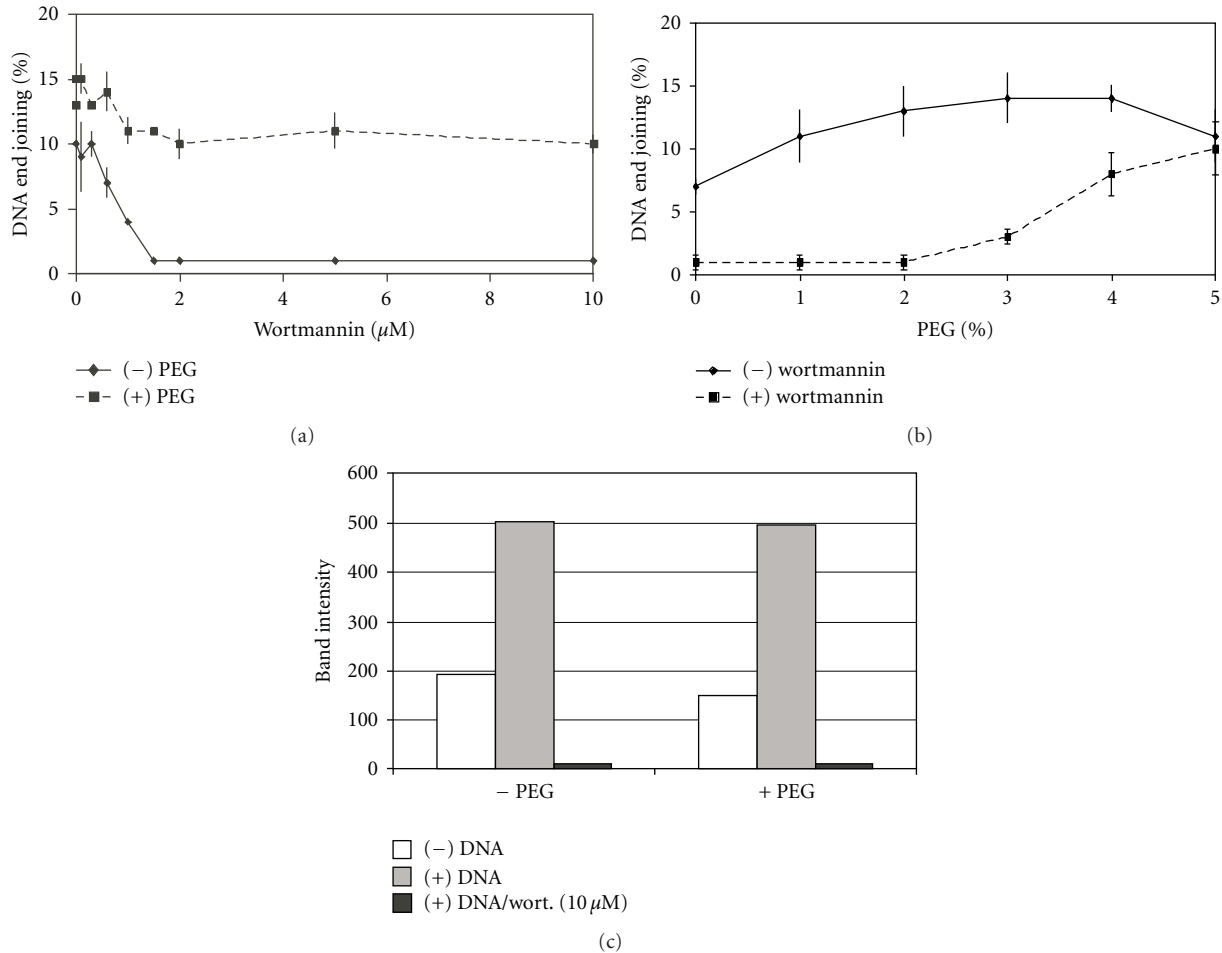


FIGURE 2: DNA end-joining activity and DNA-PK activity responses in PEG and/or wortmannin. (a) Wortmannin dose response. DNA end-joining reactions were run using HeLa WCE under standard conditions with or without 5% PEG and wortmannin for 1 hr at 30°C. Reactions contained 0 to 10  $\mu\text{M}$  wortmannin in 1% DMSO. Error bars indicate the standard deviation for triplicate reactions. (b) PEG dependence of wortmannin sensitivity. DNA end-joining reactions were run in triplicate with and without 10  $\mu\text{M}$  wortmannin at 0–5% PEG. (c) DNA-PK kinase activity under DNA end-joining reaction conditions in the presence and absence of PEG. Standard DNA end-joining reactions were run with HeLa WCE for 10 min at 30°C in the presence of a DNA-PK peptide substrate and [ $\gamma$ - $^{32}\text{P}$ ] ATP. The peptide was isolated on a 16% PAGE gel and the intensity of the radiolabeled band, a measure of DNA-PK kinase activity, was detected by autoradiography. The presence or absence of 5% PEG during the end-joining reaction did not affect DNA-PK kinase activity, nor did it affect the ability of wortmannin to inhibit DNA-PK kinase activity. The mean activity of duplicate reactions is plotted.

concentration of KCl from 25 mM to 120 mM [70]. High concentrations of chloride have been reported earlier to reduce protein-DNA interactions [71, 72]. Of the NHEJ proteins, only Ku can bind directly to DNA in 75 mM KCl [73]. However, since both the NHEJ-dependent and -independent pathways utilize Ku, a reduction in the number of nonspecific protein-DNA interactions competing with Ku for the DNA ends should enhance both NHEJ pathways. However, high-chloride concentrations can also inhibit protein-protein interactions and have indeed been shown to inhibit DNA-PK holoenzyme formation [72, 74].

Variable concentrations of the divalent cations  $\text{Mg}^{2+}$  and  $\text{Mn}^{2+}$  were also examined for their effect on DNA end-joining activity. Increasing  $\text{MgCl}_2$  concentration from its optimum at 5 mM, up to a final concentration of 10 mM (by steps of 1, 2, and 5 mM additions of  $\text{MgCl}_2$ ) had little

effect on DNA end-joining activity with or without PEG (data not shown). Addition of up to 5 mM  $\text{MnCl}_2$  in addition to the 5 mM  $\text{MgCl}_2$  already in the standard reaction buffers, increased DNA-PK-dependent end-joining activity (without PEG) and reduced DNA-PK-independent end joining (with PEG) (as shown in Figure 4(b)). To further study the effect of manganese on DNA end joining, various concentrations of  $\text{MnCl}_2$  were added to reactions with 5% PEG and 10  $\mu\text{M}$  wortmannin (Figure 4(c)). As observed previously in the absence of  $\text{MnCl}_2$  and presence of PEG, a small decrease in DNA end-joining activity occurred with the addition of 10  $\mu\text{M}$  wortmannin. Without wortmannin, DNA end-joining activity was reduced at low  $\text{MnCl}_2$  concentrations but partially recovered with the addition of 0.5 to 1 mM  $\text{MnCl}_2$ . This recovery in activity, however, was inhibited by wortmannin, indicating that even in the presence of

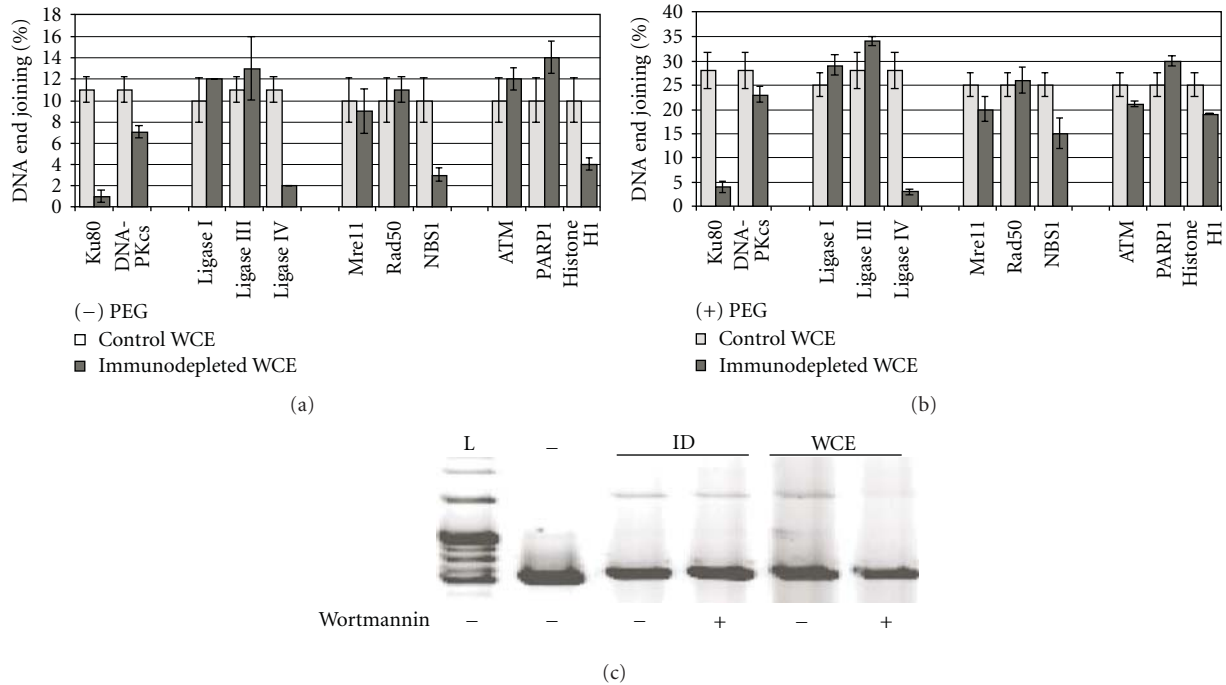


FIGURE 3: DNA end joining with immunodepleted extracts. HeLa WCE was immunodepleted for the various potential NHEJ proteins indicated, and immunodepletion ( $\geq 3$ -fold) of the target protein was confirmed by western blot (data not shown). The individual immunodepleted extracts were then assayed for DNA end-joining activity at 30°C for 2 hrs. (a) Results of DNA end-joining reactions performed in the absence of 5% PEG. (b) Results of DNA end-joining reactions performed in the presence of 5% PEG. All reactions were performed in triplicate and error bars indicate the standard deviation. (c) Wortmannin-insensitive DNA end joining is detectable in the DNA-PK<sub>cs</sub> immunodepleted HeLa WCE in the absence of PEG. Reactions were run in the absence of 5% PEG and where indicated, in the presence of 10  $\mu$ M wortmannin at 30°C for 2 hrs. (L) T4 DNA ligase positive control; (-) negative control; (ID) DNA-PK<sub>cs</sub>-immunodepleted WCE.

5% PEG, a small fraction of the observed DNA end-joining activity results from the DNA-PK-dependent pathway or at least one that is dependent on the DNA-PK kinase activity. Furthermore, the addition of  $MnCl_2$  increases the activity of this wortmannin-sensitive pathway. Previous studies have shown that one factor that could alter the relative influence of a particular end-joining pathway in the reaction is the concentration of divalent cations, particularly  $Mg^{2+}$  and  $Mn^{2+}$  [75]. We observe that the DNA-PK-dependent NHEJ activity present in our system is sensitive to the reaction concentration of  $Mg^{2+}$  and particularly,  $Mn^{2+}$ . Elevated concentrations of these divalent cations stimulate overall end-joining activity and mask the requirement for DNA-PK, suggesting the involvement of a DNA-PK-independent NHEJ pathway. Thus, the relative contribution of a particular pathway to the overall end-joining activity observed in WCEs seems to depend on, and in turn reflect, the *in vitro* reaction conditions used. Taken as a whole, differential reaction buffer preference and variable responses to divalent cations observed in this study emphasize the existence of distinct biochemical differences between the DNA-PK-independent and -dependent NHEJ activities observed in the presence and absence of PEG, respectively.

#### 3.4. Functional Changes Are Associated with DNA-PK-Dependent and -Independent Reaction Conditions. Previous

studies have suggested that DNA-PK-dependent and -independent repair pathways may be functionally distinct, possibly preferentially interacting with certain subclasses of DNA DSBs and/or having different DSB repair fidelity [18, 49–51, 58]. We therefore chose to investigate DSB repair fidelity under our DNA-PK-dependent and -independent reaction conditions. To test DSB repair fidelity, the ability of the HeLa WCE to accurately end-join DSBs with various DSB-end overhang configurations was determined. Standard DNA end joining assays run both with and without 5% PEG were conducted using substrate plasmid DNA that had been linearized by restriction digestion with, *StuI* (blunt ends), *EcoRI* (4 nucleotide 5'-overhang), *HinII* (2 nucleotide 5'-overhang), or *PvuI* (2 nucleotide 3'-overhang). The products of these end-joining reactions were then subjected to redigestion with their corresponding restriction enzyme (Figure 5). Accurate DSB end-joining restores the enzyme recognition sequence at the end-joining junction sites, resulting in product DNA that is susceptible to recutting with the restriction enzyme originally used to linearize the plasmid. DSB repair fidelity is defined as the frequency with which the DNA end-joining assays accurately join DSB ends, and is reported here as the percent of total end-joined product DNA cleaved following redigestion with the appropriate restriction enzyme. As shown in Figure 5, substantial functional differences were detected between DSB

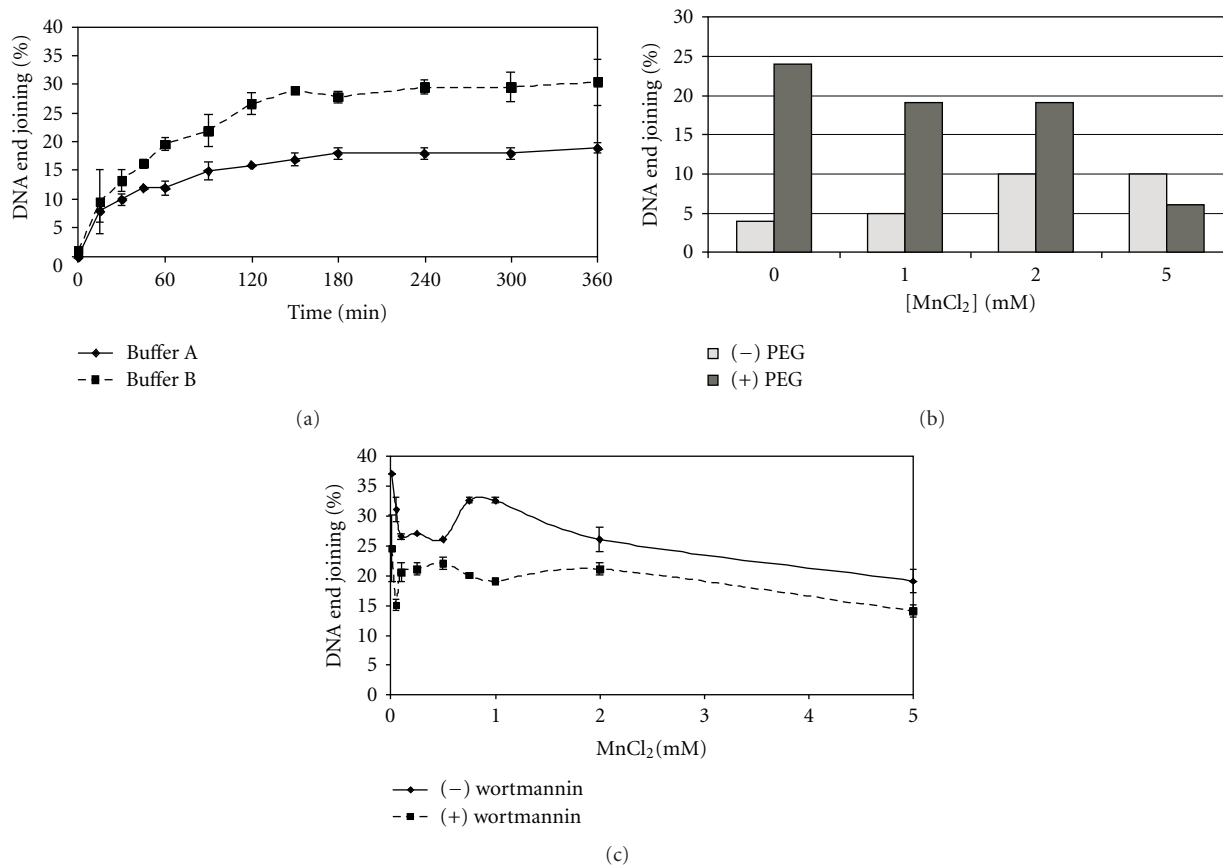


FIGURE 4: Effects of reaction conditions on DNA end-joining activity. (a) Reaction buffer composition effects on HeLa WCE end-joining activity time course reactions in the presence of 5% PEG. Reactions were run at 30°C for the times indicated in either of the two standard reaction buffers as described in the text. The mean values of triplicate reactions were plotted and the error bars indicate standard deviation. (b) Effects of MnCl<sub>2</sub> on HeLa WCE DNA end-joining activity. Reactions were run with the addition of 0–5 mM MnCl<sub>2</sub> to standard DNA end-joining reactions containing 5 mM MgCl<sub>2</sub> for 2 hrs at 30°C in the presence or absence of 5% PEG as indicated. (c) The DNA end-joining reactions employing MnCl<sub>2</sub> (0–5 mM) in the presence of PEG were repeated with and without 10 μM wortmannin (6 hrs at 30°C). Reactions were run in triplicate and the error bars indicate standard deviation.

repair reactions catalyzed by the DNA-PK-dependent and -independent NHEJ pathways. End joining under DNA-PK-dependent reaction conditions (without PEG) resulted in substantially higher DSB repair fidelity than reactions (with PEG) favoring the DNA-PK-independent end-joining pathway, and these results are consistent with the pathway-dependent DSB repair fidelity reported by others [51].

#### 4. Conclusion

In summary, we have demonstrated *in vitro* assay conditions that permit coincident and differential analysis of DNA-PK-dependent and -independent NHEJ activities under conditions in which functional DNA-PK<sub>cs</sub> is present. Establishing and defining these reaction conditions facilitates biochemical analysis of these important subpathways of NHEJ regardless of the cellular source of enzyme activities, and irrespective of intrinsic DNA-PK<sub>cs</sub> expression status. We found that reactions containing 5% PEG favored DNA-PK-independent NHEJ while reactions lacking PEG favored DNA-PK-dependent NHEJ. The biochemically distinct nature of the

pathways represented by these two reaction conditions is borne out by the differential end-joining activity observed in response to the DNA-PK inhibitor wortmannin, immunodepletion of individual proteins that may participate in NHEJ, and the pathway specific responses to divalent cations, and reaction buffer composition.

In addition to these results that indicate the biochemically distinct nature of the end-joining mechanisms represented by the DNA-PK-dependent and -independent NHEJ assays, we also observe functional differences between the two pathways. We find that DNA-PK-dependent DSB end joining is a higher fidelity process than DNA-PK-independent end joining. This latter finding is consistent with *in vivo* results reported by others using cell lines that lack expression of DNA-PK<sub>cs</sub> [51, 52, 54], or following depletion of DNA-PK<sub>cs</sub> from extracts of cells that do express the protein [54].

*In vitro* end joining of restriction enzyme-cut plasmid DNA is routinely reported as a measure of NHEJ activity, yet these reports are often conflicting with respect to what enzymes are involved in the repair of DNA DSBs. Our

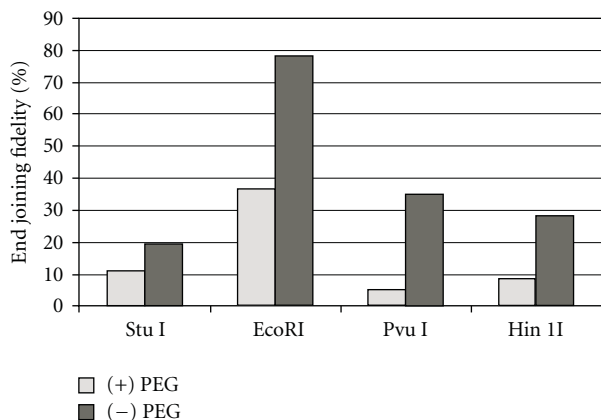


FIGURE 5: DNA end-joining fidelity reactions run in the presence or absence of 5% PEG. DNA DSB end joining was performed with each of the four different restriction enzyme linearized plasmid DNA substrates indicated to assess the effects of different DSB overhang configurations (see text) upon the fidelity of DSB repair occurring under DNA-PK-independent and -dependent reaction conditions. DSB repair fidelity is measured as the fraction of total DNA end-joining reaction products that are capable of being recut with the restriction enzyme that was originally used to linearize the end-joining substrate DNA. All reactions were run in triplicate. Bars represent the average restriction enzyme redigestion efficiency of the end-joining reaction products, which is reported as % fidelity.

results indicate that multiple pathways may simultaneously contribute to the production of linear plasmid multimers *in vitro*. Consequently, the ability to selectively shift the mechanism of product formation by altering reaction conditions not only suggests the need for care when evaluating data obtained by the wide variety of *in vitro* DSB repair assays currently in use, but also provides a means by which greater control may be achieved over the repair mechanism through which this end point is reached.

Application of the reaction conditions described in this report may permit concurrent investigations of the relative contributions of DNA-PK-dependent and -independent NHEJ pathways to DSB repair in any mammalian cell. This approach could be helpful in identifying proteins involved in the DNA-PK-dependent and -independent NHEJ DSB repair subpathways, and characterizing their individual roles in these multiprotein repair complexes. Information such as this is likely to be useful in identifying new and more effective approaches for manipulating cellular DSB repair activity.

## Abbreviations

DSB:	Double-strand break.
DNA-PK:	DNA-protein kinase.
DNA-PK <sub>cs</sub> :	DNA-protein kinase catalytic subunit.
NHEJ:	nonhomologous end joining.
DMSO:	dimethylsulfoxide.
PEG:	polyethylene glycol.
WCE:	whole cell extract.

## Acknowledgment

This research was supported in part by the Intramural Research Program of the NIH, through the Warren Grant Magnuson Clinical Center.

## References

- [1] D. C. van Gent, J. H. J. Hoeijmakers, and R. Kanaar, "Chromosomal stability and the DNA double-stranded break connection," *Nature Reviews Genetics*, vol. 2, no. 3, pp. 196–206, 2001.
- [2] L. F. Povirk, "DNA damage and mutagenesis by radiomimetic DNA-cleaving agents: bleomycin, neocarzinostatin and other enediynes," *Mutation Research*, vol. 355, no. 1-2, pp. 71–89, 1996.
- [3] E. Weterings and D. J. Chen, "The endless tale of non-homologous end-joining," *Cell Research*, vol. 18, no. 1, pp. 114–124, 2008.
- [4] P. A. Jeggo, "Identification of genes involved in repair of DNA double-strand breaks in mammalian cells," *Radiation Research*, vol. 150, no. 5, pp. S80–S91, 1998.
- [5] P. Baumann and S. C. West, "DNA end-joining catalyzed by human cell-free extracts," *Proceedings of the National Academy of Sciences of the United States of America*, vol. 95, no. 24, pp. 14066–14070, 1998.
- [6] Y. Ma, U. Pannicke, K. Schwarz, and M. R. Lieber, "Hairpin opening and overhang processing by an Artemis/DNA-dependent protein kinase complex in nonhomologous end joining and V(D)J recombination," *Cell*, vol. 108, no. 6, pp. 781–794, 2002.
- [7] Y. M. Ma, H. Lu, B. Tippin et al., "A biochemically defined system for mammalian nonhomologous DNA end joining," *Molecular Cell*, vol. 16, no. 5, pp. 701–713, 2004.
- [8] S. P. Lees-Miller, R. Godbout, D. W. Chan et al., "Absence of p350 subunit of DNA-activated protein kinase from a radiosensitive human cell line," *Science*, vol. 267, no. 5201, pp. 1183–1185, 1995.
- [9] J. Smith, E. Riballo, B. Kysela et al., "Impact of DNA ligase IV on the fidelity of end joining in human cells," *Nucleic Acids Research*, vol. 31, no. 8, pp. 2157–2167, 2003.
- [10] D. van Heemst, L. Bruggmans, N. S. Verkaik, and D. C. van Gent, "End-joining of blunt DNA double-strand breaks in mammalian fibroblasts is precise and requires DNA-PK and XRCC4," *DNA Repair*, vol. 3, no. 1, pp. 43–50, 2004.
- [11] P. Ahnesorg, P. Smith, and S. P. Jackson, "XLF interacts with the XRCC4-DNA Ligase IV complex to promote DNA nonhomologous end-joining," *Cell*, vol. 124, no. 2, pp. 301–313, 2006.
- [12] D. Buck, L. Malivert, R. de Chasseval et al., "Cernunnos, a novel nonhomologous end-joining factor, is mutated in human immunodeficiency with microcephaly," *Cell*, vol. 124, no. 2, pp. 287–299, 2006.
- [13] P. A. Jeggo and M. Löbrich, "Artemis links ATM to double strand break rejoining," *Cell Cycle*, vol. 4, no. 3, pp. 359–362, 2005.
- [14] Y. Ma, K. Schwarz, and M. R. Lieber, "The Artemis:DNA-PKcs endonuclease cleaves DNA loops, flaps, and gaps," *DNA Repair*, vol. 4, no. 7, pp. 845–851, 2005.
- [15] A. A. Goodarzi, Y. Yu, E. Riballo et al., "DNA-PK autophosphorylation facilitates Artemis endonuclease activity," *The EMBO Journal*, vol. 25, no. 16, pp. 3880–3889, 2006.

- [16] K. Akopiants, R.-Z. Zhou, S. Mohapatra et al., "Requirement for XLF/Cernunnos in alignment-based gap filling by DNA polymerases  $\lambda$  and  $\mu$  for nonhomologous end joining in human whole-cell extracts," *Nucleic Acids Research*, vol. 37, no. 12, pp. 4055–4062, 2009.
- [17] S. Yamanaka, E. Katayama, K.-I. Yoshioka, S. Nagaki, M. Yoshida, and H. Teraoka, "Nucleosome linker proteins HMGB1 and histone H1 differentially enhance DNA ligation reactions," *Biochemical and Biophysical Research Communications*, vol. 292, no. 1, pp. 268–273, 2002.
- [18] E. Riballo, M. Kühne, N. Rief et al., "A pathway of double-strand break rejoining dependent upon ATM, Artemis, and proteins locating to  $\gamma$ -H2AX foci," *Molecular Cell*, vol. 16, no. 5, pp. 715–724, 2004.
- [19] J. R. Huang and W. S. Dynan, "Reconstitution of the mammalian DNA double-strand break end-joining reaction reveals a requirement for an Mre11/Rad50/NBS1-containing fraction," *Nucleic Acids Research*, vol. 30, no. 3, pp. 667–674, 2002.
- [20] W. S. Dynan and S. Yoo, "Interaction of Ku protein and DNA-dependent protein kinase catalytic subunit with nucleic acids," *Nucleic Acids Research*, vol. 26, no. 7, pp. 1551–1559, 1998.
- [21] T. M. Gottlieb and S. P. Jackson, "The DNA-dependent protein kinase: requirement for DNA ends and association with Ku antigen," *Cell*, vol. 72, no. 1, pp. 131–142, 1993.
- [22] S. Yoo and W. S. Dynan, "Geometry of a complex formed by double strand break repair proteins at a single DNA end: recruitment of DNA-PKcs induces inward translocation of Ku protein," *Nucleic Acids Research*, vol. 27, no. 24, pp. 4679–4686, 1999.
- [23] A. Kurimasa, S. Kumano, N. V. Boubnov et al., "Requirement for the kinase activity of human DNA-dependent protein kinase catalytic subunit in DNA strand break rejoining," *Molecular and Cellular Biology*, vol. 19, no. 5, pp. 3877–3884, 1999.
- [24] L. G. DeFazio, R. M. Stansel, J. D. Griffith, and G. Chu, "Synapsis of DNA ends by DNA-dependent protein kinase," *The EMBO Journal*, vol. 21, no. 12, pp. 3192–3200, 2002.
- [25] U. Grawunder, M. Wilm, X. Wu et al., "Activity of DNA ligase IV stimulated by complex formation with XRCC4 protein in mammalian cells," *Nature*, vol. 388, no. 6641, pp. 492–495, 1997.
- [26] P. Calsou, C. Delteil, P. Frit, J. Drouet, and B. Salles, "Coordinated assembly of Ku and p460 subunits of the DNA-dependent protein kinase on DNA ends is necessary for XRCC4-ligase IV recruitment," *Journal of Molecular Biology*, vol. 326, no. 1, pp. 93–103, 2003.
- [27] L. Chen, K. Trujillo, P. Sung, and A. E. Tomkinson, "Interactions of the DNA ligase IV-XRCC4 complex with DNA ends and the DNA-dependent protein kinase," *Journal of Biological Chemistry*, vol. 275, no. 34, pp. 26196–26205, 2000.
- [28] H.-L. Hsu, S. M. Yannone, and D. J. Chen, "Defining interactions between DNA-PK and ligase IV/XRCC4," *DNA Repair*, vol. 1, no. 3, pp. 225–235, 2002.
- [29] R. A. Izzard, S. P. Jackson, and G. C. M. Smith, "Competitive and noncompetitive inhibition of the DNA-dependent protein kinase," *Cancer Research*, vol. 59, no. 11, pp. 2581–2586, 1999.
- [30] D. Merkle, P. Douglas, G. B. G. Moorhead et al., "The DNA-dependent protein kinase interacts with DNA to form a protein-DNA complex that is disrupted by phosphorylation," *Biochemistry*, vol. 41, no. 42, pp. 12706–12714, 2002.
- [31] K. Meek, P. Douglas, X. Cui, Q. Ding, and S. P. Lees-Miller, "Trans autophosphorylation at DNA-dependent protein kinase's two major autophosphorylation site clusters facilitates end processing but not end joining," *Molecular and Cellular Biology*, vol. 27, no. 10, pp. 3881–3890, 2007.
- [32] Q. Ding, Y. V. R. Reddy, W. Wang et al., "Autophosphorylation of the catalytic subunit of the DNA-dependent protein kinase is required for efficient end processing during DNA double-strand break repair," *Molecular and Cellular Biology*, vol. 23, no. 16, pp. 5836–5848, 2003.
- [33] B. L. Mahaney, K. Meek, and S. P. Lees-Miller, "Repair of ionizing radiation-induced DNA double-strand breaks by non-homologous end-joining," *Biochemical Journal*, vol. 417, no. 3, pp. 639–650, 2009.
- [34] X. Cui, Y. Yu, S. Gupta, Y.-M. Cho, S. P. Lees-Miller, and K. Meek, "Autophosphorylation of DNA-dependent protein kinase regulates DNA end processing and may also alter double-strand break repair pathway choice," *Molecular and Cellular Biology*, vol. 25, no. 24, pp. 10842–10852, 2005.
- [35] P. Douglas, G. P. Sapkota, N. Morrice et al., "Identification of in vitro and in vivo phosphorylation sites in the catalytic subunit of the DNA-dependent protein kinase," *Biochemical Journal*, vol. 368, no. 1, pp. 243–251, 2002.
- [36] P. Douglas, X. Cui, W. D. Block et al., "The DNA-dependent protein kinase catalytic subunit is phosphorylated in vivo on threonine 3950, a highly conserved amino acid in the protein kinase domain," *Molecular and Cellular Biology*, vol. 27, no. 5, pp. 1581–1591, 2007.
- [37] N. Uematsu, E. Weterings, K.-I. Yano et al., "Autophosphorylation of DNA-PKcs regulates its dynamics at DNA double-strand breaks," *Journal of Cell Biology*, vol. 177, no. 2, pp. 219–229, 2007.
- [38] D. W. Chan, R. Q. Ye, C. J. Veillette, and S. P. Lees-Miller, "DNA-dependent protein kinase phosphorylation sites in Ku 70/80 heterodimer," *Biochemistry*, vol. 38, no. 6, pp. 1819–1828, 1999.
- [39] R. Leber, T. W. Wise, R. Mizuta, and K. Meek, "The XRCC4 gene product is a target for and interacts with the DNA-dependent protein kinase," *Journal of Biological Chemistry*, vol. 273, no. 3, pp. 1794–1801, 1998.
- [40] Y. P. Yu, W. Wang, Q. Ding et al., "DNA-PK phosphorylation sites in XRCC4 are not required for survival after radiation or for V(D)J recombination," *DNA Repair*, vol. 2, no. 11, pp. 1239–1252, 2003.
- [41] J. Drouet, C. Delteil, J. Lefrançois, P. Concannon, B. Salles, and P. Calsou, "DNA-dependent protein kinase and XRCC4-DNA ligase IV mobilization in the cell in response to DNA double strand breaks," *Journal of Biological Chemistry*, vol. 280, no. 8, pp. 7060–7069, 2005.
- [42] B. Kysela, M. Chovanec, and P. A. Jeggo, "Phosphorylation of linker histones by DNA-dependent protein kinase is required for DNA ligase IV-dependent ligation in the presence for histone H1," *Proceedings of the National Academy of Sciences of the United States of America*, vol. 102, no. 6, pp. 1877–1882, 2005.
- [43] M. Hammel, Y. Yu, B. L. Mahaney et al., "Ku and DNA-dependent protein kinase dynamic conformations and assembly regulate DNA binding and the initial non-homologous end joining complex," *Journal of Biological Chemistry*, vol. 285, no. 2, pp. 1414–1423, 2010.
- [44] B. L. Sibanda, D. Y. Chirgadze, and T. L. Blundell, "Crystal structure of DNA-PKcs reveals a large open-ring cradle comprised of HEAT repeats," *Nature*, vol. 463, no. 7277, pp. 118–121, 2010.
- [45] K. Meek, V. Dang, and S. P. Lees-Miller, "DNA-PK: the means to justify the ends?" *Advances in Immunology*, vol. 99, pp. 33–58, 2008.

- [46] M. J. Difilippantonio, J. Zhu, H. T. Chen et al., "Dna repair protein Ku80 suppresses chromosomal aberrations and malignant transformation," *Nature*, vol. 404, no. 6777, pp. 510–514, 2000.
- [47] K. M. Frank, N. E. Sharpless, Y. Gao et al., "DNA ligase IV deficiency in mice leads to defective neurogenesis and embryonic lethality via the p53 pathway," *Molecular Cell*, vol. 5, no. 6, pp. 993–1002, 2000.
- [48] E. B. Kabotyanski, L. Gomelsky, J.-O. Han, T. D. Stamato, and D. B. Roth, "Double-strand break repair in Ku86- and XRCC4-deficient cells," *Nucleic Acids Research*, vol. 26, no. 23, pp. 5333–5342, 1998.
- [49] N. Cheong, A. R. Perrault, H. Wang et al., "DNA-PK-independent rejoining of DNA double-strand breaks in human cell extracts in vitro," *International Journal of Radiation Biology*, vol. 75, no. 1, pp. 67–81, 1999.
- [50] M. Löbrich, B. Rydberg, and P. K. Cooper, "Repair of X-ray-induced DNA double-strand breaks in specific Not I restriction fragments in human fibroblasts: joining of correct and incorrect ends," *Proceedings of the National Academy of Sciences of the United States of America*, vol. 92, no. 26, pp. 12050–12054, 1995.
- [51] S. J. DiBiase, Z.-C. Zeng, R. Chen, T. Hyslop, W. J. Curran Jr., and G. Iliakis, "DNA-dependent protein kinase stimulates an independently active, nonhomologous, end-joining apparatus," *Cancer Research*, vol. 60, no. 5, pp. 1245–1253, 2000.
- [52] H. C. Wang, A. R. Perrault, Y. Takeda, W. Qin, H. Wang, and G. Iliakis, "Biochemical evidence for Ku-independent backup pathways of NHEJ," *Nucleic Acids Research*, vol. 31, no. 18, pp. 5377–5388, 2003.
- [53] S. E. Lee, R. A. Mitchell, A. Cheng, and E. A. Hendrickson, "Evidence for DNA-PK-dependent and -independent DNA double-strand break repair pathways in mammalian cells as a function of the cell cycle," *Molecular and Cellular Biology*, vol. 17, no. 3, pp. 1425–1433, 1997.
- [54] R. Perrault, H. Wang, M. Wang, B. Rosidi, and G. Iliakis, "Backup pathways of NHEJ are suppressed by DNA-PK," *Journal of Cellular Biochemistry*, vol. 92, no. 4, pp. 781–794, 2004.
- [55] G. Iliakis, "Backup pathways of NHEJ in cells of higher eukaryotes: cell cycle dependence," *Radiotherapy and Oncology*, vol. 92, no. 3, pp. 310–315, 2009.
- [56] K. W. Caldecott, C. K. McKeown, J. D. Tucker, S. Ljungquist, and L. H. Thompson, "An interaction between the mammalian DNA repair protein XRCC1 and DNA ligase III," *Molecular and Cellular Biology*, vol. 14, no. 1, pp. 68–76, 1994.
- [57] M. Audebert, B. Salles, and P. Calsou, "Involvement of poly(ADP-ribose) polymerase-1 and XRCC1/DNA ligase III in an alternative route for DNA double-strand breaks rejoining," *Journal of Biological Chemistry*, vol. 279, no. 53, pp. 55117–55126, 2004.
- [58] H. Wang, B. Rosidi, R. Perrault et al., "DNA ligase III as a candidate component of backup pathways of nonhomologous end joining," *Cancer Research*, vol. 65, no. 10, pp. 4020–4030, 2005.
- [59] M. Wang, W. Wu, W. Wu et al., "PARP-1 and Ku compete for repair of DNA double strand breaks by distinct NHEJ pathways," *Nucleic Acids Research*, vol. 34, no. 21, pp. 6170–6182, 2006.
- [60] B. Rosidi, M. Wang, W. Wu, A. Sharma, H. Wang, and G. Iliakis, "Histone H1 functions as a stimulatory factor in backup pathways of NHEJ," *Nucleic Acids Research*, vol. 36, no. 5, pp. 1610–1623, 2008.
- [61] R. Okayasu, K. Suetomi, and R. L. Ullrich, "Wortmannin inhibits repair of DNA double-strand breaks in irradiated normal human cells," *Radiation Research*, vol. 149, no. 5, pp. 440–445, 1998.
- [62] S. B. Chernikova, R. L. Wells, and M. M. Elkind, "Wortmannin sensitizes mammalian cells to radiation by inhibiting the DNA-dependent protein kinase-mediated rejoining of double-strand breaks," *Radiation Research*, vol. 151, no. 2, pp. 159–166, 1999.
- [63] M. Bryans, M. C. Valenzano, and T. D. Stamato, "Absence of DNA ligase IV protein in XR-1 cells: evidence for stabilization by XRCC4," *Mutation Research*, vol. 433, no. 1, pp. 53–58, 1999.
- [64] L. D. Murphy and S. B. Zimmerman, "Macromolecular crowding effects on the interaction of DNA with *Escherichia coli* DNA-binding proteins: a model for bacterial nucleoid stabilization," *Biochimica et Biophysica Acta*, vol. 1219, no. 2, pp. 277–284, 1994.
- [65] S. B. Zimmerman and B. H. Pfeiffer, "Macromolecular crowding allows blunt-end ligation by DNA ligases from rat liver or *Escherichia coli*," *Proceedings of the National Academy of Sciences of the United States of America*, vol. 80, no. 19, pp. 5852–5856, 1983.
- [66] A. P. Minton, "The influence of macromolecular crowding and macromolecular confinement on biochemical reactions in physiological media," *Journal of Biological Chemistry*, vol. 276, no. 14, pp. 10577–10580, 2001.
- [67] E. Pastwa, R. D. Neumann, and T. A. Winters, "In vitro repair of complex unligatable oxidatively induced DNA double-strand breaks by human cell extracts," *Nucleic Acids Research*, vol. 29, no. 16, article e78, 2001.
- [68] K. K. Leuther, O. Hammarsten, R. D. Kornberg, and G. Chu, "Structure of DNA-dependent protein kinase: implications for its regulation by DNA," *The EMBO Journal*, vol. 18, no. 5, pp. 1114–1123, 1999.
- [69] K. Datta, R. D. Neumann, and T. A. Winters, "An in vitro nonhomologous end-joining assay using linear duplex oligonucleotides," *Analytical Biochemistry*, vol. 358, no. 1, pp. 155–157, 2006.
- [70] D. A. Ramsden and M. Geliert, "Ku protein stimulates DNA end joining by mammalian DNA ligases: a direct role for Ku in repair of DNA double-strand breaks," *The EMBO Journal*, vol. 17, no. 2, pp. 609–614, 1998.
- [71] S. Leirmo, C. Harrison, D. S. Cayley, R. R. Burgess, and M. T. Record Jr., "Replacement of potassium chloride by potassium glutamate dramatically enhances protein-DNA interactions in vitro," *Biochemistry*, vol. 26, no. 8, pp. 2095–2101, 1987.
- [72] M. G. Cacace, E. M. Landau, and J. J. Ramsden, "The Hofmeister series: salt and solvent effects on interfacial phenomena," *Quarterly Reviews of Biophysics*, vol. 30, no. 3, pp. 241–277, 1997.
- [73] O. Hammarsten and G. Chu, "DNA-dependent protein kinase: DNA binding and activation in the absence of Ku," *Proceedings of the National Academy of Sciences of the United States of America*, vol. 95, no. 2, pp. 525–530, 1998.
- [74] M. A. Griep and C. S. McHenry, "Glutamate overcomes the salt inhibition of DNA polymerase III holoenzyme," *Journal of Biological Chemistry*, vol. 264, no. 19, pp. 11294–11301, 1989.
- [75] Q. Zhong, T. G. Boyer, P.-L. Chen, and W.-H. Lee, "Deficient nonhomologous end-joining activity in cell-free extracts from Brca1-null fibroblasts," *Cancer Research*, vol. 62, no. 14, pp. 3966–3970, 2002.

## Research Article

# Selective Incision of the $\alpha$ - $N^5$ -Methyl-Formamidopyrimidine Anomer by *Escherichia coli* Endonuclease IV

Plamen P. Christov, Surajit Banerjee, Michael P. Stone, and Carmelo J. Rizzo

Departments of Chemistry and Biochemistry, Center in Molecular Toxicology, Vanderbilt University,  
VU Station B 351822, Nashville, N 37235-1822, USA

Correspondence should be addressed to Carmelo J. Rizzo, c.j.rizzo@vanderbilt.edu

Received 13 April 2010; Accepted 4 June 2010

Academic Editor: Ashis Basu

Copyright © 2010 Plamen P. Christov et al. This is an open access article distributed under the Creative Commons Attribution License, which permits unrestricted use, distribution, and reproduction in any medium, provided the original work is properly cited.

Formamidopyrimidines (Fapy) lesions result from ring opening of the imidazole portion of purines. Fapy lesions can isomerize from the natural  $\beta$ -anomeric stereochemistry to the  $\alpha$ -configuration. We have unambiguously demonstrated that the  $\alpha$ -methyl-Fapy-dG (MeFapy-dG) lesion is a substrate for *Escherichia coli* Endonuclease IV (Endo IV). Treatment of a MeFapy-dG-containing 24 mer duplex with Endo IV resulted in 36–40% incision. The catalytic efficiency of the incision was comparable to that of  $\alpha$ -dG in the same duplex sequence. The  $\alpha$ - and  $\beta$ -MeFapy-dG anomers equilibrate to  $\sim 21 : 79$  ratio over  $\sim 3$  days. Related studies with a duplex containing the  $\alpha$ -Fapy-dG lesion derived from aflatoxin B<sub>1</sub> epoxide ( $\alpha$ -AFB-Fapy-dG) showed only low levels of incision. It is hypothesized that the steric bulk of the aflatoxin moiety interferes with the binding of the substrate to Endo IV and the incision chemistry.

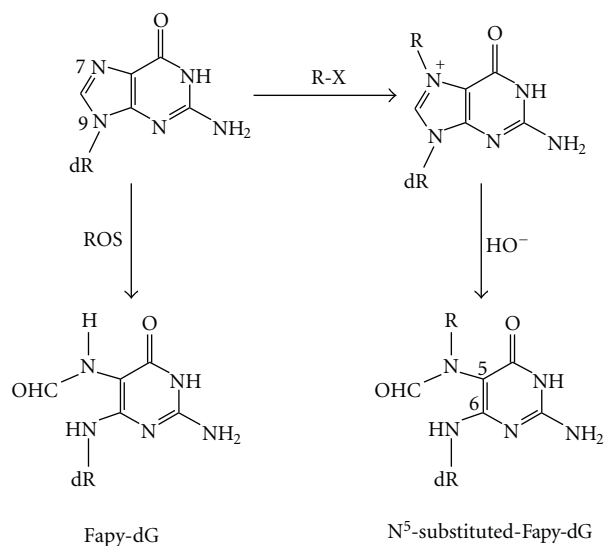
## 1. Introduction

Formamidopyrimidines (Fapy) are DNA lesions that result from ring opening of the imidazole portion of purines. Fapy lesions derived from dG can form by either initial oxidation or N7-alkylation of the guanine base (Scheme 1) [1–6]. These are structurally related lesions that differ by the substitution at the  $N^5$ -formamide. The formyl nitrogen of the Fapy-dG derived from oxidative damage is unsubstituted, and it has been proposed that recognition of this lesion by human OGG involves hydrogen-bonding interactions between the protein and this functional group [7]. The formyl nitrogen is substituted with the alkylating agent from the alkylative pathway, and this substitution is likely to change the conformation of the adduct and its interaction with repair proteins and DNA polymerases. The corresponding Fapy-dG adducts were shown to be the persistent DNA lesions resulting from exposure to methylating agents (MeFapy-dG) and aflatoxin B<sub>1</sub> (AFB-Fapy-dG) [8–10].

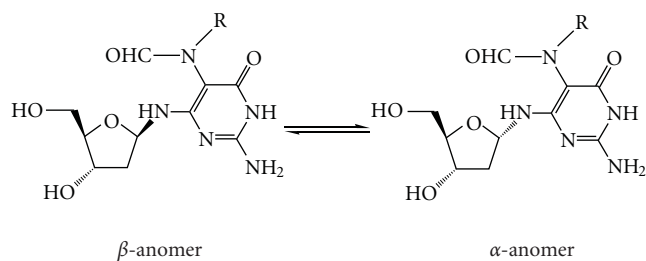
An unusual property of Fapy lesions is that the C1' stereochemistry can interconvert between the  $\beta$ - and  $\alpha$ -anomers. This presumably occurs through the  $N^6$ -C1' imine

intermediate [11, 12]; the pyranose form can also result at the nucleoside level [13, 14]. The  $\alpha$ -anomer of dA, dT, and dC results from  $\gamma$ -radiolysis of DNA [15, 16]; however, the  $\alpha$ -stereochemistry of these lesions is static once it is formed.

*Escherichia coli* Endonuclease IV (Endo IV) is a double-strand specific AP endonuclease that hydrolyzes the phosphodiester bond on the 5'-side of abasic sites and accounts for  $\sim 10\%$  of the AP endonuclease activity in *E. coli* [17–19]. The incision of the damaged strand results in a 5'-terminal ribosyl-5'-phosphate on the downstream fragment and a free 3'-hydroxyl group of the upstream fragment. Endo IV also possesses 3'-diesterase activity and can remove 3'-blocking groups such as 3'-phosphates, 3'-phosphoglycolate, and the 3'-(4-hydroxy-2-pentenal)-5-phosphate group that results from  $\beta$ -elimination of abasic sites. Endo IV was also found to possess 3'  $\rightarrow$  5' exonuclease activity and can generate a single base gap at the 5'-side of a damaged base [20, 21]. Endo IV contains three Zn<sup>2+</sup> atoms in its active site and recognizes the damage site by a double nucleotide-flipping mechanism [22–24]. Oligonucleotides containing the  $\alpha$ -dA,  $\alpha$ -dT,  $\alpha$ -dC,  $\alpha$ -Fapy-dA, and  $\alpha$ -Fapy-dG lesions as well as the configurationally stable  $N^6$ -carbon Fapy analogues



SCHEME 1: Fapy-dG lesions derived from oxidative or alkylative damage to dG.



SCHEME 2: The  $\beta$ - and  $\alpha$ -anomers of Fapy-dG.

$\alpha$ -C-Fapy-dA have been shown to be substrates for Endo IV [25–29]. Oligonucleotides containing MeFapy-dG have also been examined as potential substrates for Endo IV. Asagoshi et al. reported that a MeFapy-dG-containing oligonucleotide was not a substrate for Endo IV and concluded that this lesion existed as the  $\beta$ -MeFapy-dG anomer [30, 31]. However, Ishchenko et al. [32] reported incision of the MeFapy-dG lesion with a catalytic efficiency comparable to that reported for  $\alpha$ -C-Fapy-dA [29]. Interestingly, evidence that Endo IV plays a role in the repair of deoxyribosylurea lesions has also been reported [33]; this lesion can also undergo anomerization, and it is likely that the  $\alpha$ -anomer is a substrate for Endo IV [34–36].

We recently described the synthesis of a phosphoramidite reagent of the MeFapy-dG lesion and its utility in the site-specific synthesis of modified oligonucleotides [11]. Two transitions were observed in the thermal melting curve of a 12-mer duplex containing a MeFapy-dG lesion. The lower melting transition was assigned as the  $\alpha$ -MeFapy-dG anomer and the higher melting transition as the  $\beta$ -anomer. These assignments were based on a similar thermal melting profile of the AFB-Fapy-dG adduct for which the conformations of the  $\alpha$ - and  $\beta$ -anomers (Scheme 2) have been determined by

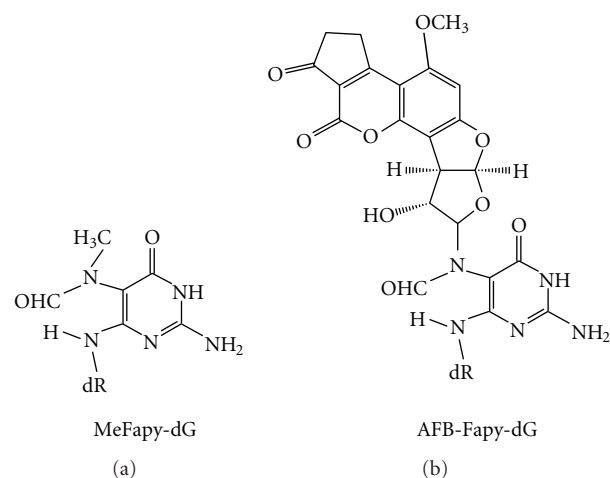


FIGURE 1: Structures of the methyl and aflatoxin B<sub>1</sub> Fapy-dG lesions.

NMR [37, 38]. The  $\alpha$  :  $\beta$  anomeric ratio of the MeFapy-dG adduct was estimated to be  $\sim$ 40:60. We report here the selective incision of the  $\alpha$ -MeFapy-dG anomer from duplex DNA by Endo IV.

## 2. Materials and Methods

$\alpha$ -dG was purchased from Berry and Associates, Inc. and was converted to its phosphoramidite reagent using standard protocols [39]. T4 polynucleotide kinase and *E. coli* Endo IV were purchased from New England Biolabs.  $\gamma$ -<sup>32</sup>P-ATP was purchased from PerkinElmer Life Sciences. Unmodified oligonucleotides were purchased from Midland Certified Reagents. MALDI-TOF mass spectra were recorded using a 3-hydroxypicolinic acid (HPA) and ammonium hydrogen citrate matrix.

**Oligonucleotide Synthesis.** The MeFapy-dG and AFB-Fapy-dG modified oligonucleotides were synthesized as previously described [11, 40]. The  $\alpha$ -dG-containing oligonucleotide was synthesized via the phosphoramidite method. The purity of all oligonucleotides was judged to be >99% by capillary gel electrophoresis. Oligonucleotides were characterized by MALDI-TOF mass spectrometry and enzymatic digestion.

5'-ACCACGCTAGC-( $\alpha/\beta$ -MeFapy-dG)-AGTCCTAACAAC-3'. It was purified by reversed-phase HPLC using gradient 1 and further purified by PAGE. MALDI-TOF MS (HPA)  $m/z$  calcd for (M-H), 7304.4; found 7305.4.

5'-ACCACGCTAGC-( $\alpha$ -dG)-AGTCCTAACAAC-3'. It was purified by reversed-phase HPLC using gradient 2. MALDI-TOF MS (HPA)  $m/z$  calcd for (M-H), 7272.2; found 7272.3.

5'-ACCACTACTAT-( $\alpha$ -AFB-Fapy-dG)-ATTTCATAACAAC-3'. It was purified by reverse-phase HPLC using gradient 3.

MALDI-TOF MS (HPA)  $m/z$  calcd for (M-H), 7593.2; found 7594.1.

**HPLC Purification.** A YMC ODS-AQ column (250 × 4.6 mm, flow rate 1.5 mL/min; 250 × 10 mm, flow rate 5 mL/min) or Phenomenex Gemini-C18 column (250 × 4.6 mm, flow rate 1.5 mL/min; 250 × 10 mm, flow rate 5 mL/min) was used for oligonucleotide purifications and to monitor reactions. Oligonucleotides were detected by their UV absorbance at 254 nm. The mobile phase consisted of CH<sub>3</sub>CN and 100 mM ammonium formate buffer (v/v).

**Gradient 1.** Initial conditions were 1% CH<sub>3</sub>CN; a linear gradient to 8% CH<sub>3</sub>CN over 5 minute; a linear gradient to 13% CH<sub>3</sub>CN over 15 minute; a linear gradient to 80% CH<sub>3</sub>CN over 2 minute; isocratic at 80% CH<sub>3</sub>CN for 2 minute; then a linear gradient to the initial conditions over 3 minute.

**Gradient 2.** Initial conditions were 1% CH<sub>3</sub>CN; a linear gradient to 5% CH<sub>3</sub>CN over 5 minute; a linear gradient to 10% CH<sub>3</sub>CN over 15 minute; a linear gradient to 80% CH<sub>3</sub>CN over 2 minute; isocratic at 80% CH<sub>3</sub>CN for 2 minute; then a linear gradient to the initial conditions over 3 minute.

**Gradient 3.** Initial conditions were 6% CH<sub>3</sub>CN; a linear gradient to 25% CH<sub>3</sub>CN over 25 minute; a linear gradient to 80% CH<sub>3</sub>CN over 2 minute; isocratic at 80% CH<sub>3</sub>CN for 2 minute; then a linear gradient back to the initial conditions over 3 minute.

**LC-ESI-MS Analysis.** MS analysis was performed in the Vanderbilt University facility on a Waters Acquity UPLC system connected to a Finnigan LTQ mass spectrometer (ThermoElectron) equipped with an Ion Max API source and a standard electrospray probe using an Acquity UPLC BEH C18 column (1 μm, 1.0 mm × 100 mm). LC conditions were as follows: buffer A contained 10 mM NH<sub>4</sub>CH<sub>3</sub>CO<sub>2</sub> plus 2% CH<sub>3</sub>CN (v/v), and buffer B contained 10 mM NH<sub>4</sub>CH<sub>3</sub>CO<sub>2</sub> plus 95% CH<sub>3</sub>CN (v/v). The following gradient program was used with a flow rate of 150 μL/min: initially 0% B, 3 minute linear gradient to 3% B, 1.5 minute linear gradient to 20% B, 0.5 minute linear gradient to 100% B, isocratic at 100% B for 0.5 minute, 1 minute linear gradient to 0% B, and isocratic at 0% B for 3 minute. The temperature of the column was maintained at 50°C, and the samples (10 μL) were infused with an autosampler. The electrospray conditions were as follows: source voltage: 4 kV; source current: 100 μA; N<sub>2</sub> was used as the auxiliary gas at a flow rate setting of 20; sweep gas flow-rate setting, 5; sheath gas flow setting: 34; capillary voltage: -49 V; capillary temperature, 350°C; and tube lens voltage: -90 V. The automatic gain control (AGC) setting in full MS was 10000. The maximum injection time in full MS was 10 ms. The MS data were acquired in negative mode. The number of μscan used for data acquisition in full MS was 2. Product ion spectra were acquired over the range of  $m/z$  345–2000.

**Oligonucleotide Labeling and Annealing.** The labeling of the MeFapy-dG oligonucleotide was performed as previously described using T4 polynucleotide kinase and γ-<sup>32</sup>P-ATP [41]. Electrophoresis gels were exposed to a PhosphorImager screen (Imaging Screen K, Bio-Rad) overnight. The bands were visualized with a PhosphorImaging system (Bio-Rad, Molecular Imager FX) using the manufacturer's Quantity One software, version 4.3.0. Unless otherwise noted, the oligonucleotide duplexes were formed by annealing the 5'-<sup>32</sup>P-labeled MeFapy-dG-containing oligonucleotide (200 nM) with its complementary strand (600 nM) in Tris buffer (100 μL, 50 mM, pH 8.0) at 95°C for 5 minute; the solution was then slowly cooled to ambient temperature over 1 h.

**Time Course Incision of the MeFapy-dG and α-dG-Containing Duplexes by Endo IV.** The oligonucleotide duplex (4 μL, 0.8 pmols) was added to the Endo IV reaction buffer (74 μL of 1X: 100 mM NaCl, 50 mM Tris-HCL, 10 mM MgCl<sub>2</sub>, and 1 mM dithiothreitol, pH 7.9) and warmed to 37°C. Endo IV (0.08 nM) was added; aliquots (5 μL) were removed at the appropriate times, added to 10 μL of 95% formamide loading buffer containing xylene cyanol and bromophenol blue dyes, and heated for 1 minute at 90°C. Aliquots (6 μL) from the samples were separated by electrophoresis on a denaturing gel.

To determine the extent of background deglycosylation of the lesion, aliquots of the MeFapy-dG-containing oligonucleotide were treated with 0.1 M NaOH and incubated at 37°C for 20 minute. The samples were neutralized by addition of 0.1 M HCl, diluted with loading buffer, and analyzed by gel electrophoresis. The amount of the cleavage in this control experiment was subtracted from the amount of incision in the Endo IV reactions. Reactions were carried out in duplicate. The same procedure was used for the incision of the 5'-<sup>32</sup>P-labeled α-dG-containing duplex.

**Incision of the α-AFB-Fapy-dG-Containing Duplex by Endo IV.** The 5'-<sup>32</sup>P-labeled α-AFB-Fapy-dG oligonucleotide (120 nM) was annealed to its complementary strand (160 nM) in Tris buffer (100 μL, 50 mM, pH 8.0) at room temperature. Aliquots (10 μL, 120 nM) were taken every 5 minute and added to a mixture of Endo IV enzyme buffer (10X, 6 μL), water (40 μL), and Endo IV (0.4 nM) at 37°C; the incision reactions were incubated at 37°C and pH 7.9. Aliquots (5 μL) were taken every 2 minute and added to 10 μL of 95% formamide loading buffer containing xylene cyanol and bromophenol blue dyes and heated for 1 minute at 90°C. Aliquots (6 μL) were separated by electrophoresis on a denaturing gel. The extent of background deglycosylation of the α-AFB-Fapy-dG lesion was determined as described above. The amount of the cleavage in the control experiment was subtracted from the amount of incision in the Endo IV reactions. Reactions were carried out in duplicate.

**Kinetics for the Incision of the MeFapy-dG- and α-dG-Containing Duplexes by Endo IV.** The duplex was annealed

as described above with the following modifications. The 5'-<sup>32</sup>P-labeled MeFapy-dG and its complementary strand were 100 and 150 nM, respectively. Endo IV (0.08 nM) was added to varying concentrations of the DNA duplex (0.5–35 nM in 1X Endo IV reaction buffer, pH 7.9) to a final volume 50  $\mu$ L. Reactions were run at 37°C for up to 10 minute. Aliquots (5  $\mu$ L) were taken at 1 minute intervals, added to loading buffer (10  $\mu$ L), and heated at 90°C for 1 minute. Separation was achieved by gel electrophoresis. The kinetics parameters were calculated using KaleidaGraph 4.0. Reactions were carried out in duplicate. The same procedure was used for incision of the  $\alpha$ -dG-containing duplex.

*Time Course Incision of the MeFapy-dG-Containing Duplex by Endo IV at pH 7.0.* The oligonucleotide duplex (12  $\mu$ L, 2.4 pmols) was added to the Endo IV reaction buffer (100 mM NaCl, 50 mM Tris-HCl, 10 mM MgCl<sub>2</sub>, 1 mM dithiothreitol, pH 7, 222  $\mu$ L), followed by addition of Endo IV (0.08 nM). The reaction was incubated at 37°C for 5 days. A fresh portion of Endo IV (0.08 nM) was added every 24 h. Aliquots (5  $\mu$ L) were removed 30 minute after the Endo IV addition, added to 10  $\mu$ L of 95% formamide loading buffer containing xylene cyanol and bromophenol blue dyes, and heated for 1 minute at 90°C. The incision reaction was analyzed by gel electrophoresis. The experiment was run in duplicate.

*Incision of the MeFapy-dG-Containing Duplex after Denaturation and Reannealing.* The DNA duplex was formed as described above with the following modifications. The 5'-<sup>32</sup>P-labeled MeFapy-dG and its complementary strand were 200 and 400 nM, respectively. The oligonucleotide duplex (8  $\mu$ L, 1.6 pmols) was added to 1X Endo IV reaction buffer (148  $\mu$ L), followed by addition of Endo IV (0.08 nM). The reaction was run at 37°C for 40 minute and aliquots (5  $\mu$ L) were removed periodically, added to 10  $\mu$ L of 95% formamide loading buffer containing xylene cyanol and bromophenol blue dyes and heated for 1 minute at 90°C. The remaining reaction mixture was heated at 95°C for 5 minute, cooled to 75°C for 30 minute, then cooled to ambient temperature over 1 h. The reannealed DNA duplex incubated at 37°C and Endo IV (0.08 nM) was added. Aliquots were taken as previously described, and the level of incision was analyzed by gel electrophoresis. The denaturation and reannealing cycles were repeated one more time.

*LC-ESI-MS Analysis of the Incision of the MeFapy-dG-Containing Duplex by Endo IV.* MeFapy-dG-containing 24 mer oligonucleotide (0.774 nmol) was annealed to its complementary strand (1.5 eq., 1.161 nmol) in Tris buffer (100  $\mu$ L, 50 mM, pH 8.0) as described above. To this solution Endo IV reaction buffer (13  $\mu$ L, 10X) was added followed by addition of Endo IV (0.8 nM). The reaction mixture was incubated at 37°C for 2 h. The reaction mixture was then passed through a spin column (Bio-spin 6 Tris columns) and lyophilized. The white residue was dissolved in water and analyzed by LC-ESI-MS.

*Incision of the MeFapy-dG-Containing Duplex by Endo IV at pH 7.0.* The DNA duplex was annealed as described above in Tris buffer (50 mM, pH 7.0). The oligonucleotide duplex (12  $\mu$ L, 2.4 pmols) was added to the Endo IV reaction buffer (222  $\mu$ L, 100 mM NaCl, 50 mM Tris-HCl, 10 mM MgCl<sub>2</sub>, and 1 mM dithiothreitol, pH 7.0). The reaction was incubated at 37°C. Aliquots (50  $\mu$ L) were removed after 1, 3, 5, 7, and 10 days and treated with Endo IV (0.08 nM). Aliquots (8  $\mu$ L) were added to 10  $\mu$ L of 95% formamide loading buffer containing xylene cyanol and bromophenol blue dyes and heated for 1 minute at 90°C. The experiment was run in duplicate.

*Thermal Melting ( $T_m$ ) Analysis of the MeFapy-dG-Containing 12 mer Duplex.* A 1:1 mixture of MeFapy-dG containing 12 mer oligonucleotide and its complementary strand (0.25 A<sub>260</sub> units) were placed in melting buffer (0.5 mL, 10 mM Na<sub>2</sub>HPO<sub>4</sub>/NaH<sub>2</sub>PO<sub>4</sub>, 1.0 M NaCl, and 50  $\mu$ M Na<sub>2</sub>EDTA, pH 7.2). The UV absorbance of the duplex was monitored 260 nm as a function of temperature. Absorbance measurements were taken at 1 minute intervals with a 1°C/min temperature gradient. The temperature was cycled between 15 and 85°C. The first derivative of the melting curve was used to establish  $T_m$  values. After running the first  $T_m$ , the sample was incubated at 37°C for 5 days, then  $T_m$  experiment was repeated.

### 3. Results and Discussion

*3.1. Incision of MeFapy-dG-Containing Duplex by Endo IV.* The MeFapy-dG lesion was site specifically incorporated at position 12 of the 24 mer oligonucleotide shown in Figure 2 (X = MeFapy-dG) and annealed to its complementary strand. The activity of Endo IV toward the MeFapy-dG lesion when paired with dC was examined. PAGE analysis of the reaction mixture typically showed between 36% and 40% of the 5'-<sup>32</sup>P-ACCACGCTAGC-3' incision product after 30 minute (Figure 2(a)). Increasing the initial concentration of Endo IV or addition of a second portion of enzyme after the initial 30 minute incubation period did not increase the amount of incised product. The incision reaction was also followed by LC-ESI-MS with nonradiolabeled oligonucleotides (Figure 3). In addition to the MeFapy-dG-containing oligonucleotide ( $m/z$  = 1825.4 [M-4H] and 1460.3 [M-5H]) and its complementary strand ( $m/z$  = 1484.9 [M-5H] and 1237.2 [M-6H]), the 5'-ACCACGCTAGC-3' ( $m/z$  = 1094.1 [M-3H] and 820.3 [M-4H]) and 5'-p(MeFapy-dG)-AGTCCTAACAAAC-3' ( $m/z$  = 1345.2 [M-3H] and 1009.0 [M-4H]) incision products were observed.

After the initial incision of the MeFapy-dG-containing duplex, the remaining 24 mer duplex, which was presumably highly enriched in the  $\beta$ -MeFapy-dG anomer, was denatured by heating to 90°C, then slowly cooled to reanneal the duplex. The heating and annealing cycle is expected to equilibrate the  $\alpha$ - and  $\beta$ -anomers of the MeFapy-dG lesion [29]. Additional Endo IV was added and the 5'-<sup>32</sup>P-ACCACGCTAGC-3' incision product was found to be ~59% (Figure 2(b)); the 23% increase of the incision

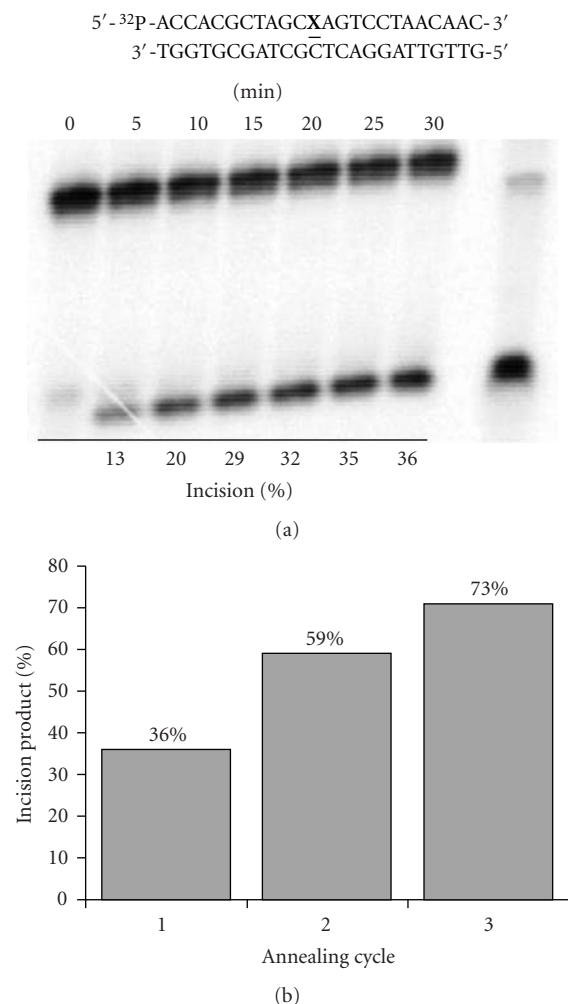


FIGURE 2: Gel electrophoretic analysis of the incision of the MeFapy-dG containing duplex with *E. coli* Endo IV. (a) Incision after the annealing of the 5'-<sup>32</sup>P-labelled MeFapy-dG containing oligonucleotide (24 mer) with its complement. The right lane is a standard of the 5'-<sup>32</sup>P-ACCACGCTAGC-3' incision product. (b) Percentage of the incision product after subsequent denaturation-reannealing and additional Endo IV.

products represents ~36% cleavage of the MeFapy-dG duplex remaining (64%) after the initial Endo IV incision. A subsequent denaturation-reannealing cycle followed by addition of a third aliquot of Endo IV resulted in an additional 14% increase of the incision product (73% total), representing ~34% cleavage of the MeFapy-dG-containing duplex remaining after the prior two rounds of Endo IV treatment (41%). These results are similar to those reported by Patro et al. for the incision of the Fapy-dA containing duplex and is consistent with selective incision of the  $\alpha$ -MeFapy-dG anomer [29].

The MeFapy-dG-containing oligonucleotide was also hybridized to complementary strands in which the lesion was mismatched with dG, dA, and dT. Treatment of these duplexes with Endo IV and PAGE analysis resulted in 30%, 32%, and 30% incision, respectively. The reactions products

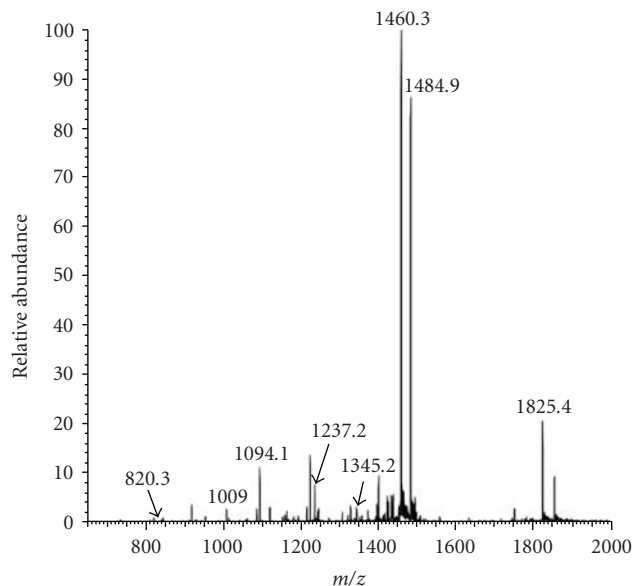


FIGURE 3: Full-can mass spectrum of the Endo IV incision of the MeFapy-dG containing duplex;  $m/z$  1825.4 [M-4H] and 1460.3 [M-5H] are the 5'-ACCACGCTAGC-(MeFapy-dG)-AGTCCTAACAAAC-3',  $m/z$  1484.9 [M-5H] and 1237.2 [M-6H] are the 5'-GTTGTAGGACTCGCTAGCGTGGT-3',  $m/z$  1094.1 [M-3H] and 820.3 [M-4H] are the 5'-ACCACGCTAGC-3', and  $m/z$  1345.2 [M-3H] and 1009.0 [M-4H] is the 5'-p(MeFapy-dG)-AGTCCTAACAAAC-3' oligonucleotide.

from the mismatched duplexes were also characterized by LC-ESI-MS analyses.

**3.2. Steady-State Analysis for the Endo IV Incision of the MeFapy-dG-Containing Duplex.** Figure 4 shows the steady-state kinetic analysis for the incision of MeFapy-dG strand when paired with dC. The modified strand was incised with a  $k_{cat} = 5.5 \pm 0.5 \text{ min}^{-1}$  and  $K_m = 17.8 \pm 3.8 \text{ nM}$  ( $k_{cat}/K_m = 0.33 \pm 0.12 \text{ nM}^{-1} \text{ min}^{-1}$ ; filled circles). When the DNA concentration used in the rate calculation was adjusted to reflect only the amount of the  $\alpha$ -MeFapy-dG adduct (~40%, open circles), the catalytic efficiency improved to  $0.78 \pm 0.33 \text{ nM}^{-1} \text{ min}^{-1}$  by virtue of a lower  $K_m$  ( $7.1 \pm 1.5 \text{ nM}$ ). This treatment of the rate data assumes that the  $\beta$ -MeFapy-dG-containing duplex does not inhibit Endo IV and is based on the observation that the incision of duplex DNA containing  $\alpha$ -dA was not inhibited by the addition of an unmodified duplex, even at concentrations 30-fold higher than the substrate DNA [25]. For comparison, the phosphoramidite reagent of  $\alpha$ -dG was prepared and incorporated into the same 24 mer sequence;  $\alpha$ -dG was chosen for this comparison because of the commercial availability of the nucleoside. The catalytic efficiency for the incision of the  $\alpha$ -dG-containing duplex ( $k_{cat}/K_m$ ) was  $0.69 \pm 0.5 \text{ nM}^{-1} \text{ min}^{-1}$  ( $k_{cat} = 4.9 \pm 0.5 \text{ min}^{-1}$  and  $K_m = 7.1 \pm 1.0 \text{ nM}$ ) (Figure 4 (b)).

**3.3. Equilibration of the MeFapy-dG Anomers in DNA.** The  $\alpha$ -MeFapy-dG lesion was excised from the 24 mer duplex, and the equilibration of the remaining  $\beta$ -MeFapy-dG to

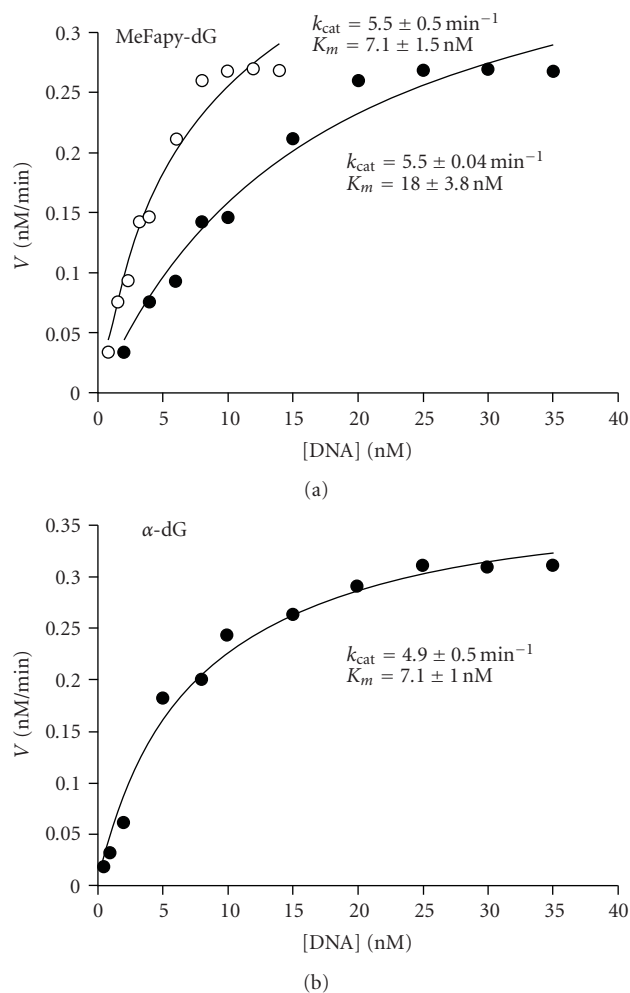


FIGURE 4: Steady-state kinetic analysis for the incision of the MeFapy-dG-(a) and  $\alpha$ -dG-(b) containing duplexes when the modified base was opposite dC. The Endo IV concentration was 0.08 nM.

a mixture of  $\alpha$ - and  $\beta$ -anomers was monitored at 37°C (Figure 5). Aliquots were taken every 24 h after the initial incision reaction and additional Endo IV was added; the increase in the 5'-<sup>32</sup>P-ACCACGCTAGC-3' was attributed to the anomerization of the  $\beta$ -MeFapy-dG remaining after initial incision. The prolonged exposure of the incision product to Endo IV resulted in its conversion to a product one nucleotide shorter. We attribute this observation to the 3' → 5' exonuclease activity of Endo IV, and the product is presumably 5'-<sup>32</sup>P-ACCACGCTAG-3' [20]. Virtually no anomerization was observed at pH 8.0, consistent with studies that showed that the anomerization of the AFB-Fapy-dG lesion was acid catalyzed [40]. We found that the anomeric stereochemistry of the  $\beta$ -MeFapy-dG equilibrated over ~5 days to an  $\alpha$  :  $\beta$  ratio of ~21 : 79 at pH 7.0 and 37°C. To insure that the additional cleavage of the duplex was not due to fortuitous deglycosylation of the MeFapy-G base, the MeFapy-dG-containing duplex was incubated at 37°C for 5 days, then *E. coli* Endonuclease V was added, which is known to cleave abasic sites. No cleavage was observed.

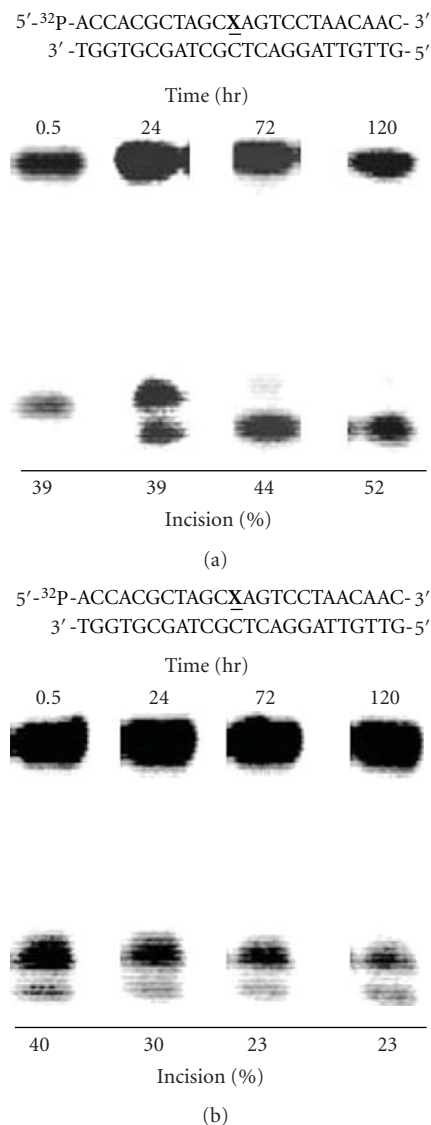


FIGURE 5: Gel electrophoretic analysis of the equilibration of the  $\beta$ - and  $\alpha$ -MeFapy-dG anomers in duplex DNA. (a) Anomerization of the  $\beta$ -MeFapy-dG after initial incision with Endo IV. Aliquots were treated with additional Endo IV every 24 h; the increase in the incision product is attributed to equilibration of the  $\beta$ -MeFapy-dG to the  $\alpha$ -anomer. (b) Treatment of the MeFapy-dG-containing duplex with Endo IV after incubation at 37°C, pH 7.0 for up to 5 days.

The duplex that resulted from annealing the MeFapy-dG modified oligonucleotide with its complement initially contained ~36%–40% of the  $\alpha$ -MeFapy-dG. The equilibration of the  $\alpha$ -MeFapy-dG anomer to the  $\beta$ -anomer was monitored by incubating the annealed duplex at 37°C and treating aliquots with Endo IV (Figure 5 (b)). We observed that the  $\alpha$  :  $\beta$  anomeric ratio was ~30 : 70 after 24 h and 23 : 77 after 3 days; the reaction was monitored up to 10 days, and the percentage of incision product remained at ~23%. These results are in good agreement with those starting from the  $\beta$ -anomer.

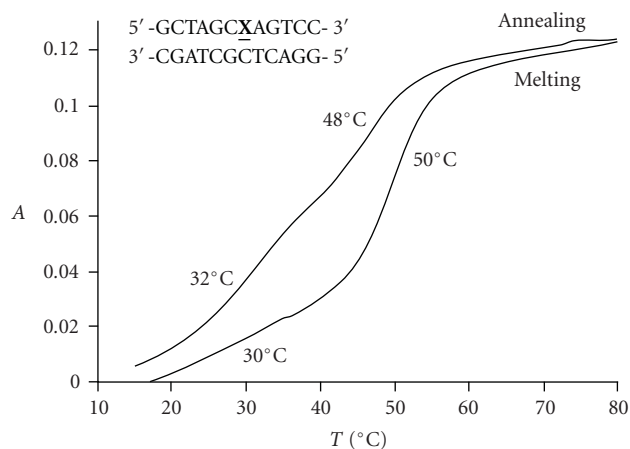


FIGURE 6: Thermal melting analysis of the 12 mer duplex containing the MeFapy-dG lesion opposite dC after 5 days at 37°C. The  $T_m$  for the unmodified duplex was 59°C.

We initially reported that the thermal melting ( $T_m$ ) curve of a 12 mer duplex containing the MeFapy-dG lesion did not change over time [11]; these studies were conducted at 5°C. The thermal melting temperature of the 12 mer duplex 5'-GCTAGC-(MeFapy-dG)-AGTCC-3' · 5'-GGACTCGCTAGC-3' was reexamined by monitoring the hyperchromicity of the DNA UV absorption at 260 nm as a function of temperature (Figure 6). This duplex has the same local sequence as the 24 mer duplex used for the Endo IV incision studies. The duplex was incubated at 37°C for 5 days then analyzed. The  $T_m$  values were determined by taking the first derivative of the melting and annealing curves. As previously reported, two transitions were present in the melting cycle; however, the relative proportions of the transitions differed after 5 days at 37°C. The higher melting transition ( $T_m = 50^\circ\text{C}$ ), which was assigned as the  $\beta$ -MeFapy-dG anomer, made up ~80% of the duplex after the incubation period. The  $T_m$  curve for the annealing cycle was displaced from the heating cycle, reflecting that the reannealing of the MeFapy-dG oligonucleotide with its complement resulted in a different  $\alpha : \beta$  anomeric ratio than after equilibration for 5 days. Similar melting and annealing profiles were recently reported for a duplex containing the AFB-Fapy-dG lesion [38]. These studies are consistent with the Endo IV incision data.

The initial anomeric ratio (~36:64) after annealing the MeFapy-dG-containing oligonucleotide with its complement may reflect the ratio in single-strand DNA. The  $\alpha$ - and  $\beta$ -MeFapy-dG anomers equilibrate over several days and reach a final  $\alpha : \beta$  ratio of ~21:79. The equilibration studies may provide insight to the conflicting reports by Asagoshi et al. regarding the Endo IV incision of the MeFapy-dG lesion in DNA. The MeFapy-dG-containing duplexes were prepared differently. Ishchenko et al. prepared the MeFapy-dG lesion by treating a single-stranded oligonucleotide containing a single dG with a methylating agent [32]; the resulting 7-methyl-dG was then subjected to base treatment

to generate the MeFapy-dG lesion. Annealing of the MeFapy-dG-containing oligonucleotide is expected to contain both the  $\alpha$ - and  $\beta$ -anomers as demonstrated in our studies. Asagoshi et al. prepared a DNA duplex by incorporating 7-methyl-dGTP opposite a template strand containing a single dC with a DNA polymerase [30, 31]; alkali treatment of the duplex produced the MeFapy-dG lesion. It is likely that ring opening of  $\beta$ -7-methyl-dG in duplex DNA produced largely or exclusively the  $\beta$ -MeFapy-dG anomer. We demonstrated that the anomerization of the  $\beta$ -MeFapy-dG anomer is slow at pH 7.0 and is expected to be slower at pH 7.5, the conditions reported by Asagoshi et al. for the attempted Endo IV incision [30]. It is possible that the  $\beta$ -MeFapy-dG anomer had not equilibrated when treated with Endo IV, and consequently, no incision was observed.

The MeFapy-dG lesion was shown to be the persistent DNA lesion in rats treated with methylnitrosourea, 1,2-dimethylhydrazine, and N,N-dimethylnitrosamine [8, 9]. The MeFapy-dG lesion was reported to be present 21 days after exposure; these studies detected the MeFapy-G base, thus information regarding the anomeric stereochemistry was lost. As noted above, the MeFapy-dG lesion is likely to be initially formed as the  $\beta$ -anomer; our observation that  $\beta$ -MeFapy-dG will slowly equilibrate to ~21% of the  $\alpha$ -anomer over 3–5 days suggests that the  $\alpha$ -anomer is present in cells due to the long-lived nature of this lesion and therefore may be biologically relevant.

**3.4. Incision of AFB-Fapy-dG by Endo IV.** The 24 mer oligonucleotide containing the AFB-Fapy-dG lesion, 5'-ACCCTACTAT-(AFB-Fapy-dG)-ATTTCATAACAAC-3', was synthesized as previously described, and the  $\alpha$ - and  $\beta$ -AFB-Fapy-dG-containing oligonucleotides were separated by HPLC [38]. The oligonucleotide containing the  $\alpha$ -AFB-Fapy-dG lesion was 5'-<sup>32</sup>P-end labeled and hybridized to its complementary strand in which the lesion was opposite dC. Treatment of this duplex (20 nM) with Endo IV (0.08 nM) under the same conditions used for incision of the MeFapy-dG-containing duplex resulted in ~5% incision of  $\alpha$ -AFB-Fapy-dG modified strand after 30 minute (Figure 7); the level of incision did not increase after 90 minute. The level of incision reached ~9% when the Endo IV concentration was increased by 10-fold.

The activity of Endo IV toward the AFB-Fapy-dG lesion was low in comparison to the MeFapy-dG lesion. The  $\alpha$ -AFB-Fapy-dG was reported to have completely isomerized to the  $\beta$ -anomer over several days at pH 7.0 and 5°C [37]. It is possible that the low level of incision observed for the AFB-Fapy-dG-containing 24 mer duplex was due to rapid isomerization of the  $\alpha$ -anomer to the  $\beta$ ; however, HPLC analysis indicated that the level on the  $\beta$ -AFB-Fapy-dG anomer was less than 5% over the 90 minute reaction time and conditions used to <sup>32</sup>P-label the substrate. In Figure 1 a recent NMR structure of the  $\alpha$ -AFB-Fapy-dG lesion in a 5'-CTAT-(AFB-Fapy-dG)-ATTTC-3' · 5'-TGAATCATAG-3' 10 mer duplex revealed that the AFB moiety was intercalated to the 5'-side of the modified  $\alpha$ -Fapy-dG base [38] and well stacked (Figure 8). The modified  $\alpha$ -AFB-Fapy-dG base was

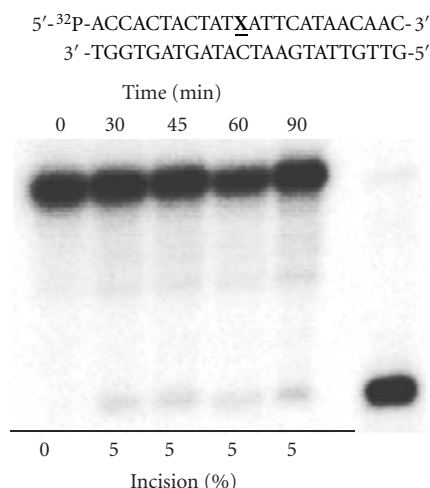


FIGURE 7: Gel electrophoretic analysis of the incision of the  $\alpha$ -AFB-Fapy-dG-containing 5'-<sup>32</sup>P-labeled 24 mer duplex by Endo IV. The right lane is a standard of the 5'-<sup>32</sup>P-ACCACTACTAT-3' incision product.

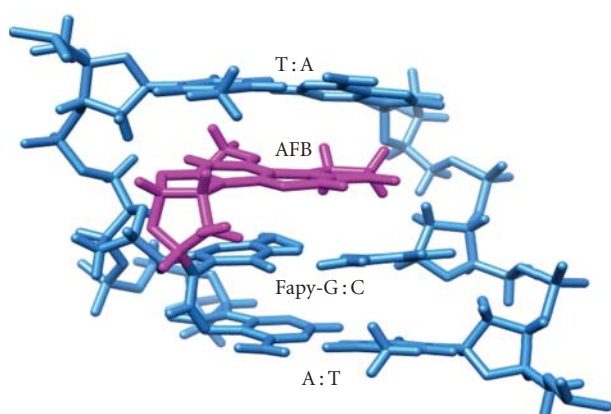


FIGURE 8: Conformation of the  $\alpha$ -AFB-Fapy-dG-containing 10 mer duplex. The AFB moiety (magenta) was intercalated to the 5'-side of the Fapy-G base, which was paired with its complement (pdb code 2KH3).

paired with its complementary dC, and both bases were intrahelical. The 10 mer sequence possesses the same local sequence as the AFB-Fapy-dG containing 24 mer used in this study. The insertion of the Tyr-72 side chain of Endo IV into the DNA helix plays an important role in the recognition and catalytic mechanism by promoting the flipping of the abasic nucleotide along with its partner nucleotide into the active site of the enzyme, stabilizing a 90° bend in the DNA and positioning the phosphate for hydrolysis. The position of the bulky AFB group may severely interfere with the binding of the substrate DNA to Endo IV and the incision reaction [22, 23]. Alternatively, a solvent accessible pocket in the active site of Endo IV is hypothesized to accommodate  $\alpha$ -nucleotides, and it is plausible that bulky lesions such as the  $\alpha$ -AFB-Fapy-dG cannot be readily accommodated in this pocket [22]. Chromatographic evidence for a minor

conformation of the  $\alpha$ -AFB-Fapy-dG in single strand was reported [38]; the nature of this conformation is not clear but the possibilities include geometric isomers of the amide or atropisomers [14, 40, 42]. It is possible that Endo IV is selectively incising this minor  $\alpha$ -AFB-Fapy-dG conformer.

#### 4. Conclusion

We unambiguously observed that the  $\alpha$ -MeFapy-dG lesion is a substrate for Endo IV. This activity was exploited to probe the anomeric configuration of the MeFapy-dG lesion in duplex DNA. Endo IV was used to follow the equilibration of the  $\alpha$ - and  $\beta$ -MeFapy-dG lesions, and we estimate the  $\alpha$  :  $\beta$ -ratio to be ~21 : 79. Although the equilibration was slow, it was faster than the repair of the MeFapy-dG lesion from the DNA of rats. We conclude that the  $\alpha$ -MeFapy-dG will be present in mammalian cells, and its repair and replication are therefore of interest. Only low levels of incision were observed for the  $\alpha$ -AFB-Fapy-dG-containing duplex. It is likely that the bulk of the AFB moiety, which was intercalated on the 5'-side of the modified base, interferes with substrate recognition and the incision reaction by Endo IV.

The MeFapy-dG lesion has been shown to be a substrate for the Fpg/Nei family of glycosylases [3, 30, 43–45]. It is possible that Endo IV and the Fpg/Nei glycosylases have distinct roles during the repair of the MeFapy-dG with Endo IV incising the  $\alpha$ -anomer and Fpg/Nei glycosylases excising the  $\beta$ -anomer. The specificity of Endo IV for the  $\alpha$ -MeFapy-dG anomer may provide a valuable tool for uncovering the mechanistic details of the repair of MeFapy-dG and related lesions.

#### Acknowledgments

The authors thank Professor Marc M. Greenberg for helpful discussions. This work was supported by NIH Research Grants P01 ES05355 (Carmelo J. Rizzo and Michael P. Stone) and R01 CA55678 (Michael P. Stone), and Center Grant P30 ES00267 (Carmelo J. Rizzo and Michael P. Stone).

#### References

- [1] M. M. Greenberg, "In vitro and in vivo effects of oxidative damage to deoxyguanosine," *Biochemical Society Transactions*, vol. 32, no. 1, pp. 46–50, 2004.
- [2] D. Pluskota-Karwatka, "Modifications of nucleosides by endogenous mutagens-DNA adducts arising from cellular processes," *Bioorganic Chemistry*, vol. 36, no. 4, pp. 198–213, 2008.
- [3] M. Dizdaroglu, G. Kirkali, and P. Jaruga, "Formamidopyrimidines in DNA: mechanisms of formation, repair, and biological effects," *Free Radical Biology and Medicine*, vol. 45, no. 12, pp. 1610–1621, 2008.
- [4] B. Tudek, "Imidazole ring-opened DNA purines and their biological significance," *Journal of Biochemistry and Molecular Biology*, vol. 36, no. 1, pp. 12–19, 2003.
- [5] K. S. Gates, T. Nooner, and S. Dutta, "Biologically relevant chemical reactions of N7-alkylguanine residues in DNA," *Chemical Research in Toxicology*, vol. 17, no. 7, pp. 839–856, 2004.

- [6] G. Boysen, B. F. Pachkowski, J. Nakamura, and J. A. Swenberg, "The formation and biological significance of N7-guanine adducts," *Mutation Research*, vol. 678, no. 2, pp. 76–94, 2009.
- [7] L. T. Burgdorf and T. Carell, "Synthesis, stability, and conformation of the formamidopyrimidine G DNA lesion," *Chemistry—A European Journal*, vol. 8, no. 1, pp. 293–301, 2002.
- [8] F. F. Kadlubar, D. T. Beranek, C. C. Weis, F. E. Evans, R. Cox, and C. C. Irving, "Characterization of the purine ring-opened 7-methylguanine and its persistence in rat bladder epithelial DNA after treatment with the carcinogen N-methylnitrosourea," *Carcinogenesis*, vol. 5, no. 5, pp. 587–592, 1984.
- [9] D. T. Beranek, C. C. Weis, F. E. Evans, C. J. Chetsanga, and F. F. Kadlubar, "Identification of N<sup>5</sup>-methyl-N<sup>5</sup>-formyl-2,5,6-triamino-4-hydroxypyrimidine as a major adduct in rat liver DNA after treatment with the carcinogens, N,N-dimethylnitrosamine or 1,2-dimethylhydrazine," *Biochemical and Biophysical Research Communications*, vol. 110, no. 2, pp. 625–631, 1983.
- [10] J. M. Essigmann, R. G. Croy, R. A. Bennett, and G. N. Wogan, "Metabolic activation of aflatoxin B<sub>1</sub>: patterns of DNA adduct formation, removal, and excretion in relation to carcinogenesis," *Drug Metabolism Reviews*, vol. 13, no. 4, pp. 581–602, 1982.
- [11] P. P. Christov, K. L. Brown, I. D. Kozekov, M. P. Stone, T. M. Harris, and C. J. Rizzo, "Site-specific synthesis and characterization of oligonucleotides containing an N<sup>6</sup>-(2-deoxy-D-erythro-pentofuranosyl)-2,6-diamino-3,4-dihydro-4-oxo-5-N-methylformamidopyrimidine lesion, the ring-opened product from N7-methylation of deoxyguanosine," *Chemical Research in Toxicology*, vol. 21, no. 12, pp. 2324–2333, 2008.
- [12] F. Büsch, J. C. Pieck, M. Ober et al., "Dissecting the differences between the  $\alpha$  and  $\beta$  anomers of the oxidative DNA lesion FaPydG," *Chemistry—A European Journal*, vol. 14, no. 7, pp. 2125–2132, 2008.
- [13] M. Berger and J. Cadet, "Isolation and characterization of the radiation-induced degradation products of 2'-deoxyguanosine in oxygen-free aqueous solutions," *Zeitschrift für Naturforschung*, vol. 40, no. 11, pp. 1519–1531, 1985.
- [14] M. Tomasz, R. Lipman, M. S. Lee, G. L. Verdine, and K. Nakanishi, "Reaction of acid-activated mitomycin C with calf thymus DNA and model guanines: elucidation of the base-catalyzed degradation of N7-alkylguanine nucleosides," *Biochemistry*, vol. 26, no. 7, pp. 2010–2027, 1987.
- [15] K. B. Lesiak and K. T. Wheeler, "Formation of  $\alpha$ -deoxyadenosine in polydeoxynucleotides exposed to ionizing radiation under anoxic conditions," *Radiation Research*, vol. 121, no. 3, pp. 328–337, 1990.
- [16] A. Bonicel, N. Mariaggi, E. Hughes, and R. Teoule, "In vitro  $\gamma$  irradiation of DNA: identification of radioinduced chemical modifications of the adenine moiety," *Radiation Research*, vol. 83, no. 1, pp. 19–26, 1980.
- [17] P. W. Doetsch and R. P. Cunningham, "The enzymology of apurinic/apyrimidinic endonucleases," *Mutation Research*, vol. 236, no. 2-3, pp. 173–201, 1990.
- [18] D. Ramotar, "The apurinic-apyrimidinic endonuclease IV family of DNA repair enzymes," *Biochemistry and Cell Biology*, vol. 75, no. 4, pp. 327–336, 1997.
- [19] S. Ljungquist, T. Lindahl, and P. Howard-Flanders, "Methyl methane sulfonate sensitive mutant of *Escherichia coli* deficient in an endonuclease specific for apurinic sites in deoxyribonucleic acid," *Journal of Bacteriology*, vol. 126, no. 2, pp. 646–653, 1976.
- [20] S. M. Kerins, R. Collins, and T. V. McCarthy, "Characterization of an endonuclease IV 3'-5' exonuclease activity," *Journal of Biological Chemistry*, vol. 278, no. 5, pp. 3048–3054, 2003.
- [21] G. Golan, A. A. Ishchenko, B. Khassenov, G. Shoham, and M. K. Saparbaev, "Coupling of the nucleotide incision and 3' → 5' exonuclease activities in *Escherichia coli* endonuclease IV: structural and genetic evidences," *Mutation Research*, vol. 685, no. 1-2, pp. 70–79, 2010.
- [22] D. J. Hosfield, Y. Guan, B. J. Haas, R. P. Cunningham, and J. A. Tainer, "Structure of the DNA repair enzyme endonuclease IV and its DNA complex: double-nucleotide flipping at abasic sites and three-metal-ion catalysis," *Cell*, vol. 98, no. 3, pp. 397–408, 1999.
- [23] E. D. Garcin, D. J. Hosfield, S. A. Desai et al., "DNA apurinic-apyrimidinic site binding and excision by endonuclease IV," *Nature Structural and Molecular Biology*, vol. 15, no. 5, pp. 515–522, 2008.
- [24] I. Ivanov, J. A. Tainer, and J. A. McCammon, "Unraveling the three-metal-ion catalytic mechanism of the DNA repair endonuclease IV," *Proceedings of the National Academy of Sciences of the United States of America*, vol. 104, no. 5, pp. 1465–1470, 2007.
- [25] H. Ide, K. Tedzuka, H. Shimzu et al., " $\alpha$ -Deoxyadenosine, a major anoxic radiolysis product of adenine in DNA, is a substrate for *Escherichia coli* endonuclease IV," *Biochemistry*, vol. 33, no. 25, pp. 7842–7847, 1994.
- [26] J. M. Aramini, S. H. Cleaver, R. T. Pon, R. P. Cunningham, and M. W. Germann, "Solution structure of a DNA duplex containing an  $\alpha$ -anomeric adenosine: insights into substrate recognition by endonuclease IV," *Journal of Molecular Biology*, vol. 338, no. 1, pp. 77–91, 2004.
- [27] L. Gros, A. A. Ishchenko, H. Ide, R. H. Elder, and M. K. Saparbaev, "The major human AP endonuclease (Ape1) is involved in the nucleotide incision repair pathway," *Nucleic Acids Research*, vol. 32, no. 1, pp. 73–81, 2004.
- [28] S. Daviet, S. Couvé-Privat, L. Gros et al., "Major oxidative products of cytosine are substrates for the nucleotide incision repair pathway," *DNA Repair*, vol. 6, no. 1, pp. 8–18, 2007.
- [29] J. N. Patro, K. Haraguchi, M. O. Delaney, and M. M. Greenberg, "Probing the configurations of formamidopyrimidine lesions Fapy · dA and Fapy · dG in DNA using endonuclease IV," *Biochemistry*, vol. 43, no. 42, pp. 13397–13403, 2004.
- [30] K. Asagoshi, T. Yamada, H. Terato et al., "Distinct repair activities of human 7,8-dihydro-8-oxoguanine DNA glycosylase and formamidopyrimidine DNA glycosylase for formamidopyrimidine and 7,8-dihydro-8-oxoguanine," *Journal of Biological Chemistry*, vol. 275, no. 7, pp. 4956–4964, 2000.
- [31] K. Asagoshi, H. Terato, Y. Ohyama, and H. Ide, "Effects of a guanine-derived formamidopyrimidine lesion on DNA replication. Translesion DNA synthesis, nucleotide insertion, and extension kinetics," *Journal of Biological Chemistry*, vol. 277, no. 17, pp. 14589–14597, 2002.
- [32] A. A. Ishchenko, G. Sanz, C. V. Privezentzev, A. V. Maksimenko, and M. Saparbaev, "Characterisation of new substrate specificities of *Escherichia coli* and *Saccharomyces cerevisiae* AP endonucleases," *Nucleic Acids Research*, vol. 31, no. 21, pp. 6344–6353, 2003.
- [33] M. F. Laspia and S. S. Wallace, "Excision repair of thymine glycols, urea residues, and apurinic sites in *Escherichia coli*," *Journal of Bacteriology*, vol. 170, no. 8, pp. 3359–3366, 1988.
- [34] V. Gervais, J. A. H. Cognet, A. Guy, J. Cadet, R. Téoule, and G. V. Fazakerley, "Solution structure of N-(2-deoxy-D-erythro-pentofuranosyl)urea frameshifts, one intrahelical and the other extrahelical, by nuclear magnetic resonance and

- molecular dynamics,” *Biochemistry*, vol. 37, no. 4, pp. 1083–1093, 1998.
- [35] I. Dubey, G. Pratiel, A. Robert, and B. Meunier, “Convenient method for the preparation of 2′-deoxyribosylurea by thymidine oxidation and NMR study of both anomers,” *Nucleosides, Nucleotides and Nucleic Acids*, vol. 20, no. 8, pp. 1463–1471, 2001.
- [36] S. Baillet and J.-P. Behr, “Deoxyribosylurea and deoxyribosylformamide oligonucleotides,” *Tetrahedron Letters*, vol. 36, no. 49, pp. 8981–8984, 1995.
- [37] H. Mao, Z. Deng, F. Wang, T. M. Harris, and M. P. Stone, “An intercalated and thermally stable FAPY adduct of aflatoxin B<sub>1</sub> in a DNA duplex: structural refinement from <sup>1</sup>H NMR,” *Biochemistry*, vol. 37, no. 13, pp. 4374–4387, 1998.
- [38] K. L. Brown, M. W. Voehler, S. M. Magee, C. M. Harris, T. M. Harris, and M. P. Stone, “Structural perturbations induced by the α-anomer of the aflatoxin B<sub>1</sub> formamidopyrimidine adduct in duplex and single-strand DNA,” *Journal of the American Chemical Society*, vol. 131, no. 44, pp. 16096–16107, 2009.
- [39] E. R. Marinelli, F. Johnson, C. R. Iden, and P.-L. Yu, “Synthesis of 1,N<sup>2</sup>-(1,3-propano)-2′-deoxyguanosine and incorporation into oligodeoxynucleotides: a model for exocyclic acrolein-DNA adducts,” *Chemical Research in Toxicology*, vol. 3, no. 1, pp. 49–58, 1990.
- [40] K. L. Brown, J. Z. Deng, R. S. Iyer et al., “Unraveling the aflatoxin-FAPY conundrum: structural basis for differential replicative processing of isomeric forms of the formamidopyrimidine-type DNA adduct of aflatoxin B<sub>1</sub>,” *Journal of the American Chemical Society*, vol. 128, no. 47, pp. 15188–15199, 2006.
- [41] J. S. Stover, G. Chowdhury, H. Zang, F. P. Guengerich, and C. J. Rizzo, “Translesion synthesis past the C8- and N<sup>2</sup>-deoxyguanosine adducts of the dietary mutagen 2-amino-3-methylimidazo[4,5-f]quinoline in the *NarI* recognition sequence by prokaryotic DNA polymerases,” *Chemical Research in Toxicology*, vol. 19, no. 11, pp. 1506–1517, 2006.
- [42] S. Boiteux, J. Belleney, B. P. Roques, and J. Laval, “Two rotameric forms of open ring 7-methylguanine are present in alkylated polynucleotides,” *Nucleic Acids Research*, vol. 12, no. 13, pp. 5429–5439, 1984.
- [43] S. Boiteux, T. R. O’Connor, F. Lederer, A. Gouyette, and J. Laval, “Homogeneous *Escherichia coli* FPG protein. A DNA glycosylase which excises imidazole ring-opened purines and nicks DNA at apurinic/apyrimidinic sites,” *Journal of Biological Chemistry*, vol. 265, no. 7, pp. 3916–3922, 1990.
- [44] A. Katafuchi, T. Nakano, A. Masaoka et al., “Differential specificity of human and *Escherichia coli* endonuclease III and VIII homologues for oxidative base lesions,” *Journal of Biological Chemistry*, vol. 279, no. 14, pp. 14464–14471, 2004.
- [45] M. Liu, V. Bandaru, J. P. Bond et al., “The mouse ortholog of NEIL3 is a functional DNA glycosylase in vitro and in vivo,” *Proceedings of the National Academy of Sciences of the United States of America*, vol. 107, no. 11, pp. 4925–4930, 2010.

## Review Article

# Regulation of HuR by DNA Damage Response Kinases

**Hyeon Ho Kim,<sup>1,2</sup> Kotb Abdelmohsen,<sup>1</sup> and Myriam Gorospe<sup>1</sup>**

<sup>1</sup>Laboratory of Cellular and Molecular Biology, NIA-IRP, NIH, Baltimore, MD 21224, USA

<sup>2</sup>Samsung Biomedical Research Institute, Samsung Medical Center, Sungkyunkwan University School of Medicine, Seoul 135-710, Republic of Korea

Correspondence should be addressed to Kotb Abdelmohsen, abdelmohsenk@grc.nia.nih.gov

Received 15 April 2010; Accepted 17 May 2010

Academic Editor: Ashis Basu

Copyright © 2010 Hyeon Ho Kim et al. This is an open access article distributed under the Creative Commons Attribution License, which permits unrestricted use, distribution, and reproduction in any medium, provided the original work is properly cited.

As many DNA-damaging conditions repress transcription, posttranscriptional processes critically influence gene expression during the genotoxic stress response. The RNA-binding protein HuR robustly influences gene expression following DNA damage. HuR function is controlled in two principal ways: (1) by mobilizing HuR from the nucleus to the cytoplasm, where it modulates the stability and translation of target mRNAs and (2) by altering its association with target mRNAs. Here, we review evidence that two main effectors of ataxia-telangiectasia-mutated/ATM- and Rad3-related (ATM/ATR), the checkpoint kinases Chk1 and Chk2, jointly influence HuR function. Chk1 affects HuR localization by phosphorylating (hence inactivating) Cdk1, a kinase that phosphorylates HuR and thereby blocks HuR's cytoplasmic export. Chk2 modulates HuR binding to target mRNAs by phosphorylating HuR's RNA-recognition motifs (RRM1 and RRM2). We discuss how HuR phosphorylation by kinases including Chk1/Cdk1 and Chk2 impacts upon gene expression patterns, cell proliferation, and survival following genotoxic injury.

## 1. Introduction

Damage to the cellular DNA can transiently inhibit the activity of RNA polymerase II at a time when DNA damage response (DDR) proteins and DNA repair proteins are critically needed [1]. As transcription is reduced, there is increased need to regulate the production of proteins from the pre-existing pool of mRNAs. Two main posttranscriptional mechanisms control protein expression following genotoxic damage: mRNA turnover and translational regulation [2, 3]. These two sets of events are potently influenced by RNA-binding proteins (RBPs) and noncoding RNAs (primarily microRNAs), which interact with mRNAs and modulate their half-lives and translation rates [4–6].

During the DDR, several RBPs showing altered levels or subcellular localization have been implicated in controlling gene expression. For example, many RBPs that control RNA metabolism showed altered expression in response to ionizing radiation (IR) and ultraviolet radiation (UV) [7]; in another study, several members of the heterogeneous ribonuclear protein (hnRNP) family were found to participate in the response to IR [8]. Specific RBPs have also been shown to participate in different types of DDR; for example,

the RBPs AU-binding factor 1 (AUF1) and T cell-restricted intracellular antigen-related protein (TIAR) controlled the expression of the growth arrest- and DNA damage-inducible (gadd)45a protein in response to alkylating DNA damage [9], the RBPs nucleolin and nucleophosmin participated in the cellular responses to IR and UV [10], and the RBP Sam68 modulated alternative splicing following DNA damage [11]. One of the best characterized RBPs that control expression of DDR genes, HuR, is the subject of this review.

## 2. Stress-Response Protein HuR

HuR is the ubiquitous member of the embryonic lethal abnormal vision (ELAV)/Hu family of RBPs, which also contains the primarily neuronal members HuB, HuC, and HuD [12]. Although HuR is predominantly nuclear, its translocation to the cytoplasm is linked to its ability to stabilize target mRNAs and/or modulate their translation [13, 14]. The 326-aa long HuR binds target mRNAs through its three RNA recognition motifs (RRMs); located between RRM2 and RRM3 is a hinge region that encompasses a nucleocytoplasmic shuttling sequence (HNS, spanning

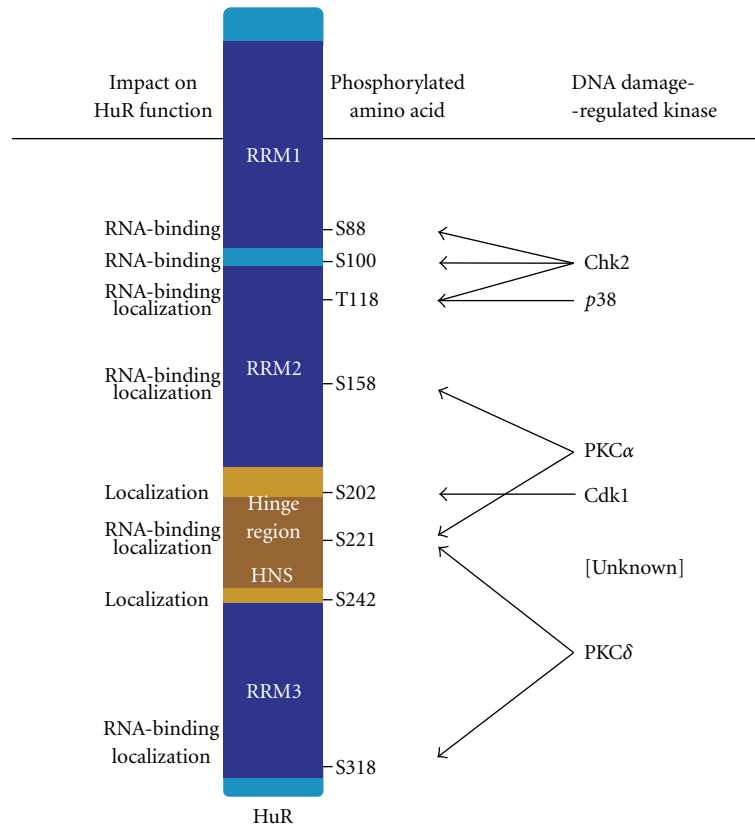


FIGURE 1: Sites of HuR phosphorylation by DNA damage-inducible kinases. Schematic of HuR depicting the RNA recognition motifs (RRMs, dark blue), the hinge region (brown) with the HuR nucleocytoplasmic shuttling sequence (HNS), the sites of phosphorylation (under “Phosphorylated Amino Acids”), and the DNA Damage-Regulated Kinases responsible, including an unknown kinase predicted to phosphorylate S242. The consequences of HuR phosphorylation at the different sites are indicated under “Impact on HuR Function”. More details in the text.

residues 205–237 [15]) (Figure 1). The nuclear export of HuR is mediated by its association with transportin 1 (Trn1) and Trn2 [16] and with nuclear ligands pp32 and APRIL, which contain nuclear export signals that are recognized by the export receptor CRM1 [17, 18].

HuR target mRNAs encode many proteins implicated in the cellular response to DNA damage, including tumor suppressors (p53, pVHL), cyclins (A, B1, and D1), proto-oncogenes (c-fos, c-myc), growth factors (VEGF), cytokines (TGF- $\beta$ , TNF- $\alpha$ ), cyclin-dependent kinase (cdk) inhibitors (p21, p27), antiapoptotic factors [prothymosin  $\alpha$  (ProT $\alpha$ ), Bcl-2, and Mcl-1], and signaling molecules like the mitogen-activated protein (MAP) kinase phosphatase MKP-1 [19–30] (Table 1); most of these transcripts contain one or several copies of a U-rich RNA signature motif [31]. Given the functions of the proteins encoded by HuR-regulated mRNAs, HuR has been implicated in processes such as carcinogenesis, proliferation, immune function, differentiation, and responsiveness to oxidative and genotoxic damage [14, 26, 32–38].

With a few exceptions [38, 44], acute changes in HuR function do not involve changes in protein abundance but rely instead on two regulatory steps: (1) the subcellular localization of HuR and (2) the interaction of HuR with

target mRNAs. In response to DNA-damaging stresses, the past few years have uncovered a signaling pathway that jointly affects both of these processes, HuR’s subcellular distribution and its interaction with target transcripts. DNA damage is recognized by sensor proteins, such as the Rad9-Rad1-Hus1 complex (also termed “9-1-1 complex”) that recognizes certain types of DNA damage and is mediated by proteins such as those that comprise the Mre11-Rad50-Nbs1 complex (MRN), which recruits the transducer protein DNA damage-activated ataxia telangiectasia mutated (ATM) to sites of DNA damage [45]. The transducer proteins include the kinases ATM and ATM- and Rad3-related (ATR); ATM/ATR phosphorylates and thereby activates the checkpoint kinases Chk1 and Chk2, which control HuR cytoplasmic abundance and RNA binding, respectively. ATM is primarily activated by double-strand breaks in DNA, such as those caused by IR [46] while ATR is activated in response to other damaging agents, including UV, alkylating agents, and chemical inhibitors of DNA replication [47, 48], but there is extensive evidence that both kinases work in tandem [49]. As these kinases are essential for genomic integrity, deficiencies in ATM/ATR and other components of DNA damage checkpoints cause debilitating diseases such as ataxia telangiectasia, Fanconi’s anemia, and Seckel syndrome,

TABLE 1: HuR target mRNAs showing altered expression after DNA damage. Partial list of HuR target mRNAs encoding proteins that change following DNA damage (first column), the region of interaction with HuR (second column), and the genotoxic damage that was shown to affect HuR regulation of the mRNA (third column); “n.r.”: no reported. The HuR kinases linked to the regulation of the mRNAs in the first column are indicated (fourth column).

	Target mRNA after DNA damage	Binding region	DNA damage conditions affecting regulation by HuR	HuR Kinase	References
	<i>c-fos</i>	3'UTR	n.r.	n.r.	[-]
	<i>p21</i>	3'UTR	UVC, arsenite, IR	Chk2, p38	[27, 39]
	<i>cyclin A2</i>	3'UTR	H <sub>2</sub> O <sub>2</sub>	Chk2, Cdk1	[27, 29]
	<i>cyclin B1</i>	3'UTR	H <sub>2</sub> O <sub>2</sub>	n.r.	[40]
	<i>cyclin D1</i>	3'UTR	UVC	Chk2	[27]
	<i>iNOS</i>	3'UTR	n.r.	n.r.	[-]
	<i>VEGF</i>	3'UTR	n.r.	n.r.	[-]
mRNA stabilization	<i>SIRT1</i>	3'UTR	H <sub>2</sub> O <sub>2</sub>	Chk2	[27]
	<i>TNF-<math>\alpha</math></i>	3'UTR	n.r.	n.r.	[-]
	<i>bcl-2</i>	3'UTR	n.r.	Cdk1	[28]
	<i>mcl-1</i>	3'UTR	n.r.	Cdk1	[28]
	<i>COX-2</i>	3'UTR	n.r.	PKC, p38	[41, 42]
	<i>uPA</i>	3'UTR	n.r.	n.r.	[-]
	<i>uPAR</i>	3'UTR	n.r.	n.r.	[-]
	<i>IL-3</i>	3'UTR	n.r.	n.r.	[-]
	<i>MKP-1</i>	3'UTR	H <sub>2</sub> O <sub>2</sub>	Cdk1	[43]
	<i>p53</i>	3'UTR	UVC	n.r.	[-]
† Translation	<i>ProT<math>\alpha</math></i>	3'UTR	UVC	Chk2, Cdk1	[29]
	<i>cytochrome c</i>	3'UTR	n.r.	Chk2	[27]
	<i>MKP-1</i>	3'UTR	H <sub>2</sub> O <sub>2</sub>	Cdk1	[29]
	<i>HIF-1<math>\alpha</math></i>	3'UTR	n.r.	Cdk1	[29]
	<i>p27</i>	5'UTR	n.r.	n.r.	[-]
	<i>IGF-IR</i>	5'UTR	n.r.	n.r.	[-]
‡ Translation	<i>Wnt5a</i>	3'UTR	n.r.	n.r.	[-]
	<i>HuR</i>	3'UTR	n.r.	n.r.	[-]
	<i>c-Myc</i>	3'UTR	n.r.	n.r.	[-]

thereby contributing to premature aging and carcinogenesis [50, 51]. Given that HuR target transcripts encode proteins implicated in the DDR, HuR control by ATM/ATR is rising as a major gene regulatory paradigm in the pathophysiology of DNA damage (Figure 2). Consequently, even in the presence of normal HuR levels in the cell, HuR's ability to regulate DDR gene expression posttranscriptionally is impaired in cells with aberrant ATM/ATR signaling.

### 3. Regulation of HuR by ATM/ATR → Chk1 → Cdk1

During DDR such as that resulting from exposure to UV, oxidants, or IR, Chk1 is phosphorylated by ATM/ATR at serine (S)317 and S345 [52]. Chk1 plays a pivotal role in the regulation of the cell division cycle by phosphorylating proteins such as the cyclin-dependent kinase 1 (Cdk1, also named Cdc2). ATM/ATR → Chk1 signaling leads to the inactivation of a dual-specificity phosphatase, Cdc25, which

consists of three members (A, B, and C). Chk1 phosphorylates Cdc25A at S76, a modification that triggers the degradation of Cdc25A via SCF $\beta$ -TRCP-mediated ubiquitination [53]. Chk1 also associates with Cdc25B and Cdc25C and inactivates these phosphatases through phosphorylation at S309/323 and S216, respectively, in turn causing their nuclear exclusion through association with 14-3-3 [54]. Cdk1 is fully activated in two steps: by phosphorylation at threonine (T)161 via the kinase Cdk7 and by dephosphorylation of phosphor- (p-) tyrosine (Y)15 via the phosphatase Cdc25. Thus, by inhibiting Cdc25, ATM/ATR → Chk1 inactivates Cdk1. Additionally, Chk1 activates the kinase Wee1, which is responsible for the inhibitory phosphorylation of Cdk1 at Y15 [55]. As recently reported, during mitosis Cdk1 phosphorylates Chk1 at S286 and S301; the mitotic phosphorylation of Chk1 is accompanied by the translocation of Chk1 to the cytoplasm [56]. Phosphorylation of Chk1 resulting in its removal from chromatin has been shown to modify cytoplasmic substrates and plays a role at the centrosome during cell division [57].

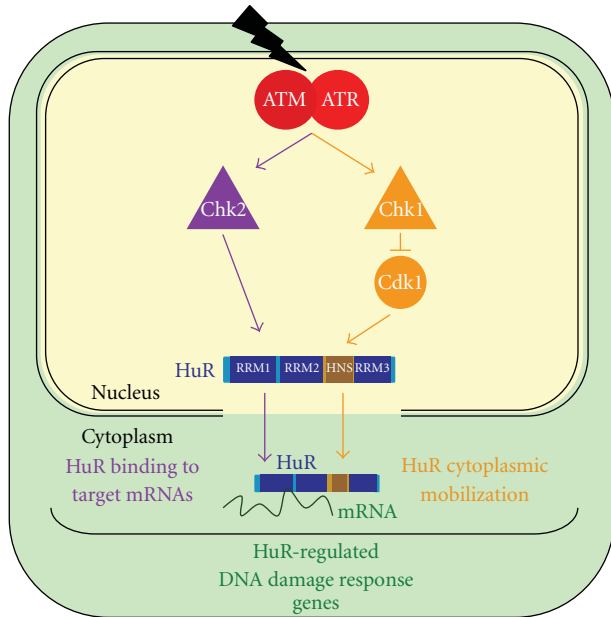


FIGURE 2: Regulation of HuR function by ATM/ATR  $\rightarrow$  Chk1/Chk2. ATM/ATR regulates HuR function through the activation of Chk1 and Chk2. Active Chk1 phosphorylates (and hence inactivates) Cdk1, a kinase that phosphorylates HuR at S202; in turn, unphosphorylated HuR(S202) can be transported to the cytoplasm (orange). Active Chk2 phosphorylates HuR at S88, S100, and T118 (at RRM1 and RRM2); in turn, HuR association with target mRNAs is altered (purple). Jointly, ATM/ATR  $\rightarrow$  Chk1/Chk2 modulates the amount of HuR in the cytoplasm and its interaction with target mRNAs (green).

The cellular DDR dynamically regulates the subcellular presence of HuR. Although predominantly nuclear, exposure to UV or oxidants triggers the accumulation of HuR in the cytoplasm [20, 24, 43], where it modulates the stability and/or translation of numerous target mRNAs, as explained above. We recently reported that HuR was a direct substrate for Cdk1, which phosphorylated HuR at S202 [29]. HuR subcellular localization during the cell division cycle followed fluctuations in Cdk1 activity [29]. The reduction in Cdk1 activity that followed UV irradiation of HeLa cells resulted in the loss of HuR phosphorylation at S202, which in turn promoted the cytoplasmic accumulation of HuR. HuR translocation following Cdk1 inhibition was linked to the nuclear interaction of p-HuR(S202) and 14-3-3 [29]. Inhibition or silencing of Cdk1 enhanced the cytoplasmic level of HuR and increased its interaction with target mRNAs, including those that encode anti-apoptotic proteins like Bcl-2, Mcl-1, and prothymosin- $\alpha$ ; therefore, lowering Cdk1 also diminished the proapoptotic influence of etoposide or staurosporine. Given that DNA damage triggered by many agents reduces Cdk1 activity and increases the cytoplasmic presence of HuR, it is likely that the ATM/ATR  $\rightarrow$  Chk1  $\rightarrow$  Cdk1 pathway is broadly responsible for controlling the cytoplasmic levels of HuR after different types of DDR.

Other DNA damage-activated pathways also affect HuR localization through Cdk1. Activation of the MAP kinase (MAPK) p38 by DNA damage phosphorylates Cdc25B and thus triggers it for degradation. In this manner, p38 affects Cdk1 levels through its influence on Cdc25B abundance. DNA damage induces the cleavage of PKC $\delta$  and generates a constitutively active catalytic fragment termed PKC $\delta$ -cat. PKC $\delta$ -cat can also phosphorylate Cdk1 at Y15, thereby inactivating Cdk1 and inducing G2/M arrest. Moreover, PKC $\delta$  can phosphorylate directly HuR at S221 and S318 (see below), triggering the cytoplasmic translocation of HuR [58]. Overall, DNA damage inactivates Cdk1, which increases cytoplasmic HuR level and thus enhances mRNA stability and translation of DNA damage response proteins.

#### 4. Regulation of HuR by ATM/ATR $\rightarrow$ Chk2

One of the main roles of the ATM/ATR  $\rightarrow$  Chk2 pathway is to induce cell cycle arrest, allowing cells to repair damaged DNA [59]; see [60] for a recent review on Chk2 and Chk1. Activated Chk2 phosphorylates downstream effectors such as p53, BRCA1, and Cdc25 and Cdc25A, which are involved in cellular processes such as apoptosis, DNA repair, and growth arrest [61].

Exposure of human diploid fibroblasts to genotoxic doses of hydrogen peroxide (H<sub>2</sub>O<sub>2</sub>) activated Chk2, which in turn phosphorylated HuR [27]. HuR phosphorylation by Chk2 triggered the dissociation of the longevity and stress-response protein SIRT1 from HuR ribonucleoprotein (RNP) complexes; this dissociation rendered the *SIRT1* mRNA unstable and triggered a decrease in the abundance of *SIRT1* mRNA and protein. Three putative Chk2 phosphorylation sites were identified: HuR residues S88, S100, and T118. In human diploid fibroblasts, mutating S100 to a nonphosphorylatable residue (S100A) promoted the continued association of *SIRT1* mRNA with HuR after oxidative damage, indicating that phosphorylation at residue S100 (located between RRM1 and RRM2) was critical for dissociation of the mRNA [27]. A more stable target transcript, the *prothymosin*  $\alpha$  (*PTMA*) mRNA, also showed increased binding to HuR(S100A) compared to wild-type HuR following H<sub>2</sub>O<sub>2</sub> treatment. Interestingly, mutation of T118 (located within RRM2) to a nonphosphorylatable site (T118A) generally showed reduced binding to all target mRNAs, suggesting that phosphorylation at T118 enhanced HuR binding to target mRNAs. Additional studies are needed to elucidate if other DNA-damaging agents also act upon Chk2 to phosphorylate HuR and how these modifications affect HuR function following genotoxic stress. Further work is also necessary to investigate how other HuR target mRNAs are regulated following HuR phosphorylation by Chk2.

Unexpectedly, HuR phosphorylation by Chk2 in response to heat shock helped to prevent its degradation in this stress paradigm [38]. Following heat shock, the nonphosphorylatable HuR mutants (S88A, S100A, and T118A) were more labile while HuR phosphomimetic mutants (S88D, S100D, and T118D) were more resistant

to degradation [38]. Although details of this process await further analysis, Chk2 phosphorylation of HuR appeared to block HuR proteolysis mediated by ubiquitination at HuR residue K182 [38]. Whether DNA damage also helps to increase HuR stability via Chk2-mediated phosphorylation also warrants careful consideration.

In addition, since Chk2 phosphorylates HuR, and Chk2 mutations influence Chk2 function, it is important to study in detail the influence of Chk2 upon HuR function on target mRNAs, just as was done for *SIRT1* mRNA [27]. Chk2 was found to be mutated in the Li-Fraumeni cancer syndrome and in cancer [62, 63]; these mutations modified Chk2's ability to interact with substrates, Chk2 kinase activity, and Chk2 subcellular localization [59, 64]. How the role of HuR in gene expression is affected in Chk2 mutant cells remains unclear and will be an important aim of future studies.

## 5. Other HuR Kinases Regulated by DNA Damage

Genotoxic damage also activates additional kinases that control HuR function, including protein kinase C (PKC) and the MAPK p38. Although less is known about their influence on HuR function after DNA damage, they are also expected to be intimately linked to this response (Figure 1).

**5.1. PKC.** Protein kinase C (PKC) $\alpha$  was reported to phosphorylate HuR at S158 and S221 while PKC $\delta$  was phosphorylated HuR at S221 and S318 [41, 58, 65, 66]. PKC $\alpha$  and PKC $\delta$  were implicated in the cytoplasmic export of HuR, its enhanced association with target transcripts (e.g., *COX-2*, *cyclin D1*, and *cyclin A* mRNAs), and their stabilization [41, 58, 65, 66]. Doller and coworkers primarily examined the effect of angiotensin II (AngII) in human mesangial cells, uncovering a complex set of regulatory features. However, PKC is a *bona fide* DNA damage response kinase [39, 67]. The influence of PKC on HuR-modulated gene expression is a promising area for future study.

**5.2. p38.** The MAPK p38 plays a key role in the growth arrest that follows exposure to DNA-damaging agents [68–70]. An important mediator of this effect is the cdk inhibitor p21, whose levels increase in response to genotoxins such as IR. The Nebreda laboratory recently showed that following IR, p38 phosphorylated HuR at T118, leading to the cytoplasmic accumulation of HuR, and increased the binding of HuR to *p21* mRNA. *p21* mRNA was thus stabilized, leading to increased expression of p21 protein and to the activation of the G1/S checkpoint [71]. Inhibiting p38 or using the non-phosphorylatable mutant HuR(T118A) prevented the p38-mediated increase in p21 expression after IR, which abrogated the G1/S arrest. The effect of p38 upon HuR translocation and binding to target mRNAs appears to require the p38 downstream substrate MAPKAPK-2 (MK2), as shown in cells responding to taxanes or oxidants [42, 72], although MK2 does not appear to phosphorylate HuR

directly. While a direct influence of p38 on HuR after H<sub>2</sub>O<sub>2</sub> has not been studied to date, the mutant HuR(T118A) also showed reduced binding to *p21* mRNA in H<sub>2</sub>O<sub>2</sub>-treated cells [27], suggesting that H<sub>2</sub>O<sub>2</sub>-activated p38 could similarly change HuR binding to target mRNAs.

**5.3. Additional Kinases Affecting HuR Function.** The AMP-activated protein kinase (AMPK) does not phosphorylate HuR directly, but it phosphorylates and enhances the acetylation of importin  $\alpha$ 1 [42]; in turn, importin  $\alpha$ 1 favors the nuclear import of HuR. Stress conditions that reduce AMPK activity can suppress this import pathway, thus allowing cytoplasmic HuR to accumulate [73]. How DNA damage affects importin  $\alpha$ -mediated localization of HuR remains to be tested directly. Finally, an as-yet unidentified kinase was reported to phosphorylate HuR at S242, promoting its nuclear retention [40, 74] (Figure 1).

## 6. Concluding Remarks

HuR function is regulated by several kinases that play central roles in the DNA damage response, notably those in the ATM/ATR  $\rightarrow$  Chk1/Chk2 pathway. Together with PKC and p38, these signaling cascades govern HuR's cytoplasmic abundance and interaction with target mRNAs. It is intriguing that these kinases converge on a shared substrate protein, HuR, which potently influences gene expression patterns posttranscriptionally. A deeper understanding of the signaling pathways that govern HuR function is helping to elucidate HuR's role in the overall DDR and in the gene expression changes that ensue.

The emergence of HuR a key effector of the DDR program has important biological and clinical implications. First, it suggests that modulation of gene expression by ATM/ATR  $\rightarrow$  Chk1/Chk2 is strongly influenced by HuR; consequently, cells with impaired ATM/ATR  $\rightarrow$  Chk1/Chk2 signaling could express different subsets of proteins due to aberrant HuR function (localization and RNA-binding activity). Second, since lowering HuR levels or preventing its phosphorylation reduced cell survival following genotoxic damage [26, 27, 75], HuR could be a promising target for therapeutic intervention. Third, the high levels of HuR observed in many cancers (which appear to underlie HuR's role in tumorigenesis [76, 77]) could engender an effective DDR in cancer cells. Thus, cancer treatments that do not rely on DNA damage might be advantageous when tumoral HuR levels are elevated.

In sum, the posttranscriptional control of gene expression is particularly important during the DDR, when transcription may be depressed to avoid the synthesis of aberrant transcripts. Through post-translational modification by the kinases reviewed here (primarily ATM/ATR  $\rightarrow$  Chk1/Chk2, but also PKC and p38), HuR helps to orchestrate protein expression from pre-existing mRNAs following damage to DNA. In this capacity, HuR is a key factor that helps to ensure the maintenance of cellular homeostasis following genotoxic injury.

## Abbreviations

ATM: Ataxia-telangiectasia-mutated  
 ATR: ATM- and Rad3-related  
 ELAV: Embryonic lethal abnormal vision  
 IR: Ionizing radiation  
 UV: Ultraviolet irradiation  
 RBP: RNA-binding protein  
 UTR: Untranslated region.

## Acknowledgments

This work was supported by the Intramural Research Program of the National Institute on Aging and National Institutes of Health.

## References

- [1] J. Q. Svejstrup, "Mechanisms of transcription-coupled DNA repair," *Nature Reviews Molecular Cell Biology*, vol. 3, no. 1, pp. 21–29, 2002.
- [2] P. Mitchell and D. Tollervey, "mRNA stability in eukaryotes," *Current Opinion in Genetics and Development*, vol. 10, no. 2, pp. 193–198, 2000.
- [3] G. Orphanides and D. Reinberg, "A unified theory of gene expression," *Cell*, vol. 108, no. 4, pp. 439–451, 2002.
- [4] M. J. Moore, "From birth to death: the complex lives of eukaryotic mRNAs," *Science*, vol. 309, no. 5740, pp. 1514–1518, 2005.
- [5] J. D. Keene, "RNA regulons: coordination of post-transcriptional events," *Nature Reviews Genetics*, vol. 8, no. 7, pp. 533–543, 2007.
- [6] D. P. Bartel, "MicroRNAs: target recognition and regulatory functions," *Cell*, vol. 136, no. 2, pp. 215–233, 2009.
- [7] K. E. Rieger and G. Chu, "Portrait of transcriptional responses to ultraviolet and ionizing radiation in human cells," *Nucleic Acids Research*, vol. 32, no. 16, pp. 4786–4803, 2004.
- [8] B. Haley, T. Paunesku, M. Protic, and G. E. Woloschak, "Response of heterogeneous ribonuclear proteins (hnRNP) to ionising radiation and their involvement in DNA damage repair," *International Journal of Radiation Biology*, vol. 85, no. 8, pp. 643–655, 2009.
- [9] A. Lal, K. Abdelmohsen, and R. Pullmann et al., "Posttranscriptional derepression of GADD45 $\alpha$  by genotoxic stress," *Molecular Cell*, vol. 22, no. 1, pp. 117–128, 2006.
- [10] C. Yang, D. A. Maignel, and F. Carrier, "Identification of nucleolin and nucleophosmin as genotoxic stress-responsive RNA-binding proteins," *Nucleic Acids Research*, vol. 30, no. 10, pp. 2251–2260, 2002.
- [11] R. Busà, R. Geremia, and C. Sette, "Genotoxic stress causes the accumulation of the splicing regulator Sam68 in nuclear foci of transcriptionally active chromatin," *Nucleic Acids Research*, vol. 38, no. 9, pp. 3005–3018, 2010.
- [12] M. N. Hinman and H. Lou, "Diverse molecular functions of Hu proteins," *Cellular and Molecular Life Sciences*, vol. 65, no. 20, pp. 3168–3181, 2008.
- [13] J. D. Keene, "Why is Hu where? Shuttling of early-response-gene messenger RNA subsets," *Proceedings of the National Academy of Sciences of the United States of America*, vol. 96, no. 1, pp. 5–7, 1999.
- [14] C. M. Brennan and J. A. Steitz, "HuR and mRNA stability," *Cellular and Molecular Life Sciences*, vol. 58, no. 2, pp. 266–277, 2001.
- [15] X. C. Fan and J. A. Steitz, "HNS, a nuclear-cytoplasmic shuttling sequence in HuR," *Proceedings of the National Academy of Sciences of the United States of America*, vol. 95, no. 26, pp. 15293–15298, 1998.
- [16] S. Güttinger, P. Mühlhäusser, R. Koller-Eichhorn, J. Brennecke, and U. Kutay, "Transporting functions as importin and mediates nuclear import of HuR," *Proceedings of the National Academy of Sciences of the United States of America*, vol. 101, no. 9, pp. 2918–2923, 2004.
- [17] I.-E. Gallouzi and J. A. Steitz, "Delineation of mRNA export pathways by the use of cell-permeable peptides," *Science*, vol. 294, no. 5548, pp. 1895–1901, 2001.
- [18] A. Rebane, A. Aab, and J. A. Steitz, "Transportins 1 and 2 are redundant nuclear import factors for hnRNP A1 and HuR," *RNA*, vol. 10, no. 4, pp. 590–599, 2004.
- [19] N. S. Levy, S. Chung, H. Furneaux, and A. P. Levy, "Hypoxic stabilization of vascular endothelial growth factor mRNA by the RNA-binding protein HuR," *Journal of Biological Chemistry*, vol. 273, no. 11, pp. 6417–6423, 1998.
- [20] W. Wang, H. Furneaux, and H. Cheng et al., "HuR regulates p21 mRNA stabilization by UV light," *Molecular and Cellular Biology*, vol. 20, no. 3, pp. 760–769, 2000.
- [21] W. Wang, M. C. Caldwell, S. Lin, H. Furneaux, and M. Gorospe, "HuR regulates cyclin A and cyclin B1 mRNA stability during cell proliferation," *EMBO Journal*, vol. 19, no. 10, pp. 2340–2350, 2000.
- [22] L. B. Nabors, G. Y. Gillespie, L. Harkins, and P. H. King, "HuR, a RNA stability factor, is expressed in malignant brain tumors and binds to adenine- and uridine-rich elements within the 3' untranslated regions of cytokine and angiogenic factor mRNAs," *Cancer Research*, vol. 61, no. 5, pp. 2154–2161, 2001.
- [23] M. Kullmann, U. Göpfert, B. Siewe, and L. Hengst, "ELAV/Hu proteins inhibit p27 translation via an IRES element in the p27 5'UTR," *Genes and Development*, vol. 16, no. 23, pp. 3087–3099, 2002.
- [24] K. Mazan-Mamczarz, S. Galbán, and I. López de Silanes et al., "RNA-binding protein HuR enhances p53 translation in response to ultraviolet light irradiation," *Proceedings of the National Academy of Sciences of the United States of America*, vol. 100, no. 14, pp. 8354–8359, 2003.
- [25] A. Lal, K. Mazan-Mamczarz, T. Kawai, X. Yang, J. L. Martindale, and M. Gorospe, "Concurrent versus individual binding of HuR and AUF1 to common labile target mRNAs," *EMBO Journal*, vol. 23, no. 15, pp. 3092–3102, 2004.
- [26] A. Lal, T. Kawai, X. Yang, K. Mazan-Mamczarz, and M. Gorospe, "Antiapoptotic function of RNA-binding protein HuR effected through prothymosin  $\alpha$ ," *EMBO Journal*, vol. 24, no. 10, pp. 1852–1862, 2005.
- [27] K. Abdelmohsen, R. Pullmann Jr., and A. Lal et al., "Phosphorylation of HuR by Chk2 regulates SIRT1 expression," *Molecular Cell*, vol. 25, no. 4, pp. 543–557, 2007.
- [28] K. Abdelmohsen, A. Lal, H. H. Kim, and M. Gorospe, "Post-transcriptional orchestration of an anti-apoptotic program by HuR," *Cell Cycle*, vol. 6, no. 11, pp. 1288–1292, 2007.
- [29] H. H. Kim, K. Abdelmohsen, and A. Lal et al., "Nuclear HuR accumulation through phosphorylation by Cdk1," *Genes and Development*, vol. 22, no. 13, pp. 1804–1815, 2008.
- [30] H. H. Kim, Y. Kuwano, S. Srikantan, E. K. Lee, J. L. Martindale, and M. Gorospe, "HuR recruits let-7/RISC to repress c-Myc expression," *Genes and Development*, vol. 23, no. 15, pp. 1743–1748, 2009.

- [31] I. López de Silanes, M. Zhan, A. Lal, X. Yang, and M. Gorospe, "Identification of a target RNA motif for RNA-binding protein HuR," *Proceedings of the National Academy of Sciences of the United States of America*, vol. 101, no. 9, pp. 2987–2992, 2004.
- [32] I. López de Silanes, J. Fan, and X. Yang et al., "Role of the RNA-binding protein HuR in colon carcinogenesis," *Oncogene*, vol. 22, no. 46, pp. 7146–7154, 2003.
- [33] M. Gorospe, "HuR in the mammalian genotoxic response: post-transcriptional multitasking," *Cell Cycle*, vol. 2, no. 5, pp. 412–414, 2003.
- [34] A. Figueroa, A. Cuadrado, and J. Fan et al., "Role of HuR in skeletal myogenesis through coordinate regulation of muscle differentiation genes," *Molecular and Cellular Biology*, vol. 23, no. 14, pp. 4991–5004, 2003.
- [35] K. van der Giessen, S. Di-Marco, E. Clair, and I. E. Gallouzi, "RNAi-mediated HuR depletion leads to the inhibition of muscle cell differentiation," *Journal of Biological Chemistry*, vol. 278, no. 47, pp. 47119–47128, 2003.
- [36] V. Katsanou, O. Papadaki, and S. Milatos et al., "HuR as a negative posttranscriptional modulator in inflammation," *Molecular Cell*, vol. 19, no. 6, pp. 777–789, 2005.
- [37] K. Abdelmohsen, Y. Kuwano, H. H. Kim, and M. Gorospe, "Posttranscriptional gene regulation by RNA-binding proteins during oxidative stress: implications for cellular senescence," *Biological Chemistry*, vol. 389, no. 3, pp. 243–255, 2008.
- [38] K. Abdelmohsen, S. Srikantan, and X. Yang et al., "Ubiquitin-mediated proteolysis of HuR by heat shock," *EMBO Journal*, vol. 28, no. 9, pp. 1271–1282, 2009.
- [39] A. Basu, "Involvement of protein kinase C- $\delta$  in DNA damage-induced apoptosis," *Journal of Cellular and Molecular Medicine*, vol. 7, no. 4, pp. 341–350, 2003.
- [40] H. H. Kim, X. Yang, Y. Kuwano, and M. Gorospe, "Modification at HuR(S242) alters HuR localization and proliferative influence," *Cell Cycle*, vol. 7, no. 21, pp. 3371–3377, 2008.
- [41] A. Doller, A. Huwiler, R. Müller, H. H. Radeke, J. Pfeilschifter, and W. Eberhardt, "Protein kinase C $\alpha$ -dependent phosphorylation of the mRNA-stabilizing factor HuR: implications for posttranscriptional regulation of cyclooxygenase-2," *Molecular Biology of the Cell*, vol. 18, no. 6, pp. 2137–2148, 2007.
- [42] K. Subbaramaiah, T. P. Marmo, D. A. Dixon, and A. J. Dannenberg, "Regulation of cyclooxygenase-2 mRNA stability by taxanes: evidence for involvement of p38, MAPKAPK-2, and HuR," *Journal of Biological Chemistry*, vol. 278, no. 39, pp. 37637–37647, 2003.
- [43] Y. Kuwano, H. H. Kim, and K. Abdelmohsen et al., "MKP-1 mRNA stabilization and translational control by RNA-binding proteins HuR and NF90," *Molecular and Cellular Biology*, vol. 28, no. 14, pp. 4562–4575, 2008.
- [44] R. Mazroui, S. Di Marco, and E. Clair et al., "Caspase-mediated cleavage of HuR in the cytoplasm contributes to pp32/PHAP-I regulation of apoptosis," *Journal of Cell Biology*, vol. 180, no. 1, pp. 113–127, 2008.
- [45] H. Niida and M. Nakanishi, "DNA damage checkpoints in mammals," *Mutagenesis*, vol. 21, no. 1, pp. 3–9, 2006.
- [46] M. B. Kastan and D.-S. Lim, "The many substrates and functions of ATM," *Nature Reviews Molecular Cell Biology*, vol. 1, no. 3, pp. 179–186, 2000.
- [47] W. A. Cliby, C. J. Roberts, and K. A. Cimprich et al., "Overexpression of a kinase-inactive ATR protein causes sensitivity to DNA-damaging agents and defects in cell cycle checkpoints," *EMBO Journal*, vol. 17, no. 1, pp. 159–169, 1998.
- [48] R. S. Tibbetts, K. M. Brumbaugh, and J. M. Williams et al., "A role for ATR in the DNA damage-induced phosphorylation of p53," *Genes and Development*, vol. 13, no. 2, pp. 152–157, 1999.
- [49] B. Shiotani and L. Zou, "Single-stranded DNA orchestrates an ATM-to-ATR switch at DNA breaks," *Molecular Cell*, vol. 33, no. 5, pp. 547–558, 2009.
- [50] Y. Shiloh and M. B. Kastan, "ATM: genome stability, neuronal development, and cancer cross paths," *Advances in Cancer Research*, vol. 83, pp. 209–254, 2001.
- [51] N. Motoyama and K. Naka, "DNA damage tumor suppressor genes and genomic instability," *Current Opinion in Genetics and Development*, vol. 14, no. 1, pp. 11–16, 2004.
- [52] H. Zhao and H. Piwnica-Worms, "ATR-mediated checkpoint pathways regulate phosphorylation and activation of human Chk1," *Molecular and Cellular Biology*, vol. 21, no. 13, pp. 4129–4139, 2001.
- [53] J. Jin, T. Shirogane, and L. Xu et al., "SCF $\beta$ -TRCP links Chk1 signaling to degradation of the Cdc25A protein phosphatase," *Genes and Development*, vol. 17, no. 24, pp. 3062–3074, 2003.
- [54] M. Donzelli and G. F. Draetta, "Regulating mammalian checkpoints through Cdc25 inactivation," *EMBO Reports*, vol. 4, no. 7, pp. 671–677, 2003.
- [55] J. Lee, A. Kumagai, and W. G. Dunphy, "Positive regulation of Wee1 by Chk1 and 14-3-3 proteins," *Molecular Biology of the Cell*, vol. 12, no. 3, pp. 551–563, 2001.
- [56] M. Enomoto, H. Goto, and Y. Tomoro et al., "Novel positive feedback loop between Cdk1 and Chk1 in the nucleus during G2/M transition," *Journal of Biological Chemistry*, vol. 284, no. 49, pp. 34223–34230, 2009.
- [57] V. A. J. Smits, P. M. Reaper, and S. P. Jackson, "Rapid PIKK-dependent release of Chk1 from chromatin promotes the DNA-damage checkpoint response," *Current Biology*, vol. 16, no. 2, pp. 150–159, 2006.
- [58] A. Doller, E.-S. Akool, and A. Huwiler et al., "Posttranslational modification of the AU-rich element binding protein HuR by protein kinase C $\delta$  elicits angiotensin II-induced stabilization and nuclear export of cyclooxygenase 2 mRNA," *Molecular and Cellular Biology*, vol. 28, no. 8, pp. 2608–2625, 2008.
- [59] B.-B. S. Zhou and S. J. Elledge, "The DNA damage response: putting checkpoints in perspective," *Nature*, vol. 408, no. 6811, pp. 433–439, 2000.
- [60] H. C. Reinhardt and M. B. Yaffe, "Kinases that control the cell cycle in response to DNA damage: Chk1, Chk2, and MK2," *Current Opinion in Cell Biology*, vol. 21, no. 2, pp. 245–255, 2009.
- [61] J. Bartek, J. Falck, and J. Lukas, "Chk2 kinase—a busy messenger," *Nature Reviews Molecular Cell Biology*, vol. 2, no. 12, pp. 877–886, 2001.
- [62] D. W. Bell, J. M. Varley, and T. E. Szydlo et al., "Heterozygous germ line hCHK2 mutations in Li-Fraumeni syndrome," *Science*, vol. 286, no. 5449, pp. 2528–2531, 1999.
- [63] P. Vahteristo, J. Bartkova, and H. Eerola et al., "A CHEK2 genetic variant contributing to a substantial fraction of familial breast cancer," *American Journal of Human Genetics*, vol. 71, no. 2, pp. 432–438, 2002.
- [64] X. Wu, S. R. Webster, and J. Chen, "Characterization of tumor-associated Chk2 mutations," *Journal of Biological Chemistry*, vol. 276, no. 4, pp. 2971–2974, 2001.
- [65] A. Doller, K. Schlepckow, H. Schwalbe, J. Pfeilschifter, and W. Eberhardt, "Tandem phosphorylation of serines 221 and 318 by protein kinase C $\delta$  coordinates mRNA binding and nucleocytoplasmic shuttling of HuR," *Molecular and Cellular Biology*, vol. 30, no. 6, pp. 1397–1410, 2010.

- [66] A. Doller, J. Pfeilschifter, and W. Eberhardt, "Signalling pathways regulating nucleo-cytoplasmic shuttling of the mRNA-binding protein HuR," *Cellular Signalling*, vol. 20, no. 12, pp. 2165–2173, 2008.
- [67] K. Yoshida, "Nuclear trafficking of pro-apoptotic kinases in response to DNA damage," *Trends in Molecular Medicine*, vol. 14, no. 7, pp. 305–313, 2008.
- [68] Á. Molnár, A. M. Theodoras, L. I. Zon, and J. M. Kyriakis, "Cdc42Hs, but not Rac1, inhibits serum-stimulated cell cycle progression at G1/S through a mechanism requiring p38/RK," *Journal of Biological Chemistry*, vol. 272, no. 20, pp. 13229–13235, 1997.
- [69] A. Cuenda and S. Rousseau, "p38 MAP-kinases pathway regulation, function and role in human diseases," *Biochimica et Biophysica Acta*, vol. 1773, no. 8, pp. 1358–1375, 2007.
- [70] T. M. Thornton and M. Rincon, "Non-classical p38 map kinase functions: cell cycle checkpoints and survival," *International Journal of Biological Sciences*, vol. 5, no. 1, pp. 44–52, 2009.
- [71] V. Lafarga, A. Cuadrado, I. López de Silanes, R. Bengoechea, O. Fernandez-Capetillo, and A. R. Nebreda, "p38 mitogen-activated protein kinase- and HuR-dependent stabilization of p21Cip1 mRNA mediates the G1/S checkpoint," *Molecular and Cellular Biology*, vol. 29, no. 16, pp. 4341–4351, 2009.
- [72] H. Tran, F. Maurer, and Y. Nagamine, "Stabilization of urokinase and urokinase receptor mRNAs by HuR is linked to its cytoplasmic accumulation induced by activated mitogen-activated protein kinase-activated protein kinase 2," *Molecular and Cellular Biology*, vol. 23, no. 20, pp. 7177–7188, 2003.
- [73] W. Wang, X. Yang, and T. Kawai et al., "AMP-activated protein kinase-regulated phosphorylation and acetylation of importin  $\alpha$ 1: involvement in the nuclear import of RNA-binding protein HuR," *Journal of Biological Chemistry*, vol. 279, no. 46, pp. 48376–48388, 2004.
- [74] H. H. Kim and M. Gorospe, "Phosphorylated HuR shuttles in cycles," *Cell Cycle*, vol. 7, no. 20, pp. 3124–3126, 2008.
- [75] K. Abdelmohsen, S. Srikantan, Y. Kuwano, and M. Gorospe, "miR-519 reduces cell proliferation by lowering RNA-binding protein HuR levels," *Proceedings of the National Academy of Sciences of the United States of America*, vol. 105, no. 51, pp. 20297–20302, 2008.
- [76] K. Abdelmohsen, M. M. Kim, S. Srikantan, et al., "miR-519 suppresses tumor growth by reducing HuR levels," *Cell Cycle*, vol. 9, no. 7, pp. 1354–1359, 2010.
- [77] K. Abdelmohsen and M. Gorospe, "Post-transcriptional regulation of cancer traits by HuR," *WIRES RNA*. In press.

## Review Article

# DNA Mismatch Repair in Eukaryotes and Bacteria

**Kenji Fukui**

RIKEN SPring-8 Center, Harima Institute, 1-1-1 Kouto, Sayo-cho, Sayo-gun, Hyogo 679-5148, Japan

Correspondence should be addressed to Kenji Fukui, k.fukui@spring8.or.jp

Received 14 May 2010; Accepted 24 June 2010

Academic Editor: Shigenori Iwai

Copyright © 2010 Kenji Fukui. This is an open access article distributed under the Creative Commons Attribution License, which permits unrestricted use, distribution, and reproduction in any medium, provided the original work is properly cited.

DNA mismatch repair (MMR) corrects mismatched base pairs mainly caused by DNA replication errors. The fundamental mechanisms and proteins involved in the early reactions of MMR are highly conserved in almost all organisms ranging from bacteria to human. The significance of this repair system is also indicated by the fact that defects in MMR cause human hereditary nonpolyposis colon cancers as well as sporadic tumors. To date, 2 types of MMRs are known: the human type and *Escherichia coli* type. The basic features of the former system are expected to be universal among the vast majority of organisms including most bacteria. Here, I review the molecular mechanisms of eukaryotic and bacterial MMR, emphasizing on the similarities between them.

## 1. Introduction

DNA mismatch repair (MMR) is a highly conserved DNA repair system (Table 1) that greatly contributes to maintain genome stability through the correction of mismatched base pairs. The major source of mismatched base pairs is replication error, although it can arise also from other biological processes [1]. In *Escherichia coli*, MMR increases the accuracy of DNA replication by 20–400-fold [2]. Mutations and epigenetic silencing in MMR genes have been implicated in up to 90% of human hereditary nonpolyposis colon cancers [3–8], indicating the significance of this repair system. Postreplicative MMR is performed by the long-patch MMR mechanism in which multiple proteins are involved and a relatively long tract of the oligonucleotide is excised during the repair reaction [9, 10]. In contrast, particular kinds of mismatched base pairs are repaired through very short-patch MMR in which a short oligonucleotide tract is excised to remove the lesion [11–13]. In this paper, I refer to long-patch MMR as MMR.

Currently, 2 types of MMR mechanisms have been elucidated: one is expected to be employed by eukaryotes and the majority of bacteria, and the other is specific to *E. coli* and closely related bacteria. As shown in Figures 1(a) and 1(b), MMR in eukaryotes and most bacteria directs the repair to the error-containing strand of the mismatched duplex by recognizing the strand discontinuities. On the other hand,

as shown in Figure 1(c), *E. coli* MMR reads the absence of methylation as a strand discrimination signal. In both MMR systems, strand discrimination is conducted by nicking endonucleases. MutL homologues from eukaryotes and most bacteria incise the discontinuous strand to introduce the entry or termination point for the excision reaction. In *E. coli*, MutH nicks the unmethylated strand of the duplex to generate the entry point of excision.

Here, I first review the overviews of MMR systems in *E. coli*, eukaryotes, and the majority of bacteria. Second, I refer to the molecular features of MutS and MutL homologues, the key enzymes in MMR. Third, molecular mechanisms for strand-discrimination and excision reaction are discussed. Finally, I introduce the cellular functions of MMR other than postreplication mismatch correction.

## 2. Overview of Methyl-Directed MMR in *E. coli*

The *E. coli* MMR system has been well characterized and reconstituted using recombinant proteins (Figure 1(c)) [14]. In this system, a mismatched base is recognized by a MutS homodimer. A MutL homodimer interacts with the MutS-DNA complex, and then a MutH restriction endonuclease is activated by MutL. The MMR system needs to discriminate the newly-synthesized/error-containing strand; however, a mismatched base itself contains no such signal. The *E. coli*

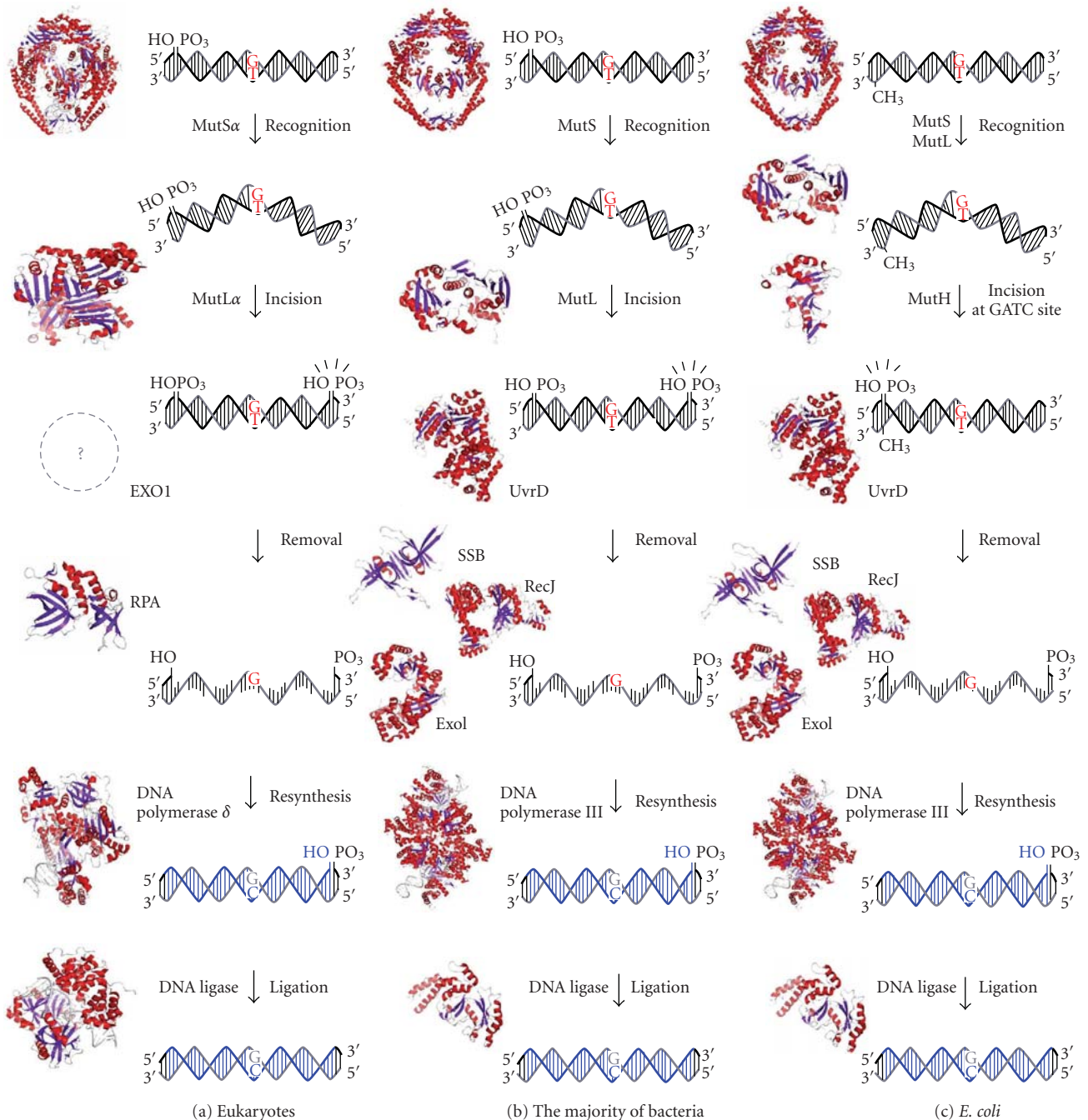


FIGURE 1: A schematic representation of MMR pathway models. (a) Eukaryotic MMR. A DNA mismatch is generated by the misincorporation of a base during DNA replication. MutS $\alpha$  recognizes base-base mismatches and MutL $\alpha$  nicks the 3'- or 5'-side of the mismatched base on the discontinuous strand. The resulting DNA segment is excised by the EXO1 exonuclease, in cooperation with the single-stranded DNA-binding protein RPA. The DNA strand is resynthesized by DNA polymerase  $\delta$  and DNA ligase 1. (b) MMR in *mutH*-less bacteria. Mismatched bases are recognized by MutS. After the incision of discontinuous strand by MutL, the error-containing DNA strand is removed by the cooperative functions of DNA helicases, such as UvrD, the exonucleases RecJ and ExoI, and the single-stranded DNA-binding protein SSB. DNA polymerase III and DNA ligase fill the gap to complete the repair. (c) *E. coli* MMR. MutS recognizes mismatched bases, and MutL interacts with and stabilizes the complex. Then, MutH endonuclease is activated to incise the unmethylated GATC site to create an entry point for the excision reaction. DNA helicase, a single-stranded DNA-binding protein, and several exonucleases are involved in the excision reaction. PDB IDs of crystal structures in this figure are 2O8B (human MutS $\alpha$ ), 1H7S (human MutL $\alpha$ ), 1L1O (human RPA), 3IAY (human DNA polymerase  $\delta$ ), 1X9N (human DNA ligase 1), 1E3M (bacterial MutS), 1B63 (bacterial MutL), 2AZO (*E. coli* MutH), 2ISI (bacterial UvrD), 2ZXO (bacterial RecJ), 3C95 (bacterial ExoI), 2CWA (bacterial SSB), 2HQA (bacterial DNA polymerase III), and 2OWO (bacterial DNA ligase).

TABLE 1: Distribution of MMR proteins.

Molecular function	<i>Thermus thermophilus</i>	<i>Escherichia coli</i>	<i>Saccharomyces cerevisiae</i>	<i>Homo sapiens</i>
Mismatch recognition	MutS	MutS	MutS $\alpha$ (MSH2/MSH6) MutS $\beta$ (MSH2/MSH3)	MutS $\alpha$ (MSH2/MSH6) MutS $\beta$ (MSH2/MSH3)
Strand incision	$\beta$ -clamp* <sup>1</sup> clamp-loader* <sup>1</sup>	—	PCNA RFC	PCNA RFC
Strand incision	MutL	MutH	MutL $\alpha$ (MLH1/PMS1) MutL $\gamma$ * <sup>2</sup> (MLH1/MLH3)	MutL $\alpha$ (MLH1/PMS2) MutL $\gamma$ * <sup>2</sup> (MLH1/MLH3)
Match making	—	—	—	—
Match making	MutL	MutL	MutL $\alpha$ (MLH1/PMS1) MutL $\beta$ (MLH1/MLH2) MutL $\gamma$ (MLH1/MLH3)	MutL $\alpha$ (MLH1/PMS2) MutL $\beta$ (MLH1/PMS1) MutL $\gamma$ (MLH1/MLH3)
Strand excision (single-stranded DNA-binding)	SSB	SSB	RPA	RPA
Strand excision (exonuclease)	RecJ ExoI	RecJ ExoI ExoVII ExoX	EXO1* <sup>3</sup>	EXO1* <sup>3</sup>
Strand excision (helicase)	UvrD	UvrD	—	—
Repair synthesis	DNA polymerase III	DNA polymerase III	DNA polymerase $\delta$	DNA polymerase $\delta$

\*<sup>1</sup>The involvement of bacterial clamp and clamp-loader in the strand incision reaction has not yet been confirmed. \*<sup>2</sup>It is demonstrated that the endonuclease motif in MLH3 is responsible for *in vivo* MMR [83]; however, the endonuclease activity of MutL $\gamma$  has not yet been confirmed biochemically. \*<sup>3</sup>In yeast and human, EXO1 has the 5'-flap endonuclease activity in addition to 5'-3' exonuclease activity.

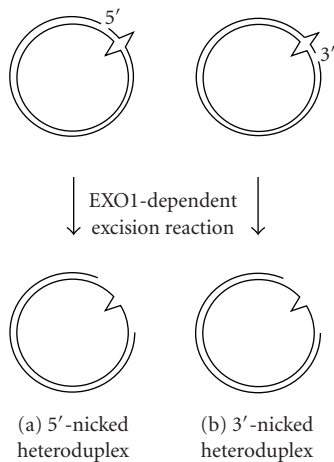


FIGURE 2: Bidirectionality of eukaryotic MMR. The 5'-nicked (a) and 3'-nicked (b) heteroduplexes are used as model substrate. The shorter path is chosen to remove the mismatched base. The 5'-3' exonuclease activity of EXO1 is required for excision reaction in both 5'- and 3'-nicked heteroduplexes.

MMR system utilizes the absence of methylation at the restriction site to direct the repair to the newly synthesized strand. MutH nicks the unmethylated strand at the hemimethylated GATC site to introduce an entry point for the excision reaction [15–17]. The error-containing strand is removed by helicases [18] and exonucleases [19–21], and a new strand is synthesized by DNA polymerase III and ligase. The absence of methylation serves as a signal for the

discrimination of the error-containing strand, and hence, *E. coli* MMR is called methyl-directed MMR. Although homologues of *E. coli* MutS and MutL exist in almost all organisms, no homologue of *E. coli* MutH has been identified in the majority of organisms including eukaryotes and most bacteria (Table 1) [22].

### 3. Overview of Eukaryotic MMR

In eukaryotes, strand discontinuity serves as a signal that directs MMR to the discontinuous strand of a mismatched duplex (Figure 1(a)). In newly synthesized strands, discontinuities can exist as 3'-ends or termini of Okazaki fragments. These termini of the DNA strand may function as strand discrimination signals *in vivo*. For the biochemical characterization of eukaryotic MMR, nicked plasmid DNAs have been used as a model substrate containing a strand discontinuity, on which several reviews elaborated [10, 23, 24]. For this assay system, the shorter path from a nick to the mismatch is removed by the excision reaction, indicating that 5'- and 3'-directed MMRs are distinct (Figure 2) [25–27]. Intriguingly, the 5'-3' exonuclease activity of exonuclease 1 (EXO1) is required for both 5'- and 3'-directed strand removals [28, 29]. The reason for the apparently contradictory requirement of 5'-3' exonuclease activity for the 3'-discontinuity-directed excision reaction had been unknown because it was thought that strand discontinuity was also the entry point for excision reaction. This issue was resolved by the discovery that the human MutL homologue MutL $\alpha$  (MLH1-PMS2 heterodimer) and yeast MutL $\alpha$  (MLH1-PMS1 heterodimer)

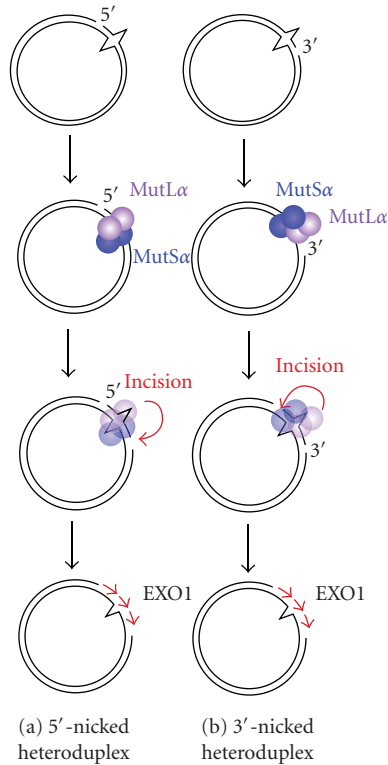


FIGURE 3: The 5'-nick-(a) and 3'-nick-(b) directed eukaryotic MMR. After recognition of a mismatched base by MutS $\alpha$ , MutL $\alpha$  incises the discontinuous strand of the heteroduplex in a mismatch-MutS $\alpha$ -, PCNA-, RFC-, and ATP-dependent manner [10, 30, 31]. Incisions by MutL $\alpha$  occur dominantly on the distal side of the mismatched base relative to the pre-existed strand break although it can also occur proximal to the mismatch [30].

harbor latent endonuclease activity that nicks the discontinuous strand of the mismatched duplex in a MutS $\alpha$ -, PCNA-, RFC-, and ATP-dependent manner (Figure 3) [10, 30, 31]. In eukaryotic 5'- and 3'-directed MMR, the 3'- and 5'-sides of a mismatch are incised, respectively, by MutL $\alpha$ , and the 5'-3' exonuclease activity of EXO1 removes the DNA segment spanning the mismatch, that is, in eukaryotic 3'-directed MMR, the preexisting strand discontinuity does not serve as an entry point for the excision reaction, and the entry point is introduced by the endonuclease activity of MutL $\alpha$  (Figure 3(b)).

Intriguingly, MutL $\alpha$  is essential for 3'-nick-directed MMR but it is dispensable for 5'-nick-directed MMR, although MutL $\alpha$  possesses an enhancing effect on 5'-nick-directed MMR [32, 33]. This result indicates that there is an alternative pathway for 5'-nick-directed MMR. *In vitro* experiments suggest that MutL $\alpha$ -independent 5'-nick-directed human MMR requires at least 3 proteins, MutS $\alpha$ , EXO1, and replication protein A (RPA) [32].

#### 4. Overview of MMR in *mutH*-Less Bacteria

The DQHA(X)<sub>2</sub>E(X)<sub>4</sub> motif in the C-terminal domain of the PMS2 subunit of human MutL $\alpha$  comprises a metal-binding

site that is essential for the endonuclease activity of MutL $\alpha$  and MMR activity of nuclear extract [30]. Except for *E. coli* and closely related bacteria, most *mutH*-lacking bacteria possess MutL homologues that contain this metal-binding motif [30, 34]. Therefore, the molecular mechanism established on the basis of the results obtained from eukaryotic MMR systems is expected to be universal for organisms lacking *mutH*. In agreement with this prediction, several studies demonstrated that MutL homologues from *mutH*-less bacteria, for example, *Thermus thermophilus*, *Aquifex aeolicus*, and *Neisseria gonorrhoeae*, possess endonuclease activity that is dependent on the DQHA(X)<sub>2</sub>E(X)<sub>4</sub> motif [34–36]. Furthermore, in *T. thermophilus*, it is clarified that the endonuclease activity of MutL is essential for *in vivo* DNA repair activity [34]. Thus, the molecular mechanism of MMR in *mutH*-less bacteria is expected to resemble that of eukaryotic one (Figure 1(b)).

#### 5. Molecular Functions of MutS Homologues

The amino acid sequence of MutS is highly conserved among bacteria regardless of the presence and absence of *mutH* [37–39]. Bacterial MutS forms a homodimer and recognizes mispaired bases and short insertion/deletion loops [9, 40, 41]. Eukaryotes possess several mismatch-recognizing MutS homologues: MSH2, MSH3, and MSH6. These 3 homologues contain amino acid sequences homologous to bacterial MutS and form 2 heterodimers, namely, MutS $\alpha$  (MSH2/MSH6) and MutS $\beta$  (MSH2/MSH3). MutS $\alpha$  recognizes single base-base mismatches and short insertion/deletion loops while MutS $\beta$  is responsible for the repair of relatively large insertion/deletion loops that contain ~16-mer excess nucleotides [42].

The crystal structures of C-terminal dimerization domain-deleted bacterial MutS [37, 38] and human MutS $\alpha$  [43] were solved in complex with mismatched DNA (Figure 4). The structures revealed that the mismatch-recognition mechanisms of bacterial MutS and eukaryotic MutS $\alpha$  fundamentally resemble each other. The bacterial MutS homodimer/DNA complex shows a functionally asymmetric protein dimer in which only 1 of the 2 subunits recognizes the mismatched or unpaired base. Thus, although bacterial MutS binds to double-stranded DNA as a homodimer, its functionality is heterodimeric.

Bacterial MutS and human MutS $\alpha$  recognize the heteroduplex by stacking the mismatched base with a phenylalanine residue (Phe36 and Phe432 in *E. coli* MutS and human MSH6, resp.) that is intercalated from the minor groove side [38] (Figure 4). This phenylalanine residue is perfectly conserved among bacterial MutS homologues and eukaryotic MSH6 [37], and the alteration of this residue to an alanine results in a drastic decrease in the mismatch-recognition ability of *Thermus aquaticus* MutS [49]. The adjacent glutamate residue (Glu38 and Glu434 in *E. coli* MutS and human MSH6, resp.) also plays a central role in mismatch recognition by forming a hydrogen bond with the mismatched base (Figures 5(a)–3(c)) [38]. This glutamate

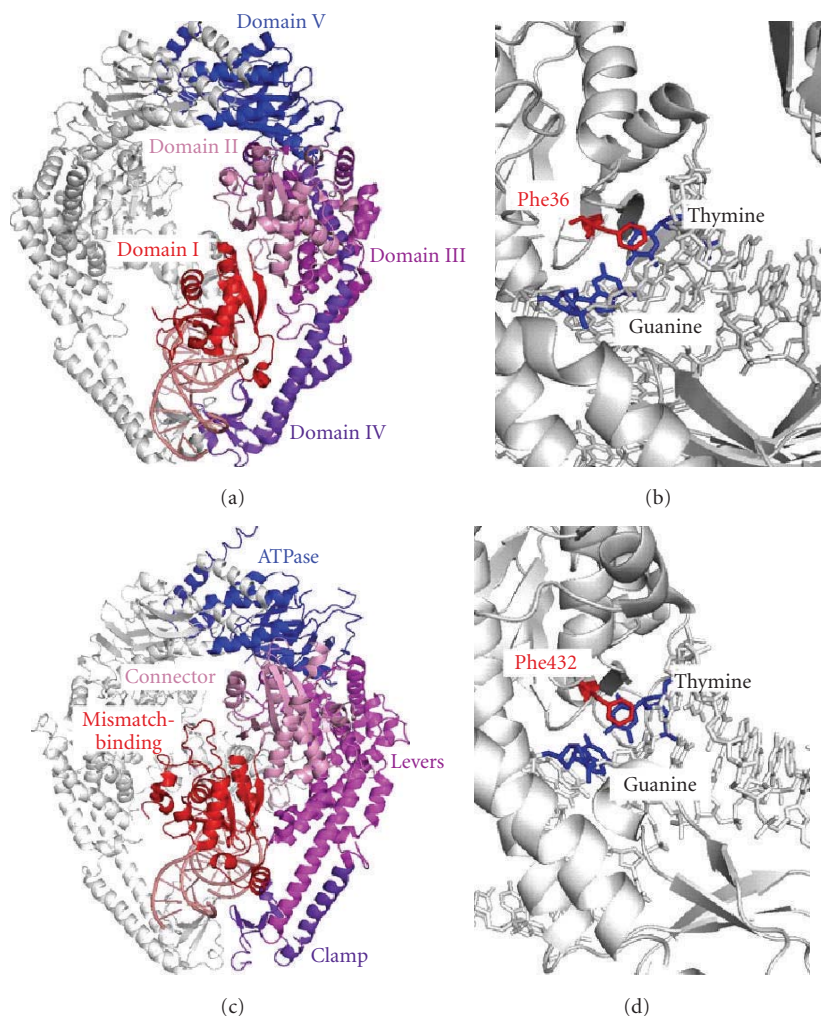


FIGURE 4: Crystal structures of MutS-mismatch complex. (a) Crystal structure of *E. coli* MutS bound to a G:T-mismatched heteroduplex (PDB ID: 1E3M). One of the 2 subunits of *E. coli* MutS is shown in color. DNA is shown in salmon. Domains I, II, III, IV, and V are shown in red, pink, violet, purple blue, and blue, respectively. Domains I, IV, and V are responsible for mismatch recognition, double-stranded DNA binding, and dimerization/ATP binding, respectively. (b) The mismatch-recognition site in *E. coli* MutS-G:T mismatch complex. The mismatch-recognizing phenylalanine residue (Phe36) and G:T mismatch are shown in red and blue, respectively. (c) Crystal structure of human MutS $\alpha$  (PDB ID: 2O8B), which is comprised of full-length MSH2 and a protease-resistant fragment of MSH6 lacking the first 340 amino acid residues. MSH2 is shown in white and MSH6 is in color. Mismatch-binding, Connector, Levers, Clamp, and ATPase domains are colored in red, pink, magenta, purple, and blue, respectively. (d) The mismatch-recognition site in human MutS $\alpha$ -G:T mismatch complex. Phe432 and G:T mismatch is shown in red and blue, respectively.

residue is also conserved among bacterial MutS and eukaryotic MSH6 [37], and the mutation of this glutamate into an alanine or a glutamine abolishes *in vivo* MMR activity [50–52]. Elimination of this hydrogen bond by replacing the thymidine with 2,4-difluorotoluene, which lacks the N3, resulted in the decrease in mismatch selectivities of *E. coli* MutS and yeast MutS $\alpha$  [50, 52].

The excellent crystallographic analyses of *E. coli* MutS complexes with various kinds of mismatched heteroduplexes remarkably enhanced our understanding of the mismatch recognition mechanism at an atomic resolution [53]. MutS recognizes a wide range of mismatches in a common manner. Heteroduplexes bound by MutS homologues are sharply kinked with the minor groove wide-opened (Figure 5(d)),

which allows the mismatched base to be in close contact with the phenylalanine and the glutamate residues of the mismatch-recognition domain. The carbonyl oxygen (OE2) of Glu38 in *E. coli* MutS forms a hydrogen bond with N3 of mismatched pyrimidine or N7 of mismatched purine base [53]. It is expected that N7 of mismatched purine or OE2 of the glutamate is protonated. As previously discussed, this might be the reason why the mutation of Glu38 to Gln in *E. coli* MutS eliminates MMR activity though Gln also can form hydrogen bonds [53]. The acidity of the glutamate but not glutamine might be suitable for the required  $pK_a$  shift. Interestingly, E38A mutant of *E. coli* MutS exhibited the enhanced DNA-binding activity to a perfectly matched homoduplex DNA [50]. Schofield et al. proposed the idea

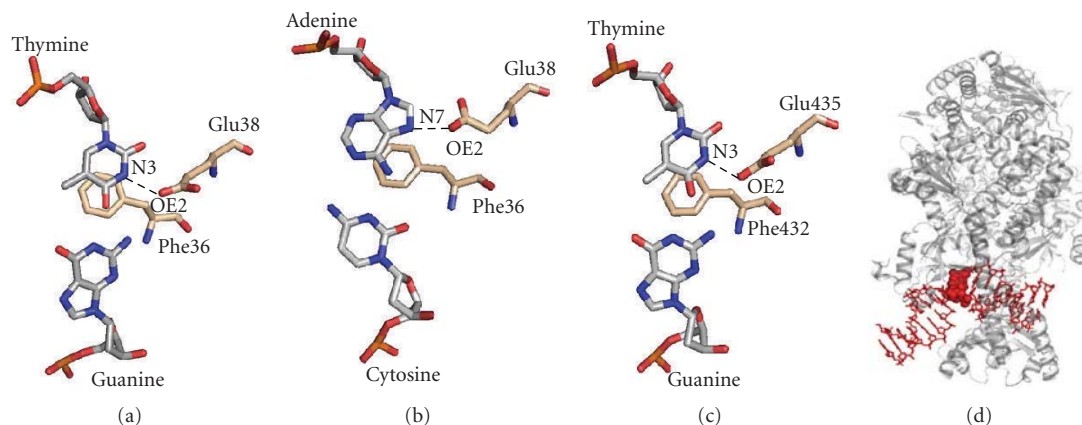


FIGURE 5: Mismatch recognition mode of MutS. (a) G:T mismatch bound to *E. coli* MutS (PDB ID: 1E3M). (b) C:A mismatch bound to *E. coli* MutS (PDB ID: 1OH5). Cytosine residue is in a syn conformation. (c) G:T mismatch bound to human MutS $\alpha$  (PDB ID: 2O8B). (d) Side view of the *E. coli* MutS-mismatch complex (PDB ID: 1E3M). The mismatched duplex is sharply kinked in the complex with MutS. MutS and mismatched DNA are colored grey and red, respectively. The mismatched G and T are shown in the sphere model.

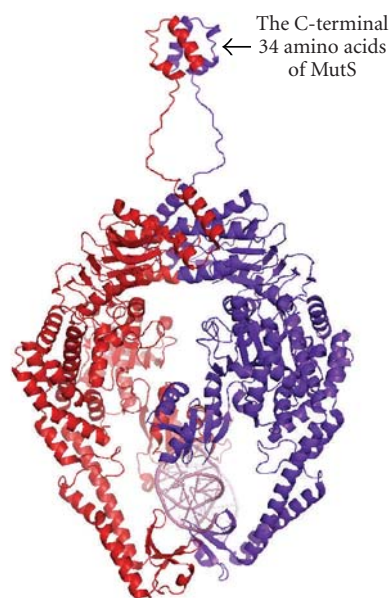


FIGURE 6: The model for full length of *E. coli* MutS dimer. The crystal structure of the C-terminal 34 amino acids of *E. coli* MutS (2OK2) [44] was connected to the C-termini of *E. coli* MutS (residues 2-800) structure (1E3M).

that Glu38 would take part in the promotion of DNA kinking by destabilizing the unkinked DNA-MutS complex through the electrostatic repulsion of the Glu side-chain with phosphate backbone [50].

The lack of a crystal structure for MutS homologues with a homoduplex has prevented us from further understanding the mechanism; however, atomic force microscopy is a powerful tool that can be used to investigate the events that occur during the initial substrate binding by MutS homologues. Observations of the *E. coli* MutS-DNA complex using atomic force microscopy revealed that the DNA is bent

at the perfectly matched site while it is bent and unbent at the mismatched site [54]. Taken together with previous biochemical and crystallographic data, it is proposed that MutS nonspecifically binds to DNA and bends it in order to search for a mismatch, when it encounters a mismatch it kinks the DNA at the mismatched site and finally forms an ultimate recognition complex in which the DNA is unbent [54]. In order to explain why an unbent conformation is more stable at a mismatch than at a homoduplex site, Wang et al. speculated the possibility that a mismatched base is flipped out upon mismatch recognition by MutS [54]. Base flipping is one of the major base-recognition mechanisms observed among base-processing enzymes such as DNA glycosylases or methyltransferases [55]. Although further experimental evidence should be required, this idea may be attractive especially when we remember the recent report that a nonenzymatic protein, alkylguanine alkyltransferase-like protein, also flips out the methylated base upon substrate recognition [56, 57].

The mismatch-recognizing property of MutS homologues is closely related to their ATP-binding/hydrolyzing activity [58–63]. MutS homologues contain a Walker's ATP-binding motif in each subunit that is formed through the association of the subunits. It has been shown that *E. coli* MutS exchanges ADP to ATP upon mismatch binding then undergoes a conformational change to form a sliding clamp [61, 63]. The ATP-binding-dependent formation of the sliding clamp was also confirmed in eukaryotic MutS homologues [63–66]. Several studies revealed that the ATPase activity of the *E. coli* MutS homodimer is also heterodimeric [67, 68]. One of the 2 nucleotide-binding sites exhibits a high affinity to ADP, and the other shows a high affinity to ATP [60, 69, 70], therefore, we should discriminate between the different adenine nucleotide-binding forms of MutS homologues in MMR. Recently, a computational study using normal-mode analysis was applied to assess the conformational dynamics of *E. coli* MutS and human MutS $\alpha$  [71]. Normal-mode analysis is one of the simulation

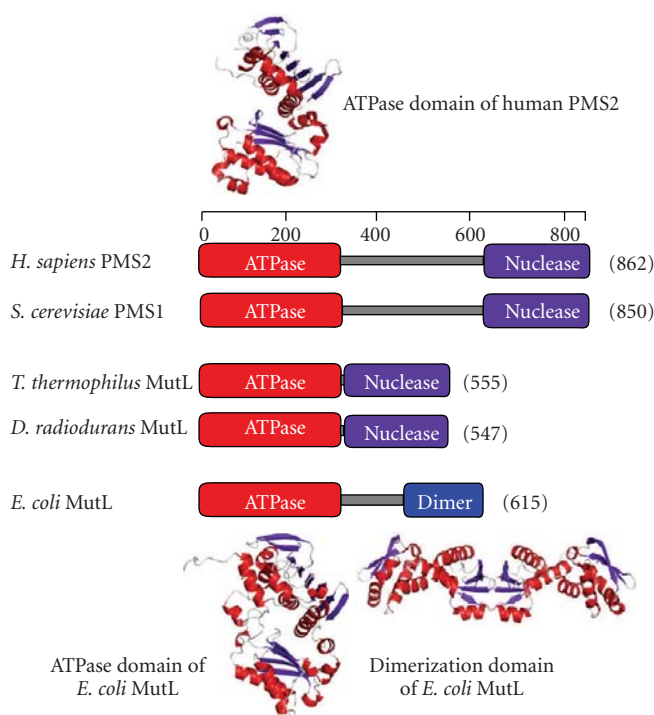


FIGURE 7: (a) A schematic representation of the domain structure of MutL homologues. ATPase, nuclease, and dimer indicate the ATPase, endonuclease, and dimerization domains, respectively. The crystal structures of N-terminal ATPase domain of human PMS2 (PDB ID: 1EA6) [45], ATPase domain of *E. coli* MutL (PDB ID: 1B63) [46], and C-terminal dimerization domain of *E. coli* MutL (PDB ID: 1X9Z) [47, 48] are shown.

methodologies which can deal with the dynamics of large molecules [72]. The analyses suggested the existence of the distinct conformational states which are expected to reflect the functional cycles including DNA scanning, mismatch recognition, repair initiation, and sliding along DNA after mismatch recognition [71]. These computational studies can provide start points for further experiments.

It is thought that the sliding clamp of MutS leaves the mismatch and diffuses along the DNA to activate the downstream reactions, which is called the “moving” or “*cis*” model [23, 74]. The “moving” model is supported by the result that blockages between the mismatch and the nick prevent *in vitro* *E. coli* MMR [75]. In contrast, another mechanism, which is called the “stationary” or “*trans*” model, is also proposed to account for the activation of downstream reactions [23, 74]. In the “stationary” model, MutS remains bound at the mismatch after recognition, and the ATPase activity of MutS is required for verification of mismatch recognition. The “stationary” model is supported by the observation that MutS-mismatch complex can activate MutH on separate homoduplex molecule [67].

The dynamism and transiency of the ternary complex of MutS (MutS $\alpha$ )-MutL (MutL $\alpha$ )-mismatch had prevented us from characterizing their physical interactions. Hydrogen/deuterium exchange mass spectrometry (DXMS) is suitable to study the interactions in large and transient complexes. DXMS analysis of the formation of *E. coli* MutS-MutL-mismatch complex revealed that a relatively small region in domain II (Figure 4) of MutS serves as an interface

for binding MutL [76]. On the basis of the structural analyses of the MutS and MutL N-terminal domains, Wei Yang and coworkers also predicted this region to be a MutL-interacting site [37]. Although the sequence similarity of this region is limited, a structurally conserved region in the MSH2 subunit of *Saccharomyces cerevisiae* MutS $\alpha$  is also essential for interaction with MutL $\alpha$  [76].

*E. coli* MutS proteins exist not only in a dimeric form but also in a tetrameric form at high concentrations [41, 77]. The C-terminal domain (the last 53 amino acids in *E. coli* MutS) is responsible for the tetramerization of full-length MutS. Although the crystallographic analyses were achieved by using C-terminal truncations, it has been pointed out that the deletion of the C-terminal domain causes defects in mismatch recognition, MutH stimulation, and *in vivo* MMR activity [77–79]. On the basis of the crystallographic analysis of the C-terminal domain (Figure 6), tetramer-disrupting mutants of *E. coli* MutS were prepared [44]. Examination of the effects of those mutations revealed that dimerization but not tetramerization of the MutS C-terminal domain is essential for *in vivo* mismatch repair [44].

## 6. Molecular Functions of MutL Homologues

Bacterial MutL homologues exist as homodimers [47] while eukaryotic MutL homologues form the heterodimers MutL $\alpha$ , MutL $\beta$ , and MutL $\gamma$  [80–83]. It is suggested that a large portion of eukaryotic MMR is performed by MutL $\alpha$ . In contrast,

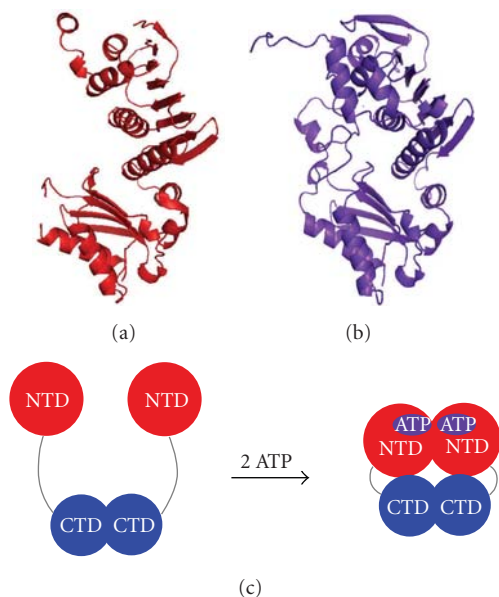


FIGURE 8: Crystal structures of the apo form ((a) PDB ID: 1BKN) and ADPNP-bound form ((b) PDB ID: 1B63) of the *E. coli* MutL N-terminal domain. (c) A schematic representation of a model for the ATP-dependent conformational change of full-length MutL $\alpha$  [73]. NTD and CTD indicate the N-terminal ATPase domain and the C-terminal endonuclease domain, respectively. In the apo form of MutL $\alpha$ , the PMS2 and MLH1 subunits dimerize via their C-terminal domains. ATP binding induces the dimerization of the N-terminal domain and condensation of the molecule.

there is only a slight effect of inactivation of MutL $\beta$  or MutL $\gamma$  on *in vivo* MMR activity. Crystallographic and biochemical analyses revealed that the bacterial MutL homodimer is comprised of an N-terminal ATPase/DNA-binding domain and a C-terminal dimerization/DNA-binding domain (Figure 7) [47, 84]. Eukaryotic MutL homologues are expected to have the same domain organization as bacterial MutL, except for the prolonged interdomain linker (Figure 7) [45, 85].

The N-terminal ATPase domain contains a single ATP-binding motif per subunit. MutL homologues belong to the GHKL ATPase superfamily that includes homologues of DNA gyrase, Hsp90, and histidine kinase in addition to MutL homologues [46, 86]. The GHKL superfamily proteins undergo large conformational changes upon ATP binding and/or hydrolysis. X-ray crystallographic analysis clarified the ATP-binding-dependent conformational change of the N-terminal domain of *E. coli* MutL (Figure 8(a)) [46]. In addition, study using atomic force microscopy revealed that full-length *S. cerevisiae* MutL $\alpha$  can exist in several ATP-binding species with specific conformations in a solution [73]. The conformational change of the full-length MutL homologue seems to involve the interaction between the N-terminal and C-terminal domains (Figure 8(c)). ATP-dependent conformational changes are also implicated for bacterial MutL endonucleases [34, 87]. Such ATPase-cycle-dependent conformational changes in MutL homologue should be necessary to perform the MMR reaction [88–90].

The C-terminal domain of MutL homologues is the endonuclease domain in *mutH*-less organisms [30, 31]. The inactivation of the metal-binding motif in the C-terminal domain of *Homo sapiens* PMS2, *S. cerevisiae* PMS1, *T. thermophilus* MutL, *A. aeolicus* MutL, and *N. gonorrhoeae* MutL diminishes their endonuclease activity [34–36]. Eukaryotic MutL $\alpha$  and bacterial MutL show apparently nonspecific endonuclease activity against lesionless DNA, indicating that MMR requires the sequence- or structure-nonspecific endonuclease activity to introduce excision entry point wherever it is needed [30, 34]. The regulatory mechanism of this apparently nonspecific endonuclease activity has been argued [10, 91].

The endonuclease activity of MutL homologues is affected by the binding of ATP to their N-terminal domain. Isolated *T. thermophilus* MutL tightly binds ATP in the absence of the MutS-mismatch complex and the ATP-binding form of MutL has decreased endonuclease activity against perfectly matched substrates *in vitro* [34]. The *in vitro* endonuclease activities of *A. aeolicus* and *N. gonorrhoeae* MutL are also suppressed by the addition of ATP [34, 35]. In addition, *T. thermophilus* MutL is stably associated with a MutS-mismatch complex in the presence of ATP [34]. Since it has been known that the ATPase activity of MutL is activated by its interaction with MutS, formation of MutS-mismatch-MutL complex is expected to stimulate the endonuclease activity of MutL by canceling the ATP-dependent suppression (Figure 9). In other words, ATP may be utilized to suppress the apparently nonspecific endonuclease activity of MutL until it is required. However, it remains to be determined whether the regulatory mechanism is used by other MutL homologues, including eukaryotic MutL $\alpha$ , because the endonuclease activity of MutL $\alpha$  is enhanced by the addition of ATP instead of being suppressed [30, 31]. Interestingly, it is clarified that ATP stimulates the endonuclease activity of a relatively high concentration of *A. aeolicus* MutL in the absence of a MutS-mismatch complex [36], suggesting that the effect of ATP on the MutL endonuclease activity depends on the concentration of MutL. This finding also strongly indicates that the ATPase activity of MutL is required for its endonuclease activity, that is, ATP is utilized not only to suppress the nonspecific endonuclease activity of MutL but also to actively enhance its activity.

The C-terminal endonuclease domain of MutL homologues contains the highly conserved motif, CPHGRP. Mutations in this motif result in the deficiency of *in vivo* and *in vitro* MMR activities [34, 85]. Bioinformatic analysis indicated that this motif takes part in the formation of the metal-binding motif and it resembles a metal-dependent transcriptional regulator [85]. Using biochemical procedures, the C-terminal domain of the human PMS2 subunit of MutL $\alpha$  was demonstrated to bind a zinc ion [85]. Although the detailed functions of this zinc ion remain unknown, the involvement of the CPHGRP motif in the ATP-dependent conformational change in *T. thermophilus* MutL is suggested [34].

As mentioned above, recent biochemical studies on the endonuclease activity of MutL homologues have been achieved by using homologues from thermophilic bacteria, such as *T. thermophilus*, *A. aeolicus*, and *Thermotoga*

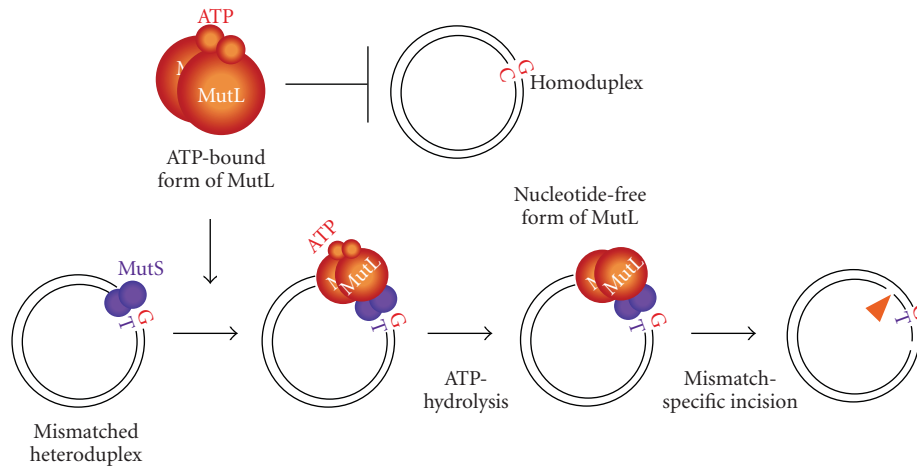


FIGURE 9: A model for the ATPase-cycle-dependent regulation of bacterial MutL endonuclease activity. Free MutL exists as an ATP-bound form whose endonuclease activity is inactive, but preferably binds to a MutS-mismatch complex. The interaction with the MutS-mismatch complex induces the ATP hydrolysis of MutL, resulting in the stimulation of its endonuclease activity. Adapted from the work of Fukui et al. [34].

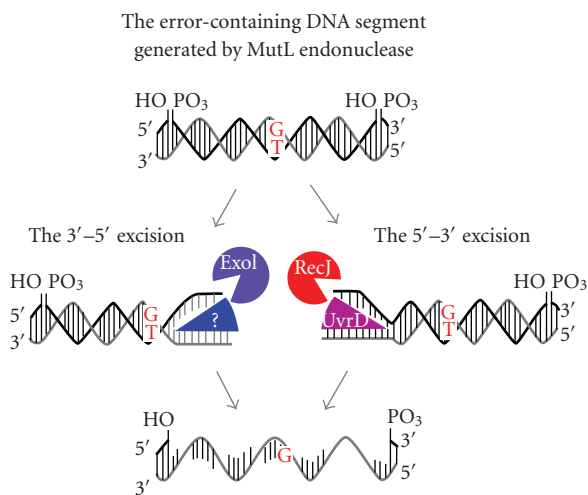


FIGURE 10: Two parallel pathways of excision reaction in *T. thermophilus*. RecJ (red) and ExoI (purple) are thought to be responsible for the 5'- and 3'-directed excision, respectively. UvrD helicase (magenta) functions in cooperation with RecJ. DNA helicase (blue) which translocates 5' to 3' direction has been unknown.

*maritima* [34, 36, 87, 92]. Proteins from these bacteria are extremely stable and suitable for physicochemical examinations including crystallographic analysis. In addition, a variety of gene manipulating procedures are established in *T. thermophilus*. *T. thermophilus* may be one of the ideal model organisms for the study of nick-directed MMR.

## 7. Strand Discrimination in Nick-Directed MMR

Accumulating evidence indicates that a pre-existing strand break can serve as a signal to discriminate the

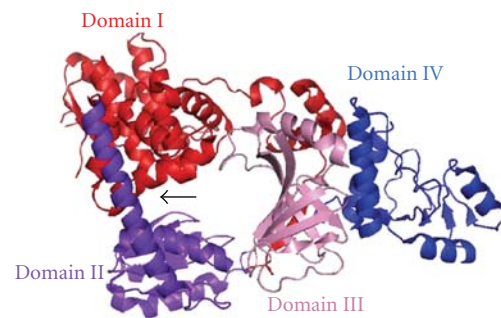


FIGURE 11: Crystal structure of *T. thermophilus* RecJ (PDB ID: 2ZXR). Full-length *T. thermophilus* RecJ is comprised of domains I–IV and forms a ring-like structure. The catalytic active site is located in the cavity between domains I and II as indicated by an arrow. Domain III shows a structural similarity to the oligonucleotide/oligosaccharide-binding fold that is often found in single-stranded DNA-binding proteins. The ring-like structure and oligonucleotide/oligosaccharide-binding fold will ensure the high processivity and strict specificity for single-stranded DNA.

error-containing strand in eukaryotic MMR [27, 30]. Since newly synthesized strands always contain strand break as 3'-ends or 5'-termini of Okazaki fragments, these ends can be utilized as strand discrimination signals *in vivo*. This is consistent with the observation that MutS $\alpha$ -dependent yeast MMR corrects mismatches more efficiently in the lagging strand than in the leading strand [93]. As mentioned above, MutL $\alpha$  is responsible for the strand-discrimination by nicking the discontinuous strand of the mismatched duplex (Figures 1 and 3). Interestingly, it is demonstrated that MutL $\alpha$  incises the discontinuous strand at a distal site from the pre-existing strand break. How does MutL $\alpha$  discriminate the discontinuous strand at a site distant from the strand-discrimination signal? One possible explanation is that MutS $\alpha$  (or MutS $\beta$ ) and MutL $\alpha$  are loaded onto

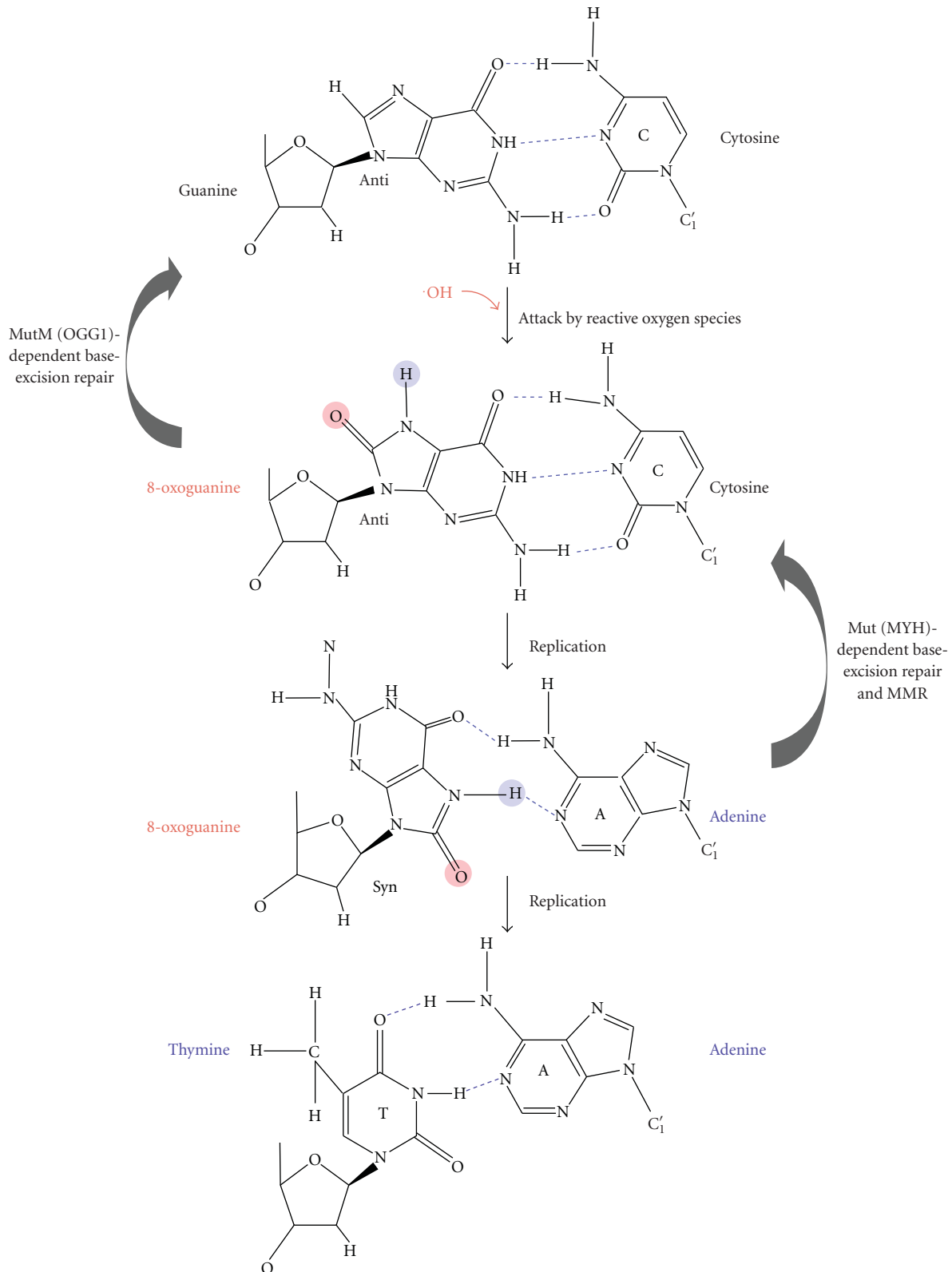


FIGURE 12: Prevention of 8OG-induced G:C-T:A transversion mutations. The 8OG base is one of the major forms of oxidative DNA damage and can be generated by reactive oxygen species. Since 8OG can pair not only with C but also with A, it causes a G:C-T:A transversion through DNA replication. MutM (OGG1)- and MutY (MYH)-dependent base-excision repair pathways are known to remove the 8OG and A from 8OG:C and 8OG:A pairs, respectively. MMR is also responsible for the removal of A from 8OG.

the substrate DNA through their interactions with the replication machinery such as proliferating cell nuclear antigen (PCNA), replication factor C (RFC), and/or DNA polymerase  $\delta$  to render the newly synthesized strand in the catalytic site of the MutL $\alpha$  endonuclease domain [23, 94, 95]. It is known that MSH3 and MSH6 contain the PCNA-interacting motif QX<sub>2</sub>(L/I)X<sub>2</sub>FF [96]. In fact, several studies have demonstrated the associations of MutS $\alpha$  and MutS $\beta$  with PCNA [95, 97, 98]. In addition, PCNA and RFC are necessary not only for repair synthesis [99] but also for the mismatch-provoked incision and excision reactions [30, 100]. Inhibitors of PCNA abolish 3'-nick-directed excision and 40–50% of 5'-nick-directed excision [99–101]. The excision reaction of MutL $\alpha$ -independent 5'-nick-directed MMR may be performed independently of PCNA. In *mutH*-less bacteria, the C-terminal region of MutS contains the putative  $\beta$ -clamp-binding motif QLSFF [102]. The deletion of this region abolishes the *in vitro* interaction of MutS with the  $\beta$ -clamp and *in vivo* MMR activity [103]; furthermore, this interaction is necessary for the *in vivo* localization of MutS and MutL in response to mismatches [103]. These interactions may also be responsible for the strand discrimination in bacterial nick-directed MMR.

## 8. Downstream Events in Nick-Directed MMR

The excision reaction of *in vitro* eukaryotic MMR is performed by the 5'–3' single-stranded DNA-specific exonuclease EXO1. To date, EXO1 is a unique exonuclease that is involved in eukaryotic MMR [30, 104]. In addition, no reports have identified the MMR-related eukaryotic DNA helicase. The exonuclease activity of EXO1 is enhanced by its direct interaction with MutS $\alpha$  [99]. As mentioned above, MutS $\alpha$  forms a sliding clamp and diffuses along the DNA after mismatch recognition. The purpose of the diffusion of MutS $\alpha$  from the mismatch may be to activate EXO1 at the 5'-terminus. In *mutH*-less bacteria, *A. aeolicus* MutL enhances the DNA helicase activity of UvrD [105] whose amino acid sequence is ubiquitous among bacteria. Furthermore, a genetic study implied the simultaneous involvements of the 5'–3' exonuclease RecJ and a 3'–5' exonuclease ExoI in *T. thermophilus* MMR [106]. In *mutH*-less bacteria, the error-containing DNA segment generated by the endonuclease activity of MutL may be removed bi-directionally by the cooperative function of multiple exonucleases and helicases (Figure 10).

The termination of the EXO1-dependent excision reaction in eukaryotic 3'-nick-directed and MutL $\alpha$ -dependent 5'-nick-directed MMR can be directed by 3'-termini that are pre-existing and newly introduced by MutL $\alpha$ , respectively (Figure 3). In contrast, excision termination in MutL $\alpha$ -independent 5'-nick-directed MMR appears to employ a relatively complicated mechanism, because the termination of the excision reaction is not directed by the terminus of the DNA strand. Excision termination in MutL $\alpha$ -independent 5'-nick-directed MMR is conducted by the inhibitory function of RPA, a single-stranded DNA-binding protein [32]. In *mutH*-less bacteria, the mechanism for terminating the

excision reaction remains unknown. The implication of the involvements of 5'–3' and 3'–5' exonucleases [106] raises the possibility that the excision termination of 5'- and 3'-nick-directed MMR in *mutH*-less bacteria is directed by the 3'- and 5'-termini of the DNA strand that are introduced by MutL (Figure 10). Biochemical and structural studies on the exonucleases are required to further understand the excision reaction. Structural analyses of the RecJ 5'–3' exonuclease from *T. thermophilus* were successfully performed [20, 107]; thus, proteins from *T. thermophilus* are known to be suitable for physicochemical examinations [108, 109]. The structure of RecJ consists of 4 domains that form a ring-like structure with the catalytic site in the center of the ring (Figure 11). Based on this structure, the molecular basis for the high processivity and substrate specificity of this enzyme was discussed [107]. In addition, a detailed biochemical study on the *T. thermophilus* ExoI was also performed [106]. It is expected that, unlike other model organisms, *T. thermophilus* possesses only a single set of 5'–3' and 3'–5' exonucleases [106]. Hence, *in vitro* and *in vivo* experiments concerning the excision reaction would be relatively straightforward in this bacterium. It will be intriguing to examine whether MutS can stimulate the exonuclease activities of RecJ and ExoI.

## 9. Other Functions

Mismatch base pairs can arise not only from replication error but also from other biological processes including homeologous recombination, oxidation, and methylation of bases. Long-patch MMR also has a role in the repair machinery for those mismatches.

The involvement of MMR proteins in the suppression of homeologous recombination, that is, the strand exchange between nonidentical DNA molecules, has been reported [110, 111]. Inhibition of homeologous recombination contributes to genome integrity by limiting the invasion of foreign replicons and the excessive intracellular rearrangement of genome. Although the requirement of MutS and MutL homologues for this inhibitory function has been demonstrated, the downstream reactions following the recognition of the mismatch had not been described. Recently, it is suggested that the endonuclease activity of MutL $\alpha$  is required for this system [112].

Oxidative damage is one of the major spontaneously arising forms of DNA damage. Aerobic cells yield reactive oxygen species via respiration events that attack biomolecules such as proteins, lipids, and DNAs [113]. The attack of reactive oxygen species on DNA bases generates oxidized bases including 8-oxoguanine (8OG) (Figure 12) [114]. An 8OG base can pair not only with cytosine but also with adenine [115]. An 8OG:A pair can be converted to a T:A pair through replication, forming a G:C-T:A transversion mutation. To prevent this mutational process, base-excision repair employs MutM (OGG1 in eukaryotes) and MutY (MYH in eukaryotes) glycosylases that excise 8OG and adenine from 8OG:C and 8OG:A pairs, respectively [115]. *In vitro* and *in vivo* studies indicated that bacterial and eukaryotic MMR can recognize an 8OG:A pair as a substrate

and remove the adenine residue because the mismatched adenine residue exists in the newly synthesized strand [116, 117], that is, MMR can perform the same role as the MutY (MYH)-dependent base-excision repair pathway (Figure 12).

$O^6$ -methylguanine ( $O^6$ MeG) is generated by the action of  $S_N1$ -alkylating agents, such as  $N$ -methyl- $N$ -nitrosourea and  $N$ -methyl- $N'$ -nitro- $N$ -nitrosoguanidine that are used in cancer chemotherapy [118].  $O^6$ MeG can pair with thymine, resulting in a G:C-A:T transition mutation through replication. Although the major repair activity for  $O^6$ MeG is derived from  $O^6$ MeG methyltransferase and/or its homologues [56, 119], MutS $\alpha$  can also bind to an  $O^6$ MeG:T mismatch [43, 120]. However, if the  $O^6$ MeG is in the template strand of the duplex, MMR does not remove the lesion. The accumulation of the complex of unrepaired  $O^6$ MeG with MMR proteins is thought to result in the induction of apoptosis [121] through the crosstalk between MMR proteins and check point kinases [120].

## 10. Conclusions

In this paper, the molecular mechanism of widely conserved human-type MMR has been described. Since the accumulating evidence indicates the similarities of basic features among bacterial and eukaryotic MMR, *mutH*-less bacteria may serve as a model organism for biochemical and structural studies of MMR proteins.

The structural analyses on initial recognition complex should be required for further understanding of mismatch-recognition mechanism of MutS homologues. It would be beneficial to identify the amino acid residue which is responsible for the kinking of heteroduplex by MutS homologues. Such mutant might be utilized for the crystallographic analysis of the initial recognition complex. In order to understand the ATP-dependent functional cycles of MutL endonucleases, structural analyses on the full-length MutL homologues should be necessary. Since MutL endonucleases from several thermophilic bacteria have relatively short linker region between N-terminal and C-terminal domains [34, 36, 92, 105], these proteins are expected to be suitable for crystallographic analyses. However, we should not underestimate the importance of this interdomain linker region. This region might be responsible for the protein-protein interaction or domain-domain interaction just like intrinsically disordered proteins [122]. It also remains to be clarified how MutL endonucleases discriminate the discontinuous strand of mismatched heteroduplex. Further experiments using *in vitro* reconstituted system may provide the key findings to understand the mechanism. Discrimination between the "moving" and "stationary" models should also be argued in this context.

## Acknowledgments

The author thanks Drs. Seiki Kuramitsu and Taisuke Wakamatsu for critical reading of this paper.

## References

- [1] E. C. Friedberg, G. C. Walker, and W. Siede, *DNA Repair and Mutagenesis*, American Society for Microbiology, Washington, DC, USA, 2nd edition, 2005.
- [2] R. M. Schaaper, "Base selection, proofreading, and mismatch repair during DNA replication in *Escherichia coli*," *Journal of Biological Chemistry*, vol. 268, no. 32, pp. 23762–23765, 1993.
- [3] R. Fishel and R. D. Kolodner, "Identification of mismatch repair genes and their role in the development of cancer," *Current Opinion in Genetics and Development*, vol. 5, no. 3, pp. 382–395, 1995.
- [4] C. M. Suter, D. I. K. Martin, and R. L. Ward, "Germline epimutation of MLH1 in individuals with multiple cancers," *Nature Genetics*, vol. 36, no. 5, pp. 497–501, 2004.
- [5] M. F. Kane, M. Loda, G. M. Gaida et al., "Methylation of the hMLH1 promoter correlates with lack of expression of hMLH1 in sporadic colon tumors and mismatch repair-defective human tumor cell lines," *Cancer Research*, vol. 57, no. 5, pp. 808–811, 1997.
- [6] P. Modrich and R. Lahue, "Mismatch repair in replication fidelity, genetic recombination, and cancer biology," *Annual Review of Biochemistry*, vol. 65, pp. 101–133, 1996.
- [7] R. Fishel, M. K. Lescoe, M. R. S. Rao et al., "The human mutator gene homolog MSH2 and its association with hereditary nonpolyposis colon cancer," *Cell*, vol. 75, no. 5, pp. 1027–1038, 1993.
- [8] F. S. Leach, N. C. Nicolaides, N. Papadopoulos et al., "Mutations of a mutS homolog in hereditary nonpolyposis colorectal cancer," *Cell*, vol. 75, no. 6, pp. 1215–1225, 1993.
- [9] R. R. Lyer, A. Pluciennik, V. Burdett, and P. L. Modrich, "DNA mismatch repair: functions and mechanisms," *Chemical Reviews*, vol. 106, no. 2, pp. 302–323, 2006.
- [10] P. Modrich, "Mechanisms in eukaryotic mismatch repair," *Journal of Biological Chemistry*, vol. 281, no. 41, pp. 30305–30309, 2006.
- [11] F. Hennecke, H. Kolmar, K. Brundl, and H.-J. Fritz, "The *vsr* gene product of *E. coli* K-12 is a strand- and sequence-specific DNA mismatch endonuclease," *Nature*, vol. 353, no. 6346, pp. 776–778, 1991.
- [12] S. E. Tsutakawa, H. Jingami, and K. Morikawa, "Recognition of a TG mismatch: the crystal structure of very short patch repair endonuclease in complex with a DNA duplex," *Cell*, vol. 99, no. 6, pp. 615–623, 1999.
- [13] S. E. Tsutakawa, T. Muto, T. Kawate et al., "Crystallographic and functional studies of very short patch repair endonuclease," *Molecular Cell*, vol. 3, no. 5, pp. 621–628, 1999.
- [14] R. S. Lahue and P. Modrich, "DNA mismatch correction in a defined system," *Science*, vol. 245, no. 4914, pp. 160–164, 1989.
- [15] P. Modrich, "Methyl-directed DNA mismatch correction," *Journal of Biological Chemistry*, vol. 264, no. 12, pp. 6597–6600, 1989.
- [16] F. Längle-Rouault, G. Maenhaut-Michel, and M. Radman, "GATC sequences, DNA nicks and the MutH function in *Escherichia coli* mismatch repair," *EMBO Journal*, vol. 6, no. 4, pp. 1121–1127, 1987.
- [17] R. S. Lahue and P. Modrich, "Methyl-directed DNA mismatch repair in *Escherichia coli*," *Mutation Research*, vol. 198, no. 1, pp. 37–43, 1988.
- [18] L. E. Mechanic, B. A. Frankel, and S. W. Matson, "*Escherichia coli* MutL loads DNA helicase II onto DNA," *Journal of Biological Chemistry*, vol. 275, no. 49, pp. 38337–38346, 2000.

- [19] V. Burdett, C. Baitinger, M. Viswanathan, S. T. Lovett, and P. Modrich, "In vivo requirement for RecJ, ExoVII, ExoI, and ExoX in methyl-directed mismatch repair," *Proceedings of the National Academy of Sciences of the United States of America*, vol. 98, no. 12, pp. 6765–6770, 2001.
- [20] A. Yamagata, Y. Kakuta, R. Masui, and K. Fukuyama, "The crystal structure of exonuclease RecJ bound to Mn<sup>2+</sup> ion suggests how its characteristic motifs are involved in exonuclease activity," *Proceedings of the National Academy of Sciences of the United States of America*, vol. 99, no. 9, pp. 5908–5912, 2002.
- [21] A. Yamagata, R. Masui, Y. Kakuta, S. Kuramitsu, and K. Fukuyama, "Overexpression, purification and characterization of RecJ protein from *Thermus thermophilus* HB8 and its core domain," *Nucleic Acids Research*, vol. 29, no. 22, pp. 4617–4624, 2001.
- [22] J. A. Eisen, "A phylogenomic study of the MutS family of proteins," *Nucleic Acids Research*, vol. 26, no. 18, pp. 4291–4300, 1998.
- [23] T. A. Kunkel and D. A. Erie, "DNA mismatch repair," *Annual Review of Biochemistry*, vol. 74, pp. 681–710, 2005.
- [24] C. P. Spampinato, R. L. Gomez, C. Gales, and L. D. Lario, "From bacteria to plants: a compendium of mismatch repair assays," *Mutation Research*, pp. 110–128, 2009.
- [25] W.-H. Fang and P. Modrich, "Human strand-specific mismatch repair occurs by a bidirectional mechanism similar to that of the bacterial reaction," *Journal of Biological Chemistry*, vol. 268, no. 16, pp. 11838–11844, 1993.
- [26] L. Dzantiev, N. Constantin, J. Genschel, R. R. Iyer, P. M. Burgers, and P. Modrich, "A defined human system that supports bidirectional mismatch-provoked excision," *Molecular Cell*, vol. 15, no. 1, pp. 31–41, 2004.
- [27] N. Constantin, L. Dzantiev, F. A. Kadyrov, and P. Modrich, "Human mismatch repair: reconstitution of a nick-directed bidirectional reaction," *Journal of Biological Chemistry*, vol. 280, no. 48, pp. 39752–39761, 2005.
- [28] J. Genschel, L. R. Bazemore, and P. Modrich, "Human exonuclease I is required for 5' and 3' mismatch repair," *Journal of Biological Chemistry*, vol. 277, no. 15, pp. 13302–13311, 2002.
- [29] K. Wei, A. B. Clark, E. Wong et al., "Inactivation of exonuclease I in mice results in DNA mismatch repair defects, increased cancer susceptibility, and male and female sterility," *Genes and Development*, vol. 17, no. 5, pp. 603–614, 2003.
- [30] F. A. Kadyrov, L. Dzantiev, N. Constantin, and P. Modrich, "Endonucleolytic function of mutL $\alpha$  in human mismatch repair," *Cell*, vol. 126, no. 2, pp. 297–308, 2006.
- [31] F. A. Kadyrov, S. F. Holmes, M. E. Arana et al., "Saccharomyces cerevisiae MutL $\alpha$  is a mismatch repair endonuclease," *Journal of Biological Chemistry*, vol. 282, no. 51, pp. 37181–37190, 2007.
- [32] J. Genschel and P. Modrich, "Functions of MutL $\alpha$ , replication protein A (RPA), and HMGB1 in 5'-directed mismatch repair," *Journal of Biological Chemistry*, vol. 284, no. 32, pp. 21536–21544, 2009.
- [33] J. T. Drummond, A. Anthoney, R. Brown, and P. Modrich, "Cisplatin and adriamycin resistance are associated with MutL $\alpha$  and mismatch repair deficiency in an ovarian tumor cell line," *Journal of Biological Chemistry*, vol. 271, no. 33, pp. 19645–19648, 1996.
- [34] K. Fukui, M. Nishida, N. Nakagawa, R. Masui, and S. Kuramitsu, "Bound nucleotide controls the endonuclease activity of mismatch repair enzyme MutL," *Journal of Biological Chemistry*, vol. 283, no. 18, pp. 12136–12145, 2008.
- [35] V. Duppatla, C. Bodda, C. Urbanke, P. Friedhoff, and D. N. Rao, "The C-terminal domain is sufficient for endonuclease activity of *Neisseria gonorrhoeae* MutL," *Biochemical Journal*, vol. 423, no. 2, pp. 265–277, 2009.
- [36] J. Mauris and T. C. Evans Jr., "Adenosine triphosphate stimulates *Aquifex aeolicus* MutL endonuclease activity," *PLoS ONE*, vol. 4, no. 9, article no. e7175, 2009.
- [37] G. Obmolova, C. Ban, P. Hsieh, and W. Yang, "Crystal structures of mismatch repair protein MutS and its complex with a substrate DNA," *Nature*, vol. 407, no. 6805, pp. 703–710, 2000.
- [38] M. H. Lamers, A. Perrakis, J. H. Enzlin, H. H. K. Winterwerp, N. De Wind, and T. K. Sixma, "The crystal structure of DNA mismatch repair protein MutS binding to a G·T mismatch," *Nature*, vol. 407, no. 6805, pp. 711–717, 2000.
- [39] H. Tachiki, R. Kato, R. Masui et al., "Domain organization and functional analysis of *Thermus thermophilus* MutS protein," *Nucleic Acids Research*, vol. 26, no. 18, pp. 4153–4159, 1998.
- [40] H. Tachiki, R. Kato, and S. Kuramitsu, "DNA binding and protein-protein interaction sites in MutS, a mismatched DNA recognition protein from *Thermus thermophilus* HB8," *Journal of Biological Chemistry*, vol. 275, no. 52, pp. 40703–40709, 2000.
- [41] S. Takamatsu, R. Kato, and S. Kuramitsu, "Mismatch DNA recognition protein from an extremely thermophilic bacterium, *Thermus thermophilus* HB8," *Nucleic Acids Research*, vol. 24, no. 4, pp. 640–647, 1996.
- [42] S. D. McCulloch, L. Gu, and G.-M. Li, "Nick-dependent and -independent processing of large DNA loops in human cells," *Journal of Biological Chemistry*, vol. 278, no. 50, pp. 50803–50809, 2003.
- [43] J. J. Warren, T. J. Pohlhaus, A. Changela, R. R. Iyer, P. L. Modrich, and L. Beese, "Structure of the human MutS $\alpha$  DNA lesion recognition complex," *Molecular Cell*, vol. 26, no. 4, pp. 579–592, 2007.
- [44] M. L. Mendillo, C. D. Putnam, and R. D. Kolodner, "Escherichia coli MutS tetramerization domain structure reveals that stable dimers but not tetramers are essential for DNA mismatch repair in vivo," *Journal of Biological Chemistry*, vol. 282, no. 22, pp. 16345–16354, 2007.
- [45] A. Guarné, M. S. Junop, and W. Yang, "Structure and function of the N-terminal 40 kDa fragment of human PMS2: a monomeric GHL ATPase," *EMBO Journal*, vol. 20, no. 19, pp. 5521–5531, 2001.
- [46] C. Ban, M. Junop, and W. Yang, "Transformation of MutL by ATP binding and hydrolysis: a switch in DNA mismatch repair," *Cell*, vol. 97, no. 1, pp. 85–97, 1999.
- [47] A. Guarné, S. Ramon-Maiques, E. M. Wolff et al., "Structure of the MutL C-terminal domain: a model of intact MutL and its roles in mismatch repair," *EMBO Journal*, vol. 23, no. 21, pp. 4134–4145, 2004.
- [48] J. Kosinski, I. Steindorf, J. M. Bujnicki, L. Giron-Monzon, and P. Friedhoff, "Analysis of the quaternary structure of the MutL C-terminal domain," *Journal of Molecular Biology*, vol. 351, no. 4, pp. 895–909, 2005.
- [49] V. A. Malkov, I. Biswas, R. D. Camerini-Otero, and P. Hsieh, "Photocross-linking of the NH<sub>2</sub>-terminal region of Taq MutS protein to the major groove of a heteroduplex DNA," *Journal of Biological Chemistry*, vol. 272, no. 38, pp. 23811–23817, 1997.

- [50] M. J. Schofield, F. E. Brownnewell, S. Nayak, C. Du, E. T. Kool, and P. Hsieh, "The Phe-X-Glu DNA binding motif of MutS. The role of hydrogen bonding in mismatch recognition," *Journal of Biological Chemistry*, vol. 276, no. 49, pp. 45505–45508, 2001.
- [51] M. S. Junop, W. Yang, P. Funchain, W. Clendenin, and J. H. Miller, "In vitro and in vivo studies of MutS, MutL and MutH mutants: correlation of mismatch repair and DNA recombination," *DNA Repair*, vol. 2, no. 4, pp. 387–405, 2003.
- [52] K. Drotschmann, W. Yang, F. E. Brownnewell, E. T. Kool, and T. A. Kunkel, "Asymmetric recognition of DNA local distortion. Structure-based functional studies of eukaryotic Msh2-Msh6," *Journal of Biological Chemistry*, vol. 276, no. 49, pp. 46225–46229, 2001.
- [53] G. Natrajan, M. H. Lamers, J. H. Enzlin, H. H. K. Winterwerp, A. Perrakis, and T. K. Sixma, "Structures of *Escherichia coli* DNA mismatch repair enzyme MutS in complex with different mismatches: a common recognition mode for diverse substrates," *Nucleic Acids Research*, vol. 31, no. 16, pp. 4814–4821, 2003.
- [54] H. Wang, Y. Yang, M. J. Schofield et al., "DNA bending and unbending by MutS govern mismatch recognition and specificity," *Proceedings of the National Academy of Sciences of the United States of America*, vol. 100, no. 25, pp. 14822–14827, 2003.
- [55] R. J. Roberts and X. Cheng, "Base flipping," *Annual Review of Biochemistry*, vol. 67, pp. 181–198, 1998.
- [56] R. Morita, N. Nakagawa, S. Kuramitsu, and R. Masui, "An O<sup>6</sup>-methylguanine-DNA methyltransferase-like protein from *Thermus thermophilus* interacts with a nucleotide excision repair protein," *Journal of Biochemistry*, vol. 144, no. 2, pp. 267–277, 2008.
- [57] J. L. Tubbs, V. Latypov, S. Kanugula et al., "Flipping of alkylated DNA damage bridges base and nucleotide excision repair," *Nature*, vol. 459, no. 7248, pp. 808–813, 2009.
- [58] L. J. Blackwell, D. Martik, K. P. Bjornson, E. S. Bjornson, and P. Modrich, "Nucleotide-promoted release of hMutS $\alpha$  from heteroduplex DNA is consistent with an ATP-dependent translocation mechanism," *Journal of Biological Chemistry*, vol. 273, no. 48, pp. 32055–32062, 1999.
- [59] L. J. Blackwell, K. P. Bjornson, D. J. Allen, and P. Modrich, "Distinct MutS DNA-binding modes that are differentially modulated by ATP binding and hydrolysis," *Journal of Biological Chemistry*, vol. 276, no. 36, pp. 34339–34347, 2001.
- [60] K. P. Bjornson and P. Modrich, "Differential and simultaneous adenosine di- and triphosphate binding by MutS," *Journal of Biological Chemistry*, vol. 278, no. 20, pp. 18557–18562, 2003.
- [61] S. Acharya, P. L. Foster, P. Brooks, and R. Fishel, "The coordinated functions of the *E. coli* MutS and MutL proteins in mismatch repair," *Molecular Cell*, vol. 12, no. 1, pp. 233–246, 2003.
- [62] R. Kato, M. Kataoka, H. Kamikubo, and S. Kuramitsu, "Direct observation of three conformations of MutS protein regulated by adenine nucleotides," *Journal of Molecular Biology*, vol. 309, no. 1, pp. 227–238, 2001.
- [63] M. L. Mendillo, C. D. Putnam, A. O. Mo et al., "Probing DNA- and ATP-mediated conformational changes in the MutS family of mismatch recognition proteins using deuterium exchange mass spectrometry," *Journal of Biological Chemistry*, vol. 285, no. 17, pp. 13170–13182, 2010.
- [64] S. Gradia, D. Subramanian, T. Wilson et al., "hMSH2-hMSH6 forms a hydrolysis-independent sliding clamp on mismatched DNA," *Molecular Cell*, vol. 3, no. 2, pp. 255–261, 1999.
- [65] I. Iaccarino, G. Marra, P. Dufner, and J. Jiricny, "Mutation in the magnesium binding site of hMSH6 disables the hMutS $\alpha$  sliding clamp from translocating along DNA," *Journal of Biological Chemistry*, vol. 275, no. 3, pp. 2080–2086, 2000.
- [66] J. Jiang, L. Bai, J. A. Surtees, Z. Gemici, M. D. Wang, and E. Alani, "Detection of high-affinity and sliding clamp modes for MSH2-MSH6 by single-molecule unzipping force analysis," *Molecular Cell*, vol. 20, no. 5, pp. 771–781, 2005.
- [67] M. S. Junop, G. Obmolova, K. Rausch, P. Hsieh, and W. Yang, "Composite active site of an ABC ATPase: MutS uses ATP to verify mismatch recognition and authorize DNA repair," *Molecular Cell*, vol. 7, no. 1, pp. 1–12, 2001.
- [68] M. H. Lamers, H. H. K. Winterwerp, and T. K. Sixma, "The alternating ATPase domains of MutS control DNA mismatch repair," *EMBO Journal*, vol. 22, no. 3, pp. 746–756, 2003.
- [69] D. Martik, C. Baitinger, and P. Modrich, "Differential specificities and simultaneous occupancy of human MutS $\alpha$  nucleotide binding sites," *Journal of Biological Chemistry*, vol. 279, no. 27, pp. 28402–28410, 2004.
- [70] E. Antony and M. M. Hingorani, "Mismatch recognition-coupled stabilization of Msh2-Msh6 in an ATP-bound state at the initiation of DNA repair," *Biochemistry*, vol. 42, no. 25, pp. 7682–7693, 2003.
- [71] S. Mukherjee, S. M. Law, and M. Feig, "Deciphering the mismatch recognition cycle in MutS and MSH2-MSH6 using normal-mode analysis," *Biophysical Journal*, vol. 96, no. 5, pp. 1707–1720, 2009.
- [72] F. Tama, M. Valle, J. Frankt, and C. L. Brooks III, "Dynamic reorganization of the functionally active ribosome explored by normal mode analysis and cryo-electron microscopy," *Proceedings of the National Academy of Sciences of the United States of America*, vol. 100, no. 16, pp. 9319–9323, 2003.
- [73] E. J. Sacho, F. A. Kadyrov, P. Modrich, T. A. Kunkel, and D. A. Erie, "Direct visualization of asymmetric adenine nucleotide-induced conformational changes in MutL $\alpha$ ," *Molecular Cell*, vol. 29, no. 1, pp. 112–121, 2008.
- [74] G.-M. Li, "Mechanisms and functions of DNA mismatch repair," *Cell Research*, vol. 18, no. 1, pp. 85–98, 2008.
- [75] A. Pluciennik and P. Modrich, "Protein roadblocks and helix discontinuities are barriers to the initiation of mismatch repair," *Proceedings of the National Academy of Sciences of the United States of America*, vol. 104, no. 31, pp. 12709–12713, 2007.
- [76] M. L. Mendillo, V. V. Hargreaves, J. W. Jamison et al., "A conserved MutS homolog connector domain interface interacts with MutL homologs," *Proceedings of the National Academy of Sciences of the United States of America*, vol. 106, no. 52, pp. 22223–22228, 2009.
- [77] K. P. Bjornson, L. J. Blackwell, H. Sage, C. Baitinger, D. Allen, and P. Modrich, "Assembly and molecular activities of the MutS tetramer," *Journal of Biological Chemistry*, vol. 278, no. 36, pp. 34667–34673, 2003.
- [78] M. A. Calmann, A. Nowosielska, and M. G. Marinus, "Separation of mutation avoidance and antirecombination functions in an *Escherichia coli* mutS mutant," *Nucleic Acids Research*, vol. 33, no. 4, pp. 1193–1200, 2005.
- [79] M. A. Calmann, A. Nowosielska, and M. G. Marinus, "The MutS C terminus is essential for mismatch repair activity in vivo," *Journal of Bacteriology*, vol. 187, no. 18, pp. 6577–6579, 2005.
- [80] H. Flores-Rozas and R. D. Kolodner, "The *Saccharomyces cerevisiae* MLH3 gene functions in MSH3-dependent

- suppression of frameshift mutations," *Proceedings of the National Academy of Sciences of the United States of America*, vol. 95, no. 21, pp. 12404–12409, 1998.
- [81] S. M. Lipkin, V. Wang, R. Jacoby et al., "MLH3: a DNA mismatch repair gene associated with mammalian microsatellite instability," *Nature Genetics*, vol. 24, no. 1, pp. 27–35, 2000.
- [82] B. D. Harfe, B. K. Minesinger, and S. Jinks-Robertson, "Discrete *in vivo* roles for the MutL homologs Mlh2p and Mlh3p in the removal of frameshift intermediates in budding yeast," *Current Biology*, vol. 10, no. 3, pp. 145–148, 2000.
- [83] K. T. Nishant, A. J. Plys, and E. Alani, "A mutation in the putative MLH3 endonuclease domain confers a defect in both mismatch repair and meiosis in *Saccharomyces cerevisiae*," *Genetics*, vol. 179, no. 2, pp. 747–755, 2008.
- [84] C. Ban and W. Yang, "Crystal structure and ATPase activity of MutL: implications for DNA repair and mutagenesis," *Cell*, vol. 95, no. 4, pp. 541–552, 1998.
- [85] J. Kosinski, G. Plotz, A. Guarné, J. M. Bujnicki, and P. Friedhoff, "The PMS2 subunit of human MutL $\alpha$  contains a metal ion binding domain of the iron-dependent repressor protein family," *Journal of Molecular Biology*, vol. 382, no. 3, pp. 610–627, 2008.
- [86] R. Dutta and M. Inouye, "GHKL, an emergent ATPase/kinase superfamily," *Trends in Biochemical Sciences*, vol. 25, no. 1, pp. 24–28, 2000.
- [87] T. G. Kim, H. J. Cha, H. J. Lee et al., "Structural insights of the nucleotide-dependent conformational changes of *Thermotoga maritima* Mutl using small-angle X-ray scattering analysis," *Journal of Biochemistry*, vol. 145, no. 2, pp. 199–206, 2009.
- [88] C. Spampinato and P. Modrich, "The MutL ATPase is required for mismatch repair," *Journal of Biological Chemistry*, vol. 275, no. 13, pp. 9863–9869, 2000.
- [89] M. Räschle, P. Dufner, G. Marra, and J. Jiricny, "Mutations within the hMLH1 and hPMS2 subunits of the human MutL $\alpha$  mismatch repair factor affect its ATPase activity, but not its ability to interact with hMutSa," *Journal of Biological Chemistry*, vol. 277, no. 24, pp. 21810–21820, 2002.
- [90] M. C. Hall, P. V. Shcherbakova, and T. A. Kunkel, "Differential ATP binding and intrinsic ATP hydrolysis by amino-terminal domains of the yeast Mlh1 and Pms1 proteins," *Journal of Biological Chemistry*, vol. 277, no. 5, pp. 3673–3679, 2002.
- [91] W. Yang, "Human MutL $\alpha$ : the jack of all trades in MMR is also an endonuclease," *DNA Repair*, vol. 6, no. 1, pp. 135–139, 2007.
- [92] T. G. Kim, S.-D. Heo, J. K. Ku, and C. Ban, "Functional properties of the thermostable *mutL* from *Thermotoga maritima*," *BMB Reports*, vol. 42, no. 1, pp. 53–58, 2009.
- [93] Y. I. Pavlov, I. M. Mian, and T. A. Kunkel, "Evidence for preferential mismatch repair of lagging strand DNA replication errors in yeast," *Current Biology*, vol. 13, no. 9, pp. 744–748, 2003.
- [94] P. J. Masih, D. Kunnev, and T. Melendy, "Mismatch repair proteins are recruited to replicating DNA through interaction with Proliferating Cell Nuclear Antigen (PCNA)," *Nucleic Acids Research*, vol. 36, no. 1, pp. 67–75, 2008.
- [95] R. R. Iyer, T. J. Pohlhaus, S. Chen et al., "The MutSa-proliferating cell nuclear antigen interaction in human DNA mismatch repair," *Journal of Biological Chemistry*, vol. 283, no. 19, pp. 13310–13319, 2008.
- [96] G.-L. Moldovan, B. Pfander, and S. Jentsch, "PCNA, the maestro of the replication fork," *Cell*, vol. 129, no. 4, pp. 665–679, 2007.
- [97] S. S. Shell, C. D. Putnam, and R. D. Kolodner, "The N terminus of *Saccharomyces cerevisiae* Msh6 is an unstructured tether to PCNA," *Molecular Cell*, vol. 26, no. 4, pp. 565–578, 2007.
- [98] P. J. Lau and R. D. Kolodner, "Transfer of the MSH2·MSH6 complex from proliferating cell nuclear antigen to mismatched bases in DNA," *Journal of Biological Chemistry*, vol. 278, no. 1, pp. 14–17, 2003.
- [99] J. Genschel and P. Modrich, "Mechanism of 5'-directed excision in human mismatch repair," *Molecular Cell*, vol. 12, no. 5, pp. 1077–1086, 2003.
- [100] A. Umar, A. B. Buermeier, J. A. Simon et al., "Requirement for PCNA in DNA mismatch repair at a step preceding DNA resynthesis," *Cell*, vol. 87, no. 1, pp. 65–73, 1996.
- [101] S. Guo, S. R. Presnell, F. Yuan, Y. Zhang, L. Gu, and G.-M. Li, "Differential requirement for proliferating cell nuclear antigen in 5' and 3' nick-directed excision in human mismatch repair," *Journal of Biological Chemistry*, vol. 279, no. 17, pp. 16912–16917, 2004.
- [102] B. P. Dalrymple, K. Kongsuwan, G. Wijffels, N. E. Dixon, and P. A. Jennings, "A universal protein-protein interaction motif in the eubacterial DNA replication and repair systems," *Proceedings of the National Academy of Sciences of the United States of America*, vol. 98, no. 20, pp. 11627–11632, 2001.
- [103] L. A. Simmons, B. W. Davies, A. D. Grossman, and G. C. Walker, " $\beta$  clamp directs localization of mismatch repair in *Bacillus subtilis*," *Molecular Cell*, vol. 29, no. 3, pp. 291–301, 2008.
- [104] J. Genschel and P. Modrich, "Analysis of the excision step in human DNA mismatch repair," *Methods in Enzymology*, vol. 408, pp. 273–284, 2006.
- [105] J. Mauris and T. C. Evans Jr., "A human PMS2 homologue from *Aquifex aeolicus* stimulates an ATP-dependent DNA helicase," *Journal of Biological Chemistry*, vol. 285, no. 15, pp. 11087–11092, 2010.
- [106] A. Shimada, R. Masui, and N. Nakagawa, "A novel single-stranded DNA-specific 3'-5' exonuclease, *Thermus thermophilus* exonuclease I, is involved in several DNA repair pathways," *Nucleic Acids Research*. In press.
- [107] T. Wakamatsu, Y. Kitamura, Y. Kotera, N. Nakagawa, S. Kuramitsu, and R. Masui, "Structure of RecJ exonuclease defines its specificity for single-stranded DNA," *The Journal of Biological Chemistry*, vol. 285, pp. 9762–9769, 2010.
- [108] H. Iino, H. Naitow, Y. Nakamura et al., "Crystallization screening test for the whole-cell project on *Thermus thermophilus* HB8," *Acta Crystallographica Section F*, vol. 64, no. 6, pp. 487–491, 2008.
- [109] S. Yokoyama, H. Hirota, T. Kigawa et al., "Structural genomics projects in Japan," *Nature Structural Biology*, vol. 7, supplement, pp. 943–945, 2000.
- [110] B. D. Harfe and S. Jinks-Robertson, "DNA mismatch repair and genetic instability," *Annual Review of Genetics*, vol. 34, pp. 359–399, 2000.
- [111] B. D. Harfe and S. Jinks-Robertson, "Mismatch repair proteins and mitotic genome stability," *Mutation Research*, vol. 451, no. 1-2, pp. 151–167, 2000.
- [112] N. Erdeniz, M. Nguyen, S. M. Deschênes, and R. M. Liskay, "Mutations affecting a putative MutL $\alpha$  endonuclease motif impact multiple mismatch repair functions," *DNA Repair*, vol. 6, no. 10, pp. 1463–1470, 2007.
- [113] J. Cadet, T. Douki, D. Gasparutto, and J.-L. Ravanat, "Oxidative damage to DNA: formation, measurement and biochemical features," *Mutation Research*, vol. 531, no. 1-2, pp. 5–23, 2003.

- [114] S. V. Jovanovic and M. G. Simic, "The DNA guanyl radical: kinetics and mechanisms of generation and repair," *Biochimica et Biophysica Acta*, vol. 1008, no. 1, pp. 39–44, 1989.
- [115] S. S. David, V. L. O'Shea, and S. Kundu, "Base-excision repair of oxidative DNA damage," *Nature*, vol. 447, no. 7147, pp. 941–950, 2007.
- [116] P. Macpherson, F. Barone, G. Maga, F. Mazzei, P. Karran, and M. Bignami, "8-Oxoguanine incorporation into DNA repeats *in vitro* and mismatch recognition by MutSa," *Nucleic Acids Research*, vol. 33, no. 16, pp. 5094–5105, 2005.
- [117] A. Mazurek, M. Berardini, and R. Fishel, "Activation of human MutS homologs by 8-oxo-guanine DNA damage," *Journal of Biological Chemistry*, vol. 277, no. 10, pp. 8260–8266, 2002.
- [118] R. B. Roth and L. D. Samson, "Gene transfer to suppress bone marrow alkylation sensitivity," *Mutation Research*, vol. 462, no. 2-3, pp. 107–120, 2000.
- [119] A. E. Pegg, "Mammalian O<sup>6</sup>-alkylguanine-DNA alkyltransferase: regulation and importance in response to alkylating carcinogenic and therapeutic agents," *Cancer Research*, vol. 50, no. 19, pp. 6119–6129, 1990.
- [120] K. Yoshioka, Y. Yoshioka, and P. Hsieh, "ATR kinase activation mediated by MutSa and MutLa in response to cytotoxic O<sup>6</sup>-methylguanine adducts," *Molecular Cell*, vol. 22, pp. 501–510, 2006.
- [121] D. R. Duckett, S. M. Bronstein, Y. Taya, and P. Modrich, "hMutSa and hMutLa-dependent phosphorylation of p53 in response to DNA methylator damage," *Proceedings of the National Academy of Sciences of the United States of America*, vol. 96, pp. 12384–12388, 1999.
- [122] V. N. Uversky and A. K. Dunker, "Understanding protein non-folding," *Biochimica et Biophysica Acta*, vol. 1804, no. 6, pp. 1231–1264, 2010.

## Review Article

# H2AX Phosphorylation: Its Role in DNA Damage Response and Cancer Therapy

Monika Podhorecka,<sup>1</sup> Andrzej Skladanowski,<sup>2</sup> and Przemyslaw Bozko<sup>3</sup>

<sup>1</sup>Department of Haematology and Bone Marrow Transplantation, Medical University of Lublin, 20081 Lublin, Poland

<sup>2</sup>Laboratory of Molecular and Cellular Pharmacology, Department of Pharmaceutical Technology and Biochemistry, Gdansk University of Technology, 80233 Gdansk, Poland

<sup>3</sup>Institute of Experimental Internal Medicine, Medical Faculty, Otto von Guericke University, 39120 Magdeburg, Germany

Correspondence should be addressed to Przemyslaw Bozko, przemyslaw.bozko@med.ovgu.de

Received 16 April 2010; Revised 28 June 2010; Accepted 5 July 2010

Academic Editor: Ashis Basu

Copyright © 2010 Monika Podhorecka et al. This is an open access article distributed under the Creative Commons Attribution License, which permits unrestricted use, distribution, and reproduction in any medium, provided the original work is properly cited.

Double-strand breaks (DSBs) are the most deleterious DNA lesions, which, if left unrepaired, may have severe consequences for cell survival, as they lead to chromosome aberrations, genomic instability, or cell death. Various physical, chemical, and biological factors are involved in DSB induction. Cells respond to DNA damage by activating the so-called DNA damage response (DDR), a complex molecular mechanism developed to detect and repair DNA damage. The formation of DSBs triggers activation of many factors, including phosphorylation of the histone variant H2AX, producing  $\gamma$ H2AX. Phosphorylation of H2AX plays a key role in DDR and is required for the assembly of DNA repair proteins at the sites containing damaged chromatin as well as for activation of checkpoints proteins which arrest the cell cycle progression. In general, analysis of  $\gamma$ H2AX expression can be used to detect the genotoxic effect of different toxic substances. When applied to clinical samples from cancer patients, evaluation of  $\gamma$ H2AX levels may allow not only to monitor the efficiency of anticancer treatment but also to predict of tumor cell sensitivity to DNA damaging anticancer agents and toxicity of anticancer treatment toward normal cells.

## 1. DNA Double-Strand Breaks

DNA double-strand break (DSB) is a type of DNA damage in which two complementary strands of the double helix of DNA are damaged simultaneously, in locations close to each other. DSB is the most dangerous type of DNA damage, because it is believed that a single unrepaired DSB is sufficient for the induction of cell death process [1, 2]. Many different physical, chemical, and biological factors may lead to DSB formation. DSBs also occur in cells, for example, during differentiation of reproductive cells or lymphocytes [3, 4]. The factors leading to the formation of DSB include endogenous factors, that are associated with physiological processes occurring in the cell, and the exogenous ones [5, 6].

In living cells, DNA is subject to a constant process of oxidative damage by oxygen free radicals (reactive oxygen species—ROS) that are produced inside the cell as a result of metabolic processes [6, 7]. It is estimated that in a single cell cycle at least 5000 single-stranded DNA breaks can

occur as a result of ROS production. Approximately 1% of these DNA breaks is converted into DSBs, mainly during DNA replication, while the remaining 99% is repaired. Thus, during the cell cycle in a single nucleus, about 50 so-called “endogenous” DSBs are formed. Accumulation of unrepaired DNA damage induced by ROS leads to cell aging and may be responsible for the induction of neoplastic transformation [6, 8].

One of the first exogenous factors involved in inducing DSBs was ionizing radiation. Among the various types of DNA damage caused by X-rays, formation of DSB seems to be the most important mechanism of reproductive cell damage or in changing genome integrity that leads to malignancy [9]. Similar changes may be induced by UV radiation [9, 10].

DNA damage is also induced by many anticancer drugs, among them the most effective appear to be inhibitors of topoisomerases. DNA topoisomerases are enzymes that regulate DNA over- and underwinding and remove knots

and tangles from the genetic material by creating transient breaks in DNA double-helix [11, 12]. There are two classes of topoisomerases: type I enzymes introduce single-strand breaks in DNA and type II ones introduce double-strand breaks [11–13]. Type I topoisomerases modulate DNA under- and overwinding, but cannot remove knots and tangles from duplex DNA, while type II topoisomerases modulate DNA supercoiling and also remove DNA knots and tangles [14]. Since a single unrepaired DSB has potentially lethal consequences, type II topoisomerases, being necessary for cell survival, also have the capacity to fragment the genome [14]. When a nucleic acid tracking system, such as a replication or transcription complex, attempts to traverse the cleavable complex between topoisomerase and DNA, it may convert this transient enzyme-DNA intermediate to a permanent DSB in the genetic material, leading to DNA aberrations [15].

Inhibitors of DNA topoisomerase I (camptothecin and topotecan) and II (etoposide, doxorubicin, and mitoxantrone) belong to the most effective antitumor drugs. Their mode of action involves stabilization of cleavable complexes between topoisomerase and DNA. It leads to collisions of the progressing DNA replication forks or RNA polymerase with the drug-stabilized topoisomerase-DNA complexes and conversion them into DSBs, which trigger apoptosis [16, 17].

In eukaryotic cells, the efficient repair of DSB is essential for survival. Two major pathways have evolved to deal with these lesions, homologous recombination (HR), and non homologous end-joining (NHEJ). The mechanism of HR is based on using the genetic information from a corresponding undamaged region present on the second DNA molecule or homologous chromosomes and therefore is active mainly during S and G2 phases of cell cycle. NHEJ is based on a direct ligation of the two ends of damaged DNA molecules and repairs DSBs mainly in G1 phase [2].

## 2. H2AX Phosphorylation

It was reported several years ago, that in mammalian cells the phosphorylation of the subtype of histone H2A, called H2AX, in the position of Ser139 occurs in response to DSB formation. The phosphorylated form of H2AX is called  $\gamma$ H2AX [18, 19]. Since then, many researchers focused on the explanation of mechanisms which induce phosphorylation of H2AX and its role in DNA damage signaling and repair.

Histone H2AX is a substrate of several phosphoinositide 3-kinase-related protein kinases (PIKKs), such as ATM (ataxia teleangiectasia mutated), ATR (ATM and Rad3-related), or DNA-dependent protein kinase (DNA-PK). ATM kinase is considered as a major physiological mediator of H2AX phosphorylation in response to DSB formation [20, 21]. ATM is activated by its autophosphorylation at Ser1981 position, which leads to dissociation of the inactive ATM dimers into single protein molecules with increased kinase activity [18–21]. A tri-protein complex called MRN complex (MRE11-RAD50-NBS1) recognizes DNA damage, recruits ATM to the site of damage and also functions in targeting ATM to initiate phosphorylation of the respective

substrates [22–24]. It is also reported that ATM activation requires prior ATM acetylation, mediated by Tip60 histone acetyltransferase [24, 25]. Apart from H2AX, the target substrates phosphorylated by ATM are BRCA1, 53BP1, and MDC1 as well as checkpoint proteins, Chk1 and Chk2. These processes are aimed to stop the progression of the cell cycle and to activate proteins responsible for DNA repair, as is described in details below.

H2AX can also be phosphorylated by ATR and DNA-dependent protein kinases. ATR phosphorylates H2AX in response to single-stranded DNA breaks and during replication stress, such as replication fork arrest [26, 27]. DNA-PK mediates phosphorylation of H2AX in cells under hypertonic conditions and during apoptotic DNA fragmentation [28, 29]. However, DNA damage caused by ionizing radiation leads to phosphorylation of H2AX that is mediated by all PIKK kinases, ATM, ATR, and DNA-PK [30].

Recently, it was reported that some other events occur before H2AX phosphorylation in mammalian cells. Ayoub et al. [31] observed that DNA breaks mobilize heterochromatin protein 1 $\beta$  (HP1- $\beta$ ), a chromatin factor bound to histone H3 methylated on lysine 9 (H3K9me). In response to DNA damage, HP1- $\beta$  was rapidly phosphorylated at threonine 51 (Thr51) by casein kinase 2 (CK2). This phosphorylation leads to releasing HP1- $\beta$  from chromatin by disrupting hydrogen bonds that fold its chromodomain around H3K9me, resulting in its transient mobilization from chromatin. Although it is still not known what signals CK2 to phosphorylate HP1, the phosphorylation and mobilization of HP1 seems to be important for H2AX phosphorylation [31].

Based on the results of Ayoub et al. [31] and Goodarzi et al. [32, 33], it is expected that the loss of HP1 is beneficial to repair in heterochromatin. However, another recent study by Luijsterburg et al. [34], that also addressed the role of HP1 proteins in DNA damage response, suggested an apparently active and positive role for HP1 in DNA repair. These authors demonstrate that HP1 proteins accumulate de novo at sites of DNA damage, and this recruitment was independent of binding to H3K9me. It cannot be excluded that there is a partial HP1 dissociation from H3K9me at damaged sites, however the accumulation of HP1 reflects H3K9me-independent binding to damage sites rather than the rebinding of HP1 to H3K9me sites [34, 35]. Despite these controversies, the findings presented above illustrate the important role of HP1 proteins in DNA damage and open up a new direction of research to characterize the role of HP1 in H2AX phosphorylation and DNA damage response.

## 3. $\gamma$ H2AX and Its Role in DNA Damage Response

*3.1. Accumulation of DNA Damage Signaling and Repair Proteins at DSBs.* Unrepaired DSBs induce genome instability and promote tumorigenesis. Thus, cells have mechanisms responsible for recognition of DNA damage and activation of cell cycle checkpoints leading to DNA repair. The generation of DSBs triggers the relocalization of many DNA damage response (DDR) proteins such as MRE11/NBS1/RAD50,

MDC1, 53BP1, and BRCA1 to nuclear foci where these proteins colocalize and interact with  $\gamma$ H2AX [36–46]. Presumably,  $\gamma$ H2AX foci specifically attract repair factors, leading to higher concentration of repair proteins surrounding a DSB site [47, 48]. Specific recognition of  $\gamma$ H2AX by these repair factors requires the presence of protein domains, which bind to the phosphorylated carboxy terminus of  $\gamma$ H2AX. So far, two domains, which are frequently found in proteins involved in DDR, have been described to specifically recognize phosphorylated amino acid residues. The forkhead-associated (FHA) domain recognizes phosphorylated threonine residues in a specific amino acid sequence context [49]. In addition, two consecutive BRCT domains (BRCA1 C-terminal domain) can create a structural element with phospho-peptide binding capacity [50–63]. It was shown that the BRCT repeats of mediator of DNA damage checkpoint protein 1 (MDC1) build the predominant recognition module of  $\gamma$ H2AX [39, 43, 54, 55]. Interaction between MDC1 and  $\gamma$ H2AX can be recognized as the first step in which the site of the DSB is prepared for DNA damage signaling and repair. This is because there is experimental evidence that MDC1 also directly interacts in a highly dynamic manner with NBS1 [43, 56], which together with other proteins of the MRN complex is required for the activation of ATM [57, 58]. This interaction is mediated through phosphorylation of MDC1 by CK2 that, in turn, promotes phosphorylation-dependent interactions with NBS1, through its closely opposed FHA domain and two BRCA repeats [59]. In this way, a positive feed-back loop is generated that extends H2AX phosphorylation to large DNA regions (millions of base pairs).

Several lines of evidence suggest the critical role of H2AX phosphorylation at DSB sites for nuclear foci formation and induction of DSB repair.

- (i) H2AX-knockout cells manifested impaired recruitment of NBS1, 53BP1, and BRCA1 to irradiation-induced foci [45].
- (ii) Both H2AX+/- and H2AX-/- mouse thymocytes show an increase in chromosomal aberrations [60–62].
- (iii) Mouse embryonic stem (ES) cells deficient in H2AX phosphorylation have alterations in efficiency of DNA repair by NHEJ or HR [60–64]. As a result of these defects in DNA damage repair, such cells have increased sensitivity to DNA damage [60–65].
- (iv) H2AX knock-out mice show male-specific infertility and reduced levels of secondary immunoglobulin isotypes, suggesting defects in class switch recombination (CSR) [45]. It was shown that efficient resolution of DSBs induced during CSR in lymphocytes requires H2AX [61, 63], and its absence is associated with chromosome abnormalities involving the immunoglobulin locus [61].

All these facts suggest that  $\gamma$ H2AX might serve as a docking site for DNA damage/repair proteins and functions to promote DSB repair and genome stability ([60–68] and Figure 1).

**3.2. Signal Amplification and Induction of DNA Damage-Sensitive Cell Cycle Checkpoints.** One of most important kinases-activating cell cycle checkpoints following DNA damage is ATM. Mutations in the ATM gene results in the genomic instability and cancer predisposition syndrome Ataxia-Telangiectasia (AT) syndrome. In response to DSBs, ATM phosphorylates many cell cycle checkpoint-related factors such as p53, Chk2, SMC1 and NBS1 [69]. In the absence of DNA damage, ATM forms inactive homodimers, but chromatin remodeling following generation of DSBs leads to autophosphorylation of ATM at serine 1981 and dimer dissociation [18–21]. Next, phosphorylated ATM is recruited to DSB sites by its interaction with NBS1 and this recruitment is critical for phosphorylation of checkpoint proteins by ATM [57]. Mutations in the NBS1 gene result in Nijmegen breakage syndrome (NBS). Cells from both NBS and AT patients show similar phenotypes such as radio-resistant DNA synthesis, radiation hypersensitivity and genome instability [38]. As it was previously described, NBS1 forms a complex with hMRE11 and hRAD50. Since such a complex is involved in DNA double-strand break repair by homologous recombination (HR), one of the reasons of the genomic instability in NBS patients may be the defect in HR. Moreover, it was shown that this function of NBS1 requires DNA damage-induced focus formation of the NBS1/hMRE11/hRAD50 complex through direct interaction of NBS1 with  $\gamma$ H2AX at DNA damage sites [37, 70].

As mentioned above, the recruitment of ATM to DSBs is dependent on NBS1 and NBS1 forms the complex with both ATM and  $\gamma$ H2AX. Thus, both  $\gamma$ H2AX and NBS1 contribute to the recruitment of ATM to DSB sites and its activation of cell cycle checkpoints. Molecular mechanism involved in ATM recruitment to DSBs was recently investigated in detail by Kobayashi and colleagues [38]. These authors provide a line of evidence that  $\gamma$ H2AX plays an important role in the recruitment of ATM to DSB sites and the subsequent activation of ATM-related cellular response. Moreover, H2AX is a component of the complex containing ATM at DSBs and is important for activation of the ATM kinase. Importantly, H2AX-knockout cells displayed a defect in DSB-induced cell cycle checkpoint response. These results provide strong evidence that H2AX is one of essential components of the active ATM complex and participates in the activation of ATM-dependent cell cycle checkpoints. Moreover, Kobayashi and colleagues showed that ATM forms a complex with  $\gamma$ H2AX via NBS1 or MDC1 and this might be crucial for the recruitment of ATM to DSB sites and induction of ATM-dependent checkpoints [38].

**3.3.  $\gamma$ -H2AX and Chromatin Remodeling to Prevent Dissociation of Break Ends and Enhance DSB Processing and Repair Efficiency.** During last few years several groups suggested that  $\gamma$ H2AX has an important function as a docking site for protein complexes that bind to broken DNA ends and promote chromatin remodeling to keep broken chromosomal DNA ends together [60, 63, 71]. The critical role of  $\gamma$ H2AX in chromatin reorganization following DNA damage and preventing the separation of DNA ends, thus

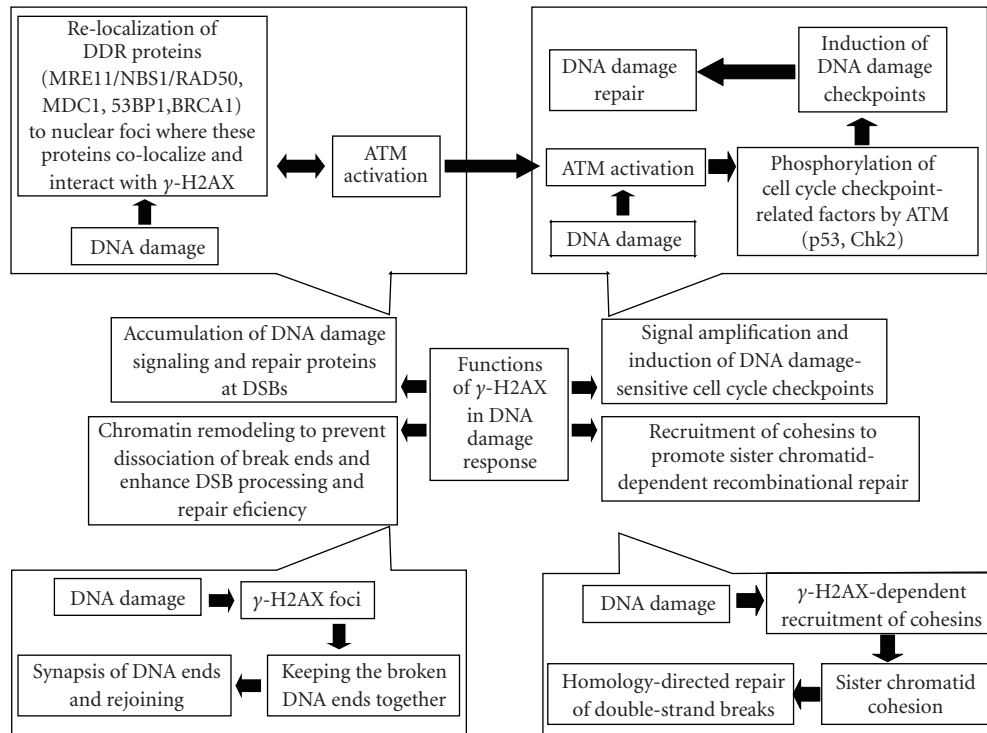


FIGURE 1: H2AX phosphorylation and its role in DNA damage response upon phosphorylation H2AX became critical player in DNA damage response. Activity of  $\gamma$ H2AX could be summarized to following main points: accumulation of DNA damage signaling and repair proteins at DSBs The generation of DSBs triggers the relocalization of many DNA damage response (DDR) proteins such as MRE11/NBS1/RAD50, MDC1, 53BP1 and BRCA1 to nuclear foci where these proteins colocalize and interact with  $\gamma$ H2AX. Signal amplification and induction of DNA damage-sensitive cell cycle checkpoints  $\gamma$ H2AX contribute to the recruitment of ATM to DSB sites and activation of ATM-dependent cell cycle checkpoints. Chromatin remodeling to prevent dissociation of break ends and enhance DSB processing and repair efficiency The  $\gamma$ H2AX foci help keeping the broken DNA ends together and make successful and faithful repair more likely. Recruitment of cohesins to the site of DNA damage to promote sister chromatid-dependent recombinational repair DNA cohesion induced by double-strand DNA break and mediated by  $\gamma$ H2AX has an important function during repair of double-strand breaks following DNA replication by holding the damaged chromatid close to its undamaged sister template.

facilitating DNA end rejoining, can be important not only in the repair of DSBs but also during V(D)J recombination. According to hypothesis put forward by Bassing and colleagues,  $\gamma$ H2AX behaves like an anchor that facilitates the assembly of multiple DNA-protein interactions involving 53BP1, MDC1/NFBD1, and MRN complexes. Formation of such complexes prevents dissociation of broken DNA ends and subsequent error-prone repair of DSBs (reviewed in [71]). Moreover, this specific “anchoring” function of H2AX at sites containing DSBs, would inhibit the irreversible disassociation of broken DNA ends and promote chromatin compaction to facilitate error-free repair, thereby suppressing inappropriate translocations of chromatin fragments. In this way,  $\gamma$ H2AX-mediated mechanisms prevent DNA ends from drifting apart, inappropriate rejoining of chromatin fragments, resulting in genetic translocations and other abnormalities (Figure 1 and reviewed in [71]).

**3.4. Recruitment of Cohesins to the Site of DNA Damage to Promote Sister Chromatid-Dependent Recombinational Repair.**  $\gamma$ H2AX might be important for processes occurring further

away from the break that are required for efficient repair. One of such processes can be sister chromatid cohesion, that in addition to its essential role in chromosome segregation, is important for efficient postreplicative double-strand DNA break repair [72]. Sister chromatid cohesion is established during S phase by cohesins. In the absence of cohesin complex, chromosomes cannot segregate properly. It was also shown that cohesins play an important role in DNA repair and recombination. Cells with mutated cohesins are oversensitive to irradiation and deficient in postreplicative DNA repair [72, 73]. Moreover, cohesins have been shown to accumulate at laser-induced DNA damage during S and G2 phases in a Mre11/Rad50- dependent manner [74]. In parallel, it was shown that DNA cohesion induced by double-strand DNA breaks and mediated by  $\gamma$ H2AX is not only important to maintain sister chromatids. It is also likely to function during repair of double-strand breaks following DNA replication by holding the damaged chromatid close to its undamaged sister template [64]. The use of genetic information present in an undamaged sister chromatid to mediate error-free recombination repair of a DSB would prevent gross chromosomal alterations, which are frequently

observed, for example, in cancer cells. Thus, this form of homology-directed DNA repair of double-strand breaks helps to maintain a high level of genome stability, even though immediate cell survival may be only minimally affected in its absence, because of other repair mechanisms (Figure 1 and reviewed in [75]).

#### 4. Methods of $\gamma$ H2AX Detection

The quantitative assessment of DSBs was initially based on methods, such as pulse-field gel electrophoresis (PFGE), DNA elution tests, or the so-called “comet assay” (single cell gel electrophoresis—SCGE). Among these methods, the comet assay is a versatile, sensitive, and widely used one. In this method individual cells with damaged DNA embedded in agarose gels are subjected to an electric field and generate a characteristic pattern of DNA distribution forming a tail that, after staining with fluorescence dye, can be analyzed by fluorescence microscopy. The extent and length of the comet’s tail correlates with the severity of DNA damage [76]. The sensitivity of the comet assay, however, depends on proper calibration and its specificity is not absolute [77, 78].

Development of an antibody, that is specific to  $\gamma$ H2AX, made it possible to detect H2AX phosphorylation and thus detection of DNA damage and repair *in situ* in individual cells. The presence of  $\gamma$ H2AX in chromatin can be detected shortly after induction of DSBs in the form of discrete nuclear foci. Since each focus represents a single DSB, their frequency reports the incidence of DSBs (reviewed in [79]). Compared with alternative methods of DNA damage assessment mentioned above, the immunocytochemical approach is less cumbersome and offers much greater sensitivity [79, 80]. The presence of  $\gamma$ H2AX-containing nuclear foci can be measured by microscopy, flow cytometry, and possibly Western blotting of cell/tissue lysates, with normalization for the total H2AX levels. Measurement of  $\gamma$ H2AX with the use of multiparameter flow or laser scanning cytometry seems to be particularly advantageous as H2AX phosphorylation can be determined in individual cells with high sensitivity and accuracy and  $\gamma$ H2AX expression in cell populations can be correlated with DNA content or induction of apoptosis [79, 80].

#### 5. Applications of $\gamma$ H2AX Detection

Assessment of H2AX phosphorylation as a reporter of DNA damage can be clinically useful. The most important clinical application of  $\gamma$ H2AX measurements is to follow DSBs levels induced by radio- and chemotherapy as a marker of treatment efficacy [81, 82] and in dose/scheduling estimation as well as to determine the efficiency of DNA repair to predict possible tumor sensitivity or resistance to DNA damaging anticancer agents. By assessing DSB levels induced by anticancer treatment in normal cells, one may also predict toxicity of anticancer treatment.

Exposure to endogenous or environmental mutagens results in DNA damage which in turn activates the DDR cascade [83, 84]. Once activated, the DDR machinery

functions as an “anticancer barrier” and delays or suppresses tumor development by inducing cell death or replicative senescence [83, 85]. However, prolonged activation of DDR may sometimes lead to survival of malignant cells if only these cells are able to bypass cell growth barrier imposed by the DDR pathway [79]. Thus, activated components of the DDR can be used as cancer biomarkers, with  $\gamma$ H2AX being the most sensitive one. In this way,  $\gamma$ H2AX level measurements may help to detect precancerous lesions or cancer at its early stages [86–88]. In this case, increased background levels of  $\gamma$ H2AX or the presence of DSBs on telomere ends may be indicative for replicative senescence, including premature senescence induced by anticancer drugs [89] or cancer progression. Finally, other possible practical applications of  $\gamma$ H2AX include screening for effects of environmental pollutants (air- or food-borne etc.) or follow-up of DNA lesions induced by mutagenic substances at work places, including nurses distributing anticancer drugs [90]. Similarly,  $\gamma$ H2AX may help to evaluate effects of chemopreventive agents.

Endogenous  $\gamma$ H2AX levels may also reflect genomic instability phenotype since optimal protection against cancer requires full functionality of both alleles of H2AX gene (*H2AFX*). Several different tumor types have been reported to possess mutations, including single gene polymorphism, amplification, or deletion in the region 11q23 that maps for *H2AFX* [62, 91]. Other groups reported alterations in H2AX gene copy number or changes in its promoter region to be associated with the risk of sporadic breast cancer and lymphomas [81, 92]. In this way, one may also relate *H2AFX* mutations or deletions with the susceptibility of individuals to tumors, such as lymphoma, acute myeloid leukemia, and head and neck cell carcinomas for tumor risk assessment studies [92–95].

#### 6. Conclusions

As discussed above, determination of  $\gamma$ H2AX levels is not only important from the fundamental perspective as a sensitive marker of the DNA damage response, including DNA repair processes. It has also many potential practical applications in monitoring effects induced by anticancer therapy and assessing tumor risk as well as in determination of DNA lesions resulting from exposure of animals and humans to environmental pollutants. However, it is important to discuss not only advantages but also potential limitations and problems of the application of  $\gamma$ H2AX in clinical practice. An obvious advantage of  $\gamma$ H2AX compared to other DNA damage markers is its extremely high sensitivity that enables one to detect very small changes in genome integrity on a single cell level. However, the lower limit of  $\gamma$ H2AX detection depends on many factors, including background levels of nuclear foci observed in unstressed cells, which are associated with DNA replication and progression through mitosis [96, 97]. In addition, background  $\gamma$ H2AX levels may differ between various tumor cells and, more importantly, between tumor and normal cells due to changed functionality of *H2AFX* discussed above. This can make it more complicated to predict the toxicity of anticancer treatment in patients

based on the direct comparison of DSBs induced in tumor *versus* normal cells.

Timing of  $\gamma$ H2AX measurements after drug treatment may also be critical for the appropriate data analysis and interpretation. Induction of H2AX phosphorylation is, at least for some agents, very rapid and this requires quick methods of patient sample acquisition and analysis. In some situations, the choice between of different sample material may be crucial for the assay (PBMLs *versus* tumor cells—leukemia, normal tissue, and tumor samples for solid tumors etc.). Moreover, anticancer treatment may lead to increased phosphorylation of H2AX due to death-associated DNA fragmentation, especially after long time periods after drug treatment or in case of agents which induce rapid apoptosis. However, cell death-related H2AX phosphorylation can be discriminated from that induced by anticancer treatment based on focal and diffuse or soluble  $\gamma$ H2AX signals [98]. This requires selection of appropriate diagnostic methods and application of biparametric flow cytometry, scanning cytometry, or fluorescence microscopy to estimate  $\gamma$ H2AX levels.

## Acknowledgments

This work was supported by a research Grant from Polish Ministry of Science and Higher Education (Grant no. N402 208535) and statutory funds from the Faculty of Chemistry, Gdansk University of Technology.

## References

- [1] S. P. Jackson, "Sensing and repairing DNA double-strand breaks," *Carcinogenesis*, vol. 23, no. 5, pp. 687–696, 2002.
- [2] E. Sonoda, H. Hohegger, A. Saberi, Y. Taniguchi, and S. Takeda, "Differential usage of non-homologous end-joining and homologous recombination in double strand break repair," *DNA Repair*, vol. 5, no. 9-10, pp. 1021–1029, 2006.
- [3] V. Smider and G. Chu, "The end-joining reaction in V(D)J recombination," *Seminars in Immunology*, vol. 9, no. 3, pp. 189–197, 1997.
- [4] S. P. Jackson, "Detecting, signalling and repairing DNA double-strand breaks," *Biochemical Society Transactions*, vol. 29, no. 6, pp. 655–661, 2001.
- [5] T. Tanaka, H. D. Halicka, X. Huang, F. Traganos, and Z. Darzynkiewicz, "Constitutive histone H2AX phosphorylation and ATM activation, the reporters of DNA damage by endogenous oxidants," *Cell Cycle*, vol. 5, no. 17, pp. 1940–1945, 2006.
- [6] T. Tanaka, X. Huang, H. D. Halicka et al., "Cytometry of ATM activation and histone H2AX phosphorylation to estimate extent of DNA damage induced by exogenous agents," *Cytometry Part A*, vol. 71, no. 9, pp. 648–661, 2007.
- [7] M. M. Vilenchik and A. G. Knudson, "Endogenous DNA double-strand breaks: production, fidelity of repair, and induction of cancer," *Proceedings of the National Academy of Sciences of the United States of America*, vol. 100, no. 22, pp. 12871–12876, 2003.
- [8] A. Takahashi and T. Ohnishi, "Does  $\gamma$ H2AX foci formation depend on the presence of DNA double strand breaks?" *Cancer Letters*, vol. 229, no. 2, pp. 171–179, 2005.
- [9] T. Tanaka, M. Kajstura, H. D. Halicka, F. Traganos, and Z. Darzynkiewicz, "Constitutive histone H2AX phosphorylation and ATM activation are strongly amplified during mitogenic stimulation of lymphocytes," *Cell Proliferation*, vol. 40, no. 1, pp. 1–13, 2007.
- [10] M. Cuadrado, B. Martinez-Pastor, and O. Fernandez-Capetillo, "ATR activation in response to ionizing radiation: still ATM territory," *Cell Division*, vol. 1, article 7, pp. 1–4, 2006.
- [11] J. C. Wang, "DNA topoisomerases," *Annual Review of Biochemistry*, vol. 65, pp. 635–692, 1996.
- [12] J. C. Wang, "Cellular roles of DNA topoisomerases: a molecular perspective," *Nature Reviews Molecular Cell Biology*, vol. 3, no. 6, pp. 430–440, 2002.
- [13] J. L. Nitiss, "DNA topoisomerase II and its growing repertoire of biological functions," *Nature Reviews Cancer*, vol. 9, no. 5, pp. 327–337, 2009.
- [14] J. E. Dewese and N. Osheroff, "The DNA cleavage reaction of topoisomerase II: wolf in sheep's clothing," *Nucleic Acids Research*, vol. 37, no. 3, pp. 738–748, 2009.
- [15] A. K. McClendon and N. Osheroff, "DNA topoisomerase II, genotoxicity, and cancer," *Mutation Research*, vol. 623, no. 1-2, pp. 83–97, 2007.
- [16] Y. Pommier, "DNA topoisomerase I Inhibitors: chemistry, biology, and interfacial inhibition," *Chemical Reviews*, vol. 109, no. 7, pp. 2894–2902, 2009.
- [17] Y. Pommier, "Topoisomerase I inhibitors: camptothecins and beyond," *Nature Reviews Cancer*, vol. 6, no. 10, pp. 789–802, 2006.
- [18] E. P. Rogakou, D. R. Pilch, A. H. Orr, V. S. Ivanova, and W. M. Bonner, "DNA double-stranded breaks induce histone H2AX phosphorylation on serine 139," *Journal of Biological Chemistry*, vol. 273, no. 10, pp. 5858–5868, 1998.
- [19] C. E. Helt, W. A. Cliby, P. C. Keng, R. A. Bambara, and M. A. O'Reilly, "Ataxia telangiectasia mutated (ATM) and ATM and Rad3-related protein exhibit selective target specificities in response to different forms of DNA damage," *Journal of Biological Chemistry*, vol. 280, no. 2, pp. 1186–1192, 2005.
- [20] M. B. Kastan and D.-S. Lim, "The many substrates and functions of ATM," *Nature Reviews Molecular Cell Biology*, vol. 1, no. 3, pp. 179–186, 2000.
- [21] C. J. Bakkenist and M. B. Kastan, "DNA damage activates ATM through intermolecular autophosphorylation and dimer dissociation," *Nature*, vol. 421, no. 6922, pp. 499–506, 2003.
- [22] A. Dupré, L. Boyer-Chatenet, and J. Gautier, "Two-step activation of ATM by DNA and the Mre11-Rad50-Nbs1 complex," *Nature Structural and Molecular Biology*, vol. 13, no. 5, pp. 451–457, 2006.
- [23] N. Srivastava, S. Gochhait, P. de Boer, and R. N. K. Bamezai, "Role of H2AX in DNA damage response and human cancers," *Mutation Research*, vol. 681, no. 2-3, pp. 180–188, 2009.
- [24] Y. Sun, X. Jiang, S. Chen, N. Fernandes, and B. D. Price, "A role for the Tip60 histone acetyltransferase in the acetylation and activation of ATM," *Proceedings of the National Academy of Sciences of the United States of America*, vol. 102, no. 37, pp. 13182–13187, 2005.
- [25] Y. Sun, Y. Xu, K. Roy, and B. D. Price, "DNA damage-induced acetylation of lysine 3016 of ATM activates ATM kinase activity," *Molecular and Cellular Biology*, vol. 27, no. 24, pp. 8502–8509, 2007.
- [26] I. M. Ward and J. Chen, "Histone H2AX is phosphorylated in an ATR-dependent manner in response to replicational stress," *Journal of Biological Chemistry*, vol. 276, no. 51, pp. 47759–47762, 2001.

- [27] I. M. Ward, K. Minn, and J. Chen, "UV-induced ataxia-telangiectasia-mutated and Rad3-related (ATR) activation requires replication stress," *Journal of Biological Chemistry*, vol. 279, no. 11, pp. 9677–9680, 2004.
- [28] B. Mukherjee, C. Kessinger, J. Kobayashi et al., "DNA-PK phosphorylates histone H2AX during apoptotic DNA fragmentation in mammalian cells," *DNA Repair*, vol. 5, no. 5, pp. 575–590, 2006.
- [29] T. Reitsemá, D. Klovov, J. P. Banáth, and P. L. Olive, "DNA-PK is responsible for enhanced phosphorylation of histone H2AX under hypertonic conditions," *DNA Repair*, vol. 4, no. 10, pp. 1172–1181, 2005.
- [30] H. Wang, M. Wang, H. Wang, W. Böcker, and G. Iliakis, "Complex H2AX phosphorylation patterns by multiple kinases including ATM and DNA-PK in human cells exposed to ionizing radiation and treated with kinase inhibitors," *Journal of Cellular Physiology*, vol. 202, no. 2, pp. 492–502, 2005.
- [31] N. Ayoub, A. D. Jeyasekharan, J. A. Bernal, and A. R. Venkataraman, "HP1- $\beta$  mobilization promotes chromatin changes that initiate the DNA damage response," *Nature*, vol. 453, no. 7195, pp. 682–686, 2008.
- [32] A. A. Goodarzi, A. T. Noon, D. Deckbar et al., "ATM signaling facilitates repair of DNA double-strand breaks associated with heterochromatin," *Molecular Cell*, vol. 31, no. 2, pp. 167–177, 2008.
- [33] A. A. Goodarzi, A. T. Noon, and P. A. Jeggo, "The impact of heterochromatin on DSB repair," *Biochemical Society Transactions*, vol. 37, no. 3, pp. 569–576, 2009.
- [34] M. S. Luijsterburg, C. Dinant, H. Lans et al., "Heterochromatin protein 1 is recruited to various types of DNA damage," *Journal of Cell Biology*, vol. 185, no. 4, pp. 577–586, 2009.
- [35] C. Dinant and M. S. Luijsterburg, "The emerging role of HP1 in the DNA damage response," *Molecular and Cellular Biology*, vol. 29, no. 24, pp. 6335–6340, 2009.
- [36] T. T. Paull, E. P. Rogakou, V. Yamazaki, C. U. Kirchgessner, M. Gellert, and W. M. Bonner, "A critical role for histone H2AX in recruitment of repair factors to nuclear foci after DNA damage," *Current Biology*, vol. 10, no. 15, pp. 886–895, 2000.
- [37] J. Kobayashi, H. Tauchi, S. Sakamoto et al., "NBS1 localizes to  $\gamma$ -H2AX foci through interaction with the FHA/BRCT domain," *Current Biology*, vol. 12, no. 21, pp. 1846–1851, 2002.
- [38] J. Kobayashi, A. Antocchia, H. Tauchi, S. Matsuura, and K. Komatsu, "NBS1 and its functional role in the DNA damage response," *DNA Repair*, vol. 3, no. 8–9, pp. 855–861, 2004.
- [39] G. S. Stewart, B. Wang, C. R. Bigneli, A. M. R. Taylor, and S. J. Elledge, "MDC1 is a mediator of the mammalian DNA damage checkpoint," *Nature*, vol. 421, no. 6926, pp. 961–966, 2003.
- [40] M. Stucki and S. P. Jackson, " $\gamma$ H2AX and MDC1: anchoring the DNA-damage-response machinery to broken chromosomes," *DNA Repair*, vol. 5, no. 5, pp. 534–543, 2006.
- [41] I. M. Ward, K. Minn, K. G. Jorda, and J. Chen, "Accumulation of checkpoint protein 53BP1 at DNA breaks involves its binding to phosphorylated histone H2AX," *Journal of Biological Chemistry*, vol. 278, no. 22, pp. 19579–19582, 2003.
- [42] L. B. Schultz, N. H. Chehab, A. Malikzay, and T. D. Halazonetis, "p53 binding protein 1 (53BP1) is an early participant in the cellular response to DNA double-strand breaks," *Journal of Cell Biology*, vol. 151, no. 7, pp. 1381–1390, 2000.
- [43] M. Stucki, J. A. Clapperton, D. Mohammad, M. B. Yaffe, S. J. Smerdon, and S. P. Jackson, "MDC1 directly binds phosphorylated histone H2AX to regulate cellular responses to DNA double-strand breaks," *Cell*, vol. 123, no. 7, pp. 1213–1226, 2005.
- [44] Z. Lou, K. Minter-Dykhouse, S. Franco et al., "MDC1 maintains genomic stability by participating in the amplification of ATM-dependent DNA damage signals," *Molecular Cell*, vol. 21, no. 2, pp. 187–200, 2006.
- [45] A. Celeste, S. Petersen, P. J. Romanienko et al., "Genomic instability in mice lacking histone H2AX," *Science*, vol. 296, no. 5569, pp. 922–927, 2002.
- [46] K. Minter-Dykhouse, I. Ward, M. S. Y. Huen, J. Chen, and Z. Lou, "Distinct versus overlapping functions of MDC1 and 53BP1 in DNA damage response and tumorigenesis," *Journal of Cell Biology*, vol. 181, no. 5, pp. 727–735, 2008.
- [47] T. Kouzarides, "Chromatin modifications and their function," *Cell*, vol. 128, no. 4, pp. 693–705, 2007.
- [48] S. D. Taverna, H. Li, A. J. Ruthenburg, C. D. Allis, and D. J. Patel, "How chromatin-binding modules interpret histone modifications: lessons from professional pocket pickers," *Nature Structural and Molecular Biology*, vol. 14, no. 11, pp. 1025–1040, 2007.
- [49] D. Durocher, J. Henckel, A. R. Fersht, and S. P. Jackson, "The FHA domain is a modular phosphopeptide recognition motif," *Molecular Cell*, vol. 4, no. 3, pp. 387–394, 1999.
- [50] I. A. Manke, D. M. Lowery, A. Nguyen, and M. B. Yaffe, "BRCT repeats as phosphopeptide-binding modules involved in protein targeting," *Science*, vol. 302, no. 5645, pp. 636–639, 2003.
- [51] X. Yu, C. C. S. Chini, M. He, G. Mer, and J. Chen, "The BRCT domain is a phospho-protein binding domain," *Science*, vol. 302, no. 5645, pp. 639–642, 2003.
- [52] J. A. Clapperton, I. A. Manke, D. M. Lowery et al., "Structure and mechanism of BRCA1 BRCT domain recognition of phosphorylated BACH1 with implications for cancer," *Nature Structural and Molecular Biology*, vol. 11, no. 6, pp. 512–518, 2004.
- [53] R. S. Williams, M. S. Lee, D. D. Hau, and J. N. M. Glover, "Structural basis of phosphopeptide recognition by the BRCT domain of BRCA1," *Nature Structural and Molecular Biology*, vol. 11, no. 6, pp. 519–525, 2004.
- [54] C. Lukas, F. Melander, M. Stucki et al., "Mdc1 couples DNA double-strand break recognition by Nbs1 with its H2AX-dependent chromatin retention," *EMBO Journal*, vol. 23, no. 13, pp. 2674–2683, 2004.
- [55] M. Rodriguez, X. Yu, J. Chen, and Z. Songyang, "Phosphopeptide Binding Specificities of BRCA1 COOH-terminal (BRCT) Domains," *Journal of Biological Chemistry*, vol. 278, no. 52, pp. 52914–52918, 2003.
- [56] M. Goldberg, M. Stucki, J. Falck et al., "MDC1 is required for the intra-S-phase DNA damage checkpoint," *Nature*, vol. 421, no. 6926, pp. 952–956, 2003.
- [57] J. Falck, J. Coates, and S. P. Jackson, "Conserved modes of recruitment of ATM, ATR and DNA-PKcs to sites of DNA damage," *Nature*, vol. 434, no. 7033, pp. 605–611, 2005.
- [58] Z. You, C. Chahwan, J. Bailis, T. Hunter, and P. Russell, "ATM activation and its recruitment to damaged DNA require binding to the C terminus of Nbs1," *Molecular and Cellular Biology*, vol. 25, no. 13, pp. 5363–5379, 2005.
- [59] J. R. Chapman and S. P. Jackson, "Phospho-dependent interactions between NBS1 and MDC1 mediate chromatin retention of the MRN complex at sites of DNA damage," *EMBO Reports*, vol. 9, no. 8, pp. 795–801, 2008.

- [60] A. Celeste, S. Difilippantonio, M. J. Difilippantonio et al., "H2AX haploinsufficiency modifies genomic stability and tumor susceptibility," *Cell*, vol. 114, no. 3, pp. 371–383, 2003.
- [61] S. Petersen, R. Casellas, B. Reina-San-Martin et al., "AID is required to initiate Nbs1/ $\gamma$ -H2AX focus formation and mutations at sites of class switching," *Nature*, vol. 414, no. 6864, pp. 660–665, 2001.
- [62] C. H. Bassing, K. F. Chua, J. Sekiguchi et al., "Increased ionizing radiation sensitivity and genomic instability in the absence of histone H2AX," *Proceedings of the National Academy of Sciences of the United States of America*, vol. 99, no. 12, pp. 8173–8178, 2002.
- [63] B. Reina-San-Martin, S. Difilippantonio, L. Hanitsch, R. F. Masilamani, A. Nussenzweig, and M. C. Nussenzweig, "H2AX is required for recombination between immunoglobulin switch regions but not for intra-switch region recombination or somatic hypermutation," *Journal of Experimental Medicine*, vol. 197, no. 12, pp. 1767–1778, 2003.
- [64] A. Xie, N. Puget, I. Shim et al., "Control of sister chromatid recombination by histone H2AX," *Molecular Cell*, vol. 16, no. 6, pp. 1017–1025, 2004.
- [65] J. Kao, M. T. Milano, A. Javaheri et al., " $\gamma$ -H2AX as a therapeutic target for improving the efficacy of radiation therapy," *Current Cancer Drug Targets*, vol. 6, no. 3, pp. 197–205, 2006.
- [66] S. Franco, M. Gostissa, S. Zha et al., "H2AX prevents DNA breaks from progressing to chromosome breaks and translocations," *Molecular Cell*, vol. 21, no. 2, pp. 201–214, 2006.
- [67] A. R. Ramiro, M. Jankovic, E. Callen et al., "Role of genomic instability and p53 in AID-induced c-myc-Igh translocations," *Nature*, vol. 440, no. 7080, pp. 105–109, 2006.
- [68] A. Kinner, W. Wu, C. Staudt, and G. Iliakis, "Gamma-H2AX in recognition and signaling of DNA double-strand breaks in the context of chromatin," *Nucleic Acids Research*, vol. 36, no. 17, pp. 5678–5694, 2008.
- [69] S. Matsuoka, B. A. Ballif, A. Smogorzewska et al., "ATM and ATR substrate analysis reveals extensive protein networks responsive to DNA damage," *Science*, vol. 316, no. 5828, pp. 1160–1166, 2007.
- [70] S. Sakamoto, K. Iijima, D. Mochizuki et al., "Homologous recombination repair is regulated by domains at the N- and C-terminus of NBS1 and is dissociated with ATM functions," *Oncogene*, vol. 26, no. 41, pp. 6002–6009, 2007.
- [71] C. H. Bassing and F. W. Alt, "H2AX may function as an anchor to hold broken chromosomal DNA ends in close proximity," *Cell Cycle*, vol. 3, no. 2, pp. 149–153, 2004.
- [72] C. Sjögren and K. Nasmyth, "Sister chromatid cohesion is required for postreplicative double-strand break repair in *Saccharomyces cerevisiae*," *Current Biology*, vol. 11, no. 12, pp. 991–995, 2001.
- [73] E. Sonoda, T. Matsusaka, C. Morrison et al., "Scc1/Rad21/Mcd1 is required for sister chromatid cohesion and kinetochore function in vertebrate cells," *Developmental Cell*, vol. 1, no. 6, pp. 759–770, 2001.
- [74] J.-S. Kim, T. B. Krasieva, V. LaMorte, A. M. Taylor, and K. Yokomori, "Specific recruitment of human cohesin to laser-induced DNA damage," *Journal of Biological Chemistry*, vol. 277, no. 47, pp. 45149–45153, 2002.
- [75] N. F. Lowndes and G. W.-L. Toh, "DNA repair: the importance of phosphorylating histone H2AX," *Current Biology*, vol. 15, no. 3, pp. R99–R102, 2005.
- [76] O. Ostling and K. J. Johanson, "Microelectrophoretic study of radiation-induced DNA damages in individual mammalian cells," *Biochemical and Biophysical Research Communications*, vol. 123, no. 1, pp. 291–298, 1984.
- [77] A. R. Collins, A. A. Oscoz, G. Brunborg et al., "The comet assay: topical issues," *Mutagenesis*, vol. 23, no. 3, pp. 143–151, 2008.
- [78] D. G. McArt, G. McKerr, C. V. Howard, K. Saetzier, and G. R. Wasson, "Modelling the comet assay," *Biochemical Society Transactions*, vol. 37, no. 4, pp. 914–917, 2009.
- [79] X. Huang, H. D. Halicka, F. Traganos, T. Tanaka, A. Kurose, and Z. Darzynkiewicz, "Cytometric assessment of DNA damage in relation to cell cycle phase and apoptosis," *Cell Proliferation*, vol. 38, no. 4, pp. 223–243, 2005.
- [80] Z. Darzynkiewicz, X. Huang, and M. Okafuji, "Detection of DNA strand breaks by flow and laser scanning cytometry in studies of apoptosis and cell proliferation (DNA replication)," *Methods in Molecular Biology*, vol. 314, pp. 81–93, 2006.
- [81] J. A. Downs, "Chromatin structure and DNA double-strand break responses in cancer progression and therapy," *Oncogene*, vol. 26, no. 56, pp. 7765–7772, 2007.
- [82] N. Taneja, M. Davis, J. S. Choy et al., "Histone H2AX phosphorylation as a predictor of radiosensitivity and target for radiotherapy," *Journal of Biological Chemistry*, vol. 279, no. 3, pp. 2273–2280, 2004.
- [83] J. Bartkova, Z. Hořejší, K. Koed et al., "DNA damage response as a candidate anti-cancer barrier in early human tumorigenesis," *Nature*, vol. 434, no. 7035, pp. 864–870, 2005.
- [84] T. D. Halazonetis, V. G. Gorgoulis, and J. Bartek, "An oncogene-induced DNA damage model for cancer development," *Science*, vol. 319, no. 5868, pp. 1352–1355, 2008.
- [85] J. Campisi, "Suppressing cancer: the importance of being senescent," *Science*, vol. 309, no. 5736, pp. 886–887, 2005.
- [86] L. J. Kuo and L.-X. Yang, " $\gamma$ -H2AX—a novel biomarker for DNA double-strand breaks," *In Vivo*, vol. 22, no. 3, pp. 305–310, 2008.
- [87] O. A. Sedelnikova and W. M. Bonner, " $\gamma$ H2AX in cancer cells: a potential biomarker for cancer diagnostics, prediction and recurrence," *Cell Cycle*, vol. 5, no. 24, pp. 2909–2913, 2006.
- [88] V. G. Gorgoulis, L.-V. F. Vassiliou, P. Karakaidos et al., "Activation of the DNA damage checkpoint and genomic instability in human precancerous lesions," *Nature*, vol. 434, no. 7035, pp. 907–913, 2005.
- [89] I. B. Roninson, "Tumor cell senescence in cancer treatment," *Cancer Research*, vol. 63, no. 11, pp. 2705–2715, 2003.
- [90] P. V. Rekhadevi, N. Sailaja, M. Chandrasekhar, M. Mahboob, M. F. Rahman, and P. Grover, "Genotoxicity assessment in oncology nurses handling anti-neoplastic drugs," *Mutagenesis*, vol. 22, no. 6, pp. 395–401, 2007.
- [91] C. H. Bassing, H. Suh, D. O. Ferguson et al., "Histone H2AX: a dosage-dependent suppressor of oncogenic translocations and tumors," *Cell*, vol. 114, no. 3, pp. 359–370, 2003.
- [92] K. L. Novik, J. J. Spinelli, A. C. Macarthur et al., "Genetic variation in H2AFX contributes to risk of non-Hodgkin lymphoma," *Cancer Epidemiology Biomarkers and Prevention*, vol. 16, no. 6, pp. 1098–1106, 2007.
- [93] J. Lu, Q. Wei, M. L. Bondy et al., "Genetic variants in the H2AFX promoter region are associated with risk of sporadic breast cancer in non-Hispanic white women aged  $\leq 55$  years," *Breast Cancer Research and Treatment*, vol. 110, no. 2, pp. 357–366, 2008.

- [94] M. J. Thirman, H. J. Gill, R. C. Burnett et al., "Rearrangement of the MLL gene in acute lymphoblastic and acute myeloid leukemias with 11q23 chromosomal translocations," *New England Journal of Medicine*, vol. 329, no. 13, pp. 909–914, 1993.
- [95] R. A. Parikh, J. S. White, X. Huang et al., "Loss of distal 11q is associated with DNA repair deficiency and reduced sensitivity to ionizing radiation in head and neck squamous cell carcinoma," *Genes Chromosomes and Cancer*, vol. 46, no. 8, pp. 761–775, 2007.
- [96] Y. Ichijima, R. Sakasai, N. Okita, K. Asahina, S. Mizutani, and H. Teraoka, "Phosphorylation of histone H2AX at M phase in human cells without DNA damage response," *Biochemical and Biophysical Research Communications*, vol. 336, no. 3, pp. 807–812, 2005.
- [97] K. J. McManus and M. J. Hendzel, "ATM-dependent DNA damage-independent mitotic phosphorylation of H2AX in normally growing mammalian cells," *Molecular Biology of the Cell*, vol. 16, no. 10, pp. 5013–5025, 2005.
- [98] Y. Liu, M. Tseng, S. A. Perdreau et al., "Histone H2AX is a mediator of gastrointestinal stromal tumor cell apoptosis following treatment with imatinib mesylate," *Cancer Research*, vol. 67, no. 6, pp. 2685–2692, 2007.

## Research Article

# Differential Dynamics of ATR-Mediated Checkpoint Regulators

Daniël O. Warmerdam,<sup>1</sup> Roland Kanaar,<sup>1,2</sup> and Veronique A. J. Smits<sup>3</sup>

<sup>1</sup>Department of Cell Biology and Genetics, Cancer Genome Center, Erasmus MC, Dr. Molewaterplein 50, 3015 GE Rotterdam, The Netherlands

<sup>2</sup>Department of Radiation Oncology, Erasmus MC, Dr. Molewaterplein 50, 3015 GE Rotterdam, The Netherlands

<sup>3</sup>Unidad de Investigación, Hospital Universitario de Canarias, Ofra s/n, La Laguna 38320, Tenerife, Spain

Correspondence should be addressed to Veronique A. J. Smits, vsmits@ull.es

Received 3 May 2010; Accepted 28 June 2010

Academic Editor: Ashis Basu

Copyright © 2010 Daniël O. Warmerdam et al. This is an open access article distributed under the Creative Commons Attribution License, which permits unrestricted use, distribution, and reproduction in any medium, provided the original work is properly cited.

The ATR-Chk1 checkpoint pathway is activated by UV-induced DNA lesions and replication stress. Little was known about the spatio and temporal behaviour of the proteins involved, and we, therefore, examined the behaviour of the ATRIP-ATR and Rad9-Rad1-Hus1 putative DNA damage sensor complexes and the downstream effector kinase Chk1. We developed assays for the generation and validation of stable cell lines expressing GFP-fusion proteins. Photobleaching experiments in living cells expressing these fusions indicated that after UV-induced DNA damage, ATRIP associates more transiently with damaged chromatin than members of the Rad9-Rad1-Hus1 complex. Interestingly, ATRIP directly associated with locally induced UV damage, whereas Rad9 bound in a cooperative manner, which can be explained by the Rad17-dependent loading of Rad9 onto damaged chromatin. Although Chk1 dissociates from the chromatin upon UV damage, no change in the mobility of GFP-Chk1 was observed, supporting the notion that Chk1 is a highly dynamic protein.

## 1. Introduction

Eukaryotic cells are continuously threatened by DNA damage caused by environmental factors and intracellular metabolic processes. To protect themselves against these potential threats, cells have developed DNA damage checkpoint and repair mechanisms, which help to ensure transmission of an intact genome. Cell cycle checkpoints and DNA repair mechanisms together determine the ultimate faith of the cell after suffering DNA damage. Activation of the DNA damage checkpoint involves the activation of transducer kinases ATR/ATM and subsequently the effector kinases Chk1/Chk2 [1]. So-called mediator proteins, including Claspin and BRCA1, were additionally discovered, and function either in the recruitment of substrates to DNA lesions or as scaffolds on which protein complexes are assembled [2, 3]. In response to a variety of DNA damaging agents like UV light and replication stress, the ATR-mediated checkpoint pathway is activated. Biochemical data indicates that ATRIP, in complex with ATR, binds to RPA-coated single stranded

DNA (ssDNA) [4]. Independently, the Rad17-RFC complex is also recruited to sites of damage. The Rad17-RFC protein complex facilitates the loading of the Rad9-Rad1-Hus1 (9-1-1 complex) sliding clamp onto the DNA [5–7]. Subsequently, TopBP1 is recruited to DNA lesions by binding to the Rad9 subunit of the 9-1-1 complex, thereby locating near the ATRIP-ATR heterodimer. Through an interaction with TopBP1, ATR becomes fully active, resulting in the activation of effector kinase Chk1 and subsequent checkpoint arrest [8–10].

Detection of DNA alterations after genotoxic stress is essential for the survival of cells and gaining more insight into the early events of the DNA damage response will give a better understanding of how DNA damage checkpoints function, how genome stability is achieved, and how cancer can develop. In recent years, biochemical work has provided invaluable insight into the requirements, substrates, and activities of proteins involved in the ATR-mediated checkpoint pathway [11–13]. Although the importance for protein localization after DNA damage induction has been reported

for proteins involved in the response to double-stranded breaks (DSBs), not much is known about how the ATR-Chk1 pathway operates in living cells and moreover, how the spatio and temporal behaviour of proteins in this pathway influence the DNA damage response [14, 15]. We set out to study the behaviour of ATRIP-ATR and 9-1-1 DNA damage sensor complexes by creating cDNA constructs expressing GFP- (green fluorescent protein-) tagged proteins in human cells. The use of GFP-fusion proteins creates advantages over using standard immunofluorescence techniques as it avoids fixation methods and antibody artefacts. In addition, GFP-labelled proteins can be followed in time using live cell video microscopy. Furthermore, due to the spectral qualities of GFP and its variants it has become possible to perform quantitative fluorescent analysis [16–18]. The use of GFP-labelled proteins opens up a number of new possibilities in the DNA damage response field. First, the localization GFP-fusion proteins can be directly followed into DNA damage-induced nuclear foci. Second, the ability to measure in time makes it possible to establish an order of events occurring directly after DNA damage induction. Third, the existence of multiple spectral GFP-variants allows for the simultaneous detection of several fluorescently labelled proteins in a single cell [19–21]. Forth, live cell video microscopy in combination with GFP-photobleaching experiments can be applied to quantitatively determine changes in protein mobility in response to DNA damage. Collectively, these tools help to increase our understanding of cellular mechanisms involved in DNA damage response.

The accumulation of DNA damage response proteins at sites of damage, shown in cells as nuclear foci, is essential for downstream checkpoint events, although how, is not yet fully understood [22–24]. Many, if not most, proteins in the ATR-mediated checkpoint pathway are recruited to sites of damage into nuclear foci. As a result, a proportion of the total amount of free proteins becomes immobilized in these foci due to interactions with either the damaged chromatin or other proteins at the DNA lesion. To gain more understanding of the DNA damage-induced behaviour of a protein, its localization and mobility can be determined. The DNA damage-induced change in protein mobility has been studied for several proteins involved in the DNA damage response, mainly in DNA repair and in response to double stranded breaks (DSBs) [17, 25–27]. The studies performed on proteins involved in nucleotide excision repair (NER), for example, have been important in understanding this DNA repair process and helped explain some of the phenotypic characteristics seen in patients that harbour mutations in proteins in this pathway. This indicates the importance of these types of studies for research in cancer and related diseases associated with genome instability [28, 29].

A method was setup for the generation of stable cell lines expressing GFP-fusion proteins and different assays to validate and characterize GFP-expressing cell lines were developed. We analyzed the dynamic behaviour of multiple proteins involved in the ATR checkpoint pathway including all three components of the 9-1-1 complex, ATRIP, and of the downstream kinase Chk1. We compared the mobility changes of these proteins after UV-irradiation and together

the results indicated a distinct dynamic behaviour of the studied proteins. Whereas effector kinase Chk1 was highly mobile and did not immobilize upon DNA damage, Rad9 and ATRIP were associated to sites of DNA damage. ATRIP directly bound to DNA lesions but in a more transient manner than Rad9, which displayed a relatively slow exchange with damaged chromatin. Together these data demonstrate the importance of spatio and temporal protein regulation in the cells response to DNA damage.

## 2. Materials and Methods

**2.1. Cell Culture.** U2OS, HeLa, and 293T cells were grown using standard procedures. U2OS and HeLa cells stably expressing eGFP-fusion proteins were grown in standard medium supplemented with 350–700  $\mu\text{g}/\text{mL}$  of G418 (gentamicin).

**2.2. Antibodies.** Antibodies obtained from commercial sources were as follows: Orc2 (BD Pharmingen), Grb2 (BD Transduction), RPA (Ab2, Oncogene), Rad9 (Novus),  $\gamma\text{H2AX}$  (Upstate), Chk1-pS317 (Cell Signaling), and Chk1 (Abcam). The following antibodies were obtained from Santa Cruz Biotechnology: CENP-F (H-260), Cyclin A (H-432), Cyclin B1 (GNS1), Ku86 (C-20), Chk1 (G-4), Rad1 (N-18), Rad9 (C-20), and ATR (N-19).

Rabbit polyclonal anti-Rad9, anti-Hus1, and anti-GFP were described before and a kind gift by R. Freire (Tenerife, Spain) [30, 31]. Rabbit polyclonal anti-ATRIP was a kind gift by P. M. Reaper (UK) [32].

**2.3. Transfection.** Plasmid DNA was transfected into cells using the calcium phosphate transfection method.

siRNA oligonucleotides (Dharmacon Research) were transfected into cells using Oligofectamine (Invitrogen) according to the manufacturer's instructions and as previously described [33]. Sequences of oligonucleotides were as follows:

Luc (CGUACGCGGAAUACUUCGAdTdT),  
 Chk1 (UCGUGAGCGUUUGUUGAACdTdT)  
 Rad9 (ACCACUAUAGGCAAUGAGGdTdT)  
 Rad9 3'UTR (CCAAGAACCUGAAGCCUGUUU/  
 GAAUCCAGCUUUGACCUUUU).

**2.4. Colony Survival Assays.** Cells were counted and 1000 cells were seeded onto 60 mm diameter dishes whereafter left for 12 hours to attach. Cells were treated with different doses of UV (5, 10, 15, and 20  $\text{J}/\text{m}^2$ ) and incubated for 7–14 days, after which the colonies were fixed, stained, and counted. All experiments were performed in triplicate.

**2.5. Immunofluorescence.** For immunostaining, cells were fixed in 2% paraformaldehyde containing 0.2% Triton X-100 for 20 minutes at RT and then permeabilized with 0.1% Triton X-100 for 5 minutes at RT. Samples were blocked in 1% FCS and immunostained with antibodies as indicated. For detection of GFP-tagged proteins in U2OS cells, living

cells were studied or cells were fixed and permeabilized as above.

Images were made using a Cell Observer fluorescent microscope equipped with Axiovision software (Zeiss) or a Confocal Laser Scanning Microscope LSM 510 (Zeiss), equipped with a 488 nm Ar-laser and a 505–530 nm bandpass filter for green fluorescence. Red fluorescence was detected using a 543 nm laser and 560 nm longpass filter. For strip-FRAP experiments and time lapse imaging after UV laser induction, GFP-tagged proteins were detected in living cells using a Confocal Laser Scanning Microscope LSM 510 (Zeiss), equipped with a 488 nm Ar-laser and a 505–530 nm bandpass filter for green fluorescence.

**2.6. Whole Cell Extracts and Cell Fractionation.** For whole cell extracts, cells were washed in cold PBS, after which the cells were resuspended in Laemmli sample buffer (4% SDS, 20% glycerol, 120 mM Tris pH 6.8) and boiled for 5 minutes. Protein concentrations were determined using the Lowry protein assay. Chromatin fractionation was performed as previously described [34, 35].

**2.7. Generation of DNA Damage and Photobleaching Techniques.** UV-irradiation was performed using a 254 nm UV-C lamp (Philips) at 20 J/m<sup>2</sup> and cells were processed 1 hour posttreatment. Cells were incubated with 5  $\mu$ g/mL of aphidicolin (Sigma) for 20 hours prior to processing of samples. Cells were incubated with 200 nM camptothecin (Sigma) for 20 hours before fixation. IR (10 Gy) was induced using a <sup>137</sup>Cs source or a linear accelerator (LINAC) and cells were processed 2 hours after treatment. Local UV laser induction was performed as previously described [36]. In short, cells were grown on a 25 mm quartz coverslip. A small area inside the nucleus was exposed for ~1 second to a 2 mW pulsed (7.8 kHz) diode laser emitting at 266 nm. Time-lapse images were made every minute immediately starting after local UV induction. The time course measurements were normalized to the plateau phase. Start of UV irradiation was defined as  $t = 0$ . Assembly curves were normalized to 1 and processed as previously described [26].

In the FRAP experiments, a strip spanning the nucleus was photobleached for 20 milliseconds using an Ar-laser (488 nm) at 100% laser intensity, which irreversibly bleaches all GFP molecules in that area. Subsequently, the redistribution of fluorescence in the strip was monitored by taking confocal images every 20 milliseconds for a total of 24 seconds at low laser intensity to avoid further bleaching. The fluorescence before bleaching ( $I_{t<0}$ ) was set to 1 and the intensity immediately after bleaching ( $I_0$ ) was set to 0. The recovery of fluorescence was plotted against time.

In the FLIP experiments, half of the nucleus was continuously bleached using an Ar-laser (488 nm) at 50% laser intensity. Subsequently, the loss of fluorescence in the unbleached area was monitored taking confocal images every 10 seconds for a total of 300 seconds at low laser intensity. The fluorescence before bleaching ( $I_{t<0}$ ) was set to

1. The loss of fluorescence was plotted against time. FLIP-FRAP experiments were performed as previously described [33, 37].

### 3. Results

**3.1. Generation of Cell Lines Stably Expressing GFP-Tagged Proteins.** The limitations of conventional fixation methods were overcome by the introduction of GFP, the green fluorescent protein derived from *Aequorea Victoria*, a species of jellyfish [38, 39]. Through the cloning of the cDNA encoding GFP, it became possible to fluorescently label proteins and express them, thereby creating the opportunity for monitoring proteins in living cells. Different fluorescent versions of the GFP exist such as the red fluorescent (RFP), yellow fluorescent (YPF), and cyan fluorescent (CFP) protein, and many more spectral variants have been created since [40]. The expression of GFP and derivatives itself in mammalian cells is not harmful although the protein originates from a different species. Nonetheless, labelling of proteins with (fluorescent) epitopes can potentially influence the behaviour of the labelled protein. Validation and functional analysis of a GFP-fusion protein construct, therefore, is essential for the interpretation of experimentally obtained data.

The amount of fluorescence signal in a cell population derived from a single cell clone is in principle identical in all cells and, therefore, comparing fluorescence intensities after different treatments becomes reliable. We setup a method for the creation, generation, and validation of GFP-fusion proteins for the purpose of live cell imaging. The approach is schematically depicted in Figure 1(a) and discussed below.

**3.1.1. Creation of GFP-Tagged Protein Constructs.** After the discovery of GFP and its potential usefulness in biology, the protein itself became the subject of intensive research. Certain mutations in the GFP gene lead to different spectral variants and improvements in the protein characteristics, such as an increase in brightness (fluorescent intensity) and photo stability [41]. These qualities can be found in, for example, the GFP variant called “enhanced GFP” (eGFP). Vectors encoding for eGFP and fluorescent derivatives are commercially available (Clontech) and have been published [40]. In the studies presented here, we made use of vectors containing eGFP or eGFP with the addition of two other, nonfluorescent epitopes, namely, an HA- and His-tag (eGFP will hereafter be referred to as GFP). The additional epitope creates the possibility to detect the GFP-fusion protein with antibodies directed against the HA- and/or His-tags. Additionally, these tags can be used for immunoprecipitation experiments to identify interaction partner proteins.

For proper cellular function a protein needs to be folded correctly upon its expression. Since GFP and the cDNA of interest encode for two proteins that are attached, proper protein folding might be influenced by sterical hindrance. As a possible solution to this problem, adding a small

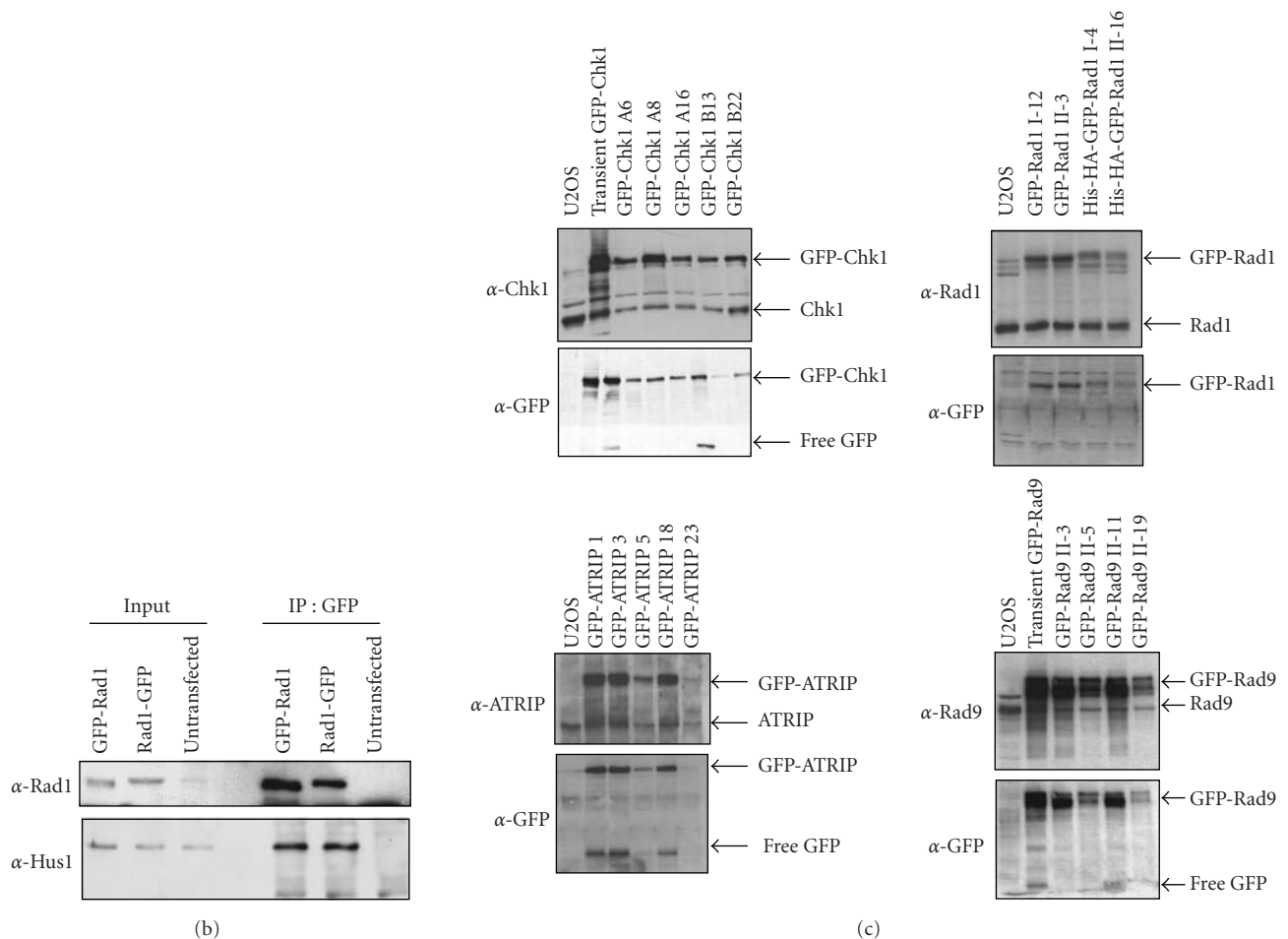
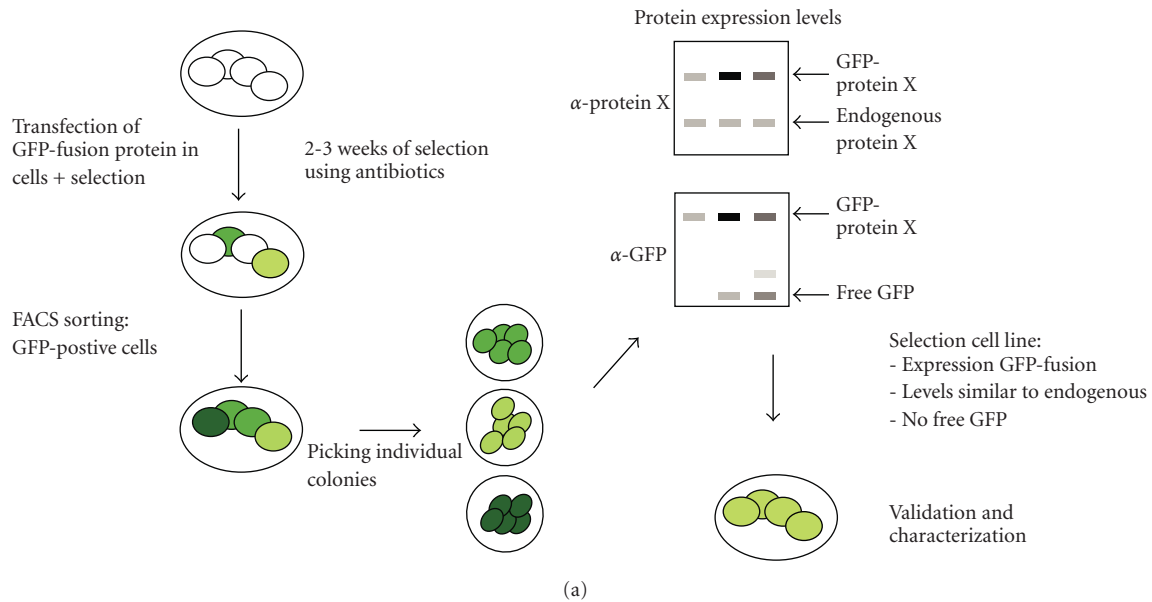


FIGURE 1: Generation of stable cell lines expressing GFP-tagged proteins. (a) Stepwise protocol for stable expression of GFP-fusion proteins in cells. (b) 293T cells were transfected with GFP-Rad1, Rad1-GFP, or mock transfected, after which cells were lysed and immunoprecipitations were carried out using anti-GFP antibody. Western blot analysis of the immunoprecipitates using the indicated antibodies. (c) Protein expression analysis of different stable clones. Western blot analysis of whole cell extracts using the indicated antibodies.

DNA sequence linker in between the sequence encoding for GFP and the cDNA this can be minimized [38, 42]. In addition, such a linker might help to restore the functionality of the protein, as a rigid tag might interfere with, for example, binding to (endogenous) partners.

In addition to a neomycin resistance cassette for selection, the GFP vectors contain a CMV promoter that is compatible with expression in immortalized cells, such as the human osteosarcoma (U2OS) and epithelial cervical cancer (Hela) cell lines used in this study. As adding a tag might influence protein functionality, it is advisable to construct both N- and C-terminal labelled versions of the proteins. cDNA was cloned into the GFP-vectors via PCR and/or restriction enzyme cutting and religating by T4 DNA ligase, resulting in plasmids encoding an in-frame sequence of GFP and the cDNA of interest. After obtaining the right plasmid DNA the functionality of the GFP-fusion protein was tested by determining the interaction with its known binding partners. In this way a reasonable choice can be made to continue with either the N- or C-terminally tagged version of the protein, or both. After transient expression of the cDNA encoding the GFP-fusion protein and the known binding partner, cell extracts were prepared for immunoprecipitation using antibodies against GFP. The interaction with the known binding partners was determined by western blotting. The N- and C-terminally labelled proteins from the Rad9-Rad1-Hus1 complex were tested in this manner. Labelling of Rad1 at either site of the protein did not influence the interaction with endogenous Hus1 (Figure 1(b)). GFP-labelling of Rad9 at the C-terminus completely abrogated the interaction with its binding partners whereas Hus1 labelling at the N-terminus decreased the binding to its partners (data not shown). When binding partners of a GFP-fusion protein are not known or do not exist and/or antibodies are not available testing for functionality must be performed in a different manner. Later in this section, different assays that can be used to validate the function of the GFP-tagged protein in living cells are described.

*3.1.2. Expression of GFP-Tagged Proteins in Human Cells.* After obtaining cDNA encoding a GFP-fusion protein, cells were transfected to achieve random integration of the GFP-fusion construct. We used the well studied human U2OS and Hela cells for the expression of the GFP-fusion protein since these cells are well-suited for both live cell imaging and siRNA-mediated downregulation of proteins. We obtained a transient transfection efficiency of ~70% in both Hela and U2OS cells using the calcium-phosphate transfection method, whereafter we started with antibiotic selection. Importantly, multiple copies of the cDNA can be incorporated in the genome and the site (s) of integration additionally may create artefacts and influence cellular behaviour. In human cells this problem can only be tackled by using retroviral constructs that integrate only once. To minimize these possible artefacts we only selected individual clones expressing low amounts of GFP-fusion proteins.

*3.1.3. Selection of GFP-Positive Cells Using an Antibiotic Selection Marker.* To obtain cells that incorporated at least one copy of the GFP-fusion cDNA we used antibiotic selection through the neomycin-resistance cassette present in the GFP vector. To achieve stable integration of the cDNA in the genome of the transfected cells, cells were seeded in different densities and selected using 700 µg/mL G418 for at least two weeks, refreshing the medium with antibiotics every 3 days.

*3.1.4. FACS Sorting of GFP-Positive Cells.* G418 selection caused cell death of cells that did not integrate the cDNA construct in their genome. GFP-positive cells were sorted from the total population by FACS. Approximately 5%–10% of the cells became GFP-positive after two weeks of G418 selection. This small percentage is most likely due to an incorrect integration the GFP-fusion cDNA causing expression of the only part of the construct including the G418 resistance cassette. The sorted GFP-positive cells were replated in different dilutions so that single cells could grow into discrete colonies. Cells were kept in similar conditions of antibiotic selection as previously used and medium was refreshed at least twice a week.

*3.1.5. Picking of Individual Cell Colonies.* After the multiplication of a single cell into a colony of around 50–100 cells, the colonies were randomly picked under sterile conditions using an inverted light microscope. At least 24 colonies were picked for every cell line. The selected colonies were kept in individual wells and were cultured until completely confluent, whereafter split into two plates. One plate was frozen and the other one was used to prepare cell lysates for expression analysis.

*3.1.6. Determining Protein Expression Levels of the GFP-Fusion.* The cell lysates from individual clones were analyzed by SDS-PAGE and western blotting using antibodies specifically against the protein of interest and GFP. Expression levels of the endogenous compared to the GFP-fusion protein was determined as well as the amount of free GFP or the existence of degradation products.

*3.1.7. Selecting Clones Expressing Relatively Low Amounts of GFP-Tagged Protein.* Clones were selected on the basis of the following criteria: low expression levels of the GFP-fusion protein (not higher than that of the endogenous protein) and the absence of free GFP or other undefined products, based on the western blotting analysis. A number of 4 clones that meet these criteria were selected and thawed for further validation. Clones were cultured in medium containing 350 µg/mL G418 to maintain expression of the GFP-fusion protein.

With the method described above stable cell lines were obtained that express a GFP-fusion from the ATR-Chk1 pathway, namely, ATRIP, Rad17, Rad9, Rad1, Hus1, and Chk1 (Figure 1(c) and data not shown). We also generated control cell lines expressing GFP and H2B-GFP-Chk1.

**3.1.8. Validation and Characterization of the Selected Stable Cell Lines.** To validate the functionality of the GFP-fusion protein and characterize the stable cell lines we utilized a number of assays.

Immunoprecipitations (IP) of the GFP-fusion protein were performed to confirm the interaction of the GFP-fusion with its known endogenous protein partners. We published before that GFP-Rad9 interacts with its endogenous partners Rad1 and Hus1 [33]. A similar experiment was performed with GFP-ATRIP, which demonstrated that the GFP-fusion was able to bind endogenous ATR (Figure 2(a)).

To check if stable expression of the GFP-fusion protein influences the cells response to DNA damage by functioning as a dominant negative, we determined the sensitivity of our cell lines to genotoxic stress. We compared the colony survival in response to UV light of the stable clones to the parental untransfected cell line. As shown in Figure 2(b), the expression of the GFP-Rad9 in both HeLa and U2OS cells did not alter the sensitivity to UV damage, indicating that GFP-Rad9 does not function as a dominant negative. The expression of GFP alone in HeLa cells also did not influence sensitivity to UV-irradiation.

The ATR-dependent checkpoint pathway is triggered in response to genotoxic stress and induces the ATR-mediated phosphorylation of Chk1, which results in a temporal cell cycle arrest [11]. To test if expression of the GFP-fusion proteins influences checkpoint activation we monitored the UV-induced phosphorylation of Chk1. Expression of GFP-ATRIP and GFP-Chk1 did not influence the levels of phosphorylated Chk1 (Figure 2(c)). GFP-Chk1 is phosphorylated in response to UV damage, indicating the GFP-tagged Chk1 behaves similarly to the endogenous one. To study the G2 phase arrest induced by DNA damage, we determined the mitotic index of cells expressing GFP-Chk1 and untransfected cells. A similar decrease in mitotic cells upon ionizing radiation (IR) was observed in GFP-Chk1 expressing and control cells, indicating that expression of GFP-Chk1 does not interfere with the DNA damage-induced G2 checkpoint (Figure 2(d)).

Although these assays demonstrate the absence of a dominant negative effect of the GFP-fusions, to definitively rule out problems due to GFP-tagging, complementation of a mutant or knock out cell line is required. Cells derived from Seckel syndrome patients that harbour a mutation in the ATR gene, leading to an abrogated expression of the ATR protein, are available [43], but most proteins in this pathway are essential for cell viability making a direct complementation impossible in human cells. In addition, knock outs of Rad9 and Hus1 in mouse embryonic stem cells are lethal, although the lethality of Hus1 disruption can be rescued by knocking out p21 [44–46]. Chicken DT40 cells can be successfully used for knocking out genes that are essential in mammalian cells, like Chk1, but are less suitable for the generation of stable GFP-fusion cell lines and live cell imaging, since these cells are genomically unstable and can only be cultured in suspension [47]. Another approach is siRNA-mediated downregulation of the endogenous protein and subsequent complementation by expression of the GFP-tagged protein. We favour this option since in this way we are able to study

both the functionality of the GFP-fusion protein as well as its mobility in the same cell line.

To specifically downregulate the endogenous protein, different siRNA-mediated approaches are available. First, as the cDNA encoding for the GFP-fusion protein does not contain a 3'UTR, the use of siRNA oligos that specifically target this region of the protein of interest should result in knock down of the endogenous protein only. We applied this approach in cells expressing GFP-Rad9. Figure 2(e) demonstrates that 48 hours after transfection with siRNA oligo number 1, endogenous Rad9 is more efficiently downregulated than the GFP-labelled Rad9 protein. At 72 hours after transfection, the efficiency of downregulation became less, demonstrating that knock down is optimal 48 hours after transfection with siRNA oligo number 1. Transfection with siRNA oligo number 2 also lowered endogenous Rad9 levels more than the GFP-labelled Rad9 protein levels and the efficiency of downregulation was similar between 48 and 72 hours after transfection. In an alternative approach, a silent mutation is made in the cDNA of the GFP-tagged protein, thereby leaving the encoded protein unchanged. By using siRNA oligos that recognize the mRNA from the endogenous but not the GFP-fusion protein, the endogenous protein can be specifically downregulated, such that the functionality of the GFP-fusion protein can be assessed [33]. Collectively the performed validation assays indicate that the introduction and stable expression of GFP-fusions of Chk1, ATRIP, Rad9, Rad1, and Hus1 did not change the response of these cells to DNA damage. These GFP-fusion proteins can therefore be seen as functional equivalents of their endogenous counterparts.

**3.2. Cellular Localization of GFP-Fusion Proteins in Response to DNA Damage.** Numerous studies over the past years indicated that the accumulation of DNA damage response proteins at sites of damage is of crucial importance for downstream checkpoint events [14, 22, 24, 48, 49]. Although for many proteins involved in checkpoint regulation a (relatively small) fraction of the total pool of proteins is bound to chromatin in unperturbed cells, the majority of these proteins relocalize and accumulate at or near sites of DNA lesions to form so-called nuclear foci [50]. GFP-Rad9, for example, localizes into foci after the treatment with different DNA damaging agents (Figure 3(a)).

To investigate the specific DNA substrate onto which a protein is recruited, different DNA damaging agents can be tested, as well as colocalization with other proteins involved in the DNA damage response. Biochemical experiments indicated that the Rad17-RFC and ATRIP-ATR protein complexes are recruited to DNA damage-induced RPA-coated ssDNA and this localization induces the activation of the downstream kinase Chk1 [4, 51, 52]. Rad9, a component of the 9-1-1 complex, is loaded onto the DNA by Rad17-RFC in response to DNA damage [5, 53]. We observed colocalization of GFP-Rad9 and RPA upon treatment of cells with both UV light and IR, suggesting that Rad9 is recruited to sites of RPA-coated ssDNA (Figure 3(a)). In response to DNA damage, histone H2AX is phosphorylated at Ser139 by ATM/ATR [54]. Although phosphorylation

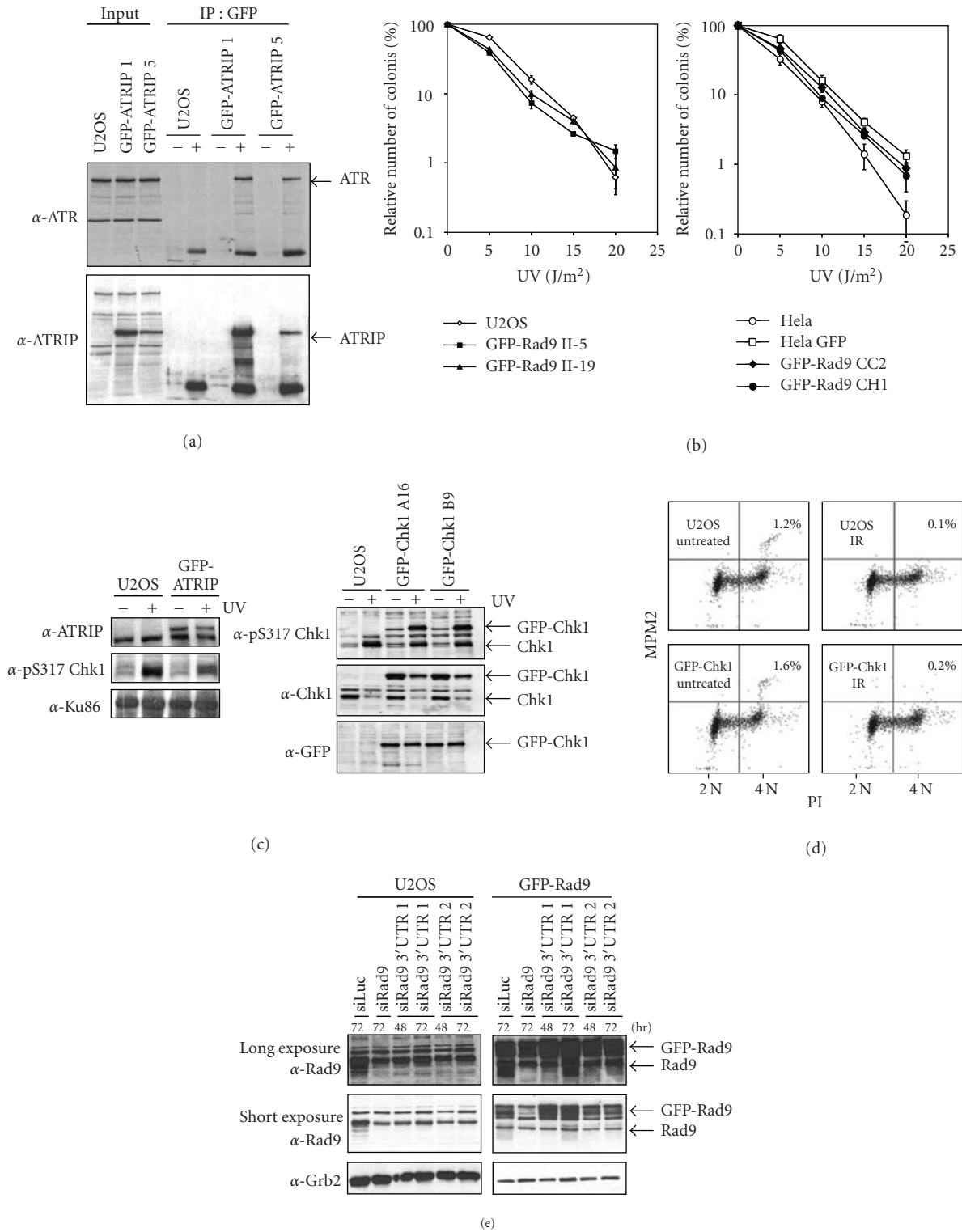


FIGURE 2: Validation and functionality of stable cells expressing GFP-fusions. (a) Two independent U2OS clones expressing GFP-ATRIP were lysed after which immunoprecipitations were carried out using anti-GFP antibody. Western blot analysis of the immunoprecipitates using the indicated antibodies. (b) U2OS and HeLa cells expressing GFP-Rad9 were seeded in low density and treated with different doses of UV. The number of surviving colonies after 10 days was counted. (c) Left panel: cells expressing GFP-ATRIP or control U2OS cells were left untreated or treated with UV. One hour later, cells were lysed and analyzed by western blotting with the indicated antibodies. Right panel: as left panel, but with two clones expressing GFP-Chk1. (d) Control U2OS cells or cells expressing GFP-Chk1 were left untreated or treated with 10 Gy IR. After 2 hours, cells were fixed and stained with PI and MPM2 and analyzed by FACS. The percentage of mitotic cells is indicated. (e) U2OS cells expressing GFP-Rad9 were transfected with siRNA oligos directed against Rad9 or the 3'UTR of Rad9 for the indicated time periods. Cell extracts were prepared and western blot analysis was performed using the indicated antibodies.

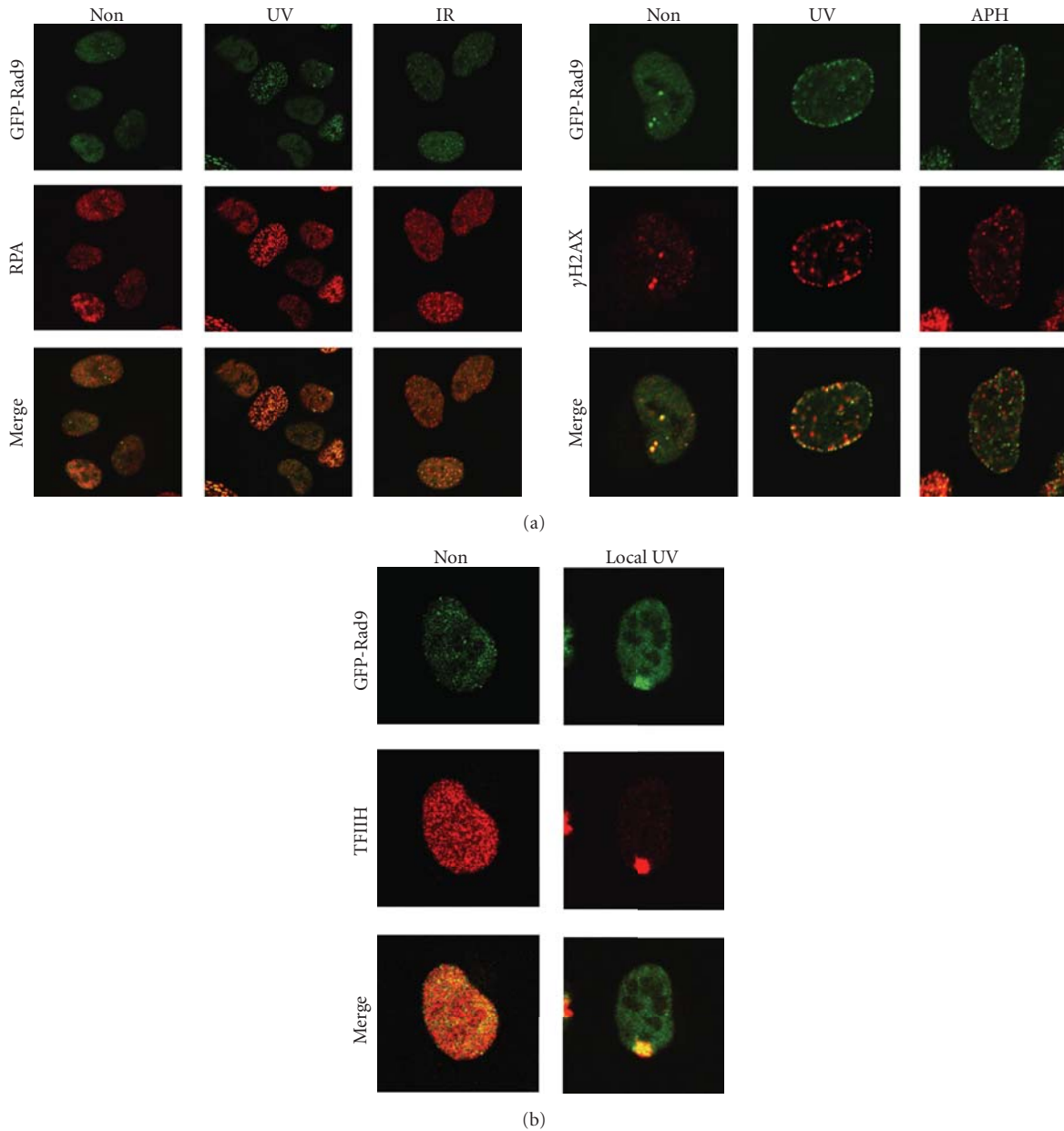


FIGURE 3: DNA damage-induced foci formation of GFP-Rad9. (a) GFP-Rad9 expressing cells were left untreated or exposed to UV, IR, or aphidicolin. GFP-Rad9 was detected by direct fluorescence and RPA and  $\gamma$ H2AX by immunofluorescence. (b) GFP-Rad9 expressing cells were treated with  $40 \text{ J/m}^2$  local UV-irradiation using an isopore filter. One hour later the cells were fixed and stained. GFP-Rad9 was detected by direct fluorescence and TFIIH by immunofluorescence.

of H2AX ( $\gamma$ H2AX) is commonly used to identify DSBs,  $\gamma$ H2AX is also induced in response to UV light or treatment with other agents that do not directly induce DSBs, like the replication inhibitor aphidicolin (Figure 3(a)) [55]. We observed colocalization of GFP-Rad9 and  $\gamma$ H2AX in all UV-induced foci whereas treatment of cells with aphidicolin or IR did not result in a complete colocalization of the two proteins (Figure 3(a) and data not shown). Close inspection demonstrated that foci induced by aphidicolin either contained both GFP-Rad9 and  $\gamma$ H2AX or  $\gamma$ H2AX only. Since the phosphorylation of H2AX is triggered in response

to a wide variety of DNA lesions, we conclude that GFP-Rad9 is only recruited to a subset of aphidicolin-induced DNA lesions.

Not all proteins accumulate into foci, even though they are recruited to sites of DNA damage. Proteins involved in nucleotide excision repair, for example, do not form foci in response to genotoxic stress. The accumulation of these proteins onto damaged DNA can be visualized by applying local UV damage in the nucleus. By irradiating the cells while covered with an isopore filter, the UV light can only penetrate the pores and as a consequence, only a small

part(s) of the nucleus contains damaged DNA [56, 57]. As shown in Figure 3(b), proteins involved in the ATR-mediated checkpoint pathway, such as Rad9, also accumulate onto local UV damage. This method requires fixation of cells and is therefore unsuitable for live cell imaging. The development of laser-induced DNA damage circumvented this problem [26, 36, 58]. Laser-induced DNA damage can be easily combined with live cell imaging and different types of lasers are commonly available [15, 59]. For example, recent studies make use of specific types of sources and lasers, specifically inducing subsets of DNA lesions such as CPDs and 6-4P induced by UV light, and DSBs [14, 36, 56, 60, 61]. Nonetheless caution is required, as often sources and lasers also produce other, unwanted, types of lesions, that may influence protein behaviour adversely [36, 62].

We did not observe the accumulation of the effector kinase Chk1 into nuclear foci in response to DNA damage nor onto locally applied UV-induced DNA damage using a filter (data not shown), in contrast to ATR, TopBP1, 9-1-1 members, and many other checkpoint mediator proteins. In this sense, Chk1 behaves similarly to Chk2, the effector kinase for the cellular response to DSBs [15]. In order to trigger a cell cycle arrest in response to DNA damage, these effector kinases phosphorylate a range of substrates that are present throughout the nucleus. Although both Chk1 and Chk2 do not associate to chromatin after DNA damage, Chk1 associates to chromatin in unperturbed cells and is released from the chromatin in response to DNA damage [35]. In the light of this, the absence of accumulated Chk1 at sites of DNA lesions was to be expected.

**3.3. Quantitative GFP-Fusion Protein Dynamics.** By measuring the change in mobility of a protein in response to DNA damage a number of parameters can be determined. First, the time the protein spends at the site of a DNA lesion and second, the fraction of the total amount of protein engaged in that process. Fluorescent Redistribution after Photobleaching (FRAP) is applied to study the mobility of GFP-fusion proteins in living cells. In a defined region (strip) of the nucleus, the fluorescence is irreversibly photobleached through brief illumination at high laser intensity (strip-FRAP). Redistribution or recovery of the total fluorescence in the bleached area is then measured in time, indicative of protein mobility [16, 63, 64].

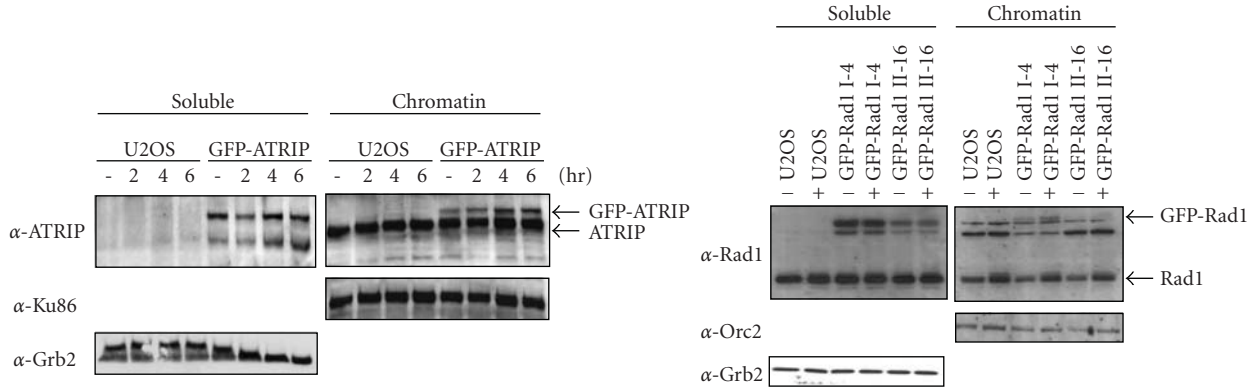
To gain further understanding of how the proteins in the ATR-pathway sense DNA lesions and subsequently respond to trigger the checkpoint-mediated cell cycle arrest, the dynamic behaviour of these proteins was studied. We demonstrated that GFP-Rad1, GFP-ATRIP, and GFP-Rad9 form foci and are recruited to chromatin in response to DNA damage, as shown by chromatin fractionation (Figure 4(a), data not shown) [21]. To address whether these proteins become immobilized at sites of DNA lesions, we determined the change in mobility of GFP-Rad1, GFP-Rad9, Hus1-GFP, and GFP-ATRIP upon UV-irradiation. Importantly, the total amount of GFP-labelled molecules could be different between cells and between GFP-fusion protein cell lines. These two discrepancies could potentially influence photobleaching results since relative immobilization is dependent

on the total amount of protein available. To adjust for cell-to-cell differences in a population, we normalized the obtained measurements as described in Section 2. Furthermore, we used saturating amounts of UV-irradiation to be sure that all possible molecules would be engaged (data not shown). Although we did not measure the exact amount of GFP-fusion molecules per cell, western blotting analysis indicates that the different GFP-fusion proteins are expressed to a similar extent (Figure 1(b)).

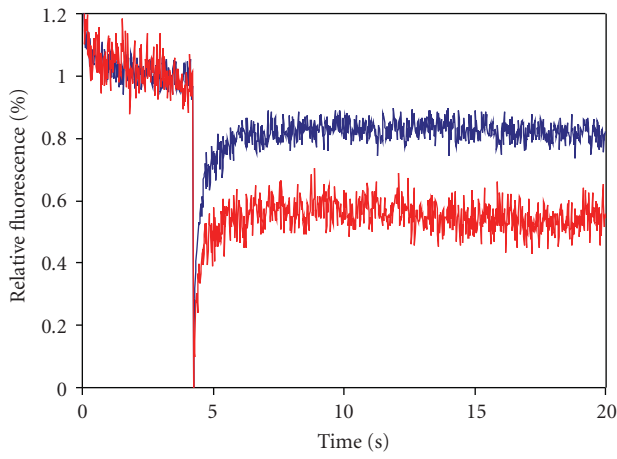
In response to UV light, 20%–40% of the 9-1-1 complex proteins become immobilized (Figures 4(b)–4(e)). The GFP-Rad1 and Hus1-GFP FRAP curves show more variability compared to the GFP-Rad9 FRAP curve, which is probably due to the fluorescent variety of the GFP-Rad1 and Hus1-GFP cell lines and the amount of cells that were measured (Figures 4(b)–4(d)). Although the ATRIP-ATR complex is also recruited to sites of DNA damage, relatively less GFP-ATRIP is immobilized (5%–10%) in response to UV damage as compared to either of the proteins of the 9-1-1 complex (Figure 4(e)). These data demonstrate that the 9-1-1 and ATRIP-ATR complexes behave differently after DNA damage and suggest that ATRIP displays a higher turnover at sites of DNA lesions.

To further investigate the possible distinct behaviour between these two putative DNA damage sensor complexes Fluorescent Loss after photobleaching (FLIP) experiments were performed. During FLIP half of the nucleus is constantly bleached and the loss of fluorescence in the unbleached half of the nucleus is measured, representing the rate of dissociation. As shown in Figure 4(f), nondamaged cells expressing either GFP-Rad9 or GFP-ATRIP completely lost fluorescence 150 seconds after start of bleaching ( $k_{1/2} \sim 15$  seconds). After UV irradiation the dissociation rates were less fast. GFP-ATRIP completely lost fluorescence after 250 seconds ( $k_{1/2} \sim 25$  seconds) whereas GFP-Rad9 after more than 300 seconds ( $k_{1/2} \sim 40$  seconds). These FLIP experiments indicate that after DNA damage induction both ATRIP and Rad9 become less mobile, but the release (dissociation) of ATRIP from sites of damage is faster than Rad9. These data are in accordance to the FRAP experiments, that show relatively less immobilization of ATRIP upon UV irradiation as compared to the proteins of the 9-1-1 complex.

The rate at which proteins associate to sites of DNA lesions was addressed by measuring the accumulation of proteins upon local UV laser irradiation. Briefly, a small area inside the nucleus is irradiated with a 266 nm UV laser. GFP-Rad9 and GFP-ATRIP fluorescence in the locally damaged area was measured every 60 seconds until a plateau was reached. GFP-ATRIP quickly started accumulating at the damaged area and reaches a plateau  $\sim 20$  minutes after damage induction ( $k_{1/2} \sim 6$  minutes) (Figure 4(g)). GFP-Rad9 accumulation in the first 8 minutes is relatively slow, but rises faster thereafter and reaches a plateau after  $\sim 30$  minutes ( $k_{1/2} \sim 12$  minutes) (Figure 4(g)). These results indicate that ATRIP and Rad9 associate very differently to UV-damaged DNA and suggest that ATRIP is recruited directly to the sites of damage in an exponential manner, following Michaelis-Menten kinetics

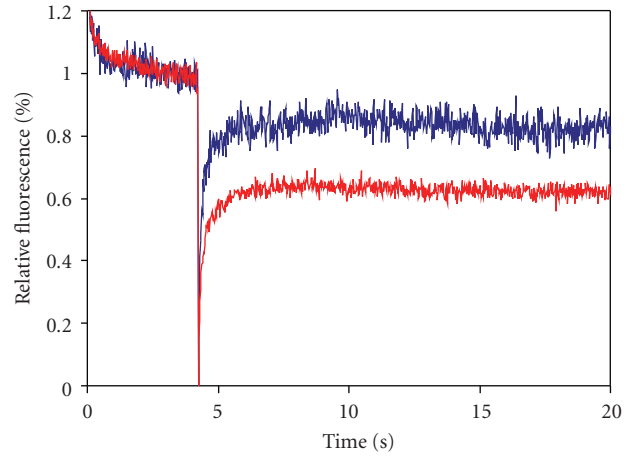


(a)



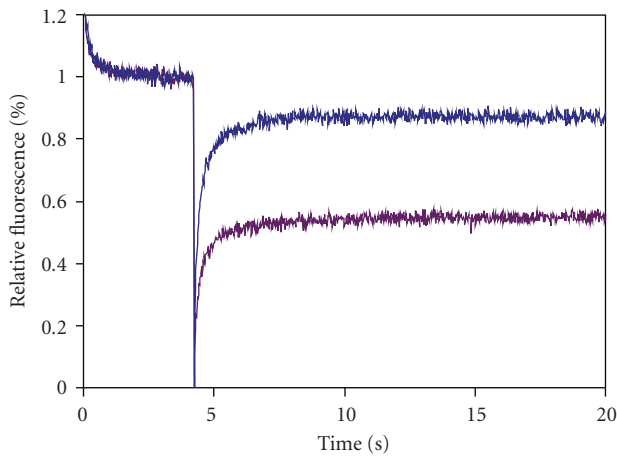
— Hus1-GFP untreated,  $n = 6$   
 — Hus1-GFP UV,  $n = 7$

(b)



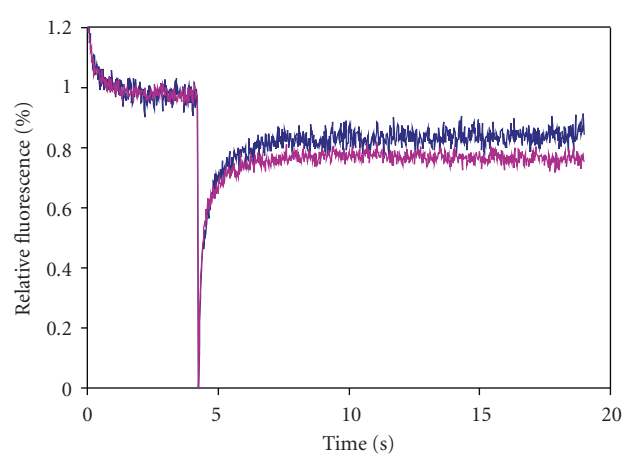
— GFP-Rad1 untreated,  $n = 8$   
 — GFP-Rad1 UV,  $n = 25$

(c)



— GFP-Rad9 untreated,  $n = 33$   
 — GFP-Rad9 UV,  $n = 36$

(d)



— GFP-ATRIP untreated,  $n = 19$   
 — GFP-ATRIP UV,  $n = 35$

(e)

FIGURE 4: Continued.

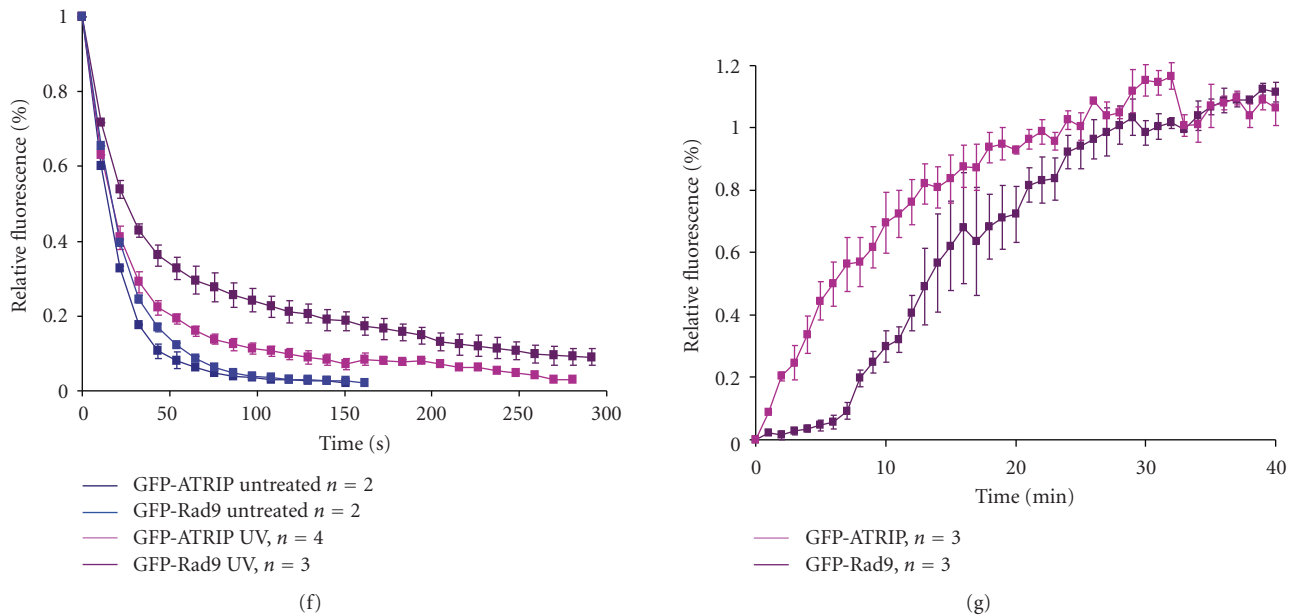


FIGURE 4: UV-induced changes in mobility of checkpoint proteins. (a) U2OS cells expressing GFP-ATRIP (left panel) and GFP-Rad1 (right panel) were left untreated or treated with UV. Two hours later, soluble and chromatin-bound proteins were isolated and analyzed by western blotting using the indicated antibodies. (b–e) Hus1-GFP (b), GFP-Rad1 (c), GFP-Rad9 (d), and GFP-ATRIP (e) expressing cells were left untreated or treated with UV and analyzed by strip-FRAP (see Section 2 for technical details). (f) U2OS cells expressing GFP-Rad9 or GFP-ATRIP were left untreated or treated with UV. After 1 hour cells were analyzed by FLIP (see Section 2 for technical details). Plotted is the loss of fluorescence during continuous bleaching. (g) U2OS cells expressing GFP-Rad9 or GFP-ATRIP were locally irradiated using a 266 nm UV laser. Plotted is the association of fluorescent signal at the locally damaged area.

[65] whereas the accumulation kinetics of Rad9 follow a sigmoidal curve (non-Michaelis-Menten kinetics), representing cooperative binding [66]. Rad17-dependent loading of Rad9 onto the DNA might explain this cooperative binding of GFP-Rad9 after DNA damage induction [67], compared to ATRIP-ATR which binds directly to RPA-coated ssDNA [4].

Chk1 is phosphorylated at or near the DNA lesion and thereafter released from the chromatin [35] and consequently, the amount of immobilized GFP-Chk1 measured by photobleaching experiments might become lower after DNA damage induction. To test this hypothesis, we performed strip-FRAP on cells expressing GFP-Chk1 treated with UV light. We compared the GFP-Chk1 mobility with that of free GFP and an artificially immobile form of Chk1, where GFP-Chk1 was fused to histone H2B (H2B-GFP-Chk1) [35]. Upon photobleaching GFP-Chk1 demonstrated a fast recovery of fluorescence both before and after UV damage (Figure 5(a)). The recovery was similar to that of free GFP, arguing against the existence of a stably bound GFP-Chk1 fraction. Since GFP-Chk1 was present in relatively high levels due to overexpression in addition to endogenous Chk1, we reasoned that the amount of Chk1 might be too high to observe any change in protein mobility upon DNA damage induction. Therefore, we lowered the total amount of Chk1 by RNA interference. Cells expressing GFP-Chk1 were transfected with either control luciferase or Chk1 siRNA oligos. Twenty four hours later cells were treated with

UV light and chromatin fractions were prepared. As shown in Figure 5(b), both endogenous and GFP-labelled Chk1 were released from chromatin upon DNA damage induction in control downregulated cells, although the GFP-tagged version less efficiently than endogenous Chk1 (endogenous 64%, GFP-labelled 16%). Transfection of Chk1 siRNA oligos resulted in downregulation of endogenous Chk1 and did not influence the release of Chk1 from chromatin. Although GFP-Chk1 is less efficiently released from the chromatin than endogenous Chk1, a small but considerable fraction of GFP-Chk1 (~15%) is released in response to DNA damage, which is comparable to the previous experiment without the depletion of endogenous Chk1.

Next, we lowered the total amount of Chk1 in GFP-Chk1 expressing cells by siRNA-mediated downregulation. Subsequent strip-FRAP analysis indicated that nondamaged GFP-Chk1 expressing cells did not contain more immobile GFP-Chk1 molecules compared to UV-treated cells (Figure 5(c)). Downregulation of Chk1 did not influence the recovery of residual GFP-Chk1 fluorescence in untreated cells and accordingly it did not change GFP-Chk1 mobility after UV-treatment.

The strip-FRAP experiments demonstrated the absence of a stably bound Chk1 pool in these conditions. Nonetheless, these experiments were performed in a relatively short period of time (20 seconds). Since Chk1 released from the chromatin in response to UV-induced DNA damage could be a more gradual and thus time-dependent process,

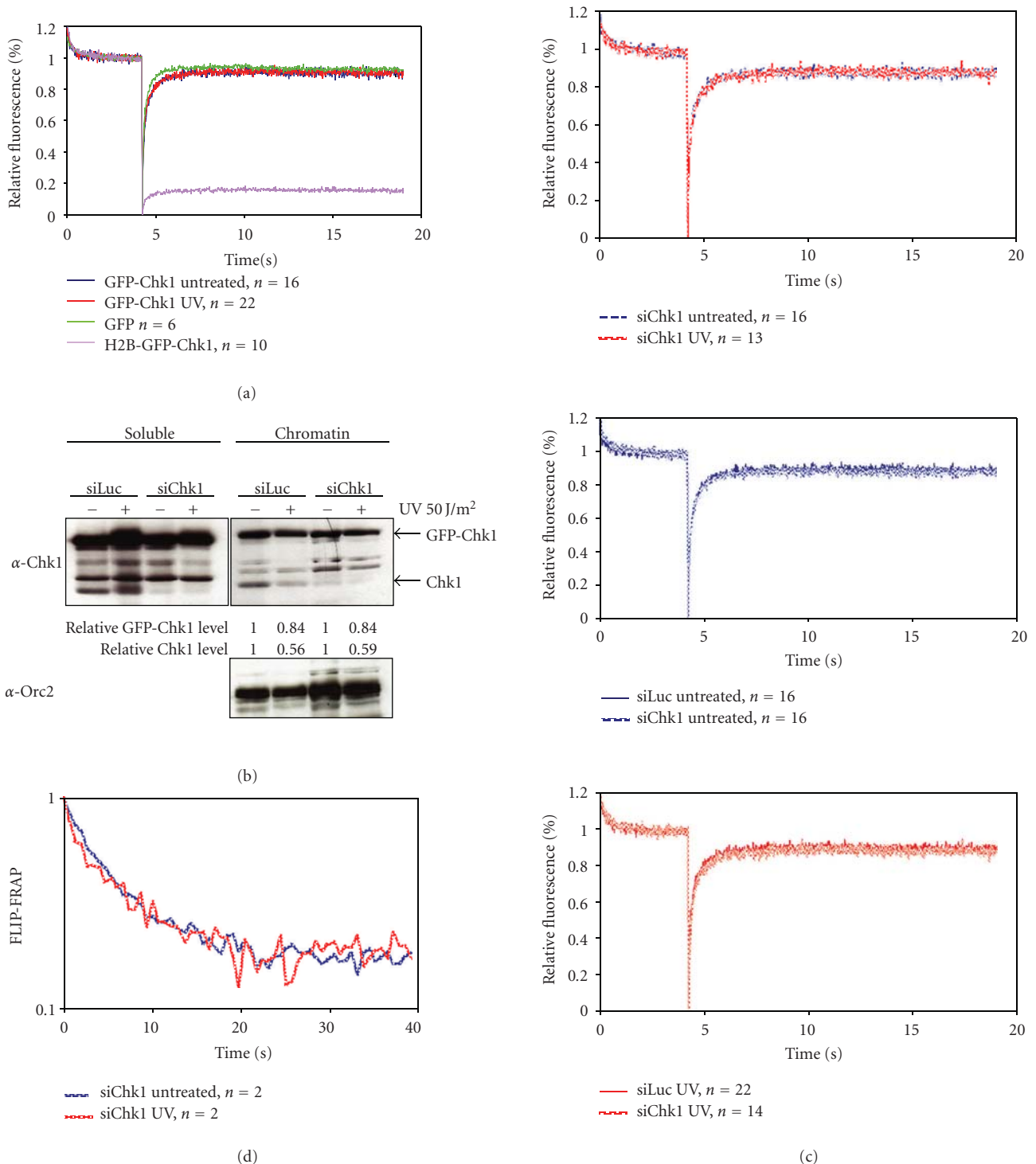


FIGURE 5: Mobility of GFP-Chk1 in response to DNA damage. (a) U2OS cells expressing GFP, H2B-GFP-Chk1, or GFP-Chk1 were left untreated or treated with UV and analyzed by strip-FRAP (see Section 2 for technical details). (b) Chromatin fractionation of GFP-Chk1 expressing cells transfected with siRNA oligos directed against luciferase or Chk1 for 24 hours before UV treatment and cell fractionation. Relative Chk1 levels as compared to untreated controls are indicated. Western blot analysis of the fractions was performed using the indicated antibodies. (c) GFP-Chk1 expressing cells were transfected with siRNA oligos against luciferase or Chk1 for 24 hours and left untreated or treated with UV. One hour later, cells were analyzed by strip-FRAP. (d) U2OS cells expressing GFP-Chk1 were transfected with Chk1 siRNA oligos for 24 hours and left untreated or treated with UV and subsequently analyzed by FLIP-FRAP (see Section 2 for technical details).

we additionally addressed GFP-Chk1 mobility by determining its residence time on DNA. Chk1 was downregulated in GFP-Chk1 expressing cells as previously described and subsequently the cells were irradiated with UV-light. Thereafter, half of the nucleus was bleached once and redistribution of GFP-Chk1 fluorescence was measured in the bleached and unbleached area over time. The time it takes to reach full fluorescent redistribution determines the proteins residence time. The results shown in Figure 5(d) indicated that GFP-Chk1 reached redistribution after 40 seconds, which is outside the timeframe of our original experiment. However, during the 40 seconds directly after bleaching we did not observe any difference in the mobility using this method. These results further indicate that Chk1 is a highly mobile protein and suggests that it only very transiently interacts with the chromatin.

#### 4. Discussion

The initial response to DNA damage is of crucial importance for cell functioning and viability, since an improper DNA damage response can eventually lead to cancer and other human diseases [1, 68]. In response to UV light, the putative DNA sensors Rad17-RFC and ATRIP-ATR are independently recruited to DNA regions containing RPA-coated ssDNA [4, 52]. Rad17-RFC is responsible for the loading of the 9-1-1 complex onto the DNA [5]. These events are required for the subsequent activation of Chk1, which results in a cell cycle arrest [12]. To gain further insight into the events that take place after a genotoxic insult in living cells, we GFP-labelled several proteins of the ATR pathway and expressed these fusion proteins in human cells. We discussed how to generate and validate stable GFP-fusion cell lines.

The quantitative analysis of GFP-fusion proteins in living cells using video microscopy allowed us to determine the dynamic behaviour of different individual proteins of the pathway in response to DNA damage. With the use of photobleaching techniques (strip-FRAP, FLIP, FLIP-FRAP, local UV laser) we determined multiple parameters of the proteins, including the rate of accumulation onto locally induced UV laser damage, rate of diffusion, immobile fraction, and the average time of immobilization (residence time) before and after global UV-irradiation. These methods are useful tools to investigate the dynamics of proteins involved in the DNA damage response, as shown in this paper, since many of the involved proteins bind DNA or proteins present at the site of damage and become immobilized to a certain extent.

GFP-Rad9, GFP-Rad1, Hus1-GFP, and GFP-ATRIP accumulate into nuclear foci in response to DNA damage. However, a relatively larger fraction of the 9-1-1 complex proteins become immobilized in response to UV as compared to ATRIP. Biochemical experiments show that the 9-1-1 complex is loaded onto the 5' ssDNA/dsDNA by Rad17-RFC, therefore, its association to DNA lesions might take some time and is the result of cooperative binding [51]. In contrast, ATRIP interacts directly with RPA-coated ssDNA, explaining its exponential binding behaviour [4]. The results obtained by FLIP suggest that a loaded 9-1-1 complex

cannot easily dissociate from the DNA. This dissociation might be slower because the 9-1-1 complex forms a ring around the DNA. It, therefore, has to either slide off a DNA end or actively dissociate, which likely is a more time-consuming process [69]. In addition, the FRAP experiments show that 20%–40% of the 9-1-1 complex molecules become immobile whereas only 5%–10% of the ATRIP molecules are immobilized after DNA damage. These results also indicate a relatively more stable association of the 9-1-1 complex with damaged chromatin which is consistent with the FLIP results.

All together, the putative DNA damage sensors Rad9-Rad1-Hus1 and ATRIP-ATR show a different dynamic behaviour directly after induction and during the presence of UV-induced DNA damage. Nonetheless, both GFP-Rad9 and GFP-ATRIP molecules are exchanging rapidly in UV-induced foci since all the mobility measurements performed on both GFP-Rad9 and GFP-ATRIP DNA damage-induced-foci do not indicate a stable immobilized fraction, suggesting that these foci are not static but highly dynamic structures.

Recruitment of the ATRIP-ATR heterodimer to sites of DNA damage results in ATR kinase activation which leads to the phosphorylation and subsequent activation of the Chk1 kinase [70, 71]. To investigate the spatio and temporal behaviour of downstream effector Chk1 in living cells, we studied the dynamic behaviour of GFP-Chk1 in response to DNA damage. *In vivo* imaging experiments confirm the absence of a stable chromatin-bound Chk1 fraction. The data presented here signify that Chk1 is a very mobile protein both in the absence or presence of DNA damage. The observed chromatin binding of Chk1 that is observed in biochemical experiments is not indicative of a stably bound Chk1 chromatin fraction [35] (Figure 5(b)). This high nuclear mobility of Chk1 was hypothesized to ensure the access of additional Chk1 molecules to ATR and the transmission of the damage signal throughout the nucleus [15, 35, 72].

Measuring protein mobility is not always as straightforward as it seems. Problems that are commonly faced when performing these types of experiments are monitor bleaching, influx of proteins from the cytoplasm, and blinking. Monitor bleaching is caused by observing the cells before, during, and after photobleaching or time lapse experiments. By using low amounts of laser power this can be avoided, although with low fluorescent protein levels this could be problematic. Lowering the laser power could result in a low resolution, which in turn results in a large variability between measurements. Monitor bleaching can be corrected for by measuring the amount of bleaching in an unbleached area of the cell, but this only applies for freely diffusion proteins [63, 73]. Another potential problem is the presence of a cytoplasmic protein fraction that could influence nuclear measurements due through the influx of fluorescence from the cytoplasm. Before the start of the actual measurement, the cytoplasmic fraction can be bleached, thereby eliminating this potential influx. Blinking is the property of fluorescent molecules to be reactivated, which can also influence photobleaching results. By keeping experimental conditions similar in all conditions the influence of blinking is constant in all measurements and,

therefore, insignificant. When comparing results obtained from different fluorescent variants, on the other hand, it needs to be taken into account that the blinking properties are different and, therefore, the amount of blinking needs to be determined for every variant and corrected for in the final analysis [63, 73].

To overcome the problem of GFP-fusion protein overexpression and the (competitive) presence of the endogenous counterpart, a GFP knock-in strategy using mice can be utilized [74] (Jeroen Essers, personal communication). This method places the GFP tag before the endogenous gene of interest in the mice genome, thereby being regulated by the endogenous promoter. As a result the expression levels of the GFP-fusion protein are identical to nontargeted protein in wild type cells, resulting in better quantitative measurements. The behaviour of proteins can additionally be studied in different tissues and cell types under physiological conditions [75]. Performing a similar approach for proteins involved in the ATR-Chk1 pathway may result in a more precise determination of the dynamic behaviour of this DNA damage checkpoint pathway. The ATR gene may act as a good candidate to start a GFP knock in approach, since it localizes to sites of damage and thereby becomes immobilized. Furthermore, ATR interacts with and phosphorylates a number of key target proteins.

Conclusively, we show that the GFP-labelling of ATRIP, Chk1, and the 9-1-1 complex proteins results in functional equivalents that can be studied by live cell video microscopy and quantitative fluorescence photobleaching. We compared the mobility changes of GFP-ATRIP, GFP-Chk1, GFP-Rad9, GFP-Rad1, and Hus1-GFP after UV-irradiation and collectively the results indicate a distinct dynamic behaviour between some of the studied proteins. Whereas effector kinase Chk1 is highly mobile and does not immobilize upon DNA damage, Rad9 and ATRIP stably associate to sites of DNA lesions. ATRIP directly binds to DNA lesions but more transiently than Rad9, which in contrast displays a more stable association with damaged chromatin. Together these data demonstrate the importance of spatio and temporal protein regulation in the DNA damage-induced ATR-Chk1 pathway.

## Acknowledgments

The authors thank Raimundo Freire for sharing reagents and technical support and Philip Reaper for reagents. This work was supported by the Association for International Cancer Research (AICR 05-005), the Dutch Cancer Society (EMCR 2005-3412), and the Ramón y Cajal Program (Ministerio de Ciencia e Innovación) to V. A. J. Smits and the integrated project 512113 from the European Commission and the Netherlands Genomics Initiative/Netherlands Organization for Scientific Research (NWO) to R. Kanaar.

## References

[1] Y. Shiloh, "ATM and related protein kinases: safeguarding genome integrity," *Nature Reviews Cancer*, vol. 3, no. 3, pp. 155–168, 2003.

[2] M. S. Y. Huen, S. M. H. Sy, and J. Chen, "BRCA1 and its toolbox for the maintenance of genome integrity," *Nature Reviews Molecular Cell Biology*, vol. 11, no. 2, pp. 138–148, 2010.

[3] M. S. Y. Huen and J. Chen, "Assembly of checkpoint and repair machineries at DNA damage sites," *Trends in Biochemical Sciences*, vol. 35, no. 2, pp. 101–108, 2010.

[4] L. Zou and S. J. Elledge, "Sensing DNA damage through ATRIP recognition of RPA-ssDNA complexes," *Science*, vol. 300, no. 5625, pp. 1542–1548, 2003.

[5] L. Zou, D. Cortez, and S. J. Elledge, "Regulation of ATR substrate selection by Rad17-dependent loading of Rad9 complexes onto chromatin," *Genes and Development*, vol. 16, no. 2, pp. 198–208, 2002.

[6] T. Kondo, T. Wakayama, T. Naiki, K. Matsumoto, and K. Sugimoto, "Recruitment of Mec1 and Ddc1 checkpoint proteins to double-strand breaks through distinct mechanisms," *Science*, vol. 294, no. 5543, pp. 867–870, 2001.

[7] J. A. Melo, J. Cohen, and D. P. Toczyski, "Two checkpoint complexes are independently recruited to sites of DNA damage in vivo," *Genes and Development*, vol. 15, no. 21, pp. 2809–2821, 2001.

[8] J. Lee, A. Kumagai, and W. G. Dunphy, "The Rad9-Hus1-Rad1 checkpoint clamp regulates interaction of TopBP1 with ATR," *Journal of Biological Chemistry*, vol. 282, no. 38, pp. 28036–28044, 2007.

[9] S. Delacroix, J. M. Wagner, M. Kobayashi, K.-I. Yamamoto, and L. M. Karnitz, "The Rad9-Hus1-Rad1 (9-1-1) clamp activates checkpoint signaling via TopBP1," *Genes and Development*, vol. 21, no. 12, pp. 1472–1477, 2007.

[10] J. Majka, A. Niedziela-Majka, and P. J. Burgers, "The checkpoint clamp activates Mec1 kinase during initiation of the DNA damage checkpoint," *Molecular Cell*, vol. 24, no. 6, pp. 891–901, 2006.

[11] B.-B. S. Zhou and S. J. Elledge, "The DNA damage response: putting checkpoints in perspective," *Nature*, vol. 408, no. 6811, pp. 433–439, 2000.

[12] B. Shiotani and L. Zou, "ATR signaling at a glance," *Journal of Cell Science*, vol. 122, no. 3, pp. 301–304, 2009.

[13] J. W. Harper and S. J. Elledge, "The DNA damage response: ten years after," *Molecular Cell*, vol. 28, no. 5, pp. 739–745, 2007.

[14] S. Bekker-Jensen, C. Lukas, R. Kitagawa et al., "Spatial organization of the mammalian genome surveillance machinery in response to DNA strand breaks," *Journal of Cell Biology*, vol. 173, no. 2, pp. 195–206, 2006.

[15] C. Lukas, J. Falck, J. Bartkova, J. Bartek, and J. Lukas, "Distinct spatiotemporal dynamics of mammalian checkpoint regulators induced by DNA damage," *Nature Cell Biology*, vol. 5, no. 3, pp. 255–260, 2003.

[16] J. Essers, A. B. Houtsmuller, and R. Kanaar, "Analysis of DNA recombination and repair proteins in living cells by photobleaching microscopy," *Methods in Enzymology*, vol. 408, pp. 463–485, 2006.

[17] J. Essers, A. B. Houtsmuller, L. Van Veelen et al., "Nuclear dynamics of RAD52 group homologous recombination proteins in response to DNA damage," *EMBO Journal*, vol. 21, no. 8, pp. 2030–2037, 2002.

[18] L. R. Van Veelen, T. Cervelli, M. W. Van De Rakt, A. F. Theil, J. Essers, and R. Kanaar, "Analysis of ionizing radiation-induced foci of DNA damage repair proteins," *Mutation Research*, vol. 574, no. 1-2, pp. 22–33, 2005.

[19] J. Lippincott-Schwartz and G. H. Patterson, "Development and use of fluorescent protein markers in living cells," *Science*, vol. 300, no. 5616, pp. 87–91, 2003.

- [20] H. P. Easwaran, H. Leonhardt, and M. C. Cardoso, "Cell cycle markers for live cell analyses," *Cell Cycle*, vol. 4, no. 3, pp. 453–455, 2005.
- [21] D. O. Warmerdam, R. Freire, R. Kanaar, and V. A. J. Smits, "Cell cycle-dependent processing of DNA lesions controls localization of Rad9 to sites of genotoxic stress," *Cell Cycle*, vol. 8, no. 11, pp. 1765–1774, 2009.
- [22] C. Y. Bonilla, J. A. Melo, and D. P. Toczyski, "Colocalization of sensors is sufficient to activate the DNA damage checkpoint in the absence of damage," *Molecular Cell*, vol. 30, no. 3, pp. 267–276, 2008.
- [23] J. Lukas, C. Lukas, and J. Bartek, "Mammalian cell cycle checkpoints: signalling pathways and their organization in space and time," *DNA Repair*, vol. 3, no. 8-9, pp. 997–1007, 2004.
- [24] E. Soutoglou and T. Misteli, "Activation of the cellular DNA damage response in the absence of DNA lesions," *Science*, vol. 320, no. 5882, pp. 1507–1510, 2008.
- [25] A. B. Houtsmuller, S. Rademakers, A. L. Nigg, D. Hoogstraten, J. H. J. Hoeijmakers, and W. Vermeulen, "Action of DNA repair endonuclease ERCC1/XPF in living cells," *Science*, vol. 284, no. 5416, pp. 958–961, 1999.
- [26] A. Zotter, M. S. Luijsterburg, D. O. Warmerdam et al., "Recruitment of the nucleotide excision repair endonuclease XPG to sites of UV-induced DNA damage depends on functional TFIIH," *Molecular and Cellular Biology*, vol. 26, no. 23, pp. 8868–8879, 2006.
- [27] M. S. Luijsterburg, J. Goedhart, J. Moser et al., "Dynamic in vivo interaction of DDB2 E3 ubiquitin ligase with UV-damaged DNA is independent of damage-recognition protein XPC," *Journal of Cell Science*, vol. 120, no. 15, pp. 2706–2716, 2007.
- [28] G. Giglia-Mari, F. Coin, J. A. Ranish et al., "A new, tenth subunit TFIIH is responsible for the DNA repair syndrome trichothiodystrophy group A," *Nature Genetics*, vol. 36, no. 7, pp. 714–719, 2004.
- [29] G. Giglia-Mari, C. Miquel, A. F. Theil et al., "Dynamic interaction of TTDA with TFIIH is stabilized by nucleotide excision repair in living cells," *PLoS Biology*, vol. 4, no. 6, article e156, 2006.
- [30] M. Toueille, N. El-Andaloussi, I. Fouin et al., "The human Rad9/Rad1/Hus1 damage sensor clamp interacts with DNA polymerase  $\beta$  and increases its DNA substrate utilisation efficiency: implications for DNA repair," *Nucleic Acids Research*, vol. 32, no. 11, pp. 3316–3324, 2004.
- [31] J. M. Rendtlew Danielson, D. H. Larsen, K. B. Schou et al., "HCLK2 is required for activity of the DNA damage response kinase ATR," *Journal of Biological Chemistry*, vol. 284, no. 7, pp. 4140–4147, 2009.
- [32] G. G. Jones, P. M. Reaper, A. R. Pettitt, and P. D. Sherrington, "The ATR-p53 pathway is suppressed in noncycling normal and malignant lymphocytes," *Oncogene*, vol. 23, no. 10, pp. 1911–1921, 2004.
- [33] A. L. Medhurst, D. O. Warmerdam, I. Akerman et al., "ATR and Rad17 collaborate in modulating Rad9 localisation at sites of DNA damage," *Journal of Cell Science*, vol. 121, no. 23, pp. 3933–3940, 2008.
- [34] J. Mendez and B. Stillman, "Chromatin association of human origin recognition complex, Cdc6, and minichromosome maintenance proteins during the cell cycle: assembly of pre-replication complexes in late mitosis," *Molecular and Cellular Biology*, vol. 20, no. 22, pp. 8602–8612, 2000.
- [35] V. A. J. Smits, P. M. Reaper, and S. P. Jackson, "Rapid PIKK-dependent release of Chk1 from chromatin promotes the DNA-damage checkpoint response," *Current Biology*, vol. 16, no. 2, pp. 150–159, 2006.
- [36] C. Dinant, M. de Jager, J. Essers et al., "Activation of multiple DNA repair pathways by sub-nuclear damage induction methods," *Journal of Cell Science*, vol. 120, no. 15, pp. 2731–2740, 2007.
- [37] J. Essers, A. F. Theil, C. Baldeyron et al., "Nuclear dynamics of PCNA in DNA replication and repair," *Molecular and Cellular Biology*, vol. 25, no. 21, pp. 9350–9359, 2005.
- [38] R. Y. Tsien, "The green fluorescent protein," *Annual Review of Biochemistry*, vol. 67, pp. 509–544, 1998.
- [39] R. Y. Tsien and A. Miyawaki, "Seeing the machinery of live cells," *Science*, vol. 280, no. 5371, pp. 1954–1955, 1998.
- [40] B. N. G. Giepmans, S. R. Adams, M. H. Ellisman, and R. Y. Tsien, "The fluorescent toolbox for assessing protein location and function," *Science*, vol. 312, no. 5771, pp. 217–224, 2006.
- [41] R. Heim, A. B. Cubitt, and R. Y. Tsien, "Improved green fluorescence," *Nature*, vol. 373, no. 6516, pp. 663–664, 1995.
- [42] M. Prescott, S. Nowakowski, P. Nagley, and R. J. Devenish, "The length of polypeptide linker affects the stability of green fluorescent protein fusion proteins," *Analytical Biochemistry*, vol. 273, no. 2, pp. 305–307, 1999.
- [43] M. O'Driscoll, V. L. Ruiz-Perez, C. G. Woods, P. A. Jeggo, and J. A. Goodship, "A splicing mutation affecting expression of ataxia-telangiectasia and Rad3-related protein (ATR) results in Seckel syndrome," *Nature Genetics*, vol. 33, no. 4, pp. 497–501, 2003.
- [44] R. S. Weiss, T. Enoch, and P. Leder, "Inactivation of mouse Hus1 results in genomic instability and impaired responses to genotoxic stress," *Genes and Development*, vol. 14, no. 15, pp. 1886–1898, 2000.
- [45] R. S. Weiss, P. Leder, and C. Vaziri, "Critical role for mouse Hus1 in an S-phase DNA damage cell cycle checkpoint," *Molecular and Cellular Biology*, vol. 23, no. 3, pp. 791–803, 2003.
- [46] K. M. Hopkins, W. Auerbach, X. Y. Wang et al., "Deletion of mouse Rad9 causes abnormal cellular responses to DNA damage, genomic instability, and embryonic lethality," *Molecular and Cellular Biology*, vol. 24, no. 16, pp. 7235–7248, 2004.
- [47] G. Zachos, M. D. Rainey, and D. A. F. Gillespie, "Chk1-dependent S-M checkpoint delay in vertebrate cells is linked to maintenance of viable replication structures," *Molecular and Cellular Biology*, vol. 25, no. 2, pp. 563–574, 2005.
- [48] R. Kitagawa, C. J. Bakkenist, P. J. McKinnon, and M. B. Kastan, "Phosphorylation of SMC1 is a critical downstream event in the ATM-NBS1-BRCA1 pathway," *Genes and Development*, vol. 18, no. 12, pp. 1423–1438, 2004.
- [49] S. Bekker-Jensen, C. Lukas, F. Melander, J. Bartek, and J. Lukas, "Dynamic assembly and sustained retention of 53BP1 at the sites of DNA damage are controlled by Mdc1/NFBD1," *Journal of Cell Biology*, vol. 170, no. 2, pp. 201–211, 2005.
- [50] J. A. Bonner and T. S. Lawrence, "Doxorubicin decreases the repair of radiation-induced DNA damage," *International Journal of Radiation Biology*, vol. 57, no. 1, pp. 55–64, 1990.
- [51] J. Majka, S. K. Binz, M. S. Wold, and P. M. J. Burgers, "Replication protein a directs loading of the DNA damage checkpoint clamp to 5'-DNA junctions," *Journal of Biological Chemistry*, vol. 281, no. 38, pp. 27855–27861, 2006.
- [52] L. Zou, D. Liu, and S. J. Elledge, "Replication protein A-mediated recruitment and activation of Rad17 complexes," *Proceedings of the National Academy of Sciences of the United States of America*, vol. 100, no. 24, pp. 13827–13832, 2003.

- [53] J. Majka and P. M. Burgers, "Function of Rad17/Mec3/Ddc1 and its partial complexes in the DNA damage checkpoint," *DNA Repair*, vol. 4, no. 10, pp. 1189–1194, 2005.
- [54] M. Modesti and R. Kanaar, "Dna repair: spot(light)s on chromatin," *Current Biology*, vol. 11, no. 6, pp. R229–R232, 2001.
- [55] J. A. Marteiijn, S. Bekker-Jensen, N. Mailand et al., "Nucleotide excision repair-induced H2A ubiquitination is dependent on MDC1 and RNF8 and reveals a universal DNA damage response," *The Journal of Cell Biology*, vol. 186, no. 6, pp. 835–847, 2009.
- [56] M. J. Moné, M. Volker, O. Nikaido et al., "Local UV-induced DNA damage in cell nuclei results in local transcription inhibition," *EMBO Reports*, vol. 2, no. 11, pp. 1013–1017, 2001.
- [57] M. Volker, M. J. Moné, P. Karmakar et al., "Sequential assembly of the nucleotide excision repair factors in vivo," *Molecular Cell*, vol. 8, no. 1, pp. 213–224, 2001.
- [58] M. J. Moné, T. Bernas, C. Dinant et al., "In vivo dynamics of chromatin-associated complex formation in mammalian nucleotide excision repair," *Proceedings of the National Academy of Sciences of the United States of America*, vol. 101, no. 45, pp. 15933–15937, 2004.
- [59] P.-O. Mari, B. I. Florea, S. P. Persengiev et al., "Dynamic assembly of end-joining complexes requires interaction between Ku70/80 and XRCC4," *Proceedings of the National Academy of Sciences of the United States of America*, vol. 103, no. 49, pp. 18597–18602, 2006.
- [60] J. A. Aten, J. Stap, P. M. Krawczyk et al., "Dynamics of DNA double-strand breaks revealed by clustering of damaged chromosome domains," *Science*, vol. 303, no. 5654, pp. 92–95, 2004.
- [61] J. Stap, P. M. Krawczyk, C. H. Van Oven et al., "Induction of linear tracks of DNA double-strand breaks by  $\alpha$ -particle irradiation of cells," *Nature Methods*, vol. 5, no. 3, pp. 261–266, 2008.
- [62] E. S. Williams, J. Stap, J. Essers et al., "DNA double-strand breaks are not sufficient to initiate recruitment of TRF2," *Nature Genetics*, vol. 39, no. 6, pp. 696–698, 2007.
- [63] A. B. Houtsmuller, "Fluorescence recovery after photobleaching: application to nuclear proteins," *Advances in Biochemical Engineering/Biotechnology*, vol. 95, pp. 177–199, 2005.
- [64] A. B. Houtsmuller and W. Vermeulen, "Macromolecular dynamics in living cell nuclei revealed by fluorescence redistribution after photobleaching," *Histochemistry and Cell Biology*, vol. 115, no. 1, pp. 13–21, 2001.
- [65] M. E. Stroppolo, M. Falconi, A. M. Caccuri, and A. Desideri, "Superefficient enzymes," *Cellular and Molecular Life Sciences*, vol. 58, no. 10, pp. 1451–1460, 2001.
- [66] J. Ricard and A. Cornish-Bowden, "Co-operative and allosteric enzymes: 20 years on," *European Journal of Biochemistry*, vol. 166, no. 2, pp. 255–272, 1987.
- [67] L. Zou and S. J. Elledge, "Sensing and signaling DNA damage: roles of Rad17 and Rad9 complexes in the cellular response to DNA damage," *Harvey Lectures*, vol. 97, pp. 1–15, 2001.
- [68] D. Hanahan and R. A. Weinberg, "The hallmarks of cancer," *Cell*, vol. 100, no. 1, pp. 57–70, 2000.
- [69] A. S. Doré, M. L. Kilkeny, N. J. Rzechorzek, and L. H. Pearl, "Crystal structure of the rad9-rad1-hus1 DNA damage checkpoint complex—implications for clamp loading and regulation," *Molecular Cell*, vol. 34, no. 6, pp. 735–745, 2009.
- [70] R. T. Abraham, "Cell cycle checkpoint signaling through the ATM and ATR kinases," *Genes and Development*, vol. 15, no. 17, pp. 2177–2196, 2001.
- [71] A. Kumagai, J. Lee, H. Y. Yoo, and W. G. Dunphy, "TopBP1 activates the ATR-ATRIP complex," *Cell*, vol. 124, no. 5, pp. 943–955, 2006.
- [72] V. A. J. Smits, "Spreading the signal: dissociation of Chk1 from chromatin," *Cell Cycle*, vol. 5, no. 10, pp. 1039–1043, 2006.
- [73] M. E. van Royen, P. Farla, K. A. Mattern, B. Geverts, J. Trapman, and A. B. Houtsmuller, "Fluorescence recovery after photobleaching (FRAP) to study nuclear protein dynamics in living cells," *Methods in Molecular Biology*, vol. 464, pp. 363–385, 2009.
- [74] G. Giglia-Mari, A. F. Theil, P.-O. Mari et al., "Differentiation driven changes in the dynamic organization of basal transcription initiation," *PLoS Biology*, vol. 7, no. 10, article e1000220, 2009.
- [75] T. L. R. Tan, J. Essers, E. Citterio et al., "Mouse Rad54 affects DNA conformation and DNA-damage-induced Rad51 foci formation," *Current Biology*, vol. 9, no. 6, pp. 325–328, 1999.

## Research Article

# Role of Topoisomerase II $\beta$ in DNA Damage Response following IR and Etoposide

Nicola J. Sunter, Ian G. Cowell, Elaine Willmore, Gary P. Watters, and Caroline A. Austin

*Institute for Cell and Molecular Biosciences, The Medical School, Newcastle University, Newcastle upon Tyne NE2 4HH, UK*

Correspondence should be addressed to Caroline A. Austin, caroline.austin@ncl.ac.uk

Received 18 June 2010; Accepted 15 July 2010

Academic Editor: Ashis Basu

Copyright © 2010 Nicola J. Sunter et al. This is an open access article distributed under the Creative Commons Attribution License, which permits unrestricted use, distribution, and reproduction in any medium, provided the original work is properly cited.

The role of topoisomerase II $\beta$  was investigated in cell lines exposed to two DNA damaging agents, ionising radiation (IR) or etoposide, a drug which acts on topoisomerase II. The appearance and resolution of  $\gamma$ H2AX foci in murine embryonic fibroblast cell lines, wild type and null for DNA topoisomerase II $\beta$ , was measured after exposure to ionising radiation (IR) or etoposide. Topoisomerase II-DNA adduct levels were also measured. IR rapidly triggered phosphorylation of histone H2AX, less phosphorylation was seen in TOP2 $\beta$ <sup>-/-</sup> cells, but the difference was not statistically significant. IR did not produce topoisomerase II-DNA adducts above control levels. Etoposide triggered the formation of topoisomerase II-DNA adducts and the phosphorylation of histone H2AX, the  $\gamma$ H2AX foci appeared more slowly with etoposide than with IR. Topoisomerase II-DNA complexes in WT cells but not TOP2 $\beta$ <sup>-/-</sup> cells increased significantly at 24 hours with the proteasome inhibitor MG132, suggesting topoisomerase II $\beta$  adducts are removed by the proteasome.

## 1. Introduction

Exogenous agents such as ionising radiation (IR) and ultraviolet light or endogenous agents such as free radicals produced within cells can damage the DNA of eukaryotic organisms. Diverse mechanisms have evolved to detect and repair DNA damage that threatens the integrity of the genome. Here, we study two DNA damaging agents used in the treatment of cancer, IR and the epipodophyllotoxin drug etoposide that acts on topoisomerase II.

Cellular DNA damage responses to IR exposure have been extensively investigated and several pathways exist within the cell to respond to double strand breaks (DSBs) induced by ionising radiation (IR). Histone H2AX is rapidly phosphorylated following IR, with foci observed within the first minute following exposure [1–3]. The phosphorylation of H2AX occurs over megabase regions of chromatin extending away from the site of DNA damage [1] and initiates assembly of several proteins involved in the DNA damage response [4]. H2AX phosphorylation has been shown to be essential for correct amplification of the DNA damage response [5–7]. At sublethal levels of DNA damage,

phosphorylated H2AX (termed  $\gamma$ H2AX) forms distinct foci within the cell nuclei. At less than 150 DSBs per nucleus, there exists a 1:1 relationship of  $\gamma$ H2AX foci:DSBs [2]. At these levels of DNA damage,  $\gamma$ H2AX can be used as an accurate and sensitive surrogate reporter of DNA DSB levels [8]. H2AX can also be phosphorylated in response to topoisomerase II-targeting agents [9–12].

Topoisomerase II is an enzyme that alters the topological state of DNA via a transient covalent enzyme-bridged double strand break in the DNA, through which a second DNA helix can pass. These protein associated breaks can be stabilised by drugs such as etoposide [13, 14]. Two isoforms of topoisomerase II exist, termed  $\alpha$  and  $\beta$  [15], these are both targeted by etoposide [16–18]. The genotoxic effects of etoposide are generally considered to be mediated through conversion of stabilised protein-DNA complexes to protein free “frank” DSBs [19, 20], possibly via collisions between the drug-stabilised topoisomerase-DNA complex and RNA polymerase during transcription or with DNA replication forks, analogous to the situation seen with topoisomerase I [21, 22]. Frank DSBs may also be generated by proteolytic degradation of the topoisomerase II moiety

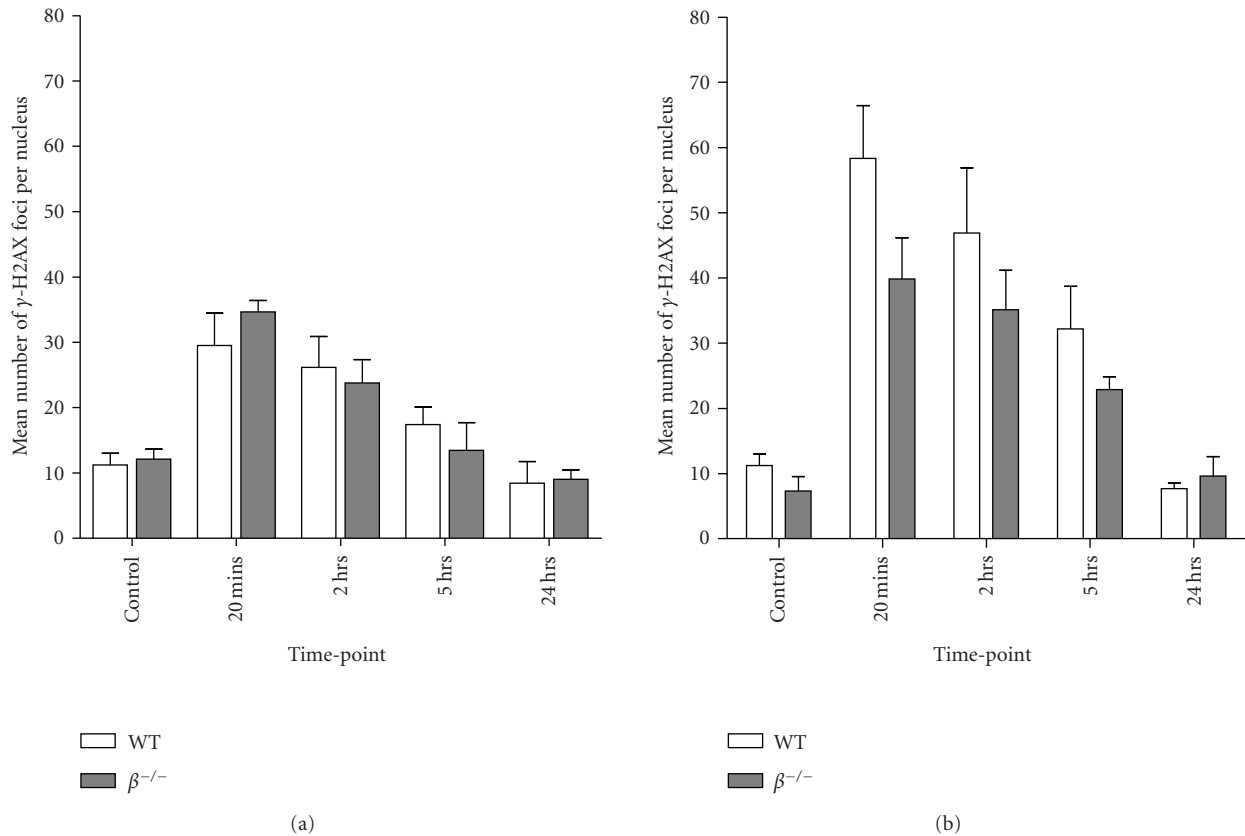


FIGURE 1: Effect of topoisomerase II $\beta$  status on  $\gamma$ H2AX focus formation in response to IR. WT and TOP2 $\beta^{-/-}$  MEFs were exposed to 1 Gy IR (a) or 2 Gy IR (b) and  $\gamma$ H2AX foci were counted at 20 minutes, 2 hours, 5 hours, and 24 hours after exposure. Data are derived from at least  $n = 3$  independent experiments.

[23–26] and topoisomerase II $\beta$  is thought to be preferentially degraded over the  $\alpha$  isoform [26]. A reduction in etoposide induced DSB levels was reported in cells cotreated with the proteasome inhibitor MG-132 [26], suggesting that the proteasome has a role in converting etoposide-stabilised protein-DNA complexes into frank DSBs [26]. Additionally a 5' tyrosyl DNA phosphodiesterase (TTRAP) has recently been identified that may play a role in generating frank DSBs ready for repair [27].

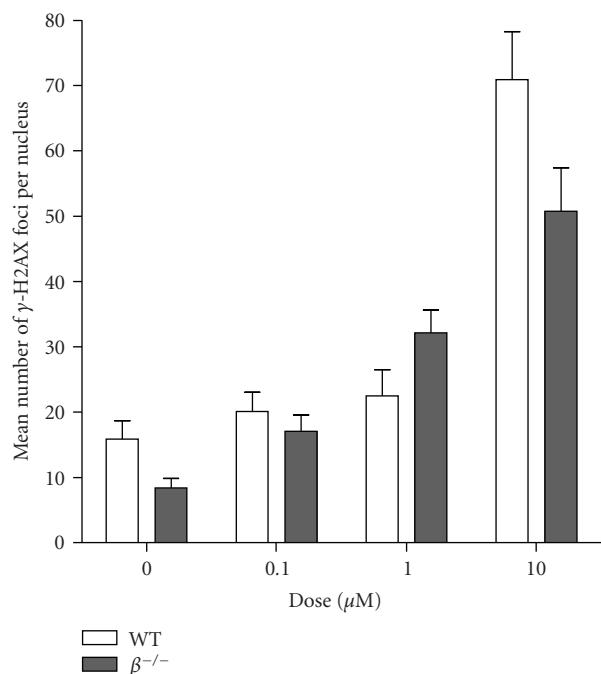
Topoisomerase II has been implicated in the cellular response to DNA DSBs. Down regulating topoisomerase II $\alpha$  by siRNA altered the response to radiation [28] whilst topoisomerase II $\beta$  has been reported to play a role in promoting DSB repair following peroxide damage [29]. The damage sensor TopBP1 was first identified as a topoisomerase II $\beta$  interacting protein [30], and WSTF (Williams syndrome transcription factor) which regulates the H2AX DNA damage response [7] interacts with WINAC, a topoisomerase II $\beta$  containing multi protein complex [31]. Thus topoisomerase II $\beta$  may be directly involved in damage detection and signalling following IR via protein-protein interactions. Alternatively, topoisomerase II $\beta$  may be required for proper regulation of genes involved in the damage responses. For example, cells downregulated for topoisomerase II $\beta$  have been reported to express reduced peroxiredoxin 2 [32].

To investigate whether topoisomerase II $\beta$  affects the cellular response to IR or etoposide induced DNA damage, we used WT and TOP2 $\beta^{-/-}$  MEFs, we used H2AX assays and in parallel the trapped in agarose DNA immunostaining (TARDIS) assay to examine the kinetics of formation and removal of topoisomerase II-DNA complexes in response to IR or etoposide treatment.

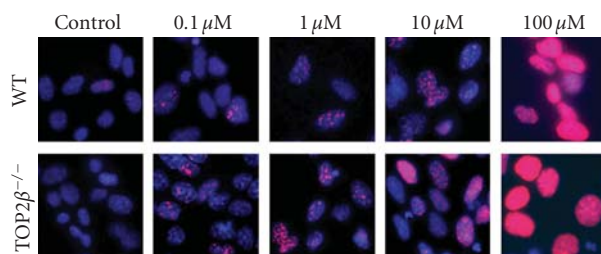
## 2. Materials and Methods

**2.1. Cell Culture.** Wild-type mTOP2 $\beta$ -4 (containing both topoisomerase II $\alpha$  and topoisomerase II $\beta$ ) [WT] and mtop2 $\beta$ -5 [TOP2 $\beta^{-/-}$ ] immortalized mouse embryonic fibroblasts (MEFs) have been described previously [17] and were maintained as monolayers in Dulbecco's Modified Eagle's Medium (DMEM) supplemented with 10% foetal bovine serum (FBS) and penicillin (50  $\mu$ g/mL)/streptomycin (50  $\mu$ g/mL). Cells were grown at 37°C in a humidified atmosphere containing 5% CO<sub>2</sub>. Cell culture reagents were obtained from Gibco BRL (Paisley, UK).

**2.2. Chemicals and DNA Damaging Agents.** All chemicals were obtained from Sigma-Aldrich (Poole, UK) and VWR International (Lutterworth, UK). Etoposide was obtained



(a)



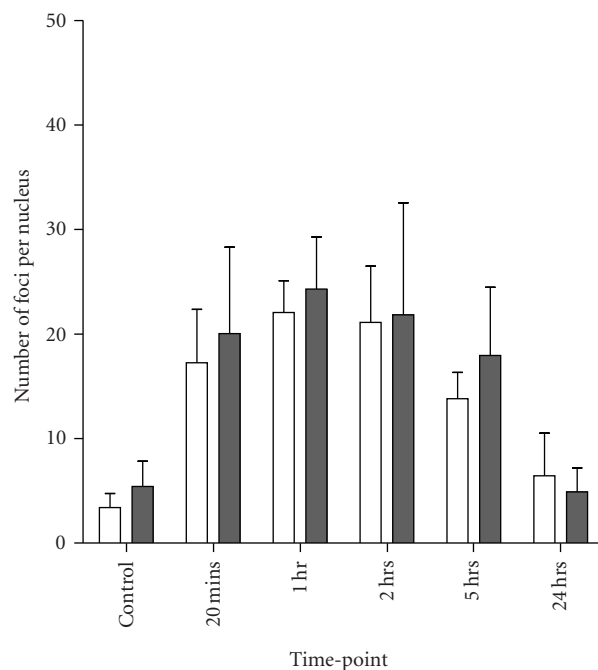
(b)

FIGURE 2:  $\gamma\text{H2AX}$  foci formed in response to increasing doses of etoposide. WT and  $\text{TOP2}\beta^{-/-}$  MEFs were exposed to 0.1, 1, 10, and 100  $\mu\text{M}$  etoposide for 2 hours and then assayed for  $\gamma\text{H2AX}$  foci. (a) Histograms of foci number  $\pm$  SEM at each dose counted. 100  $\mu\text{M}$  was not counted as foci were not distinct at this dose. Data derived from one experiment. (b) Representative images of  $\gamma\text{H2AX}$  foci (red) in nuclei stained with DAPI (blue) in WT and  $\text{TOP2}\beta^{-/-}$  MEFs.

from Sigma and was dissolved in methanol. IR exposure was carried out using a Gammacell 1000 irradiator with a  $[^{137}\text{Cs}]$  source (Nordion International, Inc.) and was delivered at a rate of approximately 3.08 Gy/min.

**2.3. H2AX Focus Assay.** The  $\gamma\text{H2AX}$  focus assay was performed as described previously in detail by Watters and colleagues [12].

**2.4. TARDIS (Trapped in Agarose DNA Immunostaining).** WT and  $\text{TOP2}\beta^{-/-}$  MEFs were seeded at  $3 \times 10^4$  cells/well into 6-well tissue culture plates and grown to approximately 80% confluency. Cells were exposed to the appropriate DNA damaging agent (IR or etoposide) and harvested by trypsinisation at specific time-points as detailed in the text.



□ WT  
 ■  $\beta^{-/-}$

FIGURE 3:  $\gamma\text{H2AX}$  foci following a 2 hour short-term exposure to etoposide. WT and  $\text{TOP2}\beta^{-/-}$  MEFs were exposed to 1  $\mu\text{M}$  etoposide and  $\gamma\text{H2AX}$  foci were counted at the indicated time points after drug removal. The data are derived from at least  $n = 3$  independent experiments, each data point shows the mean  $\pm$  SEM.

Trypsinised cells were resuspended in 1 mL of ice-cold PBS, centrifuged at 1000 rpm for 3 minutes and then resuspended in 50  $\mu\text{L}$  of ice-cold PBS. The slide preparation has been described in detail previously [17]. Slides were probed with an antibody that detects topoisomerase II $\alpha$  and  $\beta$ .

Quantification of complex levels has been described previously [16]. Statistical analyses were carried out using Graphpad Prism 4 software (Cherwell Scientific, Oxford, UK.). Two-tailed, paired, and unpaired Students  $t$ -tests were generally used to compare data sets and data sets between cell lines; analysis of variance (ANOVA) was used for multiple comparisons where appropriate, as detailed in the text. All statistical analyses were calculated using a 95% confidence interval ( $P < .05$ ).

### 3. Results and Discussion

The present study examined two DNA damaging agents, IR and etoposide.  $\gamma\text{H2AX}$  formation was used as a surrogate marker for DSBs in parallel with topoisomerase II-DNA complex measurement in both wild-type and topoisomerase II $\beta$  null murine embryo fibroblast cell lines (MEFs).

The response to three doses of IR (0.5, 1 and 2 Gy) was determined in MEFs wild type (WT) or null for topoisomerase II $\beta$  ( $\text{TOP2}\beta^{-/-}$ ). In response to 1 Gy,  $\gamma\text{H2AX}$

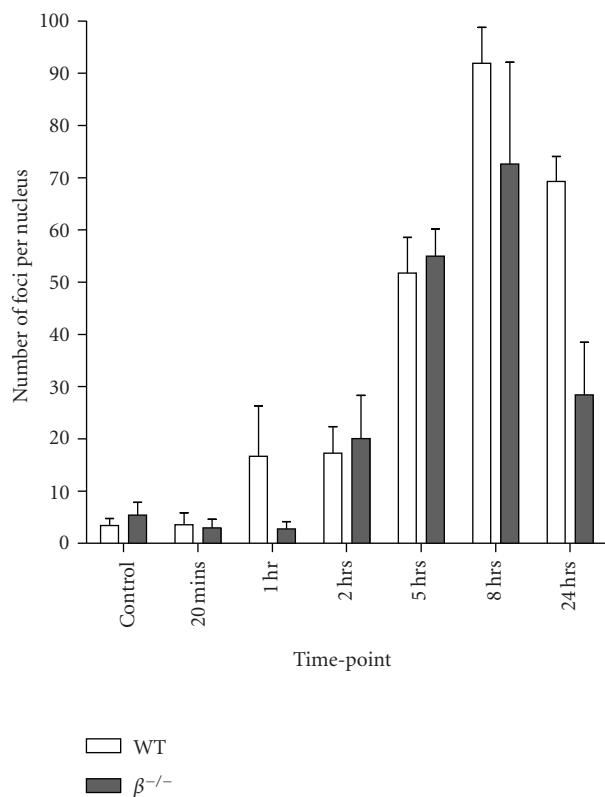


FIGURE 4:  $\gamma$ H2AX foci during continuous exposure to etoposide up to 24 hours. WT and TOP2 $\beta$ <sup>-/-</sup> MEFs were exposed to 1  $\mu$ M etoposide and  $\gamma$ H2AX foci were counted at the indicated time points up to 24 hours. The data are derived from at least  $n = 3$  independent experiments, each data point shows the mean  $\pm$  SEM.

focus numbers were similar between the two cell lines, with  $\sim 35$   $\gamma$ H2AX foci per nucleus at 20 minutes (Figure 1(a)).  $\gamma$ H2AX foci were most abundant at the 20 minute time-point after irradiation and decreased at each subsequent time-point investigated and returned to background levels at 24 hours (Figure 1(a)). Following 2 Gy (Figure 1(b)), focus numbers appeared higher in the WT cell line than the TOP2 $\beta$ <sup>-/-</sup> at 20 minutes, 2 hours, and 5 hours following exposure. The lower foci number in the TOP2 $\beta$ <sup>-/-</sup> cells suggests the initial DNA damage responses following IR are altered in these cells, however, the differences were not statistically significant by two way ANOVA or Student's  $t$ -test. Nor was there any significant difference between the levels of apoptosis following IR between the two cell lines. The trapped in agarose DNA immunostaining (TARDIS) assay was used to detect topoisomerase II protein-DNA complex levels in these cell lines following IR. Topoisomerase II complex formation did not increase in response to IR in WT or TOP2 $\beta$ <sup>-/-</sup> cells when compared to the untreated cells, as previously reported for CEM cells [18] (data not shown), thus IR had no effect upon topoisomerase II-DNA complex levels in the 24 hours following exposure to 2 Gy.

In an etoposide “dose finding” experiment topoisomerase II $\beta$  wild-type and null MEF cell lines were exposed to 0, 0.1, 1, 10, or 100  $\mu$ M etoposide for 2 hours, after

which time cells were placed in drug-free media for 20 minutes before being assayed for  $\gamma$ H2AX foci. Foci numbers per nucleus increased in both cell lines with increasing dose of drug. At 100  $\mu$ M, foci were no longer distinct and therefore uncountable (Figure 2). To ensure foci were within a countable range, subsequent experiments were performed using doses of 1  $\mu$ M and 10  $\mu$ M only.

WT and TOP2 $\beta$ <sup>-/-</sup> cells were exposed to 1.0  $\mu$ M etoposide for 2 hours, cells were then resuspended in drug-free media and assayed for  $\gamma$ H2AX at different time points after drug removal, 20 minutes, 2 hours, 5 hours, and 24 hours following removal of drug (Figure 3). The kinetics of focus formation and removal were comparable between the wild-type and TOP2 $\beta$ <sup>-/-</sup> cell lines, and by 24 hours postdrug removal foci numbers were similar to untreated controls. No statistically significant difference was found in focus numbers between the two cell lines, indicating that topoisomerase II $\beta$  status did not affect the kinetics of disappearance of  $\gamma$ H2AX phosphorylation following a 2 hour exposure to 1  $\mu$ M etoposide, this is consistent with the evidence that the cytotoxic effect of etoposide is mainly mediated via topoisomerase II $\alpha$  in these cells, since the IC50 for etoposide did not differ significantly between the two cell lines [17]. The topoisomerase II-DNA adducts levels measured by TARDIS after a 2 hour exposure to etoposide has previously been reported [17].

Wild-type and TOP2 $\beta$ <sup>-/-</sup> cells were also exposed continuously to 1.0  $\mu$ M etoposide over the course of 24 hours, and samples removed to quantify  $\gamma$ H2AX foci formation at various time points (Figure 4). After two hours of etoposide exposure the foci numbers were comparable to that seen after the two-hour short term exposure, numbers then increased further with continued exposure to etoposide. The maximal foci numbers were seen after 8 hours of etoposide, and they then decreased by 24 hours even though etoposide was still present. The focus numbers were statistically different between the two cell lines only at the 24 hours point ( $P < .05$ ), when the WT cell line had approximately double the number of foci compared to the TOP2 $\beta$ <sup>-/-</sup> cell line.

Topoisomerase II-DNA complex levels in WT and TOP2 $\beta$ <sup>-/-</sup> cells were determined using the TARDIS assay at time-points over a 24 hour continuous exposure to etoposide at 1  $\mu$ M (Figure 5(a)) or 10  $\mu$ M (Figure 5(b)). At both drug doses and in both cell lines, treatment induced a time-dependent increase in topoisomerase II DNA adduct levels (FITC immunofluorescence) up to the 8 hour time-point followed by a decrease at the 24 hour time-point (Figures 5(a) and 5(b)). With 1  $\mu$ M etoposide, the increase was significant at 8 hours in WT cells and at both 5 hours ( $P < .05$ ) and 8 hours ( $P < .01$ ) in TOP2 $\beta$ <sup>-/-</sup> cells. Although levels decreased at 24 hours, immunofluorescence was still significantly greater than background levels in both wild-type and TOP2 $\beta$ <sup>-/-</sup> cells ( $P < .05$ ). When cells were exposed to 10  $\mu$ M etoposide, immunofluorescence levels in WT cells became statistically significant at 2 hours after drug addition ( $P < .05$ ) and remained elevated at all other time-points ( $P < .01$ ). In TOP2 $\beta$ <sup>-/-</sup> cells, levels were significant at 1 hour ( $P < .01$ ), 5 hours ( $P < .05$ ), and 24 hours ( $P < .001$ ). Notably immunofluorescence levels were greater in the TOP2 $\beta$ <sup>-/-</sup>

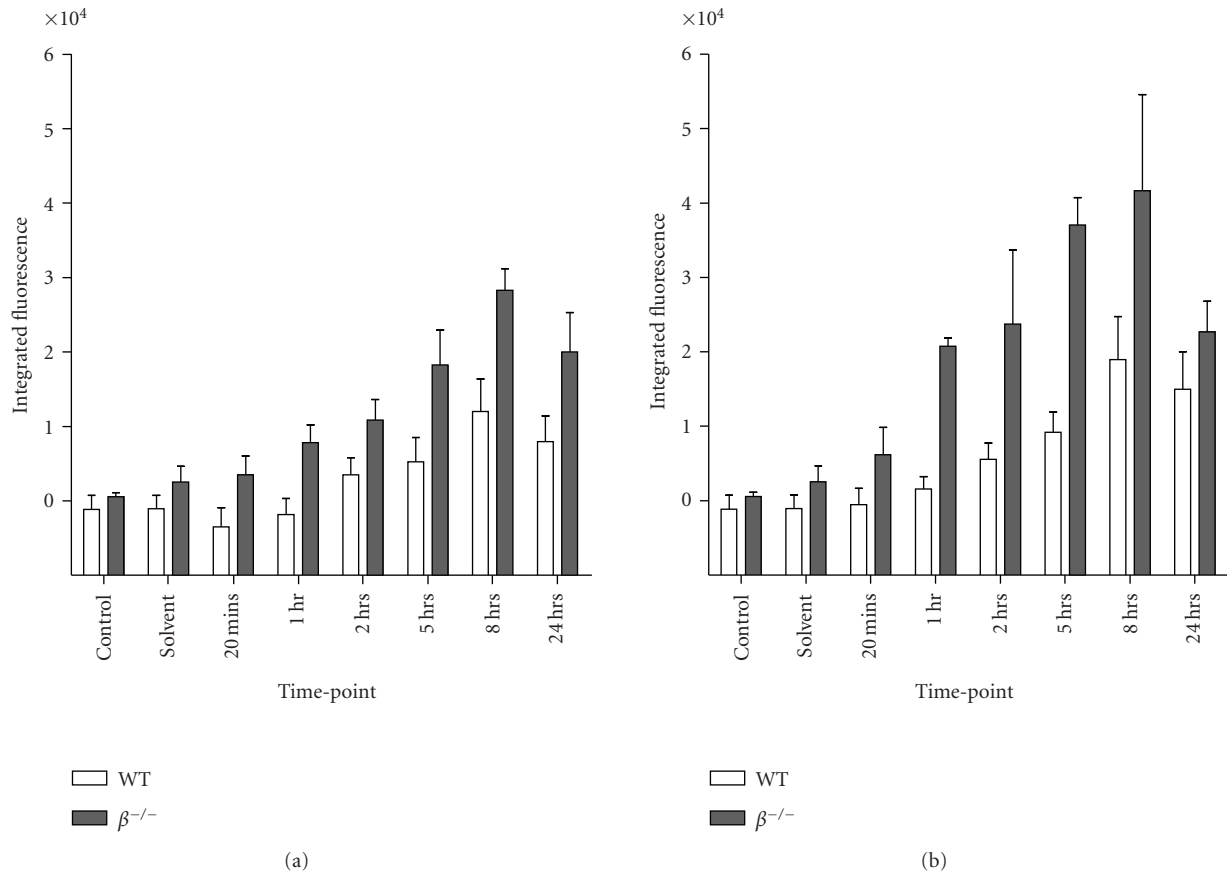


FIGURE 5: TARDIS analysis of cells treated with etoposide continuously for 24 hours. Topoisomerase II-DNA adducts were detected using an antibody that detects both isoforms in WT and TOP2 $\beta^{-/-}$  MEFs following exposure to 1  $\mu$ M (a) or 10  $\mu$ M (b). Plots show the mean of the median FITC fluorescence from at least three independent experiments.

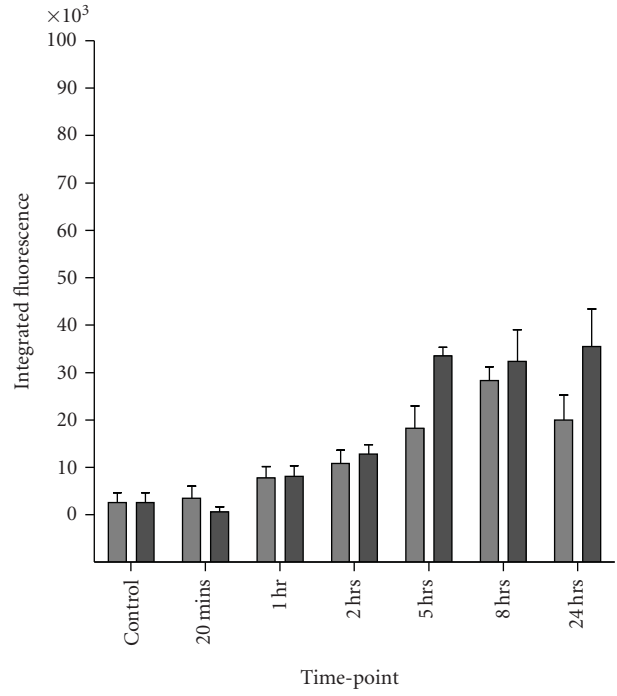
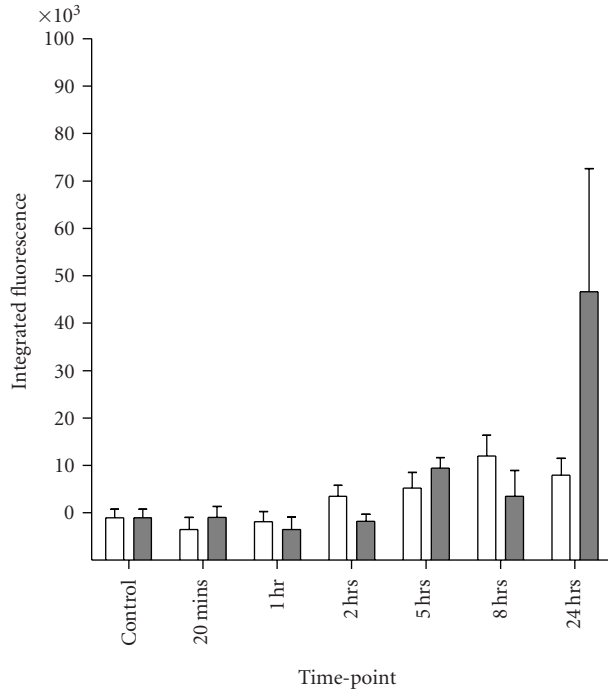
cells than the wild-type cells (Figure 5) at both drug doses and all time-points (all  $P$ -values <.05). The higher complex levels seen in cells lacking topoisomerase II $\beta$  may result from the longer half life of topoisomerase II $\alpha$  complexes [16] or be due to a role of topoisomerase II $\beta$  in sensing and/or promoting repair [29] or alternatively to downregulation of peroxiredoxins in TOP2 $\beta^{-/-}$  cells [32, 33].

To investigate whether the decrease in topoisomerase II-DNA complexes between the 8 hour and 24 hour time-points was due to proteasomal degradation of topoisomerase II, WT and TOP2 $\beta^{-/-}$  cells were incubated in the presence of the proteasome inhibitor, MG-132, for 30 minutes prior to and during 24 hour exposures to 1  $\mu$ M and 10  $\mu$ M etoposide. As shown in Figure 6(e), when treated with MG-132 alone, topoisomerase II-DNA complex levels were only significantly elevated above background levels at the 24 hour time-point. Immunofluorescence levels were comparable in the WT and TOP2 $\beta^{-/-}$  cells at all time-points considered. In cells cotreated with etoposide and MG-132, topoisomerase II-DNA complex levels did not decrease between the 8 hour and 24 hour time-points, as seen in cells treated with etoposide alone. Figure 6(a)–6(d), demonstrate that cotreatment led to increased immunofluorescence at the 24 hour time-point, in both cell lines and at both drug doses. This increase was

most dramatic in WT cells, where cotreatment led to a 6-fold increase in immunofluorescence in cells treated with 1  $\mu$ M etoposide and a 15-fold increase in cells treated with 10  $\mu$ M etoposide. In the TOP2 $\beta^{-/-}$  cells, the increase was roughly 2-fold at both doses of drug. This indicates that topoisomerase II removal at 24 hours is mediated via the proteasome, and that the effect is greatest on topoisomerase II $\beta$ , in agreement with previous studies [23, 25, 26].

#### 4. Conclusions

In response to IR phosphorylation of histone H2AX was triggered immediately, and slightly less phosphorylation was seen in TOP2 $\beta^{-/-}$  cells, which may indicate altered DNA damage sensing. As previously reported, IR did not produce topoisomerase II-DNA adducts. In response to etoposide both  $\gamma$ H2AX foci and topoisomerase II-DNA adducts were formed, with foci appearing 1 hour after treatment in WT cells and after 2 hours in TOP2 $\beta^{-/-}$  cells. This was slower than following treatment with IR, and presumably reflects the need to remove the topoisomerase II adduct to produce a frank DSB to trigger phosphorylation of histone H2AX. In both instances, levels become maximal at the 8 hour time-point and subsequently decrease at 24 hours.

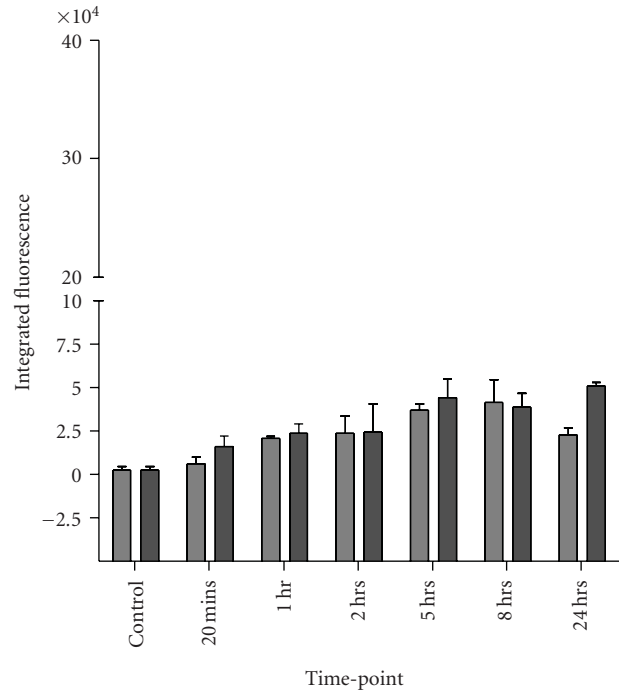
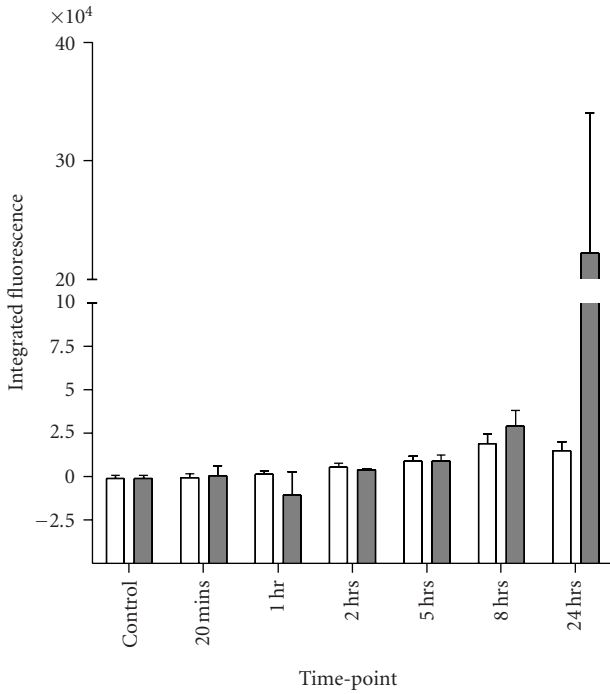


Legend for (a):  
□ WT 1  $\mu\text{M}$  Etop  
■ WT 1  $\mu\text{M}$  Etop + MG132

(a)

Legend for (b):  
■  $\beta^{-/-}$  1  $\mu\text{M}$  Etop  
■  $\beta^{-/-}$  1  $\mu\text{M}$  Etop + MG132

(b)



Legend for (c):  
□ WT 10  $\mu\text{M}$  Etop  
■ WT 10  $\mu\text{M}$  Etop + MG132

(c)

Legend for (d):  
■  $\beta^{-/-}$  10  $\mu\text{M}$  Etop  
■  $\beta^{-/-}$  10  $\mu\text{M}$  Etop + MG132

(d)

FIGURE 6: Continued.

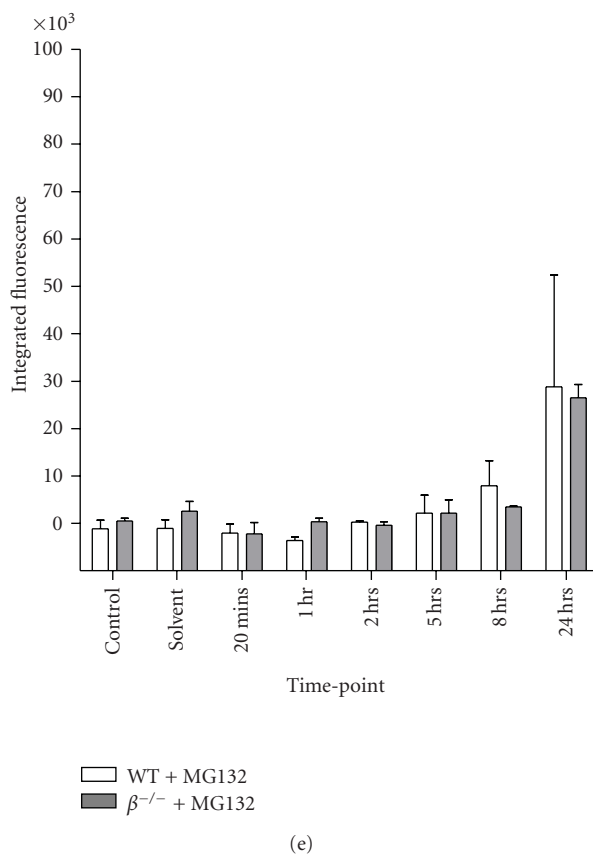


FIGURE 6: TARDIS analysis of cells treated with etoposide continuously for 24 hours plus and minus MG132 or with MG132 alone. Topoisomerase II-DNA adducts were quantified using an antibody that detects both isoforms. WT MEFs following exposure to  $1 \mu\text{M} \pm 2 \mu\text{M}$  MG132 (a), Top2 $\beta^{-/-}$  MEFs following exposure to  $1 \mu\text{M} \pm 2 \mu\text{M}$  MG132 (b), WT MEFs following exposure to  $10 \mu\text{M} \pm 2 \mu\text{M}$  MG132 (c), Top2 $\beta^{-/-}$  MEFs following exposure to  $10 \mu\text{M} \pm 2 \mu\text{M}$  MG132 (d), or WT and TOP2 $\beta^{-/-}$  MEFs following exposure to  $2 \mu\text{M}$  MG132 alone (e). Plots show the mean of the median FITC fluorescence.

Topoisomerase II complexes in WT cells but not TOP2 $\beta^{-/-}$  cells increased significantly at 24 hours when the proteasome was inhibited, suggesting that topoisomerase II $\beta$  adducts are removed by the proteasome.

## Acknowledgment

N. J. Sunter was funded on an LRF Gordon Pillar Studentship, now the LLR.

## References

- [1] E. P. Rogakou, C. Boon, C. Redon, and W. M. Bonner, "Megabase chromatin domains involved in DNA double-strand breaks in vivo," *Journal of Cell Biology*, vol. 146, no. 5, pp. 905–915, 1999.
- [2] E. P. Rogakou, D. R. Pilch, A. H. Orr, V. S. Ivanova, and W. M. Bonner, "DNA double-stranded breaks induce histone H2AX phosphorylation on serine 139," *Journal of Biological Chemistry*, vol. 273, no. 10, pp. 5858–5868, 1998.
- [3] C. H. Bassing, K. F. Chua, J. Sekiguchi et al., "Increased ionizing radiation sensitivity and genomic instability in the absence of histone H2AX," *Proceedings of the National Academy of Sciences of the United States of America*, vol. 99, no. 12, pp. 8173–8178, 2002.
- [4] M. Stucki and S. P. Jackson, " $\gamma$ H2AX and MDC1: anchoring the DNA-damage-response machinery to broken chromosomes," *DNA Repair*, vol. 5, no. 5, pp. 534–543, 2006.
- [5] A. Celeste, S. Petersen, P. J. Romanienko et al., "Genomic instability in mice lacking histone H2AX," *Science*, vol. 296, no. 5569, pp. 922–927, 2002.
- [6] I. G. Cowell, N. J. Sunter, P. B. Singh, C. A. Austin, B. W. Durkacz, and M. J. Tilby, " $\gamma$ H2AX foci form preferentially in euchromatin after ionising-radiation," *PLoS ONE*, vol. 2, no. 10, article e1057, 2007.
- [7] A. Xiao, H. Li, D. Shechter et al., "WSTF regulates the H2A.X DNA damage response via a novel tyrosine kinase activity," *Nature*, vol. 457, no. 7225, pp. 57–62, 2009.
- [8] F. Bouquet, C. Muller, and B. Salles, "The loss of  $\gamma$ H2AX signal is a marker of DNA double strand breaks repair only at low levels of DNA damage," *Cell Cycle*, vol. 5, no. 10, pp. 1116–1122, 2006.
- [9] X. Huang, F. Traganos, and Z. Darzynkiewicz, "DNA damage induced by DNA topoisomerase I- and topoisomerase II-inhibitors detected by histone H2AX phosphorylation in relation to the cell cycle phase and apoptosis," *Cell cycle (Georgetown, Tex.)*, vol. 2, no. 6, pp. 614–619, 2003.

- [10] J. P. Banáth and P. L. Olive, "Expression of phosphorylated histone H2AX as a surrogate of cell killing by drugs that create DNA double-strand breaks," *Cancer Research*, vol. 63, no. 15, pp. 4347–4350, 2003.
- [11] D. J. Smart, H. D. Halicka, G. Schmuck, F. Traganos, Z. Darzynkiewicz, and G. M. Williams, "Assessment of DNA double-strand breaks and  $\gamma$ H2AX induced by the topoisomerase II poisons etoposide and mitoxantrone," *Mutation Research*, vol. 641, no. 1-2, pp. 43–47, 2008.
- [12] G. P. Watters, D. J. Smart, J. S. Harvey, and C. A. Austin, "H2AX phosphorylation as a genotoxicity endpoint," *Mutation Research*, vol. 679, no. 1-2, pp. 50–58, 2009.
- [13] J. M. Fortune and N. Osheroff, "Topoisomerase II as a target for anticancer drugs: when enzymes stop being nice," *Progress in Nucleic Acid Research and Molecular Biology*, vol. 64, pp. 221–253, 2000.
- [14] A. C. G. Porter and C. J. Farr, "Topoisomerase II: untangling its contribution at the centromere," *Chromosome Research*, vol. 12, no. 6, pp. 569–583, 2004.
- [15] C. A. Austin and K. L. Marsh, "Eukaryotic DNA topoisomerase II $\beta$ ," *BioEssays*, vol. 20, no. 3, pp. 215–226, 1998.
- [16] F. Errington, E. Willmore, C. Leontiou, M. J. Tilby, and C. A. Austin, "Differences in the longevity of topo II $\alpha$  and topo II $\beta$  drug-stabilized cleavable complexes and the relationship to drug sensitivity," *Cancer Chemotherapy and Pharmacology*, vol. 53, no. 2, pp. 155–162, 2004.
- [17] F. Errington, E. Willmore, M. J. Tilby et al., "Murine transgenic cells lacking DNA topoisomerase II $\beta$  are resistant to acridines and mitoxantrone: analysis of cytotoxicity and cleavable complex formation," *Molecular Pharmacology*, vol. 56, no. 6, pp. 1309–1316, 1999.
- [18] E. Willmore, A. J. Frank, K. Padget, M. J. Tilby, and C. A. Austin, "Etoposide targets topoisomerase II $\alpha$  and II $\beta$  in leukemic cells: isoform-specific cleavable complexes visualized and quantified in situ by a novel immunofluorescence technique," *Molecular Pharmacology*, vol. 54, no. 1, pp. 78–85, 1998.
- [19] K. Caldecott, G. Banks, and P. Jeggo, "DNA double-strand break repair pathways and cellular tolerance to inhibitors of topoisomerase II," *Cancer Research*, vol. 50, no. 18, pp. 5778–5783, 1990.
- [20] S. H. Kaufmann, "Cell death induced by topoisomerase-targeted drugs: more questions than answers," *Biochimica et Biophysica Acta*, vol. 1400, no. 1-3, pp. 195–211, 1998.
- [21] J. Wu and L. F. Liu, "Processing of topoisomerase I cleavable complexes into DNA damage by transcription," *Nucleic Acids Research*, vol. 25, no. 21, pp. 4181–4186, 1997.
- [22] Y.-H. Hsiang, M. G. Lihou, and L. F. Liu, "Arrest of replication forks by drug-stabilized topoisomerase I-DNA cleavable complexes as a mechanism of cell killing by camptothecin," *Cancer Research*, vol. 49, no. 18, pp. 5077–5082, 1989.
- [23] A. M. Azarova, Y. L. Lyu, C.-P. Lin et al., "Roles of DNA topoisomerase II isozymes in chemotherapy and secondary malignancies," *Proceedings of the National Academy of Sciences of the United States of America*, vol. 104, no. 26, pp. 11014–11019, 2007.
- [24] Y. Mao, S. D. Desai, C.-Y. Ting, J. Hwang, and L. F. Liu, "26 S proteasome-mediated degradation of topoisomerase II cleavable complexes," *Journal of Biological Chemistry*, vol. 276, no. 44, pp. 40652–40658, 2001.
- [25] H. Xiao, Y. Mao, S. D. Desai et al., "The topoisomerase II $\beta$  circular clamp arrests transcription and signals a 26S proteasome pathway," *Proceedings of the National Academy of Sciences of the United States of America*, vol. 100, no. 6, pp. 3239–3244, 2003.
- [26] A. Zhang, Y. L. Lyu, C.-P. Lin et al., "A protease pathway for the repair of topoisomerase II-DNA covalent complexes," *Journal of Biological Chemistry*, vol. 281, no. 47, pp. 35997–36003, 2006.
- [27] F. C. Ledesma, S. F. El Khamisy, M. C. Zuma, K. Osborn, and K. W. Caldecott, "A human 5'-tyrosyl DNA phosphodiesterase that repairs topoisomerase-mediated DNA damage," *Nature*, vol. 461, no. 7264, pp. 674–678, 2009.
- [28] S. Y. A. Terry, A. C. Riches, and P. E. Bryant, "Suppression of topoisomerase II $\alpha$  expression and function in human cells decreases chromosomal radiosensitivity," *Mutation Research*, vol. 663, no. 1-2, pp. 40–45, 2009.
- [29] R. K. Mandraju, P. Kannapiran, and A. K. Kondapi, "Distinct roles of Topoisomerase II isoforms: DNA damage accelerating  $\alpha$ , double strand break repair promoting  $\beta$ ," *Archives of Biochemistry and Biophysics*, vol. 470, no. 1, pp. 27–34, 2008.
- [30] K. Yamane, M. Kawabata, and T. Tsuruo, "A DNA-topoisomerase-II-binding protein with eight repeating regions similar to DNA-repair enzymes and to a cell-cycle regulator," *European Journal of Biochemistry*, vol. 250, no. 3, pp. 794–799, 1997.
- [31] H. Kitagawa, R. Fujiki, K. Yoshimura et al., "The chromatin-remodeling complex WINAC targets a nuclear receptor to promoters and is impaired in Williams syndrome," *Cell*, vol. 113, no. 7, pp. 905–917, 2003.
- [32] K. Chikamori, J. E. Hill, D. R. Grabowski et al., "Downregulation of topoisomerase II $\beta$  in myeloid leukemia cell lines leads to activation of apoptosis following all-trans retinoic acid-induced differentiation/growth arrest," *Leukemia*, vol. 20, no. 10, pp. 1809–1818, 2006.
- [33] A. V. Kropotov, P. S. Grudinkin, N. M. Pleskach, B. A. Gavrilov, N. V. Tomilin, and B. Zhivotovsky, "Downregulation of peroxiredoxin V stimulates formation of etoposide-induced double-strand DNA breaks," *FEBS Letters*, vol. 572, no. 1–3, pp. 75–79, 2004.

## Review Article

# Structural Biology of DNA Repair: Spatial Organisation of the Multicomponent Complexes of Nonhomologous End Joining

**Takashi Ochi, Bancinyane Lynn Sibanda, Qian Wu, Dimitri Y. Chirgadze, Victor M. Bolanos-Garcia, and Tom L. Blundell**

*Department of Biochemistry, University of Cambridge, Tennis Court Road, Cambridge CB2 1GA, UK*

Correspondence should be addressed to Takashi Ochi, takashi@cryst.bioc.cam.ac.uk

Received 22 May 2010; Accepted 2 July 2010

Academic Editor: Ashis Basu

Copyright © 2010 Takashi Ochi et al. This is an open access article distributed under the Creative Commons Attribution License, which permits unrestricted use, distribution, and reproduction in any medium, provided the original work is properly cited.

Nonhomologous end joining (NHEJ) plays a major role in double-strand break DNA repair, which involves a series of steps mediated by multiprotein complexes. A ring-shaped Ku70/Ku80 heterodimer forms first at broken DNA ends, DNA-dependent protein kinase catalytic subunit (DNA-PKcs) binds to mediate synapsis and nucleases process DNA overhangs. DNA ligase IV (LigIV) is recruited as a complex with XRCC4 for ligation, with XLF/Cernunnos, playing a role in enhancing activity of LigIV. We describe how a combination of methods—X-ray crystallography, electron microscopy and small angle X-ray scattering—can give insights into the transient multicomponent complexes that mediate NHEJ. We first consider the organisation of DNA-PKcs/Ku70/Ku80/DNA complex (DNA-PK) and then discuss emerging evidence concerning LigIV/XRCC4/XLF/DNA and higher-order complexes. We conclude by discussing roles of multiprotein systems in maintaining high signal-to-noise and the value of structural studies in developing new therapies in oncology and elsewhere.

## 1. Introduction

Nonhomologous End Joining (NHEJ) and Homologous Recombination (HR) comprise the two major modes of DNA double-strand break (DSB) repair in human cells. Although HR is dominant in late S/G2 phases when a sister chromatid is available [1], NHEJ, which does not require a template [2], plays a major role in G1/early S phase [1]. It is predicted that in humans about 50 endogenous DSBs per cell during each cell cycle may occur [3]. These are mainly generated by ionizing radiation, reactive oxygen species, and DNA replication across a nick [2]. Unrepaired DSBs can cause catastrophic gene loss during cell division, leading to chromosomal translocations, increased mutation rates, and carcinogenesis [4]. The NHEJ system is also responsible for programmed DSBs in V(D)J recombination [5] and class switch recombination [6] during development of immune diversity. NHEJ has an alternative end-joining pathway, which is mostly microhomology-mediated end joining [7] and is independent of NHEJ components [8]. Here NHEJ implies the main NHEJ pathway.

The NHEJ pathway comprises three major steps: synapsis, end processing and ligation [9]. Synapsis is carried out by DNA-dependent protein kinase (DNA-PK) consisting of Ku70, Ku80, DNA-PK catalytic subunit (DNA-PKcs), and DNA. Ku70 and Ku80 form a ring-shaped heterodimer around the broken DNA ends and maintain them in proximity [10, 11]. DNA-PKcs, a very large protein belonging to the phosphatidylinositol-3-OH kinase (PI3K)-related kinase (PIKKs) family [12], is recruited through interaction with the C-terminus of Ku80 [13, 14], and causes the Ku70/80 heterodimer to move about one helical turn inward from the end [15] to make space for DNA-PKcs to bind DNA. Two DNA-PK assemblies are probably required to hold the two DNA ends close together [16]. Activated DNA-PKcs phosphorylates itself and various proteins, including the other NHEJ components [17, 18]. Synapsis induces the autophosphorylation of DNA-PKcs and allows other NHEJ proteins access to DNA ends [19, 20].

The end processing involves nucleases such as Artemis [21], which is capable of cutting an array of DNA overhangs

and is thought to be sufficient as a nuclease, although other nucleases in particular PNK, aprataxin (APTX), and PNK-APTX-like factor (PALF), a 3' exonuclease, cannot be ruled out [22]. Artemis interacts with DNA-PKcs and opens DNA hairpins in the V(D)J recombination process [23]. Mutations in *Artemis* gene cause Radiosensitive Severe Combined Immunodeficiency (RS-SCID) [21]. Polymerases Pol $\mu$  and Pol $\lambda$  use their BRCT domains to bind to Ku/DNA complexes and terminal deoxynucleotidyl transferase (TdT) is exclusively expressed in initial lymphoid cells to engage in NHEJ of the V(D)J recombination process [24–26]. Furthermore, as recently shown Ku in its role as a lyase also participates in end processing cutting DNA 3' at abasic sites, indicating that this protein, like its partner DNA-PKcs, has enzymatic properties and thus fulfils a number of roles in the NHEJ pathway [27].

The final ligation step of rejoining is mediated by DNA ligase IV (LigIV), which is associated with dimeric X-ray cross-complementation group 4 (XRCC4) [28]. These proteins form a very stable complex, which is maintained at 2 M NaCl or 7 M urea [29]. XRCC4 stimulates adenylation and ligase activity [30–32]. Knockouts of these genes in mice result in the late embryonic lethality in the p53-dependent manner [33–36] while mutations in *lig4* gene result in LIG4 syndrome characterized by radiosensitivity, unusual facial features, microcephaly, developmental and growth delay, pancytopenia, and skin abnormality [37]. XRCC4-Like Factor (XLF)/Cernunnos (XLF), mutations of which in humans cause Severe Combined Immunodeficiency, also interacts with XRCC4, and enhances the ligation by LigIV [38, 39].

Here we review what is known of the architectures of the transient multicomponent complexes that mediate Nonhomologous End Joining. Figure 1 is an attempt to construct an interaction diagram that summarises our current understanding of NHEJ protein interactions and phosphorylation by DNA-PKcs, indicating where structural information is available. Although the existence of DNA-PK—the complex between DNA-PKcs, heterodimeric Ku and DNA—is clearly defined, as is the tight complex between XRCC4 and LigIV, the temporal and spatial organisation of higher-order complexes is unclear. Do subcomplexes exist that allow the Ku to get off the DNA before ligation, or is there one supercomplex in which DNA-PK, LigIV/XRCC4, and XLF coexist to achieve ligation? In this case, how does Ku leave when ends are ligated? In this paper, we first consider what is known about the structure of the huge single chain DNA-PKcs and how this might lead to a better understanding of the target for use in structure-guided drug discovery. We then discuss the organisation of DNA-PKcs/Ku70/Ku80/DNA complex (known as DNA-PK), in order to shed light on the initial events that take place in the NHEJ pathway. We discuss the emerging evidence concerning 3D structures of LigIV/XRCC4/XLF/DNA complexes, which should give clues about the binding and functional mechanism of LigIV/XRCC4 and XLF in NHEJ. Finally we consider the spatial arrangement of higher-order complexes in order to give a picture of the NHEJ repair system as a whole.

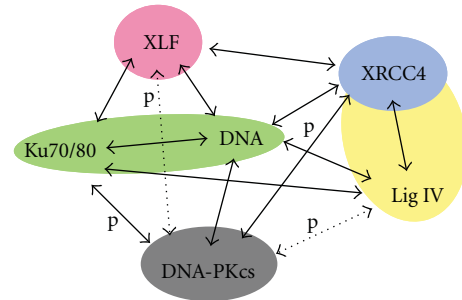


FIGURE 1: Schematic diagram of interactions of the NHEJ machinery. Colour-filled shapes indicate the proteins and complexes with known 3D structures. Solid arrows indicate confirmed whereas dashed arrows are plausible interactions. Phosphorylation events are indicated by letter “p”.

## 2. Structural Biology of Individual Components

Considerable advances have been made in the structural biology of individual components and complexes of the NHEJ repair machinery, but further work is required to understand the spatial organisation of this complicated and dynamic process. Here we discuss what is known about each component before discussing the multiprotein complexes that mediate their functions in NHEJ.

**2.1. Ku70/80.** The double-stranded (ds) DNA end-binding activity of Ku70 and Ku80 requires their association to form a heterodimer [40]. The crystal structure of the Ku70/Ku80 heterodimer reveals a similar topology and domain organisation, comprising an amino-terminal  $\alpha/\beta$  domain, a central  $\beta$ -barrel domain, and a helical C-terminal arm [10]. These proteins, when associated, form a pseudosymmetrical structure, in which residues that contribute to the dimer interface show a low level of sequence identity (approximately 15%; Figure 2), favouring heterodimer formation over Ku70-Ku70 or Ku80-Ku80 homodimerisation.

The crystal structure of the Ku70/80 heterodimer in complex with one 55-nucleotide long Y-shaped DNA fragment shows that the Ku70/80 heterodimer adopts the shape of a ring that encircles duplex DNA (Figure 3). No large conformational changes occur on binding DNA to heterodimeric Ku except for the C-terminal domains of Ku70 and Ku80. Indeed, no contacts with DNA bases and only a few interactions with the sugar-phosphate backbone are made. The DNA duplex is embraced through the Ku70/80 preformed ring in such a way that one DNA face is relatively accessible to the solvent and therefore exposed to processing enzymes that remove damaged nucleotides and fill gaps prior to ligation. These features can provide structural support to broken DNA ends and bring the DNA helix into phase across the junction during end processing and ligation. Although Ku70/80 heterodimer shows low affinity for circularized DNA [43] and does not bind any DNA substrates shorter than 14 bp, it does bind dsDNA fragments of similar length and structure in a DNA sequence-independent fashion and irrespective of whether the DNA ends are blunt, with hairpin loops, or 5' or 3' overhangs.

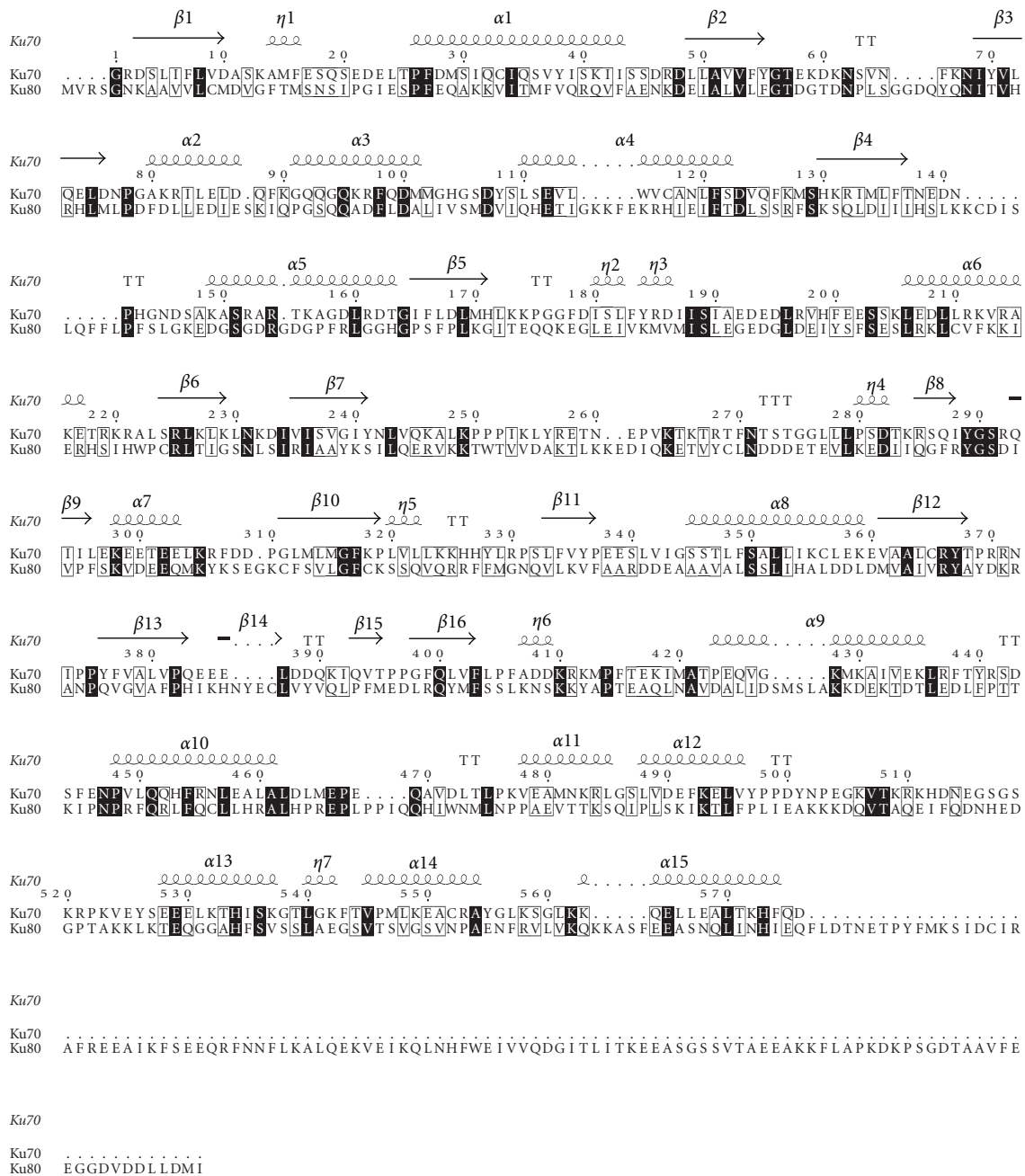


FIGURE 2: Ku70 and Ku80 aligned sequences on the basis of their structures. They show a similar domain organisation despite the low sequence identity. The alignment was created with ClustalW2 [41] and visualized with ESPript [42]. Many residues are conserved (black box) or semiconserved/similar (gray box).

**2.2. DNA-PKcs.** The structure of DNA-PKcs has proved quite elusive. Some beautiful work performed using cryo-electron microscopy single particle reconstruction of DNA-PKcs [44–47] has given a good impression of the overall structure (see Figure 4(a)). This has now been complemented by work in our laboratory. We have shown that DNA-PKcs crystals can be grown and diffract to about 8.5 Å resolution but the diffraction is better for the complexes with C-terminal fragments of Ku80, presumably due to a

stabilization of the DNA-PKcs in the complex leading to better ordering of the crystal packing. We have recently used multiwavelength anomalous dispersion with the Ta<sub>6</sub>Br<sub>12</sub><sup>2+</sup> heavy-metal cluster [48] to solve the structure of DNA-PKcs in complex with C-terminal domain of Ku80 at 6.6 Å resolution (Figure 4(b)).

Much of the DNA-PKcs polypeptide chain is constructed from HEAT repeat units (Figure 5) to form several separate domains. The DNA-PKcs tertiary structure measures 160 Å

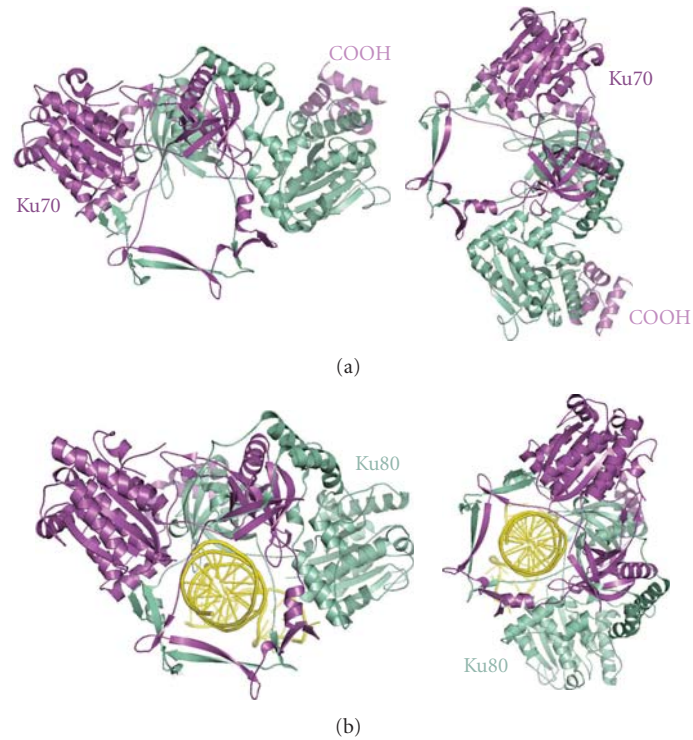


FIGURE 3: Heterodimerisation of Ku70/80 defines a ring shape that binds DNA. Crystal structures of Ku70/80 heterodimer in the absence of DNA (a) and in DNA-bound form (b). Adapted from [10].

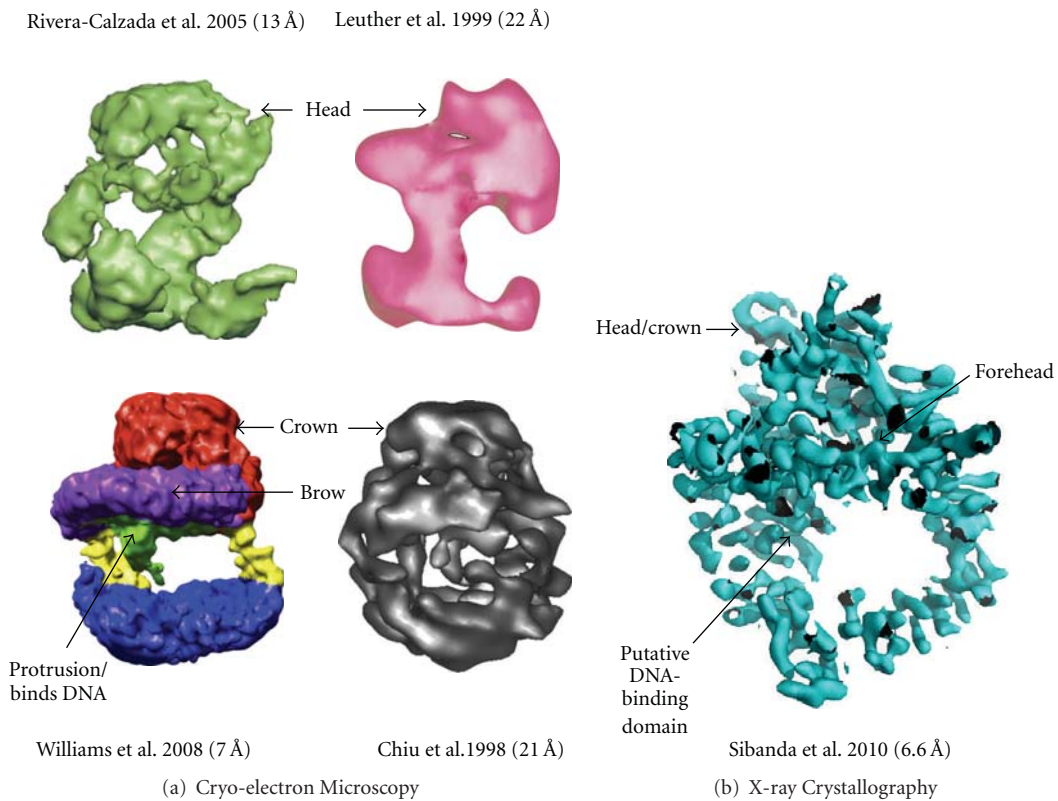


FIGURE 4: Equivalent views of DNA-PKcs as defined by (a) Cryo-electron microscopy and (b) X-ray protein crystallography. References to the publications and resolutions of the models are given above. Colour coding of these EM structures are as given in their respective publications [44–47]. The X-ray crystallographic experimental electron density map is as defined by Sibanda et al. [48].

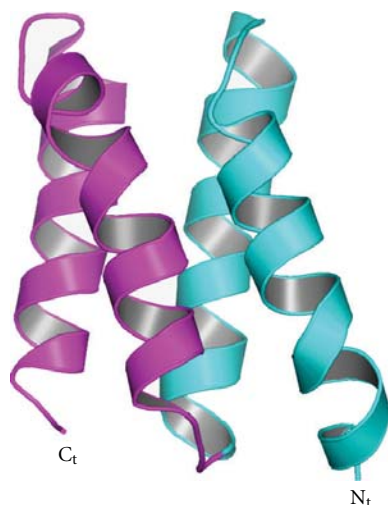


FIGURE 5: An example of HEAT-repeat motifs. Two consecutive  $\alpha$ -helical hairpins are shown.

high and 120 Å across as viewed in Figure 6(a). From the N-terminus, HEAT-repeat motifs comprising about 66  $\alpha$ -helices fold into a hollow circular structure, which when viewed from the side resembles a cradle (Figure 6(b)). The chain changes direction before the circle is complete, thus leaving a gap (Figure 6(a)). Within this circular structure the regularity of the HEAT repeats breaks down at certain points, as indicated in Figure 6(a) with blue arrows. These points of irregularity may play a part in conformational changes that have been implicated in the function of this molecule [16]. It is possible that these conformational changes could have a bearing on the size of the gap (Figure 6(a)), which may have a role in the release of DNA-PKcs from DNA ends when NHEJ is complete. The ring structure most likely acts as a platform for proteins that engage in repair of broken DNA and together with Ku holds in place the DNA while it is being repaired.

In the second part of the structure the polypeptide chain exploits HEAT repeats to fold into a small, globular, putative DNA-binding domain within the circular structure. It is known that DNA-PKcs binds both double-stranded and single-stranded DNA. Williams et al. (2008) have proposed that “the protrusion” in their cryo-EM structure binds DNA [47], and this protrusion is equivalent to the small globular domain located within the circular region of the crystal structure. This remains the best candidate for both single- and double-stranded DNA recognition, but further work on DNA-PK (DNA-PKcs, Ku, DNA complex) crystals at a higher resolution structure of DNA-PKcs will be needed to confirm this. Thirdly, the C-terminal region folds into the Head/Crown that is perched right at the top of the cradle shaped circular structure and extends further back. This part contains the FAT, kinase domain, FATC, and various parts where other proteins, as indicated by biochemical studies, may bind to form complexes with DNA-PKcs (Figure 7).

The core of the kinase structure from PI(3)K $\gamma$ , one of the family members, was superposed onto this Head/Crown

region resulting in a plausible fit to the N-lobe  $\beta$ -strands and the C-lobe  $\alpha$ -helices (Figure 8). In this location the kinase is exposed and easily accessible to substrates (Figure 8). From the location of the kinase domain the positions of the FAT and FATC regions can be inferred (Figure 7) as the kinase domain likely “snuggles” in between these two regions [62].

The size of the monomer of DNA-PKcs is predicted by small angle X-ray scattering (SAXS) to be about 155 Å [63], broadly in agreement with that of the crystallographic structure. DNA-PKcs dimerizes without DNA in a concentration-dependent manner. SAXS data indicate a large conformational change between autophosphorylated and unphosphorylated DNA-PKcs; the dimension and radius of gyration of phosphorylated DNA-PKcs increased 25 and 2 Å, respectively, compared to mock DNA-PKcs. Also, shape reconstruction of phosphorylated DNA-PKcs shows a wider cleft between head and palm domains than in the unphosphorylated enzyme.

**2.3. DNA Ligase IV.** Human LigIV has also proved difficult to study in isolation due to instability and flexibility but it is stabilised by interaction with XRCC4 [28]. In human, LigIV is one of three ATP-dependent DNA ligases, I, III, and IV, and plays a central role in eukaryotic NHEJ. LigIV can be divided into the catalytic and interaction regions. There are excellent reviews of the comparison of structures of DNA and RNA ligases, and RNA capping enzymes elsewhere [64–67].

LigIV belongs to the nucleotidyltransferase superfamily and carries out a three-step nucleotidyl transfer reaction: the formation of covalent enzyme-nucleotide monophosphate (NMP) intermediate (step 1), the transformation of the NMP to a 5'-phosphate of polynucleotide (step 2), and the joining of the 5'-phosphate with 3'-hydroxyl to seal two polynucleotides (step 3) [68]. These enzymes have four common motifs (I, III, IV, V) and in addition two more motifs (III $\alpha$  and VI), which are conserved among the cellular and ASF virus capping enzymes and eukaryotic ATP-dependent DNA ligases [69]. A recently found motif, Va, is well conserved among human DNA ligases [70]. The motif I KX(D/N)G has the catalytic lysine which forms the NMP-covalent intermediate. Motifs I-V are located in the nucleotidyltransferase domain (NTase) (Figure 9), the core of which comprises three mainly antiparallel  $\beta$ -sheets flanked by six  $\alpha$ -helices [64]. Motifs Va and VI belong to the oligonucleotide/oligosaccharide-binding domain (OBD) (Figure 9), which has the five stranded Greek-key  $\beta$ -barrel capped by an  $\alpha$ -helix [64, 71]. NTase and OBD are conserved among capping enzymes and DNA ligases [64]. Most LigIV syndrome mutations are found in the NTase and OBD [72] (Figure 9).

Many enzymes in the nucleotidyltransferase superfamily have extra domains in addition to conserved catalytic core domains. N-terminal to the NTase, for instance, the human DNA ligases have DNA-binding domain (DBD), the three-dimensional structure of which was first uncovered by Pascal et al. (2004) with the catalytic domains of human DNA ligase I (LigI) complexed with an unligatable, nicked DNA fragment [73]. This domain is also found in archaeal DNA

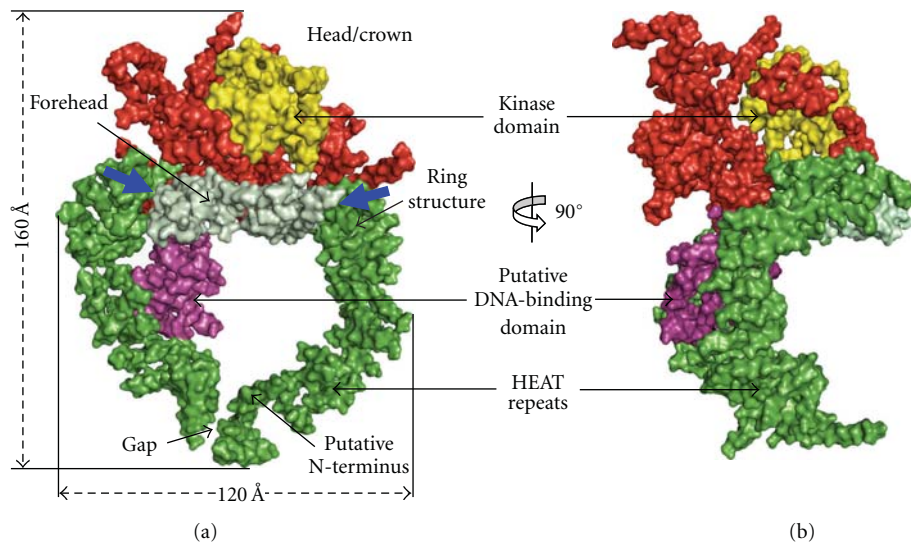


FIGURE 6: Crystal structure of DNA-PKcs. Molecular surface of the DNA-PKcs structure showing (a) front and (b) side views. Also shown in (a), is the overall size of DNA-PKcs with the potential flexible sites indicated in blue arrows. The molecule is colour coded as follows: the ring structure that is predominantly HEAT repeats is green; the forehead that is part of the ring structure is light green; the putative DNA binding domain is magenta; the larger C-terminal part that includes the FAT and FATC domains is red, and the kinase domain is yellow.

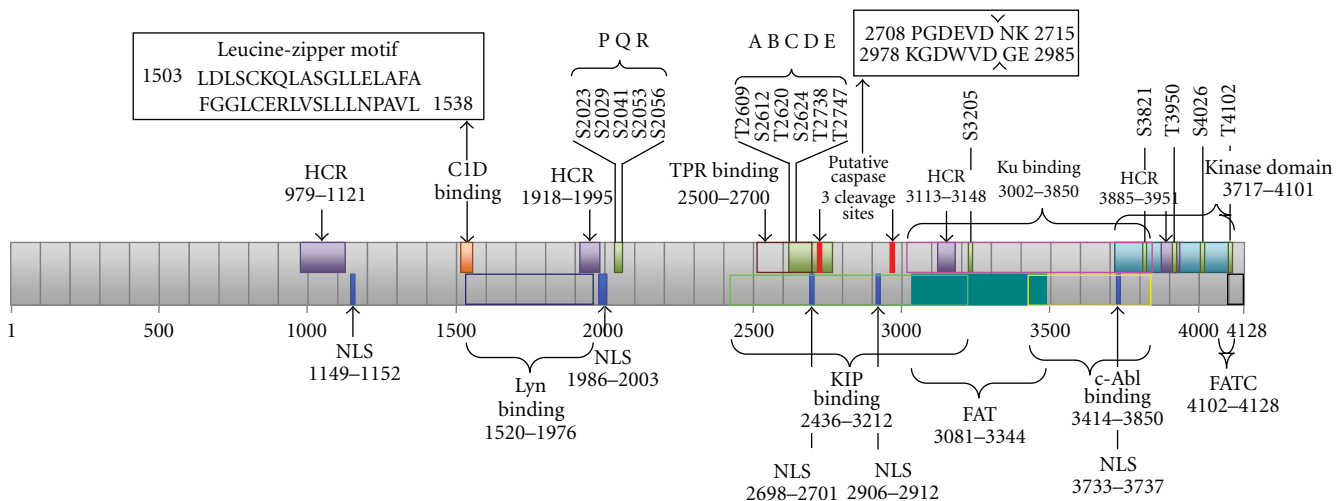


FIGURE 7: Schematic diagram of DNA-PKcs sequence-function implications. Shown are four highly conserved regions (HCR) [49]; Kinase, FAT, and FATC domains; putative sites for nuclear localization signals (NLSs) [49]; Autophosphorylation sites PQR [50], ABCDE [19], S3205 [51], S3821, S4026, T4102 [52], and T3950 [53]; cleavage sites for apoptotic protease caspase-3 [49, 54–56]; binding sites for Lyn tyrosine kinase [57], C1D protein that interacts at the leucine-zipper motif of DNA-PKcs [58], protein phosphatase-5 (PP5) that binds, using its tetratricopeptide repeat (TPR), to dephosphorylate DNA-PKcs at S2056 and T2609 [59], Ku70/80 that binds to present the damaged DNA double strand ends to DNA-PKcs [60], the kinase interacting protein (KIP) [61], and c-Abl that binds using its SH<sub>3</sub>, a binding that is triggered by DNA damage [60].

ligases [74–76] and possibly other eukaryotic, Poxvirus, and archaeal DNA ligases [77]. Pascal et al. (2004) showed that DBD is essential for LigI to bind DNA and to carry out ligation of DNA nicks [73]. However, this does not seem to be the case for DNA ligase III [78], although most DNA-binding affinity of LigIV seems to come from its DBD (T Ochi and TL Blundell, unpublished results). These results suggest that

DBD of each human DNA ligase has different DNA-binding properties, although they are likely to have similar structures [79]. Two LigIV syndrome mutations are severe only when they are combined with R278H, and they seem to have little impact on LigIV activity [37]. On the basis of structural similarities of the catalytic regions of LigI and LigIV, they are likely to bind DNA in a similar manner.

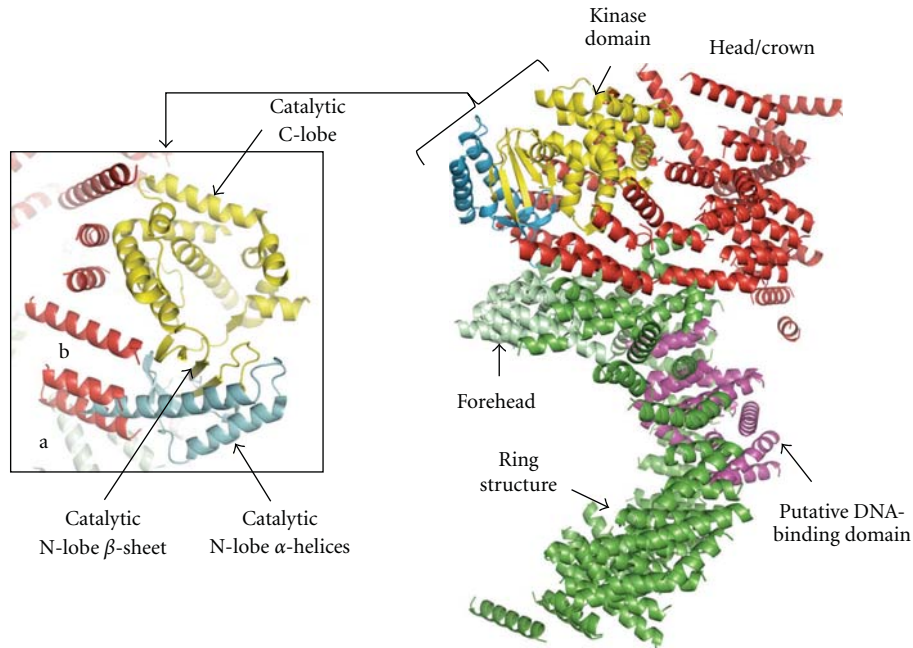


FIGURE 8: DNA-PKcs kinase domain. The figure shows a cartoon of the overall structure of DNA-PKcs depicting the position of the kinase domain. The colour coding is as shown in Figure 6. The modelling of DNA-PKcs catalytic domain was based on the crystal structure of one of its family members, the PI(3)K $\gamma$  kinase (PDB code: 1E8X). Also shown is a closeup of DNA-PKcs catalytic domain. Helices of DNA-PKcs labelled (a) and (b) could be occupied by helices from the N-lobe of PI(3)K $\gamma$ . The N-lobe helices displayed in light blue were omitted from the final structure of DNA-PKcs due to unclear electron density in this region.

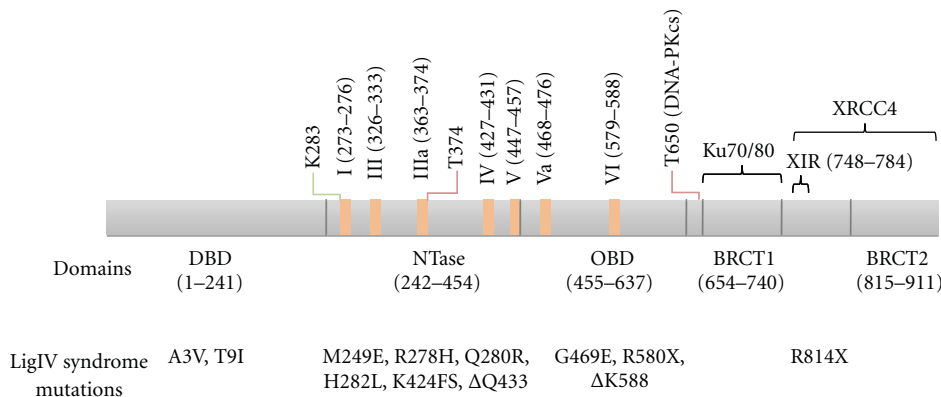


FIGURE 9: Schematic diagram of human DNA ligase IV. Domain boundaries shown in the figure are based on the crystallographic structure of human DNA ligase I [73] and BRCT domains of LigIV [94]. Conserved motifs (I, III, IIIa, IV, V, Va, and VI) are shown in orange rectangles [69, 70]. The conserved catalytic lysine is indicated in green line. Reported phosphorylation sites are indicated by red lines [81, 99]. LigIV syndrome mutations are shown under domains [72, 100]. Ku and XRCC4 interaction regions are indicated with black brackets [29, 84, 94].

In addition to the catalytic region, human DNA ligases have extra domains [79]. LigIV has a tandem BRCT domain with a linker predicted to be mostly disordered. This linker seems to be important for the catalytic activity of LigIV [80] and has a phosphorylation site at T650 by DNA-PKcs, the phosphorylation of which stabilizes LigIV [81]. The BRCT domain, which typically has four parallel  $\beta$ -strands surrounded by three  $\alpha$ -helices [82], is common in cell cycle checkpoint proteins that respond to DNA damage [83]. LigIV interacts with XRCC4 mainly through the linker

between the two BRCT [80]. As noted above, in addition to the interaction with XRCC4, the first BRCT domain (BRCT1) has been shown to interact with Ku70/80 [84].

Structures of tandem BRCT domains of human BRCA1 and MDC1, yeast Crb2, Nbs1, and Brc1, have been solved with different phosphopeptides. Four key residues that form the phospho-serine binding pocket—the (S/T)G motif at the end of the first  $\beta$ -strand ( $\beta$ 1) and the (S/T)XK motif at the beginning of the second helix ( $\alpha$ 2) [85–93] have been identified; the residues are conserved in the tandem

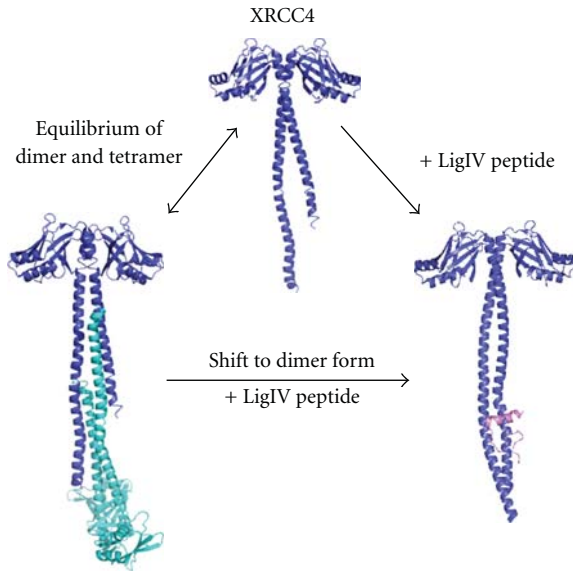


FIGURE 10: XRCC4 dimer, tetramer, and binding with DNA ligase IV peptide. The equilibrium is shifted to dimer when DNA ligase IV peptide binds to XRCC4.

BRCT domain of LigIV except that the second motif is replaced by NXR. Thus BRCT1 might bind to phosphoserines [94], although the interactions with the two proximal BRCT domains found in BRCA1, MDC1, Crb2, Nbs1, and Brcl are unlikely to occur in LigIV as the tandem BRCT domains are probably positioned apart [94, 95]. Indeed, *in vitro* phosphopeptide binding experiments showed that BRCT domains of LigIV bound phosphopeptides [96, 97]. However, the precise sequence of a phosphopeptide that binds to the BRCT domains has not yet been determined.

Since the tandem BRCT domains have a common globular arrangement of the BRCT domains, LigIV domains may interact when LigIV is in the free form. The main dimerization interface of the tandem BRCT domain is  $\alpha 2$  in BRCT1, and the first and third helices  $\alpha' 1$  and  $\alpha' 3$  in the second BRCT domain (BRCT2) [98]. Interestingly, the interaction surface of those BRCT domains and XRCC4 is similar to that of other tandem BRCT domains (as discussed below). It is possible that a BRCT domain from another protein interacts with  $\alpha 2$  of BRCT1, which is exposed to the solvent. Thus, although the tandem BRCT domains of LigIV have a long linker, they have features in common with other tandem BRCT domains.

**2.4. XRCC4.** In solution, XRCC4 exists as a salt-dependent equilibrium of dimers and tetramers [102] see Figure 10. Tail-to-tail tetramerisation was observed in XRCC4 protein crystals [103]. Binding of LigIV with the XRCC4 C-terminal ( $\alpha$ -helical coiled-coil stabilizes the XRCC4 dimer formation. The binding region between XRCC4 and LigIV overlaps with the XRCC4 tetramerisation region, which may explain why LigIV functions to shift XRCC4 to dimer form in solution [102]. Whether tetrameric XRCC4 has a function during NHEJ repair pathway is still not known.

The protein sequence of XRCC4 after residue 213 is not included in XRCC4 crystal structures due to the expected highly disordered and flexible structure of XRCC4 C-terminal domain [103]. However, EM studies have revealed that mouse XRCC4 C-terminal structure is a globular domain [104]. This domain includes putative nuclear localization sequences [105]. These authors also suggested that a cluster of acidic amino acids 229–238 is important for the auto-transcription activity. Furthermore, the XRCC4 C-terminal domain is the target for NHEJ regulatory proteins. DNA-PKcs phosphorylates XRCC4 and regulates its binding with DNA [31]. Residues S260 and S318 in the XRCC4 C-terminal region were identified to be the main phosphorylation sites by DNA-PKcs [106]. XRCC4 is also phosphorylated by CK2, residue T233 and the phosphorylation by CK2 recruits PNK, which is likely to participate in NHEJ [107]. Indeed the structure of the ForkHead-Associated (FHA) Domain of PNK with a XRCC4-derived phosphopeptide has been solved [108]. XRCC4 residue K210 was also reported to be important for small ubiquitin-like modifier (SUMO) modification, which regulates XRCC4 cellular localization [109]. The XRCC4 C-terminal region, together with the N-terminal region (residues 1–28) and central region (residues 168–200), may facilitate cooperative DNA binding [31]. Thus, definition of the structure of the C-terminal region structure will contribute to understanding how XRCC4 binds to LigIV and DNA in order to carry out its function.

**2.5. XLF.** XLF was identified through a cDNA functional complementation cloning study of patient 2BN following discovery of a group of NHEJ deficiency patients (2BN) [38, 110]. It was also independently identified through yeast two-hybrid screening for XRCC4 interactors [39]. XLF is evolutionarily conserved throughout a wide range of eukaryotes such as vertebrates, insects, and even in filamentous fungi [111]. Full-length human XLF contains 299 residues. At its extreme C-terminus, a small conserved basic cluster constitutes the nuclear localization sequence. Using immunofluorescence staining, XLF was observed localizing in nucleus of human cells [39].

The crystal structure of XLF with a C-terminal truncation, solved independently at 2.3 Å resolution by Andres et al. [112] and in our laboratory [101], exists as a homodimer containing a globular N-terminal head domain and extended coiled-coil helical tail, which is folded back around the coiled-coil (Figure 11). The N-terminal head domain starts with a single helix  $\alpha 1$ , which is followed by a seven-stranded antiparallel  $\beta$  structure sandwiching a helix-turn-helix motif between  $\beta 4$  and  $\beta 5$ . The tail structure contains three helices  $\alpha 4$ ,  $\alpha 5$ , and  $\alpha 6$ . While  $\alpha 4$  extends away from N-terminal head domain around 60 Å,  $\alpha 5$  and  $\alpha 6$  fold back and make contact with the head domain. The  $\alpha 4$  helices from the two protomers interact as a coiled-coil structure burying highly conserved and hydrophobic residues at the interface. This dimerization of XLF is further enhanced through the folding back of the  $\alpha 5$  and  $\alpha 6$  helices to encircle the  $\alpha 4$  helices of the other protomer to form a clamp, leading to burying of a surface area of  $\sim 6500$  Å<sup>2</sup>. Gel filtration, protein crosslinking and analytical ultracentrifugation are also consistent with

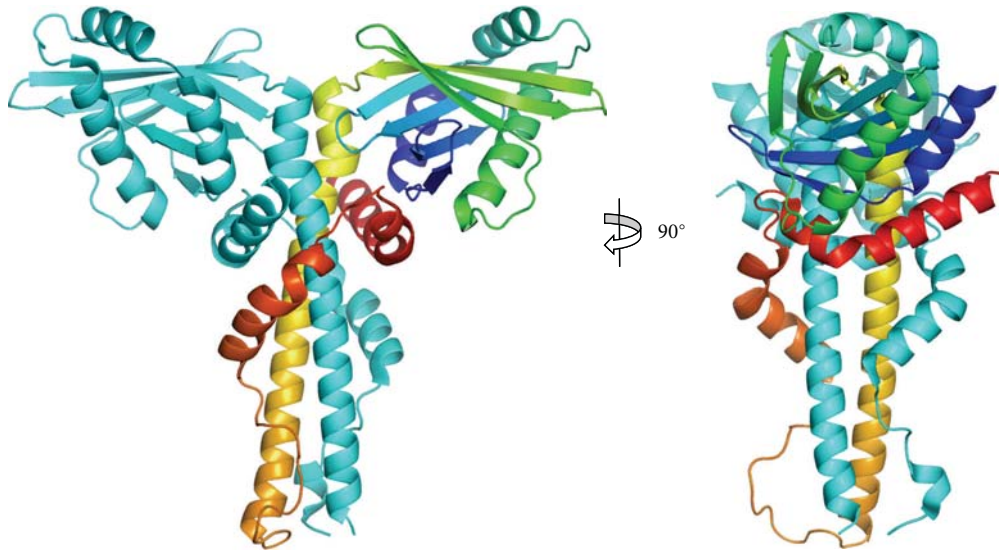


FIGURE 11: Crystal structure of XLF/Cernunnos. Ribbon diagram of the XLF/Cernunnos dimer. One protomer is rainbow colour going from N-terminus (blue) to C-terminus (red). Adapted from Li et al. [101].

a stable homodimer form of XLF in solution [101]. XLF was found to have concentration-dependent higher-order complex formation during gel filtration experiments [112]. The homodimer of XLF, however, is the smallest stable functional unit.

Due to the predicted disordered structure for the XLF C-terminal region after residue 245, around 70 residues were removed from the XLF C-terminus in the crystal structure analyses [101, 112]. The approximate location of the XLF C-terminal region, however, can be predicted to be near the N-terminal head domain region according to the helix  $\alpha 6$  direction.

Although XLF and XRCC4 have similar architectures, large structural differences from head to tail occur between these two proteins. For the head domain, both proteins contain the same seven-stranded antiparallel  $\beta$ -structure sandwiching a helix-turn-helix motif, but XLF contains an extra helix at the N-terminus. As we have seen, the tail structure of XLF contains distinct helices folding back, while the extended coiled-coil tail structure of XRCC4 contains the LigIV binding region near the C-terminus. The differences in sequence and structure between XLF and XRCC4 tails explain why LigIV does not bind to XLF in the same way as XRCC4.

The functions and mechanisms of action of XLF in NHEJ are still not fully understood. XLF not only stabilizes LigIV/XRCC4 at broken DNA ends, but also enhances the LigIV/XRCC4 end-joining process. XLF has also been found to be essential for repairing mismatched 3' overhangs and the gap-filling process together with DNA polymerase pol $\lambda$  and pol $\mu$  [113, 114]. Understanding how XLF functions in NHEJ through studying its interaction with other NHEJ proteins structurally will help unravel the exact role of XLF. It will contribute towards our current understanding of DNA repair in NHEJ and may also potentially lead to future therapeutic application for NHEJ defects patients.

### 3. Structural Biology of Complexes

**3.1. DNA-PKcs/Ku70/Ku80/DNA Ternary Complex (DNA-PK).** The crystal structure of the Ku70/80 heterodimer does not include the C-terminal DNA-PKcs interaction domain of Ku80 (Ku80CTD), which is dispensable for the binding of Ku70/80 to DNA but is required for DNA-PK recruitment to the sites of damaged DNA [13, 14]. Nuclear magnetic resonance analysis of 19 kDa Ku80CTD (residues 545–732) defines an  $\alpha$ -helical structure [115, 116]. Further structural studies of full-length Ku70/80 with and without DNA have been conducted using single-particle electron microscopy (EM) [117] and SAXS combined with live cell imaging [63]. The position of Ku80CTD was proposed to be under the  $\alpha/\beta$  domain of Ku70 by EM, but the domain was found to be flexible in the SAXS study. Molecular dynamic simulations of Ku80CTD produced an ensemble of conformations, supporting the idea of Ku80CTD being a region of high flexibility [63]. Taken together, the studies show that association of Ku70 and Ku80 to form a heterodimer is required for binding dsDNA ends, that Ku-dependent DNA binding drives the recruitment of DNA-PKcs and that the latter interaction involves the helical domain located at the C-terminus of Ku80. Although Ku80CTD was included in the crystal structure of DNA-PKcs, its position could not be unequivocally defined, presumably due to the dominance of similar alpha helical structures in the DNA-PKcs itself [48].

Insights into the DNA-PKcs/Ku70/Ku80 holoenzyme structures and possible synaptic complexes have been obtained using cryo-electron microscopy and SAXS. Boskovic et al. (2003) used electron microscopy at low resolution ( $\sim 30 \text{ \AA}$ ) to demonstrate large conformational changes in human DNA-PKcs when double-stranded DNA binds, and suggested that this may correlate with the activation of the kinase [118]. Subsequently, Spagnolo et al. (2006) have used single-particle electron microscopy at

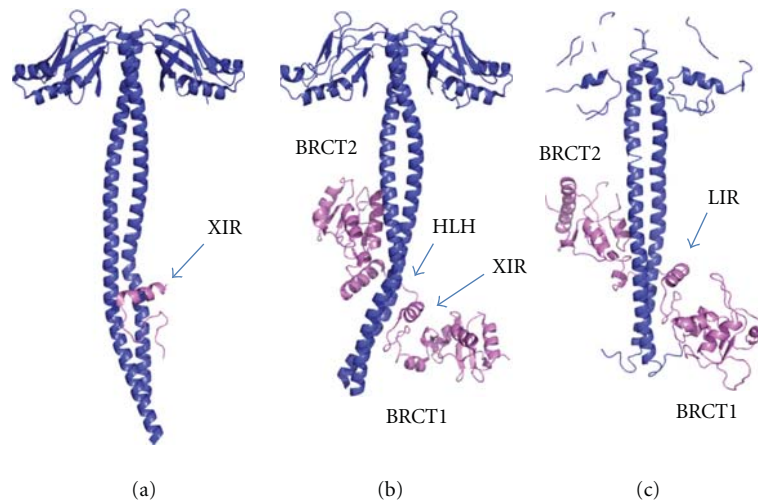


FIGURE 12: Crystal structures of LigIV/XRCC4 and Lif1p-Lig4p. Conserved XRCC4 or Lif1 interaction region of LigIV (XIR) or Lig4p (LIR) are indicated with blue arrows. (a) XRCC4(residues 1–213)(blue) and XIR (violet) (PDB code: 1IK9). (b) XRCC4(residues 1–203)(blue) and BRCT domains of LigIV(residues 654–911)(violet) (PDB code: 3II6) (c) Lif1p(residues 1–246)(blue) and BRCT domains of Lig4p(residues 680–944)(violet).

~25 Å resolution to study human DNA-PKcs/Ku70/Ku80 holoenzyme assembled on DNA [16]. They again found evidence for conformational changes on binding of Ku and DNA to DNA-PKcs. They identified dimeric particles comprising two DNA-PKcs/Ku70/Ku80 holoenzymes, which they consider are likely to be synaptic complexes, maintaining broken ends and providing a platform for other components required for end processing and ligation. A SAXS study of DNA-PK revealed that it had two different modes of dimerization as was observed previously with DNA-PKcs [63]. Depending on the presence of either 40 bp hairpin DNA or 40 bp Y-shaped DNA, DNA-PK formed the head-to-head or palm-to-palm dimer. Very recently Perry et al. (2010) have taken study of the DNA-PKcs/Ku70/Ku80 holoenzyme further by analyzing their earlier SAXS studies in the light of the crystal structure of DNA-PKcs [119]. They have impressively demonstrated that DNA-PK phosphorylation causes a large conformational change, sufficient to open the gap in the ring and provide access to or release from DNA. Ku80CTD has been shown to be flexible and to extend in solution to the benefit of recruitment of DNA-PKcs. It is possible that Ku80 interacts with DNA-PKcs on both sides of BSB [63].

**3.2. DNA Ligase IV/XRCC4 Complexes.** LigIV is stabilized by forming a tight complex with XRCC4 [28]. About 99% of LigIV is preadenylated when purified together with XRCC4 and it is difficult to readenylate after single-nick ligation [120], implying that the LigIV/XRCC4 complex is ready to ligate DNA. Unlike other human DNA ligases LigIV/XRCC4 can efficiently ligate one of the nicks of a DSB, although the other is unligatable [26], and it can ligate DNA strands across gaps and fully incompatible ends [121]. Furthermore, it has been shown that LigIV can ligate single-stranded poly-T DNA [122]. Interestingly, the ligation efficiency is higher with long DNA substrates  $\geq 157$  bp than short ones  $\leq 53$  bp

[123]. This might be related to the observation that a single LigIV/XRCC4 bridges two DNA ends [124].

The crystal structures of the XRCC4 dimer complexed with the tandem BRCT domain of LigIV shows that the linker between the two BRCT domains is well ordered and forms a helix-loop-helix (HLH) clamp around the coiled-coil [29, 94] (Figures 12(a) and 12(b)). The same interaction mode and secondary structure arrangement are observed in the orthologous yeast complex between XRCC4 (Lif1p) and LigIV (Lig4p) [95] (Figure 12(c)). The two BRCT domains in the human and yeast complexes extend the clamp, encircling the coiled-coil domain. The  $3_{10}$ -helix in BRCT1 is located close to the conserved XRCC4 interaction region of the linker (XIR: residue 748–784) between two BRCT domains. The corresponding  $3_{10}$ -helix in BRCT1 of 53BP1 participates in the interaction surface of p53 [125, 126]. The interaction of XRCC4 with LigIV produces a kink in one helix of the coiled-coil of XRCC4 dimer and switches the left-handed heptad repeat into a right-handed undecad coiled-coil; as a result, the LigIV interaction surface becomes flat [29, 94]. The kink bends in the opposite direction in the complex between XRCC4 with XIR and with the tandem BRCT domain [94]. The former structure might be an intermediate state of LigIV/XRCC4 interaction. If so, this dynamical conformational change might have a biological role *in vivo*. This kink does not appear in Lif1p/Lig4p even though the refinement of the structure against a new 3.5 Å diffraction data set was carried out (see [127], T Ochi and TL Blundell, unpublished results). Thus, the kink may be unique to human and some other higher organisms.

The second helix in HLH mediates a hydrophobic interaction with the opposite side of the flat surface of the XRCC4 to where XIR interacts [94] and a similar extensive hydrophobic interaction is observed in Lif1p/Lig4 (residues 827–839) [95]. LigIV additionally interacts with the coiled-coil of XRCC4 via  $\alpha'1$  and  $\alpha'3$  of BRCT2, in a

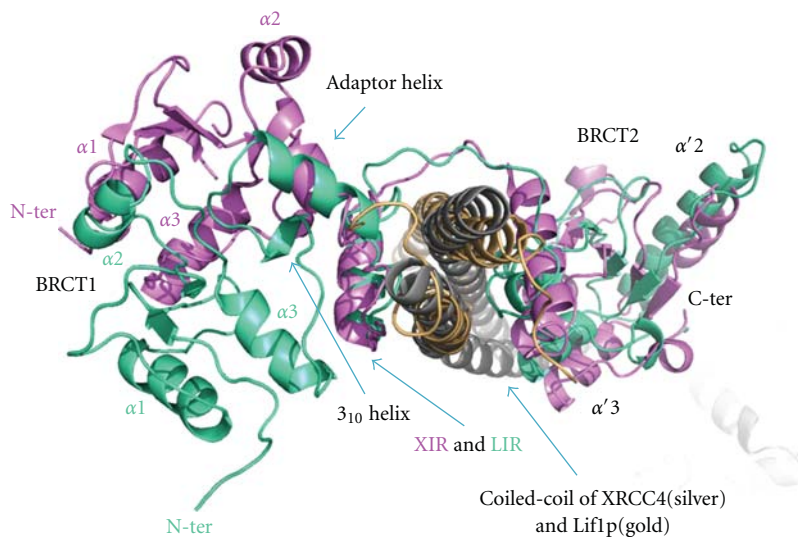


FIGURE 13: Comparison of positions of BRCT1 between LigIV/XRCC4 and Lif1p/Lig4p. Structures of LigIV/XRCC4 (violet/silver) and Lif1p/Lig4p (green/gold) were superimposed based on XIR and LIR. The figure is a view of the C- to N-terminal direction of the coiled-coils of XRCC4 and Lif1p. The N-terminals and helices of BRCT1 of LigIV and Li4p are labeled with violet and green, respectively.

manner that resembles the interaction between BRCT1 and BRCT2 of other tandem BRCT domains. Superposition of LigIV/XRCC4 and Lif1p/Lig4p based on XIR and the corresponding region of Lig4p (LIR) shows that, apart from the kink described above, a further change occurs in the position of BRCT1 (Figure 13). This may be a crystallographic artefact because BRCT1 is closely packed with BRCT2 belonging to another molecule in both human and yeast structures. However, the NMR structure of BRCT1 (PDB code: 2E2W) has the same conformation as the crystallographic one, suggesting at least human BRCT1 and the following linker is likely to have the same conformation in solution.

A recently published EM structure of the LigIV/XRCC4 complex shows the N-terminal of LigIV in proximity to the head domain of XRCC4 [128]. The authors compared two LigIV/XRCC4 constructs, one with the full-length sequences, and the other with a full-length LigIV and a truncated XRCC4 (residues 1–213). From the differences of the two EM images, they determined the position of the C-terminal of XRCC4 and by labelling the hexahistidine tag with gold, they identified the N-terminus of LigIV. Although the authors reconstructed 2D averaged images of LigIV/XRCC4, the 3D reconstruction failed partially because of heterogeneity of the LigIV/XRCC4 conformation. Thus, they proposed that the catalytic region of LigIV is connected to the C-terminal region by a flexible linker and this may have functional importance (see also Perry et al. (2010) [119]).

We have carried out SAXS studies of the tandem BRCT domain of LigIV/mutated XRCC4 (BmX4) and LigIV/mutated XRCC4 (LmX4) in order to investigate the conformation of the catalytic region in solution (Figure 14(a)) [129]. Here, mutated XRCC4 is identical to the one used for solving the structure of XIR/XRCC4 [29]. The linearity of the respective Guinier plots confirmed that the protein solutions were homogeneous and monodisperse

(Figure 14(b)). The deduced radius of gyration and the maximum molecular dimension of LmX4 are 9 Å and 43 Å larger, respectively, than those of BmX4. The simulated scattering profile using the crystallographic structure of BmX4 (PDB code: 3II6) fitted the measured SAXS curve well ( $\chi^2 = 3.687$ , data not shown). Moreover, the *ab initio* 3D shape restoration of BmX4 reproduced an overall conformation consistent with the crystal structure (Figure 14(c)). The *ab initio* shape reconstruction of LmX4 revealed that the catalytic region may contribute additional density to the head domain of XRCC4 or the tandem BRCT domain of LigIV when compared with the conformation of BmX4 (Figure 14(c)). Since the extended, open conformation of the catalytic region in solution has also been observed in an archaeal DNA ligase [74], the extra density may correspond to a similar conformation of the catalytic region of LigIV to the closed conformation observed in other archaea DNA ligases [75, 76]. As the shape restorations of LmX4 yielded a reproducible conformation (also indicated by the normalized spatial discrepancy (NSD) value after shape averaging), this finding might imply interactions between the catalytic region and BmX4. However, electrophoretic mobility shift assay and protease analysis (data not shown) indicate that the catalytic region is unlikely to have strong interactions with BmX4. Thus, although the majority of LmX4 in solution may have the extended open conformation, the catalytic region is flexibly attached to BmX4. Our observations agree with the EM study [128].

**3.3. XLF/XRCC4 Complexes.** The interaction between XLF and XRCC4 is salt sensitive, it does not depend on DNA [39, 133] and interactions occur through the head regions as shown by yeast two-hybrid study of various mutants [134]. XLF bound to beads at its C-terminal was still able to pull

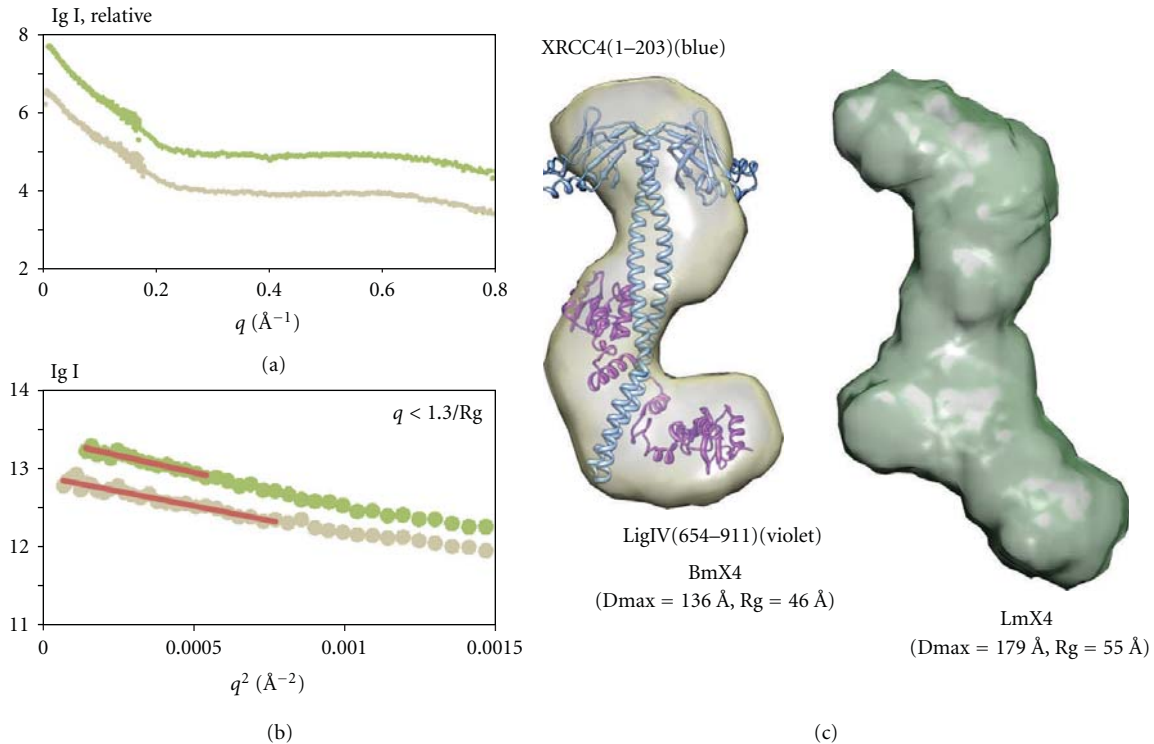


FIGURE 14: SAXS study of LmX4 and Bm4. (a) SAXS data of LmX4 (green) and BmX4 (gold) where  $q = (4\pi \sin \theta)/\lambda$ . (b) Guinier plots of LmX4 and BmX4 with liner fits (red line)  $q < 1.3/R_g$ . (c) Shape reconstructions of BmX4 (gold) and LmX4 (green) created by using Dammin [130]. Ten individual models were calculated and averaged by Damaver [131]. NSD of BmX4 and LmX4 are 0.780 and 0.814, respectively. Molecular envelopes were produced using the UCSF Chimera package from the Resource for Biocomputing, Visualization, and Informatics at the University of California, San Francisco (supported by NIH P41 RR-01081) [132]. The crystallographic model of BmX4 (PDB code: 3II6) was superimposed into its molecular envelope by using Chimera.

down LigIV/XRCC4, implying that the C-terminal of XLF is not important for interaction with LigIV/XRCC4 [135].

Mutagenesis studies indicate that the structurally exposed XLF residue L115 (Figure 16 shown in green) located in the  $\beta 6$ - $\beta 7$  loop is important for XLF/XRCC4 interaction [112]. Residues K63, K65, and K99 (Figure 15 shown in green) of XRCC4 are essential for interaction and are located on the region of the head domain close to the helical tail [112]. Nonessential interaction residues of XLF are mainly located outside the head domain region whereas the nonessential XLF/XRCC4 binding residues in XRCC4 are mainly located on the topside of N-terminal head domain and on the helical tail structure before the LigIV binding region (Figures 15 and 16 shown in grey) [112]. These studies are consistent with a linear side-by-side interaction model, in which XLF head domains slide into the space created by XRCC4 head domains and N-terminal part of the tail structure [112] (Figure 17). However, we cannot exclude a model for XLF/XRCC4, involving XLF and XRCC4 binding together in a side-by-side manner but with a degree of twist introducing curvature and possibly a circular complex. This would have the advantage of forming a finite and discrete complex. Further X-ray small angle scattering experiments may be the best approach to resolving this, especially if the complexes are dynamic as gel filtration experiments suggest. However, some encouragement that well-defined

complexes can be identified is found in the observation that XLF/XRCC4 complexes have been crystallized and X-ray data collected, albeit to low resolution (Q Wu, TL Blundell unpublished data).

**3.4. Spatial Arrangement of Higher-Order Complexes.** In order to give a picture of the spatial and temporal organisation of the NHEJ repair system as a whole, an understanding of the order of interactions during the assembly of the DNA-PKcs/Ku70/Ku80/DNA ternary complex and the LigIV/XRCC4/XLF/DNA quaternary complex will be essential.

Ku70/80 and DNA-PKcs, which have higher DNA-binding affinity compared to LigIV/XRCC4/XLF, most likely form the DNA-PKcs/Ku70/Ku80/DNA ternary complex first. For the following LigIV/XRCC4/XLF/DNA complex formation, the order and dynamics of protein assembly are still to be determined. The interaction between XRCC4 and XLF is relatively weak compared to the strong binding between XRCC4 and LigIV. It is not clear whether the XLF-dimer interactions with XRCC4-dimer are maintained when the ligase is recruited. Protein interaction assays have confirmed the XRCC4 independent, XLF recruitment to DSBs ends through interaction with Ku70/80 only in the presence of DNA. This may imply that XLF can act independently without XRCC4.

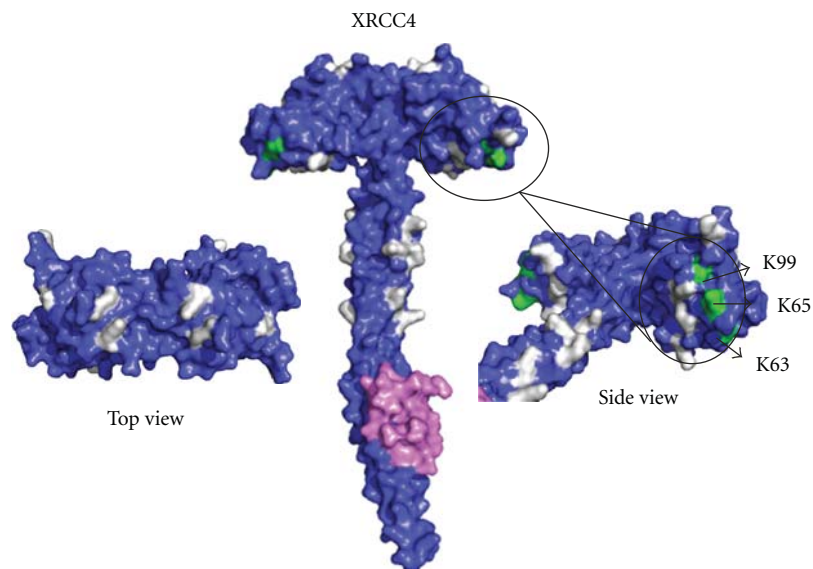


FIGURE 15: Surface views of XRCC4<sub>1-213</sub>-DNA ligase IV peptide<sub>748-784</sub> structure (PDB code:1IK9). Residues K63, K65, and K99, which are important for XLF-XRCC4 binding are labeled in green. Nonessential residues for XLF-XRCC4 interaction K26, R71, K72, K90, R107, K115, K146, R150, R153, R161, and R164 are labeled in grey [112].

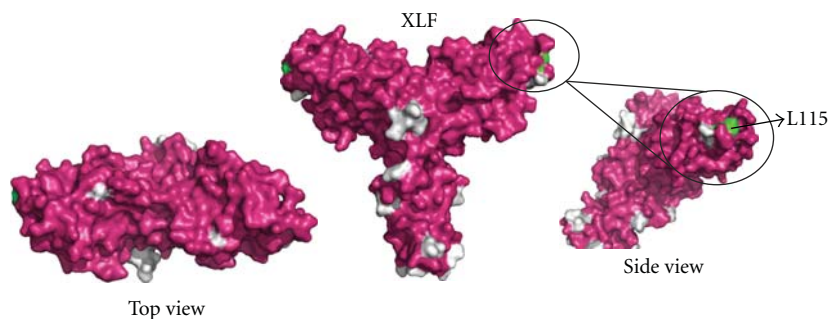


FIGURE 16: Surface views of XLF<sub>1-233</sub> (PDB code: 2QM4). Residue L115, which is important for XLF-XRCC4 binding is labeled in green. Nonessential residues for XLF-XRCC4 interaction I105, E111, E169, L174, R178, L179, E185, and I195 and residues after 224 are labeled in grey [112].

Live cell imaging techniques have identified the immediate recruitment of XLF to laser-induced DSBs with Ku70/80 protein bound [136]. XRCC4 is dispensable for XLF recruitment to DNA ends, but its presence can stabilize the XLF/DNA interaction [136]. Protein interaction assays have confirmed the interaction between Ku70/80 and XLF, and this interaction only occurs in the presence of DNA [136].

Both XRCC4 and XLF require a long piece of DNA for binding. How DNA is structurally involved in all the higher-order protein complexes is of fundamental interest. The phosphorylation of LigIV, XRCC4, and XLF by DNA-PKcs does not interfere greatly with the core functions of these proteins, but could alter the relative binding affinities of various protein-protein or protein-DNA interactions, which are important for correct spatial arrangement of the higher-order complexes. All of this uncertainty underlines the need for further studies to characterise complexes temporally as well as spatially.

#### 4. Discussion

The challenges of structural characterisation of dynamic multiprotein systems clearly demand a combination of SAXS, EM, X-ray crystallography, and other approaches. All will be advantaged by methods for stabilization and fixation of the complexes. Modified constructs, for example, phospho-mimicking mutation and truncation as well as postmodification, for example, phosphorylation and methylation, need to be explored in order to identify stable complexes. For single particle cryo-EM studies, GraFix has been successfully introduced to stabilize macromolecules [137]. This exploits glycerol gradient centrifugation into increasing concentrations of chemical fixation reagent to stabilize individual macromolecules and to prevent opportunistic aggregation. A similar approach might be used for other structural studies including X-ray crystallography, although here molecular surface modification of the complexes may prevent the formation of ordered crystals.

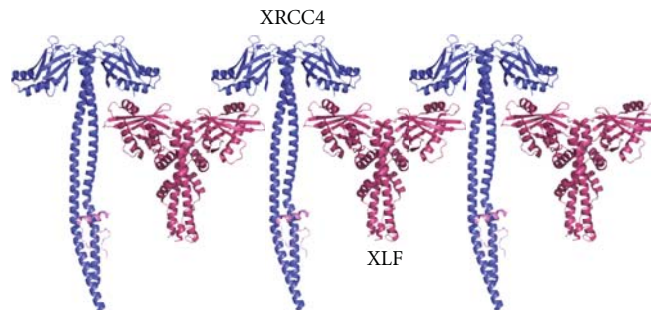


FIGURE 17: XLF/XRCC4 linear side-by-side interaction model. Adapted from [112].

Crystals of large multiprotein assemblies suitable for high-resolution X-ray diffraction remain a challenge. So the development of methods to analyse low-resolution X-ray diffraction data is essential. In this respect free-electron laser (FEL) light sources may allow single particle X-ray FEL (XFEL) imaging. X-ray crystallography with nanocrystals is also a promising method.

X-ray crystallography is still the only technique to give atomic resolution of large structures and high resolution is essential for studying the binding of small molecules. Indeed chemical tools that allow specific intervention in NHEJ should allow dissection of the roles of the various components. These tools would also likely contribute to the discovery of lead compounds and preclinical candidates for therapeutic intervention at allosteric and other regulatory interaction sites in oncology and for patients with defects in the NHEJ pathway.

The immediate interest, developing from the emerging structure of DNA-PKcs, is the improvement of design of inhibitors that bind at the ATP site of the protein kinase moiety. Such inhibitors would not only inform the development of useful therapeutic agents but should also be of immediate value in investigating the possibility of improving stability of the kinase domain, and the quality and resolution of crystals.

Eventually, we would hope to pursue a structure-guided approach to optimize the design of such inhibitors. Similar approaches could be taken with the ligase active site. In our view a more exciting and adventurous approach would be to design new chemical entities that bind at allosteric sites, templates or adaptor binding sites—so called allo-targeting—that are critical to the activation, colocalisation and/or specificity of the regulation of NHEJ. The use of fragment-based methods [138–140] in this context is attractive. Likely targets would be the head-to-head interactions of XRCC4 and XLF, the interactions of BRCT domains, and the interaction of Ku70/80 and the DNA-PKcs.

In conclusion, a spatial and temporal understanding of NHEJ should provide insights into the mechanism of this critical cellular process and also suggest approaches to designing useful chemical tools. Indeed the design of small chemical agents that noncovalently modulate interactions would also likely contribute to the discovery of lead compounds that allow therapeutic intervention in oncology and treatment of patients with defects in the NHEJ pathway.

## Acknowledgments

The authors would like to thank Dr. J. Günter Grossmann for useful discussions and comments on the SAXS data. B. L. Sibanda and D. Y. Chirgadze were supported by Wellcome Trust Programme Grant: 079281/Z/06/Z. T. Ochi was supported by Overseas Research Studentship (ORS). Molecular graphics except for Figures 4 and 14 were prepared by using PyMOL [141].

## References

- [1] M. Takata, M. S. Sasaki, E. Sonoda et al., “Homologous recombination and non-homologous end-joining pathways of DNA double-strand break repair have overlapping roles in the maintenance of chromosomal integrity in vertebrate cells,” *The EMBO Journal*, vol. 17, no. 18, pp. 5497–5508, 1998.
- [2] M. O’Driscoll and P. A. Jeggo, “The role of double-strand break repair—insights from human genetics,” *Nature Reviews Genetics*, vol. 7, no. 1, pp. 45–54, 2006.
- [3] M. M. Vilenchik and A. G. Knudson, “Endogenous DNA double-strand breaks: production, fidelity of repair, and induction of cancer,” *Proceedings of the National Academy of Sciences of the United States of America*, vol. 100, no. 22, pp. 12871–12876, 2003.
- [4] K. K. Khanna and S. P. Jackson, “DNA double-strand breaks: signaling, repair and the cancer connection,” *Nature Genetics*, vol. 27, no. 3, pp. 247–254, 2001.
- [5] M. Gellert, “V(D)J recombination: RAG proteins, repair factors, and regulation,” *Annual Review of Biochemistry*, vol. 71, pp. 101–132, 2002.
- [6] J. Chaudhuri and F. W. Alt, “Class-switch recombination: interplay of transcription, DNA deamination and DNA repair,” *Nature Reviews Immunology*, vol. 4, no. 7, pp. 541–552, 2004.
- [7] C. T. Yan, C. Boboila, E. K. Souza et al., “IgH class switching and translocations use a robust non-classical end-joining pathway,” *Nature*, vol. 449, no. 7161, pp. 478–482, 2007.
- [8] A. Nussenzweig and M. C. Nussenzweig, “A backup DNA repair pathway moves to the forefront,” *Cell*, vol. 131, no. 2, pp. 223–225, 2007.
- [9] M. R. Lieber, Y. Ma, U. Pannicke, and K. Schwarz, “The mechanism of vertebrate nonhomologous DNA end joining and its role in V(D)J recombination,” *DNA Repair*, vol. 3, no. 8-9, pp. 817–826, 2004.
- [10] J. R. Walker, R. A. Corpina, and J. Goldberg, “Structure of the Ku heterodimer bound to dna and its implications for

- double-strand break repair," *Nature*, vol. 412, no. 6847, pp. 607–614, 2001.
- [11] J. A. Downs and S. P. Jackson, "A means to a DNA end: the many roles of Ku," *Nature Reviews Molecular Cell Biology*, vol. 5, no. 5, pp. 367–378, 2004.
- [12] K. O. Hartley, D. Gell, G. C. M. Smith et al., "DNA-dependent protein Kinase catalytic subunit: a relative of phosphatidylinositol 3-Kinase and the ataxia telangiectasia gene product," *Cell*, vol. 82, no. 5, pp. 849–856, 1995.
- [13] B. K. Singleton, M. I. Torres-Arzayus, S. T. Rottinghaus, G. E. Taccioli, and P. A. Jeggo, "The C terminus of Ku80 activates the DNA-dependent protein Kinase catalytic subunit," *Molecular and Cellular Biology*, vol. 19, no. 5, pp. 3267–3277, 1999.
- [14] D. Gell and S. P. Jackson, "Mapping of protein-protein interactions within the DNA-dependent protein Kinase complex," *Nucleic Acids Research*, vol. 27, no. 17, pp. 3494–3502, 1999.
- [15] S. Yoo and W. S. Dynan, "Geometry of a complex formed by double strand break repair proteins at a single DNA end: recruitment of DNA-PKcs induces inward translocation of Ku protein," *Nucleic Acids Research*, vol. 27, no. 24, pp. 4679–4686, 1999.
- [16] L. Spagnolo, A. Rivera-Calzada, L. H. Pearl, and O. Llorca, "Three-dimensional structure of the human DNA-PKcs/Ku70/Ku80 complex assembled on DNA and its implications for DNA DSB repair," *Molecular Cell*, vol. 22, no. 4, pp. 511–519, 2006.
- [17] G. C. M. Smith and S. P. Jackson, "The DNA-dependent protein Kinase," *Genes and Development*, vol. 13, no. 8, pp. 916–934, 1999.
- [18] E. Weterings and D. J. Chen, "The endless tale of non-homologous end-joining," *Cell Research*, vol. 18, no. 1, pp. 114–124, 2008.
- [19] Q. Ding, Y. V. R. Reddy, W. Wang et al., "Autophosphorylation of the catalytic subunit of the DNA-dependent protein Kinase is required for efficient end processing during DNA double-strand break repair," *Molecular and Cellular Biology*, vol. 23, no. 16, pp. 5836–5848, 2003.
- [20] W. D. Block, Y. Yu, D. Merkle et al., "Autophosphorylation-dependent remodeling of the DNA-dependent protein Kinase catalytic subunit regulates ligation of DNA ends," *Nucleic Acids Research*, vol. 32, no. 14, pp. 4351–4357, 2004.
- [21] D. Moshous, I. Callebaut, R. de Chasseval et al., "Artemis, a novel DNA double-strand break repair/V(D)J recombination protein, is mutated in human severe combined immune deficiency," *Cell*, vol. 105, no. 2, pp. 177–186, 2001.
- [22] M. R. Lieber, "The mechanism of double-strand DNA break repair by the nonhomologous DNA end-joining pathway," *Annual Review of Biochemistry*, vol. 79, pp. 181–211, 2010.
- [23] Y. Ma, U. Pannicke, K. Schwarz, and M. R. Lieber, "Hairpin opening and overhang processing by an Artemis/DNA-dependent protein Kinase complex in nonhomologous end joining and V(D)J recombination," *Cell*, vol. 108, no. 6, pp. 781–794, 2002.
- [24] K. N. Mahajan, S. A. Nick McElhinny, B. S. Mitchell, and D. A. Ramsden, "Association of DNA polymerase  $\mu$  (pol  $\mu$ ) with Ku and ligase IV: role for pol  $\mu$  in end-joining double-strand break repair," *Molecular and Cellular Biology*, vol. 22, no. 14, pp. 5194–5202, 2002.
- [25] J. W. Lee, L. Blanco, T. Zhou et al., "Implication of DNA Polymerase  $\lambda$  in alignment-based gap filling for nonhomologous DNA end joining in human nuclear extracts," *The Journal of Biological Chemistry*, vol. 279, no. 1, pp. 805–811, 2004.
- [26] Y. Ma, H. Lu, B. Tippin et al., "A biochemically defined system for mammalian nonhomologous DNA end joining," *Molecular Cell*, vol. 16, no. 5, pp. 701–713, 2004.
- [27] S. A. Roberts, N. Strande, M. D. Burkhalter et al., "Ku is a 5'-dRP/AP lyase that excises nucleotide damage near broken ends," *Nature*, vol. 464, no. 7292, pp. 1214–1217, 2010.
- [28] M. Bryans, M. C. Valenzano, and T. D. Stamato, "Absence of DNA ligase IV protein in XR-1 cells: evidence for stabilization by XRCC4," *Mutation Research/DNA Repair*, vol. 433, no. 1, pp. 53–58, 1999.
- [29] B. L. Sibanda, S. E. Critchlow, J. Begun et al., "Crystal structure of an Xrcc4-DNA ligase IV complex," *Nature Structural Biology*, vol. 8, no. 12, pp. 1015–1019, 2001.
- [30] U. Grawunder, M. Wilm, X. Wu et al., "Activity of DNA ligase IV stimulated by complex formation with XRCC4 protein in mammalian cells," *Nature*, vol. 388, no. 6641, pp. 492–495, 1997.
- [31] M. Modesti, J. E. Hesse, and M. Gellert, "DNA binding of Xrcc4 protein is associated with V(D)J recombination but not with stimulation of DNA ligase IV activity," *The EMBO Journal*, vol. 18, no. 7, pp. 2008–2018, 1999.
- [32] Y. Wang, B. J. Lamarche, and M.-D. Tsai, "Human DNA ligase IV and the ligase IV/XRCC4 complex: analysis of nick ligation fidelity," *Biochemistry*, vol. 46, no. 17, pp. 4962–4976, 2007.
- [33] Y. Gao, Y. Sun, K. M. Frank et al., "A critical role for DNA end-joining proteins in both lymphogenesis and neurogenesis," *Cell*, vol. 95, no. 7, pp. 891–902, 1998.
- [34] K. M. Frank, J. M. Sekiguchi, K. J. Seidl et al., "Late embryonic lethality and impaired V(D)J recombination in mice lacking DNA ligase IV," *Nature*, vol. 396, no. 6707, pp. 173–177, 1998.
- [35] Y. Gao, D. O. Ferguson, W. Xie et al., "Interplay of p53 and DNA-repair protein XRCC4 in tumorigenesis, genomic stability and development," *Nature*, vol. 404, no. 6780, pp. 897–900, 2000.
- [36] K. M. Frank, N. E. Sharpless, Y. Gao et al., "DNA ligase IV deficiency in mice leads to defective neurogenesis and embryonic lethality via the p53 pathway," *Molecular Cell*, vol. 5, no. 6, pp. 993–1002, 2000.
- [37] M. O'Driscoll, K. M. Cerosaletti, P.-M. Girard et al., "DNA ligase IV mutations identified in patients exhibiting developmental delay and immunodeficiency," *Molecular Cell*, vol. 8, no. 6, pp. 1175–1185, 2001.
- [38] D. Buck, L. Malivert, R. de Chasseval et al., "Cernunnos, a novel nonhomologous end-joining factor, is mutated in human immunodeficiency with microcephaly," *Cell*, vol. 124, no. 2, pp. 287–299, 2006.
- [39] P. Ahnesorg, P. Smith, and S. P. Jackson, "XLF interacts with the XRCC4-DNA Ligase IV complex to promote DNA nonhomologous end-joining," *Cell*, vol. 124, no. 2, pp. 301–313, 2006.
- [40] E. Feldmann, V. Schmiemann, W. Goedecke, S. Reichenberger, and P. Pfeiffer, "DNA double-strand break repair in cell-free extracts from Ku80-deficient cells: implications for Ku serving as an alignment factor in non-homologous DNA end joining," *Nucleic Acids Research*, vol. 28, no. 13, pp. 2585–2596, 2000.
- [41] M. A. Larkin, G. Blackshields, N. P. Brown et al., "Clustal W and Clustal X version 2.0," *Bioinformatics*, vol. 23, no. 21, pp. 2947–2948, 2007.
- [42] P. Gouet, E. Courcelle, D. I. Stuart, and F. Métoz, "ESPrInt: analysis of multiple sequence alignments in PostScript," *Bioinformatics*, vol. 15, no. 4, pp. 305–308, 1999.

- [43] W. S. Dynan and S. Yoo, "Interaction of Ku protein and DNA-dependent protein Kinase catalytic subunit with nucleic acids," *Nucleic Acids Research*, vol. 26, no. 7, pp. 1551–1559, 1998.
- [44] C. Y. Chiu, R. B. Cary, D. J. Chen, S. R. Peterson, and P. L. Stewart, "Cryo-EM imaging of the catalytic subunit of the DNA-dependent protein Kinase," *Journal of Molecular Biology*, vol. 284, no. 4, pp. 1075–1081, 1998.
- [45] K. K. Leuther, O. Hammarsten, R. D. Kornberg, and G. Chu, "Structure of DNA-dependent protein Kinase: implications for its regulation by DNA," *The EMBO Journal*, vol. 18, no. 5, pp. 1114–1123, 1999.
- [46] A. Rivera-Calzada, J. D. Maman, L. Spagnolo, L. H. Pearl, and O. Llorca, "Three-dimensional structure and regulation of the DNA-dependent protein Kinase catalytic subunit (DNA-PKcs)," *Structure*, vol. 13, no. 243, p. 495, 2005.
- [47] D. R. Williams, K. J. Lee, D. J. Chen, J. Shi, and P. L. Stewart, "Cryo-EM structure of the DNA-dependent protein Kinase catalytic subunit at subnanometer resolution reveals alpha helices and insight into DNA binding," *Structure*, vol. 16, pp. 468–477, 2008.
- [48] B. L. Sibanda, D. Y. Chirgadze, and T. L. Blundell, "Crystal structure of DNA-PKcs reveals a large open-ring cradle comprised of HEAT repeats," *Nature*, vol. 463, no. 7277, pp. 118–121, 2010.
- [49] A. Fujimori, R. Araki, R. Fukumura et al., "Identification of four highly conserved regions in DNA-PKcs," *Immunogenetics*, vol. 51, no. 11, pp. 965–973, 2000.
- [50] C. Xiaoping, Y. Yaping, S. Gupta, Y.-M. Cho, S. P. Lees-Miller, and K. Meek, "Autophosphorylation of DNA-dependent protein Kinase regulates DNA end processing and may also alter double-strand break repair pathway choice," *Molecular and Cellular Biology*, vol. 25, no. 24, pp. 10842–10852, 2005.
- [51] P. Douglas, G. P. Sapkota, N. Morrice et al., "Identification of in vitro and in vivo phosphorylation sites in the catalytic subunit of the DNA-dependent protein Kinase," *The Biochemical Journal*, vol. 368, no. 1, pp. 243–251, 2002.
- [52] Y. Ma, U. Pannicke, H. Lu, D. Niewolik, K. Schwarz, and M. R. Lieber, "The DNA-dependent protein Kinase catalytic subunit phosphorylation sites in human artemis," *The Journal of Biological Chemistry*, vol. 280, no. 40, pp. 33839–33846, 2005.
- [53] P. Douglas, X. Cui, W. D. Block et al., "The DNA-dependent protein Kinase catalytic subunit is phosphorylated in vivo on threonine 3950, a highly conserved amino acid in the protein Kinase domain," *Molecular and Cellular Biology*, vol. 27, no. 5, pp. 1581–1591, 2007.
- [54] M. Le Romancer, S. C. Cosulich, S. P. Jackson, and P. R. Clarke, "Cleavage and inactivation of DNA-dependent protein Kinase catalytic subunit during apoptosis in *Xenopus* egg extracts," *Journal of Cell Science*, vol. 109, no. 13, pp. 3121–3127, 1996.
- [55] Q. Song, S. P. Lees-Miller, S. Kumar et al., "DNA-dependent protein Kinase catalytic subunit: a target for an ICE-like protease in apoptosis," *The EMBO Journal*, vol. 15, no. 13, pp. 3238–3246, 1996.
- [56] H. Teraoka, Y. Yumoto, F. Watanabe et al., "CPP32/Yama/apopain cleaves the catalytic component of DNA-dependent protein Kinase in the holoenzyme," *The FEBS Letters*, vol. 393, no. 1, pp. 1–6, 1996.
- [57] S. Kumar, P. Pandey, A. Bharti et al., "Regulation of DNA-dependent protein Kinase by the Lyn tyrosine Kinase," *The Journal of Biological Chemistry*, vol. 273, no. 40, pp. 25654–25658, 1998.
- [58] U. Yavuzer, G. C. M. Smith, T. Bliss, D. Werner, and S. P. Jackson, "DNA end-independent activation of DNA-PK mediated via association with the DNA-binding protein CID," *Genes and Development*, vol. 12, no. 14, pp. 2188–2199, 1998.
- [59] T. Wechsler, B. P. C. Chen, R. Harper et al., "DNA-PKcs function regulated specifically by protein phosphatase 5," *Proceedings of the National Academy of Sciences of the United States of America*, vol. 101, no. 5, pp. 1247–1252, 2004.
- [60] S. Jin, S. Kharbanda, B. Mayer, D. Kufe, and D. T. Weaver, "Binding of Ku and c-Abl at the Kinase homology region of DNA-dependent protein Kinase catalytic subunit," *The Journal of Biological Chemistry*, vol. 272, no. 40, pp. 24763–24766, 1997.
- [61] X. Wu and M. R. Lieber, "Interaction between DNA-dependent protein Kinase and a novel protein, KIP," *Mutation Research/DNA Repair*, vol. 385, no. 1, pp. 13–20, 1997.
- [62] R. Bosotti, A. Isacchi, and E. L. L. Sonhammer, "FAT: a novel domain in PIK-related Kinases," *Trends in Biochemical Sciences*, vol. 25, no. 5, pp. 225–227, 2000.
- [63] M. Hammel, Y. Yu, B. L. Mahaney et al., "Ku and DNA-dependent protein Kinase dynamic conformations and assembly regulate DNA binding and the initial non-homologous end joining complex," *The Journal of Biological Chemistry*, vol. 285, no. 2, pp. 1414–1423, 2010.
- [64] A. J. Doherty and S. W. Suh, "Structural and mechanistic conservation in DNA ligases," *Nucleic Acids Research*, vol. 28, no. 21, pp. 4051–4058, 2000.
- [65] T. Ellenberger and A. E. Tomkinson, "Eukaryotic DNA ligases: structural and functional insights," *Annual Review of Biochemistry*, vol. 77, pp. 313–338, 2008.
- [66] J. M. Pascal, "DNA and RNA ligases: structural variations and shared mechanisms," *Current Opinion in Structural Biology*, vol. 18, no. 1, pp. 96–105, 2008.
- [67] S. Shuman, "DNA ligases: progress and prospects," *The Journal of Biological Chemistry*, vol. 284, no. 26, pp. 17365–17369, 2009.
- [68] S. Shuman and C. D. Lima, "The polynucleotide ligase and RNA capping enzyme superfamily of covalent nucleotidyl-transferases," *Current Opinion in Structural Biology*, vol. 14, no. 6, pp. 757–764, 2004.
- [69] S. Shuman and B. Schwer, "RNA capping enzyme and DNA ligase: a superfamily of covalent nucleotidyl transferases," *Molecular Microbiology*, vol. 17, no. 3, pp. 405–410, 1995.
- [70] C. Marchetti, S. A. Walker, F. Odreman, A. Vindigni, A. J. Doherty, and P. Jeggo, "Identification of a novel motif in DNA ligases exemplified by DNA ligase IV," *DNA Repair*, vol. 5, no. 7, pp. 788–798, 2006.
- [71] A. G. Murzin, "OB(oligonucleotide/oligosaccharide binding)-fold: common structural and functional solution for non-homologous sequences," *The EMBO Journal*, vol. 12, no. 3, pp. 861–867, 1993.
- [72] D. A. Chistiakov, N. V. Voronova, and A. P. Chistiakov, "Ligase IV syndrome," *European Journal of Medical Genetics*, vol. 52, no. 6, pp. 373–378, 2009.
- [73] J. M. Pascal, P. J. O'Brien, A. E. Tomkinson, and T. Ellenberger, "Human DNA ligase I completely encircles and partially unwinds nicked DNA," *Nature*, vol. 432, no. 7016, pp. 473–478, 2004.
- [74] J. M. Pascal, O. V. Tsodikov, G. L. Hura et al., "A flexible interface between DNA Ligase and PCNA supports conformational switching and efficient ligation of DNA," *Molecular Cell*, vol. 24, no. 2, pp. 279–291, 2006.

- [75] H. Nishida, S. Kiyonari, Y. Ishino, and K. Morikawa, "The closed structure of an archaeal DNA Ligase from *pyrococcus furiosus*," *Journal of Molecular Biology*, vol. 360, no. 5, pp. 956–967, 2006.
- [76] D. J. Kim, O. Kim, H.-W. Kim, H. S. Kim, S. J. Lee, and S. W. Suh, "ATP-dependent DNA ligase from *archaeoglobus fulgidus* displays a tightly closed conformation," *Acta Crystallographica Section F*, vol. 65, no. 6, pp. 544–550, 2009.
- [77] I. V. Martin and S. A. MacNeill, "ATP-dependent DNA ligases," *Genome Biology*, vol. 3, no. 4, article 3005, 2002.
- [78] E. Cotner-Gohara, I.-K. Kim, A. E. Tomkinson, and T. Ellenberger, "Two DNA-binding and nick recognition modules in human DNA ligase III," *The Journal of Biological Chemistry*, vol. 283, no. 16, pp. 10764–10772, 2008.
- [79] A. E. Tomkinson, S. Vijayakumar, J. M. Pascal, and T. Ellenberger, "DNA ligases: structure, reaction mechanism, and function," *Chemical Reviews*, vol. 106, no. 2, pp. 687–699, 2006.
- [80] U. Grawunder, D. Zimmer, and M. R. Lieber, "DNA ligase IV binds to XRCC4 via a motif located between rather than within its BRCT domains," *Current Biology*, vol. 8, no. 15, pp. 873–876, 1998.
- [81] Y.-G. Wang, C. Nnakwe, W. S. Lane, M. Modesti, and K. M. Frank, "Phosphorylation and regulation of DNA ligase IV stability by DNA-dependent protein Kinase," *The Journal of Biological Chemistry*, vol. 279, no. 36, pp. 37282–37290, 2004.
- [82] X. Zhang, S. Moréra, P. A. Bates et al., "Structure of an XRCC1 BRCT domain: a new protein-protein interaction module," *The EMBO Journal*, vol. 17, no. 21, pp. 6404–6411, 1998.
- [83] P. Bork, K. Hofmann, P. Bucher, A. F. Neuwald, S. F. Altschul, and E. V. Koonin, "A superfamily of conserved domains in DNA damage-responsive cell cycle checkpoint proteins," *The FASEB Journal*, vol. 11, no. 1, pp. 68–76, 1997.
- [84] S. Costantini, L. Woodbine, L. Andreoli, P. A. Jeggo, and A. Vindigni, "Interaction of the Ku heterodimer with the DNA ligase IV/Xrcc4 complex and its regulation by DNA-PK," *DNA Repair*, vol. 6, no. 6, pp. 712–722, 2007.
- [85] E. N. Shiozaki, L. Gu, N. Yan, and Y. Shi, "Structure of the BRCT repeats of BRCA1 bound to a BACH1 phosphopeptide: implications for signaling," *Molecular Cell*, vol. 14, no. 3, pp. 405–412, 2004.
- [86] J. A. Clapperton, I. A. Manke, D. M. Lowery et al., "Structure and mechanism of BRCA1 BRCT domain recognition of phosphorylated BACH1 with implications for cancer," *Nature Structural and Molecular Biology*, vol. 11, no. 6, pp. 512–518, 2004.
- [87] R. S. Williams, M. S. Lee, D. D. Hau, and J. N. M. Glover, "Structural basis of phosphopeptide recognition by the BRCT domain of BRCA1," *Nature Structural and Molecular Biology*, vol. 11, no. 6, pp. 519–525, 2004.
- [88] M. Stucki, J. A. Clapperton, D. Mohammad, M. B. Yaffe, S. J. Smerdon, and S. P. Jackson, "MDC1 directly binds phosphorylated histone H2AX to regulate cellular responses to DNA double-strand breaks," *Cell*, vol. 123, no. 7, pp. 1213–1226, 2005.
- [89] A. K. Varma, R. S. Brown, G. Birrane, and J. A. A. Ladas, "Structural basis for cell cycle checkpoint control by the BRCA1-CtIP complex," *Biochemistry*, vol. 44, no. 33, pp. 10941–10946, 2005.
- [90] M. L. Kilkenny, A. S. Doré, S. M. Roe et al., "Structural and functional analysis of the Crb2-BRCT2 domain reveals distinct roles in checkpoint signaling and DNA damage repair," *Genes and Development*, vol. 22, no. 15, pp. 2034–2047, 2008.
- [91] R. S. Williams, G. E. Dodson, O. Limbo et al., "Nbs1 flexibly tethers Ctp1 and Mre11-Rad50 to coordinate DNA double-strand break processing and repair," *Cell*, vol. 139, no. 1, pp. 87–99, 2009.
- [92] J. Lloyd, J. R. Chapman, J. A. Clapperton et al., "A Supramolecular FHA/BRCT-repeat architecture mediates Nbs1 adaptor function in response to DNA damage," *Cell*, vol. 139, no. 1, pp. 100–111, 2009.
- [93] J. S. Williams, R. S. Williams, C. L. Dovey, G. Guenther, J. A. Tainer, and P. Russell, " $\gamma$ H2A binds Brc1 to maintain genome integrity during S-phase," *The EMBO Journal*, vol. 29, no. 6, pp. 1136–1148, 2010.
- [94] P.-Y. Wu, P. Frit, S. Meesala et al., "Structural and functional interaction between the human DNA repair proteins DNA ligase IV and XRCC4," *Molecular and Cellular Biology*, vol. 29, no. 11, pp. 3163–3172, 2009.
- [95] A. S. Doré, N. Furnham, O. R. Davies et al., "Structure of an Xrcc4-DNA ligase IV yeast ortholog complex reveals a novel BRCT interaction mode," *DNA Repair*, vol. 5, no. 3, pp. 362–368, 2006.
- [96] X. Yu, C. C. S. Chini, M. He, G. Mer, and J. Chen, "The BRCT domain is a phospho-protein binding domain," *Science*, vol. 302, no. 5645, pp. 639–642, 2003.
- [97] M. Rodriguez, X. Yu, J. Chen, and Z. Songyang, "Phosphopeptide binding specificities of BRCA1 COOH-terminal (BRCT) domains," *The Journal of Biological Chemistry*, vol. 278, no. 52, pp. 52914–52918, 2003.
- [98] J. N. M. Glover, R. S. Williams, and M. S. Lee, "Interactions between BRCT repeats and phosphoproteins: tangled up in two," *Trends in Biochemical Sciences*, vol. 29, no. 11, pp. 579–585, 2004.
- [99] K. Imami, N. Sugiyama, Y. Kyono, M. Tomita, and Y. Ishihama, "Automated phosphoproteome analysis for cultured cancer cells by two-dimensional nanoLC-MS using a calcined tania/C18 biphasic column," *Analytical Sciences*, vol. 24, no. 1, pp. 161–166, 2008.
- [100] S. Unal, K. Cerosaletti, D. Uckan-Cetinkaya, M. Cetin, and F. Gumruk, "A novel mutation in a family with DNA ligase IV deficiency syndrome," *Pediatric Blood and Cancer*, vol. 53, no. 3, pp. 482–484, 2009.
- [101] Y. Li, D. Y. Chirgadze, V. M. Bolanos-Garcia et al., "Crystal structure of human XLF/Cernunnos reveals unexpected differences from XRCC4 with implications for NHEJ," *The EMBO Journal*, vol. 27, no. 1, pp. 290–300, 2008.
- [102] M. Modesti, M. S. Junop, R. Ghirlando et al., "Tetramerization and DNA ligase IV interaction of the DNA double-strand break repair protein XRCC4 are mutually exclusive," *Journal of Molecular Biology*, vol. 334, no. 2, pp. 215–228, 2003.
- [103] M. S. Junop, M. Modesti, A. Guarné, R. Ghirlando, M. Gellert, and W. Yang, "Crystal structure of the Xrcc4 DNA repair protein and implications for end joining," *The EMBO Journal*, vol. 19, no. 22, pp. 5962–5970, 2000.
- [104] M. A. Recuero-Checa, A. S. Doré, E. Arias-Palomo et al., "Electron microscopy of Xrcc4 and the DNA ligase IV-Xrcc4 DNA repair complex," *DNA Repair*, vol. 8, no. 12, pp. 1380–1389, 2009.
- [105] R. Mizuta, H.-L. Cheng, Y. Gao, and F. W. Alt, "Molecular genetic characterization of XRCC4 function," *International Immunology*, vol. 9, no. 10, pp. 1607–1613, 1997.
- [106] Y. Yu, W. Wang, Q. Ding et al., "DNA-PK phosphorylation sites in XRCC4 are not required for survival after radiation

- or for V(D)J recombination," *DNA Repair*, vol. 2, no. 11, pp. 1239–1252, 2003.
- [107] C. A. Koch, R. Agyei, S. Galicia et al., "Xrcc4 physically links DNA end processing by polynucleotide Kinase to DNA ligation by DNA ligase IV," *The EMBO Journal*, vol. 23, no. 19, pp. 3874–3885, 2004.
- [108] N. K. Bernstein, R. S. Williams, M. L. Rakovszky et al., "The molecular architecture of the mammalian DNA repair enzyme, polynucleotide Kinase," *Molecular Cell*, vol. 17, no. 5, pp. 657–670, 2005.
- [109] V. Yurchenko, Z. Xue, and M. J. Sadofsky, "SUMO modification of human XRCC4 regulates its localization and function in DNA double-strand break repair," *Molecular and Cellular Biology*, vol. 26, no. 5, pp. 1786–1794, 2006.
- [110] Y. Dai, B. Kysela, L. A. Hanakahi et al., "Nonhomologous end joining and V(D)J recombination require an additional factor," *Proceedings of the National Academy of Sciences of the United States of America*, vol. 100, no. 5, pp. 2462–2467, 2003.
- [111] P. Hentges, P. Ahnesorg, R. S. Pitcher et al., "Evolutionary and functional conservation of the DNA non-homologous end-joining protein, XLF/Cernunnos," *The Journal of Biological Chemistry*, vol. 281, no. 49, pp. 37517–37526, 2006.
- [112] S. N. Andres, M. Modesti, C. J. Tsai, G. Chu, and M. S. Junop, "Crystal structure of human XLF: a twist in nonhomologous DNA end-joining," *Molecular Cell*, vol. 28, no. 6, pp. 1093–1101, 2007.
- [113] C. J. Tsai, S. A. Kim, and G. Chu, "Cernunnos/XLF promotes the ligation of mismatched and noncohesive DNA ends," *Proceedings of the National Academy of Sciences of the United States of America*, vol. 104, no. 19, pp. 7851–7856, 2007.
- [114] K. Akopiants, R.-Z. Zhou, S. Mohapatra et al., "Requirement for XLF/Cernunnos in alignment-based gap filling by DNA polymerases  $\lambda$  and  $\mu$  for nonhomologous end joining in human whole-cell extracts," *Nucleic Acids Research*, vol. 37, no. 12, pp. 4055–4062, 2009.
- [115] R. Harris, D. Esposito, A. Sankar et al., "The 3D solution structure of the C-terminal region of Ku86 (Ku86CTR)," *Journal of Molecular Biology*, vol. 335, no. 2, pp. 573–582, 2004.
- [116] Z. Zhang, W. Hu, L. Cano, T. D. Lee, D. J. Chen, and Y. Chen, "Solution structure of the C-terminal domain of Ku80 suggests important sites for protein-protein interactions," *Structure*, vol. 12, no. 3, pp. 495–502, 2004.
- [117] A. Rivera-Calzada, L. Spagnolo, L. H. Pearl, and O. Llorca, "Structural model of full-length human Ku70-Ku80 heterodimer and its recognition of DNA and DNA-PKcs," *EMBO Reports*, vol. 8, no. 1, pp. 56–62, 2007.
- [118] J. Boskovic, A. Rivera-Calzada, J. D. Maman et al., "Visualization of DNA-induced conformational changes in the DNA repair Kinase DNA-PKcs," *The EMBO Journal*, vol. 22, no. 21, pp. 5875–5882, 2003.
- [119] J. J. Perry, E. Cotner-gohara, T. Ellenberger, and J. A. Tainer, "Structural dynamics in DNA damage signaling and repair," *Current Opinion in Structural Biology*, vol. 20, no. 3, pp. 283–294, 2010.
- [120] X. Chen, J. D. Ballin, J. Della-Maria et al., "Distinct kinetics of human DNA ligases I, III $\alpha$ , III $\beta$ , and IV reveal direct DNA sensing ability and differential physiological functions in DNA repair," *DNA Repair*, vol. 8, no. 8, pp. 961–968, 2009.
- [121] J. Gu, H. Lu, B. Tippin, N. Shimazaki, M. F. Goodman, and M. R. Lieber, "XRCC4:DNA ligase IV can ligate incompatible DNA ends and can ligate across gaps," *The EMBO Journal*, vol. 26, no. 4, pp. 1010–1023, 2007.
- [122] J. Gu, H. Lu, A. G. Tsai, K. Schwarz, and M. R. Lieber, "Single-stranded DNA ligation and XLF-stimulated incompatible DNA end ligation by the XRCC4-DNA ligase IV complex: influence of terminal DNA sequence," *Nucleic Acids Research*, vol. 35, no. 17, pp. 5755–5762, 2007.
- [123] B. Kysela, A. J. Doherty, M. Chovanec et al., "Ku stimulation of DNA ligase IV-dependent ligation requires inward movement along the DNA molecule," *The Journal of Biological Chemistry*, vol. 278, no. 25, pp. 22466–22474, 2003.
- [124] L. Chen, K. Trujillo, P. Sung, and A. E. Tomkinson, "Interactions of the DNA ligase IV-XRCC4 complex with DNA ends and the DNA-dependent protein Kinase," *The Journal of Biological Chemistry*, vol. 275, no. 34, pp. 26196–26205, 2000.
- [125] W. S. Joo, P. D. Jeffrey, S. B. Cantor, M. S. Finnin, D. M. Livingston, and N. P. Pavletich, "Structure of the 53BP1 BRCT region bound to p53 and its comparison to the Brca1 BRCT structure," *Genes and Development*, vol. 16, no. 5, pp. 583–593, 2002.
- [126] D. J. Derbyshire, B. P. Basu, L. C. Serpell et al., "Crystal structure of human 53BP1 BRCT domains bound to p53 tumour suppressor," *The EMBO Journal*, vol. 21, no. 14, pp. 3863–3872, 2002.
- [127] T. Ochi, V.M. Bolanos-Garcia, V. Stojanoff, and A. Moreno, "Perspectives on protein crystallisation," *Progress in Biophysics and Molecular Biology*, vol. 101, no. 1–3, pp. 56–63, 2009.
- [128] M. A. Recuero-Checa, A. S. Doré, E. Arias-Palomo et al., "Electron microscopy of Xrcc4 and the DNA ligase IV-Xrcc4 DNA repair complex," *DNA Repair*, vol. 8, no. 12, pp. 1380–1389, 2009.
- [129] T. Ochi, J. G. Grossmann, V. M. Bolanos-Garcia, and T. L. Blundell, To be published.
- [130] D. I. Svergun, "Restoring Low Resolution Structure of Biological Macromolecules from Solution Scattering Using Simulated Annealing," *Biophysical journal*, vol. 76, pp. 2879–2886, 1999.
- [131] V. V. Volkov and D. I. Svergun, "Uniqueness of ab initio shape determination in small-angle scattering," *Journal of Applied Crystallography*, vol. 36, no. 3 I, pp. 860–864, 2003.
- [132] E. F. Pettersen, T. D. Goddard, C. C. Huang et al., "UCSF Chimera—a visualization system for exploratory research and analysis," *Journal of Computational Chemistry*, vol. 25, no. 13, pp. 1605–1612, 2004.
- [133] E. Riballo, L. Woodbine, T. Stiff, S. A. Walker, A. A. Goodarzi, and P. A. Jeggo, "XLF-Cernunnos promotes DNA ligase IV-XRCC4 re-adenylation following ligation," *Nucleic Acids Research*, vol. 37, no. 2, pp. 482–492, 2009.
- [134] R. A. Deshpande and T. E. Wilson, "Modes of interaction among yeast Nej1, Lif1 and Dnl4 proteins and comparison to human XLF, XRCC4 and Lig4," *DNA Repair*, vol. 6, no. 10, pp. 1507–1516, 2007.
- [135] H. Lu, U. Pannicke, K. Schwarz, and M. R. Lieber, "Length-dependent binding of human XLF to DNA and stimulation of XRCC4-DNA ligase IV activity," *The Journal of Biological Chemistry*, vol. 282, no. 15, pp. 11155–11162, 2007.
- [136] K.-I. Yano and D. J. Chen, "Live cell imaging of XLF and XRCC4 reveals a novel view of protein assembly in the non-homologous end-joining pathway," *Cell Cycle*, vol. 7, no. 10, pp. 1321–1325, 2008.
- [137] B. Kastner, N. Fischer, M. M. Golas et al., "GraFix: sample preparation for single-particle electron cryomicroscopy," *Nature Methods*, vol. 5, no. 1, pp. 53–55, 2008.

- [138] T. L. Blundell, H. Jhoti, and C. Abell, “High-throughput crystallography for lead discovery in drug design,” *Nature Reviews Drug Discovery*, vol. 1, no. 1, pp. 45–54, 2002.
- [139] T. L. Blundell, B. L. Sibanda, R. W. Montalvão et al., “Structural biology and bioinformatics in drug design: opportunities and challenges for target identification and lead discovery,” *Philosophical Transactions of the Royal Society B*, vol. 361, no. 1467, pp. 413–423, 2006.
- [140] M. Congreve, C. W. Murray, and T. L. Blundell, “Keynote review: structural biology and drug discovery,” *Drug Discovery Today*, vol. 10, no. 13, pp. 895–907, 2005.
- [141] W. L. DeLano, *The PyMOL Molecular Graphics System*, DeLano Scientific LLC, Palo Alto, Calif, USA, 2008, <http://www.pymol.org>.

## Review Article

# The Roles of Several Residues of *Escherichia coli* DNA Photolyase in the Highly Efficient Photo-Repair of Cyclobutane Pyrimidine Dimers

Lei Xu<sup>1,2</sup> and Guoping Zhu<sup>1</sup>

<sup>1</sup>Institute of Molecular Biology and Biotechnology, Anhui Normal University, Wuhu 241000, China

<sup>2</sup>Department of Basic Medicine, Wannan Medical College, Wuhu, Anhui 241002, China

Correspondence should be addressed to Guoping Zhu, gpz1996@yahoo.com

Received 14 March 2010; Revised 7 July 2010; Accepted 7 August 2010

Academic Editor: Shigenori Iwai

Copyright © 2010 L. Xu and G. Zhu. This is an open access article distributed under the Creative Commons Attribution License, which permits unrestricted use, distribution, and reproduction in any medium, provided the original work is properly cited.

*Escherichia coli* DNA photolyase is an enzyme that repairs the major kind of UV-induced lesions, cyclobutane pyrimidine dimer (CPD) in DNA utilizing 350–450 nm light as energy source. The enzyme has very high photo-repair efficiency (the quantum yield of the reaction is  $\sim 0.85$ ), which is significantly greater than many model compounds that mimic photolyase. This suggests that some residues of the protein play important roles in the photo-repair of CPD. In this paper, we have focused on several residues discussed their roles in catalysis by reviewing the existing literature and some hypotheses.

## 1. Introduction

The sun gives warmth and light to the living beings on the earth. However, the ultra-violet (UV) radiation in the sunlight stimulates lesions forming in DNA. The UV-induced lesions in DNA block the replication and transcription events in the living cells, cause growth delay, mutagenesis, or lethal effects to organisms [1]. In order to survive under the sunlight, the organisms have evolved several repair mechanisms to resist the harmfulness of UV. Direct reversal by DNA photolyases is one of the mechanisms. There are two types of DNA photolyases, CPD photolyases and (6-4) photolyases, which, respectively, reverse the two major UV-induced lesions in DNA, cyclobutane pyrimidine dimers (CPD), and (6-4) photoproducts, utilizing blue or near-UV light (350–450 nm) as energy source [1–4]. CPD photolyases can be further categorized into two subclasses, class I (microbial) and class II (animal and plant), based on their amino acid sequence similarity [3, 5, 6]. Flavin adenine dinucleotide (FAD) is catalytic cofactor of all photolyases [3]. And a second cofactor, usually a derivative of folate, deazaflavin or flavin, acts as a photoantenna to increase the repair efficiency of the enzymes under limiting light conditions [3, 7–9]. The repair reactions are proposed through a photon-induced

electron transfer mechanism which is supported by many model compounds studies. However, the quantum yields ( $\Phi = 0.7–0.98$ ) in the repair of pyrimidine dimers by DNA photolyase is significantly higher [3, 10–13] than those model compounds ( $\Phi = 0.016–0.4$ ) [14–16]. These results indicate that some amino acid residues of photolyases play important roles in the repair reactions.

*Escherichia coli* DNA photolyase is a representative of them. By reviewing the existing literature and some hypotheses, we discussed the roles of some residues of *E. coli* photolyase in the highly efficient catalysis. This paper would provide the further insights into the catalytic mechanism of the enzyme.

## 2. *Escherichia coli* DNA Photolyase

*Escherichia coli* DNA photolyase is a class I CPD photolyase [17], containing 471 amino acids [18, 19] and two cofactors, FAD [20] and a folate derivative, 5,10-methenyltetrahydropterolypolyglutamate (MTHF) [7]. The enzyme was found in 1950s by Rupert et al. [21]. Its gene was first cloned by Sancar et al. [18, 19], which settled the problem that the little expression of the gene in the cells prevents the high yield of pure enzyme for researches.

During the following years, the enzyme has been extensively studied. The physiological form of the enzyme contains a fully reduced FAD (FADH<sup>-</sup>) that is required for its activity both *in vivo* and *in vitro* [22]. It binds a CPD in DNA independent of light [17] and flips the dimer out of the double helix into the active site cavity to make a stable enzyme-substrate complex [23–26]. The light-dependent catalytic reaction was proposed through these steps: FADH<sup>-</sup> is excited directly by a photon or by the photoexcited MTHF cofactor and then transfers an electron to CPD to generate a charge-separated radical pair (FADH<sup>•</sup> + CPD<sup>•-</sup>); then the CPD radical anion cleaves, and the excess electron returns to FADH<sup>•</sup> to restore the reduced form and close the catalytic photocycle [3, 11, 22, 27–29]. By the techniques such as time-resolved spectroscopy, laser flash photolysis [30–35], and transient electron paramagnetic resonance [36, 37], this photon-induced electron transfer mechanism has been substantiated. However, the roles of the amino acid residues in the steps of the high efficient enzymatic reaction, such as substrate docking and splitting, electron transfer, and intermediate stabilization, need further investigation.

### 3. Trp277: A Residue for CPD Docking and Splitting

*E. coli* DNA photolyase contains 15 tryptophan residues. Trp277 lies in a highly conserved region Trp277-Tyr281, which is considered to be important for DNA binding [38]. By the site-directed mutagenesis studies, it was found when Trp277 was replaced with arginine or glutamate, the binding affinity for CPD substrate was lower for 300- or 1000-fold, respectively, although the photochemical properties and the quantum yields for catalyses (under the irradiation wavelengths at 366 nm and 384 nm) of the mutants were indistinguishable from the wild-type enzyme [38]. Later on, it was discovered that Trp277 can also directly and efficiently repair CPD under 280 nm light [39]. These results revealed that Trp277 is crucial for substrate binding, and under certain conditions it also acts as a catalytic residue.

The crystal structure of *E. coli* photolyase (Protein Data Bank entry 1DNP) shows that a positively charged groove on the surface of the protein which might interact with the DNA backbone and a hydrophobic cavity locates at the center. The cavity has the right dimension to hold a *cis,syn* CPD, and Trp277 forms one side wall of it [40] (Figure 1(a)). It is proposed that photolyase binds DNA chain containing a CPD, flips it out into the cavity, and Trp277 stacks with the 5' side of the CPD by  $\pi$ - $\pi$  interaction [23–26, 38]. This is confirmed by the crystal structure of the complex of CPD-like lesion in DNA and photolyase from *Anacystis Nidulans* (*Synechococcus* sp.) (Protein Data Bank entry 1TEZ) [41].

There is another tryptophan, Trp384, in the cavity forming a wedge with Trp277 (Figure 1(a)) [40]. By the examination of the cocrystal structure of *Thermus thermophilus* photolyase with a thymine, it is proposed that CPD might be sandwiched by these two tryptophans [42], and its 3' side might stack with Trp384 in a similar manner. However, from the structure 1TEZ, it is concluded that the

3' side should stack with a methionine residue, Met345, but not Trp384. Met345 is to be discussed in the next section.

### 4. Met345: A Discriminating Residue of CPD Photolyase from Photolyase-Cryptochrome Super Family

A methionine residue in the active cavity of *Saccharomyces cerevisiae* photolyase, which corresponds to Met345 of *E. coli* photolyase, was predicted to interact with CPD [24]. By the structure of the complex of *Anacystis Nidulans* photolyase and CPD-like lesion, it was confirmed that Met345 should stack with the 3' side of CPD [41] (Figure 1(a)). Methionine is a sulfur-containing amino acid. From the studies of the crystal structures of many proteins, Morgan and coworkers proposed that the sulfur atoms might interact with aromatic rings by the so-called sulfur- $\pi$  interaction [43–51]. Although the mechanism of this interaction is still controversial, it does exist. For example, in the structure of the flavodoxin of *Clostridium beijerinckii* (Protein Data Bank entry 5ULL), a methionine residue is located near the xylene ring side of the flavin cofactor [52] the conformations are just like those of Met345 and the 3' side of CPD (Figure 1(b)). The sulfur- $\pi$  stack might also contribute to substrate-binding affinity. In addition, this interaction together with that between Trp277 and the 5' side of CPD might have some effects on substrate splitting.

The electron transfer from excited FADH<sup>-</sup> to CPD is now considered to be through a direct pathway [33, 53, 54]. However, a theoretical calculation with the CPD-photolyase complex structure shows that the indirect electron transfer via protein mediators is as important as the direct electron transfer [55]. The electron-tunneling pathway analysis suggested that there were two typical electron-tunneling routes for the electron transfer of photolyase, one was an adenine route, and the other was through a methionine corresponding to Met345 of *E. coli* photolyase [55]. It is widely accepted that the electron transfers from FADH<sup>-</sup> to the 5' side of CPD first, then to the 3' side [3, 32]. And the pathway for excess electron transfer back to FADH<sup>•</sup> remains unclear till now. Considering Met345 adjacent to the 3' side of CPD, we speculate that it might be an electron back transfer pathway.

It is intriguing that Met345 is proposed to be a residue for the discrimination of CPD photolyase from the photolyase-cryptochrome super family [55]. The super family contains CPD photolyases, (6-4) photolyases, and cryptochromes, all of which are flavoproteins. (6-4) photolyases repair (6-4) photoproduct but not CPD [4]. Cryptochromes play roles in photomorphogenesis in plants and entrain the circadian biological clocks in animal [2, 3, 56]. Recently, it is found that some cryptochromes in insects and birds might function as light-activated magnetoreceptors [57–61]. Although these proteins are functionally diverse, they have relatively high degree of homology. Met345 is conserved in all CPD photolyase whereas in (6-4) photolyases, it is replaced by a histidine which is also important for catalysis [62]. In cryptochromes, it is replaced by histidine, valine, glutamine, and so forth. It might be one of the residues responsible for

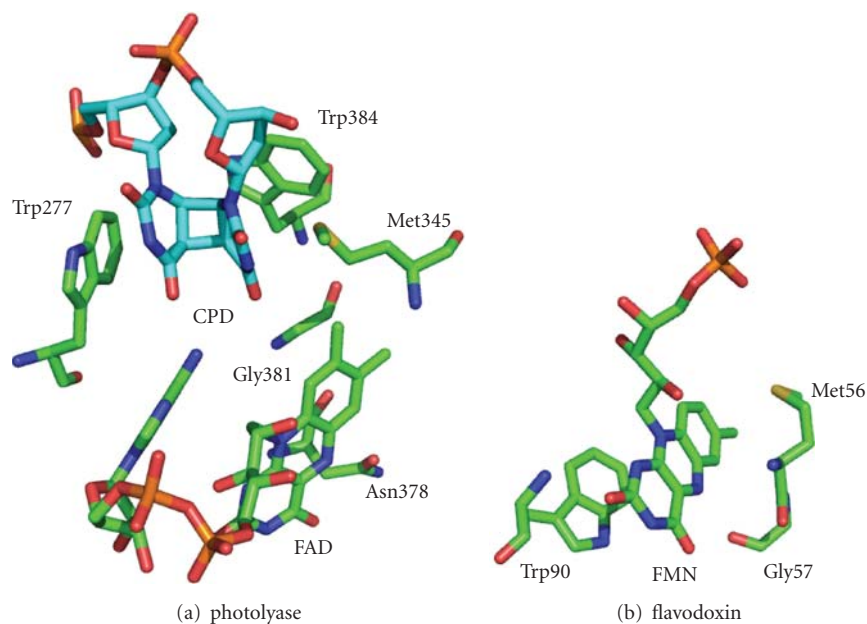


FIGURE 1: Conformations of (a) active sites of photolyase and (b) FMN binding sites of *Clostridium beijerinckii* flavodoxin. The CPD structure was extracted from the PDB entry 1SNH and coupled with *E. coli* DNA photolyase structure 1DNP according to the CPD like lesion-photolyase complex structure 1TEZ. The FMN binding sites of flavodoxin were extracted from the PDB entry 5ULL. This figure was prepared with PyMOL (<http://www.pymol.org/>).

the function diversity of the proteins in this super family [55].

### 5. Asn378: A Stabilizer of the Neutral FAD Radical

Although *E. coli* photolyase contain reduced FAD *in vivo*, it is usually purified with FAD in the blue neutral radical form (FADH<sup>•</sup>). It is known that *E. coli* photolyase is one of the unusual flavoproteins in which the radical is extremely stable [63]. The purified enzyme can hold its radical flavin cofactor unoxidized in aerobic conditions for several days whereas it hardly exists free in aqueous solutions because the dismutation of the radical is favored. These results indicate that the protein environment gives a strong stabilization to the radical. *Clostridium beijerinckii* flavodoxin is another example that has the ability to hold stable radical flavin cofactor. It was proposed that a hydrogen bond between the flavin N(5)H group and the backbone carbonyl oxygen of Gly57 in the flavodoxin is important for the modulation of the redox potentials of the cofactor and the stabilization of the radical form (Figure 1(b)) [64, 65]. Interestingly, there is a similar hydrogen bond between the flavin N(5)H group and the side carbonyl of the Asn378 residue (Figure 1(a)). We had replaced the asparagine residue with serine and found that the mutant has no stable radical state [66]. Moreover, the catalytic activity of the mutant was lost [66]. These experiments show that Asn378 is crucial both for the stabilizing the neutral flavin radical cofactor and for catalysis. It is convincing because the catalytic reaction of CPD splitting is through a radical mechanism: FADH<sup>•</sup> gives

an electron to CPD and becomes FADH<sup>•</sup>. If the transient radical intermediate is well stabilized, it will give enough time for cleavage of the cyclobutane ring to achieve high repair efficiency [33, 67]. When the stabilizing effect is disrupted, the unwanted back electron transfer might be accelerated, leading to low repair efficiency.

Asn378 is a highly conserved residue in photolyases. In most class I CPD photolyases and (6-4) photolyases, the residues are unchanged or replaced with aspartate [6, 68]. The residue is also conserved in mammalian cryptochromes [69]. In a plant cryptochrome *Arabidopsis thaliana* CRY1, it is replaced with aspartate that is proposed to be responsible for the down shift of the flavin redox potentials which make the difference between the cryptochrome and photolyases [70]. Meanwhile, some insect cryptochromes have replaced the residue with cysteine, which may be responsible for a red anionic radical (FAD<sup>•-</sup>) state but not the blue neutral radical state in photolyases [69, 71]. However, in many class II CPD photolyases, the asparagine residues are not conserved [6, 72]. There is evidence that class II CPD photolyases have the similar photochemical properties and the FAD binding environments as compare to class I CPD and (6-4) photolyases [72]. Thus, a stabilizer near the flavin N(5)H group is also required in a class II enzyme. By examining a model structure of a class II enzyme (*Oryza sativa* CPD photolyase) calculated by comparative modeling (<http://modbase.compbio.ucsf.edu/modbase-cgi/index.cgi>) [72, 73], we find another asparagine residue, Asn421, might be an alternative candidate for the stabilization function, which is also highly conserved in class II CPD photolyases.

From the model structure of *Oryza sativa* CPD photolyase, it is of interest to find that the residue corresponding to Trp277 in *E. coli* photolyase is not conserved, which is considered to be crucial for substrate binding (*vide ante*). It indicates that the class II CPD photolyases might use a different substrate binding mechanism as compared to class I group. However, it seems that the residues corresponding to Met345 and Trp384 in *E. coli* photolyase are conserved in the substrate binding cavity, emphasizing their important roles for substrate binding and/or catalysis. Therefore, to fully uncover details of substrate binding and FAD usage, a real crystal structure of a class II photolyase is highly awaited [72].

A mutagenesis study on *Anacystis nidulans* photolyase shows that two residues (Trp384 and Gly381 of *E. coli* photolyase) are crucial for the kinetics stability of the neutral flavin radical in the enzyme (Figure 1(a)) [74]. In *Synechocystis* sp. PCC6803 CRY-DASH, these residues are replaced with tyrosine and asparagine, respectively [74]. The difference might also be a reason for the diverse functions of photolyases and cryptochromes.

## 6. Perspectives

Although the first photolyase has been discovered more than 50 years [21], photolyases still occupies a unique position in biochemistry [1, 2]. Photolyases bind the substrate in a light-independent manner, but the catalysis is absolutely dependent on light that makes the possible to analyze the binding and catalysis steps of the enzymes independently [2, 3]. Furthermore, the level of substrate in the cell can be controlled easily by simply changing the UV dose, and the repairing of the bound substrate is ultrafast by a single light flash. All characteristics make the photolyases to be useful tools for biochemical research, especially the *in vivo* enzymology [2]. Cryptochromes are homologues of photolyases, which are widely concerned now for their functions in the circadian clocks of animal, the photomorphogenesis of plants and the migration of birds and insects by acting as light-activated magnetoreceptors [2, 3, 56–61]. The action mechanisms of cryptochromes are still unclear at present. However, as photolyases, flavin radical is also proposed to be crucial for their functions [57–61, 69–71, 74–76]. Thus, further exploring the photolyase system might give new insights into the researches of both photolyases and cryptochromes.

## 7. Summary

In this paper, we have discussed some of important residues of *E. coli* DNA photolyase. Evidence suggests that they play significant roles in substrate docking and splitting, electron transfer, and intermediate stabilization. Of course, due to the limits of our knowledge, there must be a lot of amino acid residues that might be much more important in the catalysis of enzyme, which are not discussed here. Together with all these amino acid residues and the cofactors of the enzyme, they built a very high efficient system for the photo-repair

of cyclobutane pyrimidine dimers in DNA. Further research on this system will not only contribute to understanding its efficient catalytic mechanism, but also give new insights to the other biochemical research in the future.

## Acknowledgments

The work was supported by the National Natural Science Foundation of China (30900243; 30870062) and Bilingual Teaching Project of the Education Ministry of China.

## References

- [1] R. Beukers, A. P. M. Eker, and P. H. M. Lohman, "50 years thymine dimer," *DNA Repair*, vol. 7, no. 3, pp. 530–543, 2008.
- [2] A. Sancar, "Structure and function of photolyase and *in vivo* enzymology: 50th anniversary," *Journal of Biological Chemistry*, vol. 283, no. 47, pp. 32153–32157, 2008.
- [3] A. Sancar, "Structure and function of DNA photolyase and cryptochrome blue-light photoreceptors," *Chemical Reviews*, vol. 103, no. 6, pp. 2203–2237, 2003.
- [4] S.-T. Kim, K. Malhotra, C. A. Smith, J.-S. Taylor, and A. Sancar, "Characterization of (6-4) photoproduct DNA photolyase," *Journal of Biological Chemistry*, vol. 269, no. 11, pp. 8535–8540, 1994.
- [5] A. Yasui, A. P. M. Eker, S. Yasuhira et al., "A new class of DNA photolyases present in various organisms including aplacental mammals," *EMBO Journal*, vol. 13, no. 24, pp. 6143–6151, 1994.
- [6] S. Kanai, R. Kikuno, H. Toh, H. Ryo, and T. Todo, "Molecular evolution of the photolyase-blue-light photoreceptor family," *Journal of Molecular Evolution*, vol. 45, no. 5, pp. 535–548, 1997.
- [7] J. L. Johnson, S. Hamm-Alvarez, G. Payne, G. B. Sancar, K. V. Rajagopalan, and A. Sancar, "Identification of the second chromophore of *Escherichia coli* and yeast DNA photolyases as 5,10-methenyltetrahydrofolate," *Proceedings of the National Academy of Sciences of the United States of America*, vol. 85, no. 7, pp. 2046–2050, 1988.
- [8] A. P. M. Eker, P. Kooiman, J. K. C. Hessels, and A. Yasui, "DNA photoreactivating enzyme from the cyanobacterium *Anacystis nidulans*," *Journal of Biological Chemistry*, vol. 265, no. 14, pp. 8009–8015, 1990.
- [9] T. Ueda, A. Kato, S. Kuramitsu, H. Terasawa, and I. Shimada, "Identification and characterization of a second chromophore of DNA photolyase from *Thermus thermophilus* HB27," *Journal of Biological Chemistry*, vol. 280, no. 43, pp. 36237–36243, 2005.
- [10] G. Payne and A. Sancar, "Absolute action spectrum of E-FADH2 and E-FADH2-MTHF forms of *Escherichia coli* DNA photolyase," *Biochemistry*, vol. 29, no. 33, pp. 7715–7727, 1990.
- [11] P. F. Heelis, "Photochemical properties of *Escherichia coli* DNA photolyase: a flash photolysis study," *Biochemistry*, vol. 25, no. 25, pp. 8163–8166, 1986.
- [12] A. J. Ramsey, J. L. Alderfer, and M. S. Jorns, "Energy transduction during catalysis by *Escherichia coli* DNA photolyase," *Biochemistry*, vol. 31, no. 31, pp. 7134–7142, 1992.
- [13] S.-T. Kim, P. F. Heelis, and A. Sancar, "Energy transfer (deazaflavin → FADH2) and electron transfer (FADH2 → T ↔ T) kinetics in *Anacystis nidulans* photolyase," *Biochemistry*, vol. 31, no. 45, pp. 11244–11248, 1992.

- [14] S. T. Kim, R. F. Hartman, and S. D. Rose, "Solvent dependence of pyrimidine dimer splitting in a covalently linked dimer-indole system," *Photochemistry and Photobiology*, vol. 52, no. 4, pp. 789–794, 1990.
- [15] R. Epple, E.-U. Wallenborn, and T. Carell, "Investigation of flavin-containing DNA-repair model compounds," *Journal of the American Chemical Society*, vol. 119, no. 32, pp. 7440–7451, 1997.
- [16] Q.-H. Song, W.-J. Tang, X.-M. Hei, H.-B. Wang, Q.-X. Guo, and S.-Q. Yu, "Efficient photosensitized splitting of thymine dimer by a covalently linked tryptophan in solvents of high polarity," *European Journal of Organic Chemistry*, no. 6, pp. 1097–1106, 2005.
- [17] D. E. Brash, W. A. Franklin, G. B. Sancar, A. Sancar, and W. A. Haseltine, "Escherichia coli DNA photolyase reverses cyclobutane pyrimidine dimers but not pyrimidine-pyrimidone (6-4) photoproducts," *Journal of Biological Chemistry*, vol. 260, no. 21, pp. 11438–11441, 1985.
- [18] A. Sancar, F. W. Smith, and G. B. Sancar, "Purification of Escherichia coli DNA photolyase," *Journal of Biological Chemistry*, vol. 259, no. 9, pp. 6028–6032, 1984.
- [19] G. B. Sancar, F. W. Smith, and A. Sancar, "Identification and amplification of the E. coli phr gene product," *Nucleic Acids Research*, vol. 11, no. 19, pp. 6667–6678, 1983.
- [20] A. Sancar and G. B. Sancar, "Escherichia coli DNA photolyase is a flavoprotein," *Journal of Molecular Biology*, vol. 172, no. 2, pp. 223–227, 1984.
- [21] C. S. Rupert, S. H. Goodgal, and R. M. Herriott, "Photoreactivation in vitro of ultraviolet-inactivated Hemophilus influenzae transforming factor," *The Journal of General Physiology*, vol. 41, pp. 451–471, 1958.
- [22] G. Payne, P. F. Heelis, B. R. Rohrs, and A. Sancar, "The active form of Escherichia coli DNA photolyase contains a fully reduced flavin and not a flavin radical, both in vivo and in vitro," *Biochemistry*, vol. 26, no. 22, pp. 7121–7127, 1987.
- [23] I. Husain, G. B. Sancar, S. R. Holbrook, and A. Sancar, "Mechanism of damage recognition by Escherichia coli DNA photolyase," *Journal of Biological Chemistry*, vol. 262, no. 27, pp. 13188–13197, 1987.
- [24] B. J. Vande Berg and G. B. Sancar, "Evidence for dinucleotide flipping by DNA photolyase," *Journal of Biological Chemistry*, vol. 273, no. 32, pp. 20276–20284, 1998.
- [25] K. S. Christine, A. W. MacFarlane IV, K. Yang, and R. J. Stanley, "Cyclobutylpyrimidine dimer base flipping by DNA photolyase," *Journal of Biological Chemistry*, vol. 277, no. 41, pp. 38339–38344, 2002.
- [26] K. Yang and R. J. Stanley, "Differential distortion of substrate occurs when it binds to DNA photolyase: a 2-aminopurine study," *Biochemistry*, vol. 45, no. 37, pp. 11239–11245, 2006.
- [27] G. B. Sancar, M. S. Jorns, and G. Payne, "Action mechanism of Escherichia coli DNA photolyase. III. Photolysis of the enzyme-substrate complex and the absolute action spectrum," *Journal of Biological Chemistry*, vol. 262, no. 1, pp. 492–498, 1987.
- [28] M. S. Jorns, E. T. Baldwin, G. B. Sancar, and A. Sancar, "Action mechanism of Escherichia coli DNA photolyase. II. Role of the chromophores in catalysis," *Journal of Biological Chemistry*, vol. 262, no. 1, pp. 486–491, 1987.
- [29] M. S. Jorns, B. Wang, and S. P. Jordan, "DNA repair catalyzed by Escherichia coli DNA photolyase containing only reduced flavin: elimination of the enzyme's second chromophore by reduction with sodium borohydride," *Biochemistry*, vol. 26, no. 21, pp. 6810–6816, 1987.
- [30] S.-T. Kim, P. F. Heelis, T. Okamura, Y. Hirata, N. Mataga, and A. Sancar, "Determination of rates and yields of interchromophore (folate → flavin) energy transfer and intermolecular (flavin → DNA) electron transfer in Escherichia coli photolyase by time-resolved fluorescence and absorption spectroscopy," *Biochemistry*, vol. 30, no. 47, pp. 11262–11270, 1991.
- [31] T. Okamura, A. Sancar, P. F. Heelis, T. P. Begley, Y. Hirata, and N. Mataga, "Picosecond laser photolysis studies on the photorepair of pyrimidine dimers by DNA photolyase. 1. Laser photolysis of photolyase-2-deoxyuridine dinucleotide photodimer complex," *Journal of the American Chemical Society*, vol. 113, no. 8, pp. 3143–3145, 1991.
- [32] T. Langenbacher, X. Zhao, G. Bieser, P. F. Heelis, A. Sancar, and M. E. Michel-Beyerle, "Substrate and temperature dependence of DNA photolyase repair activity examined with ultrafast spectroscopy," *Journal of the American Chemical Society*, vol. 119, no. 43, pp. 10532–10536, 1997.
- [33] Y.-T. Kao, C. Saxena, L. Wang, A. Sancar, and D. Zhong, "Direct observation of thymine dimer repair in DNA by photolyase," *Proceedings of the National Academy of Sciences of the United States of America*, vol. 102, no. 45, pp. 16128–16132, 2005.
- [34] A. W. MacFarlane IV and R. J. Stanley, "Evidence of powerful substrate electric fields in DNA photolyase: implications for thymidine dimer repair," *Biochemistry*, vol. 40, no. 50, pp. 15203–15214, 2001.
- [35] A. W. MacFarlane IV and R. J. Stanley, "Cis-Syn thymidine dimer repair by DNA photolyase in real time," *Biochemistry*, vol. 42, no. 28, pp. 8558–8568, 2003.
- [36] S. T. Kim, A. Sancar, C. Essenmacher, and G. T. Babcock, "Evidence from photoinduced EPR for a radical intermediate during photolysis of cyclobutane thymine dimer by DNA photolyase," *Journal of the American Chemical Society*, vol. 114, no. 11, pp. 4442–4443, 1992.
- [37] R. R. Rustandi and M. S. Jorns, "Photoinduced spin-polarized radical pair formation in a DNA photolyase-substrate complex at low temperature," *Biochemistry*, vol. 34, no. 7, pp. 2284–2288, 1995.
- [38] Y. F. Li and A. Sancar, "Active site of Escherichia coli DNA photolyase: mutations at Trp277 alter the selectivity of the enzyme without affecting the quantum yield of photorepair," *Biochemistry*, vol. 29, no. 24, pp. 5698–5706, 1990.
- [39] S.-T. Kim, Y. F. Li, and A. Sancar, "The third chromophore of DNA photolyase: Trp-277 of Escherichia coli DNA photolyase repairs thymine dimers by direct electron transfer," *Proceedings of the National Academy of Sciences of the United States of America*, vol. 89, no. 3, pp. 900–904, 1992.
- [40] H.-W. Park, S.-T. Kim, A. Sancar, and J. Deisenhofer, "Crystal structure of DNA photolyase from Escherichia coli," *Science*, vol. 268, no. 5219, pp. 1866–1894, 1995.
- [41] A. Mees, T. Klar, P. Gnau et al., "Crystal structure of a photolyase bound to a CPD-like DNA lesion after in situ repair," *Science*, vol. 306, no. 5702, pp. 1789–1793, 2004.
- [42] H. Komori, R. Masui, S. Kuramitsu et al., "Crystal structure of thermostable DNA photolyase: pyrimidine-dimer recognition mechanism," *Proceedings of the National Academy of Sciences of the United States of America*, vol. 98, no. 24, pp. 13560–13565, 2001.
- [43] R. S. Morgan, C. E. Tatch, R. H. Gushard, J. McAdon, and P. K. Warne, "Chains of alternating sulfur and pi-bonded atoms in eight small proteins," *International Journal of Peptide and Protein Research*, vol. 11, no. 3, pp. 209–217, 1978.

- [44] R. S. Morgan and J. M. McAdon, "Predictor for sulfur-aromatic interactions in globular proteins," *International Journal of Peptide and Protein Research*, vol. 15, no. 2, pp. 177–180, 1980.
- [45] B. L. Bodner, L. M. Jackman, and R. S. Morgan, "NMR study of 1:1 complexes between divalent sulfur and aromatic compounds: a model for interactions in globular proteins," *Biochemical and Biophysical Research Communications*, vol. 94, no. 3, pp. 807–813, 1980.
- [46] G. Némethy and H. A. Scheraga, "Strong interaction between disulfide derivatives and aromatic groups in peptides and proteins," *Biochemical and Biophysical Research Communications*, vol. 98, no. 2, pp. 482–487, 1981.
- [47] K. S. C. Reid, P. F. Lindley, and J. M. Thornton, "Sulphur-aromatic interactions in proteins," *FEBS Letters*, vol. 190, no. 2, pp. 209–213, 1985.
- [48] M. Lebl, E. E. Sugg, and V. J. Hruby, "Proton n.m.r. spectroscopic evidence for sulfur-aromatic interactions in peptides," *International Journal of Peptide and Protein Research*, vol. 29, no. 1, pp. 40–45, 1987.
- [49] A. R. Viguera and L. Serrano, "Side-chain interactions between sulfur-containing amino acids and phenylalanine in  $\alpha$ -helices," *Biochemistry*, vol. 34, no. 27, pp. 8771–8779, 1995.
- [50] D. S. Spencer and W. E. Stites, "The M32L substitution of staphylococcal nuclease: disagreement between theoretical prediction and experimental protein stability," *Journal of Molecular Biology*, vol. 257, no. 3, pp. 497–499, 1996.
- [51] R. J. Zauhar, C. L. Colbert, R. S. Morgan, and W. J. Welsh, "Evidence for a strong sulfur-aromatic interaction derived from crystallographic data," *Biopolymers*, vol. 53, no. 3, pp. 233–248, 2000.
- [52] L. J. Druhan and R. P. Swenson, "Role of methionine 56 in the control of the oxidation-reduction potentials of the *Clostridium beijerinckii* flavodoxin: effects of substitutions by aliphatic amino acids and evidence for a role of sulfur-flavin interactions," *Biochemistry*, vol. 37, no. 27, pp. 9668–9678, 1998.
- [53] T. R. Prytkova, D. N. Beratan, and S. S. Skourtis, "Photoselected electron transfer pathways in DNA photolyase," *Proceedings of the National Academy of Sciences of the United States of America*, vol. 104, no. 3, pp. 802–807, 2007.
- [54] A. Acocella, G. A. Jones, and F. Zerbetto, "What is adenine doing in photolyase?" *Journal of Physical Chemistry B*, vol. 114, no. 11, pp. 4101–4106, 2010.
- [55] Y. Miyazawa, H. Nishioka, K. Yura, and T. Yamato, "Discrimination of class I cyclobutane pyrimidine dimer photolyase from blue light photoreceptors by single methionine residue," *Biophysical Journal*, vol. 94, no. 6, pp. 2194–2203, 2008.
- [56] C. Lin and T. Todo, "The cryptochromes," *Genome Biology*, vol. 6, no. 5, article 220, 2005.
- [57] M. Liedvogel, K. Maeda, K. Henbest et al., "Chemical magnetoreception: bird cryptochrome 1a is excited by blue light and forms long-lived radical-pairs," *PLoS One*, vol. 2, no. 10, Article ID e1106, 2007.
- [58] R. J. Gegear, A. Casselman, S. Waddell, and S. M. Reppert, "Cryptochrome mediates light-dependent magnetosensitivity in *Drosophila*," *Nature*, vol. 454, no. 7207, pp. 1014–1018, 2008.
- [59] H. Zhu, I. Sauman, Q. Yuan et al., "Cryptochromes define a novel circadian clock mechanism in monarch butterflies that may underlie sun compass navigation," *PLoS Biology*, vol. 6, no. 1, p. e4, 2008.
- [60] C. T. Rodgers and P. J. Hore, "Chemical magnetoreception in birds: the radical pair mechanism," *Proceedings of the National Academy of Sciences of the United States of America*, vol. 106, no. 2, pp. 353–360, 2009.
- [61] T. Biskup, E. Schleicher, A. Okafuji et al., "Direct observation of a photoinduced radical pair in a cryptochrome blue-light photoreceptor," *Angewandte Chemie. International Edition*, vol. 48, no. 2, pp. 404–407, 2009.
- [62] K. Hitomi, H. Nakamura, S.-T. Kim et al., "Role of two histidines in the (6-4) photolyase reaction," *Journal of Biological Chemistry*, vol. 276, no. 13, pp. 10103–10109, 2001.
- [63] M. S. Jorns, G. B. Sancar, and A. Sancar, "Identification of a neutral flavin radical and characterization of a second chromophore in *Escherichia coli* DNA photolyase," *Biochemistry*, vol. 23, no. 12, pp. 2673–2679, 1984.
- [64] W. W. Smith, R. M. Burnett, G. D. Darling, and M. L. Ludwig, "Structure of the semiquinone form of flavodoxin from *Clostridium* MP. Extension of 1.8 Å resolution and some comparisons with the oxidized state," *Journal of Molecular Biology*, vol. 117, no. 1, pp. 195–225, 1977.
- [65] M. L. Ludwig, K. A. Patridge, A. L. Metzger et al., "Control of oxidation-reduction potentials in flavodoxin from *Clostridium beijerinckii*: the role of conformation changes," *Biochemistry*, vol. 36, no. 6, pp. 1259–1280, 1997.
- [66] L. Xu, W. Mu, Y. Ding et al., "Active site of *Escherichia coli* DNA photolyase: Asn378 is crucial both for stabilizing the neutral flavin radical cofactor and for DNA repair," *Biochemistry*, vol. 47, no. 33, pp. 8736–8743, 2008.
- [67] P. F. Heelis, R. F. Hartman, and S. D. Rose, "Photoenzymic repair of UV-damaged DNA: a chemist's perspective," *Chemical Society Reviews*, vol. 24, no. 4, pp. 289–297, 1995.
- [68] N. Goosen and G. F. Moolenaar, "Repair of UV damage in bacteria," *DNA Repair*, vol. 7, no. 3, pp. 353–379, 2008.
- [69] A. Berndt, T. Kottke, H. Breitzkreuz et al., "A novel photoreaction mechanism for the circadian blue light photoreceptor *Drosophila* cryptochrome," *Journal of Biological Chemistry*, vol. 282, no. 17, pp. 13011–13021, 2007.
- [70] V. Bolland, M. Byrdin, A. P. M. Eker, M. Ahmad, and K. Brettel, "What makes the difference between a cryptochrome and DNA photolyase? A spectroelectrochemical comparison of the flavin redox transitions," *Journal of the American Chemical Society*, vol. 131, no. 2, pp. 426–427, 2009.
- [71] N. Öztürk, S.-H. Song, C. P. Selby, and A. Sancar, "Animal type I cryptochromes: analysis of the redox state of the flavin cofactor by site-directed mutagenesis," *Journal of Biological Chemistry*, vol. 283, no. 6, pp. 3256–3263, 2008.
- [72] A. Okafuji, T. Biskup, K. Hitomi et al., "Light-induced activation of class II cyclobutane pyrimidine dimer photolyases," *DNA Repair*, vol. 9, no. 5, pp. 495–505, 2010.
- [73] U. Pieper, N. Eswar, H. Braberg et al., "MODBASE, a database of annotated comparative protein structure models, and associated resources," *Nucleic Acids Research*, vol. 32, pp. D217–D222, 2004.
- [74] M. J. Damiani, G. N. Yalloway, J. Lu, N. R. McLeod, and M. A. O'Neill, "Kinetic stability of the flavin semiquinone in photolyase and cryptochrome-DASH," *Biochemistry*, vol. 48, no. 48, pp. 11399–11411, 2009.
- [75] S.-H. Song, N. Öztürk, T. R. Denaro et al., "Formation and function of flavin anion radical in cryptochrome 1 blue-light photoreceptor of monarch butterfly," *Journal of Biological Chemistry*, vol. 282, no. 24, pp. 17608–17612, 2007.

- [76] N. Hoang, E. Schleicher, S. Kacprzak et al., "Human and *Drosophila* cryptochromes are light activated by flavin photoreduction in living cells," *PLoS Biology*, vol. 6, no. 8, Article ID e160, 2008.

## Research Article

# Parameters of Reserpine Analogs That Induce MSH2/MSH6-Dependent Cytotoxic Response

**Aksana Vasilyeva,<sup>1</sup> Jill E. Clodfelter,<sup>1</sup> Michael J. Gorczynski,<sup>2</sup> Anthony R. Gerardi,<sup>2</sup> S. Bruce King,<sup>2</sup> Freddie Salisbury,<sup>3</sup> and Karin D. Scarpinato<sup>1,4</sup>**

<sup>1</sup> Department of Cancer Biology, Wake Forest University School of Medicine, Winston-Salem, NC 27157, USA

<sup>2</sup> Department of Chemistry, Wake Forest University, Winston-Salem, NC 27109, USA

<sup>3</sup> Department of Physics, Wake Forest University, Winston-Salem, NC 27109, USA

<sup>4</sup> Comprehensive Cancer Center, Wake Forest University School of Medicine, Winston-Salem, NC 27157, USA

Correspondence should be addressed to Karin D. Scarpinato, kscarpin@wfubmc.edu

Received 22 March 2010; Revised 2 June 2010; Accepted 18 June 2010

Academic Editor: Ashis Basu

Copyright © 2010 Aksana Vasilyeva et al. This is an open access article distributed under the Creative Commons Attribution License, which permits unrestricted use, distribution, and reproduction in any medium, provided the original work is properly cited.

Mismatch repair proteins modulate the cytotoxicity of several chemotherapeutic agents. We have recently proposed a “death conformation” of the MutS homologous proteins that is distinguishable from their “repair conformation.” This conformation can be induced by a small molecule, reserpine, leading to DNA-independent cell death. We investigated the parameters for a small reserpine-like molecule that are required to interact with MSH2/MSH6 to induce MSH2/MSH6-dependent cytotoxic response. A multidisciplinary approach involving structural modeling, chemical synthesis, and cell biology analyzed reserpine analogs and modifications. We demonstrate that the parameters controlling the induction of MSH2/MSH6-dependent cytotoxicity for reserpine-analogous molecules reside in the specific requirements for methoxy groups, the size of the molecule, and the orientation of molecules within the protein-binding pocket. Reserpine analog rescinnamine showed improved MSH2-dependent cytotoxicity. These results have important implications for the identification of compounds that require functional MMR proteins to exhibit their full cytotoxicity, which will avoid resistance in MMR-deficient cells.

## 1. Introduction

Mismatch repair is one of the key DNA repair systems in the cell that repair incorrectly formed base pairs and insertion/deletion loops during replication, significantly increasing the stability of the genome [1–5]. Additional importance comes from the contribution of defects in MMR proteins to cancer development, progression and therapeutic success. In addition to the recognition of replication errors, key MMR proteins MSH2/MSH6 recognize a number of DNA lesions that are irreparable by these proteins, which, in turn, initiate a cell death pathway. The role of MMR proteins in the cell death response to cytotoxic agents has been the subject of much debate [6, 7]. Whether DNA damage is recognized in form of a mismatch at the site of the damage, or DNA damage itself is recognized remains subject of investigation and may vary with the nature of the

damage. Recent data suggest that some types of DNA lesions are recognized without the requirements for a mismatch [8]. As a result of their ability to recognize certain DNA lesions and their participation in the initiation of cell death, MMR proteins modulate the response to certain chemotherapeutic agents. This participation is particularly evident in cells with defects in MMR proteins which reduce the sensitivity to chemotherapeutic agents sufficiently to prove to be a problem for the treatment of tumors [1, 6, 9–12].

The exact mechanism of the cytotoxic response initiated by MSH2/MSH6 interactions with DNA damage remains under investigation and speculation. Recent data suggest that the response pathway depends on the nature of the lesion rather than the unification of different signals into a common pathway [13]. At least two hypotheses have been put forward to address the mechanism behind the MMR protein-dependent cell death: The “futile cycles of

repair” hypothesis is based on the formation of a mismatch opposite the DNA damage, followed by attempted repair events that retain the damage and the formation of DNA strand breaks as factual initiators of cell death [1, 4, 14]. The second hypothesis suggests a direct involvement of MMR proteins in the initiation of the cell death event. We and others have identified separation-of-function mutants that demonstrate that repair-defective mutants of MMR proteins retain the ability to induce cell death, suggesting that repair is not required for cytotoxic response to all types of DNA damage [8, 15–17], but also suggesting that specific MMR proteins form recognition complexes for both mismatch repair, and at least some types of DNA damage. Computational modeling predicted the formation of a “death conformation” with distinctly different features to the “repair conformation” of MutS and its homologs (MSH). This model of a MutS “death conformation” was validated in extensive mutational analyses on eukaryotic proteins [8]. Although the mechanistic details of this pathway are largely unknown, targeting the apparent recognition complex for cell death, that is, the “death conformation,” has shown initial successes [18]. Hence, we aim to exploit this pathway via small molecule binding to the “death conformation.”

Recently, we have demonstrated that the MSH2-dependent cell death response can be induced by small molecules that mimic binding to DNA damage and promote the induction of this cell death [18]. The prototype for this induction of MSH2-dependent cell death without genotoxic insult is reserpine, a drug previously in clinical use for hypertension. The predicted binding of the molecule to the protein occurs in the DNA binding pocket and induces specific conformational changes that allow access to the “death conformation” of the protein [18]. At present, the direct binding of reserpine, and its derivatives, to the “death conformation” has been predicted, and the ability of reserpine and rescinnamine to induce MSH2-dependent apoptosis has been verified experimentally in this work as well as in an earlier study [18]. Unfortunately, it does not seem possible, with present technology, to unequivocally demonstrate physical association between MSH2/MSH6 and either reserpine or rescinnamine. Attempts to use SPR and calorimetry (data not shown) have lacked the precision to detect these small alkaloids binding to such a large protein complex. We expect that the technology used to detect such direct binding of small molecules to large protein complexes will be refined over the next few years, and that presently challenging complexes, such as the proposed MSH2/MSH6/rescinnamine or reserpine complex, will be directly studied. For now, given the circumstantial evidence reported herein and in [18] we consider the hypothesis that reserpine binds to MSH2/MSH6 as predicted to be a reasonable starting point for further studies. Here, we determine the parameters for small molecules to initiate the MMR protein-dependent cell-death response, where the cell-death response is measured via two distinct standard assays, MTS assay and caspase activation, which provide multiple pieces of evidence for the induction of cell-death. Based on our models, we have hypothesized that specific structural parameters are required of a small molecule to mimic the interaction of MSH2/MSH6

with DNA damage, show the correct orientation in the protein-binding pocket and initiate MSH2-dependent cell death. In a combination of computer-based structural modeling, chemical synthesis, and cell biology, we have identified these distinct requirements, which consist of the size of the molecule, the presence and location of methoxy groups, and the orientation of the molecule within the protein-binding pocket. While the computational modeling assumes that the small molecules bind in a specific pocket and in specific orientations, as predicted, the cellular assays do not require such assumptions. These small-molecule structural parameters will provide the foundation for any subsequent searches for new small molecule compounds that initiate the specific MSH2-dependent cell death targeted in this approach.

## 2. Materials and Methods

**2.1. Virtual Screening.** AutoDock 3.0 was used to perform 3D docking into structural models generated from the molecular dynamics simulations. Docking grids from vdW and electrostatic interactions were generated using standard AutoDock charges, vdW, and electrostatic parameters on cubic grids, 18.75 Å on a side. The grids were centered on the midpoint of the line connecting the two guanine nitrogens that are crosslinked in the platinated simulation, but the grids were generated in the absence of DNA and the platinum adduct. The mol2 files for the small molecules were generated using MARVIN and assigned charges and rotatable bonds using AutoDock, which was also used to perform the preparatory work for the grid docking. The ligands were docked using default Autodock Lamarckian genetic algorithm parameters except the number of runs was increased to 256. The structure with the lowest estimated inhibition constant,  $K_i$ , as calculated by AutoDock was used as the docked pose [15].

**2.2. Molecular Dynamics Simulations.** The structures used for the docking are the centroids from the final equilibrated clusters of two molecular dynamics simulations. The clusters were obtained by  $K$ -means clustering with a 1 Å radius cutoff on the alpha-carbon positions of structures in the molecular dynamics trajectories. The simulation protocol is largely the same as described elsewhere, differing only in the use of a constant pressure algorithm, and differing simulation lengths, and is briefly summarized here. The X-ray structure of *Escherichia coli* MutS in complex with DNA was the initial starting point; hydrogen atoms were added using the building facility of CHARMM and TIP3P water molecules and counterions were added using the solvate package of the visual molecular dynamics (VMD) package. The CHARMM27 force field was used for the entire complex with additional parameters added based on preexisting cisplatin parameters. The platinum crosslinks two adjacent guanines. The simulation was performed in NAMD using standard parameters: a 2.0 fs timestep using SHAKE on all bonds to hydrogen atoms, a 12 Å cutoff, Particle Mesh Ewald with a 128 grid points on a side, Berendsen’s constant

pressure algorithm with a target pressure of 1.01325 bar, a compressibility of 45.7 mbar, a relaxation time of 1 ps, and a pressure frequency of 40 fs, and a coordinate save frequency of 200 fs; all as implemented in NAMD. The simulation protocol consisted of 250 ps of thermal equilibration to 300 K, followed by a 10 ns production simulation. The partition coefficients were calculated using extended group contribution approach. In this approach, a chemical structure is automatically decomposed into fragments and atom types, and the contributions of different fragments and atom types are summed together, along with correction terms to account for interactions between different fragments [19].

**2.3. Chemical Synthesis.** Methyl reserpate and benzoyl reserpine were prepared from reserpine as previously described [20]. All other reserpine analogs were generated in a similar fashion by condensation of methyl reserpate with the commercially available acid chloride. All new compounds were purified by flash chromatography and characterized by proton and carbon NMR spectroscopy and mass spectrometry (see Supplementary Material for specific compounds).

**2.4. Cell Viability Assays.** HEC59 cells (*msh2* deficient) and the paired cell line with chromosome 2 transfer HEC59 (2) have been extensively characterized previously [21]. In addition to their *msh2* defect, these cells contain dysfunctional p53. The cells were grown in standard growth media of DMEM-F12 +10% FBS. Cells were plated in 96 well plates at an appropriate concentration in 100  $\mu$ l media and incubated overnight. Media was replaced with fresh media containing drug and allowed to incubate for 24 hours at indicated concentrations. Untreated cells received fresh media with vehicle only. One solution reagent (CellTiter 96(r) AQueous One Solution) was added to existing media (20  $\mu$ l/well) and allowed to incubate 3-4 hrs. A plate reader was used to record the absorbance at 490 nm.

Dose-dependent response to nineteen increasing concentrations of the respective compound was determined. OD measurements were used to determine cell viability at each of the concentrations as percentage of control and analyzed for IC<sub>50</sub> values using GraphPad Prism 4™. Each compound was analyzed in triplicate. Graphs represent the mean values and standard deviations of three independent experiments.

### 3. Results

**3.1. Functional MSH2- and MSH6 Are Required to Induce Full Cytotoxic Response to Reserpine and Rescinnamine.** Reserpine (Figure 1(a)), a small molecule identified through computational modeling has been predicted to bind MutS homologs mimicking DNA damage [18]. We have used LC-MS total ion chromatography to provide evidence for the binding of reserpine to yeast Msh2/Msh6 (see Figure 1 in Supplementary Material available online at doi:10.4061/2011/162018). Data analysis was performed for *m/z* 609, which is characteristic of reserpine alone. The chromatogram of pure reserpine

standard showed one prominent peak that eluted at 1.62 minutes with a mass/charge of 609.325 (suppl. Figure 1). This peak was fragmented by the later MS sectors and two fragments—397.08 and 194.82 were reproducibly observed. When the reserpine was mixed in a one-to-one ratio with the protein sample, the peak very reproducibly eluted with a longer retention time (1.88 minutes) relative to pure reserpine. The fact that we detected the peak at 609 could lead to several conclusions: The detected reserpine may represent never bound or excess unbound reserpine. However, no consistent longer migration times would be expected. If the presence of protein simply blocked sites of interaction on the stationary phase, it would be surprising to see this as a highly reproducible effect. An alternate explanation would be that the detected reserpine indeed had protein bound, but that the bound reserpine had been liberated (unbound) during the electrospray stage of the analysis. Since no excess reserpine was present in the mix, we would not expect two peaks (unbound, excess, and bound reserpine). Taken together, our data indicate that reserpine was bound to protein through the LC column, and freed during the electrospray stage. These data indicate a relatively weak binding of reserpine to the protein. The weakness of interaction may not be surprising, given that the compound is much smaller than the normal DNA substrate, and hence provides much fewer opportunities for interactions. This does provide indirect evidence that reserpine does bind, albeit, potentially weakly to the protein complex, which suggests that modification of reserpine may be fruitful to improve targeting of the MSH2-dependent pathway.

Cell viability assays show that even though reserpine decreases viability of both *MSH2*-deficient (IC<sub>50</sub> 93  $\mu$ M) and *MSH2*-proficient (IC<sub>50</sub> 61  $\mu$ M) cells after 24-hr treatment, it preferentially kills *MSH2*-proficient cells (Figure 1(b)). The 1.5-fold difference in cell viability between proficient and deficient cells is reminiscent of the activity of cisplatin, though reserpine activity is observed considerably earlier. Rescinnamine (Figure 1(a)), a derivative of reserpine that adds additional length via the substitution of the trimethoxybenzoyl group with a trimethoxycinnamoyl group, likewise requires functional *MSH2* for full reduction of cell viability (*MSH2*-deficient: IC<sub>50</sub> 115  $\mu$ M; *MSH2*-proficient: IC<sub>50</sub> 38  $\mu$ M) (Figure 1(b)). The increase in length, without alteration of functional groups, doubled *MSH2*-dependent cytotoxicity to a 3-fold difference in cell viability between proficient and deficient cells.

We next determined if the decrease in mitochondrial integrity, as determined by the MTS assay for cell viability is indicative of the induction of an apoptotic response pathway. Cell extracts of treated cells were analyzed for the specific activation of caspase-3, a proapoptotic protein commonly used as an indicator for apoptotic cell death. The treatment of *MSH2*-deficient cells with reserpine (85  $\mu$ M), rescinnamine (60  $\mu$ M) or the control compound Staurosporine for 24 hours induces caspase-3 cleavage equally and only weakly above the untreated background control (Figure 1(c)). Drug concentrations were chosen based on the IC<sub>50</sub> in these cells, which is reflective of the different toxicity of the compounds. In contrast, in *MSH2*-proficient cells, caspase-3 activation

is significantly stronger. The difference in the efficiency in inducing cell death response between reserpine and rescinnamine is apparent, as rescinnamine induces stronger caspase-3 activation than reserpine (Figure 1(c)).

MSH2 forms a functional heterodimer with MSH6 in its ability to recognize DNA lesions and initiate response pathways. We next determined if MSH6 is also required in the initiation of proper responses to small molecules, such as reserpine and rescinnamine. *MSH6*-deficient and *MSH6*-deficient cells were treated with reserpine (85  $\mu\text{M}$ ) and rescinnamine (60  $\mu\text{M}$ ) for 24 hours. The detection of cleaved caspase-3 in extracts from both cell lines revealed activation primarily in the *MSH6*-proficient cells, consistent with a functional requirement of the protein for cytotoxic response (Figure 1(d)).

**3.2. Combinatorial Treatment of Cisplatin and Rescinnamine Abrogates *MSH2*-Dependence of Cytotoxic Response and Eliminates Chemotolerance.** Cisplatin is a chemotherapeutic that primarily forms (1,2)-intrastrand crosslinks between adjacent guanines in DNA. This compound was previously used as a model agent to characterize the *MSH2*/*MSH6*-dependent induction of a protein “death conformation” and cytotoxic response [8]. Since reserpine was predicted to likewise stabilize the *MSH2*/*MSH6* “death conformation” [18], and rescinnamine showed an improved activity over reserpine, we asked whether a combination of rescinnamine with cisplatin would improve the activity of either drug alone.

*MSH2*-deficient and *MSH2*-proficient cells were treated with sublethal doses of cisplatin (10  $\mu\text{M}$ ) and increasing concentrations of rescinnamine (0–25  $\mu\text{M}$ ). Cell viability was determined after 24, 48, and 72 hours by MTS assay (Figure 2). Twenty-four hours after treatment (Figure 2(a)), a rapid decrease in cell viability was observed that led to the complete elimination of viable cells after 48 hours at much lower concentration of either cisplatin or rescinnamine alone (Figure 1(b)) [18]. This effect on cell viability was indistinguishable for *MSH2*-proficient and *MSH2*-deficient cells. Overall cell viability was reminiscent of the treatment of *MSH2*-proficient cells with rescinnamine alone, and increased tolerance to the drug was eliminated by the concomitant treatment with cisplatin (Figure 2(a)). Increased exposure to the combination treatment eradicated cell viability entirely (Figures 2(b) and 2(c)), which was previously not observed for much higher concentrations of either drug alone [13, 18]. Full eradication of cells was observed after 48 or 72 hour treatment with 20  $\mu\text{M}$  cisplatin and 15  $\mu\text{M}$  rescinnamine.

The  $\text{IC}_{50}$  values of the combination treatment confirm this result. The addition of cisplatin resulted in a 7.3-fold decrease in  $\text{IC}_{50}$  value for rescinnamine after 24 hours, and a 9.7-fold decrease after 48 hours in *MSH2*-deficient cells. The same levels of rescinnamine reduced cell viability in *MSH2*-proficient cells (Table 1). An additional 24 hours of treatment for a total of 72 hours did not significantly alter the  $\text{IC}_{50}$  any further. The combination treatment results in a rapid, *MSH2*-independent demise of cell viability. These

findings are confirmed by immunoblotting; upon treatment with 24 hours of rescinnamine (60  $\mu\text{M}$ ) and cisplatin (10  $\mu\text{M}$ ) comparable levels of caspase-3 cleavage in *MSH2*-deficient and *MSH2*-proficient cells are observed (Figure 2(d)). At 48 and 72 hours, all cells treated with the combination treatment were eliminated and no lysates could be collected and assessed for caspase-3 cleavage.

**3.3. Structural Predictions and Validation of Parameters Required for *MSH2*-Dependent Cell Death.** Next, we wanted to identify the specific parameters that are required for the *MSH2*-dependent induction of cell death, and when altered, reduce or abolish this function. Modeling of reserpine and rescinnamine into the MutS structure (Figure 3) predicted functional groups and parts of the molecules with favorable (red) or unfavorable (blue) interactions with the protein. Green depicts intermediate importance in the interaction.

Differences in the predicted favorable and unfavorable interactions of reserpine and rescinnamine, respectively, represent the difference in their activity. The methoxy group on ring 1 of reserpine is predicted to be nonessential for interactions, while, in rescinnamine, it is proposed to be important for interactions. As for ring 6, all three methoxy groups in reserpine are predicted to have favorable interactions, but only two of them are highly favorable for interactions between rescinnamine and MutS/*MSH* proteins. In reserpine, the carbon of ring 5 that connects to carbon chain leading to ring 6 is pertinent for interactions. Nonetheless, in rescinnamine, that system is unfavorable.

These computational predictions were subsequently experimentally analyzed to determine the validity of the prediction. Derivatives of reserpine and rescinnamine were purchased or synthesized (if not commercially available) (see Table 1). Through structural predictions, the compounds were subdivided into four distinct modes of binding to MutS/*MSH* proteins: reserpine-like conformation, flipped conformation, mismatch-like conformation, and nonspecific conformation (see Figure 5).

**3.3.1. Reserpine-Like Conformation.** Reserpine was identified utilizing the cisplatin-induced “death conformation” of *MSH2*/*MSH6* [8, 18], predicting a similar interaction with the DNA-binding pocket of MutS (Figure 3(a)). Likewise, rescinnamine is predicted to show similar interactions (Figure 3(b)). The space occupied by either molecule largely overlaps with that of DNA. The molecules are stabilized by hydrogen bonds between their methoxy groups and at least three amino acids (G38, R58, R108 of MutS). These residues were previously identified as being important for the interaction with cisplatinated DNA [8]. The phenylalanine (F36) shown to be indispensable for mismatch repair is far removed from the small molecules and shows no significant binding activity [8, 22]. This lack of significance is reminiscent of its failure to exhibit a significant effect on the binding to cisplatinated DNA or, when mutated, on the cytotoxic response to cisplatin [8]. Both molecules show a characteristic bend. Previously, it was suggested that an acquired or preexisting bend in the ligand for

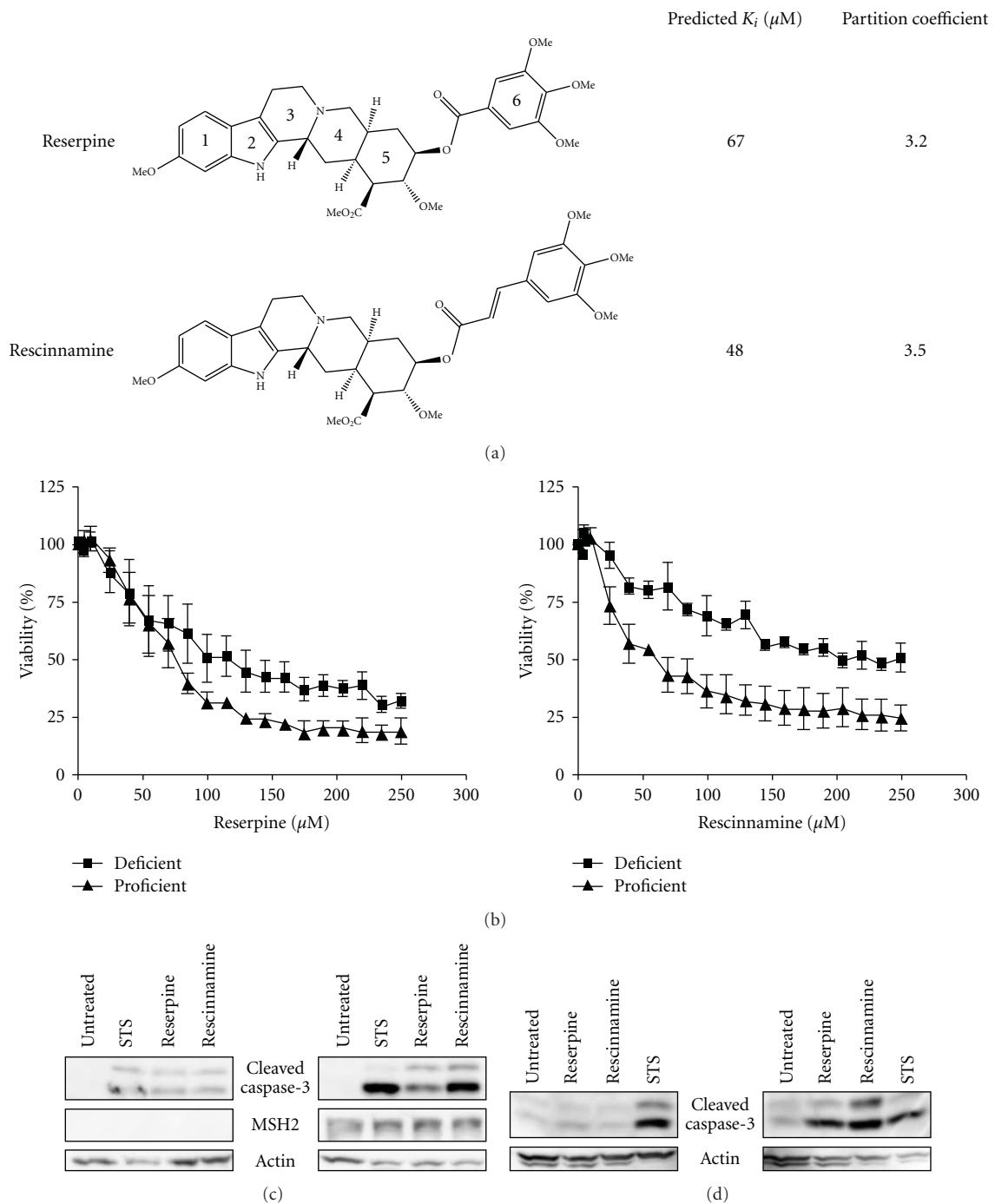


FIGURE 1: (a) Structures of reserpine and rescinnamine with their binding constants and calculated partition coefficients (see Methods for details). (b) MTS cell survival assay shows *MSH2*-dependent cell viability after concentration-dependent reserpine (left) and rescinnamine (right) treatments. *MSH2*-deficient cell response is shown with squares, proficient response with triangles. (c) Western blot shows caspase-3 cleavage in Hec59 (*MSH2*-deficient; left panel) and Hec59(2) (*MSH2*-proficient; right panel) cells upon treatment with reserpine (85  $\mu\text{M}$ ) and rescinnamine (60  $\mu\text{M}$ ). The 17 and 19 kDa cleavage products of caspase-3 are depicted. Staurosporine (STS) was used as a positive control; actin was used as a loading control. (d) Western blot displays caspase-3 cleavage in DLD1 (*MSH6*-deficient; left panel) and DLD1(2) (*MSH6*-proficient; right panel) cells treated with reserpine and rescinnamine.

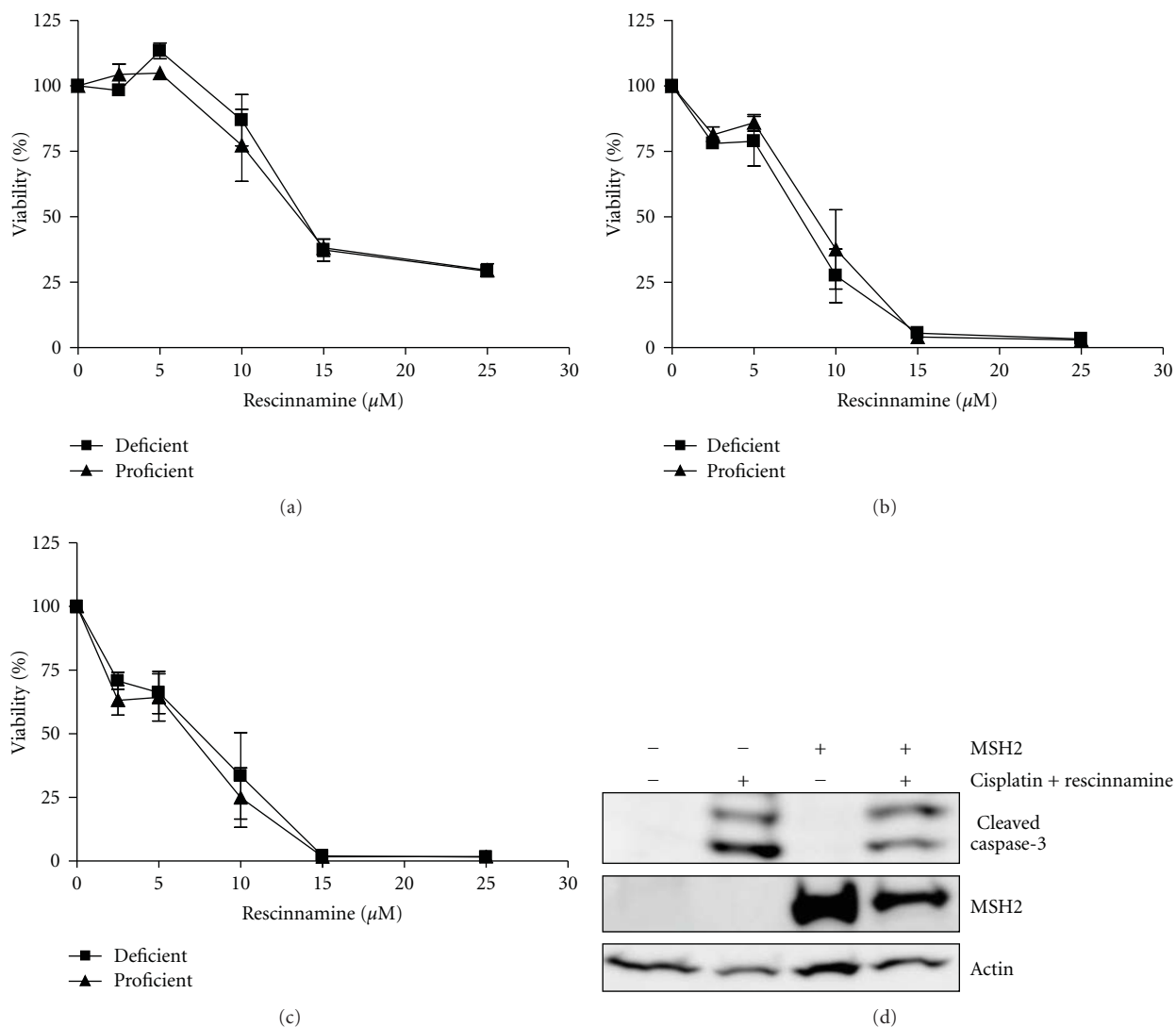


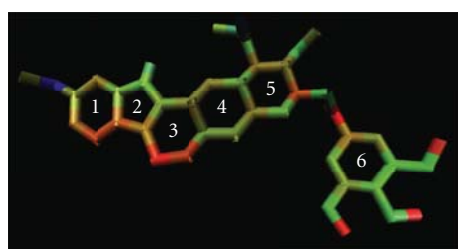
FIGURE 2: Combination treatment of cisplatin and rescinamine drastically reduces cell viability within 24 hours (a) and completely eliminates all cells at 48 and 72 hours (b and c, resp.) when cells are treated with cisplatin ( $10\ \mu\text{M}$ ) and increasing concentrations of rescinamine ( $0\text{--}25\ \mu\text{M}$ ). Cell viability is accessed via MTS assays; MSH2-deficient cells (■) and MSH2-proficient (▲) cell response is shown. Mean values and standard deviations of three independent experiments are shown. (d) Immunoblotting demonstrates caspase-3 cleavage in Hec59 (*MSH2*-deficient; lanes 1 and 2) and Hec59(2) (*MSH2*-proficient; lanes 3 and 4) cells upon treatment with 24 hours of cisplatin ( $10\ \mu\text{M}$ ) and rescinamine ( $60\ \mu\text{M}$ ). The 17 and 19 kDa cleavage products of caspase-3 are depicted. Staurosporine (STS) was used as a positive control; actin was used as a loading control.

MutS homologous proteins is required for robust binding to their substrates [23]. The existence of such a bend may be a prerequisite for small molecules to specifically bind to MutS homologous proteins and induce a specific response. However, the predicted orientation of the bend in the small molecules appears to be inverted compared to DNA, which may suggest that the actual presence of a bend is not a requirement for cytotoxic response. Among all the compounds tested, reserpine and rescinamine are the only molecules predicted to preferentially bind in this specific conformation and exhibit these specific interactions with the protein binding pocket.

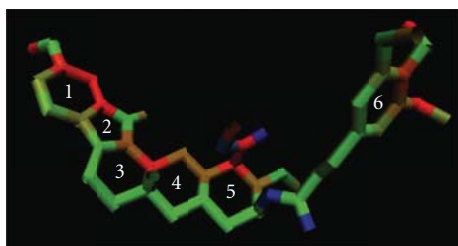
**3.3.2. Flipped Conformation.** To determine the functional requirements of a small molecule to induce MSH2-dependent cell death, we constructed a number of analogs based on the reserpine structure. We hypothesized, based on the structural predictions, that the methoxy groups on ring 6 will have significant impact. We constructed several compounds that either lack all or some of the methoxy groups, resulting in seven different molecules: benzoyl, 3-methoxybenzoyl, 4-methoxybenzoyl, 3,4-dimethoxybenzoyl, 3,5-dimethoxybenzoyl, methylenedioxybenzoyl, and cinnamoyl reserpine (Figure 4(a)). Interestingly, the structural predictions suggest a preferred altered binding

TABLE 1: IC<sub>50</sub> values for response of MSH2-deficient and MSH2-proficient cells to Reserpine analogs.

Compound	IC <sub>50</sub> [ $\mu$ M]				Fold difference
	MSH2-deficient	95% CL	MSH2-proficient	95% CL	
cisplatin	75	46–130	47	35–64	1.6
<b>reserpine</b>	<b>93</b>	<b>74–120</b>	<b>61</b>	<b>54–70</b>	<b>1.5</b>
<b>rescinnamine</b>	<b>87</b>	<b>53–150</b>	<b>39</b>	<b>32–47</b>	<b>2.6</b>
rescinnamine + 10 $\mu$ M cisplatin (24 h)	12	11–13	11	10–13	1.1
rescinnamine + 10 $\mu$ M cisplatin (48 h)	9.1	7–12	9.7	9–11	0.94
rescinnamine + 10 $\mu$ M cisplatin (72 h)	9.9	9–11	9.8	5 <sup>-13</sup> –2 <sup>14</sup>	1.01
benzoyl	110	100–120	132	107–160	0.83
3-methoxy benzoyl	83	74–92	88	75–104	0.94
4-methoxy benzoyl	68	58–81	67	59–75	1.01
<b>3,4-dimethoxy benzoyl</b>	<b>85</b>	<b>78–93</b>	<b>66</b>	<b>59–74</b>	<b>1.3</b>
3,5-dimethoxy benzoyl	36	28–48	38	30–49	0.95
cinnamoyl	150	92–250	130	107–160	1.2
methylenedioxybenzoyl	36	32–41	51	45–58	0.71
deserpidine	59	51–69	48	46–51	1.2



(a)



(b)

FIGURE 3: Structures of reserpine (a) and rescinnamine (b) analyzed by computational modeling depicting favorable (red) and unfavorable (blue) interactions with amino acids within MutS-binding pocket. Green indicates interactions of intermediate binding relevance.

orientation of these molecules, even for those lacking only one methoxy group (3,4-dimethoxy benzoyl; 3,5-dimethoxy benzoyl). This altered binding mode would flip the molecule and have it oriented the opposite way to the reserpine/rescinnamine. The binding of each one of the five molecules in this orientation is predicted to be strong, with predicted  $K_i$  values of 15–32  $\mu$ M. Experimental determination of the cell death demonstrates the ability of these compounds to induce cell death, however in an MSH2-independent manner (Figure 6(a), Table 1). The

3,4-dimethoxy benzoyl compound is an exception and the only molecule that initiates a significant MSH2-dependent cell death response. The IC<sub>50</sub> values for this compound result in 85  $\mu$ M in MSH2-deficient cells versus 66  $\mu$ M in MSH2-proficient cells, with a 1.3-fold difference, reminiscent of the response observed with reserpine (Table 1). When forced by computational modeling into the “correct” orientation, the predicted binding constant is 93  $\mu$ M, which would substantiate the cell biology data and suggest a poorer binding to MutS than reserpine. The limitations of the resolution of structural modeling make it impossible to distinguish the binding affinity of this compound from the one of other methoxy compounds in the “correct” orientation.

Since ring 6 is attached to the remainder of the protein by a rotatable bond, the 3,4-dimethoxy benzoyl compound is indistinguishable from the 4,5-dimethoxy molecule. Whether the presence of two methoxy groups on this ring is sufficient for the induction of MSH2-dependent cell death, or this rotation and the resulting presence of methoxy groups in all three positions enable the appropriate response is unknown.

Methylenedioxybenzoyl has an additional ring system on ring 6. This compound is predicted to bind to MutS with a  $K_i$  of 19  $\mu$ M; however, the predicted binding is also found to be in a flipped conformation. The cell death response is opposite to the damage response generally observed in dependence of mismatch repair proteins. MSH2-deficient cells show a higher sensitivity to the compound than proficient ones (IC<sub>50</sub> of 36  $\mu$ M in MSH2-deficient ones, versus 51  $\mu$ M in MSH2-proficient cells, Table 1), reversing the resistance phenotype seen with cisplatin and reserpine/rescinnamine.

Cinnamoyl reserpine is a rescinnamine derivative that lacks the methoxy groups on ring 6, similar to the reserpine analog benzoyl. Again, similar to the corresponding reserpine analog, the predicted binding of cinnamoyl reserpine to MutS is predicted to occur in the flipped conformation with

		Predicted $K_i$ ( $\mu\text{M}$ )	Partition coefficient
Benzoyl		32	3.8
3-methoxybenzoyl		15	3.5
4-methoxybenzoyl		28	3.5
3,4-dimethoxybenzoyl		25	3.3
3,5-dimethoxybenzoyl		22	3.3
Methylenedioxy		19	ND
Cinnamoyl		14	ND

(a) Flipped Conformation

FIGURE 4: Continued.

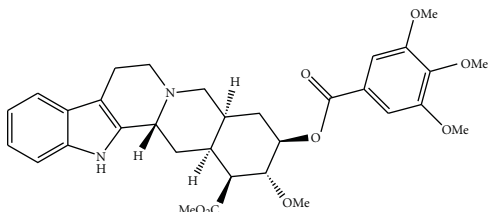
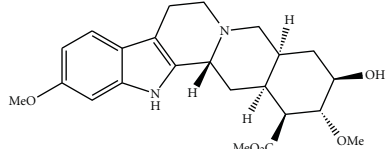
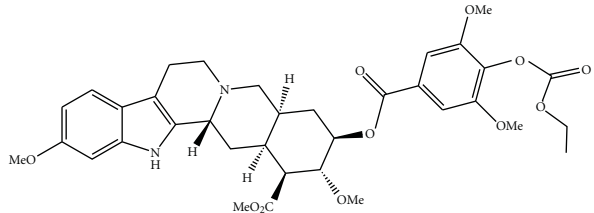
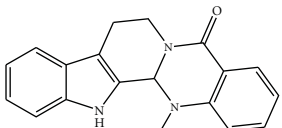
		Predicted $K_i$ ( $\mu\text{M}$ )	Partition coefficient
Deserpidine		133	3.6
(b) Mismatch-like binding			
Methyl reserpate		101	1*
Syrosingopine		1310	3.6
Evodiamine		ND	3.4
(c) Nonspecific and altered binding			

FIGURE 4: Structures of reserpine and rescinnamine derivatives are shown on the left and their corresponding predicted (calculated, as described in Section 2) binding constants and partition coefficients are displayed on the right. Derivatives are subdivided into their predicted binding modes: (a) flipped; (b) mismatch-like; and (c) nonspecific or altered (see also Figure 5).

a binding constant of  $14 \mu\text{M}$ . The compound induces cell death that is independent of functional MSH2 ( $\text{IC}_{50}$  value of  $150 \mu\text{M}$  in *MSH2*-deficient cells versus  $130 \mu\text{M}$  in *MSH2*-proficient cells; Figure 6(a), Table 1). This result confirms the structural prediction.

Together, these results suggest that the absence of essential methoxy groups on ring 6 that appear to position the molecules in the correct conformation triggers a different binding mode (Figure 5(b)) that does not result in MSH2-dependent cell death. Removal of these suggested, essential functional groups eliminates the MSH2-dependent cell death response.

**3.3.3. Mismatch-Like Binding.** The methoxy group on ring 1 was predicted to show unfavorable interactions with the MutS protein for reserpine, but not rescinnamine (Figure 3). A clinically relevant compound exists that has the general structure of reserpine, but lacks this methoxy group (deserpidine, Figure 4(b)). Though eliminating a suggestively unfavorable interaction, the predicted binding constant is

roughly 2-fold worse than that for reserpine ( $130 \mu\text{M}$ ), which suggests that even an “unfavorable” interaction may be required to correctly orient the molecule in the binding pocket.

The predicted binding mode for deserpidine is reminiscent of the binding of mismatched DNA to the protein. The molecule shows a stronger bending than other compounds and altered orientation that results in the molecule wrapping around the phenylalanine involved in coordinating mismatch binding (F36) (Figure 5(c)). The predicted specificity for the “death conformation” is reduced for this molecule, which would further confirm the predicted “mismatched DNA”-like binding mode.

The cell biology of this compound revealed cell death induction with no significant specificity for the presence of MSH2 ( $\text{IC}_{50}$  values of  $56 \mu\text{M}$  in *MSH2*-deficient versus  $49 \mu\text{M}$  in *MSH2*-proficient cells; Figure 6(b), Table 1), confirming the structural predictions. This result suggests that binding in the “mismatched DNA mode” eliminates MSH2-dependent cytotoxic response.

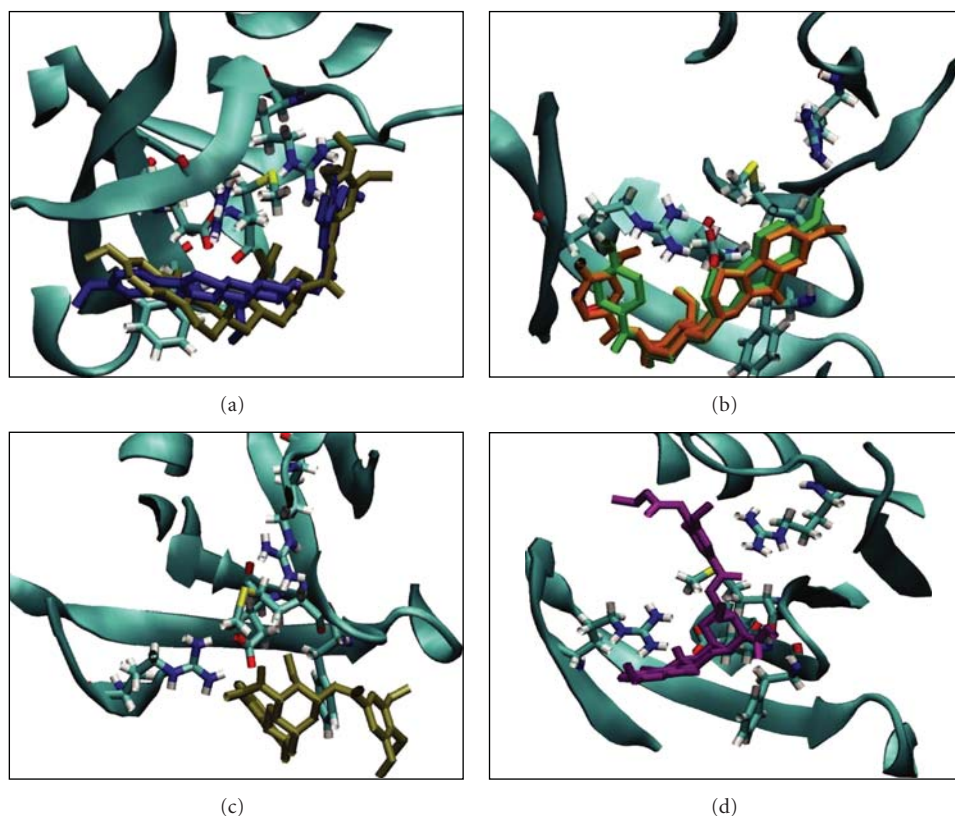


FIGURE 5: Predicted modes of binding of reserpine and rescinnamine derivatives include: (a) reserpine-like; (b) flipped; (c) mismatch-like; (d) nonspecific or altered.

**3.3.4. Nonspecific and Altered Binding.** Some compounds are predicted to bind MutS in an entirely altered conformation. Though binding is still observed in or close to the DNA-binding pocket, the general orientation of these compounds is altered when compared to the binding of reserpine/rescinnamine (Figure 5(d)).

Methyl Reserpate lacks the entire ring 6. This compound is predicted to bind in a distance to the actual binding pocket with a  $K_i$  of  $101 \mu\text{M}$ . The molecule only weakly induces cell death in either *MSH2*-proficient and *MSH2*-deficient cells with no preference for either cell line. The cell death response was not sufficient to reliably determine  $\text{IC}_{50}$  values.

Syrosingopine is a commercially available reserpine analog that has found application as an antihypertensive drug. Its predicted binding to the mismatch repair protein is the worst among the tested compounds, with a predicted  $K_i$  of  $1310 \mu\text{M}$ . This is largely due to the fact that its substitution on position 4 of ring 6 increases its length considerably, which interferes with the binding to the protein (Figures 4(c) and 5(d)). The binding of the molecule is hence highly “distorted” when compared to the interaction of reserpine/rescinnamine with the protein (compare Figures 5(a) and 5(d)).

Evodiamine, a compound described as aiding in diet-induced obesity [24], only contains ring systems 1-5 and lacks all methoxy groups seen in reserpine/rescinnamine.

This compound shows no specific binding in the computational docking experiments, and hence does not result in a predictable binding constant. In the cell system, this molecule shows no significant cytotoxic effect, in either the presence or absence of *MSH2* (Figure 6(a)). This is presumably due to the fact that evodiamine cannot establish any of the required interactions with the MMR protein.

Cells were treated with selected reserpine derivatives to determine their effect on cell viability and caspase-3 cleavage. *MSH2*-proficient and *MSH2*-deficient cells were treated with increasing concentrations ( $0$ – $250 \mu\text{M}$ ) of 3-methoxy reserpine, 3,4-dimethoxybenzoyl reserpine, 3,5-dimethoxybenzoyl reserpine, evodiamine, and deserpidine for 24 hours after which time their viability was assessed via MTS assay (Figure 6(a) and data not shown). Upon treatment with 3,5-dimethoxybenzoyl, no *MSH2*-dependent cell death was observed (data not shown). Upon treatment with 3,4-dimethoxybenzoyl reserpine, however, a 1.3-fold difference between *MSH2*-proficient and *MSH2*-deficient cells was observed, reminiscent of the increase in resistance to cisplatin in *MSH2*-deficient cells. This result indicates the importance of two methoxy groups on ring 6 of the small molecule. This cellular result provides further indirect evidence that the computational model, which is one of direct binding to a specific protein conformation, is valid.

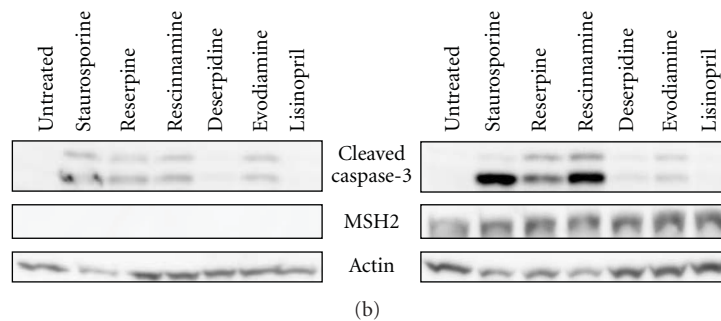
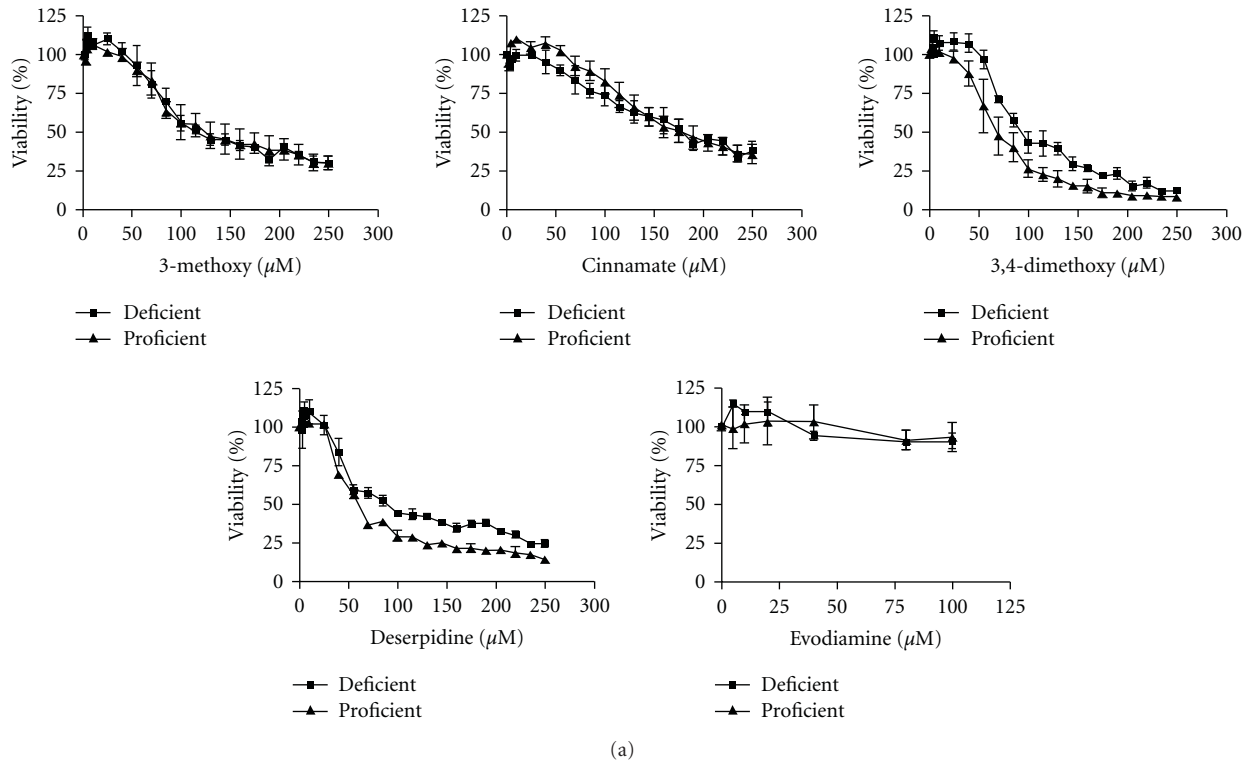


FIGURE 6: (a) Derivatives of reserpine and rescinnamine diminish cell viability in an *MSH2*-independent manner as shown by MTS assays with an exception of 3,4-dimethoxy reserpine, which demonstrates a slight dependence on *MSH2*. Evodiamine has an insignificant effect on cell viability. One representative from each of the predicted binding mode groups is shown. *MSH2*-deficient cells (■) and *MSH2*-proficient (▲) cell response is shown. (b) Caspase-3 cleavage was assessed in Hec59 (*MSH2*-deficient; left panel) and Hec59(2) (*MSH2*-proficient; right panel) cells when treated with various compounds. The 17 and 19 kDa cleavage products of caspase-3 are depicted. Staurosporine (STS) was used as a positive control; actin was used as a loading control. Lisinopril is an ACE inhibitor, like rescinnamine, and demonstrates rescinnamine's action as being independent of its antihypertensive properties.

Since rescinnamine exhibits the activity of an ACE inhibitor, we determined if the observed effect on cell viability is due to this activity. In comparison, another, structurally different ACE inhibitor, lisinopril [25], was added and cell viability determined. No effect on cell viability and caspase-3 activation was observed in either *MSH2*-proficient and *MSH2*-deficient cells (Figure 6(b)), suggesting a different function for rescinnamine in *MSH2*-dependent cell death.

#### 4. Discussion

MMR is one of the primary DNA repair pathways that maintain genome stability within every cell. Its significance is displayed by its contribution to carcinogenesis in cells deficient for a key MMR protein. Based on the increasing number of additional protein interactions MMR proteins undergo, they may participate in numerous other cellular functions that remain to be understood. Among these,

their participation in the response to cytotoxic agents and the initiation of cell death is of importance, particularly since defects in MMR proteins increase resistance to certain chemotherapeutic agents and lead to the clonal selection of MMR-deficient cells. We have previously described the response of MMR proteins to the chemotherapeutic agent cisplatin and predicted a “death conformation” that is selectively targeted. This “death conformation” can be accessed by a small molecule, reserpine that induces DNA damage-independent cell death. Our multiple cellular assays have provided indirect evidence that this model, which required direct binding of reserpine, is indeed correct. However, we do look forward to the day when direct binding can be observed with either refinements of current technologies, or with brand new technologies. We have here determined the particular parameters that allow reserpine and its analogs to access the predicted “death conformation” of MSH2/MSH6 and induce cell death. These parameters, although predicted based on our model, were verified by cellular assays, which provided indirect evidence for the appropriateness of our model. Our experimental data indicates that the length of the molecule and specific functional groups are required for the induction of cell death. In our model, these parameters are critical to maintain the correct orientation of the small molecules within the MSH2/MSH6-binding pocket. Small changes in this structure of reserpine abrogate the ability to induce MSH2-dependent cell death; which would not be surprising if our model of direct binding were correct. These results suggest that the development of an improved molecule for the induction of cell death that is based on reserpine will need to be closely designed upon the original structure of the molecule. Since rescinnamine proved to be the best compound, future designs would do well to be based on this structure. Since cinnamate, a derivative of rescinnamine without the trimethoxy groups on ring system 6, abrogates the MSH2-dependent cell death response, these groups are required for the observed activity.

## 5. Conclusions

Our data demonstrate the combining virtual screening with conformational modeling is a novel, valid approach to identify compounds that target highly specific structures and pathways. We show that, in at least the case, molecular dynamics simulations provide molecular conformations that are sufficiently accurate as to allow for targeting of specific conformations associated with specific molecular functions. In particular, we have shown that cell death can be induced by small molecules that have been screened against models for a specific “death” conformation of the MSH2/MSH6 complexes. We have demonstrated the effects of these small molecules, reserpine-analogs, via two distinct cell assays; MTS assay and caspase-activation, which are standard and commonly used tests for cell viability and apoptotic cell death. Furthermore, the combinatorial treatment of reserpine and cisplatin resulted in rapid, MSH2-independent cell death, suggesting that the combination treatment “overloads” the MSH2-dependent system, and the cell induces

death via a different pathway. This observation suggests that future mechanistic studies, well beyond the scope of this paper as few of the actors involved are known, would be fruitful in determining the precise signaling pathways induced in the MSH2-dependent and MSH2-independent cell-death pathways. A more detailed mechanistic study of the MSH2-dependent pathway would be useful in potentially providing another protein target. Understanding the mechanism of the MSH2-dependent pathway may provide treatment options for MMR-deficient tumors, which are found in many patients with colorectal cancers.

Taken together, our data determine the parameters required of reserpine analogs to induce MMR-dependent cell death that can be utilized to further develop chemicals targeting this particular cell death pathway.

## Acknowledgments

The authors thank Dr. Christa Colyer for valuable discussions and providing LC-MS experiments. The project described was supported by Grants nos. CA101829 and CA129373 from the National Cancer Institute. The content is solely the responsibility of the authors and does not necessarily represent the official views of the National Cancer Institute or the National Institutes of Health. Further support was provided from the Comprehensive Cancer Center and the Translational Science Institute at Wake Forest University Health Sciences. The computations were performed on the WFU DEAC cluster (<http://www.deac.wfu.edu/>), which is supported in part by WFU IS and WFU’s Associate Provost for Research. Additional storage was provided by IBM through a SUR grant. The authors thank WFU and IBM for their support. S. B. King, F. Salsbury, and K. D. Scarpinato contributed equally to the paper.

## References

- [1] L. Stojic, R. Brun, and J. Jiricny, “Mismatch repair and DNA damage signalling,” *DNA Repair*, vol. 3, no. 8-9, pp. 1091–1101, 2004.
- [2] R. Fishel and T. Wilson, “MutS homologs in mammalian cells,” *Current Opinion in Genetics and Development*, vol. 7, no. 1, pp. 105–113, 1997.
- [3] R. D. Kolodner and G. T. Marsischky, “Eukaryotic DNA mismatch repair,” *Current Opinion in Genetics and Development*, vol. 9, no. 1, pp. 89–96, 1999.
- [4] A. Bellacosa, “Functional interactions and signaling properties of mammalian DNA mismatch repair proteins,” *Cell Death and Differentiation*, vol. 8, no. 11, pp. 1076–1092, 2001.
- [5] T. A. Kunkel and D. A. Erie, “DNA mismatch repair,” *Annual Review of Biochemistry*, vol. 74, pp. 681–710, 2005.
- [6] J. A. E. Irving and A. G. Hall, “Mismatch repair defects as a cause of resistance to cytotoxic drugs,” *Expert Review of Anticancer Therapy*, vol. 1, no. 1, pp. 149–158, 2001.
- [7] J. Jiricny, “The multifaceted mismatch-repair system,” *Nature Reviews Molecular Cell Biology*, vol. 7, no. 5, pp. 335–346, 2006.
- [8] F. R. Salsbury Jr., J. E. Clodfelter, M. B. Gentry, T. Hollis, and K. D. Scarpinato, “The molecular mechanism of DNA damage recognition by MutS homologs and its consequences for cell

- death response," *Nucleic Acids Research*, vol. 34, no. 8, pp. 2173–2185, 2006.
- [9] S. Aebi, B. Kurdi-Haidar, R. Gordon et al., "Loss of DNA mismatch repair in acquired resistance to cisplatin," *Cancer Research*, vol. 56, no. 13, pp. 3087–3090, 1996.
- [10] P. Modrich, "Strand-specific mismatch repair in mammalian cells," *The Journal of Biological Chemistry*, vol. 272, no. 40, pp. 24727–24730, 1997.
- [11] S. Aebi, D. Fink, R. Gordon et al., "Resistance to cytotoxic drugs in DNA mismatch repair-deficient cells," *Clinical Cancer Research*, vol. 3, no. 10, pp. 1763–1767, 1997.
- [12] D. Fink, S. Nebel, S. Aebi et al., "The role of DNA mismatch repair in platinum drug resistance," *Cancer Research*, vol. 56, no. 21, pp. 4881–4886, 1996.
- [13] R. P. Topping, J. C. Wilkinson, and D. Scarpinato, "Mismatch repair protein deficiency compromises cisplatin-induced apoptotic signaling," *The Journal of Biological Chemistry*, vol. 284, no. 21, pp. 14029–14039, 2009.
- [14] P. Karran, "Mechanisms of tolerance to DNA damaging therapeutic drugs," *Carcinogenesis*, vol. 22, no. 12, pp. 1931–1937, 2001.
- [15] D. P. Lin, Y. Wang, S. J. Scherer et al., "An MSH2 point mutation uncouples DNA mismatch repair and apoptosis," *Cancer Research*, vol. 64, no. 2, pp. 517–522, 2004.
- [16] K. Drotschmann, R. P. Topping, J. E. Clodfelter, and F. R. Salsbury, "Mutations in the nucleotide-binding domain of MutS homologs uncouple cell death from cell survival," *DNA Repair*, vol. 3, no. 7, pp. 729–742, 2004.
- [17] G. Yang, S. J. Scherer, S. S. Shell et al., "Dominant effects of an Msh6 missense mutation on DNA repair and cancer susceptibility," *Cancer Cell*, vol. 6, no. 2, pp. 139–150, 2004.
- [18] A. Vasilyeva, J. E. Clodfelter, B. Rector, T. Hollis, K. D. Scarpinato, and F. R. Salsbury Jr., "Small molecule induction of MSH2-dependent cell death suggests a vital role of mismatch repair proteins in cell death," *DNA Repair*, vol. 8, no. 1, pp. 103–113, 2009.
- [19] G. Klopman, J. Li, S. Wang, and M. Dimayuga, "Computer automated logP calculations based on an extended group contribution approach," *Journal of Chemical Information and Computer Sciences*, vol. 34, no. 4, pp. 752–781, 1994.
- [20] H. L. Pearce, A. R. Safa, N. J. Bach, M. A. Winter, M. C. Cirtain, and W. T. Beck, "Essential features of the P-glycoprotein pharmacophore as defined by a series of reserpine analogs that modulate multidrug resistance," *Proceedings of the National Academy of Sciences of the United States of America*, vol. 86, no. 13, pp. 5128–5132, 1989.
- [21] A. Umar, M. Koi, J. I. Risinger et al., "Correction of hypermutability, N-Methyl-N'-nitro-N-nitrosoguanidine resistance, and defective dna mismatch repair by introducing chromosome 2 into human tumor cells with mutations in MSH2 and MSH6," *Cancer Research*, vol. 57, no. 18, pp. 3949–3955, 1997.
- [22] K. Drotschmann, W. Yang, F. E. Brownell, E. T. Kool, and T. A. Kunkel, "Asymmetric recognition of DNA local distortion," *The Journal of Biological Chemistry*, vol. 276, no. 49, pp. 46225–46229, 2001.
- [23] H. Wang, Y. Yang, M. J. Schofield et al., "DNA bending and unbending by MutS govern mismatch recognition and specificity," *Proceedings of the National Academy of Sciences of the United States of America*, vol. 100, no. 25, pp. 14822–14827, 2003.
- [24] Y. Kobayashi, Y. Nakano, M. Kizaki, K. Hoshikuma, Y. Yokoo, and T. Kamiya, "Capsaicin-like anti-obese activities of evodiamine from fruits of *Evodia rutaecarpa*, a vanilloid receptor agonist," *Planta Medica*, vol. 67, no. 7, pp. 628–633, 2001.
- [25] F. H. Messerli and U. R. Kaesser, "Lisinopril in the treatment of hypertension," *Journal of Human Hypertension*, vol. 3, no. 1, pp. 17–21, 1989.

## Review Article

# Early Steps in the DNA Base Excision Repair Pathway of a Fission Yeast *Schizosaccharomyces pombe*

**Kyoichiro Kanamitsu and Shogo Ikeda**

*Department of Biochemistry, Faculty of Science, Okayama University of Science, 1-1 Ridai-cho, Kita-ku, Okayama 700-0005, Japan*

Correspondence should be addressed to Shogo Ikeda, ikeda@dbc.ous.ac.jp

Received 21 June 2010; Accepted 12 August 2010

Academic Editor: Ashis Basu

Copyright © 2010 K. Kanamitsu and S. Ikeda. This is an open access article distributed under the Creative Commons Attribution License, which permits unrestricted use, distribution, and reproduction in any medium, provided the original work is properly cited.

DNA base excision repair (BER) accounts for maintaining genomic integrity by removing damaged bases that are generated endogenously or induced by genotoxic agents. In this paper, we describe the roles of enzymes functioning in the early steps of BER in fission yeast. Although BER is an evolutionarily conserved process, some unique features of the yeast repair pathway were revealed by genetic and biochemical approaches. AP sites generated by monofunctional DNA glycosylases are incised mainly by AP lyase activity of Nth1p, a sole bifunctional glycosylase in yeast, to leave a blocked 3' end. The major AP endonuclease Apn2p functions predominantly in removing the 3' block. Finally, a DNA polymerase fills the gap, and a DNA ligase seals the nick (Nth1p-dependent or short patch BER). Apn1p backs up Apn2p. In long patch BER, Rad2p endonuclease removes flap DNA containing a lesion after DNA synthesis. A UV-specific endonuclease Uve1p engages in an alternative pathway by nicking DNA on the 5' side of oxidative damage. Nucleotide excision repair and homologous recombination are involved in repair of BER intermediates including the AP site and single-strand break with the 3' block. Other enzymes working in 3' end processing are also discussed.

## 1. Introduction

DNA molecules in cells always suffer from chemical decay due to exposure to endogenous and environmental agents [1–3]. Cells die when the damage to DNA obstructs replication and transcription. Moreover, base damage causes mutations, which are responsible for cancer, aging, and the hereditary diseases [3–5]. Base excision repair (BER) is a DNA repair pathway directed mainly at nonbulky lesions, such as, alkylated and oxidized bases, and at some types of mismatched bases that are produced during replication or by deamination [3, 5–7]. The BER pathway is usually initiated by DNA glycosylase that removes damaged bases to leave apurinic/apyrimidinic (AP) sites. The AP sites are further processed by an AP endonuclease that cleaves phosphodiester bonds 5' to the AP site to leave a 3' OH and 5'-deoxyribose phosphate (5'-blocked end). Bifunctional DNA glycosylase associated with AP lyase removes damaged bases and cleaves 3' to the AP site, leaving a 3'- $\alpha$ , $\beta$ -unsaturated aldehyde (3'-blocked end) and a 5' phosphate. These blocked ends are subsequently converted into 3' OH and 5'

phosphate by appropriate enzymes. Finally, a repair DNA polymerase fills the gap, and a DNA ligase seals the nick.

The basic mechanism of BER was first elucidated in *Escherichia coli* [3]. Subsequent studies showed that the process is conserved in eukaryotes including the budding yeast *Saccharomyces cerevisiae* and mammals. Fission yeast (*Schizosaccharomyces pombe*) is an ascomycetous yeast that shares many fundamental cellular properties with higher multicellular eukaryotes [8]. Although *S. pombe* has been used as a prominent model organism, research of the BER pathway in yeast has started late. Completion of the *S. pombe* genome project in 2002 provided a list of the yeast BER machineries including DNA glycosylases and AP endonucleases, which are evolutionarily conserved from bacteria to man [9]. Over the past decade, the BER pathway of *S. pombe* has been fairly well characterized by genetic approaches using many BER-defective mutants constructed by gene targeting. Biochemical properties of BER enzymes were also examined using purified recombinant proteins. In this paper, we describe the roles of the enzymes involved in the early steps of BER in fission yeast with an emphasis on

TABLE 1: DNA glycosylases in bacteria, yeasts, and human cells.

<i>E. coli</i>	<i>S. cerevisiae</i>	<i>S. pombe</i>	Human	AP lyase
Ung	Ung1p	Ung1p	hUNG	
Mug		Thp1p	hTDG hSMUG1 hMBD4	–
AlkA	Mag1p	Mag1p Mag2p		
TagA			hMPG	
MutY		Myh1p	hMYH	
Nth1	Ntg1p Ntg2p	Nth1p	hNTH1	
	Ogg1p		hOGG1	+
Fpg				
Nei			hNEIL1 hNEIL2 hNEIL3	

outlining common features as well as differences with other model organisms.

## 2. DNA Glycosylases in *S. pombe*

DNA glycosylases identified in *E. coli*, *S. cerevisiae*, *S. pombe*, and the human are classified in Table 1 on the basis of their substrate specificities and structural features [3, 7, 10]. Monofunctional DNA glycosylase simply hydrolyzes the *N*-glycosidic bond to release damaged bases and leaves the AP site. Nth1 and Ogg1 DNA glycosylases are associated with AP lyase activity, which cleaves 3' to the AP site by  $\beta$  elimination, leaving a 3'- $\alpha,\beta$ -unsaturated aldehyde. *E. coli* Fpg and Nei and human NEILs are other types of bifunctional glycosylases which cleave the AP site by  $\beta,\delta$  elimination and generate a 3'-phosphate end. *S. pombe* has five monofunctional DNA glycosylases (Ung1p, Thp1p, Mag1p, Mag2p, and Myh1p) [11]. Unlike other organisms, Nth1p is a sole DNA glycosylase with AP lyase activity in *S. pombe* cells. Nth1 DNA glycosylase is  $\beta$  lyase and does not possess  $\delta$  lyase activity [2, 5, 7].

**2.1. Uracil DNA Glycosylases Ung1p and Thp1p Function in Avoidance of Spontaneous Mutation.** Deamination of cytosine residues in DNA occurs spontaneously in pH- and temperature-dependent reactions, and results in conversion to uracil [1, 3]. Cytosine deamination is estimated to produce 400 uracil residues per mammalian genome per day [12]. Promutagenic U:G mispair causes C:G to T:A transition mutations, if not repaired prior to DNA replication.

Uracil also occurs in DNA through incorporation of dUMP instead of dTMP by DNA polymerase during replication. Deamination of 5-methylcytosine in DNA results in the formation of thymine, and hence T:G mispairs. Uracil residues can be removed through the activity of uracil DNA glycosylase (UDG), which consists of four distinct families in mammalian cells: the UNG family (the major activity of UDG in cells), the MUG (mismatch-specific uracil DNA glycosylase)/TDG (thymine DNA glycosylase) family, the SMUG (single strand-specific monofunctional uracil-DNA glycosylase) family, and the MBD4 (methyl-binding domain 4) family [3, 5, 13]. The UDGs, other than MBD4, form a single protein superfamily with a common  $\alpha/\beta$ -fold structure and must have been evolved from a common ancestor [14].

*S. pombe* has two UDG genes, *ung1* (systematic name SPCC1183.06) and *thp1* (SPCC965.05c). The Ung1p protein is highly conserved (51% identity to human UNG) and localizes predominantly to the nucleus [15]. The bacterially expressed protein showed an apparent enzyme activity for uracil-containing DNA, which was inhibited by an inhibitor protein (UGI). Overexpression of *ung1* induces a DNA checkpoint-dependent cell cycle delay and causes cell death [15]. Human MUG/TDG was first isolated as an enzyme that excises thymine from T:G mispairs as well as uracil from U:G mispairs [16, 17]. *S. pombe* Thp1p is a member of the MUG family, and maintains a high level of glycosylase activity towards substrates containing U, 5-fluorouracil, 3,*N*<sup>4</sup>-ethenocytosine, and 5-hydroxyuracil [18]. Unlike human enzyme, Thp1p cannot excise thymine residues from the T:G mispair substrate. Since cytosine methylation is undetectable in fission yeast cells, the potential to process this substrate appears to be correlated with the degree of cytosine methylation in the genome of organisms [19]. Thp1p can also remove deaminated purine bases: xanthine and oxanine from guanine and hypoxanthine from adenine [20]. Both *ung1* and *thp1* mutants showed a moderate mutator phenotype [21]. Double mutation of the genes additively increased the mutation frequency. Moreover, expression of Ung1p and Thp1p suppressed spontaneous mutagenesis in UDG-deficient cells. These results indicate that both proteins play important roles in the prevention of spontaneous mutagenesis of *S. pombe* cells.

**2.2. Two AlkA Homologs Mag1p and Mag2p Function in Removal of Alkylated Base.** Alkylating agents such as methyl methanesulfonate (MMS) generate covalent modifications at nitrogen residues of DNA bases, in particular N3-methyladenine (3-meA) and N7-methylguanine (7-meG), which account for 11% and 83% among the alkylation bases by MMS, respectively [1, 3]. In contrast, 7-meG appears to be a harmless alteration while 3-meA is a cytotoxic lesion that blocks both replication and transcription. *S*-adenosylmethionine, which is a common cosubstrate involved in methyl group transfer, also takes part in the nonenzymatic methylation of DNA [1]. In a human cell, 3-mA and 7-mG spontaneously generate 600 and 4,000 residues a day, respectively [12].

In *E. coli*, alkylation products such as 3-meA and 7-meG are mainly removed by two structurally different

monofunctional DNA glycosylases, AlkA and TagA [3]. The *S. pombe* genome encodes two *alkA* paralogs *mag1* (SPAPB24D3.04c) and *mag2* (SPBC23G7.11). The amino acid sequences of Mag1p and Mag2p share 44.8% similarity. The *S. pombe mag1* gene was cloned by its ability to reverse the MMS-sensitive phenotype of an *E. coli alkA/tagA* double mutant [22]. The substrate range of Mag1p overproduced in *E. coli* is limited to the main alkylation products, such as, 3-meA, 3-meG, and 7-meG, whereas no significant activity was found toward deamination products, ethenoadducts, or oxidation products [23]. The efficiency of 3-meA and 3-meG removal was 5–10 times slower for Mag1p than for *E. coli* AlkA, whereas the two enzymes remove 7-meG at a similar rate. On the other hand, biochemical analysis of Mag2p has not been performed yet because the recombinant protein expressed in *E. coli* showed no glycosylase activity [23].

Mutant strains *mag1Δ* and *mag2Δ* hardly showed MMS sensitivity [23–25]. The BER mutants *nth1Δ*, *apn2Δ*, and *rad2Δ* were sensitive to MMS, while the double mutants *nth1Δ/mag1Δ*, *apn2Δ/mag1Δ*, and *rad2Δ/mag1Δ* restored resistance to MMS [23, 25]. This showed that Mag1p is involved in the initial step of MMS-damaged repair both by the Nth1p-dependent short patch BER pathway and by the Rad2p (flap endonuclease)-dependent long patch BER pathway (Figure 1). Moreover, double mutant *nth1Δ/mag2Δ* was more resistant to MMS than *nth1Δ*, indicating that Mag2p also functions in the removal of alkylated bases [25]. *rad16* encodes an XPF homolog that functions as a DNA repair endonuclease in nucleotide excision repair (NER). The double mutant of *rad16* with *mag1* or *mag2* increased sensitivity to MMS [25]. In addition, the *rad16Δ/mag1Δ/mag2Δ* triple mutant exhibited the highest MMS sensitivity. Expression of Mag1p or Mag2p in the triple mutant restored tolerance to MMS. These results showed that BER and NER could independently repair the alkylation DNA damage. Comparison of the substrate specificity and kinetic parameters of Mag1p and Mag2p will be needed to dissect the precise roles of these redundant enzymes in MMS resistance. *rhp51* encodes a RecA-like protein that functions in homologous recombination (HR). The double mutant of *rhp51* with *mag1* decreased the sensitivity to chronic MMS exposure compared with *rhp51Δ* single mutant [24]. In addition, spontaneous intrachromosomal recombination frequencies increased 3-fold in the *mag1* mutant [23]. These results show that both Mag1p and HR contribute to repair of the alkylation base. Deletion of *mag1* from *nth1*, *rad16*, or *rad2* decreased the recombination frequency, indicating that AP sites generated by Mag1p removal of spontaneous base lesions are substrates of short patch BER, long patch BER, NER, and HR [23].

### 2.3. Nth1p Is the Major Contributor for Incision of the AP Site.

An 8-oxoguanine (8-oxoG) produced by the oxidation of the guanine residue in G:C could pair not only with cytosine but also with adenine, and the G:C to T:A mutation occurs during the next stage of replication [3, 5, 7]. In a human cell, about 1,000 residues of 8-oxoG are generated per genome in a day [12]. Bifunctional DNA glycosylases Fpg (MutM) in *E. coli* and OGG1 in budding yeast and mammals can

excise 8-oxoG paired with cytosine. Thymine glycol (Tg), which is the oxidation product of thymine, interrupts DNA replication and transcription. In human cells, production of Tg and similar oxidized pyrimidines is estimated to be 500 residues per genome per day [12]. In *E. coli* endonuclease III (Nth) and endonuclease VIII (Nei) excise Tg and oxidized pyrimidines from DNA and subsequently cleave the strand by AP lyase activity [3]. *S. pombe* has no homolog of Fpg, OGG1, or Nei [11].

The *S. pombe nth1* gene (SPAC30D11.07) was cloned on the basis of homology to *E. coli nth* [26]. Nth1 family proteins have a helix-hairpin-helix motif in the vicinity of the active lysine residue and an iron-sulfur cluster [4Fe-4S] at the C terminal. In addition, a eukaryote's enzyme has a nuclear localization signal. Indeed, fusion protein of *S. pombe* Nth1p with green fluorescent protein was predominantly localized in the nucleus [27]. Unlike budding yeast Ntg1p and the enzyme in mammals, *S. pombe* Nth1p was not observed in mitochondria.

A recombinant *S. pombe* Nth1p expressed in *E. coli* shows a broad substrate specificity. Mass spectrometry of released bases from oxidized DNA by treatment of Nth1p revealed that the enzyme efficiently excised five pyrimidine-derived lesions: 5-hydroxycytosine, Tg, 5-hydroxy-6-hydrothymine, 5, 6-dihydroxycytosine, and 5-hydroxyuracil [28]. *S. pombe* Nth1p could remove 5-formyluracil and 5-hydroxymethyluracil as efficiently as *E. coli* Nth [29]. Moreover, 8-oxoG in 8-oxoG:G and 8-oxoG:A mispair is also the substrate for *S. pombe* Nth1p. The expression of *S. pombe* Nth1p reduced hydrogen peroxide (H<sub>2</sub>O<sub>2</sub>) toxicity and the frequency of spontaneous mutations in the *E. coli nth/nei* double mutant [29]. Although the *S. pombe nth1Δ* is sensitive to MMS, Nth1p did not remove 3-meA and 7-meG [30]. However, methyl-formamidepyrimidine, a cytotoxic lesion generated from 7-meG by opening the imidazole ring, was excised efficiently by Nth1p. Nicking activity to oligonucleotides containing Tg and the AP site virtually disappeared in the extract from *nth1Δ* cells, indicating that these lesions are mainly incised by Nth1p in the yeast cell [27].

An *nth1Δ* strain was tolerant to oxidative damage (H<sub>2</sub>O<sub>2</sub> and menadione) and UV irradiation, but exhibited moderate sensitivity to MMS [27, 30, 31]. In addition, the mutant strain exhibited a more than 6-fold increase in the frequency of interchromosomal recombination [30]. Epistasis analysis of the *nth1* gene versus *rad2*, *rad16*, and *rhp55* showed that MMS damage could be repaired through NER and HR other than the BER pathway [30]. Although a mutant of the major AP endonuclease gene *apn2* showed hypersensitivity to MMS, double mutation of *nth1* and *apn2* became tolerant to MMS [31]. This shows that Nth1p functions upstream of Apn2p in the same pathway; that is, the 3'-blocked end generated by Nth1p is converted to 3' OH by phosphodiesterase activity of Apn2p (Figure 1). In *S. pombe* cells, Nth1p not only removes the oxidized base as DNA glycosylase, but also incises a large portion of the AP site generated by the action of Mag1p and Mag2p DNA glycosylases. Thus, Nth1p plays a central role during early steps of the BER pathway in the fission yeast [27].

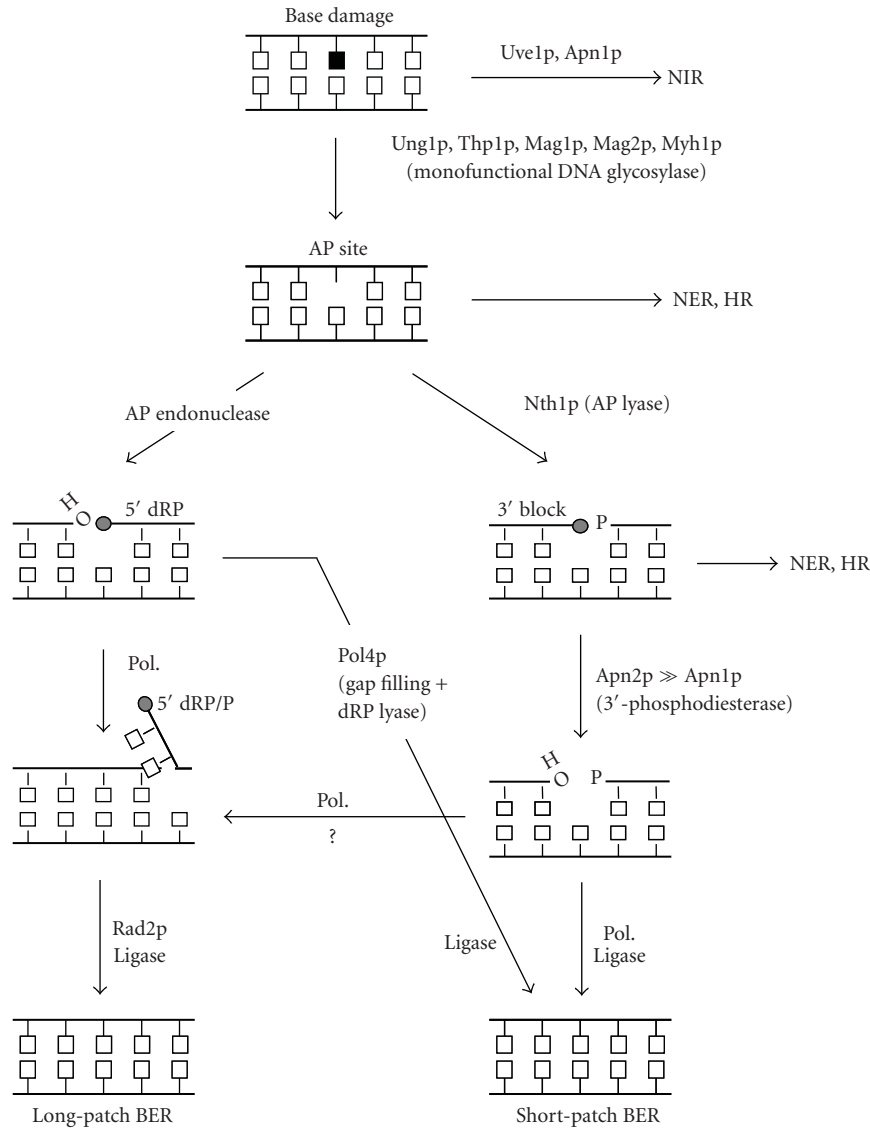


FIGURE 1: A schematic illustration of the BER pathway in *S. pombe*. In the Nth1p-dependent (or short patch) pathway, repair of the AP site is initiated by incision of Nth1p leaving the 3'-block. Apn2p functions primarily in the removal of the 3'-block, and poorly in the incision of AP sites. Apn1p is a back-up enzyme for 3'-phosphodiesterase activity of Apn2p. Finally, a DNA polymerase (Pol.) fills the gap, and a DNA ligase seals the nick. NER and HR could repair a part of the AP sites and single-strand breaks with 3' blocks. AP endonuclease incises the AP site leaving 5'-dRP end, which will be removed by 5'-dRP lyase activity of Pol4p to feed into short-patch BER. In the long patch pathway, Rad2p incises the flap DNA containing the lesion after DNA synthesis. Uve1p and Apn1p are possibly involved in the NIR pathway. Details are discussed in the text.

**2.4. DNA Glycosylase for Mismatch.** An 8-oxoG:A mispair in DNA, which is generated by incorporation of an adenine residue opposite to 8-oxoG, leads to a G:C to T:A mutation [3, 5]. The repair of this mismatch is initiated by excision of an adenine residue by adenine-specific mismatch DNA glycosylase (MutY in *E. coli*). The *mutY* homolog of *S. pombe*, namely, *myh1* (SPAC26A3.02), has been cloned [32]. Expression of Myh1p in the *mutY* mutant of *E. coli* could reduce the spontaneous mutation frequency of the cells. Purified Myh1p recognized A:G and A:8-oxoG, as well as 2-aminopurine:G and A:2-aminopurine [32]. In addition,

Myh1p probably prevents a C:G to G:C transversion mutation because it can remove the guanine from G:8-oxoG [33]. The *myh1Δ* strain displays a 36-times higher frequency of spontaneous mutation than the wild strain [34]. Moreover, *myh1Δ* showed sensitivity to H<sub>2</sub>O<sub>2</sub>. Myh1p binds to proliferative cell nuclear antigen (PCNA) and PCNA-like heterotrimer Rad9p/Rad1p/Hus1p [35–37]. All subunits of the latter complex are required for proper functioning of the checkpoint and DNA replication under stress [38]. Myh1p may act as an adaptor to recruit checkpoint proteins to the DNA lesion [36].

TABLE 2: AP endonucleases in bacteria, yeasts, and human cells.

<i>E. coli</i>	<i>S. cerevisiae</i>	<i>S. pombe</i>	Human
<b>Xth</b>			<b>hAPE1</b>
	Apn2p	<b>Apn2p</b>	hAPE2
Nfo	<b>Apn1p</b>	Apn1p (Uve1p)	

AP endonucleases showed in boldface contribute to the major activities in each organism.

### 3. AP Endonucleases in *S. pombe*

AP sites are generated by removal of damaged bases by monofunctional DNA glycosylase and more frequently by nonenzymatic hydrolysis of the *N*-glycosidic bond of DNA [1, 3]. In a human cell, about 9,000 residues of the AP sites arise per genome in a day [12]. AP endonuclease hydrolyzes phosphodiester bonds 5' to the AP site to leave 3' OH and 5'-deoxyribose phosphate (dRP). *E. coli* has two types of AP endonuclease, exonuclease III (Xth), and endonuclease IV (Nfo) [3, 39]. AP endonucleases from various organisms are classified on the basis of structural similarity to Xth and Nfo (Table 2). APE1 in mammals is an Xth-type homolog, which accounts for more than 90% of the AP endonuclease activity in cells [3, 39]. A second Xth-type homolog APE2 was found [40, 41], but no Nfo-type enzymes were present in mammalian cells. On the other hand, yeasts have an Nfo-type homolog Apn1p other than Apn2p with similarity to mammalian APE2. In the budding yeast, Apn1p is the major contributor of AP endonuclease activity [39]. Both Xth and Nfo types of AP endonuclease could also convert 3' blocked ends (e.g., 3'- $\alpha$ , $\beta$ -unsaturated aldehyde, phosphoglycolate, and phosphate termini) to 3' OH. Therefore, 3'-phosphodiesterase and 3'-phosphatase activity of AP endonuclease is essential for the repair of single-strand breaks induced by reactive oxygen species (ROS), ionized radiation, and bleomycin [39, 42].

**3.1. Apn2p Predominantly Functions in the Removal of 3' Blocks.** The *S. pombe* *apn2* gene (SPBC3D6.10) encodes an AP endonuclease with homology to *S. cerevisiae* Apn2p and human APE2 [40, 41, 43, 44]. The N-terminal region of the protein has homology with Xth. Notably, Apn2p maintains the entire critical catalytic residue of hAPE1, which is also conserved in several proteins recently predicted to maintain the four-layered  $\alpha/\beta$  of Xth and the "nonspecific" nuclease DNase I [45, 46]. The C-terminal region of Apn2p protein contains a binding motif similar to PCNA and a sequence homologous to DNA topoisomerase III (TOP3) family [40, 41, 47]. Physical interaction of *S. cerevisiae* Apn2p with PCNA stimulates the 3' to 5' exonuclease and 3'-phosphodiesterase activities of Apn2p *in vitro* [47]. However, the PCNA-binding motif and the TOP3-homologous region of *S. pombe* Apn2p are dispensable for BER of MMS damage in cells [44, 48]. It remains to be elucidated whether Apn2p binds to *S. pombe* PCNA *in vitro* and *in vivo*. Apn2p is predominantly localized in the nucleus [49].

Cells lacking Apn2p exhibit severe hypersensitivity to treatment with MMS and bleomycin analogues [31, 44, 49]. The mutation rate of *apn2* $\Delta$  cells rose remarkably by MMS [44]. Incision activity to oligonucleotides containing an AP site (or tetrahydrofuran) was significantly reduced in the extract from *apn2* $\Delta$  cells [44, 49]. These results show that Apn2p is the major contributor of AP endonuclease activity in *S. pombe* cells. Disruption of *nth1* in *apn2* $\Delta$  cells restored tolerance to MMS, indicating that Apn2p functions downstream of Nth1p in the same pathway (Figure 1). Although overexpression of Apn2p in *nth1* $\Delta$  failed to suppress MMS sensitivity, hAPE1 and *S. cerevisiae* Apn1p reduced the MMS sensitivity of *nth1* $\Delta$  cells to the wild type level [27, 49]. This result suggests that Apn2p cannot begin repair of the AP site in cells in spite of the fact that the enzyme can cleave the AP site *in vitro*. *S. pombe* Apn2p predominantly functions in the removal of 3' blocks induced by Nth1p. *Trans*-complementation of *S. cerevisiae* Apn1p strongly reflects differences in the major pathway for processing the AP sites between *S. cerevisiae* and *S. pombe* cells.

**3.2. Other AP Endonucleases of *S. pombe*.** *apn1* (SPCC622.17) encodes an Nfo-type AP endonuclease [50]. Although the *APN1* mutant of *S. cerevisiae* is hypersensitive to MMS, the *S. pombe* *apn1* mutant exhibited no sensitivity to MMS and oxidative stress. In addition, the *nth1* $\Delta$ /*apn1* $\Delta$  double mutant showed the same MMS sensitivity as the *nth1* $\Delta$  single mutant [30]. However, the *apn2* $\Delta$ /*apn1* $\Delta$  double mutant was more sensitive than the *apn2* $\Delta$  single mutant [44]. Moreover, when Apn1p was overexpressed in *apn2* $\Delta$  cells, MMS sensitivity was partially restored [49]. Therefore, Apn1p removes the 3'-blocked end as a back-up function of the major enzyme Apn2p (Figure 1). Since Apn1p was observed in both the nucleus and cytoplasm, it possibly functions in more than just nuclear DNA repair [49]. *S. cerevisiae* Apn1p has been shown to move into the mitochondria to maintain genomic stability [51].

Uve1p (SPBC19C7.09c), which is primarily a UV-photoproduct specific endonuclease of *S. pombe*, could recognize non-UV-induced DNA damage (e.g., the AP site and dihydrouracil) and mismatched bases *in vitro*, and hydrolyze immediately 5' to the damage [52, 53]. The protein has a TIM barrel fold that is very similar to the structure of Nfo [54]. *S. cerevisiae* has no reported Uve1p homolog. Deletion of the *uve1* gene in *apn2* $\Delta$  significantly increased MMS sensitivity [44]. *Neurospora crassa* Uve1p could complement *E. coli* *xth* $\Delta$ /*nfo* $\Delta$  with respect to sensitivity to MMS and *t*-butyl hydroperoxide [55]. The mutation frequency of *uve1* $\Delta$  increased when treated with H<sub>2</sub>O<sub>2</sub> [56]. This effect was additively elevated by the deletion of *apn2*, indicating that both Uve1p and Apn2p contribute to the avoidance of H<sub>2</sub>O<sub>2</sub>-induced mutagenesis, but these enzymes define a distinct oxidative damage repair pathway. *E. coli* Nfo and *S. cerevisiae* Apn1p can nick DNA on the 5' side of several oxidized base lesions, generating a 3' OH and a 5' dangling damaged nucleotide, which provide an alternative nucleotide incision repair (NIR) pathway to the classic BER [57, 58]. Therefore, *S. pombe* Uve1p and Apn1p possibly engage in the NIR

pathway by nicking oxidative damage on DNA in an Nth1p-independent manner (Figure 1). In such a case, damaged bases might be removed by a flap endonuclease, Rad2p, after long-patch repair DNA synthesis is primed by the actions of Uve1p and Apn1p [59, 60]. Uve1p works efficiently in mitochondria as well as in the nucleus [61].

**3.3. Short- and Long-Patch Repair Subpathways.** In the Nth1-dependent repair pathway, 3'-phosphodiesterase activity of AP endonuclease removes 3'-blocked end resulting in a 1-nt gap, which will be refilled via short-patch BER (Figure 1). However, it is not known whether the BER synthesis extends beyond a single nucleotide, with incorporation of two or more nucleotides (long-patch BER). When AP endonuclease incises the AP site, single-strand break with 3'-OH and 5'-dRP ends is generated. The dRP moiety is released by combined action of a DNA polymerase and Rad2p endonuclease (long-patch BER). An X-family DNA polymerase of *S. pombe*, Pol4p, has been shown to contain an intrinsic 5'-dRP lyase activity like mammalian DNA polymerases  $\beta$  and  $\lambda$ , suggesting another AP endonuclease pathway to feed into short-patch BER (Figure 1) [62]. *S. cerevisiae* Trf4 protein plays a similar role in short-patch BER of the yeast [63]. In mammalian cells, the choice of short-patch or long-patch BER may depend on the state of the 5' terminal moiety and protein-protein interaction of BER components [64]. *In vitro* analyses of repair synthesis with whole cell extracts or purified enzymes are needed to clarify the relative contribution of short-patch and long-patch BER in *S. pombe* cells.

#### 4. Enzymes for Removing 3' Blocked Ends in *S. pombe* Cells

Single-strand breaks with 3' phosphate ends in DNA are induced by chemical attacks of endogenous ROS and environmental oxidants [3]. Fpg/Nei-type DNA glycosylases cleave the AP site by  $\beta, \delta$  elimination and generate DNA strand breaks with a 3'-phosphate end. In human cells, removal of 3' phosphate is dependent on 3'-DNA phosphatase (hPNK), and not the major AP endonuclease hAPE1 [65]. Unlike bacteria and humans, *S. pombe* does not possess Fpg/Nei-type DNA glycosylase, and the physiological source of 3' phosphate in the yeast is probably due to the action of tyrosyl-DNA phosphodiesterase I (TDP1). TDP1 catalyzes the hydrolysis of 3'-phosphotyrosyl bonds of the irreversible topoisomerase I (Top1)-DNA covalent complex to generate a 3'-phosphate end [66, 67]. A 3'-DNA phosphatase (Pnk1p; SPAC23C11.04c) has been purified from *S. pombe* on the basis of its ability to process H<sub>2</sub>O<sub>2</sub>-damaged DNA to allow DNA synthesis by DNA polymerase [68]. Like human PNK, Pnk1p localizes in nuclei and has both 5'-DNA kinase and 3'-DNA phosphatase activities [69]. The *pnk1* mutant showed hypersensitivity to ionizing radiation and camptothecin, an inhibitor Top1, but not to MMS. It remains to be elucidated whether Pnk1p is the major 3'-DNA phosphatase in *S. pombe* cells.

TDP1 has been implicated in the repair of the irreversible Top1-DNA covalent complex, which can be generated by

either exogenous or endogenous factors [67]. Additionally, TDP1 hydrolyses a variety of 3' lesions, including 3' phosphoglycolate [70, 71]. A recessive mutation in the human (*TDPI*) gene is responsible for the inherited disorder, spinocerebellar ataxia with axonal neuropathy (SCAN1) [72]. A *tdp1* (SPCP31B10.05) mutant of *S. pombe* was completely sensitive to camptothecin [73]. Moreover, the mutant cells progressively accumulate DNA damage and rapidly lose viability in nondividing conditions [73]. Low cellular respiration levels protected the *tdp1* $\Delta$  cells, indicating that the production of endogenous ROS is a major cause for the accumulation of DNA lesions in the absence of Tdp1p [73]. Therefore, Tdp1p with Pnk1p processes the same naturally occurring 3' ends, produced from oxidative DNA damage. Rapid and extensive death of the *tdp1* $\Delta$ /*rhp51* $\Delta$  double mutant strain suggested the pivotal role of the HR process in DNA repair in *tdp1* $\Delta$  cells [73].

#### 5. BER in a Catalase-Deficient Mutant of *S. pombe*

The BER mutants of *S. pombe* are substantially resistant to H<sub>2</sub>O<sub>2</sub>. A catalase-deficient mutant (*ctt1* $\Delta$ ), in which ROS scavenging activity is extensively reduced, became sensitive to H<sub>2</sub>O<sub>2</sub> [74, 75]. Deletion of the BER gene (*nth1*, *apn1*, *apn2*, or *uve1*) from *ctt1* $\Delta$  further increased the sensitivity to H<sub>2</sub>O<sub>2</sub>, indicating that catalase activity obscures the functions of BER enzymes *in vivo* [75]. Double mutants in both *ctt1* and BER genes showed extremely high spontaneous mutation rates, especially in the *ctt1/nth1* mutant. Vitamin C relieved the mutator phenotype of the *ctt1/nth1* mutant [75]. The results provide evidence that BER enzymes as well as catalase and an antioxidant contribute *in vivo* to avoidance of ROS-induced mutagenesis and cell death.

#### 6. Conclusion

In this paper, we described the early steps of BER in the fission yeast highlighting the key roles of DNA glycosylases, AP endonucleases, and other end-cleaning activities in maintenance of genomic integrity. Although the yeast BER pathway consists of evolutionarily conserved enzymes, the major activity for processing the AP site is different from these of the budding yeast and mammals. AP sites generated by monofunctional glycosylase are mainly repaired via the Nth1p-dependent BER pathway [23, 27, 30, 31]. Unlike other model organisms, the major AP endonuclease of this yeast is assigned to Apn2p, which works primarily in the removal of the 3' block, and poorly in the incision of AP sites [23, 44, 49]. Uve1p engages in an Nth1p-independent pathway by nicking DNA on the 5' side of oxidative damage [56, 75]. Genetic interactions of BER genes with NER and HR genes suggest synergism among the different DNA repair pathways in the protection of alkylation and oxidative damage [23–25, 30]. NER and HR probably repair the intermediates of BER such as, the AP site and single-strand breaks with 3' blocks. BER operates most efficiently when specific protein-protein coordination occurs [76]. A study of physical interaction

of the BER proteins will facilitate an understanding of the regulation of BER protein activities and crosstalk between BER and other DNA transaction pathways in yeast cells. Upon nitrogen-starvation, mostly G<sub>2</sub> vegetative *S. pombe* cells promote two rounds of division and enter the G<sub>0</sub> state with 1C DNA [77]. The *S. pombe* G<sub>0</sub> state will provide an excellent model to reconsider the roles of BER and other DNA pathways in resting and nondividing physiological conditions [73, 78].

## Acknowledgment

This work was supported in part by the Ministry of Education, Culture, Sports, Science and Technology of Japan through a Financial Assistance Program of the Social Cooperation Study (2006-2010).

## References

- [1] T. Lindahl, "Instability and decay of the primary structure of DNA," *Nature*, vol. 362, no. 6422, pp. 709–715, 1993.
- [2] R. De Bont and N. van Larebeke, "Endogenous DNA damage in humans: a review of quantitative data," *Mutagenesis*, vol. 19, no. 3, pp. 169–185, 2004.
- [3] E. C. Friedberg, G. C. Walker, W. Siede, R. D. Wood, R. A. Schultz, and T. Ellenberger, *DNA Repair and Mutagenesis*, ASM Press, Washington, DC, USA, 2nd edition, 2006.
- [4] M. S. Cooke, M. D. Evans, M. Dizdaroglu, and J. Lunec, "Oxidative DNA damage: mechanisms, mutation, and disease," *FASEB Journal*, vol. 17, no. 10, pp. 1195–1214, 2003.
- [5] D. E. Barnes and T. Lindahl, "Repair and genetic consequences of endogenous DNA base damage in mammalian cells," *Annual Review of Genetics*, vol. 38, pp. 445–476, 2004.
- [6] H. Nilsen and H. E. Krokan, "Base excision repair in a network of defence and tolerance," *Carcinogenesis*, vol. 22, no. 7, pp. 987–998, 2001.
- [7] M. L. Hegde, T. K. Hazra, and S. Mitra, "Early steps in the DNA base excision/single-strand interruption repair pathway in mammalian cells," *Cell Research*, vol. 18, no. 1, pp. 27–47, 2008.
- [8] M. Yanagida, "The model unicellular eukaryote, *Schizosaccharomyces pombe*," *Genome Biology*, vol. 3, no. 3, pp. 2003.1–2003.4, 2002.
- [9] V. Wood, R. Gwilliam, M.-A. Rajandream et al., "The genome sequence of *Schizosaccharomyces pombe*," *Nature*, vol. 415, no. 6874, pp. 871–880, 2002.
- [10] K. Hitomi, S. Iwai, and J. A. Tainer, "The intricate structural chemistry of base excision repair machinery: implications for DNA damage recognition, removal, and repair," *DNA Repair*, vol. 6, no. 4, pp. 410–428, 2007.
- [11] O. Fleck, "DNA repair pathway," in *The Molecular Biology of Schizosaccharomyces pombe*, R. Egel, Ed., pp. 101–115, Springer, Berlin, Germany, 2004.
- [12] T. A. Kunkel, "The high cost of living," *Trends in Genetics*, vol. 15, no. 3, pp. 93–94, 1999.
- [13] S.-I. Yonekura, N. Nakamura, S. Yonei, and Q.-M. Zhang-Akiyama, "Generation, biological consequences and repair mechanisms of cytosine deamination in DNA," *Journal of Radiation Research*, vol. 50, no. 1, pp. 19–26, 2009.
- [14] L. Aravind and E. V. Koonin, "The alpha/beta fold uracil DNA glycosylases: a common origin with diverse fates," *Genome Biology*, vol. 1, no. 4, pp. research0007.1–research0007.87, 2000.
- [15] R. T. Elder, X. Zhu, S. Priet et al., "A fission yeast homologue of the human uracil-DNA-glycosylase and their roles in causing DNA damage after overexpression," *Biochemical and Biophysical Research Communications*, vol. 306, no. 3, pp. 693–700, 2003.
- [16] K. Wiebauer and J. Jiricny, "In vitro correction of G·T mispairs to G·C pairs in nuclear extracts from human cells," *Nature*, vol. 339, no. 6221, pp. 234–236, 1989.
- [17] P. Neddermann, P. Gallinari, T. Lettieri et al., "Cloning and expression of human G/T mismatch-specific thymine-DNA glycosylase," *The Journal of Biological Chemistry*, vol. 271, no. 22, pp. 12767–12774, 1996.
- [18] U. Hardeland, M. Bentele, J. Jiricny, and P. Schär, "The versatile thymine DNA-glycosylase: a comparative characterization of the human, Drosophila and fission yeast orthologs," *Nucleic Acids Research*, vol. 31, no. 9, pp. 2261–2271, 2003.
- [19] D. Cortázar, C. Kunz, Y. Saito, R. Steinacher, and P. Schär, "The enigmatic thymine DNA glycosylase," *DNA Repair*, vol. 6, no. 4, pp. 489–504, 2007.
- [20] L. Dong, R. Mi, R. A. Glass, J. N. Barry, and W. Cao, "Repair of deaminated base damage by *Schizosaccharomyces pombe* thymine DNA glycosylase," *DNA Repair*, vol. 7, no. 12, pp. 1962–1972, 2008.
- [21] M. Ikeda, R. Ikeda, and S. Ikeda, "Spontaneous mutation in uracil DNA glycosylase-deficient cells of a fission yeast *Schizosaccharomyces pombe*," *Current Topics in Biochemical Research*, vol. 11, no. 1, pp. 55–60, 2009.
- [22] A. Memisoglu and L. Samson, "Cloning and characterization of a cDNA encoding a 3-methyladenine DNA glycosylase from the fission yeast *Schizosaccharomyces pombe*," *Gene*, vol. 177, no. 1-2, pp. 229–235, 1996.
- [23] I. Alseth, F. Osman, H. Korvald et al., "Biochemical characterization and DNA repair pathway interactions of Mag1-mediated base excision repair in *Schizosaccharomyces pombe*," *Nucleic Acids Research*, vol. 33, no. 3, pp. 1123–1131, 2005.
- [24] A. Memisoglu and L. Samson, "Contribution of base excision repair, nucleotide excision repair, and DNA recombination to alkylation resistance of the fission yeast *Schizosaccharomyces pombe*," *Journal of Bacteriology*, vol. 182, no. 8, pp. 2104–2112, 2000.
- [25] K. Kanamitsu, H. Tanihigashi, Y. Tanita, S. Inatani, and S. Ikeda, "Involvement of 3-methyladenine DNA glycosylases Mag1p and Mag2p in base excision repair of methyl methanesulfonate-damaged DNA in the fission yeast *Schizosaccharomyces pombe*," *Genes and Genetic Systems*, vol. 82, no. 6, pp. 489–494, 2007.
- [26] T. Roldán-Arjona, C. Anselmino, and T. Lindahl, "Molecular cloning and functional analysis of a *Schizosaccharomyces pombe* homologue of *Escherichia coli* endonuclease III," *Nucleic Acids Research*, vol. 24, no. 17, pp. 3307–3312, 1996.
- [27] T. Sugimoto, E. Igawa, H. Tanihigashi, M. Matsubara, H. Ide, and S. Ikeda, "Roles of base excision repair enzymes Nth1p and Apn2p from *Schizosaccharomyces pombe* in processing alkylation and oxidative DNA damage," *DNA Repair*, vol. 4, no. 11, pp. 1270–1280, 2005.
- [28] B. Karahalil, T. Roldán-Arjona, and M. Dizdaroglu, "Substrate specificity of *Schizosaccharomyces pombe* Nth protein for products of oxidative DNA damage," *Biochemistry*, vol. 37, no. 2, pp. 590–595, 1998.

- [29] S.-I. Yonekura, N. Nakamura, T. Doi et al., "Recombinant *Schizosaccharomyces pombe* Nth1 protein exhibits DNA glycosylase activities for 8-oxo-7,8-dihydroguanine and thymine residues oxidized in the methyl group," *Journal of Radiation Research*, vol. 48, no. 5, pp. 417–424, 2007.
- [30] F. Osman, M. Björås, I. Alseth et al., "A new *Schizosaccharomyces pombe* base excision repair mutant, nth1, reveals overlapping pathways for repair of DNA base damage," *Molecular Microbiology*, vol. 48, no. 2, pp. 465–480, 2003.
- [31] I. Alseth, H. Korvald, F. Osman, E. Seeberg, and M. Björås, "A general role of the DNA glycosylase Nth1 in the abasic sites cleavage step of base excision repair in *Schizosaccharomyces pombe*," *Nucleic Acids Research*, vol. 32, no. 17, pp. 5119–5125, 2004.
- [32] A.-L. Lu and W. P. Fawcett, "Characterization of the recombinant MutY homolog, an adenine DNA glycosylase, from yeast *Schizosaccharomyces pombe*," *The Journal of Biological Chemistry*, vol. 273, no. 39, pp. 25098–25105, 1998.
- [33] T. Doi, S.-I. Yonekura, K. Tano, S. Yasuhira, S. Yonei, and Q.-M. Zhang, "The *Schizosaccharomyces pombe* homolog (SpMYH) of the *Escherichia coli* MutY is required for removal of guanine from 8-oxoguanine/guanine mispairs to prevent G:C to C:G transversions," *Journal of Radiation Research*, vol. 46, no. 2, pp. 205–214, 2005.
- [34] D.-Y. Chang, Y. Gu, and A.-L. Lu, "Fission yeast (*Schizosaccharomyces pombe*) cells defective in the mutY-homologous glycosylase activity have a mutator phenotype and are sensitive to hydrogen peroxide," *Molecular Genetics and Genomics*, vol. 266, no. 2, pp. 336–342, 2001.
- [35] D.-Y. Chang and A.-L. Lu, "Functional interaction of MutY homolog with proliferating cell nuclear antigen in fission yeast, *Schizosaccharomyces pombe*," *The Journal of Biological Chemistry*, vol. 277, no. 14, pp. 11853–11858, 2002.
- [36] D.-Y. Chang and A.-L. Lu, "Interaction of checkpoint proteins Hus1/Rad1/Rad9 with DNA base excision repair enzyme MutY homolog in fission yeast, *Schizosaccharomyces pombe*," *The Journal of Biological Chemistry*, vol. 280, no. 1, pp. 408–417, 2005.
- [37] K. Jansson, J. Warringer, A. Farewell et al., "The tumor suppressor homolog in fission yeast, *myh1*<sup>+</sup>, displays a strong interaction with the checkpoint gene *rad1*<sup>+</sup>," *Mutation Research*, vol. 644, no. 1–2, pp. 48–55, 2008.
- [38] T. Caspari, M. Dahlen, G. Kanter-Smoler et al., "Characterization of *Schizosaccharomyces pombe* Hus1: a PCNA-related protein that associates with Rad1 Rad9," *Molecular and Cellular Biology*, vol. 20, no. 4, pp. 1254–1262, 2000.
- [39] B. Demple and L. Harrison, "Repair of oxidative damage to DNA: enzymology and biology," *Annual Review of Biochemistry*, vol. 63, pp. 915–948, 1994.
- [40] M. Z. Hadi and D. M. Wilson III, "Second human protein with homology to the *Escherichia coli* abasic endonuclease exonuclease III," *Environmental and Molecular Mutagenesis*, vol. 36, no. 4, pp. 312–324, 2000.
- [41] D. Tsuchimoto, Y. Sakai, K. Sakumi et al., "Human APE2 protein is mostly localized in the nuclei and to some extent in the mitochondria, while nuclear APE2 is partly associated with proliferating cell nuclear antigen," *Nucleic Acids Research*, vol. 29, no. 11, pp. 2349–2360, 2001.
- [42] J. L. Parsons, I. I. Dianova, and G. L. Dianov, "APE1 is the major 3'-phosphoglycolate activity in human cell extracts," *Nucleic Acids Research*, vol. 32, no. 12, pp. 3531–3536, 2004.
- [43] R. E. Johnson, C. A. Torres-Ramos, T. Izumi, S. Mitra, S. Prakash, and L. Prakash, "Identification of APN2, the *Saccharomyces cerevisiae* homolog of the major human AP endonuclease HAP1, and its role in the repair of abasic sites," *Genes and Development*, vol. 12, no. 19, pp. 3137–3143, 1998.
- [44] B. Ribar, T. Izumi, and S. Mitra, "The major role of human AP-endonuclease homolog Apn2 in repair of abasic sites in *Schizosaccharomyces pombe*," *Nucleic Acids Research*, vol. 32, no. 1, pp. 115–126, 2004.
- [45] M. Dlakić, "Functionally unrelated signalling proteins contain a fold similar to Mg<sup>2+</sup>-dependent endonucleases," *Trends in Biochemical Sciences*, vol. 25, no. 6, pp. 272–273, 2000.
- [46] M. Z. Hadi, K. Ginalski, L. H. Nguyen, and D. M. Wilson III, "Determinants in nuclease specificity of Ape1 and Ape2, human homologues of *Escherichia coli* exonuclease III," *Journal of Molecular Biology*, vol. 316, no. 3, pp. 853–866, 2002.
- [47] I. Unk, L. Haracska, X. V. Gomes, P. M. J. Burgers, L. Prakash, and S. Prakash, "Stimulation of 3'→5' exonuclease and 3'-phosphodiesterase activities of yeast Apn2 by proliferating cell nuclear antigen," *Molecular and Cellular Biology*, vol. 22, no. 18, pp. 6480–6486, 2002.
- [48] E. Igawa, H. Tanihigashi, A. Yamada, and S. Ikeda, "Functions of conserved motifs in the major AP endonuclease Apn2p of *Schizosaccharomyces pombe* for base excision repair of alkylation DNA damage," *Current Topics in Biochemical Research*, vol. 10, no. 1, pp. 101–105, 2008.
- [49] H. Tanihigashi, A. Yamada, E. Igawa, and S. Ikeda, "The role of *Schizosaccharomyces pombe* DNA repair enzymes Apn1p and Uve1p in the base excision repair of apurinic/aprimidinic sites," *Biochemical and Biophysical Research Communications*, vol. 347, no. 4, pp. 889–894, 2006.
- [50] D. Ramotar, J. Vadnais, J.-Y. Masson, and S. Tremblay, "*Schizosaccharomyces pombe* Apn1 encodes a homologue of the *Escherichia coli* endonuclease IV family of DNA repair proteins," *Biochimica et Biophysica Acta*, vol. 1396, no. 1, pp. 15–20, 1998.
- [51] R. Vongsamphanh, P.-K. Fortier, and D. Ramotar, "Pir1p mediates translocation of the yeast Apn1p endonuclease into the mitochondria to maintain genomic stability," *Molecular and Cellular Biology*, vol. 21, no. 5, pp. 1647–1655, 2001.
- [52] A. M. Avery, B. Kaur, J.-S. Taylor, J. A. Mello, J. M. Essigmann, and P. W. Doetsch, "Substrate specificity of ultraviolet DNA endonuclease (UVDE/Uve1p) from *Schizosaccharomyces pombe*," *Nucleic Acids Research*, vol. 27, no. 11, pp. 2256–2264, 1999.
- [53] B. Kaur, J. L. A. Fraser, G. A. Freyer, S. Davey, and P. W. Doetsch, "A Uve1p-mediated mismatch repair pathway in *Schizosaccharomyces pombe*," *Molecular and Cellular Biology*, vol. 19, no. 7, pp. 4703–4710, 1999.
- [54] N. Goosen and G. F. Moolenaar, "Repair of UV damage in bacteria," *DNA Repair*, vol. 7, no. 3, pp. 353–379, 2008.
- [55] S.-I. Kanno, S. Iwai, M. Takao, and A. Yasui, "Repair of apurinic/aprimidinic sites by UV damage endonuclease; a repair protein for UV and oxidative damage," *Nucleic Acids Research*, vol. 27, no. 15, pp. 3096–3103, 1999.
- [56] J. L. A. Fraser, E. Neill, and S. Davey, "Fission yeast Uve1 and Apn2 function in distinct oxidative damage repair pathways in vivo," *DNA Repair*, vol. 2, no. 11, pp. 1253–1267, 2003.
- [57] A. A. Ischenko and M. K. Sapparbaev, "Alternative nucleotide incision repair pathway for oxidative DNA damage," *Nature*, vol. 415, no. 6868, pp. 183–187, 2002.

- [58] A. A. Ishchenko, G. Sanz, C. V. Privezentzev, A. V. Maksimenko, and M. Saparbaev, "Characterisation of new substrate specificities of *Escherichia coli* and *Saccharomyces cerevisiae* AP endonucleases," *Nucleic Acids Research*, vol. 31, no. 21, pp. 6344–6353, 2003.
- [59] R. Yonemasu, S. J. McCready, J. M. Murray et al., "Characterization of the alternative excision repair pathway of UV-damaged DNA in *Schizosaccharomyces pombe*," *Nucleic Acids Research*, vol. 25, no. 8, pp. 1553–1558, 1997.
- [60] J. L. Alleva, S. Zuo, J. Hurwitz, and P. W. Doetsch, "In vitro reconstitution of the *Schizosaccharomyces pombe* alternative excision repair pathway," *Biochemistry*, vol. 39, no. 10, pp. 2659–2666, 2000.
- [61] S. Yasuhira and A. Yasui, "Alternative excision repair pathway of UV-damaged DNA in *Schizosaccharomyces pombe* operates both in nucleus and in mitochondria," *The Journal of Biological Chemistry*, vol. 275, no. 16, pp. 11824–11828, 2000.
- [62] S. González-Barrera, A. Sánchez, J. F. Ruiz et al., "Characterization of SpPol4, a unique X-family DNA polymerase in *Schizosaccharomyces pombe*," *Nucleic Acids Research*, vol. 33, no. 15, pp. 4762–4774, 2005.
- [63] L. Gellon, D. R. Carson, J. P. Carson, and B. Demple, "Intrinsic 5'-deoxyribose-5-phosphate lyase activity in *Saccharomyces cerevisiae* Trf4 protein with a possible role in base excision DNA repair," *DNA Repair*, vol. 7, no. 2, pp. 187–198, 2008.
- [64] P. Fortini and E. Dogliotti, "Base damage and single-strand break repair: mechanisms and functional significance of short- and long-patch repair subpathways," *DNA Repair*, vol. 6, no. 4, pp. 398–409, 2007.
- [65] L. Wiederhold, J. B. Leppard, P. Kedar et al., "AP endonuclease-independent DNA base excision repair in human cells," *Molecular Cell*, vol. 15, no. 2, pp. 209–220, 2004.
- [66] S.-W. Yang, A. B. Burgin Jr., B. N. Huiyenga, C. A. Robertson, K. C. Yao, and H. A. Nash, "A eukaryotic enzyme that can disjoin dead-end covalent complexes between DNA and type I topoisomerases," *Proceedings of the National Academy of Sciences of the United States of America*, vol. 93, no. 21, pp. 11534–11539, 1996.
- [67] T. S. Dexheimer, S. Antony, C. Marchand, and Y. Pommier, "Tyrosyl-DNA phosphodiesterase as a target for anticancer therapy," *Anti-Cancer Agents in Medicinal Chemistry*, vol. 8, no. 4, pp. 381–389, 2008.
- [68] A. Jilani and D. Ramotar, "Purification and partial characterization of a DNA 3'-phosphatase from *Schizosaccharomyces pombe*," *Biochemistry*, vol. 41, no. 24, pp. 7688–7694, 2002.
- [69] M. Meijer, F. Karimi-Busheri, T. Y. Huang, M. Weinfeld, and D. Young, "Pnk1, a DNA kinase/phosphatase required for normal response to DNA damage by  $\gamma$ -radiation or camptothecin in *Schizosaccharomyces pombe*," *The Journal of Biological Chemistry*, vol. 277, no. 6, pp. 4050–4055, 2002.
- [70] K. V. Inamdar, J. J. Pouliot, T. Zhou, S. P. Lees-Miller, A. Rasouli-Nia, and L. F. Povirk, "Conversion of phosphoglycolate to phosphate termini on 3' overhangs of DNA double strand breaks by the human tyrosyl-DNA phosphodiesterase hTdp1," *The Journal of Biological Chemistry*, vol. 277, no. 30, pp. 27162–27168, 2002.
- [71] H. Interthal, H. J. Chen, and J. J. Champoux, "Human Tdp1 cleaves a broad spectrum of substrates, including phosphoamide linkages," *The Journal of Biological Chemistry*, vol. 280, no. 43, pp. 36518–36528, 2005.
- [72] H. Takashima, C. F. Boerkoel, J. John et al., "Mutation of TDP1, encoding a topoisomerase I-dependent DNA damage repair enzyme, in spinocerebellar ataxia with axonal neuropathy," *Nature Genetics*, vol. 32, no. 2, pp. 267–272, 2002.
- [73] S. Ben Hassine and B. Arcangioli, "Tdp1 protects against oxidative DNA damage in non-dividing fission yeast," *EMBO Journal*, vol. 28, no. 6, pp. 632–640, 2009.
- [74] N. Mutoh, C. W. Nakagawa, and K. Yamada, "The role of catalase in hydrogen peroxide resistance in fission yeast *Schizosaccharomyces pombe*," *Canadian Journal of Microbiology*, vol. 45, no. 2, pp. 125–129, 1999.
- [75] Y. Hida and S. Ikeda, "Base excision repair of oxidative DNA damage in a catalase-deficient mutant of *Schizosaccharomyces pombe*," *Genes and Environment*, vol. 30, no. 3, pp. 86–91, 2008.
- [76] J. Fan and D. M. Wilson III, "Protein-protein interactions and posttranslational modifications in mammalian base excision repair," *Free Radical Biology and Medicine*, vol. 38, no. 9, pp. 1121–1138, 2005.
- [77] S. S. Y. Su, Y. Tanaka, I. Samejima, K. Tanaka, and M. Yanagida, "A nitrogen starvation-induced dormant G<sub>0</sub> state in fission yeast: the establishment from uncommitted G<sub>1</sub> state and its delay for return to proliferation," *Journal of Cell Science*, vol. 109, no. 6, pp. 1347–1357, 1996.
- [78] S. Mochida and M. Yanagida, "Distinct modes of DNA damage response in *S. pombe* G<sub>0</sub> and vegetative cells," *Genes to Cells*, vol. 11, no. 1, pp. 13–27, 2006.

## Review Article

# Nonhomologous DNA End Joining in Cell-Free Extracts

**Sheetal Sharma and Sathees C. Raghavan**

*Department of Biochemistry, Indian Institute of Science, Bangalore 560 012, India*

Correspondence should be addressed to Sathees C. Raghavan, sathees@biochem.iisc.ernet.in

Received 2 June 2010; Revised 14 July 2010; Accepted 5 August 2010

Academic Editor: Ashis Basu

Copyright © 2010 S. Sharma and S. C. Raghavan. This is an open access article distributed under the Creative Commons Attribution License, which permits unrestricted use, distribution, and reproduction in any medium, provided the original work is properly cited.

Among various DNA damages, double-strand breaks (DSBs) are considered as most deleterious, as they may lead to chromosomal rearrangements and cancer when unrepaired. Nonhomologous DNA end joining (NHEJ) is one of the major DSB repair pathways in higher organisms. A large number of studies on NHEJ are based on *in vitro* systems using cell-free extracts. In this paper, we summarize the studies on NHEJ performed by various groups in different cell-free repair systems.

## 1. Introduction

Maintenance of genomic integrity and stability is of prime importance for the survival of an organism. Upon exposure to different damaging agents, DNA acquires various lesions such as base modifications, single-strand breaks (SSBs), and double-strand breaks. Organisms have evolved specific repair pathways in order to efficiently correct such DNA damages. Examples include base excision repair (base level changes), nucleotide excision repair (distortions in the DNA); and single-strand break repair. DSBs are considered as the most deleterious type of DNA damages, among different lesions. It can result in chromosomal rearrangements like translocations and cancer or cell death when unrepaired [1, 2].

DSBs can be generated by pathological or physiological agents. Pathological agents can be exogenous such as ionizing radiation, or chemotherapeutic agents like bleomycin (Figure 1). They can also be endogenous like oxidative free radicals, replication across a nick, inadvertent enzyme action at fragile sites (Figure 1), mechanical shearing at anaphase bridges, metabolic by products, and so forth [3–5]. Physiological processes such as V(D)J recombination, class switch recombination (CSR); and meiosis also introduce DSBs in our genome.

DSB repair pathways in mammals can be broadly classified into two categories, namely, homologous recombination (HR) and nonhomologous DNA end joining. NHEJ needs

little or no homology and is usually imprecise, while HR requires a region of extensive homology [6–8]. HR occurs in S and G2 phases of the cell cycle and is accurate as it uses the sister chromatid as a template to repair the damaged strand [8–10]. The protein machinery involved in HR includes RAD50, MRE11, NBS1, RAD51, and RAD54 [6, 11, 12]. On the other hand, NHEJ operates throughout the cell cycle and is error prone [4, 10, 13]. The errors introduced during NHEJ in higher eukaryotes pose little threat to the organism as only a small percentage of the genome encodes for proteins whereas entering into S or G2 phase with unrepaired DNA strands is a major risk.

## 2. NHEJ Proteins

Genetic studies using radiosensitive mammalian cell lines deficient in DSB rejoining in conjunction with biochemical evidences have led to the discovery of many NHEJ proteins. Ku proteins, which play a major role in NHEJ, were originally discovered as a target for autoantibodies in patients with autoimmune diseases [14–16]. Subsequently, studies using various DNA end structures provided the evidence that Ku proteins recognize the DNA ends [17]. The first evidence for the involvement of Ku proteins in NHEJ came from the discovery that Ku80 subunit was defective in X-ray sensitive mammalian cell mutants in the XRCC5 group [18–20]. Ku70 was identified initially as an interaction partner for Ku80 by biochemical assays [16, 21]. Later, *in vivo* studies confirmed

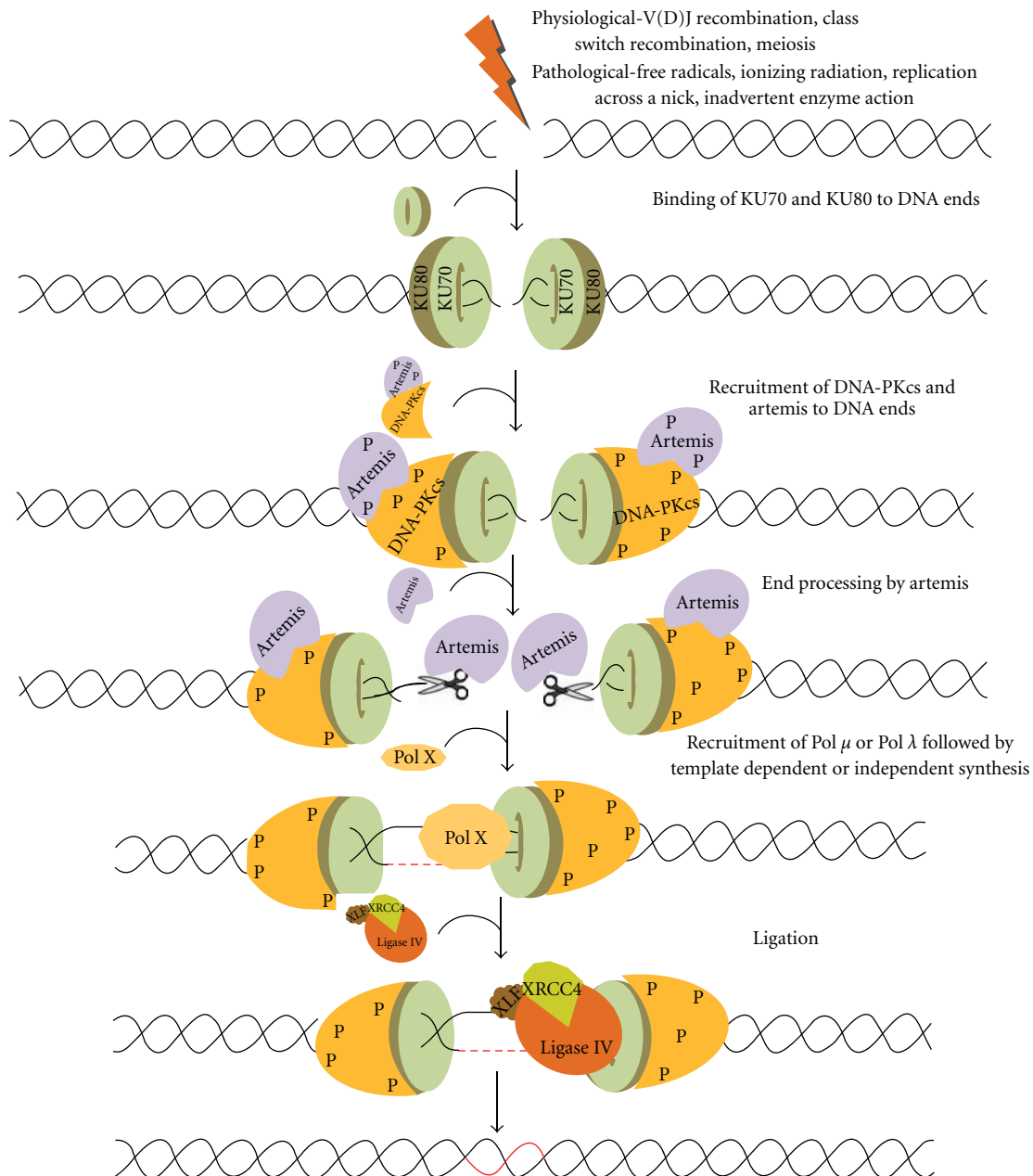


FIGURE 1: Double-strand breaks (DSBs) are generated exogenously by ionizing radiation, or endogenously by free radicals or during V(D)J recombination in pre-B (bone marrow) and pre-T cells (thymus) by RAG complex or also during class switch recombination in activated B cells (in the peripheral lymphoid tissues such as spleen, lymph nodes, and Peyer's patches). NHEJ involves the binding of Ku70 and Ku80 heterodimeric complex to the DNA ends, and DNA-PKcs in association with ARTEMIS. ARTEMIS is a 5'-3' exonuclease in an unphosphorylated form while it is an endonuclease in a phosphorylated form. Artemis protein acts as an exonuclease and helps in resection of the ends. Polymerase X family members are then recruited for DNA synthesis, which includes both template dependent and independent DNA synthesis. The resulting DNA ends are ligated by a specific DNA LIGASE IV with stimulatory factors (XRCC4-LIGASE IV-XLF complex) that restores the integrity of DNA.

this observation [22]. DNA-PKcs was first identified during a biochemical screen for kinases that were stimulated by double-stranded DNA [17]. Chinese hamster ovary cell lines lacking *XRCC7* showed 10-fold higher sensitivity to radiation and later the protein coded by the gene was identified as DNA-PK [16, 23, 24]. The critical finding

that Ku protein is the regulatory component of DNA-PKcs unified both areas of research and gave a new dimension to the NHEJ field. The *in vivo* role of Ku and DNA PKcs was later confirmed by many studies [2, 25–29].

More or less at the same time, a distinct DNA ligase, named DNA Ligase IV, having ATP dependent ligase activity

was purified from HeLa cell nuclei with substrate specificity to both single- and double-stranded breaks [30]. Later, the same ligase was identified as the enzyme responsible for NHEJ both in mammals and yeast [31–33]. Another, NHEJ protein, XRCC4 was identified based on radiosensitivity shown by mammalian cells deficient for XRCC4 gene [21, 34–36]. Later using biochemical assays it was reported that XRCC4, small nuclear phosphoprotein, forms a tight, specific complex with DNA Ligase IV and stimulates its activity by many folds [32, 33]. More recently, it was identified that an XRCC4-like protein, XLF (also known as Cernunnos), is an interaction partner of the DNA Ligase IV/XRCC4 complex, facilitating the ligation of the ends [37, 38].

In early 2000, Artemis, a novel protein involved in V(D)J recombination and DSB repair, was identified [39]. It was reported that a mutation in the Artemis was responsible for the SCID phenotype [39]. Later, using an elegant biochemical assay system, it was shown that phosphorylated Artemis in conjunction with DNA-PKcs complex has the ability to cleave the hairpin intermediate of V(D)J recombination, besides its ability to cleave 5'-overhangs, 3'-overhangs, and other DNA structures [40–43]. In addition, Artemis on its own possesses an exonuclease activity [42]. Polymerases involved in NHEJ, Pol  $\mu$  and Pol  $\lambda$ , both belonging to the polX family were also identified later [44, 45].

### 3. Mechanism of NHEJ

The key players of NHEJ recognize the broken DNA ends and further process and ligate them [4, 6, 13, 46]. To begin with, the DNA with DSBs is recognised by the Ku70/Ku80 heterodimeric complex, which then recruits DNA-PKcs in association with Artemis [47–49] (Figure 1). DNA-PKcs and Ku complex play an important role in forming a synaptic complex that brings the two DNA ends together and also interacts with the Ku heterodimer. DNA-PKcs further autophosphorylates itself and phosphorylates Artemis as well. Artemis-DNA-PKcs complex can cleave 5'-overhangs and 3'-overhangs while Artemis alone can function as an exonuclease [40–42]. After processing, the ends are filled using Pol  $\mu$  and Pol  $\lambda$  [44, 45]. Finally, the ends are ligated by XLF:XRCC4:DNA Ligase IV complex [31, 32, 37] (Figure 1). Since NHEJ is not precise, although the integrity is maintained, it may lead to mutations which may further help in evolution of the organism.

### 4. Alternative NHEJ

In the absence of key NHEJ proteins, a less-characterized pathway has been shown to play an important role in joining of DSBs, which is now classified as alternative NHEJ or backup NHEJ or microhomology-mediated end joining (MMEJ). Although recent studies indicate that this pathway is distinct and error prone, the exact mechanism is yet to be uncovered. A classic paper which introduced the term alternative NHEJ describes it as a possible source of chromosomal translocation and the authors showed coamplification of

c-Myc and IgH locus from pro-B lymphomas in mice deficient for p53 and Xrcc4 [50]. Another interesting study showed a reduced level of class switch recombination and increased number of chromosomal breaks at IgH locus in mouse B cells, which were deficient for XRCC4 and Ligase IV [51]. Another study showed the occurrence of robust alternative end joining in the absence of XRCC4 and upon removal of certain portions of murine RAG proteins [52]. Besides, a residual joining mediated by microhomology towards the end of DSBs was also identified in Xrcc4 defective cells [53]. The protein machinery for this kind of backup joining in the absence of key NHEJ proteins is still not very clear although studies suggest the role of MRE11-RAD50-NBS1 complex in a subset of alternative NHEJ junctions [54, 55]. Another study has deciphered the role of PARP1 in repairing switch regions through a microhomology-mediated pathway while PARP2 suppresses IgH/c-myc translocations during immunoglobulin class switch recombination [56]. DNA Ligase III $\alpha$  and WRN have also been shown to contribute to the repair of DSBs by alternative NHEJ [57]. Therefore, canonical NHEJ requires XRCC4-Ligase IV complex while alternative NHEJ is characterized by joining mediated through microhomology regions, which is prominent in the absence of canonical NHEJ proteins. Recently, an interesting study has shown the role of XRCC4-Ligase IV in suppressing alternative end joining during chromosomal translocations [58]. Another study has shown the role of alternative end joining in robust IgH locus deletions and translocations in the combined absence of Ku70 and Ligase IV [59].

We further discuss NHEJ catalysed by crude extracts which includes joining mediated by classical NHEJ, single-strand annealing, alternative NHEJ, or microhomology-mediated end joining.

### 5. NHEJ Assays

Since NHEJ is the major pathway of DSB repair in higher organisms, extensive studies have been done to understand its mechanism. Various *in vitro* and *in vivo* assays have been designed to study NHEJ in different cell lines, which were derived from different cancers. In this section, we will discuss different types of NHEJ assays used in the literature, so far. Intracellular (*ex vivo*) assays have been generally based on transfection of mammalian cells with restriction enzyme linearized plasmid DNA [60–62]. Following transfection, cells were allowed to grow for several hours and plasmid DNA was harvested using either alkaline lysis or a high-salt-based nondenaturing method. The NHEJ products were analysed by Southern hybridization. The joining junctions were then characterized by PCR amplification followed by cloning and sequencing. In one of the first studies, the authors' transfected linear SV40 genome with mismatched ends into cultured monkey kidney cells and checked for the presence of recombinants [60, 61, 63]. Some other studies used vectors that overexpress I-SceI endonuclease within the cells to induce DSBs on a plasmid containing I-SceI site, which has an advantage that the DSBs can be induced within the cells [64, 65].

The intracellular assays, although widely used, have many shortcomings. Generally, the quantity of NHEJ products obtained are very low and hence, various end-joined products such as dimer, trimer, and other forms of multimers cannot be visualized on a gel even after Southern hybridization. PCR amplification could be used for detecting the NHEJ products; however, it may not be able to distinguish between different types of joined products. Besides, while extracting DNA out of the cell, many linear products could be lost and hence one would not get the actual efficiency of joining. Nevertheless, it is an excellent system because the role of different proteins can be studied as one could generate knockout for different NHEJ genes in cell lines.

*In vitro* assays, on the other hand, use a different strategy. They use a cell-free system containing different cellular proteins or selected purified proteins [41, 66–71]. Such assays have been instrumental in studying NHEJ both at the biochemical and molecular level. Cell-free system includes either total protein, cytoplasmic, or nuclear extracts prepared generally from cell lines or rarely from tissues [67–69, 72, 73]. Cell-free system is better because it provides greater flexibility in selecting the types of DSB end configurations. The sequences at or adjacent to DSBs can be easily manipulated to study different junctional features of NHEJ. *In vitro* assays have used two types of DNA substrates, plasmids and oligomers. Although plasmid substrates are most commonly used, genomic DNA has also been studied [41, 68, 73–76] (Figure 2). DSBs are generated either by restriction enzyme digestion, by treatment with chemicals such as bleomycin, or by irradiation with x-rays or  $\gamma$ -rays [68, 73, 74, 77–79]. The joining products can be visualised on agarose gel following purification of products or after Southern hybridization, depending on the quantity of the substrates used [67, 68, 73, 74]. An oligomer based system has also been used recently for studying NHEJ [41, 76, 80]. In this assay, appropriate oligomers can be designed, synthesized, and annealed to generate substrates containing different DSBs (Figure 2(b)). These substrates can be end-labelled with [ $\gamma$ -<sup>32</sup>P] ATP, incubated with the extracts or purified proteins, and then resolved on a polyacrylamide gel (Figure 2(a)). In both cases, all the joining products can be visualised and the efficiency of the joining between the substrates can be easily compared as it is proportional to the intensity of bands. The standard NHEJ products observed are dimers, trimers, multimers, and circular products [67, 68, 74]. Similar to intracellular studies, NHEJ junctions can be PCR amplified, cloned, and sequenced. The extent of joining can also be determined by using quantitative PCR [75]. Oligomeric DNA substrates provide more flexibility with respect to end configurations of DSBs as compared to plasmid substrates, where restriction enzyme sites are used to generate DSBs. However, size of the oligomers could be a limiting factor in certain studies.

## 6. Preparation of Cell-Free Extracts from Different Sources

Manley et al. described the protocol for the preparation of cell-free extracts of *in vitro* cultured cells for the first

time [81]. They precipitated the proteins using ammonium sulphate following lysis of the cells using hypotonic buffer and mechanical pressure. Later, many studies adopted modifications to Manley's protocol to prepare cell extracts from different sources. In one of the studies, the concentration of ammonium sulphate was changed in order to reduce the nonspecific nuclease activity present in the extracts [82]. Wood et al. introduced several changes to the cell extract preparation while studying nucleotide excision repair [83]. Later, the protocol was modified to prepare cell-free extracts from tissues (testicular cells) to study DSB repair pathways [68, 84]. Another method of preparation of cell-free extracts involves cellular lysis, followed by removal of cell debris by ultracentrifugation [74]. Although both methods are different in many ways, the overall repair efficiency of the cell-free extracts is similar. One of the major drawbacks of these methods is with respect to the number of cells required for the extract preparation. Both require very high number of cells ( $> 1-5 \times 10^8$ ). In contrast, a recent study has scaled down the number of cells required to  $5-10 \times 10^6$  [85]. The NHEJ efficiency was found to be optimum after testing in different cell lines including MO59K (glioblastoma), HepG2 (liver), HeLa (cervix), MCF-7 (breast), A549 (lungs), HCT116 (colon), and RT112 (bladder). This microscale assay can be used for clinical samples and thus the role of DNA DSB repair in tumorigenesis can be studied [85].

## 7. NHEJ Using Different Cell-Free Systems

Many studies have used different cell-free systems to study NHEJ. One of the first studies to report NHEJ *in vitro* using cell-free extracts was done using fertilized or activated *Xenopus* eggs. End joining was observed using different plasmid substrates containing DSBs with varying end configurations [71, 86]. NHEJ has also been reported from germinal vesicles (oocyte nuclei) of *Xenopus* where ligation of compatible ends was tested and the efficiency of joining was compared among different stages of oocyte development. Authors found that interestingly only the stage VI oocytes showed NHEJ, which was in presence of dNTPs. Deletions were also seen at the junctions of the end-joined products [87].

Mammalian cells have been extensively used for *in vitro* and *in vivo* end joining reactions. Nuclear extracts from MRC5V1 (immortalised control fibroblasts cell line) were found to catalyze the efficient joining of compatible overhangs as compared to blunt ends [67, 88]. Nuclear extracts from HeLa cells could join linear plasmid substrates, in both head-to-head and tail-to-tail configurations [69]. Another study compared the NHEJ activity of both nuclear and cytoplasmic extracts from three human and one mouse cell line. Interestingly, they observed that the extent of deletion and mechanism of joining was similar to *Xenopus* oocytes [89]. A study using extracts prepared from human lymphoblastoid cell line, GM00558B, described a precise and LIGASE IV-dependent NHEJ on a BamHI digested plasmid DNA. For the first time, authors showed a direct role for Ku70, Ku80, and DNA-PKcs in NHEJ using an *in vitro* cell-free system [74]. Sequence analysis of NHEJ junctions

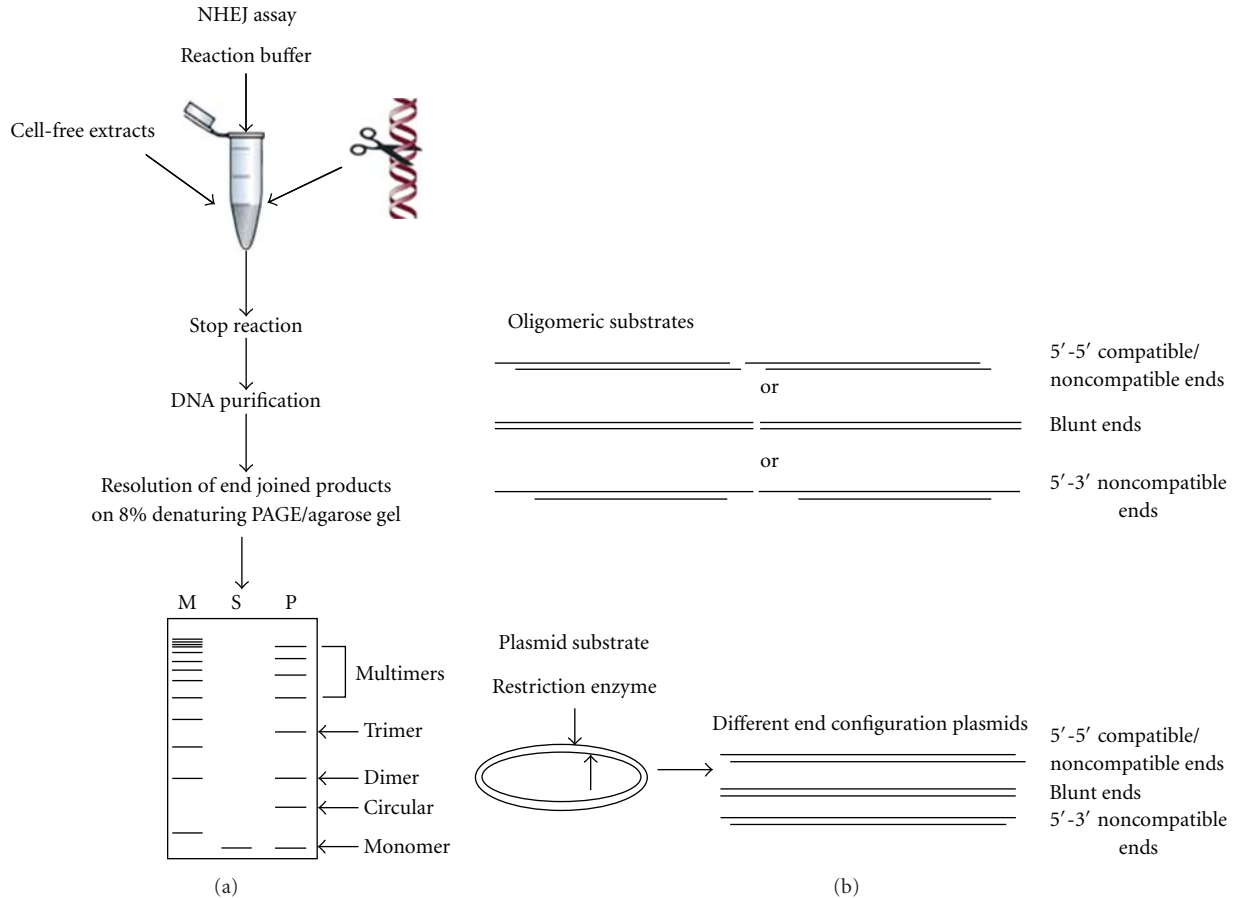


FIGURE 2: Schematic representation of NHEJ reaction using cell-free extracts. (a) Cell-free extract is incubated with one of the 5'-end-labelled DNA substrate (oligomer) or restriction enzyme-digested plasmid DNA as shown in the figure along with NHEJ buffer. The reaction is stopped by adding proteinase K and EDTA, DNA is purified by phenol:chloroform extraction, precipitated with glycogen and ethanol, resuspended in TE, and run on 8% denaturing PAGE or agarose gel. After end joining, dimers, trimers, and multimers can be seen. "M" is marker, "S" is substrate, and "P" indicates products. (b) Oligomeric or plasmid DNA substrates.

by another study showed that deletions occur exclusively between short direct repeats in nuclear extracts prepared from AT5BIVA (derived from ATM patient) and MRC5V1 (derived from a normal individual) [88]. SupT1 cells (human T cell lymphoblastic lymphoma) catalyzed efficient joining without deletions or insertions, when complementary ligatable ends were used for the study. However, interestingly, even in the case of noncomplementary ends, the joining took place without deletions [73]. Chinese hamster ovary cell line was used to demonstrate that  $^{125}\text{I}$ -Triplex forming oligonucleotide containing radiation-induced DSBs was repaired at approximately 10-fold lower efficiency as compared to restriction enzyme generated DSBs [90].

In an independent study, different cell lines were employed while standardizing the clinical samples for analysing NHEJ and it was observed that the efficiency of NHEJ varied among the cells [85]. Cell-free assay was also used to compare the efficiency of 11 sporadic breast cancer cell lines (BCCLs) with normal fibroblasts and it was found that only 2 BCCLs showed a reduced NHEJ *in vitro* [91].

Attempts were also made to study NHEJ in tissues using cell-free extracts. In one of the first studies using a mice

testicular cell-free system, it was shown that NHEJ is efficient in male germ cells [68, 84]. Based on plasmid rejoining assay, the authors reported end-joining leading to dimers, trimers, and other forms of multimers, while circularization was absent [68]. The joining of complementary and noncomplementary ends took place with minimum alterations [84]. In continuation to this study, we have recently compared the efficiency of NHEJ in mice and rat testicular extracts, using an oligomer-based assay system. We noticed that there was no major difference in the joining efficacy when mice or rat testicular extracts were used (Figure 3). More recently, we compared the NHEJ efficiencies between testis and other somatic tissues using cell-free extracts. Interestingly, we found that similar to testis, lungs also showed efficient NHEJ (unpublished, SS & SCR). Efficiency of NHEJ was moderate in case of brain, thymus, and spleen while it was weaker in case of kidney, liver, and heart. An independent study showed an efficient NHEJ activity in rat neurons, while it was also shown that efficiency of NHEJ in rat neurons can go down in an age-dependent manner [92, 93]. NHEJ activity of nuclear extracts prepared from cortical neurons of patients suffering from Alzheimer's disease (AD) was also compared

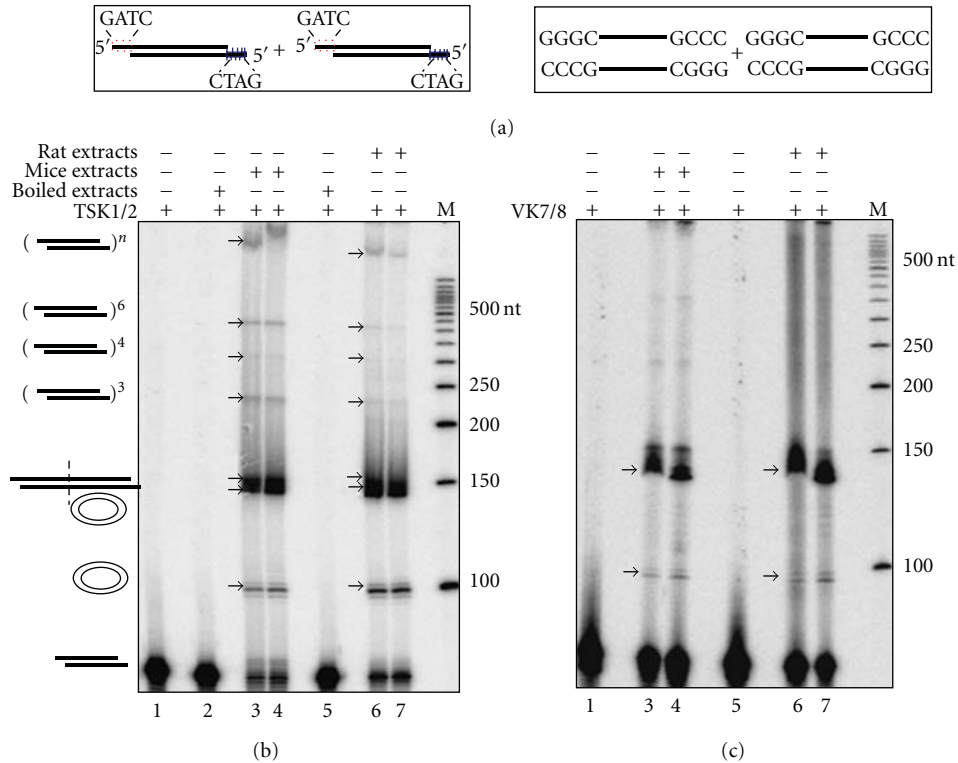


FIGURE 3: Comparison of efficiencies of NHEJ in rat and mice testis. Cell-free extract was prepared from age-matched rat and mice testes and protein profile was normalized between both animals. 5  $\mu$ g of protein was incubated with 4 nM of 5'-end labelled with [ $\gamma$ - $^{32}$ P] DNA containing both compatible and blunt termini against each lane (a) which are represented schematically along with buffer containing 30 mM HEPES-KOH, pH 7.9, 7.5 mM MgCl<sub>2</sub>, 1 mM DTT, 2 mM ATP, 50  $\mu$ M dNTPs, and 0.1  $\mu$ g BSA. End joining reaction using (b) compatible end and (c) blunt end DNA. Lane 1 shows negative control that contains substrate alone, Lane 2 shows heat-inactivated control which is mice testis cell-free extract-boiled for 10 min and used for the reaction, and Lanes 3 and 4 are the end joining reactions with cell-free extract from mice testis. Lane 5 is the heat-inactivated control which is boiled rat testicular extract as described previously. Lanes 6 and 7 are the end joining reactions with rat testicular cell-free extracts. "M" indicates 5'-end-labelled 50 bp ladder. The efficiency of joining is similar in both mice and rat testicular extracts. Different types of end-joined products formed are indicated.

with that of normal human subjects and it was reported that DNA-PKcs activity was significantly lower in AD brains when compared to healthy controls [94].

NHEJ activity was also studied *in vivo* by transfecting adenovirus DNA fragments into A549 (lung carcinoma cell line) and it was found that the joining was efficient irrespective of the ends [72]. Previously, monkey kidney cell lines have been used for studying NHEJ using transfection assays [60, 61, 63, 95]. Thus, the mechanistic aspects of NHEJ have been studied using different cell lines both *in vitro* and *in vivo*.

## 8. NHEJ Mechanisms in Cell-Free System

Various studies described above helped in unravelling the mechanistic aspects of NHEJ (Figure 4). Using monkey kidney cells transfected with SV40 T-antigen containing episome, it was noted that single-strand extensions are stable and few nucleotides present at the terminal end of a DSB are important for the joining [60, 63]. The authors proposed three independent mechanisms for the end-joining based on the sequence at the junctions, which were single-stranded

DNA ligation, template-directed ligation, and postrepair ligation [60]. Later, other studies helped in deciphering the fine mechanistic details of NHEJ pathway. If the ends were compatible, joining was predominantly conservative and mostly required only LigaseIV or LigaseIV-XRCC4 complex (Figure 4(a)) [68, 75]. In this case, following the alignment, the ends were simply ligated. However, the involvement of a separate protein for alignment is still not clear. The joining mechanism was mostly the same for DSBs with blunt ends as well (Figure 4(b)). In this case also, the joining generally did not involve any modifications at the junctions, although the efficiency was many fold lower as compared to compatible ends. In case of noncomplementary ends with 5'-5' overhangs, ligation was dependent on end-filling of one end and deletion of the other (Figure 4(c)) [96]. Alternatively, joining could occur after end-filling of each end independently followed by ligation or joining of one overhang with a second overhang which was end filled (Figure 4(d)) [63]. When DSBs with 5' and 3' overhangs were used for the study, a different mechanism was used, in which single-strand ligation of protruding 5' and 3' ends occurred initially, followed by template dependent

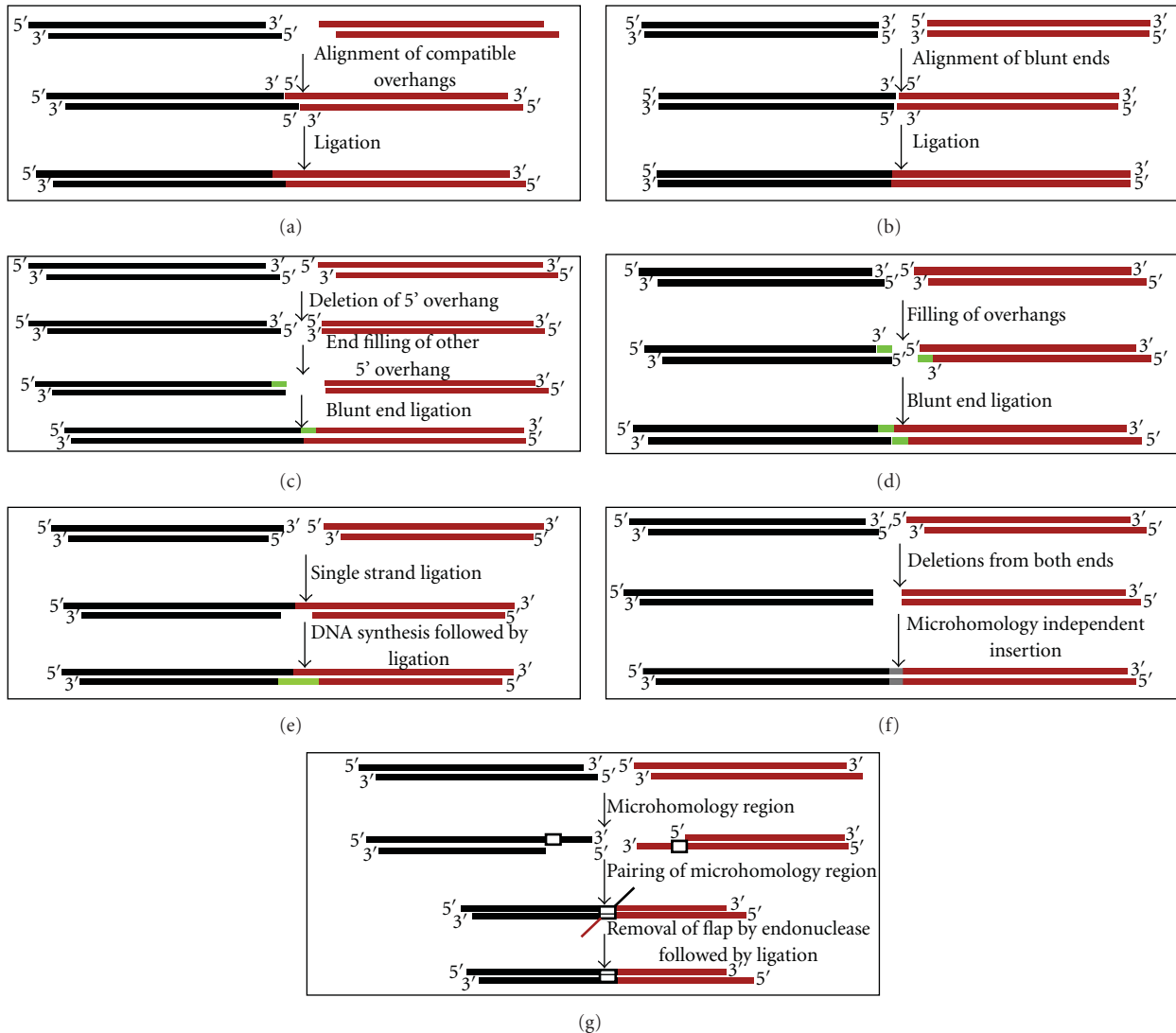


FIGURE 4: Schematic representation of possible mechanisms involved in repair for DNA termini. (a) In case of compatible ends, ligation usually does not involve much modification. Here, the two termini are aligned and ligated by DNA LIGASE IV. (b) Similarly, alignment of DNA ends in case of blunt ends take place and are ligated by DNA LIGASE IV as it does not need end modifications. On the other hand, modifications take place for non-compatible ends. There are different possibilities in case of 5'-5' substrate which includes (c) deletion of nucleotides from both ends and insertion of nucleotides followed by ligation or (d) deletion of 5'-overhang from one end, end-filling of other 5'-end followed by blunt end ligation. (e) Another possibility includes end filling of both the overhangs followed by ligation. (f) In case of 5'-3' overhangs, single strand ligation of overhangs is followed by template dependent synthesis and ligation. (g) Microhomology dependent joining can take place in any of the overhangs which is characterized by pairing of microhomology region followed by removal of flap by an endonuclease and then ligation.

strand synthesis (Figure 4(e)). In an interesting study using *Xenopus* oocytes cell-extracts as a model system, a novel end alignment mechanism, in which alignment of 3' protruding ends followed polymerisation and ligation of two DNA ends, was described [86]. During joining of certain noncompatible ends, deletion from both ends followed by blunt end ligation has also been proposed (Figure 4(f)) [60, 71].

A microhomology-mediated joining has also been reported by different groups irrespective of the termini (Figure 4(g)) [84, 88, 96]. This mechanism involves exonuclease digestion of one of the strands till the microho-

mology region is exposed, followed by the alignment of microhomology sequence. The flap region is deleted by Artemis/DNAPKcs or FEN endonuclease. Template dependent DNA synthesis takes place and nicks are then ligated by using LigaseIV complex [75]. Recent studies have suggested that in case of classical NHEJ, the microhomology box normally consists of 1–4 nucleotides [97]. If the size of microhomology used is more than 6–8 nucleotides, the joining is categorised as an alternative NHEJ as discussed above, which is proposed as the repair mechanism involved in the generation of many chromosomal translocations [51, 97].

## 9. Future Prospects

Numerous studies have utilized cell lines as a model system to understand the mechanism of NHEJ. Cell lines give an opportunity to study NHEJ at intracellular level. In addition, cell lines grow much faster than the original tissues from where they are derived. Therefore, it is difficult to extrapolate these findings to the *in vivo* scenario, where most of the cells of somatic tissues do not grow actively. It has been shown that glioma cell lines possess lower DNA repair capacity compared to the ascitic fluid collected from tumour [98]. Moreover, studies have also shown that expression of proteins in a cell line is different from that of the tissue of its origin [99]. Besides, cell lines are derived from tumour tissues and, therefore, their origin itself is controversial as most of the tumours are metastatic [100]. Therefore, studies using primary tissues to understand the mechanism of NHEJ are important in the coming years.

It is known that tissues of various origins have differential sensitivity towards radiation. It appears that there could be a correlation between radiosensitivity and the rate of cell division. The tissues with replicating cells, such as blood, testis, bone marrow, ovaries, and intestine, are highly sensitive, while others are less radiosensitive [101, 102].  $\gamma$ -H2AX formation could be correlated with radiosensitivity in complex tissues, however, this requires more investigation. Studies on NHEJ and the recently discovered alternative NHEJ, at the tissue level could help in understanding the mechanism of radiosensitivity and susceptibility to cancer in complex tissues and organs.

Although end-alignment issues related to NHEJ have been studied extensively, still many questions are unanswered. Identification of novel proteins in NHEJ may help facilitate addressing such questions. The signalling which follows DNA damage could be another area of interest in the context of human diseases.

## Conflict of Interest

Authors disclose that there is no conflict of interest.

## Acknowledgments

The authors thank Mridula Nambiar, Nishana M. and other members of SCR laboratory for critical reading of the manuscript. to “This work was supported by grant from DAE, India (2008/37/5/BRNS) and IISc start-up grant for S. C. Raghavan, S. Sharma acknowledges SRF from DBT, India.

## References

- [1] M. R. Lieber, K. Yu, and S. C. Raghavan, “Roles of nonhomologous DNA end joining, V(D)J recombination, and class switch recombination in chromosomal translocations,” *DNA Repair*, vol. 5, no. 9-10, pp. 1234–1245, 2006.
- [2] D. O. Ferguson and F. W. Alt, “DNA double strand break repair and chromosomal translocation: lessons from animal models,” *Oncogene*, vol. 20, no. 40, pp. 5572–5579, 2001.
- [3] M. R. Lieber, “The mechanism of double-strand DNA break repair by the nonhomologous DNA end-joining pathway,” *Annual Review of Biochemistry*, vol. 79, pp. 181–211, 2010.
- [4] M. L. Hefferin and A. E. Tomkinson, “Mechanism of DNA double-strand break repair by non-homologous end joining,” *DNA Repair*, vol. 4, no. 6, pp. 639–648, 2005.
- [5] E. Weterings and D. J. Chen, “The endless tale of non-homologous end-joining,” *Cell Research*, vol. 18, no. 1, pp. 114–124, 2008.
- [6] C. Wyman and R. Kanaar, “DNA double-strand break repair: all’s well that ends well,” *Annual Review of Genetics*, vol. 40, pp. 363–383, 2006.
- [7] S. P. Jackson, “Sensing and repairing DNA double-strand breaks,” *Carcinogenesis*, vol. 23, no. 5, pp. 687–696, 2002.
- [8] M. Takata, M. S. Sasaki, E. Sonoda et al., “Homologous recombination and non-homologous end-joining pathways of DNA double-strand break repair have overlapping roles in the maintenance of chromosomal integrity in vertebrate cells,” *EMBO Journal*, vol. 17, no. 18, pp. 5497–5508, 1998.
- [9] E. Sonoda, M. S. Sasaki, J.-M. Buerstedde et al., “Rad51-deficient vertebrate cells accumulate chromosomal breaks prior to cell death,” *EMBO Journal*, vol. 17, no. 2, pp. 598–608, 1998.
- [10] M. R. Lieber, Y. Ma, U. Pannicke, and K. Schwarz, “Mechanism and regulation of human non-homologous DNA end-joining,” *Nature Reviews Molecular Cell Biology*, vol. 4, no. 9, pp. 712–720, 2003.
- [11] A. J. Hartlerode and R. Scully, “Mechanisms of double-strand break repair in somatic mammalian cells,” *Biochemical Journal*, vol. 423, no. 2, pp. 157–168, 2009.
- [12] S. C. West, “Molecular views of recombination proteins and their control,” *Nature Reviews Molecular Cell Biology*, vol. 4, no. 6, pp. 435–445, 2003.
- [13] K. K. Chiruvella, S. K. Sankaran, M. Singh, M. Nambiar, and S. C. Raghavan, “Mechanism of DNA Double-Strand Break Repair,” *The ICAFI Journal of Biotechnology*, vol. 1, pp. 7–22, 2007.
- [14] W. H. Reeves, “Use of monoclonal antibodies for the characterization of novel DNA-binding proteins recognized by human autoimmune sera,” *Journal of Experimental Medicine*, vol. 161, no. 1, pp. 18–39, 1985.
- [15] T. Mimori, J. A. Hardin, and J. A. Steitz, “Characterization of the DNA-binding protein antigen Ku recognized by autoantibodies from patients with rheumatic disorders,” *Journal of Biological Chemistry*, vol. 261, no. 5, pp. 2274–2278, 1986.
- [16] W. S. Dynan and S. Yoo, “Interaction of Ku protein and DNA-dependent protein kinase catalytic subunit with nucleic acids,” *Nucleic Acids Research*, vol. 26, no. 7, pp. 1551–1559, 1998.
- [17] A. I. Walker, T. Hunt, R. J. Jackson, and C. W. Anderson, “Double-stranded DNA induces the phosphorylation of several proteins including the 90 000 mol. wt. heat-shock protein in animal cell extracts,” *EMBO Journal*, vol. 4, no. 1, pp. 139–145, 1985.
- [18] V. Smider, W. K. Rathmell, M. R. Lieber, and G. Chu, “Restoration of X-ray resistance and V(D)J recombination in mutant cells by Ku cDNA,” *Science*, vol. 266, no. 5183, pp. 288–291, 1994.
- [19] G. E. Taccioli, T. M. Gottlieb, T. Blunt et al., “Ku80: product of the XRCC5 gene and its role in DNA repair and V(D)J recombination,” *Science*, vol. 265, no. 5177, pp. 1442–1445, 1994.

- [20] W. K. Rathmell and G. Chu, "Involvement of the Ku autoantigen in the cellular response to DNA double-strand breaks," *Proceedings of the National Academy of Sciences of the United States of America*, vol. 91, no. 16, pp. 7623–7627, 1994.
- [21] P. A. Jeggo, "DNA-PK: at the cross-roads of biochemistry and genetics," *Mutation Research*, vol. 384, no. 1, pp. 1–14, 1997.
- [22] Y. Gu, S. Jin, Y. Gao, D. T. Weaver, and F. W. Alt, "Ku70-deficient embryonic stem cells have increased ionizing radiosensitivity, defective DNA end-binding activity, and inability to support V(D)J recombination," *Proceedings of the National Academy of Sciences of the United States of America*, vol. 94, no. 15, pp. 8076–8081, 1997.
- [23] S. P. Lees-Miller, R. Godbout, D. W. Chan et al., "Absence of p350 subunit of DNA-activated protein kinase from a radiosensitive human cell line," *Science*, vol. 267, no. 5201, pp. 1183–1185, 1995.
- [24] D. W. Chan and S. P. Lees-Miller, "The DNA-dependent protein kinase is inactivated by autophosphorylation of the catalytic subunit," *Journal of Biological Chemistry*, vol. 271, no. 15, pp. 8936–8941, 1996.
- [25] S. Rooney, J. Sekiguchi, C. Zhu et al., "Leaky Scid phenotype associated with defective V(D)J coding end processing in Artemis-deficient mice," *Molecular Cell*, vol. 10, no. 6, pp. 1379–1390, 2002.
- [26] T. Blunt, N. J. Finnie, G. E. Taccioli et al., "Defective DNA-dependent protein kinase activity is linked to V(D)J recombination and DNA repair defects associated with the murine scid mutation," *Cell*, vol. 80, no. 5, pp. 813–823, 1995.
- [27] Z. E. Karanjawala, N. Adachi, R. A. Irvine et al., "The embryonic lethality in DNA ligase IV-deficient mice is rescued by deletion of Ku: implications for unifying the heterogeneous phenotypes of NHEJ mutants," *DNA Repair*, vol. 1, no. 12, pp. 1017–1026, 2002.
- [28] C. Zhu, M. A. Bogue, D.-S. Lim, P. Hasty, and D. B. Roth, "Ku86-deficient mice exhibit severe combined immunodeficiency and defective processing of V(D)J recombination intermediates," *Cell*, vol. 86, no. 3, pp. 379–389, 1996.
- [29] K. M. Frank, N. E. Sharpless, Y. Gao et al., "DNA ligase IV deficiency in mice leads to defective neurogenesis and embryonic lethality via the p53 pathway," *Molecular Cell*, vol. 5, no. 6, pp. 993–1002, 2000.
- [30] P. Robins and T. Lindahl, "DNA ligase IV from HeLa cell nuclei," *Journal of Biological Chemistry*, vol. 271, no. 39, pp. 24257–24261, 1996.
- [31] T. E. Wilson, U. Grawunder, and M. R. Lieber, "Yeast DNA ligase IV mediates non-homologous DNA end joining," *Nature*, vol. 388, no. 6641, pp. 495–498, 1997.
- [32] U. Grawunder, M. Wilm, X. Wu et al., "Activity of DNA ligase IV stimulated by complex formation with XRCC4 protein in mammalian cells," *Nature*, vol. 388, no. 6641, pp. 492–495, 1997.
- [33] S. E. Critchlow, R. P. Bowater, and S. P. Jackson, "Mammalian DNA double-strand break repair protein XRCC4 interacts with DNA ligase IV," *Current Biology*, vol. 7, no. 8, pp. 588–598, 1997.
- [34] L. H. Thompson and P. A. Jeggo, "Nomenclature of human genes involved in ionizing radiation sensitivity," *Mutation Research*, vol. 337, no. 2, pp. 131–134, 1995.
- [35] P. A. Jeggo, J. Tesmer, and D. J. Chen, "Genetic analysis of ionizing radiation sensitive mutants of cultured mammalian cell lines," *Mutation Research*, vol. 254, no. 2, pp. 125–133, 1991.
- [36] J. Thacker and R. E. Wilkinson, "The genetic basis of resistance to ionising radiation damage in cultured mammalian cells," *Mutation Research*, vol. 254, no. 2, pp. 135–142, 1991.
- [37] P. Ahnesorg, P. Smith, and S. P. Jackson, "XLF interacts with the XRCC4-DNA Ligase IV complex to promote DNA nonhomologous end-joining," *Cell*, vol. 124, no. 2, pp. 301–313, 2006.
- [38] D. Buck, L. Malivert, R. de Chasseval et al., "Cernunnos, a novel nonhomologous end-joining factor, is mutated in human immunodeficiency with microcephaly," *Cell*, vol. 124, no. 2, pp. 287–299, 2006.
- [39] D. Moshous, I. Callebaut, R. de Chasseval et al., "Artemis, a novel DNA double-strand break repair/V(D)J recombination protein, is mutated in human severe combined immune deficiency," *Cell*, vol. 105, no. 2, pp. 177–186, 2001.
- [40] Y. Ma, U. Pannicke, K. Schwarz, and M. R. Lieber, "Hairpin opening and overhang processing by an Artemis/DNA-dependent protein kinase complex in nonhomologous end joining and V(D)J recombination," *Cell*, vol. 108, no. 6, pp. 781–794, 2002.
- [41] Y. Ma, H. Lu, B. Tippin et al., "A biochemically defined system for mammalian nonhomologous DNA end joining," *Molecular Cell*, vol. 16, no. 5, pp. 701–713, 2004.
- [42] Y. Ma, K. Schwarz, and M. R. Lieber, "The Artemis:DNA-PKcs endonuclease cleaves DNA loops, flaps, and gaps," *DNA Repair*, vol. 4, no. 7, pp. 845–851, 2005.
- [43] S. M. Yannone, I. S. Khan, R.-Z. Zhou, T. Zhou, K. Valerie, and L. F. Povirk, "Coordinate 5' and 3' endonucleolytic trimming of terminally blocked blunt DNA double-strand break ends by Artemis nuclease and DNA-dependent protein kinase," *Nucleic Acids Research*, vol. 36, no. 10, pp. 3354–3365, 2008.
- [44] H.-M. Tseng and A. E. Tomkinson, "A physical and functional interaction between yeast Pol4 and Dnl4-Lif1 links DNA synthesis and ligation in nonhomologous end joining," *Journal of Biological Chemistry*, vol. 277, no. 47, pp. 45630–45637, 2002.
- [45] K. N. Mahajan, S. A. Nick McElhinny, B. S. Mitchell, and D. A. Ramsden, "Association of DNA polymerase  $\mu$  (pol  $\mu$ ) with Ku and ligase IV: Role for pol  $\mu$  in end-joining double-strand break repair," *Molecular and Cellular Biology*, vol. 22, no. 14, pp. 5194–5202, 2002.
- [46] M. R. Lieber, H. Lu, J. Gu, and K. Schwarz, "Flexibility in the order of action and in the enzymology of the nuclease, polymerases, and ligase of vertebrate non-homologous DNA end joining: relevance to cancer, aging, and the immune system," *Cell Research*, vol. 18, no. 1, pp. 125–133, 2008.
- [47] R. B. West, M. Yaneva, and M. R. Lieber, "Productive and nonproductive complexes of Ku and DNA-dependent protein kinase at DNA termini," *Molecular and Cellular Biology*, vol. 18, no. 10, pp. 5908–5920, 1998.
- [48] M. Falzon, J. W. Fewell, and E. L. Kuff, "EBP-80, a transcription factor closely resembling the human autoantigen Ku, recognizes single- to double-strand transitions in DNA," *Journal of Biological Chemistry*, vol. 268, no. 14, pp. 10546–10552, 1993.
- [49] T. Mimori and J. A. Hardin, "Mechanism of interaction between Ku protein and DNA," *Journal of Biological Chemistry*, vol. 261, no. 22, pp. 10375–10379, 1986.
- [50] C. Zhu, K. D. Mills, D. O. Ferguson et al., "Unrepaired DNA breaks in p53-deficient cells lead to oncogenic gene amplification subsequent to translocations," *Cell*, vol. 109, no. 7, pp. 811–821, 2002.

- [51] C. T. Yan, C. Boboila, E. K. Souza et al., "IgH class switching and translocations use a robust non-classical end-joining pathway," *Nature*, vol. 449, no. 7161, pp. 478–482, 2007.
- [52] B. Corneo, R. L. Wendland, L. Deriano et al., "Rag mutations reveal robust alternative end joining," *Nature*, vol. 449, no. 7161, pp. 483–486, 2007.
- [53] J. Guirouilh-Barbat, E. Rass, I. Plo, P. Bertrand, and B. S. Lopez, "Defects in XRCC4 and KU80 differentially affect the joining of distal nonhomologous ends," *Proceedings of the National Academy of Sciences of the United States of America*, vol. 104, no. 52, pp. 20902–20907, 2007.
- [54] M. Dinkelmann, E. Spehalski, T. Stoneham et al., "Multiple functions of MRN in end-joining pathways during isotype class switching," *Nature Structural and Molecular Biology*, vol. 16, no. 8, pp. 808–813, 2009.
- [55] L. Deriano, T. H. Stracker, A. Baker, J. H. J. Petrini, and D. B. Roth, "Roles for NBS1 in alternative nonhomologous end-joining of V(D)J recombination intermediates," *Molecular Cell*, vol. 34, no. 1, pp. 13–25, 2009.
- [56] I. Robert, F. Dantzer, and B. Reina-San-Martin, "Parp1 facilitates alternative NHEJ, whereas Parp2 suppresses IgH/c-myc translocations during immunoglobulin class switch recombination," *Journal of Experimental Medicine*, vol. 206, no. 5, pp. 1047–1056, 2009.
- [57] A. Sallmyr, A. E. Tomkinson, and F. V. Rassool, "Up-regulation of WRN and DNA ligase IIIalpha in chronic myeloid leukemia: consequences for the repair of DNA double-strand breaks," *Blood*, vol. 112, no. 4, pp. 1413–1423, 2008.
- [58] D. Simsek and M. Jasin, "Alternative end-joining is suppressed by the canonical NHEJ component Xrcc4-ligase IV during chromosomal translocation formation," *Nature Structural and Molecular Biology*, vol. 17, no. 4, pp. 410–416, 2010.
- [59] C. Boboila, M. Jankovic, C. T. Yan et al., "Alternative end-joining catalyzes robust IgH locus deletions and translocations in the combined absence of ligase 4 and Ku70," *Proceedings of the National Academy of Sciences of the United States of America*, vol. 107, no. 7, pp. 3034–3039, 2010.
- [60] D. B. Roth and J. H. Wilson, "Nonhomologous recombination in mammalian cells: role for short sequence homologies in the joining reaction," *Molecular and Cellular Biology*, vol. 6, no. 12, pp. 4295–4304, 1986.
- [61] D. B. Roth and J. H. Wilson, "Relative rates of homologous and nonhomologous recombination in transfected DNA," *Proceedings of the National Academy of Sciences of the United States of America*, vol. 82, no. 10, pp. 3355–3359, 1985.
- [62] U. Grawunder, D. Zimmer, S. Fugmann, K. Schwarz, and M. R. Lieber, "DNA ligase IV is essential for V(D)J recombination and DNA double-strand break repair in human precursor lymphocytes," *Molecular Cell*, vol. 2, no. 4, pp. 477–484, 1998.
- [63] D. B. Roth, T. N. Porter, and J. H. Wilson, "Mechanisms of nonhomologous recombination in mammalian cells," *Molecular and Cellular Biology*, vol. 5, no. 10, pp. 2599–2607, 1985.
- [64] M. Honma, M. Sakuraba, T. Koizumi, Y. Takashima, H. Sakamoto, and M. Hayashi, "Non-homologous end-joining for repairing I-SceI-induced DNA double strand breaks in human cells," *DNA Repair*, vol. 6, no. 6, pp. 781–788, 2007.
- [65] H. Willers, J. Husson, L. W. Lee et al., "Distinct mechanisms of nonhomologous end joining in the repair of site-directed chromosomal breaks with noncomplementary and complementary ends," *Radiation Research*, vol. 166, no. 4, pp. 567–574, 2006.
- [66] J. Thacker, "The role of homologous recombination processes in the repair of severe forms of DNA damage in mammalian cells," *Biochimie*, vol. 81, no. 1-2, pp. 77–85, 1999.
- [67] P. North, A. Ganesh, and J. Thacker, "The rejoining of double-strand breaks in DNA by human cell extracts," *Nucleic Acids Research*, vol. 18, no. 21, pp. 6205–6210, 1990.
- [68] C. R. Sathees and M. J. Raman, "Mouse testicular extracts process DNA double-strand breaks efficiently by DNA end-to-end joining," *Mutation Research*, vol. 433, no. 1, pp. 1–13, 1999.
- [69] A. L. Nicolas and C. S. H. Young, "Characterization of DNA end joining in a mammalian cell nuclear extract: junction formation is accompanied by nucleotide loss, which is limited and uniform but not site specific," *Molecular and Cellular Biology*, vol. 14, no. 1, pp. 170–180, 1994.
- [70] G. Pont-Kingdon, R. J. Dawson, and D. Carroll, "Intermediates in extrachromosomal homologous recombination in *Xenopus laevis* oocytes: characterization by electron microscopy," *EMBO Journal*, vol. 12, no. 1, pp. 23–34, 1993.
- [71] P. Pfeiffer and W. Vielmetter, "Joining of nonhomologous DNA double strand breaks in vitro," *Nucleic Acids Research*, vol. 16, no. 3, pp. 907–924, 1988.
- [72] M. K. Derbyshire, L. H. Epstein, C. S. H. Young, P. L. Munz, and R. Fishel, "Nonhomologous recombination in human cells," *Molecular and Cellular Biology*, vol. 14, no. 1, pp. 156–169, 1994.
- [73] S.-O. Boe, J. Sodroski, D. E. Helland, and C. M. Farnet, "DNA end-joining in extracts from human cells," *Biochemical and Biophysical Research Communications*, vol. 215, no. 3, pp. 987–993, 1995.
- [74] P. Baumann and S. C. West, "DNA end-joining catalyzed by human cell-free extracts," *Proceedings of the National Academy of Sciences of the United States of America*, vol. 95, no. 24, pp. 14066–14070, 1998.
- [75] J. Budman and G. Chu, "Processing of DNA for nonhomologous end-joining by cell-free extract," *EMBO Journal*, vol. 24, no. 4, pp. 849–860, 2005.
- [76] J. Gu, H. Lu, B. Tippin, N. Shimazaki, M. F. Goodman, and M. R. Lieber, "XRCC4:DNA ligase IV can ligate incompatible DNA ends and can ligate across gaps," *EMBO Journal*, vol. 26, no. 4, pp. 1010–1023, 2007.
- [77] P. Labhart, "Nonhomologous DNA end joining in cell-free systems," *European Journal of Biochemistry*, vol. 265, no. 3, pp. 849–861, 1999.
- [78] V. Manova, K. Gecheff, and L. Stoilov, "Efficient repair of bleomycin-induced double-strand breaks in barley ribosomal genes," *Mutation Research*, vol. 601, no. 1-2, pp. 179–190, 2006.
- [79] E. Pastwa, R. D. Neumann, and T. A. Winters, "In vitro repair of complex unligatable oxidatively induced DNA double-strand breaks by human cell extracts," *Nucleic Acids Research*, vol. 29, no. 16, p. E78, 2001.
- [80] S. Sharma, B. Choudhary, and S.C. Raghavan, "Efficiency of nonhomologous DNA end joining varies among somatic tissues, despite similarity in mechanism," *Cellular and Molecular Life Sciences*. In press.
- [81] J. L. Manley, A. Fire, A. Cano, P. A. Sharp, and M. L. Gelfer, "DNA-dependent transcription of adenovirus genes in a soluble whole-cell extract," *Proceedings of the National Academy of Sciences of the United States of America*, vol. 77, no. 7, pp. 3855–3859, 1980.

- [82] F. Coudoré, P. Calsou, and B. Salles, "DNA repair activity in protein extracts from rat tissues," *FEBS Letters*, vol. 414, no. 3, pp. 581–584, 1997.
- [83] R. D. Wood, P. Robins, and T. Lindahl, "Complementation of the xeroderma pigmentosum DNA repair defect in cell-free extracts," *Cell*, vol. 53, no. 1, pp. 97–106, 1988.
- [84] S. C. Raghavan and M. J. Raman, "Nonhomologous end joining of complementary and noncomplementary DNA termini in mouse testicular extracts," *DNA Repair*, vol. 3, no. 10, pp. 1297–1310, 2004.
- [85] C. P. Diggle, J. Bentley, and A. E. Kiltie, "Development of a rapid, small-scale DNA repair assay for use on clinical samples," *Nucleic Acids Research*, vol. 31, no. 15, p. e83, 2003.
- [86] S. Thode, A. Schafer, P. Pfeiffer, and W. Vielmetter, "A novel pathway of DNA end-to-end joining," *Cell*, vol. 60, no. 6, pp. 921–928, 1990.
- [87] C. W. Lehman, M. Clemens, D. K. Worthylake, J. K. Trautman, and D. Carroll, "Homologous and illegitimate recombination in developing *Xenopus* oocytes and eggs," *Molecular and Cellular Biology*, vol. 13, no. 11, pp. 6897–6906, 1993.
- [88] J. Thacker, J. Chalk, A. Ganesh, and P. North, "A mechanism for deletion formation in DNA by human cell extracts: the involvement of short sequence repeats," *Nucleic Acids Research*, vol. 20, no. 23, pp. 6183–6188, 1992.
- [89] P. Daza, S. Reichenberger, B. Göttlich, M. Hagmann, E. Feldmann, and P. Pfeiffer, "Mechanisms of nonhomologous DNA end-joining in frogs, mice and men," *Biological Chemistry*, vol. 377, no. 12, pp. 775–786, 1996.
- [90] A. Odersky, I. V. Panyutin, I. G. Panyutin et al., "Repair of sequence-specific 125I-induced double-strand breaks by nonhomologous DNA end joining in mammalian cell-free extracts," *Journal of Biological Chemistry*, vol. 277, no. 14, pp. 11756–11764, 2002.
- [91] P. Mérel, A. Prieur, P. Pfeiffer, and O. Delattre, "Absence of major defects in non-homologous DNA end joining in human breast cancer cell lines," *Oncogene*, vol. 21, no. 36, pp. 5654–5659, 2002.
- [92] K. Ren and S. Peña de Ortiz, "Non-homologous DNA end joining in the mature rat brain," *Journal of Neurochemistry*, vol. 80, no. 6, pp. 949–959, 2002.
- [93] V. N. Vyjayanti and K. S. Rao, "DNA double strand break repair in brain: reduced NHEJ activity in aging rat neurons," *Neuroscience Letters*, vol. 393, no. 1, pp. 18–22, 2006.
- [94] D. A. Shackelford, "DNA end joining activity is reduced in Alzheimer's disease," *Neurobiology of Aging*, vol. 27, no. 4, pp. 596–605, 2006.
- [95] D. B. Roth and J. H. Wilson, Eds., *Genetic Recombination*, American Society for Microbiology, Washington, DC, USA, 1988.
- [96] R. M. Mason, J. Thacker, and M. P. Fairman, "The joining of non-complementary DNA double-strand breaks by mammalian extracts," *Nucleic Acids Research*, vol. 24, no. 24, pp. 4946–4953, 1996.
- [97] M. McVey and S. E. Lee, "MMEJ repair of double-strand breaks (director's cut): deleted sequences and alternative endings," *Trends in Genetics*, vol. 24, no. 11, pp. 529–538, 2008.
- [98] S. C. Short, C. Martindale, S. Bourne, G. Brand, M. Woodcock, and P. Johnston, "DNA repair after irradiation in glioma cells and normal human astrocytes," *Neuro-Oncology*, vol. 9, no. 4, pp. 404–411, 2007.
- [99] F. Carlomagno, N. G. Burnet, I. Turesson et al., "Comparison of DNA repair protein expression and activities between human fibroblast cell lines with different radiosensitivities," *International Journal of Cancer*, vol. 85, no. 6, pp. 845–849, 2000.
- [100] R. Sandberg and I. Ernberg, "Assessment of tumor characteristic gene expression in cell lines using a tissue similarity index (TSI)," *Proceedings of the National Academy of Sciences of the United States of America*, vol. 102, no. 6, pp. 2052–2057, 2005.
- [101] S. M. Bentzen, "Preventing or reducing late side effects of radiation therapy: radiobiology meets molecular pathology," *Nature Reviews Cancer*, vol. 6, no. 9, pp. 702–713, 2006.
- [102] E. J. Hall and A. J. Giaccia, *Clinical Responses of Normal Tissues*, Lippincott, Williams and Wilkins, 2005.

## Research Article

# BRCA1 Forms a Functional Complex with $\gamma$ -H2AX as a Late Response to Genotoxic Stress

Susan A. Krum,<sup>1</sup> Esther de la Rosa Dalugdugan,<sup>2</sup> Gustavo A. Miranda-Carboni,<sup>2</sup>  
and Timothy F. Lane<sup>1,2,3</sup>

<sup>1</sup> Molecular Biology Institute, Jonsson Comprehensive Cancer Center, David Geffen School of Medicine at UCLA, Los Angeles, CA 90095, USA

<sup>2</sup> Department of Obstetrics and Gynecology, Jonsson Comprehensive Cancer Center, David Geffen School of Medicine at UCLA, Los Angeles, CA 90095, USA

<sup>3</sup> Department of Biological Chemistry, Jonsson Comprehensive Cancer Center, David Geffen School of Medicine at UCLA, Los Angeles, CA 90095, USA

Correspondence should be addressed to Timothy F. Lane, [tlane@mednet.ucla.edu](mailto:tlane@mednet.ucla.edu)

Received 3 April 2010; Accepted 7 June 2010

Academic Editor: Ashis Basu

Copyright © 2010 Susan A. Krum et al. This is an open access article distributed under the Creative Commons Attribution License, which permits unrestricted use, distribution, and reproduction in any medium, provided the original work is properly cited.

Following genotoxic stress, the histone H2AX becomes phosphorylated at serine 139 by the ATM/ATR family of kinases. The tumor suppressor BRCA1, also phosphorylated by ATM/ATR kinases, is one of several proteins that colocalize with phospho-H2AX ( $\gamma$ -H2AX) at sites of active DNA repair. Both the precise mechanism and the purpose of BRCA1 recruitment to sites of DNA damage are unknown. Here we show that BRCA1 and  $\gamma$ -H2AX form an acid-stable biochemical complex on chromatin after DNA damage. Maximal association of BRCA1 with  $\gamma$ -H2AX correlates with reduced global  $\gamma$ -H2AX levels on chromatin late in the repair process. Since BRCA1 is known to have E3 ubiquitin ligase activity *in vitro*, we examined H2AX for evidence of ubiquitination. We found that H2AX is ubiquitinated at lysines 119 and 119 *in vivo* and that blockage of 26S proteasome function stabilizes  $\gamma$ -H2AX levels within cells. When BRCA1 levels were reduced, ubiquitination of H2AX was also reduced, and the cells retained higher levels of phosphorylated H2AX. These results indicate that BRCA1 is recruited into stable complexes with  $\gamma$ -H2AX and that the complex is involved in attenuation of the  $\gamma$ -H2AX repair signal after DNA damage.

## 1. Introduction

One of the first observable responses to DNA damage is activation of DNA-PK family kinases and resulting phosphorylation of the histone variant H2AX on S<sub>139</sub> [1]. Due to the availability of excellent antibodies to S<sub>139</sub>-phosphorylated H2AX (a form of the protein called  $\gamma$ -H2AX), this modification is a widely recognized early marker of both genotoxic stress and normal DNA replication [2]. The tail region of H2AX includes a conserved SQ motif (S<sub>139</sub>Q<sub>140</sub>) that is recognized as the core target motif of DNA-PK family serine/threonine kinases (ATM [3], ATR [4], and DNA-PK [3, 5]).

Within minutes after DNA damage,  $\gamma$ -H2AX becomes identifiable and is localized to discrete nuclear foci [6]. The foci actually include large areas of chromatin flanking points of DNA damage [6]. After DNA damage, several

proteins are recruited to regions of  $\gamma$ -H2AX staining. These include the breast cancer susceptibility gene BRCA1, RAD51 [7], the NBS1/RAD50/MRE11 complex [1, 8], 53BP1 [9, 10], and MDC1 [11, 12]. Recruitment of most proteins to radiation-induced foci is dependent on ATM/ATR activity and formation of  $\gamma$ -H2AX, indicating that H2AX phosphorylation plays a key role in maintenance of irradiation-induced foci [13]. ATM is the major H2AX kinase in response to  $\gamma$ -irradiation [3] while ATR plays a larger role during DNA synthesis [4]. S<sub>139</sub> phosphorylation of H2AX is greatly reduced in ATM/ATR knockout cells and is completely blocked by treatment with wortmannin [3], an inhibitor of DNA-PK kinases.

Genetic and biochemical experiments support roles for BRCA1 in homologous recombination [7, 14], nonhomologous end joining [15, 16], and transcription-coupled repair [17]. BRCA1 null cells are extremely sensitive to  $\gamma$ -irradiation

and other types of genotoxic stress [18, 19]. Although the role of BRCA1 in DNA repair is not known, the N-terminal ring finger of BRCA1 interacts with the ring finger of BARD1 [20], and the complex has been shown to possess E3 ubiquitin ligase activity *in vitro* [21]. The E2 ubiquitin-conjugating enzyme (UbcH5c) has been shown to associate with this complex [21, 22], and several *in vitro* substrates have been identified, including monoubiquitinated histones H2AX, H2A, H2B, H3, and H4 (but not H1) [22]. So far, *in vivo* targets of the complex have been less clearly defined.

BRCA1 association with chromatin is properly considered an intermediate or late event in chromatin repair [1, 23]. Here we demonstrate by differential fractionation of chromatin bound BRCA1 complexes that BRCA1 and  $\gamma$ -H2AX form a biochemical complex in the chromatin fraction of cells as a late event following DNA damage. The complex is resistant to nonionic detergent extraction and is dependent on wortmannin-sensitive kinases, features that are distinct from BRCA1 prior to genomic stress. We show that a phosphomimetic of H2AX (H2AX-E<sub>139</sub>) is ubiquitinated *in vivo*, and the major site of ubiquitination is on K<sub>118</sub> and/or K<sub>119</sub>. When BRCA1 levels were reduced using an antisense morpholino knockdown strategy, we observed substantially reduction in H2AX ubiquitination and increased amounts of H2AX S<sub>139</sub> phosphorylation. These results are consistent with the hypothesis that BRCA1 is present in non-chromatin-associated complexes (including processive RNA polymerase II) prior to genotoxic stress; it becomes phosphorylated, moves into a stable chromatin-associated complex containing  $\gamma$ -H2AX, and then targets  $\gamma$ -H2AX for turnover as a late phase of DNA repair.

## 2. Materials and Methods

**2.1. Plasmids.** H2AX, H2AX-A<sub>139</sub>, and H2AX-E<sub>139</sub>, were generated by RT-PCR from human RNA using primers, described in the supplemental data (see Table 1 in Supplementary Material available online at doi: 10.4061/2011/801594), and cloned into pcDNA3.1D-V5-H6 (Invitrogen) to generate epitope-tagged variants. PCR-mediated mutagenesis was performed [24] using primers described in the supplementary data to generate additional mutations. pMT-HA-Ub (hemagglutinin tagged- ubiquitin) was the generous gift of Dr. Dirk Bohmann (University of Rochester).

**2.2. Cell Culture.** 293T, MCF-7, and HBL100 were maintained as described in [25].

**2.3. DNA Damage and Wortmannin.** Damage—randomly cycling HBL100 cells were treated with 4  $\mu$ M adriamycin or were exposed to 10 Gy ionizing radiation using a <sup>137</sup>Cs source (Mark 1 irradiator, Shepherd and Associates). Following treatments, cells were returned to a 5% CO<sub>2</sub> incubator for the indicated amount of time. Cells treated with wortmannin were first pretreated with 100  $\mu$ M wortmannin for 15 minutes [3].

**2.4. Immunoprecipitations and Immunoblotting.** Nuclei were prepared by extracting cells in EBC buffer (50 mM Tris pH 8.0, 120 mM NaCl, and 0.5% NP-40) as described in [25]. Nuclei were then treated with 0.1 M HCl for 30 minutes and neutralized with 0.1 M NaOH. This acid soluble “chromatin fraction” was centrifuged for 5 minutes at 14,000 RPM to remove insoluble material. Lysates were precleared with protein A or G beads and then incubated overnight with primary antibodies to  $\gamma$ -H2AX (Upstate Biotechnology) or BRCA1 (Ab-4, EMD Biosciences). Extracts were run on a 5% or 14% SDS-PAGE gel. Proteins were then transferred to nitrocellulose membranes, blocked in 5% nonfat dry milk, and incubated with a primary antibody generated against BRCA1 (Ab-4, EMD Biosciences),  $\gamma$ -H2AX (Upstate Biotechnology), H2A (H-124, Santa Cruz Biotechnology), RNA polymerase II (N-20, Santa Cruz Biotechnology or 8WG16 (provided by Dr. Michael Carey (UCLA)), FCP1 (provided by Dr. Michael E. Dahmus (UC Davis)), or  $\beta$ -actin (Sigma), followed by a goat antirabbit (or anti-mouse) horseradish peroxidase-conjugated secondary antibody (Pierce). Blots were developed with a chemiluminescence detection substrate (SuperSignal, Pierce).

**2.5. Immunocytochemistry.** Cells were fixed in 4% paraformaldehyde (PFA) for 30 minutes on ice.  $\gamma$ -H2AX was detected with an antibody from Upstate Biotechnology. Alexa-488-conjugated secondary antibodies (Molecular Probes) were used to visualize immune complexes, and photomicrographs were prepared as described in [25]. Quantitation of fluorescent  $\gamma$ -H2AX foci was accomplished using a Laser Scanning Cytometer (LSC, CompuCyte). Potential autofluorescence was carefully gated by tuning the lasers to optimize signal.

**2.6. Proteasome and Phosphatase Inhibitors.** Human MCF-7 or 293T cells were treated with 5  $\mu$ M adriamycin for 1 hour. Following adriamycin treatment, the cells were washed then treated with or without lactacystin (Sigma) or a serine/threonine phosphatase inhibitor cocktail [(−)-p-Bromotetramisole Oxalate, Cantharidin and Microcystin-LR] (EMD Biosciences) for 4 hours, after which the cells were fixed in 4% PFA.  $\gamma$ -H2AX was immunostained as described above. Quantitation of fluorescent  $\gamma$ -H2AX foci was accomplished using a Laser Scanning Cytometer (LSC, CompuCyte).

**2.7. Antisense Morpholino Oligos.** Two antisense morpholino oligos (Gene Tools, Inc.) were designed against BRCA1 (AS1 5′-GCGAAGAGCAGATAAATCCATTTCT-3′ and AS2 5′-TGTGCTGACTTACCAGATGGGACAC-3′). 20  $\mu$ L of each of the two 500  $\mu$ M morpholino antisense oligos were delivered into the cells using the EPEI delivery solution according to the manufacturer’s protocol. The remaining cells were treated with a serum-free media control, EPEI delivery solution (Gene Tools, Inc.), or 40  $\mu$ L of a 500  $\mu$ M scrambled control oligo (5′-CCTCTTACCTCAGTTACAATTTATA-3′). After a two-hour treatment, the media were replaced with serum-containing media. The cells were allowed to

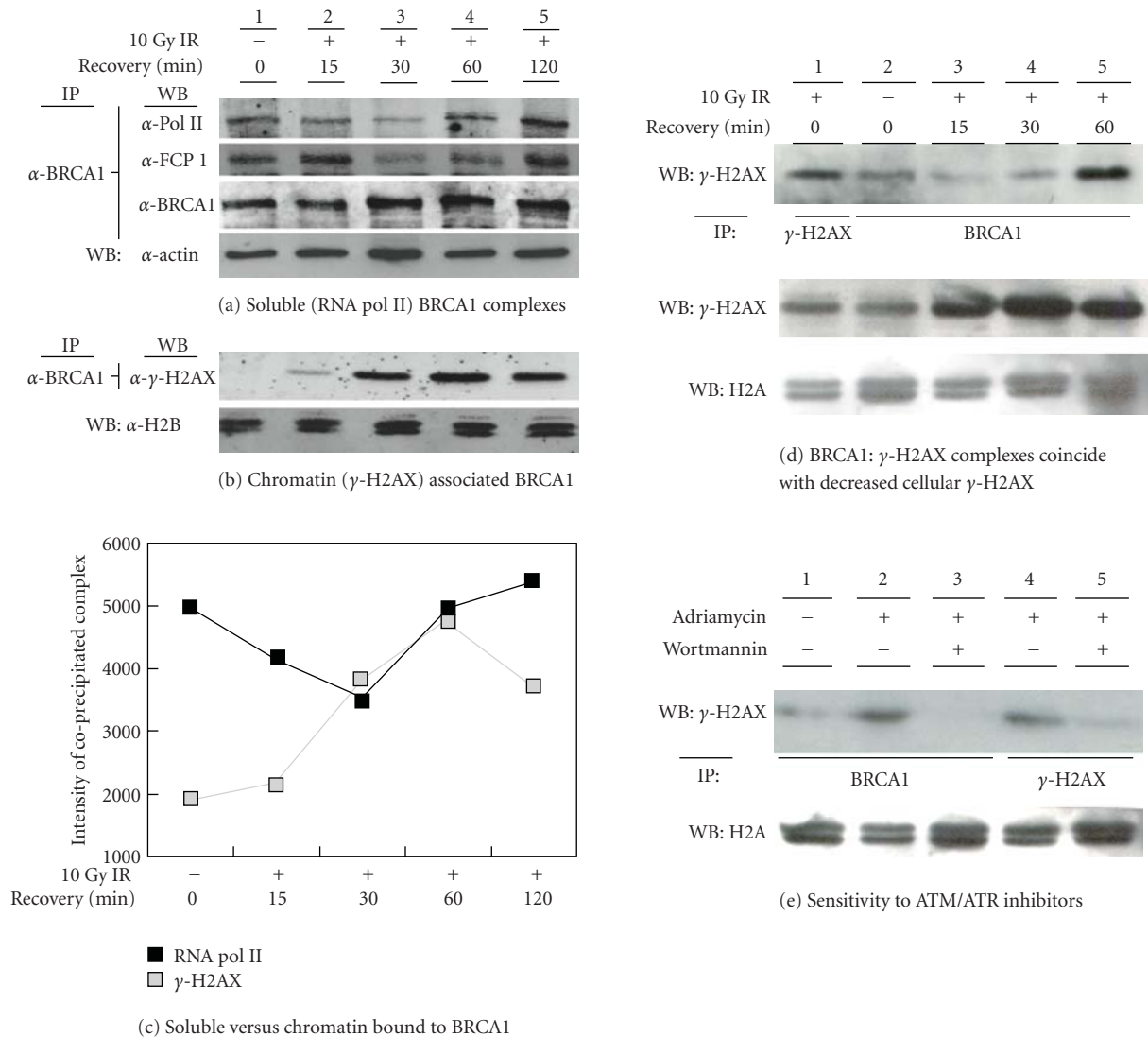


**FIGURE 1: BRCA1 moves into a chromatin complex containing S<sub>139</sub> phosphorylated H2AX ( $\gamma$ -H2AX) after DNA damage *in vivo*.** HBL100 cells were exposed to 10 Gy  $\gamma$ -irradiation (IR) or 4  $\mu$ M adriamycin then allowed to recover for the indicated time before isolation of protein complexes. (a) Nonchromatin (soluble) nuclear proteins from panel (a) were immunoprecipitated (IP) with antisera to BRCA1. Immunoprecipitates were treated with phosphatase (CIP) and immunoblotted (WB) using antibodies to RNA polymerase II (Pol II, 8WG16), FCP1, or BRCA1. 10% of the lysate was immunoblotted directly and probed for  $\beta$ -actin. (b) Total  $\gamma$ -H2AX and BRCA1-associated  $\gamma$ -H2AX were immunoprecipitated from the chromatin fraction of cells following IR. 10% of the chromatin fraction was blotted directly and probed for total H2B. (c) BRCA1 complexes identified in (a) and (b) were quantified and graphed as a function of time. (d) Chromatin-associated protein complexes were extracted (chromatin fraction) of cells exposed to IR as indicated. BRCA1 was immunoprecipitated (IP) from 90% of the chromatin extract, and immunoblots (WB) were probed with an antibody to  $\gamma$ -H2AX (S<sub>139</sub> phosphorylated H2AX). 10% of the chromatin fraction was blotted directly and probed for total H2A. (e) Cells were pretreated with wortmannin for 15 minutes prior to treatment with 4  $\mu$ M adriamycin for 1 hr. 90% of the chromatin fraction was immunoprecipitated (IP) with antibodies to either BRCA1 or  $\gamma$ -H2AX and blotted (WB) with an antibody to  $\gamma$ -H2AX. 10% of the chromatin fraction was blotted directly and probed for total H2A.

recover for 24 hours at which time they were lysed with EBC buffer. Data related to dose and effectiveness are provided (see supplementary data)

### 3. Results

**3.1. BRCA1 Interacts with  $\gamma$ -H2AX.** BRCA1 and  $\gamma$ -H2AX form a physical complex on chromatin following DNA

damage. Before DNA damage, small amounts of BRCA1 are present in the chromatin fraction, consistent with the percentage of S-phase nuclei in this population of cells [4, 7, 26]. After treatment with the DNA-damaging agent adriamycin, there is a substantial increase in acid-stable nuclear BRCA1:  $\gamma$ -H2AX complexes (Figure 1(a)). Stable interaction is minimal at early times following DNA damage then increases to the maximum at about 60 minutes. The

association is blocked by the ATM/ATR inhibitor wortmannin (Figure 1(b)). This data supports the hypothesis that interaction of BRCA1 and H2AX occurs well after DNA damage, requires phosphorylation by ATM or ATR [3, 27], and provides evidence that the interaction requires the formation of a stable complex.

**3.2. Time Course of the BRCA1 Complex Formation.** In order to analyze the kinetics of BRCA1 interactions, we examined BRCA1 complexes present in undamaged cells and in cells responding to DNA damage. In undamaged cells, we had previously demonstrated that BRCA1 interacts with the phosphorylated, transcriptionally active form of RNA polymerase II (RNA pol II) [25]. Following  $\gamma$ -irradiation, we found that the BRCA1:  $\gamma$ -H2AX complex was enhanced (Figure 1(a)) whereas the BRCA1:RNA pol II interaction is disrupted (Figure 1(c)). This shift accompanies the movement of BRCA1 from an easily extractable form in undamaged cells to a chromatin-associated form in damaged cells. The association between BRCA1 and  $\gamma$ -H2AX peaks about 30–60 minutes after DNA damage whereas the association between BRCA1 and RNA polymerase II is at the lowest 30–60 minutes after DNA damage (Figure 1(d)). FCP1, a protein that is part of the elongating pol II complex, has a similar pattern of association with BRCA1 as that of pol II (Figure 1(c)), illustrating the reciprocal functionality between BRCA1:  $\gamma$ -H2AX complex and the BRCA1:RNA pol II complex.

Further analysis of the timing of the BRCA1:  $\gamma$ -H2AX complex shows that this complex coincides with a decreased level of cellular  $\gamma$ -H2AX. When the BRCA1:  $\gamma$ -H2AX complex is at its highest level (about 60 minutes after DNA damage), the level of  $\gamma$ -H2AX has begun to decrease, as demonstrated by immunoblot of the total chromatin extract (Figure 1(e)).

**3.3. H2AX Is Ubiquitinated In Vivo.** Because BRCA1 is an E3 ubiquitin ligase, we hypothesized that the reduction of  $\gamma$ -H2AX seen following association with BRCA1 could be the result of ubiquitin-mediated proteasomal degradation. If this were true, then proteasome inhibitors should result in stabilized levels of  $\gamma$ -H2AX. BRCA1 has been shown to ubiquitinate H2AX *in vitro* [22]; therefore, we wanted to determine if  $\gamma$ -H2AX turnover was proteasome mediated. To test whether  $\gamma$ -H2AX was degraded by the 26S proteasome, MCF-7 mammary epithelial cells were treated with the DNA-damaging agent adriamycin then treated with or without the proteasome inhibitor lactacystin for an additional hour before fixation. Cells were fixed and immunostained to identify  $\gamma$ -H2AX high and  $\gamma$ -H2AX low cells. As shown in Figure 2(a), lactacystin increased the percentage of  $\gamma$ -H2AX high cells in the population of cells recovering from adriamycin treatment.

By this  $\gamma$ -H2AX immunofluorescence assay, 20% of untreated cells were found to be positive for high levels of  $\gamma$ -H2AX (Figure 2(b)). When cells were treated with adriamycin for 1 hour followed by 1 hour recovery,  $\gamma$ -H2AX immunofluorescence showed a 2-fold increase over

control cells, consistent with the view that H2AX was dynamically phosphorylated in response to DNA damage. The proteasome inhibitor lactacystin had a similar effect as adriamycin, when added alone, consistent with the hypothesis that  $\gamma$ -H2AX formation in normal cycling cells could be stabilized by proteasome inhibitors. When adriamycin-induced damage was followed by lactacystin treatment, there was a fourfold increase in the amount of  $\gamma$ -H2AX over control, resulting in over 80% of cells containing high levels of  $\gamma$ -H2AX by two hours. Addition of a phosphatase inhibitor cocktail also stabilized  $\gamma$ -H2AX level, suggesting that there may be additional ways to attenuate H2AX phosphorylation in cells. However, the phosphatase inhibitors alone did not cause stabilization or activation of  $\gamma$ -H2AX, indicating that proteasome-mediated turnover was a general mechanism to be addressed in further detail. These results provide evidence that  $\gamma$ -H2AX is degraded by the proteasome and potentially by other mechanisms requiring dephosphorylation of one or more components after DNA damage.

**3.4. H2AX Is Ubiquitinated at Lysine 118 and/or 119.** Previous reports have shown that histone H2A is polyubiquitinated on K<sub>119</sub>, and H2B had shown evidence of ubiquitination on K<sub>120</sub> [28]. To examine the role of ubiquitin modifications in  $\gamma$ -H2AX turnover we created a series of modifications intended to model phosphorylation at S<sub>139</sub> and the roles of various lysine (K) residues in the C terminus (Figure 3(a) and supplementary Figure 1). H2AX-V5-H6 was first mutagenized to replace S<sub>139</sub> with alanine (A) or glutamic acid (E), to mimic the negative charge of phosphorylation at S<sub>139</sub>. As predicted, H2AX-S<sub>139</sub>-V5-H6 localized to chromatin but was moderately less stable than the wild-type H2AX-V5-H6 or A<sub>139</sub> mutation products (not shown). Cotransfection of H2AX-S<sub>139</sub>-V5-H6 with a cytosolic form of BRCA1 lacking a nuclear localization sequence (BRCA1- $\Delta$ 11-GFP) resulted in nuclear localization of both proteins and rapid turnover (not shown). For these reasons, we hypothesized that H2AX-S<sub>139</sub> was mimicking S<sub>139</sub> phosphorylation and recruiting binding of BRCA1.

We then replaced each lysine (K) residue found in the conserved C-terminus of H2AX-E<sub>139</sub> with arginine (R) and tested for ubiquitination *in vivo* (Figure 3). K<sub>118</sub> and K<sub>119</sub> (which align with K<sub>119</sub> and K<sub>120</sub> of H2A) were mutated individually (Figure 3(c), lanes 6 and 7) and in combination (lane 8). K<sub>133</sub> and K<sub>134</sub> were also mutated individually (Figure 3(c), lanes 9 and 10) and in combination (lane 11) to arginine. Mutation of K<sub>128</sub> to R<sub>128</sub> was also prepared as part of this series but had no effect (data not shown). 293T cells were transfected with wild-type or mutagenized pcDNA3-H2AX-V5-H6 in addition to HA-tagged ubiquitin. H6-tagged complexes were purified using nickel-chelated beads, and bound proteins were analyzed by immunoblotting for the presence of HA-tagged H2AX (Ub-H2AX). As shown, V5 immunoblotting identified modified and ubiquitinated H2AX only when extracts from cotransfected cells were purified and blotted (Figure 3(b)). Reprobing these blots with anti-HA antisera revealed that the upper band contained ubiquitin (Figure 3(b)). While the

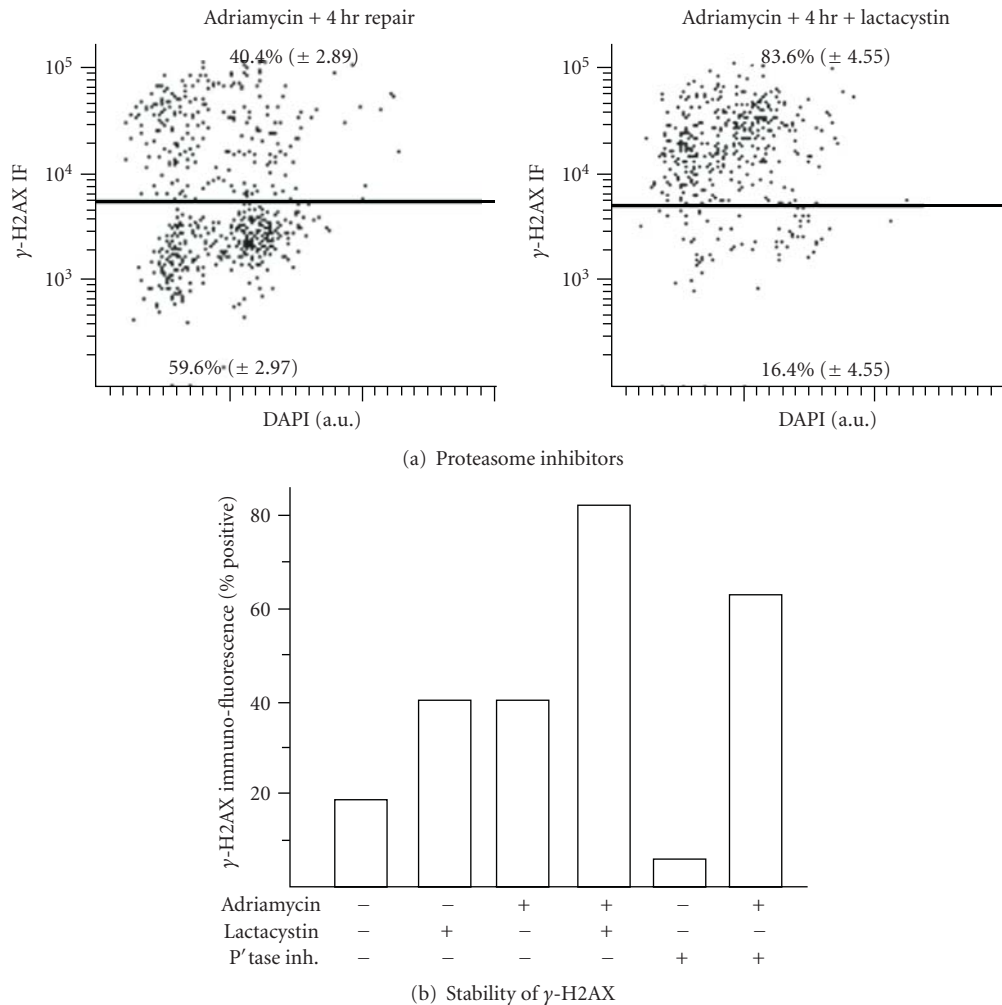


FIGURE 2: H2AX is dephosphorylated following DNA damage. MCF-7 cells were treated with adriamycin for 1 hour then treated with lactacystin or a phosphatase inhibitor (P'tase inh.) cocktail, as indicated. Cells were fixed and stained for  $\gamma$ -H2AX and quantitated using a Laser Scanning Cytometer.

major band migrated in a fashion consistent with that of monoubiquitinated H2AX, there were additional bands of immunoreactivity at higher molecular weights that suggested polyubiquitination as well (Figure 3(b) arrowheads). H2AX mutated at both K<sub>118</sub> and K<sub>119</sub> showed no ubiquitination (lane 8), indicating that H2AX is ubiquitinated at either K<sub>118</sub> or K<sub>119</sub>, whereas other point mutations showed levels of ubiquitination similar to wild type. These results show that H2AX-E<sub>139</sub> is ubiquitinated at either K<sub>118</sub> or K<sub>119</sub>.

**3.5. BRCA1 Knockdown Increases Steady State Levels of  $\gamma$ -H2AX Buy Reduction of Ubiquitination in Cells Undergoing Replicative Stress.** To functionally examine the interaction between BRCA1 and  $\gamma$ -H2AX, we used antisense morpholino oligonucleotides to knockdown BRCA1 expression. Treatment of cells with BRCA1 antisense oligonucleotides reduced the amount of BRCA1 to under 3% of normal levels (Figure 4(a), and supplemental data). Reduction of

BRCA1 protein resulted in increased levels of  $\gamma$ -H2AX expression by both immunofluorescence (Figure 4(a)) and immunoblotting (Figure 4(b)).

Cells treated with antisense oligos directed at BRCA1 mRNA were transfected with H2AX-V5-H6 and HA-tagged ubiquitin. The epitope-tagged H2AX product was then isolated using nickel-chelated beads and analyzed by immunoblotting for the presence of HA-tagged ubiquitin. Cells treated with BRCA1 antisense oligos had a reduction in the global amount of H2AX ubiquitination detected (Figure 4(c)). Efforts to examine the role of double-strand break repair on this process are underway but are complicated by the extreme sensitivity of BRCA1 deficient cells to genotoxic agents.

It has been shown previously that BRCA1 deficiency is associated with G2/M checkpoint and other defects [29–32]. To examine the relationship between BRCA1 and genotoxic stress more carefully, we examined cells treated with BRCA1

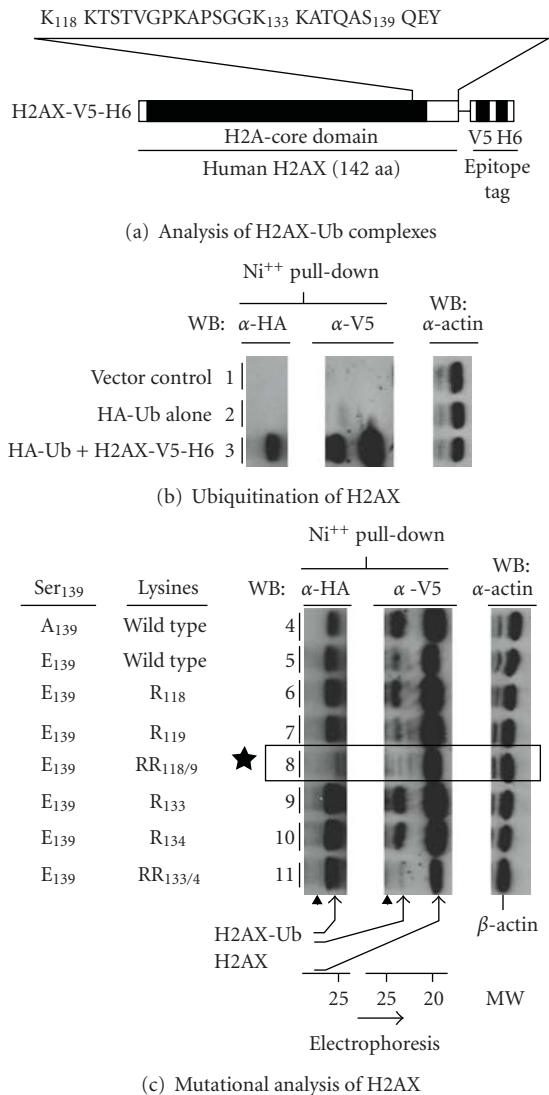


FIGURE 3: H2AX-E<sub>139</sub> is ubiquitinated at K<sub>118</sub> or K<sub>119</sub>. (a) Critical amino acids within the C-terminus are shown. (b) HA-tagged ubiquitin (HA-Ub) was transfected into cells with or without H2AX-V5-H6. His-tagged (H6) proteins were purified from chromatin fractions then probed sequentially for the presence of HA-ubiquitin and V5 epitopes (WB). 10% of the unfractionated extract was blotted directly and probed for  $\beta$ -actin. (c) H2AX variants containing E<sub>139</sub> (to mimic S<sub>139</sub> phosphorylation) and various lysine (K) to arginine (R) Substitutions were transfected with HA-tagged ubiquitin. Histidine-tagged proteins were purified from chromatin fractions then probed sequentially for the presence of HA-ubiquitin and V5 epitopes. 10% of the unfractionated extract was blotted directly and probed for  $\beta$ -actin. The star (lane 8) indicates the absence of HA-tagged ubiquitin. Arrows indicate unmodified and ubiquitinated H2AX.

antisense oligos for evidence that  $\gamma$ -H2AX stabilization correlated with replicative defects. We found that early in the response to BRCA1 knockdown,  $\gamma$ -H2AX expression was confined to cells in G2/M or late S-phase of the cell cycle (Figure 4(d)). Most cells with 2N DNA, as measured by DAPI fluorescence, had normal  $\gamma$ -H2AX staining patterns

## 4. Discussion

These results suggest that BRCA1 deficiency is associated with defective clearance of  $\gamma$ -H2AX from cells following replication and other types of genotoxic stress (Figure 5). We propose that BRCA1 interacts with processive RNA pol II in undamaged cells as part of a role in genomic surveillance (Figure 5(a)) [25, 33]. Following genotoxic stress, phosphorylation of BRCA1 by ATM/ATR and potentially by chk1 results in its dissociation from stalled RNA pol II complexes. We propose that an early repair complex forms on DNA as a consequence of ATM/ATR phosphorylation. Early targets for ATM/ATR include phosphorylation of H2AX to form  $\gamma$ -H2AX [34, 35].  $\gamma$ -H2AX then serves as a template to aid in the recruitment of early and late components of the repair machinery, including 53BP1 (Figure 5(b)) [36]. We propose that BRCA1 is recruited at later times, potentially after break repair has been affected. One target for BRCA1 recruitment is  $\gamma$ -H2AX, which is directly or indirectly ubiquitinated on K<sub>118</sub> or K<sub>119</sub> and degraded through the actions of the 26S proteasome (Figure 5(c)).

We have shown that BRCA1 is in a biochemical complex with  $\gamma$ -H2AX after DNA damage. This interaction is dependent on the DNA-PK family of kinases (ATM and/or ATR), as the interaction is disrupted by the inhibitor wortmannin. This data agrees with previous data that BRCA1 colocalizes with repair proteins and suggests a function for BRCA1 in the chromatin fraction of nuclei. BRCA1 becomes part of the BRCA1-associated surveillance complex (BASC), which includes many proteins involved in DNA repair, including MSH2, MSH6, MLH1, ATM, BLM, and the RAD50-MRE11-NBS1 protein complex [37]. BRCA1 and the BASC complex are localized at the site of DNA damage (nuclear foci). The repair factors are thus at the site of damage where they can perform their particular enzymatic activities and repair the DNA.

Using a mutant from of H2AX (H2AX-E<sub>139</sub>) designed to mimic phosphorylation at S<sub>139</sub> in  $\gamma$ -H2AX, we performed mutagenesis of several conserved lysine residues in the C-terminal end of H2AX. Results from these experiments suggest that ubiquitination is suppressed following mutation of both K<sub>118</sub> and K<sub>119</sub>, but not by mutation of other lysines either alone or in combination. Previously reports also showed that BRCA1 was capable of supporting ubiquitination of H2AX, but those studies were carried out in cell-free reactions *in vitro* [22]. Ubiquitination of K<sub>118</sub> and K<sub>119</sub> agrees with tryptic peptide data [38] that showed ubiquitination between residues 118 and 127.

We propose that a major function of BRCA1 is to decrease the levels of  $\gamma$ -H2AX in cells as a mechanism for signaling an end to early events in DNA repair. BRCA1 activity is then critical for timely attenuation of active repair phase. Defective production of BRCA1 in tumor cells would be expected to result in less ordered diminution of the repair signal and lead to problems in progression though G2/M phases of the cell cycle.

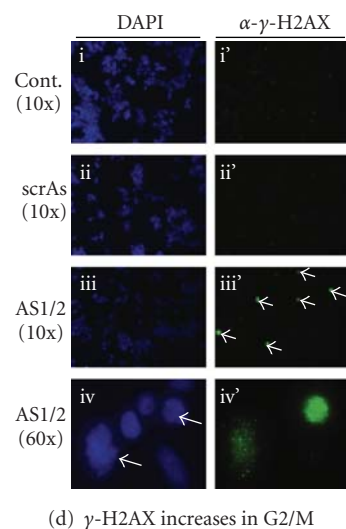
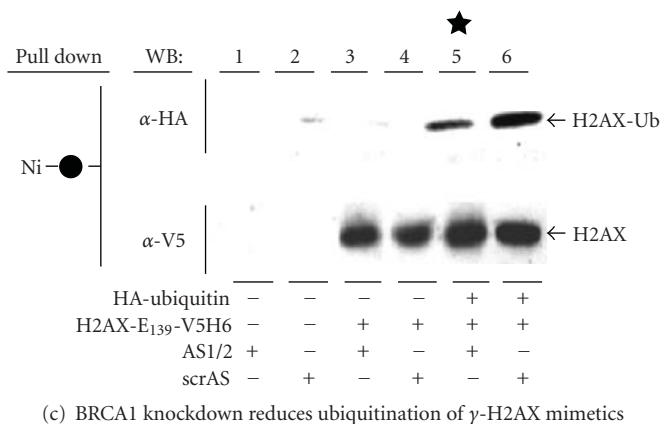
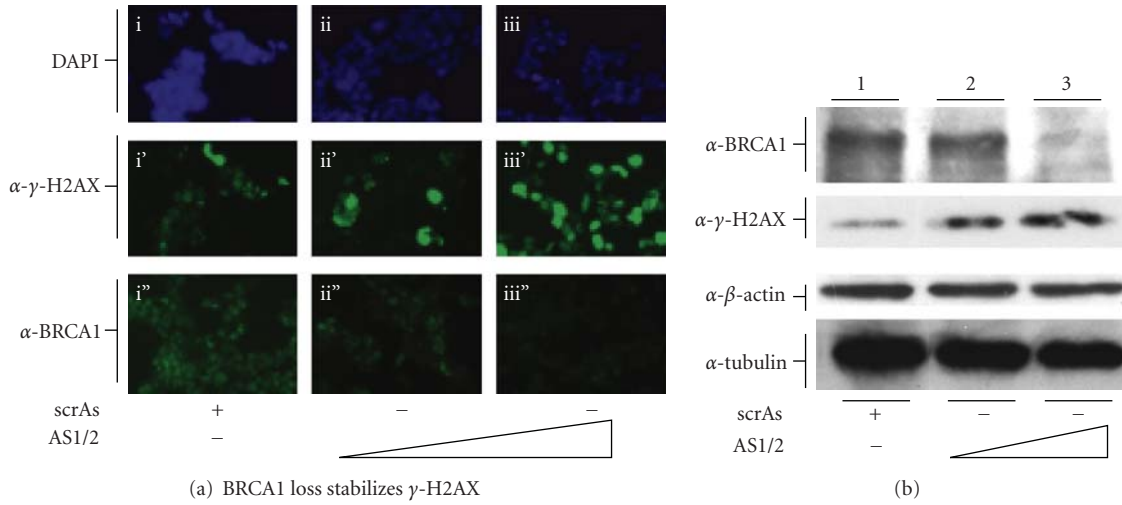


FIGURE 4: BRCA1 knockdown stabilizes  $\gamma$ -H2AX and reduces ubiquitination of  $\gamma$ -H2AX. (a) Cells treated with different amounts of antisense morpholino oligos (AS1 and AS2) or a scrambled antisense morpholino (scrAS) were stained with DAPI or immunostained for  $\gamma$ -H2AX. A second set of morpholino-treated cells was immunostained for BRCA1 to show dose-dependent knockdown of BRCA1 protein. (b) Cells treated with scrambled antisense morpholino (lane 1, scrAS) or increasing amounts of antisense morpholino oligos (AS1/2, lanes 2 and 3) were lysed and separated by SDS-PAGE and probed (WB) for BRCA1,  $\gamma$ -H2AX,  $\beta$ -actin, or  $\beta$ -tubulin. (c) 293T cells were treated with control (scrambled antisense (scrAS) or BRCA1 antisense morpholino oligos (AS1/2) and then transfected with control vector, HA-ubiquitin alone, and/or H2AX-E139-V5-H6. Histidine- (H6-) tagged H2AX was purified from chromatin fractions then probed for HA-ubiquitin. The blot was stripped and reprobred for V5-tag on H2AX. (d) Cells treated with a scrambled antisense morpholino (scrAS) or anti-BRCA1 morpholino oligos (AS1/2) were stained with DAPI (i–iv) or immunostained for  $\gamma$ -H2AX (i’–iv’). Micrographs were captured with either 10x (i–iii) or 60x (iv) objectives. Final magnification was 100x or 600x.

**Acknowledgments**

The authors are grateful for an NRSA predoctoral fellowship (no. GM07185) to Susan A. Krum. Esther de la Rosa Dalugdugan was supported by the UCLA CARE Program and by a Howard Hughes Medical Institute grant to the Undergraduate Biological Sciences Education Program of UCLA. Initial funding came from the UCLA Human Gene

Medicine Program, and the Stop Cancer Foundation, to Timothy F. Lane. The project also received support from the Ovarian Cancer Research Fund, the DOD C.D.M.R.P Breast Cancer Initiative, and the Cancer Research Coordinating Committee of the University of California. The authors thank Robert Lurvey for assistance with mutagenesis of H2AX and members of the Lane Lab for many helpful discussions.

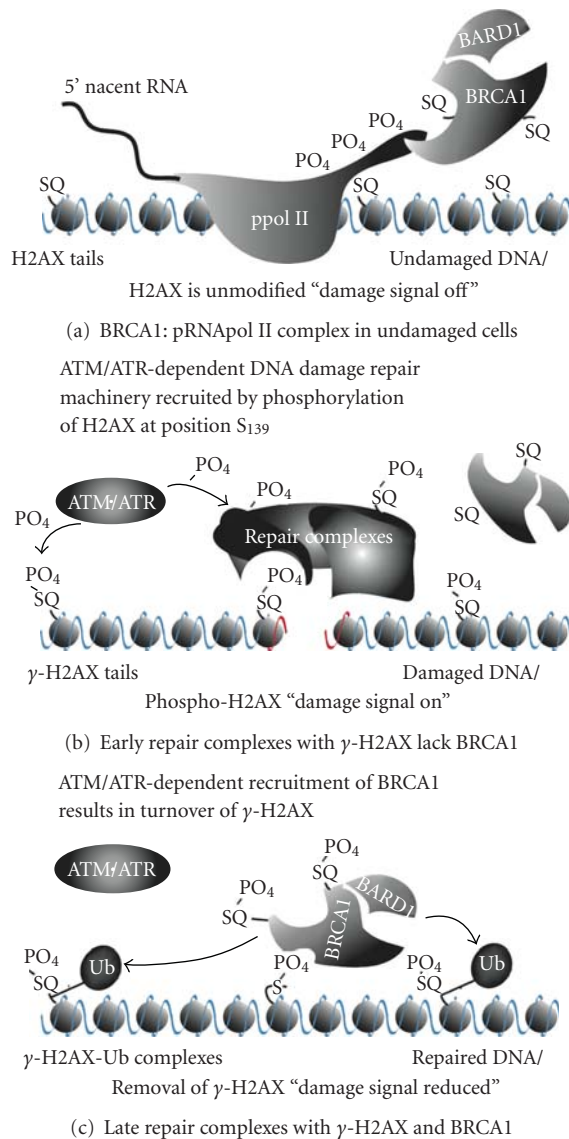


FIGURE 5: Model of BRCA1 interactions with RNA polymerase II and γ-H2AX in distinct biochemical complexes. See text for details.

## References

- [1] T. T. Paull, E. P. Rogakou, V. Yamazaki, C. U. Kirchgessner, M. Gellert, and W. M. Bonner, "A critical role for histone H2AX in recruitment of repair factors to nuclear foci after DNA damage," *Current Biology*, vol. 10, no. 15, pp. 886–895, 2000.
- [2] E. P. Rogakou, D. R. Pilch, A. H. Orr, V. S. Ivanova, and W. M. Bonner, "DNA double-stranded breaks induce histone H2AX phosphorylation on serine 139," *The Journal of Biological Chemistry*, vol. 273, no. 10, pp. 5858–5868, 1998.
- [3] S. Burma, B. P. Chen, M. Murphy, A. Kurimasa, and D. J. Chen, "ATM phosphorylates histone H2AX in response to DNA double-strand breaks," *The Journal of Biological Chemistry*, vol. 276, no. 45, pp. 42462–42467, 2001.
- [4] I. M. Ward and J. Chen, "Histone H2AX is phosphorylated in an ATR-dependent manner in response to replicational stress," *The Journal of Biological Chemistry*, vol. 276, no. 51, pp. 47759–47762, 2001.
- [5] E.-J. Park, D. W. Chan, J.-H. Park, M. A. Oettinger, and J. Kwon, "DNA-PK is activated by nucleosomes and phosphorylates H2AX within the nucleosomes in an acetylation-dependent manner," *Nucleic Acids Research*, vol. 31, no. 23, pp. 6819–6827, 2003.
- [6] E. P. Rogakou, C. Boon, C. Redon, and W. M. Bonner, "Megabase chromatin domains involved in DNA double-strand breaks in vivo," *Journal of Cell Biology*, vol. 146, no. 5, pp. 905–915, 1999.
- [7] R. Scully, J. Chen, A. Plug et al., "Association of BRCA1 with Rad51 in mitotic and meiotic cells," *Cell*, vol. 88, no. 2, pp. 265–275, 1997.
- [8] T. Furuta, H. Takemura, Z.-Y. Liao et al., "Phosphorylation of histone H2AX and activation of Mre11, Rad50, and Nbs1 in response to replication-dependent DNA double-strand breaks induced by mammalian DNA topoisomerase I cleavage complexes," *The Journal of Biological Chemistry*, vol. 278, no. 22, pp. 20303–20312, 2003.
- [9] S. Fan, J.-A. Wang, R. Yuan et al., "BRCA1 inhibition of estrogen receptor signaling in transfected cells," *Science*, vol. 284, no. 5418, pp. 1354–1356, 1999.
- [10] O. Fernandez-Capetillo, S. K. Mahadevaiah, A. Celeste et al., "H2AX is required for chromatin remodeling and inactivation of sex chromosomes in male mouse meiosis," *Developmental Cell*, vol. 4, no. 4, pp. 497–508, 2003.
- [11] G. S. Stewart, B. Wang, C. R. Bigneli, A. M. R. Taylor, and S. J. Elledge, "MDC1 is a mediator of the mammalian DNA damage checkpoint," *Nature*, vol. 421, no. 6926, pp. 961–966, 2003.
- [12] A. Peng and P.-L. Chen, "NFB1, like 53BP1, is an early and redundant transducer mediating Chk2 phosphorylation in response to DNA damage," *The Journal of Biological Chemistry*, vol. 278, no. 11, pp. 8873–8876, 2003.
- [13] A. Celeste, O. Fernandez-Capetillo, M. J. Kruhlak et al., "Histone H2AX phosphorylation is dispensable for the initial recognition of DNA breaks," *Nature Cell Biology*, vol. 5, no. 7, pp. 675–679, 2003.
- [14] M. E. Moynahan, J. W. Chiu, B. H. Koller, and M. Jasint, "Brca1 controls homology-directed DNA repair," *Molecular Cell*, vol. 4, no. 4, pp. 511–518, 1999.
- [15] H. Wang, Z.-C. Zeng, T.-A. Bui et al., "Nonhomologous end-joining of ionizing radiation-induced DNA double-stranded breaks in human tumor cells deficient in BRCA1 or BRCA2," *Cancer Research*, vol. 61, no. 1, pp. 270–277, 2001.
- [16] C. Baldeyron, E. Jacquemin, J. Smith et al., "A single mutated BRCA1 allele leads to impaired fidelity of double strand break end-joining," *Oncogene*, vol. 21, no. 9, pp. 1401–1410, 2002.
- [17] L. C. Gowen, A. V. Avrutskaya, A. M. Latour, B. H. Koller, and S. A. Leadon, "BRCA1 required for transcription-coupled repair of oxidative DNA damage," *Science*, vol. 281, no. 5379, pp. 1009–1012, 1998.
- [18] N. Chiba and J. D. Parvin, "Redistribution of BRCA1 among four different protein complexes following replication blockage," *The Journal of Biological Chemistry*, vol. 276, no. 42, pp. 38549–38554, 2001.
- [19] R. Scully, J. Chen, R. L. Ochs et al., "Dynamic changes of BRCA1 subnuclear location and phosphorylation state are initiated by DNA damage," *Cell*, vol. 90, no. 3, pp. 425–435, 1997.
- [20] L. C. Wu, Z. W. Wang, J. T. Tsan et al., "Identification of a RING protein that can interact in vivo with the BRCA1 gene product," *Nature Genetics*, vol. 14, no. 4, pp. 430–440, 1996.

- [21] R. Hashizume, M. Fukuda, I. Maeda et al., "The RING heterodimer BRCA1-BARD1 is a ubiquitin ligase inactivated by a breast cancer-derived mutation," *The Journal of Biological Chemistry*, vol. 276, no. 18, pp. 14537–14540, 2001.
- [22] D. L. Mallery, C. J. Vandenberg, and K. Hiom, "Activation of the E3 ligase function of the BRCA1/BARD1 complex by polyubiquitin chains," *The EMBO Journal*, vol. 21, no. 24, pp. 6755–6762, 2002.
- [23] A. Rothfuss and M. Grompe, "Repair kinetics of genomic interstrand DNA cross-links: evidence for DNA double-strand break-dependent activation of the Fanconi anemia/BRCA pathway," *Molecular and Cellular Biology*, vol. 24, no. 1, pp. 123–134, 2004.
- [24] M. Carey and S. T. Smale, *Transcriptional Regulation in Eukaryotes: Concepts, Strategies, and Technique*, Cold Spring Harbor Laboratory, 2001.
- [25] S. A. Krum, G. A. Miranda, C. Lin, and T. F. Lane, "BRCA1 associates with processive RNA polymerase II," *The Journal of Biological Chemistry*, vol. 278, no. 52, pp. 52012–52020, 2003.
- [26] Y. Chen, A. A. Farmer, C.-F. Chen, D. C. Jones, P.-L. Chen, and W.-H. Lee, "BRCA1 is a 220-kDa nuclear phosphoprotein that is expressed and phosphorylated in a cell cycle-dependent manner," *Cancer Research*, vol. 56, no. 14, pp. 3168–3172, 1996.
- [27] D. Cortez, Y. Wang, J. Qin, and S. J. Elledge, "Requirement of ATM-dependent phosphorylation of Brca1 in the DNA damage response to double-strand breaks," *Science*, vol. 286, no. 5442, pp. 1162–1166, 1999.
- [28] L. J. M. Jason, S. C. Moore, J. D. Lewis, G. Lindsey, and J. Ausió, "Histone ubiquitination: a tagging tail unfolds?" *BioEssays*, vol. 24, no. 2, pp. 166–174, 2002.
- [29] R.-H. Wang, H. Yu, and C.-X. Deng, "A requirement for breast-cancer-associated gene 1 (BRCA1) in the spindle checkpoint," *Proceedings of the National Academy of Sciences of the United States of America*, vol. 101, no. 49, pp. 17108–17113, 2004.
- [30] X. Wang, R.-H. Wang, W. Li et al., "Genetic interactions between Brca1 and Gadd45a in centrosome duplication, genetic stability, and neural tube closure," *The Journal of Biological Chemistry*, vol. 279, no. 28, pp. 29606–29614, 2004.
- [31] M. Ouchi, N. Fujiuchi, K. Sasai et al., "BRCA1 phosphorylation by Aurora-A in the regulation of G<sub>2</sub> to M transition," *The Journal of Biological Chemistry*, vol. 279, no. 19, pp. 19643–19648, 2004.
- [32] L. M. Starita, Y. Machida, S. Sankaran et al., "BRCA1-dependent ubiquitination of  $\gamma$ -tubulin regulates centrosome number," *Molecular and Cellular Biology*, vol. 24, no. 19, pp. 8457–8466, 2004.
- [33] P. Čabart, H. K. Chew, and S. Murphy, "BRCA1 cooperates with NUFIP and P-TEFb to activate transcription by RNA polymerase II," *Oncogene*, vol. 23, no. 31, pp. 5316–5329, 2004.
- [34] P. J. McKinnon, "ATM and ataxia telangiectasia. Second in molecular medicine review series," *EMBO Reports*, vol. 5, no. 8, pp. 772–776, 2004.
- [35] N. Motoyama and K. Naka, "DNA damage tumor suppressor genes and genomic instability," *Current Opinion in Genetics and Development*, vol. 14, no. 1, pp. 11–16, 2004.
- [36] B. Wang, S. Matsuoka, P. B. Carpenter, and S. J. Elledge, "53BP1, a mediator of the DNA damage checkpoint," *Science*, vol. 298, no. 5597, pp. 1435–1438, 2002.
- [37] Y. Wang, D. Cortez, P. Yazdi, N. Neff, S. J. Elledge, and J. Qin, "BASC, a super complex of BRCA1-associated proteins involved in the recognition and repair of aberrant DNA structures," *Genes and Development*, vol. 14, no. 8, pp. 927–939, 2000.
- [38] M. H. P. West, R. S. Wu, and W. M. Bonner, "Polyacrylamide gel electrophoresis of small peptides," *Electrophoresis*, vol. 5, no. 3, pp. 133–138, 1984.

## Research Article

# Modulation of the Ribonucleotide Reductase-Antimetabolite Drug Interaction in Cancer Cell Lines

Jun Zhou,<sup>1,2</sup> Paula Oliveira,<sup>1,2</sup> Xueli Li,<sup>1</sup> Zhengming Chen,<sup>1,2</sup> and Gerold Bepler<sup>1,2</sup>

<sup>1</sup>Department of Thoracic Oncology, Moffitt Cancer Center, Tampa, FL 33612, USA

<sup>2</sup>Department of Oncology, Karmanos Cancer Institute, Detroit, MI 48201, USA

Correspondence should be addressed to Gerold Bepler, bepler@karmanos.org

Received 29 March 2010; Revised 14 July 2010; Accepted 1 September 2010

Academic Editor: Caroline Kisker

Copyright © 2010 Jun Zhou et al. This is an open access article distributed under the Creative Commons Attribution License, which permits unrestricted use, distribution, and reproduction in any medium, provided the original work is properly cited.

RRM1 is a determinant of gemcitabine efficacy in cancer patients. However, the precision of predicting tumor response based on RRM1 levels is not optimal. We used gene-specific overexpression and RNA interference to assess RRM1's impact on different classes of cytotoxic agents, on drug-drug interactions, and the modulating impact of other molecular and cellular parameters. RRM1 was the dominant determinant of gemcitabine efficacy in various cancer cell lines. RRM1 also impacted the efficacy of other antimetabolite agents. It did not disrupt the interaction of two cytotoxic agents when combined. Cell lines with truncation, deletion, and null status of p53 were resistant to gemcitabine without apparent relationship to RRM1 levels. Pemetrexed and carboplatin sensitivity did not appear to be related to p53 mutation status. The impact of p53 mutations in patients treated with gemcitabine should be studied in prospective clinical trials to develop a model with improved precision of predicting drug efficacy.

## 1. Introduction

The regulatory subunit of ribonucleotide reductase (RRM1) has been identified as the key molecular determinant of gemcitabine efficacy both *in vitro* and *in vivo* [1–7]. Human lung and pancreatic cancer cell lines and a serially transplanted mouse colon cancer made resistant to gemcitabine through continuous exposure to increasing amounts of drug overexpressed RRM1 [1, 3, 5]. RRM1 overexpression through transfection of a lung cancer cell line likewise resulted in gemcitabine resistance [4]. Reduction of RRM1 expression through RNA interference abrogated the induced gemcitabine resistance and increased drug sensitivity in otherwise sensitive cell lines [4, 5].

An association between intratumoral RRM1 levels and efficacy of systemic therapy that includes gemcitabine as a single-agent or in combination with a platinum-agent or pemetrexed has also been reported [8]. However, the addition of a vinca-alkaloid (vinorelbine) to a gemcitabine-containing combination in patients with non-smallcell lung cancer (NSCLC) appeared to abrogate the RRM1-gemcitabine efficacy association [2]. Although gemcitabine therapy is statistically significantly more efficacious

in patients with low tumoral RRM1 levels, the scatter plots reported and correlation coefficients are less than optimal for precise predictions on whether or not gemcitabine will result in tumor shrinkage in individual patients [7].

Here we studied associations between RRM1 expression levels and sensitivities to frequently used chemotherapeutic single agents and combinations as well as cell lines characteristics in an effort to determine the impact of RRM1 on relevant classes of agents and to identify parameters that might modify the RRM1-gemcitabine efficacy interaction.

## 2. Material and Methods

**2.1. Cell Lines and Culture Conditions.** The cell lines used in this study were obtained from the American Type Culture Collection (ATCC) or the originators. MCF7 human mammary adenocarcinoma cells were maintained in MEM- $\alpha$  supplemented with 10% fetal bovine serum, penicillin/streptomycin, nonessential aminoacids (0.1 mM), sodium pyruvate (1 mM), sodium bicarbonate (1.5 g/L), and bovine pancreatic insulin (Sigma Aldrich, 0.01 mg/mL). All NSCLC cell lines and HCT8 (human colonic adenocarcinoma cells) were maintained in RPMI 1640 supplemented

with L-glutamine (2 mM), penicillin/streptomycin (100 units/100  $\mu$ g per mL), and 10% fetal bovine serum. Unless otherwise specified, all reagents were purchased from Gibco (Invitrogen). All cell lines were free of mycoplasma contamination (Stratagene), their authenticity was confirmed by DNA fingerprint analysis, and testing was performed within 6 months of *in vitro* propagation for experiments described herein. They were harvested at 70% confluency for subsequent experiments.

**2.2. RRM1 and p53 Transfected Cell Lines.** We have generated three human cell line models derived from lung (H23), breast (MCF7), and colon (HCT8) cancers, with increased and decreased RRM1 expression by stable transfection as previously described [9]. In general, stably overexpressing RRM1 cell lines and their controls were generated by transfection with full-length human RRM1 cDNA cloned into the expression plasmid pCMV-Tag2 (Stratagene). Stably down-regulated RRM1 cell lines were generated by transfection with pSUPER-GFP (oligoEngine) containing RRM1-specific target sequence (GACGCTAGAGCGGTCTTAT) or, as a control, scramble sequence that had no similarity to any known gene using FuGENE HD (Roche Applied Science). The overexpression and down regulation of RRM1 were confirmed by real-time RT-PCR and immunoblotting. A stably TP53 wild-type expressing cell line (H358-p53+) was generated by transfection with a pcDNA3 vector containing full-length TP53 cDNA (a gift from Dr. Jiandong Chen).

**2.3. Target Gene Expression Reduction.** Dharmacon on-TARGETplus Smartpool siRNA to TP53, ERCC1, and RRM1 (Dharmacon RNAi Technologies) were delivered to H23, A549, H292, and H460 NSCLC cell lines using Lipofectamine RNAiMAX (Invitrogen) following manufacturer's instructions. Nontarget Pool siRNA was used as control.

**2.4. Isolation of Total Cellular RNA and Real-Time PCR.** Total RNA was isolated from cultured cells with TRIzol reagent (Invitrogen), and cDNA was synthesized with the Superscript amplification kit (Invitrogen). Quantitative real-time PCR was employed to measure the expression of RRM1 using 18s-rRNA as internal reference standard. The RRM1 primers were forward AAGAG CAGCG TGCCA GAGAT, reverse ACACA TCAAA GACCA GTCCT GATTA G, and probe 5' TTTGC TCTTT GGATT CCGGA TCTCT TCA 3'. 18s-rRNA was detected using commercial primers and probes (Applied Biosystems). For each sample, the target RRM1 and 18s-rRNA concentrations were determined by interpolation to a standard curve. The normalized RRM1 quantity was then derived by dividing the RRM1 value by the 18s-rRNA value.

**2.5. Drug Sensitivity and In Vitro Proliferation Assay.** The following anticancer drugs were tested: gemcitabine and pemetrexed (Eli Lilly), methotrexate, carboplatin, hydroxyurea, and 5-fluorouracil (Sigma Aldrich); docetaxel (Sanofi-Aventis); cisplatin (Ben Venue Laboratory), vinorelbine (Sicor), and etoposide (Bedford Laboratory). At the time of

use, the drugs were freshly prepared and diluted stepwise to the desired concentration in the proper solvent or culture medium.

Cell viability in response to various drugs was assessed with a cell proliferation 3-(4,5-dimethylthiazol-2-yl)-5-(3-carboxymethoxyphenyl)-2-(4-sulfophenyl)-2H-tetrazolium (MTS) assay in 96-well plates (Corning). Briefly, 1,000–4,000 viable cells were seeded in triplicate in 100  $\mu$ L of growth medium and allowed to attach for 24 h. The cells were then continuously exposed to 0.01 nM–1 mM of each drug (0.1 nM–10 mM for hydroxyurea) for 3–10 days. Thereafter, cells were exposed to CellTiter96 AQ<sub>ueous</sub> One Solution Reagent (Promega) for 2 h at 37°C, and formazan absorbance was measured at 490 nm using a microplate reader (Benchmark Plus, Bio-Rad). Each experiment was repeated 3 times on different days with separate preparations of cells and drugs.

Alternately, drug activity was assessed using the CellTiter-Blue viability assay in 384-well plates (Promega). In this format, 800 or 1,200 cells (for 5-day or 3-day experiments, respectively) were plated in each well by using a Precision XS automated pipetting system (Bio-Tek Instruments) and allowed to attach overnight at 37°C. The respective drugs and combinations were serially diluted in growth medium, and 5  $\mu$ L were then added to wells. Four replicate wells were used for each drug concentration and an additional four control wells received media without drug. After 3 or 5 days of incubation, 5  $\mu$ L CellTiter-Blue solution was added to each well. Cell viability was assessed by the ability of the metabolically active cells to reduce resazurin to the highly fluorescent resorufin. The resulting fluorescence (560Ex/590Em) was measured with a Synergy HT microplate reader (Bio-Tek Instruments).

For both, the 96-well and 384-well experiments, fluorescence data were transferred to a spreadsheet program to calculate the percent viability relative to the replicate control cell wells that did not receive drug. Data analysis for IC<sub>50</sub> value calculations was performed using SigmaPlot (Systat Software).

For drug combination experiments, the IC<sub>50</sub> values obtained from single drug assays were used to design the experiments, and the cell viability assays were performed as described above. The results were analyzed for synergistic, additive, or antagonistic effects using the combination index (CI) method developed by Chou [10]. For the application of this method, the drug concentration dilutions were used at fixed dose ratios (e.g., 50 : 1, 2 : 5, 1 : 250). Briefly, the dose-effect curve for each drug alone was determined based on experimental observations using the median-effect principle and compared to the effect achieved with a combination of two drugs to derive a CI value. The method involves plotting dose-effect curves, for each agent and their combination, using the median-effect equation:  $f_a/f_u = (D/D_m)^m$ , where  $D$  is the dose of the drug,  $D_m$  the dose required for a 50% effect (equivalent to IC<sub>50</sub>),  $f_a$  and  $f_u$  the affected and unaffected fractions ( $f_a = 1 - f_u$ ), and  $m$  the exponent signifying the sigmoidicity of the dose-effect curve. The computer software XLfit was used to calculate the values of  $D_m$  and  $m$ . The CI used for the analysis of the drug combinations

was determined by the isobologram equation for mutually nonexclusive drugs that have different modes of action:  $CI = (D)_1/(Dx)_1 + (D)_2/(Dx)_2 + (D)_1(D)_2/(Dx)_1(Dx)_2$ , where  $(Dx)_1$  and  $(Dx)_2$  in the denominators are the doses (or concentrations) for drug 1 and drug 2 alone that gives  $x\%$  inhibition, whereas  $(D)_1$  and  $(D)_2$  in the numerators are the doses of drug 1 and drug 2 in combination that also inhibited  $x\%$  (i.e., isoeffective). Combination indices  $CI < 1$ ,  $CI = 1$ , and  $CI > 1$  indicate synergism, additive effects, and antagonism, respectively.

**2.6. Immunoblotting and Antibody Reagents.** Tumor cells were cultured as described above. Crude cell extract proteins were suspended in RIPA buffer in the presence of a protease inhibitor cocktail. After determination of the protein concentration, extracts were separated on 8%–10% SDS-PAGE gels, transferred to membranes, and the expression profiles analyzed by immunoblotting. Monoclonal antibodies or antisera to RRM1 (T-16, cat # sc-11733, lot # H0608), RRM2a (I-15, cat # sc-10848, lot # G1806), RRM2b (N-16, cat # sc-10840, lot # E2107), P38 (H-147, cat # sc-7149, lot # I149), ERCC1 (FL-297, cat # sc-10785, lot # G1103), and MCM2 (N-19, cat # sc-9839, lot # I1907) were purchased from Santa Cruz Biotechnology, and monoclonal antibody to TS (TS-106, cat # MS-471-p1, lot # 471P708B) was from Anatomical Pathology and to TP53 (p53, cat # 554293, lot # 0000045190) from BD Bioscience. The bound antibody was detected using the ECL detection system according to manufacturer's instructions (Amersham Pharmacia Biotech). The intensity values of specific bands were quantified with a Personal Densitometer SI (Molecular Dynamics). To compare expression values among the different cell lines, the target protein values were normalized by comparison with the house keep gene  $\beta$ -actin. These adjusted measures were then assigned the value 1.0 in cell line H23 to obtain relative adjusted values for all other cell lines.

**2.7. DNA Sequencing.** DNA sequencing of the p53 and K-ras genes was done using the Applied Biosystems 3130XL genetic analysis system. Genomic DNA from tumor cell lines was obtained with PureLink Genomic DNA kits (Invitrogen). Exons of the p53 gene were amplified using previously reported primers with minor modifications [11]. For K-ras, codon 12 and 13 were sequenced bidirectionally. For p53, all 11 exons were sequenced in both directions. All sequence data were confirmed with publicly available information.

### 3. Results

**3.1. Impact of RRM1 Modulation on Different Classes of Agents.** We had previously described the stably transfected RRM1 up- and down-regulated clones of NSCLC cell line H23 [4]. To expand and complement this model, we generated similar clones for the human breast cancer cell line MCF7 and colon cancer cell line HCT8. RRM1 expression at the mRNA and protein level was variable among clones. For drug testing, clones with a greater than 2-fold increase (for up regulation) or a greater than 2-fold decrease (expression

<50% of control) in RRM1 expression at the mRNA and protein level were selected (Figures 1(a), 1(b)).

To evaluate the impact of RRM1 on different classes of chemotherapeutic agents, clones with high and low RRM1 levels and their respective controls were treated with each agent over a broad range of concentrations. Dose response blots were generated and mean  $IC_{50}$  values calculated from at least 3 independent experiments (Table 1). For all agents, a dose-dependent inhibition was observed (Figure 1(c)). The relative impact of RRM1 was assessed by dividing the  $IC_{50}$  values of RRM1 modulated clones with those of control clones (Table 1). High RRM1 levels resulted in resistance and low levels in sensitivity to gemcitabine and 5-FU in NSCLC cell line H23, breast cancer cell line MCF7, and colon cancer cell line HCT8. Similarly, high RRM1 induced resistance to methotrexate and pemetrexed in H23, but low levels induced only a minimal increase in sensitivity. In MCF7 and HCT8, no effect on methotrexate was observed and the effect on pemetrexed was in the opposite direction; that is, high RRM1 was associated with increased sensitivity and low levels with resistance. Hydroxyurea was not affected by RRM1 in H23, but low levels resulted in increased sensitivity in MCF and HCT8.

For the platinum agents cisplatin and carboplatin, high or low RRM1 induced minimal resistance or sensitivity in H23 and had no consistent impact in MCF7 and HCT8. There was no observable relationship between RRM1 levels and efficacy of docetaxel, vinorelbine, and etoposide in all three model systems.

**3.2. Impact of RRM1 Modulation on Drug Combinations in H23.** We next assessed if RRM1 modulation would impact on the cytotoxicity of combinations of two agents. For this, we chose four commonly used chemotherapy doublets focused on antimetabolites in NSCLC; that is, gemcitabine + carboplatin, gemcitabine + docetaxel, gemcitabine + pemetrexed, and pemetrexed + carboplatin. The assays and analyses were as described using synchronous drug exposure, and a combination index (CI) was calculated from three separate experiments (Table 2). We observed synergy for the two platinum combinations and antagonism for the two nonplatinum combinations. RRM1 expression levels did not abrogate or reverse these interactions, although the CI values differed slightly among the RRM1 modulated clones.

**3.3. Down Regulation of RRM1 by RNA Interference Increases Gemcitabine Sensitivity in Other NSCLC Cell Lines.** To confirm if RRM1 downregulation would increase gemcitabine efficacy in other NSCLC cell lines, we transfected 20 nM of target-specific short interfering RNA (siRNA) and nonspecific random siRNA for control purposes into cell lines A549, H292, and H460. Since ERCC1 (excision repair cross complementing group 1) expression levels in lung cancers are positively correlated with those of RRM1, we also used ERCC1-specific siRNA as a control. Immunoblot analysis demonstrated efficient knock-down of the specific target proteins RRM1 and ERCC1 in all three cell lines

TABLE 1:  $IC_{50}$  ratios of clones with high and low RRM1 expression of three cell lines for different cytotoxic agents.\*

	H23			MCF7			HCT8			
	RRM1 up	RRM1 down	Control	RRM1 up	RRM1 down	Control	RRM1 up	RRM1 down	Control	
	IC50 Ratio Mean SE	IC50 Ratio Mean SE	IC50 $\mu$ M	IC50 Ratio Mean SE	IC50 Ratio Mean SE	IC50 $\mu$ M	IC50 Ratio Mean SE	IC50 Ratio Mean SE	IC50 $\mu$ M	
<b>Antimetabolites</b>										
Gemcitabine	1.80*	0.22	0.44*	0.06	0.47*	0.013	1.80*	0.16	0.49*	0.08
Hydroxyurea	0.87	0.01	1.18	0.05	0.50*	1547.900	1.20	0.10	0.57*	0.02
Methotrexate	2.30*	0.21	0.87	0.26	1.14	0.026	1.03	0.12	1.03	0.17
Pemetrexed	2.49*	0.25	0.80	0.02	1.20	0.109	0.49*	0.07	2.10*	0.38
5-Fluorouracil	2.09*	0.97	0.23*	0.05	0.59*	39.223	5.56*	0.50	0.44*	
<b>Platinum Compounds</b>										
Cisplatin	1.54*	0.06	0.75*	0.02	0.80	5.653	0.79*	0.04	1.04	0.11
Carboplatin	1.31*	0.61	0.59*	0.16	1.15	21.558	no data		no data	
<b>Mitosis Inhibitors</b>										
Docetaxel	1.21	0.44	0.90	0.17	0.79	0.013	0.94	0.16	1.18	0.04
Vinorelbine	0.96	0.16	1.00	0.21	0.98	0.072	0.98	0.10	1.14	0.14
<b>Topoisomerase Inhibitors</b>										
Etoposide	1.15	0.06	1.14	0.06	1.06	0.183	1.18	0.14	1.03	0.17

\*  $IC_{50}$  values for the wild-type cell lines for each of the drugs tested are listed in the column labeled "Control". The  $IC_{50}$  ratios for RRM1 up- and down-regulated clones for cell lines H23, MCF7, and HCT8 were calculated as described in the Material and Methods section. Values greater than 1 indicated that higher drug concentrations are required to reach the  $IC_{50}$ ; that is, drug resistance. Values smaller than 1 indicated that the lower drug concentrations are required to reach the  $IC_{50}$ ; that is, drug sensitivity. \* Indicates values considered to be significantly changed.

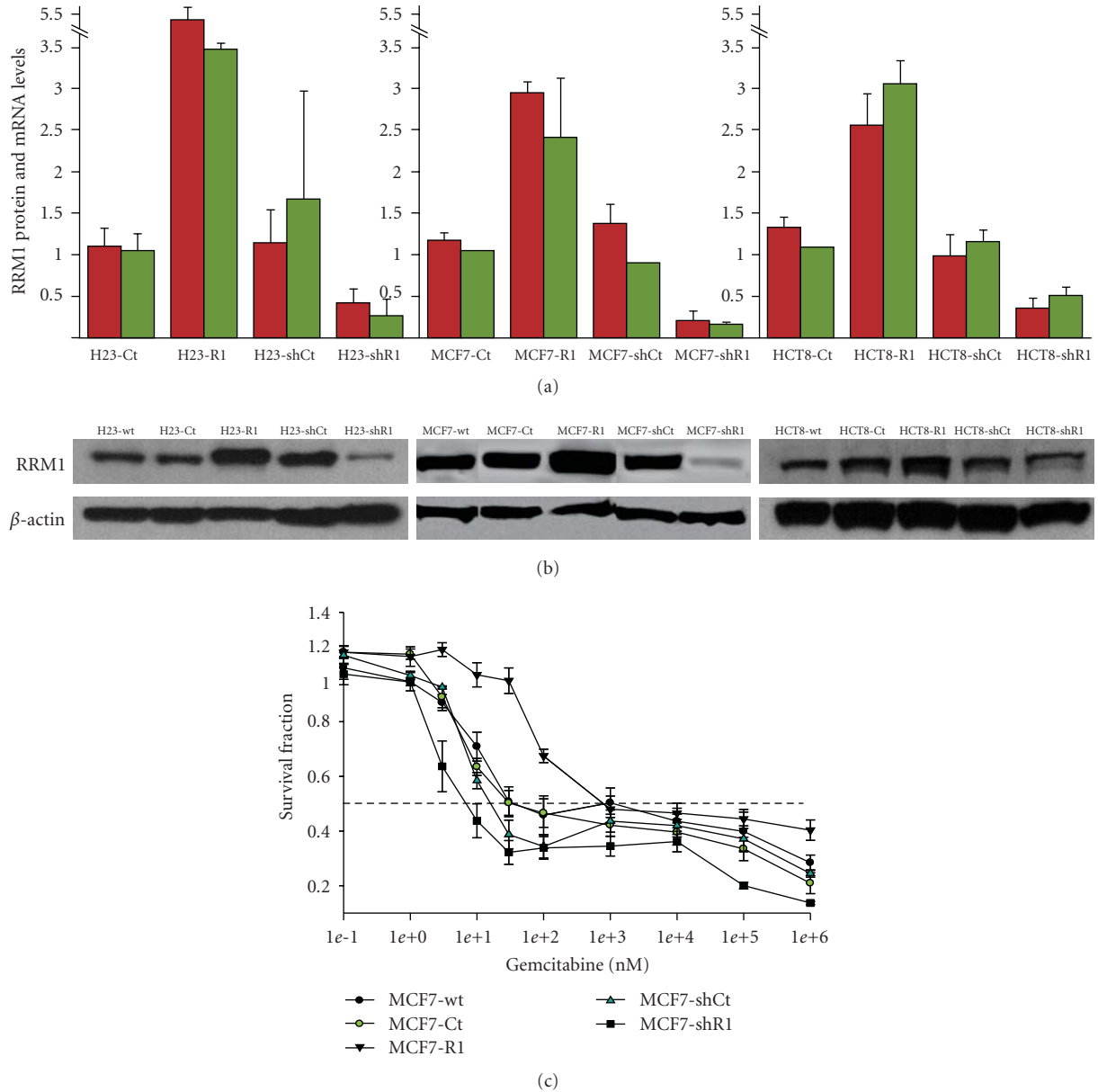


FIGURE 1: Modification of RRM1 expression by stable transfection with RRM1 and shRRM1 expression vectors in cell lines H23, MCF7, and HCT. Wt, wild-type cell lines, R1, clones of cell lines transfected with RRM1; Ct, clones transfected with an out-of-frame RRM1 vector; shR1, clones transfected with a small hair-pin RRM1 vector; shCt, clones transfected with a random control small hair-pin vector. (a) RRM1 protein (red) and mRNA (green) expression in stably transfected clones of H23, MCF7, and HCT8. (b) Western blots of H23, MCF7, and HCT8 clones. (c) Cytotoxicity of MCF7 clones following gemcitabine treatment for 6 days. Each point is the mean of at least three independent experiments. The dashed line indicates the 50% survival fraction.

(Figure 2(a)). We observed a 5- to 20-fold increase in gemcitabine efficacy with RRM1 down-regulation (Figure 2(b)); carboplatin efficacy was not notably affected.

**3.4. Endogenous RRM1 Expression, Drug Sensitivity, and Cell Line Characteristics in a Panel of NSCLC Cell Lines.** Since tumoral RRM1 levels and therapeutic efficacy of chemotherapy vary widely [7], we sought to investigate parameters that might influence the RRM1-gemcitabine efficacy interaction. For this, we used a random series of 26 NSCLC cell lines

with a diverse range of properties. In these cell lines, we determined the endogenous levels of RRM1, RRM2a, RRM2b, and other molecules associated with nucleotide metabolism and cell proliferation in exponentially growing, subconfluent, and unsynchronized cultures. The relative expression levels were determined by densitometry of specific bands on a single, large immunoblot adjusted for  $\beta$ -actin expression and normalized to the level of each target protein in cell line H23 (levels arbitrarily set to 1.00). We also determined the p53 and K-ras mutational status,

TABLE 2: Impact of RRM1 expression on drug combinations.\*

Drug combination	Clones of H23			
	H23-Ct control	H23-R1 R1 increased	H23-shCt control	H23-shR1 R1 decreased
Gemcitabine & Carboplatin	0.93 (+/-)	0.83 (++)	0.56 (+++)	0.72 (++)
Gemcitabine & Docetaxel	2.8 (- - -)	2.1 (- - -)	3.1 (- - -)	1.4 (- - -)
Gemcitabine & Pemetrexed	1.5 (- - -)	1.4 (- - -)	1.7 (- - -)	1.7 (- - -)
Pemetrexed & Carboplatin	0.79 (++)	0.94 (+/-)	0.73 (++)	0.64 (+++)

\*The combination index (CI) was calculated according to Chou [10] and averaged from three separate experiments. Combination indices  $CI < 1$ ,  $CI = 1$ , and  $CI > 1$  indicate synergism, additive effects, and antagonism, respectively. Ranking symbols within parenthesis indicate relative antagonism, additivity, or synergy: (- - -: strong antagonism; - -: moderate antagonism; +/-: nearly additive; ++: moderate synergy; +++: strong synergy).

the doubling time (calculated with CurveExpert software), and the  $IC_{50}$  and maximum achievable cytotoxicity with gemcitabine, pemetrexed, and carboplatin (Table 3).

We did not observe a statistically significant correlation between RRM1 levels and the gemcitabine  $IC_{50}$  values (Spearman rank correlation coefficient  $r = 0.10$ ,  $P = .65$ ). There was also no significant correlation between RRM1 levels and those of the other 7 proteins analyzed or the doubling time. Of note, TS levels and pemetrexed  $IC_{50}$  values were not correlated ( $r = 0.003$ ,  $P = .99$ ), neither were ERCC1 levels and carboplatin  $IC_{50}$  values ( $r = 0.07$ ,  $P = .75$ ).

However, the median  $IC_{50}$  values for gemcitabine were approximately 10-fold higher in the group of 8 cell lines with p53 truncations, deletions, or null status ( $0.3 \mu M$ ) compared to the 18 cell lines without such mutations ( $0.03 \mu M$ ;  $P = .06$  by rank sum test). A similar trend was not observed for pemetrexed or carboplatin. The K-ras mutation status did not impact efficacy of the three agents tested.

The doubling time of cell lines was significantly correlated with gemcitabine  $IC_{50}$  values; that is, cell lines with long doubling times had higher  $IC_{50}$  values (Spearman rank correlation coefficient  $r = 0.63$ ,  $P < .001$ ), and it was not correlated with the  $IC_{50}$  values of pemetrexed or carboplatin.

**3.5. TP53 Levels and Gemcitabine Cytotoxicity.** In order to study if wild-type p53 contributes to gemcitabine efficacy, we delivered p53-specific siRNA and nonspecific random siRNA to cell lines H23, A549, H292, and H460. We obtained near complete knock down in A549 and H292, a partial reduction in H460, and a minimal reduction in H23 using 20 nM siRNA concentrations and 24 hrs of exposure (Figure 3). Higher siRNA concentrations and longer exposure times did not yield better p53 reduction in H23 and H460. Gemcitabine  $IC_{50}$  values increased 2.0-fold in A549 (p53 wild-type) to 3.4-fold in H292 (p53 wild-type) and remained essentially unchanged in H23 (1.3-fold, p53 M246I missense) and H460 (1.1-fold, p53 wild-type).

To corroborate this result, we used the p53-null cell line H358 and its stably transfected and wild-type p53-expressing counterpart H358p53<sup>+</sup> (Figure 4). We observed a statistically

significant reduction in the gemcitabine  $IC_{50}$  from 15.3 nM in H358 to 10.7 nM in H358p53<sup>+</sup> ( $P = .03$  by *t*-test; values are means of three independent experiments using 5 days of exposure), while the  $IC_{50}$  values for pemetrexed and carboplatin were not significantly different between these cell lines.

#### 4. Discussion

The use of unselected double-agent chemotherapy has resulted in an approximately 50% improvement in overall median survival of patients with advanced NSCLC [12]. The only criteria currently used for selection of agents are histology [13], toxicity profiles, and convenience of delivery. Two recent prospective clinical trials have demonstrated the feasibility of selecting individualized chemotherapy based on RRM1 and/or ERCC1 expression levels in tumor biopsy specimens [14, 15]. Both trials also reported favorable response rates for patients receiving molecularly-based selected compared to unselected therapy. In two additional prospective trials in patients with metastatic stage III or stage IV disease, a statistically significant association between the tumoral expression levels of RRM1 and the magnitude of change in tumor burden with gemcitabine single-agent or gemcitabine and carboplatin double-agent therapy have been reported; that is, the lower the levels the better the response [4, 7].

The antitumoral activity of gemcitabine is a result of at least two separate actions. One is a presumed direct interaction with RRM1, with a resulting reduction of ribonucleotide reductase function and deoxynucleotide levels, and the other is incorporation into newly synthesized DNA, with a resulting chain termination. It is the presumed interaction with RRM1 that explains the direct and linear association between RRM1 levels and gemcitabine  $IC_{50}$  levels in experimental model systems. However, as can be gleaned from the published scatter plots depicting the association between intratumoral RRM1 levels and tumor response in cancer patients [4, 7], it is difficult to be precise in predicting whether an individual patient will actually derive benefit from the selected therapy.

TABLE 3: Endogenous RRM1 levels and gemcitabine, pemetrexed, and carboplatin efficacy in 26 NSCLC cell lines.

Cell Line	ATCC #	Histological Subtype*	p53 mutation (* = stop) based on CCDS11118.1 cod on 72 either proline or arginine	K-ras mutation	Doubling Time (hr)	RRM1	RRM2a	RRM2b	ERCC1	TS	TP53	P38	MCM2	Gem IC50 (uM)	Pem IC50 (uM)	Carbo IC50 (uM)
A549	CLL-185	AD-BAC	wt	G12S	48	2.30	1.08	1.23	2.49	0.90	0.53	0.91	0.83	0.010	0.103	41.003
ADLC5M2	—	AD	wt	wt	24	2.42	1.79	0.30	2.40	0.66	0.12	0.58	1.22	0.079	0.044	6.678
EPLC65H	—	SQ	wt	wt	47	2.83	1.07	0.55	3.92	1.23	0.12	1.22	0.97	0.019	0.039	7.590
H125	CRL-5801	AD/SQ	N239*	wt	70	1.65	2.53	1.05	3.64	0.60	0.00	0.92	0.87	>1000	0.374	39.678
H1299	CRL-5803	NSCLC-NOS	homozygous deletion	wt	46	1.92	2.43	2.18	1.31	0.91	0.00	2.01	1.37	0.024	0.236	27.273
H1355	CRL-5865	AD	E258K	G13C	36	2.04	2.32	1.08	3.68	1.12	0.58	0.54	0.94	0.006	0.355	30.651
H157	CRL-5802	SQ	E298*	G12R	58	2.22	2.80	1.16	0.73	0.73	0.03	1.65	1.01	0.036	0.433	21.766
H1648	CRL-5882	AD	frame shift codon 35;D42*	wt	57	2.26	1.14	1.32	0.27	0.08	0.00	1.55	1.58	>1000	>1000	19.730
H1650	CRL-5883	AD	wt	wt	49	0.83	1.58	1.07	1.09	0.08	0.02	0.97	0.81	0.020	0.053	14.535
H1703	CRL-5889	AD	wt	wt	42	0.91	2.45	1.45	0.73	0.66	0.04	0.64	1.02	0.002	0.173	28.421
H1975	CRL-5908	AD	R273H	wt	39	1.94	2.24	1.05	0.13	0.15	1.01	1.25	1.05	0.145	0.051	19.250
H2122	CRL-5985	AD	Q16L; C176F	G12C	72	1.04	1.42	0.61	0.90	0.05	0.37	0.95	0.92	>1000	0.054	56.217
H2172	CRL-5930	NSCLC-NOS	frame shift codon 72;V122*	wt	45	1.99	0.29	2.20	1.21	0.00	0.00	0.94	1.00	0.435	0.533	10.800
H2228	CRL-5935	AD	Q331*	wt	50	0.68	0.12	0.25	1.53	0.09	0.55	0.63	1.18	0.023	0.039	11.036
H226	CRL-5826	SQ	wt	wt	76	2.30	0.45	3.28	0.79	0.24	0.45	1.63	0.96	7.491	>1000	37.317
H23	CRL-5800	AD	M246I	G12C	45	1.00	1.00	1.00	1.00	1.00	1.00	1.00	1.00	0.008	0.125	21.220
H292	CRL-1848	ME	wt	wt	31	2.11	1.90	1.13	2.08	0.93	0.61	1.26	0.73	0.011	0.026	30.326
H322	CRL-5806	AD-BAC	R248L	wt	36	1.26	1.65	1.06	1.65	0.38	0.72	0.76	1.02	0.016	0.118	41.434
H358	CRL-5807	AD-BAC	homozygous deletion	G12C	74	1.61	1.36	1.22	3.80	0.29	0.00	2.02	1.20	0.135	0.030	23.634
H441	HTB-174	AD	R158L	G12V	58	1.86	1.91	4.49	0.99	0.05	0.47	2.77	1.87	0.033	0.093	23.545
H460	HTB-177	LC	wt	Q61H	35	2.47	2.13	1.30	1.15	0.84	0.76	0.79	0.94	0.053	0.183	85.373
H522	CRL-5810	AD	frame shift codon 191 with deletion of P	wt	108	1.08	3.17	0.73	7.04	1.10	0.22	1.74	0.89	>1000	>1000	21.298
H596	HTB-178	AD/SQ	G245C	wt	49	1.61	1.98	1.00	3.00	0.53	0.68	1.25	0.93	0.031	0.012	28.626
H650	CRL-5835	AD	K164N	wt	83	1.25	1.34	1.57	1.55	0.13	0.66	0.77	0.91	>1000	>1000	32.422
H661	HTB-183	LC	R158L; S215I	wt	47	1.34	1.05	0.86	2.06	0.88	0.54	0.88	1.23	0.024	>1000	57.253
H820	HTB-181	AD	T284P	wt	68	—	—	—	—	—	—	—	—	6.883	>1000	32.116

\* AD: adenocarcinoma, AD-BAC: adenocarcinoma with bronchoalveolar features, LC: large cell carcinoma, SQ: squamous cell carcinoma, ME: mucoepidermoid bronchial gland carcinoma, AD/SQ: mixed adenocarcinoma cell carcinoma, NSCLC-NOS: nonsmall cell lung cancer; not otherwise specified. IC50 values are the means of at least three experiments; 3–6 wells per experiment and dose level: 4,000 cells per well; 96 hr exposure.

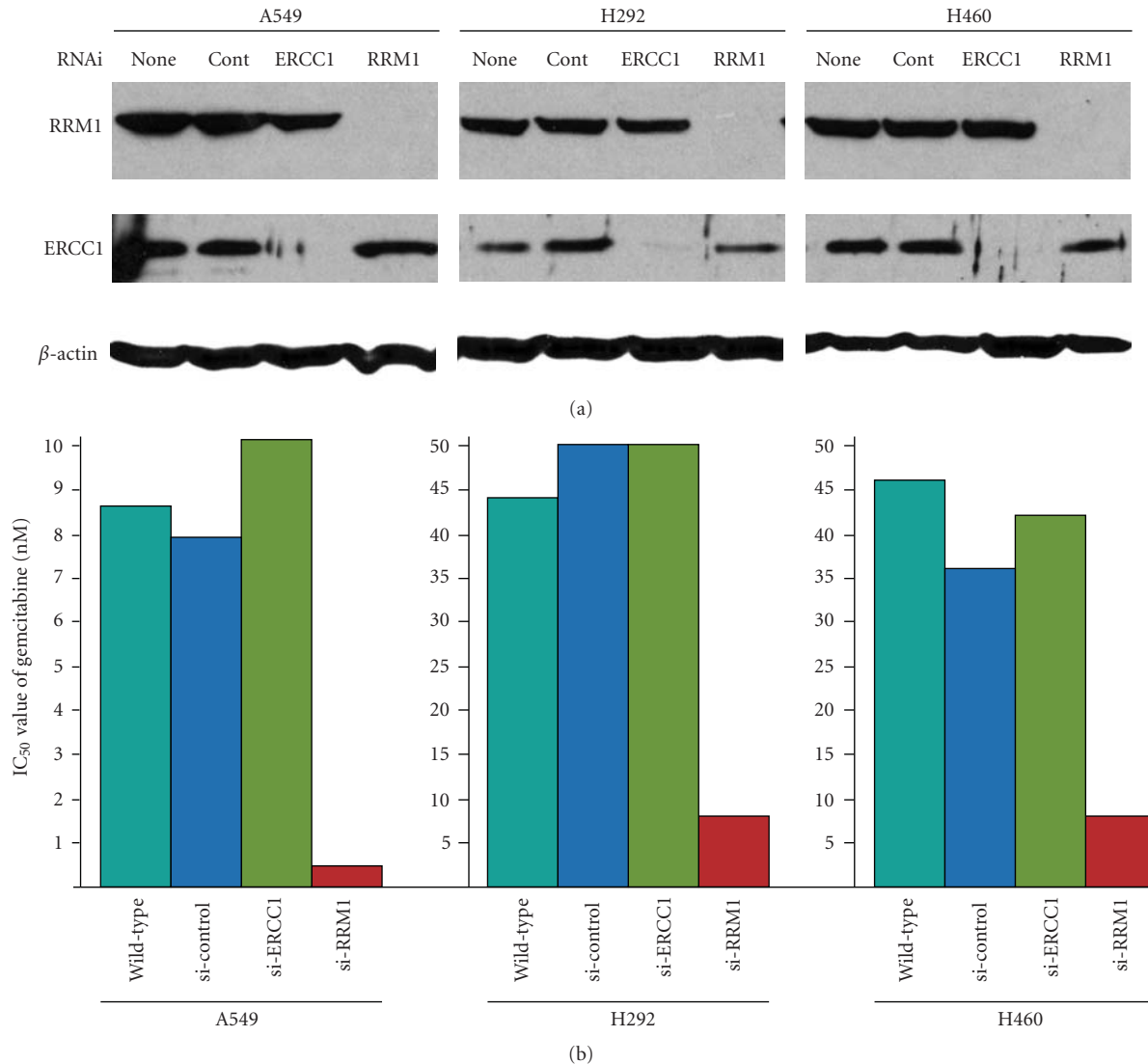


FIGURE 2: Knock-down of RRM1 and ERCC1 expression in three NSCLC cell lines by RNA interference and impact on gemcitabine efficacy. (a) Western blots showing that RRM1-specific siRNA reduced RRM1 protein expression to undetectable levels, while random control and ERCC1-specific siRNAs did not affect RRM1 expression. Likewise, ERCC1-specific siRNA reduced ERCC1 protein expression to undetectable levels, while random control and RRM1-specific siRNAs did not affect ERCC1 expression. (b)  $IC_{50}$  values of gemcitabine cytotoxicity in cell lines A549, H292, and H460. Wt, wild-type cell lines; si-control, cell lines transfected with nonspecific siRNA; si-ERCC1; cell lines transfected with ERCC1-specific siRNA; si-RRM1, cell lines transfected with RRM1-specific siRNA.

Given the molecular complexity of NSCLC, this is not surprising and strongly suggests that a variety of other tumor-specific and host-specific parameters substantially impact the gemcitabine-RRM1 interaction. Our results in a lung, breast, and colon cancer cell line with genetically modified RRM1 levels demonstrate that RRM1 expression levels are the dominant determinant of gemcitabine efficacy despite diverse molecular backgrounds. This result is consistent with prior reports of increased RRM1 levels in pancreatic and colon cancer models upon induction of gemcitabine resistance [3, 5]. In our cell line models, we further demonstrate that RRM1 levels can impact efficacy of other cytotoxic agents in the class of antimetabolites. Since this effect was not observed in all cell lines, other parameters

may dominate over the interaction between RRM1 and 5FU, pemetrexed, and methotrexate. For instance, a significant role for TS on 5FU and dihydrofolate reductase on methotrexate efficacy has been established, and a role for TS and other enzymes involved in nucleotide synthesis on pemetrexed efficacy is evolving. However, an explanation for the increased pemetrexed sensitivity of RRM1 transfected MCF7 and HCT8 cell lines is elusive. We also demonstrate that RRM1 levels do not impact on efficacy of spindle-disrupting agents or etoposide, which are frequently used in lung cancer therapy. In fact, an earlier report on a small subset of patients treated with vinorelbine, gemcitabine, and platinum had suggested that the addition of vinorelbine may abrogate the therapeutic benefit of gemcitabine in patients

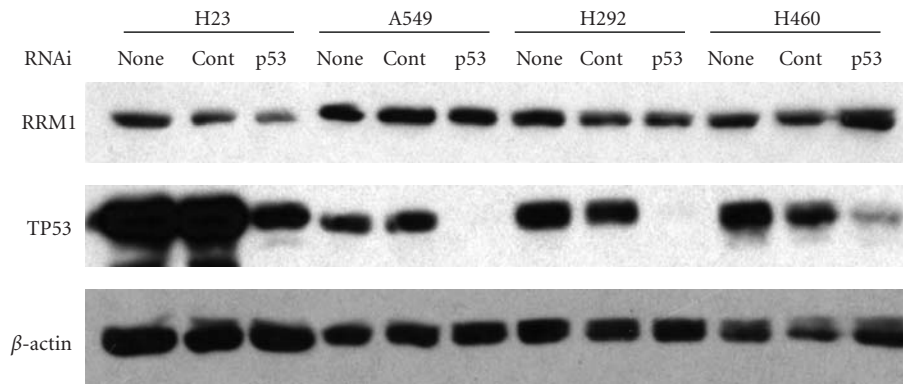


FIGURE 3: Western blots of knock-down of TP53 expression in four NSCLC cell lines by RNA interference. TP53-specific siRNA reduced TP53 protein expression to undetectable levels in A549 and H292 and greater than 10-fold in H23 and H460, while random control siRNA did not affect TP53 or RRM1 expression.

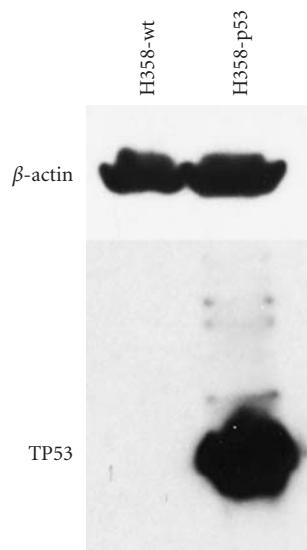


FIGURE 4: Western blots of cell line H358. There is no detectable TP53 expression in wild-type cells; while transfected cells clearly show TP53 expression.

with low levels of RRM1 expression [2]. Our *in vitro* results on combination therapy suggest that RRM1 does not disrupt drug-drug interactions when gemcitabine is combined with carboplatin, docetaxel, or pemetrexed.

Since RRM1 is often combined with ERCC1 in trials seeking to enhance therapeutic efficiency through agent selection and because both molecules are frequently coexpressed [2, 4, 7, 16, 17], we tested in three cell lines if ERCC1 expression reduction through RNA interference would alter gemcitabine efficacy and found no evidence for this.

Using a panel of lung cancer cell lines with diverse features and molecular characteristics, we identified two variables that significantly impacted gemcitabine efficacy

without being associated with RRM1 levels. We found that cell lines with functional p53-impairing mutations, that is, null, truncation, and deletion mutations, displayed a pattern of resistance to gemcitabine. We corroborated this result through transfection of wild-type p53 into a null cell line (H358), which resulted in a statistically significant improvement in gemcitabine efficacy, and through abrogation of p53 by RNA interference in other cell lines, which resulted in gemcitabine resistance. This was not explained by RRM1 expression levels, since no association between RRM1 levels and p53 was observed. In contrast, pemetrexed and platinum efficacy did not seem to be influenced by p53 expression modulation. To our knowledge, the impact of p53 mutations on gemcitabine efficacy has not been studied in clinical trials. It is important to corroborate these results in prospective trials since a potential clinical implication might be that tumoral RRM1 levels may not be predictive of gemcitabine efficacy in patients whose tumors harbor functionally significant p53 mutations.

Finally, our *in vitro* data demonstrated a statistically significant correlation between gemcitabine efficacy and the doubling time; that is, cell lines with long doubling times were more resistant to gemcitabine. Although we used a 4-day continuous exposure to gemcitabine, which should allow for all cells to proceed through at least one complete cell cycle, we cannot exclude that this result is caused by the experimental conditions. However, a similar phenomenon was not observed for pemetrexed or carboplatin, which suggests that a true association between the speed of cellular replication and gemcitabine efficacy exists. It is not explained by RRM1 expression levels or p53, since a significant correlation between these and the doubling time was not observed. However, we had previously reported that overexpression of RRM1 through stable transfection in cell lines resulted in slow growth predominantly through G2 arrest [18]. It is thus possible that the increased gemcitabine efficacy is a result of a decreased ability of cells to repair newly synthesized DNA with incorporated 2', 2'-difluorodeoxycytidine that leads to chain termination [19].

## 5. Conclusions

We demonstrated a dominant role for RRM1 in gemcitabine efficacy and also a role in efficacy of other antimetabolites in selected cell lines. RRM1 did not disrupt the interaction between gemcitabine and other cytotoxic agents when combined. The mutational status of p53 and cell line doubling time were significant and independent determinants of gemcitabine efficacy. Their impact on gemcitabine efficacy in patients with lung cancer in the context of RRM1 expression requires investigations in prospective clinical trials.

## Abbreviations

RR: Ribonucleotide reductase  
 RRM1: RR subunit M1  
 RRM2a: RR subunit M2a  
 RRM2b: p53-inducible RR subunit M2b, encoded by the p53R2 gene  
 ERCC1: Excision repair cross-complementation group 1  
 TP53: p53 tumor suppressor gene  
 TS: Thymidylate synthase  
 MCM2: Minichromosome maintenance protein 2  
 MTS: 3-(4,5-dimethylthiazol-2-yl)-5-(3-carboxymethoxyphenyl)-2-(4-sulfophenyl)-2H-tetrazolium  
 NSCLC: Nonsmall cell lung cancer.

## Acknowledgment

This work was supported by R01-CA129343 from the NCI.

## References

- [1] J. D. Davidson, L. Ma, M. Flagella, S. Geeganage, L. M. Gelbert, and C. A. Slapak, "An increase in the expression of ribonucleotide reductase large subunit 1 is associated with gemcitabine resistance in non-small cell lung cancer cell lines," *Cancer Research*, vol. 64, no. 11, pp. 3761–3766, 2004.
- [2] R. Rosell, K. D. Danenberg, V. Alberola et al., "Ribonucleotide reductase messenger RNA expression and survival in gemcitabine/cisplatin-treated advanced non-small cell lung cancer patients," *Clinical Cancer Research*, vol. 10, no. 4, pp. 1318–1325, 2004.
- [3] A. M. Bergman, P. P. Eijk, V. W. T. Ruiz van Haperen et al., "In vivo induction of resistance to gemcitabine results in increased expression of ribonucleotide reductase subunit M1 as the major determinant," *Cancer Research*, vol. 65, no. 20, pp. 9510–9516, 2005.
- [4] G. Bepler, I. Kusmartseva, S. Sharma et al., "RRM1 modulated in vitro and in vivo efficacy of gemcitabine and platinum in non-small-cell lung cancer," *Journal of Clinical Oncology*, vol. 24, no. 29, pp. 4731–4737, 2006.
- [5] S. Nakahira, S. Nakamori, M. Tsujie et al., "Involvement of ribonucleotide reductase M1 subunit overexpression in gemcitabine resistance of human pancreatic cancer," *International Journal of Cancer*, vol. 120, no. 6, pp. 1355–1363, 2007.
- [6] H. Akita, Z. Zheng, Y. Takeda et al., "Significance of RRM1 and ERCC1 expression in resectable pancreatic adenocarcinoma," *Oncogene*, vol. 28, no. 32, pp. 2903–2909, 2009.
- [7] C. Reynolds, C. Obasaju, M. J. Schell et al., "Randomized phase III trial of gemcitabine-based chemotherapy with in situ RRM1 and ERCC1 protein levels for response prediction in non-small-cell lung cancer," *Journal of Clinical Oncology*, vol. 27, no. 34, pp. 5808–5815, 2009.
- [8] G. Bepler, K. E. Sommers, A. Cantor et al., "Clinical efficacy and predictive molecular markers of neoadjuvant gemcitabine and pemetrexed in resectable non-small cell lung cancer," *Journal of Thoracic Oncology*, vol. 3, no. 10, pp. 1112–1118, 2008.
- [9] A. Gautam, Z.-R. Li, and G. Bepler, "RRM1-induced metastasis suppression through PTEN-regulated pathways," *Oncogene*, vol. 22, no. 14, pp. 2135–2142, 2003.
- [10] T.-C. Chou, "Theoretical basis, experimental design, and computerized simulation of synergism and antagonism in drug combination studies," *Pharmacological Reviews*, vol. 58, no. 3, pp. 621–681, 2006.
- [11] M. Behn and M. Schuermann, "Sensitive detection of p53 gene mutations by a 'mutant enriched' PCR-SSCP technique," *Nucleic Acids Research*, vol. 26, no. 5, pp. 1356–1358, 1998.
- [12] T. D. Shanafelt, C. Loprinzi, R. Marks, P. Novotny, and J. Sloan, "Are chemotherapy response rates related to treatment-induced survival prolongations in patients with advanced cancer?" *Journal of Clinical Oncology*, vol. 22, no. 10, pp. 1966–1974, 2004.
- [13] G. V. Scagliotti, P. Parikh, J. Von Pawel et al., "Phase III study comparing cisplatin plus gemcitabine with cisplatin plus pemetrexed in chemotherapy-naive patients with advanced-stage non-small-cell lung cancer," *Journal of Clinical Oncology*, vol. 26, no. 21, pp. 3543–3551, 2008.
- [14] G. Simon, A. Sharma, X. Li et al., "Feasibility and efficacy of molecular analysis-directed individualized therapy in advanced non-small-cell lung cancer," *Journal of Clinical Oncology*, vol. 25, no. 19, pp. 2741–2746, 2007.
- [15] M. Cobo, D. Isla, B. Massuti et al., "Customizing cisplatin based on quantitative excision repair cross-complementing 1 mRNA expression: a phase III trial in non-small-cell lung cancer," *Journal of Clinical Oncology*, vol. 25, no. 19, pp. 2747–2754, 2007.
- [16] P. Ceppi, M. Volante, S. Novello et al., "ERCC1 and RRM1 gene expressions but not EGFR are predictive of shorter survival in advanced non-small-cell lung cancer treated with cisplatin and gemcitabine," *Annals of Oncology*, vol. 17, no. 12, pp. 1818–1825, 2006.
- [17] Z. Zheng, T. Chen, X. Li, E. Haura, A. Sharma, and G. Bepler, "DNA synthesis and repair genes RRM1 and ERCC1 in lung cancer," *New England Journal of Medicine*, vol. 356, no. 8, pp. 800–808, 2007.
- [18] A. Gautam and G. Bepler, "Suppression of lung tumor formation by the regulatory subunit of ribonucleotide reductase," *Cancer Research*, vol. 66, no. 13, pp. 6497–6502, 2006.
- [19] P. Huang, S. Chubb, L. W. Hertel, G. B. Grindey, and W. Plunkett, "Action of 2',2'-difluorodeoxycytidine on DNA synthesis," *Cancer Research*, vol. 51, no. 22, pp. 6110–6117, 1991.

## Review Article

# Overview of DNA Repair in *Trypanosoma cruzi*, *Trypanosoma brucei* and *Leishmania major*

**Danielle Gomes Passos-Silva, Matheus Andrade Rajão, Pedro Henrique Nascimento de Aguiar, João Pedro Vieira-da-Rocha, Carlos Renato Machado, and Carolina Furtado**

*Departamento de Bioquímica e Imunologia, Instituto de Ciências Biológicas, Universidade Federal de Minas Gerais, Av. Antônio Carlos, 6627, Pampulha, Belo Horizonte, MG, 31270-901, Brazil*

Correspondence should be addressed to Carolina Furtado, carolfts@gmail.com

Received 17 June 2010; Revised 29 July 2010; Accepted 25 August 2010

Academic Editor: Ashis Basu

Copyright © 2010 Danielle Gomes Passos-Silva et al. This is an open access article distributed under the Creative Commons Attribution License, which permits unrestricted use, distribution, and reproduction in any medium, provided the original work is properly cited.

A wide variety of DNA lesions arise due to environmental agents, normal cellular metabolism or intrinsic weaknesses in the chemical bonds of DNA. Diverse cellular mechanisms have evolved to maintain genome stability, including mechanisms to repair damaged DNA, to avoid the incorporation of modified nucleotides and to tolerate lesions (translesion synthesis). Studies of the mechanisms related to DNA metabolism in trypanosomatids have been very limited. Together with recent experimental studies, the genome sequencing of *Trypanosoma brucei*, *Trypanosoma cruzi* and *Leishmania major*, three related pathogens with different life cycles and disease pathology, has revealed interesting features of the DNA repair mechanism in these protozoan parasites, which will be reviewed here.

## 1. Introduction

The trypanosomatids *Trypanosoma cruzi*, *Trypanosoma brucei*, and *Leishmania major* are the causative agents of Chagas disease, African sleeping sickness and leishmaniasis, respectively. These protozoan pathogens affect over 27 million people, primarily in developing countries within tropical and subtropical regions. There are no vaccines for these diseases and only a few drugs, which are largely ineffective due to toxicity and resistance [1].

These three pathogens (herein collectively referred to as Trityps) share many general characteristics, especially the presence of the unique mitochondrion, which contains a dense region named as kinetoplast. This mitochondrial region is composed by a network of several thousand minicircles and a few dozen maxicircles that form the kinetoplast DNA (kDNA) [2]. Minicircles encode guide RNAs that modify maxicircle transcripts by RNA editing while maxicircles are correspondent to the mitochondrial DNA in higher eukaryotes that encodes rRNAs and the subunits of respiratory complexes [2]. The mitochondrion replicates its DNA, maintains its structural integrity, and

undergoes division. Actually, kDNA replication always takes place earlier than mitosis, indicating that the kDNA may be needed for cell division, either by signaling a successful replication or by affecting the structure [3]. Furthermore, the trypanosome mitochondrion may hold vital metabolic pathways besides a possible role in Ca<sup>2+</sup> homeostasis, fatty acid metabolism, and apoptosis [3]. In fact, kDNA function and integrity may play a crucial role in the survival of some stages of Trityps lifecycles [3–5]. However, the kDNA is subjected to large amounts of endogenous oxidative damage generated by oxidative phosphorylation. Thus, an efficient kDNA maintenance mechanism is necessary to repair and avoid oxidative lesions in the mitochondrial DNA.

The draft genome sequences of the Trityps, released in 2005, have allowed a better understanding of the genetic and evolutionary characteristics of these parasites [6–9]. A comparison of gene content and genome architecture of *T. cruzi*, *T. brucei*, and *L. major* revealed large syntenic polycistronic gene clusters. In addition, many species-specific genes, such as large surface antigen families, occur at nonsyntenic chromosome-internal and subtelomeric regions. Syntenic discontinuities are associated with retroelements, structural

RNAs, and gene family expansion. Along with these factors, gene divergence, acquisition and loss, and rearrangement within the syntenic regions help to shape the genome of each parasite [8]. Expansion of gene families by tandem duplication is a potential mechanism by which parasites can increase expression levels to compensate for a general lack of transcriptional control due to polycistronic structure and the absence of general transcription factors [7].

Concerning the individual features of each parasite, which reflect differences in their lifecycles, *T. brucei* has large subtelomeric arrays that contain variant surface glycoprotein (VSG) genes used by the parasite to evade the mammalian immune system. Meanwhile, over 50% of the *T. cruzi* genome consists of repeated sequences, such as genes for large families of surface molecules, which might function in immune evasion and adaptation to an intracellular environment. *Leishmania* spp. has a simpler genome but also has the ability to amplify genomic regions. This genus contains genes for the synthesis of complex surface glycoconjugates that are likely to enhance survival in the macrophage phagolysosome [8].

Analyses of the Trityps genomes have identified differences in the DNA maintenance mechanisms (nuclear and mitochondrial) between Trityps and other eukaryotes. DNA repair systems are responsible for preserving the genome stability *via* correcting DNA lesions caused by damaging agents both from the environment and endogenous metabolic processes [10–14]. This system embraces several distinct pathways: (1) sanitization of the nucleotide pool, (2) direct reversal of the base modifications by demethylation processes, by the action of photolyases or dioxygenases, or (3) excision of (i) oxidized, methylated, or misincorporated bases by base excision repair (BER), (ii) bulky damage by nucleotide excision repair (NER), and (iii) misincorporated bases in the newly replicated DNA strand by mismatch repair (MMR). DNA is also susceptible to single-strand breaks (SSBs) and double-strand breaks (DSBs), which can be repaired by homologous recombination (HR) and nonhomologous end joining (NHEJ). Even though these mechanisms repair the majority of DNA lesions, some of the damage remains, leading to mutations or block of the DNA replication. Alternative DNA polymerases can bypass these lesions in an error-free or error-prone fashion using a tolerance process known as translesion synthesis (TLS) [14]. Basic knowledge of DNA damage repair and tolerance processes is crucial to understanding how and why the genome is affected during the organism lifespan and how the cells will deal with it.

*T. cruzi*, *T. brucei*, and *L. major* appear to be able to catalyze most of the DNA repair pathways [6–9]. Here, we briefly review the current information on DNA repair mechanisms in Trityps with an emphasis on experimentally characterized genes (Table 1). We highlight the main features of the major DNA repair pathways and report the presence or absence of key genes in Trityps. Most of the genes were previously identified by their genome projects [6–9, 15], and few of them were identified through similarity screening and domain analysis. The gene “absence” could truly represent a nonoccurrence of the gene (whose function

could be compensated or not by another gene), a large sequence divergence, or even an annotation error, which made the search for a homolog difficult.

## 2. Direct Repair

Two mechanisms of direct repair are present in Trityps: alkylation reversal and oxidative damage repair [6–9]. These pathways perform immediate chemical reversals of specific forms of DNA damage. Single homologs of O<sup>6</sup>-methylguanine alkyltransferase (MGMT) can be found in the three genomes. This enzyme catalyzes the repair of O<sup>6</sup>-meG, a critical mutagenic lesion that yields G:C to A:T transitions [41]. AlkB, an iron-dependent dioxygenase that reverses DNA lesions (1-meA and 3-meC) in single-strand DNA (ssDNA) or RNA [42], is also present in Trityps. The third mechanism of direct repair utilizes photolyases, which catalyze the splitting of pyrimidine dimers into the constituent monomers, a process called photoreactivation [43]. *T. cruzi* does not contain a clear photolyase homolog although *T. brucei* and *L. major* are thought to perform photoreactivation because they have a gene that contains an N-terminal photolyase domain [6–9]. The absence of photoreactivation as a repair mechanism for pyrimidine dimers in *T. cruzi* could be associated with the availability of transcription-coupled repair (TCR), which would efficiently deal with such lesions. This subject is discussed further in a later section.

## 3. Base Excision Repair

BER is the predominant pathway for dealing with a wide range of lesions that modify individual bases without large effects on the double helix structure. Such modifications on DNA bases can arise as a result of oxidation, alkylation, and/or deamination. The BER pathway consists of modified base recognition and removal by a DNA glycosylase, cleavage of the sugar-phosphate backbone, and excision of the abasic (apurinic-apyrimidinic, AP) site by a DNA AP endonuclease, followed by DNA synthesis and ligation steps [44].

The gapfilling and rejoining steps can occur by either of two subpathways: short-patch BER or long-patch BER. In the short-patch BER subpathway, only one nucleotide is replaced by DNA Pol $\beta$  and the nick is sealed by LIG3, all steps being coordinated by XRCC1 [45]. In long-patch BER, 2–13 nucleotides are replaced with the involvement of the replicative polymerases  $\delta$  (Pol $\delta$ ) or  $\epsilon$  (Pol $\epsilon$ ) [46]. This polymerization gives rise to a “flap” structure that is removed by FEN1 through a single-stranded break for subsequent nick ligation by ligase 1 (LIG1) [47]. The long-patch mechanism also involves PCNA, which interacts and coordinates the enzymes involved, and poly ADP-ribose polymerase (PARP), that binds to DNA SSBs preventing DSBs and facilitates access for the long-patch machinery [48].

The primary components of the BER pathway have been identified in *T. cruzi*, *T. brucei* and *L. major* genomes [6–9] and are organized in the *TritypDB* database [15]. The Trityps possess the enzymes required to effectively

TABLE 1

Gene	Function	Organism (Gene ID)	Experimental data	Ref.
<i>BER Genes</i>				
Uracyl-DNA glycosylase (UNG)	Excision of uracil in DNA	<i>T. cruzi</i> (Tc00.1047053511277.330)	(i) <i>In vitro</i> activity (enhanced by AP endonuclease) (ii) Heterologous complementation of <i>E. coli</i>	[16, 17]
AP endonuclease1	Cleavage of the phosphodiester bond at the 5' side of AP site	<i>T. cruzi</i> (Tc00.1047053507083.30)	(i) Heterologous complementation of <i>E. coli</i>	[18]
		<i>L. major</i> (LmjF16.0680)	(i) Heterologous complementation of <i>E. coli</i> (ii) Increment of H <sub>2</sub> O <sub>2</sub> and methotrexate resistance	[18–20]
POL $\beta$	Polymerization of DNA Strand displacement (long-patch) Cleavage of the 5' - dRP	<i>T. cruzi</i> (Tc00.1047053503955.20)	(i) <i>In vitro</i> activity	[21]
		<i>T. brucei</i> (Tb927.5.2780)	(ii) Kinetoplast localization	[22]
PARP	Binding to ssDNA Stimulation of DNA synthesis and strand displacement	<i>T. cruzi</i> (Tc00.1047053509721.60)	(i) <i>In vitro</i> activity (enhanced by SSB)	[23]
<i>NER Genes</i>				
TFIIH-TFB1	Component of TFIIH	<i>T. brucei</i> (Tb11.01.1200)	(i) Essential for initiating synthesis of spliced leader RNA	[24]
TFIIH-TFB2		<i>T. brucei</i> (Tb927.10.5210)		
TFIIH-TFB4		<i>T. brucei</i> (Tb11.01.7730)		
TFIIH-TFB5		<i>T. brucei</i> (Tb10.61.2600)		
TFIIH-XPB	Component of TFIIH (helicase)	<i>T. brucei</i> (Tb11.01.7950Tb927.3.5100)	(i) Interaction with TSP1 and TSP2	
TFIIH-XPB		<i>T. brucei</i> (Tb927.8.5980)	(i) Nuclear localization	
TFIIH-TSP1	Trypanosomatid-specific component of TFIIH	<i>T. brucei</i> (Tb927.1.1080)	(i) Essential for initiating synthesis of spliced leader RNA	[24]
TFIIH-TSP2		<i>T. brucei</i> (Tb11.01.5700)	(i) Nuclear localization (ii) Essential for initiating synthesis of spliced leader RNA	
XAB2*	May function as a scaffold for protein complex formation	<i>T. cruzi</i> (Tc00.1047053509767.40)	(i) Putative	—
		<i>T. brucei</i> (Tb927.5.1340)	(i) Putative	—
		<i>L. major</i> (LmjF23.1550)	(i) Putative	—
<i>MMR Genes</i>				
MSH2	Repair of single base-base and IDL mismatches Heterodimers with MSH3 or MSH6	<i>T. cruzi</i> (Tc00.1047053507711.320)	(i) Three isoforms with different efficiencies (ii) Involvement in oxidative stress response (independently from MLH1)	[25, 26]
		<i>T. brucei</i> (Tb927.10.11020)	(i) Involvement in oxidative stress response (independently from MLH1) (ii) Microsatellite instability and MNNG tolerance in <i>MSH2/MLH1</i> double mutants (iii) Regulatory role in HR	[26–28]
MLH1	Heterodimers with MutL homologs Matchmaker for coordinating events from mismatch binding to DNA synthesis	<i>T. brucei</i> (Tb927.8.6840)	(i) Microsatellite instability and MNNG tolerance in <i>MSH2/MLH1</i> double mutants (ii) Regulatory role in HR	[27, 28]

TABLE 1: Continued.

Gene	Function	Organism (Gene ID)	Experimental data	Ref.
<i>NHEJ Genes</i>				
Ku70	DSB recognition DSB bridging nucleolytic processing of the ends	<i>T. brucei</i> (Tb927.3.5030)	(i) Telomere maintenance	[29, 30]
Ku80	Telomere maintenance	<i>T. brucei</i> (Tb927.6.1760)		
<i>HR Genes</i>				
Mre11	DSB end resection Nuclease activities	<i>T. brucei</i> (Tb927.2.4390)	(i) Mre11 mutations cause impairment of HR and increased DNA damage sensitivity	[31, 32]
		<i>T. cruzi</i> (Tc00.1047053503801.30)	(i) Gene expression induced by DNA damaging agents (ii) Involved in DSBs and oxidative lesions repair	[33]
Rad51	Recombinases	<i>T. brucei</i> (Tb11.01.0360)	(i) Null mutants led to impairments in VSG switch and DNA transformation, besides a higher sensitivity to genotoxic agents	[34]
		<i>L. major</i> (LmjF28.0550)	(i) Gene expression induced by DNA-damaging agents	[35]
Dmc1	Recombinases	<i>T. brucei</i> (Tb09.211.1210)	(i) DMC1 mutation does not affect HR or VSG switching	[36]
BRCA2	ssDNA binding Recombination mediator	<i>T. brucei</i> (Tb927.1.640)	(i) Expansion in the number of BRC repeats (ii) BRCA2 mutants display antigenic variation impairment and genome instability	[37]
Rad51-3		<i>T. brucei</i> (Tb11.02.0150)	(i) Rad51-3 mutations resulted in reduced levels of VSG switching, altered RAD51 localization following DNA damage and DNA damage sensitized parasites	[38]
Rad51-5	ssDNA binding Recombination mediator activity	<i>T. brucei</i> (Tzb10.389.1770)	(i) Rad51-5 mutations caused altered RAD51 localization following DNA damage and DNA damage sensitized parasites	[38]
<i>TLS Genes</i>				
Pol $\eta$	Error-free bypass of cis-syn cyclobutane pyrimidine dimers (CPDs)	<i>T. cruzi</i> (Tc00.1047053511911.120)	(i) Heterologous complementation of <i>S. cerevisiae</i> (ii) <i>In vitro</i> bypass of 8-oxoG (iii) Overexpression increases H <sub>2</sub> O <sub>2</sub> resistance	[39]
Pol $\kappa$	Bypass of N2-adducted dG lesions Extension of mismatched primer termini	<i>T. cruzi</i> (Tc00.1047053503755.30)	(i) Mitochondrial localization (ii) <i>In vitro</i> bypass of 8-oxoG (iii) DNA synthesis within recombination intermediates (iv) Overexpression increases zeocin, gamma radiation, and H <sub>2</sub> O <sub>2</sub> resistance	[40]

perform BER of different base lesions. However, it is not clear whether they can perform short-patch and long-patch BER since the homologs of LIG3 and XRCC1, which are supposedly essential for the short-patch mechanism [46, 49, 50], have not yet been identified in the three organisms.

However, these BER components are also absent in plants, and Córdoba-Cañero et al. [51] recently demonstrated that BER of uracil and abasic sites occurs in *Arabidopsis thaliana* whole-cell extracts by both single-nucleotide insertion and long-patch DNA synthesis. In contrast to the other Trityps,

the *L. major* genome allegedly does not encode for the PARP enzyme, which could play a role in the long-patch subpathway [7].

Different DNA glycosylases involved in the removal of modified bases from DNA have been characterized in Trityps. The Uracyl-DNA glycosylase from *T. cruzi* (TcUNG) was the first one to be characterized by Fárez-Vidal and coworkers [16]. They demonstrated that the enzyme activity was enhanced by the addition of an AP endonuclease from *L. major*, suggesting that there could be a functional interaction between the two enzymes [16]. Recently, Peña-Dias and colleagues [17] reported that TcUNG is able to complement *E. coli ung* mutants, and that the trypanosome enzyme has a catalytic activity similar to human UNG. Surprisingly, their results indicated that TcUNG is able to excise uracil in DNA *via* short-patch BER using a polymerase that follows a Pol $\beta$ -like pattern of inhibition. The characterization of the TcUNG protein sequence suggested that it has a probable PCNA-binding motif and could be directed either to the mitochondrion or nucleus [17].

Another glycosylase found in Trityps is 8-oxoG-DNA glycosylase (OGG1), an enzyme that removes the oxidative lesion 7,8-dihydro-8-oxoguanine (also known as 8-oxoguanine or 8-oxoG) when it is paired with cytosine. Among the DNA damage caused by reactive oxygen species (ROS), 8-oxoG is of outstanding interest because of its highly mutagenic potential and abundance [52]. This lesion has the ability to mimic thymine functionally, forming a stable 8-oxoG:A base pair. This conformation allows the replicative DNA polymerases to efficiently bypass 8-oxoG failing to detect this damaged DNA base [53]. A functional homolog of OGG1 in *T. cruzi* has been studied *in vivo* by Furtado and colleagues (unpublished data). This gene is able to complement yeast OGG1 mutants, reducing the mutation rate of these cells. The expression of OGG1-GFP fusion protein in *T. cruzi* revealed that the intracellular localization of OGG1 is both nuclear and mitochondrial. In fact, overexpression of the OGG1 in *T. cruzi* diminishes the levels of 8-oxoG within the nucleus and mitochondrion after hydrogen peroxide (H<sub>2</sub>O<sub>2</sub>) treatment. The unusual localization of OGG1 in the mitochondrion could indicate the importance of the maintenance of the kDNA integrity in this parasite.

In addition to OGG1 glycosylase, MutT and MutY also contribute to counteract the mutagenesis effects of 8-oxoG. These three enzymes constitute the so-called GO-system [54]. MutT degrades 8-oxo-dGTP from the nucleotide pool to 8-oxo-dGMP, preventing mutations that arise from the misincorporation of this oxidized form of dGTP. On the other hand, the DNA glycosylase MutY removes adenine from the 8oxoG:A pair [54]. When 8-oxo-dGTP is misincorporated opposite adenine in template DNA, MutY can fix an A:T to C:G mutation because it removes the correct adenine from the A:8oxoG pair. Therefore, when MutY is present, the action of MutT is crucial because oxidized nucleotides must be eliminated from the nucleotide pool [54]. At the time the genome sequence was released, homologs of 8-oxoguanine hydrolase MutT were not encountered in the Trityps genome [6–9]. A more

accurate search of the Trityps genomes revealed that MutT homologs are present in *T. brucei*, *L. major*, and possibly in *T. cruzi* [15]. This is not unexpected given that these parasites have putative MutY homologs [15]. Indeed, a *T. cruzi* MutY homolog has been characterized (Kunrath-Lima, unpublished data). This gene is able to complement MutY-deficient bacteria, diminishing its mutation rates. Moreover, the *T. cruzi* MutY recombinant protein removes the adenine paired with 8-oxoG *in vitro* from a 30 mer fluorescent substrate.

The AP endonucleases 1 from *T. cruzi* and *L. major* have also been characterized [18–20]. Both were able to efficiently complement AP endonuclease-deficient *E. coli*, conferring resistance to alkylating and oxidizing agents [18]. The *L. major* AP endonuclease was more extensively studied, and the purified protein exhibited endonuclease and high 3' phosphodiesterase activities on AP DNA *in vitro*. Moreover, *Leishmania* parasites overexpressing the AP endonuclease showed increased H<sub>2</sub>O<sub>2</sub> and methotrexate resistance as well as reduced DNA fragmentation [19]. The structural characteristics of the *L. major* enzyme exhibited similarities with previously characterized homologs [20].

Among the polymerases, Pol $\beta$  from *T. cruzi* and *T. brucei* have already been characterized [21, 22]. The TcPol $\beta$  localizes to the parasite kinetoplast and exhibits DNA polymerization and 5' dRP lyase activity [21]. Similarly, the TbPol $\beta$  characterization also showed that, in addition to a mitochondrial localization, it is active as a DNA polymerase and as a lyase [22]. The cellular localization of these polymerases highlights an important feature of the Trityps: the presence of kDNA. The kDNA structure is so complex that it requires an unusual replication mechanism, which differs from higher eukaryotes [55, 56]. This complexity is reflected in the DNA repair and replication machinery that can be localized to this organelle [7]. Pol $\beta$  is an example of a polymerase that shows a nuclear localization in higher eukaryotes [57] but is addressed to the kinetoplast in the Trityps [21, 22]. The *L. major* Pol $\beta$  has not yet been experimentally characterized; however, a Pol $\beta$  from *L. infantum* was shown to have a nuclear localization [58], which could indicate that the *L. major* polymerase is also nuclear, as their primary protein sequences showed 100% identity. The possibility that *L. major* possesses a nuclear Pol $\beta$ , combined with the fact that this parasite does not have the PARP enzyme [7, 15], suggests that short-patch BER could play an important role in nuclear DNA repair for this organism. As *Leishmania* proliferates inside macrophage phagolysosomes, a well-coordinated nuclear short-patch BER is essential to combat oxidative DNA damage during parasite nuclear DNA replication [58]. The Trityps genomes apparently do not encode for the other X-family polymerases, DNA polymerase lambda (Pol $\lambda$ ), and mu (Pol $\mu$ ) [7, 15]; thus, *L. major* may be the only Trityps parasite that has an X-family polymerase in the nucleus, reinforcing the importance of short-patch BER in this organelle.

PARP from *T. cruzi*, another enzyme that is involved in long-patch BER pathway, has also been characterized. The activity of this enzyme has been shown to be dependent on the presence of DNA and was enhanced by SSB in DNA

in a concentration-dependent manner. Moreover, it was demonstrated that DNA-damaging agents, such as H<sub>2</sub>O<sub>2</sub> and  $\beta$ -lapachone, induced PAR synthesis in the parasite nucleus, indicating that this enzyme could be involved in the signaling of this phenomenon [23].

#### 4. Nucleotide Excision Repair

Nucleotide excision repair is one of the most versatile DNA repair mechanisms, responsible for repairing lesions that alter the tridimensional DNA conformation, such as cisplatin adducts [59] and UV-induced lesions (pyrimidine dimers and pyrimidine photoproducts [60]). This mechanism can be divided into two major pathways: global genome repair (GGR), which operates in the noncoding parts of the genome and in the nontranscribed strand of active genes, and TCR, which is activated when a lesion appears in a gene that is being transcribed, ensuring that the transcribed strand of active genes has a higher priority for being repaired than the rest of the genome [61].

The GGR-NER mechanism comprises several steps: (i) distortion detection, performed by XPC and HR23B [62] or alternatively by the complex DDB1/XPE-DDB2 [63]; (ii) double-strand opening by the TFIIH complex *via* its XPB and XPD helicase subunits [64]; (iii) recruitment of XPA complexed with the three heterotrimeric replication protein A (RPA) subunits [65]; (iv) DNA incision by the XPG endonuclease (3' side of lesion [66]) and by the XPF-ERRC1 heterodimer (5' side of the lesion [67]); (v) gap filling by the replicative polymerases  $\delta$  and  $\epsilon$  associated with PCNA [68, 69]; (vi) nick sealing by ligase III together with XRCC1 (in quiescent cells) or at a lower level by ligase I (in actively replicative cells) [70].

TCR-NER has a mechanism similar to GGR, but it differs in the initial steps because it lacks the XPC and DDB1 complexes. TCR-NER is triggered by the stalling of RNA polymerase II, which subsequently recruits CSA, CSB, and XAB2. The following steps are performed by the TFIIH complex as in GGR [71].

Although the entire NER mechanism is well conserved in nature, there is no sequence homology between the NER proteins from bacteria and eukaryotes. Despite the sequence conservation shared by the eukaryotic NER proteins, not all the genes that encode those proteins are found among distantly related phylogenetic groups. The most remarkable examples are the lack of XPA in *Arabidopsis thaliana* and the lack of XPA, XPC, and XPE in *Plasmodium falciparum* [72], which suggest that the NER mechanism can have slight variations between different taxa.

The Trityps genomes contain the majority of the NER components [7, 15], but the biochemical mechanisms of this pathway may present some minor differences from the higher eukaryotes. Some of the genes are duplicated. For example, Trityps have two copies of XPB and DDB1 appear duplicated in *T. cruzi*. However, others such as XPA could not be identified in Trityps. It is also possible that the Trityps ligation step is different from the ligation step from higher eukaryotes. The Trityps lack a recognizable

ligase III, which together with its partner XRCC1 plays a major role in this final step. However, because their genomes encode ligase I, it might be possible that the ligation step is performed exclusively by this protein in those parasites. DDB2, which interacts with DDB1 and recognizes UV-induced lesions, and RPA3, a component of the RPA heterotrimer, also could not be identified in the genomes of these trypanosomatids. The TFIIH complex shows some differences when compared to yeast and mammals because it does not contain the cyclin-activating kinase (CAK) sub-complexes. In addition to that, a recent study showed that *T. brucei* TFIIH contains two trypanosomatid-specific subunits of TFIIH (TSP1 and TSP2), which are indispensable for parasite viability and transcription of splice-leader gene [24]. These subunits are also present in the genomes of *T. cruzi* and *L. major*.

Protein-coding genes are constitutively transcribed in trypanosomatids [73]. This peculiarity implies that TCR could be one of the most crucial mechanisms involved in repairing DNA damage in those parasites. Surprisingly, the Trityps genomes apparently lack the gene that encodes CSA. Although the role of CSA in TCR is not clear, recent evidence indicates that CSA is involved in CSB ubiquitination and degradation following UV irradiation [74], which would restore transcription at a normal rate after the repair. The absence of an evident CSA in Trityps implies that the trypanosomatid TCR differs from the standard TCR mechanism, either by the lack or divergence of this component, or by the presence of an alternative protein to perform this step. This could be related to the peculiar constitutive transcription of Trityps. In fact, overexpression of *T. cruzi* DNA polymerase  $\eta$  (Pol $\eta$ ), involved in the translesion synthesis of pyrimidine dimers, and overexpression or haploinsufficiency of RAD51, a key protein in HR, do not confer any protection against UV irradiation, which could suggest that the UV-induced lesions are fully repaired before the cell enters the S-phase ([39], Passos-Silva et al., submitted). In addition, results obtained by our group show that *T. cruzi* repairs cisplatin-induced lesions at an extremely high rate, with total lesion removal in less than an hour (Rajão, unpublished data). Taken together, these results led us to hypothesize that, in *T. cruzi*, lesions that cause DNA distortions are readily detected and repaired by TCR because the great majority of the protein-coding genes are transcribed constitutively. Whether the CSA absence or the presence of an alternative CSA is an adaptation to this distinctive repair is a topic for future investigation. When compared to other taxa, GGR-NER in trypanosomatids seems to be similar to the GGR pathway encountered in plants, as both groups of organisms share peculiarities regarding the presence and absence of some NER genes. Although plants encode all the TFIIH subunits and CSA, the plant genome, like Trityps, does not possess an identifiable XPA, RPA3, or ligase 3. In addition, the plant genome also carries two copies of XPB [72]. Interestingly, these DNA repair similarities found in Trityps and plants can also be observed in the MMR pathway, which could suggest that both groups might share some commonalities in their DNA repair mechanisms.

## 5. Mismatch Repair

Postreplicative DNA mismatch repair promotes genetic stability by repairing DNA replication errors (single base-base mismatches and insertion or deletion loops, IDLs), inhibiting recombination between nonidentical DNA sequences and participating in responses to DNA damage induced by genotoxic agents, such as H<sub>2</sub>O<sub>2</sub>, cisplatin, and N-methyl-N'-nitro-N-nitrosoguanidine (MNNG) [75].

The fundamental aspects of the pathway have been highly conserved throughout evolution. In essence, postreplicative MMR operates through (i) DNA mismatch recognition by MutS $\alpha$  (MSH2-MSH6) or MutS $\beta$  (MSH2-MSH3), (ii) excision of the damaged DNA section mainly by ExoI, and (iii) DNA resynthesis by DNA Pol $\delta$  and ligation. Steps after DNA mismatch recognition are coordinated by MLH heterodimers that bind to MSH proteins and probably recruit and assemble downstream repair complexes. Strand discontinuities associated with DNA replication can serve as entry points for strand excision, conferring strand specificity to MMR [75].

Each trypanosomatid encodes a set of MMR proteins, which suggests they are fully competent for mismatch recognition and repair [7, 15]. Components of the MMR pathway are major players in processes known to generate genetic diversity, such as mutagenesis and DNA recombination. Evidences suggest that differences in MMR efficiency could be an important source of genetic diversity in organisms [76–79].

*T. cruzi* has a highly heterogeneous population, composed of a pool of strains with distinct characteristics such as morphology, growth rate, virulence, and sensitivity to drugs [80]. Despite its broad genetic diversity, three major lineages, named *T. cruzi* I, II and III, have been identified in the parasite population [81]. Studies with a number of molecular markers revealed that parasites belonging to the *T. cruzi* I lineage have lower genetic variability compared to *T. cruzi* II, and III [82–84]. The great genetic diversity observed in *T. cruzi* (and more precisely, in *T. cruzi* II strains) may play an important role in pathogenesis and survival of the parasite within its different hosts.

It is conceivable that components of DNA repair pathways participate in processes that resulted in increasing genetic variability within the parasite population [85]. MSH2, the core eukaryotic mismatch repair gene, has been characterized in *T. cruzi* [25, 26, 86]. Sequence analyses of TcMSH2 showed the existence of three distinct isoforms, named TcMSH2A, B, and C, encoded in the genome of *T. cruzi* I, III, and II strains, respectively [25]. It is possible that these isoforms have distinct protein activity, leading to variations in the efficiency of MMR. In fact, parasites that have TcMSH2A show increased sensitivity to cisplatin and MNNG, increased microsatellite instability, and greater resistance to H<sub>2</sub>O<sub>2</sub> when compared to parasites expressing TcMSH2B or TcMSH2C ([25], Campos et al., submitted). Further studies are needed to determine if these variations in MMR efficiency have a broader impact on genetic variation and behavior in *T. cruzi* strains. Attempts to generate TcMSH2-null mutants indicate that, in addition to its role

in MMR, TcMSH2 acts in the parasite response to oxidative DNA damage in an MMR independent manner [26].

In *T. brucei*, MSH2 has been studied along with MLH1 [27]. Mutations in both genes give rise to increased microsatellite instability and lead to increased tolerance to the alkylating agent MNNG [27]. Both phenotypes are consistent with an impairment of nuclear MMR activity [75]. These results indicate that MMR in trypanosomatids is active in repairing errors that arise during replication and in response to chemical damage.

MMR also plays a regulatory role in homologous recombination in *T. brucei* [28]. Double mutants of MSH2 and MLH1 show an increased frequency of homologous recombination, both between perfectly matched DNA molecules and between DNA molecules with divergent sequences. However, MMR has little influence on antigenic variation in this parasite [28]. This topic is discussed in detail in the “Double strand break section”.

*T. brucei* MSH2-null mutants are more sensitive to H<sub>2</sub>O<sub>2</sub> than wild-type cells [26]. Because MLH1-null mutants do not show this phenotype, TbMSH2 seems to have an additional role in dealing with oxidative damage, which may occur independently of MMR [26]. Interestingly, the heterologous expression of MSH2 from *T. cruzi* was able to counteract the increased sensitivity to H<sub>2</sub>O<sub>2</sub> in the *T. brucei* MSH2-null mutant. However, it did not affect the classical MMR-deficient phenotypes, such as microsatellite instability and resistance to MNNG [26]. This differential activity of MSH2 has also been reported in colon adenocarcinoma cell lines where MSH2, but not MLH1, has been implicated in the repair of 8-oxoG [87]. In addition, *Helicobacter pylori*, which is suggested to be MMR-defective due to the lack of MutH and MutL homologs, presents a MutS homolog that is involved in repairing oxidative damage [88].

Four additional MSH-like genes can be found in the trypanosomatids: MSH3, MSH4, MSH5, and MSH6 [7, 15, 27]. The predicted MSH6 polypeptides in Trityps have N-terminal truncations relative to eukaryotic orthologues [27]. In comparison, MSH7, unique to plants, bears similar truncations in the N-terminus along with the conserved mismatch interaction residues indicative of the MSH6 subgrouping [89]. MSH4 and MSH5 predicted proteins that appear to lack an N-terminal mismatch interaction, indicating an absence of function in the mismatch repair and a possible role in meiotic recombination [27].

Concerning MutL-related genes, Trityps contain PMS1 and MLH1 [27]. Other MutL homologs, such as PMS2, MLH2, and MLH3, appear to be absent. Trypanosomatid MMR is therefore likely to involve only an MLH1-PMS1 heterodimer whereas the functions performed by the dimers formed between MLH1 and its three other binding partners in yeast are either absent or fulfilled by MLH1-PMS1.

## 6. Repair of Double-Strand Breaks

DNA DSBs are a particularly dangerous type of lesion. DSBs can arise when replication forks encounter blocking lesions, which leads to fork collapse, or can be induced by ionizing

radiation and radiomimetic chemicals. Failure to accurately repair such damage can result in cell death or large-scale chromosome changes, including deletions, translocations, and chromosome fusions that enhance genome instability. Two distinct and evolutionarily conserved pathways for DSB repair exist: homologous recombination and nonhomologous end joining [90].

**6.1. Nonhomologous End Joining.** NHEJ is frequently imprecise. The two ends of the DSB are held together and religated, often following the loss of some sequence by nucleolytic degradation or addition by polymerization [90].

Eukaryotic NHEJ is a multistep pathway beginning with limited end processing by the MRE11/RAD50/NBS1 (MRN) complex and initial recognition of DSBs through end binding by Ku, a ring comprised of the Ku70, and Ku80 subunits. In higher eukaryotes, the DNA-dependent protein kinase catalytic subunit (DNA-PKcs) is also recruited. In the final step, DNA ligase IV with its binding partners XRCC4 (Lif1 in yeast) and XLF (also called Cernunnos) seals the break [90].

NHEJ seems to be absent in trypanosomatids. With the exception of Mre11, Rad50, KU70 and KU80, no other factors implicated in NHEJ could be identified in these organisms. KU70 and KU80 have been identified in *T. brucei*, *T. cruzi*, and *L. major*. Studies in *T. brucei* have shown that these genes act in telomere maintenance [29, 30], a function they provide in addition to NHEJ [91]. However, the mutants of KU70 and KU80 did not display higher sensitivity to DNA-damaging agents, suggesting that they play, at most, a minor role in DSBs repair possibly due to the absence of NHEJ in this organism. The most striking absences are DNA ligase IV and XRCC4/Lif1 [92]. These absences in Trityps suggest one of two possibilities: either NHEJ is absent from these organisms or its catalytic components have been modified beyond recognition, perhaps using a distinct DNA ligase. These possibilities should be further investigated.

**6.2. Homologous Recombination.** HR is required for DNA DSBs repair and provides critical support for DNA replication in the recovery of stalled or broken replication forks. In addition, HR is involved in the repair of incomplete telomeres and in the correct segregation of homologous chromosomes during meiosis. The broad reaction scheme [93, 94] can be considered in three steps: initiation (or presynapsis) when the nucleolytic resection of DSBs occurs, generating single-stranded tails with 3'-OH ends; strand exchange (synapsis), when the end(s) of the DSB invades the intact DNA molecule *via* regions of sequence homology; resolution (postsynapsis), when strand exchange intermediates are separated and the DSB is repaired.

Homologous recombination is the major pathway of DSB repair in lower eukaryotes [95]. Essential components of this mechanism have been identified in the genome of *T. cruzi*, *T. brucei*, and *L. major*. HR can contribute to different strategies evolved by trypanosomatids to create genetic variability that is needed for survival in their hosts. Antigenic variation is used by *T. brucei* to evade the host immune system through the switch of surface proteins (VSGs). This

mechanism is regulated by HR, allowing the switch of one VSG at time to the expression site [85]. Meanwhile, *T. cruzi* displays a wide range of surface molecules that are highly polymorphic and may represent a useful arsenal to evade immune systems [85]. Recent works have been suggesting that HR is responsible for creating mosaic genes of surface molecules through segmental gene conversion and for decreasing the divergence between duplicated regions such as surface multigenic families [83, 96]. In addition, experiments with genetic manipulation have shown that homologous recombination is the main mechanism for integration of transformed DNA in these organisms [97–100].

The complex of proteins involved in the presynapsis step of HR can be found in Trityps, such as MRE11, Rad50, NSB1, and RPA. However, only MRE11 from *T. brucei* has been fully characterized. Mutation of MRE11 causes impairment in *T. brucei* homologous recombination, increases DNA damage sensitivity, and leads to gross chromosomal rearrangements [31, 32]. MRE11 does not contribute to recombination during antigenic variation, an important mechanism used by *T. brucei* to escape host immune response as mentioned before [32].

The core step of HR is the search for homology, homologous DNA pairing, and strand exchange reaction that is mediated by recombinases, such as RAD51 and DMC1. Both enzymes are present in Trityps. DMC1, a putative meiosis-specific recombinase, has only been studied in *T. brucei*. The lack of DMC1 does not affect HR repair or VSG switching in this parasite [36]. The presence of genes involved in meiosis is an intriguing feature of Trityps because they reproduce primarily through clonal reproduction [101]. Even though the population structure of each parasite is largely clonal [101], evidence of genetic exchange in the wild-type populations of *T. brucei* [102], *T. cruzi* [103, 104], and *L. major* [105] has been presented. However, it is unclear whether or not the existence of meiotic recombination genes implies that the trypanosomatids use meiosis.

RAD51 has been characterized in the three trypanosomatids. The expression of RAD51 in *T. cruzi* and *L. major* is induced by DNA-damaging agents [33, 35]. Moreover, the overexpression of RAD51 in *T. cruzi* confers a faster recovery and a more efficient DNA repair of DSBs formed after genotoxic treatment [33]. In addition, *T. cruzi* RAD51 accumulates in the nucleus after exposure to gamma radiation (Passos-Silva et al., submitted). Besides, the levels of Rad51 in *T. cruzi* reflect its susceptibility to oxidative agents. The overexpression of TcRad51 confers a greater resistance to H<sub>2</sub>O<sub>2</sub> whereas the deletion of one of the TcRad51 alleles increases the sensitivity when compared to wild-type parasites (Passos-Silva et al., submitted). Thus, Rad51 seems to be involved in a greater resistance to oxidative damage in *T. cruzi* DNA. An active response to oxidative stress is an important feature of *T. cruzi* and *L. major* because they have an intracellular stage in the host that is subjected to a rigorous oxidizing environment [106]. For *T. brucei*, RAD51, and consequently HR, is directly involved in antigenic variation. Null mutants of RAD51 led to impairments in VSG switch and DNA transformation and

a higher sensitivity to genotoxic agents [34]. However, an RAD51-independent recombination pathway is also present, as evidenced by two mechanisms detected in *T. brucei* RAD51 mutants: (i) antigenic variation by gene conversion [34] and (ii) integration of transformed DNA by homology-based recombination although the frequency of detection is low [29]. Interchromosomal HR is the major pathway used by *T. brucei* to repair DSBs, as demonstrated by Glover and colleagues [107]. After the generation of single DSB through SceI endonuclease, RAD51 accumulates into the foci and a G2M checkpoint is activated [107]. In addition, Tritryps show intriguing differences concerning gamma radiation treatment, which generates high levels of DSBs. *T. cruzi* and *L. major* are highly resistant to gamma radiation when compared to other eukaryotes [33, 108, 109]. However, this resistance is not seen in *T. brucei* (unpublished data). In fact, after gamma radiation treatment, the expression of RAD51 in *T. cruzi* and *L. major* are induced [33, 35] whereas the RAD51 levels in *T. brucei* do not increase [34]. As mentioned before, these intriguing differences concerning the efficiency of recombination in Tritryps could be due to the distinct mechanisms used by these organisms to create genetic variability and to evade the mammalian immune system.

The loading of recombinases in the ssDNA is a rate-limiting process that is enhanced by recombination mediators [93]. BRCA2, the RAD51 paralogs, and RAD54 are among the recombination mediators present in trypanosomatids. RAD52, however, seems to be absent in these organisms. Whether or not this has a significant impact on recombination is unclear. Unlike the yeast mutant, in which RAD52 is a key protein for HR, mouse RAD52 mutants display an exceedingly mild recombination defect and no ionizing radiation sensitivity [110]. It is unclear which proteins functionally replace the yeast RAD52 protein in mammalian cells or trypanosomatids. One candidate is BRCA2, which is not found in budding yeast. BRCA2 can interact with RAD51 through the BRC repeat motifs [111–113] and unrelated sequences. BRCA2 from *T. cruzi* and *Leishmania* have two nonidentical BRC repeats [37]. On the other hand, *T. brucei* BRCA2 has undergone an expansion in the number of BRC repeats (15 BRC repeats), and these elements are crucial for the efficiency of HR and RAD51 localization. In addition, *T. brucei* BRCA2 mutants display antigenic variation impairment and genome instability [37]. Four RAD51 paralogs appear to be encoded by *T. brucei* and *T. cruzi*, one of which appears to be missing in *L. major*. Two of the *T. brucei* RAD51-like proteins play a role in DNA repair and recombination [38].

Studies in *T. brucei* have been showing that HR in this organism is regulated by MMR through the rejection of HR between insufficiently homologous DNA sequences. This has been evidenced by experiments done with MSH2 mutants which are able to recombine mismatched substrates more efficiently than wild type cells. Around 100 bp of homology are required for an efficient Rad51-mediated recombination [28]. In contrast, the HR that occurs during VSG switching uses a short and divergent substrate such as the 70 bp repeats upstream of VSG genes. Thus, the VSG switching may

happen through a specific recombination pathway that is independent of MMR or the suppression of MMR would be necessary [100, 114].

## 7. Translesion Synthesis

Lesions in DNA can block replicative DNA polymerases (Pol $\delta$  and Pol $\epsilon$ ), causing the stall of the replication fork. This halt leads to PCNA monoubiquitination by Rad6/Rad18 complex, promoting the switch from replicative DNA polymerase to TLS DNA polymerase, which catalyses nucleotide insertion opposite the lesion. Then, nucleotide extension is performed mostly by DNA polymerase zeta (Pol $\zeta$ ). After the extension step, replicative DNA polymerases return to DNA synthesis [115]. TLS DNA polymerases contain a minimally stringent catalytic site, allowing for the accommodation of templates containing damaged bases. Moreover, this group of specialized DNA polymerases has lost 3'-5' proofreading activity, having a highly mutagenic character [116].

*T. cruzi*, *T. brucei*, and *L. major* genomes encode for a wide variety of translesion synthesis proteins. Pol $\kappa$ , Pol $\eta$ , Rev1, and Pol $\zeta$  homologs are found in these species. PCNA and Rad6 homologs are also present. These parasites show an expansion of Pol $\kappa$  gene, present in two, ten, and three copies in *T. cruzi*, *T. brucei*, and *L. major* genomes, respectively [6–9]. The gene duplication/amplification displayed by Tritryps Pol $\kappa$  gene could result in an increment of Pol $\kappa$  gene expression level which would compensate the lack of pretranscriptional mechanisms in these organisms [9].

Pol $\eta$  from *T. cruzi* has been characterized *in vitro* and *in vivo* [39]. TcPol $\eta$  is able to complement yeast Rad30 mutant (Pol $\eta$ -null mutant), increasing yeast resistance to UV radiation, which indicates that Pol $\eta$  is able to bypass UV lesions. Parasites overexpressing TcPol $\eta$  show a higher resistance to H<sub>2</sub>O<sub>2</sub> treatment. This resistance could be associated with the ability of TcPol $\eta$  to bypass 8-oxoG lesions *in vitro*, suggesting that this enzyme is able to incorporate nucleotides opposite oxidative lesions as well. In contrast to the result seen in yeast, parasites overexpressing this nuclear polymerase do not show a higher resistance to UV radiation. The lack of conferred resistance might be related to the number of lesions remaining during S phase because it is possible that the majority of UV lesions would be repaired by TCR-NER prior to DNA replication, as the majority of the protein-coding genes are constitutively transcribed in this organism [39].

*T. cruzi* DNA polymerase kappa has been studied by our group. One copy of TcPol $\kappa$  localizes in the *T. cruzi* mitochondrion [40]. This result indicates that *T. cruzi* is the first organism described in the literature to contain one exclusively mitochondrial Pol $\kappa$ . Mitochondrial TcPol $\kappa$  bypasses 8-oxoG *in vitro*, which correlates with the increase in H<sub>2</sub>O<sub>2</sub> resistance observed in parasites overexpressing this protein. This DNA polymerase could also participate in the homologous recombination pathway in *T. cruzi* because it synthesizes DNA within recombination intermediates. Reinforcing this hypothesis, TcPol $\kappa$  overexpression confers higher resistance to gamma radiation and zeocin, which are

agents known to cause DSBs [40]. Recent results have shown that the other copy of TcPolk has nuclear localization (Rajão, unpublished results).

TLS deals with DNA damage that blocks the replication fork, thus rescuing the cell from death. This accounts for the survival increase displayed by TcPolk-overexpressing parasites when treated with agents that cause DSBs. In addition, TcPolk- and TcPol $\eta$ -overexpressing cells also presented increased resistance to H<sub>2</sub>O<sub>2</sub> treatment [39, 40]. The presence of TLS DNA polymerases that efficiently bypass oxidative lesions might be important during *T. cruzi* lifecycle, especially in the intracellular amastigote phase, when this organism deals with ROS generated by the infected host cell [117]. Moreover, because TLS can operate in an error-prone fashion, TLS can generate DNA punctual mutations in the parasite genome [116]. This can be correlated with the generation of genetic variability in Trityps, notably in surface molecules. In fact, mutation is considered one of the main driving forces that increase the divergence between genes from multigenic families in *T. cruzi*, in contrast to the genetic conversion, another main driving force that decreases this divergence [83, 96]. A variable repertoire of surface molecules is a key strategy for *T. cruzi* to achieve a successful rate of infection. These proteins interact with different molecules on the host cell membranes and the extracellular matrix, increasing its chance to adapt to distinct cell types and hosts [83, 96]. Besides, the polymorphism of *T. cruzi* surface proteins contributes to evade cellular immune response of the mammalian host through the presentation of a broad range of possible target epitopes to CD8+T cells. This can result in an inefficient activation of naïve CD8+T cells, leading to a delayed protective immune response [118]. Thus, TLS can affect the general diversity in the organism, which is important for acquiring evolutionary novelty and for adaptation to the parasitic lifestyle.

## 8. Conclusion

The genome sequencing of *T. cruzi*, *T. brucei*, and *L. major* has provided insight into the DNA maintenance mechanisms in these pathological protozoa [6–9]. Experimental data have revealed additional particular features of these systems in the Trityps, which presumably reflect the distinct aspects of the infectious cycle that shape the survival strategies of each protozoa pathogen. Among these particularities, the unexpected mitochondrial localization of some typically nuclear proteins (Furtado, unpublished data) [21, 22, 40] and the additional roles of a few proteins in response to oxidative treatment were highlighted in this paper (Passos-Silva, submitted) [26, 39, 40]. The former is important during the replicative stages of the parasites when the metabolic activity is higher and the unique mitochondrion is then exposed to higher amounts of ROS generated by oxidative phosphorylation [3–5]. The later feature is particularly critical during the intracellular stage of the parasites *L. major* and *T. cruzi* when they are subjected to the immune response of mammalian host cells through oxidative stress [106, 119].

The DNA damage repair and tolerance mechanisms of Trityps are also involved in the generation of genetic variability which raises the successful rate of infection through the increasing of surface molecules diversity in *T. cruzi* and the expanding of the repertoire of VSGs in *T. brucei* [85]. Indeed, strains of *T. cruzi* that have a higher genetic variability (possibly a reflection of a less efficient MMR—Campos et al., unpublished data) are frequently associated with human infection [120, 121]. On the other hand, HR regulates antigenic variation in *T. brucei*, the strategy used by this parasite to evade mammalian immune system [106]. A clear association between DNA repair in *L. major* and evasion of the mammalian immunological response has not been established yet possibly due to a relatively narrow range of studies that investigate DNA repair in this organism.

Essentially, with the exception of NHEJ, the major DNA repair pathways appear to be present in Trityps [7]. Further studies are necessary to clarify the information about DNA repair pathways in Trityps, specifically the differences in Trityps machinery from the typical eukaryotic machinery for DNA repair, which could provide potential points of attack against the parasites.

## Acknowledgments

This work is supported by funds from CNPq, Fundação de Amparo a Pesquisa do Estado de Minas Gerais—FAPEMIG (Brazil), and the Howard Hughes Medical Institute.

## References

- [1] K. Nussbaum, J. Honek, C. M. Cadmus, and T. Efferth, “Trypanosomatid parasites causing neglected diseases,” *Current Medicinal Chemistry*, vol. 17, no. 15, pp. 1594–1617, 2010.
- [2] W. de Souza, “Structural organization of *Trypanosoma cruzi*,” *Memorias do Instituto Oswaldo Cruz*, vol. 104, no. 1, pp. 89–100, 2009.
- [3] A. Schnauffer, G. J. Domingo, and K. Stuart, “Natural and induced dyskinetoplastic trypanosomatids: how to live without mitochondrial DNA,” *International Journal for Parasitology*, vol. 32, no. 9, pp. 1071–1084, 2002.
- [4] A. O. M. Stoppani, R. Docampo, J. F. de Boiso, and A. C. C. Frasc, “Effect of inhibitors of electron transport and oxidative phosphorylation on *Trypanosoma cruzi* respiration and growth,” *Molecular and Biochemical Parasitology*, vol. 2, no. 1, pp. 3–21, 1980.
- [5] R. Dey, C. Meneses, P. Salotra, S. Kamhawi, H. L. Nakhasi, and R. Duncan, “Characterization of a Leishmania stage-specific mitochondrial membrane protein that enhances the activity of cytochrome c oxidase and its role in virulence,” *Molecular Microbiology*, vol. 77, no. 2, pp. 399–414, 2010.
- [6] M. Berriman, E. Ghedin, C. Hertz-Fowler et al., “The genome of the African trypanosome *Trypanosoma brucei*,” *Science*, vol. 309, no. 5733, pp. 416–422, 2005.
- [7] N. M. El-Sayed, P. J. Myler, D. C. Bartholomeu et al., “The genome sequence of *Trypanosoma cruzi*, etiologic agent of chagas disease,” *Science*, vol. 309, no. 5733, pp. 409–415, 2005.
- [8] N. M. El-Sayed, P. J. Myler, G. Blandin et al., “Comparative genomics of trypanosomatid parasitic protozoa,” *Science*, vol. 309, no. 5733, pp. 404–409, 2005.

- [9] A. C. Ivens, C. S. Peacock, E. A. Wortley et al., "The genome of the kinetoplastid parasite, *Leishmania major*," *Science*, vol. 309, no. 5733, pp. 436–442, 2005.
- [10] J. H. J. Hoeijmakers, "Genome maintenance mechanisms for preventing cancer," *Nature*, vol. 411, no. 6835, pp. 366–374, 2001.
- [11] D. Branzei and M. Foiani, "Maintaining genome stability at the replication fork," *Nature Reviews Molecular Cell Biology*, vol. 11, no. 3, pp. 208–219, 2010.
- [12] P. Huertas, "DNA resection in eukaryotes: deciding how to fix the break," *Nature Structural & Molecular Biology*, vol. 17, no. 1, pp. 11–16, 2010.
- [13] K. D. Arczewska and J. T. Kuśmierk, "Bacterial DNA repair genes and their eukaryotic homologues: 2. Role of bacterial mutator gene homologues in human disease. Overview of nucleotide pool sanitization and mismatch repair systems," *Acta Biochimica Polonica*, vol. 54, no. 3, pp. 435–457, 2007.
- [14] L. S. Waters, B. K. Minesinger, M. E. Wiltrout, S. D'Souza, R. V. Woodruff, and G. C. Walker, "Eukaryotic translesion polymerases and their roles and regulation in DNA damage tolerance," *Microbiology and Molecular Biology Reviews*, vol. 73, no. 1, pp. 134–154, 2009.
- [15] M. Aslett, C. Aurrecochea, M. Berriman et al., "TriTrypDB: a functional genomic resource for the Trypanosomatidae," *Nucleic Acids Research*, vol. 38, supplement 1, pp. D457–D462, 2009.
- [16] M. E. Fárez-Vidal, C. Gallego, L. M. Ruiz-Pérez, and D. González-Pacanowska, "Characterization of uracil-DNA glycosylase activity from *Trypanosoma cruzi* and its stimulation by AP endonuclease," *Nucleic Acids Research*, vol. 29, no. 7, pp. 1549–1555, 2001.
- [17] J. Peña-Díaz, M. Akbari, O. Sundheim et al., "*Trypanosoma cruzi* contains a single detectable uracil-DNA glycosylase and repairs uracil exclusively via short patch base excision repair," *Journal of Molecular Biology*, vol. 342, no. 3, pp. 787–799, 2004.
- [18] J. Pérez, C. Gallego, V. Bernier-Villamor, A. Camacho, D. González-Pacanowska, and L. M. Ruiz-Pérez, "Apurinic/aprimidinic endonuclease genes from the trypanosomatidae *Leishmania major* and *Trypanosoma cruzi* confer resistance to oxidizing agents in DNA repair-deficient *Escherichia coli*," *Nucleic Acids Research*, vol. 27, no. 3, pp. 771–777, 1999.
- [19] C. Gallego, A. M. Estévez, E. Fárez, L. M. Ruiz-Pérez, and D. González-Pacanowska, "Overexpression of AP endonuclease protects *Leishmania major* cells against methotrexate induced DNA fragmentation and hydrogen peroxide," *Molecular and Biochemical Parasitology*, vol. 141, no. 2, pp. 191–197, 2005.
- [20] A. E. Vidal, M. Harkiolaki, C. Gallego et al., "Crystal Structure and DNA Repair Activities of the AP Endonuclease from *Leishmania major*," *Journal of Molecular Biology*, vol. 373, no. 4, pp. 827–838, 2007.
- [21] D. d. O. Lopes, B. L. F. Schamber-Reis, C. G. Regis-da-Silva et al., "Biochemical studies with DNA polymerase  $\beta$  and DNA polymerase  $\beta$ -PAK of *Trypanosoma cruzi* suggest the involvement of these proteins in mitochondrial DNA maintenance," *DNA Repair*, vol. 7, no. 11, pp. 1882–1892, 2008.
- [22] T. T. Saxowsky, G. Choudhary, M. M. Klingbeil, and P. T. Englund, "*Trypanosoma brucei* has two distinct mitochondrial DNA polymerase beta enzymes," *The Journal of biological chemistry*, vol. 278, no. 49, pp. 49095–49101, 2003.
- [23] S. H. Fernández Villamil, R. Baltanás, G. D. Alonso, S. C. Vilchez Larrea, H. N. Torres, and M. M. Flawiá, "TcPARP: a DNA damage-dependent poly(ADP-ribose) polymerase from *Trypanosoma cruzi*," *International Journal for Parasitology*, vol. 38, no. 3–4, pp. 277–287, 2008.
- [24] J. H. Lee, H. S. Jung, and A. Günzl, "Transcriptionally active TFIIH of the early-diverged eukaryote *Trypanosoma brucei* harbors two novel core subunits but not a cyclin-activating kinase complex," *Nucleic Acids Research*, vol. 37, no. 11, pp. 3811–3820, 2009.
- [25] L. Augusto-Pinto, S. M. R. Teixeira, S. D. J. Pena, and C. R. Machado, "Single-nucleotide polymorphisms of the *Trypanosoma cruzi* MSH2 gene support the existence of three phylogenetic lineages presenting differences in mismatch repair efficiency," *Genetics*, vol. 164, no. 1, pp. 117–126, 2003.
- [26] A. Machado-Silva, S. M. R. Teixeira, G. R. Franco et al., "Mismatch repair in *Trypanosoma brucei*: heterologous expression of MSH2 from *Trypanosoma cruzi* provides new insights into the response to oxidative damage," *Gene*, vol. 411, no. 1–2, pp. 19–26, 2008.
- [27] J. S. Bell, T. I. Harvey, A.-M. Sims, and R. McCulloch, "Characterization of components of the mismatch repair machinery in *Trypanosoma brucei*," *Molecular Microbiology*, vol. 51, no. 1, pp. 159–173, 2004.
- [28] J. S. Bell and R. McCulloch, "Mismatch repair regulates homologous recombination, but has little influence on antigenic variation, in *Trypanosoma brucei*," *Journal of Biological Chemistry*, vol. 278, no. 46, pp. 45182–45188, 2003.
- [29] C. Conway, C. Proudfoot, P. Burton, J. D. Barry, and R. McCulloch, "Two pathways of homologous recombination in *Trypanosoma brucei*," *Molecular Microbiology*, vol. 45, no. 6, pp. 1687–1700, 2002.
- [30] C. J. Janzen, F. Lander, O. Dreesen, and G. A. M. Cross, "Telomere length regulation and transcriptional silencing in KU80-deficient *Trypanosoma brucei*," *Nucleic Acids Research*, vol. 32, no. 22, pp. 6575–6584, 2004.
- [31] K. S. W. Tan, S. T. G. Leal, and G. A. M. Cross, "*Trypanosoma brucei* MRE11 is non-essential but influences growth, homologous recombination and DNA double-strand break repair," *Molecular and Biochemical Parasitology*, vol. 125, no. 1–2, pp. 11–21, 2002.
- [32] N. P. Robinson, R. McCulloch, C. Conway, A. Browitt, and J. D. Barry, "Inactivation of Mre11 does not affect VSG gene duplication mediated by homologous recombination in *Trypanosoma brucei*," *Journal of Biological Chemistry*, vol. 277, no. 29, pp. 26185–26193, 2002.
- [33] C. G. Regis-da-Silva, J. M. Freitas, D. G. Passos-Silva et al., "Characterization of the *Trypanosoma cruzi* Rad51 gene and its role in recombination events associated with the parasite resistance to ionizing radiation," *Molecular and Biochemical Parasitology*, vol. 149, no. 2, pp. 191–200, 2006.
- [34] R. McCulloch and J. D. Barry, "A role for RAD51 and homologous recombination in *Trypanosoma brucei* antigenic variation," *Genes and Development*, vol. 13, no. 21, pp. 2875–2888, 1999.
- [35] P. G. McKean, J. K. Keen, D. F. Smith, and F. E. Benson, "Identification and characterisation of a RAD51 gene from *Leishmania major*," *Molecular and Biochemical Parasitology*, vol. 115, no. 2, pp. 209–216, 2001.
- [36] C. Proudfoot and R. McCulloch, "*Trypanosoma brucei* DMC1 does not act in DNA recombination, repair or antigenic variation in bloodstream stage cells," *Molecular and Biochemical Parasitology*, vol. 145, no. 2, pp. 245–253, 2006.

- [37] C. L. Hartley and R. McCulloch, "Trypanosoma brucei BRCA2 acts in antigenic variation and has undergone a recent expansion in BRC repeat number that is important during homologous recombination," *Molecular Microbiology*, vol. 68, no. 5, pp. 1237–1251, 2008.
- [38] C. Proudfoot and R. McCulloch, "Distinct roles for two RAD51-related genes in *Trypanosoma brucei* antigenic variation," *Nucleic Acids Research*, vol. 33, no. 21, pp. 6906–6919, 2005.
- [39] M. B. De Moura, B. L. F. Schamber-Reis, D. G. P. Silva et al., "Cloning and characterization of DNA polymerase  $\eta$  from *Trypanosoma cruzi*: roles for translesion bypass of oxidative damage," *Environmental and Molecular Mutagenesis*, vol. 50, no. 5, pp. 375–386, 2009.
- [40] M. A. Rajão, D. G. Passos-Silva, W. D. DaRocha et al., "DNA polymerase kappa from *Trypanosoma cruzi* localizes to the mitochondria, bypasses 8-oxoguanine lesions and performs DNA synthesis in a recombination intermediate," *Molecular Microbiology*, vol. 71, no. 1, pp. 185–197, 2009.
- [41] A. E. Pegg, "Repair of O6-alkylguanine by alkyltransferases," *Mutation Research*, vol. 462, no. 2-3, pp. 83–100, 2000.
- [42] L. Aravind and E. V. Koonin, "The DNA-repair protein AlkB, EGL-9, and leprecan define new families of 2-oxoglutarate- and iron-dependent dioxygenases," *Genome Biology*, vol. 2, no. 3, p. RESEARCH0007, 2001.
- [43] A. Sancar, "Structure and function of photolyase and in vivo enzymology: 50th anniversary," *Journal of Biological Chemistry*, vol. 283, no. 47, pp. 32153–32157, 2008.
- [44] A. B. Robertson, A. Klungland, T. Rognes, and I. Leiros, "Base excision repair: the long and short of it," *Cellular and Molecular Life Sciences*, vol. 66, no. 6, pp. 981–993, 2009.
- [45] Y. Kubota, R. A. Nash, A. Klungland, P. Schär, D. E. Barnes, and T. Lindahl, "Reconstitution of DNA base excision-repair with purified human proteins: interaction between DNA polymerase  $\beta$  and the XRCC1 protein," *EMBO Journal*, vol. 15, no. 23, pp. 6662–6670, 1996.
- [46] G. Frosina, P. Fortini, O. Rossi et al., "Two pathways for base excision repair in mammalian cells," *Journal of Biological Chemistry*, vol. 271, no. 16, pp. 9573–9578, 1996.
- [47] K. Kim, S. Biade, and Y. Matsumoto, "Involvement of flap endonuclease 1 in base excision DNA repair," *Journal of Biological Chemistry*, vol. 273, no. 15, pp. 8842–8848, 1998.
- [48] D. D'Amours, S. Desnoyers, I. D'Silva, and G. G. Poirier, "Poly(ADP-ribosylation) reactions in the regulation of nuclear functions," *Biochemical Journal*, vol. 342, no. 2, pp. 249–268, 1999.
- [49] I. I. Dianova, K. M. Sleeth, S. L. Allinson et al., "XRCC1-DNA polymerase  $\beta$  interaction is required for efficient base excision repair," *Nucleic Acids Research*, vol. 32, no. 8, pp. 2550–2555, 2004.
- [50] Y. Uchiyama, R. Takeuchi, H. Kodera, and K. Sakaguchi, "Distribution and roles of X-family DNA polymerases in eukaryotes," *Biochimie*, vol. 91, no. 2, pp. 165–170, 2009.
- [51] D. Córdoba-Cañero, T. Morales-Ruiz, T. Roldán-Arjona, and R. R. Ariza, "Single-nucleotide and long-patch base excision repair of DNA damage in plants," *Plant Journal*, vol. 60, no. 4, pp. 716–728, 2009.
- [52] S. Boiteux and J. P. Radicella, "The human OGG1 gene: structure, functions, and its implication in the process of carcinogenesis," *Archives of Biochemistry and Biophysics*, vol. 377, no. 1, pp. 1–8, 2000.
- [53] G. W. Hsu, M. Ober, T. Carell, and L. S. Beese, "Error-prone replication of oxidatively damaged DNA by a high-fidelity DNA polymerase," *Nature*, vol. 431, no. 7005, pp. 217–221, 2004.
- [54] T. Tsuzuki, Y. Nakatsu, and Y. Nakabeppu, "Significance of error-avoiding mechanisms for oxidative DNA damage in carcinogenesis," *Cancer Science*, vol. 98, no. 4, pp. 465–470, 2007.
- [55] R. Woodward and K. Gull, "Timing of nuclear and kinetoplast DNA replication and early morphological events in the cell cycle of *Trypanosoma brucei*," *Journal of Cell Science*, vol. 95, no. 1, pp. 49–57, 1990.
- [56] M. M. Klingbeil, S. A. Motyka, and P. T. Englund, "Multiple mitochondrial DNA polymerases in *Trypanosoma brucei*," *Molecular Cell*, vol. 10, no. 1, pp. 175–186, 2002.
- [57] D. N. Foster and T. Gurney Jr., "Nuclear location of mammalian DNA polymerase activities," *Journal of Biological Chemistry*, vol. 251, no. 24, pp. 7893–7898, 1976.
- [58] S. Taladriz, T. Hanke, M. J. Ramiro et al., "Nuclear DNA polymerase beta from *Leishmania infantum*. Cloning, molecular analysis and developmental regulation," *Nucleic Acids Research*, vol. 29, no. 18, pp. 3822–3834, 2001.
- [59] E. E. Trimmer and J. M. Essigmann, "Cisplatin," *Essays in Biochemistry*, vol. 34, pp. 191–211, 1999.
- [60] M. Tijsterman, R. De Pril, J. G. Tasseront-De Jong, and J. Brouwer, "RNA polymerase II transcription suppresses nucleosomal modulation of UV-induced (6-4) photoproduct and cyclobutane pyrimidine dimer repair in yeast," *Molecular and Cellular Biology*, vol. 19, no. 1, pp. 934–940, 1999.
- [61] T. Nospikel, "Nucleotide excision repair: variations on versatility," *Cellular and Molecular Life Sciences*, vol. 66, no. 6, pp. 994–1009, 2009.
- [62] M. Araki, C. Masutani, M. Takemura et al., "Centrosome protein centrin 2/caltractin 1 is part of the xeroderma pigmentosum group C complex that initiates global genome nucleotide excision repair," *Journal of Biological Chemistry*, vol. 276, no. 22, pp. 18665–18672, 2001.
- [63] J. Tang and G. Chu, "Xeroderma pigmentosum complementation group E and UV-damaged DNA-binding protein," *DNA Repair*, vol. 1, no. 8, pp. 601–616, 2002.
- [64] F. Coin, V. Oksenyh, and J.-M. Egly, "Distinct roles for the XPB/p52 and XPD/p44 subcomplexes of TFIIH in damaged DNA opening during nucleotide excision repair," *Molecular Cell*, vol. 26, no. 2, pp. 245–256, 2007.
- [65] K. Sugawara, J. M. Y. Ng, C. Masutani et al., "Xeroderma pigmentosum group C protein complex is the initiator of global genome nucleotide excision repair," *Molecular Cell*, vol. 2, no. 2, pp. 223–232, 1998.
- [66] A. O'Donovan, A. A. Davies, J. G. Moggs, S. C. West, and R. D. Wood, "XPG endonuclease makes the 3' incision in human DNA nucleotide excision repair," *Nature*, vol. 371, no. 6496, pp. 432–435, 1994.
- [67] D. Mu, D. S. Hsu, and A. Sancar, "Reaction mechanism of human DNA repair excision nuclease," *Journal of Biological Chemistry*, vol. 271, no. 14, pp. 8285–8294, 1996.
- [68] O. Popanda and H. W. Thielmann, "The function of DNA polymerases in DNA repair synthesis of ultraviolet-irradiated human fibroblasts," *Biochimica et Biophysica Acta*, vol. 1129, no. 2, pp. 155–160, 1992.
- [69] M. K. K. Shivji, M. K. Kenny, and R. D. Wood, "Proliferating cell nuclear antigen is required for DNA excision repair," *Cell*, vol. 69, no. 2, pp. 367–374, 1992.

- [70] J. Moser, H. Kool, I. Giakzidis, K. Caldecott, L. H. F. Mullenders, and M. I. Foustier, "Sealing of chromosomal DNA nicks during nucleotide excision repair requires XRCC1 and DNA ligase III $\alpha$  in a cell-cycle-specific manner," *Molecular Cell*, vol. 27, no. 2, pp. 311–323, 2007.
- [71] S. Tornaletti, "DNA repair in mammalian cells: transcription-coupled DNA repair: directing your effort where it's most needed," *Cellular and Molecular Life Sciences*, vol. 66, no. 6, pp. 1010–1020, 2009.
- [72] R. M. A. Costa, V. Chiganças, R. D. S. Galhardo, H. Carvalho, and C. F. M. Menck, "The eukaryotic nucleotide excision repair pathway," *Biochimie*, vol. 85, no. 11, pp. 1083–1099, 2003.
- [73] S. Martínez-Calvillo, J. C. Vizuet-de-Rueda, L. E. Florencio-Martínez, R. G. Manning-Cela, and E. E. Figueroa-Angulo, "Gene expression in trypanosomatid parasites," *Journal of Biomedicine & Biotechnology*, vol. 2010, Article ID 525241, 15 pages, 2010.
- [74] R. Groisman, I. Kuraoka, O. Chevallier et al., "CSA-dependent degradation of CSB by the ubiquitin-proteasome pathway establishes a link between complementation factors of the Cockayne syndrome," *Genes and Development*, vol. 20, no. 11, pp. 1429–1434, 2006.
- [75] M. J. Schofield and P. Hsieh, "Dna mismatch repair: molecular mechanisms and biological function," *Annual Review of Microbiology*, vol. 57, pp. 579–608, 2003.
- [76] K. Drotschmann, P. V. Shcherbakova, and T. A. Kunkel, "Mutator phenotype due to loss of heterozygosity in diploid yeast strains with mutations in MSH2 and MLH1," *Toxicology Letters*, vol. 112–113, pp. 239–244, 2000.
- [77] J. E. LeClerc, B. Li, W. L. Payne, and T. A. Cebula, "High mutation frequencies among *Escherichia coli* and *Salmonella* pathogens," *Science*, vol. 274, no. 5290, pp. 1208–1211, 1996.
- [78] O. Tenaillon, F. Taddei, M. Radman, and I. Matic, "Second-order selection in bacterial evolution: selection acting on mutation and recombination rates in the course of adaptation," *Research in Microbiology*, vol. 152, no. 1, pp. 11–16, 2001.
- [79] O. Tenaillon, B. Toupance, H. L. Nagard, F. Taddei, and B. Godelle, "Mutators, population size, adaptive landscape and the adaptation of asexual populations of bacteria," *Genetics*, vol. 152, no. 2, pp. 485–493, 1999.
- [80] A. M. Macedo, C. R. Machado, R. P. Oliveira, and S. D. J. Pena, "*Trypanosoma cruzi*: genetic structure of populations and relevance of genetic variability to the pathogenesis of Chagas disease," *Memorias do Instituto Oswaldo Cruz*, vol. 99, no. 1, pp. 1–12, 2004.
- [81] J. M. de Freitas, L. Augusto-Pinto, J. R. Pimenta et al., "Ancestral genomes, sex, and the population structure of *Trypanosoma cruzi*," *PLoS Pathogens*, vol. 2, no. 3, p. e24, 2006.
- [82] C. A. Buscaglia and J. M. Di Noia, "*Trypanosoma cruzi* clonal diversity and the epidemiology of Chagas' disease," *Microbes and Infection*, vol. 5, no. 5, pp. 419–427, 2003.
- [83] G. C. Cerqueira, D. C. Bartholomeu, W. D. DaRocha et al., "Sequence diversity and evolution of multigene families in *Trypanosoma cruzi*," *Molecular and Biochemical Parasitology*, vol. 157, no. 1, pp. 65–72, 2008.
- [84] F. Mathieu-Daudé, M.-F. Bosseno, E. Garzon et al., "Sequence diversity and differential expression of Tc52 immuno-regulatory protein in *Trypanosoma cruzi*: potential implications in the biological variability of strains," *Parasitology Research*, vol. 101, no. 5, pp. 1355–1363, 2007.
- [85] C. R. Machado, L. Augusto-Pinto, R. McCulloch, and S. M. R. Teixeira, "DNA metabolism and genetic diversity in *Trypanosomes*," *Mutation Research*, vol. 612, no. 1, pp. 40–57, 2006.
- [86] L. Augusto-Pinto, D. C. Bartholomeu, S. M. R. Teixeira, S. D. J. Pena, and C. R. Machado, "Molecular cloning and characterization of the DNA mismatch repair gene class 2 from the *Trypanosoma cruzi*," *Gene*, vol. 272, no. 1–2, pp. 323–333, 2001.
- [87] P. Pitsikas, D. Lee, and A. J. Rainbow, "Reduced host cell reactivation of oxidative DNA damage in human cells deficient in the mismatch repair gene hMSH2," *Mutagenesis*, vol. 22, no. 3, pp. 235–243, 2007.
- [88] G. Wang, P. Alamuri, M. Z. Humayun, D. E. Taylor, and R. J. Maier, "The *Helicobacter pylori* MutS protein confers protection from oxidative DNA damage," *Molecular Microbiology*, vol. 58, no. 1, pp. 166–176, 2005.
- [89] K. M. Culligan and J. B. Hays, "*Arabidopsis* MutS homologs - AtMSH2, AtMSH3, AtMSH6, and a novel AtMSH7—form three distinct protein heterodimers with different specificities for mismatched DNA," *Plant Cell*, vol. 12, no. 6, pp. 991–1002, 2000.
- [90] M. Shrivastav, L. P. De Haro, and J. A. Nickoloff, "Regulation of DNA double-strand break repair pathway choice," *Cell Research*, vol. 18, no. 1, pp. 134–147, 2008.
- [91] B. Williams and A. J. Lustig, "The paradoxical relationship between NHEJ and telomeric fusion," *Molecular Cell*, vol. 11, no. 5, pp. 1125–1126, 2003.
- [92] P. Burton, D. J. McBride, J. M. Wilkes, J. D. Barry, and R. McCulloch, "Ku heterodimer-independent end joining in *Trypanosoma brucei* cell extracts relies upon sequence microhomology," *Eukaryotic Cell*, vol. 6, no. 10, pp. 1773–1781, 2007.
- [93] C. Wyman, D. Ristic, and R. Kanaar, "Homologous recombination-mediated double-strand break repair," *DNA Repair*, vol. 3, no. 8–9, pp. 827–833, 2004.
- [94] B. O. Krogh and L. S. Symington, "Recombination proteins in yeast," *Annual Review of Genetics*, vol. 38, pp. 233–271, 2004.
- [95] M. K. Bhattacharyya, D. E. Norris, and N. Kumar, "Molecular players of homologous recombination in protozoan parasites: implications for generating antigenic variation," *Infection, Genetics and Evolution*, vol. 4, no. 2, pp. 91–98, 2004.
- [96] D. C. Bartholomeu, G. C. Cerqueira, A. C. A. Leão et al., "Genomic organization and expression profile of the mucin-associated surface protein (masp) family of the human pathogen *Trypanosoma cruzi*," *Nucleic Acids Research*, vol. 37, no. 10, pp. 3407–3417, 2009.
- [97] C. E. Clayton, "Genetic manipulation of kinetoplastida," *Parasitology Today*, vol. 15, no. 9, pp. 372–378, 1999.
- [98] S. M. Beverley, "Protozomics: trypanosomatid parasite genetics comes of age," *Nature Reviews Genetics*, vol. 4, no. 1, pp. 11–19, 2003.
- [99] R. McCulloch, E. Vassella, P. Burton, M. Boshart, and J. D. Barry, "Transformation of monomorphic and pleomorphic *Trypanosoma brucei*," *Methods in Molecular Biology*, vol. 262, pp. 53–86, 2004.
- [100] R. L. Barnes and R. McCulloch, "*Trypanosoma brucei* homologous recombination is dependent on substrate length and homology, though displays a differential dependence on mismatch repair as substrate length decreases," *Nucleic Acids Research*, vol. 35, no. 10, pp. 3478–3493, 2007.

- [101] M. Tibayrenc and F. J. Ayala, "The clonal theory of parasitic protozoa: 12 years on," *Trends in Parasitology*, vol. 18, no. 9, pp. 405–410, 2002.
- [102] A. Tait, "Evidence for diploidy and mating in trypanosomes," *Nature*, vol. 287, no. 5782, pp. 536–538, 1980.
- [103] A. R. Bogliolo, L. Lauria-Pires, and W. C. Gibson, "Polymorphisms in *Trypanosoma cruzi*: evidence of genetic recombination," *Acta Tropica*, vol. 61, no. 1, pp. 31–40, 1996.
- [104] H. J. Carrasco, I. A. Frame, S. A. Valente, and M. A. Miles, "Genetic exchange as a possible source of genomic diversity in sylvatic populations of *Trypanosoma cruzi*," *American Journal of Tropical Medicine and Hygiene*, vol. 54, no. 4, pp. 418–424, 1996.
- [105] J. M. Kelly, J. M. Law, C. J. Chapman, G. J. J. M. Van Eys, and D. A. Evans, "Evidence of genetic recombination in *Leishmania*," *Molecular and Biochemical Parasitology*, vol. 46, no. 2, pp. 253–264, 1991.
- [106] C. Bogdan and M. Röllinghoff, "How do protozoan parasites survive inside macrophages?" *Parasitology Today*, vol. 15, no. 1, pp. 22–28, 1999.
- [107] L. Glover, R. McCulloch, and D. Horn, "Sequence homology and microhomology dominate chromosomal double-strand break repair in African trypanosomes," *Nucleic Acids Research*, vol. 36, no. 8, pp. 2608–2618, 2008.
- [108] G. K. Takeda, R. Campos, J. Kieffer et al., "Effect of gamma rays on blood forms of *Trypanosoma cruzi*. Experimental study in mice," *Revista do Instituto de Medicina Tropical de Sao Paulo*, vol. 28, no. 1, pp. 15–18, 1986.
- [109] M. Seo, D. K. Chun, S. T. Hong, and S. H. Lee, "Influence of heat shock, drugs, and radiation on karyotype of *Leishmania major*," *Korean Journal of Parasitology*, vol. 31, no. 3, pp. 277–283, 1993.
- [110] T. Rijkers, J. Van Den Ouweland, B. Morolli et al., "Targeted inactivation of mouse RAD52 reduces homologous recombination but not resistance to ionizing radiation," *Molecular and Cellular Biology*, vol. 18, no. 11, pp. 6423–6429, 1998.
- [111] A. K. C. Wong, R. Pero, P. A. Ormonde, S. V. Tavtigian, and P. L. Bartel, "RAD51 interacts with the evolutionarily conserved BRC motifs in the human breast cancer susceptibility gene *brca2*," *Journal of Biological Chemistry*, vol. 272, no. 51, pp. 31941–31944, 1997.
- [112] P.-L. Chen, C.-F. Chen, Y. Chen, J. Xiao, Z. D. Sharp, and W.-H. Lee, "The BRC repeats in BRCA2 are critical for RAD51 binding and resistance to methyl methanesulfonate treatment," *Proceedings of the National Academy of Sciences of the United States of America*, vol. 95, no. 9, pp. 5287–5292, 1998.
- [113] L. Y. Marmorstein, T. Ouchi, and S. A. Aaronson, "The BRCA2 gene product functionally interacts with p53 and RAD51," *Proceedings of the National Academy of Sciences of the United States of America*, vol. 95, no. 23, pp. 13869–13874, 1998.
- [114] P. A. Blundell, G. Rudenko, and P. Borst, "Targeting of exogenous DNA into *Trypanosoma brucei* requires a high degree of homology between donor and target DNA," *Molecular and Biochemical Parasitology*, vol. 76, no. 1-2, pp. 215–229, 1996.
- [115] A. R. Lehmann, A. Niimi, T. Ogi et al., "Translesion synthesis: Y-family polymerases and the polymerase switch," *DNA Repair*, vol. 6, no. 7, pp. 891–899, 2007.
- [116] S. Prakash, R. E. Johnson, and L. Prakash, "Eukaryotic translesion synthesis DNA polymerases: specificity of structure and function," *Annual Review of Biochemistry*, vol. 74, pp. 317–353, 2005.
- [117] S. Gupta, V. Bhatia, J.-J. Wen, Y. Wu, M.-H. Huang, and N. J. Garg, "*Trypanosoma cruzi* infection disturbs mitochondrial membrane potential and ROS production rate in cardiomyocytes," *Free Radical Biology and Medicine*, vol. 47, no. 10, pp. 1414–1421, 2009.
- [118] R. L. Tarleton, "Immune system recognition of *Trypanosoma cruzi*," *Current Opinion in Immunology*, vol. 19, no. 4, pp. 430–434, 2007.
- [119] S. Gupta, J. J. Wen, and N. J. Garg, "Oxidative Stress in Chagas Disease," *Interdisciplinary Perspectives on Infectious Diseases*, vol. 2009, Article ID 190354, 8 pages, 2009.
- [120] J. M. Freitas, E. Lages-Silva, E. Crema, S. D. J. Pena, and A. M. Macedo, "Real time PCR strategy for the identification of major lineages of *Trypanosoma cruzi* directly in chronically infected human tissues," *International Journal for Parasitology*, vol. 35, no. 4, pp. 411–417, 2005.
- [121] O. Fernandes, R. H. Mangia, C. V. Lisboa et al., "The complexity of the sylvatic cycle of *Trypanosoma cruzi* in Rio de Janeiro state (Brazil) revealed by the non-transcribed spacer of the mini-exon gene," *Parasitology*, vol. 118, no. 2, pp. 161–166, 1999.

## Review Article

# DNA Damage Induced by Alkylating Agents and Repair Pathways

Natsuko Kondo,<sup>1</sup> Akihisa Takahashi,<sup>2</sup> Koji Ono,<sup>1</sup> and Takeo Ohnishi<sup>3</sup>

<sup>1</sup> Particle Radiation Oncology Research Center, Research Reactor Institute, Kyoto University, Kumatori-cho, Sennan-gun, Osaka 590-0494, Japan

<sup>2</sup> Department of Biology, School of Medicine, Nara Medical University, 840 Shijo-cho, Kashihara, Nara 634-8521, Japan

<sup>3</sup> Department of Radiation Oncology, School of Medicine, Nara Medical University, 840 Shijo-cho, Kashihara, Nara 634-8521, Japan

Correspondence should be addressed to Akihisa Takahashi, atakahas@naramed-u.ac.jp

Received 8 June 2010; Revised 26 August 2010; Accepted 12 October 2010

Academic Editor: Ashis Basu

Copyright © 2010 Natsuko Kondo et al. This is an open access article distributed under the Creative Commons Attribution License, which permits unrestricted use, distribution, and reproduction in any medium, provided the original work is properly cited.

The cytotoxic effects of alkylating agents are strongly attenuated by cellular DNA repair processes, necessitating a clear understanding of the repair mechanisms. Simple methylating agents form adducts at *N*- and *O*-atoms. *N*-methylations are removed by base excision repair, AlkB homologues, or nucleotide excision repair (NER). *O*<sup>6</sup>-methylguanine (MeG), which can eventually become cytotoxic and mutagenic, is repaired by *O*<sup>6</sup>-methylguanine-DNA methyltransferase, and *O*<sup>6</sup>MeG:T mispairs are recognized by the mismatch repair system (MMR). MMR cannot repair the *O*<sup>6</sup>MeG/T mispairs, which eventually lead to double-strand breaks. Bifunctional alkylating agents form interstrand cross-links (ICLs) which are more complex and highly cytotoxic. ICLs are repaired by complex of NER factors (e.g., endonuclease xeroderma pigmentosum complementation group F-excision repair cross-complementing rodent repair deficiency complementation group 1), Fanconi anemia repair, and homologous recombination. A detailed understanding of how cells cope with DNA damage caused by alkylating agents is therefore potentially useful in clinical medicine.

## 1. Introduction

Alkylating drugs are the oldest class of anticancer drugs still commonly used; they play an important role in the treatment of several types of cancers [1]. Most alkylating drugs are monofunctional methylating agents (e.g., temozolomide [TMZ], *N*-methyl-*N'*-nitro-*N*-nitrosoguanidine [MNNG], and dacarbazine), bifunctional alkylating agents such as nitrogen mustards (e.g., chlorambucil and cyclophosphamide), or chloroethylating agents (e.g., nimustine [ACNU], carmustine [BCNU], lomustine [CCNU], and fotemustine).

Simple methylating agents form adducts at the *N*- and *O*-atoms in DNA bases. *N*-methylation adducts comprise more than 80% of methylated bases. These alkyl DNA base adducts exhibit different stabilities. For example, *N*<sup>7</sup>-methylguanine (*N*<sup>7</sup>MeG) is the most stable *N*-methylation adduct in vitro with a half-life ( $t_{1/2}$ ) no longer than 80 h [2]. Although *O*<sup>6</sup>-methylguanine (*O*<sup>6</sup>MeG) accounts for only 0.3% (for methyl methanesulfonate) to 8% (for methyl nitrosourea) of

the total DNA methyl adducts, it is stable and persists in the absence of the DNA repair protein *O*<sup>6</sup>-methylguanine-DNA methyltransferase (MGMT) [3–5]. *O*<sup>4</sup>-methylthymine (*O*<sup>4</sup>MeT) is produced at a much lower level (<0.4%) [2], and its mutagenicity and cytotoxicity are unclear. In general, *O*-alkylations (e.g., *O*<sup>6</sup>alkylG and *O*<sup>4</sup>alkylT) are highly mutagenic and genotoxic, whereas *N*-alkylations (e.g., *N*<sup>3</sup>alkylA and *N*<sup>1</sup>alkylA) are cytotoxic, but less mutagenic [6–9]. The primary products of methylating agents, *N*-alkylated purines, are efficiently removed by base excision repair (BER) or human AlkB homologues (hABH). BER repairs *N*<sup>7</sup>MeG, *N*<sup>3</sup>MeA, and *N*<sup>3</sup>MeG, whereas hABH repairs *N*<sup>1</sup>MeA, *N*<sup>3</sup>MeC, *N*<sup>3</sup>MeT, and *N*<sup>1</sup>MeG [10].

One-step repair of *O*<sup>6</sup>MeG involves transferring the alkyl group from the oxygen in the guanine to a cysteine residue in the catalytic pocket of MGMT [10]. Nucleotide excision repair (NER) is an elaborate repair system that removes bulky lesions from DNA in 27-nt to 29-nt oligomers. Because it is also capable of removing nonbulky lesions such as apurinic/apyrimidinic sites and *O*<sup>6</sup>MeG residues, NER plays

a backup role for other repair systems [11]. Mismatch repair (MMR) is also important in the repair of  $O^6$ MeG. If it is left unrepaired, replication over the  $O^6$ MeG results in an  $O^6$ MeG:T mismatch or  $O^6$ MeG:C ambiguous pair [12]. In the next round of replication, the  $O^6$ MeG:T becomes an A:T transition mutation, or the  $O^6$ MeG:C is replicated again as an  $O^6$ MeG:C pair or becomes an  $O^6$ MeG:T mismatch [13]. The  $O^6$ MeG:T or  $O^6$ MeG:C is recognized by the MutS $\alpha$  complex (hMSH2 and hMSH6), which initiates MMR to create a gapped duplex by incision of the newly replicated strand [13]. If  $O^6$ MeG remains in the template, a futile repair loop can eventually result in highly toxic double-strand breaks (DSBs), which are intermediates in apoptotic and DSB repair pathways [13]. Accordingly, DSB repair pathways are activated by methylating agents [14, 15].

Bifunctional alkylating agents, such as chlorambucil or BCNU, are commonly used anticancer drugs. DNA lesions produced by these agents require complex repair mechanisms. The primary chloroethyl adducts at  $O^6$ G are repaired by MGMT, but the secondary interstrand cross-links (ICLs) require NER factors (e.g., endonuclease xeroderma pigmentosum complementation group F-excision repair cross-complementing rodent repair deficiency complementation group 1 (XPB-ERCC1)) for incision, Fanconi anemia (FA) repair, and homologous recombination (HR) for complete repair [16].

This paper will focus on the repair pathways for  $O^6$ MeG generated by methylating agents and those for ICLs generated by bifunctional alkylating agents. We will also briefly discuss other alkylation damage defense and processing functions (hABH and BER).

## 2. DNA Repair Mechanisms for DNA Damage Induced by Methylating Agents

**2.1. MGMT (Figure 1(a)).** MGMT repairs  $O^6$ -alkylation adducts but irreversibly inactivates MGMT itself in the process. In the absence of active MGMT,  $O^6$ MeG forms  $O^6$ MeG/T mismatches during replication. Early studies demonstrated that MGMT-deficient cells unable to repair  $O^6$ MeG damage were more sensitive to the effects of methylating agents than normal cells expressing MGMT [17]. This observation has been utilized experimentally and clinically to target cells with an MGMT inhibitor, the  $O^6$ MeG analogue  $O^6$ benzylG [18]. However, in some tumors, *p53* dysfunction suppresses MGMT expression [19, 20] or hypermethylation of the MGMT promoter results in gene silencing [21]. The low basal MGMT activity makes these cells less vulnerable to the effects of  $O^6$ benzylG. Kaina et al. reported that about 5% of all solid tumors assayed in their laboratory were completely deficient in MGMT [10]. In particular, 17% to 30% of gliomas lack MGMT [22, 23]. Because drug efficacy is likely to be limited if only MGMT is targeted in these tumors, new molecular targets are being sought.

**2.2. MMR (Figure 1(b)).** The cytotoxicity of monofunctional alkylating agents requires a functional MMR in the target cells. In fact, mammalian cells proficient in MMR are

generally about 100-fold more sensitive to alkylating agents than their MMR-deficient counterparts [24, 25]. In MMR-deficient cells, DNA damage accumulates but does not trigger cell death. Thus, resistance to these cytotoxic agents is associated with loss of MMR activity, particularly in the absence of MGMT [26, 27]. The mechanism of action of monofunctional alkylating agents has been studied in cell lines and mouse models; results indicate that replication over unrepaired  $O^6$ MeG:C results in an  $O^6$ MeG:T mismatch (or possibly an  $O^6$ MeG:C ambiguous pair). In the next round of replication, an  $O^6$ MeG:T mismatch becomes an A:T transition mutation. An  $O^6$ MeG:T or  $O^6$ MeG:C pair is recognized by the MutS $\alpha$  complex, which initiates MMR. MMR creates a gapped duplex after incision of the newly replicated strand. The mere presence of MeG in the genomic DNA of MMR-proficient cells is not cytotoxic, even if the cells are allowed to undergo a round of replication during which MeG:C and MeG:T pairs form. To activate the  $G_2/M$  DNA damage checkpoint, these mispairs must be recognized and processed. Cells treated with MNNG are not arrested in the first  $G_2/M$  checkpoint, but  $G_2/M$  arrest is commonly observed in the second cell cycle [28].

**2.3. DSB Repair (Figure 1(c)).** Although alkylating agents do not directly induce DSBs, DSBs are detected in wild-type cells and other cell culture systems after the processing of DNA lesions induced by alkylating agents [14, 15, 29, 30]. DSBs lead to cell death; therefore, cells defective in DSB repair are thought to be more sensitive to alkylating agents. Consistent with this hypothesis, studies have reported that DSB repair pathways are involved in the repair of DNA damage induced by alkylating agents [14, 15, 29].

DSBs are repaired through the HR and nonhomologous end joining (NHEJ) pathways [31]. In human cells, HR proteins include members of the MRN complex, which consist of meiotic recombination 11 (MRE11)/radiation-sensitive mutant 50 (Rad50)/Nijmegen breakage syndrome 1 (NBS1) as well as Rad51, the Rad51 paralogs (Rad51B, Rad51C, Rad51D, X-ray repair cross-complementing group 2 (XRCC2), and XRCC3), Rad54, and Rad54B [31]. Proteins involved in the NHEJ pathway include Ku70/80, the DNA-dependent protein kinase catalytic subunit (DNA-PKcs), ligase IV (Lig4), XRCC4 and Artemis [31].

HR, which is a generally error-free pathway, uses DNA homology to direct DNA repair; an undamaged chromatid serves as template for the repair of a broken sister chromatid. The products of the breast cancer susceptibility genes, BRCA1 and BRCA2 (also known as FA complementation group D1 or FANCD1), are also involved in the HR pathway [32].

HR is required for MNNG-treated cells to transition into the second cell cycle. Most mammalian cells that undergo cell cycle arrest after the second S phase die; however, the surviving cells show a high frequency of sister chromatid exchanges (SCEs), indicative of DSB repair at collapsed replication forks [33]. Roos et al. reported that BRCA2/XRCC2-dependent HR, but not NHEJ, protects against  $O^6$ MeG-triggered DSBs and chromosomal aberrations, leading to SCEs [14].

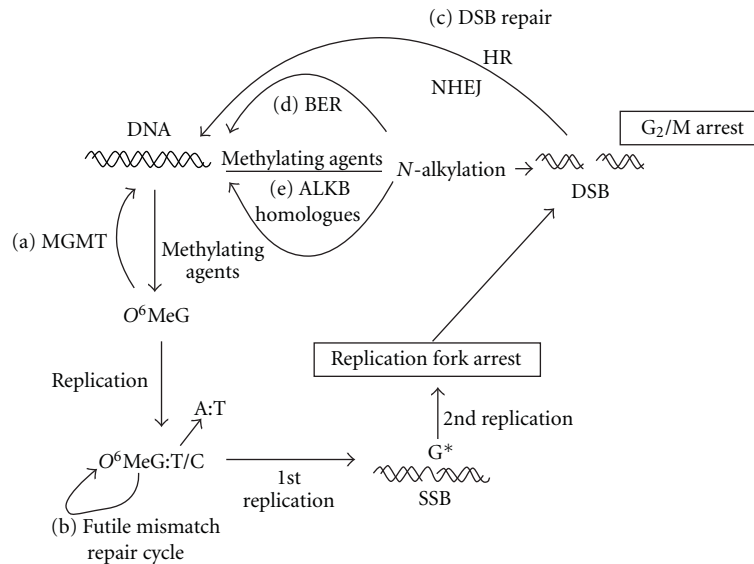


FIGURE 1: Pathways for DNA damage induced by methylating agents. (a) *O*<sup>6</sup>-methylguanine-DNA methyltransferase (MGMT) removes the methyl adduct from *O*<sup>6</sup>MeG in one step. If left unrepaired, *O*<sup>6</sup>MeG:C ambiguous pairs or *O*<sup>6</sup>MeG:T mismatch pairs can form during replication. In the next round of replication, *O*<sup>6</sup>MeG:T pairs can become A:T transition mutations. (b) *O*<sup>6</sup>MeG:T and *O*<sup>6</sup>MeG:C pairs are recognized by the mismatch repair (MMR) system, which creates a single-strand break (SSB), cause replication arrest, and finally leads to a double-strand break (DSB). *O*<sup>6</sup>MeG:T/C does not induce cell cycle arrest at the first G<sub>2</sub>/M DNA damage checkpoint, but G<sub>2</sub>/M arrest is commonly observed in the second cell cycle. (c) Homologous recombination (HR) and nonhomologous end joining (NHEJ) may play a role in the repair of DSBs. *N*-alkylations are repaired by either (d) base excision repair (BER), or (e) AlkB homologues, and if not repaired, DSBs occur.

NHEJ, which is the simplest way to repair a DSB, involves the religation of broken DNA ends without a template; this type of repair does not preserve the original genetic information. NHEJ eliminates DSBs during the G<sub>1</sub> phase of the cell cycle, when the lack of sister chromatids prevents HR [34].

Results of a clonogenic survival study showed that Lig4 plays a more important role in the repair of TMZ-induced DSBs than XRCC2 or Rad54 [15]. DSBs, which may arise from adducts other than *O*<sup>6</sup>MeG, such as TMZ-induced *N*-methylpurines, are repaired within 24 h in *Lig4*-proficient cells. In contrast, up to 80% of the DSBs in *Lig4*<sup>-/-</sup> cells were not repaired [15]. In A172 glioblastoma cells, siRNA silencing of *Lig4* increased cellular sensitivity to TMZ. After TMZ treatments, A172 cells with silenced *Lig4* exhibited a 62.5% decrease in survival compared with control A172 cells; thus, modulating Lig4 activity may enhance tumor sensitivity to TMZ [15].

**2.4. BER (Figure 1(d)).** The alkylation adducts *N*<sup>7</sup>MeG, *N*<sup>3</sup>MeA, and *N*<sup>3</sup>MeG are repaired by the BER system, the main DNA repair system in mammalian cells used to eliminate small DNA base lesions [16]. Damaged bases are removed by a lesion-specific DNA glycosylase, in this case alkyladenine DNA glycosylase (Aag). The resulting abasic site is recognized by an apurinic/aprimidinic endonuclease, APE1, which incises the damaged strand, leaving 3'-OH and 5'-deoxyribose phosphate (5'-dRP) groups at the margins. A DNA polymerase β- (*pol*-β)-mediated DNA synthesis step fills the single nucleotide gap [35, 36] and removes

the cytotoxic 5'-dRP group [37, 38]. Alternatively, DNA polymerase λ (*pol*-λ) or DNA polymerase-ι (*pol*-ι), both of which possess 5'-dRP lyase activity, may participate in BER to remove this toxic repair intermediate [39–41]. Finally, DNA ligase I, or a complex of DNA ligase III and XRCC1, conducts the final, nick-sealing step in the pathway [42].

In the absence of *pol*-β, cells cannot repair the BER intermediate 5'dRP and are thus hypersensitive to the alkylating agent methyl methanesulfonate [37, 38, 43, 44]. For example, fibroblasts from a *pol*-β-null mutant mouse are highly sensitive to monofunctional alkylating agents, but not to BCNU [45]. Similarly, RNA interference-mediated *pol*-β suppression boosts TMZ efficacy, although a deficiency in *pol*-ι or *pol*-λ does not increase TMZ-mediated cytotoxicity [46]. Furthermore, loss of *pol*-β coupled with TMZ treatment triggers H2AX phosphorylation, indicating activation of the DNA damage response pathway by unrepaired lesions [46]. H2AX is a histone protein that is rapidly phosphorylated on Ser139 (γH2AX) when DNA breaks are introduced in mammalian cells following external damage and replication fork collapse [47, 48]. Poly(ADP-ribose) polymerase-1 (PARP-1) is activated by strand breaks and participates in gap sealing with DNA ligase III and XRCC1, but deficiencies in the subsequent steps of BER increase sensitivity to alkylating agents. Inhibition of PARP-1 by the inhibitor AG14361 restores sensitivity to TMZ in MMR-deficient cells that have lost killing sensitivity to *O*<sup>6</sup>MeG via the MGMT/MMR pathway [49]. The combination of TMZ with PARP-1 inhibitors is currently under investigation in several Phase I-II clinical trials.

2.5. *Direct Reversal of Alkylation Damage by AlkB Homologues (Figure 1(e)).* The *E. coli* protein AlkB is an oxidative DNA demethylase that repairs the cytotoxic lesions  $N^1\text{MeA}$  and  $N^3\text{MeC}$ . A detailed mapping of the human genome has identified eight hABH homologues. ABH2 and ABH3 belong to the alpha-ketoglutarate- and Fe(II)-dependent dioxygenase superfamily. These proteins repair  $N^1\text{MeA}$ ,  $N^3\text{MeC}$ ,  $N^3\text{MeT}$ , and  $N^1\text{MeG}$  by oxidative demethylation [50, 51]. Although hABH2 preferentially repairs double-stranded DNA, hABH3 acts more efficiently on single-stranded nucleic acids. Accordingly, hABH2 relocates to replication foci during S-phase, which suggested that hABH2 repairs DNA close to replication forks, whereas hABH3 maintains nuclear single-stranded DNA and RNA, potentially targeting genes undergoing transcription.

### 3. Repair of Cross-links Induced by Bifunctional Alkylating Agents

Bifunctional alkylating agents (e.g., nitrogen mustards (melphalan, chlorambucil, cyclophosphamide, and ifosfamide) and chloroethylnitrosoureas (BCNU and CCNU)) possess two reactive sites. These agents cross-link DNA with proteins or, alternatively, cross-link two DNA bases within the same DNA strand (intrastrand cross-links) or on opposite DNA strands (ICLs). ICLs, which block replication forks, are the most serious cytotoxic lesions produced by most bifunctional drugs. Accordingly, the extent of ICLs correlates well with the cytotoxicity of nitrogen mustard drugs [52].

Nitrogen mustards form  $N^7\text{G}:N^7\text{G}$  cross-links, and chloroethylnitrosoureas form  $N^1\text{G}:N^3\text{C}$  cross-links [53]. The chloroethylated  $O^6\text{G}$  of the  $N^1\text{G}:N^3\text{C}$  cross-link can be repaired by MGMT; however, this adduct is unstable and undergoes intramolecular rearrangement producing an intermediary  $N^1\text{-}O^6\text{-ethanoG}$ . The  $N^1\text{-}O^6\text{-ethanoG}$  adduct may react with cytosine in the complementary strand to yield a highly toxic ICL between position 1 in the guanine residue and position 3 in the cytosine residue (1-(3-cytosinyl)-2-(1-guanosinyl)-ethane) [53].

ICL repair mechanisms are complex; therefore, they are only briefly summarized here. An ICL represents a formidable block to the DNA replication machinery and is unique in requiring a combination of FA repair, NER, translesion synthesis (TLS), and HR repair for efficient repair [54]. Although the FA pathway was initially characterized in terms of DNA cross-link repair, this pathway is also involved in homologous recombination and resolution of the replication arrest [55, 56]. Thirteen FA genes have been identified [54], although the precise function of many of these FA proteins is unclear. The FA core complex, which consists of eight FA proteins, is activated by DNA damage. Specifically, the FA proteins FANCM and FANCA Associating Polypeptide 24 form a heterodimer that binds DNA [57, 58] and appears to be involved in sensing DNA replication forks blocked at cross-links. The NER proteins ERCC1 and XPF make incisions on either side of the cross-link to generate a gap. The gap is then filled by translesion synthesis (TLS) polymerases  $\zeta$  (Rev3 and Rev7 subunits)

and Rev1 (part of the Rev3-Rev7 complex [59]). The FA core complex monoubiquitinates FANCD2 and its paralog FANCI, and the ubiquitinated FANCD2 then interacts with FANCD1 to promote HR [54].

Incision at the ICL could occur before or after lesion bypass, leaving a DSB subject to HR or NHEJ [60]. As expected, XRCC2 and Rad54 are involved in the repair of ACNU-induced DSBs, but surprisingly Lig4 plays the most important role in this process [29]. In  $\text{Lig4}^{-/-}$  cells, levels of phosphorylated histone  $\gamma\text{H2AX}$  increased more than 4-fold at 12 h and 6-fold at 24 h after ACNU treatment compared to its initial levels. In contrast,  $\gamma\text{H2AX}$  levels were not markedly altered by ACNU in normal cells. In addition, ACNU treatment markedly reduced the colony-forming ability of A172 glioblastoma cells transfected with siRNA against Lig4 or XRCC2 compared to controls [29]. However, *Lig4* siRNA rendered cells more sensitive to the effects of ACNU than did *XRCC2* siRNA [29]. These data suggest NHEJ may also be involved in removing DSBs formed by unrepaired ICLs.

### 4. Conclusion

DNA repair pathways attenuate the therapeutic effects of alkylating agents; therefore, characterization of the repair pathways is essential for developing new treatments. For example, MGMT promoter hypermethylation results in gene silencing and therefore decreased MGMT activity; therefore, MGMT promoter hypermethylation may be a useful way to enhance the therapeutic efficacy of TMZ [61, 62].

Currently, clinical trials are testing DNA repair inhibitors that target PARP, BER, or MGMT in combination with alkylating agents [63]. In the case of  $O^6\text{benzylG}$ , a phase I clinical trial has defined the maximum tolerated dose of a single dose of TMZ when combined with  $O^6\text{benzylG}$  and has determined the dose of  $O^6\text{benzylG}$  that depletes tumor MGMT activity for 48 h [64]. In addition, when combined with cytotoxic chemotherapy, myelosuppression appears to be significantly enhanced by  $O^6\text{benzylG}$ , significantly reducing the required doses of alkylating agents [65]. The success of such approaches will depend on selective targeting of the tumor. Locoregional chemotherapy has recently been shown to improve the survival of glioma patients [66]. Therefore, combining a locoregional delivery system with the simultaneous downregulation of DNA repair pathways may decrease the amount of alkylating agent needed for chemotherapy, thereby reducing the severe side effects. In addition, new inhibitors against specific repair proteins, such as pol- $\beta$ , BRCA2, or Lig4, should be developed because resistance against currently available inhibitors may develop.

### Acknowledgments

This work was supported by Grants-in-Aid for Scientific Research from the Ministry of Education, Culture, Sports, Science and Technology of Japan. This work was also funded in part by a grant from the Central Research Institute of the Electric Power Industry in Japan and by a grant for Exploratory Research for Space Utilization from the Japan Space Forum.

## References

- [1] S. G. Chaney and A. Sancar, "DNA repair: enzymatic mechanisms and relevance to drug response," *Journal of the National Cancer Institute*, vol. 88, no. 19, pp. 1346–1360, 1996.
- [2] D. T. Beranek, "Distribution of methyl and ethyl adducts following alkylation with monofunctional alkylating agents," *Mutation Research*, vol. 231, no. 1, pp. 11–30, 1990.
- [3] R. Goth and M. F. Rajewsky, "Persistence of O<sup>6</sup> ethylguanine in rat brain DNA: correlation with nervous system specific carcinogenesis by ethylnitrosourea," *Proceedings of the National Academy of Sciences of the United States of America*, vol. 71, no. 3, pp. 639–643, 1974.
- [4] R. Goth-Goldstein, "Inability of Chinese hamster ovary cells to excise O<sup>6</sup>-alkylguanine," *Cancer Research*, vol. 40, no. 7, pp. 2623–2624, 1980.
- [5] B. Kaina, A. A. van Zeeland, A. de Groot, and A. T. Natarajan, "DNA repair and chromosomal stability in the alkylating agent-hypersensitive Chinese hamster cell line 27-1," *Mutation Research*, vol. 243, no. 3, pp. 219–224, 1990.
- [6] G. P. Margison, M. F. Santibáñez-Koref, and A. C. Povey, "Mechanisms of carcinogenicity/chemotherapy by O<sup>6</sup>-methylguanine," *Mutagenesis*, vol. 17, no. 6, pp. 483–487, 2002.
- [7] M. Christmann, M. T. Tomicic, W. P. Roos, and B. Kaina, "Mechanisms of human DNA repair: an update," *Toxicology*, vol. 193, no. 1-2, pp. 3–34, 2003.
- [8] M. D. Wyatt, J. M. Allan, A. Y. Lau, T. E. Ellenberger, and L. D. Samson, "3-Methyladenine DNA glycosylases: structure, function, and biological importance," *BioEssays*, vol. 21, no. 8, pp. 668–676, 1999.
- [9] H. E. Krokan, R. Standal, and G. Slupphaug, "DNA glycosylases in the base excision repair of DNA," *Biochemical Journal*, vol. 325, no. 1, pp. 1–16, 1997.
- [10] B. Kaina, M. Christmann, S. Naumann, and W. P. Roos, "MGMT: key node in the battle against genotoxicity, carcinogenicity and apoptosis induced by alkylating agents," *DNA Repair*, vol. 6, no. 8, pp. 1079–1099, 2007.
- [11] A. Sancar, "Excision repair in mammalian cells," *The Journal of Biological Chemistry*, vol. 270, no. 27, pp. 15915–15918, 1995.
- [12] H. T. Chen, A. Bhandoola, M. J. Difilippantonio et al., "Response to RAG-mediated V(D)J cleavage by NBS1 and  $\gamma$ -H2AX," *Science*, vol. 290, no. 5498, pp. 1962–1964, 2000.
- [13] G. P. Margison and M. F. Santibáñez-Koref, "O<sup>6</sup>-alkylguanine-DNA alkyltransferase: role in carcinogenesis and chemotherapy," *BioEssays*, vol. 24, no. 3, pp. 255–266, 2002.
- [14] W. P. Roos, T. Nikolova, S. Quiros et al., "Brca2/Xrcc2 dependent HR, but not NHEJ, is required for protection against O<sup>6</sup>-methylguanine triggered apoptosis, DSBs and chromosomal aberrations by a process leading to SCEs," *DNA Repair*, vol. 8, no. 1, pp. 72–86, 2009.
- [15] N. Kondo, A. Takahashi, E. Mori et al., "DNA ligase IV as a new molecular target for temozolomide," *Biochemical and Biophysical Research Communications*, vol. 387, no. 4, pp. 656–660, 2009.
- [16] F. Drabløs, E. Feyzi, P. A. Aas et al., "Alkylation damage in DNA and RNA—repair mechanisms and medical significance," *DNA Repair*, vol. 3, no. 11, pp. 1389–1407, 2004.
- [17] R. S. Day III, C. H. J. Ziolkowski, and D. A. Scudiero, "Defective repair of alkylated DNA by human tumour and SV40-transformed human cell strains," *Nature*, vol. 288, no. 5792, pp. 724–727, 1980.
- [18] N. Hosoya and K. Miyagawa, "Clinical importance of DNA repair inhibitors in cancer therapy," *Memo—Magazine of European Medical Oncology*, vol. 2, no. 1, pp. 9–14, 2009.
- [19] M. D. Blough, M. C. Zlatescu, and J. G. Cairncross, "O<sup>6</sup>-methylguanine-DNA methyltransferase regulation by p53 in astrocytic cells," *Cancer Research*, vol. 67, no. 2, pp. 580–584, 2007.
- [20] S. J. Russell, Y.-W. Ye, P. G. Waber, M. Shuford, S. C. Schold Jr., and P. D. Nisen, "p53 Mutations, O<sup>6</sup>-alkylguanine DNA alkyltransferase activity, and sensitivity to procarbazine in human brain tumors," *Cancer*, vol. 75, no. 6, pp. 1339–1342, 1995.
- [21] M. Esteller, S. R. Hamilton, P. C. Burger, S. B. Baylin, and J. G. Herman, "Inactivation of the DNA repair gene O<sup>6</sup>-methylguanine-DNA methyltransferase by promoter hypermethylation is a common event in primary human neoplasia," *Cancer Research*, vol. 59, no. 4, pp. 793–797, 1999.
- [22] I. Preuss, I. Eberhagen, S. Haas et al., "O<sup>6</sup>-methylguanine-DNA methyltransferase activity in breast and brain tumors," *International Journal of Cancer*, vol. 61, no. 3, pp. 321–326, 1995.
- [23] N. P. Lees, K. L. Harrison, E. Hill, C. Nicholas Hall, A. C. Povey, and G. P. Margison, "Heterogeneity of O<sup>6</sup>-alkylguanine-DNA alkyltransferase activity in colorectal cancer: implications for treatment," *Oncology*, vol. 63, no. 4, pp. 393–397, 2002.
- [24] P. Karran, "Mechanisms of tolerance to DNA damaging therapeutic drugs," *Carcinogenesis*, vol. 22, no. 12, pp. 1931–1937, 2001.
- [25] L. Stojic, R. Brun, and J. Jiricny, "Mismatch repair and DNA damage signalling," *DNA Repair*, vol. 3, no. 8-9, pp. 1091–1101, 2004.
- [26] P. Branch, G. Aquilina, M. Bignami, and P. Karran, "Defective mismatch binding and a mutator phenotype in cells tolerant to DNA damage," *Nature*, vol. 362, no. 6421, pp. 652–654, 1993.
- [27] A. Kat, W. G. Thilly, W.-H. Fang, M. J. Longley, G.-M. Li, and P. Modrich, "An alkylation-tolerant, mutator human cell line is deficient in strand-specific mismatch repair," *Proceedings of the National Academy of Sciences of the United States of America*, vol. 90, no. 14, pp. 6424–6428, 1993.
- [28] S. Quiros, W. P. Roos, and B. Kaina, "Processing of O<sup>6</sup>-methylguanine into DNA double-strand breaks requires two rounds of replication whereas apoptosis is also induced in subsequent cell cycles," *Cell Cycle*, vol. 9, no. 1, pp. 168–178, 2010.
- [29] N. Kondo, A. Takahashi, E. Mori et al., "DNA ligase IV is a potential molecular target in ACNU sensitivity," *Cancer Science*, vol. 101, no. 8, pp. 1881–1885, 2010.
- [30] S. C. Naumann, W. P. Roos, E. Jöst et al., "Temozolomide- and fotemustine-induced apoptosis in human malignant melanoma cells: response related to MGMT, MMR, DSBs, and p53," *British Journal of Cancer*, vol. 100, no. 2, pp. 322–333, 2009.
- [31] T. Ohnishi, E. Mori, and A. Takahashi, "DNA double-strand breaks: their production, recognition, and repair in eukaryotes," *Mutation Research*, vol. 669, no. 1-2, pp. 8–12, 2009.
- [32] A. A. Davies, J. Y. Masson, M. J. McIlwraith et al., "Role of BRCA2 in control of the RAD51 recombination and DNA repair protein," *Molecular Cell*, vol. 7, no. 2, pp. 273–282, 2001.
- [33] N. Mojas, M. Lopes, and J. Jiricny, "Mismatch repair-dependent processing of methylation damage gives rise to

- persistent single-stranded gaps in newly replicated DNA," *Genes and Development*, vol. 21, no. 24, pp. 3342–3355, 2007.
- [34] T. Helleday, J. Lo, D. C. van Gent, and B. P. Engelward, "DNA double-strand break repair: from mechanistic understanding to cancer treatment," *DNA Repair*, vol. 6, no. 7, pp. 923–935, 2007.
- [35] R. W. Sobol and S. H. Wilson, "Mammalian DNA  $\beta$ -polymerase in base excision repair of alkylation damage," *Progress in Nucleic Acid Research and Molecular Biology*, vol. 68, pp. 57–74, 2001.
- [36] S. H. Wilson, R. W. Sobol, W. A. Beard, J. K. Horton, R. Prasad, and B. J. Vande Berg, "DNA polymerase  $\beta$  and mammalian base excision repair," *Cold Spring Harbor Symposia on Quantitative Biology*, vol. 65, pp. 143–155, 2000.
- [37] R. W. Sobol, J. K. Horton, R. Kühn et al., "Requirement of mammalian DNA polymerase- $\beta$  in base-excision repair," *Nature*, vol. 379, no. 6561, pp. 183–186, 1996.
- [38] R. W. Sobol, R. Prasad, A. Evenski et al., "The lyase activity of the DNA repair protein  $\beta$ -polymerase protects from DNA-damage-induced cytotoxicity," *Nature*, vol. 405, no. 6788, pp. 807–810, 2000.
- [39] R. Prasad, K. Bebenek, E. Hou et al., "Localization of the deoxyribose phosphate lyase active site in human DNA polymerase  $\beta$  by controlled proteolysis," *The Journal of Biological Chemistry*, vol. 278, no. 32, pp. 29649–29654, 2003.
- [40] K. Bebenek, A. Tissier, E. G. Frank et al., "5'-deoxyribose phosphate lyase activity of human DNA polymerase L *in vitro*," *Science*, vol. 291, no. 5511, pp. 2156–2159, 2001.
- [41] M. García-Díaz, K. Bebenek, T. A. Kunkel, and L. Blanco, "Identification of an intrinsic 5'-deoxyribose-5-phosphate lyase activity in human DNA polymerase  $\lambda$ : a possible role in base excision repair," *The Journal of Biological Chemistry*, vol. 276, no. 37, pp. 34659–34663, 2001.
- [42] T. Lindahl and R. D. Wood, "Quality control by DNA repair," *Science*, vol. 286, no. 5446, pp. 1897–1905, 1999.
- [43] R. W. Sobol, M. Kartalou, K. H. Almeida et al., "Base excision repair intermediates induce p53-independent cytotoxic and genotoxic responses," *The Journal of Biological Chemistry*, vol. 278, no. 41, pp. 39951–39959, 2003.
- [44] R. W. Sobol, D. E. Watson, J. Nakamura et al., "Mutations associated with base excision repair deficiency and methylation-induced genotoxic stress," *Proceedings of the National Academy of Sciences of the United States of America*, vol. 99, no. 10, pp. 6860–6865, 2002.
- [45] J. K. Horton, D. F. Joyce-Gray, B. F. Pachkowski, J. A. Swenberg, and S. H. Wilson, "Hypersensitivity of DNA polymerase  $\beta$  null mouse fibroblasts reflects accumulation of cytotoxic repair intermediates from site-specific alkyl DNA lesions," *DNA Repair*, vol. 2, no. 1, pp. 27–48, 2003.
- [46] R. N. Trivedi, K. H. Almeida, J. L. Fornsgaglio, S. Schamus, and R. W. Sobol, "The role of base excision repair in the sensitivity and resistance to temozolomide-mediated cell death," *Cancer Research*, vol. 65, no. 14, pp. 6394–6400, 2005.
- [47] E. P. Rogakou, D. R. Pilch, A. H. Orr, V. S. Ivanova, and W. M. Bonner, "DNA double-stranded breaks induce histone H2AX phosphorylation on serine 139," *The Journal of Biological Chemistry*, vol. 273, no. 10, pp. 5858–5868, 1998.
- [48] I. M. Ward and J. Chen, "Histone H2AX is phosphorylated in an ATR-dependent manner in response to replicational stress," *The Journal of Biological Chemistry*, vol. 276, no. 51, pp. 47759–47762, 2001.
- [49] N. J. Curtin, L.-Z. Wang, A. Yiakoukaki et al., "Novel poly(ADP-ribose) polymerase-1 inhibitor, AG14361, restores sensitivity to temozolomide in mismatch repair-deficient cells," *Clinical Cancer Research*, vol. 10, no. 3, pp. 881–889, 2004.
- [50] T. Duncan, S. C. Trewick, P. Koivisto, P. A. Bates, T. Lindahl, and B. Sedgwick, "Reversal of DNA alkylation damage by two human dioxygenases," *Proceedings of the National Academy of Sciences of the United States of America*, vol. 99, no. 26, pp. 16660–16665, 2002.
- [51] P. A. Aas, M. Otterlei, P. O. Falnes et al., "Human and bacterial oxidative demethylases repair alkylation damage in both RNA and DNA," *Nature*, vol. 421, no. 6925, pp. 859–863, 2003.
- [52] P. M. O'Connor and K. W. Kohn, "Comparative pharmacokinetics of DNA lesion formation and removal following treatment of L1210 cells with nitrogen mustards," *Cancer Communications*, vol. 2, no. 12, pp. 387–394, 1990.
- [53] M. R. Middleton and G. P. Margison, "Improvement of chemotherapy efficacy by inactivation of a DNA-repair pathway," *Lancet Oncology*, vol. 4, no. 1, pp. 37–44, 2003.
- [54] L. H. Thompson and J. M. Hinz, "Cellular and molecular consequences of defective Fanconi anemia proteins in replication-coupled DNA repair: mechanistic insights," *Mutation Research*, vol. 668, no. 1-2, pp. 54–72, 2009.
- [55] K. Yamamoto, M. Ishiai, N. Matsushita et al., "Fanconi anemia FANCG protein in mitigating radiation- and enzyme-induced DNA double-strand breaks by homologous recombination in vertebrate cells," *Molecular and Cellular Biology*, vol. 23, no. 15, pp. 5421–5430, 2003.
- [56] K. Nakanishi, Y.-G. Yang, A. J. Pierce et al., "Human Fanconi anemia monoubiquitination pathway promotes homologous DNA repair," *Proceedings of the National Academy of Sciences of the United States of America*, vol. 102, no. 4, pp. 1110–1115, 2005.
- [57] A. R. Meetei, A. L. Medhurst, C. Ling et al., "A human ortholog of archaeal DNA repair protein Hef is defective in Fanconi anemia complementation group M," *Nature Genetics*, vol. 37, no. 9, pp. 958–963, 2005.
- [58] A. Ciccia, C. Ling, R. Coulthard et al., "Identification of FAAP24, a Fanconi Anemia Core Complex Protein that Interacts with FANCM," *Molecular Cell*, vol. 25, no. 3, pp. 331–343, 2007.
- [59] Y. Masuda, M. Ohmae, K. Masuda, and K. Kamiya, "Structure and enzymatic properties of a stable complex of the human REV1 and REV7 proteins," *The Journal of Biological Chemistry*, vol. 278, no. 14, pp. 12356–12360, 2003.
- [60] M. L. G. Dronkert and R. Kanaar, "Repair of DNA interstrand cross-links," *Mutation Research*, vol. 486, no. 4, pp. 217–247, 2001.
- [61] M. E. Hegi, A.-C. Diserens, T. Gorlia et al., "MGMT gene silencing and benefit from temozolomide in glioblastoma," *The New England Journal of Medicine*, vol. 352, no. 10, pp. 997–1003, 2005.
- [62] M. Esteller, J. Garcia-Foncillas, E. Andion et al., "Inactivation of the DNA-repair gene MGMT and the clinical response of gliomas to alkylating agents," *The New England Journal of Medicine*, vol. 343, no. 13, pp. 1350–1354, 2000.
- [63] T. Helleday, E. Petermann, C. Lundin, B. Hodgson, and R. A. Sharma, "DNA repair pathways as targets for cancer therapy," *Nature Reviews Cancer*, vol. 8, no. 3, pp. 193–204, 2008.
- [64] J. A. Quinn, A. Desjardins, J. Weingart et al., "Phase I trial of temozolomide plus O<sup>6</sup>-benzylguanine for patients with recurrent or progressive malignant glioma," *Journal of Clinical Oncology*, vol. 23, no. 28, pp. 7178–7187, 2005.

- [65] O. Khan and M. R. Middleton, "The therapeutic potential of  $O^6$ -alkylguanine DNA alkyltransferase inhibitors," *Expert Opinion on Investigational Drugs*, vol. 16, no. 10, pp. 1573–1584, 2007.
- [66] A. Giese, T. Kucinski, U. Knopp et al., "Pattern of recurrence following local chemotherapy with biodegradable carmustine (BCNU) implants in patients with glioblastoma," *Journal of Neuro-Oncology*, vol. 66, no. 3, pp. 351–360, 2004.

## Review Article

# Molecular Mechanisms of Ultraviolet Radiation-Induced DNA Damage and Repair

Rajesh P. Rastogi,<sup>1</sup> Richa,<sup>1</sup> Ashok Kumar,<sup>2</sup> Madhu B. Tyagi,<sup>3</sup> and Rajeshwar P. Sinha<sup>1</sup>

<sup>1</sup>Laboratory of Photobiology and Molecular Microbiology, Centre of Advanced Study in Botany, Banaras Hindu University, Varanasi 221005, India

<sup>2</sup>School of Biotechnology, Banaras Hindu University, Varanasi 221005, India

<sup>3</sup>Mahila Maha Vidyalaya, Banaras Hindu University, Varanasi 221005, India

Correspondence should be addressed to Rajeshwar P. Sinha, r.p.sinha@gmx.net

Received 11 June 2010; Revised 15 August 2010; Accepted 28 September 2010

Academic Editor: Shigenori Iwai

Copyright © 2010 Rajesh P. Rastogi et al. This is an open access article distributed under the Creative Commons Attribution License, which permits unrestricted use, distribution, and reproduction in any medium, provided the original work is properly cited.

DNA is one of the prime molecules, and its stability is of utmost importance for proper functioning and existence of all living systems. Genotoxic chemicals and radiations exert adverse effects on genome stability. Ultraviolet radiation (UVR) (mainly UV-B: 280–315 nm) is one of the powerful agents that can alter the normal state of life by inducing a variety of mutagenic and cytotoxic DNA lesions such as cyclobutane-pyrimidine dimers (CPDs), 6-4 photoproducts (6-4PPs), and their Dewar valence isomers as well as DNA strand breaks by interfering the genome integrity. To counteract these lesions, organisms have developed a number of highly conserved repair mechanisms such as photoreactivation, base excision repair (BER), nucleotide excision repair (NER), and mismatch repair (MMR). Additionally, double-strand break repair (by homologous recombination and nonhomologous end joining), SOS response, cell-cycle checkpoints, and programmed cell death (apoptosis) are also operative in various organisms with the expense of specific gene products. This review deals with UV-induced alterations in DNA and its maintenance by various repair mechanisms.

## 1. Introduction

The stratospheric ozone layer is continuously depleting due to the release of atmospheric pollutants such as chlorofluorocarbons (CFCs), chlorocarbons (CCs), and organobromides (OBs). Consequently there is an increase in the incidence of UV radiation (UVR) on the Earth's surface [1] which is one of the most effective and carcinogenic exogenous agents that can interact with DNA and alter the genome integrity and may affect the normal life processes of all organisms ranging from prokaryotes to mammals [2–10]. However, wide variations in tolerance to UV-B among species and taxonomic groups have been reported. Moreover, ozone depletion followed by increased UV exposure has been predicted to continue throughout most of this century [11]. In all the groups of UVR (i.e., UV-A: 315–400 nm; UV-B: 280–315 nm; UV-C: <280 nm) UV-B radiation produces adverse effects on diverse habitats, even though most of the

extraterrestrial UV-B is absorbed by the stratospheric ozone [12]. UV-A radiation has a poor efficiency in inducing DNA damage, because it is not absorbed by native DNA. UV-A and visible light energy (up to 670–700 nm) are able to generate singlet oxygen ( $^1O_2$ ) that can damage DNA via indirect photosensitizing reactions [13]. UV-C radiation is quantitatively absorbed by oxygen and ozone in the Earth's atmosphere, hence does not show much harmful effects on biota. Solar UV radiation is responsible for a wide range of biological effects including alteration in the structure of protein, DNA, and many other biologically important molecules, chronic depression of key physiological processes, and acute physiological stress leading to either reduction in growth and cell division, pigment bleaching,  $N_2$  fixation, energy production, or photoinhibition of photosynthesis in several organisms [3, 9, 10]. It has been documented that UV-B severely affects survival, fecundity, and sex-ratio in several intertidal copepods [14]. One of the most prominent

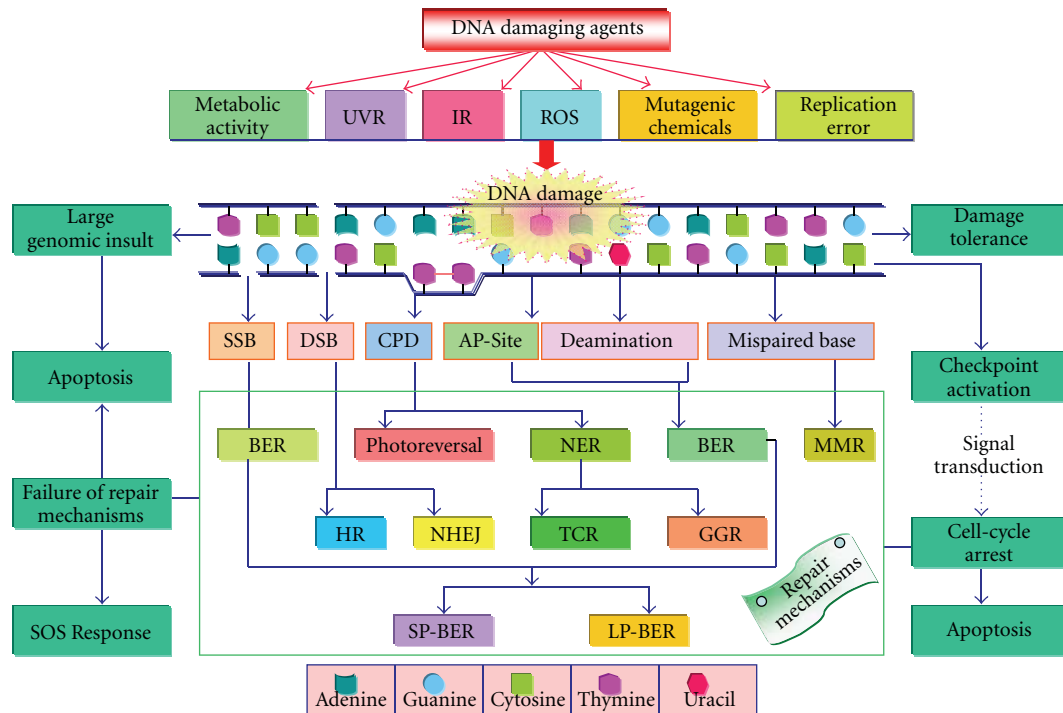


FIGURE 1: DNA damage and maintenance. Genomic lesions produced by various DNA damaging agents trigger several specific repair machinery to conserve the genomic integrity. In case of severe damage and/or failure of repair mechanisms, cells undergo apoptosis or induce a complex series of phenotypic changes, that is, SOS response. Sometimes the potentiality of lesions in the genome is mitigated by a phenomenon known as damage tolerance, during which DNA lesions are recognized by certain repair machinery, allowing the cells to undergo normal replication and gene expression. The cellular response to DNA damage may activate cell-cycle checkpoint by means of a network of signaling pathway that gives the cell extra time to repair the genomic lesions or may induce cell suicide response/programmed cell death (PCD).

targets of solar UV-radiation is cellular DNA, which absorbs UV-B radiation and causes adverse effects on living systems such as bacteria [15, 16], cyanobacteria [17], phytoplankton [18], macroalgae [19], plants [20], animals, and humans [21–23].

Although UV-B radiation has less than 1% of total solar energy, it is a highly active component of the solar radiation that brings about chemical modification in DNA and changes its molecular structure by the formation of dimers. Certain UV-absorbing pigments are produced by a number of organisms as a first line of defense; however, they are unable to avoid UV-radiation completely from reaching DNA in superficial tissue [28–32]. Certain enzymes, such as superoxide dismutase (SOD), catalase (CAT), peroxidase (POD), and scavengers such as vitamin C, B, and E, cysteine, and glutathione play an additional role in defense against UV radiation [33]. However, as a second line of defense several organisms have developed a number of specific and highly conserved repair mechanisms such as photoreactivation, excision repair, mismatch repair (MMR), double strand break (DSB) repair and certain other mechanisms like damage tolerance (dimer bypass), SOS (save our soul) response, checkpoint activation, and programmed cell death (PCD) or apoptosis (Figure 1) that efficiently remove DNA lesions ensuring the genomic integrity [22]. Plants are unique in the obligatory nature of their exposure

to UVR; it is also conceivable that they may also have evolved certain efficient repair mechanisms for the elimination of UV-induced DNA damage. However, a number of questions concerning the basic phenomena of the DNA repair in plants remain to be elucidated. In the following, we discuss the molecular mechanisms of UV-induced DNA damage and repair mechanism (s) operative in various organisms.

## 2. UV-Induced DNA Damage

Induction of DNA damage by solar UVR is a key event that drastically influences the normal life processes of all organisms. A number of endogenous factors such as free radicals [34] generated during metabolic processes as well as exogenous factors such as UV or ionizing radiations [35] are known to interfere with genome integrity. DNA damage results in (i) misincorporation of bases during replication process, (ii) hydrolytic damage, which results in deamination of bases, depurination, and depyrimidination [36], (iii) oxidative damage, caused by direct interaction of ionizing radiations (IR) with the DNA molecules, as well as mediated by UV radiation-induced free radicals or reactive oxygen species [37, 38], and (iv) alkylating agents that may result in modified bases [36, 39]. The hydrolytic deamination (loss of an amino group) can directly convert

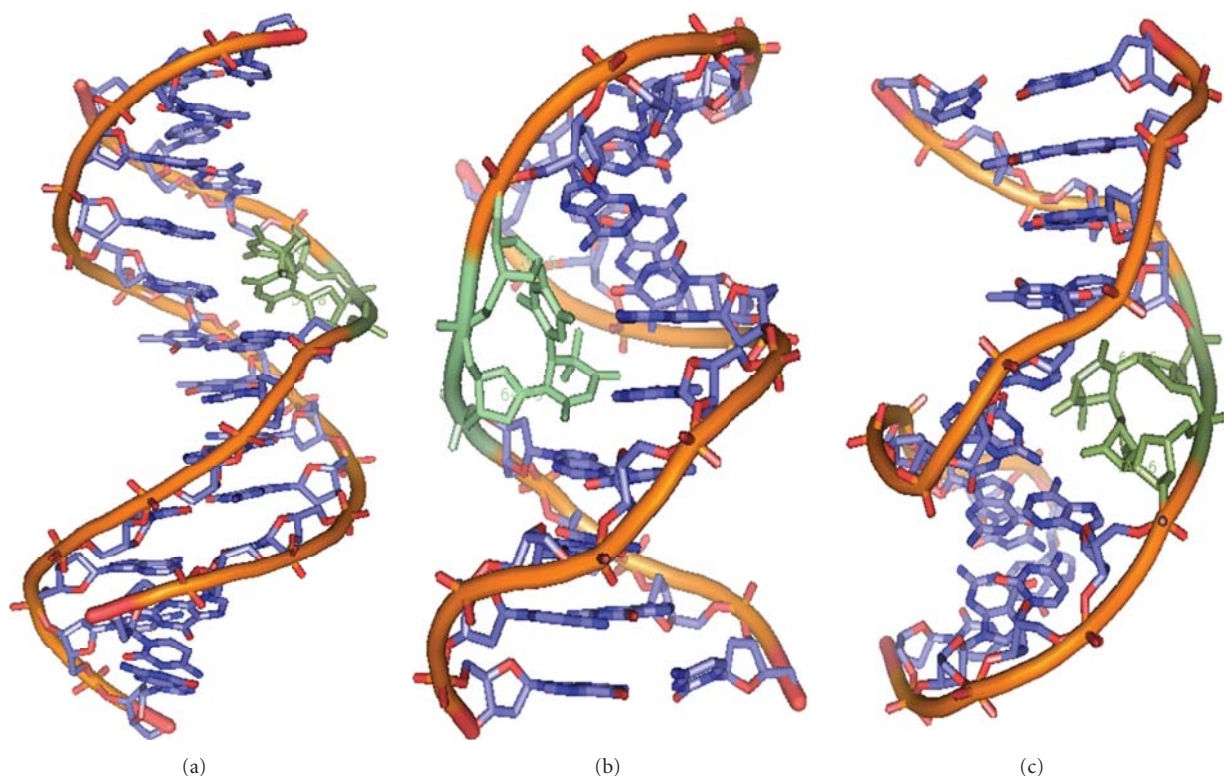


FIGURE 2: Structures of DNA duplexes showing the presence of lesions (in green) such as CPD (a), 6-4PP (b), and 6-4 Dewar dimer (c). Hydrogen atoms are not shown, prepared from PDB entries 1TTD [24], 1CFL [25], and 1QKG [26] using PyMol. (version 1.1r1) [27].

one base to another; for example, deamination of cytosine results in uracil and at much lower frequency adenine to hypoxanthine. In depurination/depyrimidination, there are complete removals of purine/pyrimidine bases, leaving the deoxyribose sugar depurinated/depyrimidinated, that may cause breakage in the DNA backbone. The exposure of UVR, IR, and certain genotoxic chemicals may result in single as well as double DNA strand breaks. Among different types of damages, DNA double strand breaks (DSBs) are the most deleterious, since they affect both strands of DNA and can lead to the loss of genetic material. At high concentrations oxygen-free radicals or, more frequently, reactive oxygen species (ROS) can induce damage to cell structure, lipids, proteins as well as DNA and results in oxidative stress which has been implicated in a number of human diseases [40]. The hydroxyl radicals ( $\text{OH}^\bullet$ ) can damage all components of DNA molecules such as purine and pyrimidine bases and also the deoxyribose backbone, inhibiting the normal functions of the cell [37, 38].

### 3. UV-Induced Pyrimidine Photoproducts

UV-B radiation is one of the most important energetic solar components that may lead to the formation of three major classes of DNA lesions, such as cyclobutane pyrimidine dimers (CPDs), pyrimidine 6-4 pyrimidone photoproducts (6-4PPs), and their Dewar isomers (Figure 2) [5, 22, 23, 41–43]. CPDs correspond to the formation of a four-member

ring structure involving C5 and C6 of both neighboring bases whereas 6-4PPs are formed by a noncyclic bond between C6 (of the 5'-end) and C4 (of the 3'-end) of the involved pyrimidines via spontaneous rearrangement of the oxetane (when the 3'-end is thymine) (Figure 3(a)) or azetidone (when the 3'-end is cytosine) (Figure 3(b)) intermediates [5, 44]. The 6-4PPs are eagerly converted into their Dewar valence isomers upon exposure to UV-B or UV-A radiation that may further undergo reversion to the 6-4PPs upon exposure to short-wavelength UV radiation [45]. Two adjacent cytosines are considered as mutation hotspots of UVB and UVC radiations [42]. It has been found that T-T and T-C sequences are more photoreactive than C-T and C-C sequences [46]. The diastereoisomers of pyrimidine dimers (Figure 4) can be observed in free solution that differ in the orientation of the two pyrimidine rings relative to the cyclobutane ring, and on the relative orientations of the C5–C6 bonds in each pyrimidine base [44]. It has been demonstrated that the main photoproducts are *cis-syn*-configured CPD lesions, while *trans-syn*-configured CPD lesions are formed in much less quantity [47]. In double stranded B-DNA, where the dimer entails two adjoining pyrimidine bases on the same DNA strand, only the *syn* isomers can be generated, whereas the *cis* isomer is preferred over the *trans* isomer to a great extent [42]. The incidence of *trans-syn* isomer in single-stranded or denatured DNA is more common because of the increased flexibility of the DNA backbone. A few CPD lesions (i.e., *cis-syn* or *trans-anti* isomers) can also be detected in aqueous

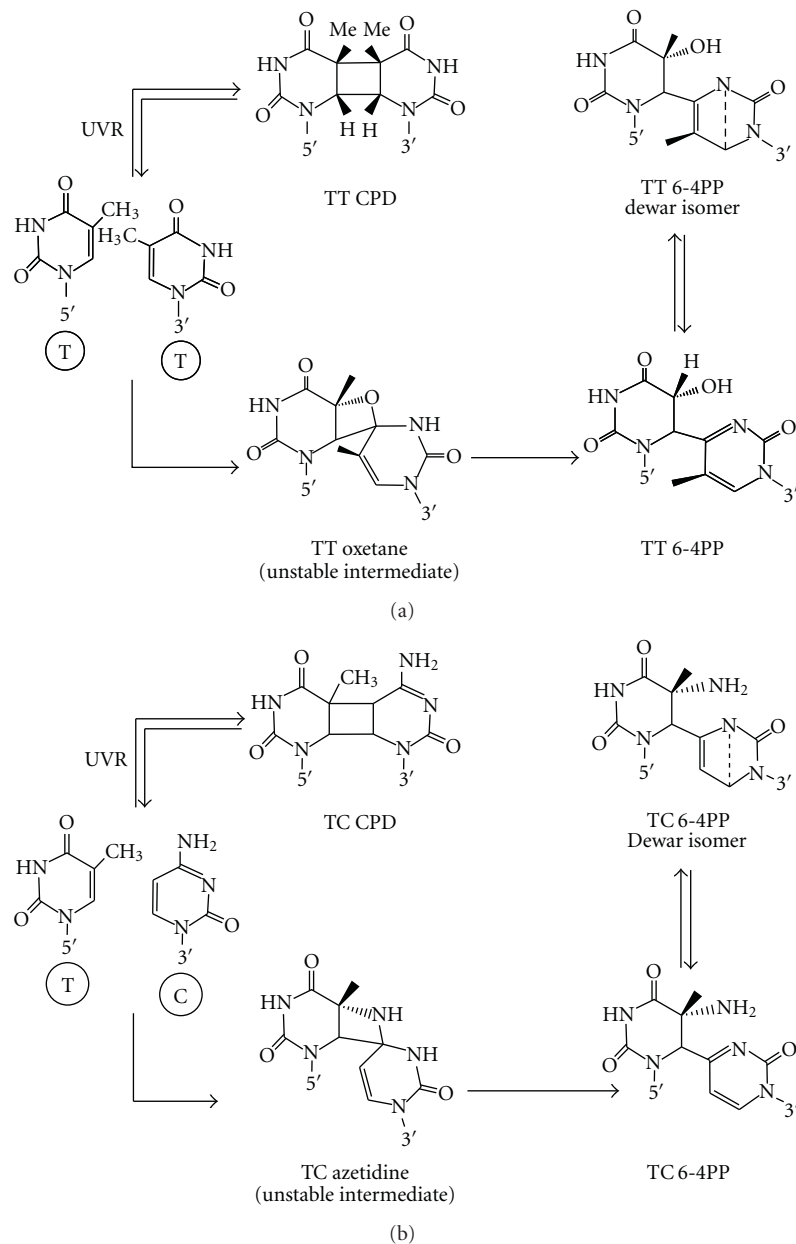


FIGURE 3: Pathway of UVR-induced T-T (a) and T-C (b) CPD, 6-4PPs, and their Dewar isomers.

solutions by UV-C irradiation [48]. The formation of “spore photoproduct” has been detected in UV-irradiated bacterial spores by the addition of methyl group of one thymine residue to the C5 position of an adjacent thymine. In most cellular environments, there is no much significance of this photoproduct, since it requires anhydrous conditions for its formation [49].

The base damage by UVR is determined by the flexibility of the DNA strand as well as nature and position of the base. CPDs are formed at higher quantity by cycloaddition reaction between two pyrimidine bases [47] in single-stranded DNA (ssDNA) and at the flexible ends of poly (dA)-(dT) tracts, but not at their rigid centre [50, 51]. Bending of DNA towards the minor groove reduces CPDs

formation [52]. One of the transcription factors, TATA-box binding protein (TBP), promotes the selective formation of 6-4PPs in the TATA-box, where the DNA is bent, but CPDs are formed preferentially at the edge of the TATA box and outside where the DNA is not bent [53]. The amounts of CPDs and 6-4PPs are about 75 and 25%, respectively, of the total UV-mediated DNA damage products [22]; however, the ratio between the yield of CPDs and 6-4PPs mainly depends upon the two adjacent bases involved in the formation of dimers [54]. Thus the heterogeneous distribution of the UV-induced photolesions in the DNA depends on the sequences that facilitate DNA bending as well as the chromatin modulation through the binding of specific protein [55]. Mapping of CPDs in the nucleosome core

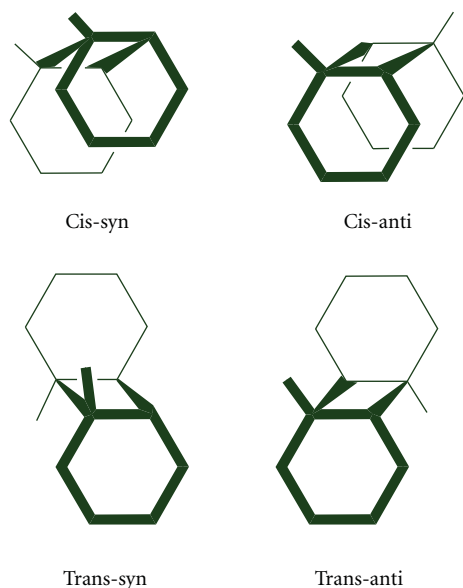


FIGURE 4: Possible diastereoisomers of pyrimidine T  $\diamond$  T dimer.

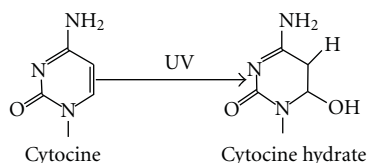


FIGURE 5: Formation of cytosine photohydrate (6-hydroxy-5,6-dihydrocytosine) as a result of photohydration reaction.

regions of UV-treated chromatin has revealed the formation of CPDs with an average distance of 10.3 bases, away from the surface of histones [56]. The formation of photoproducts is not restricted to cells exposed to UV-B or UV-B + UV-A radiations; UV-A-induced formation of CPDs has also been observed in bacteria as well as in eukaryotic cells and whole skin [57–59]. Recent studies on the effects of UV-A radiation on rodent and human skin cells have revealed that CPDs are in larger yields than 8-oxo-7,8-dihydroguanine (the most frequent UVA-induced DNA lesion) and DNA strand breaks [48, 60]. The occurrence of 5-methylcytosine-containing photoproducts in UV-irradiated DNA is still controversial. However, Su et al. [61] have reported a new photoproduct of 5-Methylcytosine and Adenine characterized by high-performance liquid chromatography and mass spectrometry. An additional photochemical characteristic for cytosine is the formation of monomeric pyrimidine photoproduct “cytosine photohydrate” (6-hydroxy-5,6-dihydrocytosine) as a result of photohydration reaction (Figure 5) [62]. There is little information concerning the formation of cytosine hydrates in UV-irradiated DNA due to instability of the resulting photoproduct [63]. The oxidation product of pyrimidine bases such as pyrimidine glycols is also formed by means of hydration reaction [42].

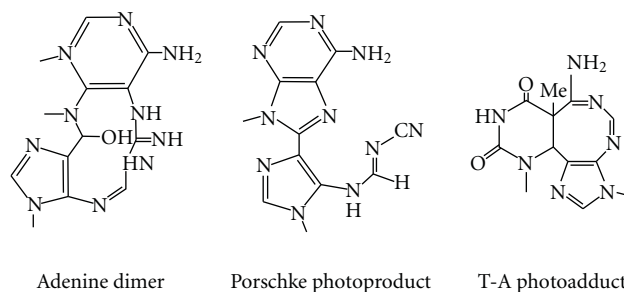


FIGURE 6: Structure of purinic photoproduct, that is, adenine dimer, porschke photoproduct and thymine-adenine photoadduct.

#### 4. UV-Induced Purine Photoproducts

Although dipyrimidine photoproducts are the preferential outcome of UV-B radiation, the biological importance of UV radiation-induced modifications of DNA purine bases has also been recognized [64]. These comprise the photoproducts that involve, at least, one adenine residue that undergoes photocycloaddition reactions with contiguous adenine or thymine (Figure 6) upon exposure to UV-B radiation [65, 66]. The extent of adenine-containing photoproduct (A-T) is very low ( $1 \times 10^{-5}$  in native DNA) but these lesions may contribute to the biological effects of UV radiation in view of the fact that the A-T adduct has been shown to be mutagenic [67, 68]. Photodimerization of adenine (A) involves the cycloaddition of N7-C8 double bond of the 5'-A across the C6 and C5 positions of the 3'-A [65, 69] and generates a very unstable azetidine intermediate. This intermediate photoproduct undergoes competing reaction pathways to form two distinct adenine photoproducts such as adenine dimer (A=A) and Porschke photoproduct (Figure 6) [70]. Conversion of both these photoproducts into 4,6-diamino-5-guanidinopyrimidine (DGPY) and 8-(5-aminoimidazol-4-yl)adenine (8-AIA), respectively, can be detected from individual acid hydrolysates of UV-irradiated polynucleotides and DNA [71]. It has been found that complexing of UV-irradiated poly(dA)-poly(dT) effectively reduces the formation of A=A photoproduct [71]. Moreover, photoreactivity of adjoining adenine bases in DNA is strongly suppressed by the complementary base pairing [50, 72]. UV-induced ROS acts as a powerful oxidant that may cause oxidative DNA damage. A number of oxidation products of purine bases such as 8-oxo-7,8-dihydroguanyl (8-oxoGua), 8-oxo-Ade, 2,6-diamino-4-hydroxy-5-formamidoguanine (FapyGua), FapyAde, and oxazolone have been reported to form upon exposure of DNA to UV radiation [44, 73, 74].

Overall, it has been concluded that UV-induced DNA lesions such as CPDs, 6-4PPs, abasic site, strand breaks, and oxidative product are the predominant and most persistent lesions and if not repaired may cause severe structural distortions in the DNA molecule, thereby affecting the important cellular processes such as DNA replication and transcription, compromising cellular viability and functional integrity and ultimately leading to mutagenesis, tumorigenesis, and cell death [30, 36].

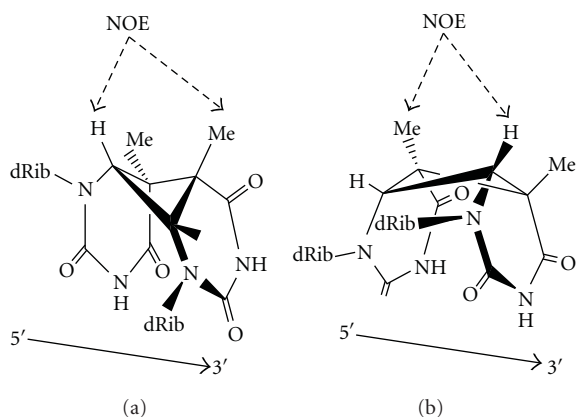


FIGURE 7: *Cis-syn* CPD showing the right-handed or left-handed twist in DNA duplex. Dotted arrows elucidate the strongest nuclear overhauser enhancement (NOE) interaction in both cases (Adopted from Lukin and de los Santos [75]).

## 5. Differential Effects of CPDs and 6-4PPs on DNA Conformation

UV-induced DNA lesions such as CPDs and 6-4PPs show differential effects on DNA conformation, impairing their regulatory functions and other dynamic processes [24, 26, 75, 76]. Nuclear Magnetic Resonance (NMR) spectroscopy has presented new insights on UV radiation-induced nucleic acid conformation. It has been well established that the comparative orientation of damaged residues is unusual from that observed in unmodified DNA duplexes [75]. Nuclear overhauser enhancement (NOE) study of interactions among the photoadduct H6 and methyl ( $\text{CH}_3$ ) groups has established that the *cis-syn* CPD changes the cyclobutane conformation from a left-handed twist (observed in the isolated dimer) to a right-handed twist in DNA duplex [46] (Figure 7). Assessment of the chemical shift data suggests that the DNA helix is disturbed more along the 3'- and 5'-side of the *cis-syn* and *trans-syn* dimer, respectively. It was revealed that the presence of *trans-syn* CPD causes distortion to a great extent than the *cis-syn* product by means of a kink or dislocation at the 5'-side of the dimer in double-stranded DNA [77]. NMR and X-ray diffraction studies of the ultraviolet photoproduct, *cis-syn* CPD, with the S-cyanoethyl phosphotriester have revealed that the two pyrimidine bases are rotated by  $-29^\circ$  base twist, contrasting to the right-handed  $36^\circ$  value observed in B-form DNA [78, 79]. Moreover, in contrast to the *cis-syn* CPD, the duplex spectra of the *trans-syn* lesion illustrated no abnormally shifted  $^{31}\text{P}$  or imino proton signal, signifying the absence of major distortions in the conformation of the sugar-phosphate backbone [75]. The thymine (T) residues of the CPD form stable wobble pairs with the opposite guanine (G) residues. The T6-G15 wobble pair of the CPD formed hydrogen bonds between the T6-imino and G15-O6 and between the G15-imino and T6-O2. The two T (T5, T6) residues of the CPD in the CPD/GG duplex form wobble

base pairs with the opposite G residues, similar to the T6-G15 base pair in the CPD/GA duplex [80]. It has been reported that the preexisting CPDs in the DNA molecule can influence its rotational setting on the histone surface during nucleosome formation [81]. Recently, Rumora et al. [82] have examined the thymine dimer-induced structural changes to the DNA duplex with several small, base-selective reactive chemical probes. The formation of 6-4PPs and their Dewar isomers cause remarkable change in the conformation of DNA duplex. The one- and two-dimensional NMR data on the (6-4)-adduct-containing DNA duplex decamer was analyzed in  $\text{H}_2\text{O}$  and  $\text{D}_2\text{O}$  solutions to elicit the base pairing and unusual conformation in the vicinity of the lesion [76, 83, 84]. The distortion of the double helix caused by the 6-4PP is much greater than that of the CPD [85].

The main conformational perturbations caused by the (6-4) adduct and Dewar product are concerned with their effects on global DNA curvature. Both duplex decamers are significantly bent at the lesion sites. In contrast to the 6-4PPs, the 5,6-dihydro-5-hydroxythymine base is the most perturbed part of the 6-4 Dewar lesion. Even though there are no hydrogen bonds between 5,6-dihydro-5-hydroxythymine and its partner adenine residue, this lesion produces minor distortions in comparison to the 6-4PP. In general helical bending induced by the (6-4) adducts and the Dewar product is  $44^\circ$  and  $21^\circ$ , respectively [76]. All the supplementary imino proton resonances from the flanking base pairs were observed in the hydrogen-bonded region, which indicate that the structure of the (6-4) adduct inside the duplex shows a distinctive base orientation due to (6-4) covalent linkage which makes a normal Watson-Crick-type hydrogen bonding unfavorable at the 3'-side of the lesion site with an empty space between the 3'-thymine (T6) and its opposite base (A15) [76]. Contrary to the duplex (6-4) decamer which retains a hydrogen-bonded imino proton at the 5'-side (T5) of the (6-4) lesion, the T5 imino proton of the Dewar lesion is not hydrogen-bonded. The NMR characterization of a 6-4PP dimer containing duplex showed that the 5'-residue of the lesion remains essentially unperturbed. However, the 5'-pyrimidine residue loses aromaticity and acquires an additional hydrophilic group [75, 83]. The glycosyl bond torsion angle at the T5 residue of the (6-4) lesion and the Dewar lesion prevails in the anti and high-anti conformation, respectively, and thus both the lesions exhibit considerable differential effects on DNA backbone conformation. It has been observed that the large structural distortion induced by the (6-4) lesion may ensure a favorable recognition by the repair enzyme, which may possibly elucidate the correlation with the elevated repair rate of the T-T (6-4) adduct than of the T-T Dewar product and the T-T *cis-syn* dimer [76].

## 6. UV-Induced DNA Double Strand Breaks

The generation of DNA double strand breaks (DSBs) in UV-irradiated cells, specifically in replicating DNA, has been known for a long time [86]. DNA strand breaks are observed extensively in cells under UV-B irradiation [87, 88]. UV-B-induced ROS [89] as well as DNA lesions

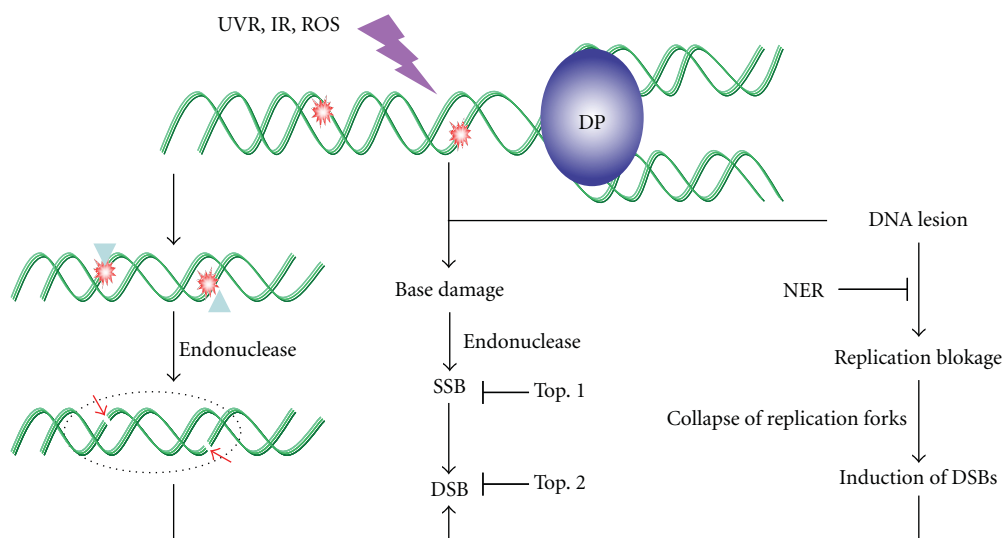


FIGURE 8: Schematic representation showing different pathways of DSBs.

(CPDs and 6-4PPs) may cause primary as well as secondary breaks, respectively. These lesions are commonly associated with transcription/replication blockage that may lead to production of DNA double-strand breaks (DSBs) at the sites of collapsed replication forks of CPDs-containing DNA [90, 91] (Figure 8). Dunkern and Kaina [92] also observed UV-C-induced DNA DSBs, arising from replication of damaged DNA. A significantly low amount of DSBs was found in the cell where replication was inhibited. It was assumed that initial photoproducts are converted into DSBs during DNA replication, due to not a distinct process, that is, “collapse of replication forks” [93]. After labeling of replicating DNA of UV-irradiated SV40-transformed human cell lines with radioactive precursors, an increased number of DSBs was observed in NER deficient cells in comparison to NER proficient cells. These results further support the view that DSBs are produced during the replication of unrepaired UV-induced DNA lesions [91]. DSBs can be formed in response to the repair of single strand breaks (SSBs) passing through base excision repair (BER) [94, 95]. Overall, it seems that UV radiation does not directly produce DNA DSBs but rather produces pyrimidine dimers and other photoproducts leading to replication arrest and DSBs. UV-induced replication arrest in the xeroderma pigmentosum variant (XPV) followed by the accumulation of Mre11/Rad50/Nbs1 complex and phosphorylated histone H2AX ( $\gamma$ -H2AX) in large nuclear foci at sites of stalled replication forks also suggests that UV damage leads to the formation of DSBs during the course of replication arrest [90, 95].

A number of pathways have been considered for the formation of DSBs at a stalled replication fork. It was shown that when the DNA replication machinery encounters a replication-blocking lesion, DNA polymerase (DP) enzyme is stalled at the blocked site resulting in the formation of a Y-shaped DNA structure, which may be recognized by a specific endonuclease, that successively makes a nick in the template strand resulting in the induction of a DSB close to the

replication-blocking lesion [144]. Furthermore, replication stresses may trap topoisomerase I (Top1) cleavage complexes leading to generation of DSBs by preventing Top1-mediated DNA religation [145]. Free radicals may also cause DSBs [146] by preventing the topoisomerase II (Top2)-mediated DNA religation [144, 147]. Recently, Harper et al. [148] have shown that radiation-induced SSBs and non-DSB DNA damage contribute to the formation of replication-induced DSBs. In spite of the above possible facts regarding the formation of DSBs, more experimental evidences are still needed.

## 7. Detection of DNA Damage

Several workers have attempted to detect different types of DNA lesions and presently a number of detection strategies are widely used (Table 1). An alkaline gel method for quantitating single-strand breaks (SSBs) in nanogram quantities of nonradioactive DNA was developed by Freeman et al. [149]. Mitchell et al. [150] have developed a method for the detection of CPDs, where DNA is labeled with radioactive substances followed by agarose gel electrophoresis and densitometric analysis and finally digesting with endo. III and endo.V before analyzing on sequencing gels. UV-B induced DNA damage in mammalian genome was reported by Wang et al. [96] using the PCR-based short interspersed DNA element- (SINE-) mediated detection method. For analyzing the 6-4PPs, terminal transferase-dependent PCR (TD-PCR) has been used [97]. UV-induced decrease in template activity of genomic DNA of cyanobacterium *Anabaena* strain BT2 was documented by Kumar et al. [98] using the PCR-based assays such as random amplified polymorphic DNA (RAPD) and rDNA amplification. Similarly, UV-B-induced DNA damage was also detected in *Anabaena variabilis* PCC 7937 and *Rivularia* sp. HKAR-4 by PCR (data not published). The formation of thymine dimer ( $T^{\wedge}T$ ) within

TABLE 1: Various strategies for the detection of damaged DNA.

DNA damage detection strategies	Types of lesions detected	References
PCR based assay (TDPCR, LMPCR, ICPCR, SINE)	Decrease in DNA template activity, T $\leftrightarrow$ T CPDs, 6-4PPs	[96–99]
Commet assay (Single-cell gel Electrophoresis)	Oxidative DNA damage and single/double strand break	[100, 101]
Halo assay/AHA/FHA	Chromatin fragility/single strand breaks at the single cell level	[102, 103]
TUNEL assay	Single/double strand breaks, apoptosis	[104, 105]
HPLC-MS/MS	Oxidative DNA damage; CPDs, 6-4PPs and their related Dewar valence isomers; 5-hydroxy-2-deoxyuridine,8-oxo-7,8-dihydro-2-Deoxyadenosine; 5-Methylcytosine and adenine	[48, 54, 61, 106]
FISH	Chromosomes with numerical aberrations	[107, 108]
FCM	Chromosomal aberrations, sister chromatid exchange, chemical adducts to DNA and DNA strand breakage	[109, 110]
Annexin V labeling	Chromatin condensation, DNA fragmentation, radiation-induced apoptosis	[109, 111]
Immuno-dot-blot assay	CPDs, 6-4PPs and their Dewar valence isomers	[17, 59, 112, 113]
RIA	CPDs and 6-4PPs	[114, 115]
GC-MS	Strand break, modified bases, abasic sites, DNA-protein crosslinks and other oxidative DNA damage.	[39]
FADU	Single/double strand breaks and alkali-labile sites	[88, 116]
NMR spectroscopy	Lesions induced distortions of DNA duplex	[78–80]

PCR: polymerase chain reaction; TDPCR: terminal transferase dependent PCR; LMPCR: ligation-mediated PCR; ICPCR: immuno-coupled PCR; SINE: short interspersed DNA element; AHA: alkaline-halo assay; FHA: fast halo assay; TUNEL: terminal deoxyribonucleotidyl transferase mediated deoxyuridine triphosphate nick end labeling; HPLC-MS/MS: high-performance liquid chromatography coupled to tandem mass spectrometry; FISH: fluorescence *in situ* hybridization; FCM: flow cytometry; RIA: radio immunoassay; ELISA: enzyme-linked immunosorbent assay; GC-MS: gas chromatography-mass spectrometry; NMR: nuclear magnetic resonance spectroscopy.

human genomic DNA has been detected by immunocoupled PCR (IC-PCR) [99]. DNA damage such as SSBs, DSBs, and oxidative DNA damage caused by UVR, ultrasound electromagnetic frequency radiation, and so forth may be detected by comet assay [100]. Recently, a modified version of comet assay (apo/necro-comet assay) has been developed that differentiates viable, apoptotic, and necrotic cells and also correlates the DNA fragmentation pattern [101]. Both single and DSBs as well as apoptosis can also be detected by TUNEL assay [104, 105]. However, it has been experienced that TUNEL assay is not able to distinguish various types of cell death; hence, an alternate method based on flow cytometry (FCM) has been developed for the detection of apoptosis [109]. Recently, apoptosis in tumor cells caused by X-rays has been analyzed using  $^{125}\text{I}$ -labeled annexin V [111]. FCM assay is useful in detecting chromosomal aberrations, sister chromatid exchange, chemical adducts to DNA, and DNA strand breakage [110]. Alkaline unwinding FCM (AU-FCM) may be used to detect nucleotide excision repair (NER) [151]. The changes in DNA organization in the individual cells can be determined by halo assay [102]. SSBs at the single cell level can be assessed by alkaline-halo assay (AHA), where cells are embedded in melted agarose and spread on the microscope slide and then incubated in a high-salt alkaline lysis solution followed by another incubation in a hypotonic alkaline solution and, finally, stained with ethidium bromide (EtBr). Under

these conditions, single-stranded DNA fragments diffuse radically from the nuclear cage [103]. DNA strand breaks (SSBs, DSBs, and alkali-labile sites) induced by genotoxic agent such as UVR can also be detected by fluorometric analysis of DNA unwinding (FADU) assay, which was first reported by Birnboim and Jevcak [116] to detect X-ray-induced DNA damage in mammalian cells. Numerical aberrations in chromosome can be detected efficiently by fluorescence *in situ* hybridization (FISH) method [107]. Recently, immuno-dot-blot assay is used extensively to detect UV-induced photoproducts in various organisms such as mammals, cyanobacteria, phytoplankton, macroalgae, and liverwort [17, 59, 112, 113]. This technique is based on use of thymine-dimer specific antibodies followed by blotting and chemiluminescence method. Another detection strategy includes radio-immunoassay (RIA) which is used to estimate CPDs and 6-4PPs [114]. The very low amount of CPDs caused by UVR in bacterioplankton and marine viruses may be detected very efficiently using RIA method [115]. Kara et al. [152] have studied the electrochemical detection of DNA damage by direct and indirect irradiation with radioactive technetium (TC-99m) and iodine (I-131). Certain photoproducts such as 5-Methylcytosine and adenine can be detected by high-performance liquid chromatography and mass spectrometry [61]. Recently, Kumari et al. [108] have made an attempt to dissect various strategies for detection of DNA lesions produced by a number of genotoxic agents.

TABLE 2: Photolyase enzymes in four different kingdoms.

Kingdom	Organism	CPD Photolyase	6-4PP Photolyase	References
Archaeobacteria	<i>Halobacterium halobium</i>	+	–	[117]
	<i>Methanobacterium thermoautotrophicum</i>	+	–	[118, 119]
	<i>Sulfolobus tokodaii</i>	+	–	[120]
Eubacteria	<i>Bacillus firmus</i>	+	–	[121]
	<i>Escherichia coli</i>	+	–	[122, 123]
	<i>Salmonella typhimurium</i>	+	–	[122]
	<i>Anacystis nidulans</i>	+	–	[124]
	<i>Synechocystis sp. PCC 6803</i>	+	–	[125]
	<i>Streptomyces griseus</i>	+	–	[126]
	<i>Myxococcus xanthus</i>	+	–	[127]
	<i>Vibrio cholerae</i>	+	–	[128]
Eukaryotes	<i>Saccharomyces cerevisiae</i>	+	–	[122]
	<i>Neurospora crassa</i>	+	–	[129, 130]
	<i>Drosophila melanogaster</i>	+	+	[131]
	<i>Homo sapiens</i>	?	?	[118, 132]
	<i>Carassius auratus</i>	+	–	[133]
	<i>Oryzias latipes</i>	+	–	[118]
	<i>Monodelphis domestica</i>	+	–	[134]
	<i>Potorous tridactylis</i>	+	–	[118]
	<i>Xenopus laevis</i>	+	+	[135]
	<i>Arabidopsis thaliana</i>	+	+	[136]
	<i>Chlamydomonas reinhardtii</i>	+	–	[137]
	<i>Cucumis sativus</i>	+	–	[138, 139]
	<i>Ginkgo biloba</i>	+	–	[140]
<i>Medicago sativa</i>	+	–	[20]	
<i>Triticum sp.</i>	+	–	[141]	
Viruses	<i>Fowl pox virus</i> (FPV)	+	–	[142]
	<i>Melanoplus sanguinipes</i> entomopox virus (MsEPV)	+	–	[143]
	<i>Chrysodeixis chalcites</i> nucleopolyhedrovirus (ChchNPV)	+	–	[106]

## 8. DNA Repair

The idea about the ability of living beings to overcome the lethal effects of UV-radiation emerged as early as the mid 1930s [153], but the existence of repair mechanisms was observed by Kelner [154] and Dulbecco [155] independently. The determination of a particular repair pathway within the cell mainly depends on the types and location of lesions in the genome [156]. The biochemical and molecular studies on repair pathways have been extensively investigated in some model organisms such as *E. coli*, *S. cerevisiae*, and human, where specialized repair proteins scan the genome continuously and encounter the DNA lesions by triggering several distinct repair mechanisms such as photoreactivation, excision repair (BER and NER), mismatch repair (MMR), and some specialized forms of repair system such as SOS response, damage tolerance, and apoptosis.

## 9. Photoreactivation

The process of photoreactivation is executed by means of a photoreactivating enzyme known as “photolyase”, which is well conserved and found throughout the three domains of life (Table 2). The enzyme binds specifically to the CPDs (CPD photolyase) or 6-4PPs (6-4 photolyase) and directly monomerizes the cyclobutane ring of the pyr > pyr, using the energy of visible/blue-light and protects the genome from deleterious effects of UVR [157, 158]. The absorption of every blue-light photon may split approximately one dimer [159]. CPD photolyases have been reported in diverse groups such as archaea, bacteria, fungi, virus, plants, invertebrates, and many vertebrates including aplacental mammals (Table 2). On the other hand, 6-4 photolyases have been identified in certain organisms like *Drosophila*, silkworm, *Xenopus laevis*, and rattle snakes [22]. Photolyases seem to be

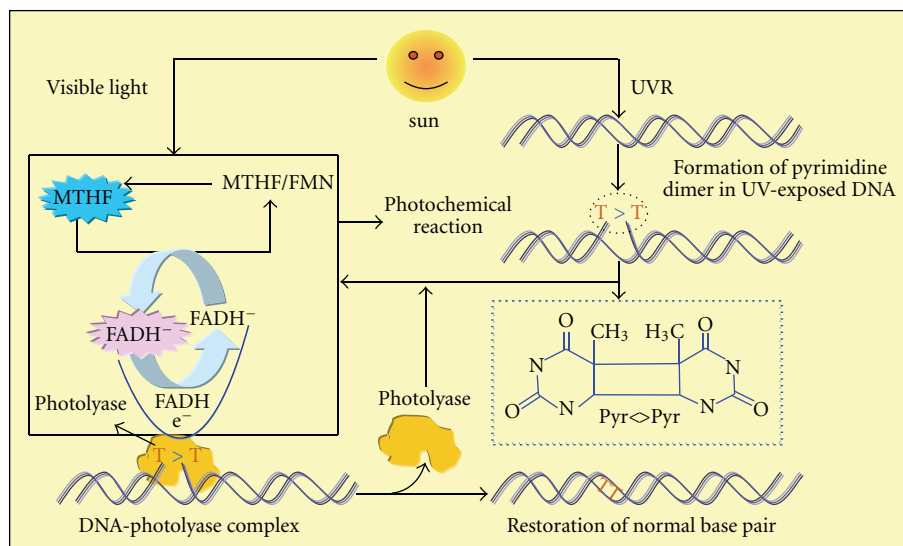


FIGURE 9: Photoreactivation: incidence of ultraviolet radiation (UVR) results in pyrimidine lesion (thymine dimer), which is recognized by a photoreactivating enzyme “photolyase”. The light energy (>380 nm) is trapped by the antenna molecules of photolyase (such as MTHF/8-HDF/FMN) and transfers them to catalytic cofactor FADH<sup>-</sup> which becomes excited and transfers energy to the pyrimidine dimer in the form of e<sup>-</sup>, splitting the CPD into two monomeric unit, and then electron is transferred back to the flavin molecule.

absent or nonfunctional in placental mammals like human [118, 132, 160]. However, Sutherland [161], Sutherland and Bennett [162], and Harm [163] have demonstrated photolyase activity in cells and tissues, including white blood cells (WBCs) of several placental mammals, such as humans, ox, cat, and mouse. A number of workers have identified a human photolyase which shows homology with *Cry* gene (plant blue-light receptor) and about 40% sequence identity to the *Drosophila* 6-4 photolyase, but their exact roles in repair process, whether it acts as a photolyase or as a photoreceptors, are still under investigation [164].

DNA photolyases (45–66 kDa) having 420–616 amino acid residues [158] are monomeric flavin-dependent repair enzymes, consisting of two known cofactors, a catalytic cofactor and a light-harvesting cofactor. Till date, 5,10-methenyltetrahydrofolate (MTHF) [122], 8-hydroxy-5-deaza-riboflavin (8-HDF) [124], and FMN [165] are known as light-harvesting cofactors, which absorb light energy efficiently and transfer them to FADH<sup>-</sup> [166]. Deprotonated reduced flavin adenine dinucleotide (FADH<sup>-</sup>) is found in all known photolyases as a catalytic cofactor, which transfers energy in the form of an electron to the CPD, splitting the cyclobutane ring with the generation of two monomeric bases [157, 167] (Figure 9).

In comparison to other eukaryotic systems, reports on the repair of UV-induced DNA damage in plants are still very limited. To avoid the deleterious effects of UVR, plants have acquired two main protective strategies; shielding by flavonoids and phenolic compounds [168, 169] and DNA repair by photoreactivation. Photoreactivation mediated by the enzyme photolyases is thought to be the major DNA repair pathway in several higher plants such as rice, *Arabidopsis*, wheat, and maize [170–172]. Studies on *Arabidopsis* seedling, rice, and alfalfa indicate that photoreactivation

greatly enhances the rate of removal of dimers, although, in the absence of photoreactivating (blue) light, dimers are slowly eliminated from bulk DNA and 6-4PPs are generally observed to be repaired more quickly than CPDs [173, 174]. Plants grown in the presence of photoreactivating radiation can eliminate the majority of both 6-4 products and CPD lesion within hours, or in some cases minutes, of their induction [30]. The structural information about the interaction between CPD lesions and photolyases became clear with the help of X-ray crystallography [175] and nuclear magnetic resonance (NMR) spectroscopy [176]. However, how DNA photolyases find lesions in the DNA molecule is still not clear [158]. It has been observed that about 240 kJ/mol of energy is captured upon absorption, out of which about 125 kJ/mol energy is consumed during the initial electron transfer from the excited FADH to CPD lesions [177]. The splitting of CPD lesion proceeds rapidly within 0.6 nanosecond [167, 178]. The back-transfer of electrons from the CPD lesion to the FADH radical is efficiently avoided by the enzyme before completion of cleavage of the cyclobutane ring [157]. With the help of ultrafast femtosecond laser spectroscopy, MacFarlane and Stanley [178] have suggested that photolyase enzyme is indeed left in the semiquinonid state after accomplishment of repair of the CPD lesion. However, Kavakli and Sancar [179] have analyzed the role of intraprotein electron transfer in photoreactivation by DNA photolyase and found that photoreduction process is not a regular part of the photolyase photocycle under physiological conditions, because the enzyme may undergo at least 25 repair cycles before losing its activity. After completion of DNA repair, a thymine pair is flipped back into the duplex DNA to form a hydrogen bond with their complementary adenine base. Fourier transform infrared spectroscopy (FTIR) has revealed that the relaxation of DNA backbone proceeds very slowly

than the repair of CPD lesions [180]. In the absence of photoreactivating light, the enzyme binds to pyr  $\diamond$  pyr and stimulates the removal of UV damage by stimulating the NER system in vivo or in vitro and defense against DNA damage even in the absence of light [181].

## 10. Excision Repair

Unlike photoreactivation, excision repair is a multistep, dark repair pathway, where an abnormal or damaged base is removed by two major subpathways: (i) base excision repair (BER) and (ii) nucleotide excision repair (NER).

**10.1. Base Excision Repair (BER).** BER is the predominant DNA repair pathway against base lesions arising from hydrolytic deamination, strong alkylating agents, ionizing radiation (IR), or by different intracellular metabolites and, indirectly, also by UV radiation via generation of ROS [182–184] and proceeds through a series of repair complexes that act at the site of DNA damage [185, 186]. The efficiency and specificity of the repair pathway are determined by several forms of DNA glycosylase which removes different types of modified bases (Table 3) by cleaving the N-glycosidic bond between the abnormal base and deoxyribose creating either an abasic site or an SSB [187]. Recently, Parsons et al. [188] have discovered that the formation of DNA repair complexes on damaged DNA stabilizes BER proteins. On the contrary, BER proteins that are not involved in repair are ubiquitinated by carboxyl terminus of Hsc70 interacting protein (CHIP) and subsequently degraded by the proteasome.

The extent of BER conservation among *E. coli* and mammals has led to progress in our understanding of mammalian BER and here, a general overview of the mammalian BER pathway will be discussed. As a result of multiple interactions with a number of repair proteins XRCC1 plays a crucial role in the coordination of BER and SSB repair [189]. The interaction between XRCC1 and polymerase  $\beta$  (Pol.  $\beta$ ) and its functional aspects was confirmed after UV-A-induced oxidative damage in living mammalian cells [190]. The AP-site is removed by the action of AP endonuclease-1 (APE-1) along with phosphodiesterase that breaks the DNA strand along 5' or 3' to the AP site, respectively, and subsequently the gap is filled by a repair DNA polymerase and the strand is joined by a DNA ligase (Figure 10) [182, 191]. It has been reported that the repair Pol.  $\beta$  itself has the capacity to excise the 5' deoxyribose phosphate residues, that is, generated by the combined actions of DNA glycosylase and ClassII AP endonuclease [192]. The major APE-1 that was discovered independently as an abasic site-specific endonuclease homologous to the *E. coli* Xth protein [193] incises duplex oligonucleotides containing 5,6-dihydroxyuracil (DHU), 5-hydroxyuracil (5-ohU), and alpha-anomeric 2'-deoxynucleosides (i.e.,  $\alpha$ dA and  $\alpha$ T) residues in human cells [194].

DNA having one nucleotide lesion is removed by short-patch BER (SP-BER) whereas two/more nucleotide lesion is repaired by long-patch BER (LP-BER) pathway [195] (Figure 10). Recently, Almeida and Sobol [184] have

proposed a unified model of SP-BER and LP-BER. On the basis of measuring the BER efficiency and presence of a single modified base in a plasmid molecule transfected into mammalian cells, Sattler et al. [196] made the first attempt to verify the occurrence of LP-BER in vivo. It is assumed that majority of repair takes place through SP-BER, initiated either by monofunctional or by bifunctional glycosylase [184]. The pathway of SP-BER after excision of damaged base involves the recruitment of poly (ADP-ribose) polymerase-1 (PARP-1) followed by scaffold protein XRCC1 and DNA pol.  $\beta$  to replace the damaged nucleotide. DNA ligase III (Lig. III) seals the nick and restores the intact DNA.

It has been observed that radiation- (X-rays,  $\gamma$ -rays) induced breaks exist mainly as 5'p and 3'p at the margin of the gap [197, 198] which is converted by the polynucleotide kinase (PNK) or APE1 into 5'P and 3'OH moieties, necessary for the DNA synthesis [199]. Unlike SP-BER, LP-BER involves proliferating cell nuclear antigen (PCNA) coupled with DNA pol.  $-\delta/\epsilon$  or  $\beta$  which extends and fills the gap by inserting 2–13 nucleotide [184]. The replication factor C (RF-C) is required to load PCNA onto the damaged DNA [195]. The flap endonuclease (Fen1) protein then displaces the ensuing DNA flap leaving a nick which is ligated by DNA ligase I (Lig. I) [200, 201].

In several plant species, some of the genes requisite for dark repair have been identified [171, 172, 202–204]. The available evidence supports the additional existence of enzyme-mediated excision-repair mechanisms in a variety of systems including pollen, whole seedlings and plants, and protoplasts derived from leaves and cultured cells [205, 206]. The formation of AP sites has been observed in seeds of *Zea mays* during early germination. This phenomenon was attributed to the action of DNA glycosylases on lesions accumulated during seed storage [207], implying the presence of BER in this species. Likewise, an enzyme activity attributed to uracil-DNA glycosylase was found in cultured cells of *Daucus carota* [208]. Recently, it has been reported that the mechanisms of BER and NER (but not photoreactivation) in higher plants are active in proliferating cells [172].

**10.2. Nucleotide Excision Repair (NER).** NER is critically important in the repair of UV-induced DNA lesions and is one of the most versatile and flexible repair systems found in most organisms but highly conserved in eukaryotes. It sorts out a wide range of structurally unrelated DNA lesions, such as CPDs and 6-4PPs caused by UVR, bulky chemical adducts, DNA-intrastrand crosslinks, and some forms of oxidative damage, that cause helical distortion of the DNA double helix as well as modification of the DNA chemistry and interfere with DNA duplication and transcription [209, 210]. Although both 6-4PPs and CPDs are removed presumably by the same NER proteins, the relative repair efficiency of both of these lesions varies considerably in mammalian cells. It has been established that in human and hamster cells, the elimination of 6-4PP is at least fivefold faster than that of CPDs [211].

Discovery of NER was first described in *E. coli* [212, 213] where about six proteins such as UvrA, B, and C

TABLE 3: DNA glycosylases and their probable substrate in bacteria, yeast, and human (modified from Sinha and Häder [22]).

Glycosylases	Organisms	Genes	Substrate
(1) Uracil DNA glycosylase	<i>E. coli</i>	<i>Ung</i>	uracil from ss- and ds-DNA
		<i>Dug/mug</i>	U from U : G, ethenocytosine, hypoxanthine and 5-hydroxycytosine
		<i>Dut</i>	?
	<i>S. cerevisiae</i>	<i>UNG</i>	Uracil
	Human	<i>UNG1/UNG2</i> <i>SMUG1</i>	uracil from ss- and ds-DNA uracil from ss-DNA, hydroxymethyluracil, formyluracil
(2) 3-methyl adenine DNA glycosylase	<i>E. coli</i>	<i>tag</i>	3-methyladenine
		<i>alkA</i>	3-methyladenine, 7-methylguanine, 2-methylcytosine, 5-formyluracil
	<i>S. cerevisiae</i>	<i>MAG1</i>	3-methyladenine, 7-methylguanine
	Human	<i>MPG</i>	3-methyladenine hypoxanthine
		<i>Aag</i>	
(3) UV-endonuclease	T4	<i>den V</i>	<i>cis-syn</i> -cyclobutane-type pyrimidine dimer
	<i>E. coli</i>	?	?
	<i>Bacillus subtilis</i>	<i>UVDE</i>	Pyrimidine dimers
	<i>S. cerevisiae</i>	?	?
	<i>S. pombe</i>	<i>UVDE</i>	Pyrimidine dimers
(4) Endonuclease III/thymine glycol DNA glycosylase	<i>E. coli</i>	<i>Nth</i>	5-hydroxycytosine, thymine glycol, urea oxidative DNA damage, thymine glycol and formamido-pyrimidines, oxidized pyrimidines, 2 formamido-pyrimidine-G, Me <sup>7</sup> -formamido-pyrimidine-G
		<i>NTG1</i>	oxidative DNA damage, Thymine glycol and formamido-pyrimidines residues, 5-hydroxycytosine, oxidized pyrimidines, Me <sup>7</sup> -fapy-G
	Human	<i>NTG2</i>	oxidized guanine lesions
		<i>NTH1</i>	
	(5) Endonuclease VIII	<i>E. coli</i>	<i>nei</i>
<i>S. cerevisiae</i>		?	?
Human		<i>NEIL1</i>	5-hydroxyuracil, 5-hydroxycytosine, 5,6-dihydrouracil, thymine glycol, formamido-pyrimidines (FapyA/G)
		<i>NEIL2</i>	5-hydroxyuracil and 5-hydroxycytosine
		<i>NEIL3</i>	?
(6) fapy/8-oxoguanine DNA glycosylase	<i>E. coli</i>	<i>fpg/mutM</i>	2,6-diamino-5-formamidopyrimidine 8-oxo-7,8-dihydroguanine, 5-hydroxycytosine
	<i>S. cerevisiae</i>	<i>OGG1</i>	2,6-diamino-5-formamidopyrimidine 8-oxoG, 2 formamidopyrimidine-G, Me <sup>7</sup> -formamidopyrimidine-G
	Human	<i>hOGG1</i>	8-hydroxyguanine, Me <sup>7</sup> -formamidopyrimidine-G
(7) A-G-mismatch DNA glycosylase	<i>E. coli</i>	<i>mut Y</i>	Adenine/C
	<i>S. pombe</i>	<i>spMYH</i>	2-aminopurine/G and A/2-aminopurine, Adenine/C
	Human	<i>MYH</i>	Adenine from G : A, 8-oxoG : A, 2-hydroxyadenine
(8) G-T-mismatch DNA glycosylase	<i>E. coli</i>	?	?
	<i>M. thermoautrophicum</i>	<i>Mig-Mth</i>	Thymine residues from T-G mismatches
	<i>S. pombe</i>	<i>thp1</i>	Uracil from G : U
	Human	<i>MBD4</i> ( $\approx$ <i>MED1</i> )	Thymine from T : G
		<i>TDG</i>	Recognizes a G : T mispair in a CpG sequence

TABLE 3: Continued.

Glycosylases	Organisms	Genes	Substrate
(9) Formyluracil DNA glycosylase	<i>E. coli</i>	<i>mug</i>	Formyluracil mispaired with A & G
		<i>mutM</i>	?
		<i>mutS</i>	Formyluracil mispaired with G
	<i>S. cerevisiae</i>	?	?
	Human	<i>MBD4</i> <i>hNTH1</i>	Formyluracil mispaired with G ?
(10) Hydroxymethyl uracil DNA glycosylase	<i>E. coli</i>	?	?
	<i>S. cerevisiae</i>	?	?
	Human	?	5-hydroxymethyluracil mispaired with G

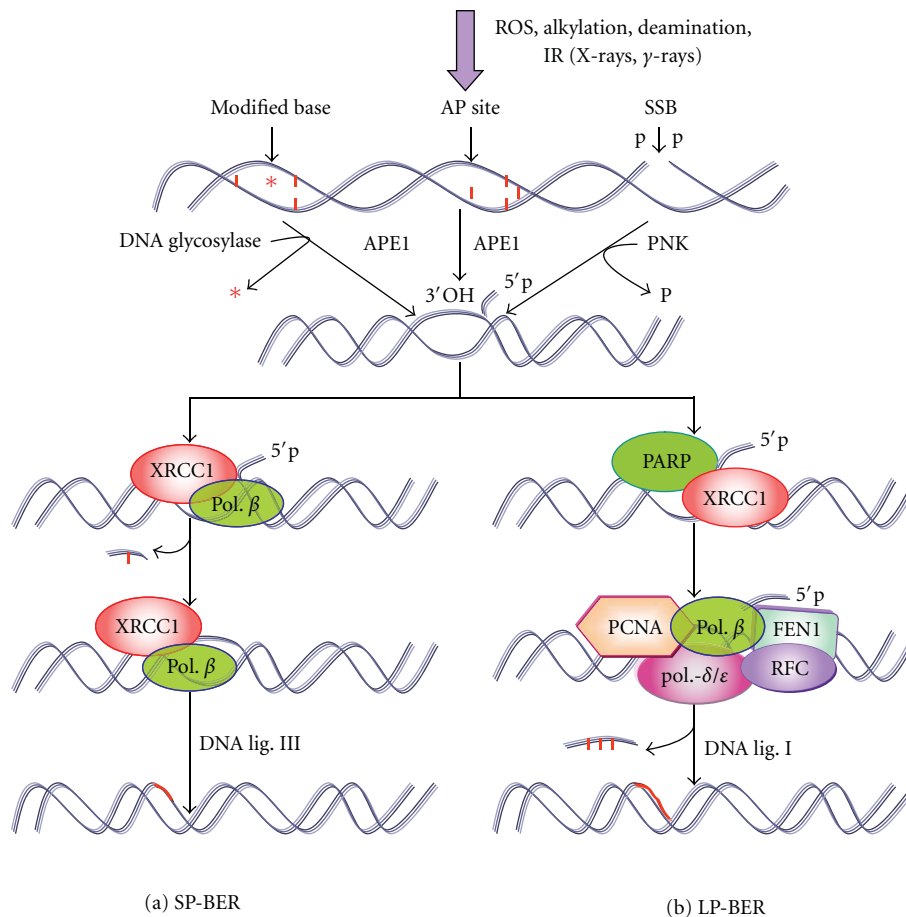


FIGURE 10: Schematic overview of mammalian SP-BER (a), and LP-BER (b). SP-BER is initiated by the activity of glycosylase and APE1, followed by scaffold protein XRCC1 and pol.  $\beta$  to remove the damaged nucleotide and DNA ligase III seals the nick. In case of LP-BER, after DNA damage by ionizing radiation, PNK is recruited to convert the damaged ends to 3' OH and 5' P moieties. Here PARP1/2, followed by XRCC1, is involved. PCNA and DNA pol.  $\beta$  and/or pol.  $-\delta/\epsilon$  extend and fill the gap by >2 nucleotides. Replication factor-C (RFC) is required to load the PCNA on DNA. Ultimately the resulting 5' flap of DNA is removed by the flap endonuclease I (FEN1) and subsequently the nick is sealed by DNA ligase I.

(known as ABC-complex, which shows excinuclease activity), UvrD (helicase II), DNA polymerase I (pol. I), and DNA ligase are recruited to complete the repair [214, 215]. Eukaryotic NER is known to be similar to prokaryotes regarding the biochemical strategy used but differs widely

in the nature and number of proteins used [210]. The eukaryotic NER pathway has extensively been studied at the molecular level in yeast and human cells. A schematic representation of the NER pathway in human is illustrated in Figure 11.

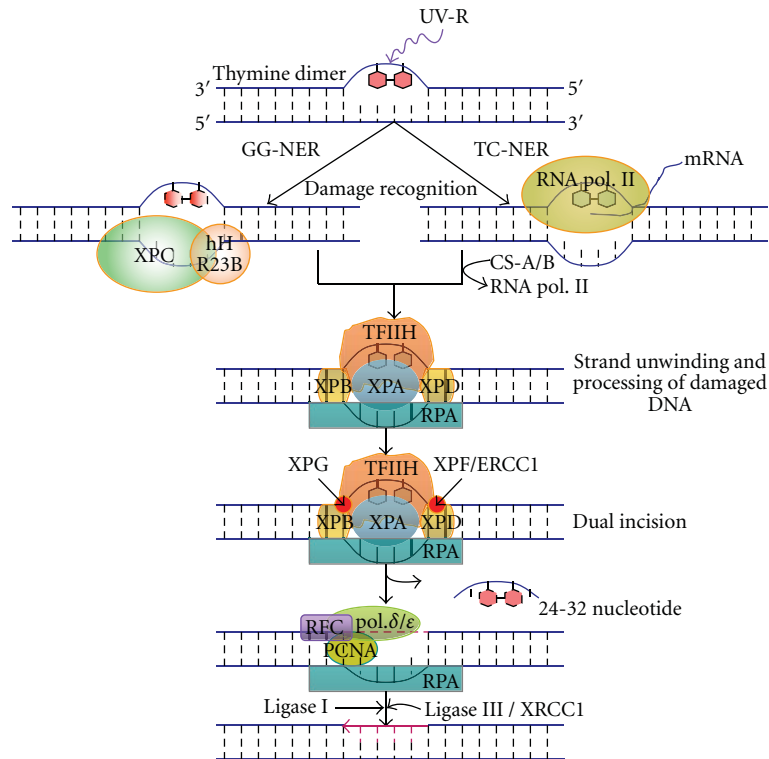


FIGURE 11: Molecular mechanisms of global genome nucleotide excision repair (GG-NER) and transcriptional coupled nucleotide excision repair (TC-NER) in mammals. For details see the text.

NER can be subdivided into differentially regulated subpathways such as global genome NER (GG-NER) and transcription-coupled NER (TC-NER): repair of lesions over the entire genome, referred to as global genome repair (GGR), and repair of transcription-blocking lesions present in transcribed DNA strands, referred to as transcription coupled repair (TCR). Both repair systems removed a wide range of UV-induced DNA lesions in a sequential way that includes damage recognition, opening of DNA double helix at damage site, and dual incisions on both sides of the lesion followed by resynthesis and ligation [210, 216] (Figure 11). In human XP-C cells, where the removal of 6-4PP takes place through the TCR pathway, the repair seems to be threefold slower as compared to normal cells. This indicates that the GGR is the most preferred and efficient pathway for 6-4PP removal [211].

## 11. Mechanistic Differences between GG- and TC-NER in Mammalian Cells

Global genome repair (GGR) is a random process that occurs gradually, whereas TCR, which is firmly linked to RNA polymerase II (RNA pol II) transcription, is highly specific and efficient. NER defects are associated with a surprisingly wide clinical heterogeneity.

It is assumed that TC-NER proceeds when the transcription machinery RNA pol II encounters a lesion. To progress the transcription-coupled repair (TCR), the stalled

polymerase must be displaced, which is brought about by the recruitment of two proteins CSA and CSB. The CSA protein (44 kDa) which belongs to “WD repeat” family of proteins exhibits structural and regulatory roles and CSB proteins (168 kDa) which belong to SWI/SNF family of proteins exhibit DNA-stimulated ATPase activity [217–219]. As stated earlier, elongation of active RNA pol II is prerequisite for efficient TCR; the CSA and CSB gene products are required for efficient repair only during the elongation stages of RNA pol II transcription. It has been suggested that the RNA pol II backs up some nucleotides upon encountering the lesion to facilitate the accessibility of the repair machinery to the lesion site [220, 221]. It is expected that the CSB protein ubiquitinates the stalled elongating RNA pol II complex at the lesion and enhances the assembly of repair factors [222]. However, the fate and the role of ubiquitylated RNA pol II have yet to be clarified [223]. Recently, Fousteri et al. [224] has revealed that CSB is a prerequisite factor in vivo to assemble NER proteins while it is not essential to recruit TFIIH or NER complex in vitro. In living human cells, Proietti-De-Santis et al. [225] have shown that CSB is required during the first phases of RNA pol II transcription initiation. At higher dose of UV radiation (i.e., used for 6-4PP detection), elongation of RNA pol II is greatly impaired, affecting the efficiency of TCR. Hence, at higher UV radiation the GGR overrules the TCR pathway [55]. The probable relationship between TCR and blockage of RNA transcription subsequent to UV-irradiation may possibly be due to CSB which acts as a chromatin remodeling

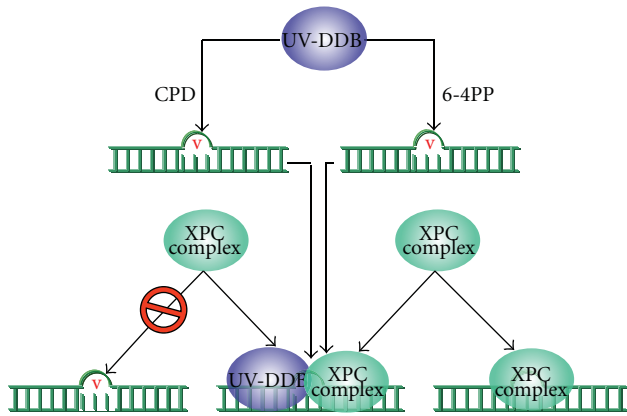


FIGURE 12: Different pathway for recognition of DNA lesions such as CPD and 6-4PP. In case of CPD photoproduct (cause little distortion), XPC complex binds to the lesion after recruitment of UV-DDB whereas 6-4PP that distorts the DNA helix to a great extent can be recognized either by interacting with prebound UV-DDB or directly by XPC complex.

factor at both levels, allowing either the recruitment of the transcription machinery at the initiation sites or the remodeling of the stalled RNA polymerase allowing the NER factors to access the lesion [223].

In GG-NER pathway, lesions produced in transcriptionally silent areas of the genome are recognized by hHR23B-XPC protein complex in an energy-independent manner. The rate of GGR strongly depends on the type of lesion. For instance, 6-4PPs are removed much faster from the genome than CPDs, possibly because of disparity in affinity of the damage sensor hHR23B-XPC. XPC is the sole XP factor not essential for TCR and is restricted to GGR [211]. It is supposed that XPC binds preferentially to the stretch of ssDNA that occurs in the nondamaged strand, opposite to a lesion [252]. However, association of UV-damaged DNA-binding protein (UV-DDB) with a cullin-based ubiquitin ligase has revealed novel mechanistic and regulatory aspects of mammalian GG-NER. It was reported that XPC and UV-DDB materialize to assist for the efficient recognition of UV-induced photolesions and that both factors are ubiquitinated [250, 253]. Lesions that cause little distortion can be recognized by the DDB complex which is also part of an E3 ubiquitin (Ub) ligase that poly-ubiquitinates XPC and XPE [216]. A mechanistic pathway for recruitment of XPC complex to the major UV-induced photolesions (i.e., CPDs and 6-4PPs) has recently been elucidated [216, 253]. It was shown that DDB complex is recruited first to the lesion (CPD) before the XPC complex, on little distorted DNA helix; however, in case of large distortion of the DNA helix caused by 6-4PPs, direct recognition by XPC is also possible for this lesion (Figure 12) [216, 253]. However, the method by which XPC locates a lesion in the vast excess of undamaged DNA in the enormous mammalian genome is not clear [254] and it needs more investigation. On the basis of DNase I footprinting, Sugawara et al. [226] showed that hHR23B-XPC attaches directly to DNA damage and alters the DNA conformation around the lesion. The

XPC protein (125 kDa) is complexed with hHR23B protein (58 kDa). These two proteins are human homologs of the yeast (*S. cerevisiae*) NER factor Rad4 and Rad23, respectively (Table 4). In mammalian cells, the quantity of hHR23B is higher than the XPC [255] and *in vitro* activation of the later protein is stimulated by hHR23B possibly in a structural quite than a catalytic way [256, 257]. It has been assumed that hHR23A can substitute for hHR23B in complex formation and stimulation of XPC repair activity [258]. Both hHR23A and -B harbor a ubiquitin-like moiety at their amino terminus [230]. hHR23B-XPC complex or only XPC exhibits a similar high affinity for both UV-induced single-stranded DNA (ssDNA) and double-stranded DNA (dsDNA) [230, 259], preferentially binds to DNA with various lesions [259] and even to small bubble structures with or without a lesion [260]. hHR23B-XPC is absolutely required for dual incision as well as for open complex formation during GG-NER [243, 261]. Overall, it has been distinguished that RNA pol II with the recruitment of two proteins (i.e., CSA and CSB) proceeds the TCR while hHR23B-XPC complex is the first factor in NER that initiates GGR by sensing and binding lesions, locally distorting the DNA double helix and recruiting the other factors of the system [227].

After initial steps of damage recognition, the subsequent pathway for both GGR and TCR system is almost similar. The unwinding of DNA double helix at the site of lesion takes place by the components of multi-subunit transcription factor-IIH (TFIIH). TFIIH is a ten-subunit protein complex (Table 4) composed of a core complex (XPB, XPD, p62, p44, p34, p52, p8) and of a cdk activating kinase (CAK) subunit (Mat1, Cdk7, CyclinH) [236]. TFIIH is usually involved in initiation of RNA Pol II transcription, but upon DNA damage can be employed in cell cycle regulation and NER (both in global genome and TC-NER) [228, 235]. Two subunits of TFIIH such as XPB (3' to 5' helicase) and XPD (5' to 3' helicase) are responsible for opening of DNA double helix around the lesion in an energy (ATP) dependent manner. It has been found that the XPD helicase activity is dispensable for *in vitro* transcription [262] but seems to play an additional architectural role within the complex by connecting the core TFIIH with the CAK subunit [228, 236]. After opening of DNA double helix by TFIIH, three proteins such as RPA, XPA, and XPG are recruited. The exact order of assembly of these proteins is not clear. Both XPA and RPA can recruit with the DNA lesions in absence of XPG, and similarly XPG can also join the damage sites in the absence of XPA [238, 239]. Moreover, XPA and heterotrimeric replication protein A (RPA; RPA70, 32 and 14) are recruited to confirm the presence of DNA damage and form a more stable preincision complex [185]. RPA was found to be required both for the dual incision and for the repair synthesis steps of NER [263]. It was assumed that RPA binds the nondamaged strand of the opened DNA bubble, thus allowing exact positioning and stimulation of the endonuclease activities of XPG and ERCC1-XPF [246, 247]. XPG, which belongs to flap endonuclease-1 (FEN-1) family of structure-specific endonucleases [264], is not only involved in performing the 3' incision in NER but also required for stabilizing the fully open DNA bubble structure

TABLE 4: NER proteins and their probable role in human and *S. cerevisiae*.

NER Factors	Name		Size (a.a)	Function	References
	Human	Yeast <i>S. cerevisiae</i>			
XPC-hHR23B	XPC	Rad4	940	Binds damaged DNA; recruits other NER proteins; works with hHR23B. involved only in GGR	[22, 226, 227]
	hHR23B	Rad23	409	Stimulates XPC activity <i>in vitro</i> ; contains ubiquitin domain	[22, 227–229]
	hHR23A	Rad23	363	Can substitute for hHR23B <i>in vitro</i>	[227, 230]
	CEN2	—	172	Stabilizes the XPC-hHR23B complex	[216, 231]
TFIIH	XPB	Rad25/SSL2	782	3' → 5' helicase	[227, 232, 233]
	XPD	Rad3	760	5' → 3' helicase	[227, 233, 234]
	p34	TFB4	303	DNA binding?	[227, 228, 235]
	p44	SSL1	395	DNA binding?	[227, 228, 233]
	p62	TFB1	548	Core TFIIH subunit	[227, 228, 236]
	p52	TFB2	462	Core TFIIH subunit	[227, 228, 233, 236]
	Mat1	TFB3	309	CDK assembly factor; CAK subcomplex	[227, 228]
	Cdk7	Kin28	346	CDK, C-terminal domain kinase; (CAK) subcomplex; phosphorylates RNA pol. II and other substrates	[227, 228]
	Cyclin H	CCL1	323	Cyclin; CAK subcomplex	[227, 228]
	TFB5/TTDA (p8)	Tfb5	71	Stabilizing subunit	[228, 237]
XPA	XPA	Rad14	273	Binds damaged DNA and facilitates repair complex assembly; affinity for ssDNA	[183, 238, 239]
RPA	RPA70	Rfa1	616	Stabilizes opened DNA complex; positions nucleases; ssDNA binding	[227, 240–242]
	RPA32	Rfa2	270	Stabilizes opened DNA complex; positions nucleases; ssDNA binding	[227, 240–242]
	RPA14	Rfa3	121	Stabilizes open complex (with XPA/Rad14)	[22, 240, 241]
XPG	XPG	Rad2	1186	Endonuclease (catalyzes 3' incision); stabilizes full open complex	[228, 243–245]
ERCC1-XPF	ERCC1	Rad10	297	Part of structure-specific endonuclease; catalyzes 5' incision; interstrand cross-link repair	[227, 246–248]
	XPF	Rad1	905	Part of endonuclease (5'-incision); recombination via single-strand annealing	[227, 246, 249]
DDB	DDB1	—	1140	CPD recognition?	[228, 250, 251]
	DDB2	—	428	Chromatin remodeling?	[228, 251]

and to permit the 5' incision by ERCC1- XPF [265]. Subsequently, the injured part of the DNA is removed by cleaving the damaged strand towards 3' and 5' of the lesion by endonuclease XPG and XPF/ERCC1 complex, respectively, generating a 24–32 base oligonucleotide fragment [183]. It has been found that E2F1 plays a direct, non-transcriptional role in DNA repair involving increased recruitment of NER factors to sites of UV-induced DNA damage [266]. Finally the gap is filled by DNA polymerase  $\delta$  or  $\epsilon$  (along with some accessory proteins, like PCNA and RFC) and sealed

by DNA ligase. It is assumed that ligase-I is responsible for ligation of remaining nick [267], but very recently it has been reported that mostly ligase III, in cooperation with its partner XRCC1 seals the DNA nicks and ligase I plays a minor role in actively replicating cells, but not in quiescent cells [268]. Recently, several workers have tried to dissect the molecular mechanisms of TC-NER [216, 223, 244, 269]. In spite of the above facts, more investigations are still required to improve our understanding of the GGR and TCR pathways.

Several observations provide evidence that “dark” repair of UV-induced NER is a significant DNA repair mechanisms in plants that is capable of excising dimers, particularly 6-4PPs [30, 270]. Genetic and genomic analysis indicates that plant NER pathway is homologous to that of mammals and fungi and unrelated to the bacterial system [204, 271–273]. Based on the reduction of nuclear CPD frequency, the presence of NER has been reported to occur in several plants such as *Glycine max* and cultivars of *Oryza sativa* [274, 275]. Furthermore, CPDs were found to be excised from the nuclear DNA of *Daucus carota* and *Wolffia microscopia* at rates dependent on damage levels and comparable to those in animal cells [205, 275]. A UV-specific endonuclease resembling UvrABC nuclease in activity was partially characterized from spinach [206]. Classical genetic analysis has resulted in the identification of at least four complementation groups required for this repair in *Arabidopsis* (*UVR1*, *UVR5*, *UVR7* and *UVR1*) [276–278] and many more UV-sensitive mutants await further genetic and phenotypic characterization [206]. Moreover, a plant homologue of human NER gene of the endonuclease, *ERCC1*, has been cloned from *Lilium longiflorum* which showed a similar role in DNA repair in plants [279].

## 12. Recombinational Repair

It is one of the widespread mechanisms which efficiently repair double-strand breaks (DSBs) and single-strand gaps in damaged DNA by a series of complex biochemical reactions, as a result of ionizing radiation, UVR, ROS, and chemotherapeutic genotoxic chemicals [5]. The lethal effects of double strand breaks (DSBs) can be conquered by the existence of two independent pathway, such as homologous recombination (HR) and non-homologous end joining (NHEJ). Multiple proteins are required for DSB repair by recombination, which are conserved among all eukaryotes and deficiencies in this repair mechanism can cause hereditary diseases. For instance, mutation of at least one of these repair proteins, called BRCA1 may lead to hereditary breast cancer [280]. Evidence suggests that BRCA1 could be one of the key players in DNA damage response [281]. DSB repair through HR process is an error free pathway, since, it requires an extensive region of sequence homology between the damaged and template strands, whereas NHEJ is an error prone, alternate pathway for the repair of DSBs, essentially joins broken chromosomal ends independent of sequence homology.

**12.1. Homologous Recombination.** Repair of DSBs by HR requires the genes of “RAD52 epistasis group” such as *RAD50*, *RAD51*, *RAD52*, *RAD54*, *RAD55*, *RAD57*, *RAD59*, *MRE11* and *XRS2*, which were first defined in yeast *Saccharomyces cerevisiae* mutants. Homologues of most of the genes are highly conserved among all eukaryotes including human [282, 283] highlighting these genes for cell survival. Among all, *E. coli recA* gene and its eukaryotic homologs *RAD51s* are the best recombination genes [284]. The *recA* gene encodes a DNA-dependent ATPase that binds to

ssDNA and promotes strand invasion and exchange between homologous DNA molecules [285]. Among eukaryotes, the yeast *S. cerevisiae* and *Schizosaccharomyces pombe* have four *RAD51*-like genes (*RAD51*, *DMC1*, *RAD55/rhp55*, and *RAD57/rhp57*) [286, 287] whereas vertebrate animals and plants have seven types of *RAD51*-like genes (*RAD51*, *-51B*, *-51C*, *-51D*, *DMC1*, *XRCC2*, and *XRCC3*) [288]. The eukaryotic *RAD51s* play a significant role in HR, maintaining genome integrity in both mitotic as well as meiotic cell cycle [288, 289]. There are 59% identity between *S. cerevisiae*, human and mouse in the case of Rad51 protein (Rad51p) and 30% identity to RecA protein of bacteria [290], whereas yeast and human proteins are 60% identical in case of Rad52 proteins (Rad52p) [291]. Yeast cell can exhibit both “allelic” [292, 293] as well as “ecotopic recombination” [294, 295] to repair a broken chromosome. Recombinational repair is a significant UV-tolerance mechanism in plants where UV-induced chromosomal rearrangements including homologous intrachromosomal recombination events have been found [296]. In mammalian cells the recombinational pathway of DSBs, seems to be operated in late S- and G2-phase, when DNA molecules are replicated and spatially juxtaposed [297].

The first step of DSB repair *via* HR is the resection of 5′ ends to produce a 3′ ssDNA overhang by means of an exonuclease (such as RecBCD in *E. coli*, MRX-complex in *S. cerevisiae* and MRN-complex in vertebrates). Rad51 (a functional homolog of the *E. coli* RecA) [298] is the central protein in HR, binds the exposed single-stranded tails forming a nucleoprotein filament and this early step is promoted by a Rad55/Rad57 protein heterodimer [299] by overcoming the inhibitory effects of the heterotrimeric single-stranded DNA binding protein RPA [300]. Recently, it has been reported that a member of the histone H2A family,  $\gamma$ -H2AX protein plays an important role in the recruitment of Rad51 protein in HR in eukaryotes [301]. The Rad51 nucleoprotein filament in association with other repair protein searches the genome for an intact copy of the broken DNA on the sister chromatid to form a heteroduplex joint molecules or D-loop that is matured in to a Holliday junctions (HJs). HJ is then resolved to give crossover products (Figure 13). In *E. coli*, this HJ is resolved by the positioning of RuvABC resolvasome, however in eukaryotic cell, how this HJ is resolved to give crossover products is not known. In *S. cerevisiae*, DNA DSB repair by forming noncrossover product has been reported which does not involve the processing of a double HJ structure. Virtually, the joint molecule formation is followed by extension of the incoming strand by DNA polymerases and branch migration, leading to restoration of the genetic information [283, 302].

**12.2. Non-Homologous End Joining.** When HR is inactivated, an alternate pathway, that is, NHEJ becomes operative for the repair of DSBs [303], that also involves a multi-protein complex and has been found in organisms ranging from a few prokaryotes to mammals. This suggests that this mechanism has been conserved during the course of

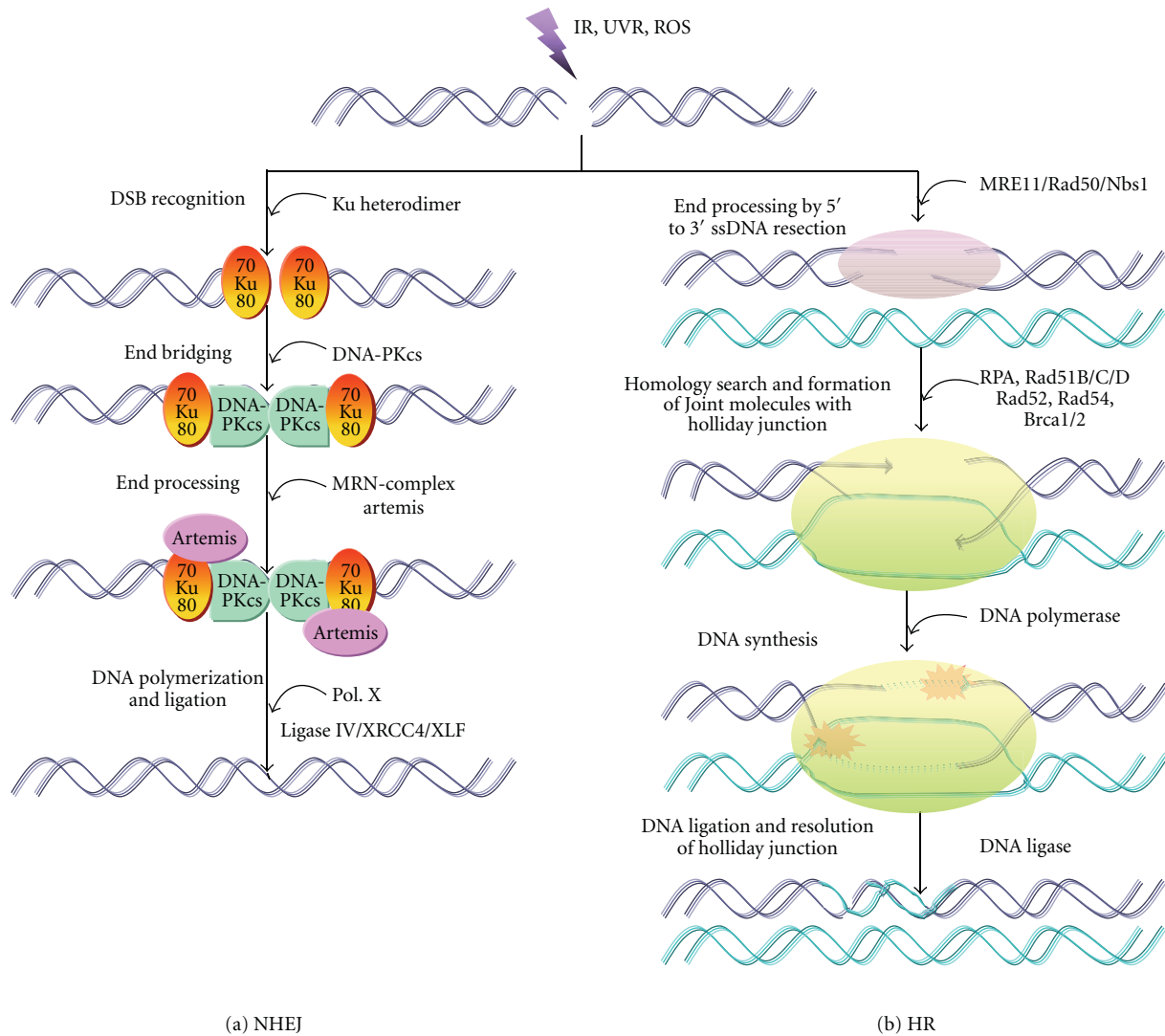


FIGURE 13: Schematic representation of recombinational repair by (a) non-homologous end joining (NHEJ), and (b) homologous recombination (HR).

evolution, although, most of the protein factors, involved in NHEJ were initially identified in the mammalian cells [304]. Most of the DSBs produced by DNA damaging agents, do not have ligatable termini, hence requires the action of nucleases and DNA polymerases to generate them. The participation of DNA polymerase in the NHEJ pathways is still a matter of debate, however in vitro biochemical analysis in mammals, suggest that DNA polymerase  $\lambda$  (Pol.  $\lambda$ ) and/or polymerase  $\mu$  (Pol.  $\mu$ ) participates in NHEJ process at incompatible DNA ends [80, 305, 306]. The NHEJ process is initiated by the binding of specific protein to the broken ends, which may acts as end bridging factor [307]. It has been shown that Ku complex (a heterodimer of Ku70/Ku80 [ $\approx 86$ ]) is a major end binding factor in mammalian cells, possess end bridging activity [308, 309]. The catalytic subunit of DNA protein kinase (DNA-PKcs) is required in mammalian NHEJ to bridge the DNA ends through their protein-protein interactions [310, 311]. Cells lacking functional DNA-PK

components are known to have elevated sensitivity toward UV irradiation [312].

Association of DNA-PKcs is followed by the recruitment of other repair proteins (such as ligaseIV/Xrcc4, Artemis, PNK and Polymerase X) to proceed the NHEJ repair [304] (Figure 13). Recently, a third protein, designated as XLF or Cernunnos [313] that has homology to Xrcc4, has been identified and shown to co-associate with the DNA ligaseIV/Xrcc4 complex [314, 315]. Artemis, a member of  $\beta$ -lactamase superfamily, has 5'  $\rightarrow$  3' exonuclease activity. In the presence of DNA-PKcs, Artemis can also function as a 5'  $\rightarrow$  3' endonuclease. It has been found that Artemis dependant DSB rejoining also requires ATM, Mre11-Rad50-Nbs1 (MRN) complex, 53BP1 and H2AX [316–318]. The yeast Hdf1/2 and Dnl4/Lif1 are the functional homology of mammalian Ku and DNA ligaseIV/Xrcc4, respectively. DNA ligase IV is absent in bacteria, however, in *Bacillus subtilis*, the gene *ykou/v* has been found that encodes a

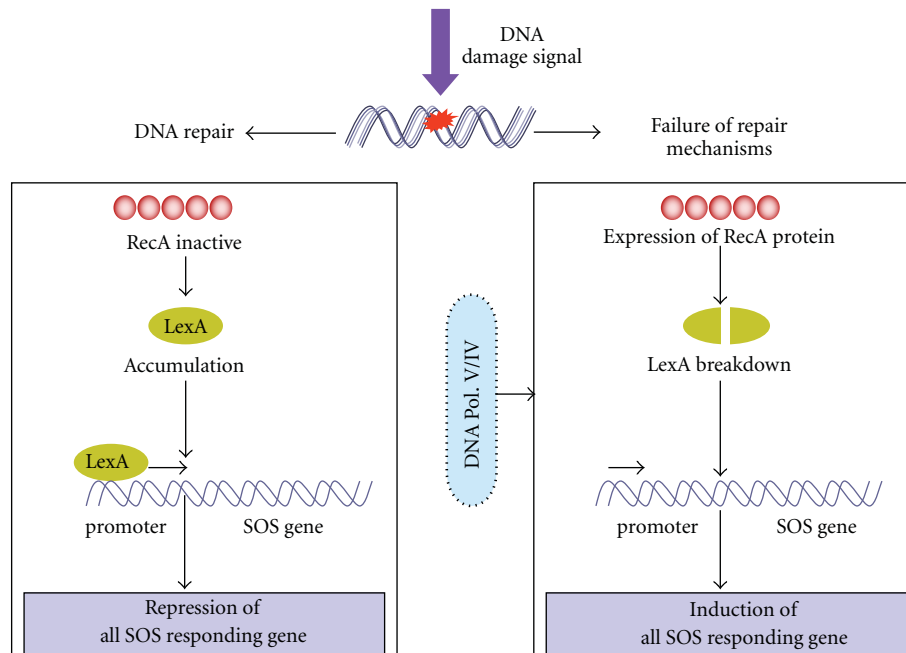


FIGURE 14: SOS response: As a result of massive DNA damage and failure of all possible repair mechanisms, RecA proteins is expressed, which activate the auto breakdown of LexA proteins, allowing the induction of all SOS responding genes. The pathway of SOS response is reversed when damages are repaired through the damage specific mechanisms. Here the inactivation of RecA protein allows the accumulation of LexA, which bind to SOS promoters and repress all SOS responding genes. SOS response is highly mutagenic due to involvement of DNA polymerase V/IV.

polypeptide with ligase, primase and nuclease domains. Genetic and biochemical evidence suggest that Mre11-Rad50-Xrs2 (MRX) act as end bridging factor in yeast NHEJ, since DNA-PKcs is absent in them [319, 320]. In case of bacteria, the Ku proteins occur in homodimeric forms and exhibits homology with eukaryotic Ku protein in some extent [321]. Recombinational repair is a significant UV tolerance mechanism in plants where UV-induced chromosomal rearrangements including homologous intrachromosomal recombination events have been found [296]. Very few of the plant genes involved in DSB repair have been identified. The sequence of an *Arabidopsis* Rad51 homologue has been made available [322]. It has been suggested that as in mammals, breaks are repaired by nonhomologous recombination far more frequently than *via* HR [202, 323].

### 13. SOS Repair/Response

The accumulation of massive amount of DNA lesions within the cells under different specific physiological responses [324] may lead to the occurrence of SOS repair system which was well described in *E. coli*, where the involvement of more than 40 genes have been found [325]. It has been found that the bacterial NER is linked with all DNA damage response through a network of reactions, known as SOS response [326].

The accumulation of DNA lesions may interfere with replication process, prompting cells to stop division, therefore giving time to the cell to repair damaged DNA and

proceeds DNA replication process [324]. SOS repair system is initiated by interaction of two crucial proteins the RecA and the LexA repressor which curbs the expression of SOS genes by binding to their promoters [327] (Figure 14). The proteolytic activity of RecA protein inactivates the LexA repressor and induces all the genes to which LexA is associated. A number of genes (or operon) collectively known as din (damage inducible) gene such as *uvrA*, *uvrB*, *cho* (*uvrC* homolog) and *uvrD* of *E. coli* NER take part in SOS response [325, 328]. The SOS response is induced with damage signal but it is highly mutagenic due to engagement of error-prone DNA polymerase V (UmuC/UmuD<sub>2</sub> complex) [329] and DNA polymerase IV [330] in *E. coli*. Interestingly, it has been found that DNA polymerase IV (*dinB*) is also involved in translesion synthesis in *E. coli* [331]. Majchrzak et al. [324] examined the effects of SOS response on genome stability of trinucleotide repeat sequences (TRS) in *E. coli* and observed that SOS response genes destabilized the TRS tracts and also altered the superhelical density of the plasmids. Recently, the genes *imuA* and *imuB* have been described that induce SOS mutagenesis in *Caulobacter crescentus*, but absent in *E. coli* [332]. However, the number of genes responsible for SOS repair system has still to be investigated.

### 14. Cell-Cycle Checkpoint Activation

In response to diverse genotoxic stresses such as UV radiation, IR, chemicals used in medical therapy, by-products of intra-cellular metabolism, several protective mechanisms

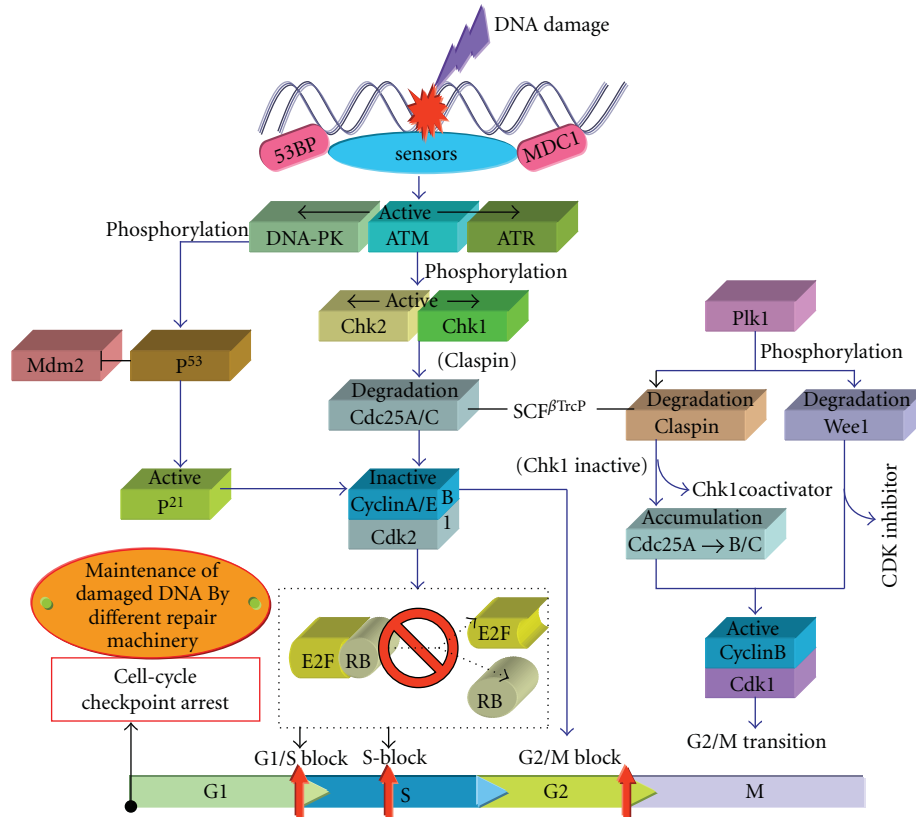


FIGURE 15: Schematic illustration of DNA damage-induced cell-cycle checkpoint activation (for details, see text).

including processes of DNA repair, Cell-cycle checkpoint arrest and apoptosis (programmed cell death) develop within the organisms to secure the genomic integrity. DNA damage such as altered DNA bases, abasic site, DNA lesions (CPDs/6-4PPs), strand breaks (DSBs/SSBs) may stop the progression of cell-cycle temporarily to give opportunities to the cell for DNA repair before replication or segregation of the affected chromosome [333], or may induce an apoptotic program to eliminate the damaged cells to avoid their carcinogenic potential [334]. ROS may induce several types of DNA lesions such as DSBs and SSBs, DNA-DNA and DNA-protein cross links and base modifications [335]. It has been shown that most of the chromosomal translocations produce via aberrant processing of a DNA DSBs. Hence forth, we discuss the DSBs/SSBs-induced cell-cycle checkpoint arrest in eukaryotes mainly in mammals that play a critical role in preventing chromosomal instability. Regulation of cell-cycle checkpoint proceeds through a network of damage sensors, signal transducers, mediators, and various effector proteins [183]. Phosphatidylinositol-3 (PI3)-kinase related kinases (PIKKs) ATM (ataxia telangiectasia mutated) protein, ATR (ATM and Rad3 related) protein, and DNA-PK, with effector proteins mediated cell-cycle checkpoint arrest (at G1/S, G2/M, and intra S-phase), DNA repair and cell death have been observed in mammalian cells [336]. It has been shown that ATM and DNA-PK are activated by the presence of DSBs where as activation of ATR takes place by single strand regions of DNA [337, 338]. Activation of both ATM

and ATR results in phosphorylation of Chk2 and Chk1 respectively which transfer the DNA damage signal to the cell-division cycle proteins Cdc25(A-C). Phosphorylation of Cdc25 by Chk1/Chk2 leads to its ubiquitin mediated degradation that results in G1 and S-phase arrest (Figure 15). The prevailing evidence suggests that damage response mediated activation of ATM/ATR either directly or *via* Chk2 phosphorylates p53, which transcriptionally activates the Cdk inhibitor, p21, which arrest G1/S cell-cycle checkpoint [336]. Recently, it has been reported that DNA damage caused by UV radiation or ROS such as hydroxyl (OH) free-radical results in ATM mediated phosphorylation of BID protein that induce cell-cycle arrest in S-phase [339, 340]. The occurrence of DNA damage response in G2-phase, leads to checkpoint mediator (claspin) dependent activation of Chk1/2, followed by SCF<sup>βTrcP</sup> mediated degradation of CDK-activating phosphatase Cdc25A [341, 342], that results in arrest of multiple cell-cycle transition including the G2 checkpoint [343, 344]. The ubiquitin mediated destruction of claspin and WEE1 (both proteins have conserved β-TrcP phosphodegrons) eliminates the essential coactivator of Chk1 and CDK inhibitor respectively allowing reaccumulation of Cdc25A followed by Cdc25B and C, which results in activation of cyclin-Cdk (cyclinB-Cdk1) complex [345]. Under normal conditions, this latter complex being active promotes G2/M transition and upon inactivation due to DNA damage, blocks the G2 cell-cycle and unlike the G1/S checkpoint this arrest seems to be partly p53/p21

independent [183]. The intermediate component of this pathway is  $\beta$ -TrcP (an adaptor protein) that links both WEE1 [346] and claspin [347–349] with the SCF ubiquitin ligase complex and this SCF <sup>$\beta$ TrcP</sup> acts as trigger of checkpoint initiation where recognition of phosphodegron  $\beta$ -TrcP is exposed after Chk1 mediated Phosphorylation of Cdc25A [350], as well as checkpoint recovery which is linked with Plk1 mediated phosphorylation of claspin and WEE1 [347, 348]. Although, the exact mechanism(s) regarding the reactivation of Plk1 during checkpoint recovery is still in dispute. The malfunctioning of cell-cycle checkpoint as a result of chronic damage and/or defects in DNA damage response (DDR) components such as p53, p21, ATM, Chk2, BRCA1/2 tumor suppressors, may induce several types of human disorder at the expense of enhanced genomic instability [351].

In addition to the above mentioned repair mechanisms several other repair machineries such as mutagenic repair (or lesion bypass) and programmed cell death (PCD) or apoptosis may become effective for the recovery of genome against constant attack of numerous genotoxins. UV-radiation, ionizing radiation and various chemicals are responsible for most of the mutagenesis due to a process of translesion synthesis in which a polymerase or replicative assembly encounters a noncoding or miscoding lesion, inserts an incorrect nucleotide opposite the lesion and then continues elongation [5]. It has been reported that translesion synthesis past a CPD, facilitated by pol.  $\eta$ , with the insertion of adenines opposite both bases of a T<sup>^</sup>T CPD [352], where as 6-4TT may lead to a G insertion. In *Saccharomyces cerevisiae*, pol.  $\eta$  and pol.  $\zeta$  (consisting of Rev3 and Rev7 proteins) has been reported to replicate across a T<sup>^</sup>T CPD [353]. Polymerase  $\eta$  (pol.  $\eta$ ) can also replicate across a basic sites, AAF (acetylaminofluorene), guanine adducts and cis-platinated guanines [352].

When the repair mechanisms are unsuccessful, it may cause cellular senescence (permanent cell cycle arrest), oncogenesis or apoptosis [354]. Apoptosis plays an essential role in survival of the organisms by preventing the multiplication of mutated chromosomes, normal embryonic development, elimination of indisposed cells and maintenance of cell homeostasis.

## Acknowledgments

R. P. Rastogi acknowledges University Grants Commission, New Delhi, India, for financial support in the form of a fellowship. Works related to UV-B radiation effects are partly supported by the project grant sanctioned by Department of Science and Technology, Govt. of India, New Delhi (SR/SO/PS-49/09).

## References

- [1] D. Lubin and E. H. Jensen, "Effects of clouds and stratospheric ozone depletion on ultraviolet radiation trends," *Nature*, vol. 377, no. 6551, pp. 710–713, 1995.
- [2] R. P. Sinha, H. D. Kumar, A. Kumar, and D. P. Häder, "Effects of UV-B irradiation on growth, survival, pigmentation and nitrogen metabolism enzymes in cyanobacteria," *Acta Protozoologica*, vol. 34, no. 3, pp. 187–192, 1995.
- [3] R. P. Sinha, R. P. Rastogi, N. K. Ambasht, and D.-P. Häder, "Life of wetland cyanobacteria under enhancing solar UV-B radiation," *Proceedings of the National Academy of Sciences, India B*, vol. 78, pp. 53–65, 2008.
- [4] D.-P. Häder and R. P. Sinha, "Solar ultraviolet radiation-induced DNA damage in aquatic organisms: potential environmental impact," *Mutation Research*, vol. 571, no. 1-2, pp. 221–233, 2005.
- [5] E. C. Friedberg, G. C. Walker, W. Siede, R. D. Wood, R. A. Schultz, and T. Ellenberger, *DNA Repair and Mutagenesis*, ASM Press, Washington, DC, USA, 2006.
- [6] D.-P. Häder, H. D. Kumar, R. C. Smith, and R. C. Worrest, "Effects of solar UV radiation on aquatic ecosystems and interactions with climate change," *Photochemical and Photobiological Sciences*, vol. 6, no. 3, pp. 267–285, 2007.
- [7] M. Norval, A. P. Cullen, F. R. De Grujil et al., "The effects on human health from stratospheric ozone depletion and its interactions with climate change," *Photochemical and Photobiological Sciences*, vol. 6, no. 3, pp. 232–251, 2007.
- [8] K. R. Solomon, "Effects of ozone depletion and UV-B radiation on humans and the environment," *Atmosphere—Ocean*, vol. 46, no. 1, pp. 185–202, 2008.
- [9] M. Zeeshan and S. M. Prasad, "Differential response of growth, photosynthesis, antioxidant enzymes and lipid peroxidation to UV-B radiation in three cyanobacteria," *South African Journal of Botany*, vol. 75, no. 3, pp. 466–474, 2009.
- [10] M. Llabrés, S. Agustí, P. Alonso-Laita, and G. J. Herndl, "*Synechococcus* and *Prochlorococcus* cell death induced by UV radiation and the penetration of lethal UVR in the Mediterranean Sea," *Marine Ecology Progress Series*, vol. 399, pp. 27–37, 2010.
- [11] A. Tabazadeh, M. L. Santee, M. Y. Danilin et al., "Quantifying denitrification and its effect on ozone recovery," *Science*, vol. 288, no. 5470, pp. 1407–1411, 2000.
- [12] R. L. McKenzie, L. O. Björn, A. Bais, and M. Ilyasd, "Changes in biologically active ultraviolet radiation reaching the Earth's surface," *Photochemical and Photobiological Sciences*, vol. 2, no. 1, pp. 5–15, 2003.
- [13] R. G. Alscher, J. L. Donahue, and C. L. Cramer, "Reactive oxygen species and antioxidants: relationships in green cells," *Physiologia Plantarum*, vol. 100, no. 2, pp. 224–233, 1997.
- [14] L. Chalker-Scott, "Survival and sex ratios of the intertidal copepod, *Tigriopus californicus*, following ultraviolet-B (290–320 nm) radiation exposure," *Marine Biology*, vol. 123, no. 4, pp. 799–804, 1995.
- [15] M. J. Peak and J. G. Peak, "Single-strand breaks induced in *Bacillus subtilis* DNA by ultraviolet light: action spectrum and properties," *Photochemistry and Photobiology*, vol. 35, no. 5, pp. 675–680, 1982.
- [16] M. J. Peak, J. G. Peak, M. P. Moehring, and R. B. Webb, "Ultraviolet action spectra for DNA dimer induction, lethality, and mutagenesis in *Escherichia coli* with emphasis on the UVB region," *Photochemistry and Photobiology*, vol. 40, no. 5, pp. 613–620, 1984.
- [17] R. P. Sinha, M. Dautz, and D.-P. Häder, "A simple and efficient method for the quantitative analysis of thymine dimers in cyanobacteria, phytoplankton and macroalgae," *Acta Protozoologica*, vol. 40, no. 3, pp. 187–195, 2001.
- [18] A. G. J. Buma, M. K. De Boer, and P. Boelen, "Depth distributions of DNA damage in antarctic marine phyto and bacterioplankton exposed to summertime UV radiation," *Journal of Phycology*, vol. 37, no. 2, pp. 200–208, 2001.

- [19] H. Pakker, C. A. C. Beekman, and A. M. Breeman, "Efficient photoreactivation of UVBR-induced DNA damage in the sublittoral macroalga *Rhodomenia pseudopalmeta* (Rhodophyta)," *European Journal of Phycology*, vol. 35, no. 2, pp. 109–114, 2000.
- [20] F. E. Quate, B. M. Sutherland, and J. C. Sutherland, "Quantitation of pyrimidine dimers in DNA from UVB-irradiated alfalfa (*Medicago sativa* L.) seedlings," *Applied and Theoretical Electrophoresis*, vol. 2, no. 6, pp. 171–175, 1992.
- [21] B. Stein, H. J. Rahmsdorf, A. Steffen, M. Litfin, and P. Herrlich, "UV-induced DNA damage is an intermediate step in UV-induced expression of human immunodeficiency virus type 1, collagenase, c-fos, and metallothionein," *Molecular and Cellular Biology*, vol. 9, no. 11, pp. 5169–5181, 1989.
- [22] R. P. Sinha and D.-P. Häder, "UV-induced DNA damage and repair: a review," *Photochemical and Photobiological Sciences*, vol. 1, no. 4, pp. 225–236, 2002.
- [23] K. M. D. Lima-Bessa, M. G. Armelini, V. Chiganças et al., "CPDs and 6–4PPs play different roles in UV-induced cell death in normal and NER-deficient human cells," *DNA Repair*, vol. 7, no. 2, pp. 303–312, 2008.
- [24] K. McAteer, Y. Jing, J. Kao, J.-S. Taylor, and M. A. Kennedy, "Solution-state structure of a DNA dodecamer duplex containing a cis-syn thymine cyclobutane dimer, the major UV photoproduct of DNA," *Journal of Molecular Biology*, vol. 282, no. 5, pp. 1013–1032, 1998.
- [25] J.-H. Lee, G.-S. Hwang, and B.-S. Choi, "Solution structure of a DNA decamer duplex containing the stable 3' T·G base pair of the pyrimidine(6–4)pyrimidone photoproduct [(6–4) adduct]: implications for the highly specific 3' T → C transition of the (6–4) adduct," *Proceedings of the National Academy of Sciences of the United States of America*, vol. 96, no. 12, pp. 6632–6636, 1999.
- [26] J.-H. Lee, S.-H. Bae, and B.-S. Choi, "The Dewar photoproduct of thymidyl(3' → 5')-thymidine (Dewar product) exhibits mutagenic behavior in accordance with the "A rule"," *Proceedings of the National Academy of Sciences of the United States of America*, vol. 97, no. 9, pp. 4591–4596, 2000.
- [27] DeLano Scientific LLC, 400 Oyster Point Blvd., Suite 213, South San Francisco, CA 94080-1918, USA. <http://www.pymol.org/>.
- [28] R. P. Sinha, M. Krywult, and D.-P. Häder, "Effects of ultraviolet, monochromatic and PAR waveband on nitrate reductase activity and pigmentation in a rice field cyanobacterium, *Anabaena* sp.," *Acta Hydrobiologica*, vol. 2, pp. 105–112, 1998.
- [29] R. P. Sinha, S. P. Singh, and D.-P. Häder, "Database on mycosporines and mycosporine-like amino acids (MAAs) in fungi, cyanobacteria, macroalgae, phytoplankton and animals," *Journal of Photochemistry and Photobiology B*, vol. 89, no. 1, pp. 29–35, 2007.
- [30] A. B. Britt, "Repair of DNA damage induced by solar UV," *Photosynthesis Research*, vol. 81, no. 2, pp. 105–112, 2004.
- [31] R. P. Rastogi, Richa, R. P. Sinha, S. P. Singh, and D.-P. Häder, "Photoprotective compounds from marine organisms," *Journal of Industrial Microbiology and Biotechnology*, vol. 37, no. 6, pp. 537–558, 2010.
- [32] R. P. Rastogi, Richa, S. P. Singh, D.-P. Häder, and R. P. Sinha, "Mycosporine-like amino acids profile and their activity under PAR and UVR in a hot-spring cyanobacterium *Scytonema* sp. HKAR-3," *Australian Journal of Botany*, vol. 58, no. 4, pp. 286–293, 2010.
- [33] Z. Xie, Y. Wang, Y. Liu, and Y. Liu, "Ultraviolet-B exposure induces photo-oxidative damage and subsequent repair strategies in a desert cyanobacterium *Microcoleus vaginatus* Gom.," *European Journal of Soil Biology*, vol. 45, no. 4, pp. 377–382, 2009.
- [34] H. Wiseman and B. Halliwell, "Damage to DNA by reactive oxygen and nitrogen species: role in inflammatory disease and progression to cancer," *Biochemical Journal*, vol. 313, no. 1, pp. 17–29, 1996.
- [35] J.-S. Taylor, "DNA, sunlight, and skin cancer," *Journal of Chemical Education*, vol. 67, no. 10, pp. 833–841, 1990.
- [36] T. Lindahl, "Instability and decay of the primary structure of DNA," *Nature*, vol. 362, no. 6422, pp. 709–715, 1993.
- [37] M. Valko, C. J. Rhodes, J. Moncol, M. Izakovic, and M. Mazur, "Free radicals, metals and antioxidants in oxidative stress-induced cancer," *Chemico-Biological Interactions*, vol. 160, no. 1, pp. 1–40, 2006.
- [38] B. Halliwell and J. Gutteridge, *Free Radicals in Biology and Medicine*, Oxford University Press, Oxford, UK, 4th edition, 2007.
- [39] M. Dizdaroglu, "Oxidative damage to DNA in mammalian chromatin," *Mutation Research*, vol. 275, no. 3–6, pp. 331–342, 1992.
- [40] M. Valko, D. Leibfritz, J. Moncol, M. T. D. Cronin, M. Mazur, and J. Telser, "Free radicals and antioxidants in normal physiological functions and human disease," *International Journal of Biochemistry and Cell Biology*, vol. 39, no. 1, pp. 44–84, 2007.
- [41] Y.-H. You, P. E. Szabo, and G. P. Pfeifer, "Cyclobutane pyrimidine dimers form preferentially at the major p<sup>53</sup> mutational hotspot in UVB-induced mouse skin tumors," *Carcinogenesis*, vol. 21, no. 11, pp. 2113–2117, 2000.
- [42] J.-L. Ravanat, T. Douki, and J. Cadet, "Direct and indirect effects of UV radiation on DNA and its components," *Journal of Photochemistry and Photobiology B*, vol. 63, no. 1–3, pp. 88–102, 2001.
- [43] J. Cadet, E. Sage, and T. Douki, "Ultraviolet radiation-mediated damage to cellular DNA," *Mutation Research*, vol. 571, no. 1–2, pp. 3–17, 2005.
- [44] D. I. Pattison and M. J. Davies, "Actions of ultraviolet light on cellular structures," in *Cancer: Cell Structures, Carcinogens and Genomic Instability*, L. P. Bignold, Ed., Birkhäuser, Switzerland, 2006.
- [45] J. S. Taylor, H. F. Lu, and J. J. Kotyk, "Quantitative conversion of the (6–4) photoproduct of TpdC to its Dewar valence isomer upon exposure to simulated sunlight," *Photochemistry and Photobiology*, vol. 51, no. 2, pp. 161–167, 1990.
- [46] S. Courdavault, C. Baudouin, M. Charveron et al., "Repair of the three main types of bipyrimidine DNA photoproducts in human keratinocytes exposed to UVB and UVA radiations," *DNA Repair*, vol. 4, no. 7, pp. 836–844, 2005.
- [47] T. Carell and R. Epple, "Repair of UV light induced DNA lesions: a comparative study with model compounds," *European Journal of Organic Chemistry*, no. 7, pp. 1245–1258, 1998.
- [48] T. Douki, A. Reynaud-Angelin, J. Cadet, and E. Sage, "Bipyrimidine photoproducts rather than oxidative lesions are the main type of DNA damage involved in the genotoxic effect of solar UVA radiation," *Biochemistry*, vol. 42, no. 30, pp. 9221–9226, 2003.
- [49] J. E. Donnellan Jr. and R. B. Setlow, "Thymine photoproducts but not thymine dimers found in ultraviolet-irradiated bacterial spores," *Science*, vol. 149, no. 3681, pp. 308–310, 1965.

- [50] M. M. Becker and Z. Wang, "Origin of ultraviolet damage in DNA," *Journal of Molecular Biology*, vol. 210, no. 3, pp. 429–438, 1989.
- [51] V. Lyamichev, "Unusual conformation of (dA)n.(dT)n-tracts as revealed by cyclobutane thymine-thymine dimer formation," *Nucleic Acids Research*, vol. 19, no. 16, pp. 4491–4496, 1991.
- [52] J. R. Pehrson and L. H. Cohen, "Effects of DNA looping on pyrimidine dimer formation," *Nucleic Acids Research*, vol. 20, no. 6, pp. 1321–1324, 1992.
- [53] A. Aboussekhra and F. Thoma, "TATA-binding protein promotes the selective formation of UV-induced (6–4)-photoproducts and modulates DNA repair in the TATA box," *EMBO Journal*, vol. 18, no. 2, pp. 433–443, 1999.
- [54] T. Douki and J. Cadet, "Individual determination of the yield of the main UV-induced dimeric pyrimidine photoproducts in DNA suggests a high mutagenicity of CC photolesions," *Biochemistry*, vol. 40, no. 8, pp. 2495–2501, 2001.
- [55] A. S. Balajee and V. A. Bohr, "Genomic heterogeneity of nucleotide excision repair," *Gene*, vol. 250, no. 1–2, pp. 15–30, 2000.
- [56] J. M. Gale, K. A. Nissen, and M. J. Smerdon, "UV-induced formation of pyrimidine dimers in nucleosome core DNA is strongly modulated with a period of 10.3 bases," *Proceedings of the National Academy of Sciences of the United States of America*, vol. 84, no. 19, pp. 6644–6648, 1987.
- [57] R. M. Tyrrell, "Induction of pyrimidine dimers in bacterial DNA by 365 nm radiation," *Photochemistry and Photobiology*, vol. 17, no. 1, pp. 69–73, 1973.
- [58] E. Kvam and R. M. Tyrrell, "Induction of oxidative DNA base damage in human skin cells by UV and near visible radiation," *Carcinogenesis*, vol. 18, no. 12, pp. 2379–2384, 1997.
- [59] D. Perdiz, P. Gróf, M. Mezzina, O. Nikaido, E. Moustacchi, and E. Sage, "Distribution and repair of bipyrimidine photoproducts in solar UV-irradiated mammalian cells: possible role of dewar photoproducts in solar mutagenesis," *Journal of Biological Chemistry*, vol. 275, no. 35, pp. 26732–26742, 2000.
- [60] S. Courdavault, C. Baudouin, M. Charveron, A. Favier, J. Cadet, and T. Douki, "Larger yield of cyclobutane dimers than 8-oxo-7,8-dihydroguanine in the DNA of UVA-irradiated human skin cells," *Mutation Research*, vol. 556, no. 1–2, pp. 135–142, 2004.
- [61] D. G. T. Su, J.-S. A. Taylor, and M. L. Gross, "A new photoproduct of 5-methylcytosine and adenine characterized by high-performance liquid chromatography and mass spectrometry," *Chemical Research in Toxicology*, vol. 23, no. 3, pp. 474–479, 2010.
- [62] K. L. Wierzchowski and D. Shugar, "Photochemistry of cytosine nucleosides and nucleotides, II," *Acta Biochimica Polonica*, vol. 8, pp. 219–234, 1961.
- [63] R. J. Boorstein, T. P. Hilbert, R. P. Cunningham, and G. W. Teebor, "Formation and stability of repairable pyrimidine photohydrates in DNA," *Biochemistry*, vol. 29, no. 46, pp. 10455–10460, 1990.
- [64] N. J. Duker and P. E. Gallagher, "Purine photoproducts," *Photochemistry and Photobiology*, vol. 48, no. 1, pp. 35–39, 1988.
- [65] S. Kumar, N. D. Sharma, R. J. Davies, D. W. Phillipson, and J. A. McCloskey, "The isolation and characterisation of a new type of dimeric adenine photoproduct in UV-irradiated deoxyadenylates," *Nucleic Acids Research*, vol. 15, no. 3, pp. 1199–1216, 1987.
- [66] T. M. G. Koning, R. J. H. Davies, and R. Kaptein, "The solution structure of the intramolecular photoproduct of d(TpA) derived with the use of NMR and a combination of distance geometry and molecular dynamics," *Nucleic Acids Research*, vol. 18, no. 2, pp. 277–284, 1990.
- [67] S. N. Bose, R. J. H. Davies, S. K. Sethi, and J. A. McCloskey, "Formation of an adenine-thymine photoadduct in the deoxydinucleoside monophosphate d(TpA) and in DNA," *Science*, vol. 220, no. 4598, pp. 723–725, 1983.
- [68] S. N. Bose and R. J. Davies, "The photoreactivity of T-A sequences in oligodeoxyribonucleotides and DNA," *Nucleic Acids Research*, vol. 12, no. 20, pp. 7903–7914, 1984.
- [69] P. H. Clingen, R. Jeremy, and H. Davies, "Quantum yields of adenine photodimerization in poly(deoxyadenylic acid) and DNA," *Journal of Photochemistry and Photobiology B*, vol. 38, no. 1, pp. 81–87, 1997.
- [70] D. Porschke, "A specific photoreaction in polydeoxyadenylic acid," *Proceedings of the National Academy of Sciences of the United States of America*, vol. 70, no. 9, pp. 2683–2686, 1973.
- [71] N. D. Sharma and R. J. H. Davies, "Extent of formation of a dimeric adenine photoproduct in polynucleotides and DNA," *Journal of Photochemistry and Photobiology B*, vol. 3, no. 2, pp. 247–258, 1989.
- [72] R. O. Rahn, "Search for an adenine photoproduct in DNA," *Nucleic Acids Research*, vol. 3, no. 4, pp. 879–890, 1976.
- [73] P. W. Doetsch, T. H. Zastawny, A. M. Martin, and M. Dizdaroglu, "Monomeric base damage products from adenine, guanine and thymine induced by exposure of DNA to ultraviolet radiation," *Biochemistry*, vol. 34, pp. 737–742, 1995.
- [74] D. B. Hall, R. E. Holmlin, and J. K. Barton, "Oxidative DNA damage through long-range electron transfer," *Nature*, vol. 382, no. 6593, pp. 731–735, 1996.
- [75] M. Lukin and C. de los Santos, "NMR structures of damaged DNA," *Chemical Reviews*, vol. 106, no. 2, pp. 607–686, 2006.
- [76] J.-H. Lee, G.-S. Hwang, J.-K. Kim, and B.-S. Choi, "The solution structure of DNA decamer duplex containing the Dewar product of thymidylyl(3' → 5')thymidine by NMR and full relaxation matrix refinement," *FEBS Letters*, vol. 428, no. 3, pp. 269–274, 1998.
- [77] S. N. Rao, J. W. Keepers, and P. Kollman, "The structure of d(CGCGAAT[ ]TCGCG)-d(CGCGAATTCGCG): the incorporation of a thymine photodimer into a B-DNA helix," *Nucleic Acids Research*, vol. 12, no. 11, pp. 4789–4807, 1984.
- [78] F. E. Hruska, D. J. Wood, K. K. Ogilvie, and J. L. Charlton, "A proton magnetic resonance study of the ultraviolet photoproduct of d(TpT) in aqueous solution," *Canadian Journal of Chemistry*, vol. 53, pp. 1193–1203, 1975.
- [79] L.-S. Kan, L. Voituriez, and J. Cadet, "Nuclear magnetic resonance studies of Cis-Syn, Trans-Syn, and 6–4 photodimers of thymidylyl(3'–5')thymidine monophosphate and Cis-Syn photodimers of thymidylyl(3'–5')thymidine cyanoethyl phosphotriester," *Biochemistry*, vol. 27, no. 15, pp. 5796–5803, 1988.
- [80] J.-H. Lee, C.-J. Park, J.-S. Shin, T. Ikegami, H. Akutsu, and B.-S. Choi, "NMR structure of the DNA decamer duplex containing double T.G mismatches of cis-syn cyclobutane pyrimidine dimer: implications for DNA damage recognition by the XPC-hHR23B complex," *Nucleic Acids Research*, vol. 32, no. 8, pp. 2474–2481, 2004.
- [81] C. Suquet and M. J. Smerdon, "UV damage to DNA strongly influences its rotational setting on the histone surface of reconstituted nucleosomes," *Journal of Biological Chemistry*, vol. 268, no. 32, pp. 23755–23757, 1993.

- [82] A. E. Rumora, K. M. Kolodziejczak, A. M. Wagner, and M. E. Núñez, "Thymine dimer-induced structural changes to the DNA duplex examined with reactive probes," *Biochemistry*, vol. 47, no. 49, pp. 13026–13035, 2008.
- [83] J.-K. Kim and B.-S. Choi, "The solution structure of DNA duplex-decamer containing the (6–4) photoproduct of thymidylyl(3' → 5')thymidine by NMR and relaxation matrix refinement," *European Journal of Biochemistry*, vol. 228, no. 3, pp. 849–854, 1995.
- [84] G.-S. Hwang, J.-K. Kim, and B.-S. Choi, "NMR structural studies of DNA decamer duplex containing the Dewar photoproduct of thymidylyl(3' → 5')thymidine: conformational changes of the oligonucleotide duplex by photoconversion of a (6–4) adduct to its Dewar valence isomer," *European Journal of Biochemistry*, vol. 235, no. 1-2, pp. 359–365, 1996.
- [85] D. A. Pearlman, S. R. Holbrook, D. H. Pirkle, and S.-H. Kim, "Molecular models for DNA damaged by photoreaction," *Science*, vol. 227, no. 4692, pp. 1304–1308, 1985.
- [86] T. V. Wang and K. C. Smith, "Postreplication repair in ultraviolet-irradiated human fibroblasts: formation and repair of DNA double-strand breaks," *Carcinogenesis*, vol. 7, no. 3, pp. 389–392, 1986.
- [87] T. A. Slieman and W. L. Nicholson, "Artificial and solar UV radiation induces strand breaks and cyclobutane pyrimidine dimers in *Bacillus subtilis* spore DNA," *Applied and Environmental Microbiology*, vol. 66, no. 1, pp. 199–205, 2000.
- [88] C. Baumstark-Khan, U. Hentschel, Y. Nikandrova, J. Krug, and G. Horneck, "Fluorometric analysis of DNA unwinding (FADU) as a method for detecting repair-induced DNA strand breaks in UV-irradiated mammalian cells," *Photochemistry and Photobiology*, vol. 72, no. 4, pp. 477–484, 2000.
- [89] R. P. Rastogi, S. P. Singh, D.-P. Häder, and R. P. Sinha, "Detection of reactive oxygen species (ROS) by the oxidant-sensing probe 2',7'-dichlorodihydrofluorescein diacetate in the cyanobacterium *Anabaena variabilis* PCC 7937," *Biochemical and Biophysical Research Communications*, vol. 397, no. 3, pp. 603–607, 2010.
- [90] C. L. Limoli, E. Giedzinski, W. M. Bonner, and J. E. Cleaver, "UV-induced replication arrest in the xeroderma pigmentosum variant leads to DNA doublestrand breaks,  $\gamma$ -H2AX formation, and Mre11 relocalization," *Proceedings of the National Academy of Sciences of the United States of America*, vol. 99, no. 1, pp. 233–238, 2002.
- [91] L. F. Z. Batista, B. Kaina, R. Meneghini, and C. F. M. Menck, "How DNA lesions are turned into powerful killing structures: insights from UV-induced apoptosis," *Mutation Research*, vol. 681, no. 2-3, pp. 197–208, 2009.
- [92] T. R. Dunkern and B. Kaina, "Cell proliferation and DNA breaks are involved in ultraviolet light-induced apoptosis in nucleotide excision repair-deficient Chinese hamster cells," *Molecular Biology of the Cell*, vol. 13, no. 1, pp. 348–361, 2002.
- [93] W. P. Roos and B. Kaina, "DNA damage-induced cell death by apoptosis," *Trends in Molecular Medicine*, vol. 12, no. 9, pp. 440–450, 2006.
- [94] M. M. Vilenchik and A. G. Knudson, "Endogenous DNA double-strand breaks: production, fidelity of repair, and induction of cancer," *Proceedings of the National Academy of Sciences of the United States of America*, vol. 100, no. 22, pp. 12871–12876, 2003.
- [95] A. Takahashi and T. Ohnishi, "Does  $\gamma$ H2AX foci formation depend on the presence of DNA double strand breaks?" *Cancer Letters*, vol. 229, no. 2, pp. 171–179, 2005.
- [96] G. Wang, L. M. Hallberg, E. Saphier, and E. W. Englander, "Short interspersed DNA element-mediated detection of UVB-induced DNA damage and repair in the mouse genome, in vitro, and in vivo in skin," *Mutation Research*, vol. 433, no. 3, pp. 147–157, 1999.
- [97] G. Wang, L. M. Hallberg, E. Saphier, and E. W. Englander, "Pyrimidine (6–4) pyrimidone photoproduct mapping after sub-lethal UVC doses: nucleotide resolution using terminal transferase-dependent PCR," *Photochemistry and Photobiology*, vol. 82, pp. 1370–1376, 2006.
- [98] A. Kumar, M. B. Tyagi, and P. N. Jha, "Evidences showing ultraviolet-B radiation-induced damage of DNA in cyanobacteria and its detection by PCR assay," *Biochemical and Biophysical Research Communications*, vol. 318, no. 4, pp. 1025–1030, 2004.
- [99] A. Karakoula, M. D. Evans, I. D. Podmore, P. E. Hutchinson, J. Lunec, and M. S. Cooke, "Quantification of UVR-induced DNA damage: global- versus gene-specific levels of thymine dimers," *Journal of Immunological Methods*, vol. 277, no. 1-2, pp. 27–37, 2003.
- [100] P. L. Olive, J. P. Banath, and R. E. Durand, "Heterogeneity in radiation-induced DNA damage and repair in tumor and normal cells measured using the 'comet' assay," *Radiation Research*, vol. 122, no. 1, pp. 86–94, 1990.
- [101] N. Morley, A. Rapp, H. Dittmar et al., "UVA-induced apoptosis studied by the new apo/necro-Comet-assay which distinguishes viable, apoptotic and necrotic cells," *Mutagenesis*, vol. 21, no. 2, pp. 105–114, 2006.
- [102] J. L. R. Roti and W. D. Wright, "Visualization of DNA loops in nucleoids from HeLa cells: assays for DNA damage and repair," *Cytometry*, vol. 8, no. 5, pp. 461–467, 1987.
- [103] P. Sestili, C. Martinelli, and V. Stocchi, "The fast halo assay: an improved method to quantify genomic DNA strand breakage at the single-cell level," *Mutation Research*, vol. 607, no. 2, pp. 205–214, 2006.
- [104] J. Chen, K. Jin, M. Chen et al., "Early detection of DNA strand breaks in the brain after transient focal ischemia: implications for the role of DNA damage in apoptosis and neuronal cell death," *Journal of Neurochemistry*, vol. 69, no. 1, pp. 232–245, 1997.
- [105] C. Stecco, A. Porzionato, V. Macchi et al., "Detection of apoptosis in human brainstem by TUNEL assay," *Italian Journal of Anatomy and Embryology*, vol. 110, no. 4, pp. 255–260, 2005.
- [106] F. Xu, J. M. Vlak, A. P. M. Eker, and M. M. van Oers, "DNA photolyases of *Chrysodeixis chalcites* nucleopolyhedrovirus target to the nucleus and interact with chromosomes and mitotic spindle structures," *Journal of General Virology*, vol. 91, pp. 907–914, 2010.
- [107] S. K. Murthy and D. J. Demetrick, "New approaches to fluorescence in situ hybridization," *Methods in Molecular Biology*, vol. 319, pp. 237–259, 2006.
- [108] S. Kumari, R. P. Rastogi, K. L. Singh, S. P. Singh, and R. P. Sinha, "DNA damage: detection strategies," *EXCLI Journal*, vol. 7, pp. 44–62, 2008.
- [109] G. Koopman, C. P. Reutelingsperger, G. A. Kuijten, R. M. Keehnen, and S. T. Pals, "Annexin V for flow cytometric detection of phosphatidylserine expression on B cells undergoing apoptosis," *Blood*, vol. 4, pp. 1415–1420, 1994.
- [110] J. W. Bickham, "Flow cytometry as a technique to monitor the effects of environmental genotoxins on wild life populations," in *In Situ Evaluation of Biological Hazards of Environmental Pollutants*, S. S. Sandhu, W. R. Lower, F. J. de

- Serres, W. A. Suk, and R. R. Tice, Eds., pp. 97–108, Plenum Press, New York, NY, USA, 1990.
- [111] H. Watanabe, Y. Murata, M. Miura, M. Hasegawa, T. Kawamoto, and H. Shibuya, “In-vivo visualization of radiation-induced apoptosis using 125I-annexin V,” *Nuclear Medicine Communications*, vol. 27, no. 1, pp. 81–89, 2006.
- [112] M. Klisch, R. P. Sinha, E. W. Helbling, and D.-P. Häder, “Induction of thymine dimers by solar radiation in natural freshwater phytoplankton assemblages in Patagonia, Argentina,” *Aquatic Sciences*, vol. 67, no. 1, pp. 72–78, 2005.
- [113] S. Otero, E. Núñez-Olivera, J. Martínez-Abaiagar, R. Tomás, M. Arróniz-Crespo, and N. Beaucourt, “Effects of cadmium and enhanced UV radiation on the physiology and the concentration of UV-absorbing compounds of the aquatic liverwort *Jungermannia exsertifolia* subsp. *cordifolia*,” *Photochemical and Photobiological Sciences*, vol. 5, no. 8, pp. 760–769, 2006.
- [114] D. L. Mitchell, C. A. Haipek, and J. M. Clarkson, “(6–4)photoproducts are removed from the DNA of UV-irradiated mammalian cells more efficiently than cyclobutane pyrimidine dimers,” *Mutation Research*, vol. 143, no. 3, pp. 109–112, 1985.
- [115] W. H. Jeffrey, P. Aas, M. M. Lyons, R. B. Coffin, R. J. Pledger, and D. L. Mitchell, “Ambient solar radiation-induced photodamage in marine bacterioplankton,” *Photochemistry and Photobiology*, vol. 64, no. 3, pp. 419–427, 1996.
- [116] H. C. Birnboim and J. J. Jevcak, “Fluorometric method for rapid detection of DNA strand breaks in human white blood cells produced by low doses of radiation,” *Cancer Research*, vol. 41, no. 5, pp. 1889–1892, 1981.
- [117] T. Iwasa, S. Tokutomi, and F. Tokunaga, “Photoreactivation of *Halobacterium halobium*: action spectrum and role of pigmentation,” *Photochemistry and Photobiology*, vol. 47, pp. 267–270, 1988.
- [118] A. Yasui, A. P. M. Eker, S. Yasuhira et al., “A new class of DNA photolyases present in various organisms including aplacental mammals,” *EMBO Journal*, vol. 13, no. 24, pp. 6143–6151, 1994.
- [119] A. Kiener, I. Husain, A. Sancar, and C. Walsh, “Purification and properties of *Methanobacterium thermoautotrophicum* DNA photolyase,” *Journal of Biological Chemistry*, vol. 264, no. 23, pp. 13880–13887, 1989.
- [120] M. Fujihashi, N. Numoto, Y. Kobayashi et al., “Crystal structure of archaeal photolyase from *Sulfolobus tokodaii* with two FAD molecules: implication of a novel light-harvesting cofactor,” *Journal of Molecular Biology*, vol. 365, no. 4, pp. 903–910, 2007.
- [121] K. Malhotra, S.-T. Kim, and A. Sancar, “Characterization of a medium wavelength type DNA photolyase: purification and properties of photolyase from *Bacillus firmus*,” *Biochemistry*, vol. 33, no. 29, pp. 8712–8718, 1994.
- [122] J. L. Johnson, S. Hamm-Alvarez, G. Payne, G. B. Sancar, K. V. Rajagopalan, and A. Sancar, “Identification of the second chromophore of *Escherichia coli* and yeast DNA photolyases as 5,10-methenyltetrahydrofolate,” *Proceedings of the National Academy of Sciences of the United States of America*, vol. 85, no. 7, pp. 2046–2050, 1988.
- [123] G. B. Sancar, F. W. Smith, M. C. Lorence, C. S. Rupert, and A. Sancar, “Sequences of the *Escherichia coli* photolyase gene and protein,” *Journal of Biological Chemistry*, vol. 259, no. 9, pp. 6033–6038, 1984.
- [124] A. P. M. Eker, P. Kooiman, J. K. C. Hessels, and A. Yasui, “DNA photoreactivating enzyme from the cyanobacterium *Anacystis nidulans*,” *Journal of Biological Chemistry*, vol. 265, no. 14, pp. 8009–8015, 1990.
- [125] W.-O. Ng, R. Zentella, Y. Wang, J.-S. A. Taylor, and H. B. Pakrasi, “*phrA*, the major photoreactivating factor in the cyanobacterium *Synechocystis* sp. strain PCC 6803 codes for a cyclobutane-pyrimidine-dimer-specific DNA photolyase,” *Archives of Microbiology*, vol. 173, no. 5-6, pp. 412–417, 2000.
- [126] A. P. Eker, R. H. Dekker, and W. Berends, “Photoreactivating enzyme from *Streptomyces griseus*-IV. On the nature of the chromophoric cofactor in *Streptomyces griseus* photoreactivating enzyme,” *Photochemistry and Photobiology*, vol. 33, no. 1, pp. 65–72, 1981.
- [127] K. A. O’Connor, M. J. McBride, M. West et al., “Photolyase of *Myxococcus xanthus*, a Gram-negative eubacterium, is more similar to photolyases found in archaea and “higher” eukaryotes than to photolyases of other eubacteria,” *Journal of Biological Chemistry*, vol. 271, no. 11, pp. 6252–6259, 1996.
- [128] E. N. Worthington, I. H. Kavakli, G. Berrocal-Tito, B. E. Bondo, and A. Sancar, “Purification and characterization of three members of the photolyase/cryptochrome family blue-light photoreceptors from *Vibrio cholerae*,” *Journal of Biological Chemistry*, vol. 278, no. 40, pp. 39143–39154, 2003.
- [129] H. Yajima, H. Inoue, A. Oikawa, and A. Yasui, “Cloning and functional characterization of a eucaryotic DNA photolyase gene from *Neurospora crassa*,” *Nucleic Acids Research*, vol. 19, no. 19, pp. 5359–5362, 1991.
- [130] A. P. M. Eker, H. Yajima, and A. Yasui, “DNA photolyase from the fungus *Neurospora crassa*. Purification, characterization and comparison with other photolyases,” *Photochemistry and Photobiology*, vol. 60, no. 2, pp. 125–133, 1994.
- [131] T. Todo, H. Takemori, H. Ryo et al., “A new photoreactivating enzyme that specifically repairs ultraviolet light-induced (6–4)photoproducts,” *Nature*, vol. 361, no. 6410, pp. 371–374, 1993.
- [132] A. Sancar, “No “End of history” for photolyases,” *Science*, vol. 272, no. 5258, pp. 48–49, 1996.
- [133] S. Yasuhira and A. Yasui, “Visible light-inducible photolyase gene from the goldfish *Carassius auratus*,” *Journal of Biological Chemistry*, vol. 267, no. 36, pp. 25644–25647, 1992.
- [134] T. S. Mikkelsen, M. J. Wakefield, B. Aken et al., “Genome of the marsupial *Monodelphis domestica* reveals innovation in non-coding sequences,” *Nature*, vol. 447, no. 7141, pp. 167–177, 2007.
- [135] T. Todo, S.-T. Kim, K. Hitomi et al., “Flavin adenine dinucleotide as a chromophore of the *Xenopus* (6–4)photolyase,” *Nucleic Acids Research*, vol. 25, no. 4, pp. 764–768, 1997.
- [136] Q. Pang and J. B. Hays, “UV-B-inducible and temperature-sensitive photoreactivation of cyclobutane pyrimidine dimers in *Arabidopsis thaliana*,” *Plant Physiology*, vol. 95, no. 2, pp. 536–543, 1991.
- [137] J. L. Petersen, D. W. Lang, and G. D. Small, “Cloning and characterization of a class II DNA photolyase from *Chlamydomonas*,” *Plant Molecular Biology*, vol. 40, no. 6, pp. 1063–1071, 1999.
- [138] S. Takahashi, N. Nakajima, H. Saji, and N. Kondo, “Diurnal changes of cucumber CPD photolyase gene (CsPHR) expression and its physiological role in growth under UV-B irradiation,” *Plant and Cell Physiology*, vol. 43, pp. 342–349, 2002.

- [139] Y. Takeuchi, T. Inoue, K. Takemura et al., "Induction and inhibition of cyclobutane pyrimidine dimer photolyase in etiolated cucumber (*Cucumis sativus*) cotyledons after ultraviolet irradiation depends on wavelength," *Journal of Plant Research*, vol. 120, pp. 365–374, 2007.
- [140] J. E. Trosko and V. H. Mansour, "Photoreactivation of ultraviolet light-induced pyrimidine dimers in *Ginkgo* cells grown in vitro," *Mutation Research*, vol. 7, no. 1, pp. 120–121, 1969.
- [141] R. Taylor, A. Tobin, and C. Bray, "Nucleotide sequence of an *Arabidopsis* cDNA At-phrII encoding a protein with high homology to the class II CPD photolyases present in higher eukaryotes," *Plant Physiology*, vol. 112, pp. 862–863, 1996.
- [142] V. Srinivasan, W. M. Schnitzlein, and D. N. Tripathy, "Fowlpox virus encodes a novel DNA repair enzyme, CPD-photolyase, that restores infectivity of UV light-damaged virus," *Journal of Virology*, vol. 75, no. 4, pp. 1681–1688, 2001.
- [143] C. L. Afonso, E. R. Tulman, Z. Lu, E. Oma, G. F. Kutish, and D. L. Rock, "The genome of *Melanoplus sanguinipes* entomopoxvirus," *Journal of Virology*, vol. 73, no. 1, pp. 533–552, 1999.
- [144] T. Ohnishi, E. Mori, and A. Takahashi, "DNA double-strand breaks: their production, recognition, and repair in eukaryotes," *Mutation Research*, vol. 669, no. 1–2, pp. 8–12, 2009.
- [145] D. Strumberg, A. A. Pilon, M. Smith, R. Hickey, L. Malkas, and Y. Pommier, "Conversion of topoisomerase I cleavage complexes on the leading strand of ribosomal DNA into 5'-phosphorylated DNA double-strand breaks by replication runoff," *Molecular and Cellular Biology*, vol. 20, no. 11, pp. 3977–3987, 2000.
- [146] H. C. Box, J. B. Dawidzik, and E. E. Budzinski, "Free radical-induced double lesions in DNA," *Free Radical Biology and Medicine*, vol. 31, no. 7, pp. 856–868, 2001.
- [147] J. P. Banáth and P. L. Olive, "Expression of phosphorylated histone H2AX as a surrogate of cell killing by drugs that create DNA double-strand breaks," *Cancer Research*, vol. 63, no. 15, pp. 4347–4350, 2003.
- [148] J. V. Harper, J. A. Anderson, and P. O'Neill, "Radiation induced DNA DSBs: contribution from stalled replication forks?" *DNA Repair*, vol. 9, pp. 907–913, 2010.
- [149] S. E. Freeman, A. D. Blackett, and D. C. Monteleone, "Quantitation of radiation-, chemical-, or enzyme-induced single strand breaks in nonradioactive DNA by alkaline gel electrophoresis: application to pyrimidine dimers," *Analytical Biochemistry*, vol. 158, no. 1, pp. 119–129, 1986.
- [150] D. L. Mitchell, J. Jen, and J. E. Cleaver, "Relative induction of cyclobutane dimers and cytosine photohydrates in DNA irradiated in vitro and in vivo with ultraviolet-C and ultraviolet-B light," *Photochemistry and Photobiology*, vol. 54, no. 5, pp. 741–746, 1991.
- [151] B. Thyagarajan, K. E. Anderson, C. J. Lessard et al., "Alkaline unwinding flow cytometry assay to measure nucleotide excision repair," *Mutagenesis*, vol. 22, no. 2, pp. 147–153, 2007.
- [152] P. Kara, K. Dağdeviren, and M. Özsöz, "An electrochemical DNA biosensor for the detection of DNA damage caused by radioactive iodine and technetium," *Turkish Journal of Chemistry*, vol. 31, no. 3, pp. 243–249, 2007.
- [153] A. Hollaender and J. T. Curtis, "Effects of sublethal doses of monochromatic ultraviolet radiation on bacteria in liquid suspension," *Proceedings of the Society for Experimental Biology and Medicine*, vol. 33, pp. 61–62, 1935.
- [154] A. Kelner, "Effects of visible light on the recovery of *Streptomyces griseus* conidia from ultraviolet irradiation injury," *Proceedings of the National Academy of Sciences of the United States of America*, vol. 35, pp. 73–79, 1949.
- [155] R. Dulbecco, "Reactivation of ultra-violet-inactivated bacteriophage by visible light," *Nature*, vol. 163, no. 4155, pp. 949–950, 1949.
- [156] J. Essers, W. Vermeulen, and A. B. Houtsmuller, "DNA damage repair: anytime, anywhere?" *Current Opinion in Cell Biology*, vol. 18, no. 3, pp. 240–246, 2006.
- [157] S.-T. Kim, P. F. Heelis, and A. Sancar, "Energy transfer (deazaflavin → FADH2) and electron transfer (FADH2 → T<>T) kinetics in *Anacystis nidulans* photolyase," *Biochemistry*, vol. 31, no. 45, pp. 11244–11248, 1992.
- [158] L. O. Essen and T. Klar, "Light-driven DNA repair by photolyases," *Cellular and Molecular Life Sciences*, vol. 63, no. 11, pp. 1266–1277, 2006.
- [159] A. B. Britt, "DNA damage and repair in plants," *Annual Review of Plant Physiology and Plant Molecular Biology*, vol. 47, no. 1, pp. 75–100, 1996.
- [160] T. Todo, "Functional diversity of the DNA photolyase/blue light receptor family," *Mutation Research*, vol. 434, no. 2, pp. 89–97, 1999.
- [161] B. M. Sutherland, "Photoreactivating enzyme from human leukocytes," *Nature*, vol. 248, no. 5444, pp. 109–112, 1974.
- [162] B. M. Sutherland and P. V. Bennett, "Human white blood cells contain cyclobutyl pyrimidine dimer photolyase," *Proceedings of the National Academy of Sciences of the United States of America*, vol. 92, no. 21, pp. 9732–9736, 1995.
- [163] H. Harm, "Damage and repair in mammalian cells after exposure to non-ionizing radiations. III. Ultraviolet and visible light irradiation of cells of placental mammals, including humans, and determination of photorepairable damage in vitro," *Mutation Research*, vol. 69, no. 1, pp. 167–176, 1980.
- [164] D. S. Hsu, X. Zhao, S. Zhao et al., "Putative human blue-light photoreceptors hCRY1 and hCRY2 are flavoproteins," *Biochemistry*, vol. 35, no. 44, pp. 13871–13877, 1996.
- [165] T. Ueda, A. Kato, S. Kuramitsu, H. Terasawa, and I. Shimada, "Identification and characterization of a second chromophore of DNA photolyase from *Thermus thermophilus* HB27," *Journal of Biological Chemistry*, vol. 280, no. 43, pp. 36237–36243, 2005.
- [166] C. Saxena, A. Sancar, and D. Zhong, "Femtosecond dynamics of DNA photolyase: energy transfer of antenna initiation and electron transfer of cofactor reduction," *Journal of Physical Chemistry B*, vol. 108, no. 46, pp. 18026–18033, 2004.
- [167] Y.-T. Kao, C. Saxena, L. Wang, A. Sancar, and D. Zhong, "Direct observation of thymine dimer repair in DNA by photolyase," *Proceedings of the National Academy of Sciences of the United States of America*, vol. 102, no. 45, pp. 16128–16132, 2005.
- [168] A. E. Stapleton and V. Walbot, "Flavonoids can protect maize DNA from the induction of ultraviolet radiation damage," *Plant Physiology*, vol. 105, no. 3, pp. 881–889, 1994.
- [169] R. Schmitz-Hoerner and G. Weissenböck, "Contribution of phenolic compounds to the UV-B screening capacity of developing barley primary leaves in relation to DNA damage and repair under elevated UV-B levels," *Phytochemistry*, vol. 64, pp. 243–255, 2003.
- [170] G. Kaiser, O. Kleiner, C. Beisswenger, and A. Batschauer, "Increased DNA repair in *Arabidopsis* plants overexpressing CPD photolyase," *Planta*, vol. 230, no. 3, pp. 505–515, 2009.

- [171] N. Tuteja, M. B. Singh, M. K. Misra, P. L. Bhalla, and R. Tuteja, "Molecular mechanisms of DNA damage and repair: progress in plants," *Critical Reviews in Biochemistry and Molecular Biology*, vol. 36, no. 4, pp. 337–397, 2001.
- [172] S. Kimura, Y. Tahira, T. Ishibashi et al., "DNA repair in higher plants; photoreactivation is the major DNA repair pathway in non-proliferating cells while excision repair (nucleotide excision repair and base excision repair) is active in proliferating cells," *Nucleic Acids Research*, vol. 32, pp. 2760–2767, 2004.
- [173] J. J. Chen, D. L. Mitchell, and A. B. Britt, "A light-dependent pathway for the elimination of UV-induced pyrimidine (6–4) pyrimidinone photoproducts in *Arabidopsis*," *Plant Cell*, vol. 6, no. 9, pp. 1311–1317, 1994.
- [174] H.-S. Kang, J. Hidema, and T. Kumagai, "Effects of light environment during culture on UV-induced cyclobutyl pyrimidine dimers and their photorepair in rice (*Oryza sativa* L.)," *Photochemistry and Photobiology*, vol. 68, no. 1, pp. 71–77, 1998.
- [175] A. Mees, T. Klar, P. Gnau et al., "Crystal structure of a photolyase bound to a CPD-like DNA lesion after in situ repair," *Science*, vol. 306, no. 5702, pp. 1789–1793, 2004.
- [176] T. Torizawa, T. Ueda, S. Kuramitsu et al., "Investigation of the cyclobutane pyrimidine dimer (CPD) photolyase DNA recognition mechanism by NMR analyses," *Journal of Biological Chemistry*, vol. 279, no. 31, pp. 32950–32956, 2004.
- [177] P. F. Heelis, R. F. Hartman, and S. D. Rose, "Photoenzymic repair of UV-damaged DNA—a chemist's perspective," *Chemical Society Reviews*, vol. 24, no. 4, pp. 289–297, 1995.
- [178] A. W. MacFarlane and R. J. Stanley, "Cis-Syn thymidine dimer repair by DNA photolyase in real time," *Biochemistry*, vol. 42, no. 28, pp. 8558–8568, 2003.
- [179] I. H. Kavakli and A. Sancar, "Analysis of the role of intraprotein electron transfer in photoreactivation by DNA photolyase in vivo," *Biochemistry*, vol. 43, no. 48, pp. 15103–15110, 2004.
- [180] E. Schleicher, B. Heßling, V. Illarionova et al., "Light-induced reactions of *Escherichia coli* DNA photolyase monitored by Fourier transform infrared spectroscopy," *FEBS Journal*, vol. 272, no. 8, pp. 1855–1866, 2005.
- [181] G. B. Sancar and F. W. Smith, "Interactions between yeast photolyase and nucleotide excision repair proteins in *Saccharomyces cerevisiae* and *Escherichia coli*," *Molecular and Cellular Biology*, vol. 9, no. 11, pp. 4767–4776, 1989.
- [182] E. Seeberg, L. Eide, and M. Bjørås, "The base excision repair pathway," *Trends in Biochemical Sciences*, vol. 20, no. 10, pp. 391–397, 1995.
- [183] J. H. Houtgraaf, J. Versmissen, and W. J. van der Giessen, "A concise review of DNA damage checkpoints and repair in mammalian cells," *Cardiovascular Revascularization Medicine*, vol. 7, no. 3, pp. 165–172, 2006.
- [184] K. H. Almeida and R. W. Sobol, "A unified view of base excision repair: lesion-dependent protein complexes regulated by post-translational modification," *DNA Repair*, vol. 6, no. 6, pp. 695–711, 2007.
- [185] K. Hitomi, S. Iwai, and J. A. Tainer, "The intricate structural chemistry of base excision repair machinery: implications for DNA damage recognition, removal, and repair," *DNA Repair*, vol. 6, no. 4, pp. 410–428, 2007.
- [186] A. B. Robertson, A. Klungland, T. Rognes, and I. Leiros, "Base excision repair: the long and short of it," *Cellular and Molecular Life Sciences*, vol. 66, no. 6, pp. 981–993, 2009.
- [187] D. E. Barnes and T. Lindahl, "Repair and genetic consequences of endogenous DNA base damage in mammalian cells," *Annual Review of Genetics*, vol. 38, pp. 445–476, 2004.
- [188] J. L. Parsons, P. S. Tait, D. Finch, I. I. Dianova, S. L. Allinson, and G. L. Dianov, "CHIP-mediated degradation and DNA damage-dependent stabilization regulate base excision repair proteins," *Molecular Cell*, vol. 29, no. 4, pp. 477–487, 2008.
- [189] K. W. Caldecott, "XRCC1 and DNA strand break repair," *DNA Repair*, vol. 2, no. 9, pp. 955–969, 2003.
- [190] L. Lan, S. Nakajima, Y. Oohata et al., "In situ analysis of repair processes for oxidative DNA damage in mammalian cells," *Proceedings of the National Academy of Sciences of the United States of America*, vol. 101, no. 38, pp. 13738–13743, 2004.
- [191] K. Sakumi and M. Sekiguchi, "Structures and functions of DNA glycosylases," *Mutation Research*, vol. 236, no. 2-3, pp. 161–172, 1990.
- [192] Y. Matsumoto and K. Kim, "Excision of deoxyribose phosphate residues by DNA polymerase  $\beta$  during DNA repair," *Science*, vol. 269, no. 5224, pp. 699–702, 1995.
- [193] B. Demple and L. Harrison, "Repair of oxidative damage to DNA: enzymology and biology," *Annual Review of Biochemistry*, vol. 63, pp. 915–948, 1994.
- [194] L. Gros, A. A. Ishchenko, H. Ide, R. H. Elder, and M. K. Saparbaev, "The major human AP endonuclease (Ape1) is involved in the nucleotide incision repair pathway," *Nucleic Acids Research*, vol. 32, no. 1, pp. 73–81, 2004.
- [195] P. Fortini and E. Dogliotti, "Base damage and single-strand break repair: mechanisms and functional significance of short- and long-patch repair subpathways," *DNA Repair*, vol. 6, no. 4, pp. 398–409, 2007.
- [196] U. Sattler, P. Frit, B. Salles, and P. Calsou, "Long-patch DNA repair synthesis during base excision repair in mammalian cells," *EMBO Reports*, vol. 4, no. 4, pp. 363–367, 2003.
- [197] W. D. Henner, S. M. Grunberg, and W. A. Haseltine, "Enzyme action at 3' termini of ionizing radiation-induced DNA strand breaks," *Journal of Biological Chemistry*, vol. 258, no. 24, pp. 15198–151205, 1983.
- [198] W. D. Henner, L. O. Rodriguez, S. M. Hecht, and W. A. Haseltine, "gamma Ray induced deoxyribonucleic acid strand breaks. 3' Glycolate termini," *Journal of Biological Chemistry*, vol. 258, no. 2, pp. 711–713, 1983.
- [199] A. Jilani, D. Ramotar, C. Slack et al., "Molecular cloning of the human gene, PNKP, encoding a polynucleotide kinase 3'-phosphatase and evidence for its role in repair of DNA strand breaks caused by oxidative damage," *Journal of Biological Chemistry*, vol. 274, no. 34, pp. 24176–24186, 1999.
- [200] R. Gary, K. Kim, H. L. Cornelius, M. S. Park, and Y. Matsumoto, "Proliferating cell nuclear antigen facilitates excision in long-patch base excision repair," *Journal of Biological Chemistry*, vol. 274, no. 7, pp. 4354–4363, 1999.
- [201] P. Fortini, B. Pascucci, E. Parlanti, R. W. Sobol, S. H. Wilson, and E. Dogliotti, "Different DNA polymerases are involved in the short- and long-patch base excision repair in mammalian cells," *Biochemistry*, vol. 37, no. 11, pp. 3575–3580, 1998.
- [202] A. B. Britt, "Molecular genetics of DNA repair in higher plants," *Trends in Plant Science*, vol. 4, no. 1, pp. 20–25, 1999.
- [203] J. B. Hays, "*Arabidopsis thaliana*, a versatile model system for study of eukaryotic genome-maintenance functions," *DNA Repair*, vol. 1, no. 8, pp. 579–600, 2002.
- [204] E. Hefner, S. B. Preuss, and A. B. Britt, "*Arabidopsis* mutants sensitive to gamma radiation include the homologue of the human repair gene ERCC1," *Journal of Experimental Botany*, vol. 54, no. 383, pp. 669–680, 2003.

- [205] A. G. McLennan, "The repair of ultraviolet light-induced DNA damage in plant cells," *Mutation Research*, vol. 181, no. 1, pp. 1–7, 1987.
- [206] E. J. Vonarx, H. L. Mitchell, R. Karthikeyan, I. Chatterjee, and B. A. Kunz, "DNA repair in higher plants," *Mutation Research*, vol. 400, no. 1-2, pp. 187–200, 1998.
- [207] E. Dandoy, R. Schyns, R. Deltour, and W. G. Verly, "Appearance and repair of apurinic/apyrimidinic sites in DNA during early germination of *Zea mays*," *Mutation Research*, vol. 181, no. 1, pp. 57–60, 1987.
- [208] M. Talpaert-Borlè and M. Liuzzi, "Base-excision repair in carrot cells," *European Journal of Biochemistry*, vol. 124, no. 3, pp. 435–440, 1982.
- [209] R. T. Hess, U. Schwitter, M. Petretta, B. Giese, and H. Naegeli, "Bipartite substrate discrimination by human nucleotide excision repair," *Proceedings of the National Academy of Sciences of the United States of America*, vol. 94, no. 13, pp. 6664–6669, 1997.
- [210] R. M. A. Costa, V. Chigaças, R. D. S. Galhardo, H. Carvalho, and C. F. M. Menck, "The eukaryotic nucleotide excision repair pathway," *Biochimie*, vol. 85, no. 11, pp. 1083–1099, 2003.
- [211] A. Van Hoffen, J. Venema, R. Meschini, A. A. Van Zeeland, and L. H. F. Mullenders, "Transcription-coupled repair removes both cyclobutane pyrimidine dimers and 6–4 photoproducts with equal efficiency and in a sequential way from transcribed DNA in xeroderma pigmentosum group C fibroblasts," *EMBO Journal*, vol. 14, no. 2, pp. 360–367, 1995.
- [212] R. P. Boyce and P. Howard-Flanders, "Release of ultraviolet light-induced thymine dimers from DNA in *E. coli* K-12," *Proceedings of the National Academy of Sciences of the United States of America*, vol. 51, pp. 293–300, 1964.
- [213] D. E. Pettijohn and P. C. Hanawalt, "Evidence for repair-replication of ultraviolet damaged DNA in bacteria," *Journal of Molecular Biology*, vol. 9, pp. 395–410, 1964.
- [214] J.-J. Lin and A. Sancar, "Reconstitution of nucleotide excision nuclease with UvrA and UvrB proteins from *Escherichia coli* and UvrC protein from *Bacillus subtilis*," *Journal of Biological Chemistry*, vol. 265, no. 34, pp. 21337–21341, 1990.
- [215] D. K. Orren, P. Selby, J. E. Hearst, and A. Sancar, "Post-incision steps of nucleotide excision repair in *Escherichia coli*. Disassembly of the UvrBC-DNA complex by helicase II and DNA polymerase I," *The Journal of Biological Chemistry*, vol. 267, pp. 780–788, 1992.
- [216] T. Nospikel, "Nucleotide excision repair: variations on versatility," *Cellular and Molecular Life Sciences*, vol. 66, no. 6, pp. 994–1009, 2009.
- [217] S. W. Matson, D. W. Bean, and J. W. George, "DNA helicases: enzymes with essential roles in all aspects of DNA metabolism," *BioEssays*, vol. 16, no. 1, pp. 13–22, 1994.
- [218] K. A. Henning, L. Li, N. Iyer et al., "The Cockayne syndrome group A gene encodes a WD repeat protein that interacts with CSB protein and a subunit of RNA polymerase II TFIIF," *Cell*, vol. 82, no. 4, pp. 555–564, 1995.
- [219] C. P. Selby and A. Sancar, "Human transcription-repair coupling factor CSB/ERCC6 is a DNA-stimulated ATPase but is not a helicase and does not disrupt the ternary transcription complex of stalled RNA polymerase II," *Journal of Biological Chemistry*, vol. 272, no. 3, pp. 1885–1890, 1997.
- [220] P. C. Hanawalt, B. A. Donahue, and K. S. Sweder, "Repair and transcription: collision or collusion?" *Current Biology*, vol. 4, no. 6, pp. 518–522, 1994.
- [221] S. Tornaletti and P. C. Hanawalt, "Effect of DNA lesions on transcription elongation," *Biochimie*, vol. 81, no. 1-2, pp. 139–146, 1999.
- [222] J. N. Ratner, B. Balasubramanian, J. Corden, S. L. Warren, and D. B. Bregman, "Ultraviolet radiation-induced ubiquitination and proteasomal degradation of the large subunit of RNA polymerase II: implications for transcription-coupled DNA repair," *Journal of Biological Chemistry*, vol. 273, no. 9, pp. 5184–5189, 1998.
- [223] A. Sarasin and A. Stary, "New insights for understanding the transcription-coupled repair pathway," *DNA Repair*, vol. 6, no. 2, pp. 265–269, 2007.
- [224] M. Foustieri, W. Vermeulen, A. A. van Zeeland, and L. H. F. Mullenders, "Cockayne syndrome A and B proteins differentially regulate recruitment of chromatin remodeling and repair factors to stalled RNA polymerase II in vivo," *Molecular Cell*, vol. 23, no. 4, pp. 471–482, 2006.
- [225] L. Proietti-De-Santis, P. Drané, and J.-M. Egly, "Cockayne syndrome B protein regulates the transcriptional program after UV irradiation," *EMBO Journal*, vol. 25, no. 9, pp. 1915–1923, 2006.
- [226] K. Sugawara, J. M. Y. Ng, C. Masutani et al., "Xeroderma pigmentosum group C protein complex is the initiator of global genome nucleotide excision repair," *Molecular Cell*, vol. 2, no. 2, pp. 223–232, 1998.
- [227] W. L. De Laat, N. G. J. Jaspers, and J. H. J. Hoeijmakers, "Molecular mechanism of nucleotide excision repair," *Genes and Development*, vol. 13, no. 7, pp. 768–785, 1999.
- [228] L. C. J. Gillet and O. D. Schärer, "Molecular mechanisms of mammalian global genome nucleotide excision repair," *Chemical Reviews*, vol. 106, no. 2, pp. 253–276, 2006.
- [229] C. Petit and A. Sancar, "Nucleotide excision repair: from *E. coli* to man," *Biochimie*, vol. 81, no. 1-2, pp. 15–25, 1999.
- [230] C. Masutani, K. Sugawara, J. Yanagisawa et al., "Purification and cloning of a nucleotide excision repair complex involving the xeroderma pigmentosum group C protein and a human homologue of yeast RAD23," *EMBO Journal*, vol. 13, no. 8, pp. 1831–1843, 1994.
- [231] M. Araki, C. Masutani, M. Takemura et al., "Centrosome protein centrin 2/caltractin 1 is part of the xeroderma pigmentosum group C complex that initiates global genome nucleotide excision repair," *Journal of Biological Chemistry*, vol. 276, no. 22, pp. 18665–18672, 2001.
- [232] L. Schaeffer, R. Roy, S. Humbert et al., "DNA repair helicase: a component of BTF2 (TFIIH) basic transcription factor," *Science*, vol. 260, pp. 58–63, 1993.
- [233] F. Coin, V. Oksenysh, and J.-M. Egly, "Distinct roles for the XPB/p52 and XPD/p44 subcomplexes of TFIIH in damaged DNA opening during nucleotide excision repair," *Molecular Cell*, vol. 26, no. 2, pp. 245–256, 2007.
- [234] L. Schaeffer, V. Moncollin, R. Roy et al., "The ERCC2/DNA repair protein is associated with the class II BTF2/TFIIH transcription factor," *EMBO Journal*, vol. 13, no. 10, pp. 2388–2392, 1994.
- [235] J. Chen, S. Larochelle, X. Li, and B. Suter, "Xpd/Ercc2 regulates CAK activity and mitotic progression," *Nature*, vol. 424, no. 6945, pp. 228–232, 2003.
- [236] P. Schultz, S. Fribourg, A. Poterszman, V. Mallouh, D. Moras, and J. M. Egly, "Molecular structure of human TFIIH," *Cell*, vol. 102, no. 5, pp. 599–607, 2000.
- [237] J. A. Ranish, S. Hahn, Y. Lu et al., "Identification of TFB5, a new component of general transcription and DNA repair factor IIIH," *Nature Genetics*, vol. 36, no. 7, pp. 707–713, 2004.

- [238] C. J. Jones and R. D. Wood, "Preferential binding of the xeroderma pigmentosum group A complementing protein to damaged DNA," *Biochemistry*, vol. 32, no. 45, pp. 12096–12104, 1993.
- [239] T. Matsuda, M. Saijo, I. Kuraoka et al., "DNA repair protein XPA binds replication protein A (RPA)," *Journal of Biological Chemistry*, vol. 270, no. 8, pp. 4152–4157, 1995.
- [240] E. Stigger, R. Drissi, and S.-H. Lee, "Functional analysis of human replication protein A in nucleotide excision repair," *Journal of Biological Chemistry*, vol. 273, no. 15, pp. 9337–9343, 1998.
- [241] Z. He, L. A. Henricksen, M. S. Wold, and C. J. Ingles, "RPA involvement in the damage-recognition and incision steps of nucleotide excision repair," *Nature*, vol. 374, no. 6522, pp. 566–569, 1995.
- [242] J. L. Burns, S. N. Guzder, P. Sung, S. Prakash, and L. Prakash, "An affinity of human replication protein A for ultraviolet-damaged DNA: implications for damage recognition in nucleotide excision repair," *Journal of Biological Chemistry*, vol. 271, no. 20, pp. 11607–11610, 1996.
- [243] E. Evans, J. G. Moggs, J. R. Hwang, J.-M. Egly, and R. D. Wood, "Mechanism of open complex and dual incision formation by human nucleotide excision repair factors," *EMBO Journal*, vol. 16, no. 21, pp. 6559–6573, 1997.
- [244] A. H. Sarker, S. E. Tsutakawa, S. Kostek et al., "Recognition of RNA polymerase II and transcription bubbles by XPG, CSB, and TFIIH: insights for transcription-coupled repair and Cockayne syndrome," *Molecular Cell*, vol. 20, no. 2, pp. 187–198, 2005.
- [245] K. G. Cloud, B. Shen, G. F. Strniste, and M. S. Park, "XPG protein has a structure-specific endonuclease activity," *Mutation Research*, vol. 347, no. 2, pp. 55–60, 1995.
- [246] W. L. De Laat, E. Appeldoorn, N. G. J. Jaspers, and J. H. J. Hoeijmakers, "DNA structural elements required for ERCC1-XPF endonuclease activity," *Journal of Biological Chemistry*, vol. 273, no. 14, pp. 7835–7842, 1998.
- [247] J. H. Enzlin and O. D. Schärer, "The active site of the DNA repair endonuclease XPF-ERCC1 forms a highly conserved nuclease motif," *EMBO Journal*, vol. 21, no. 8, pp. 2045–2053, 2002.
- [248] R. D. Wood, "Nucleotide excision repair in mammalian cells," *Journal of Biological Chemistry*, vol. 272, no. 38, pp. 23465–23468, 1997.
- [249] D. Mu, D. S. Hsu, and A. Sancar, "Reaction mechanism of human DNA repair excision nuclease," *Journal of Biological Chemistry*, vol. 271, no. 14, pp. 8285–8294, 1996.
- [250] K. Sugawara, Y. Okuda, M. Saijo et al., "UV-induced ubiquitylation of XPC protein mediated by UV-DDB-ubiquitin ligase complex," *Cell*, vol. 121, no. 3, pp. 387–400, 2005.
- [251] J. Tang and G. Chu, "Xeroderma pigmentosum complementation group E and UV-damaged DNA-binding protein," *DNA Repair*, vol. 1, no. 8, pp. 601–616, 2002.
- [252] O. Maillard, S. Solyom, and H. Naegeli, "An aromatic sensor with aversion to damaged strands confers versatility to DNA repair," *PLoS Biology*, vol. 5, no. 4, article no. e79, 2007.
- [253] K. Sugawara, "UV-induced ubiquitylation of XPC complex, the UV-DDB-ubiquitin ligase complex, and DNA repair," *Journal of Molecular Histology*, vol. 37, no. 5-7, pp. 189–202, 2006.
- [254] D. Hoogstraten, S. Bergink, V. H. M. Verbiest et al., "Versatile DNA damage detection by the global genome nucleotide excision repair protein XPC," *Journal of Cell Science*, vol. 121, no. 17, pp. 2850–2859, 2008.
- [255] P. J. Van der Spek, A. Eker, S. Rademakers et al., "XPC and human homologs of RAD23: intracellular localization and relationship to other nucleotide excision repair complexes," *Nucleic Acids Research*, vol. 24, no. 13, pp. 2551–2559, 1996.
- [256] K. Sugawara, C. Masutani, A. Uchida et al., "hHR23B, a human Rad23 homolog, stimulates XPC protein in nucleotide excision repair in vitro," *Molecular and Cellular Biology*, vol. 16, no. 9, pp. 4852–4861, 1996.
- [257] C. Masutani, M. Araki, K. Sugawara et al., "Identification and characterization of XPC-binding domain of hHR23B," *Molecular and Cellular Biology*, vol. 17, no. 12, pp. 6915–6923, 1997.
- [258] K. Sugawara, J. M. Y. Ng, C. Masutani et al., "Two human homologs of Rad23 are functionally interchangeable in complex formation and stimulation of XPC repair activity," *Molecular and Cellular Biology*, vol. 17, no. 12, pp. 6924–6931, 1997.
- [259] J. T. Reardon, D. Mu, and A. Sancar, "Overproduction, purification, and characterization of the XPC subunit of the human DNA repair excision nuclease," *Journal of Biological Chemistry*, vol. 271, no. 32, pp. 19451–19456, 1996.
- [260] K. Sugawara, T. Okamoto, Y. Shimizu, C. Masutani, S. Iwai, and F. Hanaoka, "A multistep damage recognition mechanism for global genomic nucleotide excision repair," *Genes and Development*, vol. 15, no. 5, pp. 507–521, 2001.
- [261] A. Aboussekhra, M. Biggerstaff, M. K. K. Shivji et al., "Mammalian DNA nucleotide excision repair reconstituted with purified protein components," *Cell*, vol. 80, no. 6, pp. 859–868, 1995.
- [262] F. Tirode, D. Busso, F. Coin, and J.-M. Egly, "Reconstitution of the transcription factor TFIIH: assignment of functions for the three enzymatic subunits, XPB, XPD, and cdk7," *Molecular Cell*, vol. 3, no. 1, pp. 87–95, 1999.
- [263] D. Mu, C.-H. Park, T. Matsunaga, D. S. Hsu, J. T. Reardon, and A. Sancar, "Reconstitution of human DNA repair excision nuclease in a highly defined system," *Journal of Biological Chemistry*, vol. 270, no. 6, pp. 2415–2418, 1995.
- [264] M. R. Lieber, "The FEN-1 family of structure-specific nucleases in eukaryotic DNA replication, recombination and repair," *BioEssays*, vol. 19, no. 3, pp. 233–240, 1997.
- [265] A. Constantinou, D. Gunz, E. Evans et al., "Conserved residues of human XPG protein important for nuclease activity and function in nucleotide excision repair," *Journal of Biological Chemistry*, vol. 274, no. 9, pp. 5637–5648, 1999.
- [266] R. Guo, J. Chen, F. Zhu et al., "E2F1 Localizes to sites of UV-induced DNA damage to enhance nucleotide excision repair," *The Journal of Biological Chemistry*, vol. 285, pp. 19308–19315, 2010.
- [267] S. Nocentini, "Rejoining kinetics of DNA single- and double-strand breaks in normal and DNA ligase-deficient cells after exposure to ultraviolet C and gamma radiation: an evaluation of ligating activities involved in different DNA repair processes," *Radiation Research*, vol. 151, no. 4, pp. 423–432, 1999.
- [268] J. Moser, H. Kool, I. Giakzidis, K. Caldecott, L. H.F. Mullenders, and M. I. Foustieri, "Sealing of chromosomal DNA nicks during nucleotide excision repair requires XRCC1 and DNA ligase III $\alpha$  in a cell-cycle-specific manner," *Molecular Cell*, vol. 27, no. 2, pp. 311–323, 2007.
- [269] S. Tornaletti, "Transcription-coupled DNA repair: directing your effort where it's most needed," *Cellular and Molecular Life Sciences*, vol. 66, no. 6, pp. 1010–1020, 2009.

- [270] G. R. Harlow, M. E. Jenkins, T. S. Pittalwala, and D. W. Mount, "Isolation of *uvh1*, an *Arabidopsis* mutant hypersensitive to ultraviolet light and ionizing radiation," *Plant Cell*, vol. 6, no. 2, pp. 227–235, 1994.
- [271] A. L. Fidantsef, D. L. Mitchell, and A. B. Britt, "The *Arabidopsis UVH1* gene is a homolog of the yeast repair endonuclease RAD1," *Plant Physiology*, vol. 124, no. 2, pp. 579–586, 2000.
- [272] Z. Liu, G. S. Hossain, M. A. Islas-Osuna, D. L. Mitchell, and D. W. Mount, "Repair of UV damage in plants by nucleotide excision repair: *Arabidopsis UVH1* DNA repair gene is a homolog of *Saccharomyces cerevisiae* Rad1," *Plant Journal*, vol. 21, no. 6, pp. 519–528, 2000.
- [273] Z. Liu, J. D. Hall, and D. W. Mount, "*Arabidopsis UVH3* gene is a homolog of the *Saccharomyces cerevisiae* RAD2 and human XPG DNA repair genes," *Plant Journal*, vol. 26, no. 3, pp. 329–338, 2001.
- [274] G. C. Cannon, L. A. Hedrick, and S. Heinhorst, "Repair mechanisms of UV-induced DNA damage in soybean chloroplasts," *Plant Molecular Biology*, vol. 29, no. 6, pp. 1267–1277, 1995.
- [275] J. Hidema, T. Kumagai, J. C. Sutherland, and B. M. Sutherland, "Ultraviolet B-sensitive rice cultivar deficient in cyclobutyl pyrimidine dimer repair," *Plant Physiology*, vol. 113, no. 1, pp. 39–44, 1997.
- [276] M. E. Jenkins, G. R. Harlow, Z. Liu, M. A. Shotwell, J. Ma, and D. W. Mount, "Radiation-sensitive mutants of *Arabidopsis thaliana*," *Genetics*, vol. 140, no. 2, pp. 725–732, 1995.
- [277] C.-Z. Jiang, C.-N. Yen, K. Cronin, D. Mitchell, and A. B. Britt, "UV- and gamma-radiation sensitive mutants of *Arabidopsis thaliana*," *Genetics*, vol. 147, no. 3, pp. 1401–1409, 1997.
- [278] S. Kimura and K. Sakaguchi, "DNA repair in plants," *Chemical Reviews*, vol. 106, no. 2, pp. 753–766, 2006.
- [279] H. Xu, I. Swoboda, P. L. Bhalla et al., "Plant homologue of human excision repair gene *ERCC1* points to conservation of DNA repair mechanisms," *Plant Journal*, vol. 13, no. 6, pp. 823–829, 1998.
- [280] E. C. Friedberg, "DNA damage and repair," *Nature*, vol. 421, no. 6921, pp. 436–440, 2003.
- [281] J. Wu, L.-Y. Lu, and X. Yu, "The role of BRCA1 in DNA damage response," *Protein Cell*, vol. 1, pp. 117–123, 2010.
- [282] P. Sung, K. M. Trujillo, and S. Van Komen, "Recombination factors of *Saccharomyces cerevisiae*," *Mutation Research*, vol. 451, no. 1-2, pp. 257–275, 2000.
- [283] G. A. Cromie, J. C. Connelly, and D. R. F. Leach, "Recombination at double-strand breaks and DNA ends: conserved mechanisms from phage to humans," *Molecular Cell*, vol. 8, no. 6, pp. 1163–1174, 2001.
- [284] J. Thacker, "The RAD51 gene family, genetic instability and cancer," *Cancer Letters*, vol. 219, no. 2, pp. 125–135, 2005.
- [285] K. McEntee, G. M. Weinstock, and I. R. Lehman, "recA protein-catalyzed strand assimilation: stimulation by *Escherichia coli* single-stranded DNA-binding protein," *Proceedings of the National Academy of Sciences of the United States of America*, vol. 77, no. 2, pp. 857–861, 1980.
- [286] D. K. Bishop, D. Park, L. Xu, and N. Kleckner, "DMC1: a meiosis-specific yeast homolog of *E. coli* recA required for recombination, synaptonemal complex formation, and cell cycle progression," *Cell*, vol. 69, no. 3, pp. 439–456, 1992.
- [287] S. T. Lovett, "Sequence of the RAD5 gene of *Saccharomyces cerevisiae*: similarity of RAD55 to prokaryotic RecA and other RecA-like proteins," *Gene*, vol. 142, no. 1, pp. 103–106, 1994.
- [288] W. Li and H. Ma, "Double-stranded DNA breaks and gene functions in recombination and meiosis," *Cell Research*, vol. 16, no. 5, pp. 402–412, 2006.
- [289] M. Kawabata, T. Kawabata, and M. Nishibori, "Role of recA/RAD51 family proteins in mammals," *Acta Medica Okayama*, vol. 59, no. 1, pp. 1–9, 2005.
- [290] Y. Aylon and M. Kupiec, "New insights into the mechanism of homologous recombination in yeast," *Mutation Research*, vol. 566, no. 3, pp. 231–248, 2004.
- [291] M. S. Park, "Expression of human RAD52 confers resistance to ionizing radiation in mammalian cells," *Journal of Biological Chemistry*, vol. 270, no. 26, pp. 15467–15470, 1995.
- [292] Y. Aylon and M. Kupiec, "The checkpoint protein Rad24 of *Saccharomyces cerevisiae* is involved in processing double-strand break ends and in recombination partner choice," *Molecular and Cellular Biology*, vol. 23, no. 18, pp. 6585–6596, 2003.
- [293] S. Palmer, E. Schildkraut, R. Lazarin, J. Nguyen, and J. A. Nickoloff, "Gene conversion tracts in *Saccharomyces cerevisiae* can be extremely short and highly directional," *Nucleic Acids Research*, vol. 31, no. 4, pp. 1164–1173, 2003.
- [294] O. Inbar and M. Kupiec, "Homology search and choice of homologous partner during mitotic recombination," *Molecular and Cellular Biology*, vol. 19, no. 6, pp. 4134–4142, 1999.
- [295] Y. Aylon, B. Liefshitz, G. Bitan-Banin, and M. Kupiec, "Molecular dissection of mitotic recombination in the yeast *Saccharomyces cerevisiae*," *Molecular and Cellular Biology*, vol. 23, no. 4, pp. 1403–1417, 2003.
- [296] H. Puchta, P. Swoboda, and B. Hohn, "Induction of intrachromosomal homologous recombination in whole plants," *Plant Journal*, vol. 7, no. 2, pp. 203–210, 1995.
- [297] P. A. Jeggo, "Studies on mammalian mutants defective in rejoining double-strand breaks in DNA," *Mutation Research*, vol. 239, no. 1, pp. 1–16, 1990.
- [298] G. Ira, A. Pelliccioli, A. Balijja et al., "DNA end resection, homologous recombination and DNA damage checkpoint activation require CDK1," *Nature*, vol. 431, no. 7011, pp. 1011–1017, 2004.
- [299] P. Sung, "Yeast Rad55 and Rad57 proteins form a heterodimer that functions with replication protein A to promote DNA strand exchange by Rad51 recombinase," *Genes and Development*, vol. 11, no. 9, pp. 1111–1121, 1997.
- [300] B. Wolner, S. Van Komen, P. Sung, and C. L. Peterson, "Recruitment of the recombinational repair machinery to a DNA double-strand break in yeast," *Molecular Cell*, vol. 12, no. 1, pp. 221–232, 2003.
- [301] E. Sonoda, G. Y. Zhao, M. Kohzaki et al., "Collaborative roles of  $\gamma$ H2AX and the Rad51 paralog Xrcc3 in homologous recombinational repair," *DNA Repair*, vol. 6, no. 3, pp. 280–292, 2007.
- [302] F. Pâques and J. E. Haber, "Multiple pathways of recombination induced by double-strand breaks in *Saccharomyces cerevisiae*," *Microbiology and Molecular Biology Reviews*, vol. 63, no. 2, pp. 349–404, 1999.
- [303] S. E. Critchlow and S. P. Jackson, "DNA end-joining: from yeast to man," *Trends in Biochemical Sciences*, vol. 23, no. 10, pp. 394–398, 1998.
- [304] M. L. Hefferin and A. E. Tomkinson, "Mechanism of DNA double-strand break repair by non-homologous end joining," *DNA Repair*, vol. 4, no. 6, pp. 639–648, 2005.

- [305] S. A. McElhinny, J. M. Havener, M. Garcia-Diaz et al., "A gradient of template dependence defines distinct biological roles for family X polymerases in nonhomologous end joining," *Molecular Cell*, vol. 19, no. 3, pp. 357–366, 2005.
- [306] J.-P. Capp, F. Boudsocq, P. Bertrand et al., "The DNA polymerase  $\lambda$  is required for the repair of non-compatible DNA double strand breaks by NHEJ in mammalian cells," *Nucleic Acids Research*, vol. 34, no. 10, pp. 2998–3007, 2006.
- [307] S. Thode, A. Schäfer, P. Pfeiffer, and W. Vielmetter, "A novel pathway of DNA end-to-end joining," *Cell*, vol. 60, no. 6, pp. 921–928, 1990.
- [308] R. B. Cary, S. R. Peterson, J. Wang, D. G. Bear, E. M. Bradbury, and D. J. Chen, "DNA looping by Ku and the DNA-dependent protein kinase," *Proceedings of the National Academy of Sciences of the United States of America*, vol. 94, no. 9, pp. 4267–4272, 1997.
- [309] D. A. Ramsden and M. Geliert, "Ku protein stimulates DNA end joining by mammalian DNA ligases: a direct role for Ku in repair of DNA double-strand breaks," *EMBO Journal*, vol. 17, no. 2, pp. 609–614, 1998.
- [310] P. Baumann and S. C. West, "DNA end-joining catalyzed by human cell-free extracts," *Proceedings of the National Academy of Sciences of the United States of America*, vol. 95, no. 24, pp. 14066–14070, 1998.
- [311] H. Yajima, K.-J. Lee, S. Zhang, J. Kobayashi, and B. P. C. Chen, "DNA double-strand break formation upon UV-induced replication stress activates ATM and DNA-PKcs kinases," *Journal of Molecular Biology*, vol. 385, no. 3, pp. 800–810, 2009.
- [312] C. Muller, P. Calsou, P. Frit, C. Cayrol, T. Carter, and B. Salles, "UV sensitivity and impaired nucleotide excision repair in DNA-dependent protein kinase mutant cells," *Nucleic Acids Research*, vol. 26, no. 6, pp. 1382–1389, 1998.
- [313] P. Hentges, P. Ahnesorg, R. S. Pitcher et al., "Evolutionary and functional conservation of the DNA non-homologous end-joining protein, XLF/Cernunnos," *Journal of Biological Chemistry*, vol. 281, no. 49, pp. 37517–37526, 2006.
- [314] P. Ahnesorg, P. Smith, and S. P. Jackson, "XLF interacts with the XRCC4-DNA ligase IV complex to promote DNA nonhomologous end-joining," *Cell*, vol. 124, no. 2, pp. 301–313, 2006.
- [315] D. Buck, L. Malivert, R. De Chasseval et al., "Cernunnos, a novel nonhomologous end-joining factor, is mutated in human immunodeficiency with microcephaly," *Cell*, vol. 124, no. 2, pp. 287–299, 2006.
- [316] E. Riballo, M. Kühne, N. Rief et al., "A pathway of double-strand break rejoining dependent upon ATM, Artemis, and proteins locating to  $\gamma$ -H2AX foci," *Molecular Cell*, vol. 16, no. 5, pp. 715–724, 2004.
- [317] J. Lloyd, J. R. Chapman, J. A. Clapperton et al., "A supramolecular FHA/BRCT-repeat architecture mediates Nbs1 adaptor function in response to DNA damage," *Cell*, vol. 139, no. 1, pp. 100–111, 2009.
- [318] R. S. Williams, G. E. Dodson, O. Limbo et al., "Nbs1 is an extended flexible arm binding to Ctp1 and Mre11-Rad50 to coordinate dsDNA break processing," *Cell*, vol. 139, pp. 87–99, 2009.
- [319] T. T. Paull and M. Gellert, "A mechanistic basis for Mre11-directed DNA joining at microhomologies," *Proceedings of the National Academy of Sciences of the United States of America*, vol. 97, no. 12, pp. 6409–6414, 2000.
- [320] L. Chen, K. Trujillo, W. Ramos, P. Sung, and A. E. Tomkinson, "Promotion of Dnl4-Catalyzed DNA end-joining by the Rad50/Mre11/Xrs2 and Hdf1/Hdf2 complexes," *Molecular Cell*, vol. 8, no. 5, pp. 1105–1115, 2001.
- [321] L. Aravind, V. M. Dixit, and E. V. Koonin, "Apoptotic molecular machinery: vastly increased complexity in vertebrates revealed by genome comparisons," *Science*, vol. 291, no. 5507, pp. 1279–1284, 2001.
- [322] M.-P. Doutriaux, F. Couteau, C. Bergounioux, and C. White, "Isolation and characterisation of the RAD51 and DMC1 homologs from *Arabidopsis thaliana*," *Molecular and General Genetics*, vol. 257, no. 3, pp. 283–291, 1998.
- [323] A. C. Vergunst and P. J. J. Hooykaas, "Recombination in the plant genome and its application in biotechnology," *Critical Reviews in Plant Sciences*, vol. 18, no. 1, pp. 1–31, 1999.
- [324] M. Majchrzak, R. P. Bowater, P. Staczek, and P. Parniewski, "SOS repair and supercoiling influence the genetic stability of DNA triplet repeats in *Escherichia coli*," *Journal of Molecular Biology*, vol. 364, no. 4, pp. 612–624, 2006.
- [325] J. Courcelle, A. Khodursky, B. Peter, P. O. Brown, and P. C. Hanawalt, "Comparative gene expression profiles following UV exposure in wild-type and SOS-deficient *Escherichia coli*," *Genetics*, vol. 58, pp. 41–64, 2001.
- [326] B. Michel, "After 30 years of study, the bacterial SOS response still surprises us," *PLoS Biology*, vol. 3, no. 7, pp. 1174–1176, 2005.
- [327] M. Martins-Pinheiro, R. C. P. Marques, and C. F. M. Menck, "Genome analysis of DNA repair genes in the alpha proteobacterium *Caulobacter crescentus*," *BMC Microbiology*, vol. 7, article no. 17, 2007.
- [328] B. Van Houten, J. A. Eisen, and P. C. Hanawalt, "A cut above: discovery of an alternative excision repair pathway in bacteria," *Proceedings of the National Academy of Sciences of the United States of America*, vol. 99, no. 5, pp. 2581–2583, 2002.
- [329] R. P. Fuchs, S. Fujii, and J. Wagner, "Properties and functions of *Escherichia coli* Pol IV and Pol V," *Advances in Protein Chemistry*, vol. 69, pp. 229–264, 2004.
- [330] M. F. Goodman, "Coping with replication 'train wrecks' in *Escherichia coli* using Pol V, Pol II and RecA proteins," *Trends in Biochemical Sciences*, vol. 25, no. 4, pp. 189–195, 2000.
- [331] B. S. Strauss, R. Roberts, L. Francis, and P. Pouryazdanparast, "Role of the dinB gene product in spontaneous mutation in *Escherichia coli* with an impaired replicative polymerase," *Journal of Bacteriology*, vol. 182, no. 23, pp. 6742–6750, 2000.
- [332] R. S. Galhardo, R. P. Rocha, M. V. Marques, and C. F. M. Menck, "An SOS-regulated operon involved in damage-inducible mutagenesis in *Caulobacter crescentus*," *Nucleic Acids Research*, vol. 33, no. 8, pp. 2603–2614, 2005.
- [333] L. H. Hartwell and T. A. Weinert, "Checkpoints: controls that ensure the order of cell cycle events," *Science*, vol. 246, no. 4930, pp. 629–634, 1989.
- [334] H.-L. Lo, S. Nakajima, L. Ma et al., "Differential biologic effects of CPD and 6–4PP UV-induced DNA damage on the induction of apoptosis and cell-cycle arrest," *BMC Cancer*, vol. 5, article no. 135, 2005.
- [335] J. Mercer, M. Mahmoudi, and M. Bennett, "DNA damage, p<sup>53</sup>, apoptosis and vascular disease," *Mutation Research*, vol. 621, no. 1–2, pp. 75–86, 2007.
- [336] J. Lukas, C. Lukas, and J. Bartek, "Mammalian cell cycle checkpoints: signalling pathways and their organization in space and time," *DNA Repair*, vol. 3, no. 8–9, pp. 997–1007, 2004.

- [337] Y. Shiloh, "ATM and related protein kinases: safeguarding genome integrity," *Nature Reviews Cancer*, vol. 3, no. 3, pp. 155–168, 2003.
- [338] P. A. Jeggo and M. Löbrich, "Contribution of DNA repair and cell cycle checkpoint arrest to the maintenance of genomic stability," *DNA Repair*, vol. 5, no. 9–10, pp. 1192–1198, 2006.
- [339] S. S. Zinkel, K. E. Hurov, C. Ong, F. M. Abtahi, A. Gross, and S. J. Korsmeyer, "A role for proapoptotic BID in the DNA-damage response," *Cell*, vol. 122, no. 4, pp. 579–591, 2005.
- [340] I. Kamer, R. Sarig, Y. Zaltsman et al., "Proapoptotic BID is an ATM effector in the DNA-damage response," *Cell*, vol. 122, no. 4, pp. 593–603, 2005.
- [341] J. Jin, T. Shirogane, L. Xu et al., "SCF $\beta$ -TRCP links Chk1 signaling to degradation of the Cdc25A protein phosphatase," *Genes and Development*, vol. 17, no. 24, pp. 3062–3074, 2003.
- [342] Y. Kanemori, K. Uto, and N. Sagata, " $\beta$ -TrCP recognizes a previously undescribed nonphosphorylated destruction motif in Cdc25A and Cdc25B phosphatases," *Proceedings of the National Academy of Sciences of the United States of America*, vol. 102, no. 18, pp. 6279–6284, 2005.
- [343] N. Mailand, J. Falck, C. Lukas et al., "Rapid destruction of human Cdc25A in response to DNA damage," *Science*, vol. 288, no. 5470, pp. 1425–1429, 2000.
- [344] N. Mailand, A. V. Podtelejnikov, A. Groth, M. Mann, J. Bartek, and J. Lukas, "Regulation of G<sub>2</sub>/M events by Cdc25A through phosphorylation-dependent modulation of its stability," *EMBO Journal*, vol. 21, no. 21, pp. 5911–5920, 2002.
- [345] J. Bartek and J. Lukas, "DNA damage checkpoints: from initiation to recovery or adaptation," *Current Opinion in Cell Biology*, vol. 19, no. 2, pp. 238–245, 2007.
- [346] N. Watanabe, H. Arai, Y. Nishihara et al., "M-phase kinases induce phospho-dependent ubiquitination of somatic Wee1 by SCF $\beta$ -TrCP," *Proceedings of the National Academy of Sciences of the United States of America*, vol. 101, no. 13, pp. 4419–4424, 2004.
- [347] N. Mailand, S. Bekker-Jensen, J. Bartek, and J. Lukas, "Destruction of claspin by SCF $\beta$ TrCP restrains Chk1 activation and facilitates recovery from genotoxic stress," *Molecular Cell*, vol. 23, no. 3, pp. 307–318, 2006.
- [348] A. Peschiaroli, N. V. Dorrello, D. Guardavaccaro et al., "SCF $\beta$ TrCP-mediated degradation of claspin regulates recovery from the DNA replication checkpoint response," *Molecular Cell*, vol. 23, no. 3, pp. 319–329, 2006.
- [349] I. Mamely, M. A. van Vugt, V. A. Smits et al., "Polo-like kinase-1 controls proteasome-dependent degradation of Claspin during checkpoint recovery," *Current Biology*, vol. 16, no. 19, pp. 1950–1955, 2006.
- [350] L. Busino, M. Donzelli, M. Chiesa et al., "Degradation of Cdc25A by  $\beta$ -TrCP during S phase and in response to DNA damage," *Nature*, vol. 426, no. 6962, pp. 87–91, 2003.
- [351] M. B. Kastan and J. Bartek, "Cell-cycle checkpoints and cancer," *Nature*, vol. 432, no. 7015, pp. 316–323, 2004.
- [352] C. Masutani, R. Kusumoto, S. Iwai, and F. Hanaoka, "Mechanisms of accurate translesion synthesis by human DNA polymerase  $\eta$ ," *EMBO Journal*, vol. 19, no. 12, pp. 3100–3109, 2000.
- [353] R. E. Johnson, S. Prakash, and L. Prakash, "Efficient bypass of a thymine—thymine dimer by yeast DNA polymerase, Pol $\eta$ ," *Science*, vol. 283, no. 5404, pp. 1001–1004, 1999.
- [354] R. P. Rastogi, Richa, and R. P. Sinha, "Apoptosis: molecular mechanisms and pathogenicity," *EXCLI Journal*, vol. 8, pp. 155–181, 2009.

## Research Article

# Repair of DNA Alkylation Damage by the *Escherichia coli* Adaptive Response Protein AlkB as Studied by ESI-TOF Mass Spectrometry

Deyu Li,<sup>1,2,3</sup> James C. Delaney,<sup>1,2,3,4</sup> Charlotte M. Page,<sup>1,2,3,5</sup> Alvin S. Chen,<sup>1,2,3</sup> Cintyu Wong,<sup>2,3,6,7,8</sup> Catherine L. Drennan,<sup>2,3,6,7</sup> and John M. Essigmann<sup>1,2,3</sup>

<sup>1</sup> Department of Biological Engineering, Massachusetts Institute of Technology, Cambridge, MA 02139, USA

<sup>2</sup> Center for Environmental Health Sciences, Massachusetts Institute of Technology, Cambridge, MA 02139, USA

<sup>3</sup> Department of Chemistry, Massachusetts Institute of Technology, Cambridge, MA 02139, USA

<sup>4</sup> Visterra Inc., Cambridge, MA 02142, USA

<sup>5</sup> Department of Chemistry, Yale University, New Haven, CT 06520, USA

<sup>6</sup> Department of Biology, Massachusetts Institute of Technology, Cambridge, MA 02139, USA

<sup>7</sup> Howard Hughes Medical Institute, USA

<sup>8</sup> Johnson & Johnson Pharmaceutical Research & Development, 930 Route 202 South, Raritan, NJ 08869, USA

Correspondence should be addressed to John M. Essigmann, jessig@mit.edu

Received 5 August 2010; Accepted 15 September 2010

Academic Editor: Ashis Basu

Copyright © 2010 Deyu Li et al. This is an open access article distributed under the Creative Commons Attribution License, which permits unrestricted use, distribution, and reproduction in any medium, provided the original work is properly cited.

DNA alkylation can cause mutations, epigenetic changes, and even cell death. All living organisms have evolved enzymatic and non-enzymatic strategies for repairing such alkylation damage. AlkB, one of the *Escherichia coli* adaptive response proteins, uses an  $\alpha$ -ketoglutarate/Fe(II)-dependent mechanism that, by chemical oxidation, removes a variety of alkyl lesions from DNA, thus affording protection of the genome against alkylation. In an effort to understand the range of acceptable substrates for AlkB, the enzyme was incubated with chemically synthesized oligonucleotides containing alkyl lesions, and the reaction products were analyzed by electrospray ionization time-of-flight (ESI-TOF) mass spectrometry. Consistent with the literature, but studied comparatively here for the first time, it was found that 1-methyladenine, 1,*N*<sup>6</sup>-ethenoadenine, 3-methylcytosine, and 3-ethylcytosine were completely transformed by AlkB, while 1-methylguanine and 3-methylthymine were partially repaired. The repair intermediates (epoxide and possibly glycol) of 3,*N*<sup>4</sup>-ethenocytosine are reported for the first time. It is also demonstrated that *O*<sup>6</sup>-methylguanine and 5-methylcytosine are refractory to AlkB, lending support to the hypothesis that AlkB repairs only alkyl lesions attached to the nitrogen atoms of the nucleobase. ESI-TOF mass spectrometry is shown to be a sensitive and efficient tool for probing the comparative substrate specificities of DNA repair proteins *in vitro*.

## 1. Introduction

Nuclear and mitochondrial DNA is vulnerable to chemical modification from exogenous and endogenous sources. Exogenous sources include radiation, oxidation and alkylation by organic and inorganic chemical agents; endogenous cellular processes that contribute to the burden of genomic damage include enzyme-promoted oxidation, alkylation, and deamination of DNA [1, 2]. Because DNA has many potential nucleophilic reaction sites, such as the nitrogen and oxygen atoms on the bases and the oxygen atoms on

the sugar and phosphodiester backbone, small alkylating agents from the environment or from internally generated sources form a remarkably vast array of covalent alkyl-DNA adducts [3]. These adducts challenge the cell in several ways. They can cause mutations and hence irreversibly reprogram the destiny of a somatic or germ cell. They jeopardize the epigenetic pattern that imprints long term gene regulation. Moreover, adducts can block DNA and RNA synthesis, inhibit mRNA transcription and translation, and lead to strand breaks. To avoid the undesired effects of alkyl-DNA lesions, living systems have developed a host of DNA repair

systems that act as front line defenses against the threats that these adducts pose to cellular welfare [1, 2].

The cellular response of *E. coli* to alkylation is an intricate and fascinating system that includes a specific sensor of DNA alkylation burden (monitored as the alkyl phosphotriester concentration) that, when triggered, results in the expression of four proteins that afford a robust global defense against a broad array of alkyl DNA adducts [4–6]. When *E. coli* experiences a low dose of a methylating agent, the alkylation damage to DNA creates a signal for transcriptional activation of the genes encoding the Ada, AlkA, AlkB, and AidB proteins, each of which combats selective features of the alkylation threat. The accumulation of those four proteins affords *E. coli* resistance to the mutagenicity and toxicity of subsequent higher doses of the alkylating agent [7]. This process in *E. coli* is called the adaptive response, which is activated by the Ada protein following its alkylation by the aforementioned DNA backbone alkyl phosphotriester that serves as the cellular barometer for alkylation stress [4, 5]. The AlkA enzyme is a DNA glycosylase and works against selected alkylated bases, such as 3-methyladenine and 7-methylguanine, among others [2]. The AidB protein is proposed to be a defensive operative that sequesters or chemically inactivates alkylating agents before they can react with DNA; its exact enzymatic activity and mechanism, however, are still unknown [8]. The AlkB protein was discovered to be an  $\alpha$ -ketoglutarate- and Fe(II)-dependent oxidizing enzyme that can efficiently repair various DNA and RNA alkyl lesions [9, 10] (Figure 1). The reported substrate scope for the AlkB enzyme encompasses either simple methylated or ethylated DNA lesions, such as 1MeA, 3MeC, 3EtC, 1MeG, and 3MeT, or even lesions with bridged two-carbon units, such as eA, eC, and ethanoA [2, 4, 11, 12] (Figure 2). AlkB has many mammalian homologs, including ABH1 through ABH8 and FTO, some of which have also been proposed or proved to act upon alkylated DNA and RNA [2, 4, 11, 12]. Since the discovery of the enzymatic properties of AlkB, research on this protein and its homologs has become a fertile research area.

In this work we utilized chemical synthesis to prepare structurally defined lesions at specific sites within oligonucleotides. The site-specifically modified oligonucleotides were incubated with purified AlkB protein to allow a head-to-head comparison of the substrate properties of various alkyl lesions in the same DNA sequence context. This method enabled us to monitor efficiently the ability of AlkB to repair alkylation damage by a mass spectrometry tool employed by us earlier in a limited manner with three DNA lesions [13, 14]. This tool is demonstrated to have promise for the high throughput comparative analysis of multiple and diverse DNA repair substrates.

## 2. Materials and Methods

**2.1. Oligonucleotide Synthesis.** Oligonucleotides containing the lesions in Figure 2 were made using solid-phase phosphoramidite chemistry, and were deprotected, purified and characterized as described previously [13, 15–17]. For all nine lesions, the 16 mer oligonucleotide

sequence was 5'-GAAGACCTXGGCGTCC-3', ( $X$  = lesion); for  $O^6$ MeG, an additional sequence was made (5'-GAAGACCGXTGCGTCC-3',  $X = O^6$ MeG). The calculated MWs of the oligonucleotides are shown in Table 1. DNA concentration was determined by UV absorbance using the extinction coefficients ( $\epsilon$ ) at 260 nm (For any alkylated base, we substituted its extinction coefficient with the extinction coefficient of its unmodified counterpart due to the small difference between the values in the context of 16 mer DNA.).

**2.2. In Vitro Reactions of Lesions with AlkB.** All assays were carried out with AlkB $\Delta$ N11, a truncated form of AlkB in which the first eleven residues are deleted. AlkB $\Delta$ N11 was purified as described [14] and shown previously to have similar activity to wild-type protein [14, 18]. All AlkB reactions used similar conditions as previously described [13], the major change being that all the reactions were performed in HEPES buffer. Reactions were performed at 37°C in 45 mM HEPES (pH 8.0), 67  $\mu$ M Fe(NH<sub>4</sub>)<sub>2</sub>(SO<sub>4</sub>)<sub>2</sub>·6H<sub>2</sub>O, 0.9 mM  $\alpha$ -ketoglutarate and 1.8 mM ascorbate. DNA 16 mer substrates were as described in the previous section. Reactions were conducted with 5  $\mu$ M DNA (see Figures 3-5 for detailed information) and with or without 2.5  $\mu$ M AlkB in a 10  $\mu$ L volume. Reaction mixtures were kept on dry ice until ESI-TOF MS analysis.

**2.3. LC-ESI-TOF/MS Analysis.** Oligonucleotide analyses were performed on an Agilent ESI-TOF mass spectrometer (Palo Alto, CA). ESI was conducted using a needle voltage of 3.5 kV. Nitrogen gas was used with a setting of drying 10 L/min and setting of nebulizer 15 psig and a heated capillary at 325°C. Liquid chromatographic separations were performed using a Zorbax SB-Aq column (2.1  $\times$  150 mm; 3.5  $\mu$ m; Agilent Technologies, Palo Alto, CA) with a flow rate of 0.2 mL/min. Solvent A was 10 mM ammonium acetate in water and solvent B was 100% acetonitrile. A linear gradient was performed in the following steps: 2% to 30% B over 30 minutes, 30% to 2% B over 5 minutes, and 2% to 2% B over 10 minutes. Data analyses were performed using Agilent MassHunter Workstation software. For each individual lesion, we assumed the 16 mer DNA oligo with the lesion and the oligo with the undamaged counterpart have identical extinction coefficients. In an effort to achieve unbiased quantification of the repair reaction, we first extracted the UV chromatogram by using two  $m/z$  values that bracket all expected oligonucleotide species. The time interval encompassing all extracted UV peaks was used to generate the ion chromatogram containing all expected oligonucleotide species. We found the  $-4$  charge envelope of each target oligonucleotide. Then we chose the highest peak in each envelope to generate oligonucleotide-specific UV profiles, from which we selected the maximum UV absorbance at 260 nm to extract the ion abundance, whose maximum peak in the envelope was used to calculate the relative ratio between the oligonucleotides with the lesion or the undamaged/transformed counterpart.

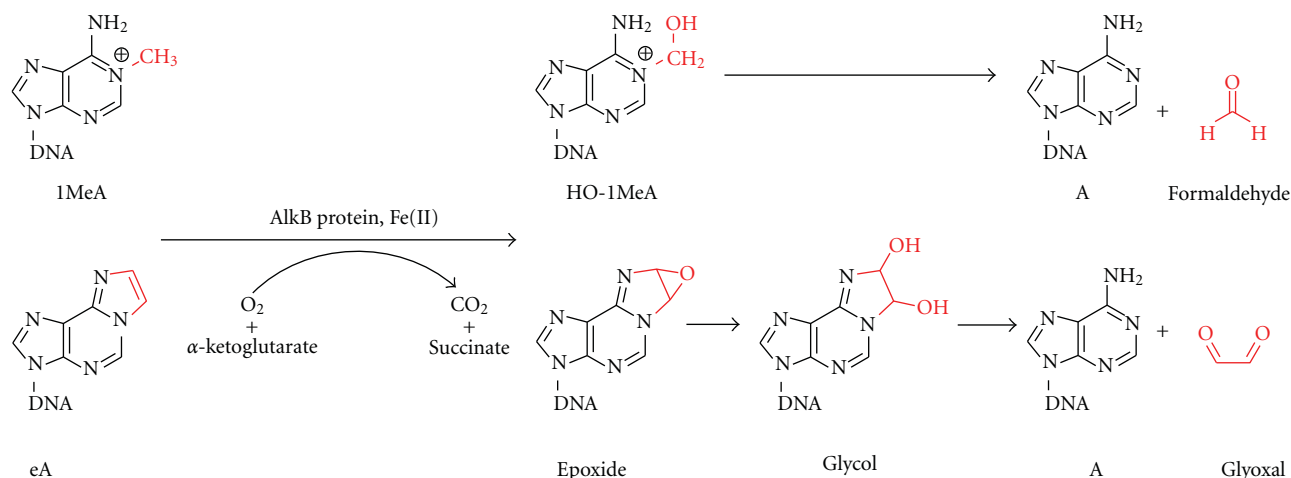


FIGURE 1: Proposed mechanisms and examples (1MeA and eA) of AlkB-mediated enzymatic repair of alkyl DNA lesions.

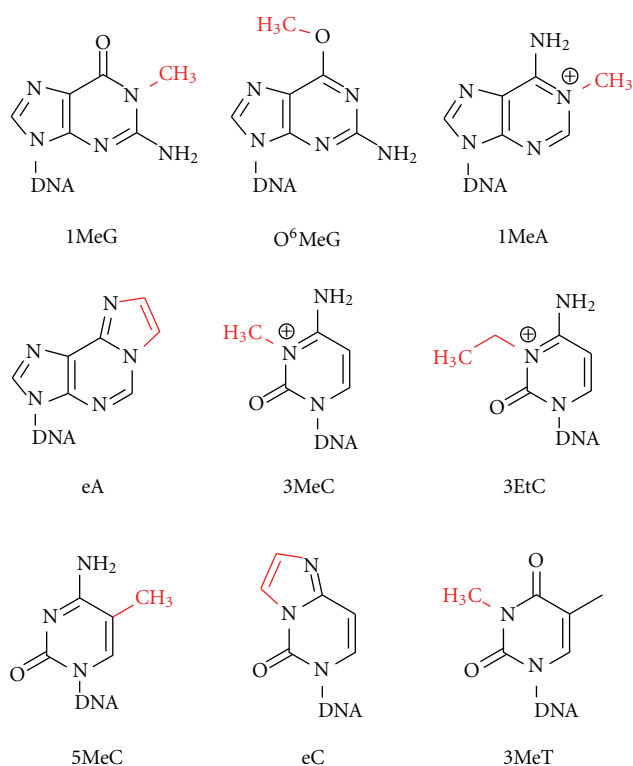


FIGURE 2: Chemical structures and abbreviations of DNA lesions screened as possible repair substrates for the AlkB protein using ESI-TOF mass spectrometry. The repair target within each base is highlighted in red.

### 3. Results

Nine 16 mer oligonucleotides were chemically synthesized containing the alkyl-DNA adducts shown in Figure 2. The sequence used was 5'-GAAGACCTXGGCGTCC-3'; the flanking sequence of each lesion (X) was identical, fixing the sequence context for the repair reaction. The 16 mers with each lesion were incubated in HEPES buffer with the known

cofactors for the AlkB reaction:  $\alpha$ -ketoglutarate, iron in the +2 oxidation state, and ascorbate (see Section 2 for details). For each lesion, two sets of experiments were conducted, one with the AlkB protein and one in the reaction buffer without the AlkB protein. Following the repair reaction, ESI-TOF mass spectrometry was used to detect the reaction products. The 16 mer oligonucleotides demonstrated a good signal in the -4 charge envelope of the ESI-TOF spectra. To give one example to illustrate the method of analysis, the molecular weight (MW) of the 1MeG lesion in the 16 mer is calculated as 4918.87 Daltons for the neutral species, and the MW of its monoisotopic peak (all <sup>12</sup>C, <sup>14</sup>N, etc) when migrating with 4 negative charges (the -4 charge envelope) in the electric field of the spectrometer is *calculated* as having an *m/z* of 1228.71 (all MW information is shown in Table 1). The multiple peaks in each -4 charge envelope reflect the number of <sup>13</sup>C or other heavier isotopes (Figure 3). Again using 1MeG as the example, its monoisotopic peak is *observed* as 1228.62. This experimental result is considered consistent with the theoretical calculation. The next peak in that envelope has an *m/z* of 1228.87, 0.25 amu larger than the 1228.62 peak, which indicates a species containing <sup>13</sup>C, <sup>15</sup>N or another isotope that adds a nominal mass of 1.0 to the total weight of the 16 mer (e.g., 0.25 = *m/z* = one <sup>13</sup>C/a charge state of 4). Additional peaks in the spectrum represent additional heavy isotopes within the parental 16 mer.

**3.1. N1-Methylguanine.** N1-Methylguanine (1MeG) (Figure 2) has been found both *in vitro* [19] and *in vivo* [20]. The glycosylase AAG can repair the 1MeG lesion *in vitro* [21]. Our group and others have observed that the AlkB protein can repair 1MeG both *in vivo* and *in vitro* [15, 22]. In the *in vivo* assay, AlkB can partially overcome the strong block of 1MeG to replication (lesion bypass increases from 2% in AlkB- cells to 16% in AlkB+ cells). Similarly, AlkB causes a reduction in the mutagenicity of 1MeG from a high frequency of 80% in AlkB- cells to 4% in AlkB+ cells [15].

In the *in vitro* incubation reaction without AlkB protein, we observed the monoisotopic peak of the 1MeG 16mer

TABLE 1: Calculated and observed monoisotopic molecular weight of oligonucleotides and intermediates present in the AlkB repair reactions.

Lesion or base	MW (calculated)	m/z (calculated)		m/z (observed)
	of neutral species	−4 charge monoisotopic peak		−4 charge monoisotopic peak
G	4904.86	1225.21		1225.11
1MeG	4918.87	1228.71		1228.61/2
O <sup>6</sup> MeG	4918.87	1228.71		1228.62/3
A	4888.86	1221.21		1221.12/33
1MeA	4902.88	1224.71		1224.67
eA	4912.86	1227.21		1227.22/4
eA epoxide	4928.86	1231.21		1231.23
eA glycol	4946.87	1235.71		1235.72
C	4864.85	1215.20		1215.20/1
3MeC	4878.87	1218.71		1218.72
3EtC	4892.88	1222.21		1222.23
5MeC	4878.87	1218.71		1218.73
eC	4888.85	1221.20		1221.21/2
eC epoxide	4904.84	1225.20		1225.19
eC glycol	4922.86	1229.71		1229.69
T	4879.85	1218.95		1218.97
3MeT	4893.87	1222.46		1222.49

oligonucleotide for the −4 charge state at m/z of 1228.62 (Figure 3(a)), which correlates well with the calculated value for the −4 charge monoisotopic peak (m/z = 1228.71). In the presence of the AlkB protein (Figure 3(b)), we found 47% of the 1MeG was repaired to the undamaged guanine base (−4 charge m/z = 1225.11) and 53% of the 1MeG (−4 charge m/z = 1228.61) was unchanged. Whereas many other lesions, such as 1MeA, 3MeC, 3EtC, or eA [13, 15], are fully transformed, 1MeG is not. It is noteworthy that its incomplete repair observed here is also in line with studies done on the same lesion *in vivo*, which showed that 1MeG has a relatively low efficiency of lesion bypass (16% for AlkB+ *E. coli*) [15].

**3.2. O<sup>6</sup>-Methylguanine.** O<sup>6</sup>-Methylguanine (O<sup>6</sup>MeG) (Figure 2) is formed when the genome is under alkylation attack [23] and is an especially potent driver of G → A transition mutations [24]. O<sup>6</sup>MeG is formed both endogenously [25, 26] and exogenously [27]. *E. coli* has two repair proteins for such damage. The constitutive Ogt and the inducible Ada proteins reverse methylation damage by transferring the methyl group to one of the internal cysteine residues on each protein. This transfer is a stoichiometric (“suicidal”) reaction that irreversibly inactivates the repair proteins [5]; thus, Ogt and Ada are not true enzymes since their active sites cannot be regenerated. The mismatch repair (MMR) pathway has also been reported to play an important role in the response to O<sup>6</sup>MeG [28]. In the present work, it was our goal to test whether AlkB can also act upon and possibly repair O<sup>6</sup>MeG.

For the O<sup>6</sup>MeG lesion, we synthesized two sets of 16mers and named them as TXG and GXT according to the neighboring nucleosides (see Section 2). In the mass spectra of both TXG (Figure 3(c)) and GXT (Figure 3(e)) in the absence of the AlkB enzyme, we observed m/z values of 1228.62 (TXG) and 1228.63 (GXT) for the −4 charge

monoisotopic peak, which are in good agreement with the calculated m/z of 1228.71. For the reactions with AlkB protein, we did not observe any repaired product nor any structural modifications (as shown below, AlkB sometimes fully removes the alkyl group but it sometimes can create stable oxidized products that are distinct from both the starting material and an unmodified base product). The observed products of the reaction were identical to the starting material: m/z of 1228.62 for TXG (Figure 3(d)) and of 1228.62 for GXT (Figure 3(f)). These results indicate O<sup>6</sup>MeG is not a substrate for AlkB in the *in vitro* experiments under the reaction conditions tested, which provide for full transformation of other lesions, such as 1MeA and eA.

**3.3. N1-Methyladenine.** N1-Methyladenine (1MeA) (Figure 2) is formed mainly in single-stranded DNA by alkylating agents and has been detected *in vitro* [3, 9, 10, 19, 29–31] and *in vivo* [3, 32–35]. These alkylating agents include S<sub>N</sub>2 agents, such as methylmethanesulfonate (MMS) and the naturally occurring methyl halides [5]. The AlkB enzyme repairs 1MeA both *in vitro* and *in vivo* [15]. Studies of 1MeA *in vivo* reveal that the lesion imposes a severe block to DNA replication in AlkB− cells, which is completely removed in AlkB+ cells. These results underscore the physiological relevance of the AlkB system for countering the toxicity of this base. While very toxic, 1MeA is only weakly mutagenic in both AlkB− and AlkB+ cells [15].

In our *in vitro* study of 1MeA repair, the lesion was completely repaired to the undamaged base adenine (Figure 3(h), m/z = 1221.12), while no change occurred in the absence of the AlkB protein (Figure 3(g), m/z 1224.67). The *in vitro* results confirm that 1MeA is a good substrate for AlkB. Moreover, the current observations correlate very well with the strong reparability of 1MeA suggested by earlier *in vivo* lesion bypass studies [15].

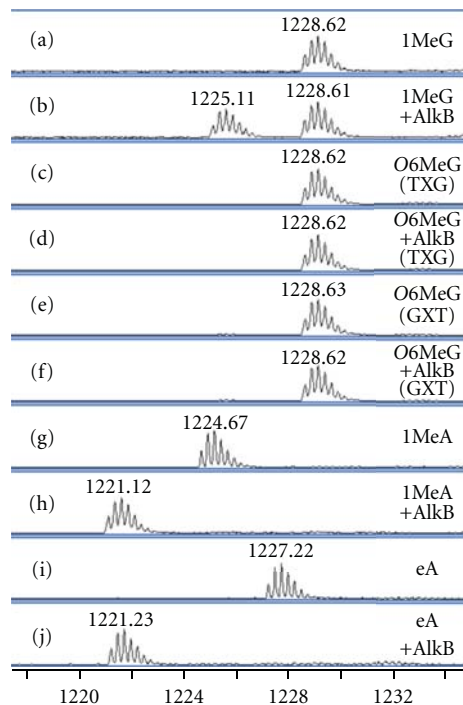


FIGURE 3: ESI-TOF analysis of 16mer reactants and products from the *in vitro* incubation reactions of alkylated lesions and AlkB protein. Data represent the  $-4$  charge envelopes; multiple ion mass peaks associated with each envelope reflect mostly the number of  $^{13}\text{C}$  atoms in each  $-4$  charged packet. The monoisotopic peak (all  $^{12}\text{C}$ ,  $^{14}\text{N}$ , etc.) value is labeled above each peak envelope. (a) 1MeG; (b) 1MeG + AlkB; (c)  $\text{O}^6\text{MeG}$  (TXG); (d)  $\text{O}^6\text{MeG}$  (TXG) + AlkB; (e)  $\text{O}^6\text{MeG}$  (GXT); (f)  $\text{O}^6\text{MeG}$  (GXT) + AlkB; (g) 1MeA; (h) 1MeA + AlkB; (i) eA; (j) eA + AlkB.

3.4.  $1, N^6$ -Ethenoadenine. The formation of  $1, N^6$ -ethenoadenine (eA) (Figure 2) may result from the reaction of adenine with products of unsaturated lipid peroxidation [36–39] or arise from normal physiological conditions in both rodents and humans [40, 41]. The eA lesion is believed to be a good biomarker of inflammation and oxidative stress. This lesion may also be formed by exposure to the common industrial agent vinyl chloride and its metabolites, such as chloroacetaldehyde [42]. In duplex DNA, eA can be repaired by the base excision repair (BER) pathway *in vitro* [21, 43] and *in vivo* [44, 45]. Recently, it was shown that AlkB and its human homolog ABH2 and ABH3 can repair eA *in vitro* [13, 46, 47]. The direct reversal mechanism is also likely to be operative *in vivo*. In AlkB $-$  cells, eA is 35% mutagenic, but less than 0.3% mutagenic in AlkB $+$  cells [13].

In our present *in vitro* study using mass spectrometry to monitor the repair reaction, the oligonucleotide with eA was observed at  $m/z$  of 1227.22 for its  $-4$  charge monoisotopic peak in the absence of AlkB (Figure 3(i)). In the presence of AlkB, the eA lesion was mostly converted to the undamaged product, adenine ( $m/z = 1221.23$ , Figure 3(j)). The  $m/z$  difference at the  $-4$  charge state between the eA and A is 5.99 Daltons, which corresponds to the  $\sim 24$  Dalton MW difference (two carbon atoms) of

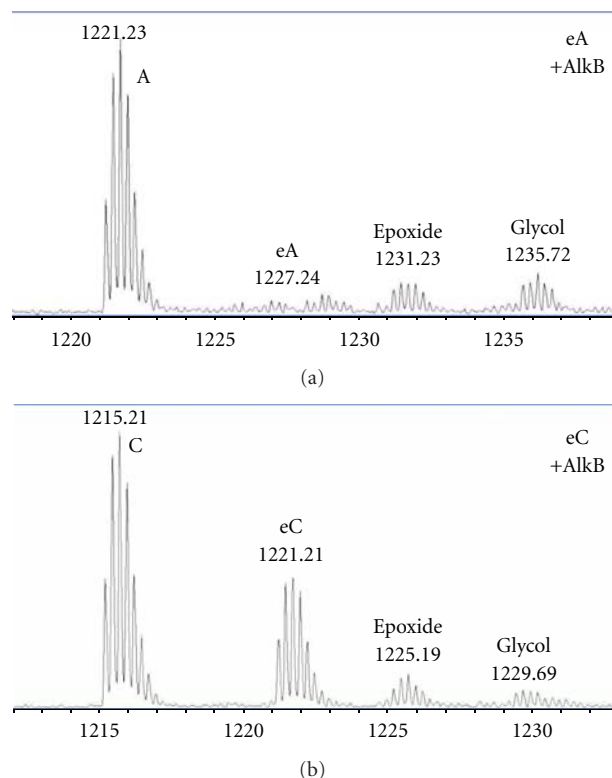


FIGURE 4: ESI-TOF analysis of 16mer reactants and products from the *in vitro* incubation reactions of eA and eC lesions with the AlkB protein. Data represent the  $-4$  charge envelopes; multiple ion mass peaks associated with each envelope reflect mostly the number of  $^{13}\text{C}$  atoms in each  $-4$  charged packet. The monoisotopic peak (all  $^{12}\text{C}$ ,  $^{14}\text{N}$ , etc.) value is labeled above each peak envelope. (a) eA + AlkB; (b) eC + AlkB.

the two products. We also observed peak clusters consistent in MW with epoxide and glycol intermediates (Figures 1 and 4(a)), which are consistent with previous observations [13].

3.5.  $N^3$ -Methylcytosine and  $N^3$ -Ethylcytosine.  $N^3$ -Methylcytosine (3MeC) (Figure 2) has been detected both *in vitro* [3, 9, 19, 29–31, 48, 49] and *in vivo* [3, 20, 34, 49]. The corresponding ethyl homolog,  $N^3$ -ethylcytosine (3EtC) (Figure 2), also has been detected *in vitro* [3, 29] and *in vivo* [3, 50]. In *E. coli*, the AlkB protein has good activity against 3MeC and 3EtC both *in vitro* and *in vivo* [9, 10, 15]. The mutation frequency of 30% for both 3MeC and 3EtC in AlkB $-$  cells dropped to  $<2\%$  in AlkB $+$  cells [15].

The  $m/z$  values of the starting material for 3MeC and 3EtC in the ESI-TOF mass spectra were 1218.72 (Figure 5(a)) and 1222.23 (Figure 5(c)), respectively. After incubation with AlkB protein, the 3MeC and 3EtC residues were completely repaired to the undamaged cytosine ( $m/z$  of 1215.21 for 3MeC, Figure 5(b); and of 1215.20 for 3EtC, Figure 5(d)). The complete *in vitro* repair of these lesions establishes both as good substrates for AlkB, consistent with findings from previous *in vivo* bypass and mutagenesis assays [15].

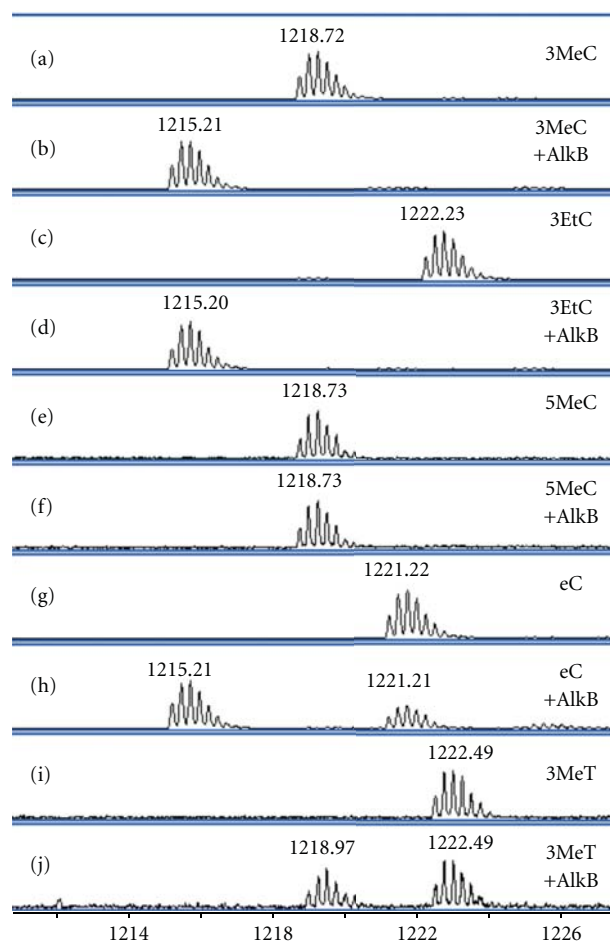


FIGURE 5: ESI-TOF analysis of 16 mer reactants and products from the *in vitro* incubation reactions of alkylated lesions and AlkB protein. Data represent the  $-4$  charge envelopes; multiple ion mass peaks associated with each envelope reflect mostly the number of  $^{13}\text{C}$  atoms in each  $-4$  charged packet. The monoisotopic peak (all  $^{12}\text{C}$ ,  $^{14}\text{N}$ , etc.) value is labeled above each peak envelope. (a) 3MeC; (b) 3MeC + AlkB; (c) 3EtC; (d) 3EtC + AlkB; (e) 5MeC; (f) 5MeC + AlkB; (g) eC; (h) eC + AlkB; (i) 3MeT; (j) 3MeT + AlkB.

**3.6. 5-Methylcytosine.** 5-Methylcytosine (5MeC) (Figure 2) is the naturally methylated form of cytosine seen in prokaryotes and eukaryotes. This methylation does not disturb the Watson-Crick base pairing ability of cytosine, and it is not recognized as DNA damage. 5MeC is an important epigenetic biomarker for mammalian development. It also occurs in bacterial systems as a marker for restriction endonucleases and as a marker used in a specialized type of mismatch repair [51]. Recently, researchers found TET1, an  $\alpha$ -ketoglutarate- and Fe(II)-dependent enzyme, that can oxidize 5MeC to 5-hydroxymethylcytosine [52]. We assessed the ability of AlkB to act similarly on 5MeC.

In the reaction without the AlkB protein, the monoisotopic  $-4$  charge peak of 5MeC appeared at  $m/z = 1218.73$  (Figure 5(e)). In the incubation reaction with 5MeC plus AlkB, the only peak in the spectrum corresponded to 5MeC ( $m/z = 1218.73$ , Figure 5(f)). No peak corresponding to

5-hydroxymethylcytosine or the fully demethylated product, cytosine, was observed, indicating that 5MeC is not an AlkB substrate under the conditions of analysis.

**3.7. 3, $N^4$ -Ethenocytosine.** 3, $N^4$ -Ethenocytosine (eC) (Figure 2) is produced from the same precursors and by the same pathways that generate eA in DNA [36–38, 53]. The BER pathway (human thymine-DNA-glycosylase (hTDG) in human and double-stranded uracil-DNA-glycosylase (dsUDG) in *E. coli*) has been shown to suppress the occurrence of this adduct [44, 53]. In *E. coli*, AlkB has a modest effect on eC toxicity, but reduces the mutation of eC from 82% in AlkB $-$  cells to 37% in AlkB $+$  cells [13].

In our *in vitro* studies, the reaction of eC oligonucleotide without the AlkB protein gave a  $-4$  envelope signal at  $m/z = 1221.22$  (Figure 5(g)). The reaction with AlkB showed eC to be a significant substrate for AlkB protein, although the lesion was not fully repaired under conditions that fully repaired other adducts, such as 1MeA and 3MeC. Only 67% of the eC lesion was consumed (to cytosine, epoxide, and glycol) and 33% of the eC remained intact (signal at  $m/z = 1221.21$ , Figure 5(h)). We also observed a small amount of the epoxide and possibly glycol products (Figure 4(b)), comparable to the products found in the eA repair reaction by AlkB [13]. These results strongly support the conclusions from earlier *in vivo* experiments, and further show that eC may be repaired by AlkB via an epoxide intermediate, which is hydrolyzed to a glycol and then may be released as glyoxal (Figure 1). This ESI-TOF analysis of eC with AlkB is the first demonstration of the detailed mechanism and intermediates of this lesion repaired by the AlkB protein *in vitro*.

**3.8. N3-Methylthymine.** N3-Methylthymine (3MeT) (Figure 2) has been found both *in vitro* [3, 19, 29, 31, 54] and *in vivo* [54, 55] and is formed through the reaction of thymine with  $S_N2$  alkylating agents such as MMS. This adduct has been reported as a very weak substrate for AlkB *in vivo* [15]. Recently, another  $\alpha$ -ketoglutarate- and Fe(II)-dependent demethylase, FTO (fat mass and obesity associated) protein has been reported as an enzyme that can efficiently repair 3MeT in ssDNA [12, 56, 57].

Our *in vitro* experiments confirm the ability of AlkB to effectuate the partial repair of 3MeT as shown in the *in vivo* assays. In the absence of the AlkB protein, the  $-4$  envelope monoisotopic peak of 3MeT appeared at  $m/z$  of 1222.49 (Figure 5(i)). In the reaction with AlkB protein, 47% of 3MeT was converted to thymine ( $m/z = 1218.97$ , Figure 5(j)), leaving 53% unrepaired ( $m/z = 1222.49$ , Figure 5(j)).

## 4. Discussion

**4.1. Advantages of Chemical Synthesis and ESI-TOF Mass Spectrometry.** In the *in vitro* experiments described above, purified AlkB protein was incubated with oligonucleotides containing individual DNA lesions within the same sequence context. There are two ways commonly used to generate alkyl lesions in DNA. The first is by treatment of an unmodified oligonucleotide of known sequence with alkylating agents,

such as MMS and N-methyl-N'-nitro-N-nitrosoguanidine (MNNG), to generate a spectrum of alkyl lesions within the oligomer. The second approach, which was used in this work, utilizes chemical synthesis to incorporate a modified DNA base into a defined sequence, thus providing homogeneous targeted damage to be used as a substrate for repair, replication, or other biochemical assays. All nine lesions investigated in this paper were synthesized in the same 16 mer background, thus eliminating sequence context as a variable for rank-ordering the extent to which each lesion may be repaired by the AlkB protein. We then utilized high-resolution liquid chromatography-mass spectrometry (LC-MS) to detect the reaction products. The ESI-TOF mass spectrometry method utilized here allowed us to achieve good signal with only 20 pmol of oligonucleotide, establishing it as a viable tool for DNA repair studies.

**4.2. Substrate Scope for AlkB and Correlation of In Vitro Data with In Vivo Results.** As reported in the above sections, we observed that the AlkB protein can repair different alkyl lesions to varying extents. Under the current experimental condition, good substrates for AlkB were 1MeA, eA, 3MeC, and 3EtC, which were completely repaired or transformed after a one-hour incubation at 37°C, which mimics human physiological temperature. The 1MeG, eC, and 3MeT lesions are less efficient substrates for AlkB under the conditions tested, and the extent of their transformation varied from 47% to 67%. The repair efficiency trends from the *in vitro* experiments performed here are in line with previously published *in vivo* results from lesion bypass and mutagenesis assays performed in our laboratory using single-stranded viral genomes site-specifically modified with each lesion, which were passaged through AlkB<sup>-</sup> and AlkB<sup>+</sup> *E. coli* [13, 15]. The oxygen-attached lesion O<sup>6</sup>MeG in two sequence contexts and the carbon-attached lesion 5MeC were not repaired or transformed at all in the AlkB reactions under the conditions tested. These results, combined with others in the literature, suggest that AlkB repairs only those alkyl-DNA lesions that are attached via the nitrogen atoms of the bases and not lesions bound to carbon or oxygen atoms.

## 5. Conclusions

There were two goals to the present study. The first was to expand our earlier study of DNA repair in which we used ESI-TOF to study repair of eA [13]. That work was a systematic enzymatic analysis including demonstration that this tool can capture real-time snapshots of the repair reaction as it progresses from starting material, through intermediates, and to products. In the present work, for the sake of simplicity, one time point was chosen (that at which eA repair was complete in the previous kinetic analysis). At that time point (one hour), the ESI-TOF method is shown to be of great value as a tool for rapid comparison of many structurally different substrates. Having shown the potential of this technology for real-time monitoring of DNA

repair reactions, future studies can use ESI-TOF and isotope-labeling with multiple time points for each lesion to define more accurately the kinetic parameters of their individual repair reactions.

The second goal of this work was to probe, more completely and systematically than in the past, the structural requirements of the AlkB enzyme. Among the nine lesions studied, we present direct new evidence for AlkB repair of eC by a direct reversal mechanism, and buttress the growing body of evidence that lesions connected to bases at nitrogens are the major targets of this enzyme. Similar analyses using the same substrate library as in the present study could be performed using the eight known human AlkB homologs as well as the FTO protein, TET1, and other  $\alpha$ -ketoglutarate- and Fe(II)-dependent enzymes. Such studies will help further to define how this class of proteins helps to protect the genome from DNA damage or helps to modify gene expression programs.

## Acknowledgments

This work was supported by National Institutes of Health Grants CA080024, CA26731, and ES02109. Authors would also like to thank Dr. John. S. Wishnok for helpful discussions.

## References

- [1] L. A. Loeb and C. C. Harris, "Advances in chemical carcinogenesis: a historical review and prospective," *Cancer Research*, vol. 68, no. 17, pp. 6863–6872, 2008.
- [2] N. Shrivastav, D. Li, and J. M. Essigmann, "Chemical biology of mutagenesis and DNA repair: cellular responses to DNA alkylation," *Carcinogenesis*, vol. 31, no. 1, pp. 59–70, 2010.
- [3] B. Singer and D. Grunberger, *Molecular Biology of Mutagens and Carcinogens*, Plenum, New York, NY, USA, 1983.
- [4] B. Sedgwick, P. A. Bates, J. Paik, S. C. Jacobs, and T. Lindahl, "Repair of alkylated DNA: recent advances," *DNA Repair*, vol. 6, no. 4, pp. 429–442, 2007.
- [5] B. Sedgwick, "Repairing DNA-methylation damage," *Nature Reviews Molecular Cell Biology*, vol. 5, no. 2, pp. 148–157, 2004.
- [6] B. Sedgwick and T. Lindahl, "Recent progress on the Ada response for inducible repair of DNA alkylation damage," *Oncogene*, vol. 21, no. 58, pp. 8886–8894, 2002.
- [7] L. Samson and J. Cairns, "A new pathway for DNA repair in *Escherichia coli*," *Nature*, vol. 267, no. 5608, pp. 281–283, 1977.
- [8] T. Bowles, A. H. Metz, J. O'Quin, Z. Wawrzak, and B. F. Eichman, "Structure and DNA binding of alkylation response protein AidB," *Proceedings of the National Academy of Sciences of the United States of America*, vol. 105, no. 40, pp. 15299–15304, 2008.
- [9] S. C. Trewick, T. F. Henshaw, R. P. Hausinger, T. Lindahl, and B. Sedgwick, "Oxidative demethylation by *Escherichia coli* AlkB directly reverts DNA base damage," *Nature*, vol. 419, no. 6903, pp. 174–178, 2002.
- [10] P. Ø. Falnes, R. F. Johansen, and E. Seeberg, "AlkB-mediated oxidative demethylation reverses DNA damage in *Escherichia coli*," *Nature*, vol. 419, no. 6903, pp. 178–182, 2002.
- [11] Y. Mishina, E. M. Duguid, and C. He, "Direct reversal of DNA alkylation damage," *Chemical Reviews*, vol. 106, no. 2, pp. 215–232, 2006.

- [12] C. Yi, C. G. Yang, and C. He, "A non-heme iron-mediated chemical demethylation in DNA and RNA," *Accounts of Chemical Research*, vol. 42, no. 4, pp. 519–529, 2009.
- [13] J. C. Delaney, L. Smeester, C. Wong et al., "AlkB reverses etheno DNA lesions caused by lipid oxidation *in vitro* and *in vivo*," *Nature Structural and Molecular Biology*, vol. 12, no. 10, pp. 855–860, 2005.
- [14] L. E. Frick, J. C. Delaney, C. Wong, C. L. Drennan, and J. M. Essigmann, "Alleviation of 1,N6-ethanoadenine genotoxicity by the *Escherichia coli* adaptive response protein AlkB," *Proceedings of the National Academy of Sciences of the United States of America*, vol. 104, no. 3, pp. 755–760, 2007.
- [15] J. C. Delaney and J. M. Essigmann, "Mutagenesis, genotoxicity, and repair of 1-methyladenine, 3-alkylcytosines, 1-methylguanine, and 3-methylthymine in alkB *Escherichia coli*," *Proceedings of the National Academy of Sciences of the United States of America*, vol. 101, no. 39, pp. 14051–14056, 2004.
- [16] J. C. Delaney and J. M. Essigmann, "Context-dependent mutagenesis by DNA lesions," *Chemistry and Biology*, vol. 6, no. 10, pp. 743–753, 1999.
- [17] J. C. Delaney and J. M. Essigmann, "Effect of sequence context on O6-methylguanine repair and replication *in vivo*," *Biochemistry*, vol. 40, no. 49, pp. 14968–14975, 2001.
- [18] B. Yu, W. C. Edstrom, J. Benach et al., "Crystal structures of catalytic complexes of the oxidative DNA/RNA repair enzyme AlkB," *Nature*, vol. 439, no. 7078, pp. 879–884, 2006.
- [19] C.-J. Chang, J. D. Gomes, and S. R. Byrn, "Chemical modification of deoxyribonucleic acids: a direct study by carbon-13 nuclear magnetic resonance spectroscopy," *Journal of Organic Chemistry*, vol. 48, no. 26, pp. 5151–5160, 1983.
- [20] L. A. Culp, E. Dore, and G. M. Brown, "Methylated bases in DNA of animal origin," *Archives of Biochemistry and Biophysics*, vol. 136, no. 1, pp. 73–79, 1970.
- [21] C.-Y. I. Lee, J. C. Delaney, M. Kartalou et al., "Recognition and processing of a new repertoire of DNA substrates by human 3-methyladenine DNA glycosylase (AAG)," *Biochemistry*, vol. 48, no. 9, pp. 1850–1861, 2009.
- [22] P. Ø. Falnes, "Repair of 3-methylthymine and 1-methylguanine lesions by bacterial and human AlkB proteins," *Nucleic Acids Research*, vol. 32, no. 21, pp. 6260–6267, 2004.
- [23] T. Lindahl, B. Sedgwick, M. Sekiguchi, and Y. Nakabeppu, "Regulation and expression of the adaptive response to alkylating agents," *Annual Review of Biochemistry*, vol. 57, pp. 133–157, 1988.
- [24] E. L. Loechler, C. L. Green, and J. M. Essigmann, "In vivo mutagenesis by O6-methylguanine built into a unique site in a viral genome," *Proceedings of the National Academy of Sciences of the United States of America*, vol. 81, no. 20, pp. 6271–6275, 1984.
- [25] P. Taverna and B. Sedgwick, "Generation of an endogenous DNA-methylating agent by nitrosation in *Escherichia coli*," *Journal of Bacteriology*, vol. 178, no. 17, pp. 5105–5111, 1996.
- [26] D. E. G. Shuker and G. P. Margison, "Nitrosated glycine derivatives as a potential source of O6-methylguanine in DNA," *Cancer Research*, vol. 57, no. 3, pp. 366–369, 1997.
- [27] A. Loveless, "Possible relevance of O-6 alkylation of deoxyguanosine to the mutagenicity and carcinogenicity of nitrosamines and nitrosamides," *Nature*, vol. 223, no. 5202, pp. 206–207, 1969.
- [28] L. J. Rasmussen and L. Samson, "The *Escherichia coli* MutS DNA mismatch binding protein specifically binds O6-methylguanine DNA lesions," *Carcinogenesis*, vol. 17, no. 9, pp. 2085–2088, 1996.
- [29] D. T. Beranek, C. C. Weis, and D. H. Swenson, "A comprehensive quantitative analysis of methylated and ethylated DNA using high pressure liquid chromatography," *Carcinogenesis*, vol. 1, no. 7, pp. 595–606, 1980.
- [30] J. D. Gomes and C. J. Chang, "Reverse-phase high-performance liquid chromatography of chemically modified DNA," *Analytical Biochemistry*, vol. 129, no. 2, pp. 387–391, 1983.
- [31] D. J. Ashworth, W. M. Baird, C. J. Chang et al., "Chemical modification of nucleic acids. Methylation of calf thymus DNA investigated by mass spectrometry and liquid chromatography," *Biomedical Mass Spectrometry*, vol. 12, no. 7, pp. 309–318, 1985.
- [32] G. P. Margison, J. M. Margison, and R. Montesano, "Methylated purines in the deoxyribonucleic acid of various Syrian golden hamster tissues after administration of a hepatocarcinogenic dose of dimethylnitrosamine," *Biochemical Journal*, vol. 157, no. 3, pp. 627–634, 1976.
- [33] E. M. Faustman and J. I. Goodman, "A method for the rapid quantitation of methylated hepatic DNA-purines using high pressure liquid chromatography," *Journal of Pharmacological Methods*, vol. 4, no. 4, pp. 305–312, 1980.
- [34] D. T. Beranek, R. H. Heflich, R. L. Kodell, S. M. Morris, and D. A. Casciano, "Correlation between specific DNA-methylation products and mutation induction at the HGPRT locus in Chinese hamster ovary cells," *Mutation Research*, vol. 110, no. 1, pp. 171–180, 1983.
- [35] E. M. Faustman-Watts and J. I. Goodman, "DNA-purine methylation in hepatic chromatin following exposure to dimethylnitrosamine or methylnitrosourea," *Biochemical Pharmacology*, vol. 33, no. 4, pp. 585–590, 1984.
- [36] F. El Ghissassi, A. Barbin, J. Nair, and H. Bartsch, "Formation of 1,N6-ethanoadenine and 3,N4-ethenocytosine by lipid peroxidation products and nucleic acid bases," *Chemical Research in Toxicology*, vol. 8, no. 2, pp. 278–283, 1995.
- [37] F.-L. Chung, H.-J. C. Chen, and R. G. Nath, "Lipid peroxidation as a potential endogenous source for the formation of exocyclic DNA adducts," *Carcinogenesis*, vol. 17, no. 10, pp. 2105–2111, 1996.
- [38] L. J. Marnett, "Oxyradicals and DNA damage," *Carcinogenesis*, vol. 21, no. 3, pp. 361–370, 2000.
- [39] I. A. Blair, "Lipid hydroperoxide-mediated DNA damage," *Experimental Gerontology*, vol. 36, no. 9, pp. 1473–1481, 2001.
- [40] J. Nair, A. Barbin, Y. Guichard, and H. Bartsch, "1,N6-ethenodeoxyadenosine and 3,N4-ethenodeoxycytidine in liver DNA from humans and untreated rodents detected by immunoaffinity/32P-postlabelling," *Carcinogenesis*, vol. 16, no. 3, pp. 613–617, 1995.
- [41] A. Barbin, H. Ohgaki, J. Nakamura, M. Kurrer, P. Kleihues, and J. A. Swenberg, "Endogenous deoxyribonucleic acid (DNA) damage in human tissues: a comparison of ethenobases with aldehydic DNA lesions," *Cancer Epidemiology Biomarkers and Prevention*, vol. 12, no. 11, pp. 1241–1247, 2003.
- [42] A. Barbin, "Etheno-adduct-forming chemicals: from mutagenicity testing to tumor mutation spectra," *Mutation Research*, vol. 462, no. 2-3, pp. 55–69, 2000.
- [43] M. Sapparbaev, K. Kleibl, and J. Laval, "*Escherichia coli*, *Saccharomyces cerevisiae*, rat and human 3-methyladenine DNA glycosylases repair 1,N6-ethanoadenine when present in DNA," *Nucleic Acids Research*, vol. 23, no. 18, pp. 3750–3755, 1995.
- [44] B. P. Engelward, G. Weeda, M. D. Wyatt et al., "Base excision repair deficient mice lacking the Aag alkyladenine DNA glycosylase," *Proceedings of the National Academy of Sciences of*

- the United States of America*, vol. 94, no. 24, pp. 13087–13092, 1997.
- [45] A.-J. L. Ham, B. P. Engelward, H. Koc et al., “New immunoaffinity-LC-MS/MS methodology reveals that Aag null mice are deficient in their ability to clear 1,N6-etheno-deoxyadenosine DNA lesions from lung and liver *in vivo*,” *DNA Repair*, vol. 3, no. 3, pp. 257–265, 2004.
- [46] Y. Mishina, C.-G. Yang, and C. He, “Direct repair of the exocyclic DNA adduct 1,N6-etheno-adenine by the DNA repair AlkB proteins,” *Journal of the American Chemical Society*, vol. 127, no. 42, pp. 14594–14595, 2005.
- [47] J. Ringvoll, M. N. Moen, L. M. Nordstrand et al., “AlkB homologue 2-mediated repair of etheno-adenine lesions in mammalian DNA,” *Cancer Research*, vol. 68, no. 11, pp. 4142–4149, 2008.
- [48] S. Boiteux and J. Laval, “Mutagenesis by alkylating agents: coding properties for DNA polymerase of poly (dC) template containing 3-methylcytosine,” *Biochimie*, vol. 64, no. 8-9, pp. 637–641, 1982.
- [49] H. Kawasaki, S. Ninomiya, and H. Yuki, “High-performance liquid chromatographic determination of 3-methylcytosine in deoxyribonucleic acid treated with carcinogenic methylating agents *in vitro* and *in vivo*,” *Chemical and Pharmaceutical Bulletin*, vol. 33, no. 3, pp. 1170–1174, 1985.
- [50] J. V. Frei, D. H. Swenson, W. Warren, and P. D. Lawley, “Alkylation of deoxyribonucleic acid *in vivo* in various organs of C57BL mice by the carcinogens N-methyl-N-nitrosourea, N-ethyl-N-nitrosourea and ethyl methanesulphonate in relation to induction of thymic lymphoma,” *Biochemical Journal*, vol. 174, no. 3, pp. 1031–1044, 1978.
- [51] P. T. Rye, J. C. Delaney, C. Netirojjanakul, D. X. Sun, J. Z. Liu, and J. M. Essigmann, “Mismatch repair proteins collaborate with methyltransferases in the repair of O<sup>6</sup>-methylguanine,” *DNA Repair*, vol. 7, no. 2, pp. 170–176, 2008.
- [52] M. Tahiliani, K. P. Koh, Y. Shen et al., “Conversion of 5-methylcytosine to 5-hydroxymethylcytosine in mammalian DNA by MLL partner TET1,” *Science*, vol. 324, no. 5929, pp. 930–935, 2009.
- [53] M. Saparbaev and J. Laval, “3,N4-ethenocytosine, a highly mutagenic adduct, is a primary substrate for *Escherichia coli* double-stranded uracil-DNA glycosylase and human mismatch-specific thymine-DNA glycosylase,” *Proceedings of the National Academy of Sciences of the United States of America*, vol. 95, no. 15, pp. 8508–8513, 1998.
- [54] L. Den Engelse, G. J. Menkveld, R.-J. De Brij, and A. D. Tates, “Formation and stability of alkylated pyrimidines and purines (including imidazole ring-opened 7-alkylguanine) and alkylphosphotriesters in liver DNA of adult rats treated with ethylnitrosourea or dimethylnitrosamine,” *Carcinogenesis*, vol. 7, no. 3, pp. 393–403, 1986.
- [55] B. Singer, J. Sági, and J. T. Kuśmierk, “*Escherichia coli* polymerase I can use O<sup>2</sup>-methyldeoxythymidine or O<sup>4</sup>-methyldeoxythymidine in place of deoxythymidine in primed poly(dA-dT).poly(dA-dT) synthesis,” *Proceedings of the National Academy of Sciences of the United States of America*, vol. 80, no. 16, pp. 4884–4888, 1983.
- [56] T. Gerken, C. A. Girard, Y.-C. L. Tung et al., “The obesity-associated FTO gene encodes a 2-oxoglutarate-dependent nucleic acid demethylase,” *Science*, vol. 318, no. 5855, pp. 1469–1472, 2007.
- [57] G. Jia, C.-G. Yang, S. Yang et al., “Oxidative demethylation of 3-methylthymine and 3-methyluracil in single-stranded DNA and RNA by mouse and human FTO,” *FEBS Letters*, vol. 582, no. 23-24, pp. 3313–3319, 2008.

## Research Article

# Aflatoxin B<sub>1</sub>-Associated DNA Adducts Stall S Phase and Stimulate Rad51 foci in *Saccharomyces cerevisiae*

Michael Fasullo,<sup>1,2,3</sup> Yifan Chen,<sup>1</sup> William Bortcosh,<sup>3</sup> Minzeng Sun,<sup>1</sup> and Patricia A. Egner<sup>4</sup>

<sup>1</sup>Ordway Research Institute, Center for Medical Sciences, 150 New Scotland Avenue, Albany, NY 12209, USA

<sup>2</sup>Department of Biomedical Sciences, State University of New York at Albany, 150 New Scotland Avenue, Albany, NY 12209, USA

<sup>3</sup>Albany Medical College, 47 New Scotland Avenue, Albany, NY 12208, USA

<sup>4</sup>Bloomberg School of Public Health, Johns Hopkins University, 615 North Wolfe Street, Baltimore, MD 21205, USA

Correspondence should be addressed to Michael Fasullo, mfasullo@ordwayresearch.org

Received 15 August 2010; Accepted 9 September 2010

Academic Editor: Ashis Basu

Copyright © 2010 Michael Fasullo et al. This is an open access article distributed under the Creative Commons Attribution License, which permits unrestricted use, distribution, and reproduction in any medium, provided the original work is properly cited.

AFB<sub>1</sub> is a potent recombinagen in budding yeast. AFB<sub>1</sub> exposure induces *RAD51* expression and triggers Rad53 activation in yeast cells that express human CYP1A2. It was unknown, however, when and if Rad51 foci appear. Herein, we show that Rad53 activation correlates with cell-cycle delay in yeast and the subsequent formation of Rad51 foci. In contrast to cells exposed to X-rays, in which Rad51 foci appear exclusively in G2 cells, Rad51 foci in AFB<sub>1</sub>-exposed cells can appear as soon as cells enter S phase. Although *rad51* and *rad4* mutants are mildly sensitive to AFB<sub>1</sub>, chronic exposure of the NER deficient *rad4* cells to AFB<sub>1</sub> leads to increased lag times, while *rad4 rad51* double mutants exhibit synergistic sensitivity and do not grow when exposed to 50 μM AFB<sub>1</sub>. We suggest *RAD51* functions to facilitate DNA replication after replication fork stalling or collapse in AFB<sub>1</sub>-exposed cells.

## 1. Introduction

Hepatocellular carcinoma (HCC) ranks fifth in worldwide cancer mortality (for review, see [1]) and sixth in the United States [2]. High-risk factors for HCC include exposure to genotoxins, such as the mycotoxin aflatoxin B<sub>1</sub> (AFB<sub>1</sub>), and infection with hepatitis B and C viruses [3]. Exposure to AFB<sub>1</sub> is endemic in particular areas of China and sub-Saharan Africa due to *Aspergillus flavus* (mold) contamination of food and water [3]. A current hypothesis is that regeneration of liver cells following chronic liver injury renders liver cells susceptible to AFB<sub>1</sub>-associated carcinogenesis [4].

HCC pathogenesis is correlated with the accumulation of mutations and chromosomal rearrangements leading to either an inactivation of tumor suppressor genes or activation of oncogenes (for review, see [5]). MicroRNA-221 (MiR-221) overexpression contributes to liver tumorigenesis [6] and correlates with downregulation of cyclin dependent kinase inhibitors p21 and p57 [7]; however, there is no

known correlation with AFB<sub>1</sub> exposure. The p53(Ser)249 substitution mutation frequently occurs in liver cancer, where AFB<sub>1</sub> exposure is highest [8–10]; however, there are conflicting reports whether the p53 249 codon is a direct hot spot for AFB<sub>1</sub>-associated mutagenesis [11]. Gross chromosomal translocations and gene amplifications have also been observed [12], and 10%–20% of HCCs contain cyclin D amplifications [13]. Although HCC associated with AFB<sub>1</sub> exposure exhibits more genetic instability compared to HCC in nonendemic regions [14], it is unclear which types of genetic instability are directly caused by AFB<sub>1</sub>-associated DNA damage.

AFB<sub>1</sub> is not genotoxic *per se* but requires metabolic activation. In humans, AFB<sub>1</sub> metabolic activation in the liver is catalyzed by CYP1A2 and CYP3A4 [15] to form the highly unstable AFB<sub>1</sub>-8,9-exo-epoxide, which reacts primarily with the N<sup>7</sup> position of guanine, present in the major groove of DNA [16]. The resulting adduct, 8,9-dihydro-8-(N<sup>7</sup>-guanyl)-9-hydroxyaflatoxin B<sub>1</sub> (AFB<sub>1</sub>-N<sup>7</sup>-Guanine) is unstable and converts to either formamidopyrimidine

(FAPY) derivatives or an apurinic site [16], both potentially mutagenic [17]. Both the FAPY derivatives and AFB<sub>1</sub>-N<sup>7</sup>-Guanine adducts are repaired by the nucleotide excision repair (NER) genes [18, 19]. The FAPY adducts also hinder DNA replication [20], which could lead to chromosomal breaks and require DNA repair genes that function in double-strand break and X-ray repair (XRCC). Thus, repair of AFB<sub>1</sub>-associated DNA damage may require both NER and XRCC genes.

Interestingly, a subset of known polymorphisms [21] in both NER gene XPD and the X-ray repair gene XRCC3 correlate with higher incidence in liver cancer in endemic areas of AFB<sub>1</sub> exposure [22, 23]. Defective NER could lead to an increase in DNA adducts, while XRCC3 polymorphisms could confer defective repair of double-strand breaks (for review, see [24]). However, the polymorphism in XRCC3, Thr241Met, which is correlated with higher levels of AFB<sub>1</sub>-associated HCC [23], has not been correlated with a defect in double-strand break repair [25], suggesting that other functions in DNA damage or repair may be defective in cells containing this allele. Considering that recombinational repair may also participate in DNA damage-tolerance pathways, it is important to elucidate whether there are competing DNA repair pathways for AFB<sub>1</sub>-associated adducts.

*Saccharomyces cerevisiae* (budding yeast) is useful in elucidating the genetics of DNA repair of AFB<sub>1</sub>-DNA adducts. Yeast strains that express human *CYP1A1* or *CYP1A2* cDNAs on multicopy 2  $\mu$  plasmids can measure the genotoxicity of metabolically active carcinogens [26–30]. Interestingly, AFB<sub>1</sub> increases recombination frequencies more than mutation frequencies in cells expressing these cDNAs [26, 29].

The genotoxicity of AFB<sub>1</sub> in yeast [26–29] correlates with the transcription of DNA repair genes involved in recombination, including *RAD51* [27, 30] and *RAD54* [30]. *RAD51* induction has been observed in log phase cells exposed to AFB<sub>1</sub> [30], and *RAD51* overexpression partially suppresses recombination defects in the *mec1* null checkpoint mutant [27]. *RAD51* is also required for AFB<sub>1</sub>-associated sister chromatid exchange (SCE) [29]. These results indicate that increased expression of *RAD51* likely stimulates recombination when cells are exposed to AFB<sub>1</sub>-associated DNA adducts.

In log-phase yeast cultures, AFB<sub>1</sub> is a mutagen [28]. Microarray analysis reveals not only a strong induction of *RAD51* and *RAD54* but also a downregulation of gene transcripts encoding histones [30]. *rad51* mutants exhibit an increase in AFB<sub>1</sub>-associated mutations [28]. Both AFB<sub>1</sub>-associated mutations and recombination events require checkpoint genes [28, 29]. Considering that AFB<sub>1</sub> exposure triggers both checkpoint activation and S phase delay, it seems possible that the genotoxic responses to AFB<sub>1</sub> result from stalled replication forks.

In this paper, we show that Rad53 activation correlates with S phase delay and subsequent Rad51 foci formation in yeast. A *RAD51* deletion in NER defective strains results in high levels of lethality. We suggest that Rad51 foci formation may occur in S phase and be associated with error-free bypass of DNA lesions.

## 2. Materials and Methods

**2.1. Strains and Media.** Standard media were used for the culture of yeast cells. YPD (yeast extract, peptone, and dextrose), SC-TRP (synthetic complete lacking tryptophan), and SC-URA (synthetic complete lacking uracil) and FOA (5-fluoro-orotic acid) were described in Burke et al. [31]. The genotypes of yeast strains used in this study are listed in Table 1. *rad4*, *rad51* and *rad4 rad51* strains for measuring SCE and AFB<sub>1</sub> sensitivity are derived from YB163, which contains *his3* recombination substrates in tandem at *TRP1* [32]. Ura<sup>-</sup> derivatives of *rad4*, and *rad4 rad51* strains were selected on FOA medium. LSY1957 was a gift of Fung et al. [33]. pRS424-CYP1A2 was constructed by inserting the *SacI* CYP1A2 fragment from pCS316 into pRS424 and introduced into yeast strains by selecting for Trp<sup>+</sup> transformants.

**2.2. Measuring DNA AFB<sub>1</sub>-Associated Recombination and Rad51 foci.** To measure AFB<sub>1</sub>-associated genotoxic events, log-phase yeast cells ( $A_{600} = 0.5-1$ ) were centrifuged and concentrated five-fold in selective media (SC-URA or SC-TRP). Cells were exposed to 50  $\mu$ M AFB<sub>1</sub>, previously dissolved in DMSO. To synchronize cells in G1, log-phase cells were exposed to 10<sup>-4</sup> M alpha factor (Sigma Co.) for two hours, and G1 cells were visualized in the light microscope. Cells were maintained in selective media (SC-URA or SC-TRP) during the carcinogen exposure and then washed twice in H<sub>2</sub>O. To measure SCE frequencies, recombinants were selected on SC-HIS, and viability was determined by plating an appropriate dilution on YPD. To visualize Rad51 foci formation, cells were resuspended in selective media (SC-TRP or SC-URA) and immobilized on glass slides.

To determine whether ionizing radiation stimulates the formation of Rad51 foci, cells were washed once in H<sub>2</sub>O, resuspended in 10 ml of H<sub>2</sub>O, and placed in a 81 mm diameter Petri dish. Cells were irradiated at 6 krad using a Nordion 1.8 kCi <sup>137</sup>Cs irradiator (6 krad/hr). After irradiation cells were concentrated in YPD medium and immobilized on glass slides.

**2.3. Live Cell Epifluorescence and Microscopy Analysis.** Cells for microscopic analysis were grown to early-mid-log phase overnight in synthetic medium. After exposure to the genotoxin, cells were harvested by centrifugation, washed twice, and resuspended in YPD. Immobilization of cells was performed by mixing equal volumes of cell suspension and 1.4% low-melt agarose. Cover slips were sealed with a wax mixture as described by Lisby et al. [35]. Slides were visualized using a Zeiss LSM 510 META confocal microscope.

**2.4. FACS Analyses.** Cells were visualized by the fluorescent activated cell sorter (FACS) to directly correlate their DNA content with their cell-cycle phases. After AFB<sub>1</sub> exposure, cells were washed, resuspended in 0.1 M sodium citrate, and treated with 1 mg/ml RNase A at 50°C for 1 hr. The cells were incubated at 50°C for 5 hr in 8  $\mu$ g/ml proteinase K. An equal volume of 25  $\mu$ g/ml propidium iodide (PI) diluted in 0.1 M sodium citrate was then added to the cells prior to the

TABLE 1: Yeast strains.

Strain (source)	Genotype	Plasmid introduced	Reference
Strains isogenic to S288c*			
YB401	<i>MATa-inc ura3-52 his3- Δ200 ade2-101 lys-801 trp1- Δ1 gal3-trp1:: [his3- Δ3'::HOcs, his3- Δ5']</i>	pCS316	This laboratory
YB402	<i>MATα leu2-Δ1 rad51</i>	pCS316	[34]
YB403	<i>MATa-inc ura3 rad4::KanMX</i>	pCS316	[34]
YB404	<i>MATa-inc ura3 rad51::URA3 rad4::KanMX rad51</i>	pCS316	[34]
Strains isogenic to W303			
YB405	<i>MATa YFP-rad51-I345T-URA3-RAD51 ADE2 leu2 trp1 ura3 his3</i>	PRS424-CYP1A2	L.Symington (LSY1957) [33]

\*Strains under this heading are isogenic to S288c. All genotypes are the same as YB163, unless indicated.

FACS analysis, to a final concentration of 12.5  $\mu\text{g/ml}$  PI, and analyzed for fluorescence content with the use of a BD LSR II Flow cytometer.

**2.5. Detection and Quantification of DNA Adducts.** To measure the AFB<sub>1</sub>-associated DNA adducts in yeast, we used liquid chromatography-electrospray ionization tandem mass spectrometry (LC-ESI/MS/MS) [36]. Log-phase cultures of yeast-expressing human CYP1A2 (pCS316) were exposed to 50  $\mu\text{M}$  AFB<sub>1</sub> for 4 h. Because standard protocols for isolating yeast DNA involve alkaline buffers, rendering the highly unstable AFB<sub>1</sub>-N<sup>7</sup>-Guanine DNA adducts labile, we have modified the “smash-and-grab” protocol [37] so that we are using a neutral buffer containing 10 mM Tris-HCl, 1 mM EDTA, 100 mM NaCl, 2% Triton X-100, and 1% SDS, pH 7. DNA was isolated from two independent samples of yeast cells. The DNA adducts were identified and measured by high-performance liquid chromatography and tandem mass spectrometry (LC-ESI/MS/MS) after acid hydrolysis [36].

**2.6. Determining Rad53 Activation.** Activation of Rad53 was determined by Western blots. Cells were inoculated in SC-URA medium. Log-phase cells ( $A_{600} = 0.5-1$ ) were concentrated three fold in SC-URA and exposed to 50  $\mu\text{M}$  AFB<sub>1</sub> for 4 h. After washing cells twice in H<sub>2</sub>O, aliquots were plated directly on SC-HIS to measure recombination, appropriately diluted and plated on YPD to measure viability. Protein extracts were prepared as previously described by Foiani et al. [38], separated on 10% acrylamide/0.266% bis-acrylamide gels for Rad53 detection and transferred to nitrocellulose membranes. Rad53 was detected by Western blotting using goat anti-Rad53 (yC-19, Santa Cruz, Biotechnology, Santa Cruz, CA). The secondary antibody was antigoat IgG-HRP (Santa Cruz).

### 3. Results

**3.1. Delay in Cell-Cycle Progression Correlated with Rad53 Activation.** We previously observed that log-phase cells

exposed to AFB<sub>1</sub> exhibit Rad53 activation [29], which can result from replication blockage or delay. We measured Rad53 activation and cell-cycle delay in log-phase cells after continuous exposure to 50  $\mu\text{M}$  AFB<sub>1</sub>. The data show that there is a peak activation of Rad53 after 3 hrs exposure to AFB<sub>1</sub>. Three hrs of exposure was also sufficient time to observe SCE recombinants (Figure 1). After 4 hrs of AFB<sub>1</sub> exposure, there was less Rad53 activation and cell-cycle progression continued. The transient delay in the cell cycle is consistent with a previous study that indicated that AFB<sub>1</sub>-exposed yeast exhibit a transient S phase delay [30]. The data suggest that there is a correlation between AFB<sub>1</sub>-associated Rad53 activation and S phase delay. Because AFB<sub>1</sub> adducts are detected in cycling cells after the S phase delay [29], we speculate that cells actively tolerate AFB<sub>1</sub>-associated DNA lesions during DNA replication.

Rad53 not only delays cell-cycle progression but is also required for the phosphorylation of the Rad51 paralogs, Rad55, and Rad57, which may facilitate replication restart at stalled replication forks [39]. Rad55 and Rad57 facilitate the formation of DNA repair foci at double-strand breaks [40]. Previous data indicate that RAD53 is required for DNA damage associated SCE [41], including AFB<sub>1</sub>-associated SCE [29]. We, therefore, determined whether AFB<sub>1</sub> exposure also stimulates Rad51 foci formation in yeast.

**3.2. Exposure to AFB<sub>1</sub> Results in Rad51 foci Formation in Cells that Are Entering S Phase.** To visualize Rad51 foci that result from AFB<sub>1</sub>-associated DNA damage, we introduced pRS424-CYP1A2 into strain LSY1957 [33] to metabolically activate AFB<sub>1</sub>. This strain (YB405) contains *rad51-I345T*, an allele of *RAD51*, which when tagged with YFP, is still capable of conferring radiation resistance [33]. As a positive control, cells were exposed to either X rays (2 krad) or gamma rays (6 krad). After exposure, cells were returned to growth medium (YPD), and live cells were imaged for Rad51 foci. After 2 hrs of growth in YPD, most irradiated cells arrested in G2 and exhibited the dumb-bell shape (Figure 2). Cells were then visualized with the confocal microscope. Nearly 90% of

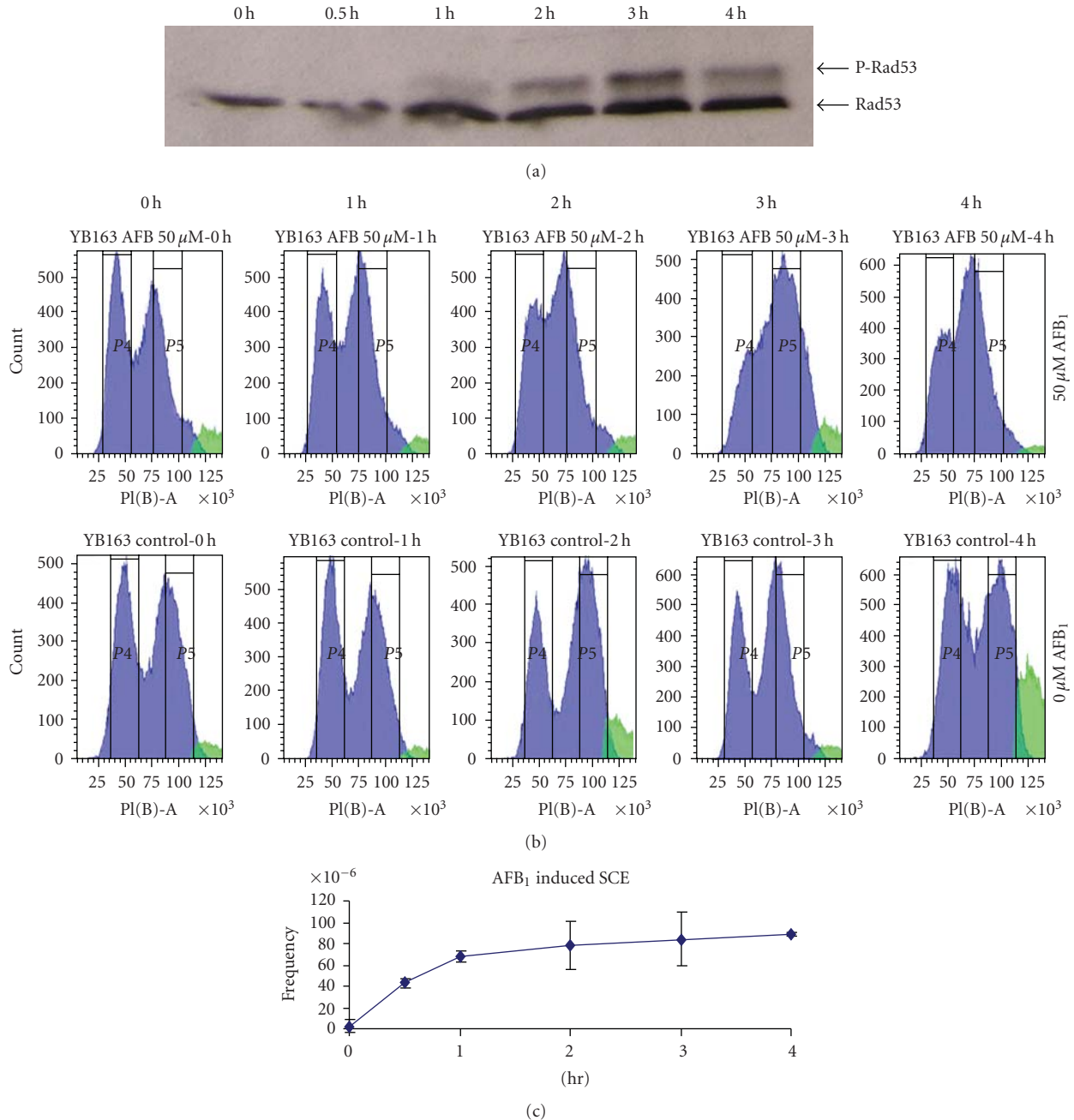


FIGURE 1: Rad53 checkpoint activation, cell cycle progression, and recombination after log-phase cells were exposed to 50  $\mu\text{M}$  AFB<sub>1</sub>. At indicated times, cells were collected for FACS analysis to measure frequencies of SCE and to make extracts to measure Rad53 activations. (a) Rad53 checkpoint activation was monitored after AFB<sub>1</sub> exposure at the indicated times. Rad53 and the activated checkpoint protein, Rad53p, are indicated by arrows. (b) FACS analysis was performed at indicated time periods after exposure. The G1 and G2 cells are indicated by P4 and P5. The peak to the right of the G2 peak indicates bloated cells due to enlarged vacuoles. (c) AFB<sub>1</sub>-associated SCE were measured by selecting for His<sup>+</sup> recombinants that result from unequal recombination between two truncated *his3* fragments. Net recombination frequencies = recombination frequency after AFB<sub>1</sub> exposure—spontaneous recombination frequency.

the G2-arrested cells contain Rad51 foci, in agreement with Lisby et al. [40].

Similarly, we determined whether Rad51 foci appear in cells after exposure to 50  $\mu\text{M}$  AFB<sub>1</sub> for 3 hrs. To first confirm the presence of AFB<sub>1</sub> adducts, we extracted DNA from LSY197 cells after AFB<sub>1</sub> exposure and observed approx-

imately the same number of DNA adducts (Table 2) as previously observed in strains used to measure recombination [29]. After 3 hr of AFB<sub>1</sub> exposure, we also observed that nearly 90% of the cells exhibited Rad51 foci. However, the difference with irradiated cells was that many AFB<sub>1</sub>-exposed cells that exhibited Rad51 foci were not G2 arrested. In

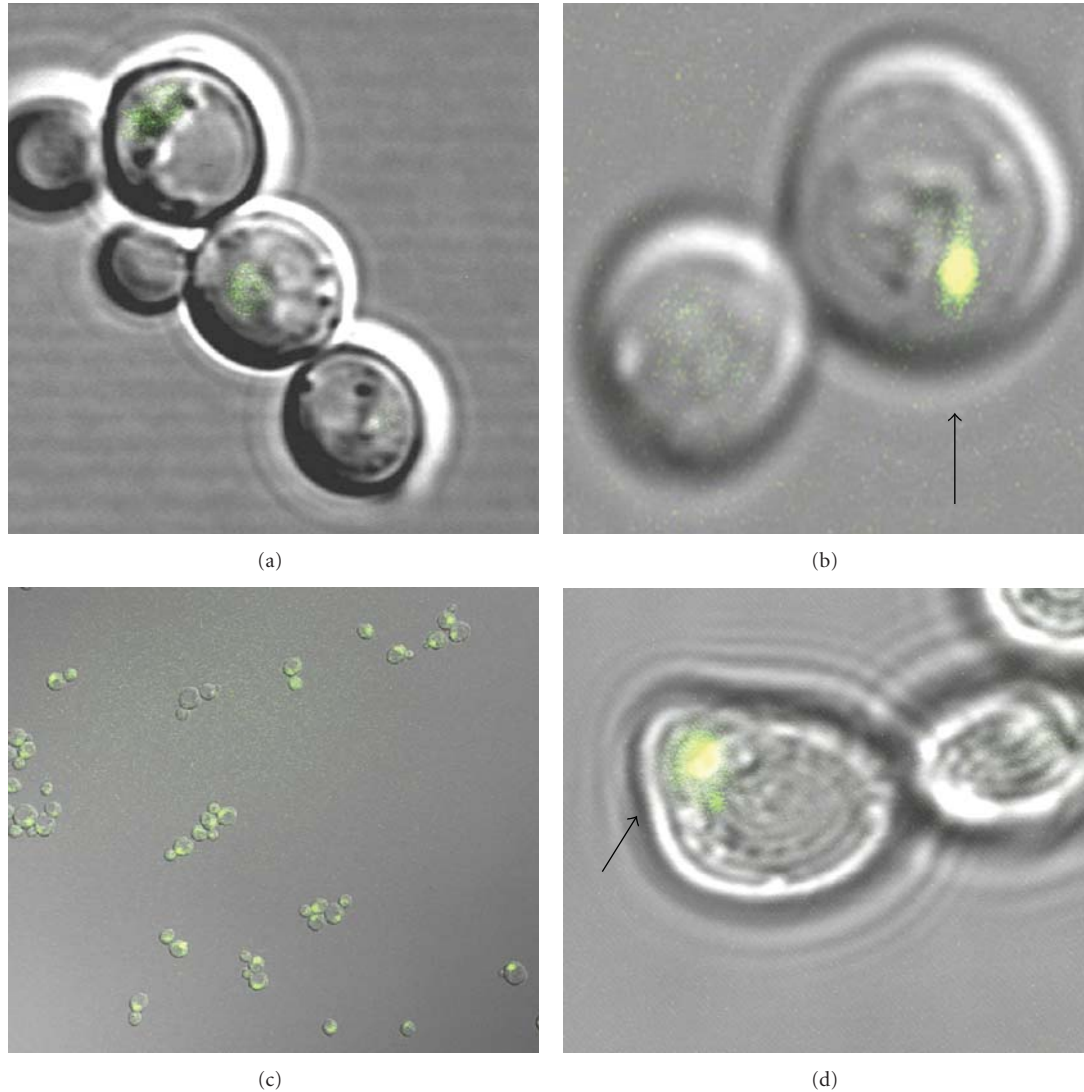


FIGURE 2: Confocal imaging of Rad51-YFP foci in live AFB<sub>1</sub>-exposed yeast cells. (a) Control, no AFB<sub>1</sub> exposure, (b) Rad51-foci after exposure to X-rays, (c) Rad51 foci in logarithmically growing cells exposed to 50  $\mu$ M AFB<sub>1</sub>, wide view, and (d) Rad51 focus in a synchronized cell after alpha factor arrest and exposure to AFB<sub>1</sub>.

addition, many cells exhibited Rad51 foci in both mother and daughter bud (Figure 2). These data indicate that AFB<sub>1</sub>-associated Rad51 foci are not restricted to the G2 phase of the cell cycle. Because daughter buds are not always visible in the confocal microscope, we decided to synchronize cells in G1, expose the cells to AFB<sub>1</sub> and then determine when Rad51 foci could be detected.

To determine whether cells can express Rad51 foci in S phase, cells were first arrested in G1 with alpha factor, and then exposed to AFB<sub>1</sub> for three hours. Cells were then washed and returned to growth medium without AFB<sub>1</sub>. We observed that newly budded cells (90%) contain Rad51 foci. Rad51 foci were not evident after 30 minutes or 1 hr incubation time, but were evident after 1.5 hrs of incubation; after three hours of incubation, there were few Rad51 foci. These data indicate that Rad51 foci can be observed in cycling cells that are entering S phase.

TABLE 2: AFB<sub>1</sub>-N<sup>7</sup> Guanine adducts in wild type and the *rad4* mutant.

Genotype (Strain) <sup>a</sup>	Total AFB <sub>1</sub> -N <sup>7</sup> Guanine adducts/mg DNA <sup>b</sup>	Ratio <sup>c</sup>
<i>RAD4</i> (YB163)	$7.2 \times 10^{-3}$ nmol	1
<i>rad4::KanMX</i> (YB225)	$21.7 \times 10^{-3}$ nmol	3
Rad51-YFP (LSY1957)	$4.6 \times 10^{-3}$ nmol	0.7

<sup>a</sup> Relevant genotype, see Table 1 for complete genotype,

<sup>b</sup>  $n = 2$ ,

<sup>c</sup> Ratio: AFB<sub>1</sub> adduct in strain or *rad* mutant/AFB<sub>1</sub> adduct in wild type (YB163).

3.3. *rad4* Cells Are Defective in the Excision of AFB<sub>1</sub> DNA Adducts. NER and recombinational repair mutants are modestly sensitive to AFB<sub>1</sub> [27, 28]. Both *rad4* and *rad51* mutants exhibit higher rates of AFB<sub>1</sub>-associated mutagenesis

[29, 30]. Measurements of DNA adducts indicated there are about three-fold higher levels of AFB<sub>1</sub>-N<sup>7</sup>-Guanine adducts in *rad4*, compared to wild type (Table 2). Consistent with the notion that AFB<sub>1</sub> adducts persist longer in *rad4* mutants, we observed by FACS analysis a delayed S phase after exposure to 10 μM AFB<sub>1</sub>. We asked whether wild type, *rad4*, and *rad51* mutants could tolerate DNA adducts.

We used a growth assay in microtiter dishes [42] to determine differences in growth curves of wild type (YB401), *rad4* (YB403), *rad51* (YB402), and *rad4 rad51* (YB404) strains during chronic exposure to AFB<sub>1</sub>. Approximately 10<sup>5</sup> cells were inoculated in 96 well plates and exposed to 0 μM, 25 μM and 50 μM of AFB<sub>1</sub>; the experiments were done in triplicate. Growth was measured by A<sub>600</sub> (Figure 3). The lag time [42] for wild type was ~3 hrs and similar to *rad51*. Whereas the *rad4* mutants exhibited a longer lag period, ~13 hrs, the *rad4 rad51* mutant exhibited little, if any, growth. The data suggest that *RAD51* function is critical in conferring AFB<sub>1</sub> resistance in the *rad4* mutant. This result is consistent with previous results that *rad14 rad51* cells are also synergistically more sensitive to AFB<sub>1</sub> [30].

To further investigate whether *rad4* cells can progress through S phase in the presence of DNA adducts, we arrested *rad4* cells in G1 with alpha factor and exposed cells to AFB<sub>1</sub> for 3 hrs. Cells were then washed, diluted, and inoculated on YPD plates to visualize the growth of single colonies every three hours under the microscope. After 12 hrs, ~70% (46/67) of cells that were not exposed to AFB<sub>1</sub> formed colonies. However, only ~16% (46/268) of cells exposed to AFB<sub>1</sub> (10 μM or 50 μM) formed colonies. 60% (*n* = 2) of either wild type or *rad4* cells that do form colonies retain the *URA3*-containing plasmid expressing *CYP1A2*, indicating that colony formation occurred in cells that could still metabolically activate AFB<sub>1</sub>. Many of the *rad4* cells that do not form colonies were arrested in early S phase, as evident by the presence of small daughter buds (Figure 3(f)). These data indicate that a few NER-deficient cells can progress through the cell cycle in the presence of AFB<sub>1</sub>-associated DNA adducts.

#### 4. Discussion

AFB<sub>1</sub> is a very potent liver carcinogen. The metabolic activation of AFB<sub>1</sub> generates AFB<sub>1</sub>-associated DNA adducts which both stimulate mutagenesis and recombination in a variety of organisms. Polymorphisms in both XPD and XRCC3 are correlated with greater HCC risk [22, 23], thus underscoring the need to elucidate the role of recombinational repair in AFB<sub>1</sub> metabolism. In budding yeast, well-conserved RAD and checkpoint genes are required for AFB<sub>1</sub>-associated mutation and recombination [28, 29]. Higher frequencies of AFB<sub>1</sub>-associated mutations in *rad51* mutants [28, 29] and synergistic increase in the AFB<sub>1</sub> sensitivity of double mutants defective in both recombinational and NER suggest that there are redundant pathways in conferring resistance to AFB<sub>1</sub>. AFB<sub>1</sub> is highly recombinogenic and induces *RAD51* in yeast [27]; however, it was unclear when and if Rad51 foci form. The salient conclusions from this study are (1) cells

are delayed in S phase after AFB<sub>1</sub> exposure, and there is a correlation with Rad53 checkpoint activation and cell cycle delay; (2) Rad51 foci form after AFB<sub>1</sub>-exposed cells enter S phase; (3) *rad4* mutants accumulate AFB<sub>1</sub>-N<sup>7</sup>-Guanine adducts, and many exposed cells arrest or are delayed in S phase. This is the first study to show that AFB<sub>1</sub> exposure leads to Rad51 foci formation.

Previous studies indicated that *RAD53* is required for both AFB<sub>1</sub>-associated recombination and mutagenesis in yeast [29]. The coincident timing of recombination, Rad53 checkpoint activation, and S phase delay suggest that checkpoint activation is required to trigger AFB<sub>1</sub>-associated recombination in yeast. A possible link is that Rad53 is required for the DNA damage-associated phosphorylation of the Rad51 paralogs Rad55 and Rad57 [39], which participate in recombinational repair between sister chromatids [34]. We do not yet know how the checkpoint activation would trigger mutagenesis, but several studies suggest a role for checkpoint genes in DNA damage tolerance and translesion synthesis [43–46].

The identification of AFB<sub>1</sub>-associated Rad51 foci was performed by detecting YFP fluorescence in the confocal microscope. Rad51 is not known to bind to specific DNA adducts, so we presume that the AFB<sub>1</sub> N<sup>7</sup>-Guanine adducts and resulting FAPY and apurinic sites are further converted into recombinogenic lesions, including double-strand breaks or single-strand gaps. It is unlikely that all the lesions that initiate AFB<sub>1</sub>-associated Rad51 foci are the same as for X-ray-associated Rad51 foci, since we observed Rad51 foci in newly cycling cells entering S phase whereas we only observed X-ray-initiated Rad51-foci in G2-arrested cells. However, double-strand breaks or single-strand gaps could also result after replication forks stall or collapse in S phase, and AFB<sub>1</sub> lesions have been reported to stall or hinder DNA replication in *Escherichia coli* [17]. Thus, an attractive model is that Rad51 foci form as AFB<sub>1</sub>-exposed cells transition through S phase.

We suggest that *RAD51* confers AFB<sub>1</sub> resistance in NER defective mutants by two possible functions. First, *RAD51* would function in repairing double-strand breaks that indirectly results from AFB<sub>1</sub>-associated DNA damage. Considering that one double-strand break could confer lethality [47], one would estimate that at least one break occurs in every *rad4 rad51* double mutant cell during chronic exposure to 50 μM AFB<sub>1</sub>. Second, *RAD51* could actively participate in tolerating AFB<sub>1</sub>-associated DNA lesions; previous studies have indicated that the *RAD52* pathway is involved in tolerating UV-associated damage [48]. Growth curves of wild-type cells indicate that some AFB<sub>1</sub>-associated DNA adducts can be tolerated without affecting doubling time. This second possibility is supported by observations that *rad14 rad51* mutants exhibit extremely high frequencies of AFB<sub>1</sub>-associated mutagenesis [28]. Further speculation would suggest that the Rad51-paralog, XRCC3, has a similar function.

#### 5. Conclusions

AFB<sub>1</sub>-associated DNA adducts stimulate both checkpoint activation and Rad51 focus formation. The timing of the

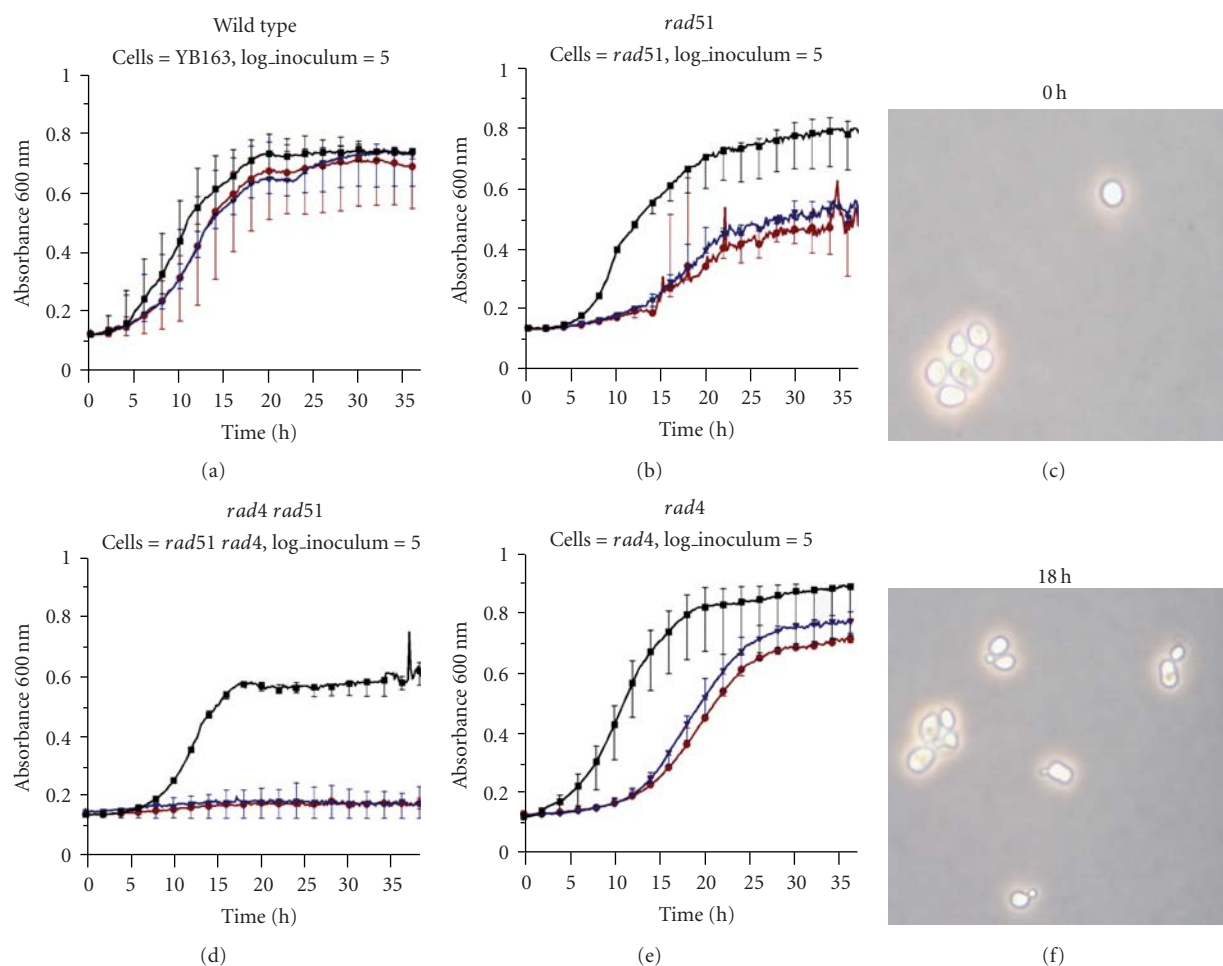


FIGURE 3: Growth of wild type (a), *rad51* (b), *rad4* (e), and *rad4 rad51* (d) cells after exposure to AFB<sub>1</sub>. (Left) Growth of cells containing pCS316 and expressing CYP1A2 after chronic exposure to 0 μM (black), 25 μM (blue), and 50 μM (red) AFB<sub>1</sub>. The relevant genotype is given below the panel (see Table 1, for complete genotype). 10<sup>5</sup> log-phase cells were inoculated in each well, *n* = 3. *A*<sub>600</sub> is plotted against time (h). (Right) *rad4* cells synchronized in G1 were exposed to 50 μM AFB<sub>1</sub> for 3 hrs, washed, and inoculated on YPD. Cell growth was monitored from 0–18 hrs. Bars indicate the actual range of measurements.

Rad51 foci during the cell cycle in early S phase suggests a different mechanism of foci formation, compared to that of ionizing radiation. Understanding the function of these Rad51 foci will elucidate how polymorphisms in XRCC3 correlate with higher rates of liver cancer in endemic areas exposed to AFB<sub>1</sub>. It will thus be interesting if Rad51 foci also occur in mammalian cells after AFB<sub>1</sub> exposure.

## Acknowledgments

This work was supported by Grants nos. ES015954 and PO1ES006052 from the National Institutes of Health. The authors are thankful to Gary Schools for his expertise on the confocal microscope, Autumn Smith and Cinzia Cera for assistance with the microplate reader, and Cinzia Cera for critically reading this paper. We thank Chang-Uk Lim for assistance with the flow cytometer.

## References

- [1] S. A. Hussain, D. R. Ferry, G. El-Gazzaz et al., "Hepatocellular carcinoma," *Annals of Oncology*, vol. 12, no. 2, pp. 161–172, 2001.
- [2] A. Jemal, R. Siegel, J. Xu, and E. Ward, "Cancer statistics," *CA A Cancer Journal for Clinicians*, vol. 60, no. 5, pp. 277–300, 2010.
- [3] K. A. McGlynn and W. T. London, "Epidemiology and natural history of hepatocellular carcinoma," *Best Practice and Research*, vol. 19, no. 1, pp. 3–23, 2005.
- [4] M. C. Kew, "Synergistic interaction between aflatoxin B<sub>1</sub> and hepatitis B virus in hepatocarcinogenesis," *Liver International*, vol. 23, no. 6, pp. 405–409, 2003.
- [5] D. Moradpour and H. E. Blum, "Pathogenesis of hepatocellular carcinoma," *European Journal of Gastroenterology and Hepatology*, vol. 17, no. 5, pp. 477–483, 2005.
- [6] P. Pineau, S. Volinia, K. McJunkin et al., "miR-221 overexpression contributes to liver tumorigenesis," *Proceedings of the National Academy of Sciences of the United States of America*, vol. 107, no. 1, pp. 264–269, 2010.

- [7] F. Fornari, L. Gramantieri, M. Ferracin et al., "MiR-221 controls CDKN1C/p57 and CDKN1B/p27 expression in human hepatocellular carcinoma," *Oncogene*, vol. 27, no. 43, pp. 5651–5661, 2008.
- [8] I. C. Hsu, R. A. Metcalf, T. Sun, J. A. Welsh, N. J. Wang, and C. C. Harris, "Mutational hotspot in the p53 gene in human hepatocellular carcinomas," *Nature*, vol. 350, no. 6317, pp. 427–428, 1991.
- [9] H.-M. Shen and C.-N. Ong, "Mutations of the p53 tumor suppressor gene and ras oncogenes in aflatoxin hepatocarcinogenesis," *Mutation Research*, vol. 366, no. 1, pp. 23–44, 1996.
- [10] G. N. Wogan, "Aflatoxin as a human carcinogen," *Hepatology*, vol. 30, no. 2, pp. 573–575, 1999.
- [11] V. Paget, F. Sichel, D. Garon, and M. Lechevrel, "Aflatoxin B<sub>1</sub>-induced TP53 mutational pattern in normal human cells using the FASAY (Functional Analysis of Separated Alleles in Yeast)," *Mutation Research*, vol. 656, no. 1-2, pp. 55–61, 2008.
- [12] D. B. Zimonjic, M. E. Durkin, C. L. Keck-Waggoner, S.-W. Park, S. S. Thorgeirsson, and N. C. Popescu, "SMAD5 gene expression, rearrangements, copy number, and amplification at fragile site FRA5C in human hepatocellular carcinoma," *Neoplasia*, vol. 5, no. 5, pp. 390–396, 2003.
- [13] E. Pang, N. Wong, P. B.-S. Lai, K.-F. To, W.-Y. Lau, and P. J. Johnson, "Consistent chromosome 10 rearrangements in four newly established human hepatocellular carcinoma cell lines," *Genes Chromosomes and Cancer*, vol. 33, no. 2, pp. 150–159, 2002.
- [14] P. Pineau, A. Marchio, C. Battiston et al., "Chromosome instability in human hepatocellular carcinoma depends on p53 status and aflatoxin exposure," *Mutation Research*, vol. 653, no. 1-2, pp. 6–13, 2008.
- [15] D. L. Eaton and E. P. Gallagher, "Mechanisms of aflatoxin carcinogenesis," *Annual Review of Pharmacology and Toxicology*, vol. 34, pp. 135–172, 1994.
- [16] C. N. Martin and R. C. Garner, "Aflatoxin B oxide generated by chemical or enzymic oxidation of aflatoxin B<sub>1</sub> causes guanine substitution in nucleic acids," *Nature*, vol. 267, no. 5614, pp. 863–865, 1977.
- [17] M. E. Smela, M. L. Hamm, P. T. Henderson, C. M. Harris, T. M. Harris, and J. M. Essigmann, "The aflatoxin B<sub>1</sub> formamidopyrimidine adduct plays a major role in causing the types of mutations observed in human hepatocellular carcinoma," *Proceedings of the National Academy of Sciences of the United States of America*, vol. 99, no. 10, pp. 6655–6660, 2002.
- [18] Y. O. Alekseyev, M. L. Hamm, and J. M. Essigmann, "Aflatoxin B<sub>1</sub> formamidopyrimidine adducts are preferentially repaired by the nucleotide excision repair pathway in vivo," *Carcinogenesis*, vol. 25, no. 6, pp. 1045–1051, 2004.
- [19] L. L. Bedard and T. E. Massey, "Aflatoxin B<sub>1</sub>-induced DNA damage and its repair," *Cancer Letters*, vol. 241, no. 2, pp. 174–183, 2006.
- [20] K. L. Brown, M. W. Voehler, S. M. Magee, C. M. Harris, T. M. Harris, and M. P. Stone, "Structural perturbations induced by the  $\alpha$ -anomer of the aflatoxin B<sub>1</sub> formamidopyrimidine adduct in duplex and single-strand DNA," *Journal of the American Chemical Society*, vol. 131, no. 44, pp. 16096–16107, 2009.
- [21] M. Manuguerra, F. Saletta, M. R. Karagas et al., "XRCC3 and XPD/ERCC2 single nucleotide polymorphisms and the risk of cancer: a HuGE review," *American Journal of Epidemiology*, vol. 164, no. 4, pp. 297–302, 2006.
- [22] X. D. Long, Y. Ma, D. Y. Qu et al., "The polymorphism of XRCC3 codon 241 and AFB1-related hepatocellular carcinoma in Guangxi population, China," *Annals of Epidemiology*, vol. 18, no. 7, pp. 572–578, 2008.
- [23] X. D. Long, Y. Ma, Y. F. Zhou et al., "XPD codon 312 and 751 polymorphisms, and AFB1 exposure, and hepatocellular carcinoma risk," *BMC Cancer*, vol. 17, no. 9, article no. 400, 2009.
- [24] R. D. Johnson and M. Jasin, "Double-strand-break-induced homologous recombination in mammalian cells," *Biochemical Society Transactions*, vol. 29, no. 2, pp. 196–201, 2001.
- [25] F. D. Araujo, A. J. Pierce, J. M. Stark, and M. Jasin, "Variant XRCC3 implicated in cancer is functional in homology-directed repair of double-strand breaks," *Oncogene*, vol. 21, no. 26, pp. 4176–4180, 2002.
- [26] C. Sengstag, B. Weibel, and M. Fasullo, "Genotoxicity of aflatoxin B<sub>1</sub>: evidence for a recombination-mediated mechanism in *Saccharomyces cerevisiae*," *Cancer Research*, vol. 56, no. 23, pp. 5457–5465, 1996.
- [27] M. U. Keller-Seitz, U. Certa, C. Sengstag, F. E. Würzler, M. Sun, and M. Fasullo, "Transcriptional response of yeast to aflatoxin B<sub>1</sub>: recombinational repair involving RAD51 and RAD1," *Molecular Biology of the Cell*, vol. 15, no. 9, pp. 4321–4336, 2004.
- [28] Y. Guo, L. L. Breeden, H. Zarbl, B. D. Preston, and D. L. Eaton, "Expression of a human cytochrome P450 in yeast permits analysis of pathways for response to and repair of aflatoxin-induced DNA damage," *Molecular and Cellular Biology*, vol. 25, no. 14, pp. 5823–5833, 2005.
- [29] M. Fasullo, M. Sun, and P. Egner, "Stimulation of sister chromatid exchanges and mutation by aflatoxin B<sub>1</sub>-DNA adducts in *Saccharomyces cerevisiae* requires MEC1 (ATR), RAD53, and DUN1," *Molecular Carcinogenesis*, vol. 47, no. 8, pp. 608–615, 2008.
- [30] Y. Guo, L. L. Breeden, W. Fan, L. P. Zhao, D. L. Eaton, and H. Zarbl, "Analysis of cellular responses to aflatoxin B<sub>1</sub> in yeast expressing human cytochrome P450 1A2 using cDNA microarrays," *Mutation Research*, vol. 593, no. 1-2, pp. 121–142, 2006.
- [31] D. Burke, D. Dawson, and T. Stearns, *A Cold Spring Harbor Laboratory Course Manual, Methods in Yeast Genetics*, Cold Spring Harbor Press, New York, NY, USA, 2000.
- [32] M. T. Fasullo and R. W. Davis, "Recombinational substrates designed to study recombination between unique and repetitive sequences in vivo," *Proceedings of the National Academy of Sciences of the United States of America*, vol. 84, no. 17, pp. 6215–6219, 1987.
- [33] C. W. Fung, A. M. Mozlin, and L. S. Symington, "Suppression of the double-strand-break-repair defect of the *Saccharomyces cerevisiae* rad57 mutant," *Genetics*, vol. 181, no. 4, pp. 1195–1206, 2009.
- [34] Z. Dong and M. Fasullo, "Multiple recombination pathways for sister chromatid exchange in *Saccharomyces cerevisiae*: role of RAD1 and the RAD52 epistasis group genes," *Nucleic Acids Research*, vol. 31, no. 10, pp. 2576–2585, 2003.
- [35] M. Lisby, U. H. Mortensen, and R. Rothstein, "Colocalization of multiple DNA double-strand breaks at a single Rad52 repair center," *Nature Cell Biology*, vol. 5, no. 6, pp. 572–577, 2003.
- [36] P. A. Egner, J. D. Groopman, J.-S. Wang, T. W. Kensler, and M. D. Friesen, "Quantification of aflatoxin-B<sub>1</sub>-N7-guanine in human urine by high-performance liquid chromatography and isotope dilution tandem mass spectrometry," *Chemical Research in Toxicology*, vol. 19, no. 9, pp. 1191–1195, 2006.

- [37] C. S. Hoffman and F. Winston, "A ten-minute DNA preparation from yeast efficiently releases autonomous plasmids for transformation of *Escherichia coli*," *Gene*, vol. 57, no. 2-3, pp. 267-272, 1987.
- [38] M. Foiani, F. Marini, D. Gamba, G. Lucchini, and P. Plevani, "The B subunit of the DNA polymerase  $\alpha$ -primase complex in *Saccharomyces cerevisiae* executes an essential function at the initial stage of DNA replication," *Molecular and Cellular Biology*, vol. 14, no. 2, pp. 923-933, 1994.
- [39] K. Herzberg, V. I. Bashkirov, M. Rolfmeier et al., "Phosphorylation of Rad55 on serines 2, 8, and 14 is required for efficient homologous recombination in the recovery of stalled replication forks," *Molecular and Cellular Biology*, vol. 26, no. 22, pp. 8396-8409, 2006.
- [40] M. Lisby, J. H. Barlow, R. C. Burgess, and R. Rothstein, "Choreography of the DNA damage response: spatiotemporal relationships among checkpoint and repair proteins," *Cell*, vol. 118, no. 6, pp. 699-713, 2004.
- [41] M. Fasullo, Z. Dong, M. Sun, and L. Zeng, "*Saccharomyces cerevisiae* RAD53 (CHK2) but not CHK1 is required for double-strand break-initiated SCE and DNA damage-associated SCE after exposure to X rays and chemical agents," *DNA Repair*, vol. 4, no. 11, pp. 1240-1251, 2005.
- [42] M. Toussaint and A. Conconi, "High-throughput and sensitive assay to measure yeast cell growth: a bench protocol for testing genotoxic agents," *Nature Protocols*, vol. 1, no. 4, pp. 1922-1928, 2006.
- [43] H. Neecke, G. Lucchini, and M. P. Longhese, "Cell cycle progression in the presence of irreparable DNA damage is controlled by a Mec1- and Rad53-dependent checkpoint in budding yeast," *EMBO Journal*, vol. 18, no. 16, pp. 4485-4497, 1999.
- [44] S. Sabbioneda, I. Bortolomai, M. Giannattasio, P. Plevani, and M. Muzi-Falconi, "Yeast Rev1 is cell cycle regulated, phosphorylated in response to DNA damage and its binding to chromosomes is dependent upon MEC1," *DNA Repair*, vol. 6, no. 1, pp. 121-127, 2007.
- [45] V. Pagès, S. R. Santa Maria, L. Prakash, and S. Prakash, "Role of DNA damage-induced replication checkpoint in promoting lesion bypass by translesion synthesis in yeast," *Genes and Development*, vol. 23, no. 12, pp. 1438-1449, 2009.
- [46] F. Conde, D. Ontoso, I. Acosta, A. Gallego-Sánchez, A. Bueno, and P. A. San-Segundo, "Regulation of tolerance to DNA alkylating damage by Dot1 and Rad53 in *Saccharomyces cerevisiae*," *DNA Repair*, vol. 9, no. 10, pp. 1038-1049, 2010.
- [47] C. B. Bennett, A. L. Lewis, K. K. Baldwin, and M. A. Resnick, "Lethality induced by a single site-specific double-strand break in a dispensable yeast plasmid," *Proceedings of the National Academy of Sciences of the United States of America*, vol. 90, no. 12, pp. 5613-5617, 1993.
- [48] V. Gangavarapu, S. Prakash, and L. Prakash, "Requirement of RAD52 group genes for postreplication repair of UV-damaged DNA in *Saccharomyces cerevisiae*," *Molecular and Cellular Biology*, vol. 27, no. 21, pp. 7758-7764, 2007.

## Research Article

# Expression of $O^6$ -Alkylguanine-DNA Alkyltransferase in Normal and Malignant Bladder Tissue of Egyptian Patients

Abir A. Saad,<sup>1,2</sup> Heba Sh. Kassem,<sup>1,3</sup> Andrew C. Povey,<sup>4</sup> and Geoffrey P. Margison<sup>1</sup>

<sup>1</sup> Cancer Research UK Carcinogenesis Group, Paterson Institute for Cancer Research, The University of Manchester, Manchester M20 4BX, UK

<sup>2</sup> Institute of Graduate Studies and Research, University of Alexandria, Alexandria 21526, Egypt

<sup>3</sup> Pathology Department and Clinical Genomics Center, Faculty of Medicine, University of Alexandria, Alexandria 21526, Egypt

<sup>4</sup> Centre for Occupational and Environmental Health, Faculty of Medical and Human Sciences, The University of Manchester, Manchester M13 9PL, UK

Correspondence should be addressed to Geoffrey P. Margison, gmargison@picr.man.ac.uk

Received 12 June 2010; Accepted 17 August 2010

Academic Editor: Ashis Basu

Copyright © 2010 Abir A. Saad et al. This is an open access article distributed under the Creative Commons Attribution License, which permits unrestricted use, distribution, and reproduction in any medium, provided the original work is properly cited.

Bladder tumour tissues and corresponding uninvolved mucosa (normal tissue) of Egyptian bladder cancer patients were assessed for  $O^6$ -alkylguanine-DNA-alkyltransferase (MGMT) activity by functional assay of tissue extracts (36 paired samples), and distribution by immunofluorescence (IF) microscopy of fixed material (24 paired samples). MGMT varied widely from 42–253 fmoles/mg protein and from 3.2–40 fmoles/ $\mu$ g DNA in normal and 58–468 fmoles/mg protein and 2.5–49.5 fmoles/mg protein, in the tumour tissues; only one tumour had undetectable activity. Pairwise comparison of MGMT activity in tumour and adjacent normal tissue showed no significant difference based on DNA content but was 1.75-fold higher in tumour ( $P < .01$ ) based on protein. There was no effect of gender or bilharzia infection status. IF showed that in tumours, both the mean percentage of positive nuclei ( $57.3 \pm 20.3\%$ ) and mean integrated IF ( $5.47 \pm 3.66$ ) were significantly higher than those in uninvolved tissues ( $42.8 \pm 13.5\%$   $P = .04$ ) and ( $1.89 \pm 1.42$ ;  $P < .01$ ), respectively. These observations suggest that, overall, MGMT levels are increased during human bladder carcinogenesis and that MGMT downregulation is not a common feature of bladder cancers. Based on this, bladder cancers would be expected to be relatively resistant to chemotherapy which involved  $O^6$ -guanine alkylating antitumour agents.

## 1. Introduction

Carcinoma of the urinary bladder is the most common malignancy among Egyptian males, accounting for 16% of total cancer incidence while in females it ranks second to breast cancer [1, 2]. The high incidence of bladder cancer in Egypt is associated with chronic urinary infection with *Schistosoma haematobium* [2, 3] which is thought to lead to endogenous nitrosation and the formation of N-nitroso compounds [4–6]. Such compounds have been shown to alkylate DNA causing a range of DNA adducts with differing mutagenic, and carcinogenic potential [7].  $O^6$ -alkylguanine is one such adduct which has been shown to be a toxic, mutagenic and carcinogenic lesion. This damage can be processed by the DNA repair protein,  $O^6$ -alkylguanine-DNA-alkyltransferase (MGMT), which transfers the alkyl

group to a cysteine residue at its catalytic site in a process that leads to the inactivation of the protein. Since each MGMT molecule acts only once, cells have a limited capacity to repair  $O^6$ -alkylguanine lesions, which is determined by the steady state number of MGMT molecules at the time of alkylating agent exposure. Further repair following depletion of the pool requires *de novo* synthesis of the protein [8, 9].

While MGMT may be an important factor in the aetiology of bladder cancer, it may also play an important role in cellular defence against the toxic effects of certain types of alkylating agents used in cancer chemotherapy, usually referred to as  $O^6$ -alkylating agents [10, 11]. In this context, cytosine methylation of the MGMT promoter has generally been accepted to result in loss of MGMT expression [12, 13], but this is reported to be rare in bladder tumours occurring in 2–9% of those examined [14, 15]. Tumour

MGMT activity has also been reported to be higher [16] or lower [4] than normal bladder tissue. The reasons for these conflicting results are not clear but may reflect the underlying pathogenesis of bladder cancer or the use of normal bladder tissue from different patients as controls instead of the corresponding uninvolved mucosa from the same subject. Studies of tumour extracts also give no indication of possible regional heterogeneity or intracellular localisation of MGMT. We have therefore determined the distribution and levels of immunoreactive MGMT and MGMT activity in human bladder tumour tissues and corresponding uninvolved mucosa using immunohistochemistry and a functional assay for MGMT activity. The results were examined in relation to tumour type, gender, and schistosomiasis status. There was no significant difference in activity between samples from men and women and from those with or without evidence of bilharzia infection. But overall, tumour samples displayed higher levels of MGMT expression than associated normal tissues.

## 2. Materials and Methods

**2.1. Human Tissue Specimens.** Tissue samples were collected during radical cystectomy of 36 Egyptian bladder cancer patients attending the department of Urology, Faculty of Medicine, Alexandria University following taking informed consent and ensuring non compromise of pathologic diagnosis. All samples were taken from the urinary face of the bladder mucosa and were frozen immediately on dry ice and stored at  $-70^{\circ}\text{C}$ . Samples were collected, in pairs, each pair comprised a sample of bladder tumour and a sample of bladder mucosa with no macroscopic sign of tumour invasion (referred to as uninvolved tissue). Schistosomiasis infection was established from a self-reported clinical history of schistosomiasis or schistosoma ova detected in histological specimens. Most (32) patients had evidence of bilharzia infection: 23 had a transitional cell carcinoma (TCC), 5 a squamous cell carcinoma (SCC), and 4 a TCC with SCC foci; of the four patients without infection, 2 had adenocarcinomas (Ad), 1 a SCC, and 1 a TCC with SCC foci.

**2.2. Assay of Tissue Levels of MGMT.** MGMT activity in bladder tissue extracts was assayed in all 36 paired samples by measuring the transfer of [ $^3\text{H}$ ] from a [ $^3\text{H}$ ]-methylated DNA substrate to protein in the tissue extract using the methods described by Watson and Margison [17]. MGMT activity was expressed as fmoles of methyl groups transferred per mg of protein and per  $\mu\text{g}$  of DNA in the tissue extract. MGMT activity in paired uninvolved and tumour tissue from the same patient were compared using a paired sample *t*-test.

**2.3. Tissue Localisation of Human MGMT.** Frozen bladder tissues were fixed in 4% neutral buffered formalin then processed to paraffin wax. Sections ( $3\mu\text{m}$ ) were cut and mounted onto APES-subbed slides, dewaxed in xylene, and rehydrated in graded ethanol. Tissues were then microwaved (650 watts) in 10 mM citrate buffer (pH 6.0) to retrieve the immunoreactivity of the cross-linked proteins. Slides

were treated with 3%  $\text{H}_2\text{O}_2$  in TBS to block endogenous peroxidase, washed in dd $\text{H}_2\text{O}$  and TBS, and incubated with 10% normal swine serum. Sections were incubated at  $4^{\circ}\text{C}$  with antihuman MGMT  $1^{\circ}\text{Ab}$  (diluted to 1:1000). Slides were then washed in TBS, followed by application of swine-antirabbit biotinylated IgG and ABC peroxidase. The sections were developed with DAB/ $\text{H}_2\text{O}_2$ , washed, dehydrated, and mounted. As a negative control, adjacent sections were incubated with preimmune serum instead of the MGMT antiserum.

**2.4. Quantitative Immunohistochemistry.** Quantitation of MGMT in tissue sections was performed using immunofluorescence (IF) in 24 paired samples. Sections were stained for MGMT as above except that the ABC complex and DAB visualisation steps were omitted and replaced by Cy3/DAPI fluorescent staining; samples were stained with Avidin-Cy3 (1:1000) followed by TBS wash then counterstained with DAPI (0.2  $\mu\text{g}/\text{ml}$ ). Samples were then washed with dd $\text{H}_2\text{O}$  and mounted in PBS-buffered glycerol (9:1).

Fluorescent microscopy images of the mounted slides were generated using a Nikon microscope equipped with a mercury arc lamp and with red and blue filter sets (for Cy3 and DAPI fluorescence resp.). Images were captured using a Hitachi HVC20 camera and analysed with the Lucia G image analysis software package using a macro that automated data collection and performed calculations of the number of positive nuclei, the mean and integrated fluorescence, and mean area.

The macro operated the following steps: (i) highlighting the position of nuclei in tissue sections by the use of a DAPI filter, (ii) superimposing the nuclear outline on the Cy3 image (through TRITC filter), (iii) capturing this image and comparing it against negative control sections, and (iv) measuring the fluorescence intensity of MGMT-Cy3 staining and the area of each nucleus within the nuclear boundaries recorded from the DAPI image.

For each sample, data were averaged from 10 to 20 fields (depending on the size of the section). MGMT expression in the tissue sections was quantified using 3 parameters: (1) the percentage of immunoreactive MGMT positive nuclei which indicates the fraction of cells containing detectable levels of nuclear MGMT, (2) the mean fluorescence intensity of Cy3 MGMT staining which corresponds to the average amount of MGMT protein per unit nuclear area in the positively staining cells, and (3) the integrated fluorescence (area fraction of Cy3 positive nuclei  $\times$  mean fluorescence) which represents the total amount of MGMT protein in the tissue. These fluorescent parameters were compared in paired uninvolved and tumour tissue from the same patient were compared using a paired sample *t*-test

## 3. Results

All uninvolved (normal) bladder tissue samples contained measurable MGMT activity which ranged from 3.2 to 39.8 fmoles/ $\mu\text{g}$  DNA (12.4-fold variation). MGMT activity was detected in 35/36 tumour samples with the activity

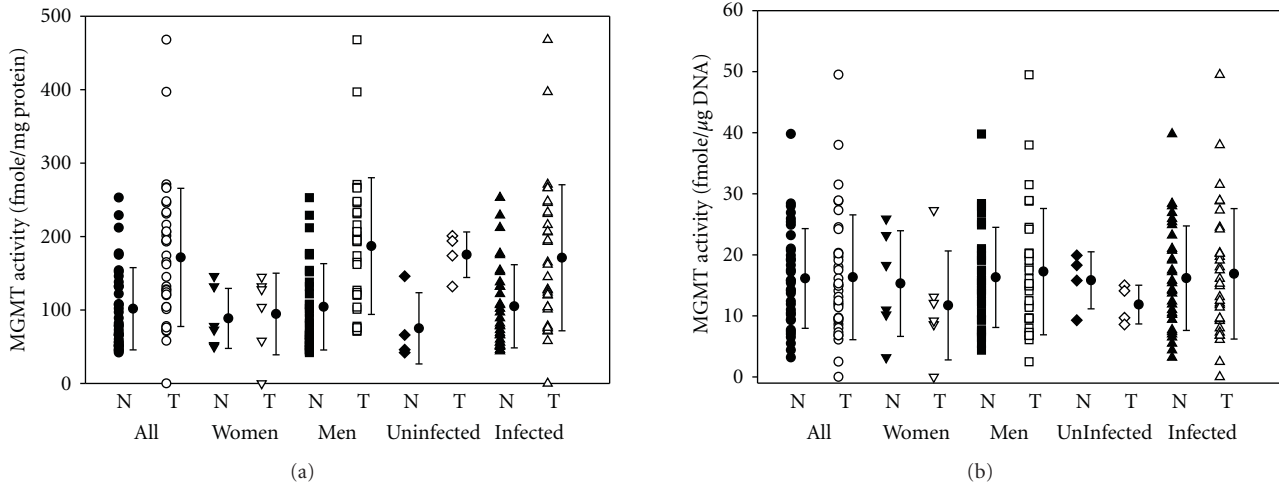


FIGURE 1: Relationships between MGMT activity (upper: fmole/mg protein, lower: fmole/ug DNA) in normal (N) and tumour (T) tissues of Egyptian bladder cancer patients. Data are also subdivided according to gender and bilharzia status. Statistical analyses are presented in Table 1.

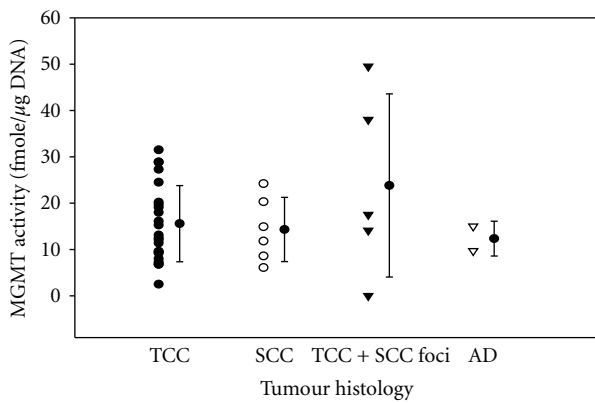


FIGURE 2: Relationship between MGMT activity (fmole/μg of cellular DNA: means indicated by asterisks, error bars indicate standard error) and tumour histology. TCC, transitional cell carcinoma; SCC, squamous cell carcinoma; AD, adenocarcinoma.

ranging up to 49.5 fmole/μg DNA. There was no significant difference in activity between samples from men and women and from those with or without evidence of bilharzia infection (Table 1; Figure 1) or in activity from samples of different histological tumours (Figure 2). Tumour MGMT activity when expressed as fmole/mg protein was significantly higher than that in uninvolved tissue from the same patient (Table 1). However, when MGMT was expressed as fmole/μg DNA there was, overall, no significant difference between tumour and normal tissue (Table 1). Breaking this down, tumour MGMT activity based on protein content was 1.5–5-fold higher in 22 sample pairs, 10 pairs of samples had similar levels of activities in tumour and normal tissue, while 3 tumour samples had 1.5-fold lower activity compared to uninvolved tissue. On the other hand, based on DNA content, the MGMT activities of 9 tumour samples were up to 3-fold higher than the corresponding controls; in

16 patients, there were similar levels, while in 10 patients tumour samples had 1.5- to 2-fold lower activities than control.

Representative examples of the inter- and intracellular distribution and intensity of MGMT staining in the bladder sections are illustrated in Figure 3. MGMT antiserum staining showed mild upregulation of MGMT expression in the metaplastic epithelium (2b) in comparison with the normal urothelium (2a). The intensity of tumour staining showed marked variation between patients' samples. One SCC bladder sample (2a) showed relatively homogenous pattern and intense nuclear staining as well as some cytoplasmic staining, whereas another SCC sample (moderately differentiated and keratinised) presented a heterogeneous pattern and less intense nuclear staining with some faint cytoplasmic staining (2b). The invasive TCC sample showed more intense but less uniform staining of the tumour nuclei (3a) than did the papillary TCC sample (3b). In all cases, no cellular staining was observed with preimmune serum and all nuclei acquired the blue colour of the haematoxylin counterstain. There was an obvious inconsistent pattern of staining in the tumour tissue relative to the uninvolved mucosa. In some of the samples, differences in the intensity of MGMT nuclear staining were observed between normal urothelium and the corresponding tumour tissue from the same patient (4 and 5). While in some cases the urothelial nuclei showed heavy staining compared to the tumour tissue (4a) and (4b), in other cases the bladder urothelium showed heterogeneous and generally reduced nuclear staining in comparison to its corresponding tumour (5a) and (5b).

Twenty four paired bladder samples from the previous series of tumour and uninvolved tissues were stained for MGMT using IF Cy3 staining with DAPI counterstain. In tumour tissues, there was no association between the % positive nuclei and either the mean fluorescence ( $r = 0.10$ ;  $P = .64$ ) or the integrated fluorescence ( $r = 0.37$ ;  $P = .21$ ), but there was an association between the mean and integrated

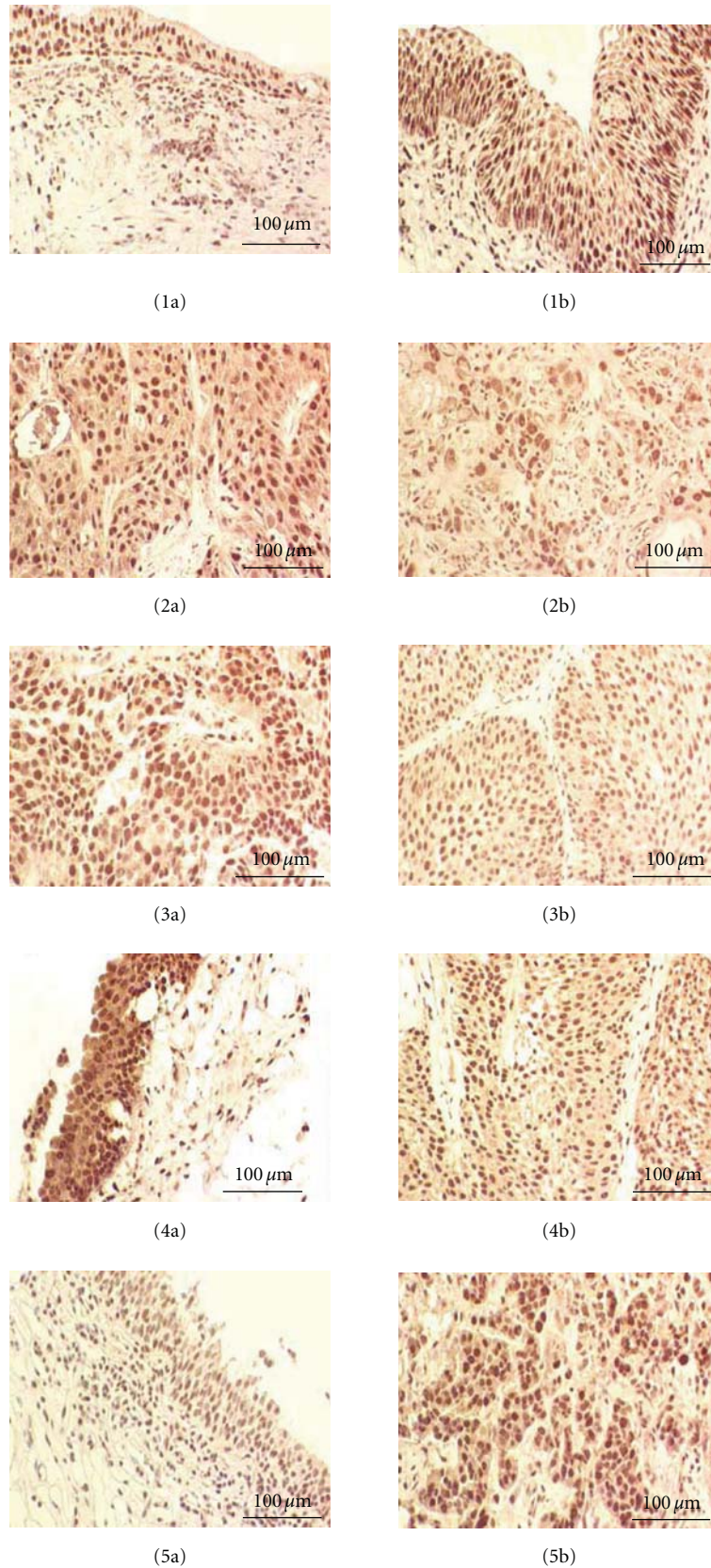


FIGURE 3: Immunohistochemical detection of MGMT in bladder tissue from patients with bladder cancer: normal urothelium (1a) and squamous metaplastic epithelium I(b); SCC (2a) and moderately differentiated SCC (2b) sections of bilharzial bladder; invasive TCC (3a) and low grade papillary TCC (3b); non neoplastic urothelium with some dysplastic changes (4a) and grade II papillary TCC (4b); normal urothelium (5a) and invasive TCC (5b). Note that the intensity of staining is highest in the high grade section (5b). Scale bars = 100  $\mu$ m.

TABLE 1: MGMT activity in extracts of bladder tumours and uninvolved tissue.

	<i>n</i>	MGMT activity (mean $\pm$ SD)					
		Fmoles/mg protein			Fmoles/ $\mu$ g DNA		
		Uninvolved tissue	Tumour tissue	Difference (tumour uninvolved)	Uninvolved tissue	Tumour tissue	Difference (tumour uninvolved)
Total	36	101.6 $\pm$ 55.9	171.6 $\pm$ 94.0	70.0 $\pm$ 75.8*	16.1 $\pm$ 8.2	16.3 $\pm$ 10.2	0.2 $\pm$ 8.5
Males	30	104.3 $\pm$ 58.7	187.0 $\pm$ 93.1	82.7 $\pm$ 73.6*	16.3 $\pm$ 8.2	17.3 $\pm$ 10.3	1.0 $\pm$ 8.9
Females	6	88.5 $\pm$ 40.8	94.5 $\pm$ 55.6	6.0 $\pm$ 54.1	15.3 $\pm$ 8.7	11.7 $\pm$ 8.9	-3.6 $\pm$ 5.2
Schistosomiasis infected	32	105.0 $\pm$ 56.6	171.1 $\pm$ 94.4	66.1 $\pm$ 75.6*	16.2 $\pm$ 8.6	16.9 $\pm$ 10.7	0.7 $\pm$ 8.6
Schistosomiasis negative	4	75.0 $\pm$ 48.5	175.3 $\pm$ 31.0	100.3 $\pm$ 79.3	15.8 $\pm$ 4.7	11.9 $\pm$ 3.2	-4.0 $\pm$ 7.3

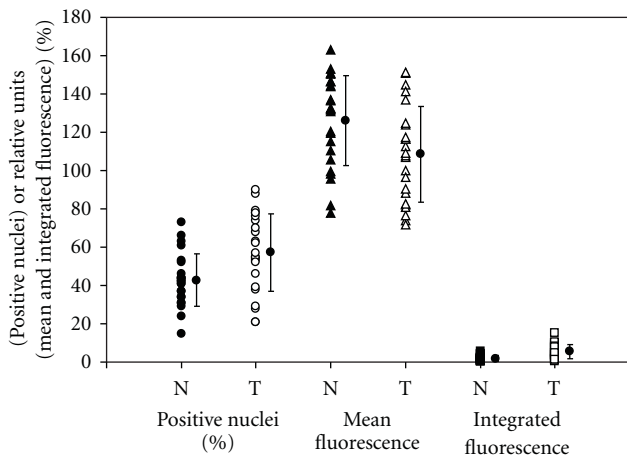
\* $P < .001$ 

FIGURE 4: Ranges and means (asterisks, error bars indicate standard error) in immunofluorescence values for MGMT in normal (N) and tumour (T) tissue. Values for positive nuclei are shown as %, and for mean fluorescence and integrated fluorescence as relative units.

fluorescence ( $r = 0.45$ ;  $P = .03$ ). In contrast, in uninvolved tissues there were significant associations between the % positive nuclei and both the mean fluorescence ( $r = 0.54$ ;  $P = .006$ ) and the integrated fluorescence ( $r = 0.90$ ;  $P < .001$ ) and also between the mean and integrated fluorescence ( $r = 0.54$ ;  $P = .006$ ). This probably reflects a higher degree of heterogeneity in the tumour tissues.

The percentage of MGMT positive nuclei varied from 21 to 90% in tumour tissues, and from 15 to 73% in uninvolved bladder tissues. The mean percentage positive nuclei for tumours was significantly higher ( $P = .002$ ) than that for the corresponding uninvolved tissues (Table 2; Figure 4). In contrast, the average of the mean fluorescence was significantly lower in tumours than in normal tissues ( $P = .004$ ; Table 2; Figure 4). However, integrated MGMT fluorescence varied from 0.56 to 15.43 in bladder tumours (27.6-fold variation) and from 0.29 to 5.78 in uninvolved bladder tissue (19.9-fold variation). The mean of this parameter was again significantly higher in tumours than in the corresponding normal tissue ( $P < .001$  Table 2; Figure 4). There were no

differences in these parameters in tumour tissues of different histology (data not shown).

In normal (uninvolved) bladder tissues, MGMT activity was correlated with the % positive nuclei and integrated fluorescence but not with the mean fluorescence (Figure 5) whereas in tumour tissue, MGMT activity was only correlated with the mean fluorescence (Figure 5).

MGMT activity in normal tissue was highly correlated with that found in tumour tissue (Figure 6) whereas there were no correlations between immunofluorescence parameters in normal tissue and the corresponding parameters in tumour tissue (Figure 6).

The marked variations in MGMT expression levels within and between patient tumour samples, along with the numbers of samples in the study, have precluded testing any correlation between MGMT expression and other factors such as gender and bilharzial infection.

#### 4. Discussion

In this study, MGMT protein was measured in bladder tissues using quantitative IF and MGMT activity using a functional assay. A wide range in immunoreactive protein levels was detected; not all cells were stained and in positively staining cells intensity varied but was mainly confined within the nucleus. Only one tumour sample had no detectable MGMT activity; whether or not this may have been due to promoter methylation was not investigated. Also, we cannot exclude the possibility that the unstained or low MGMT-expressing cells in the examined population may be completely or partially MGMT-promotor methylated. The results presented here are consistent with those of other reports examining other tumour types and showing that staining with MGMT antibody is predominantly nuclear [18, 19]. MGMT staining also varied markedly from one patient to another. Whilst there was interindividual variation in the cellular distribution of reaction, staining was present in all cell types in most samples. In some TCC as well as SCC cases, most of the cells expressed the protein in a relatively homogenous pattern, whereas in others, marked intercellular heterogeneity was observed. In addition, cytoplasmic

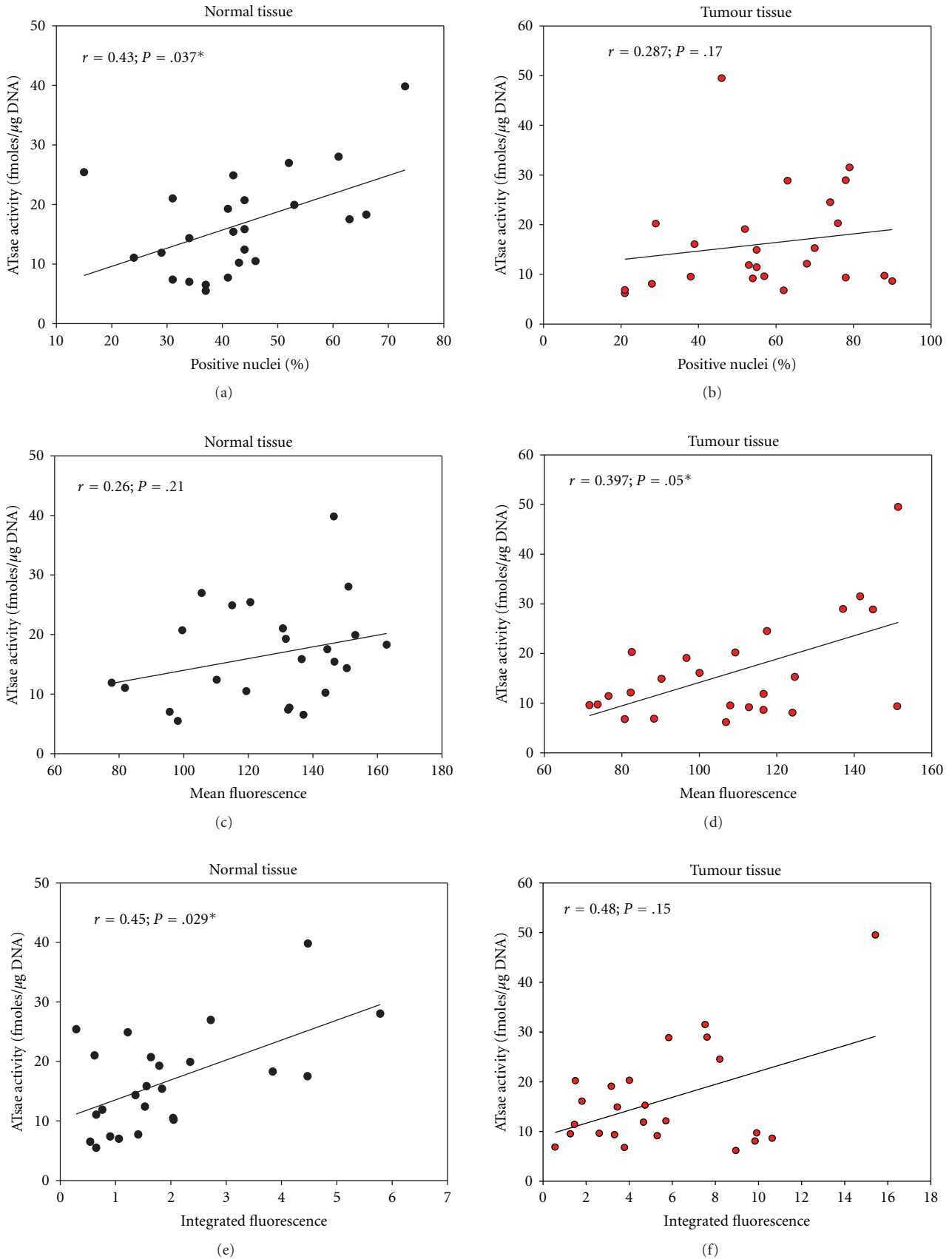


FIGURE 5: Relationship between MGMT activity (fmole/ $\mu$ g of cellular DNA) and immunofluorescence parameters of MGMT content (top: %positive nuclei, middle: mean fluorescence, bottom: integrated fluorescence) in normal and tumour tissue.

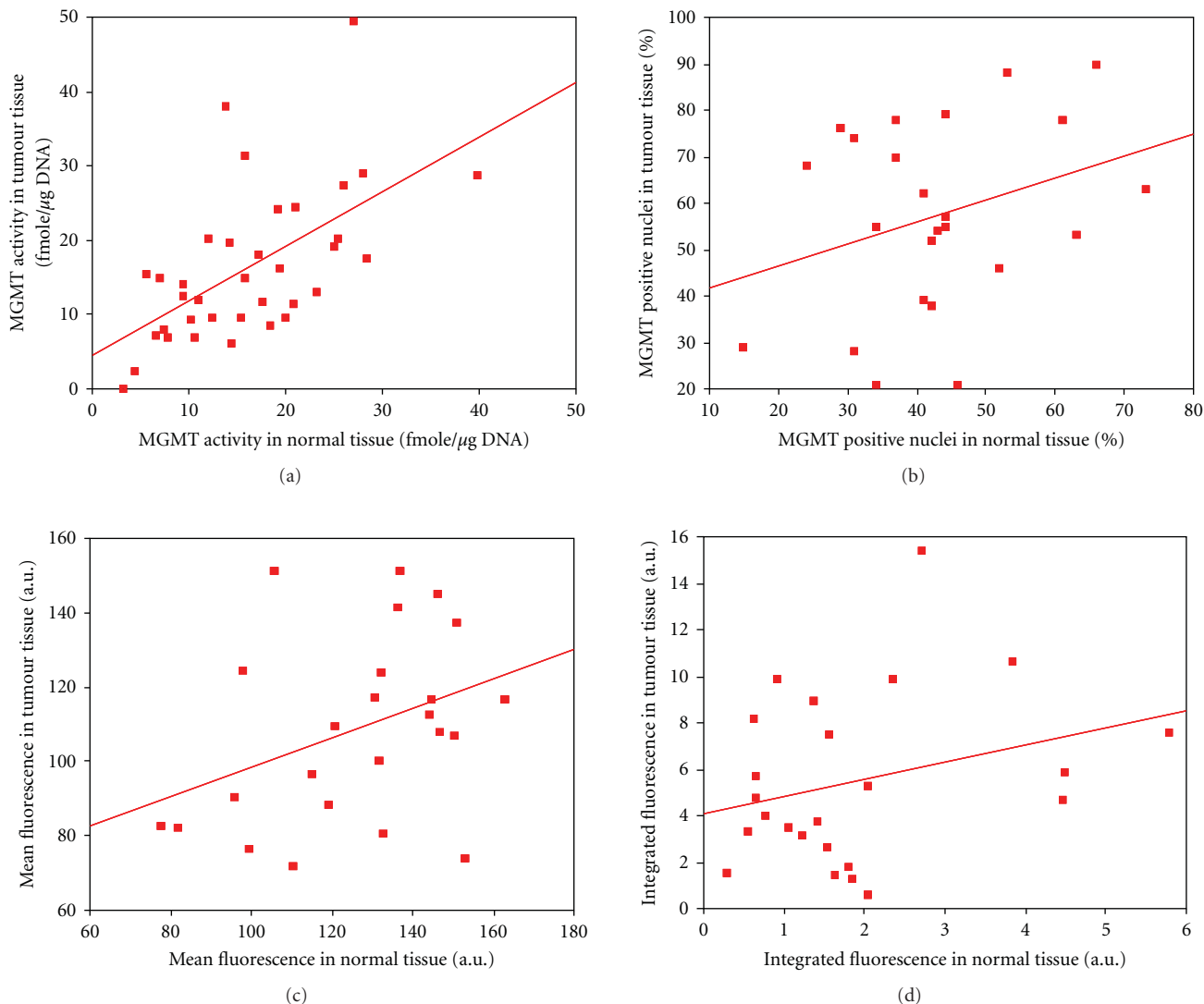


FIGURE 6: Relationship between tumour and normal tissue MGMT activity (fmole/ug DNA, (a)), % positive nuclei (b), mean fluorescence (c) and integrated fluorescence (d), parameters of MGMT content.

TABLE 2: MGMT content in bladder tumours and uninvolved tissues measured by quantitative immunofluorescence.

Variable	Uninvolved tissue	Tumour tissue	Difference tumour uninvolved	<i>P</i>
% positive nuclei	$42.8 \pm 13.5$	$57.3 \pm 20.3$	$14.5 \pm 20.5$	.002
Mean fluorescence	$126.0 \pm 23.5$	$108.5 \pm 24.9$	$-17.5 \pm 27.1$	.004
Integrated fluorescence	$1.9 \pm 1.4$	$5.5 \pm 3.7$	$3.6 \pm 3.5$	<.001

staining of MGMT was observed in many samples with variable intensities. Previous studies have reported a nuclear localisation for MGMT with only occasional mention of cytoplasmic staining [18, 20] while others reported the presence of high levels of cytoplasmic MGMT in cancer [21, 22]. The significance of cytoplasmic immunoreactive MGMT protein is unclear, but it may be that cytoplasmic staining reflects a relative inefficiency in the ubiquitin-mediated MGMT degradation pathway [23] giving rise to more persistent inactive cytoplasmic protein.

The wide range of MGMT activity observed in uninvolved tissues and bladder cancer tissues is similar to that previously reported for bladder tissue [24–27]. In the present study, although differences in functional activity were observed between tumour tissue and uninvolved bladder tissue from the same patient when expressed per unit protein, no differences were seen when expressed per unit DNA. Normalisation per unit DNA is generally considered to be more appropriate as cells vary greatly in protein content and because MGMT acts on  $O^6$ -alkylguanine lesions

in DNA; it also provides an indication of the number of MGMT molecules per cell. Differences between different sets of published data are thus likely to reflect the use of different normalisation procedures (per unit protein or per unit DNA). It is worth noting, however, that bladder tumours have a very high frequency (more than 50%; [28]) of polyploid cells, so that using DNA as a parameter, the number of MGMT molecules per cell may be grossly underestimated. Basing the results on either protein or DNA content, together with the % positive nuclei or integrated MGMT fluorescence, which are indications of the overall level of MGMT expression, would thus suggest that tumour cells contain substantially higher levels of MGMT than normal cells. The basis of this apparent MGMT upregulation remains to be established.

There is a large body of evidence to suggest that MGMT activity can be an important determinant in the efficacy of chemotherapy involving the "O<sup>6</sup>-alkylating" agents [10, 29], and it is reasonable to consider if bladder cancer patients might benefit from such chemotherapy. There was marked heterogeneity of MGMT distribution with, in some cases, the majority of the tumour cells expressing relatively low levels of MGMT. If bladder tumour patients were to be treated with O<sup>6</sup>-alkylating agents, this would likely lead to an initial beneficial response in terms of tumour reduction, but later, disease recurrence from those cells and areas of highest MGMT expression. Indeed, such alkylating agents are not used in bladder cancer treatment although a prospective study to investigate the pretreatment expression of MGMT and response to therapy employing appropriate alkylating agents is feasible. Bladder cancer treatment might, however, benefit from the use of MGMT inactivating agents such as BeG [30] or Lomeguatrib [31] which would potentially ablate MGMT activity in bladder cells, relatively increasing the sensitivity of the tumours cells to chemotherapy with Temozolomide or Dacarbazine. Clinical studies of these agents have established that MGMT activity can be depleted by systemic administration of such agents, but this increases the myelosuppressive effect of the chemotherapeutic agent [11]. Given our present results, intravesical administration of MGMT inactivators prior to systemic, or even local, chemotherapy using O<sup>6</sup>-alkylating agents seems a feasible proposition.

## Abbreviations

MGMT:	O <sup>6</sup> -alkylguanine-DNA-alkyltransferase
ABC complex:	Avidin-biotin complex
APES:	3-aminopropyltriethoxysilane
DAB:	3', 3'-diaminobenzidine
DAPI:	4,6-diamidino 2-phenylindole
PBS:	Phosphate buffer saline
TBS:	Tris-buffered saline.
IF:	Immunofluorescence.

## Acknowledgments

This work was supported in part by Cancer Research-UK and by a grant to A. A. Saad from the Egyptian Government.

Contacts between Alexandria University and Manchester University were facilitated by the British Council. The authors thank Don Cooper, Peter O'Connor, and Gill Forster for help and advice.

## References

- [1] H. M. Khaled, "Systemic management of bladder cancer in Egypt: revisited," *Journal of the Egyptian National Cancer Institute*, vol. 17, no. 3, pp. 127–131, 2005.
- [2] S. A. Fedewa, A. S. Soliman, K. Ismail et al., "Incidence analyses of bladder cancer in the Nile delta region of Egypt," *Cancer Epidemiology*, vol. 33, no. 3-4, pp. 176–181, 2009.
- [3] International Agency for Research on Cancer, *IARC Monographs on the Evaluation of the Carcinogenic Risk to Humans*, vol. 61 of *schistosomes, Liver Flukes and Helicobacter Pylori*, IARC, Lyon, France, 1994.
- [4] A. F. Badawi, M. H. Mostafa, T. Aboul-Azm, N. Y. Haboubi, P. J. O'Connor, and D. P. Cooper, "Promutagenic methylation damage in bladder DNA from patients with bladder cancer associated with schistosomiasis and from normal individuals," *Carcinogenesis*, vol. 13, no. 5, pp. 877–881, 1992.
- [5] M. H. Mostafa, S. A. Sheweita, and P. J. O'Connor, "Relationship between schistosomiasis and bladder cancer," *Clinical Microbiology Reviews*, vol. 12, no. 1, pp. 97–111, 1999.
- [6] M. A. Abdel Mohsen, A. A. M. Hassan, S. M. El-Sewedy et al., "Human bladder cancer, schistosomiasis, N-Nitroso compounds and their precursors," *International Journal of Cancer*, vol. 88, no. 4, pp. 682–683, 2000.
- [7] G. Margison and P. O'Connor, "Biological consequences of reactions with DNA: role of specific lesions," in *Handbook of Experimental Pharmacology*, C.S. Cooper and P.L. Grover, Eds., vol. 94I, pp. 547–571, Springer, Berlin, Germany, 1990.
- [8] G. P. Margison and A. C. Povey, "Chemical carcinogenesis," in *Oxford Textbook of Oncology*, R. L. Souhami, I. Tannock, P. Hohenberger, and J.-C. Horiot, Eds., pp. 129–149, 2nd edition, 2002.
- [9] G. P. Margison, A. C. Povey, B. Kaina, and M. F. Santibáñez Koref, "Variability and regulation of O<sup>6</sup>-alkylguanine-DNA alkyltransferase," *Carcinogenesis*, vol. 24, no. 4, pp. 625–635, 2003.
- [10] M. R. Middleton and G. P. Margison, "Enhancing chemotherapy by inactivation of a DNA repair pathway," *The Lancet Oncology*, vol. 4, no. 1, pp. 37–44, 2003.
- [11] B. Verbeek, T. D. Southgate, D. E. Gilham, and G. P. Margison, "O<sup>6</sup>-Methylguanine-DNA methyltransferase inactivation and chemotherapy," *British Medical Bulletin*, vol. 85, no. 1, pp. 17–33, 2008.
- [12] X. Qian, M. A. von Wronski, and T. P. Brent, "Localization of methylation sites in the human O<sup>6</sup>-methylguanine DNA methyltransferase promoter: correlation with gene suppression," *Carcinogenesis*, vol. 16, no. 6, pp. 1385–1390, 1995.
- [13] F. V. Jacinto and M. Esteller, "MGMT hypermethylation: a prognostic foe, a predictive friend," *DNA Repair*, vol. 6, no. 8, pp. 1155–1160, 2007.
- [14] R. Maruyama, S. Toyooka, K. O. Toyooka et al., "Aberrant promoter methylation profile of bladder cancer and its relationship to clinicopathological features," *Cancer Research*, vol. 61, no. 24, pp. 8659–8663, 2001.
- [15] M. W. Y. Chan, L. W. Chan, N. L. S. Tang et al., "Hypermethylation of multiple genes in tumor tissues and voided urine in urinary bladder cancer patients," *Clinical Cancer Research*, vol. 8, no. 2, pp. 464–470, 2002.

- [16] E. I. Saygili, T. Akcay, Y. Dinçer, C. Öbek, A. R. Kural, and C. Çakalir, "Methylguanine DNA methyl transferase activities, glutathione S transferase and nitric oxide in bladder cancer patients," *Cancer Investigation*, vol. 24, no. 3, pp. 256–260, 2006.
- [17] A. J. Watson and G. P. Margison, "*O*<sup>6</sup>-alkylguanine-DNA-alkyltransferase assay," in *Methods in Molecular Biology. DNA repair protocols: Prokaryotic systems*, P. Vaughan, Ed., vol. 152, pp. 49–61, Human press, otowa, NJ, USA, 2000.
- [18] S. M. Lee, J. A. Rafferty, R. H. Elder et al., "Immunohistochemical examination of the inter- and intracellular distribution of *O*<sup>6</sup>-alkylguanine DNA-alkyltransferase in human liver and melanoma," *British Journal of Cancer*, vol. 66, no. 2, pp. 355–360, 1992.
- [19] T. C. Ayi, K. C. Loh, R. B. Ali, and B. F. L. Li, "Intracellular localization of human DNA repair enzyme methylguanine-DNA methyltransferase by antibodies and its importance," *Cancer Research*, vol. 52, no. 23, pp. 6423–6430, 1992.
- [20] S.-M. Lee, M. Harris, J. Rennison et al., "Expression of *O*<sup>6</sup>-alkylguanine-DNA-alkyltransferase in situ in ovarian and Hodgkin's tumours," *European Journal of Cancer Part A*, vol. 29, no. 9, pp. 1306–1312, 1993.
- [21] D. M. Kokkinakis, M. M. Ahmed, R. Delgado, M. M. Fruitwala, M. Mohiuddin, and J. Albores-Saavedra, "Role of *O*<sup>6</sup>-methylguanine-DNA methyltransferase in the resistance of pancreatic tumors to DNA alkylating agents," *Cancer Research*, vol. 57, no. 23, pp. 5360–5368, 1997.
- [22] T. Ishibashi, Y. Nakabeppu, H. Kawate, K. Sakumi, H. Hayakawa, and M. Sekiguchi, "Intracellular localization and function of DNA repair methyltransferase in human cells," *Mutation Research*, vol. 315, no. 3, pp. 199–212, 1994.
- [23] K. S. Srivenugopal, X.-H. Yuan, H. S. Friedman, and F. Ali-Osman, "Ubiquitination-dependent proteolysis of *O*<sup>6</sup>-methylguanine-DNA methyltransferase in human and murine tumor cells following inactivation with *O*<sup>6</sup>-benzylguanine or 1,3-bis(2-chloroethyl)-1-nitrosourea," *Biochemistry*, vol. 35, no. 4, pp. 1328–1334, 1996.
- [24] B. Myrnes, K. E. Giercksky, and H. Krokan, "Interindividual variation in the activity of *O*<sup>6</sup>-methyl guanine-DNA methyltransferase and uracil-DNA glycosylase in human organs," *Carcinogenesis*, vol. 4, no. 12, pp. 1565–1568, 1983.
- [25] R. C. Grafstrom, A. E. Pegg, B. F. Trump, and C. C. Harris, "*O*<sup>6</sup>-Alkylguanine-DNA alkyltransferase activity in normal human tissues and cells," *Cancer Research*, vol. 44, no. 7, pp. 2855–2857, 1984.
- [26] S. A. Kyrtopoulos, B. Vrotsou, and B. Golematis, "*O*<sup>6</sup>-Methylguanine-DNA transmethylase activity in extracts of human gastric mucosa," *Carcinogenesis*, vol. 5, no. 7, pp. 943–947, 1984.
- [27] O. Wiestler, P. Kleihues, and A. E. Pegg, "*O*<sup>6</sup>-alkylguanine-DNA alkyltransferase activity in human brain and brain tumors," *Carcinogenesis*, vol. 5, no. 1, pp. 121–124, 1984.
- [28] D. Bollman, M. Bollmann, A. Bankfalvi et al., "Quantitative molecular grading of bladder tumours: a tool for objective assessment of the biological potential of urothelial neoplasias," *Oncology Reports*, vol. 21, no. 1, pp. 39–47, 2009.
- [29] S. L. Gerson, "Clinical relevance of MGMT in the treatment of cancer," *Journal of Clinical Oncology*, vol. 20, no. 9, pp. 2388–2399, 2002.
- [30] H. S. Friedman, J. A. Quinn, S. X. Jiang et al., "Phase II Trial of Temozolomide Plus *O*<sup>6</sup>-Benzylguanine in Adults with Recurrent, Temozolomide-Resistant Malignant Glioma," *Journal of Clinical Oncology*, vol. 27, no. 8, pp. 1262–1267, 2009.
- [31] A. J. Watson, A. Sabharwal, M. Thorncroft et al., "Tumor *O*<sup>6</sup>-methylguanine-DNA methyltransferase inactivation by oral lomeguatrib," *Clinical Cancer Research*, vol. 16, no. 2, pp. 743–749, 2010.

## Review Article

# Lung Cancer Risk and Genetic Polymorphisms in DNA Repair Pathways: A Meta-Analysis

Chikako Kiyohara,<sup>1</sup> Koichi Takayama,<sup>2</sup> and Yoichi Nakanishi<sup>2</sup>

<sup>1</sup>Department of Preventive Medicine, Graduate School of Medical Sciences, Kyushu University, 3-1-1 Maidashi, Higashi-ku, Fukuoka 812-8582, Japan

<sup>2</sup>Research Institute for Diseases of the Chest, Graduate School of Medical Sciences, Kyushu University, 3-1-1 Maidashi, Higashi-ku, Fukuoka 812-8582, Japan

Correspondence should be addressed to Chikako Kiyohara, chikako@phealth.med.kyushu-u.ac.jp

Received 31 May 2010; Revised 21 July 2010; Accepted 27 July 2010

Academic Editor: Ashis Basu

Copyright © 2010 Chikako Kiyohara et al. This is an open access article distributed under the Creative Commons Attribution License, which permits unrestricted use, distribution, and reproduction in any medium, provided the original work is properly cited.

Genetic variations in DNA repair genes are thought to modulate DNA repair capacity and are suggested to be related to lung cancer risk. We conducted a meta-analysis of epidemiologic studies on the association between genetic polymorphisms in both base excision repair and nucleotide excision repair pathways, and lung cancer. We found xeroderma pigmentosum complementation group A (*XPA*) G23A (odds ratio (OR) = 0.76, 95% confidence interval (CI) = 0.61–0.94), 8-oxoguanine DNA glycosylase 1 (*OGG1*) Ser326Cys (OR = 1.22, 95% CI = 1.02–1.45), and excision repair cross-complementing group 2 (*ERCC2*) Lys751Gln (OR = 1.27, 95% CI = 1.10–1.46) polymorphisms were associated with lung cancer risk. Considering the data available, it can be conjectured that if there is any risk association between a single SNP and lung cancer, the risk fluctuation will probably be minimal. Advances in the identification of new polymorphisms and in high-throughput genotyping techniques will facilitate the analysis of multiple genes in multiple DNA repair pathways. Therefore, it is likely that the defining feature of future epidemiologic studies will be the simultaneous analysis of large samples of cases and controls.

## 1. Introduction

Sporadic cancer is a multifactorial disease that results from complex interactions between many genetic and environmental factors [1]. This means that there will not be a single gene or single environmental factor that has large effects on cancer susceptibility. Environmental factors (e.g., tobacco smoke, dietary factors, infectious agents, and radiation) add to the carcinogenic load to which humans are exposed, but exact numbers for added risk are generally less well established.

Cigarette smoke contains several thousand chemicals that are known to chemically modify DNA [2] and lead to the formation of mutations [3]. Most of these compounds are procarcinogens that must be activated by Phase I enzymes, such as cytochrome P450s. All activated carcinogens can bind to DNA and form DNA adducts that are capable of

inducing mutations and initiating carcinogenesis. The capacity to repair DNA damage induced by activated carcinogens appears to be one of the host factors that may influence lung cancer risk. A critical cellular response that counteracts the carcinogenic effects of DNA damage is DNA repair.

Several studies have investigated whether reduced DNA repair capacity (DRC) is associated with an increased risk of cancer [4]. The reduced DRC of benzo(a)pyrene-7,8-diol-9,10-epoxide (an active form of benzo(a)pyrene)-DNA adducts is associated with an increased risk of lung cancer (2.1-fold, 95% confidence interval (CI) = 1.5–3.0) [5]. The reduced DRC has been shown to be associated with a 5.7-fold (95% CI = 2.1–15.7) increased risk of developing lung cancer [6]. Likewise, the reduced DRC of bleomycin-induced damage was found to be associated with an increased risk of lung cancer [7]. These studies suggested that a low DRC of various DNA repair mechanisms predisposes individuals to

lung cancer, and this realization prompted us to search for defined DNA repair activities that may be risk factors for lung cancer. Polymorphisms in DNA repair genes may be associated with differences in the DRC of DNA damage and may influence an individual's risk of lung cancer, because the variant genotype in those polymorphisms might destroy or alter repair function.

At least four pathways of DNA repair operate on specific types of damaged DNA. Base excision repair (BER) operates on small lesions, while the nucleotide excision repair (NER) pathway repairs bulk lesions. Mismatch repair corrects replication errors. Double-strand DNA break repair (DSBR) actually consists of two pathways, homologous recombination (HR) and nonhomologous end-joining (NHEJ). The NHEJ repair pathway involves direct ligation of the two double strand break ends, while HR is a process by which double-strand DNA breaks are repaired through the alignment of homologous sequences of DNA. The following sections review the literature on DNA repair genes in more detail, specifically those involved in the NER and BER pathways.

It is believed that the predominant pathway used for removal of oxidized and many of the alkylated bases is BER. The process of BER is initiated by DNA glycosylases [e.g., 8-oxoguanine DNA glycosylase 1 (OGG1), endonuclease III homolog 1, thymine glycol-DNA-glycosylase], which are often promiscuous as far as their substrate specificity is concerned. The BER pathway can proceed through two different subpathways: short-patch and long-patch BER. These pathways are differentiated by the enzymes involved and the number of nucleotides removed. Short-patch BER replaces a single nucleotide by polymerase  $\beta$  and the newly synthesized DNA sealed by DNA ligase III/X-ray cross-complementing group 1 (XRCC1) heterodimer [8]. Long-patch BER inserts 2–13 nucleotides by concordant action of polymerase  $\delta$ , proliferating cell nuclear antigen, flap endonuclease 1, and ligase I.

NER is a versatile DNA repair system that removes a wide range of DNA lesions including UV-induced lesions. There are two subpathways in NER. One is transcription-coupled DNA repair (TCR), which preferentially removes DNA damage that blocks ongoing transcription in the transcribed DNA strand of active genes. The other is global genome repair (GGR), which removes lesions throughout the genome, including those from the nontranscribed strand in the active gene [9]. Three rare, autosomal recessive inherited human disorders are associated with impaired NER activity: XP, CS, and trichothiodystrophy (TTD) [10]. XP has been studied most extensively. Seven different DNA NER genes, which correct seven distinct genetic XP complementation groups (*XPA*, *XPB* (excision repair cross-complementing group 3, *ERCC3*), *XPC*, *XPD* (*ERCC2*), *XPE*, *XPV* (*ERCC4*) and *XPG* (*ERCC5*, this gene causes CS)) and *XPV* have been identified [10]. *XPA*, *ERCC3/XPB*, *ERCC2/XPD*, *ERCC4/XPF* and *ERCC5/XPG* have a defect in TCR and GGR, while *XPC* and *XPE* have a defect in GGR only. *ERCC6* and *ERCC8* are also known as *CS type B (CSB)* and *CSA*, respectively.

The aim of this article is to review and evaluate associations between genes in the BER and NER pathways,

focusing on genetic polymorphisms in *OGG1*, *XRCC1*, *XPA*, and *ERCC2* genes, which have been reported a sufficient number of studies to conduct a meta-analysis. The details of the *OGG1*, *XRCC1*, *XPA*, and *ERCC2* genes are given in Table 1

## 2. Materials and Methods

**2.1. Identification and Eligibility of Relevant Studies.** We conducted MEDLINE, Current Contents, and Web of Science searches using “OGG1”, “XRCC1”, “XPA”, “ERCC2/XPD”, “lung cancer”, and “polymorphism” as keywords to search for papers published (from January 1, 1966 through December 31, 2009). Additional articles were identified through the references cited in the first series of articles selected. Articles included in the meta-analysis were in English language, with human subjects. Case-control studies were eligible if they had determined the distribution of the relevant genotypes in lung cancer cases and in concurrent controls using a molecular method for genotyping. For overlapping studies, only the first published one was selected. Using the MEDLINE database, we identified 18 genetic epidemiological studies that provided information on lung cancer occurrence associated with the *OGG1* Ser326Cys polymorphism. Also, we identified 22 studies of the *XRCC1* Arg399Gln polymorphism, 12 studies of *XRCC1* Arg194Trp polymorphism, and 10 studies of the *XRCC1* Arg280His polymorphism. As for NER polymorphisms, we identified 6 studies for the *XPA* G23A polymorphism, 16 studies for the Asp312Asn polymorphism, and 19 studies for the Lys751Gln polymorphism. No additional articles through Current Contents or Web of Science have been identified.

**2.2. Data Extraction and Assessment of Study Quality.** For each study, characteristics such as authors, year of publication, ethnic group of the study population, source of control population, number of genotyped cases and controls, crude odds ratio (OR), and the method for quality control of genotyping were noted. For studies including subjects of different ethnic groups, data were extracted separately for each ethnic group whenever possible.

Methods for defining study quality in genetic studies are more clearly delineated than those for observational studies. We combined only studies with allelic frequencies being in Hardy-Weinberg equilibrium (HWE) (Pearson  $\chi^2$  test,  $P \geq .05$ ) because departure from HWE can imply the presence of genotyping error, possible ethnic admixture in the population, or selection bias (lack of representativeness of the general population). We assessed the homogeneity of the study population (Caucasian or Asian).

**2.3. Meta-Analysis.** Data were combined using both a fixed effects (the inverse variance-weighted method) and a random effects (DerSimonian and Laird method) models [11]. The Cochran Q statistics test is used for the assessment of heterogeneity. The fixed effects model is used when the effects are assumed to be homogenous, while the random effects model is used when they are heterogenous.

TABLE 1: The details of the *OGGI*, *XRCCI*, *XPA*, and *ERCC2/XPD* genes.

Gene symbol	Gene name	Gene location	Polymorphism	DNA repair capacity
<i>OGGI</i>	8-oxoguanine DNA glycosylase	3p26.2	Ser326Cys (rs1052133)	The Cys/Cys genotype may be associated with a lower DNA repair capacity
<i>XRCCI</i>	X-ray repair complementing defective repair in Chinese hamster cells 1	19q13.2	Arg194Trp (rs1799782), Arg280His (rs25489), Arg399Gln (rs25487)	Although the Arg399Gln, Arg194Trp, and Arg280His polymorphisms have been suggested to be functional, there is no direct evidence on its functional consequences
<i>XPA</i>	Xeroderma pigmentosum, complementation group A	9q22.3	G23A (rs 1800975)	The G allele may be associated with a higher DNA repair capacity
<i>ERCC2/XPD</i>	Excision repair cross-complementing group 2/ Xeroderma pigmentosum, complementation group D	19q13.3	Asp312Asn (rs1799793), Lys751Gln (rs13181)	The 312Asn and 751Gln alleles are reported to be associated with lower DNA repair capacity

In the absence of between-study heterogeneity, the two methods provide identical results. The presence of heterogeneity can result from differences in the selection of controls, age distribution, prevalence of lifestyle factors, histological type of lung cancer, stage of lung cancer, and so on. The random effects model incorporates an estimate of the between-study variance and tends to provide wider CIs when the results of the constituent studies differ among themselves. As the random effects model is more appropriate when heterogeneity is present [11], the summary OR and prevalence were essentially based on the random effects model. The meta-analyses were performed on crude ORs, since the adjusted ORs were not comparable because of the inclusion of different covariates in the multivariate regression models. Using individuals with the homozygous common genotype as the reference group, we calculated ORs for individuals with the heterozygous genotype and homozygous rare genotype separately whenever possible (information available in at least two studies). In some cases, we combined the heterozygous genotype with the homozygous rare genotype due to a low prevalence of the rare allele in several polymorphisms. The *Q* statistic was considered significant for  $P < .10$  [12, 13]. Publication bias is always a concern in meta-analysis. The presence of publication bias indicates that nonsignificant or negative findings remain unpublished. To test for publication bias, both Begg's [14] and Egger's [15] tests are commonly used to assess whether smaller studies reported greater associations than larger studies. Publication bias is considered significant for  $P < .10$ . For each genetic comparison, subgroup analysis was stratified by the ethnicity and, if possible, histological type of lung cancer. All of the calculations were performed using STATA Version 10.1 (Stata Corporation, College Station, TX) software.

### 3. Results

**3.1. *OGGI* Ser326Cys Polymorphism.** Table 2 shows the individual ORs from each study and summary ORs of the *OGGI* Ser326Cys polymorphism [16–33]. Two studies [24, 26] were excluded from the meta-analysis because genotype

distribution in control population significantly deviates from HWE. Combining data from all 17 populations on the basis of 6,181 cases and 7,331 controls, the summary ORs were 1.04 (95% CI = 0.94–1.23) for Ser/Cys carriers and 1.22 (95% CI = 1.02–1.45) for Cys/Cys carriers. The Cys/Cys genotype was significantly associated with lung cancer risk in all populations combined. The summary ORs for the Cys/Cys genotype in Caucasians (mostly composed of Caucasians) and Asians were 1.24 (95% CI = 0.84–1.83) and 1.24 (95% CI = 1.00–1.55,  $P = .052$ ), respectively. There was a marginally significant association between lung cancer risk and the *OGGI* Ser326Cys polymorphism among Asians. Publication bias was absent in all analyses. Heterogeneity was present in the analyses of all studies combined and Caucasian studies combined.

A further analysis on histological type was performed to assess whether the impact of the *OGGI* Ser326Cys polymorphism between adenocarcinoma and squamous cell carcinoma cases (the two histological types present most often in the data set) was similar or not. Among the seven case-control studies (2,052 lung cancer cases and 3,032 controls), the summary OR for the Cys/Cys genotype in adenocarcinoma was 1.38 (95% CI = 1.12–1.75) (data not shown). Among both Caucasians (612 cases and 2,618 controls) [17, 22, 25] and Asians (1,440 cases and 864 controls) [16, 19, 28, 32], subjects with the Cys/Cys genotype were at increased risk of adenocarcinoma. Summary ORs for Caucasians and Asians were 1.90 (95% CI = 0.99–3.63,  $P = .054$ ) and 1.30 (95% CI = 1.00–1.29,  $P = .049$ ), respectively (data not shown). It was found that increased risk associated with the Cys/Cys genotype was not evident for squamous cell lung cancer risk among Caucasians [17, 22, 25]. The available data on squamous cell carcinoma are insufficient for Asians.

**3.2. *XRCCI* Polymorphism.** Table 3 shows that summary ORs of the *XRCCI* Arg399Gln polymorphism on the basis of 8,684 cases and 10,913 controls [23, 25–27, 30, 33–49]. The summary OR for the 399Gln/Gln genotype among 24 different ethnic populations was 1.00 (95% CI = 0.86–1.17). The Cochran *Q* test for heterogeneity showed a statistical

TABLE 2: Genetic polymorphisms in the BER pathway and lung cancer risk: *OGG1* Ser326Cys polymorphism.

Author, published year (reference no.)	Ethnicity	No. of Cases/Controls	Source of controls	OR (95% CI)*		Quality control of genotyping	
				Ser/Cys	Cys/Cys		
Sugimura et al., 1999 [16]	Asian	241/197	Hospital	0.80 (0.52–1.21)	1.13 (0.63–2.02)	Sequencing	
Wikman et al., 2000 [17]	Caucasian	105/105	Hospital	0.66 (0.37–1.17)	2.20 (0.41–11.8)	Sequencing	
Ito et al., 2002 [18]	Asian	138/240	Hospital	1.02 (0.63–1.67)	0.85 (0.46–1.56)	None	
Sunaga et al., 2002 [19]	Asian	198/152	Hospital	1.49 (0.91–2.43)	0.98 (0.54–1.77)	None	
Le Marchand et al., 2002 [20]	Admixed population	298/405	Population	0.90 (0.65–1.26)	1.76 (1.15–2.71)	Sequencing	
Lan et al., 2004 [21]	Asian	118/109	Population	1.96 (1.10–3.48)	1.84 (0.83–4.06)	None	
Park et al., 2004 [22]	Mostly composed of Caucasians	179/350	Screening	1.89 (1.27–2.80)	4.10 (1.65–10.2)	Sequencing	
Vogel et al., 2004 [23]	Caucasian	256/269	Population	1.09 (0.75–1.60)	0.78 (0.35–1.72)	Replication (random samples)	
Liang et al., 2005 [24]†	Asian	227/227	Hospital	0.94 (0.63–1.41)	0.98 (0.33–2.87)	Sequencing	
Hung et al., 2005 [25]	Mostly composed of Caucasians	2,155/2,163	Hospital	0.90 (0.79–1.03)	1.15 (0.84–1.57)	Replication (random samples)	
Zienolddiny et al., 2006 [26]‡	Caucasian	326/386	Population	0.91 (0.64–1.29)	0.63 (0.40–0.97)	Replication (all samples)	
Matullo et al., 2006 [27]	Caucasian	116/1094	Population	1.26 (0.83–1.91)	0.82 (0.21–2.33)	Replication (random samples)	
Kohno et al., 2006 [28]	Asian	1097/394	Hospital	1.24 (0.94–1.63)	1.43 (1.02–2.01)	None	
Sørensen et al., 2006 [29]	Caucasian	431/796	Population	1.04 (0.80–1.35)	1.18 (0.63–2.21)	Replication (random samples)	
De Ruyck et al., 2007 [30]	Caucasian	110/110	Hospital	0.58 (0.33–1.02)	0.61 (0.13–2.82)	None	
Karahlil et al., 2008 [31]	Turkish	165/250	Hospital	0.82 (0.54–1.24)	0.65 (0.32–1.29)	None	
Miyaishi et al., 2009 [32]	Asian	108/121	Hospital	1.47 (0.79–2.73)	1.34 (0.65–2.77)	None	
Chang et al., 2009 [33]	Latino	112/296	Population	0.91 (0.56–1.47)	1.05 (0.45–2.32)	Replication (random samples)	
Chang et al., 2009 [33]	African- American	254/280	Population	1.32 (0.89–1.98)	0.89 (0.25–3.00)	Replication (random samples)	
Summary**	No. of populations					Cochran Q test for heterogeneity	
All	17	6,181/7,331		1.04 (0.94–1.23)	1.22 (1.02–1.45)	0.004	0.220
Caucasian (mostly composed of Caucasians)	7	3,352/4,887		1.02 (0.81–1.29)	1.24 (0.84–1.83)	0.004	0.133
Asian	6	1,900/1,213		1.23 (0.97–1.55)	1.24 (1.00–1.55)†	0.159	0.572

\*Crude odds ratio and 95% confidence interval.

\*\*Based on random effects model.

† $P = .052$ .

‡Excluded from the meta-analysis because genotype distribution of control population was not in Hardy-Weinberg equilibrium. NA, not available.

TABLE 3: Genetic polymorphisms in the BER pathway and lung cancer risk: *XRCC1* Arg399Gln polymorphism.

Author, published year (reference no.)	Ethnicity	No. of Cases/Controls	Source of controls	OR (95% CI)*		Quality control of genotyping	
				Arg/Gln	Gln/Gln		
Ratnasinghe et al., 2001 [34]	Asian	107/208	Population	1.00 (0.60–1.60)	1.40 (0.50–1.70)	Replication (random sample)	
David-Beabes and London , 2001 [35]	African- American	154/243	Population	1.03 (0.66–1.60)	0.52 (0.14–1.97)	Replication (random sample)	
David-Beabes and London , 2001 [35]	Caucasian	180/461	Population	0.75 (0.52–1.08)	0.63 (0.34–1.14)	Replication (random sample)	
Divine et al., 2001 [36]	Caucasian	172/143	Hospital	0.76 (0.47–1.22)	1.64 (0.80–3.36)	None	
Chen et al., 2002 [37]	Asian	109/109	Population	1.02 (0.57–1.80)	0.67 (0.20–2.26)	None	
Park et al., 2002 [38]	Asian	192/135	Hospital visitors	1.27 (0.81–2.04)	2.30 (0.87–6.09)	Sequencing	
Misra et al., 2003 [39]	Caucasian	315/313	Population	1.10 (0.78–1.54)	0.84 (0.45–1.58)	Replication (random sample)	
Zhou et al., 2003 [40]	Caucasian	1,091/1,240	Hospital visitors	1.00 (0.80–1.20)	1.30 (1.00–1.70)	Replication (random sample)	
Ito et al., 2004 [41]	Asian	178/449	Hospital	1.01 (0.70–1.45)	1.39 (0.70–2.76)	None	
Popanda et al., 2004 [42]	Caucasian	463/460	Hospital	0.89 (0.67–1.17)	0.87 (0.58–1.29)	Replication (random sample)	
Harms et al., 2004 [43]	Caucasian	110/119	Hospital	0.73 (0.44–1.25)	1.07 (0.39–2.96)	Replication (all samples)	
Zhang et al., 2005 [44]	Asian	1,000/1,000	Hospital	0.95 (0.79–1.14)	1.14 (0.84–1.55)	Replication (all samples)	
Hung et al., 2005 [25]	Mostly composed of Caucasians	2,049/2,015	Hospital	1.12 (0.98–1.28)	1.01 (0.83–1.23)	Replication (random sample)	
Vogel et al., 2004 [23]	Caucasian	256/269	Population	0.79 (0.54–1.17)	0.81 (0.46–1.41)	Replication (random sample)	
Schneider et al., 2005 [45]	Caucasian	446/622	Hospital	0.94 (0.72–1.23)	0.83 (0.54–1.26)	None	
Shen et al., 2005 [46]	Asian	116/109	Population	0.59 (0.33–1.05)	0.75 (0.13–4.23)	None	
Zienolddiny et al., 2006 [26]	Caucasian	331/391	Population	1.08 (0.78–1.49)	0.67 (0.39–1.14)	Replication (all samples)	
Matullo et al., 2006 [27]	Caucasian	116/1,094	Population	1.14 (0.75–1.73)	0.52 (0.19–1.19)	Replication (random sample)	
Yin et al., 2007 [47]	Asian	205/193	Hospital	1.20 (0.77–1.85)	0.21 (0.05–1.00)	None	
López-Cima et al., 2007 [48]	Caucasian	516/533	Hospital	0.91 (0.70–1.20)	0.89 (0.61–1.31)	Sequencing	
Pachouri et al., 2007 [49]	Asian	103/122	Population	0.36 (0.20–0.64)	0.47 (0.20–1.09)	None	
De Ruyck et al., 2007 [30]	Caucasian	109/109	Hospital	1.28 (0.69–2.28)	1.68 (0.67–4.23)	None	
Chang et al., 2009 [33]	Latino	112/296	Population	1.30 (0.73–2.30)	3.03 (1.11–7.83)	Replication (random sample)	
Chang et al., 2009 [33]	African- American	254/280	Population	1.02 (0.62–1.65)	1.19 (0.24–5.13)	Replication (random sample)	
Summary**	No. of populations					Cochran Q test for heterogeneity	
All	24	8,684/10,913		0.97 (0.89–1.05)	1.00 (0.86–1.17)	0.153	0.004
Caucasian (mostly composed of Caucasians)	13	6,154/7,769		1.00 (0.92–1.08)	0.95 (0.83–1.10)	0.433	0.218
Asian	8	2,010/2,325		0.90 (0.72–1.13)	1.08 (0.78–1.49)	0.024	0.030

\*Crude odds ratio and 95% confidence interval..

\*\*Based on random effects model.

TABLE 4: Genetic polymorphisms in the BER pathway and lung cancer risk: *XRCC1* Arg194Trp polymorphism.

Author, published year (reference no.)	Ethnicity	No. of Cases/control	Source of controls	OR (95% CI)*		Quality control of genotyping	
				Arg/Trp	Trp/Trp		
Ratnasinghe et al., 2001 [34]	Asian	108/216	Population	0.70 (0.40–1.20)	0.70 (0.30–1.60)	Replication (random sample)	
David-Beabes and London , 2001 [35]	African- American	154/234	Population	0.40 (0.19–0.83)	1.44 (0.20– 10.37)	Replication (random sample)	
David-Beabes and London , 2001 [35]	Caucasian	180/461	Population	1.05 (0.62–1.78)	—	Replication (random sample)	
Chen et al., 2002 [37]	Asian	109/109	Population	1.31 (0.73–2.32)	2.61 (0.85– 8.04)	None	
Hung et al., 2005 [25]	Mostly composed of Caucasians	2,147/2,132	Hospital	0.86 (0.72–1.03)	0.81 (0.35–1.88)	Replication (random sample)	
Schneider et al., 2005 [45]	Caucasian	446/622	Hospital	0.99 (0.67–1.46)	1.86 (0.31–12.8)	None	
Shen et al., 2005 [46]	Asian	118/112	Population	1.01 (0.56–1.83)	1.48 (0.51–4.45)	None	
Zienolddiny et al., 2006 [26]	Caucasian	336/405	Population	0.88 (0.50–1.55)	0.60 (0.01–11.5)	Replication (all samples)	
Matullo et al., 2006 [27]	Caucasian	116/1094	Population	1.10 (0.59–1.94)	9.70 (0.69– 134.6)	Replication (random samples)	
Yin et al., 2007 [47]	Asian	241/249	Hospital	0.89 (0.60–1.32)	1.09 (0.54–2.18)	None	
Pachouri et al., 2007 [49] <sup>†</sup>	Asian	103/122	Population	0.97 (0.54–1.76)	1.36 (0.67–2.75)	None	
De Ruyck et al., 2007 [30]	Caucasian	110/110	Hospital	0.43 (0.15–1.12)	—	None	
Chang et al., 2009 [33]	Latino	112/296	Population	0.73 (0.37–1.49)	—	Replication (random samples)	
Chang et al., 2009 [33]	African- American	254/280	Population	1.23 (0.64–2.30)	—	Replication (random samples)	
Summary**	No. of populations					Cochran Q test for heterogeneity	
						Arg/Trp	Trp/Trp
All	13	4,431/6,320		0.89 (0.79– 1.00) <sup>†</sup>	1.15 (0.80–1.67)	0.467	0.510
Caucasian (mostly composed of Caucasians)	6	3,335/4,824		0.89 (0.77–1.03)	1.24 (0.50–3.11)	0.653	0.315
Asian	4	576/686		0.93 (0.72–1.20)	1.18 (0.72–1.93)	0.476	0.305

\*Crude odds ratio and 95% confidence interval.

\*\*Based on random effects model.

<sup>†</sup> $P = .047$ .

<sup>‡</sup>Excluded from the meta-analysis because genotype distribution of control population was not in Hardy-Weinberg equilibrium.

significance ( $P = .004$ ). Both the Egger's and Begg's tests were not statistically significant, however. The summary ORs for the 339Gln/Gln genotype among Caucasians and Asians were 0.95 (95% CI = 0.83–1.10) and 1.08 (95% CI = 0.78–1.49), respectively. Evidence for publication bias was absent in subgroup analyses by ethnic. The Cochran Q test for heterogeneity showed a statistical significance among Asians.

A further analysis on histological type (adenocarcinoma and squamous cell carcinoma) was carried out. Although available data were not sufficient, there were no statistically significant differences in risk associated with the *XRCC1* Arg399Gln polymorphism and adenocarcinoma or squamous cell both Caucasians and Asians [25, 38, 42, 44, 45, 49].

Table 4 shows summary ORs of the *XRCC1* Arg194Trp polymorphism [25–27, 30, 33–35, 37, 45–47, 49]. One study

TABLE 5: Genetic polymorphisms in the BER pathway and lung cancer risk: *XRCC1* Arg280His polymorphism.

Author, published year (reference no.)	Ethnicity	No. of Cases/ controls	Source of controls	OR (95% CI)*		Quality control of genotyping	
				Arg/His	Arg/His or His/His	Arg/His	Arg/His or His/His
Ratnasinghe et al., 2001 [34]	Asian	106/209	Population	1.40 (0.70–2.60)	1.60 (0.90–2.90)	Replication (random sample)	
Mirsa et al., 2003 [39]	Caucasian	309/302	Population	1.12 (0.70–1.80)	1.17 (0.73–1.87)	Replication (random samples)	
Hung et al., 2005 [25]	Mostly composed of Caucasians	2,088/2,092	Hospital	0.95 (0.77–1.18)	0.95 (0.77–1.17)	Replication (random samples)	
Vogel et al., 2004 [23]	Caucasian	256/269	Population	0.98 (0.53–1.79)	1.01 (0.56–1.85)	Replication (random samples)	
Schneider et al., 2005 [45]	Caucasian	446/622	Hospital	0.93 (0.59–1.44)	0.97 (0.63–1.53)	None	
Shen et al., 2005 [46]	Asian	111/110	Population	1.14 (0.60–2.18)	1.29 (0.69–2.41)	None	
Zienolddiny et al., 2006 [26]‡	Caucasian	324/377	Population	1.53 (0.85–2.78)	1.45 (0.82–2.56)	Replication (All samples)	
Yin et al., 2007 [47]	Asian	238/242	Hospital	0.73 (0.46–1.16)	0.72 (0.46–1.12)	None	
De Ruyck et al., 2007 [30]	Caucasian	110/110	Hospital	0.26 (0.06–0.87)	0.26 (0.06–0.87)	None	
Chang et al., 2009 [33]	Latino	112/296	Population	1.11 (0.53–2.20)	1.08 (0.53–2.10)	Replication (random samples)	
Chang et al., 2009 [33]	African- American	254/280	Population	—	—	Replication (random samples)	
Summary**	No. of populations					Cochran Q test for heterogeneity	
						Arg/His	Arg/His or His/His
All	10	4,030/4,532		0.96 (0.83–1.11)	0.99 (0.83–1.19)	0.525	0.281
Caucasian (mostly composed of Caucasians)	5	3,209/3,395		0.95 (0.80–1.13)	0.96 (0.80–1.17)	0.400	0.357
Asian	3	455/561		0.99 (0.66–1.48)	1.10 (0.66–1.84)	0.236	0.076

\*Crude odds ratio and 95% confidence interval.

\*\*Based on random effects model.

‡Excluded from the meta-analysis because genotype distribution of control population was not in Hardy-Weinberg equilibrium.

[49] was excluded from the meta-analysis because allelic frequency in control population is not in HWE. Based on 11 studies in 13 different ethnic populations on the basis of 4,431 cases and 6,320 controls, the summary ORs for the Arg/Trp genotype and Trp/Trp genotype were 0.89 (95% CI = 0.79–1.00,  $P = .047$ ) and 1.15 (95% CI = 0.80–1.67), respectively. The ORs for the Trp/Trp genotype were 1.24 (95% CI = 0.50–3.11) in Caucasians and 1.18 (95% CI = 0.72–1.93) in Asians. This polymorphism was not associated with lung cancer risk among both Caucasians and Asians. Evidence for heterogeneity and publication bias was absent in any analysis.

Table 5 shows summary ORs of the *XRCC1* Arg280His polymorphism [23, 25, 26, 30, 33, 34, 39, 45–47]. One study [26] was excluded from the meta-analysis because genotype distribution in control population does not fulfill HWE. The summary OR for the Arg/His versus the Arg/Arg

genotype among 9 studies on the basis of 4,030 cases and 4,532 controls was 0.96 (95% CI = 0.83–1.11). The summary OR for the Arg/His and His/His genotypes combined versus the Arg/Arg genotype was 0.99 (95% CI = 0.83–1.19). The summary ORs for the Arg/His and His/His genotypes combined versus the Arg/Arg genotype in Caucasians and Asians were 0.96 (95% CI = 0.80–1.17) and 1.10 (95% CI = 0.66–1.84), respectively. There was no ethnic difference in the association between lung cancer risk and the *XRCC1* Arg280His polymorphism. Evidence for heterogeneity and publication bias was absent in subgroup analyses by ethnic.

3.3. *XPA G23A Polymorphism.* Table 6 shows summary ORs of the *XPA G23A* polymorphism on the basis of 2,025 cases and 1,991 controls [26, 30, 42, 50–52]. SNP alleles with higher frequencies are more likely to be ancestral than less frequently occurring alleles although there may be some

TABLE 6: Genetic polymorphisms in the NER pathway and lung cancer risk: XPA G23A polymorphism.

Author, published year (reference no.)	Ethnicity	No. of Cases /controls	Source of controls	OR (95% CI)*		Quality control of genotyping	
				G/A	G/G		
Park et al., 2002 [50]	Asian	265/185	Population	1.00 (0.62–1.62)	0.62 (0.35–1.10)	Sequencing	
Wu et al., 2003 [51]	Caucasian	564/581	Population	0.65 (0.48–0.87)	0.74 (0.55–1.01)	None	
Wu et al., 2003 [51]	Mexican- American	50/47	Population	0.31 (0.09–1.00)	0.40 (0.13–1.25)	None	
Wu et al., 2003 [51]	African- American	71/67	Population	0.54 (0.16–1.68)	0.49 (0.15–1.49)	None	
Popanda et al., 2004 [42]	Caucasian	461/457	Hospital	0.77 (0.48–1.21)	0.82 (0.52–1.30)	Replication (random samples)	
Vogel et al., 2005 [52]	Caucasian	256/269	Population	0.78 (0.41–1.49)	0.57 (0.30–1.06)	None	
Zienolddiny et al., 2006 [26]	Caucasian	248/276	Population	0.87 (0.48–1.57)	1.41 (0.79–2.52)	Replication (all samples)	
De Ruyck et al., 2007 [30]	Caucasian	110/109	Hospital	1.00 (0.34–2.92)	1.02 (0.34–3.03)	None	
Summary**	No. of populations					Cochran Q test for heterogeneity	
						G/A	G/G
All	8	2,025/1,991		0.74 (0.61–0.90)	0.76 (0.61–0.94)	0.640	0.345
Caucasian	5	1,639/1,692		0.73 (0.59–0.90)	0.83 (0.64–1.08)	0.855	0.266

\*Crude odds ratio and 95% confidence interval.

\*\* Based on random effects model.

exceptions. As the 23G allele was more prevalent than the 23A allele [53], we regarded the 23G allele as ancestral (wild-type or major) allele for descriptive purposes (the XPA 23 polymorphism caused by the G-to-A substitution is the XPA G23A polymorphism). Summary ORs for the G/A genotype and G/G genotype among 6 studies in 8 populations were 0.74 (95% CI = 0.61–0.90) and 0.76 (95% CI = 0.61–0.94), respectively (Table 6, Figure 1). Among Caucasian studies, the summary ORs for the G/A genotype and the A/A genotype were 0.73 (95% CI = 0.59–0.90) and 0.83 (95% CI = 0.64–1.08), respectively. The Cochran Q test for heterogeneity did not show a statistical significance. The Egger's test was statistically significant for publication bias in a subgroup analysis of Caucasians ( $P = .024$ , G/A genotype versus G/G genotype).

**3.4. ERCC2/XPD Polymorphism.** Table 7 shows summary ORs of the ERCC2 Asp312Asn polymorphism on the basis of 6,346 cases and 7,792 controls [26, 27, 30, 39, 42, 48, 54–63]. The summary OR for the Asn/Asn genotype among 17 different ethnic populations was 1.19 (95% CI = 1.03–1.38). Caucasians with the Asn/Asn genotype and Asian with the Asn/Asn genotype had a marginal 1.15-fold (95% CI = 0.98–1.32,  $P = .079$ ) and a significant 8.26-fold (95% CI = 1.50–45.6,  $P = .015$ ) risk of developing lung cancer,

respectively. No significant association between lung cancer and the heterozygous Asp/Asn genotype was found for all of the studies combined or by ethnicity. The impact of the heterozygous genotype on lung cancer was similar between Caucasians and Asians. The Cochran Q test for heterogeneity did not show a statistical significance in all analyses. Although no evidence of publication bias was found in overall analyses, both Begg's ( $P = .040$ ) and Egger's ( $P = .010$ ) tests showed a statistical significance in a subgroup analysis of Caucasians (Asn/Asn genotype versus Asp/Asp genotype).

Table 8 shows summary ORs of the ERCC2 Lys751Gln polymorphism [26, 27, 30, 37, 39, 42, 43, 48, 55–65]. One study [26] was excluded from the meta-analysis because genotype distribution in control population significantly deviates from HWE. Based on 6,941 cases and 8,595 controls, summary ORs for the Gln/Gln genotype and Lys/Gln genotype were 1.09 (95% CI = 1.04–1.18) and 1.27 (95% CI = 1.10–1.46), respectively. The Gln/Gln genotype was significantly associated with an increased risk of lung cancer in Caucasians (OR = 1.24, 95% CI = 1.06–1.45) (Figure 2) but not in Asians (OR = 1.16, 95% CI = 0.48–2.80). The Cochran Q test for heterogeneity showed a statistical significance among Asian studies. Evidence of publication bias was absent in all of the analyses.

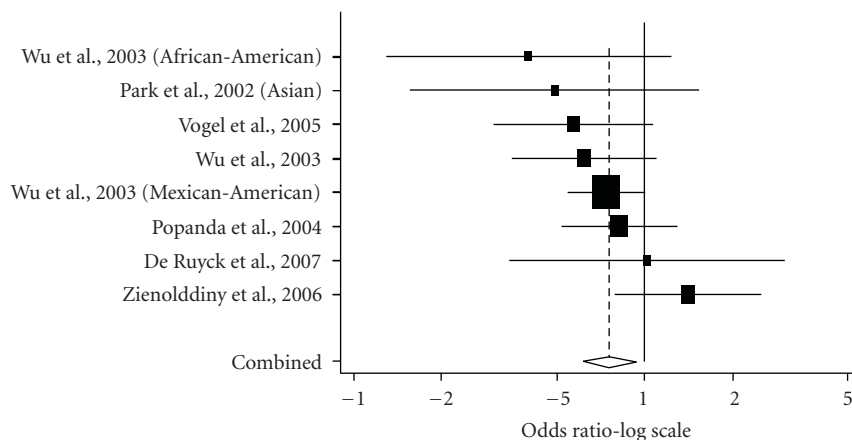


FIGURE 1: Meta-analysis of 8 studies (5 Caucasian studies and 3 non-Caucasian studies) of lung cancer and the *XPA* G23A polymorphism (GG versus AA). The center of a box and the horizontal line (logarithm) indicate the odds ratio (OR) and the 95% confidence interval (CI) in each study, with the areas of the boxes representing the weight of each study. The summary OR based on random effects model is represented by the middle of a diamond whose width indicated the 95% CI. The summary OR is shown by the dotted vertical line. Statistical heterogeneity between studies was assessed with Cochran Q test ( $Q = 7.86$ ,  $P = .35$ ). Summary: OR = 0.76 (95% CI = 0.61–0.94).

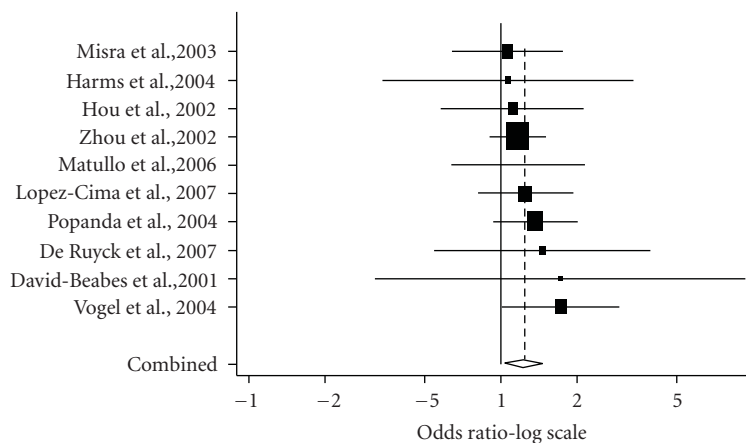


FIGURE 2: Meta-analysis of 10 Caucasian studies of lung cancer and the *ERCC2* Lys751Gln polymorphism (Gln/Gln versus Lys/Lys). The center of a box and the horizontal line (logarithm) indicate the odds ratio (OR) and the 95% confidence interval (CI) in each study, with the areas of the boxes representing the weight of each study. The summary OR based on random effects model is represented by the middle of a diamond whose width indicated the 95% CI. The summary OR is shown by the dotted vertical line. Statistical heterogeneity between studies was assessed with Cochran Q test ( $Q = 2.75$ ,  $P = .97$ ). Summary: OR = 1.24 (95% CI = 1.06–1.45).

#### 4. Discussion

Epidemiological studies of common polymorphisms in DNA repair genes, if large and unbiased, can provide insight into the *in vivo* relationships between DNA repair genes and lung cancer risk. Such studies may identify empirical associations which indicate that a polymorphism in a gene of interest has an impact on lung cancer, independent of metabolic regulatory mechanisms and other genetic and environmental variability. Findings from epidemiological studies can complement *in vitro* analyses of the various polymorphisms, genes, and pathways. In addition, epidemiological studies of common polymorphisms can lead to an increased understanding of the public health dimension of DNA-repair variation.

We conducted a systematic literature review to evaluate the associations between sequence variants in DNA repair genes and lung cancer risk. We found an increased risk of lung cancer among subjects carrying the *ERCC2* 751 Gln/Gln genotype in Caucasians (OR = 1.24, 95% CI = 1.06–1.45). The meta-analysis by Hu et al., showed that the Gln/Gln genotype had a significant 23% (95% CI = 3%–47%) increased risk of lung cancer compared with individuals with the Lys/Lys genotype among Caucasians [66]. The meta-analysis by Benhamou and Sarasin reported that the summary OR for the Gln/Gln genotype was 1.25 (95% CI = 1.03–1.52) in the United States (stratified by geographic region) [67]. Both of the meta-analyses were based on the same published data from 8 individual case-control (five Caucasian and three Asians) studies [37, 39, 55–58, 64, 65].

TABLE 7: Genetic polymorphisms in the NER pathway and lung cancer risk: *ERCC2* Asp312Asn polymorphism.

Author, published year (reference no.)	Ethnicity	No. of Cases/controls	Source of controls	OR (95% CI)*		Quality control of genotyping	
				Asp/Asn	Asn/Asn		
Butkiewicz et al., 2001 [54]	Caucasian	96/94	Population	0.49 (0.24–0.98)	0.71 (0.29–1.74)	Sequencing	
Spitz et al., 2001 [55]	Admixed population	195/257	Population	0.92 (0.62–1.36)	1.54 (0.78–3.05)	None	
Hou et al., 2002 [56]	Caucasian	184/162	Population	1.27 (0.78–2.05)	0.88 (0.43–1.84)	Replication (random samples)	
Zhou et al., 2002 [57]	Caucasian	1,092/1,240	Population	0.98 (0.82–1.17)	1.41 (1.06–1.86)	Replication (random samples)	
Liang et al., 2003 [58]	Asian	1,006/1,020	Population	0.98 (0.76–1.28)	11.2 (1.45–87.2)	Replication (random samples)	
Misra et al., 2003 [39]	Caucasian	313/312	Population	0.76 (0.53–1.07)	0.94 (0.56–1.59)	Replication (random samples)	
Popanda et al., 2004 [42]	Caucasian	463/460	Hospital	1.14 (0.77–1.68)	1.03 (0.70–1.51)	Replication (random samples)	
Vogel et al., 2004 [59]	Caucasian	252/263	Population	1.27 (0.86–1.89)	1.09 (0.63–1.86)	None	
Shen et al., 2005 [60]	Asian	118/113	Population	0.58 (0.21–1.52)	—	Replication (random samples)	
Zienolddiny et al., 2006 [26]	Caucasian	275/290	Population	0.85 (0.58–1.25)	1.11 (0.68–1.81)	Replication (all samples)	
Matullo et al., 2006 [27]	Caucasian	116/1094	Population	0.81 (0.52–1.26)	0.95 (0.51–1.71)	Replication (random samples)	
Hu et al., 2006 [61]	Asian	970/986	Hospital	1.07 (0.81–1.43)	4.11 (0.41– 202.7)	None	
López-Cima et al., 2007 [48]	Caucasian	516/533	Hospital	1.04 (0.80–1.35)	1.39 (0.88–2.20)	Sequencing	
De Ruyck et al., 2007 [30]	Caucasian	110/109	Hospital	1.28 (0.70–2.35)	1.03 (0.40–2.66)	None	
Chang et al., 2008 [62]	Latino	108/297	Population	1.37 (0.83–2.26)	2.13 (0.72–5.96)	Replication (random samples)	
Chang et al., 2008 [62]	African- American	247/277	Population	1.10 (0.71–1.70)	0.68 (0.10–3.57)	Replication (random samples)	
Yin et al., 2009 [63]	Asian	285/285	Hospital	1.31 (0.77–2.77)	—	Replication (random samples)	
Summary**	No. of populations					Cochran Q test for heterogeneity	
						Asp/Asn	Asn/Asn
All	17 (15)	6,346/7,792		1.00 (0.92–1.10)	1.19 (1.03–1.38)	0.510	0.510
Caucasian	10	3,417/4,557		0.98 (0.86–1.11)	1.15 (0.98–1.34)	0.257	0.770
Asian	4 (2)	2,379/2,404		1.02 (0.85–1.22)	8.26 (1.50–45.6)	0.565	0.597

\* Crude odds ratio and 95% confidence interval.

\*\* Based on random effects model.

These meta-analyses also indicate that the excess lung cancer risk from the Gln/Gln genotype may be about 20%. The Gln allele of the *ERCC2* Lys751Gln polymorphism is associated with a higher DNA adduct level or lower DNA repair efficiency [56, 68, 69], except in research published by Duell et al., who found no correlation between the *ERCC2* Lys751 Gln

polymorphism and the level of polyphenol-DNA adducts in human blood samples [70]. Thus, it is biologically plausible that subjects with the Gln/Gln genotype are at increased risk of lung cancer. As with the two meta-analyses, in our meta-analysis the Gln/Gln genotype was not associated with an increased risk of lung cancer among Asians. The Cochran

TABLE 8: Genetic polymorphisms in the NER pathway and lung cancer risk: ERCC2 Lys751Gln polymorphism.

Author, published year (reference no.)	Ethnicity	No. of Cases/controls	Source of controls	OR (95% CI)**		Quality control of genotyping	
				Lys/Gln	Gln/Gln		
David-Beabes et al., 2001 [64]	Caucasian	178/453	Population	1.14 (0.77–1.71)	1.72 (1.00–2.94)	Replication (random samples)	
David-Beabes et al., 2001 [64]	African- American	153/234	Population	1.14 (0.73–1.78)	1.39 (0.54–3.55)	Replication (random samples)	
Spitz et al., 2001 [55]	Admixed population	341/360	Population	1.07 (0.78–1.46)	1.36 (0.84–2.20)	None	
Chen et al., 2002 [37]	Asian	109/109	Population	0.79 (0.17–1.11)	0.44 (0.17–1.11)	None	
Hou et al., 2002 [56]	Caucasian	185/162	Population	1.22 (0.75–2.00)	1.11 (0.58–2.13)	Replication (random samples)	
Zhou et al., 2002 [57]	Caucasian	1,092/1,240	Population	1.01 (0.84–1.21)	1.17 (0.90–1.51)	Replication (random samples)	
Park et al., 2002 [65]	Asian	250/163	Population	1.06 (0.55–2.11)	—	None	
Liang et al., 2003 [58]	Asian	1,006/1,020	Population	0.93 (0.73–1.18)	2.36 (0.90–6.17)	Replication (random samples)	
Misra et al., 2003 [39]	Caucasian	310/302	Population	0.87 (0.60–1.26)	1.06 (0.64–1.76)	Replication (random samples)	
Popanda et al., 2004 [42]	Caucasian	463/459	Hospital	1.14 (0.86–1.52)	1.37 (0.93–2.02)	Replication (random samples)	
Harms et al., 2004 [43]	Caucasian	110/119	Population	1.34 (0.79–2.49)	1.07 (0.34–3.38)	Replication (all samples)	
Vogel et al., 2004 [59]	Caucasian	256/269	Population	1.57 (1.05–2.34)	1.73 (1.01–2.96)	None	
Shen et al., 2005 [60]	Asian	118/108	Population	0.44 (0.18–1.03)	—	Replication (random samples)	
Zienolddiny et al., 2006 [26]‡	Caucasian	317/386	Population	1.20 (0.84–1.73)	1.56 (1.06–2.31)	Replication (all samples)	
Matullo et al., 2006 [27]	Caucasian	116/1094	Population	1.23 (0.78–1.96)	1.17 (0.63–2.11)	Replication (random samples)	
Hu et al., 2006 [61]	Asian	975/997	Hospital	1.16 (0.89–1.52)	1.46 (0.40–5.87)	None	
De Ruyck et al., 2007 [30]	Caucasian	110/109	Hospital	1.07 (0.58–1.97)	1.46 (0.55–3.94)	None	
López-Cima et al., 2007 [48]	Caucasian	516/533	Hospital	1.08 (0.83–1.41)	1.25 (0.80–1.95)	Sequencing	
Chang et al., 2008 [62]	Latino	113/299	Population	1.01 (0.61–1.66)	2.89 (1.20–6.91)	Replication (random samples)	
Chang et al., 2008 [62]	African American	255/280	Population	1.20 (0.83–1.74)	1.01 (0.41–2.43)	Replication (random samples)	
Yin et al., 2009 [63]	Asian	285/285	Hospital	1.68 (1.06–2.67)	1.47 (0.24–10.1)	Replication (random samples)	
Summary**	No. of populations					Cochran Q test for heterogeneity	
All	20 (18)	6,941/8,595		1.09 (1.04–1.18)	1.27 (1.10–1.46)	0.613	0.727
Caucasian	10	3,336/4,740		1.10 0.99–1.22)†	1.24 (1.06–1.45)	0.702	0.973
Asian	6 (4)	2,743/2,682		1.04 (0.81–1.35)	1.16 (0.48–2.80)	0.085	0.096

\* Crude odds ratio and 95% confidence interval. \*\* Based on random effects model. †  $P = .051$ 

‡ Excluded from the meta-analysis because genotype distribution of control population was not in Hardy-Weinberg equilibrium.

Q test for heterogeneity showed a statistical significance among Asian studies. The presence of heterogeneity may compromise the interpretation of meta-analyses and result in erroneous and potentially misleading conclusions [71, 72]. The presence of significant heterogeneity suggests that the estimated OR in each study is not homogeneous and the estimated ORs are close to 1.0 in the larger studies. Possible sources of heterogeneity are ethnicity (the prevalence of the “at risk” allele, ethnic differences in roles of the polymorphism), study design, and so on. Another possible reason for heterogeneity is linkage disequilibrium, with additional allelic variants of this gene that modulate overall enzyme activity. Furthermore, it is possible that interaction with polymorphisms at other genes may be important. Heterogeneity can be taken into account by applying the random effects model, however. This discrepancy between Caucasian studies and Asian studies may only be due to a difference in sample sizes. Reasons for this difference in risk among different ethnic populations are as yet unknown but, if real, may be related to other genetic or environmental factors.

In contrast to the Lys751Gln polymorphism, the Asp312Asn polymorphism was not associated with an increased risk of lung cancer among Caucasians. Both Begg’s and Egger’s tests were statistically significant for publication bias in a subgroup analysis of Caucasians. Publication bias may be always a possible limitation of combining data from various sources as in a meta-analysis. The idea of adjusting the results of meta-analyses for publication bias and imputing “fictional” studies into a meta-analysis is controversial at the moment [73]. Although publication bias is always a possible limitation of combining data from various sources as in a meta-analysis, Sutton et al., concluded that publication or related biases did not affect the conclusions in most meta-analyses because missing studies changed the conclusions in less than 10% of meta-analyses [73]. Two meta-analyses have been published in 2004 [66] and 2005 [67], respectively. Both of them are based on the same published data from 6 individual case-control (five Caucasian and one Asian) studies [54–58, 74]. The first meta-analysis showed that individuals with the Asn/Asn genotype were associated with an increased risk of lung cancer among Caucasians (OR = 1.22, 95% CI = 0.99–1.49). The second meta-analysis was somewhat different from the first one, because unadjusted ORs were summarized in the first one. A significantly increased risk of lung cancer associated with the Asn/Asn genotype of the *ERCC2* Asp312Asn polymorphism in the United States was found (OR = 1.43, 95% CI = 1.11–1.83) [67]. The study of Zhou et al., [57], which was based on a large sample size and observed the significant result (OR = 1.5, 95 % CI = 1.1–2.0), made a significant influence on the summary OR of the United States. In this study, a significant 8.26-fold (95% CI = 1.50–45.6) risk of developing lung cancer was observed among Asians. This finding was entirely due to the study of Liang et al. [58]. Although no clear association between *ERCC2* Asp312Asn polymorphism and lung cancer can be found, the Asn allele of the *ERCC2* Asp312Asn polymorphism has been reported to be associated with a higher DNA adduct

level or lower DNA repair efficiency [56]. Therefore, it is plausible that the Asn allele is associated with an increased risk of lung cancer. The Lys751Gln polymorphism has been more studied than the Asp312Asn polymorphism because the frequency of the 751Gln allele is more prevalent than the 312Asn allele. Moreover, the Asp312Asn polymorphism is in linkage disequilibrium with the Lys751Gln polymorphism [54, 55, 58]. As absence of association with lung cancer risk and Asp312Asn polymorphism may be partly due to the low prevalence of the 312Asn allele (low statistical power), the finding on the *ERCC2* Asp312Asn polymorphism should be interpreted with caution before being confirmed in future studies.

In contrast, we found a protective effect of the *XPG* G23A G/G genotype (OR = 0.76, 95% CI = 0.61–0.94) on lung cancer risk. The *XPA* G23A polymorphism itself may alter the transcription and/or translation of the gene. Because this polymorphism is located in the vicinity of the translation initiation codon, it may alter translation efficiency. The nearby proximal nucleotides to the AUG initiation codon are important for the initiation of translation because the 40S ribosomal subunit binds initially at the 5′-end of the mRNA [75]. The consensus sequence around the start codon is GCCRCCAUGG, which is known as the Kozak consensus sequence [76]. The R at position –3 and the G just downstream of the start codon are especially important, and the lack of these bases leads to read-through of the start codon [77]. However, there has been no precise explanation of the mechanism by which the recognition of the start codon is aided by a purine at position –3 [76], which is the core nucleotide of the Kozak consensus. The polymorphism *XPA* G23A is a G/A transversion occurring four nucleotides upstream of the start codon of *XPA* and possibly improving the Kozak sequence [50]. The sequences (CCAGAGAUGG) around the predicted initiator methionine codon of the *XPA* gene agree with the Kozak’s consensus sequence at positions –3 and +4 [78]. Although both the A and polymorphic variant G nucleotides at the –4 position of the *XPA* gene do not correspond to the original consensus Kozak sequence containing the nucleotide C at position –4, it is possible that a nucleotide substitution of A to G at position-4 preceding the AUG codon may affect ribosomal binding and thus alter the efficiency of *XPA* protein synthesis. To investigate whether the transition from G to A changes the translation efficiency, an *in vitro* transcription/translation analysis and a primer extension assay of the initiation complex will be necessary in the future. Furthermore, a functional association between the G23A polymorphism and DRC was reported [51], which showed significantly higher repair efficiency in healthy subjects with at least one G allele. An alternative explanation could be that the protective *XPA* 23G allele is in linkage disequilibrium with an allele from an adjacent gene which is the true susceptibility gene. The *XPA* G23A polymorphism may be a promising SNP for lung cancer. It is thought that cigarette smoking modifies the association between DNA repair polymorphisms, as well as metabolic polymorphisms, and lung cancer risk. Since interactions between the *XPA* G23A polymorphism and smoking have not been fully elucidated, further studies are

needed to better understand the associations between the XPA G23A polymorphism and lung cancer risk.

The Cys/Cys genotype of the *OGG1* Ser326Cys polymorphism was significantly associated with lung cancer risk in all of the studies combined (OR = 1.22, 95% CI = 1.02–1.45) and was marginally associated with lung cancer risk in Asian populations (OR = 1.24, 95% CI = 1.00–1.55,  $P = .052$ ). In the stratified analysis by histological type of lung cancer, a significant association was found for adenocarcinoma. In a narrative review, the Ser326Cys polymorphism has inconsistently been associated with risk of lung cancer [79]. There was an increased risk of lung cancer among subjects with the *OGG1* 326Cys/Cys genotype, which is consistent with experimental evidence that this isoform exhibits decreased the BER activity [80, 81]. The meta-analysis of Hung et al. showed that the summary OR was 1.37 (95% CI = 1.02–1.82) for the Cys/Cys genotype in various ethnic populations combined [82]. The meta-analysis of Li et al. showed that individuals carrying the Cys/Cys genotype did not have significantly increased risk of lung cancer in all populations combined but, in the stratified analysis by ethnicity, a significantly increased risk was found among Asians (OR = 1.18, 95% CI = 1.01–1.38) [83]. Ethnic difference in the association between lung cancer risk and the *OGG1* Ser326Cys polymorphism was suggested. Large studies including different ethnic groups with a careful matching between cases and controls should be considered in future association studies to confirm results from the meta-analyses.

None of the *XRCC1* polymorphisms was associated with an increased risk of lung cancer among both Caucasians and Asians. Our result for the *XRCC1* Arg280His and Arg399Gln polymorphisms replicated the results of the meta-analysis by Hung et al. [82]. Results of previous studies that examined the association between the *XRCC1* polymorphisms and lung cancer risk were inconsistent, possibly owing to the large random error in several small studies. This inconsistency might be due, in part, to differences in the prevalence of smokers. Lunn et al., [84] measured higher levels of aflatoxin B1 adducts in the *XRCC1* Arg399Gln polymorphism and suggested that this might result in a deficient DRC. Two other *XRCC1* polymorphisms, Arg194Trp and Arg280His, have been also determined and the functional effect of these polymorphisms is also unclear, even though some studies have revealed that amino acid changes at the evolutionary conserved regions can alter its function [85]. Although these polymorphisms result in amino acid substitutions, there is no direct evidence on its functional consequences. The *XRCC1* Arg399Gln polymorphism has been associated with risk of breast cancer among African Americans, but not among Caucasians [86, 87], indicating that the *XRCC1* Arg399Gln polymorphism may be linked to another biologically effective mutation. Further investigations of the combined effects of polymorphisms within these DNA repair genes, smoking, and other risk factors may help to clarify the influence of genetic variation in the carcinogenic process.

Several DNA repair pathways are involved in the maintenance of genetic stability. The most versatile and important one is the NER pathway, which detects and removes bulky

DNA adducts, including those induced by cigarette smoking [88]. However, there are several conflicting reports on the association between this polymorphism and lung cancer risk among various populations. Although the reasons for the inconsistencies in the studies are not clear, possible explanations are (1) low frequency of the “at-risk” genotype, which would reduce the statistical power of the studies and (2) small size of the studies. Ethnic differences in the roles of the polymorphism may be caused by gene-gene interactions, different linkages to the polymorphisms determining lung cancer risk, and different lifestyles.

The most important problems facing lung cancer research are identifying “at-risk” individuals and implementing clinical surveillance, prevention practices, and follow-up care. Repair pathways play an important role in lung cancer risk, and genetic variations may contribute to decreased DRC and lung cancer susceptibility. Although the increased/decreased risk associated with individual DNA repair SNPs may be small compared to that conferred by high-penetrance cancer genes, their public health implication may be large because of their high frequency in the general population. It is thus essential that epidemiological investigations of DNA repair polymorphisms are adequately designed. Unfortunately a fairly good number of studies are limited by their sample size and subsequently suffer from too low power to detect effects that may truly exist. Also, given the borderline significance of some associations and multiple comparisons that have been carried out, there is a possibility that one or more findings are false-positives [89]. Large and combined analyses may be preferred to minimize the likelihood of both false-positive and false-negative results. In addition, controls should be chosen in such a way that, if they were cases, they would be included in the case group; when controls are matched to cases, it is essential to account for matching in the analysis. When appropriate, confounding factors should be controlled for, with particular consideration of race and ethnicity. An additional major concern is the grouping of genotypes for calculation of ORs. Without functional data to dictate genotype groupings, it seems prudent to present two ORs per polymorphism (one for heterozygotes versus common-allele homozygotes and one for rare-allele homozygotes versus common-allele homozygotes) so that dominant, codominant, or recessive patterns may be elucidated.

Continued advances in SNP maps and in high-throughput genotyping methods will facilitate the analysis of multiple polymorphisms within genes and the analysis of multiple genes within pathways. The effects of polymorphisms are best represented by their haplotypes. Data from multiple polymorphisms within a gene can be combined to create haplotypes, the set of multiple alleles on a single chromosome. None of the studies reviewed here reported haplotype associations, although several studies analyzed multiple polymorphisms within a gene, sometimes with inconsistent results. The analysis of haplotypes can increase the power to detect disease associations because of higher heterozygosity and tighter linkage disequilibrium with disease-causing mutations. In addition, haplotype analysis offers the advantage of not assuming that any

of the genotyped polymorphisms is functional; rather, it allows for the possibility of an ungenotyped functional variant to be in linkage disequilibrium with the genotyped polymorphisms [90]. An analysis of data from multiple genes within the same DNA-repair pathway (particularly those known to form complexes) can provide more comprehensive insight into the studied associations. Such an analysis may shed light on the complexities of the many pathways involved in DNA repair and lung cancer development, providing hypotheses for future functional studies. Because of concerns over inflated type I error rates in pathway-wide or genome-wide association studies, methods of statistical analysis seeking to obviate this problem are under development [91]. The ability to include haplotype information and data from multiple genes, and to model their interactions, will provide more powerful and more comprehensive assessments of the DNA repair pathways.

This review, which is limited by the bias against publication of null findings, highlights the complexities inherent in epidemiological research and, particularly, in molecular epidemiological research. There is evidence that some polymorphisms in DNA repair genes play a role in carcinogenesis, most notably the *ERCC2* Lys751Gln and *XPA* G23A polymorphisms. The variant allele of each of the three polymorphisms was associated with about a 30% decrease or increase in lung cancer risk. Although the summary risk for developing lung cancer in individuals of each genotype may not be large, lung cancer is such a common malignancy that even a small increase in risk can translate to a large number of excess lung cancer cases. Therefore, polymorphisms, even those not strongly associated with lung cancer, should be considered as potentially important public health issues. In addition, it is important to keep in mind that a susceptibility factor in one population may not be a factor in another. There are differences in the prevalence of DNA repair polymorphisms across populations. In a population where the prevalence of an “at-risk” genotype in a given polymorphism is very low, the “at-risk” allele or “at-risk” genotype may be too infrequent to assess its associated risk. At a population level, the attributable risk must be small simply because it is an infrequent allele. Finally, the major burden of lung cancer in the population probably results from the complex interaction between many genetic and environmental factors over time. Most environmental carcinogens first require metabolic activation by Phase I enzymes to their ultimate forms which then bind to DNA, forming aromatic-DNA adducts that are thought to be an early step in tumorigenesis. On the other hand, these activated forms are detoxified by Phase II enzymes. Thus, genetically determined susceptibility to lung cancer may depend on the metabolic balance among Phase I enzymes, Phase II enzymes, and DNA repair enzymes [92]. Further investigations of the combined effects of polymorphisms between DNA repair genes and drug-metabolizing genes may also help to clarify the influence of genetic variation in the carcinogenic process. Consortia and international collaborative studies, which may be a way to maximize study efficacy and overcome the limitations of individual studies, are needed to help further illuminate

the complex landscape of lung cancer risk and genetic variations.

## Acknowledgment

This study was funded in part by a Grant-in-Aid for Scientific Research (B) (21390190) from the Ministry of Education, Science, Sports and Culture, Japan.

## Conflict of Interests

The authors have declared that no conflict of interests exists.

## References

- [1] P. D. P. Pharoah, A. M. Dunning, B. A. J. Ponder, and D. F. Easton, “Association studies for finding cancer-susceptibility genetic variants,” *Nature Reviews Cancer*, vol. 4, no. 11, pp. 850–860, 2004.
- [2] S. S. Hecht, “Tobacco smoke carcinogens and lung cancer,” *Journal of the National Cancer Institute*, vol. 91, no. 14, pp. 1194–1210, 1999.
- [3] Z. Livneh, “DNA damage control by novel DNA polymerases: translesion replication and mutagenesis,” *Journal of Biological Chemistry*, vol. 276, no. 28, pp. 25639–25642, 2001.
- [4] M. Berwick and P. Vineis, “Markers of DNA repair and susceptibility to cancer in humans: an epidemiologic review,” *Journal of the National Cancer Institute*, vol. 92, no. 11, pp. 874–897, 2000.
- [5] Q. Wei, L. Cheng, C. I. Amos et al., “Repair of tobacco carcinogen-induced DNA adducts and lung cancer risk: a molecular epidemiologic study,” *Journal of the National Cancer Institute*, vol. 92, no. 21, pp. 1764–1772, 2000.
- [6] Q. Wei, L. Cheng, W. K. Hong, and M. R. Spitz, “Reduced DNA repair capacity in lung cancer patients,” *Cancer Research*, vol. 56, no. 18, pp. 4103–4107, 1996.
- [7] N. Rajae-Behbahani, P. Schmezer, A. Risch et al., “Altered DNA repair capacity and bleomycin sensitivity as risk markers for non-small cell lung cancer,” *International Journal of Cancer*, vol. 95, no. 2, pp. 86–91, 2001.
- [8] A. E. Tomkinson and Z. B. Mackey, “Structure and function of mammalian DNA ligases,” *Mutation Research*, vol. 407, no. 1, pp. 1–9, 1998.
- [9] P. C. Hanawalt, “Subpathways of nucleotide excision repair and their regulation,” *Oncogene*, vol. 21, no. 58, pp. 8949–8956, 2002.
- [10] D. Bootsma, K. H. Kraemer, J. E. Cleaver, and J. H. Hoeijmakers, “Nucleotide excision repair syndromes: xeroderma pigmentosum, Cockayne syndrome, and trichothiodystrophy,” in *The Genetic Basis of Human Cancer*, B. Vogelstein and K. W. Kinzler, Eds., pp. 245–274, McGraw-Hill, New York, NY, USA, 1998.
- [11] R. DerSimonian and N. Laird, “Meta-analysis in clinical trials,” *Controlled Clinical Trials*, vol. 7, no. 3, pp. 177–188, 1986.
- [12] W. Cochran, “The combination of estimates from different experiments,” *Biometrics*, vol. 10, pp. 101–129, 1954.
- [13] A. Whitehead and J. Whitehead, “A general parametric approach to the meta-analysis of randomized clinical trials,” *Statistics in Medicine*, vol. 10, no. 11, pp. 1665–1677, 1991.
- [14] C. B. Begg and M. Mazumdar, “Operating characteristics of a rank correlation test for publication bias,” *Biometrics*, vol. 50, no. 4, pp. 1088–1101, 1994.

- [15] M. Egger, G. Davey Smith, M. Schneider, and C. Minder, "Bias in meta-analysis detected by a simple, graphical test," *British Medical Journal*, vol. 315, no. 7109, pp. 629–634, 1997.
- [16] H. Sugimura, T. Kohno, K. Wakai et al., "hOGG1 Ser326Cys polymorphism and lung cancer susceptibility," *Cancer Epidemiology, Biomarkers and Prevention*, vol. 8, no. 8, pp. 669–674, 1999.
- [17] H. Wikman, A. Risch, F. Klimek et al., "hOGG1 polymorphism and loss of heterozygosity (LOH): significance for lung cancer susceptibility in a caucasian population," *International Journal of Cancer*, vol. 88, no. 6, pp. 932–937, 2000.
- [18] H. Ito, N. Hamajima, T. Takezaki et al., "A limited association of OGG1 Ser326Cys polymorphism for adenocarcinoma of the lung," *Journal of Epidemiology*, vol. 12, no. 3, pp. 258–265, 2002.
- [19] N. Sunaga, T. Kohno, N. Yanagitani et al., "Contribution of the NQO1 and GSTT1 polymorphisms to lung adenocarcinoma susceptibility," *Cancer Epidemiology, Biomarkers and Prevention*, vol. 11, no. 8, pp. 730–738, 2002.
- [20] L. Le Marchand, T. Donlon, A. Lum-Jones, A. Seifried, and L. R. Wilkens, "Association of the hOGG1 Ser326Cys polymorphism with lung cancer risk," *Cancer Epidemiology, Biomarkers and Prevention*, vol. 11, no. 4, pp. 409–412, 2002.
- [21] Q. Lan, J. L. Mumford, M. Shen et al., "Oxidative damage-related genes AKR1C3 and OGG1 modulate risks for lung cancer due to exposure to PAH-rich coal combustion emissions," *Carcinogenesis*, vol. 25, no. 11, pp. 2177–2181, 2004.
- [22] J. Park, L. Chen, M. S. Tockman, A. Elahi, and P. Lazarus, "The human 8-oxoguanine DNA N-glycosylase 1 (hOGG1) DNA repair enzyme and its association with lung cancer risk," *Pharmacogenetics*, vol. 14, no. 2, pp. 103–109, 2004.
- [23] U. Vogel, B. A. Nexø, H. Wallin, K. Overvad, A. Tjønneland, and O. Raaschou-Nielsen, "No association between base excision repair gene polymorphisms and risk of lung cancer," *Biochemical Genetics*, vol. 42, no. 11–12, pp. 453–460, 2004.
- [24] G. Liang, Y. Pu, and L. Yin, "Rapid detection of single nucleotide polymorphisms related with lung cancer susceptibility of Chinese population," *Cancer Letters*, vol. 223, no. 2, pp. 265–274, 2005.
- [25] R. J. Hung, P. Brennan, F. Canzian et al., "Large-scale investigation of base excision repair genetic polymorphisms and lung cancer risk in a multicenter study," *Journal of the National Cancer Institute*, vol. 97, no. 8, pp. 567–576, 2005.
- [26] S. Zienoldiny, D. Campa, H. Lind et al., "Polymorphisms of DNA repair genes and risk of non-small cell lung cancer," *Carcinogenesis*, vol. 27, no. 3, pp. 560–567, 2006.
- [27] G. Matullo, A. M. Dunning, S. Guarrera et al., "DNA repair polymorphisms and cancer risk in non-smokers in a cohort study," *Carcinogenesis*, vol. 27, no. 5, pp. 997–1007, 2006.
- [28] T. Kohno, H. Kunitoh, K. Toyama et al., "Association of the OGG1-Ser326Cys polymorphism with lung adenocarcinoma risk," *Cancer Science*, vol. 97, no. 8, pp. 724–728, 2006.
- [29] M. Sørensen, O. Raaschou-Nielsen, R. D. Hansen, A. Tjønneland, K. Overvad, and U. Vogel, "Interactions between the OGG1 Ser326Cys polymorphism and intake of fruit and vegetables in relation to lung cancer," *Free Radical Research*, vol. 40, no. 8, pp. 885–891, 2006.
- [30] K. De Ruyck, M. Szaumkessel, I. De Rudder et al., "Polymorphisms in base-excision repair and nucleotide-excision repair genes in relation to lung cancer risk," *Mutation Research*, vol. 631, no. 2, pp. 101–110, 2007.
- [31] B. Karahalil, E. Emerce, B. Koçer, S. Han, N. Alkiş, and A. E. Karakaya, "The association of OGG1 Ser326Cys polymorphism and urinary 8-OHdG levels with lung cancer susceptibility: a hospital-based case-control study in Turkey," *Arhiv za Higijenu Rada i Toksikologiju*, vol. 59, no. 4, pp. 241–250, 2008.
- [32] A. Miyaishi, K. Osawa, Y. Osawa et al., "MUTYH Gln324His gene polymorphism and genetic susceptibility for lung cancer in a Japanese population," *Journal of Experimental and Clinical Cancer Research*, vol. 28, no. 1, article 10, 2009.
- [33] J. S. Chang, M. R. Wrensch, H. M. Hansen et al., "Base excision repair genes and risk of lung cancer among San Francisco Bay Area Latinos and African-Americans," *Carcinogenesis*, vol. 30, no. 1, pp. 78–87, 2009.
- [34] D. Ratnasinghe, S.-X. Yao, J. A. Tangrea et al., "Polymorphisms of the DNA repair gene XRCC1 and lung cancer risk," *Cancer Epidemiology, Biomarkers and Prevention*, vol. 10, no. 2, pp. 119–123, 2001.
- [35] G. L. David-Beabes and S. J. London, "Genetic polymorphism of XRCC1 and lung cancer risk among African-Americans and Caucasians," *Lung Cancer*, vol. 34, no. 3, pp. 333–339, 2001.
- [36] K. K. Divine, F. D. Gilliland, R. E. Crowell et al., "The XRCC1 399 glutamine allele is a risk factor for adenocarcinoma of the lung," *Mutation Research*, vol. 461, no. 4, pp. 273–278, 2001.
- [37] S. Chen, D. Tang, K. Xue et al., "DNA repair gene XRCC1 and XPD polymorphisms and risk of lung cancer in a Chinese population," *Carcinogenesis*, vol. 23, no. 8, pp. 1321–1325, 2002.
- [38] J. Y. Park, S. Y. Lee, H.-S. Jeon et al., "Polymorphism of the DNA repair gene XRCC1 and risk of primary lung cancer," *Cancer Epidemiology, Biomarkers and Prevention*, vol. 11, no. 1, pp. 23–27, 2002.
- [39] R. R. Misra, D. Ratnasinghe, J. A. Tangrea et al., "Polymorphisms in the DNA repair genes XPD, XRCC1, XRCC3, and APE1/ref-1, and the risk of lung cancer among male smokers in Finland," *Cancer Letters*, vol. 191, no. 2, pp. 171–178, 2003.
- [40] W. Zhou, G. Liu, D. P. Miller et al., "Polymorphisms in the DNA repair genes XRCC1 and ERCC2, smoking, and lung cancer risk," *Cancer Epidemiology, Biomarkers and Prevention*, vol. 12, no. 4, pp. 359–365, 2003.
- [41] H. Ito, K. Matsuo, N. Hamajima et al., "Gene-environment interactions between the smoking habit and polymorphisms in the DNA repair genes, APE1 Asp148Glu and XRCC1 Arg399Gln, in Japanese lung cancer risk," *Carcinogenesis*, vol. 25, no. 8, pp. 1395–1401, 2004.
- [42] O. Popanda, T. Schattenberg, C. T. Phong et al., "Specific combinations of DNA repair gene variants and increased risk for non-small cell lung cancer," *Carcinogenesis*, vol. 25, no. 12, pp. 2433–2441, 2004.
- [43] C. Harms, S. A. Salama, C. H. Sierra-Torres, N. Cajas-Salazar, and W. W. Au, "Polymorphisms in DNA repair genes, chromosome aberrations, and lung cancer," *Environmental and Molecular Mutagenesis*, vol. 44, no. 1, pp. 74–82, 2004.
- [44] X. Zhang, X. Miao, G. Liang et al., "Polymorphisms in DNA base excision repair genes ADPRT and XRCC1 and risk of lung cancer," *Cancer Research*, vol. 65, no. 3, pp. 722–726, 2005.
- [45] J. Schneider, V. Classen, U. Bernges, and M. Philipp, "XRCC1 polymorphism and lung cancer risk in relation to tobacco smoking," *International Journal of Molecular Medicine*, vol. 16, no. 4, pp. 709–716, 2005.
- [46] M. Shen, S. I. Berndt, N. Rothman et al., "Polymorphisms in the DNA base excision repair genes APEX1 and XRCC1 and lung cancer risk in Xuan Wei, China," *Anticancer Research*, vol. 25, no. 1B, pp. 537–542, 2005.
- [47] J. Yin, U. Vogel, Y. Ma, R. Qi, Z. Sun, and H. Wang, "The DNA repair gene XRCC1 and genetic susceptibility of lung cancer in

- a northeastern Chinese population," *Lung Cancer*, vol. 56, no. 2, pp. 153–160, 2007.
- [48] M. F. López-Cima, P. González-Arriaga, L. García-Castro et al., "Polymorphisms in XPC, XPD, XRCC1, and XRCC3 DNA repair genes and lung cancer risk in a population of Northern Spain," *BMC Cancer*, vol. 7, article 162, 2007.
- [49] S. S. Pachouri, R. C. Sobti, P. Kaur, and J. Singh, "Contrasting impact of DNA repair gene XRCC1 polymorphisms Arg399Gln and Arg194Trp on the risk of lung cancer in North-Indian population," *DNA and Cell Biology*, vol. 26, no. 3, pp. 186–191, 2007.
- [50] J. Y. Park, S. H. Park, J. E. Choi et al., "Polymorphisms of the DNA repair gene xeroderma pigmentosum group A and risk of primary lung cancer," *Cancer Epidemiology, Biomarkers and Prevention*, vol. 11, no. 10, part 1, pp. 993–997, 2002.
- [51] X. Wu, H. Zhao, Q. Wei et al., "XPA polymorphism associated with reduced lung cancer risk and a modulating effect on nucleotide excision repair capacity," *Carcinogenesis*, vol. 24, no. 3, pp. 505–509, 2003.
- [52] U. Vogel, K. Overvad, H. Wallin, A. Tjønneland, B. A. Nexø, and O. Raaschou-Nielsen, "Combinations of polymorphisms in XPD, XPC and XPA in relation to risk of lung cancer," *Cancer Letters*, vol. 222, no. 1, pp. 67–74, 2005.
- [53] C. Kiyohara and K. Yoshimasu, "Genetic polymorphisms in the nucleotide excision repair pathway and lung cancer risk: a meta-analysis," *International Journal of Medical Sciences*, vol. 4, no. 2, pp. 59–71, 2007.
- [54] D. Butkiewicz, M. Rusin, L. Enewold, P. G. Shields, M. Chorazy, and C. C. Harris, "Genetic polymorphisms in DNA repair genes and risk of lung cancer," *Carcinogenesis*, vol. 22, no. 4, pp. 593–597, 2001.
- [55] M. R. Spitz, X. Wu, Y. Wang et al., "Modulation of nucleotide excision repair capacity by XPD polymorphisms in lung cancer patients," *Cancer Research*, vol. 61, no. 4, pp. 1354–1357, 2001.
- [56] S.-M. Hou, S. Fält, S. Angelini et al., "The XPD variant alleles are associated with increased aromatic DNA adduct level and lung cancer risk," *Carcinogenesis*, vol. 23, no. 4, pp. 599–603, 2002.
- [57] W. Zhou, G. Liu, D. P. Miller et al., "Gene-environment interaction for the ERCC2 polymorphisms and cumulative cigarette smoking exposure in lung cancer," *Cancer Research*, vol. 62, no. 5, pp. 1377–1381, 2002.
- [58] G. Liang, D. Xing, X. Miao et al., "Sequence variations in the DNA repair gene XPD and risk of lung cancer in a Chinese population," *International Journal of Cancer*, vol. 105, no. 5, pp. 669–673, 2003.
- [59] U. Vogel, I. Laros, N. R. Jacobsen et al., "Two regions in chromosome 19q13.2-3 are associated with risk of lung cancer," *Mutation Research*, vol. 546, no. 1-2, pp. 65–74, 2004.
- [60] M. Shen, S. I. Berndt, N. Rothman et al., "Polymorphisms in the DNA nucleotide excision repair genes and lung cancer risk in Xuan Wei, China," *International Journal of Cancer*, vol. 116, no. 5, pp. 768–773, 2005.
- [61] Z. Hu, L. Xu, M. Shao et al., "Polymorphisms in the two helicases ERCC2/XPD and ERCC3/XPB of the transcription factor IIH complex and risk of lung cancer: a case-control analysis in a Chinese population," *Cancer Epidemiology, Biomarkers and Prevention*, vol. 15, no. 7, pp. 1336–1340, 2006.
- [62] J. S. Chang, M. R. Wrensch, H. M. Hansen et al., "Nucleotide excision repair genes and risk of lung cancer among San Francisco Bay Area Latinos and African Americans," *International Journal of Cancer*, vol. 123, no. 9, pp. 2095–2104, 2008.
- [63] Z. Yin, M. Su, X. Li et al., "ERCC2, ERCC1 polymorphisms and haplotypes, cooking oil fume and lung adenocarcinoma risk in Chinese non-smoking females," *Journal of Experimental and Clinical Cancer Research*, vol. 28, no. 1, article 153, 2009.
- [64] G. L. David-Beabes, R. M. Lunn, and S. J. London, "No association between the XPD (Lys751Gln) polymorphism or the XRCC3 (Thr241Met) polymorphism and lung cancer risk," *Cancer Epidemiology, Biomarkers and Prevention*, vol. 10, no. 8, pp. 911–912, 2001.
- [65] J. Y. Park, S. Y. Lee, H.-S. Jeon et al., "Lys751Gln polymorphism in the DNA repair gene XPD and risk of primary lung cancer," *Lung Cancer*, vol. 36, no. 1, pp. 15–16, 2002.
- [66] Z. Hu, Q. Wei, X. Wang, and H. Shen, "DNA repair gene XPD polymorphism and lung cancer risk: a meta-analysis," *Lung Cancer*, vol. 46, no. 1, pp. 1–10, 2004.
- [67] S. Benhamou and A. Sarasin, "ERCC2/XPD gene polymorphisms and lung cancer: a HuGE review," *American Journal of Epidemiology*, vol. 161, no. 1, pp. 1–14, 2005.
- [68] G. Matullo, M. Peluso, S. Polidoro et al., "Combination of DNA repair gene single nucleotide polymorphisms and increased levels of DNA adducts in a population-based study," *Cancer Epidemiology, Biomarkers and Prevention*, vol. 12, no. 7, pp. 674–677, 2003.
- [69] D. Palli, A. Russo, G. Masala et al., "DNA adduct levels and DNA repair polymorphisms in traffic-exposed workers and a general population sample," *International Journal of Cancer*, vol. 94, no. 1, pp. 121–127, 2001.
- [70] E. J. Duell, J. K. Wiencke, T.-J. Cheng et al., "Polymorphisms in the DNA repair genes XRCC1 and ERCC2 and biomarkers of DNA damage in human blood mononuclear cells," *Carcinogenesis*, vol. 21, no. 5, pp. 965–971, 2000.
- [71] S. G. Thompson, "Why sources of heterogeneity in meta-analysis should be investigated," *British Medical Journal*, vol. 309, no. 6965, pp. 1351–1355, 1994.
- [72] S. C. Faddy, "Significant statistical heterogeneity in a meta-analysis of the usefulness of acetylcysteine for prevention of contrast nephropathy," *American Journal of Cardiology*, vol. 94, no. 3, p. 414, 2004.
- [73] A. J. Sutton, S. J. Duval, R. L. Tweedie, K. R. Abrams, and D. R. Jones, "Empirical assessment of effect of publication bias on meta-analyses," *British Medical Journal*, vol. 320, no. 7249, pp. 1574–1577, 2000.
- [74] R. R. Misra, D. Ratnasinghe, J. A. Tangrea et al., "Polymorphisms in the DNA repair genes XPD, XRCC1, XRCC3, and APE/ref-1, and the risk of lung cancer among male smokers in Finland," *Cancer Letters*, vol. 191, no. 2, pp. 171–178, 2003.
- [75] M. Kozak, "Role of ATP in binding and migration of 40S ribosomal subunits," *Cell*, vol. 22, no. 2, part 2, pp. 459–467, 1980.
- [76] M. Kozak, "Initiation of translation in prokaryotes and eukaryotes," *Gene*, vol. 234, no. 2, pp. 187–208, 1999.
- [77] M. Kozak, "Adherence to the first-AUG rule when a second AUG codon follows closely upon the first," *Proceedings of the National Academy of Sciences of the United States of America*, vol. 92, no. 15, p. 7134, 1995.
- [78] K. Tanaka, N. Miura, I. Satokata et al., "Analysis of a human DNA excision repair gene involved in group A xeroderma pigmentosum and containing a zinc-finger domain," *Nature*, vol. 348, no. 6296, pp. 73–76, 1990.
- [79] J. M. Weiss, E. L. Goode, W. C. Ladiges, and C. M. Ulrich, "Polymorphic variation in hOGG1 and risk of cancer: a review of the functional and epidemiologic literature," *Molecular Carcinogenesis*, vol. 42, no. 3, pp. 127–141, 2005.

- [80] T. Kohno, K. Shinmura, M. Tosaka et al., "Genetic polymorphisms and alternative splicing of the hOGG1 gene, that is involved in the repair of 8-hydroxyguanine in damaged DNA," *Oncogene*, vol. 16, no. 25, pp. 3219–3225, 1998.
- [81] A. Dhénaut, S. Boiteux, and J. P. Radicella, "Characterization of the hOGG1 promoter and its expression during the cell cycle," *Mutation Research*, vol. 461, no. 2, pp. 109–118, 2000.
- [82] R. J. Hung, J. Hall, P. Brennan, and P. Boffetta, "Genetic polymorphisms in the base excision repair pathway and cancer risk: a HuGE review," *American Journal of Epidemiology*, vol. 162, no. 10, pp. 925–942, 2005.
- [83] H. Li, X. Hao, W. Zhang, Q. Wei, and K. Chen, "The hOGG1 Ser326Cys polymorphism and lung cancer risk: a meta-analysis," *Cancer Epidemiology, Biomarkers and Prevention*, vol. 17, no. 7, pp. 1739–1745, 2008.
- [84] R. M. Lunn, R. G. Langlois, L. L. Hsieh, C. L. Thompson, and D. A. Bell, "XRCC1 polymorphisms: effects on aflatoxin B1-DNA adducts and glycophorin A variant frequency," *Cancer Research*, vol. 59, no. 11, pp. 2557–2561, 1999.
- [85] S. Savas, D. Y. Kim, M. F. Ahmad, M. Shariff, and H. Ozelik, "Identifying functional genetic variants in DNA repair pathway using protein conservation analysis," *Cancer Epidemiology, Biomarkers and Prevention*, vol. 13, no. 5, pp. 801–807, 2004.
- [86] E. J. Duell, R. C. Millikan, G. S. Pittman et al., "Polymorphisms in the DNA repair gene XRCC1 and breast cancer," *Cancer Epidemiology, Biomarkers and Prevention*, vol. 10, no. 3, pp. 217–222, 2001.
- [87] B. A. Nexø, U. Vogel, A. Olsen et al., "A specific haplotype of single nucleotide polymorphisms on chromosome 19q13.2-3 encompassing the gene RAI is indicative of post-menopausal breast cancer before age 55," *Carcinogenesis*, vol. 24, no. 5, pp. 899–904, 2003.
- [88] A. Sarasin, "An overview of the mechanisms of mutagenesis and carcinogenesis," *Mutation Research*, vol. 544, no. 2-3, pp. 99–106, 2003.
- [89] S. Wacholder, S. Chanock, M. Garcia-Closas, L. El Ghormli, and N. Rothman, "Assessing the probability that a positive report is false: an approach for molecular epidemiology studies," *Journal of the National Cancer Institute*, vol. 96, no. 6, pp. 434–442, 2004.
- [90] M. Khoury, T. H. Beaty, and B. H. Cohen, *Fundamentals of Genetic Epidemiology*, Monographs in Epidemiology and Biostatistics, Oxford University Press, New York, NY, USA, 1993.
- [91] J. Hoh, A. Wille, and J. Ott, "Trimming, weighting, and grouping SNPs in human case-control association studies," *Genome Research*, vol. 11, no. 12, pp. 2115–2119, 2001.
- [92] C. Kiyohara, A. Otsu, T. Shirakawa, S. Fukuda, and J. M. Hopkin, "Genetic polymorphisms and lung cancer susceptibility: a review," *Lung Cancer*, vol. 37, no. 3, pp. 241–256, 2002.

## Review Article

# Molecular Mechanisms of the Whole DNA Repair System: A Comparison of Bacterial and Eukaryotic Systems

Rihito Morita,<sup>1</sup> Shuhei Nakane,<sup>1</sup> Atsuhiko Shimada,<sup>1</sup> Masao Inoue,<sup>1</sup> Hitoshi Iino,<sup>1,2</sup>  
Taisuke Wakamatsu,<sup>3</sup> Kenji Fukui,<sup>2</sup> Noriko Nakagawa,<sup>1,2</sup> Ryoji Masui,<sup>1,2</sup>  
and Seiki Kuramitsu<sup>1,2,3</sup>

<sup>1</sup> Department of Biological Sciences, Graduate School of Science, Osaka University, 1-1 Machikaneyama-cho, Toyonaka, Osaka 560-0043, Japan

<sup>2</sup> RIKEN SPring-8 Center, Harima Institute, 1-1-1 Kouto, Sayo-cho, Sayo-gun, Hyogo 679-5148, Japan

<sup>3</sup> Graduate School of Frontier Biosciences, Osaka University, 1-3 Yamadaoka, Suita, Osaka 565-0871, Japan

Correspondence should be addressed to Seiki Kuramitsu, kuramitsu@bio.sci.osaka-u.ac.jp

Received 15 June 2010; Accepted 27 July 2010

Academic Editor: Shigenori Iwai

Copyright © 2010 Rihito Morita et al. This is an open access article distributed under the Creative Commons Attribution License, which permits unrestricted use, distribution, and reproduction in any medium, provided the original work is properly cited.

DNA is subjected to many endogenous and exogenous damages. All organisms have developed a complex network of DNA repair mechanisms. A variety of different DNA repair pathways have been reported: direct reversal, base excision repair, nucleotide excision repair, mismatch repair, and recombination repair pathways. Recent studies of the fundamental mechanisms for DNA repair processes have revealed a complexity beyond that initially expected, with inter- and intrapathway complementation as well as functional interactions between proteins involved in repair pathways. In this paper we give a broad overview of the whole DNA repair system and focus on the molecular basis of the repair machineries, particularly in *Thermus thermophilus* HB8.

## 1. Introduction

It is essential for all living organisms to warrant accurate functioning and propagation of their genetic information. However, the genome is constantly exposed to various environmental and endogenous agents, which produce a large variety of DNA lesions (Figure 1) [1, 2]. Environmental damage can be induced by several chemical reactive species and physical agents. Endogenous damages occur spontaneously and continuously even under normal physiologic conditions through intrinsic instability of chemical bonds in DNA structure. The biological consequences of these damages usually depend on the chemical nature of the lesion. Most of these lesions affect the fidelity of DNA replication, which leads to mutations. Some of human genetic diseases are associated to defects in DNA repair (Table 1).

To cope with these DNA damages, all organisms have developed a complex network of DNA repair mechanisms [1, 3]. A variety of different DNA repair pathways have been reported: direct reversal, base excision repair, nucleotide

excision repair, mismatch repair, and recombination repair pathways. Most of these pathways require functional interactions between multiple proteins. Furthermore, recent studies have revealed inter- and intra-pathway complementation.

Although there are a number of model organisms representing different kingdoms, such as *Escherichia coli*, *Saccharomyces cerevisiae*, *Arabidopsis thaliana*, and *Mus musculus* (Table 1), we selected the bacterial species *Thermus thermophilus* HB8 for use in our studies of basic and essential biological processes. *T. thermophilus* is a Gram-negative eubacterium that can grow at temperatures over 75°C [4]. *T. thermophilus* HB8 was chosen for several reasons: (i) it has a smaller genome size than other model organisms; (ii) proteins from *T. thermophilus* HB8 are very stable suitable for *in vitro* analyses of molecular function; and (iii) the crystallization efficiency of the proteins is higher than for those of other organisms [5]. Moreover, since each biological system in *T. thermophilus* is only constituted of fundamentally necessary enzymes, *in vitro* reconstitution of a particular system should be easier and more understandable.

Our group has constructed overexpression plasmids for most *T. thermophilus* HB8 ORFs [6], and those plasmids are available from The DNA Bank, RIKEN Bioresource Center (Tsukuba, Japan) ([http://www.brc.riken.jp/lab/dna/en/thermus\\_en.html](http://www.brc.riken.jp/lab/dna/en/thermus_en.html)). Approximately 80% of the ORFs have been completely cloned into the overexpression vectors pET-11a, pET-11b, pET-3a, and/or pET-HisTEV. Furthermore, plasmids for gene disruption are also available from the Structural-Biological Whole Cell Project (<http://www.thermus.org/>). Protein purification profiles and gene disruption methods can be downloaded from the RIKEN Bioresource Center. Therefore, it is a relatively simple matter to initiate an analysis of proteins of interest in this species.

*T. thermophilus* HB8 has all of the fundamental enzymes known to be essential for DNA repair, and most of these show homology to human enzymes. Biological and structural analyses of DNA repair in *T. thermophilus* will therefore provide a better understanding of DNA repair pathways in general. Moreover, these analyses are aided by the high efficiency of protein crystallization and stability of purified proteins in this species. In this paper we give a broad overview of the whole DNA repair system and focus on the molecular basis of the repair machineries, especially in *T. thermophilus* HB8.

## 2. Direct Reversal of DNA Damage

UV-induced pyrimidine dimers and alkylation adducts can be directly repaired by DNA photolyases and alkyl transferases, respectively. These repair systems are not followed by incision or resynthesis of DNA.

**2.1. Photolyases.** UV-induced pyrimidine dimers, such as cyclobutane pyrimidine dimers (CPDs) and (6-4) photoproducts, disturb DNA replication and transcription. Some species make use of DNA photolyases to repair these lesions (Figure 2(a)). The FADH<sup>-</sup> in the photolyase donates an electron to the CPD, which induces the breakage of the cyclobutane bond [7].

CPD photolyases repair UV-induced CPDs utilizing photon energy from blue or near-UV light [8]. To absorb light, CPD photolyases have two different chromophoric cofactors. One of these, FAD, acts as the photochemical reaction center in the repair process. An electron is transferred from an exogenous photoreductor to FAD, which is changed to the fully reduced, active form FADH<sup>-</sup> [9]. Although only this chromophore is necessary for the reaction, photolyases have a second chromophore as an auxiliary antenna to harvest light energy, which is transferred to the reaction center. The identity of the second chromophore differs among species. To date, reduced folate (5,10-methenyl-tetrahydrofolate, MTHF), 8-hydroxy-5-deazaflavin (8-HDF), FMN, and riboflavin have been identified as secondary chromophores.

A CPD photolyase (ORF ID, TTB102) of *T. thermophilus* (ttPhr) was identified as the first thermostable photolyase in 1997 [10]. The crystal structures of photolyases from *E.*

*coli* and *Aspergillus nidulans* were reported in 1995 and 1997, respectively [11, 12]. Those of ttPhr and the complex it forms with thymine, a part of its substrate, were reported in 2001 [13]. NMR analysis showed that the CPD is flipped out from the double-stranded DNA (dsDNA) into a cavity in ttPhr [14]. Likewise, the thymine dimer interacts with the active site in the crystal structure of *A. nidulans* photolyase complexed with substrate dsDNA [15]. NMR analysis also showed the distance between FAD and CPD, which is important for understanding the CPD repair reaction by ttPhr [16]. In 2005, an overexpression analysis using *E. coli* identified the second chromophore of ttPhr as FMN [17]. Photolyases usually have a specific binding site for cofactors, but the second chromophore, FMN, of ttPhr shows promiscuous binding with riboflavin or 8-HDF [18].

Placental mammals lack photoreactivation activity, but they do have nucleotide excision repair (NER) systems for repairing CPDs [21]. NER has two sub-pathways: global genomic repair (GGR) and transcription-coupled repair (TCR) [3]. These sub-pathways are versatile repair systems and are highly conserved across species. Thus, the absence of photoreactivation activity would not have a significant effect on DNA repair efficiency in placental mammals. The mechanisms of NER are detailed in the later section. It should be noted that mammals, birds, and plants have photolyase-like proteins, the so-called cryptochromes, which have no ability to repair damaged DNA but function as blue-light photoreceptors [22].

**2.2. Reversal of O<sup>6</sup>-Alkylguanine-DNA.** O<sup>6</sup>-alkylguanine is one of the most harmful alkylation adducts and can induce mutation and apoptosis [23–25]. Almost all species possess mechanisms to repair this adduct (Figures 2(b) and 2(c)). O<sup>6</sup>-alkylguanine-DNA alkyltransferase (AGT) accepts an alkyl group on a cysteine residue at its active site (PC<sub>HR</sub>) in a stoichiometric fashion, and this alkylated AGT is inactive (Figure 2(b)) [26–28]. AGT acts as a monomer and transfers the alkyl group from DNA without a cofactor [29–31]. The structure of human AGT, MGMT, indicates that a helix-turn-helix motif mediates binding to the minor groove of DNA and that O<sup>6</sup>-methylguanine (O<sup>6</sup>-meG) is flipped out from the base stack into this active site [32, 33]. Tyrosine and arginine residues in the active site of the enzyme mediate nucleotide flipping.

The cysteine residue in the active site (PC<sub>HR</sub>) of AGT is necessary for the methyltransferase activity. Some AGT-like proteins lack cysteine residues in their active sites (PX<sub>HR</sub>) [34–40]. Alkyltransferase-like (ATL) proteins are a type of AGT homologue and are present in all three domains of life. ATL proteins from *E. coli*, *Schizosaccharomyces pombe*, and *T. thermophilus* can bind to DNA and show preferential binding to O<sup>6</sup>-meG-containing DNA, but they are unable to transfer a methyl group from the modified DNA [37–39]. This binding activity inhibits AGT activity in a competitive manner [38]. *E. coli* has three AGT homologues, AGT, Ada, and the ATL protein, but *S. pombe* and *T. thermophilus* have only the ATL protein. Therefore, *S. pombe* or *T. thermophilus* are particularly suitable for studies of ATL proteins.

TABLE 1: Distribution of DNA repair genes. \*<sup>1</sup>Related human diseases are listed by referencing the following databases: KEGG disease (<http://www.genome.jp/kegg/disease/>), GeneCards (<http://www.genecards.org/>), and Online Mendelian Inheritance in Man (<http://www.ncbi.nlm.nih.gov/omim>). \*<sup>2</sup>Descriptions in the parentheses indicate the subunit organizations of holoenzymes.

Repair pathways	Molecular functions	<i>T. thermophilus</i>	<i>E. coli</i>	<i>S. cerevisiae</i>	<i>A. thaliana</i>	<i>M. musculus</i>	<i>H. sapiens</i>	Related disease* <sup>1</sup>
<i>Direct reversal</i>								
<i>Photoreactivation</i>								
Alkyltransfer	Alkyltransfer or recognition alkyltransfer	Phr (TTHB102) ATL (TTHA1564)	PhrA Ada, AGT, ATL AlkB	PHR1 MGTI	PhrB	MGMT ALKBH1	MGMT ALKBH2, ALKBH3	
<i>Base excision repair</i>								
Base excision	Remove ring-saturated or fragmented pyrimidines remove 3-meA, ethenoA, hypoxanthine Remove U	EndoIII (TTHA0112) AlkA (TTHA0329) UDGA (TTHA0718) UDGB (TTHA1149)	Nth (EndoIII) AlkA, TagA Ung	Ntg1p, Ntg2p Mag1p Ung1p	AT1G05900 AT3G12040 (MAG) AT3G18630 uracil DNA glycosylase family protein	Nthl1 Mpg Ung	NTHL1 MPG, (MAG, AAG) Ung	Hyper IgM syndromes, autosomal recessive type
	Remove U, hydroxymethyl U Remove U or T opposite G at CpG sequences Remove U, T, or ethenoC opposite G Remove 8-oxoG opposite C Remove A opposite 8-oxoG Remove thymine glycol Remove oxidative products of C, U Not known	MutM (TTHA1806) MutY (TTHA1898)	Fpg (MutM) MutY Nei (EndoVIII)	Ogg1p	OGG1 AT4G12740 (MYH-related)	Ogg1 MUTYH Neil1	OGG1 MUTYH NEIL1 NEIL2 NEIL3	Lung cancer

TABLE 1: Continued.

Repair pathways	Molecular functions	<i>T. thermophilus</i>	<i>E. coli</i>	<i>S. cerevisiae</i>	<i>A. thaliana</i>	<i>M. musculus</i>	<i>H. sapiens</i>	Related disease*1
Alternative strand incision	Incision 3' of hypoxanthine and uracil	EndoV (TTHA1347)	Nfi (EndoV)		EndoV	EndoV	EndoV	
AP site processing and resynthesis	AP endonuclease	EndoIV (Nfo) (TTHA0834)	Nfo (EndoIV)	Apn1p				
	AP endonuclease		XthA (ExoIII)	Apn2p (Eyh1)	ARP	Apex1	APEX1 (APE1, APEX, HAP1, REF1), APEX2	
	AP endonuclease				AT4G36050	Apex2		
	AP endonuclease	PolX (TTHA1150)				Polβ	Polβ	
	DNA polymerase, 5' flap endonuclease	PolI (TTHA1054)	PolI					
	replication and BER in mitochondrial DNA			Mip1p			Poly	
	NAD-dependent DNA ligase	LigA (TTHA1097)	LigA					
	ATP-dependent DNA ligase				AT1G66730 (ATP-dependent)	Lig3 (ATP-dependent)	LIG3 (ATP-dependent)	
	accessory factor for LIG3 and BER				AT1G80420 (putative XRCC1)	Xrcc1	XRCCI	
	poly (ADP-ribose) polymerase				PARP2	Parp1	PARP1 (ADPRT)	
	ADPRT-like enzyme				APP (Arabidopsis poly(ADP-ribose) polymerase)	Parp2	PARP2 (ADPRTL2)	
<i>Nucleotide excision repair</i>								
DNA binding	Bind damaged DNA in complex with UvrB	UvrA (TTHA1440)	UvrA					

TABLE 1: Continued.

Repair pathways	Molecular functions	<i>T. thermophilus</i>	<i>E. coli</i>	<i>S. cerevisiae</i>	<i>A. thaliana</i>	<i>M. musculus</i>	<i>H. sapiens</i>	Related disease*1
	Catalyze unwinding in preincision complex	UvrB (TTHA1892)	UvrB					
	Bind disordered DNA as complex			RAD4	RAD4	Xpc	XPC	Xeroderma pigmentosum (XP)
	Bind disordered DNA as complex			RAD23	RAD23	Rad23b (Hr23b)	RAD23B (HR23B)	
	Bind DNA and proteins in preincision complex			RAD14		Rad23a (Hr23a)	RAD23A (HHR23A)	
						Xpa	XPA	XP,
TFIIH subunits	3'-5' DNA helicase TFIIH subunit			SSL2 (RAD25)	XPB2	Xpb (Ercc3)	XPB (ERCC3)	XP, Cockayne syndrome (CS), Trichothiodystrophy (TTD)
	5'-3' DNA helicase TFIIH subunit			RAD3	UVH6	Xpd (Ercc2)	ERCC2	XP, CS, TTD
	TFIIH subunit p62			TFB1	AT1G55750	Gtf2h1	GTF2H1	
	TFIIH subunit p44			SSL1	GTF2H2	Gtf2h2	GTF2H2	
	TFIIH subunit p34			TFB4	AT1G18340	Gtf2h3	GTF2H3	
	TFIIH subunit p52			TFB2	AT4G17020	Gtf2h4	GTF2H4	
	TFIIH subunit p8			TFB5	AT1G12400	Gtf2h5	GTF2H5 (TTDA)	TTD
	Kinase subunits of TFIIH			KIN28	CDKD1;3	Cdk7	CDK7	
	Kinase subunits of TFIIH			CCL1	CYCH;1	Ccnh	CCNH	
	TFIIH subunit			TFB3	AT4G30820	Mnat1 (Mat1)	MNAT1 (MAT1)	
Strand incision and excision	3' and 5' incision nuclease	UvrC (TTHA1548)	UvrC					
	3' incision nuclease		Cho					
	3' incision nuclease			RAD2	UVH3	Xpg (Ercc5)	ERCC5	XP, CS
	5' incision nuclease subunits			RAD10	ERCC1	Ercc1	ERCC1	XP
	5' incision nuclease subunits			RAD1	UVH1	Xpf (Ercc4)	ERCC4	XP
Separating two annealed strands	DNA helicase	UvrD (TTHA1427)	UvrD					

TABLE 1: Continued.

Repair pathways	Molecular functions	<i>T. thermophilus</i>	<i>E. coli</i>	<i>S. cerevisiae</i>	<i>A. thaliana</i>	<i>M. musculus</i>	<i>H. sapiens</i>	Related disease*1
Other factors	Transcription- repair coupling factor	Mfd (TTHA0889)	Mfd		ERCC6	Csb (Ercc6)	CSB (ERCC6)	CS, UV-sensitive syndrome (UVS)
	Cockayne syndrome, needed for TC-NER				AT1G19750	Csa (Ckn1, Ercc8)	CSA (ERCC8)	CS
	Cockayne syndrome, needed for TC-NER				DDB1	Ddb1	DDB1 (XPE)	
	P127 subunit of DDB				DDB2	Ddb2 (Xpe)	DDB2 (XPE)	XP
	P48 subunit of DDB, defective in XP-E				AT5G48120	Mms19	MMS19	
	transcription and NER							
<i>Mismatch repair</i>								
Mismatch recognition	DNA-binding ATPase	MutS (TTHA1324)	MutS	MutSα (MSH2/MSH6) MutSβ (MSH2/MSH3)	MutSα (MSH2/MSH6) MutSβ (MSH2/MSH3)	MutSα (MSH2/MSH6) MutSβ (MSH2/MSH3)	MutSα (MSH2/MSH6) MutSβ (MSH2/MSH3)	Colorectal cancer, Ovarian cancer
Strand incision	Activation of MutL homologue	DNA polymerase III, β subunit (TTHA0001)	—	PCNA	PCNA	PCNA	PCNA	
	Activation of MutL homologue	DNA polymerase III, δ, δ', γ, τ subunits (TTHA0788, 1860, 1952)	—	RFC (RFC1-5)*2	RFC (RFC1-5)*2	RFC (RFC1-5)*2	RFC (RFC1-5)*2	
	Endonuclease ATPase	MutL (TTHA1323)	—	MutLα (MLH1/PMS1) MutLβ (MLH1/MLH2) MutLγ (MLH1/MLH3)	MutLα (MLH1/PMS1) MutLβ (MLH1/PMS1) MutLγ (MLH1/MLH3)	MutLα (MLH1/PMS2) MutLβ (MLH1/PMS1) MutLγ (MLH1/MLH3)	MutLα (MLH1/PMS2) MutLβ (MLH1/PMS1) MutLγ (MLH1/MLH3)	Colorectal cancer, Endometrial cancer, Ovarian cancer
Match making	ATPase	—	MutL	—	—	—	—	
Strand excision	5'-3' exonuclease	RecJ (TTHA1167)	RecJ	—	—	—	—	
	3'-5' exonuclease	ExoI (TTHB178)	ExoI	—	—	—	—	
	5'-3' exonuclease	ExoVII	ExoVII	—	—	—	—	
	3'-5' exonuclease	ExoX	ExoX	—	—	—	—	
	5'-3' exonuclease	SSB (TTHA0244)	SSB	—	AT1G29630	Exo1	EXO1	
	Single-stranded DNA binding protein	—	—	—	—	—	—	
	Single-stranded DNA binding protein complex	—	—	—	—	—	—	
	DNA helicase	UvrD (TTHA1427)	UvrD	RFA (RFA1-3)*2	RPA (RPA1-3)*2	Rpa (Rpa1-3)*2	RPA (RPA1-3)*2	

TABLE 1: Continued.

Repair pathways	Molecular functions	<i>T. thermophilus</i>	<i>E. coli</i>	<i>S. cerevisiae</i>	<i>A. thaliana</i>	<i>M. musculus</i>	<i>H. sapiens</i>	Related disease*1
<i>Recombination repair</i>								
End resection and recombinase loading	5'-3' exonuclease	RecJ (TTHA1167)	RecJ					
	5'-3' exonuclease			EXO1	AT1G29630	Exo1	EXO1	
	5'-flap endonuclease			DNA2	AT1G08840	Dna2	DNA2	
	RECQ family DNA helicase		RecQ	SGS1	AT1G10930 (RECQ4A)	Blm	BLM	Bloom syndrome
	Endonuclease, interact with MRN complex			SAE2	AT3G52115 (ATGR1)	CtIP (Rbbp8)	CTIP (RBBP8)	
	SMC-like ATPase, complex with SbcD (Mre11)	SbcC (TTHA1288)	SbcC	RAD50	AT2G31970 (RAD50)	Rad50	RAD50	Nijmegen breakage syndrome-like disorder
	3'-5' exonuclease, endonuclease, complex with SbcC (Rad50)	SbcD (TTHA1289)	SbcD	MRE11	AT5G54260 (MRE11)	Mre11a	MRE11A	Ataxia telangiectasia-like disorder
	Accessory protein for MR complex			XRS2	AT3G02680 (NBS1)	Nbn (Nbs1)	NBN (NBS1)	Nijmegen breakage syndrome
	SMC-like ATPase	RecN (TTHA1525)	RecN					
	Helicase/nuclease complex		RecB					
	Helicase/nuclease complex		RecC					
	Helicase/nuclease complex		RecD					
	5'-3' exonuclease		RecE					
	ssDNA annealing		RecT					
	Single-stranded DNA binding protein	SSB (TTHA0244)	Ssb					
	Single-stranded DNA binding protein complex							
	ATPase, complex with RecR	RecF (TTHA0264)	RecF					
	Recombinase mediator, ssDNA annealing	RecO (TTHA0623)	RecO					
				RFA (RFA1-3)	RPA (RPA1-3)	Rpa (Rpa1-3)	RPA (RPA1-3)	

TABLE 1: Continued.

Repair pathways	Molecular functions	<i>T. thermophilus</i>	<i>E. coli</i>	<i>S. cerevisiae</i>	<i>A. thaliana</i>	<i>M. musculus</i>	<i>H. sapiens</i>	Related disease*1
	DNA binding, complex with RecF and RecO	RecR (TTHA1600)	RecR					
	Recombinase mediator, ssDNA annealing	Rad52-like (TTHA0081)		RAD52		Rad52	RAD52	Pancreatic cancer, Ovarian cancer, Breast cancer, Fanconi anemia
	Recombinase mediator				AT5G01630 (BRCA2B)	Brca2	BRCA2	Adenocarcinoma, Non-Hodgkin lymphoma
	RAD54 family DNA translocase, recombinase mediator			RAD54	AT3G19210 (ATRrad54)	Rad54l	RAD54L	Colon cancer, Non-Hodgkin lymphoma
	RAD54 family DNA translocase, recombinase mediator			RDH54		Rad54b	RAD54B	Colon cancer, Non-Hodgkin lymphoma
	RAD51-like, recombinase mediator				AT5G64520 (XRCC2)	Xrcc2	XRCC2	Breast cancer
	RAD51-like, recombinase mediator				AT5G57450 (XRCC3)	Xrcc3	XRCC3	Breast cancer, Melanoma
	RAD51-like, recombinase mediator			RAD57	AT2G28560 (RAD51B)	Rad51ll	RAD51LI	Uterine leiomyoma
	RAD51-like, recombinase mediator				AT2G45280 (RAD51C)	Rad51c	RAD51C	Fanconi anemia-like disorder, Breast-Ovarian cancer

TABLE 1: Continued.

Repair pathways	Molecular functions	<i>T. thermophilus</i>	<i>E. coli</i>	<i>S. cerevisiae</i>	<i>A. thaliana</i>	<i>M. musculus</i>	<i>H. sapiens</i>	Related disease*
	RAD51-like, recombinase mediator			RAD55	AT1G07745 (RAD51D)	Rad51l3	RAD51L3	
Strand exchange	Recombinase	RecA (TTHA1818)	RecA	RAD51	AT2G19490 (recA) AT5G20850 (ATRAD51)	Rad51	RAD51	
Branch migration	Branch migration complex	RuvA (TTHA0291)	RuvA					
	Branch migration complex	RuvB (TTHA0406)	RuvB					
	DNA helicase	RecG (TTHA1266)	RecG		AT2G01440 (RecG)			
	RecA-like ATPase	RadA/Sms (TTHA0541)	RadA/Sms		AT5G50340			
	RAD54 family DNA translocase, recombinase mediator			RAD54	AT3G19210 (ATRAD54)	Rad54l	RAD54L	Adenocarcinoma, Non-Hodgkin lymphoma
	RAD54 family DNA translocase, recombinase mediator			RDH54		Rad54b	RAD54B	Colon cancer, Non-Hodgkin lymphoma
	RECQ family DNA helicase		RecQ	SGS1	AT1G10930 (RECQ4A)	Blm	BLM	Bloom syndrome

TABLE 1: Continued.

Repair pathways	Molecular functions	<i>T. thermophilus</i>	<i>E. coli</i>	<i>S. cerevisiae</i>	<i>A. thaliana</i>	<i>M. musculus</i>	<i>H. sapiens</i>	Related disease*
	RECQ family DNA helicase					Wrn	WRN	Werner syndrome
	RECQ family DNA helicase				AT1G31360 (RECQL2)	Recql	RECQL	
	RECQ family DNA helicase			MPH1	AT1G35530	Fancm	FANCM	Fanconi anemia
Holliday junction resolution	HJ resolvase	RuvC (TTHA1090)	RuvC					
	HJ resolvase		RusA					
	HJ resolvase			YEN1	AT1G01880	Gen1	GEN1	
	Structure-specific endonuclease			MUS81	AT4G30870 (MUS81)	Mus81	MUS81	
	complex with MUS81			MMS4	AT2G22140 (ATEME1B)	Eme1	EME1	Xeroderma pigmentosum
	Structure-specific endonuclease			RAD1	AT5G41150 (UVH1)	Erc4	ERCC4	Cerebro-oculo-facio-skeletal syndrome
	complex with ERCC4 (RAD1)			RAD10	AT3G05210 (ERCC1)	Erc1	ERCC1	
	HJ resolvase			SLX1	AT2G30350	Slx1 (Giyd2)	SLX1 (GIYD2)	
	Accessory protein for structure-specific nucleases			SLX4		Slx4 (Btbd12)	SLX4 (BTBD12)	
Anti-recombination	Recombinase inhibitor	RecX (TTHA0848)	RecX		AT3G13226 (RecX)			
	DNA helicase	UvrD (TTHA1427)	UvrD	SRS2	AT4G25120			
	Structure-specific endonuclease	MutS2 (TTHA1645)			AT1G65070 (MutS2)			

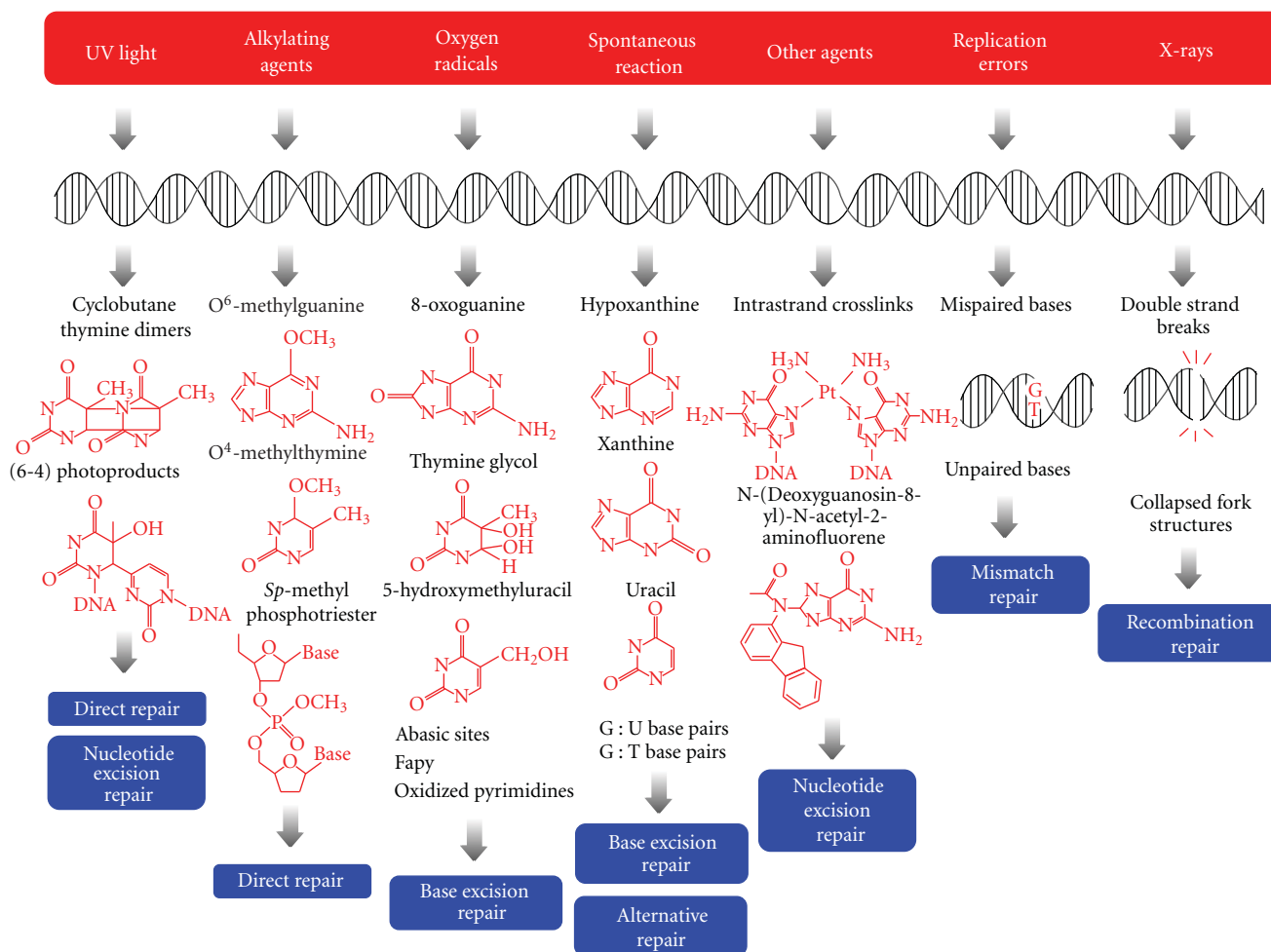


FIGURE 1: Different repair systems for the principal types of DNA lesion produced by a wide range of factors. UV-light induces cyclobutane pyrimidine dimers or (6-4) photoproducts that are repaired by nucleotide excision repair and direct reversal systems. Alkylating agents can modify all of the bases and the phosphates of the DNA, and some repair proteins remove these alkyl adducts in a direct manner. Oxygen radicals modify DNA, and the base excision repair system acts to reverse these changes. The main cause of spontaneous mutation is deamination, and base excision repair and alternative repair systems remove the lesions. Other bulky adducts or interstrand cross-links are repaired by the nucleotide excision repair system. The mismatch repair pathway repairs replication errors. Double-strand breaks and four-way junctions are induced by X-rays and are repaired by recombinational repair.

The tyrosine and arginine residues involved in base flipping are also conserved in ATL proteins. A fluorescence assay of the *T. thermophilus* ATL protein (TTHA1564) suggested that it can also recognize  $O^6$ -meG and flips out the target residue into its active site (Figure 2(c)) [37]. The crystal and NMR structures of ATL proteins indicate that the  $O^6$ -meG residue is flipped out from the base stacks into the active site [34, 40]. Mutational analysis demonstrated that the tyrosine and arginine residues of ATL proteins are also involved in base flipping [34].

A comparison of their 3D structures showed that the lesion-binding pocket of ATL proteins is approximately three times larger than that of AGTs [34, 40]. The *S. pombe* ATL protein (Atl1) can bind to the bulky  $O^6$ -adduct,  $O^6$ -4-(3-pyridyl)-4-oxobutylguanine ( $O^6$ -pobG), with higher affinity than to  $O^6$ -meG [34]. Additionally, AGT repairs  $O^6$ -pobG with lower efficiency than  $O^6$ -meG. In species that have both

AGT and ATL protein, for example, *E. coli*, it is possible that AGT repairs  $O^6$ -meG while the ATL protein is involved in the repair of bulky  $O^6$ -adducts such as  $O^6$ -pobG.

It is known that the action of ATL proteins is linked with the NER pathway (Figure 2(c)) [34, 36, 37, 40]. The ATL protein of *T. thermophilus*, TTHA1564, can interact with UvrA, while that of *E. coli* can interact with UvrA and UvrC [36, 37, 40]. MNNG caused an increased mutation frequency in the *ttha1564*-deficient mutant compared with the wild type (unpublished data). Genetic analysis of *S. pombe* Atl1 showed that *atl1* is epistatic to *rad13* (the fission yeast orthologue of human ERCC5) and *swi10* (the ERCC1 orthologue) but not to *rhp14* or *rad2* for *N*-methyl-*N'*-nitro-*N*-nitrosoguanidine (MNNG) toxicity [40]. Analyses of the spontaneous mutation rate of *rad13* and *rad13 atl* mutants suggested that ATL-DNA complexes block an alternative repair pathway probably because ATL proteins form a highly

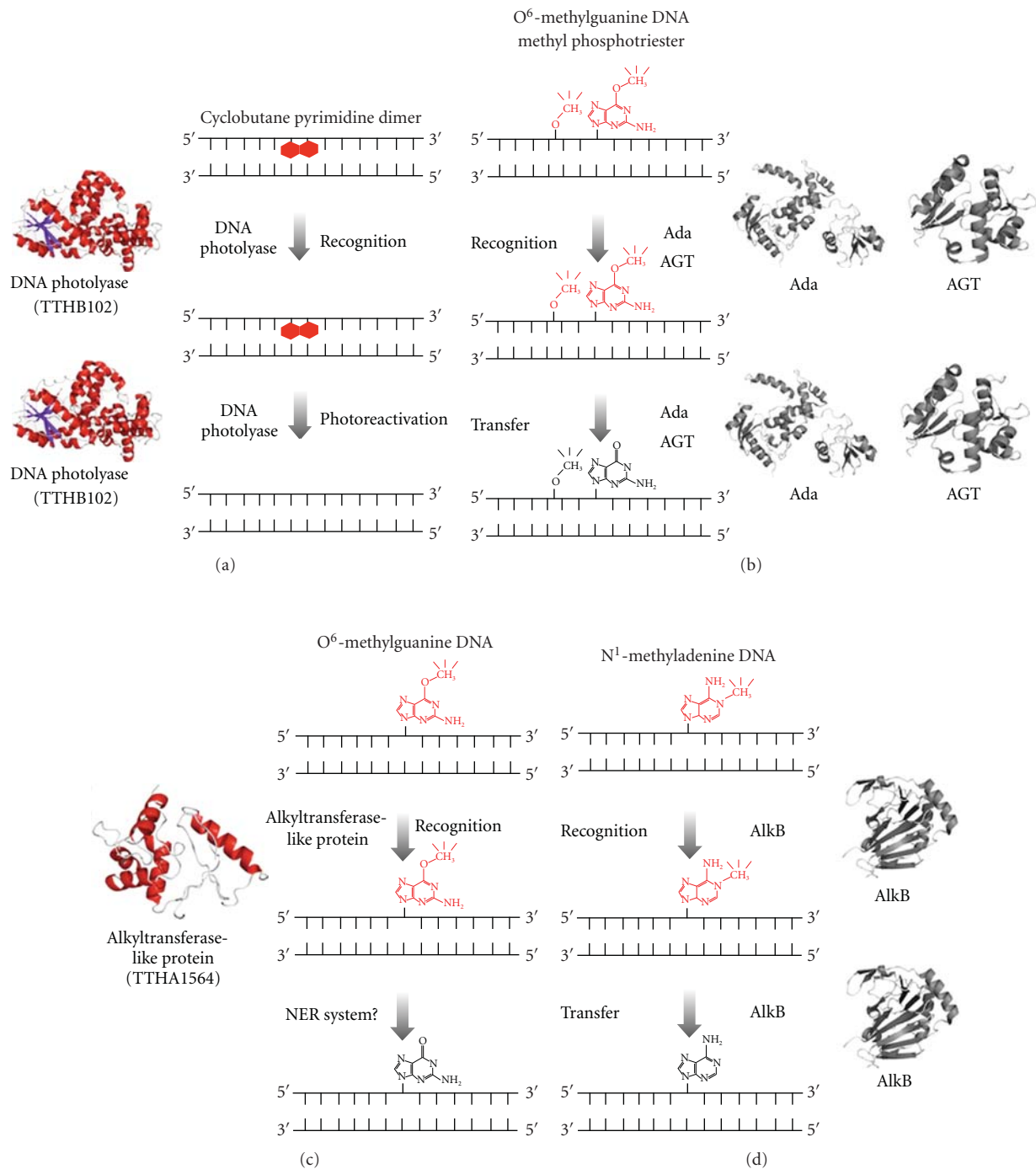


FIGURE 2: A schematic representation of models for direct reversal of DNA damage. The structure of the ATL proteins was modeled by SWISS-MODEL (the template structure is *Sulfolobus tokodaii* Ogt) [19, 20]. AGT, Ada, and AlkB are not conserved in *T. thermophilus*. (a) Cyclobutane pyrimidine dimers are recognized by photolyase (TTHB102; PDB ID: 1IQR) and repaired by photolyase. (b) O<sup>6</sup>-methylguanines are recognized by AGT (PDB ID: 1EH6) in most species and by the C-terminal domain of Ada (PDB ID: 1SFE) in *E. coli*. Methyl phosphotriesters are recognized by the N-terminal domain of Ada (PDB ID: 1WPK) in *E. coli*. These enzymes directly accept a methyl group, and the alkyl adducts are removed from the DNA. (c) O<sup>6</sup>-alkyl adducts including O<sup>6</sup>-methylguanines are recognized by ATL proteins (TTHA1564; predicted model) in several species. It is predicted that NER proteins are involved in this pathway after recognition of the adducts by ATL proteins. (d) N<sup>1</sup>-methyladenines and N<sup>3</sup>-methylcytosines are recognized by AlkB (PDB ID: 2IUW). Methyl group transfer by AlkB depends on  $\alpha$ -ketoglutarate and Fe(II).

stable complex with DNA in the absence of Rad13 or other NER proteins [40]. However, the mechanism by which ATL proteins repair lesions in collaboration with NER proteins is not well understood.

The protein Ada repairs alkylated lesions in the same manner as AGTs in *E. coli* (Figure 2(b)) [27]. The amino acid sequence and the molecular function of the C-terminal domain of Ada (C-Ada) show similarity to those of AGTs. The N-terminal domain of Ada (N-Ada) can repair a methyl phosphotriester lesion in DNA *in vitro* [44]. Methylated N-Ada specifically binds to the promoter region of the *ada-alkB* operon and the *alkA* and *aidB* genes and C-Ada can bind to RNA polymerase [45, 46]. Thus, the methylated Ada acts as a transcriptional activator.

**2.3. AlkB.** AlkB homologues are conserved in many organisms including humans and *E. coli*. As described above, *alkB* is one of the genes regulated by Ada. AlkB requires  $\alpha$ -ketoglutarate and Fe(II) as cofactors to repair  $N^1$ -methyladenine or  $N^3$ -methylcytosine via an oxidative demethylation mechanism [46]. These properties are consistent with the fact that AlkB has sequence motifs in common with 2-oxoglutarate and iron-dependent dioxygenases (Figure 2(d)) [47]. AlkB oxidizes the methyl group using nonheme  $Fe^{2+}$ ,  $O_2$ , and  $\alpha$ -ketoglutarate to restore undamaged bases with subsequent release of succinate,  $CO_2$ , and formaldehyde. The detailed mechanisms of substrate recognition and catalysis were identified by structural and mutational analyses.

Eight AlkB homologues are known in humans, [48] and, of these, ALKBH1, ALKBH2, and ALKBH3 have been identified as repair enzymes, each of which has a different substrate specificity [49, 50]. *E. coli* AlkB can repair a lesion in both single-stranded DNA (ssDNA) and dsDNA, whereas ALKBH3 repairs lesions only in ssDNA. ALKBH1 and ALKBH2 can act only on DNA whereas *E. coli* AlkB and ALKBH3 can act on both DNA and RNA [51]. The crystal structures of AlkB-dsDNA and ALKBH2-dsDNA complexes explain distinct preferences of AlkB homologues for substrates [51]. Cell cycle-dependent subcellular localization experiments suggested that ALKBH2 and ALKBH3 repair mainly newly synthesized DNA and mRNA, respectively, and withhold demethylation of modified rRNA or tRNA.

### 3. Base Excision Repair

DNA is altered and damaged by various endogenous and exogenous reactions [52]. With regard to endogenous reactions, deamination of cytosine, adenine and guanine produce uracil, hypoxanthine, and xanthine, respectively. Depurination and depyrimidination result in the formation of an apurinic/apyrimidinic site (AP site). Reactive oxygen species (ROs) convert guanine to 7,8-dihydro-8-oxoguanine (8-oxoguanine, 8-oxoG, or its isomeric form 8-hydroxyguanine) and purine bases to 2,6-diamino-4-hydroxy-5-formamidopyrimidine (FaPyG) and 4,6-diamino-5-formamidopyrimidine (FaPyA). Thymine glycol, cytosine hydrates, and etheno adducts of adenine, cytosine,

and guanine are also generated as a result of oxygen damage. DNA replication errors also introduce lesions into the DNA. For example, DNA polymerases sometimes incorporate mismatched bases or damaged nucleotides (such as dUMP and 8-oxo-dGMP) [53–55]. With regard to exogenous reactions, DNA is susceptible to damage by agents such as UV radiation and alkylating compounds. The lesions caused by endogenous and exogenous reactive species can be repaired through the base excision repair (BER) pathway described below.

**3.1. General Mechanism of BER.** BER is probably the most frequently used DNA repair pathway in the cell (Figure 3, Table 1) [56, 57]. Bases damaged as described above are specifically recognized by various DNA glycosylases to initiate BER [58]. Monofunctional DNA glycosylases catalyze the hydrolysis of N-glycosyl bonds and generate an AP site. Bi- and trifunctional DNA glycosylases have AP lyase activity via a  $\beta$ - or  $\beta/\delta$ -elimination mechanism using an  $\epsilon$  amino group of a lysine residue or  $\alpha$ -imino group in addition to DNA glycosylase activity [59]. However, it is still unclear whether this lyase activity is the primary *in vivo* mechanism. AP sites are targeted by both AP endonuclease and AP lyase. AP endonuclease nicks an AP site through a hydrolytic reaction to generate a 3'-OH and 5'-deoxyribosephosphate (dRP) [60–62]. This 5' block is removed by deoxyribophosphodiesterase (dRPase) or dRP lyase using hydrolytic or lyase ( $\beta$ -elimination) mechanisms, respectively [63–65]. When the AP lyase incises an AP site, it produces 3'- $\alpha,\beta$ -unsaturated aldehyde (by  $\beta$ -elimination) or 3'-phosphate (by  $\beta/\delta$ -elimination) and 5'-phosphate [66]. These 3'-blocking groups must be removed by 3'-phosphoesterase to allow DNA polymerase activity. A one-nucleotide gap typically remains after AP site processing. When repair synthesis is performed by incorporation of a single nucleotide, this pathway is called single nucleotide-BER (SN-BER) [67]. Some DNA polymerases can synthesize DNA of more than 2 bases by strand displacement activity, followed by cleaving flap DNA via flap endonuclease activity. This pathway is called long-patch BER (LP-BER) [67]. In both pathways, the resulting nick is sealed by DNA ligase.

**3.2. BER in *T. thermophilus*.** The *T. thermophilus* HB8 genome contains the genes for all the fundamental BER enzymes. The genome includes the following monofunctional DNA glycosylases: 3-methyl-adenine DNA glycosylase, TTHA0329 (ttAlkA); uracil DNA glycosylase A, TTHA0718 (ttUDGA); uracil DNA glycosylase B, TTHA1149 (ttUDGB). It also includes the following bifunctional DNA glycosylases: endonuclease III (Nth), TTHA0112 (ttEndoIII); adenine DNA glycosylase, TTHA1898 (ttMutY); formamidopyrimidine DNA glycosylase, TTHA1806 (ttMutM). AP endonucleases are classified on the basis of their structure as members of either the exonuclease III family or the endonuclease IV (Nfo) family. The only AP endonuclease in *T. thermophilus* is the EndoIV, TTHA0834 (ttEndoIV); a similar restriction occurs in other bacterial and archaeal species. *T. thermophilus* has been found to have two DNA polymerases, TTHA1054

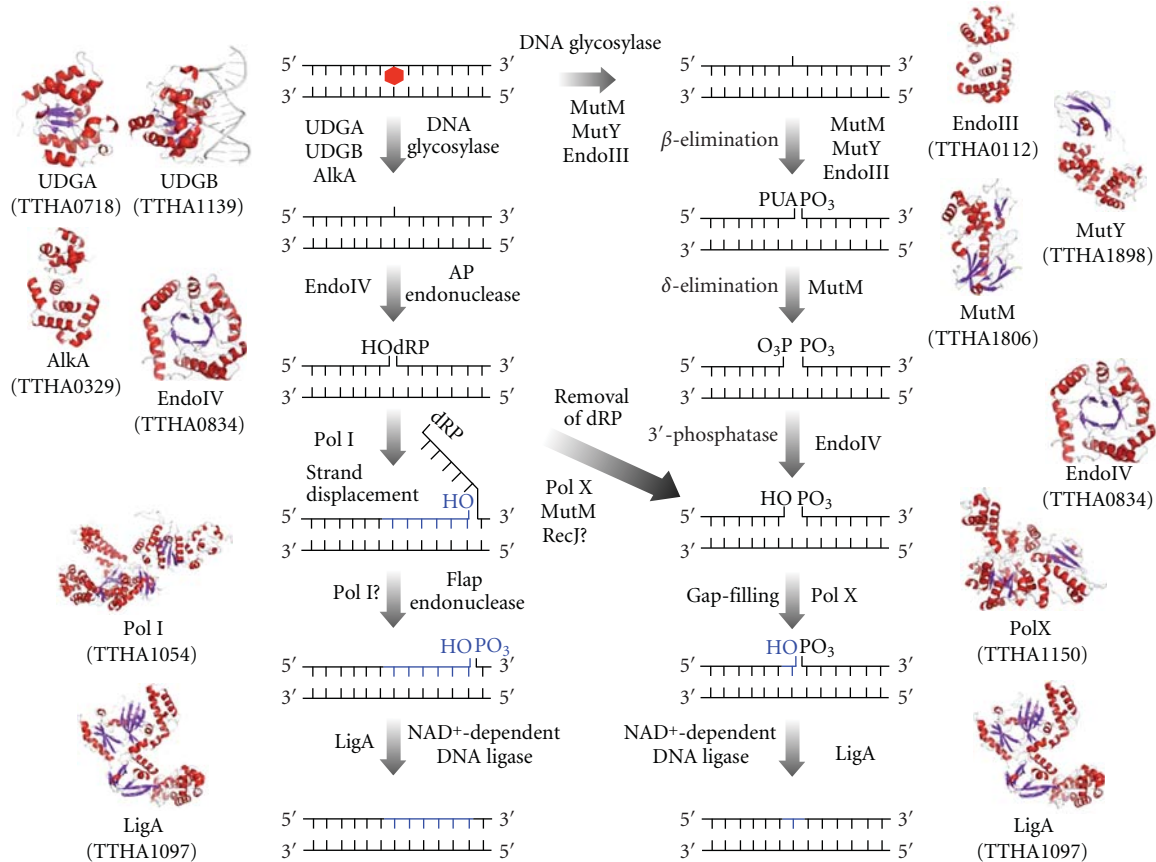


FIGURE 3: General mechanism of the BER pathway in *T. thermophilus*. UDGA, UDGB, and Alka are monofunctional DNA glycosylases. UDGA (PDB ID: 1UII0) and UDGB (PDB ID: 2DDG) remove uracil from DNA. Alka removes 3-methyladenine in *E. coli*. MutY and EndoIII are bifunctional DNA glycosylases and have both DNA glycosylase and AP lyase activities. MutY removes adenine opposite 8-oxoG, and EndoIII removes pyrimidine residues damaged by ring saturation, fragmentation, and contraction [41], by which 3'-phospho  $\alpha,\beta$ -unsaturated aldehyde (3'-PUA) remains. MutM (PDB ID: 1EE8) is a trifunctional DNA glycosylase that removes 8-oxoG from oxidatively damaged DNA and 3'-phosphate remains. An AP site resulting from DNA glycosylase activity is processed by EndoIV or multifunctional DNA glycosylases. EndoIV has both AP endonuclease activity and 3'-esterase activity in *E. coli* [42, 43]. PolX or MutM removes 5'-dRP by dRP lyase activity. In addition, 5'-3' exonuclease (RecJ) may have dRPase activity. The resulting gap is filled by PolI or PolX followed by sealing of the nick by LigA. The structures of Alka, EndoIII, MutY, PolI, PolX, and LigA were obtained using SWISS-MODEL [19, 20] (PDB ID: 2H56, 2ABK, 3FSP, 1TAU, 2W9M, and 1V9P, resp.) based on amino acids sequences of *T. thermophilus* HB8.

(ttPolI) and TTHA1150 (ttPolX), and an NAD<sup>+</sup>-dependent DNA ligase, TTHA1097 (ttLigA). The crystal structures of ttUDGA [68], ttUDGB [69], ttMutM [70], and ttEndoIV (unpublished data) have been determined.

Uracil-DNA glycosylases (Ungs or UDGs) remove uracil from DNA by cleaving the N-glycosylic bond. These enzymes are classified into several families on the basis of similarities in their amino acid sequences [71, 72]. *T. thermophilus* HB8 has two Ungs that belong to families 4 (ttUDGA) and 5 (ttUDGB). ttUDGA removes uracil from not only U:G but also U:C, U:A, and U:T and can also remove uracil from ssDNA. Moreover, the crystal structure of ttUDGA with uracil indicates that the mechanism by which family 4 Ungs remove uracils from DNA is similar to that of family 1 enzymes [68]. The crystal structures of apo-form ttUDGB and ttUDGB complexed with AP site containing DNA have been solved [69]. The active site structures suggest that this enzyme uses both steric force and water activation for its

excision reaction. Based on the absence of a significant open-closed conformational change upon binding to DNA, it was proposed that Ungs recognize the damaged base by sliding along the target-containing strand [69].

MutM is a trifunctional DNA glycosylase which removes 8-oxoG from oxidatively damaged DNA [73]. ttMutM was cloned, characterized, and crystallized. Based on crystal structure and biochemical experiments of ttMutM, DNA-binding mode and catalytic mechanism of MutM were proposed [70].

In mammalian cells, SN-BER is the principal BER sub-pathway and is catalyzed mainly by Pol $\beta$  [74, 75]. Nevertheless, LP-BER also occurs *in vivo* [76]. The selection of which sub-pathway to use is dependent on the nature of the damaged base, the 5'-blocking structure, and the enzymes involved [74, 77–82]. Bacteria have both SN- and LP-BER pathways [83]. Bacterial PolIs, including ttPolI, have strand displacement [84] and flap endonuclease-like

activities (structure-specific 5'-nuclease activity) [85–89]. Therefore, PolI is probably the main DNA polymerase in bacterial LP-BER. Furthermore, the fact that the  $\beta$ -clamp, the  $\beta$  subunit of DNA polymerase III holoenzyme, interacts with some DNA repair enzymes, such as PolI and LigA [90], indicates that it is possibly involved in bacterial LP-BER in a similar manner to mammalian PCNA clamp [77].

Many bacteria have PolX, which belongs to the X-family DNA polymerases; the mammalian homologues of this enzyme are Pol $\beta$ , Pol $\lambda$ , Pol $\mu$ , TdT, and Pol $\sigma$  [91]. PolXs can efficiently fill a short DNA gap in mammals [79, 92] and bacteria [93] and are therefore thought to be the main DNA polymerases in the SN-BER pathway [74, 75, 94]. Although PolX is conserved in many bacteria, including *T. thermophilus*, *E. coli* does not have this enzyme. Therefore, *T. thermophilus* has an advantage as a model organism in understanding human and bacterial BER. ttPolX has two principal active regions, the N-terminal POLX core (POLXc) domain and the C-terminal polymerase and histidinol phosphatase (PHP) domain. These domains are conserved in many bacteria, but eukaryotic PolXs lack the PHP domain. Furthermore, it is thought that only PHP domain-containing PolXs have 3'-5' exonuclease activity [95, 96]. The PHP domain has nine catalytic residues and is mainly responsible for the nuclease activity; however, the POLXc domain is also needed for this activity [97]. Although the PHP domain is thought to have a phosphoesterase activity, details of the function of the PHP domain remain to be clarified. Bacterial PolXs may play more than two roles in the BER pathway whereas these functions might be performed in eukaryotes by two or more separate enzymes. Identifying the role of the PHP domain of bacterial PolXs in BER will be important for understanding both bacterial and eukaryotic BERs.

**3.3. Eukaryotic-Specific BER Enzymes.** Eukaryotes have many functional homologues of bacterial BER enzymes, and the mechanism of BER is similar to that of prokaryotes. However, eukaryotes also have specific BER enzymes. To date, poly(ADP-ribose) polymerase (PARP) and X-ray cross-complementing group 1 (XRCC1) have been identified as eukaryotic-specific enzymes. PARP1 uses NAD to add branched ADP-ribose chains to proteins. PARP1 functions as a DNA nick-sensor in DNA repair and as a negative regulator of the activity of Pol $\beta$  in LP-BER [98]. XRCC1 interacts with DNA ligase III and PARP through its two BRCT domains and with Pol $\beta$  through an N-terminal domain. XRCC1 also interacts with many other proteins and forms a large DNA repair complex [99, 100].

## 4. Nucleotide Excision Repair

Nucleotide excision repair (NER) is one of the most important repair systems and is conserved from prokaryotes to higher eukaryotes [101, 102]. The most important feature of the NER system is its broad substrate specificity: NER can excise DNA lesions such as UV-induced pyrimidine dimers or more bulky adducts [103].

In the prokaryotic NER system, recognition and excision of DNA lesions are mediated by UvrABC excinucleases (Figure 4) [101, 102]. After the incision event, UvrD helicase removes the nucleotide fragment, PolI synthesizes the complementary strand, and then DNA ligase completes the repair process. NER has two sub-pathways, global genomic repair (GGR) and transcription-coupled repair (TCR) [104, 105]. In GGR, recognition of DNA lesions by UvrAB initiates the initiation of the repair reaction, whereas, in TCR, stalling of the RNA polymerase is responsible for the initiation of repair [106]. When a transcribing RNA polymerase meets a bulky DNA lesion, the polymerase stalls. Transcription-repair coupling factor (TRCF) releases the stalled RNA polymerase from the template DNA and then recruits UvrA. After UvrA has bound to the DNA, the subsequent reactions proceed in the same fashion as in GGR.

Most eukaryote species, including humans, possess an NER system. The amino acid sequences of the proteins that act in eukaryotic NER are very different from those of bacterial proteins, but the functions of these proteins are nevertheless similar [101]. The molecular mechanism of NER is more complicated in eukaryotes than bacteria. The eukaryotic NER pathway involves more than ten proteins, including some that are functional homologues of those required for bacterial NER [107].

**4.1. Global Genomic Repair (GGR).** Bacterial GGR is a multistep process that removes a wide variety of DNA lesions. In solution, UvrA and UvrB form UvrA<sub>2</sub>B or UvrA<sub>2</sub>B<sub>2</sub> that can recognize lesions in DNA and can make a stable complex with the DNA [108, 109]. When UvrB detects a lesion, it hydrolyzes ATP to form the pro-preincision complex. After UvrA is released, UvrB binds tightly to DNA and makes a stable UvrB-DNA complex, that is, a pre-incision complex. In this state, UvrB hydrolyzes ATP and can then specifically recognize damage in the absence of UvrA [110]. In *E. coli*, UvrB can hydrolyze ATP in this step with UvrA but not without UvrA [111]. In *T. thermophilus* HB8, the UvrB protein (ttUvrB; TTHA1892) shows ATPase activity at its physiological temperature even in the absence of UvrA (ttUvrA; TTHA1440) [112, 113]. Finally, a new pre-incision complex is formed by binding new ATP [110]. UvrC can bind to the pre-incision complex to incise both sides of a DNA lesion. The first incision is made at the fourth or fifth phosphodiester bond on the 3' side of the lesion and is immediately followed by incision at the eighth phosphodiester bond on the 5' side [114, 115]. The catalytic sites for 3' and 5' incisions are located in different domains of UvrC. It has been reported that the expression levels of *uvrA* and *uvrB* are approximately three times higher than that of *uvrC* (*ttha1548*) in *T. thermophilus* [116].

UvrD is a DNA helicase that releases lesion-containing DNA fragments from dsDNA. The purification and characterization of UvrD from *T. thermophilus* (ttUvrD; TTHA1427) have been reported [117]. After removing the nucleotide fragment, PolI synthesizes a new strand with the same sequence as the removed nucleotide fragment. The

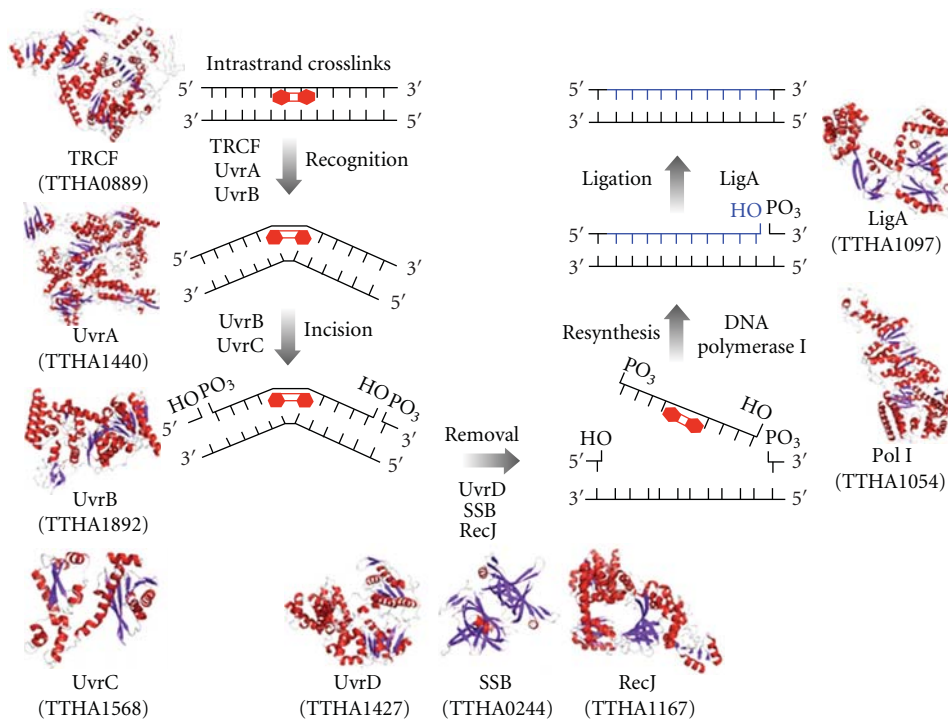


FIGURE 4: A schematic representation of models for the nucleotide excision repair pathway controlled by Uvr proteins. All of the predicted protein structures were modeled using SWISS-MODEL. The template structures used in the model building were *Geobacillus stearothermophilus* UvrA, the N- and C-terminal domain of *Thermotoga maritime* UvrC, *G. stearothermophilus* UvrD, *Thermus aquaticus* DNA polymerase I, *Thermus filiformis* DNA ligase, and *E. coli* TRCF. UvrA (TTHA1440; predicted model) and UvrB (TTHA1892; PDB ID: 1D2M) recognize the DNA lesion. In transcribing strand, TRCF (TTHA0889; predicted model) is also involved in recognition of the lesion. UvrC (TTHA1568; predicted model) incises both sides of the lesion. The DNA fragment containing the lesion is excised by UvrD (TTHA1427; predicted model), SSB (TTHA0244; 2CWA), and exonuclease RecJ (TTHA1167; PDB ID: 2ZXO). A new strand is resynthesized by DNA polymerase I (TTHA1054; predicted model) and ligated by DNA ligase (TTHA1097; predicted model).

newly synthesized sequence is ligated to the adjacent strand by DNA ligase, and all of the repair steps are completed.

**4.2. Transcription-Coupled Repair (TCR).** Bacterial TCR is a highly efficient NER system. In 1985, it became apparent that the DNA lesion in the transcribed strand is preferentially repaired [118]. The first consequence of this mechanism is that a stalled RNA polymerase interacts with UvrA with high affinity. Interestingly, however, a stalled RNA polymerase interrupts the NER repair system *in vitro* [119]. Hence, it was suspected that an unknown factor must release the stalled RNA polymerase and recruit NER proteins. Selby et al. showed in *E. coli* that the gene product (transcription-repair coupling factor, TRCF) of the *mfd* gene is the factor involved [106, 120].

TRCF can release a stalled elongation complex but not an initiation complex [106]. The activity for releasing an elongation complex is dependent on ATP hydrolysis. After the complex is released, TRCF can recruit UvrA to the DNA lesion. TRCF has a UvrB homology module, which interacts with UvrA [106, 121]. After recruiting UvrA to the DNA lesion, the subsequent reactions are the same as in GGR. UvrB and DNA form a pre-incision complex, and then UvrC incises both sides of the DNA strand.

The broad substrate specificity of TCR is similar to that of GGR, but TCR repairs lesions with a higher efficiency [106]. In TCR, UvrA can be more rapidly directed to the DNA lesion because the stalled RNA polymerase and TRCF mediate binding of UvrA, whereas, in GGR, UvrA needs to search for DNA lesions across the whole genome without the aid of cofactors. An increased efficiency in finding the substrate also increases the efficiency of the repair system.

**4.3. Crystal Structures and Functions of Key Enzymes.** The overall crystal structures of UvrA, UvrB, and TRCF and the two domains of UvrC were determined some years ago [122–128]. In 1999, UvrB was the first of the proteins involved in NER to have its crystal structure established [124, 125, 127]. Later, in 2006, the 3D structure of the UvrB-DNA complex was reported [129]. It was suggested by limited proteolysis that ttUvrB is comprised of four domains, whereas analysis of the 3D structure identified five domains, 1a, 1b, 2, 3, and 4 (Figure 5(a)) [125, 130]. Domain 2 interacts with UvrA, and domain 4 interacts with both UvrA and UvrC. Domains 1a and 3 contain helicase motifs and share high structural similarity to the DNA helicases NS3, PcrA, and Rep. The flexible  $\beta$ -hairpin-connecting domains 1a and 1b are predicted to play important roles in DNA binding.

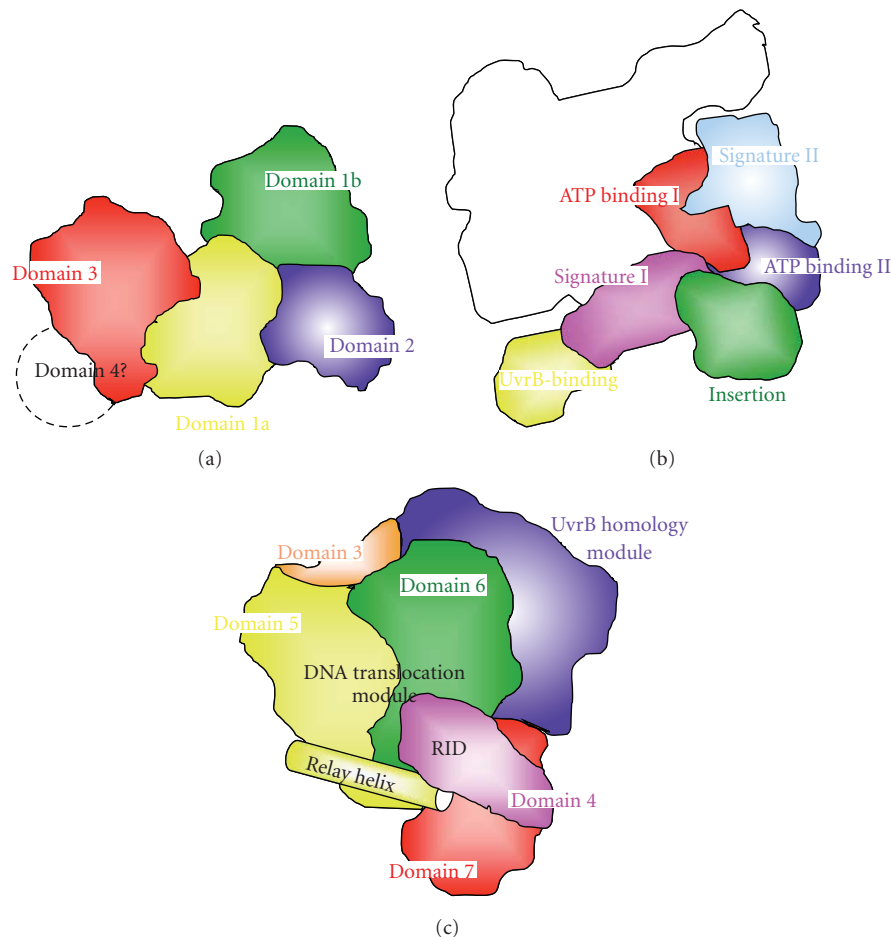


FIGURE 5: The domain architectures of UvrB, UvrA, and TRCF. (a) UvrB is comprised of five domains. Domains 1a (yellow) and 3 (red) contain helicase motifs. Domain 1b (green) has the flexible  $\beta$ -hairpin involved in substrate recognition. Domain 2 (blue) interacts with UvrA. Domain 4 is disordered in the crystal structures. (b) UvrA is comprised of six domains: ATP-binding I (red), ATP-binding II (blue), signature I (pink), signature II (cyan), UvrB-binding (yellow), and insertion (green) domain. The white region is the other subunit of the dimer. (c) TRCF is comprised of seven domains. Domains 1 and 2 (not separated in the figure) comprise UvrB homology module (blue). Domains 5 (yellow) and 6 (green) comprise DNA translocation module. Relay helix (yellow) interacts with domain 4 (pink), RNA polymerase interaction domain (RID). The functions of domain 3 (orange) and domain 7 (red) are unclear.

The structure of the UvrB-DNA complex shows that the nucleotide directly behind the  $\beta$ -hairpin is flipped out and inserted into a small pocket in UvrB [129].

The crystal structures of the N-terminal and C-terminal domains of UvrC were reported in 2005 and 2007, respectively, but the 3D structure of the interdomain loop and of full-length UvrC is still unclear [123, 128]. The N-terminal domain of UvrC catalyzes the 3' incision reaction and shares homology with the catalytic domain of GIY-YIG family endonucleases. The C-terminal domain of UvrC is responsible for the 5' incision [123]. It includes an endonuclease domain and an (HhH)<sub>2</sub> domain. Despite the lack of sequence homology, the endonuclease domain has an RNase H-like fold. We established the methods of purification of UvrC from *T. thermophilus* (ttUvrC; TTHA1568), and Hori et al. developed an *in vitro* reconstitution system of NER using purified ttUvrA, ttUvrB, and ttUvrC [131]. The ttUvrABC system can recognize a (6-4) thymine dimer and

excise the affected strand; however, it does not excise a strand containing 8-hydroxy-2'-deoxyguanine or 2-hydroxy-2'-deoxyadenine [131].

The overall structure of UvrA was reported in 2008 [126]. UvrA is comprised of six domains: ATP-binding I, signature I, ATP-binding II, signature II, UvrB-binding, and insertion domains (Figure 5(b)). UvrA has two ATPase modules: one is divided into an ATP-binding domain I and a signature domain I, the other is divided into an ATP-binding domain II and a signature domain II. UvrA contains three zinc ions. It has been reported that ttUvrA and ttUvrB can recognize bulky adducts, such as tetramethylrhodamine and tetramethylrhodamine ethyl ester, and (6-4) pyrimidine dimer [113, 131]. Furthermore, it has been shown that ttUvrA can interact with the ATL protein, but the physiological significance of this interaction remains unclear [37].

The overall structure of TRCF was reported in 2006 [122]. Domains 1a, 2, and 1b comprise a UvrB homology

module, which interacts with UvrA (Figure 5(c)). Domains 5 and 6 comprise a DNA translocation module. Domain 4 is an RNA polymerase interaction domain (RID). The RID and the DNA translocation modules are linked by a long helix called the relay helix. The functions of domains 3 and 7 are unclear. The *mfd* gene from *T. thermophilus* (the gene product name is ttTRCF; TTHA0889) is listed in the genome annotation but no formal report has yet been published.

The 3D structures of these proteins show that they all contain several enzymatic domains. The NER pathways involve multi-step processes; therefore, almost all the proteins can interact in order to advance the process to the next repair step. TRCF has a UvrA-binding domain whose amino acid sequence and 3D structure are similar to those of the UvrB domain 2 [122]. Therefore, it might be expected that TRCF would bind to UvrA in the same manner as UvrB. The mechanisms of interaction of TRCF with UvrA and other proteins, such as the ATL protein, are not yet well defined.

## 5. Mismatch Repair

The DNA mismatch repair (MMR) machinery recognizes and corrects mismatched or unpaired bases that principally result from errors by DNA polymerases during DNA replication. MMR increases the accuracy of DNA replication by at least 3 orders of magnitude [132]. Mutations in the genes involved in MMR are associated with increased predisposition to human hereditary nonpolyposis colorectal cancers [133]. Postreplication MMR is achieved by removal of a relatively long tract of mismatch-containing oligonucleotides, a process called long-patch MMR. Here, we refer to long-patch MMR simply as MMR.

**5.1. Methyl-Directed MMR in *E. coli*.** In *E. coli*, the first steps in MMR are performed by the MutHLS system, which consists of three proteins, MutS, MutL, and MutH (Figure 6(a)) [134, 135]. In this system, a MutS homodimer recognizes and attaches to a mismatched base in the dsDNA [136–138]. A MutL homodimer then interacts with and stabilizes the MutS-mismatch complex and activates a MutH restriction endonuclease [139]. The MMR system needs to discriminate the newly synthesized DNA strand in order to remove the incorrect base of the mismatched pair. However the mismatch itself contains no signal for such discrimination. The *E. coli* MMR system utilizes the absence of methylation at a restriction site to direct repair to the newly synthesized strand [135]. Immediately after replication, the restriction sites in the newly synthesized strand remain unmethylated. At the site of a mismatch, the MutH endonuclease nicks the unmethylated strand at a hemimethylated GATC site to introduce an entry point for the excision reaction. The error-containing region is excised by a DNA helicase [140] and an ssDNA-specific exonuclease [141–143]. The excised tract of oligonucleotides is then replaced by DNA synthesis directed by DNA polymerase III and a ligase. Since the absence or presence of methylation provides the signal for strand discrimination, *E. coli* MMR is termed methyl-directed MMR [135]. Homologues of *E. coli* MutS and MutL

are found in almost all organisms; however, no homologue of *E. coli* MutH has been identified in the majority of eukaryotes or most bacteria.

**5.2. Nick-Directed MMR in Eukaryotes.** In eukaryotes, it has been demonstrated that strand discontinuity serves as a signal for directing MMR to a particular strand of the mismatched duplex *in vitro*. In living cells, newly synthesized strands contain discontinuities as 3'-ends or termini of Okazaki fragments. Since the presence or absence of a nick can be a strand discrimination signal, eukaryotic MMR is termed nick-directed MMR. It has also been reported that the shorter path from a nick to the mismatch is removed by the excision reaction, indicating that 5'- and 3'-nick-directed MMR are distinct [144–147]. Surprisingly, both 5'- and 3'-nick-directed strand removal requires the 5'-3' exonuclease activity of exonuclease 1 (EXO1) [148, 149]. This apparently contradictory requirement for 5'-3' exonuclease activity in 3'-nick-directed MMR was explained by the breakthrough discovery that the human MutL homologue MutL $\alpha$  (MLH1-PMS2 heterodimer) and the yeast homologue MutL $\alpha$  (MLH1-PMS1 heterodimer) harbor latent endonuclease activity, which nicks the discontinuous strand of the mismatched duplex [147, 150, 151]. In eukaryotic 5'-nick-directed and 3'-nick-directed MMR, MutL $\alpha$  incises the 3'- and 5'- sides of a mismatch, respectively, to yield a DNA segment spanning the mismatch. Then, the 5'-3' exonuclease activity of EXO1 removes the segment.

**5.3. MMR in *mutH*-Less Bacteria.** The DQHA(X)<sub>2</sub>E(X)<sub>4</sub> motif in the C-terminal domain of the PMS2 subunit of human MutL $\alpha$  comprises the metal-binding site, which is essential for endonuclease activity [150]. In *mutH*-less bacteria, the C-terminal domains of MutL homologues contain this metal-binding motif and exhibit endonuclease activity [150, 152]; moreover, in *T. thermophilus*, *Aquifex aeolicus*, and *Neisseria gonorrhoeae*, this activity is abolished by mutations in the motif [152–154]. The endonuclease activity of *T. thermophilus* MutL has been shown to be essential for *in vivo* DNA repair activity [152]. Thus, the molecular mechanism of MMR in *mutH*-less bacteria appears to resemble that of eukaryotic MMR (Figure 6(b)).

MutS homologues from *mutH*-less bacteria show fundamentally similar properties to *E. coli* MutS and eukaryotic MutS $\alpha$ . First, *T. thermophilus* MutS exhibits a high affinity for mismatched heteroduplexes [138, 155], and the mismatch-MutS complex seems to be stabilized by MutL [152]. Second, similar ATP binding-dependent conformational changes have been observed in MutS homologues from *T. thermophilus* [156], *E. coli* [157, 158], and humans [159, 160]. Third, the crystal structures of *Thermus aquaticus* MutS [137], *E. coli* MutS [136, 161], and human MutS $\alpha$  [162] exhibit a common mismatch recognition mode in which the mismatched base is recognized by the intercalated phenylalanine residue from one of the two subunits. Finally, *T. thermophilus mutS* gene complements the hypermutability of the *E. coli mutS*-deleted null mutant [138]. These results indicate that interspecies variations in MMR machinery may

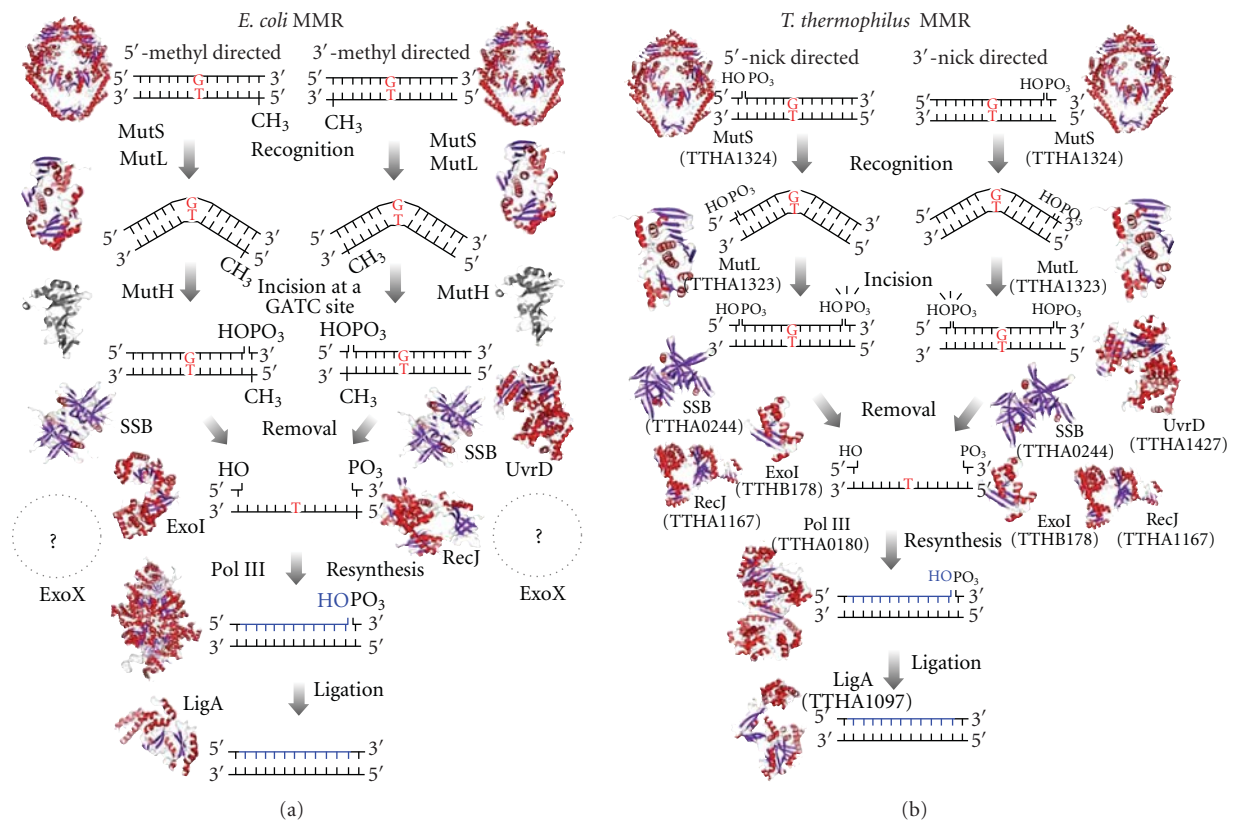


FIGURE 6: A schematic representation of models for MMR pathways in *E. coli* and *mutH*-less bacteria. (a) 5'- and 3'-methyl-directed MMR in *E. coli*. DNA mismatches principally result from misincorporation of bases during DNA replication. The MutS (PDB ID: 1E3M)/MutL (PDB ID: 1NHJ) complex recognizes a mismatch and activates the MutH endonuclease (PDB ID: 1AZO). MutH nicks the unmethylated strand of the duplex to introduce an entry point for the excision reaction. In 3'-methyl-directed MMR, one of the 5'-3' exonucleases (RecJ and exonuclease VII (ExoVII)) removes the error-containing DNA strand in cooperation with UvrD helicase (PDB ID: 2IS4) and single-stranded DNA-binding protein (SSB; PDB ID: 1EYG). By contrast, one of the 3'-5' exonucleases (exonuclease I (ExoI; PDB ID: 1FXX) and exonuclease X (ExoX)) is responsible for the 3'-5' excision reaction. DNA polymerase III (PDB ID: 2HNN) and DNA ligase (PDB ID: 2OWO) synthesize a new strand to complete the repair. (b) A predicted model for 5'- and 3'-nick-directed MMR in *T. thermophilus*. After recognition of a mismatch by MutS (TTHA1324), MutL (TTHA1323) incises the discontinuous strand of the mismatched duplex to direct the excision reaction to the newly synthesized strand. The error-containing DNA segment is excised by UvrD helicase (TTHA1427), SSB (TTHA0244), and an exonuclease (either RecJ (TTHA1167; PDB ID: 2ZZR) or ExoI (TTHB178)) followed by the resynthesis of a new strand by DNA polymerase III (TTHA0180) and DNA ligase (TTHA1097). The modeled structures of *T. thermophilus* MutS, MutL (amino acid residues 1–316), ExoI, DNA polymerase III  $\alpha$  subunit, DNA ligase, and *E. coli* RecJ were modeled using SWISS-MODEL. The template structures used for model building were *E. coli* MutS, the N-terminal domain of MutL, ExoI, UvrD, DNA polymerase III  $\alpha$  subunit, DNA ligase, and *T. thermophilus* RecJ.

principally derive from differences in the functions of the MutL homologues.

The biochemical properties of MutL endonucleases have been studied using MutL homologues from *mutH*-less thermophilic bacteria such as *T. thermophilus* and *A. aeolicus*. The endonuclease activity of *T. thermophilus* MutL is suppressed by the binding of ATP [152]. MutL homologues belong to the GHKL ATPase superfamily that also includes homologues of DNA gyrase, Hsp90, and histidine kinase [163]. GHKL superfamily proteins undergo large conformational changes upon ATP binding and/or hydrolysis. Such conformational changes are expected to affect the molecular functions of the MutL homologues [164, 165]. The endonuclease activities of MutL homologues exhibit no sequence or structure specificity [150, 152]; hence, it is thought that living cells

may have mechanisms for regulating these activities. Cells may employ ATP binding-induced suppression of MutL endonuclease activity in order to ensure mismatch-specific incision. It has also been suggested that the ATP binding form of *T. thermophilus* MutL preferably interacts with a MutS-mismatch complex [152]. Since the ATPase activity of MutL is activated by interaction with MutS, it could be speculated that the ATP binding-dependent suppression of the endonuclease activity of MutL is canceled by the interaction with a MutS-mismatch complex. Recently, it was reported that the endonuclease activity of *A. aeolicus* MutL in response to ATP depends on the concentration of the protein and that when *A. aeolicus* MutL is present at relatively high concentrations activity is stimulated, not suppressed, by ATP [154]. This result indicates that ATP is required not

only for suppression but also for active enhancement of the endonuclease activity of MutL.

**5.4. Strand Discrimination in Nick-Directed MMR.** As mentioned above, a pre-existing strand break serves as a signal to direct the excision reaction in eukaryotic nick-directed MMR [146, 150]. Since daughter strands always contain 3'- or 5'-termini during replication, these ends may act as strand discrimination signals *in vivo*. In eukaryotic nick-directed MMR, MutL $\alpha$  is responsible for strand discrimination by incising the discontinuous strand [150]. Interestingly, MutL $\alpha$  has been found to incise the discontinuous strand at a distal site from the pre-existing strand break. It remains to be elucidated how MutL $\alpha$  discriminates the discontinuous strand of the duplex at a site far removed from the strand discrimination signal. One possible explanation may lie in the association of MutS and MutL homologues with replication machinery. MSH6 and MSH3 subunits contain a PCNA-interacting motif [166], and this interaction between MutS $\alpha$  and PCNA is now well characterized [167]. Furthermore, both PCNA and replication factor C (RFC) are required for stimulation of the latent endonuclease activity of MutL $\alpha$  in eukaryotic MMR [150]. These results suggest that MutS $\alpha$  (or MutS $\beta$ ) and MutL $\alpha$  are loaded onto the substrate DNA through an interaction with PCNA in the presence of RFC to produce binding to the newly synthesized strand in the catalytic site of the MutL $\alpha$  endonuclease domain [168–170]. In *mutH*-less bacteria, it has been also demonstrated that mismatch-provoked localization of MutS and MutL is controlled through an association with  $\beta$ -clamp, a bacterial counterpart of eukaryotic PCNA [171]. These interactions may also be responsible for strand discrimination in bacterial nick-directed MMR.

**5.5. Downstream Events in Nick-Directed MMR.** EXO1 is responsible for the excision reaction in eukaryotic MMR *in vitro*. To date, EXO1 is the only ssDNA-specific exonuclease that has been reported to be involved in the reaction [150, 172]. In addition, no MMR-related eukaryotic DNA helicase has yet been identified. The exonuclease activity of eukaryotic EXO1 is enhanced by a direct interaction with MutS $\alpha$  in a mismatch- and ATP-dependent manner [173]. MutS $\alpha$  is known to form a sliding clamp that diffuses along the DNA after mismatch recognition. The diffusion of MutS $\alpha$  from the mismatch may be required for the activation of EXO1 at the 5'-terminus of the error-containing DNA segments. In contrast to eukaryotes, the MutL of *A. aeolicus* stimulates DNA helicase activity in UvrD, an enzyme that shows high conservation of amino acid sequence among bacteria [174]. Furthermore, in *T. thermophilus*, genetic analyses have indicated that 5'-3' exonuclease RecJ and 3'-5' exonuclease ExoI are involved in parallel pathways of MMR [175]. It is possible that *mutH*-less bacteria employ the cooperative function of multiple exonucleases and helicases to remove error-containing DNA segments.

Termination of the EXO1-dependent excision reaction in eukaryotic 3'-nick-directed and MutL $\alpha$ -dependent 5'-nick-directed MMR is expected to be determined by pre-existing

and newly introduced 3'-termini, respectively. In *mutH*-less bacteria, the mechanism for termination of the excision-reaction remains unknown. Since not only 5'-3' exonuclease but also 3'-5' exonuclease can be involved in the repair [175], termination of an excision reaction in 5'- and 3'-nick-directed MMR might be achieved by the 3'- and 5'-termini that are introduced by MutL.

Further biochemical and structural studies on exonucleases are required to achieve a deeper understanding of the excision reaction. Recently, the crystal structure of intact RecJ, a 5'-3' exonuclease, from *T. thermophilus* was reported [176]. The entire structure of RecJ consists of four domains that form a ring-like structure with the catalytic site in the center of the ring. One of these four domains contains an oligonucleotides/oligosaccharide-binding fold that is known as a nucleic acid-binding fold. Knowledge of these structural features increases our understanding of the molecular basis for the high processivity and specificity of this enzyme. Furthermore, two Mn<sup>2+</sup> ions in the catalytic site suggest that RecJ utilizes a two-metal ion mechanism [177] for the exonuclease activity. The understanding of a 3'-5' exonuclease in MMR has been also enhanced by the ongoing biochemical studies on *T. thermophilus* ExoI [175]. The study revealed that ExoI has extremely high  $K_M$  value compared with other exonucleases. The interactions with other MMR proteins might stimulate the DNA-binding activity of ExoI. Especially, it would be intriguing to examine the interaction between ExoI and MutS.

## 6. Recombination Repair

DNA double-strand breaks (DSBs) are the most crucial lesions in DNA for inducing loss of genetic information and chromosomal instabilities. DSBs can be caused by ionizing radiation, ROS, nuclease dysfunction, or replication fork collapse [178]. Defects in the repair of DSBs lead to cancer or other severe diseases [179–181]. There are two different pathways for repair of DSBs, homologous recombination (HR) and nonhomologous end-joining [178]. HR is the accurate pathway and makes use of undamaged homologous DNA as a template for repair. Nonhomologous end-joining directly ligates two DSB ends together, and although it is efficient, it is prone to loss of genetic information at the ligation sites. In most bacteria, the HR pathway is thought to be the major route for repair of DSBs [182–184].

Recombination repair of DSBs consists of various steps: end resection, strand invasion, DNA repair synthesis, branch migration, and Holliday junction (HJ) resolution (Figure 7). Although the repair-related components and details of each step show variations among organisms, these steps are conserved in all organisms, and there are many evolutionarily conserved functional homologues involved in recombination repair [182, 184]. The first step of recombination repair, end resection, is initiated by a 5' to 3' degradation of DSB ends to generate 3'-ssDNA tails. Next, mediator proteins bind to the 3'-tailed ssDNA and load the recombinase to promote formation of a nucleoprotein filament. The recombinase searches for a homologous DNA sequence

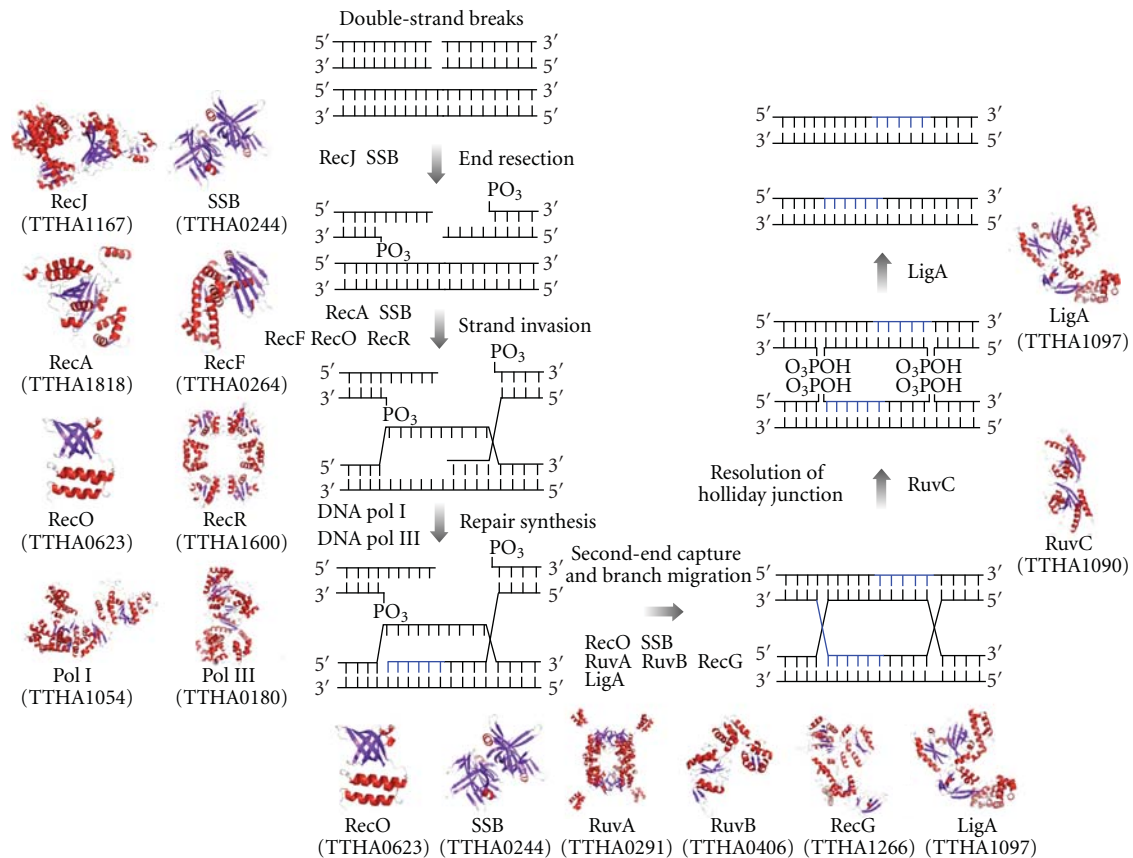


FIGURE 7: A schematic pathway of recombination repair and structures of the proteins involved in *T. thermophilus*. Recombination repair of DSBs is initiated by an end resection step in which DSB ends are processed by the concerted action of RecJ nuclease (TTHA1167; PDB ID: 2ZXR) and SSB (TTHA0244; PDB ID: 2CWA) to form 3'-ssDNA tails. After end resection, the SSB-ssDNA complex is disassembled and RecA recombinase (TTHA1818) is loaded onto ssDNA by "mediators", RecF (TTHA0264), RecO (TTHA0623), and RecR (TTHA1600), to promote strand invasion. DNA repair synthesis is primed by PolI (TTHA1054) and PolIII (TTHA0180) from the invaded strand of the D-loop structure. Alternatively, second-end capture is mediated by RecO and SSB and branch migration mediated by the RuvA-RuvB complex (TTHA0291-TTHA0406; PDB ID: 1IXR) and RecG (TTHA1266) to yield HJs. HJs are cleaved by RuvC resolvase (TTHA1090) and the nicks sealed by LigA (TTHA1097). Newly synthesized DNA is colored in blue. The model structures of *T. thermophilus* RecA, RecF, RecO, RecR, PolI, PolIII  $\alpha$  subunit, RecG, RuvC, and LigA were generated using SWISS-MODEL. The models were based on the structures of *Mycobacterium smegmatis* RecA (PDB ID: 2OE2), *D. radiodurans* RecF (PDB ID: 2O5V), RecO (PDB ID: 1U5K), RecR (PDB ID: 1VDD), *E. coli* PolI (PDB ID: 1TAU), PolIII  $\alpha$  subunit (PDB ID: 2HNH), RuvC (PDB ID: 1HJR), LigA (PDB ID: 2OWO), and *Thermotoga maritima* RecG (PDB ID: 1GM5).

and catalyzes strand invasion to yield a D-loop structure. After strand invasion, DNA synthesis occurs using the homologous DNA as the template, and the intermediates are processed through a branch migration reaction to form HJs, stable four-stranded DNA structures. Finally, HJs are endonucleolytically resolved into linear duplexes, and the nicks at cleavage site are sealed by DNA ligase to complete the repair. HR significantly contributes to retention of genome integrity; however, this mechanism is also utilized for the rearrangement of genome, such as incorporation of foreign DNAs or intrachromosomal gene conversion [185, 186]. There are various anti-recombination mechanisms to suppress excessive recombination that might cause genomic instabilities [187, 188]. These sub-pathways interact with each other to regulate the HR system.

**6.1. End Resection and Loading of Recombinase.** Recombination repair is initiated by an end resection step that processes DSB ends to generate 3'-ssDNA tails. In mammals, various nucleases and helicases have been implicated in this step, such as the MRN complex, CTIP, EXO1, DNA2, and RECQ paralogues [189]. By contrast, most bacteria have two major sub-pathways, the RecF pathway and the RecBCD/AddAB pathway [183, 190, 191]. The RecF pathway is highly conserved in many bacteria and is similar to the eukaryotic end resection pathway whereas the RecBCD/AddAB pathway differs from that of eukaryotes and also shows diversity in bacteria. In the RecF pathway, RecJ nuclease, RecQ helicase, and SSB act in concert in the processing of DSB ends. After DNA unwinding by RecQ helicase and 5' to 3' exonucleolytic degradation by RecJ nuclease, the generated 3'-ssDNA tails

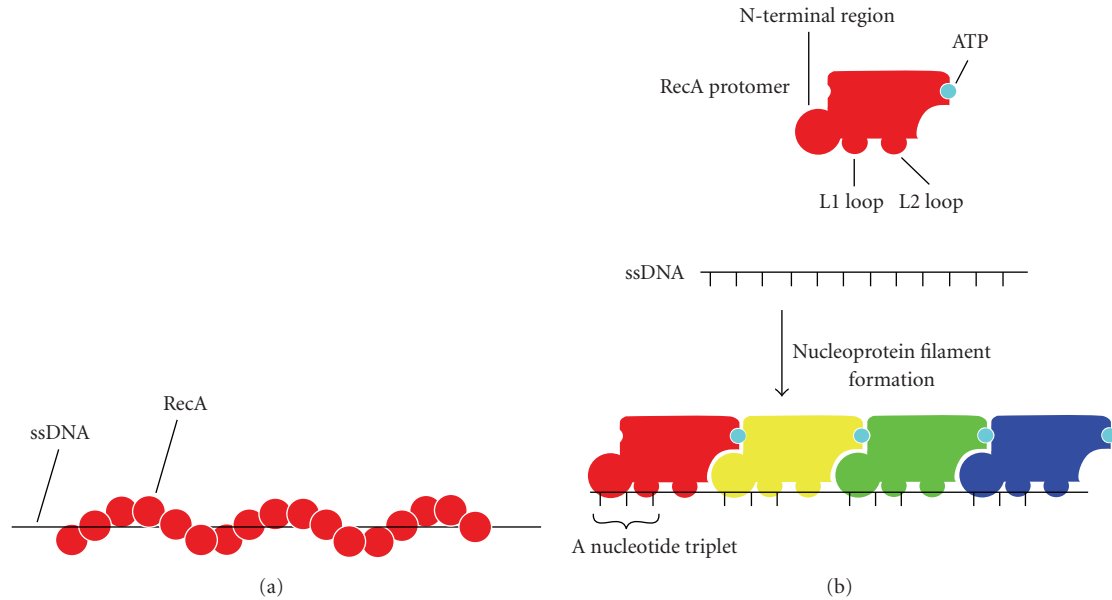


FIGURE 8: A schematic illustration of RecA-ssDNA interaction in the nucleoprotein filament. (a) A schematic representation of a RecA-ssDNA nucleoprotein filament. The filament comprises a helical structure. RecA molecules are shown as red spheres and the ssDNA as a black line. (b) A schematic model of RecA-ssDNA interaction. The RecA protomer has the L1 and L2 loops and the N-terminal region to make contact with the ssDNA. The bound ssDNA comprises a nucleotide triplet with a nearly normal B-form distance between bases followed by a long internucleotide stretch before the next triplet. The ATP binds to RecA-RecA interfaces. The schematic model was prepared from the crystal structure of RecA-ssDNA complex (PDB ID: 3CMW).

are coated and stabilized with SSB [192]. Interestingly, there is no RecQ homologue in *T. thermophilus* HB8 [193]. However, a recent *in vitro* reconstitution study of the *E. coli* RecF pathway showed that RecJ nuclease degrades dsDNA exonucleolytically in the absence of RecQ helicase [190]. Another study also showed that *Haemophilus influenzae* SSB directly interacts with RecJ nuclease and stimulates exonuclease activity [194]. Based on these results, it could be speculated that in *T. thermophilus* HB8, RecJ nuclease and SSB might synergistically perform the end resection step without involvement of a helicase. Recently, the crystal structures of *T. thermophilus* RecJ and SSB were solved [176]. By combining these structural data with biochemical analyses, it should soon be feasible to elucidate the molecular mechanism of the end resection step.

In the RecF pathway, after generation of 3'-ssDNA tails, recombination mediators, RecFOR or RecOR, disassemble the SSB-ssDNA complex and load RecA recombinase onto ssDNA to form nucleoprotein filaments [190, 195]. Structural and biochemical analyses of *T. thermophilus* RecF, RecO, and RecR proteins showed that RecR forms a tetrameric ring-like structure and acts as a DNA clamp and also binds to RecF and RecO; on the other hand, RecO can also bind to RecR, SSB, and ssDNA [196–198]. These studies found that SSB is displaced from ssDNA by RecO and that RecA loading is mediated by RecR [198]. Based on these results, there appear to be two distinct ways for SSB displacement and RecA loading [190]. The RecFOR complex binds at the ssDNA-dsDNA junction on the resected DNA and loads RecA onto ssDNA in a 5' to 3' direction. The RecOR complex binds to SSB-ssDNA complex and promotes the exchange of SSB

by RecA. These processes are very similar to the eukaryotic recombination repair pathway mediated by RAD52, RAD54, BRCA2, and RAD51 paralogues [199–202]. Recombinase loading by “mediators” is thought to be a common system of recombination repair in all three kingdoms of life.

**6.2. Strand Invasion by Recombinase.** The DNA strand exchange between homologous segments of chromosomes is catalyzed by the RecA-family recombinases, which include RecA in bacteria, RAD51 in eukaryotes, and RadA in archaea [203]. The processes catalyzed by these recombinases have been studied in detail [204–206]. In bacteria, RecA binds to ssDNA, forming helical nucleoprotein filament (Figure 8(a)). Contact between the RecA-coated ssDNA and dsDNA allows ssDNA to search sequence homology. Strand exchange is initiated by local denaturation of dsDNA in a region of homology. The invading strand forms a paranemic joint, which is an unstable intermediate. When the free end of the strand invades, the paranemic joint is converted into a plectonemic joint, in which the two strands are intertwined. Then heteroduplex formation is extended by branch migration.

The crystal structure of RecA filament determined in 1992 [207] revealed six subunits in each helical turn, but this structure contained no DNA. In 2008, Chen et al. determined the structures of both RecA complexed with ssDNA and with dsDNA [208], which are the substrate and product forms of DNA strand exchange, respectively. The RecA-ssDNA filament is different from the RecA filament primarily in the orientation of the subunit relative to the filament axis. The bound ssDNA makes contact with the

L1 and L2 loops, which had been suggested to be DNA binding sites and the N-terminal region (Figure 8(b)). It had been previously assumed that in the nucleoprotein filament ssDNA is uniformly stretched by about 1.5-fold [209]. However, unexpectedly, the DNA comprises a nucleotide triplet (three-nucleotide segment) with a nearly normal B-form distance between bases followed by a long untwisted internucleotide stretch before the next triplet. In addition, ATP binds to RecA-RecA interfaces, which can couple RecA-ATP interaction to RecA-DNA interaction.

**6.3. Postsynaptic Phase.** After strand invasion, HJs are formed through DNA repair synthesis, second-end capture, and branch migration during the postsynaptic phase. In most organisms, a range of DNA polymerases deal with the various DNA processes, and several of these DNA polymerases are involved in recombination-associated DNA repair synthesis [210]. It has been shown that the translesion synthesis (TLS) polymerase, Pol $\eta$ , and replicative polymerase, Pol $\delta$ , are involved in mammalian recombination-associated DNA synthesis [211–214]. In addition, a recent genetic study suggested the possible involvement of human Pol $\nu$ , prokaryotic PolI-like enzyme, in HR [215]. However, it is still unclear whether other DNA polymerases can synthesize the DNA strand during recombination. Interestingly, bacterial TLS polymerases, PolII, PolIV, and PolV, are also able to synthesize the DNA strand in recombination processes as well as PolI and PolIII in *E. coli*; however, the details of the relationship between TLS and HR remain to be elucidated [216]. The *Deinococcus-Thermus* group of bacteria has only two processive DNA polymerases, PolI and PolIII, and, therefore, it should be relatively straightforward to analyze the involvement of DNA polymerases in recombination-associated DNA synthesis [217, 218]. A recent study on genome repair after ionizing radiation in *Deinococcus radiodurans* showed that PolI and PolIII had distinct roles in the extensive synthesis-dependent strand annealing repair pathway [219]; therefore, it might be expected that in *T. thermophilus*, PolI and PolIII will also act in concert in recombination-associated DNA synthesis.

Second-end capture and branch migration also occur at the same time as DNA repair synthesis in the postsynaptic phase. In eukaryotes, second-end capture appears to be mediated by RAD52 and RPA, whereas their functional homologues in bacteria are RecO and SSB, respectively [220–222]. Interestingly, it has been shown that *E. coli* RecO cannot form joint molecules with the *S. cerevisiae* RPA-ssDNA complex nor can *S. cerevisiae* RAD52 promote second-end capture with either the human RPA-ssDNA complex or the *E. coli* SSB-ssDNA complex [222]. These results indicate that the second-end capture event can be performed in a species-specific manner. Various DNA translocases are involved in branch migration. There is evidence that RAD54 and RECQ paralogues process the joint molecules to generate HJs in eukaryotes. By contrast, RuvAB, RecG and RadA/Sms promote branch migration in bacteria [201, 223–225]. To date, there is no satisfactory explanation as to why a single organism might redundantly possess multiple branch migration activities. In bacteria, RuvAB are believed to be

the main branch migration proteins based on their genetic properties [223, 226]. Currently, the crystal structure of the RuvAB-HJ complex is not available. However, various crystal structures involving *T. thermophilus* RuvA and RuvB proteins have been solved and their biochemical properties determined [227–232]. In addition, an atomic model of the RuvAB-HJ complex has been proposed based on data from electron microscopic analyses [229, 233]. These structural and functional analyses of RuvAB provide insights into its molecular properties with regard to branch migration. Two RuvA tetramers sandwich an HJ forming a planar conformation while two RuvB hexameric rings are bound to the arms of the junction symmetrically via RuvA and promote branch migration using energy from ATP hydrolysis [224]. Furthermore, by combining structural and biochemical data on RuvC resolvase, it is possible to suggest a model for HJ resolution that involves the formation of a RuvABC resolvosome [224, 234–237].

Recombination repair is completed by HJ resolution and sealing of its cleavage sites. In mammals, members of a structure-specific endonuclease family, including GEN1, SLX1, MUS81-EME1, and ERCC4-ERCC1, are involved in the resolution of HJs and recombination intermediates [238]. Recent work showed that GEN1 can act as an HJ resolvase. Other studies have suggested that the SLX4 protein can form a complex with SLX1, MUS81-EME1, or ERCC4-ERCC1 and control their activities [239–243]. It has been shown that the SLX1-SLX4 complex can resolve HJs symmetrically. In bacteria, RuvC and RusA have HJ resolvase activity. RuvC forms a dimeric structure and cleaves HJs symmetrically in a sequence-specific manner [234, 244]. Biochemical analyses of RuvC in the presence of RuvAB suggest that RuvC forms a complex with RuvAB and that the HJ resolution event is coupled with the branch migration reaction [235, 236]. In *E. coli*, there is another resolvase, RusA, which has cleaved HJs symmetrically at specific sites [245, 246]. It has also been suggested that topoisomerase III can resolve HJs in *E. coli* as an alternative to the RuvABC pathway [247]. *T. thermophilus* does not have either RusA or topoisomerase III [217]. Thus, this organism will be a suitable model for analyzing this step of HJ resolution because of its simple and minimal systems.

**6.4. Anti-Recombination.** Since excessive recombination events lead to the alteration of the genetic information, various anti-recombination mechanisms are employed by organisms to regulate the frequency of recombination [188]. For example, the MMR system is present in a wide range of organisms and serves particularly to prevent homeologous recombination [187]. In bacteria, RecX acts as an anti-recombinase that inhibits RecA recombinase in both direct and indirect manners [248]. Direct interaction with RecX inhibits the recombinase activity of RecA and destabilizes the nucleoprotein filament [249, 250]. RecX also suppresses *recA* induction at the transcription level [248]. The UvrD helicase is suspected to be an anti-recombinase because of its activity to disassemble the RecA nucleoprotein filament *in vitro* [251, 252].

Recently, a novel anti-recombination mechanism was identified in *Helicobacter pylori* and *T. thermophilus*. It was found that disruption of *mutS2*, a bacterial paralogue of the MMR gene *mutS*, significantly increased the frequency of recombination events, indicating that *mutS2* had an anti-recombination function [253, 254]. It has also been shown that MutS2 is not involved in MMR, that is, MutS2 prevents recombination in an MMR-independent manner. Detailed biochemical investigation showed that *T. thermophilus* MutS2 possesses an endonuclease activity that preferably incises the D-loop structure, the primary intermediate in HR [253, 255–257]. MutS2 might suppress HR through the resolution of early intermediates.

## Acknowledgments

This work was supported in part by Grant-in-Aid for Scientific Research 20570131 (to R. Masui), 19770083 (to N. Nakagawa) and 20870042 (to K. Fukui) from the Ministry of Education, Science, Sports and Culture of Japan. R. Morita and S. Nakane are the recipients of a Research Fellowship of the Japan Society for the Promotion of Science for Young Scientists (no. 21-1019 and 22-37, resp.).

## References

- [1] O. D. Schärer, "Chemistry and biology of DNA repair," *Angewandte Chemie*, vol. 42, no. 26, pp. 2946–2974, 2003.
- [2] F. Altieri, C. Grillo, M. Maceroni, and S. Chichiarrelli, "DNA damage and repair: from molecular mechanisms to health implications," *Antioxidants and Redox Signaling*, vol. 10, no. 5, pp. 891–937, 2008.
- [3] E. C. Friedberg, G. C. Walker, and W. Siede, *DNA Repair and Mutagenesis*, ASM Press, Washington, DC, USA, 2006.
- [4] T. Oshima and K. Imahori, "Description of *Thermus thermophilus* (Yoshida and Oshima) comb. nov., a nonsporulating thermophilic bacterium from a Japanese thermal spa," *International Journal of Systematic Bacteriology*, vol. 24, no. 1, pp. 102–112, 1974.
- [5] H. Iino, H. Naitow, Y. Nakamura et al., "Crystallization screening test for the whole-cell project on *Thermus thermophilus* HB8," *Acta Crystallographica Section F*, vol. 64, no. 6, pp. 487–491, 2008.
- [6] S. Yokoyama, H. Hirota, T. Kigawa et al., "Structural genomics projects in Japan," *Nature Structural Biology*, vol. 7, supplement, pp. 943–945, 2000.
- [7] G. Payne, P. F. Heelis, B. R. Rohrs, and A. Sancar, "The active form of *Escherichia coli* DNA photolyase contains a fully reduced flavin and not a flavin radical, both in vivo and in vitro," *Biochemistry*, vol. 26, no. 22, pp. 7121–7127, 1987.
- [8] A. Sancar and G. B. Sancar, "DNA repair enzymes," *Annual Review of Biochemistry*, vol. 57, pp. 29–67, 1988.
- [9] C. Aubert, M. H. Vos, P. Mathis, A. P. M. Eker, and K. Brettel, "Intraprotein radical transfer during photoactivation of DNA photolyase," *Nature*, vol. 405, no. 6786, pp. 586–590, 2000.
- [10] R. Kato, K. Hasegawa, Y. Hidaka, S. Kuramitsu, and T. Hoshino, "Characterization of a thermostable DNA photolyase from an extremely thermophilic bacterium, *Thermus thermophilus* HB27," *Journal of Bacteriology*, vol. 179, no. 20, pp. 6499–6503, 1997.
- [11] H.-W. Park, S.-T. Kim, A. Sancar, and J. Deisenhofer, "Crystal structure of DNA photolyase from *Escherichia coli*," *Science*, vol. 268, no. 5219, pp. 1866–1872, 1995.
- [12] T. Tamada, K. Kitadokoro, Y. Higuchi et al., "Crystal structure of DNA photolyase from *Anacystis nidulans*," *Nature Structural Biology*, vol. 4, no. 11, pp. 887–891, 1997.
- [13] H. Komori, R. Masui, S. Kuramitsu et al., "Crystal structure of thermostable DNA photolyase: pyrimidine-dimer recognition mechanism," *Proceedings of the National Academy of Sciences of the United States of America*, vol. 98, no. 24, pp. 13560–13565, 2001.
- [14] T. Torizawa, T. Ueda, S. Kuramitsu et al., "Investigation of the cyclobutane pyrimidine dimer (CPD) photolyase DNA recognition mechanism by NMR analyses," *Journal of Biological Chemistry*, vol. 279, no. 31, pp. 32950–32956, 2004.
- [15] A. Mees, T. Klar, P. Gnau et al., "Crystal structure of a photolyase bound to a CPD-like DNA lesion after in situ repair," *Science*, vol. 306, no. 5702, pp. 1789–1793, 2004.
- [16] T. Ueda, A. Kato, Y. Ogawa et al., "NMR study of repair mechanism of DNA photolyase by FAD-induced paramagnetic relaxation enhancement," *Journal of Biological Chemistry*, vol. 279, no. 50, pp. 52574–52579, 2004.
- [17] T. Ueda, A. Kato, S. Kuramitsu, H. Terasawa, and I. Shimada, "Identification and characterization of a second chromophore of DNA photolyase from *Thermus thermophilus* HB27," *Journal of Biological Chemistry*, vol. 280, no. 43, pp. 36237–36243, 2005.
- [18] T. Klar, G. Kaiser, U. Hennecke, T. Carell, A. Batschauer, and L.-O. Essen, "Natural and non-natural antenna chromophores in the DNA photolyase from *Thermus thermophilus*," *ChemBioChem*, vol. 7, no. 11, pp. 1798–1806, 2006.
- [19] F. Kiefer, K. Arnold, M. Künzli, L. Bordoli, and T. Schwede, "The SWISS-MODEL repository and associated resources," *Nucleic Acids Research*, vol. 37, supplement 1, pp. D387–D392, 2009.
- [20] T. Schwede, J. Kopp, N. Guex, and M. C. Peitsch, "SWISS-MODEL: an automated protein homology-modeling server," *Nucleic Acids Research*, vol. 31, no. 13, pp. 3381–3385, 2003.
- [21] G. T. J. Van Der Horst, M. Muijtjens, K. Kobayashi et al., "Mammalian Cry1 and Cry2 are essential for maintenance of circadian rhythms," *Nature*, vol. 398, no. 6728, pp. 627–630, 1999.
- [22] M. Müller and T. Carell, "Structural biology of DNA photolyases and cryptochromes," *Current Opinion in Structural Biology*, vol. 19, no. 3, pp. 277–285, 2009.
- [23] E. L. Loechler, C. L. Green, and J. M. Essigmann, "In vivo mutagenesis by O<sup>6</sup>-methylguanine built into a unique site in a viral genome," *Proceedings of the National Academy of Sciences of the United States of America*, vol. 81, no. 20, pp. 6271–6275, 1984.
- [24] A. Loveless, "Possible relevance of O-6 alkylation of deoxyguanosine to the mutagenicity and carcinogenicity of nitrosamines and nitrosamides," *Nature*, vol. 223, no. 5202, pp. 206–207, 1969.
- [25] E. T. Snow, R. S. Foote, and S. Mitra, "Base-pairing properties of O<sup>6</sup>-methylguanine in template DNA during *in vitro* DNA replication," *Journal of Biological Chemistry*, vol. 259, no. 13, pp. 8095–8100, 1984.
- [26] T. Lindahl, B. Demple, and P. Robins, "Suicide inactivation of the *E. coli* O<sup>6</sup>-methylguanine-DNA methyltransferase," *EMBO Journal*, vol. 1, no. 11, pp. 1359–1363, 1982.

- [27] M. Olsson and T. Lindahl, "Repair of alkylated DNA in *Escherichia coli*. Methyl group transfer from O<sup>6</sup>-methylguanine to a protein cysteine residue," *Journal of Biological Chemistry*, vol. 255, no. 22, pp. 10569–10571, 1980.
- [28] O. Wiestler, P. Kleihues, and A. E. Pegg, "O<sup>6</sup>-alkylguanine-DNA alkyltransferase activity in human brain and brain tumors," *Carcinogenesis*, vol. 5, no. 1, pp. 121–124, 1984.
- [29] D. Bhattacharyya, R. S. Foote, A. M. Boulden, and S. Mitra, "Physicochemical studies of human O<sup>6</sup>-methylguanine-DNA methyltransferase," *European Journal of Biochemistry*, vol. 193, no. 2, pp. 337–343, 1990.
- [30] A. M. Boulden, R. S. Foote, G. S. Fleming, and S. Mitra, "Purification and some properties of human DNA-O<sup>6</sup>-methylguanine methyltransferase," *Journal of Biosciences*, vol. 11, no. 1–4, pp. 215–224, 1987.
- [31] B. Demple, A. Jacobsson, and M. Olsson, "Repair of alkylated DNA in *Escherichia coli*. Physical properties of O<sup>6</sup>-methylguanine-DNA methyltransferase," *Journal of Biological Chemistry*, vol. 257, no. 22, pp. 13776–13780, 1982.
- [32] D. S. Daniels and J. A. Tainer, "Conserved structural motifs governing the stoichiometric repair of alkylated DNA by O<sup>6</sup>-alkylguanine-DNA alkyltransferase," *Mutation Research*, vol. 460, no. 3–4, pp. 151–163, 2000.
- [33] D. S. Daniels, T. T. Woo, K. X. Luu et al., "DNA binding and nucleotide flipping by the human DNA repair protein AGT," *Nature Structural and Molecular Biology*, vol. 11, no. 8, pp. 714–720, 2004.
- [34] J. M. Aramini, J. L. Tubbs, S. Kanugula et al., "Structural basis of O<sup>6</sup>-alkylguanine recognition by a bacterial alkyltransferase-like DNA repair protein," *Journal of Biological Chemistry*, vol. 285, no. 18, pp. 13736–13741, 2010.
- [35] G. P. Margison, A. Butt, S. J. Pearson et al., "Alkyltransferase-like proteins," *DNA Repair*, vol. 6, no. 8, pp. 1222–1228, 2007.
- [36] G. Mazon, G. Philippin, J. Cadet, D. Gasparutto, and R. P. Fuchs, "The alkyltransferase-like ybaZ gene product enhances nucleotide excision repair of O<sup>6</sup>-alkylguanine adducts in *E. coli*," *DNA Repair*, vol. 8, no. 6, pp. 697–703, 2009.
- [37] R. Morita, N. Nakagawa, S. Kuramitsu, and R. Masui, "An O<sup>6</sup>-methylguanine-DNA methyltransferase-like protein from *Thermus thermophilus* interacts with a nucleotide excision repair protein," *Journal of Biochemistry*, vol. 144, no. 2, pp. 267–277, 2008.
- [38] S. J. Pearson, J. Ferguson, M. Santibanez-Koref, and G. P. Margison, "Inhibition of O<sup>6</sup>-methylguanine-DNA methyltransferase by an alkyltransferase-like protein from *Escherichia coli*," *Nucleic Acids Research*, vol. 33, no. 12, pp. 3837–3844, 2005.
- [39] S. J. Pearson, S. Wharton, A. J. Watson et al., "A novel DNA damage recognition protein in *Schizosaccharomyces pombe*," *Nucleic Acids Research*, vol. 34, no. 8, pp. 2347–2354, 2006.
- [40] J. L. Tubbs, V. Latypov, S. Kanugula et al., "Flipping of alkylated DNA damage bridges base and nucleotide excision repair," *Nature*, vol. 459, no. 7248, pp. 808–813, 2009.
- [41] L. H. Breimer and T. Lindahl, "DNA glycosylase activities for thymine residues damaged by ring saturation, fragmentation, or ring contraction are functions of endonuclease III in *Escherichia coli*," *Journal of Biological Chemistry*, vol. 259, no. 9, pp. 5543–5548, 1984.
- [42] B. Demple, A. Johnson, and D. Fung, "Exonuclease III and endonuclease IV remove 3' blocks from DNA synthesis primers in H<sub>2</sub>O<sub>2</sub>-damaged *Escherichia coli*," *Proceedings of the National Academy of Sciences of the United States of America*, vol. 83, no. 20, pp. 7731–7735, 1986.
- [43] J. D. Levin, A. W. Johnson, and B. Demple, "Homogeneous *Escherichia coli* endonuclease IV. Characterization of an enzyme that recognizes oxidative damage in DNA," *Journal of Biological Chemistry*, vol. 263, no. 17, pp. 8066–8071, 1988.
- [44] T. V. McCarthy and T. Lindahl, "Methyl phosphotriesters in alkylated DNA are repaired by the Ada regulatory protein of *E. coli*," *Nucleic Acids Research*, vol. 13, no. 8, pp. 2683–2698, 1985.
- [45] P. Landini and M. R. Volkert, "Regulatory responses of the adaptive response to alkylation damage: a simple regulon with complex regulatory features," *Journal of Bacteriology*, vol. 182, no. 23, pp. 6543–6549, 2000.
- [46] B. Sedgwick and T. Lindahl, "Recent progress on the Ada response for inducible repair of DNA alkylation damage," *Oncogene*, vol. 21, no. 58, pp. 8886–8894, 2002.
- [47] S. C. Trewick, T. F. Henshaw, R. P. Hausinger, T. Lindahl, and B. Sedgwick, "Oxidative demethylation by *Escherichia coli* AlkB directly reverts DNA base damage," *Nature*, vol. 419, no. 6903, pp. 174–178, 2002.
- [48] M. A. Kurowski, A. S. Bhagwat, G. Papaj, and J. M. Bujnicki, "Phylogenomic identification of five new human homologs of the DNA repair enzyme AlkB," *BMC Genomics*, vol. 4, no. 1, article no. 48, 2003.
- [49] T. Duncan, S. C. Trewick, P. Koivisto, P. A. Bates, T. Lindahl, and B. Sedgwick, "Reversal of DNA alkylation damage by two human dioxygenases," *Proceedings of the National Academy of Sciences of the United States of America*, vol. 99, no. 26, pp. 16660–16665, 2002.
- [50] Y.-F. Wei, K. C. Carter, R.-P. Wang, and B. K. Shell, "Molecular cloning functional analysis of a human cDNA encoding an *Escherichia coli* AlkB homolog, a protein involved in DNA alkylation damage repair," *Nucleic Acids Research*, vol. 24, no. 5, pp. 931–937, 1996.
- [51] P. A. Aas, M. Otterlei, P. Ø. Falnes et al., "Human and bacterial oxidative demethylases repair alkylation damage in both RNA and DNA," *Nature*, vol. 421, no. 6925, pp. 859–863, 2003.
- [52] K. S. Gates, "An overview of chemical processes that damage cellular DNA: spontaneous hydrolysis, alkylation, and reactions with radicals," *Chemical Research in Toxicology*, vol. 22, no. 11, pp. 1747–1760, 2009.
- [53] M. D. Gibbs, R. A. Reeves, D. Mandelman, Q. Mi, J. Lee, and P. L. Bergquist, "Molecular diversity and catalytic activity of *Thermus* DNA polymerases," *Extremophiles*, vol. 13, no. 5, pp. 817–826, 2009.
- [54] K. Makiela-Dzbenka, M. Jaszczur, M. Banach-Orlowska, P. Jonczyk, R. M. Schaaper, and I. J. Fijalkowska, "Role of *Escherichia coli* DNA polymerase I in chromosomal DNA replication fidelity," *Molecular Microbiology*, vol. 74, no. 5, pp. 1114–1127, 2009.
- [55] K. Yoshiyama, K. Higuchi, H. Matsumura, and H. Maki, "Directionality of DNA replication fork movement strongly affects the generation of spontaneous mutations in *Escherichia coli*," *Journal of Molecular Biology*, vol. 307, no. 5, pp. 1195–1206, 2001.
- [56] B. Dalhus, J. K. Laerdahl, P. H. Backe, and M. Bjørås, "DNA base repair—recognition and initiation of catalysis," *FEMS Microbiology Reviews*, vol. 33, no. 6, pp. 1044–1078, 2009.
- [57] D. O. Zharkov, "Base excision DNA repair," *Cellular and Molecular Life Sciences*, vol. 65, no. 10, pp. 1544–1565, 2008.

- [58] T. Visnes, B. Doseth, H. S. Pettersen et al., "Uracil in DNA and its processing by different DNA glycosylases," *Philosophical Transactions of the Royal Society B*, vol. 364, no. 1517, pp. 563–568, 2009.
- [59] J. C. Fromme, A. Banerjee, and G. L. Verdine, "DNA glycosylase recognition and catalysis," *Current Opinion in Structural Biology*, vol. 14, no. 1, pp. 43–49, 2004.
- [60] A. A. Ischenko and M. K. Saparbaev, "Alternative nucleotide incision repair pathway for oxidative DNA damage," *Nature*, vol. 415, no. 6868, pp. 183–187, 2002.
- [61] E. S. Motta, P. T. Souza-Santos, T. R. Cassiano, F. J. S. Dantas, A. Caldeira-De-Araujo, and J. C. P. De Mattos, "Endonuclease IV is the main base excision repair enzyme involved in DNA damage induced by UVA radiation and stannous chloride," *Journal of Biomedicine and Biotechnology*, vol. 2010, Article ID 376218, 9 pages, 2010.
- [62] S. T. Mundle, J. C. Delaney, J. M. Essigmann, and P. R. Strauss, "Enzymatic mechanism of human apurinic/aprimidinic endonuclease against a THF AP site model substrate," *Biochemistry*, vol. 48, no. 1, pp. 19–26, 2009.
- [63] G. Dianov, B. Sedgwick, G. Daly, M. Olsson, S. Lovett, and T. Lindahl, "Release of 5'-terminal deoxyribose-phosphate residues from incised abasic sites in DNA by the *Escherichia coli* RecJ protein," *Nucleic Acids Research*, vol. 22, no. 6, pp. 993–998, 1994.
- [64] C. E. Piersen, A. K. McCullough, and R. S. Lloyd, "AP lyases and dRPases: commonality of mechanism," *Mutation Research*, vol. 459, no. 1, pp. 43–53, 2000.
- [65] R. Prasad, V. K. Batra, X.-P. Yang et al., "Structural insight into the DNA polymerase  $\beta$  deoxyribose phosphate lyase mechanism," *DNA Repair*, vol. 4, no. 12, pp. 1347–1357, 2005.
- [66] A. K. McCullough, A. Sanchez, M. L. Dodson, P. Marapaka, J.-S. Taylor, and R. Stephen Lloyd, "The reaction mechanism of DNA glycosylase/AP lyases at abasic sites," *Biochemistry*, vol. 40, no. 2, pp. 561–568, 2001.
- [67] A. B. Robertson, A. Klungland, T. Rognes, and I. Leiros, "DNA repair in mammalian cells," *Cellular and Molecular Life Sciences*, vol. 66, no. 6, pp. 981–993, 2009.
- [68] J. Hoseki, A. Okamoto, R. Masui et al., "Crystal structure of a family 4 uracil-DNA glycosylase from *Thermus thermophilus* HB8," *Journal of Molecular Biology*, vol. 333, no. 3, pp. 515–526, 2003.
- [69] H. Kosaka, J. Hoseki, N. Nakagawa, S. Kuramitsu, and R. Masui, "Crystal structure of family 5 uracil-DNA glycosylase bound to DNA," *Journal of Molecular Biology*, vol. 373, no. 4, pp. 839–850, 2007.
- [70] M. Sugahara, T. Mikawa, R. Kato et al., "Crystallization and preliminary X-ray crystallographic studies of *Thermus thermophilus* HB8 MutM protein involved in repairs of oxidative DNA damage," *Journal of Biochemistry*, vol. 127, no. 1, pp. 9–11, 2000.
- [71] L. H. Pearl, "Structure and function in the uracil-DNA glycosylase superfamily," *Mutation Research*, vol. 460, no. 3–4, pp. 165–181, 2000.
- [72] O. D. Schäfer and J. Jiricny, "Recent progress in the biology, chemistry and structural biology of DNA glycosylases," *BioEssays*, vol. 23, no. 3, pp. 270–281, 2001.
- [73] T. Mikawa, R. Kato, M. Sugahara, and S. Kuramitsu, "Thermostable repair enzyme for oxidative DNA damage from extremely thermophilic bacterium, *Thermus thermophilus* HB8," *Nucleic Acids Research*, vol. 26, no. 4, pp. 903–910, 1998.
- [74] P. Fortini, B. Pascucci, E. Parlanti, R. W. Sobol, S. H. Wilson, and E. Dogliotti, "Different DNA polymerases are involved in the short- and long-patch base excision repair in mammalian cells," *Biochemistry*, vol. 37, no. 11, pp. 3575–3580, 1998.
- [75] A. J. Podlutzky, I. I. Dianova, S. H. Wilson, V. A. Bohr, and G. L. Dianov, "DNA synthesis and dRPase activities of polymerase  $\beta$  are both essential for single-nucleotide patch base excision repair in mammalian cell extracts," *Biochemistry*, vol. 40, no. 3, pp. 809–813, 2001.
- [76] U. Sattler, P. Frit, B. Salles, and P. Calsou, "Long-patch DNA repair synthesis during base excision repair in mammalian cells," *EMBO Reports*, vol. 4, no. 4, pp. 363–367, 2003.
- [77] R. Gary, K. Kim, H. L. Cornelius, M. S. Park, and Y. Matsumoto, "Proliferating cell nuclear antigen facilitates excision in long-patch base excision repair," *Journal of Biological Chemistry*, vol. 274, no. 7, pp. 4354–4363, 1999.
- [78] A. S. Jaiswal, R. Balusu, M. L. Armas, C. N. Kundu, and S. Narayan, "Mechanism of adenomatous polyposis coli (APC)-mediated blockage of long-patch base excision repair," *Biochemistry*, vol. 45, no. 51, pp. 15903–15914, 2006.
- [79] N. A. Lebedeva, N. I. Rechkunova, S. V. Dezhurov et al., "Comparison of functional properties of mammalian DNA polymerase  $\lambda$  and DNA polymerase  $\beta$  in reactions of DNA synthesis related to DNA repair," *Biochimica et Biophysica Acta*, vol. 1751, no. 2, pp. 150–158, 2005.
- [80] Y. Lin, W. A. Beard, D. D. Shock, R. Prasad, E. W. Hou, and S. H. Wilson, "DNA polymerase  $\beta$  and flap endonuclease 1 enzymatic specificities sustain DNA synthesis for long patch base excision repair," *Journal of Biological Chemistry*, vol. 280, no. 5, pp. 3665–3674, 2005.
- [81] R. Prasad, M. J. Longley, F. S. Sharief, E. W. Hou, W. C. Copeland, and S. H. Wilson, "Human DNA polymerase  $\theta$  possesses 5'-dRP lyase activity and functions in single-nucleotide base excision repair *in vitro*," *Nucleic Acids Research*, vol. 37, no. 6, pp. 1868–1877, 2009.
- [82] M. Stucki, B. Pascucci, E. Parlanti et al., "Mammalian base excision repair by DNA polymerases  $\delta$  and  $\epsilon$ ," *Oncogene*, vol. 17, no. 7, pp. 835–843, 1998.
- [83] J.-S. Sung and D. W. Mosbaugh, "*Escherichia coli* uracil- and ethenocytosine-initiated base excision DNA repair: rate-limiting step and patch size distribution," *Biochemistry*, vol. 42, no. 16, pp. 4613–4625, 2003.
- [84] K. Singh, A. Srivastava, S. S. Patel, and M. J. Modak, "Participation of the fingers subdomain of *Escherichia coli* DNA polymerase I in the strand displacement synthesis of DNA," *Journal of Biological Chemistry*, vol. 282, no. 14, pp. 10594–10604, 2007.
- [85] D. L. Ho, W. M. Byrnes, W.-P. Ma, Y. Shi, D. J. E. Callaway, and Z. Bu, "Structure-specific DNA-induced conformational changes in Taq polymerase revealed by small angle neutron scattering," *Journal of Biological Chemistry*, vol. 279, no. 37, pp. 39146–39154, 2004.
- [86] M. W. Kaiser, N. Lyamicheva, W. Ma et al., "A comparison of eubacterial and archaeal structure-specific 5'-exonucleases," *Journal of Biological Chemistry*, vol. 274, no. 30, pp. 21387–21394, 1999.
- [87] V. Lyamichev, M. A. D. Brow, and J. E. Dahlberg, "Structure-specific endonucleolytic cleavage of nucleic acids by eubacterial DNA polymerases," *Science*, vol. 260, no. 5109, pp. 778–783, 1993.

- [88] W.-P. Ma, M. W. Kaiser, N. Lyamicheva et al., "RNA template-dependent 5' nuclease activity of *Thermus aquaticus* and *Thermus thermophilus* DNA polymerases," *Journal of Biological Chemistry*, vol. 275, no. 32, pp. 24693–24700, 2000.
- [89] Y. Xu, N. D. F. Grindley, and C. M. Joyce, "Coordination between the polymerase and 5'-nuclease components of DNA polymerase I of *Escherichia coli*," *Journal of Biological Chemistry*, vol. 275, no. 27, pp. 20949–20955, 2000.
- [90] F. J. López de Saro and M. O'Donnell, "Interaction of the  $\beta$  sliding clamp with MutS, ligase, and DNA polymerase I," *Proceedings of the National Academy of Sciences of the United States of America*, vol. 98, no. 15, pp. 8376–8380, 2001.
- [91] J. Yamtich and J. B. Sweasy, "DNA polymerase Family X: function, structure, and cellular roles," *Biochimica et Biophysica Acta*, vol. 1804, no. 5, pp. 1136–1150, 2010.
- [92] W. W. Duym, K. A. Fiala, N. Bhatt, and Z. Suo, "Kinetic effect of a downstream strand and its 5'-terminal moieties on single nucleotide gap-filling synthesis catalyzed by human DNA polymerase  $\lambda$ ," *Journal of Biological Chemistry*, vol. 281, no. 47, pp. 35649–35655, 2006.
- [93] B. Baños, J. M. Lázaro, L. Villar, M. Salas, and M. de Vega, "Characterization of a *Bacillus subtilis* 64-kDa DNA Polymerase X Potentially Involved in DNA Repair," *Journal of Molecular Biology*, vol. 384, no. 5, pp. 1019–1028, 2008.
- [94] N. P. Khairnar and H. S. Misra, "DNA polymerase X from *Deinococcus radiodurans* implicated in bacterial tolerance to DNA damage is characterized as a short patch base excision repair polymerase," *Microbiology*, vol. 155, no. 9, pp. 3005–3014, 2009.
- [95] B. Baños, J. M. Lázaro, L. Villar, M. Salas, and M. de Vega, "Editing of misaligned 3'-termini by an intrinsic 3'-5' exonuclease activity residing in the PHP domain of a family X DNA polymerase," *Nucleic Acids Research*, vol. 36, no. 18, pp. 5736–5749, 2008.
- [96] M. Blasius, I. Shevelev, E. Jolivet, S. Sommer, and U. Hübscher, "DNA polymerase X from *Deinococcus radiodurans* possesses a structure-modulated 3' > 5' exonuclease activity involved in radioresistance," *Molecular Microbiology*, vol. 60, no. 1, pp. 165–176, 2006.
- [97] S. Nakane, N. Nakagawa, S. Kuramitsu, and R. Masui, "Characterization of DNA polymerase X from *Thermus thermophilus* HB8 reveals the POLXc and PHP domains are both required for 3' – 5' exonuclease activity," *Nucleic Acids Research*, vol. 37, no. 6, pp. 2037–2052, 2009.
- [98] M. Sukhanova, S. Khodyreva, and O. Lavrik, "Poly(ADP-ribose) polymerase 1 regulates activity of DNA polymerase  $\beta$  in long patch base excision repair," *Mutation Research*, vol. 685, no. 1-2, pp. 80–89, 2009.
- [99] M. J. Cuneo and R. E. London, "Oxidation state of the XRCC1 N-terminal domain regulates DNA polymerase  $\beta$  binding affinity," *Proceedings of the National Academy of Sciences of the United States of America*, vol. 107, no. 15, pp. 6805–6810, 2010.
- [100] ZH. K. Nazarkina, S. N. Khodyreva, S. Marsin, J. P. Radicella, and O. I. Lavrik, "Study of interaction of XRCC1 with DNA and proteins of base excision repair by photoaffinity labeling technique," *Biochemistry*, vol. 72, no. 8, pp. 878–886, 2007.
- [101] A. Sancar, "DNA excision repair," *Annual Review of Biochemistry*, vol. 65, pp. 43–81, 1996.
- [102] B. Van Houten, "Nucleotide excision repair in *Escherichia coli*," *Microbiological Reviews*, vol. 54, no. 1, pp. 18–51, 1990.
- [103] J. J. Truglio, D. L. Croteau, B. van Houten, and C. Kisker, "Prokaryotic nucleotide excision repair: the UvrABC system," *Chemical Reviews*, vol. 106, no. 2, pp. 233–252, 2006.
- [104] C. P. Selby and A. Sancar, "Mechanisms of transcription-repair coupling and mutation frequency decline," *Microbiological Reviews*, vol. 58, no. 3, pp. 317–329, 1994.
- [105] J. Q. Svejstrup, "Mechanisms of transcription-coupled DNA repair," *Nature Reviews Molecular Cell Biology*, vol. 3, no. 1, pp. 21–29, 2002.
- [106] C. P. Selby and A. Sancar, "Molecular mechanism of transcription-repair coupling," *Science*, vol. 259, no. 5104, pp. 53–58, 1993.
- [107] L. C. J. Gillet and O. D. Schärer, "Molecular mechanisms of mammalian global genome nucleotide excision repair," *Chemical Reviews*, vol. 106, no. 2, pp. 253–276, 2006.
- [108] D. K. Orren and A. Sancar, "The (A)BC excinuclease of *Escherichia coli* has only the UvrB and UvrC subunits in the incision complex," *Proceedings of the National Academy of Sciences of the United States of America*, vol. 86, no. 14, pp. 5237–5241, 1989.
- [109] E. E. A. Verhoeven, C. Wyman, G. F. Moolenaar, and N. Goosen, "The presence of two UvrB subunits in the UvrAB complex ensures damage detection in both DNA strands," *EMBO Journal*, vol. 21, no. 15, pp. 4196–4205, 2002.
- [110] G. F. Moolenaar, M. F. Herron, V. Monaco et al., "The role of ATP binding and hydrolysis by UvrB during nucleotide excision repair," *Journal of Biological Chemistry*, vol. 275, no. 11, pp. 8044–8050, 2000.
- [111] P. R. Caron and L. Grossman, "Involvement of a cryptic ATPase activity of UvrB and its proteolysis product, UvrB\* in DNA repair," *Nucleic Acids Research*, vol. 16, no. 20, pp. 9651–9662, 1988.
- [112] R. Kato, N. Yamamoto, K. Kito, and S. Kuramitsu, "ATPase activity of UvrB protein from *Thermus thermophilus* HB8 and its interaction with DNA," *Journal of Biological Chemistry*, vol. 271, no. 16, pp. 9612–9618, 1996.
- [113] A. Yamagata, R. Masui, R. Kato et al., "Interaction of UvrA and UvrB proteins with a fluorescent single-stranded DNA. Implication for slow conformational change upon interaction of UvrB with DNA," *Journal of Biological Chemistry*, vol. 275, no. 18, pp. 13235–13242, 2000.
- [114] J.-J. Lin and A. Sancar, "Active site of (A)BC excinuclease. I. Evidence for 5' incision by UvrC through a catalytic site involving Asp399, Asp438, Asp466, and His538 residues," *Journal of Biological Chemistry*, vol. 267, no. 25, pp. 17688–17692, 1992.
- [115] E. E. A. Verhoeven, M. Van Kesteren, G. F. Moolenaar, R. Visse, and N. Goosen, "Catalytic sites for 3' and 5' incision of *Escherichia coli* nucleotide excision repair are both located in UvrC," *Journal of Biological Chemistry*, vol. 275, no. 7, pp. 5120–5123, 2000.
- [116] T. Ohta, S.-I. Tokishita, R. Imazuka, I. Mori, J. Okamura, and H. Yamagata, " $\beta$ -Glucosidase as a reporter for the gene expression studies in *Thermus thermophilus* and constitutive expression of DNA repair genes," *Mutagenesis*, vol. 21, no. 4, pp. 255–260, 2006.
- [117] R. Collins and T. V. McCarthy, "Purification and characterization of *Thermus thermophilus* UvrD," *Extremophiles*, vol. 7, no. 1, pp. 35–41, 2003.
- [118] V. A. Bohr, C. A. Smith, D. S. Okumoto, and P. C. Hanawalt, "DNA repair in an active gene: removal of pyrimidine dimers from the DHFR gene of CHO cells is much more efficient than in the genome overall," *Cell*, vol. 40, no. 2, pp. 359–369, 1985.
- [119] C. P. Selby and A. Sancar, "Transcription preferentially inhibits nucleotide excision repair of the template DNA

- strand *in vitro*," *Journal of Biological Chemistry*, vol. 265, no. 34, pp. 21330–21336, 1990.
- [120] C. P. Selby, E. M. Witkin, and A. Sancar, "Escherichia coli mfd mutant deficient in "mutation frequency decline" lacks strand-specific repair: *in vitro* complementation with purified coupling factor," *Proceedings of the National Academy of Sciences of the United States of America*, vol. 88, no. 24, pp. 11574–11578, 1991.
- [121] C. P. Selby and A. Sancar, "Structure and function of transcription-repair coupling factor. I. Structural domains and binding properties," *Journal of Biological Chemistry*, vol. 270, no. 9, pp. 4882–4889, 1995.
- [122] A. M. Deaconescu, A. L. Chambers, A. J. Smith et al., "Structural basis for bacterial transcription-coupled DNA repair," *Cell*, vol. 124, no. 3, pp. 507–520, 2006.
- [123] E. Karakas, J. J. Truglio, D. Croteau et al., "Structure of the C-terminal half of UvrC reveals an RNase H endonuclease domain with an Argonaute-like catalytic triad," *EMBO Journal*, vol. 26, no. 2, pp. 613–622, 2007.
- [124] M. Machius, L. Henry, M. Palnitkar, and J. Deisenhofer, "Crystal structure of the DNA nucleotide excision repair enzyme UvrB from *Thermus thermophilus*," *Proceedings of the National Academy of Sciences of the United States of America*, vol. 96, no. 21, pp. 11717–11722, 1999.
- [125] N. Nakagawa, M. Sugahara, R. Masui, R. Kato, K. Fukuyama, and S. Kuramitsu, "Crystal structure of *Thermus thermophilus* HB8 UvrB protein, a key enzyme of nucleotide excision repair," *Journal of Biochemistry*, vol. 126, no. 6, pp. 986–990, 1999.
- [126] D. Pakotiprapha, Y. Inuzuka, B. R. Bowman et al., "Crystal Structure of *Bacillus stearothermophilus* UvrA provides insight into ATP-modulated dimerization, UvrB interaction, and DNA binding," *Molecular Cell*, vol. 29, no. 1, pp. 122–133, 2008.
- [127] K. Theis, P. J. Chen, M. Skorvaga, B. Van Houten, and C. Kisker, "Crystal structure of UvrB, a DNA helicase adapted for nucleotide excision repair," *EMBO Journal*, vol. 18, no. 24, pp. 6899–6907, 1999.
- [128] J. J. Truglio, B. Rhau, D. L. Croteau et al., "Structural insights into the first incision reaction during nucleotide excision repair," *EMBO Journal*, vol. 24, no. 5, pp. 885–894, 2005.
- [129] J. J. Truglio, E. Karakas, B. Rhau et al., "Structural basis for DNA recognition and processing by UvrB," *Nature Structural and Molecular Biology*, vol. 13, no. 4, pp. 360–364, 2006.
- [130] N. Nakagawa, R. Masui, R. Kato, and S. Kuramitsu, "Domain structure of *Thermus thermophilus* UvrB protein. Similarity in domain structure to a helicase," *Journal of Biological Chemistry*, vol. 272, no. 36, pp. 22703–22713, 1997.
- [131] M. Hori, C. Ishiguro, T. Suzuki et al., "UvrA and UvrB enhance mutations induced by oxidized deoxyribonucleotides," *DNA Repair*, vol. 6, no. 12, pp. 1786–1793, 2007.
- [132] R. M. Schaaper, "Base selection, proofreading, and mismatch repair during DNA replication in *Escherichia coli*," *Journal of Biological Chemistry*, vol. 268, no. 32, pp. 23762–23765, 1993.
- [133] R. Fishel and R. D. Kolodner, "Identification of mismatch repair genes and their role in the development of cancer," *Current Opinion in Genetics and Development*, vol. 5, no. 3, pp. 382–395, 1995.
- [134] R. R. Lyer, A. Pluciennik, V. Burdett, and P. L. Modrich, "DNA mismatch repair: functions and mechanisms," *Chemical Reviews*, vol. 106, no. 2, pp. 302–323, 2006.
- [135] P. Modrich, "Methyl-directed DNA mismatch correction," *Journal of Biological Chemistry*, vol. 264, no. 12, pp. 6597–6600, 1989.
- [136] M. H. Lamers, A. Perrakis, J. H. Enzlin, H. H. K. Winterwerp, N. De Wind, and T. K. Sixma, "The crystal structure of DNA mismatch repair protein MutS binding to a G·T mismatch," *Nature*, vol. 407, no. 6805, pp. 711–717, 2000.
- [137] G. Obmolova, C. Ban, P. Hsieh, and W. Yang, "Crystal structures of mismatch repair protein MutS and its complex with a substrate DNA," *Nature*, vol. 407, no. 6805, pp. 703–710, 2000.
- [138] S. Takamatsu, R. Kato, and S. Kuramitsu, "Mismatch DNA recognition protein from an extremely thermophilic bacterium, *Thermus thermophilus* HB8," *Nucleic Acids Research*, vol. 24, no. 4, pp. 640–647, 1996.
- [139] C. Ban and W. Yang, "Structural basis for MutH activation in *E. coli* mismatch repair and relationship of MutH to restriction endonucleases," *EMBO Journal*, vol. 17, no. 5, pp. 1526–1534, 1998.
- [140] L. E. Mechanic, B. A. Frankel, and S. W. Matson, "Escherichia coli MutL loads DNA helicase II onto DNA," *Journal of Biological Chemistry*, vol. 275, no. 49, pp. 38337–38346, 2000.
- [141] V. Burdett, C. Baitinger, M. Viswanathan, S. T. Lovett, and P. Modrich, "In vivo requirement for RecJ, ExoVII, ExoI, and ExoX in methyl-directed mismatch repair," *Proceedings of the National Academy of Sciences of the United States of America*, vol. 98, no. 12, pp. 6765–6770, 2001.
- [142] A. Yamagata, Y. Kakuta, R. Masui, and K. Fukuyama, "The crystal structure of exonuclease RecJ bound to Mn<sup>2+</sup> ion suggests how its characteristic motifs are involved in exonuclease activity," *Proceedings of the National Academy of Sciences of the United States of America*, vol. 99, no. 9, pp. 5908–5912, 2002.
- [143] A. Yamagata, R. Masui, Y. Kakuta, S. Kuramitsu, and K. Fukuyama, "Overexpression, purification and characterization of RecJ protein from *Thermus thermophilus* HB8 and its core domain," *Nucleic Acids Research*, vol. 29, no. 22, pp. 4617–4624, 2001.
- [144] W.-H. Fang and P. Modrich, "Human strand-specific mismatch repair occurs by a bidirectional mechanism similar to that of the bacterial reaction," *Journal of Biological Chemistry*, vol. 268, no. 16, pp. 11838–11844, 1993.
- [145] L. Dzantiev, N. Constantin, J. Genschel, R. R. Iyer, P. M. Burgers, and P. Modrich, "A defined human system that supports bidirectional mismatch-provoked excision," *Molecular Cell*, vol. 15, no. 1, pp. 31–41, 2004.
- [146] N. Constantin, L. Dzantiev, F. A. Kadyrov, and P. Modrich, "Human mismatch repair: reconstitution of a nick-directed bidirectional reaction," *Journal of Biological Chemistry*, vol. 280, no. 48, pp. 39752–39761, 2005.
- [147] P. Modrich, "Mechanisms in eukaryotic mismatch repair," *Journal of Biological Chemistry*, vol. 281, no. 41, pp. 30305–30309, 2006.
- [148] J. Genschel, L. R. Bazemore, and P. Modrich, "Human exonuclease I is required for 5' and 3' mismatch repair," *Journal of Biological Chemistry*, vol. 277, no. 15, pp. 13302–13311, 2002.
- [149] K. Wei, A. B. Clark, E. Wong et al., "Inactivation of exonuclease I in mice results in DNA mismatch repair defects, increased cancer susceptibility, and male and female sterility," *Genes and Development*, vol. 17, no. 5, pp. 603–614, 2003.
- [150] F. A. Kadyrov, L. Dzantiev, N. Constantin, and P. Modrich, "Endonucleolytic function of MutL $\alpha$  in human mismatch repair," *Cell*, vol. 126, no. 2, pp. 297–308, 2006.

- [151] F. A. Kadyrov, S. F. Holmes, M. E. Arana et al., "Saccharomyces cerevisiae MutL $\alpha$  is a mismatch repair endonuclease," *Journal of Biological Chemistry*, vol. 282, no. 51, pp. 37181–37190, 2007.
- [152] K. Fukui, M. Nishida, N. Nakagawa, R. Masui, and S. Kuramitsu, "Bound nucleotide controls the endonuclease activity of mismatch repair enzyme MutL," *Journal of Biological Chemistry*, vol. 283, no. 18, pp. 12136–12145, 2008.
- [153] V. Duppatla, C. Bodda, C. Urbanke, P. Friedhoff, and D. N. Rao, "The C-terminal domain is sufficient for endonuclease activity of *Neisseria gonorrhoeae* MutL," *Biochemical Journal*, vol. 423, no. 2, pp. 265–277, 2009.
- [154] J. Mauris and T. C. Evans Jr., "Adenosine triphosphate stimulates *Aquifex aeolicus* MutL endonuclease activity," *PLoS ONE*, vol. 4, no. 9, article no. e7175, 2009.
- [155] H. Tachiki, R. Kato, and S. Kuramitsu, "DNA binding and protein-protein interaction sites in MutS, a mismatched DNA recognition protein from *Thermus thermophilus* HB8," *Journal of Biological Chemistry*, vol. 275, no. 52, pp. 40703–40709, 2000.
- [156] R. Kato, M. Kataoka, H. Kamikubo, and S. Kuramitsu, "Direct observation of three conformations of MutS protein regulated by adenine nucleotides," *Journal of Molecular Biology*, vol. 309, no. 1, pp. 227–238, 2001.
- [157] S. Acharya, P. L. Foster, P. Brooks, and R. Fishel, "The coordinated functions of the *E. coli* MutS and MutL proteins in mismatch repair," *Molecular Cell*, vol. 12, no. 1, pp. 233–246, 2003.
- [158] M. L. Mendillo, C. D. Putnam, A. O. Mo et al., "Probing DNA- and ATP-mediated conformational changes in the MutS family of mispair recognition proteins using deuterium exchange mass spectrometry," *Journal of Biological Chemistry*, vol. 285, no. 17, pp. 13170–13182, 2010.
- [159] L. J. Blackwell, D. Martik, K. P. Bjornson, E. S. Bjornson, and P. Modrich, "Nucleotide-promoted release of hMutSa from heteroduplex DNA is consistent with an ATP-dependent translocation mechanism," *The Journal of Biological Chemistry*, vol. 273, no. 48, pp. 32055–32062, 1998.
- [160] L. J. Blackwell, K. P. Bjornson, D. J. Allen, and P. Modrich, "Distinct MutS DNA-binding modes that are differentially modulated by ATP binding and hydrolysis," *Journal of Biological Chemistry*, vol. 276, no. 36, pp. 34339–34347, 2001.
- [161] G. Natrajan, M. H. Lamers, J. H. Enzlin, H. H. K. Winterwerp, A. Perrakis, and T. K. Sixma, "Structures of *Escherichia coli* DNA mismatch repair enzyme MutS in complex with different mismatches: a common recognition mode for diverse substrates," *Nucleic Acids Research*, vol. 31, no. 16, pp. 4814–4821, 2003.
- [162] J. J. Warren, T. J. Pohlhaus, A. Changela et al., "Structure of the human MutSa DNA lesion recognition complex," *Molecular Cell*, vol. 26, no. 4, pp. 579–592, 2007.
- [163] R. Dutta and M. Inouye, "GHKL, an emergent ATPase/kinase superfamily," *Trends in Biochemical Sciences*, vol. 25, no. 1, pp. 24–28, 2000.
- [164] C. Ban, M. Junop, and W. Yang, "Transformation of MutL by ATP binding and hydrolysis: a switch in DNA mismatch repair," *Cell*, vol. 97, no. 1, pp. 85–97, 1999.
- [165] E. J. Sacho, F. A. Kadyrov, P. Modrich, T. A. Kunkel, and D. A. Erie, "Direct visualization of asymmetric adenine nucleotide-induced conformational changes in MutL $\alpha$ ," *Molecular Cell*, vol. 29, no. 1, pp. 112–121, 2008.
- [166] G.-L. Moldovan, B. Pfander, and S. Jentsch, "PCNA, the maestro of the replication fork," *Cell*, vol. 129, no. 4, pp. 665–679, 2007.
- [167] S. S. Shell, C. D. Putnam, and R. D. Kolodner, "The N terminus of *Saccharomyces cerevisiae* Msh6 is an unstructured tether to PCNA," *Molecular Cell*, vol. 26, no. 4, pp. 565–578, 2007.
- [168] T. A. Kunkel and D. A. Erie, "DNA mismatch repair," *Annual Review of Biochemistry*, vol. 74, pp. 681–710, 2005.
- [169] P. J. Masih, D. Kunnev, and T. Melendy, "Mismatch repair proteins are recruited to replicating DNA through interaction with Proliferating Cell Nuclear Antigen (PCNA)," *Nucleic Acids Research*, vol. 36, no. 1, pp. 67–75, 2008.
- [170] R. R. Iyer, T. J. Pohlhaus, S. Chen et al., "The MutSa-proliferating cell nuclear antigen interaction in human DNA mismatch repair," *Journal of Biological Chemistry*, vol. 283, no. 19, pp. 13310–13319, 2008.
- [171] L. A. Simmons, B. W. Davies, A. D. Grossman, and G. C. Walker, " $\beta$  clamp directs localization of mismatch repair in *Bacillus subtilis*," *Molecular Cell*, vol. 29, no. 3, pp. 291–301, 2008.
- [172] J. Genschel and P. Modrich, "Analysis of the excision step in human DNA mismatch repair," *Methods in Enzymology*, vol. 408, pp. 273–284, 2006.
- [173] J. Genschel and P. Modrich, "Mechanism of 5'-directed excision in human mismatch repair," *Molecular Cell*, vol. 12, no. 5, pp. 1077–1086, 2003.
- [174] J. Mauris and T. C. Evans Jr., "A human PMS2 homologue from *Aquifex aeolicus* stimulates an ATP-dependent DNA helicase," *Journal of Biological Chemistry*, vol. 285, no. 15, pp. 11087–11092, 2010.
- [175] A. Shimada, R. Masui, N. Nakagawa et al., "A novel single-stranded DNA-specific 3'–5' exonuclease, *Thermus thermophilus* exonuclease I, is involved in several DNA repair pathways," *Nucleic Acids Research*, vol. 38, no. 17, pp. 5792–5705, 2010.
- [176] T. Wakamatsu, Y. Kitamura, Y. Kotera, N. Nakagawa, S. Kuramitsu, and R. Masui, "Structure of RecJ exonuclease defines its specificity for single-stranded DNA," *Journal of Biological Chemistry*, vol. 285, no. 13, pp. 9762–9769, 2010.
- [177] W. Yang, "An equivalent metal ion in one- and two-metal-ion catalysis," *Nature Structural and Molecular Biology*, vol. 15, no. 11, pp. 1228–1231, 2008.
- [178] M. Shrivastav, L. P. De Haro, and J. A. Nickoloff, "Regulation of DNA double-strand break repair pathway choice," *Cell Research*, vol. 18, no. 1, pp. 134–147, 2008.
- [179] M. E. Moynahan and M. Jasin, "Mitotic homologous recombination maintains genomic stability and suppresses tumorigenesis," *Nature Reviews Molecular Cell Biology*, vol. 11, no. 3, pp. 196–207, 2010.
- [180] T. Helleday, J. Lo, D. C. van Gent, and B. P. Engelward, "DNA double-strand break repair: from mechanistic understanding to cancer treatment," *DNA Repair*, vol. 6, no. 7, pp. 923–935, 2007.
- [181] L. H. Thompson and D. Schild, "Recombinational DNA repair and human disease," *Mutation Research*, vol. 509, no. 1–2, pp. 49–78, 2002.
- [182] A. Nowosielska, "Bacterial DNA repair genes and their eukaryotic homologues: 5. The role of recombination in DNA repair and genome stability," *Acta Biochimica Polonica*, vol. 54, no. 3, pp. 483–494, 2007.
- [183] E. P. C. Rocha, E. Cornet, and B. Michel, "Comparative and evolutionary analysis of the bacterial homologous recombination systems," *PLoS Genetics*, vol. 1, no. 2, article no. e15, pp. 0247–0259, 2005.
- [184] G. A. Cromie, J. C. Connelly, and D. R. F. Leach, "Recombination at double-strand breaks and DNA ends: conserved

- mechanisms from phage to humans," *Molecular Cell*, vol. 8, no. 6, pp. 1163–1174, 2001.
- [185] M. Sasaki, J. Lange, and S. Keeney, "Genome destabilization by homologous recombination in the germ line," *Nature Reviews Molecular Cell Biology*, vol. 11, no. 3, pp. 182–195, 2010.
- [186] C. M. Thomas and K. M. Nielsen, "Mechanisms of, and barriers to, horizontal gene transfer between bacteria," *Nature Reviews Microbiology*, vol. 3, no. 9, pp. 711–721, 2005.
- [187] G.-M. Li, "Mechanisms and functions of DNA mismatch repair," *Cell Research*, vol. 18, no. 1, pp. 85–98, 2008.
- [188] P. Sung and H. Klein, "Mechanism of homologous recombination: mediators and helicases take on regulatory functions," *Nature Reviews Molecular Cell Biology*, vol. 7, no. 10, pp. 739–750, 2006.
- [189] P. Huertas, "DNA resection in eukaryotes: deciding how to fix the break," *Nature Structural and Molecular Biology*, vol. 17, no. 1, pp. 11–16, 2010.
- [190] N. Handa, K. Morimatsu, S. T. Lovett, and S. C. Kowalczykowski, "Reconstitution of initial steps of dsDNA break repair by the RecF pathway of *E. coli*," *Genes and Development*, vol. 23, no. 10, pp. 1234–1245, 2009.
- [191] J. T.P. Yeeles and M. S. Dillingham, "The processing of double-stranded DNA breaks for recombinational repair by helicase-nuclease complexes," *DNA Repair*, vol. 9, no. 3, pp. 276–285, 2010.
- [192] R. D. Shereda, D. A. Bernstein, and J. L. Keck, "A central role for SSB in *Escherichia coli* RecQ DNA helicase function," *Journal of Biological Chemistry*, vol. 282, no. 26, pp. 19247–19258, 2007.
- [193] H. Brüggemann and C. Chen, "Comparative genomics of *Thermus thermophilus*: plasticity of the megaplasmid and its contribution to a thermophilic lifestyle," *Journal of Biotechnology*, vol. 124, no. 4, pp. 654–661, 2006.
- [194] R. Sharma and D. N. Rao, "Orchestration of *Haemophilus influenzae* RecJ exonuclease by interaction with single-stranded DNA-binding protein," *Journal of Molecular Biology*, vol. 385, no. 5, pp. 1375–1396, 2009.
- [195] K. Morimatsu and S. C. Kowalczykowski, "RecFOR proteins load RecA protein onto gapped DNA to accelerate DNA strand exchange: a universal step of recombinational repair," *Molecular Cell*, vol. 11, no. 5, pp. 1337–1347, 2003.
- [196] M. Honda, T. Fujisawa, T. Shibata, and T. Mikawa, "RecR forms a ring-like tetramer that encircles dsDNA by forming a complex with RecF," *Nucleic Acids Research*, vol. 36, no. 15, pp. 5013–5020, 2008.
- [197] M. Honda, J. Inoue, M. Yoshimasu, Y. Ito, T. Shibata, and T. Mikawa, "Identification of the RecR Toprim domain as the binding site for both recF and recO: A role of recR in recFOR assembly at double-stranded DNA-single-stranded DNA junctions," *Journal of Biological Chemistry*, vol. 281, no. 27, pp. 18549–18559, 2006.
- [198] J. Inoue, M. Honda, S. Ikawa, T. Shibata, and T. Mikawa, "The process of displacing the single-stranded DNA-binding protein from single-stranded DNA by RecO and RecR proteins," *Nucleic Acids Research*, vol. 36, no. 1, pp. 94–109, 2008.
- [199] A. Carreira and S. C. Kowalczykowski, "BRCA2: shining light on the regulation of DNA-binding selectivity by RAD51," *Cell Cycle*, vol. 8, no. 21, pp. 3445–3447, 2009.
- [200] S. L. Gasiot, H. Olivares, U. Ear, D. M. Hari, R. Weichselbaum, and D. K. Bishop, "Assembly of RecA-like recombinases: distinct roles for mediator proteins in mitosis and meiosis," *Proceedings of the National Academy of Sciences of the United States of America*, vol. 98, no. 15, pp. 8411–8418, 2001.
- [201] A. V. Mazin, O. M. Mazina, D. V. Bugreev, and M. J. Rossi, "Rad54, the motor of homologous recombination," *DNA Repair*, vol. 9, no. 3, pp. 286–302, 2010.
- [202] M. J. McIlwraith, E. Van Dyck, J.-Y. Masson, A. Z. Stasiak, A. Stasiak, and S. C. West, "Reconstitution of the strand invasion step of double-strand break repair using human Rad51 Rad52 and RPA proteins," *Journal of Molecular Biology*, vol. 304, no. 2, pp. 151–164, 2000.
- [203] Z. Lin, H. Kong, M. Nei, and H. Ma, "Origins and evolution of the recA/RAD51 gene family: evidence for ancient gene duplication and endosymbiotic gene transfer," *Proceedings of the National Academy of Sciences of the United States of America*, vol. 103, no. 27, pp. 10328–10333, 2006.
- [204] D. A. McGrew and K. L. Knight, "Molecular design and functional organization of the RecA protein," *Critical Reviews in Biochemistry and Molecular Biology*, vol. 38, no. 5, pp. 385–432, 2003.
- [205] M. M. Cox, "Motoring along with the bacterial RecA protein," *Nature Reviews Molecular Cell Biology*, vol. 8, no. 2, pp. 127–138, 2007.
- [206] J. San Filippo, P. Sung, and H. Klein, "Mechanism of eukaryotic homologous recombination," *Annual Review of Biochemistry*, vol. 77, pp. 229–257, 2008.
- [207] R. M. Story, I. T. Weber, and T. A. Steitz, "The structure of the *E. coli* recA protein monomer and polymer," *Nature*, vol. 355, no. 6358, pp. 318–325, 1992.
- [208] Z. Chen, H. Yang, and N. P. Pavletich, "Mechanism of homologous recombination from the RecA-ssDNA/dsDNA structures," *Nature*, vol. 453, no. 7194, pp. 489–494, 2008.
- [209] T. Nishinaka, Y. Ito, S. Yokoyama, and T. Shibata, "An extended DNA structure through deoxyribose-base stacking induced by RecA protein," *Proceedings of the National Academy of Sciences of the United States of America*, vol. 94, no. 13, pp. 6623–6628, 1997.
- [210] M. D. Sutton and G. C. Walker, "Managing DNA polymerases: coordinating DNA replication, DNA repair, and DNA recombination," *Proceedings of the National Academy of Sciences of the United States of America*, vol. 98, no. 15, pp. 8342–8349, 2001.
- [211] T. Kawamoto, K. Araki, E. Sonoda et al., "Dual roles for DNA polymerase  $\eta$  in homologous DNA recombination and translesion DNA synthesis," *Molecular Cell*, vol. 20, no. 5, pp. 793–799, 2005.
- [212] X. Li, C. M. Stith, P. M. Burgers, and W.-D. Heyer, "PCNA is required for initiation of recombination-associated DNA synthesis by DNA polymerase  $\delta$ ," *Molecular Cell*, vol. 36, no. 4, pp. 704–713, 2009.
- [213] M. J. McIlwraith and S. C. West, "DNA repair synthesis facilitates RAD52-mediated second-end capture during DSB repair," *Molecular Cell*, vol. 29, no. 4, pp. 510–516, 2008.
- [214] M. J. McIlwraith, A. Vaisman, Y. Liu et al., "Human DNA polymerase  $\eta$  promotes DNA synthesis from strand invasion intermediates of homologous recombination," *Molecular Cell*, vol. 20, no. 5, pp. 783–792, 2005.
- [215] G.-L. Moldovan, M. V. Madhavan, K. D. Mirchandani, R. M. McCaffrey, P. Vinciguerra, and A. D. D'Andrea, "DNA polymerase POLN participates in cross-link repair and homologous recombination," *Molecular and Cellular Biology*, vol. 30, no. 4, pp. 1088–1096, 2010.
- [216] S. Delmas and I. Matic, "Interplay between replication and recombination in *Escherichia coli*: impact of the alternative DNA polymerases," *Proceedings of the National Academy of*

- Sciences of the United States of America*, vol. 103, no. 12, pp. 4564–4569, 2006.
- [217] A. Henne, H. Brüggemann, C. Raasch et al., “The genome sequence of the extreme thermophile *Thermus thermophilus*,” *Nature Biotechnology*, vol. 22, no. 5, pp. 547–553, 2004.
- [218] O. White, J. A. Eisen, J. F. Heidelberg et al., “Genome sequence of the radioresistant bacterium *Deinococcus radiodurans* R1,” *Science*, vol. 286, no. 5444, pp. 1571–1577, 1999.
- [219] D. Slade, A. B. Lindner, G. Paul, and M. Radman, “Recombination and replication in DNA repair of heavily irradiated *Deinococcus radiodurans*,” *Cell*, vol. 136, no. 6, pp. 1044–1055, 2009.
- [220] N. Kantake, M. V. V. M. Madiraju, T. Sugiyama, and S. C. Kowalczykowski, “*Escherichia coli* RecO protein anneals ssDNA complexed with its cognate ssDNA-binding protein: a common step in genetic recombination,” *Proceedings of the National Academy of Sciences of the United States of America*, vol. 99, no. 24, pp. 15327–15332, 2002.
- [221] T. Sugiyama, N. Kantake, Y. Wu, and S. C. Kowalczykowski, “Rad52-mediated DNA annealing after Rad51-mediated DNA strand exchange promotes second ssDNA capture,” *EMBO Journal*, vol. 25, no. 23, pp. 5539–5548, 2006.
- [222] A. V. Nimonkar, R. A. Sica, and S. C. Kowalczykowski, “Rad52 promotes second-end DNA capture in double-stranded break repair to form complement-stabilized joint molecules,” *Proceedings of the National Academy of Sciences of the United States of America*, vol. 106, no. 9, pp. 3077–3082, 2009.
- [223] J. M. Martínez-Salazar, J. Zuñiga-Castillo, and D. Romero, “Differential roles of proteins involved in migration of Holliday junctions on recombination and tolerance to DNA damaging agents in *Rhizobium etli*,” *Gene*, vol. 432, no. 1–2, pp. 26–32, 2009.
- [224] K. Yamada, M. Ariyoshi, and K. Morikawa, “Three-dimensional structural views of branch migration and resolution in DNA homologous recombination,” *Current Opinion in Structural Biology*, vol. 14, no. 2, pp. 130–137, 2004.
- [225] C. J. Rudolph, A. L. Upton, G. S. Briggs, and R. G. Lloyd, “Is RecG a general guardian of the bacterial genome?” *DNA Repair*, vol. 9, no. 3, pp. 210–223, 2010.
- [226] C. E. Beam, C. J. Saveson, and S. T. Lovett, “Role for radA/sms in recombination intermediate processing in *Escherichia coli*,” *Journal of Bacteriology*, vol. 184, no. 24, pp. 6836–6844, 2002.
- [227] M. Ariyoshi, T. Nishino, H. Iwasaki, H. Shinagawa, and K. Morikawa, “Crystal structure of the holliday junction DNA in complex with a single RuvA tetramer,” *Proceedings of the National Academy of Sciences of the United States of America*, vol. 97, no. 15, pp. 8257–8262, 2000.
- [228] Y. Fujiwara, K. Mayanagi, and K. Morikawa, “Functional significance of octameric RuvA for a branch migration complex from *Thermus thermophilus*,” *Biochemical and Biophysical Research Communications*, vol. 366, no. 2, pp. 426–431, 2008.
- [229] K. Yamada, T. Miyata, D. Tsuchiya et al., “Crystal structure of the RuvA-RuvB complex: a structural basis for the holliday junction migrating motor machinery,” *Molecular Cell*, vol. 10, no. 3, pp. 671–681, 2002.
- [230] K. Yamada, N. Kunishima, K. Mayanagi et al., “Crystal structure of the Holliday junction migration motor protein RuvB from *Thermus thermophilus* HB8,” *Proceedings of the National Academy of Sciences of the United States of America*, vol. 98, no. 4, pp. 1442–1447, 2001.
- [231] T. Ohnishi, T. Hishida, Y. Harada, H. Iwasaki, and H. Shinagawa, “Structure-function analysis of the three domains of RuvB DNA motor protein,” *Journal of Biological Chemistry*, vol. 280, no. 34, pp. 30504–30510, 2005.
- [232] T. Ohnishi, H. Iwasaki, Y. Ishino, S. Kuramitsu, A. Nakata, and H. Shinagawa, “Identification and characterization of *Thermus thermophilus* HB8 RuvA protein, the subunit of the RuvAB protein complex that promotes branch migration of Holliday junctions,” *Genes and Genetic Systems*, vol. 75, no. 5, pp. 233–243, 2000.
- [233] K. Mayanagi, Y. Fujiwara, T. Miyata, and K. Morikawa, “Electron microscopic single particle analysis of a tetrameric RuvA/RuvB/Holliday junction DNA complex,” *Biochemical and Biophysical Research Communications*, vol. 365, no. 2, pp. 273–278, 2008.
- [234] M. Ariyoshi, D. G. Vassylyev, H. Iwasaki, H. Nakamura, H. Shinagawa, and K. Morikawa, “Atomic structure of the RuvC resolvase: a Holliday junction-specific endonuclease from *E. coli*,” *Cell*, vol. 78, no. 6, pp. 1063–1072, 1994.
- [235] A. K. Eggleston and S. C. West, “Cleavage of holliday junctions by the *Escherichia coli* RuvABC complex,” *Journal of Biological Chemistry*, vol. 275, no. 34, pp. 26467–26476, 2000.
- [236] A. J. Van Gool, N. M. A. Hajibagheri, A. Stasiak, and S. C. West, “Assembly of the *Escherichia coli* RuvABC resolvosome directs the orientation of Holliday junction resolution,” *Genes and Development*, vol. 13, no. 14, pp. 1861–1870, 1999.
- [237] D. Zerbib, C. Mézard, H. George, and S. C. West, “Coordinated actions of RuvABC in Holliday junction processing,” *Journal of Molecular Biology*, vol. 281, no. 4, pp. 621–630, 1998.
- [238] J. M. Svendsen and J. W. Harper, “GEN1/Yen1 and the SLX4 complex: solutions to the problem of Holliday junction resolution,” *Genes and Development*, vol. 24, no. 6, pp. 521–536, 2010.
- [239] S. L. Andersen, D. T. Bergstralh, K. P. Kohl, J. R. LaRocque, C. B. Moore, and J. Sekelsky, “*Drosophila* MUS312 and the vertebrate ortholog BTBD12 interact with DNA structure-specific endonucleases in DNA repair and recombination,” *Molecular Cell*, vol. 35, no. 1, pp. 128–135, 2009.
- [240] S. Fekairi, S. Scaglione, C. Chahwan et al., “Human SLX4 is a holliday junction resolvase subunit that binds multiple DNA repair/recombination endonucleases,” *Cell*, vol. 138, no. 1, pp. 78–89, 2009.
- [241] I. M. Muñoz, K. Hain, A.-C. Déclais et al., “Coordination of structure-specific nucleases by human SLX4/BTBD12 is required for DNA repair,” *Molecular Cell*, vol. 35, no. 1, pp. 116–127, 2009.
- [242] T. T. Saito, J. L. Youds, S. J. Boulton, and M. P. Colaiácovo, “*Caenorhabditis elegans* HIM-18/SLX-4 interacts with SLX-1 and XPF-1 and maintains genomic integrity in the germline by processing recombination intermediates,” *PLoS Genetics*, vol. 5, no. 11, article no. e1000735, 2009.
- [243] J. M. Svendsen, A. Smogorzewska, M. E. Sowa et al., “Mammalian BTBD12/SLX4 assembles a Holliday junction resolvase and is required for DNA repair,” *Cell*, vol. 138, no. 1, pp. 63–77, 2009.
- [244] H. Iwasaki, M. Takahagi, T. Shiba, A. Nakata, and H. Shinagawa, “*Escherichia coli* RuvC protein is an endonuclease that resolves the Holliday structure,” *EMBO Journal*, vol. 10, no. 13, pp. 4381–4389, 1991.
- [245] E. L. Bolt and R. G. Lloyd, “Substrate specificity of RuvA resolvase reveals the DNA structures targeted by RuvAB and RecG in vivo,” *Molecular Cell*, vol. 10, no. 1, pp. 187–198, 2002.

- [246] S. N. Chan, L. Harris, E. L. Bolt, M. C. Whitby, and R. G. Lloyd, "Sequence specificity and biochemical characterization of the RusA Holliday junction resolvase of *Escherichia coli*," *Journal of Biological Chemistry*, vol. 272, no. 23, pp. 14873–14882, 1997.
- [247] C. R. Lopez, S. Yang, R. W. Deibler et al., "A role for topoisomerase III in a recombination pathway alternative to RuvABC," *Molecular Microbiology*, vol. 58, no. 1, pp. 80–101, 2005.
- [248] D. Sheng, R. Liu, Z. Xu, P. Singh, B. Shen, and Y. Hua, "Dual negative regulatory mechanisms of RecX on RecA functions in radiation resistance, DNA recombination and consequent genome instability in *Deinococcus radiodurans*," *DNA Repair*, vol. 4, no. 6, pp. 671–678, 2005.
- [249] K. Jimbo, J. Inoue, T. Masuda, T. Shibata, and T. Mikawa, "Purification and characterization of the *Thermus thermophilus* HB8 RecX protein," *Protein Expression and Purification*, vol. 51, no. 2, pp. 320–323, 2007.
- [250] S. Ragone, J. D. Maman, N. Furnham, and L. Pellegrini, "Structural basis for inhibition of homologous recombination by the RecX protein," *EMBO Journal*, vol. 27, no. 16, pp. 2259–2269, 2008.
- [251] R. Lestini and B. Michel, "UvrD controls the access of recombination proteins to blocked replication forks," *EMBO Journal*, vol. 26, no. 16, pp. 3804–3814, 2007.
- [252] X. Veaute, S. Delmas, M. Selva et al., "UvrD helicase, unlike Rep helicase, dismantles RecA nucleoprotein filaments in *Escherichia coli*," *EMBO Journal*, vol. 24, no. 1, pp. 180–189, 2005.
- [253] K. Fukui, N. Nakagawa, Y. Kitamura, Y. Nishida, R. Masui, and S. Kuramitsu, "Crystal structure of Muts2 endonuclease domain and the mechanism of homologous recombination suppression," *Journal of Biological Chemistry*, vol. 283, no. 48, pp. 33417–33427, 2008.
- [254] A. V. Pinto, A. Mathieu, S. Marsin et al., "Suppression of homologous and homeologous recombination by the bacterial MutS2 protein," *Molecular Cell*, vol. 17, no. 1, pp. 113–120, 2005.
- [255] K. Fukui, Y. Takahata, N. Nakagawa, S. Kuramitsu, and R. Masui, "Analysis of a nuclease activity of catalytic domain of *Thermus thermophilus* MutS2 by high-accuracy mass spectrometry," *Nucleic Acids Research*, vol. 35, no. 15, article no. e100, 2007.
- [256] K. Fukui, H. Kosaka, S. Kuramitsu, and R. Masui, "Nuclease activity of the MutS homologue MutS2 from *Thermus thermophilus* is confined to the Smr domain," *Nucleic Acids Research*, vol. 35, no. 3, pp. 850–860, 2007.
- [257] K. Fukui, R. Masui, and S. Kuramitsu, "*Thermus thermophilus* MutS2, a MutS paralogue, possesses an endonuclease activity promoted by MutL," *Journal of Biochemistry*, vol. 135, no. 3, pp. 375–384, 2004.

## Review Article

# Prevention of Mutation, Cancer, and Other Age-Associated Diseases by Optimizing Micronutrient Intake

**Bruce N. Ames**

*Nutrition and Metabolism Center, Children's Hospital Oakland Research Institute, 5700 Martin Luther King Jr. Way, Oakland, CA 94609, USA*

Correspondence should be addressed to Bruce N. Ames, bames@chori.org

Received 8 June 2010; Accepted 30 July 2010

Academic Editor: Ashis Basu

Copyright © 2010 Bruce N. Ames. This is an open access article distributed under the Creative Commons Attribution License, which permits unrestricted use, distribution, and reproduction in any medium, provided the original work is properly cited.

I review three of our research efforts which suggest that optimizing micronutrient intake will in turn optimize metabolism, resulting in decreased DNA damage and less cancer as well as other degenerative diseases of aging. (1) Research on delay of the mitochondrial decay of aging, including release of mutagenic oxidants, by supplementing rats with lipoic acid and acetyl carnitine. (2) The triage theory, which posits that modest micronutrient deficiencies (common in much of the population) accelerate molecular aging, including DNA damage, mitochondrial decay, and supportive evidence for the theory, including an in-depth analysis of vitamin K that suggests the importance of achieving optimal micronutrient intake for longevity. (3) The finding that decreased enzyme binding constants (increased  $K_m$ ) for coenzymes (or substrates) can result from protein deformation and loss of function due to an age-related decline in membrane fluidity, or to polymorphisms or mutation. The loss of enzyme function can be compensated by a high dietary intake of any of the B vitamins, which increases the level of the vitamin-derived coenzyme. This dietary remediation illustrates the importance of understanding the effects of age and polymorphisms on optimal micronutrient requirements. Optimizing micronutrient intake could have a major effect on the prevention of cancer and other degenerative diseases of aging.

## 1. Lipoic Acid and Acetyl-Carnitine Supplements Decrease the Oxidative Mitochondrial Decay of Aging

Mitochondrial decay appears to be a major contributor to aging and its associated degenerative diseases including cancer and neural decay [1, 2]. Mitochondria from old rats compared with those from young rats generate increased amounts of mutagenic [3–5] oxidant by-products [6] and have decreased membrane potential, respiratory control ratio, cellular oxygen consumption, and cardiolipin (a key lipid found in mitochondria). Oxidative damage to DNA, RNA, proteins, and mitochondrial membrane lipids contributes to this decay [6–10] and leads to functional decline of mitochondria, cells, tissues, and eventually organs such as the brain, with an accompanying loss of cognition and ambulatory activity [6–10].

Decreased capacity to produce ATP and increased oxidant production are two properties of aging mitochondria

supported by multiple lines of direct and indirect observations. First, the analysis of gene expression profiles in mice showed significant age-associated declines in the mRNA levels of mitochondrially encoded subunits of complex I, III, IV, and V in old compared to young mice [11]. Second, in addition to reduced gene expression, the levels of mutagenic [3, 4] aldehydes [12] and oxidants increase in aging tissues.

The importance of optimizing metabolic function to prevent mitochondrial decay is illustrated by feeding the mitochondrial metabolites acetyl carnitine (ALC) [13–15] and R-alpha lipoic acid (LA) [16] to old rats. Carnitine is used for transporting fatty acids into the mitochondria; the main short-chain acyl-carnitine is ALC [17]. In humans at rest, ALC accounts for roughly a quarter of total carnitine in plasma, muscle, and liver tissues [17]. LA is a mitochondrial coenzyme and is preferentially reduced in the mitochondria to a potent antioxidant. LA is also an effective inducer of the transcription factor Nrf2, which in turn induces the glutathione synthesis enzymes [18–20]. Nrf2 induces over

200 phase-2 antioxidant and thiol-protective enzymes [21, 22]. ALC and LA, when added as a supplement, can act in some cases synergistically, to restore much of the lost mitochondrial function in old rats [6–9].

One possible mechanism of mitochondrial decay is that with age, stiffer membranes due to lipid oxidation or increased oxidative damage to mitochondrial proteins cause structural deformation of key enzymes such as carnitine acyl transferase that lowers their affinity for the enzyme substrate [9]. Feeding old rats the substrate ALC with LA for a few weeks decreases oxidative damage, allowing the synthesis of new carnitine acyl transferase with normal binding affinity ( $K_m$ ) [9]. This partially restores mitochondrial function, decreases mutagenic oxidants, neuronal RNA oxidation, and mutagenic aldehydes, and increases rat ambulatory activity and cognition [6–9]. ALC and LA are not usually thought of as micronutrients, as they can be synthesized in the body, but they are illustrative of many normal metabolites that decline with age and may be beneficial as supplements in the elderly.

Park et al. [23] used DNA microarrays to identify transcriptional markers of aging that are differentially expressed in young versus old mice of multiple inbred strains. They then fed the mice various metabolites, mostly antioxidants, to see if they would oppose these transcriptional markers of aging, comparing effectiveness to caloric restriction, a known potent method for delaying aging. ALC was as effective as caloric restriction in the heart and LA was as effective in the cerebellum. These experiments suggest that ALC + LA is an effective caloric restriction mimetic and that tuning up metabolism may help in slowing down the aging process. The tissue specific effects of caloric restriction-mimetic agents suggest that a combinatory approach may be needed.

## 2. Triage Theory Suggests a Cause of Much Preventable Mutation and Cancer

The “trriage theory” [24–26] provides a unifying rationale for a causal link between chronic modest deficiency of a micronutrient (~40 essential minerals, vitamins, amino acids, and fatty acids) and the many degenerative diseases accompanying aging such as cancer, immune dysfunction, cognitive decline, cardiovascular disease, and stroke. If the theory is correct, the incidence of these diseases might be reduced by an inexpensive micronutrient intervention [24–26].

Triage theory [24, 25] posits that during evolution, as a result of periods of shortage of micronutrients required by various proteins for function, nature was selected for a rebalancing of metabolism (e.g., by selection for strong micronutrient binding constants for critical proteins). This rebalancing ensured survival of the organism at the expense of metabolism whose lack caused the accumulation of insidious damage leading to longer-term consequences, that I proposed including chronic diseases of aging. That nature may have developed such a system is logically consistent with the consensus that natural selection favors short-term survival for reproduction over long-term health [27]. During evolution micronutrient shortages were likely to be

very common. For example, the 15 essential minerals are not distributed evenly on the earth; dietary sources and availability also fluctuated markedly [28].

The triage theory predicts that optimizing intake of the ~40 essential micronutrients will reduce the risk of chronic diseases associated with aging and increase lifespan [24]. Micronutrients are remarkably inexpensive. Micronutrient intakes below recommended levels are unusually widespread in poor countries, but also in the US population in all segments of society, especially the poor, children, adolescents, the obese, and the elderly. High consumption of calorie-rich, micronutrient-poor unbalanced diets exacerbates the problem [24]. For example, over half of the US population have inadequate intakes of magnesium [24], almost all African-Americans are extremely low in vitamin D [29], and much of the population is low in a variety of other micronutrients, (e.g., omega-3 fatty acids, potassium, calcium, vitamin C, vitamin E, vitamin K) [24, 30, 31]. There is little societal concern because no overt pathologies have been associated with marginal to moderate levels of deficiency. The triage theory predicts that the pathology is insidious, but we believe that it is measurable. We hypothesize that two of the many insidious, but measurable, consequences of moderate micronutrient inadequacy are increased DNA damage (future cancer) and mitochondrial decay (mutagenic oxidant release, future cancer, and cognitive dysfunction) as aspects of a triage response. These consequences are known to increase with age. In addition, evidence from our own work and that of others, as briefly reviewed below, indicates that sensitive assays targeted at these endpoints have a high likelihood of detecting changes in individuals with moderate micronutrient deficiencies. Other age-related diseases, such as cardiovascular disease and immune dysfunction [25] are also increased by micronutrient deficiencies and are discussed elsewhere [25, 30].

*2.1. Vitamin K as an Example of the Utility of Triage Theory [30].* For 16 known vitamin K-dependent (VKD) proteins, we evaluated the relative lethality of 11 known mouse knockout mutants to categorize essentiality. Results indicated that 5 VKD proteins required for coagulation had critical functions (knockouts were embryonic lethal), whereas the knockouts of 5 less critical VKD proteins [osteocalcin, matrix Gla protein (Mgp), growth arrest specific protein 6 (Gas6), transforming growth factor  $\beta$ -inducible protein (Tgfb1 or  $\beta$ ig-h3), and periostin] survived at least through weaning. The VKD  $\gamma$ -carboxylation of the 5 essential VKD proteins in the liver and the 5 nonessential proteins in nonhepatic tissues sets up a dichotomy that takes advantage of the preferential distribution of dietary vitamin K1 to the liver to preserve coagulation function when vitamin K1 is limiting. Genetic loss of less critical VKD proteins, dietary vitamin K inadequacy, human polymorphisms or mutations, and vitamin K deficiency induced by chronic anticoagulant (warfarin/coumadin) therapy are all linked to age-associated conditions [30]: bone fragility after estrogen loss (osteocalcin); increased risk of type 2 diabetes (Gas6) [32]; arterial calcification (Mgp) [33, 34]; calcific aortic valve disease (periostin) [35]; increased chromosomal aberrations and spontaneous

cancer with mitotic spindle abnormalities (Tgfb1) [30, 36]. Studies on vitamin K deficiency as a cause of cancer are few but are suggestive [36, 37]. A triage perspective reinforces recommendations of some experts that much of the population and warfarin/coumadin patients may not receive sufficient vitamin K for optimal function of VKD proteins that are important to maintain long-term health [30].

**2.2. DNA Damage and Cancer.** Deficiency in each of the 7 micronutrients (iron, magnesium, zinc, and vitamins B6, C, folic acid, and biotin) that we have so far examined results in increased DNA damage in rodents, primary human cells in culture, or humans [24, 38–42]. Deficiency was severe in many of these studies, but further evidence discussed below suggests that modest levels of deficiency also can result in DNA damage and cancer.

*Folate deficiency* at moderate levels was the first micronutrient inadequacy to be clearly established as a mutagenic hazard for a considerable percentage of the US population. Low folate in mice was shown to cause chromosome breaks [43] and cancer [44]. Folate deficiency in human cells in culture was accompanied by chromosome breaks, cell cycle arrest in the S-phase, apoptosis, and high uracil incorporation into DNA, a likely cause of the breaks [38, 45–47]. A comparison of folate deficiency with radiation in breaking chromosomes has been done by us [38] and others [48, 49]. Folate deficiency in ex vivo human lymphocytes causes aneuploidy [50] and increased DNA oxidation and decreased DNA repair in rats [51]. Moderate deficiency of folate in humans (before folate supplementation of flour in the US) caused chromosome breaks at levels of deficiency present in 10% of the US population and in half of low income adolescents and elderly [47, 52, 53]. A study of human folate deficiency and micronuclei (chromosome breaks) [52] should have been the seminal paper in the nutrition-cancer field but has not been sufficiently appreciated. Micronuclei as a measure of chromosome breaks have been validated as a predictor of future human cancer [54]. In studies of Australian healthy adults, the third of the population with the lowest folate levels had a significantly increased level of chromosome breaks [55, 56]. Moderate folate deficiency has also been associated with human cancer, as reviewed in [51, 57, 58]. Moderate deficiency in B12 causes chromosome breaks in humans, apparently by the same mechanism as folate deficiency [53, 55].

*Magnesium Deficiency.* Magnesium intakes for ~56% of adults in the United States are below the Estimated Average Requirement (EAR), the current measure of micronutrient inadequacy (the RDA is set at 2 standard deviations above the EAR). Intakes below the EAR are especially prevalent among the poor, teenagers (78% of 14- to 18-year-old males and 91% of 14- to 18-year-old females), the obese, African Americans, and the elderly (81%) [31, 59–63]. Moderate magnesium deficiency causes genetic instability [64]. In humans, moderate magnesium deficiency has been associated with colorectal and other cancers [64–69], hypertension, stroke, osteoporosis, diabetes, and the metabolic syndrome [67, 70–72]. In a study of 4,035 men followed for 18 years, the highest quartile with serum magnesium at

baseline compared with the lowest had a 40% decrease in all-cause mortality and cardiovascular disease and a 50% decrease in cancer deaths [69]. In primary human cells in culture, magnesium deficiency leads to accelerated telomere shortening, activation of cell-cycle arrest proteins, premature senescence [41], and mitochondrial DNA damage (D. W. Killilea, B. N. A., unpublished observations). Magnesium deficiency in rats leads to chromosome breaks [73] and cancer [64]. In rats, a diet moderately deficient in magnesium increased mortality, blood pressure, inflammation, and oxidants and decreased resistance to oxidants compared with a standard or magnesium-supplemented diet [74]. This evidence suggests that supplementation programs should be considered because there is little risk of magnesium toxicity [70]. Good sources of magnesium are greens (magnesium is in the center of the chlorophyll molecule), whole grains, and nuts. A standard multivitamin-mineral (MVM) supplement does not contain sufficient magnesium (or calcium) because it would make the supplement too bulky.

*Vitamin B6 deficiency*, as measured by pyridoxal phosphate (PLP) levels in plasma, is associated with colorectal cancer; colorectal cancer decreased by 49% for every 100-pmol/mL increase in blood PLP level [75]. Serum levels of PLP were inversely associated with lung cancer in both smokers and nonsmokers in the EPIC study (100,000 person years) [76]. A significant inverse association between PLP level and gastric cancer has been shown in a large cohort study [77]. One possible mechanism is deficiency of B6 causing interference with heme biosynthesis causing release of mutagenic oxidants [24] though other mechanisms are also possible [78]. A sizeable percentage of the population not using supplements has inadequate PLP levels [79]; 49% of elderly women have inadequate (<EAR) B6 intake [31]. Low PLP levels are also associated with depression [80] and stroke [81].

*Moderate deficiencies* of calcium, niacin, vitamin E, retinol [56], or vitamins A, C, or E [82] are associated with chromosome damage. Severe deficiencies in rodents or human cell cultures for selenium, copper, niacin, choline, pantothenate, or riboflavin are also associated with chromosome breaks [24, 56]. Many of these and other moderate micronutrient deficiencies, when studied epidemiologically, are associated with cancer [24, 69, 83–93]. A number of human intervention studies with micronutrients report a decrease in DNA damage or cancer [52, 94–96] though more studies are needed to reach a definitive conclusion. The limitations of experimental approaches available for demonstrating a causal relation between micronutrient deficiency and cancer have been pointed out [97, 98]; a critical analysis of this large literature is not attempted here.

**2.3. Mitochondrial Oxidant Release.** A large literature, as discussed in Section 1, provides evidence that mitochondrial decay occurs with age and results in increased production of mutagenic oxidant byproducts of electron transport. To the extent that the DNA damage is caused by oxidants released from mitochondria, mtDNA will be damaged before nuclear DNA and should be more easily detected. Mitochondrial

decay appears to be a major contributor to both aging and its associated degenerative diseases, such as cancer and brain dysfunction, for example, complex I and Parkinson's disease, complex IV and Alzheimer's disease [24]. In mice, or human cells in culture, we found that severe deficiencies in zinc [42], iron [40], biotin [39], or vitamin B6 resulted in increased mitochondrial oxidative decay [24]. In all 4 cases, the mechanism could involve inhibition of heme synthesis which lowers levels of complex IV [24, 39], as discussed below.

*2.4. Some Micronutrient Deficiencies Impair Heme Synthesis, Which Can Result in Oxidative Stress, Mitochondrial Decay, DNA Damage, and Cell Senescence.* Seven micronutrients (biotin, pantothenate, pyridoxine, riboflavin, copper, iron, and zinc) are required for heme synthesis in mitochondria. A severe deficiency in any of these seven will cause a deficit of heme and therefore of complex IV, of which heme-a is an essential component [39, 99–103]. This mechanism is compatible with a triage response if complex IV is sensitive to modest deficiencies as well. The normal complement of complex IV keeps oxidants to a minimum; deficits of complex IV result in oxidant leakage, DNA damage, accelerated mitochondrial decay, and cellular aging [39, 99–103]. Deficiencies of iron, zinc, and biotin are discussed below.

*Iron.* Iron deficiency is the most common micronutrient deficiency in the world, and anemia is widespread in underdeveloped countries [104]. Iron intake in US menstruating women is low; ~16% are below the EAR, the standard measure of inadequacy [31]. Hispanic women and the obese are at greater risk of being iron deficient [105]. In humans, iron deficiency anemia is associated with poor cognitive development in toddlers [106–110], suggesting that iron deficiency in humans during critical periods of development harms the developing brain [107, 108, 111]. Severe iron deficiency causes loss of mitochondrial complex IV in selected regions in the brain of neonatal rats [112] as well as other changes in function, morphology, and physiology of the brain [107, 113]. Iron deficiency or excess in rats damages mitochondria and causes oxidant release, oxidative DNA damage, and decreased mitochondrial efficiency at levels both below and above the optimum [40].

Functional iron deficiency also is associated with diminished immune function and neuromuscular abnormalities [114, 115]. The effects of iron deficiency occur along a continuum [40, 107, 116]. Mitochondrial oxidant release resulting from nonsevere iron deficiency [40] could possibly be due to effects on heme-a biosynthesis [102, 103]. Iron deficiency without anemia can also occur in newborns exposed to intrauterine hypoxia, such as infants of preeclamptic or diabetic mothers [117]. In such cases, iron is prioritized to erythroid and hemoglobin synthesis, putting the nonerythroid tissues at risk of iron deficiency and hence heme deficiency [118, 119]. Dietary iron deficiency in the absence of anemia decreases aerobic capacity and physical work performance, which are improved by iron supplementation [120]. Iron deficiency has not been adequately

studied as a possible risk factor for cancer and the results are discordant [121, 122]. Many studies are looking for a monotonic relationship and do not take into account that one might expect cancer at levels of iron that are *both too low and too high* [40], as in hereditary hemochromatosis, a known risk factor for cancer [123]. Both iron deficiency and excess iron (excess iron may cause zinc or copper deficiency) in mice cause oxidant leakage from mitochondria, oxidative mtDNA damage, and mitochondrial dysfunction [40]. Iron accumulates with age and causes mitochondrial damage and early senescence in human cells in culture [124] and in rats [125]. Excess iron in human cells causes mitochondrial dysfunction, which can be ameliorated by ALC and LA [126].

*Zinc.* Zinc inadequacy is common in adults, ~12% of whom are below the EAR [31]. In human cells in culture, severe zinc deficiency causes complex IV deficiency and the release of oxidants, resulting in significant oxidative damage to DNA [42, 127, 128]. Zinc deficiency also causes chromosome breaks in rats [73] and is associated with cancer in both rodents and humans [129]. As discussed above, these observations reinforce the need to determine what degree of deficiency in humans results in DNA damage. We think it is likely that the trigger for decreased heme synthesis is the inactivation of the second enzyme of the pathway,  $\delta$ -aminolevulinate dehydratase, which contains 8 atoms of zinc [102, 130]. Zinc deficiency in human cells also inactivates other zinc-containing proteins such as the tumor suppressor protein p53 and the DNA base excision repair enzyme, apyrimidinic/apurinic endonuclease, with a resulting synergistic effect on genetic damage [42, 127].

*Biotin.* Biotin deficiency is more common than previously thought; ~40% of pregnant women who do not take a multivitamin show metabolic signs of deficiency [131]. Marginal biotin deficiency is teratogenic in mice [131]. Biotin is a prosthetic group in 4 biotin-dependent carboxylases (3 of which are solely present in mitochondria) that replenish intermediates in the tricarboxylic acid cycle [132]. Biotin deficiency decreases the activity of these enzymes, leading to a decrease of 2 heme precursors, mitochondrial succinyl-CoA, and glycine, thus resulting in heme deficiency [39]. Biotin deficiency in normal human lung fibroblasts in culture caused a 40–50% decrease in heme content, oxidant release, premature senescence, and DNA damage [39]. The relationship of these effects to human intake amounts needs to be determined [133].

Despite the promise of decreasing mutation rates by optimizing metabolism, a cautionary note is that too much of some micronutrients, such as iron [40] or selenium [134, 135], as well as too little, can be harmful. Several micronutrients, for example, folate [58, 136, 137] or vitamin K [30, 138], may stimulate previously existing cancer cells. It should not be assumed that “too much of a good thing is wonderful.” Mae West, who said that, was not thinking about micronutrients.

### 3. Ameliorating Some Consequences of Mutation: Enzymes Lose Binding Affinity (Increased Km) for Coenzymes and Substrate with Mutation or Age

We reviewed [139] about 50 human genetic diseases due to defective enzymes, which were remedied or ameliorated by the administration of high doses of the vitamin component of the corresponding coenzyme, thus partially restoring enzyme activity. Up to a quarter of mutations in a gene result in the corresponding enzyme having a decreased binding constant (increased Km) for a coenzyme resulting in a lower rate of reaction [139]. The review points out that many of the B vitamins, given at levels 10–100 times the RDA, can raise coenzyme activity levels by an order of magnitude or more, usually with minimal toxicity. Several single-nucleotide polymorphisms (SNPs) with a deleterious phenotype, under some conditions, decrease binding constants and thus may also be remediable by raising cellular concentrations of the cofactor by high-dose vitamin therapy. Our review raised the issue of whether some appreciable percentage of the population may require a higher level of a particular vitamin or substrate for optimum function.

A follow-up review [140] points out that it is common for proteins to become deformed with age, for example, membranes become stiffer by oxidation, deforming membrane proteins, and particularly in mitochondria. This raises the question of whether high dose B vitamins may be beneficial in the elderly. Deformation of an enzyme commonly decreases binding affinity (increased Km) for its coenzyme or substrate. Enzyme substrates and vitamin precursors of coenzymes can be elevated by feeding and may enhance the activity of a deformed enzyme. These observations also reinforce the importance of including age in dietary recommendations. For example, for vitamin B12, there is a special recommendation for the elderly based on their increased requirement, due to loss of uptake [141]. It also raises the question whether many metabolites, as well as vitamins, might be fed to improve functioning of enzymes in the elderly. The remediation of deformed enzymes, whether due to mutation or aging, is a field that shows promise and may be an inexpensive way to improve health.

The substrate binding affinities of complex I, III, and IV in mitochondria isolated from muscle of young and old mice were examined [142]. A kinetic analysis of complex III revealed a significant 29% age-associated increase in the Km (decreased binding) for ubiquinone-2. More recent work [143] reported a defect in the ubiquinone-binding site of cytochrome *b* in complex III in the interfibrillary mitochondria isolated from old rats [143]. The resulting defect in ubiquinone binding affinity is likely to increase superoxide production at this site. One possible mechanism of mitochondrial decay is that with age, stiffer membranes due to lipid oxidation or increased oxidative damage to mitochondrial proteins causes structural deformation of key enzymes such as carnitine acyl transferase that lowers their affinity for the enzyme substrate. Feeding old rats the substrate ALC with LA for a few weeks decreases

oxidative damage, allowing the synthesis of new carnitine acyl transferase with normal binding affinity (Km) [9]. This partially restores mitochondrial function, decreases oxidants, neuronal RNA oxidation, and mutagenic aldehydes, and increases rat ambulatory activity and cognition [6–9]. Mitochondrial complexes were examined [144] in the brain of young and old rats, with and without dietary ALC and LA. ALC and LA partially restored function of complex I to the level of the young, but by restoring Vmax, not Km for CoQ and NADH [144]. Increased levels of CoQ and niacin might overcome the increased Km. The Km mechanism for restoring function is not the only possible one; decreased oxidants may increase protein activity by increasing stability as well [6, 9, 144]. ALC and LA are not micronutrients, as they are made in the mitochondria, but they are illustrative of many normal metabolites that may be useful in the elderly.

### 4. Conclusion

The work on acetyl carnitine and lipoic acid suggests that decay of mitochondria leading to cancer and a variety of other diseases of aging is not inevitable but can be delayed by various interventions to improve metabolism. Understanding the mechanisms will suggest still other interventions. For example, if the effectiveness of lipoic acid is because it induces the ~200 enzymes in the phase-2 defense system against oxidants, as seems likely, then the whole area of optimizing our various inducible defense systems for longevity by hormetic mechanisms becomes attractive and we are at the start of the discovery of many interventions.

If the triage hypothesis proves to be correct, as the vitamin K analysis suggests, it will demonstrate the importance for a long and healthy life of avoiding modest micronutrient deficiencies for minimizing cancer and other age-related diseases, and for changing how people think about nutrition and health. Most of the world's population, including that of the US, is inadequate in one or more micronutrients according to current intake recommendations. Yet, because there is no overt pathology associated with these levels of deficiency, there has been little public concern. The triage hypothesis framework may facilitate the discovery of sensitive and specific biomarkers of micronutrient insufficiencies that can be used to optimize metabolism at a personal and population level. Current recommendations do not take into account the insidious biochemical consequences of metabolic triage. We think that we can show that insidious damage is indeed occurring at modest levels of deficiency and that this damage will increase the risk of cancer, cardiovascular disease, cognitive dysfunction, and the other diseases associated with aging.

The genomic variability between individuals is being explored at a rapid rate, but a correct understanding as to how to intervene awaits bringing nutrition, particularly micronutrient-dependent proteins into the picture. We believe that the analysis of binding constants is the beginning of a large field that will make it possible to overcome a large class of deleterious genetic changes by nutritional interventions.

Various lines of evidence reviewed here suggest that healthier lives are to be gained by optimizing our metabolism. More attention to balanced diets and optimizing micronutrient intake could have a major effect on delaying the degenerative diseases of aging. My vision is that this will be done in the future by individuals measuring their own levels of micronutrients from a finger prick of blood in a machine in their local pharmacy (<http://www.reliadiagnostics.com/>), and tuning up their metabolism by adjusting diet or taking supplements—the beginning of an age of true preventive medicine.

### Conflict of Interest

Dr. Ames is one of the founders of Juvenon (<http://juvenon.com/>), a company that has licensed the University of California patent on acetyl carnitine + lipoic acid for rejuvenating old mitochondria (Ames and T. Hagen, inventors), sells acetyl carnitine + lipoic acid supplements, and does clinical trials on them. Ames founder's stock was put in a nonprofit foundation at the founding in 1999. He is director of Juvenon's Scientific Advisory Board, but reimbursement for that from Juvenon is given to the foundation.

### Acknowledgments

The author is indebted to J. McCann, D. Killilea, S. Shenvi, and J. Suh for helpful criticisms and to the many excellent students and colleagues who have contributed to this work. This paper has been adapted in part from [26].

### References

- [1] M. K. Shigenaga, T. M. Hagen, and B. N. Ames, "Oxidative damage and mitochondrial decay in aging," *Proceedings of the National Academy of Sciences of the United States of America*, vol. 91, no. 23, pp. 10771–10778, 1994.
- [2] K. B. Beckman and B. N. Ames, "Mitochondrial aging: open questions," *Annals of the New York Academy of Sciences*, vol. 854, pp. 118–127, 1998.
- [3] L. J. Marnett, H. K. Hurd, M. C. Hollstein, D. E. Levin, H. Esterbauer, and B. N. Ames, "Naturally occurring carbonyl compounds are mutagens in *Salmonella* tester strain TA104," *Mutation Research*, vol. 148, no. 1-2, pp. 25–34, 1985.
- [4] T. Douki and B. N. Ames, "An HPLC-EC assay for 1,N2-propano adducts of 2'-deoxyguanosine with 4-hydroxynonenal and other  $\alpha,\beta$ -unsaturated aldehydes," *Chemical Research in Toxicology*, vol. 7, no. 4, pp. 511–518, 1994.
- [5] A. M. S. Lezza, F. P. Fallacara, V. Pesce, C. Leeuwenburgh, P. Cantatore, and M. N. Gadaleta, "Localization of abasic sites and single-strand breaks in mitochondrial DNA from brain of aged rat, treated or not with caloric restriction diet," *Neurochemical Research*, vol. 33, no. 12, pp. 2609–2614, 2008.
- [6] T. M. Hagen, J. Liu, J. Lykkesfeldt et al., "Feeding acetyl-L-carnitine and lipoic acid to old rats significantly improves metabolic function while decreasing oxidative stress," *Proceedings of the National Academy of Sciences of the United States of America*, vol. 99, no. 4, pp. 1870–1875, 2002.
- [7] T. M. Hagen, R. Moreau, J. H. Suh, and F. Visioli, "Mitochondrial decay in the aging rat heart: evidence for improvement by dietary supplementation with acetyl-L-carnitine and/or lipoic acid," *Annals of the New York Academy of Sciences*, vol. 959, pp. 491–507, 2002.
- [8] J. Liu, E. Head, A. M. Gharib et al., "Memory loss in old rats is associated with brain mitochondrial decay and RNA/DNA oxidation: partial reversal by feeding acetyl-L-carnitine and/or R- $\alpha$ -lipoic acid," *Proceedings of the National Academy of Sciences of the United States of America*, vol. 99, no. 4, pp. 2356–2361, 2002.
- [9] J. Liu, D. W. Killilea, and B. N. Ames, "Age-associated mitochondrial oxidative decay: improvement of carnitine acetyltransferase substrate-binding affinity and activity in brain by feeding old rats acetyl-L-carnitine and/or R- $\alpha$ -lipoic acid," *Proceedings of the National Academy of Sciences of the United States of America*, vol. 99, no. 4, pp. 1876–1881, 2002.
- [10] B. N. Ames, J. Liu, H. Atamna, and T. M. Hagen, "Delaying the mitochondrial decay of aging in the brain," *Clinical Neuroscience Research*, vol. 2, no. 5-6, pp. 331–338, 2003.
- [11] M. Manczak, Y. Jung, B. S. Park, D. Partovi, and P. H. Reddy, "Time-course of mitochondrial gene expressions in mice brains: implications for mitochondrial dysfunction, oxidative damage, and cytochrome c in aging," *Journal of Neurochemistry*, vol. 92, no. 3, pp. 494–504, 2005.
- [12] J. H. Suh, S.-H. Heath, and T. M. Hagen, "Two subpopulations of mitochondria in the aging rat heart display heterogenous levels of oxidative stress," *Free Radical Biology and Medicine*, vol. 35, no. 9, pp. 1064–1072, 2003.
- [13] M. N. Gadaleta, A. Cormio, V. Pesce, A. M. S. Lezza, and P. Cantatore, "Aging and mitochondria," *Biochimie*, vol. 80, no. 10, pp. 863–870, 1998.
- [14] M. N. Gadaleta, V. Petruzzella, M. Renis, F. Fracasso, and P. Cantatore, "Reduced transcription of mitochondrial DNA in the senescent rat. Tissue dependence and effect of L-carnitine," *European Journal of Biochemistry*, vol. 187, no. 3, pp. 501–506, 1990.
- [15] T. M. Hagen, R. T. Ingersoll, C. M. Wehr et al., "Acetyl-L-carnitine fed to old rats partially restores mitochondrial function and ambulatory activity," *Proceedings of the National Academy of Sciences of the United States of America*, vol. 95, no. 16, pp. 9562–9566, 1998.
- [16] T. M. Hagen, R. T. Ingersoll, J. Lykkesfeldt et al., "(R)- $\alpha$ -lipoic acid-supplemented old rats have improved mitochondrial function, decreased oxidative damage, and increased metabolic rate," *FASEB Journal*, vol. 13, no. 2, pp. 411–418, 1999.
- [17] R. Gatti, C. B. de Palo, P. Spinella, and E. F. de Palo, "Free carnitine and acetyl carnitine plasma levels and their relationship with body muscular mass in athletes," *Amino Acids*, vol. 14, no. 4, pp. 361–369, 1998.
- [18] J. H. Suh, S. V. Shenvi, B. M. Dixon et al., "Decline in transcriptional activity of Nrf2 causes age-related loss of glutathione synthesis, which is reversible with lipoic acid," *Proceedings of the National Academy of Sciences of the United States of America*, vol. 101, no. 10, pp. 3381–3386, 2004.
- [19] J. H. Suh, H. Wang, R.-M. Liu, J. Liu, and T. M. Hagen, "(R)- $\alpha$ -lipoic acid reverses the age-related loss in GSH redox status in post-mitotic tissues: evidence for increased cysteine requirement for GSH synthesis," *Archives of Biochemistry and Biophysics*, vol. 423, no. 1, pp. 126–135, 2004.

- [20] A. R. Smith, S. V. Shenvi, M. Widlansky, J. H. Suh, and T. M. Hagen, "Lipoic acid as a potential therapy for chronic diseases associated with oxidative stress," *Current Medicinal Chemistry*, vol. 11, no. 9, pp. 1135–1146, 2004.
- [21] M.-K. Kwak, N. Wakabayashi, K. Itoh, H. Motohashi, M. Yamamoto, and T. W. Kensler, "Modulation of gene expression by cancer chemopreventive dithiolethiones through the Keap1-Nrf2 pathway: identification of novel gene clusters for cell survival," *Journal of Biological Chemistry*, vol. 278, no. 10, pp. 8135–8145, 2003.
- [22] N. Wakabayashi, A. T. Dinkova-Kostova, W. D. Holtzclaw et al., "Protection against electrophile and oxidant stress by induction of the phase 2 response: fate of cysteines of the Keap1 sensor modified by inducers," *Proceedings of the National Academy of Sciences of the United States of America*, vol. 101, no. 7, pp. 2040–2045, 2004.
- [23] S.-K. Park, K. Kim, G. P. Page, D. B. Allison, R. Weindruch, and T. A. Prolla, "Gene expression profiling of aging in multiple mouse strains: identification of aging biomarkers and impact of dietary antioxidants," *Aging Cell*, vol. 8, no. 4, pp. 484–495, 2009.
- [24] B. N. Ames, "A theory of evolutionary allocation of scarce micronutrients by enzyme triage: adequate micronutrient nutrition to delay the degenerative diseases of aging," *Proceedings of the National Academy of Sciences of the United States of America*, vol. 103, pp. 17589–17594, 2006.
- [25] B. N. Ames and J. C. McCann, "Foreword: prevention of cancer, and the other degenerative diseases of aging, through nutrition," in *Chemoprevention of Cancer and DNA Damage by Dietary Factors*, S. Knasmüller, D. DeMarini, I. Johnson, and C. Gerhäuser, Eds., Wiley-VCH, Weinheim, Germany, 2009.
- [26] B. N. Ames, "Optimal micronutrients delay mitochondrial decay and age-associated diseases," *Mechanisms of Ageing and Development*, vol. 131, no. 7-8, pp. 473–479, 2010.
- [27] T. B. L. Kirkwood, "Understanding ageing from an evolutionary perspective," *Journal of Internal Medicine*, vol. 263, no. 2, pp. 117–127, 2008.
- [28] S. B. Eaton and M. Konner, "Paleolithic nutrition. A consideration of its nature and current implications," *New England Journal of Medicine*, vol. 312, no. 5, pp. 283–289, 1985.
- [29] J. C. McCann and B. N. Ames, "Is there convincing biological or behavioral evidence linking vitamin D deficiency to brain dysfunction?" *FASEB Journal*, vol. 22, no. 4, pp. 982–1001, 2008.
- [30] J. C. McCann and B. N. Ames, "Vitamin K, an example of triage theory: is micronutrient inadequacy linked to diseases of aging?" *American Journal of Clinical Nutrition*, vol. 90, no. 4, pp. 889–907, 2009.
- [31] A. Moshfegh, J. Goldman, and L. Cleveland, "What We Eat in America, NHANES 2001-2002: Usual Nutrient Intakes from Food Compared to Dietary Reference Intakes," U.S. Department of Agriculture, Agricultural Research Service, 2005.
- [32] Y. J. Hung, C. H. Lee, N. F. Chu, and Y. S. Shieh, "Plasma protein growth arrest-specific 6 levels are associated with altered glucose tolerance, inflammation, and endothelial dysfunction," *Diabetes Care*, vol. 33, no. 8, pp. 1840–1844, 2010.
- [33] R. J. Renneberg, P. W. de Leeuw, A. G. H. Kessels et al., "Calcium scores and matrix Gla protein levels: association with vitamin K status," *European Journal of Clinical Investigation*, vol. 40, no. 4, pp. 344–349, 2010.
- [34] R. J. Renneberg, B. J. van Varik, L. J. Schurgers et al., "Chronic coumarin treatment is associated with increased extracoronary arterial calcification in humans," *Blood*, vol. 115, no. 24, pp. 5121–5123, 2010.
- [35] T. V. Tkatchenko, R. A. Moreno-Rodriguez, S. J. Conway, J. D. Molkenkin, R. R. Markwald, and A. V. Tkatchenko, "Lack of periostin leads to suppression of Notch1 signaling and calcific aortic valve disease," *Physiological Genomics*, vol. 39, no. 3, pp. 160–168, 2009.
- [36] Y. Zhang, G. Wen, G. Shao et al., "TGFB1 deficiency predisposes mice to spontaneous tumor development," *Cancer Research*, vol. 69, no. 1, pp. 37–44, 2009.
- [37] K. Nimptsch, S. Rohrmann, A. Nieters, and J. Linseisen, "Serum undercarboxylated osteocalcin as biomarker of vitamin K intake and risk of prostate cancer: a nested case-control study in the Heidelberg cohort of the European prospective investigation into cancer and nutrition," *Cancer Epidemiology Biomarkers and Prevention*, vol. 18, no. 1, pp. 49–56, 2009.
- [38] C. Courtemanche, A. C. Huang, I. Elson-Schwab, N. Kerry, B. Y. Ng, and B. N. Ames, "Folate deficiency and ionizing radiation cause DNA breaks in primary human lymphocytes: a comparison," *FASEB Journal*, vol. 18, no. 1, pp. 209–211, 2004.
- [39] H. Atamna, J. Newberry, R. Erlitzki, C. S. Schultz, and B. N. Ames, "Biotin deficiency inhibits heme synthesis and impairs mitochondria in human lung fibroblasts," *Journal of Nutrition*, vol. 137, no. 1, pp. 25–30, 2007.
- [40] P. B. Walter, M. D. Knutson, A. Paler-Martinez et al., "Iron deficiency and iron excess damage mitochondria and mitochondrial DNA in rats," *Proceedings of the National Academy of Sciences of the United States of America*, vol. 99, no. 4, pp. 2264–2269, 2002.
- [41] D. W. Killilea and B. N. Ames, "Magnesium deficiency accelerates cellular senescence in cultured human fibroblasts," *Proceedings of the National Academy of Sciences of the United States of America*, vol. 105, no. 15, pp. 5768–5773, 2008.
- [42] E. Ho and B. N. Ames, "Low intracellular zinc induces oxidative DNA damage, disrupts p53, NFκB, and AP1 DNA binding, and affects DNA repair in a rat glioma cell line," *Proceedings of the National Academy of Sciences of the United States of America*, vol. 99, no. 26, pp. 16770–16775, 2002.
- [43] J. T. MacGregor, R. Schlegel, C. M. Wehr, P. Alperin, and B. N. Ames, "Cytogenetic damage induced by folate deficiency in mice is enhanced by caffeine," *Proceedings of the National Academy of Sciences of the United States of America*, vol. 87, no. 24, pp. 9962–9965, 1990.
- [44] E. Knock, L. Deng, Q. Wu, A. K. Lawrance, X.-L. Wang, and R. Rozen, "Strain differences in mice highlight the role of DNA damage in neoplasia induced by low dietary folate," *Journal of Nutrition*, vol. 138, no. 4, pp. 653–658, 2008.
- [45] C. Courtemanche, I. Elson-Schwab, S. T. Mashiyama, N. Kerry, and B. N. Ames, "Folate deficiency inhibits the proliferation of primary human CD8+ T lymphocytes in vitro," *Journal of Immunology*, vol. 173, no. 5, pp. 3186–3192, 2004.
- [46] S. T. Mashiyama, C. M. Hansen, E. Roitman et al., "An assay for uracil in human DNA at baseline: effect of marginal vitamin B6 deficiency," *Analytical Biochemistry*, vol. 372, no. 1, pp. 21–31, 2008.

- [47] B. C. Blount, M. M. Mack, C. M. Wehr et al., "Folate deficiency causes uracil misincorporation into human DNA and chromosome breakage: implications for cancer and neuronal damage," *Proceedings of the National Academy of Sciences of the United States of America*, vol. 94, no. 7, pp. 3290–3295, 1997.
- [48] M. Fenech, "The Genome Health Clinic and Genome Health Nutrigenomics concepts: diagnosis and nutritional treatment of genome and epigenome damage on an individual basis," *Mutagenesis*, vol. 20, no. 4, pp. 255–269, 2005.
- [49] P. Leopardi, F. Marcon, S. Caiola et al., "Effects of folic acid deficiency and MTHFR C677T polymorphism on spontaneous and radiation-induced micronuclei in human lymphocytes," *Mutagenesis*, vol. 21, no. 5, pp. 327–333, 2006.
- [50] J. Ni, L. Lu, M. Fenech, and X. Wang, "Folate deficiency in human peripheral blood lymphocytes induces chromosome 8 aneuploidy but this effect is not modified by riboflavin," *Environmental and Molecular Mutagenesis*, vol. 51, no. 1, pp. 15–22, 2010.
- [51] S. J. Duthie, G. Grant, L. P. Pirie, A. J. Watson, and G. P. Margison, "Folate deficiency alters hepatic and colon MGMT and OGG-1 DNA repair protein expression in rats but has no effect on genome-wide DNA methylation," *Cancer Prevention Research*, vol. 3, no. 1, pp. 92–100, 2010.
- [52] R. B. Everson, C. M. Wehr, G. L. Erexson, and J. T. MacGregor, "Association of marginal folate depletion with increased human chromosomal damage *in vivo*: demonstration by analysis of micronucleated erythrocytes," *Journal of the National Cancer Institute*, vol. 80, no. 7, pp. 525–529, 1988.
- [53] J. T. MacGregor, C. M. Wehr, R. A. Hiatt et al., "'Spontaneous' genetic damage in man: evaluation of interindividual variability, relationship among markers of damage, and influence of nutritional status," *Mutation Research*, vol. 377, no. 1, pp. 125–135, 1997.
- [54] E. Murgia, M. Ballardini, S. Bonassi, A. M. Rossi, and R. Barale, "Validation of micronuclei frequency in peripheral blood lymphocytes as early cancer risk biomarker in a nested case-control study," *Mutation Research*, vol. 639, no. 1-2, pp. 27–34, 2008.
- [55] M. F. Fenech, I. E. Dreosti, and J. R. Rinaldi, "Folate, vitamin B12, homocysteine status and chromosome damage rate in lymphocytes of older men," *Carcinogenesis*, vol. 18, no. 7, pp. 1329–1336, 1997.
- [56] M. F. Fenech, "Dietary reference values of individual micronutrients and nutrients for genome damage prevention: current status and a road map to the future," *American Journal of Clinical Nutrition*, vol. 91, no. 5, pp. 1438S–1454S, 2010.
- [57] B. N. Ames and P. Wakimoto, "Are vitamin and mineral deficiencies a major cancer risk?" *Nature Reviews Cancer*, vol. 2, no. 9, pp. 694–704, 2002.
- [58] A. J. Levine, J. C. Figueiredo, W. Lee et al., "A candidate gene study of folate-associated one carbon metabolism genes and colorectal cancer risk," *Cancer Epidemiology Biomarkers and Prevention*, vol. 19, no. 7, pp. 1812–1821, 2010.
- [59] E. S. Ford, "Race, education, and dietary cations: findings from the third national health and nutrition examination survey," *Ethnicity and Disease*, vol. 8, no. 1, pp. 10–20, 1998.
- [60] C. H. Fox, M. C. Mahoney, D. Ramsoomair, and C. A. Carter, "Magnesium deficiency in African-Americans: does it contribute to increased cardiovascular risk factors?" *Journal of the National Medical Association*, vol. 95, no. 4, pp. 257–262, 2003.
- [61] "Data Tables: Food and Nutrient Intakes by Income, 1994–1996," U.S. Department of Agriculture, Agricultural Research Services, 1999, <http://www.ars.usda.gov/ba/bhnrc/ndl>.
- [62] M. P. Vaquero, "Magnesium and trace elements in the elderly: intake, status and recommendations," *Journal of Nutrition, Health and Aging*, vol. 6, no. 2, pp. 147–153, 2002.
- [63] P. Wakimoto and G. Block, "Dietary intake, dietary patterns, and changes with age: an epidemiological perspective," *Journals of Gerontology A*, vol. 56, no. 2, pp. 65–80, 2001.
- [64] A. Hartwig, "Role of magnesium in genomic stability," *Mutation Research*, vol. 475, no. 1-2, pp. 113–121, 2001.
- [65] J. M. Blondell, "The anticarcinogenic effect of magnesium," *Medical Hypotheses*, vol. 6, no. 8, pp. 863–871, 1980.
- [66] A. R. Folsom and C.-P. Hong, "Magnesium intake and reduced risk of colon cancer in a prospective study of women," *American Journal of Epidemiology*, vol. 163, no. 3, pp. 232–235, 2006.
- [67] K. He, K. Liu, M. L. Daviglius et al., "Magnesium intake and incidence of metabolic syndrome among young adults," *Circulation*, vol. 113, no. 13, pp. 1675–1682, 2006.
- [68] S. C. Larsson, L. Bergkvist, and A. Wolk, "Magnesium intake in relation to risk of colorectal cancer in women," *Journal of the American Medical Association*, vol. 293, no. 1, pp. 86–89, 2005.
- [69] N. Leone, D. Courbon, P. Ducimetiere, and M. Zureik, "Zinc, copper, and magnesium and risks for all-cause, cancer, and cardiovascular mortality," *Epidemiology*, vol. 17, no. 3, pp. 308–314, 2006.
- [70] Institute of Medicine, *Committee on the Scientific Evaluation of Dietary Reference Intakes, Food and Nutrition Board*, National Academy of Sciences, National Academy Press, Washington, DC, USA, 1997.
- [71] R. M. van Dam, F. B. Hu, L. Rosenberg, S. Krishnan, and J. R. Palmer, "Dietary calcium and magnesium, major food sources, and risk of type 2 diabetes in U.S. black women," *Diabetes Care*, vol. 29, no. 10, pp. 2238–2243, 2006.
- [72] S. C. Larsson, M. J. Virtanen, M. Mars et al., "Magnesium, calcium, potassium, and sodium intakes and risk of stroke in male smokers," *Archives of Internal Medicine*, vol. 168, no. 5, pp. 459–465, 2008.
- [73] L. T. Bell, M. Branstrator, C. Roux, and L. S. Hurley, "Chromosomal abnormalities in maternal and fetal tissues of magnesium or zinc deficient rats," *Teratology*, vol. 12, no. 3, pp. 221–226, 1975.
- [74] D. Blache, S. Devaux, O. Joubert et al., "Long-term moderate magnesium-deficient diet shows relationships between blood pressure, inflammation and oxidant stress defense in aging rats," *Free Radical Biology and Medicine*, vol. 41, no. 2, pp. 277–284, 2006.
- [75] S. C. Larsson, N. Orsini, and A. Wolk, "Vitamin B6 and risk of colorectal cancer: a meta-analysis of prospective studies," *Journal of the American Medical Association*, vol. 303, no. 11, pp. 1077–1083, 2010.
- [76] M. Johansson, C. Relton, P. M. Ueland et al., "Serum B vitamin levels and risk of lung cancer," *Journal of the American Medical Association*, vol. 303, no. 23, pp. 2377–2385, 2010.
- [77] S. J. P. M. Eussen, S. E. Vollset, S. Hustad et al., "Vitamins B2 and B6 and genetic polymorphisms related to one-carbon metabolism as risk factors for gastric adenocarcinoma in the European Prospective Investigation into Cancer and Nutrition," *Cancer Epidemiology Biomarkers and Prevention*, vol. 19, no. 1, pp. 28–38, 2010.

- [78] K. Matsubara, S.-I. Komatsu, T. Oka, and N. Kato, "Vitamin B6-mediated suppression of colon tumorigenesis, cell proliferation, and angiogenesis," *Journal of Nutritional Biochemistry*, vol. 14, no. 5, pp. 246–250, 2003.
- [79] M. S. Morris, M. F. Picciano, P. F. Jacques, and J. Selhub, "Plasma pyridoxal 5'-phosphate in the US population: the National Health and Nutrition Examination Survey, 2003–2004," *American Journal of Clinical Nutrition*, vol. 87, no. 5, pp. 1446–1454, 2008.
- [80] A.-M. Hvas, S. Juul, P. Bech, and E. Nexø, "Vitamin B6 level is associated with symptoms of depression," *Psychotherapy and Psychosomatics*, vol. 73, no. 6, pp. 340–343, 2004.
- [81] P. J. Kelly, V. E. Shih, J. P. Kistler et al., "Low vitamin B6 but not homocyst(e)ine is associated with increased risk of stroke and transient ischemic attack in the era of folic acid grain fortification," *Stroke*, vol. 34, no. 6, pp. e51–e54, 2003.
- [82] D. F. Smith, J. T. MacGregor, R. A. Hiatt et al., "Micronucleated erythrocytes as an index of cytogenetic damages in humans: demographic and dietary factors associated with micronucleated erythrocytes in splenectomized subjects," *Cancer Research*, vol. 50, no. 16, pp. 5049–5054, 1990.
- [83] M. F. Holick, "Vitamin D: its role in cancer prevention and treatment," *Progress in Biophysics and Molecular Biology*, vol. 92, no. 1, pp. 49–59, 2006.
- [84] J. Ishihara, T. Otani, M. Inoue, M. Iwasaki, S. Sasazuki, and S. Tsugane, "Low intake of vitamin B-6 is associated with increased risk of colorectal cancer in Japanese men," *Journal of Nutrition*, vol. 137, no. 7, pp. 1808–1814, 2007.
- [85] M. V. Grau, J. A. Baron, R. S. Sandler et al., "Prolonged effect of calcium supplementation on risk of colorectal adenomas in a randomized trial," *Journal of the National Cancer Institute*, vol. 99, no. 2, pp. 129–136, 2007.
- [86] J. E. Chavarro, M. J. Stampfer, H. Li, H. Campos, T. Kurth, and J. Ma, "A prospective study of polyunsaturated fatty acid levels in blood and prostate cancer risk," *Cancer Epidemiology Biomarkers and Prevention*, vol. 16, no. 7, pp. 1364–1370, 2007.
- [87] Q. Dai, M. J. Shrubsole, R. M. Ness et al., "The relation of magnesium and calcium intakes and a genetic polymorphism in the magnesium transporter to colorectal neoplasia risk," *American Journal of Clinical Nutrition*, vol. 86, no. 3, pp. 743–751, 2007.
- [88] R. B. Franklin and L. C. Costello, "Zinc as an anti-tumor agent in prostate cancer and in other cancers," *Archives of Biochemistry and Biophysics*, vol. 463, no. 2, pp. 211–217, 2007.
- [89] C. C. Abnet, B. Lai, Y.-L. Qiao et al., "Zinc concentration in esophageal biopsy specimens measured by X-ray fluorescence and esophageal cancer risk," *Journal of the National Cancer Institute*, vol. 97, no. 4, pp. 301–306, 2005.
- [90] L. Y. Fong, Y. Jiang, and J. L. Farber, "Zinc deficiency potentiates induction and progression of lingual and esophageal tumors in p53-deficient mice," *Carcinogenesis*, vol. 27, no. 7, pp. 1489–1496, 2006.
- [91] A. S. Jaiswal and S. Narayan, "Zinc stabilizes adenomatous polyposis coli (APC) protein levels and induces cell cycle arrest in colon cancer cells," *Journal of Cellular Biochemistry*, vol. 93, no. 2, pp. 345–357, 2004.
- [92] A. S. Prasad, F. W. J. Beck, T. D. Doerr et al., "Nutritional and zinc status of head and neck cancer patients: an interpretive review," *Journal of the American College of Nutrition*, vol. 17, no. 5, pp. 409–418, 1998.
- [93] K.-Y. Liaw, P.-H. Lee, F.-C. Wu, J.-S. Tsai, and S.-Y. Lin-Shiau, "Zinc, copper, and superoxide dismutase in hepatocellular carcinoma," *American Journal of Gastroenterology*, vol. 92, no. 12, pp. 2260–2263, 1997.
- [94] M. Fenech, C. Aitken, and J. Rinaldi, "Folate, vitamin B12, homocysteine status and DNA damage in young Australian adults," *Carcinogenesis*, vol. 19, no. 7, pp. 1163–1171, 1998.
- [95] Y. I. Goh, E. Bollano, T. R. Einarson, and G. Koren, "Prenatal multivitamin supplementation and rates of pediatric cancers: a meta-analysis," *Clinical Pharmacology and Therapeutics*, vol. 81, no. 5, pp. 685–691, 2007.
- [96] M. L. Ribeiro, D. P. Arçari, A. C. Squassoni, and J. Pedrazzoli Jr., "Effects of multivitamin supplementation on DNA damage in lymphocytes from elderly volunteers," *Mechanisms of Ageing and Development*, vol. 128, no. 10, pp. 577–580, 2007.
- [97] J. C. McCann and B. N. Ames, "Evidence required for causal inferences about effects of micronutrient deficiencies during development on brain health—DHA, choline, iron, and vitamin D," in *Micronutrients and Brain Health*, L. Packer, H. Sies, M. Eggersdorfer, and E. Cadenas, Eds., chapter 30, CRC Press, London, UK, 2009.
- [98] B. N. Ames, J. C. McCann, M. J. Stampfer, and W. C. Willett, "Evidence-based decision making on micronutrients and chronic disease: long-term randomized controlled trials are not enough," *American Journal of Clinical Nutrition*, vol. 86, no. 2, pp. 522–524, 2007.
- [99] B. N. Ames, "Increasing longevity by tuning up metabolism," *EMBO Reports*, vol. 6, no. 1, pp. S20–S24, 2005.
- [100] B. N. Ames, H. Atamna, and D. W. Killilea, "Mineral and vitamin deficiencies can accelerate the mitochondrial decay of aging," *Molecular Aspects of Medicine*, vol. 26, no. 4–5, pp. 363–378, 2005.
- [101] D. A. Richert and M. P. Schulman, "Vitamin interrelationships in heme synthesis," *American Journal of Clinical Nutrition*, vol. 7, pp. 416–425, 1959.
- [102] H. Atamna, "Heme, iron, and the mitochondrial decay of ageing," *Ageing Research Reviews*, vol. 3, no. 3, pp. 303–318, 2004.
- [103] H. Atamna, J. Liu, and B. N. Ames, "Heme deficiency selectively interrupts assembly of mitochondrial complex IV in human fibroblasts: relevance to aging," *Journal of Biological Chemistry*, vol. 276, no. 51, pp. 48410–48416, 2001.
- [104] World Health Organization, *Iron Deficiency Anaemia: Assessment, Prevention, and Control. A Guide for Programme Managers*, World Health Organization, Geneva, Switzerland, 2001.
- [105] K. G. Nead, J. S. Halterman, J. M. Kaczorowski, P. Auinger, and M. Weitzman, "Overweight children and adolescents: a risk group for iron deficiency," *Pediatrics*, vol. 114, no. 1, pp. 104–108, 2004.
- [106] J. C. McCann and B. N. Ames, "DHA and cognitive development," *Pediatric Basics*, vol. 117, pp. 16–22, 2007.
- [107] J. L. Beard and J. R. Connor, "Iron status and neural functioning," *Annual Review of Nutrition*, vol. 23, pp. 41–58, 2003.
- [108] S. Grantham-McGregor and C. Ani, "A review of studies on the effect of iron deficiency on cognitive development in children," *Journal of Nutrition*, vol. 131, no. 2, supplement 2, pp. 649S–668S, 2001.
- [109] E. K. Hurtado, A. H. Claussen, and K. G. Scott, "Early childhood anemia and mild or moderate mental retardation," *American Journal of Clinical Nutrition*, vol. 69, no. 1, pp. 115–119, 1999.

- [110] B. Lozoff, E. Jimenez, J. Hagen, E. Mollen, and A. W. Wolf, "Poorer behavioral and developmental outcome more than 10 years after treatment for iron deficiency in infancy," *Pediatrics*, vol. 105, no. 4, article E51, 2000.
- [111] H. Atamna, D. W. Killilea, A. N. Killilea, and B. N. Ames, "Heme deficiency may be a factor in the mitochondrial and neuronal decay of aging," *Proceedings of the National Academy of Sciences of the United States of America*, vol. 99, no. 23, pp. 14807–14812, 2002.
- [112] M. DeUngria, R. Rao, J. D. Wobken, M. Luciana, C. A. Nelson, and M. K. Georgieff, "Perinatal iron deficiency decreases cytochrome c oxidase (CytOx) activity in selected regions of neonatal rat brain," *Pediatric Research*, vol. 48, no. 2, pp. 169–176, 2000.
- [113] M. B. Youdim and S. Yehuda, "The neurochemical basis of cognitive deficits induced by brain iron deficiency: involvement of dopamine-opiate system," *Cellular and Molecular Biology*, vol. 46, no. 3, pp. 491–500, 2000.
- [114] M. L. Failla, "Trace elements and host defense: recent advances and continuing challenges," *Journal of Nutrition*, vol. 133, no. 5, pp. 1443S–1447S, 2003.
- [115] F. E. Viteri and H. Gonzalez, "Adverse outcomes of poor micronutrient status in childhood and adolescence," *Nutrition Reviews*, vol. 60, no. 5, pp. S77–S83, 2002.
- [116] P. R. Dallman, "Biochemical basis for the manifestations of iron deficiency," *Annual Review of Nutrition*, vol. 6, pp. 13–40, 1986.
- [117] U. M. Chockalingam, E. Murphy, J. C. Ophoven, S. A. Weisdorf, and M. K. Georgieff, "Cord transferrin and ferritin values in newborn infants at risk for prenatal uteroplacental insufficiency and chronic hypoxia," *Journal of Pediatrics*, vol. 111, no. 2, pp. 283–286, 1987.
- [118] R. Rao and M. K. Georgieff, "Perinatal aspects of iron metabolism," *Acta Paediatrica*, vol. 91, no. 438, pp. 124–129, 2002.
- [119] S. F. Guiang III, M. K. Georgieff, D. J. Lambert, R. L. Schmidt, and J. A. Widness, "Intravenous iron supplementation effect on tissue iron and hemoproteins in chronically phlebotomized lambs," *American Journal of Physiology*, vol. 273, no. 6, pp. R2124–R2131, 1997.
- [120] T. D. Brutsaert, S. Hernandez-Cordero, J. Rivera, T. Viola, G. Hughes, and J. D. Haas, "Iron supplementation improves progressive fatigue resistance during dynamic knee extensor exercise in iron-depleted, nonanemic women," *American Journal of Clinical Nutrition*, vol. 77, no. 2, pp. 441–448, 2003.
- [121] S. Hercberg, C. Estaquio, S. Czernichow et al., "Iron status and risk of cancers in the SU.VI.MAX cohort," *Journal of Nutrition*, vol. 135, no. 11, pp. 2664–2668, 2005.
- [122] D. Pra, S. I. Rech Franke, J. A. Pegas Henriques, and M. Fenech, "A possible link between iron deficiency and gastrointestinal carcinogenesis," *Nutrition and Cancer*, vol. 61, no. 4, pp. 415–426, 2009.
- [123] M. Elmberg, R. Hultcrantz, A. Ekbom et al., "Cancer risk in patients with hereditary hemochromatosis and in their first-degree relatives," *Gastroenterology*, vol. 125, no. 6, pp. 1733–1741, 2003.
- [124] D. W. Killilea, H. Atamna, C. Liao, and B. N. Ames, "Iron accumulation during cellular senescence in human fibroblasts in vitro," *Antioxidants and Redox Signaling*, vol. 5, no. 5, pp. 507–516, 2003.
- [125] A. Y. Seo, J. Xu, S. Servais et al., "Mitochondrial iron accumulation with age and functional consequences," *Aging Cell*, vol. 7, no. 5, pp. 706–716, 2008.
- [126] A. Lal, W. Atamna, D. W. Killilea, J. H. Suh, and B. N. Ames, "Lipoic acid and acetyl-carnitine reverse iron-induced oxidative stress in human fibroblasts," *Redox Report*, vol. 13, no. 1, pp. 2–10, 2008.
- [127] E. Ho, C. Courtemanche, and B. N. Ames, "Zinc deficiency induces oxidative DNA damage and increases P53 expression in human lung fibroblasts," *Journal of Nutrition*, vol. 133, no. 8, pp. 2543–2548, 2003.
- [128] P. I. Oteiza, M. S. Clegg, M. P. Zago, and C. L. Keen, "Zinc deficiency induces oxidative stress and AP-1 activation in 3T3 cells," *Free Radical Biology and Medicine*, vol. 28, no. 7, pp. 1091–1099, 2000.
- [129] L. Y. Y. Fong, L. Zhang, Y. Jiang, and J. L. Farber, "Dietary zinc modulation of COX-2 expression and lingual and esophageal carcinogenesis in rats," *Journal of the National Cancer Institute*, vol. 97, no. 1, pp. 40–50, 2005.
- [130] E. K. Jaffe, "The porphobilinogen synthase catalyzed reaction mechanism," *Bioorganic Chemistry*, vol. 32, no. 5, pp. 316–325, 2004.
- [131] D. M. Mock, "Marginal biotin deficiency is teratogenic in mice and perhaps humans: a review of biotin deficiency during human pregnancy and effects of biotin deficiency on gene expression and enzyme activities in mouse dam and fetus," *Journal of Nutritional Biochemistry*, vol. 16, no. 7, pp. 435–437, 2005.
- [132] D. M. Mock, *Biotin. Present Knowledge in Nutrition*, ILSI Press, Washington, DC, USA, 7th edition, 1996.
- [133] S. L. Stratton, A. Bogusiewicz, M. M. Mock, N. I. Mock, A. M. Wells, and D. M. Mock, "Lymphocyte propionyl-CoA carboxylase and its activation by biotin are sensitive indicators of marginal biotin deficiency in humans," *American Journal of Clinical Nutrition*, vol. 84, no. 2, pp. 384–388, 2006.
- [134] D. J. Waters, S. Shen, L. T. Glickman et al., "Prostate cancer risk and DNA damage: translational significance of selenium supplementation in a canine model," *Carcinogenesis*, vol. 26, no. 7, pp. 1256–1262, 2005.
- [135] J. Wu, G. H. Lyons, R. D. Graham, and M. F. Fenech, "The effect of selenium, as selenomethionine, on genome stability and cytotoxicity in human lymphocytes measured using the cytokinesis-block micronucleus cytome assay," *Mutagenesis*, vol. 24, no. 3, pp. 225–232, 2009.
- [136] M. Ebbing, K. H. Bønaa, O. Nygård et al., "Cancer incidence and mortality after treatment with folic acid and vitamin B12," *Journal of the American Medical Association*, vol. 302, no. 19, pp. 2119–2126, 2009.
- [137] C. M. Ulrich and J. D. Potter, "Folate and cancer—timing is everything," *Journal of the American Medical Association*, vol. 297, no. 21, pp. 2408–2409, 2007.
- [138] C. Ma, Y. Rong, D. R. Radloff et al., "Extracellular matrix protein  $\beta$ g-h3/TGFBI promotes metastasis of colon cancer by enhancing cell extravasation," *Genes and Development*, vol. 22, no. 3, pp. 308–321, 2008.
- [139] B. N. Ames, I. Elson-Schwab, and E. A. Silver, "High-dose vitamin therapy stimulates variant enzymes with decreased coenzyme binding affinity (increased  $K_m$ ): relevance to genetic disease and polymorphisms," *American Journal of Clinical Nutrition*, vol. 75, no. 4, pp. 616–658, 2002.
- [140] B. N. Ames, J. H. Suh, and J. Liu, "Enzymes lose binding affinity (increase  $K_m$ ) for coenzymes and substrates with age: a strategy for remediation," in *Nutrigenomics: Discovering the Path to Personalized Nutrition*, J. K. R. Rodriguez, Ed., pp. 277–293, John Wiley & Sons, Hoboken, NJ, USA, 2006.

- [141] Institute of Medicine, *Committee on the Scientific Evaluation of Dietary Reference Intakes, Food and Nutrition Board*, National Academy of Sciences, National Academy Press, Washington, DC, USA, 1998.
- [142] R. J. Feuers, "The effects of dietary restriction on mitochondrial dysfunction in aging," *Annals of the New York Academy of Sciences*, vol. 854, pp. 192–201, 1998.
- [143] S. Moghaddas, C. L. Hoppel, and E. J. Lesnefsky, "Aging defect at the QO site of complex III augments oxyradical production in rat heart interfibrillar mitochondria," *Archives of Biochemistry and Biophysics*, vol. 414, no. 1, pp. 59–66, 2003.
- [144] J. Long, F. Gao, L. Tong, C. W. Cotman, B. N. Ames, and J. Liu, "Mitochondrial decay in the brains of old rats: ameliorating effect of alpha-lipoic acid and acetyl-L-carnitine," *Neurochemical Research*, vol. 34, no. 4, pp. 755–763, 2009.

## Review Article

# Role of Nicotinamide in DNA Damage, Mutagenesis, and DNA Repair

Devita Surjana, Gary M. Halliday, and Diona L. Damian

Discipline of Dermatology, Sydney Cancer Centre, Bosch Institute, University of Sydney at Royal Prince Alfred Hospital, Camperdown, Sydney, NSW 2006, Australia

Correspondence should be addressed to Gary M. Halliday, gary.halliday@sydney.edu.au

Received 16 April 2010; Accepted 13 June 2010

Academic Editor: Ashis Basu

Copyright © 2010 Devita Surjana et al. This is an open access article distributed under the Creative Commons Attribution License, which permits unrestricted use, distribution, and reproduction in any medium, provided the original work is properly cited.

Nicotinamide is a water-soluble amide form of niacin (nicotinic acid or vitamin B3). Both niacin and nicotinamide are widely available in plant and animal foods, and niacin can also be endogenously synthesized in the liver from dietary tryptophan. Nicotinamide is also commercially available in vitamin supplements and in a range of cosmetic, hair, and skin preparations. Nicotinamide is the primary precursor of nicotinamide adenine dinucleotide (NAD<sup>+</sup>), an essential coenzyme in ATP production and the sole substrate of the nuclear enzyme poly-ADP-ribose polymerase-1 (PARP-1). Numerous *in vitro* and *in vivo* studies have clearly shown that PARP-1 and NAD<sup>+</sup> status influence cellular responses to genotoxicity which can lead to mutagenesis and cancer formation. This paper will examine the role of nicotinamide in the protection from carcinogenesis, DNA repair, and maintenance of genomic stability.

## 1. Introduction

Nicotinamide (pyridine-3-carboxamide; Figure 1(a) is an amide active form of Vitamin B3 or niacin (pyridine-3-carboxylic acid; Figure 1(b). Both nicotinamide and niacin are precursors for the synthesis of nicotinamide adenine dinucleotide (NAD<sup>+</sup>) and the phosphorylated derivative NADP<sup>+</sup> [1] (Figure 2). Nicotinamide and niacin are readily available from plant and animal foods, and niacin can be endogenously synthesized from the amino acid tryptophan [2], which constitutes ~1% of protein in the diet [1]. The main dietary sources of nicotinamide and niacin are various meats, liver, yeast, dairy products, legumes, beans, nuts, seeds, green leafy vegetables, fortified bread, cereals, coffee, and tea [1, 3]. Uncooked foods mostly contain NAD<sup>+</sup> and NADP<sup>+</sup>, which can be enzymatically hydrolysed to nicotinamide in the process of cooking [1]. Studies in adult humans in the 1950s estimated that around 60 mg of tryptophan is hepatically converted to 1 mg of niacin, which is equal to 1 niacin equivalent (NE) [1]. Vitamins B2 (riboflavin) and B6 (pyridoxine) in addition to iron are needed as cofactors for conversion of tryptophan to niacin [1, 3]. The ability to convert tryptophan to niacin varies greatly between individuals and is enhanced by

protein and tryptophan deficiency, and it is depressed by excessive dietary leucine [1]. The adult recommended daily intake expressed as niacin equivalent is 16 NE/day for men, 14 NE/day for women and 18 NE/day and 17 NE/day for pregnant and lactating women, respectively [4]. In humans, dietary nicotinamide and niacin are absorbed from stomach and intestine via both sodium-dependent and passive diffusions [1]. Most tissues take up both forms of vitamins to synthesize NAD<sup>+</sup> and NADP<sup>+</sup>, although nicotinamide is the preferable substrate [5]. Dietary NAD<sup>+</sup> and NADP<sup>+</sup> are hydrolyzed by intestinal mucosal and hepatic NAD glycohydrolases to release nicotinamides into the portal or systemic circulation [1]. Niacin is also endogenously synthesized from dietary tryptophan via kynurenine pathway and quinolinate (Figure 2), and this supplies most of the body's niacin requirements [1]. Niacin and quinolinate are further converted to nicotinic acid ribonucleotides and then into NAD<sup>+</sup> [1]. Excess nicotinamide and niacin are methylated in the liver to form N<sup>1</sup>-methylnicotinamide (NMN) and N<sup>1</sup>-methylnicotinic acid (NMNA), respectively [1]. NMN is further oxidised into N<sup>1</sup>-methyl-4-pyridone-3-carboxamide (4-pyr) and N<sup>1</sup>-methyl-2-pyridone-5-carboxamide (2-pyr) [1]. Niacin is also metabolized in the liver into glycine conjugate and nicotinuric acid [6]. These metabolites are

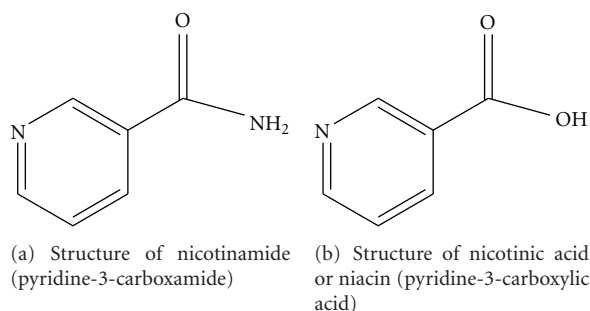


FIGURE 1

then renally excreted [1]. Some cosmetic preparations also contain nicotinamide. Systemic absorption of topical nicotinamide has been reported to be approximately 10% depending on the vehicle used [7]. Adverse effects of nicotinamide are rare and have occurred mainly with high oral doses ( $\geq 6$  gram/day), which include nausea, vomiting, liver toxicity, headache, fatigue, and dizziness [8–10]. Unlike niacin, nicotinamide is not a vasodilator, thus it rarely causes flushing [11].

Severe nicotinamide deficiency in humans causes the disease pellagra (*Italian* “*pelle agra*”; “*rough skin*”), which is characterised by photosensitive dermatitis, diarrhoea, dementia, and death [3]. It was thought that the clinical manifestations of pellagra arise from the deficient  $\text{NAD}^+$  and  $\text{NADP}^+$  levels in maintaining energy for cellular functions [13]. However, understanding of these multiple symptoms has progressed with the finding of  $\text{NAD}^+$  as a substrate for poly(ADP-ribose)polymerases (PARPs) [14]. PARP has been recognized to play multitude roles in DNA damage responses, including DNA repair, maintenance of genomic stability, transcriptional regulation, signaling pathways involving apoptosis, telomere functions, and other multiple cellular functions [15]. Several members of the PARP family have been identified, of which PARP-1 is the most reported and is the focus of this paper.  $\text{NAD}^+$  has also been shown to be a free radical scavenger [16–20] and is directly used for the synthesis of cyclic ADP-ribose, which may be involved in calcium signaling pathways leading to apoptosis or necrosis [21, 22]. Cellular  $\text{NAD}^+$  status has been increasingly demonstrated to alter the cell susceptibility to genotoxic damage [23], highlighting the crucial role of nicotinamide as a  $\text{NAD}^+$  precursor in modulating pathways involved in carcinogenesis. This paper will first discuss nicotinamide and carcinogenesis in humans and whole animal models. Next, the roles of nicotinamide in relation to DNA repair, genomic stability, and mutagenesis will be examined.

## 2. Nicotinamide, Niacin, and Cancer in Humans

There are relatively few epidemiological studies on the association between nicotinamide intake and cancer in humans. Deficiency of nicotinamide and other micronutrients including riboflavin, zinc, and magnesium have been linked to the increased frequency of oesophageal cancer in certain

populations in China and Italy [24, 25]. Low dietary niacin has also been associated with an increased frequency of oral, gastric, and colon cancers, as well as oesophageal dysplasia [25–27]. In the Linxian trial in China, involving nearly 30,000 residents, 40 mg niacin and 3.2 mg riboflavin were supplemented in one of the treatment arms daily for over 5 years. It was shown that this combined supplementation decreased oesophageal cancer incidence and mortality by 14% and 10%, respectively [24]. Most human studies have examined the dietary intake or supplementation of niacin in combination with other micronutrients [24, 25, 28–32]. The impact of niacin on human carcinogenesis is therefore confounded by the effect of other micronutrients. Analysis from a large Western population within The Malmö Diet and Cancer Study in Sweden showed that approximately 15%–20% of individuals in this population were niacin deficient [33]. While severe niacin deficiency resulting in pellagra is uncommon in Western populations, suboptimal niacin intake may be relevant in populations at risk such as cancer patients and individuals with high occupational or environmental exposure to genotoxic agents including ionizing radiation, ultraviolet radiation (UVR), and alkylating agents. Limited studies indicate that cancer patients are at risk of niacin deficiency [34, 35]. In one trial involving 42 patients with various primary cancers, it was shown that 40% of these patients were niacin deficient as measured by abnormally low urine levels of the niacin metabolite  $\text{N}^1$ -methylnicotinamide [34]. Chemotherapy may also depress  $\text{NAD}^+$  levels [35] and precipitate pellagra by promoting anorexia and malabsorption. Some chemotherapeutic agents (e.g., 5-fluorouracil, 6-mercaptopurine) also interfere with tryptophan conversion to niacin [36]. Moreover, chemotherapeutic alkylating agents have been shown to cause miscoding lesions, chromosomal aberrations [37], and secondary cancer, particularly leukemia, which complicates chemotherapy in 10%–15% of cancer survivals [38]. More direct evidence comes from studies in rats, which showed that niacin deficiency significantly increases the risk of chemotherapeutic-induced secondary leukemia [39]. Niacin and  $\text{NAD}^+$  levels are important determinants of genomic responses to genotoxic insults [23]. Maintaining an optimum nicotinamide level is therefore essential in cancer patients and individuals at risk of exposure to genotoxic agents.

## 3. Nicotinamide Supplementation and Animal Models of Carcinogenesis

Animal models show that nicotinamide supplements influence carcinogenesis in a dose-dependent and organ-specific manner (Table 1). Nicotinamide is not carcinogenic by itself at doses more than 300-fold above requirement, administered to mice throughout their life span [40]. Overall, low-dose nicotinamide (dose range of 150–200  $\mu\text{M}$ , topical; 0.25%–2.5%, oral; 30 mg/kg body weight (bw) intraperitoneal) appears to be protective in various chemical- and UVR-induced carcinogenesis models in animals. Nicotinamide at dietary concentrations of 0.25%–2.5% is protective against urethane-induced pulmonary adenoma in

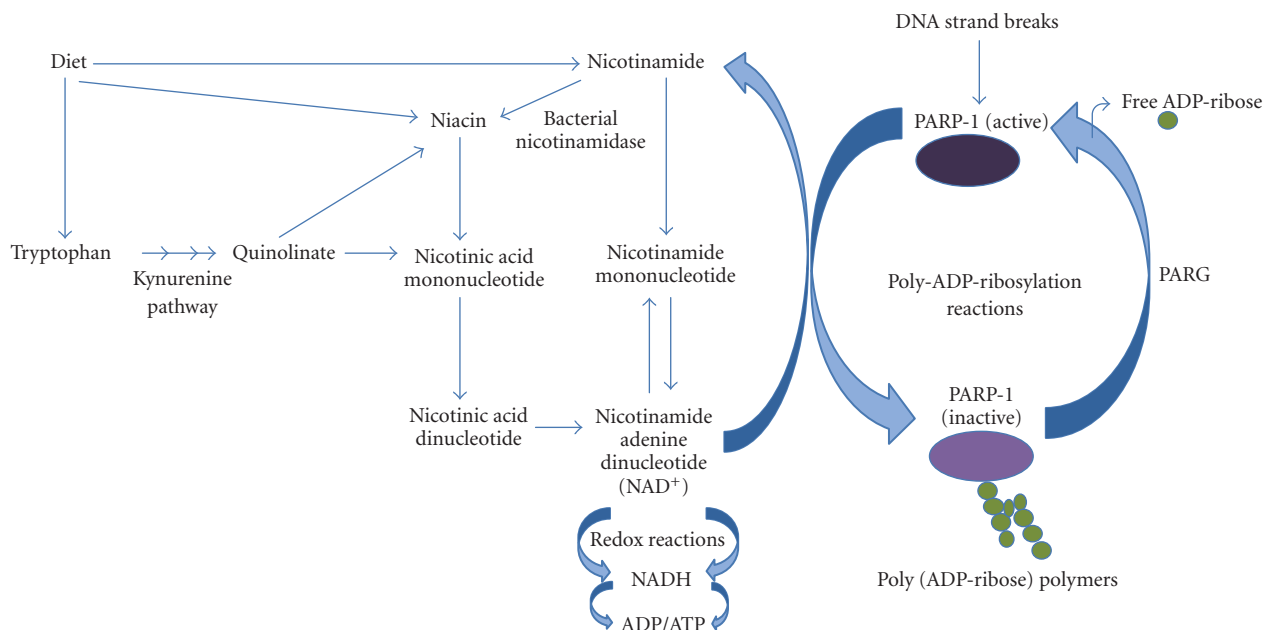


FIGURE 2: The simplified pathways for nicotinamide, niacin, NAD<sup>+</sup>, and PARP-1 metabolism. Dietary nicotinamide, niacin, and tryptophan are precursors for the synthesis of NAD<sup>+</sup>, essential in ATP production and PARP-1 activation. Nicotinamide can be converted to niacin by bacterial nicotinamidase in the intestinal lumen. PARP-1 is activated by DNA strand breaks, cleaving NAD<sup>+</sup> into nicotinamide and ADP-ribose. Poly(ADP-ribose) glycohydrolase (PARG) reactivates PARP-1 by removing poly(ADP-ribose) polymers, allowing for continuous NAD<sup>+</sup> utilization. Figure is adapted from Jacobson et al., in 1995 [6] and Meyer-Ficca et al., in 2004 [12].

mice, whereas 0.25% niacin did not show the same protection [41, 42]. However, higher concentrations of dietary niacin (0.4%) caused a 6% reduction in the incidence of nonlymphocytic leukemia induced by ethylnitrosourea in Weanling male Long-Evans rats [43]. Nicotinamide has also been shown to inhibit the growth of transplanted murine breast adenocarcinoma in mice, although the doses required are higher (2.5% and 5% diet; 1000 mg/kg bw intraperitoneal) than those needed to suppress carcinogen-induced cancers [44, 45]. The effect of nicotinamide on diethylnitrosamine (DEN)-, streptozotocin-, and heliotrine-induced carcinogenesis seems to be organ-specific. Massive doses of nicotinamide (350–500 mg/kg bw intraperitoneal, multiple dosing) inhibited DEN-induced liver tumours (34% reduction), but promoted DEN-induced kidney neoplasia (44% increase) in Wistar rats [46]. However, in another study of DEN-induced carcinogenesis, even low-dose nicotinamide (0.082% and 0.37% oral) increased the incidence of DEN-induced kidney tumours from 5% in controls (DEN only) to 28% and 59%, respectively, in male F344 rats [47]. 0.37% nicotinamide by itself had no effect on tumour formation [47], suggesting that the presence of carcinogen is required for the tumour promoting or inhibiting effect of nicotinamide.

Intraperitoneal nicotinamide (350 mg/kg) increased the incidence of streptozotocin-induced pancreatic islet-cell tumours in male Holtzman rats from 4% in controls (streptozotocin only) to 64% [48], but it decreased the incidence of renal adenomas from 77% to 18% [49]. Nicotinamide administered intraperitoneally at 500 mg/kg to

white male weanling rats before and after administration of pyrrolizidine alkaloid heliotrine increased pancreatic islet-cell tumours [50]. The varying effects of nicotinamide with different carcinogens and target organs may reflect the differential susceptibility of each organ to DNA damaging agents. Furthermore, it has been shown that PARP-1 protein expression is tissue- and/ or cell-type specific [51], and there are tissue and species differences in requirements for NAD<sup>+</sup> precursors. Tissues with high cellular turnover including breast, lung, and skin have higher NAD<sup>+</sup> requirements, and mice are relatively more resistant to niacin deficiency compared to rats or humans [23]. Hence, the breast, lung, and skin tissues of rats and humans likely required higher doses of NAD<sup>+</sup> precursors in the face of genomic insults.

#### 4. Nicotinamide: Photoimmunosuppression and Skin Cancer

The immune system is an important defense mechanism that prevents potentially cancerous cells from developing into tumors. In humans, the importance of immunity in preventing cancer is observed in renal transplant recipients on immunosuppressive medications. In this population, there is an increased incidence of all cancer type (13.7-fold increase), nonmelanoma skin cancer (33-fold increase), and melanoma (3.3-fold increase) compared to age-matched immune competent individuals [58]. Ultraviolet (UV) radiation in sunlight is the primary initiator of skin cancer by

TABLE 1: Animal models of nicotinamide or niacin effect on carcinogenesis.

Animal	Carcinogen	Form of nicotinamide (dose)	Organ	Effect on tumor	Ref.
Mouse	None	Oral	All	None	[40]
Mouse	UV	Topical(200 $\mu$ M)	Skin	Inhibition	[52]
Mouse	UVB	Oral (niacin)(0.5%; 1% diet)	Skin	Inhibition	[53]
Mouse	TPA	Topical (150 $\mu$ M)	Skin	Inhibition	[54]
Mouse	DMBA and Croton oil	Oral(0.2% diet)	Skin	None	[55]
Mouse	Urethane	Oral (0.25%; 0.4% diet)	Lung	Inhibition	[41]
		Oral (niacin) (0.25% diet)	Lung	None	
Mouse	Urethane	Oral (1%; 2.5% diet)	Lung	Inhibition	[42]
Rat	ENU	Oral (niacin) (0.4% diet)	Bone marrow (haemopoietic cells)	Inhibition	[43]
Rat	Bracken fern	Oral (0.5% diet)	Intestine	Inhibition	[56]
			Bladder	Inhibition	
Hamster	BOB	ip (30 mg/kg bw)	Pancreas	Inhibition	[57]
Rat	DEN	ip (350–500 mg/kg bw)	Kidney	Increase	[46]
			Liver	Inhibition	
Rat	DEN	Oral (0.082%; 0.37%)	Kidney	Increase	[47]
Rat	Streptozotocin	ip (350 mg/kg bw)	Pancreas	Increase	[48]
Rat	Streptozotocin	ip (350 mg/kg bw)	Kidney	Inhibition	[49]
Rat	Helioirine	ip (500 mg/kg bw)	Pancreas	Increase	[50]
Mouse	Transplanted murine breast adenocarcinoma	Oral (2.5%; 5%)	Recipient subcutaneous tissue	Inhibition	[44]
Mouse	Transplanted murine breast adenocarcinoma	ip (1000 mg/kg bw)	Recipient subcutaneous tissue	Inhibition	[45]

causing DNA damage in the skin and also by suppressing cutaneous immunity, even at exposure doses 25% to 50% of those required to cause mild sunburn [59]. Both UVB (290–320 nm) and UVA (320–400 nm) in sunlight are immune suppressive [60, 61]. UV-induced DNA damage, particularly in the form of cyclobutane pyrimidine dimers (CPDs), is an important molecular trigger for UV-induced immunosuppression [62]. Agents that can modulate DNA repair and prevent UV-induced immunosuppression may thus reduce skin cancer.

In mice, 200  $\mu$ M topical nicotinamide [52] and 0.5% and 1% niacin-supplemented diets [53] have both been shown to markedly protect against UV-induced immunosuppression and significantly reduce the incidence of UV-induced skin tumours. In these studies, UV-induced immunosuppression was measured by passive transfer assay, whereby splenocytes from irradiated mice enhanced the growth of antigenic tumours in unirradiated, recipient mice [52, 53]. Topical nicotinamide also slowed down the rate of skin tumour development [52] and the effect of oral niacin on tumour inhibition was greater with increasing dose [53]. Oral niacin increased skin NAD<sup>+</sup> levels, which were reduced by UVR in mice not receiving niacin, and this was thought to contribute to tumour prevention [52, 53]. It was also suggested that protection from photoimmunosuppression is a mechanism by which nicotinamide and niacin prevent UV-induced carcinogenesis [52, 53].

Using the Mantoux model of delayed-type hypersensitivity (DTH) in healthy volunteers, we have shown that nicotinamide protects from UV-induced immunosuppression in humans [63, 64]. 5% topical nicotinamide, applied 15 minutes before or after each of 3 daily exposures to low-dose solar-simulated (ss) UV (equivalent to less than  $\sim$ 8 minutes exposure to Sydney spring sunlight [65]), prevented UV-induced suppression of Mantoux reactions [63]. 5% topical nicotinamide, applied immediately after a single exposure to narrowband UVB (300 nm) or UVA (385 nm), protected against immunosuppression by both wavebands [66]. Using the same model, oral nicotinamide has also been shown to protect skin immunity in humans [64].

## 5. Nicotinamide, PARP-1 and DNA Repair

The role of nicotinamide in DNA repair and maintenance of genomic stability is tightly related to its functions as an NAD<sup>+</sup> precursor and a substrate for PARP-1. PARP-1 is a nuclear enzyme which detects DNA damage, binds to DNA single or double strand breaks, and then uses NAD<sup>+</sup> as a substrate to form nicotinamide and ADP-ribose. Subsequent enzymatic reactions lead to the formation of branched ADP-ribose polymers on a nuclear acceptor protein [67, 68] (Figure 2). Poly(ADP-ribosylation) of the acceptor protein has been hypothesized to function in DNA repair by modifying structural proteins proximal to DNA

strand breaks, facilitating the opening of the condensed chromatin structure, which is required for the recruitment of DNA repair complexes [69, 70]. The major acceptor proteins of poly(ADP-ribose) are PARP-1 itself, and auto-poly(ADP-ribosylation) results in downregulation of the enzyme [70]. Other major acceptor proteins reported are histone, topoisomerase I and II, DNA polymerase  $\alpha$  and  $\beta$ , DNA ligase I and II, nuclear retinoid X receptor, nuclear factor (NF)- $\kappa$ B, and p53 [70, 71]. Poly(ADP-ribose) glycohydrolase (PARG) is the main enzyme involved in catabolism of poly(ADP-ribose), cleaving it into free ADP-ribose monomers [70]. PARP-1 itself is also known to be part of chromatin structure and involved in maintaining a compact chromatin structure, preventing inadvertent transcription from occurring [72]. Unfolding of the compact chromatin structure allows DNA regulatory and repair processes access to the damaged sites as well as to replication and transcription initiation sites [73]. PARP-1 has been reported to play a key role in the nucleotide excision repair (NER) pathway used to remove bulky DNA adducts [74] and in the base excision repair (BER) pathway by interacting with BER protein XRCC1 (X-ray repair cross-complementing 1) [75–78]. PARP-1 is involved in maintaining chromosomal integrity by protecting broken DNA from inappropriate homologous recombination during DNA repair and replication [79, 80]. PARP knockout mice exhibited dramatically increased sensitivity to ionizing radiation and alkylating agents [81–83] and showed a 2–3-fold increase in spontaneous sister chromatid exchange (SCE) and amplified SCE and micronuclei (MN) formation induced by carcinogens [83, 84]. PARP-null mice also showed extreme sensitivity to nitrosamine-induced carcinogenesis [85], had shorter telomeres, and increased end-to-end chromosomal fusions, aneuploid cells, and chromosome fragments [86]. Thus, nicotinamide is involved in maintenance of genomic stability by providing a substrate for PARP-1, preserving a cellular energy reserve for ATP-dependent DNA repair [87] and enabling preservation of PARP-1 integrity [88].

## 6. The Influence of NAD<sup>+</sup> Status on Genomic Stability and DNA Repair

**6.1. In Vitro Studies.** A large number of *in vitro* studies reported that NAD<sup>+</sup> status influences genomic stability and sensitivity to cytotoxic effects of DNA-damaging agents. Nicotinamide (50–500  $\mu$ M) increased intracellular NAD<sup>+</sup> and enhanced the repair of DNA damage induced by N-methyl-N'-nitro-N-nitrosoguanidine (MNNG) in cultured primary human mammary epithelial cells [23]. Preincubation with 74  $\mu$ M nicotinamide prevented NAD<sup>+</sup> depletion after dimethyl sulphate (DMS) exposure and increased strand break rejoining rate [89]. Increasing NAD<sup>+</sup> status by the addition of nicotinamide thus improved the capacity of DNA repair. NAD<sup>+</sup> is also an important determinant of skin cell survival following UV radiation. 0.1 and 33  $\mu$ M nicotinamide added to UV-irradiated cultured human skin fibroblasts increased cell survival 7 days post irradiation in a dose-dependent manner [90]. Even in the absence of genotoxic stress, NAD<sup>+</sup> depletion increased spontaneous

DNA damage in human HaCaT keratinocytes, which was reversible with the addition of nicotinamide [91]. NAD<sup>+</sup> status is therefore critical in preserving genomic function of skin cells. Furthermore, it was shown that skin NAD<sup>+</sup> levels are negatively correlated with malignant phenotype in human skin cancers. Normal skin from patients with premalignant actinic keratoses had significantly higher NAD<sup>+</sup> than normal skin from patients with cutaneous squamous cell cancers [23].

Exposure of *ex vivo* human lymphocytes to oxygen radicals [92], UVB [93, 94],  $\gamma$ -irradiation [95], N-methyl-N'-nitro-N-nitrosoguanidine (MNNG) [93, 94], or dimethyl sulfate (DMS) [93] resulted in reduced intracellular NAD<sup>+</sup>, with numbers of DNA-strand breaks inversely correlated with NAD<sup>+</sup> levels [92]. Addition of 2–5 mM nicotinamide prevented this lowering of NAD<sup>+</sup> levels, stimulated unscheduled DNA synthesis (UDS), and increased DNA repair [93–95]. The ability of nicotinamide to enhance DNA repair depends on the presence of functional repair mechanisms. Xeroderma pigmentosum is an autosomal recessive genetic disorder of DNA repair, in which the ability to repair DNA damage caused by UVR is deficient. [96]. In the presence of 2 mM nicotinamide, lymphocytes from these patients exhibited increased UDS after MNNG treatment but failed to show increased UDS after UVB irradiation. Normal lymphocytes incubated with the same dose of nicotinamide, in contrast, showed increased UDS and enhancement of DNA repair after UVB or MNNG exposures [97].

In HaCaT cells (human keratinocyte cell line) NAD<sup>+</sup> depletion upregulated NADPH oxidase activity with consequent increase in reactive oxygen species (ROS) production. NAD<sup>+</sup> repletion with nicotinamide completely reversed the ROS accumulation [91]. In support of these findings, niacin deficiency, which results in intracellular NAD<sup>+</sup> depletion in rats, also caused an increase in both protein carbonyls and 8-oxo-7,8-dihydro-2'-deoxyguanosine (8-oxo-dG) in bone marrow [98]. Oxidative-induced DNA damage 8-oxo-dG is a miscoding lesion, which generates GC  $\rightarrow$  TA transversion mutations by pairing with an adenine instead of a cytosine during replication [99]. ROS also damages other cellular components including cell membranes by peroxidation of fatty acids within the phospholipid bilayer and proteins by forming carbonyl derivatives [100]. Lipid peroxidation increases production of prostaglandins (PG), including PGE<sub>2</sub>, which is known to play an important role in inflammation. Inflammation in premalignant actinic keratoses has been reported to be a marker of progression to squamous cell carcinoma [101]. It was also postulated that ROS may cause gene mutations in actinic keratoses, driving their progression to squamous cell carcinoma [101]. Regulation of ROS levels by maintenance of intracellular NAD<sup>+</sup> is therefore important in preventing oxidative DNA damage and gene mutation.

**6.2. In Vivo Studies.** Administration of 100 mg/day niacin to two volunteers for 8 weeks protected against *ex vivo* lymphocyte DNA strand breaks induced by hypoxanthine/xanthine oxidase. The supplementation increased NAD<sup>+</sup> concentrations by nearly 5 times baseline levels and significantly

reduced oxygen radical-induced DNA strand breaks in the lymphocytes [92].

The impact of niacin deficiency in rats has been extensively studied by the Kirkland group [98, 102–106]. Wenling Long-Evans rats were kept niacin-deficient (ND) or were pair-fed (PF) either normal dietary niacin or supplemental 4 mg/gram niacin (NA) (0.4% of diet). The DNA-alkylating agent ethylnitrosurea (ENU) or the topoisomerase II inhibitor etoposide (ETO) was then administered to these rats orally. Bone marrow is a good indicator of niacin intake. ND diets caused 72%–80% [102, 104] reduction in bone marrow NAD<sup>+</sup> content, whereas NA diets produced a 240% increase [103]. Basal poly(ADP-ribose) levels were also significantly lower in ND rats. After ENU- or ETO-treatment, poly(ADP-ribose) levels were not increased in bone marrow of ND rats whereas in PF and NA rats, the level of bone marrow poly(ADP-ribose) rose significantly [102, 104]. Adequate NAD<sup>+</sup> is therefore essential for the increase in ADP-ribose polymer metabolism activated by DNA damage. Niacin deficiency alone causes increased micronuclei (MN) formation (6.2-fold), SCE frequency (2.8-fold) [103], chromosomes breaks (4-fold), and chromatid breaks (2-fold). With ENU- or ETO-treatment, there were much greater increases in MN formation, SCE, and chromosomal aberrations (CA) in bone marrow of ND rats [103, 105]. The increased genomic instability in ND rats is further evidenced by the reduction in latency and the increase in the incidence of developing ENU-induced leukemia [102]. Niacin deficiency significantly delayed DNA repair in bone marrow after ENU- or ETO-treatment [103, 105] and was shown to alter p53 expression and impair ETO-induced cell cycle arrest and apoptosis [104].

## 7. Nicotinamide, PARP-1, and Cellular Responses to DNA Damage

The activation of PARP-1 by DNA strand breaks can lead to three cellular pathways depending on the intensity of DNA-damaging stimuli [70] (Figure 3). In the case of relatively mild DNA damage, PARP-1 activation enhances DNA repair by interacting with p53 protein, signaling cell-cycle arrest, and facilitating DNA repair enzymes, including XRCC1 and DNA-dependent protein kinases to access damaged DNA [70]. When DNA damage is irreparable, PARP-1 activation induces apoptotic cell death by activating NF- $\kappa$ B pathway and preventing ATP depletion and DNA repair through caspase-mediated PARP-1 cleavage [70, 107]. In contrast, extensive DNA damage leads to PARP-1 overactivation, depleting its substrate (NAD<sup>+</sup>). As cells consume ATP in an attempt to replenish NAD<sup>+</sup>, this leads to a cellular energy crisis, which precipitates necrotic cell death [70]. Apoptosis is an energy-dependent process [108–111] thus cells severely deficient in energy are unable to proceed through apoptotic cell death.

PARP-1 is inhibited by nicotinamide and its analogues such as 3-aminobenzamide and metoclopramide [112, 113]. PARP-1 inhibition by nicotinamide *in vitro* has been reported to delay the rejoining of DNA strand breaks [95, 114, 115],

induce UDS [95, 97, 116], and increase the frequency of spontaneous SCE [117, 118]. It has been suggested that high dose of nicotinamide (5 mM or more) inhibits DNA repair through PARP-1 inhibition while low dose nicotinamide enhances rejoining of DNA strand breaks through provision of NAD<sup>+</sup> [114]. However, it is argued that nicotinamide is unlikely to inhibit PARP *in vivo* [119]. Rats fed nicotinamide 33 times above normal requirements exhibited 2-fold increases in basal poly(ADP-ribose). After exposure to a hepatocarcinogen, induction of poly(ADP-ribose) was only marginally higher in the nicotinamide supplemented rats [120], suggesting that a much higher dose of nicotinamide is required to possibly inhibit PARP-1 in the whole organism.

Excessive PARP activity is however detrimental to cells. Augmented PARP activity caused by reactive oxygen injury to cultured pulmonary-artery endothelial cells resulted in NAD<sup>+</sup> and ATP depletion and necrotic cell death, which was prevented by the PARP-1 inhibitors nicotinamide and 3-aminobenzamide (3-AB) [121]. *Ex vivo* murine lung exposed to bleomycin, a DNA-cleaving antitumor antibiotic, caused acute lung injury through sustained PARP activation and NAD<sup>+</sup> depletion. This injury was prevented in the presence of 3-AB [122]. The topical PARP inhibitor, BGP-15M (O-(3-piperidino-2-hydroxy-1-propyl) pyrimide-3-carboxylic acid amidoxime monohydrochloride) reduced UVB-induced DNA strand breaks in hairless mouse skin and prevented excessive production of poly(ADP-ribose) induced by moderate UV doses. These findings suggest that the inhibition of PARP-1 overactivation, and therefore of NAD<sup>+</sup> and ATP depletion, can occur without negative consequence to DNA repair [123].

PARP-1 inhibition by nicotinamide has been shown to switch the mode of cell death from necrosis to apoptosis in *ex vivo* human lymphocytes treated with hydrogen peroxide [124]. In addition, it has been widely reported that in the cells exposed to oxidative stress, both ATP and NAD<sup>+</sup> levels serve as crucial molecular switches between apoptosis and necrosis [125–133]. Nicotinamide as a precursor of NAD<sup>+</sup>, ATP, and as an endogenous inhibitor of PARP-1 therefore plays significant roles in cellular protection and in determining cellular fate in response to genotoxic DNA damage.

## 8. Nicotinamide, PARP-1, and Regulation of Gene Expression

PARP-1 has been reported to frequently associate with transcriptionally active regions of chromatin [134, 135]. PARP-1 is a transcription coactivator of nuclear factor- $\kappa$ B (NF- $\kappa$ B) [136], a transcription factor that plays a significant role in regulation of genes involved in a variety of cellular processes including immune and inflammatory responses, apoptosis, cell proliferation, and differentiation [137, 138]. There is a large amount of literature supporting the involvement of NF- $\kappa$ B in cutaneous carcinogenesis [136, 139]. Epidermal inflammation promotes tumor progression [101] and NF- $\kappa$ B is known to be one of the mediators involved [139]. PARP-1 knockout mice are much less sensitive to inflammatory stress [140, 141] and PARP-1 deficient mice exhibited

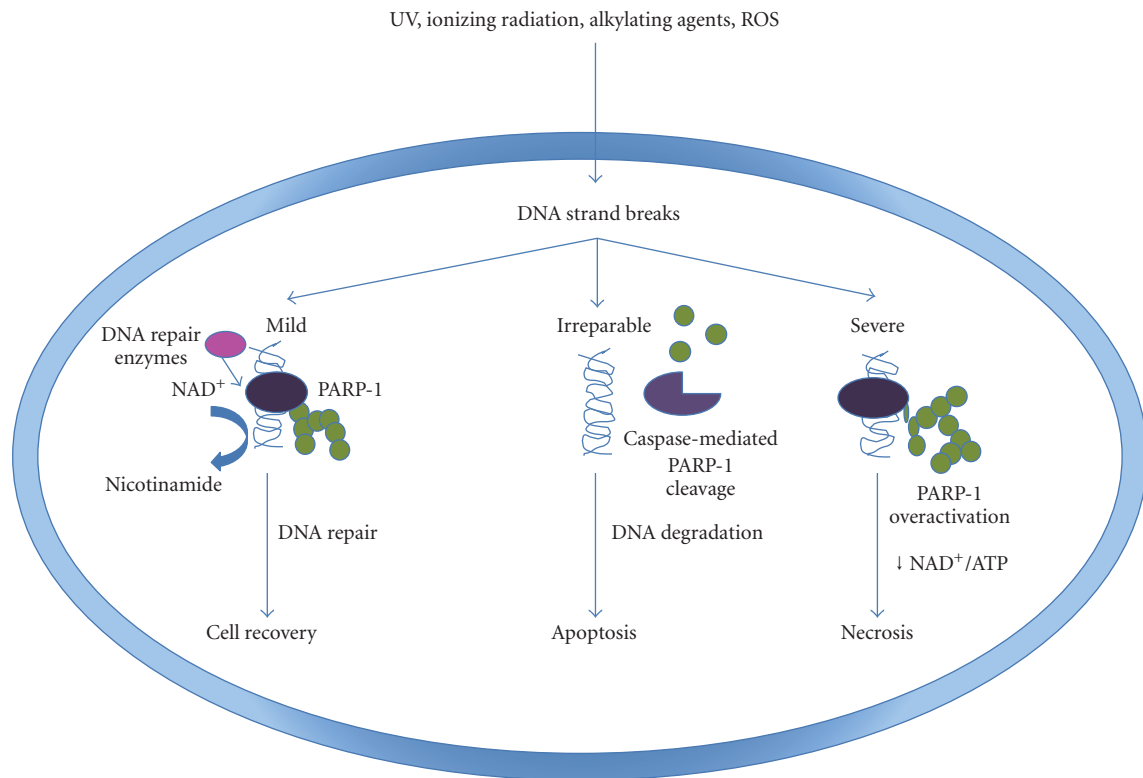


FIGURE 3: PARP-1 and cellular responses to DNA damage. The intensity of DNA damage determines cellular pathways: survival, apoptosis, or necrosis. In the case of mild DNA damage, poly(ADP-ribosylation) enhances DNA repair and thus cell survival. When the damage is beyond repair, PARP-1 facilitates apoptosis, preventing ATP depletion and DNA repair through PARP-1 caspase-mediated cleavage. Severe DNA damage leads to PARP-1 overactivation, cellular energy depletion, and necrotic cell death. Figure is adapted from Virág and Szabó, in 2002 [70].

substantially reduced sensitivity to the carcinogenic effect of DMBA and TPA on the skin [136]. In PARP-1 null (*parp-1<sup>-/-</sup>*) mice, the development of skin papillomas induced by DMBA and TPA was significantly delayed and reduced in numbers compared to control (*parp-1<sup>+/+</sup>*) mice. PARP-1 inhibition in mice with 3,4-dihydro-5-[4-(1-piperidinyl)butoxy]-1(2H)-isoquinoline (DPQ) also had the same effect [142]. PARP-1 inhibition with nicotinamide and benzamides was also shown to inhibit NF- $\kappa$ B in vitro and suppress lipopolysaccharide-induced TNF- $\alpha$  production in mice [143]. Indirect inhibition of NF- $\kappa$ B by elimination or inhibition of PARP-1 may prevent activation of  $\kappa$ B-target genes, leading to suppression of inflammation and expression of genes associated with tumor progression [136]. Although PARP-1 knockout mice as mentioned previously have increased genomic instability in response to alkylating agents and ionizing radiation [81–83] and were more recently shown to be more sensitive to nitrosamine- [85] and azoxymethane-induced cancers [144], it is thought that this controversy can be explained by the unique environmental and intrinsic factors involved in tumorigenesis of differing genotoxic agents and organs [136].

PARP-1 inhibition by DPQ or by genetic deletion of PARP-1 in mice was also found to normalize or downregulate some upregulated genes in DMBA/TPA-treated skin, including several tumor-associated genes in mouse and human

and genes involved in oxidative stress, inflammation, and the immune response. Of particular importance is the absence of induction of Hif (Hypoxia inducible factor)-1 $\alpha$  in the PARP-1 deficient and DPQ-treated murine skin [142]. The transcription factor Hif-1 $\alpha$  promotes the adaptation of tumour cells to hypoxia, including angiogenesis, vasodilation, glucose transport, and anaerobic metabolism [145]. It was also noted that in the tumours of DPQ-treated mice, there were increased apoptotic cells, suggesting that inhibition of Hif-1 $\alpha$  may contribute to tumour death through failure of these cells to adapt to hypoxia [142]. In our research group, topical nicotinamide was found to normalize subsets of apoptosis, energy metabolism, and immune function-related genes that are downregulated by UVR in human skin [63]. Low dose of ssUV was shown in this study to downregulate apoptotic genes BCL2, TP53, IGF1R, PRKCA, and AKT1, which are also involved in the regulation of telomerase activity, and thought to play important roles in the initiation of skin carcinogenesis [63, 146]. Normalisation of these subsets of genes by nicotinamide suggests its involvement in apoptosis and early events in skin carcinogenesis. The downregulation of genes for energy production in ssUV-treated skin supports evidence for the cellular energy decline known to be induced by UVR [90]. As previously mentioned, DNA repair requires ATP [87], and an adequate NAD<sup>+</sup> level is critical in maintaining the genomic integrity of skin

cells during UV radiation [90]. Consistent with its role as an NAD<sup>+</sup> and ATP precursor, nicotinamide protects the cell from UVR-induced energy depletion. Nicotinamide also normalized ssUV downregulation of TP53 genes. p53 is a key regulator of cell cycle arrest and apoptosis in response to DNA damage [147]. In response to genotoxic stress, p53 is stabilized and activated by posttranslational modifications, including poly(ADP-ribosyl)ation, phosphorylation, and acetylation [148, 149]. Niacin deficiency in rats [104] and nicotinamide depletion in cultured cells derived from breast, lung, and skin cells [23] caused decreased expression of the tumor suppressor protein, p53. PARP-1 inhibition has been shown to decrease basal p53 levels and impairs p53 stabilization after DNA damage [150]. In addition, PARP-1 deficient cell lines exhibit a significant reduction in both baseline p53 expression and its activity compared to normal wild type cells [150]. Diminished p53 function is highly associated with malignancy in breast, lungs, and skin [151]. Nicotinamide prevented UV-induced downregulation of p53, suggesting its mode of protection from genotoxic effect of UVR. The effect of nicotinamide on p53 regulation has also been reported to be independent of PARP [152].

## 9. Conclusion

Nicotinamide, which is the dietary precursor for NAD<sup>+</sup>, provides a substrate for PARP-1 activity. The activation of nuclear enzyme PARP-1 by DNA strand breaks during cellular genotoxic stress responses leads to complex signaling pathway that can enhance DNA repair, result in apoptotic cell death, or cause cellular energy loss leading to necrotic cell death. *In vivo* and *in vitro* studies showed that NAD<sup>+</sup> content of the cells influences responses to DNA damaging agents. NAD<sup>+</sup> depletion impairs ADP-ribose polymer metabolism and increases genomic instability in the face of genotoxic and oxidative stress challenges. Nicotinamide deficiency in humans may also contribute to increased frequency of gastrointestinal cancers in certain populations although other micronutrient deficiencies are likely to be involved as well. Nicotinamide supplementation in animal models has opposing effect on carcinogenesis, depending on the type of carcinogens and target organs. Nicotinamide protected against UV-induced immunosuppression in mice and humans and UV-induced carcinogenesis in mice. Limited study in humans indicates that skin NAD<sup>+</sup> content is an important determinant of malignant phenotype. Thus, nicotinamide supplementation may influence the progression of premalignant actinic keratoses to malignant squamous cell cancers. PARP-1 plays a key role in regulation of genes involved in inflammation, apoptosis, and cellular differentiation. While PARP-1 inhibition could impair its role in DNA repair, PARP-1 overactivation is detrimental to the cells by depleting its substrate NAD<sup>+</sup>, which leads to cellular energy crisis and necrotic cell death. In various murine models, PARP-1 inhibition was shown to favor apoptotic cell death, reduce inflammatory response, and reduce genomic sensitivity to various carcinogens. However, extrapolation of these data to human, particularly when

physiological regimes involved in human carcinogenesis, should be done cautiously. Further studies are needed to determine the effect of high-dose nicotinamide on *in vivo* carcinogenesis and genomic stability of the cancer cells and the surrounding normal cells.

## Abbreviations

BOB	N-nitrosobis(2-oxopropylamine)
DEN:	diethylnitrosamine
DMBA:	9,10-dimethyl-12-benzanthracene
DMS:	dimethyl sulphate
DTH:	delayed-type hypersensitivity
ETO:	etoposide; FBS, fetal bovine serum
MN:	micronuclei
MNNG:	N-methyl-N'-nitro-N-nitrosoguanidine
NAD <sup>+</sup> :	nicotinamide adenine dinucleotide
PARP:	poly-ADP-ribose polymerase
ROS:	reactive oxygen species
SCE:	sister chromatid exchange
ssUV:	solar-simulated ultraviolet
TPA:	12-O-tetradecanoylphorbol-13-acetate
UDS:	unscheduled DNA synthesis
UVR:	ultraviolet radiation.

## References

- [1] R. A. Jacob and M. E. Swendseid, "Niacin," in *Present Knowledge in Nutrition*, E. E. Ziegler and L. J. Filer, Eds., pp. 184–190, ILSI Press, Washington, DC, USA, 1996.
- [2] C. A. Benavente, M. K. Jacobson, and E. L. Jacobson, "NAD in skin: therapeutic approaches for niacin," *Current Pharmaceutical Design*, vol. 15, no. 1, pp. 29–38, 2009.
- [3] K. Karthikeyan and D. M. Thappa, "Pellagra and skin," *International Journal of Dermatology*, vol. 41, no. 8, pp. 476–481, 2002.
- [4] "Nutrient Reference Values for Australian and New Zealand, including recommended dietary intake," pp.1–329, National Health and Medical Research Council publication, Canberra, Australia, 2006.
- [5] T. M. Jackson, J. M. Rawling, B. D. Roebuck, and J. B. Kirkland, "Large supplements of nicotinic acid and nicotinamide increase tissue NAD<sup>+</sup> and poly(ADP-ribose) levels but do not affect diethylnitrosamine-induced altered hepatic foci in Fischer-344 rats," *Journal of Nutrition*, vol. 125, no. 6, pp. 1455–1461, 1995.
- [6] E. L. Jacobson, A. J. Dame, J. S. Pyrek, and M. K. Jacobson, "Evaluating the role of niacin in human carcinogenesis," *Biochimie*, vol. 77, no. 5, pp. 394–398, 1995.
- [7] Cosmetic Ingredient Review (CIR) Expert Panel, "Final report of the safety assessment of niacinamide and niacin," *International Journal of Toxicology*, vol. 24, pp. 1–31, 2005.
- [8] J. Denekamp and J. F. Fowler, "ARCON—current status: summary of a workshop on preclinical and clinical studies," *Acta Oncologica*, vol. 36, no. 5, pp. 517–525, 1997.
- [9] S. L. Winter and J. L. Boyer, "Hepatic toxicity from large doses of vitamin-B3 (Nicotinamide)," *New England Journal of Medicine*, vol. 289, no. 22, pp. 1180–1182, 1973.
- [10] J. H. A. M. Kaanders, M. R. L. Stratford, J. Liefers et al., "Administration of nicotinamide during a five- to seven-week course of radiotherapy: pharmacokinetics, tolerance,

- and compliance," *Radiotherapy and Oncology*, vol. 43, no. 1, pp. 67–73, 1997.
- [11] R. E. Ranchoff and K. Tomecki, "Niacin or niacinamide? Nicotinic acid or nicotinamide? What is the difference?" *Journal of the American Academy of Dermatology*, vol. 15, no. 1, pp. 116–117, 1986.
- [12] M. L. Meyer-Ficca, R. G. Meyer, E. L. Jacobson, and M. K. Jacobson, "Poly(ADP-ribose) polymerases: managing genome stability," *International Journal of Biochemistry and Cell Biology*, vol. 37, no. 5, pp. 920–926, 2005.
- [13] W. M. Hendricks, "Pellagra and pellagralike dermatoses: etiology, differential diagnosis, dermatopathology, and treatment," *Seminars in Dermatology*, vol. 10, no. 4, pp. 282–292, 1991.
- [14] P. Chambon, J. D. Weill, and P. Mandel, "Nicotinamide mononucleotide activation of a new DNA-dependent polyadenylic acid synthesizing nuclear enzyme," *Biochemical and Biophysical Research Communications*, vol. 11, no. 1, pp. 39–43, 1963.
- [15] F. J. Oliver, J. Menissier-de Murcia, and G. De Murcia, "Poly(ADP-Ribose) polymerase in the cellular response to DNA damage, apoptosis, and disease," *American Journal of Human Genetics*, vol. 64, no. 5, pp. 1282–1288, 1999.
- [16] J. P. Kamat and T. P. A. Devasagayam, "Methylene blue plus light-induced lipid peroxidation in rat liver microsomes: inhibition by nicotinamide (vitamin B3) and other antioxidants," *Chemico-Biological Interactions*, vol. 99, no. 1–3, pp. 1–16, 1996.
- [17] K. Yamada, K. Nonaka, T. Hanafusa, A. Miyazaki, H. Toyoshima, and S. Tarui, "Preventative and therapeutic effects of large-dose nicotinamide injections on diabetes associated with insulinitis—an observation in non-obese diabetic (NOD) mice," *Diabetes*, vol. 31, no. 9, pp. 749–753, 1982.
- [18] D. M. Abdallah, "Nicotinamide alleviates indomethacin-induced gastric ulcers: a novel antiulcer agent," *European Journal of Pharmacology*, vol. 627, no. 1–3, pp. 276–280, 2010.
- [19] A. M. Vincent, M. J. Stevens, C. Backus, L. L. Mclean, and E. L. Feldman, "Cell culture modeling to test therapies against hyperglycemia-mediated oxidative stress and injury," *Antioxidants and Redox Signaling*, vol. 7, no. 11–12, pp. 1494–1506, 2005.
- [20] G. L. Wilson, N. J. Patton, and J. M. McCord, "Mechanisms of streptozotocin- and alloxan-induced damage in the rat B-cells," *Diabetologia*, vol. 27, no. 6, pp. 587–591, 1984.
- [21] C. Q. Vu, D. L. Coyle, H. H. Tai, E. L. Jacobson, and M. K. Jacobson, "Intramolecular ADP-ribose transfer reactions and calcium signalling," in *ADP-Ribosylation in Animal Tissue: Structure, Function, and Biology of Mono-ADP-Ribosyltransferases and Related Enzymes*, F. Haag and F. Koch-Nolte, Eds., pp. 381–388, Plenum Press, New York, NY, USA, 1997.
- [22] C. O. Vu, D. L. Coyle, E. L. Jacobson, and M. K. Jacobson, "Intracellular signaling by cyclic ADP-Ribose in oxidative cell injury," *FASEB Journal*, vol. 11, no. 9, p. 1522, 1997.
- [23] E. L. Jacobson, W. M. Shieh, and A. C. Huang, "Mapping the role of NAD metabolism in prevention and treatment of carcinogenesis," *Molecular and Cellular Biochemistry*, vol. 193, no. 1–2, pp. 69–74, 1999.
- [24] W. J. Blot, J.-Y. Li, P. R. Taylor et al., "Nutrition intervention trials in Linxian, China. Supplementation with specific vitamin/mineral combinations, cancer incidence, and disease-specific mortality in the general population," *Journal of the National Cancer Institute*, vol. 85, no. 18, pp. 1483–1492, 1993.
- [25] S. Franceschi, E. Bidoli, A. E. Baron, and C. La Vecchia, "Maize and risk of cancers of the oral cavity, pharynx, and esophagus in Northeastern Italy," *Journal of the National Cancer Institute*, vol. 82, no. 17, pp. 1407–1411, 1990.
- [26] E. Negri, S. Franceschi, C. Bosetti et al., "Selected micronutrients and oral and pharyngeal cancer," *International Journal of Cancer*, vol. 86, no. 1, pp. 122–127, 2000.
- [27] F. Siassi, Z. Pouransari, and P. Ghadirian, "Nutrient intake and esophageal cancer in the caspian littoral of Iran: a case-control study," *Cancer Detection and Prevention*, vol. 24, no. 3, pp. 295–303, 2000.
- [28] G. C. Kabat, A. B. Miller, M. Jain, and T. E. Rohan, "Dietary intake of selected B vitamins in relation to risk of major cancers in women," *British Journal of Cancer*, vol. 99, no. 5, pp. 816–821, 2008.
- [29] L. B. Zablotska, Y. Chen, J. H. Graziano et al., "Protective effects of B vitamins and antioxidants on the risk of arsenic-related skin lesions in Bangladesh," *Environmental Health Perspectives*, vol. 116, no. 8, pp. 1056–1062, 2008.
- [30] C. Pelucchi, I. Tramacere, P. Bertuccio, A. Tavani, E. Negri, and C. La Vecchia, "Dietary intake of selected micronutrients and gastric cancer risk: an Italian case-control study," *Annals of Oncology*, vol. 20, no. 1, pp. 160–165, 2009.
- [31] C.-X. Qu, F. Kamangar, J.-H. Fan et al., "Chemoprevention of primary liver cancer: a randomized, double-blind trial in Linxian, China," *Journal of the National Cancer Institute*, vol. 99, no. 16, pp. 1240–1247, 2007.
- [32] C. Bosetti, L. Scotti, L. Dal Maso et al., "Micronutrients and the risk of renal cell cancer: a case-control study from Italy," *International Journal of Cancer*, vol. 120, no. 4, pp. 892–896, 2007.
- [33] E. L. Jacobson, "Niacin deficiency and cancer in women," *Journal of the American College of Nutrition*, vol. 12, no. 4, pp. 412–416, 1993.
- [34] R. I. Inculet, J. A. Norton, and G. E. Nichoalds, "Water-soluble vitamins in cancer patients on parenteral nutrition: a prospective study," *Journal of Parenteral and Enteral Nutrition*, vol. 11, no. 3, pp. 243–249, 1987.
- [35] S. Dreizen, K. B. McCredie, M. J. Keating, and B. S. Andersson, "Nutritional deficiencies in patients receiving cancer chemotherapy," *Postgraduate Medicine*, vol. 87, no. 1, pp. 163–170, 1990.
- [36] H. P. Stevens, L. S. Ostlere, R. H. J. Begent, J. S. Dooley, and M. H. A. Rustin, "Pellagra secondary to 5-fluorouracil," *British Journal of Dermatology*, vol. 128, no. 5, pp. 578–580, 1993.
- [37] C. W. Op Het Veld, S. Van Hees-Stuivenberg, A. A. Van Zeeland, and J. G. Jansen, "Effect of nucleotide excision repair on hprt gene mutations in rodent cells exposed to DNA ethylating agents," *Mutagenesis*, vol. 12, no. 6, pp. 417–424, 1997.
- [38] C. A. Felix, "Secondary leukemias induced by topoisomerase-targeted drugs," *Biochimica et Biophysica Acta*, vol. 1400, no. 1–3, pp. 233–255, 1998.
- [39] J. B. Kirkland, "Niacin and carcinogenesis," *Nutrition and Cancer*, vol. 46, no. 2, pp. 110–118, 2003.
- [40] B. Toth, "Lack of carcinogenicity of nicotinamide and isonicotinamide following lifelong administration to mice," *Oncology*, vol. 40, no. 1, pp. 72–75, 1983.
- [41] F. A. French, "The influence of nutritional factors on pulmonary adenomas in mice," in *Inorganic and Nutritional*

- Aspects of Cancer*, G. N. Schrauzer, Ed., Plenum Press, New York, NY, USA, 1978.
- [42] H. Gotoh, T. Nomura, H. Nakajima, C. Hasegawa, and Y. Sakamoto, "Inhibiting effects of nicotinamide on urethane-induced malformations and tumors in mice," *Mutation Research*, vol. 199, no. 1, pp. 55–63, 1988.
- [43] A.-P. Bartleman, R. Jacobs, and J. B. Kirkland, "Niacin supplementation decreases the incidence of alkylation-induced nonlymphocytic leukemia in long-evans rats," *Nutrition and Cancer*, vol. 60, no. 2, pp. 251–258, 2008.
- [44] H. Gotoh, T. Nomura, and C. Hasegawa, "Growth-inhibition of transplanted murine-breast cancer by nicotinamide in C3H/HEJ mice," *Cancer Research Therapy and Control*, vol. 3, no. 2, pp. 121–126, 1993.
- [45] M. R. Horsman, A. A. Khalil, D. J. Chaplin, and J. Overgaard, "The ability of nicotinamide to inhibit the growth of a C3H mouse mammary carcinoma," *Acta Oncologica*, vol. 34, no. 3, pp. 443–446, 1995.
- [46] R. Schoental, "The role of nicotinamide and of certain other modifying factors in diethylnitrosamine carcinogenesis: fusaria mycotoxins and spontaneous tumors in animals and man," *Cancer*, vol. 40, no. 4, pp. 1833–1840, 1977.
- [47] M. R. Rosenberg, D. L. Novicki, and R. L. Jirtle, "Promoting effect of nicotinamide on the development of renal tubular cell tumors in rats initiated with diethylnitrosamine," *Cancer Research*, vol. 45, no. 2, pp. 809–814, 1985.
- [48] N. Rakieten, B. S. Gordon, A. Beaty, D. A. Cooney, R. D. Davis, and P. S. Schein, "Pancreatic islet cell tumors produced by the combined action of streptozotocin and nicotinamide," *Proceedings of the Society for Experimental Biology and Medicine*, vol. 137, no. 1, pp. 280–283, 1971.
- [49] N. Rakieten, B. S. Gordon, and A. Beaty, "Modification of renal tumorigenic effect of streptozotocin by nicotinamide: spontaneous reversibility of streptozotocin diabetes," *Proceedings of the Society for Experimental Biology and Medicine*, vol. 151, no. 2, pp. 356–361, 1976.
- [50] R. Schoental, "Pancreatic islet cell and other tumors in rats given heliotrine, a monoester pyrrolizidine alkaloid, and nicotinamide," *Cancer Research*, vol. 35, no. 8, pp. 2020–2024, 1975.
- [51] V. Burkart, Z.-Q. Wang, J. Radons et al., "Mice lacking the poly(ADP-ribose) polymerase gene are resistant to pancreatic beta-cell destruction and diabetes development induced by streptozocin," *Nature Medicine*, vol. 5, no. 3, pp. 314–319, 1999.
- [52] H. L. Gensler, "Prevention of photoimmunosuppression and photocarcinogenesis by topical nicotinamide," *Nutrition and Cancer*, vol. 29, no. 2, pp. 157–162, 1997.
- [53] H. L. Gensler, T. Williams, A. C. Huang, and E. L. Jacobson, "Oral niacin prevents photocarcinogenesis and photoimmunosuppression in mice," *Nutrition and Cancer*, vol. 34, no. 1, pp. 36–41, 1999.
- [54] A. Ludwig, M. Dietel, G. Schafer, K. Muller, and H. Hilz, "Nicotinamide and nicotinamide analogues as antitumor promoters in mouse skin," *Cancer Research*, vol. 50, no. 8, pp. 2470–2475, 1990.
- [55] F. J. C. Roe, "Effect of massive doses of riboflavin, and other vitamins of the B group, on skin carcinogenesis in mice," *British Journal of Cancer*, vol. 16, pp. 252–257, 1964.
- [56] A. M. Pamukcu, U. Milli, and G. T. Bryan, "Protective effect of nicotinamide on bracken fern inducec carcinogenicity in rats," *Nutrition and Cancer*, vol. 3, p. 86, 1981.
- [57] P. M. Pour and T. Lawson, "Modification of pancreatic carcinogenesis in the hamster model. XV. Preventive effect of nicotinamide," *Journal of the National Cancer Institute*, vol. 73, no. 3, pp. 767–770, 1984.
- [58] F. J. Moloney, H. Comber, P. O'Lorcain, P. O'Kelly, P. J. Conlon, and G. M. Murphy, "A population-based study of skin cancer incidence and prevalence in renal transplant recipients," *British Journal of Dermatology*, vol. 154, no. 3, pp. 498–504, 2006.
- [59] G. M. Halliday and H. Honigsmann, "Sunscreens, photoimmunosuppression, and photoaging," in *Clinical Guide to Sunscreens and Photoprotection*, H. W. Lim and Z. D. Draelos, Eds., pp. 101–116, Informa Healthcare USA, Inc, New York, NY, USA, 2009.
- [60] G. M. Halliday, R. Bestak, K. S. Yuen, L. L. Cavanagh, and R. S. C. Barnetson, "UVA-induced immunosuppression," *Mutation Research*, vol. 422, no. 1, pp. 139–145, 1998.
- [61] D. L. Damian, R. S. C. Barnetson, and G. M. Halliday, "Low-dose UVA and UVB have different time courses for suppression of contact hypersensitivity to a recall antigen in humans," *Journal of Investigative Dermatology*, vol. 112, no. 6, pp. 939–944, 1999.
- [62] L. A. Applegate, R. D. Ley, J. Alcalay, and M. L. Kripke, "Identification of the molecular target for the suppression of contact hypersensitivity by ultraviolet radiation," *Journal of Experimental Medicine*, vol. 170, no. 4, pp. 1117–1131, 1989.
- [63] D. L. Damian, C. R. S. Patterson, M. Stapelberg, J. Park, R. S. C. Barnetson, and G. M. Halliday, "UV radiation-induced immunosuppression is greater in men and prevented by topical nicotinamide," *Journal of Investigative Dermatology*, vol. 128, no. 2, pp. 447–454, 2008.
- [64] E. Yiasemides, G. Sivapirabu, G. M. Halliday, J. Park, and D. L. Damian, "Oral nicotinamide protects against ultraviolet radiation-induced immunosuppression in humans," *Carcinogenesis*, vol. 30, no. 1, pp. 101–105, 2009.
- [65] D. L. Damian and G. M. Halliday, "Measurement of ultraviolet radiation-induced suppression of recall contact and delayed-type hypersensitivity in humans," *Methods*, vol. 28, no. 1, pp. 34–45, 2002.
- [66] G. Sivapirabu, E. Yiasemides, G. M. Halliday, J. Park, and D. L. Damian, "Topical nicotinamide modulates cellular energy metabolism and provides broad-spectrum protection against ultraviolet radiation-induced immunosuppression in humans," *British Journal of Dermatology*, vol. 161, no. 6, pp. 1357–1364, 2009.
- [67] G. De Murcia, V. Schreiber, M. Molinete et al., "Structure and function of poly(ADP-ribose) polymerase," *Molecular and Cellular Biochemistry*, vol. 138, no. 1-2, pp. 15–24, 1994.
- [68] G. De Murcia and J. Menissier-de Murcia, "Poly(ADP-ribose) polymerase: a molecular nick-sensor," *Trends in Biochemical Sciences*, vol. 19, no. 4, pp. 172–176, 1994.
- [69] S. Shall and G. De Murcia, "Poly(ADP-ribose) polymerase-1: what have we learned from the deficient mouse model?" *Mutation Research*, vol. 460, no. 1, pp. 1–15, 2000.
- [70] L. Virág and C. Szabó, "The therapeutic potential of poly(ADP-ribose) polymerase inhibitors," *Pharmacological Reviews*, vol. 54, no. 3, pp. 375–429, 2002.
- [71] G. J. Hageman and R. H. Stierum, "Niacin, poly(ADP-ribose) polymerase-1 and genomic stability," *Mutation Research*, vol. 475, no. 1-2, pp. 45–56, 2001.
- [72] M. Y. Kim, S. Mauro, N. Gévy, J. T. Lis, and W. L. Kraus, "NAD<sup>+</sup>-dependent modulation of chromatin structure and transcription by nucleosome binding properties of PARP-1," *Cell*, vol. 119, no. 6, pp. 803–814, 2004.

- [73] S. D. Skaper, "Poly(ADP-ribose) polymerase-1 in acute neuronal death and inflammation—a strategy for neuroprotection," in *Neuroprotective Agents*, W. Slikkerand, J. Andrews, and B. Tremblay, Eds., pp. 217–228, The New York Academy of Sciences, New York, NY, USA, 2003.
- [74] R. H. Stierum, M. H. M. Van Herwijnen, G. J. Hageman, and J. C. S. Kleinjans, "Increased poly(ADP-ribose) polymerase activity during repair of ( $\pm$ )-anti-benzo[a]pyrene diolepoxide-induced DNA damage in human peripheral blood lymphocytes in vitro," *Carcinogenesis*, vol. 15, no. 4, pp. 745–751, 1994.
- [75] C. Trucco, F. J. Oliver, G. De Murcia, and J. Menissier-de Murcia, "DNA repair defect in poly(ADP-ribose) polymerase-deficient cell lines," *Nucleic Acids Research*, vol. 26, no. 11, pp. 2644–2649, 1998.
- [76] M. Molinete, W. Vermeulen, A. Burkle, et al., "Overproduction of the poly(ADP-ribose)polymerase DNA-binding domain blocks alkylation-induced DNA-repair synthesis in mammalian-cells," *Embo Journal*, vol. 12, no. 5, pp. 2109–2117, 1993.
- [77] R. Ding and M. Smulson, "Depletion of nuclear poly(ADP-ribose)polymerase by antisense RNA expression-influences on genomic stability, chromatin organization and DNA-repair," *Faseb Journal*, vol. 8, no. 7, p. A1409, 1994.
- [78] F. Dantzer, H. P. Nasheuer, J. L. Vonesch, G. de Murcia, and J. Menissier-de Murcia, "Functional association of poly(ADP-ribose) polymerase with DNA polymerase alpha-primase complex: a link between DNA strand break detection and DNA replication," *Nucleic Acids Research*, vol. 26, no. 8, pp. 1891–1898, 1998.
- [79] M. S. Satoh, G. G. Poirier, and T. Lindahl, "Dual function for poly(ADP-ribose) synthesis in response to DNA strand breakage," *Biochemistry*, vol. 33, no. 23, pp. 7099–7106, 1994.
- [80] S. Chatterjee, S. J. Berger, and N. A. Berger, "Poly(ADP-ribose) polymerase: a guardian of the genome that facilitates DNA repair by protecting against DNA recombination," *Molecular and Cellular Biochemistry*, vol. 193, no. 1-2, pp. 23–30, 1999.
- [81] C. Trucco, V. Rolli, F. J. Oliver et al., "A dual approach in the study of poly (ADP-ribose) polymerase: in vitro random mutagenesis and generation of deficient mice," *Molecular and Cellular Biochemistry*, vol. 193, no. 1-2, pp. 53–60, 1999.
- [82] M. Masutani, T. Nozaki, K. Nakamoto et al., "The response of Parp knockout mice against DNA damaging agents," *Mutation Research*, vol. 462, no. 2-3, pp. 159–166, 2000.
- [83] Z.-Q. Wang, L. Stingl, C. Morrison et al., "PARP is important for genomic stability but dispensable in apoptosis," *Genes and Development*, vol. 11, no. 18, pp. 2347–2358, 1997.
- [84] J. Menissier-de Murcia, C. Niedergang, C. Trucco et al., "Requirement of poly(ADP-ribose) polymerase in recovery from DNA damage in mice and in cells," *Proceedings of the National Academy of Sciences of the United States of America*, vol. 94, no. 14, pp. 7303–7307, 1997.
- [85] M. Tsutsumi, M. Masutani, T. Nozaki et al., "Increased susceptibility of poly(ADP-ribose) polymerase-1 knockout mice to nitrosamine carcinogenicity," *Carcinogenesis*, vol. 22, no. 1, pp. 1–3, 2001.
- [86] F. D. Di Fagagna, M. P. Hande, W.-M. Tong, P. M. Lansdorp, Z.-Q. Wang, and S. P. Jackson, "Functions of poly(ADP-ribose) polymerase in controlling telomere length and chromosomal stability," *Nature Genetics*, vol. 23, no. 1, pp. 76–80, 1999.
- [87] M. A. Osley, T. Tsukuda, and J. A. Nickoloff, "ATP-dependent chromatin remodeling factors and DNA damage repair," *Mutation Research*, vol. 618, no. 1-2, pp. 65–80, 2007.
- [88] F. Li, Z. Z. Chong, and K. Maiese, "Cell life versus cell longevity: the mysteries surrounding the NAD<sup>+</sup> precursor nicotinamide," *Current Medicinal Chemistry*, vol. 13, no. 8, pp. 883–895, 2006.
- [89] B. W. Durkacz, O. Omidiji, D. A. Gray, and S. Shall, "(ADP-ribose)<sub>n</sub> participates in DNA excision repair," *Nature*, vol. 283, no. 5747, pp. 593–596, 1980.
- [90] E. L. Jacobson, P. U. Giacomoni, M. J. Roberts, G. T. Wondrak, and M. K. Jacobson, "Optimizing the energy status of skin cells during solar radiation," *Journal of Photochemistry and Photobiology B*, vol. 63, no. 1–3, pp. 141–147, 2001.
- [91] C. A. Benavente and E. L. Jacobson, "Niacin restriction upregulates NADPH oxidase and reactive oxygen species (ROS) in human keratinocytes," *Free Radical Biology and Medicine*, vol. 44, no. 4, pp. 527–537, 2008.
- [92] A. B. Weitberg, "Effect of nicotinic acid supplementation in vivo on oxygen radical-induced genetic damage in human lymphocytes," *Mutation Research*, vol. 216, no. 4, pp. 197–201, 1989.
- [93] N. A. Berger and G. W. Sikorski, "Nicotinamide stimulates repair of DNA damage in human lymphocytes," *Biochemical and Biophysical Research Communications*, vol. 95, no. 1, pp. 67–72, 1980.
- [94] J. L. Sims, S. J. Berger, and N. A. Berger, "Effects of nicotinamide on NAD and poly(ADP-ribose) metabolism in DNA-damaged human lymphocytes," *Journal of Supramolecular and Cellular Biochemistry*, vol. 16, no. 3, pp. 281–288, 1981.
- [95] E. Kjellen, G. G. Jonsson, R. W. Pero, and P.-I. Christensson, "Effects of hyperthermia and nicotinamide on DNA repair synthesis, ADP-ribosyl transferase activity, NAD<sup>+</sup> and ATP pools, and cytotoxicity in  $\gamma$ -irradiated human mononuclear leukocytes," *International Journal of Radiation Biology*, vol. 49, no. 1, pp. 151–162, 1986.
- [96] J. E. Cleaver and J. E. Trosko, "Defective stage of DNA repair in a human disease, xeroderma pigmentosum," *Radiation Research*, vol. 39, no. 2, p. 471, 1969.
- [97] M. Miwa, M. Kanai, T. Kondo, H. Hoshino, K. Ishihara, and T. Sugimura, "Inhibitors of poly(ADP-ribose)polymerase enhance unscheduled DNA-synthesis in human peripheral lymphocytes," *Biochemical and Biophysical Research Communications*, vol. 100, no. 1, pp. 463–470, 1981.
- [98] K. Tang, H. Sham, E. Hui, and J. B. Kirkland, "Niacin deficiency causes oxidative stress in rat bone marrow cells but not through decreased NADPH or glutathione status," *Journal of Nutritional Biochemistry*, vol. 19, no. 11, pp. 746–753, 2008.
- [99] V. O. Melnikova and H. N. Ananthaswamy, "Cellular and molecular events leading to the development of skin cancer," *Mutation Research*, vol. 571, no. 1-2, pp. 91–106, 2005.
- [100] A. Svobodova, D. Walterova, and J. Vostalova, "Ultraviolet light induced alteration to the skin," *Biomedical papers of the Medical Faculty of the University Palacký, Olomouc, Czechoslovakia*, vol. 150, no. 1, pp. 25–38, 2006.
- [101] G. M. Halliday, "Inflammation, gene mutation and photoimmunosuppression in response to UVR-induced oxidative damage contributes to photocarcinogenesis," *Mutation Research*, vol. 571, no. 1-2, pp. 107–120, 2005.
- [102] A. C. Boyonoski, J. C. Spronck, L. M. Gallacher et al., "Niacin deficiency decreases bone marrow poly(ADP-ribose) and the latency of ethylnitrosourea-induced carcinogenesis in rats," *Journal of Nutrition*, vol. 132, no. 1, pp. 108–114, 2002.

- [103] J. C. Spronck and J. B. Kirkland, "Niacin deficiency increases spontaneous and etoposide-induced chromosomal instability in rat bone marrow cells *in vivo*," *Mutation Research*, vol. 508, no. 1-2, pp. 83–97, 2002.
- [104] J. C. Spronck, J. L. Nickerson, and J. B. Kirkland, "Niacin deficiency alters p53 expression and impairs etoposide-induced cell cycle arrest and apoptosis in rat bone marrow cells," *Nutrition and Cancer*, vol. 57, no. 1, pp. 88–99, 2007.
- [105] L. M. Kostecki, M. Thomas, G. Linford et al., "Niacin deficiency delays DNA excision repair and increases spontaneous and nitrosourea-induced chromosomal instability in rat bone marrow," *Mutation Research*, vol. 625, no. 1-2, pp. 50–61, 2007.
- [106] J. B. Kirkland, "Niacin status and treatment-related leukemogenesis," *Molecular Cancer Therapeutics*, vol. 8, no. 4, pp. 725–732, 2009.
- [107] V. Rolli, R. Armin, A. Augustin, G. Schulz, J. Menissier-de Murcia, and G. de Murcia, *Poly ADP-Ribosylation Reactions: From DNA Damage and Stress Signalling to Cell Death*, Oxford University Press, Oxford, UK, 2000.
- [108] G. E. N. Kass, J. E. Eriksson, M. Weis, S. Orrenius, and S. C. Chow, "Chromatin condensation during apoptosis requires ATP," *Biochemical Journal*, vol. 318, no. 3, pp. 749–752, 1996.
- [109] C. Richter, M. Schweizer, A. Cossarizza, and C. Franceschi, "Control of apoptosis by the cellular ATP level," *FEBS Letters*, vol. 378, no. 2, pp. 107–110, 1996.
- [110] C. Stefanelli, F. Bonavita, I. Stanic' et al., "ATP depletion inhibits glucocorticoid-induced thymocyte apoptosis," *Biochemical Journal*, vol. 322, no. 3, pp. 909–917, 1997.
- [111] D. Ferrari, A. Stepczynska, M. Los, S. Wesselborg, and K. Schulze-Osthoff, "Differential regulation and ATP requirement for caspase-8 and caspase-3 activation during CD95- and anticancer drug-induced apoptosis," *Journal of Experimental Medicine*, vol. 188, no. 5, pp. 979–984, 1998.
- [112] S. D. Park, C. G. Kim, and M. G. Kim, "Inhibitors of poly(ADP-ribose) polymerase enhance DNA strand breaks, excision repair, and sister chromatid exchanges induced by alkylating agents," *Environmental Mutagenesis*, vol. 5, no. 4, pp. 515–525, 1983.
- [113] R. W. Pero, B. Axelsson, D. Siemann, D. Chaplin, and G. Dougherty, "Newly discovered anti-inflammatory properties of the benzamides and nicotinamides," *Molecular and Cellular Biochemistry*, vol. 193, no. 1-2, pp. 119–125, 1999.
- [114] E. Riklis, R. Kol, and R. Marko, "Trends and developments in radioprotection: the effect of nicotinamide on DNA repair," *International Journal of Radiation Biology*, vol. 57, no. 4, pp. 699–708, 1990.
- [115] H. Zheng and P. L. Olive, "Reduction of tumor hypoxia and inhibition of DNA repair by nicotinamide after irradiation of SCCVII murine tumors and normal tissues," *Cancer Research*, vol. 56, no. 12, pp. 2801–2808, 1996.
- [116] F. R. Althaus, S. D. Lawrence, G. L. Sattler, and H. C. Pitot, "The effect of nicotinamide on unscheduled DNA synthesis in cultured hepatocytes," *Biochemical and Biophysical Research Communications*, vol. 95, no. 3, pp. 1063–1070, 1980.
- [117] A. Oikawa, H. Tohda, M. Kanai, M. Miwa, and T. Sugimura, "Inhibitors of poly(adenosine diphosphate ribose) polymerase induce sister chromatid exchanges," *Biochemical and Biophysical Research Communications*, vol. 97, no. 4, pp. 1311–1316, 1980.
- [118] T. Utakoji, K. Hosoda, K. Umezawa, and M. Sawamura, "Induction of sister chromatid exchanges by nicotinamide in chinese-hamster lung fibroblasts and human-lymphoblastoid cells," *Biochemical and Biophysical Research Communications*, vol. 90, no. 4, pp. 1147–1152, 1979.
- [119] J. B. Kirkland, "Niacin status, NAD distribution and ADP-ribose metabolism," *Current Pharmaceutical Design*, vol. 15, no. 1, pp. 3–11, 2009.
- [120] P. W. Rankin, E. L. Jacobson, R. C. Benjamin, J. Moss, and M. K. Jacobson, "Quantitative studies of inhibitors of ADP-ribosylation *in vitro* and *in vivo*," *Journal of Biological Chemistry*, vol. 264, no. 8, pp. 4312–4317, 1989.
- [121] R. L. Thies and A. P. Autor, "Reactive oxygen injury to cultured pulmonary artery endothelial cells: mediation by poly(ADP-ribose) polymerase activation causing NAD depletion and altered energy balance," *Archives of Biochemistry and Biophysics*, vol. 286, no. 2, pp. 353–363, 1991.
- [122] D. G. Hoyt and J. S. Lazo, "NAD depletion after *in vitro* exposure of murine lung slices to bleomycin," *Biochemical Pharmacology*, vol. 46, no. 10, pp. 1819–1824, 1993.
- [123] B. Farkas, M. Magyarlaki, B. Csete et al., "Reduction of acute photodamage in skin by topical application of a novel PARP inhibitor," *Biochemical Pharmacology*, vol. 63, no. 5, pp. 921–932, 2002.
- [124] V. A. Tronov, E. M. Konstantinov, E. Petrakou, S. Tsilimigaki, and S. M. Piperakis, "Nicotinamide "protects" resting lymphocytes exposed to hydrogen peroxide from necrosis but not from apoptosis," *Cell Biology and Toxicology*, vol. 18, no. 6, pp. 359–367, 2002.
- [125] S. Coppola, C. Nosseri, V. Maresca, and L. Ghibelli, "Different basal NAD levels determine opposite effects of poly(ADP-ribose)polymerase inhibitors on H<sub>2</sub>O<sub>2</sub>-induced apoptosis," *Experimental Cell Research*, vol. 221, no. 2, pp. 462–469, 1995.
- [126] L. K. Klaidman, S. K. Mukherjee, T. P. Hutchin, and J. D. Adams, "Nicotinamide as a precursor for NAD<sup>+</sup> prevents apoptosis in the mouse brain induced by tertiary-butylhydroperoxide," *Neuroscience Letters*, vol. 206, no. 1, pp. 5–8, 1996.
- [127] M. Leist, B. Single, A. F. Castoldi, S. Kühnle, and P. Nicotera, "Intracellular adenosine triphosphate (ATP) concentration: a switch in the decision between apoptosis and necrosis," *Journal of Experimental Medicine*, vol. 185, no. 8, pp. 1481–1486, 1997.
- [128] M. Leist, B. Single, H. Naumann et al., "Inhibition of mitochondrial ATP generation by nitric oxide switches apoptosis to necrosis," *Experimental Cell Research*, vol. 249, no. 2, pp. 396–403, 1999.
- [129] S. K. Mukherjee, L. K. Klaidman, R. Yasharel, and J. D. Adams Jr., "Increased brain NAD prevents neuronal apoptosis *in vivo*," *European Journal of Pharmacology*, vol. 330, no. 1, pp. 27–34, 1997.
- [130] J. L. Lelli Jr., L. L. Becks, M. I. Dabrowska, and D. B. Hinshaw, "ATP converts necrosis to apoptosis in oxidant-injured endothelial cells," *Free Radical Biology and Medicine*, vol. 25, no. 6, pp. 694–702, 1998.
- [131] W. Lieberthal, S. A. Menza, and J. S. Levine, "Graded ATP depletion can cause necrosis or apoptosis of cultured mouse proximal tubular cells," *American Journal of Physiology*, vol. 274, no. 2, pp. F315–F327, 1998.
- [132] Z.-H. Ran, B. Rayet, J. Rommelaere, and S. Faisst, "Parvovirus H-1-induced cell death: influence of intracellular

- NAD consumption on the regulation of necrosis and apoptosis," *Virus Research*, vol. 65, no. 2, pp. 161–174, 1999.
- [133] C. L. Crowley, C. M. Payne, H. Bernstein, C. Bernstein, and D. Roe, "The NAD<sup>+</sup> precursors, nicotinic acid and nicotinamide protect cells against apoptosis induced by a multiple stress inducer, deoxycholate," *Cell Death and Differentiation*, vol. 7, no. 3, pp. 314–326, 2000.
- [134] G. De Murcia, A. Huletsky, and D. Lamarres, "Modulation of chromatin superstructure induced by poly(ADP-ribose) synthesis and degradation," *Journal of Biological Chemistry*, vol. 261, no. 15, pp. 7011–7017, 1986.
- [135] T. Lindahl, M. S. Satoh, G. G. Poirier, and A. Klungland, "Post-translational modification of poly(ADP-ribose) polymerase induced by DNA strand breaks," *Trends in Biochemical Sciences*, vol. 20, no. 10, pp. 405–411, 1995.
- [136] D. Martín-Oliva, F. O'Valle, J. A. Muñoz-Gámez et al., "Crosstalk between PARP-1 and NF- $\kappa$ B modulates the promotion of skin neoplasia," *Oncogene*, vol. 23, no. 31, pp. 5275–5283, 2004.
- [137] A. S. Baldwin, "The transcription factor NF- $\kappa$ B and human disease," *Journal of Clinical Investigation*, vol. 107, no. 1, pp. 3–6, 2001.
- [138] K. Brand, P. A. Bauerle, A. K. Walli, and D. Neumeier, "The role of NF-kappa B in the pathogenesis of atherosclerosis," *Journal of Physiology*, vol. 491P, pp. S2–S2, 1996.
- [139] I. V. Budunova, P. Perez, V. R. Vaden, V. S. Spiegelman, T. J. Slaga, and J. L. Jorcano, "Increased expression of p50-NF- $\kappa$ B and constitutive activation of NF- $\kappa$ B transcription factors during mouse skin carcinogenesis," *Oncogene*, vol. 18, no. 52, pp. 7423–7431, 1999.
- [140] P. O. Hassa and M. O. Hottiger, "A role of poly (ADP-Ribose) polymerase in NF- $\kappa$ B transcriptional activation," *Biological Chemistry*, vol. 380, no. 7-8, pp. 953–959, 1999.
- [141] F. J. Oliver, J. Menissier-de Murcia, C. Nacci et al., "Resistance to endotoxic shock as a consequence of defective NF- $\kappa$ B activation in poly (ADP-ribose) polymerase-1 deficient mice," *EMBO Journal*, vol. 18, no. 16, pp. 4446–4454, 1999.
- [142] D. Martín-Oliva, R. Aguilar-Quesada, F. O'Valle et al., "Inhibition of poly(ADP-ribose) polymerase modulates tumor-related gene expression, including hypoxia-inducible factor-1 activation, during skin carcinogenesis," *Cancer Research*, vol. 66, no. 11, pp. 5744–5756, 2006.
- [143] R. W. Pero, B. Axelsson, D. Siemann, D. Chaplin, and G. Dougherty, "Newly discovered anti-inflammatory properties of the benzamides and nicotinamides," *Molecular and Cellular Biochemistry*, vol. 193, no. 1-2, pp. 119–125, 1999.
- [144] T. Nozaki, H. Fujihara, M. Watanabe et al., "Parp-1 deficiency implicated in colon and liver tumorigenesis induced by azoxymethane," *Cancer Science*, vol. 94, no. 6, pp. 497–500, 2003.
- [145] E.-J. Yeo, Y.-S. Chun, and J.-W. Park, "New anticancer strategies targeting HIF-1," *Biochemical Pharmacology*, vol. 68, no. 6, pp. 1061–1069, 2004.
- [146] M. Ueda, "Telomerase in cutaneous carcinogenesis," *Journal of Dermatological Science*, vol. 23, no. 1, pp. S37–S40, 2000.
- [147] M. Oren, "Decision making by p53: life, death and cancer," *Cell Death and Differentiation*, vol. 10, no. 4, pp. 431–442, 2003.
- [148] C. L. Brooks and W. Gu, "Ubiquitination, phosphorylation and acetylation: the molecular basis for p53 regulation," *Current Opinion in Cell Biology*, vol. 15, no. 2, pp. 164–171, 2003.
- [149] C. M. Simbulan-Rosenthal, D. S. Rosenthal, R. Luo, and M. E. Smulson, "Poly(ADP-ribosylation) of p53 during apoptosis in human osteosarcoma cells," *Cancer Research*, vol. 59, no. 9, pp. 2190–2194, 1999.
- [150] C. M. Whitacre, H. Hashimoto, M.-L. Tsai, S. Chatterjee, S. J. Berger, and N. A. Berger, "Involvement of NAD-poly(ADP-Ribose) metabolism in p53 regulation and its consequences," *Cancer Research*, vol. 55, no. 17, pp. 3697–3701, 1995.
- [151] L. A. Donehower, M. Harvey, B. L. Slagle et al., "Mice deficient for p53 are developmentally normal but susceptible to spontaneous tumours," *Nature*, vol. 356, no. 6366, pp. 215–221, 1992.
- [152] K. G. McLure, M. Takagi, and M. B. Kastan, "NAD<sup>+</sup> modulates p53 DNA binding specificity and function," *Molecular and Cellular Biology*, vol. 24, no. 22, pp. 9958–9967, 2004.

## Research Article

# Preparation of DNA Ladder Based on Multiplex PCR Technique

**Tian-Yun Wang, Li Guo, and Jun-he Zhang**

*Department of Biochemistry and Molecular Biology, Xinxiang Medical University, Henan 453003, China*

Correspondence should be addressed to Tian-Yun Wang, wtianyuncn@126.com

Received 14 February 2010; Revised 26 April 2010; Accepted 11 May 2010

Academic Editor: Ashis Basu

Copyright © 2010 Tian-Yun Wang et al. This is an open access article distributed under the Creative Commons Attribution License, which permits unrestricted use, distribution, and reproduction in any medium, provided the original work is properly cited.

DNA molecular weight standard control, also called DNA marker (ladder), has been widely used in the experiments of molecular biology. In the paper, we report a method by which DNA marker was prepared based on multiple PCR technique. 100–1000 bp DNA fragments were amplified using the primers designed according to the 6631 ~ 7630 position of lambda DNA. Target DNA fragments were amplified using Touchdown PCR combined with hot start PCR, respectively, followed extracted by phenol/chloroform, precipitated with ethanol and mixed thoroughly. The results showed that the 100–1000 bp DNA fragments were successfully obtained in one PCR reaction, the bands of prepared DNA marker were clear, the size was right and could be used as control in the molecular biology experiment. This method could save time and be more inexpensive, rapid, simple when compared with the current DNA Ladder prepared means.

## 1. Introduction

It is necessary to determine the molecular weight (mw) or the base pair (bp) length of nucleic acids in the field of molecular biology. This need encompasses weights or lengths of nucleic acids from sizes ranging from mega bps down to very short oligonucleotides of only a few bp's. Traditionally the base pair length of the nucleic acid has been obtained by comparing the behavior of a nucleic acid under analysis with the behavior of another nucleic acid of defined length and usually but not necessarily of known sequence. Such methods may be electrophoresis, gel filtration chromatography, ultracentrifugation and like methods well known to those in the art. Because of the simplicity of the equipment, ease of use and resolving power to the technique, electrophoresis is the technique most frequently employed to determine the size of nucleic acids.

Double stranded DNA standards were typically prepared from DNA of bacteriophages or plasmids [1, 2]. This process requires the propagation of the virus or plasmid in the appropriate host organism, the purification of the viral or plasmid DNA from the nucleic acids of the host, the digestion of the purified DNA with restriction endonucleases, and the purification of the resulting fragments from undigested DNA

and the restriction enzyme. This process was labor, material, and equipment intensive, especially for preparation of large quantities of DNA. Restriction enzyme digested bacteriophage DNA such as Lambda was frequently employed as molecular weight markers. The array of fragment lengths in obtained bp's depended on the nature of the restriction enzyme, the DNA sequence composition, and the conditions employed. Each combination of restriction enzymes, DNA, and conditions provided a unique array of DNA fragments of defined lengths [3, 4].

The polymerase chain reaction (PCR) has been widely applied to the fields of molecular biology, genetics, biochemistry, genetic engineering, forensics, and the like. PCR is a simple, effectively and conveniently method and could prepare amount oligonucleotides in a very short time. However, preparing DNA ladder using common PCR was laborious. Different standard fragments were mixed according to some proportion, which were amplified and concentrated from many PCR products. So, different bands may be a standard to identify and evaluate the length of samples. However, most of DNA ladder had too many bands to be amplified by PCR, respectively, which led to great human resource, material resource, and wealth resource though which was industrialization, industry and sequencing. It is very important to

TABLE 1: Primers used in the experiment.

Length (bp)	Primer	Position
1000	5'-GCGGCACGGAGTGGAGCAAG-3'	6631
900	5'-GTTTCGATCCGAAAGGCTGGGCGCT-3'	6731
800	5'-AAAGACCTGGGCAAAGCGGTGT-3'	6831
700	5'-TCCTGCCGCACAACACGATG-3'	6931
600	5'-ACGCCTCTGCCCGTTACCCGAA-3'	7031
500	5'-GATGAGTTTCGTGTCCGTACAACGTG-3'	7131
400	5'-CCGCTCGCTGGGTGAACAA-3'	7231
300	5'-ACGGATGAAACTGCCGGTCAGGACA-3'	7331
200	5'-TGGATACGTCTGAACTGGTCACGGT-3'	7521
100	5'-AACGGCGTTTCGTGTCTCTGCCGGT-3'	7531
0:	5'-GTTATCGAAATCAGCCACAGGGC-3'	7630

find a new method to produce DNA ladder with a rapid, simple way to reduce costs and improve production. A new way for batch production will be described firstly in this study.

## 2. Materials and Methods

**2.1. PCR Primers.** According to the lambda phage DNA sequence (GenBank accession no: J02459), the sequences from 6631–7630 bp were selected and covered. The 1 000 bp primer represents the region in length from 6631–7630, 900 bp primer from 6731–7630, 800 bp primer from 6831–7630, 700 bp primer from 6931–7630, 600 bp primer from 7031–7630, 500 bp primer from 7131–7630, 400 bp primer from 7231–7630, the 300 bp primer from 7331–7630, the 200 bp primer from 7431–7630, and the 100 bp primer from 7531–7630 of the lambda target sequence. Deoxyoligonucleotides were synthesized using phosphoramidite chemistry and were obtained from Shanghai Sangon Company, China. The primers were shown as in Table 1.

**2.2. PCR Amplification and Preparation of DNA Ladder.** 100–1000 bp fragments were amplified by multiplex PCR using ten primer pairs in one PCR tube with the same sense primer. The template DNA (15–35 ng) was added to a 25  $\mu$ l reaction mixture containing 50 mM KCl, 10 mM Tris-HCl(pH 8.3), 2.0 mM MgCl<sub>2</sub>, 75 pmol of sense primer, 5 pmol of each 100–500 bp antisense primer, 10 pmol of each 600–1000 bp anti-sense primer, 0.3 mM dNTPs, and 5 unit of Taq DNA polymerase. Taq DNA polymerase was added using hot start method. PCR was performed using a PxE (Thermo) thermocycler with a temperature profile of 35 cycles, which contained 2 cycles at 95°C for 30 s, 56°C for 30 s, and 72°C for 1 min, 2 cycles 95°C for 30 s, 54°C for 30 s and 72°C for 1 min, 2 cycles for every annealing temperature interval 2 temperature, until 44°C polishing 35 cycles. PCR products were detected by 2% agarose gel with 120 V voltages for 40 min.

5  $\mu$ l of each PCR reaction mixture was screened on 2% agarose gel electrophoresis and the length was estimated by comparing the known size DNA marker (Sangon), then

was purified and sequenced by Sangon Company. The PCR products were extracted through phenol/chloroform and precipitated with ethanol, and then analyzed their UV absorbance under 260 nm. 5  $\mu$ l aliquot of the material was electrophoresed and no change in the band migration pattern or band intensities was observed following ethidium bromide staining. The marker was then frozen at –20°C.

## 3. Results and Discussion

All fragments of 100–1000 bp were amplified successfully with multiplex PCR way by optimizing process in the PCR reaction system and temperature profile (Figure 1). Finally, with the help of touch down PCR and hot start PCR technique, all the ten DNA fragments were obtained by multiplex PCR. At first, the same amount of ten primer pairs were added to a reaction system, and the annealing temperature profile from 58°C to 48°C for 30 cycles (Figure 1(a)), and the annealing temperature profile from 58°C to 48°C for 35 cycles (Figure 1(b)), 100–500 bp fragments were amplified by this method. Adjusting the amount of the ten anti-sense primers and the annealing temperature profile from 56°C to 46°C, most of target fragments were detected. (Figure 1(c)) Finally, raising the amount of 600–700 bp anti-sense primers and using the annealing temperature profile from 56°C to 44°C, all the target fragments were amplified and nonspecific fragments disappeared (Figure 1(d)).

PCR has become a widely used tool for detection, identification, and differentiation of pathogenic microorganisms in diagnosis of animal and human diseases or other studies [5]. More and more derived PCR techniques were devised for different study purpose, for instance, multiplex PCR technique, which has been widely used to detect and identify some unknown and possible pathogenic microorganisms in some diseases. Using several primer pairs, each having a particular specificity, in the same reaction added a multidimensional perspective to the diagnostic potential of PCR. Such a procedure allowed simultaneous detection of two or more different microbial agents in a single sample and the inclusion of internal controls. As multiplex PCR involved a far more complex reaction system than the normal

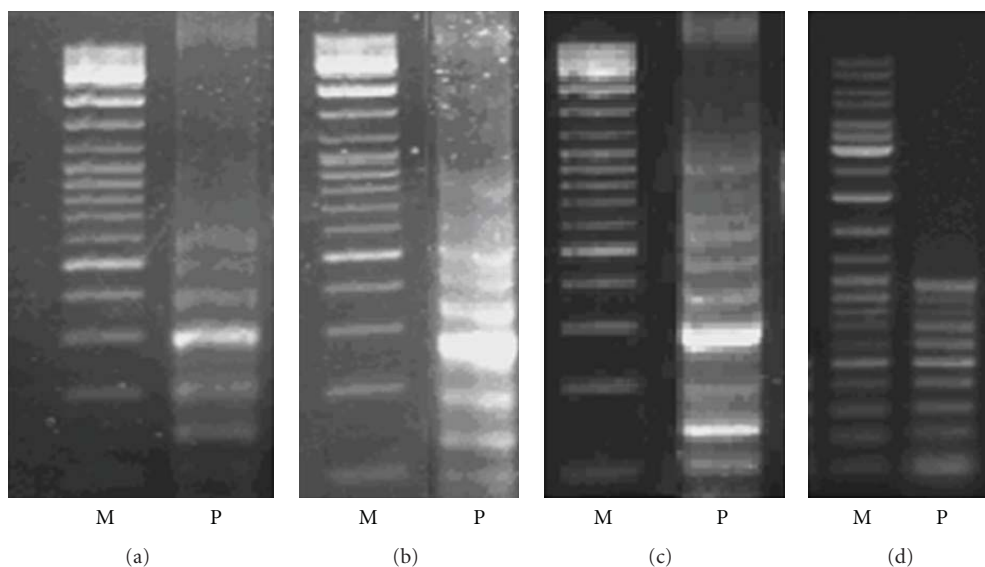


FIGURE 1: Illustrations of the PCR products for adjusting reaction system and temperature profile. 100–1000 bp fragments were amplified by multiplex PCR using 10 primer pairs in a PCR tube which have the same sense primer. (a) the annealing temperature profile from 58°C to 48°C for 30 cycles; (b) 100–500 bp fragments were amplified under the annealing temperature profile from 58°C to 46°C for 35 cycles. (c) Adjusting the amount of the ten anti-sense primers and the annealing temperature profile from 56°C to 46°C, most of target fragments were detected; (d) Raising the amount of 600–700 bp anti-sense primers and using the annealing temperature profile from 56°C to 44°C, all the target fragments were amplified and nonspecific fragments disappeared.

simplex mode, so its performance was more difficult to predict and could be assessed only after extensive trials [5]. Thus, quite a number of currently used protocols could be further optimized to exclude nonspecific reactions. In the present paper, ten primer pairs was added to a reaction system to amplify ten different fragments. We optimized the reaction system and reaction to avoid nonspecific reactions and primer dimer, target sequences as defined by primer binding sites had been checked carefully in order to insure high specificity of detection. In addition, using hot start and touch down PCR method, adjusting the quantity of each primer and annealing temperature were available to improve the performance of the amplification reaction. The basic idea of hot-start PCR was to reduce nonspecific amplification in the initial phase by releasing active enzyme only immediately before the first primer binding step [6]. Another kind of PCR, touch down PCR could design a continuous and touchdown annealing temperature range to amplify some fragments [7]. This approach was designed to prevent primer dimer formation, mispriming, and spontaneous initiation of DNA strand synthesis [8]. Finally, with the undisputed success ten fragments based on the multiplex PCR with touch down PCR and hot start were amplified and detected clearly (Figure 1).

Compared with conventional methods for producing DNA Marker, multiplex PCR method could reduce costs and raise production in laboratory once. Undoubtedly the demand for multiplex PCR method is going to increase further purpose in future because of the potential to reduce costs, human and material resource, and raise throughput in the same time for batch production.

## Acknowledgments

This work was partly supported by the grants from the Natural Science Foundation of Henan Province, China (no. 511042300, 624410041) and Science & Technology Innovation Talents in University of Henan Province (2008HASTIT026).

## References

- [1] L. J. Wei, Y. T. Wei, X. F. Huang, X. Q. Wei, and R. B. Huang, "Construction of a new kind of DNA marker vector," *Biotechnology*, vol. 14, no. 5, pp. 33–35, 2004.
- [2] C. J. Zhu, Q. Y. Wei, W. L. Qu, and H. Ding, "Experimental study on making a new DNA marker from positive and negative DNA samples," *Acta Medicinæ Sinica*, vol. 18, pp. 937–938, 2005.
- [3] Hyman, "DNA ladders," US Patent no. 5,840,575, 1999.
- [4] A-li W. Hu, J. L. Hartley, and H. J. Jordan, "Nucleic acid ladders," US Patent no. 6,924,098, 2005.
- [5] J. L. Hartley, "Nucleic acid marker ladder for estimating mass," US Patent no. 7,132,520, 2006.
- [6] Dawson, "Method for the multiplexed preparation of nucleic acid molecular weight markers and resultant products," US Patent no. 5,714,326, 1998.
- [7] D. J. Korbie and J. S. Mattick, "Touchdown PCR for increased specificity and sensitivity in PCR amplification," *Nature Protocols*, vol. 3, no. 9, pp. 1452–1456, 2008.
- [8] I. Smolina, C. Lee, and M. Frank-Kamenetsk II, "Detection of low-copy-number genomic DNA sequences in individual bacterial cells by using peptide nucleic acid-assisted rolling-circle amplification and fluorescence in situ hybridization," *Applied and Environmental Microbiology*, vol. 73, no. 7, pp. 2324–2328, 2007.